

BLM - ALASKA RESOURCES LIBRARY
Permafrost
3-0 55 0091-2083 2

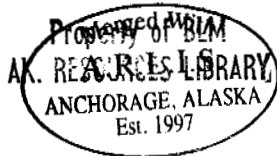
**North American
Contribution**

Permafrost

**Second International
Conference**

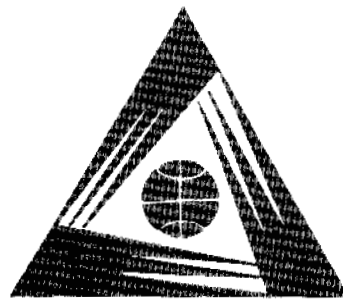


**NATIONAL ACADEMY
OF SCIENCES**



NOV 10 1973

GB
641
.I6
1973a



North American
Contribution

Permafrost

Second International
Conference

Yakutsk

13-28 July 1973
Yakutsk, U.S.S.R.

ORGANIZING COMMITTEE OF CANADA,
National Research Council of Canada
and
UNITED STATES PLANNING COMMITTEE,
U.S. National Academy of Sciences
National Academy of Engineering
National Research Council

NATIONAL ACADEMY OF SCIENCES
Washington, D.C. 1973

ARLIS

Alaska Resources
Library & Information Services
Anchorage, Alaska

Library of Congress Cataloging in Publication Data

International Conference on Permafrost, 2d, Yakutsk,
Siberia, 1973.

Permafrost: North American contribution [to the]
Second International Conference.

Includes bibliographies.

1. Frozen ground--North America--Congresses.
 2. Frozen ground--Antarctic regions--Congresses.
- I. Organizing Committee of Canada for the 2d International Conference on Permafrost. II. United States Planning Committee for the 2d International Conference on Permafrost. III. Title.

GB643.I57 1973 551.3'84 73-7881
ISBN 0-309-02115-4

Available from

Printing and Publishing Office, National Academy of Sciences
2101 Constitution Avenue, N.W., Washington, D.C. 20418

Printed in the United States of America

PREFACE

On behalf of the many North American scientists and technologists of the permafrost research community, the Organizing Committee of Canada and the United States Planning Committee present this contribution to the Second International Conference on Permafrost in order to further the international exchange of information among the many relevant disciplines and to focus attention on research needs.

The Second International Conference on Permafrost stems from a resolution adopted by participants in the First International Conference held in 1963. That resolution called for the organization of a second conference with the objective of furthering interdisciplinary exchange of information in the field.

The First International Conference on Permafrost, held at Purdue University in the United States, was presented by the Building Research Advisory Board of the U.S. National Research Council. This was the first international, interdisciplinary conference attended by research scientists and technologists to be devoted exclusively to scientific and developmental problems associated with perennially frozen ground.

Accelerated developmental activities in the cold regions of the earth have greatly increased the need for fundamental knowledge and for knowledge of sound developmental practices. For this reason, at the request of the Organizing Committee of Canada and the United States Planning Committee, the planned scope of the second conference was broadened to include consideration of environmental, ecological, and resource development issues.

Cooperation between the Canadian Organizing Committee and the U.S. Planning Committee for the conference has

resulted in this joint presentation of the North American contribution. This cooperative effort stems from the request of the conference host, the U.S.S.R. Conference Organizing Committee, for seven summary review papers from North America covering the seven main conference topics. Inasmuch as the papers were to cover all North American permafrost-related research, both a United States and a Canadian permafrost research expert were selected to co-author each of these seven papers. The decision to include all of the North American contribution in a single presentation followed.

The review papers, which appear at the beginning of each session, represent the basis for oral presentations at the conference by the 14 summary review paper co-authors. The methods by which these papers were prepared vary because of the nature of the subject matter and disciplines covered and the extent of research in the respective countries.

The remaining papers that appear in each session are summarized in the review papers and were accepted by the Canadian and the United States committees for their contribution to an understanding of permafrost in North America. However, each of these papers are the individual contribution of the author(s) and the findings and conclusions reported in each are those of the author(s).

The committee chairmen gratefully acknowledge the efforts and cooperation of the members of the committees, the summary review authors, the authors of the 79 papers, the agencies and organizations, and the committees' sponsors who have made this contribution to the Second International Conference possible.

TROY L. PÉWÉ, *Chairman*
United States Planning Committee

J. ROSS MACKAY, *Chairman*
Organizing Committee of Canada

CONTENTS

Session I Thermal Aspects of Permafrost Formation and Evolution

Thermal Conditions in Permafrost—A Review of North American Literature <i>Lorne W. Gold and Arthur H. Lachenbruch</i>	3
Influence of Climatic and Terrain Factors on Ground Temperatures at Three Locations in the Permafrost Region of Canada <i>Roger J. E. Brown</i>	27
Deep Temperature Observations in the Canadian North <i>A. S. Judge</i>	35
A General Solution for the Two-Dimensional, Transient Heat Conduction Problem in Permafrost, Using Implicit, Finite Difference Methods <i>Raymond Milton Kliewer</i>	41
Thermal Disturbance Due to Channel Shifting, Mackenzie Delta, N.W.T., Canada <i>M. W. Smith and C. T. Hwang</i>	51
Ecological Effects of River Flooding and Forest Fires on Permafrost in the Taiga of Alaska <i>Leslie A. Viereck</i>	60

Session II Regional Distribution and Characteristics of Permafrost

Distribution of Permafrost in North America and Its Relationship to the Environment: A Review, 1963-1973 <i>Roger J. E. Brown and Troy L. Péwé</i>	71
A Geoecological Terrain Analysis of Discontinuously Frozen Ground in the Upper Mackenzie River Valley, Canada <i>C. B. Crampton and N. W. Rutter</i>	101
A Spatial Correlation between Plant Distribution and Unfrozen Ground within a Region of Discontinuous Permafrost <i>Don Gill</i>	105
Indirect Mapping of the Snowcover for Permafrost Prediction at Schefferville, Quebec <i>Hardy B. Granberg</i>	113
Permafrost and Its Relationship to Other Environmental Parameters in a Midlatitude, High-Altitude Setting, Front Range, Colorado Rocky Mountains <i>Jack D. Ives</i>	121
Postglacial Permafrost Features in Eastern Canada <i>Daniel Lagarec</i>	126
The Occurrence and Characteristics of Nearshore Permafrost, Northern Alaska <i>Robert I. Lewellen</i>	131
Geophysical Identification of Frozen and Unfrozen Ground, Antarctica <i>L. D. McGinnis, K. Nakao, and C. C. Clark</i>	136
Permafrost Considerations in Land Use Planning Management <i>Curtis V. McVee</i>	146
Permafrost and Snowcover Relationships near Schefferville <i>Frank H. Nicholson and Hardy B. Granberg</i>	151

viii CONTENTS

Studies at the Timmins 4 Permafrost Experimental Site <i>Frank H. Nicholson and Bruce G. Thom</i>	159
Geochemistry of Permafrost and Quaternary Stratigraphy <i>Troy L. Péwé and Paul V. Sellmann</i>	166
Stratigraphy and Diagenesis of Perennially Frozen Sediments in the Barrow, Alaska, Region <i>Paul V. Sellmann and Jerry Brown</i>	171

Session III Genesis, Composition, and Structure of Frozen Ground and Ground Ice

† Origin, Composition, and Structure of Perennially Frozen Ground and Ground Ice: A Review <i>J. Ross Mackay and Robert F. Black</i>	185
Growth of Patterned Ground in Victoria Land, Antarctica <i>Robert F. Black</i>	193
† Thermokarst Development, Banks Island, Western Canadian Arctic <i>H. M. French and P. Egginton</i>	203
Glacial Permafrost and Pleistocene Ice Ages <i>T. Hughes</i>	213
Problems in the Origin of Massive Icy Beds, Western Arctic, Canada <i>J. Ross Mackay</i>	223
A Simulation Sensitivity Analysis of the Needle Ice Growth Environment <i>Samuel I. Outcalt</i>	228
Rates of Mass Wasting in the Ruby Range, Yukon Territory <i>Larry W. Price</i>	235
Soil Development and Patterned Ground Evolution in Beacon Valley, Antarctica <i>F. C. Ugolini, J. G. Bockheim, and Duwayne M. Anderson</i>	246

Session IV Physics, Physical Chemistry, and Mechanics of Frozen Ground and Ice

Physics, Chemistry, and Mechanics of Frozen Ground: A Review <i>Duwayne M. Anderson and N. R. Morgenstern</i>	257
The Unfrozen Water and the Apparent Specific Heat Capacity of Frozen Soils <i>Duwayne M. Anderson, Allen R. Tice, and Harlan L. McKim</i>	289
Mechanical Properties of Frozen Ground under High Pressure <i>Edwin Chamberlain</i>	295
Effect of Porosity on Amount of Soil Water Transferred in a Freezing Silt <i>Alfreds R. Jumikis</i>	305
Evaluation of <i>in situ</i> Creep Properties of Frozen Soils with the Pressuremeter <i>B. Ladanyi and G. H. Johnston</i>	310
Shock-Wave Studies of Ice and Two Frozen Soils <i>Donald B. Larson, Glenn D. Bearson, and James R. Taylor</i>	318
Thaw Consolidation of Alaskan Silts and Granular Soils <i>Ulrich Luscher and Sherif S. Afifi</i>	325
Mechanical Properties of Rocks at Low Temperatures <i>Malcolm Mellor</i>	334
Soil Freezing in Relation to Pore Water Pressure and Temperature <i>Robert D. Miller</i>	344
Ionic Mobility in Permafrost <i>Richard P. Murrmann</i>	352
Sound and Shock Transmission in Frozen Soils <i>Yoshisuke Nakano and Nilson H. Froula</i>	359

Practical Extensions to a Theory of Consolidation for Thawing Soils <i>J. F. Nixon and N. R. Morgenstern</i>	369
Experimental Pressure Studies of Frost Heave Mechanisms and the Growth-Fusion Behavior of Ice <i>F. J. Radd and D. H. Oertle</i>	377
Triaxial and Creep Tests on Frozen Ottawa Sand <i>Francis H. Sayles</i>	384
Sample Disturbance and Thaw Consolidation of a Deep Sand Permafrost <i>Wayne S. Smith, Keshavan Nair, and Robert E. Smith</i>	392
Viscoelastic Properties of Frozen Soil under Vibratory Loads <i>Henry W. Stevens</i>	400
Pore Water and Heaving Pressures Developed in Partially Frozen Soils <i>Hugh B. Sutherland and Paul N. Gaskin</i>	409
Shear Strength at a Thaw Interface <i>Stanley Thomson and Edward F. Lobacz</i>	419
Some Aspects of Surficial Salt Treatment for Attenuation of Frost Heaving <i>Raymond N. Yong, John C. Osler, and Paul V. Janiga</i>	426
 Session V Groundwater in Permafrost Areas	
Groundwater Investigations in Permafrost Regions of North America: A Review <i>John R. Williams and Robert O. van Everdingen</i>	435
Effects of Permafrost on Stream Flow Characteristics in the Discontinuous Permafrost Zone of Central Alaska <i>S. Lawrence Dingman</i>	447
Groundwater Pore Pressures Adjacent to Subarctic Streams <i>Douglas L. Kane, Robert F. Carlson, and C. Edward Bowers</i>	453
Recharge of a Central Alaska Lake by Subpermafrost Groundwater <i>Douglas L. Kane and Charles W. Slaughter</i>	458
Risk of Uncontrolled Flow from Wells through Permafrost <i>Kenneth A. Linell</i>	462
A Groundwater Supply for an Oil Camp near Prudhoe Bay, Arctic Alaska <i>Richard G. Sherman</i>	469
The Nature of the Seawater-Freshwater Interface during Breakup in the Colville River Delta, Alaska <i>H. J. Walker</i>	473
 Session VI Surveying and Predicting Permafrost Conditions	
Mapping and Predicting Permafrost in North America: A Review, 1963-1973 <i>Oscar J. Ferrians, Jr., and George D. Hobson</i>	479
An Examination of Mariner 6 and 7 Imagery for Evidence of Permafrost Terrain on Mars <i>Duwayne M. Anderson, Lawrence W. Gatto, and Fiorenzo Ugolini</i>	499
<i>In situ</i> Physicomechanical Properties of Permafrost Using Geophysical Techniques <i>Om P. Garg</i>	508
Electromagnetic Probing of Permafrost <i>Pieter Hoekstra and Duncan McNeill</i>	517
The Application of Shallow Seismic Methods to Mapping of Frozen Surficial Materials <i>J. A. M. Hunter</i>	527
Investigation of Sampling Perennially Frozen Alluvial Gravel by Core Drilling <i>G. Robert Lange</i>	535
Potential Use of Airborne Dual-Channel Infrared Scanning To Detect Massive Ice in Permafrost <i>Leonard A. LeSchack, Frederick H. Morse, Wm. R. Brinley, Jr., Nancy G. Ryan, and Robert B. Ryan</i>	542

Session VII Principles of Construction in Permafrost Regions

Engineering Design and Construction in Permafrost Regions: A Review <i>Kenneth A. Linell and G. H. Johnston</i>	553
Water Supply and Waste Disposal Concepts Applicable in Permafrost Regions <i>Amos J. Alter</i>	577
Some Passive Methods of Controlling Geocryological Conditions in Roadway Construction <i>Richard L. Berg and George W. Aitken</i>	581
Environmental Considerations for the Utilization of Permafrost Terrain <i>Jerry Brown</i>	587
Solid Waste Disposal in Permafrost Areas <i>Jules B. Cohen</i>	590
Settlement Associated with the Thawing of Permafrost <i>Frederick E. Crory</i>	599
Control of Permafrost Degradation beneath a Roadway by Subgrade Insulation <i>D. C. Esch</i>	608
Thermal Regime in an Arctic Earthfill Dam <i>Charles W. Fulwider</i>	622
Control of Culvert Icing <i>David A. Gaskin and Leonard E. Stanley</i>	629
Analysis of the Proposed Little Chena River, Earthfill Nonretention Dam, Fairbanks, Alaska <i>Warren George</i>	636
Some Effects of Surface Disturbance on the Permafrost Active Layer at Inuvik, N.W.T., Canada <i>John Alan Heginbottom</i>	649
Corps of Engineers Technology Related to Design of Pavements in Areas of Permafrost <i>Frank B. Hennion and Edward F. Lobacz</i>	658
A Sanitary Service Complex for Villages in Permafrost Regions: A Demonstration Project at Wainwright, Alaska <i>Charles L. Hoar and Lloyd K. Clark</i>	664
Permafrost Protection for Pipelines <i>H. O. Jahns, T. W. Miller, L. D. Power, W. P. Rickey, T. P. Taylor, and J. A. Wheeler</i>	673
Permafrost-Related Engineering Geology Problems Posed by the Trans-Alaska Pipeline <i>Reuben Kachadoorian and Oscar J. Ferriars, Jr.</i>	684
Long-Term Effects of Vegetative Cover on Permafrost Stability in an Area of Discontinuous Permafrost <i>Kenneth A. Linell</i>	688
Designing Friction Piles for Increased Stability at Lower Installed Cost in Permafrost <i>Erwin L. Long</i>	693
Stability of an Underground Room in Frozen Gravel <i>Howard C. Pettibone</i>	699
A Sewage-Treatment Concept for Permafrost Areas <i>Sherwood C. Reed and Timothy D. Buzzell</i>	706
Vertical and Lateral Pile Load Tests in Permafrost <i>Raymond K. Rowley, George H. Watson, and Branko Ladanyi</i>	712
Design and Construction of Practical Sanitation Facilities for Small Alaskan Communities <i>William L. Ryan</i>	721
Encountering Massive Ground Ice during Road Construction in Central Alaska <i>North Smith and Richard Berg</i>	730
The Use of Polyurethane Foam Plastics in the Construction of Expedient Roads on Permafrost in Central Alaska <i>North Smith, Richard Berg, and Larry Muller</i>	736
Effects of Ground-Ice Variability and Resulting Thaw Settlements on Buried Warm-Oil Pipelines <i>T. L. Speer, G. H. Watson, and R. K. Rowley</i>	746
Performance of the Thule Hangar Soil Cooling Systems <i>Wayne Tobiasson</i>	752

Performance of a Warm-Oil Pipeline Buried in Permafrost <i>George H. Watson, Raymond K. Rowley, and William A. Shusarchuk</i>	759
Biological Considerations for Construction in the Canadian Permafrost Region <i>Ross W. Wein and L. C. Bliss</i>	767

Appendixes

United States Planning Committee	773
Sponsors of the United States Planning Committee	775
Organizing Committee of Canada	775
Authors of Summary Review Papers	777
Authors of the United States Papers	779
Authors of the Canadian Papers	781
Standard Symbols and Units, Selected Metric Conversions	783

I THERMAL ASPECTS OF PERMAFROST FORMATION AND EVOLUTION

Permafrost formation and evolution as related to energy exchange, heat flow, geothermal gradients, secular variations, thermal properties, thermal response to nature and man-made perturbations (theoretical aspects), computer simulations

THERMAL CONDITIONS IN PERMAFROST—A REVIEW OF NORTH AMERICAN LITERATURE

Lorne W. Gold

NATIONAL RESEARCH COUNCIL OF CANADA
Ottawa, Ontario

Arthur H. Lachenbruch

U.S. GEOLOGICAL SURVEY
Menlo Park, California

INTRODUCTION

Increasing interest and activity in Alaska and northern Canada, particularly concerning oil and gas exploration and development of other natural resources, have resulted in a more general appreciation of permafrost as a thermal condition of the ground that must be given careful consideration and often requires special treatment. Appropriate methods, for example, had to be developed for excavating and handling ice-rich ore from the iron mines of Labrador and northern Quebec. The settlement that occurs as a result of the thawing of permafrost had to be taken into consideration in the design, construction, and operation of dikes for the Nelson River power development in northern Manitoba. Potential settlement and stability of ice-rich ground are causing challenging problems for the design of future oil and gas lines in Alaska, the Mackenzie Valley of the Canadian Northwest Territories, and Arctic Archipelago. Concern for the arctic environment is causing both government and industry to increase greatly the rate of accumulation of information on northern terrain and to give more attention to developing suitable methods for constructing and operating in permafrost areas.

Thermal conditions in permafrost will be discussed in this paper, in two sections—"The Surface Boundary Condition" (prepared by LWG) and "Subsurface Thermal Conditions" (prepared by AHL). The use of computerized numerical methods for ground temperature calculations is reviewed in an appendix prepared by L. E. Goodrich. For those topics that were reviewed in the First International Permafrost Symposium, the discussion emphasizes studies reported in the 10 years that have elapsed.

To most people, "permafrost" means earth material in which the moisture is predominantly in the solid state as ice, both winter and summer. A variety of more precise definitions is adopted as needed in special applications with rather little confusion. In general discussions of temperature it is useful to define permafrost as the region of perennially negative Celsius earth temperatures, and this will be adequate for most of our discussion. This is at least a necessary condition for permafrost by almost any definition, and it emphasizes the fact that permafrost is primarily a thermal state. It will, of course, include dry earth materials and

those in which part or all of the moisture is liquid as a result of freezing-point depression by solutes, surface forces, or confining pressures in excess of 1 atm.

In principle, the ground thermal regime can be determined for any time at a given location if the boundary conditions are specified. A particularly complex set of conditions exists at the surface where the earth is in contact with the atmosphere. At this boundary the temperature is continually changing in order to maintain a balance between heat lost or gained by radiation, evaporation, convection, conduction, and precipitation. The most satisfactory method of establishing this upper boundary condition appears to be by direct measurement of the temperature at some depth with respect to the surface. Although attempts are being made to determine the time dependence of the surface temperature by measuring the components of the surface heat exchange, the greatest benefit of these measurements has been to provide a general qualitative to semiquantitative appreciation of the influence of relief and surface factors, such as vegetation, type of soil, snowcover, and presence of water, on the relationships between ground temperature and weather or climate. This appreciation, along with an understanding of the dependence of the ground thermal regime on the properties of the soil, is necessary to predict the consequences of surface disturbance such as that associated with human activity.

Superimposed on the effects of changes in surface temperature are those due to heat flow from the interior of the earth. Although this amount of heat is small relative to the cyclical contributions at the surface, it has a significant influence on the temperature gradient at depths greater than that to which the annual temperature changes propagate and, therefore, on the thickness of permafrost. Attention has been given to measuring geothermal heat flow in Alaska, northern Canada, and the Arctic Basin primarily because of its scientific interest. Such measurements in permafrost areas are usually easier to interpret than ones made in non-permafrost areas, because they are not usually disturbed by groundwater movement.

A description of temperature changes and their effects in porous ground is complicated by movement of the fluid and gaseous phases of water. Additional complicating effects are caused by the phase change that occurs in bulk

water at 0 °C and at lower temperatures for water under the influence of the surface of the solid. Good progress has been made in taking into account phase changes in ground temperature calculations and in understanding their effects on the ground thermal regime, but both the qualitative and quantitative understanding of the contribution and effects of water and vapor movement are still in a primitive state.

Knowledge of thermal properties is a basic requirement for a proper interpretation and description of thermal conditions in permafrost. The need to calculate the temperature changes that occur in permafrost due to given imposed boundary conditions has revealed the lack of knowledge concerning these properties and their dependence on soil type, density, water content, and ice content. Increasing attention is now being given to their measurement both in the laboratory and in the field.

THE SURFACE BOUNDARY CONDITION

Climatological Balance

The average temperature and heat content of the ground are determined by the cyclical exchange of heat and moisture at the earth's surface. These thermal characteristics at a given site are primarily representative of the local climate, which, in turn, is a function of the large-scale atmospheric circulation, and of the organic and inorganic structure of the surfaces. They are affected to a secondary degree by local effects, such as type of surface material, surface slope, and availability of water.

The exchange of heat and moisture at the surface is driven by the radiation received from the sun. In the absence of climatic change, the net annual change in the heat content of the ground must, on the average, be zero; the net annual gain in solar radiation just equals the sum of the net long-wave radiation, sensible heat loss, and evaporative loss. Similarly, from a short-term climatological point of view, it can be assumed that there is no change in the amount of water stored in the ground and that the average annual precipitation equals the sum of runoff, evaporation, and evapotranspiration.

It is useful for many scientific and engineering problems to have an appreciation of the climatological values of the components of heat exchange. Incoming global solar radiation is measured on a regular basis at eight stations in the permafrost region of Canada and at three in Alaska. Titus and Truhlar¹⁰³ have summarized the Canadian data in map form. Radiation values calculated from sunshine records for 15 additional Canadian stations and data from four Alaskan stations were also used in the preparation of the maps.

Vowinckel and Orvig¹⁰⁹ and Hay^{44,45} calculated incoming solar radiation, as well as the other components of the radiation balance, and prepared maps presenting mean values. Hay's calculations showed that no land area in Canada and Alaska has a net negative annual balance.

McFadden and Ragotzkie⁸² have carried out extensive measurements of the average surface albedo in northern areas from an aircraft flying at a height of about 300 m. Their measurements show the significant influence of surface characteristics on the annual variation in the radiation balance. The tundra region, because of its lack of trees, has the largest seasonal range in albedo from an average high of about 80 percent during the period of snowcover to an average low of about 20 percent during the snow-free period. Kung *et al.*,⁶⁴ who were associated with the same project as McFadden and Ragotzkie, present maps of the average albedo of North America, including the permafrost regions, for various times of the year. They discuss the dependence of albedo on surface texture.

McFadden and Ragotzkie,⁸² pointed out that melting of snow occurs rapidly in spring in the tundra and that the amount of solar radiation absorbed by the surface can increase 600 percent within 3 weeks during the period of high daily incoming solar radiation. Melting is less rapid in the boreal forest region because of the sheltering effect of the tree cover, even though the average albedo during the period of snowcover is lower than for the tundra. Consideration was given by McFadden and Ragotzkie to the effect of these albedo conditions on climate. Observations in the U.S. Tundra Biome Project¹⁰⁵ are providing more detailed information on radiation effects during the snowmelt period on the tundra and the very rapid change in ground temperature associated with them.

At present, very few evaporation or runoff measurements are being made in the Canadian and Alaskan Arctic; none are being made in the Canadian Arctic Archipelago. Estimates of average values of the components of the heat and moisture balance at the surface are based primarily on standard meteorological observations. Hay⁴⁴ and Hare and Hay⁴² have studied the large-scale water balance. Maps of mean annual precipitation and runoff have been prepared based primarily on information from the Canadian Atmospheric Environmental Service, U.S. Environmental Data Service, and the *Hydrologic Atlas of Canada*.⁴⁹ They have also considered the evaporation field both as the difference between precipitation and runoff and as calculated values with reference to a study on evaporation from small lakes carried out by Ferguson *et al.*³⁶ The mean annual convective heat field was determined as the difference between the net radiation and evaporation fields. Their analysis indicates a discrepancy in northern areas that they consider to be due to an undermeasurement of snowfall. Similar difficulties in measuring snowfall in northern exposed areas using standard measurement techniques have been reported in the Soviet literature.

The marked similarity in the regional dependence of the isolines for various climatic and surface elements is evidence of their interaction. Hare⁴¹ and Hare and Ritchie⁴³ discuss these interactions with respect to the boundaries of the tundra and boreal forest regions. Factors of major impor-

tance are the control exerted by forest cover on the albedo, particularly during the period of snowcover and spring melt, and the average position of the arctic front, which determines the distribution of water vapor and cloud cover. The regional dependence of the boundaries of the discontinuous and continuous permafrost zones^{19,37} demonstrates the importance of these interactions for the ground thermal regime.

Components of the Surface Heat Balance

Measurement of the components of the surface heat balance is required to confirm and improve climatological estimates based on standard weather observations and to increase knowledge of the relative importance of factors controlling the ground thermal regime. Few such measurements have been made in the permafrost areas of Canada and the United States in the past 10 years.

The relative values of the components of the heat balance are quite sensitive to the characteristics of the surface, particularly albedo, availability of water, and type and areal extent of the cover. Ahrnsbrak¹ found for the tundra west of Hudson Bay that the sensible heat loss was appreciably greater than the evaporative loss during summer periods. This observation is consistent with the low annual precipitation that occurs in that region. Further south at sites immediately adjacent to Hudson Bay, Rouse and Stewart⁹² found the evaporative loss to be about equal to or a little greater than the sensible heat loss in lichen-heath terrain. Their observations indicated that the lichen surface had a high resistance for the movement of moisture through it. Brown¹⁷ measured a potential evaporation of about 20 cm of water for a grass site from 30 June to 17 September 1960 at Norman Wells, N.W.T. The corresponding values for nearby moss, lichen, and wooded sites for the same period were between 10 and 13 cm.

Kelley and Weaver⁶¹ carried out a heat balance for a study of ground temperatures in well-drained tundra near Barrow, Alaska. They found the total net radiation for the year to be $49\,800\text{ J cm}^{-2}$, of which $3\,340\text{ J cm}^{-2}$ was utilized in melting the snowcover. This value is close to the climatological estimate given by Hare and Hay⁴² for the Barrow area. Observations of the components of the surface heat balance are also being measured at Barrow as part of the Tundra Biome Project.¹¹⁴

Vowinckel and Orvig^{110,111} are calculating annual values for the components of the heat balance for specific sites from standard radiosonde and synoptic weather observations combined with information concerning such characteristics of the ground as soil depth and vegetation type. These values should provide an appreciation of the relative and absolute values of the components of the exchange, and how they depend on factors such as precipitation, runoff, and type of surface cover.

Brown^{22,23} is conducting a detailed study of ground

temperature and weather at Thompson, Manitoba, located at the southern edge of the discontinuous-permafrost region. His observations show that the thermal characteristics of the surface are a major determining factor in the occurrence or nonoccurrence of permafrost at a given location.

The U.S. Tundra Biome Project at Barrow demonstrated that models of the heat balance must take into account not only the characteristics of the surface at the measurement site but also other factors such as the horizontal inhomogeneity caused by lakes, polygonal ground, marshes, and topographic highs.¹⁰⁵ These areal features also have a marked influence on the ground thermal regime and changes induced in it by daily and annual weather and climatic temperature cycles (e.g., ref. 74).

Dependence of Ground Temperature on Surface Conditions

It is now well established that a difference of about $1\text{--}6\text{ }^{\circ}\text{C}$ exists in northern latitudes between the average annual air and ground surface temperatures. Observations have shown that this difference is due to the effects of such near-surface factors as snowcover, vegetation, time-varying ground thermal properties, relief, slope and orientation of the surface, and surface and subsurface drainage. In conformance with this, the southern boundary of the discontinuous-permafrost zone is found to coincide approximately with the $-1\text{ }^{\circ}\text{C}$ annual air temperature isotherm; continuous permafrost can be expected north of the $-6\text{ }^{\circ}\text{C}$ isotherm.^{16,19,21} Most of the investigations carried out during the past 10 years on the factors that determine the occurrence of permafrost in the discontinuous zone and the thickness of the active layer in the continuous zone, i.e., the ground temperature conditions in permafrost areas, have been qualitative to semi-quantitative in nature.

If the nonlinear contribution to the heat flow of freezing and thawing of water is negligible, the depth at which the amplitude of a cyclical temperature disturbance of angular frequency (ω) is reduced by a given amount in a semi-infinite medium is proportional to $\sqrt{\alpha/\omega}$, where α , the effective diffusivity of the medium, equals $K/\rho c$, where K , ρ , and c are its thermal conductivity, density, and mass specific heat, respectively. For a given frequency, therefore, the total heat capacity of the depth affected is proportional to $\rho c \sqrt{\alpha} = \sqrt{\rho c K}$. This quantity, sometimes called the conductive capacity or contact coefficient, is of particular significance for calculations of periodic heat flow in layered systems. Typical value of it for near surface materials are presented in Table I.

Table I provides an appreciation of the ability of natural materials to respond or adjust to imposed temperature changes. New snow, for example, offers a significantly higher resistance to change than wet sand and a much higher resistance than turbulent water. As neutral and unstable air can accept heat more readily than most surface materials,

TABLE 1 Representative Values of the Conductive Capacity^a

	$\sqrt{\rho c k}$ $\left(\frac{\text{cal}}{\text{cm}^2 \text{ s}^{1/2}}\right)^b$
New snow	0.002
Old snow	0.012
Dry sand	0.011
Wet sand	0.04
Sandy clay	0.037
Organic soil	0.04
Wet marshy soil	0.038
Ice	0.05
Still water	0.039
Stirred water	
great stability; moderate current	0.32
moderate stability; strong current	7.0
homogeneous; strong current	17.0
Still air	1.3×10^{-4}
Stirred air	
very stable	0.01
neutral	0.1
very unstable	1.0

^aAfter Priestley.⁸⁵

^b $\frac{1 \text{ cal}}{\text{cm}^2 \text{ s}^{1/2}} \sim \frac{42 \text{ kJ}}{\text{m}^2 \text{ s}^{1/2}}$

the heat carried away by the air will be appreciably greater than that conducted into the ground. During the period of the year when the ground is being warmed, for example, the total heat flow into it is usually less than 10 percent of the net radiation received at the surface. It is for this reason that it is so difficult, if not impractical, to determine the ground thermal regime from observations of only the components of the surface heat exchange.

Not only does the conductive capacity of the surface cover have a great influence on the thermal response of the ground but it also affects the ability of a particular surface type to thermally modify the air above. Because the atmosphere undergoes considerable turbulent mixing and usually has a larger conductive capacity than ground, lateral variations in average annual air temperature are associated with greater distances than corresponding variations in the average annual ground temperature, i.e., the atmosphere has a greater averaging capability. Most weather observations, therefore, are representative of appreciably larger areas than ground temperature measurements.

Lachenbruch⁶⁸ shows that, for a layered system, the ratio of the amplitude of a temperature disturbance at the interface between the two layers to that imposed on the surface of the upper layer depends on the thickness and thermal properties of the layer, the frequency of the disturbance, and the ratio $\sqrt{K_1 \rho_1 c_1} / \sqrt{K_2 \rho_2 c_2}$, where subscripts 1 and 2 refer to the upper and lower layers, re-

spectively. Qualitatively, if a semi-infinite medium is covered by a layer with a lower conductive capacity, the decrease with depth of the amplitude of a temperature disturbance imposed on the surface will be greater than if the layer were not present. Conversely, if the layer has a higher conductive capacity, the decrease of the amplitude with depth will not be as great.

At present, it is not possible to interpret unambiguously and correlate the semi-quantitative observations of ground temperatures and the occurrence of permafrost because of insufficient knowledge concerning the heat transfer properties of ground and surface materials and how these properties depend on such factors as water content, thermal state, and density. In the boreal forest and taiga areas of the southern part of the discontinuous zone, permafrost is usually encountered only in peatland or bog areas in association with peat plateaus of palsas. It does not generally occur in low areas with water at or near the surface or in high, well-drained regions.^{16,18,20} This clearly indicates the important influence of the thermal properties of moss, lichen, and peat on the ground thermal regime. The thermal conductivity of dry moss and peat is about a factor of 10 smaller than their value when wet. The difference in their resistance to heat flow for a dry summer condition and a wet, frozen winter condition can be sufficient to cause permafrost to be established in marginal areas.

The availability of water to the surface is particularly important with respect to the ground thermal regime, because evaporation is such an effective method of dissipating heat. Brown¹⁷ found at Norman Wells that evapotranspiration from sedge, moss, and lichen was appreciably less than from grass covers. The surface temperature of the moss and lichen was often several degrees higher than the air temperature because of reduced evaporative cooling. He also observed that the thickness of the active layer under sedge was greater than under the moss or lichen covers, indicating that sedge had a larger effective thermal diffusivity. The depth of thaw, of course, decreased with increasing thickness of peat, and there was evidence that this was also true of the average annual ground temperature.

Brown²² found no permafrost in Precambrian rock outcrops in the Thompson, Manitoba, area where the average annual air temperature is -3.3°C . At Yellowknife, N.W.T., with an average annual air temperature of -5.5°C , permafrost does not occur in exposed Precambrian rock, but is found in rock covered with overburden. The range in average annual ground temperature at Yellowknife at the 15-m depth was $1-1.8^\circ\text{C}$ in Precambrian granite, $0.8-1^\circ\text{C}$ in beach and till deposits, and -0.5 to -1.0°C in sedge and spruce peatlands. Permafrost was found in all terrain, including exposed Precambrian rock on Devon Island, but the rock had the thickest active layer.

The thermal conductivity of rock is about the same in summer as in winter; thus, a conductivity effect cannot con-

tribute to any difference that exists between the average annual ground surface and air temperatures. Other factors must be responsible, of which snowcover is probably the most important. A second factor is higher surface temperatures in summer for exposed rock than for vegetated ground, due to reduced evaporative cooling.

The Subarctic Laboratory at Schefferville, Quebec, run by McGill University (average annual air temperature -4.3°C), has given particular attention to the effect of snowcover, vegetation, and relief on the ground thermal regime.^{3,52,101,102} This region is much more exposed than the discontinuous zones studied in western Canada. A strong interdependence was found between permafrost, exposure, relief, snowcover, and vegetation. Permafrost was always observed beneath exposed, wind-swept ridges. Areas with sufficient shelter to allow brush to grow were always found to be warmer in summer and appeared to have a higher average annual ground temperature than surrounding areas completely lacking vegetation. Snowcover was found to be the major factor determining the presence of permafrost. In general, no permafrost was found in areas where the thickness of the snow exceeded about 40 cm.

Under some conditions, the contribution of one surface factor can be masked by that of a second. Price⁸⁸ found from a study in the Yukon that the active layer was shallower on slopes facing southeast than those facing north, because there was better development of the vegetation on slopes with a southern exposure. In this case, plant cover was more important than exposure in determining the depth of thaw.

Observations on the ground thermal regime, although few in number and still relatively primitive in scope and approach, are beginning to define the effect of surface factors such as relief, vegetation, drainage, soil type, and snowcover.³⁵ They indicate clearly that changes in ground temperature can be caused not only by variations in weather and climate but also by modifications to the characteristics of the surface. The surface disturbance and changes associated with man's activity in the Arctic in recent years and the realization of the need to preserve the permafrost condition in many situations have caused considerable attention to be focused on this aspect of the ground thermal problem.

Effect of Surface Changes

Several studies have been undertaken to document the thermal effects of surface changes and to establish the practice that must be followed to prevent the terrain damage that will unacceptably interfere with natural processes, transportation, and performance of structures (e.g., ref. 2).

Terrain damage due to degradation of permafrost is significant only in those soils that have a high ice content and a surface cover whose characteristics are sensitive to mechanical disturbance. Sandy and gravelly upland areas

with little vegetative cover, particularly in the high Arctic, are relatively insensitive thermally to transient surface activity, although traces of that activity may linger for a very long time due to the slow rate of recovery in the northern environment. Serious damage occurs primarily in terrain with a significant cover of peat overlain by mosses, lichens, sedge, dwarf shrub, and similar, sensitive, arctic organic surface vegetation.

Surface disturbance can affect the ground thermal regime in both a symmetric and an asymmetric manner. In the symmetric case, only the amplitude of the annual surface temperature variation is changed, and the average annual ground temperature remains the same. An increase in amplitude will cause the depth of the active layer to increase and possible subsidence due to melting of ice in permafrost. Most surface disturbances, however, cause an asymmetric effect, modifying the difference between the average annual air and ground surface temperature in addition to possibly changing the amplitude in the annual surface temperature variation. Because the geothermal gradient is appreciably smaller than the maximum average temperature gradient in soil near the surface in summer, a change in the average value of the annual ground surface temperature will (in sufficient time) have a greater effect on the thickness of permafrost than a comparable change in its amplitude. In many areas, this change can be large enough to cause complete degradation of the underlying permafrost.

Attention is being given to the consequences of past disturbances of both human and natural origin. Observations of seismic lines for which the organic layer was removed by bulldozer have indicated increases in the thickness of the active layer of 150 percent or more, the amount depending on the thickness removed and its effective thermal resistance. Increase in the thickness of the active layer was often accompanied by extensive settlement and erosion.^{10,11,77,79,112} Bliss and Wein¹¹ observed in the Mackenzie Delta area that, for seismic lines through spruce-alder forest, the depth of the active layer increased 62 percent; through the more fragile willow-alder cover, it was about 117 percent. Because of the serious terrain damage that has occurred, the practice of preparing seismic lines with a bulldozer has been stopped.

Winter roads constructed on frozen ground have a much smaller effect on the thickness of the active layer than bulldozed roads, although some increase may occur due to compaction. Bliss and Wein¹¹ also found that damage due to such roads is less through wet sedge areas than over upland terrain covered with small shrubs that are more susceptible to compaction in winter.

Investigations are being conducted by Radforth⁹⁰ on the effect of vehicles on the terrain in summer in order to establish information required for land use regulations. These observations show how the rate of deterioration of the surface depends on the nature of the cover, moisture content,

depth of thaw, weight of vehicle, aggressiveness of track, etc. Similar observations are being made in Alaska.^{15,91} Brown *et al.*¹⁴ have studied the consequences of specified surface disturbances at sites near Livengood, Alaska, and along the proposed Alaskan pipeline route. Removing the entire peat layer increased the thickness of the active layer for the undisturbed condition from 32 to 75 cm. If the entire peat layer was removed and replaced by a mulch, or if the living cover was sheared, the thickness of the active layer increased to about 60 cm. The depth of thaw under trails bulldozed in the spring was found to be 100 percent greater than in adjacent undisturbed sites. Very significant depression of the surface occurred due to melting of ice and erosion. The increase in depth of thaw under recently burned-over areas was found to be about 50 percent.

Kallio and Rieger⁵⁹ investigated the consequences of surface modifications at Fairbanks, Alaska. The upper vegetation was removed from three plots; two were cultivated—one with grass and the second with potatoes. For the site that was cleared only, the period of thaw was the same as for a fourth, undisturbed control site, but the depth of thaw was greater. In the grass and potato sites, thawing began earlier, and freezing was completed later than the control site. A permanent, unfrozen zone developed under the potato plot. The average annual ground temperature was greater than 0 °C above the permafrost table for all plots; the highest value was at the site planted with potatoes.

Observations made in burned-out areas showed an increase in the thickness of the active layer of between 30 and 60 percent.^{10,14,46,107} Heginbottom found the depth of thaw was significantly greater (80 percent) under bulldozed firelines because of greater damage to the organic cover. Fire in the northern environment was reviewed recently at a symposium held at the University of Alaska.¹⁰⁴

Water is one of the most effective modifiers of the ground surface condition. If a body of freshwater is sufficiently deep, the temperature at the bottom will always be 0 °C or higher. This creates a thawed zone whose depth and extent depends on the size of the body of water.^{25,67} If the water is eroding, as, for example, along the shore of a river or the coast of the Arctic Ocean, it continuously encroaches upon permafrost and induces a thawing condition.^{80,98} In the case of the river, erosion may be associated with exposure of thawed ground on the opposite bank. As the erosion process continues, vegetation will grow on the exposed ground on the slipoff side and the frozen condition will be restored, resulting in a gradation in maturity in both the permafrost and surface cover.^{86,98} In some cases the influence of water is periodic (e.g., floodplains), subjecting the soil not only to a transient change in surface temperature but also to the effects associated with flood damage.^{106,107}

Other types of natural process that affect the ground thermal regime are sedimentation, solifluction (particularly overriding of the surface by material involved in downslope

movement), and vegetation changes. A review of information on degradation of permafrost due to surface effects is given by Mackay.^{77,79}

Methods of controlling changes to the ground temperature caused by structures is another matter under review. The effects on ice-rich ground of removal or compaction of the organic cover may be lessened or completely prevented by using rigid insulation or an appropriate thickness of non-frost-susceptible material.^{7,16,40,63,87,93} An extensive study has been undertaken at Fairbanks, Alaska, on the effect of gravel and paved surfaces on the ground temperature. One of the paved surfaces was painted white to evaluate the effect of changing the albedo. Degradation of the permafrost was greatest under the gravel section and least under the paved surface painted white.⁷ Ferrians *et al.*³⁸ present a good review of problems that have occurred in Alaska due to surface disturbance associated with the construction of roads, railways, bridges, and buildings.

Most of the information collected in the past 10 years on the effect of surface changes on the ground thermal regime has been of a qualitative nature. It is quite possible such studies will never be more than semiquantitative because of the great natural variability in the weather and characteristics and properties of surface and near-surface materials. Attention should be given, however, to experiments and observations that will determine the range of the characteristics and properties that are important and the factors on which they depend. Such information is necessary from the science point of view to develop a full understanding of the permafrost condition and the processes that affect it and from the engineering point of view to give a rational basis for design and the conduct of human activity in permafrost areas.

SUBSURFACE THERMAL CONDITIONS

General

To understand the distribution of permafrost and the factors controlling it, it is necessary to understand the distribution of temperature in those portions of the earth in which it is likely to occur. The distribution of temperature and heat flux over the ground surface is controlled by complex and poorly understood processes, as discussed above. Nevertheless, the earth's surface is relatively accessible for measurements, and useful generalizations for these quantities can be made there. On the other hand, our direct knowledge of the thermal regime of the subsurface is limited to measurements in isolated boreholes and a few mines. In the absence of heat transfer by moving fluids, the temperature throughout the interior of a solid can be obtained by heat conduction theory from a thorough knowledge of its surface conditions and very limited information about its interior. In temperate and tropical climates, the application of heat

conduction theory to the thermal regime of the outer few hundred metres of the earth is severely limited by the effects of heat transferred by groundwater circulating through pores and fractures. In regions of continuous permafrost, however, the groundwater is largely immobilized either as ice or by surface forces, and heat conduction theory can often be applied with confidence to within a metre or so of the surface. As a result of this fact and of the importance of earth temperature in permafrost terrane, there is probably no other area of earth science in which known or easily derived analytical results from classical heat conduction theory yield more useful information. The richest English-language source of these results is the well-known book by Carslaw and Jaeger.²⁹ Whereas these analytical results yield insight and an overall understanding of the gross aspects of temperatures in permafrost, the more refined calculations usually required for engineering design are generally intractable analytically, and they must be treated by numerical methods. In such cases, however, the related exact analytical results provide useful insight and an invaluable means of verifying the computer programs.

The main features of the temperature regime in permafrost can be understood in terms of four rather distinct heat-transfer problems:

1. The steady one-dimensional flow of heat from the earth's interior to its isothermal surface, and the depth of the bottom of permafrost;
2. The periodic seasonal variation of surface temperature and the depth to the top of permafrost;
3. Long-term variations of surface temperature, the evolution of permafrost, and the effects of climatic change; and,
4. Lateral variations in the surface temperature and the effects of bodies of water, variable surface cover, topography, and engineering structures placed on the surface.

For steady-state problems or transient ones that do not involve appreciable movement of an ice-rich permafrost boundary, the governing equations are linear, and the individual solution to each of the four problems may be superimposed to obtain a complete description of the thermal regime. Even where this condition is violated for one or more of the problems, useful approximate results can often be obtained by superposition. In the following paragraphs, each of the four problems will be outlined briefly, referring where possible to the more recent work on each in North America.

Steady Heat Flow and the Depth of Permafrost

This is probably the most important of the four problems, and, in spite of the fact that it involves only simple arithmetic and forms the starting point for almost every discus-

sion of earth temperatures, it is probably the most widely misunderstood. Other discussions relating primarily to permafrost are included in the references.^{32,54,57,70,72-75,100}

If the earth is losing heat steadily by conduction through its outer layers at the rate q^* per unit area, then in any horizontal layer with thermal conductivity K_1 the Fourier heat conduction law requires:

$$q^* = K_1 G_1, \quad (1)$$

where G_1 is the thermal gradient in the layer, i.e.,

$$G_1 = \frac{dT}{dz}, \quad z \text{ in layer 1.} \quad (2)$$

Through any other layer with conductivity K_2 and gradient G_2 , the same amount of heat q^* must be flowing; hence:

$$q^* = K_1 G_1 = K_2 G_2 = \text{etc.}, \quad (3)$$

and the gradient in each layer varies inversely with its conductivity and directly with the regional heat flow. The temperature drop across layer 1 of thickness Δz_1 is:

$$\Delta T_1 = G_1 \Delta z_1 = \frac{q^*}{K_1} \Delta z_1. \quad (4)$$

If this homogeneous layer should extend from the ground surface, $z = 0$, where the long-term mean surface temperature is $-T_0$ °C, to the base of permafrost, $z = z_p$, where the temperature is 0 °C, then the gradient will be uniform, and the temperature $T(z)$ is given by:

$$T(z) = \frac{q^*}{K} z - T_0, \quad 0 < z < z_p, \quad (5)$$

and the permafrost depth z_p is:

$$z_p = \frac{K}{q^*} T_0, \quad -T_0 \text{ in } ^\circ\text{C}. \quad (6)$$

Refinements of this simple picture are easily established, e.g., if the permafrost is stratified with n layers, then K in Eq. (6) is replaced by the harmonic mean conductivity given by:

$$K = \left\{ \frac{1}{z_p} \sum_{i=1}^n \frac{\Delta z_i}{K_i} \right\}^{-1}. \quad (7)$$

It is frequently assumed, tacitly, that permafrost depth (z_p) can be estimated from the surface temperature $-T_0$, perhaps because that is the only quantity in Eq. (6) observable at the earth's surface. However, Eq. (6) expresses the important fact that permafrost depth is equally sensitive to

thermal conductivity K and heat flow q^* . It is seen from Eq. (3) that the heat flow, q^* , can be determined from an equilibrium measurement of the gradient G in any deep layer penetrated by a borehole if the conductivity, K , of that layer is also determined from a piece of core. This may be any convenient horizon; whether or not it lies within the permafrost zone is irrelevant to the problem. It is fortunate that q^* can be determined with very little subsurface information, because very little is available.^{57,75,99} It is also fortunate that data from all of the continents indicate that, for the most part, q^* varies only by a factor of about 2 (from 1 to 2×10^{-6} cal/cm²s). Over lateral distances on the order of 100 km, the variation is usually much less. By contrast, the thermal conductivity, K , in Eq. (6) can vary by a factor of 3 or more over relatively short distances.

The relation in Eq. (6) is illustrated in Figure 1, which presents generalized temperature observations at four Alaskan arctic coastal locations (data are from ref. 12, 72,

74 and Lachenbruch, Sass, Munroe, and Moses, unpublished). For this discussion, only the linear portions of the observed profiles and their dashed extrapolations should be considered. It is seen that the correlation between surface temperature, $-T_0$, and permafrost depth, z_p , is poor. At Cape Thompson, where $-T_0$ is about -7°C , the permafrost is 25 percent deeper than at Cape Simpson, where the long-term mean surface temperature is -12°C . Permafrost is 60 percent thicker at Prudhoe Bay than at Barrow in spite of the warmer surface conditions at Prudhoe. Existing data indicate that the heat flow, q^* , is about the same at all four sites (probably within 10 percent of 1.4×10^{-6} cal/cm²s); hence, variations in permafrost thickness depend mainly on K and T_0 [Eq. (6)]. The profiles of Figure 1 are quite predictable from Eq. (6) when measured and estimated values of thermal conductivity (K) are considered for each location. The increased gradient near the bottom of the Prudhoe Bay profile corresponds to a decrease in conductivity in accordance with Eq. (3). At this depth, ice is replaced by water; more will be said of this later [Eq. (35), below]. In the other holes, the moisture content is too low to display this effect.

Seasonal Temperature Variations

Next in importance to the steady heat flow, which determines the base of permafrost, is the periodic variation in surface temperature from summer to winter. It determines the position of the top of permafrost and generates the active layer upon which man's activities take place. This variation is also responsible for periodic thermal stress in the surficial permafrost layers that causes them to crack with profound geomorphic consequences.

It is common knowledge that the temperature at the earth's surface is strongly influenced by systematic diurnal and annual periodicities—predictable results of the earth's rotation and revolution. Superimposed on these are the incompletely understood effects of energy transmission between the outer limits of the earth's atmosphere and its solid surface. Variations in the latter cause perturbations in these periodicities (warm spells and cold snaps, mild and severe summers and winters, and so on) that, over intervals of a few years, generally appear to occur in random sequence. Thus, the depth of thawing in permafrost terrains, too, will tend to vary randomly from year to year as will the mean temperature at the ground surface for any successive 12-month period. Over longer periods, systematic variations (climatic changes) may be observable; their effects on permafrost is the subject of the next section. In discussing the seasonal effects on permafrost temperature, it is useful to assume at first that the surface temperature fluctuations are truly periodic with a period (P_y) of one year and that they vary about an annual mean value denoted by $-T'_0$.

The periodic variation at the surface, denoted by $\theta\left(0, \frac{2\pi t}{P_y}\right)$

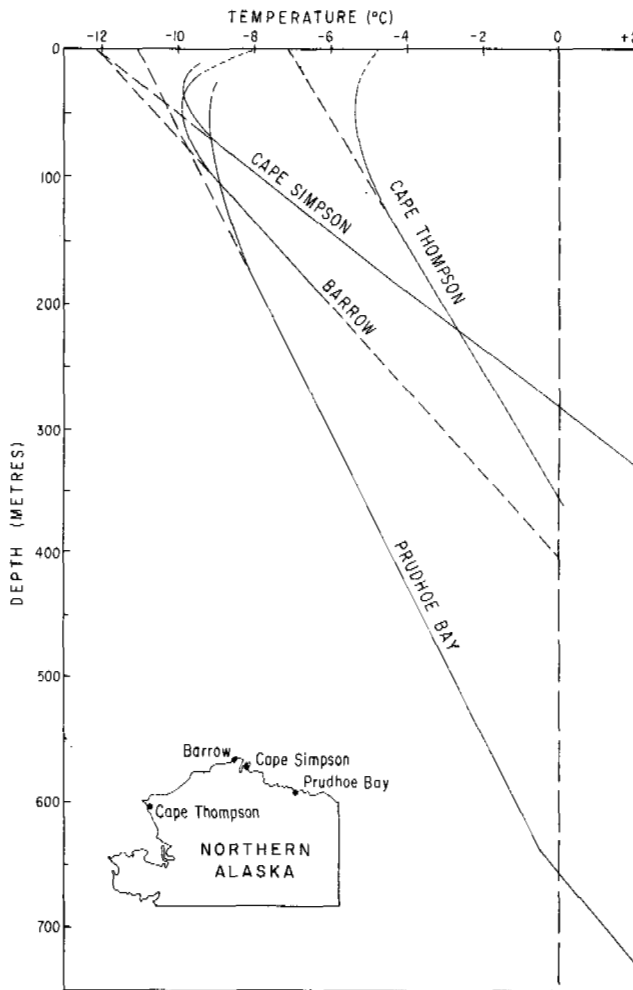


FIGURE 1 Generalized profiles of measured temperature on the Alaskan arctic coast (solid lines). Dashed lines represent extrapolations. See Eq. (5), (17), and (36).

will give rise to temperature variation with the same period, $\theta\left(z, \frac{2\pi t}{P_y}\right)$, at any depth z beneath the surface. In this discussion the effects of steady flux, q^* , at depth are unimportant, and the temperature $T(z, t)$ at any depth z at time t is given by:

$$T(z, t) = -T'_0 + \theta\left(z, \frac{2\pi t}{P_y}\right). \quad (8)$$

Denote by $\theta_m(z)$ the maximum value attained each year by θ at any depth z . In virtually all permafrost areas, some thawing occurs at the surface in summer and, hence, $\theta_m(0) > T'_0$, where it is understood that temperatures are measured in degrees Celsius. As the seasonal fluctuations attenuate with depth, $\theta_m(z)$ will generally decrease with z . The depth to the top of permafrost z_a (equivalent in this case to the depth to the bottom of the active layer) is therefore given implicitly by:

$$\theta_m(z_a) = T'_0. \quad (9)$$

The gross features of the temperature field in the zone of annual variation are given by the simple heat conduction model of a semi-infinite homogeneous medium ($z > 0$) with sinusoidal surface temperature, $\theta\left(0, \frac{2\pi t}{P_y}\right) = A_0 \sin \frac{2\pi t}{P_y}$; in which case Eq. (8) becomes:

$$T(z, t) = -T'_0 + A_0 e^{-z\sqrt{\frac{\pi}{\alpha P_y}}} \sin\left(\frac{2\pi t}{P_y} - z\sqrt{\frac{\pi}{\alpha P_y}}\right), \quad (10)$$

and Eq. (9) becomes:

$$A_0 e^{-z_a\sqrt{\frac{\pi}{\alpha P_y}}} = T'_0; \quad (11a)$$

$$z_a = \sqrt{\frac{\alpha P_y}{\pi}} \ln \frac{A_0}{T'_0}, \quad (11b)$$

where the thermal diffusivity (α), the density (ρ), and the mass specific heat (c) are related by:

$$\alpha = \frac{K}{\rho c}.$$

These much-discussed results (see, e.g., ref. 29 and 58) describe the exponential attenuation of the seasonal wave with depth and the linear lag in phase. A refinement in which the surface temperature $\theta\left(0, \frac{2\pi t}{P_y}\right)$ is represented by a Fourier series describes the rapid attenuation of high frequency components in surficial layers and consequent smoothing of the waves to simple sinusoidal form with in-

creasing depth. For a typical value of α ($0.01 \text{ cm}^2/\text{s}$), Eq. (10) indicates an attenuation of the annual wave by 10^{-1} for every 7-m depth. It is seen that comparable attenuation of a diurnal wave (of period $P_y/365$) would occur in 35 cm. As the surface amplitude, A_0 , of the annual wave is typically on the order of $15\text{--}30^\circ\text{C}$ and that of the diurnal wave is commonly considerably less, the annual wave can generally be expected to dominate, even near the base of the active layer. From the foregoing the seasonal variation will typically be $\sim 10^{-2}^\circ\text{C}$ at a depth of 20 m, and the phase lag there will be about 1 year. For thermal computations at greater depths, the surface temperature can be considered to be simply $-T'_0$. From Eq. (5), the neglected effect of uniform heat flow, q^* , at 20 m is typically less than 1°C . The geothermal gradient, of course, may be added to the seasonal effects, but in the seasonally varying layer, it usually is not warranted by other uncertainties.

Although extremely useful for insight and order-of-magnitude estimates, the simple solution [Eq. (10)] generally fails in more refined applications (e.g., to estimates of z_a or α from temperature observations) because of effects of inhomogeneity, latent heat, and longer term aperiodicities.

For surface conditions, similar to those on the Alaskan arctic coast ($A_0 \sim 16^\circ\text{C}$, $-T'_0 \sim -8^\circ$) and $\alpha \sim 8 \times 10^{-3} \text{ cm}^2/\text{s}$, Eq. (11b) gives the value of $z_a \approx 2 \text{ m}$. This is a reasonable approximation of observed depths of a dry active layer there or of the depth of a gravel fill required to maintain permafrost at its lower surface. A simple refinement to account for the change in properties at the base of the active layer yields in place of Eq. (11b) the transcendental equation [ref. 68, Eq. (21)]:

$$z_a = \sqrt{\frac{\alpha_1 P_y}{\pi}} \ln \left[\frac{A_0}{T'_0} \left(\frac{1+M}{\sqrt{S}} \right) \right], \quad (12a)$$

where

$$M = \frac{\sqrt{K_1 \rho_1 c_1} - \sqrt{K_2 \rho_2 c_2}}{\sqrt{K_1 \rho_1 c_1} + \sqrt{K_2 \rho_2 c_2}} \quad (12b)$$

and

$$S = 1 + 2M e^{-2z_a\sqrt{\frac{\pi}{\alpha_1 P_y}}} \cos 2z_a\sqrt{\frac{\pi}{\alpha_1 P_y}} + M^2 e^{-4z_a\sqrt{\frac{\pi}{\alpha_1 P_y}}}. \quad (12c)$$

The subscript 1 refers to the surficial layer and 2 refers to the underlying permafrost. Equation (12) illustrates the point made in a previous section that the "insulating" property of an active layer (or gravel fill) is sensitive to the properties of the underlying permafrost that is being insulated. It has been shown⁶⁸ that, if the permafrost were typical icy silt, Eq. (12) would indicate that the 2 m dry active layer

(or gravel fill) thickness obtained above from Eq. (11b) would be too large by about 50 percent. Equation (12) has provided a rationale for design of many gravel roads on the Alaskan arctic slope.

A further analytical refinement accounting for three layers shows that a gravel fill thickness can be reduced substantially by a thin layer of rigid insulation at its base.⁶⁸ However, a comparison of Eq. (11b) and (12) shows that even simple refinements lead quickly to cumbersome results. Furthermore, none of these solutions takes account of the often important effects of latent heat of freezing and thawing moisture in the active layer; as a result, they indicate falsely that the active layer should thicken indefinitely as the mean temperature, $-T'_0$, approaches 0°C in the subarctic. Although no analytical solutions are known for heat conduction in a two-phase medium with moving interface and periodic surface temperature, simple approximations based on Neumann's solution are often successful in estimating frost and thaw penetration in a wet active layer.^{26,27,58} Quite naturally in recent years considerable attention has been given to the application of numerical methods to these difficult and important problems.^{48,58,60,84}

An important characteristic of temperatures in permafrost beneath a wet active layer is the asymmetry generated in the thermal wave by the effects of latent heat.⁷³ The active layer warms readily past the freezing point in the spring, but its unfrozen lower portion is maintained at the freezing point throughout the autumn freezeup. As a result, the top of permafrost is maintained at 0°C until it comes in contact with the downward growing seasonal frost. By that time, the surface temperature is generally very low, and large gradients in the newly frozen active layer cause anomalously rapid cooling in the surficial permafrost immediately after freezeup. This rapid cooling may play an important role in the generation of thermal tension and ice-wedge cracks in permafrost. An analysis of this thermal stress is one of the more important applications of a study of the seasonal temperature variation (θ).⁶⁹ It is likely that this stress depends on the rate of cooling $\left(\frac{d\theta}{dt}\right)$, as well as the amount of cooling ($T'_0 - \theta$). For if it did not, the stress would be thermoelastic, and too large by an order of magnitude to explain the common observation that active ice wedges generally do not crack every year⁶⁹ (see Mackay and Black, this volume). For the reasonable assumption of power law type flow deformation (with power m) the thermal tension (σ) in permafrost is given approximately by:

$$\sigma \approx \eta(\theta) \left[\gamma \frac{d\theta}{dt} \right]^{\frac{1}{m}}, \quad (13)$$

where γ is the coefficient of expansion and η is a quasi-viscous parameter very sensitive to θ . Hence an understand-

ing of the stress and cracking in permafrost will probably require a detailed knowledge of θ and its time derivative.

Long-Term Variations of Surface Temperatures

It has been shown that if heat is flowing steadily from the earth's interior through homogeneous permafrost materials, the temperature profile beneath the zone of annual fluctuations is a straight line [Eq. (5)] that intersects the surface at the mean annual surface temperature $-T_0$. If the delicate thermal balance that determines $-T_0$ changes systematically, the net flux across the earth's surface will change, and the mean surface temperature will change to accommodate it. Suppose that such a change results in a shift in the mean surface temperature from an initial long-standing stable value, $-T_0$, to a new stable value $-T_0 + \Delta T_0$. After thermal equilibrium is achieved in the permafrost, the new temperature profile, of course, will be given by:

$$T(z) = \frac{q^*}{K} z - T_0 + \Delta T_0, \quad (14)$$

and the permafrost will have thinned from the bottom by $\Delta T_0/G$. (For $G = 20^\circ\text{C}/\text{km}$, $\Delta T_0 = 3^\circ\text{C}$; this would amount to 150 m.) During the transition between these two steady states, the temperature profile will trace a family of curves bracketed by the lines defined by Eq. (5) and (14). We assume the change at the surface takes place between time $t = 0$ and $t = t_0$, according to some function $\Delta T(0, t)$, and denote the total change $\Delta T(0, t_0)$ by ΔT_0 . The corresponding effect at depth is denoted by $\Delta T(z, t)$ and the transient profile is then given by:

$$T(z, t) = \frac{q^*}{K} z - T_0 + \Delta T(z, t). \quad (15)$$

A useful general discussion of this problem is given by Carslaw and Jaeger.²⁹ For a surface temperature change of the form:

$$\Delta T(0, t) = D t^{\frac{1}{2}n}, \quad n = 0, 1, 2, \dots, \quad (16)$$

where D is a constant. The complete temperature disturbance is given by:

$$\Delta T(z, t) = \Delta T(0, t) \frac{i^n \operatorname{erfc} \frac{z}{2\sqrt{\alpha t}}}{i^{n-1} \operatorname{erfc} 0}, \quad 0 < t < t_0, \quad (17)$$

where $(i^n \operatorname{erfc})y$ is the repeated integral of the error function for argument y . The net unbalanced downward heat flux, $F(t)$, through the earth's surface associated with this change is given by:

$$F(t) = \frac{\Gamma\left(\frac{1}{2}n+1\right)}{\Gamma\left(\frac{1}{2}n+\frac{1}{2}\right)\sqrt{\alpha}} K Dt^{\frac{1}{2}(n-1)} \quad (18a)$$

$$= \frac{\Gamma\left(\frac{1}{2}n+1\right)}{\Gamma\left(\frac{1}{2}n+\frac{1}{2}\right)\sqrt{\alpha t}} K \Delta T(0, t). \quad (18b)$$

By superimposing these results for different values of n , an arbitrary history of surface temperature or unbalanced flux can be represented in terms of a power series, and its effects on permafrost temperature can be calculated directly.²⁹ General formulations can also be made in terms of Fourier series using results like Eq. (10) or in terms of step functions as described by Birch.^{8,55}

Results of this kind can be used directly or inversely to study the evolution or temperature history of permafrost. In both cases, we make the reasonable assumption that the geothermal flux, q^* , is uniform; hence, the initial temperature is given by Eq. (5). The direct method poses no difficulty in concept, and the growth, deterioration, and temperature structure of permafrost can be calculated directly for any assumed hypothetical temperature or flux history at the surface. If thickening or thinning of ice-rich permafrost is involved, useful analytical results will not be available, but there are no serious obstacles to direct calculation by numerical methods. In the more interesting inverse problem, we are given an observed temperature profile [Eq. (15)] at some point in time ($t = t_0$), and from it we attempt

to reconstruct the temperature history, $\Delta T(0, t)$, or unbalanced flux history, $F(t)$, at the surface. Quite apart from any analytical difficulties, the inverse problem contains two basic conceptual ambiguities: the uncertainty in identifying the transient contribution $\Delta T(z, t_0)$ [Eq. (15)] in the observed temperature profile and the uncertainty in selecting from a broad range of temperature histories, $\Delta T(0, t)$, consistent with the empirically determined disturbance, $\Delta T(z, t_0)$.

The inverse problem is simplest for surface changes in which $F(t)$ is at least of the order of the geothermal flux, q^* , and which have occurred so recently that their effects have not penetrated to the base of permafrost. In such cases, if the permafrost is homogeneous, the first type of ambiguity is not serious, and the analytical difficulties associated with latent heat at the base of permafrost do not occur. In Figure 1 the effects of such a change in its early stages can be seen in all four profiles. There, $\Delta T(z, t_0)$ is clearly represented by the horizontal distance between the upward extrapolated dashed lines and the curved solid lines. It is seen that ΔT_0 evidently ranges from 2 to 4 °C and that $-T_0$ is about -12 °C at Barrow and Cape Simpson, -11 °C at Prudhoe Bay, and -7 °C at Cape Thompson. Recent changes such as these have been reported from many areas,^{6,30,50,51} but for reasons already given, they can probably be studied best by conduction theory in regions of continuous permafrost.³⁴

Ambiguity of the second type is illustrated by Figure 2, where the climatic disturbance $\Delta T(z, t_0)$ for Cape Thompson (Figure 1) is shown in the inset.^{74,75} The climatic histories, inferred from Eq. (17) for $n = 0, 1, 2, 3$, and 4, are

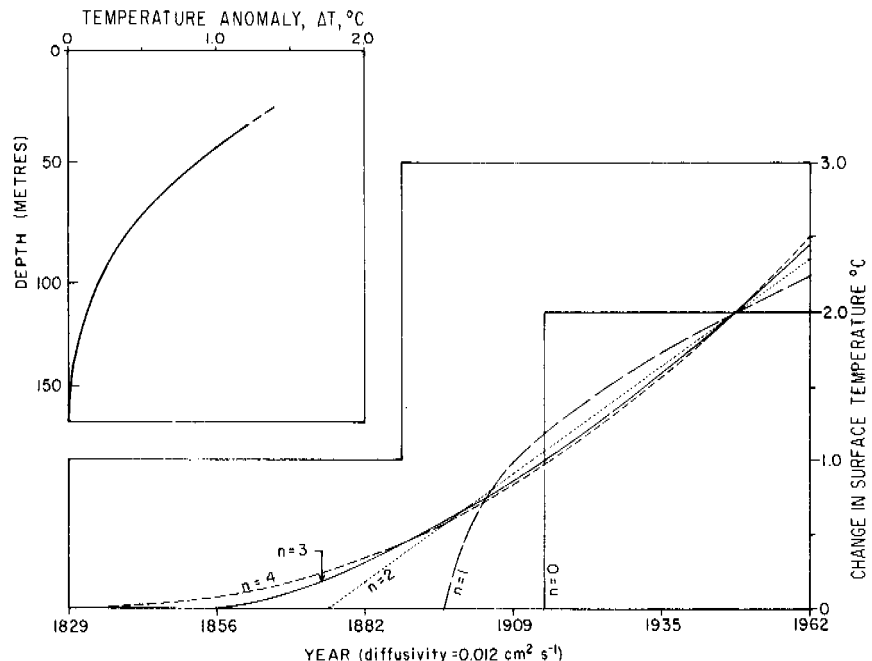


FIGURE 2 The measured climatic temperature anomaly at Cape Thompson (inset) and surface temperature histories consistent with it [Eq. (17)].

also illustrated in Figure 2. The cases $n = 0, 1, 2, 3$, each reproduce the observations (inset) with a standard error (0.01°C) close to the limit of uncertainty of the measurements, and the case $n = 4$ is only slightly worse. Although it is not possible to select from among them, all of the models clearly indicate that the climatic warming is essentially a product of the last 100 years.

In our search for a cause of this secular change, it would be useful to know the history of the unbalanced flux, $F(t)$, at the surface, and it is seen from Eq. (18a) that each of the models has quite different consequences in this respect. The case $n = 0$ implies a very large initial flux imbalance that subsequently decays as $t^{-1/2}$; $n = 1$ implies a constant flux imbalance throughout the period of surface warming, and larger values of n imply that $F(t)$ increased progressively during the event.

For the case $n = 1$ (Figure 2), it is seen that ΔT_0 is slightly greater than 2°C and that $t_0 \sim 65$ years (equivalent to $\alpha t_0 \sim 2.5 \times 10^7 \text{ cm}^2$). Using the measured conductivity value ($K \approx 7 \times 10^{-3} \text{ cal/cm s } ^\circ\text{C}$), it is seen from Eq. (18b) that the observed effect could be accounted for by a uniform heat imbalance F of about 80 cal/cm^2 per year for the past six decades. Thus, it is remarkable that this temperature anomaly, conspicuous to a depth of 150 m, results from a cumulative input of heat at the earth's surface sufficient only to melt 0.6 m of ice since the turn of this century.

The foregoing numerical example serves to illustrate the potential value of analysis of permafrost temperatures to the study of secular changes in heat balance at the earth's surface. A straightforward method of reducing ambiguity (of the second type) in determining the form of $F(t)$ is illustrated in Figure 3. Here data are presented from the well designated as "Barrow" (Figure 1), where temperatures were monitored for a period of 8 years.^{72,73,75} This permitted a determination of both the temperature anomaly $\Delta T(z, t_0)$ and its time derivative:

$$\left. \frac{d\Delta T(z, t)}{dt} \right|_{t=t_0}$$

It can be shown from differentiation of Eq. (17) that the ambiguity in the determination of n is sharply reduced if both the temperature anomaly and its time derivative are constrained by depth observations. The dots in Figure 3a represent the empirically determined values of the temperature anomaly and its time derivative; the solid curves represent the corresponding calculated values for the temperature history shown in Figure 3b. Although, as in the previous example, several values of n [Eq. (17)] described the temperature anomaly, a specific history rather like $n=3$ or the broken line illustrated was required to account for the combined data. It is seen that the broken line (Figure 3b) provides an acceptable fit, implying a substantial increase in F

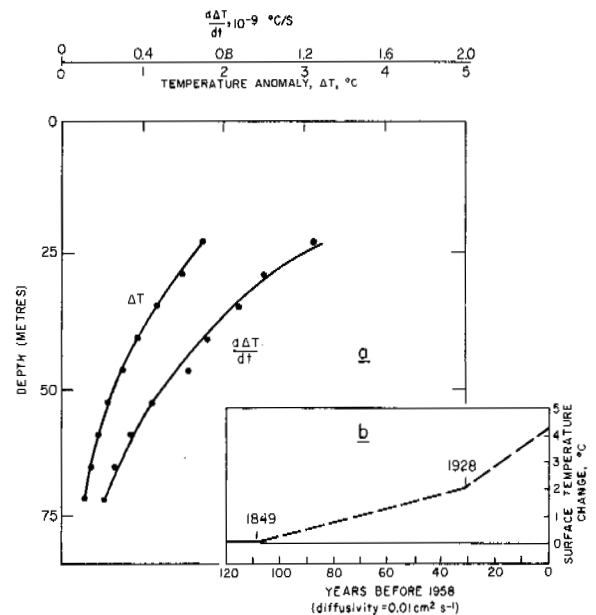


FIGURE 3 Climatic temperature anomaly at Barrow, Alaska. Dots in *a* represent observed values of anomaly (ΔT) and its observed rate of change. Solid lines represent corresponding computed values for the temperature history at the surface shown in *b*.

during the climatic event. In analyses of these second-order effects, it is important that the medium be homogeneous or that the variation in properties with depth be known.

For each of the stations represented in Figure 1, a more recent secular cooling is indicated by near-surface observations, but the data are partially obscured by seasonal variations, and no new principles would be illustrated by discussing them. It was pointed out in an earlier discussion that the difference in gradient at the four stations is a result of the difference in thermal conductivity, K , at each; those with the greater K have the smaller G . This observation, obtained from the problem of steady flow, is qualitatively consistent with the present discussion if the climatic changes at each are roughly synchronous. It is seen from Figure 1 that the maximum depth of the transient disturbance $\Delta T(z, t_0)$ increases from station to station as the gradient decreases, i.e., as K increases. It is seen from Eq. (17) that the depth of the disturbance is determined by the value of the quantity $\frac{z}{\sqrt{\alpha t_0}} = \frac{z}{\sqrt{K}} \frac{\sqrt{\rho c}}{\sqrt{t_0}}$. The quantity ρc varies little among permafrost materials and, hence, the depth z at which the climatic disturbance vanishes should increase with $(K)^{1/2}$. As q^* is relatively uniform, the depth should vary as $G^{-1/2}$ [Eq. (1)] approximately as observed (Figure 1).

As an illustration of the first type of ambiguity in the inverse problem, we consider the important problem of estimating the age of permafrost from a temperature profile.

Here the difficulty is distinguishing between the steady and transient contributions [first and third terms on the right in Eq. (15)] to observed gradients in profiles that are nearly linear deep in the permafrost. To take an extreme example, suppose permafrost is generated in a time interval t_0 from an initial state in which the mean surface temperature ($-T_0$) [Eq. (5)] was 0°C . If we assume that the surface temperature decrease was the step function $n = 0$, then Eq. (17) yields:

$$\Delta T(z, t_0) = \Delta T_0 \operatorname{erfc} \frac{z}{2\sqrt{\alpha t_0}}, \quad t = t_0 \quad (19a)$$

$$\approx \Delta T_0 \left[1 - \frac{z}{\sqrt{\pi \alpha t_0}} \right], \quad \frac{z_p}{2\sqrt{\alpha t_0}} < 0.3. \quad (19b)$$

In this example, ΔT_0 is, of course, a negative quantity. Substituting Eq. (19b) in Eq. (15) yields for an observation at $t = t_0$:

$$T(z, t_0) \approx \left[\frac{q^*}{K} - \frac{\Delta T_0}{\sqrt{\pi \alpha t_0}} \right] z + \Delta T_0, \quad \frac{z_p}{2\sqrt{\alpha t_0}} < 0.3. \quad (20)$$

Similar results apply for other values of n . Hence, long before thermal equilibrium is approached in permafrost, the transient disturbance [represented by the second term in brackets, Eq. (19b) and (20)] becomes linear, and we no longer have the curvature to distinguish its effect from the steady flux. Denoting by M the fractional departure from equilibrium at the ultimate base of permafrost (z_p), we obtain from Eq. (19b):

$$M \equiv 1 - \frac{\Delta T(z_p, t_0)}{\Delta T_0} \approx \frac{z_p}{\sqrt{\pi \alpha t_0}}$$

$$t_0 \approx \frac{z_p^2}{\pi \alpha M^2}, \quad \text{provided } M \lesssim 0.3, n = 0$$

$$\approx \frac{2.5 \times 10^3}{M^2} \text{ years at Prudhoe Bay.}$$

Thus at Prudhoe Bay where the profile is linear, we cannot distinguish between a permafrost age of 25 000 years ($M = 30$ percent) and one of 250 000 years ($M = 10$ percent). The best way to resolve this ambiguity is to compare the computed heat flow in permafrost with values determined at great depths, or at nearby locations where the properties are different.^{55,95} On the basis of fragmentary evidence of this sort, and when the effects of latent heat are considered, it seems likely that permafrost in the Prudhoe Bay area has been continually frozen on the order of 10^5 years or longer.

If a climatic warming results in a change from $-T_0 < 0^\circ\text{C}$ to $-T_0 + \Delta T_0 > 0^\circ\text{C}$, permafrost will be unstable, but the history of its disappearance will be extremely sensi-

tive to the distribution of moisture content with depth and local variability of ΔT_0 . Melting surfaces will encroach on the transient permafrost from above and below, and it will soon become isothermal at its melting point. The length of time the permafrost will persist can vary greatly from place to place, depending on the amount of latent heat that must be supplied from below by q^* and from above by $F(t)$. The result is discontinuous permafrost that is at, or close to, 0°C at all depths (Figure 3),⁷⁰ a condition produced throughout much of the subarctic by recent climatic warming. Under these conditions, moving groundwater can become an important heat transfer agent, and the applicability of conduction theory is limited.

Lateral Variations in the Surface Temperature

To this point, we have considered only one-dimensional problems, i.e., permafrost temperatures have been treated as if they depend only on distance beneath the ground surface. Clearly, this can be true only if the temperature over the earth's surface at any time can be considered uniform for lateral distances equal to several times the permafrost depth. It has been emphasized above that the temperature at the earth's solid surface is sensitive to moisture conditions, thermal properties, and geometric parameters of the surface and near-surface materials. Thus, the mean annual temperature and the thermal response of the surface to the passage of the seasons can vary significantly in a restricted locality as one passes laterally from dry to wet habitats, gravel beaches, ponds, lakes, rivers, or bodies of salt water.^{12,13} Even at a fixed point on the surface, these conditions might change significantly with time, e.g., as plant communities change or as shorelines shift, river channels migrate, or lakes are drained by thermal erosion of ice wedges. In general, engineering modifications of the surface, such as clearing timber, compressing the tundra mat, or constructing a heated building, roadway, or airstrip, also cause perturbations to the temperature over restricted areas of the earth's surface.³⁹

If we are interested in the temperature 50 m beneath a lake basin at a point 500 m from the shoreline, the effects of lateral heat flow to the cold shoreline will be negligible, and the one-dimensional considerations previously discussed will suffice; e.g., a rapid draining of the lake can be considered as a climatic change. However, if our concern is the effect of the lake on the depth of permafrost a few hundred metres beneath the same point, the cold shoreline and lateral heat flow will play an important role, and a two- or three-dimensional model will be indicated. Many important natural phenomena—such as the orientation of ice-wedge polygons,⁶⁹ the distribution of permafrost beneath the ocean's edge, or the formation of lake basins and pingos—cannot be understood without a consideration of the controlling two- or three-dimensional heat conduction prob-

lems. The same can be said of many engineering problems, such as the distribution of water supplies in continuous permafrost areas or the thaw settlement of a gravel pad or heated building.

As in the previous problems, a simple heat conduction model describes the gross aspects of this problem and provides physical insight into complex thermal conditions. It will be useful to consider the surface temperature to have a normal or ambient regime described by two parameters—the mean annual temperature, $-T'_0$, and the amplitude, A_0 , of seasonal fluctuations, which is assumed to be sinusoidal. Then, the normal temperature at any time and depth will be given by Eq. (10). Assume that at $t = 0$ a disturbance originates in a region (R) of the surface and that it shifts the mean annual temperature by δT_0 and the amplitude by δA_0 . Then, the temperature at the surface ($z = 0$) is described by:

$$T(x,y,0,t) = -T'_0 + \delta T_0 + (A_0 + \delta A_0) \sin \frac{2\pi t}{P_y}, \quad (x,y,0) \text{ in } R, t \geq 0 \quad (21a)$$

$$= -T'_0 + A_0 \sin \frac{2\pi t}{P_y}, \quad (x,y,0) \text{ not in } R, -\infty < t < +\infty \quad (21b)$$

$$(x,y,0) \text{ in } R, t < 0.$$

These perturbations at the surface in R will result in a disturbance of the normal temperature given by Eq. (10) at any point (x,y,z) beneath the surface. (The effects of temperature in R varying linearly with time are discussed by Birch.⁸) The mean shift at the surface δT_0 will cause a similar shift at any subsurface point denoted by $\delta T(x,y,z,t)$ and referred to as the “principal disturbance.” The amplitude change at the surface δA_0 will cause a periodic disturbance at depth denoted by $\delta \theta(x,y,z,t)$ and referred to as the “seasonal disturbance.” (The special case of no seasonal change in R , as in a permanently ice-covered lake or thermostatically controlled building is obtained by setting $\delta A_0 = -A_0$.)

Discussion of the seasonal disturbance can be found elsewhere.⁶⁷ It is much less important in general considerations than the principal disturbance or mean shift, which for homogeneous materials is given quite generally by [ref. 67, Eq. (26)]:

$$T(x,y,z,t) = \frac{\delta T_0}{2\pi} \iint_R \left[\frac{r}{\sqrt{\pi \alpha t}} e^{-\frac{r^2}{4\alpha t}} + \operatorname{erfc} \frac{r}{2\sqrt{\alpha t}} \right] d\Omega. \quad (22)$$

Here, $d\Omega$ is the element of solid angle subtended at the point of interest (x,y,z) by an element of surface area $dx dy$ in R . The distance between this surface element and the field point (x,y,z) is denoted by r . Equation (22) leads to simple integrated results for regions, R , of the polar coordi-

nate system⁶⁷ (a circle, annulus, sector, etc.) and for a two-dimensional half plane or strip.⁶⁶ They give the distribution of temperature in time and space beneath lakes, buildings, ocean shorelines, or linear features, such as rivers, roadways, and gravel spits.

If the lateral dimensions of the disturbed surface region, R , are small relative to the distance r of the point of interest (x,y,z) , then r can be represented by its mean value over R and:

$$\delta T(x,y,z,t) \approx \left[\frac{r}{\sqrt{\pi \alpha t}} e^{-\frac{r^2}{4\alpha t}} + \operatorname{erfc} \frac{r}{2\sqrt{\alpha t}} \right] \delta T_0 \frac{\Omega}{2\pi}, \quad (23)$$

where Ω is the solid angle subtended by R at (x,y,z) . If R is too large relative to r to permit Eq. (23), it can always be broken into subregions R_i , $i = 1, 2, 3 \dots$ that will permit it. There are two other valid reasons for breaking the disturbed surface region into subregions: if parts, R_i , have different mean temperatures $\delta_i T_0$ (e.g., a furnace room of a heated building, shallow and deep parts of lakes, etc.) or if the boundaries of R have been changing so that in each subregion, R_i , the disturbance $\delta_i T_0$ has been in existence a different time t_i (e.g., a migrating river channel, transgressing sea, or a wing added to a heated building). Therefore, Eq. (22) leads to the extremely useful and general result:

$$\delta T(x,y,z,t) = \sum_i \left[\frac{2}{\sqrt{\pi}} \beta_i e^{-\beta_i^2} + \operatorname{erfc} \beta_i \right] \frac{\Omega_i}{2\pi} \delta_i T_0, \quad (24a)$$

$$\text{where} \quad \beta_i = \frac{r_i}{2\sqrt{\alpha t_i}}. \quad (24b)$$

The expression in brackets is a transient factor representing the fractional approach to equilibrium of the disturbance in R_i at the point (x,y,z) at time t_i . Effects are negligible (i.e., the factor is $\lesssim 0.05$) for $\beta \gtrsim 2$ and close to equilibrium (factor $\gtrsim 0.95$) for $\beta < 0.5$ (ref. 67, Figure 22). The equilibrium result ($\beta \rightarrow 0$) is well known from potential theory:

$$\delta T(x,y,z) = \sum_i \frac{\Omega_i}{2\pi} \delta_i T_0. \quad (25)$$

Analytical results for Ω are available for the rectangle [see, e.g., ref. 67, Eq. (32)], as well as the strip and half plane and for figures in polar coordinates. The effects of arbitrary regions can be approximated by combining them.^{24,28,66,67}

Figure 4 illustrates the effect, δT , of three important types of anomalous surface regions. The mean annual temperature on the sea bottom beyond the shore-fast ice (2–3 m isobath) is generally close to 0°C at high latitudes. During the ice-covered period, it is close to the freezing point of seawater (approximately -1.8°C); during the short ice-free period, however, it can be much larger (up to 10 or 12°C ;

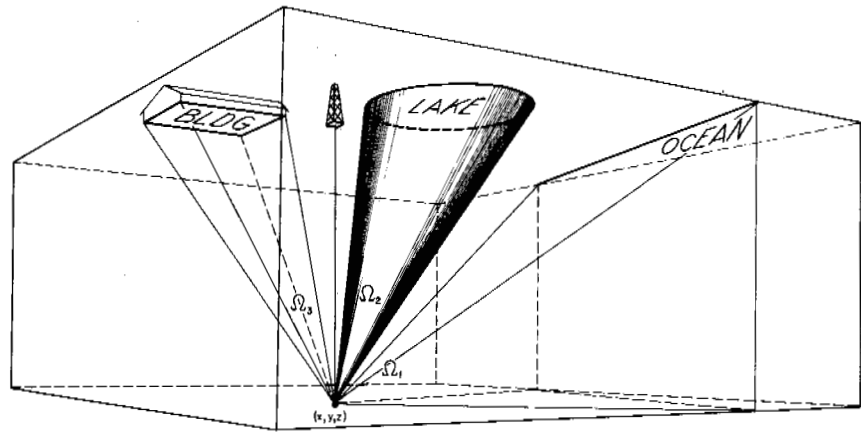


FIGURE 4 Representation of the solid angle, Ω , that determines the disturbance at any point (x, y, z) caused by thermally anomalous surface features. See Eq. (24) and (25).

Brewer, unpublished). The mean annual value at Barrow has been estimated at about $-\frac{1}{2}^{\circ}\text{C}$ ⁶⁶ and at Cape Thompson, farther south, it is probably about $+\frac{3}{4}^{\circ}\text{C}$ ⁷⁴ (see inset Figure 1). Thus equilibrium permafrost would extend out under the ocean at Barrow, and, at Cape Thompson, it would not. As the mean annual temperature of the emergent surface at high latitudes is on the order of -5 to -15°C , $\delta_1 T_0$ (Figure 4) is of this magnitude, and the effect of the ocean can be quite large at points (x, y, z) where it subtends a large solid angle Ω_1 . Near Barrow, the measured permafrost temperatures were found to be consistent with Eq. (25), indicating that the shoreline has been relatively stable there in recent times.⁷³ Near Cape Thompson, however, temperatures are too low for equilibrium conditions, and application of the transient theory⁷⁴ yields an estimate for the rate of shoreline transgression of the past few 1 000 years. Disequilibrium was indicated also near aggrading shoals at the mouth of the Mackenzie River.⁷⁸

Lakes whose depth exceeds the maximum fresh-ice thickness (~ 2 m at high latitudes) must have positive mean bottom temperatures (in $^{\circ}\text{C}$). They are underlain by perennially thawed sediments and, like the oceans, are associated with a large surface anomaly, $\delta_2 T_0$. Shallower lakes that freeze to the bottom typically have much lower mean temperatures and produce smaller anomalies.¹³ As with the ocean, the history of lakes can be studied by analyzing their transient anomalies in nearby boreholes. Two lakes studied at Barrow and one in the Mackenzie Delta were consistent with equilibrium theory.^{56,73}

The mean temperature at the base of a heated structure is likely to be 5 or 10°C greater than that of a deep lake, and the associated surface anomaly $\delta_3 T_0$ will be correspondingly larger. For the proportions shown in Figure 4, however, the effect of a building constructed in historic time would be negligible at (x, y, z) because β_3 [Eq. (24)] would be very large.

Effects of topographic relief (not shown in Figure 4) can also be represented simply with Eq. (24) by replacing the

relief by an equivalent temperature disturbance on a plane surface.^{8,71} When applying Eq. (24) to calculate the temperatures beneath the ocean, e.g., to calculate distribution of offshore permafrost,^{66,73,81} it is usually more convenient to consider the emergent land to be the anomalous surface region.

Summary of Temperature Effects

In summary, the gross aspects of the thermal regime in permafrost at high latitudes (or very high altitudes⁵³) can be described in terms of simple heat conduction models. They provide insight needed to understand the relation between the temperature and distribution of permafrost and the dynamic climatologic and geomorphic processes that modify the surface of the terrain in which it occurs. The more important of the foregoing results can be combined into a summary equation for the temperature, T , in continuous permafrost:

$$T = \frac{q^*}{K} z - T_0 + \Delta T_0 \left[\frac{i^n \operatorname{erfc} \frac{z}{2\sqrt{\alpha t_0}}}{i^{n-1} \operatorname{erfc} 0} \right] + A_0 e^{-z\sqrt{\frac{\pi}{\alpha P_y}}} \sin \left(\frac{2\pi t}{P_y} - z\sqrt{\frac{\pi}{\alpha P_y}} \right) + \sum_{i=1}^N \left[\frac{r_i}{\sqrt{\pi \alpha t_i}} e^{-\frac{r_i^2}{4\alpha t_i}} + \operatorname{erfc} \frac{r_i}{2\sqrt{\alpha t_i}} \right] \frac{\Omega_i}{2\pi} \delta_i T_0. \quad (26)$$

The first two terms represent effects of steady geothermal flux, q^* , to the surface whose long-term mean temperature is $-T_0$. The third term represents the important climatic change in the amount ΔT_0 of the last century (t_0). (For some purposes, it might be desirable to add a second term of this kind to account for the more recent secular cooling.)

The fourth term corresponds to seasonal fluctuations with surface amplitude A_0 , and the fifth is the effect of N surface regions with anomalous temperatures $\delta_i T_0$ that have existed for a time t_i . The present mean surface temperature ($-T_0 + \Delta T_0$) and A_0 may be estimated from surface observations. T_0 and q^*/K are obtained from temperature measurements in boreholes; K must be measured on laboratory samples or estimated from lithologic information. $\delta_i T_0$ is obtained from measurements or estimates of surface temperatures in anomalous regions. For superficial anomalies, it should be referred to the present mean surface temperature ($-T_0 + \Delta T$); for effects at depths little affected by the recent climatic change, it should be referred to the previously existing long-term value $-T_0$. A trivial refinement of the fourth term in Eq. (26) can account for the two- and three-dimensional effects of secular change in the rare cases where it might be necessary [see, e.g., ref. 66, Eq. (8)].

Setting $T = 0^\circ\text{C}$ in Eq. (26) and replacing the sine factor in the second term by unity yield an implicit equation for the boundary surface of permafrost. A schematic illustration of such a surface is presented in Figure 5 for a case in which the mean sea bottom temperature is greater than 0°C .

Thermal Properties

In the preceding section, the general relations for temperature in permafrost contain two basic thermal parameters— ρc , the volumetric specific heat, and K , the thermal conductivity. These quantities are the subject of a very extensive literature, and we shall consider here only a few aspects, more or less unique to permafrost. In general, they relate to the presence of water and ice close to their transition tem-

perature. When water changes to ice, its conductivity increases by a factor of 4, its volumetric specific heat decreases by a factor of $\frac{1}{2}$, and it releases enough heat to raise the temperature of an equal volume of rock by 150°C . Because of this behavior and because many thermal and mechanical problems in permafrost involve freezing and thawing, water content plays an important role in any thermal considerations of frozen and thawed earth materials.

The volumetric specific heat, ρc , is a measure of the amount of heat that must accumulate in a unit volume to produce a unit increase in temperature (ρ is the bulk density and c is the mass specific heat). For an aggregate of N constituents with constant phase composition, it is simply the sum of the values for each constituent $(\rho c)_i$ weighted by their respective volume fractions Φ_i ; thus:

$$\rho c = \sum_{i=1}^N (\rho c)_i \Phi_i. \tag{27}$$

It is convenient that practically all common rock-forming minerals, including ice, have a value of ρc within 10 or 15 percent of $0.5 \text{ cal/cm}^3 \text{ }^\circ\text{C}$.⁴ Water, of course, has a volume specific heat of $1.0 \text{ cal/cm}^3 \text{ }^\circ\text{C}$. If we denote the volume fraction of water in thawed saturated earth materials by Φ , Eq. (27) yields:

$$(\rho c)_t \approx \frac{1}{2} (1 + \Phi), \tag{28}$$

and for the same material completely frozen

$$(\rho c)_f \approx \frac{1}{2}. \tag{29}$$

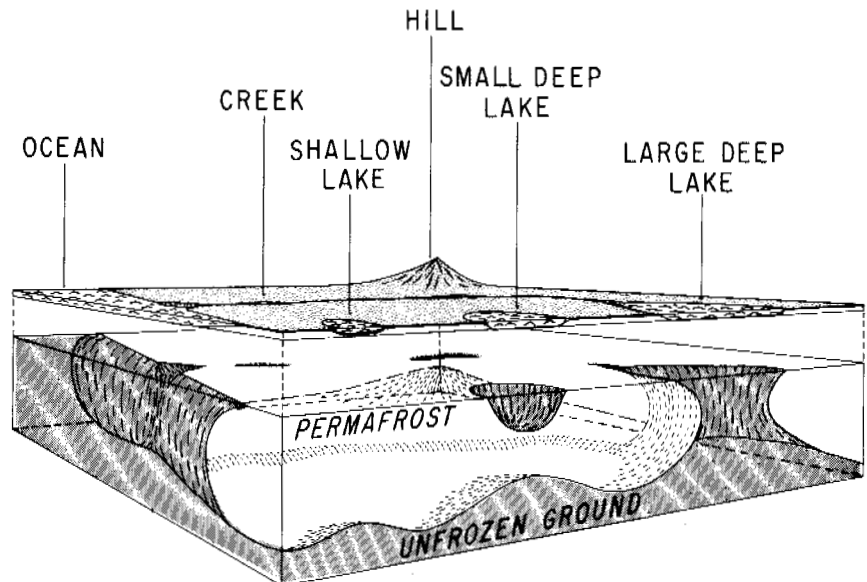


FIGURE 5 Schematic representation of permafrost distribution in a continuous-permafrost region where the mean ocean bottom temperature is greater than 0°C . See Eq. (26).

It will be understood that the units of ρc in these and subsequent relations are $\text{cal/cm}^3 \text{ }^\circ\text{C}$. The subscript “t” will refer throughout to materials that are thawed and “f” to those that are completely frozen. Thus, for completely frozen or thawed materials, the volumetric specific heat is determined adequately for most thermal calculations by a knowledge of the moisture content alone. However, if the interstitial water is saline, or if the permafrost is so fine grained as to subject appreciable volumes of water to the effects of surface forces, it may contain temperature-dependent quantities of unfrozen water. In this case, Eq. (29) might be unsatisfactory.⁷⁶ This is primarily because ρc is defined in terms of a temperature change, which for such continuous two-phase systems involves a temperature-dependent contribution of latent heat.

The thermal conductivity, K , is a measure of the rate at which heat is driven through a medium under a unit thermal gradient. It is commonly measured either by the steady state (“flux-plate” or “divided-bar”) method or by the transient (“probe” or “line-source”) method. In the steady method, the temperature drop across a layer (or disk) of material of known conductivity is compared with that across an overlying layer of the unknown, under conditions of steady, linear flow perpendicular to the layers.^{5,9,96,97,115} The conductivity is then determined from Eq. (3). (A variant using radial geometry was employed by Kersten.⁶²) In the transient method, a long thin probe, containing an axial heater filament and a temperature sensor, is inserted in the medium of unknown conductivity. Heat is supplied to the filament at a constant rate, and the conductivity is determined by comparing the observed temperature rise with the appropriate radial heat conduction model.^{85,108,113,116} The theory of the steady method is simple, but maintaining linear flow (i.e., eliminating radial losses) presents operational difficulties. By contrast, the theory of the transient method may be complicated, but it is relatively simple in operation. The transient method is generally preferred for *in situ* measurements in permafrost because of its convenience.⁶⁵

It is important that, unlike the volume specific heat, the thermal conductivity does not require a changing temperature for its operational definition. (There is no steady-state method for measuring specific heat.) Thus, where temperature-dependent quantities of unfrozen water occur in permafrost, the transient method can give erroneous results, but the thermal conductivity of the system can still be defined uniquely by the steady technique.

Many formulas have been proposed to account for the thermal conductivity of an aggregate in terms of the constituent conductivities K_i and their respective volume fractions Φ_i .^{83,116} Some are very cumbersome, and none has a completely satisfactory theoretical rationale. The major problem arises when the constituent conductivities K_i contrast by several orders of magnitude. Such is the case, for

example, in an undersaturated soil containing appreciable volumes of air and highly conducting mineral grains. In a saturated soil, however, the maximum contrast is less than a factor of 20. It has been verified experimentally^{96,117} that under these conditions no formula is more successful than the simplest one of all, the weighted geometric mean:

$$K = K_1^{\Phi_1} K_2^{\Phi_2} K_3^{\Phi_3} \dots \quad (30)$$

If we denote the geometric mean conductivity of all the mineral constituents by K_r and the thermal conductivity of water by K_w (about $1.3 \text{ mcal/cm s } ^\circ\text{C}$ near $0 \text{ }^\circ\text{C}$), then Eq. (30) yields for saturated thawed material:

$$\begin{aligned} K_t &\approx K_w^\Phi K_r^{1-\Phi} \\ &= (1.3)^\Phi K_r^{(1-\Phi)} \text{ mcal/cm s } ^\circ\text{C}. \end{aligned} \quad (31)$$

(The units of conductivity will not be repeated in the dimensional relations that follow.) Taking the conductivity of ice as $5.2 \text{ cal/cm s } ^\circ\text{C}$ and neglecting the change in volume on freezing, the same material when completely frozen is described by:

$$K_f \approx (5.2)^\Phi K_r^{(1-\Phi)}. \quad (32)$$

The change in the value of Φ on freezing, of course, can be accommodated if the required precision warrants. Because the conductivity is defined by a steady-state process, it is also possible, in concept, to account for a volume fraction of unfrozen water $\Delta\Phi$ co-existing with a volume of ice $\Phi - \Delta\Phi$:

$$K_{f,t} = (5.2)^{\Phi - \Delta\Phi} (1.3)^{\Delta\Phi} K_r^{1-\Phi}, \quad (33)$$

where the subscript “f,t” denotes that the water occurs in both states. It is assumed in Eq. (33) that the conductivity of water is not significantly influenced by the forces that depress its freezing temperature. It can be shown that Eq. (33) applies reasonably well to the interesting recent results of Penner.⁸⁵

From Eq. (31) and (32), K can be approximated for saturated frozen and thawed earth materials from a knowledge of Φ and K_r , quantities that are normally easier to measure or estimate than natural state conductivity. K_r can be determined from Eq. (30) by analysis of the mineral constituents of a dry sample or drill cuttings and reference to tabulated conductivity values.^{31,33,47,94} Common mineral conductivities vary from about $3 \text{ mcal/cm s } ^\circ\text{C}$ for some micas and glass to about 18 for randomly oriented quartz. Values of K_r typically range from about 5 to 15.

Combining Eq. (31) and (32) yields the useful simple result, depending only on moisture content:

$$\frac{K_f}{K_t} \approx 4^\Phi. \quad (34)$$

As an example of its application, let G_f denote the geothermal gradient in permafrost and G_t the gradient in the material immediately beneath its base. We assume that both gradients are uniform and that the difference between the materials results from the state of the water in each. Thus, from Eq. (3):

$$q^* = K_f G_f = K_t G_t. \quad (35)$$

Applying Eq. (34) yields an expression for Φ in terms of the observable gradient ratio:

$$\begin{aligned} \Phi &= (\ln 4)^{-1} \ln \frac{G_t}{G_f} \\ &= 0.72 \ln \frac{G_t}{G_f}. \end{aligned} \quad (36)$$

In the profile illustrated for Prudhoe Bay (Figure 1), the gradient changes at a temperature corresponding approximately to the pressure-melting point of water in a hydrostatic system. Presumably, this gradient change is of the type described in Eq. (36). Substituting the observed value, $G_t/G_f \approx 1.8$ yields $\Phi \approx 42$ percent, which is consistent with fragmentary information obtained from frozen cores at this location. With this information, an analysis of K_r from drill cuttings leads to estimates of K_t and K_f [Eq. (31) and (32)] and q^* [Eq. (35)].

It has been shown that K and ρc frequently appear in the combinations $\alpha = K/\rho c$ and $\sqrt{K\rho c} \equiv K\sqrt{\alpha}$. The first is the thermal diffusivity, important in transient calculations, as it governs the rate of propagation of a temperature disturbance through a medium. The second is variously referred to as the "thermal inertia," "contact coefficient," or "conductive capacity." It governs the heat flux across a surface on which the temperature conditions are prescribed [Eq. (18)] or the interaction between dissimilar layers in transient problems [Eq. (12)]. Combining Eq. (28), (29), (31), and (32) yields useful approximations for these quantities for materials in the common saturated condition:

$$\alpha_f \approx 2K_f \text{ cm}^2/\text{s}, \quad (37a)$$

$$\alpha_t \approx \frac{2K_t}{1+\Phi} \text{ cm}^2/\text{s}, \quad (37b)$$

and

$$\frac{\alpha_f}{\alpha_t} \approx (4)^\Phi (1+\Phi). \quad (37c)$$

It is noted that the contrast in diffusivity [Eq. (37c)] is even greater than the contrast in conductivity [Eq. (34)] when saturated materials freeze. Similarly:

$$(K\rho c)_f^{1/2} \approx \left(\frac{1}{2}K_f\right)^{1/2}, \text{ cal/cm}^2 \text{ }^\circ\text{C s}^{1/2} \quad (38a)$$

$$(K\rho c)_t^{1/2} \approx \left[\frac{1}{2}(1+\Phi)K_t\right]^{1/2}, \text{ cal/cm}^2 \text{ }^\circ\text{C s}^{1/2} \quad (38b)$$

and

$$\frac{(K\rho c)_f^{1/2}}{(K\rho c)_t^{1/2}} = \frac{2\Phi}{\sqrt{1+\Phi}}. \quad (38c)$$

It is seen that the thermal inertia is less sensitive to freezing than the conductivity. The ratio in Eq. (38c) governs the "heat-valve" effect wherein seasonally changing properties at the surface favor heat conduction out of the earth in winter to heat conduction into it in summer.

AREAS OF FUTURE RESEARCH

Methods of calculating ground temperatures for given boundary conditions are now relatively well developed (see Appendix). A major lack is detailed knowledge concerning the actual temperature distribution in permafrost regions and concerning the relative and absolute values of the climatological elements that control it. Obtaining this information is not so much a matter of research, which tends to provide detailed information at only a very small number of sites, but of the establishment of an adequate synoptic weather and ground temperature observation network. The importance of such a network in providing the appreciation of the permafrost condition required for engineering, land use, and scientific programs is often overlooked.

The ground thermal regime is dependent on the nature and characteristics of the surface cover. Little progress has been made in defining this dependence in a quantitative manner. Investigations should be undertaken to establish the relationship between the characteristics of the surface and near-surface material and the components of the surface heat exchange. Because the interest is primarily with respect to temperatures in the ground below the influence of diurnal variations, the relationships obtained should be for time periods of 1 week or more.

Man cannot operate in permafrost areas without affecting the surface in some way. It is imperative that a proper understanding be obtained of the consequences to the ground thermal regime due to such disturbances. Research is required to develop practical models for expressing these consequences in a quantitative way suitable for engineering and land use purposes. Such models would also be of great benefit to the scientist in his investigations of the mechanisms of heat and moisture transfer at the ground surface.

Ground temperature calculations depend on reliable values of the thermal properties of the ground. Measurements of these properties and of their temperature, ice,

and water content dependence are required for many types of earth material.

A very challenging problem is to obtain evidence of past climate from ground temperature measurements. Good and numerous records are required for this method of investigating the past. The application of it to permafrost areas, where it has probably the best possibility of being successful, has only just begun to be exploited.

A knowledge of the steady flow of heat from the earth's interior is fundamental to estimates of the temperature and distribution of permafrost. Consequently, heat-flow measurements should be made whenever the opportunity arises until the regional trends in permafrost regions can be established.

Computerized numerical methods are proving to be powerful tools for modeling the ground thermal regime. Their development should be continued in parallel with complete and well-designed field observation programs. These methods should also be used for parametric investigations to help define the significance to the ground temperature of changes in the thermal properties of the ground and heat transfer characteristics of the surface. Such investigations would help clarify the factors determining the difference between the average annual air and ground surface temperatures.

REFERENCES

- Ahrnsbrack, W. F. 1968. Summertime radiation balance and energy budget of the Canadian tundra. University of Wisconsin, Dept. Meteorology, Tech. Rep. 37, Madison.
- Alur. 1972. Reports of the arctic land use research program. Dept. of Indian and Northern Affairs, Ottawa, Canada.
- Annersten, L. 1966. Interaction between surface cover and permafrost. *Biul. Peryglaj.* 15:27-33.
- Beck, A. E., F. M. Anglin, and J. H. Sass. 1971. Analysis of heat flow data—in situ Thermal conductivity measurements. *Can. J. Earth Sci.* 8:1-19.
- Beck, A. E., and J. M. Beck. 1958. On the measurement of the thermal conductivities of rocks by observations on a divided bar apparatus. *Am. Geophys. Union Trans.* 39:1111-1123.
- Beck, A. E., and A. S. Judge. 1969. Analysis of heat flow data—I, Detailed observations in a single borehole. *Roy. Astron. Soc. Geophys. J.* 18:145-158.
- Berg, R. L., and G. W. Aitkin. Passive methods of controlling geocryological conditions in roadway construction. This volume.
- Birch, F. 1948. The effects of Pleistocene climatic variations upon geothermal gradients. *Am. J. Sci.* 238:529-558.
- Birch, F. 1950. Flow of heat in the Front Range, Colorado. *Geol. Soc. Am. Bull.* 61:567-630.
- Bliss, L. C., and R. W. Wein. 1971. Changes in the active layer caused by surface disturbance, p. 37-46. *In* Proceedings, Conference on permafrost active layer. Tech. Memo. 103. National Research Council of Canada, Ottawa.
- Bliss, L. C., and R. W. Wein. 1972. Plant community responses to disturbances in the western Arctic. *Can. J. Bot.* 50:1097-1109.
- Brewer, M. C. 1958. Some results of geothermal investigations of permafrost in Northern Alaska. *Am. Geophys. Union Trans.* 39:19-26.
- Brewer, M. C. 1958. The thermal regime of an Arctic lake. *Am. Geophys. Union Trans.* 39:278-284.
- Brown, J., W. Richard, and D. Victor. 1969. The effect of disturbance on permafrost terrain. SR 138, U.S. Corps Engineers, Cold Regions Research and Eng. Laboratory, Hanover, New Hampshire.
- Brown, J., and G. C. West. 1970. Tundra biome research in Alaska. U.S. Int. Biol. Prog. Tundra Biome, Rep. 70-1.
- Brown, R. J. E. 1964. Permafrost investigations on the Mackenzie Highway in Alberta and Mackenzie District. Tech. Paper 175. National Research Council of Canada, Division of Building Research, Ottawa.
- Brown, R. J. E. 1965. Some observations on the influence of climatic and terrain features on permafrost at Norman Wells, N.W.T., Canada. *Can. J. Earth Sci.* 2:15-31.
- Brown, R. J. E. 1967. Permafrost investigations in British Columbia and Yukon Territory. Tech. Paper 253. National Research Council of Canada, Division of Building Research, Ottawa.
- Brown, R. J. E. 1967. Permafrost in Canada. Map published by Div. Bldg. Res., Natl. Res. Coun. (NRC 9769) and Geol. Surv. Can. (Map 1246A).
- Brown, R. J. E. 1968. Permafrost investigations in Northern Ontario and Northeastern Manitoba. Tech. Paper 291. National Research Council of Canada, Division of Building Research, Ottawa.
- Brown, R. J. E. 1970. Permafrost as an ecological factor in the subarctic. Proceedings, Conference on ecology of subarctic regions, Helsinki, 1966. p. 129-138.
- Brown, R. J. E. Influence of climatic and terrain factors on ground temperatures at three locations in the permafrost region of Canada. This volume.
- Brown, R. J. E., and G. P. Williams. 1972. The freezing of peatlands. Tech. Paper 381. National Research Council of Canada, Division of Building Research, Ottawa.
- Brown, W. G. 1963. Graphical determination of temperature under heated or cooled areas on the ground surface. Tech. Paper 163. National Research Council of Canada, Division of Building Research, Ottawa. 58 p.
- Brown, W. G. 1963. The temperature under heated and cooled areas on the ground surface. *Trans. Eng. Inst. Can.* 6(B-14).
- Brown, W. G. 1964. Difficulties associated with predicting depth of freeze or thaw. *Can. Geotech. J.* 1:215-226.
- Brown, W. G., and G. H. Johnston. 1970. Dikes on permafrost: Predicting thaw and settlement. *Can. Geotech. J.* 7:365-371.
- Brown, W. G., G. H. Johnston, and R. J. E. Brown. 1964. Comparison of observed and calculated ground temperatures with permafrost distribution under a northern lake. *Can. Geotech. J.* 1:147-154.
- Carslaw, H. S., and J. C. Jaeger. 1947. *Conduction of heat in solids.* Clarendon Press, Oxford. 386 p.
- Cermak, V. 1971. Underground temperature and inferred climatic temperature of the past millenium. *Palaeogeogr. Palaeoclimatol. Palaeoecol.* 10:1-19.
- Clark, S. P., Jr. 1966. Thermal conductivity, p. 459-482. *In* Handbook of physical constants. Geological Society of America, Inc., New York.
- Crawford, C. B., and G. H. Johnston. 1971. Construction on permafrost. *Can. Geotech. J.* 8:236-251.
- Diment, W. H. 1964. Thermal conductivity of serpentinite from Mayaguez, Puerto Rico, and other localities. A Study of Serpentinite: The AMSOC Core Hole near Mayaguez, Puerto Rico. National Academy of Sciences, Washington, D.C. p. 92-106.

34. Diment, W. H. 1965. Comments on paper by E. A. Lubimova, "Heat flow in the Ukrainian Shield in relation to recent tectonic movements." *J. Geophys. Res.* 70:2466-2467.
35. Dingman, S. L. Relations among vegetation, permafrost and potential isolation in Central Alaska. (In press)
36. Ferguson, H. L., A. D. J. O'Neill, and H. F. Cork. 1970. Mean evaporation over Canada. *Water Resour. Res.* 6:1618-1633.
37. Ferrians, O. J., Jr. 1965. Permafrost map of Alaska. U.S. Geological Survey, Misc. Geol. Investigations, Map 1-445.
38. Ferrians, O. J., Jr., R. Kachadoorian, and G. W. Greene. 1969. Permafrost and related engineering problems in Alaska. *Geol. Survey Prof. Paper 678*. U.S. Geological Survey, Washington, D.C.
39. Gold, L. W. 1967. Influence of surface conditions on ground temperature. *Can. J. Earth Sci.* 4:199-208.
40. Gold, L. W., G. H. Johnston, W. A. Slusarchuk, and L. E. Goodrich. 1972. Thermal effects in permafrost. *Proceedings, Canadian northern pipeline Research Conference*. Tech. Memo. 104. National Research Council of Canada, Ottawa. p. 25-45.
41. Hare, F. K. 1970. The tundra climate. *Trans. Roy. Soc. Can. Ser. IV* 8:393-399.
42. Hare, F. K., and J. E. Hay. 1971. Anomalies in the large-scale annual water balance over Northern North America. *Can. Geogr.* 15:79-94.
43. Hare, F. K., and J. C. Ritchie. 1972. The boreal bioclimatis. *Geogr. Rev.* July:333-364.
44. Hay, J. E. 1970. Aspects of the heat and moisture balance of Canada. Ph.D. thesis. University of London, London, England. (Quoted by Hare and Hay, 1971)
45. Hay, J. E. 1970. Modelling the radiation climate of Canada. Presented to Annual Conference, Canadian Association of Geographers, Winnipeg, Manitoba.
46. Heginbottom, J. A. 1971. Some effects of a forest fire on the permafrost active layer at Inuvik, N.W.T. Conference on permafrost active layer. Tech. Memo. 103. National Research Council of Canada, Ottawa.
47. Horai, Ki-iti, and G. Simmons. 1969. Thermal conductivity of rock-forming minerals. *Earth Planet. Sci. Lett.* 6:359-368.
48. Hwang, C. T., D. W. Murray, and E. W. Brooker. 1972. A thermal analysis for structures on permafrost. *Can. Geotech. J.* 9:33-46.
49. Canadian National Committee for the International Hydrological Decade. 1969. Hydrologic atlas of Canada. National Research Council of Canada, Ottawa.
50. Hyndman, R. D., and J. E. Everett. 1968. Heat flow measurements in a low radioactivity area of the western Australian Pre-Cambrian shield. *Roy. Astron. Soc. Geophys. J.* 14:479-486.
51. Hyndman, R. D., J. C. Jaeger, and J. H. Sass. 1969. Heat flow measurements on the southeast coast of Australia. *Earth Planet. Sci. Lett.* 7:12-16.
52. Ives, J. D. 1961. A project for permafrost investigations in Central Labrador-Ungava. *Geogr. Paper 28*. Dept. Mines and Tech. Surveys, Geogr. Branch, Ottawa.
53. Ives, J. D., and B. D. Fahey. 1971. Permafrost occurrence in the Front Range, Colorado Rocky Mountains, U.S.A. *J. Glaciol.* 10:105-111.
54. Jessop, A. M. 1970. How to beat permafrost problems. *Oilweek Jan.*
55. Jessop, A. M. 1971. The distribution of glacial perturbation of heat flow in Canada. *Can. J. Earth Sci.* 8:162-166.
56. Johnston, G. H., and R. J. E. Brown. 1964. Some observations on permafrost distribution at a lake in the Mackenzie Delta, N.W.T., Canada. *Arctic* 17:162-175.
57. Judge, A. 1972. Predicting permafrost depth. *Oilweek July.*
58. Jumkis, A. R. 1966. The frost penetration problem in highway engineering. Rutgers University Press, New Brunswick, New Jersey. 162 p.
59. Kallio, A., and S. Rieger. 1969. Recession of permafrost in a cultivated soil of interior, Alaska. *Proc. Soil Sci. Soc. Am.* 33:430-432.
60. Kazemi, H., and T. K. Perkins. 1971. A mathematical model of thaw-freeze cycles beneath drilling rigs and production platforms in cold regions. *J. Pet. Tech.* March:381-390.
61. Kelley, J. J., and D. F. Weaver. 1969. Physical processes at the surface of the Arctic tundra. *Arctic* 22:425-437.
62. Kersten, M. 1949. Thermal properties of soils. *Univ. Minn. Eng. Exp. Sta. Bull.* 28.
63. Keyes, P. E. 1971. Arctic and subarctic road construction, p. 122-154. *Proceedings, symposium on cold regions engineering*. University of Alaska, College.
64. Kung, E. C., R. A. Bryson, and D. H. Lenshaw. 1964. Study of a continental surface albedo on the basis of flight measurements and structure of the earth's surface cover over North America. *Mon. Weather Rev.* 92:543-564.
65. Lachenbruch, A. H. 1957. A probe for measurement of thermal conductivity of frozen soils in place. *Am. Geophys. Union Trans.* 38:691-697.
66. Lachenbruch, A. H. 1957. Thermal effects of the ocean on permafrost. *Geol. Soc. Am. Bull.* 68:1515-1530.
67. Lachenbruch, A. H. 1957. Three-dimensional heat conduction in permafrost beneath heated buildings. *U.S. Geol. Surv. Bull.* 1052-B. p. 51-69.
68. Lachenbruch, A. H. 1959. Periodic heat flow in a stratified medium with application to permafrost problems. *U.S. Geol. Surv. Bull.* 1083-A. 36 p.
69. Lachenbruch, A. H. 1962. Mechanics of thermal contraction cracks and ice-wedge polygons in permafrost. *Geol. Soc. Am. Spec. Paper* 70. 69 p.
70. Lachenbruch, A. H. 1968. Permafrost, p. 833-839. *In Encyclopedia of geomorphology.*
71. Lachenbruch, A. H. 1968. Rapid estimation of the topographic disturbance to superficial thermal gradients. *Rev. Geophys.* 6:365-400.
72. Lachenbruch, A. H., and M. C. Brewer. 1959. Dissipation of the temperature effect of drilling a well in Arctic Alaska. *U.S. Geol. Surv. Bull.* 1083-C. p. 73-109.
73. Lachenbruch, A. H., M. C. Brewer, G. W. Greene, and B. V. Marshall. 1962. Temperatures in permafrost. p. 791-803. *In Temperature—Its measurement and control in science and industry*. Vol. 3. Reinhold Publishing Corp., New York.
74. Lachenbruch, A. H., G. W. Greene, and B. V. Marshall. 1966. Permafrost and the geothermal regimes. Environment of the Cape Thompson region, Alaska. *USAEC Div. Tech. Information*. p. 149-163.
75. Lachenbruch, A. H., and B. V. Marshall. 1969. Heat flow in the Arctic. *Arctic* 22:300-311.
76. Low, P. F., D. M. Anderson, and P. Hoekstra. 1968. Some thermodynamic relationships for soils at or below the freezing point. 1. Freezing point depression and heat capacity. *Water Resour. Res.* 4:379-394.
77. Mackay, J. R. 1966. Tundra and taiga, future environments of North America. F. Darling and J. P. Milton [ed.]. *Natural History Press*, New York. p. 151-171.
78. Mackay, J. R. 1967. Permafrost depths, lower Mackenzie Valley, Northwest Territories. *Arctic* 20:21-26.
79. Mackay, J. R. 1970. Disturbances to the tundra and forest tundra environment of the western Arctic. *Can. Geotech. J.* 7:420-432.

80. Mackay, J. R. 1971. The origin of massive icy beds in permafrost. *Can. J. Earth Sci.* 8:397-422.
81. Mackay, J. R. 1972. Offshore permafrost and ground ice, southern Beaufort Sea, Canada. *Can. J. Earth Sci.* 9:1550-1561.
82. McFadden, J. D., and R. A. Ragotzkie. 1967. Climatological significance of albedo in Central Canada. *J. Geophys. Res.* 72:1135-1143.
83. McGaw, R. 1969. Heat conduction in saturated granular materials. Special Rept. 103. U.S. Army Corps Engineers, Cold Regions Research and Engineering Laboratory, Hanover, New Hampshire. 131 p.
84. Meyer, G. H., H. H. Keller, and E. G. Couch. 1972. Thermal model for roads, airstrips and building foundations in permafrost regions. *J. Can. Pet. Tech.* 11:13-25.
85. Penner, E. 1970. Thermal conductivity of frozen soils. *Can. J. Earth Sci.* 7:982-987.
86. Péwé, T. L. 1970. Permafrost and vegetation on flood plains of subarctic rivers (Alaska). Symposium on the ecology of the subarctic regions, UNESCO, Helsinki, 1966. p. 141-142.
87. Peyton, H. R. 1969. Thermal design in permafrost soils. Proceedings, 3rd Canadian permafrost conference. Tech. Memo. 96. National Research Council of Canada, Ottawa. p. 85-119.
88. Price, L. W. 1971. Vegetation, microtopography and depth of active layer on different exposures in subarctic alpine tundra. *Ecology* 52:638-647.
89. Priestley, C. H. B. 1959. Turbulent transfer in the lower atmosphere. The University of Chicago Press, Chicago.
90. Radforth, J. R. 1971. Effects of off-road vehicle trials on the active layer in Tundra. Proceedings, Conference on permafrost active layer. Tech. Memo. 103. National Research Council of Canada, Ottawa. p. 48-49.
91. Rickard, W. 1972. Preliminary ecological evaluation of the effects of air cushion vehicle tests on the arctic tundra of Northern Alaska. Spec. Rep. 22. U.S. Corps Engineers, Cold Regions Research and Engineering Laboratory, Hanover, New Hampshire.
92. Rouse, W. R., and R. B. Stewart. 1972. A simple model for determining evaporation from high latitude upland sites. *J. Appl. Meteorol.* 11:1063-1070.
93. Sanger, F. J. 1969. Foundation of structures in cold regions. Mono. III C-4. U.S. Corps Engineers, Cold Regions Research and Engineering Laboratory. Hanover, New Hampshire.
94. Sass, J. H. 1965. The thermal conductivity of fifteen feldspar specimens. *J. Geophys. Res.* 70:4064-4065.
95. Sass, J. H., A. H. Lachenbruch, and A. M. Jessop. 1971. Uniform heat flow in a deep hole in the Canadian shield and its paleoclimatic implications. *J. Geophys. Res.* 76:8586-8596.
96. Sass, J. H., A. H. Lachenbruch, and R. J. Munroe. 1971. Thermal conductivity of rocks from measurements on fragments and its application to heat-flow determinations. *J. Geophys. Res.* 76:3391-3401.
97. Schwerdtfeger, P. 1970. The measurement of heat flow in the ground and the theory of heat flux meters. Tech. Rept. 232. U.S. Army Corps Engineers, Cold Regions Research and Engineering Laboratory, Hanover, New Hampshire. 31 p.
98. Smith, M. W., and C. T. Hwang. Thermal disturbance due to channel shifting, Mackenzie Delta, N.W.T. This volume.
99. W. H. K. Lee [ed.]. Terrestrial heat flow. 1965. American Geophysical Union, Washington, D.C.
100. Terzaghi, K. 1952. Permafrost. *Boston Soc. Civ. Eng. J.* 39:1-50.
101. Thom, B. G. 1969. Permafrost in the Knob Lake iron mining region. Proceedings, 3rd permafrost conference. Tech. Memo. 96. National Research Council of Canada, Ottawa. p. 9-14.
102. Thom, B. G. 1969. New permafrost investigations near Schefferville, P.Q. *Rev. Geogr. (Montreal)* 23:317-327.
103. Titus, R. L., and E. J. Truhlar. 1969. A new estimate of average global solar radiation in Canada. Dept. of the Environment, Atmospheric Environmental Service, CL17-69.
104. University of Alaska. 1971. Fire in the northern environment. U.S. Dept. of Agric., Portland, Oregon.
105. Bowen, S. [ed.] 1971. U.S. tundra biome project. Progress Rep. Vol. 1.
106. Viereck, L. A. 1970. Forest succession and soil development adjacent to the Chena River in interior Alaska. *Arctic Alp. Res.* 2:1-26.
107. Viereck, L. A. Ecological effects of river flooding and forest fires on permafrost in the taiga of Alaska. This volume.
108. Von Herzen, R. P., and A. E. Maxwell. 1959. The measurement of thermal conductivity of deep-sea sediments by a needle-probe method. *J. Geophys. Res.* 64:1557-1563.
109. Vowinckel, E., and S. Orvig. 1965. Energy balance of the Arctic I incoming and absorbed solar radiation at the ground in the Arctic. *Arch. Meteorol. Geophys. Biokl. B* 13:352-377.
110. Vowinckel, E., and S. Orvig. 1971. Synoptic heat budgets at three polar stations. *J. Appl. Meteorol.* 10:387-396.
111. Vowinckel, E., and S. Orvig. 1972. FBBA—An energy budget programme. Meteor. No. 105. McGill University, Montreal, Quebec.
112. Watmore, T. G. 1969. Thermal erosion problems in pipelining. Proceedings, 3rd Canadian conference on permafrost. Tech. Memo. 96. National Research Council of Canada, Ottawa. p. 142-162.
113. Wechsler, A. E. 1966. Development of thermal conductivity probes for soils and insulations. Tech. Rep. 182. U.S. Army Materiel Command, Cold Regions Research and Engineering Laboratory, Hanover, New Hampshire. 83 p.
114. Weller, G., and J. Brown. 1971. The structure and function of the tundra ecosystem. Progress Rep. Vol. 1. U.S. Tundra Biome Program, U.S. Int. Biol. Program.
115. Woodside, W. 1957. Deviations from one-dimensional heat flow in guarded hot-plate measurements. *Rev. Sci. Instrum.* 28:1033-1037.
116. Woodside, W., and J. H. Messmer. 1961. Thermal conductivity of porous media. I. Unconsolidated sands. *J. Appl. Phys.* 32:1688-1698.
117. Woodside, W., and J. H. Messmer. 1961. Thermal conductivity of porous media. II. Consolidated rocks. *J. Appl. Phys.* 32:1699-1706.

LIST OF CONVERSIONS

$$1 \text{ cal} = 4.2 \text{ J}$$

$$1 \text{ cal/cm}^3 \text{ } ^\circ\text{C} = 4.2 \text{ MJ/m}^3 \cdot \text{K}$$

$$1 \text{ cal/cm} \cdot \text{sec} \text{ } ^\circ\text{C} = 420 \text{ W/m} \cdot \text{K}$$

$$1 \text{ cal/cm}^2 \cdot \text{sec} = 42 \text{ kW/m}^2$$

$$1 \text{ cal/cm}^2 \cdot \text{sec}^{1/2} = 42 \text{ kJ/m}^2 \cdot \text{s}^{1/2}$$

APPENDIX

COMPUTER SIMULATION

L. E. Goodrich

NATIONAL RESEARCH COUNCIL OF CANADA
Ottawa, Ontario, Canada.

For many problems of engineering or scientific interest, calculation of the ground thermal regime by analytic

methods is either impossible or excessively cumbersome. In North America, the usual approach in such cases is to use computerized numerical methods.

Numerical models have been, and continue to be, developed by universities, government institutions, and industry. Recent interest in hot oil pipelines in the north has spurred efforts in the field of numerical modeling of the ground thermal regime, but much of this work remains proprietary. The following is an outline of the major considerations and problems relevant to modeling the ground thermal regime and the various numerical techniques used to treat them, illustrated by examples from recent literature.

Choice of the numerical method depends on the problem under consideration. For one-dimensional analyses, finite-difference methods are in common use. These fall into three categories: ordinary forward difference (explicit); backward difference (implicit); and alternating direction (explicit).

Although simple to program, the ordinary forward-difference method has a major drawback in that the time-steps chosen must be small enough to guarantee stable solutions. This requirement is often so stringent as to render the method inefficient for practical computations. This is particularly true when modeling surface boundary conditions of the heat-balance type encountered in geothermal problems. The method has been used, however, in a recent work by Dempsey² concerned with freezing and thawing in road pavements.

Backward-difference methods, although more complicated to program, are unconditionally stable. Longer time-steps may be used but since a greater number of calculations per time-step is required than for explicit methods, the computational advantage of implicit methods is not always ensured.

Alternating-direction methods are unconditionally stable and require few calculations per time-step. In the most widely known method of this type (that due to Saul'yev¹² and employed, for example, by Doherty³ and Lachenbruch⁹ in a model for the thermal regime around a buried pipeline in permafrost), accuracy considerations force the use of rather small time-steps. A new alternating-direction explicit method now being developed by the author retains the advantages of the Saul'yev method while giving an accuracy nearly identical with that of the implicit methods.

Although finite-difference methods, such as the alternating-direction implicit method of Peaceman and Rachford¹¹ used, for example, by Fleming⁴ or the alternating-direction explicit method as used by Doherty,³ are used for two-dimensional problems, the recent trend is toward the use of finite-element methods. In the latter, the differential equation and associated initial and boundary conditions are replaced by an equivalent variational problem, the solution of which may then be found approximately by numerical methods. The principal advantage of the technique, which is a consequence of the use of triangular-shaped node elements,

is the ease, accuracy, and efficiency with which complicated geometrical boundaries can be treated. A recent program of this type, intended specifically for geothermal problems, is that of Hwang *et al.*⁶ based on the fundamental work of Wilson and Nickell.¹³

Common to all models of interest to permafrost problems is some means of taking account of the effects of latent heat. The simplest approach is to assume that the phase change takes place over a small temperature range and introduce an effective heat capacity for the nodal volume undergoing phase change. Although easy to program, the method may require the use of a very fine space-grid in order to determine the position of a phase front with adequate accuracy. The time-step may then also have to be reduced to ensure that the phase boundary does not "miss" a node, thus creating an error in the results. With the time-step thus limited, there may be little or no advantage of an implicit over an explicit finite-difference formulation. The method produces distortion of the temperature field in the neighborhood of the phase boundary and keeping this within reasonable limits again requires suitably small space- and time-steps.

An example of an implicit one-dimensional formulation involving this type of latent heat treatment, but with the refinement of introducing a subgrid for evaluation of the effective heat capacity of the phase node, is the model of Nakano and Brown,¹⁰ which was designed to study seasonal thaw in Fairbanks peat and silt. Another model using this approach is the one-dimensional simultaneous heat and mass transfer model of Harlan,⁵ which was devised primarily for theoretical studies of moisture migration during soil freezing.

Although considerably more complicated to program much greater accuracy can be obtained for a given grid-spacing and time-step if, instead of introducing the artifice of an effective heat capacity for the node undergoing phase change, one models the actual boundary conditions at the moving phase boundary. This is achieved, for example, in the author's one-dimensional explicit finite-difference model, in the one-dimensional implicit model of Kazemi and Perkins,⁷ and in the two-dimensional finite-element model of Hwang *et al.*⁶

All models mentioned either take account, or are potentially capable of taking account, of the effects of latent heat release over a temperature range, as occurs in fine-grained materials. Whether such refinement is either necessary or justified is debatable. Freezing in fine-grained soils in nature is usually accompanied by considerable moisture redistribution and volume changes whether or not one is dealing with an open or closed system; unless provision is made to properly account for the resulting heat transfer and modification to the thermal properties, the model is not physically consistent. Attempts to include some of the major effects of moisture redistribution during freezing of idealized theoretical materials have been made. The simul-

taneous heat and moisture transfer model of Harlan may be cited as an example.⁵

During thawing of permafrost materials, considerable consolidation may occur. Whether it is important to attempt to model such effects again depends on the problem to be considered. For example, if one intends to use the model for the optimum design of insulated roadways in which little or no thawing below the insulation is to be permitted, then thaw consolidation is not a consideration. On the other hand, models that attempt to describe the thermal regime around hot buried pipelines in permafrost most probably should take account of thaw settlement as well as movement of the pipe. Models that attempt to do this are under development, for example, the finite element analysis of Charlwood and Svec.¹

All the numerical models mentioned are capable of handling space-, time-, and temperature-dependent thermal properties. Thermal conductivities for calculations are usually estimated from empirical formulas, such as those of Kersten⁸ for inorganic clays and sands, assuming constant values of dry density and water content.

These formulas are incapable of accounting for the effects of ice inclusions and temperature-dependent phase composition that may be of major importance to temperature calculations in frozen permafrost materials. For thaw calculations in permafrost, however, this may be of little consequence, inasmuch as such problems are dominated by the heat flow in the thawed zone and are therefore relatively insensitive to changes in thermal properties of the frozen materials.

Although capable of handling a range of external boundary conditions, most thermal numerical models assume that surface temperature is a known function of time. Very often the assumption is made that surface temperature equals air temperature. Except for problems involving strong internal heat sources or sinks (hot or cold buried pipelines may be in this category), such an assumption may lead to errors that considerably outweigh those due to the approximate treatment of internal phenomena. A surface heat balance boundary treatment can be incorporated in most models, but adequate information on the various parameters involved and their variations with time is generally unavailable. This approach is attempted, for example, in the one-dimensional model of Dempsey for dry road pavements.²

For dry surfaces the difference between air and surface temperatures may be considerable, whereas wet surfaces

more closely follow air temperatures, at least for time scales of the order of days or weeks, and, in this case, equating the two is not unreasonable. In view of the uncertainty of surface temperature values and since this is the single most important parameter in determining the near-surface ground thermal regime in many cases of interest, further refinement of the internal heat exchange aspects of numerical models is generally not warranted. For design calculations, it is seldom that one can do more than assume that surface temperature equals air temperature or some empirical function of it. This may nevertheless be adequate since such calculations are generally concerned with finding the response to possible extreme conditions.

REFERENCES

1. Charlwood, R. G., and O. Svec. 1972. Northern pipelines: An application for numerical analysis, Part II. Symposium on applications of solid mechanics. University of Waterloo, Waterloo, Ontario.
2. Dempsey, B. J. 1970. A heat transfer model for evaluating frost action and temperature related effects in multilayered pavement systems. Ph.D. Thesis. University of Illinois, Urbana.
3. Doherty, P. C. 1970. Geological Survey computer contribution No. 4, "Hot Pipe." U.S. Geological Survey, Computer Center Division, Washington, D.C.
4. Fleming, A. K. 1971. The numerical calculation of freezing processes. Presented at International Institute of Refrigeration meeting, Washington, D.C.
5. Harlan, R. L. 1972. Ground conditioning and the groundwater response to winter conditions. Presented at W.M.O.-UNESCO Symposia on the Role of Snow and Ice in Hydrology, Banff, Alberta, Canada.
6. Hwang, C. T., D. W. Murray, and E. W. Brooker. 1972. A thermal analysis for structures on permafrost. *Can. Geotech. J.* 9:33-46.
7. Kazemi, H., and T. K. Perkins. 1971. Mathematical model of freeze-thaw cycles beneath drilling rigs and production platforms in cold regions. *J. Pet. Tech.* March:381-390.
8. Kersten, M. 1949. Thermal properties of soils. *Univ. Minn. Eng. Exp. Sta. Bull.* 28.
9. Lachenbruch, A. H. 1970. Some estimates of the thermal effects of a heated pipeline in permafrost. *U.S. Geol. Surv. Circ.* 632.
10. Nakano, Y., and J. Brown. 1971. Effect of a freezing zone of finite width on the thermal regime of soils. *Water Resour. Res.* 7:1226-1233.
11. Peaceman, D. W., and H. H. Rachford. 1955. The numerical solution of parabolic and elliptic differential equations. *J. Soc. Appl. Math.* 3:28-45.
12. Saul'yev, V. K. 1960. Integration of equations of parabolic type by the method of nets. Macmillan Co. (for Pergamon Press), New York. Translated from the Russian (1964) by G. J. Tee.
13. Wilson, E. L., and R. E. Nickell. 1966. Application of the finite-element method to heat conduction analysis. *Nuclear Engineering and Design* No. 4. North Holland, Amsterdam. p. 276-286.

INFLUENCE OF CLIMATIC AND TERRAIN FACTORS ON GROUND TEMPERATURES AT THREE LOCATIONS IN THE PERMAFROST REGION OF CANADA

Roger J. E. Brown

NATIONAL RESEARCH COUNCIL OF CANADA

Ottawa, Ontario

INTRODUCTION

Regular periodic measurements (at least monthly) of ground temperatures are being taken by the Division of Building Research, National Research Council of Canada, at three locations in northern Canada to assess the influence of climatic and terrain factors on permafrost. These are Thompson, Manitoba ($55^{\circ}48'N$, $97^{\circ}52'W$), situated in the southern part of the discontinuous permafrost zone, Yellowknife, Northwest Territories ($62^{\circ}28'N$, $114^{\circ}27'W$), in the northern part of the discontinuous permafrost zone, and Devon Island ($76^{\circ}N$), located in the Canadian Arctic Archipelago (Queen Elizabeth Islands) in the northern part of the continuous zone.^{1,2} Ground temperature measurements with thermocouple cables down to the 15-m depth in various types of terrain are being taken at these locations and analyzed to determine the range of mean annual ground temperatures that may exist at any one site in the permafrost region.

TERRAIN CONDITIONS AND DESCRIPTION OF SITES

Thompson, Manitoba

Thompson, 200 m above sea level with a mean annual air temperature of $-3.3^{\circ}C$, is located in the Precambrian shield region in northern Manitoba. It is situated near the northern margin of glacial Lake Agassiz where the glaciolacustrine varved silts and clays are about 30 m thick overlying a thin layer of till on bedrock. The generally subdued relief is interrupted only by river valleys, cut into the overburden, scattered rock outcrops, and glaciofluvial deposits.

Permafrost occurs in scattered islands varying in extent from a few tens of square metres to several hectares and in thickness from about 1 to 15 m or greater, averaging between 3 and 5 m.³ The permafrost table is generally encountered anywhere from about 0.5 to 2 m below the ground surface. Much ice, primarily in the form of horizontal lenses up to 20 cm thick (the average thickness being less than 2.5 cm), is found throughout the frozen glaciolacustrine silts and clays underlying the area. No permafrost

occurs in the Precambrian rock outcrops scattered throughout the region.³

Five sites were selected for study in a program of investigation of microclimatic and terrain factors affecting the distribution and characteristics of permafrost, which includes measurements of ground temperatures.⁴ Four of the sites on the glaciolacustrine soils are located within a distance of a few hundred metres of each other, two with permafrost and two with none. Weekly measurements of ground temperatures have been undertaken since June 1968 on 12-point thermocouple cables installed in augered holes to a depth of 7.5 m. The fifth site is located in a rock (pegmatite) outcrop where weekly measurements of ground temperatures have been undertaken since February 1968 on thermocouple cables installed in drilled holes to a depth of 6 m. Air temperature, ground surface temperature, snow depth, and density measurements also have been taken regularly at all sites.

Of the four sites, site A supports black spruce up to 6 m high and dense growth, 0.5–1.5 m between trees, growing on a 10-cm-thick layer of feathermoss and forest litter overlying brown clayey soil (grain-size analysis at a depth of 15–23 cm: clay, 59 percent; silt, 39 percent; sand, 2 percent). No permafrost exists at this site.

Site B supports open stunted black spruce up to 4 m high with 1.5–3 m between trees growing on a 10-cm-thick layer of *Sphagnum* over 10 cm of peat, 23 cm of black organic clay (31 percent organic content by weight) overlying brown clayey soil (grain-size analysis at a depth of 30–53 cm: clay, 77 percent; silt, 22 percent; sand, 1 percent). There is no permafrost at this site.

Site C (Figure 1) supports open stunted black spruce similar to that at site B growing on an 18-cm-thick layer of hummocky *Sphagnum* over 18 cm of peat, 10 cm of black organic clay (26 percent organic content by weight) overlying brown clayey soil (grain-size analysis at a depth of 35–60 cm: clay, 85 percent; silt, 14 percent; sand, 1 percent). There is permafrost at this site. The permafrost table in 1968 at the beginning of the observations was at a depth of about 48 cm, almost coincident with the base of the organic soil. The permafrost is about 2.7 m thick.

Site D supports dense black spruce similar to that at site



FIGURE 1 Site C, at Thompson, Manitoba, June 1968.

A that grows on a 13-cm-thick layer of *Sphagnum* over 18 cm of black organic silt (77 percent organic content by weight) overlying brown clayey soil (grain-size analysis for the organic silt: clay, 28 percent; silt, 62 percent; sand, 10 percent; in the brown clay at 33–48 cm: clay, 87 percent; silt, 12 percent; sand, 1 percent). The permafrost table is at a depth of about 75 cm and the permafrost exceeds 6 m in thickness.

A thermocouple cable was installed in the fall of 1971 in a peat plateau with permafrost to a depth of 22.5 m. The tree vegetation is similar to that at site A with a ground cover of hummocky *Sphagnum*, lichen, and peat about 0.5 m thick overlying brown clayey soil similar to the other soil sites. Temperature measurements through part of 1 year indicate that the permafrost is 12 m thick and cooler than the permafrost at site D.

Yellowknife, Northwest Territories

Yellowknife, 180 m above sea level with a mean annual air temperature of -5.5°C , is located in the Precambrian shield on the north shore of Great Slave Lake. The terrain consists mainly of rock outcrops with scattered pockets of till, glaciofluvial deposits including sand and gravel outwash, and beach deposits. Peat bogs and small lakes occupy many of the rock basins.

Permafrost is widespread, but not continuous, and extends to depths exceeding 50 m in some areas.⁵ It does not occur in the exposed bedrock, but it is found where the rock is covered with overburden. Its greatest extent is in peatlands supporting spruce and sedge vegetation where the active layer is about 1 m. Little information is available on ground ice. Random bodies of massive ice some tens of

centimetres thick have been found in pockets of silt and clay, and thin ice layers have been observed at depth in bedrock fissures.

Eight sites were selected for study in a program of investigation of microclimatic and terrain factors affecting the distribution and characteristics of permafrost, which includes measurements of ground temperatures. A 12-point thermocouple cable was installed at each site to a depth of 15 m, four in September 1969 and the remainder 1 year later. Weekly or monthly measurements of ground temperatures have been undertaken since those dates. Air temperature, ground surface temperature, snow depth, and density measurements also have been taken regularly at all sites.

Three of the sites are situated on exposed bedrock supporting a few scattered stunted black spruce trees. The first (termed “black rock” site) is greenstone having a thermal conductivity [1] (wet) of 2.72 W/mk and porosity by volume of 0.2 percent. The second is a white granite (termed “white rock” site) having a thermal conductivity (wet) of 3.70 W/mk and porosity by volume of 0.8 percent. The third (Figure 2) is a pink granodiorite (termed “red rock” site) having a thermal conductivity (wet) of 2.60 W/mk and porosity by volume of 0.7 percent. No permafrost occurs in these sites.

Three sites in overburden where no permafrost was found are located on till, a beach ridge, and burned peatland. The till site supports open groves of birch and alder up to 7 m high with a ground cover of scattered berry plants, mosses, and lichens and an organic layer about 3 cm thick overlying a brown sandy stony till. The beach ridge site supports a dense growth of birch, jackpine, alder, and willow up to 8 m high with ground cover of berry plants, mosses, and lichens and organic layer about 3 cm thick overlying brown sandy



FIGURE 2 Red rock site at Yellowknife, N.W.T., September 1970.

gravel. The burned peatland site supports a dense growth of spindly black spruce up to 8 m high containing many dead and burned trees with ground cover of mosses and Labrador tea and a layer of wet peat 30 cm thick overlying wet fine sand. This material forms a 6-m-thick layer on greenstone bedrock.

The remaining two sites both contain permafrost. One site (termed "sedge peatland" site) is located in a peat bog supporting very scattered and stunted black spruce and tamarack up to 3 m high with willow and alder shrubs and ground cover of sedges, mosses, and peat 1 m thick overlying wet fine to medium sandy soil (Figure 3). The active layer is about 68 cm and the permafrost is about 30 m

thick. The other site (termed "spruce peatland" site) is located in a peat bog supporting black spruce and some tamarack up to 7 m high with scattered willow and alder underbrush and ground cover of hummocky *Sphagnum* and lichen and peat 1.3 m thick overlying silty fine sand with stones. Greenstone bedrock occurs at a depth of 3 m. The active layer is 30 cm, and the permafrost is about 50 m thick.

Devon Island, Northwest Territories

The ground temperature observation sites are located on the north coast of Devon Island in a lowland near sea level



FIGURE 3 Sedge peatland site at Yellowknife, N.W.T., September 1970.

measuring about 6 × 8 km. The terrain consists of groups of beach ridges interspersed with lowlying tundra meadows. The northwest corner of the lowland consists of a Palaeozoic limestone bedrock plain, and Precambrian granite outcrops are scattered throughout the eastern portion. The lowland is bounded on the east and south landward margins by 300- to 400-m-high uplands of Cambro-Ordovician interbedded limestones and sandstones and Precambrian granite, respectively.¹

Permafrost occurs everywhere beneath the ground surface to an estimated thickness of 450–600 m.² The active layer varies from a maximum of about 2.2 m in the granite bedrock to a minimum of about 12 cm in wet peaty meadow sites. Surface features, characteristic of high latitude continuous permafrost, abound including tundra ice-wedge polygons, 2-m-high polygonal peat mounds with 1-m-deep trenches, stony earth circles, and stone nets. Little information is available on the occurrence and distribution of ground ice, but it has been observed to exist in layers up to 1 m thick in the peat mounds and in vertical wedges beneath the trenches between these mounds.

Eleven holes were drilled in these major terrain units in June and July 1971 to obtain information on the perennially frozen soils and bedrock and to install thermocouple cables for monitoring ground temperatures in the permafrost. Monthly ground temperature measurements were taken from July to October 1971 inclusive. They were resumed in May 1972 and will be continued until summer of 1973 to furnish one 12-month period. Air temperature, ground surface temperature, snow depth, and density measurements also are being taken regularly at all sites. Data on the depths of the thermocouple cables, thickness of active layer and other information are given in Table I.

TABLE I Terrain Type and Active Layer Thickness at Thermocouple Cable Sites, Devon Island

Terrain Type	Elevation above Sea Level (m)	Depth of Cable (m)	Thickness of Active Layer (m)
Beach ridge			
south slope	38	1.45	1.1
top	38	1.20	0.9
north slope	38	0.75	0.6
Peat mound			
summit	30	1.35	0.3
trench	30	1.65	0.3
trench	30	1.05	0.3
Meadow	52	2.80	0.7
Limestone			
coast	1	8.70	1.2
inland	9	6.90	1.4
Granite-gneiss	75	6.45	2.2
Upland plateau	306	7.90	0.3

Four thermocouple cables, having sensors at intervals from 0.75 to 1.5 m, were installed in bedrock. Two of these are located in the limestone plain in the northwest section of the lowland, one at the coast about 1 m above sea level (Figure 4) and the other 0.5 km inland, 9 m above sea level. The rock down to a depth of about 4.5 m consists of pitted (vesicular) limestone having thermal conductivity values ranging from about 4.62 to 5.04 W/mk and porosity of about 3 percent. Below, the rock is a dolomitic limestone having thermal conductivity values ranging from about 4.20 to 4.62 W/mk and porosity of about 13 to 7 percent, respectively. One hole was drilled in a granite-gneiss outcrop, 75 m above sea level, having a thermal conductivity of 2.52 W/mk



FIGURE 4 Coastal site on limestone plain at Devon Island, N.W.T., July 1971.

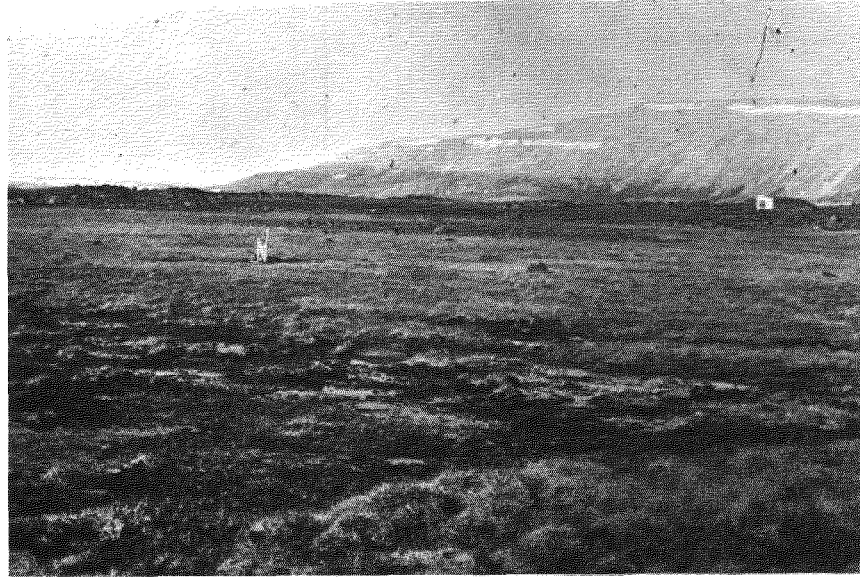


FIGURE 5 Tundra meadow site on Devon Island, N.W.T., July 1971.

and porosity of 0.3 percent. The fourth thermocouple cable was installed on the 300-m-high upland plateau east of the lowland. Although this site is virtually devoid of vegetation, the ground surface is covered with stone nets. The soil to a depth of 1.5 m is stony silt overlying fissured sandstone and dolomite and has thermal conductivity values ranging from 3.11 to 3.71 W/mk and porosity of 10 to 3 percent, respectively.

Three of the thermocouple cables that had sensors at 15-cm intervals were installed on the south and north slopes and at the top of a gravel beach ridge about 38 m above sea level. This land form, typical of the beach ridges on the lowland, is virtually devoid of vegetation, except for scattered clumps of mosses and small flowering plants.

Another set of three cables, with sensors at 15-cm intervals, was placed in a nearby area of polygonal peat mounds, 30 m above sea level, one on the summit of a mound and two in trenches. The vegetation on the mounds consists of mosses, lichens, and sedges. The mounds consist of peat 2 m thick and contain irregular ice layers up to 1 m thick overlying stony till.

One cable with sensors at 0.75- to 1.5-m intervals was installed in a tundra meadow, 52 m above sea level. The ground vegetation is a continuous carpet of sedges and mosses and 12.5 cm of peat overlying sandy stony till containing granite boulders (Figure 5).

ANALYSIS OF GROUND TEMPERATURE OBSERVATIONS

Mean annual ground temperature values and envelopes for selected years at Thompson and Yellowknife were plotted versus depth to obtain profiles characteristic of the various terrain types (Figures 6-9). At Thompson, Manitoba, mean

annual ground temperature values were plotted for 1969 for the four soil sites and for 1969 and 1970 for the pegmatite rock site. Temperature values at Yellowknife were plotted for 1970 for the greenstone rock site, burned peatland, sedge peatland, and spruce peatland sites and for all sites in 1971. At Devon Island, it was not possible to calculate annual means but the available values for July to October 1971 were averaged to obtain characteristics of the summer and fall ground thermal regimes (Figure 10).

Several correlations and generalizations can be made, the principal one being that the mean annual ground temperatures at depths down to 15 m may vary 2 °C among various types of terrain at any one location in the permafrost region.

At Thompson, the mean annual ground temperature profiles vary from the lowest at site D, which has the thickest permafrost, to site C, with thinner permafrost, to the two soil sites, with no permafrost, to the warmest, which is the bedrock site. The temperature differences between adjacent installations at the soil sites range from 0.5 to about 1 °C. The rock site is about 1.5 degrees warmer than the warmest soil site and nearly 3 degrees warmer than the coldest permafrost site. The amplitude of the annual temperature change appears to increase from the coldest hole to the warmest.

At site D, which has the thickest and coldest permafrost, the amplitude from the 2-m depth to the bottom of the hole is about 1 °C and increases to the warmest soil site hole where it is about 2 °C. The amplitude at the bedrock hole is much greater, being about 4.5 °C at the 6-m depth.

The relations of snow depth and density to ground temperatures are not straightforward. The least snow accumulation does occur at site D, but it is almost as low at site A, a nonpermafrost site. Site C, the other permafrost site, is the

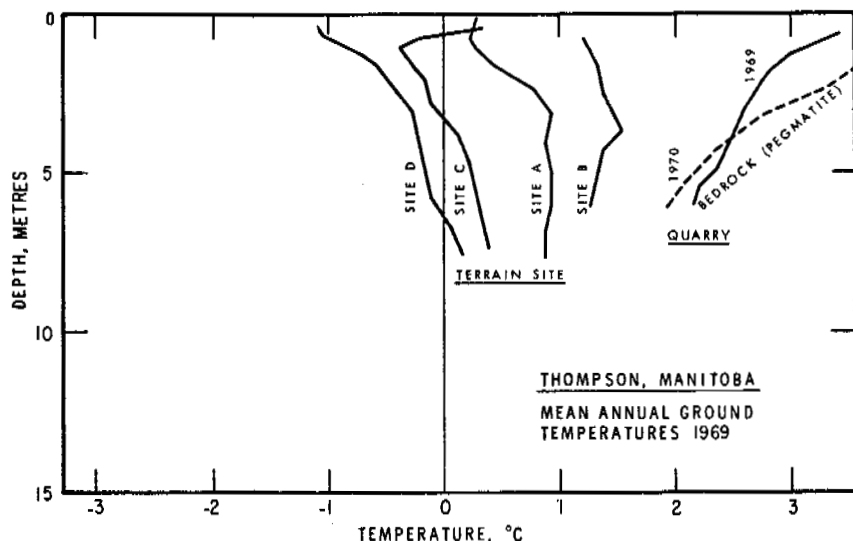


FIGURE 6 Mean annual ground temperatures, Thompson, Manitoba, July 1971.

highest of the four. Sites A and D have denser tree growth than B or C, and snow density values are generally about 10 percent lower at sites B and C. The snowfall in the early winter of 1969-1970 was greater than in 1970-1971, which appears to be reflected in the minimum temperatures at the bedrock site being slightly warmer in 1969 than in 1970.

At Yellowknife, the mean annual ground temperature profiles vary from the lowest at the spruce peatland site, which has the thickest permafrost, to the warmest holes in the bedrock. The temperature differences between adjacent installations average about 0.25 °C; the total range is about 2 °C. This is considerably less than the range between the coldest permafrost hole and bedrock hole at Thompson. The coarse-grained till and beach sites have annual means similar to the bedrock holes. The white rock (granite) has

the lowest mean annual temperature (about 0.5 °C) and the highest thermal conductivity (3.68 W/mk); the red rock (granodiorite) has the highest mean annual temperature (about 1.5 °C) and the lowest thermal conductivity (2.59). The black rock (greenstone) has mean annual temperatures of about 1 °C and a thermal conductivity value of about 2.72

The amplitude of the annual temperature change is greatest in the bedrock holes and is similar in the three holes. The difference between maximum and minimum temperatures is much greater than at Thompson, as illustrated by the temperature at the 6-m depth, which is 9.0 °C at Yellowknife and 4.5 °C at Thompson. The amplitude from the 7- to 15-m depth in the till and beach holes is much less, averaging 0.5-1 °C in the former and 1.0-1.5 °C in the

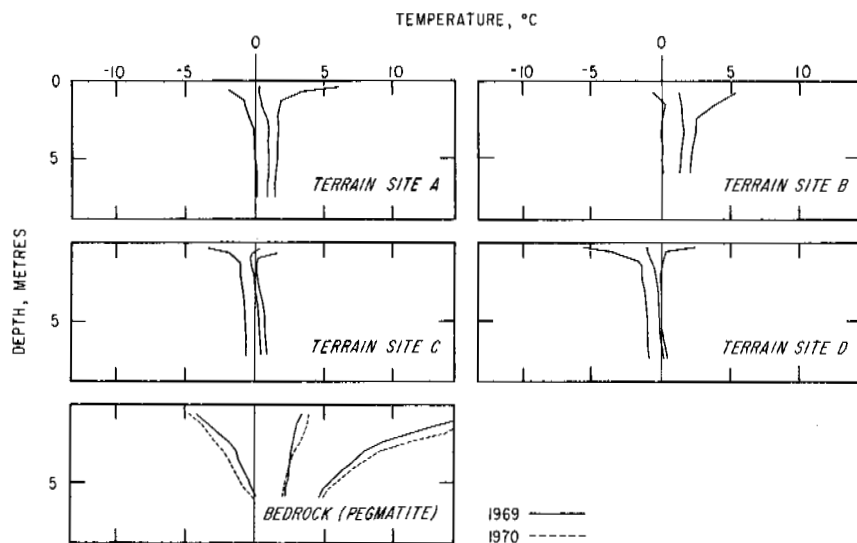


FIGURE 7 Ground temperature envelopes, Thompson, Manitoba, 1969 and 1970.

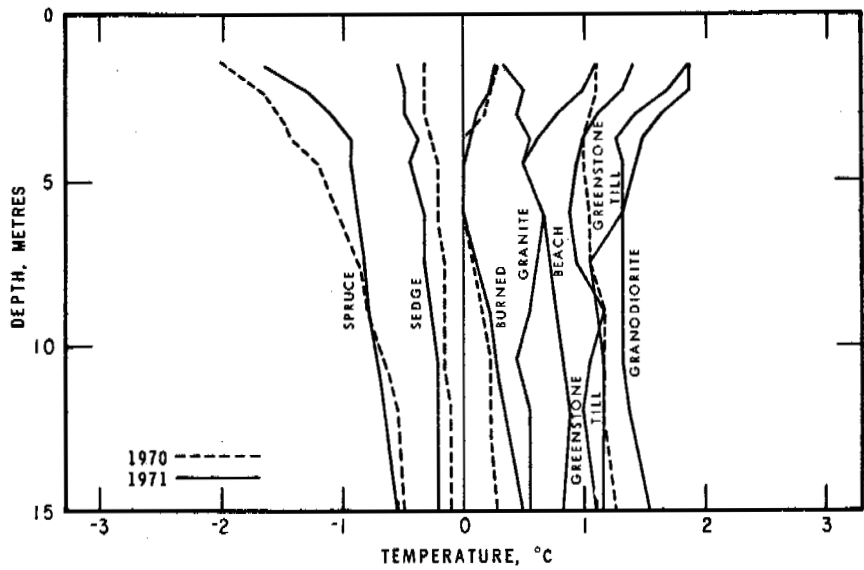


FIGURE 8 Mean annual ground temperatures, Yellowknife, N.W.T., 1970 and 1971.

latter. It is even smaller in the burned sedge and spruce peatland sites that range from 0.25 to 0.5 °C. The amplitudes in the last three holes decrease abruptly in the 1- to 3-m depth and to a lesser extent in the till and beach holes in contrast to the bedrock holes where the amplitudes decrease smoothly with depth. In all of the holes, there is a noticeable fluctuation of temperature through the year at the 15-m depth that ranges from 2 °C at the black rock site to 0.25 °C in the sedge peatland.

The relation of snow depth and density to ground temperatures is again not straightforward. The maximum snow-cover in the winter of 1970-1971 ranged from 33 cm at the black rock site to 45 cm in the burned and sedge peatland sites. The rock sites generally had slightly less accumulation than the other sites and densities about 5 percent higher.

Snowfall was greater in 1970-1971 than in 1969-1970 which appeared to be reflected in the ground temperature regimes. For example, the annual mean and minimum temperatures were slightly warmer in the second year at the black rock and spruce peatland sites.

At Devon Island, ground temperature observations are available only for July to October 1971. Nevertheless, some characteristics of the summer and fall ground thermal regime are evident. Significant variations occurred in the thickness of the active layer in different types of terrain ranging from the deepest (2.2 m) in granite-gneiss to the shallowest (0.3 m) in the peat mounds and the upland plateau. Variations due to slope orientation are very evident in the beach ridge. There did not appear to be significant variation in the peat mounds between the mound summit and the trenches. The

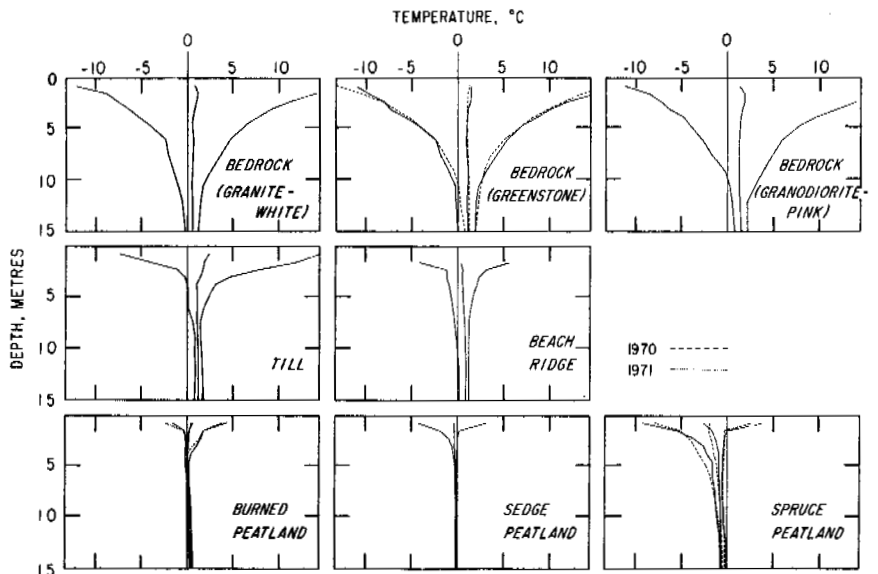


FIGURE 9 Ground temperature envelopes, Yellowknife, N.W.T., 1970 and 1971.

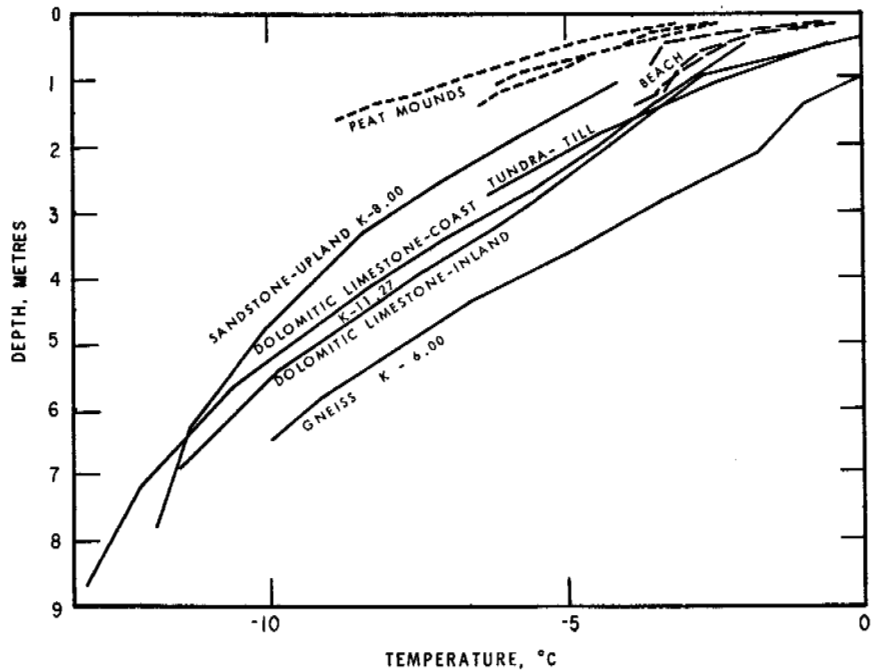


FIGURE 10 Average of mean monthly ground temperatures, Devon Island, N.W.T., July to October 1971 (inclusive).

active layer in the meadow was less than in the beach ridges (except the steep north slope) and rock outcrops because of the surface vegetation. The active layer in the limestone (especially at the coast) was considerably less than in the granite-gneiss possibly because of the former area's proximity to the cold ocean water.

These variations in depth of active layer are reflected in the ground temperature averages for the summer months. In the peat mounds, these values were nearly 3°C lower than in the beach ridges in the active layer and top metre of the permafrost. Further down, the upland was coldest, probably because of its high elevation relative to the other stations, the tundra meadow was colder than the limestone, and the granite-gneiss was considerably warmer. The relative effect of variations in thermal conductivity for the rock is not clear nor is the influence of snow depth and density.

All sites experienced a marked drop in ground temperature near the surface from August to September, and freeze-back of the active layer was completed during this period. At the bottom of the holes, the warmest temperatures were experienced in October as the effect of summer atmospheric heating penetrated downward.

CONCLUSION

These observations at Thompson, Yellowknife, and Devon Island indicate that mean annual ground temperatures at depths down to 15 m may differ over a 2°C range among various types of terrain at any one location in the permafrost region. These variations are reflected in different depths of active layer that may range from less than 0.5 m

to more than 2 m, even in the northern part of the continuous zone. Variations greater than 1°C may occur even between sites only a few tens of metres apart. These local differences can reflect significant differences in the extent and thickness of permafrost and the susceptibility to thawing. Many more observations are required from other parts of the permafrost region to correlate terrain type and ground temperature conditions.

REFERENCES

1. Brown, R. J. E. 1972. In L. C. Bliss [ed.] Permafrost investigations on Devon Island, N.W.T. Canadian Tundra Biome Study Site (IBP), Devon Island I.B.P. Project-High Arctic Ecosystem, Project Report 1970 and 1971. p. 30-45.
2. Brown, R. J. E. 1972. Permafrost in the Canadian Arctic Archipelago. *Z. Geomorphol. Suppl.* 13:102-130.
3. Johnston, G. H., R. J. E. Brown, and D. N. Pickersgill. 1963. Permafrost investigations at Thompson, Manitoba: Terrain studies. Tech. Paper No. 158. Division of Building Research, National Research Council of Canada, Ottawa. 51 p.
4. Brown, R. J. E., and G. P. Williams. 1972. The freezing of peatland. Tech. Paper No. 381. Division of Building Research, National Research Council of Canada, Ottawa. 24 p.
5. Brown, R. J. E. 1970. Permafrost in Canada—Its influence on northern development. University of Toronto Press, Toronto. 234 p.

NOTE

[1] All thermal conductivity determinations in this paper were made by the Geothermal Studies Section, Seismology Division, Earth Physics Branch, Department of Energy, Mines and Resources, Ottawa, Canada.

DEEP TEMPERATURE OBSERVATIONS IN THE CANADIAN NORTH

A. S. Judge

EARTH PHYSICS BRANCH, No. 437, DEPARTMENT
OF ENERGY, MINES AND RESOURCES
Ottawa, Ontario

INTRODUCTION

Until very recently, information on permafrost thickness in northern Canada has been very sparse; for example, Brown⁶ lists thickness for only two sites in the arctic islands. The increased drilling activity in the north, particularly for oil and gas exploration in the past 3 years, has greatly increased the available information. Many estimates have been made of deep permafrost thickness using geophysical well logs, but much of this material is not in the public domain. Permafrost thickness based on temperature measured in boreholes in, or nearly in, thermal equilibrium are still relatively rare.

As part of the terrestrial heat flow measurement programme of the geothermal group of the federal Department of Energy, Mines and Resources and with considerable assistance from petroleum and mining companies, boreholes of depths of 300 m or more have been preserved for temperature observations at 22 locations within the permafrost, of which 11 are in the arctic islands. In addition, multisensor cables have been installed in 17 boreholes, drilled by the Geological Survey of Canada, varying in depth from 20 to 60 m. The latter sites are along the Mackenzie River.

BOREHOLE PRESERVATION

The problems associated with temperature measurements in northern boreholes are considerable, including those of either preserving an open borehole or instrumenting it with multisensor cables and yet fulfilling the requirements of regulatory agencies, the cost and difficulty of access to some areas, and the length of time that a northern borehole may take to return to thermal equilibrium with its surroundings.

Usually, boreholes greater than 120 m in length must comply with conservation regulations of the Department of Indian and Northern Affairs, which administers the Canada Oil and Gas Land Regulations in the Northwest Territories and the Yukon Territory. These regulations require surface casing to be placed through the permafrost and left in place as part of the abandonment. Normally, to abandon a borehole, the regulations require the usual cement plugs to isolate porous horizons, a 30-m cement plug bridging the base of the surface casing and the open hole below, and a further cement plug a metre below the surface. The drilling mud is

left in the hole and allowed to freeze. Initially, the approach to preserving open holes for temperature measurements was, at the completion of drilling and logging, to have the usual plugs placed, up to and including that at the base of the surface casing, the drilling mud displaced by arctic diesel fuel, and the surface plug left out until completion of the measurements. This technique has worked very successfully, but does have several drawbacks: Diesel fuel can be very expensive in the Arctic, particularly at sites serviced only by aircraft. Convective overturn occurs in the bore fluid over high temperature gradient sections of boreholes. Subsequent efforts to eliminate both problems by freezing home-made cables into the drilling mud have been unsuccessful. Methods of gelling the diesel fuel around a multisensor cable or installing smaller diameter tubing in the bore have proven too expensive. In industry, efforts to strap multisensor cables to the outside of the surface casing at the time of its installation have been partially successful and are being investigated further. Over much of the mainland of the Northwest Territories and the Yukon Territory the required surface casing is to a depth of 200 m or less. In such cases 5-cm-diameter tubing was installed. The bottom of the tubing and the annulus are both filled with cement, the bore with diesel fuel. For some reason, small diameter mining boreholes in the north do not have to be cased over their entire length. Multithermistor cables have been successfully installed in these by displacing the drilling fluid with diesel fuel and then lowering the cable into the hole. Cables have been frozen directly into short boreholes of less than 60 m with no adverse effects.

MEASUREMENT OF UNDERGROUND TEMPERATURES

All temperature measurements have been made using glass-bead thermistors as sensors, either by building them into a multiconductor cable at predetermined intervals, or by a single thermistor on a portable cable. The portable cable system, used in open wells that are visited periodically, has a probe containing a single thermistor that is lowered in steps to obtain a series of temperature readings down the hole. The multithermistor cable is usually lowered into the borehole shortly after completion of drilling and is left as a

permanent or semipermanent installation. There are definite advantages to the multisensor installation, both for ease of visit and if some blockage should occur in the hole at a later date. Disadvantages are the lack of flexibility of the measurement depth, the possibility of thermistor drift, and the need to compare results from different thermistors to determine the temperature gradient.

All thermistors used are calibrated against a platinum resistance standard thermometer in a constant temperature bath. Absolute accuracy of calibration is believed to be 0.01°C , but differences in temperature can be resolved to a few millidegrees. Observations of the secular drift of the glass-bead thermistors, used for most applications, over a period of 4 years indicate an average drift of calibration toward decreasing apparent temperature of approximately $5 \times 10^{-3}^{\circ}\text{C}$ per year.

Measurements of the thermistor resistances are made in the field with a modified Wheatstone bridge. The essential features of the bridge are that it is well insulated, that it limits the power applied to the thermistor to $10 \mu\text{W}$ or less, it uses high stability, low-temperature coefficient precision resistors throughout, and has inputs for 2-, 3- or 4-lead systems. A commercially available null detector is used to balance the bridge. The entire assembly, mounted in an insulated wooden box, has been successfully operated over the entire range of ambient temperatures, i.e., 30 to -40°C ,

encountered in Canada. At very low temperatures, an external battery pack, which is carried inside the observer's clothing, is used to power the bridge.

RETURN OF BOREHOLE TO EQUILIBRIUM

The return of the sections of the borehole within the permafrost to thermal equilibrium with the surrounding formations may be prolonged over that for a similar borehole in southern Canada if, during the drilling, the permafrost was thawed around the hole and if the formations encountered are porous. Examples of the re-establishment of equilibrium can be seen in the results for two northern boreholes that have been monitored for 9 and 6 years, respectively. The first example is a hole drilled at Winter Harbour on Melville Island. It was drilled to a depth of $3\,823\text{ m}$ in a total drilling time of 195 days, 28 of which were spent drilling through permafrost. At the completion of drilling and testing in 1962, the well was abandoned below and up to the base of the 24.5-cm -diameter surface casing, and the mud in the casing was displaced by arctic diesel fuel. Four months later a multithermistor cable was installed to a depth of 605 m by the United States Geological Survey. Spacers were incorporated into the cable to inhibit convection in the bore fluid. The first temperature readings were taken over a period of several days after the installation and further

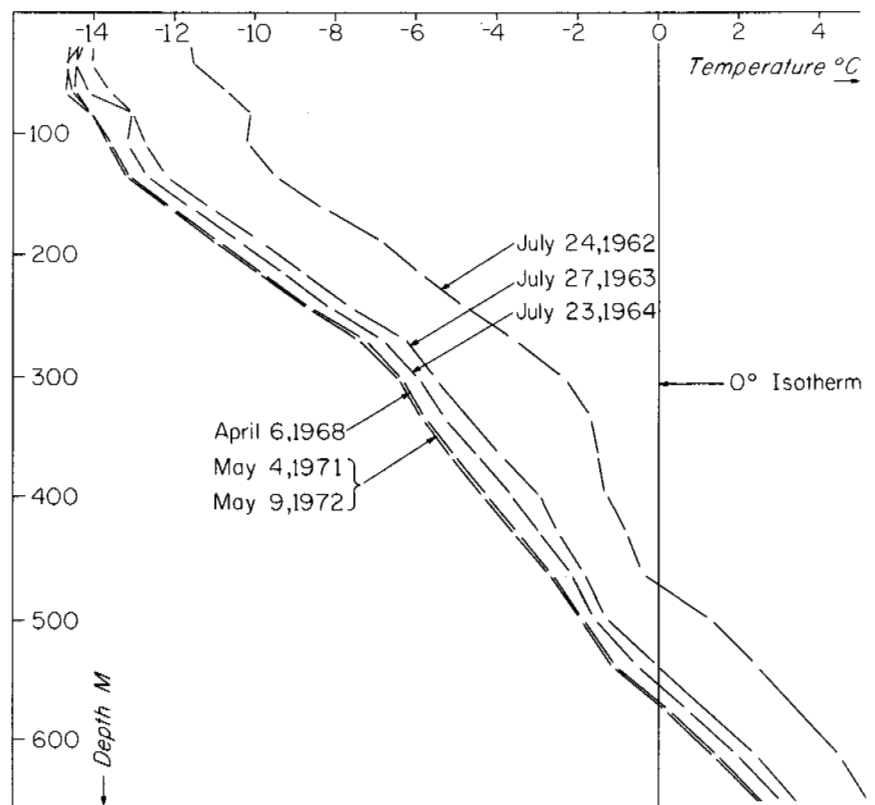


FIGURE 1 The return to equilibrium in the Winter Harbour well located at $74^{\circ}48'\text{N}$ and $110^{\circ}30.5'\text{W}$. Well completed May 24, 1962, after total drilling time of 208 days.

readings have been taken intermittently ever since. Results are shown on Figure 1. Since the first measurements, the borehole has cooled on average by 3–4 °C and, using the relationship for a logarithmic return to equilibrium suggested by Lachenbruch and Brewer,¹⁷ it is projected that the borehole is still, almost 10 years after its completion and 14 times the drilling time, 0.3 °C above the equilibrium temperatures. If the relationship continues to hold, the bore will not be within 0.05 °C of the equilibrium rock temperatures until the year 2010. In this borehole, the temperatures in the permafrost section were already below 0 °C and the geothermal gradient partially re-established when readings were taken 4 months after well completion.

If the bore through the permafrost is heated to above 0 °C during the drilling process and the rock adjacent to the bore is porous and contains ice, the ice will melt. When the bore cools again to equilibrium, it will cool to the freezing temperature and remain at constant temperature until the moisture is all frozen and the latent heat dissipated, at which point it will commence to cool once more. The rocks encountered in the Winter Harbour borehole, therefore, must be of low porosity. This is not the case, however, in the Reindeer borehole drilled on Richards Island in the Mackenzie Delta. It was drilled to a depth of 3 860 m in 181 days. On completion, it was plugged back to 628 m and 5-cm-diameter tubing run inside the 24.5-cm surface casing

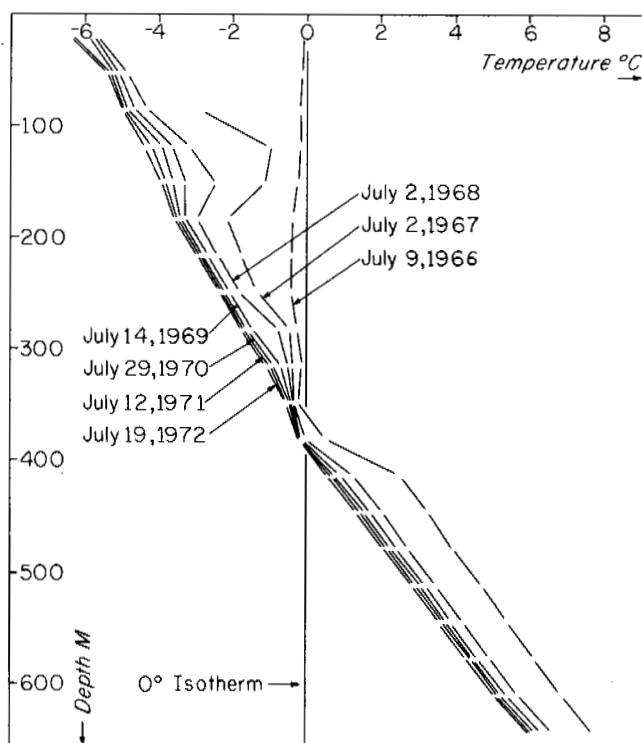


FIGURE 2 The return to equilibrium in the Richards Island well located at 69°06'N and 134°36.9'W. Well completed November 28, 1965, after total drilling time of 143 days.

with spacers on each joint to locate the pipe centrally in the bore. The drilling mud in the annulus was displaced with diesel fuel and the inner tube filled with methanol. Six months after completion, a single thermistor log, using a portable cable, was made in the borehole and a multi-thermistor cable then installed in the inner tubing to a depth of 597 m. Both sets of results shown in Figure 2 indicate that the entire length of the hole between 18 and 323 m, i.e., most of the section through the permafrost, was at temperatures between –0.1 and –0.4 °C. Thus, the porosity of the formations encountered by this borehole must be considerably greater than those encountered at the Winter Harbour location.

The section of the Richards Island hole below the permafrost is returning to equilibrium at a similar rate to the Winter Harbour hole. This return is a remarkably good fit to the logarithmic relationship mentioned earlier. Four years after completion, the temperatures were still 0.5 °C above the predicted equilibrium and will not be within 0.05 °C of equilibrium until after the year 2000. These very long settling times have very little bearing on the well being within the permafrost, but are related to the length of time required to drill the well and the total depth. Other boreholes in the Canadian arctic in which the drilling time was shorter and the total depth shallower have returned to equilibrium within 3 years. A great deal of slumping occurred in the top 150 m of the Richards Island hole during drilling, resulting in a 1.2-m-diameter hole and complicating the interpretation in these sections.

UNDERGROUND TEMPERATURES IN NORTHERN CANADA

The temperature of the earth's surface is the upper boundary condition for ground temperatures. This surface temperature, which varies both spatially across Canada and temporally from day to day, is essentially governed by energy sources external to the solid earth, e.g., incident solar radiation. The influx of solar radiation to the surface is some 6 000 times greater than the heat reaching the earth's surface from the interior. Excluding for the moment consideration of the range of the temporal variations during the year, it is possible to contour mean annual surface temperatures across Canada.^{5,13} In general, the isotherms roughly follow the lines of latitude—the surface gets cooler toward higher latitudes. It is also apparent, as illustrated by the positions of the 0 °C isotherms in Figure 3, that over much of northern Canada the surface temperature isotherms are displaced to the north of the equivalent air temperature isotherms. This displacement is 6.4 °C at Fort Vermillion in Alberta, where the mean annual air temperature is –2.1 °C and the mean annual surface temperature is 4.3 °C. On average, the displacement is smaller than this. Using surface and air temperatures for 38 sites across Canada, 20 within the

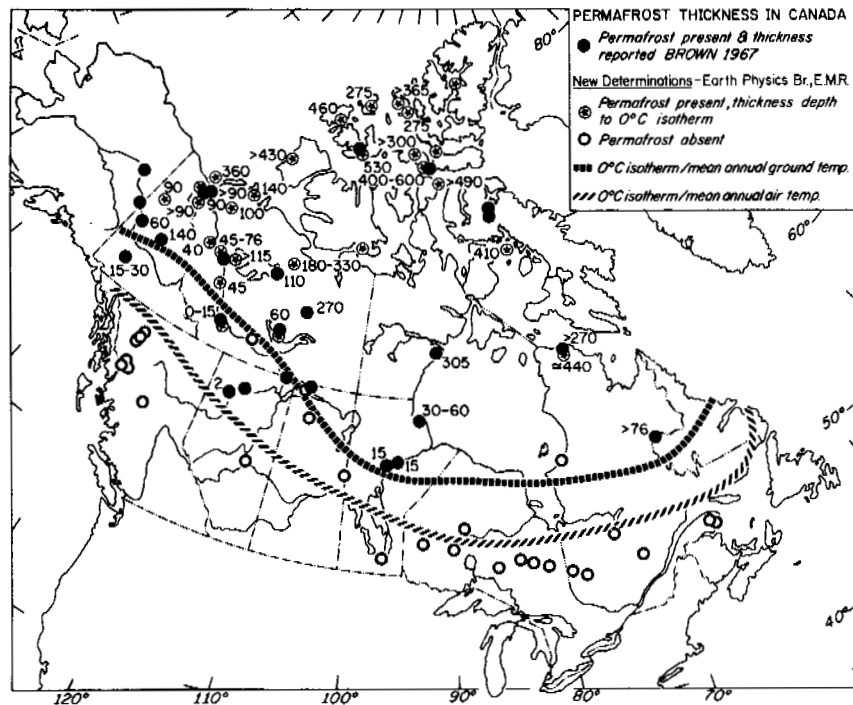


FIGURE 3 Permafrost thickness in Canada.

permafrost and 18 outside of it, the mean displacement of the isotherms is 3.3°C , with a standard deviation of 1.5°C . Much of the difference in the temperature is believed to be due to the insulating qualities of the winter snow blanket and its time of persistence.^{1,14} Local variations in surface vegetation, exposure, topography, and moisture content also contribute to variations of mean surface temperature.⁵

The rate of rise of temperature with depth below the surface—the geothermal gradient—is due to two main factors: the thermal conductivity of the subsurface rocks and the heat flow from greater depths in the earth. This internal heat is generated partly by the decay of radioactive isotopes present, particularly in the rocks that compose the earth's lithosphere, and partly by physical and chemical processes occurring at greater depths. Terrestrial heat flow varies typically across Canada from 29 to 105 mWm^{-2} , roughly a factor of 4, depending on the geological age, radioactivity, and tectonic framework of the region. The application of a thermal gradient across a material gives rise to a flow of heat in the opposite direction. In normal insulators, such as rocks, the heat flow is carried by lattice waves; the ability of the material to conduct heat in a steady state is the thermal conductivity. Thermal conductivities of rocks vary typically from $1.2\text{ Wm}^{-1}\text{K}^{-1}$ for shales to $4.8\text{ Wm}^{-1}\text{K}^{-1}$ for quartz sandstones.

Although the surface temperature at a northern site may be very low, underground temperatures at a depth of several hundred metres may be considerably higher than those of a more southerly site with a high surface temperature. This is

because the temperature gradient is a function of the thermal conductivity of the rocks in which it is measured. For example, the temperatures at depths of 600 m beneath a sequence of shales in the Sverdrup Basin may be as high as 30°C , whereas those at a similar depth beneath the gneisses of the Canadian Shield at Yellowknife, 16° further south, are only 10°C . Thus, it can be said that the internal heat flow does not affect surface temperatures and, conversely, that physical processes occurring at depths of tens of kilometres, where temperatures of several hundred degrees may occur, are not significantly affected by the spatial variation of mean annual surface temperatures across Canada of some 30°C . Refraction of heat flow occurs due to lateral variations of conductivity and thus major structures may greatly distort the isotherms.²⁰

CLIMATIC CHANGES AND UNDERGROUND TEMPERATURES

The observed distribution of geothermal gradients is not, however, quite as simple as presented above. While the thermal properties of rocks and the earth's heat flow remain relatively constant over periods of tens of thousands of years, the surface temperature does not. It varies with the highly variable factors of incident solar radiation and weather. Depth penetration of these variations is dependent on the time scale involved and the thermal properties of the ground. In general, the diurnal variation only penetrates a few centimetres—variations due to passing weather systems

to a few metres and the annual variation to depths of 20 m. Longer period and aperiodic surface temperature changes, such as those due to long period changes of climate or of surface conditions, may modify the thermal regime to many hundreds of metres.

Many boreholes across Canada, the United States, and Europe show reductions or even inversions in the temperature gradient at depths close to the surface, but at depths below that to which the annual wave penetrates. Roy *et al.*²¹ have suggested that these effects are connected with such factors as groundwater movement, changes in surface temperature due to human activities, and vegetation contrasts. However, an analysis of such an inversion in a borehole at London, Ontario, by Beck and Judge³ revealed a close correlation between the shape of the inversion curve and the known pattern of change of air temperature in London during the past 100 years. Lachenbruch *et al.*¹⁹ and Lachenbruch and Marshall¹⁸ have discussed the evidence for climatic changes in Alaska within the last 100 years that have resulted in increases of ground temperature by 2–4 °C. Most boreholes in northern Canada show a reduction in temperature gradient near the surface, but few show inversions. The occurrence of a curvature in, or reversal of, the temperature gradient simply reflects the relative values of the surface temperature increase, the geothermal gradient, and the time of onset of the change. As an example, the reduction of the temperature gradient in a borehole at Fort Providence is explained by a gradual recent increase of surface temperature by 2.2 °C, whereas the inversion in the London borehole is explained by an increase of 1.1 °C.

Changes of climate, however, are not limited to the recent past. Cermak⁷ has detected temperature perturbations of a few tenths of a degree in several boreholes penetrating uniform shield rocks. He attributes these to surface temperature changes of up to 3 °C during the Climatic Optimum of the eleventh century and the Little Ice Age of the seventeenth.

Much of Canada was covered by ice sheets until about 10 000 years ago and had been for long periods of the preceding 2 million years of the Pleistocene. These advancing and retreating ice sheets modified the surface temperatures of the ground beneath them for long periods of time. The existence of large ice sheets modified air temperatures on a worldwide scale. Although a great deal of discussion exists on the predicted perturbations to underground temperatures^{2,4,11} very little direct observational evidence of such perturbations exists.^{3,9,22} Since the response of earth materials to temperature perturbations is very slow, observational evidence of this past surface temperature history should be seen in conventional heat flow studies of 1 000- to 1 500-m boreholes as either an increasing or decreasing heat flow with depth, depending on whether the surface temperature below the ice sheet was warmer or cooler than present surface temperatures.

In some areas, in particular the Mackenzie Delta and

parts of the Sverdrup Basin, the rocks are poorly consolidated with very high moisture content. These rocks will contain a matrix composed of ice. Any change in the permafrost boundary involves the absorption or release of latent heat. The effect of this is to further slow the thermal response of the subsurface to perturbations of surface temperatures.

PERMAFROST OCCURRENCE AND THICKNESS

The permafrost base is defined as the 0 °C isotherm and the thickness as the depth from the surface to that isotherm. In fact, the soil or rock may contain water at or below 0 °C due to the effects of capillary pressure and mineralized water. Alternatively, the rock may have no porosity and thus contain no ice or water at all. In either case, it is considered to be within the permafrost if its temperature is below 0 °C.

Brown⁶ has summarized Canadian permafrost thickness measurements available prior to 1967, and Ferrians⁸ has made a similar collection of Alaskan data prior to 1965. Figure 3 shows Brown's and Ferrian's results close to the Alaska–Yukon border, together with the results of the Earth Physics Branch of the Department. Some of the observations reported previously were based on the presence of visible ice in the recovered samples rather than temperature alone, on which our measurements are based. Very few of our results are based on measured equilibrium temperatures because few of the wells are in equilibrium. However, as observed in an earlier section, quite reasonable estimates of the equilibrium temperatures can be made using non-equilibrium measurements. Brown's reported value for Winter Harbour has been updated using these arguments.

As mentioned above, water can still be present in rock pores at temperatures below 0 °C. A very preliminary examination of the temperature gradients in some of the northern boreholes suggests that the moisture in the rocks freezes at a temperature range from 0 to –2 °C.

At present, the thickest permafrost measured in Canada is 530 m at Winter Harbour on Melville Island, in a well only 1 000 m from the present shoreline. Judge,¹³ however, has predicted maximum thicknesses of 1 000 m on the basis of known rock types, surface temperature distribution, and a postulated regional heat flow distribution based on values measured in southern Canada. Very thick permafrost is to be expected if low surface temperatures occur in the areas of exposed shield rocks, or of shield rocks beneath present ice caps, and in areas where the Arctic Platform is overlain by dolostones and quartz sandstones. At present, determined thicknesses in the arctic islands range from 275 to 530 m. Thinner permafrost should be found closer to the shoreline than any of the present holes¹⁵ and beneath the shallow waters, 250 m deep or less, beneath the channels separating the islands.

Very thick permafrost is not confined to the arctic is-

lands, since a thickness of over 400 m has been projected in northern Quebec based on temperatures to depths of 260 m and a thickness of 360 m measured on Richards Island in the Mackenzie Delta. Permafrost thicker than 300 m probably occurs extensively through the shield of northern Keewatin District, since surface temperatures are -10°C or lower.

Some permafrost occurrences have been reported to the south of the present 0°C surface temperature isotherm. These may be partly a function of the surface conditions,⁵ e.g., beneath peat bogs, in which case they may be in thermal equilibrium with the present surface temperatures, or, alternatively, may represent remanent permafrost degrading in response to an increase of surface temperature to above 0°C .

Further holes are still being acquired when possible and the programme of measuring temperatures and conductivities continued in an attempt not only to measure the thickness of permafrost but also to understand its genesis and distribution in relation to the heat flow, conductivity, and surface temperature history.

ACKNOWLEDGMENTS

The author would like to thank the many people from a variety of companies and organizations who have made this work possible. Particular thanks go to the members of the Department of Indian and Northern Affairs, without whose forbearance few, if any holes could have been kept open for the observations; to the oil and mining companies who have made their holes available; to the Geological Survey of Canada for making available shallow holes along the Mackenzie Valley; and, finally, to the Polar Continental Shelf Project, without whose logistic support in the arctic islands few of the sites would have been accessible.

REFERENCES

- Annersten, L. J. 1964. *In* J. B. Bird [ed.] Permafrost studies in Labrador-Ungava. McGill Sub-Arctic Res. Laboratory Paper #16. Montreal.
- Beck, A. E. 1970. Non-equivalence of oceanic and continental heat flows and other geothermal problems. *Comments Earth Sci. Geophy.* 2:29-35.
- Beck, A. E., and A. S. Judge. 1969. Analysis of heat flow data—1. Detailed observations in a single borehole. *J. Roy. Astron. Soc.* 18:145-158.
- Birch, F. 1948. The effect of Pleistocene climatic variations upon geothermal gradients. *Am. J. Sci.* 246:729-760.
- Brown, R. J. E. 1966. Influence of vegetation on permafrost, p. 20-25. *In* Permafrost: Proceedings of an international conference. National Academy of Sciences, Washington, D.C.
- Brown, R. J. E. 1967. Permafrost in Canada. *Geol. Surv. Can. Map 1246 A*, Publ. NRC 9769. Division of Building Research, National Research Council, Ottawa, Canada.
- Cermak, V. 1971. Underground temperature and inferred climatic temperature of the past millenium. *Palaeog. Palaeoclimat. Palaeoecol.* 10:1-19.
- Ferrians, O. J. 1965. Permafrost map of Alaska. Misc. Geologic Investigations Map I-445. U.S. Geological Survey, Washington, D.C.
- Gough, D. I. 1963. Heat flow in the Southern Karroo. *Proc. Roy. Soc. Ser. A* 272:207-230.
- Jessop, A. M. 1970. How to beat permafrost problems. *Oilweek* (Jan. 12):22-25.
- Jessop, A. M. 1971. The distribution of glacial perturbation of heat flow in Canada. *Can. J. Earth Sci.* 8:162-166.
- Johnston, G. H., and R. J. E. Brown. 1964. Some observations on permafrost distribution at a lake in the Mackenzie Delta, N.W.T. *Arctic* 17:163-175.
- Judge, A. S. The prediction of permafrost thicknesses. *Can. Geotech. J.* (In press)
- Krinsley, D. B. 1963. Influence of snow cover on frost penetration. *U.S. Geol. Surv. Prof. Paper 475-B Art. 38*, B-144-147.
- Lachenbruch, A. H. 1957. Thermal effects of the ocean on permafrost. *Bull. Geol. Soc. Am.* 68:1515-1539.
- Lachenbruch, A. H. 1958. Three dimensional heat conduction in permafrost beneath heated buildings. *U.S. Geol. Surv. Bull.* 1052-B.
- Lachenbruch, A. H., and M. C. Brewer. 1959. The dissipation of the temperature effect in drilling a well in Arctic Alaska. *U.S. Geol. Surv. Bull.* 1083-C. p. 73-109.
- Lachenbruch, A. H., and B. V. Marshall. 1969. Heat flow in the Arctic. *Arctic* 22:300-311.
- Lachenbruch, A. H., G. W. Greene, and B. V. Marshall. 1966. Permafrost and geothermal regimes, p. 149-165. *In* Environment of Cape Thompson region, Alaska. U.S. Atomic Energy Commission.
- Ovnatanov, S. T., and C. P. Tamrazyan. 1970. Thermal studies in subsurface structural investigations, Apsheron Peninsula, Azerbaijan, U.S.S.R. *Am. Assoc. Petrol. Geol. Bull.* 54:1677-1685.
- Roy, R. F., D. D. Blackwell, and E. R. Decker. 1971. Continental heat flow. *In* E. Robertson [ed.] *The nature of the solid earth*. McGraw-Hill, New York.
- Sass, J. H., A. H. Lachenbruch, and A. M. Jessop. 1971. Uniform heat flow in a deep hole in the Canadian Shield and its paleoclimatic implications. *J. Geophys. Res.* 76:8586-8596.

A GENERAL SOLUTION FOR THE TWO-DIMENSIONAL, TRANSIENT HEAT CONDUCTION PROBLEM IN PERMAFROST, USING IMPLICIT, FINITE DIFFERENCE METHODS

Raymond Milton Kliwer

BROWN & ROOT, INC.
Houston, Texas

INTRODUCTION

In regions of continuous permafrost where soils may become unstable upon thawing, careful attention must be given to the response of the media when heat sources are to be placed on or near the permafrost. Knowledge of the thermal behavior of the permafrost allows appropriate design precautions to be taken. For this reason, a computer program was developed for use in modeling a large class of

problems involving the thermal response of a permafrost medium.

The soil near the surface in permafrost regions generally assumes a natural annual thaw-freeze cycle. The soil consists of a mixture of solid material and water. Different stratified layers of soil may occur having varying thermal properties depending in part on depth and geographical location. Annually, as the surface temperature increases above the freezing point, melting of the soil moisture begins at the surface. The interface between the liquid and the ice phases propagates downward into the earth during the warming season. Later, as the surface temperature decreases below the freezing point, refreezing begins at the surface and similarly propagates downward. While this occurs, the lower interface begins to move upward, having lost its heat source. Finally, the two interfaces meet, and the entire surface soil layer is again frozen. This process is repeated annually.

Several solutions to variations of this type of problem have been reported. Doherty¹ solved the two-dimensional problem using an alternating direction explicit method to obtain a temperature history. The solution did not solve the problem for soil layers having differing properties, but did allow for the change in thermal properties between the frozen and unfrozen states. Provision was made to change the grid size with respect to location. Kazemi and Perkins² solved a one-dimensional layered problem. Both analyses included latent heat and periodic temperature variation considerations.

PROBLEM DESCRIPTION

To obtain a mathematical solution, a problem amenable to such a solution must be posed; that is, a problem domain and its boundary conditions must be specified that are suitable for mathematical modeling and solution. Consider the problem domain depicted in Figure 1 within which the soil layers with different thermal properties are represented.

Along the upper boundary at the soil surface, the am-

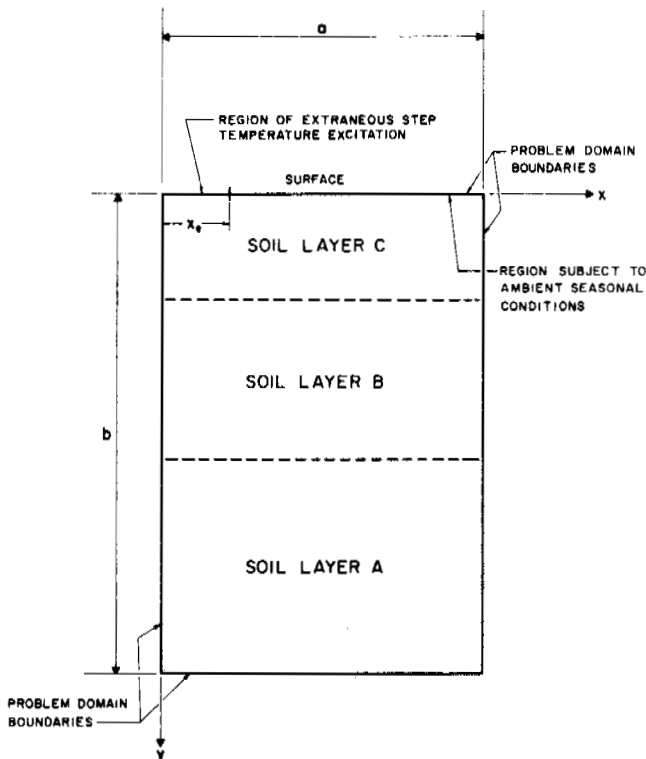


FIGURE 1 Problem domain.

bient temperature varies according to the season. A sudden-step constant-temperature disturbance is applied along the upper domain boundary from the left boundary of the domain to an intermediate point along the upper boundary; the remainder of the upper boundary continues to experience the normal seasonal temperature variation. Along the left, right, and lower boundaries, it seems appropriate to assume that there is no heat transfer across the boundary. This could either imply an insulated boundary or lines of thermal symmetry.

In addition to the domain boundary conditions, there is another discontinuity at a liquid-ice interface on the freezing isotherm. This liquid-ice interface can move throughout the domain. This might be considered to be a moving boundary condition. This movement is related to the energy liberated or absorbed by the latent heat of fusion.

GOVERNING EQUATION

The two-dimensional Cartesian partial differential equation for transient heat conduction is expressed:

$$\frac{\partial^2 T}{\partial x^2} + \frac{\partial^2 T}{\partial y^2} = \frac{1}{\alpha} \frac{\partial T}{\partial t}, \quad (1)$$

where T is temperature, α is thermal diffusivity, x is a coordinate direction, y is a coordinate direction, and t is time.

To solve the governing differential equation, appropriate mathematically defined boundary and initial conditions must be included. Along the upper boundary, it is assumed that the soil surface temperature varies according to a sinus-

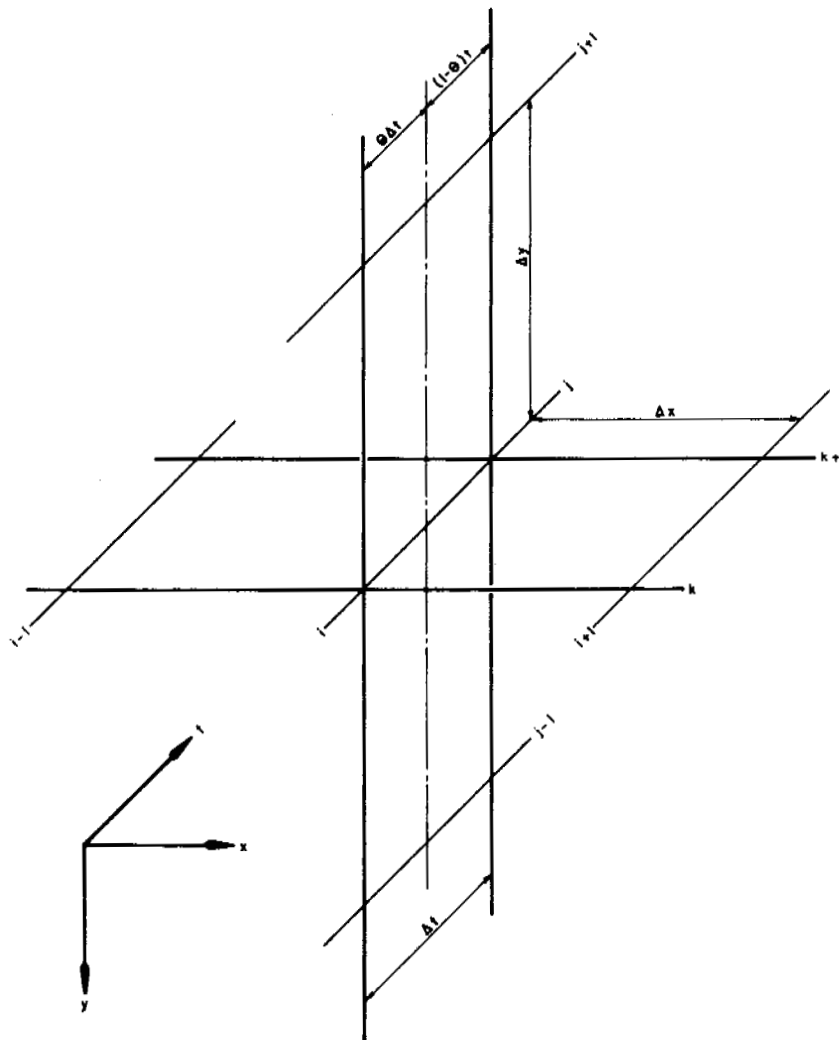


FIGURE 2 Designation of grid points.

oidal periodic function representing the annual seasonal temperature variation. This can be written as:

$$T = T_a + A \sin(\omega t - \phi), \quad (2)$$

where T_a is the average annual temperature, A is the amplitude of the seasonal temperature variation, ω is the angular frequency, and ϕ is the phase angle. Along the upper boundary, a sudden-step constant temperature is applied at a general time from the left boundary to an intermediate point:

$$T(x, t) = T_e \quad \text{when} \quad t > t_e, 0 < x < x_e, \quad (3)$$

where T_e is the temperature of the thermal step excitation, which is initiated at time t_e and replaces the sinusoidal temperature variation effect.

Along the left, lower, and right boundaries of the problem domain, the boundary condition might be expressed as:

$$\left(\frac{\partial T}{\partial n}\right)_{\text{Boundary}} = 0, \quad (4)$$

where n is the coordinate direction normal to the respective boundary. This relationship implies that no heat is transferred across the boundary.

Further, a moving discontinuity exists at the freezing isotherm. An energy balance including latent heat of fusion is included to account for thawing or freezing. The latent energy may vary between zero and a maximum value. This value might be expressed for a finite element as:

$$Q_{\max} = P\rho_w \Delta x \Delta y L, \quad (5)$$

where Q_{\max} is the maximum latent energy liberated or absorbed, P is the proportion of moisture in the soil element, ρ_w is the density of water, and L is the latent heat of fusion of water.

Thermal properties also change across the freezing isotherm, as well as across the boundaries of the different stratified layers.

NUMERICAL TECHNIQUE

Numerous finite difference schemes are available for the solution of partial differential equations. Consider the function $T_{i,j,k}$, with the subscripts i , j , and k associated with the x and y coordinates and t , respectively. The designation of grid points is shown in Figure 2. A weighting parameter, θ , with respect to time lying in the interval $0 \leq \theta \leq 1$, is introduced.

Using Taylor series expansions and dropping higher order terms, the approximate expressions [Eq. (6)-(8)] are obtained where all derivatives are evaluated at the point $[i\Delta x, j\Delta y, (k + \theta)\Delta t]$. When θ is zero, the difference approximations are explicit. For an explicit system of equations, the unknowns are found directly in terms of known quantities. If θ is not zero, then a resulting set of simultaneous equations must be solved in order to determine the values of the unknown quantities. Such a system of equations represents an implicit formulation. While it might first appear that the explicit scheme would be far simpler to use than an implicit scheme, stability, truncation, and convergence considerations reduce the desirability of the scheme. Severe stability restrictions on incremental step sizes occur with the explicit scheme greatly reducing flexibility in selecting these values.

Employing the finite difference approximations with the governing differential equation and examining the energy balance on a finite element, the resulting general difference equation is shown in Eq. (9).

$$\frac{\partial^2 T}{\partial x^2} = \frac{\theta [T_{i-1, j, k+1} - 2T_{i, j, k+1} + T_{i+1, j, k+1}] + (1-\theta) [T_{i-1, j, k} - 2T_{i, j, k} + T_{i+1, j, k}]}{\Delta x^2} \quad (6)$$

$$\frac{\partial^2 T}{\partial y^2} = \frac{\theta [T_{i, j-1, k+1} - 2T_{i, j, k+1} + T_{i, j+1, k+1}] + (1-\theta) [T_{i, j-1, k} - 2T_{i, j, k} + T_{i, j+1, k}]}{\Delta y^2} \quad (7)$$

$$\frac{\partial T}{\partial t} = \frac{T_{i, j, k+1} - T_{i, j, k}}{\Delta t} \quad (8)$$

$$\begin{aligned}
 & \frac{\theta}{2\Delta x_b^2} \left(\frac{\Delta x_b}{\Delta x_a} \right) \left[\left(\frac{K_a}{K_b} \right) \left(\frac{\Delta y_a}{\Delta y_b} \right) + 1 \right] T_{i-1, j, k+1} + \frac{\theta}{2\Delta y_b^2} \left(\frac{K_a}{K_b} \right) \left[1 + \left(\frac{\Delta x_a}{\Delta x_b} \right) \right] \left(\frac{\Delta y_b}{\Delta y_a} \right) T_{i, j-1, k+1} \\
 & - \left\{ \frac{1}{4\Delta t} \left[\left(\frac{1}{\alpha_a} \right) \left(\frac{K_a}{K_b} \right) \left[1 + \left(\frac{\Delta x_a}{\Delta x_b} \right) \right] \left(\frac{\Delta y_a}{\Delta y_b} \right) + \left(\frac{1}{\alpha_b} \right) \left[1 + \left(\frac{\Delta x_a}{\Delta x_b} \right) \right] \right] + \frac{\theta}{2\Delta x_b^2} \left[1 + \left(\frac{\Delta x_b}{\Delta x_a} \right) \right] \left[1 + \left(\frac{K_a}{K_b} \right) \right] \right. \\
 & \left. \left(\frac{\Delta y_a}{\Delta y_b} \right) \right] + \frac{\theta}{2\Delta y_b^2} \left[1 + \left(\frac{\Delta x_a}{\Delta x_b} \right) \right] \left[1 + \left(\frac{K_a}{K_b} \right) \left(\frac{\Delta y_b}{\Delta y_a} \right) \right] \right\} T_{i, j, k+1} + \frac{\theta}{2\Delta y_b^2} \left[1 + \left(\frac{\Delta x_a}{\Delta x_b} \right) \right] T_{i, j+1, k+1} \\
 & + \frac{\theta}{2\Delta x_b^2} \left[\left(\frac{K_a}{K_b} \right) \left(\frac{\Delta y_a}{\Delta y_b} \right) + 1 \right] T_{i+1, j, k+1} = - \frac{(1-\theta)}{2\Delta x_b^2} \left(\frac{\Delta x_b}{\Delta x_a} \right) \left[\left(\frac{K_a}{K_b} \right) \left(\frac{\Delta y_a}{\Delta y_b} \right) + 1 \right] T_{i-1, j, k} \\
 & - \frac{(1-\theta)}{2\Delta y_b^2} \left(\frac{K_a}{K_b} \right) \left[1 + \left(\frac{\Delta x_a}{\Delta x_b} \right) \right] \left(\frac{\Delta y_b}{\Delta y_a} \right) T_{i, j-1, k} - \left\{ \frac{1}{4\Delta t} \left[\left(\frac{1}{\alpha_a} \right) \left(\frac{K_a}{K_b} \right) \left[1 + \left(\frac{\Delta x_a}{\Delta x_b} \right) \right] \left(\frac{\Delta y_a}{\Delta y_b} \right) \right. \right. \\
 & \left. \left. + \left(\frac{1}{\alpha_b} \right) \left[1 + \left(\frac{\Delta x_a}{\Delta x_b} \right) \right] \right] - \frac{(1-\theta)}{2\Delta x_b^2} \left[1 + \left(\frac{\Delta x_b}{\Delta x_a} \right) \right] \left[1 + \left(\frac{K_a}{K_b} \right) \left(\frac{\Delta y_a}{\Delta y_b} \right) \right] - \frac{(1-\theta)}{2\Delta y_b^2} \left[1 + \left(\frac{\Delta x_a}{\Delta x_b} \right) \right] \right. \\
 & \left. \left[1 + \left(\frac{K_a}{K_b} \right) \left(\frac{\Delta y_b}{\Delta y_a} \right) \right] \right\} T_{i, j, k} - \frac{(1-\theta)}{2\Delta y_b^2} \left[1 + \left(\frac{\Delta x_a}{\Delta x_b} \right) \right] T_{i, j+1, k} - \frac{(1-\theta)}{2\Delta x_b^2} \left[\left(\frac{K_a}{K_b} \right) \left(\frac{\Delta y_a}{\Delta y_b} \right) + 1 \right] T_{i+1, j, k}. \quad (9)
 \end{aligned}$$

K is the thermal conductivity and a and b are subscripts indicating the locations shown in Figure 3.

During a phase change, the following latent heat term must be added to the right hand side of the general finite difference equation:

$$\frac{1}{4\Delta t} \left(\frac{\rho_w}{K_b} \right) \left[1 + \left(\frac{\Delta x_a}{\Delta x_b} \right) \right] \left[P_a \left(\frac{\Delta y_a}{\Delta y_b} \right) + P_b \right] [q_{i, j, k+1} - q_{i, j, k}], \quad (10)$$

where q represents liberated latent energy and lies in the interval $0 \leq q \leq L$. During the phase change, the temperature of the element remains at freezing. When no phase change occurs, the latent heat term equals zero.

EQUATION-SOLVING METHOD

With the governing equation established and expressed in finite difference form, a solution scheme can be developed to solve the difference equations. The heat conduction equation can be expressed as a group of simultaneous difference equations; there is one equation for each grid point in the finite difference mesh. In matrix form the equations can be written as:

$$HT^{k+1} = GT^k + C, \quad (11)$$

where H and G are square coefficient matrices, T^{k+1} is the column temperature matrix at the time associated with

$k+1$, T^k is the column temperature matrix at the time associated with k , and C is a column matrix evaluated for the appropriate time interval.

The coefficient matrices are banded around the diagonals. Upper triangulation can be performed on the H matrix to form a new coefficient matrix with all elements below the diagonal equal to zero. Appropriate manipulations must also be performed on the G and C matrices.

With the H matrix upper triangulated, back substitution can be performed to evaluate the element temperatures at time $k+1$. After the back substitution process, a check is made to determine whether or not a phase change is occurring. If a phase change is indeed occurring, the latent energy value and temperature are adjusted accordingly. That is, the temperature of the element is adjusted back to the freezing temperature, and the resulting specific heat energy change is added to the latent energy until the total latent energy value for the element has been reached for the appropriate phase. Readjustment of the temperature and the latent energy values is made if the latent energy value surpasses the maximum latent energy or becomes less than zero. Doherty¹ used a similar procedure.

Simply utilizing this procedure without additional manipulation is inconsistent since the current temperature of the element that is to be adjusted was determined with conduction satisfying an energy balance including specific heat capacity. This calculation involved temperatures at both the previous and current time steps. If the element temperature is merely adjusted to account for latent heat energy by balancing latent heat energy with specific heat

energy, the energy balance is no longer valid for the time step. The conduction was partially evaluated at the wrong temperature. As an illustration, consider the case of melting. Too high a temperature would be calculated for the element. If the freezing temperature had been maintained at the element, more conduction into the element would have been predicted for the current time step. Thus, not as much heat transfer was calculated as was actually occurring into the element resulting in an overly conservative prediction of the magnitude of melting.

To account for latent energy properly, the latent energy terms are added to the governing finite difference equations. These terms are a part of the *C* matrix. Iteration can be performed to appropriately adjust temperature and latent energy values.

COMPUTER PROGRAM

Actual computations are performed using a digital computer. The program was written to solve problems with any number of layered media and to coordinate step changes subject to computer size limitations. The time step size can be increased as the problem history progresses. The initial temperature distribution can be specified according to the classical solution to the problem of a steady periodic surface temperature on a semi-infinite medium. This relationship is expressed:

$$T = T_a + Ae^{-y\sqrt{\frac{\omega}{2\alpha}}} \sin(\omega t - y\sqrt{\frac{\omega}{2\alpha}} - \phi). \quad (12)$$

This does not include latent heat or layered media property variation considerations. The temperature of certain elements can be specified at a constant value within the domain. Thus a constant temperature boundary condition can be used overriding the no heat transfer lower boundary condition.

A generalized flow chart for the FORTRAN program showing the sequence of operations is presented in Figure 4. It might be noted that it is not necessary to store all temperatures at all times in the computer memory since it is possible to step in time as the solution proceeds. Thus, only temperature values at two time levels must be stored simultaneously. Further, since the coefficient matrices are sparse, only the band of elements around the diagonals need to be stored.

A larger problem space using fewer grid points can be solved because the grid mesh size can be increased at points away from the source of the thermal excitation. The selection of grid increment lengths is made more flexible by the implicit nature of the finite difference formulation. There is no restriction on the length of a problem history that can be run; however, greater computer time is required.

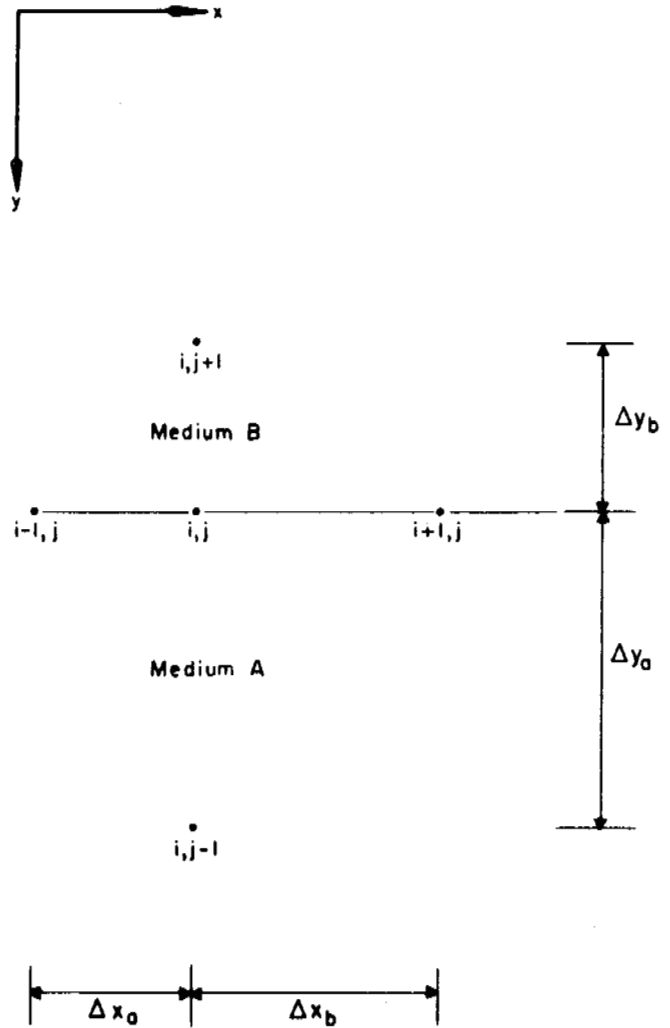


FIGURE 3 Subscript designations for difference equation [Eq. (9)].

MODELING WITH THE COMPUTER PROGRAM

A reasonable amount of discretion must be exercised when using the program to model real problems. The input data must be suitably selected so that the mathematical solution will approximate the real situation being simulated. Moisture migration is probably the most important neglected thermal phenomenon. Also, sufficient time points must be selected to depict the sinusoidal character of a surface condition. Finally, grid points should be spaced relatively closely near thermal disturbances, where large temperature changes are occurring.

A reasonable problem domain width also must be selected consistent with computer requirements. With the boundary conditions implying no heat transfer across the left, right, and lower boundaries, heat transfer can only

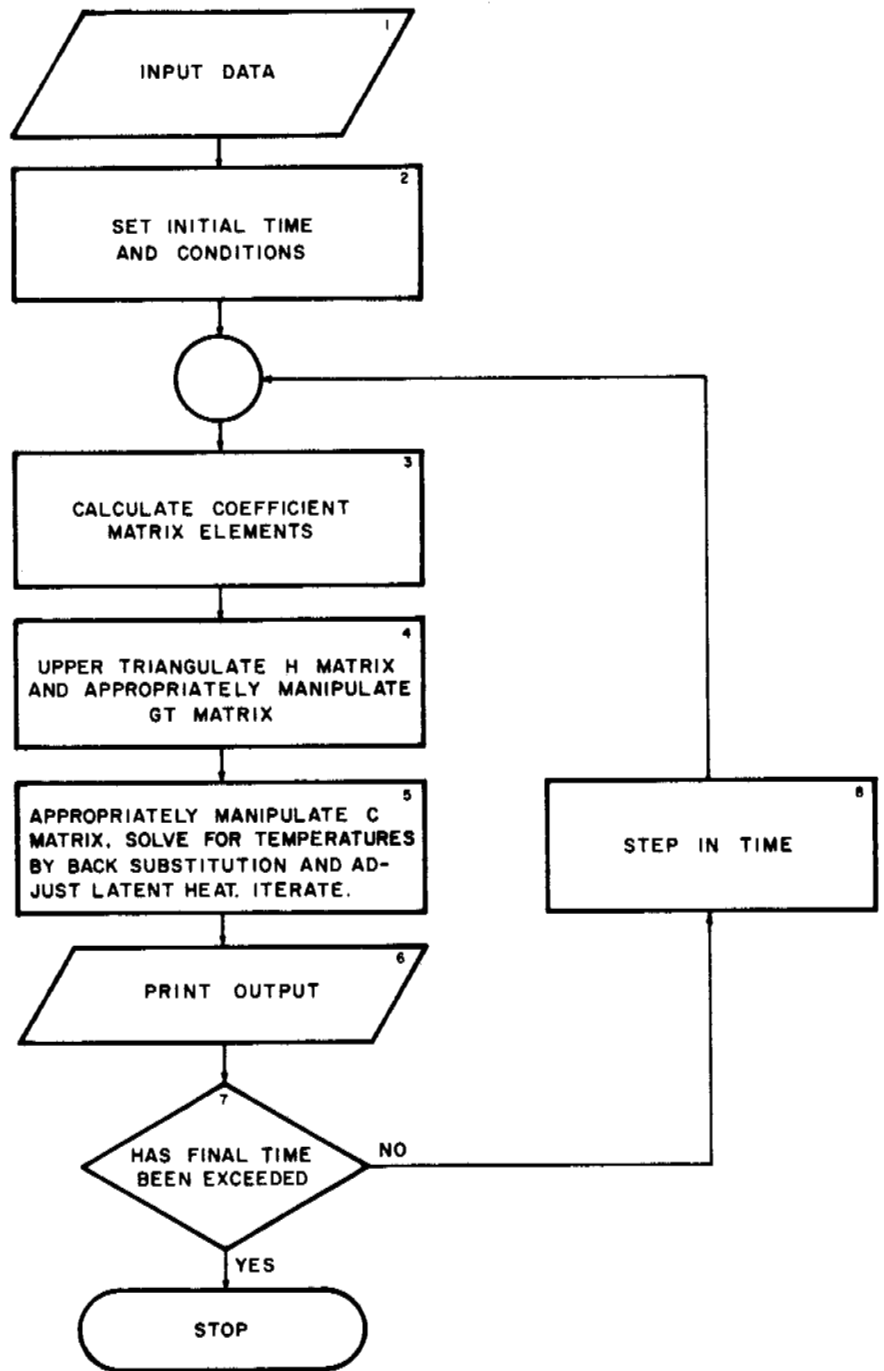


FIGURE 4 Computer flow chart.

occur across the upper boundary. The problem domain would appear to be of adequate width if the temperature response of points along the right boundary approximates the response with no extraneous thermal excitation. Admittedly, there is always some question concerning just how close these responses should be.

Another similar modeling question to be resolved is the specification of domain depth. The depth should be selected

so that the temperature along the lower boundary remains nearly constant. The selection of too narrow a domain width or too shallow a domain depth, however, would be expected to yield conservative results with respect to the prediction of the degree of melt with the no heat transfer boundary condition. Both Doherty¹ and Kazemi and Perkins² used constant temperature lower boundary condition. While this program can be used with this assumption, such

an assumption may allow a fictitiously large heat sink to be created along the lower boundary of the domain. Therefore, a constant temperature generally may not be conservative. Of course, sufficient domain depth should alleviate this problem, but the question is in the reasonableness of the depth chosen. Of course, the true lower boundary condition must lie between the extremes of the two previously mentioned.

In modeling three-dimensional problems, a two-dimensional model can be used conservatively with respect to melting depth when the most severe thermal excitation is used. The results become progressively more conservative as the length to width ratio of the extraneous thermal disturbance approaches unity. Another modeling consideration is the use of the thermal symmetry condition. A series of equally spaced thermal excitations can be modeled as depicted in Figure 1, wherein the distance "a" represents one-half the spacing of the excitations. The domain width is fixed.

EXAMPLE COMPUTER RUNS

Some computer run results are presented. The data values used are shown in Table I. The subscript 1 corresponds to the frozen state, and the subscript 2 corresponds to the unfrozen state. The values are believed to reflect those that might be encountered on the North Slope of Alaska. Hopefully, appropriate values for the various step increment lengths were selected. No special checks, such as half stepping, were performed to determine the adequacy of these values, and no undesirable solution characteristics, such as extraneous oscillations and overshooting, were noted. Further, excellent correspondence between the results obtained by the program and the classical solution to the one-dimensional problem with a steady periodic surface temperature on a semi-infinite medium has been previously observed, making the program results intuitively more satisfying. As a practical matter, it appears that an extraneous thermal disturbance with a smaller physical size and lower temperature would require a smaller domain to obtain satisfactory results.

A few times during the seasonal thawing and refreezing, some banding of the freezing isotherm has been observed. For instance along the right boundary where the freezing isotherm would be expected to remain horizontal, adjacent freezing points may appear in the vertical direction. Each of these points has an intermediate latent energy value. This situation is intuitively satisfying for the physical problem during the refreezing process where a thawed stratum lies between neighboring frozen layers, but it is difficult to justify during the melting process. The phenomenon observed is attributed to both the convergence of the iteration scheme in adjusting the latent energy values and the size of

TABLE I Computer Input Data

Soil Layer A
2.4 m < y < lower domain boundary
10% moisture
$\rho = 2.08 \text{ g/cm}^3$
$\alpha_1 = 0.0217 \text{ cm}^2/\text{s}; \alpha_2 = 0.0128 \text{ cm}^2/\text{s}$
$K_1 = 0.00992 \text{ cal/cm s }^\circ\text{C}; K_2 = 0.00744 \text{ cal/cm s }^\circ\text{C}$
Soil Layer B
0.0 m < y < 2.4 m
40% moisture
$\rho = 1.28 \text{ g/cm}^3$
$\alpha_1 = 0.0103 \text{ cm}^2/\text{s}; \alpha_2 = 0.00369 \text{ cm}^2/\text{s}$
$K_1 = 0.00488 \text{ cal/cm s }^\circ\text{C}; K_2 = 0.00269 \text{ cal/cm s }^\circ\text{C}$
Water
$\rho = 1.0 \text{ g/cm}^3$
$L = 80 \text{ cal/g}$
Freezing temperature = 0.0 °C
Conditions at Upper Boundary
$T_a = -11.1 \text{ }^\circ\text{C}$
$A = 16.9 \text{ }^\circ\text{C}$
$\omega = 1.991 \times 10^7 \text{ rad/s}$
$\phi = 2.09 \text{ rad}$
$T_e = 21.1 \text{ }^\circ\text{C}$
$x_e = 1.1 \text{ m}$
$t_e = 26.3 \text{ h}$
Computed Program Variables
Initial time $t_i = 0.0 \text{ y}$
Final time $t_f = 3.0 \text{ y}$
$\theta = 0.5$
$\Delta x = 0.3 \text{ m}, 0.0 \text{ m} < x < 2.4 \text{ m}$
$\Delta x = 0.6 \text{ m}, 2.4 \text{ m} < x < 4.9 \text{ m}$
$\Delta x = 1.2 \text{ m}, 4.9 \text{ m} < x < 7.3 \text{ m}$
$\Delta x = 2.4 \text{ m}, 7.3 \text{ m} < x < 17.1 \text{ m}$
$\Delta y = 0.3 \text{ m}, 0.0 \text{ m} < y < 3.0 \text{ m}$
$\Delta y = 0.6 \text{ m}, 3.0 \text{ m} < y < 5.5 \text{ m}$
$\Delta y = 1.2 \text{ m}, 5.5 \text{ m} < y < 7.9 \text{ m}$
$\Delta y = 2.4 \text{ m}, 7.9 \text{ m} < y < 25.0 \text{ m}$
$\Delta t = 8.766 \text{ h}, 0.0 \text{ yr} < t - t_i \leq 0.01 \text{ yr}$
$\Delta t = 87.66 \text{ h}, 0.01 \text{ yr} < t - t_i \leq 1.0 \text{ yr}$
$\Delta t = 175.32 \text{ h}, 1.0 \text{ yr} < t - t_i \leq 2.0 \text{ yr}$
$\Delta t = 350.64 \text{ h}, 2.0 \text{ yr} < t - t_i \leq t_f - t_i$
Example Computer Problem Runs
A. Soil layers A and B
B. Soil layers A and B with a constant temperature lower boundary at -11.1 °C

the time step that is related to the latent energy change for a step in time.

Run A was made with the no heat transfer lower boundary condition. Some of the results are shown in Figures 5, 6, and 7. The curves presented in the figures were estimated using the program output, which yields temperatures and

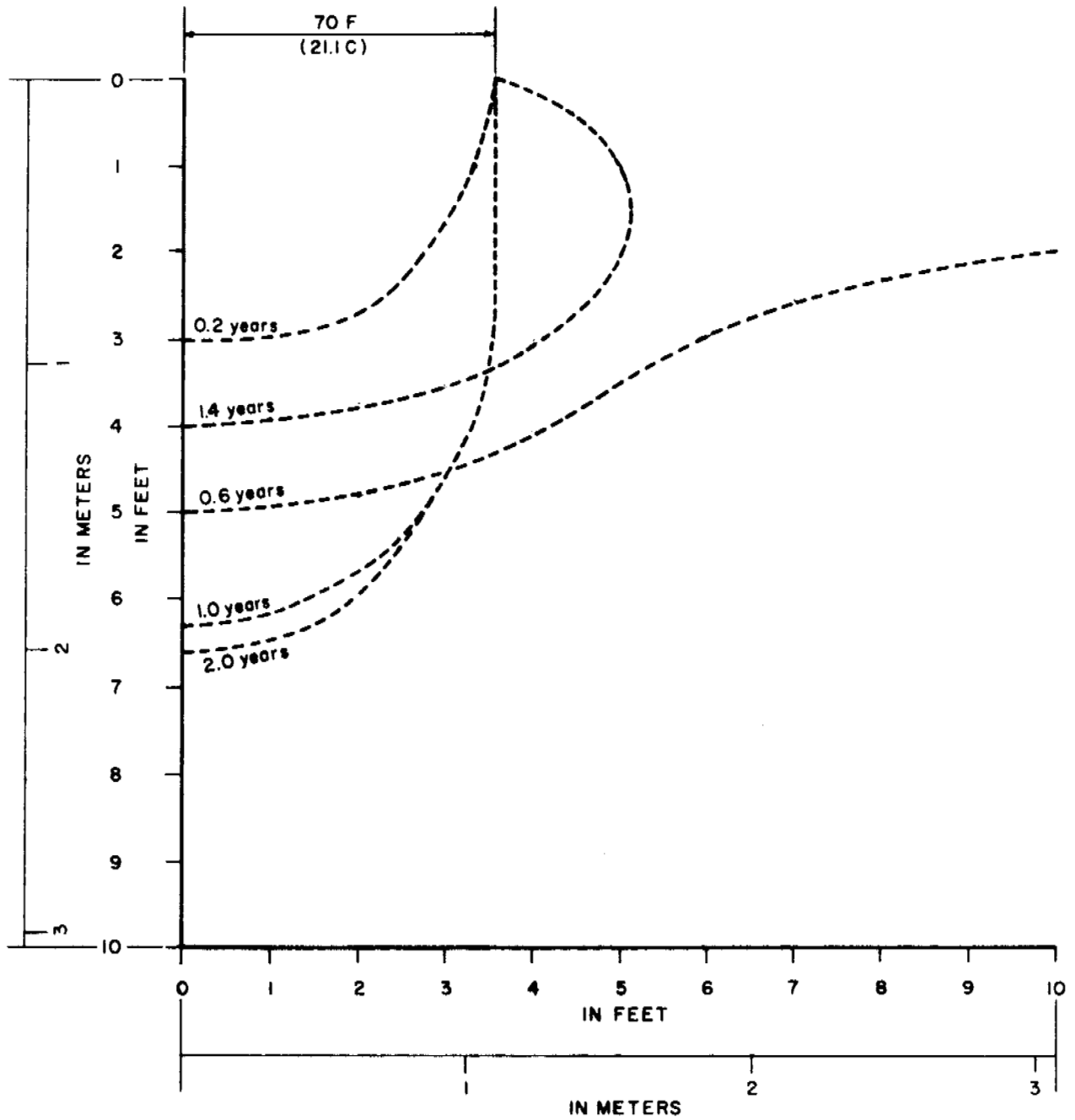


FIGURE 5 History of freezing isotherm—no heat transfer lower boundary.

latent energy values at the grid points. Figure 5 shows the history of the freezing isotherm over a 2-year period. Figure 6 shows the location of various isotherms at 2 years. It appears that the new steady periodic condition is approached after 1 year. After the first year, the location of the freezing isotherm appears to be primarily dependent upon seasonal temperature effects. Figure 7 shows the

propagation of the freezing isotherm at the left boundary under the step thermal disturbance. The rate of propagation of this isotherm is expected to be primarily dependent on the thermal diffusivity values for the soil and the amount of soil moisture present that provides the latent energy thermal inertia. Very little heating was noted along the lower boundary for a 3-year history. Additional heating might

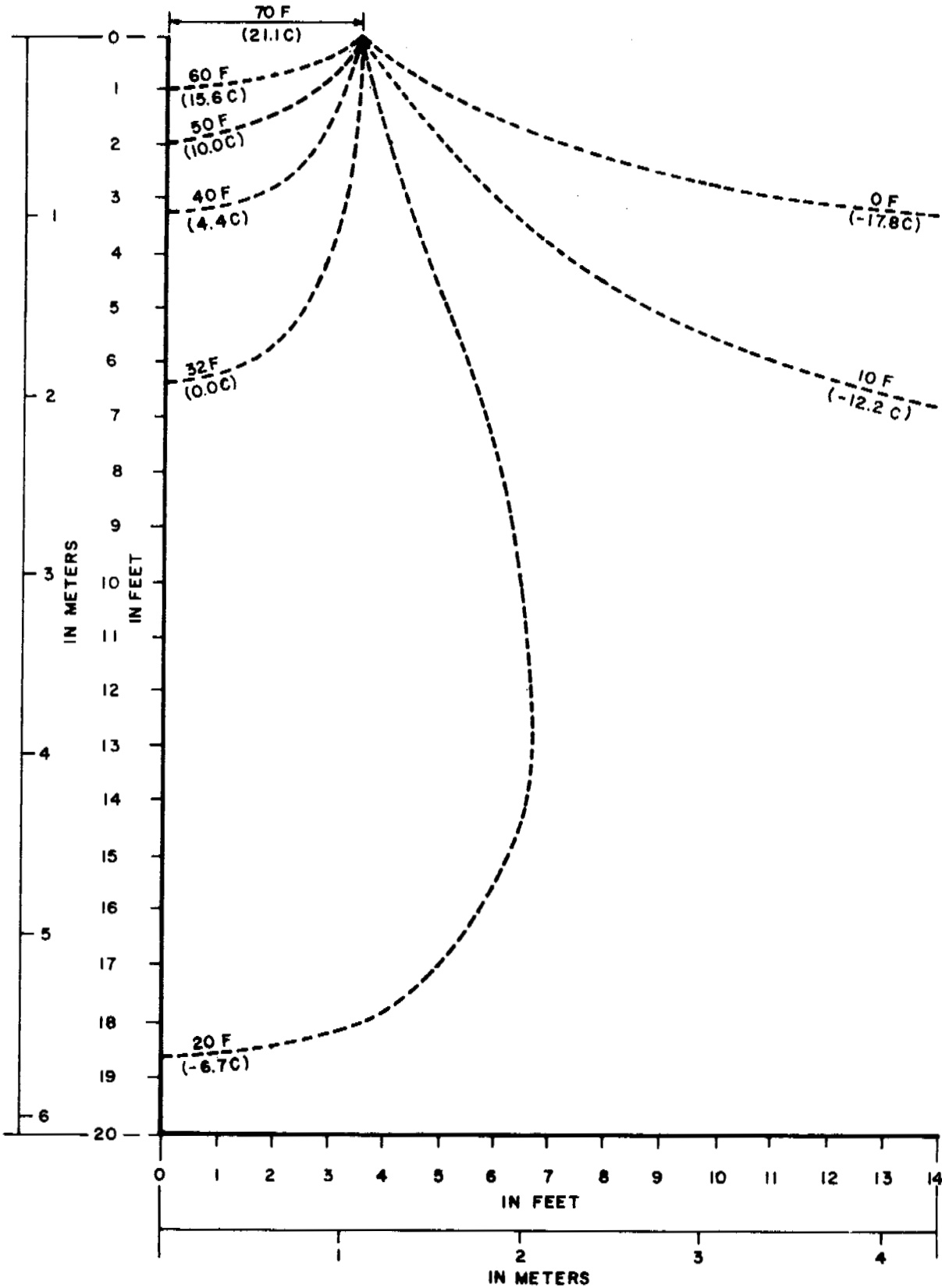


FIGURE 6 Various isotherms at 2 years—no heat transfer lower boundary.

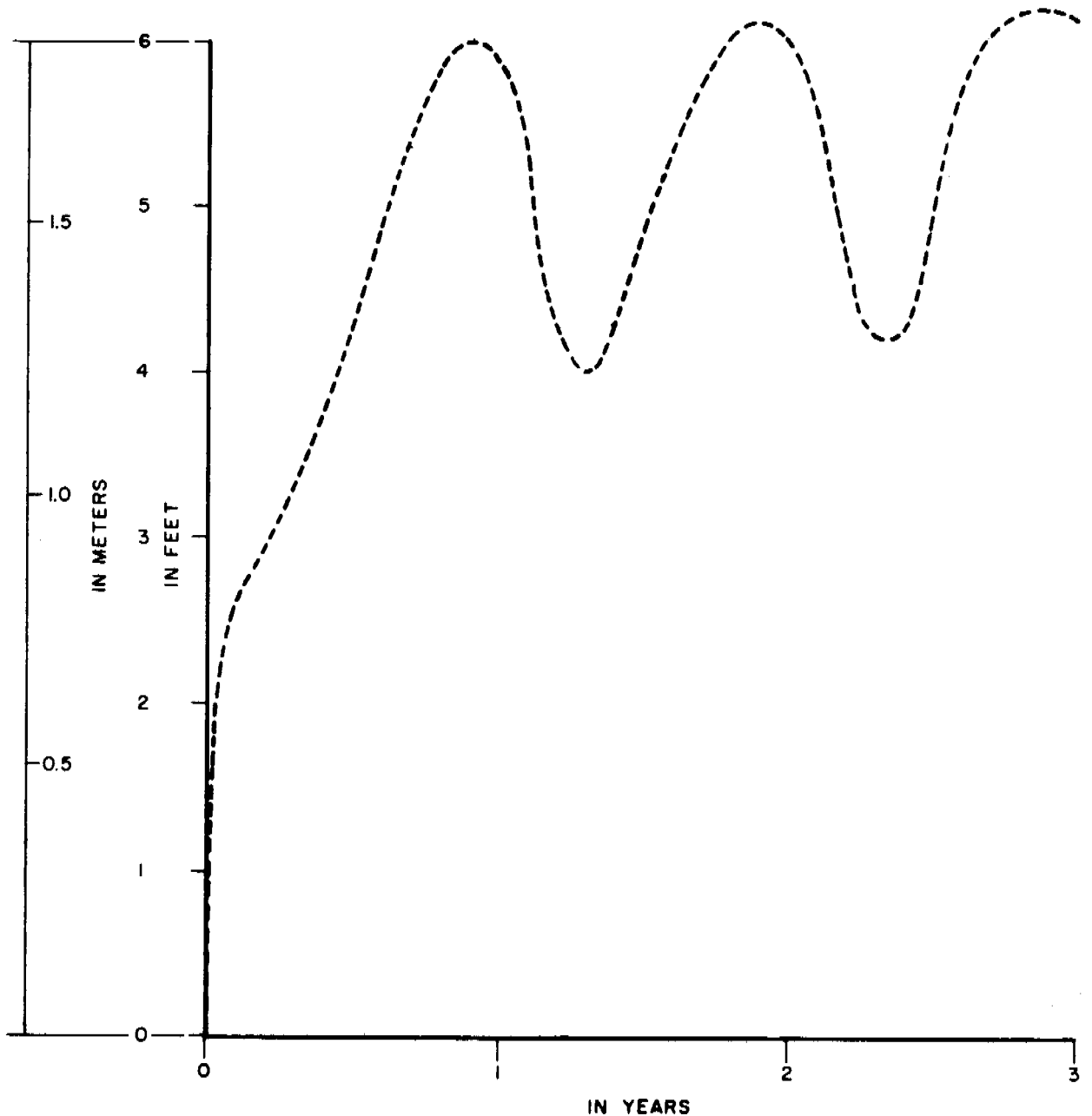


FIGURE 7 Propagation of freezing isotherm under step thermal disturbance—no heat transfer lower boundary.

occur over a longer history. The temperature variation at the lower boundary of the domain was less than 1.1°C over the 3-year history.

Run B was made with a constant temperature lower boundary, the temperature being held at the average annual ambient value. Both runs give results that are very close. For this reason, no figures corresponding to those presented for Run A are included. Run B was actually made twice. The first time, four latent heat iterations were used

for each time step over a 3-year history. The second time, eight latent heat iterations were used over a 2-year history. This is the same number of iterations as was used for the 3-year history of Run A. The two iteration schemes for Run B correlate well, the largest deviation being in the latent energy values at the freezing isotherm. For a no-heat-transfer boundary, isotherms intersect the boundary perpendicularly. For a constant temperature boundary, isotherms approach a parallel relationship, with the boundary.

with no isotherms intersecting the boundary. The boundary conditions have little effect on the freezing isotherm, provided a large domain is selected.

SUMMARY

A computer programming technique has been presented for mathematically modeling a large class of problems involving the thermal response of a permafrost medium. Allowance was made for seasonal temperature variation at the surface and also for the addition of extraneous thermal disturbances. This permits prediction of the effect of thermal disturbances on the natural variation of temperature in the permafrost. There is a provision for handling a stratified permafrost medium having layers possessing different thermal properties. Consideration also was given to changes of soil thermal properties with freezing and thawing and the latent heat of fusion was taken into account.

The transient two-dimensional heat conduction equation in Cartesian coordinates was solved using implicit finite difference methods with a weighting parameter. Finite difference step sizes may be changed with grid location. Boundary conditions for the problem domain can be varied. The output yields a time-temperature history for the domain of the solution. Results of the application of the program are included.

REFERENCES

1. Doherty, P. C. 1970. Hot pipe. Geological Survey computer contribution. U.S. Geological Survey, Washington, D.C.
2. Kazemi, H. and T. K. Perkins. 1971. A mathematical model of thaw-freeze cycles beneath drilling rigs and production platforms in cold regions. *J. Petrol. Tech.* p. 381-390.

THERMAL DISTURBANCE DUE TO CHANNEL SHIFTING, MACKENZIE DELTA, N.W.T., CANADA

M. W. Smith

CARLETON UNIVERSITY
Ottawa, Ontario

C. T. Hwang

E. W. BROOKER & ASSOCIATES
Edmonton, Alberta

INTRODUCTION

The objective of this paper is twofold: first, to study the geomorphological pattern of permafrost distribution under a shifting river channel and to analyse the matter quantitatively, in the framework of heat conduction theory. Qualitative descriptions of this situation have been reported^{3,10,13}; second, to verify against field data a computer program for predicting the effects of thermal disturbance due to engineering operations in permafrost, developed for Gas Arctic Systems.^{4,5}

STUDY AREA

The data used here are from a study carried out in the east central part of the modern Mackenzie Delta, some 50 km northwest of Inuvik.¹⁵ Aspects of the physical geography of

the region have been described by Mackay.¹¹ The climate of this part of the delta is transitional between subarctic and arctic; some climate data from Inuvik and Aklavik, the nearest stations, are presented in Table I.

Were it to conform to the broad geographical patterns of permafrost distribution, the Mackenzie Delta would lie in the continuous zone (i.e., ground temperatures at depths of 10-15 m less than -5°C).¹ On a ground temperature basis, however, the region is seen to form an outlier of the discontinuous zone; permafrost is physically discontinuous there, and maximum thickness is probably generally less than 100 m.⁷ This is due to the thermal influence of the large amounts of surface water there.^{2,14} On the nearby tundra, where these influences are not present, a permafrost thickness of 365 m has been measured.⁶

The delta is an area of active sedimentation and erosion. Shifting channel courses—as evidenced by abandoned chan-

nels, point bar deposits, and undercut banks—are a conspicuous element of the landscape (Figure 1). The channels rarely meander in the geomorphic sense, although they may be sinuous, and they do wander.¹¹ The gross topography is flat, and local relief generally does not exceed 3–4 m, excluding channel cross sections. Vegetation shows a sequential distribution: Actively forming sections near the channels are bare of vegetation; willow (*Salix* sp.) and alder (*Alnus crispa*) grow away from the rivers; and the inactive parts of the floodplain are populated by spruce (*Picea glauca*), which is the typical climax community in the lower valley and delta of the Mackenzie River.

The study area contains many lakes, ranging in size from 0.01 to 0.5 km² (Figure 1) whose depths are generally greater than the winter ice thickness. About 50 percent of the area is covered by water bodies. A major distributary, 120–170 m wide, flows through the area and is erosionally active, undergoing lateral migration.

The net total amount of shifting that has taken place during the migration cycle can be determined from the river's initial and present positions (Figure 1). The former is delineated by a fossil cut bank, which is some 230 m away from the present channel position. A second, younger, fossil cut bank shows that the river has been wandering in the recent past. Measurements from aerial photographs give an average rate of shifting of 1 m year⁻¹ over the past 30 years. In the model, however, it was decided to use a lower, "apparent" rate of shift, ν , in order to approximate the migration to an equivalent monotonic process. With $\nu = 0.5$ m year⁻¹, the migration history spans 460 years.

At present, the river is cutting into a spruce-covered surface in excess of 300 years old (as indicated by tree cores) on the outside bends of meanders, with consequent degradation of permafrost. The talik, which exists beneath the river, follows the river migration. Also as the cut bank recedes, new deposits are formed on the slipoff slope, and, under the influence of low-mean annual surface temperatures, permafrost will form there *ab initio*. The local configuration of permafrost, therefore, is closely related to the history of river migration.

The process of geomorphic change is accompanied by a vegetation succession that produces a complex interaction between topography, vegetation, microclimate, and ground temperatures.

FIELD DATA

Numerous temperature boreholes have been established in the study area, but the data used here are taken from a single transect that encompasses the geomorphological sequence described above. It must be realised that the temperature data used here represent a single transect in time for a long-term geomorphological sequence. Temperatures were measured with thermistors, and values are believed

accurate to ± 0.1 °C. In addition to the ground temperatures, data are available for mean annual lake and river temperatures [1] and for the material properties of the soils in the area [2].

THE MATHEMATICAL MODEL

To study the pattern of permafrost configuration as a long-term problem with a time-span of around 500 years, the erosional aspect of river shifting was not considered explicitly, but was absorbed into the specified rate of migration. The problem then becomes a temperature boundary value problem, and the thermal disturbance due to the channel shifting can be simulated as a temperature wave. The shape and amplitude of the wave was formed according to the measured ground and water temperature data as shown in Figure 2. (Mean annual values are used and are assumed to be representative for the long-term problem.) In this way, the changing thermal regimes associated with the river disturbance *and* the subsequent vegetation succession are accounted for. As the tail of the wave changes form over time, this simulates the decreasing surface temperatures due to increasing biomass associated with vegetation succession (Figure 2).

This wave was then moved across the surface, from some initial position to its present position, at some rate ν , thought to approximate the average rate of shift over a long period of time.

PROBLEM SOLUTION

The Thermal Code

Very few closed form mathematical solutions are currently available for thermal problems that include the effects of latent heat. The solutions that do exist are generally one-dimensional, for simple geometric configurations, uniform material properties and initial conditions, and simple disturbances of boundary temperature.¹² However, there are many complex problems involving phase change that are distinctly *two-dimensional*. In view of the difficulty of obtaining closed form solutions to such problems, numerical methods must be used. In the present paper, a finite element formulation of the transient heat conduction problem for freezing and thawing soils is used, in which latent heat is considered as a heat source in the energy balance.⁵

The finite element code was modified as follows, in order to solve a temperature boundary value problem with a moving boundary (i.e., the prescribed temperature wave disturbance): A rectangular thermal domain was assumed, with its position defined by the coordinates of prescribed corner points (Figure 3). The initial position of the river was defined by X Rear and X Front. The river was then

TABLE I Averages and Extremes of Climatic Data

	Temperature (°C)					Precipitation (cm)	
	Mean Daily	Mean Daily Maximum	Mean Daily Minimum	Extreme Maximum	Extreme Minimum	Mean Total Water	Mean Snow on Ground
Inuvik^a							
Jan	-31.1	-26.0	-36.1	1.7	-51.7	2.0	56.8
Feb	-29.8	-24.4	-35.2	2.8	-56.7	1.2	60.0
Mar	-24.7	-18.3	-31.1	6.1	-50.6	1.5	65.5
Apr	-14.5	-7.9	-21.1	13.3	-46.1	1.6	56.1
May	-0.8	4.2	-5.3	23.3	-27.8	1.7	1.3
June	10.2	16.3	4.1	31.7	-6.1	1.9	0.0
July	13.4	19.3	7.6	31.1	-3.3	3.7	0.0
Aug	10.4	15.6	5.1	29.4	-6.1	4.6	0.0
Sept	2.8	6.9	-1.4	25.6	-18.9	2.1	0.7
Oct	-8.0	-4.4	-11.6	15.0	-35.0	3.7	25.0
Nov	-21.6	-17.1	-26.2	10.6	-46.1	1.7	33.6
Dec	-26.9	-21.9	-31.9	-0.6	-50.0	1.8	46.6
YEAR	-10.1					27.5	
Aklavik^b							
Jan	-28.8	-24.9	-32.7	6.7	-50.6	1.4	
Feb	-27.6	-23.6	-31.6	9.4	-52.2	1.0	
Mar	-22.6	-17.6	-27.5	9.4	-48.9	1.0	
Apr	-12.7	-7.1	-18.3	13.9	-42.2	1.1	
May	-0.7	3.9	-5.3	25.0	-25.6	0.9	
June	9.4	14.3	4.5	30.0	-6.7	1.9	
July	13.6	18.3	8.9	33.9	-1.1	3.2	
Aug	10.4	14.6	6.1	31.1	-3.9	3.5	
Sept	3.4	6.4	0.3	24.4	-11.1	2.8	
Oct	-7.0	-4.4	-9.6	12.8	-30.0	2.6	
Nov	-19.9	-16.5	-23.3	6.7	-45.6	1.8	
Dec	-27.0	-23.2	-30.8	10.0	-47.8	1.2	
YEAR	-9.1					22.4	

^a 68° 18' N, 133° 29' W; elevation 67 m; period 1957-1971.

^b 68° 14' N, 135° 00' W; elevation 9 m; period 1931-1960.

shifted at an "apparent" rate v . Once the overall geometry has been specified, the finite element mesh (Figure 3) is automatically generated by an appropriate subroutine. The temperature wave (Figure 2) was programmed as a subroutine, which specifies the ground surface temperature variation with x and t (time).

Soil Stratigraphy and Thermal Properties

The material to a depth of 30 m consists mainly of silt, sandy-silt, and fine sand. Total moisture content, by weight, can vary from almost 100 percent in near-surface layers to 30 percent or less at depth. Other studies from the same region^{8,16} found similar results and also recorded little ice segregation and soil material well bonded by ice not visible to the eye.

Direct measurement of thermal properties was not per-

formed. Values for thermal conductivity, specific heat, and volumetric latent heat were calculated according to formulas suggested by Kersten.⁹ None of the sample boreholes were deeper than 30 m; data for the layers below this depth were taken from another study.⁸ The material properties are listed in Table II.

Initial and Boundary Conditions

INITIAL CONDITIONS

The present temperature profiles obtained from the borehole data constitute only a single time frame of the whole thermal history. To reproduce this history mathematically, assumptions have to be made regarding the thermal regime that existed when the channel was in its initial position prior to migration. Geomorphological evidence places this initial

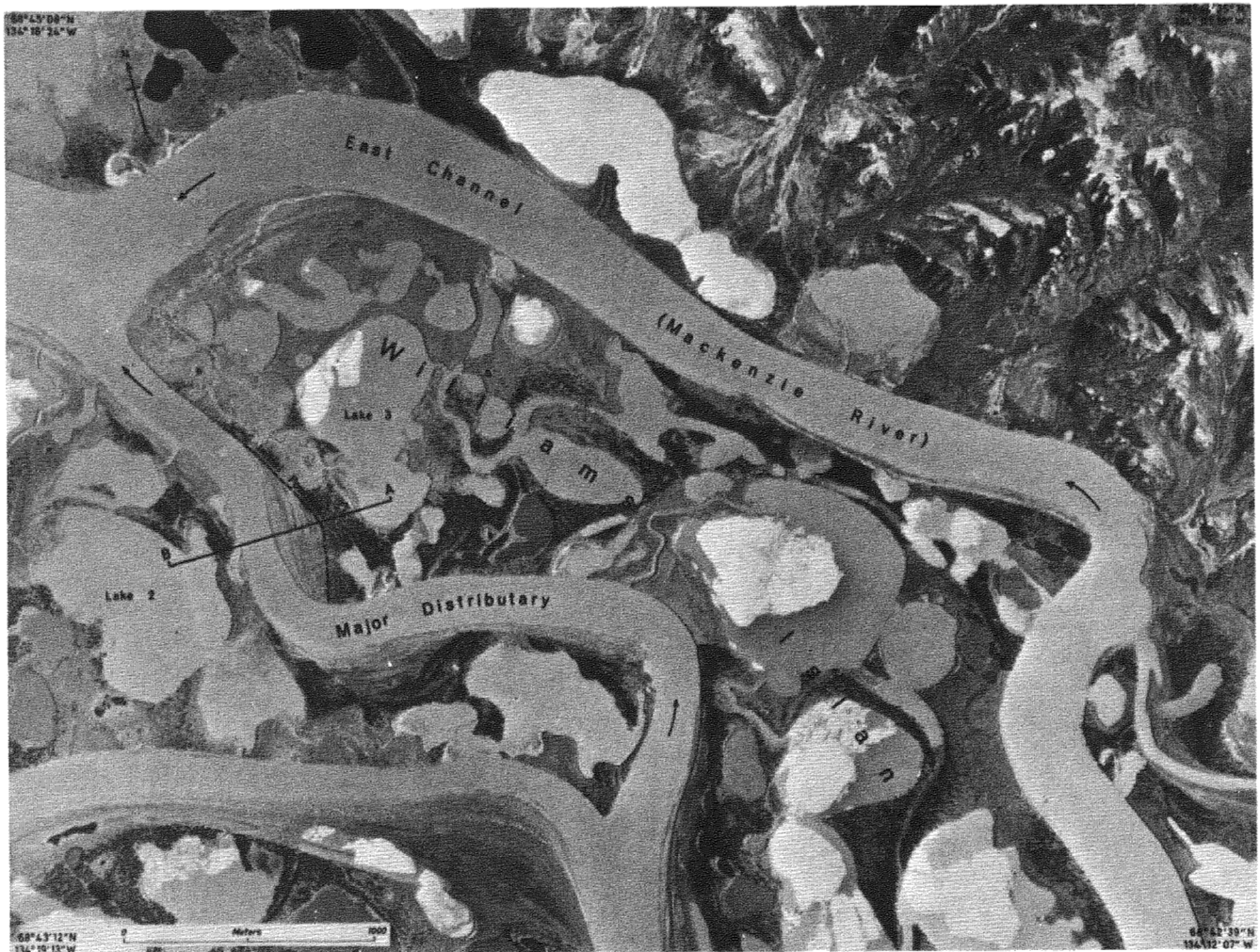


FIGURE 1 Study area and vicinity (from Canadian Government aerial photograph A 19946-13).

position 230 m back from the present position (assuming that the width of the river has not changed). The initial temperature field was obtained by assuming the river to be stationary in its initial position for 500 years prior to migration. A value of 4°C was used for the river temperature and $0.025^{\circ}\text{C m}^{-1}$ for the geothermal gradient [3]. The initial temperature field also reflects the effects of the lakes at either end of the transect A-B; a value of 3°C was used for lake temperature. The resulting permafrost configuration is shown in Figure 4a.

Starting with this initial condition, the river was shifted across the domain to its present position. With ν equal to 0.5 m year^{-1} , this would take 460 years.

BOUNDARY CONDITIONS

The ground surface, river bed, and the nearby lakes (Figure 3) were treated as boundaries with temperatures prescribed according to Figure 2.

The boundaries A-A' and B-B' (Figure 3) were assumed to be thermally insulated, i.e., there is no heat flow across them, so that the isotherms run normal to them.

The temperatures at the boundary A'-B' were assumed to be constant and were kept fixed at the values for the initial condition.

GRID SIZE AND TIME INCREMENTS

The size of the domain is set by the dimensions of the problem; the resolution of the analytical technique depends on the fineness of the grid that is imposed on this domain. This, itself, is limited by the amount of computer core available. To gain the most benefit from the core available, the grid is made finer in the upper layers, where gradients are steepest (Figure 3).

To achieve economy of computer cost for this long-term problem, logarithmic time increments were used.

The computer time required for a 400-500 year history,

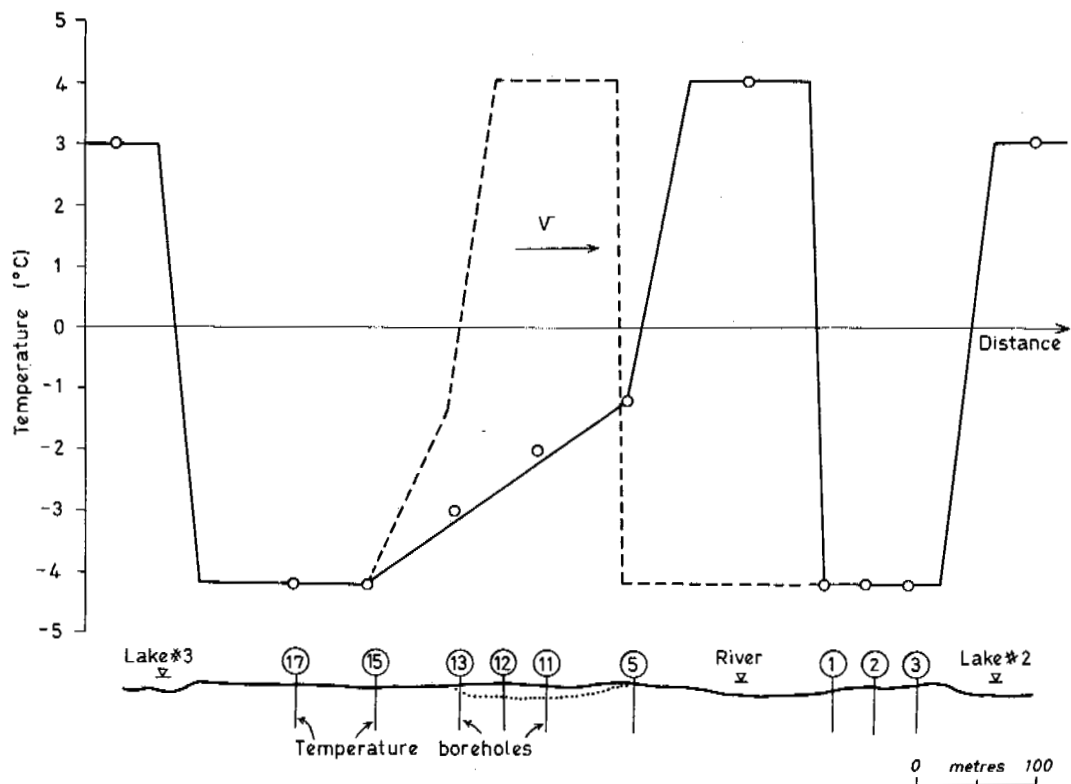


FIGURE 2 Temperature wave simulating river shifting.

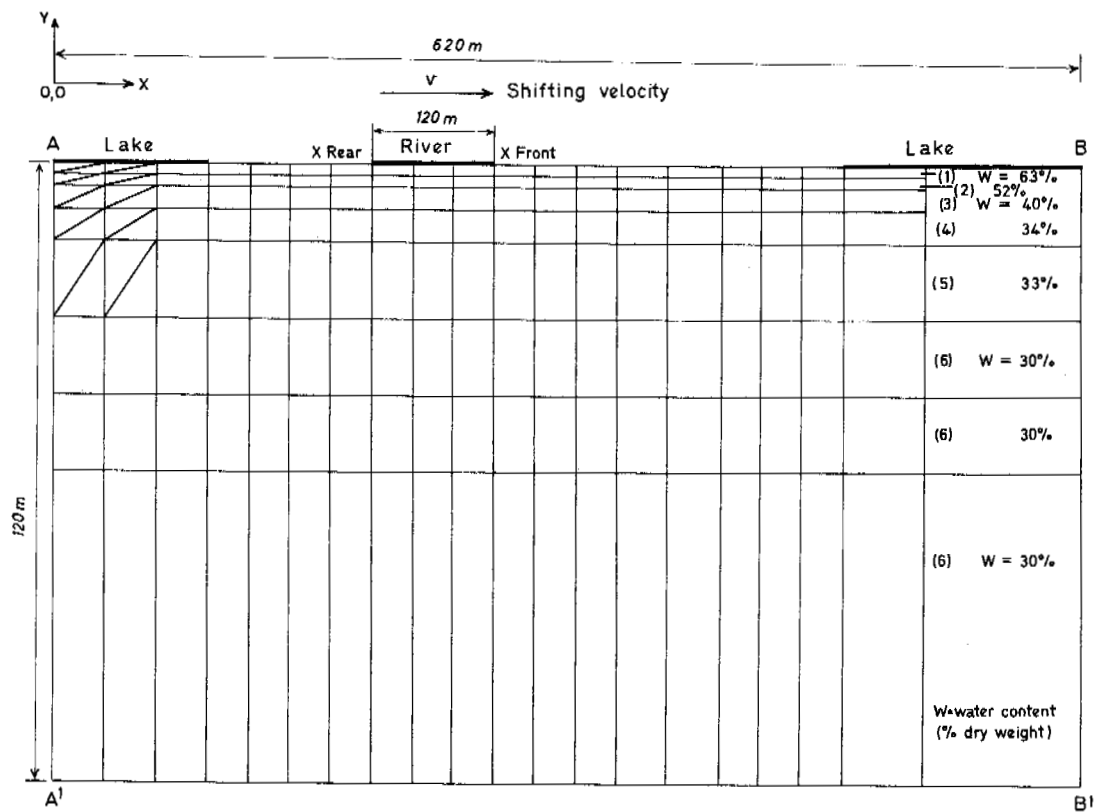


FIGURE 3 Geometry input and finite element layout.

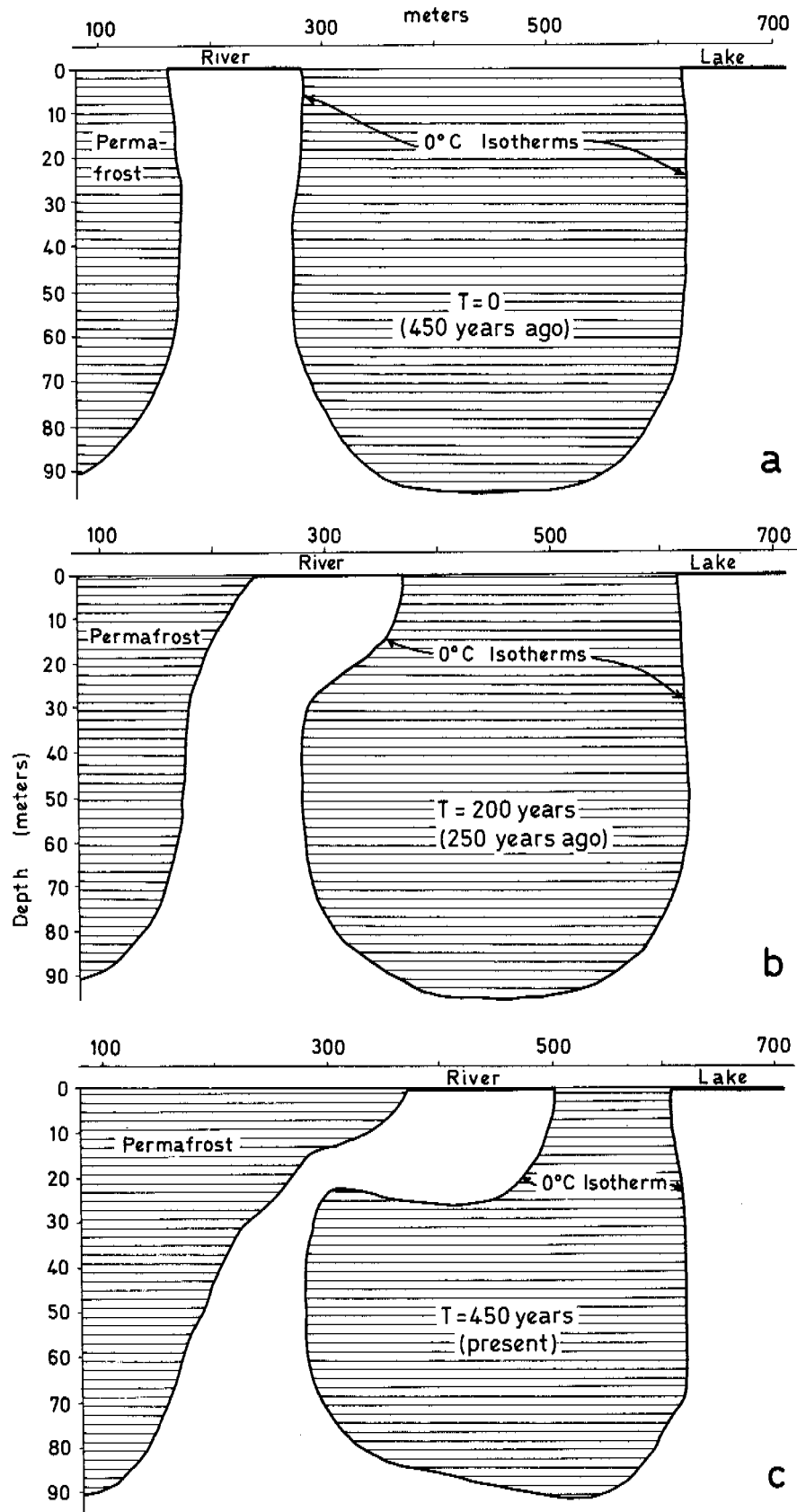


FIGURE 4 Change in permafrost configuration.

TABLE II Physical and Thermal Properties of Ground Materials

Ground Layer	Depth Interval (m)	Ground ^a Material	Total Unit Weight (kg m ⁻³) ^b	Total Moisture Content (%)	Thermal Conductivity (W m ⁻¹ K ⁻¹)		Specific Heat (J kg ⁻¹ K ⁻¹)		Volumetric Latent Heat ^c (kJ/m ³)
					Frozen	Unfrozen	Frozen	Unfrozen	
1	0-2	clayey-silt	1 698	63	3.767	1.417	1 679	2 734	261.1E + 03
2	2-4	silt	1 730	52	3.093	1.348	1 461	2 303	216.3E + 03
3	4-9	silt	1 858	40	2.626	1.279	1 227	1 800	163.4E + 03
4	9-15	silt/sand	1 922	34	2.385	1.365	1 143	1 671	143.1E + 03
5	15-30	silty-sand	1 986	33	2.315	1.417	1 097	1 616	144.7E + 03
6	30-120	sandy-silt	1 922	30	2.229	1.313	1 072	1 549	125.1E + 03

^a Grain-size classes are per USDA classification. Where only a single class appears, this indicates that neither of the other two exceeds 20 percent. When a class(es) exceeds 20 percent, but is not the main one, it appears as the modifier.

^b Values supplied by R. J. E. Brown, National Research Council of Canada (personal communication).

^c These values allow for an unfrozen water content of 5 percent.

with a 10 × 22 grid, was 23 min on the Sigma 9 computer at Carleton University.

RESULTS AND DISCUSSION

Ground Temperatures

The agreement between present-day predicted and observed temperature profiles is good on both sides of the river (Figure 5). The maximum deviation is 0.7 °C (at 30 m in No. 2), but agreement is typically within 0.2 °C. When comparing the observed and predicted profiles, one should remember that linear interpolation has been assumed between points. Consequently, where the finite element grid is coarse, below 15 m, the predicted profile may appear to deviate increasingly from the measured one, as for example, in borehole No. 13, between 15 and 30 m (Figure 5).

The predicted values are generally colder than those measured in the field, which could perhaps be due to the following:

1. Only the effects of the river and the two closest lakes have been included in the model—in view of the large amount of other surface water in the area (Figure 1), perhaps there is a significant three-dimensional effect here that has been ignored by the use of a two-dimensional model.
2. Inaccuracies in the calculated thermal properties have been used.

In the case of borehole No. 13, there is a consistent error at all depths due to an incorrectly specified surface temperature, the latter resulting from the linear approximation of the tail of the wave (see Figure 2). In most cases, the observed and predicted temperature gradients agree closely, indicating that the computational method is sound, but

that there may be errors in the input data. The average observed and predicted temperature gradients at borehole No. 12, for example, are 0.097 °C m⁻¹ and 0.100 °C m⁻¹, of which only 0.025 °C m⁻¹ is due to the earth's geothermal gradient. In other words, the river is responsible for a sizeable effect, and this is adequately reproduced in the model.

It must be pointed out that ground temperature measurements were made only to a depth of 30 m; data must be obtained to greater depths to ultimately confirm the efficacy of the mathematical model.

Permafrost Configuration

Taking the 0 °C isotherms as permafrost boundaries, the predicted changes that occur in the permafrost configuration under the migrating river are summarised in Figure 4. The predicted configurations compare well with those described by Efimov³ (Figure 6).

The permafrost history, under the influence of channel migration, may be described in general terms as follows. In the initial position, a curtain-shaped through-talik exists beneath the river, with the permafrost boundaries plunging steeply downward (Figure 4a). Through-taliks are also developed beneath the lakes. As the river migrates across the surface, this causes the talik beneath it to migrate also. There is a lag in talik formation with depth, as shown by the bulge in the 0 °C isotherm beneath the cut bank (cf. the configuration for the initial condition). This lag results from the decreasing rate of penetration of the temperature disturbance with depth. Following the river disturbance and permafrost degradation, surface temperatures on the slipoff slope gradually decrease, and permafrost "wedges" back in again. This configuration is a function of the decreasing surface temperatures away from the river, associated with the vegetation succession and the lag in the temperature re-

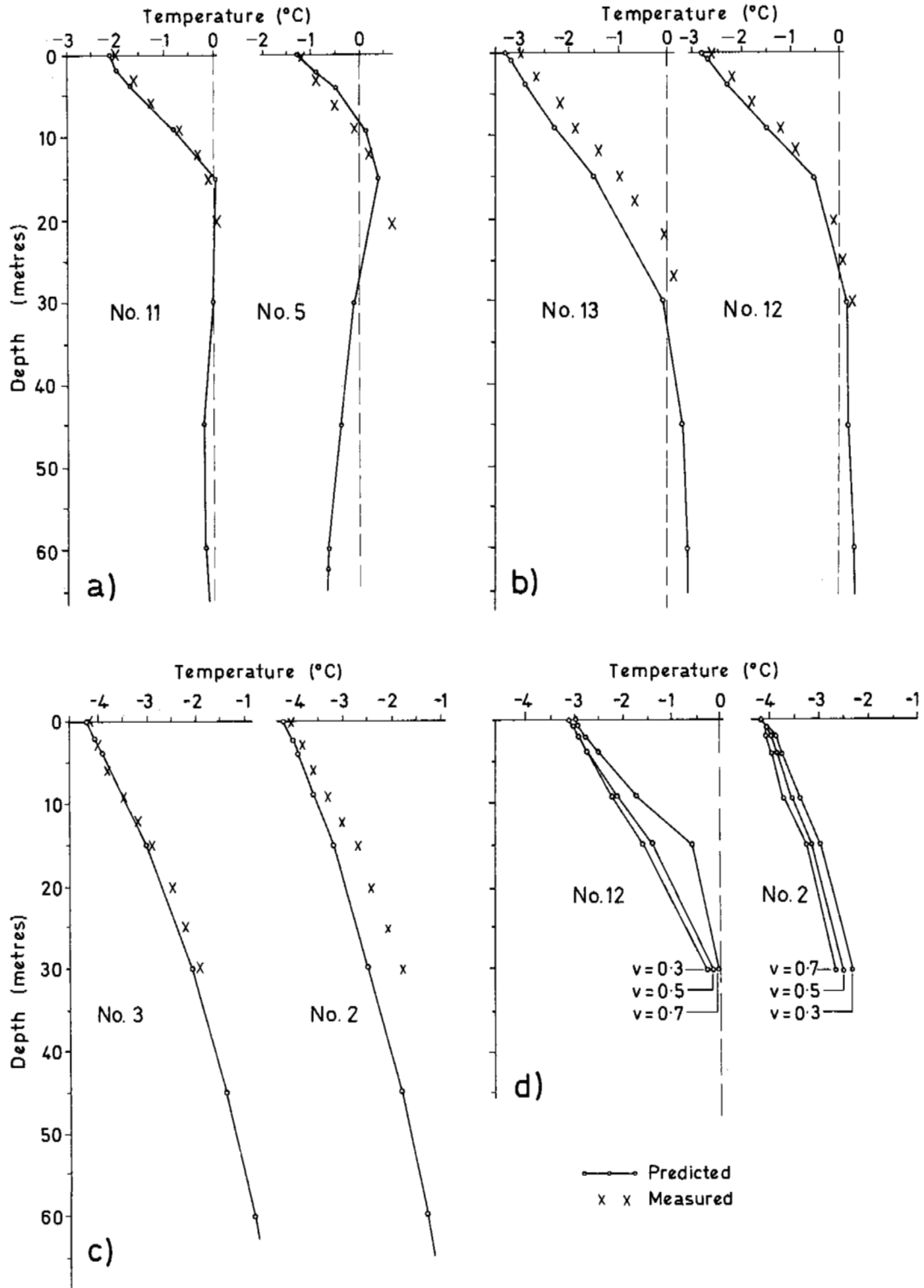


FIGURE 5 Borehole temperature profiles.

covery following disturbance. Temperatures on the cut bank side of the river are colder than those under the slipoff slope.

Effects of Varying the Shifting Rate

The thermal effects of the river on the surrounding ground temperature field depend not only on the strength of the source but also on the length of time available to the thermal processes. The latter is a function of the rate of migration. To investigate the effects of this, the program was run with various values for ν . It will suffice, here, to discuss only two of the cases— $\nu = 0.3$ and 0.7 m year^{-1} .

When ν is increased to 0.7 m year^{-1} , temperatures on the cut bank side tend to be slightly cooler, while those under the slipoff slope are a little warmer (Figure 5). For $\nu = 0.3 \text{ m year}^{-1}$, the opposite is true. For the slower migration rate, the river will have been in close proximity to the present cut bank for a longer period, as a result the warming effect is greater. On the slipoff slope, however, temperature recovery will have proceeded over a correspondingly longer time, and the temperatures there will be cooler. For the faster migration rate, the converse is the result. The solution for $\nu = 0.5 \text{ m year}^{-1}$ seems to yield the best overall result.

The thermal effects due to a varying migration rate remain to be investigated; this phase would profit from the acquisition of additional pertinent field data.

If, in the model, the river is caused to wander back and forth, the permafrost configuration thus produced is similar to that described, for such a circumstance, by Kudryavtsev.¹⁰

CONCLUSIONS

Judging from the results of this study on thermal disturbance due to channel shifting, it is concluded that:

1. The calculated variations in permafrost distribution compare well with field measurements and, in a qualitative sense, with that reported in the literature.
2. The finite element formulation of the heat conduction equation provides good temperature predictions for such a problem and demonstrates the consistency of the ground temperature field in the framework of heat conduction theory.
3. The use of a temperature wave to simulate the river migration yields satisfactory results.

ACKNOWLEDGMENTS

The fieldwork referred to in this paper was supported by the Geological Survey of Canada and by the University of British Columbia with grants to the Department of Geography from the Department of Indian and Northern Affairs and the National Research Council of Canada, under the good offices of Dr. J. R. Mackay. The authors

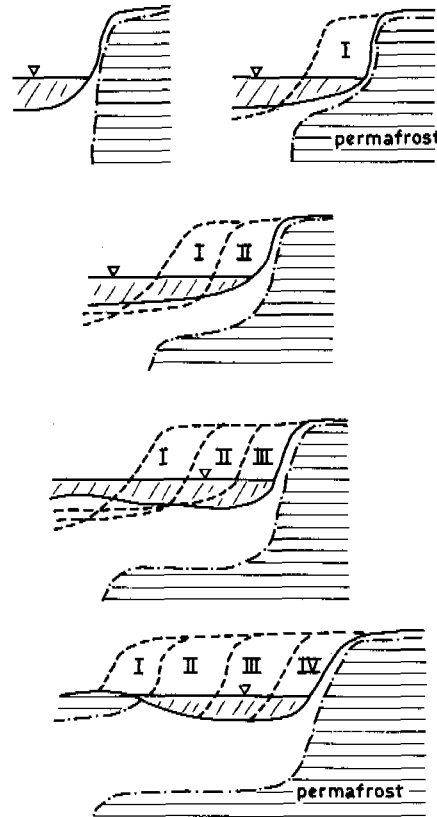


FIGURE 6 Schematic change in permafrost configuration with riverbank erosion (after Efimov³).

gratefully acknowledge the co-operation of Gas Arctic Systems, Calgary, and E. W. Brooker & Associates, Edmonton. The manuscript and illustrations were prepared in the Department of Geography, Carleton University.

REFERENCES

1. Brown, R. J. E. 1960. The distribution of permafrost and its relation to air temperature in Canada and the USSR. *Arctic* 13:163-177.
2. Brown, W. G. *et al.* 1964. Comparison of observed and predicted ground temperatures with permafrost distribution under a northern lake. *Can. Geotech. J.* 1:147-154.
3. Efimov, A. I. 1964. Hydrological and geocryological characteristics of the bed and shores of the Lena River near Yakutsk. *Akademiia Nauk SSSR, Institut Merzlotovedeniia, Geokriologicheskie Usloviia Zapodnoi Sibiri, Yakutii i Chukotki*, p. 97-110.
4. Hwang, C. T. 1972. A study of thermal disturbance due to channel shifting, Mackenzie Delta, N.W.T. Report submitted to Gas Arctic Systems by E. W. Brooker & Associates, July.
5. Hwang, C. T. *et al.* 1972. A thermal analysis for structures on permafrost. *Can. Geotech. J.* 9:33-46.
6. Jessop, A. M. 1970. How to beat permafrost problems. *Oilweek* January.
7. Johnston, G. H., and R. J. E. Brown. 1964. Some observations on permafrost distribution at a lake in the Mackenzie Delta, N.W.T., Canada. *Arctic* 17:163-175.

8. Johnston, G. H., and R. J. E. Brown. 1965. Stratigraphy of the Mackenzie River Delta, N.W.T., Canada. *Bull. Geol. Soc. Am.* 76:103-112.
9. Kersten, M. S. 1949. Laboratory research for the determination of the thermal properties of soils. *Univ. Minn. Inst. Tech. Eng. Exp. Sta. Bull. No. 28.*
10. Kudryavtsev, V. A. 1959. Temperature, thickness and discontinuity of permafrost, p. 219-273. *In Principles of geocryology. Part 1. General geocryology.* N.R.C. Tech. Transl. 1187 (1965).
11. Mackay, J. R. 1963. The Mackenzie Delta area, N.W.T. Geographical Branch, Dept. of Mines and Technical Surveys, Mem. No. 8. 202 p.
12. Muehlbauer, J. C., and J. E. Sunderland. 1965. Heat conduction with freezing or melting. *Appl. Mech. Rev.* 18:951-959.
13. Péwé, T. L. 1965. The Fairbanks Area. *In International Association for Quaternary Research, VIIth congress, Guidebook for field conference F (Central and South-Central Alaska).* p. 6-36.
14. Smith, M. W. 1972. Observed and predicted ground temperatures, Mackenzie Delta, N.W.T., p. 95-106. *In Mackenzie Delta area monograph.* 22nd International Geographical Congress.
15. Smith, M. W. 1973. Factors affecting the distribution of permafrost, Mackenzie Delta, N.W.T. Ph.D. Thesis. University of British Columbia, Vancouver. (In preparation)
16. Williams, P. J. 1968. Ice distribution in permafrost profiles. *Can. J. Earth Sci.* 5:1381-1386.

NOTES

- [1] Some of the data for lake and river temperatures were supplied by C. P. Lewis (personal communication).
- [2] The soil sample boreholes were drilled through the cooperation of Imperial Oil Ltd. and Gulf Oil Ltd.
- [3] The value for the geothermal gradient was calculated from data from W. G. Brown *et al.*² and verified with data from Jessop.⁶

ECOLOGICAL EFFECTS OF RIVER FLOODING AND FOREST FIRES ON PERMAFROST IN THE TAIGA OF ALASKA

Leslie A. Viereck

INSTITUTE OF NORTHERN FORESTRY

Fairbanks, Alaska

INTRODUCTION

In the taiga of Alaska, permafrost is one of the most important factors influencing the distribution of vegetation. Fast-growing white spruce (*Picea glauca* [Moench] Voss), quaking aspen (*Populus tremuloides* Michx.), and paper birch (*Betula papyrifera* Marsh.) are usually found on permafrost-free soils or areas with a thick active zone, whereas black spruce (*Picea mariana* [Mill.] B.S.P.), muskeg, and bog occur on permafrost soils with a thin active layer.

In general, the climate of interior Alaska is cold, with a wide temperature range and low amounts of precipitation. Yearly precipitation at Fairbanks averages 287 mm. Snow usually covers the ground from mid-October until late April and averages 1.51 m annually, with an average maximum accumulation of 0.74 m. The mean annual temperature is -3.4°C ; July, the warmest month, has a 15.5°C mean temperature and January, the coldest month, a -23.9°C mean. Permafrost, which underlies most of the forests and bogs of low-lying areas and north-facing slopes, is deep

or lacking on south-facing slopes and on newly deposited alluvium adjacent to the rivers. A detailed description of permafrost conditions and distribution in the Fairbanks area is given by Péwé.¹⁸

The vegetation-permafrost relationships of the ecosystem are not simple. The overlying vegetation also influences the distribution of permafrost, or at least the thickness of the active layer.^{1,7,19,22} Thus, if the vegetation cover is removed, as when the land is cleared for agricultural purposes, the active layer thickens and depth to the permafrost layer may change from 50 to 60 cm to over 14 m in 40 years.¹⁹ Kallio and Rieger¹³ report an increase in the active layer from 1 to 5 m only 3 years after removal of the vegetation from a black spruce type.

Both Benninghoff² and Tyrtikov²² discuss the complexities of the vegetation boundary in the taiga and show it to be poorly understood. Brown⁶ has shown that vegetation over permafrost changes the net radiation albedo and conduction-convection relations of the surface boundary and that evaporation and transpiration and their resultant cool-

ing, as well as conduction, in the organic layers are important to the effect of vegetation on the permafrost layer. Tyrtikov²² gives an excellent summary of the effects of vegetation on permafrost and the active layer thickness. Although the insulating effect of the organic layer is generally agreed to be most important in determining thickness, tree and shrub vegetation also play a role. In an earlier paper,²³ it was shown how even a single tree may produce a lens of permafrost in an open forest stand. Tyrtikov²² points out that retention of snow by tree and shrub vegetation reduces the snow cover on the ground, thus lowering winter soil temperature and that the interception of warm rain by tree, shrub, and moss vegetation may reduce summer thaw.

The importance of the overstory layers can be shown by the following: In 1969, the tree and tall shrub layer were removed from three 40 m² plots of an open black spruce/*Ledum*/moss stand near Fairbanks to determine the biomass of the overstory. The stand was located on flat terrain underlain by permafrost. The soil was Tanana silt-loam, which is approximately 22 percent sand, 72 percent silt, and 6 percent clay. The moss layer was 15 cm thick. The low shrub and moss mat was not sampled and remained relatively undisturbed during the removal of the overstory trees. Two summers later, there was a noticeable subsidence of the surface in the cleared areas. Probing for permafrost in the fall of 1972 showed that the active layer in the uncut area was from 80 cm to over 1 m thick, whereas the permafrost layer in the surrounding undisturbed forest stand was approximately 55 cm below the surface of the vegetation. In addition, the cleared areas had subsided from 30 to 50 cm below the surrounding uncleared areas, showing that the thaw had actually been more than 1 m and probably closer to 1.5 m. Tyrtikov²² reported a similar increase in the thaw depth after removal of only *Ledum palustre* shrub layer in the Igarka region of Siberia. Thus, the overstory, as well as the moss layer and organic layer, is important in maintaining a shallow active zone in taiga forest types.

FREEZE-THAW CYCLE UNDER NATURAL VEGETATION

Information is scarce for the annual freeze-thaw cycle in permafrost soils under natural vegetation. Bliss and Wein⁴

present some measurements of summer thaw rates from the tundra regions of Alaska, but similar measurements from the taiga are lacking. One reason for this is that installing measuring devices or probing in an area usually disturbs the vegetation mat, altering the thermal regime of the soil. A freeze-thaw indicator (referred to as a frost tube) used in this study was considered to cause the least disturbance of the site. It consisted of a double polyethylene tube, the inner tube of which contained sand and a 0.1 percent solution of fluorescein dye. The device has been extensively tested in the laboratory and in the field in Alaska and other northern areas by Rickard and Brown.²⁰ The holes for installing the tubes were augered at the same diameter as the outside tube. Care was taken to prevent the subsoil from spilling on the vegetation. No visible disturbance was caused by the installation of the frost tubes. Four years after installation, there were no visible changes in the vegetation mat adjacent to the frost tubes, but a depression was forming along the trail to the frost tubes.

To obtain a base line for measuring the effects of disturbance on stands, Viereck installed three frost tubes in an undisturbed open 55-year-old black spruce/*Ledum*/moss stand near Fairbanks. The soil is Minto-silt-loam, which is approximately 10 percent sand, 80 percent silt, and 10 percent clay, with an overlying organic layer 30 cm thick. Measurements were recorded weekly from October 1968 to October 1972. The annual freeze-thaw cycle for the 4 years is presented in Figure 1. The thaw begins from mid-April to early May and after mid-May progresses at an almost linear rate until the end of August, after which time little or no thaw occurs. There was little difference in thawing rates during the different years, and the maximum thaw depth (the thickness of the active layer) varied only 5 cm over the 4 years.

The freezing rate is more variable due to differences in snow depth and to the occasional occurrence of extreme cold before snow cover is deep enough to provide an insulating layer. Freezing begins from late September to late October and is usually completed by the end of January. The last 1-2 weeks of freezing is difficult to follow on the frost tubes because of a mottling of the dye color within the sand. There is slight upward freezing from the permafrost layer during this freeze-up period.

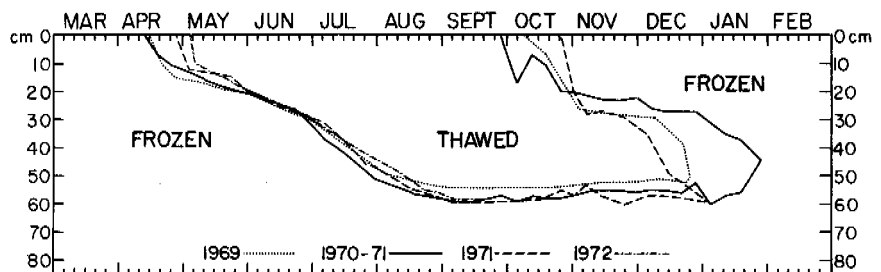


FIGURE 1 Four-year record of freeze-thaw cycle in 55-year-old open black spruce/*Ledum*/moss type near Fairbanks.

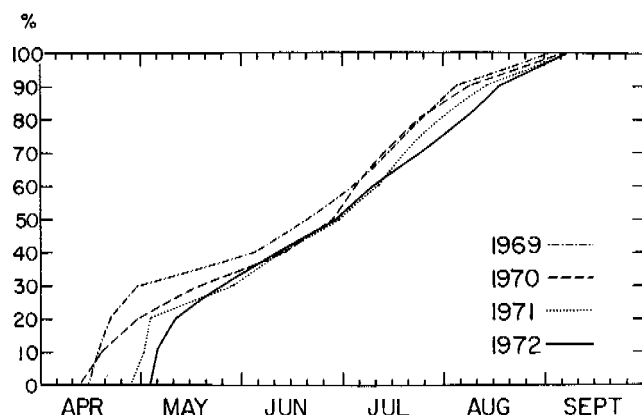


FIGURE 2 Percent of total annual thaw as related to time for four consecutive summers (from freeze-thaw curves shown in Figure 1).

From the 4-year frost-tube data, a curve was constructed (Figure 2) to show the percent of total thaw for each year. The curve shows that the total depth of thaw can be predicted within 5–10 cm by probing any time after the first of June. By mid- to late June, 50 percent of the thaw has occurred, and by mid- to late July, 75 percent of the active layer has thawed. Although overlying vegetation and soil texture affect the rate of thaw, this curve should be useful for black spruce stands under similar soil conditions in interior Alaska. It has been used to predict thaw in black spruce stands that could not be probed during September, the only period of maximum thaw when there is no surface frost to prevent probing.

EFFECTS OF FLOODING

Two naturally occurring phenomena that affect the depth of the active layer and in some cases the distribution of permafrost are seasonal and periodic flooding of river-bottom stands and burning of the vegetation and organic layers. Both of these perturbations result in thawing of previously frozen soils.

On the river floodplains in interior Alaska, permafrost is lacking beneath present river channels and in freshly deposited alluvium.^{19,24,25} As forest succession proceeds on the newly formed alluvial deposits, permafrost develops concurrently with the vegetation, and in late stages of succession, there is a gradual thinning of the active layer. Gill¹¹ has reported the same phenomena for the floodplain areas of the Mackenzie River, and Bliss and Cantlon³ found similar changes in the active layer thickness in the successional plant communities along the Colville River in northern Alaska. Tyrtikov²² reports a similar vegetation-permafrost relationship for successional plant communities colonizing a lowland lake area in northern Soviet Union.

On the floodplain of the Chena River, the author mea-

sured soil temperatures and the annual freeze-thaw cycle in four successional stands that had been established on similar alluvial deposits of different ages.^{24,25} As the forest succession proceeded and an organic layer developed, thawing and freezing rates lowered and summer soil temperatures in general were colder. The soils in the successional sequence developed from coarse gravels to silt-loams through the deposition of alluvial material. In the 250-year-old stand, the upper 20 cm had the following average particle sizes: sand 15 percent, silt 72 percent, and clay 13 percent. The soils of this stand were near saturation levels of 60–80 percent water by weight during the period of the study.

With continued forest succession and development of an insulating organic layer, summer thawing was delayed to the point that thawing was not completed: A new permafrost layer developed. In a 250-year-old floodplain spruce stand, the perennially frozen layer occurred between the depths of 60 and 90 cm. In stands on older terraces above the periodic flooding level, permafrost occurs from 50 to 60 cm below the surface to depths of at least 80 m.¹⁸

Flooding, occasional to annual, tends to prevent the development of the permafrost layer and thus maintains the productivity of the floodplain forest sites since (1) warm floodwaters provide enough input of heat into the soil to cause a warming of the soil and a thawing of the frozen layers and (2) deposition of silt kills the moss layer, preventing the buildup of a thick insulating organic layer and stopping evaporation from the moss surface.

In the Chena River study area, the author had the opportunity to observe and collect data on both these phenomena, as well as to observe the effects of an extreme flood on some of the older terraces of the floodplain. In the 250-year-old floodplain spruce stand, permafrost had been present from the time of the beginning of the study (summer 1964) until the August 12, 1967, flood. At that time, after an unusually wet summer, record rainfall in the watershed produced a flood that reached a crest of 5.7 m at Fairbanks and surpassed any previously recorded flood by 82 cm.⁸ It flooded the stand with approximately 2 m of water. A few days before the flood, the temperature profile had been similar to that of other years with a frozen layer at a depth of 60–90 cm.

On August 19, 1 week after the flood, the soil temperatures were 1–2 °C higher throughout the lower portion of the profile, and the permafrost layer had thawed (Figure 3). Thus, the floodwaters were assumed to be warm enough to thaw the frozen layer. This effect was similar to the thawing of permafrost adjacent to and under rivers in the subarctic. This effect lasted until midwinter of 1967–1968, at which time the temperatures were approximately the same as in previous winters.

A second effect of the August 1967 flood was the deposition of 1–3 cm of silt on the moss layer. Although this is not a thick layer compared with that deposited on stands

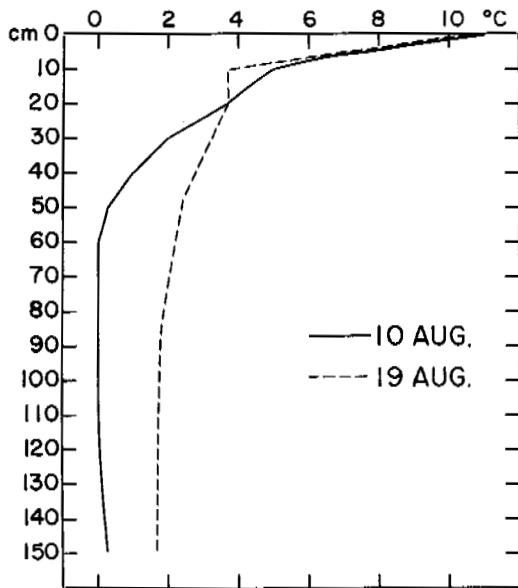


FIGURE 3 Soil temperature profile in 250-year-old white spruce/black spruce stand before and after the August 1967 flood on the Chena River.

closer to the river, it did result in the destruction of the moss mat, which only partially recovered the next summer. Soil temperatures were slightly higher and thawing was

completed; no frozen layer remained at the end of the 1968 summer. Although by 1972 the moss layer had completely recovered from the 1967 flood, there was still no re-forming of the permafrost layer.

Two other results of the 1967 flood relating to permafrost were of interest. On some of the older terraces underlain by ice-rich permafrost, the thawing of the permafrost by the floodwaters resulted in thermokarst and tipping of trees (Figure 4). After 5 years, some of these areas were still expanding and thawing, forming the beginnings of small thaw ponds similar to those described by Drury¹⁰ and Benninghoff.¹ These authors have both discussed ways in which these thaw ponds can be initiated, but neither mentions thawing as a result of flooding. Exceptional flooding of the older terraces underlain by permafrost, however, is clearly one way that these thaw ponds can become established.

Another result of the flooding was observed in a black spruce muskeg. In two locations, floodwaters had apparently separated the organic layers from the frozen substrate. The force of the flowing water had rolled and folded the vegetation and organic layer into large mounds and ridges and had left water-filled depressions where the vegetation had originally been. In the largest area observed, the force of the water created water-filled depressions 120 m wide and about 200 m long (Figure 5). At the down-slope end of the pond, the organic layers along with their moss, tree, and shrub vegetation were deposited in areas of tipped trees and ridges of peat that were as much as 3 m above the



FIGURE 4 Tipped trees resulting from the 1967 flood and surface subsidence after thawing of underlying permafrost.



FIGURE 5 Aerial view of pond and rolled and compressed vegetation and organic layers caused by the 1967 flood. (1) Pond areas that were bog and black spruce muskeg before the flood; (2) areas of compressed vegetation; and (3) old vehicle trails that may have caused break in vegetation mat.

surrounding bog surfaces (Figure 6). The pond area was 40 cm-1 m below the original surface of the bog and was thought to be at the permafrost layer at the time of the flood. Five years after the flood, the folded and rolled vegetation and peat was very similar to what it was soon after the flood.

The aerial photograph of the site after the flood (Figure

5) revealed the scar of an old vehicle road near the up-river section of the area where the surface vegetation was removed. This scar may have played a role in providing a weak point for the original rift in the vegetation mat. It is likely, however, that the phenomenon could occur at some natural break in the vegetation mat, such as that produced by a frequently used animal trail.



FIGURE 6 Rolled organic mat and disturbed vegetation caused by 1967 flood.

In bogs of the taiga, mounds of organic material occur commonly as string-like ridges or as palsas.^{10,21} In the extensive lowland bogs along the major rivers of Alaska, organic mounds may be formed by occasional catastrophic floods.

EFFECTS OF WILDFIRES ON PERMAFROST

One of the most important environmental factors affecting permafrost and vegetation in the taiga of Alaska is wildfire. Wildfires have been a part of the taiga environment for the past several thousand years and, at present, burn an average of 400 000 ha/year.

Few data are available for thickness of the active layer after fire in forest stands in Alaska, but the active layer generally is known to be thicker in the successional stands after fire than it is in unburned black spruce forests.¹⁶ The actual heat produced by the fire is probably unimportant, as the organic layer seldom burns to the permafrost boundary. Brown⁶ stated, "A fire may burn trees, brush, and even the surface of the moss without altering the underlying permafrost." After a fire, however, the changes in the surface albedo and the removal of the vegetation and some of the organic mat result in warmer soils and deeper thawing. After a fire in the black spruce stand at Inuvik, Northwest Territories, Canada, Heginbottom¹² reported that by the summer after the fire the thaw was 9 cm deeper in burned than in unburned stands. From eight permanent points within the Inuvik fire, MacKay¹⁷ reported an average increase of thaw of 24.1 cm (149 percent) by the end of the first summer after the fire and 34.8 cm (171 percent) by the end of second summer. Cody⁹ reported that, 3 years after a taiga fire in the Reindeer Grazing Reserve on the Mackenzie Delta, the permafrost had receded to a depth of 40 cm or more, and the recession of the ice had caused surface subsidence and resulted in a hummocky terrain.

At the end of the first summer after an August and September burn in eastern Alaska, Lotspeich *et al.*¹⁵ found no significant difference in thaw depth: Both burned and unburned stands had thawed to approximately 70 cm. In an *Eriophorum* tussock tundra within the taiga of Alaska, Wein²⁶ reported a 130–150 percent increase in the active layer in early summer after a fire the previous year, but only a 115–120 percent difference by the time of maximum thaw in the fall. Brown *et al.*⁵ reported an increased thaw of 160 percent and 140 percent 4 years after a fire in a black spruce/*Eriophorum* tussock type in eastern Alaska. They also reported a 141 percent and 152 percent increase in thaw depth in a 1-year-old burn in an *Eriophorum* tussock type with scattered black spruce in central Alaska.

However, at the northern limit of forest vegetation in the Soviet Union, fire may result in a thickening of the active layer followed in a few years by a rise in the permafrost upper surface. Kryuchkov¹⁴ reported that fire first

caused a thawing of the upper permafrost layers with a resultant release of moisture, creating conditions that stimulated the growth of the *Eriophorum* cover. As a result of the insulating effects of the thicker vegetation mat, the active layer was only 40–45 cm thick a few years after the fire, whereas before the fire it had been 50–70 cm thick.

At Wickersham Dome, 50 km northwest of Fairbanks, soil temperatures and the freeze–thaw cycle were studied after a fire in June of 1971. The original vegetation was a 50- to 100-year-old black spruce/*Ledum*/moss stand with a 20- to 30-cm organic layer over mineral soil. The mineral soil consisted of an Ester silt-loam with approximately 10 percent sand, 80 percent silt, and 10 percent clay. The underlying permafrost had a high percentage of ice as narrow horizontal bands. Frost tubes, probe lines, and thermistors were all used in the study. Readings were taken weekly for all units. At the time of installation of the frost tubes, the soils were completely saturated, and they remained at levels of 30–50 percent moisture by weight during the study period.

In the fall of the first summer after fire, there was no significant difference between burned and unburned stands. Probing in four stands in the burn showed thaw to an average depth of 44 cm, whereas in adjacent unburned stands the average thaw was 47 cm. The freezing cycle the next winter and the thaw cycle the next summer were recorded in one unburned 55-year-old black spruce stand and in a heavily burned adjacent area that had been the same type and age before the fire (Figure 7). In the fall after the fire, there was no significant difference in the depth of thaw—41 cm in the unburned and 43 cm in the heavily burned stand. During the first fall after the burn, freezing occurred more rapidly in the unburned than in the burned stand, and the active layer was completely frozen by December 12 in the unburned stand but not until January 15 in the burned stand.

The next summer, thawing was deeper in the burned than in the unburned stand. Although the snow melted 2 weeks earlier in the burned than in the unburned area, thawing was similar in both until June 7. Then thawing was more rapid in the burned stand. Thawing to nearly the maximum depth of 66 cm had occurred by August 23 in the burned stand and to 41 cm by September 6 in the unburned stand. Thus, thawing in the burned the first summer after the fire was 161 percent of that in the unburned stand.

Data on changes in the active layer thickness beyond the first few years after fire are limited. Undoubtedly, the active layer becomes thicker each year until the vegetation mat is re-established. Then, with increased effect of vegetation, the active layer should become progressively thinner until it eventually reaches the preburn level.

To obtain an estimate of the time involved in this sequence, some preliminary data obtained during the summer of 1972 by a vegetation survey in interior Alaska were ex-

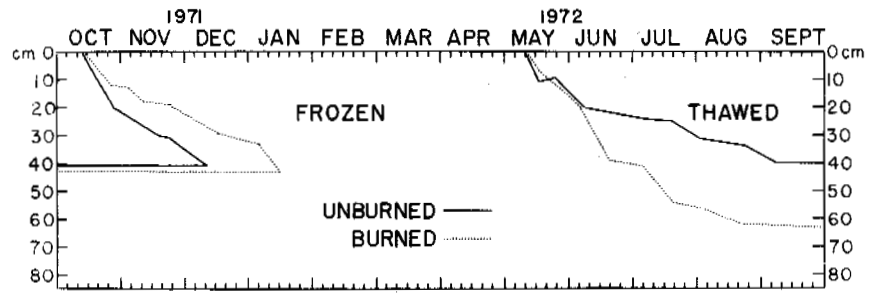


FIGURE 7 Freeze-thaw cycle in burned and unburned open stand of black spruce at Wickersham Dome for the first year after a fire.

amined. The purpose of the survey was to obtain quantitative data on revegetation after fire. As part of the survey, 20 probings to permafrost were made with a 1-m-long probe in each stand investigated. In all, 13 stands of black spruce were examined; ages since the fire ranged from 3 to 96 years. Of the seven stands in the 3- to 15-year age range, all had an active layer of more than 1 m in thickness (Table I). Unfortunately, there is a gap in stand ages in the series between 15 and 35 years. Between age 35 and 45 years, two stands had maximum thaw depths of 57 and 83 cm. At age 50 years and above, permafrost active layer thickness had returned to the preburn levels of 40-60 cm. These data indicate that the effects of fire in increasing the active layer thickness last at least 15 years after the fire. Even after 40 years, the active layer is somewhat thicker than it is in older stands. There were no significant changes in active layer thickness in stands after 55 years.

One effect of the lowering of the permafrost table after fire is the formation of thermokarst. In areas heavily underlain by ice wedges, thawing results in a subsidence of areas over the ice wedges, creating a polygonal mound and ditch pattern. The ditches or pits may be 2-3 m deep and often

remain filled with water most of the summer. Active thermokarst, with trees tipping into the ditches and fresh cracks in the mounds, occurs in successional stands of birch at least 40-50 years after fire. Eventually, with the return of black spruce, these sites may become stabilized, or small thaw ponds may develop and continue in an active cycle of pond and black spruce as has been described by Drury.¹⁰

SUMMARY

In the taiga of Alaska, permafrost and vegetation are closely related. In areas underlain by permafrost, the nature of the vegetation is important in determining the thickness of the active layer. In a black spruce/*Ledum*/moss stand, the active layer is normally 30-60 cm thick.

Flooding has been shown to have several effects on the vegetation-permafrost relationship on floodplain forest stands:

1. Flooding and water-table rise by warm water can quickly thaw existing permafrost or cause higher soil temperatures over at least the upper 150 cm of the substrate.
2. Siltation during flooding results in the compaction and death of the moss layers, thus reducing their insulating value in summer which results in higher soil temperatures and an increase in thickness of the active layer.
3. The result of thawing of frozen layers heavily laden with ice can be surface subsidence, tipping of trees, and eventually the formation of thaw ponds.
4. In some cases, flooding over permafrost results in a separation of the organic layer at the permafrost boundary and a compression and rolling of the organic layer into peat mounds.

Fire in forest types underlain by permafrost results in a temporary thickening of the active layer. Although thawing in the burned stands the year of the fire may not be significantly more than in the unburned stands, by the end of the second summer it may be as much as 160 percent of that in the unburned stands. For the first 15 years after fire, thaw is more than 1 m; return to preburn thaw levels takes about 50 years.

TABLE I Depth of Maximum Thaw for Successive Stands after Fire in the Black Spruce Type in Interior Alaska

Years since Fire	Location	Average Depth of Thaw (cm)
3	Steese Highway and Chena Hot Springs Road	>100
6	Harding Lake	>100
6	Alaska Railroad, Standard	>100
12	Badger Road, Fairbanks	>100
14	Goodpaster River	>100
14	Murphy Dome	>100
35	Chena Hot Springs Road	57
42	Alaska Highway, Milepost #1408	83
55	Wickersham Dome	41
55	Chena Hot Springs Road	60
66	Fairbanks	51
88	Chena Hot Springs Road	42
96	Alaska Highway, Milepost #1408	56

REFERENCES

1. Benninghoff, W. S. 1952. Interaction of vegetation and soil frost phenomena. *Arctic* 5:34-44.
2. Benninghoff, W. S. 1966. Relationships between vegetation and frost in soils. p. 9-12. *In* Permafrost: Proceedings of an International conference. National Academy of Sciences, Washington, D.C.
3. Bliss, L. C., and J. E. Cantlon. 1957. Succession on river alluvium in northern Alaska. *Am. Midl. Nat.* 58:452-469.
4. Bliss, L. C., and R. W. Wein. 1971. Changes in the active layer caused by surface disturbance, p. 37-47. *In* R. J. E. Brown [ed.] Proceedings of a seminar on the permafrost active layer, May 4-5, 1971. Technical Memorandum No. 103. National Research Council of Canada, Ottawa.
5. Brown, J., W. Rickard, and D. Victor. 1969. The effect of disturbance on permafrost terrain. Special Report #138. Cold Regions Research and Engineering Laboratory, Hanover, New Hampshire, 13 p.
6. Brown, R. J. E. 1965. Influence of vegetation on permafrost, p. 20-25. *In* Permafrost: Proceedings of an international conference. National Academy of Sciences, Washington, D.C.
7. Brown, R. J. E. 1970. Permafrost as an ecological factor in the subarctic, p. 129-140. *In* Ecology of subarctic regions. Proceedings of the Helsinki Symposium (Ecology and Conservation No. 1). UNESCO Paris.
8. Childers, J. M., and J. P. Meckel. 1967. Flood of August 1967 at Fairbanks, Alaska. Hydrologic Investigations Atlas HA-294. U.S. Geological Survey. [map]
9. Cody, W. J. 1964. Reindeer Range Survey 1957 and 1963. Canada Department of Agriculture, Plant Research Institute (mimeo report), 16 p.
10. Drury, W. H., Jr. 1956. Bog flats and physiographic processes in the upper Kuskokwim River region, Alaska. *Contr. Gray Herbarium (Harvard University)* 178. 130 p.
11. Gill, D. 1971. Vegetation and environment in the Mackenzie River Delta, Northwest Territories—A study in subarctic ecology. Ph.D. thesis, University of British Columbia, Vancouver. 694 p.
12. Heginbottom, A. 1971. Some effects of a forest fire on the permafrost active layer at Inuvik, N.W.T., 31-36. *In* R. J. E. Brown [ed.] Proceedings of a seminar on the permafrost active layer, May 4-5, 1971. Technical Memorandum No. 103. National Research Council of Canada, Ottawa.
13. Kallio, A., and S. Rieger. 1969. Recession of permafrost in a cultivated soil of interior Alaska. *Soil Sci. Soc. Am. Proc.* 33:430-432.
14. Kryuchkov, V. V. 1968. Soils of the far north should be conserved. *Priroda* [Museum of Soil Science, Moscow State Univ.] 12:72-74. Translated in J. Brown, W. Rickard, and D. Victor. 1969. The effect of disturbance on permafrost terrain. Special Report 138. Cold Regions Research and Engineering Laboratory, Hanover, New Hampshire. 13 p.
15. Lotspeich, F. B., E. W. Mueller, and P. J. Frey. 1970. Effects of large scale forest fires on water quality in interior Alaska. U.S. Department of the Interior, Federal Water Pollution Control Administration, Alaska Water Laboratory, Fairbanks. 155 p.
16. Lutz, H. J. 1956. Ecological effects of forest fires in the interior of Alaska. Technical Bulletin 1133. U.S. Department of Agriculture, Washington, D.C. 121 p.
17. MacKay, R. 1970. Disturbances to the tundra and forest tundra environment of the western Arctic. *Can. Geotech. J.* 7:420-432.
18. Péwé, T. L. 1954. Effect of permafrost on cultivated fields, Fairbanks area, Alaska. U.S. Geol. Survey Bull. 909-F. 40 p.
19. Péwé, T. L. 1957. Permafrost and its effect on life in the North, p. 12-25. *In* Arctic biology. Oregon State University Press, Corvallis.
20. Rickard, W., and J. Brown. 1972. The performance of a frost-tube for the determination of soil freezing and thawing depths. *Soil Sci.* 113(2):149-154.
21. Sjörs, H. 1963. Bogs and fens on Attawapishat River, Northern Ontario. *Nat. Mus. Can. Bull. Contr. Bot., 1960-1961* 186: 45-133.
22. Tyrtikov, A. P. 1959. Mnogoletnemerzlyye porodyii rastitel'nost [Perennially frozen ground and vegetation], p. 399-421. *In* P. F. Shvetsov [ed.] Osnovy geokriologii [Principles of geocryology]. Vol. I. Academy of Sciences of the USSR, Moscow. (Translated into English by the National Research Council of Canada, Ottawa, as National Research Council Technical Translation 1163, 34 p., mimeo.)
23. Viereck, L. A. 1965. Relationship of white spruce to lenses of perennially frozen ground, Mount McKinley National Park, Alaska. *Arctic* 18:262-267.
24. Viereck, L. A. 1970. Forest succession and soil development adjacent to the Chena River in interior Alaska. *Arctic Alpine Res.* 2:1-26.
25. Viereck, L. A. 1970. Soil temperatures in river bottom stands in interior Alaska, p. 223-233. *In* Ecology of the subarctic regions. Proceedings of the Helsinki Symposium (Ecology and Conservation No. 1). UNESCO Paris.
26. Wein, R. W. 1971. Fire and resources in the subarctic—Panel discussion, p. 251-253. *In* Fire in the northern environment—A symposium. Pacific Northwest Forest and Range Experiment Station, Portland, Oregon.

II

REGIONAL DISTRIBUTION AND CHARACTERISTICS OF PERMAFROST

Regional distribution, inventory, and variations of permafrost, active layer, and periglacial features (terrestrial and marine); climatic and terrain (soil, vegetation, etc.) relationships

DISTRIBUTION OF PERMAFROST IN NORTH AMERICA AND ITS RELATIONSHIP TO THE ENVIRONMENT: A REVIEW, 1963–1973

Roger J. E. Brown

NATIONAL RESEARCH COUNCIL OF CANADA
Ottawa, Ontario

Troy L. Péwé

ARIZONA STATE UNIVERSITY
Tempe, Arizona

INTRODUCTION

General Trends

Since the First International Conference on Permafrost in 1963¹⁷⁴ there has been a considerable advance in knowledge of the distribution of permafrost in North America and its relationship to the environment. The extent of the discontinuous and continuous permafrost zones in Canada has been generally determined during the past 10 years, although detailed local information is still sparse in all but a few areas. The general distribution of permafrost in Alaska was known prior to 1963, while investigations in Greenland were initiated at about that time. The relationship of permafrost distribution and occurrence to climatic and terrain factors has received much attention in the past decade, resulting in steady improvement in the ability to predict permafrost conditions in areas not previously investigated. The general correlations are now known, but much refining remains to be done. Four significant features of the investigations in North America during the past 10 years, relating to distribution of permafrost and its relationship to the environment, are the awareness of submarine permafrost extending under the seas in northern coastal areas; the origin, distribution, and amount of ground ice, especially massive ice; the increasing interest in features denoting the distribution of permafrost in past geological periods; and the distribution of permafrost at high elevations in the mountainous areas of western Canada and the United States. This review summarizes progress since 1963 in knowledge of the distribution of permafrost and the relation of environmental factors in North America.

MAJOR REVIEW PAPERS AND PERMAFROST DISTRIBUTION MAPS

From 1963 to 1973, several reviews have been published in Canada and the United States that include statements of the current level of knowledge of the distribution of permafrost and associated features and the relationship to environmental factors. The first major reviews were compiled by Péwé¹⁸⁹ and the U.S. Army Cold Regions Research and Engineering Laboratory.²⁴⁶ This was followed by Corté's review of per-

mafrost and associated engineering problems in 1969.⁶³ Laurence and Ward¹⁵⁰ compiled a shorter survey of permafrost, and in 1972 Price published a paper for the American Association of Geographers on the periglacial environment, including permafrost.²¹⁶ Péwé edited a compendium of papers concerning the periglacial environment and permafrost around the world that had been presented at the Alaska Field Symposium of International Association for Quaternary Research (INQUA) in 1965.¹⁹¹ Washburn has prepared a major monograph on principles and distribution of periglacial processes.²⁶⁸

Shorter accounts of permafrost, including its distribution and its relation to the environment, were published in Canada by Brown and Johnston.⁵⁵ Lachenbruch prepared a general statement on permafrost in 1968.¹³⁷ Péwé has two similar statements in press.^{196,197}

A book on the distribution of permafrost in Canada has been published by Brown.⁵⁰ He also published a monograph on factors influencing discontinuous permafrost in Canada in Péwé's periglacial volume⁴⁸ and a survey of permafrost conditions in the Canadian Arctic Archipelago.⁵² Péwé *et al.* presented much of the known information about permafrost and related features in central and south central Alaska for the 1965 INQUA Congress,²⁰⁰ while Ferrians *et al.* have surveyed permafrost conditions and related engineering problems in Alaska.⁸¹ In addition, Williams surveyed permafrost conditions in Alaska in relation to groundwater,²⁷⁸ and Péwé had compiled a major review of the Quaternary geology of Alaska that includes the most up-to-date compilation of permafrost conditions in that region.¹⁹⁷

Other reviews have been published on various subjects that contain information on the distribution of permafrost and related environmental aspects. Bird included considerable material on permafrost in relation to climate and terrain in his survey on the physiography of Arctic Canada, which corresponds roughly with the continuous permafrost zone.¹⁴ Péwé has prepared a monograph on geomorphic processes in polar deserts.¹⁹⁴ Hamelin and Cook prepared an illustrated glossary of periglacial phenomena.¹⁰⁰ Other more specialized monographs include a survey of the role of permafrost in the subarctic environment,⁴⁹ characteristics of the active layer,⁵¹ and midlatitude, high-altitude (alpine) permafrost.¹¹⁹

Prior to 1963, only one permafrost map of Canada had

been published (in 1948) but several were available of Alaska. In 1965, the U.S. Geological Survey published an up-to-date detailed permafrost map of Alaska, scale 1:2 500 000, showing the distribution, thickness, and ground temperatures in mountainous regions and lowlands and its relation to air temperature.⁸⁰ A somewhat similar permafrost map of Canada was published (scale 1:7 603 200), jointly by the National Research Council of Canada, and the Geological Survey of Canada.⁴⁴ It shows the location of the discontinuous and continuous permafrost zones, alpine permafrost in the western Cordillera, known thicknesses and ground temperatures, and relation to air temperature. A preliminary permafrost map of Greenland—showing the location of the discontinuous and continuous zones, some data on thickness of permafrost, and ground temperatures—has been prepared by Weidick for the Greenland Geological Survey.²⁷³ Information is available in Péwé's periglacial volume.¹⁹¹

PERMAFROST AND ITS RELATIONSHIP TO ENVIRONMENTAL FACTORS

A basic feature of investigations of permafrost that has emerged during the past decade is an improved understanding and general acceptance of the range of conditions implicit in the definition of the term. In 1943, permafrost was defined as the thermal condition of such earth materials, as soil and rock at temperatures that remain below 0 °C continuously for 2 years.¹⁷³ During the past few years, it has been recognized that permafrost includes ground that freezes in one winter, and remains frozen through the following summer and into the next winter. This is the minimum duration of permafrost; it may be only a few centimetres thick. At the other end of the scale, permafrost is thousands of years old and hundreds of metres thick. The concept of including all frozen ground, even of only 1 year's duration, is of basic importance in establishing the location of the southern limit of the permafrost region. Previously, frozen ground of 1 or a few years' duration was referred to as *pereletok* and not considered as part of the permafrost. Difficulties arise with this artificial division because of the impossibility of differentiating between a *pereletok* of, say, 3 years' duration and permafrost of 4 years' duration.

A modification of permafrost zonation in Canada was introduced in the early 1960's when the term "sporadic permafrost zone" was discarded. It became increasingly evident that both the patchy island type of permafrost and widespread discontinuous permafrost are distributional variations of discontinuous permafrost. Thus, all permafrost south of the continuous zone is considered as discontinuous, and this zone can be divided into two subzones—"southern fringe" and "widespread."

Distribution in Canada and Alaska

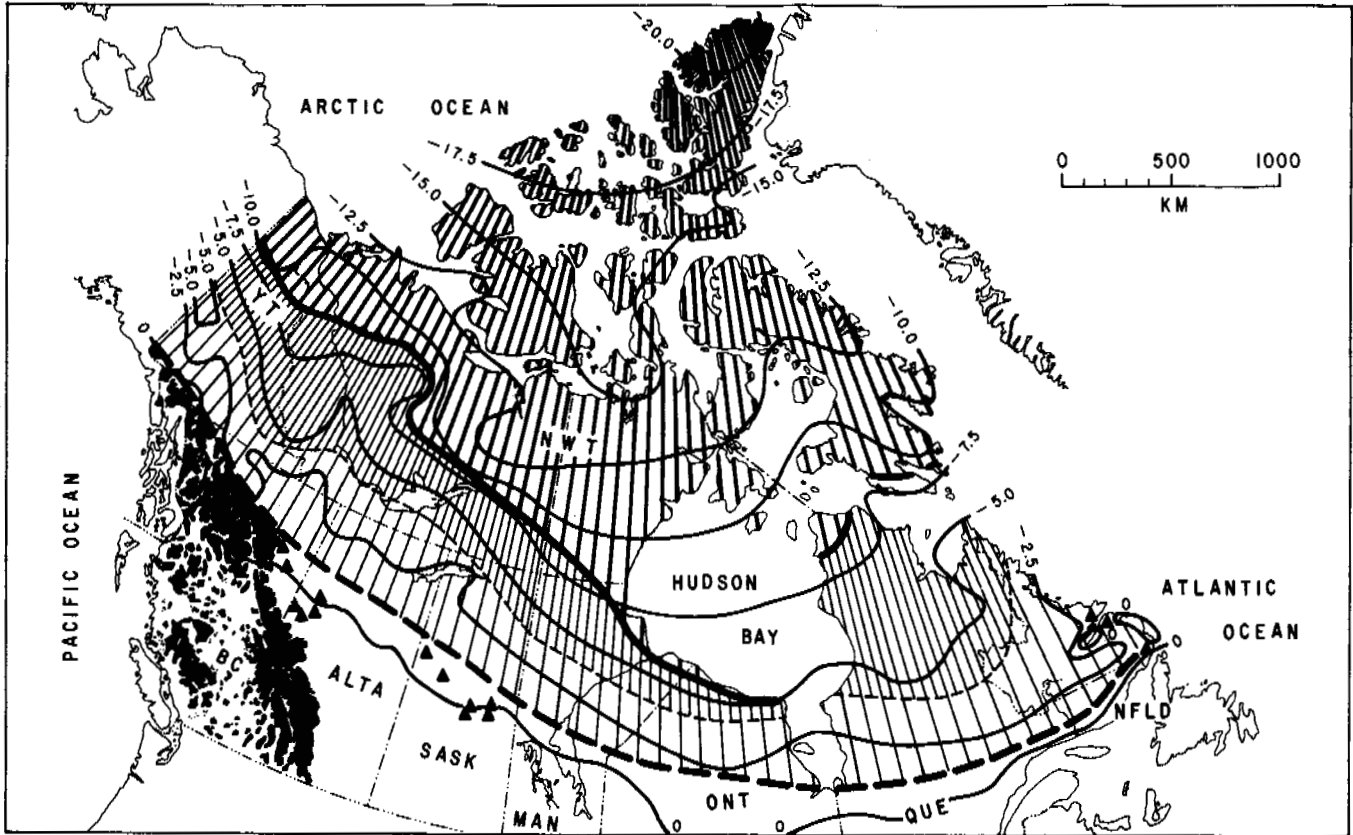
During the past 10 years, many ground and air surveys of permafrost distribution have been carried out in Canada and Alaska so that the general characteristics of these zones are now known (Figures 1 and 2).

Surveys carried out across the discontinuous zone in Canada during the first half of this decade are reported by Brown.^{41-43,45,46,54} Studies are under way in the vicinity of the boundary between the discontinuous and continuous zones⁵³ and a survey of permafrost conditions in the Canadian Arctic Archipelago in the northern part of the continuous permafrost zone was recently undertaken⁵² along with field studies by Brown⁵³ and Judge.^{129,130} Many local and regional studies have been carried out and are under way, providing information on the distribution of permafrost: Thompson, Manitoba, by Johnston *et al.*¹²⁷; northern Alberta, by Lindsay and Odynsky¹⁴⁶; York Factory, Manitoba, by Simpson²⁴⁵; Schefferville, Quebec, by Thom^{253,254} and others; northern Quebec and Baffin Island by Samson and Jordan²³¹; Yellowknife, N.W.T., by Drewe,⁷⁵ Espley,⁷⁷ and Kilgour¹³²; the large-scale studies along the Mackenzie River valley being undertaken by the Geological Survey of Canada⁶⁴ and many other government and private agencies in connection with the pipeline studies. Investigations have been initiated jointly by the National Research Council of Canada and the Department of Geography, University of British Columbia on the distribution of permafrost in the western Cordillera.

Many similar surveys and investigations have been carried out and reported in Alaska. Much of the known information about permafrost and related features in central and south central Alaska was compiled by Péwé.¹⁸⁵⁻¹⁸⁷ Ferrians *et al.* surveyed permafrost conditions in Alaska in relation to engineering problems⁸¹ and J. R. Williams made a similar survey in relation to groundwater in Alaska.²⁷⁸ Many local and regional studies have been carried out by the U.S. Geological Survey and the U.S. Army Cold Regions Research and Engineering Laboratory. Many of these studies are reported by Lachenbruch,¹³⁷⁻¹⁴¹ Péwé,¹⁸³⁻²⁰⁴ and J. Brown.²⁷⁻⁴⁰ Investigations in the western Cordillera of the continental United States by Ives¹¹⁸⁻¹²⁰ and others²²⁴ are also under way.







On the basis of the above studies it became known that in the discontinuous zone, frozen and unfrozen layers occur together. Permafrost varies in thickness from a few centimetres or metres at the southern limit to about 60-90 m at the boundary of the continuous zone. The temperature of the permafrost in the discontinuous zone at the level of zero annual amplitude generally ranges from a few tenths of a degree below 0 °C at the southern limit to -5 °C at the boundary of the continuous zone.^{53,125,197,278}



In the continuous zone, permafrost occurs everywhere beneath the ground surface, except in newly deposited un-



LEGEND

PERMAFROST

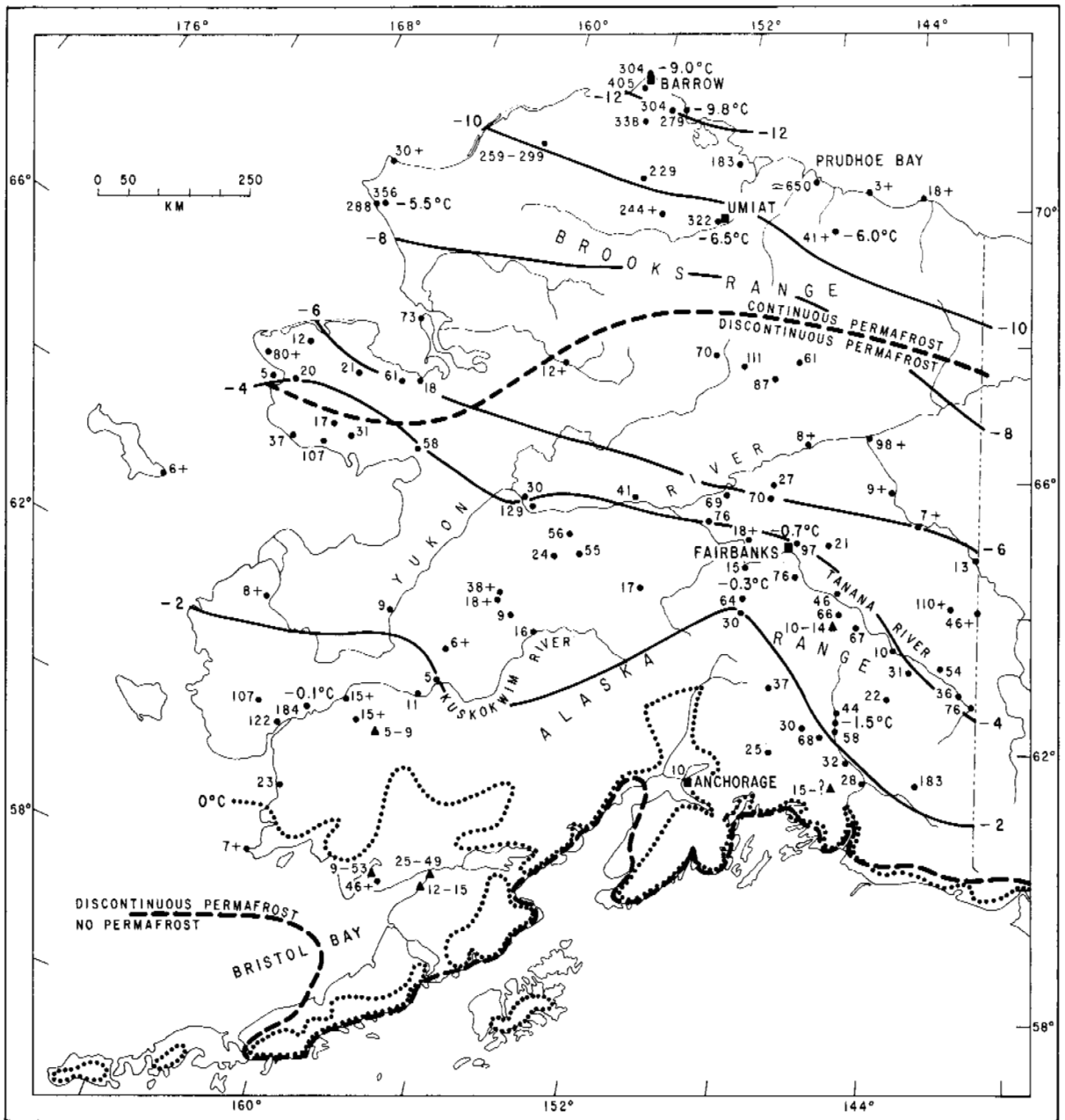
-  CONTINUOUS PERMAFROST ZONE
-  SOUTHERN LIMIT OF CONTINUOUS PERMAFROST ZONE
-  DISCONTINUOUS PERMAFROST ZONE
-  WIDESPREAD PERMAFROST
-  SOUTHERN FRINGE OF PERMAFROST REGION
-  SOUTHERN LIMIT OF PERMAFROST

-  PATCHES OF PERMAFROST OBSERVED IN PEAT BOGS SOUTH OF PERMAFROST LIMIT
-  PERMAFROST AREAS AT HIGH ALTITUDE IN CORDILLERA SOUTH OF PERMAFROST LIMIT

CLIMATE

-  MEAN ANNUAL AIR TEMPERATURE, °C

FIGURE 1 Permafrost in Canada. Adapted from "Permafrost in Canada" map, Division of Building Research, National Research Council of Canada (NRC 9769) and Geological Survey of Canada, Department of Energy, Mines and Resources (map 1246A), 1967.



LEGEND

PERMAFROST, DATA IN METERS

- 122 ● THICKNESS, DEPTH TO BASE
- 18+ ● MINIMUM THICKNESS, BASE UNKNOWN
- 12-15 ▲ RELIC PERMAFROST, GROUND FROZEN BETWEEN DEPTHS SHOWN
- 6.5°C ● TEMPERATURE OF PERMAFROST AT 15 TO 25 METERS DEPTH
- PERMAFROST ZONE BOUNDARY

CLIMATE

- APPROXIMATE POSITION OF MEAN ANNUAL AIR TEMPERATURE ISOTHERM, 0°C
- MEAN ANNUAL AIR TEMPERATURE, °C

FIGURE 2 Permafrost in Alaska.

consolidated sediments where the climate has just begun to impose its influence on the ground thermal regime. The thickness of permafrost is about 60–90 m at the southern limit of the continuous zone, possibly increasing steadily to 1 000 m in the northern part of the zone in the Canadian Arctic Archipelago^{124,129,130} and Alaska.^{113,114,247} The temperature of the permafrost in this zone—at which depth annual fluctuations become virtually imperceptible (i.e., less than about 0.1 °C), which is known as the level of zero annual amplitude—ranges from about –5 °C in the south to about –15 °C in the extreme north.

In the Cordillera, the distribution of permafrost varies with altitude as well as latitude. The lower altitudinal limit of permafrost rises progressively from north to south. Throughout northern British Columbia, south of the southern limit of permafrost on the map, field observations indicate that the lower altitudinal limit of permafrost is uniform at about 1 200 m above sea level.⁴⁴ Below this elevation, scattered permafrost islands occur only in specific types of terrain. In the southern part of the Cordillera, the lower altitudinal limit of permafrost has been estimated to increase steadily from an elevation of about 1 200 m at latitude 54°30' to about 2 100 m at the forty-ninth parallel.⁴⁴ At 52°N, permafrost was encountered at an elevation of 2 130 m in the Canadian Rocky Mountains.¹⁷⁸ The lower limit of permafrost rises steadily southward in the United States²²⁴ to 3 000 m above sea level in Colorado, where Ives is carrying out extensive investigation.^{118–120} With increasing elevation, the distribution of permafrost changes progressively from scattered islands to widespread to continuous.

In a totally different environment, submarine permafrost has been discovered in the Beaufort Sea off the arctic coasts of Canada and Alaska.^{144,157,161,223,242,243}

Climatic (Air Temperature) Relationships

Climate is a basic factor in the formation and existence of permafrost. Observations indicate a broad relation between mean annual air and ground temperatures in permafrost regions. These aspects are reviewed by Gold and Lachenbruch.⁹⁶

During the past 10 years, some broad correlations have been obtained in Canada and Alaska between the geographical distribution of the permafrost zones and air temperature on the basis of regional studies. Present knowledge of the southern limit of permafrost indicates that it coincides roughly with the –1 °C mean annual air isotherm in Canada between James Bay and the western Cordillera.⁴⁴ This is the least complex segment of the southern limit of permafrost in North America because of the subdued relief in contrast to Quebec and Labrador in the east and Alaska and the Cordillera in the west. East of Hudson Bay, there are few

field observations, and the southern limit is shown to coincide roughly with the –1 °C mean annual air isotherm. A few localized occurrences of permafrost have been encountered south of this isotherm in palsas in Labrador⁵⁴ and in the Prairie Provinces,²⁸⁴ which are either relict or due to local microclimatic conditions. In the western Cordillera, the permafrost areas shown on the permafrost map of Canada were delineated by mapping the altitudinal position of the –1 °C mean annual isotherm.⁴⁴ The situation in Alaska is complicated by the relief, although considerable information is available and has been mapped.⁸⁰ The southern limit of permafrost appears to extend south of the 0 °C isotherm due to the presence of numerous large bodies of relict permafrost not in equilibrium with the present climate; these have not been encountered on such a large scale in Canada.

North of the southern limit, between the –1 and –4 °C mean annual air isotherms in western Canada between Hudson Bay and the western Cordillera, permafrost is restricted mainly to the drier portions of peatlands and peat bogs because of the special insulating properties of the peat. In the vicinity of the –4 °C mean annual air isotherm, differences of about 3.5 °C between the mean annual air and ground temperatures produce a mean annual ground temperature of a fraction of a degree below 0 °C in most types of terrain. From the –4 °C mean annual air isotherm northward to the continuous zone, permafrost becomes increasingly widespread and thicker, and the mean annual temperature decreases. Scattered bodies of permafrost also occur on some north-facing slopes and in some heavily shaded areas. The situation in Quebec-Labrador and the western Cordillera is not known, but studies in Alaska indicate more widespread and thicker permafrost conditions in the same zone due possibly to the lack of glaciation.⁸⁰

There is little field information in Canada on the location of the boundary separating the discontinuous and continuous permafrost zones. The line on Figure 1 approximates the location of the –8.5 °C mean annual air isotherm in order to correspond with a mean annual ground temperature of –5 °C.⁹⁶ This criterion is based on earlier Soviet studies that indicated that this ground temperature is the depth of zero annual amplitude at the southern limit of the continuous permafrost zone in Eurasia. However, field observations along the coast of Hudson Bay in Ontario and Manitoba indicate a narrow band of continuous permafrost south of the –8.5 °C mean annual air isotherm. From this isotherm northward, permafrost is continuous and increasingly thicker, and the mean annual ground temperature decreases. In Alaska, the southern limit of the continuous permafrost also appears to lie south of the –8 °C isotherm, especially in the western part of the state.

Other climatic parameters, such as precipitation, wind, and the energy exchange components, are discussed by Gold and Lachenbruch.⁹⁶

Terrain Relationships

RELIEF

Relief influences the amount of solar radiation received by the ground surface and the accumulation of snow. The influence of orientation and degree of slope is particularly evident in mountainous regions.¹²⁰ In the discontinuous zone, this may result in permafrost that occurs on north-facing slopes but not on adjacent south-facing slopes. In the continuous zone, permafrost is thicker and the active layer thinner on north-facing slopes.⁸⁹ Variations in snowfall and accumulation on the ground may modify these patterns. Slope and exposure (aspect) influence the vegetation, which, in turn, affects the active layer.²¹⁵ Smaller scale variations in relief cause similar situations elsewhere in the permafrost region. Permafrost may occur, for example, in the north-facing bank of even a small stream but not in the opposite south-facing bank.⁴⁵ Similar differences can occur even in areas of intensive microrelief, such as peat mounds and peat plateaus.²⁸⁴

Permafrost affects the relief and configuration of the ground surface. Solifluction and other downslope mass movements of earth material over permafrost surfaces also alter the ground surface configuration. Thermokarst is frequently an active process in areas where large masses of ground ice exist. The melting of this ice and resulting subsidence of the ground produce undulations and hollows that alter the surface configuration considerably.

VEGETATION

Vegetation affects permafrost in various ways, and it is one of the more obvious indicators of subsurface conditions. Many of the early studies of permafrost were devoted to the role of vegetation and its relationship to the active layer. Numerous investigations have been carried out during the past decade in North America on this and other aspects of the interrelationships between permafrost and vegetation.

The role of vegetation and the associated peat in the permafrost environment has been reviewed in several papers. The influence of vegetation on permafrost in the discontinuous zone was described by Brown⁴⁸ as were the relationships between permafrost and vegetation in the Subarctic (discontinuous permafrost) reviewed.⁵⁰ Vegetation plays a much more important role in the discontinuous zone than in the continuous zone, especially in the high Arctic where it has little influence in the polar desert.⁵² Comprehensive studies of the role of vegetation have also been made by Brown and Johnson in which the environment parameters, including vegetation, were studied at Barrow, Alaska.³⁹ Raup carried out investigations of the vegetational relations of weathering, frost action, and patterned ground processes, in the Mesters Vig District of northeast Greenland.²²² The role of vegetation in the discontinuous permafrost zone of

the Mackenzie River is currently being studied by Crampton and Rutter.⁶⁴

The most obvious effect of vegetation is its role of shielding the permafrost from solar heat during the summer period; this insulating property is one of the most important factors determining the thickness of the active layer. Lindsay and Odynsky measured the active layer throughout northern Alberta and found variations that depended on vegetation and other factors.¹⁴⁶ The depth of thaw beneath various types of vegetation at Barrow, Alaska, has been plotted by Brown and Johnson.³⁹ Variations in the active layer beneath different forest cover types were recorded by Jeffrey along the lower Liard River, Northwest Territories.¹²³ The influence of vegetation in reducing the depth of the active layer was noted by Price in mountainous terrain in southwestern Yukon Territory, where the active layer was thinnest and most variable on southeast-facing slopes, which were the most densely vegetated.²¹⁵ Irregularities in the permafrost table were noted in the Mackenzie River Delta associated with variations in the vegetative cover.⁹⁵ Studies in Alaska show a strong suggestion that active layer thickness may be highly correlative to solar radiation, moss thickness, and tree shading.⁶⁹

Removal or even disturbance of the surface cover causes degradation of the underlying permafrost. In the discontinuous zone, this may result in the disappearance of bodies of permafrost, while in the continuous zone, the permafrost table will be lowered.¹⁵⁵ Many studies have been undertaken in recent years in Canada and Alaska on terrain disturbance in relation to pipeline disturbance; these are reported in the review paper by Linell and Johnston.¹⁴⁷ The predominance of moss and peat in protecting the permafrost from atmospheric heat is demonstrated by the fact that little change occurs in the depth of the permafrost table when trees and brush are removed, provided that the moss and peat are not disturbed. A fire may burn trees, brush, and even the surface of the moss, without altering the underlying permafrost as described later in this section.

The occurrence of permafrost in peatlands, but not in other types of terrain in the southern part of the discontinuous zone, was studied in the Soviet Union prior to 1963 and during the past decade in Canada by Brown.^{47,48} It appears to be related to changes in the thermal conductivity of the peat during the year. Through summer, the surface layers of peat become dry by evaporation. The thermal conductivity of the peat is low, and warming of the underlying soil is impeded. The lower peat layers gradually thaw downward and become wet as the ice layers in the seasonally frozen layer melt. In the autumn, there tends to be more moisture in the surface layers of the peat because of a decreased evaporation rate. When it freezes, the thermal conductivity of the peat is increased considerably. Thus, the peat offers less resistance to the

cooling of the underlying soil in winter than to the warming of it in summer. As a result, the mean annual ground temperature under peat will be lower than under adjacent areas without peat. When conditions under the peat are such that the ground temperature remains below 0 °C throughout the year, permafrost results and is maintained as long as the conditions leading to this thermal situation persist.

Although the influence of the ground vegetation on permafrost is dominant, trees are important. They shade the ground from solar radiation and intercept some of the snowfall in winter. The effect of even a single tree in shading the ground in summer and reducing the snowcover at its base in winter appears to influence the heat exchange at the ground surface sufficiently.²⁵⁸ The density and height of trees influence the microclimatic effects of ground surface wind velocities. Wind speeds are lower in areas of dense growth than in areas where trees are sparse or absent. The movement of air represents the transfer of heat from one area to another. In peatlands, the trees are generally stunted and scattered, and there are numerous open areas that permit higher wind speeds and the increased removal of heat per unit time. Therefore, the possibility of slightly lower air temperatures and ground temperatures, because of higher wind speeds, is greater than in areas of dense tree growth.¹²⁷ Investigations in temperate regions indicate that the nature of peat-land surfaces contributes to air temperatures being several degrees lower than over other natural adjacent surfaces.²⁷⁹ It is quite probable that the same situation prevails in permafrost regions.

Permafrost is greatly affected by changes in vegetation with time. Several significant studies have been carried out in Alaska along river valleys. Péwé traced the development of the vegetation on the floodplains of subarctic rivers and related this factor to the development of permafrost and its changes with time.¹⁹³ Viereck studied four stands of vegetation on different ages of river alluvium to show differences in soil temperatures and permafrost conditions that result from plant succession on the river floodplains in interior Alaska.²⁵⁹ He found that permafrost conditions were more extensive and severe in the early successional stands of willow and balsam poplar than in the later successional stages.²⁶⁰

Permafrost exerts considerable influence on the environment in which the subsurface organs of plants have developed.⁴⁹ The effects of permafrost are mostly detrimental to plant development because of its cold temperatures and impermeability to moisture. Permafrost impedes warming of the soil during the growing season and the temperature of the root zone is considerably below the optimum. Absorption of water by the roots is reduced, which leads to physiological dryness of the plants. On the other hand, water is gradually released to the root zone through the summer as the active layer thaws. Root development is retarded, and roots are forced to grow laterally because downward penetration is prevented by the permafrost. Many large trees cannot be

supported by these shallow root systems; they lean against each other or fall over, thus resulting in a "drunken" forest.

Permafrost forms an impermeable layer that impedes downward drainage, leading to a decline in aeration and impoverishment of nutritive substances because of the weakening of the activity of microorganisms. Soil movement in the active layer also influences the vegetation. Frost action causes unevenness in the ground surface; solifluction and other downslope mass movements of earth material disturb the vegetation; and thermokarst changes the surface configuration of the ground—all of which produce detrimental influences on the vegetation. These various influences of permafrost on vegetation increase northward as permafrost becomes increasingly widespread and the active layer becomes thinner. Kerfoot and Mackay studied the relative downslope movement across a solifluction lobe under various types of vegetation on Garry Island in the Mackenzie River Delta.¹³¹ Price noted the relationships between vegetation and solifluction in mountainous terrain in southwest Yukon Territory.²¹⁵ The tolerance of various plant communities to frost action in the active layer was studied by Raup in northeast Greenland.²²²

HYDROLOGY

Moving water is an effective thawing and erosive agent of perennially frozen soils, especially in areas of high ground ice content. Observations on this property of water are reported by Mackay and Black.¹⁶¹

Most of the study on the interaction between water and permafrost is concerned with the unfrozen layer of ground that exists under water bodies—lakes and rivers—that do not freeze to the bottom. The pioneer work in this field was done by Lachenbruch prior to 1963, but his early papers are still the basic statements and foundation for studies during the past decade in Canada and Alaska. The extent of this thawed zone varies with a large number of factors—area and depth of the water body, water temperature, thickness of winter ice and snowcover, general hydrology,⁸² and composition and history of accumulation of bottom sediments. Lachenbruch considered all of these factors in his theoretical studies and case histories. Recent work in Canada in the thawing effect of lakes is reported by Gold and Lachenbruch in their review paper.⁹⁶ The engineering problems stemming from this factor concerned with the thawing of permafrost beneath reservoirs impounded by dams and dikes are considered by Linell and Johnston.¹⁴⁷

The ocean has an important thermal influence on permafrost as evidenced by the pioneer work of Lachenbruch and other American workers in the late 1950's and early 1960's. Recent work is reported by Gold and Lachenbruch⁹⁶ and also by Mackay and Black¹⁶¹ in their accounts of submarine permafrost and the relationships to coastline changes.

Permafrost greatly influences the hydrological regime as reported by Williams and van Everdingen.²⁸¹ Its imperme-

ability to water is responsible for the existence of many small shallow lakes and ponds in the continuous zone and in the northern part of the discontinuous zone where permafrost is widespread. Beaded streams are another indication of the influence of permafrost, where irregular enlargements of stream channels result from the melting of masses of ground ice beneath the streams.

SNOWCOVER

Snowcover influences the heat transfer between the air and the ground and, hence, affects the distribution of permafrost.⁹⁶ The snowfall regime and the length of time that snow lies on the ground are critical factors. A heavy fall of snow in the autumn and early winter inhibits winter frost penetration. On the other hand, a thick snowcover that persists on the ground in the spring delays thawing of the underlying ground. The relation between these two situations determines the net effect of snowcover on the ground thermal regime.

In the discontinuous zone, particularly in the southern fringe, it can be a critical factor in the formation and existence of permafrost. For example, the thickest permafrost in the southern fringe of the permafrost region occurs in palsas on which snowcover is thin because of their exposure to wind. In the continuous zone, snowcover influences the thickness of the active layer. It was demonstrated by French that it does have the effect of temporarily lowering near-surface ground temperatures in the active layer when it falls in July or August.⁸⁹ In the Canadian Arctic Archipelago, the effect of the snowcover is considerably diminished from its influence further south in the permafrost region because of the lower snowfall, higher density, and very uneven distribution due to drifting.⁵²

Numerous earlier studies on the effect of the snowcover on permafrost were done at Fairbanks, Alaska, prior to 1963. Canadian work began in the late 1950's at Schefferville, Quebec (mean annual air temperature -4.5°C), in the discontinuous zone where the Iron Ore Company of Canada is involved in mining ore in permafrost more than 100 m thick. Early studies indicated that snowcover is a dominant factor in controlling permafrost distribution at that site. Variations in snowcover caused temperature variations greater than those resulting from the vegetation cover. It was postulated that a snow depth of about 40 cm could be regarded as the critical thickness for permafrost to persist. Beneath a greater depth either no permafrost exists or a degrading condition prevails.⁶ Studies are continuing at Schefferville and snow surveys in recently open iron mines support the above postulation in a general way although it is doubtful that strict application of the less than 40 cm snow depth as an indicator of permafrost is applicable in all cases.^{253,254} More recent analysis based on 15 years of study demonstrates that permafrost normally devel-

ops where the average snow depth for the area of influence is less than 65–75 cm.¹⁷⁶ An experimental site 1 km² is being studied to observe the effects of the snowcover,¹⁷⁷ and a computer program is being developed to map the snowcover and predict its influence on the permafrost.⁹⁷

FIRE

Fire is a transient factor that is not normally considered as affecting the permafrost. Although the time of actual burning at any given point is usually of short duration, a forest or tundra fire can have a marked influence on the ground thermal regime.^{248,261} Many fires started by lightning occur every year in the permafrost region, particularly the discontinuous zone, which is mostly forested. Through the years much, if not all, of this part of the permafrost region has been burned over more than once. Tundra fires are not as common because of the wet ground conditions and low proportion of woody material in the vegetation complex. Fires occur frequently, however, in the spruce-lichen woodlands of the forest-tundra transition where the thick dry continuous lichen may burn or smoulder for many months during the summer.²²⁷

The degree of influence of a fire on the permafrost depends on the condition of the vegetation and the rate of burning. A fire may move rapidly through an area burning trees, charring only the top surface of the ground vegetation. Palsas and peat plateaus have been observed in the Hudson Bay Lowland and northwestern Manitoba, where the trees have been burned and the surface of the moss and lichen charred by the fire. Below a depth of 2.5 cm, this vegetation layer was untouched, its insulating effect on the underlying permafrost unaltered from nearby unaffected areas that did not catch fire.^{43,46}

If dry conditions have prevailed in an area for some time prior to a fire, considerable change in the permafrost may occur. For example, a fire began on 11 August 1968 in the vicinity of Inuvik, N.W.T., located in the forested part of the continuous permafrost zone. Summer rainfall had been unusually light, and even the normally moist moss cover was dry. The fire swept through flat lands and hillsides with such intensity that even frost mounds, which occur extensively throughout the area, were denuded of all vegetation. The removal of the insulating surface cover exposed the ice-laden perennially frozen soils to thawing. Water from melting ground ice on the fire-bared hillsides northeast of Inuvik was released in sufficient quantities to cause considerable thermal erosion during the remainder of the thawing season to mid-September. Firebreaks were bulldozed to the permafrost table. In less than 1 month, water courses several feet wide had eroded 45.7 cm into the ice-laden permafrost. In the following summers, deeper thawing and thermal erosion of the permafrost continued.^{102-104,270} Measurements by J. R. Mackay of the depth of thaw from 1968, at the time of

the fire, to 1972 showed that it continued to increase despite the re-establishment of lush vegetation by 1970. The increase will probably continue into 1973 (Mackay, oral commun., Jan. 1973). The permafrost table will eventually stabilize as a new thermal equilibrium is reached, but the effects of the fire will be felt for many years.

SOIL AND ROCK

Bare soil and rock have considerable influence on the temperature of the ground because of their ability to reflect solar radiation. Reflectivity values ranging from 12 to 15 percent for rock and 15 to 30 percent for bare soil have been observed. There also will be different evaporation rates and intakes of precipitation. Variations in such thermal properties as conductivity affect the rate of permafrost accumulation. The thermal conductivity of silt, for example, is about one-half that of coarse-grained soils and several times less than that of rock. These factors assume their greatest significance in the continuous zone, where the climate is sufficiently cool to produce permafrost regardless of the type of terrain.^{53,55}

The effect of the type of soil and/or rock on the permafrost regime in the continuous zone has been observed at several locations in Canada and Alaska. Day and Rice noted that the active layer at Inuvik, N.W.T., in the southern part of the continuous zone ranged from 45 to 75 cm for clayey soils with 30 cm peat cover to 125 cm for gravelly soil with similar peat cover.⁶⁶ Observations have been conducted at several sites scattered throughout the Canadian Arctic Archipelago. Tedrow and Douglas showed that gravelly soils on Banks Island were 10 °C warmer in the top 5 cm in July than fine-grained tundra soils.²⁵² Tedrow observed that the active layer on Prince Patrick Island in gravelly sands of the polar desert exceeded 60 cm and in loamy soils it was 30–38 cm.²⁵⁰ Peters and White (personal communication)¹⁸² found the depth to the frost table on Devon Island in July to be 70 cm in Stony Arctic Brown soil (beach ridge), 47 cm in Regosol, 34 cm in Arctic Brown soil, 24 cm in Gleysol, and 13 cm in peat. In the extreme north of the archipelago, Day found the active layer on Ellesmere Island to be about 60 cm in wet silt with a 10-cm-thick peat cover.⁶⁵ The active layer in rock varies considerably from one type to another. On Devon Island the maximum active layer of 2.2 m occurs in granite in contrast to 1.5 m in limestone.⁵³

The type of earth material has also been observed to be a factor in causing variations in the thickness of permafrost. Judge postulates from currently available ground temperature and geothermal data obtained in the Canadian Arctic Archipelago that the permafrost is thickest beneath the exposed or thinly covered Precambrian rocks of northern Baffin Island, Boothia Peninsula, and Victoria Island and in the central zone beneath the high conductivity Palaeozoic rocks such as dolomites and pure quartz sandstones.¹³⁰ Thick-

nesses in these areas may be as much as 1 000 m whereas it is doubtful if thicknesses exceed 500 m in many locations.

GLACIER ICE

The growth and regime of glaciers and ice caps is determined by climate, but ice is considered as a terrain factor because—like vegetation, water, and snow—it forms a layer on the ground surface between the permafrost and the atmosphere that affects the heat exchange between them. It has been postulated by many workers that the bottom temperature beneath much of a continental ice sheet is colder than 0 °C. In temperate glacier conditions, the ice bottom temperature is at the pressure melting point. Beneath an ice sheet 1 000 m thick, for example, the temperature of the water film at the bottom of the ice would be about –0.3 °C. In polar glacier conditions, the bottom of the ice is frozen to the underlying ground and the temperature at the ice–ground interface is colder than 0 °C. Both of these glacier conditions probably occur extensively throughout an ice sheet. Consequently, beneath continental ice sheets in the northern hemisphere, permafrost was probably widespread but thin because of the proximity of bottom temperatures to 0 °C. Permafrost may have been somewhat thicker beneath the ice masses where the effect of cold air temperatures can penetrate to the underlying ground.

Only a few temperature observations at the bottom of ice caps are available in the permafrost region of North America to provide an indication of conditions prevailing during the Pleistocene. Deep core drilling in the Greenland ice sheet, 150 km east of Thule, and subsequent temperature measurements showed an ice bottom temperature of –13 °C beneath 1 387.4 m of ice overlying frozen till, indicating polar glacier conditions and thick permafrost below.^{101,143,226} In the northern part of the Canadian Arctic Archipelago, Paterson measured a bottom temperature of –16 °C beneath a small post-Wisconsinan ice cap only 121 m thick.¹⁸¹ Judge asserts that present ground surface temperatures over most of Canada's permafrost region are lower than the ice bottom temperatures during the Pleistocene.^{129,130} This means that the thickness of permafrost beneath the ice was, in general, thinner than the equilibrium value based on present surface temperatures. Temperate glacier conditions apparently may occur even in the high Arctic as evidenced by observations on Axel Heiberg Island in the north part of the Canadian Arctic Archipelago, where bottom temperatures beneath 645 m of ice seemed to be at or near 0 °C due perhaps to the possibility of abnormally high geothermal heat, or the infiltration of water from nearby warm springs.¹⁷² Philberth and Federer developed methods for estimating bottom temperatures beneath ice caps using available data from Greenland and Antarctica.²⁰⁵ It is apparent that the bottom temperature regime beneath ice caps is very complex and varied, and many more observations are required before any distributional patterns

of the underlying permafrost during the Pleistocene or at present could be attempted.

After the ice retreated, permafrost in areas covered by postglacial inundations dissipated and did not re-form until these bodies of water receded several thousand years later. In contrast with areas covered by ice sheets, much colder temperatures were imposed by the periglacial climate on ice-free areas, producing thicker and colder permafrost than that existing beneath the ice.

GROUND ICE FEATURES

Geochemistry of Permafrost and Ground Ice

A relatively new approach to the study of perennially frozen ground is the chemical investigation of ice and sediments in permafrost. This approach appears to hold a great potential for further understanding for distribution and age of frozen ground. Such work was pioneered in North America by J. Brown and his associates of the U.S. Army Cold Regions Research and Engineering Laboratory,^{2,3,27-32,34,37-40,234-236} although O'Sullivan was perhaps the first worker in the field.¹⁷⁹

Most of the work in this field has been concerned with the distribution of soluble salts of sodium, magnesium, Calcium, and potassium in perennially frozen sediments as the reflection of past thermal and leaching regimes. Relatively low concentration of soluble salts in permafrost indicate freshening as the result of local or regional thawing, leaching, and refreezing. Sellmann indicates an abrupt change of chemical concentration of extractable cations in permafrost at a stratigraphic unconformity in permafrost.^{234,235}

Péwé collected perennially frozen samples from a 40-m vertical exposure near Fairbanks. These samples were analyzed for soluble salts by Brown and Sellmann. The samples had concentrations of actions (by conductivity) from 60 to 1 285 μmho and have a close relationship to stratigraphy.^{203,204} The low content of soluble salts of the fine-grained soil probably is due to removal by groundwater during time when the sediments were unfrozen. A low conductivity figure in the upper part of permafrost probably is the result of post-Wisconsinan thawing and subsequent freezing. Also, a low figure at the base of the Wisconsinan sediments supports the suggestion of an interglacial period of no permafrost and perhaps little accumulation of silt. Preliminary geochemical analyses of frozen sediments and ice in northern and central Alaska suggest that the chemical investigation of frozen ground holds a great potential in permafrost regions for gross correlations and perhaps for interpretation of geomorphological and thermal changes in Quaternary time.

Pingos

The distribution of pingos in North America has become much better known in the last decade. The presence of

pingos are not only of value in indicating the presence of permafrost, but indicating continuous or discontinuous permafrost. With one or two exceptions, the first local maps of pingo distribution in Canada (Figure 3) and Alaska have appeared in the last 10 years,^{107,115,153,160} and the first small-scale map of pingo distribution in northwestern North America is in press¹⁹⁷ and reproduced here as Figure 4.

Considerable progress has been made on the discovery and mapping of many open system pingos in central Alaska and Yukon Territory (Figure 4), as well as the discovery of pingo-like mounds in the shallow waters of the Beaufort Sea north of the mouth of the Mackenzie River.²⁴³ The greatest advance in pingo research in the last decade has been a consideration and understanding of theory and rate of pingo growth by Mackay,^{154,156,157,159,160} Mackay and Stager,¹⁶⁴ and Mackay and Black.¹⁶¹

After restudy of the photographs of the mounds in the Yukon-Kuskokwim Delta in Alaska and an examination of palsas elsewhere in the world, Péwé¹⁹⁷ believes that the 200 so-called closed-system pingos mentioned by Burns⁵⁸ occurring on the Yukon-Kuskokwim Delta are probably not pingos but palsas.

In addition to the thousands of pingos recognized in northwestern North America, groups of pingos have been mapped on Prince Patrick Island in the Canadian Arctic Archipelago.²⁰⁷ It is still undecided whether the pingos on Prince Patrick Island are open- or closed-system types. Pingos and pingo-like mounds also have been reported on other islands of the archipelago, including Baffin, Ellesmere, Prince of Wales, and Amund Ringnes.⁶¹

Considerable research has been undertaken on open-system pingos in North America in the last 10 years. Although photographs of pingos in central Alaska were taken 60 years ago, it was only in the late 1950's that it was recognized that such pingos were widespread in the forested regions of Alaska and the Yukon Territory. Not until the work of Holmes, Hopkins, and Foster in 1968 was the existence, type, and distribution of pingos in central Alaska clearly pointed out.¹⁰⁷ Subsequently, more than 700 open-system pingos have been recognized in central Alaska^{85,136,186} and the Yukon Territory.^{93,115,116,257}

From Figure 4 it is easily seen that open-system pingos are essentially restricted to discontinuous-permafrost zones. Open-system pingos lie near the base of slopes. Evidently, water enters the subsurface system from the surface in the nonpermafrost areas upslope. Studies in the last decade indicate overwhelmingly that almost all open-system pingos in northwestern North America lie on the south- or south-east-facing slopes of alluvium-filled valleys.^{107,115} The reason for this is still unknown, although perhaps there are more opportunities for surface water to enter the ground in the nonpermafrost areas on south-facing slopes.

One of the most interesting features of the distribution of pingos in northwestern North America is the relationship

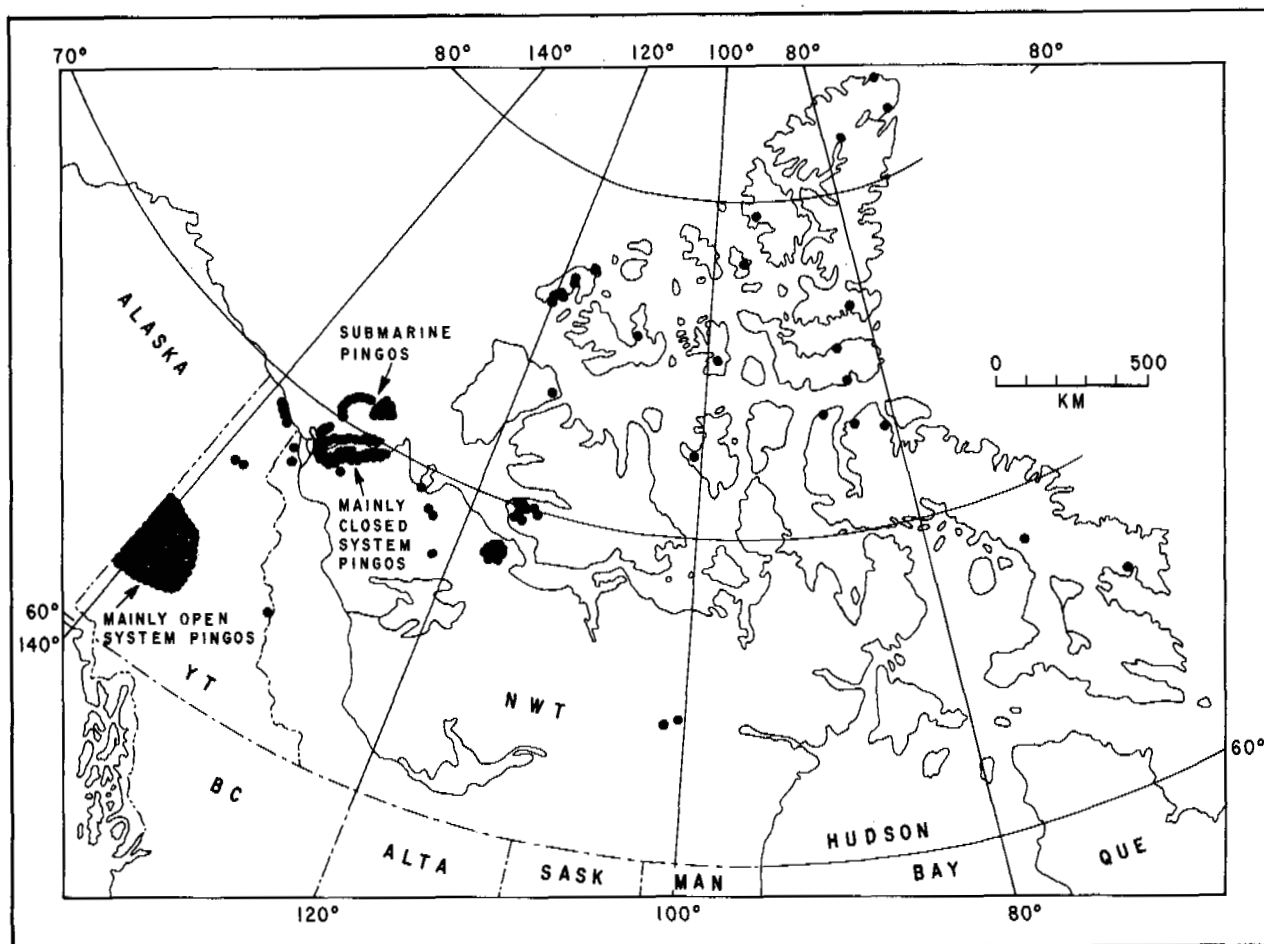
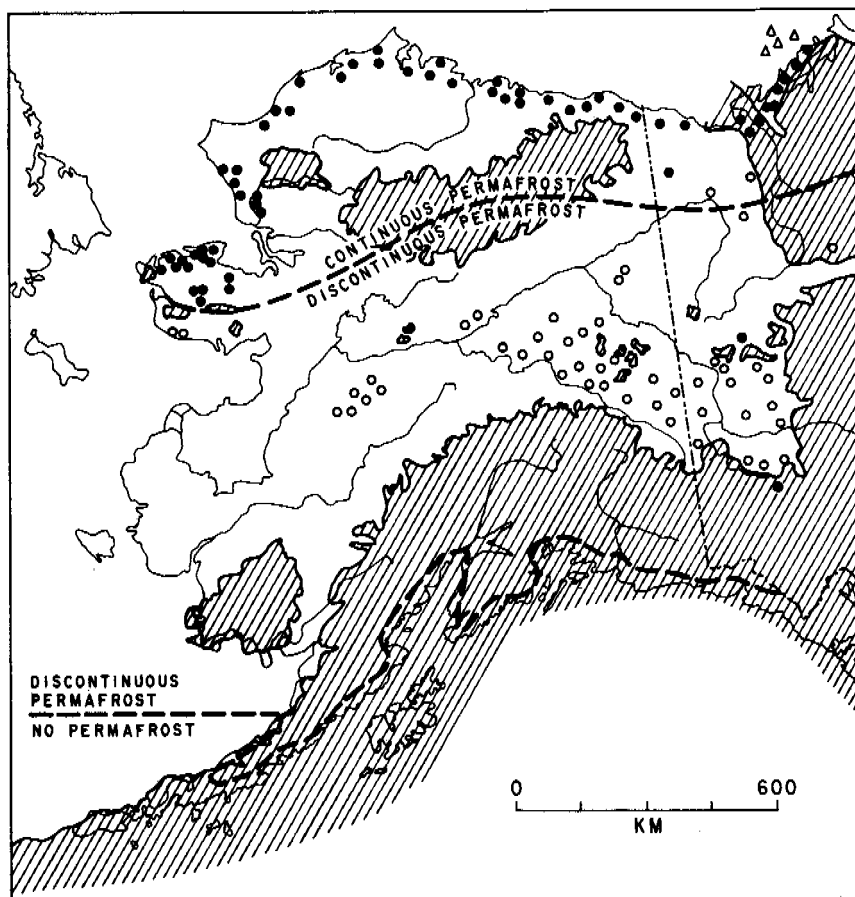


FIGURE 3 Pingos in Canada, including areas of observed open system, closed system, submarine and other type pingos, and pingo-like features. [Adapted from Geological Survey of Canada base map, Hughes (1969), Pissart (1967), Shearer (1972), and various papers from Mackay.]

of pingos to the glacial border (Figure 4). Almost all open-system pingos lie in the unglaciated part of the country (Figure 4), but a few pingos are known in areas that have been glaciated more than 25 000 years ago. Pingos are extremely rare in areas glaciated within the last 25 000 years. None are known in Alaska, and only two are known in the Yukon Territory.¹¹⁵ Perhaps about half of the 1 500 in the Mackenzie Delta, however, are in areas glaciated during the late Wisconsinan.¹⁶⁰ Hughes speculates that the absence of open pingos in the glaciated areas may be attributed to glacial modification of the topography and surficial materials necessary for their origin, or to differences in the extent and thickness of permafrost that results from glacial and postglacial history of the area.¹¹⁵ The reason for such a distribution of open-system pingos in relationship to the glacial border constitutes one of the problems that should be investigated in the near future.

Radiometric dating indicates that most pingos in North America are less than 4 000 to 7 000 years old. Mackay showed by careful field measurement over several years of four pingos that many are probably less than 1 000 years old; and some less than 25 years old.¹⁶⁰

One of the remaining problems in need of more research is a study of the water associated with open-system pingos as well as the role of artesian pressure. In 1968, Lissey began a study of hydrology of open-system pingos near Dawson, Yukon Territory, but no detailed results are yet available.¹⁴⁸ Williams and van Everdingen mentioned that one of the problems to be solved is a better understanding of the pressure developed to lift the static load of a pingo inasmuch as a total force of 0.6–2.2 MPa is thought to be required.²⁷⁹ The only work known on the chemical and biological properties of pingo lake is the preliminary study by Lotspeich, Mueller, and Frey.¹⁴⁹



LEGEND


-  LIMIT OF WISCONSIN GLACIAL AGE
- AREAS OF CLOSED SYSTEM PINGOS
- AREAS OF OPEN SYSTEM PINGOS
- △ SUBMARINE PINGOS
- PERMAFROST ZONE BOUNDARIES

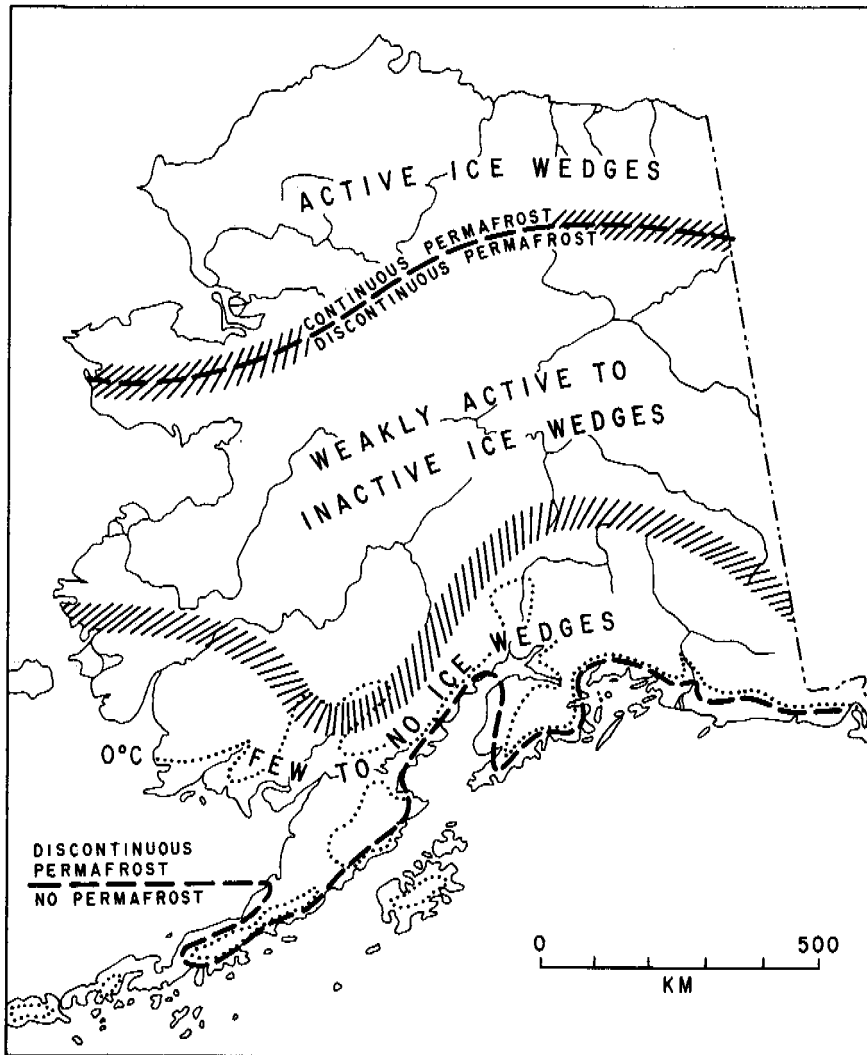
FIGURE 4 Distribution of open and closed system pingos in relation to permafrost zones and areas covered by late Wisconsin glacial ice in North America. (Map compiled from all published and unpublished sources, including personal communications from D. M. Hopkins, J. R. Mackay, I. Tailleux, O. J. Ferrians, W. Yeend, and O. L. Hughes.)

Ice Wedges

Ice wedges and the polygonal patterns they reflect on the surface of the ground are a characteristic feature of permafrost. They are termed active or inactive. Active ice wedges are defined as those that are actively growing. The area of active ice wedges in North America coincides roughly with the continuous permafrost zone; this is especially true in Alaska and northwestern Canada (Figure 5). They occur widely into the northern reaches of the Arctic Archipelago being reported in various areas including Prince Patrick

Island^{208,209} and as far north as Ellesmere Island.¹⁰⁵ It appears that the ice wedges will crack and continue to grow where the winter temperature of the ground at the top of the permafrost is about -15°C or colder; this area is almost limited to the tundra and to the continuous permafrost zone.^{16,20,122,157,158,163,208,209} Ice wedges in this zone are growing in various types of sediments; silt, sand, and gravel exhibit a polygonal pattern on the surface of the ground.

In the discontinuous-permafrost zone, especially in northwestern North America, the wedges are essentially inactive and the line dividing the zones of active and inac-



LEGEND

- — — PERMAFROST ZONE BOUNDARIES
- /////// ICE WEDGE ZONE BOUNDARIES
- APPROXIMATE POSITION OF MEAN ANNUAL AIR TEMPERATURE ISOTHERM, 0°C

FIGURE 5 Ice wedges in Alaska.

tive ice wedges is arbitrarily placed at a position where low-centered or raised-edge polygons are uncommon and where it is thought most wedges do not crack frequently (Figure 5). When more data become available concerning the temperature at the top of the permafrost, this arbitrary line may be more accurately placed.

Inactive ice wedges have no ice seam or crack extending from the wedge upward to the surface in the spring. The top of the wedge may be flat, especially if thawing has

lowered the upward surface of the wedge at some time in the past.^{186,189,194-197,234} Ice wedges in the discontinuous permafrost zone, for the most part, are present only in silt, having thawed and disappeared in many areas where they formerly existed in sand and gravel.¹⁹⁹ Large areas of ice wedges in the discontinuous zone of permafrost are covered by Holocene sediments and do not exhibit a polygonal pattern on the surface of the ground.

The age of ice wedges is being studied both from the

standpoint of absolute dating and from their geological position. Ice wedges have been radiometrically dated in northern and central Alaska and have been found to range from 14 000 to 32 000 years old.^{29,197,234,236} The writers have examined ice wedges in many countries in the world and consider all wedges seen so far to be Wisconsinan or Holocene in age.

In the last decade, a few detailed studies have been made on crystallographic investigations and on rate of growth and mechanics of cracking of frozen ground. Some of the earlier work of Black regarding crystal study was published in 1963.¹⁶ A reconnaissance examination of the crystal orientation in ice wedges in the permafrost tunnel at Fox near Fairbanks has been made,²⁶⁹ and some thermal cracking of the ground and ice wedges have been considered by Knight in connection with the stresses expected on a petroleum pipeline in northern Alaska.¹³⁴ Mackay published his observations on 5 years' continuous growth of cracks in the Mackenzie Delta and now has a continuous record for 7 years.¹⁵⁸

Although detailed measurements on cracking in the ice wedges were made earlier in Alaska, the most intense work in the last decade by workers from North America has been in Antarctica, where sand wedges and ice wedges were discovered and are currently being investigated.^{11,23,161,191}

One of the new approaches in the study of ice wedges has been a geochemical study of the ice. Although in its infancy, the examination of the ice from the standpoint of soluble salts present and other elements^{29,34,197,204} and possibly ¹⁶O/¹⁸O studies of the ice of wedges hold great promise.

Palsas

Palsas are mounds of peat and ice, 1–7 m high and 10–50 m in diameter, that occur in bogs. They protrude prominently above the level of the bog, have a rather hard and dry surface, and are more or less blown clear of snow in winter. The segregation of ice in thin layers and in bodies 2 m thick in palsas, plus the accumulation of peat, accounts for their formation. Traditionally, palsas have been thought to belong to the southern part of the discontinuous permafrost zone, but similar features have been observed in the Canadian Arctic Archipelago in the continuous permafrost zone.

Alaska and Canada are ideal places to study palsas and to learn more of their origin, age, and relationship to the glacial record and permafrost. They are well developed and abundant along the Denali Highway west of the MacLaren River Valley on the south side of the Alaska Range and are probably widespread in the nearby Susitna Valley and perhaps in the upper Kuskokwim Valley; the only investigation to date, however, is an observation by Péwé of a dissected palsa on the MacLaren River Valley. To the writers' knowledge, the dissected, 10 000-year-old palsas in the

MacLaren River Valley are the only dated ones in North America.^{100,121,185}

Péwé¹⁹⁷ believes that, from the descriptions and photographs, the grass-covered mounds reported by Burns,⁵⁸ to be pingos in the Kuskokwim–Yukon Delta near Bethel, Alaska, are, in reality, palsas.

Palsas and associated peat plateaus are widespread in the discontinuous permafrost zone of Canada, especially the southern portion where the permafrost is patchy. They are found across Canada in this subzone, having been reported in all physiographic regions from Labrador⁵⁴ to the western Cordillera.^{45,116} They are particularly prevalent in the Hudson Bay Lowland in northern Ontario and northeastern Manitoba,⁴⁶ and they have been mapped from aerial photographs at a scale of 6.4 km to 1 cm.⁷ Detailed studies have been carried out at several locations. Hamelin and Cailleux studied several palsa fields at Great Whale River, P.Q., near the east shore of Hudson Bay and observed their relationship to the local mean annual air temperature of -4 to -5 °C.⁹⁹ Their age appears to be less than 4 000 years, having formed after the postglacial thermal optimum following postglacial emergence.

A detailed ecological study of a palsa bog was made in the Hudson Bay Lowland near Winisk, Ontario, by Railton.²²⁰ The palsa bog was found to be ombrotrophic, the frozen cores of the palsas causing damming and perched water levels. Most of the better developed palsas were found in the drier regions of the bog. Evapotranspiration was the main source of heat loss, while exposure (reduced snowcover) and the low thermal conductivity of the peat were the main factors in palsa development. Palsa collapse was attributed to deterioration of the vegetation cover by rain and wind erosion, which caused the ground ice to melt.

Two important studies were carried out in Manitoba and Saskatchewan. Zoltai identified palsas and peat plateaus, indicating permafrost at present or in the recent past, in the field and on aerial photographs and traced them across Manitoba and Saskatchewan.²⁸³ The southern limit of their occurrence coincides with the 0 °C mean annual air isotherm; this is south of the -1 °C designated as the southern limit of permafrost in Canada but coincident with the designated southern limit of permafrost in Alaska. A detailed study of one wooded palsa was made in northern Manitoba and included a cross section through the perennially frozen core that was nearly 5 m thick.²⁸⁴

Mounds resembling palsas have been observed at several locations in the northern part of the continuous zone in the Canadian Arctic Archipelago and may be genetically similar. French described ice-cored hummocks or mounds that formed in the centers of ice-wedge polygons on Banks Island.⁹⁰ Peat mounds, 2–3 m high and containing 30-cm-thick layers of ice, occur in clusters on the north coast of Devon Island in low-lying tundra meadows (personal communication from W. Barr, University of Saskatchewan,

1971), the basal peat varying in age from 2 400 to 7 000 years B.P. Similar mounds have been noted also in Bathurst Island.¹⁵¹ These features may prove to be quite prevalent as more observations are reported.

Thermokarst

The thawing of ice-rich permafrost creates an uneven topography, termed thermokarst topography, that consists of mounds, sink holes, tunnels, caverns, short ravines, lake basins, and circular lowlands caused by melting of the ground ice. Thermokarst features result from disturbance or removal of the vegetation or from warming of the climate. Very small disturbances can create thermokarst features: a vehicle track across the tundra, an Eskimo dog being tied to a stake,¹⁵⁵ or the overturning of a tree.

Thermokarst topography is most commonly formed where massive ice exists in the ground, such as ice wedges or thick layers of segregated ice. It has only been in the last decade that information is becoming available in North America concerning quantitative amounts of ice in the ground. Brown made the first approximation of ground ice inventory for the Arctic Coastal Plain of Alaska³⁰ based on examination of ice in the ground from many boreholes in the Barrow area.^{29,31,33-35,39,237-239} Extrapolating from boreholes to the rest of the coastal plain by use of aerial photographs, Brown estimated that 10 percent of the volume of the upper 3.5 m of permafrost in the coastal plain is composed of ice wedges. Segregated ice is the most extensive type of ground ice, representing 75 percent of the ground by volume in places.²³⁷ Measurements made by Péwé in the Fairbanks area show that the samples of the ground may contain as much as 200-1 000 percent ice by dry weight.¹⁹⁸

Mackay has demonstrated that, for the large area of thermokarst lakes in the Mackenzie Delta, the permafrost has a great amount of ice.¹⁵⁶ There are widespread masses of ice associated with pingos and ice-wedge polygons; in addition there are hundreds of square kilometres of thick, massive ice beds. In terms of weight of ice to dry soil, the ice beds are more than 200 percent ice. Recent quantitative measurements of ice in permafrost also have been made by Hussey and Michelson¹¹⁷ and by Williams.²⁸¹

The most common thermokarst features are lakes, variously termed thaw lakes, thermokarst lakes, or cave-ins. Lakes occupying thaw basins are exceedingly abundant and widespread in arctic and subarctic North America. They occur in the lowlands and lower slopes throughout the valleys of central and northern Alaska and the northern part of Canada,⁹² especially in the Mackenzie Delta area¹⁵⁶ and elsewhere.⁶⁰ Such lakes are referred to in literature from various parts of the North.^{79,186,251,263}

Perhaps the most outstanding of the thermokarst lakes are the oriented lakes widespread on the North Slope of Alaska and east of the Mackenzie Delta on the Tuktoyak-

tuk Peninsula east to Cape Bathurst.¹⁵² A large area occurs on the west coast of Baffin Island¹⁴ and near Old Crow in Yukon Territory (Hughes, personal communication, 1972). In the 1950's and earlier, there was great discussion concerning the origin and age of these lakes in northern Alaska; however, there has been only a little work done since that time.^{21,218,219} A summary of investigation of thermokarst development on the North Slope was made by Anderson and Hussey.⁵

Despite casual or careful observations of thermokarst, investigation of thermokarst phenomena in North America is still in a beginning and descriptive stage.²² The first study in the Canadian Arctic Archipelago, on Banks Island, has just been completed by French and Egginton.⁹² For example, no continent-wide or country-wide map of thermokarst lakes exists, except for a very small-scale one for Canada.¹⁴ Nevertheless, research on thermokarst phenomena, especially the thaw lakes, is moving into a more quantitative stage.

The new work has stressed an understanding of the thermal regime associated with the thaw lakes in permafrost. Although earlier work was done in Alaska, new work has been concentrated in Canada beginning with work in the Mackenzie Delta.¹⁵² Johnston and Brown describe the distribution and temperature of the permafrost surrounding a small lake in the Mackenzie Delta.¹²⁵ Even though the lake is only 1.5 m deep and 275 m wide, it has a thawed area completely through the 70-m-thick permafrost. The thermal regime was calculated by means of a computer program.⁵⁶ A similar study was carried out on a shallow isolated lake near the delta, where a deep thaw basin was also found.¹²⁶

With increased development of the North¹⁴⁵ and construction of roads, building, and pipelines, more quantitative information is needed concerning the thermal regime of permafrost. Some of this information will be applicable to a better understanding of the development of thermokarst features.^{138,155} Several uninvestigated areas in central Alaska appear to exhibit well-developed, widespread thermokarst topography, such as the lake-pitted plains on the south side of the Yukon Flats. The same type of topography in the middle reaches of the Tozitna River may yield basic data on the origin of thermokarst topography and regional history of permafrost.

OTHER PERIGLACIAL FEATURES

Rock Glaciers

Rock glaciers—tongue-shaped or lobate masses of unsorted, angular frost-rived material with interstitial ice (if active) and with steep lichen-free fronts 10-100 m high—are one of the most spectacular deposits in the permafrost environment but are limited in areal extent. They are 150-320 m wide and 300-1 600 m long and most of them occur in cirques.

Some rock glaciers are the ablated remains of true ice glaciers, while most form independently from pre-existing glaciers.^{87,180}

Rock glaciers form under the influence of a periglacial climate in an area lacking the net accumulation of snow required for the formation of a conventional glacier. A permafrost environment must be present to enable the snow and water that trickles down into the interstices between the rock to remain as ice. Rock glaciers are indeed permafrost and move slowly downslope. Although they probably are more widely distributed, better developed, and more intensely studied in Alaska than anywhere else in North America, in the last 10 years most work on rock glaciers appears to have been done in the Rocky Mountains of the contiguous United States, Alaska, and in Canada. Rate of movement studies in the last 10 years include those by White in the Colorado Front Range, where he indicates the rock glaciers move 5-10 cm per year,^{275,276} and by Potter and Moss in the Absaroka Mountains of Wyoming, which indicate movement of 1-83 cm per year.²¹¹ In Yukon Territory measurements on some rock glaciers show movement of 50 cm per year.²¹⁶

An active rock glacier is in equilibrium with a permafrost climate to produce the frost-rived debris and to permit the interstitial ice to exist. The rock glacier becomes inactive when these climatic conditions are no longer met and thus loses its steep front, interstitial ice, and forward motion. In North America, inactive rock glaciers can be found at lower elevations than presently active ones, and no doubt they represent the lowering of snowline and changing of other climatic parameters in the past. There are both active and inactive rock glaciers in Alaska, and it is thought that all of them were active and formed in post-Wisconsinan time. Inactive rock glaciers at an elevation of 1 200 m occur along the Denali Highway in Alaska¹⁸⁵ and at an elevation of 1 200-1 500 m in Anaktuvuk Pass in the Brooks Range.²¹⁰ Two ages of rock glaciers also exist in the St. Elias Mountains, Yukon Territory.²¹⁶ Rock glaciers in North America give excellent records of late Holocene events and a great opportunity exists in most mountain regions to carefully document this span of history by a study of these features.

Altiplanation Terraces

Altiplanation (cryoplanation) terraces are large bedrock steps or terraces on ridge crests and hilltops and possess at least one scarp (ascending and/or descending) and a tread surface. The tread or "flat" area is 10 to several hundred metres wide and long. The tread is not actually flat but slopes from 1 to 5°, parallel to the ridge crests. Terrace scarps may be from 1 to 30 m high. Treads and scarps are cut into all bedrock types, but altiplanation terraces are best developed on closely jointed resistant rock, such as basalt, andesite, or hornfels. Although altiplanation terraces have been reported for more than 50 years, it is within the last decade that most widespread and detailed studies have

been undertaken to determine their distribution, orientation, and origin. In the last decade, they have been casually mentioned as occurring in various parts of North America (Figure 7)^{14,57,59,67,85,86,88,116,128,263} St. Onge describes altiplanation terraces in Canada and mentions that they are a nivation feature.^{229,230}

Reger and Péwé have been investigating in detail the origin of altiplanation terraces and relationship to bedrock and climate in central and western Alaska since 1965. The scarp retreats by nivation, forming a tread, and surficial debris is removed across and over the tread by mass movement. The terraces form perhaps a little below the general altitude of snowline²⁰² as above snowline glaciers, cirques, horns, and arêtes form. On isolated ridges and peaks not large enough to support large glaciers, however, altiplanation terraces form above snowline.

The widespread altiplanation terraces in central Alaska, and less commonly in northern Canada, occur at different altitudes and with different sharpness; in some cases, they may be traced continuously to lower altitudes on the same ridge where they are older and more rounded. Péwé^{191,192} demonstrates that pre-Illinoian altiplanation terraces still exist in rounded loess-covered forms near Fairbanks, Alaska.

The plot of the elevation of well-formed altiplanation terraces from west to east across central Alaska falls on a line below, but parallel to, past and present snowlines (Figure 6). It is not known if altiplanation terraces are actively forming in North America today, but it is known that most well-developed terraces now present formed in Wisconsinan time¹⁸⁵ and some may still be weakly active.

One of the problems remaining is the determination of the climatic conditions necessary to produce altiplanation terraces. Exact knowledge of such conditions would aid in reconstructing paleoclimatic conditions in vast areas of the nonglaciated polar areas.

Solifluction

Perhaps the most common forms of mass wasting in permafrost environments are frost creep and solifluction. Frost creep is a ratchetlike downslope movement of particles, the result of frost heaving of the ground and subsequent settling upon thawing.^{264,266} The most detailed work ever done on this subject was completed in the last decade by Washburn in northeast Greenland; there, he installed small wooden pegs in the ground and measured the amount of movement by theodolite at different times of the year.²⁶⁴ Benedict also investigated frost creep in the Colorado Rockies.⁹

Perhaps the most important form of mass wasting in the areas of rigorous climate is solifluction that has long been considered the slow flowing of debris saturated with water from higher to lower ground of masses. This process of soil flow is best developed in areas underlain by permafrost or long existing seasonal frost. Areas in which solifluction is

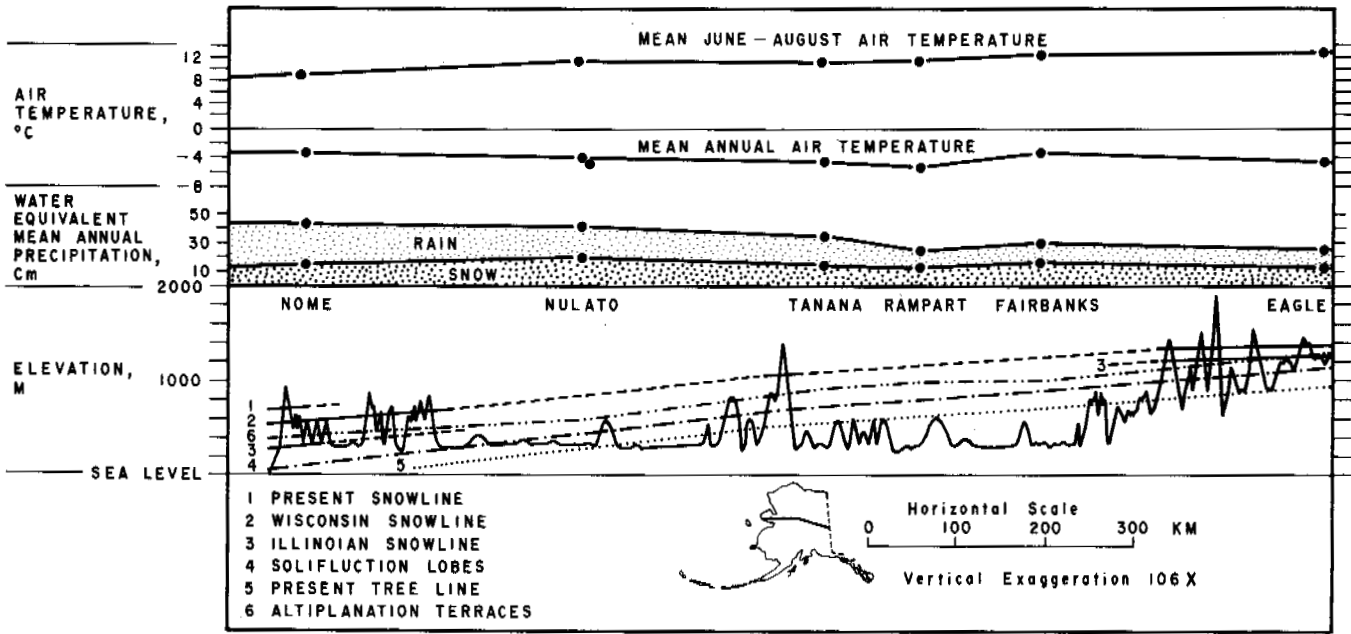


FIGURE 6 East-west section across central Alaska illustrating change of certain meteorological parameters and elevations of present snowline, snowlines of Wisconsinan and Illinoian age, solifluction lobes, present tree line, and well-developed altiplanation terraces (past snowlines were determined from the bases of cirques).

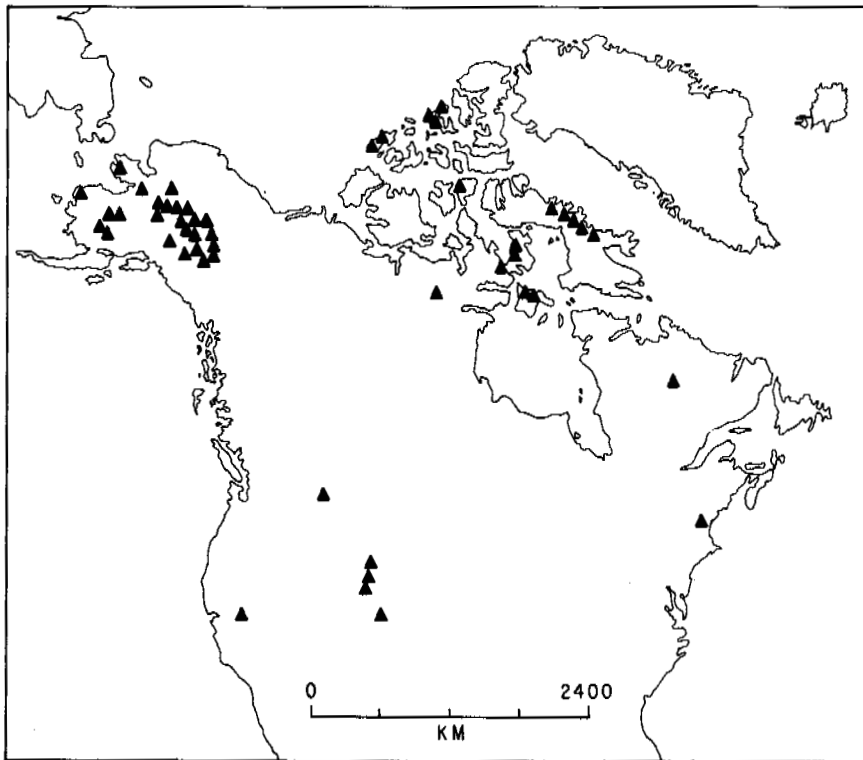


FIGURE 7 Generalized distribution of altiplanation terraces in North America. Modified from Demek (1968) and from R. Reger (unpublished data).

active lie almost entirely above or beyond the forest limit. Solifluction areas in North America are widespread and lie in the Far North. In Alaska, they are well developed in the central and northern part of the state. Well-developed solifluction lobes are at an elevation of 1 200 m in central Alaska on the Canadian border and at a progressively lower altitude to the west until on the Seward Peninsula they are only a few hundred metres above sea level^{74,76,107,162,244,249,262} (Figure 6).

Although solifluction lobes are widespread and the processes of solifluction have been observed in North America for more than 50 years, it is only within the last 10 years that the results of detailed quantitative studies on solifluction have appeared. Soil movements resulting from solifluction were investigated at Schefferville, Quebec, in the discontinuous-permafrost zone.²⁸⁰ Movements of more than 10 cm per year at the surface of a 20° bare slope were recorded. Price observed solifluction on mountain slopes in Yukon Territory.^{213,214,217} In the Canadian Arctic, Kerfoot and Mackay recorded downslope movement on a solifluction lobe of 0.25–1.40 cm per year on Garry Island in the Mackenzie River Delta located in the southern part of the continuous zone.¹³¹ Further north in the Arctic Archipelago, French noted that asymmetrical river valleys on Banks Island were forming by solifluction processes on north-facing slopes.⁹¹ In the Far North, Pissart described solifluction processes on Prince Patrick Island at 76°N lat.²⁰⁶ Everett made a short-term quantitative study on mass wasting in western Alaska.⁷⁸ Benedict studied turf-banked terraces in the U.S. Rocky Mountains,⁸ and Anderson *et al.* described bentonite flows from northern Alaska.⁴ The most detailed and rewarding study has been the careful observations and conclusions by Washburn, which is the result of many years' work in northeast Greenland.^{264–268} It is here that rates of motion were measured over slopes of different angles.

Although vegetation and rock types are important in the solifluction process, the amount of moisture remains paramount. Péwé has observed that, in the very dry areas of Antarctica, the slopes are solifluction free where moisture is less available, the rocks resistant, and highly jointed rubble fields or block fields are common. Not much work has been done recently in North America on this subject although well-developed rubble fields of Wisconsinan age have been documented overlying Illinoian till on the south side of the Alaska Range.¹⁸⁵ Also, inactive rubble fields are common in Pennsylvania and nearby states in the Appalachian region.^{133,211,240,241}

Stabilized solifluction sheets of pre-Illinoian and Wisconsinan age are widespread in the unglaciated parts of Alaska and Yukon Territory. Underlying extensive loess deposits of central Alaska are one or more sheets of solifluction material 0.3–3 m thick that blanket the hillsides.^{24,186,187,197} Work continues throughout North America to achieve a better understanding of ancient solifluction de-

posits and paleoclimatic interpretations. At archaeological sites in Alaska⁹⁴ and Canada, solifluction deposits less than a few thousands of years old have been helpful in interpreting the geologic history of the sites.

String Bogs

String bogs are boggy areas marked by a gentle undulating surface characterized by long, low, serpentine moss ridges, alternating with long, water-filled swales. The ridges or "strings" are 1–3 m wide and up to 1 m high.

There is considerable controversy at present over the origin of string bogs and their relationship to solifluction and to permafrost. Schenk²³³ states that string bogs resulted from the collapse of formerly perennially frozen bogs when permafrost disappears, but this idea has received no support from Rapp and Annersten.²²¹ Péwé mentions that string bogs are excellently developed and widespread in the lower Susitna Valley and other drainages from the Alaska Range and are well exhibited in bog flats of the western Kenai Peninsula.¹⁹⁸ String bogs are poorly developed, if at all, however, in central Alaska. They appear to be best formed near the southern limit of permafrost. Although Péwé has examined string bogs from the air and on the ground and photographs of these bogs appear in Schenk,²³³ no research has been undertaken to determine the origin or relationship to the glacial record in permafrost distribution in Alaska. In Canada, Knollenberg has mapped in a reconnaissance way the distribution of string bogs in the central part of the country, evaluated their position in relationship to the climate, and showed them to extend several hundreds of kilometres south of the permafrost limit.¹³⁵ Thom has studied string bogs near Schefferville in eastern Canada in a permafrost-free area.²⁵⁵ He emphasizes the importance of spring thaw; ice push and frost heaving are secondary. However, this is only a beginning of what should be done to further investigate string bog-permafrost relationships in North America.

Extinct Pingos

Another feature that permits an understanding of the former distribution of permafrost is the presence of collapsed pingos, sometimes called "fossil" pingos. Although collapsed pingo features have been reported from widespread localities in Europe, they have not been reported as such from the non-permafrost areas of North America. That is, the typical collapsed pingo ring, filled with pond and vegetation debris, has not been reported. However, from the nonpermafrost areas of northern British Columbia and southern Alberta and Saskatchewan, as well as from north central Illinois, there occur hundreds of pingo-like mounds.^{12,13,83,84,165,272} Although it is apparent that permafrost existed in late Quaternary time in these particular areas, based on ice-wedge casts and relationship to glacial fronts, these mounds

in themselves do not necessarily indicate permafrost or even pingos. They are unusual features, the origin of which is not completely understood. Further work is needed to demonstrate that they are remnants of late Quaternary pingo fields.

In addition to the former extent of pingos in the now non-permafrost areas, in both Alaska and northern Canada there now exists evidence of older pingos, or pingos that have collapsed and are marked today by a ring of sediment. Such old pingos are well known from central Alaska^{107,136,152,186} and often as far north as Amund Ringnes Island in the Arctic Archipelago.⁶¹

Ice-Wedge Casts

In many parts of the world, mainly temperate latitudes, the former presence of permafrost is indicated by the existence of ice-wedge casts. Such casts form when the ice wedges slowly melt, generally from warming of the climate, allowing a general collapse of the overlying sediments into the area formerly occupied by the ice wedges. The existence of these ice-wedge casts permits reconstruction of former distribution of permafrost and paleoclimates.¹⁸⁸

Although a voluminous literature has developed in Europe since 1944,¹⁹⁹ only a few examples were known in temperate North America prior to the last decade. In the last 10 years, additional examples have been described from temperate North America (Figure 7) by Clayton and Bailey,⁶² Ruhe,²²⁸ Totten,²⁵⁶ and Wayne²⁷² in the midwest United States; Black^{17-19,22} in Wisconsin; Dionne⁷⁰⁻⁷³ and Lagarec¹⁴² from southeastern Canada; Morgan^{170,171} from southern Ontario; Westgate and Bayrock²⁷⁴ from Alberta; Borns²⁵ from Nova Scotia; and Brookes²⁶ from Newfoundland. Berg describes what he believes to be "fossil" sand wedges from Alberta.¹⁰ If these examples are ice-wedge or sand-wedge casts, they indicate the existence of permafrost in late Wisconsinan time.

Although it is well known that ice wedges are common in arctic and subarctic North America, it is not generally realized that ice-wedge casts also exist there. More references have been to, and paleoclimatic inferences made from, ice-wedge casts of different ages in the Subarctic, especially Alaska, than in temperate latitudes. Evidence of the oldest permafrost in North America is from ice-wedge casts at Fairbanks^{186,187} and at Cape Deceit in western Alaska.^{98,108} It is thought that these ice-wedge casts could be 1½ million years old. The casts at Fairbanks are well developed in ancient solifluction layers and are composed of aeolian sand.¹⁹⁷

Also, in the Fairbanks area there is evidence of ice-wedge casts in loess of Illinoian age.¹⁸⁹ Such casts have also been reported by McCullough from central and western Alaska.¹⁶⁶⁻¹⁶⁸ Hopkins and Einarsson similarly record ancient and Wisconsinan ice wedges on the Pribilof Islands.¹¹¹

Ice-wedge casts of Wisconsinan age in outwash gravel and loess deposits are known in central Alaska.^{1,24,185,187} The

most thorough work on ice-wedge casts in North America is probably that of Péwé, Church, and Andreson near Big Delta in central Alaska.¹⁹⁹ In this area, the ice-wedge casts are reflected on the surface by large-scale polygons. A detailed study of the distribution, sedimentology, and paleoclimatic interpretation reveal that the climate in central Alaska at the time the large-scale contraction crack polygons formed was colder and generally more rigorous than that of today. Based on a comparison with areas where ice wedges are actively growing today, the mean annual air temperature of the Big Delta area at the time of ice-wedge growth was at least -6°C , in contrast to the mean annual air temperature of -2.8°C today. After the formation of the wedges, the climate warmed to 0°C or above, and the ice wedges as well as most of the permafrost in the outwash gravel disappeared. This interval of warmer climate was evidently rather short, inasmuch as the permafrost and ice wedges in silt in adjacent regions were only partially thawed. After this thawing, the weather cooled and frozen ground started to re-form and is still forming today.

Study of the ice-wedge casts in central Alaska near Big Delta has demonstrated that extensive areas of ice-wedge-cast polygons can occur in coarse-grained sediments in regions where permafrost is actively growing, such as in central Alaska, and where large ice wedges are still present in fine-grained sediments. Such an association supports the suggestion that the permafrost and ice wedges thaw more rapidly in coarse-grained sediments than ice-rich, fine-grained sediments. This is especially true where percolating groundwater modifies the thermal regime of the ground, such as in outwash plains, alluvial fans, and river floodplains.

PAST DISTRIBUTION OF PERMAFROST

Permafrost was more widespread in North America at different times in the past than at present; undoubtedly, at times it was also less extensive than at present. The thickness of permafrost also varied in the past. The distribution of permafrost in the past was dramatically different in the temperate latitudes than now; however, the distribution was not so different from present in the Arctic of North America. The alternating formation and disappearance of permafrost during late Cenozoic time represents a permafrost chronology.

Permafrost will form if the climate of an area cools to about or below 0°C mean annual air temperature (Figures 1 and 2). Ice wedges will form if the top of the permafrost cools to about -15 or -20°C .¹⁸⁸ This occurs in areas where the mean annual air temperature is at least -6 or -8°C (Figure 5). The exact climatic conditions for pingos are unknown (Figures 3 and 4), but they do require permafrost. Altiplanation terraces probably form only in a permafrost environment and rock glaciers do require a permafrost environment. Solifluction and sorted patterned ground are

best developed in areas of permafrost but do not require permafrost. Therefore, past existence of permafrost can be told only from the existence of past ice wedges and associated polygons, pingos, rock glaciers, and perhaps altiplanation terraces. The presence of permafrost may be suggested but not proved from stabilized solifluction deposits and small-scale patterned ground. Vegetation studies also may indicate that a rigorous environment was present but does not in itself prove the presence of permafrost. The same may be said for the presence of a continental ice sheet.

FORMER EXTENT

In the polar areas, especially unglaciated areas, permafrost was undoubtedly thicker and more extensive in Wisconsin time than now. In central Alaska, Péwé, Church, and Anderson demonstrate that many of the gravel areas are no longer perennially frozen but that the ice-rich silt areas are.¹⁹⁹ Also, in the Alaska Peninsula, permafrost occurs today only as deep-lying relicts. Permafrost was much thicker in the Cape Thompson area than now. Lachenbruch *et al.* state, for example, that only 280 m of the 357 m of permafrost observed in a drill hole in Ogoturuk Valley, 30 km southeast of Point Hope, would exist if present conditions were to persist for several thousand years.¹⁴⁰ Actually,

about 25 percent of the permafrost at Ogoturuk Valley is a product of an earlier climate.

Permafrost in central Alaska was thicker in Wisconsin time, and the now predominantly inactive ice wedges were actively growing 15 000 years ago. Although there are few supporting data, it is safe to assume that frozen ground was also thicker in the Arctic of Canada and Alaska. Permafrost definitely was present more than 40 000 years ago in the Mackenzie Delta area of northwest Canada and was deformed by glacier ice push in late Wisconsin time.¹⁶³

The distribution of permafrost in periglacial areas adjacent to the continental ice sheet in temperate latitudes of North America in late Pleistocene time is known only in the most sketchy manner.¹⁶⁹ Unlike Europe, no permafrost belt has been mapped so far in temperate North America; However, because considerable information has been accumulated in the last 10 years on the location and age of ice-wedge casts, a plotting of ice-wedge-cast distribution in Wisconsin time in North America is presented in Figure 8. From this information, the minimum former extent of permafrost in temperate North America can be deduced.

It is assumed that permafrost formed as refrigerating conditions developed in front of the expanding continental glaciers that covered all of northern North America, except western Yukon Territory and parts of Alaska. It has been

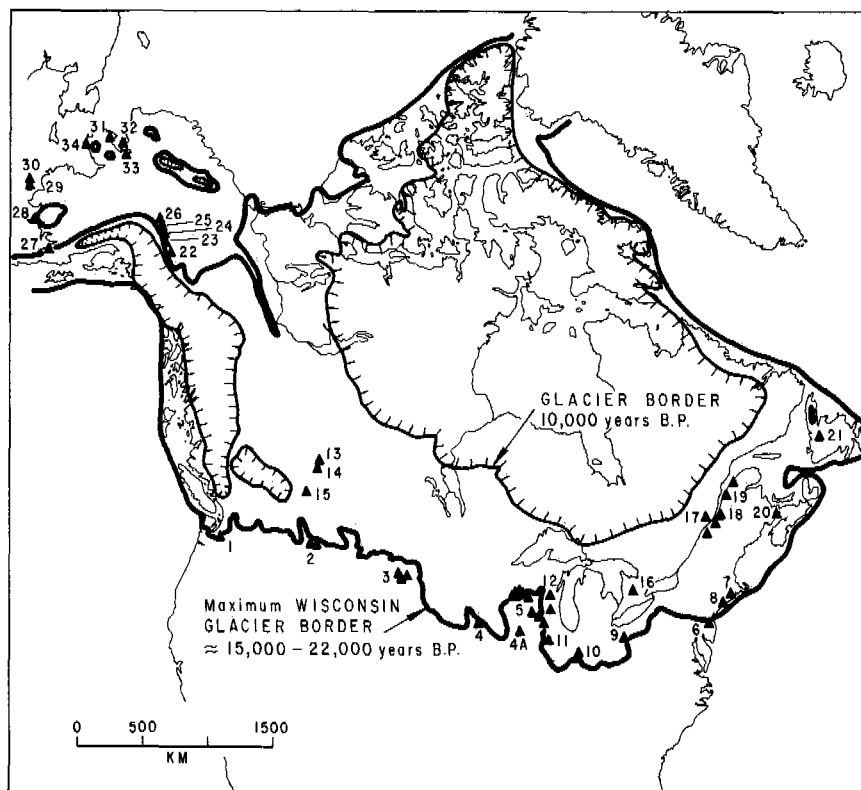


FIGURE 8 Sites of ice-wedge casts in North America. (See Table I for source of data and age of ice wedges.) Glacier ice borders generalized from V. K. Prest (1969).

postulated that permafrost existed beneath those parts of the ice sheets where the bottom temperature was colder than 0 °C either in a pressure melting situation (-2 to -1 °C) or polar glacier conditions when the ice was frozen to the underlying ground and bottom temperatures are lower. The thickness of the permafrost corresponded to the ice bottom temperatures. Perhaps part of the permafrost was thawed by running water under the temperature glaciers, but re-formed as glaciers withdrew. The permafrost adjusted to the ensuing cold periglacial conditions with the formation of ice wedges and other features as the ice sheet retreated (Figure 8).

Large areas of central Canada were inundated by post-glacial lakes (Lake Agassiz and others) beneath which existing permafrost dissipated and did not re-form until these bodies of water disappeared. Much of the Quaternary record in Canada was greatly disturbed or destroyed by Pleistocene glaciation and disturbed by postglacial submergence that made use of ancient deposits for interpreting part of permafrost conditions difficult.

One of the most logical places to find ice-wedge casts in temperate North America would be just south of the Wisconsinan ice sheet.²¹² This was the latest of the major glaciations, and features that formed at this time are the most likely to be preserved. The area adjacent to, and away from, the ice sheet for a short distance (80 to perhaps 250 km) was subjected to rigorous climate of the periglacial environment, a climate favorable for the growth of permafrost and ice wedges. Although the permafrost may form when the mean annual air temperature is 1 or 2 degrees below 0 °C, ice wedges will not form unless, as indicated earlier, the top of the permafrost becomes very cold and contracts, thus overcoming the tensile strength of the frozen ground. This generally occurs in areas where the mean annual air temperature is in the neighborhood of -6 to -8 °C today.

Many ice-wedge casts have been discovered outside of, and adjacent to, the southern border of the continental ice sheet (Figure 8).^{17-20,62,228,232}

Péwé believes that localities south of the glacial border No. 2 through No. 4 undoubtedly reflect true ice wedges in a cold continental environment; however, questions are still unanswered concerning reported ice-wedge casts along the Atlantic and Pacific coasts in temperate latitudes just in front of the ice sheet. At locality No. 1, between Seattle and Tacoma, are the widely discussed Mima Mounds. Even though Péwé,¹⁸³ Newcomb,¹⁷⁵ and Ritchie²²⁵ believe the mounds resulted from ice-wedge-polygon erosion, no typical ice-wedge casts have ever been reported with these polygonal surface structures. In northeastern United States at locality No. 6, Wolfe²⁸² (Table I) reports various periglacial features and alludes to ice-wedge casts. Péwé believes these are not true ice-wedge casts. In most instances, students of ice-wedge casts in temperate areas, especially prior to the last 5 or 10 years, were not familiar with modern ice wedges in the field

and, therefore, were hindered by lack of knowledge of what an ice wedge or ice-wedge cast should look like.

The age of the wedges that existed in front of the glacier are thought to have formed 15 000 to perhaps 22 000 years ago, although some could have formed earlier.

When the glacial ice sheet withdrew to the north, the glacial drift in most areas became perennially frozen. If climatic conditions were rigorous, ice wedges formed. As indicated on Figure 8 and Table I, ice-wedge casts have been reported from glacial deposits just north of the glacial border; this is especially true in central United States.^{18,19,112,256,271,272} These wedges formed perhaps 12 000 to 13 000 years ago.

As the continental ice sheet continued to withdraw, wedges formed at a later time farther to the north, such as reported by Berg,¹⁰ Morgan,^{170,171} Dionne,⁷⁰⁻⁷³ and Lagarec.¹⁴²

In addition, ice wedges have been reported along the eastern coast of North America. Several years ago possible ice-wedge casts in Connecticut⁶⁸ and Rhode Island¹⁵ were announced. From the nature of the descriptions, Péwé believes these are not ice-wedge casts and Denny (personal communication, December 1972) concurs that his description of periglacial features did not include ice wedges. Robert Black (personal communication, December 1972) indicates that examination of wedge forms he has seen in Connecticut and Massachusetts has not revealed any true ice-wedge casts; he believes that perhaps the climate was too mild for ice-wedge formation as the glacier withdrew. Farther north along the Atlantic Coast, typical ice-wedge casts have been reported from Nova Scotia²⁵ and Newfoundland.²⁶

In Alaska, ice-wedge casts of Wisconsinan age occur south or outside of the glacial border as reported in Bristol Bay¹¹⁰ and on the Pribilof Islands (Hopkins, personal communication, December 1972). Ice-wedge casts of Wisconsinan age also have been reported in gravel along the Tanana Valley outside of the Wisconsinan ice limits.^{1,24,199}

In addition to reconstructing the distribution of permafrost in Wisconsinan time from ice-wedge casts, these features delineate the existence of permafrost in pre-Wisconsinan (Illinoian?) and pre-Illinoian (?) times in central and western Alaska (Figure 2 and Table I).

CHRONOLOGY OF PERMAFROST

Perhaps the earliest evidence of permafrost in North America is indicated from central and western Alaska. In central Alaska on the campus of the University of Alaska are ice-wedge casts in solifluction layers (Table I and Figure 8). These ice-wedge casts are thought to be at least a million years old, inasmuch as they represent the older of two permafrost periods, both of which predate the Illinoian glaciation. Ice-wedge pseudomorphs are also reported from Cape Deceit on the south shore of Kotzebue Sound,¹⁰⁸ and Hop-

TABLE I Ice-Wedge-Cast Localities in North America

Map Location Number	Reference	Locality	Time of Ice-Wedge Formation (yr)	Distance from Glacial Border (km)
The United States of America—Outside Wisconsin Border				
1	Péwé ¹⁸³	Thurston Co., Washington	Wisconsinan ~ 14 000	at border
1	Newcomb ¹⁷⁵			
1	Ritchie ²²⁵			
2	Schafer ²³²	near Vaughn, Montana	Wisconsinan	16 km
3	Clayton and Bailey ⁶²	SW North Dakota	early Wisconsinan (?)	10–100 (?)
4	Ruhe ²²⁸	NW Iowa	Wisconsinan	10–100 (?)
4a	Ruhe ²²⁸	Tama Co., Iowa	Wisconsinan	40 (?)
5	Black ¹⁹	SW Wisconsin	~ 20 000	0.5–100
6	Wolfe ²⁸²	New Jersey ^a	Wisconsinan	<20
The United States of America—Inside Wisconsin Border				
7	Birman ¹⁵	Rhode Island ^a	late Wisconsinan	~70
8	Denny ⁶⁸	S. Connecticut ^a	late Wisconsinan	~50
9	Totten ²⁵⁶	Richland Co., Ohio	<14 000	5
10	Wayne ^{271,272}	W. Central Indiana	<14 500	75
11	Horberg ¹¹²	Bureau Co., No. Illinois	~14 000	30
12	Black ¹⁹	Outagamie Co., and Columbia Co., Wisconsin	<12 000	50
Southern Canada				
13	Westgate and Bayrock ²⁷⁴	Edmonton, Alberta	>31 000	600
14	Berg ¹⁰	Edmonton, Alberta		600
15	Morgan ¹⁷⁰	Calgary, Alberta	pre- to late-Wisconsinan	~300
16	Morgan ¹⁷¹	Toronto, Ontario		~300
17	Dionne ⁷³	15 km NW Quebec City, Quebec	12 000–11 500	~600
18	Dionne ⁷¹	South shore of St. Lawrence River	~12 000	~600
19	Lagarec ¹⁴²	SE Quebec	~12 000	~600
20	Borns ²⁵	N. Nova Scotia	~12 000	~200
21	Brookes ²⁶	Newfoundland		
Alaska				
22	Ager ¹	Healy Lake	Wisconsinan	
23	Péwé <i>et al.</i> ¹⁹⁹	Big Delta	Wisconsinan	
24	Péwé ¹⁸⁷	Shaw Creek	pre-Illinoian	
25	Blackwell ²⁴	Tanana R.	Wisconsinan	
26	Péwé ¹⁸⁶	Fairbanks	pre-Illinoian	
27	Hopkins <i>et al.</i> ¹⁰⁹	Bristol Bay	Wisconsinan	
28	Hopkins ^b	Kvichak Pa.	Wisconsinan (?)	
29	Hopkins and Einarsson ¹¹¹	Pribilof Isl.	pre-Wisconsinan [Illinoian (?)]	
30	Hopkins ^b	Pribilof Isl.	Wisconsinan	
31	Guthrie and Matthews ⁹⁸	Northern Seward Pa.	pre-Illinoian	
32	McCullough <i>et al.</i> ¹⁶⁸	Baldwin Pa. NW Alaska	pre-Wisconsinan [Illinoian (?)]	
33	McCullough and Hopkins ¹⁶⁷	NW Alaska	pre-Wisconsinan [Illinoian (?)]	
34	Hopkins <i>et al.</i> ¹¹⁰	Nome	Wisconsinan	

^a Doubtful ice-wedge casts.

^b Personal communication.

kins¹⁰⁸ believes they represent a permafrost period of 1.0 ± 0.5 million years ago. Presence of the ice wedges indicates that the mean annual air temperature was at least as cold as -6 to -8 °C.

Following this early Pleistocene cold period, there occurred a warm episode recorded in central Alaska by the withdrawal of glaciers and thawing of permafrost and melt-

ing of ice wedges. The ice wedges were replaced when wind-blown sand filtered down from the overlying sand dunes forming the ice-wedge casts.¹⁹⁷ The lowering of the permafrost table and disappearance of the ice wedges indicate that the mean annual air temperature was at least warmer than 0 °C.

In several parts of North America, there is evidence for

two or more Pleistocene cold periods of pre-Illinoian age. In central Alaska inactive solifluction deposits and altiplanation terraces show evidence of a major cold period although there is no definite proof that permafrost was present at this time. Péwé believes that the ancient altiplanation terraces are evidence of a rigorous cold period and that permafrost was present.¹⁹⁴ In fact, he further states that, barring major tectonic movement, the low-level inactive solifluction deposits and relict altiplanation terraces at Fairbanks indicate that the climate was then much more rigorous than in any later Quaternary time.

Just prior to Illinoian time, there was a period of climatic warming. It is thought that permafrost thawed at this time, and ice-wedge casts were formed in solifluction deposits near Shaw Creek in central Alaska.¹⁸⁷

Abundant evidence exists in Alaska to indicate the presence of permafrost and ice wedges during the Illinoian time (Table I and Figure 8).^{167,168,186} Again, the mean annual air temperature was colder than -7°C , which is 2 to 4°C colder than the present mean annual air temperature in central and western Alaska.

During the Sangamon interval, the climate was warmer than now, and permafrost probably completely disappeared in central Alaska; permafrost undoubtedly was much more restricted and thinner in the Arctic. Presence of ice-wedge casts in the now perennially frozen sediments of Illinoian age in both western¹⁶⁸ and central Alaska (Péwé, unpublished data) indicates that, during this interval between Illinoian and Wisconsinan time, the climate rose to give a mean annual air temperature that was warmer than 0°C , thereby causing the ice wedges to melt.

Geochemical studies of perennially frozen sediments at Fairbanks²⁰⁴ (leaching of salts, as well as other evidence of groundwater movement through now perennially frozen sediments) further support the belief that most or all of permafrost in central Alaska thawed in Sangamon time; therefore, the mean annual air temperature was higher than 0°C for a considerable length of time. Thawing of permafrost would necessarily thaw mammal carcasses preserved in the frozen ground; no carcasses of pre-Wisconsinan age are known, thereby strengthening the concept that permafrost perhaps thawed entirely in the Subarctic during Sangamon time.

Formation of weathering profiles up to 3 m thick on drift of Illinoian age in western Alaska and loess in the far west of Alaska¹⁶⁸ and in Fairbanks¹⁸⁹ further indicate that permafrost was absent.

Permafrost was more extensive during Wisconsinan time in North America than now. Deep-lying relicts of Wisconsinan permafrost are present in the glacial outwash sediments near Big Delta,^{199,201} as well as along the southern border of the permafrost area in Alaska (Figure 2). The existence of similar isolated relicts of perennially frozen ground at the southern limit of permafrost in Canada has not been definitely ascertained.

In northern North America, the ice wedges were actively growing in Wisconsinan time and are still actively growing. All that can be deduced from this information is that the climate during Wisconsinan time in the Arctic was at least as cold as now and the snowcover as thin as now. In the Subarctic, however, inactive ice wedges are widespread. If the mean annual air temperature of -6 to -8°C or colder is one requirement to form large, typical ice wedges such as are present, it would mean that, near Fairbanks as well as at Dawson, Yukon Territory, for example, the mean annual air temperature would have to be at least $3-4^{\circ}\text{C}$ lower than at present.

In western Canada, as well as central Alaska, many of the large deep-lying ice wedges have flat tops, indicating downward thawing of permafrost in ice wedges. This thawing is then dated at more than 38 000 years and is thought to represent a short, mid-Wisconsinan, or earlier, warm period with a mean annual air temperature of more than 0°C .^{197,234,237}

Radiocarbon dating of organic material in ice wedges in central Alaska indicates that the ice wedges are more than 25 000–37 000 years old.^{197,234,236} Ice-wedge growth has been active in the Barrow, Alaska, area for at least the last 10 000–15 000 years.²³⁷ Also, the frozen carcasses of extinct animals that exist in Wisconsinan permafrost suggest that the frozen ground has existed since the time of the animals' death.^{194,195} Recent work by Mackay, Rampton, and Fyles indicates that the existing permafrost in the western Arctic of Canada also dates from more than 40 000 years ago.¹⁶³

Widespread evidence from the polar areas, as well as the temperate areas, indicate that, with the warming of the climate during the last 10 000 years, permafrost has become much more restricted. All frozen ground existing prior to 10 000 years in the temperate latitudes is now gone and much of the frozen ground in central Alaska has disappeared in some areas as indicated by the presence of ice-wedge casts in Wisconsinan sediments.^{1,24,199,201}

In central Alaska, as well as the Yukon Territory, the Holocene warming of the climate produced a mean annual air temperature of 0°C or warmer for a short time, because the permafrost table and the tops of ice wedges were lowered.¹⁸⁶ Radiocarbon dates indicate that the warming began about 10 000 years ago.

Since this early warming, however, especially in the Fairbanks area, permafrost has re-formed in the sediments that were thawed starting 10 000 years ago, indicating a return to a mean annual air temperature colder than 0°C . However, the climate is not cold enough and/or snowfall is too great to permit ice-wedge growth, except in rare localities.¹⁹⁷

A study of the thermal records of deep permafrost near Barrow shows that the mean annual ground surface temperature evidently has increased about 4°C since 1850 with about half of the increase occurring since 1930. In the Ogotruk Creek area of northwestern Alaska, Lachenbruch, Green, and Marshall demonstrate by a study of a thermal record of

a borehole 357 m deep in permafrost, approximately 1 200 m from the Chukchi Sea, that the mean ground surface temperature has risen 2–2.5 °C in the last 100 years.¹⁴⁰

Lachenbruch shows that the mean annual surface temperature at Barrow 100 years ago was about –12 °C; with the recent warming, it should be about –8 °C. However, the mean annual surface temperature is slightly lower than –9 °C; recent cooling must have taken place and penetrated to a depth of only 30 m. This recent cooling is also recorded in the thermal profile from Cape Thompson (Ogotoruk Creek). Such a cooling has probably been in progress for only 10 years or so.¹⁴¹

RECOMMENDATIONS FOR FUTURE WORK

The following lines of investigations are recommended:

1. Inventory of permafrost surface features and investigations of the extent, thickness of permafrost, active layer, ground ice in local areas throughout the permafrost region;
2. Mapping permafrost by airborne remote-sensing from aircraft and satellites—Rapid mapping (identification and delineation) of permafrost bodies in the discontinuous zone and the geometry of permafrost in both zones would be a major breakthrough in the inventory of permafrost that is urgently required;
3. Improvement in aerial photographic interpretation—This must proceed, especially since accurate mapping by remote-sensing is some years away. Continual accumulation of ground truth is vital to improve the prediction of permafrost conditions in unexplored areas;
4. Dating of permafrost strata—Some work has been done in Alaska but virtually none in Canada except to relate permafrost age to past geological events, such as glaciation, postglacial submergence, and postglacial thermal optimum. More work is required to ascertain precisely the age and chronology of permafrost in various land forms to provide clues to past distribution and environmental relationships;
5. Precise ground temperature measurements and determination of mean ground temperatures—Accurate field measurements are necessary to interpret past and present distributions of permafrost and changes with time. The determination of mean ground temperature at various depths is vital in developing an understanding of the environmental relationships; and
6. Field (*in situ*) determination of thermal properties of perennially frozen soils and rock—This information is necessary to predict the distribution of permafrost in various types of earth materials.

REFERENCES

1. Ager, T. A. 1972. Surficial geology and Quaternary history of the Healy Lake area, Alaska. M.S. thesis. University of Alaska, Fairbanks. 127 p.
2. Allan, R. J. 1969. Clay mineralogy and geochemistry of soils and sediments with permafrost in interior Alaska. Ph.D. thesis. Dartmouth College, Hanover, New Hampshire. 289 p.
3. Allan, R. J. 1971. Clay mineralogy and geochemistry of soils and sediments with permafrost in interior Alaska. Dissert. Abstr. Int. B 30(7):2984-B-2985-B.
4. Anderson, D. M., R. C. Reynolds, and J. Brown. 1969. Bentonite debris flows in northern Alaska. *Science* 164(3876): 173–174.
5. Anderson, G. S., and K. M. Hussey. 1963. Preliminary investigations of thermokarst development on the North Slope, Alaska. *Iowa Acad. Sci. Proc.* 20:306–320.
6. Annersten, L. 1966. Interaction between surface cover and permafrost. *Biul. Peryglacj.* No. 15. p. 27–33.
7. Bates, D. N., and D. Simkin. 1966. Vegetation patterns of the Hudson Bay Lowlands. Map Dept. of Lands and Forests, Prov. of Ontario, Canada. Scale: 10 mi: 1 in.
8. Benedict, J. B. 1966. Radiocarbon dates from a stonebanked terrace in the Colorado Rocky Mountains, U.S.A. *Geogr. Ann. Ser. A* 48:24–31.
9. Benedict, J. B. 1970. Downslope soil movement in a Colorado alpine region: Rates, processes, and climatic significance. *J. Arctic Alp. Res.* 2(3):165–226.
10. Berg, T. E. 1969. Fossil sand wedges at Edmonton, Alberta, Canada. *Biul. Peryglacj.* No. 19. p. 325–333.
11. Berg, T. E., and R. F. Black. 1966. Preliminary measurements of growth of nonsorted polygons, Victoria Land, Antarctic, p. 61–108. *In* J. C. F. Tedrow [ed.] *Antarctic soils and soil forming processes*. Publ. 1418. National Academy of Sciences, Washington, D.C.
12. Bik, M. J. J. 1968. Morphological observations on prairie mounds. *Z. Geomorphol.* 12(4):409–469.
13. Bik, M. J. J. 1969. The origin and age of the prairie mounds of southern Alberta, Canada. *Biul. Peryglacj.* No. 19. p. 85–130.
14. Bird, J. B. 1967. *Physiography of Arctic Canada*. Johns Hopkins Press, Baltimore, Md. 336 p.
15. Birman, J. H. 1952. Pleistocene clastic dikes in weathered granite-gneiss, Rhode Island. *Am. J. Sci.* 250:721–734.
16. Black, R. F. 1963. Les coins de glace et le gel permanent dans le Nord de l'Alaska. *Ann. Geogr.* 72(391):17–271.
17. Black, R. F. 1964. Periglacial phenomena of Wisconsin, north central United States. VI Cong. Int. Assoc. Q. Res. 4:21–28.
18. Black, R. F. 1965. Ice-wedge casts of Wisconsin. *Wis. Acad. Sci. Arts Lett. Trans.* 54:187–222.
19. Black, R. F. 1965. Paleoclimatologic implications of ice-wedge casts of Wisconsin. *INQUA Ans. V., VII Congr. Boulder, Colorado*. p. 37. (Abstr.)
20. Black, R. F. 1969. Climatically significant fossil periglacial phenomena in north central United States. *Biul. Peryglacj.* 20:225–238.
21. Black, R. F. 1969. Geology, especially geomorphology of northern Alaska. *Arctic* 22:283–299.
22. Black, R. F. 1969. Thaw depressions and thaw lakes. *Biul. Peryglacj.* No. 19. p. 131–150.
23. Black, R. F. *Growth of patterned ground in Victoria Land, Antarctica*. This volume.
24. Blackwell, J. M. 1965. Surficial geology and geomorphology of the Harding Lake area, Big Delta Quadrangle, Alaska. M.S. thesis. University of Alaska, College. 91 p.
25. Borns, H. W., Jr. 1965. Late glacial ice-wedge casts in northern Nova Scotia, Canada. *Science* 148:1223–1225.
26. Brookes, I. A. 1971. Fossil ice wedge casts in western Newfoundland. *Marit. Sediments* 7(3):118–122.
27. Brown, J. 1965. Radiocarbon dating, Barrow, Alaska. *Arctic* 18:36–48.

28. Brown, J. 1965. Seasonal thaw and ground-ice morphology in tundra soils, Barrow, Alaska. *Agron. Abstr.* p. 59.
29. Brown, J. 1966. Massive underground ice in northern regions. U.S. Army Conf. Proc. 1:89-102.
30. Brown, J. 1967. An estimation of the volume of ground ice, coastal plain, northern Alaska. Tech. Note. U.S. Army Cold Regions Research Engineering Laboratory, Hanover, New Hampshire. 22 p.
31. Brown, J. 1967. Seasonal thaw chronology, Barrow, Alaska. Tech. Note. U.S. Army Cold Regions Research Engineering Laboratory, Hanover, New Hampshire. 4 p.
32. Brown, J. 1967. Tundra soils formed over ice wedges, northern Alaska. *Soil Sci. Soc. Am. Proc.* 31:686-691.
33. Brown, J. 1969. Buried soils associated with permafrost, p. 115-127. *In* Pedology and Quaternary research symposium. University of Alberta Press, Edmonton.
34. Brown, J. 1969. Ionic concentration gradients in permafrost, Barrow, Alaska. Res. Rep. 272. U.S. Army Cold Regions Research Engineering Laboratory, Hanover, New Hampshire. 25 p.
35. Brown, J. 1969. Soils of the Okpilak River region, Alaska, p. 93-128. *In* T. L. Péwé [ed.] The periglacial environment, past and present. INQUA, 7th Cong., Alaska, 1965. McGill-Queens University Press, Montreal.
36. Brown, J. 1969. Soil properties developed on the complex tundra relief of northern Alaska. *Biul. Peryglacj.* No. 18. p. 153-167.
37. Brown, J., S. Gray, and R. Allan. 1969. Evolution à la fin du Quaternaire d'un remblai de vallée a Fairbanks, Alaska, I: La géochimie et la stratigraphie du pergélisol. INQUA Congr., 8th, Résumé des Commun. p. 270. (Abstr.)
38. Brown, J., S. Gray, and W. Webster. 1967. Chemical and related properties of a permafrost section from Fairbanks, Alaska. Tech. Note. U.S. Army CRREL. 18 p.
39. Brown, J., and P. L. Johnson. 1965. Pedoecological investigations, Barrow, Alaska. Tech. Rep. 159. U.S. Army CRREL. 32 p.
40. Brown, J., and P. V. Sellmann. 1966. Radiocarbon dating of coastal peat, Barrow, Alaska. *Science* 153:299-300.
41. Brown, R. J. E. 1964. Permafrost investigations on the Mackenzie Highway and Mackenzie District. Tech. Paper 175. National Research Council of Canada, Division of Building Research, Ottawa. 27 p.
42. Brown, R. J. E. 1965. Distribution of permafrost in the discontinuous zone of Western Canada. National Research Council Assoc. Comm. on Soil and Snow Mechanics. Tech. Mem. 86. p. 1-14.
43. Brown, R. J. E. 1965. Permafrost investigations in Saskatchewan and Manitoba. Tech. Paper 193. National Research Council of Canada, Division of Building Research, Ottawa. 47 p.
44. Brown, R. J. E. 1967. Permafrost in Canada. Map NRC 9769. National Research Council of Canada, Division of Building Research, Ottawa, and Geological Survey of Canada Map 1246A.
45. Brown, R. J. E. 1967. Permafrost investigations in British Columbia and Yukon Territory. Tech. Paper 253. National Research Council of Canada, Division of Building Research, Ottawa. 43 p.
46. Brown, R. J. E. 1968. Permafrost investigations in northern Ontario and eastern Manitoba. Tech. Paper 291. National Research Council of Canada, Division of Building Research, Ottawa. 46 p.
47. Brown, R. J. E. 1968. Permafrost map of Canada. *Can. Geogr. J.* 76(2):56-63.
48. Brown, R. J. E. 1969. Factors influencing discontinuous permafrost in Canada, p. 11-53. *In* T. L. Péwé [ed.] The periglacial environment, past and present. INQUA, 7th Congr., Alaska, 1965. McGill-Queens University Press, Montreal.
49. Brown, R. J. E. 1970. Permafrost as an ecological factor in the Subarctic, p. 129-140. *In* Ecology of subarctic regions. UNESCO, Paris.
50. Brown, R. J. E. 1970. Permafrost in Canada--Its influence on northern development. University of Toronto Press, Toronto, Ontario. 234 p.
51. Brown, R. J. E. 1971. Characteristics of the active layer in the permafrost region of Canada. NRC Assoc. Committee on Geotech. Res. Tech. Mem. 103. p. 1-7.
52. Brown, R. J. E. 1972. Permafrost in the Canadian Arctic Archipelago. *Z. Geomorphol. Suppl.* 13:102-130.
53. Brown, R. J. E. Influence of climatic and terrain factors on ground temperatures at three locations in the permafrost region of Canada. This volume.
54. Brown, R. J. E. Permafrost investigations in Quebec and Newfoundland (Labrador). Tech. Paper. National Research Council of Canada, Division of Building Research, Ottawa. (In press)
55. Brown, R. J. E., and G. H. Johnston. 1964. Permafrost and related engineering problems. *Endeavour* 23(89):66-72.
56. Brown, W. G., G. H. Johnston, and R. J. E. Brown. 1964. Comparison of observed and calculated ground temperatures with permafrost distribution under a northern lake. *Can. Geotech. J.* 1:147-154.
57. Brunnenschweiler, D. 1965. Altiplanation in Alaska. INQUA Abstr. VII Congr. Boulder, Colorado. p. 51.
58. Burns, J. J. 1964. Pingos in the Yukon-Kuskokwim Delta, Alaska: Their plant succession and use by mink. *Arctic* 17:203-210.
59. Cailleux, A. 1967. Actions du vent et du froid entre le Yukon et Anchorage, Alaska. *Geogr. Ann.* 49A(Z-4):145-154.
60. Cailleux, A. 1971. Lacs en ourson, cernes et thermokarst (Bear cub and marginate lakes and thermokarst). *Cahiers Géogr. Québec* 15(34):131-138.
61. Blake, W., Jr. 1972. Personal communication. Department of Energy, Mines and Resources, Geological Survey of Canada.
62. Clayton, L., and P. K. Bailey. 1970. Tundra polygons in the northern Great Plains. *Geol. Soc. Am. Abstr.* 2(6):382.
63. Corte, A. E. 1969. Geocryology and engineering. *In* D. J. Varnes and G. Kiersch [ed.] Reviews in engineering geology. *Geol. Soc. Am.* 2:119-185.
64. Crampton, C. B., and N. W. Rutter. A geoecological terrain analysis of discontinuously frozen ground in the upper Mackenzie valley, Canada. This volume.
65. Day, J. H. 1964. Characteristics of soils of the Hazen camp area, northern Ellesmere Island, N.W.T. Rep. D Phys. R (G) Hazen. Defence Research Board, Department of National Defence, Canada. 15 p.
66. Day, J. H., and H. M. Rice. 1964. The characteristics of some permafrost soils in the Mackenzie Valley, N.W.T. *Arctic* No. 4. p. 222-236.
67. Demek, J. 1968. Summary of the occurrence of cryoplanation terraces. *Zpr. Geogr. Ustavu Csav.* No. 1. p. 10-27.
68. Denny, C. S. 1936. Periglacial phenomena in southern Connecticut. *Am. J. Sci.* 32:322-342.
69. Dingman, S. L. Relations among vegetation, permafrost, and potential insolation in central Alaska. *J. Arctic Alp. Res.* (In press)
70. Dionne, J. C. 1967. Formes de cryoturbation fossiles dans le sud-est du Québec. *Geogr. Bull.* 9(4):13-24.
71. Dionne, J. C. 1969. Nouvelles observations de fentes de gel fossiles sur la coté sud du Saint-Laurent. *Rev. Géogr. Montréal* 23(3):307-316.
72. Dionne, J. C. 1970. Fentes en coin fossile dans la région de Québec. *Rev. Géogr. Montréal* 24(3):313-318.
73. Dionne, J. C. 1971. Fentes de cryoturbation tardiglaciaires

- dans la région de Québec. *Rev. Géogr. Montréal* 25(3):245-264.
74. Drew, J. V., and R. E. Shanks. 1965. Landscape relationships of soils and vegetation in the forest-tundra ecotone, upper Firth River Valley, Alaska-Canada. *Ecol. Monogr.* 35:285-306.
 75. Drewe, J. G. 1969. Design and construction problems at the Clinton Mine of Cassiar Asbestos Corporation Limited. *Proc. Third Can. Conf. Permafrost. NRC Assoc. Committee on Geotech. Res. Tech. Mem.* 96. p. 71-78.
 76. Eakin, H. M. 1916. The Yukon-Koyukuk region, Alaska. *U.S. Geol. Surv. Bull.* 631. 88 p.
 77. Espley, G. H. 1969. Experience with permafrost in gold mining. *Proc. Third Can. Conf. Permafrost. NRC Assoc. Committee on Geotech. Res. Tech. Mem.* 96. p. 59-64.
 78. Everctt, K. R. 1966. Slope movement and related phenomena, p. 175-220. *In* N. J. Wilimovsky and J. N. Wolfe [ed.] *Environment of the Cape Thompson region, Alaska*. U.S. Atomic Energy Commission, Washington, D.C.
 79. Fernald, A. T. 1964. Surficial geology of the central Kobuk River Valley, northwestern Alaska. *U.S. Geol. Surv. Bull.* 1181-k. 31 p.
 80. Ferrians, O. J. 1965. Permafrost map of Alaska. *U.S. Geol. Surv. Misc. Geol. Inv. Map* 1-445.
 81. Ferrians, O. J., R. Kachadoorian, and G. W. Greene. 1969. Permafrost and related engineering problems in Alaska. *U.S. Geol. Surv. Prof. Paper* 678. 37 p.
 82. Feulner, A. J., and J. R. Williams. 1967. Development of a groundwater supply at Cape Lisburne, Alaska, by modification of the thermal regime of permafrost. *U.S. Geol. Surv. Prof. Paper* 575-B. p. 199-202.
 83. Flemal, R. C. 1972. Ice injection origin of the Dekalb Mounds, north-central Illinois, United States. *Proc. Int. Geol. Congr. Sect. 12.* p. 130-135.
 84. Flemal, R. C., K. Hinkley, and J. L. Hessler. 1969. Fossil pingo field in north-central Illinois. *Geol. Soc. Am. Abstr. Pt. 6.* p. 16.
 85. Foster, H. L. 1967. Geology of the Mount Fairplay area, Alaska. *U.S. Geol. Surv. Bull.* 1241-B. 18 p.
 86. Foster, H. L. 1969. Reconnaissance geology of the Eagle A-1 and A-2 quadrangles, Alaska. *U.S. Geol. Surv. Bull.* 1271-G. 30 p.
 87. Foster, H. L., and G. W. Holmes. 1965. A large transitional rock glacier in the Johnson River area, Alaska Range. *U.S. Geol. Surv. Prof. Paper* 525-B. p. B112-B116.
 88. Foster, H. L., and T. F. C. Keith. 1969. Geology along the Taylor Highway, Alaska. *U.S. Geol. Surv. Bull.* 1281. 36 p.
 89. French, H. M. 1970. Soil temperatures in the active layer, Beaufort Plain. *Arctic* 23(4):229-239.
 90. French, H. M. 1971. Ice cored mounds and patterned ground, southern Banks Island, western Canadian Arctic. *Geogr. Ann. Ser. A.* 53(1):32-38.
 91. French, H. M. 1971. Slope asymmetry of the Beaufort Plain, Northwest Banks Island, N.W.T., Canada. *Can. J. Earth Sci.* 8(7):717-731.
 92. French, H. M., and P. Egginton. Thermokarst processes and land forms of north and east central Banks Island in the Canadian Arctic Archipelago. This volume.
 93. Fyles, J. G., J. A. Heginbottom, and V. N. Rampton. 1972. Quaternary geology and geomorphology, Mackenzie Delta to Hudson Bay. *Guidebook 24th Session, Int. Geol. Congr., Field Excursion A30.* 23 p.
 94. Giddings, J. L., Jr. 1967. *Ancient men of the Arctic*. Knopf, New York. 391 p.
 95. Gill, D. Permafrost table microtopography in the Mackenzie River Delta, Northwest Territories, Canada. This volume.
 96. Gold, L. W., and A. H. Lachenbruch. Thermal conditions in permafrost. This volume.
 97. Granberg, H. B. Indirect mapping of the snow cover for permafrost prediction at Schefferville, Quebec, Canada. This volume.
 98. Guthrie, R. D., and J. V. Matthews, Jr. 1971. The Cape Deccit fauna—Early Pleistocene mammalian assemblage from the Alaskan Arctic. *Quaternary Res.* 1(4):474-510.
 99. Hamelin, L. E., and A. Cailleux. 1969. Les palscs dans le bassin de la Grande-Rivière de la Balcine. *Rev. Géogr. Montréal* 23(3): 329-337.
 100. Hamelin, L. E., and F. A. Cook. 1967. *Illustrated glossary of periglacial phenomena*. University of Quebec Press, Laval. 237 p.
 101. Hansen, B. L., and C. C. Langway, Jr. 1966. Deep core drilling in ice core analysis at Camp Century, Greenland, 1961-1966. *Antarct. J. U.S.* 1(5):207-208.
 102. Heginbottom, J. A. 1970. Erosion in a permafrost environment district of Mackenzie. *Geol. Surv. Can. Project* 690054. p. 85.
 103. Heginbottom, J. A. 1971. Some effects of a forest fire on the permafrost active layer at Inuvik, N.W.T. *NRC Assoc. Committee on Geotech. Res. Tech. Mem.* 103. p. 31-36.
 104. Heginbottom, J. A. Some effects of surface disturbance on the permafrost active layer at Inuvik, N.W.T., Canada. This volume.
 105. Hodgson, D. A. 1972. Surficial geology and geomorphology of central Ellesmere Island. *Geol. Surv. Can. Paper* 73-1. (Report of Activities, April to October)
 106. Holmes, G. W. 1959. Glacial geology of the Mt. Michelson B-2 quadrangle, Alaska, p. 47-60. *In* preliminary report of the Mt. Chamberlain-Barter Island Project, Alaska. *U.S. Geol. Surv. open-file Rep.*
 107. Holmes, G. W., D. M. Hopkins, and H. L. Foster. 1968. Pingos in central Alaska. *U.S. Geol. Surv. Bull.* 1241-H. 40 p.
 108. Hopkins, D. M. The paleogeography and climatic history of Beringia during late Cenozoic time. *Internord No. 12.* (In press)
 109. Hopkins, D. M., T. N. V. Karlstrom, *et al.* 1955. Permafrost and groundwater in Alaska. *U.S. Geol. Surv. Prof. Paper* 264-F. p. 113-145.
 110. Hopkins, D. M., F. S. MacNeil, and E. B. Leopold. 1960. The coastal plain at Nome, Alaska; a late Cenozoic type section for the Bering Strait region. *Int. Geol. Congr. 21st, Copenhagen, Proc. Pt. 4.* p. 46-57.
 111. Hopkins, D. M., and T. Einarsson. 1966. Pleistocene glaciation on St. George, Pribilof Islands. *Science* 152:343-345.
 112. Horberg, L. 1948. A possible fossil ice wedge in Bureau County, Illinois. *Ill. State Geol. Surv.* p. 132-136.
 113. Howitt, F. 1971. Permafrost geology at Prudhoe Bay. *World Pet. p.* 28.
 114. Howitt, F., and M. W. Clegg. 1970. Permafrost in the Prudhoe Bay field: Geology and physical characteristics. *Am. Assoc. Pet. Geol. Bull.* 54(12):2487. (Abstr.)
 115. Hughes, O. L. 1969. Distribution of open-system pingos in central Yukon territory with respect to glacial limits. *Geol. Surv. Can. Paper* 69-34. 8 p.
 116. Hughes, O. L., V. N. Rampton, and N. W. Rutter. 1972. Quaternary geology and geomorphology, southern and central Yukon (northern Canada). *Field excursion A11, 24th Sess. Int. Geol. Congr. (Guidebook)*
 117. Hussey, K. M., and R. W. Michelson. 1966. Tundra relief features near Point Barrow, Alaska. *Arctic* 19:162-184.
 118. Ives, J. D. 1971. Permafrost occurrence in the Front Range, Colorado Rocky Mountains, U.S.A. *J. Glaciol.* 10(58):105-111.
 119. Ives, J. D. 1973. Permafrost. *In* Arctic and alpine environments. Methuen Press, London.
 120. Ives, J. D. Permafrost and its relationship to other environmental parameters in a mid-latitude high-altitude setting, Front Range, Colorado Rocky Mountains. This volume.

121. Jahn, A. 1966. Alaska. Panstwowe Wydawnictwo Naukowe, Warsaw. 498 p.
122. Jahn, A. 1972. Tundra polygons in the Mackenzie Delta area. Hans Poser Festschrift, Gottinger Geogr. Abhandlung 60:285-293.
123. Jeffrey, W. W. 1967. Forest types along lower Liard River, Northwest Territories. Dept. of Forestry Canada. Publ. 1035. 103 p.
124. Jessop, A. M. 1970. How to beat permafrost problems. Oil-week January: 12.
125. Johnston, G. H., and R. J. E. Brown. 1964. Some observations on permafrost distribution at a lake in the Mackenzie Delta, N.W.T., Canada. *Arctic* 17:162-175.
126. Johnston, G. H., and R. J. E. Brown. 1966. Occurrence of permafrost at an arctic lake. *Nature* 211(505):952-953.
127. Johnston, G. H., R. J. E. Brown, and D. N. Pickersgill. 1963. Permafrost investigations at Thompson, Manitoba: Terrain studies. Tech. Paper 158. National Research Council of Canada, Division of Building Research. 55 p.
128. Journaux, M. A. 1969. Phénomènes périglaciaires dans le Nord de l'Alaska et du Yukon. *Geogr. Assoc. Fr. Bull.* 368-369. p. 337-350.
129. Judge, A. S. Deep permafrost observations in the Canadian North. This volume.
130. Judge, A. S. The prediction of permafrost thickness. *Can. Geotech. J.* (In press)
131. Kerfoot, D. E., and J. R. Mackay. 1972. Geomorphological process studies, Garry Island, N.W.T., p. 115-130. *In* Mackenzie Delta area Monograph. Brock University, St. Catharines, Ontario.
132. Kilgour, R. J. 1969. Mining experience with permafrost. Proc. Third Can. Conf. Permafrost, NRC Assoc. Committee on Geotech. Res. Tech. Mem. 96. p. 65-70.
133. Kirby, A. V. T. 1965. Boulder fields on Bald Eagle Mountain. *Ann. Assoc. Am. Geogr.* 55:626. (Abstr.)
134. Knight, G. R. 1971. Ice wedge cracking and related effects on buried pipelines, p. 384-395. *In* J. R. Burdick [ed.] Proceedings, Symposium on Cold Regions Engineering. University of Alaska, College.
135. Knollenberg, R. 1964. The distribution of stringbogs in central Canada in relation to climate. Tech. Rep. No. 14. University of Wisconsin, Department of Meteorology, Madison. 44 p.
136. Krinsley, D. B. 1965. Birch Creek pingo, Alaska. *U.S. Geol. Surv. Prof. Paper* 525-C. p. C113-C136.
137. Lachenbruch, A. H. 1968. Permafrost, p. 833-839. *In* R. W. Fairbridge [ed.] *The encyclopedia of geomorphology*. Reinhold, New York.
138. Lachenbruch, A. H. 1970. Some estimates of the thermal effects of a heated pipeline in permafrost. *U.S. Geol. Surv. Circ.* 632. 23 p.
139. Lachenbruch, A. H. 1970. Thermal considerations in permafrost, p. J1-J5. *In* W. L. Adkison, and M. M. Brosgé [ed.] Proceedings of the seminar on the North Slope of Alaska. American Association of Petroleum Geologists, Los Angeles.
140. Lachenbruch, A. H., G. W. Greene, and B. V. Marshall. 1966. Permafrost and the geothermal regimes, 149-163. *In* N. J. Wilimovsky [ed.] *Environment of the Cape Thompson region*. Alaska. U.S. Atomic Energy Commission, Oak Ridge, Tennessee.
141. Lachenbruch, A. H., and B. V. Marshall. 1969. Heat flow in the Arctic. *Arctic* 22(3):300-311.
142. Lagarec, D. Postglacial permafrost features in eastern Canada. This volume.
143. Langway, C. C., Jr. 1967. Stratigraphic analysis of a deep ice core from Greenland. *U.S. Army CRREL. Res. Dept.* 77. 132 p.
144. Lewellen, R. I. The occurrence and characteristics of nearshore permafrost. This volume.
145. Lewellen, R., and J. Brown. 1970. Man induced erosion on permafrost, p. 333-334. *In* Science in Alaska. Proc. 20th Alaska Sci. Conf., College, 1969.
146. Lindsay, J. D., and W. Odynsky. 1965. Permafrost in organic soils of northern Alberta. *Can. J. Soil Sci.* 45:265-269.
147. Linell, K. A., and G. H. Johnston. Principles of engineering design and construction in permafrost regions. This volume.
148. Lissey, A. 1970. Description of field work prepared for Inland Waters Branch, Canada. Annual Publication of Field Activities.
149. Lotspeich, F. B., E. W. Mueller, and P. J. Frey. 1969. Some chemical and biological properties of a pingo lake in east central Alaska. Federal Water Quality Admin., Department of the Interior, Alaska Water Lab., College, Alaska. No. 1. 12 p.
150. Lourenco, J. S., and S. H. Ward. 1970. Permafrost. NASA Tech. Dep. Contract NAS 2-5078. Item 291. 30 p.
151. Lowdon, J. A., J. G. Fyles, and W. Blake, Jr. 1967. Geological Survey of Canada radiocarbon dates VI, Radiocarbon 9:156-197.
152. Mackay, J. R. 1963. The Mackenzie River Delta area, N.W.T. Canada Dep. Mines and Tech. Surv. Geogr. Branch. Mem. 8. 202 p.
153. Mackay, J. R. 1966. Pingos in Canada, p. 71-76. *In* Permafrost: Proceedings of an international conference. National Academy of Sciences, Washington, D.C.
154. Mackay, J. R. 1968. Discussion of the theory of pingo formation by water expulsion in a region affected by subsidence. *J. Glaciol.* 7:346-357.
155. Mackay, J. R. 1970. Disturbances to the tundra and forest tundra environment of the western Arctic. *Can. Geotech. J.* 7:420-432.
156. Mackay, J. R. 1971. The origin of massive icy beds in permafrost, western arctic coast, Canada. *Can. J. Earth Sci.* 8(4):397-422.
157. Mackay, J. R. 1972. Offshore permafrost—Southern Beaufort Sea. University of British Columbia, Vancouver. 8 p.
158. Mackay, J. R. 1972. Some observations on ice-wedges, Garry Island, N.W.T., p. 131-139. *In* D. E. Kerfoot [ed.] Mackenzie Delta area monograph. 22nd Internat. Geogr. Congr. Brock University, St. Catharines, Ontario.
159. Mackay, J. R. 1972. The world of underground ice. *Ann. Assoc. Am. Geogr.* 62(1):1-22.
160. Mackay, J. R. The growth of pingos, western arctic coast, Canada. *Can. J. Earth Sci.* (In press)
161. Mackay, J. R., and R. F. Black, Origin, composition, and structure of perennially frozen ground and ground ice. This volume.
162. Mackay, J. R., W. H. Mathews, and R. S. MacNeish. 1961. Geology of the Engigstciak archeological site, Yukon Territory. *Arctic* 14:25-52.
163. Mackay, J. R., V. N. Rampton, and J. G. Fyles. 1972. Relic Pleistocene permafrost, western Arctic, Canada. *Science* 176:1321-1323.
164. Mackay, J. R., and J. K. Stager. 1966. The structure of some pingos in the Mackenzie Delta area, N.W.T. *Geogr. Bull.* 8(4):360-368.
165. Mathews, W. H. 1963. Quaternary stratigraphy and geomorphology of the Fort St. Johns area, northeastern British Columbia. *British Columbia Mines Petroleum Resources*.
166. McCulloch, D. S. 1967. Quaternary geology of the Alaskan shore of Chukchi Sea, p. 91-120. *In* D. M. Hopkins [ed.] *The Bering land bridge*. Stanford University Press, Stanford.
167. McCulloch, D. S., and D. M. Hopkins. 1966. Evidence for an early recent warm interval in northwest Alaska. *Geol. Soc. Am. Bull.* 77:1089-1108.
168. McCulloch, D. S., J. S. Taylor, and R. Meyer. 1965. Stratigraphy, non-marine mollusks, and radiometric dates from Quaternary

- deposits in the Kotzebue Sound area, western Alaska. *J. Geol.* 73:442-453.
169. Moran, J. M. 1972. An analysis of periglacial climatic indicators of late glacial time in North America. Ph.D. thesis. University of Wisconsin, Madison.
170. Morgan, A. V. 1969. Intraformational periglacial structures in the Nose Hill Gravels and Sands, Calgary, Alberta, Canada. *J. Geol.* 77(3):358-364.
171. Morgan, A. V. 1972. Late Wisconsin ice-wedge polygons near Kitchener, Ontario, Canada. *Can. J. Earth Sci.* 9(6):607-617.
172. Muller, F. 1963. Englacial temperature measurements on Axel Heiberg Island, Canadian Arctic Archipelago. I.A.S.H. Publ. No. 61. Commission of Snow and Ice. p. 168-180.
173. Muller, S. W. 1943. Permafrost or permanently frozen ground and related engineering problems. U.S. Geol. Surv. Rep. Strategic Eng. Study No. 62.
174. National Research Council. 1966. Permafrost: Proceedings of an international conference. Publ. No. 1287. National Academy of Sciences, Washington, D.C. 563 p.
175. Newcomb, R. C. 1952. Origin of the Mima Mounds, Thurston County region, Washington. *J. Geol.* 60:461-472.
176. Nicholson, F. H., and H. B. Granberg. Permafrost and snow-cover relationships near Schefferville, Quebec. This volume.
177. Nicholson, F. H., and B. G. Thom. Studies at the Timmins 4 permafrost experimental site, Schefferville, Quebec. This volume.
178. Ogilvie, R. T., and B. Baptie. 1967. A permafrost profile in the Rocky Mountains of Alberta. *Can. J. Earth Sci.* 4:744-745.
179. O'Sullivan, J. B. 1966. Geochemistry of permafrost, Barrow, Alaska. p. 20-27. *In* Permafrost: Proceedings of an international conference. National Academy of Sciences, Washington, D.C.
180. Outcalt, S. I., and J. B. Benedict. 1965. Photo-interpretation of two types of rock glacier in the Colorado Front Range, U.S.A. *J. Glaciol.* 5:849-856.
181. Paterson, W. S. B. 1968. A temperature profile through the Meighen ice cap, Arctic Canada. *Int. Assoc. Sci. Hydrol. Bull.* 79. p. 440-449.
182. Peters, T., and B. White. 1971. Personal communication.
183. Péwé, T. L. 1948. Origin of the Mima Mounds. *Sci. Mon.* 66:293-296.
184. Péwé, T. L. 1952. Geomorphology of the Fairbanks area. Ph.D. thesis. Stanford University, Stanford. 220 p.
185. Péwé, T. L. 1965. Delta River area, Alaska Range, p. 55-93. *In* T. L. Péwé, O. J. Ferrians, Jr., D. R. Nichols, and T. N. V. Karlstrom [ed.] INQUA field Conference F, Central and south central Alaska. Guidebook. Nebraska Academy of Sciences, Lincoln.
186. Péwé, T. L. 1965. Fairbanks area, p. 6-36. *In* T. L. Péwé, O. J. Ferrians, Jr., D. R. Nichols, and T. N. V. Karlstrom [ed.] INQUA field Conference F, Central and south central Alaska. Guidebook. Nebraska Academy of Sciences, Lincoln.
187. Péwé, T. L. 1965. Middle Tanana River Valley, p. 36-54. *In* T. L. Péwé, O. J. Ferrians, Jr., D. R. Nichols, and T. N. V. Karlstrom [ed.] INQUA field Conference F, Central and south central Alaska. Guidebook. Nebraska Academy of Sciences, Lincoln.
188. Péwé, T. L. 1966. Paleoclimatic significance of fossil ice wedges. *Biul. Peryglacj.* No. 15. p. 65-72.
189. Péwé, T. L. 1966. Permafrost and its effect on life in the north. Oregon State University Press, Corvallis. 40 p.
190. Péwé, T. L. 1969. Terrasses d'altiplanation du Quaternaire ancien et moyen, Fairbanks, Alaska. INQUA Congr., 8th. p. 41. (Abstr.)
191. Péwé, T. L. [ed.]. 1969. The periglacial environment: past and present. McGill-Queens University Press, Montreal. 487 p.
192. Péwé, T. L. 1970. Altiplanation terraces of early Quaternary age near Fairbanks, Alaska. *Acta Geogr. Lodz.* No. 24. p. 357-363.
193. Péwé, T. L. 1970. Permafrost and vegetation on flood-plains of sub-arctic rivers (Alaska), a summary, p. 141-142. *In* Ecology of the subarctic regions. UNESCO
194. Péwé, T. L. Geomorphic processes in polar deserts. University of Arizona, Phoenix. (In press)
195. Péwé, T. L. Permafrost. *In* Encyclopaedia britannica. (In press)
196. Péwé, T. L. Permafrost. *Geopedia.* (In press)
197. Péwé, T. L. Quaternary geology of Alaska. U.S. Geol. Surv. Prof. Paper. (In press)
198. Péwé, T. L., and J. W. Bell. Geology of the Fairbanks D-2 southwest quadrangle, Alaska. U.S. Geol. Surv. Misc. Map. (In press)
199. Péwé, T. L., R. E. Church, and M. F. Andreson. 1969. Origin and paleoclimatic significance of large scale polygons in the Donnelly Dome area, Alaska. *Geol. Soc. Am. Spec. Paper* 109. 87 p.
200. Péwé, T. L., O. J. Ferrians, Jr., D. R. Nichols, and T.N.V. Karlstrom [ed.] 1965. INQUA field conference F, Central and south-central Alaska. Guidebook. Nebraska Academy of Sciences, Lincoln. 141 p.
201. Péwé, T. L., and G. W. Holmes, 1964. Geology of the Mt. Hayes D-4 quadrangle, Alaska. U.S. Geol. Surv. Misc. Geol. Inv. Map I-394. Scale 1:63 360.
202. Péwé, T. L., and R. D. Reger. 1972. Modern and Wisconsinan snowlines in Alaska. *Proc. Int. Geol. Congr. Sect. 12.* p. 187-197.
203. Péwé, T. L., and P. V. Sellmann. 1971. Geochemistry of permafrost and Quaternary stratigraphy. *Geol. Soc. Am.* 3(7):669. (Abstr.)
204. Péwé, T. L., and P. V. Sellmann. Geochemistry of permafrost and Quaternary stratigraphy. This volume.
205. Philberth, K., and B. Federer. 1971. On the temperature profile and the age profile in the central part of cold ice sheets. *J. Glaciol.* 10(58):3-14.
206. Pissart, A. 1965-1966. Etude de quelques pentes de l'île Prince Patrick. *Ann. Soc. Géol. Belg.* 89:377-402.
207. Pissart, A. 1967. Les pingos de l'île Prince Patrick (70°N-120°W). *Geogr. Bull.* 9(3):189-217.
208. Pissart, A. 1967. Polygones de tundra de l'île Prince Patrick (Arctique Canadien 76° lat. N.), p. 151-163. *In* J. Sporek [ed.] Mélange de géographie physique, humaine, économique, appliquée, affects à M. Omer Tulippe. Vol. I.
209. Pissart, A. 1968. Les polygones de fente de gel de l'île Prince Patrick (Arctique Canadien-76° lat. N.). *Biul. Peryglacj.* No. 17. p. 171-180.
210. Porter, S. C. 1966. Geology of the Anaktuvuk Pass, central Brooks Range, Alaska. *Arctic Inst. N. Am. Tech. Paper* 18. 100 p.
211. Potter, N., Jr., and J. H. Moss. 1968. Origin of the Blue Rocks block field deposits, Berk County, Pennsylvania. *Bull. Geol. Soc. Am.* 79:255-262.
212. Prest, V. K. 1969. Wisconsin and recent ice in North America. *Geol. Surv. Can. Map* 1257. Scale 1:5 000 000.
213. Price, L. W. 1969. The collapse of solifluction lobes as a factor in vegetating blockfields. *Arctic* 22(4):395-402.
214. Price, L. W. 1970. Morphology and ecology of solifluction lobe development—Ruby Range, Yukon Territory. Ph.D. thesis. University of Illinois, Urbana. 325 p.
215. Price, L. W. 1971. Vegetation, microtopography, and depth of active layer on different exposures in subarctic alpine tundra. *Ecology* 52(4):638-647.
216. Price, L. W. 1972. The periglacial environment permafrost, and man: Resource Paper No. 14, Commission on College Geography, Association of American Geographers. 88 p.

217. Price, L. W. Rates of mass wasting in a subarctic alpine tundra environment. This volume.
218. Price, W. A. 1963. The oriented lakes of arctic Alaska: A discussion. *J. Geol.* 71:530-531.
219. Price, W. A. 1968. Oriented lakes. *Earth Sci. Encycl.* 3:784-796.
220. Railton, J. B. 1968. The ecology of palsa bogs. M.S. thesis. University of Toronto, Toronto, Ontario, 89 p.
221. Rapp, A., and L. Annersten. 1969. Permafrost and tundra polygons in northern Sweden, p. 65-91. *In* T. L. Péwé [ed.] The periglacial environment—Past and present. McGill University Press, Montreal.
222. Raup, H. M. 1971. The vegetational relations of weathering, frost action, and patterned ground processes in the Mesters Vig. District, northeast Greenland. *Medd. Grønland* 194(1):92.
223. Reimnitz, E., S. C. Wolf, and C. A. Rodeick. 1972. Preliminary interpretation of seismic profiles in the Prudhoe Bay area, Beaufort Sea, Alaska. U.S. Geol. Surv. Open-file Rep.
224. Retzer, J. L. 1965. Present soil-forming factors and processes in arctic and alpine regions. *Soil Sci.* 99(1):38-44.
225. Ritchie, A. M. 1953. The erosional origin of the mima mounds of southwest Washington. *J. Geol.* 61:41-50.
226. Robin, G. de Q. 1972. Polar ice sheets: A review. *Polar Rec.* No. 100, p. 5-22.
227. Rouse, W. R., and K. A. Kershaw. 1971. The effects of burning on the heat and water regimes of lichen-dominated subarctic surfaces. *J. Arctic Alp. Res.* 3(4):291-304.
228. Ruhe, R. V. 1969. Quaternary landscapes in Iowa. Iowa State University Press, Ames, 255 p.
229. St. Onge, D. A. 1965. La géomorphologie de l'île Ellef Ringnes, Territoires de Nord-Ouest, Canada. Canada Dep. Mines Tech. Surv. Geogr. Branch Paper No. 38, 46 p.
230. St. Onge, D. A. 1965. Nivation landforms. *Geol. Surv. Can. Paper* 69030, 12 p.
231. Samson, L., and F. Jordon. 1969. Experience with engineering site investigations in northern Quebec and northern Baffin Island. *Proc. Third Can. Conf. Permafrost.* NRC Assoc. Committee on Geotech. Res. Tech. Mem. 96, p. 21-38.
232. Schafer, J. P. 1949. Some periglacial features in Central Montana. *J. Geol.* 57:154-174.
233. Schenk, E. 1966. Origin of string bogs, p. 155-159. *In* Permafrost: Proceedings of an international conference. National Academy of Sciences, Washington, D.C.
234. Sellmann, P. V. 1967. Geology of the USA CRREL permafrost tunnel, Fairbanks, Alaska. U.S. Army CRREL Tech. Rep. 199, 33 p.
235. Sellmann, P. V. 1968. Geochemistry and ground ice structures: An aid in interpreting a Pleistocene section, Alaska. *Geol. Soc. Am. Spec. Paper* 101, p. 197-198. (Abstr.)
236. Sellmann, P. V. 1972. Additional information on the geology and properties of materials exposed in the U.S.A. CRREL permafrost tunnel. U.S. Army CRREL Spec. Rep. 16 p.
237. Sellmann, P. V., and J. Brown. Stratigraphy and diagenesis of perennally frozen sediments in the Barrow, Alaska region. This volume.
238. Sellmann, P. V., J. Brown, and R. I. Lewellen. 1964. Near-surface lithology of the Barrow, Alaska area. A preliminary report. Alaskan science conference, 14th Proc. p. 231-232.
239. Sellmann, P. V., J. Brown, and R. A. M. Schmidt. 1965. Late-Pleistocene stratigraphy, Barrow, Alaska. *INQUA Int. Congr.* 8th Abstr. Vol. p. 419-420.
240. Sevon, W. D. 1967. The Bowmanstown boulder field, Carbon County, Pennsylvania. *Proc. Penn. Acad. Sci.* 40(2):90-94.
241. Sevon, W. D. 1969. Sedimentology of some Mississippian and Pleistocene deposits of northeastern Pennsylvania, p. 214-234. *In* S. Subitzky [ed.] Geology of selected areas in New Jersey and eastern Pennsylvania and guidebook of excursions. Rutgers State University of New Jersey Press, New Brunswick.
242. Shearer, J. M. 1972. Beaufort Sea, east of Mackenzie Bay, submarine pingo-like features. *Ice No.* 38, p. 6.
243. Shearer, J. M., R. F. MacNab, B. R. Pelletier, and T. B. Smith. 1971. Submarine pingos in the Beaufort Sea. *Science* 174: 816-818.
244. Sigafos, R. S., and D. M. Hopkins. 1952. Soil instability on slopes in regions of perennally-frozen ground (Alaska). *Highw. Res. Board Spec. Rep.* 2, p. 176-192.
245. Simpson, S. J. 1971. The York factory area, Hudson Bay. Ph.D. dissertation. University of Manitoba.
246. Stearns, S. R. 1966. Permafrost. U.S. Army CRREL Pt. 1, Sect. A2, 77 p.
247. Stoneley, R. 1970. Discussion p. J2-J3. *In* W. L. Adkinson and M. M. Brosgé [ed.] Proceedings of the seminar on the North Slope of Alaska. American Association of Petroleum Geologists, Los Angeles.
248. Sykes, D. J. 1971. Effects of fire and fire control on soil and water relations in northern forests—A preliminary review. Proceedings, Fire in the northern environment—A symposium. College (Fairbanks), Alaska, p. 37-44.
249. Taber, S. 1943. Perennally frozen ground in Alaska; its origin and history. *Geol. Soc. Am. Bull.* 54:1433-1548.
250. Tedrow, J. C. F. 1966. Polar desert soils. *Soil Sci. Soc. Am. Proc.* 30(3):381-387.
251. Tedrow, J. C. F. 1969. Thaw lakes, thaw sinks and soils in northern Alaska. *Bull. Peryglaciol.* No. 20, p. 337-344.
252. Tedrow, J. C. F., and L. A. Douglas. 1964. Soil investigations on Banks Island. *Soil Sci.* 98(1):53-65.
253. Thom, B. G. 1969. New permafrost investigations near Scheferville, P.Q. *Rev. Géogr. Montreal* 23(3):317-327.
254. Thom, B. G. 1969. Permafrost in the Knob Lake iron mining region. *Proc. Third Can. Conf. Permafrost.* NRC Assoc. Committee on Geotech. Res. Tech. Mem. 96, p. 9-20.
255. Thom, B. G. 1972. The role of spring thaw in stringbog genesis. *Arctic* 25(3):236-239.
256. Totten, S. M. 1972. Glacial geology of Richland County, Ohio. *Ohio Geol. Surv. Bull.*
257. Vernon, P., and O. L. Hughes. 1966. Surficial geology, Dawson, Larsen Creek and Nash Creek map-areas, Yukon Territory. *Geol. Surv. Can. Bull.* No. 136.
258. Viereck, L. A. 1965. Relationship of white spruce to lenses of perennally frozen ground, Mount McKinley National Park, Alaska. *Arctic* 18(4):262-267.
259. Viereck, L. A. 1970. Forest succession and soil development adjacent to the Chena River in interior Alaska. *J. Arctic. Alp. Res.* 2(1):1-26.
260. Viereck, L. A. 1970. Soil temperatures in river bottom stands in interior Alaska, p. 223. *In* Ecology of the subarctic regions. UNESCO, Paris.
261. Viereck, L. A. Ecological effects of river flooding and forest fires on permafrost in the taiga on Alaska. This volume.
262. Wahrhaftig, C. 1958. Quaternary geology of the Nenana River valley and adjacent parts of the Alaska Range, p. 1-68. *In* C. Wahrhaftig and R. F. Black [ed.] Quaternary and engineering geology in the central part of the Alaska Range. U.S. Geol. Surv. Prof. Paper 293.
263. Wahrhaftig, C. 1965. Physiographic divisions of Alaska. U.S. Geol. Surv. Prof. Paper 482, 52 p.
264. Washburn, A. L. 1967. Instrumental observations of mass wasting in the Mesters Vig. district, northeast Greenland. *Medd. Grønland* 166(4):296.
265. Washburn, A. L. 1969. Patterned ground in the Mesters Vig. district, northeast Greenland. *Biul. Peryglacj.* No. 18, p. 259-330.

266. Washburn, A. L. 1969. Weathering, frost action, and patterned ground in the Mesters Vig. district, northeast Greenland. *Medd. Grønland* (4):303.
267. Washburn, A. L. 1970. Instrumental observations of mass-wasting in an Arctic climate. *Z. Geomorphol. Suppl.* 9:102-118.
268. Washburn, A. L. 1972. *Periglacial processes and environments*. Edward Arnold Ltd., London.
269. Watanabe, O. 1969. Eikyū-tōdosō no'kōri ni tsuite [On the structure of ground ice in the U.S.A. CRREL permafrost tunnel, Fairbanks, Alaska] . *Seppyō* 31(3):53-62. (in Japanese)
270. Watmore, T. G. 1969. Thermal erosion problems in pipelining. *Proc. Third Can. Conf. on Permafrost. NRC Assoc. Committee on Geotech. Res. Tech. Mem.* 96. p. 142-162.
271. Wayne, W. J. 1965. Great Lakes-Ohio River Valley-Day 4. *Guidebook G, VIIth INQUA Congr.* p. 29-36.
272. Wayne, W. J. 1967. Periglacial features and climatic gradient in Illinois, Indiana, and Western Ohio, east-central United States. *In* F. J. Cushing and H. E. Wright [ed.] *Quaternary paleoecology*. Yale University Press, Hartford, Connecticut. 433 p.
273. Weidick A. 1968. Permafrost map of Greenland. *Medd. Grønland* 165(6):73.
274. Westgate, J. A., and L. A. Bayrock. 1964. Periglacial structures in the Saskatchewan gravels and sands of central Alberta, Canada. *J. Geol.* 72(5):641-648.
275. White, S. E. 1971. Debris falls at the front of Arapaho rock glacier, Colorado Front Range, U.S.A. *Geogr. Ann.* 53A(2):86-91.
276. White, S. E. 1971. Rock glacier studies in the Colorado Front Range, 1961 to 1968. *J. Arctic Alp. Res.* 3(2):43-64.
277. Williams, G. P. 1966. Some micrometeorological observations over *Sphagnum* moss. *Proc. Eleventh Muskeg Res. Conf. Assoc. Committee on Geotech. Res. Natl. Res. Council Tech. Memo.* 87. p. 82-91.
278. Williams, J. R. 1970. Ground water in the permafrost regions of Alaska. *U.S. Geol. Surv. Prof. Paper* 696. 83 p.
279. Williams, J. R., and R. O. van Everdingen. *Groundwater investigations in permafrost regions of North America. This volume.*
280. Williams, P. J. 1966. Downslope soil movement at a sub-arctic location with regard to variations with depth. *Can. Geotech. J.* 3(4):191-203.
281. Williams, P. J. 1968. Ice distribution in permafrost profiles. *Can. J. Earth Sci.* 5(12):1381-1386.
282. Wolfe, P. E. 1953. Periglacial frost-thaw in New Jersey. *J. Geol.* 61:113-141.
283. Zoltai, S. C. 1971. Southern limit of permafrost features in peat landforms, Manitoba and Saskatchewan. *Geol. Assoc. Can. Spec. Paper No. 9.* p. 305-310.
284. Zoltai, S. C., and C. Tarnocai. 1971. Properties of a wooded palsa in northern Manitoba. *J. Arctic Alp. Res.* 3(2):115-119.

A GEOECOLOGICAL TERRAIN ANALYSIS OF DISCONTINUOUSLY FROZEN GROUND IN THE UPPER MACKENZIE RIVER VALLEY, CANADA [1]

C. B. Crampton

DEPARTMENT OF THE ENVIRONMENT
Edmonton, Alberta

N. W. Rutter

GEOLOGICAL SURVEY OF CANADA
Calgary, Alberta

INTRODUCTION

The imminent possibility of oil and gas pipeline construction along the Mackenzie River valley, Northwest Territories, Canada, an area of over 350 000 km², necessitated a reconnaissance terrain survey in two field seasons (6 months) to provide areal knowledge of geology and terrain, bearing particularly in mind the needs of government for terrain information in connection with land use planning, pipeline proposals, and other aspects of petroleum development and engineering construction. The objectives, therefore, were to map, describe, and explain the unconsolidated deposits, landforms, permafrost, ground ice, and organic cover. The upper Mackenzie River lies within the discontinuous permafrost zone¹ and so is of particular interest in that adjoining frozen and unfrozen terrain offer special construction and maintenance problems. It became apparent early in the program that a rapid method of predicting the ground ice and permafrost characteristics of the terrain from aerial photographs with a minimum amount of ground checking would be necessary. Quaternary geologists and a landscape ecologist,² each sufficiently acquainted with the other's specialty, worked together to solve the problems. The success of this cooperative study warrants the use of this approach in

other regions. The objective here is to give examples of various terrain conditions and how their permafrost characteristics, including ground ice, can be identified from aerial photographs.

The examples cited are within 60°–63°N and 118°–124°W (Figures 1 and 2). The area discussed includes broad uplands and low areas covered by thick morainal deposits that consist mostly of till forming typical morphological features. Glacial lacustrine sediments are also widespread, as are sand dunes. In the western reaches of the area, the Mackenzie Mountains are present with their associated valley deposits of glacial outwash, lacustrine sediments, and till and post-glacial alluvial terraces, fans, and colluvium. However, the landscape patterns vary in the two areas due to the distribution of permafrost, influenced by latitude and elevation that largely controls the variety and abundance of certain flora.

METHOD

Ground investigations were made by geologists and a landscape ecologist. Only about 150 spot investigations per map sheet could be made (12 000 km²) due to time and economics. The geologists identified and described the varieties of surficial deposits associated with certain land forms. Deposit thicknesses, the depth to permafrost where present, and the abundance of ground ice in certain deposits were determined also. The landscape ecologist identified the flora assemblage associated with certain geomorphic, hydrologic, and thermal conditions. Combining the information of the two disciplines, it was then possible to identify similar ground conditions by aerial photo interpretation of landscapes.

Example 1

Figure 3 illustrates alluvial fans and terraces that are typical of the major mountain valleys in the western part of the area. The alluvial fans are identified by their cone shape and relatively flat sloping surface of about 1–8°. In the stereo-pair, they overlie or have eroded the preexisting alluvial terrace that is only partially preserved. The fans consist of mostly coarse, poorly sorted, highly permeable gravels that

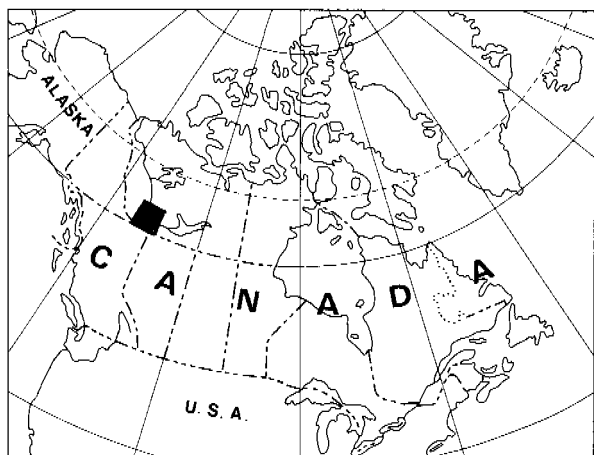


FIGURE 1 Index map of study area.

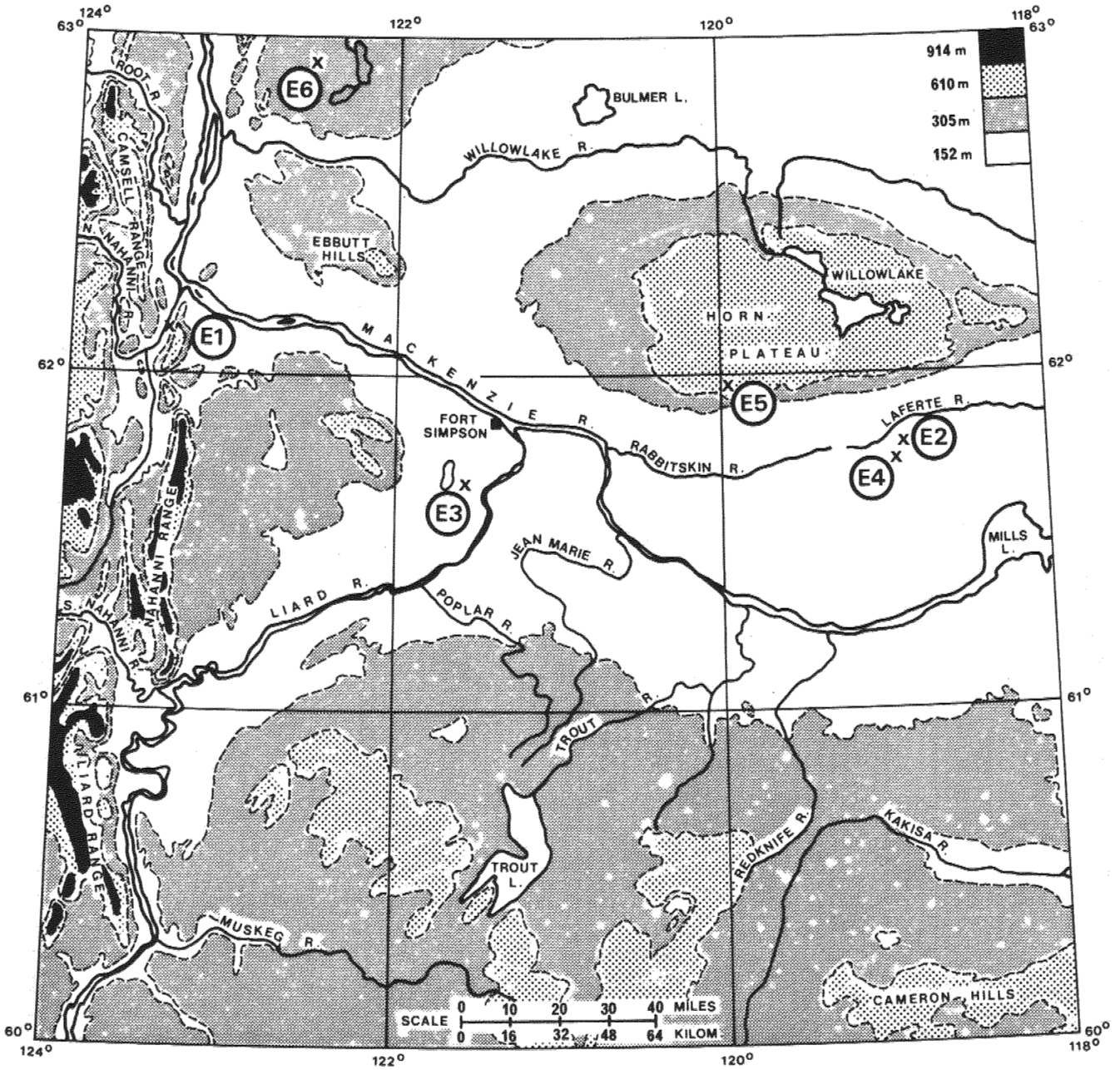


FIGURE 2 Area of study in the upper Mackenzie River valley in the discontinuous permafrost zone with location of example sites.

vary in thickness from 1 to 10 m. The alluvial terrace, on the order of 10 m thick, is composed of gravels, sand, and silt. The permeable gravels, the freely drained position of the terrace, and the shape of the fans inhibit bog development. These facts coupled with the climate of this area result in no permafrost. Similarly, freely drained sites that do not support permafrost or, at most, permafrost at 2 m or deeper include glaciofluvial sands and gravels and eolian deposits at these latitudes.

These freely drained sites possess some of the best and most dense forest stands in the area—mostly white spruce [*Picea glauca* (Moench) Voss], which sometimes grows to about 30 m, except locally, where the driest, sandiest sites (such as dunes and fans) support jack pine (*Pinus banksiana* Lamb). Therefore, the presence of high dense forest is a useful indicator of permafrost-free or deep-seated permafrost terrain that form the best construction sites.

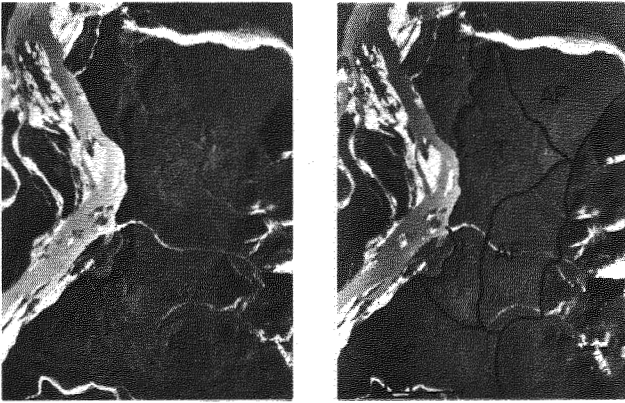


FIGURE 3 Stereopair of forested, permafrost-free alluvial fans (AF), floodplain (FP), and terraces (T). (Parts of aerial photographs A17624-52, 53; Dept. Energy, Mines and Resources: © Canadian Gov't.)

Example 2

In broad areas of relatively low elevation (300 m) in the west central area, lacustrine silts, clays and till, composed of < 5 percent pebble-sized material with a silty, clayey matrix, are common. The stereopair (Figure 4) illustrates an area underlain by a thin veneer of lacustrine silt and clay (< 1.5 m) over till. The relatively flat surface, impermeable material, and deranged surface drainage result in bog formation.

Flat lands are generally seasonally water logged; this is indicated on aerial photographs by dark tones produced by a *Sphagnum*-sedge vegetation with scattered trees and local

stands up to 15.3 m high comprised mostly black spruce [*Picea mariana* (Mill.) BSP.] and some tamarack larch [*Larix laricina* (Du Roi) (K. Koch)]. Reticulate bogs, some enclosing pools and some vegetated (Figure 4), are often present. Although the permafrost table locally occurs near the land surface, it is generally at about 2 m depth or greater, and most problems associated with construction are similar to problems encountered by engineers in wetlands in permafrost-free areas to the south.

Example 3

Figure 5 shows typical parallel to subparallel dune ridges found in the central part of the area. The dunes vary from about 2 to 5 m in height and consist of fine to medium sand. No permafrost is present, and ground ice is absent. However, between the dunes—where the drainage is deranged and where fine-grained material, mostly silt, has accumulated—peat bogs have formed; there, raised, permafrost, and ground ice occur 0.5 m below the surface.

Dune ridges support the forest stands of jackpine already described as characteristic of dry sites. Water-logged *Sphagnum*-sedge depressions and raised peat with permafrost at shallow depth occur seasonally between the dunes. The associated vegetation is described in example 4.

Example 4

Figure 6 illustrates an area of continuous permafrost in the same type of terrain as described for Figure 4. Here, however, the peat bogs have developed further, are now raised, and are more than 2.5 m thick. This results in permafrost

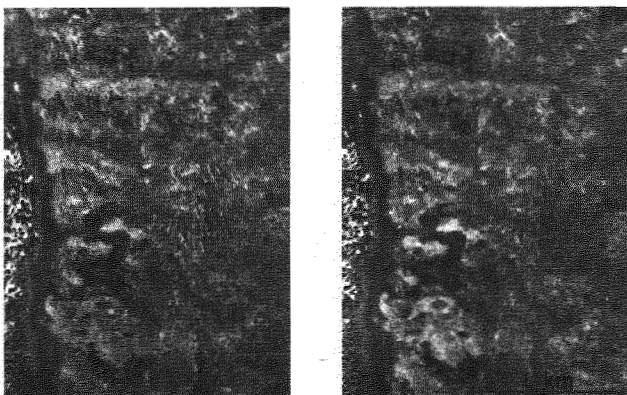


FIGURE 4 Stereopair of permafrost-free, reticulate bogs on areas of relatively low elevation consisting of lacustrine silts and clay. (Parts of aerial photographs A11378-22, 23; Dept. of Energy, Mines and Resources: © Canadian Gov't.)

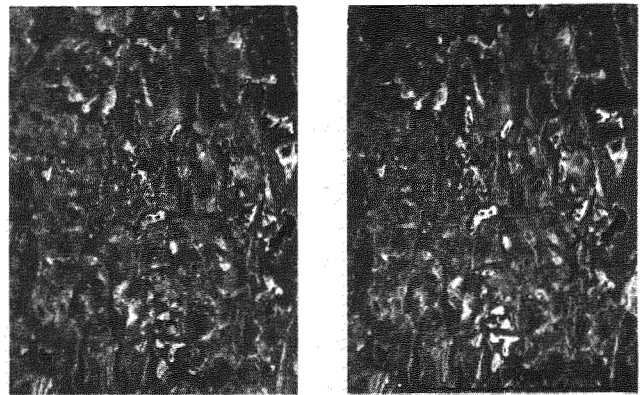


FIGURE 5 Stereopair of tree, permafrost-free, parallel to subparallel sand dunes. Between the dunes are seasonally water-logged peatland though local areas of terrazoid pattern that indicate small areas of raised peat with permafrost near the surface. (Parts of aerial photographs A11028-336, 337; Dept. of Energy, Mines and Resources: © Canadian Gov't.)

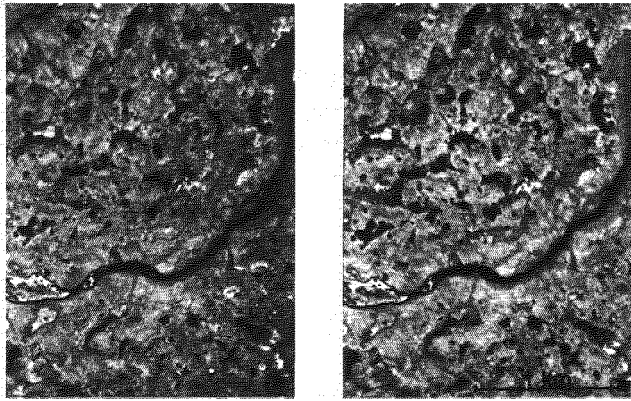


FIGURE 6 Stereopair of raised peat plateau with permafrost near the surface (0.5 m) on broad areas of relatively low elevation consisting of lacustrine silts and clay. (Parts of aerial photographs A11378-22, 23; Dept. of Energy, Mines and Resources: © Gov't. of Canada.)

about 0.5 m from the surface, with a high percentage of ground ice present. Between raised bogs are pools that may indicate discontinuities in the permafrost layer.

Associated with seasonally water-logged lands, especially over silty lacustrine deposits and noticeably scarce where morainal (or lacustrine) deposits are gravelly, these frozen peat plateaus are associated with a patchy distribution of lichen [mostly *Cladonia alpestris* (L.) Rubenh.] and Labrador tea (*Ledum groenlandicum* Oeder) on raised peat and a sphagnaceous vegetation around the pools, thus giving rise to the typical terrazoid appearance of the landscape. Stunted black spruce up to almost 8 m high are scattered across the landscape. The close juxtaposition of terrain with and without permafrost complicates construction problems.

Examples 5 and 6

Figure 7 illustrates the geomorphology of the summit area of the Horn Plateau, a prominent feature in the northern part of the study area. The plateau is composed of Cretaceous shale and sandstone capped by till that is generally over 2 m thick. The surface morphology consists of low relief subdued hummocks and ridges that form a dendritic and deranged drainage system. Permafrost and segregated ice are common in the upper part of the deposit and can be attributed to the till that contains only about 5 percent material coarser than about 4 mm, to the matrix that consists principally of silt and clay, to the elevation of the plateau greater than 700 m (the high latitude of the area), and to the insulating effect of the vegetation cover.

Figure 8 illustrates typical low angle slopes generally less than 5° that form broad uplands in the northern part of the area and the flanks of the Horn Plateau. The example illustrated is formed in Cretaceous shale modified by glacial



FIGURE 7 Stereopair of a part of the summit area of the Horn Plateau. Subdued hummocks and ridges of till underlie a polygoid network of peat with widely scattered stunted black spruce with near-surface permafrost. (Parts of aerial photographs A11342-34, 35; Dept. of Energy, Mines and Resources: © Canadian Gov't.)

activity, capped by a relatively flat cover of till not unlike that described above--although, in this case, it has been modified by a limited amount of mass wasting. The dendritic drainage pattern with small-scale ridges and mounds is a result of vegetation characteristics.

Peat polygons, or a terrain pattern approximating a polygoid network, characterizes the flatter parts (Figure 7). The vegetation is rich with lichen, giving a high albedo and, thus, suggesting that permafrost is situated at a very shallow depth. The summer thaw is minimal in this landscape; it is most pronounced in the gullies that define the polygonal pattern, where a sphagnaceous vegetation gives darker tones on aerial photographs. Slopes display a subparallel drainage pattern in the peat (up to 1 m thick) that is richly lichenous

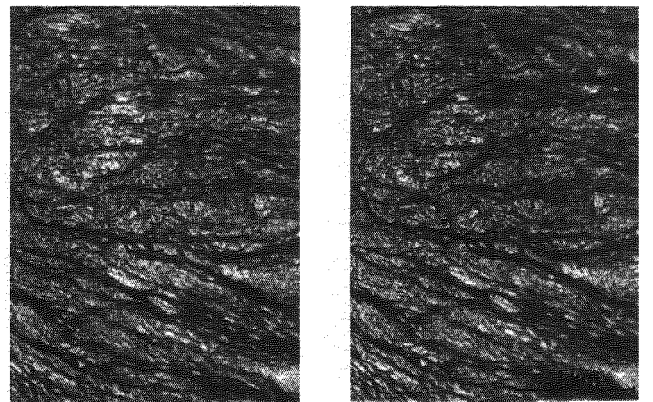


FIGURE 8 Stereopair of typical low angle slopes that are underlain by till and overlain by peat with widely scattered stunted black spruce and near-surface permafrost. (Parts of aerial photographs A17430-93, 94; Dept. of Energy, Mines and Resources: © Canadian Gov't.)

where the terrain is raised between the sphagnaceous runnels (Figure 8). Widely scattered stunted black spruce taiga characterizes both the slope and flat areas.

Permafrost causes problems for the engineer, especially where there are slopes, even the most gentle. Stripping the insulative vegetative and organic mat causes rapid thawing of the permafrost and land subsidence, and subsequent erosion can cause deep gulying. Fortunately, this terrain normally characterizes high land in the area of potential construction sites.

CONCLUSIONS

The primary aim of this study has been the rapid identification by using aerial photographs of terrain types in terms of surficial geology, microrelief, and vegetation, which is significant regarding permafrost conditions. High forest is indicative of freely drained sites, such as alluvial terraces, fans, and glaciofluvial deposits, and sand dunes, which offer the best construction sites (examples 1 and 3). Relatively featureless flats on aerial photographs, though often with local reticulate bogs, are indicative of seasonally water-logged lands on lacustrine or till deposits that present the engineer with problems typical of permafrost-free areas to the south (example 2). However, where the terrazoid pattern can be seen on aerial photographs, raised peat with near-surface

permafrost and ground ice is intricately associated with pools, often without permafrost. These patterns are characteristic of lacustrine and till deposits that contain ground ice (example 4). On uplands, with characteristic till morphology, a deranged drainage pattern on flats, especially a subparallel drainage pattern on slopes delineated by lichen on raised parts and *Sphagnum* in drainage runnels, is indicative of a shallow permafrost table and ground ice (examples 5 and 6). These areas are best avoided for most construction purposes. The examples cited are only a few of the terrain-permafrost relationships that can be identified from aerial photographs in this area.

REFERENCES

1. Brown, R. J. E. 1969. Permafrost in Canada. Geol. Surv. Can. Map 1246A. Publication NRC 9769. Division of Building Research, National Research Council of Canada, Ottawa.
2. Rowe, J. S. 1971. Why classify forest land? *Forest. Chron.* 47: 144-148.

NOTE

[1] The data for this report were obtained as a result of investigations carried out under the Environmental-Social Program, Northern Pipelines, of the Task Force on Northern Oil Development, Government of Canada.

A SPATIAL CORRELATION BETWEEN PLANT DISTRIBUTION AND UNFROZEN GROUND WITHIN A REGION OF DISCONTINUOUS PERMAFROST [1]

Don Gill

UNIVERSITY OF ALBERTA
Edmonton, Alberta

INTRODUCTION

The existence of unfrozen ground in the Mackenzie Delta has previously been recognized, but investigators have referred only to through taliks beneath water bodies. Mackay,⁷ for example, points out that, where the depth of a channel or lake exceeds the thickness of winter ice, the subjacent sediments remain unfrozen because of the thermal influence of the unfrozen pools. Because the majority of lakes and channels are sufficiently deep to prevent freezing to the

bottom and because up to 50 percent of the delta surface may be covered by water, it follows that much of the subaqueous portion of the Mackenzie Delta is underlain by unfrozen ground. Recently, Gill⁶ has shown that certain terrestrial sections of this 6 500 km² delta are also underlain by unfrozen ground. It is of interest that a Soviet worker also has given a boundary that places the delta within the discontinuous permafrost zone: Baranov¹ states that the northern boundary of "almost continuous" permafrost runs from the middle of Kotzebue Bay to the Mackenzie River

mouth, which places the delta within the discontinuous zone.

This paper demonstrates that certain terrestrial locations in the Mackenzie Delta are underlain by taliks, and hypotheses are given for their existence. Second, there is a close areal relationship between the distribution of these taliks and the distribution of one discrete plant association; explanations are given for this unusual correlation.

STUDY AREA AND DURATION

This study took place in the northeast central portion of the Mackenzie Delta (Figure 1). Field work was carried out during the 1966-1967 field seasons and was supplemented by observations during the summers of 1971 and 1972; winter measurements were made during February 1967 and March 1972.

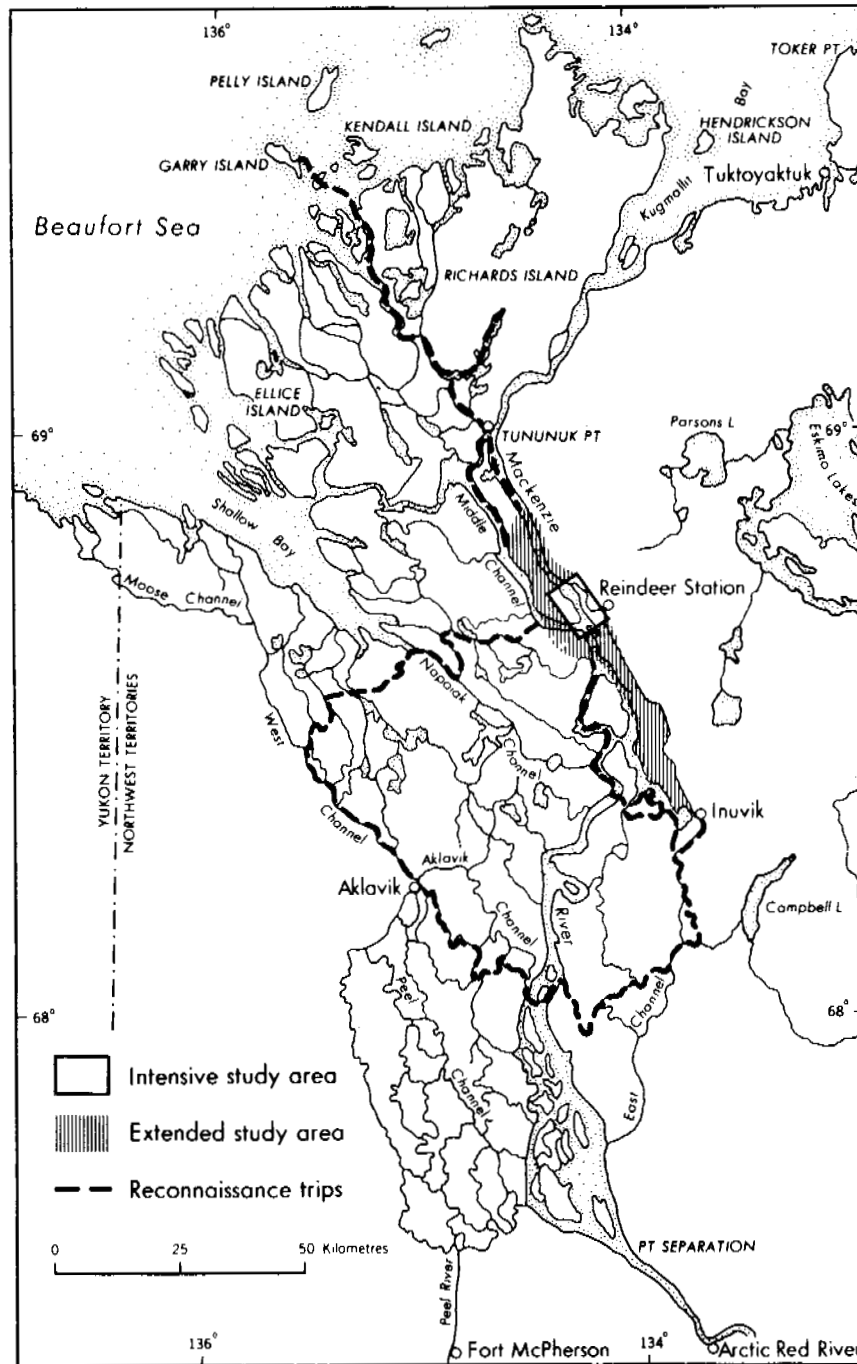


FIGURE 1 Map of study area.

PHYSICAL EVIDENCE

Discontinuous permafrost was first located beneath the *Salix-Equisetum* association shown in Figure 2. On 10 July 1966, frozen ground was encountered here at a depth of 86 cm; 3 days later, several 2-m-long dowels easily penetrated their full length without reaching permafrost. During the next 2 weeks, additional 2 m penetrations were made here and in other sites within *Salix-Equisetum* associations. On 5 August 1966, a soil pit was dug to a depth of 3 m in this location (it was impractical to go deeper because the water table was reached and the sides of the pit became unstable), and a dowel was forced downward an additional 2.5 m to give a total unfrozen depth of 5.5 m. A temperature profile was then recorded to a depth of 3.75 m; Figure 3 illustrates the results. The solid line indicates the measured soil temperature, while the broken line is an interpolated value. Since a dowel penetrated easily to a 5.5 m depth, it was assumed that ground temperatures did not reach freezing. Subsequent to this field work, a colleague working on the heat budget of permafrost at this location recorded a mean annual ground temperature of 0.7 °C at a depth of 20 m, thus verifying the existence of a talik.⁸

In 1967, the migrating lens of permafrost that bounds the channel side of the talik shown beneath the *Salix-Equisetum* association in Figure 2 was partially excavated (Figure 4) and surveyed. A temperature profile made from the soil surface through this lens (1.25 m channelward

from its edge) and downward to the 2.0-m depth indicated that the temperature of the lens was -0.8 °C at its coldest point (Figure 5). Beneath the frozen layer, the temperature increased to 0.5 °C and remained isothermal at this value for the remainder of measurable depth.

It was determined that the frozen ground channelward from the soil pit is a relatively thin lens: Probing horizontally beneath the permafrost from the soil pit showed that the ground was unfrozen for at least 3 m channelward (although the lens sloped downward; see Figure 2); by excavating a second pit through permafrost channelward of the *Salix-Equisetum* association, it was found that from 1.8 m below the ground surface the soil was not frozen; on 23 August 1967, the height of water in the pit (Figure 4) differed from that of the channel by 1 mm. On 31 August, shortly after the channel had risen some 45 cm, resurveyed levels were again similar in height (the channel was 2 mm higher than water in the pit). Thus, it is surmised that the water table level in the unfrozen ground is affected by the height of the channel; if the lens of permafrost between the bodies of water was very deep, the fluctuation response time should have been more retarded than it was (less than 1 day).

THE CREATION AND MAINTENANCE OF A TALIK

Several hypotheses are forwarded that attempt to explain why areas of unfrozen ground exist in the Mackenzie Delta. Among the youngest surfaces in the delta are incipient

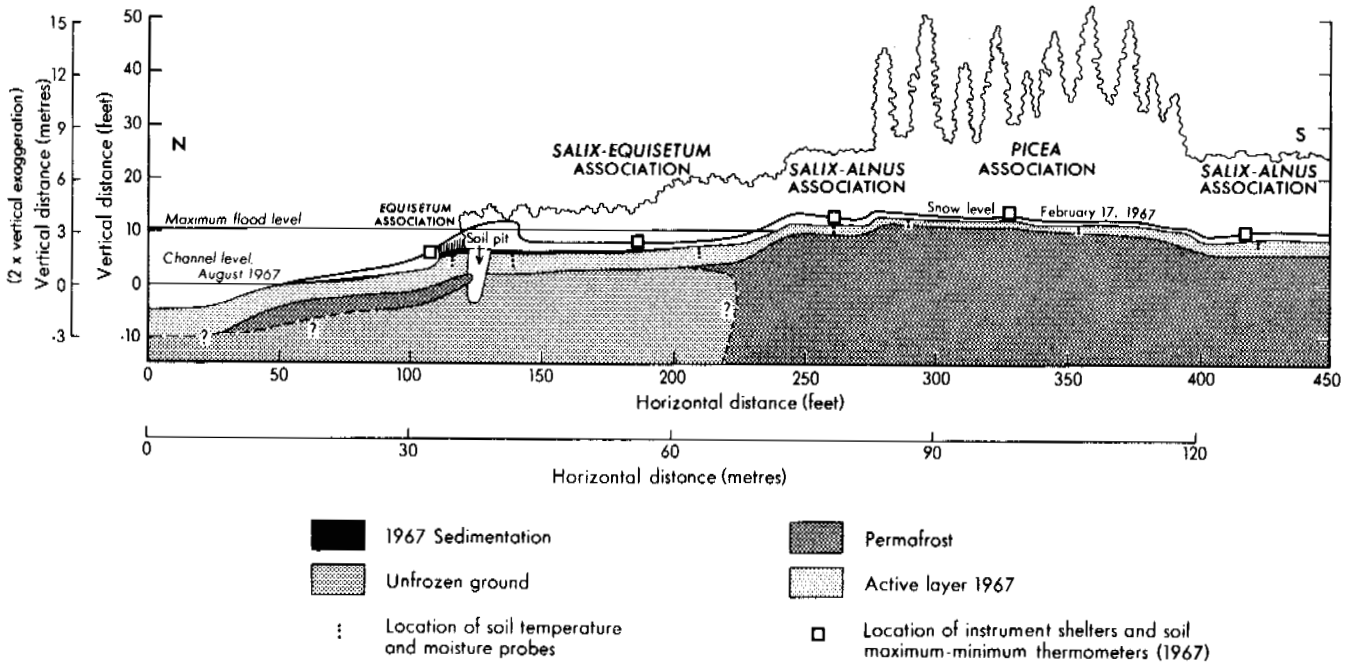


FIGURE 2 Successional associations and environmental conditions along an actively prograding channel in the Mackenzie Delta. Unfrozen ground underlies the *Salix-Equisetum* association.

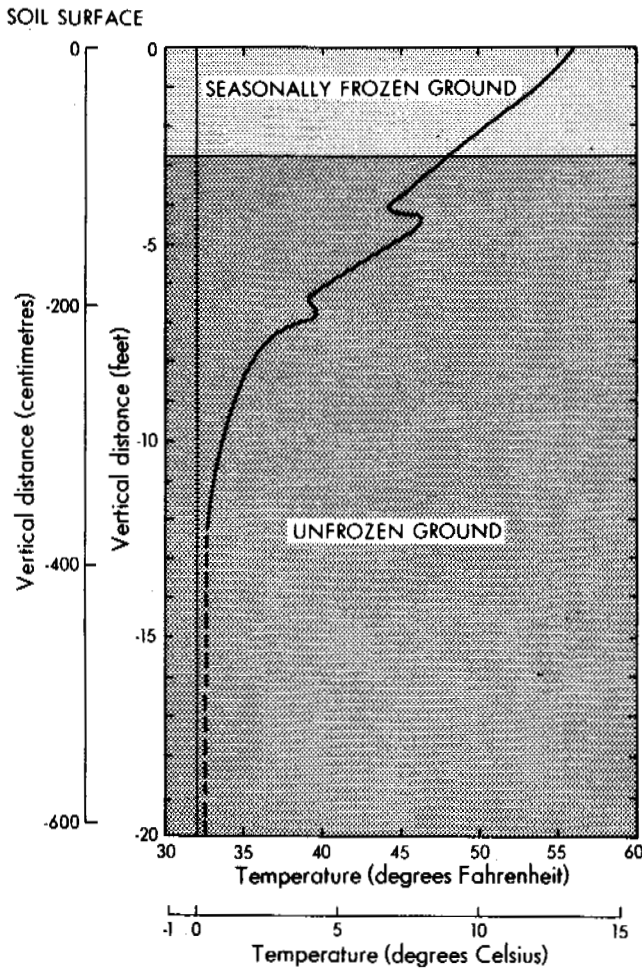


FIGURE 3 Vertical soil temperature profile in permafrost-free portion of *Salix-Equisetum* community, 5 August 1966.

levees that form on slipoff slopes along shifting channels; unfrozen zones are almost invariably found beneath these newly prograding sites. Recently deposited sediments along slipoff slopes thus occupy a thermal zone that was previously maintained by the now displaced channel at an above-freezing mean annual temperature. The distributary adjacent to the talik described above, for example, maintained a mean temperature of at least 3.5 °C during 1967 (calculating a constant water temperature during winter of 0 °C). If the position previously occupied by this channel, which is now replaced by unfrozen sediment, had been at a similar temperature, the return to a “normal” thermal condition would be very slow. Heat dissipation from a large volume of saturated sediments is further retarded by a contribution of latent heat during the phase change as permafrost slowly encroaches (Figure 2).

Smith⁸ found that the geothermal contribution of a distributary to the heat balance of adjacent sediments in the study area is approximately twice as great as the earth’s

geothermal gradient. Horizontal thermal flux from a channel with a mean annual temperature of 3.5 °C could thus be a considerable heat donor; it would certainly retard freezing of the talik.

The influence of snow is important in retarding heat loss. The insulatory properties of snow have long been recognized, particularly when it is light, dry, and free of packing or crusting. During February 1967, such snow conditions were present over most of the taliks; leafless willow stems permit an even throughfall of snow, yet have enough biomass to reduce wind drifting. Figure 2 indicates that snow thickness on one site ranged from 45 to 55 cm. In March 1971, the cover was deeper, with measurements between 55 and 70 cm. Along the channelward margin of this zone, drifts form

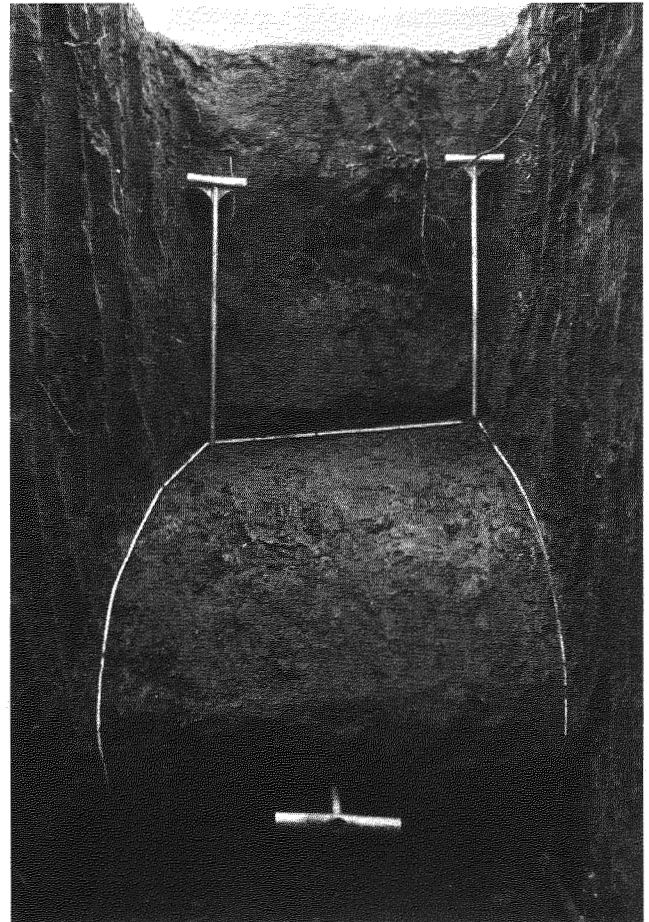


FIGURE 4 Inland edge of the 60-cm-thick lens of permafrost shown in Figure 2. Frozen sediment (1.1 m below ground level) is outlined by white rope. For scale, both metal probes extend 70 cm above the permafrost and are 70 cm apart. The probe below the lens has penetrated 1.5 m channelward, indicating that the ground is unfrozen beneath the permafrost. Note the standing water that fluctuates in stage, responding to changes in the level of the adjacent channel; 20 August 1967.

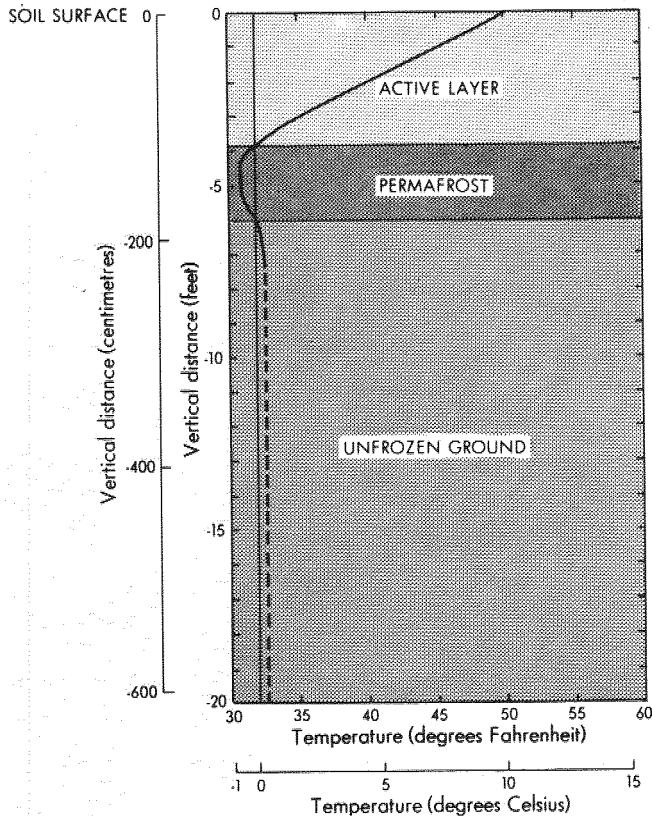


FIGURE 5 Vertical soil temperature profile through active layer and lens of permafrost, 20 August 1967.

at the leading edge of the willows; during 1967, the drift shown in Figure 2 averaged 117 cm in depth at its highest cross-sectional point (standard deviation 12 cm). In March 1971, similar measurements gave a depth of 126 cm with a standard deviation of 10 cm. These snowdrifts, which are a permanent winter feature, result from transport of snow from off an adjacent channel (snow depths on one channel section averaged 16 cm in February 1967 and 12 cm in March 1971). Contrasting types of snowcover, with extremes of depth and density, thus lie adjacent to one another. Although the drifts are compacted, their depth is sufficient that they too form an effective insulating cover: Figure 6 illustrates that on 16 February 1967 the surface of the drift shown in Figure 2 was at a temperature of -30°C , while at the snow-soil interface, it was -6.5°C . It is thus clear that the snowdrift considerably retards heat loss from the ground. Below the snow-soil interface, the remainder of the profile through the frozen and unfrozen ground is interpolated linearly from previous active layer depth measurements at this site. It is clear that the greatest temperature deflection from vertical is maintained within the drift, illustrating that compacted snow, if deep enough, will minimize the penetration of soil frost. The shallower but low-density snow that overlies the center of the talik is also an

effective insulator. Although mean daily air temperatures from 16 March through 24 March 1972 ranged from -18.5 to -27.5°C (mean daily temperature averaged over this 9-day period was -22.5°C), the temperature of the ground surface, measured 12 m inland from the drift beneath a 70-cm snowcover, was -2.5°C on 24 March.

It is doubtful that any one of the foregoing conditions singly prevents permafrost from being present under new slipoff slopes [2]; several factors probably combine to maintain these reservoirs of unfrozen ground.

FLORISTIC EVIDENCE OF UNFROZEN GROUND

Benninghoff³ maintains that commonly observed characteristics of vegetation provide neither straightforward nor universal indications of the frost characteristics of the soils beneath them. This and similar statements by other authors (cf. Brown⁴) generally hold, but there may be individual cases where certain environmental conditions affect both plant distribution and the occurrence (or lack) of perennially frozen ground. The two need not be directly linked; they may be coupled through one or more intermediaries. Such is the case in the Mackenzie Delta.

Environment of the Slipoff Slopes

New slipoff slopes that overlie taliks are at a low elevation; thus, they are influenced by a severe flood and sedimentation regime. Slipoff slopes are inundated up to 3 weeks; postflood drainage may not be complete until the third week of June. These sites receive greater volumes of sediment than any other location in the Mackenzie Delta. The rate of sedimentation on one such levee from 1955 to 1967 was 94 cm, with an average rate of 8 cm/year. In other sites, rates of alluviation are even greater. Deposition is accelerated along the leading edges of the *Salix-Equisetum* communities where thick bands of willows cause energy loss to overbank flow. During the 1967 flood period, up to 30 cm of alluvium was deposited along the outer boundary of willow stands (Figure 2); in 1972, as much as 42 cm was deposited.

Vegetation of the Slipoff Slopes

The only shrub that successfully colonizes young, rapidly alluviating slipoff slopes in the Mackenzie Delta is the felt-leaf willow (*Salix alaxensis*). It forms pure or nearly pure stands on virtually all such sites investigated in the study area (Figure 7). The more important reasons why this willow forms pure populations on slipoff slopes are that (a) *Salix alaxensis* is one of the least shade-tolerant willows, requiring sites such as new slipoff slopes that have no overstory; that (b) *Salix alaxensis* is phenologically well suited for colonizing these sites since it is one of the first willows to produce viable seeds in the spring. This species

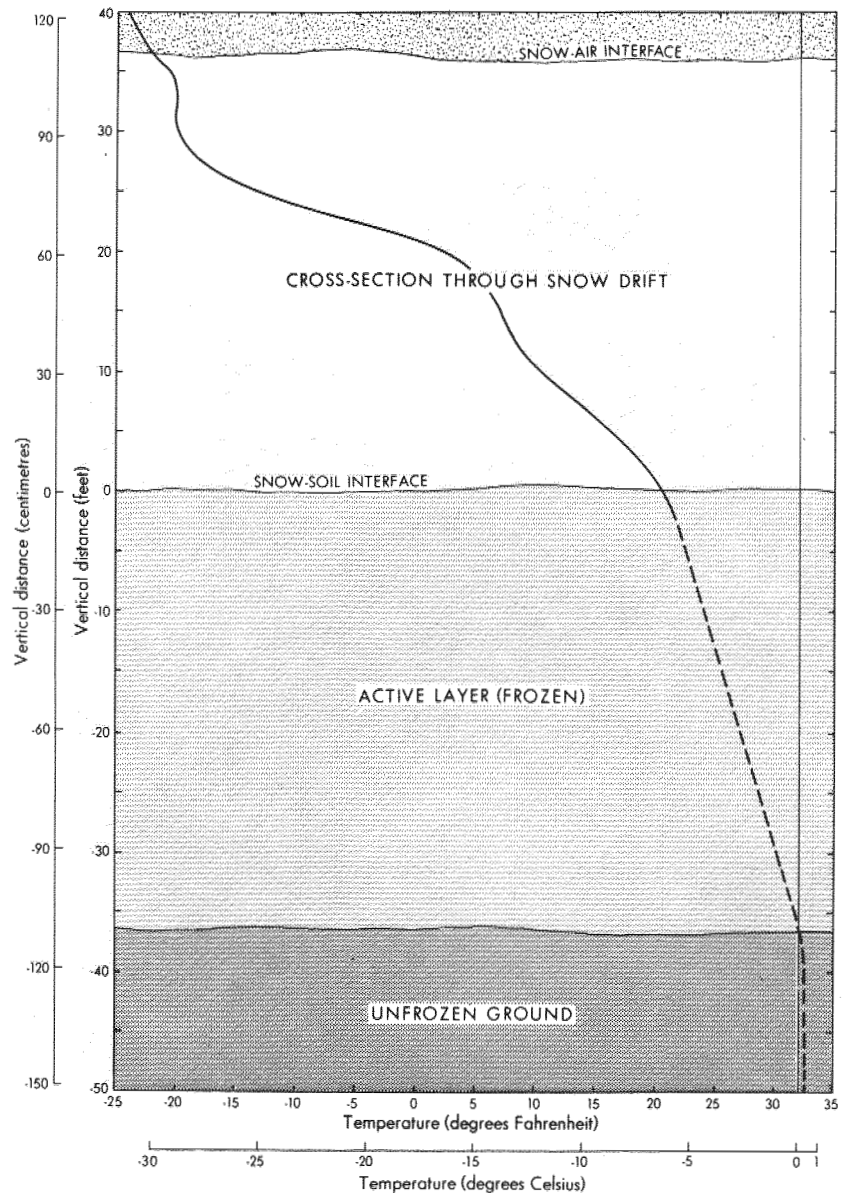


FIGURE 6 Vertical temperature profile through a snowdrift and frozen active layer in permafrost-free portion of a *Salix-Equisetum* community. Unbroken portion of temperature profile measured with a bridge and thermistor probe on 16 February 1967; broken section of profile interpolated from previous active layer measurements in this location.

flowers in early June, even while its roots remain frozen in the ground and the lower portion of its stem is submerged in floodwater. Fruit maturation occurs shortly after the receding floodwaters have deposited a new seed-bed, and the juxtaposition of these two factors aids its growth; and (c), most importantly, that this species of willow is particularly capable of developing adventitious roots (Figure 8), a necessary physiological adaptation for colonizing lower slipoff slopes.

Although the ground is not perennially frozen here, the thawing portion above the seasonally frozen ground temporarily functions as a normal active layer, affecting biotic development. During the critical period of summer growth, the thawed upper layer is relatively restricted; thus, the effective rooting zone remains as narrow as it would be if the

ground in these sites were perennially frozen. As sediment accumulates annually, the potential rooting zone migrates upward. A species unable to occupy the constantly elevating rooting area by growing new roots each year would perish.

The herb layer associated with the feltleaf willow is also largely dominated by one species, *Equisetum arvense*, the common or field horsetail, is nearly as significant in this community as *Salix alaxensis* (Figure 7). *Equisetum arvense* has a wide habitat tolerance in the Mackenzie Delta, but it especially favors the lower slipoff slopes. Similar to *Salix alaxensis*, an important reason why it is well adapted to this environment is its ability to withstand sedimentation. The perennating portions of the rhizomes of *E. arvense* are able to force their way through the overlying deposits to develop new stems. Moreover, this necessary growth is accomplished



FIGURE 7 A *Salix-Equisetum* association consistently occupies rapidly prograding slipoff slopes in the Mackenzie Delta. Taliks typically underlie this association. *Salix alaxensis* completely dominates the shrub canopy, while *Equisetum arvense* is the dominant plant of the herb layer. Grass in the foreground is *Arctagrostis latifolia*, which is occasionally present in this association.

during the critical period before newly exposed alluvium becomes too hard to penetrate. Most of the new alluvium deposited in this association begins to dry and compact after being exposed to the air for approximately 1 week (depending on weather conditions) and soon becomes too dense to penetrate.

CORRELATION BETWEEN THE DISTRIBUTION OF THE *SALIX-EQUISETUM* ASSOCIATION AND UNFROZEN GROUND

Because of the severe environment on lower slipoff slopes, only two species, which together form the *Salix-Equisetum* association (Figure 7), are able to successfully colonize this alluvial habitat. Channel migration, which is initially responsible for constructing such habitats, is also primarily

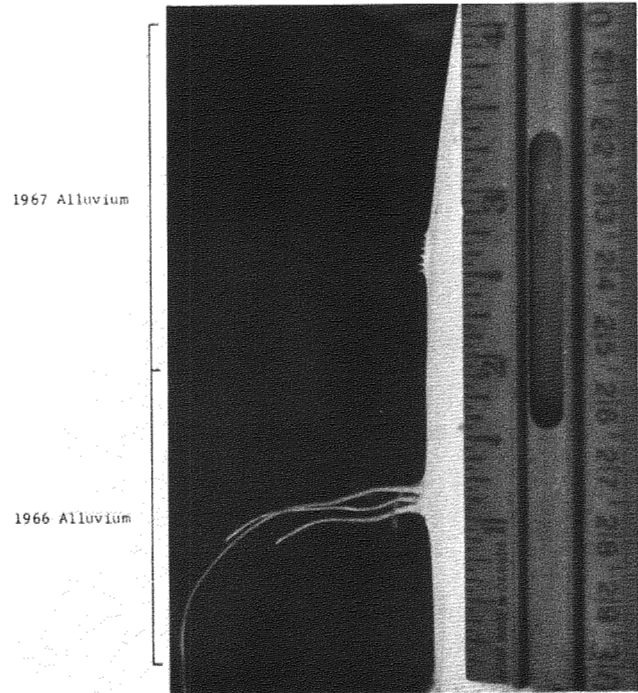


FIGURE 8 Portion of a peeled stem of feltleaf willow (*Salix alaxensis*), exhibiting the annual relationship between sedimentation and the placement of adventitious roots. Note the new roots that were initiating into the 1967 alluvium when this sample was taken in early July.

responsible for creating the zones of unfrozen ground. The final, observable result is that wherever well-developed *Salix-Equisetum* associations are established in the Mackenzie Delta, they are normally underlain by taliks. Some 300 probings were made in *Salix-Equisetum* associations during August and September of 1966, 1967, and 1971 to verify this finding, and the major portion of each association in the study area was found to be underlain by at least 2.5 m of unfrozen ground. Figure 9, which shows the distribution of two *Salix-Equisetum* associations within a portion of the study area, also indicates where unfrozen ground is located. To the writer's knowledge, no previously published map shows such a close areal relationship between the distribution of a single plant community and the thermal characteristics of the soil beneath it.

CONCLUSION

Taliks under youthful slipoff slopes in the Mackenzie Delta are undoubtedly undergoing spatial variations over time. The freezing isotherm should be prograding into the taliks from the adjacent large cells of permafrost such as that situated below the *Salix-Alnus* and *Picea* associations in Figure 2. The process of frost accretion is slow and prob-

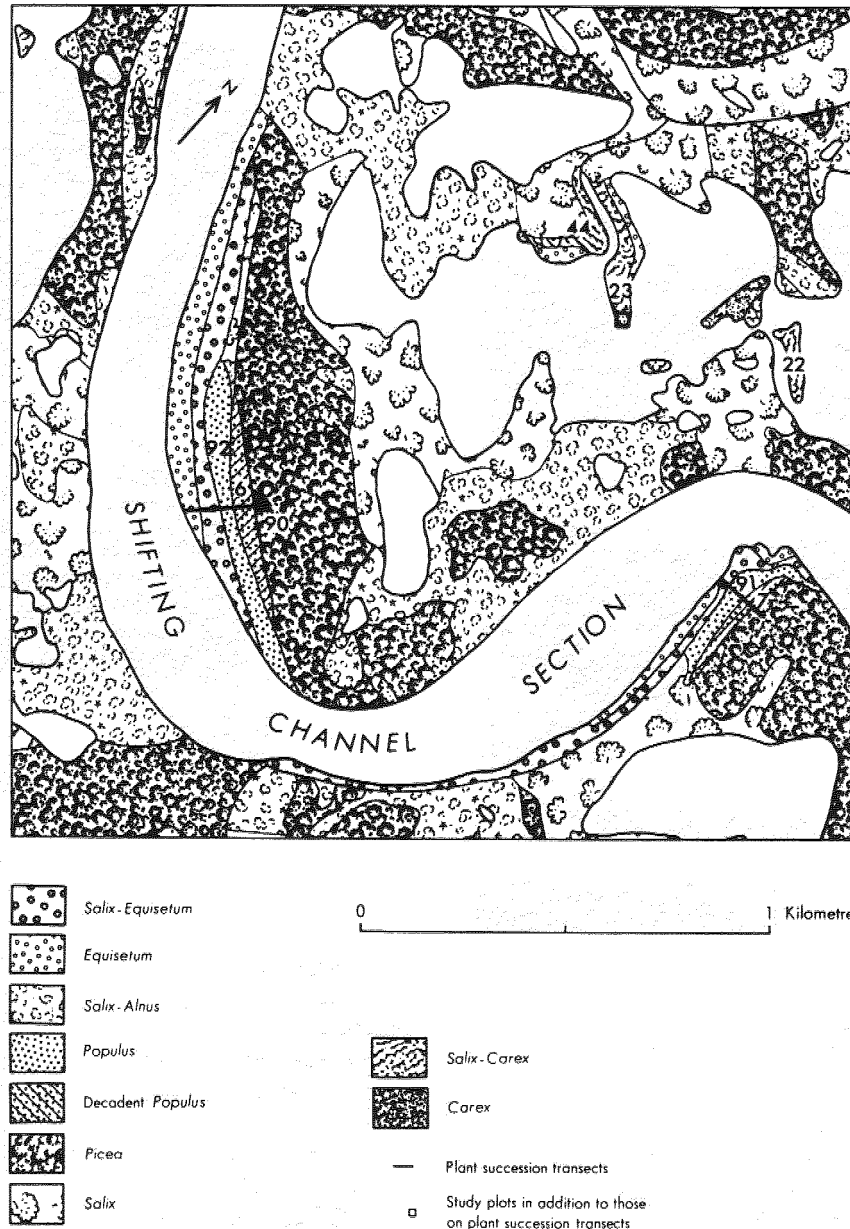


FIGURE 9 Distribution of plant associations in the Mackenzie River Delta, N.W.T. Distribution of the *Salix-Equisetum* association correlates to the zone of unfrozen ground.

ably parallels or lags behind the progradation of slipoff slopes, depending on the rate at which individual channel segments shift. Since permafrost is currently degrading along cut banks opposite such locations, it is clear that the formation and decay of perennially frozen ground in the Mackenzie Delta is a dynamic process that sees major areal displacements of permafrost bodies through time.

Finally, since the total area of unfrozen ground in the delta is substantial (approximately 8 percent of the terrestrial portion of the study area is underlain by taliks), it is argued that the boundary that marks the southern limit of continuous permafrost in northwest Canada⁵ at present should be shifted 200 km northward to include the Mackenzie River Delta within the zone of discontinuous permafrost.

ACKNOWLEDGMENTS

Most of the data on which this work was based were collected during a larger study that was supported by funds from the National Research Council of Canada, Department of Indian and Northern Affairs (via University of British Columbia Arctic and Alpine Committee), U.B.C. Research Funds, and the Department of Energy, Mines and Resources. Support for the March 1972 field work was given by Imperial Oil Ltd. Gratitude is expressed to J. Ross Mackay and V. J. Krajina, University of British Columbia, for their support during the study. Appreciation is also extended to Steve Gill, Camper Lewis, and William Yakubiec for assistance in the field.

REFERENCES

1. Baranov, I. 1959. Geographical distribution of seasonally frozen ground and permafrost, p. 193-219. *In* Principles of geocryology: Part I, General geocryology. USSR Academy of Sciences, V.A. Obuchev Institute of Permafrost Studies, Moscow. (Transl. by A. Nurklik, Ottawa, 1964: NRC TT-1121)
2. Beckel, D. Studies on seasonal changes in the temperature gradient of the active layer of soil at Fort Churchill, Manitoba. *Arctic*, 10:151-183.
3. Benninghoff, W. S. 1966. Relationships between vegetation and frost in soils, p. 9-13. *In* Permafrost: Proceedings of an international conference. National Academy of Sciences, Washington, D.C.
4. Brown, R. J. E. 1966. Influence of vegetation on permafrost,

- p. 20-25. Permafrost: Proceedings of an international conference. National Academy of Sciences, Washington, D.C.
5. Geological Survey of Canada. 1967. Permafrost in Canada. Map 1246A.
6. Gill, D. 1971. Vegetation and environment in the Mackenzie River Delta, Northwest Territories: A study in subarctic ecology. Ph.D. thesis. University of British Columbia, Vancouver. 694 p.
7. Mackay, J. R. 1963. The Mackenzie Delta area, N.W.T. Memoir 8. Geographical Branch, Mines and Technology Survey, Ottawa. 202 p.
8. Smith, M. W. 1972. Observed and predicted ground temperatures, Mackenzie Delta, N.W.T., p. 95-106. *In* D. F. Kerfoot [ed.] Mackenzie Delta monograph. 22nd Int. Geogr. Congress, Brock University, St. Catharines, Ontario.

NOTES

[1] This is a modified and expanded version of a paper presented at the Second Guelph Symposium on Geomorphology, University of Guelph, Guelph, Ontario, May 30, 1971.

[2] Taking snow as a separate condition, permafrost is present in "old" geomorphic positions, such as along stable lake shores, even where drifts accumulate to depths of 2.5 m. Snow accumulation alone is thus not an overriding factor. Furthermore, permafrost that persists adjacent to deep lakes does so despite horizontal thermal flux; thus, this factor alone is not sufficient to create or maintain unfrozen ground.

INDIRECT MAPPING OF THE SNOWCOVER FOR PERMAFROST PREDICTION AT SCHEFFERVILLE, QUEBEC

Hardy B. Granberg

MCGILL SUB-ARCTIC RESEARCH LABORATORY
Schefferville, Quebec

The distribution of discontinuous permafrost near Schefferville (54°48'N, 66°49'W) is closely related to the patterns of accumulation of the seasonal snowcover. Since the mean annual air temperature in the Schefferville area is -45 °C, extensive permafrost could be expected. However, the snowcover acts as an insulator during the cold part of the year, and where the snow is deep, it prevents the development of permafrost.

Permafrost is widespread in the upland areas, where the absence of trees allows strong redistribution of snow by wind. Thus, large parts of the terrain retain only a shallow

snowcover while deep accumulations occur locally in valleys.

In the forested lowlands, the snow is less influenced by wind and is therefore less variable in depth. Depletion of the snowcover occurs mainly in muskeg, near hill crests, and along lake shores that have a greater exposure to wind. Permafrost in the lowland areas is not common but is occasionally found in association with such areas of shallow snow.

The relationship between snow and ground temperatures is discussed in a separate paper in these proceedings.¹⁶ It

appears that a late winter snow depth between 65 and 75 cm is sufficient to prevent the development of permafrost in the Schefferville area. Figure 1 shows the distribution of snow depths in the lowland areas and the upland areas in late winter 1969. The snowfall in that year was about 100 mm greater than the average snowfall, which is 312 mm water equivalent. The figure shows that the snow conditions were more favorable for permafrost in the upland areas than in the lowlands.

Permafrost is of great economic significance to the mining industry in the area¹³ and considerable effort has been made to develop techniques whereby the three dimensional distribution of permafrost within areas of ore excavation may be determined. This research has been conducted mainly along two lines. The Iron Ore Company of Canada has undertaken experiments with geophysical techniques for direct

delineation of permafrost.⁸ The McGill Sub-Arctic Research Laboratory has, in co-operation with this company, made studies of the influence of surficial factors on the subsurface thermal regime^{1,4} so that indirect techniques of permafrost mapping may be developed. The importance of the seasonal snowcover was realized at an early stage^{6,12} and attempts were made to use snowcover information for prediction of the extent of permafrost.³ However, it is extremely difficult to map accurately the snowcover in the upland areas near Schefferville, where depths may range from 0 to 400 cm or more over distances shorter than 25 m. Direct mapping under such conditions requires a high density of sampling points and, due to the size of the areas under consideration (1 km² or more), such an approach is not feasible. Research was therefore initiated at the Timmins 4 Permafrost Experimental Site to investigate in detail the accumulation of the

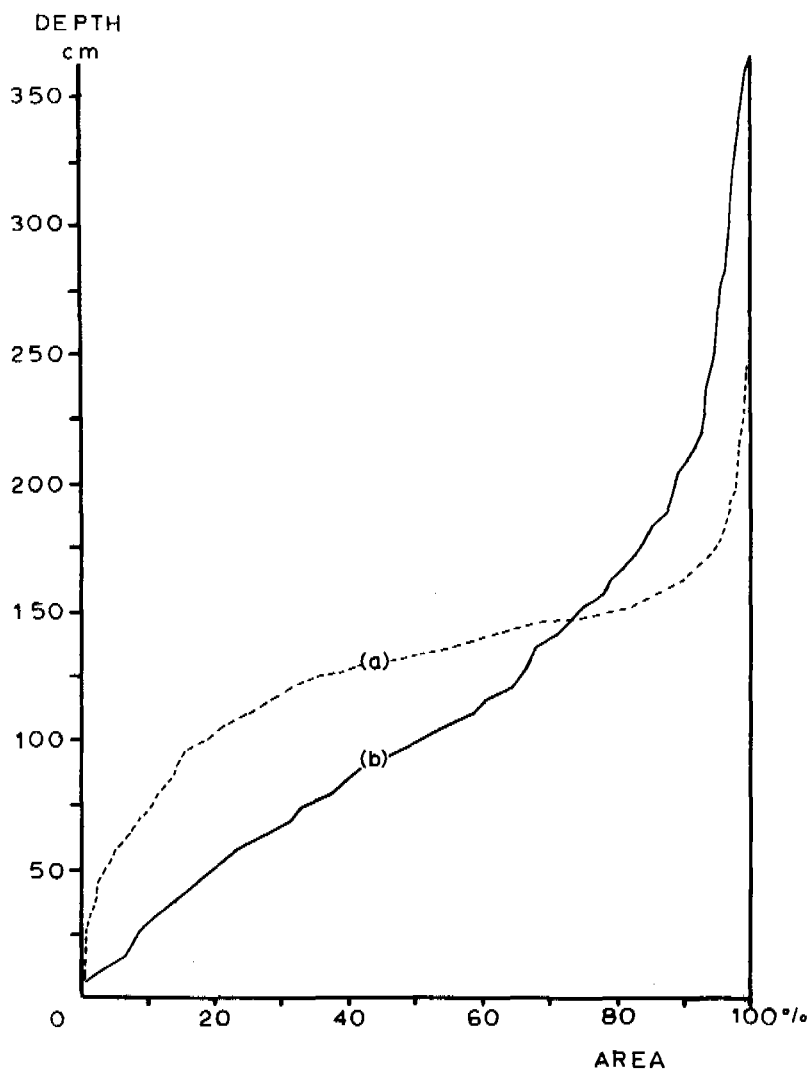


FIGURE 1 Distribution of snow depths in the lowland (a) and the upland (b) areas near Schefferville.

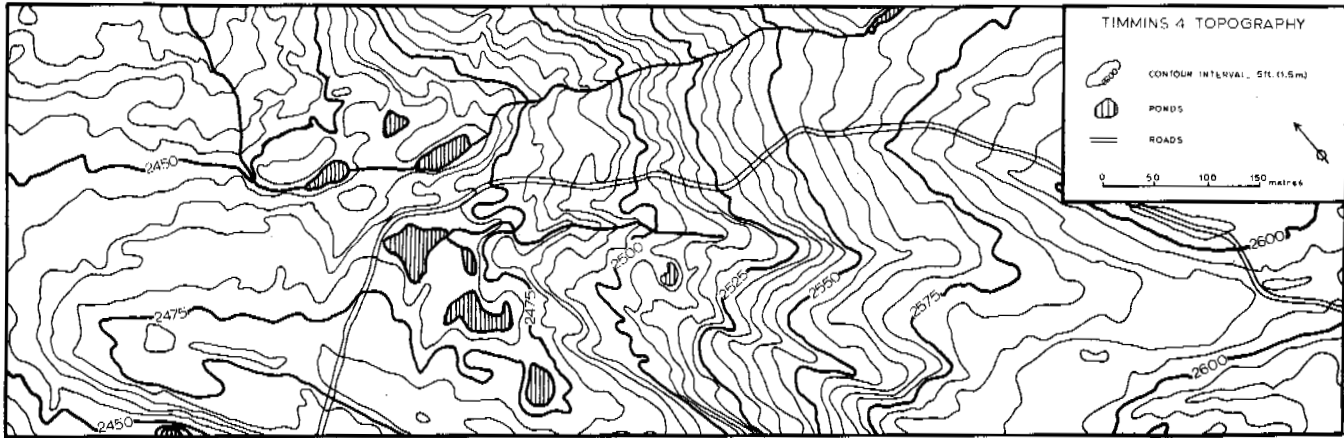


FIGURE 2 Topographic map of the Timmins 4 Permafrost Experimental Site.

seasonal snowcover and to develop indirect techniques of snowcover mapping.⁷ This paper presents some of the results of this study and describes two different techniques of indirect mapping of the snowcover that have been found useful in the Schefferville area.

THE TIMMINS 4 PERMAFROST EXPERIMENTAL SITE

The Timmins 4 site^{17,18} is located some 20 km northwest of Schefferville. Its topography (Figure 2) is characterized by a series of subparallel ridges that follow the strike of the underlying bedrock. The vegetation (Figure 3) shows an apparent relationship to the topography with sparsely vegetated ridge crests and dense dwarf birch and hygrophytic vegetation near valley bottoms. The snowcover has an important influence on the height of the bush vegetation, shielding the plants from mechanical abrasion by drifting snow.⁷ Scattered trees (not shown on the vegetation map) occur in the lower,

northwestern third of the area. Permafrost underlies the higher part of the site to a depth of at least 100 m but only small patches occur in the lower part.

Ground-temperature information is available from 28 multisensor thermocables ranging from about 10 to 110 m in depth. Multilevel snow temperatures and meteorologic data have been collected since 1968. To monitor snow depths and densities, a 147-point snow course was installed in 1968. This snow course was read before and after each major snow event in 1968-1969. In subsequent years, observations have been made at approximately bimonthly intervals.

THE RELATIONSHIP BETWEEN SURFACE ROUGHNESS AND SNOW ACCUMULATION

There is a strong relationship between terrain roughness and snow accumulation in the Schefferville area due to the strong winds associated with snowfall and the generally low temperatures during storms. These factors make the

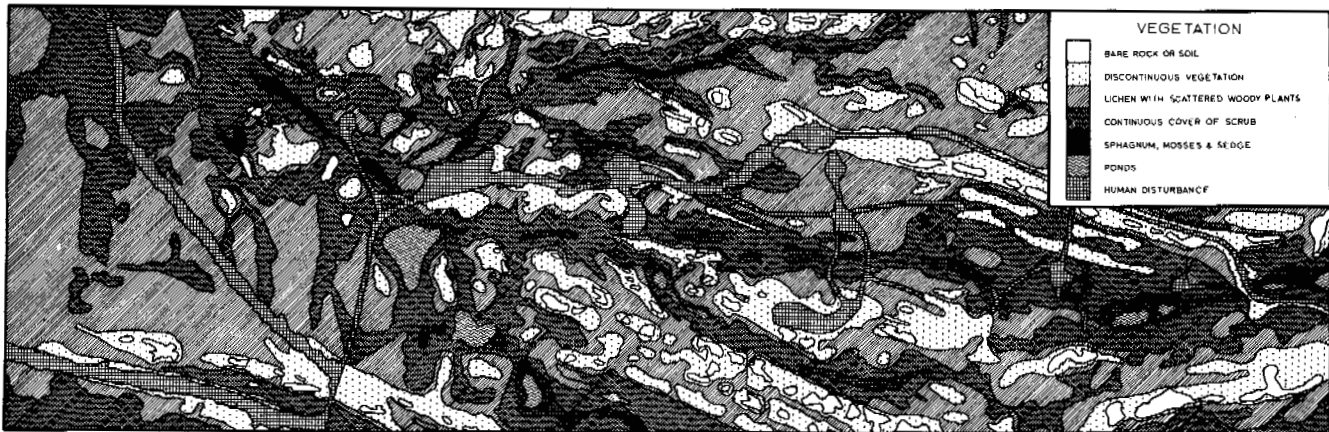


FIGURE 3 Vegetation at Timmins 4.

snow very susceptible to drift transport. The number of days with blowing snow recorded at Schefferville varies from 26 to 75 per winter over a 17-year period.

Surface roughness of varying magnitude determines the spatial variations in the wind velocity field. Near the surface, the flow field is closely controlled by small-scale roughness elements that cause variations in wind speed and direction over short distances. At higher levels, these effects become integrated, and there is a gradual transition from dominant influence by microroughness near the surface to control by larger-scale terrain features higher in the air stream. The wind speeds increase near the surface of convex elements and decrease in concave parts of the terrain. The flow at some height above the surface is subparallel to the generalized terrain profile, and the velocity at the surface can be expected to vary in relation to the difference between the generalized and the actual terrain profile. Due to inertial effects, this relationship is somewhat distorted with greater wind speeds on windward slopes than on lee slopes. Boundary-layer separations occur in association with sharp breakpoints in the terrain profile.

Differential drift transport produces variations in snow accumulation that are inversely related to the spatial variations in the wind velocity field. The total drift transport in a saturated flow is proportional to the third power of wind velocity for a given surface condition.^{2,14} A change in wind velocity with a factor of two thus changes the drift transport with a factor of eight. Snow is eroded from the surface of convex terrain elements, where the wind speed is locally increased, and deposited in concave parts, where the speed is decreased. Thus, the accumulation of snow tends to reduce surface roughness and the snow surface ultimately aligns itself to minimize accelerations and decelerations of the air stream.

A STATISTICAL MODEL FOR INDIRECT MAPPING OF SNOW DEPTHS

Previous investigations of the relationship between terrain roughness and snow accumulation in glacial environments have shown good correlations between snow accumulation and variables depicting differences between the actual and the generalized terrain profile.^{5,15} The generalization of the terrain profile has usually been a running mean along a traverse of altitudes. However, the correlations vary with direction of the profile with respect to the orientation of the terrain roughness and the direction of prevailing winds.¹⁰ Also, the scale of the most important terrain roughness varies with the amount of accumulated snow. The amount of snowfall and the influence of wind varies from year to year in an unspecified fashion. To account for these variations, the following general model was designed for use with step-by-step multiple regression⁷:

$$S = f(X_1, X_2, X_3, \dots, X_n),$$

where S is the depth of snow and $X_1, X_2, X_3, \dots, X_n$ denote terrain roughness variables that by themselves, or in any combination, contribute significantly to explaining the variation in snow depth. The terrain variables were selected to represent differences between the actual terrain profile and different degrees of generalization of this terrain profile. Asymmetry variables were used to allow for asymmetric wind effects. To account for the varying influence of winds from different directions, all variables were evaluated for eight directions. Step-by-step multiple regression was used to obtain a multivariate expression of snow depth in terms of some of the most significant terrain roughness variables.

The individual variables were calculated for each snow sampling location using a computer program. The basic terrain information was obtained from a topographic map of scale 1:1 200 and a contour interval of 1.5 m. A square grid was superimposed on the map to coincide with the snow sampling grid. Trough linear interpolation altitude readings for each grid intersection were obtained at intervals corresponding to 15 m on the ground. For brevity, the variables are only exemplified here to give the general principles of their compilation. Given the altitude matrix, A , where $A_{i,j}$ is the altitude at point i,j , the different variables were calculated as follows:

$$\begin{aligned} X_A &= A_{i,j} \\ X_B &= A_{i,j} - [(A_{i-1,j} + A_{i,j} + A_{i+1,j})/3] \\ X_C &= A_{i-1,j} - A_{i+1,j} \\ X_D &= (A_{i-1,j} - A_{i+1,j}) - (A_{i-1,j} - A_{i,j}) \\ X_E &= A_{i,j} - [(A_{i+2,j} + A_{i+1,j} + A_{i,j})/3], \end{aligned}$$

where X_A is the altitude; X_B is the difference in altitude between the actual and the generalized terrain profile. Different degrees of generalization were obtained by averaging the altitudes of 3, 5, 7, 9, 11, and 15 points along the traverse; X_C is a height difference assumed to represent general slope; X_D is the difference between general slope and the slope segment immediately "upwind" of the snow stake location; and X_E is the difference between the actual terrain profile and a generalized terrain profile that has been displaced 15 m downwind from the snow stake location.

The symmetric variables (X_B and X_C) were compiled for the four pairs of directions N-S, NE-SW, E-W, and SE-NW. The nonsymmetric variables (X_D and X_E) were computed for the eight directions individually. In all, 53 topographic roughness variables were evaluated.

Using a snow depth sample from late winter 1969, an equation was obtained that consists of four of the terrain variables:

$$S = aX_{ENE} + bX_{EW} + cX_{EN} + dX_A + e.$$

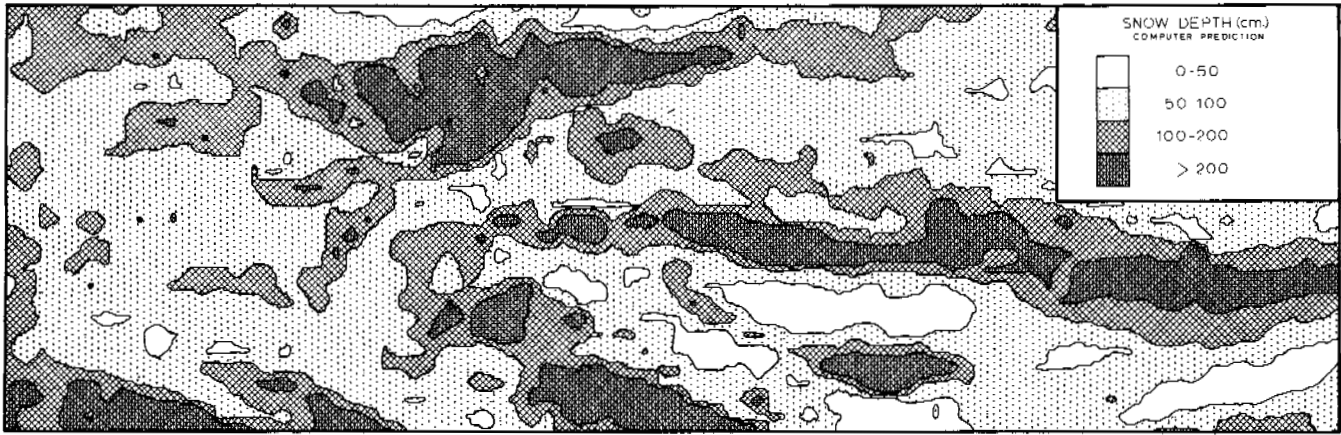


FIGURE 4 Computer prediction of snow depth at Timmins 4 in late winter 1969.

The second subscript refers to the wind direction the variable represents, and *a, b, c, d,* and *e* are the different constants. This equation explains 75 percent of the variance in snow depth. The equation was inserted as a subroutine into a computer mapping program. Using the original matrix of altitudes as input data, the program computes the variables employed in the particular equation and produces snow depth estimates for each altitude point. A snow depth map (Figure 4) was produced through linear interpolation between snow depths estimated for 2 241 points at 15-m intervals.

MAPPING OF SNOW DEPTHS FROM SEQUENCE AERIAL PHOTOGRAPHS

Five sets of aerial photographs were taken of the Timmins area during the melt period in 1969. The purpose of these flights was an attempt to develop a means of indirect map-

ping of the seasonal snow cover applicable on a regional scale. Simultaneously, snow depths were monitored at the Timmins 4 snow course. The basic assumption was that the snowmelt would take place at a sufficiently uniform rate so that the snowcover outline at the time of each flight could, with reasonable accuracy, be identified as an isoline of snow depth at the time of peak snowcover.

A snow depth map was produced for the Timmins 4 Permafrost Experimental Site by plotting the successive outlines of the snowcover onto a map (Figure 5). To find the class limits of the map, the average depth at peak snow was compiled for the snow stakes melted free from snow during the period prior to each flight. The most probable depth value for each contour was taken as the midvalue between each two such averages (Figure 6). Snowfall occurred after the peak snow and contributed to some of the error indicated by Figure 6. The influence of intermediate snowfalls between the flights was minimized by allowing

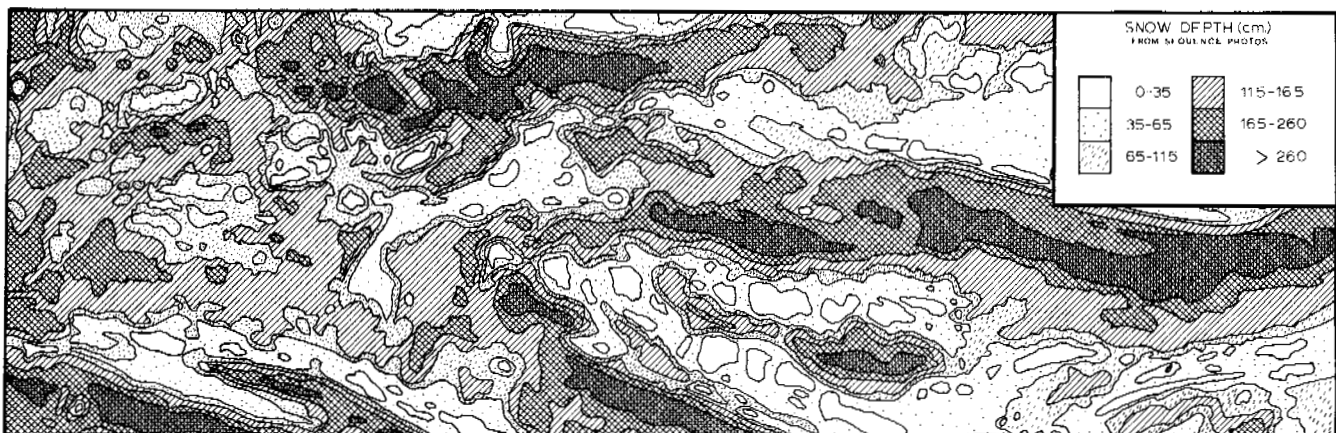


FIGURE 5 Snow depth at Timmins 4 in late winter 1969, estimated from sequence aerial photographs.

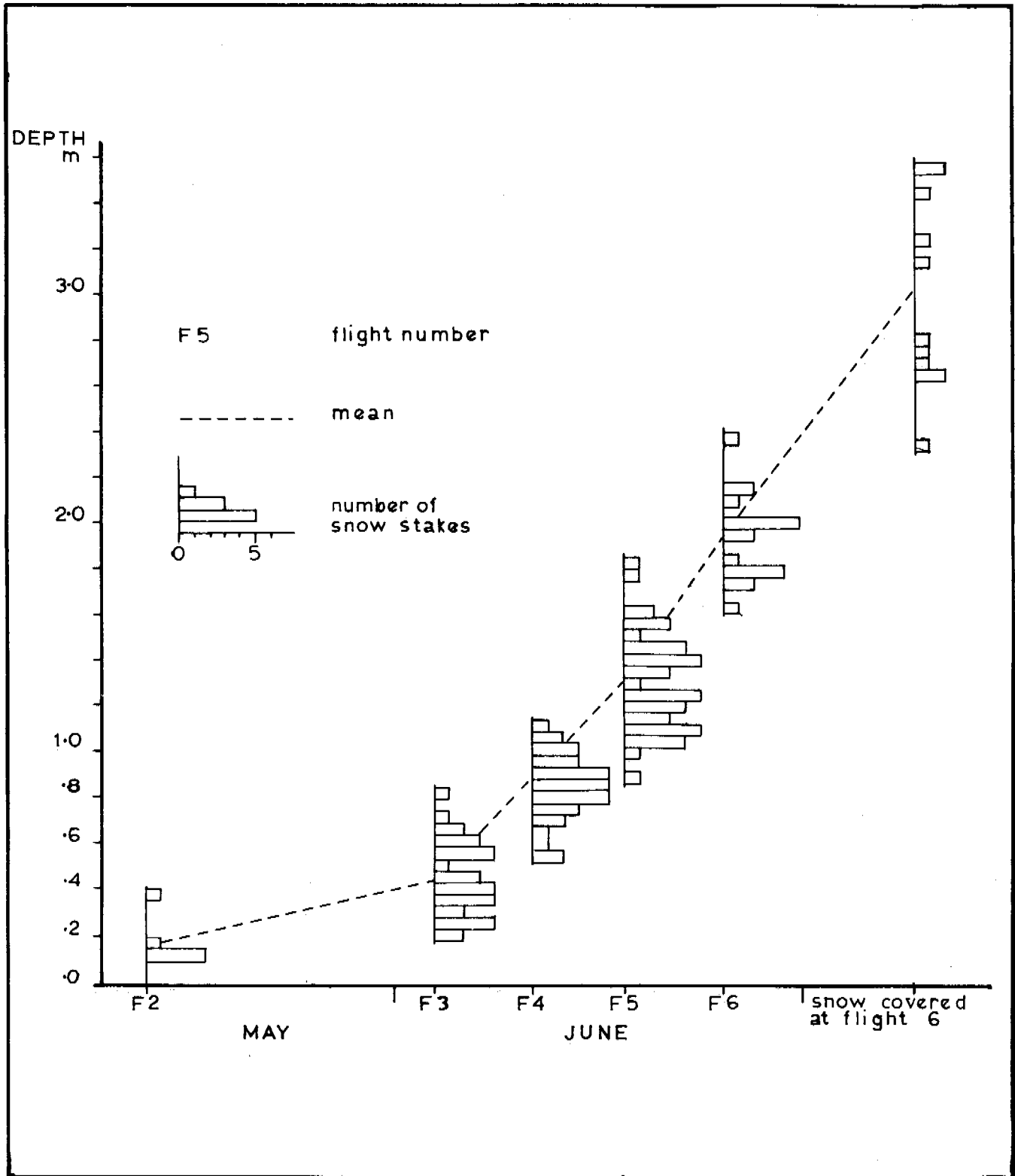


FIGURE 6 Histograms of peak snow depths for stakes melted free from snow in the period before each flight.

additional snow to melt before the next flight was undertaken. Additional error was produced by spatial variations in melt rates. The error is smallest in the shallow range of depths and increases with increasing depth.

DISCUSSION OF MAPS

The two snow depth maps (Figures 4 and 5) show a good general correspondence. The deepest parts of the snowcover are similarly shown by the two methods, and the shallow zones agree well. In the northwestern third of the site, there is a general underestimate by the computer map, probably because the influence of trees was not accounted for by the equation. The two maps have been compiled with different numbers of classes and different class limits, thus making a detailed comparison difficult. It is evident, however, that the predicted map presents a considerably improved picture of the true patterns of snow accumulation when compared with a map produced through linear interpolation between the 147 snow sampling points (Figure 7).

APPLICATION IN PERMAFROST PREDICTION

The two methods for indirect mapping of the snowcover are both valuable in permafrost prediction. The method based on sequence melt photographs is suitable for permafrost prediction on a regional scale, where only the surficial extent of permafrost is considered. Three to four flights, evenly spaced through the first 150 cm of snow depth decrease, are sufficient to obtain good information about the spatial variations in snow accumulation for the particular year. When there are appreciable regional differences in melt rates within the area photographed, additional snow measurements are required for calibration of the class limits. So far, the interpretation of the snow information has been subjective and mainly used as an aid in extrapolating thermocable information for delineation of the spatial distribution of permafrost

in ore deposits. In spring 1972, sequence melt photographs were flown for a larger portion of the ridge areas west of Schefferville for the purpose of obtaining a better picture of the regional distribution of permafrost. The interpretation of these photographs is in progress at present.

The computerized model was developed for the more detailed work on individual ore bodies, where the actual geometry of permafrost is important. A particular advantage of this model is its suitability for further modeling of the thermal effects of the snowcover and other topographically related factors. Empirical equations have been determined for the influence of the seasonal snowcover on ground temperatures.¹⁶ A map of the thermal influence of the snowcover (Figure 8) was produced by inserting the following equation into the computer mapping program:

$$T = 0.0346 S - 2.67,$$

where T ($^{\circ}\text{C}$) is the temperature at 1.5 m depth averaged over a 2-year period, and S (cm) is the average of predicted cable head snow depths at peak snow. The equation explains about 80 percent of the variance in ground temperatures within the range of snow depths from 0 to 160 cm. The information available is insufficient to determine whether the linear relationship is valid outside this range. The influence of other topographically related factors, such as direct solar radiation, can be similarly analyzed and mapped.⁹

Given a specified upper-boundary condition and a known geothermal gradient, it is possible to project the near-surface isotherms downward, provided the variations in the thermal conductivity of the ground are known. The heat flow in a steady-state condition follows the laws of potential flow and, thus, can be calculated and the isotherms delineated. However, considerable research is required before this goal can be reached. First, the accuracy of the snow mapping model must be improved. Second, more knowledge is needed about the influence of surficial factors on the near-surface

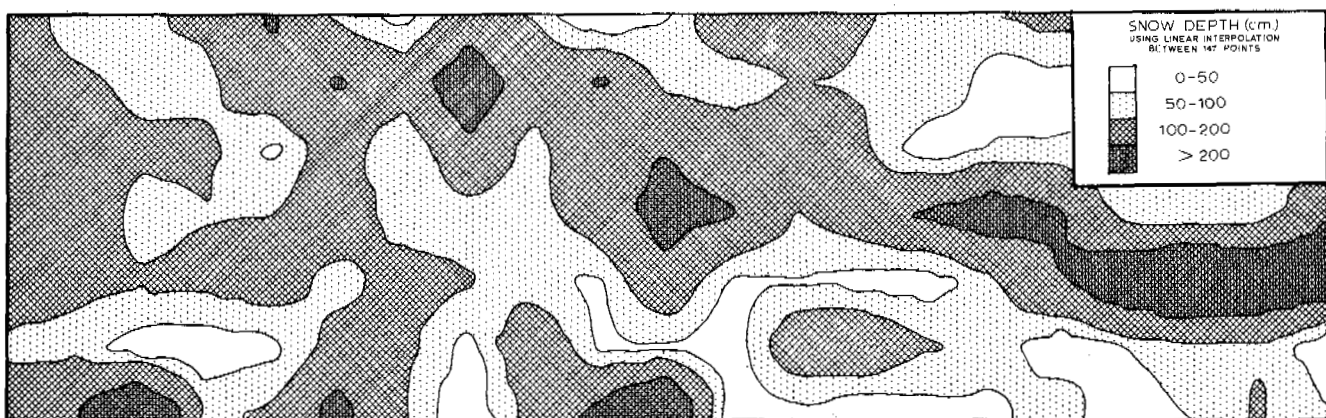


FIGURE 7 Snow depth map for late winter 1969, produced by linear interpolation between snow stake locations 60 m apart.

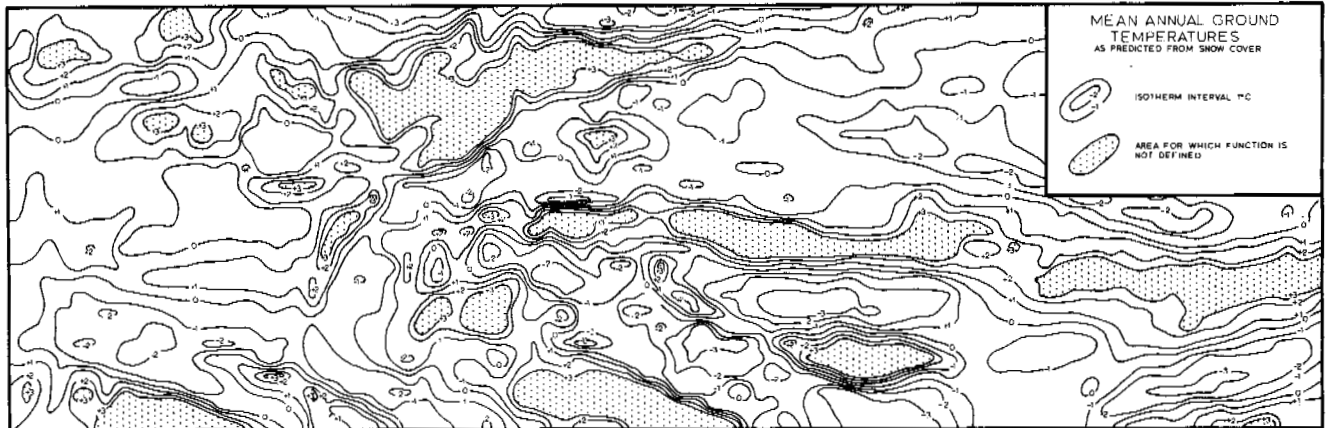


FIGURE 8 Map of the thermal influence of 2 years' snowcover at Timmins 4.

ground temperatures. Third, long-term data are needed before a steady-state assumption can be justified.

Since the snow mapping model uses information derived from topographic maps, it allows the reconstruction of snow conditions in areas that have already been mined. Usually, the extent of permafrost has been documented, but no information is available about snow conditions prior to mining. The Iron Ore Company of Canada is currently undertaking systematic mapping of ground temperatures and permafrost boundaries throughout the excavation of the Timmins mine situated 2 km southeast of Timmins 4. This information will provide an excellent means of testing quantitative models of permafrost geometry.

ACKNOWLEDGMENTS

This study was jointly sponsored by the Iron Ore Company of Canada, the National Research Council of Canada, and the McGill Sub-Arctic Research Laboratory in Schefferville.

REFERENCES

1. Annersten, L. J. 1966. Interaction between surface cover and permafrost. *Biul. Peryglacj.* 15:27-33.
2. Bagnold, R. A. 1941. *The physics of blown sand and desert dunes.* Methuen, London. 265 p.
3. Barnett, D. M. 1963. Snow depth and distribution in relation to frozen ground in the Ferriman Mine and Denault Lake areas, Schefferville. *McGill Sub-Arctic Research Papers No. 15.* p. 72-85.
4. Bird, J. B. (ed.). 1964. *Permafrost studies in central Labrador-Ungava.* McGill Sub-Arctic Research Papers No. 16. 137 p.
5. Black, H. P., and W. Budd. 1964. Accumulation in the region of Wilkes, Wilkes Land, Antarctica. *J. Glaciol.* 5 (37) 3-15.
6. Bonnlander, B. 1958. *Permafrost research.* McGill Sub-Arctic Research Papers No. 4. p. 56-58.
7. Efroymson, M. A. 1960. Multiple regression analysis. *In* A. Ralston and H. S. Wilt [ed.] *Mathematical methods for digital computers, Part V (17).* Wiley, New York.
8. Garg, O., and P. F. Stacey. Techniques used in the delineation of permafrost in the Schefferville, P.Q. area. *In* *Permafrost Thermal Regime Seminar, May 2nd-3rd, 1972.* (In press)
9. Garnier, B. J., and A. Ohmura. 1968. A method of calculating the direct shortwave radiation income of slopes. *J. Appl. Meteorol.* 7:796-800.
10. Gow, A. J., and R. Rowland. 1965. On the relationship of snow accumulation to surface topography at "Byrd Station," Antarctica. *J. Glaciol.* 5 (37):843-847.
11. Granberg, H. B. 1972. Snow depth variations in a forest-tundra environment, Schefferville, P.Q. Winter 1968-69. M.Sc. thesis. McGill University, Montreal.
12. Ives, J. D. 1960. Permafrost in Labrador-Ungava. *J. Glaciol.* 3(28):789.
13. Ives, J. D. 1962. Iron mining in permafrost, central Labrador-Ungava: A geographical review. *Geogr. Bull. No. 17.* p. 66-77.
14. Komarov, A. A. 1954. Some rules on the migration and deposition of snow in western Siberia and their application to control measures. *Tr. Transp.-Energ. Inst.* 4:89-97. (D.B.R. N.R.C. Tech. Transl. 1094, 1963, 13 p.)
15. Mock, S. J. 1968. Snow accumulation studies on the Thule Peninsula, Greenland. *J. Glaciol.* 7(49):59-76.
16. Nicholson, F. H., and H. B. Granberg. Permafrost and snowcover relationships near Schefferville. This volume.
17. Nicholson, F. H., and B. G. Thom. Studies at the Timmins 4 permafrost experimental site. This volume.
18. Thom, B. G. 1969. New permafrost investigations near Schefferville, P.Q. *Rév. Géogr. Montréal No. 23.* p. 317-327.

PERMAFROST AND ITS RELATIONSHIP TO OTHER ENVIRONMENTAL PARAMETERS IN A MIDLATITUDE, HIGH-ALTITUDE SETTING, FRONT RANGE, COLORADO ROCKY MOUNTAINS

Jack D. Ives

UNIVERSITY OF COLORADO
Boulder, Colorado

INTRODUCTION

Except for those relatively few areas where extensive ground temperature data exist,^{3-6,10,12} maps showing permafrost distribution on a worldwide scale depend on broad extrapolations and an assumed relationship between mean annual air and mean annual ground temperatures. Use of the mean annual air (screen) temperature of -1.0 to -2.0 °C to approximate the southern limit of permafrost, for instance,⁶ is justifiable for those extensive areas of the subarctic where little or no ground temperature data are available. This approach, however, may lead to inaccuracies in excess of 100 km when locating zonal boundaries.

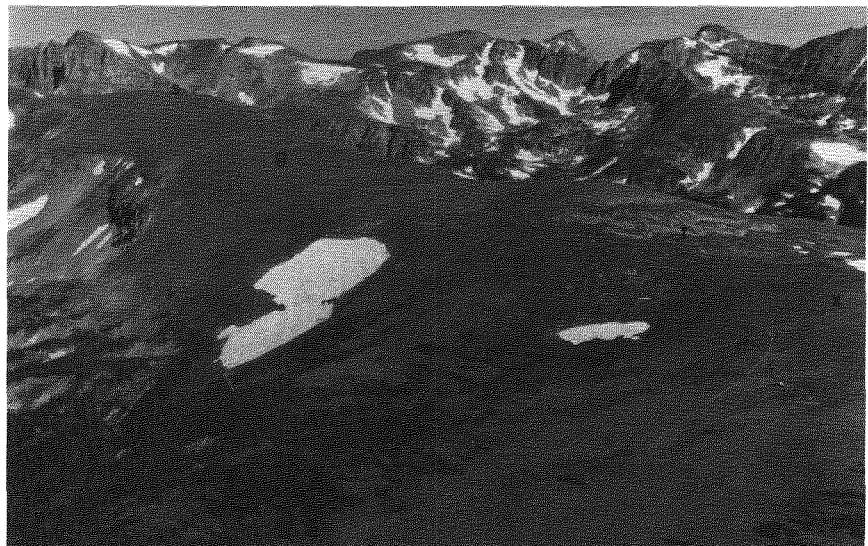
The location and extent of permafrost in high mountain areas is even more uncertain. Since an increasing number of people are using the mountain areas of the earth for recreation, it would seem logical that there should be comparable growth in our knowledge of those areas. This study represents a systematic attempt to investigate the relationships between permafrost and other environmental parameters in a midlatitude, high-altitude setting.

THE NIWOT RIDGE STUDY SITE

The site chosen for a long-term permafrost research program is Niwot Ridge and adjacent areas in the Colorado Front Range, 40 °N. Treeline lies at about 3 400 m and the Continental Divide follows the north-south crest of the range for 20 km. Individual summits exceed 4 000 m from which slopes descend precipitously into a series of cirques and U-shaped valleys. Glacial activity during the late-Cenozoic glaciations has helped produce two contrasting sets of landform assemblages—one typical of the glaciated, alpine mountains (*hochegebirge*¹³); the other characterized by broad flowing contours, enclosing low hills and ridges rising more than 300 m above treeline, and typical of a periglacial landscape. Niwot Ridge is the longest of these ridges. It is perpendicular to the Divide and 10 km in length, and the westernmost 2 km forms a knife-edged arête (Figure 1).

Eight thermistor strings, set to depths between 160 and 418 cm with a 1-m vertical spacing, were installed along the ridge in 1970 and 1971 through an altitude range of 300 m. Six supplementary sets, emplaced to depths be-

FIGURE 1 Low-level oblique air photo showing the middle section of Niwot Ridge with the forest-tundra ecotone in the foreground and Institute for Arctic and Alpine Research's access road. The 3 750-m station is shown by the letter s, and the site of the new 3 565-m station (x). Note the well-developed stone-banked lobes and terraces (t) and goletz terraces (g).



tween 100 and 150 cm with thermistors placed at 25, 50, 75, 100, and 150 cm were added in 1972. Standard climatological observations have been taken at an alpine (3 750 m) and an upper montane forest site (3 000 m) since 1952,^{11,2} and a new station for energy budget determination was established at 3 565 m in July 1972 as part of the United States Tundra Biome Program. A remote data platform, in association with analysis of the Earth Resources Technology Satellite (ERTS-1) performance, was added in October 1972 and is currently transmitting ground temperature and other data.

The available ground temperature data are still relatively sparse; more installations and a longer period of record are needed. However, sufficient data have been collected to approximate permafrost distribution and to draw some initial inferences concerning relationships between ground temperature, air temperature, precipitation and snowcover, vegetation, aspect, and short-wave radiation.

Climatic Characteristics of the Study Area

The basic climatic parameters for the 3 750-m station on Niwot Ridge, based on 19 years of record (1952-1970), are given in Table I. Data from another station, maintained for 18 months at 3 500 m, gave a specific mean annual air temperature for October 1968-September 1969 of -0.8°C . At this site, wind-swept and snow-free in winter but with a copious water supply from a nearby snow-accumulation site, depths to permafrost measured in early autumn 1968 and 1969 were 190 and 183 cm, respectively.^{7,9} From the viewpoint of possible permafrost occurrence, the most significant environmental conditions on Niwot Ridge are relatively low mean annual air temperatures (about -1.0°C at 3 500 m and -4.0°C at 3 750 m) and very high westerly winds in winter that generally maintain a snow-free condition for all but lee slopes above treeline.

TABLE I Selected Climate Data^a from Station 3 750 m, 1952-1970

Annual air temperature	-3.9°C
July temperature	8.3
January temperature	-13.2
Monthly temperature range	21.5
Annual precipitation ^b	102.1 mm
Annual wind speed ^b	10.2 m s^{-1}
Wind speed for	
November	13.4
December	13.6
January	13.9
February	11.8
March ^b	12.1

^a Values given are means.

^b Values recorded from 1965 to 1970.

During spring (April-May) low-pressure systems moving northward from the Gulf of Mexico along the eastern flank of the Rocky Mountains bring up-slope storms that produce a precipitation maximum in the form of wet snow. As a result, snowcover usually reaches its greatest extent in April and May, or early June, i.e., at a time when the mid-winter period of most extensive heat loss is well past. The wet spring snowcover is important, however, in absorbing a large proportion of the available solar energy during the melting process and, because of the ensuing high albedo, in reflecting it back into the atmosphere. The critical nature of a wet snowcover in May and June is especially important, because it usually coincides with the first half of the annual period of high-angle sun and maximum short-wave radiation.

The summer (mid-June, July, August) is characterized by clear mornings and frequent afternoon thunderstorms typical of mountain systems in continental interiors. In relation to the onset of periods of low air temperature, the incidence of first snow in September, October, or November should also be critical in terms of marginal permafrost occurrence.

Ground Temperature Conditions, 1970-1971

The 1970-1971 maximum and minimum recorded temperatures at various depths from five selected sites are shown in Figure 2. At site (a) (3 750 m), the 381-cm-deep thermistor has remained below 0°C through three summers, so that a depth to the permafrost table of approximately 340 cm has been established. At sites (b) and (c), it was impracticable to install thermistors deep enough to substantiate a permafrost table. It is possible, however, to infer the probable presence of permafrost by extending the maximum and minimum temperature curves until they intersect the 0°C level. Such extrapolation is believed justified, because at each site the temperature maxima continue to drop rapidly toward the 0°C position with increasing depth to the lowest level of effective installation (418 cm and 382 cm, respectively) and because in each case the recorded maxima are only fractionally above the freezing point. Site (d) (3 485 m), on the other hand, is probably not underlain by permafrost, and at site (e) (3 490 m) the indication is no permafrost could exist. A thermistor string was installed to 5 m on the summit of Mt. Evans (4 300 m) on a horizontal surface, and the first readings (28 August 1970) showed the ground to be frozen below 320 cm. Unfortunately, soon after these readings were taken, the installation was destroyed by tourists.

The five graphs in Figure 2 provide representative examples of the types of sites under investigation. From these data, from probing and digging, and from mining operations that encounter frozen ground in late-August and September, it is postulated that permafrost is widespread in the higher,

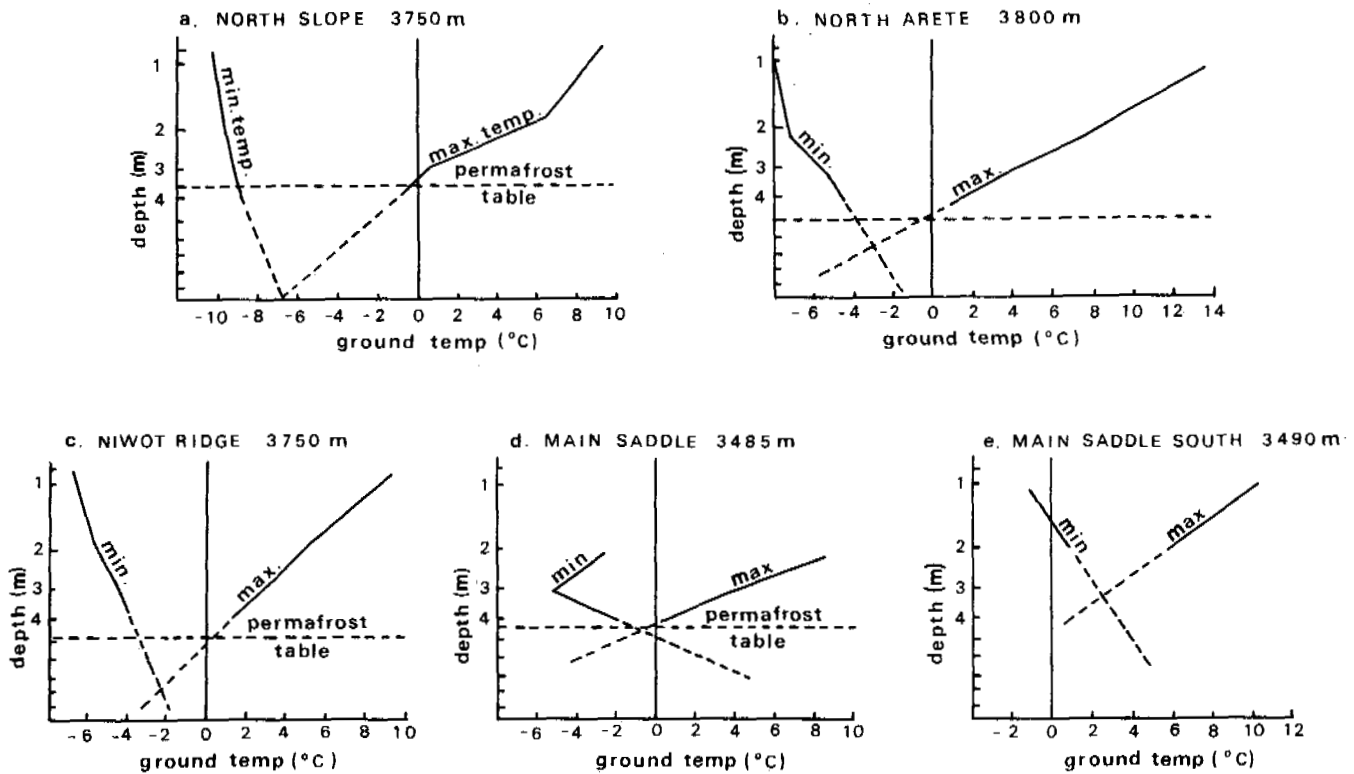


FIGURE 2 Maximum and minimum ground temperatures at various depths for 5 sites, 1970-1971, drawn on semilog paper. Permafrost either certainly or probably occurs under sites (a), (b), and (c), probably does not under site (d), and certainly does not under site (e).

wind-swept, and especially north-facing areas of the Colorado Rocky Mountains.

Comparison of Conditions, 1970-1971 and 1971-1972

Figure 3 is an 18-month temperature record from four depths on a steep (40°) north-facing slope at 3 750 m. Comparison between the two melt seasons, subject to some data limitation, indicates that the rise in ground temperatures in the spring of 1972 may have been earlier and may have been more rapid than during the preceding year. Also, the warm phase of the cycle was about 12 days longer in 1972 and maxima were slightly higher. The overturn of temperatures in the early spring occurred nearly 6 weeks earlier in 1972 and the autumn reversal 2 weeks later.

Explanation of these differences between the two seasons at the one site can be related directly to weather conditions. February and March 1972 were comparatively warm and dry with a minimal snowcover, while April and May experienced one of the lightest wet spring snowfalls during the period of record (1952-1972). In addition, solar radiative flux, determined with an actinograph maintained

at 3 750 m, was much higher for July 1972 than for July 1971 and the winter and spring periods for 1971 were much closer to normal.

The weekly observations through the middle of July 1971 caused speculation that no below-zero temperatures would be retained in the autumn. The sudden leveling off, beginning July 20, was related to a change in weather from warm and clear in the first part of the month to cloudy and very wet between July 19 and 28. This strong correlation between local weather and ground temperature trends was not repeated in 1972, yet temperatures at the 82- and 182-cm depths began to fall by the end of July, and the overall shape of the curves is very similar. The 1972 trends can be accounted for by reduced solar radiation, resulting from the progressive lowering of the sun's angle with increasing time from the summer solstice, accentuated by the northern exposure of this particular site. For comparative purposes, 1970-1971 and 1971-1972 temperature curves for a ridge crest site at 3 800 m are produced as Figure 4. The same general comparisons can be made, although the temperature decline from the summer maxima at two depths were delayed until late August, undoubtedly because of the longer exposure of the site to direct sunlight.

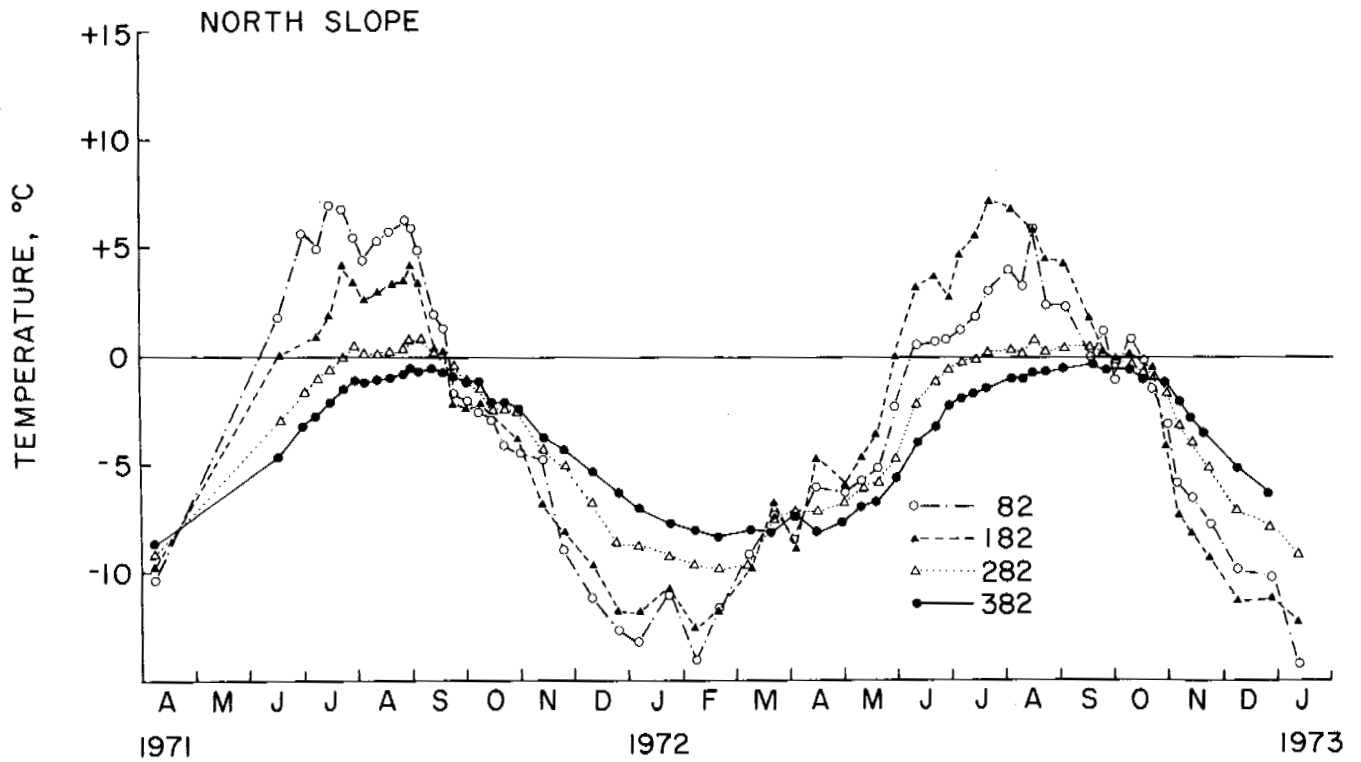


FIGURE 3 Ground temperature record from April 1971 to January 1973 for a north-facing site at 3 750 m. Following June 1971, thermistors at 82, 182, 282, and 382 cm were read weekly during the summer and approximately once every 2 weeks during the winter. The 382-cm thermistor ceased to function in December 1972.

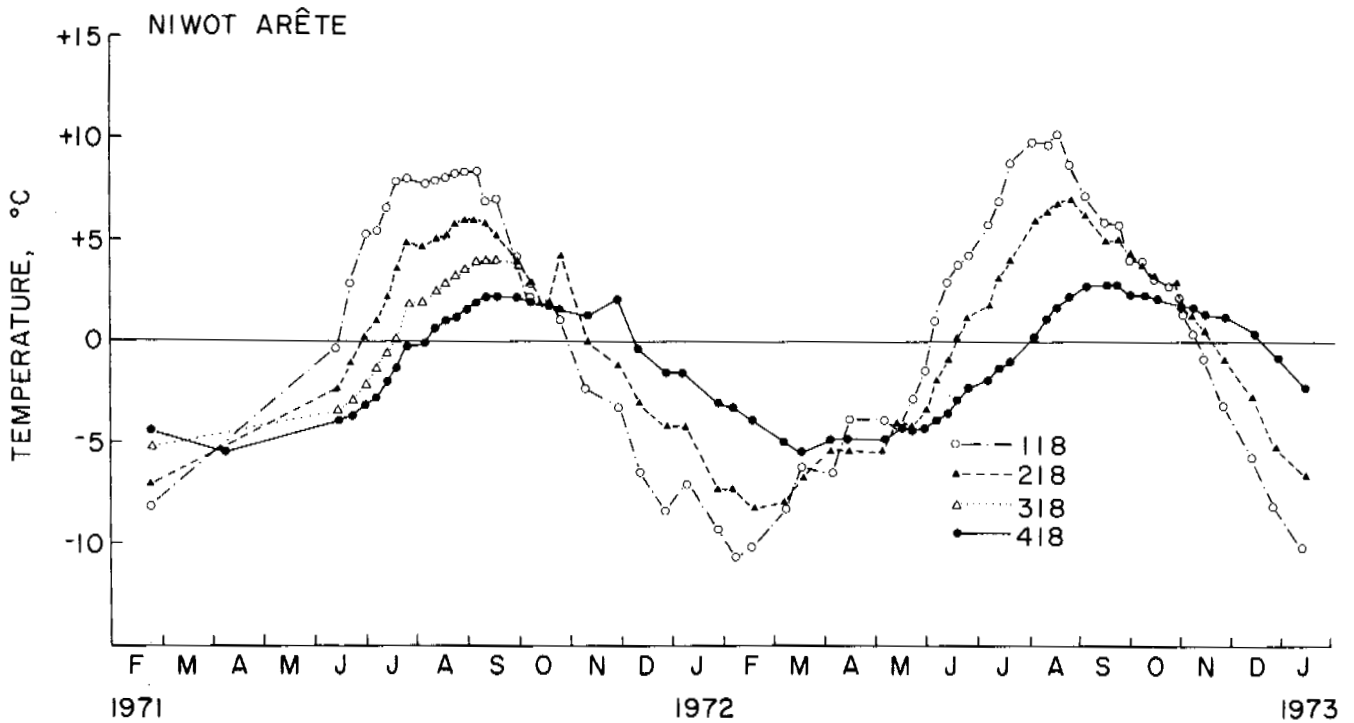


FIGURE 4 Ground temperature record for February 1971 to January 1973 from a ridge-crest site at 3 800 m for comparison with Figure 3. Thermistors were installed at 118, 218, 318, and 418 cm. The 318-cm thermistor ceased to function in October 1971.

SUMMARY

The ground temperature data presented here, together with the large number of field observations of frozen ground in late summer and autumn, indicate that permafrost occurs extensively throughout the Colorado Rocky Mountains. It is much more widespread than hitherto believed, since few of the numerous reports by the pioneer miners of the last century penetrated the scientific literature despite Weiser's¹⁴ publication of 1875 and Baranov's¹ speculation upon its existence in his world survey. Permafrost occurrence in Colorado, however, would seem marginal, although the numerous summits exceeding 4 000 m and extensive areas of north-facing slopes should retain perennially negative temperatures. One of the most important environmental parameters in this high-altitude and relatively low-latitude region is incoming short-wave radiation and hence slope angle and aspect; another is the interrelationships of wind, snow distribution, and topography. The work already accomplished is only a beginning. A second stage will be a careful analysis of the relative importance of the various secondary environmental parameters affecting permafrost distribution, and this is currently under way together with an energy balance study of a representative alpine study site. It should then be feasible to make comparisons with and extrapolations to other high-mountain regions in similar latitudes, since it is contended that the arctic and subarctic experience is not fully comparable. For the present, and despite the earlier implied criticism of the correlation between mean annual air temperature and ground temperature, it is worth reiterating that the lowest proven occurrences of permafrost in the Front Range coincide with a mean annual air temperature of approximately 1.0 °C. The following conclusions seem warranted:

1. At elevations of 3 500 m and above, i.e., immediately above treeline, patches of permafrost should be expected under wet sites that are largely blown free of snow during winter.

Thickness of the active layer may be less than 2 m and freezeback to the permafrost table may not be complete until mid-February or early March. There will be no permafrost under dry sites, south-facing slopes, and snow-accumulation sites. South-facing slopes may experience very high temperatures in late summer—11.9 °C at 115 cm and 8.6 °C at 215 cm.

2. Above about 3 750 m, permafrost will occur quite extensively under wet sites that are wind-swept in winter with an active layer less than 2 m thick. Dry south-facing slopes, and probably also wet south-facing slopes, and snow-accumulation sites will be free of permafrost. Horizontal surfaces with relatively little or no winter snowcover will probably be underlain by permafrost. North-facing slopes will be extensively underlain by permafrost, and dry sites will show a depth of 3–4 m to the permafrost table.

3. The highest summits of the Front Range (4 000–4 400 m), with an extrapolated mean annual air temperature of about –9 °C for 4 400 m, should be extensively underlain by permafrost of considerable thickness.

4. The predominantly dry conditions and extensive areas of bedrock outcrop severely limit the accumulation of significant amounts of ground ice. Nevertheless, the possible presence of permafrost is sufficient to indicate that any mountain development should take it carefully into account.

ACKNOWLEDGMENTS

The investigations described in this paper were supported by National Science Foundation Research Participation Projects in 1970–1972 and by National Science Foundation grant to the U.S. Tundra Biome Program. The assistance of many individuals is gratefully acknowledged, in particular those who assisted during the winter under sometimes severe conditions.

REFERENCES

1. Baranov, I. Ya. 1959. Geographical distribution of seasonally frozen ground and permafrost, p. 193–219. *In* Principles of geocryology. Pt. I, General geocryology. National Research Council of Canada, Ottawa. (Technical Translation 1121 by A. Nurklik.)
2. Barry, R. G. 1972. Climatic environment of the east slope of the Colorado Front Range. INSTAAR Occas. Paper No. 3, 206 p.
3. Black, R. F. 1954. Permafrost—A review. *Bull. Geol. Soc. Am.* 65:839–856.
4. Brown, R. J. E. 1960. The distribution of permafrost and its relation to air temperatures in Canada and the U.S.S.R. *Arctic* 13:163–177.
5. Brown, R. J. E. 1966. The relation between mean annual air and ground temperatures in the permafrost region of Canada, p. 214–247. *In* Permafrost: Proceedings of an international conference. National Academy of Sciences, Washington, D.C.
6. Brown, R. J. E. 1968. Permafrost map of Canada. *Can. Geogr. J.* 2:56–63.
7. Fahey, B. D. 1971. A quantitative analysis of freeze–thaw cycles, frost heave cycles and frost penetration in the Front Range of the Rocky Mountains, Boulder County, Colorado. Ph.D. thesis. University of Colorado, Boulder. 305 p.
8. Ives, J. D. 1973. Permafrost. *In* J. D. Ives and R. G. Barry [ed.] Arctic and alpine environments. Methuen, London.
9. Ives, J. D., and B. D. Fahey. 1971. Permafrost occurrence in the Front Range, Colorado Rocky Mountains, U.S.A. *J. Glaciol.* 10(58):105–111.
10. Kudryavtsev, V. A. Temperature, thickness and discontinuity of permafrost, p. 219–273. Principles of geocryology. Pt. 1: General geocryology. National Research Council of Canada, Ottawa. (Technical Translation 1187 by G. Belkov.)
11. Marr, J. W. 1961. Ecosystems of the east slope of the Front Range in Colorado. *Univ. Colo. Stud. Ser. Biol.* No. 8. 134 p.
12. Sumgin, M. I. 1937. Perennially frozen soil within the U.S.S.R. 1st edition Vladivostok, Moscow. 186 p.
13. Troll, C. 1972. Geocology and the world-wide differentiation of high-mountain ecosystems, p. 1–16. *In* C. Troll [ed.] Geocology of the high-mountain regions of Eurasia. *Erdwissenschaftliche Forschung*, Vol. 4. Franz Steiner Verlag, GMBH, Wiesbaden.
14. Weiser, S. 1875. Permanent ice in a mine in the Rocky Mountains. *Philos. Mag.* 49:322.

POSTGLACIAL PERMAFROST FEATURES IN EASTERN CANADA

Daniel Lagarec

UNIVERSITÉ LAVAL
Quebec City, Quebec

INTRODUCTION

Aerial photographic interpretation and field investigations were used in the southern parts of eastern Canada ($43^{\circ}30'$ to $49^{\circ}N$, 63° to $80^{\circ}W$), mostly in the province of Quebec, to describe several types of landforms associated with the former existence of permafrost (Figure 1). Current studies in northern Quebec (54° to $58^{\circ}N$, 68° to $78^{\circ}W$) suggest some genetic relations between recent forms observed there and similar forms observed in the south.

In those regions, tardiglacial (i.e., last period of Wisconsinan glaciation) and postglacial events were not simultaneous, and the sedimentary environments were partly similar and partly different. From the map showing the retreat of the Wisconsinan continental glacier,¹¹ deglaciation occurred about 13 500–12 000 B.P. near Halifax and Fredericton, 13 000–12 500 B.P. near Toronto, 12 500–11 800 B.P. in the Quebec region, and 10 500–9 500 B.P. in Abitibi.

After glacial retreat, the last three regions were covered by water: glacial Lake Iroquois in the Toronto region

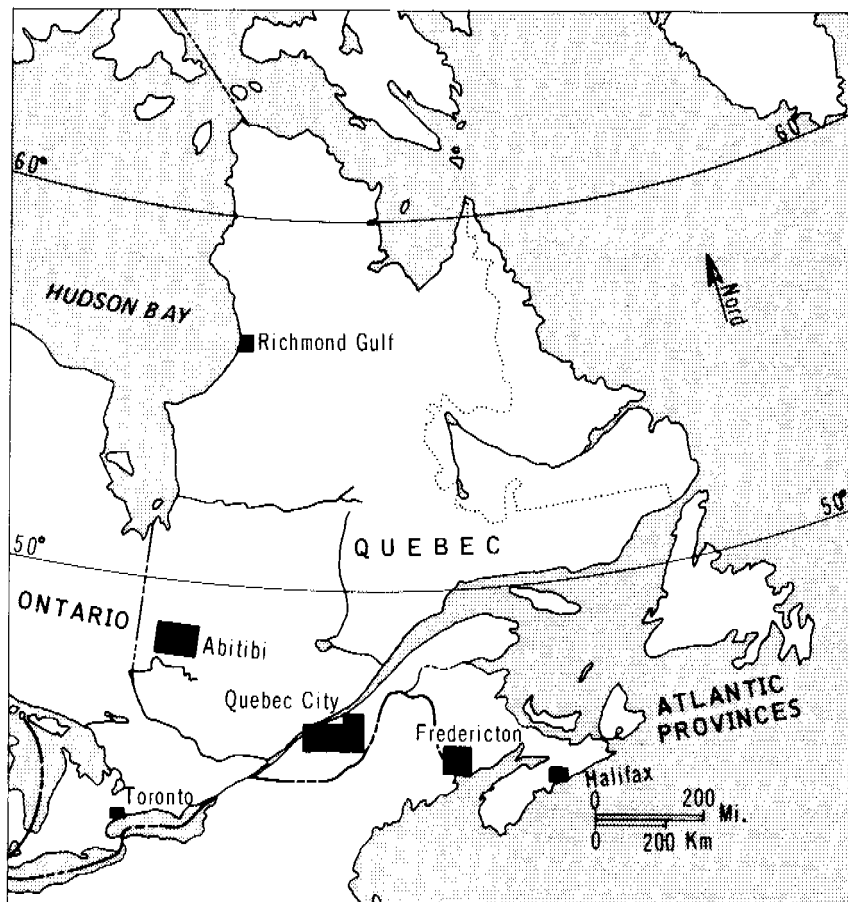


FIGURE 1 Location of investigated areas.



FIGURE 2 Aerial photograph of polygons in the Drummondville area. Small polygons exist inside larger ones in left of photograph. (Photo courtesy of Ministère des Terres et Forêts, Québec. Q 67 110-178. Enlarged to 1:5 000.)

(12 800–11 800 B.P.), Lake Barlow–Ojibway in Abitibi until 8 000 B.P., and the Champlain Sea (11 500–9 500 B.P.) near Quebec.

QUEBEC REGION

In the St. Lawrence River Valley, many traces of former permafrost were observed.⁵ Between Montreal and Quebec, in the Drummondville region, small polygons were noted on low Champlain terraces. Their greatest length is about 15 m, and they occur within larger polygons, 30–60 m long (Figure 2). Block polygons [1] were also observed near Trois-Rivières in Champlain clays next to depressions most probably thermokarst and at La Pocatière in Champlain littoral gravels. On the terraces of the Neuville region, about 30 km west of Quebec, 117 closed polygons were noted. Some were small and hexagonal, 20–30 m in diameter; others were large, pentagonal, and 40–60 m in diameter. In both cases, they occur in the alluvium of the St. Lawrence River terraces. On the higher terraces, the trenches surrounding the polygons are somewhat eroded, giving rise to a salient polygonal blocks morphology [2].

Seventy kilometres south of Quebec, the Scott–St. Gilles region has a slightly undulating relief. The eastern part has been cut by the Chaudière River and by many broad dry valleys, with gently sloping ($5\text{--}10^\circ$) sides, most probably periglacial in origin. The most characteristic features are areas of block polygons, hillocks separated by furrows, and polygons in some of the flat-floored valleys.

The most distinct polygons are located in the small valley of a meandering tributary of the Chaudière River (Figures 3 and 4). They have little relief, are outlined by narrow furrows, and measure 20–30 m in length. In some places, the furrows have determined the course of the tributary. In some dry valleys and on some benches, degraded polygons may be observed; the polygonal pattern is still apparent and the furrows are deeper.

On the $3\text{--}10^\circ$ slopes, the polygons are elongated and less distinct, and rillwash follows furrows that run parallel to the slope. On the top of the poorly developed hillocks, the relief is more chaotic. Polygonal forms are fewer, depressions are broader, thin furrows are only sporadically visible, and coalescing block polygons with small closed depressions at furrow intersections are evident.



FIGURE 3 Aerial photograph of blocks of terrane and polygons in the Scott region (southern Quebec). Note small well-preserved polygons in the lower right corner on both sides of the small valley; larger degraded blocks are evident in the centre. (Photo, Ministère des Terres et Forêts, Québec, 6016-9 L 4624. Scale, 1:15 840.)



FIGURE 4 Blocks of terrane near Scott, southern Quebec. Note the remnants of soil wedges in the depression at the left and small ponds on some blocks, two in the foreground, and one further to the left. (Photo D. Lagarec.⁷)

The forms of the hillocks may be quite variable: subdued, with only 1–3° slopes or more pronounced with 8–9° slope; more or less circular; or more complex in shape, with indentations and, in some cases, small depressions on the flanks.

The few observed profiles show no wedge-shaped cracks, but rather a type of soil wedges filled with brown, highly oxidized and frost-churned material. Cryoturbations and truncated soils may be observed in the mounds and remnants of buried soils in the depressions.

REGION WEST OF TORONTO

Near Toronto, observations were made by A. Cailleux and S. Occhietti in the northern half of the area covered by the 1:50 000 maps of Brampton (east and west sheets). Using the terminology of Veličko,¹² three principal types of morphology may be distinguished:

1. somewhat indistinct block polygons
2. microrelief of salient polygonal blocks and associated closed depressions
3. fan-shaped system of furrows

These features cover about 15 percent of the investigated territory and may be observed mainly on clayey till. The polygonal form is rarely well preserved. The furrows between the polygons are occupied by small streams that give a very distinctive pattern characteristic of this type of morphology. The block polygons average 30–50 m along the main axis (Figure 5).

The pattern of furrows is particularly evident on the ground; because of the clayey nature of the material, however, in vertical profiles, it has not been possible to discern any evidence of fossil wedges. However, some types of plastic diapirs affecting till and even the underlying Palaeozoic shales were found under certain mounds.

Aside from this type of phenomenon, there are calcite-filled wedges in deltaic sands 1 m high and 10–30 cm broad, as well as a calcareous hardpan that has been formed at or near the permafrost table or by freezing of soil solutions.

ABITIBI

Aerial photographs were investigated for the 1:50 000 maps of Landrienne, Rochebaucourt, Lac Gueguen, Val d'Or, and

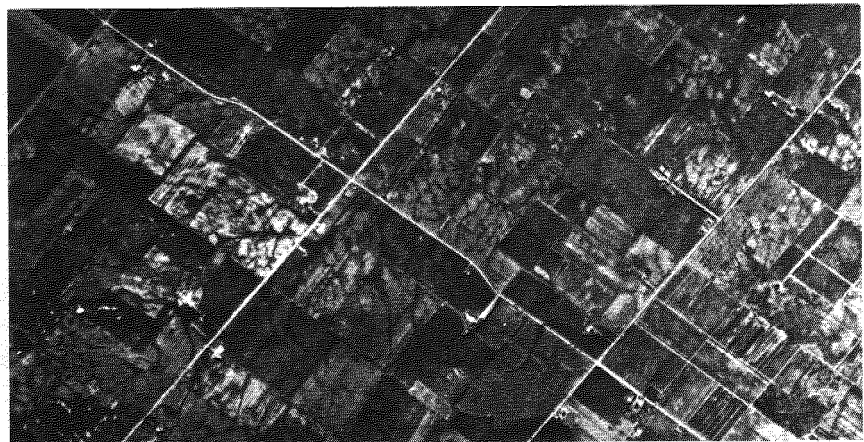


FIGURE 5 Aerial photograph of blocks of terrane west of Toronto. The more or less polygonal pattern is often accentuated by small streams flowing between the blocks and by small ponds or water at the intersections of cracks. (Photo, Department of Energy, Mines and Resources, Ottawa, A 19505-108. Scale, 1:15 840.)

Taschereau. The permafrost forms differ according to the nature of the material.

In lacustrine deposits where clay underlies a thin sand cover, block polygons 40–60 m in diameter are evident. They are quite fresh, their polygonal outline clearly preserved, and the furrows—being more moist—show darker.

String bogs are very numerous, some exhibiting peat rings enclosing ponds that may be the result of thawing of palsas. In fact, in northern Quebec, mostly near Poste-de-la-Baleine and Richmond Gulf where the permafrost is discontinuous, the thawing of palsas gives rise to a reticulate pattern that gradually accentuates and results in a patterned peat bog; thus, palsas and some types of string bog may be genetically connected (Figure 6).

Elsewhere in Abitibi, infilling of the bog has occurred, and peat rings—often accentuated by birch (*Betula*) and willow (*Salix*) stands—remain as the last trace of former palsas. It appears that some string bogs may be degradational forms of discontinuous permafrost. A differentiation in some gently sloping peat bogs may also be noted: upslope, the peat displays polygonal patterns; downslope, there are more or less rounded patches of vegetation. These aspects may possibly be interpreted as successive stages of evolution.^{7,8} The peat upslope in the polygons breaks loose and fragments float downslope to coalesce in the form of strings. The same process also appears to take place in shallow, sloping peat bogs in northern Quebec.

In Abitibi, in other peat bogs that result from infilling of lakes, polygons 10–15 m in diameter occur. Streams may be flowing in the trenches with meanders corresponding to the polygonal outlines. Such polygons may also be observed in alluvium. A statistical study of several rivers shows that the water courses have three or four preferential orientations and that the lengths of the segments vary between 15 and 30 m. In 20 percent of the cases, 25–40 m in diameter may be observed. Cuspate-banked rivers and beaded streams, with ponds 30–60 m apart, also are observed in the alluvium.

ATLANTIC PROVINCES: NEW BRUNSWICK AND NOVA SCOTIA

Flights over these currently temperate regions and aerial photographs reveal unusual land forms, mostly in lowlands and alluvial plains that are partly similar to those described above. For example, aerial photograph A 20896-48, west of Waterville, New Brunswick, shows some bead-like ponds on a left tributary of the Oromocto River that are probably due to the melting of ground ice.

Other round or egg-shaped ponds and bear-cub lakes (the outline of which shows one or several circular bow-shaped convexities) might also result from thermokarst. Other origins, such as intersections of rock fractures, mineral or organic infillings, littoral forms, or beaver dams, however, are also possible, and the question must remain open. They have been observed in the following locations: in New Brunswick, near Fredericton (photos A 11866-185 and 186), Oromocto River Valley near French Lake (A 20894 - 6 and 7), at Waterville (A 20896-46 and 48), and between the Saint John River estuary and Grand Lake (A 17865-13 and 15, A 20896-12 and 13, and an oblique air photo by J. C. Dionne²); in Nova Scotia, near Conrad (A 20307-17 and 18) and Musquodoboit Harbour (A 20307-58 and 60).

Concentrically patterned peat bogs should also be mentioned. They are minor forms, originating in a recent cool climate: in New Brunswick, near Fredericton (A 17866-117 and 118, A 21309-151 and 152); in Nova Scotia, north of Musquodoboit Harbour (A 20307-58 and 60).

INTERPRETATIONS AND CONCLUSIONS

An interpretation is proposed for the polygons and block polygons that are the most unusual forms studied by the author. These features show a great similarity with the types, also fossil, described by Veličko¹² in the Soviet plain. According to Veličko,¹² the rather good preservation

FIGURE 6 Aerial photograph of the evolution of a palsa bog (light grey mottling below centre) into a string bog (slightly above), with large ponds (black). Some palsa rings are still visible in the developing string bog. (Photo, Ministère des Terres et Forêts, Québec, 1226-8. Enlarged to approximately 1:10 000.)

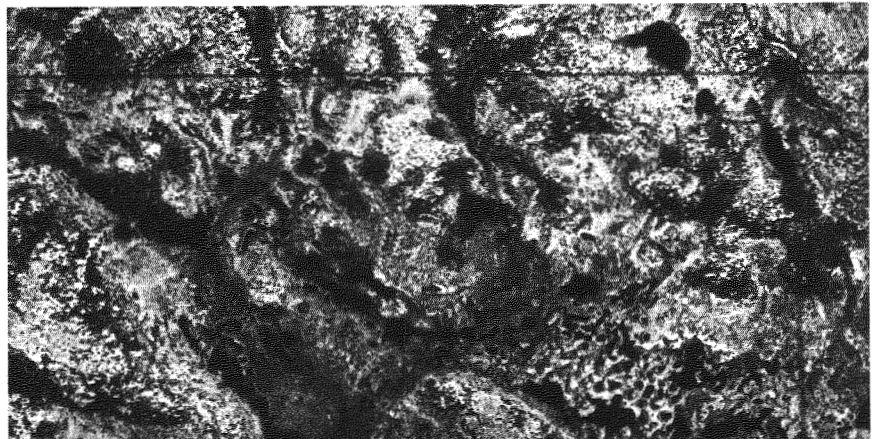


FIGURE 7 Aerial photograph of blocks of terrane visible in the center (light grey) that are forming at present in the Richmond Gulf area, northern Quebec. Ponds, which are thermokarst depressions, are more numerous at the rock contact. (Photo, Department of Energy, Mines and Resources, Ottawa. Enlargement of photo A 15618-39. Approximate scale, 1:17 000.)



of the pattern indicates that there were not broad ice wedges since the melting of large quantities of ice would have caused spreading of the edges of the polygons. Most frequently, the wedges consisted of a mixture of soil and ice or simply soil. This hypothesis is supported in Quebec by the fact that the most distinct polygons are found in coarse material. Other forms, observed chiefly in a thin sand cover overlying clay apparently derive from a polygonal pattern whose edges spread due to their greater ice content. Erosion later widened the furrows.

This morphology of salient polygonal blocks with soil wedges is developing currently in northwest Siberia under a cold, humid climate with prolonged snow melting near the southern limit of permafrost.¹⁰ It is found there in different types of material: silts, sands, and even gravels. A polygonal pattern is proof that there has been permafrost.³ Similar features have been observed in regions without permafrost or where the permafrost table is far below the ground surface. Contraction cracks form in the seasonally frozen layer during the winter; some soil falls into the cracks during the summer thaw. The resulting pattern is similar but complicated by erosion of small streams.¹⁰

Similar forms have also been observed in northern Quebec in the discontinuous permafrost zone, in a cold, humid climate (mean annual air temperature, 4.5 °C), with a thin snow cover (15–20 cm on the mounds) (Figure 7); the soil consists of 1–1.5 m thick marine sand overlying clay. The following stages result in nearly circular mounds and flat-bottomed depressions have been observed:

1. Polygonal cracking of a uniform surface in blocks 10–20 m long
2. Formation of flat-topped and steep-sided mounds, by erosion along the cracks
3. Smoothing of mound slopes by sliding of side material

These observations in northern Quebec appear to corroborate those made in the Soviet Union^{10,12} and lead to the conclusion that, in southern Quebec, these features have been formed under similar conditions, namely: discontinuous permafrost, cold humid climate, with a mean annual air temperature of –2 to –4 °C, meaning 5–7 °C cooler than the present temperature.

Fossil ice wedges and other periglacial phenomena have been ascribed to a periglacial climate following the retreat of the Champlain Sea, 9 000 years ago.² Others have postulated other cold postglacial periods:^{1,4} Such periods have been mentioned in Europe by Schove (4 500, 3 300, and 2 800 B.P.); in the Alps by Heuberger⁶ (5 500–4 000, 3 350–3 150, and 2 850–2 250 B.P.); in the Keewatin district by Nichols⁹ (2 100 B.P.), and at Porcupine Mountain, Manitoba (2 450–2 000 B.P.).

The existence of polygons at Neuville and involutions at Quebec City on the 7-m-high terrace gives a maximum age of 6 000 B.P. for those periglacial phenomena. Thus, there has been a cold period sometime in the past 6 000 years.

REFERENCES

1. Cailleux, A. 1969. Le Quaternaire du Québec. *Rev. Géogr.* 23(3): 229–232.
2. Dionne, J. C. 1971. Fentes de cryoturbation tardiglaciaires dans la région de Québec. *Rev. Géogr.* 25(3):245–264.
3. Dylík, J. 1961. Quelques problèmes du pergélisol en Pleistocène supérieur. *Bull. Soc. Sci. Lett.* 12(7):1–21.
4. Gangloff *et al.* 1971. Le problème du tardiglaciaire au Québec méridional. *Rev. Géogr.* 25(3):305–308.
5. Hamelin, L. E. 1971. Dans la plaine laurentienne, la glace du sol aurait-elle contribué au façonnement des glissements et autres formes de relief en creux? *Cahiers Géogr.* 36:439–465.
6. Heuberger, H. 1968. Die Alpengletscher in Spät- und Postglazial. *Eiszeitalter Ggw.* 19:270.

7. Lagarec, D. 1971. L'évolution des versants d'une partie de la colline de Québec. M.A. thesis. Université Laval, Quebec.
8. Lagarec, D. 1972. Paleoformes de pergélisol dans la région de Québec, Canada. C.R. Acad. Sci. Paris No. 274. p. 995-998.
9. Nichols, H. 1970. Late Quaternary pollen diagrams from the Canadian arctic barren grounds at Pelly Lake, northern Keewatin, N.W.T. *Arctic Alp. Res.* 2(1):43-62.
10. Popov, A. I., *et al.* 1966. Features of the development of frozen geomorphology in northern Eurasia. *In* Permafrost: Proceedings of an international conference. National Academy of Sciences, Washington, D.C.
11. Prest, V. K. 1969. Recent Wisconsin and Recent ice in North America. *Geol. Surv. Can. Map 1257A*. Scale 1:5 000 000.
12. Veličko, A. A. 1972. La morphologie cryogène relicte: Caractères fondamentaux et cartographie. *Z. Geomorphol. Suppl.* 13:59-72.

NOTES

[1] Block polygons or terrane blocks; term used by Veličko¹² to refer to polygonal hillocks separated by furrows.

[2] Salient polygonal blocks morphology; term used by Veličko¹² to refer to the remnants of a polygonal system whose centres are prominent due to erosion of the surrounding furrows.

THE OCCURRENCE AND CHARACTERISTICS OF NEARSHORE PERMAFROST, NORTHERN ALASKA

Robert I. Lewellen

Littleton, Colorado

INTRODUCTION

Permafrost is known to occur under the coastal waters of the Chukchi and Beaufort seas north of Alaska. However, its exact distribution and characteristics are not known. This paper discusses part of a study to determine the distribution and characteristics of the permafrost occurring nearshore from Cape Beaufort to Demarcation Point, Alaska. The approach of the study is to examine the field conditions, to obtain the necessary field measurements, and from them to model the distribution and character of this undersea permafrost.

The Physical Setting

The marine environment under investigation encompasses the shelf area adjacent to the Arctic Coastal Plain province. In general, the province represents the emergent stage of the present offshore conditions. The province lies entirely within the continuous zone of permafrost. The direct distance from Cape Beaufort to Point Barrow to Demarcation Point is approximately 1 100 km. The length of the actual coastline is much greater. Approximately 60 percent of the coast, comprising five segments, has barrier islands backed by shallow lagoons, and 40 percent of the coast, also in five

segments, is mainland exposed to the sea. Some of the barrier islands are erosional remnants of the mainland and exhibit polygonal ground and tundra. Other, older barrier islands that are not remnants have some vegetation and weakly developed ice wedge polygons.

Seawater Temperatures

An analysis of water temperature data revealed that there is a distinct difference between the Chukchi Sea and the Beaufort Sea bottom water temperatures. The former are well defined for the months of May through November, but the latter are only well defined for February, March, and July through October.

Computation of the mean annual bottom water temperature is therefore critically dependent on the value assumed for the missing months. There is growing evidence, especially in the nearshore areas with water depths less than 20 m, that the value should be approximately -1.8°C . Using this figure, the mean annual bottom water temperature in the Chukchi Sea is -0.67°C and in the Beaufort Sea -1.27°C . Using MacGinitie's Chukchi Sea data,⁵ a mean of -0.65°C was computed.

The maximum mean monthly bottom water temperature for the Chukchi Sea is 3.76°C (August) compared with

0.76 °C (July) for the Beaufort Sea.

The computed minimums are -1.84 °C (June) for the Chukchi Sea and -1.62 °C (October) for the Beaufort Sea bottom waters.

FIELD EQUIPMENT AND METHODS

Drilling

For this reconnaissance work, a light-weight drive sampler was developed, constructed, and field-tested. The unit, consisting of steel tubing with a removable center rod, is powered by a drill/breaker. The tubing is fitted with a hardened steel tapered driving shoe. The center rod is fitted with a hardened tip that matches and fits within the tapered shoe of the tubing to provide a conical bit. Upon reaching a desired level beneath the sea floor, the center rod and tip are pulled out of the tubing. A thermistor probe and soil sampler can pass through the tubing for measurements and sampling. The possible sampling depths are a function of the bottom materials. With the present design, maximum depths of 15 m are possible.

Temperature Probes

The temperature sensors are precision thermistors placed in a stainless steel probe. The probe diameter is 4.2 mm. The thermistors are located in the lower 76 mm of the 89-mm-long probe body. The top of the probe is fitted with a 0.15 m segment of 11 mm diameter, high strength, low thermal conductivity, plastic tubing. The upper end of the plastic tubing is fitted with steel tubing. The lead wires are

sheathed with woven stainless steel fibers. The sheath is attached to the steel probe body, but does not make contact with the lead wires or the thermistors. The sheathed design is useful for the dissipation of static electricity. The Wheatstone bridge metal case can be grounded to the sheath.

The resistance of the thermistors are measured with a portable precision Wheatstone bridge, equipped with an electronic null detector. The bridge voltage has been modified to prevent self-heating of the thermistors. There is an approximate 2-ohm change in resistance for each 0.01 °C change in temperature. Therefore, temperature variations as small as 0.01 °C are easily detected with this instrumentation.

During temperature measuring operations, the Wheatstone bridge is sealed into an insulated instrument box. The box has two Neoprene hood gloves attached to collars built around arm openings in the front of the box. The top of the box is fitted and sealed with a clear plastic plate. The bridge can be operated without exposing the instrument to the weather or seawater.

FIELD INVESTIGATIONS

The first area to be examined was Elson Lagoon, south and east of the Point Barrow spit. (Figure 1) This lagoon begins to flood over the ice by snowmelt by approximately June 15. The melt water moves across the areas where the ice cover is frozen to the bottom and floods the floating ice areas. Even though the ice begins to decay rapidly by June 15 the lagoon is not usually free of ice until July 15. By

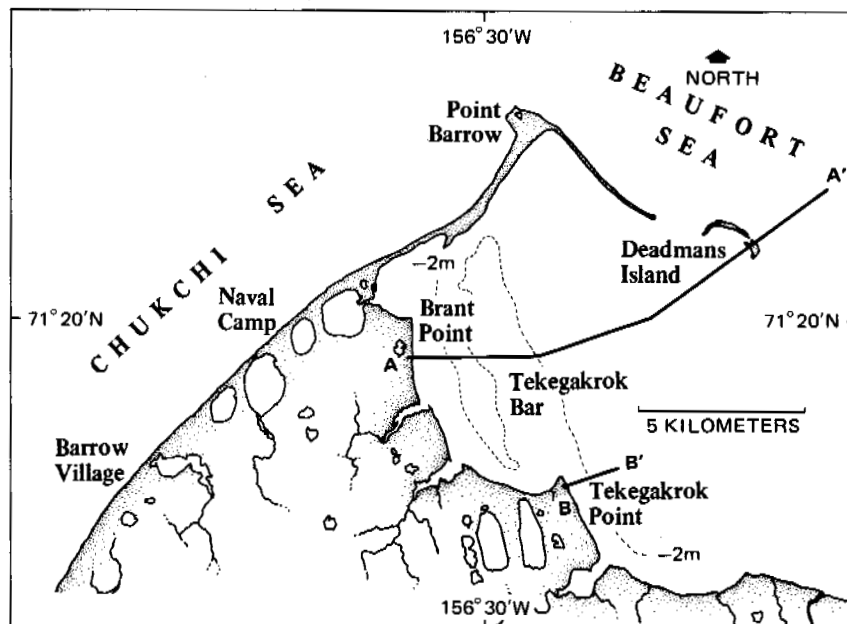


FIGURE 1 Elson Lagoon, Point Barrow, Alaska.

late September or the first of October, a cold easterly storm will build strands of frazil ice, beginning the process of freezeup.³

Northern Elson Lagoon has a maximum water depth of about 3 m. Except for sandbars and spits at the mouth of small estuaries, the western shoreline is characterized by thermal planation or truncation of permafrost. A large bar north of Tekegakrok Point has been derived from the eroding shoreline south of the point. The eastern boundary of Elson Lagoon is formed by the Plover Islands and the large sand spit that trails southeast of Point Barrow. Bottom sediments consist of fine sands and silts on the thermally truncated benches and fine organic-mineral mucks on the deeper areas.

The western shoreline is retreating and truncating, and the sudden change in environment affects the permafrost temperatures and other characteristics. Table I lists the characteristics of the permafrost along the eroding shoreline of western Elson Lagoon.⁴ The soils data for the permafrost above sea level were obtained from the unpublished field records discussed by Brown.¹ The land-area bore-hole data in Table II were summarized from approximately 500 soil moisture determinations. It appears that most of the possible settlement occurs within the upper 5 m. This implies that in a typical area of eroding shorelines, where the land is 3 m above sea level, an average of 0.26 m of settlement is possible in the first 2 m below sea level. Tables I and II exclude ice-wedge ice. The ice wedges along the western Elson Lagoon shore average from 1 to 2 m wide and from 2 to 3 m in vertical extent.

Preliminary observations have been made on five different types of permafrost environments. The first type is the shallow lagoon water area east of Brant Point. The sec-

TABLE II Ice Volume and Possible Settlement for Land Area,^a Barrow, Alaska

Depth (m)	Average Ice Volume (%)	Average Possible Settlement (m/m)
0-1	74	0.56
1-2	64	0.40
2-3	56	0.26
3-4	51	0.17
4-5	46	0.09
5-6	41	0

^a Excludes ice-wedge ice.

ond environment is the waters east of Tekegakrok Point. The third type is the flat deep lagoon floor west of the barrier islands; the fourth, the Beaufort Sea adjacent to the east side of the barrier islands; and the fifth, the large Holocene bar north of Tekegakrok Point.

Since there was no rotary drilling equipment available, it was decided that a reconnaissance would be a productive start for the study. By measuring the bottom temperatures in September (1971) and again in May and June (1972), it was possible to acquire an insight of the maximum and minimum temperatures to be encountered. The temperatures were rounded off to the nearest 0.1 °C for the purposes of this paper. The results are summarized on Figures 2 and 3.

DISCUSSION

Sea level, at or near the present level for the past years, can simulate eustatic change by the thermal erosion of the

TABLE I Permafrost Characteristics for Brant Point, Central Marsh Slough Vicinity^a

Elevation (m)	Pore Water Salinity (%)			Average Moisture Content (%)	Average Ice Volume (%)	Average Possible Settlement (m/m)	Number of Observations
	max.	ave.	min.				
3-2	2	1	1	150	82	0.68	8
2-1	8	4	1	116	77	0.61	12
1-SL	15	10	3	62	65	0.39	17
-0.6--1	58	48	32	25	42	0	10
-1--2	70	48	18	24	41	0	15
-2--3	68	37	9	23	40	0	15
-3--4	30	20	12	22	39	0	5
-4--5	33	26	23	22	39	0	3
-5--6	20	18	17	19	36	0	2
-6--6.5 ^b	24	24	24	33	49	0.13	1

^a The material averages 1.3 percent gravel, 55.3 percent sands, and 43.5 percent silts and clays. The Skull Cliff unit was 0.5 percent gravel, 44.0 percent sands, and 56.0 percent silts and clays. Observations were made from auger boring samples. The samples from -0.6 to -6.5 m were taken from 5 borings located in Elson Lagoon, at distances of 10-30 m from shore. The interval from Sea Level (SL) to -0.6 m was the lagoon ice cover.

^b Skull Cliff unit.

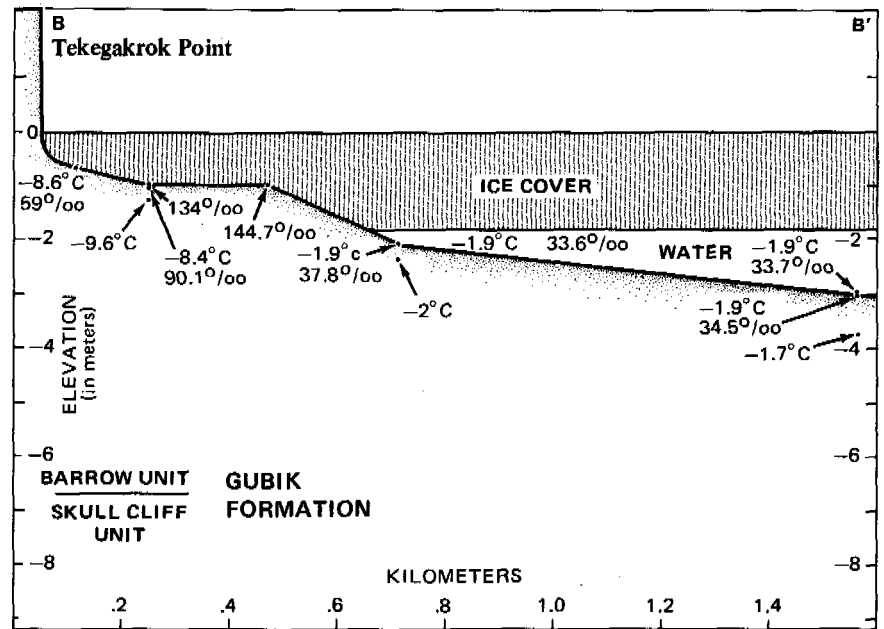


FIGURE 2 Cross section of Tekegakrok Point.

coastline. Rates of erosion ranging from 10 to 30 m per year, although operational only for the brief open-water period, can account for shoreline changes of 5-15 km in just 500 years in the Beaufort Sea region. With mean annual bottom water temperatures below -1.0°C , there is expected to be considerable expanses of offshore permafrost. Temperatures below 0°C under parts of the sea floor are enhanced by the shifting spits, bars, and barrier islands. This shifting complicates the temperature profiles. Eroded lake basins will also complicate the temperature profiles of Elson Lagoon.

The data on Chukchi and Beaufort seawater tempera-

tures and salinities are adequate for the study of offshore permafrost. However, more temperature, salinity, and ice-cover information is required for the lagoons, bars, bays, and barrier island environments. The salinities are useful guides to possible temperatures when temperature observations are missing. Fresh waters from the rivers locally affect the lagoon, bay, and sea temperatures. Information is available on the largest river in the problem area.⁷

The nearsurface brines that underlie the Barrow land area are probably related to the marine waters of the Woronzofian transgression and may interfinger with seawater and brines under the present seas. The brines were

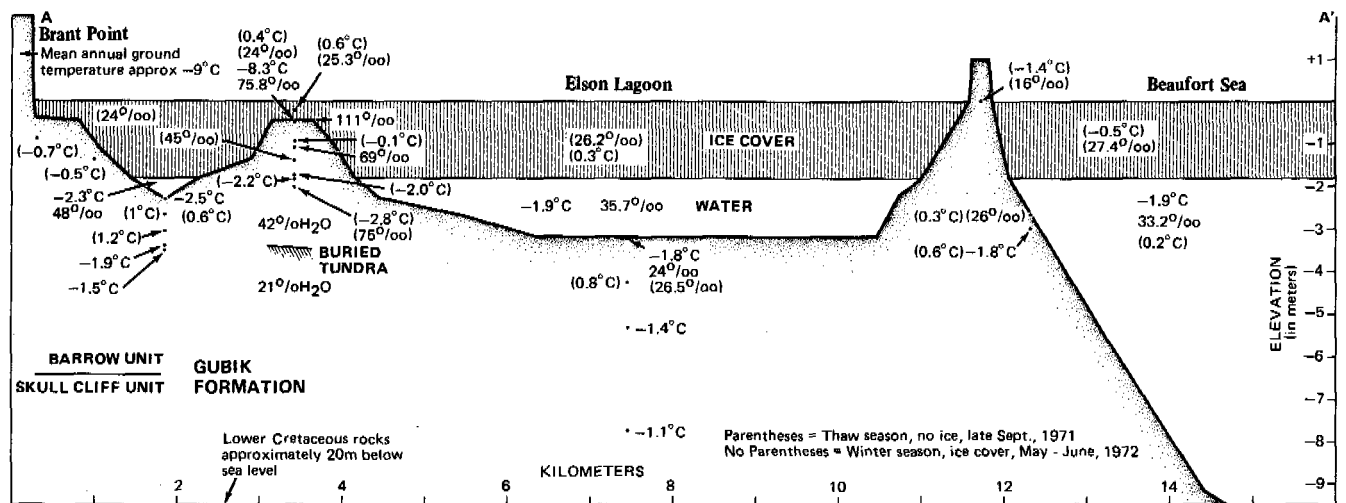


FIGURE 3 Cross section of Elson Lagoon.

probably concentrated since they were segregated from the interstitial waters by permafrost aggradation associated with the regression at the end of the Wisconsin. A brief, cold water temperature transgression could conceivably move over the low, present frozen terrain and then regress without leaving any evidence of brines or marine waters. The marine waters could have been flushed and leached out of the thin seasonal thaw zone. The only evidence that can be seen is a faint wave-cut strand. Brief high stands of sea level during the past few thousand years could be of this character.

The climate and shoreline history for the past 14 000 years is generally known. A drilling program will provide data that will refine the present knowledge. During the last glacial maximum, sea level was probably 100 m lower than the present sea level. The climate was severe enough to aggrade permafrost on the emergent land. Transgression was rapid during the approximate period of 10 000 to 5 000 years ago. Rapid and steady transgressions of seawaters, with mean annual temperatures lower than 0 °C, have probably preserved relict permafrost offshore. The sea bottom topography reveals old shorelines that are related to the last 14 000 years of eustatic changes. At distances of 6–12 km and 20 km northeast of the present geographic Point Barrow, two relict beach ridge and spit features represent the –10-m stillstand (approximately 6 000 years B.P.) and the –38-m stillstand (14 000 years B.P.), respectively.

Relict marine features similar to active features offshore can be identified within the Teshekpuk section of the Arctic Coastal Plain province. Concordant elevations, both on the land and offshore, testify to particular surfaces that are correlative in time and process.⁴

Field sites were selected on a geomorphic and thermal basis. Since it is not possible to study all locations, specific types of situations can be classified, studied, modeled, and extrapolations made from the data. The geomorphic processes, rates, and changes in the rates are important in evaluating the distribution of permafrost conditions under the sea. Field sites provide data on the aggradation of permafrost under areas of active deposition and on the lowering of the mean annual ground temperatures in these areas. Other sites provide data on the degradation of permafrost by coastal erosion and raising of the mean annual ground temperatures. Sites with a gradation of conditions between the two extreme environments also are being examined.

Mean annual bottom temperatures are more complicated along some of the more rapidly changing shorelines. More information is needed from areas where entire barrier islands have recently been eroded away. Conversely, information is needed on areas of recent sedimentation. All of the evidence examined so far indicates extensive areas of permafrost conditions under the marine waters.

The shallow nearshore bottom waters may be warmer during the summer, but these areas are much colder during

the winter than bottom waters farther out to sea. This may be especially true in areas where the circulation with the main body of seawater is restricted.

In comparison to the sea, slightly warmer summer waters may persist in the lagoons where water depths are greater than the winter ice-cover thickness. These same waters appear to be cooler in the winter. The lagoonal areas deeper than the seasonal ice cover are essentially the same thermally as the sea except for the influences of bars, barrier islands, and adjacent mainland. The marine areas where the ice cover freezes to the bottom are, in general, thermally comparable to the land areas; however, the condition quickly changes when the ice cover floats over waters that do not freeze in the winter. The detailed hydrographic surveys are being used to map the coastal areas where the annual ice cover freezes into or down to the bottom sediments. The nearshore areas that are isolated by ice barriers from the deeper waters can be identified. The smaller changes in bottom elevations can be studied from the hydrographic charts. As the seawaters transgress the coast, the bottom elevations move farther below sea level with distance away from the shoreline. This is transgression by thermal erosion or truncation without a tectonic or eustatic change. The change in bottom elevation is due, in part, to thaw subsidence and consolidation. On parts of these thermally truncated or thermal planation benches, storm waves and weak currents and tides winnow and scour fine material.

CONCLUSION

From Tables I and II it appears that there is little thaw subsidence and consolidation possible in the Brant and the Tekegakrok areas except for a small amount of ice-wedge volume loss. As the sea thermally truncates the land, modifications to the existing permafrost, at or below the level of truncation, are in the form of mean annual surface temperature change and the possible circulation of seawater in the new seasonal thaw layer. In general, a warmer but still negative mean annual temperature prevails after the shoreline passes. O'Sullivan⁶ notes that deformation could result from the brine volume changes responding to temperature changes. The situation can be further complicated by sedimentation over an area of recent thermal truncation. If thaw subsidence and consolidation occurs on truncation, then frost heaving must occur in some of the aggrading bars and spits. Rapid erosion and deposition around islands are localized problems that affect the subsea permafrost.

A thermally truncated site such as the Brant Point shoreline area is protected to a degree by the Tekegakrok bar. Truncation, the lack of any significant currents, and sedimentation have built a bench 600 m wide over the past 220 years. For the past 220 years, a truncated bench has been constructed for 510 m, perpendicular to the shoreline, off Tekegakrok Point. The east side of the bench has lost ap-

proximately 1.5 m of sediments, vertically, due to wave action and transport by currents. The Brant Point site has an average erosion rate of about 1 m per year, compared with 2.3 m per year for the Tekegakrok area.

Southeast of Point Barrow Olukralik Point, exposed to the Beaufort Sea through Ekilukruak Entrance, erodes at approximately 10 m per year. At 220 years away from the present shoreline (2.2 km) at Olukralik Point, the water depths are 3 m. This indicates that 1.5 m more of bottom sediments were eroded mechanically from the Olukralik bench than was eroded from the Tekegakrok bench. The thaw season wave action is more active at Olukralik than at Tekegakrok. Continuing southeast, the areas of Drew Point and Cape Simpson erode at a possible rate of about 30 m per year.² At 220 years off of Cape Simpson and Drew Point (6.6 km), the water depths are 7-9 m. Drew Point and Cape Simpson are fully exposed to the Beaufort Sea. The thermally truncated bench is less than 200 m wide at Cape Simpson and at Drew Point. At the present erosion rates, the 200-m-wide bench represents only 7 years of age. The 510-m-wide bench at Tekegakrok represents 220 years of age.

If the sea level has been oscillating only 1-3 m around the present level for the past 3 000 or 4 000 years, and if allowances are made for changes in coastal erosion rates, extensive areas of truncated permafrost must still exist under the Beaufort Sea floor.

ACKNOWLEDGMENTS

This work is sponsored by The Arctic Institute of North America with the approval and financial support of the Office of Naval Research under contract N00014-70-A-0219-0001 (subcontract ONR-433). Field and logistical support was provided by the Naval Arctic Research Laboratory, Barrow, Alaska.

REFERENCES

1. Brown, J. 1969. Buried soils associated with permafrost, p. 115-127. *In* Symposium on pedology and quaternary research. University of Alberta, Edmonton.
2. Leffingwell, E. deK. 1919. The Canning River region, northern Alaska. U.S. Geol. Surv. Prof. Paper 109. U.S. Geological Survey, Washington, D.C. 251 p.
3. Lewellen, R. I. 1970. Permafrost erosion along the Beaufort Sea coast. [Pub. by the author] P.O. Box 1068, Littleton, Colorado. 25 p.
4. Lewellen, R. I. 1972. Studies on the fluvial environment, Arctic Coastal Plain province, northern Alaska. Vol. I and II. [Pub. by the author] P.O. Box 1068, Littleton, Colorado. 281 p.
5. MacGinitie, G. E. 1955. Distribution and ecology of the marine invertebrates of Point Barrow, Alaska. *Smithsonian Misc. Collect.* 128(9). 201 p.
6. O'Sullivan, J. B. 1966. Geochemistry of permafrost, Barrow, Alaska, p. 30-37. *In* Permafrost: Proceedings of an international conference. National Academy of Sciences, Washington, D.C.
7. Walker, H. J. Salinity changes in the Colville River Delta, Alaska, during breakup. *In* Proceedings, Symposium on the role of snow and ice in hydrology. Banff. (In press)

GEOPHYSICAL IDENTIFICATION OF FROZEN AND UNFROZEN GROUND, ANTARCTICA

L. D. McGinnis

NORTHERN ILLINOIS UNIVERSITY
DeKalb, Illinois

K. Nakao

HOKKAIDO UNIVERSITY
Sapporo, Japan

C. C. Clark

NORTHERN ILLINOIS UNIVERSITY
DeKalb, Illinois

INTRODUCTION

The dry valleys of Victoria Land, lying 75 km west of McMurdo Station, Antarctica, contain over 4 000 km² of essentially ice-free rock exposures lying between 77 and 78°S and 160-164°E (Figure 1). The valleys, scoured by glaciers over 4 million years B.P.,⁵ are oriented east-west, are at present ice free, and contain warm and saline lakes. In a recent study,²⁰ the valleys are described as being relict

fjords, having emerged above sea level in late Pliocene time due to a general glacial withdrawal and concomitant isostatic rebound of the Transantarctic Mountains.

The dry valleys have been described as a cold desert.¹⁶ Mean annual air temperature is estimated to range from -18 to -25 °C in various parts of the valleys.^{8,16} Near-surface soil temperatures may reach 15 °C or higher for short periods during the day.

Rocks exposed in the valleys are divisible into five groups.

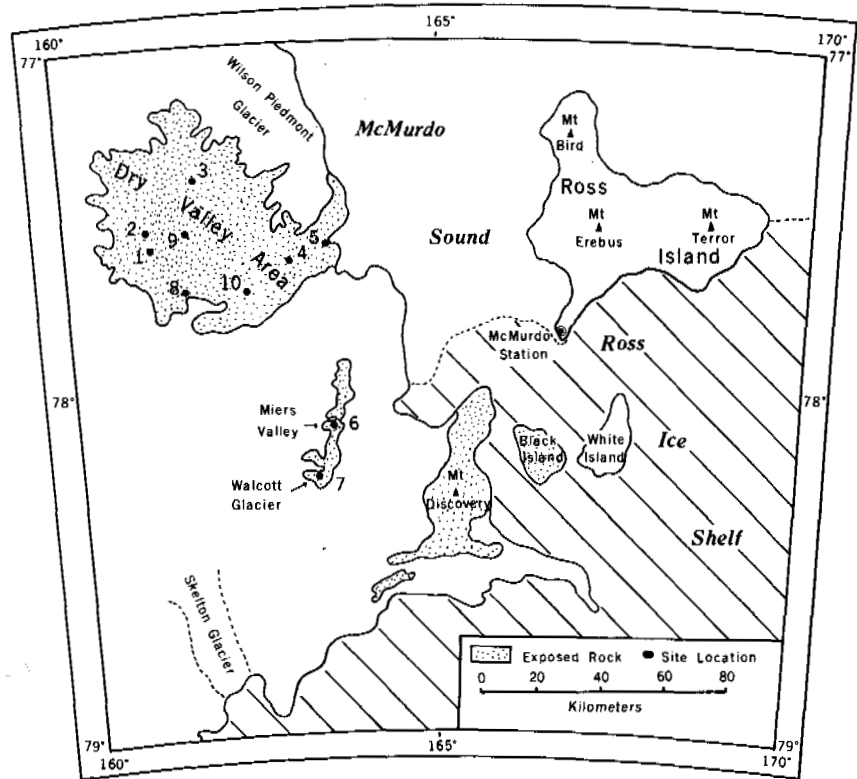


FIGURE 1 Geophysical exploration sites.

The Precambrian–Lower Cambrian crystalline basement complex contains over 4 500 m of marbles, schists, granites, and granodiorites.⁹ These igneous and metasedimentary rocks are highly folded and faulted. Beacon Supergroup sandstones unconformably overlie basement and range in age from Devonian to Cretaceous.¹ Beacon sandstones exposed in the uplands dip 3–5° westward. Ferrar dolerite sills of Jurassic age intrude the basement and Beacon Supergroup rocks.⁶ The sills were recently outlined using aeromagnetic measurements.¹³ Late Tertiary, McMurdo Volcanics—primarily basalts, trachytes, and kenytes—are present locally throughout the valleys.¹ Pliocene, Pleistocene, and recent deposits of eolian, lacustrine, glacial, and marine origin occur everywhere along the valley floors.

Surficial geophysical studies in the dry valleys of the Transantarctic Mountains were undertaken in preparation for the forthcoming Dry Valley Drilling Project (DVDP).¹¹ The project is the first of several international, multidisciplinary drilling programs now planned in Antarctica. It is hoped that the cores will permit a detailed reconstruction of Antarctic Cenozoic history.

An American and Japanese field team, utilizing reversed seismic refraction techniques and Schlumberger and Wenner electrical resistivity methods, conducted the study. In addition, laboratory sonic and electrical measurements were made on selected water, soil, and rock samples in order to better define and predict subsurface physical conditions.⁴

Geophysical studies on soils, ice, and rock in the dry valley region have been reported by several authors.^{2,10,15,19} It was concluded from previous seismic studies that velocities of frozen ground are similar to those of ice, and therefore buried ice cannot be identified by seismic methods. Although most areas are underlain by high velocity (>3 km/s) frozen ground,^{2,19} electrical resistivity measurements indicate that the frozen ground is thin near lakes and that the lakes themselves rest on unfrozen sediment.¹⁰

Laboratory geophysical measurements on frozen ground, referred to as confining permafrost in this paper (i.e., not permitting the flow of fluids¹⁰), have been made by several authors.^{10,14,17} The increase in velocity upon freezing was found to be a function of the initial porosity,¹⁷ whereas electrical resistivities in porous, saturated media were found to increase by several orders of magnitude upon freezing.¹⁰

LABORATORY GEOPHYSICAL MEASUREMENTS

Electrical resistivities were measured on surficial samples with a Wheatstone bridge, having a resistance range from 10^{-3} to 10^7 ohm. Laboratory samples were frozen into flat-ended cylinders; medical electrode jelly was applied between electrodes and the ends of samples to ensure good electrical coupling.

Electrical and seismic properties of rock, water, and soil samples were measured through temperatures ranging from

-76 to 24 °C. Resistivity measurements were made at 10 to 20 °C increments through the temperature range where electrical properties of a sample changed rapidly. Where the temperature-versus-resistivity curve became asymptotic, measurements were made at greater increments. Table I lists representative dry valley samples with resistivities at varying temperatures. Figures 2, 3, and 4 illustrate the temperature-resistivity curves of water, soils, and nonporous rock, respectively. Dilute and pure Don Juan Pond water, Lake Vanda bottom water, and triple distilled water were

used in the experiments.²¹ The general equation for these curves is:

$$\rho = ae^{b/T}, \tag{1}$$

where T is absolute temperature, and a and b are coefficients.

All ρ - T curves have the same general appearance, that is, they are concave upward on semilog plots. At temperatures greater than 0 °C, all saturated, porous soils and rocks have resistivities less than 700 ohm-m, whereas nonporous rocks

TABLE I Resistivity of Dry Valley Soils, Water, and Rock at Controlled Temperatures

Sample No.	Material	% Don Juan Pond Water in Pore Fluid	Bulk Density (kg/m ³)	Resistivity (ρ) (ohm-m) at Following Temperatures (T) (°C)											
				+24	-6	-24	-31	-41	-50	-60					
1	Saturated Lake Vida sand	100	1 720	10	11	15	24	30	43	228					
				7	10	20	28	33	143	2.6×10^4					
				9	10	23	30	54	170	2.4×10^5					
				6	9	18	27	38	86	1×10^6					
				+24	+3	-15	-27	-42	-52	-62					
5 ^a	Saturated Lake Vida sand	0	1 720	488	874	5×10^5	Too great to measure								
				+24	-8	-28	-44	-54	-64	-70					
6	Saturated Don Juan Pond soil	100	-	8	10	16	28	115	406	1.8×10^4					
				+24	+2	-15	-27	-34	-52	-60					
7	Saturated lake clay	100	-	0.1	1	2	2	2	32	473					
				+24	-2	-15	-31	-42	-65						
8 ^a	Lake silt saturated with distilled H ₂ O	0	-	7	8	23	10^3	3.1×10^4	4.7×10^5						
				+24	-3	-15	-22	-35	-42	-54	-64				
9	Distilled H ₂ O mixed with Don Juan Pond water	33	-	8	9	10	12	16	22	1010	5.1×10^4				
				7	9		13	20	37	734	1.9×10^5				
10		25	-	+24	0	-14	-20	-31	-42	-49	-58	-76			
11	Don Juan Pond water	100	-	8	13	15	15	19	21	31	35	4.8×10^4			
12	Vanda water	0	-	9	10	15	19	30	133	259	4.1×10^5	-			

^a Triple distilled water increases from 2.3×10^3 ohm-m before freezing to $>1.5 \times 10^6$ ohm-m after freezing.

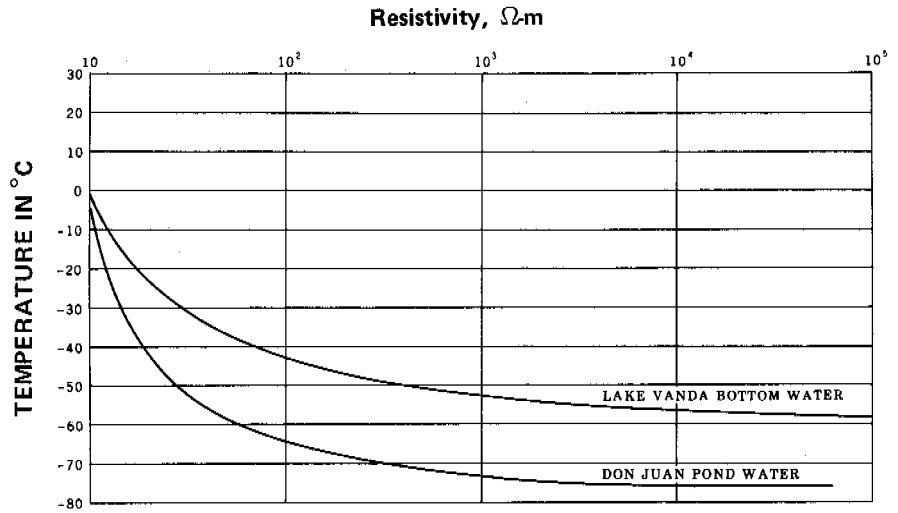


FIGURE 2 Resistivity in ohm-metres versus temperature for two saline water samples.

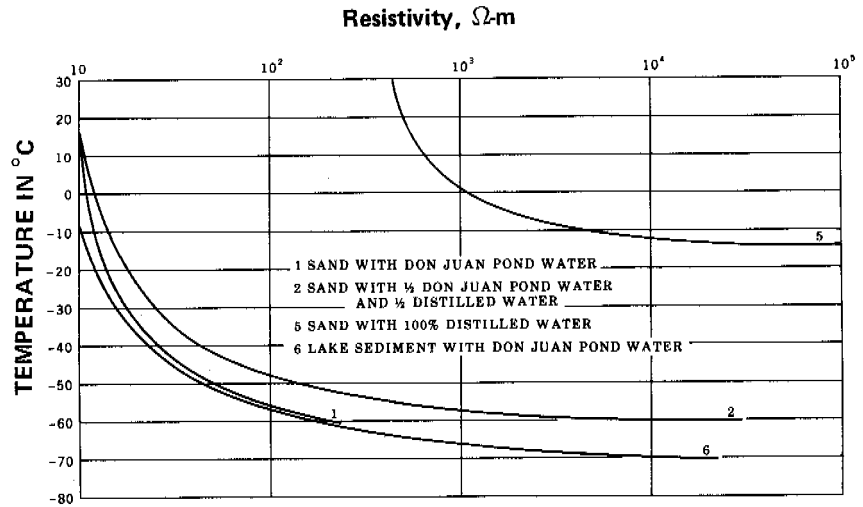


FIGURE 3 Resistivity (ohm-m) versus temperature for selected water-soil mixtures. See Table I for soil-water description.

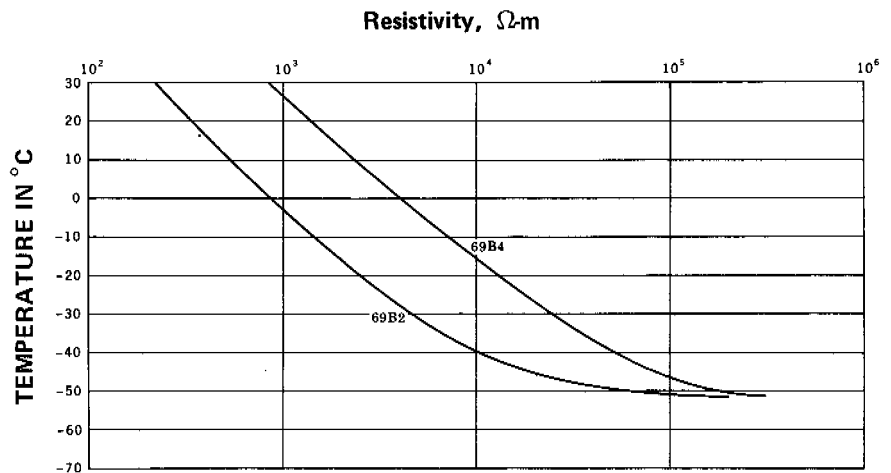


FIGURE 4 Resistivity (ohm-m) versus temperature for two rock samples. 69B2 is a vesicular basalt, and 69B4 is a granite gneiss.

may have resistivities as great as 5 000 ohm-m at 0 °C. In porous materials, the freezing point of pore water controls the point of maximum change in slope of the curves, and the freezing point is determined by water chemistry. Because of the high concentration of salts in the soils and lakes of the dry valleys, it is presumed that, where water is present in the subsurface, it will be relatively enriched in dissolved solids. It is clear from Figure 3 that, even though field measurements indicate that subsurface materials are present having resistivities less than 700 ohm-m, these materials could, given high pore water salinities, have temperatures below -60 °C. At depths in the order of 20 m below exposed soils and rocks, temperatures will be roughly equivalent to the mean annual air temperatures of -18 °C. From the curves in Figure 3, it is apparent that saturated, saline soils may have resistivities as low as 10-15 ohm-m at these temperatures. Since, by definition, permafrost consists of material below 0 °C, these soils may be properly classified as permafrost, but remain permeable to fluid flow. Thus, low resistivities (<1 000 ohm-m) are interpreted as indicating the presence of permeable soils or rock that may or may not be properly described as permafrost. This will be illustrated in the section on analysis of field exploration sites.

A seismic timer model was used for measuring seismic velocities of materials at various temperatures in the laboratory. By means of two transducers coupled to a sample, the velocity of a wave traveling through a sample was determined. A set of 200 kHz transducers is best for low-velocity materials, while 1 MHz heads are best for high-velocity rocks.

Seismic velocities in the dry valleys range from 1.5 km/s for Don Juan Pond lake sediment to 5.9 km/s for igneous basement rock. An occasional hand specimen of extrusive rock had velocities as high as 7.0 km/s. Tables II and III list dry valley seismic velocities as measured by authors. Figure 5 was constructed from published data^{17,19} for porous, frozen ground. The equation of the line (by least squares) is:

$$P = 3.63 + 0.4438V \text{ percent}, \quad (2)$$

where P is porosity and V percent is the percent velocity increase upon freezing. Nonporous rocks experience little velocity change with variations in temperature.

FIELD GEOPHYSICAL MEASUREMENTS

Interpretations in this section are based on the geology observed in the field and upon the comparison of field data with laboratory measurements reported in Tables I, II and III. In general, resistivities less than 1 000 ohm-m indicate unfrozen and usually saline-saturated materials; resistivities between 1 000 and 10 000 ohm-m are indicative of bedrock or confining permafrost conditions in unconsolidated material; and resistivities greater than 10 000 ohm-m may indicate frozen basement rock or glacial debris.

TABLE II Velocities Measured in the Field

Sample Description	Velocity (km/s)	Author
Frozen outwash, Meirs Valley	3.6-4.0	Bell ²
Frozen till		
Wright Valley	3.0-4.3	Bell ²
Meirs Valley	4.9-5.5	Bell ²
Brown Pa.	3.8-4.3	Bell ²
Taylor Valley	3.9-4.3	Bell ²
Unfrozen		
silt	0.8-1.2	Bell ²
clay	1.4-1.6	Bell ²
sandy loess	0.3-0.5	Bell ²
sandy till	1.2-1.5	Bell ²
shattered rock	1.5-2.5	Bell ²
exfoliated granite	1.1-1.3	Bell ²
broken trachyte	0.6-0.9	Bell ²
massive granite	4.6-4.9	Bell ²
Unfrozen Don Juan		
Pond sediment	1.6-1.8	This study
Basement rock under		
Don Juan Pond	4.9-5.3	This study
Frozen ground near		
Don Juan Pond	3.2	This study
Frozen ground near		
Don Quixote Pond	3.9	This study
Basement rock near		
Don Quixote Pond	5.0	This study
Frozen ground near		
Lake Vida	5.7-5.9	This study
Lake ice (Vida)	4.4	This study
Frozen ground near		
New Harbor	4.5	This study
Lake ice (Fryxell)	3.6	This study
Frozen ground near		
Lake Fryxell	4.5	This study
Frozen ground near		
Lake Vanda	3.8	This study
Basement rock west		
of Lake Vanda	5.1	This study
Frozen ground near		
Lake Bonney	4.4	This study
McMurdo Sound sediment		
2 km thick	3.1	Robinson ¹⁵
McMurdo Sound bedrock		
(basalt)	4.8	Robinson ¹⁵
Ross Island basalt	4.8	Robinson ¹⁵
Metasediments near		
Nussbaum Riegel,		
Taylor Valley	4.4-4.5	Twomey ¹⁹
Metasediments (Asgard formation),		
Taylor Valley	4.5	Twomey ¹⁹
Olympus granite,		
Wright Valley	5.1	Twomey ¹⁹
Beacon Heights		
orthoquartzite,		
Asgard Range	4.2-4.5	Twomey ¹⁹

TABLE III Laboratory Velocity Measurements of Dry Valley Materials^a

Sample Description	Temperature (°C)	Velocity (km/s)
Frozen beach sand (New Harbor)	-45	3.3
Frozen outwash (Lake Vida)	-12	3.2
Ice core (triple distilled H ₂ O)	-2	3.0
Ice-sand core (sand 30% by vol.)	-2	4.6
Ice-sand core (10% sand by vol.)	-10	3.4
Basalt	24	6.9
Fractured and weathered granite porphyry	24	3.1
	-14	3.3
Porphyritic granite	24	5.8
	-14	6.1
Lamprophyre	24	7.0
	-14	6.8
Beacon sandstone	24	3.9

^a All measurements conducted by authors of this study.

For the most part, seismic velocities less than 2.5 km/s represent unfrozen, surficial material; those up to approximately 5.0 km/s indicate frozen, unconsolidated materials; and bedrock velocities range from 4.5 to 6.0 km/s. The following sites are described in the order in which they were studied in the field. Seismic time-distance and electrical apparent resistivity curves are shown in references 4 and 10.

Site 1, Don Juan Pond

Electrical depth sounding, seismic refraction profiling, and surface resistivity measurements were conducted in the

pond basin (Figure 6). The pond is in the South Fork of Wright Valley at 77°33'3"S, 161°11'2"E in the center of a flat lacustrine plain surrounded by moraine and talus deposits. Pond water has a high concentration of CaCl₂ with total solid concentration being over 300 kg/m³. Water density is 1 380 kg/m³ and the lake remains unfrozen throughout the year. The beach area around the pond is covered with deposits of CaCl₂ and NaCl. The size of the pond on 10 December 1971 was approximately 400 m long, 200 m wide, and 23 cm deep at its center. The pond was 10 cm deeper than reported by other authors.^{12,21} Water was observed flowing from a moraine containing ice lenses on the west edge of the basin into the pond after 2 days of 10 °C air temperature.

On the east side of the pond, both Wenner and Schlumberger electrode configurations were used to delineate an interface at 30 m. Resistivities of lake sediments are less than 2 ohm-m, whereas resistivities of basement rock beneath lake sediment are in the order of 30-40 ohm-m. A seismic refraction station also located on lake sediment in the eastern side of the basin showed a near surface velocity layer of 1.5 km/s, whereas a boundary at 29.1 m is associated with a velocity increase from 1.8 to 4.9 km/s.

Along the south side of the salt flats, the bedrock surface is at an average depth of 40 m and dips to the west, as determined from a reversed, seismic refraction profile. At the western edge of the pond, the basement surface lies at a depth of 55 m. Electrical resistivity profiles located along the southern and western margins of the lake confirm the seismic interpretation. Two Schlumberger stations on the moraine west of the lake are interpreted as indicating an ice-cored moraine lying upon lower resistivity, unfrozen glacial drift, and basement. Seismic refraction profiles suggest that the basement may be faulted in places or have a highly irregular surface, possibly due to glacial scouring.

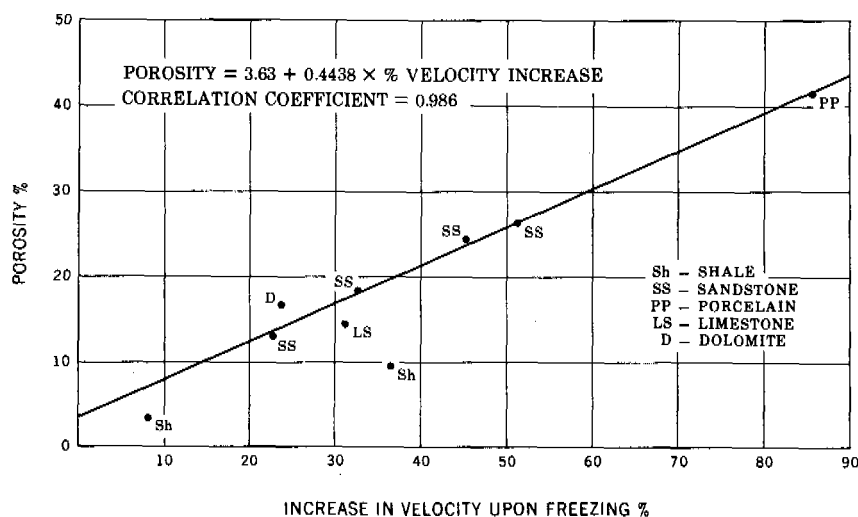


FIGURE 5 Porosity versus percent velocity increase for porous, saturated materials.

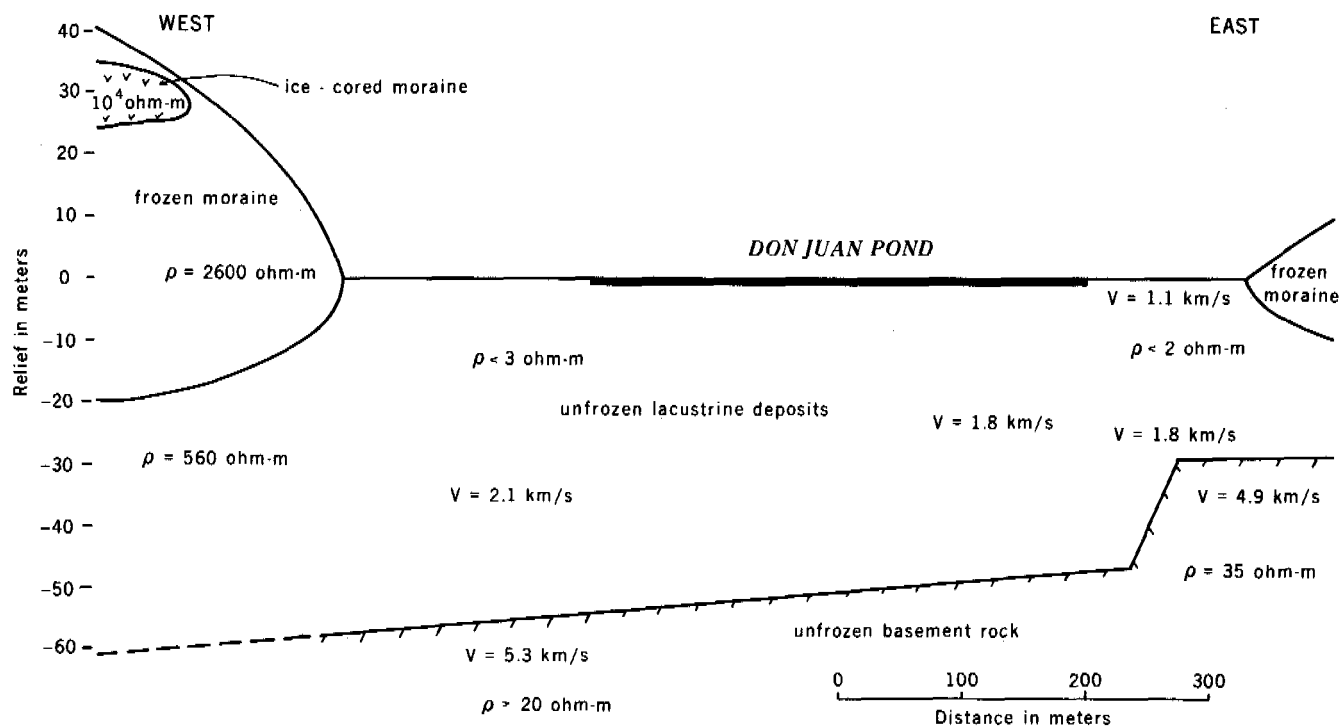


FIGURE 6 Geological cross section in the Don Juan Pond area, Wright Valley, from surface geophysical measurements.

Site 2, Don Quixote Pond

The North Fork of Wright Valley ($77^{\circ}32'6''S$, $161^{\circ}10'5''E$) has a series of five small lakes numbered from west to east; Don Quixote Pond is pond No. 1. These ponds are ephemeral as they alternate in salinities and depth from year to year.

From previous electrical studies,¹⁰ no confining permafrost near Don Quixote Pond was reported; however, both seismic and electrical data collected during the present study suggest the presence of thin, confining permafrost overlying unfrozen sediment that rests on basement at depths ranging from 30 to 40 m where the velocity increases from 3.9 to 5.0 km/s. This seismic boundary represents a change from frozen drift and lake sediments to basement. The unfrozen, intermediate layer detected from electrical measurements cannot be detected using seismic refraction techniques. Data from studies near Don Quixote Pond are included in the profile of Wright Valley in Figure 7.

Site 3, Lake Vida

Electrical stations located in the stream bed at the western end of Lake Vida ($77^{\circ}27'S$, $161^{\circ}54'E$) show confining permafrost to exist from a depth of 10 cm to below the depth of exploration (>200 m). Frozen, crystalline basement is interpreted as lying at depths in the order of 80 m. A seismic station also located in the stream bed recorded

only one layer with a velocity averaging 5.9 km/s, which is interpreted as being caused by a frozen outwash plain interbedded with relatively thick ice lenses. Presuming an unfrozen velocity of 1.8 km/s for lacustrine and outwash deposits, the plain is assumed to contain 40 percent sand and gravel, with 60 percent ice as calculated from Eq. (2). Electrical stations located around the lake and on the lake ice indicate that confining permafrost is ubiquitous.

Abnormally high seismic velocities averaging 4.4 km/s were obtained for the ice in Lake Vida. Published ice velocities rarely exceed 3.9 km/s, although pore-ice velocities have been found to be as high as 4.5 km/s.¹⁷ Auger holes drilled into Lake Vida, about 1 km from the east end, encountered sandy and silty layers at 3, 4, 10, and 11 m and an impenetrable surface of sand and gravel at 11.5 m depth.³ Experiments on compressional wave velocities through various ice-sand mixtures indicate that a sample of 30 percent sand by volume has a velocity of 4.5 km/s at $-2^{\circ}C$.

From the high velocities recorded at Lake Vida, the observed sand and gravel layers in the lake ice, and laboratory experiments, it is concluded that near the western end of Vida the lake consists of layered ice and sand lenses with as much as 20-30 percent sand and that the lake is frozen to the bottom where it lies directly on frozen glacial debris having velocities of 5.7-5.9 km/s. The lake deepens from 20 m near the west end to over 40 m near the lake center. From long Schlumberger measurements, frozen ground may be in the order of 1 000 m thick in the west end of the Lake Vida

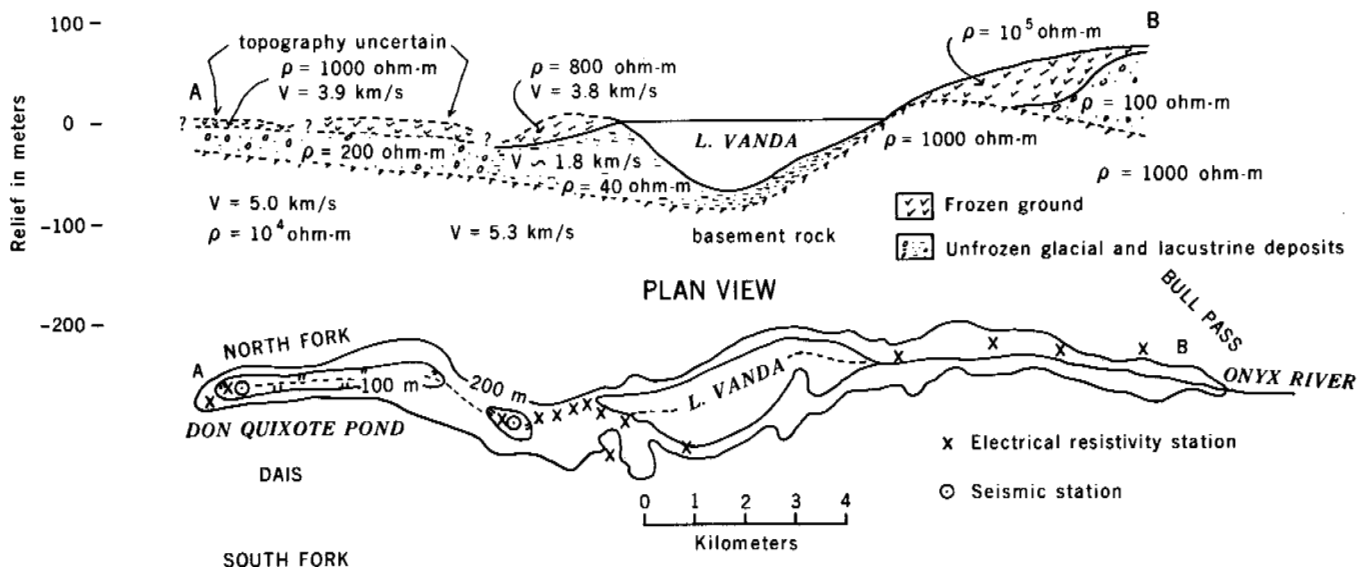


FIGURE 7 Geological cross section in the Lake Vanda area, Wright Valley, from surface geophysical measurements.

basin. Beneath the center of the lake, however, an electrical resistivity station is indicative of a low resistivity layer ($<10^3$ ohm-m), lying at depths less than 100 m. The low resistivity layer may be caused by unfrozen, saline water or lake sediment lying under the lake. A geophysical interpretation of the subsurface on the southwest end of Lake Vida is shown in Figure 8.

Site 4, Lake Fryxell

Electrical resistivity and reversed seismic refraction stations were located near a proposed drilling site on the western shores of Lake Fryxell ($77^{\circ}37'S$, $163^{\circ}06'E$) in Taylor Valley.⁷ Two seismic stations produced single-layer profiles. A velocity of 4.6 km/s was determined on land along the

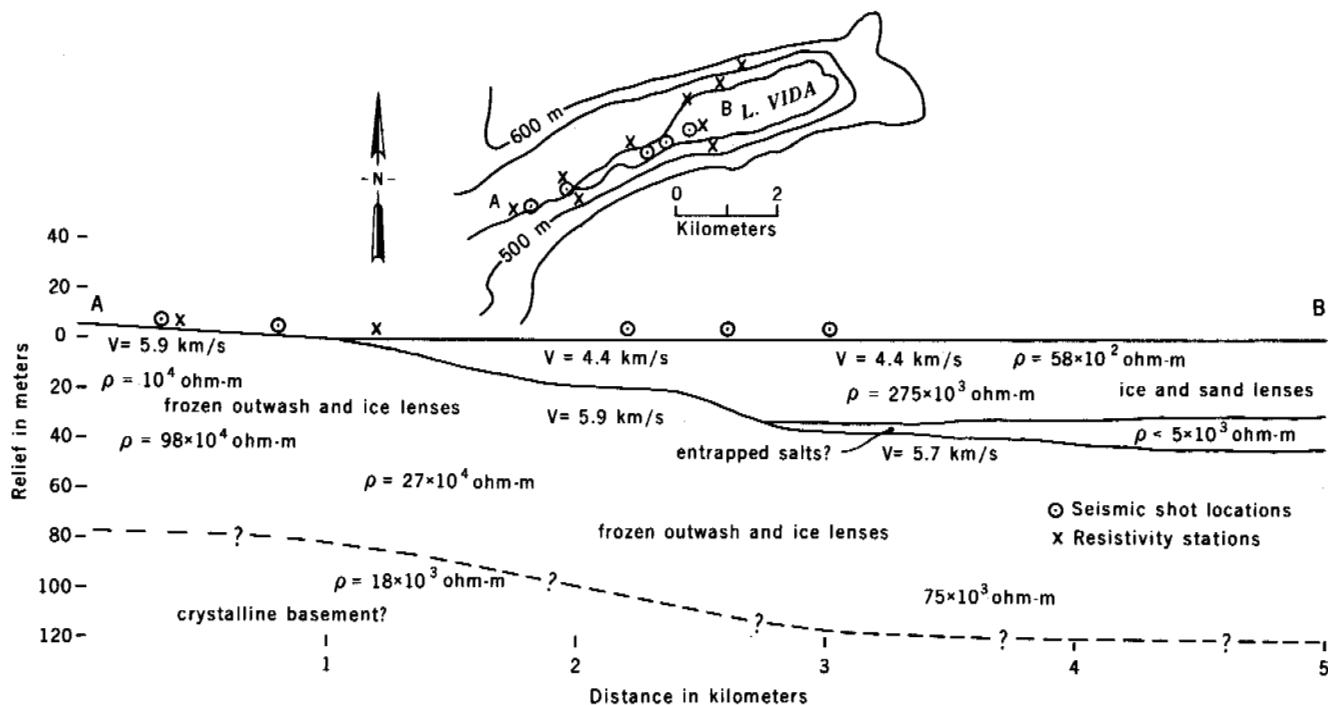


FIGURE 8 Geological cross section in the Lake Vida area, Victoria Valley, from surface geophysical measurements.

northwest shore of the lake, whereas an average velocity of 3.7 km/s was determined on the lake ice. A borehole drilled through 3 m of lake ice encountered several centimeters of water lying between lake bottom and the ice. The fact that higher velocities were not determined beneath the ice indicates the absence of frozen ground beneath the lake.

Along the shores of Lake Fryxell, electrical stations show a decrease in resistivity with increasing depth. Permafrost resistivities ($>5\,000\text{ ohm}\cdot\text{m}$) are evident in the upper 10 m on moraine near the lake. Beneath the confining permafrost, resistivities on the order of 150–400 ohm-m suggest the presence of unfrozen, saturated sands and gravels that contain water of low mineral content. A cross section of the Lake Fryxell area is shown on Figure 9.

Site 5, New Harbor Shore

A seismic station was located along a stream bed flowing eastward along the center of Taylor Valley into New Harbor ($77^{\circ}34'3''\text{S}$, $163^{\circ}28'35''\text{E}$) to supplement data from earlier electrical studies.¹⁰ A thawing effect from the Ross Sea to about 90 m inland was used to explain low resistivities near the shoreline. This analysis indicated the discontinuity was caused by a confining permafrost wedge. Further inland, permafrost greater than 150 m thick was reported.

The seismic station revealed confining permafrost beneath sand at the water's edge. Refraction profiles may be interpreted as indicating two layers, the upper having a velocity of 3.4 km/s and the lower having a velocity of 5.6

km/s. The overlying material is probably frozen outwash and sandy flood plain alluvium since this velocity compares reasonably well with the velocity obtained in the laboratory (3.3 km/s) for a core of frozen sand from the beach at New Harbor (see Table III). The thickness of confining permafrost cannot be determined; however, the lower layer of high velocities and low resistivities indicate an unfrozen basement at relatively shallow depth.

Site 6, Lake Miers

An electrical station was established about 100 m west of Lake Miers ($78^{\circ}8'29''\text{S}$, $163^{\circ}52'55''\text{E}$) on flat-lying, fine-grained outwash and lacustrine deposits. Evaporites from the area have been described¹⁸ and a bottom temperature of 5.7°C in the lake at 20 m depth was recorded. The station revealed the presence of confining permafrost extending from near the surface to the maximum depth of exploration. Resistivities ranged from 850 ohm-m near the surface to 8 500 ohm-m at depth.

Site 7, Walcott Glacier

Confining permafrost appears to be very thin or absent around the shore of the lake southwest of Walcott Glacier ($78^{\circ}14'45''\text{S}$, $163^{\circ}8'40''\text{E}$). The maximum resistivity was restricted to the top 1.6 m, below which the resistivity gradually decreased to 51.5 ohm-m. Little or no permafrost is present.

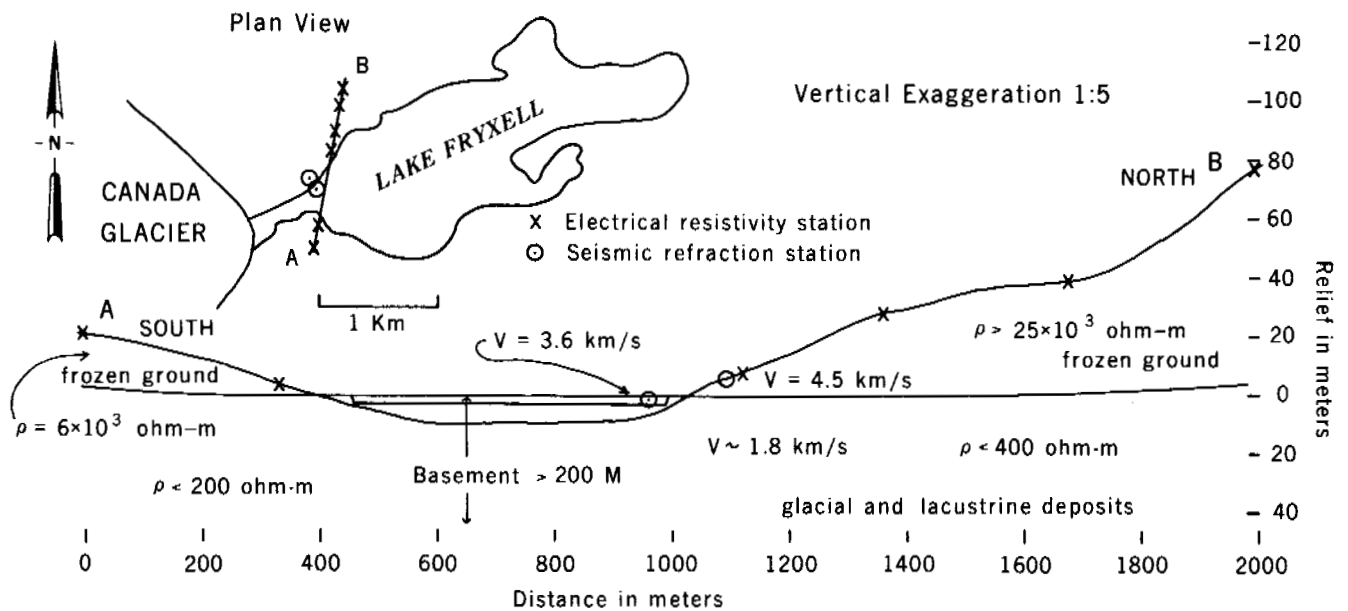


FIGURE 9 Geological cross section in the Lake Fryxell area, Taylor Valley, from surface geophysical measurements.

Site 8, Pearse Valley

An electrical resistivity station was established on the northwest shore of a small lake in Pearse Valley (77°43'22"S, 161°34'45"E). Resistivities less than 250 ohm-m to 7.4-m depth were encountered. At this boundary, the resistivity increased to 2 200 ohm-m, and at 14.7-m depth the resistivity jumped to 22 000 ohm-m, possibly indicating the depth to basement. The low, near-surface resistivities, in spite of the low ambient temperature (−11 °C on 15 January 1972), may be the result of high salinities.

Site 9, Lake Vanda Area

Electrical measurements suggest relatively thin confining permafrost in a small basin 1.5 km west of Lake Vanda. Resistivities do not exceed 800 ohm-m at any depth in the basin. Schlumberger measurements indicate a basement depth of 50 m, whereas reversed seismic refraction data indicate the basement lies under 41.3 m of glacial drift and lacustrine deposits. The seismic depth may be too small due to high velocity layering. High surface velocities and low resistivities indicate the presence of very thin confining permafrost overlying unfrozen glacial deposits, which, in turn, rest on unfrozen basement. The geologic cross section based on electrical and seismic stations in the entire Vanda basin is shown in Figure 7.

Site 10, Lake Bonney Area

A seismic station was located approximately 2 km east of Lake Bonney (77°41'19"S, 162°34'44"E) near two electrical stations.¹⁰ It revealed a one-layer time-distance curve with an average velocity of 4.3 km/s. It was suggested¹⁰ earlier that the area is characterized by an irregular thickness of confining permafrost underlain by unfrozen soils. The velocity obtained thus represents a thin layer of surficial, frozen drift. Lower velocities beneath the permafrost cannot be detected because of the high-velocity layering effect. A thick (>130-m) section of unconsolidated glacial drift and lacustrine deposits is presumed to lie on basement near the east end of the lake.

DISCUSSION

Geophysical measurements in the dry valleys of Antarctica reveal abnormally thin permafrost with respect to the present climate. Presuming a normal continental-geothermal gradient of about 18 °C/km—permafrost thicknesses should be on the order of 1 km. From laboratory studies,^{5,11} field observations,⁵ and theoretical analyses,⁸ it is inferred that the lack of development of thick confining permafrost is due to the presence of solar-heated lakes, which were much more extensive in the recent past, and to high water and

soil salinities. Even where permafrost soil temperatures are present (<0 °C), the high soil salinities depress the freezing point to such a degree that the permafrost remains unfrozen in some locations and permits the movement of pore fluids.

Both Taylor and Wright valleys contain extensive unconsolidated sediment throughout the length of their valley floors. In general, the unconsolidated deposits near the bottoms of the valleys contain a thin layer of confining permafrost resting on saturated and unfrozen sediment. It is quite likely that the unfrozen sediment forms a continuous hydrogeologic unit in the valleys and that the lakes are, therefore, part of this continuous hydrogeologic system. Studies have not been of sufficient detail between lake basins to state this with surety. It is certain, however, that all of the larger lakes in Taylor and Wright valleys are not underlain by permafrost. Therefore, groundwater does play a significant role in their replenishment, although the total hydrologic budget of the lakes is not clear from studies to date.

Beginning with Taylor Glacier in western Taylor Valley and extending eastward to the coast, all geophysical studies conducted indicate a layer of thin permafrost overlying unfrozen sediment. Along the tongue of Taylor Glacier itself, however, confining permafrost extends to depths greater than the maximum depth of exploration (150 m).¹⁰ East of Lake Bonney, confining permafrost is 20–30 m thick but is underlain by saturated, unfrozen sediment.

In Wright Valley, thin permafrost or a lack of permafrost altogether, may extend from Don Juan and Don Quixote ponds in the west to eastern Lake Vanda. Thick permafrost is associated with thin sediment cover east of the lake; however, electrical measurements indicate that thin permafrost again prevails in the vicinity of Bull Pass (Figure 7).

Victoria Valley and Lake Vida are underlain by thick and extensive permafrost. A thin layer of entrapped brine or low resistivity soil may rest on the bottom of Lake Vida as suggested by a long Schlumberger resistivity station. Subsurface conditions of Victoria Valley are thus quite different from those of Taylor and Wright valleys. Normal permafrost thicknesses of 1 km or more will obstruct passages of any subsurface fluid.

ACKNOWLEDGMENTS

This study consists of Dry Valley Drilling Project, Phase I, which was supported by the Office of Polar Programs, National Science Foundation Contract NSF-C642 and by the Japanese Antarctic Research Program. Helicopter support was provided by Antarctic Development Squadron Six (VXE-6), U.S. Navy Antarctic Support Force.

REFERENCES

1. Anderson, J. J. 1965. Bedrock geology of Antarctica: A summary of exploration, 1831–1962, p. 1–70. *In* J. B. Hadley [ed.] *Geology and paleontology of the Antarctic*. Vol. 6. American Geophysical Union, Antarctic Research Series.

2. Bell, R. A. I. 1966. A seismic reconnaissance in the McMurdo Sound region, Antarctica. *J. Glaciol.* 6:209-221.
3. Calkin, P. E., and C. Bull. 1967. Lake Vida, Victoria Land, Antarctica. *J. Glaciol.* 6:833-836.
4. Clark, C. C. 1972. Geophysical studies of permafrost in the dry valleys. M.S. thesis. Northern Illinois University, DeKalb. 97 p.
5. Denton, G. H., R. L. Armstrong, and M. Stuiver. 1969. Histoire glaciaire et chronologie de la region du detroit de McMurdo, sud de la Terre Victoria, Antarctide. *Rev. Geogr. Phys. Geol. Dynam.* 11(2):265-278.
6. Hamilton, W. 1965. Diabase sheets of the Taylor Glacier region, Victoria Land, Antarctica. U.S. Geol. Survey, Prof. Paper 456-B. 71 p.
7. Hoare, R. A., K. B. Popplewell, D. A. House, R. A. Henderson, W. M. Prebble, and A. T. Wilson. 1965. Solar heating of Lake Fryxell, a permanently ice-covered Antarctic lake. *J. Geophys. Res.* 70:1555-1558.
8. Horowitz, N. H., R. E. Cameron, and J. S. Hubbard. 1972. Microbiology of the dry valleys of Antarctica. *Science* 176: 242-245.
9. McKelvey, B. C., and P. N. Webb. 1961. Geological reconnaissance in Victoria Land, Antarctica. *Nature* 189:545-547.
10. McGinnis, L. D., and T. E. Jensen. 1971. Permafrost-hydrogeologic regimen in two ice-free valleys, Antarctica, from electrical depth sounding. *Q. Res.* 1:389-409.
11. McGinnis, L. D., T. Torii, and P. N. Webb. 1972. The Dry Valley Drilling Project. *Antarct. J. U.S.* 7:53-56.
12. Meyer, G. H., T. E. Berg, and J. L. Littlepage. 1962. Antarctica: The microbiology of an unfrozen saline pond. *Science* 138: 1103-1104.
13. Montgomery, G. E. 1972. Aeromagnetic study of part of the Ross Island and Taylor Glacier quadrangles, Antarctica. M.S. thesis. Northern Illinois University, DeKalb. 49 p.
14. Müller, G. 1961. Geschwindigkeitsbestimmungen elastischer wellen in gefrorenen gesteinen und die anwendung akustischer messungen auf untersuchungen des frostmantels and gefrierschichten. *Geophys. Prospect.* 9:276-295.
15. Robinson, E. S. 1963. Geophysical investigations in McMurdo Sound, Antarctica. *J. Geophys. Res.* 68:257-262.
16. Tedrow, J. C. F., and Ugolini, F. C. 1966. Antarctic soils, *In* J. C. F. Tedrow [ed.] *Antarctic soils and soil forming processes.* Vol. 8. American Geophysical Union, Antarctic Research Series. p. 161-177.
17. Timur, A. 1968. Velocity of compressional waves in porous media at permafrost temperatures. *Geophysics* 33:584-595.
18. Torii, T., N. Yamagata, and T. Cho. 1967. General description and water temperature for the lakes. *Antarct. Rec. No. 28* (Nat. Sci. Mus. Tokyo, Japan) p. 2225-2238.
19. Twomey, A. A. 1968. Seismic refraction studies in surficial materials of Victoria Land, Antarctica. M.S. thesis. University of Wisconsin, Madison.
20. Webb, P. N. 1972. Paleontology of late Tertiary-Quaternary sediments. Wright Valley, Antarctica. *Antarct. J. U.S.* 7:96-97.
21. Yamagata, N. T., T. Torii, and S. Murata. 1967. Chemical composition of lake waters. *Antarct. Rec. No. 29* (Nat. Sci. Mus. Tokyo, Japan) p. 2339-2361.

PERMAFROST CONSIDERATIONS IN LAND USE PLANNING MANAGEMENT

Curtis V. McVee

BUREAU OF LAND MANAGEMENT
Anchorage, Alaska

INTRODUCTION

Within the Arctic and Subarctic, the most significant universal and often dominant feature facing the resource manager is permafrost. Each land use decision, whether dealing with timber harvesting, road construction, mineral development, or urban expansion, must include a consideration of frost conditions in the ground and an analysis of the impact man's activities will have on the natural thermal equilibrium.

Thawing of permafrost is not necessarily the primary concern of the manager. In fact, it may be beneficial as in areas suitable and utilized for agriculture. The manager's concern is directed toward the effects of the thawing and not the permafrost itself.

MANAGEMENT GOALS FOR PUBLIC LANDS IN THE ARCTIC AND SUBARCTIC

The main goal is to provide resource use, protection, and extraction in harmony with environmental considerations. The purpose is to perpetuate a combination of uses of the land, compatible with the capability of the natural ecosystems, to benefit society.

Application of conventional methods usually will not protect permafrost stability. Even a minor surface disturbance may alter the thermal balance sufficiently to induce permafrost thawing, which may result in subsidence or soil erosion or both, and affect such features as surface relief, access, siltation, and wildlife habitat. Changes in surface relief, such as depressions from subsidence or gullies from

erosion by waters of melting soil ice interfere with subsequent construction or land travel. Eroding soil solids become deposited at some lower points in the watershed or drainage way, which further limit utilization of the land. Also, siltation may adversely affect water quality and the aquatic biota.

Permafrost must be considered at all times in making decisions for management of these arctic and subarctic lands if we are to enjoy their continued use. The following discussion is concerned with the factors that must be considered in the decision-making process and in the development of operational procedures.

PERMAFROST CONDITIONS AND MATERIALS SENSITIVE TO DISTURBANCE

When permafrost temperatures are near 0 °C, the slightest disturbance often is enough to induce thawing and the following consequences result: Organic mats are easily torn so they no longer provide thermal insulation; thawing of soils with segregated ice supplies water for runoff that may erode the soil; loss of ice from soils causes a volumetric reduction that results in subsidence of the surface; fine textured soils with high ice content liquefy, become unstable, and move downward on slopes. Thus, the warmer the permafrost temperature and the greater the amount of segregated ice, surplus water, and fine textured soil, the more subject the permafrost soils are to change by surface disturbance.

The effects of permafrost thawing on various environmental aspects include

1. *Soil loss* If the surface is disturbed and thawing occurs in ice-rich permafrost, ponds and small streams can form and soil flowage and erosion can occur. When the area serves for collection of surface runoff, massive erosion can occur and, if the slope is sufficient, slumps and slides result (Figure 1). Not all gullies or ruts form from soil loss. Where soil is ice-rich, the soil surface will subside as the ice melts, leaving gullies, ponds, or depressions. This is particularly evident in tundra where slopes are gentle.

Sometimes after the vegetation burns, slumps occur in silty soils on slopes underlain by permafrost. As the permafrost thaws and the soils become saturated, the weight of the soil overcomes the friction at the soil-permafrost interface and slippage or slumping results downslope. When ice lenses close to the surface melt, mass downward movement of the overlying soil follows.

2. *Water quality* Thawing of permafrost may affect water quality if there is soil movement from the thawed area to a water body.

More studies are needed to assess the relationship between thawing of permafrost and water quality. Most studies have been with the effects of wildfire and fire control



FIGURE 1 Gully erosion resulting from fireline construction in ice-rich permafrost soils.

methods (particularly firebreak construction) on water quality.⁴ Silt and organic materials and salts are the main pollutants of water following fires. Turbidity of streams frequently increases following fires. Dramatically increased turbidity can occur when tractor-constructed firebreaks intersect streams.

3. *Aesthetics* Surface disturbance in permafrost areas often has an adverse impact on scenic values. Removal of surface vegetation, differential subsidence, erosion, and gully formation may occur and have long lasting visible results of the disturbance. Disturbance caused by vehicular traffic can result in long, straight lines of impacted areas that appear highly artificial in a natural setting.

Traffic with overland vehicles on tundra does not always result in thawing permafrost. Sometimes repeated passage over tundra leaves a visible mark on the landscape, but the organic layer remains intact and there is no permafrost thawing. At other times, even a single passage is sufficient to leave a visible mark. These types of trails, although often difficult to detect on the ground, may be highly visible from the air.²

4. *Access* As permafrost thaws and erosion occurs, the resulting gullies and mudflows can damage existing roads

and trails. It is common to locate new trails adjacent to trails that have become impassable due to subsidence, thus making the relocated trail impassable too. This series of parallel thawed and eroded trails across the terrain not only impedes vehicle or foot travel but may also prove impassable for wild animals.

LAND USES INFLUENCED BY PERMAFROST

New Townsites and Village Expansion

Site selection for a new town or expansion of an established village requires consideration of permafrost conditions and materials. Prime considerations are stability of building foundations, domestic water supply, waste disposal, street systems, etc. Special location or design and construction are needed in each case.^{1,3}

Rights-of-Way

Selecting a route or site in permafrost areas must be done with knowledge of conditions and materials. Roads, railroads, airfields, pipelines, and even power transmission lines are influenced by permafrost. Most disturbances result in increased temperatures of the surface soil. In the discontinuous permafrost areas where ice is warmer, the increased temperature may be sufficient to melt the ice. This usually results in a less stable soil material, especially in areas of high moisture content or fine textured soils. Sometimes a route can be selected to avoid these areas; otherwise these conditions must be accommodated in the structure. Normally, this is done through the installation of an insulating layer of gravel or artificial material.

Mineral and Oil Development

From the Alaskan gold rush to the present activities at Prudhoe Bay, mineral and oil development in Alaska has been influenced by permafrost. Gold frequently was found at the interface of frozen alluvium and underlying bedrock, and much of the alluvium had to be thawed before removal of the gold.

Traditionally, oil activities depend on soil stability for structural or mechanical support. Yet, surface disturbance from these same activities can result in permafrost thawing, followed by subsidence and erosion. Vegetation removal and vehicular wear on the organic mat during seismic exploration have occurred in Alaska and, in some places, this has caused erosion serious enough to limit alternative land uses.⁵ Because vast quantities of gravel are used for construction pads for oil and mineral development in permafrost areas, a shortage of gravel for other purposes such as

highway maintenance or village expansion may ensue; similarly, problems attendant with large-scale gravel extraction activities may be created.

Timber Harvest

In permafrost areas, lumber and paper pulp producers need to take special precautions in tree removal. The reduction of vegetation alone can start thawing of permafrost. Transportation of the timber requires more than the usual road preparation. Either thicker roadbeds or special vehicles that spread the load over more area of the ground surface can be used.

Farming

Clearing and cultivation of permafrost-laden soils for agricultural purposes sometimes result in subsidence and changes in surface relief sufficient to make the land useless for farming and many other purposes. Again, this demonstrates the advantages of land use planning and careful selection of agricultural land through the use of a detailed soil survey.

Recreation Activities

Recreation activities, particularly those involving the use of off-road vehicles (ORV), may result in significant surface disturbance. Use of ORV's for both commercial and personal activities is one of the major influences in permafrost areas today. The types of ORV employed in Alaska vary greatly in design and have a wide range of potential for soil disturbance. Vehicles may be commercially manufactured or home-made with standard tires, tires and chains, wide tires, tire and track combination, or tracks only. Surface loading may vary from less than 400 to over 25 000 kg m⁻². Steering systems range from skid-type to center-frame joint-articulated systems. Repeated ORV traffic over the same route causes compaction of the surface vegetative layer and may expose the mineral soil. The most serious damage occurs before freezeup or during breakup in alpine terrain and in areas underlain by ice-rich permafrost. In some areas, even repeated snow machine travel over snow may cause sufficient compaction to result in thawing and erosion the following summer.

In zoning efforts, consideration should be given to priorities for ORV access, type of vehicles to be allowed, methods of vehicle operation, value of designated trails, the tolerable use level, and the best time of year for safe operation.

Studies demonstrate that the surface pressure a vehicle exerts should be less than 2 500 kg m⁻² to prevent surface disturbance that leads to permafrost thawing. Other factors to consider include steering system, track surface or shape,

number of passes, vehicle maneuvering, and soil conditions (slope, moisture, etc.).

Control of Wildfires

Wildfires caused by both lightning and man are common to interior Alaska. There were 641 occurrences in 1972 over 90 000 000 ha. While this represents the greatest number of fires ever recorded in one year, the 10-year average is 310 fires per year burning 330 000 ha annually.

One of the most effective ways of combating these fires is to construct firelines by cutting through the unfrozen organic cover to either the mineral soil or permafrost. Less trouble is generated by lines cut with hand tools. However, where fires are accessible, tractors equipped with dozer blades can be utilized. Each year bulldozers are used to construct approximately 130–160 km of firebreaks in Alaska. This equipment is very effective and control lines can be rapidly built around the perimeter of a fire. Unfortunately, however, the permafrost is exposed, and particularly in ice-rich, fine-grained soils even on gentle slopes erosion commences within days. Fireline erosion should not be confused with soil slippage on steep slopes within a burned area; it is not a result of mechanical disturbances. Although tractors equipped with dozer blades have been used to control fires in Alaska since 1958, the first concern for the effects of such practices was not recorded until 1967 when inspection of a 101 000-ha burn identified erosion of firelines and sediment flowing into streams.⁶

A detailed inventory of several fires where heavy equipment had been used established that these occurrences were not uncommon. Active erosion was evident on lines several years old. Some lines had eroded, reached slope equilibrium and stabilized. Studies are now being conducted to develop alternative techniques of firebreak construction that will not remove surface vegetation. Forced injection of fire retardants is one possibility.

Military Activities

Military activities with personnel and equipment, such as construction of buildings, landing strips, communication facilities, and roads, has often caused enough disturbance to result in permafrost thawing in Alaska. Field exercises involving travel across permafrost areas also have been followed by surface subsidence and soil erosion. Military vehicles have been designed to conquer the terrain with little consideration of avoiding permafrost thawing.

LAND REHABILITATION

Where damage has occurred from permafrost thawing, efforts should be made to rehabilitate the area. Although some techniques have been successful on firebreak rehabili-

tation, there is still much to learn about treatment of damaged areas. In addition to training fire-control personnel on the hazards of constructing firelines on ice-rich, fine grained soils and how to select alternate sites, several rehabilitation measures have been tested. The following techniques were recommended from the results of these studies:

1. Construct water bars across firebreaks where organic surface material has been removed; use solid or organic berm material and space the water bars at 20–40-m intervals (Figure 2). This can vary, depending on slope, amount of ice in the soil, and soil type. Mineral material is necessary on the uphill side of the berm to seal it against water. Debris or log dams are not effective. Bars should be 1–2 m high and angled with a slope of less than 2 percent to divert runoff into undisturbed vegetation adjacent to the firebreaks. Permafrost thawing starts almost immediately after the vegetation mat is removed. Therefore, water bars must be completed as soon after the firebreak construction as possible. Although firebreaks constructed on the contour require fewer water bars, water should always be diverted away from the burned area.

2. Seed the disturbed surface immediately after construction of the firebreaks. The goal is to establish a vegetation cover to protect soils and other resources. Both fall and



FIGURE 2 Effective water bar constructions on fireline in ice-rich permafrost.

spring seeding, using different mulches, have been tried. Applications were made on permafrost as well as on non-permafrost soils. Fall seeding is recommended utilizing a mixture of Manchar smooth brome and Kentucky Bluegrass applied at the rate of 45 kg/ha. Other species showing some promise were Reed canary grass, timothy, and sweet clover. Fertilizer is required because soils exposed by the dozer are sterile. After soil analysis, the University of Alaska recommended a 20-20-10 pellet form applied at the rate of 335 kg/ha at the time of seeding.

3. A more intensive rehabilitation treatment of an eroding trail left by repetitious movement of tracked vehicles involved the application of an excelsior mulch and seeding (Figures 3, 4, and 5). Such treatment is applicable when small restricted problem areas have developed. Other artificial insulations (e.g., chips, slash, and sawdust) may be used to retard or stop the permafrost thawing.

4. Some transplanting of brush or tree species for erosion control and screening is desirable. Willow shows more promise for such treatment than other plants.

CONCLUSIONS

Permafrost is a dominant factor that must be considered by the land manager in the Arctic. Conventional resource



FIGURE 4 Same trail identified in Figure 3 after application of seed and fertilizer covered by excelsior mulch.



FIGURE 3 Erosion commencing on untreated disturbed trail in permafrost area.

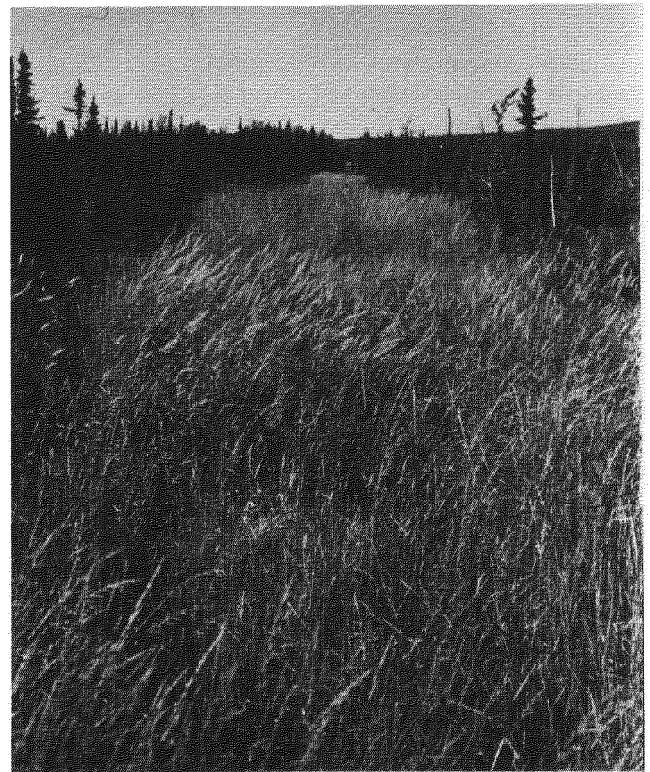


FIGURE 5 Same trail as in Figures 3 and 4 showing excellent growth of grasses and stabilization of soils.

utilization and extraction techniques must be modified to compensate for this physical phenomenon. Prior to implementing resource utilization and extraction activities, the land manager must be aware of the eventual implications of any proposed decision and its impact on future productivity and use of each finite commodity.

REFERENCES

1. Brewer, M. C. 1958. Some results of geothermal investigations of permafrost in northern Alaska. *Trans. Am. Geophys. Union* 39(1):19-26.
2. Hok, J. R. 1969. A reconnaissance of tractor trails and related phenomena on the north slope of Alaska. U.S. Department of the Interior, Bureau of Land Management, Washington, D.C. 66 p.
3. Lachenbruch, A. H. 1969. Permafrost, p. 833-839. *In* R. W. Fairbridge [ed.] *The encyclopedia of geomorphology*. Reinhold, New York.
4. Lotspeich, F. B., E. W. Mueller, and P. J. Frey. 1970. Effects of large scale forest fires on water quality in interior Alaska. Federal Water Pollution Control Administration, Northwest Region, Alaska Water Laboratory. 90 p.
5. Rickard, W., and C. Slaughter. 1972. Accelerated soil thaw and erosion under vehicle trails in permafrost landscapes. Unpublished Paper No. 72-753 prepared for the American Society of Agricultural Engineers. 8 p.
6. Wickstrom, J. C. 1968. Fire Y-34 fire recovery, water pollution and erosion observations. Unpublished report by the Bureau of Land Management, Fairbanks, Alaska. 7 p.

PERMAFROST AND SNOWCOVER RELATIONSHIPS NEAR SCHEFFERVILLE

Frank H. Nicholson and Hardy B. Granberg

McGILL SUB-ARCTIC RESEARCH LABORATORY
Schefferville, Quebec

INTRODUCTION

Fifteen years of permafrost studies at Schefferville, in the centre of the Labrador-Nouveau Québec Peninsula, have indicated important relationships between snowcover and permafrost.^{1,2,4,8,11,12} This paper presents an analysis of snow and permafrost data from the Timmins 4 Permafrost Experimental Site. The site is underlain by discontinuous permafrost that shows large variations over short distances.¹⁰

The analysis relates ground temperatures at different depths to snow variations within circular areas of different radii. For the analysis mean ground temperatures were used, based on 2-4 years' readings from 18 thermocables over ranges of depth from 10 to 110 m. The snow data have been collected from a 147-point snow course over 4 years. A technique has been developed that uses equations from point snow data to produce a map showing the full areal pattern of the snow pack.^{6,7} An alternate method of snow mapping using sequence aerial photographs during snowmelt also has been developed.

The main stimulus for the work is the need for accurate predictions of permafrost distribution for iron ore mining. The permafrost studies at Schefferville have now reached the stage when ground temperatures and the factors influencing them can be quantitatively related, and the relationships can be used to map the distribution of the permafrost.

SITE DESCRIPTION

The site of the study is the Timmins 4 Permafrost Experimental Site, an area of approximately 1 km², located about 20 km NW of Schefferville, Lat. 55°N Long. 67°W.^{10,11} The terrain includes both broad and narrow ridges in the higher parts, but has less pronounced relief in the lower parts of the site. From the higher to the lower parts of the site, the vegetation varies from bare ground, or a tundra association with occasional stunted and procumbent spruce, to very open woodland. The rocks are folded and faulted Proterozoic sedimentary, including leached iron ore deposits, overlain by a thin, discontinuous till usually less than a metre thick. The mean annual air temperature is -5 °C, and the mean annual snowfall is 315 cm.

The snowcover at the Timmins 4 site exhibits considerable spatial and temporal variations in depth and density.⁶ The snow accumulation follows a definite sequence that culminates in a smooth snowcover that is generally deeper in valleys and shallower on ridge crests. The proportional increase at different sites varies through the winter.⁶

The permafrost is uninterrupted in the higher part of the site and extends down to 100 m or more, with occasional taliks in the valleys.¹⁰ In the lower part of the site, much of the ground is unfrozen and, where permafrost is present, it is much shallower. The range of ground temperatures at

the 17 cables with long-term records is shown in Figure 1. The overall pattern of ground temperatures indicates that lateral heat flow is important.

THE EFFECTS OF SNOW ON GROUND TEMPERATURES

Snow has an important influence on ground temperatures because of its insulating effects that reduce winter heat loss. The effectiveness of the insulation depends on the thickness of the snow layer and the snow thermal conductivity. The latter varies with density. Density at the site is mainly a simple function of snow depth. The effect of snow on ground temperatures is illustrated in a test of artificial thermal amelioration on one part of the Timmins 4 site, as shown in Figures 2 and 3 and Table I.

The considerable variation in the ground temperature conditions from year to year is closely related to annual variations in snow accumulation (Figure 4). An 11-year record of ground temperatures under permafrost conditions at another site in the Schefferville area shows that in five winters the ground temperatures fell considerably lower than in other years, in a way similar to the strong contrast shown in Figure 4. Thus, years of shallow snowcover strongly affect the heat budget and are undoubtedly important to the maintenance of the permafrost.

CORRELATIONS BETWEEN PEAK SNOW DEPTH AND GROUND TEMPERATURE

The purpose of the following analysis is to investigate the spatial influence of snow depth on ground temperatures.

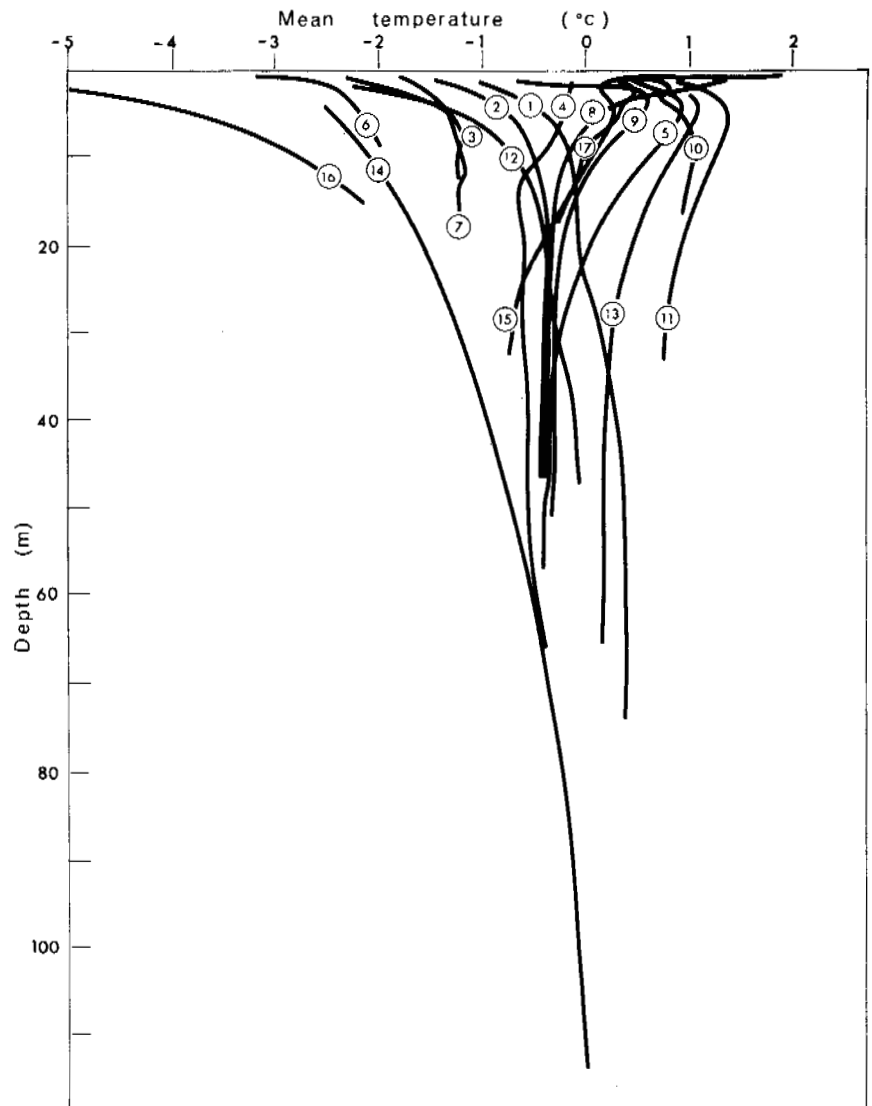


FIGURE 1 Mean temperature against depth for 17 temperature profiles, showing the range of temperature conditions at the site.

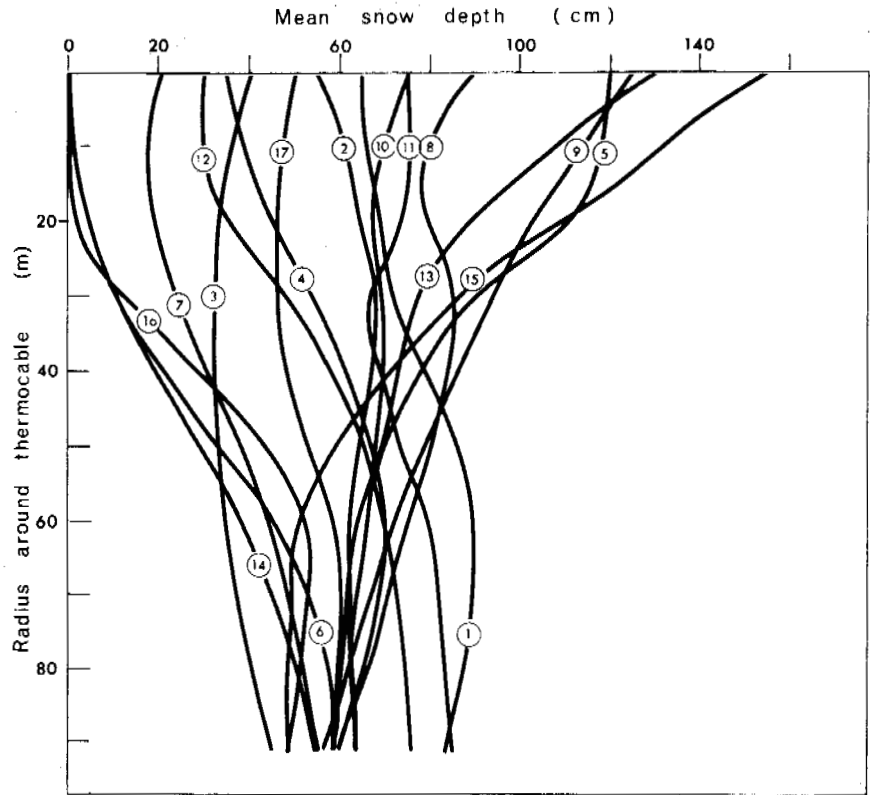


FIGURE 2 Snow conditions around the same 17 temperature profile locations given in Figure 1. It can be seen that the mean snow depth for many cables changes radically as the radius of snow area increases. Compare snow and temperature conditions at particular locations.

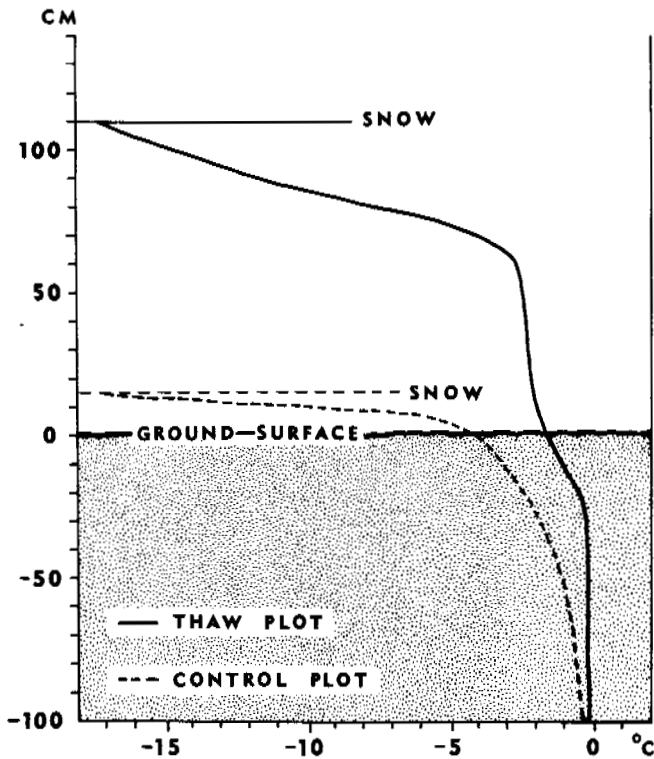


FIGURE 3 Snow and ground temperatures on a specimen day in early winter for two 5 000-m² plots—a natural control plot and a thaw plot modified by snow fences. Normal weather variations cause the irregularities.

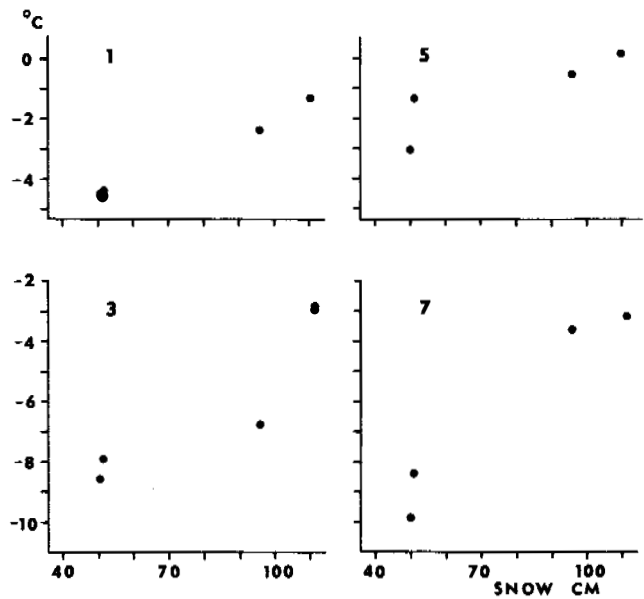


FIGURE 4 Graphs of minimum winter temperatures at 1.5-m depth against the site average snow depth from 1969 to 1972 for four different thermocables. In each case, the variations of minimum temperature from year to year are closely related to variations in the snowcover.

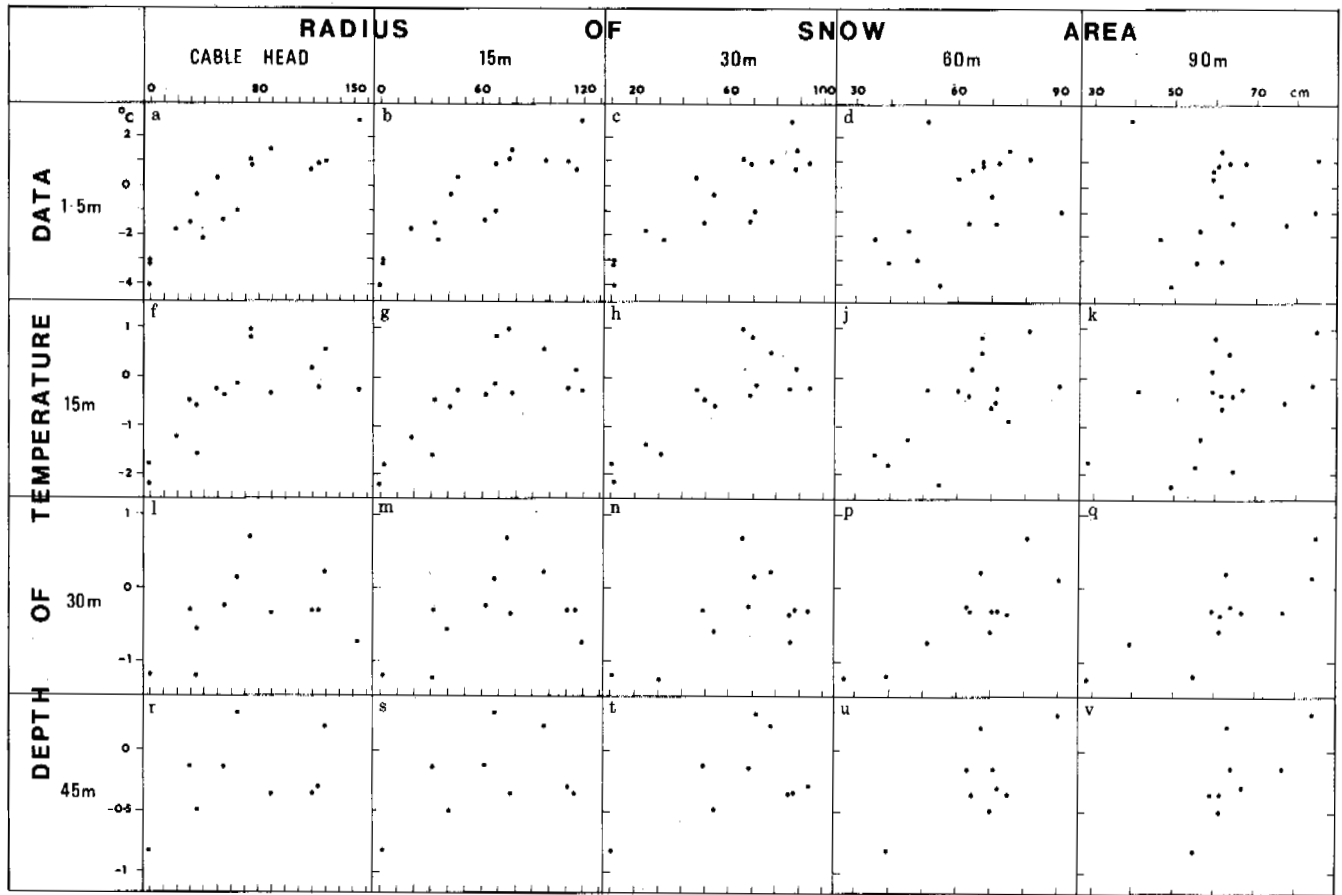


FIGURE 5 Graphs of mean ground temperatures against mean snow depth. The matrix of graphs shows correlations between temperatures at varying depth and mean snow depth of varying sized areas. Temperatures at shallow depth correlate best with small snow areas, whereas temperatures at deeper depth correlate best with larger snow areas.

The ground temperature data used were the mean ground temperatures for 18 vertical profile sites based on 2 or 4 years' data taken at monthly intervals (Figure 1). The standard depths of 1.5, 3, 6, 9, 15, 30, 45, and 60 m were chosen. Four years of snow data were used to produce a contour map of mean peak snow depths.^{6,7} The snow depths used in the analysis are the average snow depths at the cable head and over circular areas of varying radii, measured from the snow contour map. The radii chosen were 15, 30, 60, and 90 m (Figure 2).

TABLE I Minimum Ground Temperatures at Two Test Plots, Winter 1971-1972

	Snow Mean Depth (cm)	Minimum Ground Temperatures (°C)			
		50 cm Depth	1 m Depth	5 m Depth	10 m Depth
Control plot	8	-14.4	-13.2	-6.3	-3.5
Thaw plot	99	-5.5	-4.7	-2.6	-2.1

A selection of the correlation graphs are shown in Figure 5. There is a strong correlation between snow depth and mean ground temperature in some of the graphs. The matrix of correlation coefficients in Table II corresponds to the graphs in Figure 5. For the 1.5-m depth the best correlation is with the cable head snow depth. The temperature at 15 m correlates best with snow over a 30-m radius; similarly, the 30- and 45-m-depth temperatures correlate best with the snow at 60 and 90 m radii, respectively. It is not possible to be precise, but it appears that the temperature at any particular depth correlates best with the snow depth at a radius two times that depth.

A variety of more complex indices of the effect of snow were tested. The area of snow immediately above the measurement point should have a greater influence on the ground temperature than equal areas at a distance. Compound indices were calculated that weighted the snow index to give greater influence to the snow depth at smaller radii. These indices generally gave lower correlations. Other indices were calculated. The snow depth over the area of influence is frequently quite variable. The insulating effect of a uniform snowcover

TABLE II Correlation Coefficients

Temperature at Depth (m)	Radius of Snow Area				
	Cable Head	15 m	30 m	60 m	90 m
1.5	0.90	0.90	0.89	0.48	0.08
15	0.67	0.74	0.78	0.63	0.45
30	0.35	0.44	0.55	0.84	0.81
45	0.36	0.34	0.42	0.69	0.74

could be expected to differ from a variable snowcover with the same mean snow depth. In an attempt to allow for this, heat loss indices were calculated for each sample point in the circular areas, and the results summed and correlation graphs plotted. The heat loss values for varying snow depths were calculated by assuming a constant difference between air and ground surface temperatures and a constant thermal conductivity for the snow. In most cases, the correlations between heat loss indices and ground temperatures were not as close as the correlations using simple snow depth alone.

The relationships between maximum and minimum temperatures and snow depth (Figure 6) are not as good as the relationship between snow depth and mean temperature. The poorer correlation between extreme temperatures and snow is due partly to the combination of short duration of extreme temperatures at 1.5 m and the monthly interval of reading. It is also due to the variations of ground thermal properties that will affect the depth of penetration of thermal waves and therefore affect the extreme temperatures reached at any particular depth. The general trends of both maximum and minimum temperatures are similar to those described by Annersten,¹ i.e., an approximately exponential decrease of winter minimum temperature with decreasing snow depth, and a small increase in maximum temperature correlates with increasing snowcover.

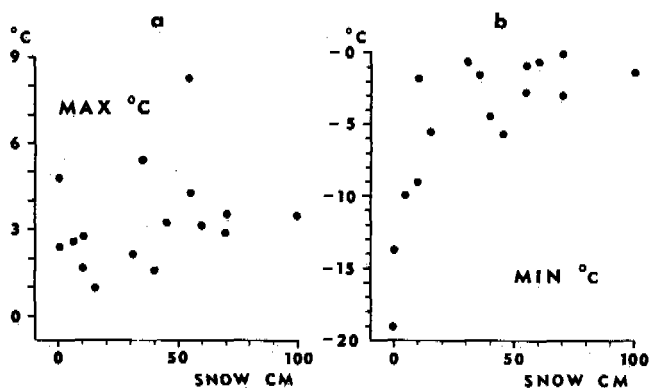


FIGURE 6 Correlations between snow depth at the cable head and (a) maximum temperatures for summer 1971 and (b) minimum temperatures for winter 1971-1972.

ERRORS DUE TO THE SNOW AND TEMPERATURE DATA

The computer technique for snow mapping produces some errors due to generalisation and local inaccuracies. These errors increase the scatter on the graphs but extensive checks against other data revealed no consistent bias due to this cause. Other errors arise because only peak snow depth was used. Variations in the accumulation pattern through the season cause variations in the heat retained in the ground that are not related to the peak snow pattern. Snow density is mainly a function of snow depth⁶; therefore, few additional errors would be caused by density variations. A 4-year period of collection of climatic data is not long enough to give a fully accurate mean. However, detailed examination of the range of snow conditions monitored over the 4 years and comparison with long-term records suggest that the mean snow data gave a reasonable estimate of the long-term pattern. The snowfall for the same period was only 2 percent higher than the 17-year mean. Mean temperatures below 15 m are accurate to 0.1 °C.¹⁰ At shallower depths, the variations from year to year are considerable, and the short period data give much less reliable mean temperatures (particularly on cables 10-17, which have only 2 years of available data), but the relative pattern of temperatures appears to be quite reliable.

DISCUSSION OF THE LINEAR RELATIONSHIPS

A straight-line relationship appears to relate mean ground temperature and snow depth data adequately. Considering only the action of snow as an insulator that prevents winter heat loss, some relationship to an exponential function might be expected. This type of relationship is indicated in Figure 6b. However, the graph of shallowest mean temperature and smallest snow area (Figure 5, graph a) shows a straight-line relationship, and this is the depth where influence of snow insulation on mean temperature should show maximum effect. Thus, there is no doubt that there is a straight-line relationship, and some explanation is necessary. On sites with extremely shallow snow, the severe conditions prevent vegetation from being established, and the resulting bare ground causes higher summer shallow ground temperatures.¹⁰ Therefore, the very low winter temperatures at sites with extremely shallow snow are partly compensated by higher summer temperatures. This appears to explain why the straight-line relationship remains satisfactory even for mean ground temperatures under very shallow snow. The straight-line relationship cannot apply to indefinitely deeper depths of snow. The data currently available does not include extensive areas with a snow depth over 90-100 cm and such areas are therefore excluded from this analysis in this paper. In the Schefferville area, this is not very important since these areas will be free of permafrost.

INFLUENCE OF SNOW DEPTH COMPARED WITH OTHER FACTORS

The correlation of ground temperature with snow alone, ignoring all other factors, must produce some errors. Other factors thought to affect the ground temperature pattern in this area are heat transport by groundwater movement, variations of vegetation cover, variations of aspect and relief, and variations in the physical properties of the rocks.

However, there is a close relationship between snow depth and relief and between snow depth and vegetation. There is also a correlation between sites with the deepest snowcover (valleys) and groundwater movement, both of which encourage higher than average temperatures. These interrelationships help to explain why the snow depth alone gives such a good explanation of the temperature distribution.

The correlation between snow and ground temperature is notably better than the correlation with any other single factor. Correlations between snow and an index of relief concavity or convexity (Figure 7) gave similar correlations to those in Figure 5 but with lower correlation coefficients (e.g., 0.67 compared with 0.78; 0.41 versus 0.84). The other factors have not been quantified sufficiently well to produce similar correlation graphs, but qualitative assessment indicates that they would give much lower correlations if considered on their own.

Transport of heat by groundwater movement affects all of the profiles in or near valley bottoms. The effect of groundwater on mean temperatures appears to be small at 1.5 m, but below that depth the trend is to hold the mean temperature between 0 and 0.5 °C. Two effects appear to be involved. First, this seems to be the characteristic temperature range for most of the groundwater circulation on this site. Second, the groundwater movement induces deep active layers that are characterised by strongly marked zero cur-

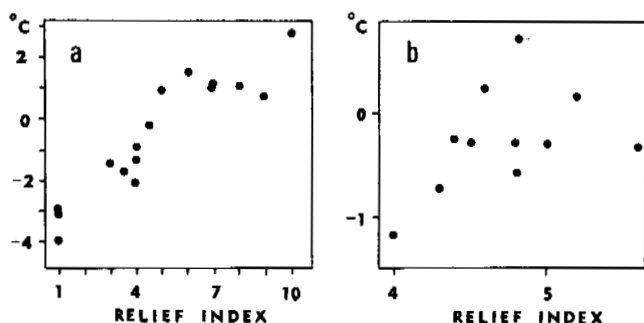


FIGURE 7 Correlations between (a) mean ground temperatures at 1.5 m and relief index for cable head (b) mean ground temperatures at 30 m and relief index for 60 m radius. The relief index scale ranges from 1 (strongly convex) to 10 (strongly concave), calculated by using deviation from average slope. The correlations are not as good as the corresponding correlations of Figure 5.

tain effects,¹⁰ and that tend to produce mean annual temperatures near to 0 °C. Most commonly, the effect is to give a temperature lower than expected, since sites with marked groundwater movement are usually also valley sites and therefore deep snow sites. The importance of groundwater effects is demonstrated by the following example. The graph for temperatures at 15 m and snow at a 30-m radius (Figure 5, graph h) shows that the four highest snow depths are anomalous in relation to the general trend. These four points are affected by groundwater, and, if they are removed, the coefficient of correlation is increased from 0.78 to 0.91.

It might be argued that anomalously low temperatures at deep snow sites in valleys are due to long-lying snow that reduces early summer heat input⁵ rather than to groundwater effects. However, long-lying snow is not thought to be important at this type of site for a variety of reasons. First, the correlations of snow with shallowest temperatures do not show anomalously low temperatures correlated with deep snow sites (Figure 5, graph a). If long-lying snow were reducing summer heat input, then it should affect shallow temperatures as well as deep temperatures. However, groundwater can affect deeper temperatures leaving the shallow temperatures almost unaltered. Second, detailed examination of the patterns of temperature change through the year at the relevant cables shows that they are consistent with groundwater effects and not with possible long-lying snow effects. Additionally, on the amelioration project plots, within a week or two of the snow melt the deep snow plot showed much higher shallow temperatures than the shallow snow plot. It appears that it is not necessarily favourable for sites to be uncovered early in the season. This reasoning may well not apply to extensive areas of deep snow, but these have already been excluded from the analysis given in this paper.

In addition to snow depth and groundwater, there are undoubtedly other influences that cannot be individually isolated from such a limited series of data.

FORMULAS RELATING SNOW AND GROUND TEMPERATURES

Discussion of the Regression Equations

Regression equations were calculated for those combinations of ground temperature and snow circle radius that showed the best correlations in the matrix of correlation coefficients (Table II). The general form of the regression equation is:

$$T = aS - w,$$

where T = mean annual temperature (°C), S = snow depth (cm), a = factor (°C/cm) for snow depth, and w = constant (°C) for mean shallow ground temperature. w/a is the snow

depth at which a temperature of 0 °C can be expected.

The data for the best regression equations at four specimen depths are given in Table III. All four regression equations show a similar depth at which a temperature of 0 °C is to be expected, the mean figure being 75 cm. The gradient of the regression, however, does vary somewhat between the equation for 1.5-m temperature against cable head snow and the equations relating to deeper depths. The gradients for the three equations relating to 15, 30, and 45 m are all similar, the mean gradient being 1:37.6.

Annersten^{1,2} came to the conclusion that 40 cm was the depth of snow sufficient to prevent permafrost formation in the Schefferville area, though he noted that some data, which he considered less reliable, indicated an alternative figure of 75 cm. The regression equations presented here are in good agreement with the latter figure.

Possible Improvements

An average of the four equations given in Table III was tested against the temperature data from all cables for 9 depths ranging from 1.5 to 60 m and involving a total sample of 123 points. It was found that the prediction of presence or absence of permafrost was correct in 82 percent of the cases. If those points known to be affected by groundwater are omitted, the level of correct predictions is then increased to 94 percent. Thus, the prediction of permafrost presence or absence will be substantially improved when a reliable groundwater factor can be incorporated into the equation.

The influence of the geothermal gradient on ground temperatures normally produces an increase in temperature at greater depths. The regression equations in Table III show that there is no consistent trend for w to increase with depth. This may mean that the geothermal gradient is masked by the inaccuracies in the data or, alternatively, that the normal geothermal gradient over this depth range may be modified by climatic change effects as demonstrated in other parts of Canada.^{3,9} A tentative estimate of the general geothermal gradient for the area is 1.1 °C/100 m, based on a thermocable with uniform snow conditions and probably limited lateral heat flow.

At the present stage, the following general model is proposed for estimating the distribution of ground temperatures:

$$T = aS + W + bD + cN$$

where S is mean snow depth (cm) over an area with a radius twice D , D is the depth in metres, b is a factor for the geothermal gradient, N is a groundwater measure, and c is the corresponding factor.

The value of a in Table III varies between 0.025 and 0.035. If the groundwater-affected points are removed from the data, the value for a falls into the range 0.028-0.035. The range of values for w is similarly altered by the removal of groundwater-affected points, and, if the necessary allowance is made for bD , the factor then lies between 2.2 and 2.7. Additionally, the shallow ground temperature of 0 °C always corresponds to a snow depth between 68 and 78 cm, i.e., $68 < w/a < 78$. The constant w could also be modified for variations of surface type if necessary. The estimate of geothermal gradient above suggests a value for b of approximately 0.01. When better estimates of the average geothermal gradient are available, the value of bD could be further modified by a factor to allow for rock thermal properties. The expression cN for groundwater influence will need to include both a measure of the size of the source area (or some other measure of discharge) and a measure of macro- and micro-permeability. A factor for aspect also could be included.

Using the values currently available, the best equation is: $T = aS + w + 0.01D$, where $0.028 < a < 0.035$, $2.2 < w < 2.7$, and $68 < w/a < 78$. For example, with a uniform snowcover 30 cm deep, this would predict the depth of permafrost to be between 123 and 163 m if the correction for geothermal gradient is accurate. Research planned and in progress will give a more accurate and comprehensive equation.

Since the main object of the study is to produce accurate permafrost predictions for practical purposes, it is essential to develop these analyses with data that can be obtained economically on a large scale. Relief data and geological data are generally available for mining sites. Peak snow data can be obtained by either of the two methods developed.⁷ The

TABLE III Regression Equation Data

Depth of Temperature Data (m)	Radius of Snow Area (m)	Regression Equation ($T = aS - w$) ^a	w/a	Correl. Coeff.	Standard Error (°C)
1.5	cable head	$T = 0.0346S - 2.67$	77.2	0.90	0.81
15	30	$T = 0.0251S - 1.84$	73.3	0.78	0.54
30	60	$T = 0.0261S - 2.00$	76.5	0.84	0.28
45	90	$T = 0.0286S - 2.11$	73.8	0.74	0.23

^a T = mean annual temperature (°C), S = snow depth (cm), a = factor (°C/cm) for snow depth, and w = constant (°C) for mean shallow ground temperature.

use of peak snow data is preferred to a more sophisticated measure of snow, because the latter would need much greater effort for the data collection. Measures of groundwater effect can probably be developed from geologic and topographic information. Data on variations of thermal properties could be related to geological information.

SUMMARY AND CONCLUSIONS

It is found that snow is the most important factor controlling permafrost distribution in the Schefferville area and that there is a linear relationship between ground temperatures and snow depth. Groundwater is an important subsidiary factor, but has not yet been quantified. The temperature at any particular depth correlates best with a snow area that has a radius two times that depth. Regression equations were calculated for combinations of temperature depth and snow radius that gave the highest correlation coefficients. The regression equations obtained were similar, and an average equation was calculated. This equation accurately predicts presence or absence of permafrost for 82 percent of a sample of 123 points, and the explanation is increased to 94 percent if points known to be affected by groundwater are removed. The depth of snow corresponding to a ground temperature of 0 °C was found to be 75 cm, though this figure may be biased by groundwater effects and perhaps should be approximately 70 cm. Various improvements and developments are suggested, and a tentative general equation is presented. It is now feasible to use the relationships between snowcover and ground temperatures for permafrost prediction for practical purposes. Current research is attempting to refine this relationship and to quantify the next most important factors.

ACKNOWLEDGMENTS

This research was carried out in cooperation with Iron Ore Company of Canada with financial assistance from the Ministère de l'Éducation, Gouvernement du Québec and the National Research Council of Canada.

REFERENCES

1. Annersten, L. J. 1964. Investigations of permafrost in the vicinity of Knob Lake, 1961-62. McGill Sub-Arctic Research Papers 16. 51-143.
2. Annersten, L. J. 1966. Interaction between surface cover and permafrost. *Biul. Peryglacj.* 15:27-33.
3. Beck, A. E., and A. S. Judge. 1969. Analysis of heat flow data—I. Detailed observations in a single borehole. *Geophys. J. R. Astr. Soc.* 18:145-148.
4. Bonnlander, B., and G. M. Major-Marothy. 1964. Permafrost and ground temperature observations, 1957. McGill Sub-Arctic Research Papers 16. p. 33-50.
5. Brown, R. J. E. 1970. Permafrost in Canada. University of Toronto Press, Toronto.
6. Granberg, H. B. 1972. Snow depth variations in a forest-tundra environment, Schefferville, P.Q. Winter 1968-69. M.Sc. thesis. McGill University, Montreal.
7. Granberg, H. B. Indirect mapping of the snowcover for permafrost prediction at Schefferville, Quebec. This volume.
8. Ives, J. D. 1960. Permafrost in Labrador-Ungava. *J. Glaciol.* 3(28):789.
9. Jessop, A. M. 1968. Three measurements of heat flow in eastern Canada. *Can. J. Earth Sci.* 5:61-68.
10. Nicholson, F. H., and B. G. Thom. Studies at the Timmins 4 Permafrost Experimental Site. This volume.
11. Thom, B. G. 1969. New permafrost investigations near Schefferville, P.Q. *Rév. Géogr. Montréal* 23:317-327.
12. Thom, B. G., and H. Granberg. 1970. Patterns of snow accumulation in a forest-tundra environment, Central Labrador-Ungava. *Proc. East. Snow Conf.* 27th Ann. Mtg. p. 76-86.

STUDIES AT THE TIMMINS 4 PERMAFROST EXPERIMENTAL SITE

Frank H. Nicholson

MCGILL SUB-ARCTIC RESEARCH LABORATORY
Schefferville, Quebec

Bruce G. Thom

AUSTRALIAN NATIONAL UNIVERSITY
Canberra, Australia

INTRODUCTION

The presence of permafrost and its effects on iron ore mining have stimulated permafrost studies in the Schefferville area over the past 15 years.^{2,3,8,9,11,12} Schefferville lies in the zone of discontinuous permafrost⁵ and the distribution of permafrost is very variable. In view of the possibility of encountering more frozen ore bodies, the Timmins 4 Permafrost Experimental Site was established in 1968 to improve the understanding of permafrost and to test methods of its delimitation.¹²

INVESTIGATION OF THE SITE

Site Surveys

The Timmins 4 site has been mapped at a scale of 1:1 200 and with a contour interval of 1.5 m. There has been a geological investigation, including numerous drill holes and test pits.⁷ The vegetation has been mapped both on the ground and from colour infrared aerial photography. The pedology of the site has been studied.

General Environmental Monitoring

Meteorological observations have been maintained at the site, using recording apparatus and visiting the site weekly since 1968. The instrumentation has been gradually increased and now includes intermittent measurement of the radiation balance. The snow has been studied in detail using a 147-point snow course to obtain a representative sample of the patterns of snow accumulation in both space and time.^{6,13} Aerial photographs taken at intervals during the snowmelt period have further documented snow changes. Distance thermographs have been used to record temperatures at varying depths in the snow and at shallow depths in the ground on several sites. Small test plots with a sequence of thermocouples to a depth of 50 cm were employed in order to evaluate the effects of different surface covers.

Deep Thermocables

Twenty-seven thermocables were installed between 1968 and 1972 to depths from 10 to 110 m. The thermocables installed

in 1968 (No. 1-9) and 1970 (No. 10-17) have 12 thermocouples spaced at varying intervals according to the length of the cables. Under the variable field measuring conditions and with long lengths of cable, individual readings may occasionally be in error by as much as 0.5 °C; however, mean temperatures and other data based on a series of readings can be corrected to be accurate to 0.1 °C. For later thermocables, it was found more satisfactory to use thermistors. The thermistors are calibrated to various accuracies according to the requirements, the most accurate being calibrated to ± 0.01 °C. The deep thermocables have been read at least once each month since installation.

Special Studies

Since the general distribution of the permafrost has been outlined, the experimental site has been used to test geophysical methods of delimiting permafrost.⁷ The geophysical work has included seismic and resistivity surveys and a wide variety of borehole geophysical tests.

For the past year, one part of the site has been used for a large-scale test of permafrost thermal amelioration using seminatural means. Snow fences have been installed to increase winter snow insulation, and the vegetation has been stripped to increase summer heat input. The amelioration is being monitored to establish both the overall change in the thermal regime and the changes in the various components of the heat balance.

The patterned ground on the site was studied in order to evaluate its significance in relation to the permafrost.¹⁴ The physiologic ecology of the site is being studied at present.

DESCRIPTION OF THE SITE

Location

The Timmins 4 Permafrost Experimental Site is in the centre of the Labrador-Nouveau Québec Peninsula at lat. 55° and is approximately 700 m above sea level (Figure 1).

Geology

The site is underlain by unmetamorphosed Proterozoic sediments that are folded and faulted. The main units are shales,

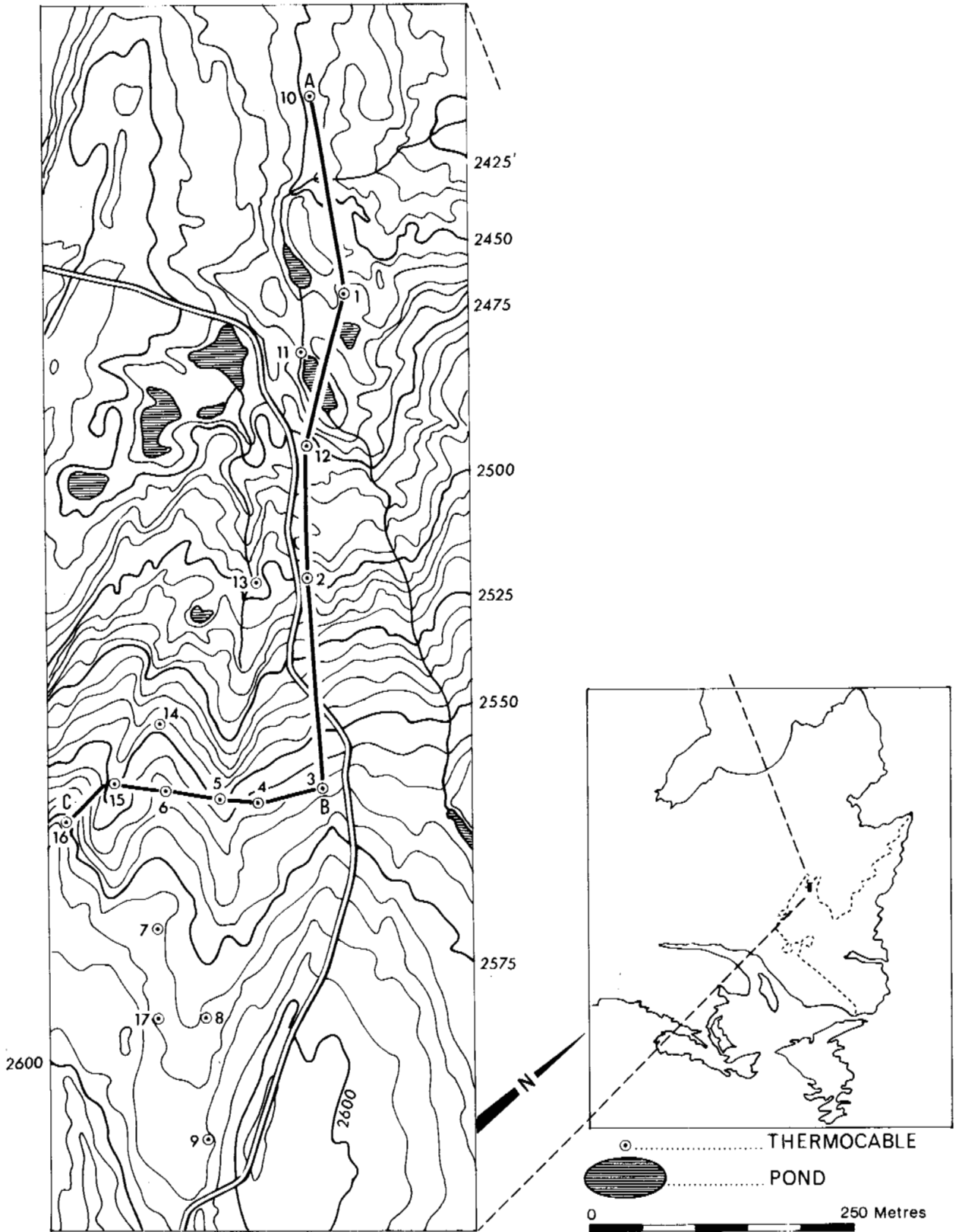


FIGURE 1 Location map and relief map of Timmins 4 Permafrost Experimental Site, showing thermocable locations and section lines.

with or without high iron content, quartzite, and the banded cherty iron formation.⁷ The economic iron deposits occur where rocks with originally high iron content have been leached, thus further increasing the percentage of iron. The leaching may affect all the rocks, including quartzites, causing a general increase in porosity. Frost shattered bedrock is exposed on parts of the ridge crests but over most of the site there is a thin, discontinuous till layer up to 1 m thick.

Topography

The topography of the site (Figure 1) is closely related to the underlying geology, and the main valleys follow fault lines. The site grades from a height of 660 m in the northwest to 720 m in the southeast, giving a range of varying topography with small ridges and valleys.

Climate

The mean annual air temperature of the Schefferville meteorological site is -4.5°C , and the mean annual precipitation is 745 mm, of which 312 mm water equivalent is snow. The mean windspeed is 5 m/s. The records from the Timmins 4 site are for too short a period to give reliable mean data, but the data available suggest that the mean annual temperature is approximately -5.5°C and the mean wind speed 50–75 percent higher than the Schefferville meteorological site.

Vegetation

The site lies in the broad transitional zone between boreal forest and tundra. In the general Schefferville area, the vegetation varies from closed spruce forest in sheltered valleys to altitudinal tundra on exposed ridges. The highest parts of the Timmins 4 site fall into the latter category.

PERMAFROST CHARACTERISTICS OF PARTICULAR INTEREST

Range of Ground Temperatures

The mean temperatures of 17 long-established thermocables show that there is a wide range of ground temperature conditions in the 1 km² site (Figure 2). This is not surprising in view of the wide range of relief, vegetation, lithology, snowcover, and many related factors. The mean temperatures at 15-m range between -2.2 and 0.8°C , with over 50 percent within the range 0 to -0.6°C . Thus, the mean ground temperature at 15 m is $4\text{--}5^{\circ}\text{C}$ higher than the mean annual air temperature of approximately -5°C . The mean temperature profiles (Figure 2) and tautochrone diagrams (Figure 3) show a considerable variety of form, as well as absolute temperature.

Influence of Snowcover

The study of snow at Timmins 4 and the correlations between snow and permafrost are discussed in separate papers of this volume. The insulating effect of snow is well known, and the importance of this factor has been previously indicated in the Schefferville area.^{1,2,4,8,12,13} The work at Timmins 4 has demonstrated that variation of snow depth is the most important factor controlling the distribution of permafrost at this site. Figure 4 shows the correlation between temperatures at a depth of 10 m and mean snow depth over a radius of 15 m. As a general approximation, the snow is shallower on the ridges and deeper in the valleys, and the permafrost is related to this general pattern. It should be noted that many other factors are related to snow distribution. Therefore correlations with snow distribution are also correlations with related factors, notably relief, vegetation, and other micrometeorological factors.⁶

The Ranges of Temperature with Depth

The depth at which the annual temperature range is only 0.1°C is used as the level of zero annual amplitude. On some sites the level of zero amplitude is at 6–8 m and on other sites the annual temperature wave penetrates as far as 25–30 m. Thermal diffusivities were calculated from the speed of penetration of the annual temperature wave, and in some cases they are surprisingly high. Figures in excess of $0.025\text{ cm}^2\text{ s}^{-1}$ are not uncommon. These high values are probably due to the nature of the iron-bearing minerals involved.

Active Layers

The average depth of active layer for the majority of sites is between 3 and 4 m. Many of the cables were not installed for the study of the active layer, and the depths given in Table I reflect this. The exceptionally deep active layer at some sites is notable; four sites have active layers between 9 and 12 m deep. These very deep active layers are found in valley sites where groundwater movement thaws much more of the frozen ground in summer. Site 5 is similar, but the thawed zone is sufficiently large to be retained through all winters yielding a talik. In some winters, the deep active layers do not freeze completely. The heat loss needed to freeze such deep active layers with relatively high water content is considerable, and undoubtedly the influence of the specially high thermal diffusivities is important.

Away from the valleys, those areas with the least snowcover, and hence lowest winter temperatures, have the deepest active layers (sites 14 and 16). Vegetation is completely absent from these areas, which are usually exposed ridge crests. Tests on small plots in a relatively dry summer demon-

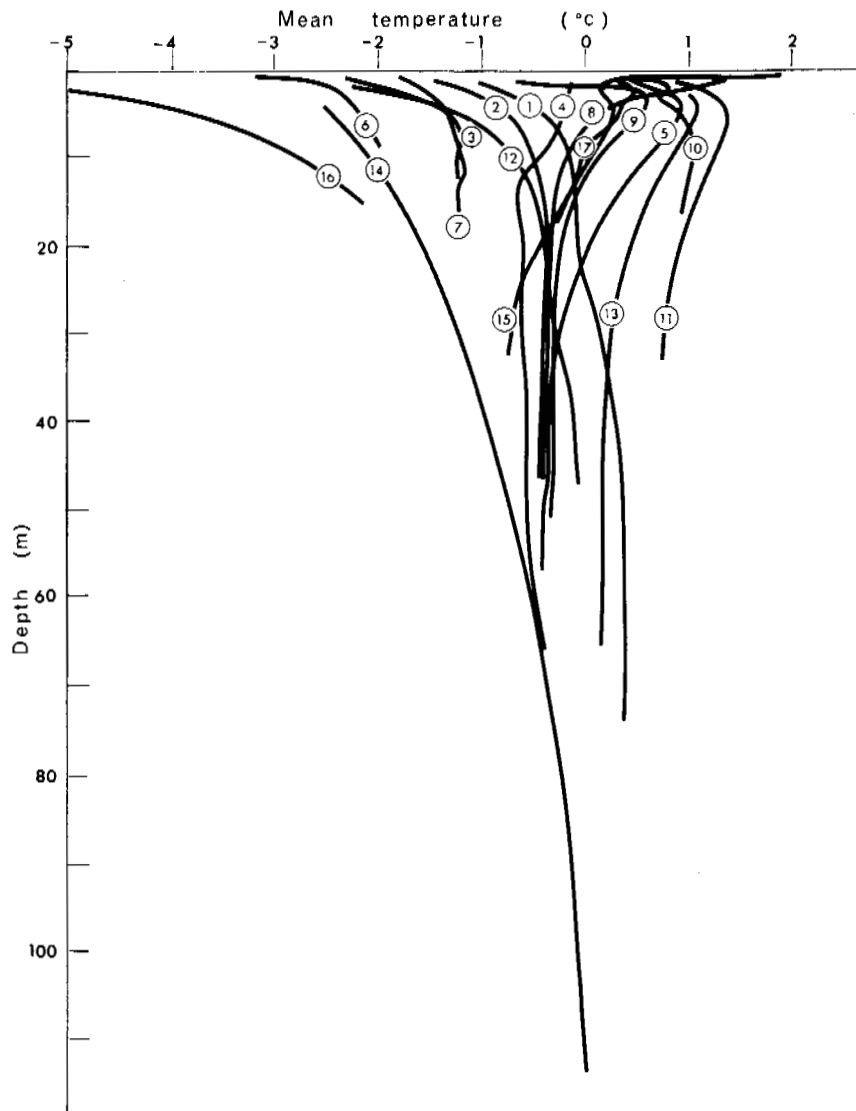


FIGURE 2 Mean temperature for cables 1-17, showing the variation of thermal conditions at different sites.

strated that ground temperatures at 50-cm depth were consistently more than 2°C higher under bare ground plots than under plots with a 5- to 10-cm-thick cover of lichen. Thus, a deeper active layer can be expected in exposed bare soil sites, despite the lower winter temperatures.

There is a suggestion that the depth of the active layer is generally greater in cool wet summers than in warmer dry summers. This would indicate that the transport of heat into the soil by downward movement of water is important, but more data are needed to provide reliable quantification. Neither the orientation of the topography nor the positioning of the thermocables is suitable for evaluating the importance of variations of active layer with different aspects. Annersten,¹

working some 16 km to the southeast, reported active layers to be only two thirds as deep on north-facing slopes.

Zero Curtains

Zero curtain effects¹⁰ have been noted in the lower parts of the active layer at all sites where there is freezing from the surface to the permafrost. These effects are particularly notable at sites with a very deep active layer. The zero curtain effects occur at 0°C , which is important in demonstrating the temperature at which the ground freezes. Thus, there is no overall depression of freezing point in the rocks of the area and the abrupt change in physical and engineering prop-

erties due to the change from frozen to unfrozen state occurs at 0 °C. This is important when evaluating thermocable data for engineering and other purposes.

Moisture Content of the Permafrost and Active Layer

Since the iron ores are leached zones of the iron formation, the permanently frozen rocks of greatest interest often have both a high porosity and a high bulk density.⁷ Moisture content measured by weight can be very misleading. In two major units of the iron formation, the average moisture content is approximately 5 percent by weight, but this figure represents approximately 15 percent by volume. It is rare for moisture content by volume to fall below 3 percent and up to 40 percent is not uncommon in frozen rocks. The moisture content of the top metre of the ground tends to be high (20-30 percent by volume) but there is neither a consistent

TABLE I Active Layer Depths

Cable No.	Depth (m)	Comments
1	3	Permafrost base at 25 m
2	3.7	
3	3	
4	3-4.5	Talík at 4.5-21.5 m
5	3-4.5	
6	3	
7	3.7-4.5	No permafrost
8	9	
9	11.7-12.3	
10	3-3.7	No permafrost
11	3	
12	3-3.7	No permafrost
13	1.5-2.1	
14	~4.5	
15	12	Talík in some years
16	5.2	
17	9.2-12.2	

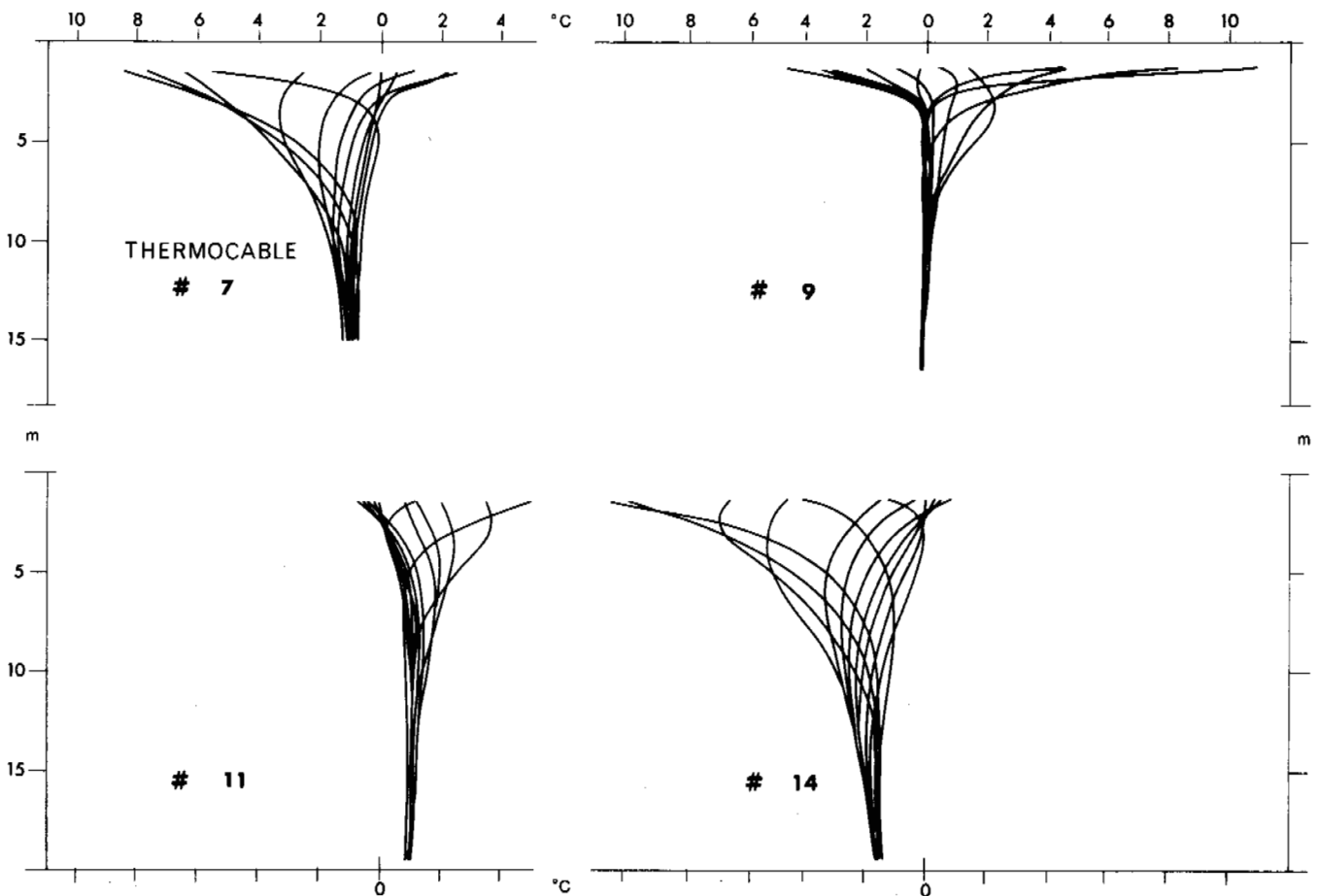


FIGURE 3 The annual pattern of ground temperature changes at four specimen thermocable sites. The diagrams are compiled from temperature readings at approximately monthly intervals during 1971.

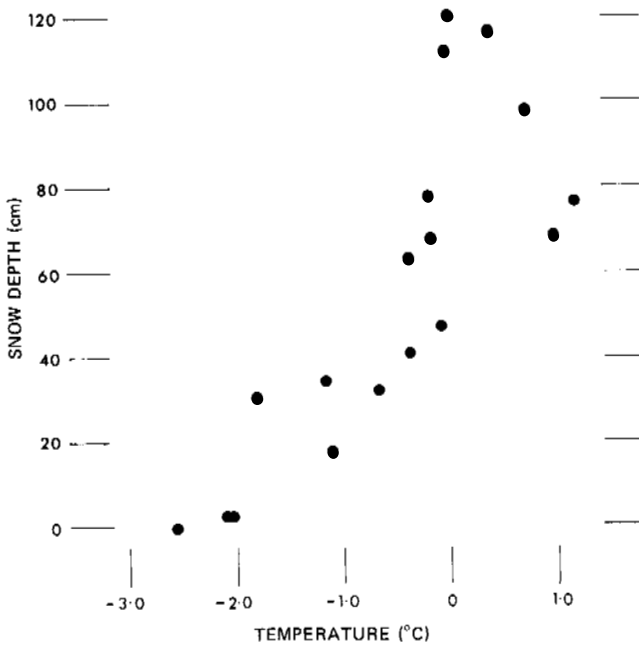


FIGURE 4 Temperatures at 10-m depth versus mean snow depth over a 15-m radius. The three points with the highest snow index represent sites that are influenced by groundwater movement.

trend of higher moisture contents throughout the active layer nor a consistent concentration of moisture just below the active layer.

DISTRIBUTION OF PERMAFROST

Figures 5 and 6 show representative sections through the permafrost. The thermocable values used are mean temperatures over 2 to 4 years. The intermediate interpolation points were produced using snow data and adjacent thermocable data.

There is at least 100 m of permafrost in the southern part of the site (section B-C, Figure 6) and possibly as much as 130 m. It is striking that most of the permafrost has a temperature higher than -1°C . The base of the permafrost is not well defined, because it proved much deeper than was expected when the investigation was planned. Towards the lower, northern part of the site, the permafrost becomes less deep and then intermittent (Figure 5). Along the line of the section, snow depths increase and vegetation cover becomes denser and taller from south (B) to north (A). In many places the isotherms are steeply inclined and even vertical, and the boundary between permafrost and unfrozen ground appears to be steeply inclined rather than wedging out slowly.

In Figure 6, the section crosses a series of ridges and valleys, showing the relationship between relief and thermal conditions. The ridges have shallower snow and the valleys

deeper snow. The valleys are also influenced by groundwater movement, and the larger valley has a talik zone.

The overall distribution demonstrates that there is a major influence of lateral heat flow. The individual ground temperature profiles seen in Figures 2 and 3 reflect this influence of lateral flow, and there appears to be some sites of net surface heat loss and others of net surface heat gain. It is possible to approximate many single temperature profiles by considering the influence of the mean snow depth at varying distances from the thermocable. A full explanation would need to take into account the overall three-dimensional thermal distribution.

Thus, the thermal pattern can be mainly explained in terms of snow distribution modified in some cases by groundwater movement. In the northern, lower part of the site, however, this explanation is less satisfactory, and other factors become important in some areas. The relative importance of other factors controlling permafrost distribution is the subject of current research.

The close relationship between environmental conditions and permafrost at the Timmins 4 site indicates that, at this site, the permafrost is in balance with modern conditions. The area has only been free of a glacial ice sheet for about 6 000 years; thus, great depths of relict permafrost would not be expected. Occasional reports of permafrost first encountered several tens of metres deep in mines may indicate relict permafrost in some cases. Annersten¹ deduced from the form of temperature profiles that degradation of permafrost was the dominant trend, but 10 years of observations on his sites have shown no clear evidence of warming. There is no suggestion of such a trend at Timmins 4. Thus it appears that not only is most of the permafrost in the Schefferville area probably in balance with the present environmental conditions but that relict permafrost also is to be expected at a relatively small number of sites.

SUMMARY

There is little doubt that snow is the most important factor controlling the distribution of the permafrost in the Schefferville area. The active layer is normally 3-4 m. Several examples of active layers up to 10 m deep have been studied, and this greater depth of thaw is thought to be due to shallow groundwater movement. The thermal diffusivity of the ground is often very high, as evidenced by the penetration of annual temperature waves as deep as 25-30 m. Moisture contents of the frozen ground range between 3 and 40 percent by volume and are commonly on the order of 15 percent. From zero curtain evidence, it is observed that the sharp change in physical properties of the rocks, due to the change from frozen to unfrozen state, occurs at 0°C . The three-dimensional pattern of the mean isotherms and the relationships between snow and ground temperatures demonstrate that lateral heat flow is particularly important. It is postulated

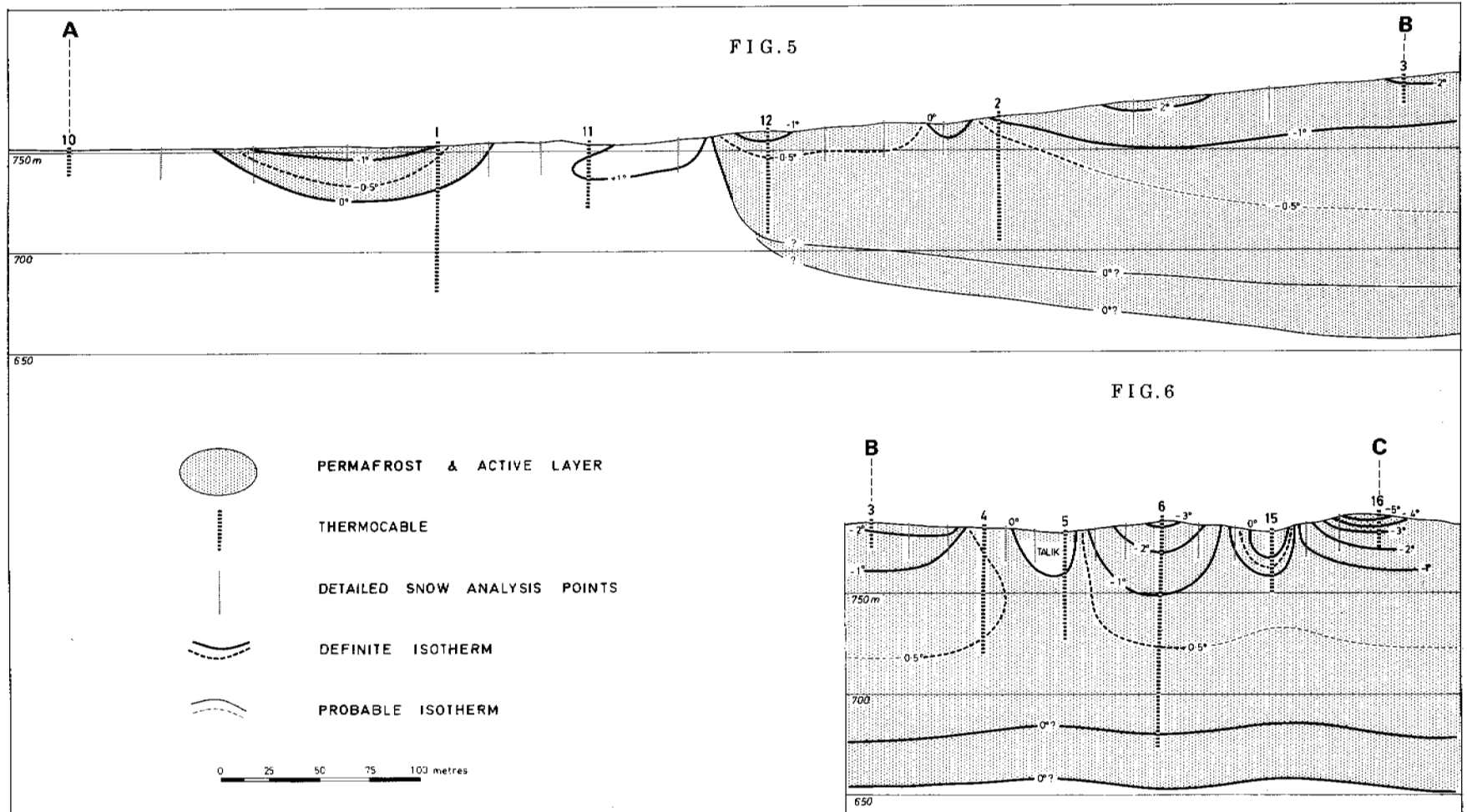


FIGURE 5 Section from lower ground to a ridge crest area. The nature of the permafrost boundary can be clearly seen. The shallow ground thermal pattern can be accounted for by snow distribution, but the deeper temperatures at sites 10 and 11 are higher than expected.

FIGURE 6 Section across a series of small ridges and valleys. The ridge crests are almost bare of snow in winter and therefore have lower mean temperatures. The valleys are affected by groundwater movement, as well as having much deeper snow.

that the present permafrost distribution in upland sites like Timmins 4 is in equilibrium with contemporary environmental conditions and that relict permafrost is not extensive.

ACKNOWLEDGMENTS

The studies were initiated in 1968 by B. G. Thom, then Director of the McGill Sub-Arctic Research Laboratory, in cooperation with L. Nichols of the Iron Ore Company of Canada. The studies have been continued since 1970 by F. H. Nicholson and others in cooperation with P. F. Stacey of the Iron Ore Company of Canada. The topography, geology, and geophysical surveys and all heavy engineering associated with the establishment and development of the site have been carried out by the Iron Ore Company of Canada. The studies of physiologic ecology and permafrost amelioration are being directed by W. C. Oechel and F. H. Nicholson, respectively. The National Research Council of Canada has provided technical assistance and advice. These studies would be impossible without the financial support of the Iron Ore Company of Canada, the Ministère de l'Éducation, Gouvernement du Québec, the National Research Council of Canada, and McGill University.

REFERENCES

1. Annersten, L. J. 1964. Investigations of permafrost in the vicinity of Knob Lake, 1961-62. McGill Sub-Arctic Research Papers 16. p. 51-143.
2. Annersten, L. J. 1966. Interaction between surface cover and permafrost. *Biul. Peryglacj.* 15:27-33.
3. Bird, J. B. [ed.] 1964. Permafrost studies in central Labrador-Ungava. McGill Sub-Arctic Research Papers 16. 137 p.
4. Bonnlander, B., and G. M. Major-Marothy. 1964. Permafrost and ground temperature observations, 1957. McGill Sub-Arctic Research Papers 16. p. 33-50.
5. Brown, R. J. E. 1970. Permafrost in Canada. University of Toronto Press, Toronto.
6. Granberg, H. B. 1972. Snow depth variations in a forest-tundra environment, Schefferville, P.Q. Winter 1968-69. M.Sc. thesis. McGill University, Montreal.
7. Iron Ore Company of Canada. Internal Rep.
8. Ives, J. D. 1960. Permafrost in Labrador-Ungava. *J. Glaciol.* 3(28):789.
9. Ives, J. D. 1962. Iron mining in permafrost, central Labrador-Ungava: A geographical review. *Geogr. Bull.* 17. p. 66-77.
10. Muller, S. W. 1947. Permafrost or permanently frozen ground and related engineering problems. J. W. Edwards, Inc., Ann Arbor, Michigan.
11. Thom, B. G. 1969. Permafrost in the Knob Lake iron mining region. *Proc. 3rd Can. Conf. Permafrost.* p. 9-20.
12. Thom, B. G. 1969. New permafrost investigations near Schefferville, P.Q. *Rév. Géogr. Montréal* 23 p. 317-327.
13. Thom, B. G., and H. Granberg. 1970. Patterns of snow accumulation in a forest tundra environment, Central Labrador-Ungava. *Proc. East. Snow Conf. 27th Ann. Mtg.* p. 76-86.
14. Thorn, C. E. 1970. Pattern and process in the development of stony earth circles near Schefferville, Quebec. M.Sc. thesis. McGill University, Montreal.

GEOCHEMISTRY OF PERMAFROST AND QUATERNARY STRATIGRAPHY

Troy L. Péwé

ARIZONA STATE UNIVERSITY
Tempe, Arizona

Paul V. Sellmann

U.S. ARMY COLD REGIONS RESEARCH AND
ENGINEERING LABORATORY
Hanover, New Hampshire

A relatively new approach to the study of permafrost is the chemical investigation of ice and sediments comprising it; this approach appears to hold a great potential. The work was initiated by O'Sullivan^{17,18} and followed up in Alaska by Brown and his associates of the U.S. Army Cold Regions Research and Engineering Laboratory (CRREL).^{1-11,25,26} Brown⁶ summarizes (p. 1):

The spatial distribution of cations and anions in near surface, earthy materials, such as soils and frozen ground, provides a means of interpreting and assessing present and past chemical regimes and geomorphological activities of a given landscape. This technique is par-

ticularly applicable to cold, perennially frozen ground in which movement of soluble ions is small and perhaps even insignificant. Therefore, the existing ionic concentration gradients and their lateral dimensions can be indicative of cold regions environments and provide a measure of conditions prior to the formation of the perennially frozen ground.

The distribution of soluble and exchangeable ions in soils, perennially frozen ground, and sediments underlying water bodies is influenced by both the materials and the present and past depositional and leaching environments. For the same material and environments, low concentrations indicate considerable leaching or freshening and high concentrations indicate lack of these active processes or enrichment by ground or surface waters. Silts and clays retain more soluble

and exchangeable ions than do sand and gravels. Ionic concentration generally increases with depth, particularly in uplifted marine sediments.

Most of the work in this field has revolved around the distribution of soluble salts of sodium, magnesium, calcium, and potassium in perennially frozen sediments as a reflection of past thermal and leaching regimes. It has been shown that a relatively low concentration of soluble salts in permafrost indicates leaching during an unfrozen state and then refreezing (Table I). At Barrow, Alaska, this low concentration in Holocene marine sediments has been interpreted as freshening due to past thaw lake migration or to local thawing, leaching, and refreezing.⁶

For the Fairbanks area, work by Sellmann^{25,26} indicates an abrupt change in chemical concentrations of extractable cations in permafrost at a stratigraphic unconformity in retransported sediments of Wisconsinan age. Preliminary interpretations suggest thawing and refreezing above the unconformity. Four cored holes, the deepest 25 m, in perennially frozen ground near Fairbanks were examined by Brown and

coworkers^{9,10} and were found to indicate an increase of soluble salts beneath an unconformity. The soluble salt content is low in the active layer and increases in step-like fashion at depth in the permafrost.

Péwé applied techniques of Brown and Sellmann to the excellent exposures of frozen ground in the mining cuts near Fairbanks that have long been under study by other means^{19-21,23} (Figure 1). Perennially frozen samples from critical points in a 30-m vertical exposure of Eva Creek, 16 km west of Fairbanks, were analyzed for soluble salts by Sellmann at CRREL²⁷ using a method described earlier¹⁰ and reported in terms of "conductivity" (micromhos). The work is continuing but preliminary results are presented here to illustrate the possible value of such studies and application elsewhere.

An examination of Figure 2 and Table 1 shows that the concentration of the cations (by conductivity) varies from 65 to 1 285 micromhos (μmho) and has a close relationship to stratigraphy. The following value ranges were obtained (Table I): 65-155 in the Holocene sediments; 235-410 in

TABLE I Conductivity and Stratigraphy of Sediments Exposed at Eva Creek Gold Placer Mining Cut, Alaska^a

Thickness (m)	Unit Surface	Conductivity (micromhos) ^b of Samples		Age
		1967	1970	
2	Loess present permafrost table		65	Holocene
			85	
	156	155		
	past permafrost table	314	235	
		249		
	252			
13	Retransported loess	285		Wisconsinan
		304		
		317		
		234		
		250		
1	Silt-forest bed	143		Sangamon
		Sangamon soil (?)	100	
			355	
			965	
		300		
19	Loess		450	Illinoian
			300	
			480	
			200	
			1 125	
	1 100			
1	Silt-forest bed	883		Yarmouth (?)
	Gravel	1 285		Pre-Yarmouth (?)

^a Conductivity examination made at U.S. Army Cold Regions Research and Engineering Laboratory, Hanover, New Hampshire, by J. Brown and P. V. Sellmann.

^b Measurements corrected to 25 °C with a cell constant of 1.0 (equivalent to micromhos centimetre).

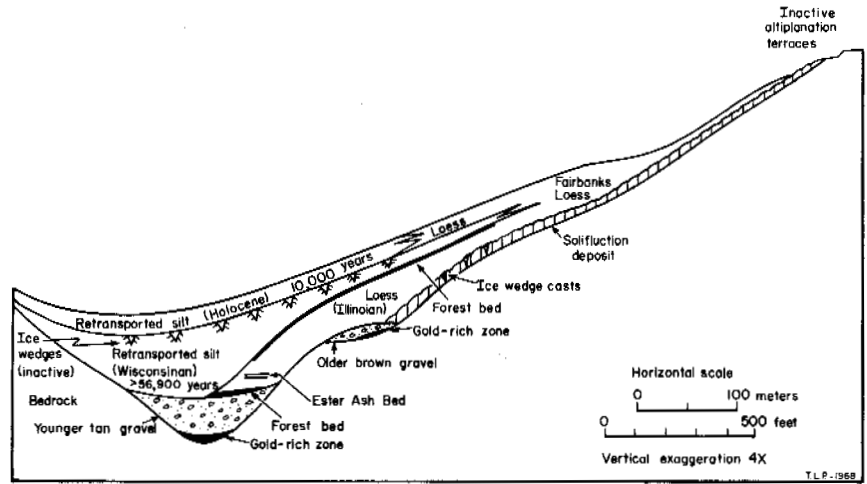


FIGURE 1 Schematic composite cross section of a creek valley in central Alaska, illustrating the relations of the Quaternary silt and gravel deposits.

the Wisconsinan retransported silt sediments; 145 in the forest bed (Sangamon); 100 for the Sangamon soil; 200-965 for the Illinoian loess; approximately 1 115 for the base of the Illinoian loess; 885 in soil and forest bed of Yarmouth (?) age; and 1 285 in gravel of pre-Yarmouth (?) age.

It is perhaps logical to assume, as Brown *et al.*¹⁰ men-

tion, that the low soluble salt content of fine-grained soil is probably due to removal by groundwater movement (leaching) during a time when the sediments are unfrozen, especially near the surface. Brown found unfrozen sediments of the present active layer at Fairbanks to have a conductivity value of 25, having been leached for many years. Also, in

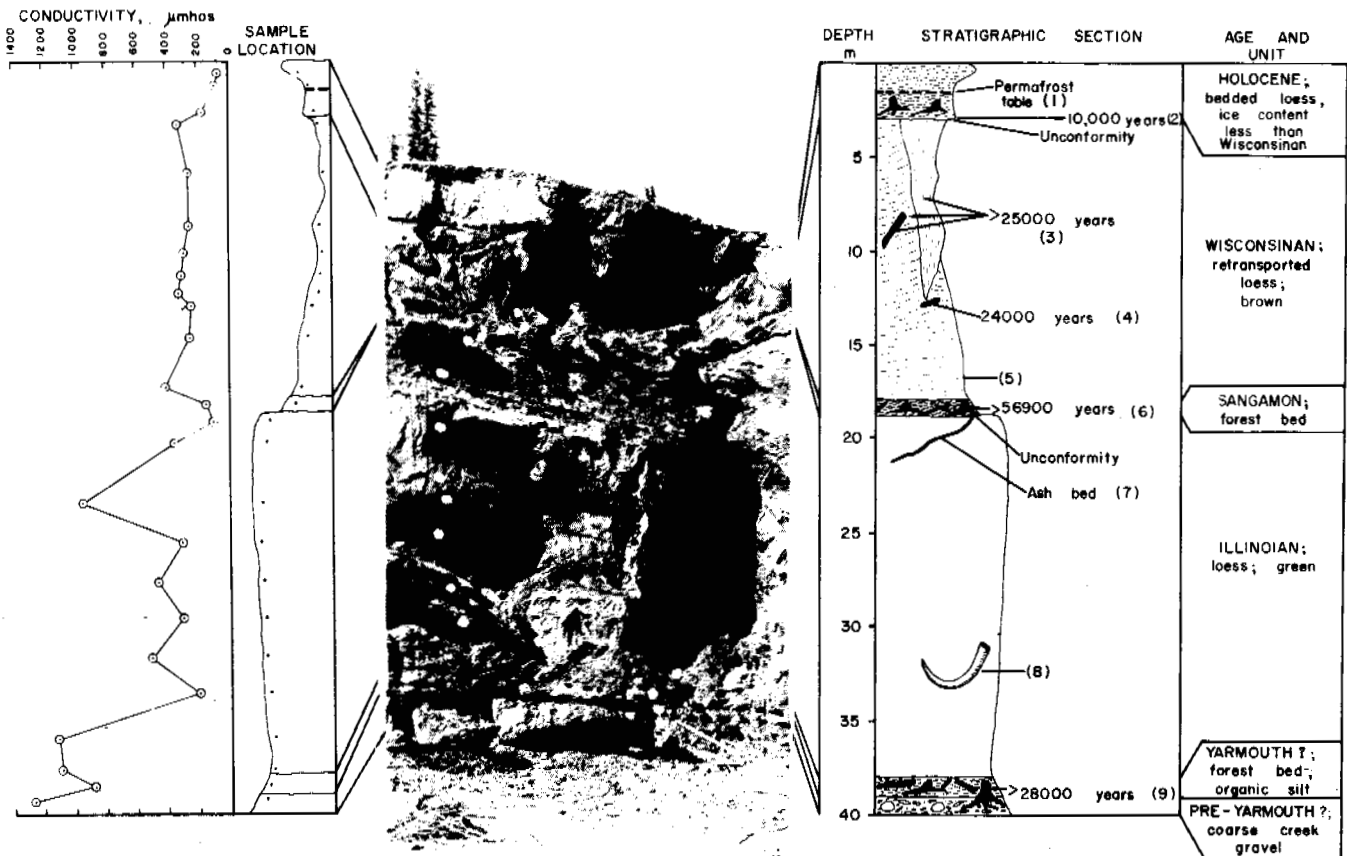


FIGURE 2 Stratigraphic section of late Quaternary perennally frozen sediments with radiocarbon dates, vertebrate occurrences, and geochemical analyses of sediment. Eva Creek, 16 km west of Fairbanks, Alaska. Numbers in parentheses refer to Notes on page 170. (Photograph No. 2540, by T. L. Pévé, July 2, 1967; see Table I.)

periods of rapid, thick accumulation, sediments have less opportunity to be leached than in periods of little or no accumulation. This has been clearly demonstrated in loess in Iowa (Ref. 12, Table 5) and Mississippi (Ref. 14, p. 9), whereas in areas of slow loess accumulation, the carbonate is almost entirely leached out, in contrast to high carbonate content in areas of rapid, thick loess accumulation.

A preliminary interpretation of the conductivity curve (Figure 2) and Table I is as follows. The present active layer is characterized by the low conductivity figure of 65–85 μmho . It has long been known that the upper 1 or 2 m of permafrost in interior Alaska thawed during early to middle Holocene time and then refroze.^{19,21,23} This cycle is supported by the relatively low conductivity figure in the perennially frozen Holocene silt—a figure that is lower than frozen Wisconsinan sediments but higher than current active layer sediments. Leaching was active during the thaw period. Conductivity jumps to 300 just below the Wisconsinan–Holocene unconformity, and all values in Wisconsinan sediments are about that magnitude, which supports the suggestion of an accumulation and freezing period. Thermal “unconformities” within the Wisconsinan sediments could be present but were missed in the sampling.

The drop in conductivity from 410 μmho at the base of Wisconsinan sediments to 195 μmho in the forest layer (Sangamon) is quite striking and supports the suggestion of an interglacial period of no permafrost and perhaps little accumulation. A period of time when the ground was unfrozen or when there was little or no loess accumulation would be favorable for leaching.²⁴

A sample at the very top of the loess section of Illinoian age yields a conductivity figure of 100 μmho . It is thought that this low figure represents the Sangamon soil and indicates thawing and leaching of Illinoian loess.

A pronounced drop in values in the forest soil layer at the base of the section relative to bounding deposits is similar to the forest layers higher in this section and strongly supports the suggestion of an interglacial or interstadial period with thawing and little deposition.

The values for conductivity of the sediments near the base of the section are much different than for the upper part (Table I). The writers' interpretation of these high figures is as follows: The base of the permafrost in many exposures in central Alaska today, and perhaps in the past, was at the base of the silt deposits, that is, at the contact between the overlying loess or retransported loess and the underlying creek gravel. Groundwater may have circulated freely in the gravel just under the silt. The circulating groundwater may have been high in soluble salts and may therefore account for the high conductivity figures at the base of the silt section, including the forest bed, and at the top of the creek gravel. In nearby exposures, there are many ironstone and calcium carbonate concretions at the contact between the silt and the gravel. Also, contemporary ground-

water analyzed from near Fairbanks has a conductivity figure of about 1 000 μmho . Therefore, perhaps the high conductivity figures at the base of the section at Eva Creek are the result of groundwater modification.

Preliminary geochemical analyses of frozen sediments and ice in northern and central Alaska suggest that the chemical investigation of frozen ground holds a great potential for gross correlations in permafrost regions and perhaps for interpretation and geomorphological and thermal changes in quaternary time.

REFERENCES

- Allan, R. J. 1969. Clay mineralogy and geochemistry of soils and sediments with permafrost in interior Alaska. Ph.D. dissertation. Dartmouth College, Hanover, New Hampshire. 289 p.
- Brown, J. 1965. Seasonal thaw and ground-ice morphology in tundra soils, Barrow, Alaska. *Agron. Abstr.* p. 59.
- Brown, J. 1966. Massive underground ice in northern regions, p. 89–102. *In* U.S. Army conference proceedings Vol. 1. West Point, New York.
- Brown, J. 1966. Ice-wedge chemistry and related frozen ground processes, Barrow, Alaska, p. 94–98. *In* Permafrost: Proceedings of an international conference. National Academy of Sciences, Washington, D.C.
- Brown, J. 1967. Tundra soils formed over ice wedges, northern Alaska. *Soil Sci. Soc. Am. Proc.* 31:686–691.
- Brown, J. 1969. Ionic concentration gradients in permafrost, Barrow, Alaska. Research Report 272. U.S. Army Cold Regions Research and Engineering Laboratory, Hanover, New Hampshire. 25 p.
- Brown, J. 1969. Soil properties developed on the complex tundra relief of northern Alaska. *Biul. Periglacialny* No. 18:153–167.
- Brown, J. 1969. Buried soils associated with permafrost, p. 115–127. *In* Pedology and Quaternary research symposium. University of Alberta Press, Edmonton.
- Brown, J., S. Gray, and R. Allan. 1969. Evolution à la fin du Quaternaire d'un remblai de vallée à Fairbanks, Alaska. I: La géochimie et la stratigraphie du pergélisol, p. 270. *In* INQUA Conference, 8th Résumé des Commun. Paris.
- Brown, J., S. Gray, and W. Webster. 1967. Chemical and related properties of a permafrost section from Fairbanks, Alaska. (Unpublished) USA CRREL Technical Note. 18 p.
- Brown, J. and P. L. Johnson. 1965. Pedoecological investigations, Barrow, Alaska. USA CRREL Technical Report 159. 32 p.
- Davidson, D. T., and R. L. Handy. 1952. Property variations in the Peorian loess of southwestern Iowa. *Iowa Acad. Sci. Proc.* 59:248–265.
- Guthrie, R. D. 1968. Paleoecology of a late Pleistocene small mammal community from interior Alaska. *Arctic* 21(4):223–244.
- Krinitzky, E. L., and W. J. Turnbull. 1967. Loess deposits of Mississippi. *Geol. Soc. Am. Spec. Paper* 94. 64 p.
- Matthews, J. V., Jr. 1968. A paleoenvironmental analysis of three late Pleistocene Coleopterous assemblages from Fairbanks, Alaska. M.S. thesis. University of Alaska, College. 59 p.
- Matthews, J. V., Jr. 1968. A paleoenvironmental analysis of three late Pleistocene Coleopterous assemblages from Fairbanks, Alaska. *Quaest. Entomol.* 4:202–224.
- O'Sullivan, J. B. 1961. Quaternary geology of the Arctic coastal plain, northern Alaska. Ph.D. thesis. Iowa State University. 191 p.
- O'Sullivan, J. B. 1966. Geochemistry of permafrost, Barrow,

- Alaska, p. 30-37. Permafrost: Proceedings of an international symposium. National Academy of Sciences, Washington, D.C.
19. Péwé, T. L. 1952. Geomorphology of the Fairbanks area. Ph.D. thesis. Stanford University, Stanford, 220 p.
 20. Péwé, T. L. 1955. Origin of the upland silt near Fairbanks, Alaska. *Geol. Soc. Am. Bull.* 66:699-724.
 21. Péwé, T. L. 1958. Geology of the Fairbanks (D-2) quadrangle, Alaska. U.S. Geol. Survey Geol. Quad. Map GQ-110, scale 1:63, 360.
 22. Péwé, T. L. 1965. Fairbanks area, p. 6-36. *In* T. L. Péwé, O. J. Ferrians, Jr., D. R. Nichols, T. N. V. Karlstrom [ed.] INQUA field conference F, central and south-central Alaska guidebook. Nebraska Academy of Sciences, Lincoln.
 23. Péwé, T. L. Quaternary stratigraphic nomenclature in central Alaska. U.S. Geol. Survey Prof. Paper, Washington, D.C. (In press)
 24. Péwé, T. L., and P. V. Sellmann. 1971. Geochemistry of permafrost and Quaternary stratigraphy. *Geol. Soc. Am. Annu. Mtg. Abstr.* 3(7):669.
 25. Sellmann, P. V. 1967. Geology of the USA CRREL permafrost tunnel, Fairbanks, Alaska. USA CRREL Technical Report 199. 33 p.
 26. Sellmann, P. V. 1968. Geochemistry and ground ice structures: An aid in interpreting a Pleistocene section, Alaska. *Geol. Soc. Spec. Paper* 101. p. 197-198. [Abstr.]
 27. Sellmann, P. V. Written communications, Dec. 28, 1967, and May 19, 1971.

NOTES TO FIGURE 2

[1] The permafrost table was lowered throughout central Alaska 1-5 m about 10 000 years ago and has subsequently risen to its present position. All sediments in the deep thaw layer were unfrozen for hundreds, if not thousands, of years. Flattop ice wedges and collapse of sediments over ice wedges remain as evidence of this thawing episode.

[2] The age of this formation in the Fairbanks area is well documented.^{19,21-23} More than a dozen samples have been dated from the Holocene loess and retransported loess in many different mining exposures; the dates range from about 3 000 to 10 000 years, with most of them in the neighborhood of 5 000-7 000 years. A date

of $3\,750 \pm 200$ years (L-117H) was obtained on a sample of wood collected by Péwé in 1951 from the base of the Holocene loess on Eva Bench mining exposure 3 m below the surface.

[3] In 1967, Péwé collected samples of ice, wood, and adjacent organic-rich silt for dating. All were dated by the radiocarbon laboratory at the University of Arizona as more than 25 000 years old. More detailed dating probably would have indicated an age between 25 000 and 30 000 years. A wood sample collected in 1951 by Péwé 2.5 m below the top of the Wisconsinan sediments on Eva Creek was dated at $23\,300 \pm 1\,000$ years (W-435). Wood samples collected by Péwé in 1952 at the base of the Wisconsinan formation and near the middle were dated as 23 000 years old (L-157A) and 30 000 years (L-163J), respectively.

[4] A radiocarbon date of $24\,400 \pm 650$ years (I-2116) was obtained on wood collected at the base of the ice wedges (Ref. 15, p. 207).

[5] Matthews^{15,16} examined fossil beetles from Wisconsinan and Sangamon deposits. Beetles, plus a pollen study by Matthews and samples collected by Péwé indicate a treeless tundra environment during Wisconsinan time. In 1949, Péwé also collected bones of mammoth and *Citellus undulatus* from Wisconsinan sediments here. Guthrie¹³ recovered *Microtus gregalis*, *Lemmus sibericus*, *Dicrostonyx torquatus*, and *Citellus undulatus* from both Wisconsinan and Illinoian deposits in this section.

[6] Péwé¹⁹ has reported a forest bed at this stratigraphic horizon from many exposures in the Fairbanks area. The oldest date obtained on this bed is reported by Matthews¹⁶ as more than 56 900 years (Hv-1328). This organic-rich silt layer with tree stumps and logs unconformably overlies the deformed loess (see Figure 1).

[7] In innumerable exposures of the contact between Wisconsinan and Illinoian silt in the Fairbanks area, a 1-cm-thick, white, vitric, volcanic ash bed occurs at the top of the Illinoian loess and is truncated by an unconformity. This ash bed is deformed by faulting and solifluction.

[8] Péwé collected (1949-1967) mammoth tusks and various bones of bison from loess of Illinoian age on Eva Creek.

[9] At Dawson mining cut and others a well developed organic silt crops out.^{19,23} This unit contains large stumps and logs that are partially flattened and deformed; it is thought to represent an interstadial or interglacial forest bed. One particularly fine white spruce stump from the organic silt of the Eva Creek section with roots in the underlying gravel is more than 28 000 years old (L-137X).

STRATIGRAPHY AND DIAGENESIS OF PERENNIALY FROZEN SEDIMENTS IN THE BARROW, ALASKA, REGION

Paul V. Sellmann and Jerry Brown

U.S. ARMY COLD REGIONS RESEARCH AND ENGINEERING LABORATORY

Hanover, New Hampshire

INTRODUCTION

The perennially frozen sediments that mantle the Barrow, Alaska, area and most of the Arctic Coastal Plain retain a record of late Quaternary events and are collectively known as the Gubik formation. The Gubik sediments are seldom more than 30 m thick and overlie rocks of Cretaceous and Tertiary age. Black² recognized three stratigraphic units in the Gubik formation. In order of increasing age they are the Barrow, Meade, and Skull Cliff units. Faas²⁰ conducted a detailed study of the Barrow Village estuary, which indicated a transition from more recent sediments to late-Pleistocene sediments based on lithologic and some paleontologic evidence. O'Sullivan²⁹ developed a sequence of depositional history based on various land surfaces and lithologies and suggested at least four major marine transgressions. McCulloch²⁸ investigated the depositional history of the northwestern part of the Arctic Coastal Plain and reported evidence for five transgressions. Hopkins'²² reviews of the Arctic Coastal Plain investigations and their correlation with other parts of coastal Alaska proposed that there appeared to be evidence for as many as seven transgressions during the Quaternary.

A series of studies on the development and modification of recent beaches in the Barrow area^{11,23,31,32} indicated their post-Wisconsinan age, and suggested possible subtle changes in sea level during the past several thousand years. Table I summarizes these observations and correlations.

Lagoons and offshore bars occur along much of the coast, with a series of old beach ridges in the Barrow area extending several kilometers inland. The Barrow area, as referred to in this report, is the small triangular-shaped land mass north of 71°15'N. Here, the land surface has a maximum relief of approximately 15 m and is covered with both drained and undrained oriented basins and a wide variety of polygonal ground patterns.³ Low, wet tundra vegetation covers the surface and is only occasionally interrupted by frost scars of bare mineral soil or wind-eroded dry peaty polygons. Permafrost under the land is generally 300 m thick.⁴ The thickness of the seasonally thawed surface zone depends primarily upon soil texture, and in the

predominantly fine-grained soils it is generally less than 0.4 m.^{9,19}

Ice volumes in the upper 3 m vary from massive buried wedges to barely visible segregated ice and decrease with depth to near saturation at 8-m depth.

Variations in soluble chemical composition of the reworked and unmodified sediments provide further documentation of depositional events and postdepositional diagenesis.⁸⁻¹⁰ Chemical concentrations from water extracts range from 0-5 meq/100 g in sediments freshened or leached in terrestrial or freshwater environments to an excess of 40 meq/100 g in primary marine sediments. Chemical, lithologic, and paleontologic findings provide supporting evidence for an interpretation of depositional environments for the Barrow region.

This paper reports on local stratigraphic investigations and is based on detailed coring and augering of the frozen sediments to a depth of some 20 m.^{8,35} Regional studies of other authors are discussed in an attempt to correlate our Barrow findings with the Quaternary events from the other arctic coastal areas.

STRATIGRAPHY

Lithology

Material was obtained from the locations shown in Figure 1 by four types of sampling techniques: small-diameter cores obtained to depths of 20 m³⁶; 3/4-m-diameter auger holes ranging from 3 to 6 m deep⁸; beach cliff exposures along Elson Lagoon and the Chukchi Sea; and underground excavations, including the meat cellar and seismic beach ridge shaft. The deeper cores provide undisturbed samples and the major stratigraphic control for the present study. The cored and augered sections were examined for morphology, grain-size distribution, density, moisture and ice contents, paleontological material, and chemical composition.

Two major lithologic units are present and are correlated with Black's² nomenclature: the upper (Barrow) unit and the lower (Skull Cliff) unit. At Barrow, the intermediate-aged Meade River unit is absent.

TABLE 1 Summary of Quaternary Transgressions for Alaskan Coastal Regions

Late Pliocene
Early Pleistocene

		Years										Investigators
2 200 000	1 900 000	700 000	300 000	175 000	170 000	100 000	50 000	25 000	10 000	5 000	2 000–Present	
Einahnuhtan. Probably about +20 m												
Beringian. Two levels higher than present but lower than Anvilian.	Anvilian. Probably much higher than Kotzebuan and Einahnuhtan <+100 m and >+20 m.			Kotzebuan. Probably about + 20 m. Shorelines at about 33 m on western coastal plain.		Pelukian. Two highs at +7–10 m.	Mid-Wisconsin. Probably a few meters below present.		Krusensternian. Within 2 m of present sea level for deposits <4 000 years old.			Hopkins ²²
Marine transgression. Sediments on wavecut bedrock platform at Kivalina.	Mid-Pleistocene. Transgression—uplift south central part of coastal plain—elevation marine sediments at least 100 m.			Pre-Illinoian. Transgressive beach deposits.		Sangamon. Marine sed. on wavecut terrace along coast.	Mid-Wisconsin. Marine sed. and ice rafted boulders—deposits raised at least 8 m by later uplift.					McCulloch ²⁸
Marine transgression. 95–160-m escarpment at the 320-m elevation at southern margin of intermediate surface.				Yarmouth. Escarpment north of intermediate surface correlated with 95-m terrace near Umiat.		Sangamon. Inner margin of coastal plain causing alluviation of major drainages.	Mid-Wisconsin. Midway on coastal plain.					O'Sullivan ²⁹
				Illinoian. Skull Cliff unit.		Sangamon. Meade River unit.	Wisconsin. Barrow unit.					Black ²
						Pelukian. Possible transgression indicated by more silty sediment under Mid-Wisconsinan unit.	Mid-Wisconsin. Marine sediment dated near Barrow—suggests extensive transgression on portions of Coastal Plain, to present 8-m level and possible deposition of inland ridge.		Krusensternian. Small fluctuations in sea level in last 2 000 years forming and modifying present Barrow spit.			Sellmann, Brown and others ^{13,23,31,36}

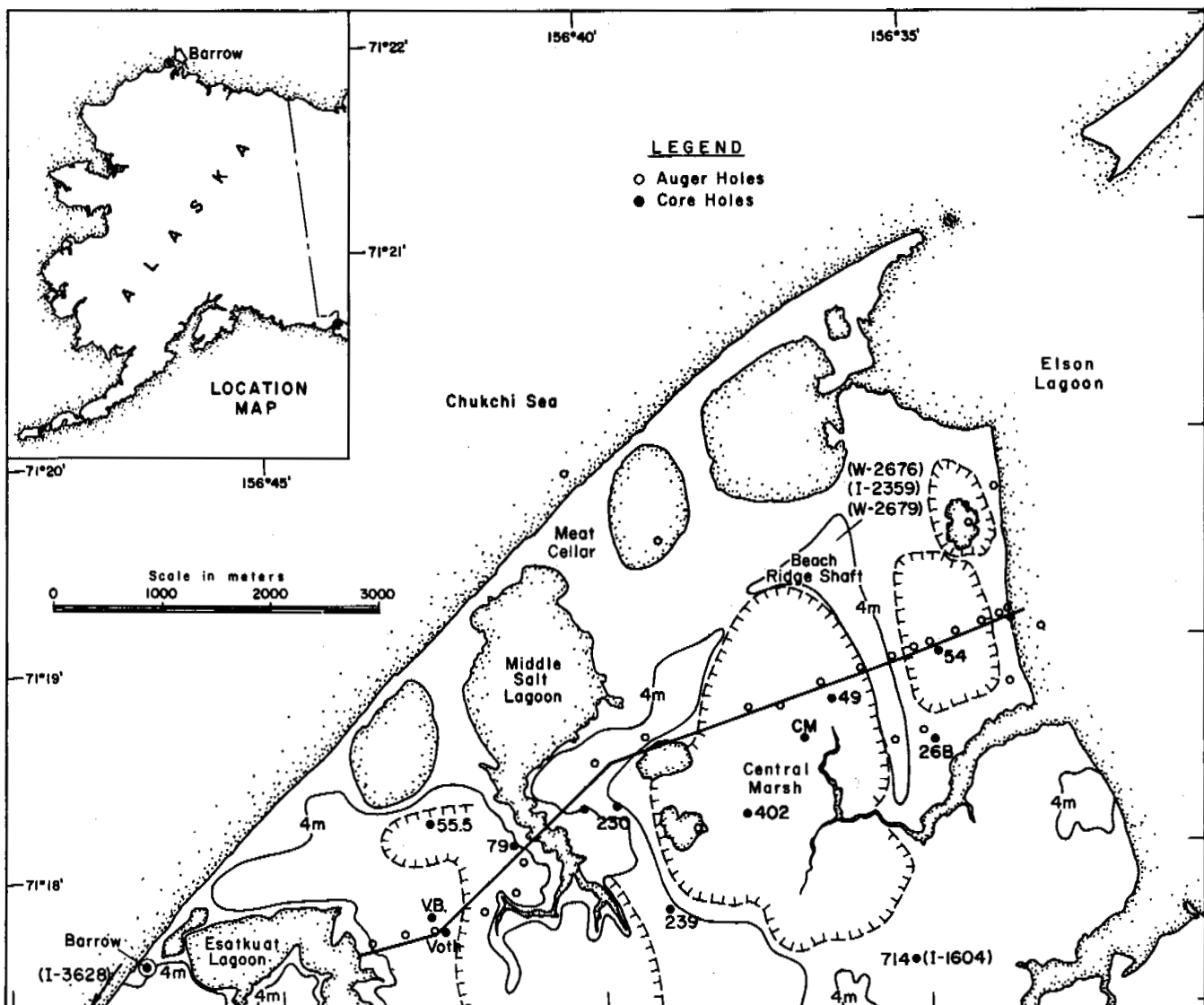


FIGURE 1 Location map for the Barrow, Alaska, sample points. Numbers in parentheses are new radiocarbon dates.

The principal characteristics of these units, as described in Black,² are as follows:

Barrow unit – poorly sorted to well-sorted mixtures of clay, silt, sand, and gravel; unit grades from yellow, tan, and brown to black; in part, contemporaneous with and grades laterally into the Meade River sand and, in part, younger; rarely deposited directly on the Upper Cretaceous rocks; mostly marine; locally, in upper part, fluvial deposits and lacustrine deposits are characteristic.

Meade River unit – white, yellow, buff, or light-tan sand; generally clean and well sorted; marine; conformable to disconformable on the Skull Cliff unit, but in places deposited directly on the Cretaceous rocks. Locally, whipped into surface dunes; in the south and southeast commonly loesslike.

Skull Cliff unit – sticky or greasy, generally poorly sorted, blue-black to dark-gray, marine clay-silt-sand-cobble unit; possibly

glacially derived, in part, and deposited unconformably on the Upper Cretaceous rocks in much of the coastal plain west of the Colville River.

From our observations at Barrow, the Barrow unit can be subdivided into the uppermost organic- and ice-rich, highly reworked sediments and the lower, well-sorted sandy portion that retains its original depositional structures. The Skull Cliff unit consists largely of silts and sandy silts. Characteristic and idealized sections are shown in Figure 2, and a fence diagram plotting all the deeper cores and the major contacts is shown in Figure 3.

The Barrow unit varies between 7 and 10 m in thickness and overlies the lower Skull Cliff unit at between 2 and 7 m below sea level. The contact between the two units dips

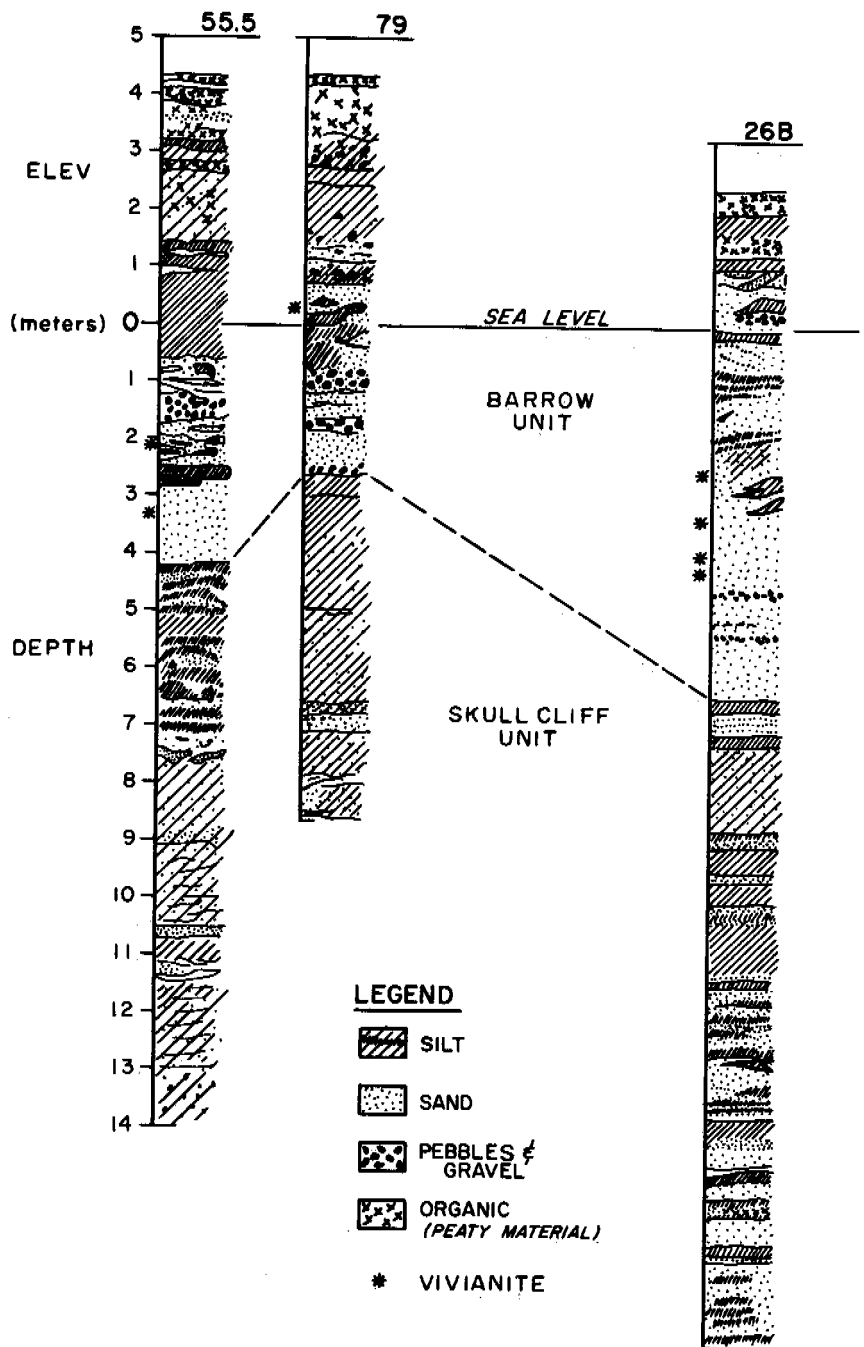


FIGURE 2 Representative and idealized stratigraphic sections from the Barrow area indicating the composition of the Barrow and Skull Cliff units. As grain size becomes finer hatched pattern becomes denser.

gently north or seaward. Average granulometric parameters for the two units are given in Table II.

BARROW UNIT

The upper portion of the Barrow unit varies considerably in thickness due principally to the topographic modifications of the original surface. Its base varies between 2 and 4 m below the present-day surface. These surface sediments contain large volumes of both segregated and ice-wedge ice.

The upper several meters contain on an average 60–70 percent segregated ice by volume, which decreases downward throughout the Barrow unit to near-saturation at about the 8-m depth.¹² In addition, active and buried ice wedges underlie almost all land surface except where recent thaw lake migration has removed older wedges.^{1,5,13} Small, contorted masses of buried peat are found throughout the ice-rich zone and decrease with depth.^{9,10}

Well-sorted sands interbedded with silts characterize

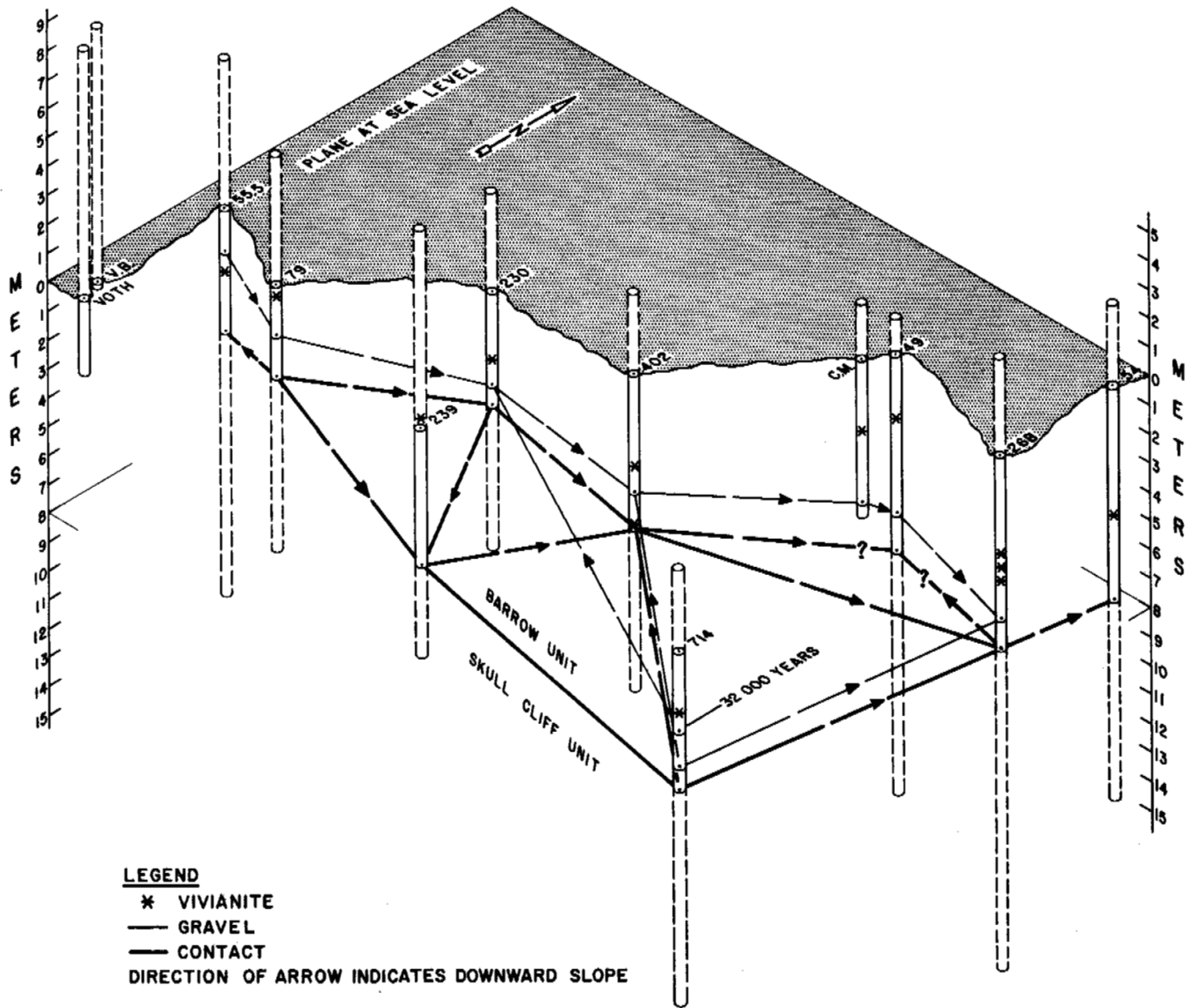


FIGURE 3 Fence diagram of the deep cores illustrating the major contact between the two units and several stratigraphic markers. The gravel line indicates the average position of thin beds (10–50 cm thick) of poorly sorted gravels.

TABLE II Average Granulometric Parameters for the Barrow and Skull Cliff Units

Parameter	Barrow Unit	Skull Cliff Unit
<0.002 mm (%)	7	28
0.002–0.05 mm (%)	12	49
>0.05 mm (%)	81	23
Median diameter (mm)	0.11	0.04
Skewness (Sk)	0.79	0.29
Sorting coefficient (So)	1.68	3.5

the lower portion of the Barrow unit; this can easily be observed in the Barrow Camp meat cellar. Small vivianite nodules occur regularly in association with the more sandy layers and prove to be reliable stratigraphic markers. Silt bands average 23 percent sand, 33 percent silt, and 44 percent clay. Thin pebble layers are found in a number of sections at about the same stratigraphic position in the lower portion of the Barrow unit.

SKULL CLIFF UNIT

This unit is composed largely of gray-black sandy silts interbedded with thin lenticular laminations of gray silty sands. The interbedded material is often contorted, yielding a marbled structure. The thickness of individual sandy

zones ranges from very thin bands (several millimeters) to layers approaching ½ m. Toward the lower portion of the sampled section (20-m depth), small interbedded layers of fibrous and well-preserved organic matter are present. In several of the sections, particularly in core 26B, the lower unit becomes sandier with depth. These sandy zones appear to be amorphous, lacking distinctive structures with the exception of contorted silty bands and stringers.

Based on our investigations the lower limit of the unit is not defined.

Paleontological Evidence

MICROFOSSIL FAUNA

Observations in this section are preliminary and were prepared by Dr. Ruth A. M. Schmidt, geologist, Anchorage, Alaska. Selected samples from the cores, cliff exposures, excavations, and current depositional environments were processed by standard sorting and flotation methods, the results of which have been partially reported.^{33,34,36}

Six species of Ostracoda were found restricted to the Barrow unit. *Normanicocythere concinella* was found in abundance in the Barrow unit and only rarely in the Skull Cliff unit. *Pteroloxa cumuloidea* and *P. venipuncta* were characteristic of the Skull Cliff unit. In some cases, they were the only Ostracoda found in the Skull Cliff units, although they were not limited to it. They occurred rarely in the Barrow unit. *Paracyprideis* and *Heterocyprideis* were present in both units. Using the 873 specimens counted as 100 percent, 85.1 percent of the Ostracoda were found in the Barrow unit and 14.9 percent in the Skull Cliff unit.

Foraminiferal assemblages also differ in each unit. The genus *Elphidium* was present in both units, although three species were more abundant in the Barrow unit and one in the Skull Cliff unit. *Buccella frigida* was found in the Barrow unit and in all cores. Ten species of Foraminifera are found in both units. Of the remaining 32 species, 27 are found only in the Barrow unit; five are confined to the Skull Cliff unit. Of the total number of Foraminifera counted (1 721), 56.8 percent were found in the Barrow unit and 43.1 percent in the Skull Cliff unit. The difference is not as great as that found between Ostracoda, but the number of species limited to the Barrow unit is greater for the Foraminifera than for the Ostracoda.

MICROFLORA

Samples for pollen analyses were obtained from both sub-surface sections and a number of surface environments. These were analyzed by Colinvaux [1] and all but the deep sections had been reported upon previously.^{14,15,16,18} The majority of the pollen analyses were associated with radiocarbon-dated samples in the upper Barrow unit and extended back to 14 000 years B.P. The modern pollen spec-

trum is dominated by grass and sedge pollens with minor amounts of willow, alder, and birch. It appears that this spectrum has undergone little major change in the past 5 000 years. Pollen samples derived from lake sediments contain large numbers of algal colonies of *Pediastrum*. The small amounts of birch and alder are explained by wind transport from nearby inland sources on the North Slope. Alder first appeared in the Barrow record around 5 000 years B.P. and birch at about 10 000 years. Willow pollen is far more abundant during the 9 000- to 14 000-year record than since that period.

The deeper stratigraphic record is derived from cores 714 and 26B with only two analyses available from the Skull Cliff unit and four in the Barrow unit (core 714). Spruce pollen was a common component of samples from core 714. The Skull Cliff sample from 26B yielded an extremely high sedge component. Black amorphous flakes and granules of carbonlike organic matter, probably coal, were found associated with the pollen in these deeper stratigraphic samples. Generally, pollen was poorly preserved in all samples associated with the lower Barrow and Skull Cliff units and occurred in such small quantities that paleoclimatic and environmental conclusions can not be drawn.

Radiocarbon Dating

Numerous radiocarbon dates and their interpretations have been previously reported for the Barrow area.^{6,7,9-11,13,23} The preponderance of samples are from surface peats and near-surface buried peats and organic residues in the upper and cryopedologically reworked Barrow unit. These dates are associated with soil development, ice-wedge stratigraphy and thaw-lake formation; the oldest date recorded was 14 000 years from plant and animal residues recovered in a buried ice wedge.⁷ Several additional and previously unreported dates from the deeper sections in the Barrow area are now available (Table III).

Pairs of samples from the same sample locations (I-1384 and W-2676; I-2359 and W-2679) were obtained at separate times and analyzed in different laboratories. Other relevant dates for stratigraphic control yield values beyond radiocarbon dating: sample I-1394 at 19-m depth in 26B⁷ and a buried frozen log from the cliffs southwest of Barrow (W-380).¹⁷

Chemical

The chemical characteristics of the near-surface permafrost were investigated in order to further define depositional events and modifications.^{8,30} Frozen samples are thawed, a solution extracted, and the chemical content or concentration of the extract determined. The assumption is made that soluble chemical constituents in the sediments remain essentially the same after freezing, particularly at lower con-

TABLE III Radiocarbon Dates of the Barrow Stratigraphy

Sample No. ^a	Location	Depth (m)	Surface Elevation (m)	Date (Years B.P.)	Description
I-1384	Beach Ridge shaft	2.1	6.3	25 300±2 300	Fibrous, thinly layered organic in beach ridge sediments
W-2676	Beach Ridge shaft	2.1	6.3	>44 000	Sample similar to I-1384
I-2359	Beach Ridge shaft	5	7	37 000+2 900 -2 000	Fine organic layer in clean sand
W-2679	Beach Ridge shaft	5	7	36 000±2 000	Sample similar to I-2359
I-1604	Core 714	6	3	31 400+3 600 -2 400	Fine organic layer in marine sediments
I-3628	Beach Cliff			>39 900	Fibrous woody fragment 2 m above sea level from cliff exposures 2 km southwest of Barrow Village

^a I, Isotopes Inc., Westwood, New Jersey; W, Isotope Geology Branch, U.S. Geological Survey Laboratory.

centrations. Sediments underlying freshwater lakes have relatively low concentrations, whereas recently emergent and quickly frozen and brackish sediments have high concentrations. The longer sediment remained unfrozen, presumably the more opportunity for freshening. Representative values for Barrow sediments follow:

Silty lagoon sediments	40-50 meq/100 g oven-dry sample
Primary, unleached permafrost	10-40 meq/100 g oven-dry sample
Present-day marine gravel	5-20 meq/100 g oven-dry sample
Freshened lake sediment	0-2 meq/100 g oven-dry sample

Using this technique and the auger samples from this study, Brown^{8,9} reconstructed the chemical profile across the Barrow peninsula. Several freshened zones under drained lakes and a freshened zone over a deeply truncated ice wedge were clearly detected.

The values in Table IV were obtained with depth from the deeper cored sites.

DEPOSITIONAL HISTORY

The data presented here, together with information previously published, allow a provisional reconstruction of the

TABLE IV Characteristic Chemical Concentrations for the Barrow Settlements

Core	Depth (Sea Level, m)	Milliequivalent/100 g Oven-Dry Sample
26B	+0.5	3.9
230	+0.5	5.5
55.5	+0.5	12.2
714	-2.0	4.6
Voth	-2.5	66.9
54	-5.3	15.7
239	-7.8	66.3

depositional and postdepositional events that have taken place during the late Quaternary in the Barrow region. These are primarily related to the complex series of marine transgressions and, secondarily, to subaerial deposition and cryologic modifications. The Barrow peninsula provides the locale that records a series of both major and minor climatically controlled events of widespread correlative value.

The least well-defined stratigraphic control is based on data from the Skull Cliff unit. Based on lithology and microfauna, this unit was deposited in a low-energy, shallow water nearshore environment, characteristic of an alternately open and closed lagoonal regime or embayment. The age of the Skull Cliff unit is still not well defined. Black² suggested an Illinoian age, and, based upon the authors' interpretation of Hopkins'²² more complex transgressional series, a younger Pelukian age (Sangamon) may be more likely. The only reliable stratigraphic sample obtained from this unit for dating (core 26B, I-1394), yielded a >36 300 years B.P. date. Microfaunal assemblages include several freshwater and brackish water forms, presumably derived from adjacent terrestrial lacustrine, fluvial, and lagoonal habitats. The quiescent nature of this sedimentary environment is also supported by the presence of well-preserved microfauna. The high percent of sedge pollen and relatively well-preserved character, based on a single sample from the Skull Cliff unit, is interpreted as indicating the close proximity of a marshy, vegetated surface during deposition of this unit and rapid deposition in a nonoxidizing sedimentary regime.

Based on the well-sorted composition of this sandy unit and the abundance of nearshore marine microfauna, the Barrow unit was deposited in a higher energy, nearshore environment. The lower Barrow unit contained no freshwater microfauna. The fact that the upper, reworked Barrow unit contained virtually no microfauna remains indicates its severe, postdepositional modification mainly due

to chemical and mechanical removal by lacustrine and soil processes. Because of the unusual assemblage, including the large abundance of spruce pollen, its poor preservation, and the appearance of having been retransported, the interpretation is that the pollen material was reworked from older deposits and brought into the area by longshore transport and therefore does not reflect a paleoenvironment that could be expected in this local area.

The pollen record in the upper, reworked Barrow unit is based on radiocarbon-dated sections and provides the most climatically sensitive interpretation for the region. The record indicates a continuing warming trend from the close of Wisconsin onward with no major change in the pollen record over the past 5 000 years. Therefore, it does not appear that a major postglacial thermal maximum occurred in the region, probably as a result of the damping influence of arctic maritime climate on this littoral region. The occurrence of a sedge tundra associated with preserved remains of lemming pellets and moss and plant fragments documents the presence of a tundra landscape as early as 14 000 years B.P. This date represents the oldest dated material in the upper Barrow unit. Buried soil peat is all less than 11 000 years old.

The age of the lower marine portion of the Barrow unit can now be assigned to the mid-Wisconsin, based on the three radiocarbon dates bracketed between 31 400 and 37 000 years B.P., and coincides with the Wisconsin transgression.

In the Barrow area, the sediments and surface relief above sea level provide evidence for a mid-Wisconsinan transgression and more recent depositional features. A topographic high represented schematically as zone D (Figure 4) and occurring above the 8-m elevation most likely persisted as an island during the invasion of the mid-Wisconsinan sea (Figure 5). The 7.5- to 8-m elevation on the coastal plain marks the upper limit for the occurrence of large ice-rafted boulders as described by MacCarthy.²⁷ Careful examination of topography of this surface indicates that the extent of this transgression was greatest on the central portion of the

coastal plain. The surface rises gently from the coast to the 8-m level, where a noticeable increase in elevation takes place. At some places this break in slope or possible escarpment is as much as 60-70 km inland. This position is in general agreement with the proposed limits of Black's² Wisconsin surface and O'Sullivan's²⁹ mid-Wisconsinan to late-Sangamon limit. McCulloch²⁸ suggests that, based on proposed sea levels at that time, the Barrow area and this extensive part of the coastal plain must have undergone post-mid-Wisconsinan uplift of more than 8 m. This assumes that the high stand of sea level during mid-Wisconsinan time was several meters below present.

Seaward of the zone D escarpment is found a younger beach ridge (zone B). This ridge overlies the dated marine portion of the Barrow unit. It seems likely this ridge was formed as the mid-Wisconsinan sea retreated seaward. Attempts to radiocarbon date this gravelly ridge are not conclusive since determinations of separately sampled organic matter yielded widely different results (25 300 versus >44 000 years), suggesting that the older dated material was reworked in origin. It is our opinion that the younger date more reliably approximates the true age of the ridge. Buried soil peats on the ridge within ½ m of the surface yield dates between 8 500 and 11 000 years, suggesting a minimum age for the feature.

The Barrow ocean shoreline, based on geothermal interpretation, has remained relatively stable over the past several thousand years.²⁴ Along the current coastline, a low series of beach ridges exists (zone A), which corresponds to the Krusensternian transgression and present-day beach building. The current beach and spit complex appears to have formed in the last several thousand years with indications of only 1- to 2-m fluctuations in sea level during its formation.^{11,21,23,31} The lagoonal shoreline during this period has been eroding inland at a rate of 0.2-2 m/year.²⁶

During post-mid-Wisconsinan time, the land surface has undergone considerable and repetitive reworking by thaw-lake formation and migration. Presumably, the near-surface permafrost formed throughout the Barrow region as the

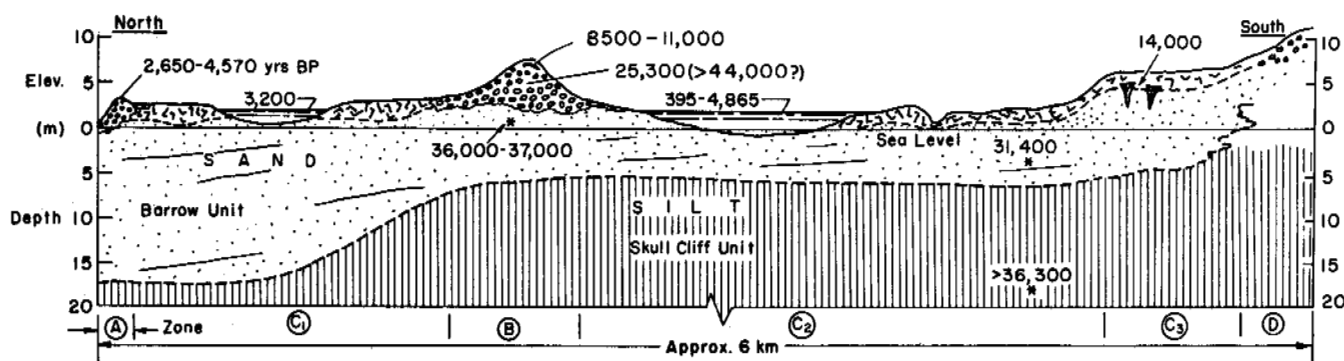


FIGURE 4 Idealized stratigraphic cross section across the Barrow Peninsula indicating the major units and their ages.

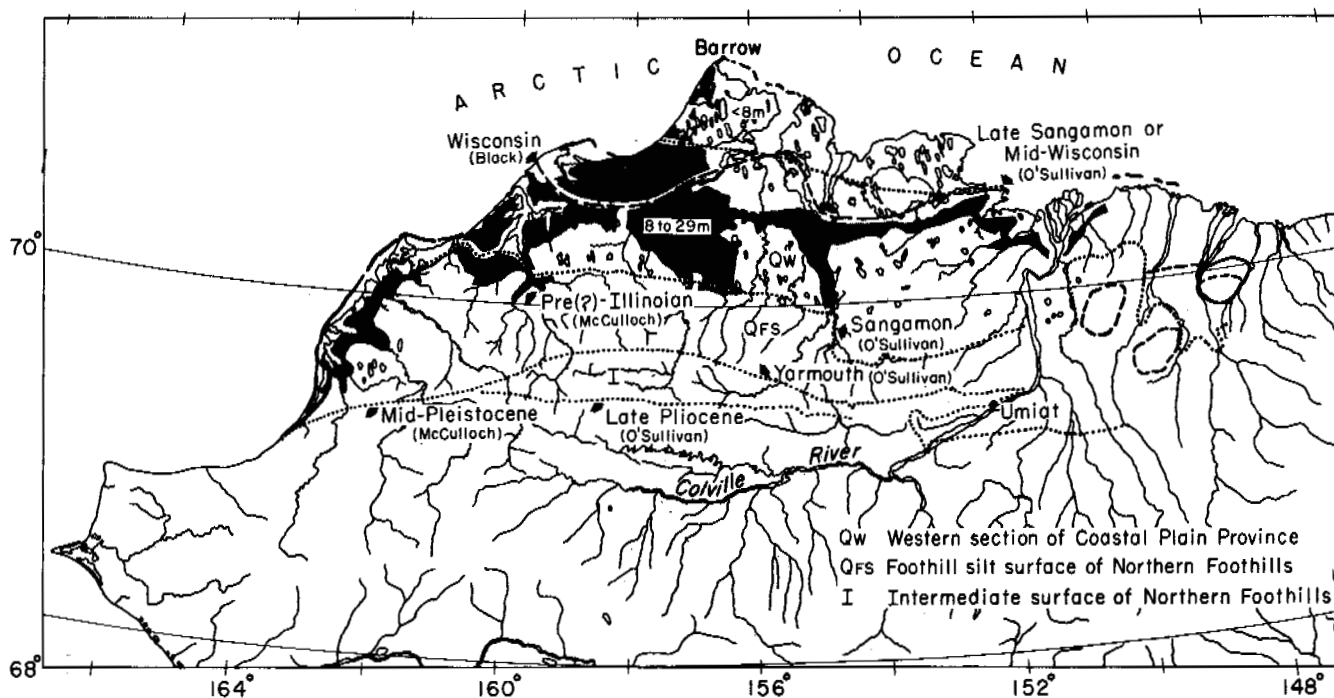


FIGURE 5 Map of northern Alaska summarizing the major transgressions and their extent on the Arctic Coastal Plain. Shaded area has 8 to 29-m elevation.

mid-Wisconsinan seas retreated, resulting in a primary land surface rich in segregated ice. Remnants of this old surface may be represented by the high ground (zone C_3) in the idealized section. At the 3-m depth, large buried masses of coalescing ice wedges occupy the major volume of the permafrost, suggesting a long period of active wedge formation. These wedges were truncated at a later time by thaw-lake migration or a minor permafrost thaw. Upon refreezing, segregated ice once again occupied a large volume of the ground in the upper several meters. The chemical content under these primary surfaces at depths of several meters and below consists of relatively high concentrations indicating the unmodified character at depth. Under other surfaces at comparable depths, concentrations are generally lower, particularly where thaw lakes have occupied the surface.

Ice-wedge and lake growth and degradation have been consistent landscape processes over the past 10 000–15 000 years. Carson's¹³ recent work suggests that regional thaw-lake development was most active during postglacial thermal time, with a contraction in thaw lakes taking place during postthermal maximum time. His radiocarbon dates for thaw-lake development cover the period 395 to 4 865 years B.P. as indicated in zone C_2 of the idealized cross section. Additional radiocarbon dates within the lacustrine sediments in zone C_1 suggest that the age of the thaw lake in this area is in the range of 3 200 years B.P.⁹

As lakes drained the bottom, sediments served as a source for local aeolian deposition that, in turn, buried some surface peats and soils. Cryopedological processes are also responsible for incorporating surface organic matter into the uppermost permafrost.

CONCLUSIONS

The late Quaternary history of the northern Alaskan Arctic Coastal Plain is now provisionally known. The last major marine transgression deposited the Barrow unit in mid-Wisconsinan time. Recession, uplift, and formation of near-surface permafrost followed. The last 10 000 years is characterized by a gradual warming, active thaw-lake formation and degradation, and burial of surface peats through cryopedologic processes. Table V summarizes our current understanding of these events.

ACKNOWLEDGMENTS

This paper presents the results of research performed by the Cold Regions Research and Engineering Laboratory under the sponsorship of the U.S. Army Corps of Engineers and the Army Materiel Command. The authors wish to express their personal appreciation to the Naval Arctic Research Laboratory and its staff for their continuing support of the authors' several Barrow-based projects. Finally, the authors recognize and acknowledge the collective assistance of the many scientists who have contributed their better understanding of the Barrow stratigraphy and permafrost environments;

TABLE V Summary of Late Quaternary Environments and Events for the Barrow, Alaska, Area

Time (year)	Climate and Permafrost	Vegetation ^{14,15,16}	Depositional	
			Marine	Lacustrine and Terrestrial
Present	Mean annual ground temperature warming of 4 °C in past 100 yr. ²⁵ Continuous formation of ice wedges from at least 14 000 yr B.P.	Pollen predominantly grass, sedge, willow; no major changes in last 5 000 yr.	Active erosion along ocean and lagoonal coastlines (0.2–2.0 m/yr). ²⁶ No major transgressions, only 1- to 2-m fluctuations in sea level resulting in formation and modifications of existing spit and drowning of Birnirk site (zone A). ^{14,21, 23,21}	Thaw-lake cycle active ^{5,7} but in contractive phase since hypsithermal expansion (zone C ₁ and C ₂). ¹³ Burial of soil organic more or less continuous since at least 11 000 yr B.P. ¹⁰
5 000	Postglacial thermal maximum but no major thaw of permafrost during past 10 000 yr. ^{10,28}	Significant alder pollen first appears.	Rapid deposition of estuary sediments. ²⁰ Rising sea level from close of Wisconsin onward and continuing uplift totaling a minimum of 8 m since mid-Wisconsin.	Expansive phase of thaw lakes between 4 000 and 8 000 yr. ¹³ Aeolian deposition at a maximum. ¹
10 000	General warming from 14 000 yr B.P. onward. ¹⁴	Willow, grasses, and sedges present; birch first appears.		
14 000–25 000	Colder and more severe than present. ¹⁴ Near-surface permafrost formation following emergence.	Grasses, sedges, mosses and willow present by 14 000 yr B.P.	Post-mid-Wisconsinan uplift of central coastal plain. Recession of mid-Wisconsinan seas and deposition of inland beach ridge (zone B) provisionally about 25 000 yr B.P.	Initiation of thaw-lake formation probably continuing into postglacial.
35 000	Mid-Wisconsinan warm period.		Deposition of Barrow unit in shallow seas during mid-Wisconsinan transgression. Ice-rafted boulders up to 7.5-m elevation. ²⁷ Sea level near that of present. ²⁸	
100 000	Sangamon warm interval.		Deposition of silty Skull Cliff unit during Illinoian ² or Pelukian transgression (zone D). ²²	

particular thanks are given to Robert Lewellen, John O'Sullivan, and David Hopkins.

REFERENCES

1. Black, R. F. 1951. Eolian deposits of Alaska. *Arctic* 4(2):8-111.
2. Black, R. F. 1964. Gubik formation of Quaternary age in northern Alaska, p. 59-91. *In* Exploration of Naval petroleum reserve No. 4, 1944-1953. Part 2. USGS Professional Paper 302-C.
3. Black, R. F. 1969. Thaw depressions and thaw lakes—A review. *Biul. Peryglacj.* 19:131-150.
4. Brewer, M. C. 1958. Some results of geothermal investigations of permafrost in northern Alaska. *Trans. Am. Geophys. Union* 39(1):19-26.
5. Britton, M. E. 1957. Vegetation of the arctic tundra. *Biol. Colloq.* (Oregon State Press) 18:26-61.
6. Brown, J. 1966. Ice-wedge chemistry and related frozen ground processes, Barrow, Alaska, p. 94-98. *In* Permafrost: Proceedings of an international conference. National Academy of Sciences, Washington, D.C.
7. Brown, J. 1965. Radiocarbon dating, Barrow, Alaska. *Arctic* 18(1):36-48.
8. Brown, J. 1969. Ionic concentration gradients in permafrost, Barrow, Alaska. CRREL Research Report 272. U.S. Army Cold Regions Research and Engineering Laboratory, Hanover, New Hampshire. 26 p.
9. Brown J. 1969. Soil properties developed on the complex tundra relief of northern Alaska. *Biul. Peryglacj.* 18:153-167.
10. Brown, J. 1969. Buried soils associated with permafrost. *In* Pedology and Quaternary research. Proceedings of a symposium, 13-14 May 1969. University of Alberta.
11. Brown, J., and P. V. Sellmann. 1966. Radiocarbon dating of coastal peat, Barrow, Alaska. *Science* 153:299-300.
12. Brown, J., and P. V. Sellmann. Permafrost and coastal plain stratigraphy, arctic Alaska. (In press)
13. Carson, C. E. 1968. Radiocarbon dating of lacustrine strands in arctic Alaska. *Arctic* 21(1):12-26.
14. Colinvaux, P. A. 1964. Origin of ice ages: Pollen evidence from arctic Alaska. *Science* 145:707-708.
15. Colinvaux, P. A. 1965. Pollen from Alaska and the origin of ice ages. *Science* 147:633.
16. Colinvaux, P. A. 1967. Quaternary vegetational history of arctic Alaska, p. 207-244. *In* The Bering land bridge. Stanford University Press, Palo Alto, California.
17. Coulter, H. W., K. M. Hussey, and J. B. O'Sullivan. 1960. Radiocarbon dates relating to Gubik formation, northern Alaska. USGS Professional Paper No. 400-B. p. B250-B251.
18. Donn, W. L., and M. Ewing. 1965. Pollen from Alaska and the origin of ice ages. *Science* 147:632-633.
19. Drew, J. V., J. C. F. Tedrow, R. E. Shanks, and J. J. Koranda. 1958. Rate and depth of thaw in arctic soils. *Trans. Am. Geophys. Union* 39(1):697-701.
20. Faas, R. W. 1966. Paleoecology of an arctic estuary. *Arctic* 19(4):343-348.
21. Ford, J. A. 1959. Eskimo prehistory in the vicinity of Point Barrow, Alaska. *Anthropol. Papers Am. Mus. Nat. His.* 272 p.
22. Hopkins, D. M. 1967. Quaternary marine transgressions in Alaska, p. 41-90. *In* The Bering land bridge. Stanford University Press, Palo Alto, California.
23. Hume, J. D. 1965. Sea-level changes during the last 2 000 years at Point Barrow, Alaska. *Science* 150:1165-1166.
24. Lachenbruch, A. H. 1957. Thermal effects of the ocean on permafrost. *Geol. Soc. Am. Bull.* 68(11):1515-1529.
25. Lachenbruch, A. H., and B. V. Marshall. 1969. Heat flow in the Arctic. *Arctic* 22(3):300-311.
26. Lewellen, R. I., and J. Brown. 1965. A retrograding lagoonal shoreline, Barrow, Alaska, p. 291. *In* Abstracts international association for Quaternary research, VII international session. Boulder, Colorado.
27. MacCarthy, G. R. 1958. Glacial boulders on the arctic coast of Alaska. *Arctic* 11(2):70-85.
28. McCulloch, D. S. 1967. Quaternary geology of the Alaskan shore of Chukchi Sea, p. 91-120. *In* The Bering land bridge. Stanford University Press, Palo Alto, California.
29. O'Sullivan, J. B. 1961. Quaternary geology of the Arctic Coastal Plain, northern Alaska. Ph.D. Thesis. Iowa State University, Ames. 191 p.
30. O'Sullivan, J. B. 1966. Geochemistry of permafrost, Barrow, Alaska, p. 30-37. *In* Permafrost: Proceedings of an international conference. National Academy of Sciences, Washington, D.C.
31. Péwé, T. L., and R. E. Church. 1962. Age of the spit at Barrow, Alaska. *Geol. Soc. Am. Bull.* 73(10):1287-1292.
32. Rex, R. W. 1964. Arctic beaches, Barrow, Alaska, p. 384-400. *In* R. L. Miller [ed.] Papers in marine geology.
33. Schmidt, R. A. M. 1967. New generic assignments for some Pleistocene Ostracoda from Alaska. *J. Paleontol.* 41(2):487-488.
34. Schmidt, R. A. M., and P. V. Sellmann. 1966. Mummified Pleistocene ostracoda in Alaska. *Science* 153:167-168.
35. Sellmann, P. V., and J. Brown. 1965. Coring of frozen ground, Barrow, Alaska: Spring 1964. CRREL Special Report 81. U.S. Army Cold Regions Research and Engineering Laboratory, Hanover, New Hampshire. 8 p.
36. Sellmann, P. V., J. Brown, and R. A. M. Schmidt. 1965. Late Pleistocene stratigraphy, Barrow, Alaska, p. 419. *In* Abstracts, international association for Quaternary research, VII international session. Boulder, Colorado.

NOTES

- [1] Unpublished observations are based on personal communications from Dr. Paul A. Colinvaux, The Ohio State University, Columbus.

III

GENESIS, COMPOSITION, AND STRUCTURE OF FROZEN GROUND AND GROUND ICE

Origin, composition, and structure of permafrost, ground ice (all forms), and periglacial features (terrestrial and marine); Quaternary history

ORIGIN, COMPOSITION, AND STRUCTURE OF PERENNIALY FROZEN GROUND AND GROUND ICE: A REVIEW

J. Ross Mackay

UNIVERSITY OF BRITISH COLUMBIA
Vancouver, British Columbia

Robert F. Black

THE UNIVERSITY OF CONNECTICUT
Storrs, Connecticut

INTRODUCTION

The origin of perennially frozen ground (permafrost) and ground ice on land in North America and beneath the sea floor of the Arctic Ocean reflects the geomorphic processes and the thermal variations of the late Quaternary period. Many review papers and books have been published on perennially frozen ground and ground ice since the First International Conference on Permafrost in 1963.^{5, 8, 10, 18, 22-24, 26, 30, 35, 50, 65, 66, 75, 78, 79} This review emphasizes massive ground ice in a brief summary of our state of knowledge of the origin, composition, and structure of permafrost. Deficiencies of knowledge are pointed out, and some recommendations for future study are made.

GROUND ICE AND THE QUATERNARY

In North America during the Quaternary, glaciers covered about 50 percent of Alaska and 97 percent of Canada.^{64, 70} It is inevitable that the age, growth, distribution, and type of ground ice are intimately related to the glacial and post-glacial history. In the unglaciated parts of Alaska and north-west Canada, permafrost has formed and disappeared in places several times during glacial and interglacial stages. In the Arctic, some permafrost may have persisted from the Illinoian Glacial Stage through the Sangamonian Interglacial Stage into the Wisconsinan Glacial Stage.¹⁸ Some pingos on Prince Patrick Island may date to the early Wisconsin.⁶⁸ Permafrost with abundant ground ice, more than 50 000 years in age, is known from the Yukon coast.⁵⁵ Late Wisconsinan ice wedges are preserved in the Fairbanks area of Alaska⁶³ and in northern Alaska.

It should be stressed that most land areas of North America now underlain by either continuous or discontinuous permafrost and nearly all marine areas between the high arctic islands were covered by glaciers less than 13 000 years ago. As recently as 8 000 years ago, ice caps partly surrounded Hudson Bay.⁶⁹ Even today, large portions of Ellesmere and Baffin islands and the western Cordillera still support alpine glaciers and ice caps. It is not known what portions of the landscape have inherited fossil permafrost or how much of existing permafrost formed since deglaciation.

The extent, age, and character of permafrost beneath the late Wisconsinan glaciers are not known. It seems likely that basal ice temperatures, like those of today, ranged from the pressure melting point of warm glaciers to the extreme cold of polar glaciers. For example, a temperature of -13°C now exists beneath 1 400 m of ice at Camp Century, Greenland,³² and -16°C is recorded at the bottom of the 120-m ice cap on Meighen Island, Arctic Canada.⁶² Thick permafrost could have formed, provided a long growth period was available. If basal temperatures were close to the pressure melting point, as in areas of discontinuous permafrost today, then very little permafrost should have formed. Consequently, wherever thin cold glaciers were present and the active layer has been thin since deglaciation, the permafrost and some ice wedges are largely inherited. Only some newer surface ice wedges can be postglacial. Although ice wedges can not grow under glaciers, ice-wedge polygons and vegetation have been observed emerging from beneath a thin ice cap on Baffin Island,²⁵ and both ice-wedge polygons and sand-wedge polygons are being exhumed from beneath perennial ice or are buried at depth in Antarctica.^{12, 58} Conversely, where warm ice conditions persisted, nearly all permafrost should be postglacial.

In many places around the margins of the continental ice sheet of North America, areas of permafrost were overrun by the expanding ice. Such permafrost may have persisted for many millenia, first as part of the glacier and later acting as an impervious layer on top of which water was trapped during the amelioration of the overlying glacier. Very likely parts of the thin outer margin of the continental ice and the accompanying permafrost below acted as a dam to melt water that existed below the thicker and warmer parts of the glacier up slope. Enormous pressures could have been generated by the hydrostatic head of the ice until a subglacial torrential discharge occurred. Such has been postulated to explain a variety of features in the Great Lakes region.⁸⁰

Glaciation also affected the surficial material, deranged drainage, and altered land-sea coastal levels. Glaciers removed the soil from hundreds of thousands of square kilometres of bedrock, and in such regions ground ice is rare. Elsewhere, and over a greater area, the deposition of till and the draining of immense proglacial and postglacial lakes have pro-

vided ideal sites for the growth of ground ice. However, the derangement of drainage, coupled with the extreme recency of deglaciation in comparison with the rate of river changes, has meant that few rivers had through-going drainage even 8 000 years ago. This applies to all of the larger rivers, with the single exception of the Yukon River. Therefore, floodplains are virtually nonexistent, and syngenetic ice wedges and ground ice, so well developed in some river valleys of the Soviet Union, are completely lacking.

Because of the enormous area of its drainage basin and its complex Quaternary history, the Yukon River deserves special mention. Its headwaters drained portions of the main continental ice sheet of North America, and the headwaters of many of its tributaries drained local small ice caps and alpine glaciers. The main trunk stream, below the headwaters, was never glaciated, yet received the outflow and debris from the various glaciers. Throughout the Quaternary, the main valley was infilled by clastic sediments whose amount and physical characteristics fluctuated with the climatic cycles. Throughout much of the drainage basin, especially in the upper tributaries, land surfaces with morphologic features characteristic of floodplains, yet modified from the effects of permafrost, were buried by floods of debris at different times. These buried surfaces commonly were underlain by networks of ice-wedge polygons and by other massive ice. Thus, in the placer workings of interior Alaska, it is common to find many superposed buried surfaces, each with its typical permafrost phenomena. In the smaller valleys of the tributaries where thick loess on the ridges has washed and flowed downslope, the well-known "muck" deposits overlie the auriferous gravels of the late Tertiary or early Quaternary. In those organic-rich silts, massive ice commonly is the dominant constituent.

Along the coast, gradual emergence of the land, as a combined result of isostatic uplift and tectonism, has added new land century by century for permafrost growth. As uplift is still continuing in the Hudson Bay and arctic islands, with rates as high as 1.3 m/100 years,¹ ground ice on an emerging coast is youngest at the shore. Thus, permafrost and ground ice commonly vary greatly in age, characteristics, and origin within short distances. For example, permafrost is now growing for the first time in the Mackenzie Delta, adjacent to ground ice of mid-Wisconsinan, or earlier, age.

OFFSHORE PERMAFROST

In general, mean annual sea-bottom temperatures in the shallow waters in the Canadian Arctic Archipelago and off the Arctic Coastal Plain of Alaska and adjacent Canada are below 0 °C. In water depths of 100 m or less, annual temperatures may be -1 °C or lower. Therefore, as permafrost is defined on a temperature basis, offshore permafrost is very extensive. Because the salinity of the pore water affects the freezing of water, however, permafrost does not necessarily

imply the presence of ice. Whether ground ice occurs in large quantities below the sea floor is not known. Theoretical considerations suggest that permafrost is thin.⁴¹ Ground ice, with lenses as much as 7 cm thick, has been encountered in offshore drilling in the southern Beaufort Sea.⁵² Ice has been recovered from a depth of at least 20 m below the sea bottom and many kilometres offshore.

Offshore underground ice could originate in several ways. During the mid- and late Wisconsinan, thick permafrost probably grew along unglaciated coasts as a result of the worldwide lowering of sea level. The Arctic Coastal Plain from northern Alaska to the north end of Banks Island was especially affected. If permafrost in unconsolidated sediments grew to a thickness exceeding several hundred metres, heat flow calculations show that some permafrost should still persist offshore, following the postglacial rise in sea level.

Rapid coastal recession of many kilometres, as is documented in northern Alaska during the past two centuries,^{43,44} also results in offshore permafrost. Water quality and oxygen isotope analyses of the ice from drill cores in the southern Beaufort Sea suggest that some of the permafrost has grown in postglacial bottom sediments, under a negative sea-bottom temperature.

On the Continental Shelf of the southern Beaufort Sea, numerous underwater mounds were discovered in 1970. The mounds average 30 m high and 400 m across. A shallow moat or depression surrounds the base of most. The mounds are believed to have formed on the sea floor subsequent to a postglacial marine transgression. According to the submarine pingo hypothesis,⁷⁴ the mounds have grown in the floors of submerged lakes following the aggradation of permafrost into the taliks of those lakes. The presence or absence of an ice core has not yet been verified by drilling. It seems quite possible, with further mapping of the Continental Shelf, that many more mounds may be found.

MAJOR GROUND-ICE FORMS

Ice in frozen ground, whether seasonal or greatly in amount from place to place, depends on material in which it is found, availability of material, rate of freezing, history of events, and so on. Geometric classification of the ice has not been universally agreed; a number of genetic classifications have been proposed.

The amount of ice in the ground, whether in the nature of the host material, is especially important in considering problems of bearing strength and particularly on thawing. Frozen ground in which ice does not fill all pores may be said to be undersaturated; saturated ground has all pores filled with ice; and supersaturated ground has more ice than pore space.⁶ By volume, the ice content of saturated material commonly ranges from 10 to 15 percent; the ice contents of undersaturated and supersaturated materials overlap the low and high ranges, respec-

tively. Undersaturated permafrost has been called "dry permafrost"; supersaturated permafrost with ice volumes approaching 100 percent is called *massive ice*.

Massive ground ice forms a continuum with decreasing amounts of ice for which no specific percentages are accepted. *Ice gneiss* and *disseminated* or *interstitial ice*⁷⁶ are locally used descriptive terms to express distinctive portions of the continuum in which well-foliated layers of ice and soil or peat occur in contrast to ice that is disseminated throughout and lacks foliation. Ice gneiss is invariably supersaturated and commonly has ice making up to 30–90 percent by volume of the material. Alternate layers of ice and organic silt are characteristic, giving the frozen ground its clearly layered appearance. In contrast, disseminated ice occurs as discrete grains and irregular films throughout the host material, providing a more homogeneous appearance. Ice distinctly takes up less volume than the host material; it commonly centers on a saturated condition. These generalizations may be applied at different scales—from samples of a few cubic centimetres to bodies involving tens of cubic metres.

For example, as ice wedges give way to composite wedges and into sand wedges, the amount of ice diminishes with no fixed boundaries established. Massive ice becomes ice gneiss and disseminated ice in the three forms. Similarly, many small mounds are mostly ice; others have foliated ice gneiss; and still others have only a small amount of disseminated ice. In all these forms their origins may follow similar lines, but reflect slightly different physical conditions. For example, ice wedges characteristically are found in humid areas where moisture can be transferred from the surface to the permafrost. In contrast, sand wedges characterize the extremely arid permafrost environment in which moisture is transferred from the permafrost to the surface. In composite wedges, both processes operate at different times during a year. In various combinations, the processes produce similar forms at similar rates, but with distinctive compositional differences. The same is true for mounds of diverse origins. Furthermore, the same terms—massive ice, ice gneiss, and disseminated ice—have been used to describe the amount and structure of permafrost in general. Ice gneiss is particularly characteristic of much permafrost with high silt content, where layers of ice alternate with layers of inorganic sediment. Infinite variations are locally possible in the amount and structure of the ice in permafrost. No adequate classifications have yet been proposed to meet all needs.

Massive Ground Ice

In recent years, primarily as a result of oil exploration and pipeline engineering studies in Alaska and Canada, data on ground ice have accumulated rapidly. Drill-hole data are available for several thousand holes, 5–15 m deep, for about 3 000 km of proposed pipeline routes. In addition, many tens of thousands of shot holes, 10–50 m deep, have been

drilled for seismic exploration in permafrost areas. Although the quality of the shot-hole records is often poor, many are very detailed and have provided excellent vertical and horizontal information on ground-ice distribution and stratigraphic relations.

Drill-hole records show that thick, tabular, and irregular bodies with much ice—here also termed *massive ice*—underlie extensive areas of the Arctic.^{47,51} The massive bodies have an ice (water) content, on a weight basis (weight of water to dry soil) of at least 250 percent, and commonly 1 000 percent, for vertical sections 10, 20, or even 30 m in thickness. The largest ice bodies are greater than 1 km² in area. The tops of most massive ice bodies are within 30 m of the ground surface, and drill holes 45 m deep have failed to penetrate through a number of such ice masses.

Stratigraphically, the material that overlies the massive ice is variable in composition, but that which underlies the ice is remarkably uniform, being mostly sand and gravel. The massive ice bodies are so large, that at first a buried origin, such as glacier ice, might be inferred. However, ice fabrics, geochemistry, and stratigraphic relations show that most ice is not buried glacial ice, but of segregated origin. For example, the systematic change in water quality of the ice with depth is identical to that of adjacent areas without massive ice, thus pointing to a common freezing and salt rejection process. Elsewhere, some buried glacial ice²¹ and pond ice have been identified.

The sands and gravels, which occur nearly universally below the massive ice, appear to have served a major role in facilitating the localization and growth of the ice. They have been the normal groundwater aquifers along which water has moved in large quantities to feed the growing ice bodies. Freezing of sands and gravels in adjacent areas may have supplied some excess water, by means of water expulsion, for the growth of the ice. At least a water table at, or just below, the growing massive ice bodies was maintained for considerable time. The mechanism envisaged is identical to that of pingo growth, where the ice core is of segregated ice and not that of freezing of a pool of water. The latter probably is the exception rather than the rule, but field studies show every conceivable gradation between the ice cores of closed-system pingos and the broad plateau created by massive ice bodies.

In Antarctica, some lake basins, such as Lake Vida, contain massive ice, stratified with clastic sediments, as part of the permafrost²⁰; in the Arctic, river icings and other forms of massive ice are occasionally buried in river valleys.

Recently, increasing attention has been paid to geochemical, radiocarbon, and stratigraphic correlations in the study of the origin and history of different permafrost sites.^{17,73} The geochemical studies have been related to the effects of climatic change, groundwater movement, and the distribution of ions during periods of freezing and thawing. Two major phenomena, which are little understood, are

the movement of water and ions in front of a freezing plane during permafrost growth and the degree to which redistribution of water and ions may take place in frozen soils. Laboratory studies indicate that short-lived thermal variations have little influence on the redistribution of ions in ice-saturated frozen materials,^{59,60} but little is known of the effect of thermal changes in the ground operating over geologic time. Ions move much more readily under diurnal and seasonal thermal gradients in dry permafrost in Antarctica.

Laboratory studies are also contributing substantially to the interpretation of structures seen in segregated ice. For example, time-lapse photography has shown the movement of clay particles through vertical columns of air in ice lenses and the infilling of the paths with clear ice.⁷¹

Ice Wedges

Because of their geometry and origin, it is convenient to discuss another form of massive ice, the ice wedge, separately. These are wedge-shaped masses, oriented vertically with their apices downward, that characteristically form polygonal patterns. Analogous patterns are produced by sand wedges that contain little ice. Sand wedges and ice wedges are end members of a continuous series of wedge-shaped forms whose ice content varies from 0 to 100 percent.^{2,11} Composite wedges, peat wedges, and other forms are distinguished. Fossil ice wedges may also leave surface polygons.⁶⁷

The principal research dealing with ice wedges and sand wedges in the past 10 years has focused on growth processes and on the mechanics of cracking in frozen ground.⁴² Comparative results are available for ice-wedge growth at Barrow, Alaska⁷; Garry Island, N.W.T.⁴⁹; and Victoria Land, Antarctica,^{2,11} but the growth of sand wedges has been measured only in Antarctica.^{2,11}

Black's studies⁷ of ice wedges and permafrost of northern Alaska were undertaken to resolve the differences in the opposing theories of Leffingwell and Taber regarding their origin. Leffingwell's contraction theory for origin of ice wedges calls for present-day segregation of ice into ice wedges after the ground is frozen to considerable depth and for moisture to come from the atmosphere and surface. Taber's concept is that ice wedges and other large masses of ice grew in the past when permafrost was forming and that the moisture was drawn up from below the downward freezing layer. Black concluded that Leffingwell's theory adequately explains the origin of ice wedges.

At Point Barrow, Alaska, ground contraction was measured between vertical iron rods driven into permafrost in five sites of different ages: old, high-centered polygons in sandy-clayey silt with ice wedges up to 6 m wide; young, flat-centered polygons in sandy-clayey silt with ice wedges up to 2 m wide; young, flat-centered polygons in sandy gravel with ice wedges up to 1 m wide; young, low-centered polygons in sandy-clayey silt with ice wedges up to 3 m

wide; and old, high-centered polygons in sandy gravel with ice wedges up to 3 m wide. In those five sites respectively, 37, 64, 70 (est.), 59, and 46 percent of the ice wedges cracked. Summer measurements showed that no contraction cracks closed completely—all cracks retained an increment of clear ice that ranged from 0.04 to 6.0 mm. A useful average increment was 2 mm; on the average, 50 percent of the wedges cracked in an area. Hence, a round-figure growth rate of 1 mm per year was obtained. This suggested an age of most surfaces of 1 000–4 000 years in the vicinity of Point Barrow; others were as much as 10 000 years old.

At Garry Island, N.W.T.,⁴⁹ at the seaward end of the Mackenzie Delta, the summer–winter growth changes at two sites with low-centered polygons have been measured for 5–7 years. The approximate time of cracking and the crack depth of 100 ice-wedge sections have also been recorded for 6 years. The summer–winter measurements show that the winter increase in separation between bench marks is abrupt, but the summer recovery is slow. Some portions of the polygons move consistently earlier or later than other portions. Maximum annual growth over 5 years was 2 mm, but most wedges grew far less than 1 mm. The percentage of ice wedges that cracked each year, during a 5-year period, for more than 100 wedges, was 40, 38, 36, 32, and 15. Most ice wedges that crack in any given year are likely to crack the next year. On a statistical basis, most cracks recur within 5–10 cm of the previous year's crack; very few cracks are continuous for more than 3 m; and most cracks are offset at each end by subparallel cracks. The frequency of cracking is related inversely to snow depth. Large troughs show less frequent cracking than the smaller ones.

Studies in Antarctica on the origin, distribution, and characteristics of ice wedges and sand wedges are the most detailed available.^{2,11} Over 500 wedges have been studied, and growth rates of 434 wedges now span 6–8 years.

Following the theoretical studies by Lachenbruch⁴² of the mechanics of ice-wedge cracking, attempts have been made to monitor the rate of ice-wedge cracking in the field. One field study of the time rate of strain-change shows that the speed of cracking is very slow compared with most published figures and to theoretical concepts.³⁸ The rate of strain increase that the cracking can propagate can be measured in units of seconds rather than in a small fraction of a second.

An attempt in Antarctica to determine whether cracks bifurcate simultaneously along both branches of a Y intersection was inconclusive.¹⁴ At one controlled intersection, only one branch cracked one year. At another, no cracking took place. Records were lost the following year. None of the studies to date monitor an initial crack—all are concerned with pre-existing cracks that exercise strong structural control of the cracking process.

In ice wedges, the most common or best developed optic-axis lineations⁶⁷ are vertical, normal to the horizontal axis

of a wedge and horizontal, normal to the horizontal axis of a wedge and inclined, and, normal to the layer in which they occur and generally normal to the horizontal axis of a wedge and inclined. Many local concentrations are found. Air bubbles and other inclusions also show marked lineation and local foliation. Inactive buried ice wedges generally can be distinguished from actively growing ice wedges by their fabrics and impurities. The former tend to have poor foliation and more equal dimensional grains and more diffuse optic-axis orientations. Ice-wedge ice almost always can be distinguished from other forms of massive ice by its external form and deployment coupled with its fabrics.

Pingos

Recent progress in the study of pingos has centered on the discovery and mapping of numerous open system pingos in interior Alaska and adjacent Yukon Territory, Canada; the discovery of pingo-like mounds under the shoal waters of the Beaufort Sea; the identification of pingo-like mounds in nonpermafrost areas; and the origin and growth rates of pingos. At present, the distribution of more than 2 500 pingos has been mapped. More than 1 500 closed-system pingos occur along the Arctic Coastal Plain of Alaska, Yukon Territory, and the Mackenzie District^{43,45} and at least 200 closed-system pingos are in the Yukon-Kuskokwim Delta of Alaska.¹⁹ Smaller groups of closed-system pingos are present in the Seward Peninsula of Alaska, on Prince Patrick Island,⁶⁸ and a few other locations.

A major concentration of more than 700 open-system pingos has recently been mapped in central Alaska and the Yukon Territory.^{34,36,40,77} These open-system pingos generally lie on gentle, south-facing slopes near the sides of alluvium-filled valleys. The pingos show a preference for southeast exposures, but just why southeast slopes are favored over south and southwest slopes is unknown. Ages of the pingos are uncertain. Some may be actively growing under present climatic conditions where mean annual ground temperatures are about -1 to -2 °C. If such is the case, these open-system pingos have been forming continuously during the Holocene.

On Prince Patrick Island, an unusual group of about 100 pingos, which may belong to neither open- nor closed-system groups, poses some puzzling genetic problems. The pingos are on the summit of the island, far from any lake or source of downslope moving water.⁶⁸ These forms may be related to some deep geological structure, with the alignment controlled by subsurface aquifers during the initial growth of permafrost, possibly in the pre-Wisconsinan stage.

The origin of pingos is becoming better known through studies on pingo structures and growth rates. One complete horizontal section of a pingo has been mapped, along with numerous partial sections.⁵⁶ The rate of pingo growth for closed-system pingos up to 25 m in height in the Mackenzie

Delta area has been determined by precise leveling over a period of up to 3 years.^{48,53} Extensive faulting also accompanies pingo growth, and a pingo summit has been observed to decrease 7.5 cm in height in 1 year and, then, increase the next.

Since the three-dimensional growth pattern of some pingos is now known, it is possible to determine where freezing occurs at depth in order to cause a rise of the surface. For instance, a pingo that grows only at the top and not on the sides can only have ice growth beneath the center. Moreover, if the growth rate equals approximately the computed rate of freezing of ice at the bottom of the ice core, then uplift is due to ice heave alone. If uplift exceeds the rate of freezing, then water injection might be inferred. The growth patterns of 11 closed-system pingos, ranging in age from 25 to about 150 years, show that actively growing pingos tend to develop mechanically induced tension cracks that extend from the pingos radially out onto the adjoining flats.^{48,53,54} Tension cracks are distinctly longer and larger than the thermally induced ice-wedge cracks. The full-grown sizes and shapes of the pingos reflect the sizes and depths of the residual ponds in which the pingos grew. The pingos attain their maximum diameters rather early, after which they grow higher rather than wider.^{48,53,54} More ice freezes beneath the centers than under the sides, as the measured growth rates show. All evidence points to growth by segregation ice, rather than freezing of a "pool" of water, as the pingos become older. The fastest growth rate from freezing of ice in the Mackenzie Delta area is estimated at about 1.5 m/year for the first year or two, after which the growth rate decreases inversely about as the square root of time. The largest pingos may take at least 1 000 years to attain full size.

In the nonpermafrost areas of northeastern British Columbia and southern Alberta and Saskatchewan, many hundred of pingo-like mounds occur.^{3,4,57} The unusual feature of these mounds is the excess of material that appears to have been moved into a mound from the surroundings during the period of permafrost growth. Thus, the mound shape still remains, unlike a collapsed ice-cored pingo, when permafrost disappears. In north central Illinois, a field of more than 500 circular to elliptical mounds has been identified.^{27,28} The hypothesis of origin, most consistent with the morphologic and stratigraphic characteristics of the mounds, is that they are deposits formed within the lakes of pingo craters. That is, the mounds are thought to be remnants of a sizeable Pleistocene pingo field.

The pingo-like mounds of northeastern British Columbia, Alberta, Saskatchewan, and Illinois are particularly puzzling, because they have no modern analog, as far as known, with the existing pingos of today. If further investigations support the pingo origin of these mounds and the submarine pingo-like mounds, then a complete restructuring of pingo terminology is required.

Palsas, Ice Laccoliths, and Other Small Ice Mounds

A perplexing array of small mounds with gradational morphology, but apparently with markedly diverse origins, has been described from the high Arctic south to the areas with only seasonal frost. The mounds are a few centimetres to many metres high and a few decimetres to tens of metres across. Their compositions are best categorized as encompassing the full range of materials expressed on a triangular diagram whose apices are represented by ice, mineral soil, and organic matter. External morphology commonly provides no clues as to the percentage of those components making up a particular mound within a mound field, yet others are reasonably distinctive and predictable. Some resemble miniature pingos and are similar in origin to them, requiring permafrost. Others are products of processes only within the active layer, and still others need only seasonal frost. Ice apparently is not a major factor in the formation of some mounds that are composed largely of frozen organic soils or peat, even though they superficially resemble forms with much ice.

Palsa is a widely used term for any mound of soil or peat with an ice core. Ice laccolith has been restricted to a small ice-cored mound formed in the active layer of the tundra in which the ice core has the shape of a laccolith. Ice forms in some by segregation and in others by injection of water to form a lens that subsequently freezes *in situ*.

In the tundra perhaps more soil or peat mounds have ice cores, either from injection of water or from ice segregation,^{29,37} than lack ice cores from doming by gas⁴⁶ or other causes. In the forests and mixed forest-tundra a variety of peaty mounds range from palsa forms to broad peat plateaus.^{16,31,72,81,82}

Discrete isolated mounds also grade into a variety of ribbed forms or elongated ridges that may be oriented downslope on hillsides and across the slope of bogs.³⁹ These also may be categorized in composition on the same triangular diagram as the mounds into which they grade morphologically.

In Antarctica, cryostatic pressure apparently is responsible for the formation of large ice masses from aperiodic saline discharges from the face of Taylor Glacier.^{9,13,15} The refreezing of seasonal ice in the annual moat developed around the perennial ice of Lake Bonney under certain circumstances forced saline lake water upward through crevasses of the terminus of the glacier.

RECOMMENDATIONS FOR FUTURE STUDY

General recommendations on permafrost and ground ice research in North America are covered in several publications.^{33,61} Recommendations for future study are listed below without regard to priority:

1. A descriptive classification and unified terminology of all ground-ice types and of related morphologic forms should be adopted before the third International Permafrost Conference meets. This classification should be accompanied by symbolization for field mapping and laboratory studies. Those should be followed by genetic classifications of both ground ice and morphologic forms;
2. Field and laboratory investigations of processes relating to freezing and thawing of soils; the movement and redistribution of water and ions within permafrost; and the role of unfrozen water in permafrost over geologic time;
3. The use of isotopes (e.g., ¹⁸O/¹⁶O) and other trace elements in interpreting the source of water now found in ground ice;
4. Detailed drilling, coring, and instrumentation of permafrost forms, such as subaerial pingos and submarine pingos, in order to answer specific questions as to their origin;
5. Geophysical and remote-sensing techniques for detecting and delimiting ground-ice bodies;
6. Computer simulation studies to analyze the growth of ground-ice forms; and
7. Origin and growth of permafrost in relation to the late Quaternary geomorphic, thermal, and groundwater history.

REFERENCES

1. Andrews, J. T. 1970. A geomorphological study of post-glacial uplift with particular reference to Arctic Canada. Special Publ. Institute of British Geographers. 156 p.
2. Berg, T. E., and R. F. Black. 1966. Preliminary measurements of growth of nonsorted polygons, Victoria Land, Antarctica, p. 61-108. *In* J. C. F. Tedrow [ed.] Antarctic soils and soil forming processes. *Antarct. Res. Ser.* 8, 177 p.
3. Bik, M. J. J. 1968. Morphoclimatic observations on prairie mounds. *Z. Geomorphol.* 12(4):409-469.
4. Bik, M. J. J. 1969. The origin and age of the prairie mounds of southern Alberta, Canada. *Periglac. Bull. No. 19.* p. 85-130.
5. Bird, J. B. 1967. The physiography of arctic Canada. Johns Hopkins Press, Baltimore. 336 p.
6. Black, R. F. 1954. Permafrost—A review. *Bull. Geol. Soc. Am.* 65:839-856.
7. Black, R. F. 1963. Les coins de glace et le gel permanent dans le nord de l'Alaska. *Ann. Geogr.* 72:257-271.
8. Black, R. F. 1969. Geology, especially geomorphology, of northern Alaska. *Arctic* 22:283-299.
9. Black, R. F. 1969. Saline discharges from Taylor Glacier, Victoria Land, Antarctica. *Antarc. J. U.S.* 4(3):89-90.
10. Black, R. F. 1969. Thaw depressions and thaw lakes—A review. *Periglac. Bull. No. 19.* p. 131-150.
11. Black, R. F. Growth of patterned ground in Victoria Land, Antarctica. This volume.
12. Black, R. F., and T. E. Berg. 1963. Glacier fluctuations recorded by patterned ground, Victoria Land, p. 107-122. *In* R. J. Aedie [ed.] Antarctic geology. North Holland, Amsterdam.
13. Black, R. F., and C. J. Bowser. 1968. Salts and associated phenomena of the termini of the Hobbs and Taylor glaciers, Victoria Land, Antarctica. *Int. Assoc. Sci. Hydrol. Publ.* 79. p. 226-238.

14. Black, R. F., and A. A. Twomey. Unpublished data.
15. Black, R. F., M. L. Jackson, and T. E. Berg. 1965. Saline discharge from Taylor Glacier, Victoria Land, Antarctica. *J. Geol.* 73:175-181.
16. Brown, R. J. E. 1968. Permafrost investigations in northern Ontario and northeastern Manitoba. National Research Council, Canada. Div. of Bldg. Res. Tech. Paper No. 291. 40 p.
17. Brown, J. 1969. Ionic concentration gradients in permafrost, Barrow, Alaska. Rep. 272. U.S. Army Cold Regions Research and Engineering Laboratory, Hanover, New Hampshire. 24 p.
18. Brown, R. J. E. 1970. Permafrost in Canada. University of Toronto Press, Toronto, Ontario. 234 p.
19. Burns, J. J. 1964. Pingos in the Yukon-Kuskokwim delta, Alaska: Their plant succession and use by mink. *Arctic* 17:203-210.
20. Calkin, P. E., and C. Bull. 1967. Lake Vida, Victoria Valley, Antarctica. *J. Glaciol.* 48:833-843.
21. Christie, R. L. 1967. Reconnaissance of the surficial geology of northeastern Ellesmere Island, Arctic Archipelago. Geological Survey of Canada Bull. 138, Ottawa, Ontario. 50 p.
22. Corte, A. E. 1969. Geocryology and engineering. *Geol. Soc. Am. Rev. Eng. Geol.* 2:119-185.
23. Dionne, J. C. 1968. A bibliography of periglacial studies in Quebec. *Rev. Géogr. Montr.* 22:175-180.
24. Dort, W., Jr., and K. Jones, Jr. [ed.]. 1970. Pleistocene and recent environments of the Great Plains. Spec. Publ. No. 3. The University Press of Kansas, Lawrence. 433 p.
25. Falconer, G. 1966. Preservation of vegetation and patterned ground under a thin ice body in northern Baffin Island, N.W.T. *Geog. Bull. (Canada)*. 8:194-200.
26. Ferrians, O. J., Jr., R. Kachadoorian, and G. W. Greene. 1969. Permafrost and related engineering problems in Alaska. Prof. Paper 678. U.S. Geological Survey, Washington, D.C. 37 p.
27. Flemal, R. C., K. C. Hinkley, and J. L. Hesler. 1969. Fossil pingo field in north-central Illinois. *Geol. Soc. Am. Pt. 6*. p. 16.
28. Flemal, R. C., K. C. Hinkley, and J. L. Hesler. The DeKalb mounds: A possible Pleistocene (Woodfordian) pingo field in north-central Illinois. *Geol. Soc. Am. Mem.* 136. (In press).
29. French, H. M. 1971. Ice cored mounds and patterned ground, southern Banks Island, western Canadian Arctic. *Geogr. Ann.* 53A:32-38.
30. Hamelin, L. E., and F. A. Cook. 1967. Le periglaciare par l'image. Les presses de l'Université Laval, Québec. 237 p.
31. Hamelin, L. E., and A. Cailleux. 1969. Les paises dans le bassin de la Grande-Rivière de la Baleine. *Rev. Géogr. Montr.* 23:329-337.
32. Hansen, B. L., and C. C. Langway, Jr. 1966. Deep core drilling in ice and core analysis at Camp Century, Greenland, 1961-1966. *Antarct. J. U.S.* 1:207-208.
33. Harwood, T. A., and R. J. E. Brown. 1970. Permafrost, p. 124-133. In C. H. Smith [ed.] Background papers on the earth sciences in Canada. *Geol. Surv. Can. Paper* 69-56.
34. Holmes, G. W., D. M. Hopkins, and H. L. Foster, 1968. Pingos in central Alaska. U.S. Geol. Surv. Bull. 1241-H, Washington, D.C. 40 p.
35. Hunt, C. B., and A. L. Washburn. 1966. Patterned ground, p. B104-B133. In C. B. Hunt *et al.* [ed.] Hydrologic basin, Death Valley, California. Prof. Paper 494-B. U.S. Geological Survey, Washington, D.C.
36. Hughes, O. L. 1969. Distribution of open-system pingos in central Yukon Territory with respect to glacial limits. Paper 69-34. Geological Survey of Canada, Ottawa, Ontario. 8 p.
37. Hussey, K. M., and R. W. Michelson. 1966. Tundra relief features near Point Barrow, Alaska. *Arctic* 19:162-183.
38. Knight, G. R. 1971. Ice-wedge cracking and related effects on buried pipelines, p. 384-395. In J. L. Burdick [ed.] Proceedings on symposium on cold regions engineering. University of Alaska, College.
39. Knollenberg, R. 1964. The distribution of string bogs in central Canada in relation to climate. Tech. Rep. No. 14. University of Wisconsin, Madison. 44 p.
40. Krinsley, D. B. 1965. Birch Creek pingo, Alaska. Prof. Paper 525-C. U.S. Geological Survey, Washington, D.C. p. C133-C136.
41. Lachenbruch, A. H. 1957. Thermal effects of the ocean on permafrost. *Bull. Geol. Soc. Am.* 68:1515-1530.
42. Lachenbruch, A. H. 1962. Mechanics of thermal contraction cracks and ice-wedge polygons in permafrost. *Geol. Soc. Am. Spec. Paper No.* 70. 69 p.
43. Leffingwell, E. De K. 1919. The Canning River region, northern Alaska. Prof. Paper. 109. U.S. Geological Survey, Washington, D.C. 251 p.
44. MacCarthy, G. R. 1953. Recent changes in the shoreline near Point Barrow, Alaska. *Arctic* 6:44-51.
45. Mackay, J. R. 1962. Pingos of the Pleistocene Mackenzie Delta area. *Geogr. Bull. Canada No.* 18, p. 20-63.
46. Mackay, J. R. 1965. Gas-domed mounds in permafrost, Kendall Island, N.W.T. *Geogr. Bull. (Canada)* 7:105-115.
47. Mackay, J. R. 1971. The origin of massive icy beds in permafrost, Western Arctic Coast, Canada. *Can. J. Earth Sci.* 4:397-422.
48. Mackay, J. R. 1972. Some observations on the growth of pingos, p. 141-148. In D. E. Kerfoot [ed.] Mackenzie Delta area monograph, 22nd international geographical congress. Brock University, St. Catharines, Ontario.
49. Mackay, J. R. 1972. Some observations on ice-wedges, Garry Island, N.W.T., p. 131-139. In D. E. Kerfoot [ed.] Mackenzie Delta area monograph. Brock University, St. Catharines, Ontario.
50. Mackay, J. R. 1972. The world of underground ice. *Ann. Assoc. Am. Geogr.* 62:1-22.
51. Mackay, J. R. Problems in the origin of massive icy beds, Western Arctic, Canada. This volume.
52. Mackay, J. R. 1972. Offshore permafrost and ground ice, southern Beaufort Sea, Canada. *Can. J. Earth Sci.* 9:1550-1561.
53. Mackay, J. R. 1973. Some aspects of permafrost growth. Paper 73-1A. Geological Survey of Canada. Ottawa. p. 232-233.
54. Mackay, J. R. 1973. The growth of pingos, western Arctic Coast, Canada. *Can. J. Earth Sci.*
55. Mackay, J. R., V. N. Rampton, and J. G. Fyles. 1972. Relic pleistocene permafrost, Western Arctic, Canada. *Science* 176:1321-1323.
56. Mackay, J. R., and J. K. Stager. 1966. The structure of some pingos in the Mackenzie Delta area, N.W.T. *Geogr. Bull. (Canada)* No. 4. p. 360-368.
57. Mathews, W. H. 1963. Quaternary stratigraphy and geomorphology of the Fort St. John area, northeastern British Columbia. B.C. Dept. Mines Petrol. Resources, Victoria, B.C. 22 p.
58. McSaveney, E. R., and M. J. McSaveney. 1972. Ancient ice wedges in Wright Valley, Antarctica. *Antarct. J. U.S.* 7:102-103.
59. Murrmann, R. P., and P. Hoekstra. 1970. Effect of thermal gradient on ionic diffusion in frozen earth materials. I: Experimental. Rep. 284. U.S. Army Cold Regions Research and Engineering Laboratory, Hanover, New Hampshire. 8 p.
60. Nakano, Y., and R. P. Murrmann. 1970. Effect of thermal gradient on ionic diffusion in frozen earth materials. II: Theoretical. U.S. Army Cold Regions Research and Engineering Laboratory, Hanover, New Hampshire. 34 p.
61. Committee on Polar Research, National Research Council, 1970.

- Polar research: A Survey. National Academy of Sciences, Washington, D.C. 204 p.
62. Paterson, W. S. B. 1968. A temperature profile through the Meighen ice cap, Arctic Canada. *Int. Assoc. Sci. Hydrol. Bull.* 79. p. 440-449.
 63. Péwé, T. L. [ed.]. 1965. Central and south central Alaska, p. 6-36. *In* Guidebook for field conference F. VII Congress, International Association for Quaternary Research. The Nebraska Academy of Sciences, Lincoln.
 64. Péwé, T. L. 1965. Notes on the physical environment of Alaska. *Proc. 15th Alaska Sci. Conf.* p. 293-310.
 65. Péwé, T. L. 1966. Permafrost and its effect on life in the north. Oregon State University Press, Corvallis. 40 p.
 66. Péwé, T. L. [ed.]. 1969. The periglacial environment, past and present. McGill-Queen's University Press, Montreal, Quebec. 544 p.
 67. Péwé, T. L., R. E. Church, and M. J. Andresen. 1969. Origin and paleoclimatic significance of large-scale patterned ground in the Donnelly Dome area, Alaska. *Geol. Soc. Am. Spec. Paper No. 103.* 87 p.
 68. Pissart, A. 1967. Les pingos de l'île Prince-Patrick (76°N-120°W) *Geogr. Bull. (Canada)* 9:189-217.
 69. Prest, V. K. 1969. Retreat of Wisconsin and recent ice in North America. Map 1257A. Geological Survey of Canada, Ottawa, Ontario.
 70. Prest, V. K. 1970. Quaternary geology of Canada, p. 675-764. *In* R. J. W. Douglas [ed.] *Geology and economic minerals of Canada. Rep. No. 1.* Geological Survey of Canada, Ottawa.
 71. Radd, F. J., and D. H. Oertle. 1971. Experimental pressure studies on frost heave mechanisms and the growth-fusion behaviour of ice in soils and glaciers. Continental Oil Company, Ponca City, Oklahoma. 39 p.
 72. Railton, J. B. 1968. The ecology of palsa bogs. M.Sc. thesis. University of Toronto, Toronto, Ontario. 89 p.
 73. Sellmann, P. V. 1967. Geology of the USA CRREL permafrost tunnel, Fairbanks, Alaska. U.S. Army Cold Regions Research and Engineering Laboratory, Hanover, New Hampshire. 22 p.
 74. Shearer, J. M., R. F. MacNab, B. R. Pelletier, and T. B. Smith. 1971. Submarine pingos in the Beaufort Sea. *Science* 174:816-818.
 75. Stearns, S. R. 1966. Permafrost. Pt. 1, Sec. A2. U.S. Army Cold Regions Research and Engineering Laboratory, Hanover, New Hampshire. 77 p.
 76. Taber, S. 1943. Perennially frozen ground in Alaska: Its origin and history. *Bull. Geol. Soc. Am.* 54:1433-1548.
 77. Vernon, P., and O. L. Hughes. 1966. Surficial geology, Dawson, Larsen Creek and Nash Creek map-areas, Yukon Territory. *Geological Survey Canada Bull.* 136, Ottawa, Ontario. 25 p.
 78. Washburn, A. L. Periglacial processes and environment. Edward Arnold, London. (In press)
 79. Wright, H. E., Jr., and W. H. Osburn. 1968. Arctic and alpine environments. *Proc. VII Cong. Int. Assoc. Quat. Res. (Indiana University Press)* 10:308 p.
 80. Wright, H. E. Tunnel valleys, glacial surges, and subglacial hydrology of the Superior Lobe, Minnesota. *Geol. Soc. Am. Mem.* 136. (In press)
 81. Zoltai, S. C. 1971. Southern limit of permafrost features in peat land forms, Manitoba and Saskatchewan. *Geol. Assoc. Can. Spec. Paper No. 9.* p. 305-310.
 82. Zoltai, S. C., and C. Tarnocai. 1971. Properties of a wooded palsa in northern Manitoba. *J. Arctic Alp. Res.* 3(2):115-119.

GROWTH OF PATTERNED GROUND IN VICTORIA LAND, ANTARCTICA

Robert F. Black

THE UNIVERSITY OF CONNECTICUT
Storrs, Connecticut

INTRODUCTION

Growth of patterned ground at 14 sites in Victoria Land, Antarctica, has been measured over an interval of 6–8 years from 1961 to 1969. This paper contains partial results of those measurements, including the latest measurements to date; some previous measurements were summarized earlier.^{1,3}

In Victoria Land, patterned ground consists of sand-wedge polygons in the inland areas and of ice-wedge polygons along the more humid coasts. These represent the end members of a continuum in which the ice content of the wedges ranges almost from 0 to 100 percent. Composite wedges, representing mixtures of ice, sand, and rubble, are most abundant and widespread. No fixed cutoffs have been established for the percent of ice for the various classes. However, ice wedges generally contain more than 90 percent ice and sand wedges less than 10 percent ice. Many composite wedges contain 30–50 percent ice. Rubble, consisting of rounded to angular gravel and cobbles, is highly variable in amount and confined mostly to the upper part of the wedges.

The wedges are oriented vertically with their apexes downward and outline polygons in plan. The wedges grow from initial contraction cracks a few millimetres wide to massive features many metres wide during old age. They are a few decimetres to several metres in vertical dimension. They are mostly in permafrost, but extensions upward through the active layer are commonly manifested at the surface.

Surface patterns reflect growth stages from narrow sharp cracks corresponding to the initial wedges through shallow rounded depressions over each wedge to wider and deeper depressions with raised rims on each side and, finally, in some places only to an irregularly mounded or pimpled surface where the mounds represent the centers of former polygons. Polygons commonly vary from 5 to 40 m in diameter. The earlier literature describes in detail the characteristics of the wedges and polygons and their significance in the evolution of the landscape.^{1,3}

Growth of patterned ground is measured by the change in width of individual wedges making up a polygon or group of polygons in a specific geomorphic setting. Most wedges widen with time. Some wedges shrink or have negative rates

of growth when the time of measurement does not coincide with maximum annual ground temperature, or when flowage of ice or squeezing of contraction cracks in wedges takes place after earlier measurements. To measure growth, permanent bench-mark rods are driven well into permafrost on opposite sides of a wedge, hairline crosses are marked on special caps, and distances between rods are measured to tenths of a millimetre with Invar bar or tape, utilizing various optical aids.¹ Ideally, measurements are made when the upper parts of permafrost attain their maximum expansion during the antarctic summer—about the beginning of the calendar year, but with variance of several weeks. This provides maximum closure of contraction cracks, which had opened the preceding winter and had been partly filled with ice or free-running sand.¹ Unfortunately, this was done rarely, so corrections need to be applied to maximize the accuracy of the results. Such corrections can be obtained empirically by frequent measurement³ or better from a detailed analysis of the thermal regime of the patterned ground.^{1–3} The two techniques combined are best. In the 1969–1970 field season in Antarctica, Thomas E. Berg had just started the repetitive measurements at the time of his unfortunate death.⁸ No corrections are applied to the growth rates given here, as the computerization of the existing thermal records² has not yet been completed.⁵ Nonetheless, the results shown permit considerable refinement of those previously determined average growth rates where very short intervals and somewhat arbitrary correction factors were employed. They also increase the accuracy of prediction of the age of the patterned ground or surface represented.^{1,3} The results quantify trends in the rate of growth in some sites that were not realized in the initial phases of the study. The trends are mostly in decreasing rates, which are tentatively related to availability of moisture.

The following discussion lists the growth of most wedges recovered in 1969 and discusses briefly the significance of the results.

GROWTH OF PATTERNED GROUND

Growth of patterned ground in Victoria Land was measured at 14 sites of different characteristics (Figure 1). Detailed descriptions and maps of most sites have been published.¹

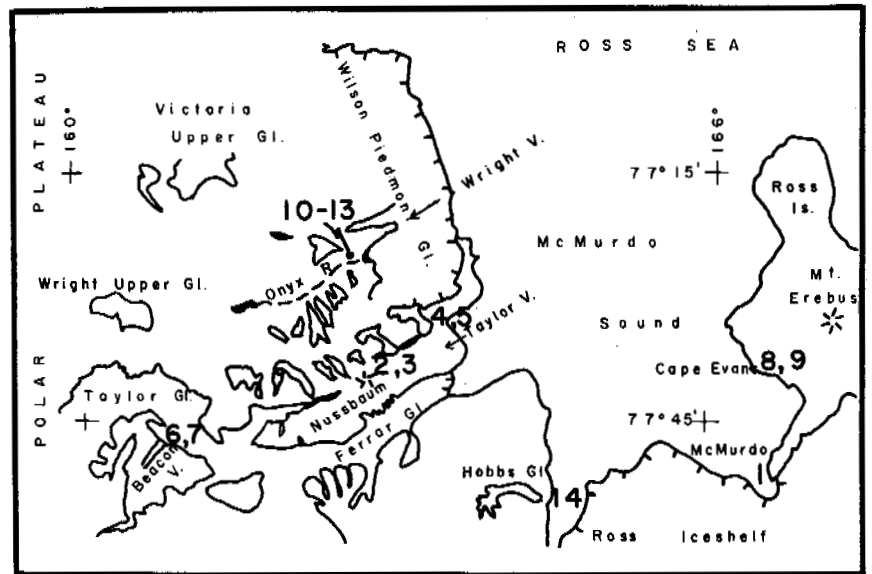


FIGURE 1 Index map of parts of Victoria Land, Antarctica, showing locations of sites where growth of patterned ground has been measured.

However, additional information on the subsurface geology of some sites is now available,⁹ and a brief description of each site is presented here for convenience of the reader. Tables I-XV contain the actual values of growth measured at each site from the first to the last available.

Site 1—Windy Crater, McMurdo, Ross Island

Windy Crater is a recent volcanic cone on Hut Point Peninsula, Ross Island. The cone is 160 m above sea level and has a double crater whose floor is 30 m below the highest point on the rim. The contraction site covers part of the east rim and part of the interior of the crater. The original location in 1960 on the west rim has been destroyed by bulldozers. A desert or windblown lag pavement of volcanic rubble, mainly scoria, covers the surface of Windy Crater. The scoria is black to reddish brown and is coated underneath the fragments with whitish mirabilite and other salts. On the rim, the scoria rests directly on lava and welded tuff at a depth of 5–20 cm; in the cone, the scoria rests on finer volcanic ash that is coated pale yellow-brown to red. Lenses of the finer ash parallel the slope and tend to increase in thickness downslope. The upper part of the unconsolidated sequence, 10–20 cm thick, generally has less than 3 percent moisture by weight; permafrost under a transition zone a few centimetres thick generally has 10–60 percent moisture by weight. Salt layers 1–5 cm thick are found locally at depths of 5–15 cm. The dry zone over permafrost is thinner on the floor of the crater than on the flanks. Perennial ice and snow banks cover a pond in each of the two craters.

Polygons are 5–10 m in diameter and have scoria-filled troughs 5–20 cm deep. Wedges range from almost 100 percent ice in the floor of the cone and adjacent to perennial

snow banks to composite wedges with 30–40 percent ice on the upper flanks and rim of the cone. The wedges average about 50 cm in width.

Table I shows that from October 29, 1962, to November 13, 1969, the average net total change per wedge of 89 wedges was -2.75 mm for an average change per wedge of -0.39 mm/year. Of those 89 wedges, 40 wedges widened an average per wedge of 5.46 mm for an average change of 0.78 mm/year; 49 wedges shrank an average per wedge of 9.45 mm for an average change of -1.35 mm/year. All wedges in the first alphabet are in the bottom of the crater or on the lowermost slope; in general, wedges of the second and third alphabet are intermediate, and those of the fourth alphabet are highest on the slope. No clear trend of positive versus negative growth shows with respect to position of a wedge in the crater or with orientation down or across slope. Most significant seems to be the nearness of two roughly parallel wedges. When they are close, one seems to grow at the expense of the other. Perennial snowbanks in 1969 were much reduced in thickness and areal extent from those present at the initiation of the project. Available moisture for growth of the ice wedges, by spring runoff into contraction cracks, has declined markedly during the period. This would seem to account for some negative growth in those wedges that shrank, but most likely not for all the total average negative change of -9.5 mm per wedge. The cause is still being investigated. Most suspect is the thermal regime of the ground at the time of measurement, but flowage of ice in the ice wedges possibly played a role too. The ground was cold and contracted in October and November,^{1,3} when measurements were made. A major thermal correction will have to be applied as was done the first year of the project, although the actual amount has not yet been determined.

TABLE 1 Growth in Width of 89 Wedges at McMurdo, Windy Crater Site, between October 29, 1962, and November 13, 1969

Wedge	Growth (mm)	Wedge	Growth (mm)	Wedge	Growth (mm)	Wedge	Growth (mm)
A	4.1	X	9.8	UU	8.8	RRR	6.9
B	3.7	Y	0.5	VV	-4.1	SSS	-4.3
C	9.8	Z	3.4	WW	1.5	TTT	-9.2
D	2.5	AA	-3.2	XX	-11.4	UUU	3.1
E	3.0	BB	-11.8	YY	-7.4	VVV	-18.5
F	10.6	CC	-0.6	ZZ	-15.3	WWW	-18.7
G	2.8	DD	8.8	AAA	-8.7	XXX	-16.0
H	2.0	EE	3.3	BBB	2.0	YYY	-11.9
H'	-9.7	FF	-6.1	CCC	-10.4	ZZZ	-6.1
J	-18.4	GG	-5.0	DDD	-5.1	AAAA	-12.6
K	1.9	HH	-2.7	EEE	6.3	BBBB	-4.3
L	-5.6	II	7.7	FFF	5.5	CCCC	-2.9
M	1.1	JJ	-8.0	GGG	8.3	DDDD	-10.8
N	-18.3	KK	-25.3	HHH	2.7	EEEE	8.2
O	7.3	LL	-2.4	III	5.8	FFFF	-0.7
P	-17.8	MM	-9.1	JJJ	7.4	GGGG	-0.5
Q	-17.1	NN	6.3	KKK	6.9	HHHH	-15.9
R	-1.9	OO	3.0	LLL	-5.9	IIII	-7.2
S	-13.6	PP	9.4	MMM	-5.9	JJJJ	-20.5
T	-12.8	QQ	9.0	NNN	3.0	KKKK	-13.7
U	-13.4	RR	-1.7	OOO	1.7		
V	-0.1	SS	-10.3	PPP	5.4	TOTAL ^a	-462.9
W	7.6	TT	6.2	QQQ	11.0		+218.3

^a +218.3 - 462.9 = -242.6 mm/89 = -2.75 mm average total change/7 = -0.39 mm/yr average change.

+218.3/40 = +5.46 mm average change/7 = +0.78 mm/yr average change.

-462.9/49 = -9.45 mm average change/7 = -1.35 mm/yr average change.

Site 2—Nussbaum Riegel, Delta Site, Taylor Valley

Taylor Valley is one of the principal east-trending lowlands in Victoria Land through which plateau ice moved eastward to the sea and later that were plugged by westward moving ice.⁷ A small sand-gravel delta 4 km east of Nussbaum Riegel in Taylor Valley was formed at a time when the shallow freshwater pond northeast of the delta was greatly enlarged.¹ The delta slopes gently to the north, is composed of sand and gravel, and has a typical desert pavement. A true active layer 25 cm thick overlies permafrost. The active layer has 2-3.5 percent moisture during the summer and stays loose in winter. Permafrost has 10-15 percent moisture by weight and is firmly cemented. A seismic profile between the delta and the present-day pond⁹ showed a 20-cm thick dry zone over 1.7 m of permafrost, with compressional wave velocity of 3 280 m/s on bedrock.

Polygons on the delta are flat centered, average 10 m in diameter, and have abrupt troughs averaging 75 cm wide. Wedges are mainly composite with more sand than ice. The top of the permafrost shows a typical double raised rim along wedges, but this does not reach the surface. The wedges average 75 cm in width.

Table II shows that from December 13, 1961, to November 12, 1969, the average net total change per wedge of 48 wedges was 2.82 mm or an average change per wedge of

0.35 mm/year. Of those 48 wedges, 40 wedges widened and only 8 wedges shrank. These measurements, however, also require a correction for thermal effect on the ground.

Table III shows measurements of change from January 14, 1961, to November 12, 1969, for seven intervals within a polygon. During the 9 years, the seven intervals shrank an average of 0.2 mm/year. This small amount can be attributed in part to the difference in temperature of the ground between the two measurements; it was colder and more contracted during the last measurement. However, no consistent relationship exists between length of interval and amount of contraction. Hence, part of the change must be attributed to the technique of measurement. Different people were involved each time with a hand-held tape. No change is expected within a polygon, so the technique seems to be capable of measuring small differences. The use of the metre bar is much more accurate.

Site 3—Nussbaum Riegel, Hill Site, Taylor Valley

A moraine-covered bedrock ridge 1 km east of the delta site lies about 450 m above sea level. Topography is irregular, large glacial erratics are common, and thickness of the dry zone averages 30 cm. A salt-rich layer locally is present 7-12 cm beneath the surface. The dry zone contains 2-3 percent moisture by weight; although permafrost exceeded

TABLE II Growth in Width of 48 Wedges at Taylor Valley, Nussbaum Riegel Delta Site, between December 13, 1961, and November 12, 1969

Wedge	Growth (mm)	Wedge	Growth (mm)
A	-2.8	AA	3.3
B	1.9	BB	6.2
C	2.6	CC	-15.2
D	4.9	DD	-0.5
E	1.6	EE	2.7
F	2.1	FF	5.2
G	3.4	GG	3.4
H	-0.3	HH	5.5
I	5.1	II	2.5
J	-1.6	JJ	1.3
K	-1.2	KK	5.6
L	6.2	LL	-4.8
M	4.4	MM	5.7
N	4.8	CE-CF	2.0
O	6.0	CH-CI	2.9
P	7.1	CJ-CK	2.0
Q	5.3	CM-CN	5.3
R	-1.4	CO-CP	1.3
S	0.6	CQ-CR	^a
T	2.2	CS-CT	5.3
U	6.5	CU-CV	3.2
V	3.7	CW-CX	3.4
W	8.9	CY-CZ	2.5
X	6.7		
Y	4.8	TOTAL ^b	-27.8
Z	5.9		+164.0

^a Not recorded.^b $+164.0 - 27.8 = +136.2 \text{ mm}/48 = +2.82 \text{ mm}$ average total change/
 $8 = +0.35 \text{ mm/yr}$ average change.

50 percent in places it generally is much less. Sand wedges commonly contained 10-15 percent moisture by weight. Wedge widths range from 50 to 160 cm and average 75 cm. Polygons are irregular in size and commonly more than 10 m in diameter. One seismic line⁹ along the ridge site showed

TABLE III Change in Width of Seven Intrapolygonal Intervals at Nussbaum Riegel, Delta Site, Taylor Valley, between January 14, 1961, and November 12, 1969

Wedge	Change (mm)
CA-CB	0.0
CC-CD	-3.9
CD-CE	-2.1
CF-CG	-2.1
CI-CD	-2.2
CD-CJ	-1.6
CK-CL	-0.6
GROWTH ^a	12.5

^a $-12.5/7 = -1.79 \text{ mm}$ average change/ $9 = -0.20 \text{ mm/yr}$ average change.

only 0.9-1.2 m of morainic rubble on metamorphic bedrock. Another line downslope showed that the rubble gradually thickened from 0.7 m at the top to 3.1 m at a distance of 185 m and out of the site. Seismic velocity increased downslope also as moisture in the morainic material increased.

Table IV shows that from November 12, 1962, to November 12, 1969, the average net total change per wedge of 37 wedges was 2.36 mm or an average change per wedge of 0.34 mm/year. Only 2 of the 37 wedges shrank during the 7 years. Although these measurements represent the same calendar time, it seems not to have been the same thermally. A correction must still be applied.

Site 4--New Harbor, Delta Site, Taylor Valley

This delta lies only 1-3 m above sea level at the mouth of Taylor Valley on the Ross Sea. The delta has been formed by a stream that flows from Commonwealth Glacier. Hence, it is subject in part to aperiodic inundations. Many polygons on the delta are rectangular, from 5 to 12 m wide and from 30 to 50 m long, parallel and normal to the main stream channel.¹ Troughs average 70 cm in width. Gravelly

TABLE IV Growth in Width of 37 Wedges at Taylor Valley, Nussbaum Riegel Hill Site, between November 12, 1962, and November 12, 1969

Wedge	Growth (mm)	Wedge	Growth (mm)
A	3.3	Y	^a
B	1.0	Z	-0.5
C	1.5	AA	1.8
D	2.8	BB	4.0
E	1.3	CC	2.8
F	1.5	DD	-1.0
G	^a	EE	1.9
H	0.9	FF	^a
I	7.4	GG	1.9
J	^a	HH	0.5
K	2.9	II	3.2
L	1.6	JJ	1.1
M	2.3	KK	1.5
N	0.5	LL	0.7
O	10.9	MM	2.2
P	2.5	NN	4.4
Q	0.8	OO	^a
R	1.6	PP	^a
S	0.8	QQ	2.6
T	3.8	RR	3.0
U	0.8		
V	5.9		
W	^a	TOTAL ^b	-1.5
X	3.2		+88.9

^a Not recorded.^b $+88.9 - 1.5 = +87.4 \text{ mm}/37 = +2.36 \text{ mm}$ average total change/ $7 = +0.34 \text{ mm/yr}$ average change.

sand of the delta has a desert pavement. Permafrost is super-saturated with 10–15 percent moisture by weight; the active layer contains 2–9 percent moisture, varying with the seasons and proximity of snowbanks or the stream.

Table V shows that from December 23, 1961, to December 31, 1969, the average net total change per wedge of 38 wedges was 7.13 mm or an average change per wedge of 0.89 mm/year. Of the 38 wedges, 11 shrank during the 8-year period, but their total change was only 13 percent of the total positive growth of the other 29 wedges. All that shrank are on the north rim of the site, closest to the stream that influences the thermal regime of the permafrost and also keeps the active layer moist so sand cannot run into contraction cracks. Growth in the site is still much faster than in the delta at Nussbaum Riegel.

Site 5—New Harbor, Moraine Site, Taylor Valley

Immediately south of the New Harbor Delta site and adjoining it is a moraine that rises to 8 m above sea level. Topography is sharply irregular in contrast to the more rounded moraine of the Nussbaum Hill site. The surface of the moraine is drier than that of the delta, except at their junction where snow is usually present. The active layer contains 1–3 percent moisture by weight and the permafrost

12 percent on the average. Polygons are 5–15 m in diameter with troughs averaging 70 cm in width.

Table VI shows that from December 23, 1961, to December 31, 1969, the average net total change per wedge of 19 wedges was 12.67 mm or an average change per wedge of 1.58 mm/year. Of the 19 wedges, 4 shrank during the 8-year period, but their total change was only 10 percent of the total positive growth. Growth is more rapid than at other sites described so far because of the abundant free-running sand at the surface and probable ice core in the moraine, which provides large contraction cracks.

Site 6—Beacon Valley, Site A

Beacon Valley is about 15 km east of the Polar Plateau and 70 km west of the Ross Sea. It trends northeasterly and is blocked at the lower end by a lobe of the Taylor Glacier. The moraine-covered floor of the valley, 17 km long and 3 km wide, rises steadily for 3 km from the Taylor Glacier at 1 250 m in elevation to 1 350 m. The valley continues to rise in undulations to an elevation of 1 900 m at its head in a series of cirques. Former glaciers from the cirques came down valley to abut ice from the formerly expanded Taylor Glacier pushing up valley. The junction is a zone several hundred metres wide. Site A is located near the axis of the

TABLE V Growth in Width of 38 Wedges at Taylor Valley, New Harbor Delta Site, between December 23, 1961, and December 31, 1969

Wedge	Growth (mm)	Wedge	Growth (mm)
M	-3.9	HH	27.0
N	18.6	II	20.7
O	-10.5	JJ	12.2
P	-11.2	KK	26.3
Q	5.8	DA-DB	-4.8
R	4.8	DD-DE	-3.9
S	-0.6	DG-DH	3.7
T	12.8	DF-DG ^a	0.8
U	17.6	DC-DN ^a	0.5
V	-1.9	DC-DD ^a	1.5
W	-1.1	DE-DF ^a	2.8
X	4.2	DI-DJ	-1.1
Y	13.5	DI-DL	5.0
Z	12.7	DJ-DK	1.5
AA	17.7	DL-DK	-0.5
BB	5.6	DM-DO	-0.7
CC	9.7	DB-DC ^a	6.4
DD	6.4		
EE	32.9		
FF	10.9	TOTAL ^b	-40.2
GG	29.4		+311.0

^a September 10, 1961.

^b +311.0 - 40.2 = +270.8 mm/38 = +7.13 mm average total change/8 = +0.89 mm/yr average change.

TABLE VI Growth in Width of 19 Wedges at Taylor Valley, New Harbor Moraine Site, between December 23, 1961, and December 31, 1969

Wedge	Growth (mm)
LL	15.1
MM	26.2
NN	15.4
OO	37.0
PP	17.9
QQ	14.5
RR	14.0
SS	14.8
TT	9.7
UU	-5.9
VV	18.3
WW	11.7
XX	19.0
YY	27.6
ZZ	-1.4
A	-1.5
B	-17.7
C	9.5
D	16.5
TOTAL ^a	-26.5
	+267.2

^a +267.2 - 26.5 = +240.7 mm/19 = +12.67 mm average total change/8 = +1.58 mm/yr average change.

TABLE VII Growth in Width of 14 Wedges at Beacon Valley, Site A, between November 12, 1961, and November 17, 1969

Wedge	Growth (mm)
A	17.3
B	6.1
C	2.4
D	0.8
E	4.5
F	11.9
G	5.5
H	6.1
I	10.1
J	2.7
K	14.8
L	0.0
M	6.0
N	3.2
TOTAL ^a	-0.0 +91.4

^a $+91.4 - 0.0 = +91.4 \text{ mm}/14 = +6.53 \text{ mm average total change}/8 = +0.82 \text{ mm/yr average change.}$

valley, 500 m southwest of Taylor Glacier and inside a prominent moraine formed by the expanded Taylor Glacier. Seismic studies⁹ show a dry zone 75–95 cm thick over ice-cored rubbly moraine, which thickens up valley from 2.4 to 10.5 m.

The morainal floor of the valley is extremely rough, with boulders of dolerite and sandstone up to 10 m in diameter scattered over the surface. Most of the surface, however, is clean quartz sand with dolerite boulders 0.5–1 m in diameter. Polygons, generally 7–12 m in diameter, cover the entire surface of the valley. In the site, troughs average 3.3 m in width, and smaller secondary wedges subdivide the larger polygons. Many of the wedges excavated show a wedge-in-wedge sequence, especially those oriented perpendicularly to the axis of the valley. Clean poorly foliated sand in the outer parts of a wedge encloses an inner wedge 50 cm wide composed of strongly foliated sand and rubble. Those wedges parallel with the sand valley have less than 2 percent moisture by weight, whereas those perpendicular to the valley with their inner wedge have 3–4 percent moisture and are noticeably more cohesive. The wedge-in-wedge sequence suggests a fairly recent hiatus in the growth of some wedges, but its cause has not been determined.

Table VII shows that from November 12, 1961, to November 16, 1969, the average total change per wedge of 14 wedges was 6.53 mm or an average change per wedge of 0.82 mm/year. One wedge did not change, but all others widened. Although the measurements were made at a similar calendar period, there were no similar thermal periods. A thermal correction should change the growth rate somewhat.

Site 7—Beacon Valley, Site B

Site B in Beacon Valley is up valley from site A and 50 m beyond the prominent moraine that separates the two sites. Site B is in moraine similar to, but slightly older than, that at site A. Polygons are the same size as in site A, but wedges average 3.4 m in width. A seismic survey⁹ showed a dry zone 30–45 cm thick over permafrost to be only 1.6–1.7 m thick on bedrock.

Table VIII shows that from November 18, 1962, to November 17, 1969, the average net total change per wedge of 18 wedges was 5.91 mm or an average change per wedge of 0.84 mm/year. A thermal correction should change the rate slightly. One wedge shrank 0.1 mm; all others widened.

Sites A and B in Beacon Valley have shown a consistently parallel growth rate that differs year to year from each other by only a few tenths of a millimetre and, in general, has decreased slowly overall since the start of the sites. Growth has been the most uniform of all the sites.

Site 8—Cape Evans, Ramp Site, Ross Island

Cape Evans on the west flank of Mount Erebus on Ross Island is triangular in shape and is bounded on the northeast by the Barne Glacier and on the other sides by McMurdo Sound. Volcanic flows and morainic debris make up the ice-free portion of the cape. The flows form knobs and

TABLE VIII Growth in Width of 18 Wedges at Beacon Valley, Site B, between November 18, 1962, and November 17, 1969

Wedge	Growth (mm)
O	7.1
P	6.7
Q	-0.1
R	4.6
S	15.3
T	5.6
U	5.6
V	15.7
W	0.9
X	2.4
Y	3.4
Z	6.6
AA	3.7
BB	7.2
CC	5.2
DD	4.4
EE	10.2
FF	1.8
TOTAL ^a	-0.1 +106.4

^a $+106.4 - 0.1 = +106.3 \text{ mm}/18 = +5.91 \text{ mm average total change}/7 = 0.84 \text{ mm/yr average change.}$

TABLE IX Growth in Width of 15 Wedges at Cape Evans, Ramp Site, between December 30, 1961, and November 13, 1969

Wedge	Growth (mm)
KA-KB	-2.1
KC-KD	19.5
KE-KF	2.2
KC-KH	-0.5
KV	-6.6
KW	1.4
KX	-0.1
KY	8.1
KZ	19.5
AA	5.7
BB	2.2
CC	14.6
DD	16.6
EE	4.8
FF	13.2
TOTAL ^a	-9.3
	+107.8

^a +107.8 - 9.3 = +98.5 mm/15 = +6.57 mm average total change/
8 = +0.82 mm/yr average change.

ridges between which are numerous shallow ponds and lakes. Moraines consist of poorly sorted black volcanic debris coated below the surface with white-yellow salts. The terminus of the Barne Glacier is an ice-cored moraine sloping steeply westward known as the "ramp." Ice is found at a depth of 40-80 cm. Debris cones rise up to 9 m above the surface.

The contraction site on the ramp contains aligned orthogonal polygons with long dimensions downslope of several tens of metres and spacing of 5-20 m. Most long fractures might be considered longitudinal tension cracks of the glacier, although no movement has been observed of the terminal area. Composite wedges vary in width, averaging 55 cm under irregular and discontinuous troughs 10-20 cm deep. In summer, the active layer has a moisture content of 2.3-4.3 percent.

Table IX shows that from December 30, 1961, to November 13, 1969, the average net total change per wedge of 15 wedges was 6.57 mm or an average change per wedge of 0.82 mm/year. That rate likely will be reduced when thermal corrections are applied. Four of the 15 wedges shrank, but they made up less than 9 percent of the total positive movement.

Site 9—Cape Evans, Base Site, Ross Island

The base site was established on relatively flat moraine at the foot of the ramp. Polygons are 5-15 m across and flat centered. Ice and composite wedges average 40 cm wide

under troughs 10-20 cm deep. The ash comprising the moraine is much finer textured than most on the ramp.

Table X shows that from December 30, 1961, to November 13, 1969, the average net total change per wedge of 15 wedges was 9.75 mm or an average change per wedge of 1.22 mm/year. That rate most likely will be reduced when thermal corrections are applied. Only 1 of the 15 wedges shrank during the interval, and its decrease was 1.1 mm. Growth over the longer period is only one-third that of the first 2 years. Snow cover decreased markedly during the period of measurement, reducing spring runoff considerably.

Site 10—Wright Valley, Site A

Wright Valley, one of the major valleys in Victoria Land, extends eastward from the Polar Plateau 70 km toward the Ross Sea, where it is filled by the Wilson Piedmont Glacier and its tributary the Wright Lower Glacier. Peaks north and south of the valley rise to more than 2 000 m. The floor of the valley at the east end is 200 m above sea level and slopes westward to its lowest point at Lake Vanda, 70 m above sea level. The lake receives most of its water from the Onyx River that drains the Wright Lower Glacier. The valley walls display a series of bedrock benches, some of which may have been formed by ice moving eastward early in the glacial history of the valley.⁶ Ice later also pushed inland from the Wright Lower Glacier area. Numerous small cirque glaciers line the upper walls of the valley. The setting

TABLE X Growth in Width of 12 Wedges at Cape Evans, Base Site, between December 30, 1961, and November 13, 1969

Wedge	Growth (mm)
KO	11.5
KP	3.0
KQ	5.3
KR	7.5
KS	2.2
KT	13.7
KU	14.5
CG	11.9
HH	6.7
II	18.7
JJ	17.0
KK	17.9
KM-KN ^a	-1.1
KK-KL ^a	6.8
KJ-KI ^a	10.7
TOTAL ^b	-1.1
	+147.4

^a April 28, 1961.

^b +147.4 - 1.1 = +146.3 mm/15 = +9.75 mm average total change/
8 = +1.22 mm/yr average change.

is geologically similar to that of Taylor Valley, the next south. Steeply dipping metasediments of Precambrian or lower-Paleozoic age form the valley walls and are capped locally by Mesozoic dolerite or Beacon sandstone. Moraines of several ages blanket most of the valley floor and extend up the valley walls.

The highest and oldest moraines on the valley walls lack patterned ground. A dry zone 2 m or more in thickness effectively prevents its formation. Moisture is generally less than 1 percent by weight. Salts are abundant in the profile, and oxidation and migration of iron are commonplace.

Site A is 7 km west of the Wright Lower Glacier and 200 m above the valley floor on the south side. It is near the base of a steep bedrock hill, the top of which is rimmed by moraine of the Denton Glacier. The area has been mapped as oldest Trilogy glacial sediments.^{1,6} The surface is covered with poorly sorted material that ranges from silt to boulders several metres across. The moraine appears youthful, with little ventifacting, some cavernous weathering, and no staining of the soil with iron oxide. No salt concentrations were seen. The contraction site slopes irregularly north and west. Polygons are 10–20 m in diameter; troughs are 70–120 cm wide and average 90 cm. Free-running sand lines the troughs 15–40 cm deep. Cones of depression along contraction cracks are common in the spring. The active layer, 20–30 cm thick, contains 1.5–3 percent moisture by weight; permafrost, only 1–1.4 m thick,⁹ has 10 percent. Metamorphic rocks underlie the site.

Table XI shows that from December 29, 1962, to November 14, 1969, the average net total change per wedge of 40 wedges was 4.87 mm or an average change per wedge of 0.70 mm/year. Only 2 of the 40 wedges shrank during the interval. A thermal correction should reduce the growth rate further.

Site 11—Wright Valley, Site B

Site B is 6 km west of the Wright Lower Glacier on an ice-cored moraine 20 m above and south of the Onyx River. The surface is very irregular. Only 30–80 cm of rubble cover 7.7 m of dead glacial ice⁹ of the intermediate Trilogy. High-centered polygons are 10–20 m in diameter. Troughs up to 4.5 m wide and 70 cm deep divide the surface. Free-running sand and cones of depression are common. Migration of contraction cracks has occurred during the past as evidenced by relic troughs separated by sections of ice-cored moraine. The overlying dry zone contains about 2 percent moisture by weight. Sand wedges average 2 m in width.

Table XII shows that from December 29, 1962, to November 14, 1969, the average net total change per wedge of 30 wedges was 9.72 mm or an average change per wedge of 1.39 mm/year. A thermal correction should reduce the

TABLE XI Growth in Width of 40 Wedges at Wright Valley, Site A, between December 29, 1962, and November 14, 1969

Wedge	Growth (mm)	Wedge	Growth (mm)
A	12.2	X	10.7
B	5.6	Y	6.7
C	1.3	Z	1.8
D	5.8	AA	11.1
E	0.3	BB	5.6
F	3.3	CC	7.7
G	4.5	DD	7.7
H	7.0	EE	4.1
I	8.9	FF	2.8
J	2.9	GG	3.5
K	3.5	HH	4.6
L	5.0	II	0.4
M	5.9	JJ	4.5
N	6.6	KK	6.6
O	2.0	LL	7.8
P	-7.3	MM	10.4
Q	^a	NN	5.9
R	1.6	OO	5.8
S	5.1	PP	^a
T	-8.3		
U	8.7		
V	4.0		
W	8.6		
		TOTAL ^b	-15.6
			+210.5

^a Not recorded.

^b +210.5 - 15.6 = 194.9 mm/40 = +4.87 mm average total change/7 = +0.70 mm/yr average change.

TABLE XII Growth in Width of 30 Wedges at Wright Valley, Site B, between December 30, 1962, and November 14, 1969

Wedge	Growth (mm)	Wedge	Growth (mm)
A	-3.5	R	18.7
B	12.8	S	19.8
C	27.8	T	14.7
D	15.9	U	11.4
E	17.1	V	6.8
F	-3.7	W	11.3
G	-3.0	X	13.9
H	16.8	Y	14.5
I	4.9	Z	6.2
J	10.7	AA	10.3
K	10.2	BB	20.7
L	16.9	CC	13.6
M	0.1	DD	-7.5
N	12.4		
O	-1.8		
P	12.4		
Q	-8.8		
		TOTAL ^a	-28.3
			+319.9

^a +319.9 - 28.3 = +291.6 mm/30 = +9.72 mm average total change/7 = +1.39 mm/yr average change.

rate further. Of the 30 wedges, 6 shrank during the period of measurement, but their movement was less than 9 percent of the positive movement. Abandonment of contraction cracks or small wedges is commonplace, as other more favorably oriented take over the growth.

Site 12—Wright Valley, Site C

Site C is on a sandy terrace on the north side of the Onyx River, opposite site B. The surface is about 3 m above water level and has not been flooded during recorded history. Well-developed double raised-rim polygons 10-30 m in diameter have troughs averaging 150 cm wide. The dry zone, 25-35 cm thick, contains 1-2 percent moisture by weight. Sand wedges are best developed near the river and decrease in width away from it toward an ice-cored moraine along which snow tends to accumulate. The increased moisture there retards the movement of sand into contraction cracks, hence, slowing their growth rate.

Table XIII shows that from December 31, 1962, to November 14, 1969, the average total change per wedge of 47 wedges was 6.29 mm or an average change per wedge of 0.90 mm/year. None of the wedges shrank during the period, although a thermal correction could reduce the growth rate somewhat. Those wedges perpendicular to the prevailing strong down-valley winds mostly grew faster than those parallel to the wind.

Site 13—Wright Valley, Site D

Site D is on top of a morainic ridge, 100 m above the valley floor, on the south side of the Onyx River and between sites A and B. Silty water-laid sand and gravel was transported in part from snow melt from a perennial snow bank to the south. At present, little water flows through the area, but the channels and deposits attest to increased flow in the past. A desert pavement of pebbles and cobbles protects the surface. Cobbles are concentrated along the sides of the polygon troughs presumably by selective removal of fines into the growing wedges. The polygons are youthful, flat centered, and bounded by shallow troughs averaging 40 cm in width. A dry zone 15-25 cm thick contains 2-4 percent moisture by weight. Seismic studies⁹ suggest that an ice core with surface relief of about 2 m is present.

Table XIV shows that from January 1, 1963, to November 14, 1969, the average net total change per wedge of 19 wedges was 3.37 mm or an average change per wedge of 0.48 mm/year. Of the 19 wedges, 6 shrank during the period; their total movement was only about 12 percent of the positive movements. Five of the wedges that shrank are in the center of the site. Nonetheless, the overall rate of growth is only about one-third that recorded for the beginning of the study and should be reduced even further when thermal corrections are applied.

TABLE XIII Growth in Width of 47 Wedges at Wright Valley, Site C, between December 31, 1962, and November 14, 1969

Wedge	Growth (mm)	Wedge	Growth (mm)
A	4.1	Z	2.1
B	3.4	AA	5.2
C	4.9	BB	3.2
D	4.5	CC	3.5
E	1.1	DD	8.7
F	1.0	EE	12.8
G	18.7	FF	5.6
H	5.7	GG	4.0
I	8.9	HH	12.8
J	10.4	II	9.9
K	2.6	JJ	3.9
L	7.2	KK	10.2
M	10.4	LL	6.4
N	3.6	MM	11.2
O	3.5	NN	10.6
P	6.9	OO	4.7
Q	9.4	PP	3.7
R	5.8	QQ	1.5
S	2.5	RR	4.7
T	4.7	SS	1.4
U	6.6	TT	4.0
V	10.1	UU	3.2
W	4.6		
X	13.5		
Y	8.2		
		TOTAL ^a	+295.6

^a +295.6/47 = +6.29 mm average total change/7 = +0.90 mm/yr average change.

TABLE XIV Growth in Width of 19 Wedges at Wright Valley, Site D, between January 1, 1963, and November 14, 1969

Wedge	Growth (mm)
A	8.9
B	8.3
C	4.9
D	-1.5
E	1.2
F	7.4
G	4.9
H	3.6
I	6.4
J	1.7
K	5.0
L	-2.1
M	-3.8
N	-0.1
O	3.9
P	10.2
Q	6.8
R	-1.0
S	-0.6
	TOTAL ^a
	+73.2

^a +73.2 - 9.1 = +64.1 mm/19 = +3.37 mm average total change/7 = +0.48 mm/yr average change.

Site 14—Hobbs Glacier Area, Moraine of Koettlitz Glacier

Directly in front of the Hobbs Glacier, on the west side of McMurdo Sound, is a large area of ice-cored moraine.⁴ Most of the ice and debris was left by the formerly expanded Koettlitz Glacier whose terminus now lies far to the south across McMurdo Sound. Only a narrow fringe immediately parallel to the front of the Hobbs Glacier has been derived from that glacier. Just outside the debris of granitic and metamorphic rocks left by the Hobbs Glacier and on one of the highest summits of the ice-cored basaltic moraine of the Koettlitz Glacier is site 14. Scoria and basaltic fragments are sand to boulder size in the site. The dry zone is generally 10–20 cm thick. Well-developed polygons are 5–20 m across, surrounded by shallow troughs 20–60 cm wide. Pond-deposited mirabilite bodies are common in the vicinity.⁴

Table XV shows that from January 16, 1963, to January 7, 1969, the average net total change per wedge of 5 wedges was 6.56 mm or an average change per wedge of 1.09 mm/year. One of the 5 wedges shrank 0.7 mm, but its movement was only 2 percent of the total positive movements. This site should require little thermal correction.

CONCLUSIONS

Table XVI summarizes the growth rates for the 14 sites, the average width of the wedges in those sites, and the age in years (rounded to the nearest 10) for the wedges, assuming constant growth rates for the life of the wedges as measured during the 6- to 8-year period. Note that these ages lack the benefit of thermal corrections; these will be applied later.

The ages obtained duplicate the results from the first year of study for sites 2 and 7 and differ by an increasing amount for sites 6, 5, and 1.³ All those initial growth rates were corrected by a factor of 4 as determined from empirical data from site 2. Those ages given in Table XVI are uncorrected. The general conformance in growth rates year after year substantiates the validity of the technique. Differences can be attributed to a number of sources of error, which have been evaluated previously.¹ Time of measurement as related to the thermal regime outweighs all others.

The general conclusion reached is that the bulk of patterned ground in Victoria Land is young, dating within the last 5 000 years (even with thermal corrections to be applied). Multicyclic wedges are recognized by the wedge-in-wedge structure, and ancient patterned ground is being exhumed today to start growing again. Hence, many surfaces are not suitable for dating with patterned ground. Still no serious problems are envisioned for dating simple wedges in stream terraces, lake beds, and the like. Other wedges fall into the gray area between the black and white cases and pose problems.

TABLE XV Growth in Width of Five Wedges at Hobbs Glacier Area, between January 16, 1963, and January 7, 1969

Wedge	Growth (mm)
EA-EB	-0.7
EC-ED	3.8
EE-EF	11.1
EG-EH	5.4
EI-EJ	13.2
TOTAL ^a	-0.7 +33.5

^a +33.5 - 0.7 = +32.8/5 = +6.56 mm average total change/6 = +1.09 mm/yr average change.

TABLE XVI Age of Patterned Ground in Victoria Land from Uncorrected Data

Site	Net Growth Rate (mm/yr)	Interval (yr)	Average Width of Wedges (mm)	Age (yr) ^a
1	-0.39	7	500	—
2	0.35	8	750	2 140
3	0.34	7	750	2 200
4	0.89	8	700	790
5	1.58	8	700	440
6	0.82	8	3 200	3 910
7	0.84	7	3 400	4 050
8	0.82	8	550	670
9	1.22	8	400	330
10	0.70	7	900	1 280
11	1.39	7	2 000	1 440
12	0.90	7	1 500	1 670
13	0.48	7	400	830
14	1.09	6	300	280

^a Rounded to nearest 10 yr.

The youthfulness of wedges in areas of glacial deposits considered to be very old^{1,3,6,7} raises problems not yet solved. However, it is not widely recognized that the patterned ground can date only that last major geomorphic event that exposes a surface, such as a lake bed or stream terrace, to the atmosphere where wedges can start to grow. A perennial cover of snow, water, or ice precludes wedge growth. Thus, youthful polygons in ancient glacial deposits date youthful events, such as the removal of perennial snow or ice or water from those surfaces. Dating with patterned ground is not necessarily incompatible with the proposed glacial chronologies. The recognition of the geomorphic events that permitted the patterned ground to start so recently in Victoria Land, however, is slow to materialize.

ACKNOWLEDGMENTS

Special acknowledgment is made posthumously to Thomas E. Berg who began field studies in Victoria Land in 1960 and carried through various parts of the study on patterned ground to the final measurement in 1969 of most wedges cited here.⁸ Many others have participated in the study for whom my warm thanks are insufficient. The field studies would not have been possible without several grants from the National Science Foundation, Office of Polar Programs (formerly office of Antarctic Programs), and support from the numerous personnel associated with it.

REFERENCES

1. Berg, T. E., and R. F. Black. 1966. Preliminary measurements of growth of nonsorted polygons, Victoria Land, Antarctica. *Am. Geophys. Union Antarct. Res. Ser.* 8:61-108.
2. Black, R. F., and T. E. Berg. 1963. Hydrothermal regimen of patterned ground, Victoria Land, Antarctica. *Int. Assoc. Sci. Hydrol. Comm. Snow Ice Publ.* 61. p. 121-127.
3. Black, R. F., and T. E. Berg. 1964. Glacier fluctuations recorded by patterned ground, Victoria Land, p. 107-122. *In* R. J. Adie [ed.] *Antarctic geology*. North-Holland, Amsterdam. 758 p.
4. Bowser, C. J., T. A. Rafter, and R. F. Black. 1970. Geochemical evidence for the origin of mirabilite deposits near Hobbs Glacier, Victoria Land, Antarctica. *Min. Soc. Am. Spec. Paper* 3. p. 261-272.
5. Burch, T. L., personal communication.
6. Calkin, P. E., R. E. Behling, and C. Bull. 1970. Glacial history of Wright Valley, southern Victoria Land, Antarctica. *Antarct. J. U.S.* 5(1):22-27.
7. Denton, G. H., R. L. Armstrong, and M. Stuiver. 1970. Late Cenozoic glaciation in Antarctica: The record in the McMurdo Sound region. *Antarct. J. U.S.* 5(1):15-21.
8. National Science Foundation. 1970. Thomas E. Berg, obituary. *Antarct. J. U.S.* 5(1):7.
9. Twomey, A. A. 1968. Seismic refraction studies in surficial materials of Victoria Land, Antarctica. M.S. thesis. University of Wisconsin, Madison. 56 p.

THERMOKARST DEVELOPMENT, BANKS ISLAND, WESTERN CANADIAN ARCTIC

H. M. French and P. Egginton

UNIVERSITY OF OTTAWA
Ottawa, Ontario

INTRODUCTION

The existence and nature of thermokarst in areas currently or previously underlain by permafrost and ground ice is now well documented both in the scientific literature^{5,7,8,10,16,21,25,32,38} and in certain textbooks.^{1,6,17,33,39} The development of thermokarst is due to the disruption of the thermal equilibrium of the permafrost and an increase in the depth of the active layer. Regions having a considerable ice content in the soil are particularly susceptible to thermokarst processes. The reason for the permafrost degradation is commonly ascribed to regional climatic change²¹ or, alternatively, to rather more localised conditions that may be either natural, such as polygonal ground development,⁵ or man induced.³¹ Although they are often intimately linked, it is sometimes useful to distinguish between thermal melting and subsidence (thermokarst *sensu stricto*)²⁹ and thermal erosion.^{9,11,40} A second distinction can be made with respect to the thermokarst process itself; Czudek and Demek,⁵ for example, have dis-

tinguished between downwearing and backwearing thermokarst processes and land forms.

In North America, the majority of studies related directly or indirectly to thermokarst have been undertaken on the mainland and, in particular, in the tundra and forest tundra environments of the Mackenzie District, Yukon coasts^{27,28} and Alaska.^{20,35} Recently, the stimulus for additional work has been provided by the increased pace of economic development of these regions.^{2,18,23,29} In the Canadian Arctic Archipelago, however, there is little information available on thermokarst processes and land forms. A notable exception is the study by Lamothe and St. Onge²⁶ on Ellef Ringnes Island. Most other geomorphological studies in the western arctic islands, however, have given little emphasis to thermokarst processes.

Within this general context, this paper describes some thermokarst land forms and processes that are to be found on Banks Island, in the western Canadian Arctic. This island, the fourth largest in the Canadian Arctic Archipelago,

lies between 71 and 75°N and is totally within the zone of continuous permafrost.³ Fieldwork, which was undertaken in the summers of 1971 and 1972, was concentrated in the vicinity of Johnson Point on the east coast and Sachs Harbour on the southwest coast.

REGIONAL THERMOKARST CONSIDERATIONS

Many of the general factors involved in thermokarst development on the island can be summarised under climate and ground ice.

Climate

Air and ground temperature conditions will influence the rate and amount of thaw and the depth of the active layer and, as such, will be important controls over the thermokarst process.²⁶ Representative climatological data for the island are presented in Table I. In view of the size of the island, regional differences in amounts of thaw between the north and the south may be expected (Table I). Based on thawing degree days, calculated for a number of western arctic stations (Table I), it may be assumed that the northern part of Banks Island experiences approximately 50 percent fewer thawing degree days than the southern part. Moreover, when the island stations are compared with the mainland, it is

clear that, in terms of thaw duration, the arctic islands have less potential for thermokarst.

Ground temperatures and insolation values, however, may be more important for the thermokarst process than air temperatures. In this respect, the month of July has the highest average of sunshine duration during the thaw period, since in August and September increasing amounts of open water in the Beaufort Sea promote overcast conditions (Table I). Ground temperature data for the island are limited, but temperatures in excess of 21 °C at the surface and 15.5 °C at the 2.5-cm depth have been recorded¹² on Banks Island. These temperatures are rather high when compared with other arctic tundra environments and reflect the high thermal conductivity and low heat capacity of sands and gravels. With respect to thermokarst, therefore, ground temperature conditions may offset the decrease in the thawing period to some extent.

Ground Ice

The importance of naturally occurring thermokarst is restricted to those areas where lithological and/or soil conditions favour a high ice content, or where massive ground ice is present. The origin of ground ice, be it buried glacial ice or segregated ice formed in association with an aggradation of the permafrost,³⁰ is complex and is regarded as a

TABLE I Selected Climatological Data of Western Arctic Stations, with Reference to Thermokarst Potential, Banks Island

Air Temperatures ^a (°C January–December)												
Sachs Harbour 1955–1960	–29.4	–31.5	–28.1	–20.0	–8.8	1.8	5.5	4.5	–1.6	12.6	–24.3	–28.0
Mould Bay 1951–1960	–33.0	–35.4	–32.7	–22.6	–10.9	0.2	4.0	1.8	–6.0	–17.0	–26.7	–31.3
Sunshine Record ^b for Sachs Harbour 1960–1970												
Average sunshine (duration, hr)	0.2	56.8	167.2	269.1	257.6	302.4	329.8	180.8	72.0	39.4	5.7	0.0
Average No. of days with no sunshine	30.9	13.5	6.1	3.2	6.5	4.6	4.5	8.3	13.1	9.4	27.5	31.0
Duration of Thaw ^c												
	Commencement				Finish							
N. Banks Island	June 15				September 1							
S. Banks Island	June 15				September 12							
Thawing Degree Days for Western Arctic Stations (1970)												
	May	June	July	August	September	October	Total					
Tuktoyaktuk, 69°N	67	273	509	458	105	6	1420					
Sachs Harbour, 71° 57'N	25	117	385	289	46		855					
Mould Bay, 76° 14'N	1	48	230	185	9		465					
Isachsen, 78° 47'N		28	183	125	1		316					

^a From H. A. Thompson, 1967. The climate of the Canadian Arctic. Meteorological Research, Department of Transport, Queen's Printer.

^b Monthly Records, Meteorological Branch, Canada Department of Transport.

^c H. A. Thompson, 1963. Freezing and thawing indices in Northern Canada. Proceedings First Canadian Permafrost Conference. N.R.C. Tech. Memo. 76. p. 18–36.

separate problem beyond the scope of this paper. As such, the restriction of the word "thermokarst" specifically to the melting of ground ice as opposed to buried glacial ice, which has been suggested by Dylík,^{7,8} is regarded as unnecessarily limiting. In terms of land-form development, the origin of the ice is relatively unimportant. Instead, the distribution of the ice (e.g., fissure ice and lenses) and the amount of "excess ice"³⁴ are more relevant.

There are several areas of Banks Island that appear to possess relatively high ice contents in the underlying material. For example, much of the western and interior lowlands are underlain by alluvial silts and fine sands and are typical thermokarst regions characterised by thaw lakes and ice-wedge polygons. A second area is in south central Banks Island where massive ice to depths in excess of 30 m inter-layered with sands and gravels has been encountered in many drill holes by Deminex Oil during the 1970-1971 seismic explorations. A third area of apparently high ice content is the eastern morainal area; this will now be discussed in detail.

THERMOKARST LAND FORMS NEAR JOHNSON POINT

An extensive belt of morainal materials extends along both sides of the Prince of Wales Strait.¹⁴ On Banks Island, it gives rise to undulating hilly terrain rising in places to over 300 m and extending for a maximum of 40-55 km inland. The ground ice of this terrain is generally hidden beneath a layer of silt or other unconsolidated material. In view of the enclosing material, it is probably of glacial origin, although no drilling information is available to confirm this or to indicate the thickness of either the ground ice or the surficial materials.

GROUND ICE MUDSLUMPS

In a number of localities, the ground ice has been exposed and, by melting, has produced localised mudflows that have excavated semicircular hollows (Figure 1). The erosion takes place through the thermal melting of the ground ice, which causes a crumbling and slipping of the overlying silts into the hollow that then liquify into mud through the addition of the melted ground ice. Excavation, therefore, by mudflow and/or solifluction, and, occasionally, if there is sufficient moisture, fluvial (thermal) erosion occurs forming a network of small channels within the hollow. The process appears to be exactly similar, therefore, to that described by Lamothe and St. Onge²⁶ on Ellef Ringnes Island and by Mackay²⁸ and Kerfoot and Mackay²⁴ in the Mackenzie Delta area.

In the area under study, the mudslumps possess a variety of forms and shapes. All features, however, are exceedingly broad and shallow, since the height of the headwall, including the ice exposure, rarely exceeds 1.5-2.5 m. As such, the features are slightly different from those on Garry Island,²⁸ where the headwall may exceed 7 m in height. Both singular and composite features can be recognised. The latter are those in which several adjacent hollows have coalesced or where a single slump possesses a distinct slump-scar within the larger feature. In addition, both actively forming hollows and stabilised ones can be identified (Figure 2).

In Figure 3, all recognisable thermokarst hollows have been plotted in the area west of Johnson Point as far as the Thompson River. Irrespective of the size of each feature, there is an average density of 0.5/km² in the area studied, which illustrates the regional importance of this process.

Ground ice slumping is probably one of the most rapid erosional agents operating in the high Arctic at present.



FIGURE 1 Active ground ice mudslump hollow, eastern Banks Island, approximately 40 km west of Johnson Point. Note the ground ice exposed in the headwall, the active slumping of material across the face, and the lobate mudflow movement within the hollow; 27 June 1972.

FIGURE 2 Relatively stabilised mudslumps hollow, eastern Banks Island, approximately 15 km west of Johnson Point. Ground ice is not directly exposed at present, but standing water upslope near the edge of the feature suggests permafrost thawing. A number of fluvial gullies have developed in the hollow. Note also the polygonal ground development and the irregular plan of the headwall; 24 July 1971.



During the summer of 1972, two active hollows were measured. Average rates of retreat of the headwall above the ground ice exposure and movement within the hollows are presented in Table II. It appears that the maximum erosion of the headwall takes place in July, the month that coincides with the highest temperature and sunshine values of the summer. The data suggest that retreat of the headwall, and thus the enlargement of the hollow, is approximately 7–10 m each summer. These values are of the same order of magnitude as those observed by Lamothe and St. Onge²⁶ (average, 7 m; maximum, 10 m) on Ellef Ringnes Island and by Kerfoot and Mackay²⁴ over a 7-year period on Garry Island (maximum retreat, 51 m; i.e., 7.3 m per annum; average, 24.4 m; i.e., 3.5 m per annum). Since no reliable ice content data are available for the Banks Island features and since the rate of retreat of the headwall is primarily a function of the ice content, it is difficult to make any definitive comparisons between the high Arctic and the tundra lowland areas.

The continued retreat of an active ground ice slump is related to the balance between the rate at which debris is supplied to, and removed from, the base of the headwall.^{23,28} Since the headwalls of the features on Banks Island rarely exceed 2 m in height, quite random increases of slumped debris may result in the stabilisation of the hollow. With the exception of composite features, the maximum size of the hollows, either active or stabilised, does not exceed 200–300 m in diameter. In view of the average retreat rates previously mentioned (see Table II), it is highly likely that the majority of the hollows become stabilised within 30–50 summers of their initiation. This is probably of the correct order of magnitude since aerial photographs from 1948 and 1962 indicate certain features to be active but, upon field examination in 1972, were found to have stabilised. Others that are active today appear on the 1962 photograph but not on the 1948 photographs.

In general, the slumps may be grouped as to their occurrence in one of three types of localities.

FIGURE 3 Terrain features of the area west of Johnson Point toward the Thomsen River. Key: 1, ground ice slump features and depressions, active or stabilized; 2, areas of badland topography and nivation processes; 3, major north-south drainage divide of the eastern morainal ridge of Banks Island; 4, present streams; 5, lakes; 6, old lake depressions and/or fluvial channels.

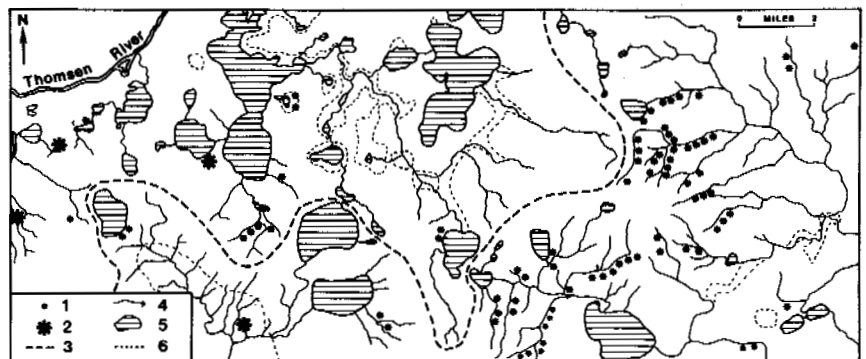


TABLE II Rates of Headwall Retreat and Mudflow Movement in Two Ground Ice Mudslumps, Eastern Banks Island, Summer 1972

Scar No.	Headwall Retreat		Mudflow Movement		
	Period of Observation	Average Rate of Retreat (m/day)	Overall Retreat (m/day)	Average Rate of Cork Movement (m/day)	
1	June 30– July 10	0.14	0.11	June 30– July 10	0.25
	July 10– July 23	0.13		July 10– July 23	0.17
	July 23– Aug. 3	0.09		July 23– Aug. 3	0.14
	Aug. 3– Aug. 13	0.08			
2	July 15– July 28	0.14	0.12	July 15– July 28	0.24
	July 28– Aug. 12	0.11		July 15– Aug. 12	0.15
				July 28– Aug. 12	0.05

Mudslumps Adjacent to Kettle Lakes and/or Depressions

Many active and stabilised hollows are found immediately adjacent to lakes and probably owe their initiation to undercutting of the bank by the lake. This would probably occur when exceptionally strong winds would concentrate wave action at one locality. Alternatively, local ice pushing in the late summer may gouge ruts and destroy vegetation along the lake shores. Numerous ice-push ridges attest to the importance of this process in this area.

Mudslumps on West- or Northwest-Facing Valley Side Slopes

Many of the small stream valleys that dissect the eastern slopes of the morainal belt are asymmetrical where the direction of the valleys is approximately north-south. In all cases, the steeper slope faces toward the west, northwest, or southwest. What makes the asymmetry so distinctive both in the field and from aerial photographs is that mudslump hollows are often associated with the steeper west-facing slope sections of the valleys (Figure 4). The cause of the feature is intimately related to the problem of the development of the asymmetry.

On the northwest part of Banks Island, the author has

drawn attention to the indirect role of wind in determining the thickness of the active layer, differential snow distribution, and, consequently, differential solifluction activity on slopes of varying orientations. These conditions promote lateral fluviothermal erosion and the development of steeper, southwest-facing slopes. A similar explanation may be appropriate in this part of Banks Island too, with the slightly different orientations of the asymmetry being explained by slightly different wind directions and snow conditions. The complexity of periglacial asymmetry forms and processes, as stressed by Kennedy and Melton,²² however, demands more detailed studies of the microclimatic factors involved in the eastern Banks Island area before any firm conclusions can be made.

Mudslumps in Random Locations

A number of mudslump features appear to be unrelated to any obvious trigger mechanism. One such feature studied in the field in 1972, however, possessed a distinct lobe of irregular topography at the downslope end of the feature on either side of the central mudflow path. In this case, and probably in others, it may be that local slope instability and slumping may have been the trigger to expose the ground ice. Such slumping has been observed by many workers in the high Arctic^{36,41} as well as by the authors on other parts of Banks Island. It occurs quite randomly in the early summer as a result of local conditions of soil saturation, mostly in years of exceptionally high snowfall and/or rapid thaw.

ICE-WEDGE POLYGONS AND ASSOCIATED FEATURES

The waning development of polygonal fissure ice bodies often leads to conical accumulations known as cemetery mounds or baydjarakhs.⁴ Where substantial amounts of the ice wedge remains, however, the mounds are extremely shallow features and may more correctly be termed high-centred polygons. As such, they often reflect the initial stages of baydjarakh formation.

On the upland areas and interflaves of the hummocky moraine, high-centred polygons dominate the terrain over large areas (Figure 5). A distinct microrelief is produced, therefore (Table III). The polygons vary in size from approximately 30 m in diameter on relatively flat terrain to over 50 m in overall dimension on better drained terrain of between 5–6°. At the same time, the linear depressions developed along the ice wedges increase in size and depth with increasing slope. Since the depressions act as channels for surface snowmelt runoff, the increase in size probably reflects thermal erosion, in addition to the initial thermal melting process.

A characteristic of this polygon terrain is the existence



FIGURE 4 Active ground ice slump developing on steeper northwest-facing slope of shallow asymmetrical valley, approximately 15 km north of Johnson Point. Note also the older thermokarst scars to right of active feature and stream at immediate foot of steeper slope. Gentle slope, in foreground, is characterised by solifluction and rillwash associated with small snow patch; 16 July 1972.

of a number of irregularly shaped ponds. They occupy the depressions formed at the junction of the ice wedges, and some of them persist throughout the summer. For example, of 26 ponds identified in one area on June 28, only 10 still remained on August 13. Average depths of thaw beneath the ponds is often less than 15 cm, while that of the ice-wedge depressions and the high-centred polygons are in excess of 30 and 40 cm, respectively (Table IV). It is debatable whether these ice-wedge junction ponds reflect thermokarst processes or are merely features associated with the spring snowmelt runoff. Ponds in between ice wedges are not uncommon in other parts of northwest Canada and Alaska and

are often interpreted as reflecting the transition from low- to high-centred polygons. As such, they are not regarded as thermokarst features. Furthermore, if it is assumed that the net active thermokarst melting is 1 cm/year, this would deepen the pond 1 m in 100 years and 10 m in 1 000 years. Clearly, therefore, the ponds do not reflect active thermokarst melting; it is more likely that their development was associated with an improvement of drainage conditions at some time in the past.

The close connection that exists between thermal erosion and thermal melting is most dramatically illustrated in localised areas of badland topography that exist in close

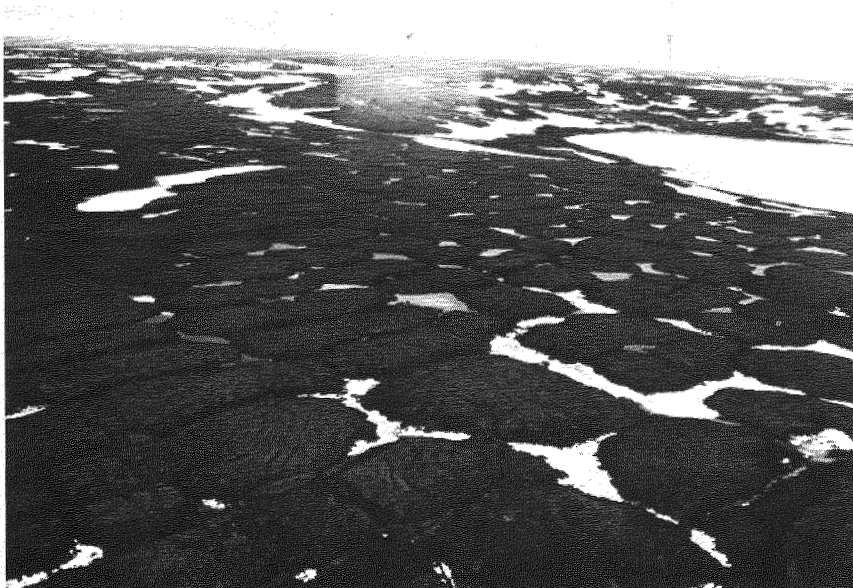


FIGURE 5 General air view of polygon terrain between Johnson Point and the Thomsen River, eastern Banks Island. Observe the small lakes developing at the junctions of the depressions, the snow distribution, and the little lake at the top right of photo; 16 June 1972.

TABLE III Microrelief Forms, Eastern Banks Island

	High-Centred Polygons			Linear (Ice-Wedge) Depressions		
	Number	Dimensions (m)	No. of Sides	Number	Width (m)	Depth (cm)
Gently sloping (<3°)	22	34.0 × 28.0	5.4	12	2.9	28
East-facing slope (5-6°)	30	57.4 × 51.4	5.7	34	7.83	38

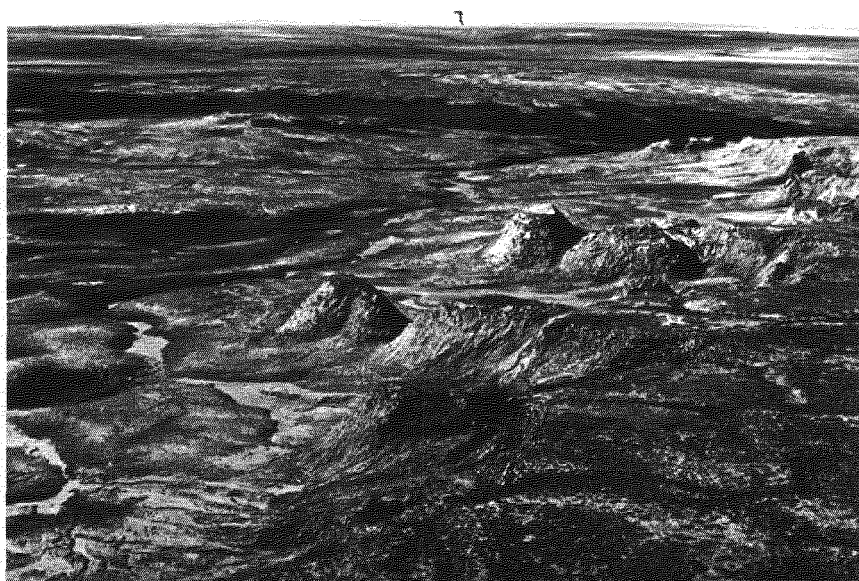
TABLE IV Average Thaw Depths under Different Terrain Conditions

Eastern Banks Island			
Date	Ice-Wedge Depressions (cm)	High-Centred Polygons (cm)	Ponds (cm)
4 July 1972	30	40	15
13 Aug. 1972	63	80	30
Sachs Harbour			
Date	Undisturbed Terrain (cm)	Airstrip Shoulder (Vegetation Removed or Flattened) (cm)	Disturbed Terrain (cm)
17 June 1972	50.0	33.0	18.5
16 July 1972	65.0	72.0	72.0
7 Sept. 1972	80.0	90.0	88.5

juxtaposition to well-developed polygon terrain and ice-wedge junction ponds. In the study area, badland topography is restricted to areas of stratified silts and sands that are locally important. In one area, a large heart-shaped amphitheatre has been developed, over 0.5 km in size (Figure 6), by a small stream draining toward the Thompson

River lowlands. A combination of nivation³⁷ and fluvial processes are excavating the hollow. However, this erosion is operating preferentially along the ice wedges (thermal erosion) to produce an irregular, serrated edge to the amphitheatre. Within the hollow, some of the polygon centres have been completely isolated to form striking conical fea-

FIGURE 6 Aerial view of badland erosion developed in association with polygonal ground, approximately 3 km from the Thomsen River, eastern Banks Island. A combination of nivation and fluviothermal erosion is operating preferentially along the ice wedges to produce irregular serrated edge to feature (bottom right), as well as to isolate, conical hills (i.e., polygon centres) within the depression (mid-foreground). In mid-distance, remnants of original polygon surface can be seen, together with thermokarst depression and irregular terrain; 24 July 1971.



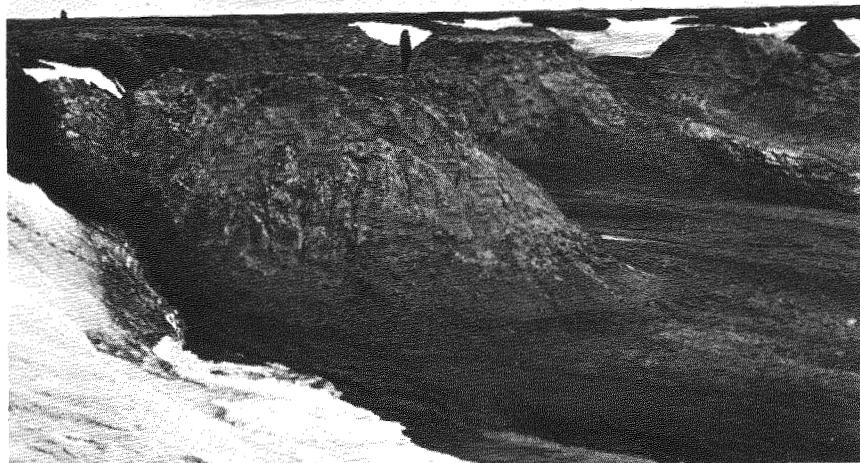


FIGURE 7 Surface view of features shown in Figure 6. Man gives scale to the features. Sediments are horizontally bedded fluviatile silts and fine sands, probably of outwash nature; 12 July 1972.

tures over 30 m high and between 7 and 10 m in diameter at the summits (Figure 7). At the same time, several standing water bodies and areas of irregular terrain on the floor of the hollow also suggest active thermokarst melting and subsidence.

THERMOKARST DEVELOPMENT AT SACHS HARBOUR

Slightly different thermokarst forms can be observed adjacent to the airstrip at Sachs Harbour, in the southwest part

of the island. During construction of the airstrip in 1962, a thin veneer of glacial sands and gravels were removed to provide material for the airstrip itself. Underlying sands and silts were thus exposed and thermokarst melting and subsidence has occurred. Average depth of thaw values taken during 1972 illustrate the increase in thaw depths of the disturbed terrain (Table IV) to be approximately 8-10 cm.

The thermokarst terrain is characterised by irregular hummocky topography, standing water, and a number of small interconnected linear depressions (Figure 8). The hummocks are often 3-5 m in diameter and give a relative



FIGURE 8 Oblique view of terrain disturbance on north of airstrip at Sachs Harbour, southwest Banks Island. The raised sections were used to transport material from the intervening depressions to the airstrip; 25 July 1971.



FIGURE 9 Surface view of disturbed terrain illustrated in Figure 8. Thermokarst melting and subsidence of the silts and sands has produced distinctive hummocky terrain with depressions and standing water. Average depth of thaw of disturbed terrain is 9–10 cm greater than the undisturbed terrain; 17 July 1972.

relief between 1 and 2 m to this terrain. Aerial photographs reveal some of the linear depressions to follow broad patterns similar to the ice-wedge polygons of adjacent undisturbed areas (Figure 9). In overall appearance, this terrain is remarkably similar to the hummocky features described by Dylík¹⁰ (Figure 2) from Siberia, and there is also some resemblance to the microtopography developing in the Inuvik area of the Northwest Territories of Canada following the forest fire of 1968.^{15,19}

CONCLUSIONS

While it may be true to argue that thermokarst is best favoured in the tundra and forest tundra environments of the Canadian north, it is equally true that in some areas of the high Arctic, thermokarst processes and land forms assume a regional importance. Certain types of thermokarst, such as ground ice slumping, are regarded as being some of the most rapid erosional processes operating in the high Arctic at present. Others, such as those related to ice-wedge polygon degradation, have received little attention in Canada to date.

ACKNOWLEDGMENTS

This research was supported by grants from the National Research Council of Canada and the Department of Indian Affairs and Northern Development. The author is also grateful to Dr. R. J. E. Brown, National Research Council of Canada, Dr. J. G. Fyles, Geological Survey of Canada, and Dr. J. R. Mackay, University of British Columbia, for their helpful advice.

REFERENCES

1. Bird, J. B. 1967. The physiography of Arctic Canada. John Hopkins University Press, Baltimore. p. 210–16.
2. Brown, J., W. Rickard, and D. Vietor. 1969. The effect of disturbance on permafrost terrain. Special Report No. 138. U.S. Army Cold Regions Research and Engineering Laboratory, Hanover, New Hampshire.
3. Brown, R. J. E. 1967. Permafrost in Canada. Map 1264A, Geological Survey Canada. Division Building Research, National Research Council Canada, Ottawa.
4. Brown, R. J. E. 1967. Comparison of permafrost conditions in Canada and the U.S.S.R. *Polar Rec.* 13:741–51.
5. Czudek, T., and J. Demek. 1970. Thermokarst in Siberia and its influence on the development of lowland relief. *Quaternary Res.* 1:103–120.
6. Dostovalov, B. N., and W. A. Kudriawcew. 1967. *Obszczeje mierzlotowiedzenie (General permafrost science)*. Moscow University. p. 224–229.
7. Dylík, J. 1964. Le thermokarst, phénomène négligé dans les études du Pleistocène. *Ann. Géogr.* 73:513–523.
8. Dylík, J. 1968. Thermokarst, p. 1149–51. *In* R. W. Fairbridge [ed.] *Encyclopedia of geomorphology*. Reinhold Book Corp., New York.
9. Dylík, J. 1969. Slope development affected by frost fissures and thermal erosion. p. 365–386. *In* T. L. Péwé [ed.] *The periglacial environment*. McGill-Queens University Press, Montreal, Quebec, Canada.
10. Dylík, J. 1970. Kras termiczny, jego istota i kierunki rozwoju. *Sprawozdania z Czynności i Posiedzeń Naukowych, Spis Tresci. Lodz. Tow. Nauk. Soc. Sci. Lodz.* 24(7):14.
11. Dylík, J. 1970. Erozja termiczna. *Sprawozdania z Czynności i Posiedzeń Naukowych, Spis Tresci. R. Lodz. Tow. Nauk. Soc. Sci. Lodz.* No. 8. 13 p.
12. French, H. M. 1970. Soil temperatures in the active layer, Beaufort Plain. *Arctic* 23(4):229–39.
13. French, H. M. 1971. Slope asymmetry of the Beaufort Plain, Northwest Banks Island, N.W.T., Canada. *Can. J. Earth Sci.* 8:717–731.

14. Fyles, J. G. 1963. Surficial geology of Victoria and Steffansson islands, District of Franklin. Geol. Surv. Can. Bull. 101. 38 p.
15. Fyles, J. G., J. A. Heginbottom, and V. Rampton. 1972. Quaternary geology and geomorphology, MacKenzie Delta to Hudson Bay. Guidebook to Field Excursion A30. 22nd International Geological Congress, Montreal. p. 23.
16. Grigorey, N. F. 1965. Thermokarst phenomena in East Antarctica, p. 174-177. *In* Soviet Antarctic expedition. Vol. 3. Elsevier, Amsterdam. (English translation)
17. Hamelin, L. D., and F. A. Cook. 1967. Illustrated glossary of periglacial phenomena. Les Presses de l'Université Laval. p. 36-41.
18. Haugen, R. K., and J. Brown. 1970. Natural and man induced disturbances of permafrost terrain, p. 139-149. *In* D. R. Coates [ed.] Environmental geomorphology. State University of New York, Binghamton.
19. Heginbottom, J. A. 1971. Some effects of a forest fire on the permafrost active layer at Inuvik, N.W.T. Proc. Sem. Permafrost active layer (Vancouver. Nat. Res. Council, Assoc. Com. Geotech. Res.) Tech. Memo. No. 103. p. 31-36.
20. Hopkins, D. M. 1949. Thaw lakes and thaw sinks in the Imuruk Lake area, Seward Peninsula, Alaska. J. Geol. 57:119-131.
21. Katchurin, S. P. 1962. Thermokarst within the territory of the U.S.S.R. Biul. Peryglacj. No. 11. p. 49-55.
22. Kennedy, B. A., and M. A. Melton. 1972. Valley asymmetry and slope forms of a permafrost area in the Northwest Territories, Canada. Spec. Publ. No. 4. Institute of British Geographers. p. 107-21.
23. Kerfoot, D. E. 1972. Topographic aspects of artificial disturbances to the tundra in the Mackenzie Delta area, N.W.T. p. 157-174. *In* Mackenzie Delta monograph. 22nd International Geographical Congress, Montreal.
24. Kerfoot, D. E., and J. R. Mackay. 1972. Geomorphological process studies, Garry Island, N.W.T., p. 115-130. *In* Mackenzie Delta monograph. 22nd International Geographical Congress, Montreal.
25. Kolasinska, J. 1970. Niektore formy krasu termicznego w Centralnej Jakucji (résumé: Certaines formes du thermokarst en Yakoutie Centrale). Prob. Czwartorzedu Acta Geogr. Lodz. 24:277-285.
26. Lamothe, C., and D. St. Onge. 1961. A note on a periglacial erosional process in the Isachsen area, N.W.T. Geogr. Bull. No. 16. p. 104-113.
27. Mackay, J. R. 1963. The Mackenzie Delta area. Geogr. Branch Mem. No. 8, 202 p.
28. Mackay, J. R. 1966. Segregated epigenetic ice and slumps in permafrost, Mackenzie Delta area, N.W.T. Geogr. Bull. 8:59-80.
29. Mackay, J. R. 1970. Disturbances to the tundra and forest tundra environment of the western Arctic. Can. Geotech. J. 7:420-432.
30. Mackay, J. R. 1971. The origin of massive icy beds in permafrost, western Arctic coast Canada. Can. J. Earth Sci. 8:397-422.
31. Péwé, T. 1954. Effect of permafrost upon cultivated fields. U.S. Geol. Surv. Bull. 989. p. 315-351.
32. Popov, A. I. 1956. Le Thermokarst. Biul. Peryglacj. No. 4. p. 319-330.
33. Price, L. W. 1972. The periglacial environment, permafrost, and man. Commission on College Geography Resource Paper No. 14. Association of American Geographers, Washington, p. 18-23.
34. Rampton, V. N., and J. R. Mackay. 1971. Massive ice and icy sediments throughout the Tuktoyaktuk Peninsula, Richards Island, and nearby areas, District of Mackenzie. Geol. Sur. Can. Paper 71-21.
35. Rex, R. W. 1960. Hydrodynamic analysis of circulation and orientation of lakes in Northern Alaska. Geol. Arctic 2:1021-1043.
36. Rudberg, S. 1963. Morphological processes and slope development in Axel Heiberg Island, N.W.T. Canada. Nach. Akad. Wis. Gottingen, 2(14):218-228.
37. St. Onge, D. A. 1969. Nivation landforms. Geol. Surv. Can. Paper 69-30.
38. Svensson, H. 1970. Thermokarst. Svensk Geogr. Arsbok 47:114-126.
39. Tricart, J. 1967. Le modelé des régions périglaciaires. SEDES, Paris. p. 284-294.
40. Walker, H. J., and L. Arnborg. Permafrost ice wedge effect on riverbank erosion, p. 164-171. *In* Permafrost: Proceedings of an international conference. National Academy of Sciences, Washington, D.C.
41. Washburn, A. L. 1947. Reconnaissance geology of portions of Victoria Island and adjacent regions, Arctic Canada. Geol. Soc. Am. Mem. 22. 142 p.

GLACIAL PERMAFROST AND PLEISTOCENE ICE AGES [1]

T. Hughes

THE OHIO STATE UNIVERSITY
Columbus, Ohio

INTRODUCTION

Permafrost defines the thermal condition existing in a material when its temperature is below the freezing point of water. In the broadest sense, therefore, materials in the permafrost state can range from cold glaciers, which contain only ice, to cold bedrock, which contains no ice. It is only necessary that the cold condition be below the freezing point of water. A common permafrost state is the frozen condition of regolith containing a significant ice fraction. This condition will be called regolith permafrost in this paper. One regolith permafrost state is the regolith-charged basal ice layer of a glacier or ice sheet, and this specific ice-regolith mix will be called glacial permafrost. Glacial permafrost has never been completely thawed and, therefore, is in a primary state. Thawed and refrozen glacial permafrost presumably cannot be distinguished from other regolith permafrost, owing to collapse and redistribution during thawing, and is no longer glacial permafrost.

Glacial permafrost will have most or all of the physical and mechanical characteristics of the regolith-charged basal ice layer of a glacier or ice sheet, even after the overlying clean ice has completely ablated. What keeps the regolith-charged basal ice from also ablating completely? The answer to this question determines whether glacial permafrost exists today in permafrost regions formerly covered by glaciers or by Pleistocene ice sheets.

Classically, permafrost has been explained as perennially frozen ground created when the mean annual ground surface temperature falls sufficiently below 0 °C so that the depth of freezing in winter exceeds the depth of thawing in summer. Hence, a layer of permafrost grows downward from the base of the active layer of seasonal frost, thickening each winter at a decreasing rate owing to the upflow of geothermal heat until a steady-state thickness of permafrost is attained. This thickness also depends on the thermal properties of the material and on the surrounding physiography, especially large, unfrozen bodies of water.¹¹ This explanation is no doubt true for much of the present global distribution of permafrost.

Another explanation of permafrost is that it is the last surviving remnant of the basal debris-filled layer of Pleistocene ice sheets. Hence, ablation of the high albedo firn or clean ice upper surface of an ice sheet during its retreat

stage eventually reaches the low albedo dirty ice basal layer of the ice sheet. Ablation of the dirty ice may rapidly form a blanket of ice-free till on the surface that is subjected to seasonal frost and becomes the active layer insulating the underlying debris-filled ice from further rapid ablation. The debris-filled ice therefore remains perennially frozen and becomes glacial permafrost. Glacial permafrost is generally unconsolidated when thawed, poorly sorted, supersaturated, contains a mixture of mineral and rock types, may have debris-rich and debris-poor layers tending to parallel bedrock at depth, includes some erratics, and may retain basal ice fabrics having strong preferred crystal orientations if creep is still occurring. Otherwise, a recrystallization ice fabric typical of the stagnant zone of retreating ice sheets may exist.²⁵ Present glacial permafrost distribution would be located in the region of permafrost that was covered by the Pleistocene glaciations. Fossil glacial permafrost would be located in the area between this region and the maximum limit of Pleistocene glaciation and will have the characteristics of basal till.

THE EFFECTIVE BED OF A SLIDING GLACIER OR ICE SHEET

Erosion and deposition by Pleistocene glaciers and ice sheets strongly suggest that these were largely wet-base ice masses since large-scale erosion and deposition seem to require a sliding bed where freeze-thaw processes can occur.²⁶ A glacier or ice sheet may cover regolith in some places and bedrock in others. Somewhere the melting point isotherm defines a thawed bed. Where is the melting point isotherm and when does it define the sliding interface that is the effective bed of the glacier or ice sheet? The answers to the questions depend on the physical and mechanical properties of the regolith permafrost.

Sliding of a glacier or ice sheet forming over either frozen or unfrozen ground will now be discussed. Consider a permafrost region where freezing extends through the regolith into bedrock. Assume that climatic changes allow some of the winter snowcover to survive through the summer so that over the years a snowfield accumulates and eventually becomes compressed into ice at sufficient depth (about 80 m). As its thickness increases, the snow-ice field becomes a cold ice sheet—that is, an ice sheet whose mean an-

nual temperature is subfreezing throughout. Under these conditions two phenomena occur in the permafrost. First, the former active layer blanketing the permafrost freezes and becomes part of the regolith permafrost layer. Second, the melting point isotherm ascends and causes thinning of the bedrock permafrost layer. When the melting point isotherm intersects or passes the bedrock-regolith interface, basal sliding becomes possible, provided the top surface slope of the ice sheet is finite. If the bedrock-regolith boundary is the sliding interface, the sliding mass consists of an upper firn layer, a middle ice layer, and a lower regolith permafrost layer; if the ice-regolith boundary is the sliding interface, it consists of an upper firn layer and a lower ice layer. The second case is equivalent to an ice sheet forming over unfrozen ground. Sliding when the melting point isotherm lies at the regolith boundaries should bracket sliding when the isotherm lies within the regolith.

Sliding at the Bedrock-Regolith Interface

In this case, sliding begins when the ascending melting point isotherm reaches the bedrock-regolith interface. It will be shown that basal sliding occurs at this interface when the regolith consists of certain representative permafrost soils, provided that ice forms the matrix of the regolith permafrost that can then flow via creep at high stresses and melts under pressure gradients in the ice fraction.

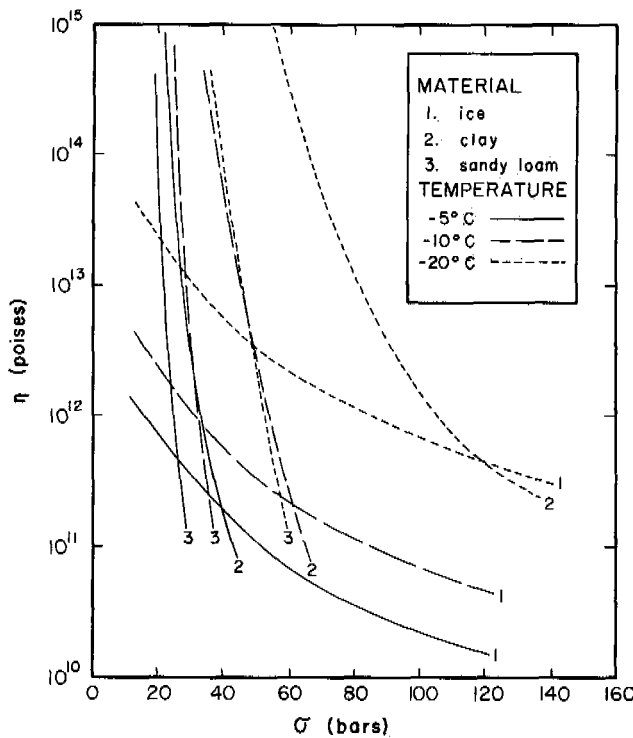


FIGURE 1 A comparison of the stress σ and temperature T variation of effective viscosity η for polycrystalline ice, clay permafrost, and sandy loam permafrost. The pertinent physical properties of these permafrost soils are presented in Tables I and II. (1 poise = 0.10 Pa·s.)

Creep tests on ice^{7,28} and permafrost soils²³ show that both these materials exhibit steady-state creep behavior below 0 °C, which can be described by the empirical equation:

$$\dot{\epsilon} = B \sigma^n, \tag{1}$$

where $\dot{\epsilon}$ is strain rate, σ is stress, n is a viscoplastic parameter, and B depends on temperature and material properties. Figure 1 shows σ versus η for ice and two representative permafrost soils, where $\eta = \sigma/\dot{\epsilon}$ is an effective viscosity that decreases with increasing stress. At stresses above 40 bars near 0 °C, these permafrost soils creep more readily than ice. The characteristics of these soils are given in Tables I and II. It seems likely that permafrost soils having a higher ice saturation would exhibit creep behavior intermediate between that of these soils and pure ice. Unfortunately, creep precisely at 0 °C is unknown.

The basal shear stress τ under an ice sheet is the product of ice density ρ , gravity acceleration g , ice thickness h , and ice sheet surface slope θ . Take x horizontal and positive downstream, y horizontal and normal to x , and z vertical and positive upward, with the coordinate origin at the central base of the ice sheet and velocities u , v , and w parallel to x , y , and z , respectively. When θ is averaged over distances $x \cong 20h$, and h changes slowly along x , Nye¹⁵ shows that,

$$\tau \cong \rho g h \tan \theta, \tag{2}$$

where h decreases as θ increases such that $\tau \cong 1$ bar.

For a dry-base ice sheet, τ is distributed rather uniformly over the bed. Figure 1 shows that ice creeps more easily than these particular permafrost soils under stress τ ; therefore, the bed of a dry-base ice sheet overlying these permafrost soils overlying bedrock will be the ice-permafrost interface.

For a wet-base ice sheet, τ cannot be transmitted across the basal water layer since water cannot support a shear stress, and basal sliding occurs. Weertman²⁴ has shown that basal sliding of ice sheets proceeds via two mechanisms—stress concentration and regelation. Stress concentration occurs because the shear stress τ is transmitted to the bed via obstacles that project upward from the bed into the ice. The ice sheet exerts a compressive stress σ on the upstream side of these obstacles and, provided cavities do not form behind obstacles, an equal tensile stress on the downstream side. This uniaxial stress is

$$\sigma = r^2 \tau, \tag{3}$$

where r is a bed roughness parameter. If L' is the average distance between obstacles and L is the average dimension

TABLE I Physical Properties of the Saturated Callovian Sandy Loam Permafrost Deformed via Creep²³

Property	Gradation (mm)	Amount (%)
Classification (%)		
sandy	0.25-0.05	70-90
silty	0.05-0.005	10-60
clayey	<0.005	2-15
Water content (%)		
maximum molecular		7.5-19.3
total		37-57
Unfrozen dry-weight water content (%)		
-0.50 °C		3.60
-1.15 °C		1.17
-3.0 °C		0.52
-5.0 °C		0
Atterberg limit (%)		
liquid limit		25.2 -36.1
plastic limit		21.4 -29.8
plasticity index		3.83- 7.23
Porosity (%)		39-44
Coefficient of permeability (m/day)		0.1-1.0
Unit weight at natural moisture content (g/cm ³)		1.2-2.1
Grain-specific gravity (g/cm ³)		2.7
Soil particle specific heat (cal/g·°C)		0.17

TABLE II Physical Properties of the Saturated Bat-Baioss Clay Permafrost Deformed via Creep²³

Property	Gradation (mm)	Amount (%)
Classification (%)		
sandy	0.25-0.05	20-25
silty	0.05-0.005	50-55
clayey	<0.005	24-75
Water content (%)		
maximum molecular		15.0-20.8
total		20-24
Unfrozen dry-weight water content (%)		
-0.60 °C		16.70
-1.05 °C		13.75
-3.00 °C		7.21
-4.35 °C		5.70
-10.10 °C		3.30
-21.2 °C		2.44
Atterberg limits (%)		
liquid limit		46.2-55.9
plastic limit		20.5-26.3
plasticity index		24.3-30.3
Porosity (%)		30-45
Coefficient of permeability (m/day)		4-6 × 10 ⁻⁵
Unit weight at natural moisture content (g/cm ³)		2.06-2.15
Grain-specific gravity (g/cm ³)		2.6 -3.2
Soil particle specific heat (cal/g·°C)		0.18

of an obstacle, then

$$r = L'/L = L'/(L_x L_y L_z)^{1/3}, \quad (4)$$

where L_x , L_y , and L_z are average obstacle lengths in directions x , y , and z , respectively. If extrapolating the Figure 1 trends to 0°C is justified, Eq. (3) requires that these permafrost soils flow more easily than ice under stress σ when $r \geq 7$ and, therefore, that the bed of a wet-base ice sheet overlying these permafrost soils overlying bedrock will be the permafrost-bedrock interface if $r \geq 7$. Weertman²⁴ argues that r is independent of obstacle size.

The expected range of r can be obtained by a further consideration of Weertman's glacier sliding theory. The stress concentration mechanism produces a basal sliding velocity u_σ in terms of B and n in Eq. (1):

$$u_\sigma \cong B r^{2n} L_x (\tau L_x / \beta L)^n, \quad (5)$$

where L_x/L is constant and $\beta = 1$ if cavities form behind obstacles and $\beta = 2$ if not. The regelation mechanism allows basal sliding because water flows around obstacles due to melting on their high-pressure upstream side and freezing on their low-pressure downstream side (increasing pressure decreases the freezing point of water). The regelation mechanism produces a basal sliding velocity u_r given by

$$u_r \cong C K r^2 \tau / \rho Q L, \quad (6)$$

where K is the thermal conductivity of the obstacle, Q is the heat of fusion of ice, and $C = \Delta T / \Delta P = 7.4 \times 10^{-3} \text{ }^\circ\text{C}/\text{bar}$ is a constant expressing the ice melting point temperature change ΔT due to a pressure change ΔP . The total basal sliding velocity occurring at $z = 0$ is

$$u_0 = u_\sigma + u_r. \quad (7)$$

From inspection of Eq. (5) and (6), it is clear that u_σ increases as obstacle size increases, whereas u_r increases as obstacle size decreases. The controlling obstacle size is $L = \Lambda$ and occurs when $u_\sigma = u_r$ so that u_0 is a maximum. Figure 2 relates u_0 , r , and Λ for these conditions. Numerous measurements confirm that $u_0 > 10 \text{ m yr}^{-1}$ is common for most wet-base glaciers, and therefore $r > 10$ is also common. Hence, r is sufficiently large to suspect that basal sliding of an ice sheet overlying certain regolith permafrost soils will occur at the bedrock-regolith interface when the melting point isotherm coincides with that interface.

The above analysis indicates that when basal sliding occurs at the bedrock-regolith interface, the regolith permafrost becomes incorporated en masse into the glacier or ice sheet. If this is a melting interface, the regolith permafrost will be eroded from below, and the eroded material will be washed toward the edge of the glacier or ice sheet. If this

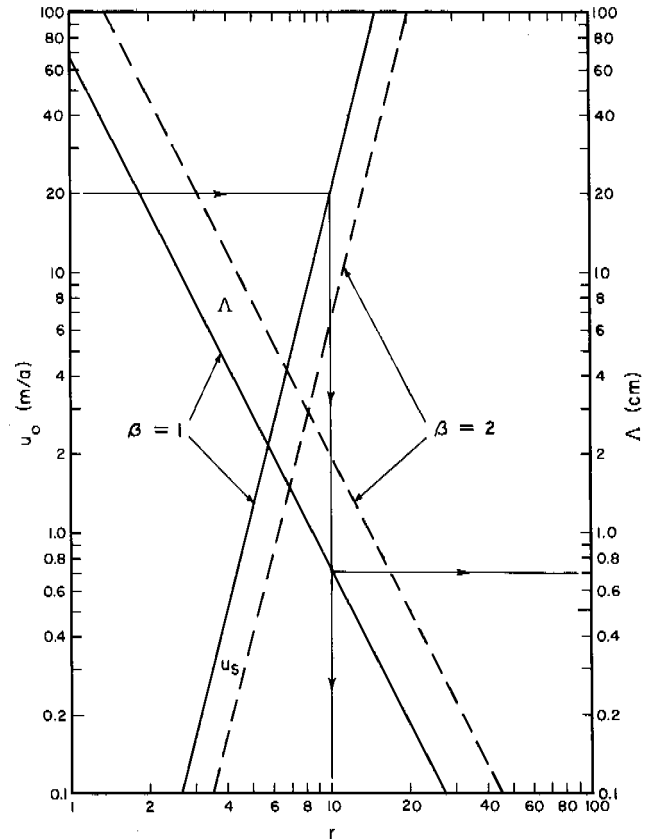


FIGURE 2 The relation of basal sliding velocity u_σ for a wet-base ice sheet to the bed roughness r and the controlling obstacle size Λ . The solid and dashed lines define the extreme range of u_σ and Λ ; the solid lines apply when cavities form on the lee side of obstacles, and the dashed lines apply when no cavities form. The arrows show how r and Λ are found for a given u_σ . For example, when $u_\sigma = 20 \text{ m yr}^{-1}$ and cavities form, $r = 10$ and $\Lambda = 0.7 \text{ cm}$. This figure is from Weertman²⁴ and is for $\tau = 1 \text{ bar}$, $\beta = 0.017 \text{ bar}^{-n} \text{ yr}^{-1}$, and $n = 3$.

is a freezing interface, the bedrock will be eroded from above, and the eroded material will be frozen onto the base of the regolith permafrost layer.

Sliding at the Ice-Regolith Interface

In this case, sliding begins when the ascending melting point isotherm reaches the ice-regolith interface. Basal sliding occurs at this interface when the regolith permafrost resists creep-regelation flow more successfully than does ice. This may be the case when ice no longer forms the regolith permafrost matrix, so that creep and regelation in the ice fraction cannot cause bulk flow of the regolith permafrost.

Basal melting under an ice sheet begins when $T_z = T_M$ at $z = 0$, where T_M is the melting point at hydrostatic pressure P . For a sliding ice sheet,

$$T_M = T_0 - P (\Delta T / \Delta P) = T_0 - \rho g h'' C, \quad (8)$$

where $T_0 = 273$ K at $P = 1$ bar, and ρ is the density averaged through thickness $z = h''$ above the bed of sliding at $z = 0$. The effective ice sheet thickness is $h'' = h$ when sliding occurs at the ice-regolith interface, and $h'' = h + d$ when sliding occurs at the bedrock-regolith interface, where d is the regolith thickness.

The ice thickness necessary to permit basal melting at the ice-regolith interface near the center of an ice sheet is given by Eq. 9¹⁸:

$$T_H - T_z = (F_G/K)(2H\alpha/w_t)^{1/2} \operatorname{erf}[(w_t/2H\alpha)^{1/2} z] \frac{H}{z}, \quad (9)$$

where

$$\operatorname{erf}(\lambda) \frac{H}{z} = \int_z^H \exp(\lambda^2) d\lambda$$

is a tabulated function

$$\left\{ \lambda = [(w_t/2H\alpha)^{1/2} z] \frac{H}{z} \right\},$$

H is the maximum ice sheet thickness, $F_G = 1.2 \times 10^{-6}$ cal/cm² s is the geothermal heat flux, $K = 5.3 \times 10^{-3}$ cal/cm s °C is the thermal conductivity, $\alpha = 1.2 \times 10^{-2}$ cm²/s is the thermal diffusivity, w_t is the top surface snow accumulation rate in ice equivalent, and the respective temperatures at H and z are T_H and T_z . The values of F_G , K , and α are typical for ice, permafrost, and bedrock.

Equations (8) and (9) can be combined to give the minimum ice thickness needed to raise the melting point isotherm to the ice-regolith interface at the center of the ice sheet. When this occurs, basal sliding becomes possible over the large central region of the ice sheet where a temperate basal ice zone exists.¹²

The viscoplastic properties of ice require that the top surface profile of an ice sheet be approximately elliptical.^{8,9,15} Therefore, if x' is the horizontal distance from the ice sheet center to its edge at $x' = X'$, and h' is the vertical distance from the x' axis to the ice sheet top surface, with $h' = H'$ at its center,

$$(h'/H')^\alpha + (x'/X')^\beta = 1, \quad (10)$$

where $\alpha = 2(n+1)/n$ and $\beta = (n+1)/n$ for a dry base,^{8,9} and $\alpha = 2(n+2)/(n+1)$ and $\beta = (n+3)/(n+1)$ for a wet base.¹⁵ These two profiles are comparable since $n = 3$ is commonly observed for polycrystalline ice.²⁸ The profiles were derived for a horizontal bed; but as the ice sheet grows, its weight will eventually depress the earth's crust to a depth equal to about one-third the ice thickness since the density of ice is about one-third the density of rock. Hence, if h is the actual ice thickness at x' , then $h' \leq h \leq 3h'/2$ (Figure 3).

Figure 3 is adapted from models developed by Weertman^{25,26} to treat the dynamics of continental ice sheets. The ice sheet slides over a wet bed that can be either an ice-bedrock interface or an ice-regolith interface. In the

latter case, Weertman²⁶ shows that the permeable regolith must be several hundred metres thick before basal melt-water would "short-circuit" through the regolith in amounts sufficient to suppress sliding at the ice-regolith interface, thereby preventing his freeze-thaw mechanism from eroding the regolith. By implication, then, the sliding and eroding bed might move down to the bedrock-regolith interface, although Weertman does not pursue this point.

The wet base of the ice sheet is a melting surface toward the center and a freezing surface toward the margin.²⁶ Water in the central zone of basal melting forms a thin sheet along the bed and flows outward toward the ice sheet margin due to the decrease of hydrostatic pressure, $P = \rho g h$, as x increases.²⁷ Hence, basal erosion occurs in the melting zone and the eroded debris is washed into the freezing zone where it is incorporated into the ice sheet, provided melt-water does not percolate through the underlying permeable regolith and drain away at the edge of the ice sheet. Weertman²⁶ has considered this problem and concludes that sheet flow in a basal water layer of thickness δ is more important than percolation flow in a regolith layer of thickness d when $d < \delta^3/12k$, where k is the regolith permeability. For a typical oil sand, $k \cong 10^{-7}$ cm² so that, if $\delta = 0.4$ cm, then $d > 0.5$ km before basal water flow is short-circuited through oil sand regolith.

The freeze-thaw erosion mechanism proposed by Weertman²⁶ creates the regolith-charged basal ice layer shown in Figure 3b. The dirty ice ablation surface on the low latitude portion of the ice sheet is caused by basal debris being frozen into the ice sheet and carried to the ablating surface along the flowlines shown in Figure 3a. These flowlines were constructed using the Haefeli^{8,9} method modified by the basal freeze-thaw mechanism of Weertman.²⁶ The thickness of the debris-filled basal ice layer is:²⁴

$$z^* = h (w_b/w_t) [1 - (x^*/x')^{\bar{u}/u^*}], \quad (11)$$

where x' is horizontal distance measured from the ice sheet center, z is vertical distance above the bed, u and w are the respective x' and z components of ice velocity, x^* marks the beginning of the debris-filled basal ice layer, z^* marks the top of the debris-filled basal ice layer, $u = u^*$ at $z = z^*$, $w = w_b$ at $z = 0$, the average horizontal ice velocity is \bar{u} , and the average vertical ice velocity from a constant snow accumulation rate w_t is \bar{w} . Equation (11) assumes that the basal freezing rate is constant and much less than the ice equivalent of the snow accumulation rate. For an equilibrium ice sheet, therefore, $\bar{u} = w_t x'/h \cong 2\bar{w} x'/h$ since $w \cong \bar{w}_t/2$.

The above analysis indicates that, when basal sliding occurs at the ice-regolith interface, the thawed regolith permafrost becomes incorporated piecemeal into the glacier or ice sheet. If this is a melting interface, the regolith will be eroded from above, and the eroded material will be washed

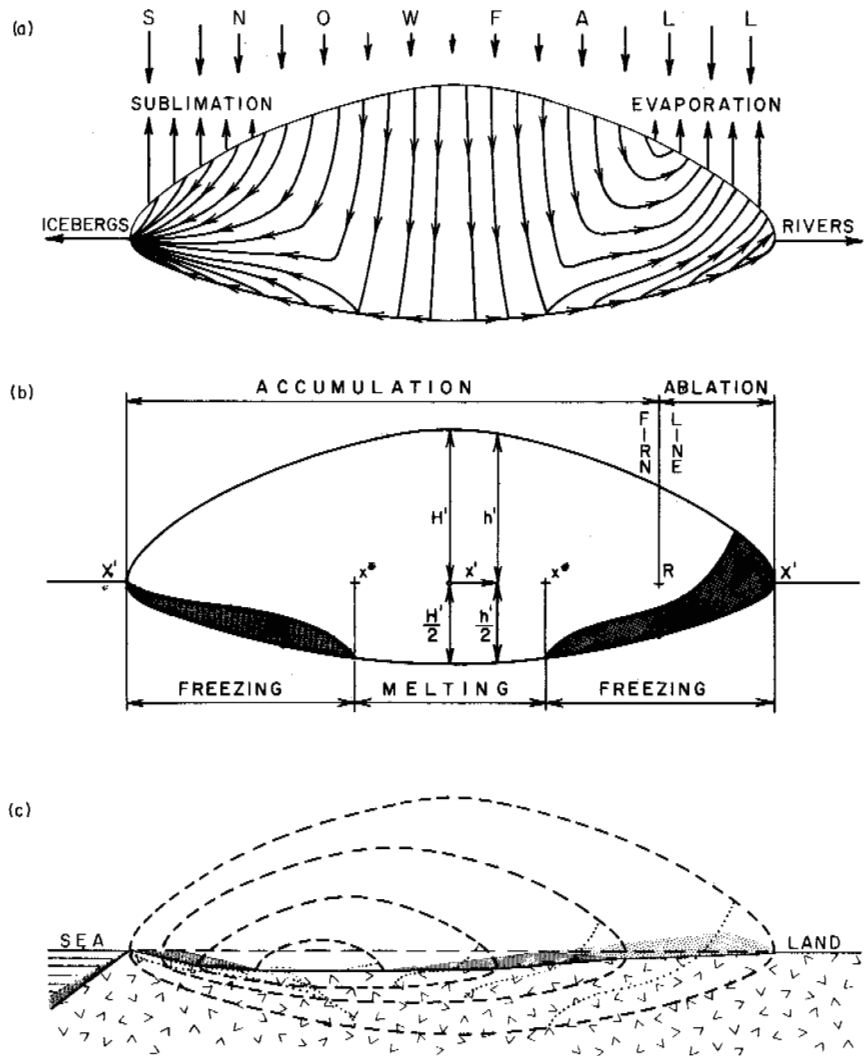


FIGURE 3 Flow, erosion, and retreat of a continental ice sheet of the ice age type. (a) The mass balance and internal flow of a steady-state ice sheet. (b) the steady-state basal dirty ice layer (shaded area) formed by the indicated mass balance pattern. (c) The basal till (dotted area) and glacial permafrost (shaded areas) derived from the basal dirty ice layer after ablation of the overlying clean ice. Basal till is thawed glacial permafrost

toward the edge of the glacier or ice sheet. If this is a freezing interface, the regolith also will be eroded from above, but the eroded material will be frozen onto the base of the ice layer. These processes occur regardless of the permeability of sufficiently thin regolith, because water from the basal melting zone tends to clog regolith pore spaces with eroded material, thereby decreasing the regolith permeability and increasing the tendency toward sheet flow of water at the base of the glacier or ice sheet.

DEPOSITION OF GLACIAL AND PREGACIAL PERMAFROST BY A RETREATING WET-BASE ICE SHEET

A fully developed, equilibrium continental ice sheet of the ice-age type occupies middle and upper latitudes. It requires 15 000–30 000 years to grow to maturity, but requires only 2 000–4 000 years to shrink to nothing.²⁵ The antarctic ice sheet moves at an average rate of about 50 m/year based on present snow accumulation rates and assuming

equilibrium.³ At such a velocity, a preglacial regolith permafrost layer incorporated en masse into the ice sheet could be transported between 750 and 1 500 km during the growth stage of an ice sheet. If basal erosion occurred at a rate of 1 cm/year, a preglacial regolith permafrost layer from 150 to 300 m thick could be eroded away during this time. Therefore, it seems likely that if any part of a preglacial regolith permafrost layer is to survive an ice age, its initial thickness must be several hundred metres.

In the basal freezing region under the ice sheet, erosion at the bedrock–regolith interface will cause a basal debris layer to grow on the bottom of the frozen preglacial regolith permafrost, and erosion at the ice–regolith interface will cause a basal debris layer to grow on the top of the thawed preglacial regolith permafrost. In both cases, this debris layer becomes glacial permafrost after degradation of the overlying ice during the shrinkage stage of the ice sheet. Hence, preglacial regolith permafrost can either cover or be covered by glacial permafrost. During the ice age, this preglacial regolith permafrost layer will have remained frozen

in the former case but will have thawed in the latter case. Whether this regolith material is permafrost after the ice age depends on subsequent climatic conditions.

Shrinkage of the steady-state ice sheet in Figure 3c begins when the firn line moves to higher altitudes.²⁵ Hence, the low latitude ablation zone moves to higher latitudes and vice versa if a high latitude ablation zone exists. The ice sheet will retreat to high elevations at high latitudes since ablation is most rapid at low elevations and latitudes. Figure 3 shows that the basal debris-filled layer gets progressively exposed to ablation as the firn line moves to higher latitudes. Initial ice ablation of this layer is rapid because debris-filled ice has a low albedo. Consequently, a thickening layer of ice-free debris would blanket the remaining debris-filled ice layer, insulating it against further rapid ice ablation. Protected in this way, the underlying debris-filled ice might persist for some time, although solar and geothermal heat could still be conducted to its respective top and bottom surfaces. The debris-filled ice layer remains in the permafrost state here defined as glacial permafrost.

Does the above scenario really occur? It should, in those cases where thick preglacial regolith permafrost is incorporated en masse into the ice sheet and retains sufficient thickness through the ice age so that, when it reaches the ablation surface, it becomes a relatively thick, stable blanket insulating the underlying glacial permafrost. Evidence favoring some such large-scale block intrusion mechanism is fairly widespread in the deposition zone of the Laurentide ice sheet.¹⁴

Preservation of glacial permafrost unprotected by a preglacial regolith permafrost blanket is unlikely on topographic highs because the ice fraction in glacial permafrost is often excessive. Hence, thawing will be accompanied by rapid water erosion. The eroded debris, however, will tend to be deposited in topographic lows and can form an insulating blanket over glacial permafrost in these regions. This blanket would then be similar to the thawed preglacial permafrost blanket described earlier.

The higher latitude portion of the basal debris-filled layer of the former ice sheet lies mostly on the polar side of the mean annual 0 °C isotherm and is therefore stable, with the freezing front perhaps even penetrating the bedrock underlying the debris-filled ice. The debris layer blanketing the top surface will be subjected to seasonal frost cycles and will gradually support life and be converted into soil. It will increasingly resemble the active layer overlying permafrost, where the permafrost would be the unmelted part of the former ice sheet.

The lower latitude portion of the basal debris-filled layer of the former ice sheet lies mostly on the equatorial side of the mean annual 0 °C isotherm and will eventually thaw completely to remain only as till deposits. These till deposits, however, may retain some evidence of their former permafrost stage, such as fossil ice wedges and relic seasonal frost patterns. The deposits also provide the best evidence

to date that preglacial regolith permafrost can be incorporated en masse into an ice sheet and can later be deposited relatively intact to provide a blanket insulating glacial permafrost.¹⁴

A remnant of the debris-filled basal ice layer is most likely to survive from one glaciation to the next if the interglacial period is short, cool, and dry. The ice sheet would then waste away from lack of nourishment rather than by melting. Ablation would be largely via sublimation, so the debris could have an opportunity to accumulate on the surface until a thickness sufficient to support a tundra ecosystem was deposited. This vegetation cover anchored to the debris layer would then help keep it from eroding should the climate warm enough to allow meltwater runoff during summers. These conditions exist today near the Arctic Circle, so glacial permafrost is most likely in that region.

HEAT FLOW THROUGH ICE SHEETS AND THE DISTRIBUTION OF GLACIAL PERMAFROST

Equation 10 and Figure 3 apply to a steady-state ice sheet. Heat conduction through steady-state ice sheets has been treated theoretically.^{3,17} These treatments can be applied to the hypothesis that glacial permafrost evolves from the basal debris-filled layer of a thinning Pleistocene ice sheet that may reach a new steady-state condition when only this layer remains. The treatments consider the effects on heat flow of surface cooling via snow accumulation and climatic cooling, surface warming via ice sheet thinning and climatic warming, basal heating via sliding friction and the geothermal flux, internal heating due to deformational friction, and internal cooling due to advection.

Figure 4 shows the expected zones of dry frozen bed, wet melting bed, and wet freezing bed that the steady-state heat flow analysis predicts for the maximum Pleistocene glaciations of North America and Antarctica, the most recent glaciation of North America, and the present glaciation of Antarctica. The ice flowline patterns are based mainly on glacially striated and grooved surfaces for Figure 4a,⁶ these plus dated ice sheet retreat contours for Figure 4b,² ancient glacial grooves and present ice flowlines for Figure 4c,⁴ and present ice sheet elevation contours for Figure 4d.³ The basic similarity of these two ice sheets is evident.

Observations after an ice sheet disappears should reveal little glacial erosion and deposition on the former dry frozen bed, much erosion and little deposition on the former wet melting bed, and much erosion and much deposition on the former wet freezing bed. These observations seem to hold for the Pleistocene ice sheet of North America since the erosion pattern deduced by White²⁹ approximately coincides with the frozen, melting, and freezing zones in Figure 4. The undisturbed zone of preglacial regolith permafrost overlying deep bedrock permafrost should roughly match the dry frozen bed portion of the steady-state ice sheet. The erosion zone of preglacial regolith permafrost

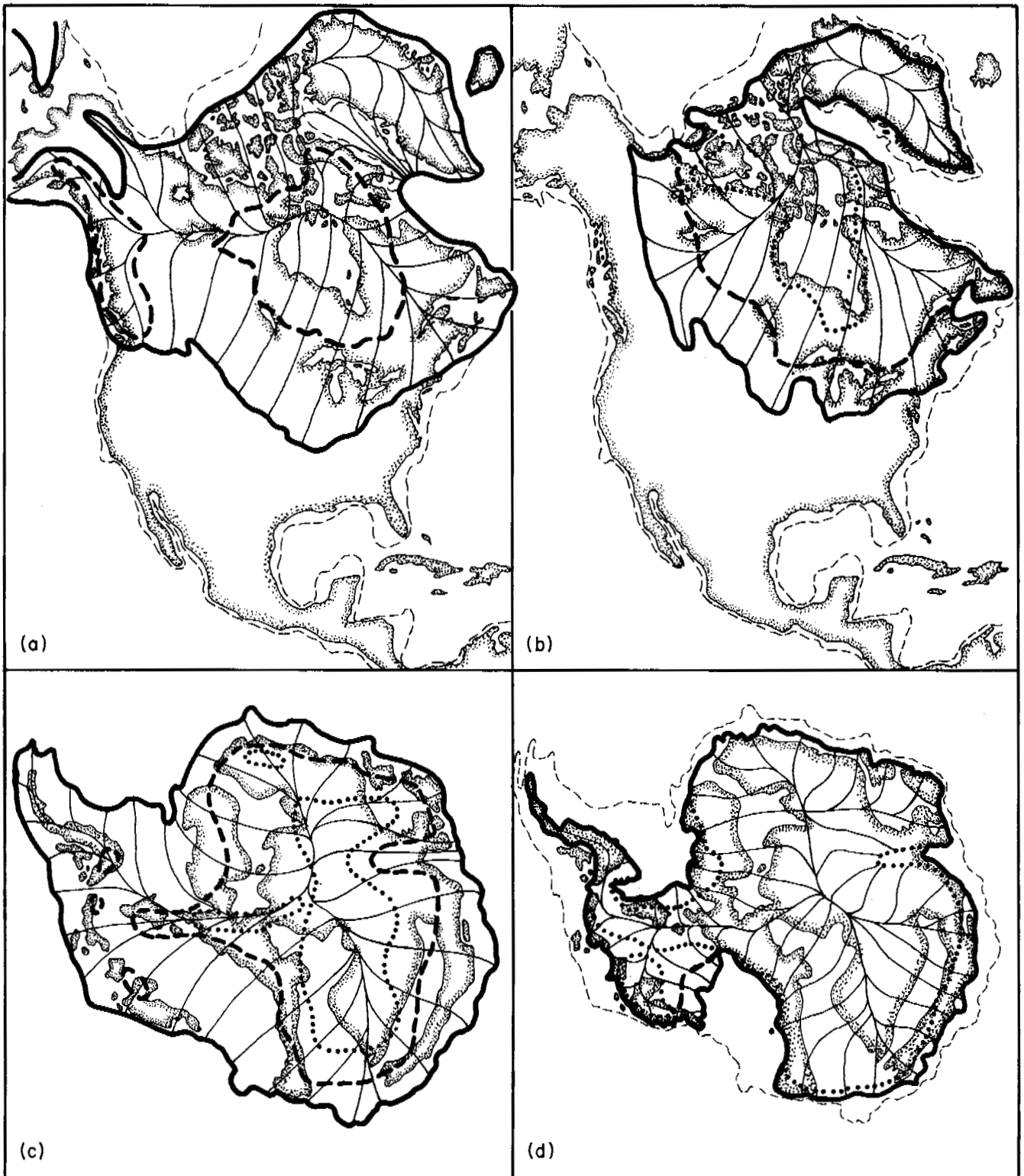


FIGURE 4 A comparison of heat flow at the base of the Laurentide and Antarctic ice sheets. For the flowlines and ice sheet dimensions shown, a dry frozen bed exists inside the dotted contour line, a wet melting bed exists between the dotted and dashed contours, and a wet freezing bed exists between the dashed and solid contours. (a) Maximum Pleistocene extent of the Laurentide ice sheet. (b) Most recent extent (late Wisconsinan) of the Laurentide ice sheet. (c) Maximum Pleistocene extent of the Antarctic ice sheet. (d) Present extent of the Antarctic ice sheet. Shaded borders are present shorelines, and thin dashed lines are continental shelves. There is no inherent difference between the behaviors of the Laurentide and Antarctic ice sheets.

that was reduced and transported toward the edge of the ice sheet should roughly match the wet melting bed portion of the growing ice sheet. The deposition zone of preglacial regolith permafrost that was reduced and transported toward the edge of the ice sheet should roughly match the wet freezing bed portion of the shrinking ice sheet. All these zones partly overlap during the growing and shrinking stages, so their boundaries for the steady-state phase shown in Figure 3 is a good compromise.

Glacial permafrost is derived from material that was eroded either from preglacial regolith permafrost or from bedrock and, subsequently, became part of the debris-filled

basal layer of the ice sheet. Thawing, reworking, and transport have been part of this process. Consequently, the thickness of glacial permafrost increases away from the frozen bed zone of the former ice sheet, except toward low latitudes where postglacial thawing has progressively reduced the original glacial permafrost thickness.

SUMMARY

The past and present distribution of glacial permafrost, as defined in this paper, is shown in Figure 5. It must be emphasized at once that widespread glacial permafrost is not

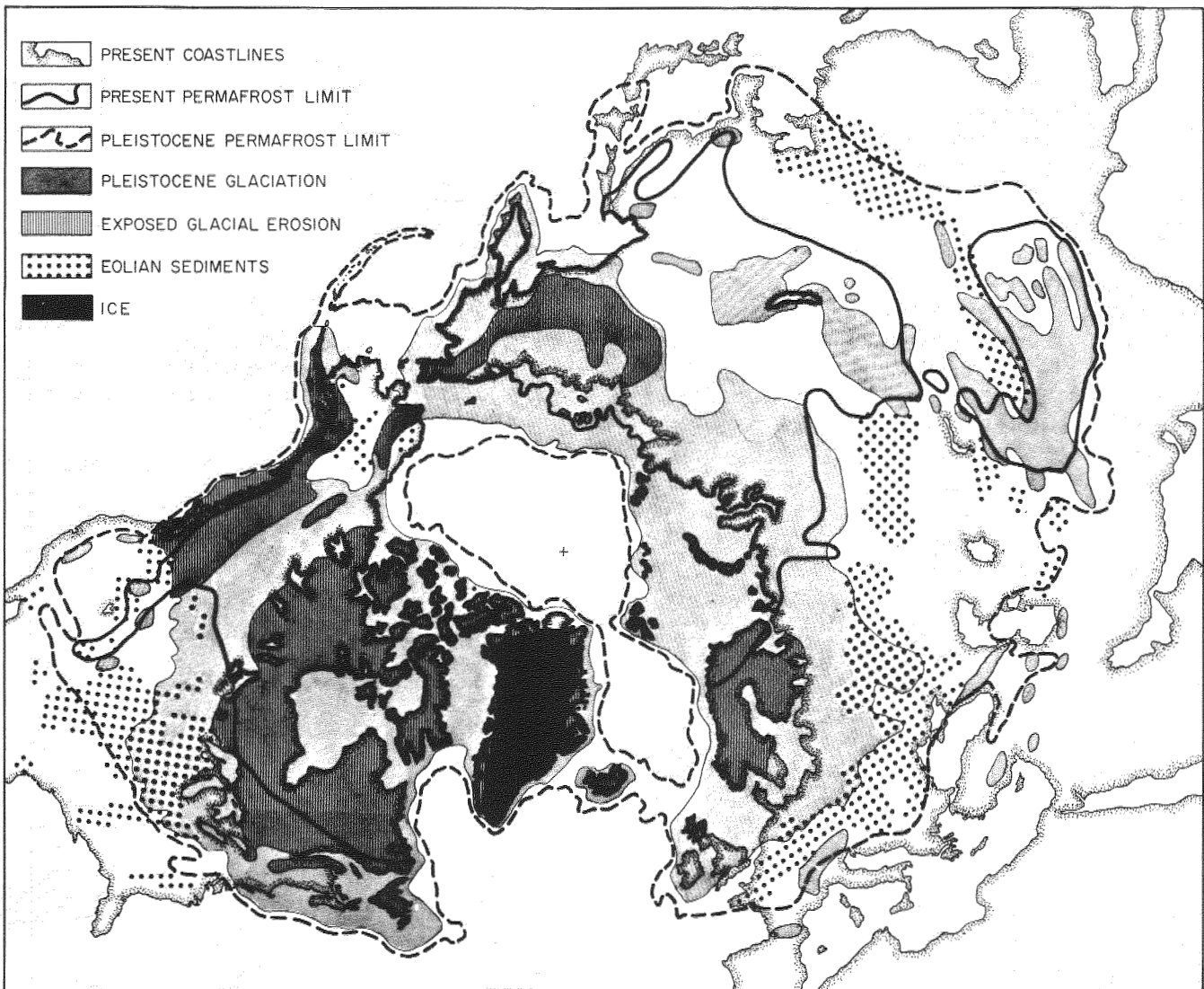


FIGURE 5 The expected region of past and present thick glacial permafrost deduced from (1) the maximum extent of known Pleistocene glaciation,^{19,22} (2) the maximum extent of known exposed Pleistocene glacial erosion surfaces,⁵ (3) the maximum extent of known Pleistocene glacial eolian sediments,⁶ (4) the probable maximum extent of Pleistocene permafrost,^{16,21} and (5) the probable maximum extent of present permafrost.¹ Present glacial permafrost is expected inside area (1) and the area bounded by (5), with the thickest deposits outside area (2). Past glacial permafrost is expected inside area (4), with the thickest deposits between areas (2) and (3). The area within the solid line (5) includes the discontinuous and continuous permafrost zones.

yet demonstrated; therefore, Figure 5 shows the area where glacial permafrost is predicted rather than established. The thickest and best developed areas of present glacial permafrost are most probably located between the exposed glacial erosion surfaces and the permafrost limit, especially the continuous permafrost limit. Such areas are regions of thick glacial deposition in the vicinity of the Arctic Circle. The Mackenzie River delta is one site satisfying these conditions, and relic Pleistocene permafrost having the expected characteristics of glacial permafrost has been found there.¹³

Glacial permafrost will preserve its similarity to the debris-filled basal layer of an ice sheet longer at depth than near the surface. Interaction with the active layer will result in ice wedging, frost heaving, patterned ground, and other surface or near-surface phenomena that obliterate most evidence relating permafrost to debris-filled glacial ice. At depth, however, many characteristics of the basal layer of a freezing wet-base ice sheet should be preserved. Icy permafrost layers should parallel the bedding, erratics should be more numerous, and any fabrics of preferred orientations for rock pebbles and ice crystals should conform to the flow direction of the former ice sheet.

Glacial permafrost might also be buried under a layer of preglacial regolith permafrost that was transported en masse but not completely eroded during the glaciation cycle.

Glacial permafrost might cover preglacial regolith permafrost or bedrock permafrost that was thawed during the glaciation cycle and, subsequently, has been refrozen. Furthermore, the lower part of a permafrost layer may be glacial permafrost that was later covered by wind- or water-borne sediments that became nonglacial permafrost. Hence, an early heretofore unexpected major Pleistocene glaciation could be detected and mapped by classifying permafrost into glacial and nonglacial varieties.

Finally, a remnant of the debris-filled basal ice layer of a Pleistocene ice sheet might survive a cool, short, dry interglacial period in the glacial permafrost state provided slow ablation via sublimation leaves an active layer thick enough to support a tundra ecosystem. These conditions prevail near the Arctic Circle. Survival prospects are greatly enhanced if preglacial regolith permafrost can be incorporated en masse into the ice sheet and is thick enough to provide an insulating blanket covering the underlying debris-filled basal ice after the overlying ice ablates. However, this requires sliding at a wet thawed bedrock-frozen regolith interface. Creep at 0 °C for ice and representative frozen regolith materials must be studied in detail before this question is answered.

REFERENCES

1. Black, R. F. 1954. Permafrost—A review. *Geol. Soc. Am. Bull.* 65:839-856.
2. Bryson, R. A., W. M. Wendland, J. D. Ives, and J. T. Andrews. 1969. Radiocarbon isochrones on the disintegration of the Laurentide ice sheet. *Arctic Alpine Res.* 1(1):1-14.
3. Budd, W., D. Jenssen, and U. Radok. 1969. The extent of basal melting in Antarctica. *Polarforschung* 6(1):293-306.
4. Cameron, R. L., and R. P. Goldthwait. 1960. The US-IGY contribution to Antarctic glaciology. *Int. Assoc. Sci. Hydrol. Publ. No. 55*, p. 7-13.
5. *Encyclopaedia Britannica World Atlas*. 1954. Geologic age and Glaciation. Plate 19. *Encyclopaedia Britannica, Inc.*, Chicago.
6. Flint, R. F. 1971. *Glacial and Quaternary geology*. Wiley, New York.
7. Glen, J. W. 1955. The creep of polycrystalline ice. *Proc. Roy. Soc. Ser. A.* 228:519-538.
8. Haefeli, R. 1961. Contribution to the movement and the form of ice sheets in the Arctic and Antarctic. *J. Glaciol.* 3:1133-1150.
9. Haefeli, R. 1963. A numerical and experimental method for determining ice motion in the central parts of ice sheets. *Int. Assoc. Sci. Hydrol. Publ. No. 61*, p. 253-260.
10. Lachenbruch, A. H. 1968. Permafrost, p. 833-839. *In* The encyclopedia of geomorphology. Reinhold, New York.
11. Lachenbruch, A. H., M. C. Brewer, G. W. Greene and B. V. Marshall. 1962. Temperatures in permafrost, p. 791-803. *Temperature—Its measurements and control in science and industry*. Vol. 3, Pt. 1. Reinhold, New York.
12. Lliboutry, L. 1966. Bottom temperatures and basal low velocity layer in an ice sheet. *J. Geophys. Res.* 71:2535-2543.
13. MacKay, J. R., V. N. Rampton, and J. G. Fyles. 1972. Relic Pleistocene permafrost, western Arctic, Canada. *Science* 176:1321-1323.
14. Moran, S. R. 1971. Glaciotectionic structures in drift, p. 127-148. *In* R. P. Goldthwait [ed.] *Till: A symposium*. Ohio State University Press, Columbus.
15. Nye, J. F. 1969. The motion of ice sheets and glaciers. *J. Glaciol.* 3:493-507.
16. Pierre Gourou atlas classique. 1956. *Le Nord du Globe*. Librairie Hachette, Paris. p. 2-3.
17. Radok, U., D. Jenssen, and W. Budd. 1970. Steady state temperature profiles in ice sheets. *Int. Assoc. Sci. Hydrol. Publ. No. 86*, p. 151-165.
18. Robin, G. deQ. 1955. Ice movement and temperature distribution in glaciers and ice sheets. *J. Glaciol.* 2:523-532.
19. Schytt, V., G. Hoppe, W. Blake, and M. G. Grosswald. 1968. The extent of the Würm glaciation in the European Arctic. *Int. Assoc. Sci. Hydrol. Publ. No. 79*, p. 207-216.
20. Stearns, S. R. 1966. Permafrost. Pt. 1, Sect. A2. U.S. Army Cold Regions Research and Engineering Laboratory, Hanover, New Hampshire.
21. Time-Life. 1961. The ice age, p. 14-15. *In* The epic of man. Time Inc., New York.
22. *The Odyssey World Atlas*. 1966. Maximum extent of Pleistocene glaciation. Odyssey Books, New York. p. 13.
23. Vialov, S. S., V. G. Gmshinskii, S. E. Gorodetskii, V. G. Grigorieva, Iu. K. Zaretskii, N. K. Pekarskaia, and E. P. Susharina. 1962. The strength and creep of frozen soils and calculations for ice-soil retaining structures. *Izdatel'stvo Akademii Nauk SSSR, Moscow*. (U.S. Army Cold Regions Research and Engineering Laboratory Translation 76)
24. Weertman, J. 1964. The theory of glacier sliding. *J. Glaciol.* 5:287-303.

25. Weertman, J. 1964. Rate of growth or shrinkage of nonequilibrium ice sheets. *J. Glaciol.* 5:145-158.
26. Weertman, J. 1966. Effect of a basal water layer on the dimensions of ice sheets. *J. Glaciol.* 6:191-207.
27. Weertman, J. 1972. General theory of water flow at the base of a glacier or ice sheet. *Rev. Geophys. Space Sci.* 10:287-333.
28. Weertman, J. 1972. Creep of ice. *In International symposium on the physics and chemistry of ice, conference proceedings.* 14-18 August 1972, Ottawa, Canada. (In press)
29. White, W. A. 1972. Deep erosion by continental ice sheets. *Geol. Soc. Am. Bull.* 83:1037-1056.

NOTES

[1] Contribution No. 240 of the Institute of Polar Studies.

PROBLEMS IN THE ORIGIN OF MASSIVE ICY BEDS, WESTERN ARCTIC, CANADA [1]

J. Ross Mackay

UNIVERSITY OF BRITISH COLUMBIA
Vancouver, British Columbia

INTRODUCTION

Massive icy beds are of widespread occurrence in the western Canadian Arctic. Natural exposures may be seen along steep coastal bluffs, river banks, lake shores, and on hill tops where disturbances have induced thawing. The prior existence of massive icy beds can also be inferred in old slump scars where the volume of debris below the headwall comprises only a fraction of the void: The missing material is ice, which was lost as water. In recent years, a vast amount of additional information on the distribution of massive ice has come from holes drilled for construction, pipeline route location, seismic, and other purposes.

At present, the most detailed information on massive icy bodies is from the Arctic Coastal Plain Province in Yukon Territory and Mackenzie District, from the Alaska-Yukon Territory boundary east for about 500 km to Cape Bathurst, N.W.T. The distribution of massive icy beds in the Canadian Arctic Archipelago is far less known, but considerable massive ice occurs on Banks Island, Prince Patrick Island, Mackenzie King Island, and Victoria Island. As exploratory drilling increases in the arctic islands, the distribution of massive ice in unconsolidated sediments and glacial deposits continues to be extended.

The massive icy beds show every conceivable gradation from icy muds to pure ice. As here defined, the massive icy beds have a minimum thickness of at least 2 m, a short diameter of at least 10 m, and an average ice content (ice to dry

soil on a weight basis) of at least 250 percent (Figure 1). More often, the ice content is upward of 500 percent. The purpose of this paper is to discuss some of the problems concerning the origin of massive icy beds in the western Canadian Arctic.

SIZE OF MASSIVE ICY BEDS

The massive icy beds vary greatly in thickness and horizontal extent. Typical slump exposures are shown in Figures 1, 2, and 3, where the average ice content exceeds 300 percent for the entire sections. The data for Figures 4, 5, and 6 have been extracted from about 15 000 shot hole logs, drilled by numerous seismic crews for different oil companies since 1960. All shot hole logs that encountered near-surface ice have been excluded because such ice would be that of ice wedges in most instances. The amount of ice that has been classified as massive ground ice is conservatively reported, because there is a common tendency among drilling crews to record only sand, silt, clay, and rock, even if ice is present.

Thickness

Figure 4 shows data on the thicknesses of 560 massive icy beds. The tops of most of the icy masses lie 10-20 m below the surface, but some have been encountered at depths of 45 m, which is at the lower limit of most drill holes. In addi-

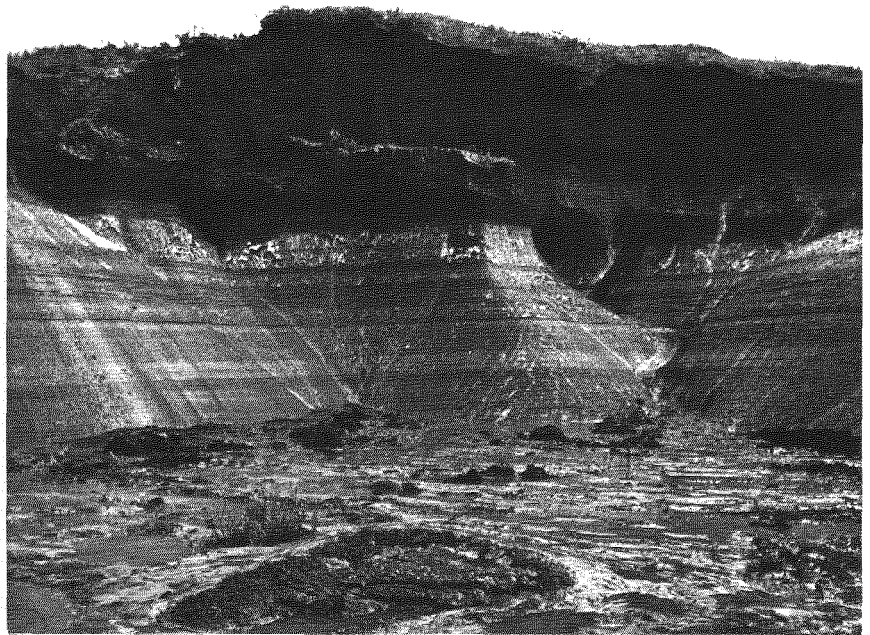


FIGURE 1 Slumping caused by the melting of massive segregated ice. The section is about 7 m high, Stanton, N.W.T.



FIGURE 2 Slump section, about 8 m high, showing two ice wedges and stony clay (glacial till), with massive ground ice at the bottom. This is part of the ice shown in Figures 3 and 5. Location, 25 km southeast of Tuktoyaktuk, N.W.T.

tion, about 90 drill holes, or 16 percent of the total, failed to bottom through the ice. Therefore, if all holes were extended, massive ice would be discovered at greater depths.

Horizontal Extent

The horizontal extent of massive icy beds ranges from a few tens of metres to over 2 km (Figure 5). Frequently, 5 or more consecutive drill holes, spaced about 200–300 m apart, will penetrate into massive ice. Some icy beds exceed 1 km² in surface area.

Materials above and below the Massive Icy Beds

The materials that lie directly above and below 640 massive icy beds, tabulated in Figure 6, are from drillers' logs. The materials have been grouped into stony clay, which is probably a till at most sites; clay, which is also usually a till; and sand and gravel. It is clear that glacial till (stony clay and clay) tends to overlie most icy beds, and sand and gravel underlie most. In view of the great range of sediments in the Western Arctic, the concentration of massive ice above sands and gravels would seem to be significant.

ORIGIN OF THE MASSIVE ICE

Syngenetic Ice Wedges

The structure and stratigraphy of the massive ice differs from that of ice wedges: The stratification is horizontal, not vertical. Uninterrupted sections have been followed



FIGURE 3 This massive icy body is a continuation of that shown in Figure 2, but about 1 km distant. Extensive drilling, as shown in Figure 5, indicates a massive ice depth exceeding 20 m. Location, 25 km southeast of Tuktoyaktuk, N.W.T.

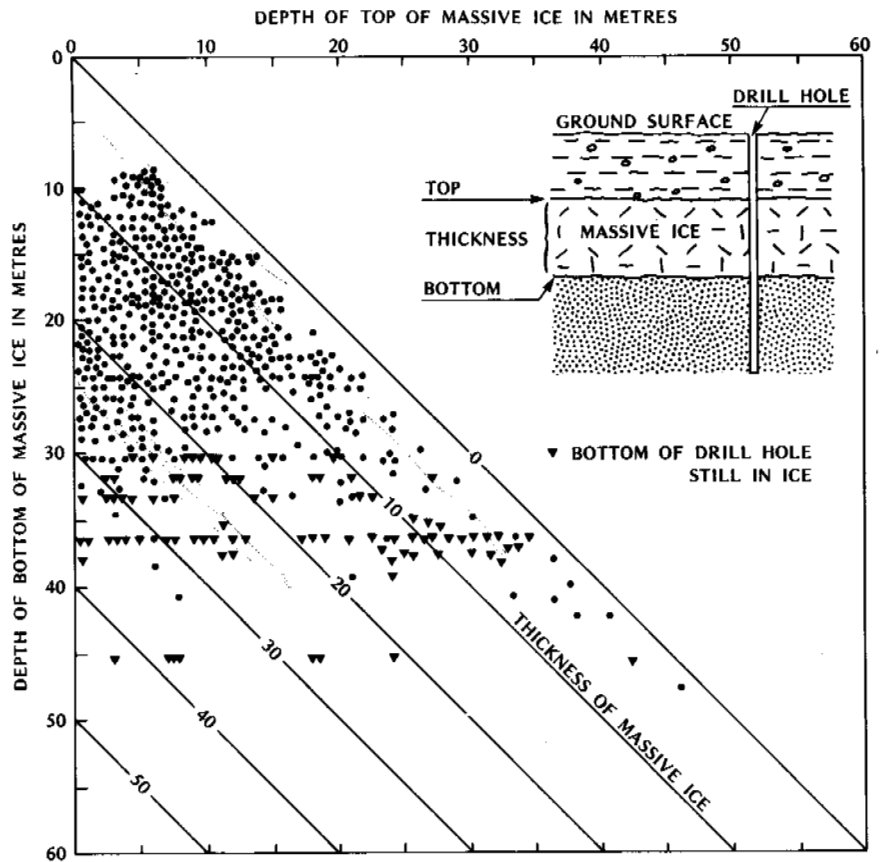


FIGURE 4 The data plotted in the graph have been obtained from shot hole logs over an extensive area in the western Canadian Arctic.

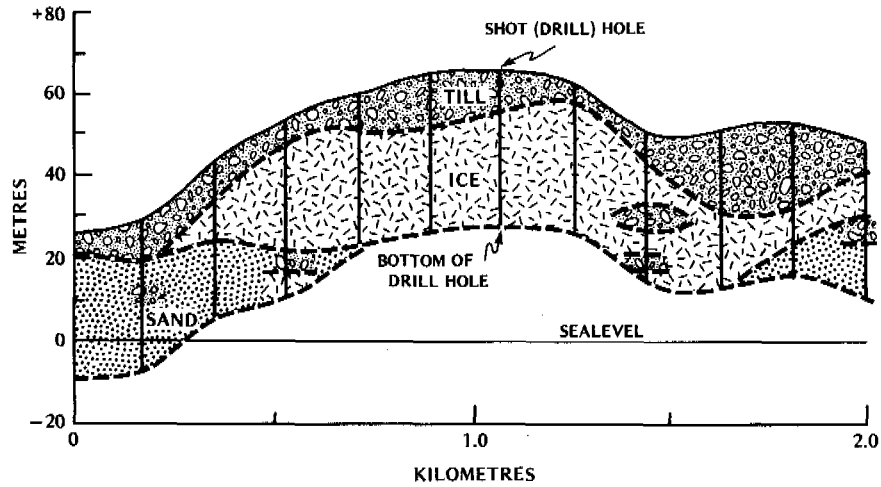


FIGURE 5 This cross section has been plotted from shot hole logs. Figures 2 and 3 show illustrations of the massive ice. Location, 25 km southeast of Tuktoyaktuk, N.W.T.

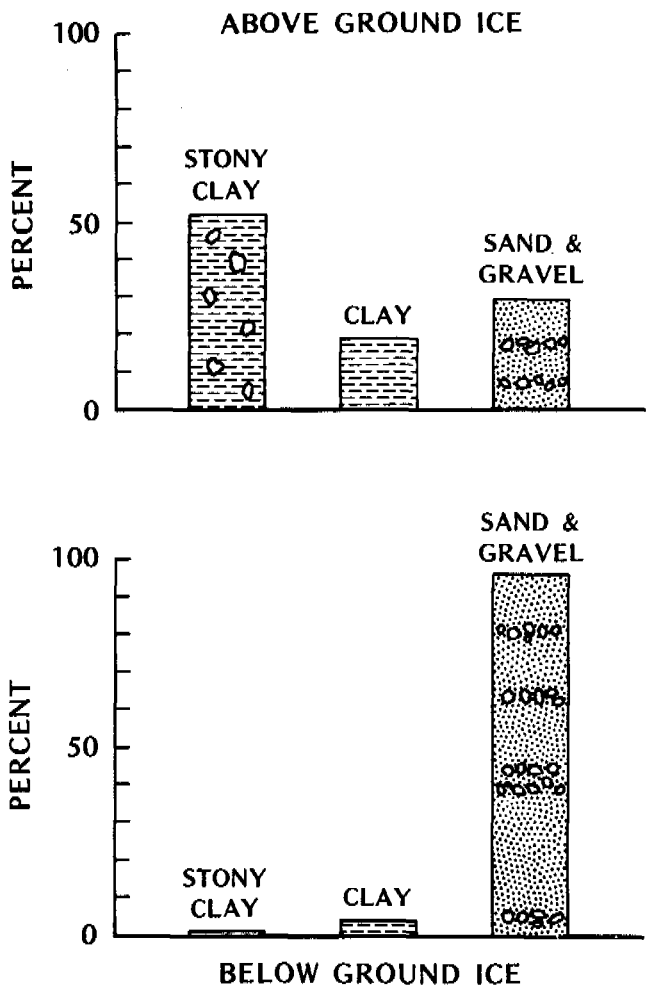


FIGURE 6 The material above and below the massive icy beds that have been completely penetrated by drill holes.

over a period of years for hundreds of metres without any evidence of vertical foliation. The massive ice may grade laterally, or interfinger, without break into glacial till, lake clays, sands, and gravels. The lower contacts can be planar or gradational; and, in a single vertical section, there may be several icy beds. The evidence overwhelmingly discredits an ice-wedge origin.

Buried Ice

Buried river, lake, and sea ice may be excluded because of the stratigraphic relationships of the massive ice and the preferred location beneath positive relief features, such as hills and plateaus. Any buried river, lake, or sea ice should occur in depressions and low sites where burial could preserve the ice.

In glaciated regions, buried ice may be expected, and has indeed been recognized in the high Arctic, a few kilometres beyond the terminus of existing glaciers. Ice-cored moraines are also well known from many glaciated areas, as are ice-disintegration features derived from the disintegration of a thin, stagnant, marginal part of a glacier. Thus some buried glacier ice could be present and go unrecognized, but the percentage is believed to be small, for several reasons:

1. Buried glacier ice should be closely associated with glaciofluvial and morainic deposits. However, the massive ice is found in a wide variety of deposits^{1,2,4,5,7,12,15}: in glacial till, typically over sands; in Pleistocene marine sediments, as at Herschel Island, N.W.T.^{3,13}; and beneath marine clays and within marine sands, both in the same section.¹⁴
2. The massive ice may be interlayered with other sediments, for example, a drill hole indicates from the surface down: gravel (0-7 m), massive ice (7-18 m), gravel (18-23 m),

massive ice (23–30 m), gravel (30–34 m), and massive ice (34–37 m, bottom of the drill hole); a stratigraphic sequence may show from the surface down: till, marine sand, massive ice, marine sand, marine clay, massive ice. Clearly, the depositional conditions are hostile to the burial of glacier ice and the subsequent thermal conditions inimical to its preservation.

3. The ice fabrics, structural minutiae, bubble patterns, etc., are atypical of glacier ice.⁹

4. Water-quality analyses of massive ice show markedly different characteristics from that of the Greenland Ice Sheet, Antarctica, and other glaciers. Ionic concentrations (Ca, Mg, Na, K, Cl) have been obtained from three drill holes 61 m deep through a hill with massive ice, similar to that in Figure 4, and from one drill hole 35 m deep on the adjacent flat. Samples were collected at 3-m intervals. The concentrations were much higher than those reported for glacier ice and the concentrations changed systematically with depth. When the ionic gradients (e.g., Ca and Mg) are plotted against depth, the trends are continuous through the till, ice, and into the underlying sands. Oxygen isotope ($H_2^{18}O:H_2^{16}O$) ratios obtained from the till (2 samples), massive ice (14 samples), and sand (1 sample) overlap and fall within a narrow range [–23.6 to –26.9 Standard Mean Ocean Water (SMOW)]. The ionic gradients and the data from the oxygen isotope ratios point to a homogeneous water source for the ice (water) in the till, massive ice, and underlying sand. The vertical ionic gradients are believed to reflect selective ionic rejection as permafrost aggraded, with the rate of rejection being a function of the freezing rate, which decreased with depth.

5. The massive ice is found in deposits of greatly differing age: in south central Banks Island, in a large area of pre-Wisconsinan glaciation¹¹; along the Yukon Coast, in glacially deformed sediments predating the late Wisconsin¹⁰; in Prince Albert Peninsula, Victoria Island, beneath late-Wisconsinan deposits; and in the Mackenzie Valley in post-glacial lacustrine clays.

The cumulative evidence indicates that most of the icy beds have grown *in situ*, even though some buried glacier ice may be present.

Segregated Ice

If the massive ice is neither ice-wedge nor buried surface ice, then a segregated origin should be considered. The ice is identical, insofar as can be determined, to small ice lenses whose origin is known. The only question is the quantity of ice.

Well-known laboratory studies have shown that very thick ice lenses can be grown, providing water is made readily available at the freezing plane. It is equally well known that pingos with ice cores 40 m thick can grow under a suitable

hydrologic regime. Drilling and field examination of pingo ice cores have shown that many are primarily of segregated ice interlayered with soil,⁸ although some are of injected water. In the growth of a pingo, a water table in contact with the ice core is maintained either by a hydrostatic head in an open system pingo or by water expulsion in a closed system pingo. The mechanism of water expulsion, which is widely accepted for pingo growth, might be extended to that of segregated ice.^{6,16}

The widespread occurrence of massive icy beds above, or in close association with, sands and gravels (Figure 6), suggest that these sediments served two purposes: a water source from water expulsion resulting from freezing of adjacent coarse-grained sediments and an aquifer. To give a specific illustration, about 150 years ago, a large lake, 8 km² in surface area, drained near Tuktoyaktuk, N.W.T. Numerous drill holes show that permafrost has now aggraded to a depth of 35 m and that water expulsion has produced artesian pressures. Precise levelling shows that the lake bottom is slowly heaving and this means ice segregation at depth. Thus, provided water is available over extensive areas, there seems to be no reason why massive bodies of segregated ice should not grow at depth, in the same manner as that of segregated ice in pingos.

ACKNOWLEDGMENT

The field work has been supported by the Geological Survey of Canada, the National Research Council of Canada, and the Department of Indian and Northern Affairs. Numerous oil companies have provided shot hole data. The Inuvik Research Laboratory and the Polar Continental Shelf Project, Department of Energy, Mines and Resources, have given logistic help in many ways. Imperial Oil Ltd. and Mr. F. H. Lane, Imperial Oil Ltd., did the drilling and sample collecting of the four holes for ionic concentration studies.

REFERENCES

1. Bouchard, M., and V. N. Rampton. 1972. Environmental geology, Tuktoyaktuk, District of Mackenzie (107 C). Geol. Surv. Can. Paper 72-1A. p. 141–143.
2. Lamothe, C., and D. St. Onge. 1961. Observations d'un processus d'érosion périglaciaire dans la région d'Isachsen, T.N.O. Geogr. Bull. Can. No. 16. p. 114–119.
3. Mackay, J. R. 1959. Glacier ice-thrust features of the Yukon Coast. Geogr. Bull. Can. No. 13. p. 5–21.
4. Mackay, J. R. 1963. The Mackenzie Delta area, N.W.T. Geographical Branch Memoir 8, Department of Mines and Technical Surveys, Ottawa, Canada. 202 p.
5. Mackay, J. R. 1966. Segregated epigenetic ice and slumps in permafrost, Mackenzie Delta area, N.W.T. Geogr. Bull. Can. 8:59–80.
6. Mackay, J. R. 1971. The origin of massive icy beds in permafrost, Western Arctic Coast, Canada. Can. J. Earth Sci. 8:397–422.
7. Mackay, J. R. 1972. The world of underground ice. Ann. Assoc. Am. Geogr. 62:1–22.
8. Mackay, J. R., and J. K. Stager. 1966. The structure of some pingos in the Mackenzie Delta area, N.W.T. Geogr. Bull. Can. No. 4. p. 360–368.

9. Mackay, J. R., and J. K. Stager. 1966. Thick tilted beds of segregated ice, Mackenzie Delta area, N.W.T. Periglac. Bull. No. 15. p. 39-43.
10. Mackay, J. R., V. N. Rampton, and J. G. Fyles. 1972. Relic Pleistocene permafrost, Western Arctic, Canada. *Science* 176: 1321-1323.
11. Prest, V. K., D. R. Grant, and V. N. Rampton. 1968. Glacial Map of Canada. Geol. Surv. Can. Map 1253A.
12. Rampton, V. N. 1971. Ground ice conditions: Yukon Coastal Plain and adjacent areas. Geol. Surv. Can. Paper 71-1B. p. 128-130.
13. Rampton, V. N. 1972. Quaternary geology, Arctic Coastal Plain, district of Mackenzie and Herschel Island, Yukon Territory. Geol. Surv. Can. Paper 72-1A. p. 171-175.
14. Rampton, V. N. 1972. Surficial deposits of the Mackenzie Delta (107 C), Stanton (107 D), Cape Dalhousie (107 E), and Mallock Hill (97 F) map-sheets, p. 15-27. In D. E. Kerfoot [ed.] Mackenzie Delta monograph. 22nd International Geographical Congress, Brock University, St. Catharines.
15. Rampton, V. N., and J. R. Mackay. 1971. Massive ice and icy sediments throughout the Tuktoyaktuk Peninsula, Richards Island, and nearby areas, District of Mackenzie. Geol. Surv. Can. Paper 71-21. 16 p.
16. Williams, P. J. 1967. Properties and behaviour of freezing soils. Publ. 72. Norwegian Geotechnical Institute, Oslo. p. 109-110.

NOTE

[1] The data for this report were obtained as a result of investigations carried out under the Environmental-Social Program, Northern Pipelines, of the Task Force on Northern Oil Development, Government of Canada.

A SIMULATION SENSITIVITY ANALYSIS OF THE NEEDLE ICE GROWTH ENVIRONMENT

Samuel I. Outcalt

UNIVERSITY OF MICHIGAN
Ann Arbor, Michigan

INTRODUCTION

Needle ice is the result of diurnal ice segregation near the soil surface. Ice segregation results from the increase in the water (ice) volume fraction of a soil layer produced by the upward migration of soil water to the freezing plane after nucleation occurs and the freezing plane remains at a fixed level in an initially unfrozen soil.^{2,3} The process of needle ice erosion produces downslope soil movement in periglacial alpine terrain⁹ and is responsible for damage to plant materials when freezing causes vertical mechanical stress within the root zone.¹

Needle ice movement of material is a major influence in the evolution of a wide spectrum of frost-sorted periglacial forms, ranging from frost boils, where the organic material has been removed or broken, to miniature stone stripes. At all points in arctic and alpine terrain where wet, heave-susceptible soil surfaces are exposed to frequent diurnal freeze-thaw events, needle ice sorting and heaving must be considered as a geomorphic agent.

In a more general sense, needle ice is of considerable theoretical interest as an extreme representative of periglacial phenomena representing very high temporal frequen-

cies and restricted spatial scales produced by local variations in soils, horizon conditions, and limited vertical dimensions of heave (10-100 mm). Thus, the successful simulation of a needle ice environment should act as a starting point for the simulation of low frequency temporal periglacial features with larger vertical spatial dimensions such as rock glaciers and the permafrost active layer. This, in fact, has been the case as the needle ice simulator provided the basic analytical framework for the production of a tundra active-layer simulator now under development at the University of Michigan.

THE SIMULATOR

The needle ice simulator is a specialized version of the equilibrium-temperature-surface-climate simulator that is described in detail in two recent publications.^{5,8} In brief, the operation of the general simulator has the following general structure based on the energy conservation equation that states that the four components of the energy budget [net radiation (R), soil heat flux (S), sensible heat flux (H), and latent heat flux (L)] must have a zero sum across a surface:

$$R + S + H + L = 0. \quad (1)$$

In turn, each of these terms is a complex function of the environmental variables that specify the radiation and thermal properties of the atmosphere and substrate media. At any instant in time, these components may be represented as functions of a limited set of environmental variables and physical constants. These controlling variables are listed with their notation in Table I.

The components of the energy budget equations can then be written in terms of these variables and the surface temperature (T) as follows:

$$R = f(Lat, Dec, D, r, Albedo, W, P, T_{sky}, T). \quad (2)$$

If the assumption is made that the soil temperature at the diurnal damping depth is approximately equal to the mean air temperature then

$$S = f(GC, GD, Ta, T), \quad (3)$$

and the turbulent transfer terms, which are corrected for stability using the Richardson number as a vehicle, may be expressed as:

$$H = f(U, ZO, P, Ta, T), \quad (4)$$

$$L = f(U, ZO, P, RH, SRH, Ta, T). \quad (5)$$

Note that in all of the above equations after specification of the input variables, the surface temperature is the only unknown. The soil temperature profile is allowed to evolve by calculating a finite difference solution of the thermal diffusion equation using the soil thermal solution from the preceding step. After the new soil thermal profile is computed, the soil heat flux [Eq. (3)] is actually calculated from the uppermost soil temperature level in place of Ta .

At each step through the diurnal cycle, the solar radiation incident on a surface may be calculated for a clear day by means of a subroutine. Subroutines are also included to calculate specific humidity gradients and to fix the free air computation level and correct the thermal properties of the atmosphere for stability.

It is apparent that, if a sequence of guesses as to the

value of the surface temperature is entered into the equation, the correct guess would bring the energy budget equation [Eq. (1)] to zero and that the correct guess would be termed the equilibrium surface temperature. The equilibrium surface temperature is that temperature which will balance the heat flux across a surface when all other relevant information is known. When the surface temperature guess produces a small residual in the energy budget equation (e.g., 1 mly/min), then all the components of the energy transfer regime (R, S, H, L) and the soil temperature vector (T) are equally good guesses and the next iteration begins with a forward solution of the finite difference form of the soil diffusion equation. (1 ly/min = 700 J/m²s.)

In the needle ice version of the simulator, it is necessary to incorporate the process of fusion and ablation in the soil and make geometric allowances for changing soil geometry (and thermal properties) due to heave. It was therefore necessary to incorporate statements into the model fabric that would produce these effects and mimic the evolution of a needle ice event. It would seem advisable at this time to trace the evolution of a synthetic needle ice event in which the critical switching values were gained from detailed micrometeorological and soil physical studies at the University of British Columbia and at the University of Virginia.^{2-4,6}

It is important to note that the object of simulation is to abstract facts about needle ice into a general model of the phenomena that is independent of location to which site specific information may be added as site variables. The basic model is site independent. Here a data set at Vancouver is being simulated. However, the process could be simulated anywhere by modifying the input variables listed in Table I. A more complete discussion of the needle ice simulator is available in the current literature.⁷

THE SEQUENCE OF A SYNTHETIC OR GENERALIZED NEEDLE ICE EVENT

During the late afternoon, the surface temperature begins to decline through time in a roughly parabolic manner. If the temperature reaches -1 °C, nucleation is assumed to occur, and ice is present near the soil surface. During needle growth, the temperature at the base of the needles is assumed to be 0 °C, and the thermal gradient through the needles and normally frozen soil cap (assumed to be 10 mm thick) is determined by the unique sequence of equilibrium temperatures at the surface.

The density of needle ice is approximately 0.2 g/cm³ and thus the thermal properties of the upper composite of soil cap and needles can be scaled accordingly. The thermal profile in the unfrozen soil beneath the base of the needles is allowed to evolve constrained by the fusion temperature at the needle bases and the mean diurnal temperature at the damping depth.

TABLE I Environmental Input Variables

Station pressure (P)	Mean air temperature (Ta)
Latitude (Lat)	Mean air relative humidity (RH)
Solar declination (Dec)	Mean air wind velocity (U)
Dust particles/cm ³ (D)	Soil thermal diffusivity (GD)
Orbital radius vector (r)	Soil volumetric heat capacity (GC)
Surface albedo ($Albedo$)	Surface roughness length (ZO)
Precipitable water (W)	Soil surface wetness (SRH)
Sky radiant temperature (T_{sky})	

The energy expended on growth (fusion) and melting (ablation) was used to calculate the vertical displacement of the needles (heave). When the surface solution was below the ice point, the energy expended on cooling or warming the soil cap-needle composite was subtracted from the soil heat flux to determine incremental and total heave. Since the writer's last publication concerning the needle ice simulation,⁷ the flux to the base of the needle mass during growth has been included in the heave equation reducing the calculated heave by approximately 50 percent and bringing the maximum diurnal heave amplitude into agreement with field observation. The phase relationships of the initial calculations were already in excellent agreement.

When the surface equilibrium temperature was greater than the ice point, the needle mass was assumed to be isothermal at 0 °C with heat flowing to it from both the warm cap surface above and the unfrozen soil layers below. The needle ice generation and ablation loop was excited when the accumulated heave reached zero and the program re-triggered to await the nucleation temperature.

It was necessary to add an additional term to the soil thermal diffusion equation to allow for the flow of soil water down the thermal gradient. The form of this modification of the diffusion equation at the computation nodes between the surfaces and the diurnal depth follows:

$$\partial T/\partial t = (\partial^2 T/\partial Z^2) + \alpha U_w (C_w/C_s) (\partial T/\partial Z), \quad (6)$$

where the temperature (T) variation with time (t) is a function of the bulk thermal diffusivity (α), depth (Z), soil water flux velocity (U_w) (known to be approximately 20 mm/h),⁶ and the ratio of the volumetric heat capacity of water to that of the bulk soil (C_w/C_s).

SENSITIVITY TESTING STRATEGY

The strategy for sensitivity testing essentially was to determine the effects of individual parameter variations on the soil surface thermal regime and heave by plotting line printer graphs of the digital computer program output. These deviations were in all cases considered to be deflections away from a standard variable set that was found to fit the mean hourly values of heave, surface temperature, and net radiation during an 11-day sequence of needle ice events at Vancouver, Canada, commencing on 6 February 1968. The values of this standard set are presented in Table II, using the notation of Table I.

Sensitivity to Air Relative Humidity and Wind Velocity

In this test, the simulation variables were arrayed in a nine point grid and contoured (Figure 1). The results are seen to be in good agreement with the actual field data at two points. Specifically, it was known that the mean diurnal

TABLE II Standard Variable Set for Vancouver

$Lat = 49.3^\circ N$	$T_a = 7^\circ C$
$Dec = -14.9^\circ$	$RH = 50$ percent
$D = 0.2/cm^3$	$U = 1.20$ m
$r = 0.98662$	$GD = 0.0056$ cgs
$Albedo = 0.15$	$GC = 0.5$ cgs
$W = 7$ mm	$ZO = 20$ mm
$T_{sky} = -20^\circ C$	$SRH = 100\%$ (or wet fraction 1.00)
$P = 1\ 020$ mbar	

maximum heave during the 11-day period was 8.7 mm, and the simulator indicates 10 mm at this point. Further, a vast amount of observational data indicated that otherwise ideal conditions needle ice did not occur when the mean nocturnal wind velocity approached 2 m/s.⁷ This work also indicates an optimum growth condition at low relative humidities centered on a wind velocity of 0.8 m/s. The empirical data have not been examined for evidence of this optimum condition that seems to be related to the evaporative-heat-loss efficiency near a critical value of the Richardson number for maintenance of mechanical turbulence that frequently occurs around 0.6 m/s.

Sensitivity to Decreasing Air Temperature

Next, the air temperature was dropped by 1 °C increments to 3 °C. It should be noted that this also affected the atmospheric vapor pressure as the air relative humidity has held constant. This appeared to have the effect of increasing heave (Figure 2). More significantly, in agreement with field data, ablation was complete by noon, even at air temperature as low as 4 °C.

Sensitivity to Soil Surface Dessication

The impact of lowering the surface wet fraction (wf) from unity to zero is graphically indicated in Figures 2 and 3. The general effect is to shift the time of nucleation radically as in the case of lowered temperature. This effect may explain the variations in total heave noted in field data when the gross meteorological environment appeared similar throughout the sequence of events.³

Sensitivity to Albedo and Surface Roughness Manipulation

The heave sensitivity to manipulation of surface roughness and solar reflectivity was examined by varying these values about the values used in the standard case. Results are listed in Table III. These results indicate that the system is much more sensitive to slight alterations in surface roughness than the range of albedo variation frequently encountered in wetting and drying cycles.

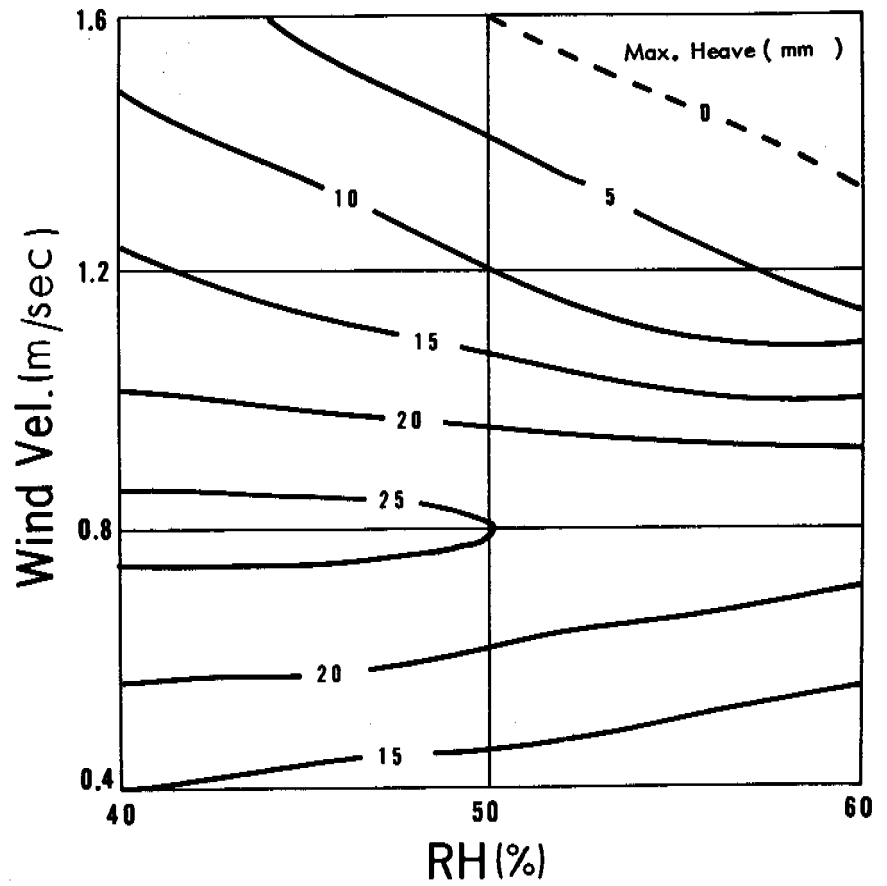


FIGURE 1 The maximum diurnal heave surface.

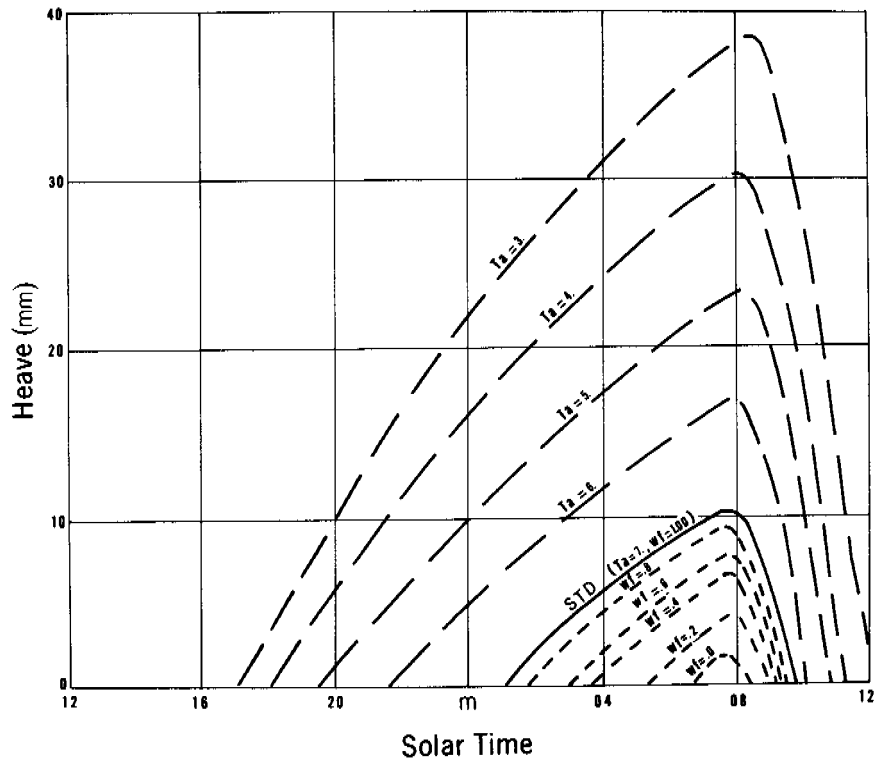


FIGURE 2 Heave variations produced by lowering the air temperature (T_a) and the soil surface wet fraction (wf).

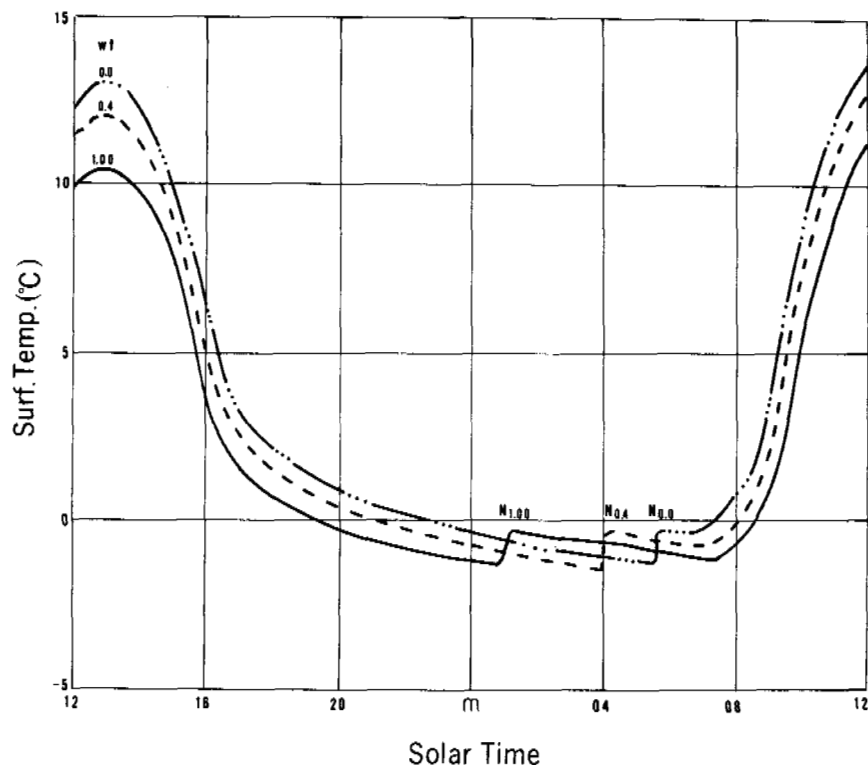


FIGURE 3 Nucleation (N) delay produced by desiccating the soil surface as the wet fraction (wf) is varied from 1.00 through 0.4 to 0.0.

POLYCYCLIC GROWTH

In earlier field studies, the polycyclic growth of needles was noted and the hypothesis advanced that the effect was the product shadowing and growth at reduced diurnal mean free air temperatures.⁶ The geomorphic evidence for this type of growth are dirty caplike layers parallel to the soil surface. These appear normally frozen and may represent a short cycle of melt-normal refreezing-continued ice segregation needle growth during the daylight hours (Figure 4).

In the simulator, shadowing is accomplished by reducing the value of beam radiation to 20 percent of its calculated value to simulate growth behind shadowing obstructions while regularly reducing the free air temperature. These results are presented in Figure 5. Note the regular increase in the length of the growth period produced by increasingly earlier nucleation. Also, as the free air temperature descends to 4 and 3 °C, the growth cycle is interrupted by a period of

ablation producing a net diurnal heave of 4 and 8 mm/day. This duplicated the geomorphic evidence precisely and is even in the correct order of magnitude for free air temperatures between 4 and 5 °C where the ablation process is complete. At higher free air temperatures (6 and 7 °C), the nucleation temperature is not reached, and no growth occurs due to a restriction of the cold sky horizon for thermal radiation.

CONCLUSION

This exercise appears to be of value in both the practical and theoretical spheres of operation. First, it indicates that needle ice damage may be attenuated by artificially mulching seedbeds with plastic sheeting or porous sand layers (10 mm thick) to reduce the surface wetness, artificially introducing roughness elements into the seedbeds, and avoiding extremely shadowed and wet natural sites. These strategies may be of extreme importance in repairing tundra and alpine meadow cover damage in alpine recreation areas. Second, it is evident that the deterministic models are capable of mimicking natural kilmageomorphic phenomena not specifically woven into the fabric of the model structure. Finally, it is evident, that as the general equilibrium temperature algorithm is spatially and temporally unconstrained dimensionally, this system of equations, when modified to include specific process information, should be applicable to the entire spectrum of periglacial phenomena.

TABLE III Roughness-Albedo Sensitivity Tests

Roughness length (mm)	20 ^a	40	60
Max. heave (mm)	10	3	0
Short wave albedo (%)	10	15 ^a	20
Max. heave (mm)	10	10	11

^a Standard case.

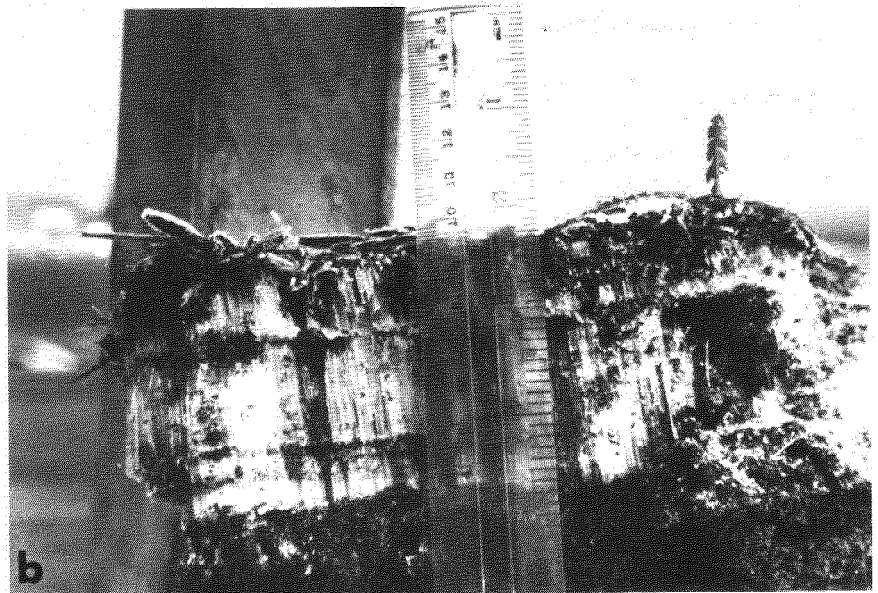


FIGURE 4 Typical structures of monocyclic (a) and polycyclic (b) needle ice. Note the normally frozen cap containing organic debris in both cases and the layered dark mineral soil debris bands parallel to the surface in the polycyclic sample.

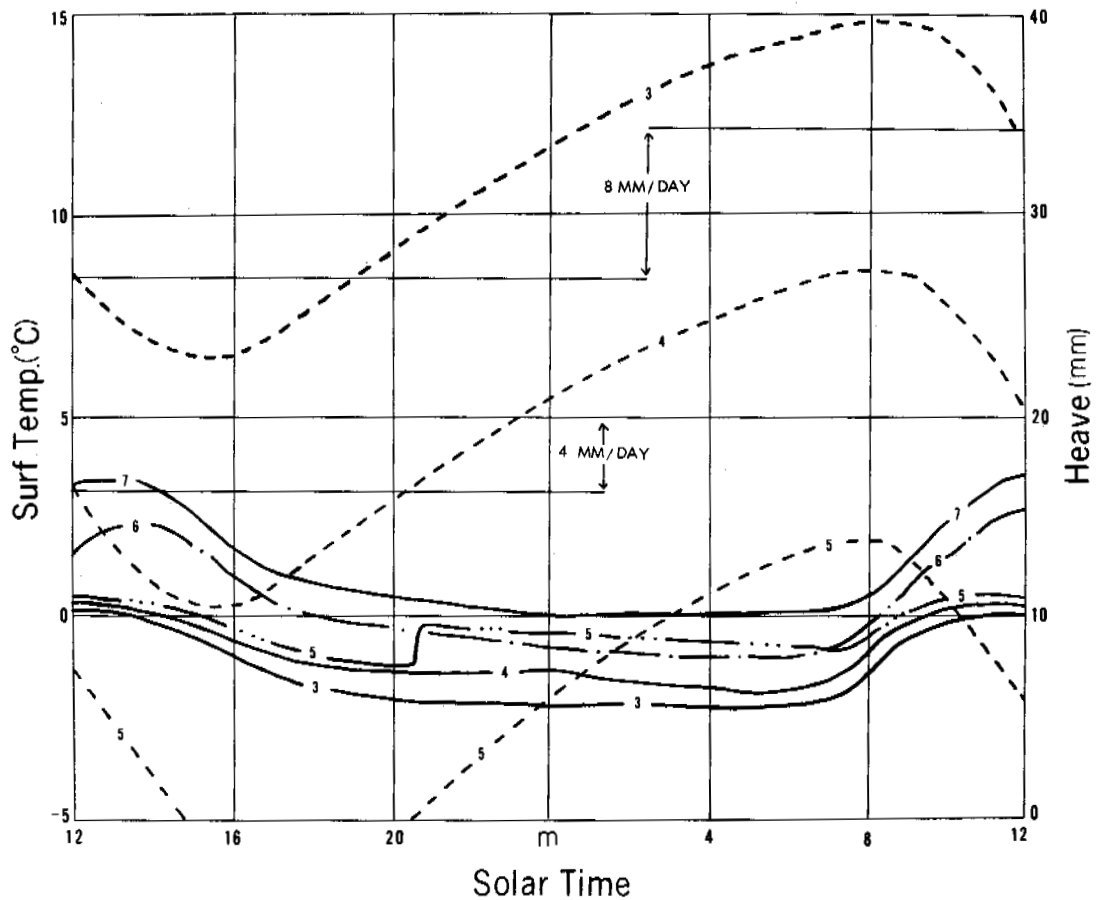


FIGURE 5 Surface temperature (solid and - - - lines) and heave (dashed lines) as functions of air temperature (labeled on lines) at a shadowed site.

REFERENCES

1. Brink, V. C., J. R. MacKay, S. Freyman, and D. G. Pearce. 1967. Needle ice and seedling establishment in southwestern British Columbia. *Can. J. Plant Sci.* 47:135-139.
2. Outcalt, S. I. 1969. Weather and diurnal frozen soil structure at Charlottesville, Virginia. *Water Resour. Res.* 5:1377-1381.
3. Outcalt, S. I. 1970. Study of time dependence during serial needle ice events. *Arch. Met. Geophys. Biokl. Ser. A* 19:329-337.
4. Outcalt, S. I. 1972. Field observations of soil temperature and water tension feedback effects on needle ice nights. *Arch. Met. Geophys. Biokl. Ser. A* 20:43-53.
5. Outcalt, S. I. 1971. A numerical surface climate simulator. *Geogr. Anal.* 3(4):379-392.
6. Outcalt, S. I. 1972. An algorithm for needle ice growth. *Water Resour. Res.* 7(2):394-399.
7. Outcalt, S. I. 1971. The climatology of a needle ice event: An experiment in simulation climatology. *Arch. Met. Geophys. Biokl. Ser. A* 19:325-338.
8. Outcalt, S. I. 1972. The development and application of a simple digital surface climate simulator. *J. Appl. Met.* 11(4):629-636.
9. Soons, J. M., and J. M. Rayner. 1960. Micro-climate and erosion processes in the Southern Alps, New Zealand. *Geogr. Ann. Ser. A* 50:1-15.

RATES OF MASS WASTING IN THE RUBY RANGE, YUKON TERRITORY

Larry W. Price

PORTLAND STATE UNIVERSITY
Portland, Oregon

INTRODUCTION

The rates of mass wasting under different environmental conditions have long fascinated geomorphologists and although the measurement of these rates seems an initially simple task, the sum total of our knowledge on the subject is surprisingly small.¹¹ This paper presents measurements of mass wasting carried out during the summers of 1967, 1968, and 1972 in the Ruby Range, Yukon Territory, Canada.^{6,9} It is the initial installment of what is hoped to be a series of reports at approximately 5-year intervals on rates of surface and subsurface slope movement under different environmental conditions in the study area.

SETTING

The Ruby Range is located in southwestern Yukon Territory at 61°23'N 138°13'W, about 215 km northwest of Whitehorse (Figure 1). It is a small granitic mountain group 130 km long by 65 km wide oriented northwest-southeast and situated along the western edge of the Yukon Plateau. Immediately to the west is Shakhwak Valley, a major structural trench dividing the older granitic rocks of the Yukon Plateau from the younger metasediments of the towering St. Elias Mountains (highest peak—Mt. Logan 6 050 m). The higher peaks of the Ruby Range average 2 130 m, and there is a distinct flattening of the upland surface that may be an old erosion surface of the Yukon Plateau.² The area has been dissected by valley glaciation, however, and is quite rugged. Although the Gulf of Alaska is located only 230 km to the west, the intervening St. Elias Mountains eliminate direct marine influence, and the Ruby Range experiences a continental climatic regime. Tree line occurs locally at about 1 200 m, and the combination of latitude, altitude, and continentality give the study area a subarctic alpine tundra environment.⁵

Intensive investigations were carried out on four slopes formed by the confluence of two ridges (Figure 2). These four slopes—facing southeast, southwest, east, and north—are all underlain by permafrost; all have the same rock type (coarse-grained biotite granodiorite) and similar gradients (14–18°) and elevations (1 675–1 980 m). The slope environments are considerably different, however, because of exposure to solar radiation and meltwater from late snow

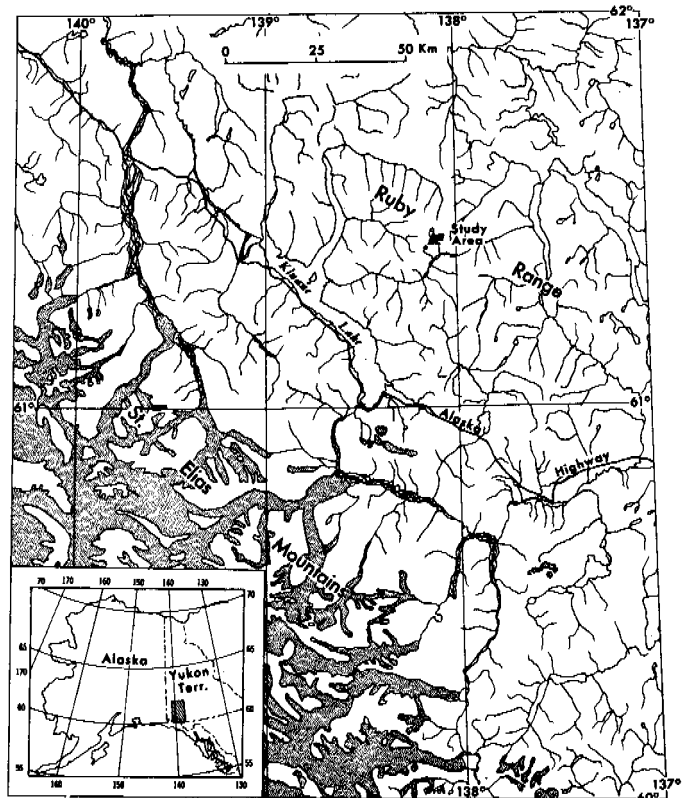


FIGURE 1 Location of study area.

melt. The tundra vegetation is best developed and the active layer is shallowest on the southeast-facing slope, and both become sequentially less so on the east-, southwest-, and north-facing slopes.⁷ Solifluction lobes are well developed on the southeast- and east-facing slopes, but become increasingly scarce on the north- and southwest-facing slopes.

RESEARCH METHODS

Weather stations were established at an elevation of 1 880 m midway up the southeast- and north-facing slopes. Soil moisture and soil temperature was determined by installing Coleman soil cells at 15-cm-interval depths to permafrost at a central site on each slope (Figure 2). The vegetation

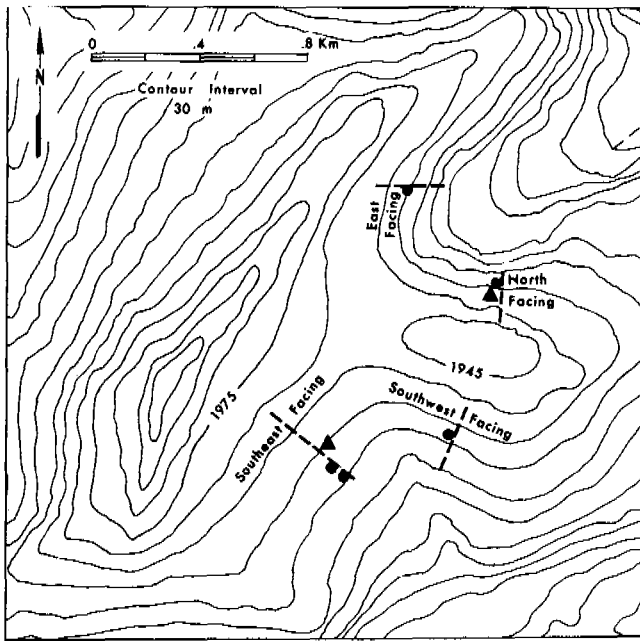


FIGURE 2 Study slopes with location of weather stations (triangles), soil moisture and temperature installations (dots), and vegetation sampling transects (dashed lines).

was sampled and analyzed along transects run across the slopes, and depth of the active layer was measured by augering at 1.5-m intervals along these same transects four times during the summer. Two major techniques were used in measuring mass-wasting: inserting polyethylene tubes vertically to frozen ground and monitoring subsequent defor-

mation with a strain gage probe; and painting *in situ* surface rocks and establishing measurement grids. The first method provides information on movement with depth, while the second is useful in determining surface movement at the risers of solifluction lobes.

The use of polyethylene tubes and strain gages for measuring slope movement was largely pioneered by Williams¹²⁻¹⁶ and Zhigarev.¹⁷ Williams' methods have been followed, except for minor modifications.⁶ Basically, this involves inserting a polyethylene tube (13 mm i.d. and 16 mm o.d.) into a small soil auger hole that is vertical to frozen ground. The tube is kept straight in the ground by a steel rod that fits snugly into the tube; after repacking the soil, the rod is removed. Subsequent deformation of the tube is measured by inserting a strain gage probe and taking readings at intervals down the tube.⁶ While remonitoring the tube measurements during summer 1972, eight of the tubes were excavated to check the accuracy of the readings. These were excavated from each of the slopes under various environmental conditions and provide a general picture of soil movement in the study area.

TUBE MEASUREMENTS

Southeast-Facing Slope

The southeast-facing slope is 900 m wide and has an average gradient of 14° . It is the alb of the glacial trough and is bounded upslope by a ridge 150–200 m high (Figure 2). Meltwater from patches of snow that accumulate in the lee of the ridge provides moisture through the summer, and

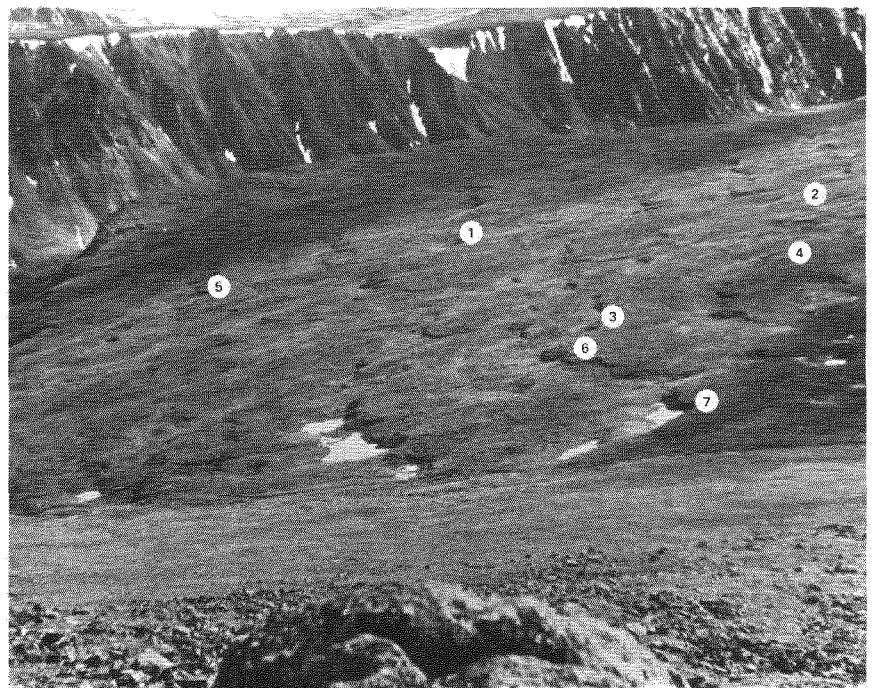


FIGURE 3 View of southeast-facing slope looking toward the southwest. Vegetation and solifluctional lobes are best developed on this slope. The lobes with snow in their lee are 4–6 m high. The circled numbers show location of the excavated tubes on this slope.

solifluction lobes are very well developed on this slope (Figure 3). The larger lobes reach a height of 4–6 m, but average height is 1–2 m. The vegetation is well developed and sharply delineated communities occur in horizontal bands across the steplike lobes.

A greater number of measurements were made on this slope than the other slopes, because the solifluction lobes were best developed here. In total, 28 tubes have been installed on the southeast-facing slope—13 during summer 1967, 10 during summer 1968, and 5 more during summer 1972. Two of the tubes were excavated during summer 1968 to check on the accuracy of the probe readings and five more were excavated during summer 1972. Their absolute and average movements are given in Table I. The collected profiles of the various excavated tubes fall into two categories: concave downslope profile indicating greatest movement at the surface and convex downslope profile suggesting greatest movement at depth (Table I and Figure 4).

TUBES WITH CONCAVE DOWNSLOPE PROFILE

Tubes one and two show greatest movement at the surface and have very similar profiles in terms of both amount and depth of movement (Figure 4a,b). Tube one was located on the tread of a small lobe 1 m upslope from a 1.3-m-high riser (Figure 3). The vegetation is well developed, consisting of mossy hummocks, and the surface organic layer is 6 cm thick. Dominant species include *Carex microchaeta*, *Salix pseudopolaris*, *S. reticulata*, and *Sphagnum* sp. Surface movement amounted to 3.7 cm, averaging 0.9 cm/year, and movement occurred to a depth of 33 cm (Figure 4a). The soil moisture is high owing to the shallow active layer (maximum depth, 85 cm).

Tube two (Figure 4b) was located on the 0.3-m-high lip or furl of a frost boil (nonsorted circle). This site is well drained, and the plant cover consists of species characteristic of drier sites, e.g., *Dryas octopetala*, *Festuca altaica*, and *Cladonia* sp. The organic layer is 3–4 cm thick and not well developed. The tube moved downslope 4.8 cm at the surface, averaging 1.2 cm/year; depth of movement was 51 cm (Table I). Frost creep is probably of considerable importance at this site, owing to its nearness to the bare area of the frost boil.

Tubes three and four were excavated during 1968, providing only 1 year's measurements, but are included for purposes of comparison. Tube three (Figure 4c) was located on the tread of a lobe 1.5 m upslope from a 1.7-m-high riser. A frost boil was present on the immediate upslope side of the tube. The soil moisture was very high, and vegetation consisted of mossy hummocks. The organic layer was 16 cm thick and well developed. Greatest movement (3.0 cm) took place at the surface and occurred to a depth of 30 cm (Figure 4c).

Tube four (Figure 4d) was located on a small lobe 1.1 m

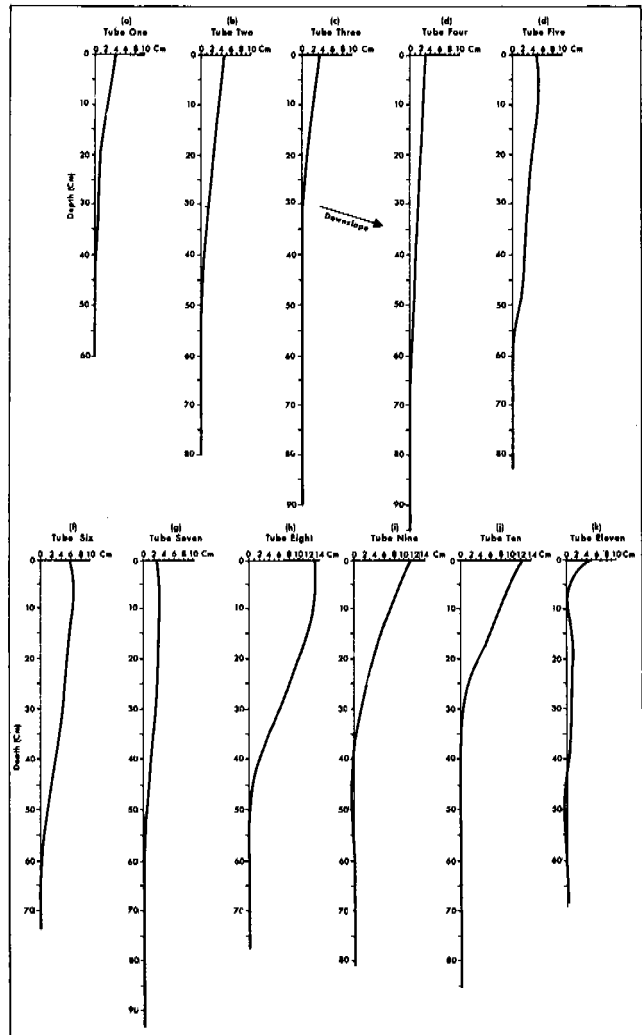


FIGURE 4 Profiles of excavated tubes.

upslope from a 0.5-m-high riser. The vegetation consisted of mossy hummocks, and the soil remained essentially saturated through the summer. The organic layer was 5 cm thick. Movement was greatest at the surface (3.5 cm) and decreased gradually to a depth of 66 cm (Figure 4d).

TUBES WITH CONVEX DOWNSLOPE PROFILE

The profiles of tubes five, six, and seven (Figure 4e,f,g) all indicate that movement was greater at depth than at the surface. Tube five was located on a lobe tread 2 m upslope from a 1.3-m-high riser (Figures 3 and 4e). The vegetation is well developed, and the organic layer is 15 cm thick. Soil moisture at this site is moderately high, and water filled the bottom of the pit during the excavation. Greatest movement occurred at a depth of 5.8 cm and decreased both above and below. The tube moved downslope 5 cm at the

TABLE I Characteristics and Results of Tube Measurement Sites

Tube	Measurement Period	Original Depth (m)	Slope Orientation	Slope Gradient (deg)	Soil Moisture Conditions	Plant Cover	Amount of Tube Upheaval (cm)	Greatest Movement		Average Annual Downslope Movement (cm)	Depth to Which Movement Occurred (cm)
								Depth (cm)	Amount (cm)		
1	17 Aug. 1968-8 Aug. 1972	0.85	southeast-facing	14	constantly wet	hummocks	7.6	surface	3.7	0.9	33
2	10 Aug. 1968-13 Aug. 1972	1.2	southeast-facing	14	moist	dry hummocks	32.4	surface	4.8	1.2	51
3	3 July 1967-10 Aug. 1968	1.08	southeast-facing	14	wet	mossy hummocks	11.8	surface	3.0	3.0	30
4	5 July 1967-10 Aug. 1968	1.05	southeast-facing	14	wet	mossy hummocks	8.9	surface	3.5	3.5	66
5	10 Aug. 1968-13 Aug. 1972	0.93	southeast-facing	14	moist	hummocks	14.8	5.8	5.3	1.1	58
6	10 Aug. 1967-13 Aug. 1972	1.1	southeast-facing	14	constantly wet	hummocks	26.3	10.1	6.2	1.2	56
7	5 July 1967-13 Aug. 1972	1.1	southeast-facing	14	moist	hummocks	25.5	23	2.8	0.6	56
8	10 Aug. 1967-7 Aug. 1972	1.1	east-facing	16	moist	hummocks	22.6	surface	13.3	2.7	48
9	10 Aug. 1972-	1.03	north-facing	22	moist	sparse	12.0	surface	13.0	2.6	36
10	30 June 1967-7 Aug. 1972	1.04	north-facing	18	moist	sparse	14.1	surface	10.7	2.1	36
11	7 July 1967-not excavated	1.1	southwest-facing	17	dry	<i>Dryas, Cladonia</i>	3.8	surface	3.4	0.7	10

surface, and movement took place to a depth of 58 cm (Figure 4e).

Tube six was placed on a lobe tread 15 m upslope from a 1.4-m-high riser on the central part of the slope. The soil moisture and temperature site for the southeast-facing slope was located only 3 m upslope from this tube and surface soil moisture always exceeded 100 percent [based on the water-to-dry soil ratio (w/w)] (Figure 5). The vegetation consists of thick mossy hummocks, and the surface organic layer is 20 cm thick. Dominant plant species include *Carex microchaeta*, *Salix pseudopolaris*, *S. reticulata*, and *Sphagnum* sp. Greatest movement (6.2 cm) occurred at a depth of 10 cm while surface movement was 5.5 cm and no movement was evident below a depth of 56 cm (Figure 4f).

Tube number seven was located on one of the largest lobes on the southeast-facing slope. The riser is 6.5 m high, bare, and rocky. The tread is well vegetated, however, and the organic layer is 5 cm thick at the tube site. Greatest movement (2.8 cm) took place at a depth of 23 cm. The tube reveals 2.5 cm of downslope movement at the surface, and movement decreases to zero at a depth of 56 cm (Figure 4g).

East-Facing Slope

The east-facing slope has an average gradient of 16° and also is the alb of the glacial trough. There is a 100-m-high ridge upslope where snow accumulates and provides meltwater for the slope until mid-July (Figure 6). Solifluction lobes are well developed on this slope, exceeded in size only by those occurring on the southeast slope. The former slope is only 300 m wide, however, compared with 900 m for the latter.

Tube eight was located 2 m upslope from a riser 1.4 m high (Figures 4h and 6). The vegetation consists of mossy hummocks, and the near-surface soil moisture exceeded 100 percent during the summer (Figure 5). The profile of this tube approximates an S curve, giving it a slight convex downslope profile near the surface. Surface movement was 13.3 cm, averaging 2.7 cm/year, and movement occurred to a depth of 48 cm (Figure 4h).

Southwest-Facing Slope

The southeast- and southwest-facing slopes, although separated only by a small stream, exhibit very great contrast between them (Figure 7). The southeast slope is the wettest of the four slopes with well-developed solifluction lobes, while the southwest-facing slope is quite dry and solifluction lobes are virtually absent, except for one narrow zone where meltwater trickles down from the ridge above. One reason for the xeric quality of the southwest slope is the

prevailing northwesterly winter wind that sweeps it clean of snow, particularly since there are very few microhabitats where snow can accumulate. The slope has an average gradient of 17° , and the surface consists of 1.5 m or more of unconsolidated weathered detritus. The plant cover is poorly developed but fairly continuous with *Dryas octopetala*, *Salix pseudopolaris* and *Cladonia* sp. dominating.

No tubes were excavated on the southwest-facing slope, but the strain gage readings have been plotted for the main measurement tube and provide movement rates (Table I). Tube eleven (Figure 4k) is not on a solifluction lobe, and the plant cover is thin with a near-surface soil moisture of only 9 percent during the summer (Figure 5). Surface movement was 3.4 cm for the 5-year period, resulting in an average of 0.7 cm/year; movement occurred to a depth of 10 cm. Due to the lack of moisture, movement here is probably more a result of frost creep than of solifluction.¹¹

North-Facing Slope

The north-facing slope (Figure 8) is the steepest (18°) and narrowest (180 m) of the study slopes. The surface consists of at least 1.5 m of weathered detritus and is strewn with large boulders 1–2 m in diameter. The sun strikes the slope at a very low angle, and mountains to the north and west prevent the sun from shining on the slope during the night hours. As a result, snow patches remain until early July; vegetation is discontinuous and sparsely developed. Solifluctional lobes occur but are not well developed; they reach a maximum height of only 1.5 m and occur singly rather than coalesced as on the southeast- and east-facing slopes.

Tube nine (Figure 4i) was located at the same site as the weather station and soil moisture and temperature site for the north-facing slope. It was not on a solifluctional lobe (Figure 8). The area was sparsely vegetated, and the near-surface soil moisture averaged 30 percent during the summer (Figure 5). Surface movement totaled 10.7 cm for an average of 2.1 cm/year, and movement gradually decreased to a depth of 36 cm, below which movement did not occur.

Tube ten was installed on a nearby north-facing slope with a steeper gradient (22°). There were several well-developed solifluction tongues, and tube ten was located on the tread of one of these, 1.5 m upslope from the 2-m-high riser. The surface is largely bare with occasional patches of vegetation, i.e., *Cassiope mertensiana* and *Carex microchaeta*. The soil is very stony and well drained, although snow patches on higher ground provided moisture throughout much of the summer. As can be seen in Figure 4j, this tube's profile is similar to that of tube nine with 13 cm of movement occurring at the surface for an average of 2.6 cm/year. The movement decreases gradually with depth and does not occur below a depth of 36 cm.

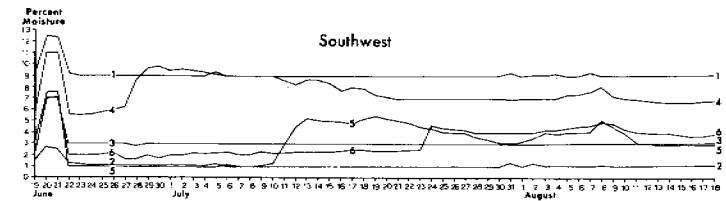
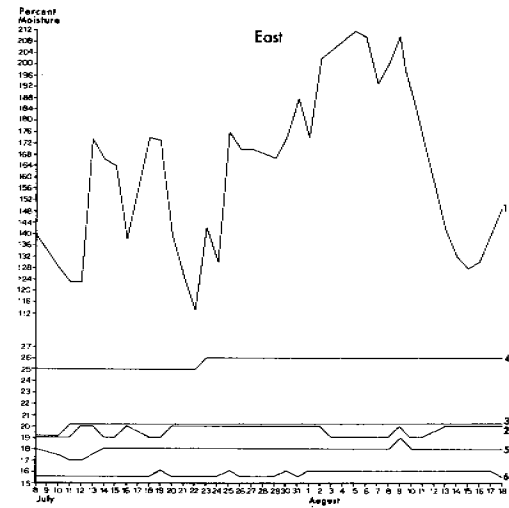
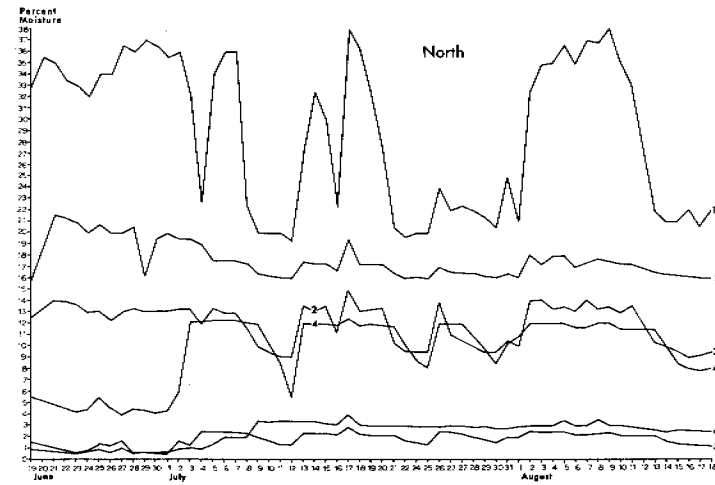
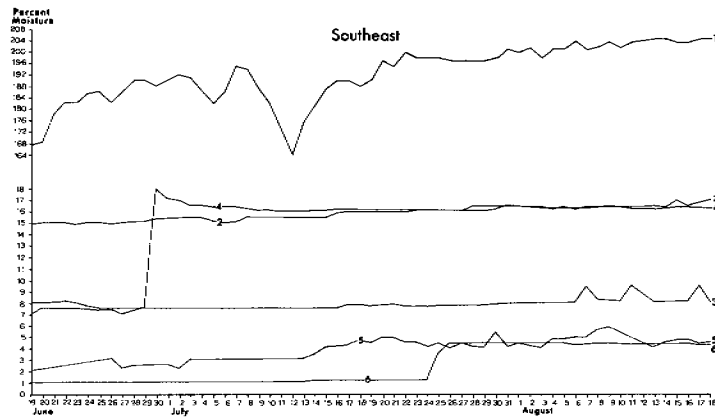


FIGURE 5 Percent soil moisture by weight on study slopes during summer 1968. The numbered lines represent daily readings from Coleman soil moisture and temperature cells that were installed at the surface (No. 1) and at successive 15-cm intervals to a depth of about 80 cm (No. 6).

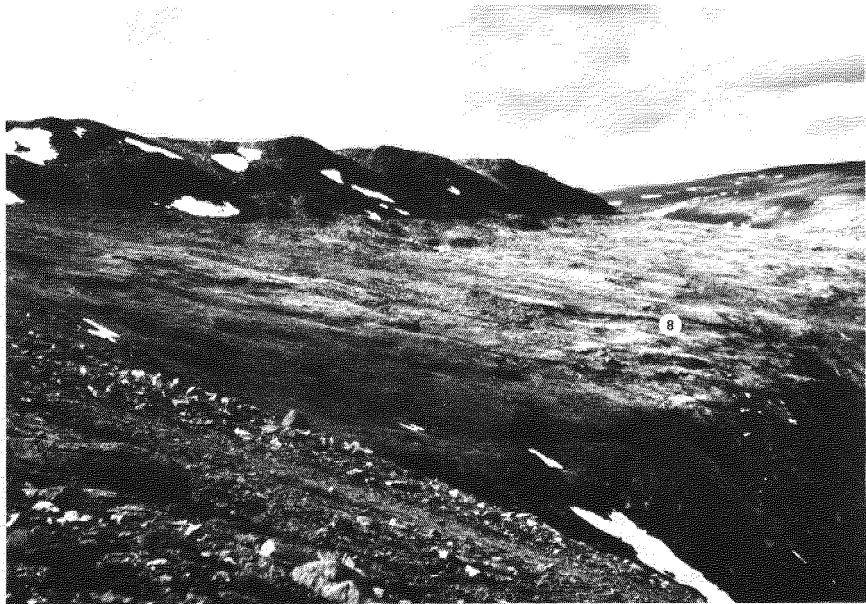


FIGURE 6 View of east-facing slope, looking toward the northwest. The vegetation is well developed and solifluctional lobes average 1-1.5 m high at the risers. The circled number is the site of the single tube excavated on this slope.

Discussion of Tube Measurements

Most of the tube profiles indicate greatest movement at the surface (Table I and Figure 4). Average annual surface movement (cm/year) for the different slopes during the measurement period are as follows:

southeast-facing slope	1.6
east-facing slope	2.7
north-facing slope	2.4
southwest-facing slope	0.7

It was originally thought that the greatest rates of movement would occur on the southeast slope since the solifluction lobes are best developed there.⁶ This has not proved to be the case, however, since, on the basis of the excavated tubes, the most rapid rates of movement occurred on the east- and north-facing slopes. It should be reiterated though that these tubes were not selected to typify movement rates but to provide a check on the accuracy of the probe readings. For example, it is felt that the rates measured for the southeast-facing slope are less than typical for the slope, while the single tube excavated on the east-facing slope may reflect a greater than average rate. This contention is sup-

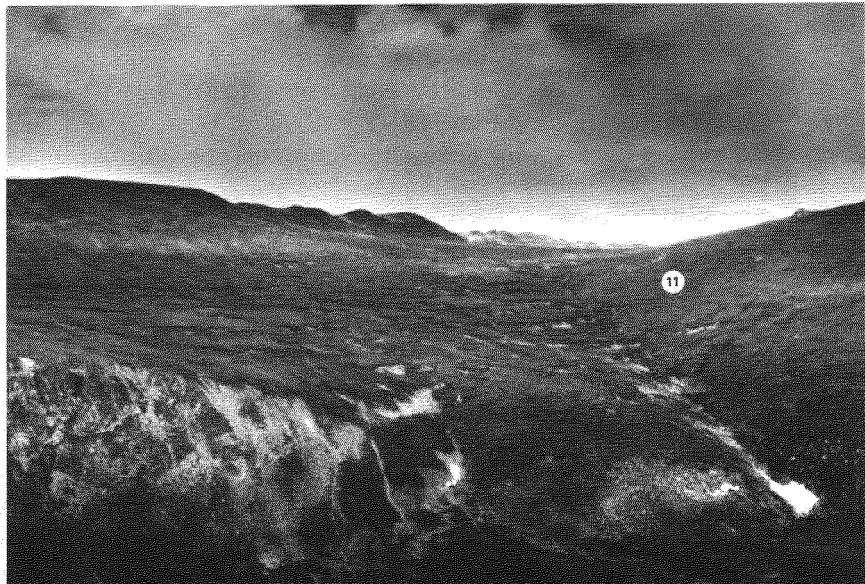


FIGURE 7 View of southeast- and southwest-facing slopes looking toward the north. The circled number indicates location of the tube measurement site on the southwest-facing slope.



FIGURE 8 View of north-facing slope looking toward the southeast. The circled number locates the excavated tube on this slope.

ported by the results of the rock measurements that are based on a larger number of sites across the slopes.

The factors controlling rates of soil movement are complex, but several of the variables in the study area have been held more or less constant since all of the slopes have the same rock type and similar elevations and slope gradients. In addition, instrumental observations were made on several other environmental factors, including weather, soil texture, soil temperature, soil moisture, depth of the active layer, and vegetational development. Each of these is inter-related, and it is difficult to isolate the effect of any single factor; on a comparative basis, however, soil moisture and plant cover appear to be the most important factors in controlling the differential rates of mass wasting on the study slopes.

The weather stations located on the southeast- and north-facing slopes indicate that summer precipitation is very similar. The winter wind is predominately northwesterly, so all of the slopes, except the southwest, receive considerable meltwater during the summer from snow patches accumulating on the ridges above. The soil moisture measurements (Figure 5) indicate highest moisture conditions occurring at the surface on the southeast- and east-facing slopes. This is largely because of the ability of the thick organic surfaces to hold considerable water in relation to their dry weight. On the other hand, the north-facing slope shows a much lower surface moisture content, owing to the lack of a well-developed organic surface. However, subsurface moisture contents are very similar for each of these slopes. The windswept southwest-facing slope, where virtually no solifluction lobes occur, shows a very low moisture content at the surface as well as at depth. The movement rates for

the southwest slope are also the lowest of any of the measurement sites.

Vegetation achieves its highest development in the study area on the southeast-facing slope. This is reflected by a greater number of species, an almost complete plant cover, and by a relatively thick organic layer.⁷ In order of decreasing vegetational development would come the east-, southwest-, and, finally, the north-facing slope, where the fewest number of species occurs, more than half of the surface is bare ground, and the turf organic layer is thin to nonexistent.

On the basis of the above comparison, it appears that vegetation has a marked effect on movement rates. This is particularly true on the southeast-, east-, and north-facing slopes where soil moisture is basically similar, but the plant cover is in great contrast, especially on the north-facing slope where vegetation is very poorly developed and the greatest rates of movement occur.

In conjunction with this, the three tubes on the southeast-facing slope with convex downslope profiles should be mentioned (see Figure 4e,f,g). To the author's knowledge, greater movement below the surface than at the surface in solifluction has not been documented by instrumental observation. Frödin³ mentions that, under a well-developed plant cover on large solifluction terraces in Swedish Lapland, an undergliding (*untergleitung*) may take place. It also has been suggested that, where the vegetation is well developed on solifluction lobes, the plant cover may act as a retaining agent and the solifluctional material would move most rapidly between the turf mat and a rocky base below.⁴ There is no rocky base in the study area, but frozen ground would serve equally well; each of the tubes indicating greater subsurface movement occurs where the vegetation

is well developed. In addition, the level of greatest movement coincides closely with the base of the organic turf layer (Figure 4e,f,g). On uniform slopes, the solifluctional material apparently becomes saturated and flows between the vegetative mat and the frozen ground without breaking or greatly distorting the roots. On the other hand, the occurrence of roots trailing downslope amidst the solifluctional material at lobe risers was occasionally noted.

The exact relationship between surface and subsurface movement is not yet known, but there is a clear indication that subsurface movement does occur and probably dominates in areas having a shallow active layer and a well-developed plant cover, especially as reflected by a thick organic turf layer. The significance of subsurface movement in solifluctional areas may be of considerable importance when dealing with engineering structures.

PAINTED ROCK MEASUREMENTS

Although the mass wasting tubes provide measurement of surface and subsurface movement on and within the lobes, they do not indicate how or at what rate the risers themselves move. To measure this very important aspect of lobe movement, over 300 *in situ* rocks in the lobe risers were painted on all slopes, except the southwest where suitable sites were lacking. The method followed was to select rocks in the riser for measurement and base rocks downslope for control. The riser rocks were painted leaving enough space to mark a small x for measurement purposes. Ideally, these rocks were *in situ*, so whatever movement occurred would accurately represent surface movement; in some cases where no rocks were available, however, rocks were placed on the surface.

It would have been better to have bedrock on which to establish permanent reference points, but the slopes were completely covered with detritus so that large, partially buried rocks below the lobes were used. These rocks were susceptible to movement as was the entire slope, but they appeared much more stable than the riser rocks. In fact, these rocks often serve as dams for the formation and perpetuation of the lobes. An x was chiseled on the base rock, and measurements were made from the center of x to the center of x on the riser rocks. Additional large embedded rocks (check rocks) were selected to help identify any movement of the base rocks. Although circumstances at each site dictated the number of rocks used, ideally more than one check rock was established—both above and below the base rock—and tied together in a measurement network. The same steel tape was used under similar temperature conditions during each measurement period. Accuracy of measurements is considered to be within ± 2 mm.

It is regrettable that location of the measurement sites was largely determined by the availability of rocks at the lobe risers, since rocks were much more prevalent on the

larger lobes. Many of the following measurements, therefore, are primarily indicative of movement on large lobes. On the basis of the tube measurements, the small lobes move more rapidly so the total picture presented by these measurements is conservative.

In analyzing the rock movement data, it became clear that rates of movement across the solifluctional lobes varied considerably from the tread to the riser to the area below the riser. Therefore, the data were analyzed on the basis of these four areas: tread, riser, near lee (within 4.5 m below riser), and far lee (4.5–30.5 m below riser). The most important and reliable measurements are those from the tread and riser (Table II). The rates of movement below the lobe are based on movement of base and check rocks and are not exactly comparable with those from riser rocks, since the former are usually much larger and more deeply embedded. Nevertheless, the near-lee and far-lee measurements provide valuable information, providing caution is used in their interpretation.

Discussion of Rock Measurements

All of the measurement sites under discussion were installed in 1967 and remeasured in 1968 and 1972. The amount of movement for the first year and the average annual movement for the last 4 years were very similar, indicating that movement rates during the 5-year period were similar.

One of the most significant aspects of the rock measurement project is the information it has provided on differential movement across the three slopes. The measurements support the evidence presented by the basic form of solifluctional lobes—that movement is more rapid on the tread than below the lobe (Figure 9). More importantly, however, they establish an order of magnitude in rate of movement from one segment of the lobe to another. For example, on the southeast-facing slope, the tread is moving at a rate eight times that of the near-lee area (Table II). The riser is moving more slowly than the tread, and movement increases again farther downslope in the far-lee area. The ratio between the tread and near-lee area on both the north- and east-facing slopes is five to one. The rates of tread movement correlate nicely to the relative development of solifluctional lobes on each of these slopes, since

TABLE II Average Annual Surface Movement in Zones across Solifluctional Lobes (cm)

Slope			Near Lee	Far Lee
	Tread	Riser	(within 4.5 m below riser)	(4.5–30.5 m below riser)
Southeast-facing	1.6	0.7	0.2	0.4
East-facing	1.4	1.0	0.3	0.2
North-facing	0.9	0.5	0.2	0.4

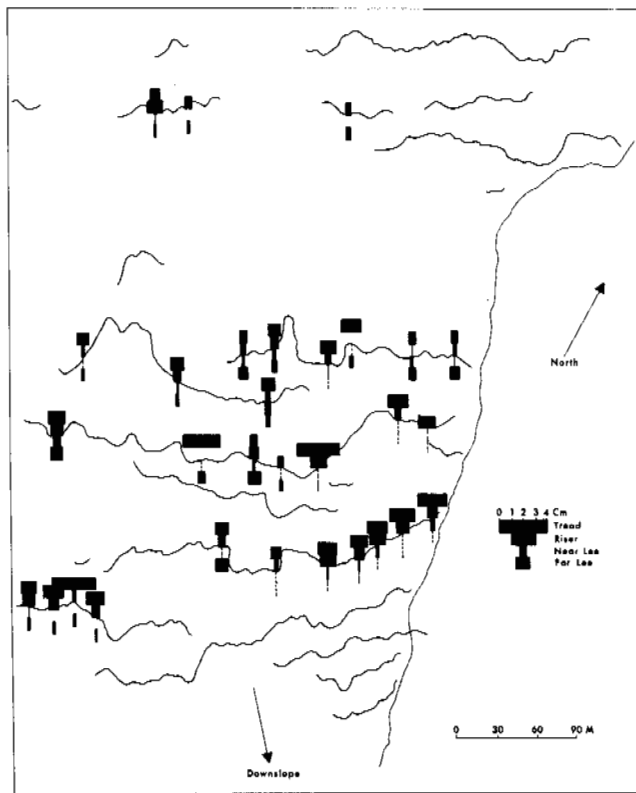


FIGURE 9 Differential movement (cm/year) across solifluctional lobes on southeast-facing slope as reflected by the rock measurement sites. A dashed line indicates zero movement, while a blank space means no data were available for that zone.

they are best developed on the southeast, followed by the east, and then the north-facing slopes (Figures 3, 6, and 9).

As mentioned earlier, some caution should be observed in a direct comparison of these figures, especially those from the near-lee and far-lee areas, since they were interpolated from inferred movement of the base and check rocks. These were usually very large rocks imbedded in the slope and gave the impression of being fairly stable. For this reason, the rates of movement are not exactly comparable. It might be more realistic, for example, to assume that the lobe treads on the southeast-facing slope are only moving four or five times faster than the near-lee areas, with similar adjustments being made for the other slopes (Table II). Nevertheless, the general trend of the relative rates of movement has been indicated.

INTEGRATION AND COMPARISON OF MOVEMENT RATES

The results of the tube and rock measurements, although not in complete agreement, present a general picture of movement rates across the study slopes (Table III).

TABLE III Movement Rates for Excavated Tubes and Rocks

Study Slope	Excavated Tubes (cm/yr)	Rock Measurements (cm/yr)
Southeast facing	1.6	1.6
East-facing	2.7	1.4
North-facing	2.4	0.9

The major disparity between the two sets of data is the measured rates for the east- and north-facing slopes. Only one tube was excavated from the east-facing slope, and it was located on one of the most active lobes on the slope as indicated by the rock measurement sites on this slope. One rock measurement was located 2 m downslope from tube eight, and it moved 10.9 cm during the 5-year period for an average of 2.5 cm/year, which compares favorably with the 2.7 cm/year indicated by the tube. The rock measurements reveal considerably lower rates for the remainder of the slope, however, as is reflected in the overall average of 1.4 cm/year.

A somewhat different situation exists for the north-facing slope. Tube nine was located on a uniform section of this slope, while the rock measurement sites were located on the treads and risers of solifluctional lobes located about 50 m upslope. The vegetation was poorly developed at both sites, and soil moisture was grossly similar, although the lobe risers were very rocky, which tended to promote better drainage. The lobes occur singly rather than coalesced as on the southeast- and east-facing slopes and appear to be largely initiated by the damming effect of large rocks. Unlike the lobes on the southeast- and east-facing slopes, the role of vegetation is insignificant to their formation or perpetuation. From the measurements just summarized, it is clear that the uniform area of the north-facing slope is moving more rapidly than the lobe area. On a cursory basis, this is an apparent paradox since the presence of solifluctional lobes provides such striking visual evidence for rapid rates of mass wasting. Nevertheless, these measurements suggest that certain slopes lacking lobes may experience greater rates of downslope movement than where lobes are well developed. In the study area, this is particularly true for north-facing slopes that have a high soil moisture content but where vegetation is poorly developed.

The measured rates of downslope movement on the study slopes emphasize the great variability that may occur within small areas, owing to microenvironmental differences. Although soil moisture appears to be the major controlling factor, other variables such as vegetation or the damming effect of rocks may alter this simple relationship. In general, however, based on the measurements made primarily on lobe treads and risers, solifluctional lobes are best de-

veloped on slopes where the greatest rates of movement occur. In the study area, these are the southeast-, east-, north-, and, finally, the southwest-facing slope (Table II).

CONCLUSION

The rates of mass wasting in the Ruby Range are, in general, somewhat less than those recorded for other solifluctional areas. These rates have been summarized by Washburn¹¹ and Benedict¹ and range between 3 and 6 cm/year, although there is considerable variation. The rates in the study area are more on the order of 1–3 cm/year (Tables I and II). The lower rates in the Ruby Range may be partially due to the fact that many of the measurements were made on large solifluctional terraces with a complete vegetation cover, whereas many of the measurements from other areas were made on individual lobes. There are, in addition, a great many environmental variables as well as differences in measurement techniques to be considered.⁸ Nevertheless, a fairly coherent picture of mass wasting in periglacial environments is beginning to emerge. Quantitative data on rates of movement have been available for only a few years. Many more measurements are needed over longer periods of time, under different environmental conditions, and from different areas of the world before the total picture of the importance of solifluction and its role in denudation come into sharp focus.

ACKNOWLEDGMENTS

Financial support was provided by the Arctic Institute of North America. Excellent logistical support was provided by the Icefield Ranges Research Project. Thanks are also due to the many people who gave encouragement and assistance in the planning and conduct of this study.

REFERENCES

- Benedict, J. B. 1970. Downslope soil movement in a Colorado alpine region: Rates, processes, and climatic significance. *Arct. Alp. Res.* 2(3):165–226.
- Bostock, H. S. 1948. Physiography of the Canadian Cordillera with special reference to the area north of the fifty-fifth parallel. *Geol. Soc. Can. Mem.* 247.
- Frödin, J. 1918. Über das Verhältnis zwischen vegetation und erdfliessen in den alpinen regionen des Schwedischen Lappland. *Lunds Univ. Arsskr.* 14(24):1–30.
- German, R. 1958. Beobachtungen zur Solifluktion in Schwedisch Lappland. *Geogr. Helv.* 13(4):295–301.
- Love, D. 1970. Subarctic and subalpine: Where and what? *Arct. Alp. Res.* 2:63–73.
- Price, L. W. 1970. Morphology and ecology of solifluction lobe development—Ruby Range, Yukon Territory. Ph.D. dissertation. University of Illinois, Urbana.
- Price, L. W. 1971. Vegetation, microtopography, and depth of active layer on different exposures in subarctic alpine tundra. *Ecology* 52:638–647.
- Price, L. W., and C. S. Alexander. 1971. Methods of measuring mass wasting; Review and critique. *Proc. Assoc. Am. Geogr.* 3:135–139.
- Price, L. W. 1972. Solifluction rates in the Ruby Mountains, Yukon Territory: A preliminary report. 22nd Int. Geogr. Union Montreal 1:56–58.
- Taylor-Barge, B. 1969. The summer climate of the St. Elias Mountain region. Research Paper No. 53. Arctic Institute of North America, Washington, D.C.
- Washburn, A. L. 1967. Instrumental observations of mass wasting in the Mesters Vig district, Northeast Greenland. *Medd. Gronland* 166(4).
- Williams, P. J. 1957. Some investigations into solifluction features in Norway. *Geogr. J.* 72:42–58.
- Williams, P. J. 1957. The direct recording of solifluction movements. *Am. J. Sci.* 255:705–714.
- Williams, P. J. 1962. An apparatus for investigation of the distribution of movement with depth in shallow soil layers. Building Note No. 39. Division of Building Research, National Research Council, Ottawa. p. 1–10.
- Williams, P. J. 1962. Quantitative investigations of soil movement in frozen ground phenomenon. *Biul. Peryglacjal.* 11:353–362.
- Williams, P. J. 1966. Downslope soil movement at a sub-arctic location with regard to variations with depth. *Can. Geotech. J.* 3(4):191–203.
- Zhigarev, L. A. 1960. Eksperimental'nye issledovaniia skorostei dvizheniia gruntovykh mass na solifliuktsionnykh sklonakh. *Trudy (Inst. Merzlotovedeniia im V. A. Obrucheva)* 16:183–190.

SOIL DEVELOPMENT AND PATTERNED GROUND EVOLUTION IN BEACON VALLEY, ANTARCTICA

F. C. Ugolini

UNIVERSITY OF WASHINGTON
Seattle, Washington

J. G. Bockheim

UNIVERSITY OF BRITISH
COLUMBIA
Vancouver, British Columbia

Duwayne M. Anderson

U.S. ARMY COLD REGIONS RESEARCH
AND ENGINEERING LABORATORY
Hanover, New Hampshire

INTRODUCTION

The outstanding feature of Antarctica is its ice sheet. Of the 14 million square kilometers—the size of the continent—only 3 percent is ice free and potentially available for soils to form.

Soil formation in Antarctica, however, is restricted not only by the limited extent of ice-free areas but also by the continuous low temperatures and the paucity of liquid water.

Soils of continental Antarctica are of the desert type; i.e., they are devoid of an organic surficial layer, display coarse textures, are extremely dry, pulverulent, and show poor horizon distinction with minor textural and structural changes and little color differentiation. The soils of Beacon Valley, southern Victoria Land, conform to these general characteristics.

DESCRIPTION OF THE STUDY AREA

Locale

Beacon Valley (77°48'S, 160°44'E) is an ice-free area in southern Victoria Land, consisting of a main valley with a broad, flat floor approximately 18 km long (Figure 1). It contains 10 lateral hanging valleys and two small cirques. Elevation of the valley floor is about 1 200 m at the north-eastern end and about 1 350 m at the southwestern end; local relief exceeds 2 400 m.

Geology

The bedrock consists of Devonian to Jurassic Beacon group sandstones, siltstones, and shale intruded by sills and dikes of Jurassic Ferrar dolerite.¹¹ The floors of the valleys are covered with various tills, consisting of dolerite, sandstone, and granitic boulders, cobbles, and pebbles. Small-scale reliefs on the main valley floor are moraine ridges.

Patterned ground in the form of nonsorted polygons is present throughout the valley. The bouldery nature of the

tills and the microrelief imposed by the polygons create a very uneven and rough valley floor.

There is evidence that the Taylor Glacier has entered Beacon Valley at least five times, including the present entry, leading to five lower Beacon glaciations (Figure 1). The upper valley was invaded by expanded Lashly and Ferrar névés, and the oldest glaciation in the upper Beacon Valley (Upper Beacon V) is represented by an exposed till synchronous with the Lower Beacon Glaciation IV (Figure 1). All the advances subsequent to Upper Beacon Glaciation V have been quite small. Although no absolute chronology for the glaciations in the Beacon Valley has been established, correlation with a general sequence as defined for the Taylor Valley by Denton *et al.*⁵ has been suggested for the lower Beacon Valley.⁹

Based on varying degrees of soil development, three major glaciations were recognized in Beacon Valley. This is in contrast to the four glaciations recognized on the basis of geomorphological consideration. The separations of the tills of Lower Beacon Glaciation III and IV, valid on the basis of surficial expressions and frequency of granitic boulders, cannot be corroborated on the basis of soil development.

Climate

Only scanty data are available for the climate of Beacon Valley. From observations made during austral summers, Berg and Black¹ report that Beacon Valley is affected by greater cloudiness, more copious snowfall, and colder soil temperature than the west-east trending valleys of the McMurdo Sound region. Meteorologic information collected at the year-around Lake Vanda Station for 1969–1970, some 40 km northeast of Beacon Valley, indicates a mean annual temperature of -20°C with an extreme maximum of 10.4°C for January, 1970, and an extreme minimum of -56.9°C for July, 1970. Measurements taken by the authors during the austral summers of 1969–1970 and 1971–1972 indicate that the air temperature for the first week of November fluctuates between -8 and -14°C .

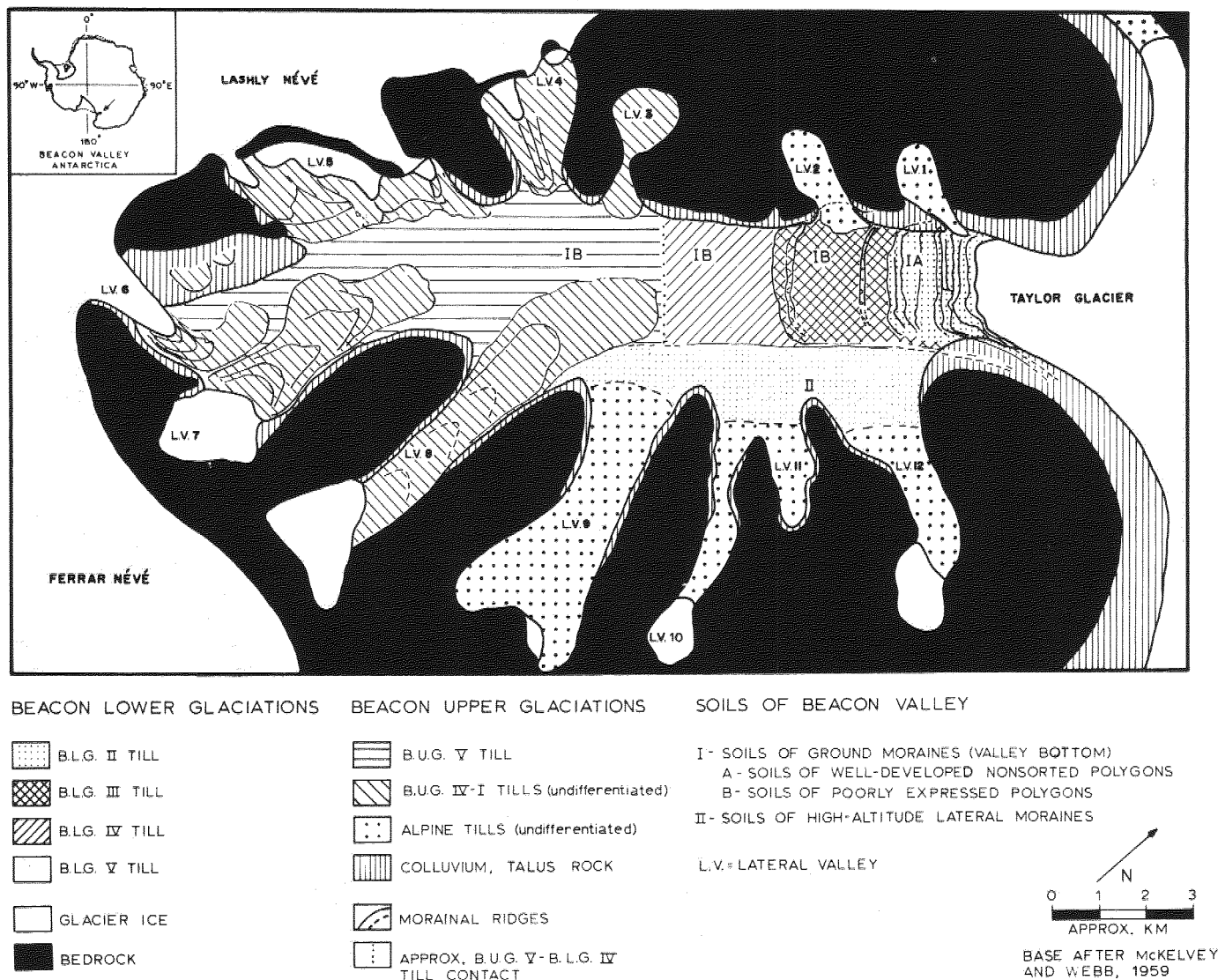


FIGURE 1 Sketch map of the Beacon Valley, south Victoria Land, Antarctica, showing geomorphic features and soil distribution.

Soil temperature at the surface fluctuates between -8 and -13 °C. According to Markov,¹⁰ the climate of Beacon Valley, like the rest of southern Victoria Land, can be classified as a cold desert.

Biota

Although no attempts were made to locate any form of living organisms, it appears that even the most obvious forms, such as mosses and lichens, are not prominent because no record was found in the Valleys, despite much terrain being covered on foot. Janetschek⁷ and Ugolini visited a lateral valley (LV10, Figure 1) during the austral summer of 1961-1962 and in 3 days of searching could find no signs of plants or insects.

PATTERNED GROUND

Patterned ground, mostly of sand-wedge, nonsorted polygons, is ubiquitous throughout the Valley. As first pointed out by Harrington and Speden,⁶ patterned ground on the floor of Beacon Valley displays different appearances, depending on age. Berg and Black¹ quantified the age of patterned ground by establishing the growth rate of wedges. Growth rates were used for dating geomorphic events during the last 5 000 to 10 000 years.

The polygons in Beacon Valley range from 3 m to over 20 m in diameter and occur both as high-center and low-center forms. The low-center forms, however, are the more prevalent. The troughs delineating the polygons range in width from approximately 2 to 6 m.

Field and Experimental Methods

Soil pits opened in the unconsolidated deposits did not penetrate below the frost table or the ice-cemented permafrost. The morphology of the soil was described following U.S. *Soil Survey Manuals*.^{14,15} Slope aspect, size and shape and microrelief of polygons, boulder frequencies, and number of ventifacts and of cavernously weathered boulders were also recorded. Samples were collected according to morphological criteria and sieved in the field through a 2-mm sieve. Volume of >2-mm fraction was recorded. Samples for moisture determination were also collected.

Soil pH was measured on a 1:5 soil-water extract using a Corning pH meter. Electrical conductivity was also determined on 1:5 soil-water extract. Iron was evaluated by extraction with sodium dithionite according to Kilmer.⁸ Chloride was determined by titration with AgNO_3 ; sulfate was determined by precipitation with BaSO_4 .¹ Carbonate was estimated by the amount of effervescence in 1 N HCl.

Mechanical analysis was performed by the hydrometer method of Day.⁴ Clays and clay-size minerals were x rayed with a Picker unit using Cu K- α radiation and a Ni filter.

Soils of Well-Developed Nonsorted Polygons

Soils of well-developed nonsorted polygons occur in the lower Beacon Valley and are associated with the Lower Beacon II till (Figure 1). The polygons have diameters ranging from 5 to 17 m, are high center, and have troughs approximately 1-2 m wide and 1 m deep (Figure 2). The polygon centers are covered with a bouldery pavement containing slightly pitted dolerite and cavernously weathered sandstone boulders. The troughs are filled with clean, well-

rounded sand, and show funnellike depression cones demonstrating the downward movement of sand in the contraction cracks. In November, when the observations were made, snow was present in the troughs and accentuated the polygonal pattern. Soil profiles were excavated in both the center of the polygon and in the troughs. Profiles 3 and 39, respectively, describe the conditions in the center and in the trough.

PROFILE 3, SOILS OF A POLYGON CENTER

The surface has (Figure 3) approximately 20 percent boulders, 5 percent cobbles, and 15 percent gravel. Boulders consist of dolerite and diorite, showing different degrees of exfoliation and pitting. Cobbles are crudely wind sculptured and have a carbonate film on their under surface.

Depth (cm)	Description
2-0	Variagated dry, coarse sand; structureless, single grain; loose, noncoherent, abrupt, and smooth boundary
0-13	Reddish yellow (SYR 6/6) dry, coarse sand; massive structure, breaking down to single grain; weakly coherent; abrupt, wavy boundary; 3 percent gravel and about 5 percent cobbles
13-28	Variagated dry, coarse sand, structureless, single grain; loose, noncoherent, abrupt, and smooth boundary; very few cobbles
28+	Ice-cemented permafrost, or frost table

PROFILE 39, SOIL OF A POLYGON TROUGH

Surface consists of smooth, dry sand with only a few cobbles that have rolled from the steep sides of the nearby high-center polygons (Figure 4).

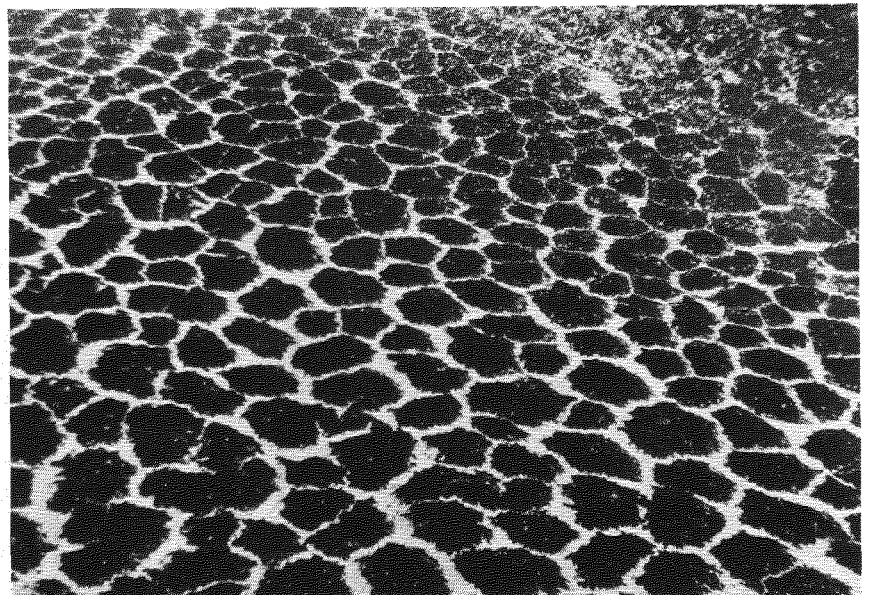


FIGURE 2 Well-developed nonsorted polygons occurring on till of the Lower Beacon Glaciation II. The average diameter of the polygons ranges from 10 to 20 m.



FIGURE 3 Soil of the center of a well-developed nonsorted polygon (Profile 3), Beacon Valley. The first 13 cm below desert pavement clearly shows massive structure and slightly coherent consistency. The subsoil, on the other hand, appears structureless, has a loose, noncoherent consistency, and is able to flow.



FIGURE 4 Soil of the trough of a well-developed, nonsorted polygon (Profile 39), Beacon Valley. The entire thickness of the soil above the ice-cemented permafrost is structureless, loose, noncoherent, and able to flow.

Depth (cm)	Description
0-26	Variegated dry, coarse sand; structureless, single grain; loose, noncoherent; abrupt, smooth boundary; no gravel or cobbles
26+	Ice-cemented permafrost, or frost table; smooth, flat surface

The descriptions of these profiles, corroborated by nine additional profiles in the same area, indicate that there is a consistent difference between the degree of soil development in the center of the polygons and in the troughs. Soils of the polygon centers have an oxidized surface horizon and have acquired some structure. The soils of the troughs, on the other hand, are unoxidized and structureless all the way through. Furthermore, in general, the soils of the center have greater thickness above the ice-cemented permafrost than the soils of the troughs. This difference is related to the degree of activity and stability of the polygon-trough complex. The center portion of the polygon is the least affected by thermal contraction, whereas the trough—the surficial expression of the sand wedge—is the most affected. The area near the wedge is further influenced by the formation of raised rims; as the wedge grows, material is pushed toward the surface. As long as the wedge grows and infilling of sand occurs, soil development in the troughs—in the pedological sense—is disrupted. Normal pedological processes reflecting the impact of local soil-forming factors continue relatively undisturbed in the center of the polygons. In the Beacon Valley, however, soils developed in the center of the well-developed nonsorted polygons are still immature. Based exclusively on field criteria, pedogenesis, as manifested by a reddening and by the acquisition of a weak coherence, has proceeded in the soils of the well-developed nonsorted polygons to a depth of some 10–15 cm. These acquired pedological properties are considered of great importance in the development of nonsorted polygons. As Figure 3 shows, the upper part of the soil has developed some cohesion, but below the structureless sand remains single grain and free to flow. This unconsolidated sand is the same that fills the depression cones in the troughs and wedges.

Soils of Poorly Expressed Nonsorted Polygons

Soils of poorly expressed polygons occur on Lower Beacon III and IV tills and on the Upper Beacon V till (Figure 1). Polygons are large (10–20 m in diameter), have troughs 1–4 m wide, and are generally low-center forms. Secondary wedges occur within some polygons. Many polygons lack a definite border and the perimeters appear diffused (Figure 5).

Compared with the well-developed polygons, the terrain associated with the poorly expressed polygons has a lower

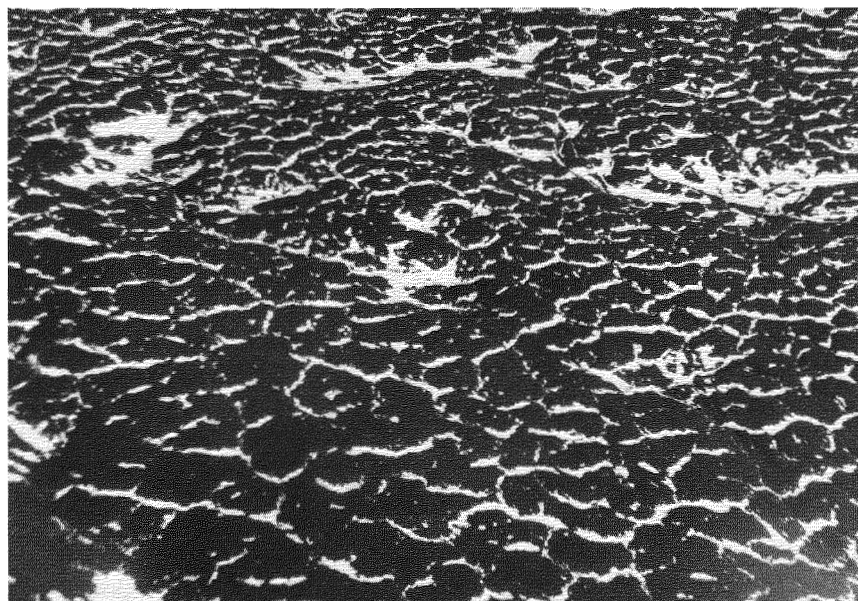


FIGURE 5 Poorly expressed, nonsorted polygons occurring on tills of the Lower Beacon III and IV and Upper Beacon V glaciations. The diameters of the polygons range from 10 to 20 m.

density of boulders larger than 0.3 m in diameter. Dolerite boulders are deeply pitted, wind-polished, and covered with desert varnish. Sandstone and diorite boulders are cavernously weathered. Ventifacts are frequent.

PROFILE 35, SOIL OF A POLYGON CENTER (FIGURE 6)

There was no sign of ice-cemented permafrost. Surface soil temperature at noon on November 12, 1969, was -10.0°C ; at 56 cm it was -20°C .

Depth (cm)	Description
1-0	Poorly defined desert pavement comprised mainly of exfoliated diorite and flaked dolerite cobbles, some exfoliated granites with desert varnish, disintegrated pink rhyolite porphyry, and rounded sandstone cobbles. Matrix comprised of variegated dry, gravelly coarse sand; structureless, single grain; loose, noncoherent; eroded in places yielding abrupt, broken boundary
0-1	Light reddish brown (5YR 6/4), dry coarse sand; massive structure, breaking down to structureless, single grain; weakly coherent; abrupt, broken boundary, 5-10 percent gravel, mostly of weathered diorite; few cobbles
1-10	Variegated dry (very faint and diffuse oxidation), coarse sand; structureless, single grain; weakly coherent; abrupt, wavy boundary; 15 percent angular and subangular gravel mostly of weathered diorite; less than 10 percent cobbles; diffuse salt pervasive
10-37	Light yellowish brown (10YR 6/4), dry, medium sand; structureless, single grain; weakly coherent; clear, wavy boundary; 15 percent gravel, about 15 percent cobbles; contains traces of weathered sandstone

Depth (cm)	Description
37-90+	Light yellowish brown (10YR 6/3), dry, gravelly medium sand; structureless, single grain; weakly coherent; 20 percent gravel, about 15-20 percent cobbles; contains streaks of weathered sandstone plates (pseudomorphs)

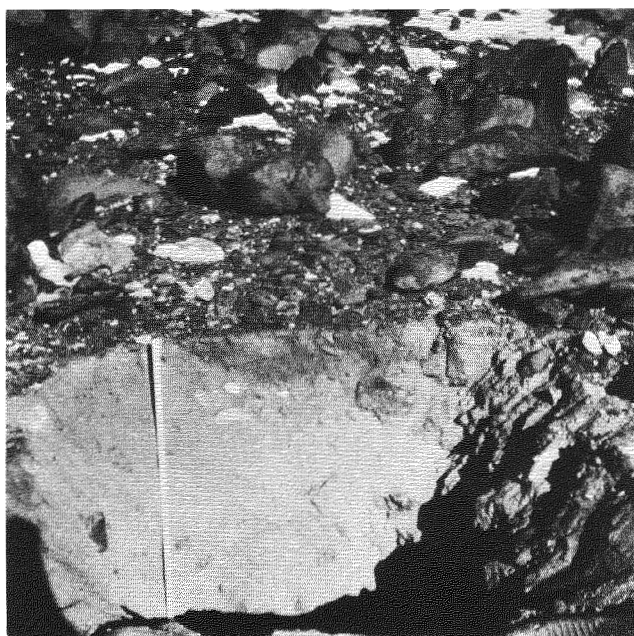


FIGURE 6 Soil of the center of a poorly expressed, nonsorted polygon (Profile 35), Beacon Valley. To a depth of 90 cm, the soil is oxidized, has massive structure, and is slightly coherent. At the surface, diorite boulders are flaked, deeply pitted, and covered by desert varnish.

PROFILE 36, SOIL OF A POLYGON TROUGH
(FIGURE 7)

Surface soil temperature at 1:30 p.m. on November 12, 1969, was -7.0°C ; at 44 cm it was -19.0°C .

Depth (cm)	Description
2-0	Poorly defined desert pavement of angular and subangular gravel and cobbles of pitted and wind-polished dolerite, exfoliated diorite, and some granodiorite and granites. Matrix comprised of variegated dry, gravelly coarse sand; structureless, single grain; loose, noncoherent; abrupt, smooth boundary
0-18	Broad, diffuse, and contorted bands of brown (7.5YR 5/5) and strong brown (7.5YR 5/6), dry, coarse sand; massive, breaking down to structureless, single grain; weakly coherent; abrupt, wavy boundary; 5 percent gravel, less than 5 percent cobbles
18-42	Variegated dry, gravelly coarse sand; structureless, single grain; weakly coherent; abrupt, wavy boundary; 30 percent gravel, about 5 percent cobbles
42+	Ice-cemented permafrost or frost table; irregular surface

Although less pronounced than in the soils of the well-developed polygons, there are differences between the soils of the center and those of the troughs. The soils of the cen-



FIGURE 7 Soil of the trough of a poorly expressed, nonsorted polygon (Profile 36), Beacon Valley. The soil shows diffuse bands imparting differences in color. The massive structure and the weak coherence is responsible for maintaining a vertical face and for preventing the soil material to flow.

ter have acquired a better coloration throughout the profile and show less banding, have a finer texture and a weaker coherence than the soils of the troughs. The ice-cemented permafrost in Profile 35 (soil from the center) was not reached at 90 cm of depth, whereas in Profile 36 (soil from the trough) it was encountered at 42 cm. More details of the chemical features of these soils follow.

RESULTS AND DISCUSSION

Soil development on the floor of the lower Beacon Valley follows a predicted pattern that is a function of age of the glacial deposits, expression of the nonsorted polygons, and position of the soil within the polygon-trough complex. Morphologically, the soils on the older terrain are more oxidized, have finer texture, contain more salt, and have a greater thickness above the ice-cemented permafrost than the soils of the young glacial deposits.³ Tables I and II show that the degree of soil development can be quantified and that the measured physical and chemical parameters go hand in hand with the morphological features. The percentage of free iron oxides are related to reddish and yellowish brown colors of the soils, whereas the clay and the salt content correlate well with the degree of structure and consistence of the soils.

The development of soils in the polygon-trough complex is related to the evolution of patterned ground. As pointed out in the description of the soils, and, as shown in Tables I and II, considerable difference exists between the soil in the polygon center and the soil in the troughs. The soil of the center contains more silt and clay, more salt and more free iron than the soil of the trough. As a result, the structure and consistency of the soil in the polygon centers are more stable. In the case of the soils in the center of the well-developed nonsorted polygons, however, pedogenesis has involved only the upper part of the soil; below the upper 15 cm, the content of silt, clay, salt, and free iron drops sharply to insignificant quantities. In the specific case of Profile 3, 14 cm of structureless, loose sand is present below the surface. This layer provides the local source of sand for filling the troughs and the thermal contraction fissures. The soil in the trough is maintained immature by the continuous addition of fresh material moving outward and downward from the higher polygon centers. Physical and chemical parameters of Profile 39 (Tables I and II) corroborate the morphological observation and demonstrate the youthful condition of the soil in the troughs. The immature soil conditions and the lack of structure and consistence, especially, are critical in allowing the sand to move into the troughs and infiltrate the contraction cracks in the lower-lying ice-cemented permafrost. Wedge growth is therefore not limited by the supply of sand.

On the older terrain where the poorly expressed polygons occur, pedogenesis is farther advanced and has affected considerable thickness of materials, which in the case of

TABLE I Some Chemical Properties of Soils from Beacon Valley, Antarctica

Position of Soil in the Polygons	Profile and Horizon	Depth (cm)	pH	Electrical Conductivity (mmho)	Fe ₂ O ₃ (%)	Cl ⁻ (%)	SO ₄ ⁻² (%)	CO ₃ ^{-2a}
Soil of well-developed nonsorted polygons								
Center	3-1	0-2	6.90	284	-	0.05	0.04	n.r.
	2	2-14	7.50	1 650	0.59	0.12	0.03	n.r.
	3	14-28	7.45	134	0.32	0.03	0.00	n.r.
	4 ^b	28+	7.45	90	0.29	0.02	0.00	n.r.
Trough	39-1	0-3	7.25	250	0.32	0.00	0.00	n.r.
	2	3-24	6.90	450	0.38	0.08	0.03	n.r.
	3 ^b	24+	7.50	80	0.29	0.01	0.00	n.r.
Soil of poorly expressed polygons								
Center	35-1	0-1	7.00	1 120	0.48	0.12	0.24	n.r.
	2	1-2	7.40	2 500	0.55	1.24	0.61	n.r.
	3	2-11	7.65	3 800	0.35	1.24	0.90	n.r.
	4	11-38	7.70	3 150	0.44	1.24	0.05	e.
	5	38-90+	7.95	1 750	0.42	0.50	0.04	e.
Trough	36-1	0-2	7.45	510	0.44	0.08	0.03	n.r.
	2	2-20	7.35	1 700	0.51	0.79	0.87	n.r.
	3	20-44	7.35	2 000	0.64	0.57	0.85	n.r.
	4 ^b	44+	7.60	640	0.41	0.17	0.11	n.r.

^a Effervescence in 1 N HCl; n.r. = no reaction; e. = slightly effervescent.

^b Ice-cemented permafrost or frost table (November, 1969).

TABLE II Some Chemical Properties of Soils from Beacon Valley, Antarctica

Position of Soil in the Polygons	Profile and Horizon	Depth (cm)	Field M.C. ^a (%)	Gravel (%)	Sand (%)	Silt (%)	Clay ^b (%)	Clay ^c Mineralogy
Soil of well-developed, nonsorted polygons								
Center	3-1	0-2	0.43	10	100	0	0	q,M,i
	2	2-14	1.36	2	94	3	3	q,m
	3	14-28	0.59	1	99	1	0	q,m,i
	4 ^d	28+	1.93	-	100	0	0	q,M,i
Trough	39-1	0-3	0.33	0	100	0	0	q,M,i,f
	2	3-24	0.45	0	100	0	0	q,M,i
	3 ^d	24+	8.89	0	100	0	0	q,M,i,f
Soil of poorly expressed polygons								
Center	35-1	0-1	0.71	-	93	4	3	q,m,i,c,f
	2	1-2	1.44	5-10	79	6	15	q,m,i,c,f
	3	2-11	2.61	15	79	10	11	q,m,i,c
	4	11-38	1.48	15	82	10	8	q,m,i,c
	5	38-90+	1.85	20	83	10	7	q,m,i,c
Trough	36-1	0-2	0.68	-	96	4	0	q,M,i,f
	2	2-20	1.41	5	94	1	5	q,m,i,f
	3	20-44	1.10	30	94	3	3	q,m,i,f
	4 ^d	44+	1.73	-	92	5	3	q,m,i,f

^a Moisture content on oven-dry basis.

^b Percent of gravel is by volume; percent of sand, silt, and clay is by weight.

^c Mineral designations: M,m = montmorillonite; Q,q = quartz; I,i = illite; C,c = chlorite; F,f = feldspars. Upper case indicates major and lower case minor amounts.

^d Ice-cemented permafrost or frost table (November 1969).

Profile 35, exceeds 90 cm. Furthermore, the soils in the troughs have also acquired pedogenic features and are considerably more developed than the soils of the troughs of the well-developed polygons (Tables I and II and Figures 4 and 7).

Two soil properties—structure and consistency—are especially important in patterned ground evolution. Both properties go hand in hand with soil development and, therefore, with the age of the land surface. Structure and consistency are controlled to a great extent by the percentage of silt and clay, the salt content, and the sesquioxides, which are iron oxides. All these constituents tend to cement the soil particles. In addition, salts induce flocculation of the clays and, therefore, increase their stability. The soils of the centers and the troughs of the poorly expressed polygons contain appreciable quantities of these constituents (Tables I and II) and display a weak structure and consistency. Therefore it is believed that the growth of the sand wedges is greatly affected by the degree of soil development in the troughs. Once the soils in the troughs have acquired a compound structure, they are unable to flow and, therefore, to fill the contraction cracks. As originally pointed out by Péwé,¹² the nonsorted polygons are actively growing by repeated contraction of the permafrost and infilling of dry sand; these polygons were named sand-wedge polygons in contrast to the common ice-wedge polygons of the Arctic. However, additional investigations by Black and Berg² show that actually wedges of ice, sand, or a composite of the two exist. In the inland ice-free areas of continental Antarctica, because of xeric conditions, sand wedges and composite wedges tend to prevail. The growth of these wedges is very much conditioned, among other things, by the source and availability of sand. As pedogenesis progresses, the availability of loose, free-moving sand is reduced and, consequently, the rate of wedge growth is no longer rectilinear. This lack of uniformity in growth rate may account for the observed discrepancy between the age of the wedges assigned by Berg and Black¹ and the degree of soil development. Based on extrapolation of the annual rate of growth of the wedges in the middle of the Beacon Valley, Berg and Black¹ estimated the age of the land surface to be approximately 6 000 years old. By comparing the morphological and chemical parameters of soils developed on surfaces of known age, in the opinion of the writers, the soils in the middle of the Beacon Valley appear to be older than 6 000 years. Indeed, if it is true that the growth of nonsorted polygons is one of the most important factors affecting pedogenesis,¹ it is also true that pedogenesis greatly affects the growth of nonsorted polygons.

SUMMARY

Two major soil units are distinguished in the northeast half of Beacon Valley, Antarctica. These two mappable units are related to the age of the glacial deposits and to the sur-

ficial expressions of nonsorted polygons. The latter are separated into well-developed, nonsorted polygons and poorly expressed, nonsorted polygons.

The soils of the well-developed polygons appear immature in contrast to the more mature conditions found in the poorly expressed polygons. This distinction is valid morphologically, physically, and chemically. The soils of the poorly expressed polygons have a fine texture, are more structured, are more oxidized, contain more salts, and have a greater thickness above the ice-cemented permafrost than the soils of the well-developed polygons. Furthermore, there is a distinction between the soils developed in the troughs and in the center of the polygons. The soils of the centers are more developed than the soils of the troughs. This distinction is more obvious in the case of the well-developed polygons. Two soil properties—structure and consistency—are of special importance in patterned ground evolution. The growth of the sand wedges is greatly affected by the degree of soil development in the troughs. Once the soils in the troughs have acquired a compound structure enhanced by the presence of salts and clays, they are not able to flow and, therefore, to fill the contraction cracks. If the availability of loose, free-moving sand is reduced, the rate of growth is no longer rectilinear. This lack of uniformity in growth rate may account for the observed discrepancy between the age of the wedges and the degree of soil development.

ACKNOWLEDGMENTS

The authors are thankful to U.S. Navy Task Force 43 for support, Dr. G. Linkletter and Mr. D. Trachte, Jr., for their congenial companionship while in the field, Mrs. Karen Trafton for some of the chemical analyses, R. A. Dayton for drafting, and Drs. M. Singer and A. L. Washburn for reviewing the manuscript.

This study was supported by NSF grant GA13835. D. M. Anderson was supported by NASA interagency order L-9715; however, part of this study was initiated when he was at the University of Washington as Distinguished Visiting Professor.

REFERENCES

1. Berg, T. E., and R. F. Black. 1966. Preliminary measurements of growth of nonsorted polygons, Victoria Land, Antarctica. *In* J. C. F. Tedrow [ed.] *Antarctica soils and soil forming processes*. Antarct. Res. Ser. 8:61-108.
2. Black, R. F., and T. E. Berg. 1963. Hydrothermal regimen of patterned ground, Victoria Land, Antarctica. *Int. Assoc. Sci. Hydrol. Comm. Snow Ice Publ.* 61. 121-127.
3. Bockheim, J. G., and F. C. Ugolini. 1972. Chronosequence of soils in the Beacon Valley, Antarctica. W. P. Adams and F. M. Helleiner [ed.] *Int. Geogr.* 1:301-303.
4. Day, P. R. 1965. Particle fractionation and particle-size analysis, p. 545-567. *In* C. A. Black [ed.] *Methods of soil analysis*, Pt. 1. Monograph 9. American Society of Agronomy, Inc., Madison, Wisconsin.
5. Denton, G. H., R. L. Armstrong, and M. Stuiver. 1970. Late Cenozoic glaciation in Antarctica. *Antarct. J. U.S.* 5:15-21.

6. Harrington, H. J., and I. G. Speden. 1961. Recent moraines of a lobe of the Taylor Glacier, Victoria Land, Antarctica. *J. Glaciol.* 3:946-948.
7. Janetschek, H. 1967. Arthropod ecology of south Victoria Land. In J. L. Gressitt [ed.] *Entomology of Antarctica*. Antarct. Res. Ser. 10:205-293.
8. Kilmer, V. J. 1960. The estimation of free iron oxides in soils. *Soil Sci. Soc. Am. Proc.* 24:420-421.
9. Linkletter, G., J. Bockheim, and F. C. Ugolini. Soils and glacial deposits in the Beacon Valley, southern Victoria Land, Antarctica. *N.Z. J. Geol. Geophys.* (In press)
10. Markov, K. K. 1956. Some facts concerning periglacial phenomena in Antarctica. *Her. Moscow Univ. Geogr.* No. 1. p. 139-148. (Text in Russian)
11. McKelvey, B. C., and P. N. Webb. 1959. Geological investigations in southern Victoria Land, Antarctica. Part 2—Geology of the upper Taylor Glacier region. *N.Z. J. Geol. Geophys.* 2:718-728.
12. Péwé, T. L. 1959. Sand-wedge polygons (tessellations) in the McMurdo Sound region, Antarctica—A progress report. *Am. J. Sci.* 257: 545-552.
13. Richards, L. A. [ed.] 1954. *Diagnosis and improvement of saline and alkali soils*. U.S. Department of Agriculture Handbook 60. U.S. Government Printing Office, Washington, D.C.
14. Soil Survey Staff. 1951. *Soil survey manual*. U.S. Department of Agriculture Handbook No. 18. U.S. Government Printing Office, Washington, D.C. 503 p.
15. Soil Survey Staff. 1962. *Supplement to Agriculture handbook No. 18, Soil survey manual*. (Replacing pages 173-188)

IV PHYSICS, PHYSICAL CHEMISTRY, AND MECHANICS OF FROZEN GROUND AND ICE

Physics, physical chemistry, and mechanics of frozen ground and ice, including geophysical properties, strength properties, unfrozen water, water migration, ice lensing, diffusion

PHYSICS, CHEMISTRY, AND MECHANICS OF FROZEN GROUND: A REVIEW

Duwayne M. Anderson

U.S. ARMY COLD REGIONS RESEARCH
AND ENGINEERING LABORATORY
Hanover, New Hampshire

N. R. Morgenstern

UNIVERSITY OF ALBERTA
Edmonton, Alberta

INTRODUCTION

The proceedings of the First International Permafrost Conference contain 23 papers and 6 extended discussions that deal with topics covered by this title. Three sessions were organized to consider these contributions: phase equilibria, thermal aspects, and physicommechanical aspects of frozen ground. Topics receiving major emphasis at that time were phase composition, theory and practical aspects of frost heaving, factors governing depth of thaw, and rheology of frozen soil. The present appraisal is concerned primarily with developments since 1963. Attention is focused on work done in North America; developments elsewhere will be reviewed by others in companion papers in this volume.

Care has been taken to avoid overlooking significant advancements and new developments. Because of spatial constraints, however, the literature citations are not exhaustive. This is regrettable, since the past decade has witnessed the appearance of a large number of contributions, each worthy of more extensive review and comment than possible in this space. Many of these have appeared in journals serving peripheral disciplines, and it is in the area of these disciplines that this review perhaps is least complete. However, this shortcoming is somewhat mitigated in that a nearly exhaustive bibliography can be constructed from the combined references contained in the publications that have been cited. Priority has been given to contributions appearing in the open literature. Communications of limited availability, such as reports distributed by corporations, academic institutions, and government agencies, are cited when no journal citation is possible and the importance of the development reported warrants it. The section on thermal aspects of frozen ground is not fully developed since this important topic is being treated in Session I.

Bouyoucos^{23,24} laid the foundation in North America for modern investigations of freezing phenomena in earth materials. He demonstrated that frozen soil retains a fraction of its total water content in the unfrozen state and correlated the amount remaining unfrozen at -4°C with the "wilting coefficient" of the soil. Since the wilting coefficient was known to be related to the specific surface area of a given

soil, Bouyoucos, by implication, correctly connected the unfrozen water with the interfacial interaction occurring between the mineral matrix and water. He also showed that the geometry of the mineral matrix and the manner in which freezing was initiated and carried out were important factors governing the state of frozen soil. During this period, the freezing and thawing of water in soils and clays were also investigated intensively by Beskow¹⁹ and Tsytoich.¹⁶¹ Nersesova and Tsytoich called attention to the three principal types of water in frozen ground: ice; strongly bound water; and water that, depending on temperature, may be either frozen or unfrozen.¹³⁰ Although, as shown below, refinements are possible, for most purposes this classification is still adequate.

THERMODYNAMIC RELATIONSHIPS

The Variables of State

Considering the heterogeneity of soils, attempts to identify all the variables that jointly determine the state of frozen ground in a comprehensive physical or thermodynamical treatment become at once extremely elaborate and cumbersome; ultimately, simplification is required. We begin by listing temperature, T (θ , when expressed in degrees below freezing), volume, V , and external pressure, P . Current practice neglects the vapor phase and divides the water into two categories: the "unfrozen water" w_u and ice w_i . Thus, the total water content w is expressed as:

$$w = w_u + w_i. \quad (1)$$

The mineralogical and chemical heterogeneity of the soil matrix usually is avoided by the artifice of regarding each soil as unique. Hence, specifying the soil by name is regarded as equivalent to specifying all its associated compositional variables, including its suite of exchangeable cations (but excluding solutes).

The geometrical aspects of the soil matrix are primarily related to the extent and nature of the interfaces present. These are discussed in some detail in a following section.

Recently, it was suggested that this complexity may be circumvented by employing, as a first approximation, the total specific surface area (internal plus external) S to represent the combined effects of soil texture and the matrix geometry of the frozen soil.¹⁵ Experimental evidence available indicates that this approximation is generally valid below about -5°C . As a governing variable, S is more important than temperature in determining the total unfrozen water content. At temperatures nearer 0°C , this approximation fails and, though seldom known in detail, the specific free energies of the interfaces, together with a geometrical description of interfacial configurations, are required to define phase composition.

The presence or absence of solutes is an important determinant also. Although not yet fully demonstrated, it appears that, in terms of phase composition, solutes create an effect equivalent to a further lowering of the freezing point of soil water roughly equal in magnitude to that calculated from their osmotic potential. Of the various types of uniform force fields that might exist, only electrical fields are sufficiently important to warrant attention; gravitational and magnetic fields are usually negligible. Frozen soils contain charge carriers either as exchangeable ions or as solutes that are free to move in the unfrozen water so that electrical currents can be sustained.

Within the framework of equilibrium thermodynamics, the static physical and mechanical state of a frozen soil-water system can be expressed in terms of γ_i , the specific free energies of the interfaces (or S , the specific surface area in favorable circumstances) w , θ , V , P , and ΣC_i , the concentration of solutes present. One usually assumes a uniform distribution of water and solutes, and this leaves a possible residual uncertainty due to neglected hysteresis.

When one is concerned with the deformation of frozen soil-water systems, the stresses, their history, and the temperature history of the system become the dominant state variables. Few investigations in which all of these factors have been controlled sufficiently well or otherwise accounted for have been reported and the need for systematic studies in which these requirements are met has often been stated but still remains.

Standard States and Water-Ice Phase Equilibria

Application of the methods of thermodynamics requires a specification of standard states for each component present in the frozen soil-water system. The standard state of the mineral matrix is taken as the "dry" solid at 1 atm and a convenient temperature. In all practical situations, the activity of this phase is taken as unity and it, as well as gaseous phases, is normally neglected. Greater attention has been given to the ice phase. Although it has been suggested that ice in frozen ground may exist in unusual phases (elsewhere in this review attention is directed to low temperature phases of

the unfrozen water), it is generally agreed that the ice present is normal, hexagonal Ice I.^{10,11} This has simplified the problem of specifying standard states for the water present: two are possible and equally convenient. The choice may be either Ice I, the solid, or the pure, supercooled liquid, at the temperature of the system and a specified pressure, usually 1 atm.

Choosing the solid (Ice I) as the standard state is convenient in circumstances where the activity of water is established by the presence of a reference "reservoir" of Ice I at a known specified temperature. For example, when water vapor adsorption isotherms are to be measured, plots of water content-relative pressure can yield the unfrozen, interfacial water content directly, since, at a given temperature and at the saturation vapor pressure of ice (a relative pressure equal to unity), the adsorbed water content may be regarded as equivalent to the unfrozen water content of a comparable soil material.¹² This is true because the activity of water in pure bulk ice at atmospheric pressure is a function of temperature only, and, at equilibrium, the activity of water in the unfrozen solution must equal that of the ice. Hence, the activity of the water in the unfrozen solution is seen to have a fixed value for each temperature at which the two phases are brought into equilibrium.

It is often assumed, as an approximation, that the water activity is not influenced significantly by interparticle geometry; at temperatures lower than about -5°C , this has been demonstrated to be true. Hence, the unfrozen liquid water content has been regarded as having fixed values for each temperature at which the two phases are in equilibrium, regardless of the amount of ice present.^{7,130} Hysteresis, while held to be important in some situations, also has been neglected in systematic formulations so far available. It is also assumed that the ice crystals formed are not small and have properties not greatly different from those of bulk ice at atmospheric pressure. Otherwise, since the properties of the ice depend on dimensions when the crystals are small, provisions for this dependence would be required. Fortunately, the ice formed in frozen ground under natural conditions produces relatively large crystals or polycrystalline lenses, and this complication is avoided.

The pure, supercooled liquid at the temperature of the system is a convenient choice for the standard state in other circumstances. Low *et al.*^{90,91} employed this choice of standard states in treating the freezing-point depression, the unfrozen water content, and the heat capacity of frozen ground. Williams and Mitchell¹⁷⁴ also used it in an analysis of isothermal volume changes in frozen ground. The principal difficulty or inconvenience involved in this choice pertains to the fact that the supercooled liquid is an unstable state; therefore, the thermodynamic arguments have a slight air of unreality. Nevertheless, the conclusions, properly derived, are equivalent in either case.

Low temperature (-30 to -50°C) phases of water in

frozen ground recently were found.¹⁴ It is probable that they represent discrete domains within the unfrozen, interfacial water complex, each with its characteristic nucleating temperature; the nature of these phases (domains), however, is not yet well characterized. On the basis of present evidence, it was concluded that these phase changes are not reversible.

The application of thermodynamic relationships to predict and describe phase equilibria has been severely hindered by a lack of suitable data. Much experimental work remains to be done before sufficient data will be available to formulate the thermodynamics of frozen ground in a complete and self-consistent way. Because of their predictive power and efficient representation of experimental data, the development of quantitative phase rules for frozen ground is of high priority in this undertaking.

Relationships from Capillary Theory

Application of the principles of capillarity to practical freeze-thaw problems is hindered by a complicated geometry. However, because it is well founded on surface and interfacial energetics, this approach has great practical utility in facilitating an understanding of frost heaving and ice segregation. Modern treatments of the physics and thermodynamics of capillarity even accommodate hysteresis phenomena and discontinuities ("Haines jumps" or "rheons").¹¹⁸ This gives promise of a quantized theory of realism and wide applicability.

Applications to permafrost and freeze-thaw phenomena to date have centered on problems of phase composition, and ice segregation and frost heaving. Miller has begun to define rules by which the water-ice phase composition of frozen ground may be extracted from soil-water characteristic curves.¹¹¹ He has found it necessary to group soils into those essentially devoid of colloidal particles and those entirely dominated by colloidal particles; no simple general rule could be formulated for intermediate compositions. Further development and comparison between predicted and experimental measurements have been provided by Williams,^{171,173} Koopmans and Miller,⁸¹ and Williams and Mitchell.¹⁷⁴

Two equations basic to any application of capillary theory to freeze-thaw phenomena are the Clausius-Clapeyron equation in its various forms and the Kelvin equation. The former is familiar.¹¹³ For large values of θ , Low *et al.* have given an exact derivation and shown how it may be applied to calculate phase composition and freezing point depressions.^{90,91}

The Kelvin equation applied to the ice-water interface is expressed:

$$(p_i - p_w) = (\sigma_{iw}/\bar{r}_{iw}) \quad (2)$$

For an ice-air interface, it is:

$$(p_i - p_a) = (2\sigma_{ai}/\bar{r}_{ai}), \quad (3)$$

where p_i , p_w , and p_a are the ice, water, and air pressures, respectively; σ is the surface tension, and \bar{r} is the mean radius of curvature of the interface; the subscripts *iw* and *ai* signify the ice-water and the air-ice interfaces, respectively. In Eq. (2), the mean radius of curvature \bar{r}_{iw} is taken as positive on the ice side of the interfaces. In calculations, it is assumed that $\sigma_{aw} : \sigma_{iw} : \sigma_{ai} = 2.2 : 1 : 3.2$.¹¹³ The ratio $\sigma_{aw} : \sigma_{iw}$ is based on the experimental work of Koopmans and Miller,⁸¹ and the ratio $\sigma_{iw} : \sigma_{ai}$ follows from the contact angle between the air-water and the ice-water interfaces.¹¹³ The role of these relationships in frost heaving and ice segregation is considered further in a subsequent section.

Heat Capacities and Latent Heats

Although frozen ground is a complicated system of many components in the gaseous, liquid, and solid states, for practical purposes in expressing the apparent heat capacity, the gaseous phases may be neglected; at constant pressure, only the soil, ice and unfrozen, interfacial water need be considered. Thus, the apparent specific heat capacity of frozen ground is expressed as a sum of the contributions by the three primary components with an additional term to account for the latent heat involved in changing the proportions of water to ice. In utilizing thermodynamic methods, it is convenient to express the properties of mixtures as partial derivatives. Thus, it is desirable to have access to values for the partial specific heats of the soil matrix, ice and unfrozen water, and values for the difference between the partial specific heat contents of ice and the unfrozen, interfacial water.^{6,9-11,45,169} Unfortunately, accurate experimental data are seldom available. Systematic measurements to obtain values for a range of representative situations, therefore, are a research topic of high priority. In practice, the partial specific heat capacities of the components are assumed to be equivalent to the ordinary specific heats, and values are approximated from handbook data. A recent investigation of the heat capacity of frozen montmorillonite-water mixtures indicated that the difference between the partial specific heat and the ordinary specific heat capacity of ice is not distinguishable.³³ The specific heat of the soil matrix, c_s , usually is estimated or, if circumstances permit, measured directly. Oster and Low¹³⁵ have reported values for the partial specific heat capacity of the unfrozen water in a number of clay-water mixtures from which it is possible to deduce corresponding values for the solid matrix. Low *et al.*⁹⁰ utilized these values to derive an apparent heat capacity-temperature relationship for Wyoming Na-bentonite. Anderson⁹ employed a sensitive microcalorimeter to obtain an experimental determination for dry Na-bentonite and reported a value of $c_s = 0.164 \text{ cal/g}^\circ\text{C}$.

The latent heat of freezing of soil water is less than that

of pure water and is equal to the difference between the partial specific enthalpies of the unfrozen water and of ice. It has been shown that values for the unfrozen water content may be derived from experimental values of heats of water vapor desorption and heats of wetting.^{6,115} A similar conclusion holds for the freezing and melting of sea ice.⁸ According to Khakimov,⁷⁶ this idea was perceived in a qualitative way by Vernadskii as early as 1933; subsequently, it was considered briefly in relation to the unfrozen water in frozen soil materials by others,^{80,101,169} but the subject still has not been fully pursued. Until recently, most North American investigators have been content to accept the conventional value and to assume that the latent heat of freezing of soil water is constant. The slight underestimates of the extent of thawing in thermal calculations and overestimates of unfrozen water contents for the most part have gone unnoticed. Errors incurred are negligible, except perhaps for soils containing large quantities of clay. Recently, mathematical modeling has become considerably more sophisticated, and although the latent heat usually is still taken as constant, refinements in accounting for the latent heat term(s) have been made.^{53,125}

The latent heat of freezing is also temperature dependent. This effect is completely negligible in most practical situations and is safely ignored. Although an empirical expression assumed to represent this temperature dependence has been incorporated into the freezing-point depression and a heat capacity equation,⁹¹ this basic relationship for silicate-water-ice interfaces has yet to be defined.

Freezing-Point Depression

Thermodynamic arguments inexorably lead to the conclusion that, at the freezing temperature θ_f of a soil at a given water content, this water content may be taken as or regarded as equal to the unfrozen water content of that soil at the same temperature, even though it may contain additional water in the form of ice. Many will recognize this as a slight oversimplification, since hysteresis here, as in the case with the soil water characteristic curve, in principle, renders the functional relationship between unfrozen water and temperature multivalued. Subject to this uncertainty, however, and looking at it from a slightly different point of view, for a given soil having ice and unfrozen water contents of w_i and w_u at a temperature corresponding to θ_i , any removal of water is accomplished at the expense of w_i so that w diminishes as $w_i \rightarrow 0$. At this point:

$$w = w_u, \quad (4)$$

and

$$\theta_i = \theta_f. \quad (5)$$

Thus $w = w_u$ at the freezing point depression θ_f .

It is probable that this relationship has occurred to a number of investigators over the years. However, since it seems to contradict Bouyoucos²⁴ early insistence that w_u appeared to be governed by freeze-thaw history and to be slightly dependent on w_i , it has not been emphasized. Sufficient data are now available, however (see subsequent paragraphs on water-ice phase composition), to support the conclusions embodied in Eq. (4) and (5). This is fortunate, because establishing this relationship leads, through other thermodynamic relationships, to a number of indirect methods of determining water-ice phase compositions for frozen soil and earth materials.

A general freezing-point depression equation has been derived and instructions for its use have been given by Low *et al.*⁹⁰ When applied to a salt-free Na-bentonite system, this equation was found to fit accurately the combined data of four different investigators, each of whom employed different experimental methods. The complete curve giving θ_f versus w down to -45°C is shown in Figure 1. This curve may be compared with the experimentally determined water-ice phase composition curve for the same system shown in Figure 6 to judge the validity of the practical conclusions drawn from Eq. (4) and (5).

Direct measurements of the freezing-point depression are complicated in the laboratory by the phenomenon of supercooling. (Remarkably, supercooling is seldom observed in the field.) The temperature of spontaneous nucleation is nearly always lower than the temperature at which the soil water is in thermodynamic equilibrium with ice. The temperatures of spontaneous nucleation of six representative clay-water systems over a wide range of water contents have been reported.¹³ The curves have shapes identical to the shape in Figure 1 and in every case they extrapolate, at low temperatures, to a characteristic water content in which freezing is extremely difficult or impossible to induce and, at high water contents, to well-defined temperatures of spontaneous nucleation of from 2 to 8 °C supercooling.

The spontaneous nucleation of supercooled soil water is an interesting topic that merits continued study because of the richness of basic information that may be revealed. Models of the silicate-water-air and silicate-water-silicate interfaces described below accommodate this phenomenon.

THE INTERFACES IN FROZEN GROUND

Much of the subject matter pertaining to the physics and chemistry of frozen ground derives from the nature and phenomenology of the interfaces present. The interfaces are of the following types: ice-ice (grain boundary), ice-water-air, silicate-water-silicate (primarily interlamellar), and silicate-water-ice (extralamellar). This terminology implies that, in contrast to the ice-ice interface, all the others possess a component with liquid-like characteristics. If, in the case of the ice-ice interface, a liquid-like component

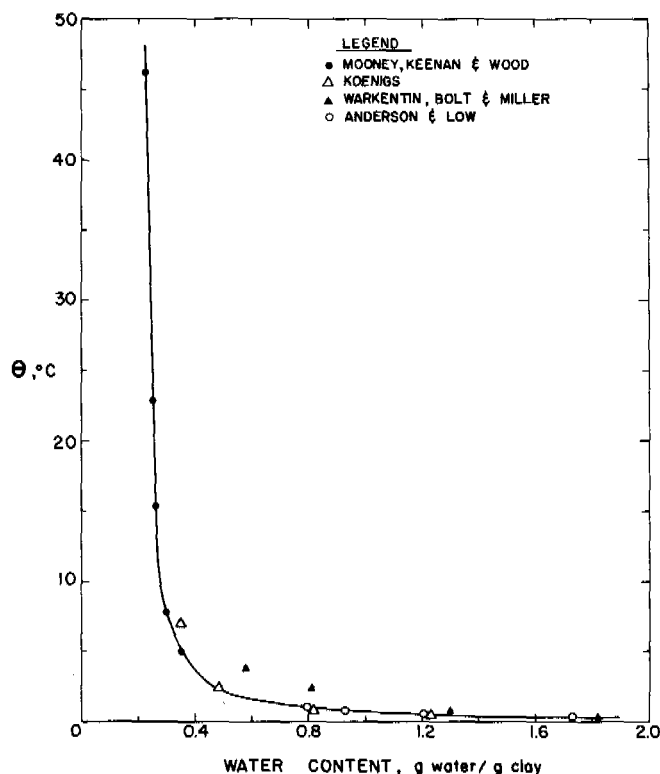


FIGURE 1 Relation between freezing-point depression and water content for Wyoming-Na bentonite.⁹⁰

were present, it should play a role in sintering and grain boundary migration. Recent discussions of sintering and grain boundary migration emphasize the rapidity of migration for small grain boundaries and the effect of bubbles or foreign particles in retarding grain boundary migration.^{28,78} Although others may remain to be discovered, two principal driving forces appear to be involved: the tendency toward a reduction of the interfacial free energy and the alleviation of intracrystalline stresses created during freezing. At present, it is generally accepted that, where no ice-air interface junction is involved, grain boundary migration occurs through lattice vacancy diffusion, and liquid-like behavior seems not to be involved.

In the case of the ice-air interface, the existence of a transition layer possessing liquid-like properties has been proposed by a number of investigators. The history of this controversial subject and a discussion of the evidence bearing on the question has been given by Jellinek⁶⁸; the subject was also treated recently by a number of other workers.^{36,54,65} Proponents of this idea point to the classic study of Nakaya and Matsumoto,¹²⁷ who showed that, when suspended from threads, two spheres of ice brought into contact at temperatures above -7°C adhere to each other and then may rotate, sliding in response to an applied torque. These observations were confirmed by Hosler *et al.*⁶³ This, it is argued, can be

explained only by assuming the existence of a liquid-like surface layer. The results of Jellinek⁶⁸—which indicate that above about -13°C adhesive breaking along the substrate is characteristic of ice bond failure, whereas below -13°C cohesive breaking within the ice occurs—also are cited. In the latter instance, however, the interface studied was a substrate-ice interface and not the ice-air interface in question. In addition, Kuroiwa's⁸² experiments on the coalescence of ice spheres in contact and the sintering experiments of Jellinek and Ibrahim⁶⁹ have been interpreted as indicating the existence of a liquid-like layer. Jellinek concludes that the existence of a liquid-like transition layer is "very likely" and that a thickness of about 100 \AA near the melting point, diminishing to practically zero near -30°C , is indicated. The viscosity of the liquid-like layer appears from the adhesion data to be at least several hundred poises at -4°C , and it is believed that the properties of this layer vary from one side of the film to the other.

Although many remain skeptical, only Hobbs and Mason⁵⁴ and Itagaki⁶⁵ in recent years have disputed the existence of a liquid-like transition layer at ice-air interfaces. Hobbs and Mason re-examined the rate of neck growth between spheres brought into contact by means of the corrected theoretical growth equations of Kuszynski.⁸³ They concluded that, for very clean ice, an evaporation-condensation mechanism is responsible for neck growth; surface or volume diffusion was found to be only 10^{-3} times as effective in mass transport to the growing neck area. Thus, they concluded that the existence of a liquid-like surface layer need not be invoked.

When ice surfaces are contaminated, as with solutes excluded from the ice during freezing, for example, the situation obviously is different. On a NaCl-contaminated ice surface, Hobbs and Mason noted that neck growth was accelerated, and they concluded that, if solutes or other contaminants are present, liquid-like transport phenomena on ice surfaces can occur. Moreover, infrared and other incident radiant energy can help create a thin, "melted" layer, unless scrupulous care is taken to shield the ice surface. This, it seems, is the crux of the matter. Since contaminants are present in most cases, the ice-air interface probably possesses a liquid-like transition layer in all but the rarest cases. The thickness and properties of this interfacial layer probably vary with temperature down to at least -20°C and probably lower.

Evidence bearing on this point may be seen in the wide-line proton nuclear magnetic resonance (NMR) spectra of a sample of fresh snow (the curve shown is the first derivative of the absorption curve) shown in Figure 2 [1]. The absorption band is made up of a narrow component of roughly 2.6 Gauss (G) in width superimposed on a very broad, 17.3-G component. The wide component (making allowances for possible instrumental broadening) is attributable to polycrystalline ice. The narrow component almost certainly must be attributed to surface and/or grain boundary protons be-

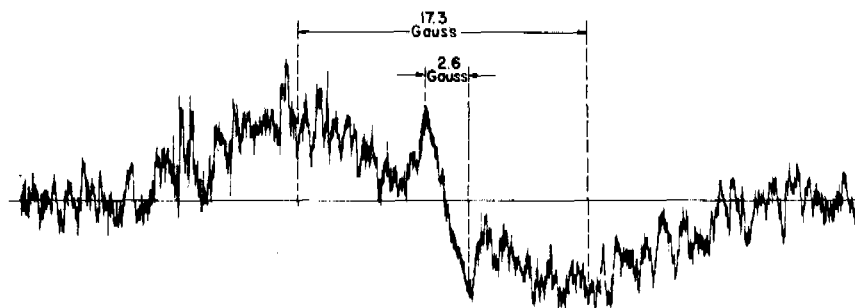


FIGURE 2 First derivative of the proton nuclear magnetic resonance of fresh snow.

cause, when the sample was stored overnight at about -30°C and then scanned at the same settings and temperature, the narrow component, although still present, had diminished considerably in intensity. During successive scans at higher temperatures, the narrow component disappeared entirely whereas the broad component remained until the sample melted. If, as is currently thought to be the case, the narrow component arises from surface protons, disappearance of the narrow component is best ascribed to sintering. As the surface area was reduced continually, the number of surface protons was reduced below that detectable by this technique.

Silicate-water interfaces are common at temperatures above freezing. Water of this type has been extensively studied. Interest in its nature and properties has been widespread, and discussions are available in several recent reviews.^{11,47,89,103} The main controversies in recent years involve the extent to which electrostatic and electrical double-layer theory is adequate to explain soil-water interaction and whether or not "clay-water forces" facilitate the build-up of hydrogen bonded water structures on clay (and more generally on soil mineral) surfaces. Evidence on the density, viscosity, thermodynamic properties of clay-sorbed water diffusion coefficients, etc., has been brought to bear; but many questions remain unanswered and to some extent poorly defined.

Soil colloids are very much more complex than has been conceded by most investigators. This is particularly true for models of the diffuse electrical double layer. Although it has been successful in similar colloidal systems, double-layer theory is not yet developed to the extent required to deal successfully in quantitative terms with all soil-water systems. The presence of hydroxy iron and aluminum complexes, adsorbed gases and other surface-moderating substances, for example,^{21,67,110,144} and the fact that clay-water systems are dynamic, delicately balanced, and seldom in equilibrium with their environment, has yet to be dealt with adequately. In this connection it was suggested recently that silicate surfaces were effective in catalyzing the formation of an anomalous phase of water (polywater). Low and White⁹² speculated that the unusual properties of clay-water systems might be a result of the presence of polywater. The phenomenology

of polywater is not unusual when viewed in the context of solutions and gels, however, and after considering the results of a flurry of investigations, Middlehurst and Fisher¹⁰⁹ and Howell⁶⁴ argue convincingly against the existence of a new anomalous phase of water.

Deductions based on conductimetric and NMR data lead to the view that the water in closest proximity to silicate surfaces is not strongly hydrogen bonded. On the contrary, it seems to be dominated by ion dipole interactions that facilitate increased proton mobility.^{50,99,100,138} Infrared absorption data support this conclusion and indicate less, not more, hydrogen bonding in the clay adsorbed water than in free water.^{86,148} Enhanced proton mobility should facilitate protonation reactions at the silicate-water interface. Observations on the conversion of chemisorbed NH_3 to NH_4^+ , the decomposition of $\text{Co}(\text{NH}_3)_6^{+3}$ on exchange sites, the transformation of triphenyl carbinol into triphenyl carbonium, the protonation of pyridine on slightly hydrated Mg-montmorillonite and the degradation of *s*-triazines confirm the existence of this "surface acidity."^{42,119,120,149,160}

An important point established in these studies is the fact that proton availability increases as the degree of mineral hydration decreases. The closer the hydrated ions and the adsorbed water are to the mineral surface, the more "acidic" is the environment created. We conclude, therefore, that the physical and chemical properties of the interfacial water continually change as the interface changes in thickness. Regions closest to the mineral surface are characterized by an interplay of adsorption forces strong enough to distort the water molecules to the point where the protons become delocalized. Rather than being "quasi-crystalline," the interface appears to be a region of great geometrical heterogeneity. Although the delocalized protons have received much attention and their existence is well established, attempts to test for the presence of the OH ion or free radical by chemical methods have not yet been reported. The role of hydroxyl groups as catalysts for reactions involving sorbed molecules, and the electron acceptor-donor role of clay minerals in the polymerization of styrene and hydroxyethyl methacrylate, however, are being investigated.^{152,153} Until more experiments of this kind are carried out, the true nature of the "surface acidity" implied by protonation reactions and by

the high apparent dissociation constant calculated from dielectric and NMR investigations for the interfacial water cannot be completely understood.

A model of the silicate-water interface developed recently to describe ice nucleation portrays a zone reaching some distance outward from the solid in which the enlargement of the hydrogen bonded flickering clusters postulated as a component in the flickering cluster-mixture model of water is promoted.¹¹ This model visualizes an extension of the lifetimes and an enlargement in the sizes of hydrogen bonded domains that then facilitate the formation and growth of embryo ice nuclei. Heterogeneous nucleation seems not to govern,¹¹ although there is evidence of epitaxy in the laminar ice formed in frozen bentonite-water pastes.^{7,11} Homogeneous nucleation of interfacial water also seems to be common to hydrophobic as well as to hydrophilic surfaces.¹⁸²

Until relatively recently, the silicate-water-ice (SWI) interface was poorly understood; however, this situation is changing rapidly. From x-ray diffraction studies of frozen montmorillonite-water mixtures, it was learned that when expanding-lattice clay-water systems are frozen, the interlamellar spacings collapse immediately to about 9 Å and with further cooling to about 6 Å at -10°C and below.⁷ When the temperature is raised in increments between -10 and 0°C , lattice re-expansion occurs, even though the normal diffraction pattern of ice persists. This is proof of the progressive melting of ice and the concomitant migration of the meltwater back into the interlamellar space. This, together with the fact that the unfrozen water content of these clay-water mixtures corresponds, with only a slight excess, to the volume of the interlamellar space, indicates that when expanding-lattice, clay-water systems are frozen, the ice crystallizes in extralamellar spaces. Two types of interfaces in frozen soils are thus defined: silicate-water-silicate (SWS) interfaces in the interlamellar space and SWI interfaces surrounding individual micelles.

The temperature dependence of the SWS interface thickness has been determined directly for various frozen clay-water systems. A direct determination for the SWI interface in these frozen systems has not been possible. It is possible to derive an estimate, however. Figure 3 gives average interfacial thicknesses as a function of temperature for kaolinite and montmorillonite obtained by dividing their respective, total unfrozen water contents by their respective specific surface areas.^{13,17} Of the two, kaolinite has the thickest interface at temperatures down to about -5°C . Since in the montmorillonite-water system interlamellar SWS interfaces predominate, whereas in the kaolinite-water system exterior SWI interfaces predominate, it follows that the SWI interface is the thicker of the two. However, the SWS interface never becomes thinner than about 6 Å, even at liquid nitrogen temperatures,⁷ whereas from Figure 3 it appears that at very low temperatures the SWI interface might become progressively thinner than that.

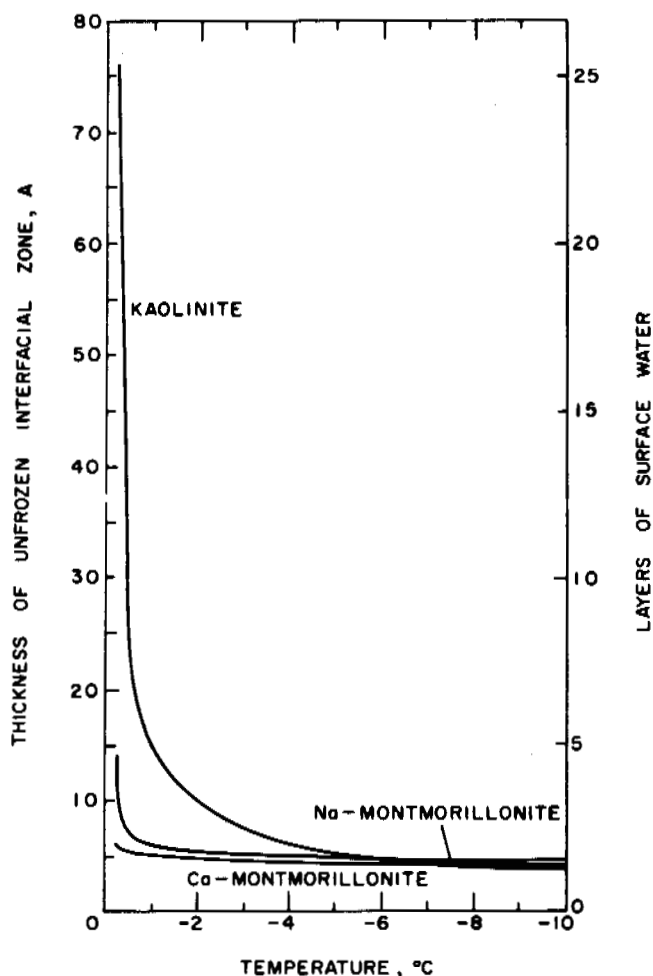


FIGURE 3 Unfrozen water content plotted against temperature for three representative clays. Redrawn from Nersesova and Tsytoich.¹³⁰

The liquid-like characteristics of the interfacial water in frozen soil materials have been well established. In brief, electrical conductance measurements have established the high mobility of charge carriers in the interfacial water. The fact that electrical and thermal osmosis of water is easily accomplished has established the high molecular mobility and the continuity of the interfacial water^{55,56}; and the fact that soil particles suspended in ice migrate through the ice along thermal gradients shows that the mineral particles are free of any but the most feeble and transitory connections to the ice phase.^{10,59}

As in the case of the SWS interface, nuclear magnetic resonance spectra of a variety of clay-water systems at temperatures far below the normal freezing point of water have confirmed the existence of high proton mobility (compared with that of ice) in the SWI interface. The data of Hecht *et al.*⁵⁰ show rapid exchange of protons with interfacial water molecules, but proton exchange with the lattice hydroxyls

is not readily accomplished.⁴⁸ It has been possible to distinguish a certain "fine structure" in the NMR absorption bands that is associated with changes in water content and the type of exchangeable ion present, but the meaning is not yet clear. Clearly, there are interacting shifts in the electrical and magnetic environment, but distinct differentiations have not yet been possible. The proton NMR spectra of Na-montmorillonite are illustrated in Figure 4 [2]. The relationship between absorption line width and temperature for a sample containing two molecular layers of interlamellar water (0.26 g H₂O/g clay) and no ice is compared with that of a sample containing two layers of interlamellar water and a substantial quantity of ice (2.0 g H₂O/g clay). Below -10 °C, all but two layers of the interlamellar water is expelled to form ice in the extralamellar space.⁷ Notice that above 0 °C the absorption lines are narrow, as is characteristic of aqueous solutions. From 0 to -20 °C, there is a perceptible but gradual increase in line width for the sample containing interlamellar water only with a slight hint of a change in inflection near -15 °C. On freezing the ice-containing sample, the line width, in contrast, rises more than fivefold over that of the ice-free sample. As the temperature is lowered further, the line width increases, but only gradually. Below -20 °C, in either case, the line widths

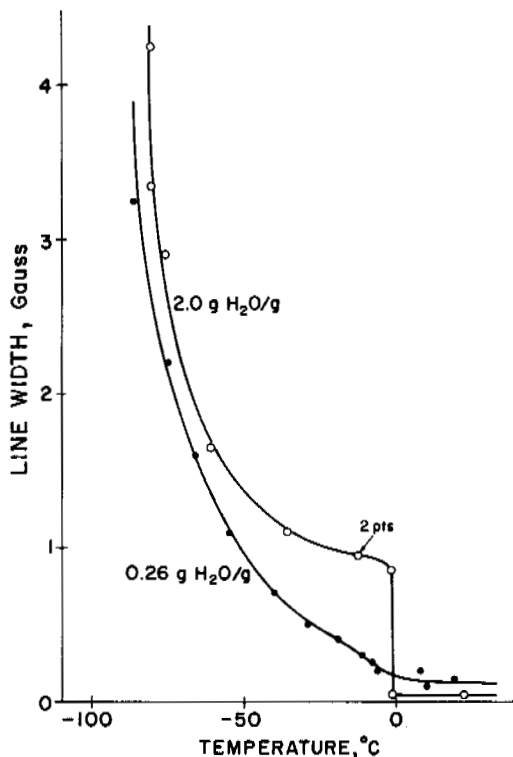


FIGURE 4 Relationship between absorption line width and temperature for proton NMR in Na-montmorillonite (Wyoming bentonite) at two selected water contents.

increase more or less exponentially with temperature, with no sharp discontinuities.

The upper line in Figure 4 is associated with the liquid-like interfacial water in the ice-containing sample. Graham *et al.*⁴⁸ have deduced the viscosity of the interfacial water in unfrozen vermiculite, montmorillonite, and hectorite from NMR resonance line widths and compared it with that of the pure water. Free water has a line width of about 0.05 mG, whereas, allowing for broadening due to field inhomogeneity and ferromagnetic constituents, the line width of interlamellar water at large $d(001)$ spacings is about 30 mG. Assuming a direct proportionality, they concluded that at ambient temperature the viscosity of interlamellar water at large interlamellar spacings is some 600 times greater than that of free water, equal roughly to that of glycerol. Using the same index of mobility, it would appear from the data of Figure 4 that the viscosity of the SWI interface could be as much as five times larger than that of the SWS interface, even though at a given temperature it is the thicker of the two.

The nature of the water-ice interface has been approached in connection with the measurement of freezing potentials by Drost-Hansen.³⁵ As he visualizes it, six zones, ranging from the bulk liquid (consisting of clusters of clathrate cages and monomers) to normal ice, may be distinguished. Separating these boundary phases is a disordered transition layer akin to Frank and Wen's region of "enhanced structure breaking around a hydrated ion."⁴⁰ Next is a zone consisting of a highly ordered layer of four coordinated water, termed "polar ice" inasmuch as many of the protons in this region are believed to be aligned perpendicular to the interface. The existence of this zone was postulated primarily to account for selective ion incorporation in ice during freezing. Immediately adjacent are two zones within the solid phase in which dipole orientations are in various stages of relaxation and the selectively incorporated anions are being neutralized by migrating protons.

By simple combination, the main features of the SWI interface as they may be deduced from the foregoing are illustrated in Figure 5. The diagram is self-explanatory for the most part, but some elaboration of the terms "order" and "disorder" is appropriate. The leading models of liquid water are "mixture models" involving monomers and either hydrogen bonded clusters, clathrate structures, or other arrangements in various proportions; to this extent, water is said to be "ordered." The zone of embryo formation mentioned earlier, synonymous with the zone of "enhanced order" in Figure 5 is believed to be more structured than that of free water in the sense that the rapidity of formation and dissolution of the clusters or cages is thought to be diminished and the sizes of the clusters or the numbers of cages are thought to be larger than in free water. The number of clusters or cages per unit volume is believed to be

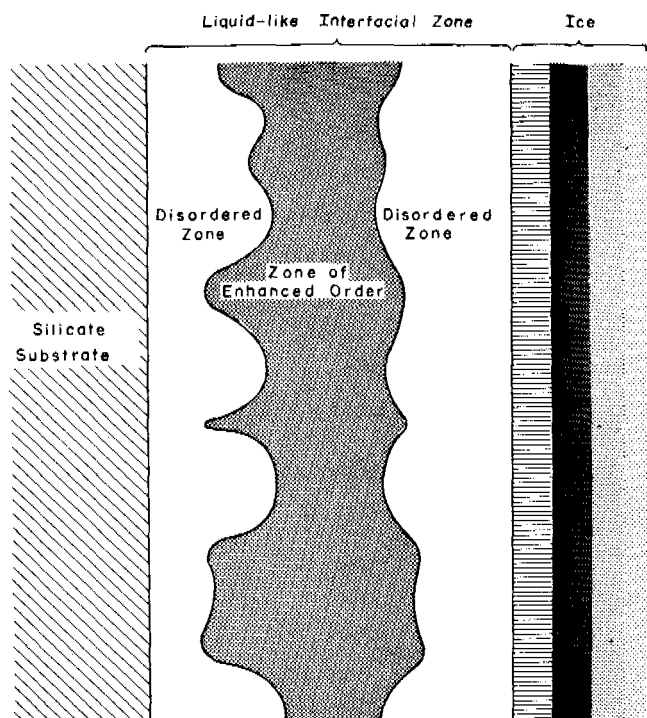


FIGURE 5 Schematic illustration of the silicate-water-ice interface.

reduced in the zones of disorder; monomers predominate there. Moreover, monomers closest to sites of surface charge, or adsorbed cations, and water coordinated to ions located in the interfacial region undergo proton delocalization that leads to a proton activity in this zone many orders of magnitude higher than that of free water. It seems a paradox that, although the viscosity of water in the silicate-water and the silicate-water-ice interfaces, on the average is higher than that of normal water, proton mobility is greatly increased; nevertheless, the evidence available at present indicates that this may be the case.

Two zones are shown in Figure 5 as "disordered." For the zone adjacent to the silicate surface, this portrayal is based on the evidence against hydrogen-bonded water networks and in favor of increased proton motion cited earlier. For the zone adjacent to the ice surface, the argument is based on the principle of microscopic reversibility.³⁵ This principle requires that the addition of water molecules to the ice lattice during interface advance must be caused by the same mechanism as the removal of water molecules during melting. If groups of water molecules are held to add on as "ice-like" units, it becomes difficult to explain the phenomena of supercooling and the large entropy of fusion. If we suggest that perhaps the units are not "ice-like" but clusters or cages of some different geometry, then there is difficulty in simultaneously incorporating large numbers of these into a con-

tinuous hexagonal lattice. One concludes, therefore, that the dominant mechanism is the addition or subtraction of monomers. Furthermore, on the molecular level there must be continual exchange of water molecules within and between zones. The species that is most compatible with the phases present is the monomer; hence, addition or subtraction of monomeric units is the most probable mechanism by which the interface is thickened and thinned. As Drost-Hansen³⁵ has argued, this view is supported by the observation that ice-like crystals grown from the melt and ice formed by vapor condensation commonly show identical morphological features, suggesting that similar mechanisms are involved in crystal formation under widely different conditions.

Since the NMR data show the SWI interface to be more structured than either bulk water or the silicate-water interface, and the above arguments require the presence of two zones in which monomers are dominant, it follows that clusters and/or cages predominate in the intervening region. Measurements of the partial specific volume of water in an SWI interface indicate a water density less than that of free water.⁵ This is in harmony with the concept of increased hydrogen bonding, but it appears that hydrogen bonding proximate to clay surfaces is less well developed than that in free water. Since monomers are held to predominate in the two "disordered zones," this is expected to increase the average interfacial water density. To bring about a net decrease in the average interfacial water density, it is necessary to invoke the existence of an intermediate zone where hydrogen-bonded clusters and/or cages predominate.

In exercising this tentative model of the SWI interface, it should be kept in mind that cations predominate in numbers over anions at the silicate surface and, during advance of the ice-water boundary, anions probably predominate next to and within the polarized "pseudoice" transition layer. It is generally conceded that all cations and most anions tend to be water structure breakers, whereas F^- and OH^- seem to be net "structure makers" in water.⁴⁰ It is thus possible that OH^- may play an important role in promoting local orientational order if delocalized protons are attracted to and tend to reside near the negatively charged silicate surfaces.

Protonation reactions have not yet been attempted at the SWI interface. However, the evidence cited above leads one to believe that attempts to carry out such reactions will be successful. The freezing of soil water is equivalent to drying the soil; in both cases water leaves the mineral matrix. Since proton delocalization is greatest at the lowest hydration states, we conclude that protonation reactions are facilitated by a thin interfacial region. Protonation reactions in the SWI interface, therefore, may be possible at quite low temperatures in systems where the water (ice) content may be high enough to inhibit reaction at normal temperatures.

WATER-ICE PHASE COMPOSITION OF FROZEN GROUND

Methods of Measurement

Recognition of the importance of the unfrozen water phase that separates ice from the mineral and organic soil matrix has created the need for methods of determining the water-ice phase composition of frozen soil throughout the whole range of temperatures of practical importance. Dilatometry, adiabatic calorimetry, x-ray diffraction, heat capacity, nuclear magnetic resonance, differential thermal analysis, isothermal calorimetry, and several indirect methods have been developed to this end. Although each technique involves a different set of approximations and assumptions, results obtained by the various methods are remarkably consistent. They also are in excellent agreement with the results of predictions based on the thermodynamic relationships discussed above.

DILATOMETRY

The dilatometer was employed by Bouyoucos²² and Bouyoucos and McCool²³ to demonstrate that all the water present in a soil is not converted to ice when the soil freezes. This method was subsequently utilized to good advantage by Buehrer and Aldrich²⁷ and Hemwall and Low⁵¹ and more recently by Koopmans and Miller.⁸¹ One of the critical assumptions involved in the dilatometer method involves the extent to which the "immiscible liquid" remains completely inert when it covers the sample and fills all the interstices. If the interface so formed is large enough and if partial solubilization or some other interaction with an associated volume change occurs, then a potentially large error can be involved. The other critical assumption is that soil water expands on freezing to the same extent as pure water in bulk. If the density of clay-adsorbed water is less than that of water in bulk in some cases⁵ and if this is generally true for all or most soils, then the dilatometer method yields a slight overestimate.⁷ Complete phase composition data by this method have not been reported, but results that have been obtained, as expected, are somewhat high when compared with those obtained by other methods.⁹ This method is most suitable in the temperature range of 0 to about -2°C .

ADIABATIC CALORIMETRY

The adiabatic calorimeter has been the device usually used to determine unfrozen water content and the principles of the method are well known.^{101,128,129,170}

Aside from the normal sources of error associated with adiabatic calorimetry, the accuracy of the determination rests entirely on the following assumptions: (a) The values of the heat capacity of all the sample components and their temperature coefficients are known; (b) during thawing, no

processes accompanied by heat effects other than absorption of the latent heat of melting are involved; and (c) the latent heat of melting ice in the frozen soil is known (79.75 cal/g). As Martynov¹⁰¹ has observed, the heat capacities of the various components of frozen soil generally are not known accurately; and, inasmuch as allowance usually is not made for the variation of heat capacity with temperature, the lower the initial sample temperature, the less reliable the result. Regarding the second assumption, it is known that when soils freeze they become differentiated into layers of segregated ice and mineral and organic matter. When the ice is melted substantial quantities of water must then be redistributed throughout the sample to achieve the original state. This process must have a heat effect. Most, if not all, of this heat corresponds to a heat of wetting or dilution when the redistributed water again attains proximity to the mineral surfaces. Thus, the third assumption is questionable. The experimental investigations required to fully define the required correction factors have not yet been done; hence, the theoretical basis of the adiabatic calorimeter method is not yet fully established. Nevertheless, it has been the preferred method. Phase composition data obtained by this means have been reported by many investigators.^{80,88,128,130,169,170} Nearly all of the data compare well with data obtained by other methods although a few of the results clearly are too high.⁹⁰

Like the dilatometer method, the adiabatic calorimeter method yields no direct information regarding the distribution, state, or properties of the unfrozen water.

X-RAY DIFFRACTION

In the x-ray diffraction method, the average distance between individual lamella in a frozen sample of a platy clay is determined at various temperatures. It is assumed that during freezing, segregated ice crystals and polycrystalline ice masses grow at the expense of the unfrozen water surrounding the soil grains. From a knowledge of the total surface area of a 2:1 lattice-expanding clay and the average distance between adjacent mineral surfaces, an estimate of the volume of the unfrozen water contained between adjacent lamella is obtained. The x-ray diffraction method does not have wide applicability. To satisfy the inherent assumptions and the instrumental requirements, it probably cannot be employed with samples other than the expanding-lattice clays. Furthermore, the method is very time-consuming and requires expensive apparatus. When uni-ionic clay-water pastes of Wyoming bentonite are frozen, the spacing between individual clay lamella decreases from very high values to small limiting values as the temperature falls through 0°C to liquid nitrogen temperature. The amounts of interlamellar water calculated at various temperatures from the observed lattice spacings and the total surface area accessible to water correspond nearly exactly to the unfrozen water contents

reported by Nersesova and Tsytoich,¹³⁰ resolving an earlier conflict in published values of unfrozen water content for this clay.⁷

The interlamellar water contents obtained from the x-ray diffraction data are slightly lower than the calorimetric unfrozen water contents. This is understandable since the x-ray diffraction method does not account for the unfrozen water bounding external surfaces. The significant fact, however, is that nearly all the unfrozen water present is accounted for as interlamellar water. This confirms the view that the unfrozen water exists in a layer intimately associated with the mineral surfaces and not as isolated pockets of soil solution. The rapidity of lattice expansion and collapse, and the concomitant movement of water observed as the temperature of the frozen sample was changed, is evidence of the high degree of fluidity of unfrozen interlamellar water, and is indicative of the liquid-like properties of unfrozen water in general.

HEAT CAPACITY

Consider the heat capacity equation:

$$c_a = c_i w + c_c + w_u (c_u - c_i) + (1/\Delta T) \int_{T_1}^{T_2} L \left[(\partial w)/\partial T \right] dT, \quad (6)$$

where c_a = the heat capacity of the mixture per degree expressed per unit weight of soil; w = the total water content; w_u = the unfrozen water content of the frozen mixture; T = temperature; c_c = the partial specific heat capacity of the soil; c_i = the partial specific heat capacity of the ice; c_u = the partial specific heat capacity of the unfrozen water; and L = the latent heat of freezing.

The first term in the brackets is the partial specific heat of the soil; to a good approximation, it can be regarded as independent of water content and constant. At a given temperature, w_u also can be taken as constant¹³⁰; hence, the second term in brackets is constant if, as is probably true, the difference between the partial specific heats of the ice and the unfrozen water is not sensitive to changes in water content. It is known that the unfrozen water content does not vary greatly with w ; hence, it is unlikely that a change in w at constant temperature will cause a significant change in the two partial specific heats. Therefore, the second term in brackets also may be taken as constant. The last term represents the heat of phase change accompanying changes in the ratio of unfrozen water to ice due to the temperature fluctuation necessitated by the measurement itself. If the conditions of the measurement are kept invariant from sample to sample, the limits of integration T_1 and T_2 will

be the same, and ΔT must be constant. Since the unfrozen water content depends principally on temperature, the functional relationship between $(\partial w_u/\partial T)$ and T and between L and T will, to a good approximation, be the same for each sample. Therefore, the numerical value of the last term in Eq. (6) may be taken as constant during an experiment.

When conditions can be arranged so that the foregoing assumptions are valid, a plot of the heat capacity of a frozen soil-water mixture versus its total water content yields a line having a slope equal to the partial specific heat capacity of ice and an intercept equal to the sum of the last two terms of Eq. (6). The plot departs from linearity whenever the total water content decreases below the point at which the ice phase disappears, for at this point the amount of unfrozen water w_u no longer can be independent of water content and the required assumptions no longer are valid. Equation (6), therefore, permits a determination of unfrozen water contents in frozen clay-water mixtures by locating the water content at which the ice phase just disappears and only the unfrozen water remains. At this point $w = w_u$, which corresponds to the point at which plots of the heat capacity versus total water content depart from linearity. Only one application of the heat capacity method has so far been reported.⁹ Results obtained corroborate those obtained by the x-ray diffraction method for Wyoming sodium bentonite and are in general agreement with results obtained in comparable samples by the adiabatic calorimeter method.

NUCLEAR MAGNETIC RESONANCE

Phase composition data can be derived from NMR spectra. Although apparently employed only once, this method has great potential. In this instance, advantage was taken of the fact that the unfrozen water has a very narrow spectral line compared with that of ice.¹⁷⁷ From a number of observations made on specimens of differing water content at selected temperatures below 0 °C, one determines the water content at which the wide ice absorption band first appears. At water contents below this value, all the water is unfrozen. Thus, a determination of the water content at which ice first appears is equivalent to a determination of the unfrozen water content at the temperature prevailing. Again, the critical assumption is that the unfrozen water content at a given temperature is independent of ice content. This assumption has been invoked in preceding sections and it will appear again. It should be possible to eliminate it by developing a more sophisticated approach based on the quantitative determination of both the ice and the unfrozen water contents from detailed line-shape analysis of the combined wide-line NMR absorption bands. Calibration samples and several spectra taken at different instrumental settings probably will be required, but eventual success seems assured. It is also possible to develop a successful method utilizing pulsed NMR techniques.

DIFFERENTIAL THERMAL ANALYSIS

Differential thermal analysis (DTA) is closely related to calorimetry. When properly calibrated, it is appropriately called differential scanning calorimetry (DSC). In DTA, the temperature of a sample is compared by means of an electrical thermometer with that of an inert reference substance while both are exposed symmetrically to a uniformly changing temperature. During a phase change, the sample temperature either lags behind or precedes that of the reference substance, depending on whether heat is being liberated or absorbed. When a moist soil is frozen during a low temperature DTA run, an exotherm corresponding to liberation of the latent heat of freezing is observed. The magnitude of the signal is proportional, in the first approximation, to the quantity of ice formed. This correspondence is the basis for an estimate of an unfrozen water content.¹⁴

Consider a sample as though it were thermally uncoupled from its surroundings; freezing liberates the latent heat of fusion L and causes a rise in sample temperature of:

$$\theta = [(w - w_u)L]/c. \quad (7)$$

The relationship between θ and total sample water content can be obtained from a series of analyses. Then, as is apparent from Eq. (7), when $\theta = 0$:

$$w = w_u. \quad (8)$$

Thus, the unfrozen water content is obtained by determining the water content at which θ for the freezing exotherm goes to zero. Although Eq. (7) does not account for all the processes involved in the evolution and disposition of energy within the DTA cell, a detailed analysis also yields Eq. (8) as the final result.¹⁴ A determination of the water content at which the sample does not yield an exotherm due to freezing is thus equivalent to determining the unfrozen water content w_u at that temperature. The value of w_u obtained is thus seen to be associated with a temperature somewhat lower than the nucleation temperature of the driest sample in the set. Invariably, this is from -10 to -30 °C. This is the range where the phase composition curve approaches its minimum value and becomes insensitive to large variations in T . Thus, the DTA method is useful primarily as a method of determining w_u at low temperatures where the dilatometer and adiabatic calorimeter methods have been most questioned. It is satisfying to note that results obtained by the DTA method are in quite good agreement and have substantiated earlier values obtained by these methods.

ISOTHERMAL CALORIMETRY

The isothermal calorimeter method of measuring the water-ice phase composition of frozen soil material was developed to exploit the relationships and to circumvent the limitations of the DTA method. To achieve equilibrium, a constant tem-

perature was provided during a premeasurement equilibration period. To extend the DTA method to obtain more than one point on the phase composition curve, control over the temperature of nucleation and the initiation of nucleation was provided.^{16,17}

Because of the difficulty of undercooling samples without spontaneous nucleation occurring before thermal equilibration is achieved, this method is limited to temperatures above about -10 °C. However, since the w versus T curve becomes quite flat at these temperatures, this is not a serious limitation. At the lower end of its temperature range, where the adiabatic calorimeter method is most liable to uncertainty, the isothermal calorimetric method, like the DTA method, is most reliable. The agreement between the results obtained by this means and those obtained for the same clays by the other methods discussed above is therefore significant. It is also significant that values of w_u are obtained after freezing in the isothermal calorimeter, the dilatometer, and DTA method, whereas they are obtained after thawing in the adiabatic calorimeter method and during either a rising or falling temperature regime in the case of the specific heat and x-ray diffraction methods. Although it is true that when redistribution of water is not allowed for or is prevented, freezing history is important¹⁴; the agreement among these diverse methods indicates that when a reasonable period (of the order of an hour or more) is allowed for water redistribution after melting and prior to refreezing, sample freezing history has only a minor influence on w_u .

THE THERMODYNAMIC METHOD

Determination of the minimum water content at which ice can exist is equivalent to a determination of the freezing point depression at that same water content. This is the relationship expressed in Eq. (8) and in Eq. (4) and (5). In addition to a direct measurement, there are a number of ways of deriving freezing-point depression curves from the soil-water characteristic curve (also known as soil-suction, matric-suction, and soil-water tension curves). We mention some experimental procedures from which the data necessary to construct this curve may be obtained without elaboration: determination of water vapor adsorption isotherms, tensiometric measurements, and pressure membrane apparatus measurements.^{52,79,81,131} Conversion into the freezing-point-depression curve via the soil-water potential function is direct and easily accomplished.⁹⁰ It is probably the most accurate indirect method available at temperatures near 0 °C, the region in which unfrozen water contents change most dramatically with temperature. This is also the range in which thermodynamic data generally are most readily available and the required assumptions most generally valid.

INDIRECT DETERMINATIONS

Although not quantitative in nature, Murrmann *et al.* found that the relationship between the self-diffusion coefficient

of sodium ion and temperature in a frozen montmorillonite-water system corresponds remarkably to the phase composition curve.¹²² While investigating the attenuation of shock waves in frozen soil, Nakano and Froula were able to estimate the phase composition of their frozen sample based on the prevailing heat balance. This work is reported elsewhere in this volume.

Summary of Recently Published Data

In the interval following the first International Permafrost Conference, a considerable number of phase composition curves have been published. Williams has given complete phase composition data down to -5°C for Leda clay, Winnipeg clay, Niagara silt, and iron ore.¹⁷¹ Similar data

for several size fractions of New Hampshire silt have been reported by Koopmans and Miller.⁸¹ Phase composition data down to -7°C have been reported for powdered basalt, powdered hematite, West Lebanon gravel, Limonite, Fairbanks silt, Dow Field silty clay, Suffield silty clay, kaolinite, Hawaiian clay, Wyoming bentonite, and Umiat bentonite.¹⁵ The latter are collected and shown in Figures 6 and 7.

During this investigation, it was found that the unfrozen water contents of most frozen soils are conveniently represented by a simple power curve:

$$w_u = m\theta^n, \quad (9)$$

where m and n are characteristic soil parameters and θ is

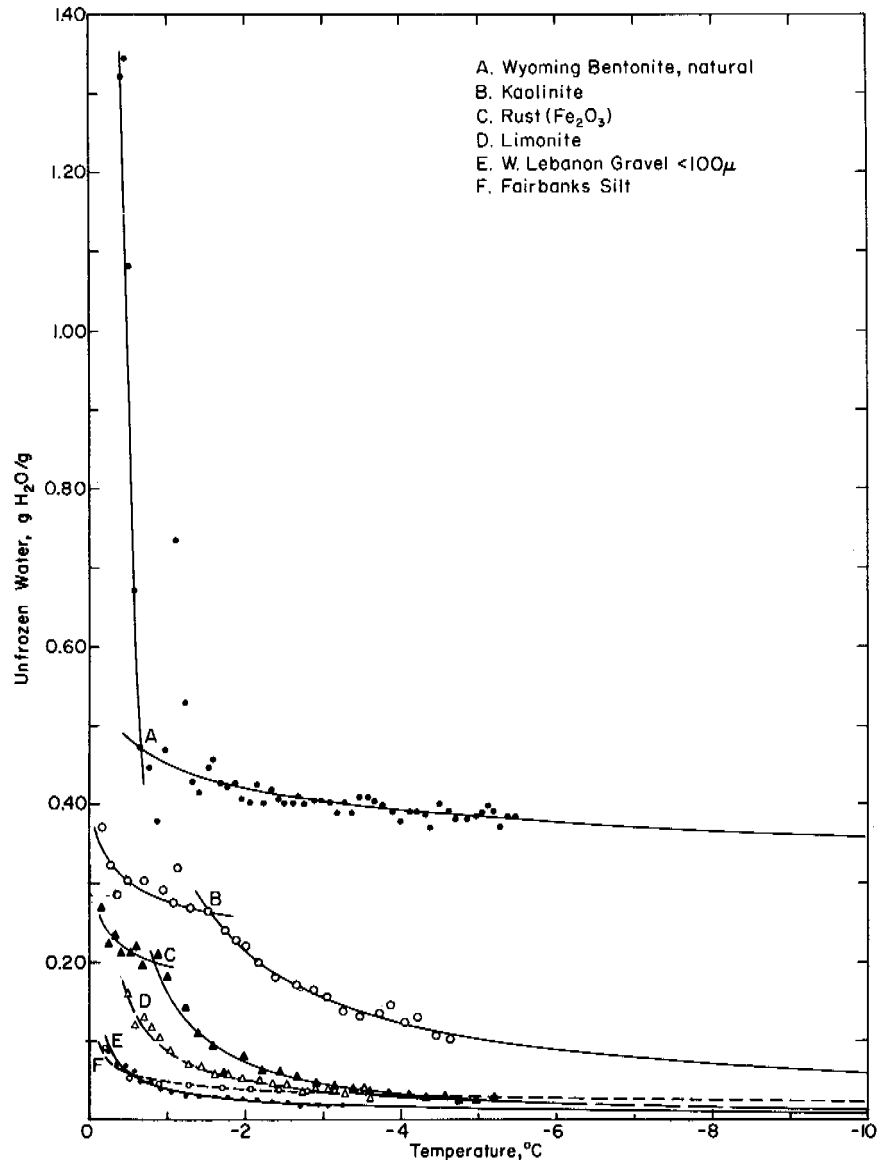


FIGURE 6 Phase composition curves for six representative soils and soil constituents.

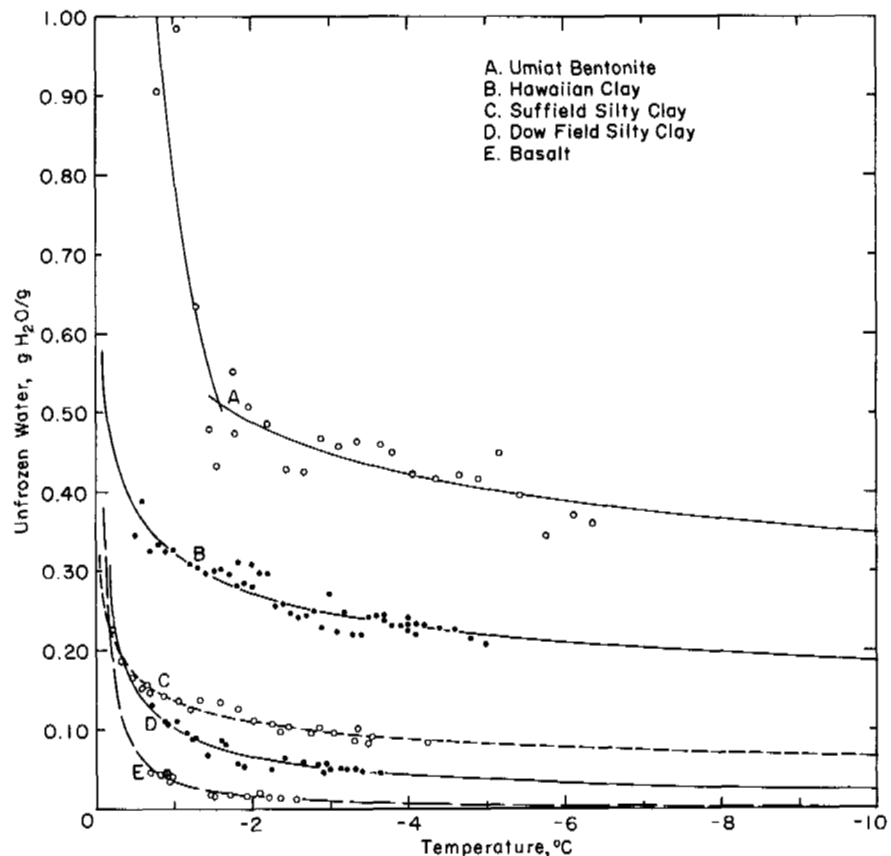


FIGURE 7 Phase composition curves for five representative soils and soil constituents.

temperature, expressed as a positive number in degrees centigrade below freezing

$$[\theta = (0 - T)].$$

Soils with extremely high clay contents, however, were found to be more complex; segments of two curves of the form of Eq. (1) with different values of α and β are required to fit the data precisely. The significance of this finding is not completely understood. It is believed, however, that it is a reflection of the existence of two distinctly different interfacial domains in platy, layered soil materials. Each domain evidently has its own characteristic freeze-thaw equilibria.

Two prediction equations giving the unfrozen water content of frozen soil as a function of temperature have been published. That of Dillon and Andersland incorporates values for the specific surface area, the Atterberg limits, the freezing-point depression of the pore water, clay mineral type, and a defined activity ratio for the soil³³; the other requires values for surface area only.¹⁵

From a regression analysis of phase composition data for a suite of representative soils having widely varying properties and characteristics, it was found that the relationship

$$\ln w_u = a + b \ln S + cS^d \ln \theta, \quad (10)$$

where a , b , c , and d are empirical constants and S is the specific surface area of the soil, holds sufficiently well to yield a good first approximation of the unfrozen water content, w_u at any temperature, θ , below freezing. Data needed to compare the relative accuracy of the two prediction equations are not available: either equation is useful for hurried estimates. The latter, because of its superior representation of experimental data throughout the entire temperature range is well suited for incorporation in mathematical models of the thermal behavior of frozen ground such as that of Ho *et al.*⁵³ and that of Nakano and Brown.^{124,125}

Effect of Overburden Pressure

The imposition of pressure at constant temperature increases the unfrozen water content of a frozen soil. This qualitative conclusion also follows inexorably from thermodynamic arguments. Early indications that the effect is significant were provided by Tsytoich.¹⁶² It also was concluded that ice in frozen soil is more easily melted by the imposition of pressure than by ice in bulk.^{11,91,147} The form of the Clausius-Clapeyron equation applicable to this situation is:

$$dp/dT = \Delta\bar{H}_{fs}/T\Delta\bar{V}. \quad (11)$$

The factors determining the solid liquid boundary on the phase diagram for ice in frozen soil involve the magnitude of the reduction in the freezing temperature T and the diminished latent heat of freezing soil water, $\Delta\bar{H}_{fs}$.¹⁶ Data are not available to fully resolve the question, but estimates indicate that, of the two opposing effects, the decrease in $\Delta\bar{H}_{fs}$ predominates. It is also necessary to consider $\Delta\bar{V}$, if there is a possibility that it can become very small. The specific volume of ice is about 10 percent greater than that of water at 0 °C; according to Anderson and Low,⁵ however, the specific volume of the interfacial water in montmorillonite is at least 3 percent greater than that of pure bulk water so that $\Delta\bar{V}$ must be reduced accordingly. This conclusion, although controversial and widely debated, has not been refuted. Moreover, there were indications in that work that, as the temperature was lowered, $\Delta\bar{V}$ for a given thickness of interfacial water was reduced still further. A final limiting value could not be determined, but it is believed that the lowering of T and the effect of a decreasing $\Delta\bar{V}$ are subordinate to the effect of decreases in $\Delta\bar{H}_{fs}$. A consequence of a decreasing slope of the solid-liquid line with decreasing water content is that ice immediately adjacent to montmorillonite surfaces is more susceptible to pressure melting than normal. The application of pressure thus tends to increase the thickness of the unfrozen water interface. This is of importance in ice segregation and frost heaving. Particle migration in ice due to thermal gradients has been shown to occur at temperatures near 0 °C.^{58,59} If the foregoing is true, the application of pressure is expected to increase the rate of particle migration at a given temperature. The application of sufficiently high pressures might even induce particle migration at temperatures lower than have so far been reported.

Indirect calculations of the magnitude of the pressure effect have yielded estimates of increases in w_u of the order of 0.3 g unfrozen water per gram montmorillonite at -1 °C and 0.02 g unfrozen water per gram clay at -10 °C for Δp 's of 100 atm.^{59,90} In a calorimetric experiment designed to test these predictions at temperatures and pressures of practical interest, Chumichev³² failed to find evidence of a significant increase in w_u for montmorillonite-water, powdered quartz-water, and loam soil-water mixtures at pressures up to about 8 kg/cm². The observed increase (average of six determinations) amounted only to about 0.002 g unfrozen water per gram clay in the case of montmorillonite at -3 °C compared with about a predicted value of the order of 0.003 under these conditions.⁹¹ This small increase was believed by Chumichev to be less than the resolution of his measurements. He concluded, therefore, that the hypothesis that an increase in confining pressure increases the unfrozen water content was unsubstantiated. The predicted value is close enough to that actually observed, however, to

render the test inconclusive. Clear-cut evidence that the thickness of the unfrozen water interface does increase with increasing pressure is provided in the observation of Hoekstra and Keune⁵⁸ that the electrical conductance of a frozen clay-water mixture increases dramatically with pressure. Nevertheless, further investigation is required to clarify questions surrounding this important topic.

Effect of Solute

The effect of solutes in the soil water on phase composition is to shift the unfrozen water content-temperature (the phase composition) curve toward lower temperatures. It is generally believed that the shift is of a magnitude comparable with the freezing-point depression of the soil solution corresponding to the osmotic potential of solutes added, although the data needed to establish a general relationship are lacking. This point of view has been resorted to by Williams¹⁷¹ in correcting phase composition data where soil solutions having freezing-point depressions ranging from 0.1 to 0.3 °C were involved. A systematic investigation of this topic also is timely.

Low Temperature Phases

Analysis of six frozen clay-water systems by low temperature DTA has revealed the existence of phase changes involving the unfrozen water component between -35 and -60 °C.¹⁴ An example is shown in Figure 8. The exotherms corresponding to these phase changes do not depend critically on ice content, but are related to clay mineral type and the exchangeable cations. Kaolinite and halloysite yielded single exotherms at -37 and -39 °C, respectively. The lithium, sodium, and calcium forms of montmorillonite yielded three at -33, -35, and -43 °C. The magnitude of each exotherm was found to be of the order of 0.1 cal/g clay. It is believed that these exotherms result from a sudden release of unfrozen interfacial water and its migration from characteristic domains to adjacent ice crystals where it freezes. Other explanations are possible, however, and the correct one remains to be established.

WATER AND IONIC MOVEMENT IN FROZEN GROUND

Water Movement in Frozen Ground

In general, water movement in frozen soil is analogous to flow in unfrozen soils but flow is confined primarily to the unfrozen interface and there is little or no contribution of vapor transport.

Soil water moves readily in response to gradients in the soil-water potential. Movement may occur in either or both the liquid and vapor state and in each phase as mass move-

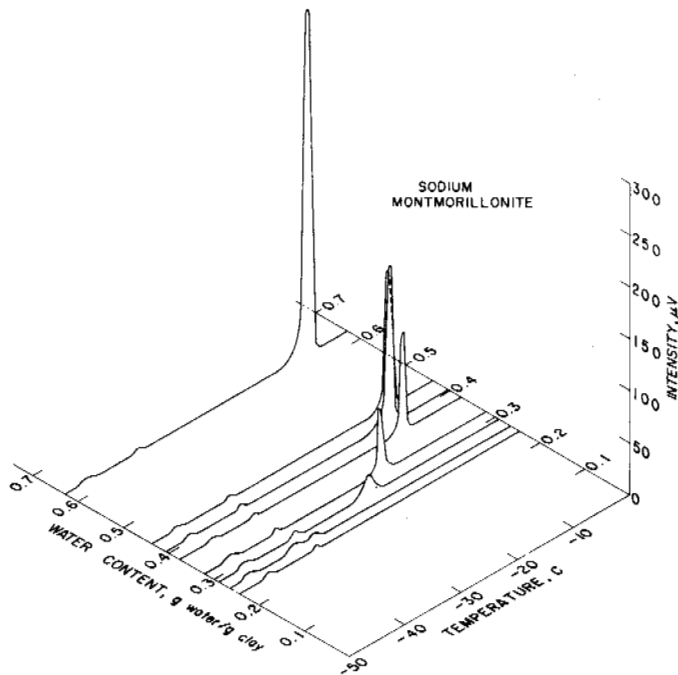


FIGURE 8 Low temperature differential thermal analysis curves for Na-montmorillonite.

ment or diffusive flow. Inasmuch as the soil-water potential is composed of pressure, gravitational, temperature, matric, compositional and electrical components, gradients in any of these tend to induce water movement. In unsaturated soils, vapor transport sometimes is significant. In unsaturated frozen soils, vapor transport also may play a role provided the interconnecting pore space is not blocked by ice. Where unfrozen channels predominate, flow is adequately described by application of the Darcy law. This aspect of the subject is considered more fully elsewhere in this volume.

When the ice content of the frozen soil is high, water movement takes place in the unfrozen, interfacial layer. While it is anticipated that this flow also obeys the Darcy law, no supporting data are available. Dirksen and Miller³⁴ verified earlier reports that frozen soil actively extracts water from unsaturated unfrozen soil by setting up a water potential gradient in the attenuated interfacial water films and demonstrated that the hydraulic flow thus induced provides the water required for ice lens growth. Vapor transport occurred but was found to be not essential to the development of heaving pressures. Ferguson *et al.*³⁹ also established the importance of liquid transport from warm to cooler regions as a consequence of temperature gradients. The effectiveness of a constant electrical field in causing the redistribution of water in frozen ground by electroosmosis has been described by Hoekstra and Chamberlain.⁵⁶ Net movement occurs toward the cathode.

In an experiment designed to confirm the perpetual existence of the unfrozen interface separating ice from soil

particles, Hoekstra⁵⁹ measured the rates of microscopic movement of soil particles through ice in which they were embedded. Movement was induced in response to small temperature gradients. Particles migrated toward the warmer regions at rates up to $7 \mu\text{m}/\text{h}$. The results were explained in terms of a continual melting of ice and a flow of water from the warm side of the particles to the cold side where the water refreezes, displacing the particles forward. The unfrozen water layer surrounding the particle was portrayed as asymmetrical, its thickness depending on the local temperature. It is thickest on the warm side and thinnest at the cold side. This asymmetry leads to an unbalanced osmotic pressure since the exchangeable ions on the particle surfaces tend to be constrained to a uniform distribution over the particle surface and the particles are thus constantly thrust forward.

Hoekstra^{59,60} also reported the migration of water in frozen soil in response to imposed thermal gradients. Flow rates up to $0.63 \times 10^{-4} \text{ cm}/\text{s}$ were measured.

A set of phenomenological equations describing both water and salt movement in unsaturated frozen ground have been reported by Cary and Mayland.³⁰ These equations were tested in a series of experiments in which temperatures ranging over the soil profiles varied from -0.5 to -5°C . Water and salt redistribution in a silt loam was followed for 6 weeks. It was found, in agreement with earlier investigators, that the dominant water flow occurred along a pressure (suction) gradient in the unfrozen water interface. A typical flux observed was $1 \times 10^{-5} \text{ cm}/\text{day}$ at an average matric potential of -10 bar. Cary and Mayland³⁰ pointed out, as did others before them, that equations such as these are applicable only when ice lensing does not occur; otherwise, established flow paths are disrupted and flow is drastically and unpredictably reduced.

As expected, the rate of water flux increased as the amount of soluble salt was increased because of the resultant enlargement of the thickness of the unfrozen interfacial layer. Since flow takes place in the unfrozen interfacial layer, the more extensive and interconnected it is, the larger is the water and salt flux. Frozen fine-grained soils, with a resulting high specific surface area, are thus expected to have relatively high capacities for water and salt redistribution compared with coarser-textured soils. The equations of Cary and Mayland do not predict the type of moisture flow associated with needle ice formation (discussed below), nor do they simultaneously connect salt and water flux with heat flux, a problem that Takagi has treated.¹⁵⁷ These problems still remain.

Ionic Migration

Inasmuch as ions and solutes tend to be rejected from the growing ice lattice, they are excluded to and confined to the domains of the unfrozen interfacial water. Here they are con-

centrated and mixed with the exchangeable ions. The mobility of these ions and solutes in this liquid-like zone is only slightly less than in a normal aqueous solution, when the tortuosity of the available migration routes is taken into account. The ability of the exchangeable cations in a frozen montmorillonite water mixture to redistribute themselves can be seen from the self-diffusion coefficient of the sodium ion. At -15°C it was determined to be about $1.7 \times 10^{-7} \text{ cm}^2/\text{s}$, only a factor of 10 less than that for the same sample at 25°C .¹²² When bentonite-silt mixtures were studied, it was found that the self-diffusion coefficient for the sodium ion ranged from $1 \times 10^{-7} \text{ cm}^2/\text{s}$ (the value for the silt-water mixture at -3°C) to $5 \times 10^{-7} \text{ cm}^2/\text{s}$ (the value for the montmorillonite-water mixture at the same temperature), respectively. The self-diffusion coefficient decreased rapidly with decreasing temperature near 0°C but by -15°C became nearly constant, closely mimicking the water-ice phase composition curve.

Ions in the unfrozen interfacial water function as charge carriers in an electrical field. It is not surprising, therefore, that the temperature dependence of the low frequency electrical conductance of frozen montmorillonite-water mixtures also is similar to the phase composition curve.^{58,59} During initial supercooling of the system, a slight decrease in conductivity corresponding to the decrease in thermal energy of the charge carriers and the increase in viscosity of the aqueous medium was observed. On nucleation, there was an abrupt drop as the charge carriers were suddenly restricted and confined to the unfrozen interfacial water layer.

Diffusion of $^{22}\text{NaCl}$ in the ice-aluminum interface behaves similarly.¹²³ Diffusion coefficients of 9.4×10^{-8} and $4.5 \times 10^{-8} \text{ cm}^2/\text{s}$ were obtained at -5 and -10°C , respectively. At these temperatures, the unfrozen interface is only 5-10 Å thick; this explains the two to three orders of magnitude reduction from the value characteristic of an aqueous solution. The observed values are still two to three orders of magnitude higher than that of ice at these temperatures, however.

In an earlier section, attention was directed to the probability that water molecules in the unfrozen interfacial zone are more readily dissociated to form hydroxyl and hydronium ions than normal. These ions also function as charge carriers. Consequently, the electrical conductance, unlike the self-diffusion coefficients for sodium ions, is somewhat dependent on total water (ice) content. The electrical conductance increases as the extent of development of interfacial zones increases.¹²² This point is discussed further by Murrmann elsewhere in this volume.

At UH and microwave frequencies, the water molecules in the interfacial regions separating ice from mineral surfaces possess sufficient degrees of motional freedom to impart a high dielectric loss to frozen ground. At high frequencies, the ice and mineral grains do not contribute to the dielectric loss and the displacement currents can be attributed

wholly to the interfacial water. The available evidence indicates that the relaxation spectra of the unfrozen interfacial water differ significantly from those of pure water in bulk.^{61,99,100} It appears that further study of the high frequency dielectric properties of frozen ground can provide additional information on the properties of the unfrozen water in frozen ground.

ICE SEGREGATION AND FROST HEAVING

A comprehensive theory of frost heaving should predict rates of heave, cumulative heave, cumulative ice-water contents, rise of heaving pressure, and ultimate (maximum) heaving pressures from a set of equations that incorporate the heat and soil water fluxes induced by prevailing thermal and water content gradients. In addition, the equations should contain one or more parameters to characterize the soil matrix. Notwithstanding the significant progress that has been made toward this end, it must be acknowledged that such a theory is not yet at hand.

The mechanism of frost heaving has been the subject of many investigations. Briefly, as heat is extracted from above and freezing is initiated, growing ice crystals coalesce into planar ice lenses. The ice lenses are enlarged by the addition of water transported from the reservoirs of soil water below. Ice-lens growth occurs at locations where the temperature is favorable and the rate of appearance and dissipation of the latent heat of freezing does not exceed the flux of soil water. Continued growth eventually leads to the buildup of heaving pressures. Growth continues until the balances between the four principal governing factors, the soil texture, the rate of heat removal, the upward flux of soil water, and the confining pressure, are disturbed.

Because of the innate perfection of the crystalline state, with few exceptions, impurities tend to be rejected and excluded from enlarging crystals on solidification of the melt; water is not exceptional in this respect. Ice crystals in a soil undergoing freezing tend to reject solutes and other foreign substances, including the smallest mineral particles associated with the soil matrix. This tendency is very strong; the more slowly crystallization proceeds the more effective it is and the larger individual crystals tend to become. The crystallization pressure associated with this process constitutes the theoretical upper limit to heaving pressures. In theory, these crystallization pressures may be exceedingly large, equivalent to that predicted by the Clausius-Clapeyron equation. In nature, however, large pressure buildups are circumvented by the existence of compliant boundaries and interruptions in the supply of liquid and disturbance of the delicate balance required between the extraction of heat, the water flux, and the configuration of the ice-water interface. Nevertheless, under optimum conditions of temperature, rate of heat extraction, soil structure, and access to a supply of liquid, enlarging ice crystals can generate high pressures.

As temperatures drop below freezing, a roughly planar 0 °C isotherm enters the soil and descends gradually. Colder soil lies above and warmer soil lies beneath. Ice forms in the colder regions above when nucleation occurs in the water filled pores. As was briefly mentioned in a preceding section, a special case of homogeneous nucleation theory seems to apply.^{10,151,182} Available evidence indicates that 2–8 °C of undercooling is required in the laboratory, but little or none in natural surroundings. In coarse-textured soils, the freezing interface closely follows the 0 °C isotherm in its downward course; in fine-textured soils it may be as much as several degrees behind, because of a larger freezing point depression.

As the freezing interface descends, one of two things may happen. On the one hand, the pore water may freeze *in situ* as growing ice crystals successively invade, fill the soil pores, and engulf the soil grains. In this case, the development of a freezing pressure results entirely from the expansion of the water as it solidifies. On the other hand, as described above, segregated ice lenses may form in a plane of favorable temperatures near, but somewhat behind, the 0 °C isotherm. These ice lenses then may enlarge by the addition of ice formed from upward-migrating soil water. The energy released on freezing is partly converted into the work of lifting the overburden; the remaining energy is dissipated as heat at the freezing interface, where its appearance tends to regulate the rate of ice formation. The lenses continue to grow and heave the earth upward as long as a favorable balance exists between the upward flux of soil water, the prevailing thermal gradients, the configuration of the ice-water interface, and the surface properties of the soil matrix. At some point, the upward heat flux required by the thermal boundary conditions may exceed the capacity of the soil-water supply. When this happens, the freezing interface descends to a new plane where ice nucleation, ice lens formation, and growth begin anew. A modern classification of all naturally occurring forms of ground ice has been given by Mackay.⁹⁷

Martin¹⁰² pointed out the similarity between periodic precipitation resulting in “Liesegang rings” and recurrent ice lenses in frozen soil. In either case, the nucleation temperature at the leading edge of a terminated layer must be lower than that further ahead where precipitation or freezing can again be initiated. In the case of frozen ground, the nucleation and freezing temperature of the water-depleted region immediately below a mature ice lens generally are lower than in more moist regions below.

There is now general agreement that the energy involved in the work of frost heaving is derived from differences between the energy states of ice and the underlying soil water. The suggestion that the work of frost heaving is a consequence of supercooling is unnecessary.⁶⁶

Kaplar⁷⁵ recently summarized the empirical relationships between rate of heave and cooling rate and surcharge loads. Takagi¹⁵⁷ has contributed theoretical relationships pertain-

ing to the development of heaving pressures and the simultaneous heat and water fluxes. A relationship successfully predicting the ultimate heaving pressure that can develop in uniform spheres was derived by Miller *et al.*¹¹⁴ and by Everett and Haynes.³⁸ A comprehensive evaluation of this and a similar equation are given by Sutherland and Gaskin in this volume. Radd¹⁴⁷ and Hoekstra *et al.*^{57,60} contributed experimental data on maximum heaving pressures developed in a number of representative soil media. Because of the free mobility of water within the network of unfrozen water interfaces, as the temperature falls, ice lenses behind the freezing front being fed from this source may continue to enlarge slowly. Although, as the temperature falls below about –5 °C, the thinness of the unfrozen interface severely restricts the quantities of water that can be transported, in theory, ice lens growth can continue until about –50 °C. At this point, for all practical purposes, the mobility of intact water molecules becomes insignificant.^{7,11} This interesting type of ice-lens enlargement, termed “secondary frost heaving” by Miller,¹¹³ also is discussed more fully elsewhere. We return to a discussion of frost heaving in connection with the mechanics of frozen ground below.

Needle-ice formation is one of the most interesting and beautiful manifestations of ice segregation near the soil surface. It is important because it often results in damage to plants, and the dissolution of needle ice accelerates soil erosion. Systematic studies of needle ice have been conducted by Soons and Greenland,¹⁵⁴ Soons and Rayner,¹⁵⁵ and Outcalt.^{136,137,139} Understanding of this type of ice segregation and frost heaving has advanced sufficiently to yield a mathematical simulation and a successful algorithm for needle-ice growth.^{138,140} Among the many morphological varieties of needle ice, the following have been successfully analyzed: ice needles capped by frozen soil, clear needles unfrozen at the base, clear needles frozen at the base, needles with incorporated mineral matter, and banded ice needles.

THERMAL ASPECTS

Inasmuch as the permafrost condition is defined solely on the basis of temperature, without reference to ice content or other compositional variables, the thermal aspect of permafrost is from any point of view a most critical one. The thermal properties of permafrost and frozen ground are central to any discussion or application in which they are involved. Hence, this topic has been accorded a prominent place elsewhere in this volume. We confine ourselves to a few brief remarks dealing with certain developments during the past decade of a basic nature.

The Apparent Specific Heat Capacity

For many substances, the specific heat capacities are tabulated and may be expressed as functions of temperature by

simple polynomials. In the case of mixtures, the specific heat capacity may be adequately represented by summing the specific heat capacities of each constituent, multiplied by its respective mass fraction. In a mixture containing constituents that undergo phase changes, additional terms containing the appropriate latent heats of phase change multiplied by the respective mass fractions of these constituents suffice to describe the situation. Thus, the term *specific heat capacity* is not strictly applicable; the term *apparent specific heat capacity* is better.

Anderson followed this approach by incorporating a term describing the progressive melting of the ice in frozen ground in the apparent specific heat capacity equation.⁹ This equation, equivalent to Eq. (6) above, was subsequently used to derive the apparent specific heat capacity of Wyoming Na-bentonite-water mixtures from thermodynamic data.⁹⁰

This expression for c_a , although in somewhat unconventional units, is convenient because the equation giving w_u as a function of T required to evaluate the last term of Eq. (6), is best expressed as weight of water per unit weight of oven-dry soil. Substituting from Eq. (9) and entering its derivative with respect to temperature in the last term yield on integration:

$$c_a = c_s + c_1 w_w + (c_u - c_1) m \theta^n + (mL/\Delta\theta) (\theta_1^n - \theta_2^n), \quad (12)$$

where, for convenience in computation, the limits of integration are expressed as $\theta_1 = [\theta - (\Delta\theta/2)]$ and $\theta_2 = [\theta + (\Delta\theta/2)]$, and $\Delta\theta = (\theta_2 - \theta_1)$. Methods for obtaining suitable values for m and n and examples of the use of Eq. (12) in situations of practical importance are described elsewhere in this volume.

Thermal Conduction

Two defined soil parameters, thermal conductivity K and thermal diffusivity α , are used to describe the conductive transfer of heat in frozen ground. (Other transfer mechanisms usually are ignored.) These parameters are related through the relationship

$$\alpha = K/\rho c_a, \quad (13)$$

where ρ is the density of the frozen medium and c_a is its apparent specific heat capacity expressed in units of energy per unit mass of the medium per degree. The treatment of heat transfer in frozen ground has been thoroughly conventional, for the most part, and standard textbooks have furnished the basic equations.²⁹ When the equations are formulated in terms of the diffusivity parameters, the gravimetric apparent specific heat capacity, defined above, is required. It can be derived from Eq. (12) by a simple rationalization of units. If the equations are formulated in terms of the thermal conduc-

tivity, an appropriate expression for the volumetric apparent specific heat capacity can be formulated.

Thus, in frozen ground, where a phase change is involved, the latent heat of phase change can be accommodated in a variable diffusivity $\alpha(T)$, or in a variable specific heat capacity. Because of the lack of a suitable function to express the phase composition of soils and the paucity of phase composition data, the conventional approach to practical heat transfer problems, until recently, has been to neglect the unfrozen water altogether, to assume that the water present freezes and melts at 0°C, and to assume constant values for the soil parameters. Many examples are to be found in the internal reports of commercial engineering firms. Jumikis⁷⁰ collected a number of these procedures and Penner¹⁴⁵ has contributed illuminating observations. More recently, Ho *et al.*⁵³ and Nakano and Brown^{124,125} have developed versatile computational methods for modeling the thermal regime of frozen ground in which the nonlinear relationship between water-ice phase composition curve can be explicitly incorporated.

ELECTRICAL PHENOMENA

Electrical Conduction and Dielectric Properties

It has been mentioned that electrical conduction in frozen ground is possible because of the presence of charge carriers in the continuous, interconnecting silicate-water-ice interfaces. These consist of the various ions present in the original soil solution, as well as the exchangeable ions associated with the mineral matrix. In addition, there is a contribution from the dissociated water proximate to electrical charge centers at mineral surfaces. The early observations of Ver-shinin¹⁶⁴ and Leonards and Andersland⁸⁷ relative to the low frequency conduction of frozen soils have been verified by Hoekstra.^{56,59} Virtually all the charge carriers present in the unfrozen soil solution, on freezing, are concentrated and confined in a continuous, interconnecting series of interfaces. The relative efficiency of the various ionic species in participating in the conduction process appears to be similar to their characteristics in aqueous solution, although this point has not been fully investigated. Migration distances and oscillatory displacements are dependent on the strength and frequency of the imposed electrical fields, as expected for unrestrained charge carriers. Because of this, the movement of water by electroosmosis is nearly as easily accomplished in frozen as in unfrozen soil. Although the total number of charge carriers remains roughly constant, as the temperature of frozen ground is lowered, the specific conductance diminishes. This is caused by progressive thinning of the unfrozen interface and perhaps its increasingly frequent interruption, both of which diminish ionic mobility. The application of pressure causes an increase in interface thickness and, consequently, the ability of individual charge carriers to move freely. Hence, the electrical conductance is

observed to increase with an increase in confining pressure at constant temperature.⁵⁸

Mamy and Chaussidon^{99,100} and Weiler and Chaussidon¹⁶⁸ made extensive measurements of the dielectric properties of soil-water systems under various conditions. This topic was pursued further by Hoekstra and Doyle.⁶¹ At 9.8×10^9 Hz, they observed a sharp break in the plot of dielectric loss-reciprocal temperature at about -50°C for Na-montmorillonite. Activation energies of about 6.0 kcal/mol and 0.3 kcal/mol for the upper and lower temperature segments were derived. For the same material at 10^5 Hz, Weiler and Chaussidon observed a break in Arrhenius plots at about -70°C with activation energies of the order of 12 kcal/mol. These are the temperatures at which large changes in proton mobility begin to be evident in the NMR spectra of frozen clay-water mixtures (Figure 4). Recall that the low temperature phase transitions in the interfacial water are completed at about -50°C .¹⁴ They may be associated with the breaks in the curvature of these plots.

Hoekstra and Doyle⁶¹ conclude that the difference in activation energy for dielectric loss at microwave frequencies as compared with radio frequencies is an indication that different charge carriers dominate in these two regions of the electromagnetic spectrum. They believe, in agreement with Fripiat *et al.*,⁴² that proton conductance dominates at radio frequencies. They observe that the data are consistent with the interfacial model illustrated earlier in this review. Other aspects of this topic, with emphasis on electromagnetic interrogation of frozen ground terrain, are discussed by Hoekstra and McNeill elsewhere in this volume.

Freeze-Thaw Potentials

The generation of a separation of electrical charge between a growing ice crystal (negatively charged) and the surrounding liquid has been observed by many investigators and by now is a well-established phenomenon.

Murphy,¹²¹ in a recent systematic study, investigated the freezing potentials arising when dilute solutions of 15 different electrolytes were frozen. At very low concentrations, he found that the freezing potential was ice-positive and, at higher concentrations, ice-negative, with respect to the unfrozen solution. In all cases, except for NH_4Cl , the freezing potential passed through zero at some concentration in the range of 10^{-6} to 10^{-5} mol. Ice positive potentials as high as 120 V were measured, but the ice negative potentials usually measured less than about 30 V.

Drost-Hansen³⁶ proposed that suitably sized ions may be incorporated into the ice lattice and tend to relieve the lattice strain caused by the opening of the hydrogen bond angle by the 2 to 4° required for a water molecule in the liquid state to add on to the ice lattice and that this results in the generation of the freezing potential. The ions are thought first to be adsorbed onto an oriented polar layer of ice at the water-ice interface and then entrapped in excess during advance-

ment of the interface. Murphy, on the other hand, visualized the process as related to the orientation of the water dipoles in the hydration hulls of the ions. For cations, the dipoles are mainly directed outward; for anions, they are directed inward. The large freezing potentials observed are thought to result from the growth of chains of partially immobilized water molecules connected together and attached to the ice surface by single hydrogen bonds. These chains later combine laterally by the formation of additional hydrogen bonds, pulling the structure together to finally form the normal ice structure. Although this explanation can account for the observations, it is rejected by Bogan and Drost-Hansen²⁰ on the grounds that the formation of chains of water molecules attached by single hydrogen bonds is—in view of the high degree of hydrogen bonding in water near the freezing point, a feature common to practically all of the leading theories of water structure—an unlikely possibility. They believe that a transient form of polar ice is not only conceptually more realistic, but more likely.

The generation of electrical potentials during the freezing of soil-water mixtures has been confirmed in a series of preliminary experiments by Anderson (unpublished). Freezing potentials of the same order of magnitude observed in the aqueous solutions were measured. In these experiments, frequent reversals of sign also were observed. Although care was taken to control freezing rates to ensure consistent electrical continuity, etc., poor reproducibility of results was experienced and the experiments have been discontinued temporarily. As in the case of freezing potentials in dilute solutions, no clear-cut explanation for the reversal of sign can be offered at present. It could be related in some unknown way to dissociation-association processes or to the governing relationships between proton mobility and the microstructure of the advancing ice front. Effort to resolve this issue should be continued; meanwhile, the possible importance of this phenomenon in influencing local geoelectrical fields during freezeup in winter should not be overlooked.

MECHANICAL PROPERTIES OF FROZEN AND THAWING GROUND

The phenomena that control the mechanical behavior of frozen and thawing ground are complex. The rheology of both frozen and unfrozen states, the influence of interfacial phenomena, the effects of heat flow, and the results of phase changes interact in ways that are not fully understood, and much further study is needed before the mechanical properties of frozen and thawing ground can be reduced to the interaction of the phases resulting from the flow of both mass and energy across the boundaries of an element of soil. The special physicochemical relations associated with the presence of ice in a porous medium have been reviewed above. Clearly, further investigations into such subjects as the temperature dependence of the creep rate of a frozen soil or the amount of

frost heave developed under certain conditions contribute in various ways to extend our understanding of these fundamental processes. At the same time, the obligation to perform engineering calculations and undertake construction in areas underlain by permafrost necessitates the development of useful theoretical methods that adequately represent the behavior of frozen or thawing ground in practice. While it is evident that a study could be undertaken to contribute not only to our understanding of mechanical properties from a fundamental point of view but to the formulation of representative phenomenological theories, the constraints in the two cases differ and studies on this subject are accordingly rare. It is more common to find a set of observations made on artificially prepared soils, tested at the laboratory scale over a limited period of time. Well-formulated studies of this type are clearly valuable, but the application of the results to problems in practice requires much caution and judgment. This is particularly so because the structure of frozen soil, *in situ*, differs markedly from that of material prepared in the laboratory.

The recent history of research into the properties of unfrozen soils is instructive. From 1950 to about 1965, most geotechnical research laboratories had extensive investigations under way into the shear strength and deformation properties of reconstituted soils prepared in a variety of ways. At the outset, linear models were used to interpret the experimental data and to develop procedures whereby they could be applied to field problems. As experimental techniques improved and as the limitations of the linear formulations became more evident, more complex models of the behavior of the artificially prepared soils that better represented the response to loading of these soils in the laboratory were developed. These formulations were more difficult to apply in practice. About 10 years ago it became apparent that there was a growing awareness among some that continuing research into reconstituted soils was yielding diminishing returns to engineering practice when it was recognized that the response of soil to loading in the field is often dominated by anisotropy, nonhomogeneity, and the presence of minor geological details such as fissures, shear planes, or silt layers. Hence, renewed attention was given to problems of size effects, anisotropy, representative sampling, and the relation between laboratory studies and the behavior of soils in the field. The interpretation of field response is often made with simpler theories since the data seldom warrant the application of complex nonlinear models. The emphasis on field studies has resulted in a much better awareness of the limitations of both laboratory and theoretical studies in practice and an increased reliance on *in situ* test procedures.

It seems likely that the development of the mechanics of frozen soils will follow a similar path. In the western hemisphere, the study of frozen soils is clearly still in the stage where most work is being done on reconstituted frozen soils and with well-controlled temperature environments. As with

unfrozen soils, a systematic exploration of the influence of dominant variables on mechanical properties is possible. For example, some of the factors controlling the strength of a frozen soil are soil type, ice content, strain rate, and temperature. The relative influence of all of these factors has been the subject of recent studies, but the actual strength of frozen ground mobilized *in situ* under the loading and thermal boundary conditions that might arise in practice is not readily estimated with accuracy. The recognition of the gap between the theory and the practice of frozen soil engineering is not new, and the reasons for it are readily understood. Until recently, there has been little foundation engineering work of consequence in the permafrost areas of North America; hence, there has been little opportunity to investigate prototype behavior. Research work in this environment is costly, and the occasions when samples of naturally frozen ground were made available to laboratories were rare. This is now changing with the growing interest in resource development in the North and we can anticipate more occasions arising to facilitate the study of the *in situ* behavior of frozen and thawing ground.

In the following, the discussion of mechanical properties is broken down under three headings: geotechnical properties of frozen ground, geotechnical properties of thawing ground, and geotechnical properties of freezing ground.

Wherever possible, the limitations to our knowledge for the solution of engineering problems will be stressed as an indication of some priorities for future work. In particular, it will be seen that field studies in all aspects of the geotechnical properties of frozen and thawing ground are likely to be of particular value.

Geotechnical Properties of Frozen Ground

The special features of the geotechnical properties of frozen soil are the dominant creep characteristics under sustained stress and the marked rate dependence of the strength. These characteristics are generally attributed to the presence of unfrozen water and the various responses of ice to loading, which can range from pressure melting to brittle fracture. The rate effects in frozen ground are obviously temperature dependent and they will vary with the amount of ice present in the mixture. Since the last International Conference on Permafrost, the western hemisphere has had the benefit of translation into English of major works by Vyalov^{165,166} and subsequent studies have been much influenced by them.

When frozen ground is subjected to a load, it will respond with an instantaneous deformation, a time-dependent deformation and, in general, if the load is high enough, will display a limiting strength. In discussing the geotechnical properties of frozen ground, it is therefore convenient to distinguish between the elastic, strength, and creep properties. All of them will depend on temperature and composition. Moreover, for

each there is concern that parameters found in the laboratory be representative of those in the field.

ELASTIC BEHAVIOR

Initial loading moduli for frozen ground of differing composition deformed at various temperatures may be found from the stress-strain curves published by Akili,² Chamberlain *et al.*,³¹ and MacFarlane,⁹⁴ but no systematic study appears to have been made. This may be a neglected area of investigation because the elastic deformation of frozen ground is likely to be small compared with the creep movements.

Goughnour and Andersland⁴⁶ reported values of Young's modulus found by unloading at the conclusion of a series of creep tests. Data for both ice and a coarse sand-ice mixture revealed a marked decrease in modulus with increasing plastic strain. This was less pronounced with a fine sand-ice mixture. Extrapolating the moduli to very small plastic strains gives values reasonably close to those found dynamically by Kaplar⁷¹ in the case of ice and coarse sand-ice. The fine sand-ice mixture has values much below those found by resonant frequency methods. The possibility of a changing elastic stiffness due to cumulative plastic strains has interesting implications for the design of machine foundations on frozen ground.

Nakano *et al.*¹²⁶ measured the ultrasonic velocities of both dilatational and shear waves in water-saturated frozen soils as a function of temperature. A strong correlation was found between the dilatational wave velocities and the unfrozen water content. Observed hysteresis in the velocities of silt and clay during a freeze-thaw cycle was thought to be caused by hysteresis in the frozen water content. A general tendency for the shear wave velocity to decrease with ascending temperature was observed, but the effect was more pronounced on the dilatational velocity. Poisson's ratio for sand was found to be almost constant but it decreased monotonically with ascending temperature for silt and clay.

The influence of low temperature on the deformability of water-saturated rocks was studied by Mellor.¹⁰⁷ In general, the initial loading moduli increased greatly as the pore water froze. This increase was attributed to the elimination of crack closure under stress since the cracks become filled with ice. The temperature dependence of the modulus, which was also detected by compressional wave velocity measurements,¹⁵⁹ is likely because of the progressive freezing in smaller and smaller pores as temperature is lowered. Limited field data on compressional velocities in frozen rock in the field are generally less than those quoted by Timur.¹⁵⁹ The difference is attributed to the presence of gas in the pores. The importance of knowing the nature and percentages of pore fluids is indicated.

STRENGTH

The strength of frozen soils has commonly been investigated by loading at constant stress, constant stress rate, or constant

strain rate. The most common configuration is unconfined cylindrical compression. It is anticipated that more complex states, such as plane strain compression or extension, would have some influence on strength since they affect separately the strength of both soils and ice. However, data on these states have not been reported. But both triaxial compression and direct shear devices have been used in testing frozen ground, the latter only infrequently.

Hoekstra⁵⁹ recently reviewed the factors influencing the strength properties of frozen ground. He quoted data illustrating the influence of soil type and temperature on the unconfined compressive strength of specimens compressed at a constant strain rate and he noted that, at least for Ottawa sand, strength is related to the rate of stress application by:

$$\sigma_{\max} = A(\dot{\sigma})^b, \quad (14)$$

where σ_{\max} = the ultimate unconfined compressive strength and $\dot{\sigma}$ = the rate of stress application. A substantial amount of data on the strength of various frozen soils loaded at different stress rates was summarized by Kaplar.⁷⁵

The strength of frozen ground tested at constant strain rate has been the subject of several investigations. MacFarlane⁹⁴ reported unconfined compression tests on frozen natural peat at -9.5°C . He found strengths of 40 kg/cm^2 at a strain rate of 1 percent/min and a strength of 47 kg/cm^2 at a strain rate of 2 percent/min. These values agree with others found in the literature. Akili² investigated the effects of soil type, temperature, and strain rate on the strength of frozen fine-grained soils. The deformation modes varied, with brittle failure being more characteristic of failure of the low plasticity soils and greater ductility associated with the high plasticity soils. Temperature and rate effects were as anticipated.

Goughnour and Andersland⁴⁶ studied the triaxial compressive strength of a sand-ice mixture over a temperature range from -4 to -12°C and over a limited range of strain rates. Of particular interest here is the systematic influence of the concentration of sand on the strength and the failure mode. They pointed out that at a sand concentration by volume of about 42 percent there was a rapid increase in shear strength due to the contribution of friction between sand particles and dilatancy. At low concentrations, a linear increase in strength with sand concentration was noted, but the data given by Kaplar⁷⁵ indicate that this need not be true in general. Andersland and Al-Nouri⁴ found no effect of confining pressure on the triaxial strength of frozen clay compressed at -12°C . Some influence was detected on a sand-ice system, and it would be of interest to isolate how much of this extra resistance was due to dilatancy. The results of Andersland and Al-Nouri⁴ were confirmed in the study undertaken by Chamberlain *et al.*³¹ They also found that at high confining pressures dilatancy was suppressed and that pressure melting developed and decreased the shear strength. At even higher pressures, an ice-water transformation took

place and the shear strength increased with increasing pressure in the manner of an undrained triaxial compression test with a slightly compressible pore fluid.

In many configurations of practical concern, the stresses are essentially constant in time since they arise from prescribed boundary loadings as in the case of building foundations or from gravity forces as in the case of slopes in frozen ground. Hence, the long-term strength of frozen ground is a matter of much concern. As is well known, the concept of a long-term strength is not appropriate for ice since ice creeps under extremely small stresses. Vyalov¹⁶⁶ pointed out that long-term strength also does not exist for "ice-saturated frozen soils" but can be applied to "structured soils" when frozen. He suggested that the variation of strength with time takes the form:

$$\sigma_{ult} = \beta / \log(t/B), \quad (15)$$

where β and B are best determined by developing a plot of $1/\sigma_{ult}$ against $\log t$ or using short-term creep tests.

Sayles,¹⁵⁰ in his comprehensive investigation into the creep of sands, investigated the ultimate strength of frozen soil; his data are in reasonable accord with the Vyalov equation. Long-term strengths based on a period of 100 years were less than 15 percent of the instantaneous strength. The relation between ultimate strength and temperature was also studied. Even in this study few tests were carried beyond 25 days; therefore, the extrapolation in time was over some three orders of magnitude.

The efficient use of frozen ground as an engineering material will not be possible without a more precise understanding of the nature of the ultimate strength of the material, particularly where natural nonhomogeneities including ice veins and lenses exist. Anisotropy also will be a factor. Special attention will also have to be given to obtaining more detailed information regarding strength and deformation properties in the temperature region of intensive phase transformations.

In his study of the effect of the low temperature on the strength of water-saturated rocks, Mellor¹⁰⁷ found that below freezing, both tensile and compressive strengths increase substantially. The filling of the pores and cracks by ice in effect reduces the size of the controlling defect structure and the strength is increased accordingly.

CREEP BEHAVIOR

Since frozen soil exhibits substantial deformation under sustained loading, engineering design usually requires that the stresses should not only be small enough to avert failure but that the deformations that develop during the lifetime of concern should also be contained within tolerable limits. Hence, the study of the creep of frozen ground is of great interest. However, creep studies are difficult to undertake. The creep behavior varies with time and long-term tests are

needed to determine clearly whether the soil is in primary or secondary creep or whether it will enter the tertiary mode or not. Since the cross-sectional area is continuously changing, loads have to be adjusted to maintain constant stress control. Creep depends on temperature; therefore, good temperature control is needed to isolate the influence of this factor. The stress history and loading path also influence creep but little systematic study of these factors has been undertaken in the western hemisphere, particularly over the temperature range of practical interest.

Recent studies on the creep of ice under low stress by Mellor and Testa¹⁰⁸ constitute a useful starting point from which to survey developments in understanding creep of frozen ground since the last International Permafrost Conference. The authors pointed out that low-stress laboratory studies in which secondary creep was assumed to have developed after a few days are doubtful. The actual relationship between stress and strain rate found in this study is of less interest here than the fact that the experiments show clearly that ice creeps at extremely small stresses. When soil is added to ice, the relation between strain rate and stress at a given temperature is modified. As the soil concentration increases, a soil structure that will inhibit creep forms; but prior to this stage there is some indication that creep rate can be augmented by the presence of some soil in an ice matrix. The variation of creep rate with composition is a matter of much practical concern since many structures that are common in permafrost areas might be founded in the upper layers of ice-rich soil. The relation between creep rates found in the laboratory and those developed *in situ* is also of the utmost interest.

Hooke *et al.*⁶² have presented results that confirm that creep rates in ice with low sand concentrations can, in some cases, rise above those of ice alone. At higher sand concentrations, they found that the creep rate decreases exponentially with increasing sand content. Qualitative field observations of convergence in an ice tunnel are quoted in support of these experimental results. Sayles¹⁵⁰ conducted an extensive series of uniaxial creep tests on two frozen sands at various stress levels related to the instantaneous strength and at temperatures from about -10 to about -0.5 °C. The duration of loading was variable. Some tests extended for over 100 days. Figure 9 gives typical strain versus time curves for both the damped and the undamped types of responses. Two empirical relations, including one from Vyalov,¹⁶⁶ were given to predict the variation in deformations with stress, time, and temperature. The porosities tested were sufficiently low to indicate that the soil structure should have influenced creep.

Creep tests of shorter duration were reported by Fukuo,⁴³ Andersland and Akili,³ MacFarlane,⁹⁴ Goughnour and Andersland,⁴⁶ Akili,¹ and Andersland and Al-Nouri.⁴ Data obtained from these tests have been used in the prediction of short-term deformations of models under more complex conditions. The flexure of a beam was studied by Fukuo⁴⁴ and the deformation of a thick hollow cylinder was investi-

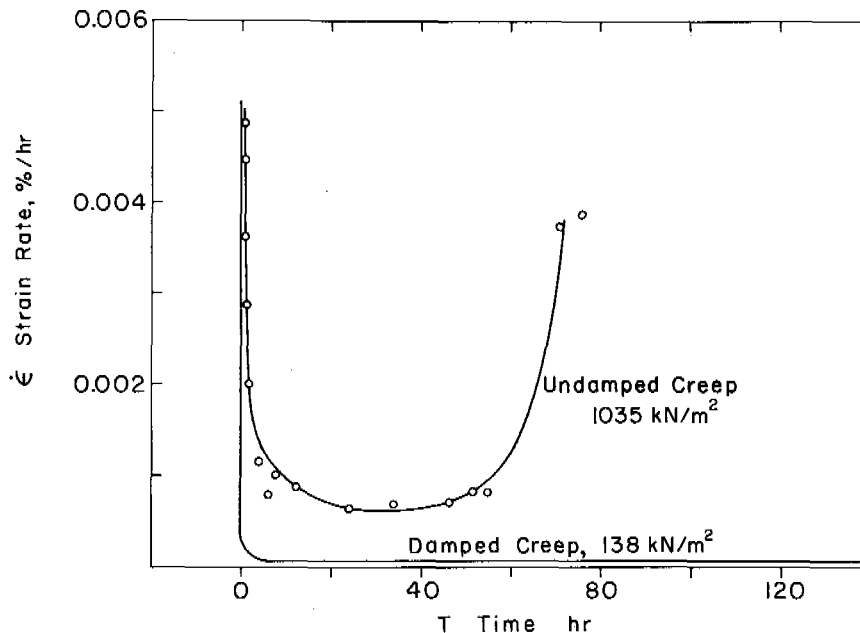


FIGURE 9 Creep rate and time, Ottawa sand (20-30), -0.5°C .

gated by Warden and Andersland.¹⁶⁷ The generalization of the simple test configuration to the more complex pattern of the models gives at best only reasonable results.

Both exponential and hyperbolic sine laws between creep rate and stress have been shown to fit experimental data over a limited range. The temperature dependence of the creep rate was analyzed in terms of the theory of rate processes by Andersland and Akili³ and Akili.¹ However, Hoekstra⁵⁹ pointed out that it is difficult to apply the concept of activation energy to a frozen soil when the temperature is lowered. The theory of rate processes can be applied when only the thermal energy of the moving molecules changes with temperature. In frozen soil, in addition to the change in thermal energy, a gradual phase change occurs.

The effect of stress and strain history on the creep rate was noted by Akili.¹ The data indicate that creep rate at a given stress decreases with increasing creep strain. Although Andersland and Al-Nouri⁴ concluded that the creep rate of frozen soil decreases exponentially with an increase in mean stress, their data are not altogether convincing and this subject deserves further study.

A study of particular importance was recently published by Thompson and Sayles,¹⁵⁸ who described the behavior and analysis of the *in situ* creep of a room in naturally frozen soil. The room was excavated in frozen gravel, the floor of the room being bedrock. However, about 20 m of frozen ice-rich silt lay above the room from ceiling level to the surface of the ground. *In situ* observations of creep within the room were taken for about 1 year. Uniaxial creep tests were made on the natural silt and gravel over an appropriate stress range

and at a temperature that was characteristic of the room. The results took the form:

$$\dot{\epsilon} = A\sigma^n, \quad (16)$$

where $\dot{\epsilon}$ = creep rate, σ = stress, and A and n = constants, which is characteristic of creep data for ice. The experimental data were generalized for use in a two-dimensional finite-element analysis. The field configuration was actually three-dimensional so some error is involved here. It was found that the form of the creep equation that was used fitted the prototype behavior quite well but the ice-rich silt deformed 3.3 times faster in the field than in the laboratory. This rate appears to be faster than is characteristic of pure ice alone. This may be the first comparison in the western hemisphere between long-term field and laboratory data, and it emphasizes the limitations of our knowledge of the behavior of frozen soils.

Ladanyi⁸⁵ explored the generalization of theories of creep on a basis similar to that of Vyalov.¹⁶⁶ As he pointed out, whether the unified theory is correct in detail or not depends on further experimental study. Generalization of uniaxial test data is not unique and more complex loading states must be studied before a comprehensive theory can be relied upon in practice.

Geotechnical Properties of Thawing Ground

In 1963, few North American geotechnical studies had been published on the behavior of permafrost subjected to thawing.

The general characteristics of high compressibility and low shear strength during the thawing of ice-rich fine-grained materials were recognized. Damage to subgrades during spring thaw was usually attributed to these features of frost-susceptible soils. Notwithstanding the lack of many investigations, major engineering structures that generated substantial thawing of permafrost were successfully designed and built.⁹³ In the interim, hydroelectric developments in areas underlain by permafrost have continued,⁹⁸ concern for disturbance of the tundra has increased,⁹⁵ and the need for a quantitative basis for design and construction of works that transmit heat into the ground has become more apparent. Lachenbruch⁸⁴ explored the implications for pipelines assuming that thawed silts and clays behave like a viscous fluid and showed that this would be a serious impediment to burying a hot pipeline in frozen fine-grained soil. This provided a substantial incentive to develop a more realistic model for the behavior of permafrost subjected to thawing.

When a soil is fully thawed and has come to equilibrium with the stresses acting on it, its subsequent response to loading can be interpreted in conventional geotechnical terms making special provision for the soil structure and stress effects associated with its freeze-thaw history. Some comments on this aspect of the behavior of thawed soils will be given later. As a soil thaws, volume changes, which are usually settlements, occur. If the thawed soil is sufficiently free draining that no excess pore pressures are sustained during thawing, then for all practical purposes the soil is always in a fully drained state. As is well known, one-dimensional volume changes due to thaw can be estimated by simple thaw settlement tests, and conventional soil testing procedures are available for determining the shear strength of the soil. Thaw rates can sometimes be estimated reliably²⁶ and the accuracy with which the settlements can be predicted is controlled mainly by the variability of the ground ice conditions and the extent of the sampling and testing program.

When the rate of generation of water exceeds its drainage capacity, excess pore pressures are generated, settlement is impeded, and the shear strength of the thawed soil is reduced. Yao and Broms¹⁷⁸ recognized that the bearing capacity of a subgrade soil is reduced by the incomplete dissipation of excess pore pressures during thawing, but their theoretical study did not fully embrace the properties of fine-grained soils. Following studies by Tsytovitich *et al.*¹⁶³ and Zaretskii,¹⁸¹ Morgenstern and Nixon¹¹⁶ developed a one-dimensional theory of thaw-consolidation based on the Terzaghi theory of consolidation with the position of the thaw front prescribed by some solution to a problem of heat conduction in solids such as the Neumann problem (e.g., Carslaw and Jaeger²⁹). The theoretical results are restricted to saturated soils because the boundary condition at the thaw line requires that the flow from the thaw line be accommodated by a change in volume of the soil. Darcy's law and a linear compressibility relation in terms of effective stress are em-

ployed. Since the theoretical relation at the interface is concerned with changes in volume, it requires the introduction of a reference state defined by σ'_0 , the initial effective stress in the soil if no volume change were permitted on thawing except that associated with the phase change of the ice. The magnitude of σ'_0 is likely to be small in ice-rich soils and since nothing was known about it at the time, it was put equal to zero for purposes of calculation. The variation of both pore pressure and settlement with time were calculated for several loading conditions. The significance of R , the thaw-consolidation ratio, was noted. This is defined by:

$$R = a/2\sqrt{c_v}, \quad (17)$$

where a = the constant of proportionality between the distance to the thaw plane and time as given by the Neumann solution and c_v = the coefficient of consolidation.

Experiments on the thaw-consolidation behavior of clays have been reported by Morgenstern and Smith.¹¹⁷ They constructed an odometer to investigate the predictions of the theory described above. This apparatus permitted the application of a step temperature change to a disk of frozen soil. One-dimensional drainage and settlement ensued. The pore pressure was measured at the base of the specimen as soon as the thaw plane reached it. Temperatures were also recorded with time at intermediate positions of the specimen. A typical set of experimental data are given in Figure 10.

The experimental results supported the thaw-consolidation theory. In particular, the settlement during thaw being proportional to the square root of time, the relation between pore pressure generation at the thaw front and the thaw-consolidation ratio R as shown in Figure 11, and the post-thaw dissipation conformed closely to the theoretical predictions. The experimental studies also proved to be useful in showing that a could be estimated reasonably well with published thermal properties of soils.

The thaw-consolidation theory may be extended in many ways, particularly with the aid of digital computers. Nixon and Morgenstern¹³³ graphically gave the solution of the equations formulated to consider more general thaw rates and, separately, a nonlinear stress-strain relationship for the soil skeleton. The former extension is applied to the consolidation beneath the centerline of a buried pipeline. Generalizations to consider nonhomogeneity, multidimensionality, and other boundary conditions are readily conceived.

An understanding of σ'_0 is central to predicting the behavior of thawed soil. The agreement between observations and theory reported above supported the assumption that σ'_0 is very nearly zero. Direct measurements made recently by Nixon¹³² confirm this conclusion. But, when a soil is subjected to cycles of freeze, thaw, and settlement, σ'_0 is found to increase substantially. We can imagine a soil subjected to thawing under an overburden less than σ'_0 increasing in volume if water is allowed to enter it. In nature,

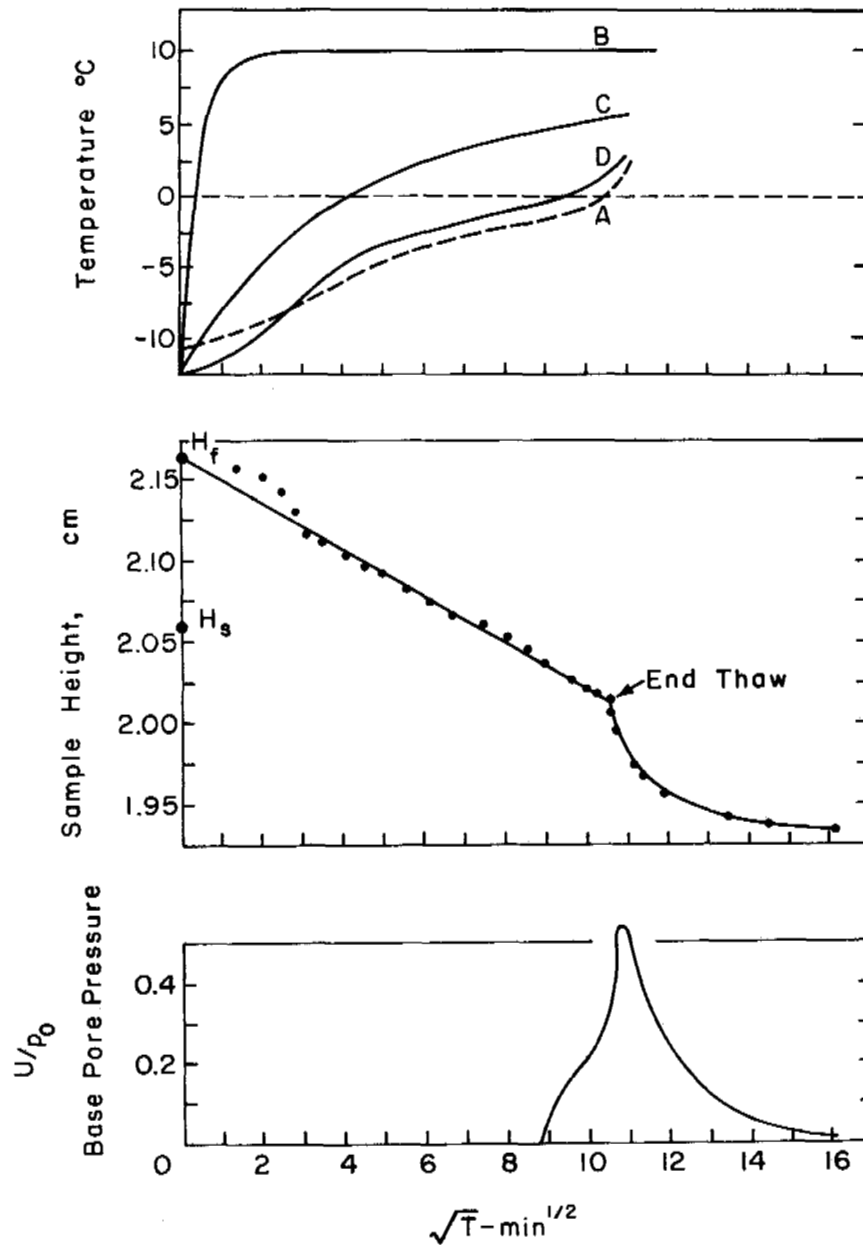


FIGURE 10 Typical one-dimensional thaw consolidation.

ice-rich soils are expected to have low values of σ'_0 , but a systematic study of the stress and climatic factors controlling it is needed before any generalizations are warranted.

The properties of the thawed soil enter into the thaw-consolidation behavior primarily through the magnitude of c_v . The coefficient of consolidation is more difficult to estimate in natural soils than the thermal properties that enter into α . Hence, our lack of knowledge of the permeability and compressibility limits our ability to determine the thaw-consolidation ratio R more than does our lack of knowledge of the thermal properties of frozen soils. Freezing of fine-grained soils changes their macrostructure, often by

aggregation, and overconsolidates the soil skeleton. All other things being equal, this should increase the permeability of the bulk soil. The compressibility of the soil depends on the amount and distribution of segregated ice as well as on the applied stresses. Few studies have been carried out on the influence of freezing and thawing on the consolidation behavior of soils. Data on the *in situ* permeability and compressibility of thawed soil are almost nonexistent. Yet such information is essential if thaw-consolidation theories are to be applied in practice with any confidence.

Stuart¹⁵⁶ described the influence of freezing and thawing on the consolidation behavior of a soft postglacial organic

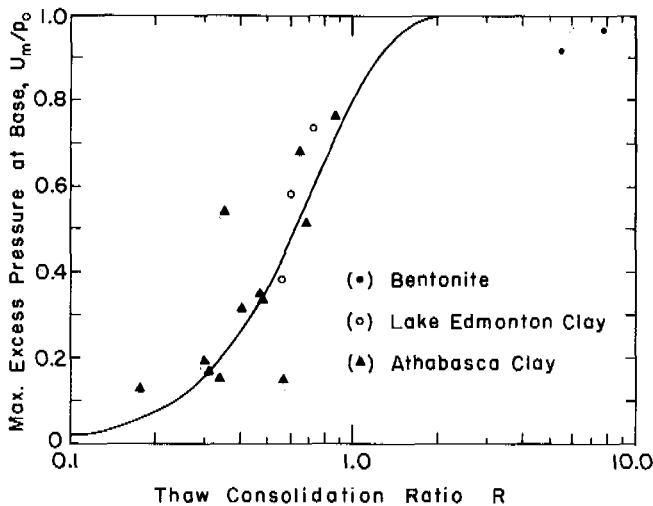


FIGURE 11 Maximum base pore pressure theory and experiment.¹¹⁵

clay. After consolidating to specific values of effective stress, the clay was frozen under essentially closed system conditions and then thawed under the same stress. During thawing, substantial rapid consolidation took place and subsequent consolidation of the soil skeleton would have the appearance of overconsolidated behavior. The test series was too limited to permit general conclusions.

The strength of naturally thawed soils is worthy of attention. These materials may be left in place in a very loose, metastable condition and have abnormally low shearing resistance as a result of their depositional conditions. The only systematic study recently undertaken in the laboratory into the influence of freezing and thawing on the strength of soils is that described by Broms and Yao,²⁵ who investigated the strength and deformation characteristics of a compacted silty clay under thawed conditions when the rate of freezing, weight of surcharge, and drainage conditions were varied. Both undrained and consolidated undrained tests were performed. The ingress of water during open system freezing greatly reduced the undrained strength of the soil when thawed. High pore pressures were observed. The shear strength in terms of effective stress was also affected by the preconsolidation pressures that developed during freezing. The effective stress paths indicated an overconsolidated condition.

While there is much to be done in the laboratory regarding the thaw-consolidation behavior of fine-grained soils and the geotechnical properties of thawed soils, correlations between prediction and field performance are of greater importance in order to establish limits of confidence to the application of thaw-consolidation theory.

Geotechnical Properties of Freezing Ground

Most saturated, fine-grained soils under low stresses exhibit an affinity for water during freezing, and ice lensing can occur.

If lensing is inhibited, substantial heave pressures can result. A comprehensive mechanistic interpretation of the factors involved in freezing moist ground was presented by Wissa and Martin¹⁷⁶ and Kaplar.⁷⁴ A detailed review of the fundamentals of these processes has been given in a previous section. Although the fundamentals of the ice-water-soil interface are complex and there are conflicting theories of ice lens formation, there is general agreement that ice lensing results when a soil has the ability to supply water to an active ice front for a sufficiently long time to build up a significant ice lens. As summarized by Wissa and Martin,¹⁷⁶ where water flow is inadequate, particle trapping and ice proliferation may result. The particle size of the soil influences the water flow to the ice front partly through its effect on the permeability of the unfrozen soil and partly through influencing the maximum stress difference that can be supported at the ice-water interface. This maximum stress difference has been the subject of much theoretical and experimental research. It can be measured for practical purposes either by finding the pore pressure at the frost line during closed system freezing¹⁷² or by observing the heave pressure during open system freezing when heave is not permitted.¹⁴² In the following remarks attention is given to some of the more applied aspects of recent research into processes associated with freezing ground.

HEAVE FORCE

Very substantial heave force can develop when frost-susceptible soils freeze. Theory indicates that this force is related to the grain size of the soil,³⁸ and laboratory studies such as those reported by Penner,¹⁴² Osler,¹³⁴ and Yong¹⁷⁹ provide supporting evidence. The exact relationship is made complex by the statistical geometry of an actual soil. Penner¹⁴³ stressed that the smaller-sized fraction has a strong influence on the maximum heaving pressures attainable.

The field studies reported by Kinoshita⁷⁷ and Penner¹⁴⁴ are of special interest in indicating how well heave pressures can be predicted in a more complex setting when compliant elements such as the creep of the frozen ground affect the results. Just prior to spring breakup, when the total measured force was highest, Penner found a heave pressure that was lower than might be calculated from theory. He commented on the role of the macrostructure of the clay in that under field conditions ice propagation probably occurs along fissures and channels. This tends to reduce the heaving pressures that are possible if ice propagates through all the pores of the soil.

Heaving pressures of natural soils are influenced by many factors that are not yet explored. Yong and Osler¹⁸⁰ drew attention to the influence of compliant restraint and pore fluid composition.

HEAVE RATE

An understanding of the factors influencing the rate of heaving associated with lensing is required to assess whether

or not such behavior may be unacceptable when freezing occurs during a limited time. It is needed also in the design of more efficient frost-susceptibility tests. There is general agreement that the water supply, the nature of the porous media, and the thermal conditions are the major factors governing the rate of heaving. The ice front propagates into the soil when the rate of heat extraction from the interface is greater than the heat made available by the supply of water and the phase change of the water-ice transformation. The supply of water can be limited by the availability of water, the low permeability of the unfrozen material, the limiting stress difference at the ice-water interface essential for lens growth, or cavitation in the pore water due to negative water pressures. Kaplar⁷⁴ described air or gas vapor bubbles emerging from solution during freezing. Provided that none of these constraints inhibit the availability of water, flow takes place to the interface and sustains lens growth. Suction at the interface apparently varies within limits, providing a driving force for the upward flow of water. Plausible as this assumption is, direct measurements substantiating it are lacking.

Studies by Penner¹⁴¹ and Kaplar⁷⁴ showed that increasing net heat flow and frost penetration rate increased the heave rate. Investigations by others were not conclusive. The influence of freezing rate on frost heaving was recently investigated in more detail by Penner.¹⁴⁶ Among his conclusions for saturated soils studied in an open system are that heaving rate increases with increasing heat removal rates and that the concept of ice segregation efficiency ratio¹⁸ is a useful indicator of frost susceptibility but it does not take into account the heave due to *in situ* freezing of pore water. The influence of water availability on heave rate was indicated in the experiments reported by McGaw.¹⁰⁵ At a given rate of penetration of the frost line, deeper water tables limit the rate of heave.

FROST-SUSCEPTIBILITY TESTS

The identification of frost-susceptible soils is a matter of practical concern in earthworks. The standard test adopted by the U.S. Army Corps of Engineers is cumbersome and time-consuming; as described by Kaplar,⁷² the test requires the freezing of a standard specimen at a constant rate of penetration for about 12 days. There is need for a more rapid test. While standardized tests are useful, their application in practice should pay attention to climatic factors. Osler¹³⁴ noted that criteria for frost susceptibility are influenced by the local depth of frost penetration. A greater quantity of fines might be permitted at depth in more northern locations, thereby utilizing the effect of overburden pressure.

An alternative approach to frost-susceptibility testing was explored by Kaplar.⁷³ In this study, freezing tests at constant temperatures indicated that testing time could be reduced to not more than a few days. Other possibilities have been noted, at least in a preliminary manner, by Wissa and Martin.¹⁷⁶ They noted that heave pressure in a constant vol-

ume test, heave rate in a constant heat extraction test, and the measurement of negative pore pressure that develops during closed-system freezing are worth considering. They described equipment that is extremely flexible in this regard, and detailed results using it will be welcome.

The recent studies by Penner¹⁴⁶ suggest that the thermal conditions imposed on testing for frost susceptibility are important and that the rate of testing should be related to the thermal conditions in the field. Tests of shorter duration than common but with rates of frost penetration both slower and faster than expected field values are advocated.

Indirect tests of frost susceptibility have been studied. Williams^{173,175} showed that air intrusion studies that reflect the pore size distribution of the soil can be utilized as a frost-susceptibility criterion. This would provide a very convenient procedure for selecting suitable soils on site if field experience provides supporting evidence.

UNSATURATED SOILS

The problem of frost heaving in unsaturated soils received attention by Dirksen and Miller,³⁴ Yong and Osler,¹⁸⁰ and Miller.¹¹³ Miller developed the concepts of secondary heaving that were discussed in a previous section and that account for the heave observed at moderate degrees of saturation. Frost heave is not a severe engineering problem with unsaturated soils. Ice segregation only occurs within a practical time scale at high degrees of saturation.

However, freezing of unsaturated soils at low degrees of saturation may result in volume shrinkage due to the increased negative pore pressures. On the basis of laboratory and field observations, Hamilton⁴⁹ concluded that compacted clays may undergo considerable freezing shrinkage depending on the moisture and density conditions prior to freezing. The maximum shrinkage occurred when the degree of saturation was between 60 and 70 percent. Expansion occurred when the degree of saturation exceeded about 90 percent. This phenomenon is worthy of more study since transverse cracking common in highways in cold climates has been attributed, in part, to the freezing shrinkage of the subgrade.

PORE WATER EXPULSION

When a coarse-grained soil is frozen in an open system, pore water is expelled. If the effective stress at the freezing front is large enough and the rate of freezing slow enough, pore water expulsion would also be expected from finer-grained soils. Wissa and Martin¹⁷⁶ among others provided direct experimental evidence for pore water expulsion from sands. Mackay⁹⁶ used this phenomenon to account for the genesis of some ground ice features. McRoberts has reported personal analysis of the physics of flow in a porous medium when a fluid flux is generated by the advance of a freezing front, and he showed that substantial pore pressures can arise. This has interesting implications for possible instability of soil during freezeback, and it deserves further study.

ACKNOWLEDGMENTS

The authors express their appreciation and thanks to their many colleagues for numerous helpful comments and critical observations offered during the preparation of this review.

REFERENCES

- Akili, W. 1970. On the stress-creep relationship for a frozen clay soil. *Mater. Res. Stand.* 10:16-22.
- Akili, W. 1971. Stress-strain behaviour of frozen fine-grained soils. *Highw. Res. Record No.* 360. p. 1-8.
- Andersland, O. B., and W. Akili. 1967. Stress effect on creep rates of a frozen clay soil. *Geotechnique* 17:27-39.
- Andersland, O. B., and I. Al-Nouri. 1970. Time-dependent strength behaviour of frozen soils. *J. Soil Mech. Found. Div. (ASCE)* 96:1249-1265.
- Anderson, D. M., and P. F. Low. 1958. The density of water adsorbed by lithium-, sodium- and potassium-bentonite. *Soil Sci. Soc. Am. Proc.* 22:99-103.
- Anderson, D. M. 1966. The latent heat of freezing soil water, p. 238-239. *In Permafrost: Proceedings of an international conference. National Academy of Sciences, Washington, D.C.*
- Anderson, D. M., and P. Hoekstra. 1965. Migration of interlamellar water during freezing and thawing of Wyoming bentonite. *Soil Sci. Soc. Am. Proc.* 29:498-504.
- Anderson, D. M. 1966. Heat of freezing and melting of sea ice. *Res. Rep.* 202. U.S. Army Cold Regions Research and Engineering Laboratory, Hanover, New Hampshire.
- Anderson, D. M. 1966. Phase composition of frozen montmorillonite-water mixtures from heat capacity measurements. *Soil Sci. Soc. Am. Proc.* 30:670-675.
- Anderson, D. M. 1967. Ice nucleation and the substrate-ice interface. *Nature* 216:563-566.
- Anderson, D. M. 1967. The interface between ice and silicate surfaces. *J. Colloid Interface Sci.* 25:174-191.
- Anderson, D. M., E. S. Gaffney, and P. F. Low. 1967. Frost phenomena on Mars. *Science* 155:314-322.
- Anderson, D. M. 1968. Undercooling, freezing point depression, and ice nucleation of soil water. *Israel J. Chem.* 6:349-355.
- Anderson, D. M., and A. R. Tice. 1971. Low-temperature phases of interfacial water in clay-water systems. *Soil Sci. Soc. Am. Proc.* 35(1):47-54.
- Anderson, D. M., and A. R. Tice. 1972. Predicting unfrozen water contents in frozen soils from surface area measurements. *Highw. Res. Record No.* 393. p. 12-18.
- Anderson, D. M., and A. R. Tice. The unfrozen interfacial phase in frozen soil water systems. *In International symposium on soil water physics and technology proceedings, Rehovot, Israel.* (In press)
- Anderson, D. M., A. R. Tice, and A. Banin. The water-ice phase composition of clay-water systems. I. The kaolinite-water system. *Soil Sci. Soc. Am. Proc.* (In press)
- Arakawa, K. 1966. Theoretical studies of ice segregation in soil. *J. Glaciol.* 6:255-260.
- Beskow, G. 1935. Soil freezing and frost heaving with special application to roads and railroads. Translated by N. Western, Tech. Inst. Evanston (1947) from the Swedish publication *Sver. Geol. Unders. Ser. C, Vol. 375.*
- Bogan, M., and W. Drost-Hansen. An investigation of some variables affecting freezing potentials. *Proc. Int. Conf. Phys. Chem. Ice, Ottawa, 14-18 Aug. 1972.* (In press)
- Bohn, H. L. 1967. The $(\text{Fe})(\text{OH})_3$ ion product in suspensions of acid soils. *Soil Sci. Soc. Am. Proc.* 31:641-644.
- Bouyoucos, G. J. 1916. The freezing point method as a new means of measuring the concentration of the soil solution directly in the soil. *Mich. Agric. Exp. Sta. Tech. Bull.* 24. p. 1-44.
- Bouyoucos, G. J., and M. M. McCool. 1916. Further studies on the freezing point lowering of soils. *Mich. Agric. Exp. Sta. Tech. Bull. No. 31.* 51p.
- Bouyoucos, G. J. 1917. Classification and measurement of the different forms of water in the soil by means of the dilatometer method. *Mich. Agric. Exp. Sta. Tech. Bull. No. 36.* 48 p.
- Broms, B. B., and Y. C. Yao. 1964. Shear strength of a soil after freezing and thawing. *J. Soil Mech. Found. Div. (ASCE)* 90:1-26.
- Brown, W. G., and G. H. Johnston. 1970. Dikes on permafrost: Predicting thaw and settlement. *Can. Geotech. J.* 7:365-371.
- Buehrer, T. F., and D. G. Aldrich. 1946. Studies in soil structure. VI. Water bound by individual soil constituents as influenced by puddling. *Univ. Ariz. Tech. Bull. No. 110.*
- Burke, J. E. 1968. Ceramics today. *Science* 161:1205-1212.
- Carlsaw, H. S., and J. C. Jaeger. 1947. Conduction of heat in solids. Clarendon Press, Oxford.
- Cary, J. W., and H. F. Mayland. 1972. Salt and water movement in unsaturated frozen soil. *Soil Sci. Soc. Am. Proc.* 36:549-555.
- Chamberlain, E., C. Groves, and R. Perham. 1972. The mechanical behaviour of frozen earth materials under high pressure triaxial test conditions. *Geotechnique* 22:469-484.
- Chumichev, B. D. 1968. Bases, foundations and structures. *Trans. Second Conf. Young Sci. Workers Sroyizdat, Moscow.* p. 122-128. (Also USA CRREL Translation No. 319)
- Dillon, H. B., and O. B. Andersland. 1966. Predicting unfrozen water contents in frozen soils. *Can. Geotech. J.* 3(2):53-60.
- Dirksen, C., and R. D. Miller. 1966. Closed system freezing of unsaturated soil. *Soil Sci. Soc. Am. Proc.* 30:168-173.
- Drost-Hansen, W. 1967. The water-ice interface as seen from the liquid side. *J. Colloid Interface Sci.* 25:131-160.
- Drost-Hansen, W., and R. W. Curry. 1970. Freezing potentials in heavy water. *J. Colloid Interface Sci.* 32:464-468.
- Ducros, P., and M. Dupont. 1962. A nuclear magnetic resonance study of water in clays in magnetic and electrical resonance and relaxation. *C. R. XI^e Colloque Ampère Eindhoven.*
- Everett, D. H., and J. M. Haynes. 1965. Capillary properties of some model pore systems with special reference to frost damage. *Révision internationale des laboratoires d'essai et de recherches sur les matériaux et les constructions bull. (Bull. Rilem) New Ser.* 27. p. 31-38.
- Ferguson, H., P. L. Brown, and D. D. Dickey. 1964. Water movement and loss under frozen soil conditions. *Soil Sci. Soc. Am. Proc.* 28:700-702.
- Frank, H. S., and W. Y. Wen. 1957. III. Ion-solvent interaction. *Disc. Faraday Soc.* 24:133-140.
- Frink, C. R., and N. Peech. 1963. Hydrolysis and exchange reactions of the aluminum ion in hectorite and montmorillonite suspensions. *Soil Sci. Soc. Am. Proc.* 27:527-530.
- Fripiat, J. J., A. Jelli, C. Poncelet, and J. Andre. 1965. Thermodynamic properties of adsorbed water molecules and electrical conduction in montmorillonites and silicas. *J. Phys. Chem.* 69:2185.
- Fukuo, Y. 1966. On the rheological behaviour of frozen soil, I. *Bull. Disaster Prev. Res. Inst. (Kyoto U.)* 15:1-7.
- Fukuo, Y. 1966. On the rheological behaviour of frozen soil, II. *Bull. Disaster Prev. Res. Inst. (Kyoto U.)* 16:31-40.
- Glasstone, S. 1916. Textbook of physical chemistry. 2nd ed. Van Nostrand, Princeton, New Jersey.
- Goughnour, R. R., and O. B. Andersland. 1968. Mechanical

- properties of a sand-ice system. *J. Soil Mech. Found. Div. (ASCE)* 94:923-950.
47. Graham, J. 1964. Adsorbed water on clay. *Rev. Pure Appl. Chem.* 14:81-90.
 48. Graham, J., G. F. Walker, and G. W. West. 1964. Nuclear magnetic resonance study of interlayer water in hydrated layer silicates. *J. Chem. Phys.* 40:540-550.
 49. Hamilton, A. B. 1966. Freezing shrinkage in compacted clays. *Can. Geotech. J.* 3:1-17.
 50. Hecht, M., M. Dupont, and P. Ducros. 1966. A study of transport phenomena of water adsorbed by certain clay minerals by nuclear magnetic resonance. *Bull. Soc. Fr. Miner. Crist.* 89:6-13.
 51. Hemwall, J. B., and P. F. Low. 1955. The hydrostatic repulsive force in clay swelling. *Soil Sci.* 82:135-145.
 52. Hillel, D. 1971. *Soil and water*. Academic Press, New York and London.
 53. Ho, D. M., M. E. Harr, and G. A. Leonards. 1969. Transient temperature distribution in insulated pavements—Predictions vs observations. *Can. Geotech. J.* 7:275-284.
 54. Hobbs, P. V., and B. J. Mason. 1964. The sintering and adhesion of ice. *Phil. Mag.* 9:181-197.
 55. Hoekstra, P. 1965. Conductance of frozen bentonite suspensions. *Soil Sci. Soc. Am. Proc.* 29:519-522.
 56. Hoekstra, P., and E. Chamberlain. 1964. Electro-osmosis in frozen soil. *Nature* 203:1406.
 57. Hoekstra, P., E. Chamberlain, and A. Frate. 1965. Frost heaving pressures. USA CRREL Res. Rep. 176.
 58. Hoekstra, P., and R. Keune. 1967. Pressure effects on the conductance of frozen montmorillonite suspensions, p. 215-225, *In Clays and clay minerals*. Vol. 15. Pergamon Press, New York.
 59. Hoekstra, P. 1969. The physics and chemistry of frozen soils. *Highw. Res. Board Spec. Rep.* 103. p. 78-90.
 60. Hoekstra, P. 1969. Water movement and freezing pressures. *Soil Sci. Soc. Am. Proc.* 33:512-518.
 61. Hoekstra, P., and W. T. Doyle. 1971. Dielectric relaxation of surface adsorbed water. *J. Colloid Interface Sci.* 36:513-521.
 62. Hooke, R. L., B. B. Dahlin, and M. T. Kauper. 1972. Creep of ice-containing dispersed fine sand. *J. Glaciol.* 11:327-336.
 63. Hosler, C. L., D. C. Jenson, and L. Goldschlak. 1957. On the aggregation of ice crystals to form snow. *J. Meteorol.* 14:415.
 64. Howell, B. 1972. Anomalous water: Is it a silica? *J. Colloid Interface Sci.* 38:633-635.
 65. Itagaki, K. 1967. Some surface phenomena of ice. *J. Colloid Interface Sci.* 25:218-227.
 66. Jackson, K. A., *et al.* 1966. Frost heave in soils. *J. Appl. Phys.* 37:848-852.
 67. Jackson, M. L. 1963. Aluminum bonding in soils: A unifying principle in soil science. *Soil Sci. Soc. Am. Proc.* 27:1-10.
 68. Jellinek, H. H. G. 1967. Liquid-like (transition) layer on ice. *J. Colloid Interface Sci.* 25:192-205.
 69. Jellinek, H. H. G., and S. H. Ibrahim. 1967. Sintering of powdered ice. *J. Colloid Interface Sci.* 25:245-254.
 70. Jumikis, A. R. 1966. *Thermal soil mechanics*. Rutgers-State University of New Jersey Press, New Brunswick.
 71. Kaplar, C. W. 1966. Laboratory determinations of dynamic moduli of frozen soils and of ice, p. 293-301. *Permafrost: Proceedings of an international conference*. National Academy of Sciences, Washington, D.C.
 72. Kaplar, C. W. 1965. A laboratory freezing test to determine the relative frost susceptibility of soils. USA CRREL Tech. Note. (Unpublished)
 73. Kaplar, C. W. 1968. New experiments to simplify frost susceptibility testing of soils. *Highw. Res. Record No.* 215. p. 48-59.
 74. Kaplar, C. W. 1970. Phenomenon and mechanism of frost heaving. *Highw. Res. Rec. No.* 304. p. 1-13.
 75. Kaplar, C. W. 1971. Some strength properties of frozen soil and effect of loading rate. USA CRREL Spcc. Rep. 159.
 76. Khakimov, Kh. R. 1957. Problems in the theory and practice of artificial freezing of soil. Academy of Science USSR, Moscow.
 77. Kinoshita, S. 1967. Heaving force of frozen soils, p. 1345-1360. *In E. H. Oura [ed.] Physics of snow and ice*. Hokkaido University.
 78. Knight, C. A. 1966. Grain boundary migration and other processes in formation of ice sheets on water. *J. Appl. Phys.* 37:568-574.
 79. Kohnke, K. 1968. *Soil physics*. McGraw-Hill, New York.
 80. Kolaian, J. H., and P. F. Low. 1963. Calorimetric determination of unfrozen water in montmorillonite pastes. *Soil Sci.* 95:376-383.
 81. Koopmans, R. W. R., and R. D. Miller. 1966. Soil freezing and soil water characteristic curves. *Soil Sci. Soc. Am. Proc.* 30:680-685.
 82. Kuroiwa, D. 1962. A study of ice sintering. USA CRREL Res. Rep. No. 86.
 83. Kuszynski, G. C. 1949. Self diffusion in sintering of metallic particles. *Trans. AIME* 9:169-178.
 84. Lachenbruch, A. H. 1970. Some estimates of the thermal effects of a heated pipeline in permafrost. *U.S. Geol. Surv. Circ.* 632.
 85. Ladanyi, B. 1972. An engineering theory of creep of frozen soils. *Can. Geotech. J.* 9:63-80.
 86. Leonard, R. A. 1968. Infrared analysis of clay-adsorbed H₂O. (Personal communication)
 87. Leonards, G. A., and O. B. Andersland. 1960. The clay-water system and the shearing resistance of clays. *Proc. conf. shear strength, soil mechanics and Found. Div. ASCE.* p. 798.
 88. Lovell, C. W. 1957. Temperature effects on phase composition and strength of partially-frozen soil. *Highw. Res. Board Bull.* 168. p. 74-95.
 89. Low, P. F. 1961. Physical chemistry of clay-water interaction. *Adv. Agron.* 13:269-327.
 90. Low, P. F., D. M. Anderson, and P. Hoekstra. 1968. Some thermodynamic relationships for soils at or below the freezing point. 1. Freezing point depression and heat capacity. *Water Resour. Res.* 4:379-394. (Also USA CRREL Res. Rep. 222, Pt. 1)
 91. Low, P. F., D. M. Anderson, and P. Hoekstra. 1968. Some thermodynamic relationships for soils at or below the freezing point. 2. Effects of temperature and pressure on unfrozen soil water. *Water Resour. Res.* 4(3):541-544.
 92. Low, P. F., and J. L. White. 1970. Hydrogen bonding and poly-water in clay-water systems. *Clays Clay Min.* 18:63-66.
 93. MacDonald, D. H. 1963. Design of Kelsey dikes, p. 492-496. *In Permafrost: Proceedings of an international conference*. National Academy of Sciences, Washington, D.C.
 94. MacFarlane, I. C. 1968. Strength and deformation tests on frozen peat, p. 143-149. *In Proceedings, 3rd International peat congress, Quebec*. National Research Council of Canada, Ottawa.
 95. Mackay, J. R. 1970. Disturbances to the tundra and forest tundra environment of the western Arctic. *Can. Geotech. J.* 7:420-432.
 96. Mackay, J. R. 1971. The origin of massive icy beds in permafrost, western Arctic Coast, Canada. *Can. J. Earth Sci.* 8:397-422.
 97. Mackay, J. R. 1972. The world of underground ice. *Ann. Assoc. Am. Geogr.* 62:1-22.
 98. Macpherson, J. G., G. H. Watson, and A. Koropatrik. 1970. Dikes on permafrost foundations in northern Manitoba. *Can. Geotech. J.* 7:356-364.
 99. Mamy, J., and J. Chaussidon. 1965. Dielectric properties of montmorillonite at low water contents. *Bull. Gr. Fr. Argiles*, 17:93-97.

100. Mamy, J., and J. Chaussidon. 1965. Conductivity of montmorillonite at low water contents and low temperatures. *Bull. Gr. Fr. Argiles* 18:41-47.
101. Martynov, G. S. 1956. The calorimetric method of determining the quantity of unfrozen water in frozen soil. *In* L. A. Meister, [ed.] *Data on the principles of the study of frozen zones on the earth's crust. Issue III. Academy of Sciences USSR, V. A. Obruchev, Inst. of Permafrost Studies, Moscow. (National Research Council of Canada, Ottawa, Tech. Translation 1088)*
102. Martin, R. T. 1959. Rhythmic ice banding in soil. *Highw. Res. Board Bull.* 218. p. 11.
103. Martin, R. T. 1962. Adsorbed water on clay: A review. *Clays Clay Min. Proc.* 9:28-70.
104. Mathieson, A. McL. 1958. Magnesium vermiculite: A refinement and re-examination of the crystal structure of the 14.36 Å phase. *Am. Min.* 43:216-217.
105. McGaw, R. 1972. Frost heaving versus depth to water table. *Highw. Res. Rec. No.* 393. p. 45-55.
106. McRoberts, E. C. 1972. Personal communication.
107. Mellor, M. 1971. Strength and deformability of rocks at low temperatures. *USA CRREL Res. Rep.* 294.
108. Mellor, M., and R. Testa. 1969. Creep of ice under low stress. *J. Glaciol.* 8:147-152.
109. Middlehurst, S., and L. R. Fisher. 1971. Polywater or silica-free substrates. *Nature* 230:575.
110. Migal, P. K., and F. M. Russu. 1965. Adsorption of organic vapors on charcoal and silica gel in the presence of added air. *Vch. Zap. Tiraspol'sk. Gas. Ped. Inst. (USSR) No. 13.* p. 136-142. [Cited in *Chem. Abstr.* 63:1718b (1965)]
111. Miller, R. D. 1966. Phase equilibria and soil freezing, p. 193-197. *In* *Permafrost: Proceedings of an international conference. National Academy of Sciences, Washington, D.C.*
112. Miller, R. D. 1970. Ice sandwich: Functional semipermeable membrane. *Science* 169:584-585.
113. Miller, R. D. 1972. Freezing and heaving of saturated and unsaturated soils. *Highw. Res. Rec. No.* 393. p. 1-11.
114. Miller, R. D., J. H. Baker, and J. H. Kolaian. 1960. Particle size, overburden pressure, pore water pressure, and freezing temperature of ice lenses in soil, p. 122-129. *In* *Proceedings, 7th International conference on soil science, Madison, Wisconsin.*
115. Mooney, R. W., R. G. Keenan, and L. A. Wood. 1952. Adsorption of water vapor by montmorillonite. I. Heat of desorption and application of BET theory. *J. Am. Chem. Soc.* 74:1367.
116. Morgenstern, N. R., and J. F. Nixon. 1971. One-dimensional consolidation of thawing soils. *Can. Geotech. J.* 8:558-565.
117. Morgenstern, N. R., and L. B. Smith. Thaw-consolidation tests on remoulded clays. *Can. Geotech. J. Vol. 10.* (In press)
118. Morrow, N. R. 1970. Physics and thermodynamics of capillarity. *Ind. Eng. Chem.* 62:32-56.
119. Mortland, M. M. Protonation of compounds at clay mineral surfaces. *In* *9th International congress of soil science proceedings. (In press)*
120. Mortland, M. M., J. J. Fripiat, J. Chaussidon, and J. Utterhoeven. 1963. Interaction between ammonia and the expanding lattice of montmorillonite and vermiculite. *J. Phys. Chem.* 67:248-258.
121. Murphy, E. J. 1969. The generation of electromotive forces during the freezing of water. *J. Colloid Interface Sci.* 32:1-11.
122. Murrmann, R. P., P. Hoekstra, and R. C. Bialkowski. 1968. Self-diffusion of sodium ions in frozen Wyoming bentonite-water paste. *Soil Sci. Soc. Am. Proc.* 32:501-506.
123. Murrmann, R. P., D. M. Anderson, and J. W. Peek. 1970. Ionic diffusion at the ice-solid interface. Snow removal and ice control research. *Highw. Res. Board Spec. Rep.* 115. p. 78-86.
124. Nakano, Y., and J. Brown. 1971. Effect of a freezing zone of finite width on the thermal regime of soils. *Water Resour. Res.* 9:1226-1233.
125. Nakano, Y., and J. Brown. 1972. Mathematical modeling and validation of the thermal regimes in tundra soils, Barrow, Alaska. *Arctic Alp. Res.* 4:19-38.
126. Nakano, Y., R. J. Martin, and M. Smith. 1972. Ultrasonic velocities of the dilatational and shear waves in frozen soils. *Water Resour. Res.* 8:1024-1030.
127. Nakaya, U., and A. Matsumoto. 1953. Evidence of the existence of a liquid-like film on ice surface. *USA SIPRE Res. Paper* 4. p. 1-6. [Also *J. Colloid Sci.* 9:41 (1954)]
128. Nersesova, Z. A. 1953. Kalorimetricheskii metod opredeleniya l'distosti gruntov (The calorimetric method of determining the ice content of soils). *Akad. Nauk SSSR, Materialy Po Laboratornym Issledovaniyam Merzlykh Gruntov.* Sb-1.
129. Nersesova, Z. A. 1954. Instruktivnye ukazaniya po apredelinyu kolichestva nezamerzshoi vody i l'da v merzlykh gruntakh (Instructions on the determination of the quantity of unfrozen water and ice in frozen soils). *Akad. Nauk SSSR, Materialy Po Laboratornym Issledovaniyam Merzlykh Gruntov.* Sb-2.
130. Nersesova, Z. A., and N. A. Tsytovich. 1966. Unfrozen water in frozen soils, p. 230-234. *In* *Permafrost: Proceedings of an international conference. National Academy of Sciences, Washington, D.C.*
131. Nielson, D. R., R. D. Jackson, J. W. Cary, and D. D. Evans. [ed.]. 1972. *Soil water. Am. Soc. Agron. and SSSA.*
132. Nixon, J. F. 1972. Personal communication.
133. Nixon, J. F., and N. R. Morgenstern. Practical extensions to a theory of consolidation for thawing soils. This volume.
134. Osler, J. C. 1967. The influence of depth of frost penetration on the frost susceptibility of soils. *Can. Geotech. J.* 4:334-346.
135. Oster, J. D., and P. F. Low. 1964. Heat capacities of clay and clay-water mixtures. *Soil Sci. Soc. Am. Proc.* 28:605-609.
136. Outcalt, S. E. 1969. Weather and diurnal frozen soil structure at Charlottesville, Va. *Water Resour. Res.* 5:1377-1381.
137. Outcalt, S. I. 1970. A study of time dependence during serial needle ice events. *Arch. Meteorol. Geophys. Bioklimatol. Ser. A* 19:329-337.
138. Outcalt, S. I. 1971. An algorithm for needle ice growth. *Water Resour. Res.* 7:394-400.
139. Outcalt, S. I. 1971. Field observations of soil temperature and water tension feedback effects on needle ice nights. *Arch. Meteorol. Geophys. Bioklimatol. Ser. A* 20:43-53.
140. Outcalt, S. I. 1971. The climatology of a needle ice event: An experiment in simulation climatology. *Arch. Meteorol. Geophys. Bioklimatol. Ser. B* 19:325-338.
141. Penner, E. 1960. The importance of freezing rate on frost action in soils. *Proc. ASTM* 60:1151-1165.
142. Penner, E. 1967. Heaving pressure in soils during unidirectional freezing. *Can. Geotech. J.* 4:398-408.
143. Penner, E. 1968. Particle size as a basis for predicting frost action in soils. *Soils Found.* 8:21-29.
144. Penner, E. 1970. Frost heaving forces in Leda Clay. *Can. Geotech. J.* 7:8-16.
145. Penner, E. 1970. Thermal conductivity of frozen soils. *Can. J. Earth Sci.* 7:982-987.
146. Penner, E. 1972. Influence of freezing rate on frost heaving. *Highw. Res. Rec. No.* 393. p. 56-64.
147. Radd, F. J., and D. H. Oertle. 1966. Experimental pressure studies on frost heave mechanics and the growth-fusion behavior of ice in soils and glaciers. Report No. 515-4-2-66. *Continental Oil Co., Ponca City, Oklahoma.*
148. Russell, J. D. 1965. Infrared study of the reactions of ammonia with montmorillonite and saponite. *Trans. Faraday Soc.* 61:2284-2294.

149. Russell, J. D., M. Cruz, and J. L. White. 1968. Mode of chemical degradation of s-triazine by montmorillonite. *Science* 160: 1340-1342.
150. Sayles, F. H. 1968. Creep of frozen sands. USA CRREL Tech. Rep. 190.
151. Scott, R. F. 1969. The freezing process and mechanics of frozen ground. USA CRREL Monogr. II-DI.
152. Smith, J. V., and J. M. Bennett. 1968. Hydroxyl groups in zeolite catalysts. *Nature* 219:1040-1041.
153. Solomon, D. H. 1968. Clay minerals as electron acceptors and/or electron donors in organic reactions. *Clays Clay Min.* 16:31-39.
154. Soons, J. M., and D. E. Greenland. 1970. Observations on the growth of needle ice. *Water Resour. Res.* 61:579-593.
155. Soons, J. M., and J. N. Raynor. 1968. Microclimate and erosion processes in the southern alps, New Zealand. *Geogr. Am.* 50:1-15.
156. Stuart, J. G. 1964. Consolidation tests on clay subjected to freezing and thawing. *Swed. Geotech. Inst. Prelim. Rep.* 7.
157. Takagi, S. 1965. Principles of frost heaving. USA CRREL Res. Rep. 140.
158. Thompson, E. G., and F. H. Sayles. 1972. In-situ creep analysis of room in frozen soil. *J. Soil Mech. Found. Div. (ASCE)* 98:899-916.
159. Timur, A. 1968. Velocity of compressional waves in porous media at permafrost temperatures. *Geophysics* 33:548-595.
160. Touillaux, R., P. Salvador, C. Vandermeersche, and J. J. Fripiat. 1968. Study of water layers adsorbed on Na and Ca-montmorillonite by the pulsed nuclear magnetic resonance technique. *Israel J. Chem.* 6:337-348.
161. Tsytoich, N. A. 1945. On the theory of the equilibrium state of water in frozen soils. *Izv. AN SSSR, Ser. Geogr.* 9(5-6).
162. Tsytoich, N. A. 1958. Bases and foundations on frozen soil. *Highw. Res. Board Spec. Rep. No.* 58.
163. Tsytoich, N. A., I. U. K. Zaretskii, V. G. Grigor'eva, and Z. G. Ter-Martirosan. 1965. Consolidation of thawing soils. *Proc. 6th Int. Conf. Soil Mech. Found. Eng.* 1:390-394.
164. Vershinin, P. V., V. V. Deriagin, and N. V. Kirilenko. 1949. The nonfreezing water in soil. *Acad. Sci. USSR Geogr. Geophys. Ser.* 13:108. [U.S. Army Arctic Construction and Frost Laboratory (USA ACFEL), Translation No. 30]
165. Vyalov, S. S. 1965. Rheological properties and bearing capacity of frozen soils. USA CRREL Translation No. 74.
166. Vyalov, S. S. 1965. The strength and creep of frozen soils and calculations for ice-soil retaining structures. USA CRREL Translation No. 76.
167. Warden, D. L., and O. B. Andersland. 1971. Soil-ice behaviour in a model retaining structure. *Can. Geotech. J.* 8:46-68.
168. Weiler, F. A., and J. Chaussidon. 1968. Surface conductivity and dielectrical properties of montmorillonite gels. *Clays Clay Min. Proc.* 16:147-155.
169. Williams, P. J. 1966. Specific heats and unfrozen water content of frozen soils. National Research Council, Canada, Assoc. Comm. on Soil and Snow Mech. Tech. Mem. No. 76. p. 109-126.
170. Williams, P. J. 1964. Specific heat and apparent specific heat of frozen soils. *Geotechnique* 14(2):133-142.
171. Williams, P. J. 1964. Unfrozen water content of frozen soils and soil moisture suction. *Geotechnique* 14(3):213-246.
172. Williams, P. J. 1966. Pore pressures at a penetrating frost line and their prediction. *Geotechnique* 16:187-208.
173. Williams, P. J. 1967. Properties and behaviour of freezing soils. *Norwegian Geotech. Inst. Publ. No.* 72.
174. Williams, P. J., and R. J. Mitchell. 1969. Isothermal volume changes of frozen soils. *In Proceedings, 22nd Soil mechanics conference. Queens University, Kingston, Alberta, Canada.*
175. Williams, P. J. 1972. Use of the ice-water surface tension concept in engineering practice. *Highw. Res. Rec. No.* 393. p. 19-29.
176. Wissa, A. E., and R. T. Martin. 1968. Behaviour of soils under flexible pavements; development of rapid frost susceptibility tests. *Can. Mil. Dept. of Civil Engineering, RR68-77, Soils Publ.* 224.
177. Wu., T. H. 1964. A nuclear magnetic resonance study of water in clay. *J. Geophys. Res.* 69:1083-1091.
178. Yao, L. Y., and B. B. Broms. 1965. Excess pore pressures which develop during thawing of frozen fine-grained subgrade soils. *Highw. Res. Rec. No.* 101. p. 39-57.
179. Yong, R. N. 1967. On the relationship between partial soil freezing and surface forces, p. 1375-1386. *In H. Oura [ed.] Physics of snow and ice. Hokkaido University.*
180. Yong, R. N., and J. C. Osler. 1971. Heave and heaving pressures in frozen soils. *Can. Geotech. J.* 8:272-282.
181. Zaretskii, Y. K. 1968. Calculation of the settlement of thawing soil. *Soil Mech. Found. Eng. No.* 3. p. 151-155.
182. Zettlemoyer, A. C. 1968. Hydrophobic surfaces. *J. Colloid Interface Sci.* 28:343-369.

NOTES

[1] The sample was taken outside the Division of Physical Chemistry Laboratory, Royal Institute of Technology, Stockholm, Sweden, 25 January 1967, during, but some hours after commencement of, the snowfall. The sample was packed into the sample container at liquid nitrogen temperature and introduced immediately into an NMR Dewar probe at -23°C . Preliminary measurements were taken to optimize the spectrometer settings. The measurements were taken at 3.5 kG, 14.8 MHz, and RF field of 100 μA , in a 50-min scan with a Varian Model V4230 LP (proton-free) probe. Some saturation effects were present and the high sweep modulation required (L-6) contributed some instrumental broadening, but not enough distortion was present to impair the qualitative value of the spectra.

[2] Measurements were taken with a Varian wide-line spectrometer using a V4230 LP probe at 3.5 kG and 14.8 MHz. RF field strengths and sweep modulations were selected for each measurement to avoid instrumentation distortion of the spectra. The sample was contained in a sealed ampoule suspended in a Dewar tube within the probe. Temperature was controlled within $\pm 0.1^{\circ}\text{C}$ at each measurement.

THE UNFROZEN WATER AND THE APPARENT SPECIFIC HEAT CAPACITY OF FROZEN SOILS

Duwayne M. Anderson, Allen R. Tice, and Harlan L. McKim

U.S. ARMY COLD REGIONS RESEARCH AND ENGINEERING LABORATORY
Hanover, New Hampshire

INTRODUCTION

Within the last decade, the pressure of technological development in arctic and subarctic environments has stimulated the development of methods to perform thermal calculations of the earth-air interface quickly and accurately. When the thermal regime of permafrost is changed as a result of engineering operations, or because of a perturbation of the local environmental conditions, the ice-water phase composition of the frozen soils also must change. The influence of this change on the stability and function of an engineering installation can be considerable. It is important, therefore, to be able to predict changes in soil temperature and in the relative ice and unfrozen water content of frozen ground resulting from various types of thermal disturbance before engineering designs are accepted and approved. This paper introduces a convenient equation for predicting the apparent specific heat capacity and the cumulative heat absorption versus temperature curve of frozen soils from their water-ice phase composition data.

UNFROZEN WATER

The existence of a continuous, unfrozen water phase separating ice from the mineral or organic matrix in frozen soils is now generally accepted. Most questions regarding the mobility of the interfacial water, the nature of the ice phase, and the factors governing the quantity of water remaining unfrozen under given conditions have been answered.^{3,4,6} The unfrozen interfacial water behaves as a two-dimensional liquid with water molecules and solutes freely mobile throughout. During the past decade, several means of obtaining phase composition curves (unfrozen water contents as a function of temperature) have been investigated.^{2,5,8,12-15,17,19-21} One result has been the development of an isothermal calorimeter method.⁶ Phase composition curves for 11 representative soils and soil constituents have been obtained by this method.⁵

In most cases, the data are well represented by a simple power equation:

$$w_u = \alpha\theta^\beta, \quad (1)$$

where w_u = unfrozen water content (g H₂O/100 g soil), θ = temperature in degrees C below zero, and α and β = parameters characteristic of each soil. The clay-water systems were somewhat more complex, however. Although Eq. (1) provides an adequate fit for practical purposes, the representation could be made exact by employing segments of two power curves of this form. In general, Eq. (1) describes the phase composition versus temperature relationship for water contents up to a weight fraction water of one. At lower water contents, one simply truncates the curve at the total water content. The corresponding value of θ is the freezing point depression of the pore water. Values of α and β were obtained for each of these 11 soils by a least squares regression of experimentally measured values of w_u versus θ . When the values of α and β obtained in this way were regressed against the specific surface area S for each soil, it was found that:

$$\ln \alpha = 0.5519 \ln S + 0.2618, \quad (2)$$

with a correlation coefficient of 0.90 and,

$$\ln (-\beta) = -0.2640 \ln S + 0.3711, \quad (3)$$

with a correlation coefficient of 0.86.

The properties of the 11 soils and soil materials selected are such as to cover the full range of possible values of specific surface area, as well as a wide range of other soil properties, excluding only dissolved solutes. Consequently, additional phase composition data, when they become available and are pooled with that considered here, are not likely to alter the values of the coefficients in Eq. (2) and (3) significantly. Therefore, Eq. (2) and (3) are entered into Eq. (1) to obtain:

$$\ln w_u = 0.2618 + 0.5519 \ln S - 1.449S^{0.264} \ln \theta. \quad (4)$$

Equation (4) is useful to compute estimates of w_u of salt-free soils with no overburden pressure for any temperature below 0 °C, provided only the surface area S of the soil is known or can be estimated.⁵

Dillon and Andersland⁸ recently constructed a somewhat similar equation for the same purpose. They collected all the factors deemed of major importance in influencing the unfrozen water content and combined them in a rational way to obtain:

$$w_u = k(T/T^{\circ})(l/A_c) S. \quad (5)$$

When written in this form, w_u , as in Eq. (4) above, is given in g H₂O/g dry soil; T/T° is the ratio of the temperature of the frozen soil to the temperature of initial freezing of the pore water in degrees K; S is the average specific surface area of the soil grains; A_c is a ratio formed between the plasticity index, I_p , and the percent soil grains less than 2 μm ; l is an adjustable parameter to account for different clay types (1 for 1:1 nonexpanding clays, 2 for 2:1 expanding clays); and k was taken as 2.8×10^{-4} g H₂O/m².

When tested against 11 soils for which unfrozen water content was available, quite good agreement was obtained. However, only one or two points on the phase composition curve for each soil, mostly at temperatures lower than -5°C , were available. This is the region where the phase composition curve varies least with temperature. When compared with the complete phase composition curves of Leonards and Andersland,¹¹ Eq. (5) was less adequate; the relationship between w_u and the soil water characteristic curve, shown by Williams²² to be a reliable predictor down to about -1°C , was recommended for the higher temperatures where Eq. (5) fails. The form of Eq. (5) is not capable of fitting complete phase composition curves well. Also, it is redundant to the degree that the plasticity index is a function of the specific surface area. In addition, although it could not have been known at the time, Eq. (5) may contain an erroneous assumption regarding the relative thickness of the unfrozen water interfaces associated with the 1:1 and 2:1 lattice clays. The coefficient k is approximately equal to an unfrozen water interface of monolayer dimensions. Combined with the factor, l , it predicts about two times more unfrozen water per unit surface area for the 2:1 expanding clays than for the 1:1 nonexpanding clays. This is contrary to a recent conclusion that kaolinite has more unfrozen water per unit surface area than two montmorillonites with which it was compared.⁵

Equation (4) is completely empirical in origin and derives its utility from the fact that it predicts the unfrozen water content of frozen soil throughout the whole temperature range remarkably well. Predictions derived from it are sufficiently accurate for a wide range of practical purposes. Although the significance of the form of Eq. (1) has not yet been fully explored, it is probable that it is of a basic nature. For this reason an application of domain theory, for example, has been facilitated by this simple relationship.⁷

HEAT CAPACITY

One of the problems encountered in performing thermal calculations has been the lack of a convenient method of incorporating the nonlinear unfrozen water versus temperature relationship of the phase composition curve into a heat capacity equation. Only recently have ways of accomplishing this been effectively proposed. Successful methods have been devised by Ho *et al.*¹⁰ and Nakano and Brown.¹⁶ In each, *ad hoc* functions were employed to represent the ice and unfrozen water content of the frozen ground. Because of its convenient form, Eq. (1) could be used in these two computational schemes and other calculations in which it is necessary to evaluate the term:

$$\int_{\theta_1}^{\theta_2} L [(\partial w_u)/(\partial \theta)] d\theta,$$

in the heat capacity equation.² This term, in which L is the conventional latent heat of phase change, accounts for the heat involved as the relative amounts of ice and unfrozen water change in the temperature interval $(\theta_2 - \theta_1)$. Disregarding its temperature dependence and taking L as constant equal to 79.7 cal/g is satisfactory in most cases, even though it is known that the latent heat of phase varies with w_u .¹ The significance of the dependence of L on w_u has been investigated by performing a series of calculations using approximate dummy functions. It was found that the necessary correction is significant only for temperatures below about -20°C .

The heat capacity of a substance, defined as the quantity of heat required to raise the temperature of a substance 1°C , expressed per unit weight is referred to as its specific heat capacity. In frozen soils, where phase change is a common, gradual occurrence, the term *specific heat capacity* is not strictly applicable, and the term *apparent specific heat capacity* is employed.²⁰ Neglecting the gas phase, a frozen soil-water mixture may be regarded as consisting of two components (soil and water) and three phases—namely, a soil particle matrix, ice, and the water that remains unfrozen. The heat capacity of this system may be expressed as the sum of the heat capacities of these three phases plus a term accounting for the latent heat involved in changing the proportion of unfrozen water to ice [1]. Thus:

$$c_a = c_s + c_i (w_w - w_u) + c_u w_u + \frac{1}{\Delta T} \int_{T_1}^{T_2} L (\partial w_u / \partial T) dT, \quad (6)$$

where c_a = apparent specific heat capacity (cal/^oC/unit weight of soil); c_s = specific heat capacity of soil matrix; c_i = specific heat capacity of ice; c_u = specific heat capacity of unfrozen water; w_w = total water content; w_u = unfrozen water content; T = temperature (^oC); $\Delta T = (T_2 - T_1)$; and L = latent heat of fusion for ice.

Because of the units employed, this expression of c_a is somewhat unconventional; it is convenient, however, because the general relationship between w_u and T required in the last term of Eq. (5) is conveniently expressed as unit weight of water per unit weight of oven-dry soil per degree.

Substituting Eq. (1) in the leading terms of Eq. (5) and entering the derivative of Eq. (1) in the last term after integration, yields:

$$c_a = c_s + c_i w_w + (c_u - c_i) \alpha \theta^\beta + (\alpha L / \Delta\theta) (\theta_1^\beta - \theta_2^\beta), \quad (7)$$

where, for computational convenience, the limits of integration are written as: $\theta_1 = [\theta - (\Delta\theta/2)]$ and $\theta_2 = [\theta + (\Delta\theta/2)]$; $\Delta\theta = (\theta_2 - \theta_1)$.

Possession of values for α and β and Eq. (6) makes it possible to compute apparent specific heat capacity versus temperature curves. Table I contains the required data for 6 of the 11 representative materials for which complete phase composition have been obtained in this laboratory. For computations, nominal values were assigned to the various parameters; $\Delta\theta$ was taken as 10^{-5} °C; c_s was taken² as 0.164 cal/g·°C; and c_i was taken⁹ as 0.5 cal/g·°C.

The fact that c_a in Eq. (7) approaches ∞ as θ goes to 0 appears to be a troublesome inconvenience, but the difficulty disappears when one recognizes that specifying a value for w_w for each soil material determines a unique, finite value for the freezing point depression, θ_f . Establishing finite values for θ_f has the effect of truncating the c_a versus T curves generated by Eq. (7) at the maximum possible value for c_a . To illustrate, the last three columns of Table I contain freezing point depressions calculated from Eq. (1) for three values of w_w . From these, together with Eq. (7), c_a versus T relationships have been computed down to $T = -15$ °C (Figures 1-3). For $0 < \theta < \theta_f$, c_a was taken simply as the sum:

$$c_a = c_s + c_w w_w, \quad (8)$$

where c_w , the specific heat of water, is taken as 1.01 cal/g·°C, the value for supercooled water at $T = 1$ to -6 °C.⁹ For $w_w = 1.0, 0.50,$ and 0.25 g H₂O/g soil, c_a in this temperature range is computed to be 1.174, 0.669, and 0.416 cal/g·°C, respectively.

Figures 1-3 illustrate that soils that have high specific surface areas have much lower apparent specific heat capacities at low water contents than the coarser soils with lower specific surface areas. This is a consequence of the relatively large value of θ_f that results when comparatively small quantities of water are distributed over large surface areas. As expected, Figures 1-3 also show that very large values of c_a occur above about -2 °C; below about -5 °C, the change in c_a with T is very gradual, and c_a is correspondingly reduced. It is reassuring to note that the curves presented in Figures 1-3 are self-consistent and in good agreement with available experimental and derived determinations.^{3,20}

Equation (7) is of immediate use in computing cumulative energies associated with temperature changes of frozen ground. The heat absorbed (positive) or extracted (negative) is given, with proper allowance for sign, by:

$$Q_{\theta_i \rightarrow \theta_j} = \int_{\theta_i}^{\theta_j} c_a d\theta + (c_s + c_w w_w) (\theta_j - \theta_i), \quad (9)$$

for subzero temperatures, where $\theta_i < \theta_f < \theta_j < 0$ °C. [The temperature dependence of $c_s, c_i, c_w, c_u,$ and L is neglected for two reasons: adequate data expressing these quantities as functions of temperature are not available, and a series of calculations using approximate dummy functions show that for the temperature of most interest (-15 to 0 °C) the appropriate corrections are insignificant.]

Curves for cumulative heats absorbed in raising the tem-

TABLE I Calculated Freezing Point Depression Values for Six Representative Soils

Soil	Specific Surface Area (m ² /g)	Experimental Values ^b		Freezing Point Depression, θ (°C)		
		α	β	$w_w = 0.25$ (g H ₂ O/g soil)	$w_w = 0.50$ (g H ₂ O/g soil)	$w_w = 1.00$ (g H ₂ O/g soil)
1 Manchester very fine sand	0.016 ^a	0.0346	-0.048	1.00×10^{-18}	1.00×10^{-25}	1.00×10^{-31}
2 Fairbanks silt	40	0.0481	-0.326	6.37×10^{-3}	7.60×10^{-4}	9.07×10^{-5}
3 Kaolinite	84	0.2380	-0.360	8.72×10^{-1}	1.27×10^{-1}	1.85×10^{-2}
4 Suffield silty clay	140	0.1392	-0.315	1.56×10^{-1}	7.3×10^{-1}	1.91×10^{-3}
5 Hawaiian clay	382	0.3242	-0.243	2.91	1.68×10^{-1}	9.7×10^{-3}
6 Umiat bentonite	800	0.6755	-0.343	18.2	2.41	3.19×10^{-1}

^a Geometrical specific surface was estimated from a grain-size distribution curve for soil No. 1, while for soils No. 2-6 the surface area was determined by the ethylene glycol retention method.

^b Values for α and β were obtained by least square regression of the data for each individual soil.

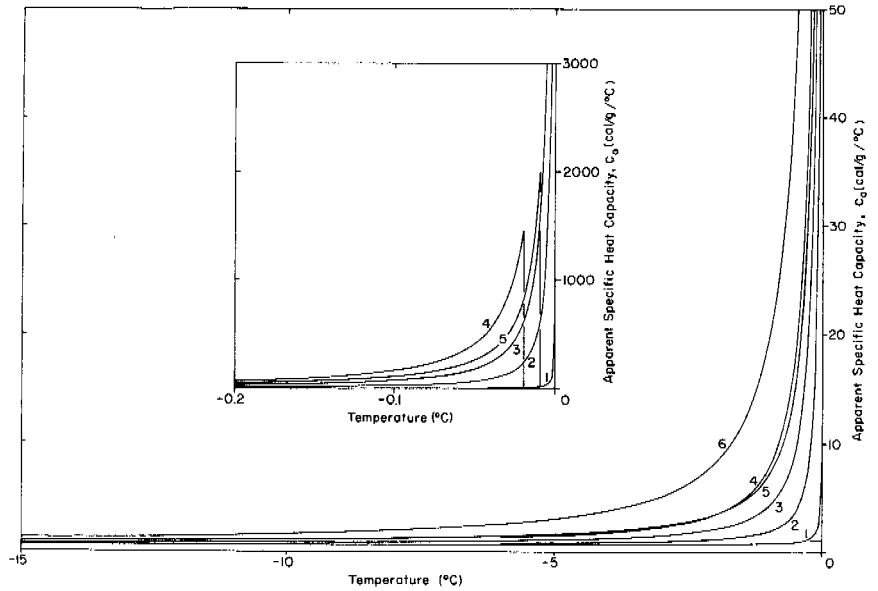


FIGURE 1 Apparent specific heat capacity of six representative soils calculated from Eq. (6) for a total water content of 1.00 g H₂O/g soil.

perature of the six representative frozen soils from -10 to 10 °C are given for water contents of 1.0, 0.5, and 0.25 g H₂O/g soil in Figures 4, 5, and 6, respectively. These curves are instructive. Soils with high specific surface areas have comparatively large cumulative heats at temperatures below θ_f . This is a consequence of their water-ice phase composition curves and indicates progressive melting of interstitial ice, beginning at temperatures below -10 °C. Even at water contents as high as 1.0 g H₂O/g soil, a large fraction of the water remains unfrozen at -5 °C in these materials, whereas in the coarse-textured soils, with low specific surface areas, a larger proportion of the water exists as ice, and

most melting occurs nearer 0 °C. As a result of this interplay, the cumulative heats of the coarse-textured soils are lower at below-zero temperatures and higher at 10 °C than those of finer-textured soils. At lower water contents (0.5 and 0.25 g H₂O/g soil), this is even more obvious. The fact that all of the cumulative heats at 0 °C are less than that calculated from the product Lw_w indicates that in all cases at least some of the water present remains unfrozen at -10 °C.

As noted above, these soils envelop the full range of possible specific surface areas and most other significant properties commonly encountered in normal soils. There-

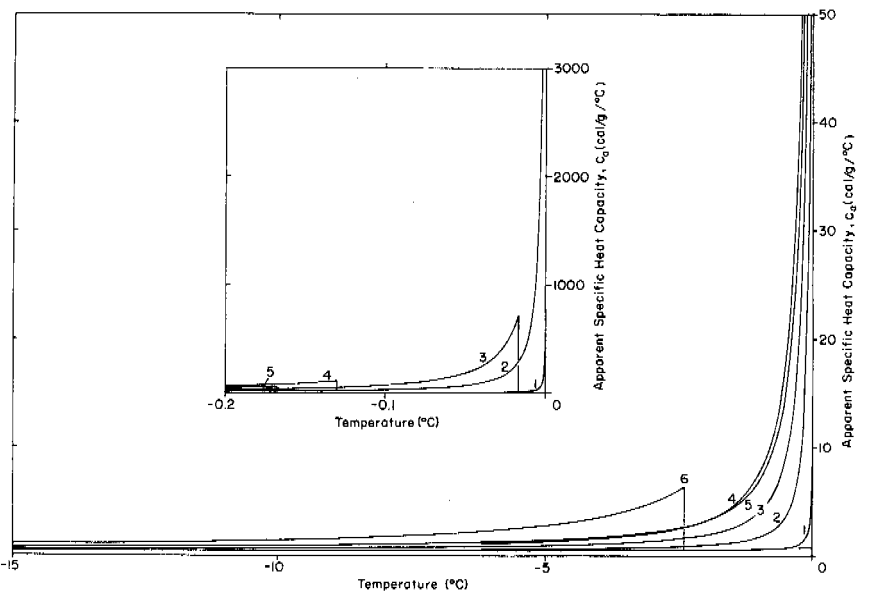


FIGURE 2 Apparent specific heat capacity of six representative soils calculated from Eq. (6) for a total water content of 0.50 g H₂O/g soil.

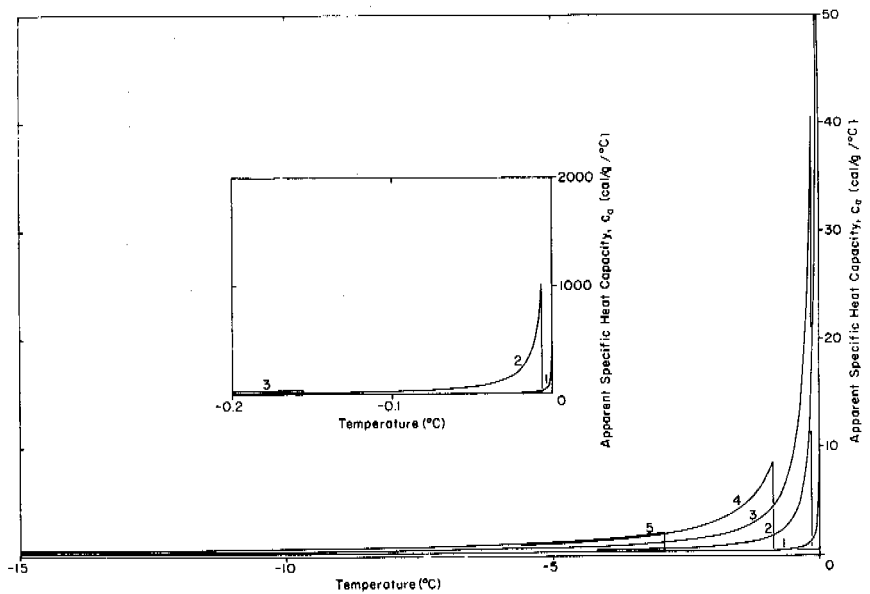


FIGURE 3 Apparent specific heat capacity of six representative soils calculated from Eq. (6) for a total water content of 0.25 g H₂O/g soil.

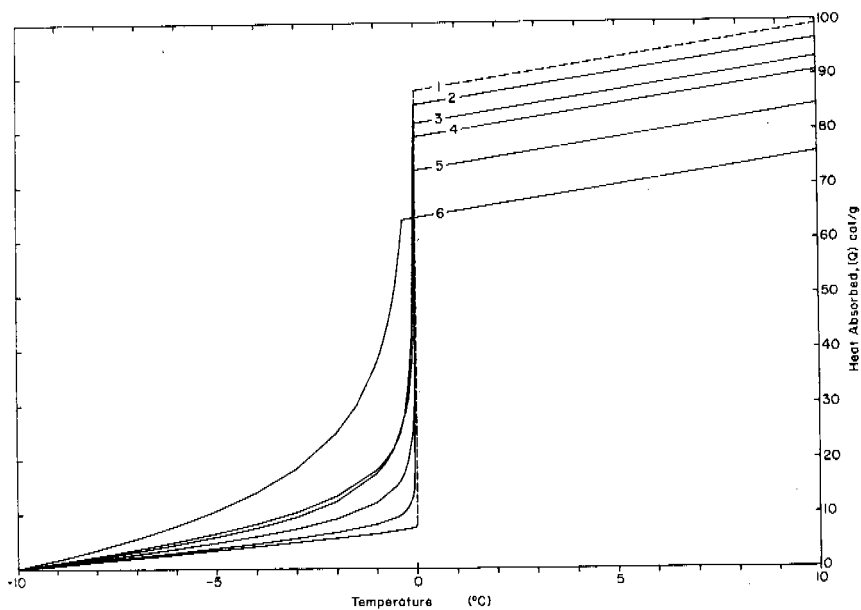


FIGURE 4 Cumulative heat absorbed in raising the frozen soil-water mixture containing 1.0 g H₂O/g soil from -10 °C through the melting point (cal/g soil).

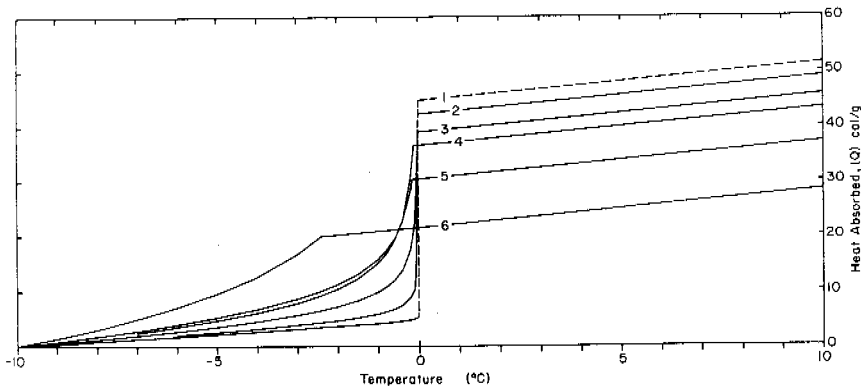


FIGURE 5 Cumulative heat absorbed in raising the frozen soil-water mixture containing 0.5 g H₂O/g soil from -10 °C through the melting point (cal/g soil).

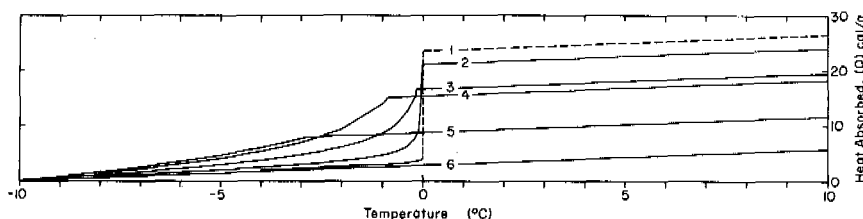


FIGURE 6 Cumulative heat absorbed in raising the frozen soil-water mixture containing 0.25 g H₂O/g soil from -10 °C through the melting point (cal/g soil)

fore, the curves in Figures 1-3 and Figures 4-6 may be regarded as defining the envelopes of possible values of the apparent specific heat versus temperature and the cumulative heat absorbed versus temperature relationships expected for all normal soils. In this way, they illustrate the desirability of using expressions equivalent to Eq. (7), (8), and (9) in performing thermal calculations. In general, the refinements proposed are most justified in situations involving fine-textured soils and temperature changes near θ_f ; because of their convenience, however, these relationships may easily be incorporated in the consideration of most, if not all, practical situations.

SUMMARY

Complete water-ice phase composition data for 11 representative soils having specific surface areas, S , ranging from 0.02 to 800 m²/g soil obtained by a newly developed isothermal calorimetric method were collected and analyzed. These data are well represented by the equation

$$w_u = \alpha\theta^\beta,$$

where w_u is the unfrozen water content, θ is the soil temperature in degrees centigrade below freezing, and α and β are empirical constants characteristic of a given soil. It was found that α and β are related to the specific surface areas (as determined by ethylene glycol retention) of the frozen soils, and the following general water phase composition equation emerged from the regression analyses:

$$\ln w_u = a + b \ln S + c S^d \ln \theta.$$

Present data indicate that $a = 0.2618$, $b = 0.5519$, $c = -1.449$, and $d = -0.2640$, when S is given in m²/g, θ is in degrees centigrade, and w_u is given in g H₂O/g soil.

The availability of these equations facilitates the calculation of thaw and frost penetration. An equation for the apparent specific heat capacity of frozen ground incorporating the relationship expressed in the first of these is derived. Apparent specific heat capacities are calculated as a function of temperature for six representative soils at each of three water contents. In addition, representative curves that

depict the cumulative heat absorbed in bringing each from -10 °C through the melting point have been computed and are given in graphical form.

ACKNOWLEDGMENTS

This paper presents the results of research performed by the U.S. Army Cold Regions Research and Engineering Laboratory under the sponsorship of the U.S. Army Corps of Engineers.

REFERENCES

1. Anderson, D. M. 1966. The latent heat of freezing soil water, 238-239. Permafrost: Proceedings of an international conference. National Academy of Sciences, Washington, D.C.
2. Anderson, D. M. 1966. Phase composition of frozen montmorillonite-water mixtures from heat capacity measurements. Soil Sci. Soc. Am. Proc. 30:670-675.
3. Anderson, D. M. 1967. The interface between ice and silicate surfaces. J. Colloid Interface Sci. 25:174-191.
4. Anderson, D. M., and A. R. Tice. 1971. Low-temperature phases of interfacial water in clay-water systems. Soil Sci. Soc. Am. Proc. 35(1):47-54.
5. Anderson, D. M., and A. R. Tice. 1972. Predicting unfrozen water contents in frozen soils from surface area measurements. Highway Research Board Record No. 393. p. 12-18.
6. Anderson, D. M., and A. R. Tice. The unfrozen interfacial phase in frozen soil water systems. International symposium on soil water physics and technology proceedings. Rehovot, Israel. (In press)
7. Banin, A., D. M. Anderson, and A. R. Tice. A multi-domain model of unfrozen water distribution in frozen clays. Colloid Interface Sci. (In press)
8. Dillon, H. B., and O. B. Andersland. 1966. Predicting unfrozen water contents in frozen soils. Can. Geotech. J. 3(2):53-60.
9. Chemical Rubber Co. 1953-1954. Handbook of chemistry and physics. 25th ed. Chemical Rubber Co., Cleveland, Ohio. p. 2079.
10. Ho, D. M., M. E. Harr, and G. A. Leonards. 1969. Transient temperature distribution in insulated pavements—predictions vs observations. Can. Geotech. J. 7:275-284.
11. Leonards, G. A., and O. B. Andersland. 1960. The clay water system and the shearing resistance of clays. Paper presented at ASLE Research Conference on Shear Strength of Cohesive Soils.
12. Lovell, C. W. 1957. Temperature effects on phase composition and strength of partially-frozen soil. Highway Research Board Bull. 168. p. 74-95.
13. Low, P. F., D. M. Anderson, and P. Hoekstra. 1968. Some thermodynamic relationships for soils at or below the freezing point.

1. Freezing point depression and heat capacity. *Water Resour. Res.* 4:379-394.
14. Low, P. F., D. M. Anderson, and P. Hoekstra. 1968. Some thermodynamic relationships for soils at or below the freezing point. 2. Effects of temperature and pressure on unfrozen soil water. *Water Resour. Res.* 4(3):541-544.
15. Martynov, G. A. 1959. Heat and moisture transfer in freezing and thawing soils, p. 153-192. *In Principles of geocryology, Part I. General geocryology.* Akad. Nauk SSSR. (Translated by E. R. Hope, National Research Council of Canada Technical Translation 1065)
16. Nakano, Y., and J. Brown. 1971. Effect of a freezing zone of finite width on the thermal regime of soils. *Water Resour. Res.* 9:1226-1233.
17. Nersesova, Z. A., and N. A. Tsytoich. 1966. Unfrozen water in frozen soils, p. 230-234. *Permafrost: Proceedings of an international conference.* National Academy of Sciences, Washington, D.C.
18. Penner, E. 1958. Soil moisture tension and ice segregation. *Highway Research Board Bull.* 168. p. 50-64.
19. Penner, E. 1966. Frost-heaving in soils, p. 197-202. *Permafrost: Proceedings of an international conference.* National Academy of Sciences, Washington, D.C.
20. Williams, P. J. 1964. Specific heat and apparent specific heat of frozen soils. *Geotechnique* 14(2):133-142.
21. Williams, P. J. 1966. Suction and its effects in unfrozen water of frozen soils, p. 225-229. *Permafrost: Proceedings of an international conference.* National Academy of Sciences, Washington, D.C.
22. Williams, P. J. 1964. Unfrozen water content of frozen soils and soil moisture suction. *Geotechnique* 14(3):231-246.

NOTE

[1] We assume the system to be at constant pressure.

MECHANICAL PROPERTIES OF FROZEN GROUND UNDER HIGH PRESSURE

Edwin Chamberlain

U.S. ARMY COLD REGIONS RESEARCH AND
ENGINEERING LABORATORY
Hanover, New Hampshire

INTRODUCTION

The evaluation of crater and crater formation and seismic waves in regions of permafrost requires considerable knowledge of the high pressure behavior of frozen soil and ice. Computer codes that have been developed to evaluate the wave motions and material states require the knowledge of many material properties, among which are the triaxial compressive strength and the isothermal compressibility. The triaxial compressive strength data are used to determine whether failure will occur in shear during the arrival of the stress wave or if it will occur in tension as the distortional strain energy is released as the wave passes. The isotherm is used to fill in the low-pressure region of the dynamic pressure-volume relationship (Hugoniot). This has been necessary since, until recently, good Hugoniot data in the low-pressure region have not been obtainable.

This paper discusses and reports the results of high-pressure triaxial compression tests ($\sigma_3 = 35\text{--}2800 \text{ kg/cm}^2$) and isothermal compressibility tests ($P_{\max} \approx 30 \text{ kbar}$) conducted at the U.S. Army Cold Regions Research and Engineering Laboratory (CRREL) over the past several years.

MATERIAL PROPERTIES

Soil

Two processed soils are tested; the first is sieved from a commercially obtained quartz sand (OWS) and the second from a glacial till (WLT). That portion of the sand used is smaller than $149 \mu\text{m}$ but larger than $74 \mu\text{m}$. The sand is well rounded, has a specific gravity of 2.63, and is classified according to the Atterberg limit system as nonplastic. The portion of the glacial till used is a silt with no particles larger than $149 \mu\text{m}$. It contains many more fines than the sand, has a liquid limit of 16 and a specific gravity of 2.87, and is classified as nonplastic. The grain-size distribution curves are shown in Figure 1.

Ice

This material is a clear polycrystalline columnar ice, having a maximum grain diameter of 0.5 cm. The density is measured as 0.917 g/cm^3 .

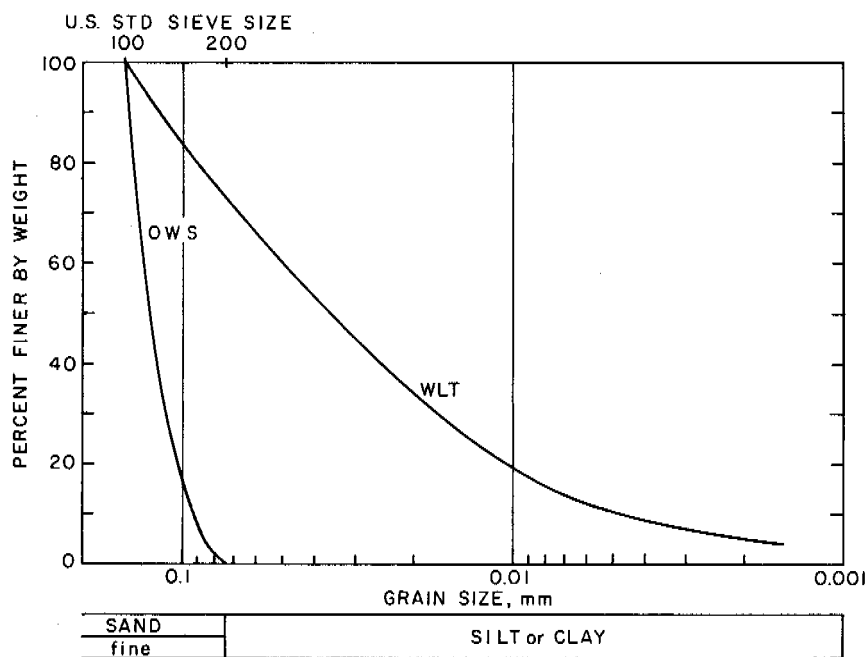


FIGURE 1 Gradations of the soils tested.

SAMPLE PREPARATION

Isothermal Compressibility Tests

The soil specimens are prepared in 1.17-cm i.d. lead capsules approximately 3.2 cm long with a wall thickness of 0.10 cm. The specimen length is approximately 2.54 cm; the excess capsule length is being used for sealing the capsule.

The WLT samples are compacted wet by tamping and the OWS samples are molded dry by vibration. The water content of each specimen is adjusted to the desired value after compaction. Saturated soil specimens are wetted under vacuum. The samples are frozen rapidly from all sides to minimize ice segregation and frost heaving and are tempered at -10°C for at least 24 h before testing.

The ice samples are frozen unidirectionally from de-aired distilled water, machined to size, and placed in the lead capsules. The ice samples also are tempered for 24 h at -10°C .

High-Pressure Triaxial Compression

The triaxial test samples are prepared in 3.58-cm i.d. Plexiglas molds—the WLT samples by compaction in layers and the OWS samples by vibration. They are degassed, saturated with degassed, distilled water under vacuum, and frozen unidirectionally from the top down in an open system; water is free to flow in or out as freezing takes place. When completely frozen, the samples are removed from their molds and the ends are machined flat and parallel. The samples are then placed in latex membranes and tempered at -10°C for at least 24 h before testing.

PROCEDURES

Isothermal Compressibility

The isothermal compressibility apparatus (Figure 2) is similar to that described by Stephens.⁷ The test sample is encapsulated in lead and compressed between two 1.27-cm-diameter carbide pistons, while confined in the bore of a carbide die. Hardened steel rings and plugs prevented extrusion of the lead. Samples, nominally 1.17 cm in diameter and 2.54 cm long, are compressed to 30 kbar (approximately $30\,000\text{ kg/cm}^2$). The pistons are loaded by a 136 000-kg universal testing machine at a rate slow enough (≈ 1 cycle/40 min) to obviate compressive heating effects. A coolant was circulated through coils attached to the die plate to maintain the temperature at $-10 \pm 0.5^{\circ}\text{C}$.

High-Pressure Triaxial Compression

The high-pressure triaxial compression apparatus (Figure 3) was developed as an outgrowth of a lower pressure device ($\sigma_{3(\text{max})} \approx 100\text{ kg/cm}^2$) being used at CRREL. In addition to its much greater capacity of $2\,800\text{ kg/cm}^2$, it provided for continuous monitoring of volume changes in the test samples. Saturated OWS and WLT samples are tested at -10°C and a strain rate of approximately 6 percent/min. The sample diameter is 3.58 cm and 8.9 cm long. Air- and hand-operated pumps are used to pressurize the kerosene used for confining fluid. A hand-operated volume compensator is used to maintain the confining pressure during the course of a test. Axial loading is applied by a 136 000-kg universal testing machine.

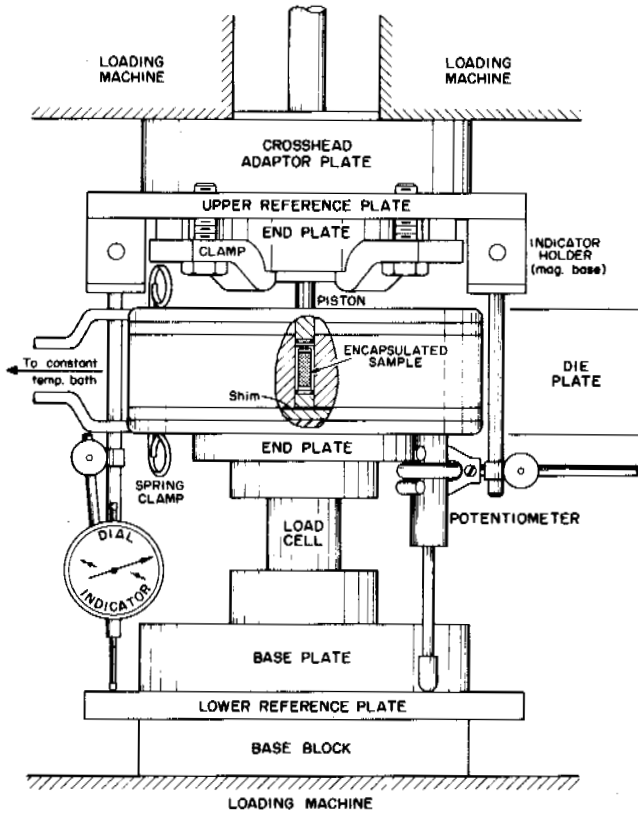


FIGURE 2 Isothermal compressibility apparatus.

RESULTS AND DISCUSSION

Isothermal Compressibility

THE COMPRESSIBILITY OF ICE

A knowledge of the compressibility of ice is essential to the understanding of the compressibility of frozen soil, since at high pressures ice has a compressibility an order of magnitude greater than that for the mineral constituents such as quartz. Earlier this century, Bridgman⁴ published many articles (republished as a collection in 1964) that remain as the definitive source for the P-V-T phase diagram of water and ice. Figure 4 illustrates the phase diagram of water as it is known today. This figure shows that several phase transitions will occur during the isothermal compression of ice at -10 °C. Ice I will melt to the liquid phase (water) at 1.11 kbar, freeze to Ice V at 4.42 kbar, undergo a polymorphic transition to Ice VI at 6.25 kbar, and transform into Ice VIII at a pressure of 20.8 kbar. The relative volume V_i^p/V_i^0 of each of these ice phases at their transition pressures is given in Table I. These data are extracted from Bridgman's work, the details of which are given by Chamberlain and Hoekstra.⁶ Typical results of isothermal compressibility tests on laboratory prepared polycrystalline ice are shown in Figure 5. The compressibility, as calculated from Bridgman's data, is plotted for comparison. The variation of the test results from Bridgman's results can be attributed primarily to rate effects. The differences are significant only in the regions of phase change and are most likely the result of the time dependency of the phase transformation process. The slightly greater compressibility in our results might be explained by the presence of microscopic air bubbles. An included air volume of approximately 1 percent would account for the differences.

Bridgman observed that Ice V nucleated only in the presence of glass splinters. Two of the three ice samples tested, however, showed the liquid-Ice V transition. For the specimen for which the data are illustrated (Figure 5), however, Ice V did not nucleate, and the liquid phase froze to Ice VI upon loading beyond the liquid-Ice V transition.

PREDICTION OF THE COMPRESSIBILITY OF FROZEN SOIL

Frozen soil can be considered as a rock made up of three components: ice, mineral particles, and air. The inclusion of organics and unfrozen water will not be considered here. The compressibility can be estimated by averaging the compressibilities of components making up the soil. Two kinds of averaging are generally used for rocks: the Reuss average and the Voigt average. The Reuss average, B_r , is given by:

$$B_r = V_a B_a + V_b B_b + V_c B_c \dots \quad (1)$$

where V_a, V_b , etc., are volume percentages of the soil com-

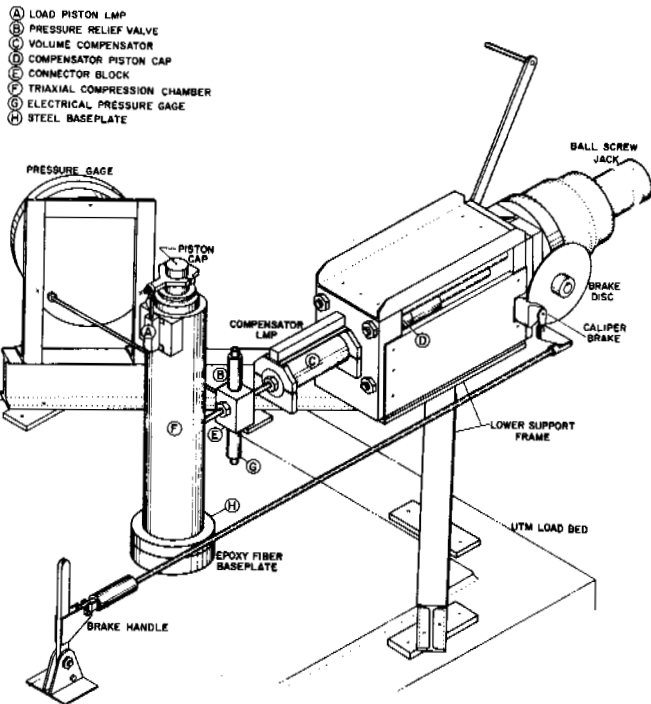


FIGURE 3 Triaxial compression apparatus.

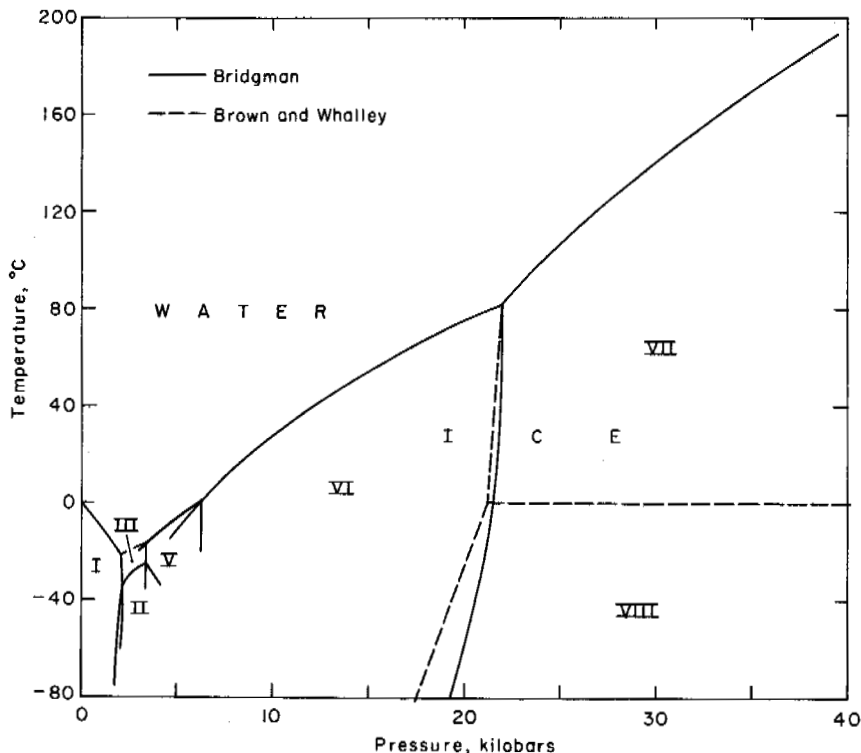


FIGURE 4 Phase diagram of water in the temperature–pressure plane. From Bridgman⁴ and Brown and Whalley.⁵

ponents, and B_a, B_b, \dots , are the volume compressibilities of the minerals. The Reuss average provides an upper bound. The lower bound, the Voigt average, B_v , is given by:

$$1/B_v = V_a/B_a + V_b/B_b + V_c/B_c + \dots \quad (2)$$

The Reuss averaging method assumes uniform distribution of stress through the matrix and neglects the difficulty in fitting grains together. The Voigt model assumes a uniform strain through the matrix and neglects the nonequilibrium stress conditions that exist.

TABLE I Compressibility of Ice at -10°C^a

Phase	Pressure (kbar)	Specific Volume (V_i^p cm ³ /g)	Relative Volume (V_i^p/V_i^o)
Ice I	0.0	1.0900	1.000
Ice I	1.11	1.0664	0.978
Water	1.11	0.9544	0.876
Water	4.42	0.8688	0.796
Ice V	4.42	0.8012	0.736
Ice V	6.25	0.7907	0.726
Ice VI	6.25	0.7522	0.690
Ice VI	20.8	0.702	0.644
Ice VIII	20.8	0.645	0.592
Ice VIII	49.1	0.60	0.550

^a Calculated by Chamberlain and Hoekstra⁶ from Bridgman⁴ and Brown and Whalley.⁵

The compressibility of frozen ground can be estimated by a form of either Eq. (1) or Eq. (2) if we assume that ice flows plastically. The problem is complicated by the four phase transitions that ice undergoes when compressed to 30 kbar at -10°C . A consequence of Eq. (1) is that the total volume change, ΔV_t , is the mere sum of the volume changes of the components, the mineral particles ΔV_m , the ice ΔV_i , and the gas ΔV_g , i.e.,

$$\Delta V_t = \Delta V_m + \Delta V_i + \Delta V_g. \quad (3)$$

A general equation for the compressibility of frozen soil, with porosity and degree of ice saturation as the main index parameters, is derived as follows: porosity (n) is defined as the ratio of the volume of voids (V_v^o) to the total volume (V_t^o) at atmospheric pressure:

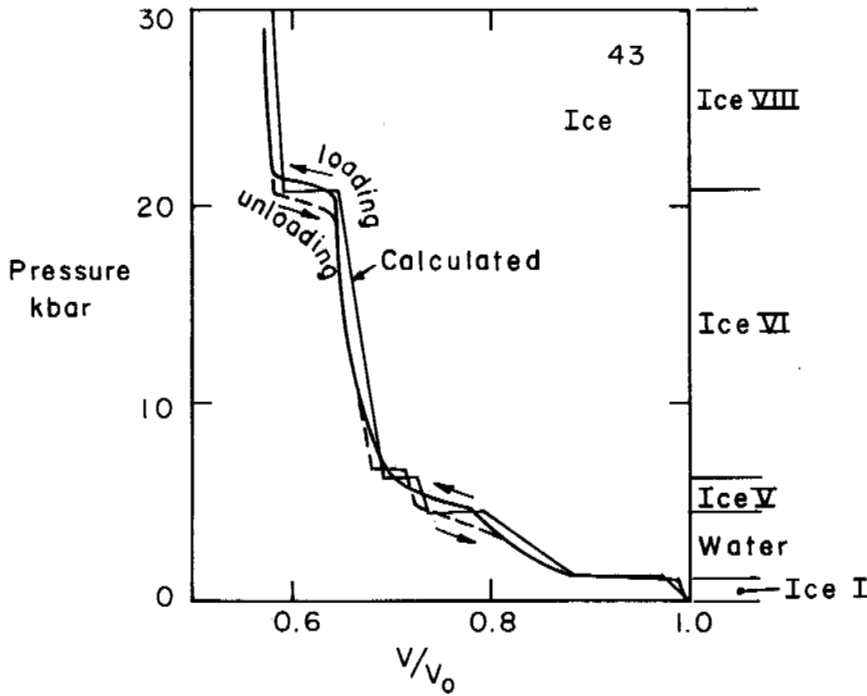
$$n = V_v^o/V_t^o. \quad (4)$$

The degree of saturation (S_i) is defined as the ratio of the volume of the voids filled with ice (V_i^o) and the total void volume (V_v^o):

$$S_i = V_i^o/V_v^o. \quad (5)$$

Thus, V_i^o can be expressed in terms of the total volume (V_t^o) and the porosity (n) by:

$$V_i^o = S_i n V_t^o. \quad (6)$$


 FIGURE 5 Isothermal compressibility of ice, specimen 43, at -10°C .

The compressibility of the mineral solids, assuming the soil to be monomineralic, is given by:

$$\Delta V_m = (V_t^0 - V_v^0)(aP + bP^2), \quad (7)$$

where a and b are compressibility coefficients and P is pressure.³ ΔV_i at pressure P is given by:

$$\Delta V_i = S_i n V_t^0 (1 - V_i^P/V_i^0), \quad (8)$$

where V_i^P/V_i^0 is the compressibility value for ice at pressure P obtained from Table I.

If we assume that all voids close with slight pressure, then ΔV_g at any pressure is

$$\Delta V_g = V_g^0 = (1 - S_i) n V_t^0. \quad (9)$$

Hence, Eq. (3) becomes:

$$\Delta V_t = (V_t^0 - V_v^0)(aP + bP^2) + S_i n V_t^0 (1 - V_i^P/V_i^0) + (1 - S_i)nV_t^0. \quad (10)$$

The isothermal compressibility of frozen ground is thus a function of the degree of saturation with ice (S_i), the porosity (n), and the compressibility of the ice and mineral components.

THE COMPRESSIBILITY OF FROZEN SAND AND SILT

The isothermal compressibilities of OWS and WLT at various degrees of saturation, but constant porosity, are shown in Figures 6 and 7. The loading curves are shown as heavy dark lines and the unloading curves, where they differ, as dashed lines. The lighter weight lines are the predicted values obtained from Bridgman's work, the loading and unloading portions being identical.

For the saturated samples, the differences in compressibility between the test results and the calculated values are subtle. The greatest differences occur in the regions of phase change and are of the same nature as those observed for ice. The onset of the Ice VI to Ice VIII transition, however, appears at a higher pressure than predicted (22.5 versus 20.8 kbar). This may be the result of nonhomogeneous pressure distribution—the mineral component taking on a higher pressure and the ice a lower; while restructuring of the soil particles occurs, the process is time dependent.

For partially saturated OWS and WLT (Figures 6b, c, and d and 7b), air void closure obscures the phase change of Ice I to water on the loading legs. At higher pressures, the phase changes are not well defined nor do they appear to be complete. The OWS unloading curves follow closely the predicted values, except above the region of the Ice VI to Ice VIII transition and below 1 kbar at an ice saturation of

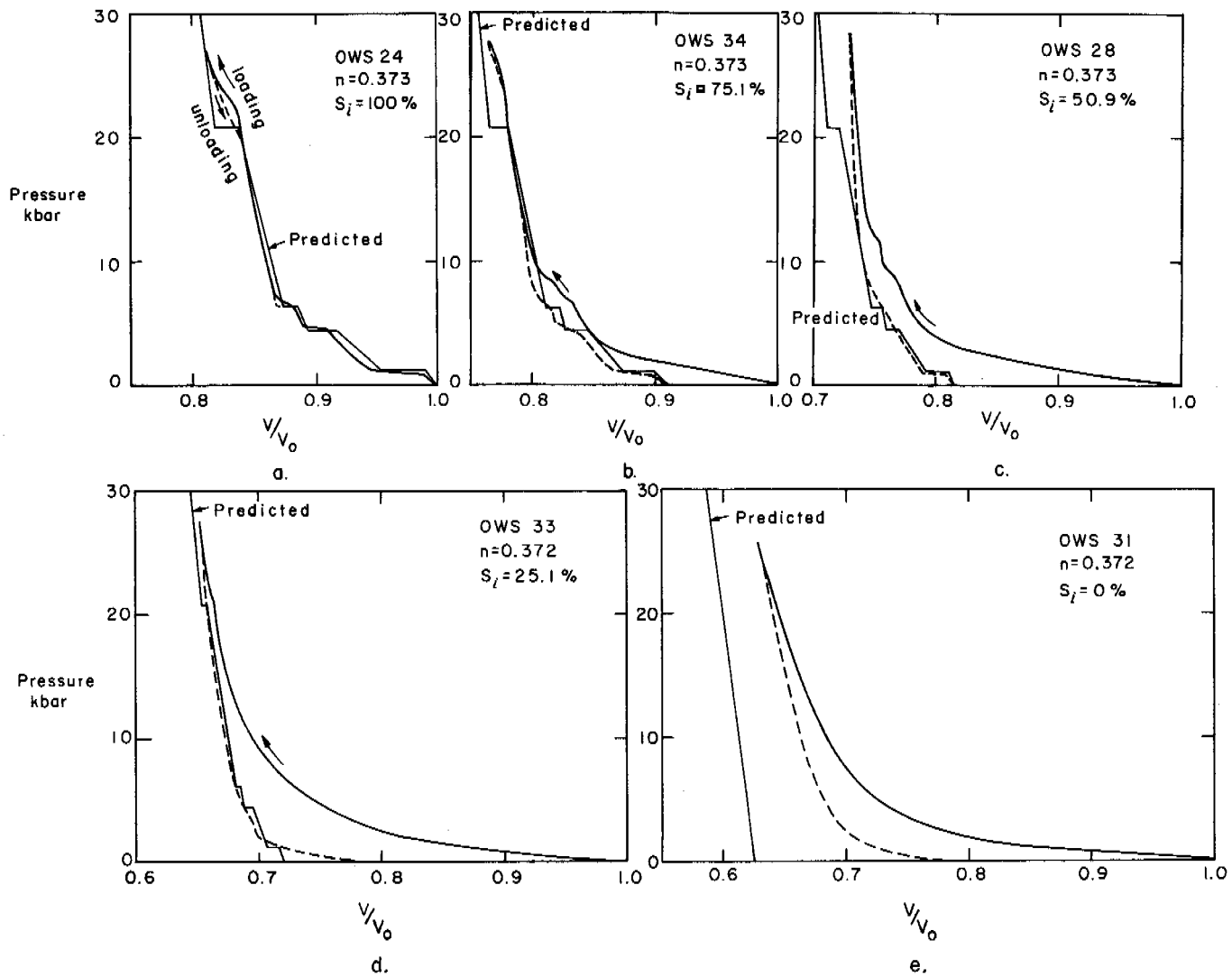


FIGURE 6 Isothermal compressibility of OWS at various degrees of ice saturation at -10°C .

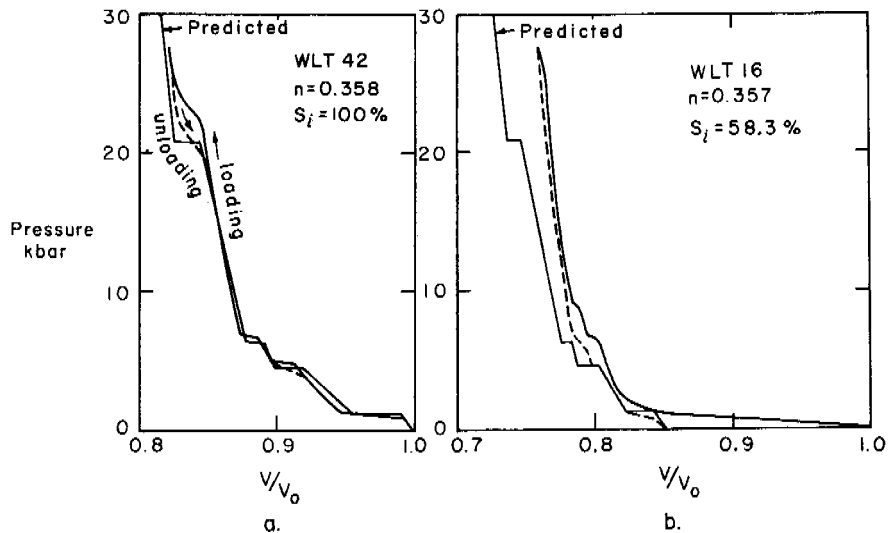


FIGURE 7 Isothermal compressibility of WLT at (a) 100 percent and (b) 58.3 percent saturation with ice at -10°C .

25 percent (Figure 6d). The former is probably the result of the nonuniform pressure distribution and the latter the result of elastic expansion of the soil structure to minimum or critical volume. The zero pressure relative volume for the release curve of dry OWS sample (Figure 6e) is identical to that of the 25 percent saturated sample ($V/V_0 \approx 0.78$).

The process of compression of frozen soil can be analyzed as follows: The initial volume reduction, in the case of partially saturated soils, occurs by rearrangement or packing of soil particles. This is followed or accompanied by crushing of the individual particles. The extent of the rearrangement and the crushing of soil particles is governed by the degree of saturation with ice. At some pressure (0 kbar for 100 percent saturated soils), ice completely fills the voids and is subjected to nearly the same overall pressure as the mineral components. The ice and the mineral components then undergo compression, much the same as they would have in pure form. As phase transformations and packing of the soil structure progress, crushing of soil particles and plastic flow of the ice occur.

The positions of the unloading curves are controlled primarily by the volume expansions of the ice and mineral components, except at low ice saturation and low pressures where the expansion of the soil structure controls.

In Figure 8, the isotherms for ice-saturated OWS and WLT at -10°C are plotted along with the Hugoniot obtained by Anderson.² The excellent agreement should be noted as the isotherms blend smoothly to the Hugoniot data. The actual low-pressure Hugoniot should be slightly to the right of the isotherms, the phase changes being somewhat obscured.

High-Pressure Triaxial Compression

Experimental results for a constant axial strain rate of approximately 6 percent/min and a temperature of -10°C are summarized in Table II. Deviator stress ($\sigma_1 - \sigma_3$) and volumetric strain ($\Delta V/V_0$) versus axial strain (ϵ_1) plots are illustrated in Figure 9. The cyclic nature of the volumetric strain curves results from the operation of the volume compensator device and is indicative of the accuracy of this measurement. One would expect a smoother curve. Nonetheless, meaningful conclusions can be drawn from the trends. The coarser grained OWS samples undergo dilation or volume expansion at confining pressures up to 525 kg/cm^2 , while the finer grained WLT samples decrease slightly in volume. At confining pressures greater than 525 kg/cm^2 , dilation is totally suppressed. Since dilation is the result of individual grains riding over one another, the reduction of dilation indicates that shearing or crushing of the individual soil particles is occurring. The resultant breakdown in particle size is illustrated in Figure 10, where the percent finer than 0.074 mm after testing is plotted versus confining pressure. The particle size reduction is propor-

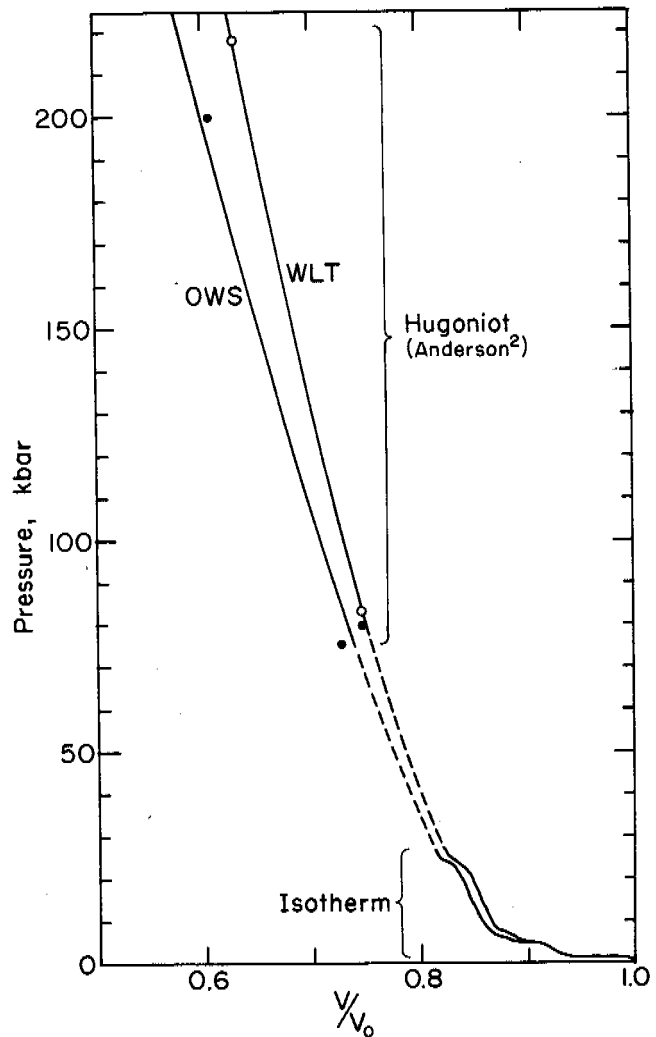


FIGURE 8 Isotherms and Hugoniot for ice-saturated OWS and WLT at -10°C .

tionally greater with increasing confining pressure as is the suppression of dilatancy. Moreover, at confining pressures greater than 525 kg/cm^2 , above which dilatancy does not occur, the particle size breakdown continues. Figure 10 also illustrates that no change in particle size for the WLT samples occurred in the entire range of confining pressures employed.

When the shear stress $[(\sigma_1 - \sigma_3)/2]$ is plotted versus mean stress $[(\sigma_1 + 2\sigma_3)/3]$ at maximum deviator stress, a trilinear relationship results (Figure 11). There appear to be two critical values of mean stress at which dramatic changes in shear stress occur (note that these are not identical for both OWS and WLT). For purposes of discussion, these values will be used to divide the shear stress versus mean stress plots into three distinct regions—low-mean stress region I, where the shear stress increases with increasing mean stress; intermediate-mean stress region II, where the

TABLE II Triaxial Test Results

Sample No.	Moisture Content (%)	Dry Density (g/cm ³)	Porosity (%)	Saturation with Ice (%)	σ_3 (kg/cm ²)	σ_1 (kg/cm ²)	Maximum Shear Stress $[(\sigma_1 - \sigma_3)/2]$ (kg/cm ²)	Mean Stress $[(\sigma_1 + 2\sigma_3)/3]$ (kg/cm ²)
OWS-6	21.0	1.649	37.3	100	35.2	249.8	107.3	106.7
12	20.1	1.674	36.3	100	70.4	306.8	118.2	149.2
3	21.8	1.620	38.4	100	178.7	527.8	174.5	295.1
5	22.0	1.618	38.5	100	351.9	894.4	271.3	532.7
13	20.2	1.671	36.5	100	525.0	1 068.3	271.6	706.1
7	21.1	1.640	37.7	100	700.9	1 139.3	219.2	847.0
16	19.9	1.672	36.4	99.6	876.1	1 256.2	190.0	1 002.8
8	20.9	1.650	37.3	100	1 052.8	1 247.0	97.1	1 117.5
9	21.8	1.624	38.2	100	1 410.3	1 620.0	104.9	1 480.0
10	21.1	1.644	37.5	100	2 114.0	2 405.3	145.7	2 111.1
11	20.2	1.666	36.7	100	2 817.7	3 134.4	158.3	2 923.3
WLT-1	18.0	1.806	36.4	97.4	38.0	203.4	82.7	93.1
2	18.6	1.770	37.7	95.3	70.4	234.3	82.0	125.0
3	18.5	1.792	36.9	98.0	182.3	350.5	84.1	238.4
4	17.9	1.816	36.0	98.3	351.9	489.1	68.6	397.6
5	18.2	1.799	36.6	97.4	527.8	666.4	69.3	574.0
6	19.0	1.783	37.2	99.3	706.5	798.0	45.7	737.0
7	19.5	1.765	37.9	99.1	876.8	925.4	24.3	893.0
8	18.6	1.798	36.7	99.4	1 055.6	1 090.8	17.6	1 067.3
9	19.1	1.781	37.3	99.5	1 410.3	1 446.9	18.3	1 422.5
10	18.4	1.784	37.2	96.2	2 108.4	2 157.6	24.6	2 124.8
11	18.7	1.787	37.1	98.3	2 814.9	2 869.8	27.4	2 833.2

shear stress decreases; and high-mean stress region III, in which the shear stress again increases.

REGION I

At very low confining pressures, the values of OWS and WLT are nearly equal. However, the coarser grained OWS is strengthened by increasing σ_3 , whereas σ_3 has little influence on the shear stress of WLT. As a result, there is a great difference in maximum shear stress in this region (shear stress ≈ 300 kg/cm² for OWS versus ≈ 80 kg/cm² for WLT). Andersland and Al-Nouri¹ have observed similar behavior for a frozen quartz sand and a highly plastic glacial lake deposit clay.

The strengthening of OWS in this region is attributed to two components: one that develops from interparticle friction and one that is related to particle interlocking. There appears to be a relationship of the total suppression of dilatancy to the peak value of shear stress that occurs at a mean stress of approximately 750 kg/cm². It suggests that particle interlocking was the primary mechanism for the development of strength for frozen OWS in this region.

The nearly horizontal failure envelope and the lack of dilation observed for WLT indicate that neither particle interlocking nor interparticle friction play significant roles in the development of strength in region I. Since at lower

confining stresses WLT would be expected to exhibit some frictional characteristics, however, the influence of interparticle friction cannot be disregarded. Its importance may be obscured by changing cohesive properties that result from an increase in unfrozen water content due to progressive pressure melting.

REGION II

Region II for both soils is characterized by decreasing shear stress. It appears, at first glance, to be a region of negative friction. More likely, the shear stress in this region is controlled by changing ice-water composition brought on by pressure melting. It is suggested that pressure melting becomes critical for OWS at $\sigma_3 = 525$ kg/cm² (mean stress = 797 kg/cm²) because of the complete suppression of dilatancy. At this confining pressure, a reversal in pore-pressure response would be expected. Rather than pore-pressure reduction with increasing shear stress, there would be an increase in pore pressure and, subsequently, pressure melting. The increase in unfrozen water content due to pressure melting should result in a decrease in shear stress such as that which has been reported for an increase in unfrozen water content due to temperature increase.⁸

The onset of shear stress reduction for WLT in region II occurs at a lower mean stress than for OWS. It is suggested

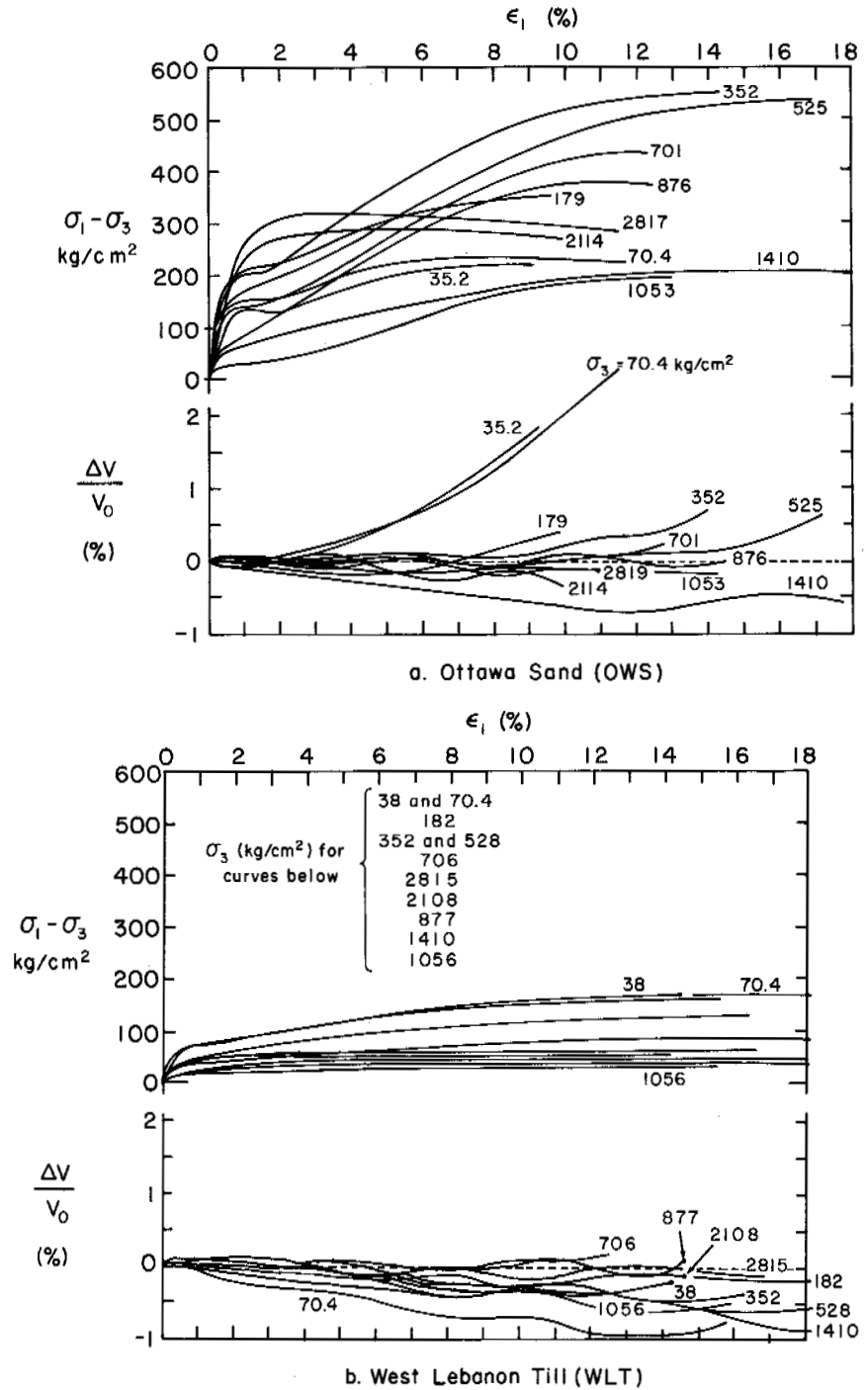


FIGURE 9 Deviator stress ($\sigma_1 - \sigma_3$) and volumetric strain ($\Delta V/V_0$) versus axial strain (ϵ_1) plots for OWS (a) and WLT (b).

that this is related to the smaller particle size, a higher unfrozen water content, and the greater sensitivity of fine grained soils—such as WLT—to pressure melting.

REGION III

As previously mentioned, the shear stress increases with increasing mean stress in region III. The breakpoint between

regions II and III occurs at $\sigma_3 \approx 1050 \text{ kg/cm}^2$, which is approximately the pressure (1130 kg/cm^2) at which the ice-water phase change takes place at -10°C (see Figure 4). It is suggested that the termination of shear stress reduction is the result of a stabilizing effect on the cohesive bonds and the partial consolidation of the soil structure brought on by complete melting of the ice component by the application

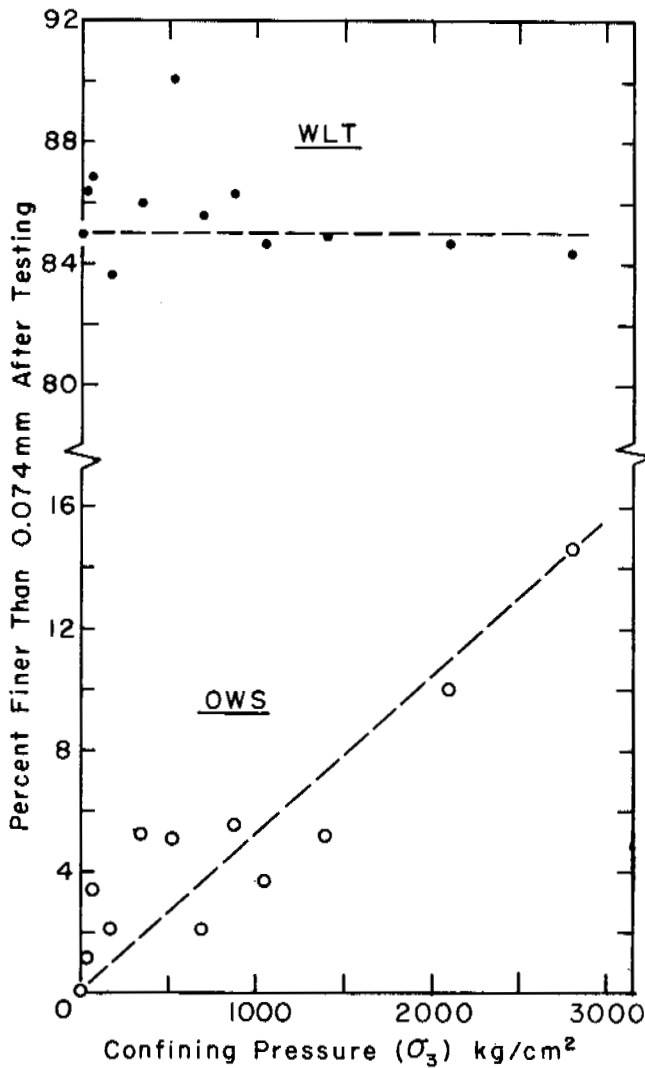


FIGURE 10 Particle-size breakdown after triaxial compression for OWS and WLT.

of the confining pressure. The resulting behavior is analogous to that of an underconsolidated, undrained triaxial test where the pore fluid is slightly compressible, the slight gain in shear stress with increasing mean stress being due to the increase in the number or area of interparticle contacts.

CONCLUSIONS

The compressibility of saturated frozen soil to 30 kbar is readily predicted from knowledge of properties, such as degree of saturation with ice, porosity, and the compressibilities of ice and mineral components. The accuracy is limited at low pressures and low degrees of saturation. The behavior of the phase transformations is somewhat obscured

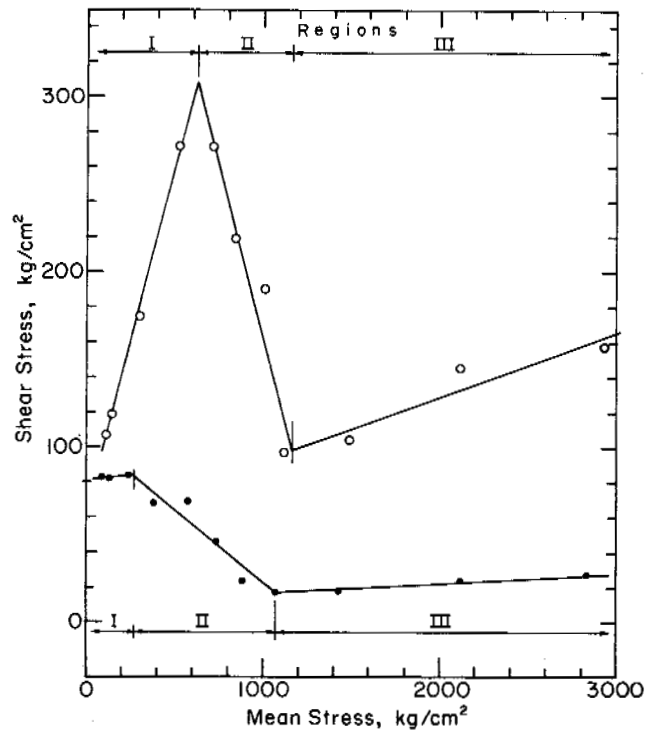


FIGURE 11 Results of the triaxial compression tests in the shear stress $[(\sigma_1 - \sigma_3)/2]$ versus mean stress $[(\sigma_1 + 2\sigma_3)]$ plane.

by rate processes and the reordering and crushing of the mineral particles.

The compressibility calculations can be applied to any frozen soil. If significant quantities of air, unfrozen water, or organics are present, then additional parameters must be added to the governing equation.

The triaxial strength tests show that confining pressure has great influence on the shear strength of frozen soils. At a temperature of -10°C and a strain rate of approximately 6 percent/min, three distinct stress regions are observed: a low-pressure region of constant or increasing shear stress, a mid-pressure region of decreasing shear stress, and a high-pressure region of slightly increasing shear stress. Confining pressure also has a profound effect on frozen sand (OWS); for example, above $\sigma_3 = 525 \text{ kg/cm}^2$, dilation is completely suppressed. It is suggested that the four elements—interparticle friction and particle interlocking, unfrozen water content, pressure melting of ice, and the ice-water phase change—control the triaxial compression behavior of saturated frozen soils.

The strength observations reported herein are limited to frozen soils, with little or no ice segregation at the strain rate and temperature reported. Significant differences in strength characteristics would be expected for frozen soils tested under other conditions.

ACKNOWLEDGMENTS

This paper presents the results of research performed by the U.S. Army Cold Regions Research and Engineering Laboratory under the sponsorship of the Advanced Research Projects Agency. The author wishes to acknowledge the participation of Dr. Pieter Hoekstra and Mr. Roscoe Perham of CRREL and of Mr. Christopher Groves, currently with Shannon & Wilson, Inc. The author is also grateful for the technical reviews provided by Dr. George Swinzow and Mr. Austin Kovacs.

REFERENCES

1. Andersland, O. B., and I. Al-Nouri. 1970. Time-dependent strength behavior of frozen soil. *J. Soil Mech. Found. Div. Proc. Am. Soc. Civil Eng.* 96:1249-1265.
2. Anderson, G. D. 1968. The equation of state of ice and composite frozen soil material. CRREL Research Report 257. U.S. Army Cold Regions Research and Engineering Laboratory, Hanover, New Hampshire.
3. Brace, W. F. 1965. Some new measurements of linear compressibility of rocks. *J. Geophys. Res.* 70(2):391-397.
4. Bridgman, P. W. 1964. Collected experimental papers. 7 Vols. Harvard University Press, Cambridge.
5. Brown, A. J., and E. Whalley. 1966. Preliminary investigation of the phase boundaries between ice VI and VII and ice VIII. *J. Chem. Phys.* 45:4360-4361.
6. Chamberlain, E., and P. Hoekstra. 1970. The isothermal compressibility of frozen soil and ice to 30 kilobars at -10°C . CRREL Technical Report 225. U.S. Army Cold Regions Research and Engineering Laboratory, Hanover, New Hampshire.
7. Stephens, D. R. 1964. The hydrostatic compression of eight rocks. *J. Geophys. Res.* 69(14):2967-2977.
8. Vyalov, S. S. 1959. Rheological properties and bearing capacity of frozen soils. *Izdatel'stvo Akad. Nauk SSSR, Moscow.* (USA CRREL Translation 74, 1965)

EFFECT OF POROSITY ON AMOUNT OF SOIL WATER TRANSFERRED IN A FREEZING SILT

Alfreds R. Jumikis

RUTGERS UNIVERSITY—THE STATE UNIVERSITY
OF NEW JERSEY
New Brunswick, New Jersey

INTRODUCTION

Because the thermal potentials taking part in soil moisture migration are by their nature periodic functions of time,^{2,6} and because the entire thermal system soil-water-temperature is a very complex one, a theoretical or mathematical analysis of the freezing soil system is a very formidable task indeed. Relative to the application of the mathematical theory of heat transfer to frost problems in soil, it must be said that such an application forces one to introduce many assumptions and simplifications, to such an extent that in many instances they are questionable or even unreal.

Because of the many unknown and obscure factors involved in the behavior of a freezing soil system, particularly concerning the effect of soil porosity on the amount of soil moisture transferred in a freezing frost-prone silty soil, and because the soil system in nature does not work with 100 percent efficiency, it is most appropriate that such freezing soil systems be studied experimentally.

This paper reports the results of the author's experimental research about porosity effects of a silty glacial outwash frost-prone soil (Dunellen soil) on the amount of soil moisture transferred from groundwater to the cold front (0°C isotherm) upon freezing. [1]

PROCEDURE

Basis

Relative to transmissibility of soil to water, it is well to remember that Darcy's law of permeability of soil to water (in bulk) does not apply to colloidal soil systems such as clay and clayey silt.¹ Also, because there is always some air and/or gas present in the soil, the soil moisture translocation from higher energy levels to lower ones may be characterized as being an unsaturated (water film) flow rather than a saturated flow of free bulk water.

Treatment

The freezing experiments were so arranged as to simulate nature as closely as possible. Each soil specimen was insulated against lateral heat flux and was frozen unidirectionally from its top down for 168 h. To facilitate comparison of experimental results, all experiments were performed under identical laboratory conditions, and all measurements comprehended the total effects of soil moisture transfer caused by all possible and simultaneously acting energy potentials.^{3,4,5}

Equipment

The freezing equipment and instrumentation used in these experiments consisted of the freezer unit, the groundwater supply and its cooling system, and associated auxiliary instruments (Figure 1).

The temperature of the groundwater in these experiments was kept at an average of 8 °C. The water cooled was automatically supplied by the burettes shown in Figure 1 in accordance with the demand of the freezing soil. These graduated burettes served as reservoirs of groundwater, maintained a constant level of groundwater table, and indicated continuously the amount of water given away and taken up by the freezing soil system.

TABLE I Basic Fractions and Physical Properties of A-2-4 Type Soil

Gravel > 1.00 mm	8%
Sand 1.00-0.05 mm	78%
Silt and clay < 0.05 mm	14%
Liquid limit (w_L)	16.5%
Plasticity index (I_p)	0
Shrinkage limit (w_S)	19.7%
Specific gravity (G)	2.68
Maximum dry density (γ_d)	1.94 g/cm ³
Optimum moisture content (m)	12.0%
Porosity at optimum moisture content (n)	37.8%
Coefficient of permeability (saturated) (k)	7.17×10^{-6} cm/s at 20 °C

Soil Samples

The soil type used in the freezing experiments was a frost-prone silty glacial outwash soil, called Dunellen soil. According to the Highway Research Board soil classification system, this soil was classified as an A-2-4 type of soil (Table I). This soil was used to prepare specimens for a porosity range from $n = 27.8$ percent to $n = 47.8$ percent (tests B-4, B-5, B-6, B-7, and B-9). The size of the cylindrically shaped soil

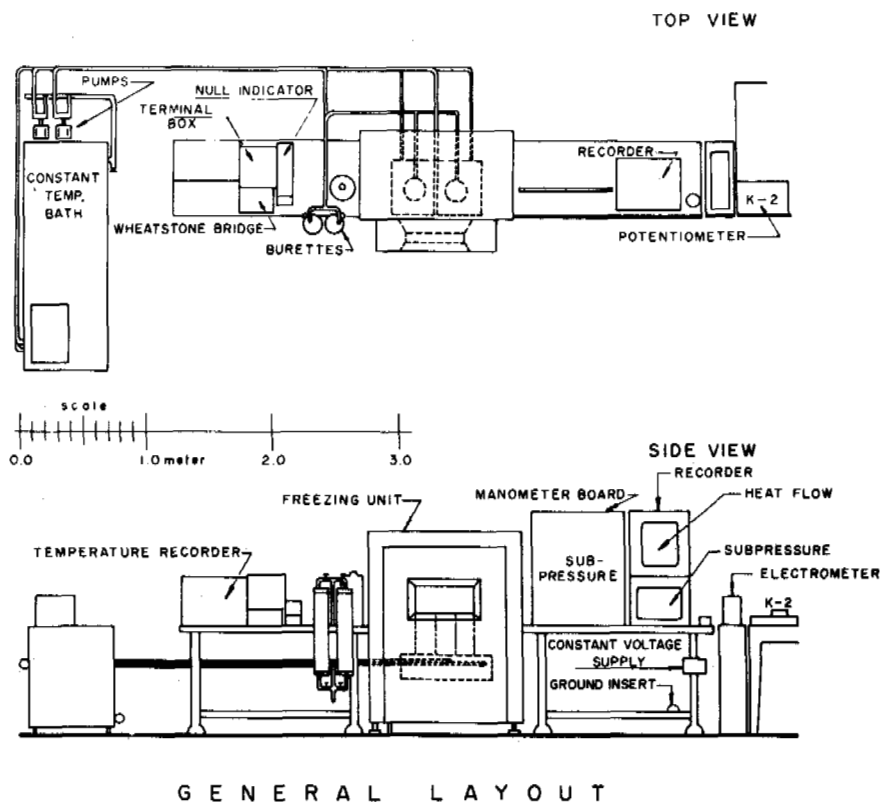


FIGURE 1 Arrangement of equipment.

specimens was 15.24 cm in diameter and 30.48 cm high (5 553 cm³).

Temperature Step-Down Schedule

In each test, the temperature in the freezing chamber was periodically lowered according to a predetermined schedule (Table II). Prior to each step-down of temperature, readings were taken of temperature, subpressure, induced electrical potential, and amount of groundwater taken up by the freezing soil system. In addition, readings were taken every 2 h from 0 900 to 1 700 h during the 7-day test period. An example of the temperature step-down for the soil tested can be seen in Figure 2a and b. Temperature and water consumption graphs for tests A-5, A-6, A-8, and B-6 are shown in Figure 2 parts a through d, respectively.

After the conclusion of a freezing experiment (after 168 h), moisture distribution tests along the height of the cylindrical soil specimen revealed that moisture had redistributed in a nonuniform way (Figure 3). A large accumulation of water was always found at the 0 °C isotherm, depending on the length of freezing during the last temperature step-down. To compare test results, two identical soil specimens were always frozen.

OBSERVATIONS ON EXPERIMENTAL RESULTS

Examples of the nature of the recorded data are shown in Figure 2. The temperature regimen of the soil systems depended greatly on the freezing surface temperature (the microclimate), the groundwater temperature, and the porosity of the soil, as reflected by such curves.

The principal results of these experiments are summarized in Figure 4. This figure summarizes the 168-h freezing-test data. It shows graphically the amount of soil moisture transferred upon freezing as a function of the initially prepared porosity *n* of the Dunellen soil. From this figure, one may draw the following inferences.

TABLE II Schedule for Periodic Temperature Reductions

Elapsed Time after Start of Test (h)	Temperature of Microclimate (°C)
0	-1.11
14	-6.67
38	-12.22
62	-17.78
86	-23.33
110-168	-28.89

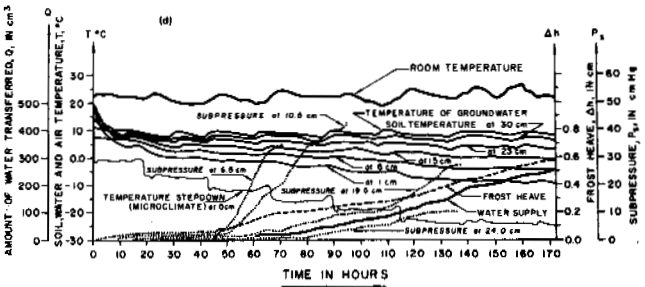
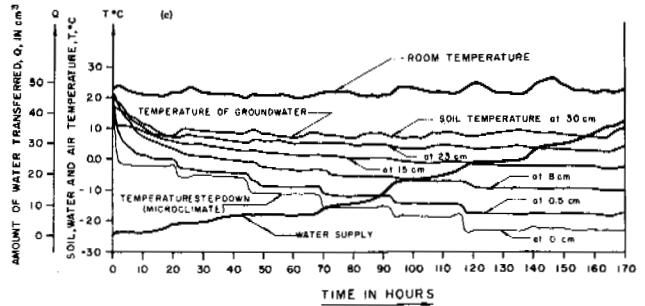
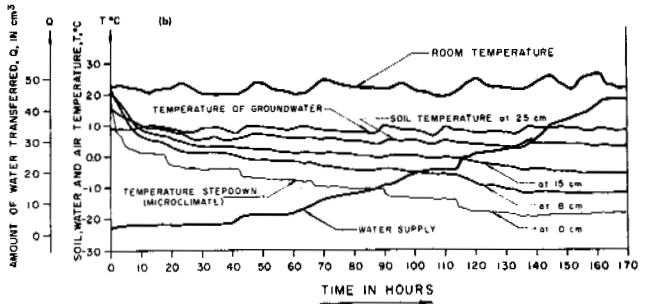
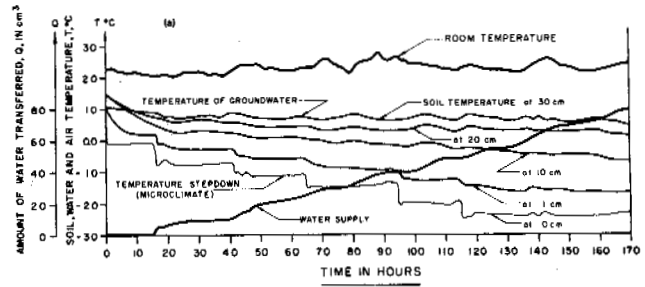


FIGURE 2 Temperature graphs. (a) Test A-5, *n* = 70 percent; (b) test A-6, *n* = 60 percent; (c) test A-8, *n* = 55 percent; (d) test B-6, *n* = 27.8 percent.

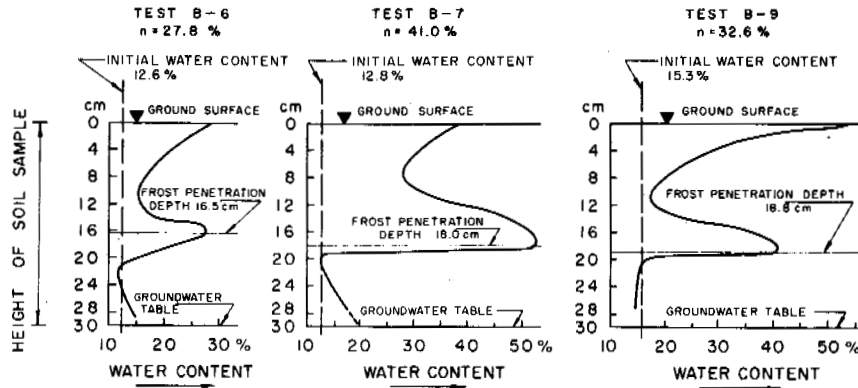


FIGURE 3 Soil moisture content before and after freezing. Tests B-6, B-7, and B-9.

1. The porosity is the primary factor controlling the amounts of heat flow, moisture transfer, and all the related phenomena, as clearly demonstrated by the similar trends of all the related factors plotted together as a function of porosity.

2. Depending on the magnitude of the porosity of the soil, moisture may be transferred upward from groundwater to the cold front by way of various moisture transfer mechanisms.

3. The effective soil moisture transfer mechanism is by way of the water-film flow (unsaturated flow) within the porosity range between $n = 27.8$ percent and $n = 47.8$ percent. The moisture transfer by the film-flow mechanism is virtually unaccompanied by vapor diffusion.

4. Figure 4 also permits one to conclude that, between porosities of $n = 60$ percent and $n = 100$ percent, the effective soil moisture transfer mechanism is vapor diffusion. The vapor transport mechanism, however, is an ineffective one.

5. As Figure 4 shows, there are no sharply defined boundaries between the various modes of soil moisture transport mechanisms and processes. It is, therefore, quite reasonable to assume that a transition from one mode to another (for example, the porosity interval from about $n = 50$ percent to about $n = 70$ percent) constitutes a combination of various modes of transport that act simultaneously.

6. For the experimental soils used in these studies, the maximum amount of soil moisture transfer from groundwater to the soil system takes place at about $n = 42$ percent porosity. This brings about the maximum frost penetration depth in these experiments and the greatest accumulation of frozen water in the frozen soil system.

7. This research has led to the identification of a consistent set of relationships among porosity and the amount

of soil moisture transferred during freezing, induced electrical potential, and frost penetration depth.

8. From these experimental studies, one also can deduce that, in reporting research results on moisture transfer in soils upon freezing, it is essential to report the porosity of the soil; for each degree of soil packing, there may be a different soil moisture transport mechanism in action.

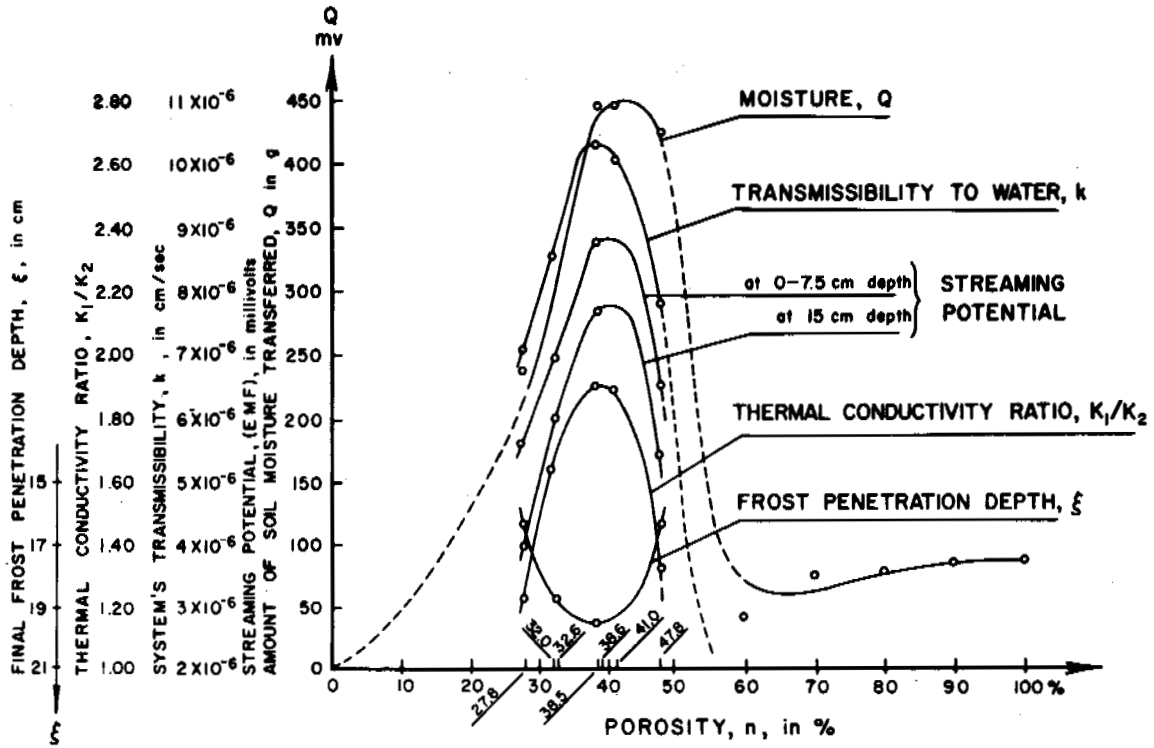
CONCLUSIONS

1. The experimental results obtained in these soil freezing-moisture transfer experiments bear out vividly the paramount effect of porosity of the freezing soil on the amount of soil moisture transferred by the thermoosmotic flow process by way of the water-film mechanism from groundwater to the cold front.

2. Although the simultaneously occurring and partaking processes in the freezing soil system are very complex and can as yet be studied qualitatively only, such a qualitative study may be considered as the first step toward a better understanding of the processes involved in a freezing soil system.

3. Popularly speaking, the soil moisture thermoosmotic migration process can be imagined and described simply as a thermal siphoning of the soil moisture from groundwater up to the cold front by means of a thermal gradient. The moisture transfer in the vapor phase is relatively ineffective as compared with soil moisture transferred by the water-film mechanism for the soil types tested.

4. As can be seen in Figure 4, this research on frost-prone soils has led to the identification of a consistent set of relationships among porosity and the amount of soil moisture transferred during freezing, induced electrical potential during freezing, and frost penetration depth.



TEST NUMBERS			B-6	B-2	B-9(3)	B-4	A-18	B-7	B-5	A-6	A-5	A-3	A-4	A-7
EFFECTIVE SOIL MOISTURE TRANSFER MECHANISMS			LOWER POROSITIES THAN n=27.8% ARE DIFFICULT TO ATTAIN IN PRACTICE			EFFECTIVE MOISTURE FILM FLOW		FILM AND VAPOR FLOW		PURE VAPOR TRANSFER				
POROSITY, n, %			27.8	32.6	32.6	38.5	41.0	47.8	60.0	70.0	80.0	90.0	100.0	
VOID RATIO, e			0.385	0.470	0.484	0.626	0.628	0.916	1.500	2.333	4.000	9.000		
OPTIMUM MOISTURE CONTENT, w, %			12.5	11.4	13.8	12.8	12.4							
MAXIMUM DRY DENSITY g / cm ³			1.92	1.78	1.64	1.57	1.39	1.06	0.68	0.53	0.26	0		
AMOUNT OF SOIL MOISTURE TRANSFERRED	ABSOLUTE AMOUNT, Q, in grams		239.0	250	246	445	424	41.9	77.0	77.8	87.8	91.6		
	RELATIVE TO MOISTURE TRANSFERRED AT n=100% POROSITY		2.61	2.73	2.78	4.88	4.87	4.63	0.46	0.84	0.85	0.98	1.00	
SYSTEMS TRANSMISSIBILITY, k, cm/sec		K ₁ for frozen soil	7.17 × 10 ⁻⁶	8.34 × 10 ⁻⁶	10.36 × 10 ⁻⁶	9.95 × 10 ⁻⁶	7.95 × 10 ⁻⁶							
STREAMING POTENTIAL { 0-7.5 cm } POTENTIAL { 15.0 cm } mv			100	200	285	340	170	275						
THERMAL CONDUCTIVITY RATIO K ₁ /K ₂		K ₂ for unfrozen soil	1.29	1.65	1.91	1.90	1.33							
FINAL FROST PENETRATION DEPTH, ξ, in cm			16.5	18.8	19.6		16.5							

FIGURE 4 Soil moisture transfer upon freezing as a function of soil porosity.

REFERENCES

1. Darcy, H. P. G. 1856. Les fontaines publiques de la Ville de Dijon. Victor Dalmont, Editeur, Paris. p. 570, 590, 594.
2. Jumikis, A. R. 1955. The frost penetration problem in highway engineering. Rutgers University Press, New Brunswick, N.J. p. 43-61.
3. Jumikis, A. R. 1959. The soil freezing experiment. Bulletin No. 135. Highway Research Board, Washington, D.C. p. 150-165.
4. Jumikis, A. R. 1962. Effective soil moisture transfer mechanisms upon freezing. Bulletin No. 317. Highway Research Board, Washington, D.C. p. 1-8.
5. Jumikis, A. R. 1966. Thermal soil mechanics. Rutgers University Press, New Brunswick, N.J. p. 11-14.
6. Lachenbruch, A. H. 1959. Periodic heat flow in a stratified medium with application to permafrost problems. U.S. Geol. Sur. Bull. 1083-A. p. 1-36.

NOTE

[1] This research was performed in the Thermal Soil Mechanics Laboratory, College of Engineering, Rutgers University-The State University of New Jersey, and was sponsored by National Science Foundations grants.

EVALUATION OF *IN SITU* CREEP PROPERTIES OF FROZEN SOILS WITH THE PRESSUREMETER

B. Ladanyi

ECOLE POLYTECHNIQUE
Montreal, Quebec

G. H. Johnston

NATIONAL RESEARCH COUNCIL OF CANADA
Ottawa, Ontario

INTRODUCTION

For the design of foundations and other engineering structures in permafrost areas, there has been a real need for new methods and instruments to determine the properties of frozen soils in the field. A research project was undertaken, therefore, in 1971 to investigate the suitability of the Ménard pressuremeter, as a tool for *in situ* evaluation of the rheological properties of frozen soils. Although the pressuremeter has been used extensively in unfrozen soils and rock, the authors were not aware of any published information that describes its use for investigating the basic creep behaviour of frozen materials.

It appeared that two kinds of problems had to be solved. First, an appropriate testing procedure had to be developed that would permit the necessary creep information to be obtained with minimum physical and thermal disturbance of the ground. Second, a theoretical interpretation method had to be found that would allow the creep information obtained in a test to be put into a useful general form.

The results of the research investigation carried out are presented in this paper.

SOIL CONDITIONS AT THE TEST SITE

Field tests were carried out during July 1971 at a permafrost site at Thompson, Manitoba. Within the depth inter-

val investigated, i.e., between 1.50 and 4.20 m, the soil was a varved clay of low to medium plasticity, composed of dark brown clay layers from 12 to 25 mm thick and tan-colored silt layers increasing in thickness with depth from 25 to 75 mm.

The most significant ice segregation was found in the top 4 m and was usually associated with the dark layers. Ice lenses were mainly horizontal and varied in thickness from hairline to a maximum of about 12 mm. Permafrost temperatures at depths between 1.50 and 9.00 m were fairly uniform, varying between -0.10 and -0.30 °C, throughout the year.

INSTRUMENTATION

The Ménard pressuremeter (Figure 1) is a special borehole dilatometer that has been used for a number of years for *in situ* measurement of stress-strain and strength properties of soils and rocks. It consists of an inflatable probe, composed of two coaxial cells, and a pressure-volume control device that allows a given pressure to be applied to the wall of the borehole and the resulting volume increase of the hole to be observed.

The tests at Thompson were performed with a type G pressuremeter fitted with a pressure-volume control device of 700 cm³ volume capacity and 0-25 bar pressure range. The NX-size probe had its rubber membrane protected by

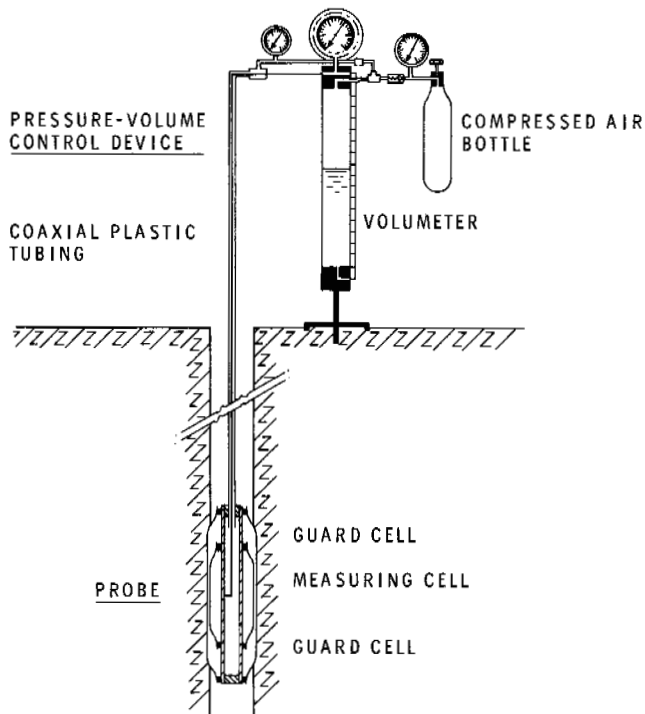


FIGURE 1 Ménard pressuremeter type G. Test setup.

an extensible overlapping metal strip jacket. For creep testing of frozen soils, the following modifications were made to the equipment:

1. A fine adjustment valve was included in the pressure control system, to provide more accurate pressure control when performing long-term creep tests.
2. Three thermocouples were fixed to the outside of the probe, so that the temperature of the soil in contact with the probe could be checked continuously during a test.
3. The complete volumeter assembly was enclosed in an insulated box that was filled with crushed ice to cool the fluid to be injected into the probe during the test.

Previous pressuremeter testing experience in unfrozen soils showed that the quality of results depends greatly on the quality and accuracy of drilling of the borehole. This is even more valid in frozen soils where not only a physical but also a thermal disturbance may occur during drilling. The method used was to auger the hole to about 0.75 m above the required test level. A special sampling tube, having its cutting edge tapered inwards to avoid disturbing the soil surrounding the hole, was then pushed into the frozen soil to make a tight hole for the probe. Owing to high air temperatures (15–25 °C), some thermal disturbance of the relatively warm permafrost at the site could not be avoided

during drilling. Temperature checks in the borehole showed, however, that the temperature at the hole wall returned to normal within about 1 h after drilling was completed. One hour was used, therefore, as a normal waiting period before starting each test.

TESTING PROGRAM

Before starting the long-term testing program, several short-term tests were conducted at the site to investigate the general character and strength range of the frozen varved soils. These short-term tests were similar to Ménard's standard or normal pressuremeter tests used in current soil testing practice. For the standard test, the pressure in the probe was increased up to the limit pressure in about 10–20 increments, the pressure being kept constant at each stage for no longer than 2 min. At each stage, volume readings were taken at 30 s, 1 min, and 2 min after the pressure was increased.

After comparing a number of different loading programs for long-term creep testing purposes, it was concluded that the following two types of pressuremeter tests might represent minimum requirements for obtaining the creep information required:

1. A one-stage creep test in which the pressure is brought rapidly to a given level and is left at that level as long as possible. In practice, because deformation is limited by the maximum volume of 700 cm³ that can be injected into the probe, the total creep time can vary from about 20 min to several hours.
2. A multistage creep test, in which the pressure is brought rapidly up to an initial creep level and then is increased to the limit in several equal stress increments, each kept constant for 15 min.

RESULTS OF SHORT-TERM TESTS

As detailed descriptions of the standard pressuremeter testing procedure including all corrections of pressure and volume readings, as well as the calibration curve determination, can be found elsewhere^{1,9} only some typical short-term results and their interpretation will be given here.

Plotting of Pressuremeter Curve

The results of a short-term pressuremeter test are usually plotted as a corrected pressuremeter curve (Figure 2A) defined as:

$$V_m = f(p_c), \quad (1)$$

where V_m denotes the total volume of fluid injected into the measuring cell from the start of pressure application,

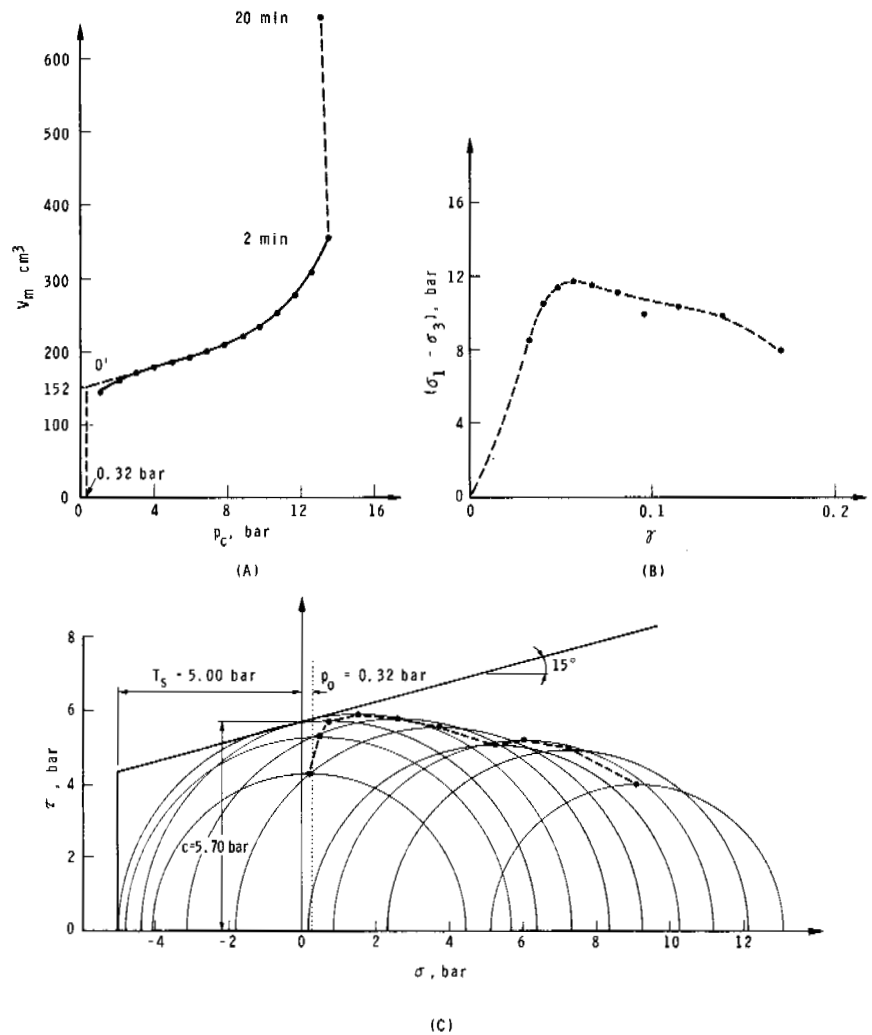


FIGURE 2 Results of a short-term pressuremeter test in a varved silt-clay soil: A, pressuremeter curve; B, stress-strain curve; C, vector curve.

and p_c is the applied pressure that has been corrected for the piezometric head and the extension resistance of the unloaded probe.

The interpretation method adopted in this paper, however, is based on the true pressuremeter curve, such as would be obtained in an ideal test starting from the original ground pressure, p_o . The true pressuremeter curve represents a relationship of the form:

$$\Delta V = f(p_c - p_o), \quad (2)$$

where p_o denotes the original total lateral ground pressure at the level of the test, and

$$\Delta V = V_m - V_{m0}, \quad (3)$$

where V_{m0} is the volume of the liquid injected in the probe up to $p_c = p_o$. The true pressuremeter curve is obtained from the corrected curve by shifting the origin from 0 to $0'$, as shown in Figures 2A and 3A.

Eleven short-term tests were carried out at the Thompson site. Two typical results are shown in Figures 2 and 3, the former obtained in a frozen varved silty soil and the latter in a frozen varved clay.

Interpretation of Short-Term Tests

From a soil mechanics point of view, a frozen soil is essentially a (c, ϕ) material having a relatively high time- and temperature-dependent cohesion and an angle of internal friction that is usually only little affected by time and temperature. Because little is yet known about the true intergranular stresses in frozen soils, c and ϕ are assumed to be total stress parameters. Moreover, if the soil is fine-grained and ice-saturated, the volumetric component of the deformation will be very small and, therefore, may be neglected. With these assumptions, a pressuremeter curve for frozen soil can be interpreted using the method proposed by Ladanyi,⁶ the main points of which are given below.

The method is based on a general solution of the problem

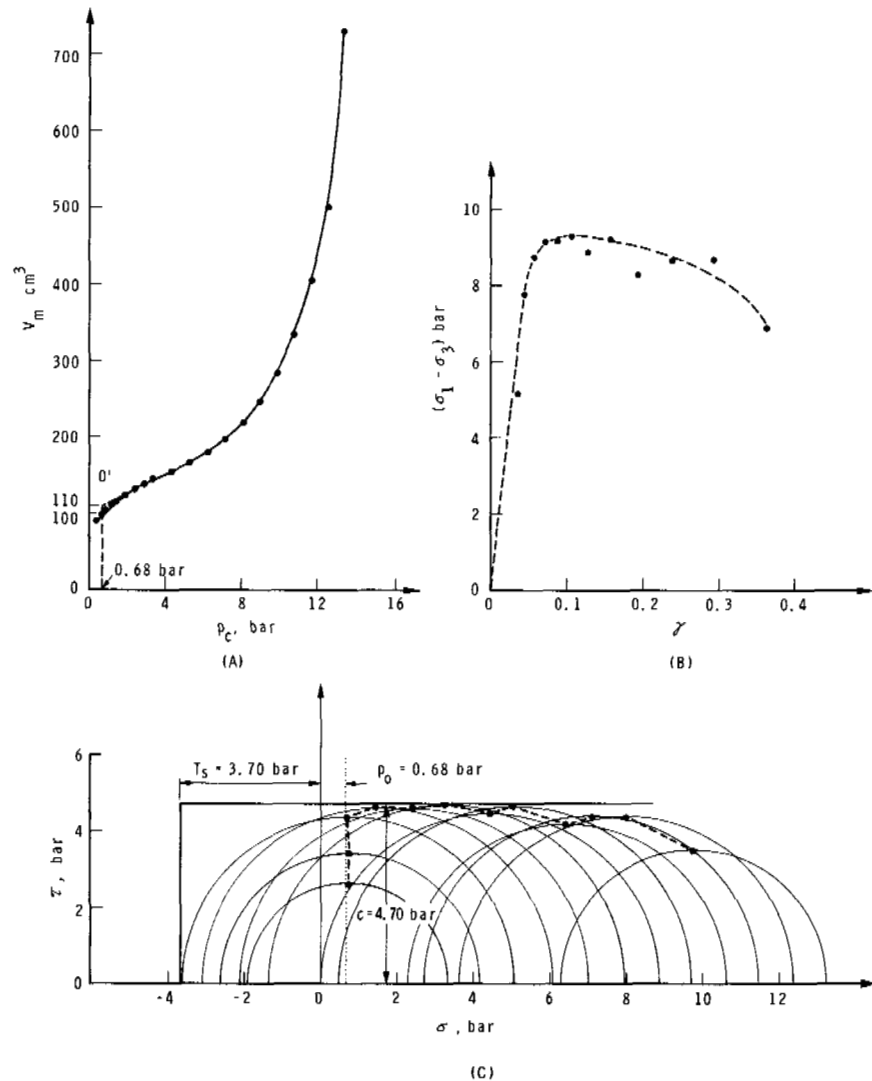


FIGURE 3 Results of a short-term pressuremeter test in a varved clay: A, pressuremeter curve; B, stress-strain curve; C, vector curve.

of expansion of a thick-walled cylinder, which is considered as an assemblage of a finite number of thin concentric cylinders, all of which respond to a common stress-strain law. By inverting the solution, it is found that not only the pressuremeter modulus and the average ultimate strength can be determined from the pressuremeter curve, as shown previously by Gibson and Anderson,² but also the whole stress-strain curve of the soil, as well as a vector curve in the Mohr plot.

Stress-Strain Curve

As shown by Ladanyi,⁶ it is possible to determine from any two points, $i, i + 1$ of the true pressuremeter curve (Figure 2A), the corresponding mobilized strength, $q_{i,i+1}$, defined as the principal stress difference:

$$q_{i,i+1} = (\sigma_1 - \sigma_3)_{i,i+1}, \quad (4)$$

and the associated average shear strain, defined as the principal normal strain difference:

$$\gamma_{i,i+1} = (\epsilon_1 - \epsilon_3)_{i,i+1}. \quad (5)$$

The principal stress difference can be calculated from the formula:

$$q_{i,i+1} = (p_i - p_{i+1}) / (1/2) [\ln(\Delta V/V)_i - \ln(\Delta V/V)_{i+1}], \quad (6)$$

and the principal normal strain difference is obtained from:

$$\gamma_{i,i+1} = (1/2) [(\Delta V/V)_i + (\Delta V/V)_{i+1}], \quad (7)$$

where p and ΔV denote the coordinates of the true pressuremeter curve at the points i and $i+1$, and the current volume V of the borehole is defined by

$$V = V_0 + \Delta V \quad (8)$$

in which

$$V_0 = V_{\text{empty}} + V_{\text{mo}} \quad (9)$$

denotes the volume of the measuring section of the probe at the moment when the pressure in the probe has attained the original ground pressure, p_0 . In this study it was found that p_0 should be determined or estimated independent of the test, since, contrary to the usual belief, the lateral pressure was usually found to be completely unrelated to the shape of the pressuremeter curve.

It should be noted that the stress-strain relationship obtained by this procedure is valid for constant volume plane-strain condition. It can, however, easily be transformed into the more usual axial symmetry case by using the von Mises yield criterion.⁶

The stress-strain curves obtained by this procedure from the pressuremeter curves (Figures 2A and 3A) are shown in Figures 2B and 3B. Some caution is necessary, however, when such stress-strain curves are compared with those obtained in a triaxial test. In fact, in brittle soils, and often in frozen soils as well, it has been found that a pressuremeter test produced radial cracking of the soil early in the test, leading to an irregular shape of the stress-strain curve.

Vector Curve in Mohr Plot

On the other hand, since both the major principal stress σ_1 (equal to the applied radial stress) and the principal stress difference ($\sigma_1 - \sigma_3$, equal to $q_{i,i+1}$) are known at any moment of the test, the information can be used for plotting a series of Mohr circles and a vector curve in the Mohr plot. In terms of plane-strain information as obtained in the test, the values of the total principal stresses σ_1 and σ_3 for any interval $i,i+1$ of the pressuremeter curve are given by:

$$\sigma_1 = (1/2)(p_{c,i} + p_{c,i+1}), \quad (10)$$

and

$$\sigma_3 = \sigma_1 - q_{i,i+1}, \quad (11)$$

where p_c is the applied radial stress and $q_{i,i+1}$ is the stress difference defined by Eq. (6).

Figures 2C and 3C show two such plots obtained for frozen varved silt and clay, respectively. To follow the sequence of Mohr circles more easily, they have been con-

nected by a vector curve, showing the variation of $(1/2)(\sigma_1 - \sigma_3)$ with $(1/2)(\sigma_1 + \sigma_3)$ in the tests.

Although a semigraphical method for plotting Mohr circles directly from a pressuremeter curve has been shown by Ménard,⁷ the true meaning of the circles has never been properly understood. To understand what the plot really means, one should remember that in a pressuremeter test the soil responds first in a pseudoelastic manner, attains failure, and then continues deforming in a plastic manner up to large deformations. In Figures 2C and 3C, the pseudoelastic behaviour is reflected by the first two or three circles that increase in diameter but remain concentric, as anticipated by the theory of expansion of a cylindrical hole in an infinite elastic medium.

The following two or three circles are failure circles and correspond to the peak strength of the soil. The remaining circles are all in the plastic domain and correspond to ever-increasing plastic deformations. The diameters of these remaining circles depend, therefore, simultaneously on the strength characteristics of the soil and on its postfailure stress-strain behaviour.

It follows, therefore, that the three kinds of Mohr circles cannot be expected to have one common failure envelope. In fact, one may be justified in drawing one failure envelope over all failure and postfailure circles only if the postfailure behaviour of the soil is very close to the ideally plastic assumption. If, on the other hand, the postfailure behaviour of the soil is either strain-hardening or strain-softening, which is most often the case, the circles will not have a common failure envelope, and the determination of failure parameters c and ϕ from one single pressuremeter curve will be very difficult or impossible. In other words, contrary to the belief expressed by Ménard⁷ and Gibson and Anderson,² a single pressuremeter test is usually insufficient for determining the failure envelope of the soil. Nevertheless, it is considered that the plotting of both the stress-strain curve and the vector curve, as described herein, is at present the best method available for a proper understanding of a short-term pressuremeter test.

In this study, the Mohr circle plots have been used only for estimating probable lower limits of the short-term tensile strength, T_s , and the cohesion, c . To estimate the two parameters, the Mohr circles were enclosed by a bilinear envelope, composed of a Coulomb straight line and a vertical tension cutoff. For the Coulomb line, a friction angle of 15° was assumed for all silty soils and 0° for all soils composed mainly of clay.

In addition, the values of the pressuremeter modulus, E_p , were calculated from the initial straight-line portions of the pressuremeter curves by using the usual formula valid for incompressible soil:

$$E_p = 3 \Delta p / \Delta(\Delta V / V). \quad (12)$$

The overall variation of the three short-term parameters in the tests was approximately as follows:

For frozen varved soil: $250 < E_p < 800$ bar; $5 < c < 14$ bar; and, $1.5 < T_s < 12$ bar.

For the same varved soil, unfrozen: $60 < E_p < 80$ bar; $2 < c < 5$ bar; and, $1 < T_s < 5$ bar.

As expected, a given type of soil is stronger and much less deformable when frozen than unfrozen. It also was noted that the tensile strength of the frozen soil tested was about the same order of magnitude as its peak shear strength. Frozen varved clay was found to be slightly weaker and more deformable than frozen varved silt at the same temperature.

INTERPRETATION OF PRESSUREMETER CREEP TESTS

According to Hult,³ there are essentially two practical methods for generalizing experimental creep information. The first method, applicable to long-term creep tests in which the steady-state creep strains greatly exceed the instantaneous and primary creep strains, consists of linearizing the creep curves and considering the total strain at any time as being the sum of the pseudoinstantaneous and the steady-state creep strain. The method was applied to the creep of frozen soils by Ladanyi⁵ and was used subsequently by Johnston and Ladanyi⁴ for generalizing creep information obtained in a series of long-term pull tests performed on grouted rod anchors in permafrost.

The second method, applicable to relatively short-term creep tests, considers the creep information as being essentially of a primary (or "stationary") creep type and attempts to extrapolate it to longer time using a convenient creep curve fitting method. As the creep time that can be realized in a pressuremeter test usually does not exceed several hours, the test should be considered as a short-term creep test to which the second method is applicable.

According to the second method, the creep data obtained in a pressuremeter test can be generalized using the solution to the problem of stationary creep under the internal pressure of a cylindrical cavity of infinite length located in an infinite medium.

The primary creep of high temperature metals, ice, and frozen soils can often conveniently be described by a law of the form

$$\epsilon^{(c)} = K \sigma^a t^b \quad (b < 1), \quad (13)$$

where K , a , and b are temperature-dependent material constants. In this report, Eq. (13) will be written in Hult's³ notation and is generalized to multiaxial state of stress:

$$\epsilon^{(c)} = [\dot{\epsilon}_c (1 + \mu)]^{1/(1+\mu)} (\sigma_e / \sigma_c)^{m/(1+\mu)} t^{1/(1+\mu)} \quad (14)$$

where ϵ_e and σ_e are the equivalent creep strain and the equivalent stress, respectively; $\dot{\epsilon}_c$ is an arbitrary, conveniently selected, strain rate; σ_c is the creep modulus in units of stress; and m and μ are creep exponents. The values of creep parameters σ_c , m , and μ can be obtained by a convenient plotting of creep curves as described by Hult.³

To solve this problem, it is convenient to introduce into Eq. (14) the transformed time unit:

$$\tau = t^{1/(1+\mu)}, \quad (15)$$

which permits Eq. (14) to be transformed into an ordinary power law:

$$d\epsilon^{(c)} / d\tau = K \sigma_e^n, \quad (16)$$

where

$$K = [\dot{\epsilon}_c (1 + \mu) / \sigma_c^m]^{1/(1+\mu)}, \quad (17)$$

and

$$n = m / (1 + \mu). \quad (18)$$

The solution of Eq. (16) for the problem of creep expansion of a cylindrical cavity under plane-strain condition can easily be obtained by analogy from the corresponding solution in nonlinear elasticity. Complete solutions of the particular problem can be found in several textbooks.⁸

To process the pressuremeter creep data, the only relationship needed from the solution is the one relating the creep cavity expansion rate with the applied internal pressure, which is, according to Odquist:⁸

$$dr/d\tau = (\sqrt{3}/2)^{n+1} K r [(2/n)(p_i - p_o)]^n, \quad (19)$$

where r is the current radius of the cavity, p_i is the constant applied internal pressure, and p_o is the pressure acting at infinity. If p_i is replaced by p_c according to the notation adopted for the corrected pressure in the borehole, Eq. (19) can be written as:

$$dr/r = G(p_c - p_o) d\tau, \quad (20)$$

where

$$G(p_c - p_o) = (\sqrt{3}/2)^{n+1} K [(2/n)(p_c - p_o)]^n, \quad (21)$$

in which K is given by Eq. (17) and n by Eq. (18).

For a finite interval of time at a constant stress, Eq. (20) can be integrated to give:

$$\ln r = G(p_c - p_o) \tau + C. \quad (22)$$

Taking $r = r_{i-1}$ at $\tau = 0$, i.e., at the beginning of the considered i th creep stage, the integration constant C can be eliminated, and Eq. (22) becomes:

$$\ln(r/r_{i-1}) = G(p_c - p_o) \tau. \quad (23)$$

Since for a cylindrical cavity:

$$(r/r_{i-1})^2 = V/V_{i-1}, \quad (24)$$

Eq. (23) becomes finally,

$$V/V_{i-1} = \exp[2G(p_c - p_o)t^{1/(1+\mu)}], \quad (25)$$

where V_{i-1} denotes the cavity volume at $t = 0$ (Figure 4), i.e., at the start of a given constant-pressure creep stage, and $V = V_{i-1} + \Delta V_c$ denotes the volume of the cavity at any time t after the step-increase of pressure ($p_c - p_o$) in the stage i .

To determine the creep parameters μ , m , and σ_c , the semigraphical procedure described by Hult³ for the primary creep case can be followed. Taking first a natural and then an ordinary logarithm of Eq. (25), one gets:

$$\log[\ln(V/V_{i-1})] = \log 2G(p_c - p_o) + (\log t)/(1 + \mu), \quad (26)$$

showing that pressuremeter creep curves should linearize if $\ln(V/V_{i-1})$ is plotted against time in a log-log plot. According to Eq. (26), in such a plot, the slope of the creep straight lines is equal to $1/(1 + \mu)$ or, from Figure 5:

$$1 + \mu = A/B. \quad (27)$$

The intercept at the unit time ($t = 1$ min in Figure 5) of any

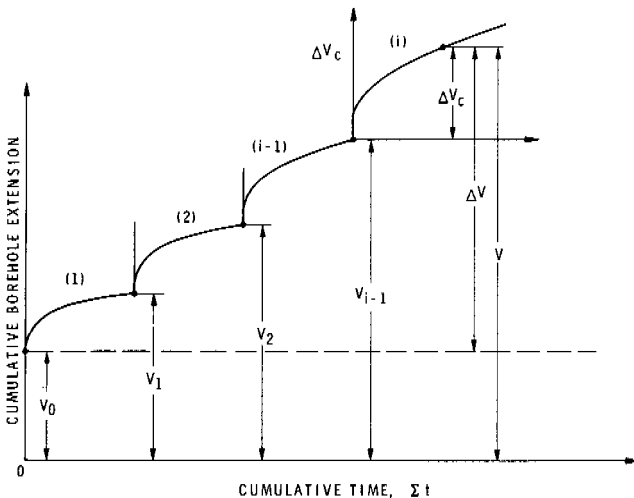


FIGURE 4 Notation for interpretation of pressuremeter creep data.

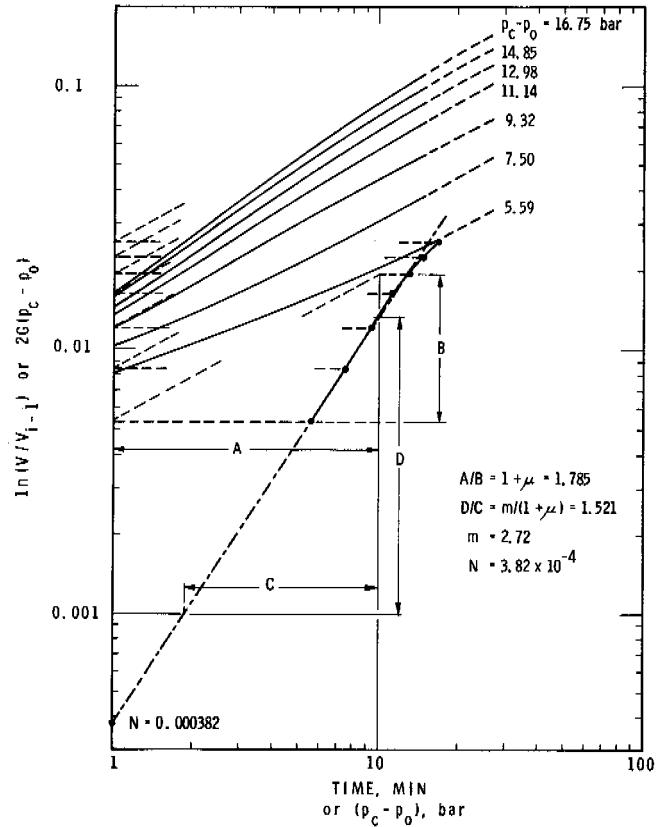


FIGURE 5 Multistage creep test in a varved silt-clay soil. Determination of creep parameters.

creep line, each of them corresponding to a different value of pressure ($p_c - p_o$), is then equal to $2G(p_c - p_o)$.

To determine the parameters m and σ_c , Eq. (21) may be written as:

$$\log 2G(p_c - p_o) = \log M - n \log \sigma_c + n \log(p_c - p_o), \quad (28)$$

where

$$\begin{aligned} \log M = & \log 2 + (1 + n) \log(\sqrt{3/2}) \\ & + (n/m) \log(\dot{\epsilon}_c m/n) + n \log(2/n). \end{aligned} \quad (29)$$

Equation (28) shows that plotting $2G(p_c - p_o)$ against $(p_c - p_o)$ in a log-log plot will give a straight line with the slope equal to n . In Figure 5 such a plot is shown superimposed on a plot of $\ln(V/V_{i-1})$ versus time. The new straight line has a slope:

$$D/C = n \equiv m/(1 + \mu) \quad (30)$$

and its intercept N , read at unit value of $(p_c - p_o)$ (at 1 bar in Figure 5), is, according to Eq. (28), equal to:

$$N = M/\sigma_c^n \tag{31}$$

Since, for an arbitrarily assumed $\dot{\epsilon}_c$, and with known μ and m , the value of M can be calculated from Eq. (29), the value of σ_c is:

$$\sigma_c = (M/N)^{(1+\mu)/m} \equiv (M/N)^{1/n} \tag{32}$$

Once the creep parameters μ , m , and σ_c have been determined, they can be substituted into Eq. (14) to get a general creep equation of the soil. The equation, subsequently, can be used either for extrapolating the pressuremeter creep data to longer time intervals or, in association with an estimated creep failure strain, serve for predicting the long-term strength of frozen soil. To predict the long-term strength, if ϵ_{ef} denotes the equivalent failure strain and σ_{ef} the equivalent creep strength, then Eq. (14) yields:

$$\sigma_{ef} = \sigma_c \epsilon_{ef}^{(1+\mu)/m} [\dot{\epsilon}_c(1+\mu)t]^{-1/m} \tag{33}$$

Figure 5 shows typical creep information obtained in a multistage pressuremeter creep test with 15 min per stage. Figure 6, in turn, shows the result of a one-stage creep test kept at a constant stress for more than 5 h. In the figures, the logarithmic creep measure, $\ln(V/V_{t-1})$, is plotted against the time, t , in a log-log plot, as required for creep parameter determination.

To apply the foregoing analysis in practice, two conditions are necessary: Creep curves should linearize in a log-log plot; and creep curves for different sustained pressures should be parallel to each other.

As can be seen in Figures 5 and 6, neither of the two conditions was completely satisfied in the tests. In fact, the

creep curves were found to curve up slightly at low pressures and curve down at high pressures. Moreover, the creep lines frequently were not quite parallel but diverged with increasing time. Nevertheless, they appeared to linearize better in one-stage tests than in multistage tests and showed a tendency to become parallel after about 15 min. With these two experimental facts in mind, it was decided, for the purpose of generalization of creep information, to consider the creep curves as becoming parallel after 15 min in each stage and having a slope $(A/B = 1 + \mu)$ average for the considered pressure interval. The creep lines were then projected back from 15 to 1 min to get the values of $2G(p_c - p_o)$, according to Eq. (26). These values were then plotted against $(p_c - p_o)$ to get a set of points through which an average (dash-dotted) line was drawn. The line, according to Eq. (28) to (31) allows the ratio $D/C = m/(1 + \mu)$ and the intercept N at $p = 1$ bar [Eq. (31)] to be determined. With these values and after calculating the value of M [Eq. (29)], the creep modulus σ_c was finally determined.

In the six tests performed in the frozen varved silt, it was found that the value of $(1 + \mu)$ remained essentially between 1.5 and 2.5, while the value of m varied from about 2 to 4. There was a much larger variation in σ_c , from about 4.5 to 24 bar.

It should be noted that in all creep calculations the arbitrary strain rate $\dot{\epsilon}_c$ was taken as equal to 10^{-5} min^{-1} .

As already explained, when the three parameters are known, one can write both the general creep equation, Eq. (14), and the time-dependent strength equation, Eq. (33). For the test shown in Figure 5, the creep equation has the form:

$$\epsilon_e = 0.87 \times 10^{-3} (\sigma_e/4.71)^{2.08} t^{0.64},$$

where σ_e is in bar and t in min, and the time-dependent

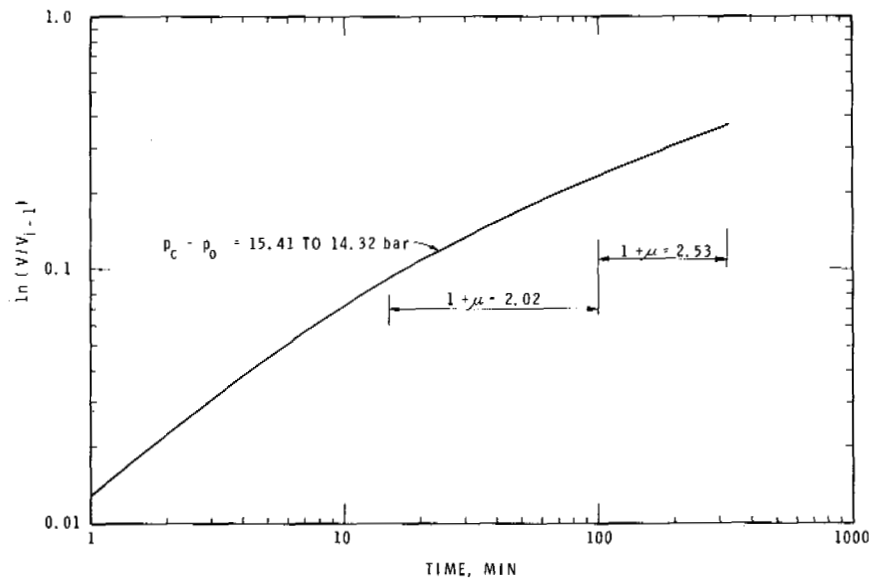


FIGURE 6 One-stage creep test in a varved silt-clay soil. Creep curve.

strength, assuming a failure strain of $\epsilon_{ef} = 0.10$, is given by:

$$\sigma_{ef} = 44.5 t^{-0.305}$$

with the same units as above. Thus, the soil would have a 30-min strength of 15.8 bar and a 1-year strength of 1.62 bar, i.e., its strength would decrease within a year to about one tenth of its short-term value.

CONCLUSIONS

The study conducted to evaluate the pressuremeter test as a means for obtaining creep information of frozen soils *in situ* indicated that:

1. After some minor modifications, the standard pressuremeter equipment proved to be suitable for performing creep tests under the conditions found at the Thompson site. It is not known, however, how the same equipment would perform at very low temperatures and in some other types of frozen soils, such as glacial till.
2. Methods used to drill and prepare the borehole for the tests were fairly satisfactory. Some temperature disturbance could not be avoided, however, and special attention must be given to this aspect in future studies.
3. A new interpretation method had to be developed in order to make use of information obtained from the short-term tests. This method permitted the determination of short-term strength parameters and the stress-strain curve from each pressuremeter test.
4. A method had also to be found for the determination

of creep parameters from the pressuremeter creep data. The method developed proved feasible for the determination of creep parameters of frozen soils *in situ* and the prediction of long-term strength. To obtain sufficient creep information for the proposed method to be applicable, however, it is recommended that, in addition to conventional short-term pressuremeter tests, the following two types of creep tests be performed: multistage creep tests with about 15 min per stage and one-stage creep tests conducted at different pressure levels to check the linearity of creep lines for long time intervals.

REFERENCES

1. Dunod. 1971. Essai pressiométrique normal. Mode opératoire MS.IS-2. Paris.
2. Gibson, R. E., and W. F. Anderson. 1961. *In situ* measurement of soil properties with the pressuremeter. Civ. Eng. Publ. Works Rev. (London) May:615-618.
3. Hult, J. A. H. 1966. Creep in engineering structures. Blaisdell Publ. Co., Waltham, Massachusetts. 115 p.
4. Johnston, G. H., and B. Ladanyi. 1972. Field tests of grouted rod anchors in permafrost. Can. Geotech. J. 9:176-194.
5. Ladanyi, B. 1972. An engineering theory of creep of frozen soils. Can. Geotech. J. 9:63-80.
6. Ladanyi, B. 1972. *In-situ* determination of undrained stress-strain behavior of sensitive clays with the pressuremeter. Can. Geotech. J. 9:313-319.
7. Ménard, L. 1957. Mesures *in-situ* des propriétés physiques des sols. Ann. Ponts Chaussées 127:357-377.
8. Odquist, F. K. G. 1966. Mathematical theory of creep and creep rupture. Oxford Math. Monogr. Clarendon Press, Oxford.
9. Société Pressiométrique Ménard. 1968. Pressiomètre type G: Description-utilisation. Paris.

SHOCK-WAVE STUDIES OF ICE AND TWO FROZEN SOILS [1]

Donald B. Larson, Glenn D. Bearson, and James R. Taylor

UNIVERSITY OF CALIFORNIA
Livermore, California

INTRODUCTION

Shock-wave experimental techniques used in conjunction with one-dimensional numerical simulation models represent a useful technique for determining high-strain-rate equations of state. These techniques can be readily employed in studying frozen materials and provide a unique

examination of the compressibilities of this important group of materials.

In the past, compressibility studies of frozen materials have included both very low and very high strain rates. The principal low-strain-rate studies were those of Bridgman²⁻⁵ on ice to 40 kbar and Chamberlain and Hoekstra⁶ on ice and several frozen soils to 30 kbar. The high-strain-rate or

shock-wave-compressibility studies were carried out by Anderson¹ on ice and several frozen soils. Anderson obtained Hugoniot states for ice in the 35- to 300-kbar stress range, and for the frozen soils ranging from 60 to 500 kbar. Unloading states from stress levels in excess of 150 kbar were also obtained. Although the past studies have covered the pressure range from 0 to 500 kbar, an important region (0–35 kbar) has not been investigated at high strain rates. These data are crucial in frozen materials, since, in the shock process, the time scale may approach that of the reaction kinetics of the phase transitions and thus limit the amount of transformation. This could cause metastable or mixed phases and result in very different compressibility curves than observed at low strain rates. Reaction kinetics could also play an important role in the high-strain-rate unloading behavior, as could the large entropy change that occurs when the frozen soils matrix is compressed.

The object of this research is to investigate the loading and unloading characteristics of frozen materials in the 0- to 15-kbar stress range, using shock-wave experimental techniques, and thereby to determine the effect reaction kinetics and a soil matrix have upon the equations of state of frozen materials.

EXPERIMENTAL TECHNIQUES AND RESULTS

Two different shock-wave loading techniques were used in the experimental investigation of polycrystalline ice—two orientations of single-crystal ice, frozen saturated Ottawa banding sand and frozen saturated West Lebanon glacial till. In all of these experiments, the frozen material had an initial temperature of $-10 \pm 2^\circ\text{C}$. In each technique, thin foils of brass were sandwiched between frozen material. Material velocity as a function of time was determined by monitoring the emf induced in these foils as they moved through an external magnetic field. Figure 1 illustrates schematically a gas-gun experiment in which the frozen material was loaded and unloaded uniaxially. Unloading occurs as a rarefaction propagates from the free surface. Figure 2 is a schematic of the second experimental technique. Spheres of LX04 high explosive embedded in the frozen material act as the energy source and give rise to radial loading. The material unloads as the shock front distributes energy over an increasing volume.

The frozen materials studied in this program, except for the polycrystalline ice, were obtained from the U.S. Army Cold Regions Research and Engineering Laboratory (CRREL), Hanover, New Hampshire [2]. The polycrystalline ice samples were made from large blocks of commercial ice. The single-crystal ice samples were obtained from Dr. K. Itagaki of CRREL. The frozen soils were made at CRREL under the supervision of E. Chamberlain. These soils were both frozen directionally to maintain grain contact. The West Lebanon glacial till had a dry density of

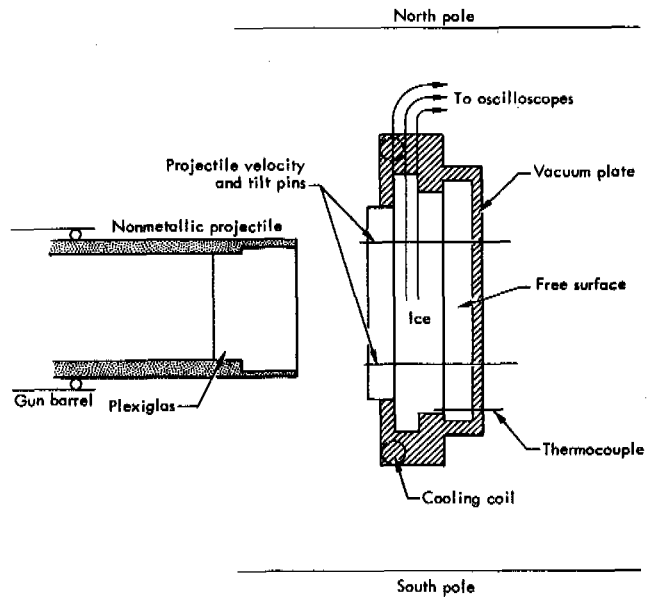


FIGURE 1 Schematic of the setup for the dynamic equation of state experiments with ice samples. The temperature is maintained at $-10 \pm 1^\circ\text{C}$ by the controlled circulation of cold N_2 vapors through the cooling coil. The Plexiglas buffer plate and vacuum plate are used to insulate the ice surfaces. The foil at the Plexiglas-ice interface records the input-particle velocity. The other two gages record the particle-velocity history when the ice is first loaded and then unloaded as the shock waves rarefy at the free surface.

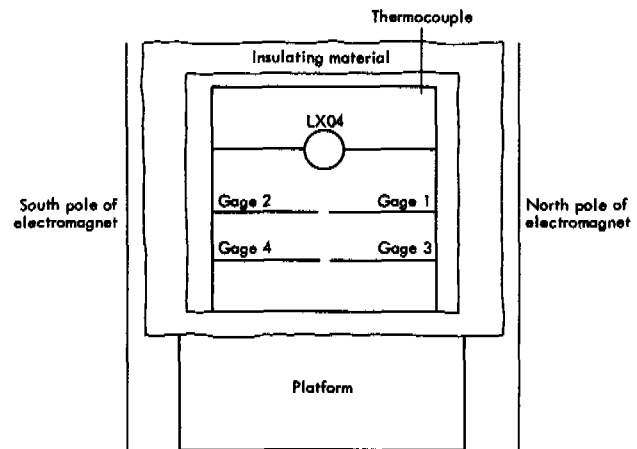


FIGURE 2 Schematic of a front cutaway view of the high-explosive experiments with frozen materials. The LX04 explosive was embedded in hemispheres cut in two plates of material; the gages were sandwiched between the other plates. A mild detonating fuse was used to initiate the LX04. The gage signals were recorded on oscilloscopes.

1.86 g/cm^3 and an expected saturated density of 2.21 g/cm^3 . Average sample density was 2.08 g/cm^3 . The Ottawa banding sand had a dry density of 1.65 g/cm^3 , a saturated density of 2.03 g/cm^3 , and an average sample density of 2.03 g/cm^3 . Porosity in both soils was about 35 percent.

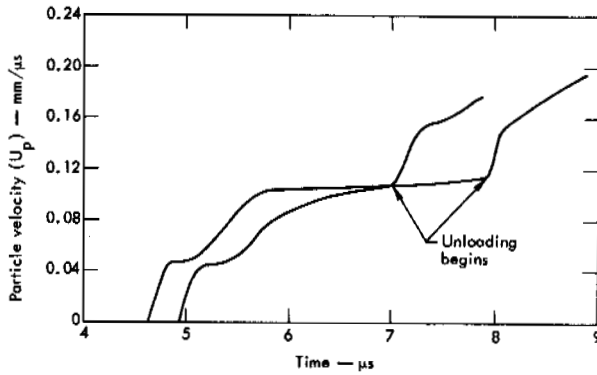


FIGURE 3 Particle-velocity history of two embedded gages in single-crystal ice loaded uniaxially perpendicular to the c -axis. The arrows indicate arrival of the rarefaction wave at the gages.

Figures 3-5 show histories of particle velocities recorded at two different positions in single-crystal ice—frozen saturated West Lebanon glacial till and frozen saturated Ottawa banding sand; each material was subjected to uniaxial compression and release. In each of these records, there are essentially three waves: The first is associated with the onset of melting of Ice I; the second is associated with the final loading state; and the broad third wave is rarefaction from the free surface. These waves are all nonsteady, except the first wave in ice and part of the first wave in the frozen soils.

The interpretation of these data requires the use of conservation of mass and momentum equations. In Lagrangian coordinates, these equations are

$$(1/V_0) (\partial V/\partial t)_h = (\partial U_p/\partial h)_t \quad (1)$$

$$\rho_0 (\partial U_p/\partial t)_h = -(\partial \sigma/\partial h)_t, \quad (2)$$

where V is the volume, $\rho_0 = 1/V_0$ is the initial density, t is the time, U_p is the mass velocity, h is the Lagrangian coordinate, and σ is the stress in the direction of motion. Analy-

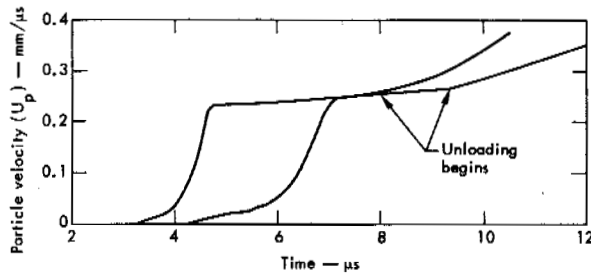


FIGURE 4 Particle-velocity history of two gages embedded in frozen saturated West Lebanon glacial till. The arrows indicate the arrival of the rarefaction wave at the gages.

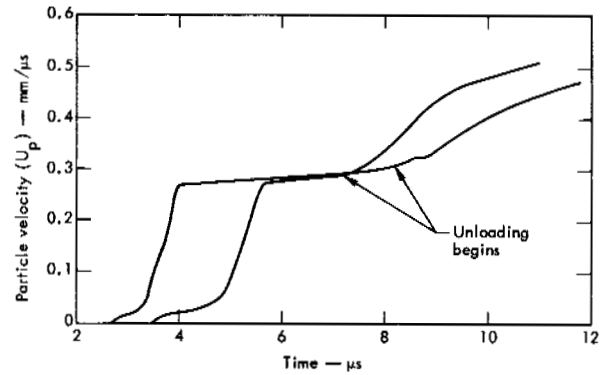


FIGURE 5 Particle-velocity history of two gages embedded in frozen saturated Ottawa banding sand. The arrows indicate the arrival of the rarefaction wave at the gages.

sis of nonsteady flow requires the integration Eq. (3) and (4):

$$(\partial V/\partial U_p)_h = -1/\rho_0 C_{U_p} \quad (3)$$

$$(\partial \sigma/\partial U_p)_h = \rho_0 C_\sigma, \quad (4)$$

which are derived from Eq. (1) and (2). (For further information on this analysis see Ref. 8.) C_{U_p} and C_σ are the phase velocities $(\partial h/\partial t)$ measured at constant particle velocity and constant stress. C_{U_p} can be calculated, and Eq. (3) and (4) can be integrated, using data such as shown in Figures 3-5 if C_σ is assumed to be equal to C_{U_p} . For steady waves, C_{U_p} is constant and equal to the shock velocity, so that integration of Eq. (3) and (4) across the shock front leads to the well-known jump conditions.

Table I gives the loading states for ice that were calculated by using Eq. (3) and (4). Figures 6 and 7 show these data along with loading and unloading paths and include the -10°C isotherm for comparison. Since both the low-strain-rate and high-strain-rate techniques produce similar compression curves (Figure 7), the first wave observed in the shock experiments is interpreted as arising from the onset of melting of Ice I.

In Figure 6, the phase transition is examined more closely. The initial, nearly straight part of the curve gives rise to a first wave or transition wave, which is steady [3], having a shock velocity of approximately 4 mm/ μs . The comparison of data from two perpendicular orientations of single-crystal ice shows no differences aside from experimental uncertainties and implies that crystal orientation is not a factor in the analysis of experimental results. The relatively large offset of the transition point is probably a strain-rate effect associated with the transition kinetics rather than due to strength effects, since differences between stress and pressures are not likely to reach the 0.5-1 kbar implied by the separation of these two curves.⁷ The unloading data

TABLE I Shock-Wave Loading Data for Various Ice Samples

Sample	First Wave				Second Wave			
	U_s (mm/ μ s)	U_p (mm/ μ s)	σ (kbar)	V (cm ³ /g)	U_p (mm/ μ s)	σ (kbar)	V (cm ³ /g)	$C_{u_p}(\sigma)$ (mm/ μ s)
<1010>	4.10	0.045	1.64	1.078	0.117	3.10	1.044	—
<1120>	3.90	0.056	1.90	1.074	0.120	3.05	1.041	2.76
<1120>	4.05	0.051	1.80	1.075	0.090	2.58	1.058	2.99
<0001>	3.76	0.049	1.58	1.075	0.125	2.85	1.035	—
<0001>	3.95	0.047	1.57	1.076	0.132	2.90	1.032	2.91
Polycrystal	3.96	0.060	2.00	1.074	0.412	6.95	0.792	—

also indicate incomplete transformation since the unloading path tends to drop toward the isotherm as the ice starts to unload.

For frozen soil, particle-velocity history records are shown in Figures 4 and 5; the first wave in both materials is interpreted as arising from the onset of melting of interstitial ice. Equations (2) and (3) were used to obtain the

data shown in Figures 8-11. Figures 8 and 9 show the results of uniaxial loading and unloading of frozen saturated Ottawa banding sand. The relatively large scatter is primarily due to experimental difficulties encountered in early experiments. Most of these difficulties were eliminated, and less scatter was observed in experiments on frozen saturated West Lebanon glacial till (Figures 10 and 11). The shock waves in frozen soils show an initial rise to approximately 1 kbar (this level varies between 0.7 and 1.2 kbar, depending on the sample) followed by a slower, nonsteady rise to 1.5-2 kbar. The main loading wave is also nonsteady. Apparently, the transition begins at approximately the same pressure in the dynamic experiment as along the isotherm in frozen soils, but the compression at the onset of the transition is somewhat smaller in the dynamic case. Beyond the initial transition point, the curves diverge, which implies a mixed phase. The nonsteady flow that characterizes these materials, like ice, appears to be a result of the influence of

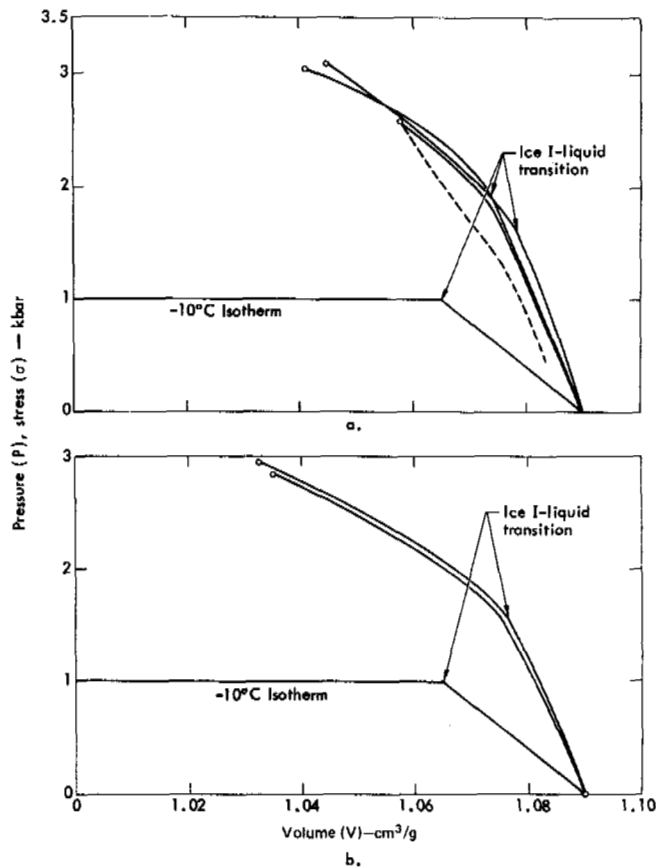


FIGURE 6 Shock-wave compression data for single-crystal ice shocked (a) perpendicular to and (b) along the <0001> axis, starting at -10°C.

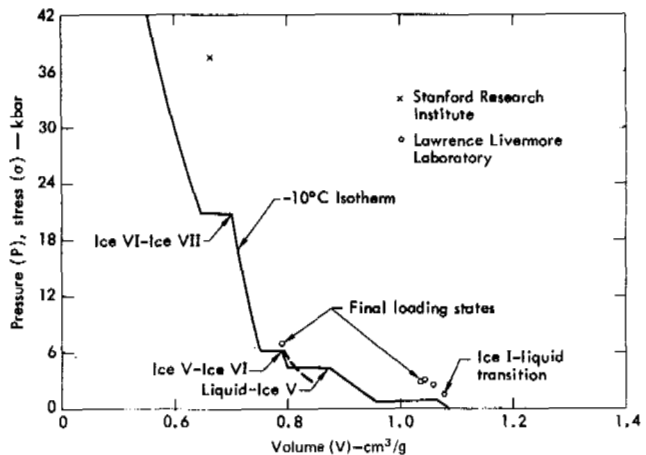


FIGURE 7 -10°C isotherm and shock-wave data for ice. The various phases are indicated along the isotherm. The dashed curve is an unloading path.

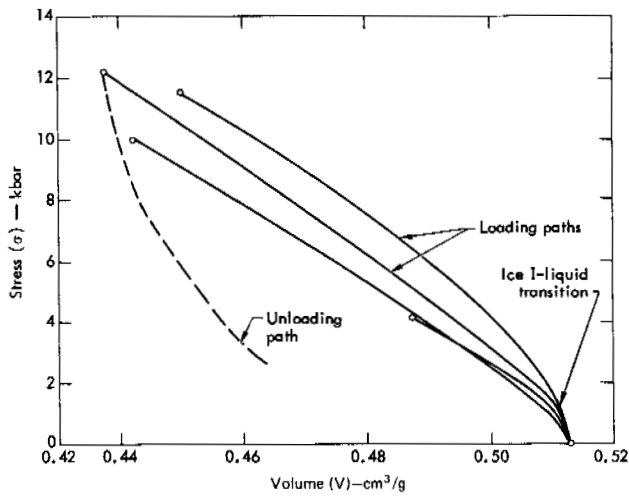


FIGURE 8 Shock-wave data for frozen saturated Ottawa banding sand. The dashed curve is an unloading path.

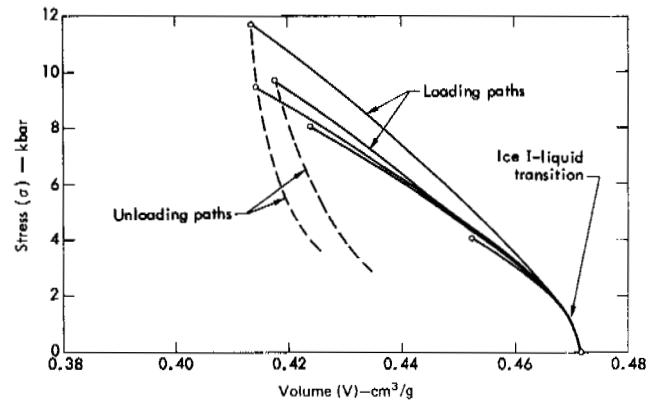


FIGURE 10 Shock-wave compression data for frozen saturated West Lebanon glacial till shocked from -10°C .

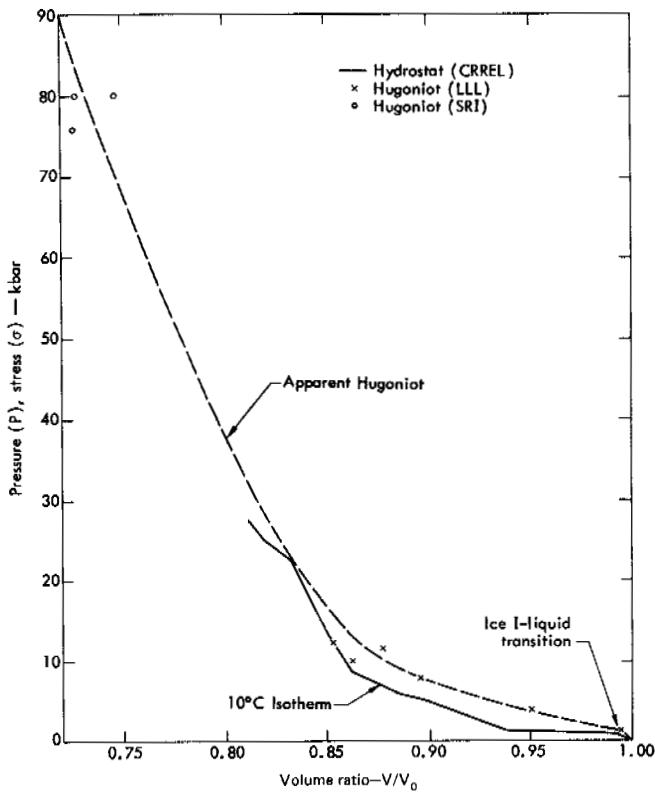


FIGURE 9 Hugoniot data and the -10°C isotherm for frozen saturated Ottawa banding sand. CRREL, Cold Regions Research and Engineering Laboratory; LLL, Lawrence Livermore Laboratory; SRI, Stanford Research Institute.

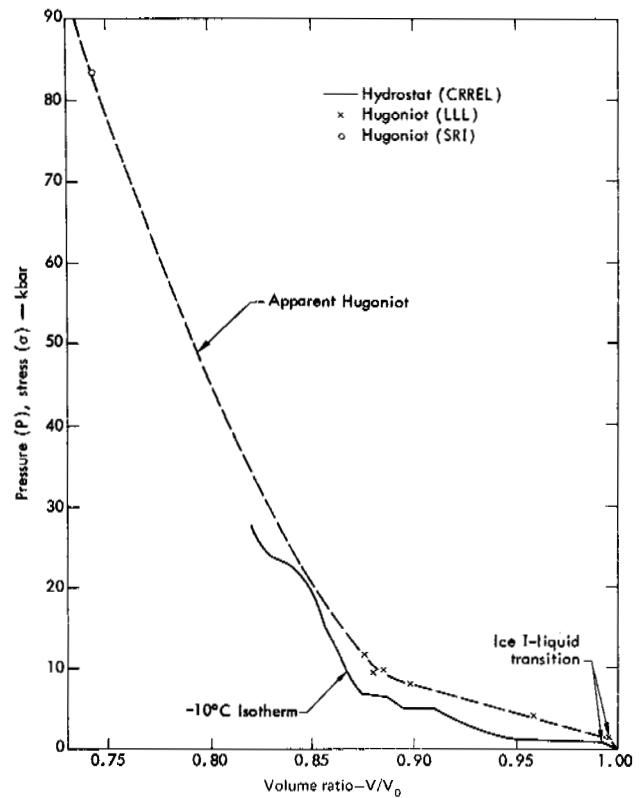


FIGURE 11 Hugoniot data and the -10°C isotherm for frozen saturated West Lebanon glacial till. CRREL, Cold Regions Research and Engineering Laboratory; LLL, Lawrence Livermore Laboratory; SRI, Stanford Research Institute.

transformation kinetics. The initially steep unloading paths observed in the neighborhood of 10 kbar suggest that the transition continues during the initial part of unloading. As unloading continues, the material expands. This expansion is an apparent partial reversion to Ice I.

Figures 12-14 show the particle-velocity history records obtained when ice, frozen saturated Ottawa banding sand, and frozen saturated West Lebanon glacial till were loaded radially with spherical high-explosive energy sources. Because energy sources of two different sizes were used, the data are given as functions of reduced radius. The reduced radius is defined as the gage initial radius divided by the radius of the high explosive.

Figure 12 shows records obtained at six different radial distances from the energy source in polycrystalline ice. The first three records were obtained from gages that were initially 3.8, 6.4, and 11.4 cm from the center of a 1.9-cm sphere of LX04 high explosive. The second set of three records is from gages 7.6, 10.2, and 14.0 cm from the center of a 0.95-cm sphere of high explosive. The arrows that appear on Figure 12 at particle velocities of 0.05-0.06 mm/μs indicate where melting should occur. Curve 1 clearly

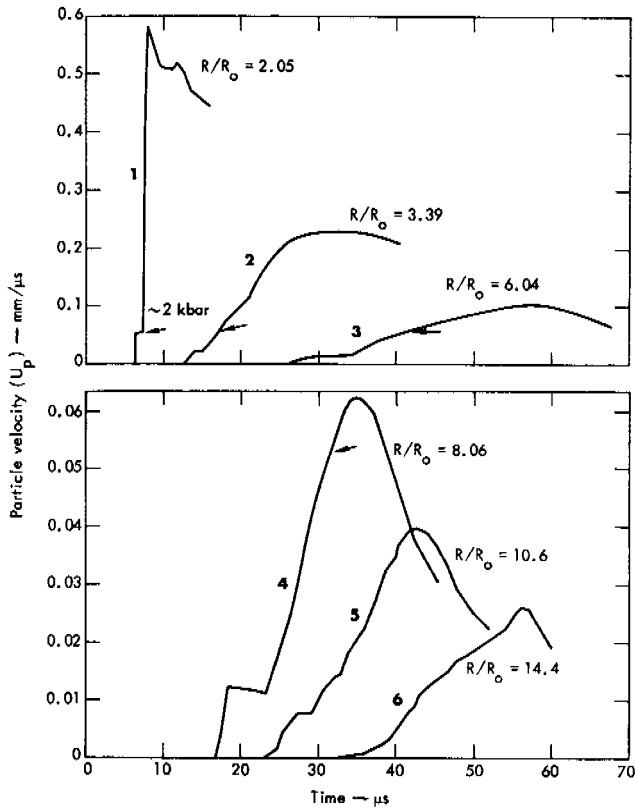


FIGURE 12 History of particle velocity in polycrystalline ice at six reduced radial distances from the high-explosive source. Reduced radius is the actual radial distance from the center of the source divided by the radius of the source.

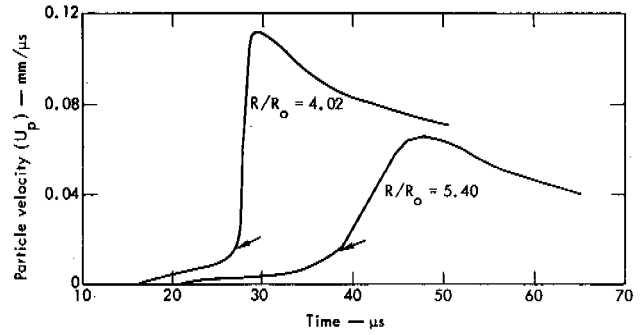


FIGURE 13 History of particle velocity in frozen saturated Ottawa banding sand at two distances from the high-explosive source.

shows the expected two-wave structure. Curves 2 and 3, which also represent material loaded above the melting point, show some indication of the two waves, but wave spreading has distorted the profiles. Curves 4, 5, and 6 are loaded at, and slightly below, the transition but show wave spreading caused by multiple waves produced in material that is closer to the source and thus loaded above the transition point. The average shock velocity recorded between gages is equal to or greater than 3.86 mm/μs, which is well above the longitudinal sound speed of 3.86 mm/μs. Thus,

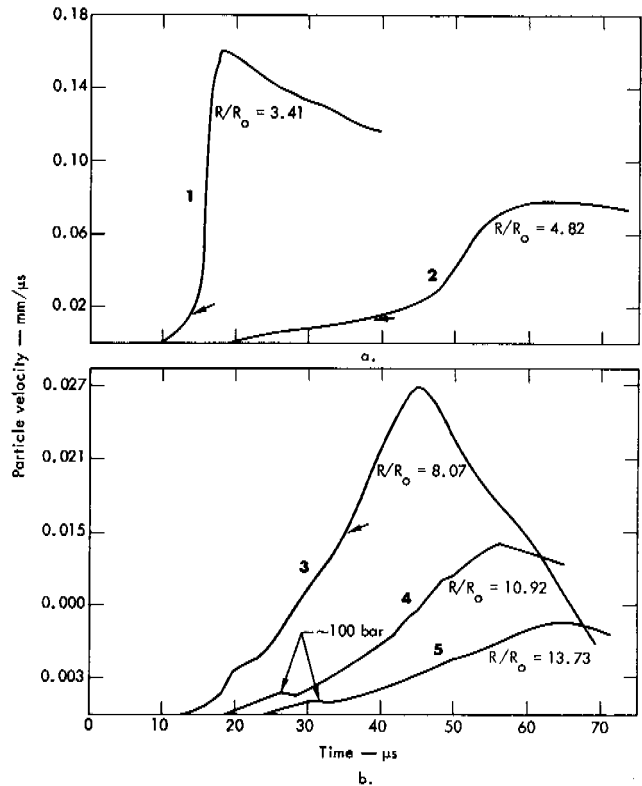


FIGURE 14 History of particle velocity in frozen saturated West Lebanon glacial till at five distances from the high-explosive source.

elastic waves were unable to propagate, and no measure of dynamic strength was possible in ice by direct measurement of a Hugoniot elastic limit.

Figure 13 shows records of mass flow in frozen saturated Ottawa banding sand at 7.6 and 10.2 cm from the center of a 1.9-cm sphere of high explosive. Both curves show spreading wave profiles. The expected onset of melting of interstitial ice is indicated by the arrow. The average precursor wave velocity between these gages was 4.29 mm/ μ s, which is above the longitudinal sound speed of 3.90 mm/ μ s.

Figure 14 shows records of particle velocity in frozen saturated West Lebanon glacial till at 6.4 and 8.9 cm from a 1.9-cm sphere of high explosive and at 7.6, 10.2 and 12.7 cm from a 0.95-cm sphere. The expected onset of melting of interstitial ice is indicated by arrows. The average precursor shock velocity for curves 1 and 2 was 4.11 mm/ μ s. Unfortunately, a meaningful value of shock velocity was not obtained for curves 3, 4, and 5. Therefore, the exact nature of the approximately 100-bar wave, appearing on curves 4 and 5, is obscure. The longitudinal sound speed or expected elastic wave velocity is 3.47 mm/ μ s.

Figure 15 shows a plot of peak particle velocity versus reduced radius for the three series of experiments on frozen materials and compares the response with that of water and the rate of attenuation of an ideal elastic wave. After an initial rapid decay rate, the attenuation in water is very similar to that of an ideal elastic wave. In contrast, ice shows a rather high and essentially constant attenuation

rate for all reduced radii. The attenuation rates in the frozen soils are also constant but considerably more rapid than in pure ice.

CONCLUSIONS

The Ice I-water phase transformation occurs during shock-wave loading both in pure ice and in the interstitial ice in saturated frozen soils. However, the observed final loading states are all in the mixed-phase region, and unloading data imply a continuation of the transformation during the initial part of this unloading. This unloading behavior creates a large energy sink whenever decaying shock waves propagate at stress levels above 2 kbar and to at least 15 kbar and also may occur at stress levels above this range. The relatively rapid attenuation of the shock wave in frozen materials, as shown in Figure 15, is directly related to this loss of energy. Numerical simulation models that duplicate this rate of attenuation are also consistent with the loading and unloading observed in the uniaxial compression experiments. The differences between ice and frozen soil are a direct result of a larger area between the loading and unloading paths in the soils. Unfortunately, complete unloading paths are not available to establish the exact explanation. However, possible reasons for this difference are a slower transformation rate upon loading, followed by relatively rapid transformation in the initial unloading or limited transformation back to Ice I after the material unloads. Temperatures behind the shock and rarefaction waves could play an important part in the reverse transformations by stabilizing part or all of the water phase.

ACKNOWLEDGMENTS

The authors thank Dr. K. Itagaki, S. Ackley, and E. Chamberlain of CRREL for the excellent frozen material samples they produced and for valuable information they provided through numerous discussions. We also acknowledge the excellent support provided by S. Spataro, W. Stutler, J. Arguello, T. Schaffer, and R. Schnetz.

REFERENCES

1. Anderson, F. 1967. The equation of state of ice and composite frozen soil material. CRREL Research Report 257. U.S. Army Cold Regions Research and Engineering Laboratory, Hanover, New Hampshire.
2. Bridgman, P. W. 1911. Water in the liquid and five solid forms, under pressure. Proc. Am. Acad. Arts Sci. 47:441-558.
3. Bridgman, P. W. 1912. Thermodynamic properties of liquid water to 80° and 12 000 kgm. Proc. Am. Acad. Arts Sci. 48:309-362.
4. Bridgman, P. W. 1914. High pressures and five kinds of ice. J. Franklin Inst. 177:315-332.
5. Bridgman, P. W. 1937. The phase diagram of water to 45 000 kg/cm². J. Chem. Phys. 5:964-966.
6. Chamberlain, E., and P. Hockstra. 1970. The isothermal compressibility of frozen soil and ice to 30 kilobars at -10 °C. CRREL

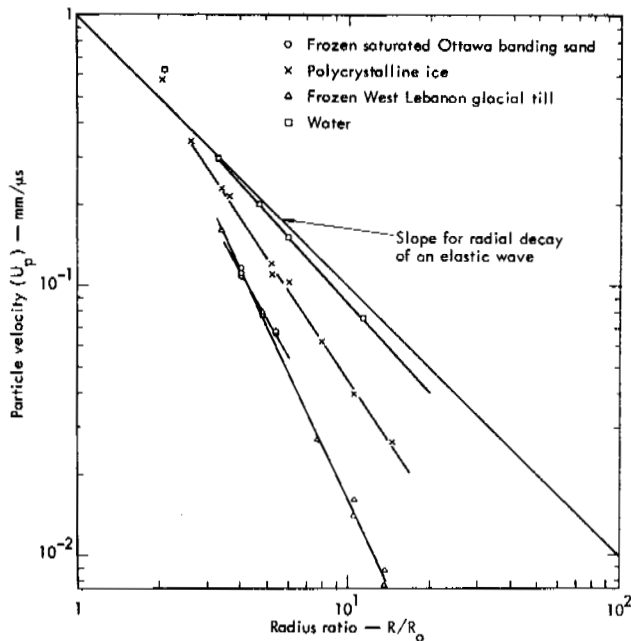


FIGURE 15 Plot of peak particle velocity versus reduced radius for frozen materials. The reduced radius is defined as the gage initial radius divided by the radius of the high-explosive source.

Technical Report 225. U.S. Army Cold Regions Research and Engineering Laboratory, Hanover, New Hampshire.

7. Chamberlain, F. 1967. Some triaxial shear strength tests on frozen soil and ice. CRREL Interim Technical Report. U.S. Army Cold Regions Research and Engineering Laboratory, Hanover, New Hampshire.
8. Cowperthwaite, M., and R. Williams. 1971. Determination of constitutive relationships with multiple gages in nondivergent waves. *J. Appl. Phys.* 42:456-462.

NOTES

- [1] Work performed under the auspices of the U.S. Atomic Energy Commission.
- [2] Reference to a company or product name does not imply approval or recommendation of the product by the University of California or the U.S. Atomic Energy Commission to the exclusion of others that may be suitable.
- [3] A steady wave is one that does not spread as it propagates.

THAW CONSOLIDATION OF ALASKAN SILTS AND GRANULAR SOILS

Ulrich Luscher and Sherif S. Afifi

WOODWARD-LUNDGREN & ASSOCIATES
Oakland, California

INTRODUCTION

To design a foundation to be placed on ground that is originally frozen but may thaw later, it is essential to know the settlement behavior of the particular soil. This problem has been recognized for a long time, and much work has been done in the past to understand and describe both the freezing phenomena and the thaw consolidation behavior of different soils.^{6,8,10,11}

Generally accepted concepts might be summarized as follows:

1. Thaw settlement behavior depends on the amount and distribution of ice in the soil. Ice may occur in frozen soil in distributed form, in lenses and veins, and as massive ice inclusions.
2. For soil with distributed ice only, a gradually advancing thaw front melts the ice. Depending on several factors, including the degree of saturation and the tendency for volume change of the soil skeleton, excess pore water may be generated at the thaw front. This excess water is dissipated according to physical laws similar to those governing consolidation phenomena in thawed soils.⁴ Hence, thaw straining may or may not occur and may or may not have a consolidation time lag associated with it.

The thaw strain T is generally believed to be composed of two components:

$$T = A_0 + a_0 \sigma \quad (1)$$

in which A_0 is a constant for a given soil and $a_0 \sigma$ is propor-

tional to the applied stress σ .^{7,8} The constants are determined by thaw consolidation tests.

3. For soil with both distributed ice and ice lenses, it is best to separate the contributions to thaw settlement due to distributed ice and ice lenses.¹ Arching reduces the settlement contribution of a lens to a value less than the lens' thickness. Alternately, thaw consolidation tests could be made on soil samples containing ice lenses, but the samples should have a lateral dimension several times that of the lenses.⁵

4. Settlement due to thawing of massive ice inclusions, including ice wedges, will be very large and irregular and must be evaluated individually.

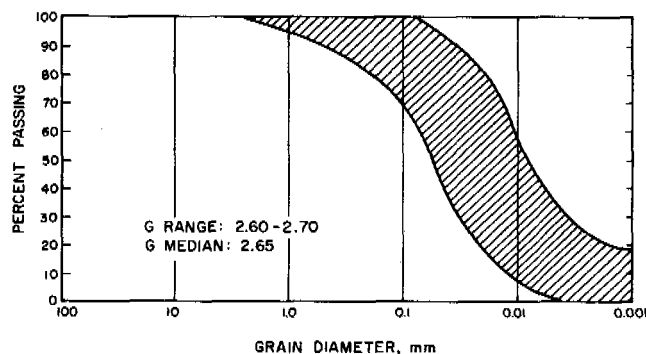
In connection with a proposed project that would traverse wide regions of Alaska, a large number of laboratory thaw consolidation tests have been made on undisturbed samples of frozen soil recovered from 0 to 20-m depth along the proposed alignment. The purpose of these tests is to establish parametric relationships between thaw strain and frozen soil index properties. That is, the purpose of the tests is not to establish precise settlement data for one specific site but to develop broad conservative relationships that could have wide applicability.

In the remainder of this paper these thaw consolidation tests are discussed, and the results and their evaluation presented. The tests discussed primarily concern soils of silt size and coarseness, with distributed ice rather than lenticular or massive ice inclusions. Emphasis is placed on final strain values rather than on time phenomena.

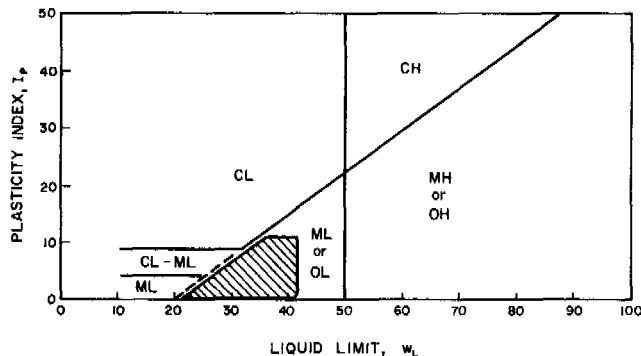
The tests included conventional uniaxial thaw consolidation tests made in standard consolidation test equipment, as well as triaxial thaw consolidation tests made in a triaxial cell. In the triaxial tests, both isotropic (uniform all around) and anisotropic loading conditions are used; the anisotropic loading condition utilizes ratios of vertical to horizontal stresses such that essentially one-dimensional deformation (as in the uniaxial test) is achieved.

MATERIALS

Four basic soil types are tested in the investigation. According to the Unified Soil Classification,³ these soils are classified as follows: low-plasticity silts (ML and OL), silt-sands, (SM, SP-SW, SW-SM, SM-ML*, and ML-SM**) [1], dirty gravels (GM and GW-GM), and clean sands and gravels (SP, SW, GP, and GW). Figure 1 shows the ranges of grain size distribution and plasticity for the silt samples tested. Organic burn tests show that the percentage of organics is less than 6 percent by weight. Figure 2 shows the ranges of grain size distribution for granular soils: silt-sands, dirty gravels, and clean sands and gravels. These soils contain negligible amounts of organics. Figures 1 and 2 also show ranges and median specific gravity values.



a.



b.

FIGURE 1 (a) Grain-size distribution and (b) plasticity range of low-plasticity silts.

TEST PROCEDURES

Uniaxial Thaw Consolidation Tests

The samples used in these tests have a diameter of about 5 cm and a height of 2-4 cm. Drainage during the test is through filter papers and porous disks placed at the top and bottom of the samples. These tests are made using a standard odometer device.²

The tests on silts consist of two major steps—thawing and consolidation under one pressure and further consolidation under additional pressures. First, the frozen sample is placed in the consolidation unit in the cold room, quickly brought to the laboratory, loaded with a vertical pressure, and left to thaw and consolidate for 24 h. The changes in sample height are recorded during this period. Next, the sample is consolidated with additional pressures. Six different pressure sequences, defined by kilonewtons per metre squared, are used to consolidate groups of six samples:

12	24	48	96	192	384
	24	48	96	192	384
		48	96	192	384
			96	192	384
				192	384
					384

The first number in each of these sequences represents the thaw pressure, and the remaining numbers represent pressure reached after thaw. All tests on silt-sands are made with a single pressure of 96 kN/m².

The uniaxial thaw consolidation test is suitable for clays, silts, and sands, where meaningful tests can be made on samples of relatively small diameter and small height. To use this test for gravel, relatively large-diameter samples would be required. Also, trimming samples to closely fit the consolidation mold is almost impossible for coarse-grained soils.

Anisotropic Thaw Consolidation Tests

The anisotropic thaw consolidation test has been devised to overcome the difficulties of the uniaxial thaw consolidation test for coarse-grained soils. In this test, the standard triaxial equipment (with some modification) is used. Samples have a diameter of 4-8 cm and a height-to-diameter ratio of 2:2.5.

In principle, a sample can be caused to consolidate purely unidimensionally (K_0 condition), either by using a confinement ring (in the standard consolidation test) or by applying principal stresses that have a certain proportion to each other (in the triaxial test). Experience has shown that the ratio K_0 of lateral stress ($\sigma_2 = \sigma_3$) to axial stress (σ_1) leading to deformation in the direction of σ_1 only ranges from 0.35 to 0.50 for granular soils. These K_0 values cor-

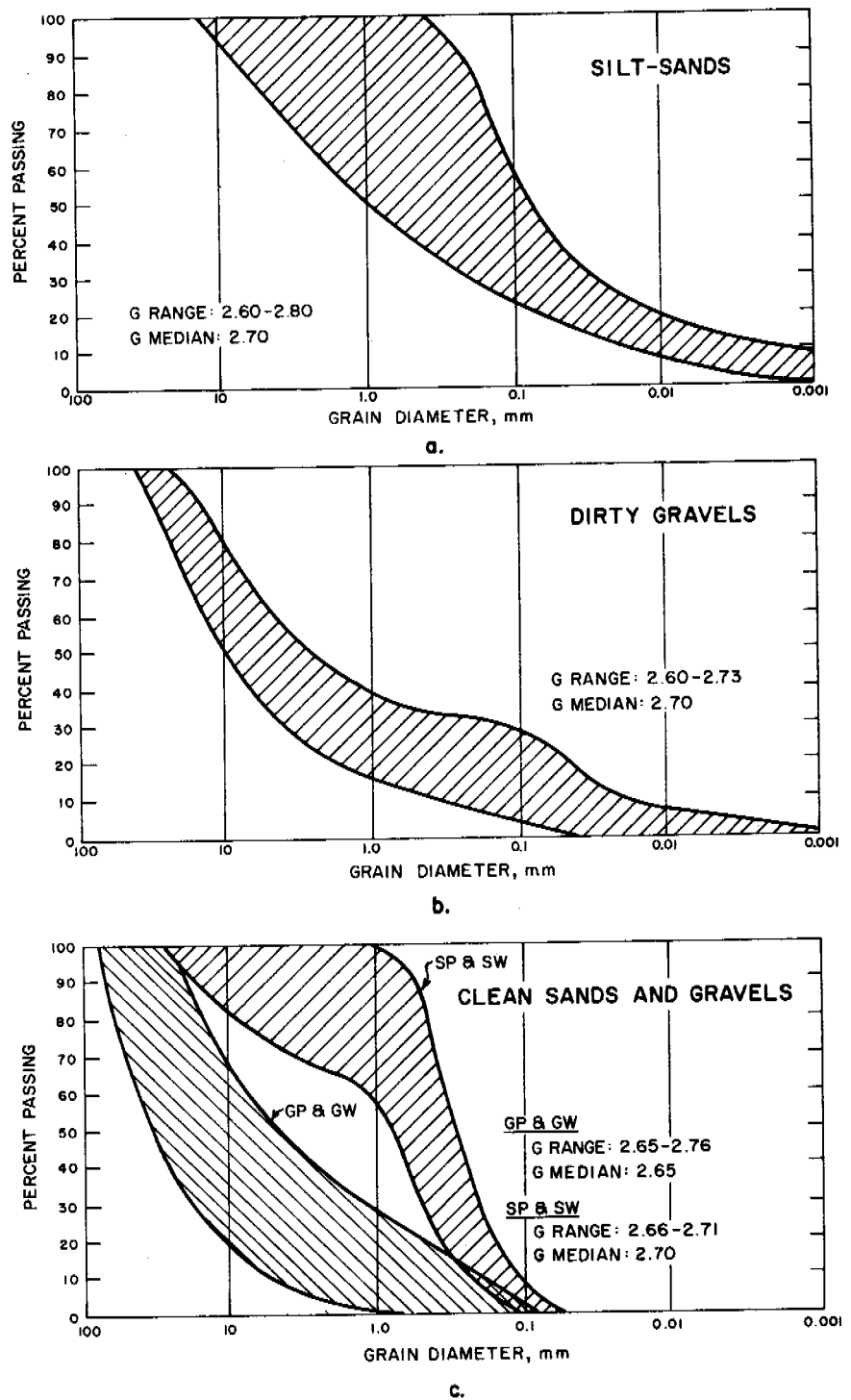


FIGURE 2 Grain-size distribution ranges for granular soils.

respond to a principal stress ratio (σ_1/σ_3) ranging from 2 to 3. Elastic theory, using values of Poisson's ratio of $1/3$ to $1/4$, leads to the same result.

The data obtained in this investigation, using anisotropic thaw consolidation for silt-sands, confirm these concepts, as will be shown in the discussion of Figure 7. Similar behavior

is expected for gravel samples that are statistically homogeneous. For practical purposes, gravel samples with a ratio of particle size to diameter of $1/3$ or less were considered statistically homogeneous and were tested using this technique.

At the beginning of this investigation, all samples are

loaded in the frozen condition and are kept frozen using refrigeration coils that surround the consolidation ring. The strains in the frozen condition obtained within 24 h are found to be insignificant, compared with the strains experienced during thaw. For this reason, the initial step of maintaining the sample frozen for 24 h under the applied load is omitted and all tests are made by allowing samples to thaw under a selected load as described for the uniaxial thaw consolidation test.

RESULTS AND DISCUSSION

Thaw Consolidation of Low-Plasticity Silts

Figure 3 is a plot of volumetric strain versus pressure for six samples of ML soil with frozen dry density that ranges from 1 250 to 1 330 kg/m^3 that are tested in the uniaxial thaw consolidation test. The samples are taken from one block sample and are nearly identical. In this figure, a solid symbol represents the volumetric thaw strain experienced

by a sample under the first applied pressure, and the open symbols of the same type represent the cumulative volumetric strain experienced by the same sample during thawed compression under additional pressures. For clarity, each unisolid point and its corresponding set of open points are connected by a dashed curve as shown. Therefore, all data connected by one dashed curve correspond to one sample.

It is seen from Figure 3 that values of volumetric strain at each pressure differ only slightly, even though they are obtained through different pressure paths. This result implies that time and loading path have insignificant effects on the thaw strain behavior of the samples tested. The plot shown in Figure 3 is typical of many others that showed similar behavior. The figure also shows that volumetric strain increased with increase in vertical pressure, though not linearly.

Figure 4 is a plot of volumetric thaw strain versus frozen dry density for ML and OL samples consolidated with pressures σ_v of 48 and 96 kN/m^2 (average of 72 kN/m^2). It is seen from this figure that thaw strain increases with de-

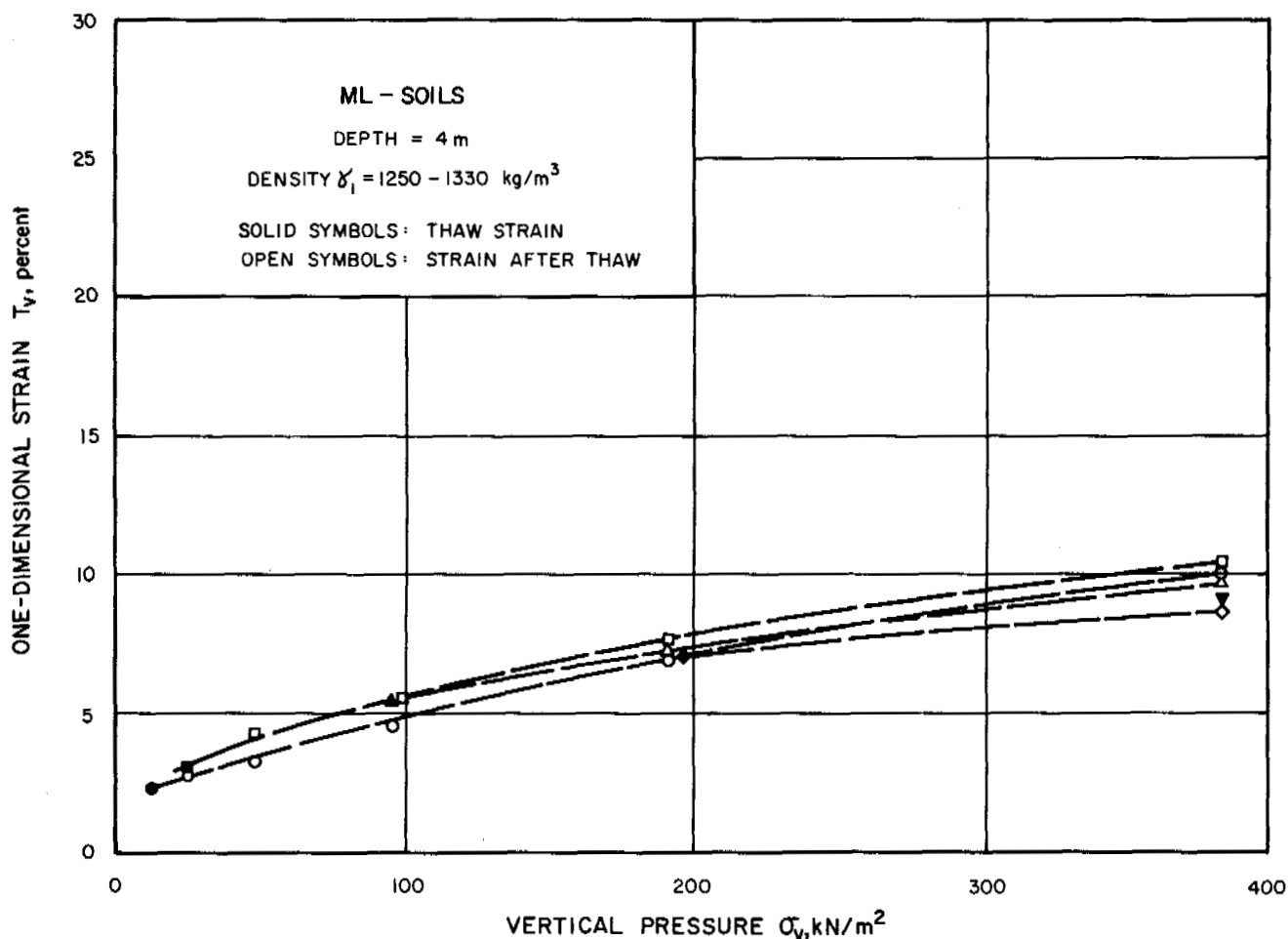


FIGURE 3 One-dimensional strain versus pressure.

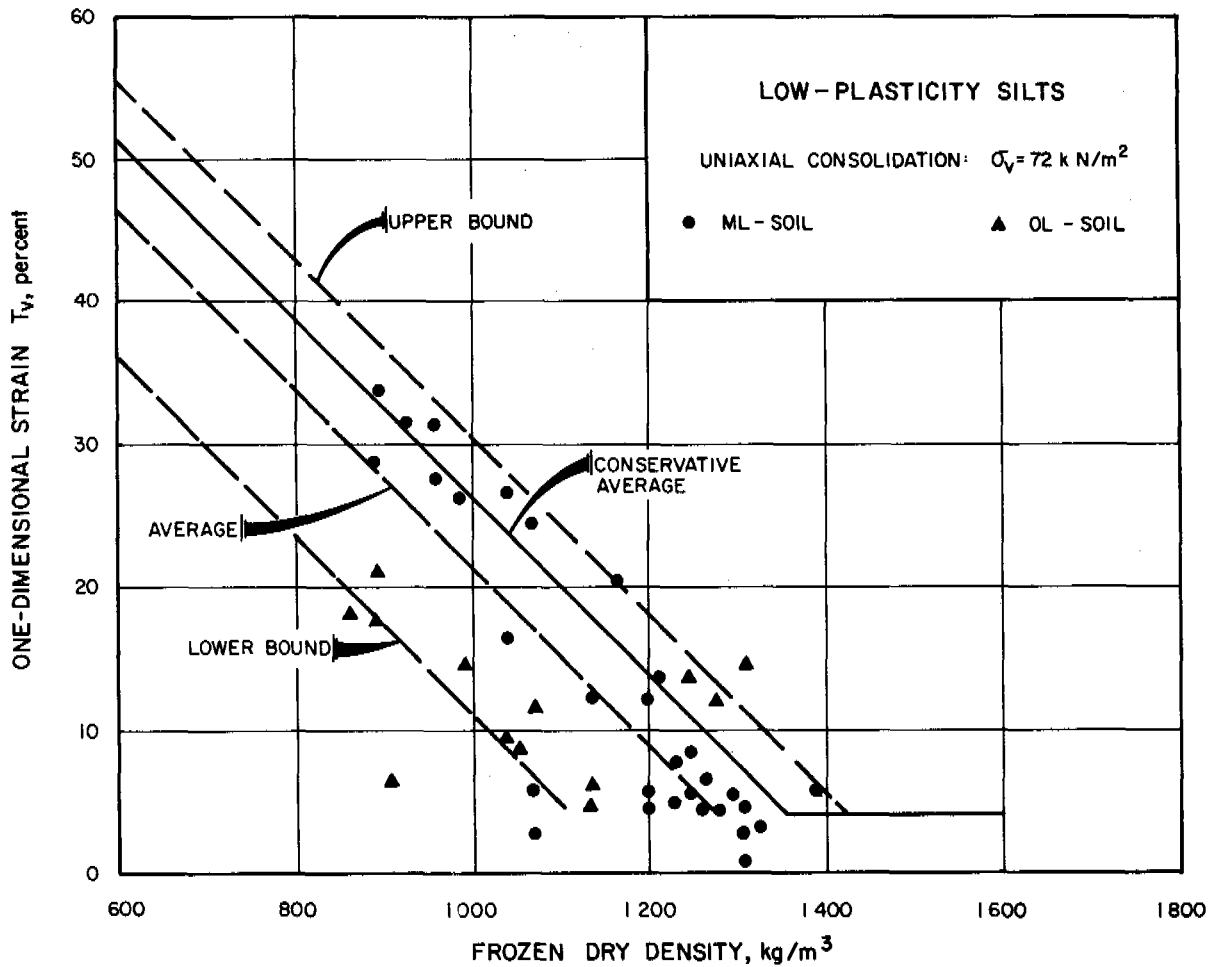


FIGURE 4 Thaw consolidation of frozen low-plasticity silts.

creasing frozen dry density in the same manner for both ML and OL samples. Based on the trend of Figure 4 and the trends observed for the remainder of the data, it is concluded that the variation of volumetric thaw strain with frozen dry density for silts can be described by upper-bound, lower-bound, and average straight lines as shown by the dashed lines in Figure 4. A "conservative average" relationship (halfway between the upper bound and the average) for design is represented by the solid line in the figure.

The remainder of the data showed similar behavior and straight lines representing conservative average thaw strain behavior are selected for average pressure of 18 kN/m² and pressures of 192 and 384 kN/m². These data are summarized in Figure 5. In the top right corner of this figure, a plot of the abscissa intercept versus thaw pressure is also shown.

As can be seen from the figure, the relationship between total strain and pressure is not linear as given by Eq. (1). Back extrapolation of the curves in the top right corner of

Figure 5 to low pressures would yield the abscissa intercept value for very low or zero consolidation pressure.

Figure 6 plots axial thaw strain obtained from triaxial consolidation tests with uniform all-around pressure ($\sigma_1 = \sigma_2 = \sigma_3$) versus frozen dry density for an average pressure σ_3 of 72 kN/m². It is again seen that thaw strain increases similarly with decreasing frozen dry density for the two soil types.

To interpret the data in Figure 6, two straight lines are shown. The dashed line is the conservative average of Figure 4, which represents the variation of volumetric thaw strain with frozen dry density for similar soils thawed one-dimensionally with a pressure σ_v of 72 kN/m². The solid line in the figure is drawn with a strain value one-third that of the dashed line. It is seen that the solid line conservatively represents the variation of axial thaw strain with frozen dry density. Theory of elasticity would indicate a ratio between axial thaw strain under isotropic stresses and volumetric thaw strain under uniaxial compression ranging from 0.43 to 0.67

for Poisson's ratio between $\frac{1}{3}$ and $\frac{1}{4}$. Considering that thaw strain is much more influenced by frozen dry density than by applied stress (see Figure 5), however, the observed one-third ratio simply means that the thaw strain pattern was essentially isotropic (i.e., similar strain in all directions) for isotropic loading of soils with randomly distributed ice.

Thaw Consolidation of Silt-Sands

Figure 7 is a plot of thaw strain data of silt-sand samples. The solid symbols in this figure represent volumetric thaw strains obtained from uniaxial thaw consolidation tests, and the open symbols represent axial thaw strains obtained from anisotropic thaw consolidation tests with a principal stress ratio of 2. In several tests, samples are thawed initially with a stress ratio of 2 and further consolidated with a stress ratio of 3. These data show that there is no significant vertical strain increase due to an increase in stress ratio from 2 to 3.

It is seen that thaw strains obtained from the uniaxial and

anisotropic thaw consolidation tests vary with frozen dry density in a similar manner. For frozen dry density greater than $1\ 680\ \text{kg/m}^3$, the data show that thaw strains are between 0 and 5 percent, with a conservative average of 4 percent. For lower frozen dry density, the thaw strain variation with frozen dry density is conservatively described by the straight line relationship shown. Thus, available data show essential agreement between results of uniaxial and anisotropic thaw consolidation tests, giving confidence in the concept that triaxial thaw consolidation tests, with stress ratio of 2 to 3, yield axial thaw strains about equal to volumetric thaw strains, i.e., the sample's area remains essentially constant.

Thaw Consolidation of Dirty Gravels

Results of about 20 anisotropic thaw consolidation tests on dirty gravels with frozen dry density between $1\ 760$ and $2\ 560\ \text{kg/m}^3$ show thaw strains between 0.7 and 3.0 per-

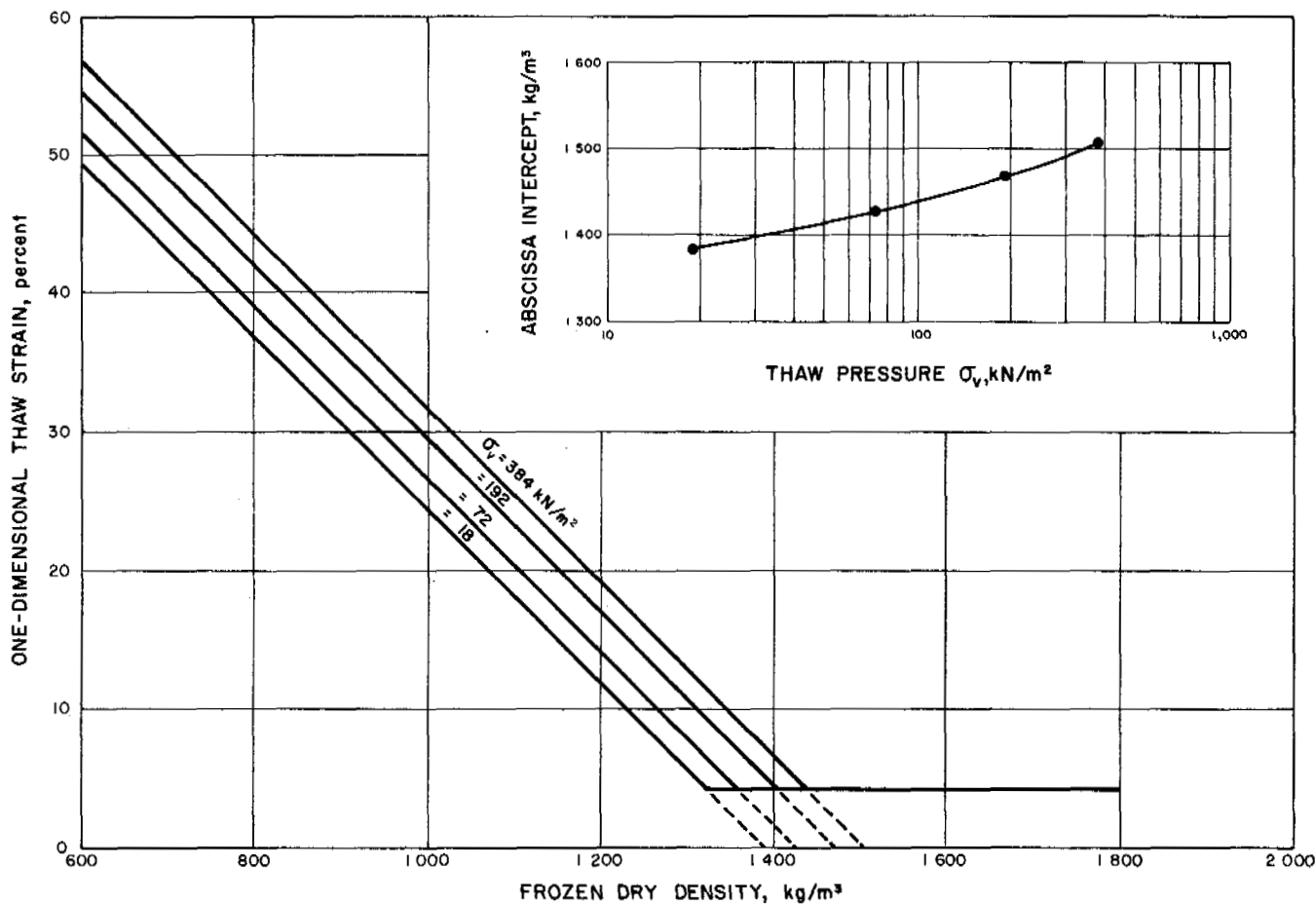


FIGURE 5 Summary plot—thaw consolidation of frozen low-plasticity silts.

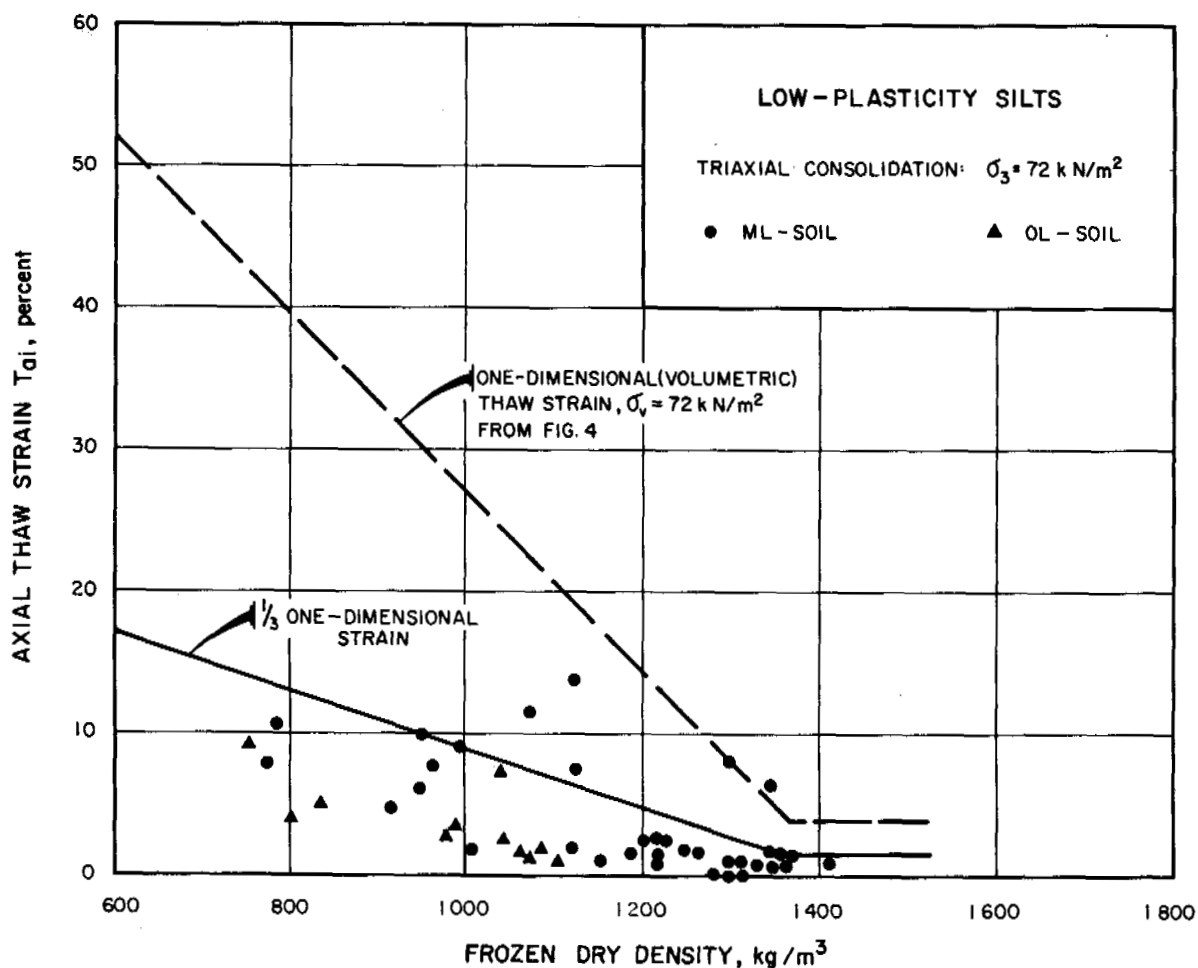


FIGURE 6 Axial thaw strain under isotropic stresses for low-plasticity silts.

cent, with a conservative average of 2.5 percent. The variability of strain with density was essentially random. (These data are not presented in a figure.)

Thaw Consolidation of Clean Sands and Gravels

Figure 8 is a plot of thaw strains obtained from anisotropic thaw consolidation tests on clean sands and gravels. Because these soils experienced lower thaw strains than others, a larger scale is used to represent strain (five times that used before). The variation of thaw strain with frozen dry density for these soils is represented by the two straight lines shown.

Most samples with frozen dry density greater than 1630 kg/m^3 have thaw strains between 0.4 and 3.0 percent, with a conservative average of 2 percent as shown by the horizontal straight line. All these samples are tested with a stress ratio of 2, and four samples were further consolidated with a stress ratio of 3 (semisolid symbols). As is seen, further

consolidation causes no significant strain increase, except where additional loading brings the strain above the 2 percent line.

The figure also shows that sands and gravels with frozen dry density less than 1630 kg/m^3 could have higher strains. It is noted that all these samples are tested with a stress ratio of 2 and that three samples are further consolidated with a stress ratio of 3. In all these cases, the resulting strains fall below the suggested relationship.

Thaw consolidation of frozen gravels may be overestimated from the tests performed, because of sample disturbance and lack of particle-to-particle contact, which is available in the field but may not be available in the small laboratory sample. Therefore, it is advisable that thaw consolidation behavior of frozen gravels be confirmed on the basis of field testing. A better idea on thaw consolidation behavior of gravels also may be obtained if large-diameter samples (e.g., 25 cm) are used.

SUMMARY

This paper presents the results of an extensive investigation of thaw consolidation behavior of undisturbed samples of frozen silts and granular soils obtained from Alaska. New procedures for thaw consolidation testing are discussed, and a wealth of data are presented. Frozen silt samples are thawed and consolidated one-dimensionally with a range of vertical pressure from 12 to 384 kN/m² using standard consolidation test equipment; these tests involve thawing with different pressures, as well as thawing with a single pressure and consolidating further with additional pressures. Frozen silt-sand samples are thawed and consolidated by two methods—one-dimensionally in the standard odometer test and anisotropically in the standard triaxial test with vertical-to-horizontal pressure ratios of 2 and 3, thus minimizing the changes in sample cross section during thawing and consolidation. Anisotropic thaw consolidation tests also are made on dirty gravels and on clean sands and grav-

els. The following conclusions can be drawn from this investigation:

1. For ML and OL samples (organics less than 6 percent by weight), the variation between volumetric thaw strain developed in the uniaxial thaw consolidation test and frozen dry density is represented conservatively by straight lines as shown in Figure 5 for consolidation pressures of 18, 72, 192, and 384 kN/m².
2. For ML and OL samples, the variation between axial thaw strain developed in the triaxial test under isotropic stresses and frozen dry density is represented by straight lines with strain values one-third the volumetric strains developed under uniaxial deformation under the same pressure. This result indicates that uniaxial (one-dimensional) thaw strains can be estimated from triaxial thaw consolidation, which is the usual initial step in a consolidated, undrained strength test. The same result also is found to be true for silt-sands.

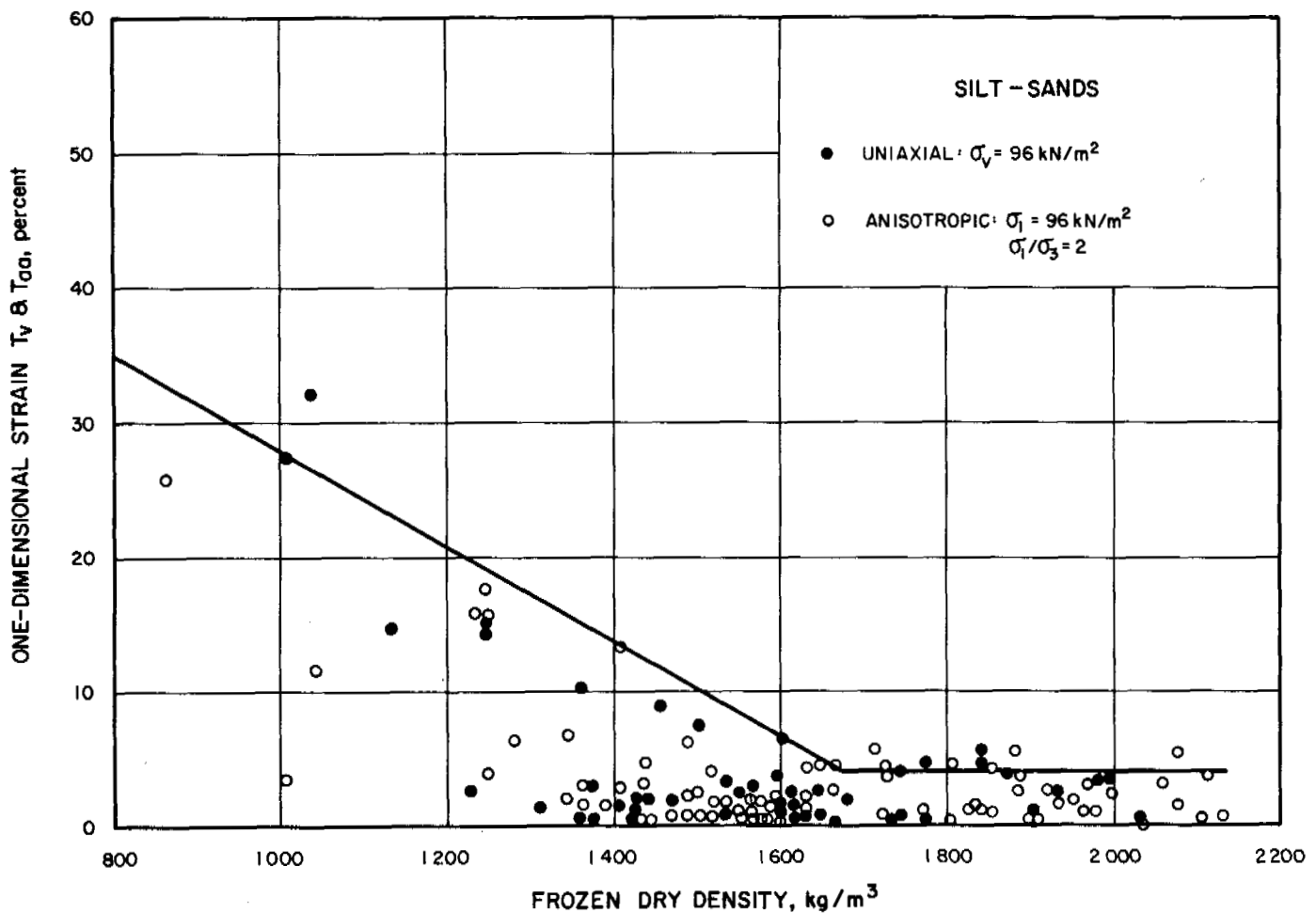


FIGURE 7 Thaw consolidation of frozen silt-sands.

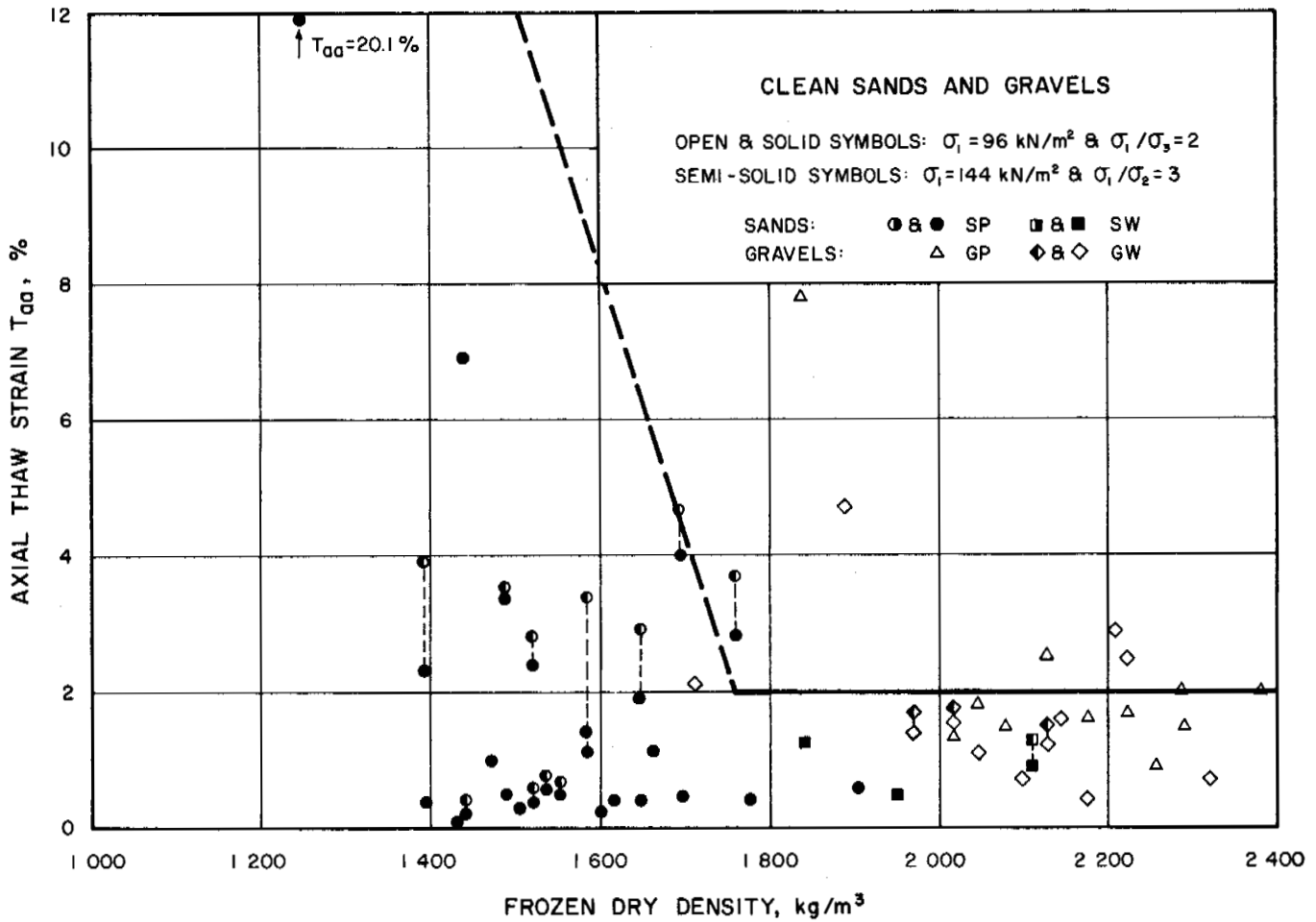


FIGURE 8 Thaw consolidation of frozen clean sands and gravels.

3. For silt-sands, results of uniaxial (one-dimensional) and anisotropic (K_0) thaw consolidation tests gave a single bilinear relationship between frozen dry density and one-dimensional thaw strain.

4. Indications are that thaw strains of dirty gravels (GM and GW-GM) are less than 2.5 percent for dry densities exceeding 1680 kg/m^3 .

5. Indications are that thaw strains of clean sands and gravels (GW, GP, GW, and GP) are less than 2 percent for dry densities exceeding 1630 kg/m^3 and fall below the straight line relationship of Figure 8 for lower density.

These data provide a tool for estimating one-dimensional thaw settlement of silts and granular soils caused by thawing of soil-ice matrix (without considering the effect of thawing of ice lenses or massive ice) from soil index properties, which can be determined by simple tests.

ACKNOWLEDGMENTS

The test program described herein was done in connection with the proposed trans-Alaska pipeline system. The support provided by the Alyeska Pipeline Service Company is acknowledged. The tests were made in the Oakland, California, laboratory of Woodward-Lundgren & Associates under the supervision of J. H. Wilson.

REFERENCES

1. Kiselev, M. F., G. I. Kostinenko, and G. A. Nyzoukin. 1965. Calculation of foundation settlements on thawing soils. Proc. 6th Int. Conf. Soil Mech. Found. Eng. 2.
2. Lambe, T. W. 1951. Soil testing for engineers. Wiley, New York.
3. Lambe, T. W., and R. V. Whitman. 1969. Soil mechanics. Wiley, New York.
4. Morgenstern, N. R., and J. F. Nixon. 1971. One-dimensional consolidation of thawing soils. Can. Geotech. J. 8:558.
5. Porkhaye, G. V., and S. G. Tsvetkova. 1972. Experimental

- methods of determining the settlement of permanently frozen ground on thawing. CRREL Draft Translation 340 (original publication 1958). U.S. Army Cold Regions Research and Engineering Laboratory, Hanover, New Hampshire.
6. Scott, R. F. 1969. The freezing process and mechanics of frozen ground. Monograph II-D1. U.S. Army Cold Regions Research and Engineering Laboratory, Hanover, New Hampshire.
 7. Shusherina, Ye. P. 1972. Studying the settling of frozen ground on thawing. CRREL Draft Translation 336 (original publication 1954). U.S. Army Cold Regions Research and Engineering Laboratory, Hanover, New Hampshire.
 8. Tsytoich, N. A. 1941. Determination of foundation settlements. Gosstroizdat.
 9. Tsytoich, N. A. 1958. Bases and foundations on frozen soils. Special Report 58. Highway Research Board, National Academy of Sciences, Washington, D.C. (Translated from Russian by C. Drashevsky, G. P. Tschebotarioff [ed.]).
 10. Tsytoich, N. A., *et al.* 1965. Consolidation of thawing soils. Proc. 6th Int. Conf. Soil Mech. Found. Eng. 1.
 11. USSR. 1962. Instructions for designing bearing media and foundations in the southern zone of the permafrost region. TT 1298. National Research Council of Canada, Ottawa.

NOTES

- [1] *SM with 40-50 percent smaller than 0.074 mm; **ML with 50-60 percent smaller than 0.074 mm.

MECHANICAL PROPERTIES OF ROCKS AT LOW TEMPERATURES

Malcolm Mellor

U.S. ARMY COLD REGIONS RESEARCH AND
ENGINEERING LABORATORY
Hanover, New Hampshire

INTRODUCTION

The effect of low temperature on mechanical properties of hard rocks has received relatively little attention, perhaps because the same kind of engineering techniques can be used on rock whether it is frozen or not. In engineering practice, however, there is evidence that rock becomes significantly stronger when it freezes; thus, a laboratory investigation of cold rock was undertaken.

Interest centered on deformation and fracture of intact rock specimens (the prime concern was excavating and drilling), but measurements were also made on fine-grained ice to provide input for possible future studies of jointed rock masses. Some thought was given to possible application of data to problems involving artificial or extraterrestrial cold environments (e.g., natural gas storage, lunar geology) and frost weathering of rocks, concrete, ceramics, etc.

EXPERIMENTAL MATERIALS

Rocks chosen for the study were Berea sandstone, Indiana limestone, and Barre granite. They are relatively uniform, with grain size small enough to ensure bulk homogeneity and representative behavior in small test specimens. They

are not very susceptible to inadvertent damage by experimental processing—e.g., by repeated wetting, drying, or freezing.

Mineralogical composition was analyzed by standard petrographic methods. Dry bulk density was determined precisely, and porosity was measured by three different methods. Pore-size distribution was estimated from high-pressure mercury intrusion, and specific surface area was measured by low-temperature gas adsorption. Thermal expansion was measured by optical extensometer and recording dilatometer, and values of thermal conductivity were taken from the literature. Failure stresses and quasi-elastic moduli were determined at room temperature from precise pseudo-static tests. Some results are summarized in Table I; complete experimental details and full results are recorded elsewhere.^{12,13} Test specimens were prepared by "clean" machining techniques.⁵

Work on ice is not reported here, but results can be found elsewhere.^{6,16,17}

PHASE COMPOSITION OF PORE WATER

Phase composition of pore water was investigated by differential thermal analysis, fluid expulsion or intrusion,

TABLE I General Properties of Test Materials

Property	Rock Type					
	Berea Sandstone		Indiana Limestone ^a		Barre Granite	
	Air-Dry	Water Saturated	Air-Dry	Water Saturated	Air-Dry	Water Saturated
Dry bulk density (g/cm ³ or Mg/m ³)	2.12		2.29		2.64	
Porosity (%)	19.8		14.1		0.69	
Water saturation	19.8		14.1		0.69	
Air pycnometer	20.6		15.0		1.20	
Mercury porosimeter	19.6				0.89	
Specific surface area (m ² /g)	1.25		0.654		0.105	
Adsorbed water content at equilibrium with 100% RH atmosphere (g water/g rock)	5 × 10 ⁻³		2 × 10 ⁻³		1.1 × 10 ⁻³	
	7 × 10 ⁻³		5 × 10 ⁻³		1.5 × 10 ⁻³	
Approx. linear expansion coeff. for air-dry rock between 10 and -50 °C (°C ⁻¹)	10 × 10 ⁻⁶		2 × 10 ⁻⁶		5 × 10 ⁻⁶	
Approx. thermal conductivity for air-dry rock [W/(m °C)]	2.4		1.8		2.8	
Approx. initial tangent modulus in uniaxial compression (23 °C, strain rate ≈ 6 × 10 ⁻⁵ s ⁻¹) (bar)	3.0 × 10 ⁴	1.0 × 10 ⁴	4.4 × 10 ⁴	2.1 × 10 ⁴	4.8 × 10 ⁵	3.5 × 10 ⁵
			2.50 × 10 ⁵	1.17 × 10 ⁵		
			2.97 × 10 ⁵			
Approx. initial tangent modulus in uniaxial tension ^b (23 °C, strain rate ≈ 10 ⁻⁵ s ⁻¹) (bar)	6.1 × 10 ⁴	2.5 × 10 ⁴	2.80 × 10 ⁵	2.7 × 10 ⁵	5.2 × 10 ⁵	3.8 × 10 ⁵
			3.9 × 10 ⁵			
Approx. tangent modulus at 50% of ultimate stress in uniaxial compression (23 °C, strain rate ≈ 6 × 10 ⁻⁵ s ⁻¹) (bar)	1.5 × 10 ⁵	1.2 × 10 ⁵	1.3 × 10 ⁵	0.95 × 10 ⁵	5.9 × 10 ⁵	4.9 × 10 ⁵
			2.46 × 10 ⁵	2.37 × 10 ⁵		
Approx. tangent modulus at 50% of ultimate stress in uniaxial tension (23 °C, strain rate ≈ 10 ⁻⁵ s ⁻¹) (bar)	1.6 × 10 ⁴	1.4 × 10 ⁴	3.0 × 10 ⁵	1.6 × 10 ⁵	3.5 × 10 ⁵	2.5 × 10 ⁵
Approx. uniaxial compressive strength (23 °C, strain rate ≈ 10 ⁻⁵ s ⁻¹) (bar)	580	470	430	330	2000	1700
	(⊥ to bedding)	(⊥ to bedding)				
Approx. uniaxial tensile strength (23 °C, strain rate ≈ 10 ⁻⁵ s ⁻¹) (bar)	12	9	59	42	135	108
	(⊥ to bedding)	(⊥ to bedding)				
	40	34				
	(to bedding)	(to bedding)				

^a Different types of this rock were tested.

^b Initial tangent moduli for tension and compression should be equal for a given strain rate.

electrical conductivity, thermal straining, and hydrostatic compression. Complete experimental details and full results have been reported by Mellor.¹²

Differential Thermal Analysis

Freezing characteristics of pore water were determined for each rock by finding the relationship between freezing point depression and total water content, which, for practical purposes, is interchangeable with the relation between unfrozen water content and temperature. Differential thermal analysis (DTA) was used; the test specimen and an inert reference were cooled at the same rate, while temperature difference between them was recorded alongside absolute specimen temperature. Phase change in the pore water pro-

duced abrupt perturbation of the temperature differential, and the resulting record gave initial nucleation temperature (supercooling), stable freezing temperature (freezing point depression), and a measure of the latent heat involved.

Freezing point depression increased as water content decreased from the saturation level, and, below a certain water content, there was no detectable evidence of abrupt phase change. Within the limits of experimental accuracy, this critical water content corresponded to that obtained by adsorption at equilibrium with a 100 percent relative humidity atmosphere, which is in agreement with previous findings by Dunn and Hudec.⁴ The relationship between freezing point depression and water content had the form of a rectangular hyperbola (Figure 1), and data plotted in logarithmic coordinates gave a straight line with a slope of -1.

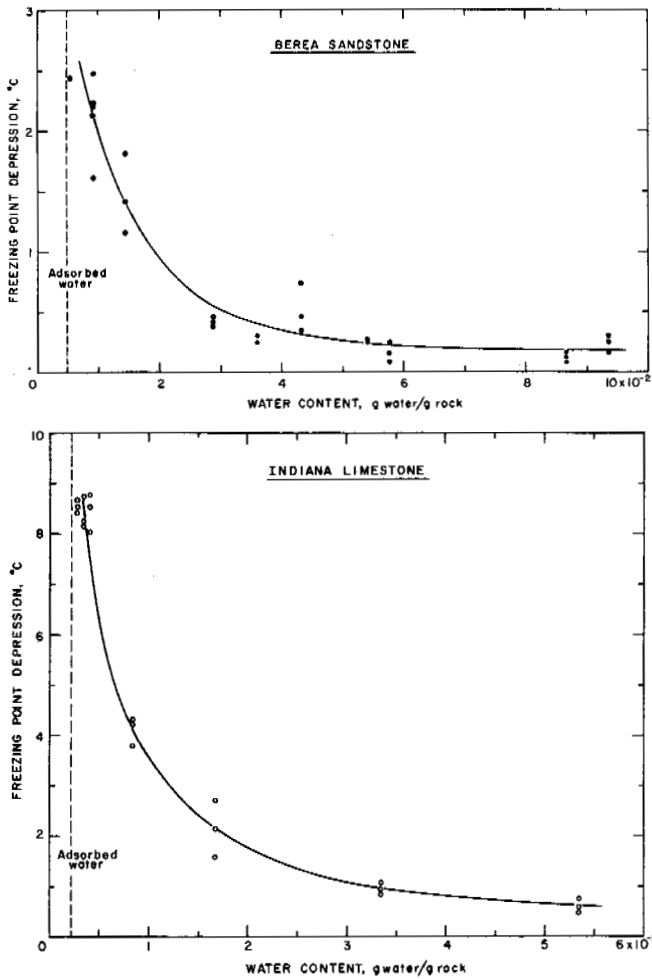


FIGURE 1 Freezing point depression as a function of water content for two rock types.

Latent heat for initial freezing was approximately proportional to water content above adsorption level, but there were no detectable exotherms at and below the adsorbed water content (Figure 2).

Maximum content of adsorbed water divided by specific surface area gave 4×10^{-3} g/m² for sandstone and limestone and 10×10^{-3} g/m² for granite. If this water were distributed uniformly over internal surfaces, there would be a layer about 14 molecules thick in sandstone and limestone and over 30 molecules thick in granite. These simple estimates of layer thickness are probably inflated by capillary condensation in small pores, which should be most noticeable in granite (cf. water and air porosity measurements in Table I).

The technique used for differential thermal analysis was awkward and inconvenient, especially for low porosity rocks, and there appear to be some drawbacks to an alternative technique used by Dunn and Hudec.³ Consequently, an attempt was made to find an easier way of estimating freezing characteristics by indirect methods.

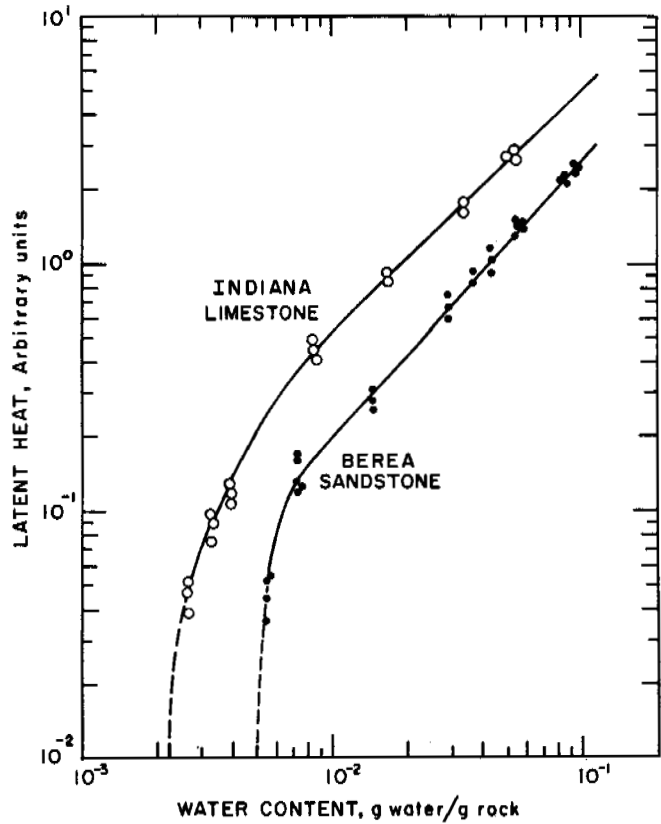


FIGURE 2 Latent heat as a function of water content for initial nucleation in two rock types.

Indirect Estimates of Freezing Characteristics

Keune and Hoekstra⁹ suggested that unfrozen water content of soils can be calculated from results of air-water penetration tests at room temperature, and they gave the relevant theory. The standard 15-bar pressure membrane apparatus, however, did not provide enough pressure to yield adequate results for rock, and agreement with DTA was rather poor. As an alternative, available results from high pressure (2 800-bar) mercury penetration measurements were used, making appropriate adjustments to the equations for surface tension and contact angle of mercury. Mercury penetration calculations appeared to give a good estimate of unfrozen water below about -1°C ; above this temperature, unfrozen water was underestimated by comparison with DTA, i.e., estimated values of freezing point depression were too small at high water contents.

Anderson and Tice¹ measured freezing characteristics of various powders—chiefly soils—and related unfrozen water to temperature by a simple power function. They correlated the two parameters of the power function to surface area by linear regression and thus derived an empirical predictive equation for freezing characteristics. Using measured values of surface areas for the three rocks, freezing characteristics

were calculated from this equation; for temperatures below -1°C , the calculated amount of unfrozen water was too small in all cases.

Electrical Conductivity

To explore unfrozen water content at very low temperatures, electrical conductivity was measured as a function of temperature at a frequency of 10^4 Hz for both dry specimens and specimens flushed and saturated with distilled water. Results are summarized in Figure 3. Above 0°C , conductivity was much higher for wet rocks than for dry rocks—by almost five orders of magnitude for sandstone and limestone and more than three orders of magnitude for granite (it was, however, considerably lower than conductivity predicted by Archie's law using constants given by Keller⁸). As pore water first froze, conductivity of wet rock dropped abruptly by a factor of approximately 20 in sandstone and limestone and 4 in Barre granite. After initial freezing, the conductivity of wet rock was still much higher than that of dry rock—by more than three orders of magnitude in sandstone and limestone and more than two orders of magnitude in granite. As temperature was lowered further, conductivity of both wet and dry rock decreased, but the curves converged so that at -195°C conductivity was the same for both wet and dry rock in granite and limestone (in sandstone, conductivity had dropped below the limit of resolution at this temperature). The low-temperature limit of conductivity for granite and limestone had almost been reached at about -100°C . At -55 to -60°C the curves have a "knee," which is most strongly marked for the dry specimens (this feature shows best when logarithm of conductivity is plotted against reciprocal of absolute temperature).

With only single frequency measurements of conductivity, it may be unwise to attach much significance to detailed shapes of the curves, but it is likely that the broad trend indicates the extent, continuity, and activity of the interfacial water film. Keller⁸ suggested that progressive freezing of pore water down to -60°C represents a reduction of conduction path, and, if changes in pore water salinity (which enters Archie's law only as a first power) are neglected, then the conductivity ratio for two different temperatures is approximately equal to the square of the ratio of unfrozen water contents. For initial freezing of sandstone, limestone, and granite, this assumption appears to hold quite well, when conductivity changes are compared with unfrozen water contents given by DTA. It also could be reasonable at -60°C , when temperature dependence of conductivity in unfrozen water is accounted for.

Thermal Strain

Thermal expansion was measured with an optical extensometer between 15 and -50°C and with a sensitive recording

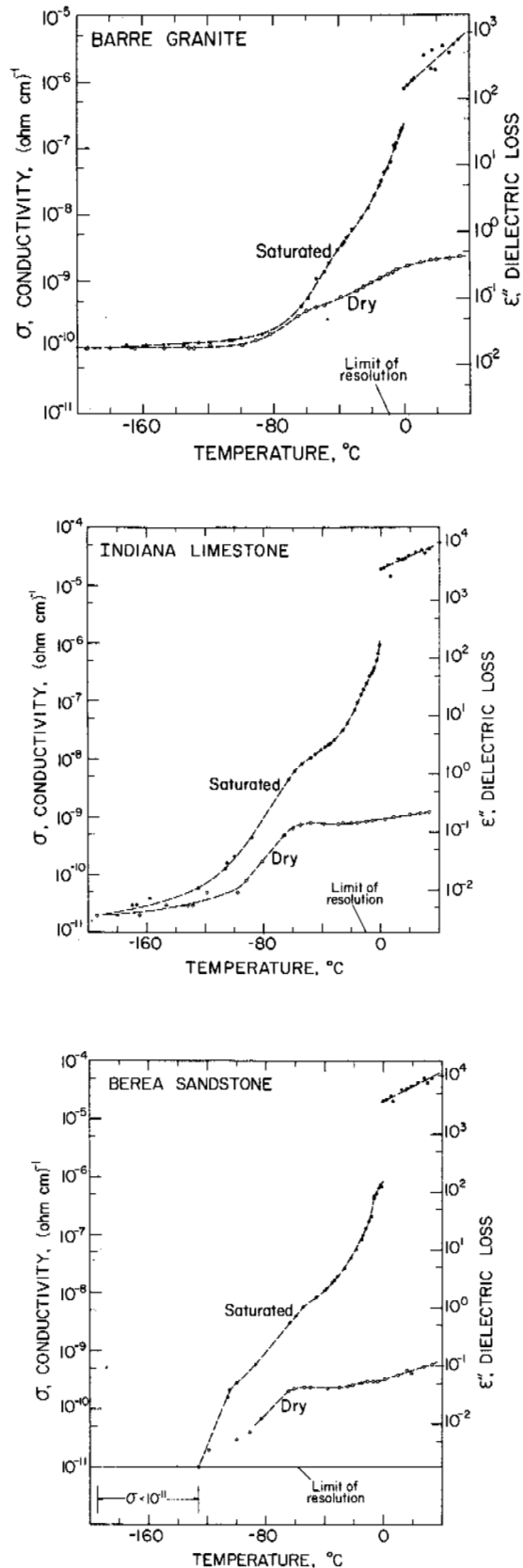


FIGURE 3 Electrical conductivity as a function of temperature for three rock types.

dilatometer down to -195°C . There were sharp discontinuities in thermal strain as pore water froze in wet rock, abrupt expansion and contraction being associated with freezing and thawing, respectively. The "freezing step" for moderately rapid cooling occurred at lower measured temperature than the "thawing step" for moderately rapid warming, and it was more abrupt. Magnitude of strain discontinuity increased with absolute water content of the rock, and it was greater for rapid freezing than for slow freezing (when water could be redistributed or extruded). Strain anomalies that were probably due to progressive change in unfrozen water content were detectable down to about -20°C .

Potential volumetric freezing strain for complete freezing of saturated rock in a closed system (ϵ_{pv}) can be expressed:

$$\epsilon_{pv} = 0.09 n / [1 + (K_I/K_R) n], \quad (1)$$

where n is porosity, and K_I and K_R are bulk moduli for ice in compression and rock in tension. The effect of elastic constraint is small in most cases, especially when the rock is not completely saturated, so that *potential* volumetric freezing strain for unsaturated ϵ'_{pv} can be written as:

$$\epsilon'_{pv} = 1.09 w \gamma_R - n, \quad (2)$$

where w is water content, γ_R is dry bulk density, and it is assumed that water can redistribute during freezing to fully utilize pore space. With this last assumption, freezing strain ought to reduce to zero when water content is $(n/1.09\gamma_R)$.

Maximum measured values of freezing strain for sandstone and limestone were almost an order of magnitude lower than ϵ_{pv} , but they were close to the tensile failure strains measured in direct mechanical tests. For granite, maximum measured values were about 70 percent of ϵ_{pv} and about 25 percent of tensile failure strain. Although freezing strain did decrease with water content, significant strains occurred at water contents lower than $(n/1.09\gamma_R)$, indicating that pore space could not be fully utilized.

Coefficient of expansion between -15 and -90°C tended to increase with water content, and it was higher for rapidly frozen rock than for slowly frozen rock. This is perhaps due to the large difference of expansion coefficients for dry rock (see Table I) and ice (linear coefficient $\approx 5 \times 10^{-5} \text{ }^{\circ}\text{C}^{-1}$).

Isothermal Hydrostatic Compression

When rock with ice-filled pores is subjected to high pressure, its pressure-volume curve ought to exhibit strain discontinuities at the points where ice undergoes high-pressure phase transformations to polymorphs of different density. To verify this experimentally, frozen specimens of water-saturated rock were encapsulated in lead and compressed

slowly to 27 kbar at -10°C , using a high-pressure die. For Berea sandstone, which had relatively high ice content, there were step discontinuities in the pressure-volume curve that appeared to correspond to successive phase changes between Ice I, water, Ice IV-V, and Ice VI; change of slope occurred at the pressure where Ice VI transforms to Ice VIII. Strain discontinuities were of the expected magnitude for ice transitions.

Compressibility of rock can be predicted with reasonable accuracy by application of Voigt-Reuss-Hill averaging methods, when individual compressibilities are known for the constituent minerals. It seems likely that effects of compressibility in pore ice can be dealt with in a similar way.

STRENGTH AND DEFORMABILITY OF COLD ROCKS

Strength was measured in tension and compression from 23 to -195°C , and deformation was measured under short-duration uniaxial compression from 23 to -60°C . Each rock type was tested "air-dry" (maximum adsorbed water content; see Table I) and "ice-saturated" (maximum water content for the frozen state: 8.6×10^{-2} , 4.9×10^{-2} , 2.4×10^{-3} for sandstone, limestone, and granite, respectively). Test techniques are described elsewhere,^{5,15} Experimental details and full results for the low-temperature work are given by Mellor.¹³

Strength as a Function of Temperature and Water Content

Results of uniaxial compression tests and Brazil tensile tests are summarized in Figures 4, 5, and 6. For all *air-dry rocks*, both compressive strength and tensile strength increased gradually, but not linearly, as temperature decreased from 23 to -195°C . Average rate was approximately $2 \times 10^{-1} \text{ }^{\circ}\text{C}^{-1}$, i.e., ≈ 0.2 percent/ $^{\circ}\text{C}$ (actual rates are given in Table II). Above-average rates appeared to prevail between 0 and -80°C . For all *saturated rocks* there were large increases in compressive and tensile strength as temperature dropped below 0°C , with abrupt increase on initial freezing of pore water and further substantial gain down to about -70°C . Maximum strength for saturated rock was reached at about -120°C , with some indication of slight decrease on further cooling to -195°C .

Strength was measured as a function of *water content* at 23 and -25°C . At 23°C , strength was highest at "zero" water content, and it decreased rapidly as water content increased to the maximum adsorbed amount, finally tending asymptotically to a limit as saturation was approached. (Table III) Normalized data are shown in Figure 7, where all results define a single curve. It appears that strength becomes highly sensitive to water content when the average thickness of the adsorbed layer drops below about 10 molecules. At

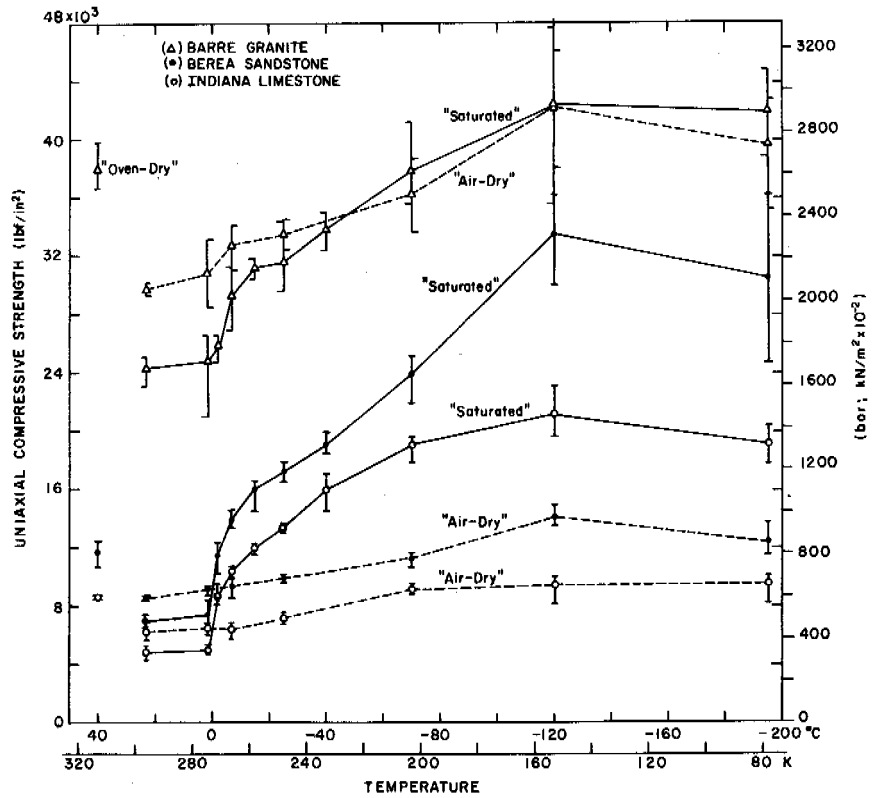


FIGURE 4 Uniaxial compressive strength as a function of temperature for three types of rock in air-dry and water-saturated conditions.

–25 °C, there was decrease in strength with increasing water content at very small water contents, but this trend reversed before maximum adsorbed water content was reached, and highest strength values were measured at saturation in sandstone and limestone. At very low water contents, strength at –25 °C was only slightly higher than at 23 °C. The strength for zero water content at temperatures above 0 °C was similar to the strength of air-dry rock at very low temperatures (see Figure 4).

Deformability as a Function of Temperature and Water Content

Stress-strain curves for air-dry and saturated rocks were recorded at temperatures ranging from 23 to –60 °C. *Initial tangent modulus of air-dry rock* tended to increase slightly with decreasing temperature at about $4 \times 10^{-3} \text{ }^\circ\text{C}^{-1}$ (i.e., 0.4 percent/°C) for sandstone and limestone, with negligible change for granite. For *air-dry rock*, *tangent modulus* at 50 percent of ultimate stress increased with decreasing temperature at rates of approximately 3×10^{-3} , 2×10^{-3} , and $5 \times 10^{-4} \text{ }^\circ\text{C}^{-1}$ for sandstone, limestone, and granite, respectively. For *saturated rocks*, the shape of the stress-strain curve was completely altered by freezing: Initial positive curvature (which is typical for porous unfrozen rocks) disappeared when pores were plugged with ice. Consequently, there was a great increase of initial tangent modu-

lus after freezing. As temperature dropped below 0 °C, stress-strain curves for wet rock became steeper, tangent modulus at 50 percent of ultimate stress increased, and for the high porosity rocks the failure strain increased.

SUMMARY

Pore water in typical rock freezes progressively, and for each rock type there is a characteristic relation between unfrozen water content and temperature, which depends to a large degree on surface area. Freezing characteristics for most rocks can probably be estimated to an acceptable degree of accuracy from fairly simple laboratory tests.

A certain amount of water, corresponding closely to the maximum adsorbed water content, remains unfrozen at temperatures of –10 °C and lower. Changes in electrical conductivity suggest that thickness, continuity and mobility of interfacial water decrease with decreasing temperature down to approximately –125 °C.

Rapid initial freezing of pore water in saturated rock can cause abrupt volumetric expansion of the rock, with strains that approach the tensile failure strain and that certainly exceed the strain where internal microcracking begins in tensile tests. These results give quantitative support to traditional ideas on frost weathering.

After initial freezing of pore water, the residual unfrozen water is free to migrate under potential gradients, but it

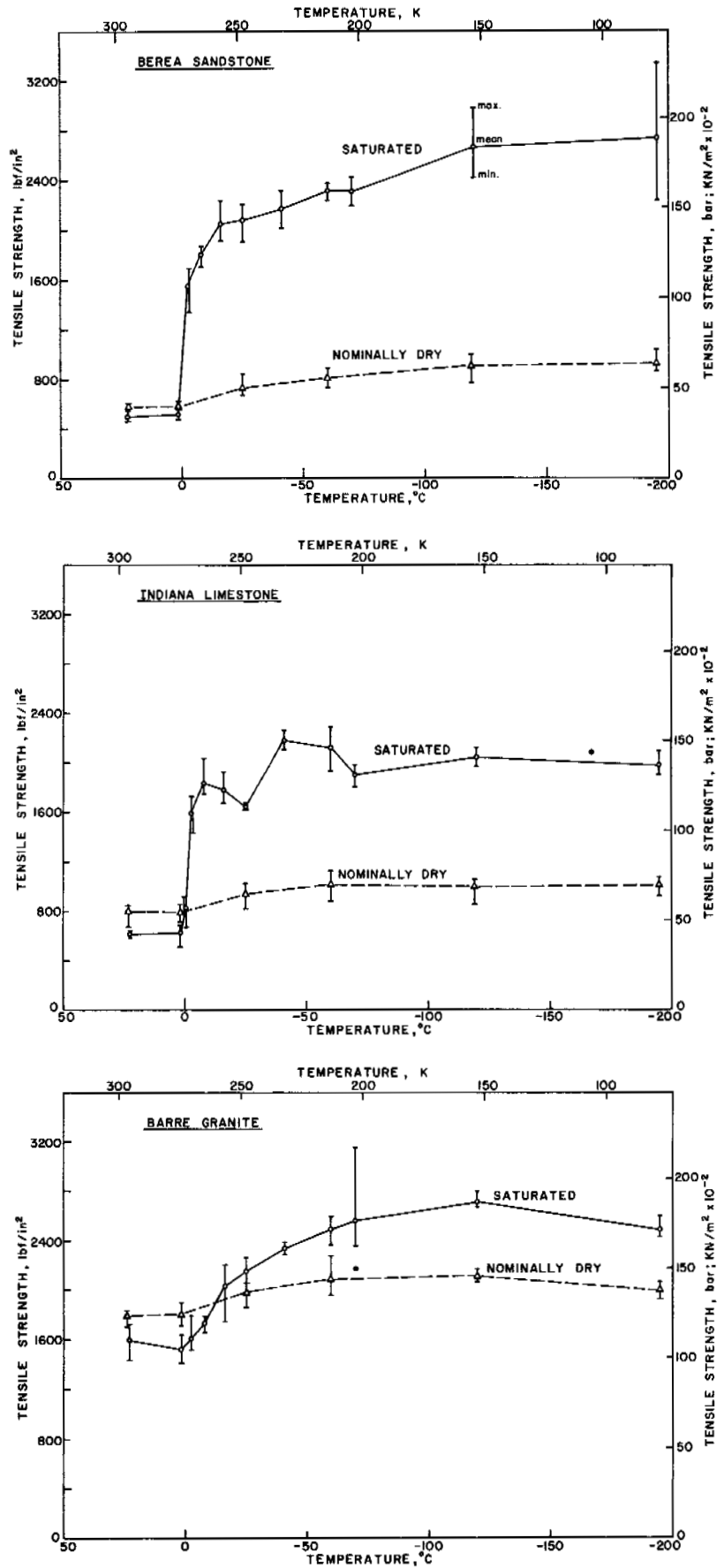


FIGURE 5 Tensile strength as a function of temperature for three types of rock in air-dry and water-saturated conditions.

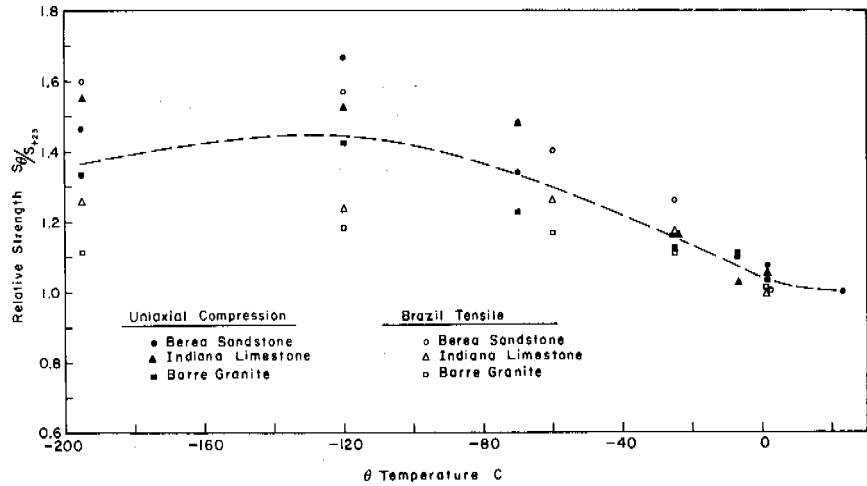


FIGURE 6 Relative strength as a function of temperature for air-dry rocks. Strength is normalized with respect to the strength at 23 °C.

will freeze (and expand) if it migrates into large cracks or cavities. Tests on Rochester shale (a frost-sensitive rock from Niagara Falls) indicated that 90 percent of the total possible water content is virtually unfreezable at typical winter ground temperatures.

When cold rock is subjected to high hydrostatic pressure, ice contained in its pores will undergo phase transformation to polymorphs of higher density. If the ice content is relatively high, this will produce significant strain discontinuities in the compressibility curve.

Dry rocks gain strength at an average rate of approximately $2 \times 10^{-3} \text{ }^\circ\text{C}^{-1}$ when cooled from 23 to -155 or -195 °C, almost irrespective of rock type (Table II). It seems unlikely that an effect of this magnitude is caused by direct thermal strain or by thermally activated diffusion processes in the bulk rock material.¹³ Since strength is

highly sensitive to adsorbed water content at 23 °C and since temperature sensitivity appears greatest between 0 and -80 °C, it seems likely that low-temperature strength is affected significantly by freezing, or ordering, of adsorbed water. In tests at 23 °C, oven-dry rock is 35–40 percent stronger than air-dry rock containing maximum adsorbed water (Figure 7); when air-dry rock with maximum adsorbed water is cooled, strength below -70 °C is 35–40 percent higher than strength at 23 °C (Figures 4, 5, and 6). In other words, oven-drying and cooling to below -70 °C have roughly the same effect on the strength of air-dry rock, which is perhaps not too surprising in view of the physical similarity of the two processes in reducing the effective thickness of the interfacial water film. In fact, temperature coefficients close to the observed values can be calculated from Figure 7 if it is assumed that effective water content

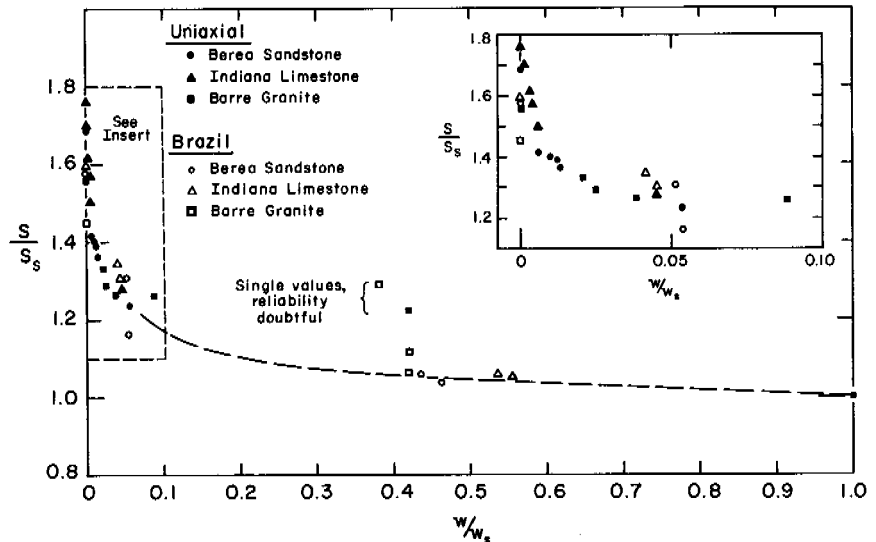


FIGURE 7 Relative strength as a function of water content at 23 °C. Strength is normalized with respect to strength for saturation water content, while water content is normalized with respect to saturation water content.

TABLE II Variation of Strength with Temperature for Nominally Dry Rocks

Rock Type	Condition (Approx. water contents in g water/g rock)	Temp Range (°C)	Type of Test	Temp Coeff ^a (%/°C)	Reference
Berea sandstone	100% RH ($\sim 5 \times 10^{-3}$)	23 to -195	Uniax. comp	0.24	Mellor ¹³
Indiana limestone	100% RH ($\sim 2 \times 10^{-3}$)	23 to -195	Uniax comp	0.24	Mellor ¹³
Barre granite	100% RH ($\sim 10^{-3}$)	23 to -195	Uniax comp	0.19	Mellor ¹³
Berea sandstone	Air-dry ($\sim 10^{-3}$)	23 to -195	Brazil	0.24	Mellor ¹³
Indiana limestone	Air-dry ($\sim 2 \times 10^{-4}$)	23 to -195	Brazil	0.15	Mellor ¹³
Barre granite	Air-dry ($\sim 3 \times 10^{-4}$)	23 to -195	Brazil	0.09	Mellor ¹³
Tholeiitic basalt	Dry ($\sim 10^{-6}$)	22 to -157	Uniax comp	0.17	Podnieks, Chamberlain, and Thill ²⁰
Tholeiitic basalt	50% RH ($\sim 5 \times 10^{-4}$)	22 to -157	Uniax comp	0.20	Podnieks, Chamberlain, and Thill ²⁰
Indiana (Salem) limestone	Dry ($\sim 10^{-6}$)	22 to -157	Uniax comp	0.26	Podnieks, Chamberlain, and Thill ²⁰
	50% RH ($\sim 10^{-5}$)	22 to -157	Uniax comp	0.30	Podnieks, Chamberlain, and Thill ²⁰
St. Cloud gray granodiorite	Dry ($\sim 5 \times 10^{-7}$)	22 to -157	Uniax comp	0.24	Podnieks, Chamberlain, and Thill ²⁰
	50% RH ($\sim 5 \times 10^{-5}$)	22 to -157	Uniax comp	0.20	Podnieks, Chamberlain, and Thill ²⁰
Devil's Hill dacite	Dry ($\sim 10^{-6}$)	22 to -157	Uniax comp	0.05	Podnieks, Chamberlain, and Thill ²⁰
	50% RH ($\sim 5 \times 10^{-4}$)	22 to -157	Uniax comp	0.28	Podnieks, Chamberlain, and Thill ²⁰
Basalt	?	23 to -196	Uniax comp	0.22	Kumar ¹¹
Granite	?	23 to -196	Uniax comp	0.20	Kumar ¹¹
Limestone	Dry	24 to -195	3-point bending	0.22	Heins and Friz ⁷
Basalt	Dry	24 to -195	3-point bending	0.18	Heins and Friz ⁷
Granite	Dry	24 to -195	3-point bending	0.08	Heins and Friz ⁷
Limestone	Dry	24 to -195	Point-breaking	0.17	Heins and Friz ⁷
Basalt	Dry	24 to -195	Point-breaking	0.19	Heins and Friz ⁷
Granite	Dry	24 to -195	Point-breaking	0.08	Heins and Friz ⁷
Concrete	Dry (oven-dried and 50% RH)	24 to -101	Uniax comp and Brazil	≈ 0.15	Monfore and Lentz ¹⁸
Fused silica		25 to -195	Uniax comp	0.15	Charles ²
Granite		25 to -195	Uniax comp	0.21	Charles ²
Albite	Vapor saturated at 25 °C, immersed in liquid nitrogen at -195 °C	25 to -195	Uniax comp	0.16	Charles ²
Spodumene		25 to -195	Uniax comp	0.38	Charles ²
Hornblende		25 to -195	Uniax comp	0.29	Charles ²
Brazilian quartz		25 to -195	Uniax comp	0.20	Charles ²
MgO crystals		25 to -195	Uniax comp	0.18	Charles ²
Sapphire		25 to -195	Bending	0.15	Charles ²
Berea sandstone		Air-dry ($\sim 10^{-3}$)	23 to -60	Ring	0.31
Indiana limestone	Air-dry ($\sim 2 \times 10^{-4}$)	23 to -60	Ring	0.31	Mellor ¹³
Borosilicate glass	? (abraded surface)	23 to -196	2-point bending 55 bars/s	0.15	Kropschot and Mikesell ¹⁰
	? (abraded surface)	23 to -196	2-point bending 0.69 bar/s	0.28	Kropschot and Mikesell ¹⁰
	? (abraded surface)	23 to -196	2-point bending 0.069 bar/s	0.32	Kropschot and Mikesell ¹⁰
	? (polished surface)	23 to -196	2-point bending 55 bars/s	0.24	Kropschot and Mikesell ¹⁰
Porphyritic tonalite	? (Believed air-dry)	25 to -191	Uniax comp 10^{-4} s^{-1}	0.27	Perkins and Green ¹⁹
	? (Believed air-dry)	25 to -191	Uniax comp 10^{-1} s^{-1}	0.26	Perkins and Green ¹⁹
	? (Believed air-dry)	25 to -191	Hopkinson split- bar $1.5 \times 10^3 \text{ s}^{-1}$	0.18	Perkins and Green ¹⁹

$$^a \text{ Temperature coefficient} = \frac{(\text{strength change}) \times 100}{(\text{Mean strength for temp range}) \times (\text{temp difference})} \% / ^\circ \text{C}.$$

TABLE III Relative Values^a of Strength and Modulus for Saturated and Air-Dry Specimens at 23 °C

Property	Rock Type		
	Berea Sandstone	Indiana Limestone	Barre Granite
Uniaxial compressive strength	0.81 (0.59) ^b	0.78 (0.57)	0.83 (0.64)
Uniaxial tensile strength	0.72	0.71	0.80
Brazil tensile strength	0.86 (0.64)	0.73 (0.63)	0.83 (0.69)
Initial tangent modulus in uniaxial compression	0.33	0.48	0.73
Tangent modulus at 50% stress in uniaxial compression	0.78	0.75	0.84
Initial tangent modulus in uniaxial tension	0.40	0.68	0.73
Tangent modulus at 50% stress in uniaxial tension	0.87	0.52	0.74

^a Figures give value for saturated rock divided by corresponding value for air-dry rock.

^b Values in parentheses give ratio of saturated strength to oven-dry strength.

is reduced to the equivalent of a monomolecular layer by cooling to -80°C .

The mechanism by which adsorbed water alters strength (a special case of the Rehbinder effect) is not well understood. Two likely possibilities are stress corrosion, which is thought to account for static fatigue in glass, and the Orowan mechanism of interfacial free energy modification during crack growth.

Temperature coefficients for quasi-elastic moduli of air-dry rocks are roughly the same as those for strength. Moduli are sensitive to water content at 23°C , but present data are insufficient for a quantitative comparison with temperature sensitivity.

Initial freezing of pore water in saturated rock brings abrupt increase of tensile and compressive strength and great increase of initial tangent modulus; these effects clearly are due to plugging of pores with ice. In simple Griffith theory, strength is controlled by the largest "cracks," or defect structures, and strength is inversely proportional to the square root of maximum crack size. If controlling defects are identified with the largest unplugged pores, strength variation with temperature can be related to pore-size distribution and freezing characteristics; simple calculations indicate that this approach may not be too unrealistic.¹³ Strength continues to increase after initial freezing, making substantial gains down to about -70°C and reaching maximum values at about -120°C —a trend that can be correlated, to some extent, to changes in unfrozen water content. Tangent modulus at 50 percent stress increases as temperature decreases to -60°C , perhaps be-

cause the effective modulus of ice in the pores is increasing. The apparent small drop in strength between -120 and -195°C needs further checking, but such a drop could be caused by opening of microcracks as ice shrinks away from the rock (expansion coefficient for ice is an order of magnitude higher than for typical rock-forming silicates).

Freezing or thawing of saturated high porosity rock is probably an important engineering factor since strength and deformability can change so drastically. Specific energy for many breaking and excavating processes, including blasting, is likely to be proportional to material strength,²⁰ and stability of slopes and tunnels is heavily dependent on strength and deformability.

ACKNOWLEDGMENTS

This paper presents the results of research performed by the Cold Regions Research and Engineering Laboratory under the sponsorship of the U.S. Army Corps of Engineers and the Army Materiel Command.

REFERENCES

- Anderson, D. M., and A. R. Tice. 1972. Predicting unfrozen water contents in frozen soils from surface area measurements. Highway Research Record, No. 393. (Presented at 51st Annual Meeting of Highway Research Board, January 1972)
- Charles, R. J. 1959. The strength of silicate glasses and some crystalline oxides, p. 225-249. B. L. Auerbach, *et al.* [ed.] Fracture. John Wiley/Chapman and Hall, New York.
- Dunn, J. R., and P. P. Hudec. 1965. Quantitative cold differential thermal analysis. Contribution 65-7. Department of Geology, Rensselaer Polytechnic Institute, Troy, New York. (New York State Department of Public Works, Physical Research Report)
- Dunn, J. R., and P. P. Hudec. 1965. The influence of clays on water and ice in rock pores (Part II). Contribution 65-8. Department of Geology, Rensselaer Polytechnic Institute, Troy, New York. (New York State Department of Public Works, Physical Research Report 65-5)
- Hawkes, I., and M. Mellor. 1970. Uniaxial testing in rock mechanics laboratories. *Eng. Geol.* 4(3):117-288.
- Hawkes, I., and M. Mellor. 1972. Deformation and fracture of ice under uniaxial stress. *J. Glaciol.* 11(61):103-131.
- Heins, R. W., and T. O. Friz. 1967. The effect of low temperature on some physical properties of rock. Paper No. SPE 1714. Society of Petroleum Engineers, American Institute of Mineralogy, Metallurgy, and Petroleum Engineers.
- Keller, G. V. 1967. Supplementary guide to the literature on electrical properties of rocks and minerals, p. 265-308. *In* E. I. Parkhomenko [ed.] Plenum Press, New York. (Translated from Russian by G. V. Keller; originally published by Nauka Press, Moscow, for O. Yu. Schmidt Institute of Physics of the Earth of the Academy of Sciences of the USSR)
- Keune, R., and P. Hoekstra. 1967. Calculating the amount of unfrozen water in frozen ground from moisture characteristic curves. CRREL Special Report 114. U.S. Army Cold Regions Research and Engineering Laboratory, Hanover, New Hampshire.
- Kropschot, R. H., and R. P. Mikesell. 1957. Strength and fatigue of glass at very low temperatures. *J. Appl. Phys.* 28(5):610-614.
- Kumar, A. 1968. The effect of stress rate and temperature on the strength of basalt and granite. *Geophysics* 33(3):501-510.

12. Mellor, M. 1970. Phase composition of pore water in cold rocks. CRREL Research Report 292. U.S. Army Cold Regions Research Engineering Laboratory, Hanover, New Hampshire.
13. Mellor, M. 1971. Strength and deformability of rocks at low temperatures. CRREL Research Report 294. U.S. Army Cold Regions Research and Engineering Laboratory. Hanover, New Hampshire.
14. Mellor, M. 1972. Normalization of specific energy values. Int. J. Rock Mech. Min. Sci. 9:661-663.
15. Mellor, M., and I. Hawkes. 1971. Measurement of tensile strength by diametral compression of discs and annuli. Eng. Geol. 5: 173-225.
16. Mellor, M., and R. Testa. 1969. Effect of temperature on the creep of ice. J. Glaciol. 8(52):131-145.
17. Mellor, M., and R. Testa. 1969. Creep of ice at low stress. J. Glaciol. 8(52):147-152.
18. Monfore, G. E., and A. E. Lentz. 1962. Physical properties of concrete at very low temperatures. J. Portland Cem. Assoc. Res. Devel. Lab. May:33-39.
19. Perkins, R. D., and S. J. Green. 1969. Uniaxial stress behavior of porphyritic tonalite at strain rates to 10^3 /second. Materials and Structures Laboratory, MSL-68-42. Manufacturing Development, General Motors Corp., for Defense Atomic Support Agency, Washington, D.C. (DASA-2200).
20. Podnieks, E. R., P. G. Chamberlain, and R. E. Thill. 1969. Environmental effects on rock properties. Paper presented at 10th symposium of rock mechanics, University of Texas, Austin, May 1968.

SOIL FREEZING IN RELATION TO PORE WATER PRESSURE AND TEMPERATURE [1]

Robert D. Miller

CORNELL UNIVERSITY
Ithaca, New York

INTRODUCTION

An analysis of freezing of saturated soils was presented at the First International Conference on Permafrost.⁶ That analysis sought to show that standard data for the drying and wetting of certain soils (the soil water characteristic curves that show water content as a function of pore water pressure) can be used to predict unfrozen water content of those same soils as a function of temperature and pore pressure (the soil freezing characteristic curves). For such predictions to be quantitative, however, it was asserted that the soil must be either essentially devoid of colloidal particles (SS soil) or entirely dominated by colloidal material (SLS soil). One rule was used for predicting unfrozen water content of SS soil; a different rule was used for SLS soil. According to that analysis, therefore, no general rule for intermediate soils (SSLS) would yield quantitative relationships between the soil water characteristic curves and soil freezing characteristic curves.

Subsequently, the predictive rules set forth in the paper mentioned were tested and confirmed in our laboratory for the range 0 to -0.2°C ⁵ (Figures 1 and 2). Ice pressure was computed from temperature and pore water pressure using the generalized Clapeyron equation:

$$\bar{V}_2(u_2 - \Pi) - \bar{V}_1 u_1 = (\Delta H/K)t, \quad (1)$$

where \bar{V}_2 is the partial molal volume of water; \bar{V}_1 is the partial molal volume of ice; ΔH is the heat of phase transition; K and t are the temperature in Kelvins and $^\circ\text{C}$, respectively; u_2 is the pore water (gage) pressure as measured (or controlled) by a tensiometer; Π is the osmotic pressure of the

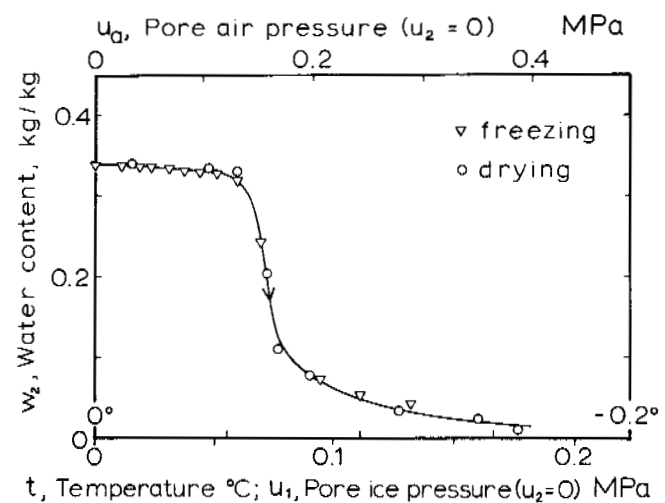


FIGURE 1 Freezing and drying characteristic data for a colloid-free soil (particle diameters, 4-8 μm) from Koopmans and Miller.⁵ Note that air pressure and ice pressure scales differ by a factor (ω_{a2}/ω_{i2}) = 2.20.

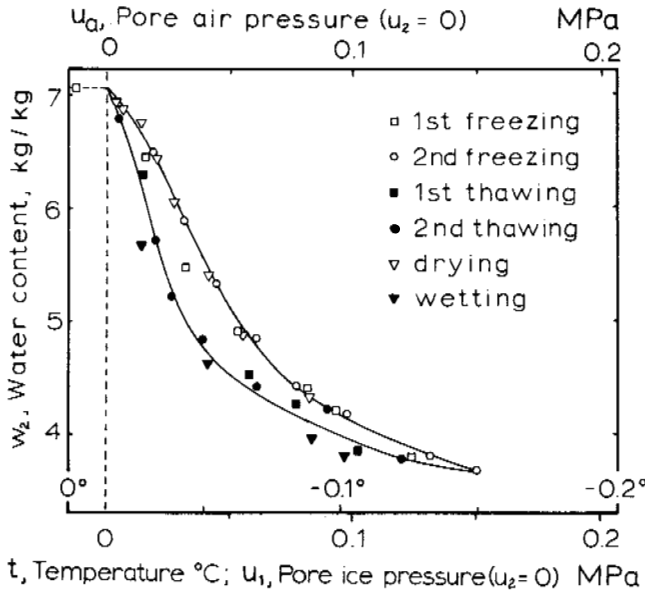


FIGURE 2 Freezing and thawing, wetting and drying data for colloidal soil (Na-saturated montmorillonite) from Koopmans and Miller.⁵ Note that air pressure scales are identical.

pore water due to free solutes, arising mainly from hydrolysis of the homoionic montmorillonite used; and u_1 is the ice (gauge) pressure.

For fractionated silt, the respective characteristic curves superimpose when $[u_a - u_2] = (\omega_{a2}/\omega_{i2}) [u_1 - (u_2 - \Pi)]$, where $(\omega_{a2})_{20^\circ\text{C}}/(\omega_{i2})_0^\circ\text{C}$ (the ratio of the surface tensions of air-water and ice-water interfaces) was found to be 2.20 ± 0.04 , i.e., in the same ratio as (72.1:33.1). On the other hand, the respective curves superimpose for the montmorillonite clay when $[u_a - u_2] = [u_1 - (u_2 - \Pi)]$.

The results obtained in studies of saturated soil demonstrated that an ice-water interface in ss soil behaved in a manner analogous to the behavior of an air-water interface in the same soil. This invites an attempt to extend the analysis of the freezing of unsaturated ss soils, where a third interface—the air-ice interface—must be considered. A preliminary and qualitative analysis of this problem was presented recently.⁷ A quantitative analysis of freezing of an unsaturated soil of very simple geometry was undertaken in order to establish a vision of the stages of progressive freezing in real soils of complex geometry. This exercise is instructive because it explains the special features that have been observed experimentally⁴ and that Globus and Nerpin^{1,2} sought to explain qualitatively. Specifically, it provides a detailed rationale for the fact that, when moist soil freezes, profound changes in the water content occur: Water moves from unfrozen to frozen soil, whereby the pores of the frozen zone become saturated and adjacent ice-free soil is desiccated. This mechanism differs from that of Globus and Nerpin in the statement of cause and effect.

In this analysis, we employ the common presumption that, under the circumstances of interest, an adsorbed film of mobile water covers the surface of a mineral particle. This film exists between the mineral particle and air or ice with which the particle is in contact (Figure 3).

The film will be thin, of the order of tens of angstrom units. Where two particles touch, whether mineral-ice or mineral-mineral contacts, there will be additional "capillary" water present, essentially unaffected by adsorption forces associated with the film, and the shape of the air-water interface will be governed by the Kelvin equation:

$$u_a - u_2 = 2\omega_{a2}/r_{a2} \tag{2a}$$

If one of the particles is ice, the ice-water interface will alter its shape by melting or freezing to achieve an equilibrium interface, and this interface also will obey the Kelvin equation:

$$u_1 - u_2 = 2\omega_{i2}/r_{i2} \tag{2b}$$

It is assumed that the air-ice interface changes its shape through sublimation, condensation, or surface migration; at equilibrium, this interface also obeys the Kelvin equation:

$$u_a - u_1 = 2\omega_{a1}/r_{a1} \tag{2c}$$

This assumption is consistent with the observed granulation that occurs in snow at temperatures near the freezing point. In these equations ω represents the surface tension of the

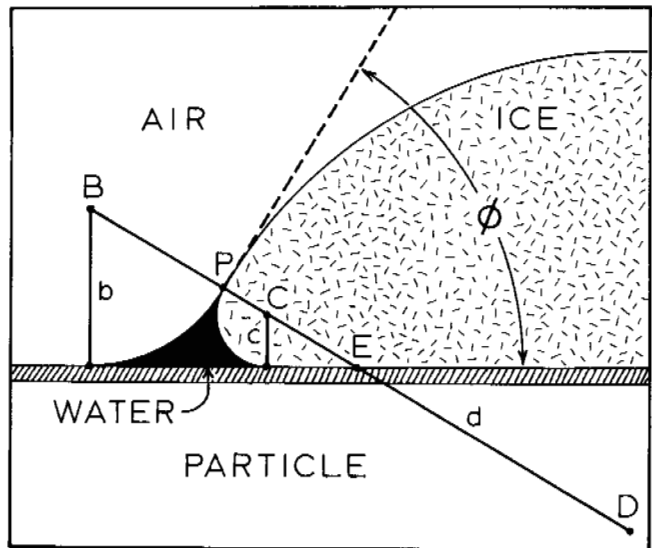


FIGURE 3 An equilibrium configuration of two-dimensional air-ice, air-water, and ice-water interfaces at the surface of a flat mineral particle having an adsorbed film. Constructed with $b:c:d = 1:0.296:3$, the resultant apparent angle of intersection ϕ is 57.1° .

appropriate interface and $1/\bar{r}$ is the mean curvature of the interface. Variations in ω associated with crystallographic orientation of the surface are neglected.

Finally, assume that these interfaces are mutually tangent at points where they converge. If this is true, it follows that

$$\omega_{a1} = \omega_{a2} + \omega_{12}. \quad (3)$$

The remainder of this paper derives from Eq. (1), (2), and (3).

APPARENT CONTACT ANGLE OF THE AIR-ICE INTERFACE

To simplify the analysis that follows, we will confine our attention to systems that can be fully diagrammed in only two dimensions and imagine that the cross sections shown in accompanying diagrams may be projected without change in directions perpendicular to the page.

Figure 3 represents the junction of air-ice, air-water, and ice-water interfaces at the surface of a flat particle having an adsorbed film of water. The three interfaces meet at point P and are mutually tangent at that point. The air-water interface and the ice-water interface are taken to be circular in cross section and tangent to the adsorbed film, which is shown as if it were a distinct entity.

For the two-dimensional surfaces involved, the kelvin equations become, if the air phase remains at atmospheric pressure ($u_a = 0$),

$$u_2 = -\omega_{a2}/b \quad (4a)$$

$$u_1 - u_2 = \omega_{12}/c \quad (4b)$$

$$u_1 = \omega_{a1}/d \quad (4c)$$

Since the three radii of curvature ($b = \overline{BP}$, $c = \overline{CP}$, $d = \overline{DP}$) are all perpendicular to the respective surfaces at their point of mutual tangency (P), the three centers of curvature (B , C , and D) lie on the same straight line \overline{BD} .

An expression for the apparent angle of intersection (ϕ) between the air-ice interface and the particle surface can be found. Observe that

$$\cos\phi = \frac{b}{b+c+CE} = \frac{c}{CE}. \quad (5a)$$

We find, by eliminating \overline{CE} , that

$$\phi = \cos^{-1} \left[\frac{b-c}{b+c} \right]. \quad (5b)$$

With appropriate substitutions involving Eq. (1), (3), and (4), various alternate expressions for ϕ may be obtained, including

$$\phi = \cos^{-1} \left[\frac{(\Delta H/K)t - (\bar{V}_2 + 1 - \omega_{12}/\omega_{a2})u_2}{(\Delta H/K)t - (\bar{V}_2 + 1 + \omega_{12}/\omega_{a2})u_2} \right], \quad (5c)$$

which gives ϕ as a function of t and u_2 . If u_2 is held constant, decreasing t causes u_1 to increase [Eq. (1)], while ϕ decreases.

GEOMETRY OF INTERFACES IN TWO-DIMENSIONAL PORES [2]

The author has succeeded in analyzing freezing of simple two-dimensional pores, specifically, those found between bundles of cylindrical particles of uniform radius (a) in orthogonal or rhombohedral packing. Where convenient, results will be normalized with respect to a . Complexities arising from the variable contact angle (ϕ), the curvature of the particle surface and the finite distance of point P from the surface seem to make it extremely difficult to analyze freezing of pores in systems of uniform spheres, for example. Nevertheless, phenomena comprehended in the analysis of freezing of two-dimensional pores provide a basis for understanding freezing in pores of other shapes.

The analysis involves extensive exercises in plane geometry indicated in this section. Some readers may wish to skip to the section headed "Critical Temperatures."

It will be assumed that pore air is always at atmospheric pressure ($u_a = 0$). It will be assumed that ω_{a2} has its handbook value at 0°C, namely $7.56 \times 10^{-3} \text{ N m}^{-1}$, that $\omega_{12} = 0.438 \omega_{a2}$, and that $\omega_{a1} = 1.438 \omega_{a2}$. It is convenient to note that this leads to $(u_1/u_2) = 0.917 (1 + 0.162 bt)$, where b is in μm .

In Figure 4, the segment \overline{AN} is perpendicular to \overline{DB} . To find a' , ($a' = \overline{AP}$), note that:

$$\begin{aligned} (a+c)^2 &= \overline{AN}^2 + \overline{NC}^2, \\ a'^2 &= \overline{AN}^2 + (\overline{NC} + c)^2, \text{ and} \\ (a+b)^2 &= \overline{AN}^2 + (\overline{NC} + c + b)^2. \end{aligned} \quad (6)$$

Eliminating \overline{AN} and \overline{NC} between these equations, we find

$$a'/a = \sqrt{1 + 4/(a/b + a/c)}. \quad (7)$$

To find z , ($z = \overline{DO}$), note that

$$\begin{aligned} z^2 &= \overline{DA}^2 - a^2, \\ \overline{DA}^2 &= a'^2 + d^2 - 2a'd \cos\theta, \text{ and} \\ (a+c)^2 &= a'^2 + c^2 - 2a'c \cos\theta. \end{aligned} \quad (8)$$

Eliminating \overline{DA} and $\cos\theta$ between these equations and normalizing with respect to a , we find that

$$z/a = -\sqrt{(d/a)^2 + (1 - d/c)(a'/a)^2 + d/c (1 + 2c/a) - 1} \quad (9a)$$

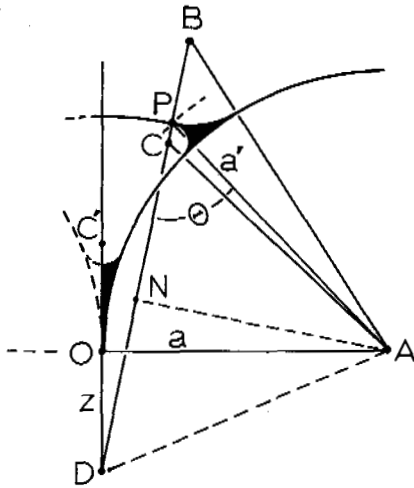


FIGURE 4 Geometry of air, ice, and water interfaces in a half-crevice between cylindrical particles of radius a . All interfaces converge at point P a distance a' from the particle center, A . Points B , C , C' , and D are centers of curvature of air-water, ice-water, and air-ice interfaces; points B , P , C , and D lie on a single straight line. The shaded areas represent water; points C and C' lie within the ice body; and point B lies in the air phase.

and that

$$\overline{OC}^0/a = \sqrt{(1 + c/a)^2 - 1}. \quad (9b)$$

It also can be shown that the radius, c^* , of a circle inscribed within a meniscus of radius b and between two particles of radius a is given by:

$$c^*/a = \frac{[\sqrt{(b/a)^2 + 2(b/a) - (b/a) + 1}]^2 + 1}{2[\sqrt{(b/a)^2 + 2(b/a) - (b/a) + 1}]} - 1. \quad (10)$$

Substituting into Eq. (4) and (1), we find that the indicated equilibrium temperature, t^* , is given by

$$at^* = (K/\Delta H) [(\bar{V}_1 - \bar{V}_2) \omega_{a2} (a/b) - \bar{V}_1 \omega_{12} (a/c^*)], \quad (11a)$$

or

$$at^* = 6.76 [0.083(a/b) - 0.438 (a/c^*)] \times 10^{-2} \mu\text{m } ^\circ\text{C}. \quad (11b)$$

In the course of computations of values of z/a , it was found that the domain of solutions that satisfy Eq. (1), (2), and (3) terminated as z/a approached zero and that for all values of b/a the quantity d/a approached a common limit, $d^{**}/a = 0.782$, as z/a approached zero. From Eq. (1), the corresponding equilibrium temperature, t^{**} , at this limit is given by:

$$at^{**} = (K/\Delta H) [\bar{V}_2 u_2 - \bar{V}_1 (\omega_{a1}/0.782a)], \quad (12a)$$

or

$$at^{**} = -8.2 \times 10^{-3} [15.2a - u_2] \mu\text{m } ^\circ\text{C}, \quad (12b)$$

when u_2 is in MPa.

For particles in orthogonal array, bodies of water at the corners of ice bodies that are growing in adjacent crevices coalesce when angle BAO in Figure 4 is 45° , i.e., when

$$[(d/a) + (b/a)]^2 - [1 + (z/a)]^2 - l^2 + \sqrt{2} l [1 + (z/a)] = 0, \quad (13)$$

where

$$l = \sqrt{2} - [1 + (b/a)].$$

When the particles are in rhombohedral array, the water bodies coalesce when angle BAO is 30° , i.e., when

$$[(d/a) + (b/a)]^2 - [(1/\sqrt{3}) + (z/a)]^2 - l^2 + l [(1/\sqrt{3}) + (z/a)] = 0. \quad (14)$$

The programs used found values of t that would satisfy, as nearly as desired, the above equations, thereby yielding temperatures to be identified below as $(t_j)_{or}$ and $(t_j)_{rh}$, respectively.

The radius, c^0 , of a cylinder inscribed between four particles in orthogonal array is given by $(c^0/a) = (\sqrt{2} - 1)$. In a rhombohedral pore between three particles, $(c^0/a) = [(2/\sqrt{3}) - 1]$. The corresponding equilibrium temperature, t^0 , in each case is given by:

$$at^0 = (K/\Delta H) [(\bar{V}_2 - \bar{V}_1) \omega_{a1} (a/b) - \bar{V}_2 \omega_{12} (a/c^0)], \quad (15)$$

which is of the same form as Eq. (11a) for t^* .

The unfrozen water content, q_2 , of a "half crevice" involves two components:

$$q_2 = q_0 + q_p, \quad (16)$$

where q_0 is the water wedge contiguous to point O and q_p is the water wedge contiguous to point P in Figure 4.

It can be shown that

$$q_0/a^2 = [W - \tan^{-1} W - (c/a)^2 \tan^{-1} (1/W)]/2, \quad (17)$$

where

$$W = [1 + (c/a)]^2 - 1.$$

It can also be shown that:

$$q_p/a^2 = \frac{\sqrt{(b/a)(c/a)[1 + (b/a) + (c/a)]}}{2} - [\cos^{-1} A + (b/a)^2 \cos^{-1} B + (c/a)^2 \cos^{-1} C]/2, \quad (18)$$

where $\cos A = [(1 + b/a)^2 + (1 + c/a)^2 - (b/a + c/a)^2] / 2(1 + b/a)(1 + c/a)$; $\cos B = [(1 + b/a)^2 + (b/a + c/a)^2 - (1 + c/a)^2] / 2(1 + b/a)(b/a + c/a)$; and $\cos C = [(1 + c/a)^2 + (b/a + c/a)^2 - (1 + b/a)^2] / 2(1 + c/a)(b/a + c/a)$.

To express results in terms of degree of pore saturation, multiply q_2/a^2 by $[8/(4 - \pi)]$ if particles are in orthogonal array or by $[12/(2\sqrt{3} - \pi)]$ if in rhombohedral array.

The ice content, q_1 , of a "half crevice" ranges upward from the minimum, q_1^* , at temperature t^* where:

$$q_1^*/a^2 = \pi(c^*/a)^2/2. \tag{19}$$

In the range between t^* and t_j or t^{**} (whichever is appropriate) an approximate value, q_1 , is given by:

$$q_1 = q' \cdot [q_0 + (q_p/2)],$$

where q' is the shaded area in Figure 5 and q_0 and q_p are found as described above. The correction term $(q_p/2)$ slightly overestimates the volume of water included in the shaded area in the vicinity of P' , but, while the magnitude of the error increases as q' increases, the relative error diminishes rapidly, and the results are satisfactory. The error can be seen as a slight step at the foot of the ascending curve in Figure 6.

To compute q' , observe that the area enclosed by $OFFP'AED$ in Figure 5 may be summed in two ways:

$$(d^2/2) \sin^{-1}(x/d) + (x/2)(y - z) + (y/2)(a - x) - z(a - x) \tag{20a}$$

$$q' + (a^2/2) \sin^{-1}(y/a) - za, \tag{20b}$$

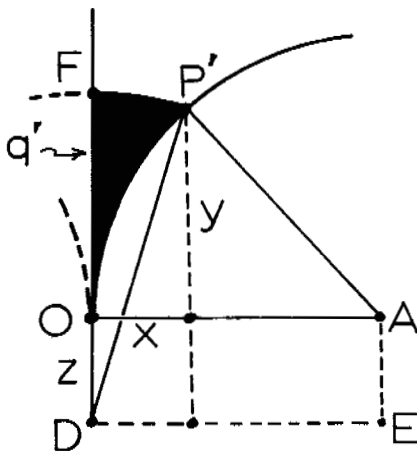


FIGURE 5 Construction used in computing approximate ice content of a half-crevice. Ice content is taken to be the shaded area shown minus the water adjacent to point O (see Figure 4) and minus half of the water adjacent to point P (Figure 4).

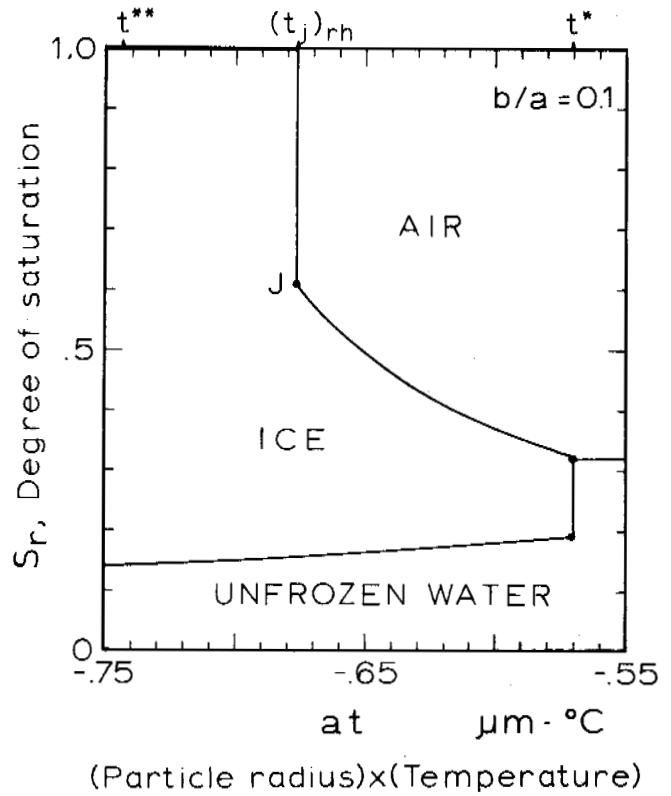


FIGURE 6 Pore contents (unfrozen water, ice, air) as functions of temperature in a rhombohedral pore with ice in all crevices during progressive freezing.

where x and y are coordinates of the intersection of the circles:

$$x^2 + (y - z)^2 = d^2$$

and

$$(x - a)^2 + y^2 = a^2.$$

To express ice content in terms of degree of pore saturation, multiply (q_1/a^2) by appropriate factors (t^* , t , or t^{**}) given above.

CRITICAL TEMPERATURES

For pore systems involving unsaturated pores between uniform cylindrical particles, four critical temperatures— t^* , t^{**} , t_j , and t^0 —will be identified, and a fifth will be mentioned.

When an ice-free soil is cooled below 0°C , stable ice cannot form until the temperature falls below a specific value, t^* . Above t^* , there is no combination of values of u_1 , u_2 , and t that will be compatible with the pore geom-

etry while simultaneously satisfying Eq. (1) and (4). In this interval ($0^\circ\text{C} > t > t^*$), the condition therefore will be as shown at the top of Figure 7.

When the temperature reaches t^* , an ice body in the form of a cylinder of radius c^* can satisfy Eq. (1) and (4), where c^* is the radius of a circle inscribed beneath the air-water meniscus and between adjacent particles as diagrammed at the right side of Figure 7. Computation of t^* is described in Eq. (11a).

An ice cylinder of radius c^* at temperature t^* will be metastable, however, in a sense similar to the instability of a critical nucleus in the theory of homogeneous nucleation. Unlike the critical nucleus, which will either grow indefinitely or evanesce as a result of fluctuations, the cylinder will evanesce sooner or later. Should it grow momentarily as a result of a local fluctuation, it will tend to return to its cylindrical shape spontaneously. If it diminishes momentarily, it will continue to diminish until it vanishes.

When the temperature falls below t^* , but not too far below that point, a stable body of ice can exist that satisfies Eq. (1) and (4). An example of such a body has been drawn to scale at the bottom of Figure 7. Computations of the quantities needed to construct the shape of ice bodies ranging from t^* to t^{**} are explained in the preceding section.

There is a finite lower limit of temperature at which air, ice, and water can coexist at equilibrium in a given pore at a given pore water pressure. The limit will be explained in terms of one of two critical temperatures (t_j or t^{**}).

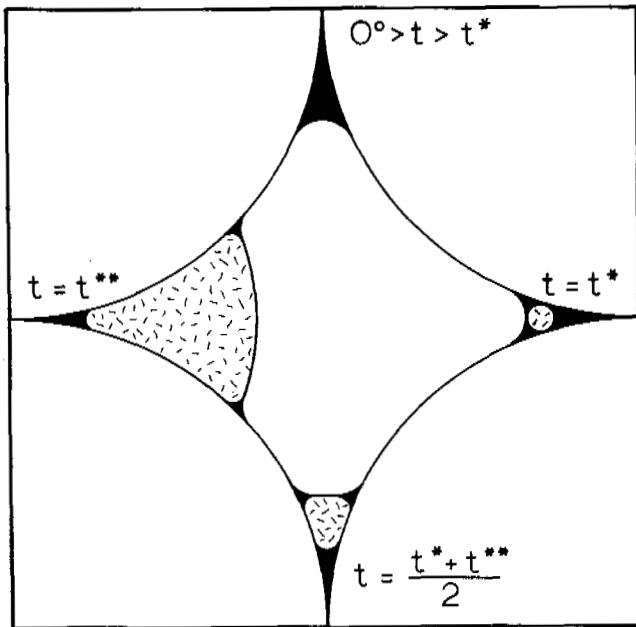


FIGURE 7 Diagrammatic representation of water and ice in crevices between cylindrical particles in equilibrium at four different temperatures for a water pressure at which $b/a = 0.1$. When t falls below t^{**} , the pore must fill with ice to reach equilibrium.

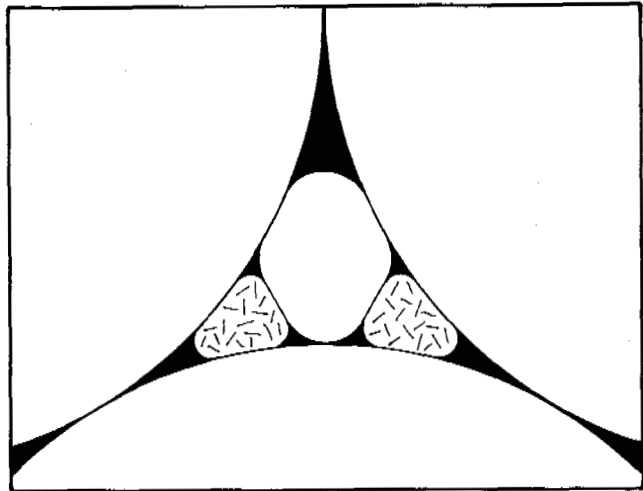


FIGURE 8 A rhombohedral pore at temperature $(t_j)_{rh}$ with ice forming in two adjacent crevices. This configuration is unstable, and the pore will fill irreversibly with ice when the state shown has been attained.

Critical temperature t_j expresses instability that develops when two bodies of ice, growing in adjacent crevices, approach one another so closely that the triangular bodies of water at the edges of the two ice bodies coalesce, as illustrated in Figure 8. This permits the pore to fill irreversibly with ice in a manner reminiscent of the "Haines jump" wherein pores fill with water when a soil is gradually wetted.³ Since the jump is initiated by ice bodies growing in adjacent crevices, the geometric proximity of the crevices is crucial, and t_j therefore is a function of the manner in which the particles are arranged in space. The configuration shown in Figure 8 satisfies Eq. (1) and (4) but is unstable since a function that causes the meniscus to rise will permit the ice-water curvature to decrease, causing more ice to form and the meniscus to rise further. This will continue until air is eliminated from the pore.

The other critical temperature, t^{**} , expresses a limit (imposed by the geometry of a single crevice) at which it becomes impossible to simultaneously satisfy Eq. (1) and (4) if an air-ice interface is present. That is, the rate of change of ice volume (in a single crevice) with decreasing temperature increases (Figure 6) and becomes infinite at temperature t^{**} . When temperature falls below t^{**} , the pore will fill irreversibly with ice if a jump situation has not previously caused the pore to fill.

In the course of computing ice-body shapes, Miller discovered that for all values of b/a , the values of d/a approach a common limit, $d^{**}/a = 0.782$, as t approaches t^{**} and as the center of curvature of the air-ice interface approaches the point of contact between particles bounding the crevice in which the ice is forming. This leads to an expression for t^{**} that is independent of u_1 (or d/a), but it does depend

on a as given in the preceding section. The ice body at the left in Figure 7 has reached this limit of equilibrium configurations. Changing b/a alters c/a and t^{**} , and d^{**}/u and the position of the air-ice interface remain unchanged.

For the values of the parameters used in my computations, it was found that $(t_j)_{rh} > (t_j)_{or} > t^{**}$ (Figure 9). Thus, if ice is nucleated in at least two adjoining crevices, the pore will fill at temperature $(t_j)_{rh}$ in a rhombohedral system or at $(t_j)_{or}$ in an orthogonal system.

If ice is nucleated in only one crevice, the pore will fill at temperature t^{**} in an orthogonal pore. If ice is nucleated in only one crevice of a rhombohedral pore, it will fill before the temperature reaches t^{**} since the air-ice interface will come in contact with the particle opposite the crevice, inducing filling. This additional critical temperature can be computed if desired.

Figure 9 presents the relationships between the critical temperatures and pore water pressure. The curves for $(at_j)_{or}$ and at^{**} are so close together that they cannot be separated at this scale, but $(at_j)_{or}$ actually lies slightly above at^{**} . For rhombohedral pores, the figure terminates at $b/a = (2/\sqrt{3}) - 1 = 0.155$, i.e., at the point where menisci

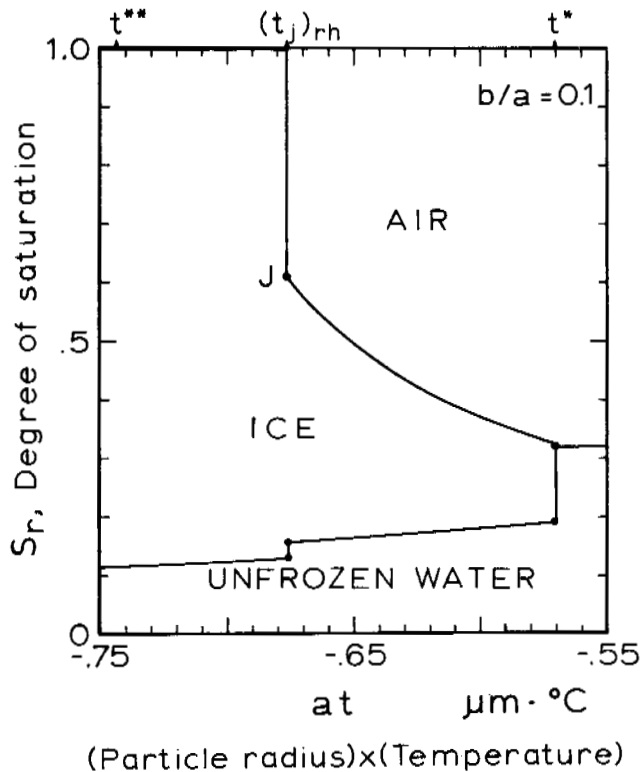


FIGURE 9 Pore contents (unfrozen water, ice, air) as functions of temperature in a rhombohedral pore with ice in all crevices during progressive freezing. The lower step in unfrozen water content is due to disappearance of the water at the corners of the ice bodies when the jump in ice content occurs.

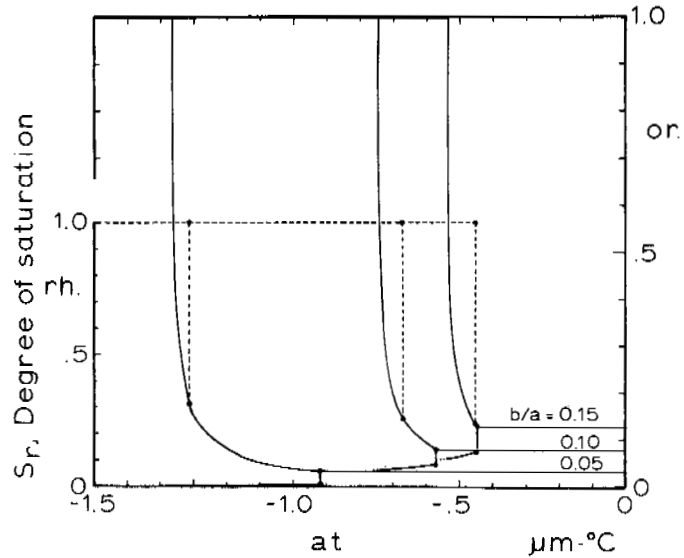


FIGURE 10 Pore contents (as in Figure 6) for orthogonal pores (right hand ordinate and solid lines) or rhombohedral pores (left hand ordinate and broken lines) as a function of temperature at three values of b/a . Jump points for orthogonal pores are omitted; the temperatures involved are indistinguishable from those at which the rising lines reach 1.0.

would coalesce with no ice present in a rhombohedral array; hence, t^* and $(t_j)_{rh}$ converge at this terminal point.

Figure 6 represents the contents of a rhombohedral pore in terms of unfrozen water, ice, and air as a function of temperature when pore water pressure is held constant. The curves were computed as described in the preceding section, assuming that ice bodies form in all crevices. The vertical portion, commencing at point J , corresponds to the jump by which the pore fills with ice and would occur at the same temperature whenever at least two adjacent crevices contain ice. If ice never occurred in adjacent crevices, however, the jump would occur at a lower temperature when the ice reached the particle on the far side. This permutation is trivial and is omitted.

Figure 10 is similar to Figure 6 and includes the curve shown in Figure 6, but is extended to include other pore water pressures (other values of b/a) and orthogonal pores.

SEQUENCE OF PORE FILLING

If a soil contains pores of various sizes, it would be of interest to know whether large pores are the first or last to fill. Table I shows critical temperatures for some large and small pores in a "soil" consisting of bundles of large rods (with large pores), together with bundles of small rods (with small pores), at uniform (and constant) pore water pressure. Inspection of the table suggests that large pores would fill first, at a temperature slightly above the filling temperature

TABLE 1 Critical Temperatures ($^{\circ}\text{C}$) Calculated for Two Pore Sizes at the Same Pore Water Pressure, $u_2 = 0.378$ MPa and $b = 0.2 \mu\text{m}$

	Small Pores ($a = 2 \mu\text{m}$)	Large Pores ($a = 4 \mu\text{m}$)
t^*	-0.285	-0.230
$(t_j)_{\text{rh}}$	-0.338	-0.328
$(t_j)_{\text{or}}$	-0.371	-0.340
t^{**}	-0.371	-0.340
$(t^{\circ})_{\text{rh}}$	-0.068	-0.020
$(t^{\circ})_{\text{or}}$	-0.008	+0.011

for small pores, providing the rate of heat extraction was so slow that every pore was very close to equilibrium at all times.

With more rapid cooling, however, the lag in filling the larger pores (which will consume more water per pore, with lower capillary conductivity expected) leads one to expect that the temperature would fall below the filling temperature for all pores, in which case the small pores might complete the filling process before the large pores. This reversal is again subject to reversal if one notices that t^* is higher for the large pores. If rapid cooling makes it impossible to maintain u_2 constant, the small pores will lose water to the large pores where ice is forming, lowering t^* for the small pores even further. Consequently, the probability seems high that large pores will tend to fill first, regardless of the rate of cooling.

THAWING-HYSTERESIS

Limitations of the two-dimensional pore analysis are encountered at the ends of the pores, where a third dimension is inevitably involved, but may be disregarded in the analysis of progressive freezing if the pores are relatively long. When we consider thawing of an ice-filled pore, the end effects become critical, and the absence of constricted pore necks, present in ordinary soils, makes the two-dimensional pore analysis inappropriate. This limitation can be disregarded by imagining that the two-dimensional pore is constricted somewhat at both ends. If the constriction is small enough to exclude air from an ice-filled pore as it is warmed, the ice-water interface will contract until it approaches the shape of a cylinder of radius c^0 inscribed within the pore, at a critical temperature t^0 as given in an earlier section. Computed values are plotted in Figure 8. The cylindrical body, like that at temperature t^* , will inevitably melt irreversibly. Since c^0 is much greater than c^* , t^0 will be a higher temperature than t^* , and we conclude that an ice-filled pore will retain some ice at temperatures well above that to which it was necessary to cool the air-filled pore to initiate ice formation, and there will be hysteresis in the

dependence of pore contents on temperature. When the ice melts at temperature t^0 , the pore may or may not empty immediately, depending on pore water pressure and the dimensions of the constriction. It also seems that, depending on the degree of constriction, air may re-enter the pore before the temperature reaches t^0 , and the system may follow the reversible path already described in the range between t_j (or t^{**}) and t^* .

If the end constrictions are small enough so that melting occurs at t^0 (see Figure 8), hysteresis effects are maximized and increase as u_2 decreases. Indeed, the ice pressure also may fall below atmospheric pressure, causing t^0 to rise above 0°C as shown.

CONCLUSIONS

From simple assumptions, it is possible to compute plausible relationships between pore water pressure, temperature, unfrozen water, and ice content of pores of simple geometry, including the microscopic geometry of air, water, and ice bodies. On a macroscopic scale, the results simulate well-known experimental data for freezing of soils of more complex geometry. Figures 9 and 10 effectively portray equilibrium ice, unfrozen water, and air content profiles at the ice front in soil with a uniform temperature gradient and pore water pressure.

While it would be instructive to develop a comparable analysis of freezing of pores between uniform spheres, for example, the exercise appears to be a formidable task. Instead, one may consider experimental measurements of families of freezing characteristic curves (like those of Figure 10) at various pore water pressures. The analysis suggests that such curves would be unique for any given soil, and, if used in conjunction with soil water characteristic curves and capillary transmission data, prediction of the ice and water content profiles during freezing of an unsaturated column of soil should be possible.

REFERENCES

1. Globus, A. M. 1962. Mechanisms of soil and ground moisture migration and of water movement in freezing soils under the effect of thermal gradients. *Pochvovedenie* 2:7-18.
2. Globus, A. M., and S. V. Nerpin. 1960. Mechanisms of soil moisture migration toward the freezing horizon. *Dokb Aked. Nauk. S.S.S.R.* 133(6):1422-1424.
3. Haines, W. B. 1930. Studies in the physical properties of soils: V. The hysteresis effect in capillary properties and the modes of moisture distribution associated therewith. *J. Agric. Sci.* 20:97-116.
4. Hutcheon, W. L. 1958. Moisture flow induced by thermal gradients within unsaturated soils, p. 113-133. *In Highway Research Board Special Report 40*. National Research Council, Washington, D.C.
5. Koopmans, R. W. R., and R. D. Miller. 1966. Soil water and soil

freezing characteristic curves. *Soil Sci. Soc. Am. Proc.* 30:680-685.

6. Miller, R. D. 1966. Phase equilibria and soil freezing, p. 193-197. *In* Permafrost: Proceedings of an international conference. National Academy of Sciences, Washington, D.C.
7. Miller, R. D. 1972. Freezing and heaving of saturated and unsaturated soils. *Highw. Res. Rec.* 393. p. 1-11.

NOTES

- [1] Agronomy Paper No. 994, New York State College of Agriculture and Life Sciences, Cornell University, Ithaca, New York.
- [2] Programs were written for the Wang 700B Programmable Computer for use in computations described in this section. These programs are available from the author on request.

IONIC MOBILITY IN PERMAFROST

Richard P. Murrmann

U.S. ARMY COLD REGIONS RESEARCH AND
ENGINEERING LABORATORY
Hanover, New Hampshire

INTRODUCTION

The migration of chemicals through unfrozen soil has been extensively investigated in the fields of soil physics and chemistry. The results of these studies have contributed not only to our understanding of fundamental processes in soils but to the solution of diverse yet related problems as well. Information on the migration of chemicals in permafrost and seasonably frozen ground is not available, although the same types of problems occur in cold regions, frequently in even more acute forms.

During the past several years, a series of experiments on the mobility of ions in frozen earth materials has been conducted at the U.S. Army Cold Regions Research and Engineering Laboratory. Approaches have included direct determination of the diffusion coefficients of ions, as well as measurement of electrical conductivity, varying such parameters as temperature, water content, and soil texture. Values for diffusion coefficients have been obtained, the significance of the effects of the parameters on the movement of dissolved substances has been determined, and information on the properties of the interfacial water through which ions diffuse has been derived. The purpose of this paper is to summarize the more significant aspects of these investigations.

ION DIFFUSION

The temperature dependence of sodium ion diffusion in Wyoming bentonite and two silt soils from permafrost regions in Alaska is shown in Figure 1. The diffusion coefficient was determined for salt-free soil materials using a video-tracer technique.¹² Ion diffusion in both the frozen

clay and silts was characterized by a rapid decrease in diffusion coefficient in the temperature range from 0 °C to about -3 °C followed by a much slower decrease to -15 °C. The data for the two silt soils corresponded very closely; however, in the higher temperature range, the ion diffusion coefficient for the soils decreased more rapidly with decreasing temperature than did the ion diffusion coefficient for the clay. The temperature dependence of the ion diffusion coefficients can be accounted for by the properties of unfrozen, interfacial water whose existence has been proved.^{1,15}

The large rate of decrease of the ion diffusion coefficient with decreasing temperature precludes the possibility that observed temperature dependence is primarily caused by a concurrent decrease in thermal energy of the ions. A plot of the unfrozen water content of bentonite and of silt soil against temperature^{3,15} is remarkably similar to the plot shown in Figure 1, indicating a relationship between unfrozen water content and the ion diffusion coefficient. Although the ion diffusion coefficients for the frozen clay and silt soils below -3 °C are about a factor of 10 less than those reported for unfrozen bentonite clay¹⁹ and soils⁶ at low moisture contents, the coefficients for the frozen samples are several orders of magnitude higher than would be expected for solid state diffusion in either ice or minerals. This shows that the water through which the ions diffuse has liquid-like properties relative to those of ice. That ions diffused as far as 5 cm across the samples proves that the films of unfrozen water are continuous throughout the sample matrix. X-ray diffraction measurements for bentonite clay² have shown that most of the unfrozen water is located in interlamellar regions. Moreover, the thickness of the interlamellar water films changes as ice forms or melts

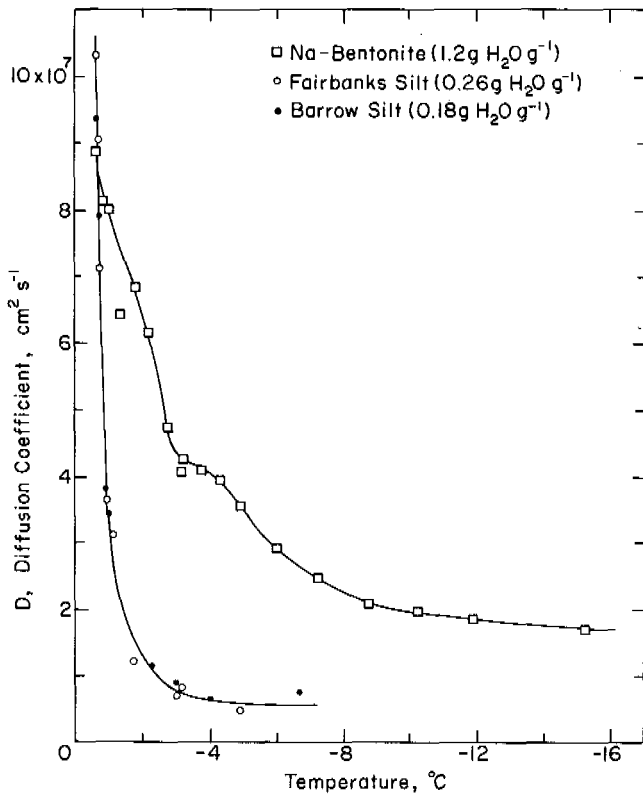


FIGURE 1 Sodium ion diffusion coefficient for frozen Wyoming bentonite, Fairbanks silt, and Barrow silt as influenced by temperature.

in response to temperature variation. Also ion diffusion coefficients for bentonite clay determined after several days as was the case in this study represent values for diffusion in the interlamellar region.⁸ It may be concluded, therefore, that ions in frozen soils are relatively mobile in continuous films of unfrozen, interfacial water.

The initial decrease in ion diffusion coefficient with temperature primarily results from a concurrent decrease in the amount of unfrozen water; however, this initial decrease in ion diffusion is not due to the increasing ice content of the soil since the value of the ion diffusion coefficient is independent of total water content over a wide range (Table I). As the film thickness of unfrozen water decreases with decreasing temperature, ionic mobility is reduced because of the increased electrical interactions of ions with mineral surfaces and/or changes in properties of the interfacial water.

The difference between the temperature dependence observed for ion diffusion in frozen clay and that observed in silts may be explained by first considering the role of the unfrozen water. Unfrozen water per unit weight of soil is higher for bentonite clay than for silt soil at a given temperature, yet the average amount of unfrozen water per unit surface area is actually higher for silts.³ Although this can

TABLE I Sodium Ion Diffusion Coefficient in Frozen Wyoming Bentonite at Different Water Contents^a

Total Water Content (g H ₂ O / g clay)	D _{avg} ^b × 10 ⁷ (cm ² s ⁻¹)
0.8	3.21
1.72	3.41
3.34	2.65
7.07	3.03
AVERAGE	3.08 ± 0.22

^a Temperature, -5.5 °C.

^b Each value represents the average of two determinations.

be interpreted to indicate a thicker film for silts, it has been proposed⁴ instead that silt has a higher proportion of the unfrozen water in pores and capillaries than clay. Hence, the thickness of the interfacial water located adjacent to mineral surfaces is believed to be about the same for both clay and silt. The ion diffusion data support this view in that, if the interfacial films of water were thicker in silt, higher rather than lower diffusion coefficients would be expected at a given temperature. In addition, the more rapid initial decrease in both the unfrozen water content and the ion diffusion coefficient for silt than for clay suggests a higher proportion of pore water in the silt. It is possible that the films of interfacial water are actually thinner in the silt than in the clay. This would account for the lower ion diffusion coefficient for the silt at a given temperature. However, there is no reason to expect that this is the case.

An alternative explanation to account for the difference between the ion diffusion coefficients for the clay and those for silt soils lies in consideration of the matrix characteristics of the two types of materials. To evaluate this, diffusion coefficients were determined for sodium ions in mixtures of bentonite clay and Barrow silt. The diffusion coefficient increased with clay content to about 30 percent clay by weight, remained relatively constant to about 70 percent clay, and then increased to the value of the ion diffusion coefficient for the pure clay (Figure 2). The electrical conductivity of the samples increased with clay content in essentially the same manner as the ion diffusion coefficient.

With the exception of the pure silt soil, the samples were carefully prepared to contain a constant amount of ice phase, even though the ion diffusion coefficient in frozen clay alone is independent of ice content (Table I). Since the mineral phase in the experiment is excluded from the ice upon freezing, the mineral matrix is considered in terms of the volumes of silt, clay, and unfrozen water, rather than in terms of the total volume including the ice phase (Figure 2). Since the silt represents at least 50 percent of the total adjusted volume in samples, with up to 40 percent clay, this region can be considered as a silt matrix to which clay is being added in increasing amounts. At higher clay contents,

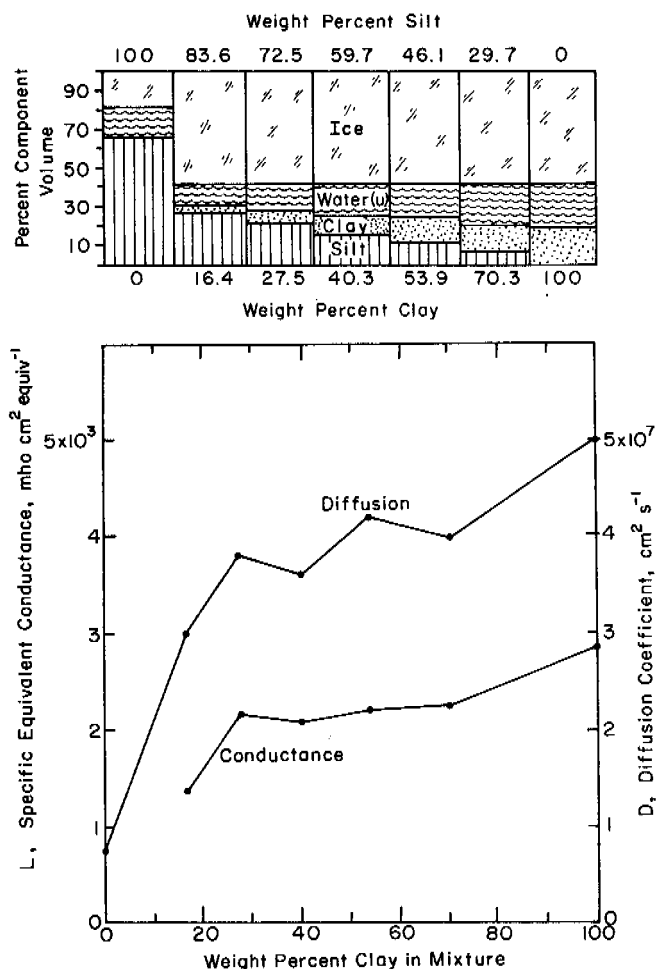


FIGURE 2 Sodium ion diffusion coefficient and specific equivalent conductance for frozen mixtures of Barrow silt and Wyoming bentonite. Temperature constant at -3.0°C .

a transition occurs after which silt can be considered as being suspended in the clay material. Based on this explanation, the ion diffusion coefficient should increase initially because of the increasing particle and film contact as clay is added to the silt. The continued increase in diffusion coefficient after the transition from a silt matrix to a clay paste is thought to reflect shorter diffusion path lengths as the silt content decreases.

Temperature dependence of ion diffusion raises a question about the possible effects of thermal gradients on ion redistribution, since both ionic and thermal gradients exist in permafrost. Experiments were conducted¹⁰ using frozen Wyoming bentonite with a linear temperature gradient of about $0.3^{\circ}\text{C cm}^{-1}$ imposed across samples ranging from -1 to -15°C . A typical ion distribution curve is shown in Figure 3 for a sample in the higher temperature range where the largest effect should occur. In addition to the experimental points, the distribution expected in the absence of a temperature gradient $D(0.5)$ and the distribution computed

using an exact solution¹³ of the diffusion equation with a distance-dependent coefficient $D(x)$ are also shown. The functionality of $D(x)$ was determined using data shown in Figure 1 $[D(T)]$ and the known thermal gradient $[T(x)]$ across the sample. The water content distribution in the sample showed no significant net movement of water toward the cold end, indicating that movement of water did not influence ion diffusion significantly. From the calculated and experimental distribution curves, it is apparent that the effect of thermal gradient on ion movement is small.

Even after 90 days, there should be little effect of a thermal gradient as can be seen by comparing the curves obtained using exact solutions of the diffusion equation, as well as a new approach¹⁴ based on the Monte Carlo method. This approach, which is applicable to true random processes, involves direct construction of random processes rather than solution of the appropriate differential equations as is normally done using the Monte Carlo method. The general approach of this method can be applied to much more complicated problems; for example, soil properties change not only with location but with time under the influence of climatic variation. Predictions of time-dependent phenomena could be made if proper geological and meteorological information were available.

The influence of salt concentration was not investigated, but the mobility of ions at a given temperature should be higher in the presence of dissolved salts because of the in-

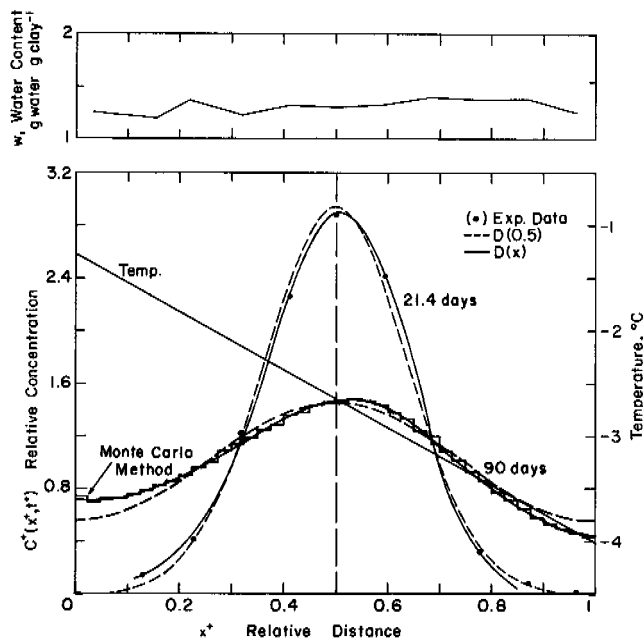


FIGURE 3 Effect of thermal gradient on sodium ion and water content distribution in frozen Wyoming bentonite after 21.4 days and 90 days. Curves were computed using exact solution of diffusion equation or Monte Carlo method as indicated.

creased amount of interfacial water with freezing point depression.⁹ Although the value of the diffusion coefficient differs somewhat for each type of cation or anion, the sodium ion diffusion coefficients shown in Figures 1 and 2 should be generally useful for estimating ion movement in permafrost or seasonally frozen ground under field conditions if temperature and textural characteristics of these soils can be defined. To verify this an ion diffusion experiment was begun in 1970 in a silt section of the CRREL permafrost tunnel.¹⁷ Unfortunately, the results are not yet available for discussion. A similar experiment was recently conducted¹⁸ in Antarctica, but no comparison of data has yet been made.

ELECTRICAL CONDUCTIVITY

Determination of diffusion coefficients is the most direct way to investigate ion migration in frozen soil; such measurements, however, are time consuming and require rather laborious procedures. Consequently, electrical conductivity studies were undertaken with the initial objective of indirectly evaluating ion mobility. The electrical conductance was obtained by measuring the resistance at 1 000 Hz by placing salt-free, Na-Wyoming bentonite samples between stainless steel electrodes in a small, cylindrical Lucite cell. Temperature measurements, accurate to within 0.05 °C, were made using a second identical cell. The electrical conductivity data were expressed in terms of the specific weight conductance to normalize the specific conductance to the number of charge carriers associated with a unit amount of dry clay but independent of the amount of clay per unit volume.

A typical curve of the temperature dependence of the electrical conductance of Wyoming bentonite is given in Figure 4. The decrease in electrical conductivity in the temperature range from 20 to -7 °C is attributed to the decreasing thermal energy of the charge carriers. The sudden drop in conductivity as nucleation occurs (NP) results from decreased film thickness in interlamellar space as water migrates to form ice in extralamellar regions of the clay paste.² Further decrease in electrical conductivity below -7 °C primarily reflects decreased thermal energy of charge carriers, since the unfrozen water thickness in the interlamellar space remains constant.²

Increasing the temperature results in an electrical conductivity curve that is essentially identical to that for ion diffusion (Figure 1). With warming, in addition to an increase in thermal energy of charge carriers, the mobility of charge carriers also increases due to an expansion of the film thickness of interlamellar water as ice melts. The fact that the freezing and cooling curves do not coincide exactly above about 2 °C is thought to reflect changes in internal geometry. It would be expected that because of freezing point depression the two curves would intersect at a temperature (MP) slightly below 0 °C. The fact that this

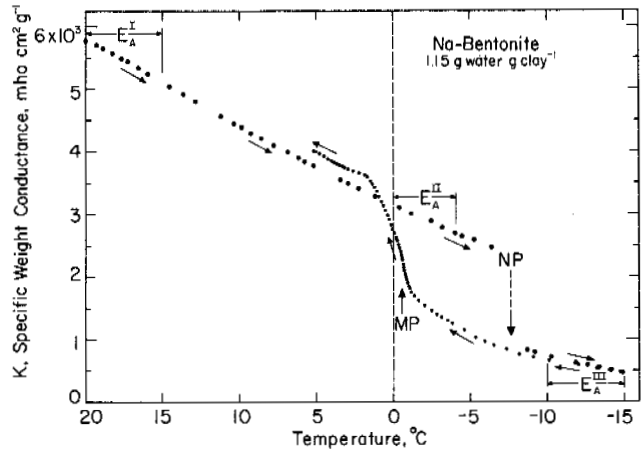


FIGURE 4 Dependence of specific weight conductance of Wyoming bentonite on temperature during freezing and thawing. E_A^I , E_A^{II} , and E_A^{III} refer to data used in calculation of activation energies given in Table II.

did not occur might be explained by the failure of the sample to equilibrate as melt occurs; however, the migration of water back into the interlamellar spaces is known to be rapid.²

A more intriguing explanation is that the melted water, although mobile, may temporarily retain a sufficient number of units with an icelike structure to reduce the mobility of the charge carriers. After warming the frozen samples, even for periods of up to 30 min at 1.5 °C, the electrical conductance generally followed the lower curve in Figure 4 when the temperature was decreased below 0 °C rather than the curve that corresponded to the supercooled condition. This suggests that ice nucleation occurred near the normal freezing point because of the presence of stable ice nuclei as in the concept of heterogeneous nucleation of water.

The temperature dependence of the specific weight conductance for frozen Wyoming bentonite, calculated from the ion diffusion coefficients shown in Figure 1, is shown in Figure 5 in comparison with experimental conductance data. The computation was made using an equation previously derived.¹⁰

Comparison of the experimental and calculated electrical conductance shows that the calculated values are too low by about 60 percent. Although the difference could be due to assumptions made in the computation, it is believed that the higher experimental conductance is largely caused by the presence of charge carriers other than exchangeable ions. It seems likely, however, that exchangeable ions account for a significant fraction of the charge carriers in frozen clay samples with a low ice content. Some investigations^{5,20} have attributed the electrical conductivity of frozen clay almost entirely to protons.

Although the ion diffusion coefficient was found to be independent of ice content in frozen Wyoming bentonite

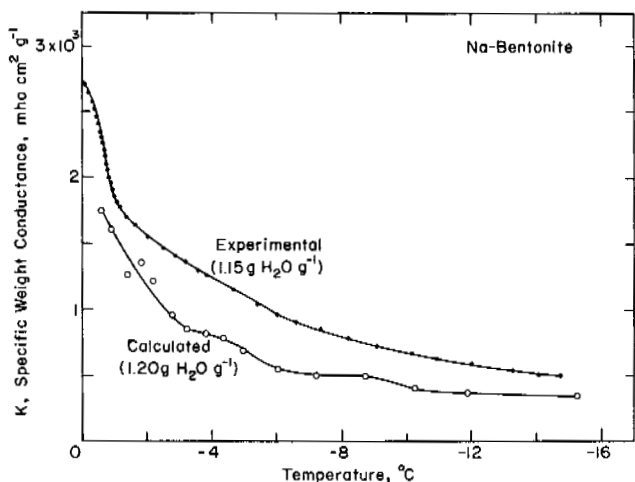


FIGURE 5 Comparison of temperature dependence of experimental specific weight conductance of frozen Wyoming bentonite with that computed from sodium ion diffusion coefficients.

(Table I), close examination of other electrical conductivity data⁷ indicate that this might not be so for the electrical conductance. This was investigated using Wyoming bentonite samples that ranged in total water content from 0.02 to 9.65 g H₂O/g clay (Table 11). Conductivity curves typical of the results are plotted in Figure 6. Clearly, the value of the electrical conductivity at a given temperature increases with ice content, since the amount of unfrozen water is virtually fixed by temperature.¹⁵ The increase in conductivity with ice content may result from several factors, including (1) decreasing tortuosity, (2) higher mobility of a

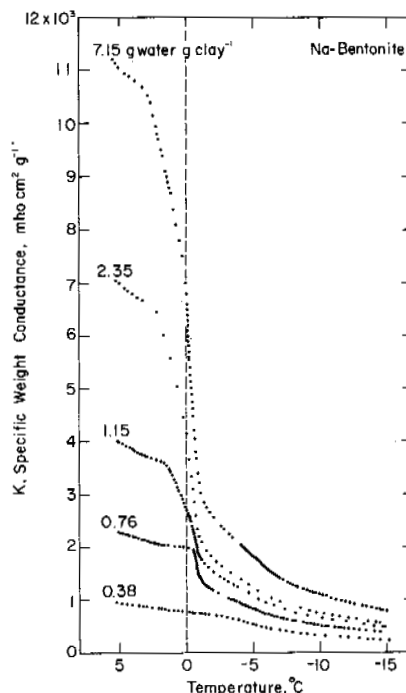


FIGURE 6 Dependence of specific weight conductance of frozen Wyoming bentonite on temperature at selected total water contents.

fixed number of charge carriers, or (3) an increase in the number of charge carriers. However, the fact that the ion diffusion coefficient did not also increase with ice content (Table I) makes the first two alternatives appear unlikely. If tortuosity decreases or more charge carriers are present,

TABLE II Activation Energies for Electrical Conductance of Frozen and Unfrozen Wyoming Bentonite at Different Water Contents

Sample No.	Total Water Content (g H ₂ O/g clay)	Activation Energy (kcal mol ⁻¹)		
		E _A ^I T = 20-15 °C (unfrozen)	E _A ^{II} T = 0 - -4 °C (supercooled)	E _A ^{III} T = -10 - -15 °C (frozen)
1	9.65	4.2	5.2	9.6
2	7.15	4.2	5.1	9.4
3	6.33	4.2	5.1	9.3
4	3.87	4.3	5.1	9.3
5	2.35	4.4	5.4	9.1
6	1.68	4.4	5.3	9.1
7	1.15	4.5	5.5	9.2
8	0.98	3.6	4.6	8.8
9	0.82	4.7	5.6	9.2
10	0.76	4.5	5.6	9.4
11	0.53	4.9	5.9	9.0
12	0.51	4.9	6.0	9.3
13	0.38	5.1	6.3	9.5
14	0.12	6.3	7.4	9.2
15	0.06	6.6	8.0	9.2
16	0.02	8.0	9.0	9.7

the activation energy for electrical conductance should remain constant. However, if ionic mobility increases because of changes in the structure of interfacial water, the activation energy should decrease. Activation energies given in Table II were computed using data in the selected temperature ranges given in Figure 4 (E_A^I , E_A^{II} , E_A^{III}) from a plot of $\log K$ versus $(1/T)$.

The activation energy for the unfrozen samples is included only to illustrate correspondence to previously reported values.¹⁶ For the supercooled samples, the activation energy was consistently about 1 kcal mol⁻¹ less than in the higher temperature range, indicating slight changes in the structure of water in the supercooled state.

The activation energies calculated for frozen samples must be viewed with some caution, because the temperature dependence of conductance reflects not only the thermal energy of the charge carriers but also the effects of the changing amounts of the interfacial water. Since both the total unfrozen water content and the interlamellar spacing remain virtually constant² from -10 to -15 °C, however, calculation of the activation energy seems justified. The activation energy of the frozen sample was about 9.0-9.5 kcal mol⁻¹, higher by a factor of 2 than that of the unfrozen sample except at the lowest water contents in the unfrozen samples. The unfrozen water content in the temperature range -10 to -15 °C is about 0.4 g H₂O/g clay.^{3,15} The activation energy for conductance in the unfrozen samples at an equivalent total water content is only about 5 kcal mol⁻¹. The implication is that the structure of interfacial films of water of equivalent thickness in frozen and unfrozen samples is significantly different. Concerning the increased electrical conductance with ice content, the constancy of the activation energy is inconsistent with the mechanism of increasing ionic mobility. It must be concluded that the enhanced electrical conductivity is caused by an increase in the number of charge carriers.

In recent years, various types of evidence¹ indicating that water adjacent to surfaces in clay systems is highly dissociated relative to bulk water have accumulated. Thus, protons and hydroxyl ions are available to participate as charge carriers. This agrees, in part, with the published results^{5,20} referred to earlier on proton conductivity. Current models² on domains of unfrozen water in frozen clay systems depict differences between properties of water located at silicate-water-silicate (SWS) interfaces and those of the water located at silicate-water-ice (SWI) interfaces. As the ice content increases, the number of SWI interfaces relative to the number of SWS interfaces per unit volume should also increase. The increased electrical conductivity indicates that interfacial water must be more highly dissociated in the SWI domain. It is proposed that, upon spontaneous freezing, the relative number of SWI interfaces that form depends on the structure of the unfrozen clay-water system, which is a function of water content. In this manner,

the number of charge carriers is fixed when freezing occurs. This view is supported by the observation that the change in relative conductance of the frozen clay with total water content is independent of temperature, as defined in Figure 7. Conversely, the relative increase in electrical conductance with temperature is independent of total water content, which primarily reflects the increased mobility of a fixed number of charge carriers.

A plot of total water content versus freezing point depression has been shown⁹ to be equivalent to the temperature dependence of unfrozen water content in frozen soil. It seems worthwhile to make such a comparison based on freezing point depression values obtained from the electrical conductivity curves shown in Figure 6. Although no sharp discontinuity appears in the electrical conductance data as might be expected at the melting point, freezing point depression is thought to be represented by the inflection of the conductance curve as the temperature approaches 0 °C upon warming the frozen samples. This possibility is indicated by the relative rates at which temperature and electrical conductance changed on warming the samples. To test this, the inflection point of the conductance curves was determined with good agreement both by observation and by fitting a curve to the experimental data. The water content of the samples was then plotted against the inflection point temperature as shown in Figure 8. Available unfrozen water content data³ were then added to the graph. The solid lines correspond only to the experimental unfrozen water content. The agreement between the two types of data supports the contention that the inflection point in the conductivity curve does represent freezing point depression. By refinement of experimental

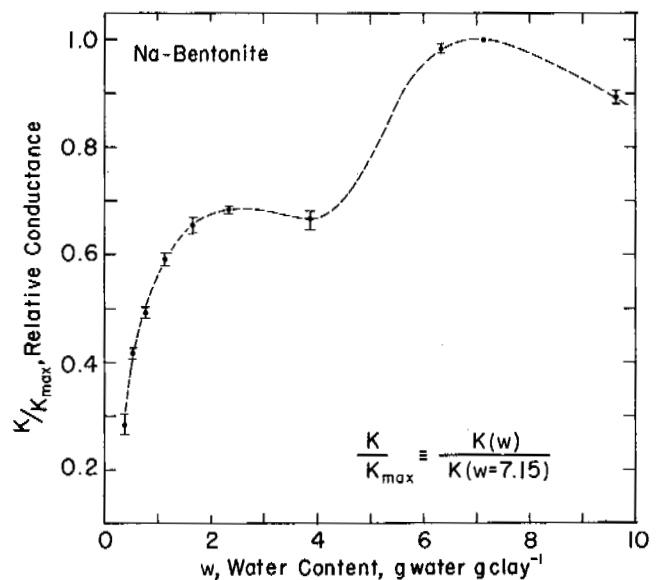


FIGURE 7 Dependence of relative specific weight conductance of frozen Wyoming bentonite on total water content.

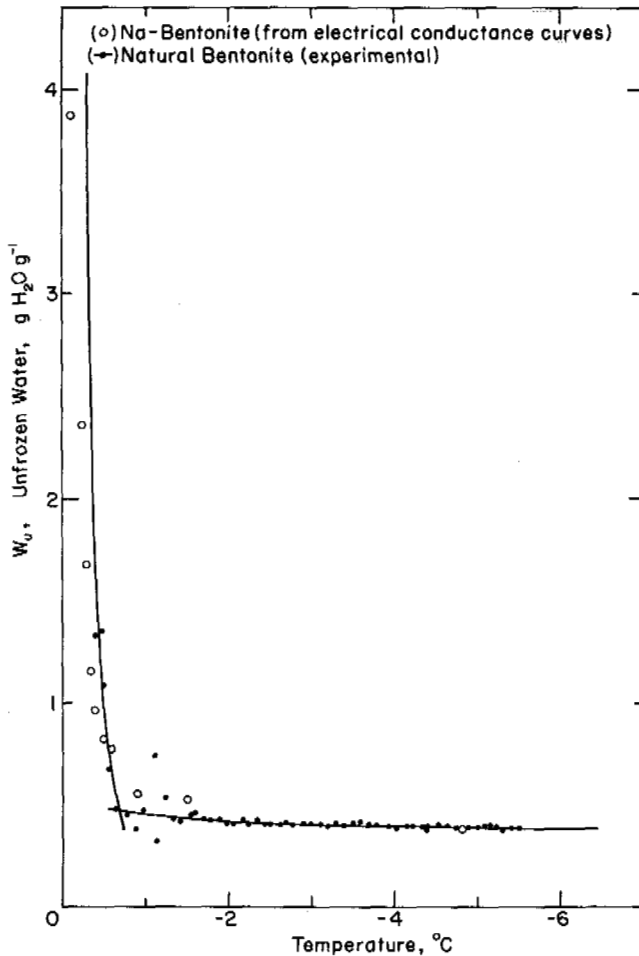


FIGURE 8 Estimate of unfrozen water content in Wyoming bentonite as a function of temperature from inflection point in electrical conductivity curve of samples with known total water content.

procedures, it might be possible to reliably estimate the unfrozen water content of soils near 0 °C where difficulty is encountered using most other methods.

SUMMARY

Despite the significance of the movement of chemical substances in relation to both natural processes and current problems of practical significance, little is known about ion migration in permafrost or seasonally frozen ground. In this work, the mobility of ions in frozen bentonite clay and frozen silts was investigated directly by determining sodium ion diffusion coefficients and indirectly by measuring electrical conductance. The results define diffusion rates, determine how soil parameters influence ion migration, and acquire supportive evidence for current concepts about the nature of unfrozen water in frozen soil.

Although ion diffusion is slower in frozen soil than in unfrozen soil, values of the diffusion coefficients in the temperature range from about 0 to -15 °C are surprisingly

high relative to those of solid state diffusion. For example, the diffusion coefficient for sodium ions in frozen bentonite at -15 °C is $1.7 \times 10^{-7} \text{ cm}^2 \text{ s}^{-1}$, only about a factor of 10 less than that expected at 25 °C. For typical silt soils the diffusion coefficient for sodium ions is about $1 \times 10^{-7} \text{ cm}^2 \text{ s}^{-1}$ at -3.0 °C. Although the rate of ion diffusion is lower in frozen silt soil than in frozen clay at a given temperature, it increases with clay content because of the decreasing tortuosity of the soil matrix. The values of the diffusion coefficient remain constant with time, and ion diffusion is not affected over a wide total water content range. The most important parameter influencing ion diffusion in a given soil is temperature, but the influence of temperature cannot be accounted for by the changing thermal energy of the ions. Despite the importance of temperature in determining the value of the ion diffusion coefficient, thermal gradients of $0.3 \text{ }^\circ\text{C cm}^{-1}$ have little perturbing influence on ion diffusion in frozen clay, even after 3 months. Generally, data reported should be applicable to any frozen soil whose texture and temperature can be specified.

The temperature dependence for the low frequency electrical conductivity of frozen Na-bentonite is strikingly similar to that for ion diffusion. Although the electrical conductivity of a sample could be reasonably estimated from ion diffusion data, electrical conductance is somewhat higher at a given temperature than can be accounted for from the diffusion coefficient of exchangeable ions in a comparable sample. Unlike diffusion, the specific weight conductance of frozen bentonite clay increases with total water content of the sample. The enhanced conductivity is due to an increased number of charge carriers, since it can not be accounted for by either increased mobility of charge carriers or decreasing sample tortuosity.

The behavior observed for ion diffusion and electrical conductance is completely consistent with current concepts proposed for the nature of unfrozen water in soils. The physical movement of ions through the frozen soil matrix and the relatively high values for diffusion coefficients can be accounted for only by the existence of continuous, thin films of interfacial water in which the molecules are relatively mobile compared with those of ice. The temperature dependence of ion diffusion and electrical conductance largely results from a higher ion mobility as interfacial films of water thicken with the melting of ice with increasing temperature. Differences between the temperature dependence of ion diffusion in frozen silt and that of frozen clay are best explained by the partition of the total unfrozen water within different domains of the soil matrix. A higher electrical conductivity than that expected from exchangeable ions arises from interfacial water, which has a higher degree of dissociation than bulk water. The increase in electrical conductivity with ice content indicates that the water at silicate-water-ice interfaces is more highly dissociated than the water at silicate-water-silicate interfaces.

ACKNOWLEDGMENTS

This paper presents the results of research performed by the U.S. Army Cold Regions Research and Engineering Laboratory under the sponsorship of the U.S. Army Corps of Engineers.

Dr. Pieter Hoekstra participated in planning and conducting many of the experiments reported. Dr. Duwayne Anderson, through many discussions, contributed to a better understanding of the relationship between the experimental results and the properties of unfrozen water. The author is indebted to both of these colleagues for their constructive criticism and helpful suggestions. Mr. Daniel Leggett assisted in obtaining and reducing much of the data.

REFERENCES

- Anderson, D. M. 1970. Phase boundary water in frozen soils. CRREL Research Report 274. U.S. Army Cold Regions Research and Engineering Laboratory, Hanover, New Hampshire, 17 p.
- Anderson, D. M., and P. Hoekstra. 1965. Migration of interlamellar water during freezing and thawing of Wyoming bentonite. *Soil Sci. Soc. Am. Proc.* 29:498-504.
- Anderson, D. M., and A. R. Tice. 1972. Predicting unfrozen water contents in frozen soils from surface area measurements. *Highway Research Record*, No. 383. p. 12-18.
- Anderson, D. M., and A. R. Tice. The unfrozen interfacial phase in frozen soil water systems. *In Proceedings, international symposium on water physics and technology*. Rehovot, Israel. (In press)
- Fripiat, J. J., A. Jelli, G. Poncelet, and J. Andre. 1965. Thermodynamic properties of adsorbed water molecules and electrical conduction in montmorillonite and silicas. *J. Phys. Chem.* 69:2185-2197.
- Graham-Bryce, I. J. 1963. Self-diffusion of ions in soil. I. Cations. *J. Soil Sci.* 14:188-194.
- Hoekstra, P. 1965. Conductance of frozen bentonite suspensions. *Soil Sci. Soc. Am. Proc.* 29:519.
- Lai, T. M., and M. M. Mortland. 1968. Cationic diffusion in clay minerals: I. Homogeneous and heterogeneous systems. *Soil Sci. Soc. Am. Proc.* 32:56-61.
- Low, P. F., D. M. Anderson, and P. Hoekstra. 1968. Some thermodynamic relationships for soils at or below the freezing point. Part I. Freezing point depression and heat capacity. *Water Resour. J.* 4:379-394.
- Murrmann, R. P., and P. Hoekstra. 1968. Ion migration in frozen soil. *Proc. Army Sci. Conf. U.S. Mil. Acad. (West Point, N.Y.)* 2:161-172.
- Murrmann, R. P., and P. Hoekstra. 1970. Effect of thermal gradient on ionic diffusion in frozen earth materials. I: Experimental. CRREL Research Report 284. U.S. Army Cold Regions Research and Engineering Laboratory, Hanover, New Hampshire. 8 p.
- Murrmann, R. P., P. Hoekstra, and R. C. Bialkowski. 1968. Self-diffusion of sodium ions in frozen Wyoming bentonite-water paste. *Soil Sci. Soc. Am. Proc.* 32:501-506.
- Nakano, Y., and R. P. Murrmann. 1970. Effect of thermal gradient on ionic diffusion in frozen earth minerals. II: Theoretical. CRREL Research Report 284. U.S. Army Cold Regions Research and Engineering Laboratory, Hanover, New Hampshire.
- Nakano, Y., and R. P. Murrmann. 1971. A statistical method for analysis of diffusion in soils. *Soil Sci. Soc. Am. Proc.* 35:397-402.
- Nersesova, Z. A., and N. H. Tsytovtich. 1963. Unfrozen water in frozen soils. p. 230-237. *Permafrost: Proceedings of an international conference*. National Academy of Sciences, Washington, D.C.
- Oster, J. D., and P. F. Low. 1963. Activation energy for ion movement in thin water films on montmorillonite. *Soil Sci. Soc. Am. Proc.* 27:369-373.
- Sellmann, P. V. 1972. Geology and properties of materials exposed in the USA CRREL permafrost tunnel. CRREL Special Report 177. 14 p.
- Ugolini, F. C., and D. M. Anderson. 1972. Ionic migration in frozen Antarctic soil. *Antarct. J.* 7:112-113.
- van Schaik, J. C., W. D. Kemper, and S. R. Olsen. 1966. Contribution of adsorbed cations to diffusion in clay-water systems. *Soil Sci. Soc. Am. Proc.* 30:17-22.
- Weiler, R. A., and J. Chaussidon. 1968. Surface conductivity and dielectric properties of montmorillonite gels. *Clays Clay Min.* 16:147-155.

SOUND AND SHOCK TRANSMISSION IN FROZEN SOILS

Yoshisuke Nakano

U.S. ARMY COLD REGIONS RESEARCH AND
ENGINEERING LABORATORY
Hanover, New Hampshire

Nilson H. Froula

SYSTEMS, SCIENCE AND SOFTWARE
La Jolla, California

INTRODUCTION

To promote better understanding of the structure and history of the earth and to develop solutions to engineering problems, stress wave propagation in earth materials has been a topic of intensive research in geophysics and geology.

In the past decade, advancements in science and technology have led to two important laboratory experimental techniques in the field of wave propagation: the ultrasonic technique to study dynamic elasticity and the high pressure technique to study shock compression of earth materials, using a gas-gun facility. Although these techniques

have been widely used for metal, plastic, and various unfrozen earth materials, only recently have they been applied to frozen earth materials.

In the first part of the paper, the experimental results obtained by the ultrasonic technique are presented and interpreted. The second half of the paper is devoted to the behavior of frozen soils under shock compression by the use of a gas-gun facility.

SOUND TRANSMISSION IN FROZEN EARTH MATERIALS

Brief Review of Literature

A summary of wave velocity data obtained in permafrost regions was compiled by Barnes.¹⁰ Zykov⁴⁷ reviewed Russian works on the subject. Several laboratory studies were reported.^{15,22,29,34,43} Frolov²² measured velocities of 30-kHz dilatational waves in four different types of soil (sand, clay, sandstone, and silt) in the temperature range from -20 to 20 °C. Muller measured the velocity in water-saturated sand and clay of various porosities. His results indicate that, with decreasing ice content, the velocity decreases for sand and increases for clay. Kaplar²⁹ measured both dilatational and shear wave velocities in various frozen earth materials in the temperature range from 0 to -20 °C by the resonant bar method, in which flexural, longitudinal, or torsional vibrations were induced by electromagnetic means. Recently, Timur⁴³ measured dilatational wave velocities in rocks between 26 and -36 °C by the pulse-transmission method. He found that the velocity measurements made during descending and ascending temperatures did not agree.

A comprehensive review of the present state of the art of experimental methods used to measure sound velocity directly or indirectly through the measurement of elastic constants of earth materials was made by Anderson and Libermann.⁴ They classified the methods into three basic types: pulse-transmission methods; resonance methods; and ultrasonic-interferometry methods.

Since multiple reflections at high frequency cannot be obtained from frozen soils due to the low quality of the specimen, the methods used for frozen soils have been either the resonance or the pulse-transmission technique. For a variety of reasons, the latter method is preferred.

Dilatational Waves in Frozen Soils

The dilatational velocities of three standard types of soil—20–30 Ottawa sand, Hanover silt, and Goodrich clay (fully water-saturated)—are presented as a function of temperature in Figure 1. The measurements were made by one of the pulse-transmission methods based on transmitting a short train of 1-MHz pulses and measuring its first arrival time through the circular cylindrical specimen. The use of suit-

able electronic devices kept the error in velocity measurements within 1 percent.³⁵

It is well known that the frozen soil generally consists of soil mineral (or organic) matter, ice, water (normal water), unfrozen water (interlamellar water), and air. In the pulse-transmission method, the received signal may be considered to be a mixture of waves traveling along various paths through the frozen soil such as the soil mineral-only path and various combinations of the soil constituents. Since the dilatational velocity obtained by the first arrival method depends on the first traveling dilatational wave, it strictly represents the characteristics of the path taken by the first wave. An understanding of the mechanism of wave propagation is crucial to the interpretation of the velocity data in terms of the physical structure of frozen soil.

In frozen granular soils, such as 20–30 Ottawa sand (Figure 1A), almost all of the water freezes at the freezing point of water. The dilatational velocity changes suddenly in a stepwise manner at 0 °C, and no hysteresis is observed in the velocity during a freeze-thaw cycle. Paterson³⁸

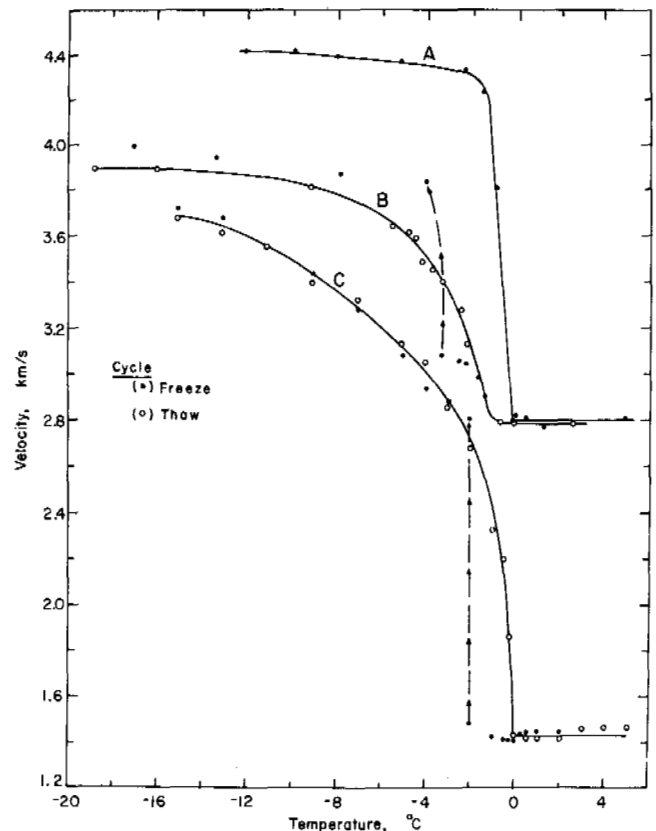


FIGURE 1 The dilatational wave velocity versus temperature for (A) 20–30 Ottawa sand, wet density $\rho = 2.20$ g/cm³, (B) Hanover silt, $\rho = 1.83$ g/cm³, and (C) Goodrich clay, $\rho = 1.80$ g/cm³ under fully water-saturated conditions. Notice the discrepancy between the freezing and thawing cycles for B and C. No discrepancy was observed for Ottawa sand.

showed that, unlike a homogeneous solid in which only two independent disturbances—the dilatational and shear waves—could be propagated, porous granular materials could support three waves: two dilatational waves—one through the mineral skeleton and one through the pore fluid—and a shear wave through the mineral skeleton. In frozen Ottawa sand, soil together with ice constitutes a mineral skeleton, and all three waves were observed.³⁶

Actually, the dilatational wave through the pore air travels with the speed of sound in air and can be clearly identified for the frozen Ottawa sand of very little ice content.

Silt and clay have fine pores, in which a significant portion of the water remains unfrozen at subfreezing temperatures.³⁷ It is evident that a strong correlation exists between dilatational wave velocity and unfrozen water content. The observed hysteresis in the velocity of both Hanover silt (Figure 1B) and Goodrich clay (Figure 1C) during a freeze-thaw cycle is considered to be caused by the hysteresis of unfrozen water content.

Since the wavelength of dilatational waves in Hanover silt and Goodrich clay is roughly 10 and 100 times larger than their average grain size, respectively, the mechanism of wave propagation in silt and clay may differ from that in sand, where the wavelength is of the same order as the grain size. It appears that the mixture theory is more appropriate to model this situation than the one applied to granular sand consisting of the mineral skeleton and the pore fluid. To examine further the hysteresis of velocities, an experimental technique was developed to measure wave velocity and unfrozen water content simultaneously.

Kaolinite clay (Kaolinite No. 7, Dixie Rubber Pit) was tested under fully water-saturated conditions. The samples were cylindrical disks, 127 mm in diameter by 6.35 mm thick and were sandwiched by two fused quartz plates 127 mm in diameter by 6.35 mm thick.

Measurements of the dilatational wave velocities were made by the pulse-first-arrival method in a refrigerated bath filled with Dow Corning 200 silicone oil used both as a cooling medium and as a medium for transmitting the input pulses across the soil specimen to the receiver.

The amount of unfrozen water contained in a frozen soil specimen was determined by monitoring the temperature of the specimen and the amount of heat exchanged between the specimen and surrounding silicone oil. The circumference of the specimen was insulated so that heat exchange occurred in the direction perpendicular to the surface of the specimen. Copper-constantan foil thermocouples 5.1 μm thick were attached near the center of both surfaces of the quartz disks to measure the temperature difference across them. A thermocouple also was placed at the center of the specimen to measure its temperature. With this arrangement, it was possible to determine the following:

The rate of heat exchange, Q , is given as

$$Q = K S(t)/(h_q h_s), \tag{1}$$

and the volumetric heat capacity, C , which includes the heat of fusion, is given as

$$C = \gamma_d [c_c + c_i w_T + (c_w - c_i)w(t) + L(t) \partial w(t)/\partial T], \tag{2}$$

where h_q = thickness of the two quartz disks (cm); h_s = thickness of the specimen (cm); $I(t)$ = ice content (g ice/g dry soil); K = thermal conductivity of fused quartz (cal/cm s °C); $L(t)$ = heat of fusion of water (cal/g); $Q(t)$ = rate of heat exchange between the unit volume of soil specimen and surrounding media (cal/cm³ s); $S(t)$ = sum of the temperature differences across two quartz disks (°C); $T(t)$ = temperature of the specimen (°C); t = time (s); $w(t)$ = water content (g water/g dry soil); $w_T = I(t) + w(t)$; γ_d = dry density of the specimen (g/cm³); c_c = specific heat capacity of clay (cal/g °C); c_i = specific heat capacity of ice (cal/g °C); and c_w = specific heat capacity of water (cal/g °C).

The value of c_i can be assumed to be equal to the value for pure bulk ice, which is obtainable at any temperature by means of the equation presented by Dorsey (1940):

$$c_i = 0.5057 + 0.001863T. \tag{3}$$

The heat of fusion, $L(t)$, is also given by Dorsey (1940):

$$L(t) = 79.62 + 0.5019T - 0.00148T^2 + 0.000012T^3. \tag{4}$$

Oster and Low (1964) have reported values for c_w for different values of w_T in unfrozen clay-water systems. Their values are averages for the temperature interval 0–30 °C. Assuming the values to be approximately correct for subzero temperatures, we used a constant value of $c_w = 1.006$ cal/g °C.

From the heat balance, we get

$$\gamma_d [c_c + c_i w_T + (c_w - c_i)w(t)] dT(t)/dt + L \gamma_d dw(t)/dt = K S(t)/(h_q h_s). \tag{5}$$

Equation 5 was solved in the following way: The total time interval (0, t_T) was divided by the points

$$0 = t_0 < t_1 < t_2 < \dots < t_{n-1} < t_n = t_T \tag{6}$$

into parts of length

$$\Delta t_i = t_i - t_{i-1}. \tag{7}$$

For each time interval (t_i, t_{i+1}), $T(t)$ and $S(t)$ were approximated by

$$T(t) = a_T^i t^2 + b_T^i t + c_T^i \tag{8}$$

$$S(t) = a_s^i t^2 + b_s^i t + c_s^i. \quad (9)$$

The constants $a_T, b_T, c_T, a_s, b_s,$ and c_s were determined by the use of experimental data. Substituting Eq. (8) and (9) into Eq. (5), an ordinary linear differential equation of the first order is derived:

$$d w(t)/dt + p^i(t) w(t) = Q^i(t) \quad t_i \leq t \leq t_{i+1}, \quad (10)$$

where

$$p^i(t) = c_w - c_i/L (2a_T^i t + b_T^i) \quad (11a)$$

and

$$Q^i(t) = K/L \gamma_d h_q h_s (a_s^i t^2 + b_s^i t + c_s) - 1/L (c_c + c_i w_T) (2a_T^i t + b_T^i). \quad (11b)$$

The solution of Eq. (10) is given as

$$w(t) = e^{-R(t)} \left[\int_{t_i}^t Q^i(t) e^{R(t)} dt + w^i e^{R(t)} \right] \quad (12)$$

$$t_i \leq t \leq t_{i+1},$$

where

$$R(t) = c_w - c_i/L (a_T^i t^2 + b_T^i t) \quad (13a)$$

and

$$w^i = w(t_i). \quad (13b)$$

The unfrozen water content, $w(t)$, was calculated from Eq. (7) for each time interval.

Figures 2 and 3 show the record of the temperature and dilatational velocity of the specimen for heating and cooling cycles, respectively. In Figure 4 the dilatational velocities are plotted as a function of temperature. The measurements of the heating and cooling cycles do not agree in the temperature range from 0 to -10°C . Similar results were observed in Figure 4, when the unfrozen water contents are plotted against temperature. In Figure 5, the dilatational wave velocities are plotted against the unfrozen water content. The relationship between the dilatational velocity and the unfrozen water content can almost be represented by a single curve, regardless of the cycle.

It should be mentioned that in calculating the unfrozen water content, the temperature dependence of the specific heat capacities of clay and water has been neglected. Also, the temperature distribution in the specimen, as well as the nonlinear effect of temperature gradient in quartz disks,

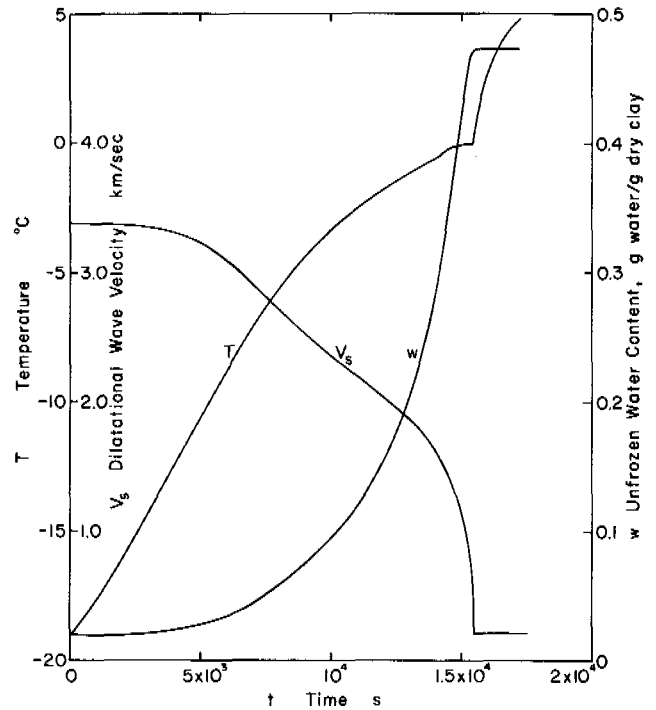


FIGURE 2 Record of the temperature of the specimen $T(t)$, the unfrozen water content $w(t)$, and the dilatational velocity V_s for a heating cycle.

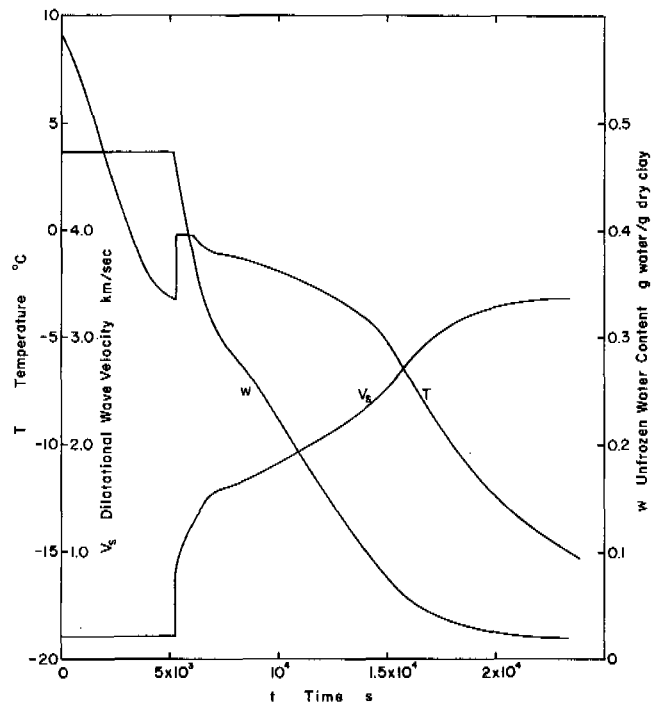


FIGURE 3 Record of the temperature of the specimen $T(t)$, the unfrozen water content $w(t)$, and the dilatational velocity V_s for a cooling cycle.

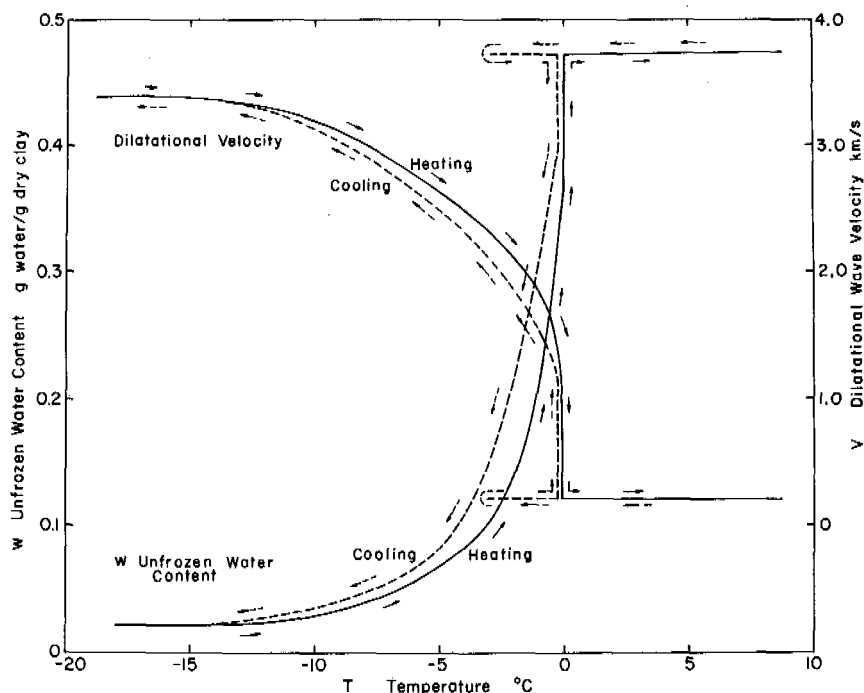


FIGURE 4 Dilatational velocity and unfrozen water content versus temperature.

was neglected. Although all these factors may add up to a certain amount of error in the final results, there is very little doubt that the unfrozen water content is a major factor contributing to a variation of the dilatational wave velocity with temperature.

Shear Waves in Frozen Soil

Two commonly used pulse-transmission techniques to measure shear wave velocities of earth material are the pulse

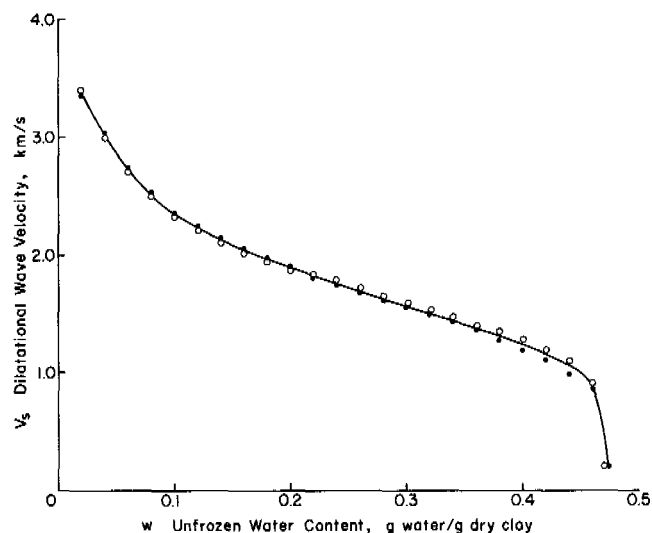


FIGURE 5 Dilatational velocity vs. unfrozen water content. The solid circles indicate the cooling cycle; the open circles, the heating cycle.

first arrival method by the use of shear transducers and the critical angle method. The quality of the specimen tends to determine the accuracy of the measurements. In the former method, since the shear wave has an inherently slow velocity, the presence of any component of the faster dilatational wave, whatever its source, tends to obscure the exact onset of the first arrival of the shear wave. Important factors influencing the accuracy of the measurement include coupling between the transducer and the specimen and proper choice of the sensitivity of the receiving transducer.

The critical angle method is based on the elementary theory of critical refraction in a solid. This method was first applied by Schneider and Burton³⁹ to metals and subsequently was used by Subbarao and Rao⁴¹ on rocks. Several studies were reported.^{5,6,25,30,46}

The shear velocities of three standard types of soils under fully water-saturated conditions are presented as a function of temperature in Figure 6. The measurements were made by the critical angle method, in which the specimen (114 mm in diameter by 25.4 mm thick) was mounted in the sample holder and was submerged in the tank filled with Dow Corning 200 silicone oil so as to intercept the ultrasonic beam. The surface of the specimen was sealed by a thin vinyl sheet. A detailed description of the critical angle method has been given in the literature.^{5,6,25} In practice, the shear critical angle was determined more accurately than the dilatational angle for the frozen soil specimens tested. Also, it was found that the dilatational wave velocities can be determined more accurately than the dilatational angle by measuring the difference in delay time between the pulses received after crossing the liquid path alone as com-

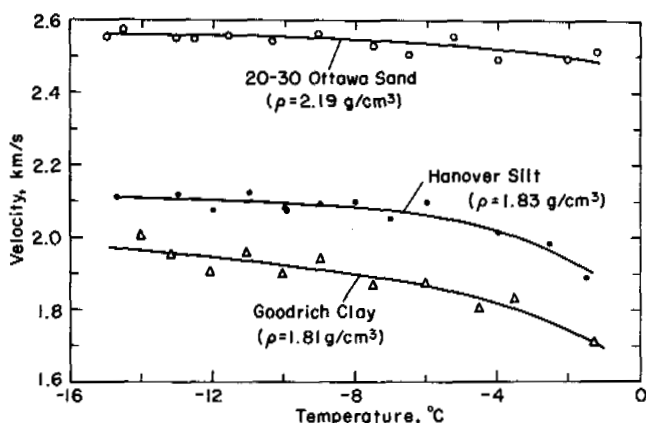


FIGURE 6 The shear wave velocity versus temperature for 20-30 Ottawa sand, Hanover silt, and Goodrich clay under fully water-saturated conditions. Wet density is ρ .

pared with their passage through liquid and specimen interposed at normal incidence.

As shown in Figure 6, the shear wave velocity tends to decrease with ascending temperature. The role of unfrozen water in shear wave propagation is not as pronounced as it is on the dilatational wave. Fluid water cannot accommodate shear, and what we consider to be shear wave propagation must result from tortuous solid-only paths and/or multiply converted shear-dilatation motion. In view of the fact that the slope of the velocity-temperature curves does not differ markedly among the tested samples, the soil mineral matrix might play a major role in shear wave propagation. The shear velocities of crystalline rock and polycrystalline ice are about 3.0 and 1.6 km/s, respectively. The measured velocities of frozen soils fall between these two bounds.

SHOCK WAVE PROPAGATION IN FROZEN SOILS

Brief Review of Literature

Over the past 20 years, considerable progress has been made in the field of research on shock wave propagation in solids.^{19,20,26} A shock wave can be introduced into a specimen by explosives and a gas gun. The gas-gun technique^{7,42} is more suited to studies in the relatively low stress range, up to 100 kbar, mainly because of controlled impacts, than are the explosively driven plate impact systems where pressures in the megabar region can be attained. The measurements that can be accurately made at present include the normal stress component by pressure transducers, such as quartz gage²⁴ and a manganin gage,^{11,23} the free-surface velocity by laser interferometry,^{8,9} and the particle velocity by electromagnetic velocity gages.¹⁷

Although advanced shock wave techniques have been widely applied to metals, plastics, and unfrozen earth mate-

rials, little attention has been directed toward frozen earth materials. Anderson³ obtained the Hugoniot data for frozen soils and ice in the pressure range from 60 to 500 kbar by using explosives to accelerate a flat plate that then impacted the specimen.

Hugoniot Equation of State

Flat-plate impact experiments by the use of a standard 102-mm-diameter bore, single stage gas gun were made on 100-200 Ottawa sand of two levels of saturation (23 and 100 percent) and two temperatures (20 and -10°C). Ottawa sand is one of the standard granular soils, is well rounded, and consists of pure quartz. The sand used in this study was the portion passed through a No. 100 sieve and retained on a No. 200 sieve. The basic properties of the specimen are tabulated in Table I. The specimen of cylindrical disk shape, 76.2 mm in diameter by 19.1 mm thick, was encapsulated in Plexiglas (polymethyl methacrylate) and held at the muzzle of the gas gun as shown in Figure 7. The specimen temperature was maintained within $\pm 0.1^{\circ}\text{C}$ during the experiment by circulating a coolant through an annular passage in the back plate using a remote control system. Manganin piezoresistive gages were used to measure incident and transmitted stress-time profiles. The details of a typical target assembly are shown in Figure 8. Note that there are relatively thin Plexiglas buffer plates between the gages and the specimen. Since the buffer plates are many solid grain diameters thick, they serve to average and smooth out irregularities in the wave fronts that arise from inhomogeneities in the soil. The projectile impact velocity was determined within an error of ± 10 ns by electronic counters that were triggered as the pins contacted annular aluminum rings on the projectile.

The relations governing the behavior of a plane, one-dimensional, steady-state shock wave propagating in a continuous medium have been derived and discussed by many investigators.²¹ The Hugoniot points were computed by the impedance match technique.⁴⁴ The measured projectile

TABLE 1 Basic Properties of Specimens

Property	1	2	3	4
Test temperature ($^{\circ}\text{C}$)	20	-10	20	-10
Degree of saturation	100	100	23	23
Density, ρ_0 (g/cm^3)	2.06 \pm 0.02	1.98 \pm 0.01	1.65 \pm 0.02	1.68 \pm 0.01
Dry density, ρ_d (g/cm^3)	1.65	1.65	1.55	1.58
Porosity, n (%)	37	37	43	42
Water (or ice) (%)	22	22	6	6

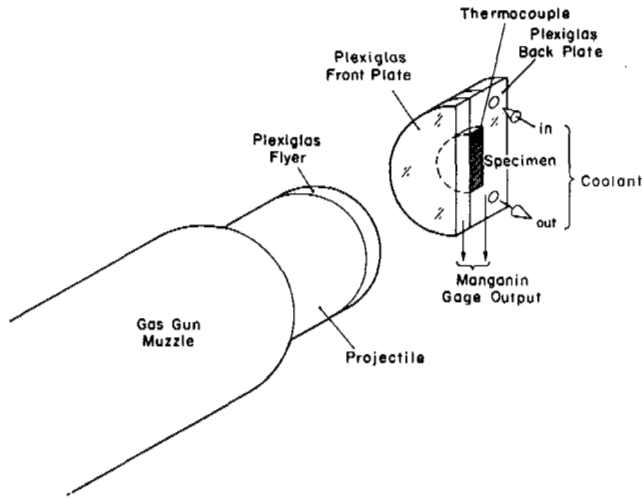
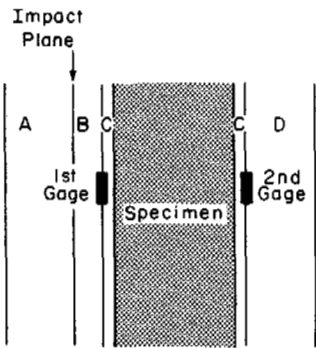


FIGURE 7 Frozen soil target configuration.

impact velocity, the known release adiabat of Plexiglas, and the stress in the specimen measured by the front gage uniquely determine a Hugoniot point in the particle-velocity and stress plane. The stress in the specimen was detected as the step change soon after the initial rise recorded by the front gage. This step change is due to a reflected shock wave at the interface between the Plexiglas and the specimen.

After propagation through the specimen, the wave entered the Plexiglas back plate. Here, after transmission by the relatively thin Plexiglas buffer plate, its stress was measured by the second manganin gage. The difference in shock impedance between the specimen and the Plexiglas plate causes a reflection to occur at this interface. The record of the rear gage was taken for the detailed analytical study on the constitutive equations of the specimen together with the release adiabat. However, here these data are used to make a qualitative comparison between the incident and the transmitted wave profiles.

The Hugoniot data derived from the front gage measurement are given in Table II and plotted in Figure 9. The stress versus time profiles for saturated unfrozen and frozen specimens are presented in Figure 10.



Design	Plexiglas Thickness mm
A (Flyer)	12.7
B (Face)	6.3
C (Buffer)	1.6
D (Back)	12.7

FIGURE 8 Details of a typical target assembly. Notice there are relatively thin Plexiglas buffer plates between the gage and the specimen.

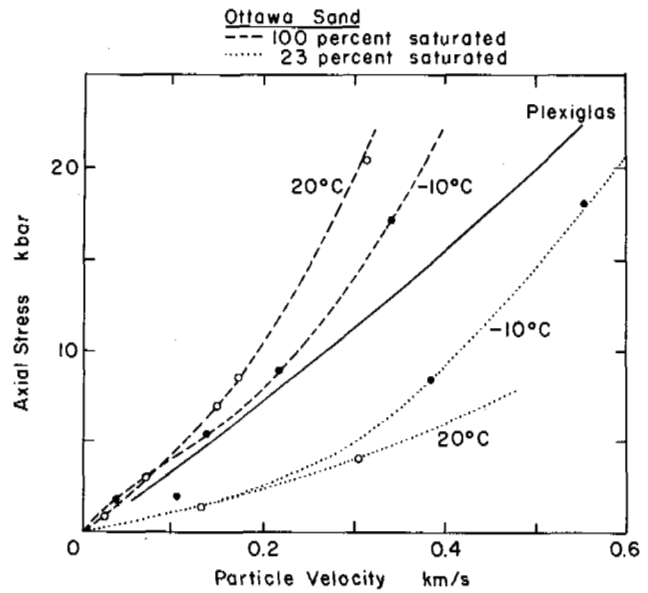


FIGURE 9 Stress versus particle velocity for Ottawa sand. The Hugoniot for Plexiglas is due to Barker and Hollenback. The equation relating the axial stress, σ (kbar), and the particle velocity, u (km/s), obtained by the least square fits are $\sigma = 35.4 u + 48.6 u^2 + 156.6 u^3$ for 20°C and $\sigma = 51.6 u - 179.5 u^2 + 711.1 u^3 - 600.7 u^4$ for -10°C .

In this figure, time is normalized to 19 mm propagation distance, and stress is scaled so that the peak stress of a transmitted wave equals the input Hugoniot stress detected by the front gage. From multiplicative factor f given in Table II the original stress time profiles can be obtained as follows:

$$\sigma \text{ (the stress record by the rear gage)} = \text{(the stress plotted in Figure 10a, b)/}f.$$

The records of the transmitted waves for 23 percent saturated specimens are destroyed shortly after shock arrival by the shocks that travel around the specimen through the container due to the extremely low shock velocity in the specimen.

Although the data points are limited, the trend of the data is clear. The 100 percent saturated, 20°C Hugoniot is a simple concave upward curve that would be expected to propagate a well-defined shock. The record of transmitted stress profiles in 100 percent saturated, -10°C specimens shows multiple shock wave structure. The Hugoniot appears to have an inflection point around 5 kbar. The concave downward Hugoniot at low stress would be expected to yield a ramped precursor, while the concave upward portion would allow steep fronted shock to form at about 3.5 kbar. This is indeed the case as is verified by the transmitted profiles in Figure 10b. In detail, the precursor shows a fairly sharp initial rise to approximately 1 kbar followed by a very slow rise creating a short plateau and the second fairly sharp rise to approximately 3.5 kbar.

TABLE II Summary of Experimental Results

Shot No.	Degree of Saturation (%)	Temperature (°C)	Impact Velocity (km/s)	Impact Stress (kbar)	Hugoniot Stress (kbar)	Hugoniot Particle Velocity (km/s)	Precursor Velocity (km/s)	Shock Velocity (km/s)	Specific Volume Ratio (V/V_0)	f	Hugoniot Particle Velocity (km/s)				Relative Error (%)
											Quartz	Water	Ice	Predicted	
1-1	100	20	0.0559	0.9	1.0	0.027		1.80	0.985	1.09	0.006	0.063		0.027	0.0
1-2	100	20	0.1517	2.6	2.8	0.071		2.04	0.965	1.25	0.018	0.159		0.069	-2.8
1-3	100	20	0.1674	6.2	6.9	0.150		2.52	0.941	1.15	0.046	0.325		0.144	-4.0
1-4	100	20	0.4009	7.5	8.5	0.175		2.41	0.927	1.27	0.056	0.380		0.169	-3.4
1-5	100	20	0.5242	16.1	20.9	0.315		2.90	0.891	1.29	0.138	0.736		0.336	6.7
2-1	100	-10	0.0846	1.5	1.7	0.037	4.41	3.53	0.990	1.45	0.012		0.065	0.030	-19.0
2-2	100	-10	0.2778	5.1	5.3	0.137	3.88	2.09	0.934	1.27	0.034		0.330	0.143	4.4
2-3	100	-10	0.4495	8.5	8.8	0.219	4.85	1.96	0.888	1.17	0.058		0.490	0.214	-2.3
2-4	100	-10	0.4781	14.9	17.0	0.343	3.73	2.31	0.852	1.08	0.112		0.750	0.334	-2.6
3-1	23	20	0.1713	3.0	1.4	0.132		1.08	0.878		0.008	0.086		0.130	-1.5
3-2	23	20	0.4174	7.8	4.0	0.305		1.21	0.748		0.026	0.213		0.224	-27.
3-3	23	20	0.5962	18.6	6.0	0.787		1.14	0.310		0.039	0.293		0.277	-64.
4-1	23	-10	0.1595	2.8	2.0	0.105		1.21	0.913		0.012		0.070	0.153	46.
4-2	23	-10	0.5916	11.2	8.0	0.384		1.34	0.713		0.052		0.460	0.326	-15.
4-3	23	-10	0.6286	20.2	18.1	0.554					0.120		0.770	0.505	-8.8

The existence of the precursor traveling with approximately the speed of sound is evidently due to ice contained in the specimen. The isothermal compression of ice at -10°C causes four phase changes up to 25 kbar,^{12,13} namely, Ice I to water at 1.11 kbar, water to Ice V at 4.42 kbar; Ice V to Ice VI at 6.25 kbar; and, finally, Ice VI to Ice VIII at 20.8 kbar. Under the isothermal compression of 100–200 Ottawa sand at -10°C , ice contained in it goes through almost the same path described above¹³ and, apparently, is free from the interference of soil minerals. The effect of phase changes on Hugoniot has been discussed.^{1,33,45} McQueen³³ classified the phase changes according to the sign of the slope, dP/dT , of the phase line and discussed their effect. For ice, the sign of the slope is positive for all phase changes, except the first one from Ice I to water, and all phase changes, if they occur under shock, are detectable by the particle and shock velocity data.³³ The rough estimate of the latent heat by the use of the Clausius-Clapeyron equation indicates that the latent heat of the first two phase changes—namely, Ice I to water and water to Ice V—are almost of the same magnitude, but those of Ice V to Ice VI and Ice VI to Ice VIII are on the order of one hundredth and one tenth of the first, respectively. Therefore, it can be anticipated that the effect of the first two phase changes on shock waves is more pronounced and more easily detectable than that of the rest of the phase changes. The initial rise to 1 kbar and the second rise to 3.5 kbar may be interpreted in connection with these first two phase changes. Accurate interpretation of wave structures, however, needs further investigation.

The effect of water content on the Hugoniot is significant as seen in Figure 9. As the water content decreases, more air fills the pores and the specimen becomes easier to compress. The construction of Hugoniot curves for porous materials was considered by many authors.^{14,16,18,27,32} Such theories are based on thermodynamic relations and differ from each other mainly in the treatment of dynamic pore-collapse relations. We calculate Hugoniot particle velocities at each experimental Hugoniot stress in Table II by using the equation derived by Doronin and Stupnikov,¹⁶ in which a complete collapse of pores by weak shock waves (to ~ 100 kbar) was assumed. The Hugoniot of quartz,²⁴ water,³² and polycrystalline ice were used in the calculations. The results of the calculations are also given in Table II. Agreement between the experimental results and the calculated values is excellent for the saturated specimens, except shot No. 2-1. However, there is a large discrepancy for the unsaturated specimens.

It is evident that further work is required to obtain a thorough understanding of the dynamic behavior of frozen earth materials. At present, our efforts are directed toward the relationships between dynamic elasticity and shock compression, which have received increased interest recently.^{2,28,31,40} The results of such work will be published soon.

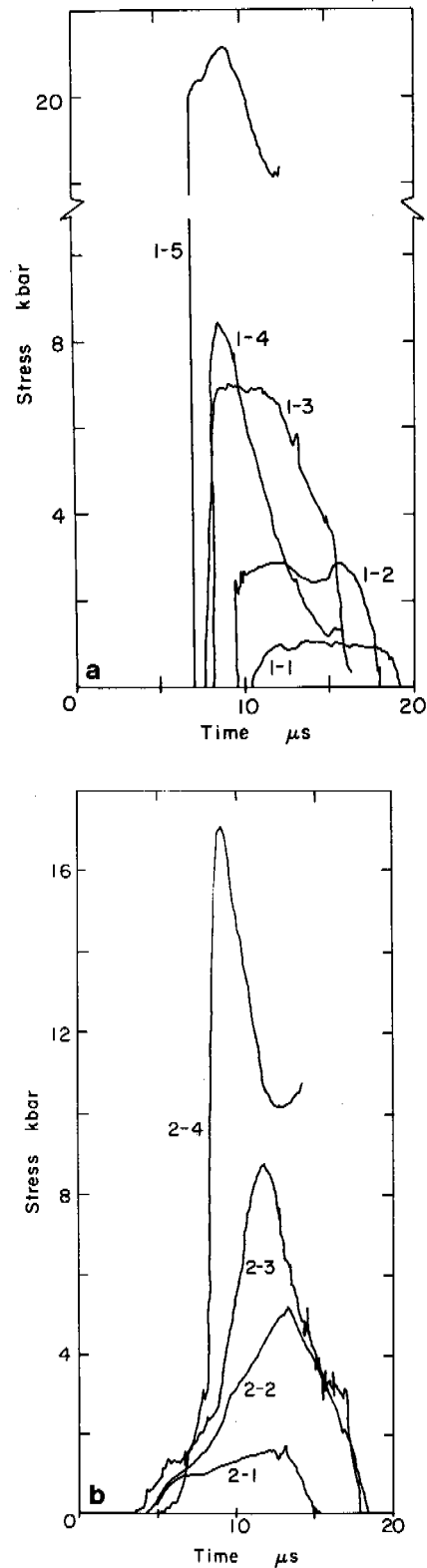


FIGURE 10 Transmitted stress profiles in Ottawa sand, 100 percent saturated (a) at 20°C and (b) at -10°C .

ACKNOWLEDGMENT

This paper presents the results of research performed by the U.S. Army Cold Regions Research and Engineering Laboratory under the sponsorship of the Advanced Research Projects Agency. The work was monitored by Dr. Stanley Ruby.

REFERENCES

1. Ahrens, T. J., D. L. Anderson, and A. E. Ringwood. 1969. Equations of state and crystal structures of high-pressure phases of shocked silicates and oxides. *Rev. Geophys.* 7(4):667-707.
2. Anderson, D. L. 1969. Bulk modulus-density systematics. *J. Geophys. Res.* 74(15):3857-3864.
3. Anderson, G. D. 1968. The equation of state of ice and composite frozen soil material. CRREL Research Report 257. U.S. Army Cold Regions Research and Engineering Laboratory, Hanover, New Hampshire.
4. Anderson, O. L., and R. C. Lieberman. 1966. Sound velocities in rocks and minerals. VESIAC State-of-the-Art Report, Willow Run Laboratory, University of Michigan, Ann Arbor.
5. Attewell, P. B. 1970. Triaxial anisotropy of wave velocity and elastic moduli in slate and their axial concordance with fabric and tectonic symmetry. *Int. J. Rock Mech. Min. Sci.* 7(2):193-207.
6. Banthia, B. S., M. S. King, and I. Fatt. 1965. Ultrasonic shear wave velocities in rocks subjected to simulated overburden pressure and internal pore pressure. *Geophysics* 30(1):117-121.
7. Barker, L. M., and R. E. Hollenback. 1964. System for measuring the dynamic properties of materials. *Rev. Sci. Instr.* 35(6):742-746.
8. Barker, L. M., and R. E. Hollenback. 1965. Interferometer technique for measuring the dynamic mechanical properties of materials. *Rev. Sci. Instr.* 36(11):1617-1620.
9. Barker, L. M. 1968. Fine structure of compressive and release wave shapes in aluminum measured by the velocity interferometer technique. *In Behavior of dense media under high dynamic pressures. Proceedings of the IUTAM symposium H.D.P., Paris, France, Sept. 1967.* Gordon and Breach, New York.
10. Barnes, D. F. 1966. A review of geophysical method for delineating permafrost, p. 349-355. *In Permafrost: Proceedings of an international conference.* National Academy of Sciences, Washington, D.C.
11. Bernstein, D., and D. D. Keough. 1964. Piezoresistivity of manganin. *J. Appl. Phys.* 35(5):1471-1474.
12. Bridgman, P. W. 1964. *Collected experimental papers.* Harvard University Press, Cambridge.
13. Chamberlain, E., and P. Hoekstra. 1970. Isothermal compressibility of frozen soil and ice to 30 kilobars at -10°C . USA CRREL Tech. Rep. 225.
14. Cowpenthwaite, M., and T. J. Ahrens. 1967. Thermodynamics of the adiabatic expansion of a mixture of two phases. *Am. J. Phys.* 35:951-955.
15. Desai, K. P., and E. J. Moore. 1967. Well log interpretation in permafrost. *Trans. Prof. Well Log Anal.* 6:1-27.
16. Doronin, G. S., and V. P. Stupnikov. 1970. Computation of Hugoniot for mixtures and for porous materials. *Izv. Sib. Otd. Ser. Tekh. Nauk.* 3(1):104-105.
17. Dremmin, A. N., and G. A. Adadurov. 1964. The behavior of glass under dynamic loading. *Soviet Phys.-Solid State* 6:1379.
18. Dremmin, A. D., and A. I. Karpukhin. 1960. A method of determining Hugoniot curves for dispersed materials. *Z. Prikl. Mekh. Tekh. Fiz.* 3:184-188.
19. Duvall, G. E. 1962. Shock waves in the study of solids. *Appl. Mech. Rev.* 15(11):849-854.
20. Duvall, G. E., and G. R. Fowles. 1963. Shock waves. *In R. S. Bradley [ed.] High pressure physics and chemistry.* Academic Press, New York.
21. Fowles, R., and R. F. Williams. 1970. Plane stress wave propagation in solids. *J. Appl. Phys.* 41(1):360-363.
22. Frolov, A. D. 1961. Rasprostranenie ul'trazubuka v merzlykh peschano glinistykh porodakh. *Izv. Akad. Nauk. SSSR Ser. Geofiz.* 5:34.
23. Fuller, P. J. A., and J. H. Price. 1964. Dynamic pressure measurements to 300 kilobars with a resistance transducer. *Br. J. Appl. Phys.* 15(6):751-758.
24. Graham, R. A., F. W. Neilson, and W. B. Benedick. 1965. Piezoelectric current from shock-loaded quartz—A submicrosecond stress gauge. *J. Appl. Phys.* 36(5):1775-1783.
25. Gregory, A. R. 1963. Shear wave velocity measurements of sedimentary rock samples under compression p. 439-471. *In C. Fairhurst [ed.] Proceedings of the fifth international symposium on rock mechanics.* University of Minnesota Press, Minneapolis.
26. Hamman, S. D. 1966. Effects of intense shock waves. *In R. S. Bradley [ed.] Advances in high pressure research.* Academic Press, New York.
27. Herrmann, W. 1969. Constitutive equation for the dynamic compaction of ductile porous materials. *J. Appl. Phys.* 40(6):2490-2499.
28. Huang, Y. K. 1971. Interrelationship between acoustic and shockwave properties of solids. *J. Appl. Phys.* 42(10):4084-4085.
29. Kaplar, C. W. 1966. Laboratory determination of dynamic moduli for frozen soils and of ice, p. 293-301. *In Permafrost: Proceedings of an international conference.* National Academy of Sciences, Washington, D.C.
30. King, M. S., and I. Fatt. 1962. Ultrasonic shear wave velocities in rocks subjected to simulated overburden pressure. *Geophysics* 27(5):590-598.
31. Lamberson, D. L., J. R. Asay, and A. H. Guenther. 1972. Equation of state of polystyrene and polymethylmethacrylate from ultrasonic measurements at moderate pressures. *J. Appl. Phys.* 43(3):976-985.
32. Lysne, P. C. 1970. A comparison of calculated and measured low-stress Hugoniot and release adiabats of dry and water-saturated tuff. *J. Geophys. Res.* 75(23):4375-4386.
33. McQueen, R. G., S. P. Marsh, and J. N. Fritz. 1967. Hugoniot equation of state of twelve rocks. *J. Geophys. Res.* 72(20):4999-5036.
34. Müller, G. 1961. Geschwindigkeitsbestimmung elastischer Wellen in geofrorenen Gesteinen und die Anwendung akustischer Messungen auf Untersuchungen des Frostmantels an Gefrierschichten. *Geophys. Prospect.* 9:276-295.
35. Nakano, Y., R. J. Martin III, and M. Smith. 1972. Ultrasonic velocities of the dilatational and shear waves in frozen soils. *Water Resour. Res.* 8(4):1024-1030.
36. Nakano, Y., and R. Arnold. Acoustic properties of frozen Ottawa sand. *Water Resour. Res.* (In press)
37. Neresova, Z. A., and N. A. Tsytoich. 1966. Unfrozen water in frozen soils. p. 230-234. *In Permafrost: Proceedings of an international conference.* National Academy of Sciences, Washington, D.C.
38. Paterson, N. R. 1956. Seismic wave propagation in porous granular media. *Geophysics* 21(3):691-714.
39. Schneider, W. C., and C. J. Burton. 1949. Determination of the elastic constants of solids by ultrasonic methods. *J. Appl. Phys.* 20(1):48-58.
40. Simmons, G., and W. F. Brace. 1965. Comparison of static and

dynamic measurements of compressibility of rocks. *J. Geophys. Res.* 70(22):5649-5656.

- 41. Subbarao, K., and B. R. Rao. 1957. A simple method of determining ultrasonic velocities in rocks. *Nature* 180:978.
- 42. Thunborg, S., Jr., G. E. Ingram, and R. A. Graham. 1964. Compressed gas gun for controlled planar impacts over a wide velocity range. *Rev. Sci. Instr.* 35(1):11-14.
- 43. Timur, A. 1968. Velocity of compressional waves in porous media at permafrost temperatures. *Geophysics* 33(4):548-595.
- 44. Walsh, J. M., M. H. Rice, R. G. McQueen, and F. L. Yarger.

1957. Shock-wave compressions of twenty-seven metals: Equations of state of metals. *Phys. Rev.* 108:196-216.

- 45. Wang, C. 1967. Phase transitions in rocks under shock compression. *Earth Planet. Sci. Lett.* 3(2):107-113.
- 46. Wyllie, M. R. J., C. H. F. Gardner, and A. R. Gregory. 1962. Studies of elastic wave attenuation in porous media. *Geophysics* 27(5):569-589.
- 47. Zykov, I. U. D. 1966. Ultrasonic methods used in the study of elastic properties of frozen ground samples. *Merzlotnye Issled.* 5:184-198.

PRACTICAL EXTENSIONS TO A THEORY OF CONSOLIDATION FOR THAWING SOILS

J. F. Nixon and N. R. Morgenstern

UNIVERSITY OF ALBERTA
Edmonton, Alberta

INTRODUCTION

When frozen ground thaws, water is released and settlements develop as the water is squeezed from the ground. If the rate of generation of water exceeds the discharge capacity of the soil, excess pore pressures will develop, and these can lead to the failure of foundations and slopes. As recognized, for example, by Tsytoich *et al.*,⁹ the development of a theory of consolidation for thawing soils is of considerable interest for the resolution of a wide variety of problems that are encountered with building on permafrost. The theory is applicable to virtually all design problems that involve a rate of settlement or a change in shear strength during thawing.

Morgenstern and Nixon⁶ have given some analytical solutions for the case of one-dimensional thawing of a uniform, homogeneous, frozen soil. As illustrated in Figure 1, the position of the thaw front is found from the Neumann solution, assuming that a step increase in temperature is applied at the surface of the soil. That is:¹

$$X(t) = \alpha\sqrt{t} \quad (1)$$

where X denotes the depth to the thaw plane, t denotes time, and α is a constant that depends on the soil thermal properties and the temperature boundary conditions.

The thawed soil is assumed to be a linearly compressible medium and the flow of water through it obeys Darcy's law. Hence, the consolidation of the thawed soil may be expressed

in terms of Terzaghi's theory of consolidation:

$$\frac{\partial u}{\partial t} = c_v \frac{\partial^2 u}{\partial x^2} \quad (2)$$

where $u(x, t)$ denotes the pore water pressure in excess of hydrostatic, c_v denotes the coefficient of consolidation, and x denotes the depth measured from the surface.

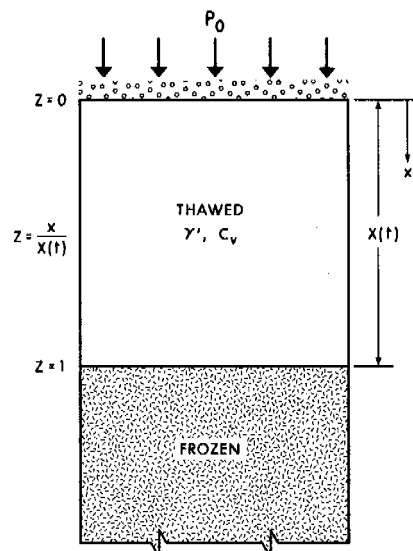


FIGURE 1 One-dimensional thaw-consolidation.

The upper surface is taken as free draining and the governing equation may be solved if the boundary condition at the thaw interface can be stated. From considerations of continuity at the interface, Morgenstern and Nixon⁶ show that the following holds:

$$(P_0 - \sigma'_0) + \gamma'X - u = -\frac{c_v}{dX} \frac{\partial u}{dt}, \quad (3)$$

where P_0 denotes an externally applied loading, σ'_0 denotes the constant initial effective stress in the thawed soil, and γ' denotes the submerged density of the soil.

In many ice-rich soils, the initial effective stress, σ'_0 , will be very close to zero; with this further assumption, which is on the safe side, solutions to Eq. (2) have been obtained for these boundary conditions that give the variation of the pore pressure distribution and settlement with time. Special attention has been paid to the limiting cases of a weightless soil and to a soil loaded by self-weight alone.

Some of the more important results of the analysis follow:

1. During thawing, the settlement is proportional to \sqrt{t} .
2. The pore pressure at the thaw interface is a function of the thaw:consolidation ratio R , where:

$$R = \frac{\alpha}{2\sqrt{c_v}}, \quad (4)$$

3. The degree of consolidation is a function of the thaw:consolidation ratio R . (When S_{\max} is the total settlement that would occur if thawing were suddenly stopped at time t and S_t is the consolidation settlement that occurs up to time t , then the degree of consolidation is defined as S_t/S_{\max} .)

4. Postthaw pore pressures may be computed using initial values given by the excess pore pressures at the end of thawing.

Morgenstern and Smith⁷ have described the results of experiments carried out in an oedometer that was specially constructed to simulate the stress and thermal boundary conditions given above. The apparatus measured settlements, temperatures at various points through the soil sample, and the excess pore pressure at the base of the sample. The predictions of the theory were generally confirmed, and, in particular, a comparison between the observed pore pressures and those calculated from the theory proved very encouraging.

In the following, this theory is extended to consider more general thaw rates and, separately, a nonlinear stress-strain relationship for the soil skeleton. This extends the range of practical problems that can be embraced by the theory.

EXTENSION TO A MORE GENERAL THAW RATE

One of the most serious limitations of the linear theory described above is the assumption that the thaw interface moves proportional to \sqrt{t} . This is, of course, a valid relationship for the important case where a step increase in temperature is applied at the surface of a homogeneous frozen mass of soil. But for reasons of nonhomogeneity, varying surface temperatures, or two dimensional effects, a more general relationship between thaw depth and time may emerge from the associated problem in heat transfer. It will be seen later how such a relationship is extracted from a solution for heat conduction around a hot pipeline in permafrost.

An analytical solution in closed form is available for the case of thaw depth proportional to \sqrt{t} , but it appears unlikely that such exact solutions might be obtained for arbitrary movements of the thaw front. Numerical methods, however, may be employed to obtain a solution for the consolidation problem to almost any required degree of accuracy.

Let the movement of the thaw front be given by:

$$X(t) = Bt^n, \quad (5)$$

and its velocity by:

$$\frac{dX}{dt} = n Bt^{n-1}. \quad (6)$$

This power law permits expression of a variety of realistic relationships between X and t , with B and n specified as constants.

Rewriting the boundary Eq. (3) at the thaw interface using Eq. (5) and (6), we obtain the set of equations:

$$t > 0; u = 0; x = 0, \quad (7)$$

$$t > 0; \frac{\partial u}{\partial t} = c_v \frac{\partial^2 u}{\partial x^2}; 0 < x < X(t), \quad (8)$$

$$t > 0; (P_0 - \sigma'_0) + \gamma' Bt^n - u = \frac{c_v}{n Bt^{n-1}} \frac{\partial u}{\partial x}; x = X(t) \quad (9)$$

$$t \geq 0; X = Bt^n \quad (5)$$

These equations may be written in finite difference form, using a scheme proposed by Crank and Nicholson,² and the moving boundary is accounted for by either of the methods described by Murray and Landis.⁸ The advantage of the Crank-Nicholson scheme is that it remains unconditionally stable for all values of the time step Δt , and the accuracy is much improved over other somewhat simpler methods.

The simultaneous equations so produced are tridiagonal

when written in matrix form, and a simple algorithm derived from the Gaussian elimination technique for simultaneous equations provides a fast efficient solution.

Excess pore pressures $u(x,t)$ were evaluated at selected times by a program written for a digital computer. The degree of consolidation in the thawed soil was evaluated as in the linear theory from the expression:

$$\frac{S_t}{S_{max}} = 1 - \frac{\int_0^x u \, dx}{(P_0 - \sigma'_0)X + \frac{\gamma'X^2}{2}} \quad (10)$$

The integral term in Eq. (10) may be evaluated using a simple numerical integration technique such as the trapezoidal rule.

Values of the normalized excess pore pressure at the thaw interface and the degree of consolidation are plotted against a time factor for the two extreme loading conditions $\gamma' = 0$, and $(P_0 - \sigma'_0) = 0$ in Figures 2, 3, 4, and 5. It was found that, for a given value of the power n , a unique relationship emerged between excess pore pressure, or settlement, and the time factor. The time factor T is defined as:

$$T = \frac{c_v t}{X(t)^2} \quad (11)$$

Values of n from zero to unity were chosen to cover the full range of physically realistic problems. A value of n equal to zero corresponds to a conventional fixed boundary consolidation problem, with the depth of consolidating soil set permanently equal to B , and an initial excess pore pressure equal to $(P_0 - \sigma'_0) + \gamma'X$. These results for $n = 0$ are

plotted for comparison purposes in order to form a lower bound to the family of curves.

The constant velocity thaw front ($n = 1$) is thought to be the upper bound for this set of curves, as this thaw rate is only achieved when, for example, the surface temperature of a homogeneous soil mass increases exponentially with time. The curious fact emerges that, for the constant velocity thaw front, the time factor T decreases with increasing time.

For thawing proportional to the square root of time ($n = 1/2$), the time factor T is constant for all time, and it may be shown to be:

$$T = \frac{1}{4R^2}, \text{ for } n = 1/2, \quad (12)$$

where R is the thaw: consolidation ratio defined by Eq. (4) for the linear theory described earlier. For $n < 1/2$, the time factor will increase with increasing time.

DISCUSSION OF RESULTS

For the loading case $\gamma' = 0$, the settlement curves are very similar for S_t/S_{max} less than 50 percent. Using the method proposed by Fox,⁴ it may be shown that these curves are well approximated by:

$$\frac{S_t}{S_{max}} = \frac{2}{\sqrt{\pi}} \sqrt{T}, \quad (13)$$

$$\left(\frac{S_t}{S_{max}} < 0.5; \gamma' = 0 \right).$$

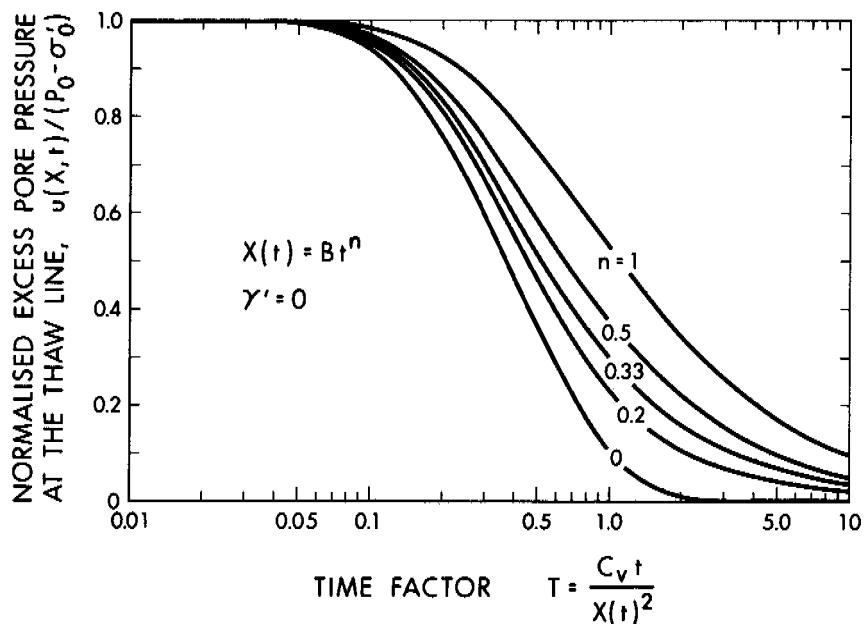


FIGURE 2 Excess pore pressures at the thaw line—applied loading.

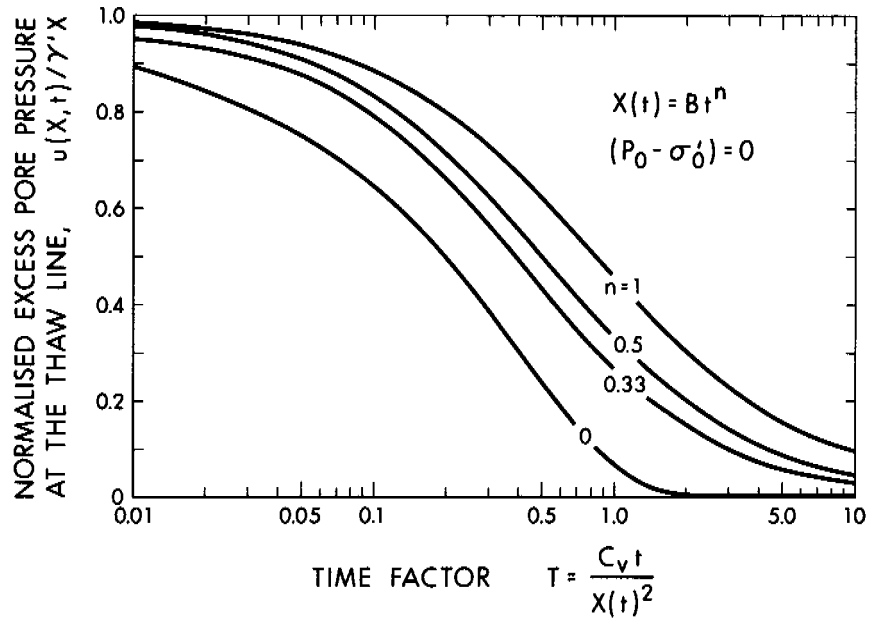


FIGURE 3 Excess pore pressures at the thaw line—self-weight loading.

For the “self-weight” loading condition $(P_0 - \sigma'_0) = 0$, no such simple relationship is valid.

The excess pore pressures at the thaw line in Figures 2 and 3 are strongly dependent on the value of n . It is clear that, in the class of problems where n is less than 0.5, excess pore pressure development at earlier times will be more critical, but stability will tend to improve as time progresses.

The solutions for any combination of the two extreme

loading conditions may be obtained by simple superposition of the excess pore pressures.

THAWING UNDER A HOT PIPELINE

A practical study of thawing under a hot oil pipeline is included to illustrate the application of the extension to the theory described above. The settlements and excess pore

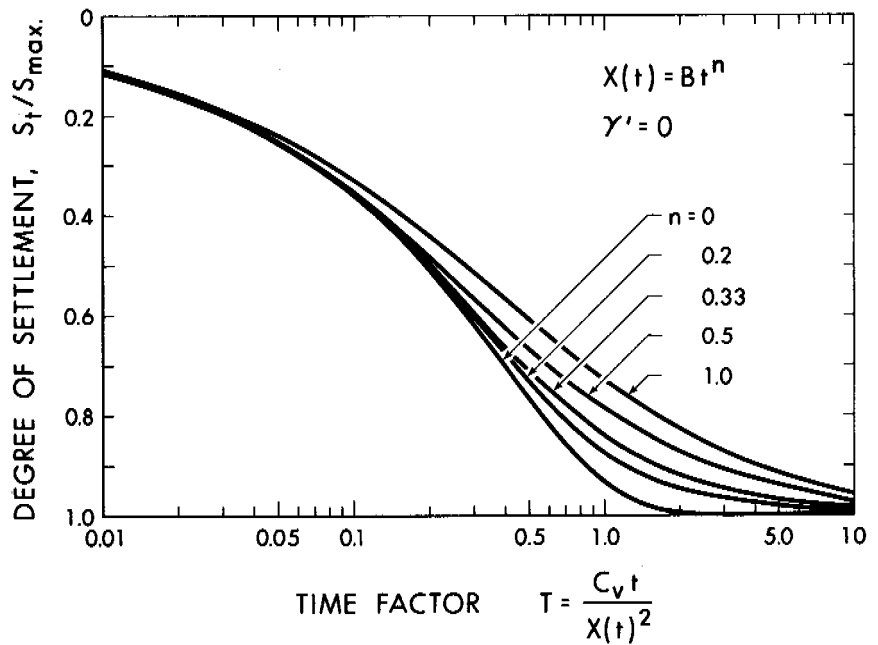


FIGURE 4 Degree of settlement—applied loading.

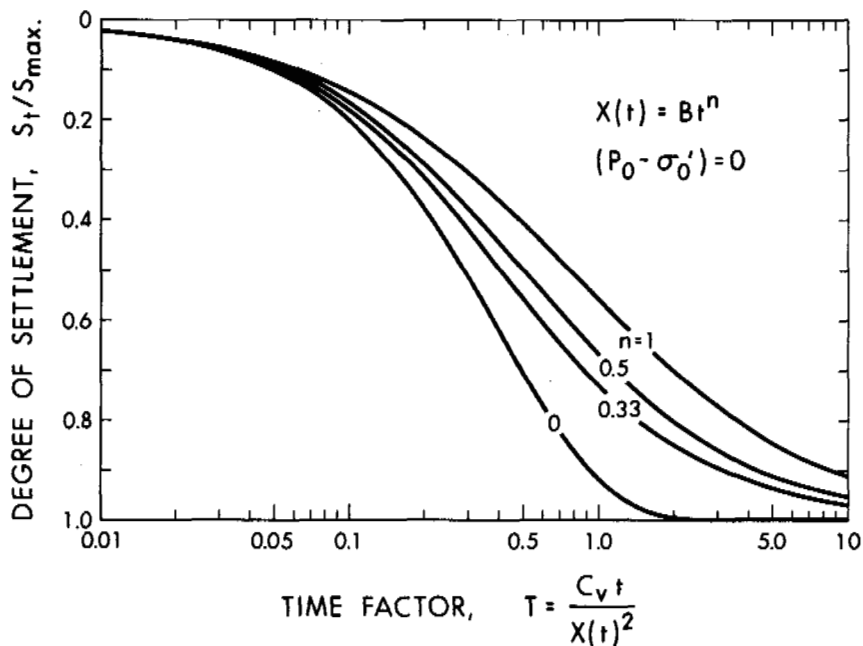


FIGURE 5 Degree of settlement—self-weight loading.

pressures under the centerline of a pipeline are analyzed, subject to the rate of thaw given by Lachenbruch.⁵ A clay substratum of 65 percent moisture content was considered by Lachenbruch in order to assess some thermal effects of a heated pipeline in permafrost. The thaw “plug” and the rate of thaw under the centerline are shown in Figure 6.

Various coefficients of consolidation c_v have been used to estimate the performance of the pipe for the first 20 years. The material overlying the pipe will be assumed to act as a surcharge loading and, for simplicity, to be comprised of a material of much higher permeability than the underlying frozen soil. It therefore does not play any active role in the drainage conditions.

From properties chosen by Lachenbruch, one finds that 2.42 m of surcharge material at a dry density of 1.75 t/m^3 causes a surcharge loading of 4.25 t/m^2 . The thawing soil at 65 percent moisture content has a submerged unit weight of 0.62 t/m^3 . The rate of thaw for the arctic (clay) case is well approximated by:

$$X = 3.56 t^{0.3}, \text{ or } B = 3.56, \text{ and } n = 0.3. \quad (14)$$

The coefficients of consolidation taken to assess the performance of the pipe are:

$$c_v = 3 \times 10^{-4}, 15 \times 10^{-4}, \text{ and } 30 \times 10^{-4} \text{ cm}^2/\text{s}.$$

Finally, the closure of the thaw plug as calculated by Lachenbruch is not assumed to affect the one-dimensional drainage under the centerline of the pipeline.

The results for the normalized excess pore pressures are

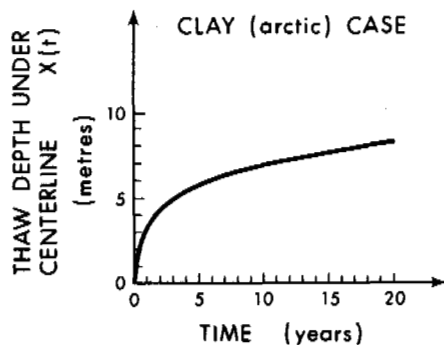
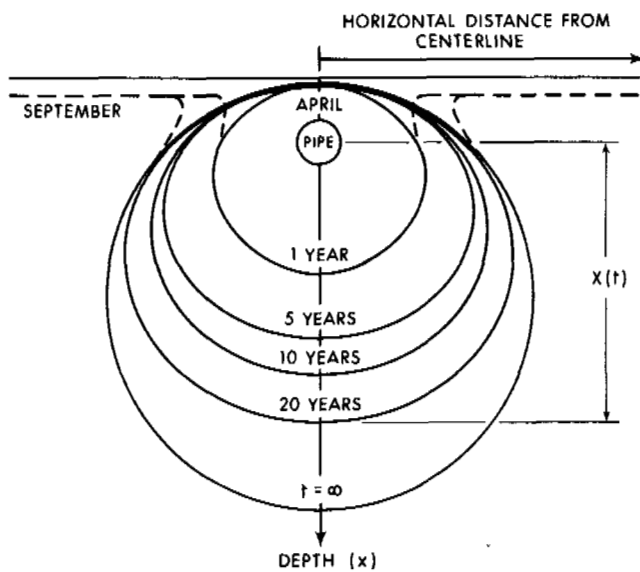


FIGURE 6 Thawing under the centerline of a hot pipeline (after Lachenbruch⁵).

shown plotted with time for different c_v values in Figure 7, for the centerline of the pipeline.

If the thaw depth against time curve is approximated by a square root of time relationship and an α value approximately calculated for the first 2 years of thawing, the dotted line in Figure 7 shows the excess pore pressures calculated using the linear theory reviewed earlier.

As expected, under these thawing conditions the excess pore water pressures are the most severe in the initial few years of thawing. For a silty clay with a c_v of $15 \times 10^{-4} \text{ cm}^2/\text{s}$, excess pore pressures equal to 50 percent of the effective overburden loading may be expected even after 2 years of operation. However, it also appears that if no severe stability problems occur in the initial years of operation, then increased stability may usually be expected as time proceeds, provided that soil conditions do not deteriorate significantly with depth.

The settlement of the pipeline is comprised of the sum of the consolidation settlement and the settlement resulting from the density change in the water phase on thawing. The consolidation settlement at any time, however, may be shown to be proportional to the product of S_r/S_{max} and the depth of thaw X . At early times, the degree of consolidation S_r/S_{max} is low. At longer times, the velocity of the thaw front decreases, and S_r/S_{max} increases. Hence, a more linear settlement-time curve is to be expected than that suggested by the thaw depth-time relationship.

INFLUENCE OF NONLINEAR EFFECTIVE STRESS-STRAIN RELATION

Many frozen soils when thawed have a high void ratio initially; over the range of stresses of engineering interest, the void ratio-effective stress relationship may be markedly non-

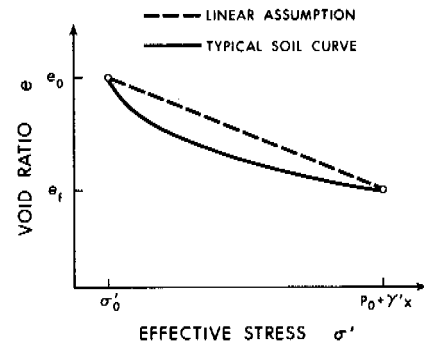


FIGURE 8 Void ratio-effective stress relationships.

linear. Figure 8 compares typical compressibility behavior with the idealized linear assumption adopted by Morgenstern and Nixon.⁶ It is of interest to investigate the influence of this nonlinearity on the consolidation of thawing soil.

If the soil is thawed and no drainage is permitted, then the effective stress in the soil is denoted by σ'_0 . If drainage is now permitted under the influence of subsequent loading increments, then the void ratio-effective stress curve may be found experimentally. Recent studies suggest that for some thawed soils tested in this manner, a straight line is obtained by plotting the void ratio (e) against the logarithm of effective stress. The same empirical relationship was incorporated by Davis and Raymond³ when formulating a theory of consolidation for normally consolidated unfrozen soils.

Although the permeability k and the slope of the stress-strain curve m_v both change over a range of loadings, it may be assumed on experimental grounds that they change in such a way as to maintain the consolidation coefficient c_v approximately constant. Following Davis and Raymond,³

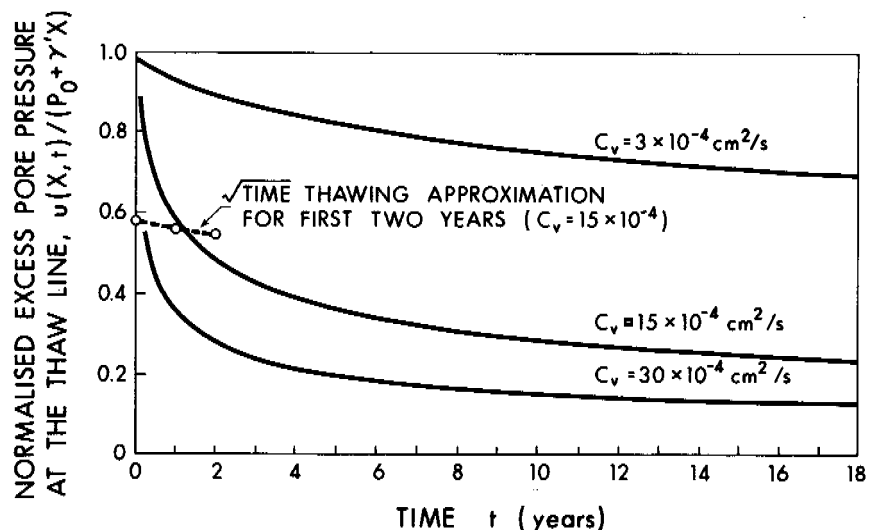


FIGURE 7 Excess pore pressures under the centerline of a hot pipeline.

a constant c_v value is adopted together with the stress-strain relationship:

$$e = e_0 - C_c \log_{10} \left(\frac{\sigma'}{\sigma'_0} \right), \quad (15)$$

where C_c is the slope of the $e/\log \sigma'$ line (compression index), and σ' is the current effective stress.

The general one-dimensional equation of consolidation for a saturated soil is then written as:

$$-c_v \left[\frac{1}{\sigma'} \frac{\partial^2 u}{\partial x^2} - \left(\frac{1}{\sigma'} \right)^2 \frac{\partial u}{\partial x} \frac{\partial \sigma'}{\partial x} \right] = \frac{1}{\sigma'} \frac{\partial \sigma'}{\partial t} \quad (16)$$

This equation is valid in the thawed soil, regardless of loading type or drainage conditions at the boundaries.

For the same loading conditions considered previously, the total and pore water stresses, respectively, are given as:

$$\sigma = P_0 + \gamma'x + \gamma_w x, \quad \text{and} \quad (17)$$

$$P_w = u + \gamma_w x. \quad (18)$$

With the water table at the surface $x = 0$, the effective stress is then the difference between these stress components:

$$\sigma' = \sigma - P_w = P_0 + \gamma'x - u. \quad (19)$$

These equations are valid for any initial effective stress σ'_0 developed on thaw, so:

$$\frac{\partial \sigma'}{\partial x} = \gamma' - \frac{\partial u}{\partial x}, \quad \text{and} \quad (20)$$

$$\frac{\partial \sigma'}{\partial t} = - \frac{\partial u}{\partial t}, \quad (21)$$

and, substituting these expressions into Eq. (16) we obtain:

$$\frac{\partial u}{\partial t} = c_v \left[\frac{\partial^2 u}{\partial x^2} - \left(\frac{\gamma' - \frac{\partial u}{\partial x}}{P_0 + \gamma'x - u} \right) \frac{\partial u}{\partial x} \right] \quad (22)$$

A linearizing transformation for this nonlinear equation, such as that used by Davis and Raymond, is only available for the case $\gamma' = 0$. This condition where applied loads dominate will be studied here. Numerical means must be employed to solve a loading combination involving self-weight stresses.

Setting $\gamma' = 0$ in Eq. (19) and (22) and linearizing the resulting equation, we obtain:

$$\frac{\partial w}{\partial t} = c_v \frac{\partial^2 w}{\partial x^2}, \quad (23)$$

where $w = \log_{10} \left(\frac{P_0 - u}{P_0} \right)$ (24)

The boundary condition at the surface is now:

$$x = 0; u = 0; w = 0. \quad (25)$$

At the thaw line, the boundary condition used previously must be now rederived for consistency. Previously, a continuity requirement generated Eq. (3).

Defining the volumetric compressibility m_v as:

$$m_v = - \frac{1}{1 + e_0} \frac{de}{d\sigma'}, \quad (26)$$

where e_0 is the initial void ratio and using the empirical Eq. (15), we obtain on differentiation:

$$m_v = \frac{0.434 I_c}{(1 + e) \sigma'}. \quad (27)$$

So,

$$\frac{e_0 - e}{1 + e} = \frac{m_v}{0.434} \sigma' \log_{10} \left(\frac{\sigma'}{\sigma'_0} \right). \quad (28)$$

The boundary condition Eq. (3) after substitution of Eq. (19), (27), and (28) becomes

$$\begin{aligned} x &= X(t); \\ \frac{P_0 + \gamma'X - u}{0.434} \log_{10} \left(\frac{P_0 + \gamma'X - u}{\sigma'_0} \right) &= \frac{c_v}{\frac{dx}{dt}} \frac{\partial u}{\partial x}; \quad t > 0 \end{aligned} \quad (29)$$

Setting $\gamma' = 0$, we obtain the boundary condition required to study the applied loading condition. And rewriting in terms of $w(x,t)$, the transformed variable, we have

$$x = X(t); \log_{10} \left(\frac{\sigma'_0}{P_0} \right) - w = \frac{c_v}{\frac{dx}{dt}} \frac{\partial w}{\partial x}; \quad t > 0. \quad (30)$$

The term $\log_{10} \left(\frac{\sigma'_0}{P_0} \right)$ is a constant, and so the Eq. (23), (25), and (30), in terms of the transformed variable w , are entirely analogous to the corresponding equations derived for the linear theory in terms of $u(x, t)$. Consequently, the solution for the linear thaw-consolidation equation may

be applied directly to obtain $w(x, t)$. For \sqrt{t} thawing:

$$W = \frac{w(z, t)}{\log_{10}\left(\frac{\sigma'_0}{P_0}\right)} = \frac{\text{erf}(Rz)}{\text{erf}(R) + \frac{e^{-R^2}}{\sqrt{\pi}R}}, \quad (31)$$

where,

$$z = \frac{x}{X(t)}, \quad (32)$$

We obtain the excess pore pressure by the modification:

$$\frac{u(z, t)}{(P_0 - \sigma'_0)} = 1 - \left(\frac{\sigma'_0}{P_0}\right)^W \quad (33)$$

Equations (31) and (33) form the exact solution for a thawing soil with consolidation occurring solely due to an applied load P_0 . The soil has an initial void ratio in the thawed state corresponding to an initial effective stress of σ'_0 .

The effects of self-weight stresses may be determined relatively simply by numerical methods, and it is considered sufficient for the scope of this paper to examine the effects of an applied load P_0 upon the excess pore pressures.

The ratio $\frac{P_0}{\sigma'_0}$ is a measure of the effective stress change in the thawing soil and, therefore, of the nonlinearity of the effective stress-strain curve. This ratio now enters as an additional dimensionless quantity, and its effect on the excess pore pressure distribution in the thawed soil may be investi-

gated. As in the linear theory, the normalised excess pore pressure distribution is unchanged throughout the thaw-consolidation process, although it is now dependent on the stress ratio $\frac{P_0}{\sigma'_0}$. The degree of settlement in the thawed soil, however, is independent of time and the ratio $\frac{P_0}{\sigma'_0}$. This fact was also recognized by Davis and Raymond³ for this type of stress-strain relationship. Consequently, the linear theory may be used equally well for calculating the degree of consolidation settlement.

Figure 9 shows the excess pore pressure at the thaw front, as a function of the stress ratio and the thaw-consolidation ratio R . It is seen that, as the stress increment ratio increases, the excess pore pressure condition at the thaw line increases to a more critical level.

In cases where high initial void ratios are present in the soil on thawing, the excess pore pressures may be underestimated considerably, if only a linear relation between void ratio and effective stress is considered.

CONCLUSION

The one-dimensional theory of consolidation of thawing soils has been extended here to consider separately problems where the thaw depth is not simply proportional to the square root of time and problems where the change of void ratio of the soil bears a semilogarithmic relationship with the change in effective stress.

For the former case expressions for the thaw depth X and its time derivative, $\frac{dX}{dt}$ may be entered into a computer

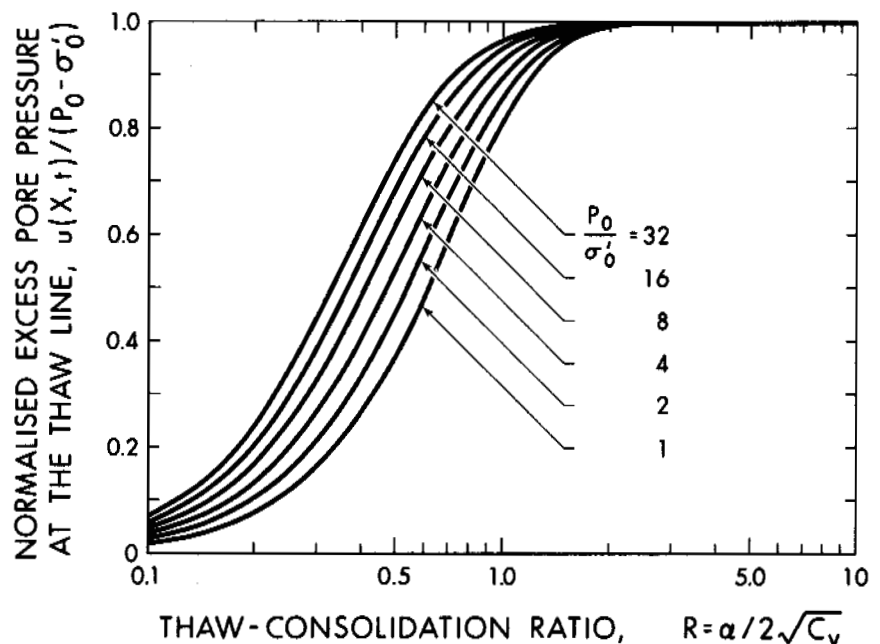


FIGURE 9 Excess pore pressures at the thaw line for nonlinear theory.

program and the excess pore pressures and settlements calculated. Curves have been presented for power law thaw depth-time relations. The approximation of a more complex thaw depth-time function by a \sqrt{t} function seems to give reasonable average pore pressure predictions, but it certainly does not predict the extremes that may be encountered.

The introduction of the nonlinear compressibility relation into the theory indicates predicted pore pressures for a given value of the thaw-consolidation ratio R that are higher than those given by the linear theory. However, these pore pressures now depend on the ratio of the final effective stress after thawing is complete to σ_0' , the effective stress in the soil following undrained thawing. Little is known as yet about σ_0' , except that it is likely small in ice-rich soils. Further study of the magnitude of σ_0' and the factors that influence it are needed before the nonlinear theory can be used with any confidence.

ACKNOWLEDGMENT

The authors are grateful to the National Research Council of Canada for their support of this study.

REFERENCES

1. Carslaw, H. S., and J. C. Jaeger. 1947. *Conduction of heat in solids*. Clarendon Press, Oxford.
2. Crank, J., and P. Nicholson. 1947. A practical method for numerical evaluation of solutions of partial differential equations of the heat conduction type. *Proc. Cambridge Phil. Soc.* 43:50-64.
3. Davis, E. H., and G. P. Raymond. 1965. A non-linear theory of consolidation. *Geotechnique* 15(2):161-173.
4. Fox, E. N. 1948. The mathematical solution for the early stages of consolidation. *Proc. 2nd Int. Conf. Soil Mech. Found. Eng.* 1:41-42.
5. Lachenbruch, A. H. 1970. Some estimates of the thermal effects of a heated pipeline in permafrost. *U.S. Geol. Surv. Cir.* 632.
6. Morgenstern, N. R., and J. F. Nixon. 1971. One-dimensional consolidation of thawing soils. *Can. Geotech. J.* 8 (4):558-565.
7. Morgenstern, N. R., and L. B. Smith. Thaw-consolidation tests on remoulded clays. *Can. Geotech. J.* (In press)
8. Murray, W. D., and F. Landis. 1959. Numerical and machine solutions of transient heat-conduction problems involving melting or freezing. *Trans. Am. Soc. Mech. Eng.* 81:106-112.
9. Tsytoovich, N. A., Y. K. Zaretskii, V. G. Grigoreva, and Z. G. Ter-Martirosyan. 1965. Consolidation of thawing soils. *Proc. 6th Int. Conf. Soil Mech. Found. Eng.* 1:390-394.

EXPERIMENTAL PRESSURE STUDIES OF FROST HEAVE MECHANISMS AND THE GROWTH-FUSION BEHAVIOR OF ICE

F. J. Radd and D. H. Oertle

CONTINENTAL OIL COMPANY
Ponca City, Oklahoma

INTRODUCTION

The various phenomena of frost heaving are well known to the agronomists, contractors, engineers, and geologists who work in the colder regions of the world. The main phenomenon appears simple: Certain fine-particle soils—clays and/or silts—will, upon freezing, heave, particularly if such soils have a good supply of groundwater. This frost heaving can damage roadbeds and building foundations. Examination of the frozen soil reveals ice segregated into layers (lenses) normal to the direction of heat flow.

Historically, there have been numerous papers on the subject of frost heaving by investigators from many nations.^{1-11, 13-19} Although considerable effort has been given

to understanding the nature of frozen soils and many theories and hypotheses advanced to explain it,^{9,16,18} the basic mechanism of frost heaving has not been established. It appeared desirable, therefore, to conduct some experimental studies based on the following basic questions: If the effects of pressure on soil freezing are examined, what is the relationship of pressure to ice lens formation? Is there evidence of a specific behavior that is not ice-limited and that is not thermodynamically predictable? Is there anything specific about fine-particle soil systems as to clay, clay-silt, or silt? How do other nonsoil solids behave? Is there anything specific about the water utilized in ice lens formation in clay and in clay-silts? Do other liquid-solid transformations show a similar behavior? How and why do ice lenses form as a

special crystal growth method? What are the relationships of pressure-volume-temperature-time in such cases?

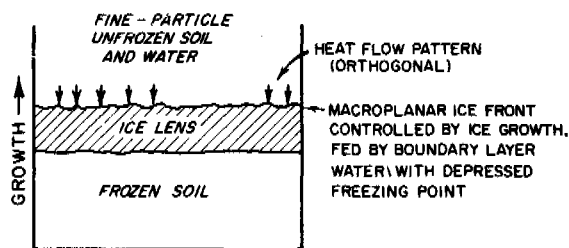
DEFINITION OF THE PROBLEMS

When frozen slowly, clays, silts, and similar fine-particle soils can show a quite remarkable volume growth if a supply of water is available. Characteristically, the final water content of such frozen soils is much greater than the original water content. The water-ice volume expansion, circa 10 percent, thus operates both on the intrinsic water content and on the drawn-in water. Sheet capillaries continuously formed and maintained at the ice-clay interface are characteristic of such ice lenses. Somehow the new, additional moisture is continuously added to the freezing interface at this sheet capillary.

The central problem is to define why and how these sheet capillaries form on the unfrozen side of an ice lens. The ice crystals' growth structure itself apparently controls the direct, axial heat flow of the fine-particle system that produces the ice lens (Figure 1a). On the one hand, the coarse-particle system offers control by the locally higher conductivity of the solid particles, compared with the thermal conductivity of the ice that is formed (Figure 1b); thus the freeze-front control appears to be based on the size, shape, packing, and properties of the coarse, solid particles and not on the growing ice front's needs. On the other hand, in a fine-particle system, the particles are of a size equal to or less than the growth steps in the ice-lens surface and so cannot project "growth" fingers of higher conductivity beyond the ice front; in this

case the entire ice-growth surface can be liquid-supplied without major heat flow disruptions, just as the ice front requires it. Even more importantly, the planar ice front is continuously maintained at the sheet capillary. Without this vital transport capacity (boundary-layer freezing-point depression and film strength) of the fine-particle system, the sheet capillary or lens type of crystal growth would not exist. The film strength of the water is no problem—this being about 1 500 to 6 000 atm. However, it appears that boundary-layer liquid-freezing-point depression makes the void and pore space crucial in the behavior of fine-particle systems, while particle size, rather than void size, is critical (because of the increased thermal conductivity of the particle) in the coarse-particle system. Accordingly, it was decided that in the pressure experiments, the growth-fusion point behavior at various pressures should be studied since this would give an accurate view of the system's transport behavior over a pressure range. Preliminarily to the pressure-temperature-time ice-lens studies, ice-lens formations were attempted in silica smoke, ordinary sand, and diatomaceous earth; formations occurred with the first and the last-named. Also tried was ice-lens formation with three nonaqueous liquids with high-purity Linde alumina. With neither water nor clay nor silica, "ice" lenses still formed in nitrobenzene, *o*-chloroaniline, and formamide. Real ice lenses were formed with fine carbon black, magnesia, and in 600-mesh carborundum. From these experiments, it was concluded that ice-lens formation is not restricted to the clay-water system but most likely represents a general crystal growth phenomenon common to any system of finely divided moisture-containing solids in the presence of a heat sink and a steady supply of moisture. Interface control by the growing ice itself, macroplanar heat flow responses, and interfacial film liquid delivery are the limiting factors, not the specific properties of the solid or of the liquid.

a. TYPE ONE, ICE STRUCTURE CONTROL



b. TYPE TWO, SOLID-PARTICLE CONTROL ICE LENS FORMATION

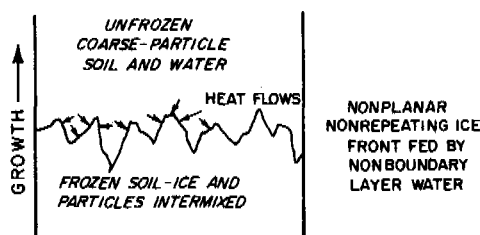


FIGURE 1 Two basic types of soil freezing.

EXPERIMENTAL APPARATUS

The apparatus design had to meet four fundamental requirements: upward force developed during ice-lens growth had to be measured despite adfreezing of the lens and soil to the cell wall; water had to be free to come and go from the soil while high soil pressures were developed in the cell, yet the soil had to be prevented from escaping; as pressure increased, some method was needed to measure the resulting soil compaction; and a reliable refrigeration source was necessary to provide close temperature control. Figure 2 is a diagram of the cell in which most of the experiments were made. Basically, it is a water-permeable, constant-volume cell [1]. By using a cell constructed from a block of Lucite with its outside faces polished, the authors were able to observe continuously and record on color film by time-lapse photographic techniques the growth of ice lenses and other physical events inside the cell. The film was studied many times after a run and proved very valuable as some physical processes and factors that were not

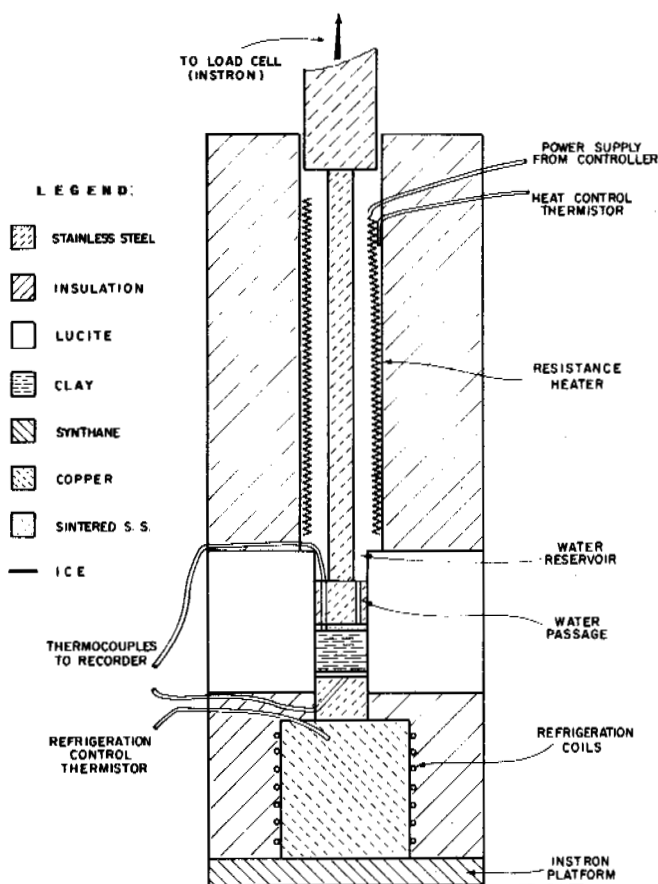


FIGURE 2 Schematic diagram of cell used for ice-lens studies.

visually noticed during a run of 30 days became obvious when viewed from the recorded film in 3½ min.

EXPERIMENTAL RESULTS

Eight experiments were performed on saturated samples of a silt-clay from the New Jersey meadows. All samples were

loaded into the Instron cell with a spatula using a spreading action across the bottom of the cell and forcing the top stainless steel plug upward until the desired thickness was obtained; the bottom stainless steel plug was then inserted. The test parameters of each experiment, shown in Table I, exhibit the additive nature of the study.

Figure 3 shows the relation between temperature, pressure, and time. The relation between volume of the ice lens, pressure, and time is shown in Figure 4. The volume data were obtained from the movie film. As can be seen from the volume curve, the film shows that the ice lens was still growing under 91.403 kg/cm², after nearly 800 h of freezing.

During the early part of the fourth run, a strange phenomenon occurred. The ice lens formed to a considerable thickness, including what appeared to be visible, vertical columns of air. As the pressure on the ice lens increased, due to the growth of the lens, small bits of the clay moved from the bottom to the top through these vertical columns. The space under the bits of clay seemed to fill with clear ice as the clay particles moved upward. Days later, when the ice became solid and clear, the clay particles no longer moved through the lens.

Subsequently, an answer was sought as to whether an ice lens would form and grow in a clay system already under a high pressure. Experiment 5 was much the same as the previous one, except that an initial pressure of 70.31 kg/cm² was applied and *maintained*. The load cycle controls were set so that a drop in the pressure, due to the compaction of the clay, would cause the unit to apply a compensating force, while a pressure increase would not cause a correction. The results of this experiment are shown graphically in Figure 5. The pressure rose to nearly 126.558 kg/cm², but there was a delay in its initiation of 275 h. The point of departure from 70.31 kg/cm² is considered the equilibrium pressure temperature (P-T) fusion point, which indicates the start of an ice lens. At the bottom of the clay, when the ice lens formed, the temperature was -7.78 °C.

Experiment 5 raised two questions: Was the delay in the start of the ice lens growth due to the lack of nucleating crys-

TABLE I Test Parameters

Experiment No.	Sample Thickness (mm)	Duration (h)	Maximum Pressure (kg/cm ²)	Remarks
1	20.32	400	<84.372	Initial pressure zero; ice-lens growth observed; found linear cold control necessary
2	20.32	200	?<68.552	Freezing front seen to be a function of pressure
3	20.32	720	?<94.215	—
4	20.32	1 000	?~105.465	Telephoto movie imagery at 5 frames/h
5	20.32	875	?~126.558	Initial pressure 70.31 kg/cm ² ; time-lapse imagery: maximum pressure after 275 h
6	18.0	5.5	105.465	Initial pressure 2.812 kg/cm ²
7	18.0	?	<175.775	Six, stepped increases of pressure
8	?	?	182.81	Limit of apparatus

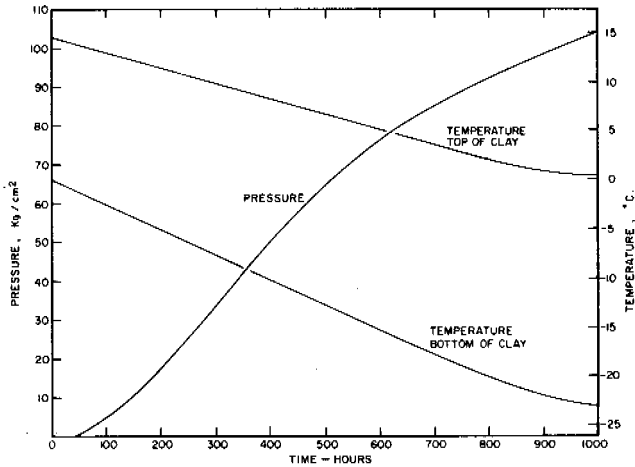


FIGURE 3 Pressure-time-temperature responses to ice-lens growth in clay-water system.

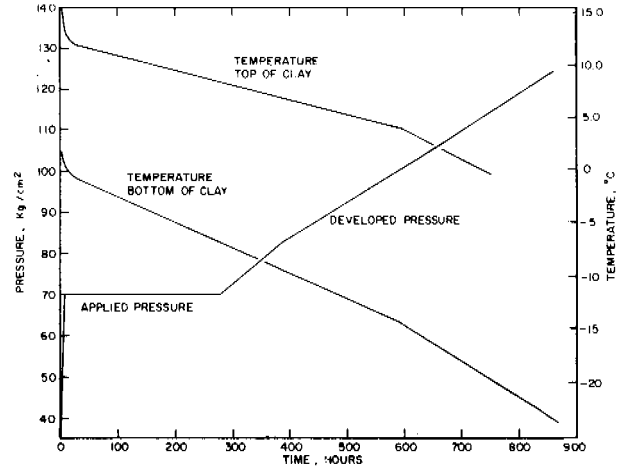


FIGURE 5 Ice-lens growth in clay-water system under 70.31 kg/cm² applied pressure.

tals that could continue to grow; or was the delay caused by a depression of the freezing point by the pressure applied to the clay? To answer these questions, it was decided to grow a sizable lens before the maintained pressure was applied and see if it continued to grow. For Experiment 6, an ice lens 2.54 mm thick was grown at the bottom of the clay with a maintained pressure of 2.812 kg/cm². When a 105.465 kg/cm² pressure was applied and maintained, the clay began to compact and the temperature at the bottom of the cell began to drop. After a 15-min lag, the temperature at the top of the cell also began to drop. After about 1 h the ice lens began to melt; after 5 h it was completely melted. These effects are shown in Figure 6, where 0 h is the time that the 105.465 kg/cm² pressure was applied. Figure 7 shows the continuation of the experiment when the lens growth caused a rise in pressure above 105.465 kg/cm² in about 200 h. This

nucleation-melting experiment confirmed that the freezing-point temperature was being depressed by the pressure in the system.

The next step was to establish a curve for freezing-point depression by pressure in the silt-clay. Temperatures for the initiation of lens growth at the bottom of the cell were known for 0, 70.31, and 105.465 kg/cm². The seventh experiment was designed to provide data at 35.155, 70.31, 105.465, 140.62, and 175.775 kg/cm². Only the 35.155, 70.31, and 175.775 kg/cm² data, with respect to temperature, were added (Figure 8).

During the eighth run, the pressure was increased from 175.775 to 182.81 kg/cm², but the refrigeration equipment did not function well enough at the low temperatures necessary to permit the expected rise to and above 210.93 kg/cm². The maximum pressure of 182.81 kg/cm² that was developed

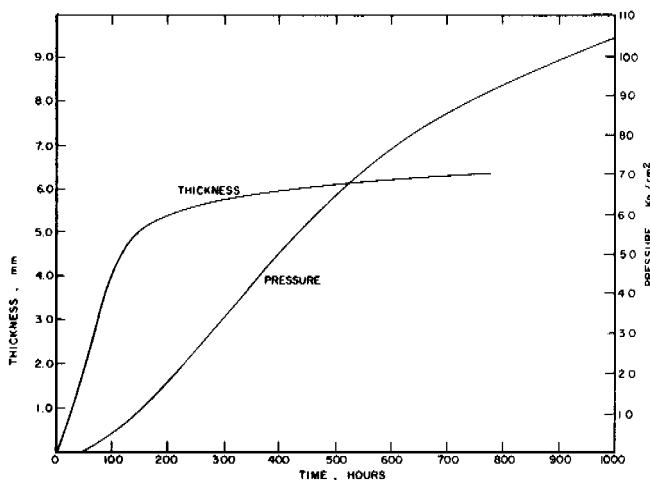


FIGURE 4 Pressure-time-thickness responses to ice-lens growth in clay-water system.

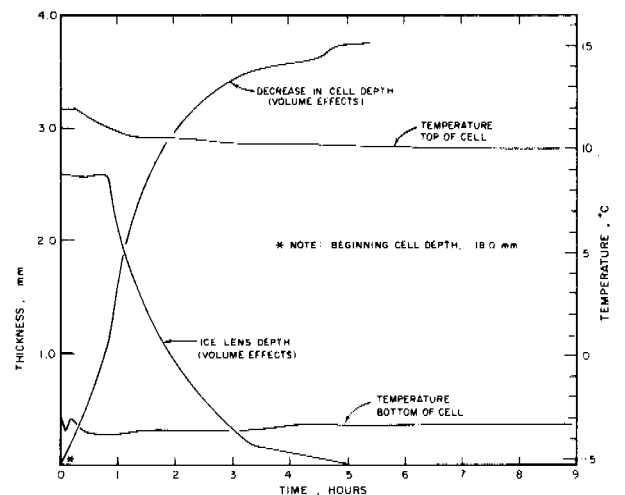


FIGURE 6 Ice-lens melting and temperature effects using 105.4 kg/cm² pressure on ice growth at about 4.2 kg/cm².

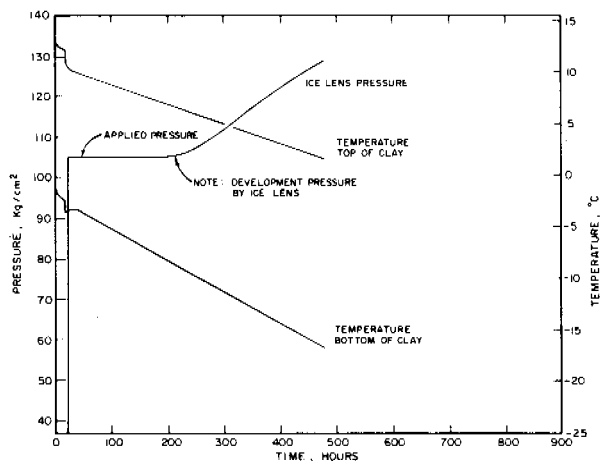


FIGURE 7 Growth of ice lens at 105.5 kg/cm².

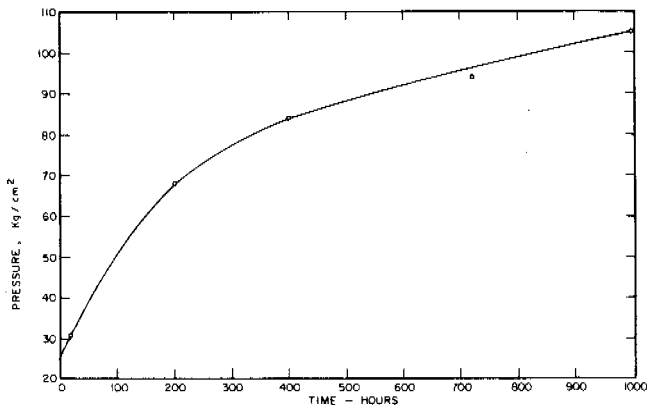


FIGURE 9 Relationship of maximum pressure reached in related runs versus freezing time, using same freezing conditions.

by an ice lens in the test soil was merely the limit of the present equipment.

DISCUSSION OF RESULTS

The systematic curve for the pressure-time response of the first six analogous runs may be expressed as $P(dV/dt) = K$ since, the lower the freezing rate, the higher the final pressure (Figure 9). Consequently, the development of ice-lens pressure at the lower temperatures (and higher pressures) confirms the boundary-layer freezing-point depression effects and the important roles played by the void spaces in the fine-particle system.

The pressures developed by freezing clay were at least 35 times those by freezing sand; the fine-particle ice front control gave a greater value than the large-particle ice-front control.

Also, no major differences were recorded between the freezing of a coarse, rounded particle sand and a sharp, regular, somewhat finer sand.

Figure 6 shows the pressure melting effects of 105.465 kg/cm² that was imposed on our ice lens grown at 2.812 kg/cm². From the temperature-time and volume-time curves involved, there can be no doubt that the sudden melting was due to the applied pressure. Other experimental explanations of this phenomenon were sought, but only the unconfined liquid, pressure-melting view explained the experimental facts.

Figure 8 shows the systematic, multipoint pressure-temperature correlation curve for making ice lenses. These data were added to the P-T fusion points of the previous seven runs to produce Figure 10. Point 3 of Figure 8, at 175.775 kg/cm², shows a valid pressure rise; however, unlike the other cases, there was no visually apparent ice lens. Graphically, however,

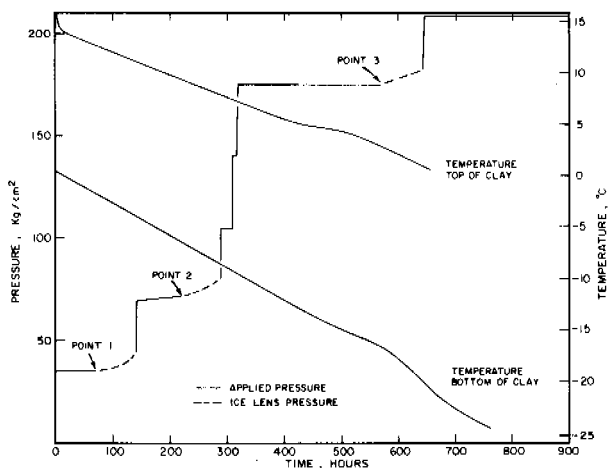


FIGURE 8 Multipoint run of freezing-point depression versus pressure on ice-lens formation.

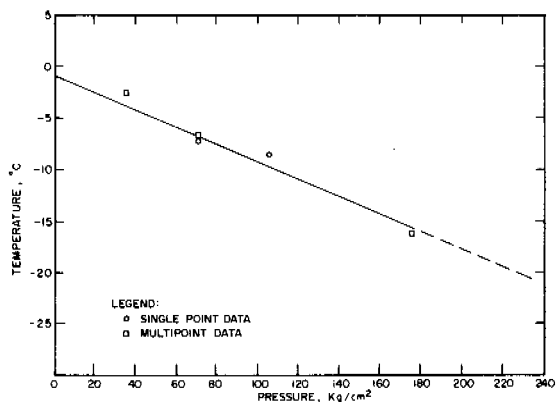


FIGURE 10 Summary of curve of freezing-point depressions versus pressure in ice-lens formation.

there was a clearly recorded pressure rise, and Figure 10 proves its full experimental validity. Water suction or drawing effects were not limiting, nor was the tensile strength of water even remotely approached in these studies.

The freezing-point depression curve in Figure 10 may be taken as an experimental confirmation of Poynting's views based on his vapor pressure calculations for water and ice.¹² Technically, to form an ice lens at a certain pressure, it is necessary to have a certain, specific temperature. Conversely, the melting point of ice in equilibrium contact with unconfined water is a linear function of the pressure.

It can be readily seen that this linear curve is a locus of equilibrium points of unconfined water and ice solid under various pressures. Accordingly, the following free energy considerations may be applied to calculate the experimental curve thermodynamically for the one-component system at its fusion point. While ice solid and water liquid are used for these derivations, the principles used herein apply to any comparable one-component system and its P-T relationships under parallel conditions, when the solid is under pressure and the liquid is not.

From a thermodynamic-free energy analysis, with S = entropy, P = absolute temperature (K), and H = enthalpy or heat content:

$$V_1 dP - S_1 dT = -S_w dT, \text{ and}$$

$$dP/dT = (S_f - S_w)/V_1 = -\Delta S_f/V_1,$$

where f = fusion; hence:

$$dT/dP = -T(V_1)/\Delta H_f \text{ or } -T(V_S)/\Delta H_f,$$

where V is the volume of the solid.

For ice at 0°C, the specific volume is 1.090 7 cm³/g, the heat of fusion 79.8 cal/g, and the cal-to-cm³/atm conversion factor 41.293; hence:

$$\begin{aligned} (dT/dP)_{0^\circ\text{C}} &= -[(273.2)(1.090\ 7)]/[(79.8)(41.293)] \\ &= -297.98/32\ 95.2 = \sim -1/11\ ^\circ\text{K/atm.} \end{aligned}$$

The pressurized solid-unpressurized liquid curve ($dT/dP = -V_S/S_f = K$) has many nonsoil implications. One is for the behavior of large glacier masses, where the foot of the glacier melts at various temperatures according to the imposed pressures. Another is within the glacier, where melting can fuse particles together. A third is for densification of powdered metals, ceramics, and salts near their fusion points. It should

be noted that this curve is independent of the nature of the insoluble solid particles in contact with the ice or of the method of applying the pressure to the ice while permitting the liquid to come or go.

The agreement between theory and experiment is most rewarding; the theory gave 0.090 4 °K/atm, and the experiment gave 0.093 8 °K/atm. This unconfined liquid-pressurized solid method might be useful in experimentally measuring the entropy of fusion for various substances. Most important, this agreement is also a double theoretical confirmation: first, the bottom-upward freezing method is justified, since a force recording error would be nonlinear with pressure and would not have permitted a fully satisfactory agreement with theory; second, the pressure-time data show that there is no appreciable specific effect from the fine-particle solid—the results are solely from the thermodynamic properties of the water-ice system, not a clay and/or silt parameter or by water structure variation.

During experiment 4, the clay particles beneath the ice lens moved vertically upward through the ice lens, perhaps with voids or gas bubbles, as if following a dislocation-vacancy flow. In these experiments pressure-temperature gradients were always present and are held to be responsible for the presumed dislocation-recovery flow. Since no solute diffusion is involved, this is markedly different from the Kirkendall metallurgical solid diffusion case.¹³

Stresses present in the formation of the ice lenses were confirmed by diffraction studies. Back reflection Laue x-ray photographs were obtained with a liquid nitrogen cooling method where the Mylar film-protected ice samples were 3 cm from the film. The splitting of the Laue spots indicates crystal fragmentation under pressure, while the smearing of the spots indicates retained residual stresses. The grain sizes of the ice lenses, determined by polarized light studies, were fairly large, so that the absence of clear Laue spots indicated severe local distortion of the ice lattices. These lattice-strain results were not unexpected, for it can be seen that by growing the ice lenses against pressure, in particular a changing pressure, a strain-free solid should not be expected.

In all of the high-pressure runs (<175.775 kg/cm²), another phenomenon was recorded on time-lapse photography—namely, the presence of liquid water that apparently exists below the freezing front. This bypassed water can contribute to ice-lens formation and is capable of movement. While only a limited supply of such boundary-layer is present, apparently in small interparticle voids, there is no question of its presence. The severely restricted amounts available of such boundary-layer depressed-freezing-point water may be one reason why the growth of ice lenses was so limited at the higher pressures. Both these water-retention effects and the clay particle diffusion effects were film-recorded, but neither phenomenon is apropos still pictures exposition. The best evidence is time-lapse movies.

CONCLUSIONS

The following conclusions are drawn from the several pressure-time-growth and/or fusion experiments on ice lens formation:

1. Maximum pressures obtained in a pressurized ice-unconfined water case are limited only by the apparatus' ability to produce low temperatures at precisely controlled rates; this is true at least to 210.93 kg/cm² and possibly to higher pressures.
2. Freezing-point depression versus temperature curves follow thermodynamic expectations. These data are more than one order of magnitude (circa 12 times) [2] larger than predicted by the Clapeyron relationship dT/dP . This original calculation should serve for many different equivalent-state, one-component systems. The experimental method of deriving this curve also shows—for this particular system—the crucial role in ice-lens actions played by boundary-layer freezing-point depressions.
3. Ice-lens formation is a special method of crystal growth, one that is neither restricted to the liquid-solid transformation of water nor to fine-particle soil solids. It appears to be a general law of nature and the result of ice growth by deposition control in fine-particle systems by action of the ice front, rather than by deposition control by the solid particles in coarse-particle systems.
4. Diffusion of solid particles up the temperature gradient can occur in ice that is recrystallizing under changing stresses and temperatures. This up-the-gradient solids-voids flow should be fully paralleled in other solid systems and represents a quite feasible method of purification.
5. Supercooled water is to be observed in frozen soils. Accordingly, ice lenses can be formed and can grow at temperatures considerably below the normal freezing point of water.
6. Observed and calculated thermodynamic data are believed to be fully applicable to ice mass (glacier) behavior at all pressure locations therein (bottom or internal points). These data also confirm the cell design (bottom-upward freezing) and the essential control of the ice-lens formation by the ice front behavior, this independently of the solid type in the fine-particle-water system.

SUMMARY

This report dealt with experimental and theoretical studies of basic frost heave mechanisms. The P-T fusion curve for ice demonstrated the non-Clapeyron case of pressure upon the solid in contact with its own unconfined liquid. This gave rise to pressure effects on ice that were about 13 times larger than the Clapeyron-predicted data of Bridgman.²¹ Ice-lens growth was demonstrated for pressures up to 182.81 kg/cm². The data are of interest to permafrost investigators, glaciologists,

metallurgists, ceramicists, as well as to basic thermodynamics. Specifically, it was shown that ice-lens formation is but a special form of crystal growth, one that is common to many liquid-solid transformations accomplished in insoluble fine-particle host systems.

ACKNOWLEDGMENTS

We wish to document the x-ray diffraction study contribution of Dr. Charles McKinney and the inspiration and the enthusiasm of Professor F. J. Sanger for the scientific understanding of the properties of frozen soils.

REFERENCES [3]

1. U.S. Army Corps of Engineers. 1958. Frost investigations 1952–1953: Cold room studies. Vol. I. Test Rep. 43. Arctic Construction and Frost Effects Laboratory, Waltham, Massachusetts. 46 p. (AD 217742)
2. Barnes, P., and D. Tabor. 1966. Plastic flow and pressure melting in the deformation of ice I. *Nature* 210 (5039): 878–882.
3. Beskov, G. 1935. Soil freezing and frost heaving with special application to railroads. *Swed. Geol. Soc. Ser. C No. 375*.
4. U.S. Army Corps of Engineers. 1952. Investigation of description, classification, and strength properties of frozen soils. Vol. I and II. Frost Effects Laboratory, Boston, Massachusetts.
5. Hoekstra, P. 1964. Electro-osmosis in frozen soil. *Nature* 203 (4952): 1406–1407.
6. Hoekstra, P. 1966. Moisture movement in soils under temperature gradients with the cold-side temperature below freezing. *Water Resour. Res.* 2(2):241–250.
7. Hoekstra, P., E. Chamberlain, and T. Frate. 1965. Frost heaving pressures. CRREL Res. Rep. 176. 12 p. (AD 626175) (Presented to 44th annual meeting of the U.S. Highway Research Board)
8. Jackson, K. A., D. R. Uhlam, and B. Chalmers. 1966. Frost heave in soils. *J. Appl. Phys.* 37:848–852.
9. Jackson, K., and B. Chalmers. 1958. Freezing of liquids in porous media with special reference to frost heave in soils. *J. Appl. Phys.* 29:1178–1181.
10. Kaplar, C. W. 1965. Some experiments to measure the frost heaving force in a silt soil. CRREL Tech. Note. U.S. Army Cold Regions Research and Engineering Laboratory, Hanover, New Hampshire.
11. Penner, E. 1966. The nature of frost heaving in soils. Permafrost: Proceedings of an international conference. National Academy of Sciences, Washington, D.C.
12. Poynting, J. H. 1881. Change of state: Solid-Liquid. *Phil. Mag.* 5 (12):32–48.
13. Kittel, C. 1956. Introduction to solid state physics. J. Wiley & Sons, New York. p. 490–491.
14. U.S. Army Corps of Engineers. 1958. Snow, ice, and permafrost establishment. Experimental study of frost heaving. Res. Rep. 45. Wilmette, Illinois.
15. Taber, S. 1930. The mechanics of frost heaving. *J. Geol.* 38:303–317.
16. Takagi, S. 1965. Principles of frost heaving. CRREL Res. Rep. No. 140. 24 p. (AD 626174) Based on Fundamentals of the theory of frost heavings, p. 203–216. In Permafrost: Proceedings of an international conference. National Academy of Sciences, Washington, D.C. (1966).

17. Tsytoich, N. A. 1963. Official papers (Soviet) of the International Conference on Permafrost, USSR Academy of Science, 105. Moscow.
18. Uhlman, D. R., B. Chalmers, and K. A. Jackson. 1964. The interaction between particles and a solid-liquid interface. *J. Appl. Phys.* 35:2986-2993.
19. Vialov, S. S. 1962. The strength and creep of frozen soils and calculations for ice-solid retaining structures. USSR Academy of Sciences, Moscow, p. 69-82.
20. Williams, P. J. 1963. Suction and its effects in unfrozen water of frozen soils. Permafrost: Proceedings of an international conference. National Academy of Sciences, Washington, D.C.
21. Bridgman, P. W. 1912. Water, in the liquid and five solid forms, under pressure. *Proc. Am. Acad. Arts Sci.* 47 (13):439-558.

NOTES

- [1] The authors will send details of the apparatus to interested individuals.
- [2] 12.473, experimental; 12.02, theoretical (thermodynamics); 11.7, via Poynting.¹²
- [3] The AD-marked publications are available from National Technical Information Services, U.S. Department of Commerce, Springfield, Virginia 22151, USA.

TRIAXIAL AND CREEP TESTS ON FROZEN OTTAWA SAND

Francis H. Sayles

U.S. ARMY COLD REGIONS RESEARCH AND
ENGINEERING LABORATORY
Hanover, New Hampshire

INTRODUCTION

Triaxial compression tests using a constant rate of applied strain and triaxial creep tests using a constant load were conducted on saturated frozen Ottawa sand (20-30 mesh) and ice to gain a better understanding of the factors that influence the strength and deformation characteristics of frozen soils. Several published results of conventional unconfined compression tests, direct shear tests, and unconfined compression creep tests^{1,2,4,5,7,8,9,12} show that the strength and deformation of a given frozen soil are strongly dependent on temperature and duration of applied stress. Although Vyalov¹⁰ discussed triaxial testing of frozen soil and suggested a generalized creep theory that takes hydrostatic pressure into account and Andersland and AlNouri² presented data from triaxial tests on Ottawa sand using confining pressures up to about 0.62×10^6 N/m², the influence of confining pressure and rate of loading on strength and deformation have not been fully assessed.

Strength and deformation of frozen soils, as with unfrozen cohesive soils, depend on both the cohesion and the internal friction of the component materials. According to Vyalov and Tsytoich,¹¹ the cohesion component in frozen soils can be attributed to molecular forces of attraction between particles, physical or chemical cementing of particles together, and cementing of particles by ice formation in

the soil voids. The cementation by ice is the result of the bonds between the ice crystals and the soil particles even though the soil particles are surrounded by a film of unfrozen water. This cementation implies that the unfrozen water under the influence of molecular forces of the soil particles is capable of transmitting normal and even some shear forces between the solid ice and the solid soil grains. The cohesion depends on the amount, strength, and area of the ice in contact with the soil particles, each of which is temperature dependent. The internal friction depends on the ice content; the soil grain arrangement, sizes, distribution, and shape; and the number of grain-to-grain contacts.^{8,11} Except for the ice content, each of these factors is independent of temperature.

The purpose of this investigation is to study the effects of hydrostatic confining pressure and the rate of applied load on the strength and deformation characteristics of frozen sands and to assess the relative influence of the cohesion of the ice matrix versus the friction between the particles of sand.

TEST PROCEDURE

The testing was conducted on cylindrical specimens about 70 mm in diameter and about 152.5 mm in length. These dimensions were chosen to ensure a large ratio between

specimen diameter and soil particle size and to use existing available testing apparatus. Each sand specimen was packed in a freezing mold, saturated with distilled, de-aired water under about 700 mm of mercury vacuum, and then frozen from the top down in an open system where free water had access to the bottom of the specimen. No expansion of the specimens was observed during the freezing process. The increase in volume, because of the change in phase of the water to ice, was absorbed in the free water supply connected to the bottom of the specimen. The ice specimens used in this study were prepared in a manner similar to that of the sand. All specimens were trimmed to ensure that the ends were perpendicular to the axis and were enclosed in two and sometimes three rubber membranes to prevent the intrusion of the confining fluid (ethylene glycol and water). The Ottawa sand specimens were saturated and had an average dry unit weight of about $1\,670\text{ kg/m}^3$, a void ratio of about 0.59, and a porosity of 37 percent; the specific gravity of the soil particles was 2.65. The average dry unit weight of the ice specimens was about 913 kg/m^3 .

Nominal hydrostatic confining pressures σ_3 of 0.34×10^6 to $8.2 \times 10^6\text{ N/m}^2$ were used; superimposed axial (deviator) stresses $(\sigma_1 - \sigma_3)[1]$ in the creep tests were 0.105×10^6 to $6.89 \times 10^6\text{ N/m}^2$; the test temperature was -3.85°C . In the compression tests, the diameter of the specimen increased with axial deformation. The resulting axial stresses were computed on the assumption that the volume of the specimen remained constant and the specimen remained a cylinder throughout each test. These assumptions were consistent with visual observation.

TRIAxIAL TESTS AT CONSTANT STRAIN RATE

Laboratory data from the constant rate of strain tests show that the shape of the stress-strain curve and the maximum or peak stresses are governed by the rate of applied strain and the magnitude of the hydrostatic confining pressure. Stress-strain curves for a rate of applied strain of about 0.03/min are shown in Figure 1. Where strains exceed about 0.1, two peak stresses occur when the confining pressure σ_3 is above about $2.7 \times 10^6\text{ N/m}^2$. The first peak occurs at strains less than 0.01, and the second peak occurs at a strain of about 0.1. The strain at which the first stress peak occurs is close to the strain at failure for columnar-grained ice specimens (i.e., where the ice crystals are columns with axes parallel to those of the cylinder specimen) also shown in Figure 1. This observation suggests that the first peak is essentially the consequence of the strength of the ice matrix, and the second peak is the development of friction between grains of sand and/or ice crystals as the strain progresses. The frictional resistance increases until the maximum dilatancy of the sand grains is reached and the second peak in the stress-strain curve is attained.

Since the strength due to internal friction of the sand in-

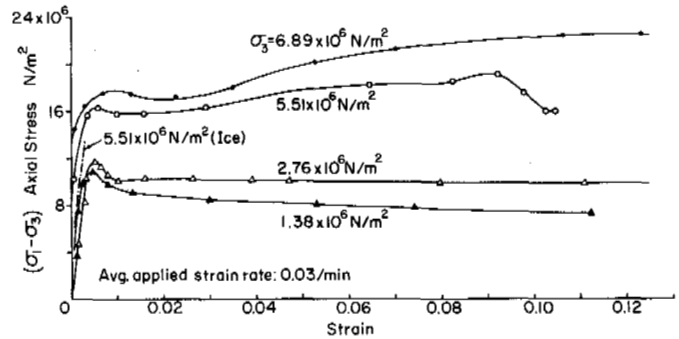


FIGURE 1 Axial stress-strain curves for Ottawa sand and ice at different confining pressures σ_3 and at large strains.

creases with confining pressure and for practical purposes the cohesion of an ice crystal does not, the second peak of the stress-strain curve may be smaller than the first peak for low confining pressures and greater than the first peak for high confining pressures. In fact, it was observed, and is shown in Figure 1, that for the lower confining pressures the frictional resistance might be considered as an apparent constant residual strength for each confining pressure.

The concept that each peak strength represents the domination of either the cohesive or frictional strength separately is reinforced by the two Mohr's strength envelopes shown in Figure 2a,b. The envelope in Figure 2b is nearly a straight line with an angle of internal friction of about 31° —a value similar to that of unfrozen Ottawa sand. The envelope in Figure 2a is curved for the lower values of confining pressure, indicating that there is some internal friction involved at these lower levels of confining pressures. However, this envelope approaches nearly a constant value at the higher confining pressures, suggesting that cohesion provides nearly all resistance at these confining pressures and small strains. The influence of confining pressure on the stress-strain curve for the first stress peak for the slightly higher constant rate of applied strain of 0.5/min is shown in Figure 3a. The first peak stresses increase with confining pressure up to about $2.7 \times 10^6\text{ N/m}^2$; above this value, the confining pressure appears to have little influence on the strength.

The Mohr's envelope for polycrystalline columnar-grained ice given in Figure 2c also shows that for lower confining pressures the ice has a strength dependency on confining pressure and at higher confining pressures the strength of the ice is nearly independent of confining pressure. The curve is consistent with the concept that the first peak stress on the stress-strain curve is a reflection of the influence of the ice matrix of the soil.

The strength dependency of polycrystalline ice on confining pressure could be attributed to the friction between the individual ice crystals. As the confining pressure is increased, the ice crystals are pressed together and tend to resist the applied stress as a single unit. The nearly constant

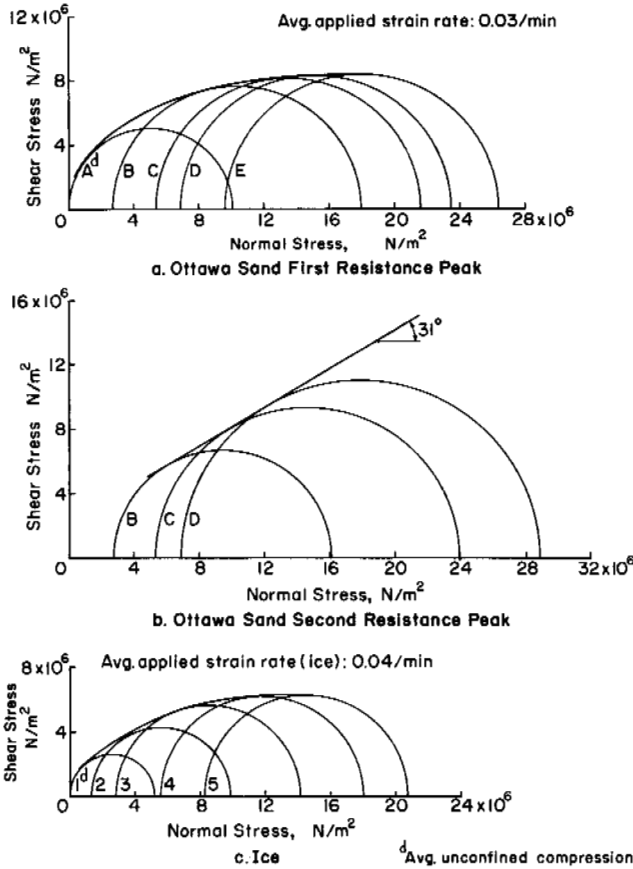


FIGURE 2 Mohr's envelopes for Ottawa sand and ice. A-E on curves indicate different specimens of sand; 1-5 on curves indicate different specimens of ice.

shearing strength of about $6.2 \times 10^6 \text{ N/m}^2$ shown in Figure 2c is greater than the values reported³ for a single ice crystal tested along the glide direction. This result is expected because it would be improbable for the glide planes of the crystals in the polycrystalline ice to have the same orientation and hence the same resistance to shear as a single crystal. Also to be noted in Figure 2a and c is the difference in Mohr's envelopes indicating that in samples of frozen sand some shearing resistance at the first peak of the stress-strain curve is contributed by the arrangement of sand grains. It should be noted that some shearing resistance in frozen sand is afforded by the structure of the sand grains at the first peak of the stress-strain curve, as indicated by the differences between the ice and the Ottawa sand Mohr's envelopes for curves shown in Figure 2a-c.

The shapes of the stress-strain curves for the first resistance peak shown in Figure 3b suggest a plastic type of failure rather than a brittle failure. These curves indicate that, as the rate of applied strain increases, the maximum peak resistance increases. It is questionable whether the resistance can increase indefinitely with the increase in strain rate before some other phenomenon such as brittle

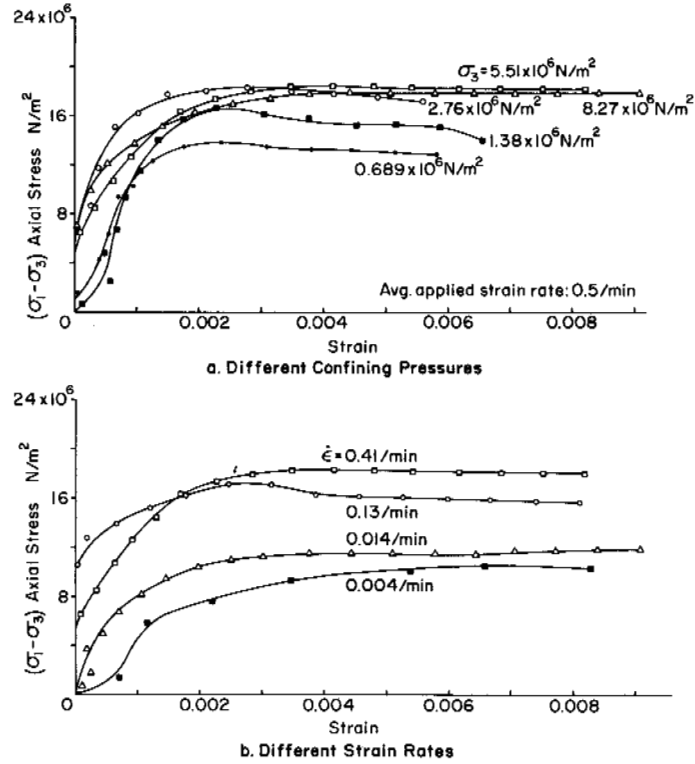


FIGURE 3 Axial stress-strain curves for Ottawa sand at small strains.

fracturing of the ice matrix limits the first peak resistance of the frozen sand. The times required to achieve peak strengths are indicated by these curves.

As shown in Figure 4, the combined effect of increasing applied strain rate $\dot{\epsilon}$ and confining pressure on the first or cohesion peak strength shows that the peak strengths for

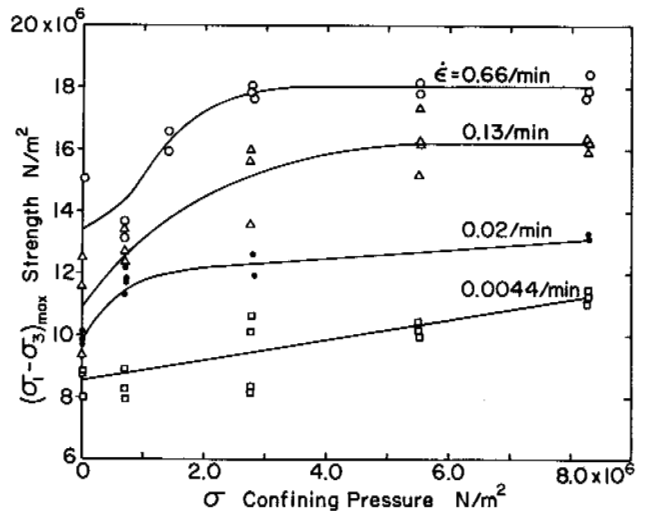


FIGURE 4 Strength versus confining pressure (σ_3) for Ottawa sand.

rates of strain above about 0.02/min increase with confining pressure up to about $2.7 \times 10^6 \text{ N/m}^2$ and then appear to be independent of confining pressure. At the slower rates of strain (below 0.02/min), the strength increases with increase in confining pressure; this suggests that friction between the sand grains is being activated possibly because the ice matrix is allowed time to creep from between the sand grains.

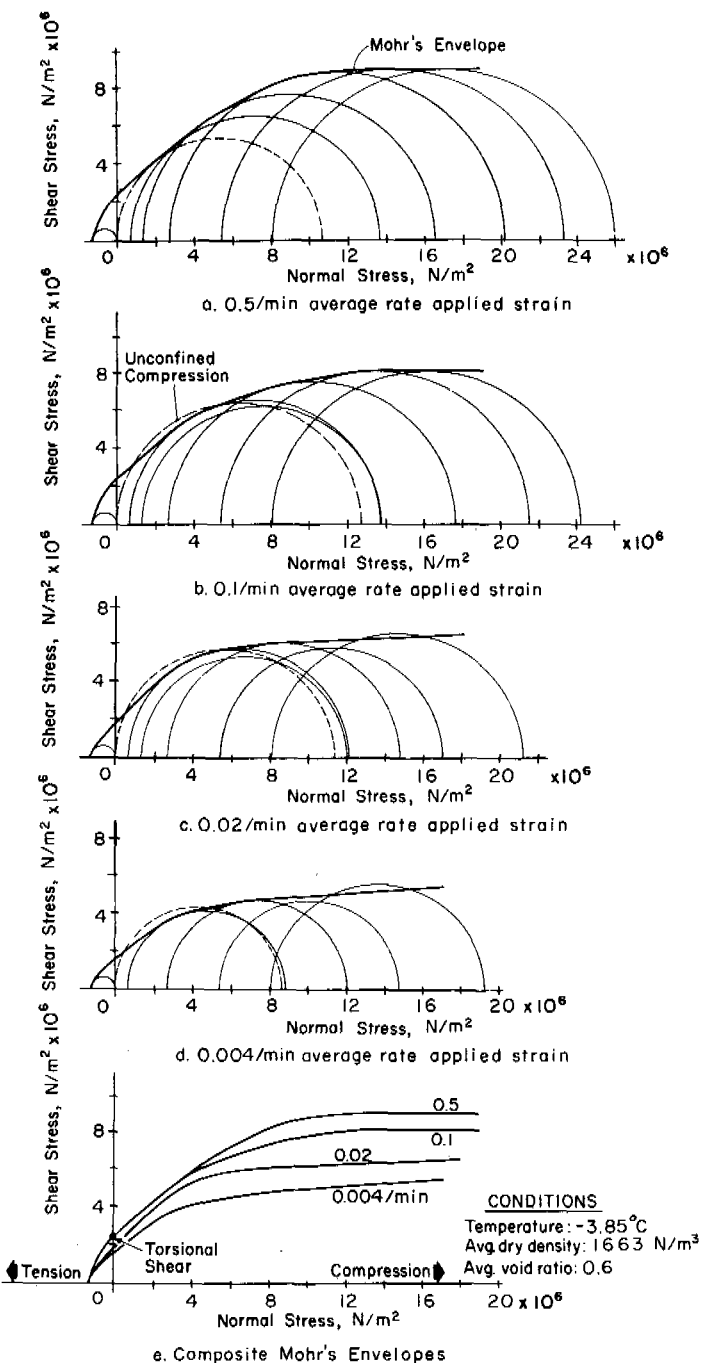


FIGURE 5 Mohr's envelopes for Ottawa sand at different strain rates.

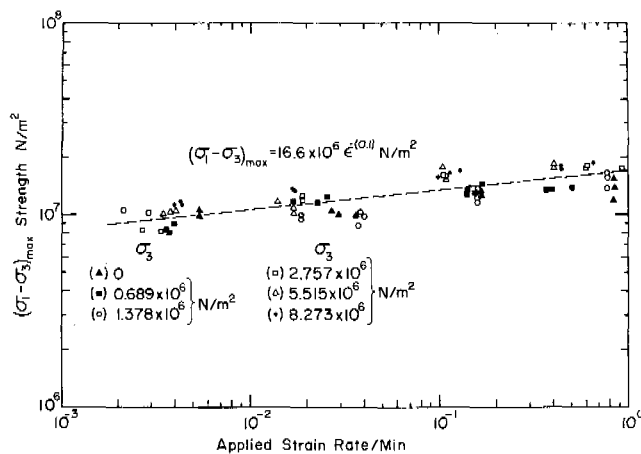


FIGURE 6 Strength versus applied strain rate for Ottawa sand.

Mohr's envelopes for the first resistance peak of frozen sand for different rates of applied axial strain are plotted in Figure 5. The figure also shows the combined effect of rate of strain and confining pressure. Again, at the higher confining pressures, the slope of the envelope is small, and the slopes are greater for the slower strain rates, possibly reflecting the friction between the ice crystals as well as the friction between the soil grains that have crept closer together.

There is evidence from unconfined compression tests that the strength of frozen Ottawa sand does not increase indefinitely as the rate of applied strain increases but is limited by a brittle type of failure at strain rates greater than 0.5/min. Nevertheless, the data obtained for confined compression in this investigation can be represented by the straight line shown in Figure 6 and the expression

$$(\sigma_1 - \sigma_3)_c = 16.6 \times 10^6 (\dot{\epsilon})^{0.1}, \quad (1)$$

where $(\sigma_1 - \sigma_3)_c$ = first peak stress or strength in N/m^2 . This expression was derived using a least-squares regression fit to all constant strain rate test data obtained in this investigation and unconfined compression data from earlier tests.⁵ Figure 6 is presented only to show that the general trend is that the strength increases as the rate of applied strain increases within the limits of the strain rates shown.

CREEP UNDER HYDROSTATIC STRESS CONDITIONS

Time versus creep strain curves for constant confining pressures shown in Figure 7 summarize data from creep tests conducted in this investigation. Where more than one specimen was tested, a single curve represents the average for the specimens. The vertical bars on the curves give the total range of strain values at the location of the bar.

Although considerable care was taken to repeat each of

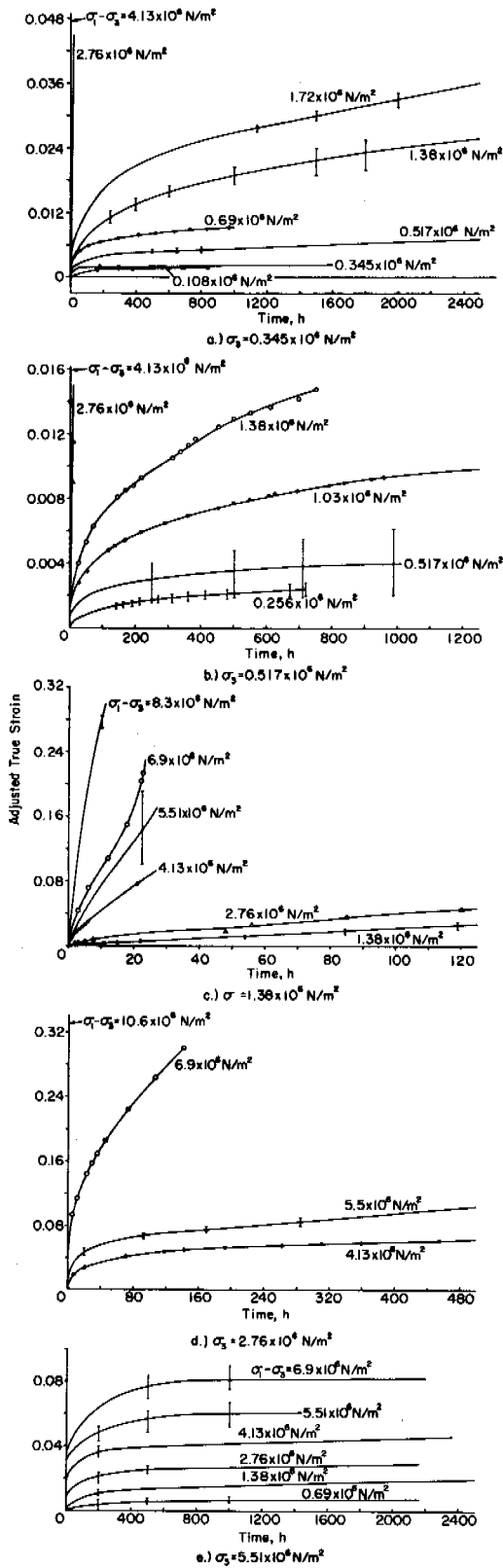


FIGURE 7 Summary creep curves for Ottawa sand at different confining pressures and axial stresses.

the tests by preparing each specimen using the same process in every detail, by testing each replication under as nearly identical conditions as possible, and by controlling the temperature within 0.1°C , there was considerable variation in the results, as shown by the size of the vertical bars on the summary creep curves. This variation is especially noticeable for the lower axial stress levels where the vertical bars overlap adjacent creep curves (Figure 7a and b).

As expected, these creep curves show that, for a given confining pressure, the magnitude of the strain at any given time increases with stress level. The effect of increasing the confining pressure is to reduce the amount of creep strain for a given period of constant axial stress application. This effect is demonstrated in Figure 8, where the axial stress is held constant and the confining pressure is increased. In comparing creep curves from triaxial tests with those from unconfined compression tests,⁸ it was noticed that the first stage or primary creep was prolonged in the triaxial tests and that strains greater than 0.2 were reached without secondary creep being attained.

An examination of the various curves of this investigation at the lower stress levels indicates that the rate of strain decreases continuously with time in a manner suggesting that an empirical power function relationship between the rate of creep strain and time may exist. The logarithmic plots of strain versus time data in Figure 9 can be represented by a straight line and the expression:

$$\dot{\epsilon} = [\dot{\epsilon}_R / (t_R)^{1/n}] (t)^{1/n}, \quad (2)$$

where $\dot{\epsilon}$ = the rate of strain at any time t greater than zero, t_R = a reference time greater than zero, $\dot{\epsilon}_R$ = a corresponding strain rate, and n = the slope of the straight line on the plot.

Any convenient value for a reference time t_R greater

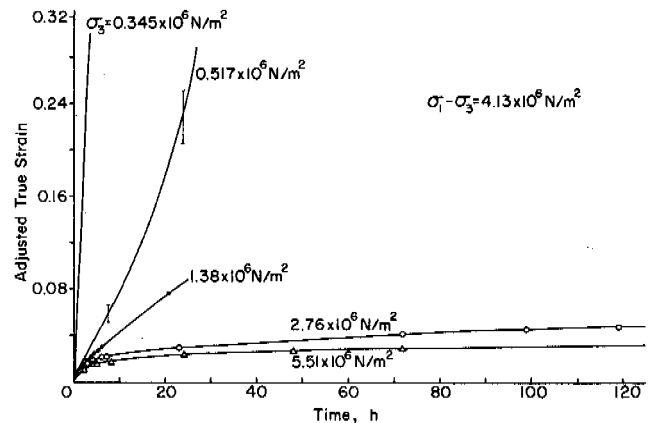


FIGURE 8 Creep curves for Ottawa sand at constant axial stress ($\sigma_1 - \sigma_3$) and different confining pressures (σ_3).

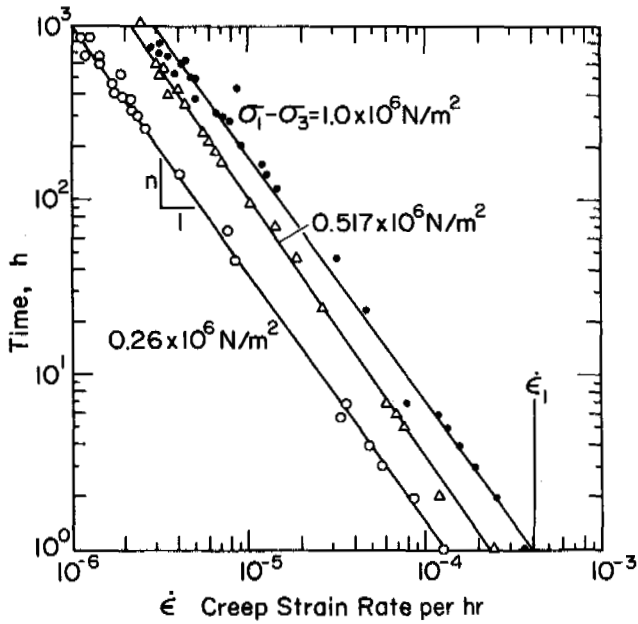


FIGURE 9 Time versus creep strain rate for Ottawa sand.

than zero can be selected. For t_R taken as 1 h, $\dot{\epsilon}_R$ becomes $\dot{\epsilon}_1$ and

$$\dot{\epsilon} = \dot{\epsilon}_1 t^{1/n} \tag{3}$$

To obtain an expression for strain at any time, Eq. (2) can be integrated:

$$\begin{aligned} \dot{\epsilon} = (d\epsilon/dt) &= [\dot{\epsilon}_R / (t_R)^{1/n}] (t)^{1/n} && t_R > 0 \\ &&& t > 0 \\ \int_{\epsilon_r}^{\epsilon} d\epsilon &= \dot{\epsilon}_R / (t_R)^{1/n} \int_{t_r}^t (t)^{1/n} dt \\ \epsilon - \epsilon_r &= [\dot{\epsilon}_R / (t_R)^{1/n}] [n / (n + 1)] [t^{(n+1)/n} - t_r^{(n+1)/n}] \\ &&& \text{for } n \neq -1 \\ &&& t_r > 0 \\ &&& t_R > 0 \end{aligned} \tag{4}$$

and

$$\epsilon - \epsilon_r = \dot{\epsilon}_R / (t_R)^{1/n} \ln(t/t_r), \text{ for } n = -1, \tag{5}$$

where t_r and ϵ_r are convenient reference time greater than zero and corresponding strain.

For t_R and t_r taken as 1 h, $\dot{\epsilon}_R = \dot{\epsilon}_1$ and $\epsilon_r = \epsilon_1$ and Eq. (4) becomes:

$$\epsilon = \epsilon_1 (n/n + 1) [t^{(n+1)/n} - 1] + \epsilon_1, \text{ for } n \neq -1, \tag{6}$$

and

$$\epsilon = \epsilon_1 (\ln t) + \epsilon_1, \text{ for } n = -1. \tag{7}$$

By determining values of $\dot{\epsilon}_1$, ϵ_1 , and n from short-term creep tests conducted under the desired stress and temperature conditions, Eq. (6) provides a means for estimating the value of strain at any time. Figure 10 compares the predicted or estimated strain with laboratory creep test data. The constants for Eq. (6) were determined from the first 8 h of each creep test.

TRIAxIAL CREEP STRENGTH

Since the soil tested in this investigation did not fail abruptly by rupture but instead deformed continuously in a plastic manner, the criterion for failure was arbitrarily taken to be the time the specimen strain reached 0.2. Assuming a strain of 0.2 as failure, strength versus time curves for different confining pressures were obtained by plotting the time to failure against the corresponding creep strength (Figure 11). These curves are drawn to approach asymptotically the maximum test stresses that did not result in specimen failure during the test period. Although limited data are available for each confining pressure and the data vary somewhat, especially for confining pressures of $1.38 \times 10^6 \text{ N/m}^2$, the test results can be represented by¹⁰:

$$\sigma_t \cong (\sigma_1 - \sigma_3)_t \cong \beta / \ln(t/B), \tag{8}$$

where β and B are parameters that can be determined by short-term creep tests under the stress and temperature

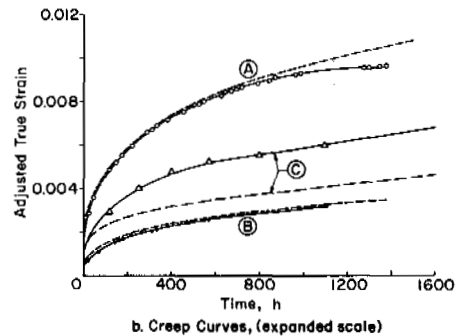
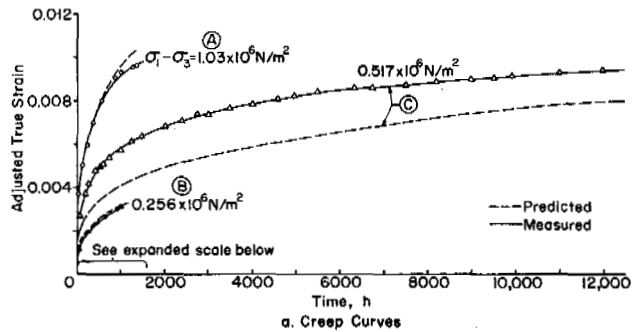


FIGURE 10 Measured compared with predicted creep strain for Ottawa sand. A, B, and C indicate different sand specimens.

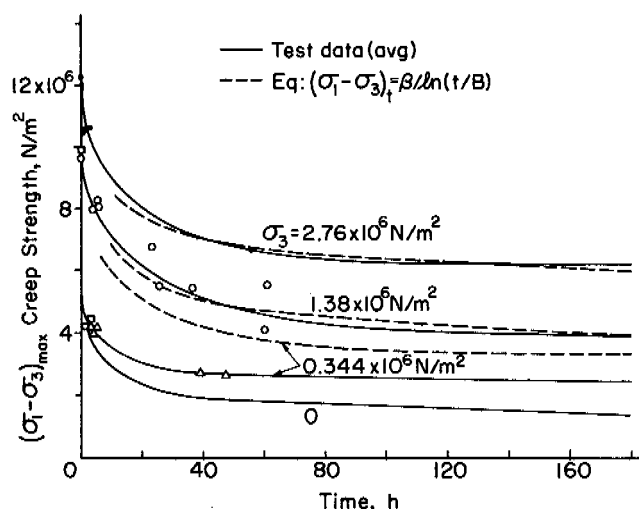


FIGURE 11 Creep strength versus time to failure for Ottawa sand.

conditions for which estimated strengths are required. The strength variations with time predicted by Eq. (8) are represented by dashed lines in Figure 11 for comparison with the test data for relatively short creep tests.

Mohr's envelopes representing creep strengths for different times after application of constant axial stress are shown in Figure 12. The curved envelopes for the shorter periods of time suggest that the strength and the friction between the ice crystals dominate the strength of the soil mass much in the manner indicated in the constant rate of applied strain tests previously described. The envelopes for the 60-h period at reduced constant axial stress approach a straight line with an angle of internal friction of about 29°. As mentioned earlier, this angle is near that of unfrozen Ottawa sand, thus implying that friction between the sand grains dominates the strength of the soil mass at the longer test times. These envelopes suggest that at lower applied axial stresses, time is available for the ice to creep from between the sand grains and allow the development of an increase in the number of soil grain contacts and firmer grain-to-grain contacts. The frictional resistance of the sand grains would thus tend to dominate the strengths of the sand over long periods. It is hypothesized that the long-term, ultimate creep strengths of frozen sands can be estimated by drained triaxial tests on sands under the same stress conditions and unit weights as those of the *in situ* material. For practical purposes Mohr-Coulomb's expression

$$\tau = C + \sigma_n \tan \phi, \tag{9}$$

where C = cohesion, σ_n = normal stress, and ϕ = angle of internal friction for the sand, would apply.

It is emphasized that Eq. (9) should be applied only to sands with low ice contents and porosity of about 37 per-

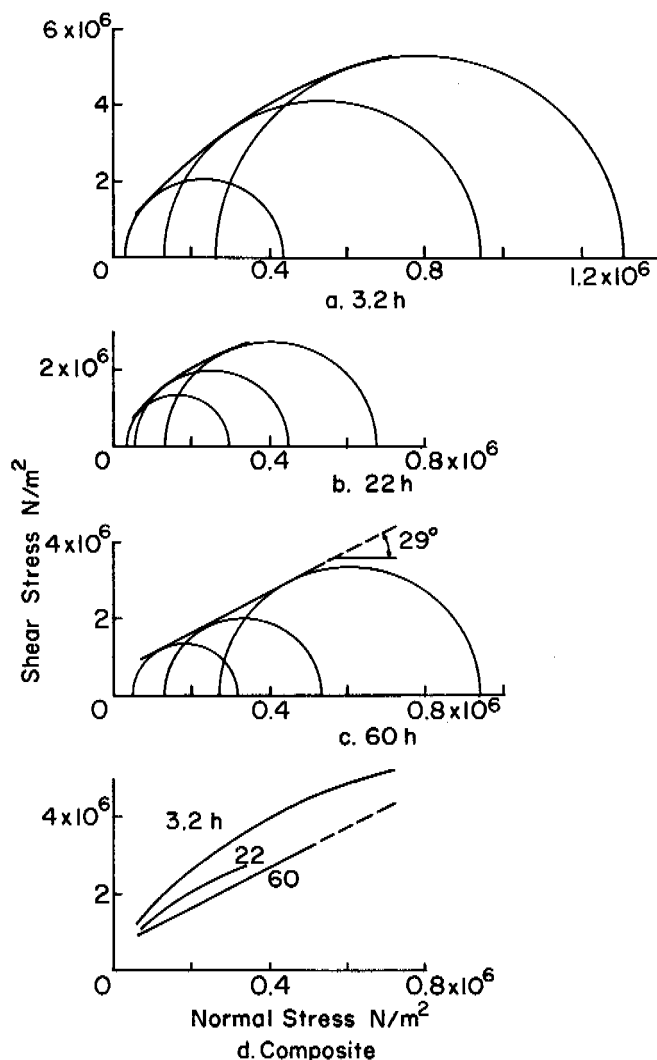


FIGURE 12 Mohr's envelopes for creep strength of Ottawa sand.

cent or less. Soils with high ice content and porosity can behave in a viscous manner.⁶

SUMMARY

The results of this investigation based on triaxial compression tests performed on saturated frozen Ottawa sand (20-30 mesh) and polycrystalline columnar-grained ice at -3.85 °C show that:

1. The resistance of saturated frozen Ottawa sand in a confined stress condition can be considered as consisting of the cohesion of the ice matrix and the frictional resistance of the sand grains. These sources of strength are nearly independent of each other when the applied rate of strain is greater than 0.02. After the ice matrix has failed at a strain less than 0.01, the soil resistance becomes a function of the

normal stress and the apparent angle of the internal friction of unfrozen sand, about 30° .

2. For a given temperature the initial or "cohesive" strength of the frozen sand increases with the rate of applied strain and can be approximated by the expression:

$$(\sigma_1 - \sigma_3)_c = 16.6 \times 10^6 (\dot{\epsilon})^{0.1},$$

where $(\sigma_1 - \sigma_3)_c$ = initial or cohesive strength and $\dot{\epsilon}$ = applied strain rate from 0.002 to 1.0.

3. The rate of increase in the initial shear strength of saturated frozen Ottawa sand and polycrystalline columnar-grained ice decreases with increasing confining pressure. At the higher confining pressures used in this investigation, the initial shear strength is nearly independent of confining pressure at rates of applied strain greater than 0.02.

4. The short-term (periods up to at least 100 h) creep strength of frozen Ottawa sand can be represented by Vyalov's¹⁰ strength equation:

$$\sigma_t \cong (\sigma_1 - \sigma_3)_t \cong \beta / \ln(t/B)$$

5. For low axial (deviator) stress levels, the creep strain rate can be represented by the empirical expression:

$$\dot{\epsilon} = [\dot{\epsilon}_R / (t_R)^{1/n}] (t)^{1/n}$$

for a given constant stress and temperature condition.

6. For low axial (deviator) stress levels, creep strain can be estimated by

$$\epsilon - \epsilon_r = [\dot{\epsilon}_R / (t_R)^{1/n}] [n/(n+1)] [t^{(n+1)/n} - t_r^{(n+1)/n}]$$

$$\text{for } \begin{array}{l} n \neq -1 \\ t_r > 0 \\ t_R > 0 \end{array}$$

and

$$\epsilon - \epsilon_r = \dot{\epsilon}_R / (t_R)^{1/n} \ln(t/t_r) \text{ for } n = -1$$

for a constant stress and temperature condition.

7. It is hypothesized that the long-term ultimate creep strength of saturated frozen sand with porosity of 37 percent or less is a function of the angle of internal friction of the sand that could be determined through triaxial tests on unfrozen sand freely drained.

ACKNOWLEDGMENTS

This paper presents the results of research performed by the U.S. Army Cold Regions Research and Engineering Laboratory under the sponsorship of the U.S. Army Corps of Engineers and the Army Materiel Command. The study was conducted for the Directorate of Military Construction (OCE) and the program was under the technical direction of the Engineering Division of this directorate, Civil Engineering Branch. The author is appreciative of assistance given by personnel in the CRREL testing laboratory.

REFERENCES

1. Andersland, O. B., and W. Akili. 1967. Stress effect on creep rates of frozen clay. *Geotechnique* 17:27-39.
2. Andersland, O. B., and I. Al-Nouri. 1970. Time-dependent strength behavior of frozen soils. *J. Soil Mech. Found. Div. (ASCE)* 96:1249-1265.
3. Muguruma, J. 1969. Effects of surface condition on the mechanical properties of ice crystals. *Br. J. Appl. Phys. (J. Phys. D)* 2(11):1517-1525.
4. Sanger, F. J., and C. W. Kaplar. 1966. Plastic deformation of frozen soils, p. 305-315. *In Permafrost: Proceedings of an international conference*. National Academy of Sciences, Washington, D.C.
5. Sayles, F. H. 1968. Creep of frozen sands. CRREL Technical Report 190. U.S. Army Cold Regions Research and Engineering Laboratory, Hanover, New Hampshire.
6. Thompson, E. G., and F. H. Sayles. 1972. In-situ creep analysis of room in frozen soil. *J. Soil Mech. Found. Div. (ASCE)* 98: 899-915.
7. Tsytoich, N. A., and M. I. Sumgin. 1957. Principles of mechanics of frozen ground. SIPRE Translation 19 (out of print). U.S. Army Snow, Ice and Permafrost Research Establishment.
8. USA SIPRE. 1952. Investigation of description, classification and strength properties of frozen soils. Prepared by USA ACFEL, U.S. Army Corps of Engineers for USA SIPRE, Report 8.
9. Vyalov, S. S. 1959. Rheological properties and bearing capacity of frozen soils. Academy of Science, USSR.
10. Vyalov, S. S. 1966. Rheology of frozen soils, p. 332-337. *In Permafrost: Proceedings of an international conference*. National Academy of Sciences, Washington, D.C.
11. Vyalov, S. S., and S. Tsytoich. 1955. Cohesion of frozen soils. *Dokl. Akad. Nauk.* 4(104):527-529.
12. Young, R. N. 1966. Soil-freezing considerations in frozen soil strength, p. 315-319. *In Permafrost: Proceedings of an international conference*. National Academy of Science, Washington, D.C.

NOTE

[1] $(\sigma_1 - \sigma_3)$ is the axial deviator stress, where σ_1 is the major principal stress and σ_3 is the hydrostatic confining pressure.

SAMPLE DISTURBANCE AND THAW CONSOLIDATION OF A DEEP SAND PERMAFROST

Wayne S. Smith and Keshavan Nair

WOODWARD-LUNDGREN AND ASSOCIATES
Oakland, California

Robert E. Smith

ATLANTIC RICHFIELD COMPANY
Dallas, Texas

INTRODUCTION

The importance of sample disturbance effects has been recognized in conventional soil mechanics for many years and a great deal of effort has been spent in correlating *in situ* properties to laboratory test results. However, similar information on the effects of sample disturbance for permafrost was not available. In the overall context of a design problem, it was necessary to evaluate the thaw-consolidation properties of permafrost at great depths (300–440 m),³ and it was considered necessary to obtain an estimate of the significance of disturbance effects on laboratory data.

To evaluate the influence of possible sample disturbance effects on the thaw-consolidation behavior, artificially frozen specimens were fabricated in the laboratory where positive control of disturbance effects was possible. Uniaxial thaw-consolidation tests were performed on both recovered

permafrost cores and artificially frozen specimens to evaluate the effect of sample disturbance on the test results.

TEST EQUIPMENT

Two major pieces of equipment were required to perform the test program. Figure 1 shows the uniaxial consolidation cell used to perform thaw-consolidation tests.

The artificial freezing device shown in Figure 2 was used to fabricate frozen specimens. This device allowed control of the total axial stress, pore water pressure, drainage conditions, and the direction of axial freezing and thawing.

UNIAXIAL TEST SPECIMEN PREPARATION

Basically two types of specimens were tested in the uniaxial consolidation cells: recovered permafrost cores kept

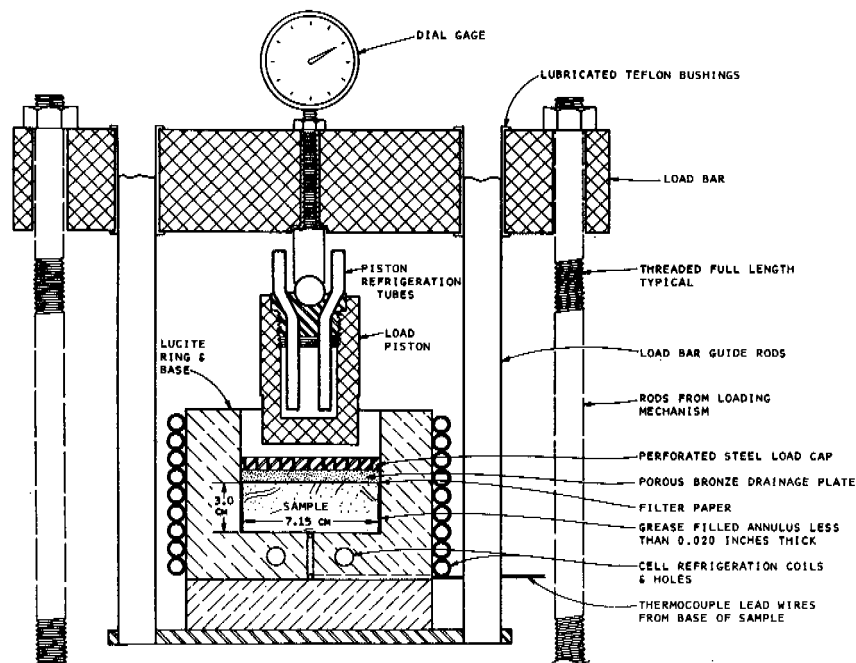


FIGURE 1 Cross section of high pressure uniaxial consolidation cell assembly.

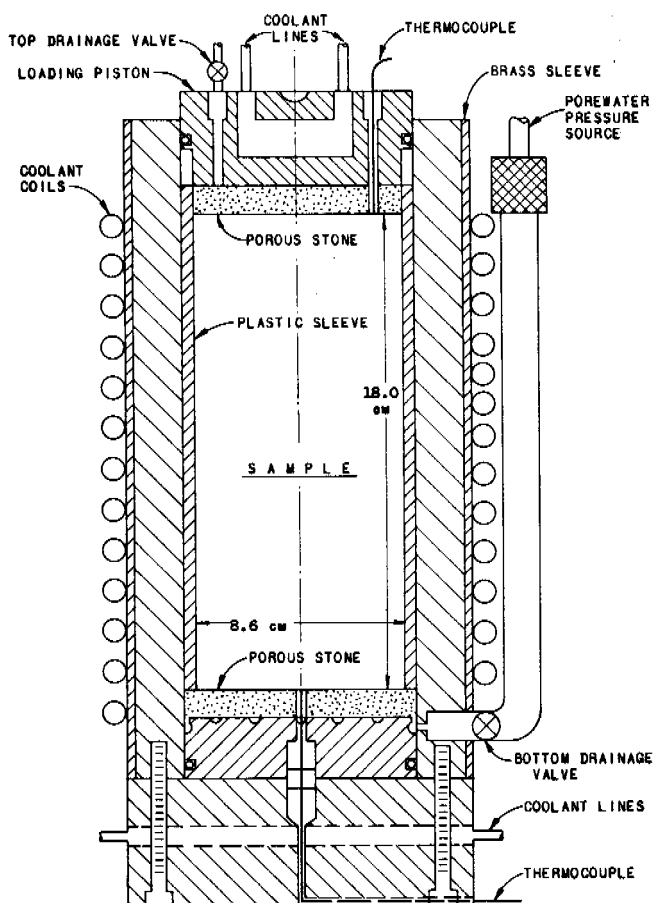


FIGURE 2 Schematic of artificial freezing device.

frozen from the time they were sampled until the final stage of thaw-consolidation testing; and artificially frozen specimens.

Recovered Permafrost Cores

Since the permafrost core samples received were of varied diameters and lengths and the test apparatus and interpretation techniques required constant diameter samples, each core selected for testing was reshaped and the ends trimmed parallel. Vaporizing liquid nitrogen provided both refrigeration and gas flow to clear cuttings during the coring process. Samples prepared by reshaping had diameters between 7.04 and 7.08 cm. The uniaxial consolidometers were 7.15 cm in diameter.

Also, because of the unavoidable small annular space between the sample and wall of the consolidometer, the sides of the samples were coated with a viscous graphite and lithium base grease. This lubricant reduced the expansion of the sample into the annular space upon loading and reduced sidewall friction. Weighing procedures provided accurate

determinations of the amount of lubricant present on each sample.

Artificially Frozen Cores

All artificially frozen specimens were fabricated from a nonplastic sand with a specific gravity of 2.66. The sand used was obtained by combining several thawed samples of recovered permafrost cores and grading was by U.S. Standard Sieves.

The artificial specimens were consolidated at a total axial stress level of 35.0 kg/cm^2 with a pore water pressure of 15.2 kg/cm^2 . The specimens were then frozen axially downward with the bottom drainage valve open approximately over a 24-h period. No claim is made that the method of freezing the specimen in the laboratory accurately simulated the freezing process that had occurred in the field. However, for soils having a small percentage of nonplastic fines, the relatively rapid rate of freezing used in the laboratory is likely to be a good approximation of the field process.

Uniaxial consolidation samples were cored from some of the artificially frozen specimens using the same procedure as described for the recovered permafrost cores. Two uniaxial consolidation specimens were obtained from one artificially frozen cylindrical specimen.

UNIAXIAL THAW-CONSOLIDATION TEST PROCEDURE

There were no generally accepted standard test procedures for thaw-consolidation testing of frozen soils; however, extensive work with frozen soils in the Soviet Union had resulted in recommended procedures.^{2,4,5} Their suggested criteria and test procedures were used, when applicable, to perform the uniaxial thaw-consolidation tests described in the following paragraphs.

The prepared samples were placed on the testing frame, and a small seating load was applied for approximately 5 s. The height of the uniaxial sample was recorded and the load applied to the frozen sample. The frozen samples were brought back approximately to their *in situ* temperature and axial stress level and allowed to come to equilibrium at that condition. In all cases it required at least 24 h to reach an equilibrium state.

This equilibrium was established from a Soviet criterion for sand permafrost⁵ when the deformation rate is less than $33.0 \times 10^{-5} \text{ cm/h}$ for specimens 2-3 cm in height. Deformation rates prior to thawing the frozen sand samples ranged from 5.1 to $23.4 \times 10^{-5} \text{ cm/h}$. Therefore, all the frozen samples reached equilibrium within 24 h.

The frozen samples were then allowed to thaw gradually under the same axial stress. During the uniaxial thawing, the loading piston was allowed to warm while the cooling

coils were maintained below freezing. This procedure combined with the thermal properties of the lucite cells ensured slow uniaxial thawing of the samples from the top to the bottom.

Typical results of a uniaxial thaw-consolidation test on a recovered sand permafrost core are shown in Figure 3. Point A is the practical equilibrium state of the frozen sample. The sample was then allowed to thaw under the same axial stress. Point B is the equilibrium state of the sample after thawing was complete. The difference in axial strain between points A and B is termed the strain on thawing or thaw strain.

At the completion of each thaw-consolidation test, the filter paper placed on top of the thaw-consolidation specimen was examined for evidence of the possible extrusion of grease that was used to fill the annular space between the sample and consolidometer wall. In every case, no evidence of grease extrusion was present. Therefore, minor errors in the axial strains calculated from changes in specimen heights due to extrusion of the side wall lubricant were effectively eliminated with the test apparatus used.

Because of the high pressures and changes in temperature occurring during a thaw-consolidation test, it was necessary to calibrate the effect of load and temperature changes on the axial deformation measurement. The load and temperature calibrations were used to account for the expansion and contraction in the test equipment. All axial deformation measurements were corrected to reflect only specimen deformations.

THAW-CONSOLIDATION RESULTS ON RECOVERED PERMAFROST CORES

The majority of the permafrost cores (the physical properties of which are presented in Table I) were recompressed

to their approximate *in situ* temperature and overburden pressure. Once the frozen samples had reached equilibrium, they were allowed to thaw gradually. The uniaxial thaw-consolidation test results are summarized in Table II. They indicated a thaw strain that varied between 1 to 4 percent, averaging 2.8 percent. Some samples were compressed more and some less than the approximate *in situ* overburden pressure to indicate the influence of the recompression pressure on the test results and did not indicate significantly different thaw strains.

These test results appeared to be at variance with an analysis of the geologic history of the region from which the permafrost cores were recovered. Geologic information indicated that the *in situ* sand permafrost was probably normally consolidated.³ Therefore, it was not expected that the axial strain on thawing would be as high as from 1 to 4 percent. Because of the depth from which these permafrost samples were recovered, it was considered necessary to investigate the possible influence of sample disturbance on the test results.

THAW-CONSOLIDATION RESULTS ON ARTIFICIALLY FROZEN SPECIMENS

The two types of artificially frozen specimens tested were distinguished by the disturbance pattern to which they were subjected after being frozen but prior to thaw-consolidation testing.

Disturbed Specimens

One set of artificially frozen specimens was subjected to a disturbance pattern similar to that which occurred with the recovered permafrost cores. Three artificial specimens were normally consolidated as described above. Once the speci-

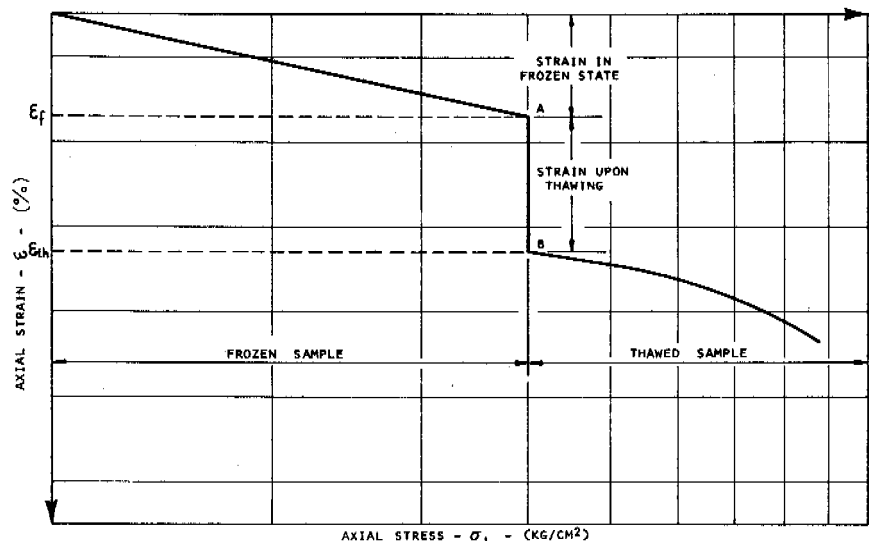


FIGURE 3 Schematic diagram of uniaxial thaw-consolidation test.

TABLE I Summary of Classification Test Results on Recovered Sand Permafrost Cores

Sample Depth (m)	Initial Dry Unit Weight (g/cm ³)	Initial ^a Water Content (%)	Initial ^b Saturation (%)	Specific Gravity	Mechanical Analysis (% Passing by Dry Weight)								Hydrometer (% Passing by Dry Weight)		
					9.2 mm	No. 4	No. 8	No. 16	No. 30	No. 50	No. 100	No. 200	5 μ	2 μ	1 μ
293	1.53	23.5	89	2.68	—	—	—	100	99	76	22	14	2	2	1
335	1.58	22.0	94	2.68	—	—	—	—	100	98	46	25	10	8	4
350	1.60	20.8	89	2.67	—	—	100	99	98	59	21	12	5	4	2
354	1.59	23.2	88	2.68	99	96	94	93	91	65	21	16	4	4	3
354	1.48	25.1	92	2.68	—	—	—	—	100	32	7	5	2	2	1
361	1.48	29.1	100	2.65	—	—	—	—	100	26	6	4	2	2	1
369	1.54	24.6	99	2.68	—	—	100	99	98	86	35	20	8	6	3
415	1.64	22.0	98	2.69	—	—	—	—	100	94	38	23	9	7	4
438 ^c	1.23	33.0	87	2.54	96	91	85	80	75	65	30	19	11	8	5

^a Water content includes frozen and unfrozen water.

^b Calculated from density determination samples, accounts for density of ice 9 percent less than density of water.

^c Samples contained much organic material.

men had been completely frozen, the total axial stress and pore water pressure were reduced simultaneously until the pore water pressure reached zero. The 19.8 kg/cm² residual axial stress was then reduced to zero in increments over 1 h to simulate the stress relief experienced during the recovery process in the field. Although the stresses were reduced to zero, some of the frozen specimens did not rebound until they were completely extruded from the artificial freezing device. This was primarily caused by the prevention of axial

expansion due to the ice that formed around the loading piston and top of the artificial freezing device during the freezing process. Nevertheless, once the specimens were extruded from the artificial freezing device, complete stress relief and subsequent rebound occurred.

Six samples were prepared from these specimens and placed in the thaw-consolidation cells. Four of the rebounded samples were recompressed to the effective axial stress at which they were frozen (19.8 kg/cm²), and two samples

TABLE II Summary of Uniaxial Sample Properties, Frozen Strains, and Strains upon Thawing for Recovered Sand Permafrost Cores

Sample No. and Depth (m)	Initial Frozen Conditions				Frozen Recompression and Thawing Pressure (kg/cm ²)	Strain in Frozen State, ϵ_f (%)	Strain upon Thawing, $\epsilon_{th} - \epsilon_f$ (%)
	Dry Unit Weight (g/cm ³)	Water ^a Content (%)	Degree of ^b Saturation (%)	Void Ratio			
293	1.61	23.5	100	0.664	27.0 ^d	3.73	0.84
293	1.76	23.5	100	0.552	8.8	0.79	2.56
335	1.54	22.0	92	0.710	28.1 ^d	3.33	3.69
350	1.55	20.8	86	0.725	37.9	2.09	3.01
350	1.54	20.8	84	0.739	8.8	1.32	4.95
354	1.59	23.3	100	0.684	32.6 ^d	1.66	1.90
354	1.51	25.1	96	0.777	32.6 ^d	2.19	4.05
354	1.49	25.1	94	0.794	32.6 ^d	4.12	3.13
354	1.49	25.1	98	0.772	32.6 ^d	3.50	4.01
354	1.49	25.1	94	0.793	8.8	2.01	3.12
354	1.49	25.1	93	0.802	63.1	8.16	4.50
369	1.49	24.6	91	0.804	8.8	1.83	1.66
438 ^c	1.28	33.0	94	0.983	40.3 ^d	6.20	1.92

^a Water content includes frozen and unfrozen water.

^b Calculated from actual samples tested and accounts for density of ice 9 percent less than density of water.

^c Sample contained much organic material.

^d Approximate overburden stress for *in situ* material.

recompressed to the total axial stress at which they were frozen (35.0 kg/cm^2). After coming to equilibrium in the frozen state, the samples were allowed to thaw. The artificial specimen fabrication data and uniaxial thaw-consolidation test results are shown in Tables III, IV, and V.

The disturbed specimens that were recompressed to their effective axial formation stress showed thaw strains varying from 3.4 to 5.1 percent. Specimens recompressed to their total axial formation stress had thaw strains of 3.3 and 4.2 percent. These thaw strains on disturbed specimens were in general agreement with the thaw strains measured with recovered permafrost cores.

Two additional specimens were fabricated in the artificial freezing device to assess the magnitude of rebound strain occurring upon complete stress relief. Both specimens were fabricated at an effective axial stress of 19.8 kg/cm^2 ; however, one specimen was formed with a zero pore water pressure and the other with a 15.2 kg/cm^2 pore water pressure. They were extruded and stored in the cold room. After 3 days, the four specimens ceased to rebound significantly. The void ratio of both specimens was then determined and indicated that both specimens had experienced a 1.0 percent volumetric rebound strain upon complete stress relief. These test results, shown in Table VI, are an indication of the magnitude of rebound strain the recovered permafrost specimens had experienced. Note that the magnitude of rebound appeared to be a function of the effective axial stress at the time they were frozen.

In summary, test results indicated that significant rebound of the frozen specimens occurs upon complete stress relief. Uniaxial thaw-consolidation tests on disturbed artificial specimens indicated that 3-5 percent thaw strains would occur for normally consolidated sand permafrost. To evaluate the effect of disturbance on the thaw strains measured in these tests, undisturbed specimens also were tested.

Undisturbed Specimens

Five specimens were used to evaluate the effects of the state of consolidation and disturbance pattern on the thaw strain. The test results for the two specimens frozen in the artificial freezing device are shown in Table VII. Artificial specimen 6 was fabricated using exactly the same procedure as used for all other specimens fabricated in the artificial freezing device. During reduction of the pore water pressure, the effective stress remained constant at 19.8 kg/cm^2 , and no rebound of the specimen occurred. The undisturbed specimen was then allowed to thaw directly in the artificial freezing device. This specimen showed only a 0.1 percent axial thaw strain.

Artificial specimen 7 was fabricated with a slightly different procedure. Upon partial freezing of the specimen, the base drainage value was closed thereby preventing flow of water out of the specimen as the freezing front advanced toward the base. The result of the base drainage prevention was axial expansion of the specimen upon the completion of

TABLE III Uniaxial Thaw-Consolidation Results for Artificial Specimens Subjected to Disturbance and Recompressed to Effective Axial Stress of Fabrication

Axial Pressure (kg/cm^2)	Pore Water Pressure (kg/cm^2)	State of Sample	Void Ratio (e)	Axial Strain $-\frac{\Delta e}{1+e_0}$ (%)	Strain upon Thawing (%)
Artificial Specimen-1					
1. 35.0	15.2	Thawed	0.549	0.0	—
2. 35.0	15.2	Frozen	0.546	0.2	—
3. 0	0	Frozen	0.544	0.3	—
Sample C1-a, Saturation = 90 Percent ^a					
1. 0	0	Frozen	0.640	0.0	—
2. 19.8	0	Frozen	0.546	5.7	—
3. 19.8	0	Thawed	0.477	9.9	4.2
Sample C1-b, Saturation = 80 Percent ^a					
1. 0	0	Frozen	0.542	0.0	—
2. 19.8	0	Frozen	0.504	2.5	—
3. 19.8	0	Thawed	0.451	5.9	3.4

^a The letter "C" before the sample number indicates that the sample was extruded from the artificial freezing device, stored, and cored. The samples cored from the artificially frozen specimen were then tested in uniaxial thaw consolidation, using the same procedure as used for recovered permafrost cores.

TABLE IV Uniaxial Thaw-Consolidation Results for Artificial Specimens Subjected to Disturbance and Recompressed to Effective Axial Stress of Fabrication

Axial Pressure (kg/cm ²)	Pore Water Pressure (kg/cm ²)	State of Sample	Void Ratio (<i>e</i>)	Axial Strain $-\frac{\Delta e}{1+e_0}$ (%)	Strain upon Thawing (%)
Artificial Specimen-2					
1. 35.0	15.2	Thawed	0.551	0.0	-
2. 35.0	15.2	Frozen	0.547	0.3	-
3. 0	0	Frozen	0.605	-3.5	-
Sample C2-a, Saturation = 92 Percent ^a					
1. 0	0	Frozen	0.611	0.0	-
2. 19.8	0	Frozen	0.539	4.5	-
3. 19.8	0	Thawed	0.463	9.2	4.7
Sample C2-b, Saturation = 89 Percent ^a					
1. 0	0	Frozen	0.653	0.0	-
2. 19.8	0	Frozen	0.577	4.6	-
3. 19.8	0	Thawed	0.492	9.7	5.1

^a The letter "C" before the sample number indicates that the sample was extruded from the artificial freezing device, stored, and cored. The samples cored from the artificially frozen specimen were then tested in uniaxial thaw-consolidation cells, using the same procedure as used for recovered permafrost cores.

TABLE V Uniaxial Thaw-Consolidation Results for Artificial Specimens Subjected to Disturbance and Recompressed to Total Axial Stress of Fabrication

Axial Pressure (kg/cm ²)	Pore Water Pressure (kg/cm ²)	State of Sample	Void Ratio (<i>e</i>)	Axial Strain $-\frac{\Delta e}{1+e_0}$ (%)	Strain upon Thawing (%)
Artificial Specimen-3					
1. 35.0	15.2	Thawed	0.577	0.0	-
2. 35.0	15.2	Frozen	0.574	0.2	-
3. 0	0	Frozen	0.579	-0.1	-
Sample C3-a, Saturation = 80 Percent ^a					
1. 0	0	Frozen	0.573	0.0	-
2. 35.0	0	Frozen	0.507	4.2	-
3. 35.0	0	Thawed	0.455	7.5	3.3
Sample C3-b, Saturation = 84 Percent ^a					
1. 0	0	Frozen	0.560	0.0	-
2. 35.0	0	Frozen	0.518	2.7	-
3. 35.0	0	Thawed	0.453	6.9	4.2

^a The letter "C" before the sample number indicates that the sample was extruded from the artificial freezing device, stored, and cored. The samples cored from the artificially frozen specimen were then tested in uniaxial thaw-consolidation cells, using the same procedure as used for recovered permafrost cores.

TABLE VI Magnitude of Rebound Strain upon Stress Relief of Artificially Frozen Specimens

Axial Pressure (kg/cm ²)	Pore Water Pressure (kg/cm ²)	State of Sample	Void Ratio (<i>e</i>)	Volumetric Strain $-\frac{\Delta e}{1+e_0}$ (%)	Volumetric Strain upon Stress Relief (%)
Artificial Specimen-4, Saturation = 97 Percent					
1. 35.0	15.2	Thawed	0.578	0.0	—
2. 35.0	15.2	Frozen	0.579	-0.1	—
3. 0	0	Frozen	0.595 ^a	-1.1	-1.0
Artificial Specimen-5, Saturation = 100 Percent					
1. 19.8	0	Thawed	0.575	0.0	—
2. 19.8	0	Frozen	0.574	0.1	—
3. 0	0	Frozen	0.589 ^a	-0.9	-1.0

^a Void ratio determined using total artificial specimen after extrusion from the artificial freezing device and storage in the cold room for 3 days.

freezing. This resulted in an underconsolidated frozen specimen. The pore water pressure and axial stress were then simultaneously reduced until the pore water pressure reached zero. The specimen was allowed to thaw and a 1.1 percent thaw strain resulted.

These two tests indicated that undisturbed normally consolidated frozen sand specimens would have only very small thaw strains in contrast to the 3-5 percent thaw strains measured on normally consolidated disturbed specimens. However, the undisturbed underconsolidated specimen showed that significant thaw strains would occur if the sand specimens were not normally consolidated in the frozen state.

Three artificial specimens (8, 9, and 10) were frozen directly in the uniaxial thaw-consolidation cells, which were modified for control of drainage at the base of specimens. The cells did not have provisions for the application of pore water pressure so all three specimens were frozen with zero pore water pressure and at an effective axial stress of 19.8 kg/cm². These artificial specimens were normally consolidated and then frozen axially downward from the top to the bottom with the base drainage valve open.

Upon completion of freezing, the specimens were allowed to thaw. The test results, shown in Table VIII, gave thaw strains of -0.1, 0.2, and 0.0 percent. The experimental accuracy of these tests was approximately 0.1 percent, and the

TABLE VII Uniaxial Thaw-Consolidation Results for Tests Performed Directly in the Artificial Freezing Device on Undisturbed Specimens

Axial Pressure (kg/cm ²)	Pore Water Pressure (kg/cm ²)	State of Sample	Void Ratio (<i>e</i>)	Axial Strain $-\frac{\Delta e}{1+e_0}$ (%)	Strain upon Thawing (%)
Artificial Specimen-6, Normally Consolidated in Frozen State					
1. 35.0	15.2	Thawed	0.563	0.0	—
2. 35.0	15.2	Frozen	0.556	0.4	—
3. 19.8	0	Frozen	0.556	0.4	—
4. 19.8	0	Thawed	0.555	0.5	0.1
Artificial Specimen-7, Underconsolidated in Frozen State					
1. 35.0	15.2	Thawed	0.592	0.0	—
2. 35.0	15.2	Frozen	0.608	-1.0	—
3. 19.8	0	Frozen	0.608	-1.0	—
4. 19.8	0	Thawed	0.590	0.1	1.1

TABLE VIII Uniaxial Thaw-Consolidation Results for Undisturbed Artificial Specimens Fabricated and Tested in the Uniaxial Consolidation Cells

Axial Pressure (kg/cm ²)	Pore Water Pressure (kg/cm ²)	State of Sample	Void Ratio (e)	Axial Strain $-\frac{\Delta e}{1+e_0}$ (%)	Strain upon Thawing (%)
Artificial Specimen-8, Saturation = 100 Percent					
1. 19.8	0	Thawed	0.547	0.0	-
2. 19.8	0	Frozen	0.541	0.4	-
3. 19.8	0	Thawed	0.542	0.3	-0.1
Artificial Specimen-9, Saturation = 100 Percent					
1. 19.8	0	Thawed	0.570	0.0	-
2. 19.8	0	Frozen	0.562	0.5	-
3. 19.8	0	Thawed	0.599	0.7	0.2
Artificial Specimen-10, Saturation = 70 Percent					
1. 19.8	0	Thawed	0.585	0.0	-
2. 19.8	0	Frozen	0.576	0.6	-
3. 19.8	0	Thawed	0.576	0.6	0.0

results once again indicated that very small thaw strain would occur in undisturbed normally consolidated frozen sand specimens.

CONCLUSIONS

The results of this investigation showed that sample disturbance effects may have a significant influence on the laboratory test results obtained with permafrost cores recovered from great depth.

It was observed that thaw-consolidation results obtained from testing normally consolidated artificially frozen specimens subjected to a disturbance pattern similar to that experienced by recovered permafrost cores produced comparable magnitudes of axial thaw strain. Since the thaw strains observed for the artificially frozen specimens subjected to disturbance were of comparable magnitude to those observed for similar recovered permafrost cores, it was felt that the artificial specimen preparation technique was a reasonable simulation of the process by which sand permafrost was formed, recovered, and tested.

Thaw-consolidation tests on undisturbed, normally consolidated, artificially frozen sand indicated that the thaw strain would be very small. This result was in direct contrast to the larger thaw strains measured on both recovered permafrost cores and disturbed normally consolidated artificially frozen specimens. Therefore, it was felt that the larger thaw strains measured on recovered permafrost cores may have been induced by sample disturbance.

Permafrost that thaws *in situ* will not experience disturbance associated with sample recovery, sample preparation, or recompression. On the basis of this initial study, it appears that such disturbance effects could be very significant. Therefore, it is felt that a detailed systematic investigation to define the correlation between *in situ* permafrost properties and properties determined in the laboratory would assist engineers in design of structures on or within permafrost. Knowledge of sample disturbance effects would lead to more economical designs for most situations.

ACKNOWLEDGMENT

The authors would like to acknowledge the assistance of John A. Shuster and Jim Wilson of Woodward-Lundgren and Associates in planning the experimental program, developing the experimental equipment, and conducting the laboratory test program.

REFERENCES

1. Nair, K., J. A. Shuster, C-Y Chang, and W. S. Smith. 1971. Investigation of the subsidence and resulting downdrag loads on an oil well casing at Prudhoe bay. Report by Woodward-Lundgren submitted to Atlantic Richfield Company, Dallas, Texas.
2. Research Institute of Foundation and Underground Structures, Academy of Construction and Architecture (USSR). 1962. Instruction for designing bearing media and foundations in the southern zone of the permafrost region. Technical Translation 1298. National Research Council of Canada, Ottawa.
3. Smith, R. E., and M. C. Clegg. 1971. Analysis and design of production wells through thick permafrost. Special Paper No. 4. In Proceedings of the 8th world petroleum congress, Moscow.

4. State Committee of the Council of Ministers (USSR) for Building Problems. 1960. Technical considerations in designing foundations in permafrost. Technical Translation 1033. National Research Council of Canada, Ottawa.

5. Vyalov, S. S., S. E. Gorodetskii, V. F. Ermakov, A. G. Zatsarnaya, and N. K. Pekarskaya. 1969. Methods of determining creep, long-term strength, and compressibility characteristics of frozen soils. Technical Translation 1364. National Research Council of Canada, Ottawa.

VISCOELASTIC PROPERTIES OF FROZEN SOIL UNDER VIBRATORY LOADS

Henry W. Stevens

U.S. ARMY COLD REGIONS RESEARCH AND
ENGINEERING LABORATORY
Hanover, New Hampshire

INTRODUCTION

Foundations for structures incorporating vibratory loads, for example heavy machinery such as turbines, compressors, or engines, must respond so that the design criteria are fully satisfied. A similar problem occurs in earthquake design where surface motion must be predicted assuming some definitive motion of the bedrock. Other examples may be cited. As the soil usually occurs in complicated layered systems often overlying bedrock, the selection of a suitable yet practical model is difficult. Dynamic stress-strain behavior of soils is approximately linear for small strains, and elastic relationships have usually been employed. Recently, a model has been suggested^{5,11} that permits the analysis of steady-state wave propagation problems in semi-infinite, linearly viscoelastic media. The model employs values of the complex modulus and of the damping property of the materials that are more accurate than those afforded by elastic theory incorporating only geometric energy dispersion or an artificial assumption of dashpot damping. The approach requires, as input, the response of the materials to dynamic loads expressed in terms of stiffness and a real damping index. Frozen soil is known to be an extremely stiff material, and it might be considered that the assumption of elastic response is adequate. Test results indicate that this is not the case. Adequate design involving stress wave propagation in frozen soils should consider such soils as effective damping materials. Also, frozen soils in nature are often present as a stiff layer overlying a soft, flexible core. A laboratory test has been adopted that subjects a right cylinder of frozen

soil to steady-state sinusoidal vibration in the longitudinal or compression mode and, again, in the torsional or shear mode. Testing is conducted in a walk-in cold room where temperatures can be controlled within $\pm 1^\circ\text{C}$. Samples are prepared by modeling to a given density and water content and are frozen in special refrigerator cabinets that allow for freezing from the top downwards. After tempering to test temperature, samples are tested in an unconfined state.

METHOD OF ANALYSIS

The desired parameters are computed from the test results using a mathematical model of the propagation of stress waves through solid bodies based on *linear* viscoelastic theory. To date, a *one-dimensional* wave propagation is assumed. Other basic assumptions are as follows:

1. The response of the solid to the propagation of the stress waves is such that there is no change in the physical properties (e.g., mass density) of the solid.
2. There are no lateral inertial effects. Although the diameter of the cylinder changes in accordance with Poisson's ratio when the wave passes, this change is so small that the inertial effects of this movement can be neglected.
3. The dynamic load is a steady-state, sinusoidal vibration.

The viscoelastic properties and terms used herein are defined as follows:

1. Complex Moduli E^* and G^* In a viscoelastic material, when the stress σ_D varies sinusoidally with time at an

angular frequency ω , the strain ϵ_D varies with time at the same frequency but there is a phase lag δ between stress and strain.

Adopting the following nomenclature:

$E^*, G^*, \epsilon^*, \sigma^*, \dots$ = complex numbers, and
 $|E^*|, |\epsilon^*|, |\sigma^*| \dots$ = modulus of complex number.

Then:

$$\begin{aligned}\sigma^* &= \sigma_1 + i\sigma_2 = |\sigma^*|e^{i\omega t}, \\ \epsilon^* &= \epsilon_1 + i\epsilon_2 = |\epsilon^*|e^{i[\omega t - (\delta)]}, \\ E^* &= E_1 + iE_2 = |E^*|e^{i\delta(\omega)},\end{aligned}$$

and

$$\frac{\sigma^*}{\epsilon^*} = \frac{|\sigma^*|e^{i\omega t}}{|\epsilon^*|e^{i(\omega t - \delta)}} = \frac{\sigma^*}{\epsilon^*} e^{i[\omega t - \omega t + \delta(i\omega)]} = \frac{\sigma^*}{\epsilon^*} e^{i\delta(\omega)},$$

where

$$\delta = \tan^{-1} \frac{E_1}{E_2}.$$

If $E^*(i\omega)$ is used to indicate a frequency-dependent phase shift between σ and ϵ , then:

$$\frac{\sigma^*}{\epsilon^*} = E^*(i\omega),$$

and E^* = complex modulus as used herein.

2. Angle of Lag, δ The angle whose tangent equals E_1/E_2 or G_1/G_2 , representing the frequency-dependent phase shift between σ and ϵ . Subscripts L and T refer to longitudinal and torsional, respectively; δ_L is not necessarily equal to δ_T .

3. Complex Poisson's Ratio, ν^* Assuming that the relationship among the elastic constants applies to the viscoelastic moduli, $\nu^* = (E^*/2G^*) - 1$, then, by substitution and arrangement of terms¹⁰:

$$\nu^* = \frac{E^*}{2G^*} - 1, |\nu^*| = [\nu_1^2 + \nu_2^2]^{1/2},$$

and

$$|\nu^*| = \frac{E_1 + iE_2}{2(G_1 + iG_2)} - 1,$$

where

$$\nu_1 = \frac{E_1 G_1 + E_2 G_2}{2(G_1^2 + G_2^2)},$$

and

$$\nu_2 = \frac{E_2 G_1 - E_1 G_2}{2(G_1^2 + G_2^2)}.$$

4. Dynamic Stress, σ_D The stress imposed by the peak sinusoidal drive force.

5. Dynamic Strain, ϵ_D The natural strain corresponding to the stress as defined under 4.

6. Damping A property of the material that causes the strain to lag in time behind the stress. Here it is expressed by $\tan \delta$.

7. Attenuation Coefficient If a plane wave is passed through a solid and the displacement amplitude at a distance from the source is A_1 and at a distance x farther along is A_2 , then $A_2 = A_1 e^{-\alpha x}$, and α = attenuation coefficient.

Subjecting one end of the specimen ($X = 0$) to a sinusoidal displacement $U(0, t) = U_0 e^{i\omega t}$ and taking into account the mass, m , resting on the other end ($X = l$), the ratio of displacements of the two ends R can be obtained.^{8,9} Recalling that $\tan \delta = E_2/E_1$ and defining the frequency ratio as $\xi = (\omega l/V_L)$, where $V_L = \sqrt{E^*/\rho}$ s $\delta/2$, the resulting equation can be written as:

$$\frac{1}{R^2} = \frac{1}{2} [Q^2 (\xi^2 + \psi^2) (\cosh 2\psi - \cos 2\xi) + 2Q(\psi \sinh 2\psi) - (\xi \sin 2\xi) + (\cosh 2\psi + \cos 2\psi)], \quad (1)$$

where $\psi = \xi \tan \delta/2$ and Q = ratio of cap mass to specimen mass.

It has been shown that the specimen is at resonance when the ratio R is a maximum.^{2,4} As the frequency is increased, the first maximum is the fundamental resonance and successive maxima indicate the harmonics. For the condition of the resonance where R is a maximum and $1/R^2$ is a minimum, Eq. (1) is differentiated with respect to ξ and set equal to zero:

$$\left(\frac{\partial}{\partial \xi}\right) \left(\frac{1}{R^2}\right) = 0,$$

as follows:

$$\begin{aligned}Q^2 \xi (1 + \psi^2 / \xi^2) (\cosh 2\psi - \cos 2\xi + \xi \sin 2\xi + \psi \sinh 2\psi) \\ + [(1 + Q)/\xi] (\psi \sinh 2\psi - \xi \sin 2\xi) \\ + (2Q/\xi) (\psi^2 \cosh 2\psi - \xi^2 \cos 2\xi) = 0.\end{aligned} \quad (2)$$

Equations (1) and (2) may be solved simultaneously with a digital computer, using an iterative process, for ξ and ψ . As values of ω and l are available, values for V (the phase velocity) and $\tan \delta$ may be obtained.

With known values of V and $\tan \delta/2$, the moduli can be

computed using the mass density ρ . As most testing to date has been with the sample resonating, σ_D and ϵ_D have been computed at the driven end of the sample ($X = 0$). If the sample is at a resonance, or fairly close to it, the stress and strain computed and used for correlation purposes are close to the maximum in the sample.

From Norris and Young⁸:

$$\sigma_D = E^* \exp(i\delta)\epsilon_D,$$

and

$$\epsilon_D = U_0 \left[\left(\frac{\tan pl + \Gamma}{1 - \Gamma \tan pl} \right) \cos px - \sin px \right] \exp(i\omega t), \quad (3)$$

where $p = \frac{\rho\omega^2}{E^*}$, $\Gamma = \frac{m\omega^2}{pAE^*(i\omega)}$, and A = cross-sectional area.

If $X = 0$, Eq. (4) becomes:

$$\epsilon_D = U_0 \left[\left(\frac{\tan pl + \Gamma}{1 - \Gamma \tan pl} \right) e^{i\omega t} \right]. \quad (4)$$

Substituting the expressions for p and Γ , after some algebraic rearrangement, Eq. (4) assumes the form:

$$\epsilon_D = \frac{U_0}{l} (\xi - i\psi) \left[\frac{\tan(\xi - i\psi) + Q(\xi - i\psi)}{1 - Q(\xi - i\psi)\tan(\xi - i\psi)} \right]. \quad (5)$$

With the input amplitude substituted for U_0 , Eq. (5) is used

to compute the strain ϵ_D . The corresponding stress σ_D is computed from:

$$\sigma_D = E^*\epsilon_D \text{ or } \sigma_D = G^*\epsilon_D. \quad (6)$$

To solve Eq. (5), the right-hand side must be separated into the real and imaginary parts, and the complex result evaluated.

The attenuation coefficient α is derived from the value of $\tan \delta$ and the velocity V , with the angular frequency as follows:

$$\alpha = \omega/V(\tan \delta/2). \quad (7)$$

TEST EQUIPMENT

The complete test apparatus includes the device for applying vibratory loads (Figure 1) and the control and readout apparatus (Figure 2). A complete description of the test equipment and test procedure is given in Reference 9.

SOILS

The majority of tests conducted to date used two soils—20-30 Ottawa sand and Manchester silt. Ottawa sand is a quartz sand with rounded grains grading between the No. 20 and the No. 30 U.S. Standard Sieves. Manchester silt is a nonplastic rock flour. Gradation is shown in Figure 3. A few specimens of other soils have been tested having grada-

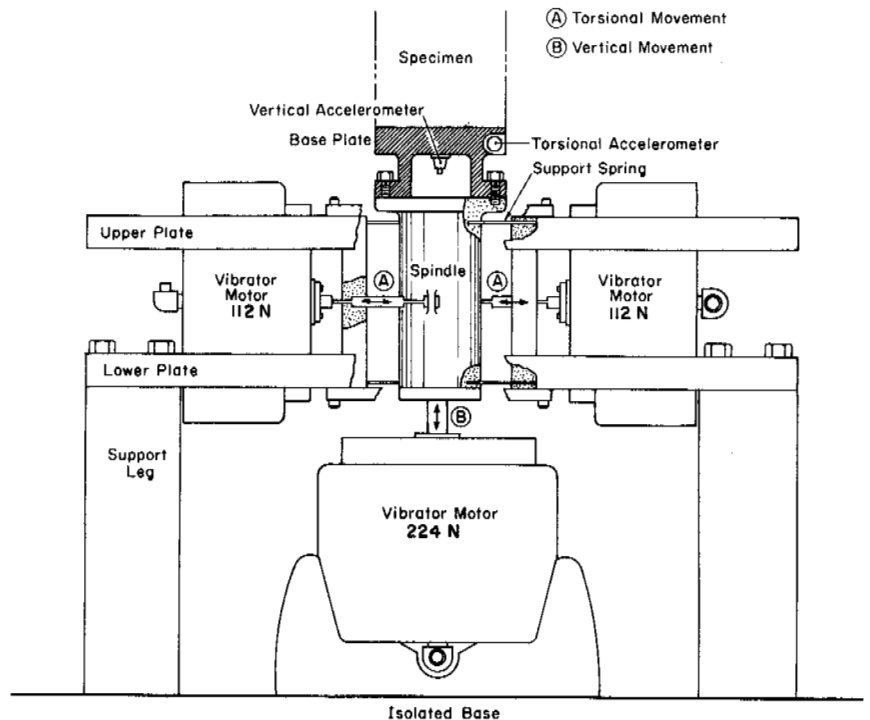


FIGURE 1 Schematic of test apparatus.

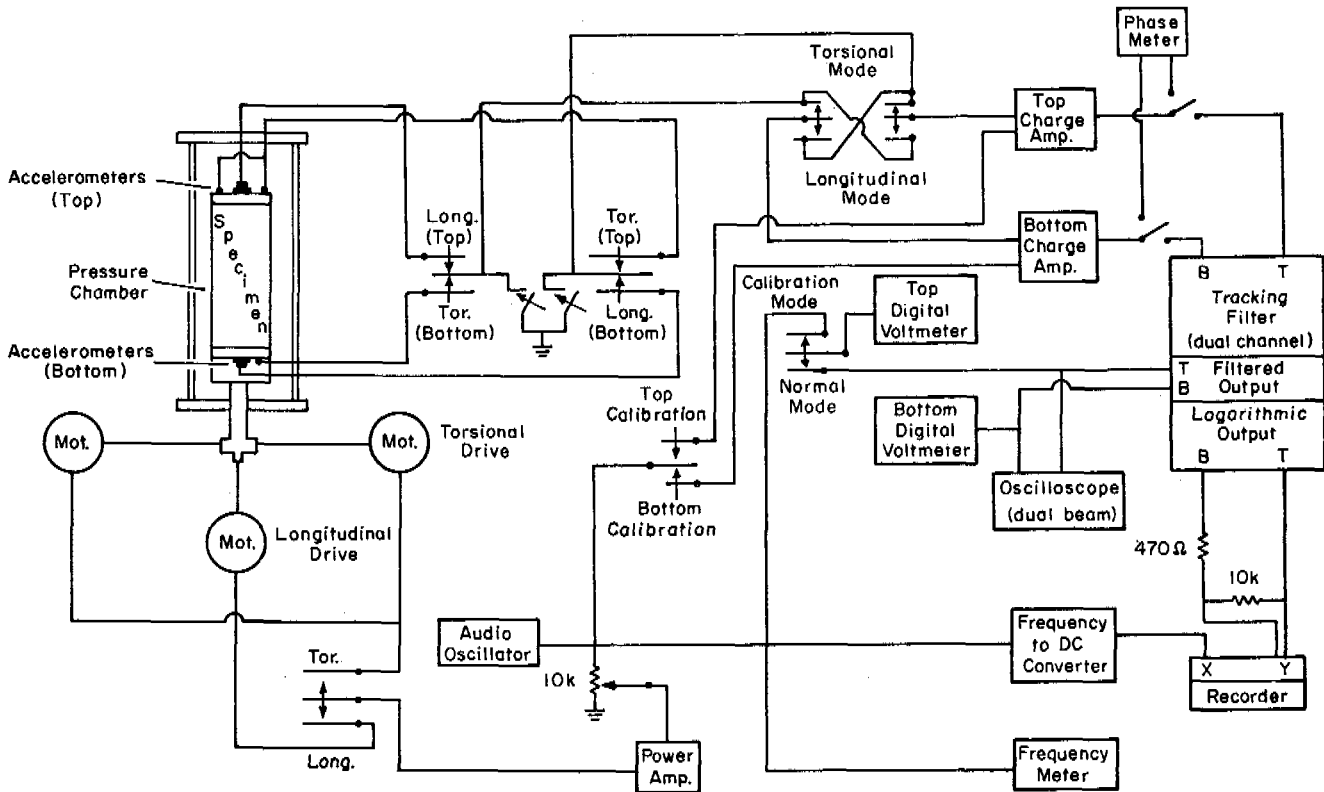


FIGURE 2 Schematic of control and readout system for dynamic test apparatus.

tions and properties as shown in Figure 3. All soils were remolded except Goodrich clay and Fairbanks silt. Goodrich clay was cored in the nonfrozen state, trimmed to size, and frozen without access to water. The Fairbanks silt was cored in the frozen state and contained various volumes of segregated ice. A few ice specimens were also tested. De-aired water was quick frozen in the same mold as the soil. Some specimens were constructed by packing saturated snow in the mold and quick freezing. In general, the latter method produced specimens with a lower density and consequent lower moduli. If possible, samples are 457 mm long and 76 mm in diameter. The theory assumes a rod condition. When the wavelength is long compared with the diameter, as is the case through the first resonance, the length:diameter ratio can be as low as 3; as higher resonances are established, however, the error increases. For the error to be insignificant at the fourth resonance a length:diameter ratio of about 6 is required.¹

TEST RESULTS

The test results show that the modulus, velocity, and damping property depend, roughly in order of importance, on the following:

1. Ice content expressed as percent saturation
2. Void ratio of soil
3. Temperature
4. Frequency of vibratory load
5. Dynamic stress and/or strain

The first two can be combined and expressed as the ratio of volume of ice to volume of soil. However, this relationship is difficult to understand as it does not readily indicate how closely the soil grains are packed. Maximum and minimum void ratios and consolidation properties in terms of void ratio are familiar. Therefore, the relationship is shown herein, as void ratio of specimens having ice saturation more than 90 percent. A second relationship shows the effect of ice saturation at a constant void ratio. As all the measured parameters cannot be shown, the shear modulus and $\tan \delta$ for shear are generally used as examples.

Effect of Void Ratio

Figure 4 relates the complex shear modulus to void ratio. All soils are nearly ice-saturated (> 90 percent). The stiffness increases with decreasing void ratio as would be expected, and the modulus of all frozen soils is greater than or

Design.		G_s	LL	PL	PI
1	20-30 Ottawa Sand	2.65	—	—	NP
2	-100 -200 Ottawa Sand	2.65	—	—	NP
3	Hanover Silt	2.74	—	—	NP
4	Fairbanks Silt	2.70	—	—	NP
5	Manchester Silt	2.73	—	—	NP
6	Suffield Clay	2.69	45.0	24.0	21.0
7	Goodrich Clay	2.82	41.0	23.0	18.0

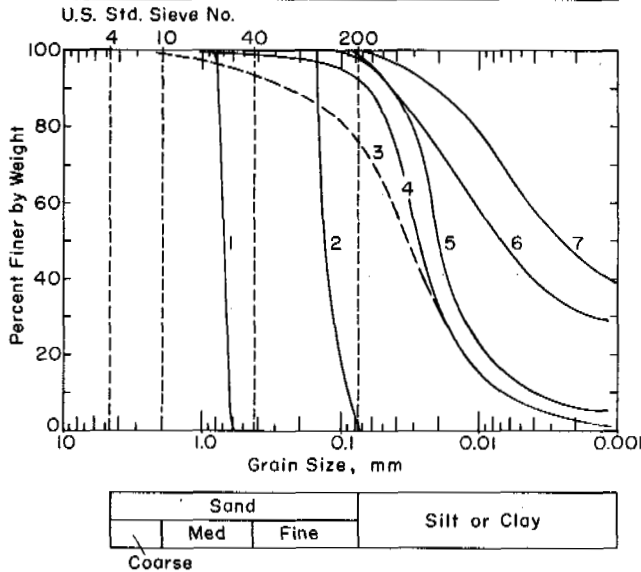


FIGURE 3 Gradation curves for frozen soils.

Design.		f kHz	σ'_0 kN/m ²	e_{min}
PG	Peabody Gravel (Kaplar ³)	4	—	0.27
MCS	McNamara Concrete Sand (Kaplar ³)	3.7	—	0.38
OS	20-30 Ottawa Sand	5	0.7	0.49
MS	Manchester Silt	5	0.7	0.65
HS	Hanover Silt	5	0.7	0.65
NHS	New Hampshire Silt (Kaplar ³)	3.1	—	0.57
FS	Fairbanks Silt (Stevens, Kaplar ³)	5	0.7	0.50
BBC	Boston Blue Clay (Kaplar ³)	2.6	—	—
SC	Suffield Clay	5	0.7	—

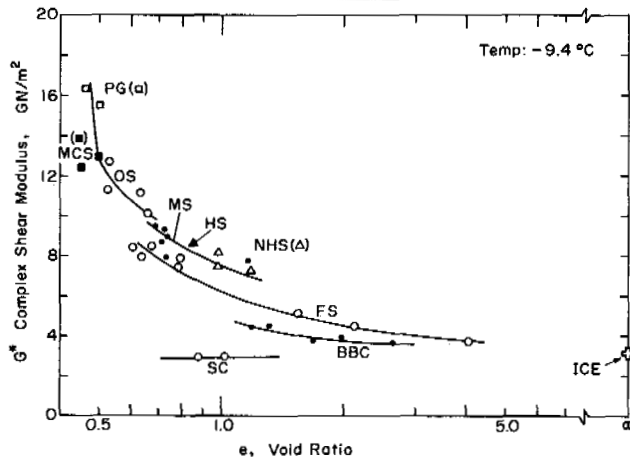


FIGURE 4 Effect of void ratio on complex shear modulus.

equal to that of ice. The coarser, nonplastic soils have the greater modulus. Each soil has a tendency to reach a peak modulus as void ratio approaches the minimum for that soil. As the void ratio increases beyond 1.0 or the volume of ice becomes significantly greater than volume of soil, the modulus tends to approach that of ice.

Effect of Ice Saturation

The rigidity of a frozen soil at a constant void ratio should vary depending on the volume of ice in the voids available to cement the soil grains together. Figure 5 shows that the degree of ice saturation strongly affects the shear modulus, with the modulus of a given soil varying from a maximum at 100 percent ice saturation to a minimum at 0 percent ice saturation, or the stiffness of the same soil unfrozen. However, there is a considerable difference in the relationship depending on soil type. The coarser-grained, nonplastic soils—typified by 20-30 Ottawa sand—show little decrease in modulus until ice saturation is less than about 50 percent. An abrupt decrease in modulus to that of the nonfrozen state occurs below 50 percent saturation. On the other hand, the increase in modulus with decreasing ice saturation for Suffield clay is nearly constant, approaching a straight line between the maximum at 100 percent and minimum at 0 percent. Manchester silt, a fine-grained, nonplastic soil, falls between these extremes.

Effect of Temperature

As temperature determines the frozen or nonfrozen state of the soil, Figure 6 gives values of the Young's and shear

Point Design.	Non-frozen Soils f kHz σ'_0 kN/m ²	W.C. %	Point Design.	Frozen Soils	f kHz	Temp °C
A	20-30 Ottawa Sand	Dry	B	Manchester Silt	1	-3.9
B'	Manchester Silt	18.3	D	20-30 Ottawa Sand (Nakano and Arnold ⁷)	1000	-10
G'	Suffield Clay	12.7	G	Suffield Clay	1	-9.4

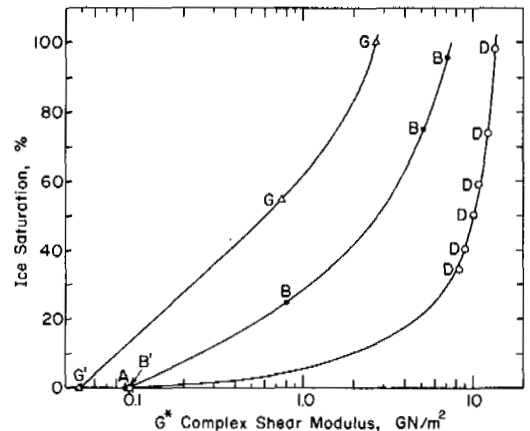


FIGURE 5 Effect of ice saturation on complex shear modulus.

Design.	S _i %	S _w %	e	
A	99.1	-	0.53	E* 20-30 Ottawa Sand
A'	-	93.8	0.60	
A''	Dry		0.50	
B	97.2	-	0.73	E* Manchester Silt
B'	-	91.4	0.73	
C	96.9	-	0.83	E* Goodrich Clay
C'	-	99.4	0.95	
D	99.1	-	0.53	
D'	-	93.8	0.60	G* 20-30 Ottawa Sand
D''	Dry		0.50	
E	97.2	-	0.73	G* Manchester Silt
E'	-	91.4	0.73	
F	96.9	-	0.83	G* Goodrich Clay
F'	-	99.4	0.96	

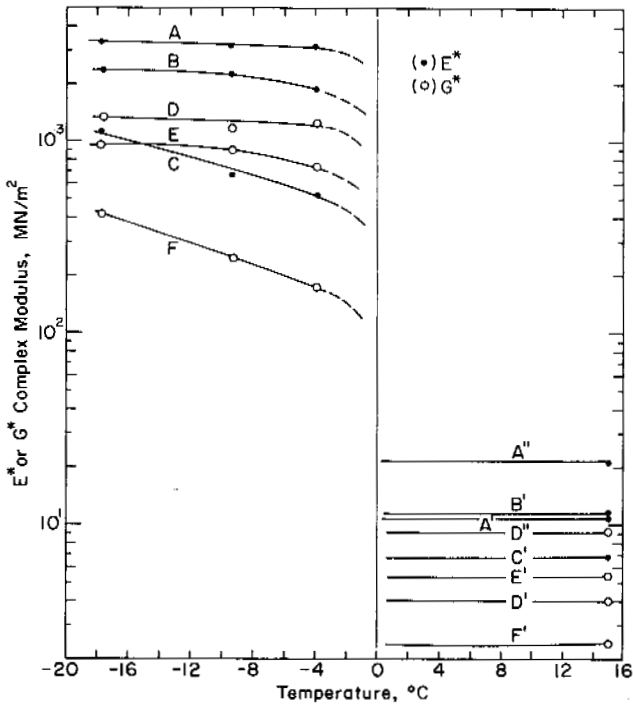


FIGURE 6 Effect of temperature on complex modulus, E* or G*; frequency = 1 kHz, dynamic stress = 0.7 kN/m².

moduli of the nonfrozen soil, as well as those for temperatures between -17 and -3 °C. Figure 7 gives the relation of temperature to tan δ. The modulus of frozen soil is approximately two orders of magnitude greater than the modulus in the nonfrozen state when saturation is better than 90 percent for both conditions. Referring to Figure 7, it is apparent that tan δ does not vary between the frozen and nonfrozen soils by any such magnitude and, in fact, is roughly equal. The tan δ (torsion) shows a tendency to be higher for the frozen condition than for the nonfrozen state. Therefore, it must be concluded that the mechanism

Design.		S _w %
A	20-30 Ottawa Sand	Dry
B	Manchester Silt	95.8
C	Goodrich Clay	98.4
D	20-30 Ottawa Sand	91.4

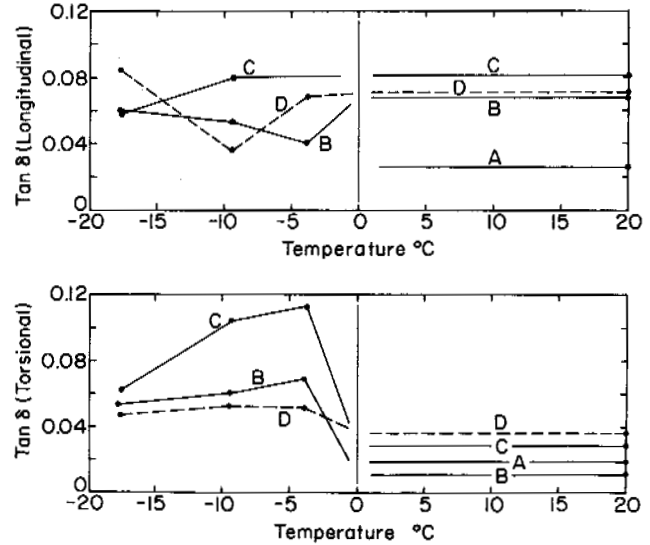


FIGURE 7 Effect of temperature on tan δ; frequency = 1 kHz, dynamic stress = 0.7 kN/m².

causing damping or attenuation of a stress wave must be quite different for the two conditions and by chance, the values are approximately equal. Considering the frozen soil only, it is shown that the modulus increases with decreasing temperature but tends to level off at about -10 °C, with only a very gradual increase as temperature decreases below that value. Between 10 and 0 °C there was only one test value at 4 °C, indicating that the decrease in modulus with increasing temperature is fairly rapid. Additional tests under close temperature control close to the freezing temperature are required to determine the effect of temperatures near 0 °C. It is, however, apparent that temperature has a greater effect on the fine-grained soils (Goodrich clay) than on the coarse-grained soils (20-30 Ottawa sand). The latter soil shows only slight decrease in modulus in the range -18 to -4 °C.

Effect of Frequency

Figures 8 and 9 show the effect of frequency (1-1 000 kHz) on the shear modulus and tan δ, respectively. While the overall effect of frequency is not great (in relation to the effect of void ratio, ice saturation and temperature), it is apparent that the shear modulus increases with increasing frequency. It is indicated that the rate of increase is greater in the 1- to 5-kHz range. It is, therefore, probable that a significant de-

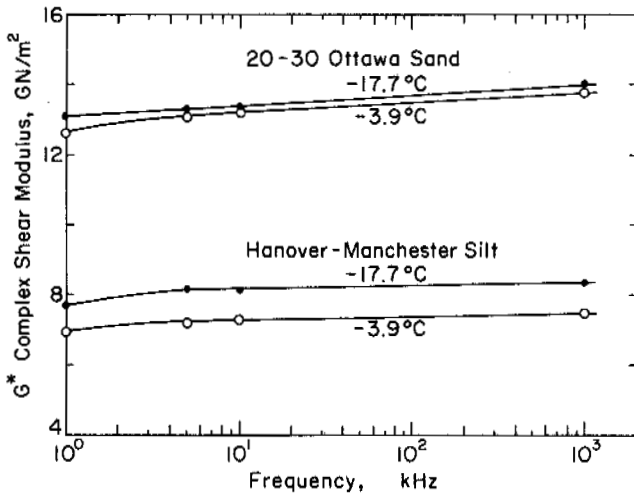


FIGURE 8 Effect of frequency on complex shear modulus; dynamic peak stress = 0.7 kN/m². Values for 20-30 Ottawa sand at 10³ kHz from Nakano and Arnold⁷; values for Hanover-Manchester silt at 10³ kHz from Nakano *et al.*⁶

crease in shear modulus might result if a vibratory load were imposed at a very low frequency. Frequency has a large effect on tan δ (Figure 9). It is suggested that damping in frozen soils may be a viscous or dashpot type reflecting the effect of ice.

Effect of Dynamic Stress

The rigidity of frozen soil, sometimes approaching that of concrete, would suggest that the threshold of nonlinearity

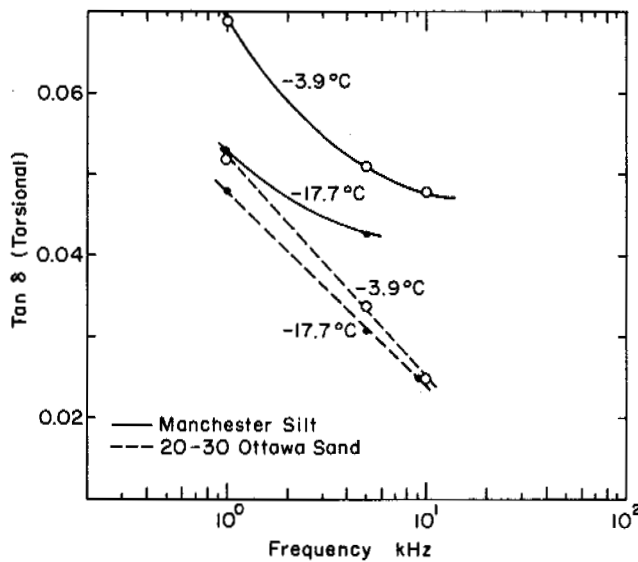


FIGURE 9 Effect of frequency on tan δ (torsion); dynamic peak stress = 0.7 kN/m².

with stress would be high in comparison with that of non-frozen soil. Figure 10 shows that the decrease in modulus with increasing stress is indeed small at least to a peak stress of 34.5 kN/m². The effect of stress is greater at higher temperatures and lower frequencies as would be expected. The shear modulus is almost independent of stress level to, at least, 34.5 kN/m² at a temperature of -18 °C. At about -4 °C, a significant nonlinearity with increasing stress commences at about 7.0 kN/m² with the greater rate of decrease at low frequency loads. There is little difference between the coarser grained Ottawa sand and finer grained silt. Figure 11 shows the effect of stress on tan δ. Again the effect is relatively small, but an increase in damping can be noted as stress increases beyond 7.0 kN/m².

Poisson's Ratio

Table I lists measured Poisson's ratios. The measurement of Poisson's ratio cannot be considered highly accurate because of the strong dependence on the accuracy of the two moduli and the question of the applicability of Poisson's ratio to viscoelastic materials. Values of the ratio greater than 0.5 are measured occasionally as shown for the Goodrich clay.

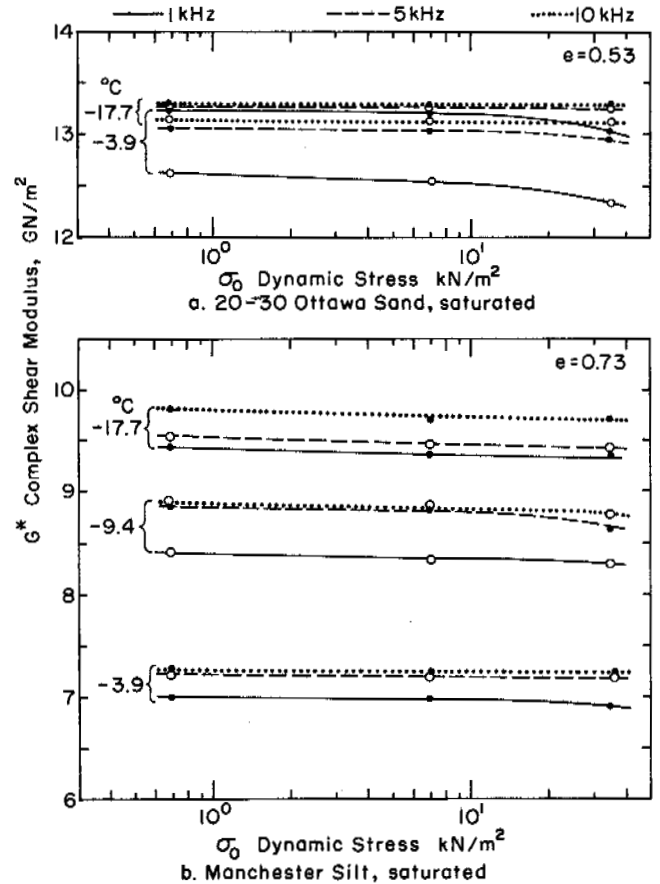


FIGURE 10 Effect of dynamic stress on complex shear modulus.

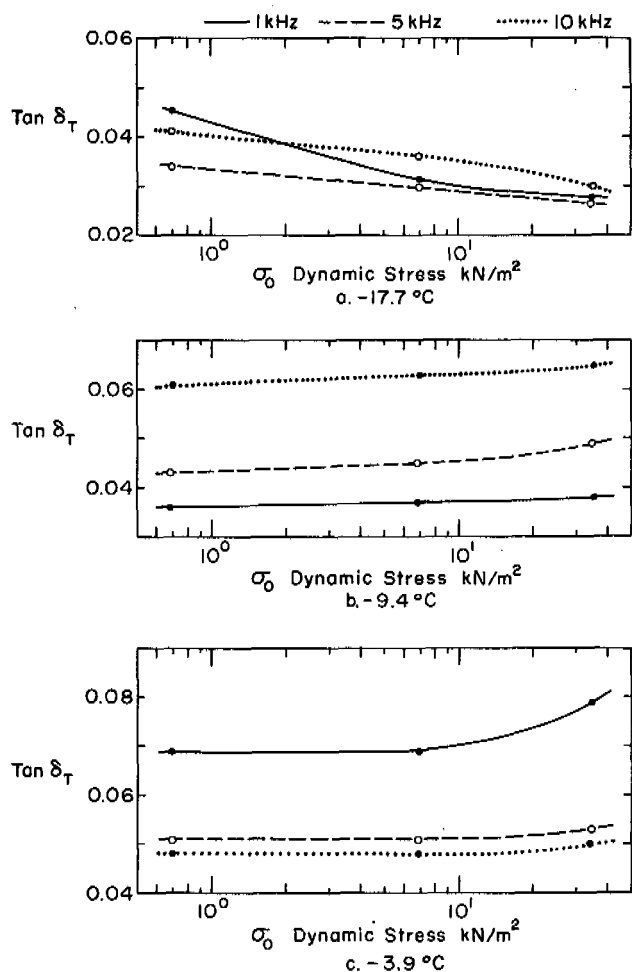


FIGURE 11 Effect of dynamic stress on $\tan \delta$ saturated Manchester silt.

Such values may be the result of inaccurate measurement, but are more likely to be the result of applying an elastic parameter to a highly viscoelastic material. In any case, the table indicates no strong relation to temperature, stress, or frequency level, except a slight trend to a decrease in Poisson's ratio with decreasing temperature and increasing frequency.

CONCLUSIONS

1. The viscoelastic properties of frozen soil may be determined by subjecting a cylinder of the soil to steady-state vibration and measuring the resonant frequency and amplitude ratio. Using the mass density and the length of the cylinder and applying linear viscoelastic theory and boundary conditions, the desired parameters can be evaluated.

2. The modulus of saturated frozen soils decreases with increasing void ratio. A void ratio of infinity or ice without soil has a lower modulus than any saturated frozen soil.

The maximum modulus for a given saturated soil depends on its minimum void ratio and the soil type. The complex shear modulus varies from 17 GN/m^2 for a clean gravel to 3 GN/m^2 for ice at -10°C with a vibratory load of 0.7 kN/m^2 stress and a 5-kHz frequency.

3. The degree of ice saturation has maximum effect on the modulus, as maximum modulus occurs with 100 percent saturation and minimum modulus occurs when no ice is contained in the voids or a nonfrozen dry state. However, the coarser grained soil (20-30 Ottawa sand) shows only a small decrease in modulus as saturation decreases from 100 percent to about 50 percent. For fine-grained soils (Goodrich clay), the rate of decrease in modulus with decreasing saturation is almost constant.

4. The modulus of frozen soil is about two orders of magnitude greater than the modulus of the same soil in the nonfrozen state. It follows that the velocity of wave propagation in frozen soil is about one order of magnitude greater than that of nonfrozen soil.

5. The damping coefficient $\tan \delta$ is approximately equal to or slightly higher for frozen soil than for nonfrozen soil.

6. The modulus of frozen soil decreases with increasing temperature, but the rate is small until temperature is higher than about -4°C . From -4 to 0°C , the rate of decrease of modulus sharply increases, but test results are not complete to determine the actual decrease.

7. Although measurements are not accurate enough to determine the relationship precisely, results to date indicate that $\tan \delta$ is relatively independent of temperature.

8. The modulus increases and $\tan \delta$ decreases with increasing temperature. The rate of increase (in modulus) is small in the frequency range 5-1 000 kHz and greater in the 1-5-kHz range. A substantial decrease in modulus may take place at frequencies less than 1 kHz.

9. Within the limits of the test procedure used (0.5 - 35 kN/m^2) the effect of stress level is small on the modulus and velocity and almost linear at temperatures less than -10°C with frequency 5 kHz or greater. It can be assumed that in the range of frequency and stress range tested, design values chosen are independent of stress level.

ACKNOWLEDGMENTS

This paper presents the results of research performed by the U.S. Army Cold Regions Research and Engineering Laboratory under the sponsorship of the U.S. Army Corps of Engineers and the Army Materiel Command. Col. J. F. Castro, CO/D, Mr. K. A. Linell, Chief, Experimental Engineering Division, and Mr. F. E. Crory, Chief, Foundations and Materials Research Branch, supervised the project for USA CRREL. There have been a number of U.S. Army enlisted men who contributed to the development of the test procedure and conducted the tests. Their excellent work is gratefully acknowledged. Thanks are expressed to Dr. T. M. Lee, Dr. D. M. Norris, Jr., and Dr. Y. Nakano for their valuable advice and assistance in developing the analysis of test data.

TABLE I Poisson's Ratio

Soil and Stress (kN/m ²)	Frequency (kHz)	Temperature (°C)		
		-3.9	-9.4	-17.8
20-30 Ottawa Sand				
0.7	1	0.25	0.34	0.28
	5	0.28	0.38	0.26
	10	0.33	0.31	0.28
7.0	1	0.25	0.36	0.28
	5	0.28	0.37	0.25
	10	0.32	0.36	0.35
34.5	1	0.28	0.30	0.27
	5	0.29	0.38	0.25
	10	0.27	0.34	0.24
Manchester Silt				
0.7	1	0.25	0.27	0.20
	5	0.27	0.26	0.20
	10	0.30	0.29	0.18
7.0	1	0.25	0.27	0.20
	5	0.29	0.26	0.20
	10	0.40	0.29	0.18
34.5	1	0.26	0.29	0.22
	5	0.30	0.31	0.22
	10	0.30	0.29	0.20
Goodrich Clay				
0.7	1	0.72	0.35	0.51
	5	0.54	0.38	0.36
	10	0.52	0.40	0.32
7.0	1	0.59	0.37	0.47
	5	0.52	0.40	0.34
	10	0.47	0.41	0.32
34.5	1	0.58	0.40	0.46
	5	0.47	0.42	0.32
	10	0.42	0.43	0.32

REFERENCES

- Bancroft, D. 1941. The velocity of longitudinal waves in cylindrical bars. *Phys. Rev.* 59.
- Brown, G. W., and D. R. Selway. 1964. Frequency response of a photoviscoelastic material. *Exp. Mech.* 4(3).
- Kaplar, C. W. 1969. Laboratory determination of dynamic modulus of frozen soils and of ice. CRREL Research Report 163. U.S. Army Cold Regions Research and Engineering Laboratory, Hanover, New Hampshire.
- Lee, T. M. 1963. Method of determining dynamic properties of viscoelastic solids employing forced vibration. CRREL Research Report 122.
- Lee, T. M. Circular footings on a viscoelastic foundation. CRREL Technical Report. (In preparation)
- Nakano, Y., M. Smith, R. Martin, H. Stevens, and K. Knuth. 1971. Determination of acoustic properties of frozen soils. CRREL report for Advanced Research Projects Agency.
- Nakano, Y., and R. Arnold. 1972. Acoustic properties of frozen Ottawa sand. *J. Water Resour. Res.* October.
- Norris, D. M., Jr., and W.-C. Young. 1970. Longitudinal forced vibration of viscoelastic bars with end mass. CRREL Special Report 135.
- Stevens, H. W. 1970. Some viscoelastic properties of materials, especially frozen and nonfrozen soils. *In* Special procedures for testing soil and rock for engineering purposes. Fifth ed.

- ASTM Special Technical Publication 479. American Society for Testing and Materials, Philadelphia.
10. Thompson, K. C. 1966. On the complex Poisson's ratio of a urethane rubber compound. Physical Sciences Research Paper No. 269. Air Force Cambridge Research Laboratory, Hanscom AFB, Bedford, Mass.
11. Waas, G. 1972. Analysis method for footing vibrations through layered media. U.S. Army Waterways Experiment Station, Technical Report S-71-14.

PORE WATER AND HEAVING PRESSURES DEVELOPED IN PARTIALLY FROZEN SOILS

Hugh B. Sutherland

UNIVERSITY OF GLASGOW
Glasgow, Scotland

Paul N. Gaskin

QUEEN'S UNIVERSITY
Kingston, Ontario

INTRODUCTION

Pressures associated with a growing ice lens in a partially frozen soil have been studied both theoretically and experimentally. Equations expressing these pressures have been derived and some experimental results supporting them have been obtained. The equations, however, were derived initially for uniform spheres and assumptions have to be made when they are applied to soils. The purpose of this investigation was to examine the validity of the equations by comparing the predicted values of the pressures with those actually measured for four soils.

When an ice lens forms in a partially frozen soil, there is a drop in the pore water pressure that is inversely proportional to the radius of the ice-water interface.^{2,4} The maximum drop in pore water pressure, $\Delta p_{w \max}$, is expressed by the following equation:

$$\Delta p_{w \max} = 2(\sigma_{iw})/r_i, \quad (1)$$

where σ_{iw} = interfacial tension, ice-water and r_i = minimum radius of the ice-water interface.

If free access of water to the growing ice lens is allowed but the soil is prevented from heaving, heaving pressure is produced. The magnitude of the heaving pressure depends on the radii of curvature of the ice-water interface that develops in the pores and also around the soil particles.

Two different equations have been previously derived for the maximum heaving pressure, $\Delta p_{h \max}$, for uniform spheres. The first equation, developed by Miller, Baker, and

Kolaian⁸ and Everett and Haynes,³ can be expressed in the form:

$$\Delta p_{h \max} = 2(\sigma_{iw})(1/r_i + 1/r)(A_s), \quad (2)$$

where r = particle radius and A_s = an area correction factor to convert the heaving force between the ice lens and the soil particles to a heaving pressure over the total cross-sectional area.

The second equation, developed by Yong¹⁹ and Osler,⁹ is given by:

$$\Delta p_{h \max} = 2(\sigma_{iw})(1/r_i + 1/r)(A_s)/(1 - V_w/V_i), \quad (3)$$

where V_w = the specific volume of water and V_i = the specific volume of ice.

To apply the three equations to soils, values of σ_{iw} , r_i , and r must be known. As yet, there is no clearly established value for σ_{iw} , and there are conflicting views as to how r_i and r should be determined. However, experimental results supporting each of the equations have previously been reported. A number of investigators have measured the drop in pore water pressure alone, but Williams¹⁸ measured drop in pore water pressure and also determined r_i from air entry tests. He worked with five silt fractions and three silts and found that his results supported Eq. (1) on the assumption that $\sigma_{iw} = 0.0305$ N/m.

The maximum heaving pressures of seven silt fractions and two fractions of glass beads measured by Penner¹¹⁻¹³ were found to support Eq. (2). Penner determined values

for r_i and r from suction-water-content curves and particle-size distribution data and assumed values of σ_{iw} between 0.025 and 0.035 N/m.

Yong,¹⁹ Osler,⁹ and Hammamji⁶ showed that the heaving pressures measured for seven silts and one silty sand supported Eq. (3). They assumed that $\sigma_{iw} = 0.03$ N/m and determined values of r_i and r from void ratio and particle-size distribution data.

Thus the experimental results of a number of investigators have supported each of the three equations, although Eq. (2) and (3), for the maximum heaving pressure, predict values that differ by a factor of about 12. The previous investigators have concerned themselves with only one of the three equations at any one time. For any one soil, there has apparently been no attempt to measure the maximum drop in pore water pressure, maximum heaving pressure, and r_i , the minimum radius of the ice-water interface.

In this investigation, the maximum heaving pressures and the maximum drops in pore water pressure have been measured for four soils, and the measured values compared with those predicted by Eq. (1), (2), and (3). The experimental work consisted of the determination of (1) the maximum drop in pore water pressure ($\Delta p_{w_{max}}$); (2) the maximum heaving pressure ($\Delta p_{h_{max}}$); (3) the minimum radius of the ice-water interface (r_i), which was found by three methods; and (4) the particle radius r .

MATERIALS

The ideal material on which to investigate the equations initially would have been one composed of uniform spherical particles but appropriately fine material is not available. Previous work¹⁶ had shown that substantial heaving pressures could be developed in samples of pulverized fuel ash, a material composed mainly of spherical particles. Pulverized fuel ash was therefore selected as soil A.

Kaolin was available in a range of suitable particle sizes and three further test materials were made up using different grades of kaolin. Soil B was composed of equal proportions of pulverized fuel ash and a kaolin. Soils C and D were composed of kaolins alone.

Table I gives pertinent details of the particle-size distributions and also gives the void ratios at which the samples were tested. Saturated specimens were used as the three equations were derived for this condition. The specimens were produced by consolidating a de-aired slurry of the soil.

DROP IN PORE WATER PRESSURE MEASUREMENT

The saturated soil specimens were frozen in a closed system so that the maximum drop in pore water pressure could be developed. The pore water was prestressed to a value

TABLE I Details of Particle Size, Specific Gravity, and Void Ratio

Soil	Effective Size, D_{10} (mm)	Uniformity Coefficient D_{60}/D_{10}	Percentage Finer than 0.02 mm	Specific Gravity	Void Ratio
A	0.004 1	3.9	73	2.18	0.87
B	0.002 1	5.2	84	2.43	0.91
C	0.001 3	5.5	96	2.67	0.81
D	0.001 1	6.5	96	2.67	0.75

greater than the anticipated drop in pore water pressure to prevent phase change in the pore water due to low pressure, as in the tests of Balduzzi¹ and Williams.¹⁸

A saturated soil specimen, 101.6 mm diameter and approximately 150 mm high, was placed on a porous stone, covered by a top cap and encased in a membrane (Figure 1). The pore water was prestressed by applying a cell air pressure of about 1050 kN/m², and the degree of saturation achieved in the specimen was checked by comparing the resulting pore water pressure with the applied cell pressure.

After the pore water had been prestressed, the cell was placed in the cold room in a cabinet containing a reservoir of water kept at a constant temperature of 4 °C. The reservoir water was level with the base of the specimen and was isolated from the specimen. Coarse dry sand was placed in the cabinet up to the level of the top of the specimen to provide lateral insulation, and the cold room temperature was lowered to -17 °C so that the freezing isotherm came to rest about halfway down the specimen. Pressure trans-

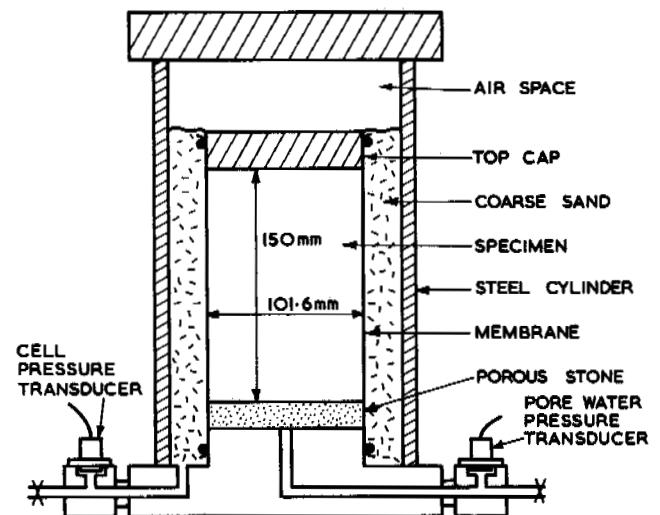


FIGURE 1 Test cell for measurement of drop in pore water pressure.

ducers measured the cell, and pore water pressures and readings were taken until the maximum drop in pore water pressure was reached.

Ice formation in the specimen was initiated by placing a thin layer of a saturated sand and pulverized fuel ash mixture on top of the specimen.

Figure 2 gives the drop in pore water pressure against time for each soil and shows that the drop in pore water pressure increased with time to a maximum value. Table II shows that the maximum drop in pore water pressure ranged from 62 kN/m² for soil A to 491 kN/m² for soil D. It can also be seen from Table II that almost complete saturation was achieved in each specimen.

HEAVING PRESSURE MEASUREMENT

The saturated soil specimens were frozen in an open system with no frost heave allowed so that the maximum heaving pressure could be developed while the pore water pressure was atmospheric. The heaving pressure apparatus is shown in Figure 3. The saturated soil specimen, 101.6 mm diameter and approximately 150 mm high, was contained in a tapered cylinder. The reaction frame with the specimen and proving ring in position was placed in the cabinet in the cold room so that the temperature conditions were the same as in the drop in pore water pressure tests. Frost heave

TABLE II Values of the Maximum Drop in Pore Water Pressure and Maximum Heaving Pressure

Soil	Applied Cell Pressure (kN/m ²)	Resulting Pore Water Pressure (kN/m ²)	Maximum Drop in Pore Water Pressure (kN/m ²)	Maximum Heaving Pressure (kN/m ²)
A	1 011	1 007	62	63
B	1 080	1 080	240	352
C	1 062	1 035	465	797
D	1 075	1 071	491	674

was prevented by the reaction frame, and free access of water to the specimen was permitted. Heaving pressure was measured by the proving ring and was recorded until the maximum value was reached.

The heaving pressure is plotted against time for each soil in Figure 4 and shows that the heaving pressure increased to

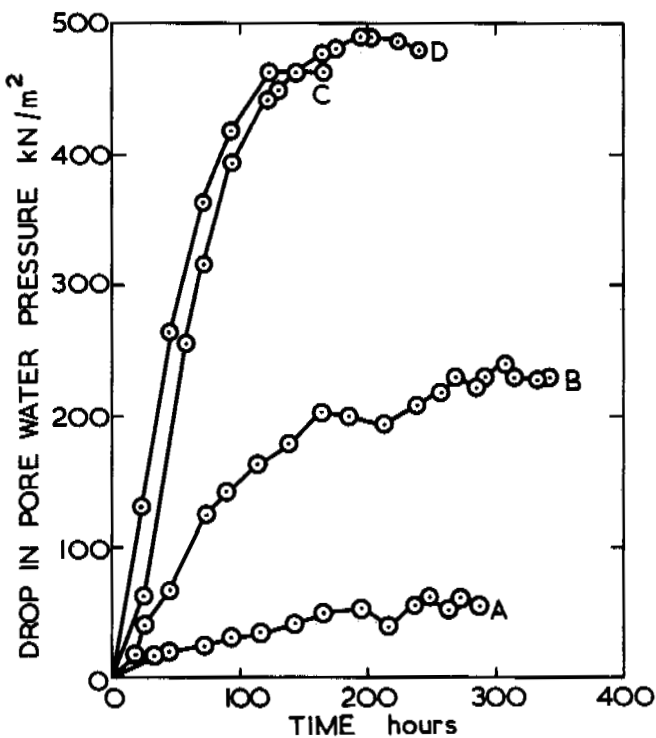


FIGURE 2 Drop in pore water pressure with time.

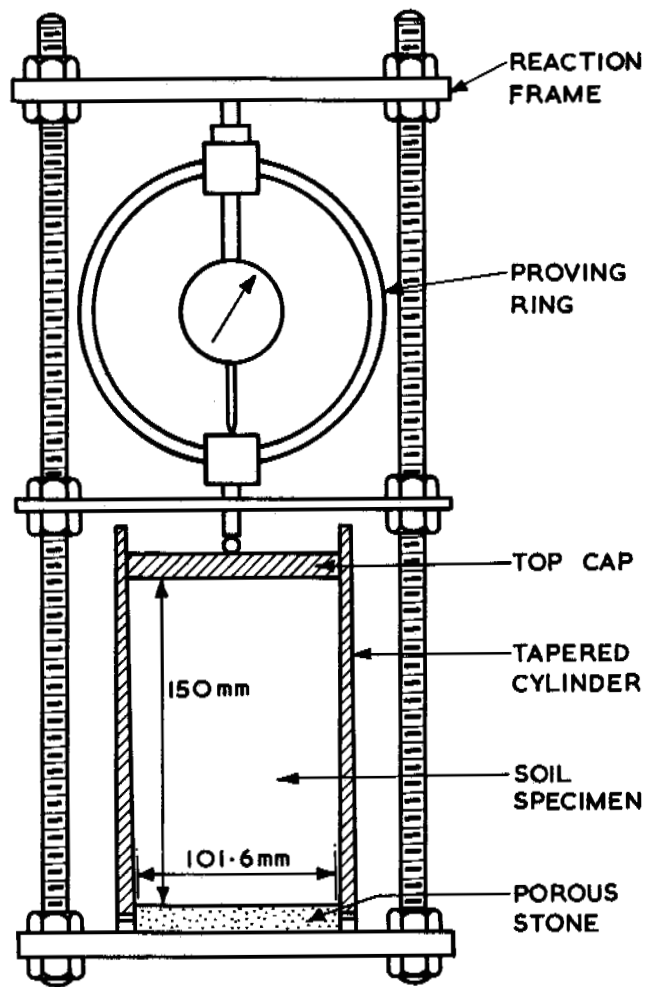


FIGURE 3 Heaving pressure apparatus.

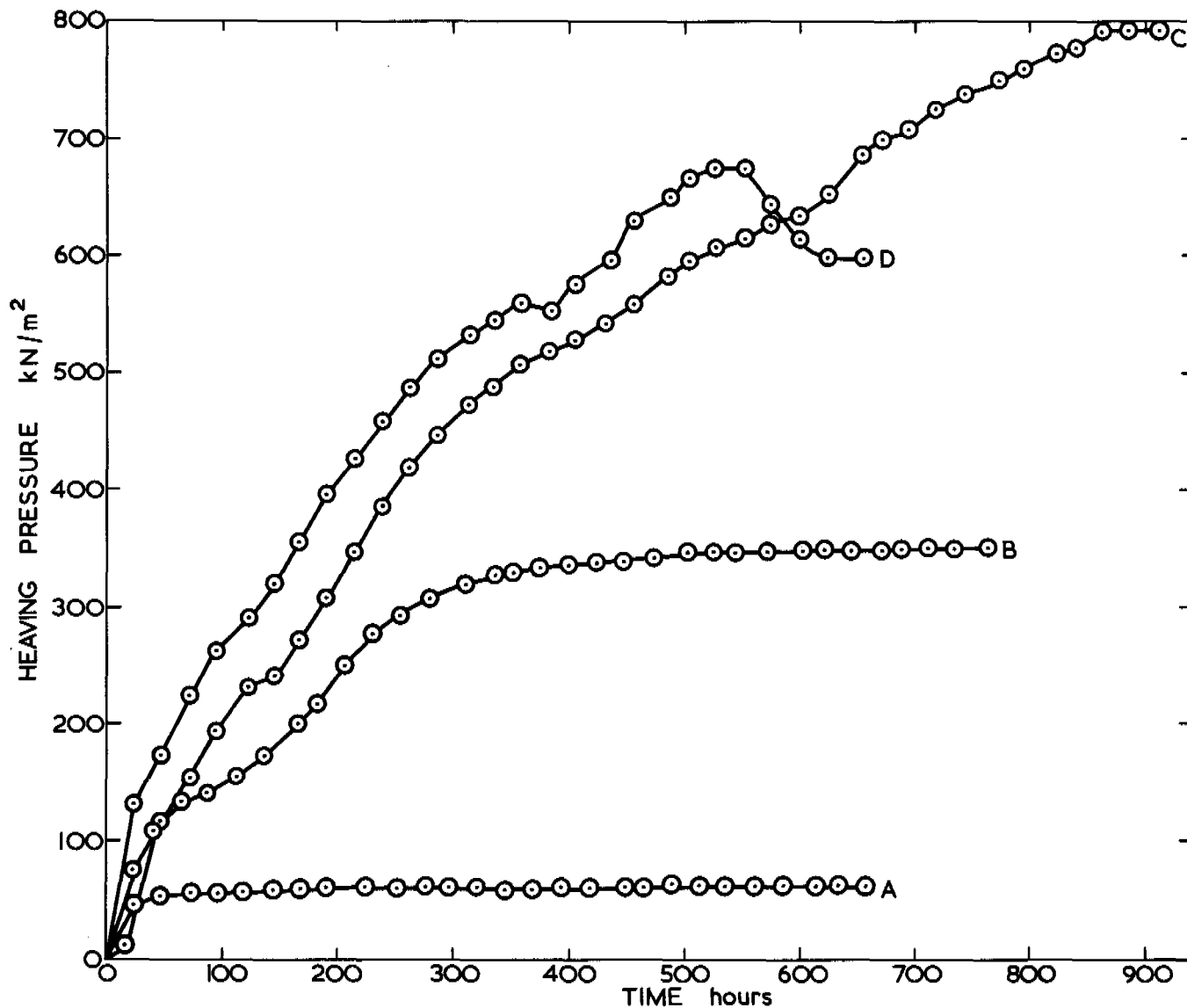


FIGURE 4 Heaving pressures developed with time.

a maximum value. The maximum heaving pressures, which are also shown in Table II, ranged from 63 kN/m^2 for soil A to 797 kN/m^2 for soil C.

PREDICTION OF MAXIMUM PORE WATER PRESSURE DROP AND HEAVING PRESSURE

To predict the maximum values of pore water pressure drop and heaving pressure, values for r_i , r , and σ_{iw} are required. It is difficult to determine these quantities, and previous investigators have used a variety of methods that can lead to substantially different results, especially when applied to soils rather than to uniform spheres. These various methods are now reviewed and then applied to the materials that were used in the present investigation.

Three methods have been used previously to obtain r_i : from particle size distribution curves; from air entry values; and from suction-water-content curves. The radius of curvature, r , of the ice-water interface around the soil particle has been obtained from the particle-size distribution curve of the material being investigated. Each of these methods is now considered.

r_i and r from Particle-Size Distribution Curves

The determination of r_i and r can be considered separately for the cases of spheres, soil fractions, and soils.

The previous work on spheres has been on spheres of equal radius, r , and of different packings. The radius of the sphere, r_i , that will just pass through the constriction be-

tween three spheres of radius r in mutual contact can be found theoretically. For open-packed spheres (six contacts per sphere), $r/r_i = 2.41$. For close-packed spheres (12 contacts per sphere), $r/r_i = 6.46$.

From tests on close-packed spheres, Haines⁵ and Everett and Haynes³ measured values of r/r_i between 5.40 and 5.87. Everett and Haynes recommended that an average value of r/r_i of 5.6 should be taken. Smith, Foote, and Busang¹⁵ determined a theoretical value of r/r_i of 9.75 for close-packed spheres, assuming that r_i was related to the reciprocal of the hydraulic radius. Their tests supported this value.

A number of investigators have worked with soil fractions and soils. Miller, Baker, and Kolaian⁸ used three silt fractions in pore water freezing-point experiments and found that their results lay between the theoretical r/r_i values of 2.41 and 6.46 for open- and close-packed spheres. They assumed that $r = 0.5(D_{50})$. Everett² and Everett and Haynes³ investigated the heaving pressures measured by Penner¹⁰ for angular particles of flint. The effective size D_{10} was used to obtain r , and, working from $r/r_i = 5.6$, they obtained general agreement with Penner's measurements. Penner¹² confirmed Everett and Haynes' proposal for $r/r_i = 5.6$, using heaving pressure measurements on uniformly graded fractions of glass beads. In his calculations, however, he used $r = 0.5(D_{50})$ and did not adopt an r value based on effective size. Next, Penner¹³ obtained reasonable agreement between predicted and measured heaving pressures for uniform gradings of angular flint particles using $r = 0.5(D_{50})$ and $r/r_i = 5.6$. Jackson, Uhlmann, and Chalmers⁷ assumed arbitrary values of $r_i = 0.05(D_{50})$ and $r = 0.5(D_{50})$. For New Hampshire silt, this gave an r/r_i value of about 75, which is far in excess of the range of r/r_i used by other investigators. Yong,¹⁹ Osler,⁹ and Hammamji⁶ proposed the relationship $r/r_i = 1/(\text{void ratio})^{1/3}$, derived from a consideration of open-packed spheres. They applied this, using $r = 0.5(D_{10})$, to heaving pressure measurements on a silty sand and six silts. Their proposed relationship for r/r_i gives values of r/r_i that are less than those derived theoretically for open- and close-packed spheres.

From the foregoing, it can be seen that a diversity of methods have been used to determine r_i and r from particle-size distribution data. The theoretical and experimental work for uniform spheres appears to agree reasonably well. Most previous investigators have considered that the values for spheres could generally be applied to soils and soil fractions but have then had to make assumptions regarding the r value to be used. For uniformly graded soil fractions, r has generally been taken as $0.5(D_{50})$, while for soils, r has often been assumed to be $0.5(D_{10})$. The assumptions made have often only been justified indirectly, and the justification has involved other assumptions such as the choice of σ_{iw} value to be used. The particle shape, grading, and pack-

ing of the soil fractions and soils undoubtedly have an influence on the r_i and r values, and while attempts have been made by some investigators to take account of some of these factors, no systematic approach has been made to consider them all.

The various methods used by previous investigators for determining r and r_i were applied to the four soils used in the present investigation. The resulting values of r and r_i are shown in Tables III and IV, respectively. It can be seen that the different methods give a large range of r and r_i for any one soil.

r_i from Air Entry Tests

Air entry tests, i.e., the measurement of the pressure at which air replaces water in a material, have been used to determine the value of r_i for arrangements of spheres of equal radius. Williams¹⁸ used air entry tests to determine r_i for five uniform silt fractions and three silts, using the following equation (see, e.g., Taylor¹⁷):

$$p_a - p_w = 2(\sigma_{aw})/r_i, \quad (4)$$

where p_a = air pressure at air entry, p_w = pore water pressure, σ_{aw} = surface tension, air-water, and r_i = minimum radius of air-water interface.

The air entry apparatus used for the test described in this paper is shown in Figure 5. Air pressure was applied to the top of the 38.1-mm-diameter and 12.7-mm-high specimen through the top cap. Leakage down the sides of the specimen was prevented by enclosing the specimen in a rubber membrane and applying a cell pressure of 70 kN/m² above the applied air pressure. The air pressure increments were between 14 and 28 kN/m², and one day was allowed for drainage between each increment. The air entry value was defined as the pressure difference between the air and the pore water when a sudden increase in drainage occurred or when air passed through the specimen into the burette.

As shown in Table V, the air entry values for the four soils ranged from 97 kN/m² for soil A to 345 kN/m² for soil D. Reasonably consistent results were obtained from the two or three tests made on each soil. The values of r_i , also shown in Table V, were calculated from Eq. (4) with p_a = air entry value of $p_w = 0$.

r_i from Suction-Water Content Curves

Penner¹¹ suggested that r_i could be determined from the suction at the point on the suction-water content curve where the drainage suddenly increased with little increase in suction, and r_i could then be calculated from Eq. (4) with $p_a - p_w = \text{suction}$.

The suction-water content curves of the four soils were determined using the conventional pressure-membrane

TABLE III Values of Particle Radius r Determined from Particle-Size Distribution Data

Method	Basis of Deriving r	Derived Value of r (μm)			
		Soil A	Soil B	Soil C	Soil D
<i>Theoretical</i>					
Open-packed spheres } Close-packed spheres }	$0.5(D_{50})$	6.5	4.5	3	2.8
<i>Experimental</i>					
Close-packed spheres Everett and Haynes Smith, Foote, and Busang }	$0.5(D_{50})$	6.5	4.5	3	2.8
Soils and soil fractions Everett Everett and Haynes Yong, Osler, and Hammamji }	$0.5(D_{10})$	2.05	1.05	0.65	0.55
Jackson, Uhlmann, and Chalmers	$0.5(D_{50})$	6.5	4.5	3	2.8

TABLE IV Values of the Minimum Radius of the Ice-Water Interface, r_i , Determined from Particle-Size Distribution Data

Method	Basis of Deriving r	Basis of Deriving r_i	Derived Value of R_i (μm)			
			Soil A	Soil B	Soil C	Soil D
<i>Theoretical</i>						
Open-packed spheres } Close-packed spheres }	$0.5(D_{50})$	$r/2.41$ $r/6.46$	2.7 1	1.87 0.696	1.25 0.46	1.16 0.433
<i>Experimental</i>						
Close-packed spheres Everett and Haynes Smith, Foote, and Busang }	$0.5(D_{50})$	$r/5.6$ $r/9.75$	1.16 0.67	0.804 0.46	0.535 0.308	0.5 0.287
Soils and soil fractions Everett Everett and Haynes Yong, Osler, and Hammamji }	$0.5(D_{10})$	$r/2.2-r/5.85$ $r/5.6$ $r(\text{void ratio})^{1/3}$	0.93-0.35 0.37 1.96	0.477-0.18 0.188 1.02	0.295-0.11 0.116 0.606	0.25-0.094 0.098 0.5
Jackson, Uhlmann, and Chalmers	$0.5(D_{50})$	$0.05(D_s)$	0.14	0.07	0.04	0.035

apparatus and are shown in Figure 6. Tangents were drawn to the portions of each curve before and after the point where the drainage suddenly increased. The intersection of these tangents gave the suction values shown in Table VI. The values of r_i shown in Table VI correspond to the suctions and were calculated from Eq. (4).

Values of σ_{iw}

A value of σ_{iw} , the interfacial tension of ice against water, must be assumed in order to calculate the predicted maximum values of drop in pore water pressure and heaving pressure. Everett² pointed to the difficulty of obtaining a reliable value of σ_{iw} and quoted a range of estimates from 0.01 to 0.04 N/m. The values assumed by previous investigators of the pressures in partially frozen soils are as follows: Everett,² 0.03 N/m; Everett and Haynes,³ 0.03

N/m; Penner,¹¹⁻¹³ 0.025-0.035 N/m; Williams,¹⁸ 0.0305 N/m; Yong,¹⁹ 0.02 N/m; Osler,⁹ 0.02 N/m; and Hammamji,⁶ 0.03 N/m. The range of values used illustrates the difficulty experienced by previous investigators in selecting σ_{iw} . The authors have had similar difficulty. In this paper, since comparisons are being made between the predictions from a number of equations, a value of $\sigma_{iw} = 0.03$ N/m has been adopted.

DISCUSSION

Predicted and Measured Values of Maximum Drop in Pore Water Pressure

Predictions of the maximum drop in pore water pressure were calculated using Eq. (1) for the four soils used in the present investigations based on r_i values determined from

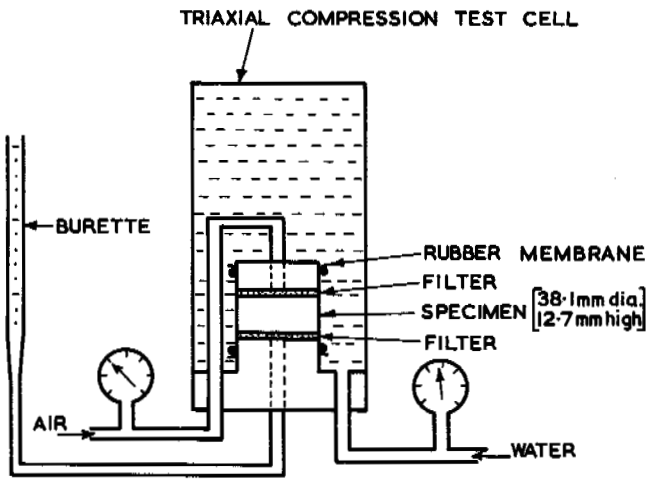


FIGURE 5 Modified air entry apparatus.

particle-size distribution data, air entry tests, and soil suction tests. Table VII shows the predicted values based on particle size. Table VIII gives the predicted values using the results from air entry and soil suction tests. In both tables, the values of maximum drop in pore water pressure actually measured are also shown.

The results based on particle-size distribution are considered first. Soil A was composed of reasonably spherical particles and was compacted to a high relative compaction. The particles were fairly uniform in size, the coefficient of uniformity being 3.9. Assuming $\sigma_{iw} = 0.03 \text{ N/m}$, Table VII shows that the measured drop in pore water pressure for soil A was fairly close to that predicted for close-packed uniform spheres. Soils B, C, and D, however, contained large percentages of a kaolin, which Smart¹⁴ has shown

TABLE V Values of Air Entry and Corresponding r_i for the Four Soils

Soil	Duration of Test (days)	Air Entry Value (kN/m ²)	Average Entry Value (kN/m ²)	r_i (μm)
A	3	90	97	1.5
	8	103		
B	13	138	138	1.06
	15	138		
C	11	255	245	0.6
	13	234		
D	4	303	345	0.42
	6	386		
	7	345		

TABLE VI Values of Suction and the Corresponding r_i for the Four Soils

Soil	Suction (pF)	Suction (kN/m ²)	r_i (μm)
A	3.0	98	1.48
B	3.4	246	0.59
C	3.5	310	0.469
D	3.77	577	0.252

by electron micrographs to be composed mainly of platy particles. Table VII shows for these three soils that the predicted drops in pore water pressure based on the theoretical and experimental work on close-packed spheres gave no agreement with those actually measured. Of the various pre-

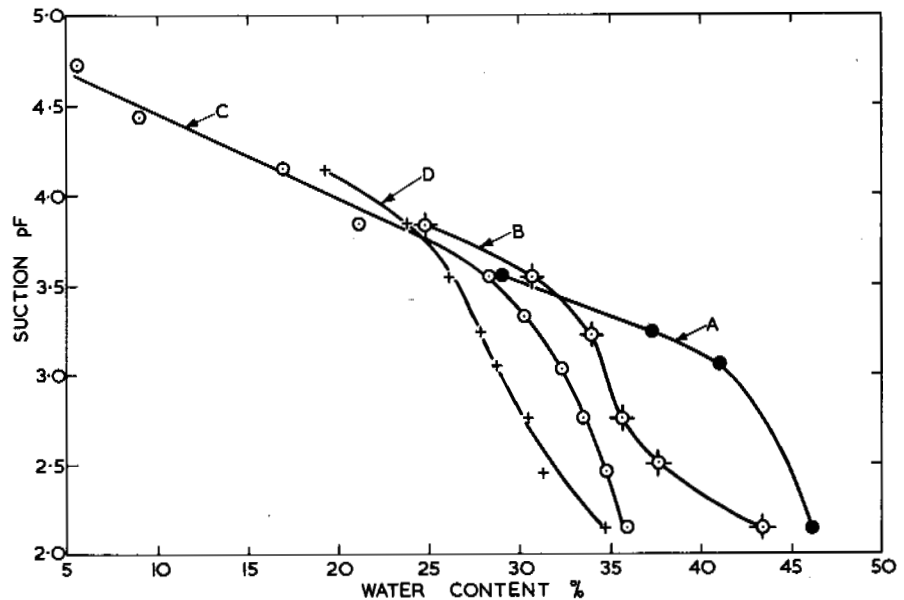


FIGURE 6 Suction-water content curves for the four soils.

TABLE VII Predicted and Measured Values of the Maximum Drop in Pore Water Pressure Based on Particle-Size Distribution Data

Method	Basis of Deriving r	Basis of Deriving r_i	Predicted Maximum Drop in Pore Water Pressure (kN/m ²)				
			Soil A	Soil B	Soil C	Soil D	
<i>Theoretical</i>							
Open-packed spheres	} $0.5(D_{50})$	$r/2.41$	23	32	48	52	
Close-packed spheres		$r/6.46$	60	86	130	139	
<i>Experimental</i>							
Close-packed spheres	} $0.5(D_{50})$	$r/5.6$	52	74	112	120	
Everett and Haynes		$r/9.75$	89	130	195	208	
Smith, Foote, and Busang							
Soils and soil fractions	} $0.5(D_{10})$	$r/2.2-r/5.85$	64-172	125-133	203-540	240-638	
Everett		$r/5.6$	162	319	517	614	
Everett and Haynes		$r(\text{void ratio})^{1/3}$	31	59	99	120	
Yong, Osler		$0.5(D_{50})$	$0.05(D_s)$	428	855	1 503	1 710
Jackson, Uhlmann, and Chalmers							
Maximum measured drop in pore water pressure (kN/m ²)			62	240	465	491	

dicted values, only those of Everett and Haynes³ based on $r/r_i = 5.6$ and using $r = 0.5(D_{10})$ gave pressures that were close to those measured. When the predicted and measured pressures for soils B, C, and D are equated and using $r = 0.5(D_{10})$, r/r_i values of 4.2, 5, and 4.5 are obtained for soils B, C, and D respectively; the average was 4.6. Assuming that $r = 0.5(D_{10})$ produces the closest agreement between predicted and measured pressures for these three soils. Everett's proposal,² therefore, that r for soils is associated with the effective size D_{10} rather than the mean particle-size D_{50} , appears to be supported from the results of the present investigation.

From Table VIII it can be seen that the predicted pore water pressures based on r_i values obtained from air entry

TABLE VIII Predicted and Measured Values of the Maximum Drop in Pore Water Pressure Based on Air Entry Tests and Suction-Water Content Curves

Soil	Predicted Maximum Drop in Pore Water Pressure Based on (kN/m ²)		Measured Maximum Drop in Pore Water Pressure (kN/m ²)
	Air Entry Values	Suction-Water Content Curves	
A	40	41	62
B	57	101	240
C	100	128	465
D	143	237	491

tests only gave near agreement with the measured values for soil A. No explanation can be offered for the lack of agreement for soils B, C, and D. It can only be noted that the materials with which Williams¹⁸ worked contained little or no clay-size particles, while soils B, C, and D were essentially kaolin with a high proportion of platy particles. The predictions based on r_i values obtained from soil suction tests are also shown in Table VIII and show that only for soil A was there approximate agreement with the measured values.

Predicted and Measured Values of Maximum Heaving Pressure

The maximum heaving pressures were predicted using Eq. (2) and (3). Both these equations contain the area correction factor A_s . A_s has been determined theoretically for spheres, and Miller, Baker, and Kolaian⁸ gave values of A_s for closed- and open-packed spheres of 0.907 and 0.785, respectively. Similar values were used by Everett and Haynes.³ Yong¹⁹ and Osler⁹ assumed that A_s could be derived from the porosity, n , of the soil and defined A_s as $A_s = (1 - n)^{2/3}$.

Using the values of r_i and r obtained from particle-size distribution data, air entry tests, and soil suction tests, the predicted maximum heaving pressures for the four soils were calculated from Eq. (2). The results are shown in Table IX along with the measured values of heaving pressure. An A_s value of 0.907 was used throughout since the four soils were

TABLE IX Predicted and Measured Maximum Heaving Pressures from Eq. (2) Based on Particle-Size Distribution Data, Air Entry Tests, and Suction-Water Content Curves

Method	Basis of Deriving r	Basis of Deriving r_i	Predicted Maximum Heaving Pressure (kN/m ²)			
			Soil A	Soil B	Soil C	Soil D
<i>Theoretical</i>						
Open-packed spheres	} $0.5(D_{50})$	$r/2.41$	29	41	61	66
Close-packed spheres		$r/6.46$	63	91	135	146
<i>Experimental</i>						
Close-packed spheres	} $0.5(D_{50})$	$r/5.6$	54	80	119	128
Everett and Haynes		$r/9.75$	90	130	195	209
Smith, Footc, and Busang	} $0.5(D_{10})$	$r/2.2-r/5.85$	85-198	163-352	269-374	317-676
Soils and soil fractions		$r/5.6$	169	340	555	657
Everett	} $0.5(D_{10})$	$r(\text{void ratio})^{1/3}$	54	105	174	208
Everett and Haynes		$r(\text{void ratio})^{1/3}$	39	76	130	158
Yong, Osler	} $0.5(D_{50})$	$0.5(D_5)$	399	793	1 413	1 586
$A_s = 0.907$						
$A_s = (1 - n)^{2/3}$	} $0.5(D_{10})$	Air entry	44	65	107	146
Jackson, Uhlmann, and Chalmers		tests	62	104	172	224
	} $0.5(D_{50})$	Suction-water	44	103	131	230
		content tests	62	141	196	309
	} $0.5(D_{10})$					
Maximum measured heaving pressure (kN/m ²)			63	352	797	674

well compacted. Since Yong and Osler had used $A_s = (1 - n)^{2/3}$, the predicted pressure obtained using this expression is also shown. For soil A, the measured heaving pressure was close to the values predicted for close-packed uniform spheres using $r = 0.5(D_{50})$. For soils B, C, and D, the only prediction that gave approximate agreement was that proposed for soils by Everett and Haynes,³ using $r/r_i = 5.6$, with $r = 0.5(D_{10})$. Assuming $r = 0.5(D_{10})$, the predicted and measured maximum heaving pressures were equal when r/r_i was 5.4 for soil B, 7.8 for soil C, and 5.4 for soil D; the average was 6.2. The results from these three soils therefore appear to support Eq. (2) when used with Everett's proposal² that r for soils is associated with the effective size D_{10} rather than the mean particle-size D_{50} .

Equation (3) has been used by Yong¹⁹ and Osler.⁹ The heaving pressures predicted by this equation are shown in Table X along with the measured heaving pressures. There was no agreement between predicted and measured pressures for soil A. Approximate agreement is indicated for soils B, C, and D for the theoretical case of open-packed uniform spheres with $r = 0.5(D_{50})$. Since these soils consisted mainly of well-compacted kaolin, it appears that the approximate agreement is fortuitous. The results from the four soils are not therefore considered to support Eq. (3).

CONCLUSIONS

The experimental work led to the following conclusions:

1. The theoretical relationship for a system of closely packed uniform spheres is $r/r_i = 6.46$. Using this ratio and taking $r = 0.5(D_{50})$, it was found that the measured pore water and heaving pressures for soil A (consisting of spherical particles) agreed closely with those predicted from Eq. (1) and (2). The predicted pore water and heaving pressures for soil A using r_i values obtained from air entry and suction-water content tests were about 70 percent of the measured values.

2. For soils B, C, and D (consisting of platy particles) the predicted pore water and heaving pressures, using the r_i values from the air entry and suction-water content tests, grossly underestimated the measured values. However, Everett and Haynes³ had previously proposed that $r/r_i = 5.6$ is applicable to soils (as distinct from the theoretical values for spheres). Substitution of the measured values of pressure into Eq. (1) and (2) gave an average value of r/r_i of 5.4 (the range for six tests being 4.2-7.8) when r was taken as $0.5(D_{10})$. This average value for r/r_i gives support to Everett's proposal² and indicates that r for soils

TABLE X Predicted and Measured Maximum Heaving Pressures from Eq. (3) Based on Particle-Size Distribution Data, Air Entry Tests, and Suction-Water Content Curve

Method	Basis of Deriving r	Basis of Deriving r_i	Predicted Maximum Heaving Pressure (kN/m ²)			
			Soil A	Soil B	Soil C	Soil D
<i>Theoretical</i>						
Open-packed spheres	} 0.5(D_{50})	$r/2.41$	353	520	775	836
Close-packed spheres		$r/6.46$	785	1 128	1 706	1 814
<i>Experimental</i>						
Close-packed spheres	} 0.5(D_{50})	$r/5.6$	686	1 000	1 500	1 598
Everett and Haynes		$r/9.75$	1 118	1 628	2 432	2 608
Smith, Foote, and Busang						
Soils and soil fractions	} 0.5(D_{10})	$r/2.2-r/5.85$	1 059-2 275	2 069-4 423	3 354-7 227	3 952-8 473
Everett		$r/5.6$	2 167	4 266	6 904	8 178
Everett and Haynes		$r(\text{void ratio})^{1/3}$	677	1 314	2 167	2 599
Yong, Osler		$r(\text{void ratio})^{1/3}$	500	941	1 628	1 971
$A_s = -0.907$ $A_s = (1 - n)^{2/3}$						
Jackson, Uhlmann, and Chalmers	0.5(D_{50})	0.05(D_s)	4 962	9 865	17 230	19 670
	0.5(D_{50})	Air entry	549	814	1 334	1 824
	0.5(D_{10})	tests	775	1 304	2 138	2 785
	0.5(D_{50})	Suction-water	549	1 285	1 638	2 883
	0.5(D_{10})	content tests	775	1 765	2 452	3 864
Maximum measured heaving pressure (kN/m ²)			63	352	797	674

is associated with the effective size of the soil rather than with the mean particle size.

3. The values of heaving pressure predicted by Eq. (3) were substantially greater than the measured values, irrespective of whether r_i was determined from particle-size distribution, air entry tests, or suction-water content values.

4. An assumed value of $\sigma_{iw} = 0.03$ N/m was used in the calculation of the predicted values. While the choice of σ_{iw} obviously affects the predictions, a much greater influence is the method of determining r_i and r . The best agreement between measured and predicted pressures was obtained when r_i was determined from particle-size distribution data rather than from air entry or suction-water content tests. For uniform spherical-shaped particles, the appropriate particle radius r was that of the sphere, while for more typical soils the appropriate r value appeared to be related to the effective size of the soil. Further investigation is required, however, on the influence of particle size, shape, grading, and packing on the r_i and r values for soils.

REFERENCES

1. Balduzzi, F. 1960. Experimental investigation of soil freezing. Tech. Transl. 912. National Research Council of Canada, Ottawa.

2. Everett, D. H. 1961. The thermodynamics of frost damage to porous solids. *Trans. Faraday Soc.* 57:1541-1551.

3. Everett, D. H., and J. M. Haynes. 1965. Capillary properties of some model pore systems with special reference to frost damage. *Re-union Internationale des Laboratoires d'Essois et de Recherches sur les Matereaux et les Constructions, Bull. New Ser.* 27. p. 31-38.

4. Gold, L. W. 1957. A possible force mechanism associated with the freezing of water in porous materials. *Highw. Res. Board Bull.* 168. p. 65-73.

5. Haines, W. B. 1930. Studies in the physical properties of soils. *J. Agric. Sci.* 20:97-116.

6. Hammamji, Y. 1969. Some factors affecting heaving pressures of frozen soils. M.Eng. thesis. McGill University, Montreal.

7. Jackson, K. A., D. R. Uhlmann, and B. Chalmers. 1966. Frost heave in soils. *J. Appl. Phys.* 37:848-852.

8. Miller, R. D., J. H. Baker, and J. H. Kolaian. 1960. Particle size, overburden pressure, pore water pressure and freezing temperature of ice lenses in soil. *Proc. 7th Int. Conf. Soil Sci. (Madison, Wis.)* p. 122-129.

9. Osler, J. C. 1967. The influence of depth of frost penetration on the frost susceptibility of soils. *Can. Geotech. J.* 4:334-346.

10. Penner, E. 1958. Pressures developed in a porous granular system as a result of ice segregation. *Highw. Res. Board, Spec. Rep.* 40. p. 191-199.

11. Penner, E. 1966. Frost heaving in soils, p. 197-202. *In Permafrost: Proceedings of an international conference.* National Academy of Sciences, Washington, D.C.

12. Penner, E. 1966. Pressures developed during the unidirectional freezing of water-saturated porous materials. Proc. Int. Conf. Low Temp. Sci. 1 (2):1401-1412.
13. Penner, E. 1967. Heaving pressure in soils during unidirectional freezing. Can. Geotech. J. 4:398-408.
14. Smart, P. 1970. Private communication.
15. Smith, W. O., P. D. Foote, and P. F. Busang. 1931. Capillary rise in sands of uniform spherical grains. Physics 1:18-26.
16. Sutherland, H. B., and P. N. Gaskin, 1970. Factors affecting the frost susceptibility characteristics of pulverized fuel ash. Can. Geotech. J. 7:69-78.
17. Taylor, D. W. 1948. Fundamentals of soil mechanics. Wiley, New York.
18. Williams, P. J. 1966. Pore pressures at a penetrating frost line and their predictions. Geotechnique 16:187-208.
19. Yong, R. N. 1966. On the relationship between partial soil freezing and surface forces. Proc. Int. Conf. Low Temp. Sci. 1(2):1375-1385.

SHEAR STRENGTH AT A THAW INTERFACE

Stanley Thomson

UNIVERSITY OF ALBERTA
Edmonton, Alberta

Edward F. Lobacz

U.S. ARMY COLD REGIONS RESEARCH AND
ENGINEERING LABORATORY
Hanover, New Hampshire

INTRODUCTION

This paper presents the results of a preliminary laboratory testing program on a remolded silty soil considered to be typical of those encountered in permafrost areas. Strength characteristics, assessed by means of conventional laboratory tests, were compared with strengths observed in direct shear tests in which a frozen-thawed interface coincided with the shear plane imposed by the direct shear apparatus. Information was obtained from undrained and drained triaxial tests on thawed samples. Inherent in this program was the development of a simple technique to yield a direct shear sample having a thawed portion and a frozen portion whose interface could be controlled to a reasonable plane.

LITERATURE REVIEW

Although considerable work has been done in the broad areas of thaw consolidation, heaving pressures of freezing soil, and the strength of thawed soil, little appears in the literature on the shearing resistance at a frozen-thawed interface.

In the past decade or so, several Soviet workers have been concerned with the loss of strength in fills during the

thawing season.^{6,9-11} Very generally, the conclusions reached as a result of laboratory studies were that the strength loss is primarily due to moisture accumulation, including that from melting ice lenses, and to structural changes in the soil mass caused by the freezing process.

Shusherina and Tsytoich⁹ reported tests conducted to determine the strength at a frozen-thawed interface. The shear plane in these tests varied relative to the orientation of ice lensing. When the direction of shearing was perpendicular to that of the ice lenses, the interface between the frozen and thawed zones was considered to be rough. In these cases, shear strengths were observed that were up to 10 times that of the unfrozen state.

If the shear plane paralleled the direction of the ice lenses, the measured strength was practically the same as that for the unfrozen soil. It was concluded that, all other things being equal, the interface between frozen and thawed soil may not be the weakest point in a thawed soil column. The zone of weakness will be that having the highest moisture content.

Vodolazkii¹¹ reported that investigations of permafrost degrading due to a buried heating line showed moisture migrating to the thawing front and upward to the ground surface where it was lost by evaporation. The result was a strength gain by consolidation.

SOIL AND SOIL SAMPLE PREPARATION

The soil used was Manchester silt, considered to be a local deltaic deposit laid down near the close of the Pleistocene. It comprises 5 percent greater than 0.06 mm (sand), 90 percent between 0.06 and 0.002 mm (silt), and 5 percent finer than 0.002 mm. The uniformity coefficient (ratio of 60 percent size to 10 percent size) is 3. It is nonplastic with a liquid limit of 26 percent. The specific gravity of the soil solids is 2.72. It is classified as a uniform inorganic silt of low compressibility. Its Unified Classification designation is ML.

All the test samples were molded using a water content of 25 percent. A reasonably high degree of saturation was achieved with adequate densities. Triaxial test samples were 36 mm diameter and 76 mm long. Direct shear samples were 100 mm diameter and on the order of 60 mm thick.

EQUIPMENT AND INSTRUMENTATION

Most of the equipment and instrumentation were of conventional design with the exceptions described below.

The triaxial samples were compacted in a four-specimen Lucite gang mold⁷ whose unique feature was a thin Lucite split liner in each mold. The sample was removed from the exterior mold by applying a force to the inner liner. Slight expansion of the liner, once it was clear of the mold, allowed the specimen to slide out without being subject to extraneous forces.

The direct shear box consisted of two Lucite rings, each approximately 100 mm i.d., 150 mm o.d., and 48 mm high. The lower ring was bolted to a steel base plate and contained two drain ports. Four sets of holes were drilled through the Lucite rings to receive thermocouple and thermistor leads. Each set consisted of three holes located 120° apart on the circumference. The sets were located 19 mm and 6.3 mm above and below the plane of separation of the two halves of the shear box. The load cap was in two parts, bolted together. The lower part remained in contact with the sample to avoid disturbing it. The upper part was composed of two interchangeable units; one was used during the consolidation phase and the other, containing a heating coil, during the shear testing phase. The upper half of the shear box was fixed and the lower half, mounted on ball bearings, was movable. In this way the normal load remained stationary.

The temperatures in the samples were monitored by 24-gage copper-constantan thermocouples arranged in four planes parallel to the shear plane. In one configuration, two thermocouples were located on each of three radii 120° apart to coincide with the holes in the shear box. The inner three thermocouples were 32 mm in from the periphery and the other three were in 10 mm. In later configurations,

thermocouples were located at 12.5-mm intervals along a diameter in each of the four planes. Also, one to three thermocouples were placed on the bottom and on the top of the sample adjacent to filter paper. The thermocouple voltages were read with a precision potentiometer or a dc null millivoltmeter with voltages converted to temperature using conversion tables.¹

The current supplied to the heating coil in the top cap, hence the heat creating the thawed portion of the sample, was controlled by a thermistor-sensing proportional controller. The thermistor was located in the center of one of the thermocouple planes.

The temperature gradient within the sample was controlled using a "box-in-box" concept. The sample and the direct shear machine were enclosed in a 50-mm-thick Styrofoam cabinet that was set up in the cold room. The shear box and the sample were wrapped with fiber glass insulation. Each successive encapsulation damped out temperature variations of the surrounding environment.

PROCEDURES

The triaxial samples were compacted in the four-specimen gang mold using a kneading compaction technique at a molding water content of 25 percent. The samples were given 15 tamps on each of five layers using the 89-N spring and a 25.4-mm-diameter foot. The specimens were subjected to an upward seepage of water to increase the degree of saturation and then frozen one-dimensionally in an open system at an ambient air temperature of -6 to -7 °C. After freezing, the samples were removed from the mold, their individual frozen unit weights were determined, and stored for testing.

Testing, either undrained or drained, was carried out after the frozen samples were set up in the triaxial cell and allowed to thaw three-dimensionally at 4 °C under the cell pressure. The compression phase of the thawed specimens followed conventional triaxial techniques.

For the direct shear samples, the apparatus was assembled, a porous ceramic stone was placed in the bottom, and the inside surfaces of the rings were coated with Teflon. The soil was compacted so that the surface of each lift coincided with the holes defining the thermocouple planes. The thermocouples were carefully positioned and their depth from the top of the upper surface of the shear ring noted. A filter paper, a porous plate, and the load cap completed the sample preparation. Saturation was in a vacuum chamber with upward seepage of de-aired water. On completion of consolidation to a preselected normal stress, the sample was frozen under the normal load, relatively rapidly, three-dimensionally, and in a closed system at -7 °C. The frozen sample and the shear box were moved to the direct shear machine

TABLE I Results of Unconsolidated, Undrained Triaxial Tests on Thawed Samples^a of Manchester Silt

Spec. No.	Confining Pressure (kg/cm ²)	Maximum Strength (kg/cm ²)	Strength at $\epsilon = 3\%$ (kg/cm ²)	Strain at Failure (%)	Moisture Content (%)	Final Dry Unit Wt (g/cm ³)	Degree of Saturation (%)
1	0.63	2.66	1.04	14.5	24.4	1.59	93.6
2	1.06	4.70	2.26	14.5	23.6	1.62	94.5
3	2.11	6.12	3.08	12.0	22.9	1.59	88.1
4	0.63	3.53	1.44	15.5	24.3	1.60	93.2
5	1.06	3.80	1.61	16.0	25.5	1.57	95.0
6	2.11	6.46	2.96	17.0	24.1	1.61	95.3
7	0.42	1.79	0.22	17.0	26.0	1.59	99.0
8	1.06	4.50	0.50	20.0	24.8	1.61	98.0
9	0.63	1.09	0.10	14.5	26.0	1.57	97.6
10	3.16	5.84	0.30	20.0	25.8	1.57	96.0
11	1.06	3.07	1.22	11.0	24.4	1.63	99.2

^a Samples frozen one-dimensionally in open system at -7°C . Samples thawed three-dimensionally under confining pressure at 4°C . Compression phase carried out at 4°C .

and readied for the shear phase. The enclosing cabinet was assembled and the setup left overnight to establish thermal equilibrium.

The following morning the thermistor-sensing proportional control device was switched on, and an estimated control setting was made. Over succeeding days, the setting was varied until a temperature gradient was obtained that indicated that the frozen-thawed interface coincided with the shear plane imposed by the shear apparatus.

The location of the frozen-thawed interface was assessed from a plot of depth versus temperature. Points representing two thermocouples located one above the other were joined and the intersection of this line and the line representing the plane of separation of the two halves of the shear box was taken as the temperature of the shear plane. Six pairs of thermocouples yielded six temperature values. Adjustments to the controller circuit were made until a straddling of the

0°C temperature line was achieved. It was assumed that the 0°C isotherm coincided with the frozen-thawed interface. Since Manchester silt is nonplastic and thus has a low percent of unfrozen water, this assumption appears acceptable.^{2,8} In addition, there was a steep temperature gradient within the sample that tended to produce a sharp interface between the frozen and thawed portions.

RESULTS

Unconsolidated, Undrained Triaxial Tests

The results of this series of tests are presented in Table I. Moisture content versus compressive strength is plotted in Figure 1, and two typical stress-strain plots are given in Figure 2.

The difference in the shape of the two stress-strain curves

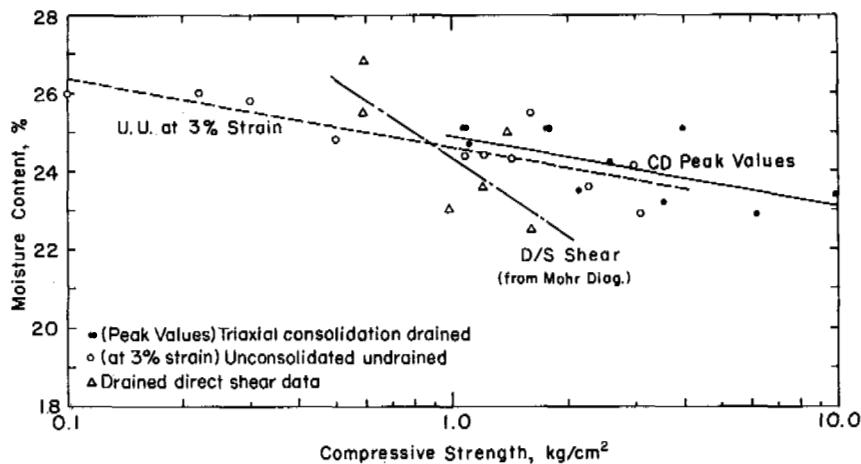


FIGURE 1 Moisture content versus compressive strength for thawed triaxial specimens of silt.

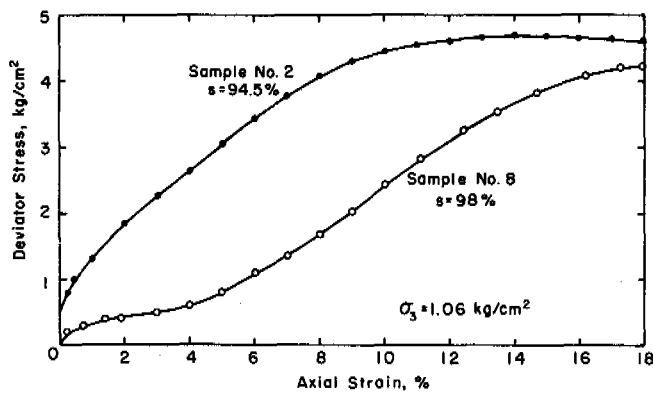


FIGURE 2 Stress versus strain; undrained triaxial tests on thawed silt samples.

of Figure 2 is anomalous. The confining pressures were the same for both samples and their densities were practically the same. However, the degree of saturation differed, sample 2 being 94.5 percent and sample 8 being 98 percent. All samples whose degree of saturation exceeded 95 percent gained strength slowly at first as evidenced by the plateau for sample 8 in Figure 2 to about 5 percent strain. Other samples whose degree of saturation was less than 95 percent gained strength steadily from the start of testing. The interpretation of these data is that the strengths at strains less than about 5 percent for samples that had a degree of saturation greater than 95 percent represented undrained behavior. At higher strains, or degrees of saturation less than 95 percent, the tests were, in fact, partially drained.

The partial drainage infers an increase in effective stress in the shear zone of the sample that, in turn, suggests migration of water within the sample. This hypothesis had observational confirmation in one test (sample 5). In this instance a clearly defined local bulging of the membrane oc-

curred around both the upper cap and lower pedestal where the O-ring seals were placed. The color difference between the bulges and the remainder of the sample strongly suggested they were full of water.

The acceptance of the hypothesis that the samples were partially drained led to choosing strengths at 3 percent strain for comparative purposes.

Although there is some scatter of the data from these tests in Figure 1, the trend of the data appears reasonably clear. An averaging line through the data has a flat slope that denotes a large strength change with a small moisture content change.

Consolidated, Drained Triaxial Tests

The results of this phase of the program are presented in Table II. Typical stress-strain and volume change-strain plots are given in Figure 3 and the moisture content-compressive strength relationship is shown in Figure 1. All the samples revealed a dilatant behavior, and, in general, the results are similar to those of unfrozen soil. The scatter of the points in Figure 1 is probably due to the inefficient technique used to achieve a high degree of saturation. However, the trend for a large change in strength to occur with a small change in moisture content is evident. The slope of an averaging line is roughly parallel to that for the undrained results.

The modified Mohr diagram in Figure 4 indicates that the effective peak angle of shearing resistance was 36° . The small effective cohesion of 0.15 kg/cm^2 is consistent with the fact that a small but noticeable dry strength existed.

Tests on Unfrozen Direct Shear Samples

A series of unfrozen samples were tested in the 100-mm-diameter shear box using conventional techniques. The procedure of reversing the direction of shear was used to accu-

TABLE II Results of Consolidated, Drained Triaxial Tests on Thawed Samples^a of Manchester Silt

Spec. No.	Confining Pressure (kg/cm ²)	Moisture Content (%)	Maximum Strength (kg/cm ²)	Strain at Failure (%)	Final Dry Unit Wt (g/cm ³)	Degree of Saturation (%)
1	0.63	23.5	2.12	7.5	1.58	86.7
2	1.06	23.2	3.55	8.5	1.58	90.0
3	2.11	22.9	6.16	10.5	1.60	88.3
4	3.16	23.4	9.73	10.0	1.58	87.6
5	0.21	24.7	1.11	8.0	1.52	85.6
6	0.42	25.1	1.75	8.0	1.50	93.8
7	1.06	25.1	3.98	9.0	1.59	96.6
8	0.63	24.3	2.56	7.5	1.61	95.9
9	0.21	25.1	1.07	8.5	1.61	100.0

^a Samples frozen one-dimensionally at -7°C in open system. Samples thawed three-dimensionally under confining pressure with drainage allowed. Compression phase carried out at 4°C .

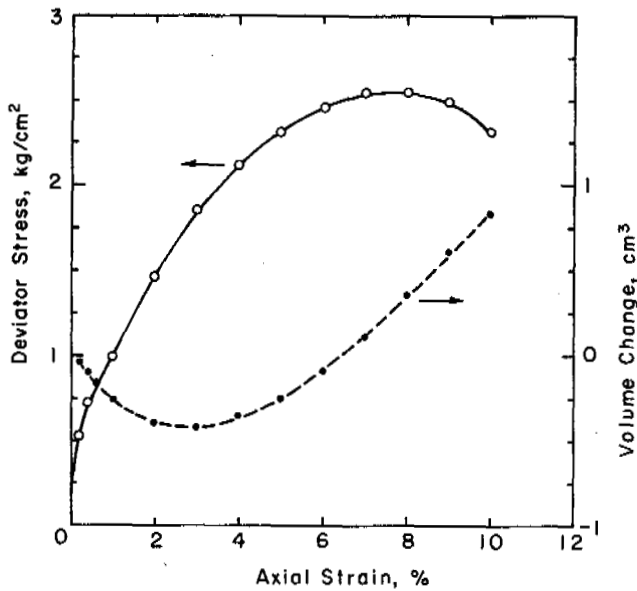


FIGURE 3 Stress versus strain; drained triaxial test on thawed sample 8.

ulate sufficient deformation to define the residual angle of shearing resistance. The effective peak (34°) and residual (32°) angles are shown on the Mohr diagram of Figure 5. The increase of 2° in the angle of shearing resistance from that observed for thawed samples (Figure 4) is attributed to differences in testing techniques.

Drained Direct Shear Tests at a Frozen-Thawed Interface

Errors associated with strength determinations of unfrozen soils are considered in most modern texts on soil mechanics.

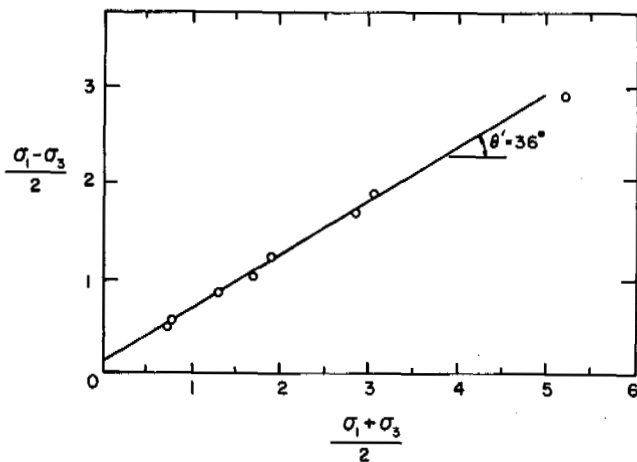


FIGURE 4 Modified Mohr diagram for drained triaxial tests on thawed samples (peak values).

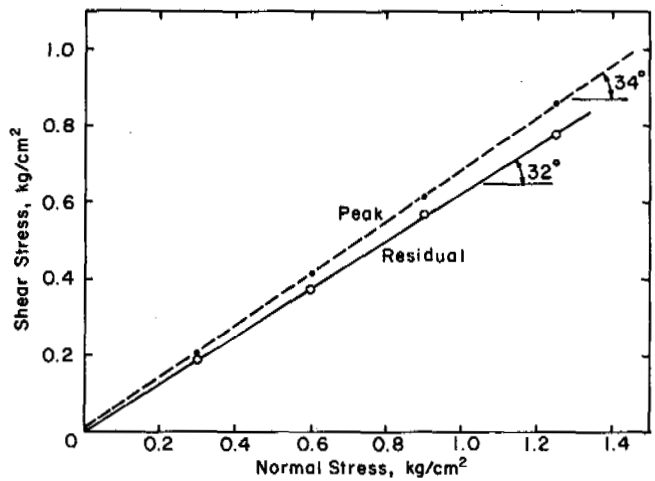


FIGURE 5 Mohr diagram for direct shear tests on unfrozen samples.

Errors inherent in the use of thermocouples and thermistors are considered in other publications.³⁻⁵

Several preliminary trials were conducted to evolve a technique that would result in a tolerable coincidence of the plane of separation of the shear box and the frozen-thawed interface. The coincidence of these two faces was possible within 1 or 2 mm. The averaging of the temperature data used to locate the 0°C isotherm appeared to offset the effects of several inherent errors in the technique.

The frozen-thawed interface was delineated during the dismantling phase by probing. It was found to be crudely convex down and somewhat undulating, with the central portions averaging about 2 mm below the periphery. In view of the premise that the shear zone within the sample has a finite thickness, it was decided to accept the slight saucering of the interface. It followed, therefore, that the actual shearing within the sample was at, or close to, the interface between the upper thawed part and the lower frozen part.

The pertinent data for the direct shear tests at a frozen-thawed interface are presented in Table III. In general, the stress-deformation curves, the temperature profiles, and the results of probing for the interface were similar for each test. A typical set of results is depicted in Figures 6 and 7.

The stress-deformation curve for sample 1 in Figure 6 was derived from a 5-mm displacement of the lower half of the shear box, immediately followed by a reversed displacement of 10 mm and a second reversal of 5 mm to the central position. This occupied the majority of a working day, and the sample was allowed to stand overnight. The following day, a second shear phase was added. The sample was dismantled, the interface located by probing, and moisture contents determined.

The curve for the first shear (Figure 6) shows a peak of 0.54 kg/cm^2 occurring at 2-mm deformation and a well-defined residual strength. The peak value for the second shear

TABLE III Results of Direct Shear Tests at a Frozen-Thawed Interface in Manchester Silt Samples

Spec. No.	Normal Stress (kg/cm ²)	Maximum Shear Stress (kg/cm ²)	Residual Shear Stress (kg/cm ²)	Moisture Content ^a (%)	As-Computed Dry Unit Weight (g/cm ³)
1	0.50	0.54	0.41	23.0	1.60
2	0.75	0.68	0.56	25.0	—
3	0.25	0.54	0.25	25.5	1.58
4	0.88	0.76	0.67	22.5	1.65
5	0.63	0.78	0.51	23.6	1.64
6	0.25	0.42	0.25	26.8	1.55

^a Moisture contents have been taken as an average value of the thawed soil adjacent to the failure plane.

phase was less clearly defined and about 10 percent higher than the residual value. The agreement of the residual values from the two phases is considered acceptable.

The temperature profile for sample 1 (Figure 7c) was typical of all samples. The thermistor-sensing proportional controller was sufficiently sensitive to shift the temperature profile laterally by about 0.1 °C. It was necessary, however, to allow a minimum of 10–12 h to allow for thermal equilibrium. When the temperature profile indicated the 0 °C isotherm was at the plane of separation of the shear box, shearing phase was started.

The results of the probing, plotted in Figure 7b, define the frozen–thawed interface. It will be noted that the predicted locations from the temperature profile agreed reasonably well with the results of probing. The undulating nature of the interface is apparent; however, the grooves were parallel to the direction of shear. Also, in this particular sample

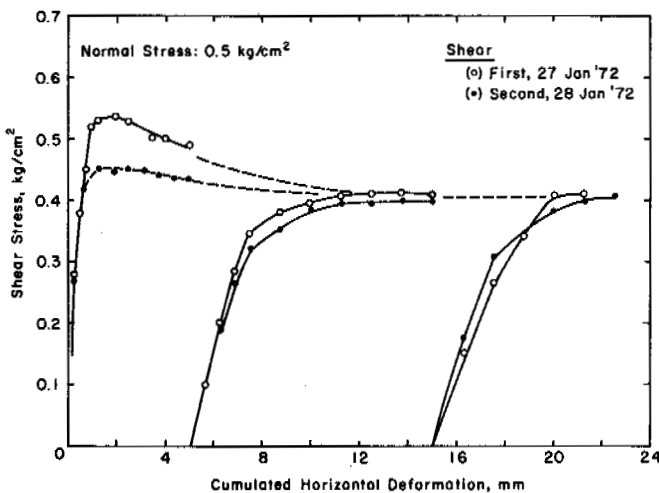
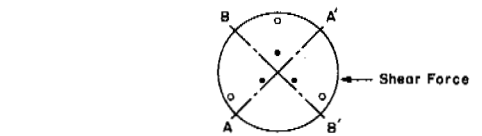
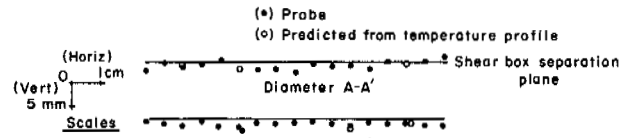


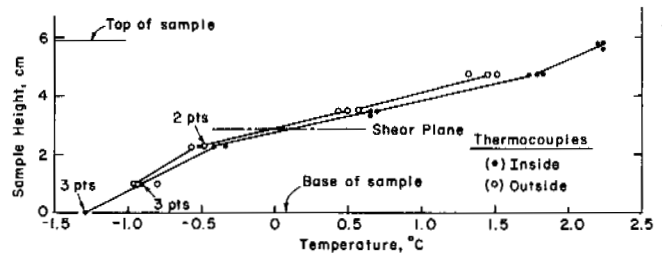
FIGURE 6 Stress versus deformation at a thaw interface for direct shear specimen 1 (normal stress 0.5 kg/cm²).



a. Plan view illustrating location of thermocouple and probe diameters. (Not to scale)



b. Location of frozen-thawed interface from probing just after shear.



c. Temperature profile just prior to shear.

FIGURE 7 Direct shear specimen 1.

the undulations were much more distinct than on the other samples.

The Mohr diagram in Figure 8 shows the direct shear data. The envelope for the residual angle of shearing resistance is reasonably unambiguous, showing an angle of 33° and a cohesion intercept of 0.09 kg/cm². This latter may represent a characteristic of shearing at a frozen–thawed interface or it may be a machine error. The fact that the unfrozen residual envelope passes through the origin of the

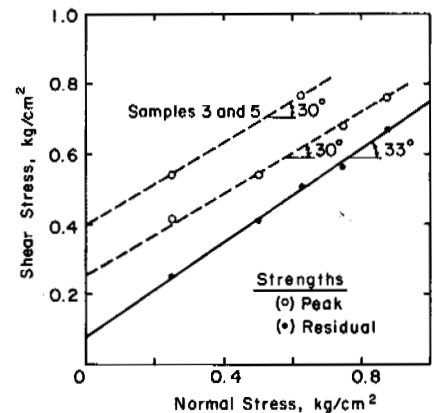


FIGURE 8 Mohr diagram for direct shear tests at a frozen–thawed interface.

Mohr diagram (Figure 5) lends weight to the former reasoning.

The peak strengths of four tests define a reasonably straight line envelope, having an angle of shearing resistance of 30° and an intercept of 0.25 kg/cm^2 . A line through the peak strengths of samples 3 and 5 is also at 30° but shows a cohesion intercept of 0.4 kg/cm^2 . With only two points, the parallelism may be simply fortuitous but also may be due to the shearing of a narrow annulus of frozen soil around the periphery of the sample.

The fact that the residual angle of shearing resistance is greater than the peak angle for shear at a thaw interface is an anomaly of some consequence. The paucity of data requires that any conclusions regarding these results be considered tentative. The following comments are, therefore, speculative in nature. The heave associated with freezing of the samples is thought to have created a quasi-stable soil structure. This soil structure was retained during subsequent one-dimensional consolidation when the upper part of the sample was thawed under the influence of the heating cap. As shear deformation occurred the thawed soil assumed a more stable configuration.

The compressive strength or deviator stress for the direct shear test was calculated from the transition equations. These values have been plotted versus moisture content in Figure 1.

SUMMARY

A central issue was to evolve a procedure for the laboratory measurement of the strength at a frozen-thawed interface within a frozen sample and to conduct tests to determine the strength of Manchester silt at that interface.

It was found possible, with the techniques used, to control the heat applied to the top of the direct shear samples in a temperature-controlled environment in such a manner that the interface between the frozen and thawed portions coincided with the plane of separation of the shear box within the tolerable limits of 2 or 3 mm.

Figures 1 and 9 and Table IV summarize the results of this preliminary testing program. The averaging lines for the triaxial data in Figure 1 are much flatter than that for the direct shear tests at a thaw interface. This infers that the moisture content is less critical in the latter type of test than in triaxial tests on thawed samples. The dramatic strength change in the thawed soils for a small amount of drainage suggested by the slopes on the lines of Figure 1 is confirmed by the curves in Figure 2. The migration of water away from the shear zone in sample 8 (Figure 2) brought about an eightfold strength increase.

The strength results are summarized in Table IV and Figure 9. The effective unfrozen peak angle (34°) is lower than the thawed peak angle (36°). The former tests were

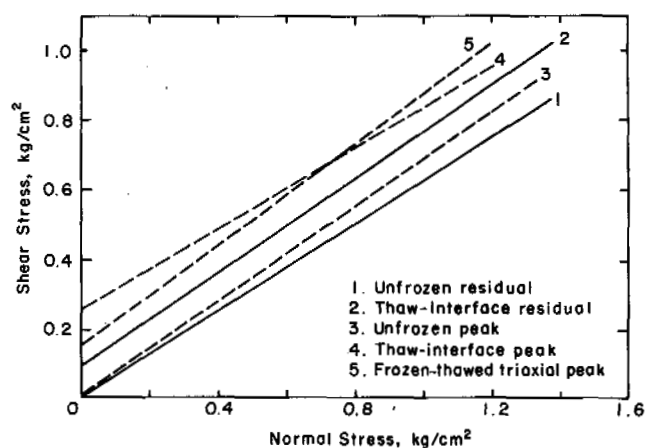


FIGURE 9 Mohr diagram summarizing results of strength tests on Manchester silt.

carried out at an ambient temperature of 22°C and the latter at 4°C . The viscosity of the pore water may have been a factor, as well as the difference, in the type of test. In addition, it is possible that there was a difference in the soil structure. The unfrozen samples were compacted and consolidated one-dimensionally. The thawed samples were compacted, frozen, then consolidated three-dimensionally. The cohesion intercept for the unfrozen envelope is negligibly small, while the thawed value is 0.11 kg/cm^2 . The preceding factors may account for the latter value.

The peak angle of 30° for the freeze-thaw interface is notably less ($4\text{--}6^\circ$) than the other comparable angles. It has been suggested that a quasi-stable soil structure and viscosity of the pore water are contributing factors. The cohesion intercept of 0.25 kg/cm^2 , in view of the postulated quasi-stable structure, appears to be due to the viscosity of the pore water. It is possible that a much lower rate of shear deformation may reduce this value.

Dilatancy of the samples may also contribute to the peak values of shear resistance, the postulated difference in soil structure being a factor in the triaxial and thawed

TABLE IV Summary of Strength Parameters for Manchester Silt

Test Conditions	Strength	Angle ($^\circ$) of Shearing Resistance	Cohesion Intercept (kg/cm^2)	Type of Shear
Unfrozen	Residual	32	0	Direct
Thaw interface	Residual	33	0.09	Direct
Unfrozen	Peak	34	0.01	Direct
Thaw interface	Peak	30	0.25	Direct
Frozen-thawed	Peak	36	0.11	Triaxial

instances and the restricted shear zone a factor in the interface tests.

The residual angles differ by one degree, the unfrozen being the lower value. The friction at a frozen-thawed interface was, in part, along the ice matrix and hence may have consisted of grain sliding. The unfrozen intergranular friction most likely involved rolling of grains. In addition, in an unfrozen sample the shear zone could develop on either side of the shear plane. At a thaw interface, the shear zone could develop only in the thawed zone. The inference is that increased work required in the latter case reflects in the slightly higher angle.

Figure 6 suggests that there is little regaining of strength after the sample has stood for approximately 18 h. The residual strength was essentially duplicated.

In light of the results of this preliminary study, it appears worthwhile to extend this study by employing automatic recording equipment and extending the program to include a wide variety of soil types. Undrained tests involving a frozen-thawed interface are also worthy of consideration.

ACKNOWLEDGMENTS

This paper presents the results of research performed by the U.S. Army Cold Regions Research and Engineering Laboratory under the sponsorship of the U.S. Army Corps of Engineers.

REFERENCES

1. Aitken, G. W. 1966. Temperature-millivolt conversion tables copper-constantan thermocouples, 32°F reference temperature. CRREL Special Report 108. U.S. Army Cold Regions Research and Engineering Laboratory, Hanover, New Hampshire.
2. Anderson, D. M., and A. R. Tice. Predicting unfrozen water contents in frozen soils from surface measurements. *In* Proceedings. Highway Research Board, Washington, D.C. (In press)
3. ASTM. 1970. Manual on use of thermocouples in temperature measurement. Special Technical Publication 470. American Society for Testing and Materials, Philadelphia.
4. ASTM. 1971. Theory and properties of thermocouple elements. Special Technical Publication 492. American Society for Testing and Materials, Philadelphia.
5. Clark, J. A., *et al.* 1967. Properties of thermistors. CRREL Technical Report 188.
6. Mikhaylov, G. D. 1966. Variation of shear strength of clayey ground during freezing and thawing. CRREL Draft Translation 264 (unpublished).
7. Sayles, F. H. 1968. Creep of frozen sands. CRREL Technical Report 190.
8. Scott, R. F. 1969. The freezing process and mechanics of frozen ground. CRREL Monograph II-D1.
9. Susharina, Ye. P., and N. A. Tsytoich. 1967. Experiments on the effects of freezing and subsequent thawing on clay strength. CRREL Draft Translation 285.
10. Titov, V. P. 1965. The strength of thawing ground. CRREL Draft Translation 156.
11. Vodolazkii, V. M. 1962. Strength characteristics of thawed clayey ground at various stages of consolidation. CRREL Draft Translation 267.

SOME ASPECTS OF SURFICIAL SALT TREATMENT FOR ATTENUATION OF FROST HEAVING

Raymond N. Yong, John C. Osler, and Paul V. Janiga

McGILL UNIVERSITY
Montreal, Quebec

INTRODUCTION

The general problems in relation to the question of treatment for alleviation of frost heaving in soils can be traced directly to lack of specific data in actual field performance of frost heaving soils treated with salt additives *added* to the soil surface (for the problem of existing railway tracks) and lack of applicable theories dealing with moisture and solute transport under transient driving gradients. Theories

of moisture and solute transfer in soil systems under thermal gradients rely on either the principles of reversible thermodynamics (classical) or those of irreversible thermodynamics. The application of classical thermodynamics requires that the system be at equilibrium. When such is achieved, it then becomes possible to apply Gibbs' relation, working directly with the partial molar frequency and the local values.² The difficulty in selecting the independent variables affecting the partial molar free energy remains a primary problem.

From the viewpoint of laboratory experimentation, it is evident that the applied temperature gradient must be constant to ultimately achieve equilibrium (or near equilibrium). In applying the classical theory, one is concerned with the specific points on the soil test sample and the local values, thus establishing the sets of forces prevailing at that particular time and at that specific point.

In applying the principles of irreversible thermodynamics to the analysis of moisture and solute transfer, the phenomenological relationships formulated require that the system under consideration not be too far from equilibrium. Thus, quasi-steady-state conditions are generally imposed (e.g., constant temperature gradient). Accuracy for analysis and predictions beyond the domain of first-order approximations become extremely doubtful, as in the case where transient conditions and reversals (such as temperature) exist. In addition, under such conditions, the choice of forces and fluxes becomes increasingly difficult.⁶⁻⁸

In the field where surface-added salt is used as treatment against frost heave temperature gradients are *not* constant. They are highly transient. In addition, temperature reversals (freeze-thaw) can occur. Overall migration is subject to freezing and thawing and long-term analysis and performance evaluation are correspondingly affected. Surficial salt treatment provides for nonuniform distribution as initial conditions for solution of the problem. Initial salt profiles immediately prior to freezeup are not well established.

OBJECTIVES

Since the specific reasons for success or failure of surface salt treatment for modification of frost heave have not been satisfactorily explained by ideal laboratory derived models, this study represents a direct field approach, utilizing the natural system with all its variations in temperature, snowfall, rainfall, cloud cover, etc. The study provides information gained over a 2-year period where field tubes of soil were placed in a constructed test embankment. Moisture and salt migration measurements, together with temperature and heave, were made throughout the freeze-thaw periods. The intent is to provide a means for deriving the necessary deterministic model that would eventually lead to a proper analysis of the field salt treatment problem with continued study.

EXPERIMENTATION

Information on soil properties was gained from direct sampling of a controlled field test site. It is pertinent to note that the study was extended over 2 years¹⁰ and that much of the information gained during the first year led to a redesign of the test apparatus and of the field examination techniques employed during the second year.

In view of the lack of information on transient temperature and freeze-thaw effects and nonuniform salt conditioning for frost heave performance, the specific items of information desired for this relate to water migration during and after the freezeup period, thereby contributing to the freeze-thaw problem; influence of salts added to the surface prior to freezeup in the overall migration and freeze-thaw phenomenon; and overall observations of ground movement due to freeze-thaw and the above factors. It is perhaps possible to begin outlining the necessary parts of the transient deterministic model with the above, which leads eventually to the analytical model.

Control Soil

The soil used was identified as "Seaway till," with an initial salt content of less than 9×10^{-4} percent dry weight of soil and with the following gradation: 100 percent finer than 0.1 mm; 65 percent finer than 0.01 mm; and 15 percent finer than 0.001 mm.

Field Placement

The soil was placed and compacted in 30.5-cm-diameter fibrecrete-coated cylinders. These cylinders, which were previously coated in the interior with a lubricant to minimize side friction, were 1.5 m long and were spaced at 0.6 m centres within a specially constructed surrounding embankment in which the tops of the cylinders were flush with the embankment's horizontal surface. The dimensions of the embankment were such that the proper simulation of one dimensional heat transfer was achieved as ascertained from thermal sensor readings.

Placement water content for the field tubes was approximately 15 percent, which was several percent above optimum as determined from a laboratory standard Proctor test. The compaction procedure used in the field involved the application of sufficient energy to achieve a wet unit weight of 19 kN/m^3 , which was about 95 percent of maximum Proctor density.

Water Regime

The three separate plastic-lined basins placed at the base of the soil pipes provided for a standing water table at 1.4 m from the ground surface. Refill standpipes extended to the ground surface and were monitored and refilled as necessary, thus ensuring that the water table did not dissipate because of water uptake and other conditions.

Each basin serviced six cylinders, therefore enabling the design possibility of introducing salts at the ground surface to two sets of six pipes without cross contamination. The three specific variables in this instance were freshwater, in-

cluding rainfall; the equivalent of 48 N/m² of NaCl added to the soil surface in each pipe; and the equivalent of 96 N/m² of NaCl added to the soil surface in each pipe.

The surfaces of the tubes were left exposed to precipitation. At no time, however, was snow accumulation on the surface allowed to exceed 15 cm.

Instrumentation

The tubes were instrumented with thermocouples with readout provided in a recording-monitoring instrument shack located adjacent to the test site. Settlement-heave plates were also placed within the cylinder with readout stakes attached.

Field Sampling

Field sampling was performed at intervals of 4-5 weeks throughout the entire test period. This consisted of coring the various tubes in each location with samples obtained at various depths.

Information Obtained

The information obtained included total water content at any time and depth, including ice as melted water; salt content at any time and depth; surface movement (monitored daily); subsoil temperature profile (monitored daily); rainfall accumulation prior to freezeup from a weather station located approximately 1.5 km from the test site; freezing index; groundwater table; and visual observations of ice segregation in cored samples and depth of frozen soil from observations during drilling. Since the intent of the study was to gain information of *in situ* behaviour of soils in the freezeup and thaw period, it was desired that conditions in

the natural state be maintained as closely as possible. The only control exercised in the field was in the preparation of the soil columns at controlled water content and density.

RESULTS AND DISCUSSIONS

Typical general pattern of frost penetration in relation to depth and surface temperature is shown in Figure 1. It is noted (but not shown in Figure 1) that approximately 80 percent of the total heave occurred in the period between December 10, 1969, and January 10, 1970. This can be compared with observations of the depth of frost penetration, which showed that approximately 70 percent of the final recorded depth of penetration during the entire freezing period had occurred by January 10, 1970. From these observations and with the aid of Figure 2, it may be directly deduced that ice segregation did not occur (actually corroborated with subsequent corings performed at a later date), and thus the heave appeared to be directly related to the volumetric expansion of pore water on freezing to ice.

Figure 2 shows the relationship between the specific heave (i.e., ratio of measured frost heave to total frozen depth) and water content. Since soil placement compaction provided for densities and water contents slightly higher than Proctor optimum, it was expected that volumetric decrease on freezing would be precluded. From the results obtained, it is apparent that the dominant frost heave mechanism is one of volumetric expansion of available pore water due to freezeup. Some scatter of data is inevitable in view of the field variability and the difficulties involved in performing field tests in winter. However, the trend toward larger specific heave with increasing amounts of fluid in the soil pores is clearly seen.

The significance of the phenomenon shown in Figure 2 is obvious—i.e., a coupled mechanism exists in freezing *in*

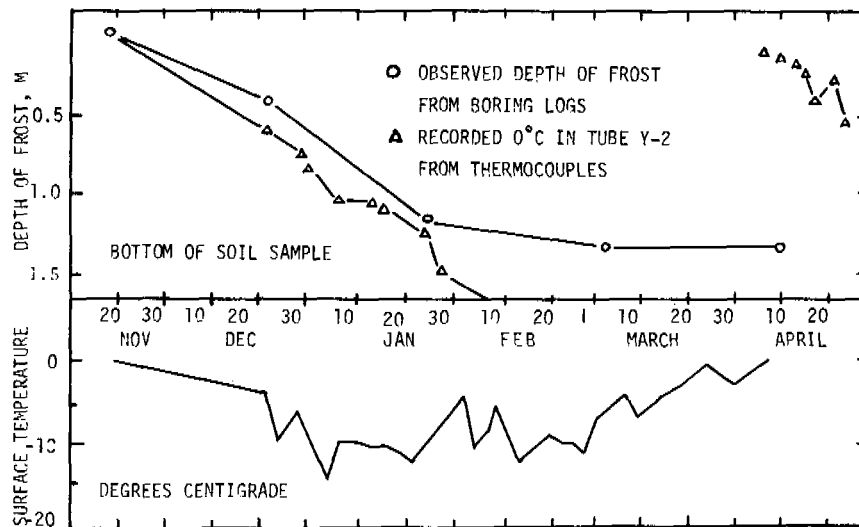


FIGURE 1 Depth of frost; surface temperature versus time.

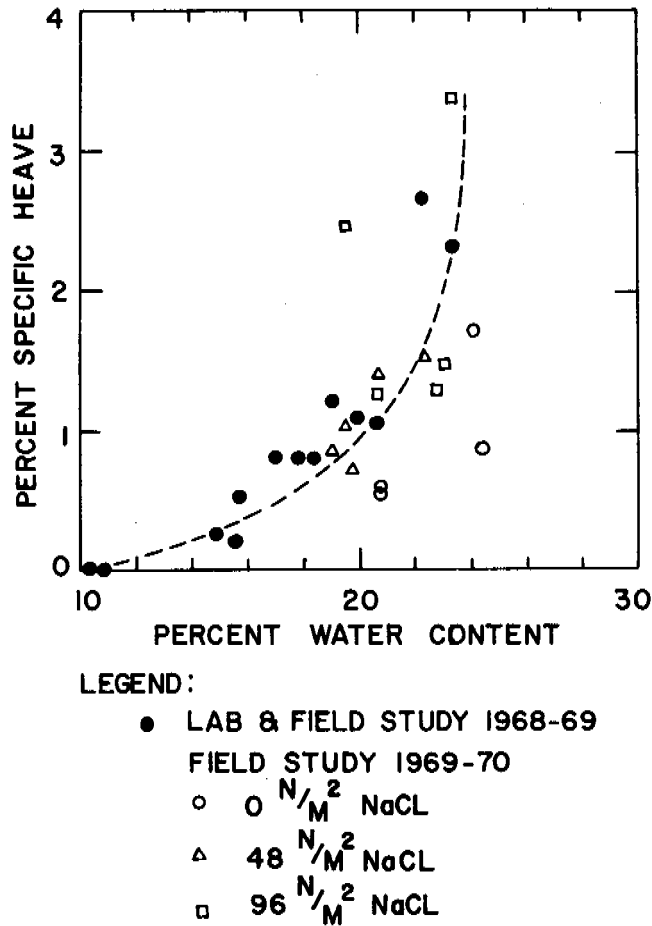


FIGURE 2 Specific heave versus water content.

situ soils. Thus the problem of frost heave and, correspondingly, of frost heaving pressures should be defined in terms of this coupling, where both phase change volumetric expansion and ice segregation can co-exist. The preponderance of one over the other will obviously depend on several factors in the field situation, including, of course, the degree of saturation. In this particular study, since saturation was relatively low (approximately 70 percent), it is apparent that phase change volumetric expansion constitutes the dominant, and primary, mechanism for frost heave; segregation plays a secondary role.

The variation in average water content in the field soil tubes with time for three representative field tubes is shown in Figure 3. This provides an indirect method of examining the water transport phenomenon since the water contents plotted represent average values for the entire frozen soil column. However, a better appreciation of water movement throughout the field tubes is obtained by examining the local distribution of water in the soil column as shown in Figure 4, which contains data from a non-salt-treated tube.

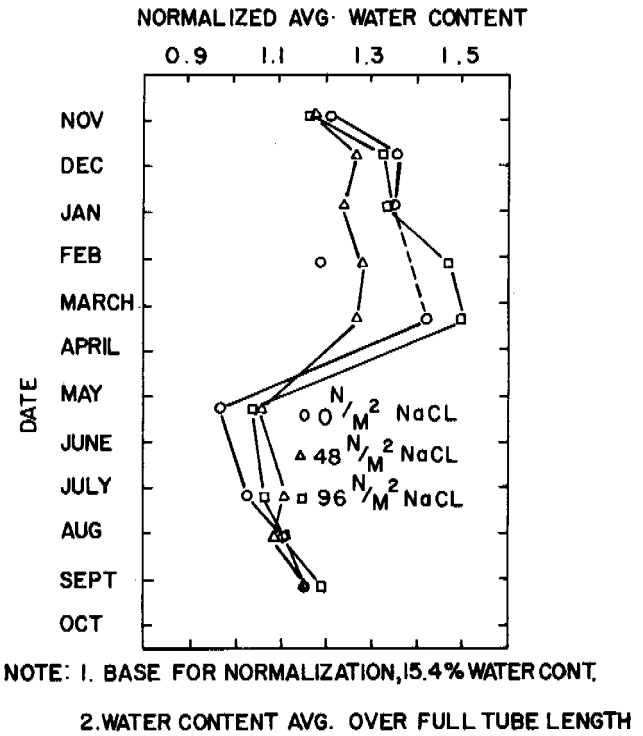


FIGURE 3 Water movement versus time. Base for normalization, 15.4 percent water content; water content average over full tube length.

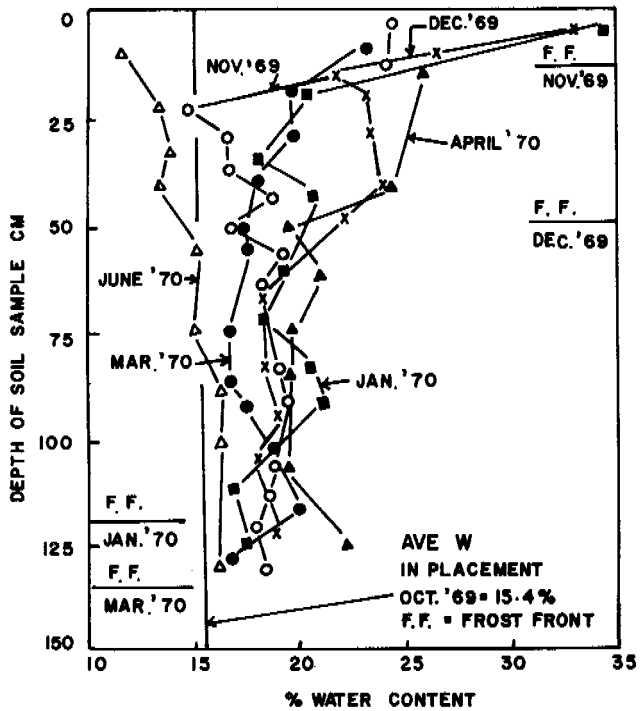


FIGURE 4 Total water movement profile between October 1969 and June 1970.

Recalling that the placement water content was about 15 percent in early October 1969, the redistribution of moisture in view of intake from rainfall and migration from the water table shows that the total water content in the frost zone is increased as freezeup begins. This phenomenon continues as the frost zone extends downward during the freeze-up period, which is consistent with theoretical expectations and predictions.¹ Similar observations have been made by other investigators^{3,4} in laboratory experiments in small columns for "closed" systems.

A reversal in water movement occurs when thaw begins, and data gathered (not shown in Figure 4) show that the water content profile in the summer months reverts to about 15 percent range as established during placement. The density of the soil columns after thaw was not checked and could have been lower than the placement value. The water transport observation is consistent, as far as trends are concerned, with theoretical expectations in regard to moisture movement from hot to cold regimes. This is generally supported by previous laboratory experience that involves water movement under thermal gradients.

Caution must be introduced here if quantitative correlations or predictions are to be made. Steady-state or constant temperature gradient theories cannot be applied to situations where transient phenomena exist if success in predictions is desired. The results in Figure 4 show that water must be moving in the frozen zone during November, December, and January, since the overall water content profile continues to develop outward in the coldest region near the ground surface.

It is significant to note in Figure 4 that most of the mea-

sured values of water content did not exceed 22 percent, which is approximately the value for full saturation at the placement density. The maximum change in water content, which was in excess of 100 percent during December and January, was restricted to the upper 10 cm of the columns and was obviously influenced by intake of surface precipitation.

The "natural" situation of variability in surface temperature (see Figure 1), availability of groundwater, and other environmental constraints involved in field experimentation render the information obtained on water transport most interesting. Specifically, the field system differs from most laboratory studies in that no control on environmental factors is exercised. Thus, steady-state and uniform conditions do not prevail, i.e., the field situation is a transient problem.

The results shown in Figure 5 provide the initial basis for an examination of salt movement in the soil tubes over a 1-year period. They indicate that, with progressive penetration of the frost front, the salt that was added at the surface will continue to migrate down the soil column toward warmer temperatures and, ultimately, enter the water table. This trend is somewhat contradictory to laboratory evidence³ obtained from samples with initially uniform salt content in steady-state-controlled experiments. Also, theoretical expectations based on ionic activities would indicate a movement of salts from the warm to the cold region. However, it must be recalled that in the field situation, fluctuations in ground temperature and perturbations in the advance of the frost front occur throughout the so-called freezing period. While ionic activity would indicate salt movement in

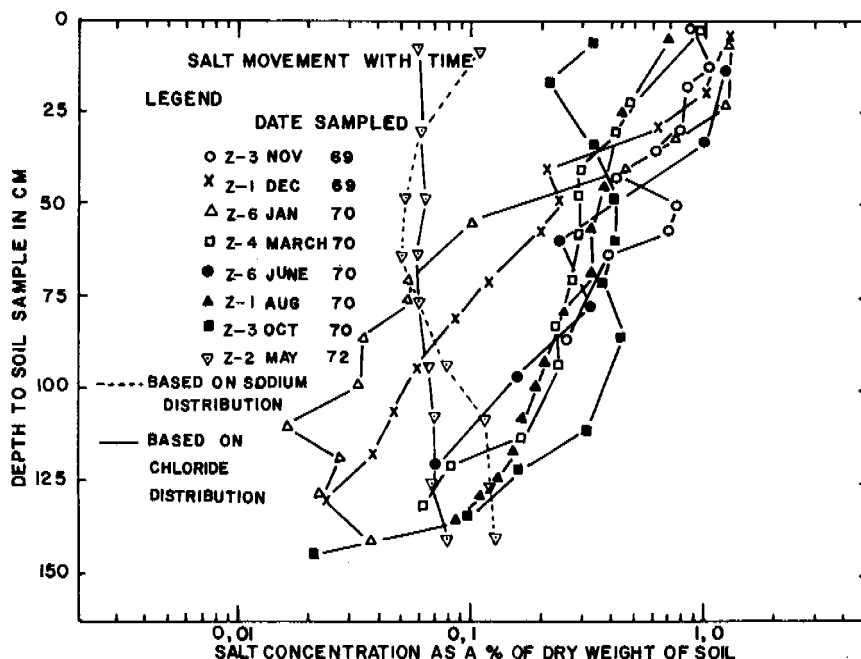


FIGURE 5 Salt movement with time; all tubes treated with 96 N/m² NaCl, October 1969.

the phase boundary layer toward the cold region, the pressure gradient realized through frost heave effects and water transport would serve to move the salts in the opposite direction. When coupled with brine exclusion in pore water freezing, it becomes obvious that the *transient* temperature situation can be most complex, i.e., general considerations of irreversible thermodynamics must now account for cross-coupling effects and counterpressure fluxes. It is apparent that the transient analysis requires application of incremental considerations in addition to non-Darcian and non-Fourier phenomena, thus resulting in nonlinear coefficients, i.e., L_{ijk} in addition to the phenomenological coefficients L_{ij} obtained on the assumption of microscopic reversibility.

Further factors to be considered in arriving at empirical or theoretical analyses require that one recalls that the field tube samples were not initially preconditioned with salts throughout. Since the purpose of the study was to assess salt treatment efficiency, surficial addition of salts was introduced as stated previously. By adding salt to the surface, a saline solution of high concentration is first created as the salt is dissolved by surface precipitation. This situation, in turn, would create large freezing-point depressions before dilution ultimately occurs from downward leaching and further precipitation. Thus, salt migration in the freeze period is seen to be also affected by partial salt effects on the freezing of the pore water in which localized thaw zones would permit migration of salts to proceed in the direction of gravity. The overall effect after a full year of environmental activity resulted in some salt leaching (approximately 35 percent) with the rest of the salts retained in the soil. In Figure 6 we note that the 2-year salt profiles begin

to assume the characteristic shapes identified with leaching in a soil with an initially uniform salt content. This contrasts sharply with the first-year profile shown in Figure 5 and by the triangular points shown in Figure 6.

The difficulty in predicting salt migration in a 1-year period, using conventional theories where simple temperature gradients and force-flux relationships hold for the surface-added salt problem, is due to the fact that initial salt profiles prior to freezeup cannot be determined in view of the nonuniform distribution of salts. The unpredictability of rainfall causing subsequent leaching contributes to the poor initial condition specification. It is clear from Figure 6 and subsequent sampling that the likelihood of success in the prediction of the salt profile using, for example, the theory of chromatography would be favorable for periods after 3 years. However, the initial values must be suitably accounted for and predictions made for salt profile development in the summer. This requires a treatment in terms of effective time period for salt transport not affected by extreme transient temperature gradients. Local gradients can be adequately treated in the analysis.

The movement of salts during the period of frost action was observed to be in the opposite direction to the water movement. Sampling before and after freeze provides only very limited information for salt distribution, and serious errors in interpretation and analysis could result. The need for continual sampling as shown from this present study is most obvious in view of the lack of complete annual performance. It is apparent that the irregularity in field performance relative to moisture and salt profile development indicates not only problems in sampling but also a lack of

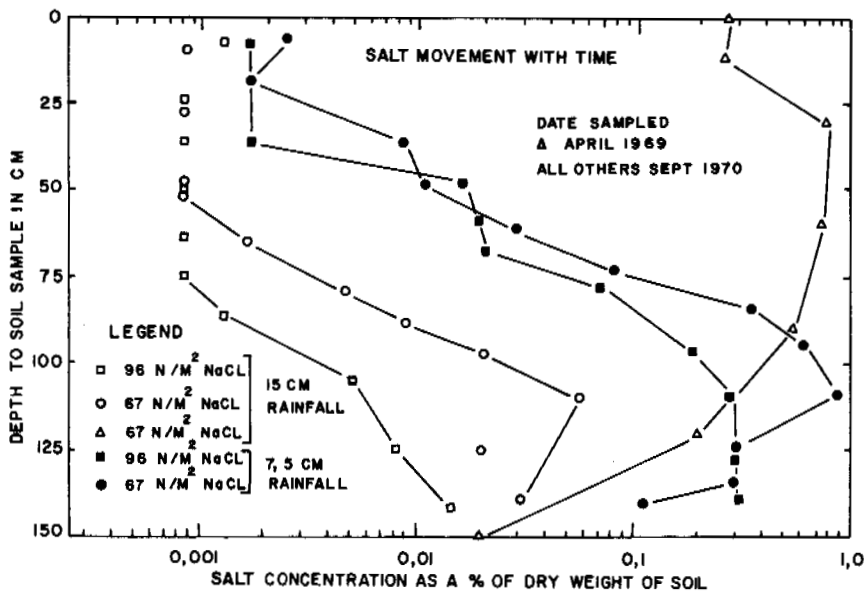


FIGURE 6 Salt movement with time for 1968-1969 field test.

understanding of the many factors defining the observed results. It is evident that ideal theories based on quasi-equilibrium and linear relationships must be modified as should laboratory experiments of similar nature in order to provide for more background to solving the problem at hand.

CONCLUSIONS

The results obtained from the field study clearly indicate that in the transient situation, i.e., where temperature and other environmental factors are transient, ideal theories relying on quasi-equilibrium and linear relationships that predict movement of water and salts must be carefully examined if predictions and analyses are to be made. The evidence shows that water transport from hot to cold does occur throughout the freeze-thaw, even for the situation of surficial salt application. In this same situation, however, salt movement does not appear to follow common expectations. Undoubtedly, much work remains to be done to isolate the surficial salt treatment phenomenon.

In regard to the actual frost heaving phenomenon, the evidence obtained indicates that volumetric and segregative performances co-exist and that volumetric expansion is the dominant mechanism in this particular study. Some of the factors contributing to this performance characteristic undoubtedly lie in the associated transport behaviour for water and salts. Thus, modification of frost heaving is seen to be relatively uncertain because of the unclear mechanisms involved in the process. Until these are identified, the proper use of modifying agents will have to be carefully examined.

ACKNOWLEDGMENTS

The authors wish to acknowledge the assistance received from the Salt Institute, Domtar Chemicals Ltd., and the Canadian Salt Co. Ltd. Field technical assistance and facilities were provided by the Canadian National Railways Technical Research Centre.

REFERENCES

1. Anderson, D. M. 1970. Phase boundary water in frozen soils. Research Report No. 274. U.S. Army Cold Regions Research and Engineering Laboratories, Hanover, New Hampshire. 17 p.
2. Bolt, G. H., and M. J. Frissel. 1960. Thermodynamics of soil moisture. *Neth. J. Agric. Sci.* 8:57-78.
3. Cary, J. W., and H. F. Mayland. 1972. Salt and water movement in unsaturated frozen soil. *Soil Sci. Soc. Am. Proc.* 36:549-555.
4. Hoekstra, P. 1966. Moisture movement in soils under temperature gradients with the cold-side temperature below freezing. *Water Resour. Res.* 2(2):241-250.
5. Johnson, A. W. 1952. Frost action in roads and airfields. Highway Research Board Special Report No. 1. 287 p.
6. Li, J. M. C. 1962. Thermodynamics for non-isothermal systems. The principle of macroscopic separability and the thermokinetic potential. *J. Appl. Phys.* 33:616-624.
7. Prigogine, I. 1961. Introduction to thermodynamics of irreversible Processes. John Wiley & Sons, New York.
8. Taylor, S. A., and J. W. Cary. 1964. Linear equations for the simultaneous flow of matter and energy in a continuous soil system. *Soil Sci. Soc. Am. Proc.* 28:167-172.
9. Yong, R. N., and D. E. Sheeran. 1971. Physics of salt intrusion—Part I, Preliminary investigation. Report No:SI-1. Soil Mechanics Laboratory, McGill University, Montreal, Quebec, Canada. 75 p.
10. Yong, R. N., and P. V. Janiga. 1970. Modification of *in-situ* frost heaving with salt—Part II. Report No:FH-SI-6. Soil Mechanics Laboratory, McGill University, Montreal, Quebec, Canada. 112 p.

V GROUNDWATER IN PERMAFROST AREAS

Surface and groundwater flow systems; recharge and discharge areas (lakes, rivers, aufeis, submarine); saltwater-freshwater interphase; thermodynamics of phase change (water to ice and reverse); groundwater in active layer; water supply, water quality, waste disposal; tracers; computer simulation

GROUNDWATER INVESTIGATIONS IN PERMAFROST REGIONS OF NORTH AMERICA: A REVIEW

John R. Williams

U.S. GEOLOGICAL SURVEY
Boston, Massachusetts

Robert O. van Everdingen

CANADA DEPARTMENT OF THE ENVIRONMENT
Calgary, Alberta

INTRODUCTION

Even though observations were made of groundwater occurrence in permafrost regions in North America as early as 1903,⁶³ it was not until 1942 that the first groundwater studies⁶¹ were undertaken to provide supplies for construction camps during construction of the Alaska Highway. Subsequent studies interpreted the local geologic framework, including distribution of permafrost, to locate well sites for towns, villages, and government installations: Some still continue on a reduced scale.^{58,69} By 1953, significant progress in mapping of the surficial deposits of Alaska permitted regional evaluations of groundwater occurrence.⁴³ The North American and available Soviet literature through 1960 was summarized in an annotated bibliography⁷⁰ and in a summary report on groundwater in permafrost regions of Alaska.⁷² Studies in the Northwest Territories, northern British Columbia, and Yukon Territory, Canada,¹² summarized the local and regional hydrogeology and provided the first attempts to relate groundwater flow systems to surface-water flow and water chemistry. Summaries of research in Alaska⁷³ and in Canada¹³ were given at the First International Conference on Permafrost in 1963.

Around this time studies of basin hydrology were begun in which groundwater was treated as a component of the hydrologic cycle.^{4,11,25-28,56} Results of some of these studies are given in the papers that follow. A natural consequence of the basin hydrology approach is the current application of mathematical and conceptual models to simulate the operation of the hydrologic cycle. Lack of data on infiltration rates, soil moisture, distribution of permafrost, and on hydraulic conductivity of the subsurface materials has prevented assessment of the groundwater component in the basins studied.

Discovery of large reserves of petroleum and natural gas in northern Alaska and northern Canada during the late 1960's and proposals for construction of pipelines through permafrost regions have led to increased support for groundwater studies as part of the evaluation of the impact of proposed developments on the environment. In these studies, less emphasis is placed on groundwater supply and more on

the role of groundwater and frost-heaving pressures developed during the freeze-thaw cycle and their effect on slope and riverbed stability and on the nature and extent of icings. Increased exploration for oil and gas in the North American Arctic has yielded extensive information on groundwater flow systems and quality of water in bedrock aquifers.

Even now, groundwater studies are limited in scope. During the nearly 30 years of study in North America, probably no more than six trained specialists have been active at any one time. From the beginning, investigators have benefited from the early Soviet work summarized in bibliographies^{62,64,70} and by studies by S. W. Muller⁵² and from recent Soviet work available in translation.

The papers that follow describe some typical recent and current studies dealing with water balance of small basins, salt-fresh water interface in arctic deltas, location of water supplies in arctic regions, and occurrence of artesian pressures and their effects on wells and pipelines in permafrost areas.

PERMAFROST AND MOVEMENT OF GROUNDWATER

Water from rain and snowmelt percolates to the water table, runs off to streams and ponds, or is lost by evapotranspiration. Groundwater flows from areas of high fluid potential to areas of low fluid potential and discharges in topographically low areas along watercourses and into the sea. Evidence of groundwater flow in permafrost regions, as in other parts of the world, is found in springs (and associated icings or aufeis), open-water reaches in otherwise frozen rivers, contributions to base flow and to dissolved mineral content of streams, and halophytic vegetation in places where mineralized water emerges.¹² Groundwater movement in permafrost areas is restricted by the presence of both perennially and seasonally frozen ground. Exchange of water between the saturated materials above and below the frozen ground is mainly accomplished through unfrozen zones that perforate the frozen layer.

It is commonly assumed that permafrost contains water only in the solid phase and that it is impermeable and,

therefore, effective in preventing movement of groundwater. These assumptions, however, are not always valid. Permafrost, defined on the basis of temperature,⁵² may be dry and contain no ice. It may contain only liquid water if pressure and/or dissolved-mineral content are high and temperature only slightly below 0 °C. Permafrost may contain a mixture of ice and liquid water, or it may be saturated with ice. Ice segregated into lenses or wedges may also be present.

When a water-bearing soil or rock material freezes, a number of its physical characteristics undergo extensive changes. Its electrical and hydraulic conductivities decrease several orders of magnitude, its apparent specific heat capacity decreases, and its thermal conductivity increases. Any water remaining in the liquid phase exhibits increased viscosity, and its dissolved-solids content generally increases as a result of fractionation during ice formation.

Observations on the behavior of soil-water-ice systems show that liquid water exists in thin films adsorbed on the surfaces of soil particles at temperatures below 0 °C. The thickness of the water films is a function of temperature³ and is, except in very dry soils, nearly independent of total water content (water plus ice).^{49,50} The water present as adsorbed films has been shown to be mobile under both electrical and thermal gradients.⁴¹ Because the liquid-water content is mainly a function of temperature, a thermal gradient that exists in a partially frozen porous medium is analogous to a water-content gradient in an unsaturated porous medium.⁴⁰ If the continuity of the unfrozen films is maintained intact, the rate of liquid transfer depends on the thermal gradient, the temperature of the system, and the available cross-sectional area of the water films. Because the thickness of the unfrozen water films decreases with temperature below 0 °C, the available cross section and thus the hydraulic conductivity also decrease. If discontinuity occurs, for example, by growth of ice lenses, flow rates are reduced even more. As the liquid-water content is independent of the total amount of water in the system, the ice phase in a freezing porous medium acts as a sink, with water moving down the thermal gradient toward the cold side where it freezes. When the temperature of the ground surface increases, heat rising from below will be used in part to melt the base of the frozen layer that now becomes a source of water for redistribution through the unfrozen part of the medium. At temperatures near 0 °C, rates of moisture transfer in the frozen and nonfrozen unsaturated parts of the same soil may be of the same order of magnitude³⁹; both are generally several orders of magnitude lower than in the same material under saturated conditions. Frozen ground, whether perennial or seasonal, thus exerts a significant retarding influence on the movement of groundwater. It, however, should not be classed indiscriminately as an impermeable material. In many cases it should be treated as a confining bed of low but finite permeability. Presence of extensive segregated ice decreases the hydraulic conductivity

to the point where the ground may become effectively impermeable.

Permafrost thus acts as a confining bed, and both its composition and distribution have a significant influence on patterns and rates of groundwater flow. In a number of basins the artesian pressure of the water confined below permafrost causes wells drilled through the permafrost to flow. Groundwater discharge may be restricted to the lower, central part of many river valleys where the permafrost is discontinuous. In some valleys, the resulting strong upward movement of groundwater causes quick conditions and instability of the affected streambeds. In the region of continuous permafrost, unfrozen zones penetrate the permafrost only where salinity of the groundwater prevents freezing, or where heat transfer from a body of surface water or from discharging subpermafrost water is sufficient to maintain the unfrozen condition.

AVAILABILITY OF GROUNDWATER

The following descriptions, summarizing results of recent investigations of groundwater occurrence in unconsolidated deposits and bedrock, illustrate some of the ways in which permafrost distribution affects groundwater flow.

Groundwater in Alluvial Deposits

Groundwater in alluvial deposits is an abundant source of supply for most of the settlements in Alaska and Canada within the discontinuous-permafrost zone.^{12,20-24,43,72} Some major valleys—such as that of the Tanana River in Alaska, where unconsolidated deposits as much as 250 m thick near Fairbanks and 610 m thick south of Minto⁴ are frozen to a maximum known depth of 81 m—contain reserves of groundwater adequate to meet any foreseeable need.²⁰ Within these aquifers, the local distribution of permafrost is affected by the history of river migration and by proximity of bodies of surface water. The older floodplain terraces, remote from the river and from lakes, are underlain by thicker and more continuous permafrost than the younger terraces and the floodplain adjacent to the stream. In the absence of some means of predicting permafrost distribution without data from closely spaced drill holes, it has been impossible so far to make a detailed assessment of the effect of permafrost on aquifer characteristics outside the Fairbanks area.

Large alluvial-fan deposits of tributaries to the Tanana, Kuskokwim, and Yukon rivers are recharged by losing (influent) streams; they contain only sporadic bodies of permafrost.^{4,72} Quality of the water in the alluvial-fan deposits is superior to that in the floodplain and terrace deposits along the major rivers, where the presence of organic material in the alluvium has caused iron, manganese, and color problems in many water supplies. Many of the small creeks in the Yukon and Tanana river watersheds in Canada and

Alaska flow in valleys that are underlain by as much as 100 m of loess and water-transported silt mixed with organic material. These deposits are separated from bedrock locally by sand and gravel. Water in unfrozen bedrock, sand, and gravel is confined under artesian head by the overlying fine material and by permafrost. As described in two papers to follow, artesian conditions in some of these valleys present problems in well construction,⁴⁸ and they appear to contribute water to swamps and ponds by upward leakage.^{23,57}

Alluvium between the active layer and the top of permafrost beneath deep lakes and rivers is the only known source of freshwater in unconsolidated deposits in the lowlands bordering the Beaufort Sea. Unfrozen alluvial aquifers beneath the Colville River and nearby terraces at Umiat^{9,43,71} could be developed. Chemical analyses of river water at Umiat in early spring 1969¹ suggest that the water is derived from storage in the riverbed or from bank storage, but does not come from the saline or brackish bedrock aquifer beneath the permafrost. A supply of water for an oil camp near Prudhoe Bay was developed from unfrozen alluvium beneath the Sagavanirktok River. Under favorable geologic conditions, perennial supplies of groundwater can be obtained from alluvial deposits beneath small intermittent streams where seasonal frost reaches the permafrost table each winter. Such a supply was developed beneath Selin Creek near Cape Lisburne, Alaska, by lowering the permafrost table over a period of years and retarding penetration of seasonal frost by inducing snow drifts to create an unfrozen zone at least 3 m thick in which a gallery was built to collect the water.³² Attempts to develop water supplies from unfrozen alluvium beneath large lakes or from coastal-plain deposits have been unsuccessful.

Major problems in the development of groundwater supplies at coastal settlements are the ease with which saline water found at shallow depth beneath coastal bars, spits, and beaches and along the outer fringes of deltas can be drawn into wells during pumping and the potential contamination of the freshwater aquifers during storm tides.

The boundary between salt water and freshwater in large coastal deltas of Alaska is still not defined, and the problem has received little study in Canada. Deposits of the largest delta in Alaska, formed by the Yukon and Kuskokwim rivers, are as much as 305 m thick, and wells have been drilled through as much as 184 m of frozen sand and silt to obtain water. The water was brackish along the outer fringes of the delta; wells farther inland produce water of the calcium bicarbonate type similar to that in the Yukon and Kuskokwim rivers above the tidal reach.³¹

Seawater invades the Colville River Delta in northern Alaska during periods of low discharge and is flushed from stream channels during the breakup flood crest.^{5,66} The position of the interface between fresh and saline groundwater in the thaw zone beneath the delta channels is unknown, but it is undoubtedly influenced by the migratory

saltwater front in the river. Salt water is reported in a lens below the freshwater aquifer beneath Sagavanirktok River about 11 km from the Arctic Ocean.⁵⁵ In the absence of temperature measurements, it is not known whether the salt water forms a lens within permafrost or whether it has a temperature above 0 °C.

At Point Spencer spit⁸ and Kotzebue, Alaska,¹⁴ seaward migration of freshwater in the suprapermafrost aquifer is prevented by permafrost that rises under beach ridges near the seaward margin of the spits. Permafrost also prevents mixing of fresh suprapermafrost water with saline subpermafrost water. Saline water within the permafrost has a temperature similar to that of the enclosing permafrost. At Kotzebue saline water in a gravel lens within the permafrost at a depth of 24–26 m is believed to represent original brackish water that became increasingly mineralized by addition of high-chloride water expelled from overlying sediments during freezing.²¹

Groundwater in Bedrock

Groundwater moves only through weathered zones and through larger fractures and faults in the crystalline rocks of the Canadian shield east of the Mackenzie River. Both its value as a source of water supply and its contribution to streamflow are negligible.¹² An extensive cover of nearly impermeable till and lacustrine deposits, much of which is perennially frozen, restricts recharge of the bedrock by infiltration of snowmelt or rainfall. Instead, most of the precipitation runs off to numerous lake- and marsh-filled depressions in the till and bedrock surface, from which it is discharged to streams or lost by evapotranspiration. Water quality is more affected by organic content than by dissolution of salts.

Continuous permafrost in unconsolidated deposits of the Arctic Coastal Plain and adjacent foothills in Alaska and Canada extends nearly everywhere into consolidated rock to depths as great as 610 m,⁴⁴ preventing downward percolation of snowmelt and rainfall. Water in the bedrock⁷² is of the sodium chloride type and may contain as much as 18.4 kg/m³ of dissolved solids, as much as 15.8 kg/m³ of chloride, and as much as 8.50 kg/m³ of sodium. A sodium bicarbonate water, with 1.02 kg/m³ of sodium and only 0.14 kg/m³ of chloride was pumped from a well 60 km northwest of Umiat.⁷² Several wells near the Colville River at Umiat produced freshwater from unconsolidated deposits and bedrock between depths of 8.5 and 148 m.⁷¹

Active groundwater flow systems in undisturbed sedimentary basins of northern Canada extend to great depths in many places. The groundwater is recharged from snowmelt and rainfall through sink holes and through unfrozen zones in the unconsolidated deposits. Water moves through solution channels and joints in gypsum and limestone and is

commonly saline where it has been in contact with salt beds. It is discharged to springs and to streams that have cut valleys in the plains. Flow rates in the bedrock become progressively slower with depth; long residence time and the availability of soluble minerals lead to high mineralization.

Groundwater in the sedimentary bedrock in northern Canada is of the sodium chloride type and may contain as much as 300 kg/m^3 dissolved solids, 183 kg/m^3 chloride, and as much as 8 kg/m^3 each of bicarbonate and sulfate. In the more highly mineralized waters, calcium concentration may exceed 25 kg/m^3 . Dissolved-solids content is seldom less than 3.5 kg/m^3 , even in the shallower formations tested in these undisturbed sedimentary basins. Springs along the Salt, Little Buffalo, Buffalo, and Saline rivers are fed by discharge from bedrock aquifers. The waters of these springs contain as much as 12.7 kg/m^3 dissolved solids, 5.2 kg/m^3 chloride, and 2.8 kg/m^3 sulfate.¹² High Na:K ratios in the water indicate that the mineralization probably results from solution of halite.³⁸ Discharge of mineralized water from bedrock affects the quality of surface waters in the Mackenzie River drainage basin.³⁸

Saline springs at Gypsum Hill, Axel Heiberg Island, typical of those elsewhere in the Canadian Arctic Archipelago, contain as much as 75 kg/m^3 dissolved solids, 42.9 kg/m^3 chloride, and 4 kg/m^3 sulfate and range in temperature from -2.9 to 6.7°C .⁷ It is not known whether these springs are points of discharge of active groundwater flow systems or the result of expulsion of connate water from sediments undergoing compaction.

Saline water under high artesian head in Cretaceous or older sedimentary rocks in the Copper River lowland, south central Alaska, migrates into overlying unconsolidated deposits. The water discharged in springs and mud volcanoes and as seepage to streams is similar to connate water of the sodium calcium chloride type and is accompanied by methane and nitrogen gas.³⁴ Three springs on the slopes of a volcano yield water of the sodium chloride bicarbonate type and carbon dioxide gas, resulting from mixing at depth of sodium calcium chloride water with water that is rich in boron, bicarbonate, and sulfate of volcanic, metamorphic, or other origin.³⁴ These waters lie within a 160-km-wide tectonically active belt extending along the Pacific coast of North America from California to Alaska.⁶ They result apparently from metamorphism of marine sedimentary rocks that, according to the plate-tectonic theory, are being underthrust beneath igneous and metamorphic rocks. The waters may serve as a hydraulic medium for tectonic activity.⁶

The groundwater flow systems in mountain ranges of northwestern Canada and Alaska benefit from higher rainfall and from relative ease of recharge through coarse unconsolidated deposits in areas protected from deep freezing by heavy snowcover.⁴³ High hydraulic gradients, causing

rapid groundwater flow and short residence times, generally result in freshwater being discharged from numerous springs.

Major Freshwater Springs

Large springs in the Brooks Range and British Mountains of northern Alaska and Yukon Territory issue from fault zones in which limestone of the Lisburne group is brought into contact with other rocks and from solution-enlarged fractures in the limestone. The springs are of interest because of the enormous icings that form downstream each winter and also because of their importance in the life cycle of certain species of anadromous fish. More than 50 known springs and icings in the Sagavanirktok, Ivishak, Canning, and other basins in the Brooks Range are under study by the U.S. Geological Survey. Discharge rates for individual springs range from 0.12 to about $1.14 \text{ m}^3/\text{s}$ and the temperature ranges from 4 to 6°C . About 0.15 m of annual basin-wide recharge is required to feed the springs in basins of the eastern Brooks Range, provided groundwater divides coincide with topographic divides [1]. Estimated annual precipitation in this part of the range is 0.5 to 1.0 m/year.² Meltwater and rainfall appear to percolate to a deep water table through unfrozen zones that perforate permafrost [1]. A spring at Cape Seppings, at the western end of the Brooks Range has a variable flow from 0.008 to $0.105 \text{ m}^3/\text{s}$ and a temperature between 4 and 5°C .⁵⁴ Streams on Seward Peninsula, Alaska, which sink into solution cavities in limestone and openings in lava flows and subsequently reappear at springs downstream, show that freezing of such underground channels can be prevented by groundwater flow. Springs have been noted along fault scarps of relatively recent age on Seward Peninsula.⁴³

Freshwater springs on the Fishing Branch of the Porcupine River north of the Ogilvie Mountains, Yukon Territory, Canada, issue from carbonate rocks of Middle Devonian age through coarse alluvium. Water temperature of the springs is 4.5°C and their specific conductance of $300 \mu\text{mho}/\text{cm}$ is only slightly higher than the $185 \mu\text{mho}/\text{cm}$ for river water upstream. After mid-July, the river upstream is dry except during extended wet periods. Downstream from the springs, the river is ice free all winter for a distance of 30 km [2]. The springs provide a major contribution to stream flow. No icings are associated with the springs, and the ice-free reach of river below the springs is an important location for spawning and overwintering of anadromous fish. The springs are being investigated for the Canadian Fisheries Service. Other large freshwater springs are present along mountainous reaches of the Liard, Snake, Arctic Red, and Porcupine rivers in northwestern Canada.¹²

The temperature of several degrees above the freezing point in the springs in both lowlands and mountains suggests that the subsurface flow path of the water must pass well

below the base of the permafrost. The warmed waters maintain unfrozen zones through permafrost to the point of discharge.

Thermal Springs

Thermal springs,⁶⁸ having a much higher temperature than those described above, may derive heat from exothermic reactions of minerals in the surrounding rocks, from anomalously high residual heat content in active tectonic zones, or from relatively young igneous intrusions or volcanic activity. Carbon dioxide gas discharged from some carbonated springs may have been formed by action of recent volcanic rocks on limestone.⁶⁸ Some of the thermal and mineral springs in northwestern Canada studied by Brandon¹² are being re-examined in current geologic and water-resource investigations. A complete inventory of thermal springs is still not available for Alaska and northern Canada, and the economic potential of the thermal waters as a source of energy has not been investigated.

ICINGS, PINGOS, AND ARTESIAN PRESSURES

Icings

Summaries of studies of icings, dealing with their origin and with methods of control and prevention,^{15,16} include results of experiments by the Alaska Department of Highways and the Cold Regions Research and Engineering Laboratory on channel modification and icing control by electrical heating and insulation. Prior to 1970 few quantitative studies were made of the hydrologic and geologic factors that affect individual icings. Studies of the pressures involved and of the relationships between icing formation and such meteorological factors as time of heavy snowfall, thickness and density of snowpack, and temperature have begun only recently.

Most icings formed by discharge of groundwater present individual problems in local hydrogeology. Local flow patterns are changed by growth and dissipation of the seasonal frost layers. Constriction of river flow and of groundwater flow through riverbeds is caused by deep freezing of the channel and by penetration of frost into the riverbed alluvium, which results in decreased transmissivity. The original distribution of transmissivity in the unfrozen materials beneath streams affects the locus of icing formation.

Investigations of river icings in northern Alaska were begun in 1969 and in the Porcupine River and Beaufort Sea drainage basins in Canada in the winter of 1971-1972. They have included aerial reconnaissance of the icings in early spring to determine points of perennial groundwater discharge from deep and shallow aquifers. The volume of a

number of icings in Alaska has been estimated to determine the amount of groundwater discharge stored as ice and its potential contribution to stream flow after the spring thaw.¹ For example, the volume of icings in the Sagavanirktok River basin is conservatively estimated at 123 000 000 m³. If accumulated uniformly over an 8-month freezing period, this volume would represent an average groundwater discharge rate of nearly 6 m³/s. Melting of these icings over a 2-month period would add an average of nearly 23 m³/s to the stream flow [3]. Studies of icings now in progress include collection of temperature and pressure data and recording of changes in volume with time, as well as an inventory of the springs that feed the icings and measurements of their water chemistry, temperature, and discharge rates [4].

Weekly measurements and photography of icing development are used in current studies of icings in the Goldstream and Caribou-Poker creek watersheds north of Fairbanks, Alaska.⁴⁶ Maximum ice buildup occurs from midwinter to early spring after the active layer is frozen to the permafrost table. Much of the water feeding the icings in the Caribou-Poker creek tributary under study is believed to be subpermafrost water, but data on depth and distribution of permafrost in both watersheds are not yet available. Release of water stored in the icings on the tributary in the Caribou-Poker creek watershed, equivalent to about 4 percent of total runoff and 40 percent of winter stream flow, is delayed until the melting period. During the 4 weeks following ablation of the snowpack, melting of the 710 000 m³ of ice would provide an average flow augmentation of about 0.28 m³/s.⁴⁶

Icings formed from mineralized spring water may carry a layer of slush with a high content of carbonate or sulfate minerals during the melting period [5]. Part of the original mineral content of the water forming the icings is apparently separated during freezing. Low temperature and low carbon dioxide content in the meltwater retard resolution, and the minerals become concentrated on the melting surface until washed away or dissolved in more aggressive rain water. Further study of this phenomenon will be necessary to determine its influence on the quality of the water released by icings during melting.

Open-System Pingos

Some 270 open-system pingos in the Yukon-Tanana upland, central Alaska,⁴² and more than 460 in central Yukon Territory, Canada,⁴⁵ are found in narrow upland valleys beyond the limits of the late Wisconsinan glaciation. They are not found in broad river valleys where continuous confining layers of permafrost or of fine-grained unconsolidated deposits are generally absent. Although both open- and closed-system pingos and recently observed underwater mounds in the Beaufort Sea are discussed in Session III, the

presumed role of artesian pressure in the development of open-system pingos warrants mention.

One of the requirements that limits the distribution of open-system pingos is a continuous confining bed that may consist of impermeable sediments or a layer of permafrost. A second requirement is restricted groundwater flow⁴²; too large a flow rate would prevent freezing of the pingo. Formation of a pingo requires that subsurface temperature be very close to 0 °C to provide the minimum tensile strength of frozen ground and to prevent premature freezing of the supply of groundwater. Calculations have shown that the static load at the base of a pingo 30 m high would be 3–4 atm; the additional force required to overcome the tensile strength of the frozen ground and to dome the pingo is cited as 2.4–17.4 atm.⁴² The total force required, 6–22 atm, is much higher than the highest artesian pressure yet measured in Alaska. It appears likely that the growth of ice lenses and the accompanying freezing pressures are largely responsible for the growth of open-system pingos. A steady slow supply of groundwater would be a prerequisite in this case. A part of the necessary uplift pressure may be supplied by the relatively low artesian pressures, increased by confinement of water under the pingo.⁴² The mechanism is still poorly understood.

A few scattered observations have been made of the hydrology of pingos, including observations on two mature open-system pingos near Dawson, Yukon Territory, Canada. These pingos have small crater lakes and basal springs. A lack of hydraulic connection between the crater lakes and the groundwater flow system is suggested by recession of lake levels at the same rate as that in evaporation pans, and by differences in temperature and specific conductance between the lake water and water from the basal springs [6].

Artesian Pressures

Current interest in stability of riverbeds and slopes has generated increased study of the artesian pressures associated with icings and open-system pingos and those found in wells in confined aquifers. Artesian heads of as much as 8.45 m above land surface have been reported in upland valleys near Fairbanks, Alaska.⁴⁸ Maximum head was 1.2 m above land surface in four holes drilled in 1972 along the Dietrich River in the Brooks Range to locate the maximum artesian head along this part of the proposed route of the trans-Alaska pipeline [1]. Studies of pore pressures in freezing alluvial deposits, to be described in a paper that follows,¹⁸ show that over the season head changes in wells are probably less than 1 m. Measurements of artesian and freezing pressures in North America have not yet revealed pressures equivalent to the 52 atm calculated for an icing mound in the Soviet Union.⁵³ Results of studies in a bog pond in one of the upland valleys near Fairbanks, described in a paper

to follow,⁵⁷ indicate feeding of the pond by upward leakage of groundwater through about 40 m of permafrost.

INFLUENCE OF PERMAFROST ON WATER QUALITY

The role of permafrost in directly imparting a particular type of mineralization to groundwater is probably minor. Reduction of the rate of groundwater movement by permafrost provides a longer residence time for reactions between groundwater and enclosing rocks than in regions without permafrost. Permafrost may separate and prevent mixing of freshwater and salt water along the coast and also of waters of different chemical composition elsewhere. Chemical reactions are retarded under low-temperature conditions, but few data are readily available. Saturation concentrations of calcium and magnesium bicarbonate will be somewhat higher in permafrost regions than elsewhere as a result of the increasing water solubility of carbon dioxide with decreasing temperature. Dissolution rates, however, decrease. Solubility of gypsum (anhydrite) also increases with decreasing temperature,¹⁰ but, again, reactions are retarded.

Shallow groundwater in the permafrost regions of Alaska and Canada is generally of the calcium or calcium magnesium bicarbonate type; some is of the magnesium bicarbonate or magnesium sulfate type. Along the coastline in some thermal springs and in the sedimentary basins described above, sodium chloride, sodium calcium chloride, and sodium bicarbonate waters predominate.^{2,4,12,29,47,72} In alluvium of interior valleys, high concentrations of iron and manganese, high organic content with resulting color and odor, as well as excess hardness, are the main objectionable qualities of the water, most of which is otherwise suitable for most domestic and industrial uses. Excessive salinity and hardness make location of potable supplies in coastal areas and in the sedimentary bedrock difficult.

The deep groundwater below permafrost is usually of a relatively constant quality. Shallow aquifers that lie above salt water in coastal areas and shallow aquifers of restricted capacity are subject to seasonal variation in water quality as a result of seasonal reduction in fresh recharge and possibly also because of fractionation by freezing of part of the aquifer. Water quality studies in Alaska of subriverbed aquifers beneath Ogotruk Creek near Cape Thompson,⁶⁷ of an aquifer developed in fractured bedrock near Cape Prince of Wales,³⁰ and of the small aquifer beneath Selin Creek near Cape Lisburne reveal pronounced increases in dissolved solids when recharge ceases in the fall. During the winter, the concentration of dissolved solids increases in the unfrozen part of the aquifer as seasonal frost penetrates; in the spring, renewed dilution by infiltration of snowmelt reduces the concentration to summer levels.

Most streams show a seasonal fluctuation in the concen-

tration of dissolved constituents as revealed by measurements of specific conductance of the water. These changes are caused by mixing varying proportions of relatively pure water from snowmelt and overland runoff with groundwater discharge. Thus, during the period of low flow in late winter, the specific conductance is highest; during peak discharge, it is lowest. If the average chemical composition of the groundwater is known, it is possible to determine the contribution of groundwater discharge to stream flow. Application of this method indicated, for example, that nearly 57 m³/s is contributed by discharge of groundwater to the flow of Liard River near the Alaska Highway crossing.¹² This method provides a means of separating stream hydrographs into components of surface runoff and groundwater discharge, using the highest specific conductance observed as that of average groundwater discharge.²⁵⁻²⁷

Accurate knowledge of groundwater temperature is important for the design of distribution systems, especially where pipes are to be laid in permafrost or within reach of seasonal freezing. Except for thermal springs and springs believed to have an exceptionally deep flow path between the areas of recharge and discharge, groundwater temperature is generally between 0 and 6 °C; average temperature of groundwater, including shallow groundwater subject to seasonal changes, is 1.7 °C at Fairbanks and 2.8 °C at Anchorage near the southern limit of permafrost. Tests near Fairbanks showed that groundwater temperature beneath permafrost increases with depth, which is consistent with the expected geothermal gradient. Temperature of deep groundwater is constant throughout the year.

METHODOLOGY

Permafrost investigations in North America have been concerned primarily with measurement of subsurface temperatures and changes in temperature distribution and with determination of ice content and structure. The questions whether the rock or soil is completely frozen and what influence perennially and seasonally frozen layers have on availability and movement of groundwater have, until recently, received only secondary consideration. Answers to these questions are, however, of great importance to the hydrogeologist. Development of methods and instrumentation for investigation of these problems is therefore receiving increasing attention.

As pointed out earlier, a perennial temperature below 0 °C need not imply that the water content of the rock or soil is even partially frozen. Elevated pressure, presence of dissolved solids in the groundwater, and the presence of appreciable percentages of some clay minerals in the porous medium will depress the freezing point and delay freezing of available liquid water until the temperature falls well below 0 °C.³ In such cases, the boundaries of the temperature-

defined permafrost do not coincide with those of frozen ground, and frost gages, of either the visual or electrical type, must be used to determine the extent of frozen ground. As described in the Soviet literature,⁶⁵ repeated installation and removal of visual frost gages disturbs the temperature field, and the current used by the electrical type heats the ground, especially when used for continuous recording.

Refinement is possible through use of soil-moisture cells^{33,37} that contain pairs of fiber glass-wrapped screen electrodes that measure changes in electrical conductivity caused by changes in liquid-water content of the surrounding medium. Each cell contains a thermistor for temperature measurement. In unfrozen, water-saturated material, the electrical resistance of the cells is mainly a function of groundwater salinity; in unfrozen, nonsaturated material, the resistance of the cells depends on the moisture content. When the material starts to freeze, the decreasing liquid-water content leads to a rapidly increasing resistance with decreasing temperature. Calibrations are necessary for each cell in combination with the material in which it is to be installed for a number of different temperatures and water contents, because response of the cells depends on moisture characteristics of the porous medium, on chemical composition of the water, and on the prevailing temperature. Development and dissipation of the frost layer at the experimental site at Calgary, Alberta, has been successfully observed with soil-moisture cells.³³

If free liquid water is present in permafrost or in seasonally freezing or thawing layers above and below permafrost, measurement of pressures in the liquid phase is of interest to detect transient hydraulic gradients that govern movement of the free groundwater. For this purpose, observation wells or piezometers often can be used, with or without continuous recorders. Antifreeze solutions can be used in the wells to prevent freezing of liquid adjacent to permafrost or the seasonally frozen layer. Problems include loss of antifreeze by evaporation and leakage into the ground when static level is below the top of the well or piezometer intake, the need to determine the changing position of the water-antifreeze interface, and the need to detect the moment of freezing of the aquifer. The use of piezometers in current studies in Alaska is discussed in two of the following papers.^{18,57}

An alternative method to measure pressures makes use of electrical, hydraulic, or pneumatic pressure transducers. These should be selected carefully to enable accurate measurement of small changes in liquid pressure and to survive the high pressures that may develop in the liquid phase during freezing of the surrounding ground. Contact between the transducer diaphragm and any solid material should be prevented by installation of the transducer in a pressure-resistant housing, allowing only liquid pressure to be transmitted to the diaphragm through small openings in the housing, via a noncom-

pressible nonfreezing liquid.⁶⁰ In undersaturated ground, the pressure registered will be equal to or below atmospheric, regardless of whether the ground is frozen or not. In saturated nonfrozen ground, positive pressures will be registered; during freezing, the liquid pressure may increase initially and then drop gradually as temperature decreases further; the reverse will occur during warming and subsequent thawing. A need exists for a relatively inexpensive method for measuring transient pressures in the transient liquid-water phase in the zone of seasonal freezing and thawing. These pressures have a significant influence on the stability of natural and man-made surfaces during freezing and thawing. Standard pressure transducers are too expensive for this type of application, because of the probability that they will be damaged or destroyed by freezing pressures or slope failure.

Borehole geophysical logging methods were tested in 1968 in holes drilled in permafrost in Isabella Creek valley near Fairbanks, Alaska [7, 8]. Natural gamma, gamma-gamma, neutron, resistivity, and caliper logs made in these holes showed that valid geophysical logs can be made in frozen, unconsolidated deposits and that interpretation is possible in terms of bulk density, organic content, moisture content, temperature, rates of freezing, resistivity of interstitial ice and water, location of ice segregations, and, possibly, migration of water during freezing and thawing. Equipment problems and poor condition of the holes affected the results, and the experimental work has not been continued. Since 1968, multielectrode equipment for quantitative resistivity measurements and an acoustic-velocity system have become available for use in boreholes [8].

In both Alaska and Canada controlled aquifer tests generally have not been justified because of availability of abundant supplies to satisfy the small demand and because of little concern over problems of well interference and aquifer depletion. Completed wells are normally given only a short aquifer test to provide information for selection of proper pump capacity.

The only known controlled aquifer tests were made on wells in alluvial deposits at Fairbanks, Alaska.²³ The tests show that alluvium can yield as much as $0.315 \text{ m}^3/\text{s}$ to a screened well 61 cm in diameter penetrating only part of the subpermafrost aquifer. Another test showed that transmissivity of the alluvium was about $9\,900 \text{ m}^3/\text{m}\cdot\text{day}$.²³ A sharp break in the plot of drawdown against time indicated an impermeable boundary that resulted from either textural changes within the alluvium²³ or the contact between unfrozen and frozen alluvium.⁷²

Tritium analyses of groundwater have been used to determine the number of years elapsed between infiltration and discharge of groundwater in the Canadian northwest.¹² Values generally were of the order of 30 ± 10 years. Velocity calculations have not been attempted, because the length of the flow systems involved was unknown.

STUDIES OF BASIN HYDROLOGY

The earliest study in which the groundwater flow system was treated as an integral part of the hydrologic system in individual basins was that of Brandon¹² in northwestern Canada. Estimates were made of the influence of mineralized groundwater on the quality of streams and of the contribution of groundwater discharge to stream flow. Estimates of groundwater storage in basins in the permafrost region require more exact knowledge of the geology and the distribution of permafrost than is now available, as well as stream-flow records covering longer periods for a greater variety of drainage basins. Existing stream-flow records in Alaska suggest that the minimum mean monthly discharge in winter is very close to zero in the continuous-permafrost zone where groundwater discharge during the winter is stored in icings. It ranges from about 0.002 to $0.005 \text{ m}^3/\text{km}^2$ in the discontinuous-permafrost zone; values exceeding $0.005 \text{ m}^3/\text{km}^2$ are characteristic of streams fed in winter by discharge from large lakes.

The hydrologic study of the basin of Delta River,²⁸ a southern tributary of the Tanana River rising in the high glacier-clad peaks of the Alaska Range, is one in which modern methods of hydrology have been applied. Results include information on flow regimen and water balance. The water balance contains figures for average surface flow of $61 \text{ m}^3/\text{s}$ and average groundwater discharge of $28 \text{ m}^3/\text{s}$. The budget includes runoff generated by net ablation of the glaciers in the Alaska Range.^{4,28}

Two small basins in the Yukon-Tanana upland, a part of the Tanana River basin, have been selected for detailed hydrologic studies,^{25,26,56} results of which are given in papers that follow.^{18,27} Study of the summer hydrology of the Glenn Creek basin did not reveal contribution to stream flow by groundwater from beneath the permafrost.²⁵⁻²⁷ The University of Alaska's Institute of Water Resources, CRREL, and other agencies are participating in studies of the Caribou-Poker creek drainage basins about 40 km north of Fairbanks, Alaska.^{18,46,56}

Hydrologic studies during four summers of a small, drained thaw-lake basin 8 km northeast of Barrow on the Arctic Coastal Plain did not include groundwater discharge, because the basin is underlain by thick, continuous permafrost at a depth of about 0.3 m.¹¹

INVESTIGATIONS FOR PIPELINE PROJECTS

The need for engineering and environmental-impact evaluations of proposed pipeline routes by which oil and gas from northern Alaska and northern Canada will be carried to market has generated extensive research in hydrogeology, ecology, and permafrost.

The proposed 789-mile trans-Alaska pipeline, which

would carry oil at about 77 °C to tidewater at Valdez, is to be buried only where foundation material is bedrock, permeable sand or gravel, or where permafrost is absent. Records of 1 700 borings along the proposed pipeline route, results of test drilling at four sites in the Brooks Range, and simple mathematical models, referred to later in this report,⁵⁹ were used to determine whether quick conditions would result from artesian pressures in alluvium between the seasonal frost and impermeable beds or permafrost beneath streams. Results of these studies and of measurements of icing pressures in the Goldstream and Caribou-Poker creek drainage basins¹⁸ indicated that occurrence of quick conditions is unlikely in the coarse material in which the pipeline is to be buried. In the only case identified by the model in which quick conditions could occur, the pipe was assumed to be buried in fine sand overlying highly permeable coarse sand and gravel. Once their potential occurrence is recognized from test-boring data, quick conditions may be avoided in this type of situation by backfilling of the trench with coarse gravel. If icing mounds develop near the pipeline, their destructive potential can be eliminated by relief of pressure if recognized early enough.

In 1971, a program was initiated to evaluate groundwater and permafrost conditions in the Mackenzie Valley transportation corridor in Canada as part of the studies of environmental impact of proposed road, railroad, and pipeline development. Hydrogeological studies are aimed at identifying principal regions of groundwater recharge and discharge and at determining regional groundwater flow patterns and rates of groundwater movement. A reconnaissance hydrogeologic study based on aerial photographic interpretation has been completed,⁵¹ and instrumentation for study of heat and water transfer has been installed in drill holes near Norman Wells and Inuvik, Northwest Territories, in late 1971. Few data on thickness and areal distribution of permafrost are available in this part of Canada, and analyses of the hydrogeology and flow systems that take into account the role of permafrost are only just starting.

HYDROLOGIC MODEL STUDIES

Hydrologic basin studies have led to the development of models that enable assessment of the relative influence of basin characteristics and hydrologic parameters on the individual components of the hydrologic cycle. The Institute of Water Resources, University of Alaska, is developing a conceptual watershed model of the Caribou-Poker creek basin¹⁷ that takes into account surface runoff, infiltration, channel storage, precipitation, evapotranspiration, and some groundwater parameters. Its output was compared with the total runoff measured during the summer of 1971. All parameters, except soil-moisture storage and groundwater

storage, operated as expected. The two storage factors increased dramatically from the thirtieth day of operation to the end of the season. Further work is being done to improve the model. Modifications may be necessary or additional measurements of the storage components may be required to verify the increase in storage. To date, subsurface data that would show the effect of permafrost on the groundwater flow system and on recharge of groundwater have not been available for this basin.

A snowmelt runoff model has been developed by the Institute of Water Resources for the Alaskan Arctic Coastal Plain.¹⁹ After tests run on data for Putuligayuk River for 1971, the model is being improved by addition of a delay factor in the snowmelt process, delineation of surface and channel storage, and provision for channel delay.

A physically based mathematical model describing the simultaneous transport of heat and water in frozen porous materials has been developed^{35,36} by the Hydrology Research Division, Canada Department of the Environment, for analysis of freezing-affected soil-water redistribution and infiltration to frozen soil. Both diffusive and viscous types of flow and their interactions with the temperature field are taken into account; the partially frozen medium can be in continuity with either saturated or unsaturated nonfrozen material. The physical basis for the model is the analogy between the mechanisms of water transport in unsaturated porous media and in partially frozen porous media.³⁶ Thermal effects that result from transport of heat by moving groundwater in permafrost terrain and the effects of surface disturbances on the configuration of upper and lower boundaries of the permafrost will be the subject of further development of this model. Test data for verification of model results are provided by experimental sites at Calgary, Alberta,³³ and near Ottawa, Ontario, as well as by observation sites recently established near Norman Wells and near Inuvik, Northwest Territories, as part of the study of groundwater and permafrost conditions in the Mackenzie Valley transportation corridor.

Simple mathematical models using finite difference approximations for equations of steady flow have been used⁵⁹ to test the probability of induced icings along buried segments of the proposed trans-Alaska pipeline. They are also used to determine whether the pressures developed beneath the seasonal frost layer would be great enough to produce quick conditions in streambed alluvium at proposed pipeline crossings.

RESEARCH NEEDS

Both theoretical and field investigations are needed to improve understanding and knowledge of groundwater hydrology and hydrogeology in permafrost regions in general.

Recommendations for further studies are listed here without regard to priority:

1. Application of the theory of irreversible thermodynamics to the problems of coupled flow of energy (heat) and mass (water and salts) in porous media subject to freezing temperatures in order to promote fuller understanding of the interaction between frozen ground and moving groundwater

2. Investigation of the effects of seasonal and long-term changes in thermal regime on the distribution of permafrost and on the groundwater regime

3. Study of the development of transient pressures in the liquid phase during freezing and thawing of near-surface layers and their effects on the stability of natural and man-made slopes, for example, failure by slumping resulting from excessive pressure buildup behind frozen surface layers and failure by "piping" due to accelerated discharge

4. Study of the development of transient pressures in riverbed alluvium and the decrease of available discharge area during freezing and their possible effect on the stability of riverbed material and on the formation of icings

5. Investigation of the influence of low temperatures, permafrost barriers, and seasonal freezing and thawing of aquifers on groundwater chemistry

6. Expanded studies of large springs, for example, in Brooks Range and British Mountains, to determine recharge areas and seasonal changes in discharge rates, temperature, and chemistry; associated icings formed downstream should be investigated to obtain a measure of groundwater discharge rates during the winter season and of contributions to stream flow during the following thawing season

7. Continued integrated study of drainage basins, using drilling and geophysical methods, to determine subsurface conditions and further development of physically based mathematical models to arrive at quantitative assessments of recharge, storage, and discharge of groundwater, and seasonality of base flow; comparison of winter stream flows in various drainage basins of similar geology could provide a measure of the relative extent of permafrost

8. Studies of regional hydrogeochemistry and influence of groundwater chemistry on the quality of surface waters

9. Study of the hydrology of open-system pingos and the mechanisms of their formation

10. Study of the economic potential of thermal waters as a source of energy

If these investigations are to be successful, they will require:

11. Further development of surface geophysical methods to define the permafrost configuration and to delineate the boundaries for groundwater flow

12. Further development of airborne or satellite remote-sensing techniques, including black-and-white and color

photography, as well as infrared sensing, to delineate major groundwater discharge areas on the basis of temperature contrasts between groundwater and surface water, snow, or ice; these methods may assist in locating the groundwater source for large icings along rivers, if applied in both summer and winter, and in delineating shallow permafrost features

13. Development of relatively low-priced instrumentation (sensors) for determining phase (liquid or solid), pressure, and groundwater chemistry in porous media subject to freezing

ACKNOWLEDGMENTS

Information on current research is acknowledged in the notes to this chapter; information was provided by D. A. Morris, C. E. Sloan, and C. R. Zenone, U.S. Geological Survey, Anchorage, Alaska; by P. V. Sellmann, U.S. Army Cold Regions Research and Engineering Laboratory, Hanover, New Hampshire; S. L. Dingman, DuBois & King Engineers, Randolph, Vermont; R. F. Carlson, University of Alaska Institute of Water Resources, College and by colleagues in the U.S. Geological Survey, Geological Survey of Canada, and Canada Department of the Environment. Sections of the report have been reviewed by C. E. Sloan and D. A. Morris of the U.S. Geological Survey and by R. L. Harlan of the Hydrology Research Division, Department of the Environment, Ottawa, Ontario. Publication authorized by the Director, U.S. Geological Survey and by Inland Waters Directorate; Environment Canada.

REFERENCES

1. Alaska District, Water Resources Division. 1969. Hydrological observations, Fairbanks to Prudhoe Bay and other arctic slope areas, May, 1969. U.S. Geol. Surv. open-file Rep.
2. Alaska District, Water Resources Division. 1969. Water resources of the arctic slope region, preliminary report. U.S. Geol. Surv. open-file Rep. 31 p.
3. Anderson, D. M., and P. Hoekstra. 1965. Crystallization of clay-adsorbed water. *Science* 49:318-319.
4. Anderson, G. S. 1970. Hydrologic reconnaissance of the Tanana Basin, central Alaska. U.S. Geol. Surv. Hydrol. Inv. Atlas HA 319.
5. Arnborg, L., H. J. Walker, and J. Peippo. 1966. Water discharge in the Colville River, 1962. *Geogr. Ann.* 48A:195-210.
6. Barnes, I. 1970. Metamorphic waters from the Pacific tectonic belt of the west coast of the United States. *Science* 168:974-975.
7. Beschel, R. E. 1963. Sulphur springs at Gypsum Hill. Preliminary Report, 1961-62. Axel Heiberg Island Res. Rep. McGill University, Montreal. p. 183-187.
8. Black, R. F. 1958. Permafrost, water-supply, and engineering geology of Point Spencer spit, Seward Peninsula, Alaska. *Arctic* 11(2):102-116.
9. Black, R. F., and W. L. Barksdale. 1948. Terrain and permafrost, Umiat area, Alaska. U.S. Geol. Surv. Permafrost Program Prog. Rep. 5. Engineer Intelligence Div., Office, Chief of Engineers, U.S. Army. 23 p.
10. Blount, C. W. 1965. The solubility of anhydrite in the systems CaSO_4 - H_2O and CaSO_4 - NaCl - H_2O and its geologic significance. PhD thesis. University of California, Los Angeles. 179 p. Univ. Microfilms, Inc., Ann Arbor. 65-15182.
11. Brown, J., S. L. Dingman, and R. I. Lewellen. 1968. Hydrology of a drainage basin on the Alaskan coastal plain. Res. Rep. 240.

- U.S. Army Cold Regions Research and Engineering Laboratory, Hanover, New Hampshire. 18 p.
12. Brandon, L. V. 1965. Groundwater hydrology and water supply in the District of Mackenzie, Yukon Territory, and adjoining parts of British Columbia. *Can. Geol. Surv. Paper* 64-39, Ottawa. 102 p.
 13. Brandon, L. V. 1966. Evidences of ground-water flow in permafrost regions, p. 176-177. *In* Permafrost: Proceedings of an international conference. National Academy of Sciences, Washington, D.C.
 14. Broadwell, J. A. 1945. How CAA engineers meet construction problems north of the Arctic Circle. *Pac. Build. Eng.* 51(4): 55-56.
 15. Carey, K. L. 1970. Icing occurrence, control, and prevention—an annotated bibliography. U.S. Army, CRREL Spec. Rep. 151. 59 p.
 16. Carey, K. L. Icings developed from surface water and ground water. U.S. Army CRREL Cold Regions Science and Eng. Monogr. III-D3. (In preparation)
 17. Carlson, R. F. 1972. Development of a conceptual model for a subarctic watershed. *Publ. IWR-28*. University of Alaska Institute of Water Resources, College. 58 p.
 18. Carlson, R. F., D. L. Kane, and C. E. Bowers. Groundwater movement adjacent to subarctic streams. This volume.
 19. Carlson, R. F., W. Norton, and R. Britch. Modeling snowmelt runoff in an Arctic coastal basin. *In* Proceedings of a symposium on properties and processes. *Int. Symp. Role Snow Ice Hydrol. Banff, Canada, Sept. 6-20, 1972.* (In press)
 20. Cederstrom, D. J. 1961. Ground-water hydrology in Alaska, p. 1014-1019. *In* *Geology of the Arctic*. Vol. 2. University of Toronto Press, Toronto, Ontario.
 21. Cederstrom, D. J. 1961. Origin of a salt-water lens in permafrost at Kotzebue, Alaska. *Geol. Soc. Am. Bull.* 72:1427-1432.
 22. Cederstrom, D. J. 1952. Summary of ground-water development in Alaska, 1950. *U.S. Geol. Surv. Circ.* 169. 37 p.
 23. Cederstrom, D. J. 1963. Ground-water resources of the Fairbanks area, Alaska. *U.S. Geol. Surv. Water-Supply Paper* 1590. 84 p.
 24. Cederstrom, D. J., P. M. Johnston, and S. Subitzky. 1953. Occurrence and development of ground water in permafrost regions. *U.S. Geol. Surv. Circ.* 275. 30 p.
 25. Dingman, S. L. 1966. Characteristics of summer runoff from a small watershed in central Alaska. *Water Resour. Res.* 2(4): 751-754.
 26. Dingman, S. L. 1971. Hydrology of the Glenn Creek watershed, Tanana River basin, central Alaska. *U.S. Army CRREL Res. Rep.* 297. 112 p.
 27. Dingman, S. L. Effects of permafrost on stream-flow characteristics in the discontinuous permafrost zone of central Alaska. This volume.
 28. Dingman, S. L., and others. 1971. Hydrologic reconnaissance of the Delta River and its drainage basin, Alaska. *U.S. Army CRREL Res. Rep.* 262. 83 p.
 29. Feulner, A. J., J. M. Childers, and V. W. Norman. 1971. Water resources of Alaska. *U.S. Geol. Surv. open-file rep.* 60 p.
 30. Feulner, A. J., and R. G. Schupp. 1963. Seasonal changes in the chemical quality of shallow ground water in northwestern Alaska. *U.S. Geol. Surv. Prof. Paper* 475-B. p. B189-B191.
 31. Feulner, A. J., and R. G. Schupp. 1964. Temperature and chemical quality of water from a well drilled through permafrost near Bethel, Alaska. *U.S. Geol. Surv. Prof. Paper* 501-D. p. D144-D147.
 32. Feulner, A. J., and J. R. Williams. 1967. Development of a groundwater supply at Cape Lisburne, Alaska, by modification of the thermal regime of permafrost. *U.S. Geol. Surv. Prof. Paper* 575-B. p. B199-B202.
 33. Freeze, R. A., and J. A. Banner. 1970. An instrumented experimental site for the investigation of soil moisture, frost, and groundwater recharge. *Tech. Bull.* 21. Canada Dept. Environment, Inland Waters Branch, Ottawa. 29 p.
 34. Grantz, A., D. E. White, H. C. Whitehead, and A. R. Tagg. 1962. Saline springs, Copper River lowland, Alaska. *Am. Assoc. Pet. Geol. Bull.* 46(11):1990-2002.
 35. Harlan, R. L. 1971. Water transport in frozen and partially frozen porous media. *Proc. 8th Can. Hydrol. Symp. Runoff Snow Ice* 1:109-129.
 36. Harlan, R. L. Ground conditioning and the groundwater response to winter conditions. *In* Proceedings of a symp. on properties and processes, *Int. Symp. Role Snow Ice Hydrol. Banff, Sept. 6-13, 1972.* (In press)
 37. Harlan, R. L., J. A. Banner, and R. A. Freeze. 1971. Interpretation of electric-resistance soil moisture data for a freeze-thaw environment. *Can. J. Soil Sci.* 51:249-259.
 38. Hitchon, B., A. A. Levinson, and S. W. Reeder. 1969. Regional variations of river water composition resulting from halite solution, Mackenzie River drainage basin, Canada. *Water Resour. Res.* 5(6):1395-1403.
 39. Hoekstra, P. 1966. Moisture movement in soils under temperature gradients with the cold side temperature below freezing. *Water Resour. Res.* 2(2):241-250.
 40. Hoekstra, P. 1967. Moisture movement to a freezing front. *IUGG, General Assembly Bern. Proc. Geochem. Precip. Evap. Soil Moisture Hydrom.* p. 411-417.
 41. Hoekstra, P., and E. Chamberlain. 1964. Electro-osmosis in frozen soil. *Nature* 203:1406-1407.
 42. Holmes, G. W., D. M. Hopkins, and H. L. Foster. 1968. Pingos in central Alaska. *U.S. Geol. Surv. Bull.* 1241-H. 40 p.
 43. Hopkins, D. M., T. N. V. Karlstrom, and others. 1955. Permafrost and ground water in Alaska. *U.S. Geol. Surv. Prof. Paper* 264-F. p. 113-146.
 44. Howitt, F. 1971. Permafrost geology at Prudhoe Bay. *World Pet.* Sept.:28.
 45. Hughes, O. L. 1969. Distribution of open-system pingos in central Yukon Territory with respect to glacial limits. *Can. Geol. Surv. Paper* 69-34. 8 p.
 46. Kane, D. L., and C. W. Slaughter. Seasonal regime and hydrological significance of stream icings in Central Alaska. *In* Proceedings of a symposium on properties and processes. *Int. Symp. Role Snow Ice Hydrol. Banff, Canada, Sept. 6-20, 1972.* (In press)
 47. Kim, S. W., P. R. Johnson, and R. S. Murphy. 1969. A ground water quality summary for Alaska. *Publ. IWR-10*. University of Alaska Institute of Water Resources, College. 32 p.
 48. Linell, K. A. Risk of uncontrolled flow from wells through permafrost. This volume.
 49. Low, P. F., D. M. Anderson, and P. Hoekstra. 1968. Some thermodynamic relationships for soils at or below the freezing point: 1. Freezing point depression and heat capacity. *Water Resour. Res.* 4:379-394.
 50. Low, P. F., P. Hoekstra, and D. M. Anderson. 1968. Some thermodynamic relationships for soils at or below the freezing point: 2. Effects of temperature and pressure on unfrozen soil water. *Water Resour. Res.* 4:541-544.
 51. Mollard, J. D., and Associates. 1972. Reconnaissance study of hydrogeology of the Mackenzie Valley region. Unpublished report to Canada Dept. Environment, Inland Waters Branch.
 52. Muller, S. W. 1947. Permafrost or perennially frozen ground and related engineering problems. *Edwards Brothers, Ann Arbor, Michigan.* 230 p.
 53. Petrov, V. G. 1934. An attempt at ascertaining the pressure of

- ground water in icing mounds (Opyt opredeleniia silyi davleniia gruntovhky vod v nalediakh). Akad. Nauk. SSSR Kom. Izuch. Vech. Merzloty Tr. 3:59-72.
54. Piper, A. M. 1966. Potential effects of Project Chariot on local water supplies, northwestern Alaska. U.S. Geol. Surv. Prof. Paper 539. 45 p.
 55. Sherman, R. G. A groundwater supply for an oil camp near Prudhoe Bay, Arctic Alaska. This volume.
 56. Slaughter, C. W. 1971. Caribou-Poker creek research watershed, interior Alaska, background and current status. Spec. Rep. 157. U.S. Army CRREL, Hanover, New Hampshire. 11 p.
 57. Slaughter, C. W., and D. L. Kane. Lake and subpermafrost groundwater interaction in a permafrost environment, central Alaska. This volume.
 58. Sloan, C. E. 1972. Water-resources reconnaissance of Anaktuvuk Pass, Alaska. U.S. Geol. Surv. open-file rep. 11 p.
 59. Sloan, C. E., and J. D. Bredehoeft. 1972. Some effects of a heated pipeline on ground-water flow in Alaska. U.S. Geol. Surv. open-file rep. 25 p.
 60. Slusarchuk, W. A., G. H. Watson, and T. L. Speer. 1972. Instrumentation around a warm oil pipeline buried in permafrost. Paper prepared for presentation at 25th Can. Geotech. Conf., Ottawa, Dec. 7-8, 1972.
 61. Theis, C. V. 1944. Thermal processes related to the formation of permafrost. U.S. Geol. Surv. open-file rep. 36 p.
 62. Tremaine, M. [ed.]. 1953 *et seq.* Arctic bibliography. Vol. 1-15. Arctic Institute of North America, Washington, D.C.
 63. Tyrrell, J. B. 1903. A peculiar artesian well in the Klondike. Eng. Mining J. 75:188.
 64. U.S. Army. 1951. *et seq.* Bibliography on snow, ice and permafrost, with abstracts. Vol. 1-24. U.S. Army CRREL Rep. 12.
 65. V. A. Obruchev Institute of Permafrost Studies. 1961. Long-term geocryological investigations. Part III of Permafrost Investigations in the Field. Academy of Sciences of the U.S.S.R. (National Research Council of Canada Tech. Transl. No. 1358, Ottawa. p. 89-113)
 66. Walker, H. J. The nature of the seawater-freshwater interface during breakup in the Colville River Delta, Alaska. This volume.
 67. Waller, R. M. 1962. Winter hydrology of a small Arctic stream, p. 134-136. *In* Proceedings 12th Alaskan science conference, 1961. College, Alaska. (Abstr.)
 68. Waring, G. A. 1917. Mineral springs of Alaska, with a chapter on the chemical character of some surface waters of Alaska by R. B. Dolc and A. A. Chambers. U.S. Geol. Surv. Water-Supply Paper 418. 114 p.
 69. Weeks, J. B. 1970. Water-resources reconnaissance of the Golovin area, Alaska. U.S. Geol. Surv. open-file rep. 10 p.
 70. Williams, J. R. 1965. Ground water in permafrost regions—An annotated bibliography. U.S. Geol. Surv. Water-Supply Paper 1792. 294 p.
 71. Williams, J. R. 1970. A review of water resources of the Umiat area, northern Alaska. U.S. Geol. Surv. Circ. 636. 8 p.
 72. Williams, J. R. 1970. Ground water in the permafrost regions of Alaska. U.S. Geol. Surv. Prof. Paper 696. 83 p.
 73. Williams, J. R., and R. M. Waller, 1966. Ground water occurrence in permafrost regions of Alaska, p. 159-164. *In* Permafrost: Proceedings of an international conference. National Academy of Sciences, Washington, D.C.

NOTES

- [1] C. E. Sloan, U.S. Geological Survey, Anchorage, Alaska, written communication, August 31, 1972.
- [2] L. V. Brandon, Department of Indian Affairs and Northern Development, Whitehorse, Yukon, written communication, January 1972.
- [3] C. E. Sloan, written communication, December 1971.
- [4] C. E. Sloan, written communication, May 26, 1972.
- [5] O. L. Hughes, Geological Survey of Canada, oral communication, August 1972.
- [6] A. Lissey, Brock University, St. Catharines, Ontario, written communication, June 20, 1972; based on work during 1968 and 1969, terminated before complete results were obtained.
- [7] W. S. Keys, July 16, 1968, "Geophysical logging in permafrost, Fairbanks, Alaska, a feasibility study." Unpublished Tech. Mem. 24, U.S. Geological Survey, Denver, Colorado.
- [8] W. S. Keys, written communication, May 3, 1972.

EFFECTS OF PERMAFROST ON STREAM FLOW CHARACTERISTICS IN THE DISCONTINUOUS PERMAFROST ZONE OF CENTRAL ALASKA

S. Lawrence Dingman

DUBOIS & KING, INC.
Randolph, Vermont

INTRODUCTION

In the Arctic and Subarctic, rational management of water resources is of special importance, due to generally low precipitation, the perennially frozen state of much of the groundwater, and the long periods during which surface water bodies are frozen. Furthermore, the detailed understanding of hydrologic processes that must form a basis for such management is limited. Thus, the objective of this study was an understanding of the hydrologic behavior of a small watershed typical of a significant portion of the discontinuous permafrost zone of the Alaskan subarctic and of the role of permafrost in influencing that behavior.

DESCRIPTION OF AREA

The watershed of Glenn Creek, 13 km NNE of Fairbanks, Alaska (Figure 1), was selected for study on the basis of its size, accessibility, lack of human disturbance, and apparent representativeness. Glenn Creek is about 1.7 km long and

flows toward the northwest. The watershed is 1.8 km² in area, ranges in elevation from 257 to 494 m MSL, and appears typical of the lower elevations of the Yukon-Tanana Uplands physiographic province in regard to its geology, soils, permafrost conditions, vegetations, and climate.³ Average slope is 0.184. The area is underlain by micaceous quartzite, with a 0-15-m-thick mantle of eolian and residual silts intermixed with gravel. Soils are well to poorly drained silt loams, and permafrost beneath a 0.3-1.0-m seasonal thaw zone is present throughout 68.5 percent of the watershed (Table I, Figure 2). Vegetation patterns are closely related to the distribution of permafrost: A white spruce-birch forest is restricted to the permafrost-free areas, while most of the rest of the area has a forest of spindly black spruce with a thick (0.15-0.30 m) moss ground cover. An area adjacent to the channel has bare ground with sedge tussocks and willow bushes (Table I, Figure 2). The normal monthly and annual precipitation and temperature at a nearby station is given in Table II. The thaw season averages 176 days (mid-April to mid-October), with an average temperature of 10.5 °C and an average precipitation of 230 mm.

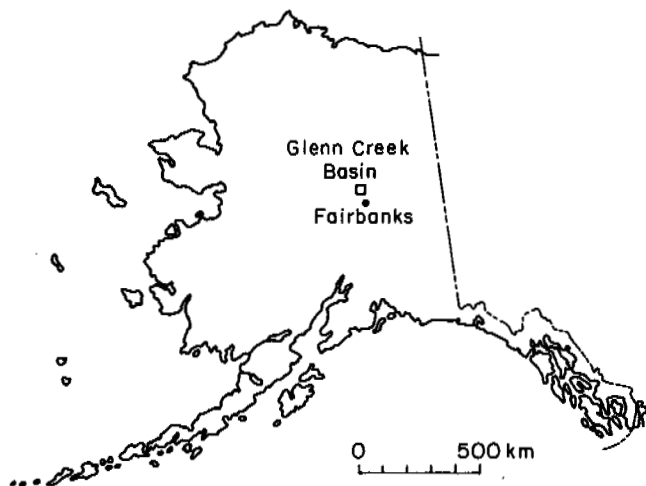


FIGURE 1 Map of Alaska, showing location of Glenn Creek drainage basin.

TABLE I Areal Distribution of Vegetation Types and Permafrost in Glenn Creek Watershed

Vegetation Type	Permafrost?	Area (km ²)	Area (%)
1. black spruce-moss	yes	0.855	47.1
1a. black spruce-birch-moss	yes	0.047	2.5
1b. open-moss	yes	0.029	1.6
2. birch-white spruce-duff and moss	no	0.544	30.0
3. birch-duff and moss	yes	0.171	9.4
3a. aspen-duff and moss	no	0.021	1.2
3b. open-duff and moss	no	0.005	0.3
4. alder-bare	yes	0.003	0.2
5. willow-sedge-bare	yes	0.021	1.1
6. black spruce-willow-sedge-bare	yes	0.119	6.6
TOTAL		1.815	100.0

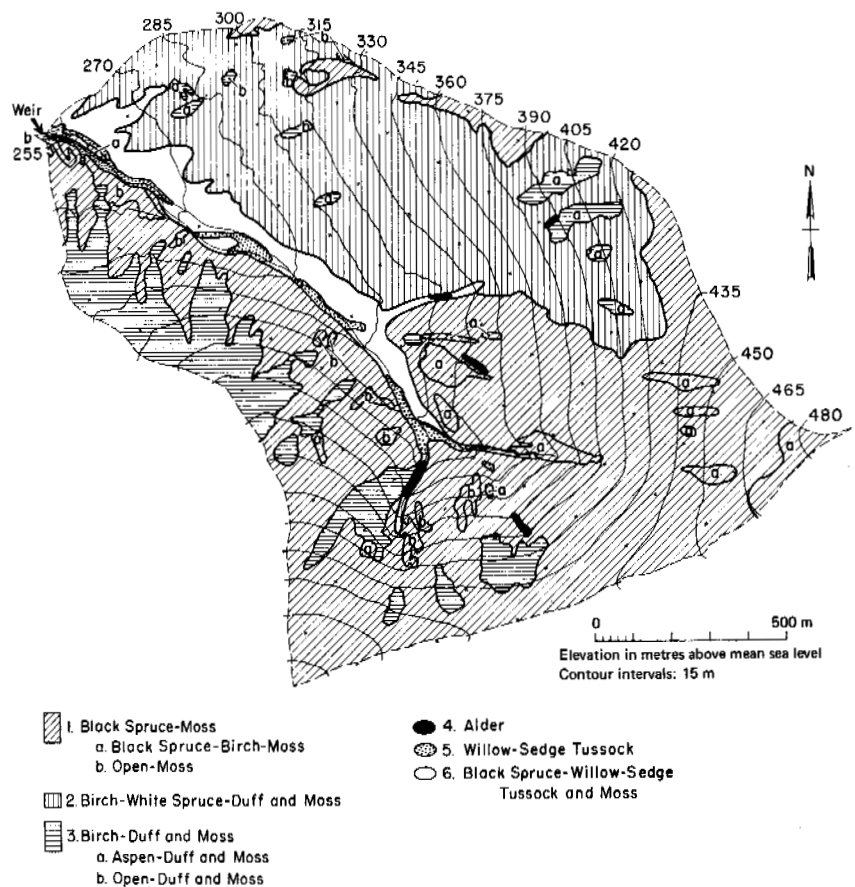


FIGURE 2 Vegetation map of Glenn Creek watershed.

METHODS OF MEASUREMENT

The study was carried out during the thaw seasons from 1964 to 1967; 1964 was near average in regard to temperature and precipitation, 1965 was the coolest thaw season of the previous 30 years, 1966 was the driest, and 1967 was

the second wettest. Stream flow was measured approximately daily with a current meter in 1964 and recorded using a V-notch weir in subsequent years. Precipitation was recorded in a standard shielded weighing gage near the watershed outlet.

TABLE II Normal Monthly Precipitation and Temperature at University Experiment Station, 16 km SW of Glenn Creek

Month	Temperature (°C)	Precipitation (mm)
January	-21.8	21
February	-17.3	13
March	-10.8	11
April	-0.7	6
May	8.3	20
June	14.8	38
July	15.4	53
August	12.6	62
September	6.9	35
October	-2.5	24
November	-14.3	16
December	-21.1	14
ANNUAL	-2.6	313

STREAM FLOW CHARACTERISTICS

Introduction

Determination of stream flow characteristics in response to rainfall requires a method for identifying the runoff from a particular storm. Some judgment is required in this; in the present case, it was found that the recessions of isolated hydrographs approximated exponential decay, and this characteristic was used in extending hydrographs from one storm when stream flow was occurring from subsequent storms. To minimize errors, however, only those stream flow rises during which flow from previous storms was minor were selected for analysis.

RAINFALL-RUNOFF RELATIONS

Table III shows monthly rainfall and runoff for the 1964 (near average) and 1966 (very dry) thaw seasons. (Data are

TABLE III Monthly Rainfall and Runoff, Glenn Creek Watershed, 1964 and 1966

Year and Month	Rainfall (mm)	Runoff (mm)	Rainfall Minus Runoff (mm)
1964			
June	62	10	52
July	74	10	64
August	95	23	72
September	17	15	2
October	7	3	4
TOTAL	255	61	194
1966			
June	54	15	39
July	31	1	30
August	29	0	29
TOTAL	114	16	98

incomplete for 1965 and 1967.) Based on these figures and the fact that about 100 mm of water is present as snow when snowmelt begins,³ it appears that the annual runoff in the area is about 150 mm, or about 50 percent of the average precipitation. The value of 150 mm for evapotranspiration may be compared with estimated Thornthwaite's actual and potential evapotranspiration data of 300 mm and 465 mm, respectively.³ Similar discrepancies have been noted by others in subarctic areas and attributed to the fact that mosses and lichens are not vascular plants and do not transpire.^{8,9,13}

For 16 individual storms, runoff:rainfall ratios ranged from 0.03 to 0.42 and averaged 0.18. Most significantly, this ratio was highly correlated with antecedent discharge (discharge just before the stream rise) (Figure 3), indicating that, the wetter the watershed, the higher the percentage of rainfall running off.

Point Design.	Date
A	22 Jun '64
B	10 Jul '64
C	28 Jul '64
D	3 Aug '64
E	15 Aug '64
F	30 Aug '64
G	5 Sep '65
H	6 Jul '66
I	9 Jul '66
J	7 Jul '67
K	8 Aug '67
L	19 Jul '67
M	21 Jul '67
N	23 Jul '67

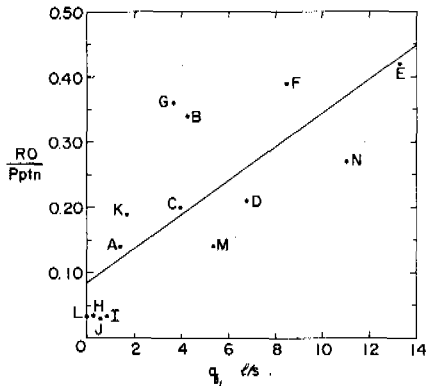


FIGURE 3 Relation between runoff/precipitation fraction RO/P_{pntn} and antecedent discharge q_1 for 14 storms in Glenn Creek Basin (1 litre = $10^{-3} m^3$).

Stream Response

In most cases, stream flow began to increase within an hour or two after the beginning of a rain of intensity greater than 0.5 mm/h. In some storms, there was a rather immediate change in the rate of stream flow increase in response to changes in rainfall intensity in the early stages of stream flow rise (Figure 4). However, immediately following an extended (7-day) period of zero stream flow, the response time was as much as 13 h. A regression analysis revealed that response time was not significantly related ($\alpha = 0.05$) to antecedent stream flow for 27 storms, indicating that, except when the basin is extremely dry, stream response time is independent of watershed wetness.

The peak stream flow generally occurred within 1 or 2 h after cessation of rain. Regression analysis indicated a highly significant correlation ($r = 0.96$) between storm duration (t_s) and duration of stream flow rise (t_p), as well as that $t_p = t_s$ at the 0.05 significance level.

Stream Flow Recessions

Stream flow recessions could generally be modeled as exponential decay curves,

$$q = q_p \exp(-t/t^*), \tag{1}$$

where q is stream flow rate at t h after peak, q_p is peak stream flow, and t^* is a decay constant (h). In spite of the generally quick response of stream flow to rainfall, stream flow recessions were very slow, with t^* averaging 39 h (22 h/km^2) and ranging from 19.6 to 76.9 h ($10.9\text{--}42.4 \text{ h/km}^2$). This may be compared with the values given by

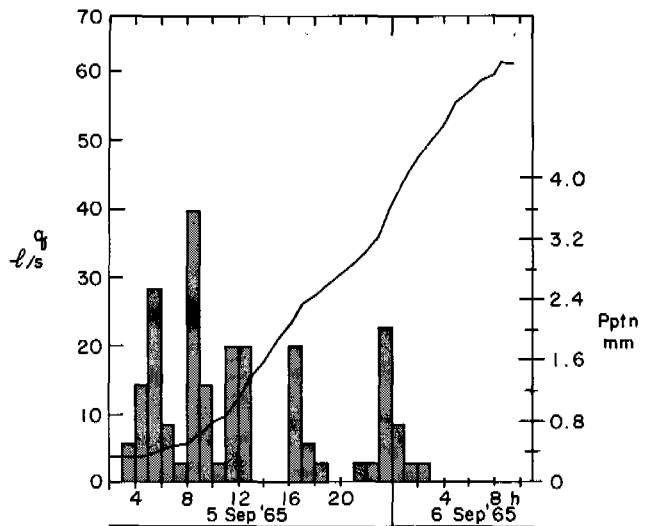


FIGURE 4 Rainfall and stream flow, Glenn Creek, 5-6 September 1965 (1 litre = $10^{-3} m^3$).

Holtan and Overton⁵ for 40 streams in the conterminous United States that range from 0.005 to 0.32 h/km². Glenn Creek clearly has a very large decay constant (t^*) for a watershed of its size.

Several investigations studying summer runoff in the Arctic and Subarctic have noted extended stream flow recessions. In his review of arctic hydrology, Straub¹² remarked on "abnormally long" recessions during which a large part of the runoff occurs. He stated that "infiltration into a surface layer of high absorptive capacity seems a plausible explanation."¹² Likes⁶ offered the same explanation for the behavior of a stream draining a 98 km² area in northwestern Alaska, where t^* was about 35 h (0.36 h/km²). The most extended recessions were reported by Brown *et al.*² for a 1.6 km² basin at Barrow, Alaska. Here, t^* was equivalent to 25 to 100 h/km². This basin had extremely low relief, with numerous small ponds, and these features were suggested as the reason for the slow recessions. Data of McCann and Cogley⁷ indicate that $t^* = 2.2$ h/km² for a 2.3 km² watershed on Devon Island, in the Canadian Arctic Archipelago.

In addition to the magnitude of t^* at Glenn Creek, its fourfold variation from storm to storm is noteworthy. There are indications that this variation is largely related to the rate of evapotranspiration during the recession. During a recession, the water-balance equation for a watershed is:

$$\frac{dV}{dt} + q + E = 0, \quad (2)$$

where V is volume of water stored in the basin, t is time, q is stream flow, and E is evapotranspiration. If q is directly proportional to V , then

$$q = (q_0 + E) \exp(-t/t^*) - E. \quad (3)$$

Figure 5 shows the effect of E on a hypothetical recession using typical values from Glenn Creek in Eq. (3). If $E > 0$, the recession is no longer a simple exponential; in the early stages (the first 20 h or so) of the recession, however, the curve does not deviate greatly from a straight line on a semi-logarithmic plot, and an "apparent" t^* can be determined for this period. Figure 6 shows this apparent t^* as a function of E for the data in Figure 5. Clearly, a fourfold variation of apparent t^* can arise from variations of E in the range found in Glenn Creek. Figure 7 shows plotted values of t^* versus panevaporation rate (an index of E) for seven recessions in Glenn Creek. There is reason to believe that the value of E shown for 22-23 July 1967 is too low.³ Thus, even though the periods for which average panevaporation rate can be determined do not coincide exactly with the recession periods, there is observational, as well as theoretical, evidence that the variation in t^* is largely caused by

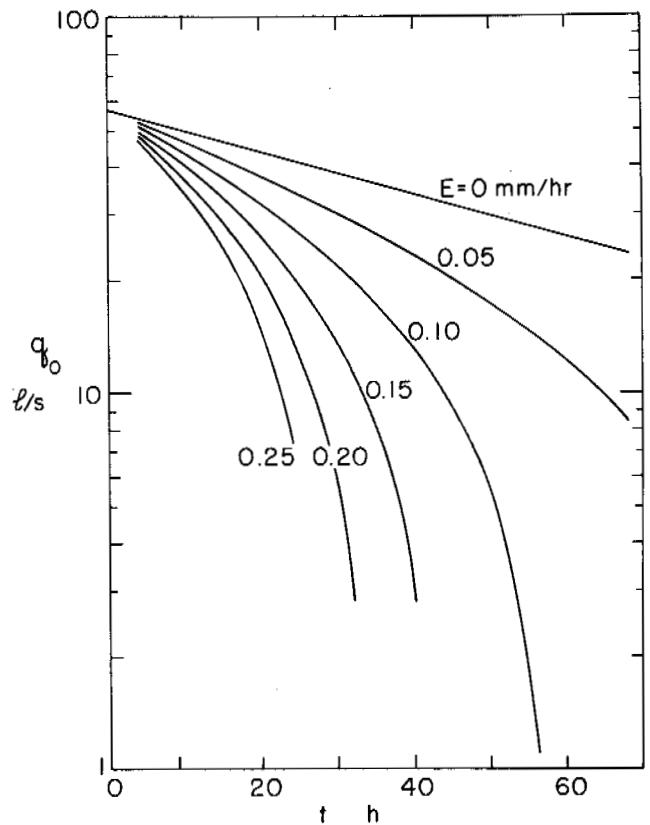


FIGURE 5 Theoretical effects of evapotranspiration rate E on recession $t^* = 77$ h, $q_0 = 0.057$ m³/s (1 litre = 10⁻³ m³).

variations in E . This leads to the suggestion that the exceptionally large values of t^* reported for arctic and subarctic watersheds are at least partially due to the low values of E in such regions compared with temperate watersheds. It is likely that vegetative cover (moss), topography, and drainage conditions also contribute to the observed differences, but the relative importance of all these factors remains to be determined.

RUNOFF SOURCES

Figure 8 illustrates schematically the physical conditions affecting runoff in Glenn Creek watershed. We can consider these as "boundary conditions" in attempting to determine the sources of stream flow that could give rise to the observed hydrograph characteristics.

Channel precipitation obviously contributes to stream flow and could conceivably contribute to the fast response to rainfall. However, the surface area of Glenn Creek is only about 0.2 percent of the total basin area, while the lowest runoff:rainfall ratio observed was more than 10 times as large (Figure 3). It can also be shown that, even if all channel precipitation occurs during the rise, it accounts for only a few percent of prepeak runoff.

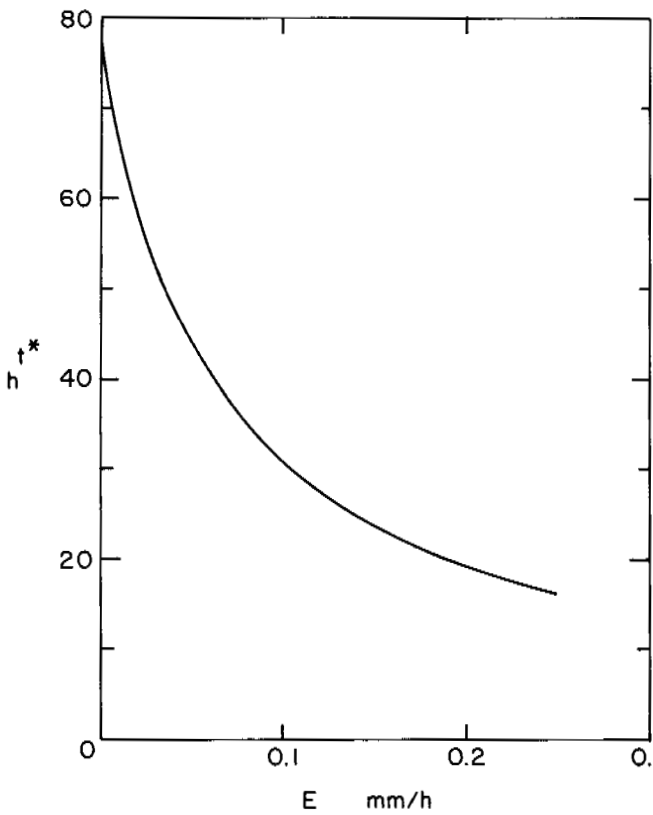


FIGURE 6 Theoretical effects of evapotranspiration rate E on apparent recession constant t^* , $q_0 = 0.057 \text{ m}^3/\text{s}$.

It is extremely unlikely that overland flow occurs on the 92.3 percent of the watershed that has continuous vegetative ground cover (Table I, Figure 2). The vertical permeability of the moss in the basin has been measured at 2.18 mm/s ,³ obviously greater than any conceivable precipitation rate. While surface infiltration rates for the areas with a duff

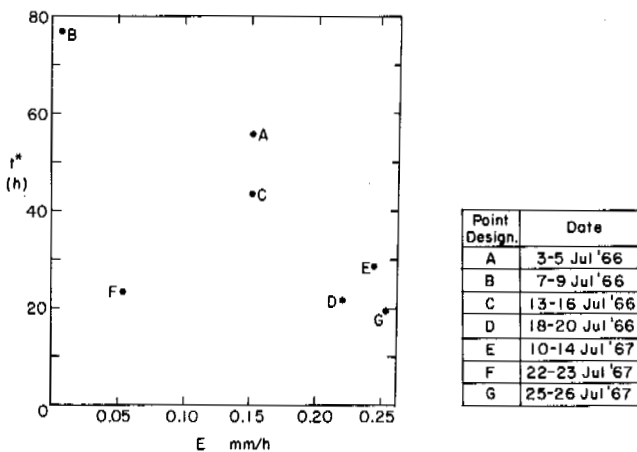


FIGURE 7 Measured recession constant t^* for 7 storms versus average class-A panevaporation rate E at Glenn Creek.

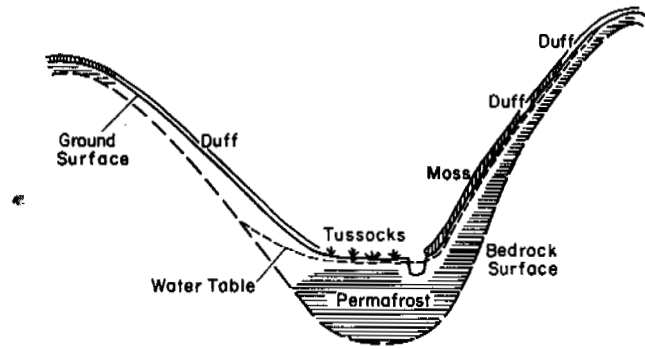


FIGURE 8 Schematic diagram, showing ground cover, water table, permafrost, and bedrock in a typical cross section of Glenn Creek watershed.

ground cover were not measured, the area was carefully examined immediately following the extraordinarily heavy and prolonged rains of mid-August 1967, and no evidence of overland flow (eroded channels, accumulations of leaves, twigs, and grasses indicating flow) was found. However, the valley bottom area (vegetation types 5 and 6), where there is no continuous ground cover and where the water table is near or above the ground surface, is a probable source of overland flow. Standing and flowing water was repeatedly observed in depressions and between tussocks in this area.

The hydrographic characteristics of fast response to initiation of rainfall and to rainfall intensity changes for all conditions of watershed wetness, except for extremely dry conditions, as well as the fact that rainfall runoff is a function of watershed wetness, all add further support to the conclusion that the valley bottom area is a significant source of runoff. These hydrographic features are consistent with a variable source area for runoff, similar to that suggested by Betson¹ and elaborated by Freeze.⁴ This mechanism is inferred to operate in the following way (Figure 9): When the watershed is relatively dry (Figure 9a), the water table in the valley bottom (vegetation types 5 and 6) is relatively low and intersects the ground surface in only a few places. These places are more common near the stream channel. Under wet conditions (Figure 9b), the water table intersects the ground over a wider portion of the valley bottom. When rain begins, overland flow to the channel begins almost immediately under both conditions, through the network of water-filled depressions. Under wet conditions, however, more of the rain falls on water standing or flowing at the surface, and less is lost in infiltration and filling detention storage. Thus, a higher percentage of rainfall runs off under wet conditions than under dry conditions, but stream flow responds rapidly to rainfall under both conditions. With extremely dry conditions (Figure 9c), the ground water table is well below the

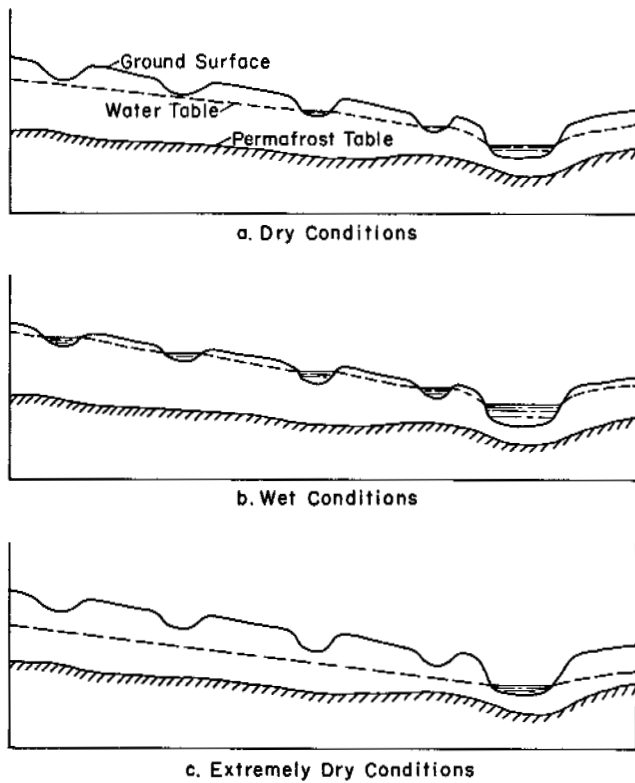


FIGURE 9 Diagram illustrating the concept of variable source area in the valley bottom of Glenn Creek watershed.

ground surface virtually everywhere, and a long period of rain is required before the stream responds.

The extremely slow recessions of Glenn Creek must be due to another runoff source. Figure 10 shows that the stream is less than a meter above the permafrost, so that it has only a very limited connection with saturated unfrozen soil. Further, the soils under the valley bottom and the north-facing slope are relatively impermeable¹⁰ and have only thin active layers. Thus direct groundwater contributions to runoff are probably minor. It has been suggested¹¹ that the thawing active layer is a significant contributor to stream flow where permafrost is present. The flow of Glenn Creek, with almost 70 percent of its watershed underlain by

permafrost, should manifest this source if it exists. However, stream flow virtually ceased for periods of several days in July and August 1966 and July 1967, following extended rainless periods, strongly suggesting that water released by thawing does not contribute to stream flow.

Thus, it appears that the principal source of delayed flow to Glenn Creek is from the moss-covered, north-facing slopes. This arises from rainfall that infiltrates the moss and flows downslope over the underlying mineral soil. As noted above, the moss is highly permeable, and, since mosses do not transpire (and since the evaporative demand on the north-facing slopes is small compared with south-facing slopes³), a relatively large fraction of the rain falling on this area probably runs off. While this has not been firmly established as a source, water was observed to be flowing in submoss channels 2 weeks after the record rains of 8-12 August 1967.

SUMMARY

The hydrographic characteristics and other observations of the physical nature of Glenn Creek watershed strongly suggest two principal sources of runoff. There is rapid runoff due to overland flow (but not Hortonian overland flow) that originates in a source area of variable size in the valley bottom; the size of the source area depends on antecedent conditions. This gives rise to almost immediate runoff when rain begins and to a close correspondence between concurrent rainfall intensities and stream flow rates. When rain ceases, this source rapidly depletes, but stream flow continues for several days as water that has infiltrated the moss on the north side of the watershed flows to the stream over the impermeable mineral soil. If evapotranspiration rates are high, this delayed source is depleted relatively rapidly, and recessions are correspondingly attenuated.

Thus, the presence of permafrost in the watershed of Glenn Creek is a major influence on the behavior of the stream, but this influence is rather indirect. Its most important roles are in supporting a high water table beneath the valley bottom area, so that overland flow derived from standing water in this area dominates the hydrograph rise and peak; restricting groundwater flow to the stream; and,

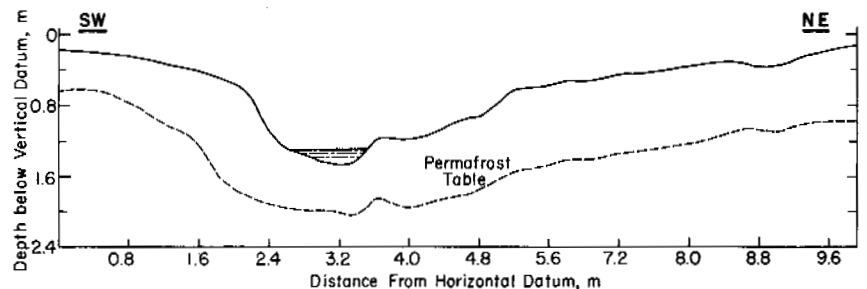


FIGURE 10 Cross section of Glenn Creek at the weir site, showing depth of permafrost, 24 August 1964.

providing an impermeable surface beneath the moss on the north-facing slopes, over which water infiltrating the moss flows to the stream to dominate the hydrographic recession.

ACKNOWLEDGMENT

The major portion of the work reported in this paper was done while the author was employed at the U.S. Army Cold Regions Research and Engineering Laboratory.

REFERENCES

1. Betson, R. 1964. What is watershed runoff? *J. Geophys. Res.* 69:1541-1551.
2. Brown, J., S. L. Dingman, and R. I. Lewellen. 1968. Hydrology of a drainage basin on the Alaskan Coastal Plain. Research Report 240. U.S. Army Cold Regions Research and Engineering Laboratory, Hanover, New Hampshire.
3. Dingman, S. L. 1971. Hydrology of the Glenn Creek watershed, Tanana River Basin, central Alaska. Research Report 297. U.S. Army Cold Regions Research and Engineering Laboratory, Hanover, New Hampshire.
4. Freeze, R. A. 1972. Role of subsurface flow in generating surface runoff: 2. Upstream source areas. *Water Resour. Res.* 8:1272-1283.
5. Holtan, H. N., and D. E. Overton. 1963. Analyses and applications of simple hydrographs. *J. Hydrol.* 1:250-264.
6. Likes, E. H. 1966. Surface-water discharge of Ogoturuk Creek, p. 125-131. *In* Environment of the Cape Thompson region, Alaska. U.S. Atomic Energy Commission, Oak Ridge, Tennessee.
7. McCann, S. B., and J. G. Cogley. 1972. Hydrological observations on a small arctic catchment, Devon Island. *Can. J. Earth Sci.* 9:361-365.
8. Nebiker, W. A. 1957. Evapotranspiration studies at Knob Lake, June-September 1956. McGill University Arctic Meteorological Research Group Publication in Meteorology No. 11.
9. Nebiker, W. A., and S. Orvig. 1958. Evaporation and transpiration from an open lichen woodland surface. International Association of Scientific Hydrology Publication No. 45. p. 379-384.
10. Ricger, S., J. A. Dement, and D. Sanders. 1963. Soil survey of the Fairbanks area, Alaska. U.S. Soil Conservation Service Series 1959, No. 25.
11. Sommer, A., and E. S. Spence. 1968. Some runoff patterns in a permafrost area of northern Canada. *Albertan Geogr.* No. 4, p. 669-676.
12. Straub, L. G. 1950. Arctic and sub-arctic hydrology. *In* V. Stefansson [ed.] *Encyclopedia Arctica*. Vol. 1, Part 1. Unpublished Ms. Stefansson Library, Dartmouth College, Hanover, New Hampshire.
13. Watts, D., J. H. Galloway, and A. Grenier. 1960. Evapotranspiration studies at Knob Lake in the Summers of 1957, 1958, and 1959. McGill University Arctic Meteorology Research Group Publication in Meteorology No. 22.

GROUNDWATER PORE PRESSURES ADJACENT TO SUBARCTIC STREAMS

Douglas L. Kane and Robert F. Carlson

UNIVERSITY OF ALASKA
Fairbanks, Alaska

C. Edward Bowers

UNIVERSITY OF MINNESOTA
Minneapolis, Minnesota

INTRODUCTION

Groundwater aquifers adjacent to subarctic streams form an important, but poorly understood, component of permafrost hydrology. They actively participate in the mechanism of aufeis formation, constitute an important unfrozen, near-surface aquifer in a permafrost region, form a possible connection for interchange with subpermafrost water, and interact with the stream flow as a storage and release mechanism. In regions of continuous permafrost, water from these aquifers may be the sole source of water throughout the winter. Because of numerous hydrologic boundary conditions, interaction with the stream, and contribution to

aufeis formation in the adjacent stream channel, the flow processes in these aquifers are very complex and ill defined.

Accelerated resource development in arctic regions has led to a renewed interest in groundwater adjacent to subarctic streams, particularly as it affects the mechanism of aufeis growth. Aufeis growth throughout the winter indicates continual flow either as subsurface flow, channel flow, or both. An understanding of the movement of water adjacent to subarctic streams is a prerequisite to understanding aufeis growth.

The primary focus of this study is to measure groundwater pore pressure and to understand its change in time and space in these stream aquifers. Impermeable boundaries

of the aquifer along a stream are numerous and complex owing to the presence of permafrost, seasonal frost, and afeis. Because of the existence of continuous winter flow, it is usually assumed that subpermafrost groundwater is discharged into the streams through unfrozen openings in the permafrost. Generally, the stream aquifer is underlain with permafrost, and the depth of the unfrozen zone is determined by the water temperature, volume of flow, and the geologic material.

As with any groundwater stream system, direct measurement of the exchange of water between the stream and the subjacent aquifer in a permafrost region is nearly impossible. Nevertheless, measurement of pore water pressure within the aquifer gives a good indication of direction of flow and a fair estimate of flow rate and volume of water exchanged.

This paper describes the exploratory phase of a program of measurement of pore water pressure and boundary conditions in the vicinity of two subarctic streams in a permafrost-dominated environment. The continuing phases of the study will expand the measurement of pore water pressure and hydraulic boundary conditions and will begin an analysis of water movement between the stream and the groundwater zone.

PREVIOUS STUDIES

The study of groundwater and its relationship with permafrost has long attracted investigators. In 1955 Hopkins *et al.*² completed one of the first comprehensive evaluations of groundwater in Alaska as it relates to permafrost. Cederstrom¹ has reported on the domestic wells in the Fairbanks, Alaska, area, including geological material penetrated, depth of well, presence of permafrost, and water quality. From these well data, he was able to define possible groundwater flow systems. Kane and Slaughter³ have also shown that small lakes in the Fairbanks area are discharge points for subpermafrost groundwater. Recent work by Williams^{6,7} and Williams and van Everdingen⁸ represents an exhaustive effort to update knowledge of groundwater and permafrost relationships.

DESCRIPTION OF STUDY SITES

The two streams selected for study are Goldstream Creek, 10 km from Fairbanks, and a tributary of Caribou-Poker Creeks, 50 km from Fairbanks (Figure 1). The drainage area above the Goldstream study site is 191 km², with a recorded minimum summer flow of approximately 0.5 m³/s. The tributary of Caribou-Poker creeks has only a small drainage area and a channel length of 250 m with the suspended source of late fall and winter flow being subpermafrost groundwater springs at the head of the channel. The average winter flow from these springs has been recorded as

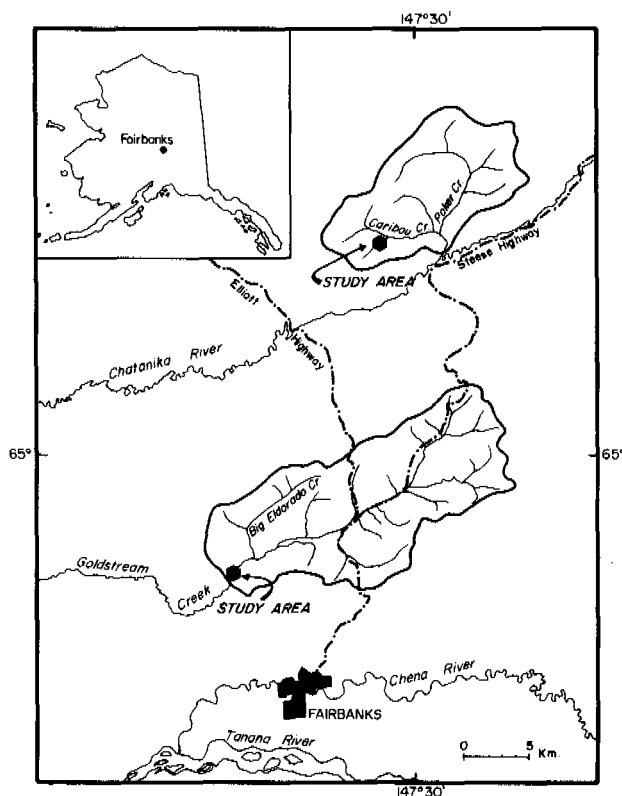


FIGURE 1 Location map of study sites on Caribou-Poker creeks and Goldstream Creek.

approximately 3.0×10^{-3} m³/s. Permafrost at both sites is assumed discontinuous with thicknesses greater than 70 m as is found elsewhere in the Fairbanks area.

A depression of the upper permafrost surface beneath and adjacent to the stream is possible because of the warming effect of the stream. The top surface of permafrost was measured to be at a depth beneath the stream of 5 m or more at the Goldstream site and 1-2 m at the Caribou-Poker site. At a cross section of newly installed piezometers on Goldstream Creek, the depth of permafrost was 4.3 m below the ground surface at 40 m from the centerline of the stream. Depending on the type of vegetation, the active layer ranges between 40 and 60 cm in this area.

Soils along both streams are a mixture of sand and silt. Where sand is dominant, the soil is well drained, and the unfrozen zone adjacent to the stream is more extensive. The unfrozen zone is more restricted where silt is dominant, resulting in less interchange of water between the stream and groundwater systems. Geology in the valley bottoms of this area consists of perennially frozen silts of eolian origin with some partially decomposed organic material. Alluvium in the flood plain adjacent to the stream is common. The major bedrock unit is schist with a highly weathered contact with the above surficial material.

STUDY PROCEDURES

Piezometers were installed to measure the groundwater pore pressure in the vicinity of the stream channel at several points at each study site within a few meters of the stream. The measured pore pressure for 1 year at one location at Goldstream Creek is shown in Figure 2.

The piezometers were constructed with a stainless steel drivepoint connected to galvanized pipe with a 3.2-cm i.d. There were hand driven to a depth of approximately 1 m below the stream bottom. Pipes heaving and water freezing in the piezometer pipes were a problem in the winter. Level surveys were run periodically to monitor movement of the pipes for appropriate corrections. An antifreeze solution of methyl alcohol and ethylene glycol was used to help prevent freezing.⁴ Since the temperature of the water in the wells is very close to 0 °C, an antifreeze with a density slightly less than 1 g/cm³ will approach the density of the water present with further dilution. Some piezometers were equipped with continuous water-level recorders; the water levels in the rest were periodically read by observers.

The upper boundary surface for the stream groundwater system consists of aufeis in the channel and seasonal frost in the soil system. The increase in thickness of the aufeis in the channel from the onset of freezeup until the spring breakup is shown in Figure 2. Variation in the elevation of the upper aufeis surface was checked by survey from an established bench mark. The only measurement of the bottom elevation of the ice was made on 17 March 1972. The ice thickness was measured at a 50-cm spacing across the stream with a steam drill. The lower surface of the ice penetrated to the stream bottom at all points except in the stippled area (Figure 3).

The depth of seasonal frost was measured using frost-tubes⁵ in conjunction with probing. The seasonal frost limits as measured 3 m back from the stream bank are shown in Figure 4.

DISCUSSION OF RESULTS

For comparative reasons, pore water pressure data were also collected during the summer. As seen in Figure 2, the pore pressure measured in the wells fluctuated quite dynamically during the winter but showed very little fluctuation during the summer. Generally, in winter, a rise in the hydrostatic head was followed by a decline. The base period and peak value of each succeeding rise increased.

Before water can be released onto the aufeis surface, the hydrostatic head elevation must be greater than the aufeis surface elevation. The increased duration between the peaks may be caused by the decrease of water available to the stream. There would also be a decrease in available water at the point of measurement as a result of water going into storage as ice upstream.

The variation in pore pressure at Caribou-Poker creeks tributary was similar to that at Goldstream Creek; however, its fluctuations were much more rapid as shown by the pressure variation for a 1-week period in January 1972 (Figure 5). During this week, an absolute change of 210 cm occurred, although the net change was only 3 cm. The relatively more rapid succession of peaks and troughs are probably due to the constant source of subpermafrost water, short length of tributary, and smaller volume of the unfrozen zone along the stream. The maximum fluctuation on the Caribou-Poker creeks tributary during the winter was 1.25 m, while at Goldstream Creek this value exceeded 2 m.

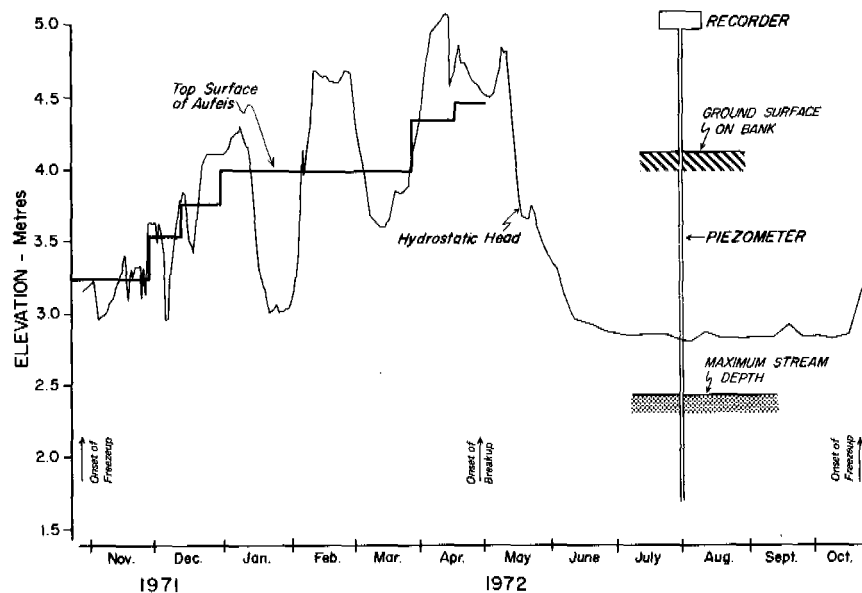


FIGURE 2 Hydrostatic head variation and aufeis accumulation for the period 1 November 1971 to 31 October 1972, Goldstream Creek.

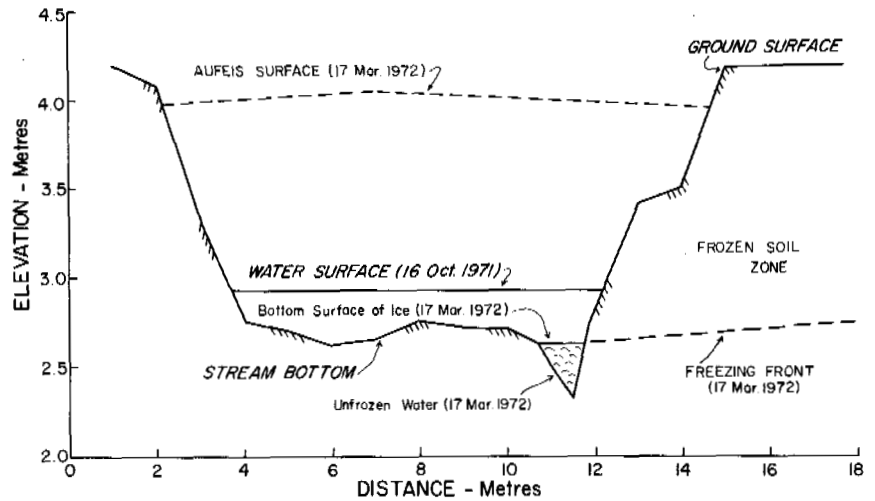


FIGURE 3 Cross section of Goldstream Creek, showing stream boundary conditions on 16 October 1971 and 17 March 1972 (4:1 vertical exaggeration).

The downward extension of seasonal frost (Figure 4) is accompanied by a general rise in the water table in the aquifer. When seasonal frost reaches the water table, the frozen ground forms an impermeable barrier that confines the groundwater. Also, the aufeis in the stream acts as the confining layer over the stream. With small increases in the volume of flow in the stream, large pressures can develop under the aufeis. These pressures gradually decrease away from the stream. Due to a lag that is directly related to the hydraulic conductivity of the soil in the stream aquifer, the water table may not be in contact with the seasonal frost boundary at points laterally removed from the stream bank.

The boundary conditions in the channel for 16 October 1972 (just prior to freezeup of the stream) and 17 March 1972 are shown in Figure 3. During the October measurement, there was no ice cover and the cross-sectional area was equal to 1.8 m². At the time of the March measurement, the freezing front had reached the bottom of the stream, except in the deeper portion of the channel. The

cross-sectional area of this unfrozen zone was calculated to be 0.2 m², a reduction greater than 90 percent of the cross-sectional area of open water on 16 October 1972.

A discharge of 1.04 m³/s was measured on 16 October 1972. No measurements of discharge in the channel could be made after the beginning of November, because of the accumulation of aufeis. Also, because of the high pressure that develops when the hydrostatic head is greater than the elevation of the aufeis surface, water will flow out of the access holes that are made for a current meter. On a small stream such disturbances would greatly affect the measured discharge. Ideally, discharge measurements during the winter should be made during a period of low pressure.

On 17 March 1972, the estimated discharge was less than 0.1 m³/s because of the decreased cross-sectional area of flow, a decrease in potential gradient, and an increase in wetted perimeter. Open channel flow will not exist when the water surface coincides with the lower ice surface. The stream water level was in contact with the bottom ice surface

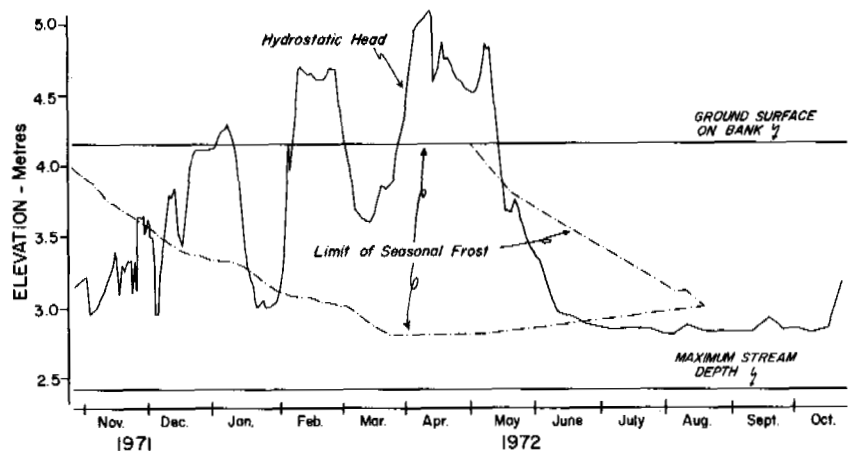


FIGURE 4 Hydrostatic head variation and the limits of seasonal frost for the period 1 November 1971 to 31 October 1972, Goldstream Creek.

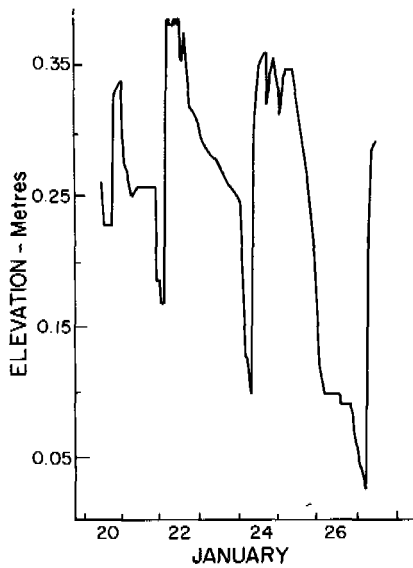


FIGURE 5 Variation in hydrostatic head from 20 January to 27 January 1972, Caribou-Poker creeks tributary.

throughout the winter from November to spring breakup (Figure 2).

Measurement of the potential gradient along the stream indicates that a greater change in potential gradient occurred when open channel conditions prevailed than during closed flow in the system. For example, in the 160 m between two wells at Goldstream Creek, the measured potential gradient of 0.0028 was typical of open channel flow conditions in the summer, while during closed system flow, this gradient often was measured to be 0.0005 or less.

Each peak in the measured piezometric head was accompanied by an increase in the aufeis thickness, with one exception in February. At this time, water did flow out through the cracks in the aufeis, but at a point downstream from the study site.

In conjunction with the changes in pore water pressure, vertical movement of the ground and ice surface has been observed. During the peak in February when no aufeis deposits occurred in the stream reach under study, the elevation of the aufeis in the center of the stream changed from 3.99 m on 4 February 1972 to 4.24 m on 26 February 1972. By 11 March 1972, the elevation of the aufeis had returned to 3.99 m. This 0.25 m change in elevation is caused by the change in pressure. The artesian aquifer with a very thin confining layer of 1-2 m will have the usual low coefficient of storage. Because of the shallow overburdens, large fluctuations in pressure may be expected in response to barometric loading, temperature expansion, and contraction of the overburden, snowfall, and aufeis in the adjacent stream.

During the initial phase, not enough piezometers were installed sufficiently far from the stream nor at various

depths to describe the flow that takes place adjacent to the stream. The program is being expanded to include more piezometers. The initial data indicate that the predominant exchange of water appears to be transverse to the stream, and to be quite unsteady. During periods of high pore pressure, the flow exchange is away from the stream and during periods of low pore pressure toward the stream. Thus, the total balance of bank storage actually increased during a winter season.

SUMMARY

Two distinct flow conditions exist in the subarctic streams. During the ice-free periods open channel flow occurs, and, when ice conditions exist (from late October to early May), closed conduit flow occurs.

During the summer, the flow conditions that exist in subarctic streams are not unusual or different from open channel flow of natural streams. During the winter months, however, very high pressures develop in the system (Figure 2), and the top surface of the water in the stream is usually in contact with a rigid lower ice surface that continually progresses downward. As a result of the high pressure, aufeis growth occurs that can fill the stream channel and extend onto the adjacent flood plain. In the soil system, the downward freezing of the seasonal frost forms an impermeable barrier when the freezing front coincides with the unfrozen water (Figure 4). The combination of the aufeis and the saturated seasonal frost zone acts as the thin overlying confining layer.

Movement of groundwater into the stream bank during the winter period results in a higher groundwater surface than exists during summer. By early June, this water is discharged into the stream when the open channel conditions again exist. If during the winter there is a net increase in bank storage along the entire stream, then the major source of stream flow is from subpermafrost groundwater. Both streams studied had extensive aufeis accumulations all along their lengths, indicating an increase in bank storage.

Movement of water down the stream channel decreases during the winter for two reasons. First, the quantity of water reaching the stream and adjacent aquifer from surface sources decreases during the winter because precipitation is being stored on the ground surface as snow. Second, a reduction in the cross-sectioned area of unfrozen water occurs in the channel as a result of downward freezing (Figure 3). This restriction of flow causes higher pressures in the stream that result in water flowing onto the surface. This water then freezes and is stored until spring breakup.

REFERENCES

1. Cederstrom, D. J. 1963. Ground-water resources of the Fairbanks area, Alaska. Water Supply Paper 1590. U.S. Geological Survey, Washington, D.C.

2. Hopkins, D. M., T. N. V. Karlstrom, and others. 1955. Permafrost and groundwater in Alaska. Professional Paper 264-F. U.S. Geological Survey, Washington, D.C.
3. Kane, D. L., and C. W. Slaughter. 1973. Recharge of a central Alaska lake by subpermafrost groundwater. This volume.
4. Mayo, L. R. 1972. Self-mixing antifreeze solution for precipitation gages. *J. Appl. Meteorol.* 11(2):400-404.
5. Rickard, W., and J. Brown. 1972. The performance of a frost-tube for the determination of soil freezing and thawing depths. *Soil Sci.* 113(2):149-154.
6. Williams, J. R. 1970. Ground water in permafrost regions—An annotated bibliography. Water Supply Paper 1792. U.S. Geological Survey, Washington, D.C.
7. Williams, J. R. 1970. Ground water in the permafrost regions of Alaska. Professional Paper 696. U.S. Geological Survey, Washington, D.C.
8. Williams, J. R., and R. O. van Everdingen. 1973. Groundwater Investigations in Permafrost Regions of North America. This volume.

RECHARGE OF A CENTRAL ALASKA LAKE BY SUBPERMAFROST GROUNDWATER

Douglas L. Kane

UNIVERSITY OF ALASKA
Fairbanks, Alaska

Charles W. Slaughter

U.S. ARMY COLD REGIONS RESEARCH AND
ENGINEERING LABORATORY
Hanover, New Hampshire

INTRODUCTION

Information on groundwater flow systems in permafrost-dominated environments is quite sparse. Review of the available literature as summarized by Williams^{10,11} indicates a dearth of quantitative data on permafrost-groundwater relationships, particularly in Alaska. Brandon¹ reports that the lack of subsurface data on permafrost has hindered the understanding of groundwater flow in permafrost environments.

Groundwater flow systems may be simply considered as comprising three components: recharge area, transmission zone, and discharge area. Typically, topographic highs constitute recharge areas, and low sites are discharge areas. Characteristics of the transmission zone, the area between recharge and discharge points, are largely determined by topography and geology.

In permafrost settings, all three components (recharge, transmission, and discharge zones) can be affected by presence of local or regional areas of frozen ground. Permafrost in the recharge area can act as a barrier to downward water movement, thus restricting aquifer recharge. The presence of permafrost can affect groundwater movement in the transmission zone. For suprapermafrost groundwater, the permafrost forms an impermeable base; for subpermafrost groundwater, the permafrost acts as an overlying confining bed and thus creates a confined aquifer. Wells that pene-

trate permafrost to the subpermafrost groundwater are commonly artesian. The presence of permafrost in discharge zones can similarly influence the groundwater movement and yield.

Presence of an unfrozen zone beneath small lakes has been reported by a number of workers.^{2,4,6,7} The presence or absence of a thawed zone linking lakes and subpermafrost aquifers has been only postulated to date.^{4,6}

OBJECTIVE

This study was undertaken to determine whether subpermafrost groundwater is a source of recharge of a small bog lake in a permafrost setting of central Alaska. This entailed determining whether the lake is underlain by frozen ground and the hydraulic potential varies with depth.

SETTING

The Isabella Creek bog lake, 0.02 km², is located in a low-lying valley, 3 km north of Fairbanks, Alaska (64°52'N, 147°40'W, elevation 145 m MSL) at the southern edge of the Yukon-Tanana Uplands physiographic province. The lake is about 90 percent covered by a floating peat mat. No surface inflow channels are evident either from ground examination or from vertical aerial photographs.

Soils in the immediate vicinity of the bog lake have been

mapped as permafrost-dominated Lemeta peat and Goldstream silt loam.⁸ The prevailing local geology consists of silt and peat-filled valley bottoms with uplands formed of Birch Creek schist.

Valley vegetation is dominated by black spruce (*Picea mariana*), intermingled with birch (*Betula papyrifera*), white spruce (*Picea glauca*), and tamarack (*Larix laricina*). Understorey species include lowbush cranberry (*Vaccinium vitis-idaea*), blueberry (*Vaccinium uliginosum*), Labrador tea (*Ledum groenlandicum*), associated willow species (*Salix* sp.), and a thick moss ground cover.

The lake is in the zone of discontinuous permafrost.⁸ Permafrost is generally present in valleys and on north-facing slopes and absent on south-facing slopes. In the immediate vicinity of the bog lake discussed here, well logs indicate that permafrost is present to a depth of 40–70 m, with an active layer in undisturbed settings as shallow as 0.2 m.^{4,8}

The Isabella bog lake was initially identified and proposed as a site for hydrogeologic investigations by Brown *et al.*³

PROCEDURES

The lake was first mapped in detail. Since the surface is almost completely covered by a floating mat of peat and vegetation, this entailed determining depth to the lake bottom and the peat mat thickness on a 20-m grid; the deepest point located in the lake was 4.5 m. The overlying peat-vegetation mat ranged from 1 to 2 m in thickness and in most places was strong enough to support a man's weight.

A simple and inexpensive way to determine whether permafrost underlies a lake is to install piezometers at varying depths to measure fluid potential. If a lake is entirely underlain by permafrost, there can be no vertical flow component, and the potential would not vary with depth; if a difference in potential exists with depth, flow must occur from zones of higher potential to zones of lower potential, and a thawed transmission zone beneath the lake would be indicated.

Near the deepest point of the lake, hydraulic and temperature observations were initiated. Four observation wells or piezometers, 32 mm in diameter, were driven into the bottom sediments to depths of 2.5, 4.0, 6.6, and 7.1 m beneath the lake floor (Figure 1). The pressure was measured through a screened opening that was 36 cm long and located at the bottom segment of the piezometer. To prevent freezing, these piezometers were charged with known amounts of oil; appropriate corrections were made in data for variations in density due to presence of this oil. Fluid level was measured relative to the top of each piezometer and was converted to a hydrostatic head measurement referenced to the lake water surface as a datum plane.

Depth of freezing in the peat mat was monitored by an array of seven frost tubes.⁹ A vertical array of thermocouples

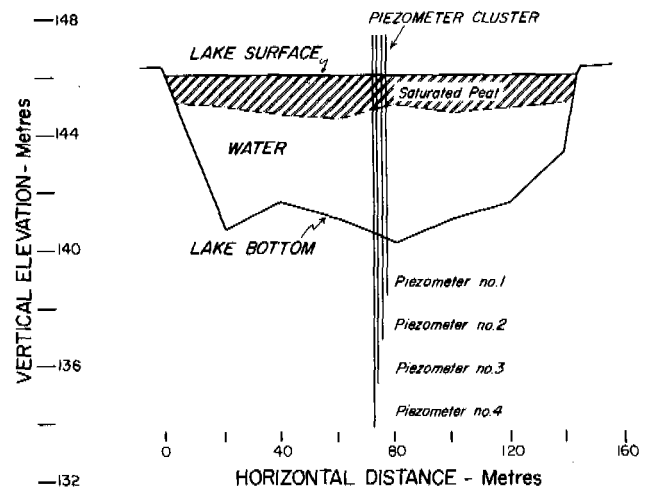


FIGURE 1 Cross section of Isabella Creek bog lake, showing the thickness of peat-vegetation, elevation of lake bottom, and the depth of piezometer installation.

was installed in the vicinity of the observation wells for temperature measurement. Thermocouples were located at seven points in the water, two points in the peat mat, one point in the lake sediments (bottom), and at two levels above ground surface. On one occasion a thermistor-tipped drive probe was utilized to determine the temperature gradient below the lake bottom.

RESULTS AND DISCUSSION

Data on the hydrostatic head as indicated by the piezometers are shown in Figure 2, where hydrostatic head is expressed as a head differential between the lake water surface and the fluid level in each piezometer (after correction for oil). These levels were measured at 3- to 4-day intervals during winter 1969–1970 and less frequently during summer 1970. These data are consistent for the period of record in showing an increase in fluid potential with depth beneath the lake bottom. Such an increase with depth indicates that water is moving from deeper zones (higher potential) to shallow zones (lower potential). Such movement would not be possible if the lake were completely underlain by permafrost; thus there does exist an unfrozen conduit, extending down to a subpermafrost aquifer.

Surface water level of the lake was measured during summer 1970; variations in level were less than 10 mm during the observation period. Precipitation averaged 1.8 mm/day throughout the same period.

As indicated previously, there was no evident surface inflow to the lake. An outflow point was located near the southwest corner of the lake through a grass and sedge covered swale in the dominant black spruce cover. Probing showed that the depth to permafrost in the swale was as

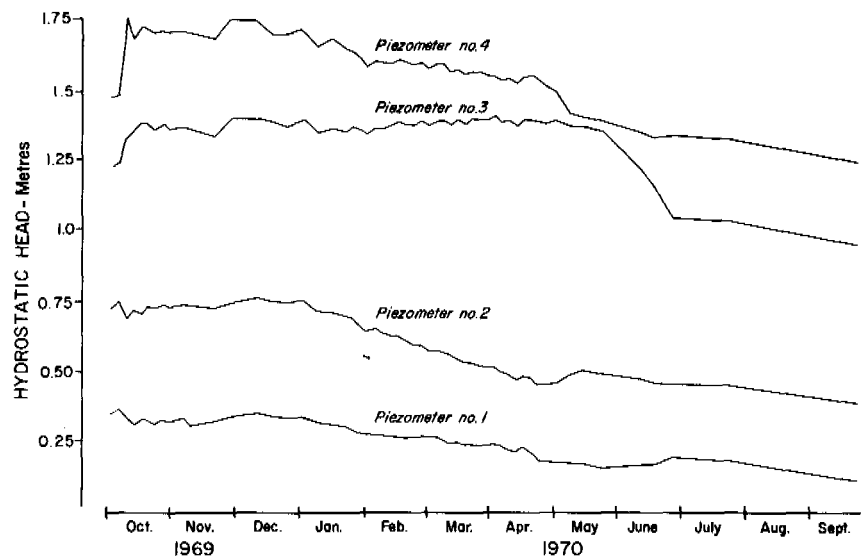


FIGURE 2 Variation of hydrostatic head with time as referenced to the lake water surface.

much as 2½ m over a width of 5–8 m. During the winter, aufeis deposits developed along this “channel,” giving evidence of groundwater movement along the course in the unfrozen zone between the seasonal frost and the permafrost.

A shallow temperature profile beneath the bottom of the lake (Figure 3) was obtained on 25 July 1969, utilizing a thermistor-tipped drive probe. Temperature measurements (throughout the year) by thermocouples yielded similar results, the only exception occurring in the top 1 m of the lake. These data show a gradual increase in temperature with depth, supporting the existence of a completely thawed zone connecting the lake with subpermafrost aquifers.

Water temperatures at the shallowest depth monitored beneath the bottom of the floating peat mat reached a minimum temperature of 0.5 °C and a maximum temperature of 1.1 °C. Higher water temperatures were observed at the deepest point, ranging from 1.3 to 1.8 °C. Since water at these latter temperatures is more dense than the cooler upper water and both are of less than maximum density (which occurs at approximately 4 °C), warming from the surface of the lake is inferred to not occur because the surface water is cooler and less dense than the bottom water.

Air temperature during the study period varied from –46 to 24 °C. Maximum depth of freezing of the floating (and saturated) peat-vegetation mat averaged 0.95 m; thus the main body of water at depth did not freeze, even during the long subarctic winter. Presence of the peat-vegetation mat over 90 percent of the lake surface precludes mechanical mixing of lake waters; thus the warmer water at deeper levels reflects higher temperatures below the lake bottom. Williams¹¹ reports that the average groundwater temperature in the Fairbanks area is near 1.7 °C, which is near the upper temperature range measured at the bottom of the lake. These

data tend to confirm the conclusion drawn from the piezometer data—that water flows into the lake from below.

Short-term fluctuations in hydrostatic head at each depth were measured (Figure 2). These fluctuations are attributed primarily to variations in barometric pressure. The data over the short period of study do not indicate any seasonal or yearly cycles in recharge of the aquifer. Rather, a gradually decreasing potential is indicated. This same trend was observed in a nearby well in 1950–1955 by Cederstrom.⁴ During the 5-year period of this study, the level in this well experienced a net drop of 1.8 m. There were short periods in early spring during which the well would recover some of the hydrostatic head loss.

In Figure 2, it can also be noted that the values of hydrostatic head converge for piezometers 3 and 4. This convergence could be caused by changes in the flow pattern in the vicinity of piezometer 3. It is more likely due to vertical movement of that piezometer relative to the others. It is suggested that, when the lake was covered with ice, the pressure within the lake built up sufficiently to heave the ice surface upward, thus also moving the piezometer upward. This upward heaving would also result in a decrease in the apparent potential.

Estimation of the volume of groundwater discharged into this lake can be determined by Darcy's equation:

$$q = k i a,$$

where q = rate of discharge, k = coefficient of permeability, i = hydraulic gradient (≈ 0.25 m/m), and a = cross-sectional area (18 200 m²).

The hydraulic gradient can be determined from the piezometer data by assuming vertical flow. Minimum horizontal cross-sectional area of the unfrozen zone below the

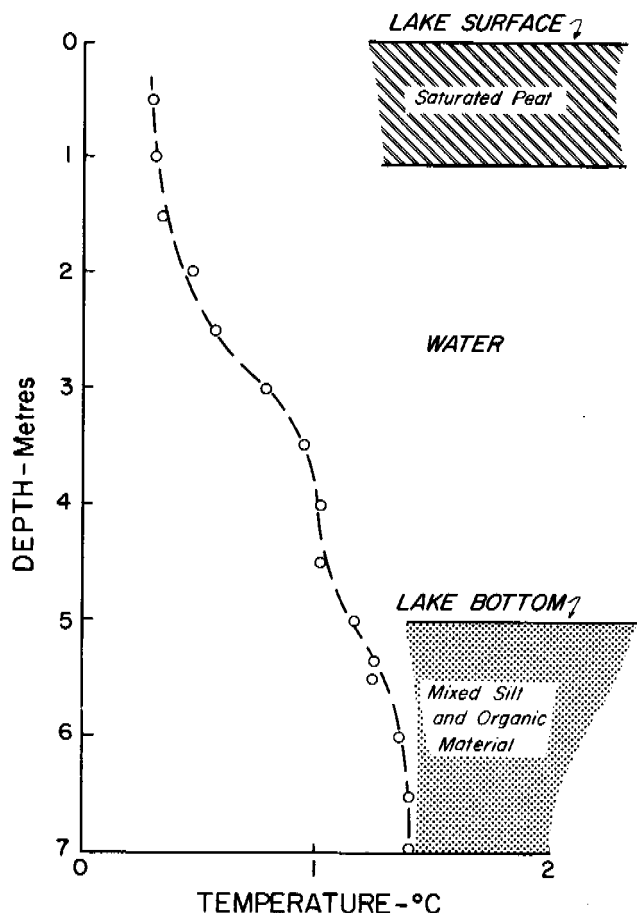


FIGURE 3 Temperature fluctuation with depth, 25 July 1969.

lake can be assumed to be nearly equal to the surface area of the lake. Well logs in the vicinity of the lake indicate that silt interspersed with sand constitutes the predominant geologic material. Using values of permeability that correspond to silty material, the rate of discharge can be estimated. The three values of permeability selected fall in the low, middle, and high range of accepted values for silt. For values of 1.1×10^{-4} m/s, 1.1×10^{-6} m/s, 1.1×10^{-8} m/s, the calculated discharges were 1 800 m³/day, 18 m³/day, and 0.18 m³/day, respectively.

During the summer of 1970, daily evaporation rates from a lake surface of a nearby body of water were determined. Hartman⁵ indicated that an average daily evaporation of 2.5 mm/day occurred for the month of August. Equating the volume of groundwater discharge per day to the average daily evaporation yielded a value of discharge equal to 44 m³/day. This is in the same order of magnitude of the discharge calculated for a middle range value of hydraulic conductivity. It should be pointed out that these values are only estimates, calculated for the purpose of determining possible magnitude.

CONCLUSIONS

Permafrost terrain is commonly characterized by abundant lakes. The role of these lakes as a surface water reservoir for precipitation and snowmelt has long been recognized. Their hydrologic role, as it pertains to groundwater flow, has been recognized only in a few cases.

The existence of an unfrozen zone beneath a lake surrounded by permafrost and recharge of the lake from subpermafrost aquifers through that thawed zone have been demonstrated in this study both by the piezometer and temperature data.

In the zone of discontinuous permafrost, including the lowlands of central Alaska, it is likely that many lakes the size of the Isabella bog lake and larger do indicate hydrologic connections between subpermafrost aquifers and the surface. Relatively warm permafrost (i.e., at a temperature of about -0.5 °C) allows increased thermal influence of even small water bodies; at the same time, lesser permafrost thicknesses (commonly less than 70 m) and existence of major permafrost-free areas increase both opportunity for thaw effect to completely penetrate permafrost and opportunity for recharge of aquifers upslope from permafrost zones.

It is thus suggested that the thousands of lakes found in the lowlands of central Alaska give evidence of a great lack of continuity of permafrost, even in low-lying, poorly drained sites. Existence of such a network of thawed zones also suggests that groundwater systems are extremely complex and that even local groundwater situations may have unsuspected hydrologic interrelations. While the Isabella Creek bog lake studied is a point of discharge for groundwater, other small lakes might comprise either recharge or discharge points for subpermafrost aquifers. Only field observations of individual cases will determine local hydrologic regimen.

REFERENCES

1. Brandon, L. V. 1966. Evidence of ground water flow in permafrost regions, p. 176-177. *In* Permafrost: Proceedings of an international conference. National Academy of Sciences, Washington, D.C.
2. Brewer, M. C. 1958. Some results of geothermal investigations of permafrost in northern Alaska. *Trans. Am. Geophys. Union.* 39(1):19-26.
3. Brown, J., P. V. Sellmann, S. L. Dingman, and S. Gray. 1966. The soils and hydrogeology of the Isabella Creek area, Fairbanks, Alaska. Study Proposal (mimeo). U.S. Army, Cold Regions Research and Engineering Laboratory, Hanover, New Hampshire.
4. Cederstrom, D. J. 1963. Ground-water resources of the Fairbanks area, Alaska. Water Supply Paper 1590. U.S. Geological Survey, Washington, D.C.
5. Hartman, C. W. Personal communication.

6. Johnston, G. H., and R. J. E. Brown. 1964. Effect of a lake on distribution of permafrost in the Mackenzie River Delta. *Arctic* 17(3):162-175.
7. Lachenbruch, A. H. 1957. Three dimensional heat conduction in permafrost beneath heated buildings. U.S. Geol. Sur. Bull. 1052-B.
8. Reiger, S., J. A. Dement, and D. Sanders. 1963. Soil survey of Fairbanks area, Alaska. U.S. Department of Agriculture, Soil Conservation Service, Washington, D.C.
9. Rickard, W., and J. Brown. 1972. The performance of a frost-tube for the determination of soil freezing and thawing depths. *Soil Sci.* 113(2):149-154.
10. Williams, J. R. 1965. Ground water in permafrost regions—An annotated bibliography. Water-Supply Paper 1792. U.S. Geological Survey, Washington, D.C.
11. Williams, J. R. 1970. Ground water in the permafrost regions of Alaska. Professional Paper 696. U.S. Geological Survey, Washington, D.C.

RISK OF UNCONTROLLED FLOW FROM WELLS THROUGH PERMAFROST

Kenneth A. Linell

U.S. ARMY COLD REGIONS RESEARCH AND
ENGINEERING LABORATORY
Hanover, New Hampshire

INTRODUCTION

Where groundwater below permafrost is under artesian pressure, risk exists that piping, erosion, uncontrolled flow, settlement of well-head facilities, and damage to the well casing may occur when a water well, oil well, or subsurface exploration boring is drilled through the permafrost. Possible consequences attending uncontrolled flow include formation of a constantly enlarging thaw and erosion pit at the well, permafrost degradation and terrain damage in the area exposed to surface and subsurface discharge from the well, ice fog and ground icing in winter, development of frost mounds, and waste of expensively developed water. Re-establishment of control may be difficult and expensive. That these potentially adverse effects are real is illustrated by the case history of a situation that occurred more than 20 years ago.

BACKGROUND

When construction of field experimental facilities was started at the Farmers Loop Road Research Area, Fairbanks, Alaska, by the U.S. Army Corps of Engineers in April 1946, one of the first investigations to be started was an effort to obtain a supply of subpermafrost water. Water was needed initially for construction purposes and later for supplying the various facilities and experiments at the station. In all,

seven wells were ultimately drilled over a period of more than 10 years in search of a supply that would be satisfactory both in quantity and quality. At well No. 3 of this series, a special group of events occurred⁴ that did not develop in any of the other wells.

As indicated in Figure 1, the site of the drilling was on a gentle, west-facing slope of about 4 percent. Permanently frozen silt of up to about 60 m thickness occurs on the valley floor, thinning out with increasing elevation on the slopes of Birch Hill. Permafrost disappears on the well-drained higher portions of the slope. Good, potable water is obtainable from relatively shallow wells in this upper zone. Water under artesian pressure is found in considerable quantity under the permafrost, except that artesian pressure is absent near and above the Steese Highway. However, this water has such a high content of minerals, organic matter, and gas as to be unusable without expensive treatment. The later drilling efforts, therefore, sought to develop a subsurface connection with the relatively unmineralized water existing higher on the slope. These efforts did not succeed. When water is allowed to discharge for extended periods from wells penetrating the permafrost, it reaches the surface at 2-3 °C.¹

The nearby Isabella Creek bog lake described by Kane and Slaughter³ is apparently a natural discharge point for such subpermafrost water. It may be noted that pingos have also been observed in the same general valley floor deposit.

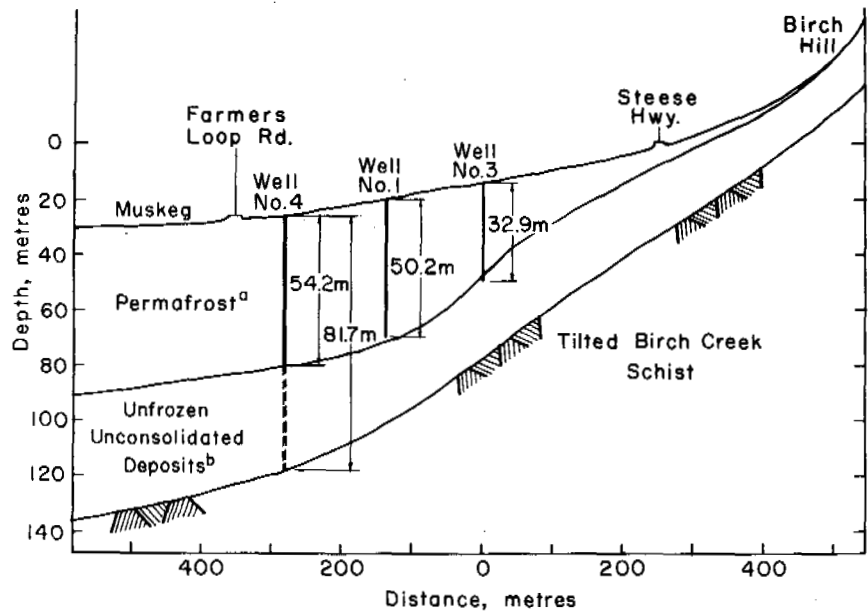


FIGURE 1 Section from Birch Hill across Alaska field station. (a) Principally silt with lenses of sand, sandy gravel, and some fractured bedrock. (b) Fractured bedrock and silt with lenses of water-deposited sand and sandy gravel; subpermafrost water under hydrostatic pressure. Ordinate depths are measured from Steese Highway data.

DRILLING THE WELL

Well No. 3 was drilled to a 12.7-cm diameter with a churn drill, using casing only for an initial length of approximately 2 m, through the annual thaw zone. Materials encountered are shown in Table I and Figure 2 and described in accordance with the soil classification system then in use. Water in considerable quantity was encountered at a depth of 32.9 m in the well on 3 May 1946. The ground was frozen through this full depth, including a 7.3-m gravel stratum drilled through immediately before encountering water. The discharge rate of 0.0085 m³/s at this time was sufficient to carry to the surface gravel-size particles up to 5 cm in diameter, and the water gushed from the well to about 1-1.2 m above the ground surface. Hydrostatic head was later measured as 82.7 kN/m² (8.44 m above ground surface). The

starter casing was withdrawn and a 10.2-cm i.d., 11.4-cm o.d. casing was placed to a depth of 33.5 m. The record indicates that during the time required to assemble and install the 11.4-cm o.d. well casing, thawing and erosive action of the flowing water enlarged the drilled hole.⁴ Jaillite,² in describing the sequence of events at the well from May to early June 1946, indicates that the hole was enlarged by thaw during drilling in addition to providing a loose fit for the casing. Probably both thaw-enlargement actions occurred. Thus, both because the outside diameter of the casing was smaller than the drilled diameter and because of thaw enlargement of the hole, the casing did not completely fill the hole, and water flowed to the surface both around and through the casing. The flow was now uncontrolled and a progressively enlarging hole was forming at the well head.

TABLE I Boring Log, Well No. 3^a

Depth below Surface (m)	Description of Soil
0.0-1.7	Peat with silt (stratified)
1.7-3.0	Silt with peat (stratified)
3.0-11.9	Silt
11.9-25.6	Silt with some peat and very fine sand
25.6-26.5	Coarse and medium sand—some silt and peat
26.5-27.4	Gravel—some silt
27.4-28.4	Gravel—some coarse sand and silt
28.4-29.3	Gravel—some silt
29.3-32.0	Gravel—some coarse sand and silt
32.0-32.9	Gravel

^a Notes: Surface elevation = 155 m; all soil frozen; visual soil classification; hole drilled, April 1946.

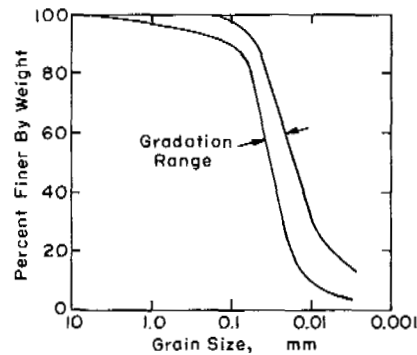


FIGURE 2 Gradation range, well No. 3, Farmers Loop Road Research Station.

EFFORTS TO CONTROL AND USE THE WELL

Measures to re-establish control of the flow of water were started at once and proceeded intensively over several weeks. About 0.76 m^3 of gravel was first placed in the developing cavity at the well head to provide a working surface. A water-cement slurry or grout containing 40 bags (1 706 kg) of cement was then pumped down the casing so that it would rise into the void between the casing and the soil. This stopped the leakage around the casing for only a few hours. Next, 1.53 m^3 of concrete were placed over the previously placed gravel at the well head; flow was controlled by pumping out of the casing with a $151 \text{ m}^3/\text{h}$ capacity pump. Seepage again appeared around the newly set concrete. A 3.05-m square slab approximately 0.3-m thick was then placed around the main casing with a secondary 15.2-cm i.d. stub casing penetrating it to permit control of the water level immediately below it. Pumping was continued from both casings until the concrete had set. A considerable amount of water was flowing from the stub casing the next day. Seepage at the edges of the concrete slab was sealed off by using drillers' mud and neat cement. At this point, flow from the main casing had completely stopped. Bailing and pumping were used to restart the flow, but subsequent grouting with another 40 bags of cement pumped down the main casing resulted in sealing the casing itself. To re-open the casing, it was dynamited at a depth of 27.4 m. Drilling through the stub casing and through the underlying concrete and gravel plug then revealed a large cavity around the main casing to a depth of 29 m. To rectify this, 1.53 m^3 of gravel was poured in through the stub casing to above the level where the casing had been dynamited and the rest of the cavity was filled with 4.59 m^3 of concrete. The main casing was again bailed out and flow again became sufficient to carry 5-cm-diameter gravel particles to the surface, with no indication of water rising outside of the main casing. Within 2 weeks after sealing was completed, the flow had decreased from 0.76 to $0.095 \text{ m}^3/\text{min}$, attributed by the field personnel to plugging of the main casing with fine sand and to reduction of peak head. Flow had completely ceased by mid-June, 6 weeks after water was struck. The well was re-opened by drilling out an ice plug in the main casing. Within 5 days the well refroze and an ice plug was again drilled out. The well then remained operative throughout the summer. At the end of the summer, the well was valved off and remained frozen throughout the winter of 1946-1947.

In 1947, the well was thawed and flowed throughout the summer. It was valved off in October. In November, the well was thawed again to install well pipes and by 13 December 1947 it had refrozen.

In January 1948, the well was thawed with steam and connected into a utilidor system. It was kept operable through the remainder of the winter, the spring, and into

summer by occasional steam-thawing in the main casing. On 10 August 1949, in an effort to correct rapid refreezing in the well, steam under 551.6 kN/m^2 pressure was introduced into the hydrojet well pumping system. In about 15 min, warm water was observed flowing from beneath the 3-m square concrete slab surrounding the casing. It was discovered that the main casing had broken at a coupling at a depth of about 2.7 m, probably as a result of frost heaving in previous winters acting on the concrete slab, which was firmly bonded to the casing. On 1 December 1948, a wooden plug was driven into the lower part of the broken casing; this appeared to stop the flow for the remainder of the winter. In view of subsequent developments, however, it appears that flow was not checked by this plugging and that water continued to flow from the ruptured casing and undoubtedly also through a thawed zone around the casing.

In 1949 water started to flow again from beneath the concrete slab shortly after the spring breakup. On 14 July the slab settled 1.2 m on its south side. Several days later the slab rotated and assumed a perpendicular position. By 21 July the slab was completely submerged and the cavity in which the slab was sinking measured $4.6 \text{ m} \times 5.5 \text{ m} \times 3.7 \text{ m}$ deep. Three weeks later the average depth of the hole was 5.2 m. By 17 September the cavity measured 7.3-8.2 m across and the water level was 0.85 m below the ground surface. The flow remained uncontrolled during the remainder of 1949 and through the winter of 1949-1950. Although records are no longer available, it is believed that the concrete slab sank to at least 7 m and possibly as much as 15 m below the surface before the flow was ultimately controlled.

ICINGS

In 1946, the well flowed most of the time from 3 May to the end of summer and, in 1947, from early summer to October. Except for a brief opening in November 1947, the well remained shut down in both the winters of 1946-1947 and 1947-1948. The record shows no report of icing or other special problems through this period. However, shortly after the well went out of control in August 1948, water was observed on the surface or close to the surface in the natural drainage way south of the Access Road, which runs from the Farmers Loop Road past the well. Unusually high precipitation in the summer had already created a general high groundwater condition.

On 27 October 1948 an active icing was observed forming in a birch forest south of the Access Road as indicated in Figure 3. A 17.8-cm thickness of ice was underlain with water 12.7 cm deep over the ground surface, and the silty soil "was in a fluid state to a depth of 2.9 m."³ Adjacent to the icing, permafrost was encountered at a depth of less than 0.6 m. From 27 October until 13 December, the icing continued to grow and, ultimately, covered the 16-

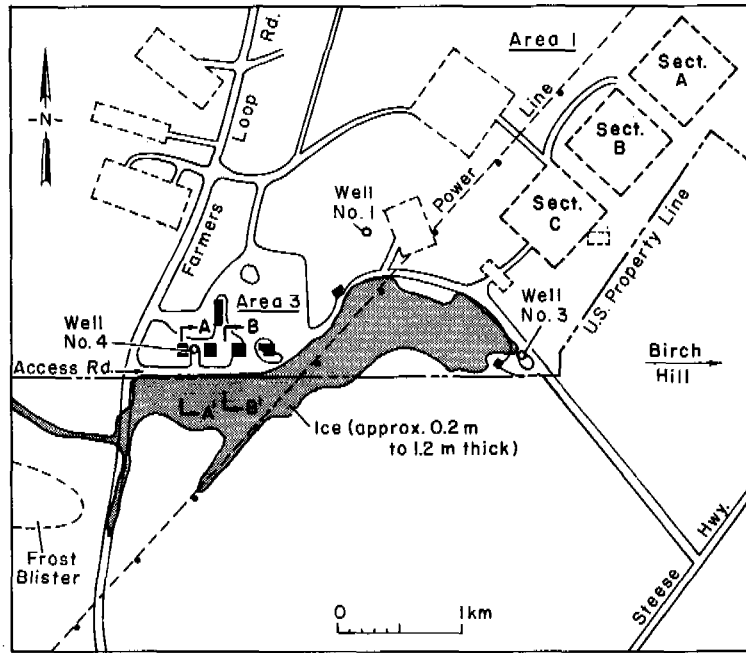


FIGURE 3 Icing extent.

20-km² shaded area indicated on Figure 3 with ice from 5 cm to 1.5 m thick, averaging about 0.45 m. At times, the growth was very rapid. For example, on the afternoon of 27 November water was filling the ditch on the uphill side of Farmers Loop Road and slush ice was about 7.5 cm below the top of the road shoulder; by 1 December a layer of ice averaging 0.4 m thick had completely covered a 65.5-m section of the road and a considerably longer section of ditch. Channels cut in the icing in an attempt to minimize ice buildup on the road rapidly iced up in air temperatures between -29 and -34 °C. Maximum ice thickness on the road was over 0.6 m. Most vigorous icing growth was observed to occur in those places having a layer of water up to 15 cm deep between the thawed underlying soil and the surface ice. Water was also observed flowing in a slushy stratum within the icing itself; that is, a cap of solid ice covered a slushy layer that was underlain again by solid ice. Points where water emerged onto the surface from below were usually characterized by one, or a combination of several, of the following surficial conditions: ground covered by a thick mat of grass or brush; bases of trees having a thick layer of needles or leaves surrounding their trunks; and contraction cracks due to extreme cold, which extended through the surface ice cap to a stratum of slushy water or saturated thawed soil. Dense ice fog developed in the vicinity of the icing when air temperature was very low, and near-by vegetation developed a coating of frost crystals.

THE FROST BLISTER

Although there had been no apparent flow from the well or icing after 13 December 1948, a low mound or frost blister

was observed in early April 1949 on the west side of Farmers Loop Road about 180 m south of the research area, at the location indicated on Figure 3. Figure 4 shows an idealized cross section of this mound. The mound was discolored and several white spruce on the north slope of the low ridge were tilted as much as 10° . The frost mound was capped with a layer of ice from 0.3 to 0.6 m thick. A deep crack, from 2.5 to 12.7 cm wide at the surface of the ice, extended for a distance of 45 m along the ridge of the mound. Most parts of the crack were sealed with ice at a depth of 0.3–0.9 m; however, it was reported that the crack extended through seasonal frost at least at those locations where water was flowing from the crack. Insoluble iron oxide was precipitated from the water on the surface of the ice, forming a greasy, chocolate-brown layer of sediment up to 2.5 cm thick.

GROUND SUBSIDENCES

As thaw progressed in the spring of 1949, a depression about 3 m long, 1.2 m wide, and 0.5 m deep appeared in Farmers Loop Road on a line between the frost blister and a point of the edge of the road right-of-way where the ground was thawed to a depth of at least 3.8 m. The ground on either side of this point was frozen to a depth of less than 1 m, indicating that the thaw was restricted to a relatively narrow channel. The depression was attributed to collapse of an underground cavity under the effects of traffic. Deposition of a considerable quantity of silt parallel to the down-slope side of Farmers Loop Road indicated that the cavity had been formed by piping silt from the road subgrade. Also, during the spring and early summer of 1949, thawing action

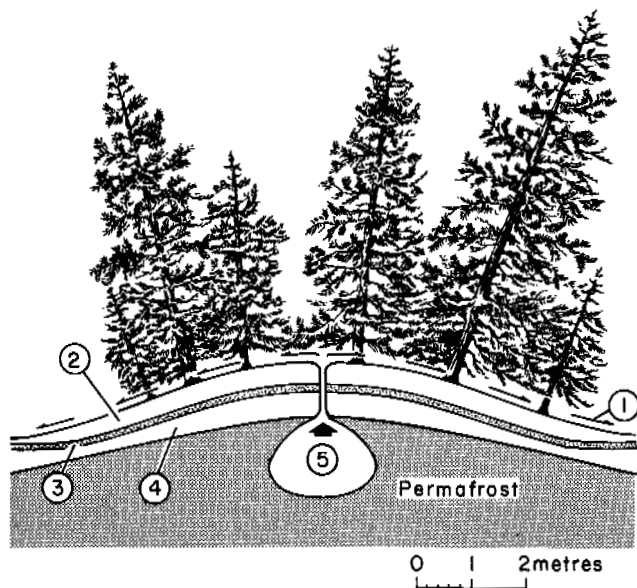


FIGURE 4 Frost blister section. Leaning trees indicating heaving action. (1) Water forced to surface from crack. (2) Surface ice cap 0.3-0.6 m thick. (3) 20-cm mantle of moss. (4) 0.5-m layer of seasonally frozen silt. (5) Water under hydrostatic head, permanent talik. Shape of aquifer may vary from a deep, narrow channel to pearshape or nearly round. In any event, the orifice at the bottom of the active layer is small.

of water leaking from the well developed cracks in the ground west of the well and a general subsidence of the surface in the channelized seepage discharge area immediately downslope from the well, averaging a few meters in width and depth. It was evident that subterranean thaw was occurring, as well as considerable erosion of silt.

FINAL RE-ESTABLISHMENT OF CONTROL

No records are available of further ground surface disturbances during the remaining period of uncontrolled flow from the summer of 1949 into 1950, except that the severity of icing conditions was less in the winter of 1949-1950 than in the previous one. The situation was finally stabilized in 1950 by installing freeze probes around the well location and circulating refrigerant brine until the area was completely refrozen and the continuity of the permafrost re-established. Plans to use well No. 3 for station water supply were abandoned.

A slight depression in the ground at the site of well No. 3 is today the only readily discernible surface evidence of these events. Probings to permafrost at the end of the 1972 thawing season on the lines designated as A-A' and B-B' on Figure 3 and plotted on Figure 5 show that no permanent degradation was produced in the wooded area south of the Access Road. Although a talik does exist under the Access Road, this could have been formed and maintained merely

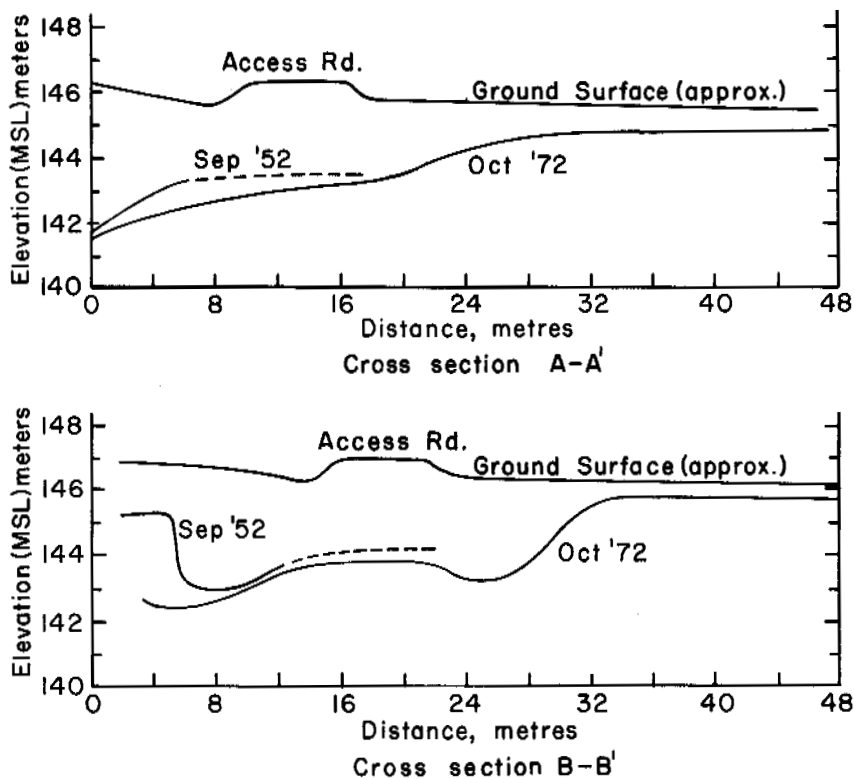


FIGURE 5 Permafrost probing sections (locations shown on Figure 3).

as a result of presence of the road, without other thermal influences.

DISCUSSION

In the case history described above, the problems might not have occurred or might not have developed so readily if a casing had been tightly installed initially through the full thickness of permafrost. Other wells drilled through the same formation at the Farmers Loop Road Research Area with casings tightly installed through permafrost have been used or allowed to flow for periods of up to several months without signs of difficulty around the casing. However, this might not have been possible in a more unfavorable permafrost formation, under more prolonged flow or under higher pumping rates, higher water temperatures, or higher pressure gradients across the permafrost layer. It should also be kept in mind that available data indicate less than 100 percent area contact with the surrounding permafrost is obtained when a steel member such as a well casing is installed in permafrost by driving because of bend and twist in the member, imperfections, or damage to the leading edge. For a casing just penetrating to the bottom of permafrost, the hydraulic head available for flow on the outside of the casing is reduced during periods of well discharge. The most critical period is likely to be at the end of a significant period of well discharge when the full artesian head is restored and an annular zone of permafrost surrounding the casing has been thawed, as indicated diagrammatically in Figure 6, by above-freezing water that has passed upward through the casing.

When a well drilled through permafrost carries subpermafrost groundwater to the surface, either ice may form inside the casing or permafrost may be thawed outside the casing; the actual result and its extent are determined by such factors as water temperature, velocity of flow, permafrost temperature, length of well in permafrost, heat transfer characteristics of the well and surrounding materials, diameter of the well, and the duration of flow. If water demand is low, thermal insulation, introduction of heat, periodic mechanical removal of ice from the well, or intentional wastage flow may be required to keep the well from freezing. From mid-June 1946 to 10 August 1948, the well described in this case history was drilled or steamed out more than eight times to remove ice that restricted or blocked flow. On the other hand, if water temperature is high, the velocity of flow is high, or excessive heat is introduced as by steam thawing, the permafrost surrounding the well may be thawed.

A reliable casing installation for an artesian well through permafrost requires accurate understanding and appropriate evaluation of the permafrost conditions. When the permafrost materials are thaw-stable soils, free of excess ice, the relative safety against flotation, piping, and blowout in a thaw zone surrounding the casing can be evaluated by stan-

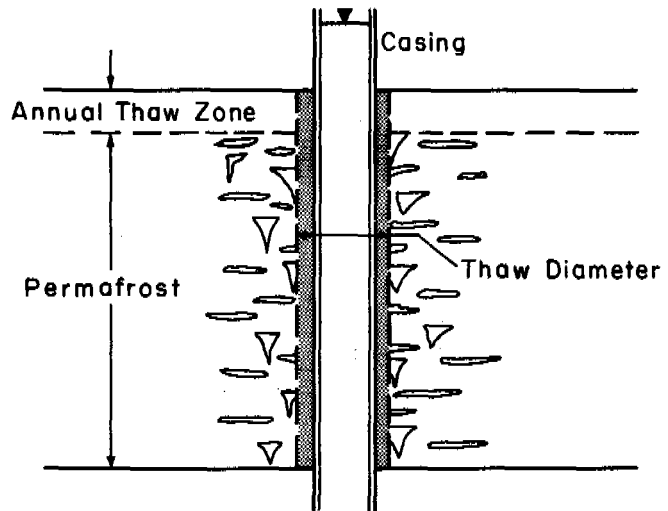


FIGURE 6 Thaw around casing.

dard soil mechanics methods, using critical hydraulic gradient or creep ratio approaches, since such soils, when thawed, will have the characteristics of ordinary unfrozen soils. Similar considerations apply for thaw-stable rock. However, when the permafrost zone contains high-ice-content soil or rock, the degree of safety may be indeterminate.

Where heavy ice-wedge concentrations exist through most of the permafrost depth, possibly formed successively over many thousands of years of surface soil accretion, it is possible that an open channel through essentially the full depth of permafrost may be formed by thawing of linking ice masses surrounding the casing. Where the permafrost consists of frozen soil containing well distributed excess ice, thawing may convert the thaw zone indicated on Figure 6 into a fluid mixture of soil and water. In either of the latter events, an unstable, expanding piping and erosion condition may result on the outside of the casing from even very small initial through seepage, with ultimate effects comparable with those described in the case history.

From the case history data, it is evident that the basic mechanism for halting flow outside the casing in 1946 was refreezing, the same as in the final re-establishment of control in 1950, and that the loss of control in 1948 undoubtedly involved thawing through of this seal. In such situations, no thaw may be permitted outside the casing. To prevent such thaw while still permitting the well to be used may require one or more special measures to be employed, such as insulation and refrigeration of the well. Insulation can at the same time serve to minimize freezing within the well. Achievement of the simultaneous freezing-nonfreezing conditions is a challenging engineering problem.

A summary analysis of well stability conditions under artesian flow for four combinations of conditions is shown in Table II. It will be seen that ensured safety against adverse

TABLE II Stability of Wells under Artesian Flow for Four Combinations of Conditions

Case No.	Type of Permafrost	Type of Casing Installation	Well Stability Condition
1	High-ice-content, thaw-unstable permafrost (extreme condition would be soil-free ice, as in drilling through a glacier)	No casing in permafrost zone or casing incompletely sealed to permafrost	Unstable; although a situation can be visualized in which flow is so slight that ice buildup occurs instead of thaw, conditions at the bottom of permafrost, where temperature is borderline, will tend to be unstable
2		Casing to bottom of permafrost zone or lower	Unstable unless thaw outside the casing is prevented. Even though penetration of casing into underlying unfrozen ground is sufficient for safety against piping or blowout within that zone and casing is in tight contact with permafrost, thaw of ice around casing by flow of warm fluid within it may allow the artesian pressure at the base of permafrost to break through
3	Thaw-stable permafrost, no excess ice	No casing in permafrost zone or casing incompletely sealed to permafrost	Unstable unless permafrost zone is thaw-stable bedrock. Frozen soils will be subject to erosion when flow thaws ice bonds
4		Casing to bottom of permafrost zone or lower	Stable, provided total casing imbedment is sufficient for safety against piping or blowout

effects under significant artesian pressures and flow rates requires wells to be fully cased through the permafrost zone except in thaw-stable bedrock, and, if the permafrost has a high ice content, thaw-unstable material requires a tight frozen seal to be maintained between the casing and the permafrost.

While the above discussion has focused on the development of water supplies from wells, the same considerations must be taken into account in subsurface exploration borings or in drilling for oil and gas development. Even though an oil or gas well is drilled to thousands of metres below permafrost, water existing under artesian pressure beneath the permafrost may rise along the outside of the casing if conditions are unfavorable. Because oil or gas rising from great depths is quite hot, especially intense thawing around the casing may occur. Whether or not risk of piping or blowout in the permafrost zone exists, the engineer must anticipate in his designs the ground settlement at the surface and the compressional forces on the casing that such thaw will entail if the permafrost zone contains excess ice.

CONCLUSIONS

Reliable, effective resistance to piping, erosion, and blowout under artesian pressure and flow conditions of significant magnitude in a well drilled through permafrost requires proper initial installation of the well casing, based on accurate knowledge and evaluation of the permafrost conditions. If the permafrost is thaw-stable, without excess ice, the casing should be tightly installed through the full permafrost zone, except that in thaw-stable bedrock casing is not needed unless for other reasons than thaw instability. If the permafrost is high-ice-content, thaw-unstable soil or rock, not only must the casing be tightly installed in the permafrost but the maintenance of a permanently frozen contact

and seal between the casing and the permafrost may also be necessary.

ACKNOWLEDGMENTS

This paper presents the results of research performed by the U.S. Army Cold Regions Research and Engineering Laboratory under the sponsorship of the U.S. Army Corps of Engineers. The information on which this paper is based represents the conscientious efforts of many individuals. The observational data on well No. 3, which are the primary basis of the case history summary, were assembled in 1950 by the Field Operations Office (Mr. B. L. Trawickey, Chief) of the Permafrost Division (Mr. Harry Carlson, Chief), St. Paul District, U.S. Army Corps of Engineers. The record of events published by W. Marks Jaillite, covering approximately the first 5 weeks after water was encountered, was also a valuable source. The 1972 probing data were obtained by the Alaskan Division, USA CRREL [Col. Elmer Clark (ret.), Chief]. Special thanks are owed to Mr. Charles W. Fulwider of USA CRREL, who gave unflinching assistance during the preparation of this paper, and to Mr. John R. Williams, U.S. Geological Survey, and to Mr. G. Robert Lange and Mr. William Quinn, USA CRREL, who reviewed the paper and gave most valuable comments.

REFERENCES

- Buzzell, T., K. Mueller, J. Contegni, and S. Reed. Water treatment experiments with a subarctic groundwater. CRREL Internal Report (unpublished). U.S. Army Cold Regions Research and Engineering Laboratory, Hanover, New Hampshire.
- Jaillite, W. M. 1947. Permafrost research area. Mil. Eng. 39:375-379.
- Kane, D. L., and C. W. Slaughter. 1973. Lake and Subpermafrost Groundwater Interaction in a Permafrost Environment, Central Alaska. This volume.
- Permafrost Division, U.S. Army Corps of Engineers. 1950. Observations of an uncontrolled artesian well, Field Research Area, Fairbanks, Alaska. Prepared by Soils Laboratory, Field Operations Office, Fairbanks, Alaska. 22 p. (Also U.S. Army Cold Regions Research and Engineering Laboratory Internal Report)

A GROUNDWATER SUPPLY FOR AN OIL CAMP NEAR PRUDHOE BAY, ARCTIC ALASKA

Richard G. Sherman

METCALF & EDDY, INC.
Boston, Massachusetts

INTRODUCTION

Attempts to locate supplies of potable water in northern Alaska have met with little success: Aquifers near the surface in unconsolidated deposits are perennially frozen to a depth of at least 150 m; ponds and streams are not resupplied during the long, cold winters; and unfrozen bedrock beneath the frozen layer is generally of low permeability and contains brackish to saline water.

Careful planning in locating campsites and in designing sanitary facilities to prevent pollution is required due to the limited water supplies, the susceptibility to contamination, and the expense of piping water in heated water lines to points of use.

In designing an oil camp on the west bank of the Sagavanirktok River 11 km south of Prudhoe Bay, the first step was to locate a year-round supply of potable water. Previous studies at Barrow,^{4,8,10} Umiat,^{2,3,11} Cape Lisburne,⁵ Antarctica, and Greenland⁷ indicate that three potential sources of water should be investigated: ponds, the river, and deep or shallow aquifers. Permafrost thickness of as much as 610 m in the campsite area⁶ eliminated consideration of deep aquifers. Potential sources in lakes and in the nearby Sagavanirktok River and in aquifers beneath the lakes and the river were explored.

INVESTIGATION IN PONDS NEAR CAMP

Holes were drilled through the ice in ponds near the proposed campsite in June 1969 to test the volume of water available in late winter and the possibility of developing an aquifer beneath the ponds. Holes in ponds A and B (Figure 1) showed that ponds less than 2 m deep were completely frozen. Ponds 2.5–3.5 m deep (D, E, F, Figure 1) had as much as 1.5 m of free water beneath 2 m of ice. Pond C was dry, having breached to the river. The fine-grained bottom deposits of these ponds were unfrozen to a depth of 4 m below the pond bottom. The sand and gravel that lies between a depth of 9 and 123 m was frozen. The small volume of free water available in late winter and the lack of any source of water to replenish that withdrawn made even the deep ponds inadequate for a camp supply and suitable

only for temporary storage for emergency supply or fire prevention. Excavating unfrozen fine-grained bottom sediments to enlarge natural storage would probably result in high turbidity for weeks or months. Even though the pond water did not exceed the quality limits recommended by U.S. Public Health Service¹² for public supplies, the free water of the deeper ponds in June 1969 was four times as hard, twice as high in chloride, and four times as high in total dissolved solids as water in the Sagavanirktok River. However, turbidity in the pond was 5 g/m³ compared with a minimum of 250 g/m³ in the river during January of 1969 when the river is at its clearest.

INVESTIGATION IN THE SAGAVANIRKTOK RIVER

Locating an intake in the Sagavanirktok River posed a number of problems. High turbidity of water during the spring breakup and early summer months would require filtration or settlement of the water before use. The principal channel followed the bank adjacent to the camp, but constantly shifting channels of this braided river might eventually migrate away from the intake. Damage to the intake structure by ice during the winter and during spring breakup might disrupt the supply. Frazil or anchor ice might block the intake during winter. Furthermore, in common with many large arctic rivers, winter flow might cease. Because of these uncertainties, exploration of the unfrozen sand and gravel aquifer beneath the river was undertaken to assess the amount of water in storage.

A straight reach of the channel along the west bank, 150–450 m downstream from the camp, had a number of deep pools in which water remained below the penetration of winter freezing. Two lines of test holes were drilled with a Mayhew 1 000 shothole rig, line A–A' (Figure 1) in January, and line B–B' in April 1969.

Drill holes along line A–A' show that an unfrozen zone ranging in thickness from 0.3 to about 7.5 m existed below the river bed. The unfrozen zone was about 105 m across and consisted of sandy gravel that contained freshwater of good quality and relatively free of the turbidity that characterizes the river water in summer. The cross-sectional area at right angles to the river channel of this aquifer was 762 m².

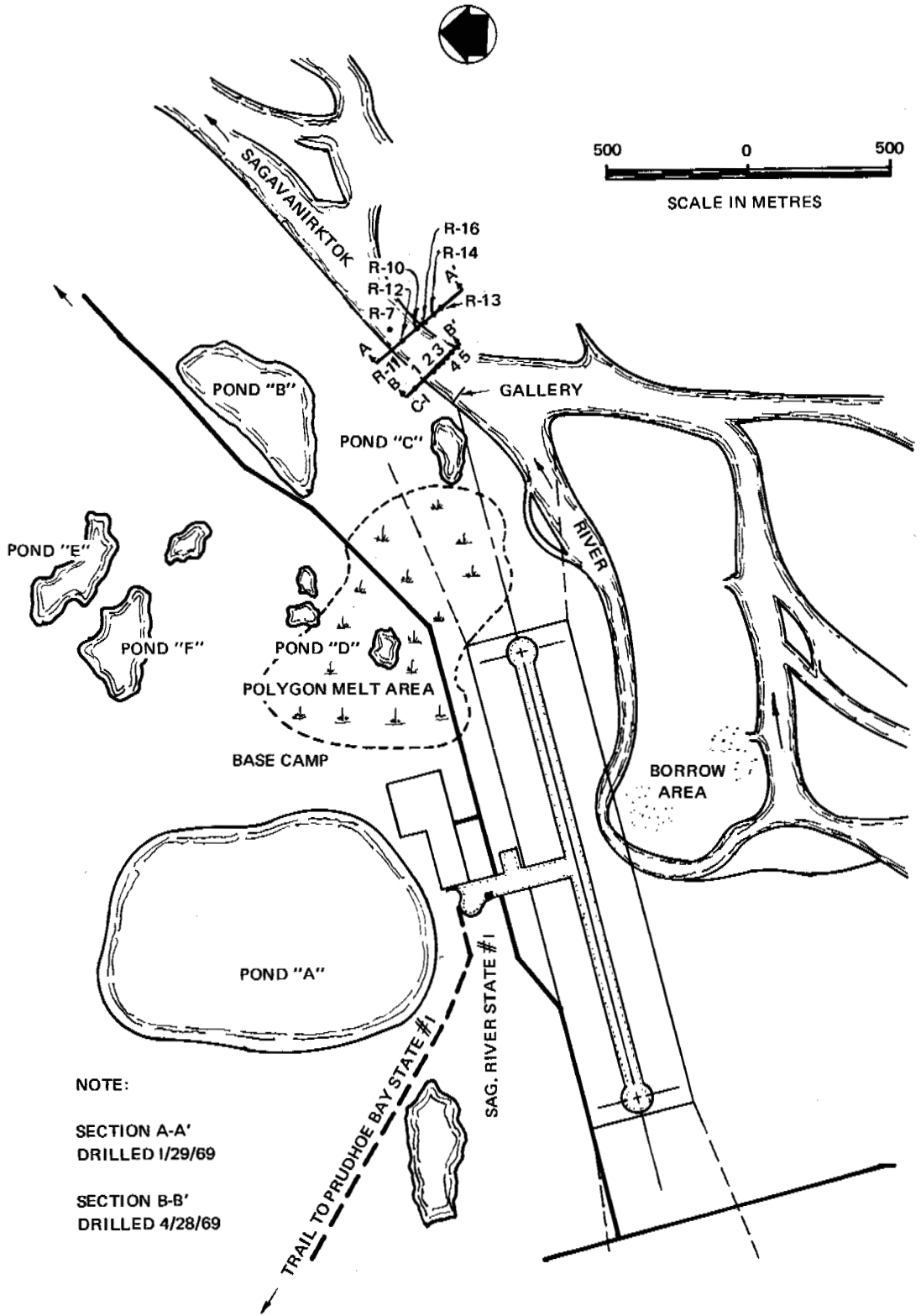


FIGURE 1 Location of test borings for water supply investigation, Sagavanirktok River, near Prudhoe Bay, Alaska.

Using a coefficient of permeability $k = 60$ and a gradient of 0.0002, according to Darcy's law, 50 000 m³/day would be moving down valley, assuming the aquifer was continuous and connected to the river.

A cross section (Figure 2) at line B-B' (Figure 1) was test drilled in April to determine progress of freezing during the critical period of late winter. The cross-sectional area of the aquifer, although much smaller (167 m²), could carry 11 000 m³/day through the section. The April measurement was probably near the minimum for 1969.

Obviously, conditions will change from year to year. In addition to natural changes in climate, they can be changed by man interfering with the natural flow and channel development of the river upstream. For example, gravel removal from the stream bed from the borrow area (Figure 1) upstream can alter flow patterns and depth of flow; on the other hand, climatic conditions can be modified by placing snow fences on the ice above the aquifers early in the winter to prevent freezing of the river to the bottom.

In the Colville River Delta, upvalley migration of the

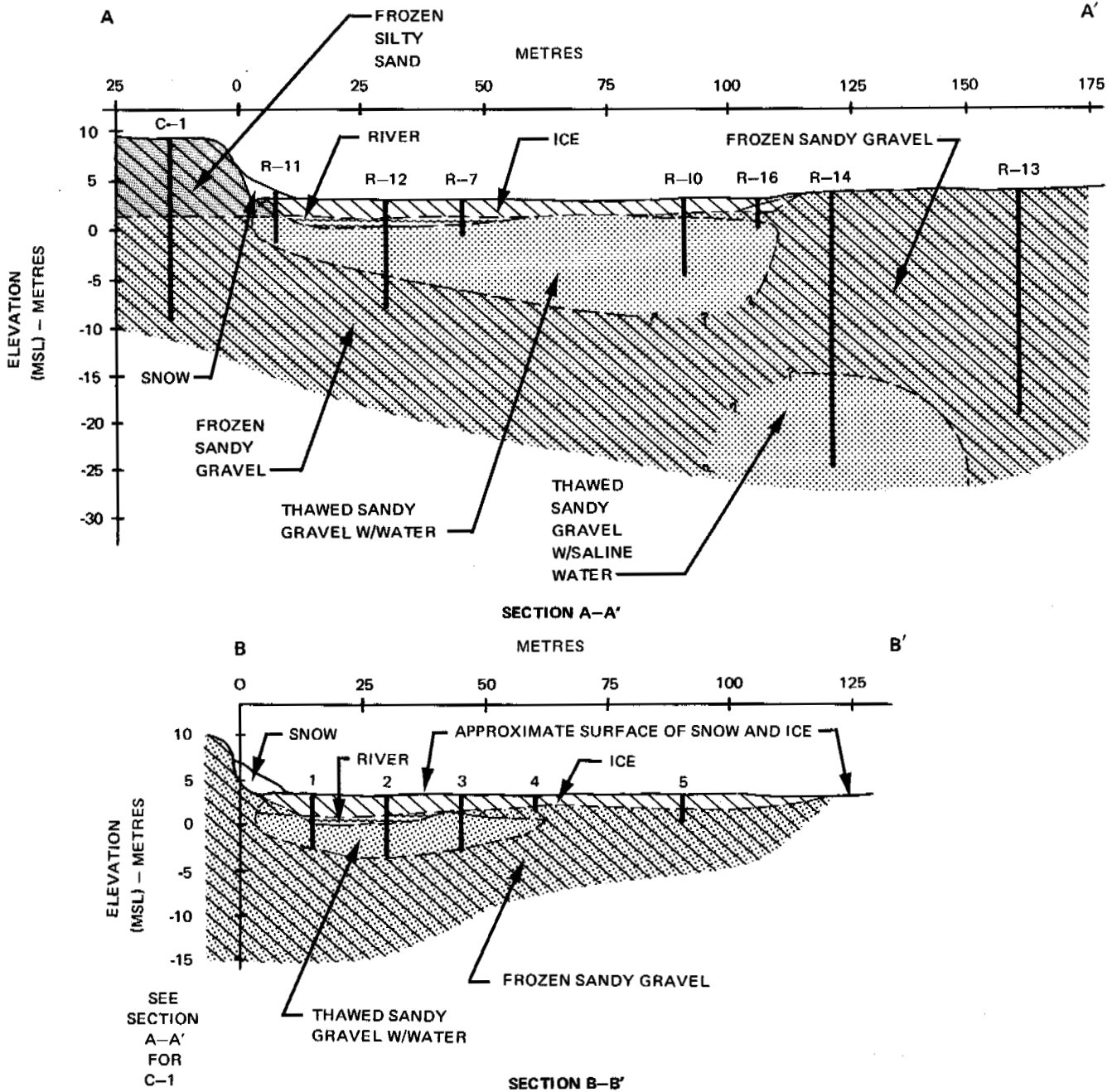


FIGURE 2 Cross sections of Sagavanirktok River, near Prudhoe Bay, Alaska.

freshwater-saltwater interface during the winter period of low flow, followed at spring breakup by flushing out the salt water,^{1,9} occurred in an environment very similar to that of the lower reaches of the Sagavanirktok River. At the Sagavanirktok River, water having a chloride concentration of 18–19 g/m³ was found at a depth of 20–24 m beneath the bar east of the channel (Figure 2). Its January temperature was –1 °C. Drilling defined neither the lower limit of the freshwater aquifer beneath the river nor the upper and westward limit of the saline water. Lateral movement of the salt water into the freshwater aquifer under heavy pumping conditions would seem possible unless further tests establish that the saltwater and freshwater are separated by an impermeable zone, such as frozen alluvium. Whether saline groundwater encroachment by upvalley migration in the unfrozen deposits beneath these rivers takes place as well has not been determined, but the presence of a saltwater aquifer beneath the lower Saganavirktok suggests the possibility of a seasonal migration of the interface.

INSTALLATION OF A GALLERY

The decision was made to install an infiltration gallery beneath the channel at a location slightly upstream from section B-B' (Figure 1). An emergency supply was developed by plugging the breach in pond C and pumping water into it from the river. According to reports, the gallery operated satisfactorily between 15 June and 15 December 1970, at which time it failed because of silting of the intake line and surrounding aquifer material. At the time of failure, a temporary intake was suspended in water through a hole in the ice for the duration of the winter. Pond C was used to supply the camp during breakup. A steel pier was installed in the summer of 1971, and the intake line suspended in the river. The gallery intake was removed. The river intake has proved satisfactory at all seasons, except breakup when pond C is used.

CONCLUSIONS

Test work shows that a year-round supply of good quality water exists in an alluvial aquifer beneath a large arctic stream. At sites near the coastline, the aquifer may be subject to saltwater encroachment, induced either by heavy pumping during periods of zero river flow or by natural upstream migration of the salt water as flushing action of the freshwater underflow supported by streamflow ceases.

SUMMARY

Subsequent to the recent discovery of oil near Prudhoe Bay, a permanent facility with a year-round potable groundwater supply was built for an oil camp on the Sagavanirktok River. The investigation for water supply considered three possible

sources: large thaw lakes, rivers, and groundwater. Problems associated with thaw lakes include freezedown, which limits storage; impurities, which can concentrate during winter to unacceptable levels; and susceptibility to contamination. The rivers are turbid in summer, have uncertain winter flow, and have channels that shift periodically. Groundwater aquifers as unfrozen zones *within* the permafrost are difficult to locate, are often saline, and usually have no recharge. Groundwater aquifers as unfrozen zones *above* the permafrost and beneath a stable river channel appeared to offer the most promise in both quantity and quality. Test drilling in mid-winter and in spring beneath part of the Sagavanirktok River showed that, during the period of maximum freezedown, the unfrozen cross-sectional area of alluvium beneath the river was at least 167 m² and would pass 11 000 m³ of water in April 1969 if the aquifer was continuous and connected to the river. The freshwater aquifer that was developed by use of a gallery in this reach of the river lies above a saltwater aquifer, but its relationship to this saline aquifer remains to be determined.

REFERENCES

1. Arnborg, L., J. J. Walker, and J. Peippo. 1962. Water discharge in the Colville River. *Geogr. Ann.* 49A:131–144.
2. Black, R. F. 1955. Arctic slope, p. 113–146. *In* D. M. Hopkins, T. N. V. Karlstrom, and others [ed.] *Permafrost and groundwater in Alaska*. Prof. Paper 264-F. U.S. Geological Survey, Washington, D.C.
3. Black, R. F., and Barksdale. 1948. Terrain and permafrost, Umiat area, Alaska. U.S. Geological Survey, Permafrost Program Progress Report 5. Engineer Intelligence Division, Office, Chief of Engineers, U.S. Army. p. 23.
4. Brewer, M. C. 1958. Some results of geothermal investigations of permafrost in northern Alaska. *Am. Geophys. Union Trans.* (39)1:19–26.
5. Feulner, A. J., and J. R. Williams. 1967. Development of a groundwater supply at Cape Lisburne, Alaska, by modification of the thermal regime of permafrost. Prof. Paper 575-B. U.S. Geol. Survey, Washington, D.C. B-199–202.
6. Howitt, F. 1971. Permafrost geology at Prudhoe Bay. *In* Second international symposium on arctic geology. AAPG, San Francisco.
7. Metcalf & Eddy, Inc. 1952. Water supply reservoir and treatment plant for lake water supply, Thule. A-E Tech. Report QRR-147 U.S. Army Engineers District, New York, Corps of Engineers.
8. Reed, J. C. 1958. Exploration of naval petroleum reserve No. 4 and adjacent areas, northern Alaska, 1944–1953. Pt. 1. Prof. Paper 301. U.S. Geological Survey, Washington, D.C.
9. Walker, H. J. 1973. The nature of the seawater-freshwater interface during breakup in the Colville River Delta, Alaska. This volume.
10. Williams, J. R. 1970. Groundwater in permafrost regions of Alaska. Prof. Paper 696. U.S. Geological Survey, Washington, D.C. p. 83.
11. Williams, J. R. 1970. A review of water resources of the Umiat area, northern Alaska. U.S. Geol. Surv. Circ. 636. p. 8.
12. U.S. Public Health Service. 1962. Public Health Service drinking water standards, 1962. PHS Publ. 956. U.S. Department of Health, Education, and Welfare, Washington, D.C. p. 61.

THE NATURE OF THE SEAWATER-FRESHWATER INTERFACE DURING BREAKUP IN THE COLVILLE RIVER DELTA, ALASKA [1]

H. J. Walker

LOUISIANA STATE UNIVERSITY
Baton Rouge, Louisiana

INTRODUCTION

One of the most important factors affecting the regimen of arctic rivers is permafrost. Rivers, such as the Ob, Yenisey, and Mackenzie, that originate outside the permafrost zone and flow across it to the Arctic Ocean flow throughout the year. In contrast, many of the rivers that have their entire drainage basin within the zone of continuous permafrost cease to flow during winter. Exceptions include rivers fed by springs (such as the Kolyma in Siberia)⁶ and by deep lakes (such as the Sadlerochit in Alaska).⁴

In the zone of continuous permafrost, low temperatures ensure that the active layer freezes, eliminating groundwater storage as a source of supply. Furthermore, the upper 1-3 m of all water bodies freeze. Thus, winter flow at the air-ice interface is restricted to those locations where water is forced to the surface usually at some point downstream from springs.¹¹ This water upon freezing becomes aufeis and is temporarily lost to river flow. Even in the zone of continuous permafrost, deep rivers have unfrozen zones beneath their beds and thus are potential contributors to winter flow beneath the ice.¹¹

The Colville River in northern Alaska (Figure 1) is such a river. No late-winter flow has been detected beneath the ice of the channels in the Colville Delta [2].^{1,8} This suggests that little, if any, of the winter flow from the springs that occur in some of the tributaries of the Colville reaches the delta. Furthermore, when considered along with the longitudinal salinity profile that prevails in late winter, it suggests that little freshwater is contributed from the unfrozen alluvium beneath the channels.

WINTER CONDITIONS

Cessation of flow during winter allows replacement by seawater of all fresh and brackish water near the mouth of the river and the penetration of seawater upstream as far as 58 km (Figure 2). In 1971, prebreakup measurements under the ice of water salinity, using a Model RS5 Beckman portable salinometer, showed that the area approximately 8 km on either side of the river mouth had salinities of over 40 ‰. These high salinities result from the expulsion of salts during the freezing of the saline water in the lower

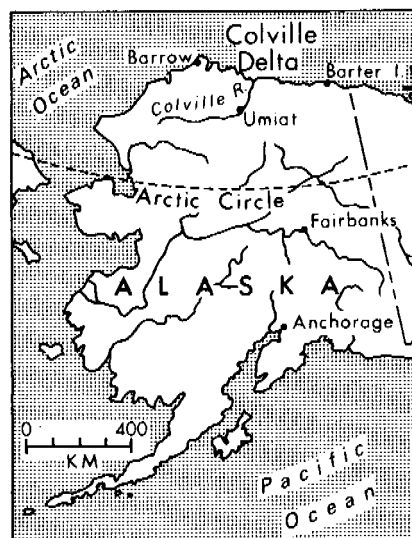


FIGURE 1 Location map.

reaches of the river channels and the shallower portions of the ocean at the delta front. Upstream there was a relatively gradual decrease to zero, whereas seaward salinities decreased to a value of about 32 ‰ at 12 km from the river mouth and then remained fairly constant farther seaward (Figure 2).

Thus, prior to breakup, the water beneath the ice of the subaqueous portion of the delta is as saline or more saline than average Arctic Ocean seawater, which indicates that

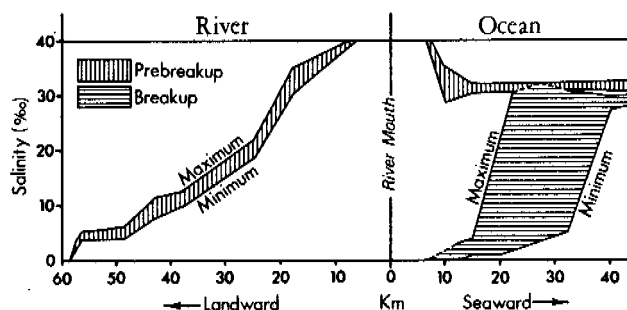


FIGURE 2 Salinity changes in the Colville River Delta.

the amount of freshwater flowing seaward in the Colville River during late winter must be minimal.

SALINITY CHANGES DURING BREAKUP

The meltwater that first accumulates on the ice is fresh because it is separated from the saline water beneath by a thick layer of ice. Ice fracturing soon follows, and mixing of the fresh and saline water occurs. In 1971, at a point 40 km upstream from the ocean, mixing began about the same time flow downstream on top of the ice was first recorded. Salinities, which had been on the order of 9–13 ‰ (Figure 2) at this location during winter, dropped rapidly as discharge increased. Complete flushing of saline water from this position in the delta took less than 2 days as had been the case in previous years.^{1,7}

In 1971, floodwater reached the front of the delta on 31 May and moved rapidly seaward both over and under the sea ice. That water moving over the ice drained through moulins and pressure ridge cracks both of which were numerous near the outer limit of over-ice flooding (Figure 3).

As in the case of the river channels, the saline water beneath the sea ice was progressively replaced by freshwater during flooding. Between 31 May and 9 June, freshwater had completely replaced seawater out to a distance of 10 km and seaward of this location had formed a wedge between

the sea ice and seawater to a distance of over 30 km (Figures 2 and 3).

The Seawater–Freshwater Interface

During breakup flooding, a helicopter was used to occupy 34 stations along the three section lines (Figure 3) that had been established by snowmobile during late winter. At each station, water salinity, conductivity, and temperature were measured at 0.6-m intervals, except across the interface between the seawater and freshwater where an interval of 0.15 m was used.

Changes in salinity at the interface were large, ranging from 0–8 ‰ to 29.5–30.5 ‰ within depth differences of less than 0.45 m. The stability of such an interface may be indexed by the densimetric Froude number, defined as:

$$U^2 / \gamma gh,$$

where *U* is the mean velocity of the floodwater as it moves seaward, γ is the density ratio, *g* is the acceleration of gravity, and *h* is the depth to the interface. The density ratio (γ) is

$$(\rho_s - \rho_f) / \rho_s,$$

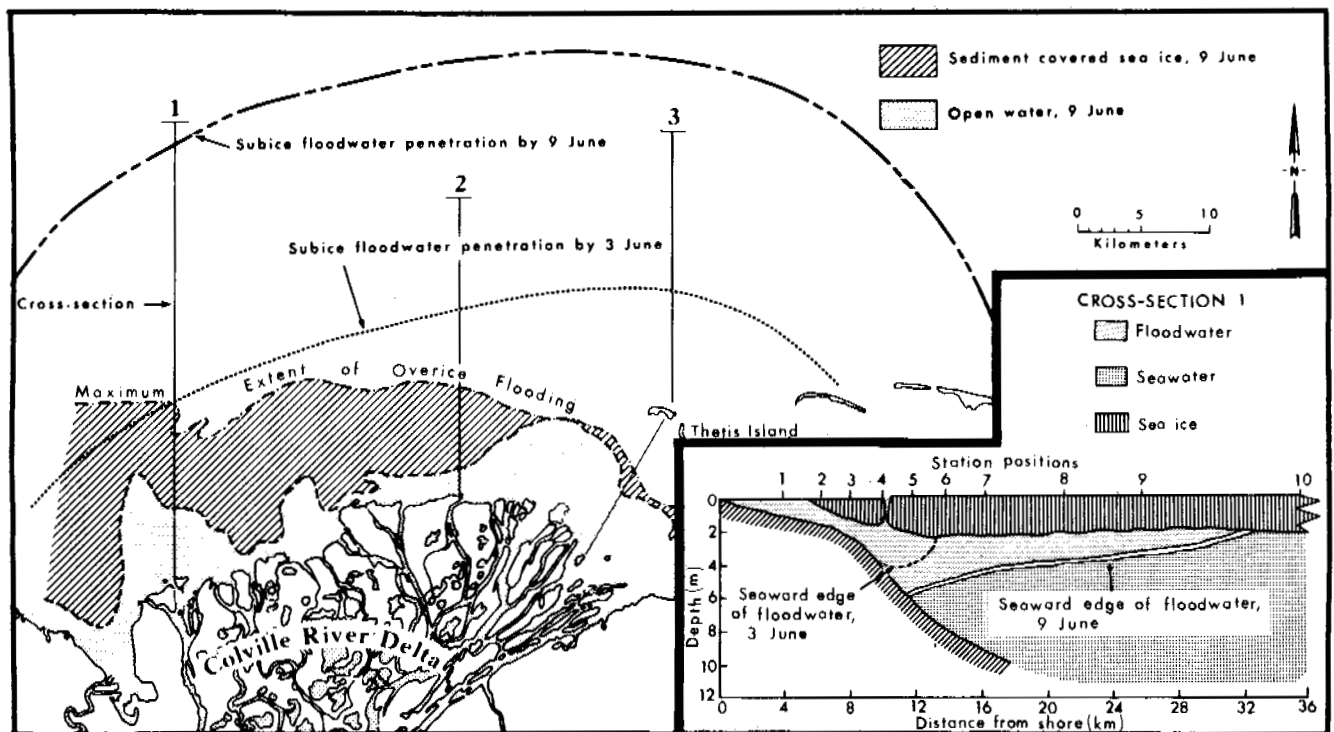


FIGURE 3 Breakup flooding, Colville River Delta, 1971.

where ρ_s is the density of the seawater and ρ_f is the density of the freshwater. Froude numbers for the interface beneath the sea ice during breakup ranged from 0.002 to 0.006 [3]. These are very low values and indicate a strong stability and little interfacial mixing. The degree of stratification in the waters off the Colville during breakup is much higher than that reported for the mouth of the Mississippi River.¹²

The Freshwater Wedge and Discharge

The replacement by seawater of all freshwater beneath the sea ice during winter and the sharpness of the interface between freshwater and seawater permit the calculation of river discharge during breakup. The volume discharged by the river to the sea prior to any particular time during breakup will equal the amount of freshwater in the system at the front of the delta, plus any water that was carried away by tidal action and longshore currents, minus the freshwater added from the melting of sea ice by that time.

The amount of freshwater in the system can be obtained by calculating the proportions of freshwater and seawater beneath the ice cover. The proportion of freshwater (C) at any level within a column of unit area is

$$1 - (S/S_0),$$

where S is the salinity at that level, and S_0 is the salinity before flooding began.

In 1971, the last date the helicopter was available was 9 June, 14 days after discharge began and 5 days before it ended. By this date the total freshwater seaward of the delta front was $4.98 \times 10^9 \text{ m}^3$ (Table I). Because of the sharpness of the freshwater-seawater interface, the configuration of the delta front, and the low tidal action along the arctic coast, it is assumed that the loss to the system either due to tidal action or longshore currents was negli-

ble. However, calculations based on snow depth and density measurements made prior to flooding on the sea ice and on the volume of sea ice melted provide a total of $0.34 \times 10^9 \text{ m}^3$ of freshwater in the system not derived from the river (Table I).

In 1971, through the first 14 days of river flow, the discharge was $4.64 \times 10^9 \text{ m}^3$. By that date, a water level recorder had been established in the river, and current measurements were being made. During the last 5 days of the flood season, discharge totaled $1.06 \times 10^9 \text{ m}^3$. Thus, the total for the flood period was $5.70 \times 10^9 \text{ m}^3$. This amount was 58 percent of the total discharge for 1971.⁹

SUMMARY

The effect of permafrost on the discharge of and/or erosion by arctic rivers has been documented in a number of studies.^{2,3,5,10,11} However, its indirect role in determining the nature of the freshwater-seawater interface near river mouths in the Arctic apparently has only recently been studied.^{1,8,9}

Permafrost, in combination with the seasonal freezing of the upper layers of all (lake, river, and sea) surface water, results in the virtual cessation of flow in many arctic rivers and the replacement of the freshwater beneath the ice by seawater in their lower reaches. During the period of flooding in spring, seawater is replaced by floodwater that progresses seaward as a wedge beneath the sea ice. The freshwater-seawater interface that develops remains sharp as the floodwater advances.

In 1971, the position and nature of the interface that developed off the Colville Delta in Alaska was established with a salinometer, and the volume of displaced seawater was calculated for the period of breakup flooding.

This technique should be usable in the determination of the initial discharge of any river that ceases flow for a period of time. However, it is especially useful in the Arctic where discharge during breakup is difficult to obtain by conventional methods.

TABLE I Freshwater Seaward of the Colville Delta by 9 June 1971

	Volume (10^9 m^3)
Location	
above interface	4.87
below interface	0.11
TOTAL	4.98
Source	
snowmelt from sea ice surface	0.04
sea ice meltwater	0.30
drainage basin discharge	4.64
TOTAL	4.98

REFERENCES

1. Arnborg, L., H. J. Walker, and J. Peippo. 1966. Water discharge in the Colville River, Alaska, 1962. *Geogr. Ann. Ser. A* 28: 195-210.
2. Brown, J., S. Dingman, and R. Lewellen. 1968. Hydrology of a drainage basin of the Alaskan Coastal Plain. CRREL Research Report 240. Cold Regions Research and Engineering Laboratory, Hanover, New Hampshire.
3. Cook, F. A. 1967. Fluvial processes in the high arctic. *Geogr. Bull.* 9:262-268.
4. Lewis, C. R. 1962. Icing mound on Sadlerochit River, Alaska. *Arctic* 15:145-150.
5. McCann, S. B., and J. G. Cogley. 1972. Hydrological observations on a small arctic catchment, Devon Island. *Can. J. Earth Sci.* 9:361-365.

6. Suslov, S. P. 1961. Physical geography of asiatic Russia. W. H. Freeman and Co., San Francisco.
7. Walker, H. J. 1970. Some aspects of erosion and sedimentation in an arctic delta during breakup. *Proc. Symp. Hydrol. Deltas (UNESCO)* 11:209-219.
8. Walker, H. J. Salinity changes in the Colville River Delta, Alaska, during breakup. *Proc. Symp. Role Snow Ice Hydrol. (Banff)* (In press)
9. Walker, H. J. Spring discharge of an arctic river determined from salinity measurements beneath sea ice. *Water Resour. Res.* (In press)
10. Walker, H. J., and L. Arnborg. 1966. Permafrost and ice-wedge effect on riverbank erosion, p. 164-171. *In Permafrost: Proceedings of an international conference*. National Academy of Sciences, Washington, D.C.
11. Williams, J. R. 1970. Ground water in permafrost regions of Alaska. Professional Paper 696. U.S. Geological Survey, Washington, D.C.
12. Wright, L., and J. Coleman. 1971. Effluent expansion and inter-

facial mixing in the presence of a salt wedge, Mississippi River Delta. *J. Geophys. Res.* 76:8649-8661.

NOTES

[1] This study was supported by the Arctic Program and Geography Programs, Office of Naval Research, under Contract N00014-69-A-0211-0003, Project NR 388 002, with Coastal Studies Institute, Louisiana State University. Logistic support was provided by the Naval Arctic Research Laboratory, Barrow, Alaska.

[2] Subice water movement is reported to occur in the Colville River at Umiat (about 150 km upstream from the ocean) during winter, although flow is too low to measure with standard current meters (Mr. L. R. Mayo, personal communication, U.S. Geological Survey).

[3] The calculation procedures used here are described in L. D. Wright, Louisiana State University, Coastal Studies Institute Technical Report 84, 1970. The computer program used is on file at Louisiana State University.

VI SURVEYING AND PREDICTING PERMAFROST CONDITIONS

Surveys, mapping, and predictions based on surface and subsurface compilation and aerial photography; state of the art and geophysical (resistivity, acoustic, electromagnetic) and multispectral techniques

MAPPING AND PREDICTING PERMAFROST IN NORTH AMERICA: A REVIEW, 1963–1973 [1]

Oscar J. Ferrians, Jr.

U.S. GEOLOGICAL SURVEY
Menlo Park, California

George D. Hobson

GEOLOGICAL SURVEY OF CANADA
Ottawa, Ontario

INTRODUCTION

Permafrost, which is soil or rock material that has remained below 0 °C (32 °F) continuously for more than 2 years, underlies approximately 20 percent of the land area of the world, including approximately 50 percent of Canada and 85 percent of Alaska. It is defined exclusively on the basis of temperature; however, one of the most important aspects of permafrost is the amount of ice that it contains. Permafrost with little or no ice generally does not cause engineering or environmental problems, but permafrost that is ice rich can cause extremely serious problems if allowed to thaw.

The recent discovery of vast amounts of oil and gas in arctic regions of North America has stimulated exploration and development and has focused attention on the many potential permafrost-related problems posed by this activity. The orderly development of these regions requires a thorough understanding of permafrost, especially the determination of its distribution and character.

Mapping and predicting permafrost are inherently difficult because permafrost occurs below the ground surface under the active layer, which generally ranges from 15 cm to 5 m (6 in. to 15 ft) in thickness. In addition, the ground conditions that determine the character of permafrost can vary greatly within short distances, both vertically and horizontally.

For this report, the methods of mapping and predicting permafrost have been divided into two broad categories: the traditional methods and the geophysical methods. In practice, the two categories overlap, and optimum results can be achieved only by utilizing aspects of both. To determine the best method or methods to use for a specific investigation, several factors must be considered—the most important of which are type and detail of information required, amount of area to be covered, complexity of the natural physical conditions in the area, and time and money available for the study.

Of primary concern to engineering in permafrost areas are the character of the permafrost soils and the way in which a proposed structure (building, pipeline, road, etc.) and these soils would interact. Wherever possible, areas that

are underlain by ice-rich permafrost should be avoided for most engineering projects; otherwise structures must be designed to accommodate the ice-rich condition of the natural foundation material, and special construction techniques acceptable for permafrost areas must be used.⁶²

The primary purpose of this report is to summarize the accomplishments in mapping and predicting permafrost in Canada and Alaska since 1963, when the First International Conference on Permafrost was held. Several papers presented at that conference¹⁵⁷ relate to methods of mapping and predicting permafrost, and a paper by Barnes⁷ described the state of the art in geophysical methods.

FACTORS THAT CONTROL AND AFFECT THE DISTRIBUTION AND CHARACTER OF PERMAFROST

The reasons for using either the traditional or geophysical methods of mapping and predicting permafrost and the attendant limitations and problems become clear once the factors that determine the distribution and character of permafrost are understood. These factors commonly are systematically appraised as a means of predicting permafrost conditions, and, even where subsurface data are available, they are used to extrapolate to adjacent areas where data are not available. Most reports that describe permafrost conditions mention at least some of these factors, and a few reports specifically treat them. For example, Brown^{27,35} describes the factors that influence permafrost, Gold⁶⁸ discusses the influence of surface conditions on ground temperature, Gold *et al.*⁶⁹ treat the thermal effects in permafrost, and Lachenbruch¹³⁰ describes the thermal conditions in permafrost.

The factors that control and affect the distribution and character of permafrost can be divided into five groups: climatic, geologic, hydrologic, topographic, and biologic.

Climatic Factors

Climate, more than anything else, determines the regional distribution and existence of permafrost. If the mean annual ground surface temperature remains below 0 °C, perma-

frost will form. The thickness of permafrost that can develop depends on the mean surface temperature and the geothermal gradient. The lower the temperature and gradient, the greater is the thickness of permafrost. The existing temperature of permafrost is commonly a reflection of past climates because permafrost at considerable depth responds very slowly to changes in surface temperature.¹²⁷

Various types of climatic data are used in predicting permafrost conditions, including mean annual air temperature, freeze and thaw indexes, precipitation, snowcover, wind, and microclimatic conditions. The importance of air temperature is self-evident, and Brown³⁰ concludes that there is a broad relationship between mean annual air temperature and permafrost temperature. Sanger¹⁹² and Thompson¹⁹⁹ discuss the usefulness of using freeze-thaw indexes and degree-days to estimate ground temperature for engineering purposes, and ground-temperature studies by Krinsley¹²⁴ in interior Alaska have demonstrated the effectiveness of snowcover as a ground insulator. Because it affects surface drainage conditions and soil moisture, precipitation must be considered; winds increase evaporation of surface water and also cause snowdrifts, which alter snowcover conditions. Local variations in microclimatic conditions can significantly affect permafrost; in fact, near the southern border of the permafrost region, these differences can determine whether or not permafrost is present.

Geologic Factors

The most important geologic factors to be considered are the character of the soil and rock materials [which determine their thermal properties, their potential for holding moisture (ice), and their behavior when thawed], the horizontal and vertical distribution of these materials, and the geothermal gradient or heat flow from the earth's interior. Differences in thermal properties, such as conductivity, diffusivity, reflectivity, and specific heat, affect the temperature and thickness of permafrost.

Lachenbruch¹³⁰ presents an excellent example of how differences in thermal properties of materials can affect the thickness of permafrost. Near Prudhoe Bay, permafrost is approximately 610 m (2 000 ft) deep, about 50 percent greater than at Barrow and about 100 percent greater than at Cape Simpson, although all three places have similar mean-surface temperatures. This difference in permafrost thickness can be explained simply in terms of an increased proportion of siliceous sediments from Cape Simpson to Barrow to Prudhoe Bay, which would cause a corresponding increase in conductivity and a decrease in geothermal gradient.

The geologic history of an area also is important if events within the last few thousand years caused changes in the surface environment—such as those produced by a trans-

gressing or regressing sea, draining of lakes, changing of stream channels, and retreating glaciers.

Hydrologic Factors

The most critical hydrologic factors are soil moisture (including the chemistry and movement of ground water), large water bodies, and glaciers and ice fields (both past and present). A review paper in this volume by Williams and van Everdingen specifically treats permafrost and ground water in North America.²¹³ The amount of soil moisture available and the rate of freezing are the principal factors that determine the amount of ice in permafrost. Because of the ability of water to hold heat, large water bodies have a significant effect on nearby permafrost. According to Lachenbruch, if a lake is at least twice as wide as the local undisturbed permafrost depth and deep enough that it does not freeze to the bottom in winter, an unfrozen “chimney” through the permafrost generally occurs beneath it.¹³⁰ Johnston and Brown¹⁰⁶ and Johnston *et al.*¹⁰⁷ have made observations on permafrost distribution at a lake in the Mackenzie Delta, Northwest Territories, and Lachenbruch¹²⁷ describes the effects of the ocean on permafrost.

The distribution of present-day glaciers and ice fields can be compiled from topographic maps, and the distribution of glaciers and ice fields during the Pleistocene epoch—when they were more extensive than at present—can be determined on the basis of the distribution of glacial deposits and features. A map showing the extent of various Pleistocene glaciations in Alaska was prepared by Coulter *et al.*,⁴⁵ and a map showing the retreatal positions and the chronology of the Wisconsin and Recent glaciers in North America was prepared by Prest.¹⁷⁷

Topographic Factors

The important topographic factors are altitude and slope, particularly the degree and orientation of the slope. Permafrost conditions and climate vary with changes in altitude, as well as with changes in latitude. At high altitudes, permafrost can exist at latitudes where it does not normally occur. The degree and orientation of a slope affect permafrost because they influence the amount of solar radiation received by the ground. In the discontinuous permafrost zone, south-facing slopes sometimes are free of permafrost, whereas nearby north-facing slopes are underlain by it. With similar slope conditions in the continuous permafrost zone, the permafrost would be thicker and colder under the north-facing slopes than it would be under the south-facing ones.

Biologic Factors

Vegetative cover, because it acts as a ground insulator, is the most important biologic factor. If it is disturbed, the

thermal regime may be upset, causing permafrost to thaw. For example, large animals disturb the vegetative cover, particularly where their movement is concentrated along trails, and forest fires destroy or alter the cover. Also, because vegetation is sensitive to ground conditions, it can serve as an important indirect indicator of permafrost conditions.

TRADITIONAL METHODS

The traditional methods for determining the distribution and character of permafrost generally involve interpretation of various kinds of data from geologic maps, aerial photographs, boreholes and wells, and extrapolation based on commonly interrelated factors, including climatic conditions, thermal properties of the various types of unconsolidated material and bedrock, drainage conditions, topographic setting, vegetative cover, proximity to large bodies of water, and permafrost-related geomorphic features.

For many years, black and white aerial photographs have been an important source of information used in these evaluations. Recently, other airborne-sensing data—including color photography, color infrared photography, thermal infrared imagery, and side-looking radar imagery—have been used with varying degrees of success. In addition, programs have been initiated to study the applicability of various types of satellite-acquired remote sensing data as an aid in determining the regional distribution and character of permafrost in Alaska.

Regional Mapping of Permafrost

Most published permafrost maps showing the regional distribution and character of permafrost are very generalized and at relatively small scales. The permafrost map of Canada by Brown^{29,32,34} is at a scale of 1 : 7 603 200 and the permafrost map of Alaska by Ferrians^{53–55} is at a scale of 1 : 2 500 000.

Two major permafrost zones are shown on the Canadian permafrost map: the continuous and the discontinuous, differentiated on the basis of the -5°C (21°F) isotherm of mean annual ground temperature measured just below the zone of seasonal variation. The discontinuous zone is subdivided into “widespread permafrost” and “southern fringe of permafrost region” on the basis of the -3.9°C (25°F) mean annual air isotherm, and the southern limit of the discontinuous permafrost zone deviates only slightly from the -1.1°C (30°F) mean annual air isotherm. Permafrost areas at high altitudes in the Cordillera and patches of permafrost in peat bogs, both south of the general limit of permafrost, are shown by special symbols. In addition, the physiographic regions are shown, and air and ground temperature and permafrost thickness are given for 24 different localities.

On the Alaskan permafrost map there are two major

divisions of the permafrost region: mountainous areas and lowland and upland areas. The thickness, distribution, and temperature of permafrost are extremely variable in the mountainous areas, but are more uniform in the lowland and upland areas.

From north to south, the mountainous areas are subdivided on the basis of climatic differences into three map units: areas generally underlain by permafrost, areas generally underlain by discontinuous permafrost, and areas generally underlain by isolated masses of permafrost.

Lowland and upland areas are subdivided into six map units that can be grouped into three broad zones: the northern zone, primarily north of the Brooks Range, is generally underlain by thick permafrost; the central zone, between the Brooks Range and the Alaska Range but including the Copper River Basin, is generally underlain by moderately thick to thin permafrost in areas where deposits are fine grained and by discontinuous permafrost or isolated masses of permafrost where the deposits are thick and coarse grained; and the southern zone, including the Bristol Bay Lowland and the northwestern Susitna Lowland, is generally underlain by numerous isolated masses of permafrost where deposits are fine grained and generally free of permafrost where the deposits are thick and coarse grained. Permafrost temperature just below the zone of seasonal variation generally ranges from -5 to -11°C (21 to 12°F) in the northern zone and from -1 to -5°C (30 to 21°F) in the central zone; it is generally above -1°C (30°F) in the southern zone.

The significance of special features within the permafrost region—such as glaciers, large bodies of water, active volcanoes, and thermal springs—is discussed, and active volcanoes and thermal springs are indicated by map symbols. In addition, permafrost data from selected wells and borings at 65 localities are presented.

Other recent permafrost maps of Alaska include small-scale, page-size maps by Williams²¹² and by Péwé,¹⁷³ both of whom recognize two major permafrost zones—the continuous and the discontinuous. The boundaries between these zones are drawn on the basis of known permafrost occurrences and mean annual air isotherms.

Local Mapping and Special Site and Area Studies

In contrast to the few regional maps covering all of Canada and Alaska, numerous local maps at a scale of 1 : 250 000 or larger have been prepared. These relatively detailed maps, which are extremely useful for land use assignments and engineering planning, generally include other important geologic environmental considerations in addition to permafrost conditions. The recently prepared 1 : 125 000-scale maps of the surficial geology of the Mackenzie River Valley transportation corridor in northwestern Canada are excellent examples of this type of mapping. At this time, maps by

Hughes *et al.*,^{92,93} Rutter *et al.*,¹⁹¹ and Rampton^{180,181} have been prepared, and maps covering the remainder of the transportation corridor will be completed in the near future. Hughes⁹¹ states that this mapping is designed to meet two main needs: “. . . need for basic terrain data for preliminary engineering assessment of transportation routes (roads, pipelines, railroads) and sites for airfields, staging areas and possibly towns” and “. . . need for a terrain classification that would permit application of appropriate land-use regulations and practices to differing terrain types.” Monroe is using the basic information presented in these maps to compile a series of “terrain classification and sensitivity” maps at a scale of 1:250 000.¹⁴⁹⁻¹⁵¹ These maps, designed to illustrate “land capability and performance,” provide information on both surficial and bedrock geology, including permafrost and ground-ice conditions, drainage characteristics, geologic hazards, and sources of construction materials.

In Alaska, the permafrost-related engineering-geologic problems posed by the trans-Alaska pipeline have been described by Kachadoorian and Ferrians,¹¹⁴ Ferrians and Kachadoorian,⁶¹ and Lachenbruch.¹³⁰ These problems were primary considerations in the engineering geologic investigations of the 1 270-km-long pipeline route extending from Prudhoe Bay on the Arctic Ocean to Valdez on the Gulf of Alaska. As an outgrowth of these investigations, a series of engineering-geologic maps at a scale of 1:125 000 were prepared by Ferrians,⁵⁶⁻⁵⁹ Kachadoorian,¹¹¹⁻¹¹³ and Weber.^{206,207} These maps show the distribution of the various types of geologic soil and rock materials and the location of special geologic features and structures. An accompanying text describes the character of these materials, the permafrost conditions, and other significant engineering-geologic conditions and processes. Other examples of geologic mapping in Alaska that include consideration of permafrost conditions are by Nichols and Yehle,¹⁵⁹ Weber and Péwé,²⁰⁸ and Péwé and Holmes.¹⁷⁵

Most of the recently published permafrost studies of special sites and areas have been made in Canada. These studies generally consist of descriptions of climate, geology, relief, drainage, vegetation, soils, permafrost observations, and, in some cases, engineering implications. To date the following areas and sites have been covered: Thompson, Manitoba,¹⁰⁷ Mackenzie Highway in Alberta and Mackenzie District,²⁶ Norman Wells, N.W.T.,²⁷ and the Kelsey Hydroelectric Generating Station in Manitoba¹⁰⁴; and investigations in British Columbia and Yukon Territory,³¹ Saskatchewan and Manitoba,²⁸ northern Ontario and northeastern Manitoba,³³ and the Canadian Arctic Archipelago.³⁷ In addition, limited permafrost studies were made by Gray in the Knob Lake area in central Labrador.⁷⁰

Dobrovolsky *et al.* made a special study along the route of the proposed trans-Alaska pipeline between Valdez and Fairbanks in south central Alaska.⁴⁸ Their report system-

atically locates and describes the significant geologic environmental factors, including permafrost, that could affect either the construction or operation of the pipeline.

Soil-Boring Investigations

A commonly used method of determining permafrost conditions directly is to bore holes through the active layer into the underlying permafrost. The character of the materials penetrated in the hole is noted and logged, and samples for laboratory analyses are collected at specified intervals. The logs of the boreholes and the results of the laboratory analyses are used to evaluate the permafrost soils. This method is commonly used to determine the suitability of the soils for engineering purposes.

A wide variety of equipment is used to bore the holes, to collect the samples, and, when necessary, to preserve the samples in their original frozen state. Recently, in Alaska, a bucket-auger device has been used very effectively in drilling large-diameter holes in permafrost to depths up to 15 m (50 ft). The holes are large enough (0.9 m in diameter) for a man to descend into the hole, collect samples, and examine the permafrost.

When it is necessary to bore a large number of holes, these investigations are time-consuming and very costly. For most building sites, the boring can be accomplished without too much difficulty, but investigations of routes for roads, pipelines, railroads, etc., generally are very difficult, because it is not practical to space holes closely enough so that the permafrost conditions can be accurately determined along the entire route. One of the most important aspects of investigating routes is to select boring sites that will provide the maximum amount of information. This is done by evaluating the distribution of the different geologic units; evaluating the drainage and slope conditions, the vegetative cover, and the special geologic features. The subsurface soil investigation of the proposed trans-Alaska pipeline route by Migliaccio and Rooney¹⁴⁷ is an excellent example of this type of study.

Geomorphic Features That Indicate the Presence of Permafrost

Several geomorphic features are excellent indicators of the presence of permafrost, and some may even indicate the character of the permafrost. Consequently, their recognition can be an important aid in mapping and predicting permafrost. However, these features must be interpreted with care because many resemble features that are found outside the permafrost region and that have modes of origin that are unrelated to permafrost. Also, some of the features are only indirectly related to permafrost. Bird discusses many permafrost-related geomorphic features and the problems of interpreting them from the air.¹⁸

The most important of these indicators are ice-wedge polygons, thaw or thermokarst pits, thaw lakes (including those that are oriented), beaded drainage, pingos, solifluction lobes and sheets, and muck or colluvial deposits rich in organic matter.

ICE-WEDGE POLYGONS

Ice-wedge polygons, honeycomb-like networks of vertical wedge-shaped ice masses in permafrost, underlie many thousands of square kilometres of northern Canada and Alaska. Individual polygons generally range from 5 to 100 m (15 to 300 ft) in diameter, and in many areas the ice wedges are overlain at the ground surface by shallow troughs that form striking polygonal patterns when viewed from the air. Studies in permafrost areas of North America relating to ice-wedge polygons and, in some cases, to other forms of patterned ground have been made by Brown,²⁵ Church *et al.*,⁴¹ French,⁶⁵ Mackay,¹⁴³ Péwé *et al.*,¹⁷⁴ Schenk,¹⁹³ Veysman,²⁰¹ and Washburn.²⁰²

THAW OR THERMOKARST PITS, THAW LAKES, AND BEADED DRAINAGE

Thaw or thermokarst pits form by the thawing of large underground ice masses that cause severe differential settlement of the surface of the ground. Lakes that occupy thaw depressions in permafrost are called thaw lakes; on the coastal plain of northwestern Canada and northern Alaska, these thaw lakes are commonly oriented in a northwesterly direction. Beaded drainage occurs in areas underlain by large masses of ground ice. The heat in the flowing surface water thaws the underlying ice masses forming depressions occupied by pools of water that are connected by the normally flowing stream. Black¹⁹ presents an excellent review of thaw depressions and thaw lakes, including oriented lakes, and Price¹⁷⁸ presents a review of all types of oriented lakes. Both supply lengthy bibliographies.

PINGOS

Pingos, which are small, ice-cored conical hills, are common in the continuous permafrost zone along the coastal plain of northern Alaska and northwestern Canada. They also occur in the discontinuous permafrost zone in central Alaska⁸⁸ and in central Yukon Territory.⁹⁰ They range from 15 to a few thousand m (45 to several thousand ft) in diameter and from 3 to about 200 m (10 to 600 ft) in height. Commonly, the summits of the pingos have craters, some of which are occupied by ponds.

J. R. Mackay and F. Müller have written numerous papers describing, classifying, and determining the modes of origin, the age, and the other pertinent aspects of pingos; however, most of these papers were published prior to the decade covered in this review. A recent paper by Mackay and Stager¹⁴⁵ describes the structure of some pingos in the Mackenzie Delta area in the Northwest Territories, and a

recent paper by Müller¹⁵³ thoroughly describes modern pingos. Other papers have been prepared by Pissart,¹⁷⁶ who describes pingos on Prince Patrick Island in the Canadian Arctic Archipelago, by Shearer *et al.*¹⁹⁶ who present evidence for submarine pingos in the Beaufort Sea, and by Krinsley,¹²⁵ who presents a detailed study of the Birch Creek pingo in interior Alaska.

SOLIFLUCTION LOBES AND SHEETS, AND MUCK DEPOSITS

Solifluction lobes and sheets, common in arctic regions, are masses of unconsolidated sediments ranging from less than a metre to a few hundred metres in width. They are formed by the gradual downslope (gravity) movement of water-saturated sediments. The surficial materials are especially mobile in the permafrost region, where these features locally cover entire valley walls because the active layer commonly is supersaturated with moisture. Solifluction plays a major role in the formation of many types of patterned ground.

Muck deposits or fine-grained colluvial deposits rich in organic matter are widespread throughout the permafrost region wherever fine-grained soils are present. Windblown silt (loess) and other fine-grained unconsolidated deposits are especially susceptible to solifluction, sheet wash, and other types of gravity movement. During downslope movement, large amounts of organic material are incorporated in these deposits, and the organic material is preserved because of the low ground temperatures.

Remote Sensing

The vastness of the permafrost region of North America and the lack of adequate transportation facilities make remote-sensing techniques especially well suited for reconnaissance studies of permafrost conditions. Rinker and Frost present a thorough discussion of the application of various types of remote sensors to environmental studies in the Arctic.¹⁸⁷ However, it must be emphasized that, for remote-sensing techniques to be fully successful, they must be done in conjunction with work on the ground that establishes "ground truth."

For many years, black and white aerial photographs have been an important source of information used in mapping and predicting permafrost conditions, and, since their use has become an accepted practice, very few reports on their use have been published during the past 10 years. An example of a recent report is one by Fletcher, who describes how aerial photographs were used for engineering soil reconnaissance in arctic Canada.⁶³ Color aerial photographs have been taken of some arctic areas but their use has been quite limited.

Greene has evaluated the applicability of using color infrared photographs and thermal infrared images to help solve permafrost-related and other arctic engineering prob-

lems.^{72,73} After evaluating three test areas along the route of the proposed trans-Alaska pipeline, Greene concludes that these types of remote-sensing surveys can provide valuable information concerning permafrost-related engineering problems and can assist the engineering geologist in site selection and route planning in the Arctic.

LeSchack and Morse have developed a technique of using dual-channel airborne infrared scanning for detecting ice in permafrost.¹³⁵ The authors conclude that they were successful in delineating massive ground ice in the form of ice-wedge polygons at a test site in interior Alaska.

Side-looking Radar (SLAR) has been used to a very limited extent in sensing permafrost, but there are possible applications. For example, ice-wedge polygons that have very little ground-surface expression might be detected by low-altitude SLAR.

Ferrians⁶⁰ and Haugen *et al.*⁷⁶ have begun studying the applicability of various types of satellite-acquired remote-sensing data as an aid in mapping the regional distribution of permafrost in Alaska. The images, which are at a scale of approximately 1:1 000 000, taken from the Earth Resources Technology Satellite (ERTS), provide an excellent synoptic view of terrain conditions, and the repetitive coverage makes it possible to monitor changing conditions.

Problems

The permafrost region of North America is vast and access to it is difficult, making permafrost investigations difficult from a logistical point of view. Coupled with the paucity of investigators, this is a basic problem that affects the advancement of all aspects of permafrost research in the field.

Some of the more important specific problems related to the traditional methods of mapping and predicting permafrost include:

- limited ground-temperature data
- inadequate *in situ* measurements of the thermal properties of soil and rock
- lack of weather observation stations to collect climatic data pertinent to permafrost studies
- inadequate knowledge of the distribution and character of the soil and rock materials, especially subsurface soil information
- lack of complete understanding of all of the interrelationships between the various factors that affect the distribution and character of permafrost
- inadequate soil-boring methods and equipment for both fine- and coarse-grained material and for both winter and summer operations
- insufficient refinements in remote-sensing techniques to detect many of the critical permafrost-related parameters in all of the different natural physical environments

GEOPHYSICAL METHODS

Temperature Measurements

The early work of Misener¹⁴⁸ in northern Canada and of Lachenbruch¹²⁸ in northern Alaska has been the starting point for many other studies in the field of heat flow and temperature measurements in permafrost. Higashi⁷⁸ measured the thermal diffusivity of frozen soils, whereas Misener measured the thermal resistance with a divided-bar apparatus to set out the thermal conductivity of frozen rock cores. At the First International Conference on Permafrost, Kersten¹¹⁹ discussed in detail the determination of thermal conductivity of frozen soil samples and set out graphs showing thermal conductivity versus moisture content with varying changes in temperature. Clark⁴² tabulates in considerable detail the thermal conductivity for various materials.

It has been demonstrated that all the water in natural soils and other porous systems does not freeze at a single freezing temperature, but that the ice content actually increases as the temperature is lowered.²¹⁴ Experiments carried out by Williams allow one to calculate the proportion of ice and unfrozen water in any given sample dependent on temperature. At a given negative temperature, the amount of unfrozen water present varies considerably with the type of soil, being greater in finer-grained soil. It also depends on whether the soil is freezing or thawing and, if thawing, it further depends on the lowest temperature reached during freezing. Penner¹⁷² measured thermal conductivity of two frozen soils at temperatures between 0 and -22°C (32 and -7.6°F). Of significance in this paper is the fact that by both measurement and estimation the same trend of increasing thermal conductivity is shown with decreasing temperature, that is, as the ice content increases. Measured values of thermal conductivity show a strong dependence on phase composition. It is noted that Penner experienced difficulty in making measurements between 0 and -2°C (32 and 29.4°F).

Jessop explains the change in temperature gradient at the base of permafrost on the basis of thermal conductivity.¹⁰⁰ The flow of heat must be the same on both sides of the boundary so that a higher gradient on one side must be accompanied by a lower conductivity on that same side. Frozen rock or sediment is expected to have a higher conductivity than unfrozen material because conductivity of ice is substantially higher than that of water. As Jessop points out, if a rock contained no water, there would be no reason for a change in temperature gradient at the permafrost base; but such a rock rarely exists in nature.

Judge¹⁰⁹ concludes that the thermal conductivity of a material is dependent on the mineral composition, the grain orientation and size, the porosity, the shape and orientation

of the voids, and the presence of any mineral infilling of the pore space. He presents a table of thermal conductivities for various rock types showing a variation from 3 $\text{mcal/cm}\cdot\text{s}\cdot^{\circ}\text{C}$ for shales, to as high as 18 for quartzites, and values below 3 for unfrozen soil. He also tabulates typical thermal conductivities and thermal diffusivities of some common rock types.¹¹⁰ Estimates of diffusivity may be made if density and thermal conductivity of the media are known; Beck *et al.*¹³ further discuss the measurement and estimation of diffusivity of rocks.

The prediction of the thickness of permafrost is the subject of several papers by authors concerned with heat flow and temperature measurements. Mean annual ground temperature both now and in the past, incoming solar radiation, thermal conductivity of the underlying material, ground-water movement, terrestrial heat flux, various conditions of soil type and vegetation cover, etc., are some of the parameters that must be considered if the thickness of permafrost is to be estimated from thermal data. Brown,³⁰ Williams,²¹¹ Jessop,¹⁰² Judge,^{109,110} and McCormick¹⁴⁶ have contributed significantly to the problem of determining permafrost thickness by considering the variables in the thermal regime above and below ground surface. Present results suggest that the permafrost is thickest beneath the exposed or thinly covered Precambrian rocks of northern Baffin Island, the Boothia Peninsula, and Victoria Island and in the central zone beneath the high-conductivity Paleozoic rocks such as dolomites and pure quartz sandstones. Thicknesses in these areas may be as much as 1 000 m (3 300 ft); it is doubtful that thicknesses exceed 500 m (1 650 ft) in most locations, and they may be considerably less in the clastic sediment of the Sverdrup Basin. Lachenbruch and Marshall underline very vividly the danger of estimating permafrost depth from surface temperature alone.¹³¹ They show that at Cape Thompson, Alaska, the surface temperature is 4 °C (7 °F) warmer than at Cape Simpson, but permafrost at the former location is 76 m (249 ft) deeper. French⁶⁴ concludes that the geomorphology of Banks Island, in many cases, seems to be influenced by the prevailing northwest winds that promote temperature variations on slopes with different exposures, thereby affecting the thickness of the permafrost. Ives⁹⁹ and Ives and Fahey⁹⁸ have used thermistors to determine the presence of permafrost in the Colorado Rocky Mountains at altitudes of 3 450 m and higher. Jessop¹⁰¹ points out that it was only with the publication of the Geological Survey of Canada map 1257A by Prest¹⁷⁷ that it became possible to calculate an approximate distribution of climatic disturbance to heat flow. Jessop presents a map that depicts a close approximation to the corrections that must be added to measured surface heat flow values to make these calculations. It is possible, then, with a knowledge of the mean annual ground temperatures, the general climatology at a given location, and the regional distribution of the

geothermal flux from the earth's interior to predict whether or not permafrost is present and how thick it is. This prediction, however, is not a simple process.

Few heat flow values have been published for the Canadian north; however, some 33 borehole values have been published for the whole of Canada.¹¹⁰ Published terrestrial heat flow values vary in Canada from 0.6 to 2.1 $\text{mcal/cm}^2\cdot\text{s}$. Thermistor cables have been installed in many boreholes and seismic shot holes to measure near-surface temperatures.^{13,100,137} Beck *et al.*¹³ conclude that considerable latitude is allowable in design and in type of material of the thermistor probes if errors of ± 10 percent can be tolerated. If an accuracy of 3–5 percent is required, very careful and detailed probe design, as well as significant modifications to the current theory, would be required, factors that, in the opinion of these authors, are not justifiable in view of the severity of other errors that enter heat flow determinations.

Thermal conductivities are measured on a routine basis on both core and chip samples using the steady-state and relative "divided-bar" method and the transient but absolute "needle-probe" methods.^{109,110}

Heat flow has been measured in the interisland waters of the Canadian Arctic Archipelago, but only to determine mean values of heat flow.^{134,167} Heat flow in M'Clure Strait is far from uniform with a mean value of 0.45 ± 0.08 $\text{mcal/cm}^2\cdot\text{s}$. These experiments were conducted to determine whether heat flow in the Canadian Arctic was uniform, not whether permafrost was present.

Acoustic Methods

One of the most discriminating acoustic properties of solids is the velocity of dilatational waves. Barnes summarized the knowledge of dilatational wave velocity data to that time as they pertained to permafrost regions.⁷ Nakano *et al.* have investigated the acoustic properties of frozen soils in great detail.¹⁵⁶ There is a decrease in dilatational wave velocity as an initially frozen water-saturated soil is thawed, and it appears to be a direct consequence of the change in state of the water. Nakano *et al.* suggest that the compressional velocity is largely determined by the compressibility of the interstitial water, rather than by the compressibility of the mineral solids. They further expect with their apparatus to be able to measure attenuation simultaneously with the elastic properties of the frozen soil. The technique should be particularly useful in discerning small variations of elastic properties as a function of temperature. These authors have dealt with the determination of dilatational and shear-wave velocities, as well as the attenuation of several standard frozen soils, by using critical angle tank. The velocity of dilatational and shear waves was measured as a function of temperature and

frequency. Frequency has no distinguishable effect on dilatational waves in the range between 300 kHz and 1.2 MHz.

Westphal conducted experiments to determine the attenuation of high frequencies by ice.²¹⁰ *In situ* studies of the propagation of compressional acoustic waves in the frequency range from 2.5 to 15 kHz have shown the presence of attenuation due to Rayleigh scattering. For frequencies above 5 kHz, this scattering is apparently due to the elastic inhomogeneity at crystal interfaces. At that time, Westphal concluded that the presence of scattering would preclude the use of frequencies above 7.5 kHz for seismic sounding through thick temperate glaciers.

Faas and Caulfield⁵² have shown that the detection of total energy and its matrix components of amplitude, frequency, and phase as a function of time can yield detailed information of the physical properties of land and marine sediment. More specifically, recent tests directed toward the measurement of porosity based on information extracted from the frequency domain have yielded results averaging a prediction error of less than 10 percent. Nelson *et al.*¹⁵⁸ take an approach that leads to a unique matching of the major acoustic parameters of energy, frequency, time, and amplitude to physical properties of the sediments. The frequency shift parameter may be the best indicator for the prediction of volumetric moisture content. Data acquired by these authors under contract to CRREL and the Geological Survey of Canada demonstrate an apparent relationship between frequency distribution and the porosity or percent of moisture as a function of depth. The system, known as LANDSCOPE, also delineates changes in the density through detection of layering as obtained in standard geophysical measurements to provide a rapid nondestructive sampling technique for determining the major physical properties of frozen soils.

A series of experiments to acquire acoustic data in the permafrost environment has been conducted at Resolute Bay, Tuktoyaktuk, Point Barrow, and in central Alaska.^{49, 160, 183-186} The objective of these programs was to establish a positive ground truth for the application of acoustic technology to permafrost. An instrument known as the LANDSCOPE system, a Raytheon Corporation instrument, was used. The last program in this series of experiments was undertaken at Thompson, Manitoba. Data acquisition proceeded as follows: acquisition of acoustic data; drilling and full coring of boreholes beneath the acoustic sites; geophysical logging of the boreholes with electric, acoustic, and neutron logging; seismic refraction profiles across the sampling area for horizontal velocity control; and a full analysis of the physical samples from the boreholes. The geophysical logging program was designed to provide bulk modulus data from the three-dimensional velocity measurements and permafrost acoustic impedance information. Time-frequency-energy relationships were developed from

the acoustic data. A Fourier analysis permits a correlation between observed frequency shift and the moisture content (by volume percent) of the reflecting soil. The frequency-response graph and the energy graph can be correlated to the percentage of moisture observed in the cores. The depth observed in the cores compared with changes in the physical sediment or soil type should correspond to acoustic reflectors at the same depth, provided the proper value of sound speed is used. Basically, the end product is the construction of an acoustic model depicting the subsurface structure at each location. The structure model for each location shows the stratigraphy, identifying ice, and other geological materials.

Radio Methods

Although most permafrost workers do not regard active glaciers as permafrost, a reference should be made to radio frequency methods of measuring thickness of glacier ice. Adey⁴ includes a rather extensive bibliography at the end of his paper describing microwave radiometry.

Seismic Methods

It has been shown above that the relation between solid and liquid water phases changes constantly in the presence of a temperature gradient. It is this fact that induces the seismic velocity gradient in permafrost. The gradient value of seismic velocity depends on temperature, moisture, ground composition, thickness of the frozen layer, and other factors. Compression of the frozen ground, which increases with depth, will cause decreased seismic velocities because the temperature of fusion of ice rises with the increasing pressure. The initial freezing temperature of the soils depends largely on the moisture content of the soil. The change of seismic velocity during freezing of the ground is caused not only by changes in the elasticity of ice and water but also changes in elasticity of the formation caused by the fissure walls being bound together. Seismic wave velocity in frozen ground is very dependent on ground temperatures.

Some of the earliest work in North America is reported by Barnes and MacCarthy,⁸ who state that a high seismic velocity is an almost sure indication of the presence of permafrost and can only be misinterpreted as bedrock. In confirmation of and in contrast to this statement, however, Hunter⁹⁴ has recorded velocities in permafrost as low as 1 525 m/s (5 000 ft/s), and Hobson⁸⁰ has reported velocities as high as 5 485 m/s (15 300 ft/s) in frozen gravel. Zelonka²¹⁷ noted that moisture content of the material traversed has a marked effect on the seismic wave velocities through frozen materials and that transmission of compressional waves through them is a function of elastic properties of both the

soil grains and the interstitial water. There is a dependence of the modulus of rigidity on temperature.

Hobson⁷⁹ and Hobson and Overton⁸² describe seismic refraction experiments in the Canadian arctic islands that require definition of permafrost in a conventional manner. Musgrave,¹⁵⁵ on the other hand, includes several papers on refraction seismic methods that have a direct application to the resolution of the permafrost problem; the curved-path and the Blondeau methods of correcting for near-surface conditions are considered in some detail in this paper.

Two papers, Bush and Schwarz³⁹ and Hobson,⁸⁰ describe shallow seismic experiments in permafrost. Both conclude that reasonably accurate interpretations of depth to bedrock can be made using refraction methods, unless there is differential thawing in the overlying material. Bush and Schwarz intimate that frozen ground should be suspected when high-frequency high-velocity early arrivals of energy are observed near the shot point that attenuates rapidly into lower frequency, lower velocity energy with distance and when total times from reversed refraction profiles are not the same, indicating that the seismic energy travels different paths depending on the direction traveled. Hobson concluded that the active layer highly attenuates seismic energy.

Roethlisberger,^{188,189} Bell and Heine,¹⁵ and Bell¹⁴ discuss seismic results from Greenland and Antarctica that do pertain to the detection of permafrost. Bell,¹⁴ in particular, in a table of seismic velocity in ice and frozen ground, shows that these two media cannot be positively distinguished by means of seismic velocity measurements. Roethlisberger¹⁸⁹ states that, in materials containing clay minerals, the energy of the direct wave along the surface will diminish rapidly with distance. Kohnen¹²³ also worked in Greenland and Antarctica and points up the interrelationship between seismic velocity and temperature.

Several authors, among them Clew *et al.*,⁴³ Hunter and Good,⁹⁷ and Hunter,⁹⁶ have studied the attenuation of seismic waves through permafrost, and all agree that there is an attenuation of both compressional and shear waves with distance both in the active layer and in the underlying permafrost. Hunter⁹⁶ concludes that the amplitude characteristics of refracted waves differ for thick and thin permafrost zones and may be a diagnostic feature in regional surveys.

The mechanical and elastic constants in frozen and thawed media have been studied in the field by Hobson and Hunter,⁸³ Hunter and Good,⁹⁷ and Garg⁶⁷ all of whom determined Poisson's ratio, Young's modulus, and other such parameters. One conclusion from these experiments is that values of the propagation velocities of elastic waves and the Poisson's ratio indicate that frozen sand is similar to solid rock with respect to its elastic properties.

Schenck¹⁹⁴ does not deal specifically with permafrost,

but considers diffractions at lenses having low velocities. This paper may have an application to the problem of interpretation of low-velocity inclusions within a permafrost layer.

Explorationists, using seismic methods in permafrost to determine petroleum potential in northern areas, in general, make use of the reflection seismic technique but are somewhat reticent about the reduction methods used to overcome the problem of highly variable horizontal and vertical extents of the medium. Boulware²² indicates that reflected energy can be recorded from the base of the permafrost but admits to several other confounding problems. Patterson¹⁶⁸ deals with the problem of near-surface velocity inversion and suggests that the problem of velocity inversions can generally be solved by using a modified Blondeau method or the curved-path method if certain principles which he specifies are taken into account. Rackets¹⁷⁹ describes how small buried explosive charges can be used to circumvent the problem of frost breaks encountered when large charges of explosives are detonated in permafrosted areas.

In considering detection of permafrost in the offshore environment, Lachenbruch^{127,128} concluded that, up to approximately 1 000 m (~3 000 ft) offshore, permafrost was not to be expected at depths below the sea bottom greater than 60–90 m (200–300 ft) unless the shoreline had undergone large transgressions in the last 1 000 years. If the shoreline has been stationary or regressing, permafrost depths are not expected to exceed 30 m (100 ft) at points more than 300–600 m (1 000–2 000 ft) offshore. Wereniskiold²⁰⁹ had concluded that frozen ground below the sea bed must extend about 100 m (300 ft) from shore. Pamerter¹⁶⁶ reports on a professional talk describing data from the CSS *Hudson* voyage through the Northwest Passage in 1970 in which it is believed that no permafrost was identified positively in the marine subsurface. There was, however, a hard reflector at the top of the deltaic unit; this could be ice or a boulder gravel beach. Ice must be considered, although it would be relict from a time of lower sea level. A number of pingo-like features were detected beneath the Beaufort Sea, remarkably similar to pingos on land. They stand 30–45 m (100–150 ft) in height and are always under 20 m (60 ft) or more of water.

Laboratory determinations of various properties of frozen soil have been undertaken by a number of authors. Yong²¹⁶ has conducted experiments to study the shear strength of frozen soils. Kaplar¹¹⁵ has studied the dynamic elastic moduli in the laboratory and concluded that, for some soils, Poisson's ratio increases with temperature, while for others this ratio decreases with temperature. King,¹²⁰ King and Bamford,¹²¹ and Kurfurst and King¹²⁶ have investigated the static and dynamic elastic properties of sandstone at permafrost temperatures. Timur has made one of the more exhaustive studies of the velocity of compressional

waves in permafrost.²⁰⁰ In all cases, samples were frozen to -21 or -22 °C (~ -7 °F), below which the velocities were independent of temperature. Velocities observed during the thawing and the freezing processes display a hysteresis effect. The shapes of the velocity-versus-temperature curves are functions of lithology, pore structure, and the nature of the interstitial fluids. The work of Watkins *et al.*²⁰³ pertains to permafrost in that it is concerned with the velocities of compressional waves in saturated and unsaturated sediments. The velocity of compressional waves in saturated and unsaturated sediments depends upon porosity and this relation must be considered in describing materials in a permafrost environment.

Borehole Logging Methods

Jessop,¹⁰⁰ Judge,^{109,110} and Johnston and Brown^{105,106} have measured temperatures in boreholes to determine thermal gradient and heat flow values at approximately 35 locations in northern Canada. Hobson *et al.*⁸¹ discussed the various geophysical logs run in two holes drilled in the Muskox Intrusion to depths in excess of 700 m (2 300 ft). A temperature profile run in a borehole on Richards Island at the mouth of the Mackenzie River shows a steep gradient at the interval between 110 and 115 m (361 and 378 ft), which has been interpreted as ice.¹⁰⁰ From this temperature log, it is concluded that a considerable thickness of ice can occur at depth.

Ladanyi and Johnston¹³² report on the application of a Menard pressuremeter, a borehole dilatometer. The experimental results show that a borehole dilatometer has the potential to determine basic creep parameters of frozen soils. Data are necessary for predicting the long-term behavior of structures embedded in permafrost.

Permafrost in the form of frozen soil and ice was penetrated in several core holes drilled in the Beaufort Sea in early 1970 by the Arctic Petroleum Operators Association.^{5,141,142} Freshwater ice was found just below the sea bed north of Tuktoyaktuk and was also recovered from the sea bottom between some Canadian arctic islands.

Probably the best publication in recent years on well log interpretation in permafrost is that published by Desai and Moore,⁴⁷ a fairly exhaustive treatment of identification and determination of properties of permafrost encountered during the drilling of oil wells. Howitt⁸⁹ reports that permafrost has been found to a depth of approximately 610 m (2 000 ft) in the Prudhoe Bay Field in Alaska. The extent of the permafrost is best seen on the sonic, resistivity, and caliper logs run in the holes immediately after drilling, while temperature surveys run in the completed well several months later clearly show the base of the permafrost.

Wyder *et al.*²¹⁵ report on the use of natural gamma, neutron, caliper, and decentralized gamma-gamma logs in shal-

low drill holes near Tuktoyaktuk, N.W.T. There is a definite correlation between sediment type and amount of natural gamma radiation; ice shows the lowest gamma content, with sand intermediate between ice and the high-count clay units. Investigations indicate that it is virtually impossible with only the gamma log to differentiate between ice-rich sediments and frozen sediments not containing excess ice. This problem can be solved if one or more other logs are contrasted with the natural gamma log. In a porous water-saturated hydrogen-free rock, the neutron log is actually a porosity measuring device. This log shows a lack of sensitivity at very high hydrogen content, which is equated with ice in this paper. The gamma-gamma log, in general, is a record of the variation of the bulk density of formations along the axis of the borehole. The gamma-gamma density logs, in conjunction with the natural gamma logs, provide a good reliable means of distinguishing between ice bodies and sediments. Opposite the low-density ice bodies, the density curve increases and the natural gamma curve decreases. This then is a means of determining the presence of ice bodies in a borehole without having to obtain an actual sample. Use of a combination of these two logs also appears to enable differentiating ice bodies containing clay, silt, and sand from either ice-rich sand or ice-rich clay and silt units.

Williams and van Everdingen²¹³ comment on borehole geophysical logging methods in permafrost at Isabella Creek near Fairbanks, Alaska. Natural gamma, gamma-gamma, neutron, resistivity, and caliper logs made in these holes showed that valid geophysical logs can be made in frozen unconsolidated deposits and that interpretation is possible in terms of bulk density, organic content, moisture content, temperature, rate of freezing, resistivity of interstitial ice and water, location of ice segregations, and, possibly, migration of water during freezing and thawing.

Gravity Methods

Gravity methods are not used to determine the presence or absence of permafrost because gravity is not affected by the freezing or thawing of soils or rock. However, gravity methods might be used locally to determine the thickness and extent of ice lenses and pingos. Rampton and Walcott¹⁸² reveal that gravity methods have been applied experimentally to investigate the distribution of ice lenses in irregular topography in the Mackenzie Delta. A Bouguer profiling technique complemented by computer analysis can reveal and delineate ice lenses. Sobczak¹⁹⁸ suggests that there may be a 2 mgal ($20 \mu\text{m/s}^2$) expression of gravity over a pingo.

Paleomagnetic Methods

There is no record to date revealed to the authors that paleomagnetic methods have been used in the study of

permafrost. However, it is suggested that the paleomagnetism of mud cores may reveal pole reversals that may be significant in the determination of paleoclimates.

Electrical Methods

Frozen rocks differ markedly from thawed ones in their true specific electrical resistance and the dielectric constant, while lithological differences in frozen rocks affect their electric resistances, particularly in the temperature range from 0 to -2°C (32 to 28.4°F). Barnes and MacCarthy⁸ have described some of the earlier field observations using electrical resistivity methods. Addison and Pounder³ and Addison² have investigated the variation of the dielectric coefficient and resistivity as a function of salinity, frequency, and temperature. Up to 100 kHz, the dielectric coefficient decreases almost as the reciprocal of the frequency, while resistivity itself decreases slowly as frequency increases.

The problem of electrode resistance has been investigated by Hessler and Franzke⁷⁷ and by Gross.⁷⁵ There is a pronounced increase in electrode resistance at temperatures below -18.3°C (0°F). Mackay¹³⁶ thoroughly describes resistivity techniques applied to permafrost investigations. He concludes that resistivity methods may be used to identify and delineate such construction materials as sands and gravels in permafrost as well as other rock and soil types or ground-ice bodies. Moisture content, temperature, and salinity are major determinants of electrical resistivity in rocks and soils. Mackay suggests that vegetative cover, topography, and drainage can be useful indicators of relative differences in near-surface resistivity. Positive identification of rock and soil types is hindered by the fact that apparent resistivities have wide ranges of overlapping values for frozen and unfrozen materials. Mackay also points out that the angles at which the resistivity traverses cross ice boundaries influence the readings.

Ostrem¹⁶⁴ underlines the fact that ice does not have the same resistivity for currents in all directions. He found that great variations in resistivity were to be observed when using dc methods and that the higher values of resistivity were obtainable at lower temperatures. A significant contribution from this paper is that every piece of ice seems to have its own specific "low resistivity direction" in that resistivity in one direction may be 100 times the resistivity in the opposite direction.

Laboratory investigations by Hoekstra⁸⁵ show that the change in resistivity of the clay sample discussed by Ogilvy¹⁶¹ is confirmed and that freezing reduces the conductivity by approximately a factor of 10. Hochstein⁸⁴ shows that resistivity depends on contact resistance between grains, which is a function of grain size and pressure. With increased grain size and increased pressure, the contact area between

grains must become larger and the contact resistance, consequently, must decrease. After eliminating the influence of hydrostatic pressure upon contact resistance, resistivity variations can be explained by temperature variations.

Several authors have investigated the possibility of studying permafrost by using the propagation of radio waves through a study of the dielectric constants, permittivity, and loss tangents as electrical properties. It has been found that these methods can generally be used with greater success the lower the average temperature in the permafrost. These electrical properties have been investigated by Jiracek and Bentley,¹⁰³ Addison,¹ Peden and Webber,¹⁷⁰ Peden and Rogers,¹⁷¹ and Hoekstra and Cappillino.⁸⁶ Evans⁵⁰ found that permittivity at high frequencies is independent of temperature and that ice, in general, has a high static permittivity value and long relaxation time. At low frequencies (300 Hz), dielectric constants decrease with increasing mineral content, while at high frequencies (30 MHz) loss tangent increases with mineral content. Bogorodskiy *et al.*²¹ show that this is due to a decrease in ice content with an increase in mineral content whose dielectric constant is greater than that of ice at high frequencies and lower at low frequencies. Other investigations have been conducted by Cook,⁴⁴ Biggs,^{16,17} and Watt *et al.*²⁰⁴

Magnetotelluric and telluric currents have not been used to any great extent to investigate permafrost. Greenhouse⁷⁴ investigated the use of telluric currents in a cursory manner.

A new method of electrical prospecting, magnetic-induced polarization, has been proposed by Siegel,¹⁹⁷ and should be of use in permafrost environments where there are electrical conductivity contrasts and where the laws of attenuation with depth pertain. The method has not been applied to permafrost as yet, presumably because Siegel has not chosen to go into the more difficult environment.

The electromagnetic method of investigating the subsurface of the permafrost environment has received considerable attention in recent years. Some of the original work in this field was conducted by Keller and Frischknecht.^{117,118} More recent investigations have been made by Pearce and Walker,¹⁶⁹ King and Harrison,¹²² Webber and Peden,²⁰⁵ and Bahar.⁶

Airborne experiments, using VLF radio stations around the world, have been used in recent studies. The principal papers in this new field of endeavor have been written by Barringer,^{9,10} Barringer and McNeill,^{11,12} Frischknecht and Stanley,⁶⁶ and Hoekstra and McNeill.⁸⁷ The general purpose is to determine whether a correlation exists between E phase, radio phase, and known permafrost occurrences, using wave tilt theory. Wave tilt measurements, both theoretically and in practice, appear to give useful information about the resistivity of the soils. One conclusion arrived at early in the investigations was that the method should be

used when the active layer is frozen. Both quadrature-phase and in-phase components of the wave tilt are determined. In effect, the technique measures the vertical and horizontal components of the electric field and the resultant magnetic field of the VLF signal. Blomquist²⁰ demonstrated that the wave tilt changed almost instantaneously when a discontinuity in the ground was traversed and that the angle of tilt is a measurement of the dielectric constant. Jones and Price¹⁰⁸ have calculated curves for the field components at the surface, which show a marked discontinuity in the horizontal electric field at the contact of two geological horizons. Frischknecht and Stanley⁶⁶ disclose that at least one ice-free locality was located using the airborne VLF data, and it was corroborated by resistivity measurements. A short survey using the VLF instrumentation by the Geological Survey of Canada at Thompson, Manitoba, failed to delineate permafrost because of the complications caused by the active layer and the use of only very low frequencies. This experience demonstrates the need for a multi-frequency approach to the problem.

Mutual coupling between loops has also been used by Keller¹¹⁶ to measure permafrost thickness. Coupling is measured at several frequencies ranging from 20 Hz to 20 kHz. Surveys at wells in the Prudhoe Bay area indicate an average uncertainty of about 6 percent for depths ranging from 100 to 700 m (330 to 2 300 ft). At lesser depths, the method loses accuracy. Keller presumes that it would be simpler to use VLF techniques when permafrost is less than 100 m (330 ft) thick.

Campbell *et al.*⁴⁰ have proposed another electromagnetic subsurface profiling (ESP) technique to accurately locate large masses of ground ice in permafrost. It is claimed that ESP will provide information on the complex internal structure and irregular upper surface of permafrost in areas where large masses of ground ice, including ice wedges, are present. Such surveys are conducted on the ground. A signal of wide frequency band width is introduced into the earth, the low frequency component propagating through the earth more easily while the higher frequency components give rise to resolution. Penetration is limited to less than 6 m (20 ft) in the Point Barrow area, but the actual penetration capability is undetermined to date.

Model Studies

Brown *et al.*,³⁸ making use of limited ground temperature measurements in the neighborhood of a small shallow lake near Inuvik, N.W.T., estimated, with the help of a computer, the entire thermal regime under and about the lake. This study forecast a completely unfrozen zone directly under the lake, and field borings under the lake and adjacent to it supported this theory. This study underlines the importance of obtaining precise knowledge of temperatures and temperature variations at ground surface.

Outcalt¹⁶⁵ describes a simulator to model the thermal contrast produced by stratification, variable sea ice, or active layer thickness in the Arctic. The probable effects of terrain modifications can be simulated so that the impact of modifications to the environment may be estimated.

Roethlisberger¹⁹⁰ describes the use of a computer program to produce a complete table of reflection and transmission coefficients for any combination of solids for angles of emergence from 90 to 0° at any desired increment. Curves and tables can be presented for various velocities, densities, and Poisson's ratios. The energy spectrum from wide-angle reflections may be of assistance in identifying the nature of a subsurface reflector. Hunter⁹⁵ has conducted a model study of reflected seismic waves from the bottom of the permafrost layer and observes that there may be two explanations for no reflections from the base of thin permafrost—overlap of wave trains and no reflector. He suggests that converted later arrivals of energy may be useful in the identification of the base of the permafrost.

Mooney *et al.*¹⁵² have computed apparent resistivity and induced polarization results for layered earth structures allowing for any type of array and any number of layers.

Shearer¹⁹⁵ has made a theoretical investigation of offshore permafrost thickness. The factors that enter such a study are thermal gradient, thermal conductivity, porosity, length of emergence, and the time of submergence. These studies allow one to determine where the base of the permafrost is at any given point on the Continental Shelf.

Applications

MINING

The development of an open-pit mine in permafrost requires a knowledge of the physical properties of the different rock types involved. Drilling conditions and costs and the propagation and attenuation of shock waves during blasting operations dictate that the elastic moduli must be determined. Lang¹³³ is concerned with experiments with blasting in permafrost at the location of an iron ore mine, while Garg⁶⁷ has applied seismic methods to the determination of elastic moduli at another location. Garg declares that the degree of leaching, ice content, and structural discontinuities in the host rocks can be predicted on a semi-quantitative basis. Operations at that mine have been greatly facilitated through the use of geophysical methods to determine permafrost conditions as they affect wall stability and the design of explosive charges in open-pit operations.

The dangers of ventilation-induced thawing around stopes and drifts underground in conventional mining are pointed up by Judge.¹¹⁰ Muller¹⁵⁴ has used ultrasonics to determine rate of freezing and changes in rock stability in a mine shaft.

Geophysical methods have been used in placer mining in the permafrost region to determine the thickness of muck and gravels and the depth to bedrock. Bedrock topography has a direct influence on the accumulation of placer gold deposits. Such investigations have been made by Hobson⁸⁰ and Green.⁷¹

GROUNDWATER

Ice, including the ice masses contained in permafrost, is part of the water budget of a country and is now the object of quantitative research as we endeavor to determine our full resources on this continent. Data available on climate, runoff, and geology are sufficient to show that groundwater is present throughout the areas of discontinuous permafrost and that rocks are saturated in the same manner as in humid temperature climates.²³ The most recent and complete paper discussing ground water in permafrost has been written by Williams and van Everdingen.²¹³

It is interesting to note at this point that artesian flows of water have been encountered in seismic shot holes in the Mackenzie Delta.^{138,140} One hole drilled in a shallow drained lake has produced considerable quantities of freshwater; because of the environment, it has been very difficult to contain the flow. Hunter⁹⁴ is measuring by means of seismic methods the depth to permafrost on gravel bars of deltas in the Beaufort Sea so that he can estimate subsurface flow of groundwater along the Yukon Coast.

PALEOCLIMATIC STUDIES

Lachenbruch and Marshall¹³¹ and Jessop¹⁰² assert that the pattern of surface temperature both now and in the past yields insight into problems peculiar to arctic heat flow measurements and provides supplementary information of considerable interest concerning climatic change in the past.

PETROLEUM EXPLORATION

In the past, improper corrections have been applied to seismic data acquired in permafrost areas in North America; it is widely believed that several wells in the Canadian Arctic may have been drilled on "permafrost anomalies." By the nature of the business, however, the corrections for permafrost conditions applied to seismic data in the petroleum industry are not widely known. Rackets¹⁷⁹ describes a unique method of not generating "frost breaks" that obliterate the arrival of reflected energy on a seismic record. This problem is alleviated by simultaneously detonating small charges in shallow shotholes. Digital processing of the great quantity of data acquired permits a more intelligent interpretation.

ENGINEERING

The detection and delineation of permafrost and the determination of its physical and mechanical properties are of paramount importance to the solution of many engineering problems currently confronting North American industry

in the Arctic. Soil boring and sampling (which are both expensive and time-consuming), geophysical methods (which are essential if horizontal sampling on a continuous basis is desired), and field and laboratory analyses of samples, all combine to define the physical properties of a site. Under certain circumstances, the solution of engineering problems requires a rapid nondestructive geophysical technique.

The production and development stages of petroleum-related work in the Arctic will require the solution of many permafrost-related problems associated with routing and constructing pipelines,¹⁴⁷ safe placing of surface casing in wells during drilling operations, and design of future production wells. If these wells and facilities are in the offshore environment, the difficulties are compounded. Geophysical methods could provide some of the necessary input needed to solve these problems.

Construction and engineering planning and design must be optimized in the arctic environment; therefore, it is essential to acquire as many data as possible on the major parameters of frozen soils. Major parameters, such as density, porosity, specific density, grain size, and elastic constants, should be available to the engineer, and several papers have been written with this in mind. Faas⁵¹ endeavors to quantify a relationship between sediment porosity and acoustic reflectivity; Hobson and Hunter⁸³ set out a method to determine elastic constants employing seismic methods; Raytheon Corp.¹⁸⁶ reports on an acoustic method that gives promise of identifying and quantifying these parameters; and Ladanyi and Johnston¹³² offer a method of determining basic creep parameters of frozen soils that are necessary for predicting the long-term behavior of structures embedded in permafrost.

The application of VLF methods by Barringer⁹ to the identification in both the vertical and horizontal directions of permafrost has been directed principally to determining the presence or absence of permafrost and the presence of ice masses and to identifying potential aggregate materials. All pipeline and highway routes could be investigated profitably in the reconnaissance stage by the application of geophysical airborne and ground methods.

There are a variety of applications of geophysics to engineering problems a few of which have been presented above. Other ones worthy of consideration are studies of shear strength with ice content of frozen soils as well as heave and heaving pressures by Osler and Yong,^{162,163} location of construction-quality gravels by Brooker and Hayley,²⁴ studies of the chemical characteristics and mechanical properties of some permafrost soils by Day and Rice,⁴⁶ analysis of the problem of liquefaction of loosely packed saturated sands and silts by seismic vibrations by Lachenbruch,¹²⁹ studies of the area of thaw around a pipeline by Lachenbruch¹²⁹ and Brown,³⁶ definition of the fine structure in the near-surface frozen materials and the occurrence of massive ice lenses by Hunter⁹⁶ and Mackay *et al.*,¹⁴⁴ the application of gravity

methods to ice-cored topography by Rampton and Walcott,¹⁸² the determination of artesian conditions with piezometric head possibly lying above the ground surface,¹⁴⁰ and the work on the problem of permafrost in the offshore environment by Mackay,^{139,141} and investigations of the change in electrical properties at interfaces permitting the use of VLF as a mapping tool by Barringer Research.¹⁰

The above descriptions of and suggestions for the application of geophysics to engineering problems in permafrost are, of necessity, very brief and superficial. It is axiomatic that several types of geophysical methods should be selected to solve a specific problem.

Problems

There are many problems related to using geophysical methods in the permafrost environment that are not completely defined or solved. The most important of these are identified by the following questions:

Can buried ice be identified by seismic methods; i.e., is ice velocity peculiar within a velocity range?

Can dry and ice-rich permafrost be differentiated, e.g., dry permafrost versus an ice lens? What is the variation in seismic velocity with lithology and temperature?

Is there a relation between velocity, porosity, saturation, and unfrozen water content?

What is the relation between compressional and shear waves within the same material?

Does the electromagnetic method indicate any frequency dependence?

How can multiple seismic and acoustic reflections be identified in the permafrost environment?

Can static and dynamic elastic moduli be compared in frozen and unfrozen soils?

What are the vertical velocity gradients?

Is there a seismic frequency variation in continuous and discontinuous zones in overburden and in bedrock?

Is the amplitude attenuation of seismic waves characteristic of the type of material and/or an indicator of a thin permafrost area?

What are the propagation velocities in various frozen and unfrozen media?

How does salinity of interstitial liquid affect geophysical methods, i.e., the seismic velocities and the apparent resistivity?

How does propagation velocity and damping coefficients of ultra sonic waves at various frequencies change with variations in lithology, temperature, moisture, mineralogy, structure, and texture?

Can the amount of ground ice present at shallow depth be estimated from surface resistivity measurements?

Can simple conduction models derived from geothermal

data permit accurate reconstruction of climatic fluctuations occurring over the past few centuries?

Can offshore thermokarst features and offshore massive ice bodies be detected by geophysical methods?

CONCLUSIONS

The recent acceleration of development activities in the vast permafrost region of Canada and Alaska and the prospect of even more development in the future attest to the urgent need for acquiring more permafrost data. Whether obtained by traditional or geophysical methods, or by a combination of both, accurate determinations of the distribution and character of permafrost are essential to the orderly development of this region. These determinations are necessary in order to make intelligent land use assignments, to find and develop groundwater supplies, to plan and achieve effective waste-disposal systems, and to expeditiously explore for and develop mineral, coal, petroleum, and natural gas resources. They are also necessary to determine the best routes and sites for engineering structures and, in areas where these structures are to be built, to make proper engineering designs and to use proper construction procedures to ensure the integrity of the structures and to minimize adverse environmental impact.

This report, a summary of the recent accomplishments and of the state of the art in mapping and predicting permafrost, focuses attention on the inherent difficulties and importance of accomplishing these objectives and on the many problems that remain to be solved. The authors hope that the information presented will encourage more work in this field and that it will aid in the solution of many of these problems.

REFERENCES

1. Addison, J. R. 1969. Electrical properties of saline ice. *J. Appl. Phys.* 40(8):3105-3114.
2. Addison, J. R. 1970. Electrical relaxation in saline ice. *J. Appl. Phys.* 41(1):54-63.
3. Addison, J. R., and E. Pounder. 1964. The electrical properties of saline ice. AFCRL-64-52. U.S. Air Force Cambridge Research Lab., Bedford, Massachusetts.
4. Adey, A. W. 1972. Microwave radiometry for surveillance from spacecraft and aircraft. C.R.C. Rep. No. 1231. Canada Department of Communication, Ottawa.
5. Arctic operators study ocean floor permafrost. *Oilweek*, June 14, 1971:13.
6. Bahar, E. 1971. Radiowave propagation over a non-uniform overburden. *In* J. R. Wait [ed.] *Electromagnetic probing in geophysics*. Golem Press.
7. Barnes, D. F. 1966. Geophysical methods for delineating permafrost. *In* *Permafrost: Proceedings of an international conference*. National Academy of Sciences, Washington, D.C.
8. Barnes, D. F., and G. R. MacCarthy. 1964. Preliminary report on tests of the application of geophysical methods to Arctic

- groundwater problems. U.S. Geological Survey open-file report. Menlo Park, California.
9. Barringer, A. 1971. Interpretational report of an airborne VLF survey in the Ilford, Long Spruce Rapids, Kelsey and Thompson areas, northern Manitoba. *Can. Geol. Surv. Intern. Rep.* 2, Ottawa.
 10. Barringer, A. 1971. Sea ice thickness measurement using wave tilt techniques. Rep. TR-71-196. U.S. Army Cold Regions Research and Engineering Laboratory, Hanover, New Hampshire.
 11. Barringer, A. R., and J. D. McNeill. 1968. Radiophase a new system of conductivity mapping, p. 157–167. *In* Fifth symposium on remote sensing of environment, Proceedings. University of Michigan, Ann Arbor.
 12. Barringer, A. R., and J. D. McNeill. 1971. Airborne surveys for measurement of permafrost and sea ice. *In* Second International symposium on arctic geology. San Francisco, California [abstr.]
 13. Beck, A. F., F. M. Auglin, and J. H. Sass. 1971. Analysis of heat flow data—*in situ* conductivity measurements. *Can. J. Earth Sci.* 8(1):1–19.
 14. Bell, R. A. I. 1966. A seismic reconnaissance in the McMurdo Sound region, Antarctica. *J. Glaciol.* 6(44):209–221.
 15. Bell, R. A. I., and A. J. Heine. 1965. Seismic refraction measurements on the McMurdo ice shelf, Antarctica. *J. Glaciol.* 5(42):880–881.
 16. Biggs, A. W. 1968. Geophysical exploration in polar areas with very low frequency phase variations. *IEEE Trans. AP-16:* 364–365.
 17. Biggs, A. W. 1971. Ground wave propagation over Arctic sea ice. *IEEE Trans. GE-9(1):*51–56.
 18. Bird, J. B. 1967. The physiography of arctic Canada. Johns Hopkins Press, Baltimore. 336 p.
 19. Black, R. F. 1969. Thaw depressions and thaw lakes—A review. *Biul. Peryglacj.* No. 19. p. 131–150.
 20. Blomquist, A. 1970. Equipment for *in-situ* measurement of the dielectric properties of ground and ice. *Int. Mtg. Glaciol.* Lyngby, Denmark.
 21. Bogorodskiy, V. V., G. P. Khokhlov, B. A. Federov, and G. V. Trepov. 1970. Electrical properties of rock-ice systems. *Dokl. Akad. Nauk. S.S.S.R.* 190(1):88–90.
 22. Boulware, R. A. 1961. How to analyse reflection data. *World Oil* April:80–84.
 23. Brandon, L. V. 1963. Groundwater in the permafrost regions of the Yukon, northern Cordillera and Mackenzie District. First Canadian conference on permafrost. National Resources Council Canada Tech. Mem. No. 76. p. 131–139. Ottawa.
 24. Brooker, E. W., and D. W. Hayley. 1970. A new look at the permafrost problem. *Oilweek* 21(21):47–52.
 25. Brown, J. 1967. Tundra soils formed over ice wedges, northern Alaska. *Soil Sci. Soc. Am. Proc.* 31:686–691.
 26. Brown, R. J. E. 1964. Permafrost investigations on the Mackenzie Highway in Alberta and Mackenzie District. Nat. Research Council Canada, Div. Bldg. Research, Tech. Paper 175, NRC 7885. 27 p. Ottawa.
 27. Brown, R. J. E. 1965. Some observations on the influence of climatic and terrain features on permafrost at Norman Wells, N.W.T., Canada. *Can. J. Earth Sci.* 2(1):15–31.
 28. Brown, R. J. E. 1965. Permafrost investigations in Saskatchewan and Manitoba. Nat. Research Council Canada, Div. Bldg. Research, Tech. Paper 193, NRC 8375, Ottawa. 36 p.
 29. Brown, R. J. E. 1965. Distribution of permafrost in the discontinuous zone of western Canada, p. 1–9. *In* Proceedings, Canadian regional permafrost conference. Tech. Memo. 86. National Research Council of Canada, Ottawa.
 30. Brown, R. J. E. 1966. Relation between mean annual air and ground temperatures in the permafrost regions of Canada, p. 241–247. *In* Permafrost: Proceedings of an international conference. National Academy of Sciences, Washington, D.C.
 31. Brown, R. J. E. 1967. Permafrost investigations in British Columbia and Yukon Territory. Tech. Paper 253, NRC 9762. National Research Council of Canada, Division of Building Research, Ottawa. 55 p.
 32. Brown, R. J. E. 1967. Permafrost in Canada. *Can. Geol. Surv. Map* 1246A. scale 1:7 603 200.
 33. Brown, R. J. E. 1968. Permafrost investigations in northern Ontario and eastern Manitoba. Tech. Paper 291, NRC 10465. National Research Council of Canada, Division of Building Research, Ottawa. 40 p.
 34. Brown, R. J. E. 1968. Permafrost map of Canada. *Can. Geogr. J.* p. 56–63.
 35. Brown, R. J. E. 1969. Factors influencing discontinuous permafrost in Canada, p. 11–53. *In* The periglacial environment, past and present. *Int. Assoc. Quaternary Res. Congr.*, 7th [1965]. McGill-Queens University Press, Montreal.
 36. Brown, R. J. E. 1971. Proceedings of a seminar on the permafrost active layer. Tech. Memo. No. 106. National Research Council of Canada, Ottawa.
 37. Brown, R. J. E. 1972. Permafrost in the Canadian Arctic Archipelago. *Z. Geomorphol. N. F. Suppl.* 13:102–130.
 38. Brown, W. G., G. H. Johnston, and R. J. E. Brown. 1964. Comparison of observed and calculated ground temperatures with permafrost distribution under a northern lake. *Can. Geotech. J.* 1(3):147–154.
 39. Bush, B. O., and S. D. Schwarz. 1964. Seismic refraction and electrical resistivity measurements over frozen ground, p. 32–37. *In* Canadian regional permafrost conference proceedings. National Research Council of Canada, Tech. Memo. No. 66. Ottawa.
 40. Campbell, K. J., C. L. Bertram, and S. S. Sandler. 1972. Determination of the distribution of large masses of ground ice in permafrost by electromagnetic subsurface profiling. Tech. Memo. 003-72. Geophysical Survey Systems, Inc., North Billerica, Massachusetts.
 41. Church, R. E., T. L. Péwé, and M. J. Andresen. 1965. Origin of large scale polygonal ground near Big Delta, Alaska. Research Rep. 159. U.S. Army Cold Regions Research Engineering Laboratory, Hanover, New Hampshire. 75 p.
 42. Clark, S. P. 1966. Thermal conductivity. *Handbook of physical constants.* Geol. Soc. Am. Mem. 97, Boulder, Colorado. p. 461–482.
 43. Clee, T. E., J. C. Savage, and K. G. Neave. 1969. Internal friction in ice near its melting point. *J. Geophys. Res.* 74(4):973–980.
 44. Cook, J. C. 1960 R.F. electrical properties of salty ice and frozen earth. *J. Geophys. Res.* 65(6):1767–1771.
 45. Coulter, H. W., D. M. Hopkins, T. N. V. Karlstrom, T. L. Péwé, C. Wahrhaftig, and J. R. Williams. 1965. Extent of glaciations in Alaska. *U.S. Geol. Surv. Misc. Geol. Inv. Map* I-415.
 46. Day, J. H., and H. M. Rice. 1964. The characteristics of some permafrost soils in the Mackenzie Valley, N.W.T. *Arctic* 17(4):222–236.
 47. Desai, K. P., and E. J. Moore. 1967. Well log interpretation in permafrost. *Soc. Prof. Well Log Anal. 8th Ann. Logging Symp. Trans. Sec. N. p.* 1–27.
 48. Dobrovolny, E., H. R. Schmoll, and L. A. Yehle. 1969. Geologic environmental factors related to TAPS (Trans Alaska Pipeline System) from Valdez to Fairbanks, Alaska. U.S. Geol. Surv. open-file report, map and table, 1 sheet. Menlo Park, California.

49. En-Tech Associates, Inc. 1969. Report on the test of an acoustical sub-bottom profiler on the sea-ice near Resolute Bay, N.W.T., Canada. Internal report to Polar Continental Shelf Project, Ottawa.
50. Evans, S. 1965. Dielectric properties of ice and snow—A review. *J. Glaciol.* 5:773-792.
51. Faas, R. W. 1969. Acoustic/mass property relationship between saturated sediments. Internal report. Raytheon Corp., Portsmouth, Rhode Island.
52. Faas, R. W., and D. D. Caulfield. 1970. Determination of bulk properties of saturated sediments through spectral analysis. *Am. Assoc. Pet. Geol. Bull.* 54(5):846. (Abstr.)
53. Ferrians, O. J., Jr. 1965. Permafrost map of Alaska. U.S. Geol. Surv. Misc. Geol. Inv. Map I-445. Scale 1:2 500 000.
54. Ferrians, O. J., Jr. 1965. Distribution and character of permafrost in the discontinuous zone of Alaska (summary), p. 15-16. *In Canadian regional permafrost conference, 1964, proceedings.* Tech. Memo. 86. National Research Council of Canada, Ottawa.
55. Ferrians, O. J., Jr. 1966. Permafrost map of Alaska, p. 172. *In Permafrost: Proceedings of an international conference.* National Academy of Sciences, Washington, D.C.
56. Ferrians, O. J., Jr. 1971. Preliminary engineering geologic maps of the proposed trans-Alaska pipeline route—Beechey Point and Sagavanirktok quadrangles. U.S. Geol. Surv. open-file report. Menlo Park, California. Scale 1:125 000.
57. Ferrians, O. J., Jr. 1971. Preliminary engineering geologic maps of the proposed trans-Alaska pipeline route—Philip Smith Mountains quadrangle. U.S. Geol. Surv. open-file report. Menlo Park, California. Scale 1:125 000.
58. Ferrians, O. J., Jr. 1971. Preliminary engineering geologic maps of the proposed trans-Alaska pipeline route—Valdez quadrangle. U.S. Geol. Surv. open-file report. Menlo Park, California. Scale 1:125 000.
59. Ferrians, O. J., Jr. 1971. Preliminary engineering geologic maps of the proposed trans-Alaska pipeline route—Gulkana quadrangle. U.S. Geol. Surv. open-file report. Menlo Park, California. Scale: 1:125 000.
60. Ferrians, O. J., Jr. 1972. ERTS and arctic engineering geology in Alaska, p. 153-154. *In Summaries. International symposium on remote sensing of environment, 8th.* Ann Arbor, Michigan.
61. Ferrians, O. J., Jr., and R. Kachadoorian. Permafrost-related engineering problems and the trans-Alaska pipeline. *Geol. Soc. Am. Abstr. Progr.* (In press)
62. Ferrians, O. J., Jr., R. Kachadoorian, and G. W. Greene. 1969. Permafrost and related engineering problems in Alaska. Prof. Paper 678. U.S. Geological Survey, Washington, D.C. 37 p.
63. Fletcher, R. J. 1964. The use of aerial photographs for engineering soil reconnaissance in Arctic Canada. *Photogr. Eng.* 30(2):210-219.
64. French, H. M. 1970. Soil temperatures in the active layer, Beaufort Plain. *Arctic* 23(4):229-239.
65. French, H. M. 1971. Ice cored mounds and patterned ground, southern Banks Island, western Canadian Arctic. *Geogr. Ann.* 53A:32-38.
66. Frischknecht, F. C., and W. D. Stanley. 1971. Airborne and ground electrical resistivity studies along proposed Trans-Alaska Pipeline System (TAPS) route. *In International symposium on arctic geology.* San Francisco, California. (Abstr.)
67. Garg, O. M. *In situ* physico-mechanical properties of permafrost using geophysical methods. This volume.
68. Gold, L. W. 1967. Influence of surface conditions on ground temperature. *Can. J. Earth Sci.* 4:199-208.
69. Gold, L. W., G. H. Johnston, W. A. Slusarchuk, and L. E. Goodrich. 1972. Thermal effects in permafrost. Tech. Paper 376. NRC 12716. National Research Council of Canada, Division of Building Research, Ottawa. 15 p.
70. Gray, J. T. 1966. Permafrost studies at Knob Lake, central Labrador—Ungava, 1964-65. McGill University Sub-Arctic Research Lab. Research Paper 21. Montreal. p. 129-134.
71. Green, H. G. 1970. A portable refraction seismograph survey of gold placer areas near Nome, Alaska. U.S. Geol. Surv. Bull. 1312-B.
72. Greene, G. W. 1971. The application of infrared remote sensing techniques to permafrost-related engineering problems, p. 59-61. *In Second international symposium on arctic geology.* San Francisco, California. Program Abstr.
73. Greene, G. W. 1972. Applications of infrared remote sensing methods to geological and engineering problems of the Arctic, p. 36. *In Annual earth resource program review, 4th.* Houston, Texas. NASA-MS-C.
74. Greenhouse, J. P. 1961. The Devon Island expedition; Measurements of electrical resistivity of ice-formations. *Arctic* 14: 259-265.
75. Gross, G. W. 1962. Four-electrode method for measuring the direct current resistivity of ice. *Science* 138:520-521.
76. Haugen, R. K., L. W. Gatto, and D. M. Anderson. 1972. Cold regions environmental analysis based on ERTS A imagery, p. 155. *In Summaries. International symposium on remote sensing of environment, 8th.* Ann Arbor, Michigan.
77. Hessler, V. P., and A. R. Franzke. 1958. Earth-potential electrodes in permafrost and tundra. *Arctic* 11(4):211-217.
78. Higashi, A. 1953. On the thermal conductivities of soils, with special reference to that of frozen soil. *Am. Geophys. Union Trans.* 34(5):737-748.
79. Hobson, G. D. 1962. Seismic exploration in the Canadian arctic islands. *Geophysics* 27(2):253-273.
80. Hobson, G. D. 1966. A shallow seismic experiment in permafrost, Klondike area, Yukon Territory, p. 10-14. *In Report of activities November 1965 to April 1966.* Geol. Surv. Can. Paper 66-2. Ottawa.
81. Hobson, G. D., A. E. Beck, and D. C. Findlay. 1966. Notes on geophysical logs and borehole temperature measurements from the Muskox drilling project, p. 108-122. *In Drilling for scientific purposes.* Geol. Surv. Can. Paper 66-13. Ottawa.
82. Hobson, G. D., and A. Overton. 1967. A seismic section of the Sverdrup Basin, Canadian arctic islands, p. 550-562. *In A. W. Musgrave [ed.] Seismic refraction prospecting.* Society of Exploratory Geophysicists, Tulsa.
83. Hobson, G. D., and J. A. Hunter. 1969. *In situ* determination of elastic constants in overburden using a hammer seismograph. *Geoexploration* 7(2):107-111.
84. Hochstein, M. 1967. Electrical resistivity measurements on ice sheets. *J. Glaciol.* 6(47):623-633.
85. Hoekstra, P. 1968. The physics and chemistry of frozen soils. Internal report. U.S. Army CRREL, Hanover, New Hampshire.
86. Hoekstra, P., and P. Capillino. 1971. Dielectric properties of sea and sodium chloride ice at H.F. and microwave frequencies. *J. Geophys. Res.* 76(20):4922-4931.
87. Hoekstra, P., and D. McNeill. Electromagnetic probing of permafrost. This volume.
88. Holmes, G. W., D. M. Hopkins, and H. L. Foster. 1968. Pings in central Alaska. U.S. Geol. Surv. Bull. 1241-H. 40 p.
89. Howitt, F. 1971. Permafrost in Prudhoe Bay Field; Geology and physical characteristics. *In International symposium on arctic geology.* San Francisco, California. (Abstr.)
90. Hughes, O. L. 1969. Distribution of open-system pings in

- central Yukon Territory with respect to glacial limits. *Can. Geol. Surv. Paper 69-34*. 8 p. Ottawa.
91. Hughes, O. L. 1972. Surficial geology and land classification, Mackenzie Valley transportation corridor, p. 17–24. *In Canadian northern pipeline research conference, Proceedings*. Tech. Memo. 104. National Research Council of Canada, Ottawa.
 92. Hughes, O. L., D. A. Hodgson, and J. Pilon. 1972. Surficial geology, Fort Good Hope (106I), Fort McPherson (106M), and Arctic Red River map sheets, District of Mackenzie. *Geol. Surv. Canada open-file report 97*, Ottawa. Scale 1:125 000.
 93. Hughes, O. L., D. A. Hodgson, and J. Pilon. 1972. Surficial geology, Ontaratué River (106J), Martin House (106K), and Travailant Lake (106O) map sheets, District of Mackenzie and Yukon Territory. *Geol. Surv. Can. open-file report 108*. Ottawa. Scale 1:125 000.
 94. Hunter, J. A. 1972. Personal communication.
 95. Hunter, J. A. 1972. A model study of reflected seismic waves from the bottom of the permafrost layer, p. 44–46. *In Report of activities, Part B; November 1971 to March 1972*. *Geol. Surv. Can. Paper 72-1, Part B*. Ottawa.
 96. Hunter, J. A. The application of shallow seismic methods to mapping of frozen surficial materials. This volume.
 97. Hunter, J. A., and R. Good. 1971. A hammer seismic investigation of the permafrost layer, Mackenzie Delta, p. 49–50. *In Report of activities, Part B; November 1970 to March 1971*. *Geol. Surv. Can. Paper 71-1, Part B*. Ottawa.
 98. Ives, J. D., and B. D. Fahey. 1971. Permafrost occurrence in the Front Range, Colorado Rocky Mountains, USA. *J. Glaciol.* 10(58):105–111.
 99. Ives, J. D. Permafrost and its relationship to other environmental parameters in a mid-latitude, high altitude setting, Front Range, Colorado Rocky Mountains. This volume.
 100. Jessop, A. M. 1970. How to beat permafrost problems. *Oilweek Jan.* 12:22–25.
 101. Jessop, A. M. 1971. The distribution of glacial perturbation of heat flow in Canada. *Can. J. Earth Sci.* 8(1):162–166.
 102. Jessop, A. M. 1972. Heat flow and permafrost. *Can. Inst. Mining Metal. Bull.* Nov:45–48.
 103. Jiracek, G. R., and C. R. Bentley. 1966. Dielectric properties of ice at 30 Mc/s. *J. Glaciol.* 6(44):319.
 104. Johnston, G. H. 1965. Permafrost studies at the Kelsey hydro-electric generating station—Research and instrumentation. *Tech. Paper 178, NRC 7943*. National Research Council of Canada, Div. Bldg. Research, Ottawa.
 105. Johnston, G. H., and R. J. E. Brown. 1964. Some observations on permafrost distribution at a lake in the Mackenzie Delta, N.W.T., Canada. *Arctic* 17(3):162–175.
 106. Johnston, G. H., and R. J. E. Brown. 1966. Occurrence of permafrost at an arctic lake. *Nature* 211(5052):952–953.
 107. Johnston, G. H., R. J. E. Brown, and D. N. Pickersgill. 1963. Permafrost investigations at Thompson, Manitoba terrain studies. *Tech. Paper 158, NRC 7568*. National Research Council of Canada, Div. Bldg. Research, Ottawa.
 108. Jones, F. W., and A. T. Price. 1971. Geomagnetic effects of sloping and shelving discontinuities of earth conductivity. *Geophysics* 36(1):58–66.
 109. Judge, A. 1972. Predicting permafrost depth. *Oilweek July* 17:62–66.
 110. Judge, A. The prediction of permafrost thickness. *Can. Geotech. J.* (In press)
 111. Kachadoorian, R. 1971. Preliminary engineering geologic maps of the proposed trans-Alaska pipeline route—Chandalar and Wiseman quadrangles. U.S. Geol. Surv. open-file report, Menlo Park, California. Scale 1:125 000.
 112. Kachadoorian, R. 1971. Preliminary engineering geologic maps of the proposed trans-Alaska pipeline route—Bettles and Beaver quadrangles. U.S. Geol. Surv. open-file report, Menlo Park, California. Scale 1:125 000.
 113. Kachadoorian, R. 1971. Preliminary engineering geologic maps of the proposed trans-Alaska pipeline route—Livengood and Tanana quadrangles. U.S. Geol. Surv. open-file report, Menlo Park, California. Scale 1:125 000.
 114. Kachadoorian, R., and O. J. Ferrians, Jr. Permafrost-related engineering geology problems posed by the trans-Alaska pipeline. This volume.
 115. Kaplar, C. W. 1966. Laboratory determination of the dynamic moduli of frozen soils and of ice, p. 293–305. *In Permafrost: Proceedings of an international conference*. National Academy of Sciences, Washington, D.C.
 116. Keller, G. V. 1971. Personal communication.
 117. Keller, G. V., and F. C. Frischknecht. 1960. Electrical resistivity studies on the Athabasca Glacier, Alberta, Canada. *J. Res. N.B.S.* 64D(5):439–448.
 118. Keller, G. V., and F. C. Frischknecht. 1961. Induction and galvanic resistivity studies on the Athabasca Glacier, Alberta, Canada. *First Int. Conf. Arctic Geol.* 2:809–832.
 119. Kersten, M. S. 1963. Thermal properties of frozen ground, p. 301–305. *In Permafrost: Proceedings of an international conference*. National Academy of Sciences, Washington, D.C.
 120. King, M. S. 1966. Wave velocities in rocks as a function of changes in overburden pressure and pore fluid saturants. *Geophysics* 31(1):50–73.
 121. King, M. S., and T. A. Bamford. 1971. Static and dynamic elastic properties of a sandstone at permafrost temperatures, p. 83–92. *In Fifth conference on Drilling and Rock Mechanics, Proceedings*.
 122. King, R. W. P., and C. W. Harrison, Jr. 1968. The transmission of electromagnetic waves and pulses into the earth. *J. Appl. Phys.* 39(9):4444–4452.
 123. Kohnen, H. 1971. The relation between seismic firm structure, temperature and accumulation. *Z. Gletscherk. Glazialgeol.* 7:1–2.
 124. Krinsley, D. B. 1963. Influence of snow cover on frost penetration, p. B144–B147. *Prof. Paper 475-B*. U.S. Geological Survey, Washington, D.C.
 125. Krinsley, D. B. 1965. Birch Creek pingo, Alaska, p. C133–C136. *Prof. Paper 525-C*. U.S. Geological Survey, Washington, D.C.
 126. Kurfurst, P. J., and M. S. King. 1972. Static and dynamic elastic properties of two sandstones at permafrost temperatures. *J. Pet. Tech.*, April:495–504.
 127. Lachenbruch, A. H. 1957. Thermal effects of the ocean on permafrost. *Geol. Soc. Am. Bull.* 68:1515–1530.
 128. Lachenbruch, A. H. 1957. A probe for measurement of thermal conductivity of frozen soils in place. *Am. Geophys. Union Trans.* 38(5):691–697.
 129. Lachenbruch, A. H. 1970. Some estimates of the thermal effects of a heated pipeline in permafrost. *U.S. Geol. Surv. Circ.* 632.
 130. Lachenbruch, A. H. 1970. Thermal considerations in permafrost, p. J1–J5. *In W. L. Adkison and M. M. Brosge [ed.] Proceedings of the geological seminar on the North Slope of Alaska*. Am. Assoc. Petroleum Geologists, Pacific Sec., Los Angeles.
 131. Lachenbruch, A. H., and B. V. Marshall. 1969. Heat flow in the Arctic. *Arctic* 22(3):300–311.

132. Ladanyi, B., and G. Johnston. 1972. *In situ* testing of frozen soils. *North. Eng.* 4(1):6-8.
133. Lang, L. C. 1966. Blasting frozen iron ore at Knob Lake. *Can. Mining J. Aug.*: 49-53.
134. Law, L. K., W. S. B. Paterson, and K. Whitham. 1965. Heat flow determinations in the Canadian Arctic Archipelago. *Can. J. Earth Sci.* 2(1):58-71.
135. LeSchack, L. A., and F. H. Morse. 1972. Dual-channel airborne I-R scanning for detection of ice in permafrost (Alaska preliminary results). *Am. Soc. Photogr. Proc.* 38:213-238.
136. Mackay, D. K. 1969. Electrical resistivity measurements in frozen ground, Mackenzie Delta area, Northwest Territories. *Association International d'Hydrologie Scientifique, Acts du Colloque de Bucarest, Paris.*
137. Mackay, J. R. 1967. Permafrost depths, Lower Mackenzie Valley, Northwest Territories. *Arctic* 20(1):21-26.
138. Mackay, J. R. 1971. The origin of massive beds in permafrost, western Arctic coast, Canada. *Can. J. Earth Sci.* 8(4):397-422.
139. Mackay, J. R. 1971. Offshore permafrost, southern Beaufort Sea. *Arctic Petroleum Operators Assoc., Calgary.*
140. Mackay, J. R. 1971. Ground ice in the active layer and the top portion of permafrost, p. 26-30. *In Seminar on permafrost active layer, Proceedings. Tech. Memo. No. 103. National Research Council of Canada, Ottawa.*
141. Mackay, J. R. 1972. Offshore permafrost and ground ice, southern Beaufort Sea, Canada. *Can. J. Earth Sci.* 9(11):1550-1561.
142. Mackay, J. R. 1972. The world of underground ice. *Assoc. Am. Geogr. Ann.* 62(1):1-22.
143. Mackay, J. R. 1972. Some observations on ice wedges, Garry Island, N.W.T., p. 131-139. *In D. E. Kerfoot [ed.] Mackenzie Delta area monograph. Int. Geog. Congr. 22d, Brock University, St. Catharines, Ontario.*
144. Mackay, J. R., V. N. Rampton, and J. G. Fyles. 1972. Relic Pleistocene permafrost in western Arctic, Canada. *Science* 176:1321-1323.
145. Mackay, J. R., and J. K. Stager. 1966. The structure of some pingos in the Mackenzie Delta area, N.W.T. *Can. Dep. Energy, Mines Resour. Geogr. Br. Geogr. Bull.* 8:360-368.
146. McCormick, G. 1972. Northern Canada; surface temperatures. *North. Eng.* 4(1):19-20.
147. Migliaccio, R. R., and J. W. Rooney. 1971. Engineering geologic and subsurface soil investigation for the Trans-Alaska Pipeline System. *In International symposium on arctic geology. San Francisco, California. Abstr.*
148. Misener, A. D. 1955. Heat flow and depths of permafrost at Resolute Bay, Cornwallis Island, N.W.T., Canada. *Am. Geophys. Union Trans.* 36(6):1055-1060.
149. Monroe, R. L. 1972. Terrain classification and sensitivity series (preliminary), Mackenzie Delta (107C), Stanton (107D), Cape Dalhousie (107E), and Malloch Hill (97F) map sheets, District of Mackenzie. *Geol. Surv. Can. open-file report 117, Ottawa. Scale 1:250 000.*
150. Monroe, R. L. 1972. Terrain classification and sensitivity series (preliminary), Demarcation Point (117C), Herschel Island (117D), Blow River (117A), Aklavik (107B, W. 1/2), Yukon Territory and District of Mackenzie. *Geol. Surv. Can. open-file report 120, Ottawa. Scale 1:250 000.*
151. Monroe, R. L. 1972. Terrain classification and sensitivity series (preliminary), Fort McPherson (106M), Arctic Red River (106N), Travailant Lake (106O), Ontaratue River (106J), and Fort Good Hope (106I), District of Mackenzie. *Geol. Surv. Can. open-file report 121, Ottawa. Scale 1:250 000.*
152. Mooney, H. M., E. Orellana, H. Pickett, and L. Tornheim. 1966. A resistivity computation method for layered earth models. *Geophysics* 31(1):192-203.
153. Müller, F. 1968. Pingos, modern, p. 845-847. *In R. W. Fairbridge [ed.] The encyclopedia of geomorphology. Reinhold Publishing Corp., New York.*
154. Muller, G. 1961. Geschwindigkeitsbestimmungen elastischer wellen in gefrorenen gesteinen und die anwendung auf untersuchungen des frostmantels an gefrierschachten. *Geophys. Prospec.* 9(2):276-295.
155. Musgrave, A. W. 1967. Seismic refraction prospecting. *Society of Exploratory Geophysicists, Tulsa, Oklahoma.*
156. Nakano, Y., M. Smith, R. Martin, H. Stevens, and K. Knuth. 1971. Determination of the acoustic properties of frozen soils. Prepared for Advanced Research Projects Agency ARPA order 1525 by CRREL.
157. National Research Council. 1966. Permafrost: Proceedings of an international conference. *National Academy of Sciences, Washington, D.C.* 536 p.
158. Nelson, J. L., D. D. Caulfield, and D. L. Bell. 1970. Application of acoustics for the determination of volumetric moisture content and physical properties in permafrost ground. *Internal report to Dept. E.M.R. Canada.*
159. Nichols, D. R., and L. A. Yehle. 1969. Engineering geologic map of the southeastern Copper River Basin, Alaska. *U.S. Geol. Surv. Misc. Geol. Inv. Map I-524. Scale 1:125 000.*
160. Oceans International. 1970. Ice data reduction. *Internal report to Geol. Surv. Can.*
161. Ogilvy, A. A. 1970. Geophysical prospecting for groundwater in the Soviet Union, p. 536-543. *In L. W. Morley [ed.] Mining and groundwater geophysics, 1967. Geol. Surv. Can. Econ. Geol. Rep. No. 26.*
162. Osler, J. C., and R. N. Yong. 1968. Engineering properties of frozen soils. *McGill University Soil Mech. Lab. Rep. to Defense Research Board Canada, grant in aid of research No. 9511-28. Montreal.*
163. Osler, J. C., and R. N. Yong. 1971. Engineering properties of frozen soils. *McGill University Soil Mech. Lab. Rep. to Defense Research Board Canada, grant in aid of research No. 9511-28. Montreal.*
164. Ostrem, G. 1967. Laboratory measurements of the resistivity of ice. *J. Glaciol.* 6(47):643-650.
165. Outcalt, S. I. 1972. The simulation of subsurface effects on diurnal surface thermal regime in cold regions. *Arctic* 25(4): 305-307.
166. Pamenter, B. 1970. G.S.C. uncovers Beaufort secrets. *Oilweek Nov.* 16:8-11.
167. Paterson, W. S. B., and L. K. Law. 1966. Additional heat flow determinations in the area of Mould Bay, Arctic Canada. *Can. J. Earth Sci.* 3(2):237-246.
168. Patterson, A. R. 1964. Datum corrections in glacial drift. *Geophysics* 29(6):957-967.
169. Pearce, D. C., and J. W. Walker. 1967. An empirical determination of the relative dielectric constant of the Greenland Ice Cap. *J. Geophys. Res.* 72(22):5743-5747.
170. Peden, I. C., and G. E. Webber. 1970. Dielectric and loss properties of the Antarctic terrain; their influence on the propagation constants of VLF modes in the earth-ionosphere waveguide. *IEEE Trans.* November.
171. Peden, I. C., and J. C. Rogers. 1971. An experiment for determining the VLF permittivity of deep Antarctic ice. *IEEE Trans. GE-9(4):224-233.*

172. Penner, E. 1970. Thermal conductivity of frozen soils. *Can. J. Earth Sci.* 7(3):982–987.
173. Péwé, T. R. Quaternary geology of Alaska. U.S. Geol. Surv. Prof. Paper. (In press)
174. Péwé, T. L., R. E. Church, and M. J. Andresen. 1969. Origin and paleoclimatic significance of large-scale patterned ground in the Donnelly Dome area, Alaska. *Geol. Soc. Am. Spec. Paper* 103. 87 p.
175. Péwé, T. L., and G. W. Holmes. 1964. Geology of the Mount Hayes D-4 quadrangle, Alaska. U.S. Geol. Surv. Misc. Geol. Inv. Map I-394.
176. Pissart, A. 1967. Les pingos de l'île Prince-Patrick (76°N-120°W). *Can. Geogr. Bull.* 9:189–217.
177. Prest, V. K. 1969. Retreat of Wisconsin and Recent ice in North America. *Geol. Surv. Can. Map* 1257A.
178. Price, W. A. 1968. Oriented lakes, p. 784–796. *In* R. W. Fairbridge [ed.] *The encyclopedia of geomorphology*. Reinhold Publishing Corp., New York.
179. Rackets, H. M. 1971. A low noise seismic method for use in permafrost regions. *Geophysics* 36(6):1150–1161.
180. Rampton, V. N. 1972. Surficial geology and landforms, Mackenzie Delta (107C), Stanton (107D), Cape Dalhousie (107E) and Malloch Hill (97F) map sheets, District of Mackenzie. *Geol. Surv. Can. open-file report* 96, Ottawa. Scale 1:125 000.
181. Rampton, V. N. 1972. Surficial geology and landforms, Aklavik. (107B, E. 1/2) map sheet, District of Mackenzie. *Geol. Surv. Can. open-file report* 119, Ottawa. Scale 1:125 000.
182. Rampton, V. N., and R. I. Walcott. The detection of ground-ice by gravity profiling. (In preparation)
183. Raytheon Corp. 1971. Phase I report, Ice Lake. Internal report to Geological Survey of Canada. Portsmouth, Rhode Island.
184. Raytheon Corp. 1971. Tuk area. Internal report to Geological Survey of Canada.
185. Raytheon Corp. 1971. Permafrost test program; a proposal prepared for Geological Survey of Canada to undertake a survey at Thompson, Manitoba. Internal report to Geological Survey of Canada.
186. Raytheon Corp. 1972. Thompson, Manitoba, permafrost. Internal report to Geological Survey of Canada.
187. Rinker, J. N., and R. E. Frost. 1970. Application of remote sensing to arctic environmental studies, p. 105–116. *In* *The use of remote sensing in conservation, development, and management of the natural resources of the State of Alaska*. Dept. Econ. Dev., Juneau, Alaska.
188. Roethlisberger, H. 1959. Seismic survey, 1957, Thule area, Greenland. Tech. Rep. No. 64. U.S. Army Cold Regions Research and Engineering Laboratory, Hanover, New Hampshire.
189. Roethlisberger, H. 1961. Seismic refraction soundings in permafrost near Thule, Greenland, First Int. Sym. Arctic Geol. Proc. 2:970–980.
190. Roethlisberger, H. 1964. Reflection and transmission coefficients at the interface ice-solid. Rep. No. 110. U.S. Army Cold Regions Research and Engineering Laboratory, Hanover, New Hampshire.
191. Rutter, N. W., G. V. Minning, and J. A. Netterville. 1972. Surficial geology and geomorphology, Trout Lake (95A), Fort Simpson (95H), Camsell Bend (95J), and Mills Lake (85E) map sheets, District of Mackenzie. *Geol. Surv. Can. open-file report* 93, Ottawa. Scale 1:125 000.
192. Sanger, F. J. 1966. Degree-days and heat conduction in soils, p. 253–262. *In* *Permafrost: Proceedings of an international conference*. National Academy of Sciences, Washington, D.C.
193. Schenk, E. 1965. Pleistozäne Eiskeil–Polygonnetze im Vergleich mit heutzutage Vorkommen in Alaska. *Nat. Mus.* 95:8–16.
194. Schenck, F. L. 1963. Delineating low-velocity lenses. *Geophysics* 28(5, pt. 2):877–881.
195. Shearer, J. A. theoretical investigation of offshore permafrost thickness. *Geol. Surv. Can.* (In press)
196. Shearer, J. M., R. F. Macnab, B. R. Pelletier, and T. B. Smith. 1971. Submarine pingos in the Beaufort Sea. *Science* 174:816–818.
197. Siegel, H. O. 1972. The magnetic induced polarization method. *West. Miner Feb.:*32–34.
198. Sobczak, L. 1972. Personal communication.
199. Thompson, H. A. 1966. Air temperature in northern Canada with emphasis on freezing and thawing indexes, p. 272–280. *In* *Permafrost: Proceedings of an international conference*. National Academy of Sciences, Washington, D.C.
200. Timur, A. 1968. Velocity of compressional waves in porous media at permafrost temperatures. *Geophysics* 33(4):584–595.
201. Veysman, J. E. 1965. Polygonal n-zhil'nyy led Alyaski i sopredel'noy territorii Kanady, in *Podzemnyy led*. Moscow University Press, Moscow. p. 51–86.
202. Washburn, A. L. 1969. Weathering frost action and patterned ground in the Mesters Vig district, Northeast Greenland. *Medd. Grønland* 176(4):313 p.
203. Watkins, J. S., L. A. Walters, and R. H. Godson. 1972. Dependence of *in-situ* compressional-wave velocity on porosity in unsaturated rocks. *Geophysics* 37(1):29–35.
204. Watt, A. D., E. L. Maxwell, and E. H. Whelan. 1959. Low frequency propagation paths in Arctic areas. *J. Res. N.B.S.* 63D(1):99–112.
205. Webber, G. E., and I. C. Peden. 1970. VLF ground-based measurements in Antarctica; their relationship to stratifications in the subsurface terrain. *Radio Sci.* 5(4):655–662.
206. Weber, F. R. 1971. Preliminary engineering geologic maps of the proposed trans-Alaska pipeline route—Fairbanks and Big Delta quadrangles. U.S. Geol. Surv. open-file report, Menlo Park, California. Scale 1:125 000.
207. Weber, F. R. 1971. Preliminary engineering geologic maps of the proposed trans-Alaska pipeline route—Mount Hayes quadrangle. U.S. Geol. Surv. open-file report, Menlo Park, California. Scale 1:125 000.
208. Weber, F. R., and T. L. Péwé. 1970. Surficial and engineering geology of the central part of the Yukon-Koyukuk Lowland, Alaska. U.S. Geol. Surv. Misc. Geol. Inv. Map I-590, Menlo Park, California. Scale 1:125 000.
209. Werenskiold, W. 1953. The extent of frozen ground under the sea bottom and glacier beds. *J. Glaciol.* 2(13):197–200.
210. Westphal, J. A. 1965. *In situ* acoustic attenuation measurements in glacial ice. *J. Geophys. Res.* 70(8):1849–1853.
211. Williams, G. P. 1971. Surface heat exchange and permafrost, p. 8–12. *In* *Seminar on permafrost active layer*, Proc. Tech. Mem. No. 103. National Research Council of Canada, Ottawa.
212. Williams, J. R. 1970. Ground water in the permafrost regions of Alaska. U.S. Geol. Surv. Prof. Paper 696. 83 p.
213. Williams, J. R., and R. O. van Everdingen. Groundwater investigations in permafrost regions of North America. This volume.
214. Williams, P. J. 1963. Specific heats and unfrozen water content of frozen soils, p. 109–126. *In* *First Canadian conference on permafrost*, Proc. Tech. Mem. No. 76. National Research Council of Canada, Ottawa.

215. Wyder, J. E., J. A. Hunter, and V. N. Rampton. Geophysical investigations of surficial materials at Tuktoyaktuk, N.W.T. Geol. Surv. Can. (In press)
216. Yong, R. 1963. Research on fundamental properties and characteristics of frozen soils, p. 84-108. *In* First Canadian conference on Permafrost, Proc. Tech. Mem. No. 76. National Research Council of Canada, Ottawa.
217. Zelonka, F. A. 1960. Determination of depth to permafrost by geophysical methods. Internal report, Defence Research Board Canada Rept. No. 193. Ottawa.

NOTE

[1] Publication authorized by the Director, U.S. Geological Survey, and by the Director, Geological Survey of Canada.

AN EXAMINATION OF MARINER 6 AND 7 IMAGERY FOR EVIDENCE OF PERMAFROST TERRAIN ON MARS

Duwayne M. Anderson and Lawrence W. Gatto

U.S. ARMY COLD REGIONS RESEARCH
AND ENGINEERING LABORATORY
Hanover, New Hampshire

Fiorenzo Ugolini

UNIVERSITY OF WASHINGTON
Seattle, Washington

INTRODUCTION

Mars poses scientific questions most likely to better our understanding of our home planet's origin, evolution, and fundamental processes, and thus to provide knowledge potentially as beneficial to human affairs as it is interesting in an absolute sense.

For these reasons given by Collins,⁷ Mariner 4 on 14 July 1965 made the first reconnaissance of Mars' surface features and returned 22 images of the planet to earth.

A more detailed and diverse reconnaissance was conducted during the photographic missions of the Mariner 6 and 7 satellites from 29 July to 5 August 1969. Two hundred and one images were telemetered to earth and computer-processed to remove electronic noise and distortion.

At near encounter (within 10 000 km of the planet) Mariner 6 and 7 wide-angle cameras (camera A) distinguished features as small as 3 km in dimension in an area approximately 1 000 km². Camera B frames at the same distances showed areas 100 km² and features 300 m or larger were resolved. Approximately 10 percent of Mars' surface was photographed during these missions; most of the coverage was of the equatorial regions and the South Pole.

CRYOSPHERES OF EARTH AND MARS

Terrestrial permafrost is defined solely on the basis of temperature without reference to ice content, lithology, or soil texture. Thus, permafrost is *any* soil or rock material, with or without moisture, that has remained continuously below 0 °C for more than 2 years.¹⁰ The mean annual temperature of Mars is well below 0 °C; it is nearly certain, therefore, that permafrost exists at all locations on the planet. The thickness of the Martian active layer (defined as the average depth of penetration of the characteristic water phase change isotherm in summer) must vary according to the prevailing local internal and external thermal regimes and the water (ice) content of the regolith.

A schematic representation of the earth's cryosphere is given in Figure 1a. It shows how variations in the continental and oceanic energy balance have created irregular, circum-polar, permafrost boundaries. On Mars, this zonation is ex-

pected to be much more regular because of the absence of oceanic thermal reservoirs. A comparable diagram for the Martian cryosphere is given in Figure 1b. During the Martian summer, surface temperatures rise daily above 0 °C between latitudes 30°N and 70°S¹³ and an active "freeze-thaw" layer (or more properly a layer where condensation-sublimation of water is active) of significant thickness can be expected. At all other locations, surface temperatures do not rise above 0 °C,^{11,18,20,24} and the upper boundary of Martian permafrost is expected to virtually coincide with the planetary surface.

The present, total atmospheric pressure on Mars is very close to the triple point on the phase diagram of water; therefore, the existence of the liquid phase is improbable.¹ If it does occur, it surely must be limited to certain favored areas, and its existence must be brief.²⁷ Thus, processes occurring in the active layer of Martian permafrost are likely to be limited to solid-vapor transitions and transitions involving water as an adsorbed surface phase or as a concentrated brine.

Relative to permafrost, the questions that concern the extent and distribution of the permafrost condition and the nature of the regolith include the following:

1. Is the permafrost dry or rich in ice?
2. Is CO₂ sometimes a major constituent? (This possibility has been suggested by Leighton and Murray¹⁵ and reinforced by the results of Mariner 6 and 7.)
3. Do hygroscopic or deliquescent salts in the regolith create unfrozen brines?

Answers to these and similar questions will begin to define the nature and characteristics of Martian permafrost.

CHAOTIC TERRAIN

Initial examinations of the imagery¹⁴ resulted in the recognition of various permanent and transitory surface features associated with the southern polar cap and three distinctly different categories of terrain: *cratered*, *featureless*, and *chaotic*. The cratered terrain was the most widespread of the three and contained craters of varying morphology and

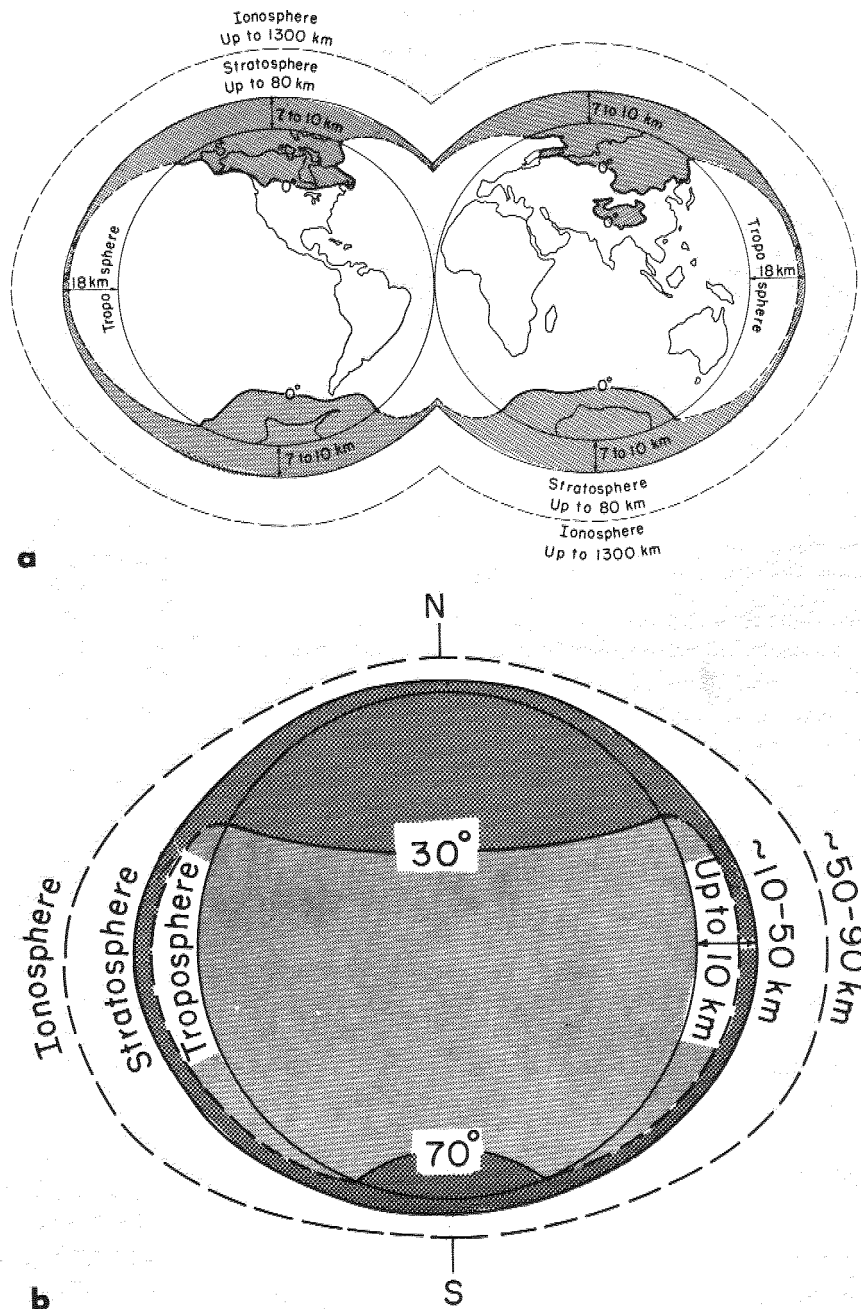


FIGURE 1 (a) Earth's cryosphere (after Baranov⁴). (b) Idealized Martian cryosphere.¹³ The region of an active layer (30°N and 70°S) corresponds to the Martian temperate zone, where daily summertime temperatures rise above 0 °C.

size. The large feature Hellas—a flat area devoid of craters or other geomorphic features—was described as featureless terrain. A terrain unit of at least $1.5 \times 10^6 \text{ km}^2$ —consisting of a rough complex of depressions, short ridges, and knobs—was found between Aurorea Sinus and Margaritifer Sinus, 10°–70° long, and 20°N to 20°S lat. Except for three very faint indications, crater outlines were not visible in this area. To avoid genetic implications until the origin of this terrain could be better established, it was designated *chaotic terrain* by Leighton *et al.*¹⁴; this term was retained by Sharp *et al.*²¹

The authors have re-examined the Mariner 6 and 7 imagery for evidence of permafrost terrains. Table I lists geomorphic features typical of terrestrial permafrost; of these, only thermokarst terrain and unusually large pingos would be expected to be detected in the Mariner imagery. The scenes of chaotic terrain (Figure 2; Table II) were examined in detail because this terrain resembles the slumped topography of a thermokarst region and because it was originally suggested that it may have been formed by the degradation of subsurface ice masses.

Photogrammetric measurements (Table III) were made

TABLE 1 Geomorphic Indicators of Permafrost^a

Feature	Typical Terrestrial Size
Patterned ground ^b	
Circles	0.5- to 3.0-m diameter; may have elevated center 0.1-1.0 m high
Nets	1.0- to 2.0-m diameter
Polygons	1.0- to 100.0-m diameter
Steps	0.3-1.5 m wide, 0.3-0.6 m high, up to 8.0 m long
Stripes	0.1-1.5 m wide, 3.0-4.6 m apart.
Pingos	Maximum height <100 m; shape and size of base variable
Thermokarst	Variable size, shape, and extent of development
Mass movement ^c	
Solifluction lobes	Variable size and shape
Rock glaciers	
Debris flows	
Valley forms ^c	
Asymmetrical valleys	Variable size and shape
Dry valleys	
Eolian ^c	
Deflation hollows/trenches	Variable size and shape
Dune fields	
Lag deposits	
Accumulation ^c	
Talus slopes	Variable size and shape
Block fields (felsenmeere)	
Moraines	
Protalus ramparts	
Block streams	

^a Not all features listed are unique to permafrost areas; some of them are formed by processes other than those accompanying permafrost formation.

^b From Washburn.²⁸

^c The dimensions of these features are controlled by the local geology.

on enlargements of the narrow-angle Camera B frames 6N6, 6N8, and 6N14. In the area of chaotic terrain, determined by planimeter to be about 1.7×10^4 km², the ridges and valleys have a distinct NE-SW orientation and vary from 1 to 5 km wide by 2 to 10 km long. Since the high sun angle and absence of shadows made it impossible to make a direct photogrammetric measurement, an estimate of maximum ridge height (1 km) was calculated from maximum discriminability pictures by assuming 30° slopes for all the ridges. To estimate collapse volume in the area of chaotic terrain shown in images 6N6, 8, and 14, the volume of the ridges was computed and subtracted from the volume obtained by multiplying the total collapse area (1.7×10^4 km²) by the estimated ridge height (1 km). The result was 2.0×10^4 km³. Approximately this much material has been withdrawn or sublimated in forming the collapsed areas.

The estimate of 1 km for the ridge height is probably too large; a more conservative figure might be about 500 m, corresponding to 15° slopes. There is at present no way to

substantiate either value, but in rectified orthographic projections (Figure 3) the chaotic terrain appears somewhat more subdued. However, the figures derived from 1-km ridge heights have been used in constructing Table III so that maximum values could be considered.

Lineaments and changes in ridge slopes are apparent on Camera B images 6N6, 8, and 14 (Figure 4). Some of these are fault scarps that border the margin of chaotic terrain. They are analogous to terrestrial, *en echelon* fault scarps that divide individual slump blocks on the border of slumping land masses (Figure 5). This was first pointed out by Sharp *et al.*,²¹ who called attention to the arcuate breakaway scarps, rotated blocks, parallel ridges, closed depressions, jumbled aspect, and surface lineaments that mimic those accompanying terrestrial slump, slide, or collapse areas.

Possible origins of chaotic terrain are deflation by winds, collapse caused by volcanism, or the decay of massive segregated bodies of ground ice.¹⁴ However, because the scale and topography of chaotic terrain are so large and varied, no terrestrial analogs have been recognized.²¹

Leighton *et al.*¹⁴ originally suggested that chaotic terrain may have formed because of the withdrawal of subsurface deposits, and Belcher *et al.*⁶ noted the similarities between chaotic terrain and terrestrial thermokarst topography. Sublimation of massive underground ice—whether buried glacier, sea, lake, or river ice, or buried snow or hydroeffusions^{16,23}—would produce a large area of surface collapse. Several of these types of ice may have been emplaced in the Martian permafrost during a more earthlike, ancient Martian environment. During this hypothetical younger stage of Martian development, outgassed juvenile water vapor may have condensed and formed large bodies of surface water, perhaps an ancient Martian sea. As the planet evolved and cooled, the sea might have solidified and become buried by windblown dust. Subsequent changes in the thermal environment at the Martian surface might then have initiated degradation of the underground ice mass.

Sublimation of a buried Martian polar cap formed under present environmental conditions on Mars should also be considered. The sizes of the Martian polar caps increase and decrease with the winter and summer seasons in the respective hemispheres. The southern cap virtually disappears after the southern summer solstice,²⁵ and only a small remnant (about 1.7×10^2 km³) of the northern cap exists after the northern summer solstice. The areas at the fullest extent of the caps, as observed from earth and satellites, are calculated to be 9.6×10^6 km² for the northern cap and 1.7×10^7 km² for the southern cap. The average depth of the caps is of the order of 1 m.^{11,17} The amounts of CO₂-water "ice" present during a winter season are of the order of 9.6×10^3 km³ and 1.7×10^4 km³ for the northern and southern caps, respectively. During each winter season relatively large areas of polar "ice" might become covered by windblown dust and thus be partially preserved throughout the following

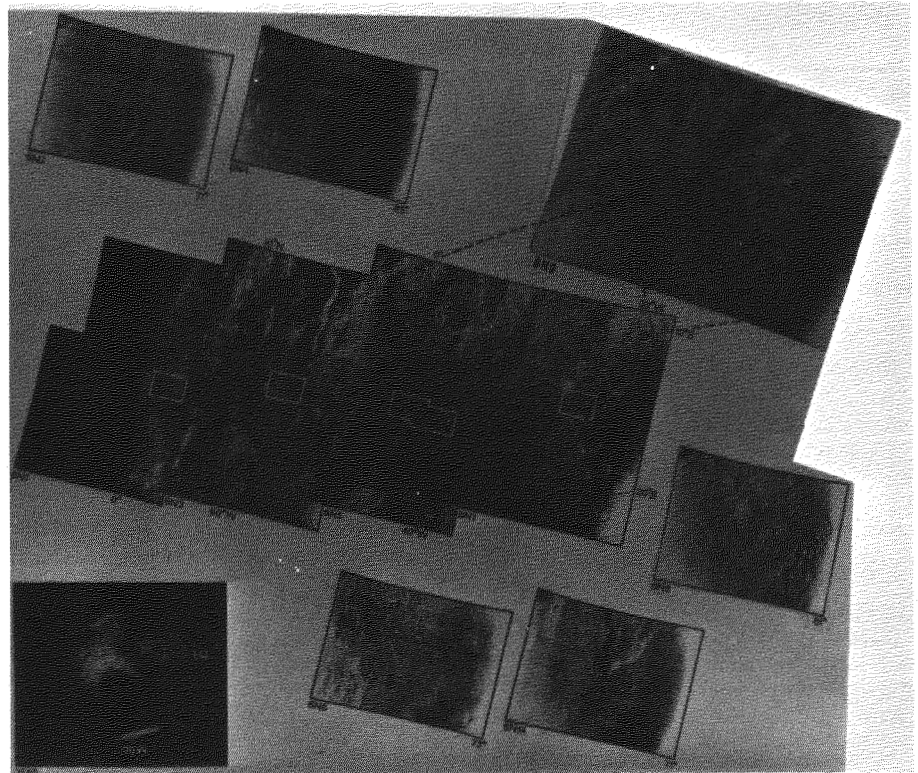


FIGURE 2 Camera A images 6N1, 6N3, 6N5, 6N7, and 6N9, showing the areal extent of chaotic terrain. Camera B images 6N6, 6N8, and 6N14, showing details of chaotic terrain

TABLE II Photographic Parameters

Picture No.	Camera	At Center of Picture						Picture Dimensions on Surface ^g (km)	
		Slant Angle ^b (km)	Phase Angle ^c (°)	Solar Zenith Angle ^d (°)	Viewing Angle ^e (°)	Long. ^f (° E)	Lat. ^f (°)	Horizontal	Vertical
Near Encounter Images ^a									
6N1 ^h	A	6 621	44	2	45	307	-6		1 292
6N2	B	7 389	52	19	70	293	4	551	143
6N3	A	6 598	44	7	57	304	-2		1 324
6N4	B	6 159	52	5	51	310	-5	238	118
6N5	A	5 699	45	11	42	317	-8	2 283	1 127
6N6	B	5 355	52	17	37	323	-10	162	103
6N7	A	5 030	51	24	30	329	-13	1 492	990
6N8	B	4 778	52	29	25	334	-14	128	92
6N9	A	4 930	51	41	41	346	0	1 511	1 228
6N14	B	4 903	80	19	62	323	-13	253	94
Far Encounter Image ⁱ									
7F69	B	535 132	23			279	-4		

^a After Dunne *et al.*⁹

^b From the spacecraft to the surface at the center of the picture.

^c Determined by the positions of the sun and the observer as measured at the center of picture.

^d Illumination angle measured from the vertical at the center of picture.

^e Direction to observer, measured from the vertical at the center of picture.

^f East longitude and latitude, on the Martian surface, of the center of picture.

^g Distance along the Martian surface of the vertical-horizontal dimensions of the field of view, measured through the picture center.

^h The center of the picture was not on the planet; therefore, the data are for the point at the center of the right edge of the frame.

ⁱ After Collins.⁷

TABLE III Photogrammetric Data from Camera B Images

	6N6	6N8	6N14	Total or Mean
Average width of ridges at base (km)	5.1	3.1	3.2	3.8
Average height of ridge (km)	1.4	0.9	0.9	1.1
Cumulative length of ridges (km)	423.1	121.3	93.2	637.6
Mean ridge length (km)	5.2	4.3	5.8	5.4
Mean orientation of ridges (°)	45	43	45	45
Area of chaotic terrain (km ²)	12 022	2 340	2 439	16 801
Volume of chaotic terrain (km ³)	17 540	2 118	2 243	21 901
Volume of ridges (km ³)	1 561	172	137	1 870
Volume of collapsed terrain (km ³)	15 979	1 946	2 106	20 031

summer. Repeated burial of CO₂ frost, together with small quantities of admixed water ice, over millennia could produce large deposits of interlayered CO₂ and water ice and windblown sediment. Because of their different sublimation temperatures over aerologic time, these deposits would become enriched with water ice as CO₂ continually escapes. In this way, one can visualize the buildup of an extensive interbedded loess-water ice deposit.

The total area of chaotic terrain recognized in all the Mariner 6 and 7 images (Figure 6) is about 1.5×10^6 km².²¹ Assuming ridge heights of 1 km, the estimated volume of chaotic terrain is about 1.5×10^6 km³. Subtracting the estimated volume of the ridges yields 1.4×10^6 km³ as the amount of material removed in the chaotic terrain so far delineated. The corresponding hypothetical "ice" mass is significantly smaller than the present terrestrial, southern polar cap (3.0×10^7 km³, including sea ice^{5,12}) and about

comparable with the northern cap (2.6×10^6 km³, including sea ice^{3,19}). The values are sufficiently comparable to invite serious consideration.

The equatorial position of chaotic terrain derived from degradation of a fossil polar cap might be accounted for in light of present-day theories for continental drift. Wells^{29,30} presented evidence for continental drift as an active tectonic process on Mars. He suggested that

The position of the circumglobal, subequatorial belt of dark areas, of Mare Acidalium and of the supposed highlands of the south pole could have resulted from dynamic processes similar to those responsible on Earth for continental drift, seafloor spreading and mountain building.

Thus, the present chaotic terrain might have been formerly in a polar position, and a shift by drifting crustal plates to a warmer environment could have initiated degradation of the "ice" and concurrent collapse of the overlying surficial material. Augmented heat flow along the aerothermal gradient in an area of active drifting could have hastened degradation of the buried ice. Similar considerations apply to massive buried ice derived from buried sea or lake ice or buried hydroeffusions, except that drifting crustal plates need not be involved.

TERRESTRIAL ANALOGS

If processes that produce thermokarst terrain produced the chaotic terrain on Mars, the most remarkable aspect is its massive scale. The most comparable terrestrial analog that we have identified is the alas thermokarst topography developed in the region of Yakutia, Siberia (Figure 7). The maximum relief developed as a result of permafrost degradation there is about 40 m, and diameters of alases vary from 100 m to 15 km.⁸ The coalescence of alases has resulted in elongated, interconnected valleys, separated by narrow inter-

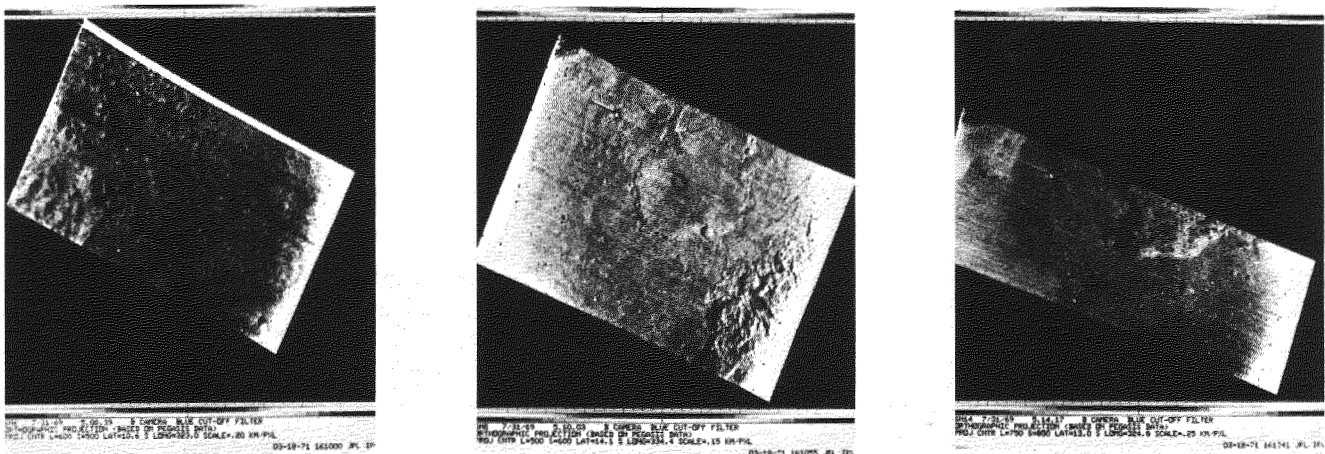


FIGURE 3 Rectified orthographic projections of camera B images 6N6, 6N8, and 6N14. North is toward the top.

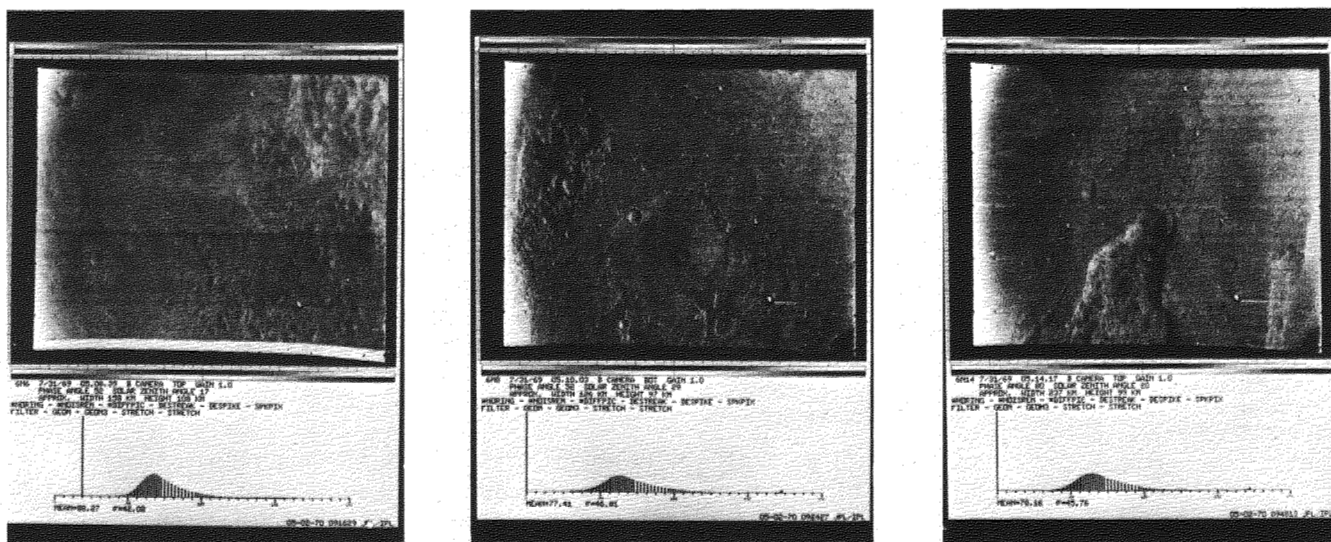


FIGURE 4 Camera B images 6N6, 6N8, and 6N14 enlarged to show the geomorphic features characteristic of chaotic terrain. North is toward the bottom.

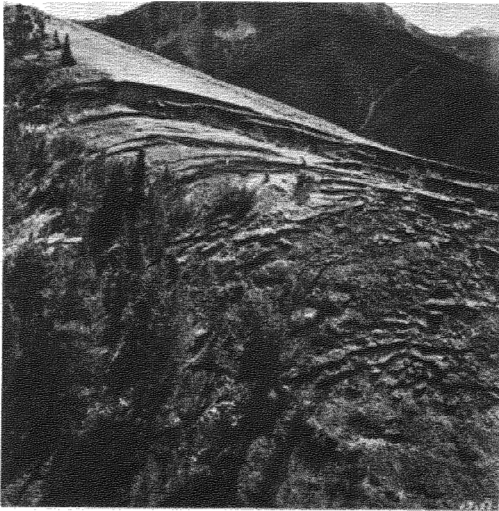
valley ridges (Figure 8). The large, massive bodies of segregated ice characteristic of this area range up to 50 m thick and the ice content of the permafrost frequently amounts to 80–90 percent by volume.⁸ Although chaotic terrain in many ways is analogous to the alas topography, there is a significant difference in scale. This might be attributed to differences in stages of development of the two areas. The thermokarst terrain of Yakutia is relatively young and, given a continuation of present thermal regime, will increase in size.

In a search for other possible terrestrial analogs, the ice-cemented permafrost adjacent to receding portions of the polar caps at Thule, Greenland, and Beacon Valley, Antarctica, have been considered.² The environmental conditions characteristic of these areas are somewhat comparable with those thought to be generally characteristic of Mars, except that the periglacial area at Thule receives 14.0 cm of precipitation in the form of rain and snow and has abundant surface water during the summer melt season. In contrast, Beacon Valley—an ice-free glacial valley exposed by retreating outlet and degrading piedmont glaciers—has little precipitation, drier air, and lower temperatures. Of the two, Beacon Valley, therefore, is considered the more apt.² Because snow accumulation is negligible and ablation occurs mainly by sublimation, liquid water there, as on Mars, is an ephemeral phase. Chemical weathering clearly is occurring, although slowly, and mechanical weathering and frost action are significant. Well-developed ventifacts sculptured by wind-blown sand or ice crystals indicate that eolian weathering is important. Soils have developed under extremely low biotic pressure and under extremely dry conditions; nevertheless,

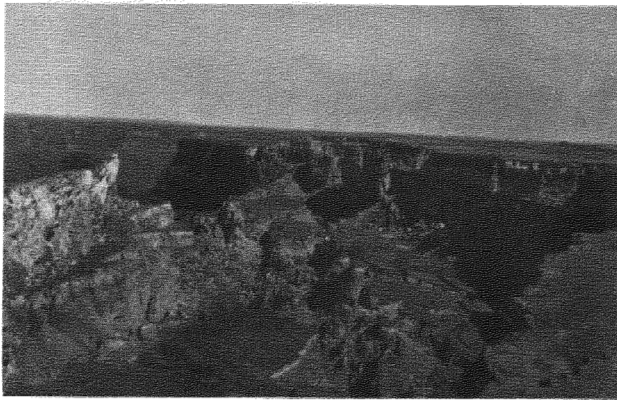
they have acquired the distinct features resulting from pedogenesis. The concentration of soluble salts near the top of the soil profile indicates that thin film migration of absorbed water is active. This terrestrial antarctic landscape is thought to possess nearly all the features of the cold, desert environment of Mars.

CONCLUSIONS

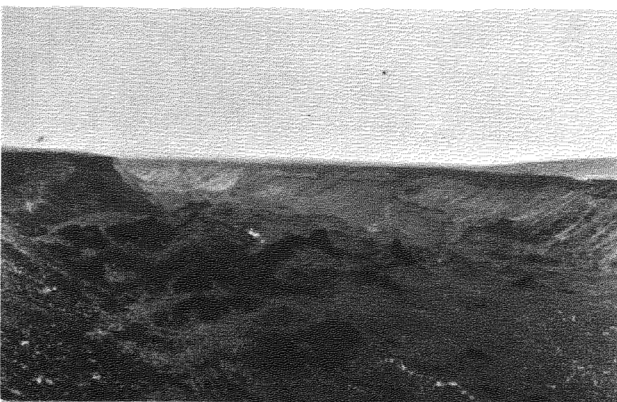
Surface indicators of terrestrial permafrost more frequently develop when water contents exceed the available pore space, producing excess ice. Patterned ground and particle sorting can also result from the filling of thermal-contraction cracks with silt and sand²⁷ and from the formation of vein ice from hoar frost accumulations, as discussed by Shumskii²² and Mackay.¹⁶ Usually, however, the development of most of the characteristic terrestrial permafrost features involves the transport of water in liquid form.¹ At present, extensive surface accumulation and movement of liquid water is not possible on Mars; only in sheltered, confined spaces is liquid water likely to occur, and its existence there is certain to be brief because of rapid evaporation and/or freezing. In other locations, strongly hygroscopic or deliquescent salts in the surface materials might prolong the occurrence of the liquid state by lowering the vapor pressure and freezing point required for the stability of the liquid phase. There is reason to believe that this may be the case on Mars for it has been observed that salts have accumulated at the surface near the edge of the arid antarctic polar cap.²⁶ Thus, active geomorphic processes associated with the existence of permafrost on Mars cannot be ruled



a



b



c

FIGURE 5 Features characteristic of terrestrial slumping: arcuate scarps (a,b), rotated blocks (b,c), parallel ridges (b,c), jumbled aspect (a,b,c), and surface lineaments (a). [Photographs by J. R. Stacy, USGS, Madison County, Montana (a); S. R. Capps, USGS, Twin Falls County, Idaho (b); and W. C. Mendenhall, USGS, Twin Falls County, Idaho (c).]

out. Furthermore, it is quite possible that Mars had a hydro-sphere at a warmer stage of its thermal history; hence, relict forms of all types of ground ice with their associated geomorphic features could have formed and been preserved or could be undergoing degradation or regeneration at present.

Since Martian surface temperatures are such that permafrost must be present, the fact that surface geomorphic expressions have not been detected may be explained simply as due to inadequate resolution in the Mariner imagery. At best, the resolution is of the order of 300 m. As mentioned earlier, the only permafrost features large enough to be detected under these circumstances are exceptionally large pingos and large-scale thermokarst topography. Mariner 9 imagery, with improved resolution of about 100 m, may perhaps show patterned ground and other permafrost indicators, but it will require imagery with a resolution of about 1 m to reveal the presence or absence of features characteristic of ice-cemented permafrost.

In spite of alternative suggestions, the original suggestion of Leighton *et al.*¹⁴ that chaotic terrain might have resulted from the degradation of massive permafrost deposits, resulting in slumping on a regional scale, has withstood re-examination; at present, Leighton's suggestion remains the leading and most plausible explanation. The occurrence of thermokarst terrain someplace on the planet is a near certainty. Additional evidence bearing on this question most likely will emerge from a detailed analysis of the results of Mariner '71, now in progress.

SUMMARY

The Mariner 6 and 7 satellite imagery of Mars was processed by computer techniques for maximum discriminability and examined for geomorphic evidence of permafrost. Particular attention was given to the region lying between 10°-70° long. and 20°N to 20°S lat., a region described as chaotic terrain by Leighton *et al.*¹⁴ This region is within the Martian temperate zone (30°N to 70°S lat.) where daily summertime surface temperatures rise above 0 °C and an active freeze-thaw layer of significant thickness can be expected. Permafrost may exist over the entire planet, however, since the mean annual temperature at all latitudes is believed to be well below 0 °C. Narrow-angle Mariner camera B frames 6N6, 6N8, and 6N14 reveal an area of chaotic terrain of about 1.7×10^4 km² in the region lying between Aureora Sinus and Margaritifer Sinus. This terrain consists of alternating ridges and valleys 1-5 km wide by 2-10 km long. The maximum ridge height was deduced to be of the order of 1 km, and a distinct NE-SW orientation was discovered from detailed photogrammetric measurements. For comparison, the alas thermokarst topography in Yakutia, Siberia, was identified as the best known terrestrial analog. The general appearance of chaotic terrain is similar but exists on a much larger scale. The depth of individual alases around Yakutia

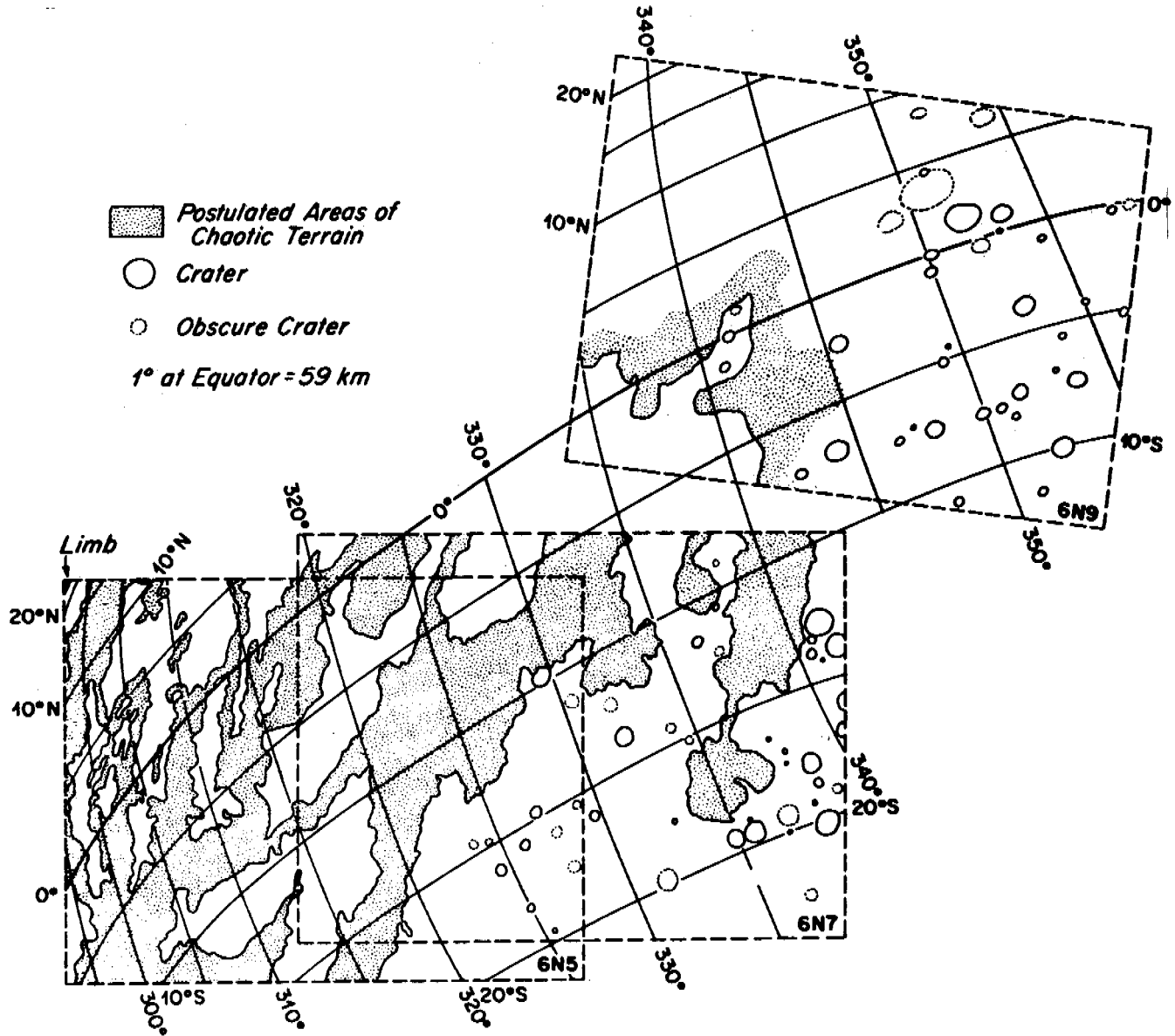


FIGURE 6 The scale and distribution of chaotic terrain.²¹

is 3–40 m with diameters varying from 100 m to 15 km. The coalescence of alases has resulted in elongated, interconnected valleys, separated by narrow intervalley ridges. It is suggested, therefore, that chaotic terrain may be Martian thermokarst terrain caused by sublimation of buried ice.

The geomorphic features characteristic of the ice-cemented permafrost adjacent to receding portions of the polar ice caps at Thule, Greenland, and Beacon Valley, Antarctica, were also studied as analogous to Martian permafrost terrain. The environmental conditions characteristic of these areas were compared with those thought to be generally characteristic of Mars. The periglacial area at Thule receives 144 mm of precipitation yearly and has abundant surface water during the

summer melt season. In contrast, Beacon Valley has little precipitation, drier air, and lower temperatures and, of the two, is considered the most apt analogy for the cold desert environment of Mars.

ACKNOWLEDGMENTS

This paper presents the results of research performed by the U.S. Army Cold Regions Research and Engineering Laboratory under the sponsorship of the National Aeronautics and Space Administration. This research is funded by the Planetology Program Office, Office of Space Science, NASA Headquarters, under grant NGR W-13,277, PR:10-9336, R/D 80X0108(71) 384-50-80.



FIGURE 7 Thermokarst terrain near Yakutia, Siberia. This is part of an extensive thermokarst depression system on the kilometre scale in areal dimensions. Relief developed is measured in tens of metres, but would be considerably greater if the depth of degradation of the 1-km thick underlying permafrost were to proceed further. (Photograph by J. Brown.)

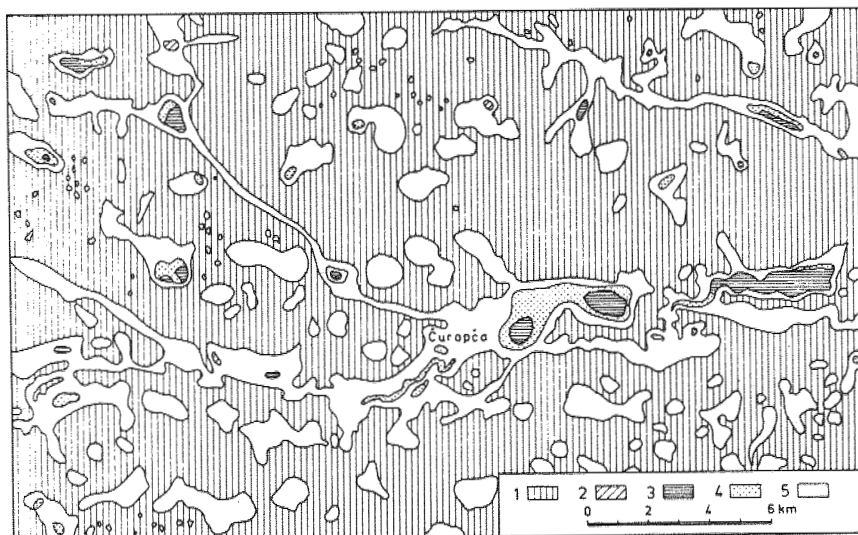


FIGURE 8 Map of thermokarst relief in the central Yakutian Lowland.⁸ 1, Original surface with ice wedges intact; 2, young lakes; 3, lakes in alases; 4, recently desiccated lakes in alases; and 5, old alases.

REFERENCES

1. Anderson, D. M., E. S. Gaffney, and P. F. Low. 1967. Frost phenomena on Mars. *Science* 155:319-322.
 2. Anderson, D. M., L. W. Gatto, and F. C. Ugolini. 1972. An antarctic analog of Martian permafrost terrain. *Antarct. J. U.S.* 7(4):114-116.
 3. Bader, H. 1961. The Greenland ice sheet. USA CRREL Report I-B2. U.S. Army Cold Regions Research and Engineering Laboratory, Hanover, New Hampshire.
 4. Baranov, I. Ya. 1959. Geographical distribution of seasonally frozen ground and permafrost. *In Principles of geocryology.*

Part 1. V. A. Obruchev Institute of Permafrost Studies, Academy of Science, U.S.S.R.
 5. Bardin, V. I., and I. A. Suyetova. 1967. Basic morphometric characteristics for Antarctica and budget of the antarctic ice cover. p. 92-100. *In* T. Nagata [ed.] *Proceedings of the symposium on pacific-antarctic science.*
 6. Belcher, D., J. Veverka, and C. Sagan. 1971. Mariner photography of Mars and aerial photography of earth: Some analogies. *Icarus* 15:241-252.
 7. Collins, S. A. 1971. The Mariner 6 and 7 pictures of Mars. NASA SP-263. 159 p.
 8. Czudek, T., and J. Demek. 1970. Thermokarst in Siberia and its

- influence on the development of lowland relief. *Quaternary Res.* 1(1):103-120.
9. Dunne, J. A., W. D. Stromberg, R. M. Ruiz, S. A. Collins, and T. E. Thorpe. 1971. Maximum discriminability versions of the near encounter Mariner pictures. *J. Geophys. Res.* 76(2):438-472.
 10. Ferriars, O. J., R. Kachadoorian, and G. W. Greene. 1969. Permafrost and related engineering problems in Alaska. U.S. Geological Survey Professional Paper 678. U.S. Government Printing Office, Washington, D.C. 37 p.
 11. Glasstone, S. 1968. The book of Mars. NASA SP-179. Office of Technology Utilization, Washington, D.C. 315 p.
 12. Gow, A. J. 1965. The ice sheet in Antarctica. T. Hatherton [ed.]. New Zealand Antarctic Society, Methuen, London. p. 221-258.
 13. Jet Propulsion Laboratory. 1968. Mars scientific model. Vol. 1. JPL Document No. 606-1. 309 p.
 14. Leighton, R. B., N. H. Horowitz, G. C. Murray, R. P. Sharp, A. G. Herriman, A. T. Young, B. A. Smith, M. E. Davies, and C. G. Leovy. 1969. Mariner 6 and 7 television pictures: Preliminary analysis. *Science* 166:49-67.
 15. Leighton, R. B., and B. C. Murray. 1966. Behavior of carbon and other volatiles on Mars. *Science* 153:136-144.
 16. Mackay, J. R. 1972. The world of underground ice. *Ann. Assoc. Am. Geogr.* 62(1):1-22.
 17. Michaux, C. M. 1967. Handbook of the physical properties of the planet Mars. NASA SP-3030. U.S. Government Printing Office, Washington, D.C. 167 p.
 18. Morrison, D., C. Sagan, and J. B. Pollack. 1969. Martian temperatures and thermal properties. *Icarus* 11:36-45.
 19. Nagarov, V. S. 1963. Quantity of ice in the world ocean and its variation. (Translation). *Okeanologia* 2:234-249. (Summarized in *Polar Rec.* 12:205)
 20. Neugebauer, G., C. Munch, S. C. Chase, Jr., H. Hatzenbeler, E. Miner, and D. Schofield. 1969. Mariner 1969: Preliminary results of the infrared radiometer experiment. *Science* 166:98-99.
 21. Sharp, R. P., L. A. Soderblom, B. C. Murray, and J. A. Cutts. 1971. The surface of Mars: Un cratered terrains. *J. Geophys. Res.* 76: 331-342.
 22. Shumskii, P. A. 1964. Principles of structural glaciology (English translation). Dover Publications, Inc., New York.
 23. Shumskii, P. A., and B. I. Vtyurin. 1963. Underground ice, p. 108-113. *In* Permafrost: Proceedings of an international conference. National Academy of Sciences, Washington, D.C.
 24. Sinton, V. M., and J. Stron. 1960. Radiometric observations of Mars. *Astrophys. J.* 131:459-469.
 25. Slipher, E. C. 1962. Mars, the photographic story. Sky Publishing Corp., Cambridge, Massachusetts, and Northland Press, Flagstaff, Arizona.
 26. Ugolini, F. C. 1963. Soil investigations in the lower Wright Valley, Antarctica, p. 55-61. *In* Permafrost: Proceedings of an international conference. National Academy of Sciences, Washington, D.C.
 27. Wade, F. A., and J. N. de Wys. 1968. Permafrost features on the Martian surface. *Icarus* 9:175-185.
 28. Washburn, A. L. 1956. Classification of patterned ground and review of suggested origins. *Geol. Soc. Am. Bull.* 67:823-866.
 29. Wells, R. A. 1967. Morphology of the Martian surface and its structural implications. Ph.D. thesis. University of London, England.
 30. Wells, R. A. 1971. Martian surface harmonics and continental drift. *Phys. Earth Planet. Inter.* 4:273-285.

IN SITU PHYSICOMECHANICAL PROPERTIES OF PERMAFROST USING GEOPHYSICAL TECHNIQUES

Om P. Garg

IRON ORE COMPANY OF CANADA
Schefferville, Quebec

INTRODUCTION

Adequate knowledge of permafrost must exist, preferably during the planning stages of such resource developments as exploration and mining, design of mine shafts, and the construction of roads, pipelines, and foundations. The three-dimensional distribution of frozen ground in the discontinuous zone is clearly much more complex and variable than in the continuous zone. Thus, work in the former zone requires a detailed understanding of various parameters affect-

ing permafrost in a given area.⁶ Some of the problems encountered during the design and the construction of dikes²³ and mine railroads³³ in the discontinuous zone of permafrost have already been investigated. The general aspects of engineering geology in permafrost have been discussed by Swinow,³⁵ among others.

This paper mainly deals with determining *in situ* physico-mechanical properties of frozen ground as a by-product of a permafrost delineation program using geophysical techniques in the Schefferville (54°49'N and 66°50'W) mining area of

subarctic Canada. Until recently, permafrost studies in the area mainly related to a program of measuring ground temperatures and their relationship to topography, drainage, vegetation, and snow depth.^{5,6,36} However, during the mining of iron ore in permafrost the physicomechanical properties of the material are very helpful in the analysis and the solution of various problems. Some investigations have been carried out related to the mechanical properties, including those related to blasting of frozen ground^{3,4,7,10,13,27,29}; however, additional knowledge of these properties is required.

GEOPHYSICAL TECHNIQUES USED IN PERMAFROST

The basic tool for quantitative delineation of permafrost has been the measurement of ground temperatures. Temperature measurements, however, provide the information at one point only and are expensive, especially if the cost of drilling is to be included. Therefore, other physical properties of the ground material have been investigated to supplement the temperature measurements.

Unlike such properties as density, radioactivity, and magnetism, there is a marked increase in the sonic and electrical properties of rocks during the freezing process. Thus, to predict the distribution of frozen ground, use is made of the appreciable changes in sonic velocities and electrical resistivities of the material. These two methods have been frequently used for delineating the top and bottom of the permafrost with a varying degree of success.^{3,8,12,15,19,21}

Seismic refraction surveys using a multichannel seismograph and resistivity soundings using a dc portable unit are used to determine the depth of the permafrost table and the base of frozen ground, respectively. The depth of penetration achieved in delineating the bottom of permafrost depends on the resistivity contrasts between different layers and the structural and lithological complexities of the area. The various grids and methods to be used in mapping permafrost vary, depending on the purpose, accuracy desired, and the area to be covered. The resistivity penetration achieved in the Schefferville area is in the order of 80 m. The three-dimensional distribution of permafrost within an 11.88 m mining lift, as well as for an ore body as a whole, is being determined on a routine basis.¹⁵

IN SITU MECHANICAL PROPERTIES

In many northern engineering projects, the mechanical properties of large volumes of frozen rocks must be considered. Dynamic rather than static methods are more suitable for determining elastic properties.²⁴ Further, it has been found that, with static and dynamic laboratory testing results, *in situ* dynamic testing techniques are nondestructive in nature, faster, cheaper, and more representative over a wider range of geological conditions.^{20,22} The dynamic method relates

the sonic velocities to the elastic properties. Seismic refraction surveys, therefore, are used to provide *in situ* elastic properties of the frozen ground.

ELASTIC CONSTANTS

Compressional and shear-wave velocities provide the various elastic constants using the following relationships¹¹:

$$E = \rho V_s^2 [(3V_p^2 - 4V_s^2)/(V_p^2 - V_s^2)], \quad (1)$$

$$\nu = \left[\left\{ \frac{1}{2}(V_p/V_s)^2 \right\} - 1 \right] / [(V_p - V_s)^2 - 1], \quad (2)$$

$$K = \rho (V_p^2 - 4/3 V_s^2), \quad (3)$$

$$\mu = \rho (V_s^2), \quad (4)$$

where V_p = compressional wave velocity, V_s = shear-wave velocity, ρ = density of the material, E = dynamic Young's modulus, ν = Poisson's ratio, K = bulk modulus, and μ = shear modulus.

It should be remembered that the above formulas are strictly applicable only to an isotropic elastic solid complying with Hooke's law. Dynamic Young's modulus, E , can also be calculated knowing V_p , ν , and ρ by the following:

$$E = (V_p^2) (\rho) [(1 + \nu)(1 - 2\nu)/(1 - \nu)]. \quad (5)$$

It should be noted that Eq. (5) does not require V_s . Finally, E , can be obtained only from V_p and ρ using Eq. (5), provided ν has been established from field data.

PREVIOUS INVESTIGATIONS RELATED TO SEISMIC VELOCITIES

The parameters that are known to influence the compressional (V_p) and shear-wave velocities (V_s) include lithology and grain size, total moisture content and the nature of interstitial fluid, temperature and degree of freezing of interstitial water, porosity and pore structure, confining pressure, and matrix composition and degree of cementation. Many of the earlier studies have shown that porosity is usually the dominant parameter affecting V_p in dry and/or saturated rock at a given pressure.^{14,25,26,31,37,38,40} The conclusions pertinent to this particular paper include the following: (a) There is a general increase in V_p and V_s with decreasing temperature mainly over the range 0 to -2°C in saturated material. However, changes in V_p and V_s are minimal in rocks at very low water content when measured as a function of temperature³⁷; (b) compared with velocities in water saturated rocks, V_p is lower in unsaturated rocks with up to 20 percent porosity and even lower in the 20–80 percent porosity range³⁸; (c) the increase in velocities in saturated material below 0°C is probably caused by the cementing action of ice formed first

in the largest pore spaces and then in progressively smaller ones as the temperature is reduced further.²⁶

ANALYSIS OF SEISMIC VELOCITIES IN PERMAFROST

There have been few investigations of the problems associated with seismic refraction surveys in the permafrost areas.^{3,9,16,17,19} This paper analyses some of the data on seismic velocities of the frozen and unfrozen rocks from the Schefferville area. Further, the relationship of elastic constants calculated from the field velocities with some of the problems encountered during open pit mining is discussed.

For the analysis of the ore, data on unfrozen and frozen middle iron formation (MIF) have mainly been used. This lithologic unit, which forms the bulk of the ore, is essentially fine to medium grained, granular, and composed mainly of blue hematite and silica with a moisture content generally varying between 5 and 8 percent by weight. The alteration is by leaching of silica resulting in a highly porous (up to 40 percent), sandy, and friable product.

DEGREE OF LEACHING IN FROZEN AND THAWED STATES

One of the main problems in interpreting the seismic survey results in the Schefferville area is the overlapping range of velocities for the frozen leached rocks on one side and the unfrozen unaltered iron formation on the other.¹⁵ Table I lists a set of typical values of compressional wave velocities both for leached and unaltered iron formation (IF), as well as for frozen and thawed conditions.

Based on Table I, it is concluded that, on freezing V_p increases at a faster rate in leached IF than in unaltered IF. Because of a fourfold increase of V_p in frozen leached IF, a more precise delineation is possible.

Furthermore, the velocity ratio of unaltered to altered IF of 2.2 in the unfrozen state is more pronounced than that of 1.1 in the frozen state. Therefore, it is concluded that a decrease in temperature (unfrozen to frozen) overrides the variations caused by the degree of leaching. In other words, perma-

frost conditions tend to create homogeneous material. Finally, velocities could possibly be used to supplement a program of mineralogical textural studies for quantitative assessment of the degree of leaching in altered iron ores.

VELOCITY CONTRASTS IN FROZEN MIF ORE

The compressional wave velocities of thawed and frozen MIF for three stations are listed in Table II. These are computed from standard time distance plots, an example of which is given in Figure 1.

In Table II, V_1 corresponds to the surface material that is thawed and saturated, while V_2 and V_3 indicate frozen layers. The ratio of V_2/V_1 , also listed in the table, indicates a rather sharp contact between the permafrost table and the bottom of the active layer. Furthermore, V_3/V_2 reflects the intensity of permafrost. These categories of permafrost are based on three distinct velocity layers. This type of delineation, although essentially qualitative in nature, has proved to be of considerable help in the mining operations.

COMPARISON OF ELASTIC CONSTANTS FOR FROZEN AND UNFROZEN MIF ORE

Various elastic constants (E , ν , K , and μ) for MIF have been calculated using average values of field velocities. The average values for frozen and thawed states appear in Table III. The temperature limits used for various ground categories are based on field temperature measurements.

The following conclusions are drawn from Table III: The values of E , ν , K , and μ are larger for frozen than for unfrozen ground; the increase of ν and K with the presence of permafrost indicate that frozen ground has a greater overall rigidity and hardness, compared with unfrozen ground. This increase is more pronounced from the marginally frozen to the frozen category than from unfrozen to marginally frozen rock. The opposite is the case for E and μ ; the value of K for frozen MIF is generally 5–11 times greater than in the unfrozen state, while the corresponding increase in E and μ is 2–4 times only; and the increase in E indicates that a frozen rock is capable of withstanding an increased load for the same strain. Thus, the

TABLE I Compressional-Wave Velocities for Iron Formation—Frozen and Thawed States

Iron Formation	Velocities (m/s)		
	Frozen	Unfrozen	Frozen-Unfrozen
Altered, leached	5 486	1 372	4.0
Unaltered	6 096	3 048	2.0
Unaltered-altered	1.1	2.2	

TABLE II Velocity Contrasts in Frozen MIF Ore

Velocities ^a (m/s)				
V_1	V_2	V_3	V_2/V_1	V_3/V_2
320	3 048	5 944	9.5	2.0
323	2 164	6 096	6.7	2.8
381	3 048	6 096	8.0	2.0

^a V_1 , V_2 , and V_3 and the velocities for first, second, and third layers, respectively.

○ FORWARD SHOT
 x BACKWARD SHOT
 VELOCITIES IN METERS/SEC.

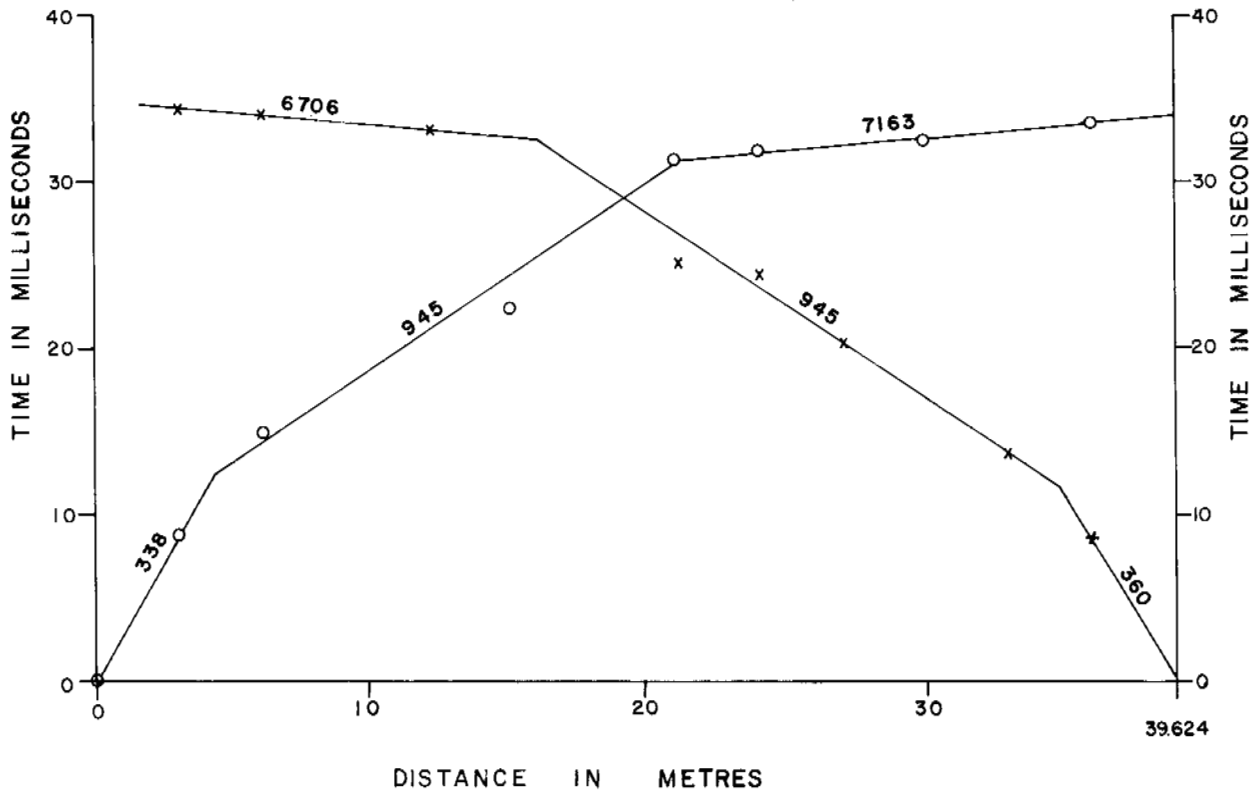


FIGURE 1 A typical distance-time plot in frozen MIF ore.

TABLE III Elastic Constants for Frozen and Unfrozen MIF

	V_p (m/s)	V_s (m/s)	ρ (g/cm ³)	$E \times 10^5$ (kg/cm ²)	ν	$K \times 10^5$ (kg/cm ²)	$\mu \times 10^5$ (kg/cm ²)
Unfrozen (>0 °C)	2 103	1 098	3.6	1.16	0.31	1.03	0.44
Marginally frozen (0 to -0.6 °C)	3 383	1 623	3.6	2.61	0.35	2.91	0.97
Frozen (<-0.6 °C)	6 096	2 033	3.6	4.36	0.44	11.60	1.52

3.76-fold increase in E for highly leached MIF on freezing has great bearing on the strength of rocks, in general, and could play a significant role in the design of pit slopes in permafrost areas.

One of the limitations in using the velocities is the effect of unfrozen water on the field measurements at temperatures below 0 °C. The importance of this aspect has been discussed in terms of the phase composition of unfrozen pore water.¹ The range of the marginal permafrost category could be minimized if the quantitative effect of unfrozen water on velocity measurements were known.

ELASTIC CONSTANTS AND DEGREE OF FROZEN GROUND

Table IV lists two sets of typical velocities (V_p) in MIF. V_p/V_s ratios of 2 and 2.5 for frozen and 2.5 and 3 for unfrozen material are assumed. The average density of the material is 3.6 g/cm³. It can be seen that the compressional-wave velocities peak at 2 164, 3 048, 4 878, and 5 944 m/s. These indicate a decreasing temperature. Although the precise temperature readings at the site of the survey are not available, the range of ground temperatures (between 2.2 and -4.4 °C) tend to confirm the general relationship—i.e., the higher the velocities, the lower the temperature. If the laboratory controlled values of V_p as a function of temperature become available, *in situ* temperature and hence severity of permafrost can be estimated based on the above analysis. Also, it would be useful to measure *in situ* temperatures in the vicinity of the seismic survey at least initially in order to confirm the relationship between temperatures and velocities as established from laboratory data.^{24,26,37}

ESTIMATION OF STRENGTH

To estimate the strength of MIF after freezing, ratios of E for different categories of frozen ground are listed in Table V. The ratios of E increase from 1.41 for marginally frozen-unfrozen to 5.31 for solidly frozen-unfrozen. This tends to confirm the laboratory results obtained by Kurfurst and King²⁶ and also confirms the general theory of Simmons and Brace³⁴ that E increases with higher pressure because of the closure of cracks in unfrozen material. In the permafrost state, all the void spaces, cracks, and openings may be filled with ice, thus creating a solid medium.

Finally, a relationship could be established between the dynamic modulus of elasticity, E' , as obtained from the field, and the compressive strength of frozen soil as suggested by Kaplar²⁴ and Mellor.³⁰

SUMMARY—SEISMIC VELOCITIES

Some of the salient features that result from the above discussion include:

1. Seismic refraction surveys provide a cheap and convenient method of determining the *in situ* mechanical properties of frozen ground, as a by-product of permafrost delineation;
2. Various elastic constants are useful in evaluating the mechanical state of the frozen material, particularly the use of dynamic Young's modulus, E , in determining the compressive strength;
3. The variation of V_p as a function of temperature within the range from 0 to -5 °C for various degrees of saturation

TABLE IV Variation of Elastic Constants in Frozen and Unfrozen MIF

V_p (m/s)	V_s (m/s)	$E \times 10^5$ (kg/cm ²)	ν	$\mu \times 10^5$ (kg/cm ²)	$K \times 10^5$ (kg/cm ²)	Remarks
MIF—unfrozen						
2 164	866	0.77	0.41	0.27	1.34	Weak
2 164	722	0.55	0.44	0.19	1.48	Weak
MIF—marginally frozen						
3 048	1 016	1.09	0.44	0.38	2.88	
3 048	1 219	1.55	0.41	0.55	2.67	
MIF—frozen						
4 878	2 438	5.84	0.33	2.18	5.84	Very strong
4 878	1 951	3.94	0.41	1.41	6.89	Strong
MIF—solidly frozen						
5 944	2 972	8.65	0.33	3.23	8.65	Very strong
5 944	2 377	5.84	0.41	2.11	10.19	Very strong

TABLE V Ratio of Young's Modulus with Severity of Permafrost

Severity of Permafrost		E_a/E_b	Assumed V_p/V_s
a	b		
Marginally frozen/unfrozen		1.40	3.0
		1.41	2.5
Frozen/marginally frozen		1.79	2.5
Solidly frozen/marginally frozen		2.65	2.5
Solidly frozen/unfrozen		5.31	2.5

is by far the most significant parameter for which controlled laboratory and field data are required. This would considerably improve the interpretation of field data; and

4. Further use could be made of seismic velocities in permafrost as related to propagation and dissipation of blast energy with a view to arriving at an optimum delay time and for improved fragmentation, response of the frozen foundation material to loading, and variation in the strength of excavated slopes subjected to freezing and thawing cycles.

ELECTRICAL RESISTIVITY IN PERMAFROST

The marked increase in the electrical resistance of partially or completely saturated rocks upon freezing is detected by resistivity surveys involving horizontal profiling and vertical soundings. Using the Schlumberger configuration of electrodes in the field, the apparent resistivity, ρ_a , is obtained by the following relationship:

$$\rho_a = \pi/4 [(L^2 - \ell^2)/\ell] \Delta V/I, \quad (6)$$

where L = distance between current electrodes, ℓ = distance between potential electrodes, and ΔV = measured potential difference for current I .

Resistivity techniques have been used not only for the lateral and vertical extent of frozen ground but also for the degree to which the ground is frozen. The variation in resistivity depends among others on lithology, temperature, moisture content, nature of the electrolyte, pore size, and lateral inhomogeneity.^{3,18,21,28,39}

COMPARISON AND ANALYSIS OF RESISTIVITY VALUES IN FROZEN AND UNFROZEN STATES

The basic data on the resistivity values of various rock types¹⁵ came as a by-product of the three-dimensional permafrost delineation program for the mining of iron ore in the Schefferville area. Typical plots of field resistivity data and temperature measurements at the time of the survey are

shown in Figures 2 and 3, respectively. These resistivity values have been analyzed with a view to indirectly evaluating the *in situ* engineering properties of permafrost in the area. Table VI lists the average resistivities for the unfrozen and frozen state for MIF and lower iron formation (LIF). This latter lithologic unit is essentially thinly bedded, composed primarily of fine- to medium-grained silica and red and blue hematite.

Table VI confirms the following conclusions: (a) That in frozen ground, the drastic increase in resistivity is due to the freezing of water in the pore spaces. Water in the unfrozen state is conductive while in permafrost it is highly resistive; (b) this factor of increase depends on the moisture content and varies in the area from 15 times in MIF with 5–8 percent moisture to as high as 50 in LIF with 10–15 percent moisture content; and (c) variations due to lithology, nature of electrolyte, and lateral inhomogeneity in these rocks seem negligible as compared with the increase due to freezing of water.

CLASSIFICATION OF FROZEN GROUND BASED ON RESISTIVITY SURVEY RESULTS

Based on the results of resistivity surveys, the frozen ground in the Schefferville discontinuous permafrost zone can be classified into three types that correspond to three layer cases used in delineating permafrost. For all the cases, ρ_1 , ρ_2 , and ρ_3 are the resistivities of the first, second, and third layers, respectively.

For Case 1, $\rho_2 > \rho_3$ and ρ_1 corresponds to thawed active layer (ρ_1) → permafrost (ρ_2) → unfrozen ground (ρ_3). This represents a common case in the Schefferville area. For Case 2, $\rho_1 \approx \rho_3 > \rho_2$ corresponds to ground frost (ρ_1) → talik (ρ_2) → permafrost (ρ_3). This is the case during the months of May and early June, when the ground frost still exists, and in areas of talik zones. Finally, for Case 3, ρ_1 and $\rho_2 > \rho_3$ corresponds to ground frost (ρ_1) → permafrost (ρ_2) → unfrozen ground (ρ_3). Two subcases $\rho_2 > \rho_1$ and $\rho_1 > \rho_2$ represent the relative intensity of ground frost and permafrost with respect to unfrozen ground. Typical field values for each case appear in Table VII.

LIMITATIONS IN INTERPRETATION TECHNIQUES

All the results used in this study were obtained by matching Orellana and Mooney multilayer curves.³² The two greatest limitations in using resistivity techniques for permafrost studies are: (a) the lack of laboratory-controlled resistivity data as a function of temperature at various degrees of saturation for different rock types. Therefore, ranges of resistivity values are used in delineation and in assessing the *in situ* engineering properties of frozen ground. This could be particularly useful in estimating the total ice content from field

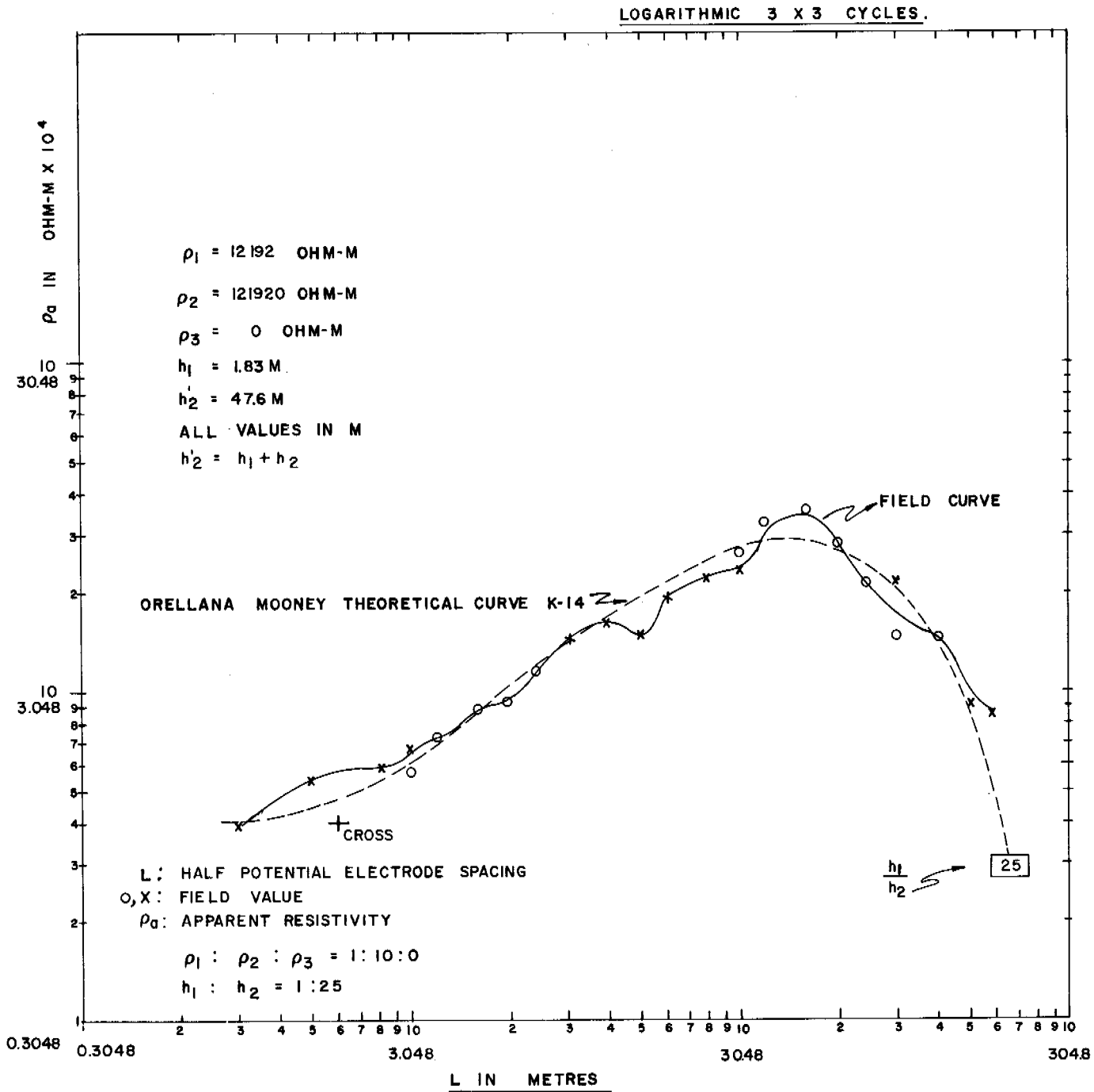


FIGURE 2 Resistivity depth data at hole No. 2 and interpretation.

resistivity ratios; and (b) nonavailability of theoretical curves to match the higher resistivity contrasts frequently encountered in the Schefferville area. Limited resistivity model experiments and theoretical studies have been undertaken and with extension could be used to minimize the above problem.^{2,28}

CONCLUSIONS

Based on this paper, it is concluded that the determination of *in situ* physicommechanical properties of frozen ground seem possible using seismic refraction resistivity surveys. However, detailed laboratory investigations on the variation of seismic

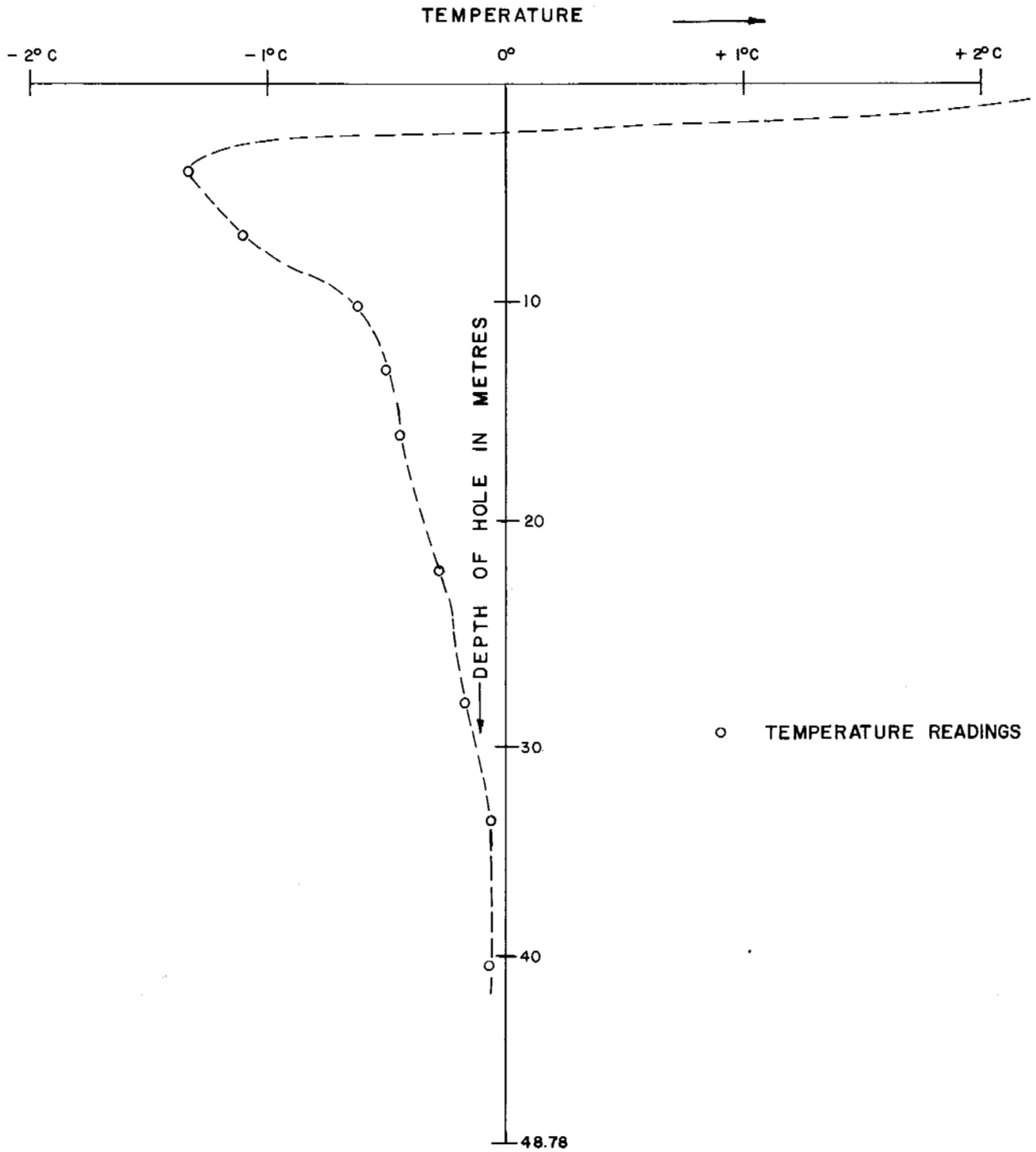


FIGURE 3 Temperature-depth plot for hole No. 2.

TABLE VI Average Resistivity Values for Unfrozen and Frozen States

	Resistivity (kohm-m)		Factor	Moisture Weight (%)
	Unfrozen	Frozen		
MIF	1.53	23.6	15	5-8
LIF ^a	0.55	26.4	50	10-15

^a LIF is generally more fine grained and has a higher moisture content than MIF.

TABLE VII Threefold Classification of Frozen Ground Based on Resistivity Values

Resistivity (kohm-m)				Estimated Permafrost Depth (m)
ρ_1	ρ_2	ρ_3	$\rho_1 : \rho_2 : \rho_3$	
CASE 1 - $\rho_2 > \rho_3$ and ρ_1 , where $\rho_1 > \rho_3$, which corresponds to active layer → permafrost → unfrozen				
13.4	120.7	13.4	1:9:1	8
11.9	106.7	0	1:9:0	20
CASE 2 - $\rho_1 = \rho_3 > \rho_2$, which corresponds to ground frost → talik → permafrost				
25.6	6.1	25.6	4:1:4	50
27.4	1.4	27.4	20:1:20	50
CASE 3 - ρ_1 and $\rho_2 > \rho_3$, which corresponds to ground frost → permafrost → unfrozen ground				
33.5	14.3	6.1	6:2:1	18
15.2	61.0	0	1:4:0	50
11.9	106.7	0	1:9:0	20

velocities and resistivity as a function of temperature are required for precise quantitative analysis and interpretation of field data.

ACKNOWLEDGMENTS

I would like to thank the Iron Ore Company of Canada for providing the facilities and the permission to publish this paper, and Mr. P. F. Stacey, Supervisor, Geotechnical Engineering, and Mr. D. S. Campbell, Superintendent, Mining Engineering, for many helpful suggestions during its preparation.

REFERENCES

- Anderson, D. M., and A. R. Tice. 1970. Low temperature phases of interfacial water in clay-water systems. Res. Rep. 290. U.S. Army CRREL, Hanover, New Hampshire.
- Apparav, A., A. Roy, and K. Mallick. 1969. Resistivity Model Experiments. Geosurveying 7(1):45-54.
- Barnes, D. F. 1966. Geophysical methods for delineating permafrost. In Permafrost: Proceedings of an international conference. National Academy of Sciences, Washington, D.C.

- Bauer, A. 1959. Rock-mechanics-blasting characteristics of frozen iron ores and overburden. Explosives Division, Canadian Industries Limited, Montreal, Quebec.
- Bird, J. B. 1964. Permafrost studies in central Labrador-Ungava. McGill Sub-Arctic Research Paper 16. Montreal, Quebec.
- Brown, R. J. E. 1970. Permafrost in Canada. University of Toronto Press, Toronto.
- Burshtein, L. S., and A. N. Kurochkin. 1970. Study of the physico-mechanical properties of frozen bedrock. U.S. Army CRREL, Hanover, New Hampshire.
- Bush, B. O., and S. D. Schwarz. 1965. Seismic Refraction and electrical resistivity measurements over frozen ground. Tech. Memo 86. National Research Council of Canada, Ottawa, p. 32-39.
- Desai, K. P., and F. J. Moore. 1967. Well log interpretation in permafrost. Proceeding SPWLA eighth annual logging symposium. Sect. N. p. 1-27.
- Dick, R. A. 1969. Evaluating blasting techniques in frozen gravel. Min. Congr. J. Sept:30-36.
- Dobrin, M. D. 1960. Introduction to geophysical prospecting. 2nd ed. McGraw-Hill, New York.
- Domzalski, W. 1955. Some problems of shallow refraction investigations. Ninth Meeting of EAEG, London.
- Farnam, H. E., Jr., 1961. New applications for explosives. American Mining Congress, Seattle, Washington.
- Garg, O. P. 1969. Static and dynamic mechanical properties of a sandstone. M.Sc. thesis. University of Saskatchewan, Saskatoon.
- Garg, O. P., and P. F. Stacey. 1972. Techniques used in the delineation of permafrost in the Schefferville, P.Q. area. National Research Council of Canada Seminar, Saskatoon. May.
- Hans, R. 1960. Seismic refraction soundings in permafrost near Thule, Greenland. International symposium on arctic geology. Calgary, Alberta. p. 970-981.
- Hans, R. 1961. Applicability of seismic refraction soundings in permafrost near Thule, Greenland. Tech. Rep. 81. U.S. Army CRREL, Hanover, New Hampshire.
- Henriet, J. P. 1971. Resistivity soundings in the Condroz (Belgium) with Schlumberger and dipole arrays; Application to limestone aquifer evaluation. Bull. Int. Assoc. Sci. Hydrol. 16:25-37.
- Hobson, G. D. 1962. Seismic exploration in the Canadian arctic islands. Geophysics 27:253-273.
- Hobson, G. D., and J. A. Hunter, August 1969. *In situ* determination of elastic constants in overburden using a hammer seismograph. Geosurveying 7:107-112.
- Joesting, H. R. 1954. Geophysical exploration in Alaska. Arctic 7(3 and 4):165-175.
- Johnson, W. S., and J. S. Nelson. 1971. Dynamic rock properties from *in situ* field seismic studies. Proc. Twelfth Symp. Rock Mech., AIME, New York.
- Johnston, G. H. 1969. Dykes on permafrost, Kelsey Generating Station, Manitoba. Can. Geotech. J. 6.
- Kaplar, C. W. 1969. Laboratory determination of dynamic moduli of frozen soils and of ice. Res. Rep. 163. U.S. Army CRREL.
- King, M. S. 1970. Static and dynamic elastic moduli of rocks under pressure. Proc. Eleventh Symp. Rock Mech., Berkeley, California.
- Kurfurst, P. J., and M. S. King. 1972. Static and dynamic elastic properties of two sandstones at permafrost temperatures. J. Pet. Tech. April:495-504.
- Lang, L. C. 1966. Blasting frozen ore at Knob Lake. Can. Min. J. August:49-53.
- Mackay, D. K. 1969. Electrical resistivity measurements in frozen ground, MacKenzie Delta area NWT. Reprint Ser. No. 82. Inland Waters Branch, E.M.R., Ottawa.

29. Mellor, M., and P. V. Sellman. 1970. Experimental blasting in frozen ground. SR 153. U.S. Army CRREL.
30. Mellor, M. 1971. Strength and deformation of rocks at low temperatures. RR 294. U.S. Army CRREL.
31. Nakano, Y., R. J. Martin III, and M. Smith. 1972. Ultrasonic velocities of the dilatational and shear waves in frozen soils. *Water Resour. Res.* 8(4).
32. Orellana, E., and H. M. Mooney. 1966. Master tables and curves for vertical electrical soundings over layered structures. *Inter-ciencia*, Madrid.
33. Pryer, R. W. J. 1966. Mine railroads in Labrador-Ungava. *In Permafrost: Proceedings of an international conference*. National Academy of Sciences, Washington, D.C.
34. Simmons, G., and W. F. Brace. 1965. Comparison of static and dynamic measurements of compressibility of rocks. *J. Geophys. Res.* 70:5649-5656.
35. Swinzow, G. K. 1969. Certain aspects of engineering geology in permafrost. *Eng. Geol.* 3:177-215.
36. Thom, B. G. 1969. New permafrost investigations near Schefferville, P.Q. *Rev. Geogr.* 23(3):317-327.
37. Timur, A. 1968. Velocity of compressional waves in porous media at permafrost temperatures. *Geophysics* 33:584-595.
38. Watkins, J. S., L. A. Walters, and R. H. Godson. 1972. Dependence of *in situ* compressional-wave velocity on porosity in unsaturated rocks. *Geophysics* 37(1):29-35.
39. Wyder, J. E. 1968. Surface resistivity surveys in southeastern Manitoba. Paper 67-44. E.M.R., Geological Survey of Canada, Ottawa.
40. Wyllie, M. R. J., A. R. Geogory, and G. H. F. Gardner. 1958. An experimental investigation of factors affecting elastic wave velocities in porous media. *Geophysics* 23:459-493.

ELECTROMAGNETIC PROBING OF PERMAFROST

Pieter Hoekstra [1]

U.S. ARMY COLD REGIONS RESEARCH AND
ENGINEERING LABORATORY
Hanover, New Hampshire

Duncan McNeill

BARRINGER RESEARCH LTD.
Toronto, Ontario

INTRODUCTION

Comprehensive Soviet geophysical mapping programs using dc resistivity techniques in permafrost have shown that three important objectives can be derived from ground resistivity: measurement of depth of permafrost; mapping of frozen sections in areas of discontinuous permafrost; and mapping of high-ice-content ground.

Resistivity surveys have the disadvantage of being relatively expensive and time-consuming. Therefore, a geophysical technique that can measure the electrical properties of the ground remotely, i.e., without the use of contacting electrodes, should have important applications in mapping permafrost, particularly if such a technique can be employed from an aircraft. This paper describes the potential application of ground and airborne low frequency electromagnetic sensors to map the electrical resistivity of ground.

This paper also summarizes existing knowledge of the resistivity of permafrost with particular emphasis on temperature dependence. The values of resistivity are used as a basis for calculating the behavior of both plane wave and dipole-

dipole electromagnetic sensors to determine the potential application, the limitations, and the range of frequencies to be used in surveys for mapping permafrost.

THE RESISTIVITY OF FROZEN GROUND

The temperature of interest in natural permafrost profiles ranges from 10 to -20°C . Parkhomenko¹³ summarized the comprehensive studies of Ananyan on the electrical resistivity of frozen and unfrozen ground over this temperature range. The behavior of resistivity with temperature is closely related to the phase composition of the frozen ground.

Figure 1 illustrates typical resistivity-temperature data for several soils and one rock type derived from the work of Ananyan,¹³ Hoekstra,⁷ Ogilvy,¹² Morgan,¹¹ and Parkhomenko.¹³ Within each soil type there is a difference of approximately a factor of 10 between the resistivity of the soil at 1°C and that at -10°C , and the resistivity at -5°C is at least a factor of 3 greater than that of the unfrozen soil. However, differentiating between frozen and unfrozen ground solely on the basis of resistivity is not always pos-

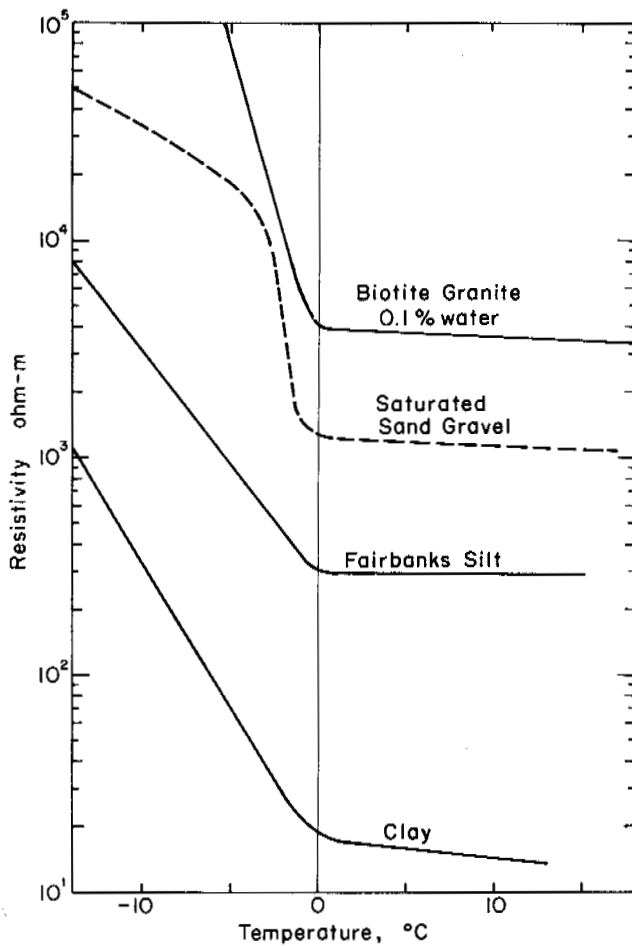


FIGURE 1 Resistivity for several soils and one rock type as a function of temperature.

sible; the resistivity of frozen clay can be less than the resistivity of unfrozen silt, sand, or rock. Therefore, resistivity surveys alone will not form the basis for mapping permafrost; they must be accompanied by other geological information.⁴

The presence of the active layer and general layering may also cause difficulties in interpretation. Figure 2 gives the envelope of maximum annual temperature variations in permafrost. The temperature profile is typical, but the magnitude of the maximum and minimum temperatures and the depth to the zero level of annual variation are a function of location. In the summer, the temperature in the top 0.5 m of the ground rises above 0 °C, and the ground thaws. This active layer often consists of water-saturated organic matter with a resistivity of less than 100 ohm-m.

Also shown in Figure 2 is a resistivity profile based on the variation of the resistivity of Fairbanks silt with temperature. Thus, in the summer the resistivity regime of the upper permafrost layers is characterized by a thin layer

TABLE I Resistivity Variation in a Permafrost Profile^a

	Summer	Winter
Active layer 0.2 m < d ₁ < 3.0 m	1 < ρ ₁ < 100	ρ ₁ > 500
Layer of annual temperature variation 5 m < d ₂ < 30 m	10 ² < ρ ₂ < 10 ⁴ (increases with depth)	5 · 10 ² < ρ ₂ < 10 ⁵ (decreases with depth)
Permafrost below annual temperature variation 50 m < d ₃ < 2 000 m	10 ² < ρ ₃ < 10 ⁴	10 ² < ρ ₃ < 10 ⁴
Unfrozen ground d ₄ < ∞	ρ ₄ < ρ ₃	ρ ₄ < ρ ₃

^a ρ₁, ρ₂, ρ₃, and ρ₄ are the resistivities of four earth layers; d₁, d₂, d₃, and d₄ are the thicknesses of the layers.

(< 5 m) of low resistivity (100 ohm-m), which overlies a layer with increasing resistivity that, in turn, overlies a region of relatively constant resistivity. In the winter, the top layer is frozen and thus has a high resistivity that gradually decreases to the depth of zero annual temperature variation.

Table I gives the resistivity variation in a permafrost profile. Evidence for the relatively complicated resistivity structure shown here is present in many Soviet dc resistivity surveys.² However, in many ways Table I is considerably oversimplified because different geological strata may cause

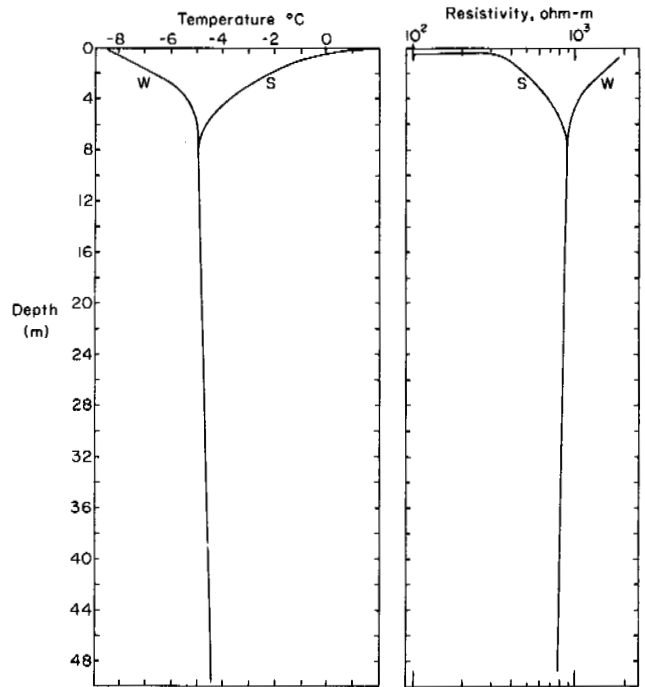


FIGURE 2 Temperature and resistivity profile of permafrost as a function of depth. The resistivity variation is for Fairbanks silt. W, winter; S, summer.

additional resistivity layering. Nevertheless, it illustrates several important features that will dictate the design of electromagnetic systems for mapping permafrost.

Within certain soil types the data seem to indicate conclusively that the resistivity increases with the ice content of the ground. In profiling with a dc resistivity method, Dement'ev² showed that high-ice-content regions are associated with resistivity highs. The anomalies in many instances exceed a factor of 5.

ELECTROMAGNETIC METHODS

Two electromagnetic methods are discussed in this section: measurement of the wave tilt of radio surface waves and measurement of the inductive coupling between low frequency dipole antennas. The main difference between these methods is that the wave tilt technique uses propagating plane waves with the receiver located in the far field of the transmitter, whereas the dipole-dipole technique locates the transmitter and receiver dipoles in close proximity so that at the relatively low frequency used the instrument functions as an electromagnetometer. Since the latter technique has been extensively used in mining geophysics, the theory is well covered in textbooks. Because the wave tilt method is not similarly well covered, it is treated here in greater detail than the dipole-dipole technique. Computer modeling of permafrost profiles were made for both techniques.

Wave Tilt Measurements

The wave tilt method uses vertically polarized radio surface waves. The electromagnetic field components of the surface wave are given in Figure 3. At frequencies below about 500 kHz—the range of resistivities and dielectric constants normally encountered in the earth's surface—the conduction

currents are large enough to increase the (complex) index of refraction of the earth many times over that of free space. According to Snell's law, this results in the refracted waves propagating virtually perpendicularly into the earth regardless of the angle of incidence. Thus, in addition to the vertical electric field E_z and the horizontal magnetic field H_y , normally found in free space, there is found a horizontal (radial) electric field component E_x .

Since the vector product of the horizontal electric and magnetic field components determines the power flow (Poynting vector) into the earth, the horizontal electric field is strongly dependent on such electrical characteristics of the earth as resistivity and the presence of layering. The horizontal component of the electric field is continuous across the air-earth interface; since the rate of falloff above the earth is relatively slow, particularly at low frequencies, the horizontal component can be measured at a substantial distance from the earth's surface, thus permitting remote sensing of the subsurface resistivity. The relationship between the field components and the subsurface resistivity will be explored in more detail later.

Beneath the surface of the earth, which is assumed to be an infinite half space of uniform resistivity, the horizontal electric field component decays with increasing depth z as:

$$E_x(z) = E_x(0)e^{-\gamma z}, \quad (1)$$

where γ is the propagation constant in the earth and is given by:

$$\gamma = [(j\mu_0\omega)/\rho - \epsilon_r\epsilon_0\mu_0\omega^2]^{1/2}, \quad (2)$$

where $j = (-1)^{1/2}$; μ_0 = permeability of free space = $4\pi \times 10^{-7}$ H/m; ϵ_0 = permittivity of free space = $1/36\pi \times 10^{-9}$ F/m; ω = angular frequency (rad/s); ρ = ground resistivity; and ϵ_r = ground dielectric constant.

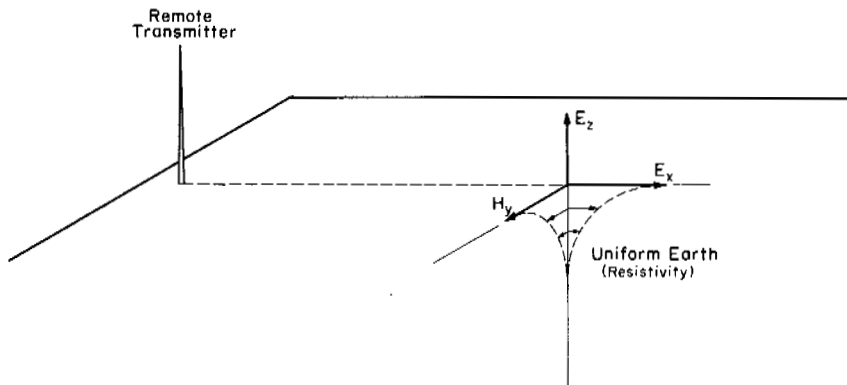


FIGURE 3 Electromagnetic field components of a vertically polarized radio surface wave.

Insertion of typical values for ρ and ϵ_r immediately reveals that at frequencies up to 5×10^5 Hz the second term in Eq. (2) is negligible compared with the first, so that:

$$\gamma \approx [(j \mu_0 \omega) / \rho]^{1/2}. \quad (3)$$

This approximation amounts to the conclusion that displacement currents are negligible compared with conduction currents.

Thus the skin depth, which is defined as the depth in the earth at which the electromagnetic field decays to e^{-1} of the value at the surface, is given by:

$$\sigma = |\gamma|^{-1} = (2\rho / \mu_0 \omega)^{1/2}. \quad (4)$$

The skin depth is a significant parameter in that it indicates the effective depth of electromagnetic wave penetration into the earth and thus the effective depth to which resistivity is sensed, since large changes in resistivity occurring at depths many times the skin depth do not greatly affect the value of the horizontal electric field at the earth's surface. Figure 4 shows the behavior of the skin depth as a function of frequency and earth resistivity. One important point is that the *effective depth of investigation can be altered by changing the frequency*. Conversely, a survey may be made with several frequencies simultaneously, thus sensing the

resistivity to a variety of depths. Another important point is that the horizontal electric field component E_x is a characteristic of the refracted wave penetrating into the earth *at the location of the receiver*. Measurement of E_x gives the *local resistivity*, independent of resistivity variations, found in the wave propagation from the transmitter to the measurement site.

Wait¹⁵ showed that the wave tilt W , defined as the ratio E_x/E_z , when measured over a homogeneous ground, is related to the ground resistivity by:

$$W = E_x/E_z = (1 + j)[(\omega \epsilon_0 \rho) / 2]^{1/2}, \quad (5)$$

from which several important facts emerge. The factor $(1 + j)$ indicates that the horizontal electric field component E_x electrically leads the vertical electric field component E_z by 45° . Thus, the electric field is elliptically polarized with its plane of polarization vertical and directed toward the transmitter. The electrical phase angle of 45° implies that the horizontal electric field has equal in-phase and quadrature-phase components with respect to the vertical electric field. Thus, in the case of a uniform half space, either component is proportional to the square root of the resistivity of the underlying earth. The horizontal component of the electric field is generally at least an order of magnitude smaller than the vertical component. Figure 5

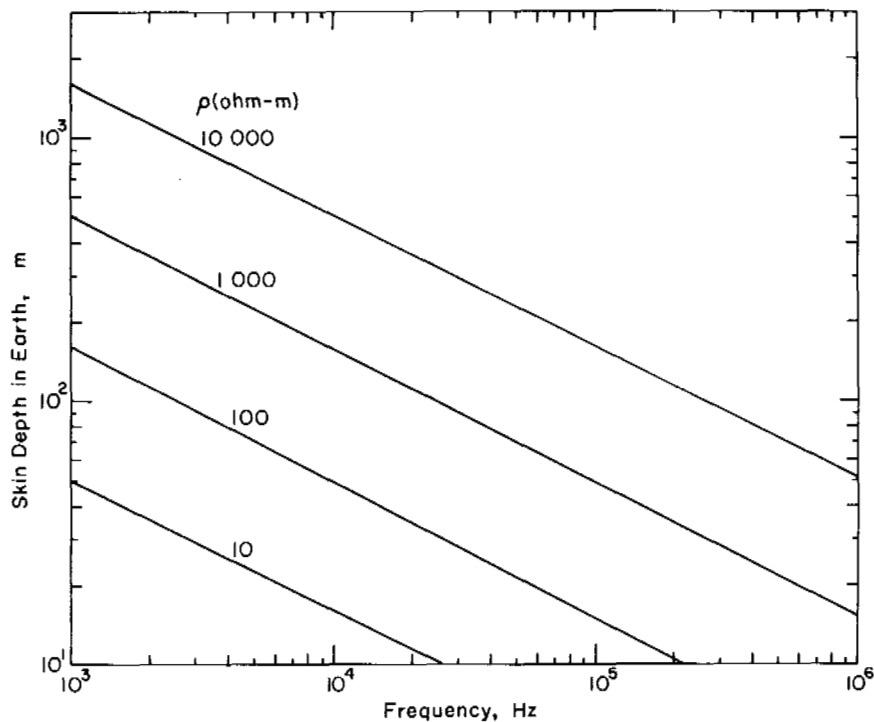


FIGURE 4 Skin depth of electromagnetic plane waves as a function of frequency.

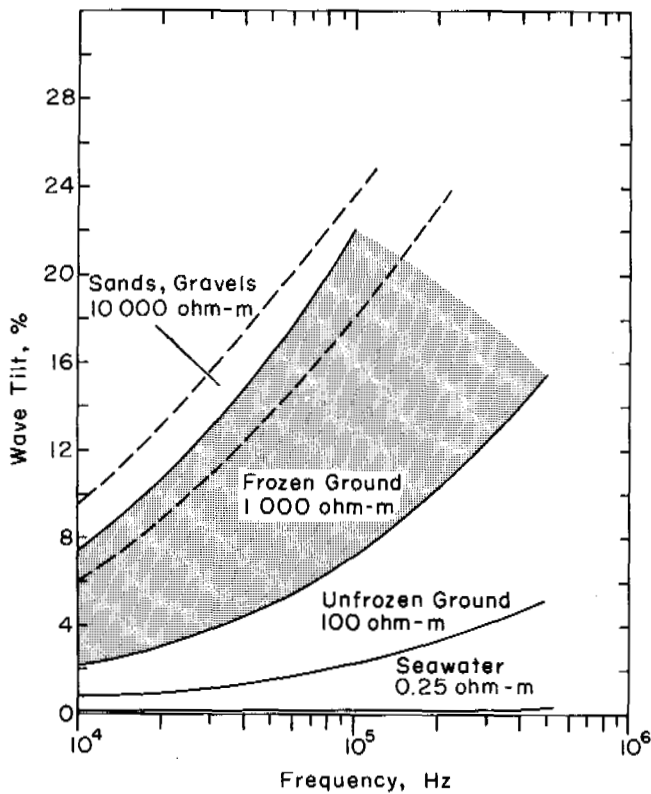


FIGURE 5 Magnitude of wave tilt as a function of frequency over typical homogeneous earth.

gives the magnitude of the wave tilt expected in a permafrost environment.

When the resistivity of the earth is layered,⁹ for example, when it has four layers of different resistivities and thicknesses, the expression for the wave tilt is given by:

$$W = \frac{j\omega\sqrt{\epsilon_0\mu_0}}{\gamma_1} \coth \left[\gamma_1 d_1 + \coth^{-1} \left\{ \frac{\gamma_1}{1} \coth \left(\gamma_2 d_2 + \coth^{-1} \left[\frac{\gamma_2}{\gamma_3} \coth \left(\gamma_3 d_3 + \coth^{-1} \frac{\gamma_3}{\gamma_4} \right) \right] \right) \right\} \right], \quad (6)$$

where $\gamma_1, \gamma_2, \gamma_3,$ and γ_4 are the propagation constants in successive layers of thicknesses $d_1, d_2, d_3,$ and the last layer is assumed to be of infinite thickness. The in-phase and quadrature-phase component of the wave tilt are generally unequal for layered earth.

Surface waves of the type described above are generated by vertical dipole antennas situated on the earth's surface.¹⁶ Enormously powerful VLF transmitters around the world provide sufficient field strength for wave tilt measurements ranging from 15 to 25 kHz over the entire Arctic. Powerful military transmitters are often found within the frequency range 50-100 kHz and navigational aid transmitters within

the frequency band 200-400 kHz. Thus, in most instances surveys can be made at three frequencies ideally spaced for effective resistivity sounding. At the frequencies of 200-400 kHz, inexpensive local transmitters can be erected near the survey site if necessary. For permafrost surveys, frequencies much higher than 400 kHz are not recommended since at these frequencies the depth of electromagnetic wave penetration becomes less than 5-10 m and displacement currents can no longer be neglected; this causes difficulties in interpretation of the survey results.

That a local resistivity is measured in this way has been shown by Blomquist,¹ who demonstrated that at a wavelength of 30 m the wave tilt changed virtually instantaneously when a discontinuity in the ground was traversed. The same conclusion was reached by McNeill and Hoekstra¹⁰ in measurements at 15-km wavelengths (VLF) over sea ice. Also, the results of many airborne surveys made at very low to 1-MHz frequencies using a technique described below clearly indicate that the resistivities measured are local and that edge effects, at least from the air, are negligible.

Several alternative methods exist for measuring the wave tilt on the ground. Since the vertical and horizontal components of the electric field are not in phase with each other, the resulting electric field vector describes an ellipse with the plane of the ellipse in the plane of incidence. A simple dipole receiving antenna, rotated in the plane of incidence about a horizontal axis perpendicular to the plane of incidence, can sense the minimum and maximum induced voltages and the angle of the minor axis with the horizontal axis. These parameters completely define the wave tilt; this method was used by Eliassen³ and Blomquist¹ in studies of the wave tilt method. This method requires only one antenna and simple receiving equipment, because it makes no phase measurements. However, careful measurements must be made of a small angle of the minor axis with the horizontal axis; this precludes using this technique from an airborne platform.

An alternative way of measuring the wave tilt is to determine the amplitude and phase of the horizontal electric field with respect to the vertical electric field. This is thus a direct measurement of the magnitude and phase of the wave tilt. This technique requires a horizontal and a vertical antenna, two separate receiving systems, and phase comparison electronic circuitry. A single frequency unit has been built that operates at VLF and allows measurement of the horizontal component to an accuracy of 0.01 percent of the vertical electric field. An improved version of this device that will permit simultaneous measurements of the same field components from 15 to 400 kHz frequencies is currently under construction. This new unit also will enable the vertical electric field or the horizontal magnetic field to be used as phase reference and the horizontal electric field to be measured in the air or in the ground through contact-

ing probes. The increased versatility of this instrument will permit an exhaustive examination of the interaction of electromagnetic fields with the ground over a wide range of frequencies.

At low frequencies and for low values of ground resistivity, the horizontal electric field component is of the order of 1 percent of the vertical electric field. Thus, a substantial error can result from measuring the in-phase component if the horizontal electric field antenna is not perfectly horizontal. This effect can be overcome on the ground by rotating the horizontal electric field antenna about a vertical axis; however, use of such a technique is obviously not practicable from an airborne platform.

Measurement of only the quadrature-phase component of the horizontal electric field can be made completely insensitive to leakage of the vertical electric field, since all leakage of the vertical field is in phase. The technique of measuring only the quadrature-phase components, which is entirely suitable for operation from airborne platforms, has been extensively used. In measuring only the quadrature-phase component, the resistivity of a uniformly stratified earth is given by:

$$\rho = (2W_{\text{quad}}^2)/(\omega\epsilon_0). \quad (7)$$

Where the earth consists of horizontally stratified layers of differing resistivity, the in-phase and quadrature-phase components are no longer equal and an apparent resistivity is defined by Eq. (7).

Figure 6 gives an example of an airborne resistivity survey made simultaneously at 17.8 kHz and 1 MHz frequencies. The interline spacing was of the order of 160 m and the aircraft mean terrain clearance was approximately 60 m. The survey was flown on the edge of a large kame moraine to explore subsurface gravel. Anomaly A shows the advantage of using two or more frequencies. The resistivity anomaly, which appears only at 1 MHz, was interpreted to indicate the presence of gravel from the near surface to a depth of 3 or 4 m, underlain by relatively conductive clay or silt. Subsequent ground followup proved this interpretation to be correct. Surveys of this type have demonstrated the lack of topographic and tree cover effects, relatively high resolution, and the presence of gravel in areas where no gravel was thought to exist. Permafrost airborne resistivity surveys in this location are planned for the near future.

Plane Wave Computer Modeling Studies

The quadrature-phase component of the wave tilt in a layered permafrost situation was modeled on the basis of Eq. (6) and (7) to evaluate the behavior of the system for measuring the thickness of permafrost, to delineate high-ice-content ground, and to map in areas of discontinuous permafrost.

Measurements of permafrost thickness made in the winter when the active layer is frozen can be represented by a two-layer earth. Figure 7 plots the apparent resistivity ρ_a versus frequency for permafrost thicknesses of 100,

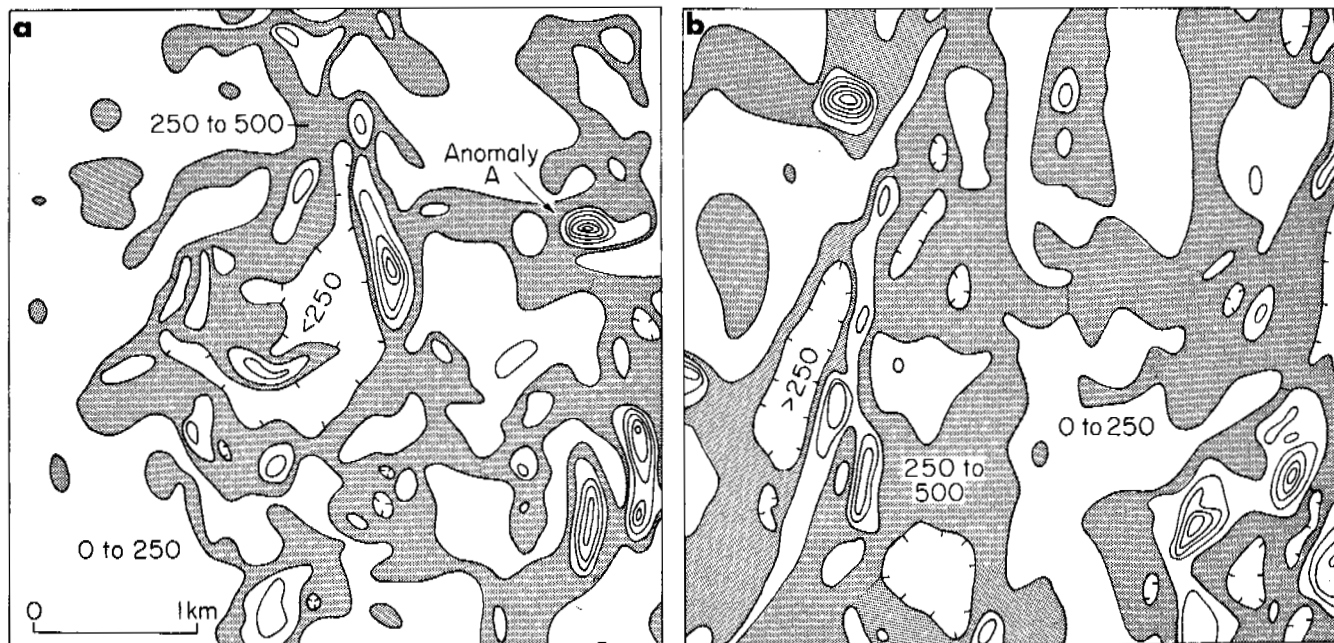


FIGURE 6 Example of an airborne resistivity survey at 17.8 kHz (b) and 1 MHz (a) flown on the edge of a large kame moraine in Ontario, Canada.

300, and 1 000 m. As would be expected from skin-depth considerations, the apparent resistivity approaches the frozen ground resistivity at high frequencies and the unfrozen ground resistivity at low frequencies. The overshoot in apparent resistivity is an artifact that arises from measuring only the quadrature-phase component of the wave tilt. The frequency range that would be diagnostic of differences in thickness would be $10\text{--}10^3$ Hz. Since plane wave electromagnetic fields at these frequencies are not available, wave tilt methods could not satisfactorily distinguish the various depths shown in Figure 7. Usually, where the depth of the feature to be distinguished is more than 100 m, other methods must be used.

The existence of high ice content in the ground seems to be mainly limited to the first 100 m of permafrost and in many instances is found in the top 20–50 m. Figure 8a gives a dc resistivity traverse reported by Dement'ev² in which the high values of resistivity were associated with high-ice-content ground. To model such a horizontal traverse the resistivity anomalies are approximated by the dotted line in Figure 8. Furthermore, the high-ice-content ground is assumed to occur to a depth of 30 m and to be underlain by permafrost with a resistivity of 500 ohm-m. The low-ice-content sections are assumed to be uniform to a considerable depth with a resistivity of 500 ohm-m. The active layer is assumed to be 1.5 m thick with a resistivity of 100 ohm-m in the summer and 10 000 ohm-m in the winter.

In Figure 8b, ρ_a obtained from computer modeling is plotted versus horizontal distance at frequencies of 20, 100, and 400 kHz. The solid line represents ρ_a when the active layer is thawed and the dotted line when the active layer is frozen. The active layer significantly screens the underlying ground, with the screening effect virtually complete at 400 kHz. When the active layer is frozen, all three frequencies show measurable contrast. At 400 kHz the maximum reso-

lution is shown. When the active layer is frozen, wave tilt surveys seem to be well suited to delineating high-ice-content ground. Space limitation does not permit the illustration of all modeling results; but, as would be expected, changing the depth of high-ice-content ground from 20 to 100 m, or adding unfrozen ground under the permafrost, below 100 m, did not affect the conclusions reached. Note that these calculations did not incorporate the edge effects resulting from the vertical discontinuities between the various regions of high and low resistivity.

To determine the effectiveness of the system for mapping discontinuous permafrost, the resistivity profiles indicated in Figure 9a were modeled. Sections with lenses of frozen and thawed ground, which cause great difficulties in construction, were also included. In Figure 9b, ρ_a is given at 20, 100, and 400 kHz. All sections would give measurably different values for apparent resistivity at 20 kHz. The presence of a frozen lens in unfrozen ground seems to be most difficult to detect. All three frequencies would clearly distinguish between the thawed and the frozen ground. In the winter or early spring, the presence of frozen ground on a thawed section would have no measurable influence on the apparent resistivity.

Frischknecht and Stanley⁶ used an airborne *E*-phase system at very low frequencies in two test areas in Alaska to delineate the permafrost regime. In each test area, at least one ice-free area was located using the airborne VLF data, and this was corroborated by resistivity measurements. A short survey made by the Geological Survey of Canada using similar equipment in the Thompson, Manitoba, area failed to delineate permafrost because of active-layer complications and the use of only very low frequencies; this shows the need for a multifrequency approach to the problem.

In summary, wave tilt surveys seem to be useful in delineating permafrost features such as high ice content and

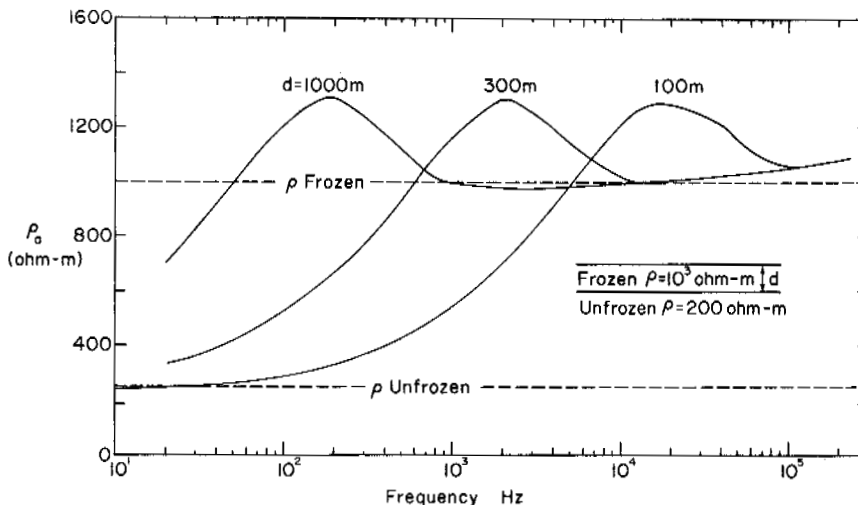


FIGURE 7 Apparent resistivity of a two-layer earth as a function of frequency.

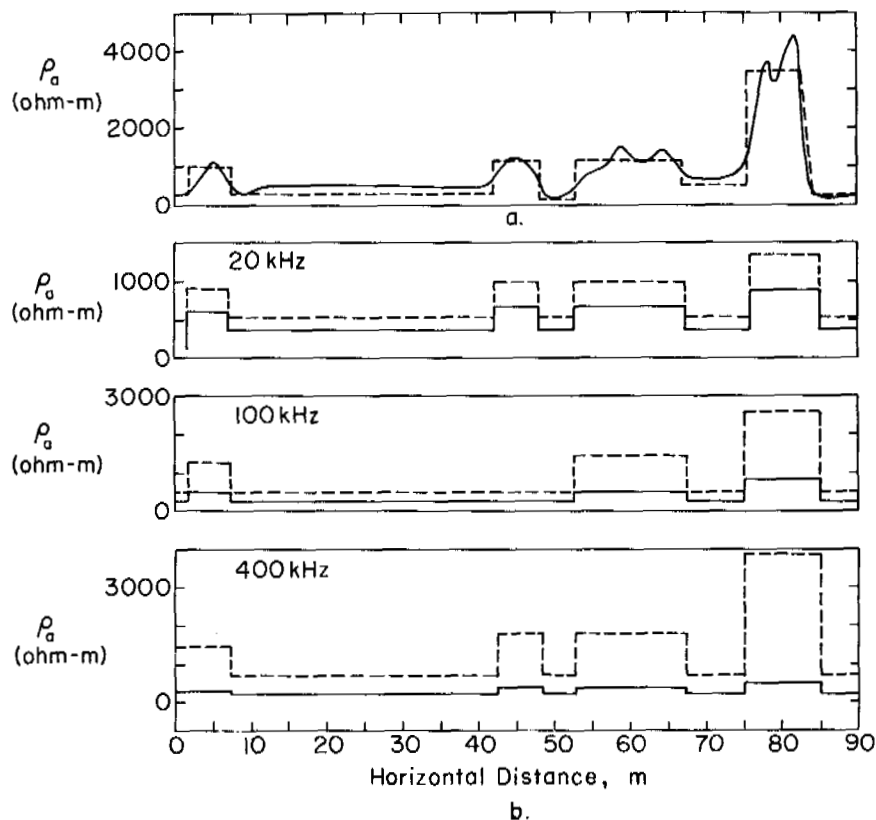


FIGURE 8 Variation in horizontal apparent resistivity of a three-layer earth. The solid and dotted lines represent the results when the active layer is thawed and frozen, respectively. (a) Apparent resistivity measured in a traverse with a Wenner array.² (b) Results of computer modeling the resistivity traverse for an airborne wave tilt survey at three frequencies.

thawed or frozen ground to a depth of 100 m. This method, however, is not suited to distinguish such deep permafrost features as thicknesses of frozen ground exceeding 100 m. These surveys should be made when the active layer is frozen because the low resistivity expected for the active layer screens the underlying ground and several frequencies must be employed.

Low Frequency Inductive Loop Measurements

The wave tilt method was shown to be unsuited to measuring the depth of permafrost because the effective penetration depth even at very low frequencies was insufficient. This difficulty was surmounted, at least on the ground, by using low frequency inductive loop techniques; theoretical calculations indicate that it should be quite feasible to employ these techniques from an airborne platform.

Keller⁸ used two large loops, separated by approximately 1 500 m and placed horizontally on the ground, to effectively sound permafrost to depths in excess of 1 000 m. In this technique, one loop is selected as a transmitter loop and is driven from sine wave oscillators over a wide range of frequencies. Another loop is used as a receiver, and either the magnitude of the secondary field (the primary field

having been electronically canceled out) or the in-phase and quadrature-phase components of the secondary field are recorded as a function of frequency.

A good deal of theoretical work has been done by Wait,¹⁵ Frischknecht⁵ and Vanyan¹⁴ using loops on or above a horizontally stratified earth. Keller's⁸ measurements, performed over a large number of survey sites, generally showed excellent agreement with theoretical curves for a two-layered earth with the upper layer resistivity about 300 ohm-m and the substrate 10 ohm-m (since the permafrost was underlain by brine-soaked shale). The depth to the bottom of the permafrost table was calculated from the measurements and confirmed by subsequent drilling to be accurate to 5 or 10 percent.

Inductive electromagnetic techniques have been employed to map resistivity for some time; however, it is only relatively recently that such techniques have appeared to be practical for use from an airborne platform. In newly developed equipment, the primary field is both electronically and mechanically canceled out at the receiver coil in such a way as to result in good base-line zeros. Airborne systems of this type can measure a change in the induced magnetic field at the receiver coil on the order of 1 ppm.

The inductive coupling method has several characteristics

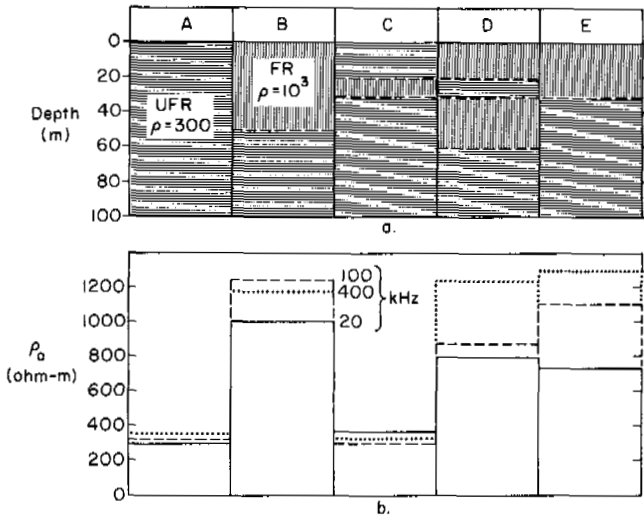


FIGURE 9 Typical permafrost resistivity profiles. (a) Typical resistivity cross sections that might occur in permafrost environments. (b) Results of computer modeling the resistivity cross section for an airborne wave tilt survey at three frequencies.

that make it a good technique for backing up wave tilt surveys:

1. Since the instruments can measure down to frequencies on the order of 100 Hz, very deep penetrations can be made, and the method is therefore suited to exploring deep features such as the depth of permafrost.
2. The variability of the frequency of the transmitting coil makes the method useful for depth sounding, i.e., for

determining the thicknesses and resistivities of different permafrost layers.

3. The two-loop inductive coupling system can be packaged in a convenient hand-held instrument. The wave tilt ground device is normally considerably heavier than this instrument and must have structures for the alignment and rotation of the horizontal and vertical antennas. This simple hand-held instrument would be of much use in surveying areas limited in size such as building and dam sites.

The potential application of airborne inductive loop techniques is illustrated in Figure 10, which shows the in-phase and quadrature-phase responses expected, over a two-layer, horizontally stratified half space. It is assumed that the transmitter and receiver coils are mounted in a towed "bird" beneath a helicopter, that the intercoil distance is 10 m and that the height of the bird above the terrain is 30 m. The curves were calculated from a computer program supplied by Frischknecht.⁵

PROJECTIONS

There are no apparent technological obstacles in applying the two electromagnetic survey methods—the measurement of wave tilt and the measurement of coupling between two loop antennas—to permafrost problems. The theory is well developed, and equipment design has probably reached a satisfactory level.

A large amount of work remains to be done in correlating ground truth with the results of resistivity surveys employing electromagnetic techniques. It would be particularly useful to obtain *in situ* resistivity profiles from borehole

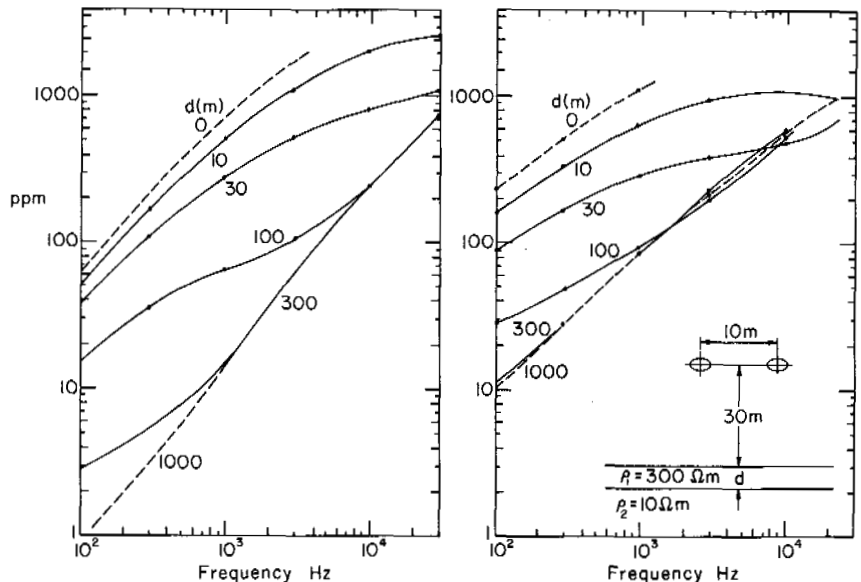


FIGURE 10 In-phase and quadrature-phase response of a two-loop inductive coupling system above a two-layer earth.

logging or from measurements on cores. If this information is processed through existing computer programs, the geological noise factor, i.e., the extent to which local variations obscure the essential objective, can then be evaluated.

The two electromagnetic methods both have the advantage over the dc resistivity probing method in that they can be used from an airborne platform. The chief advantage is that reconnaissance surveys can be conducted over large areas at a relatively low cost on a per-unit-area basis and in a fraction of the time required for the more conventional ground resistivity surveys. The experience to date has indicated that knowledge of ground resistivity over large areas is of great value and that it very much improves the interpretability of the results of ground resistivity surveys. As is always the case with geophysical exploration, the ground truth must be corroborated at sufficient intervals to maintain confidence in the airborne results.

ACKNOWLEDGMENTS

This paper presents the results of research performed by the U.S. Army Cold Regions Research and Engineering Laboratory and Barringer Research, Ltd., under the sponsorship of the U.S. Army Corps of Engineers. Most of the electromagnetic modeling work was performed at the Laboratory of Electromagnetic Theory, Technical University of Denmark, Lyngby, Denmark, while Dr. Hoekstra was on leave from USA CRREL.

REFERENCES

1. Blomquist, A. 1970. Equipment for in-situ measurement of the dielectric properties of ground and ice, p. 54-70. *In Proceedings of the International Meeting on Radioglaciology*. Lyngby, Denmark.
2. Dement'ev, A. I. 1959. Principles of geocryology. Part II. Technical Translation 1287. National Research Council of Canada, Ottawa.
3. Eliassen, K. E. 1956. A survey of ground conductivity and dielectric constant in Norway within the frequency range 0.2-10 Mc. *Geofys. Publ. (Oslo)* 19(11):1-30.
4. Ferrians, O. J., R. Kachadoorian, and G. W. Greene. 1969. Permafrost and related engineering problems in Alaska. Professional Paper 678. U.S. Geological Survey, Washington, D.C.
5. Frischknecht, F. C. 1967. Fields about an oscillating magnetic dipole over a two-layer earth. *Q. Colo. Sch. Mines* 62(1).
6. Frischknecht, F. C., and W. D. Stanley. 1971. Airborne and ground electrical resistivity studies along proposed TAPS route. *In Second international symposium on arctic geology*. San Francisco (Abstr.)
7. Hoekstra, P. 1965. Conductance of frozen bentonite suspensions. *Soil Sci. Soc. Am. Proc.* 29:519-523.
8. Keller, G. V. 1972. Personal communication.
9. Keller, G. V., and F. C. Frischknecht. 1966. Electrical methods in geophysical prospecting. Pergamon Press, New York.
10. McNeill, D., and P. Hoekstra. In-situ measurement of the conductivity and surface impedance of sea ice at VLF frequencies. *Radio Sci.* (In press)
11. Morgan, R. R. 1968. Preparation of a worldwide VLF effective conductivity map. Report No. 80133F-1. Westinghouse Research Corp., Environmental Science and Technology Dept. Boulder, Colorado.
12. Ogilvy, A. A. 1967. Geophysical studies in permafrost regions in USSR. *Mining Groundwater Geophys. (Geol. Survey Canada, Econ. Geol) No. 26.* p. 641-650.
13. Parkhomenko, E. I. 1967. Electrical properties of rock. (English Translation) Pergamon Press, New York.
14. Vanyan, L. L. 1965. Electromagnetic depth soundings. (English Translation) Consultants Bureau, New York.
15. Wait, J. R. 1962. *Electromagnetic waves in stratified media*. Pergamon Press, New York.
16. Watt, A. D. 1967. *VLF radio engineering*. Pergamon Press, New York.

NOTE

[1] Most of the electromagnetic modeling work was performed at the Laboratory of Electromagnetic Theory, Technical University of Denmark, Lyngby, Denmark, while this author was on leave from USA CRREL.

THE APPLICATION OF SHALLOW SEISMIC METHODS TO MAPPING OF FROZEN SURFICIAL MATERIALS [1]

J. A. M. Hunter

GEOLOGICAL SURVEY OF CANADA
Ottawa, Ontario

INTRODUCTION

The rapid development of the Canadian Arctic in recent years has led to the interest in, and demand for, new methods of measuring physical properties of permafrost. One of the promising geophysical techniques available is the seismic method.

The Geological Survey of Canada has recently undertaken experiments in seismic mapping of permafrost in surficial materials. The aims of the program are to detect the presence of permafrost in areas of discontinuous or patchy occurrences, to map structure at depth in frozen overburden, to measure *in situ* characteristic seismic velocities for type materials, and to measure the thickness of the permafrost layer.

PREVIOUS WORK

Much of the early laboratory experimentation on seismic properties of permafrost has been done by Soviet workers,^{1,2,6} who established the compressional velocity-temperature relationships for frozen soils and examined their attenuation characteristics. Recent laboratory work on frozen soils and rocks has been published by Nakano *et al.*,¹² Timur,²⁰ and Kurfurst and King.⁹

Early field experiments in North America were done by Roethlisberger¹⁸ where he applied seismic refraction techniques to obtain thickness of frozen surficial materials. It is interesting to note that on some of his records he attributes rapid attenuation of the first arrival energy to a negative velocity gradient with depth resulting in dissipation of seismic energy into the lower velocity regions.

A good summary of field determinations of seismic velocities in permafrost in North America is given by Barnes.³ These correlate well to determinations made on similar materials in laboratory studies mentioned above. In general, permafrost seismic velocities in surficial materials increase with the grain size of the material. Clays yield some of the lowest velocities while ice-saturated gravels yield some of the highest.

In Canada, early experiments in the application of seismic to frozen surficial deposits were done by Bush and Schwarz.⁴

Their surveys in the discontinuous permafrost zone showed that high velocities were associated with permafrost occurrences. They found that depth determinations to the top of bedrock beneath permafrost were difficult in the presence of a thick frozen zone overlying an unfrozen zone within the overburden, since the prominent event from the frozen zone masked arrivals from the unfrozen overburden. They found, however, that refractions from a thin permafrost zone exhibited velocities that increased with the suspected thickness of the zone as well as rapid attenuation of the first arrival.

Hobson⁷ utilized the hammer refraction seismograph to obtain estimates of frozen overburden thickness in relation to placer deposit mining surveys in the Yukon. Refraction techniques can map bedrock topography where positive velocity depth gradients exist in permafrost.

EXPERIMENTAL PROGRAM

The experimental program of the Geological Survey of Canada is oriented toward surveying the near-surface surficial materials to a depth less than 30 m. Type areas have been studied in various parts of the arctic and subarctic regions of Canada. Emphasis has been placed on permafrost areas where possible future oil and gas pipeline routes are under study.

The equipment used in shallow seismic studies in permafrost was originally designed for near-surface work in overburden. Figure 1 shows a seismograph used extensively in Canada. The FS-3 hammer seismograph is essentially an event marker instrument where positive portions of waves arriving at the geophone are recorded as 2 ms marks on facsimile paper by a moving high voltage stylus. The stylus is triggered by a momentary contact switch fixed to the hammer source. The recording geophone is maintained at one location, while the source (a hammer striking a plate) is moved away to produce a refraction seismogram. A typical field seismogram from a permafrost area is shown in Figure 2. This type of display has the advantage of an unbiased picking of first and later arrivals on the record. The shear wave can be seen clearly as a later event following the arrival of the first compressional wave group.

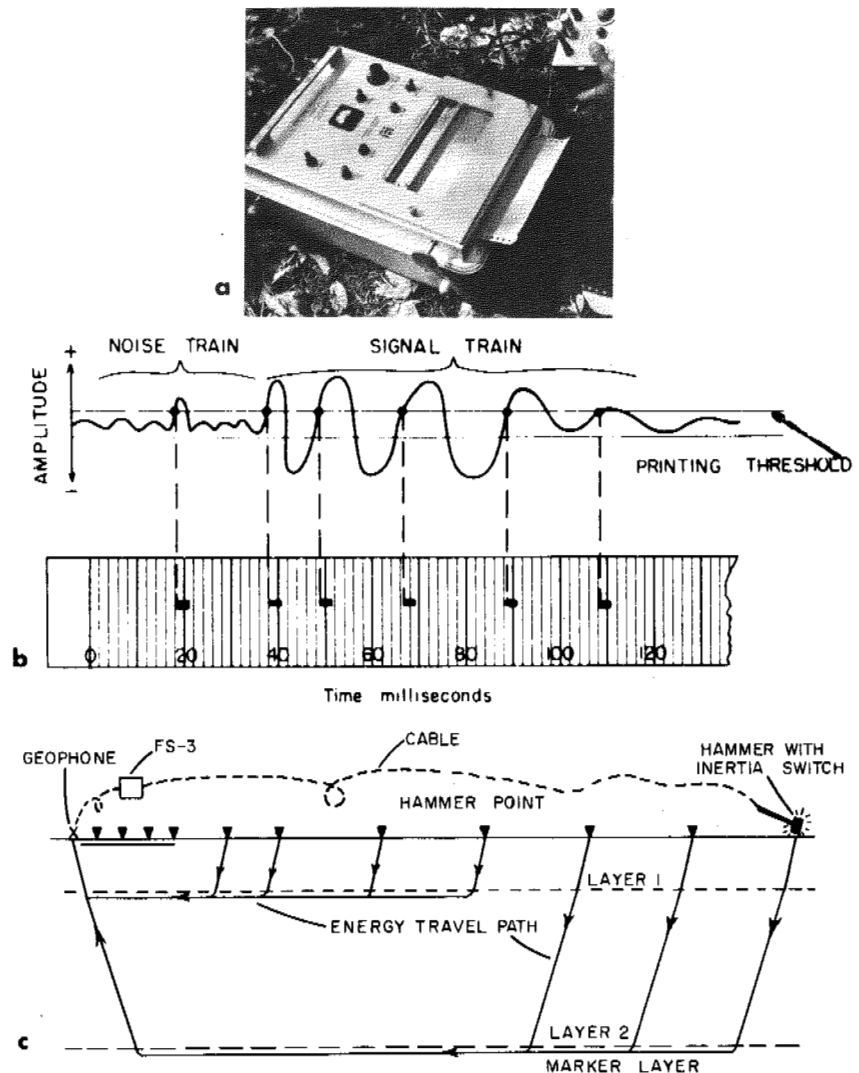


FIGURE 1(a) A single-geophone hammer seismograph used in shallow surveying. **(b)** The single geophone records the onset of signals as marks on facsimile paper from a high-voltage sweep stylus. **(c)** The hammer seismograph survey procedure employs a stationary geophone and a moving hammer source.

Another instrument used is the S.I.E. RS-4 12-channel seismograph shown in Figure 3. This is one of several similar instruments designed for shallow refraction work. A 12-geophone array of 100 or 200 m length is used with a small (0.25 kg) dynamite charge as a source. The length of the refraction speed used is much longer than that used to probe comparable depths in nonpermafrost areas. A typical record suite shot in permafrost is shown in Figure 4. Extensions of the seismogram to greater shot-detector distances is accomplished by offsetting the shot from the geophone array. Amplitude correlations can be made on each successive seismogram. The wiggle trace presentation has the advantage of amplitude measurement of events for attenuation analysis. Care must be maintained to use a matched set of amplifiers and galvanometers to reduce instrumental errors.

Both of the instruments mentioned have been operated in summer and winter arctic conditions. For extremely low

temperatures, the instrument must be kept warm. Shallow seismic instrumentation is extremely lightweight and portable, and operations can be carried out readily using small helicopters, motorized toboggans, or light trucks. The resulting survey technique is most rapid and efficient.

MAPPING OF THE OCCURRENCE OF PERMAFROST

In the discontinuous permafrost zone of Canada where frozen ground occurrences are scattered, the seismic refraction method can successfully delineate the boundaries of these areas. Figure 5 shows a test survey near Ft. Simpson, N.W.T. Permafrost is confined in this location to a low swampy area. Profiles on both sides of the road (profiles A and C) detected a high velocity near-surface layer that has been interpreted as permafrost. Profiles on both sides of the swampy area (profiles D and E) did not record high veloci-

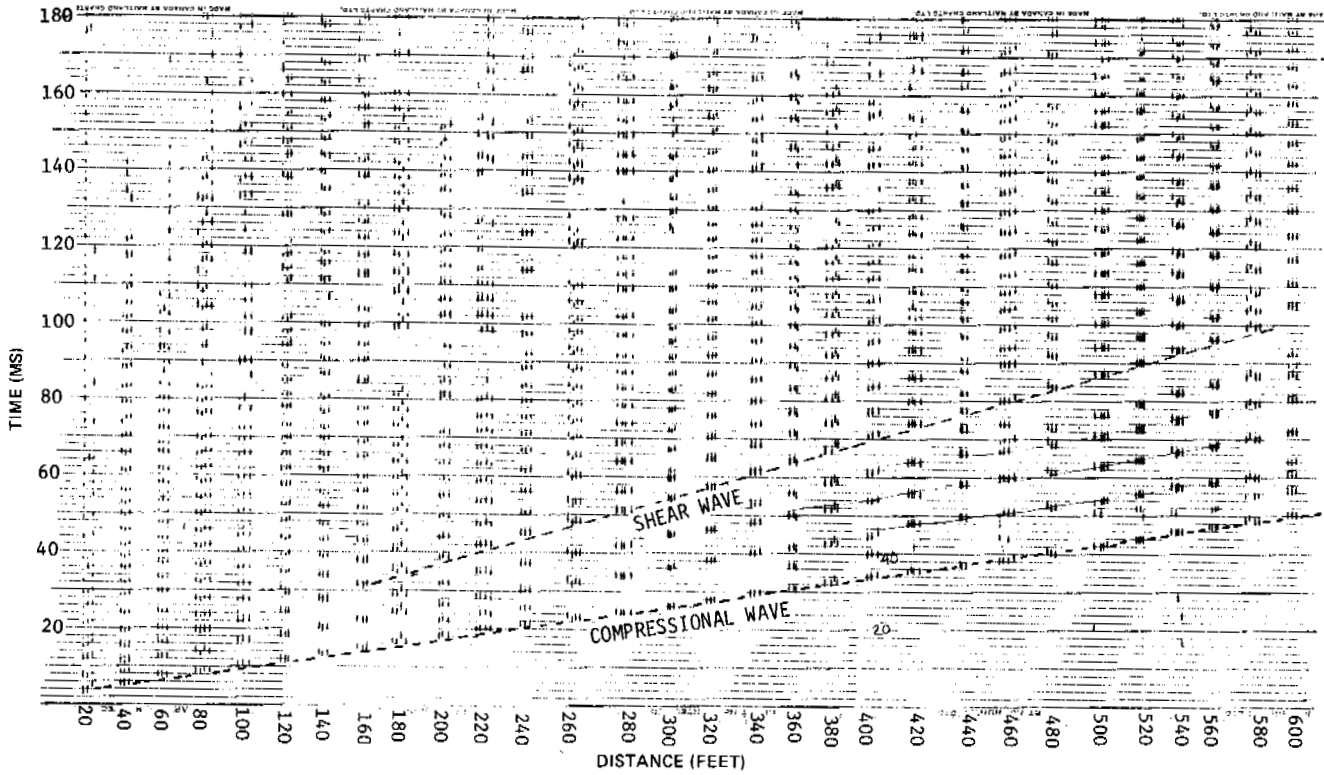


FIGURE 2 A hammer refraction seismogram recorded on the Tuktoyaktuk Peninsula, showing high velocity first arrivals from permafrost. The later event marked with the dashed line is interpreted to be the shear wave.

ties at the surface; hence, permafrost was interpreted to be absent. The lack of a definite high velocity directly beneath the road bed (profile B) suggests that permafrost is either absent or at great depth (> 40 m). This implies that the

permafrost layer has been disturbed by the presence of the road.

A further example of the refraction method applied to mapping the occurrence of permafrost is shown in Figure 6. This area is close to Norman Wells, N.W.T., in an area of widespread discontinuous permafrost. The road was built during World War II and abandoned in 1945. The roadbed was laid on existing surface humus and mosses that were disturbed only minimally during construction. The seismic profiles shot on both sides of the road detected permafrost velocities near the ground surface. The profiles shot along the road bed detected a high velocity, interpreted to be permafrost, at an average depth of 17 m. The interpretation suggests a sharp discontinuity in the permafrost layer at the edge of the road bed. Drilling in the area gave permafrost thicknesses of 15 m in adjacent areas beside the road. However, the profiles on both sides of the road display apparent velocity inversions on the time-distance plot that result from rapid attenuation of first arrivals, thus suggesting a thin permafrost layer. An interesting aspect of this study is that refraction of seismic energy off the permafrost layer along the side of the road is not detected by the vertical component geophones, although the roadbed is no wider than 10 m.

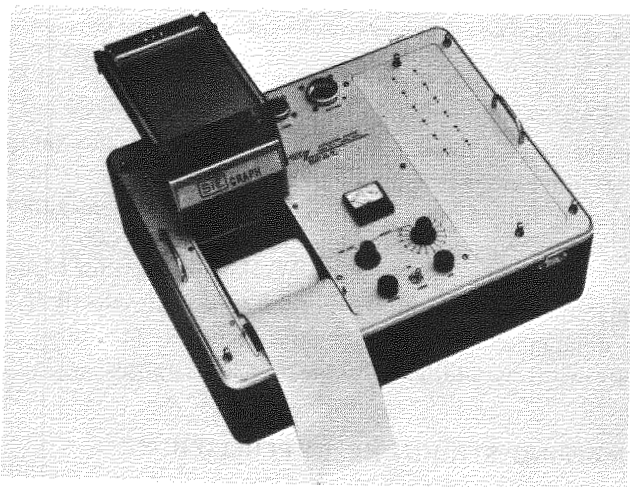


FIGURE 3 A 12-channel shallow seismograph employing the conventional oscillograph display. Recordings are made on instantaneously developed photographic paper.

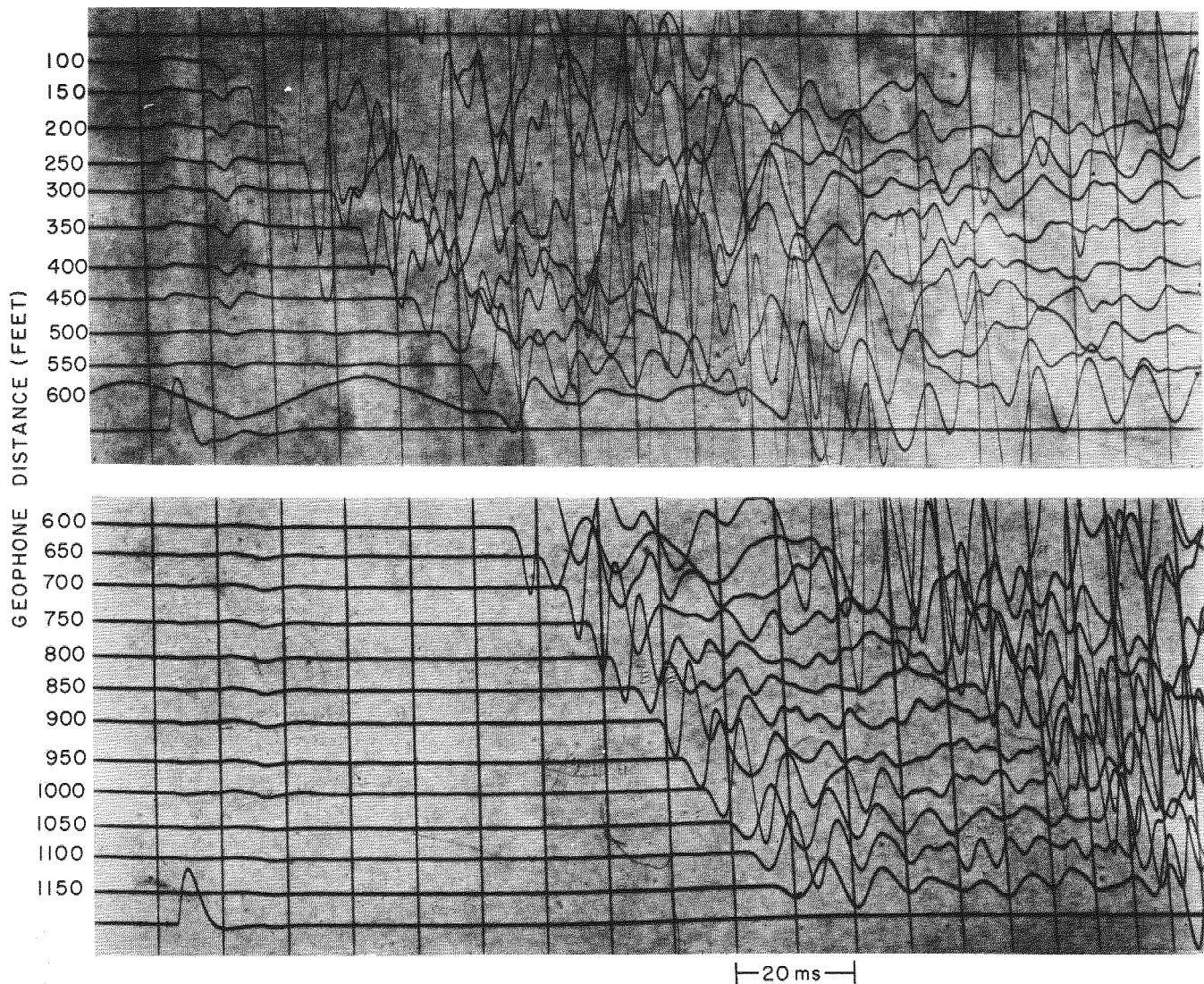


FIGURE 4 A shallow refraction record suite obtained with the 12-channel seismograph on the Tuktoyaktuk Peninsula. Amplifier gains are equal for each channel on the record but vary between records.

The seismic method has been demonstrated to be a useful tool in mapping the occurrence of frozen ground. In the discontinuous zone, profiling should be done only in the summertime in the presence of a thawed active layer. Seasonal frost acts as a high velocity screening layer event on seismic records, through which the lower velocity unfrozen material must be interpreted. If seasonal frost thickness is substantial, interpretation of low velocities on records shot in permafrost-free zones in winter may not be possible.

VELOCITY MEASUREMENTS

Velocity measurements made in the course of surveying in the various permafrost areas confirm the laboratory results referred to above. Frozen clays (below 0 °C) give velocities

in the range 1 500–2 100 m/s. Ice-saturated silts give velocities in the range of 1 800–3 100 m/s. Saturated sands, in general, range from 3 200 to 4 000 m/s, and water-saturated gravels have been measured in the range from 3 600 to 4 700 m/s. There is an overlap in velocity ranges for type materials, and identification of soil type from velocity information alone can only be done accurately in a survey area with the addition of some borehole control.

MAPPING STRUCTURE IN PERMAFROST

In many cases, the velocity structure of overburden materials in permafrost are amenable to refraction surveying techniques. For accurate delineation, velocities must increase with depth, and the thickness of the layering must be

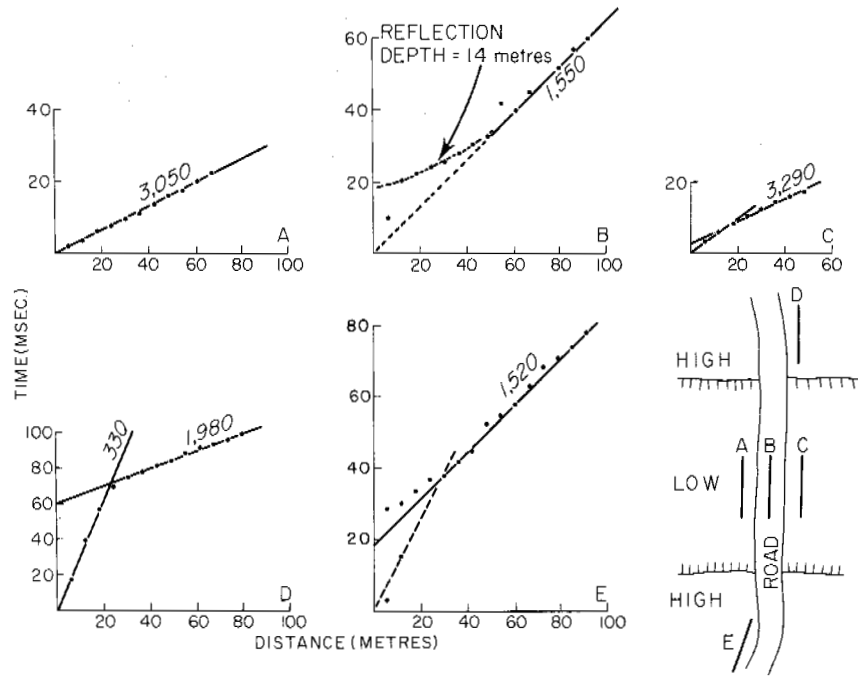


FIGURE 5 A seismic survey in the discontinuous permafrost zone, Ft. Simpson, N.W.T. Profiles A and B detected high velocities (permafrost); profiles C, D, and E did not.

at least one quarter of the length of the seismic wavelengths used. This suggests that most layers 3 m thick or more can be detected by the refraction method in permafrost.

Figure 7 shows an example of a refraction profile from the Sans Sault area of the Mackenzie River Valley. An apparent velocity decrease on the refractor results from rapid attenuation of the first arrival amplitude from relatively thin permafrost; hence travel time to the first significant arrival appears to increase. The refraction results are shown

in the form of a velocity–depth function as determined from the travel-time plots. This interpretation is discussed by Hunter,⁸ and involves smoothing of the travel-time distance function to a continuous curve while preserving abrupt changes of slopes due to velocity layering. Data points on the plot of Figure 8 result from one travel-time event. It is felt that this type of presentation of velocities best shows the depth resolution obtained.

In this plot, there is a broad correlation between the geo-

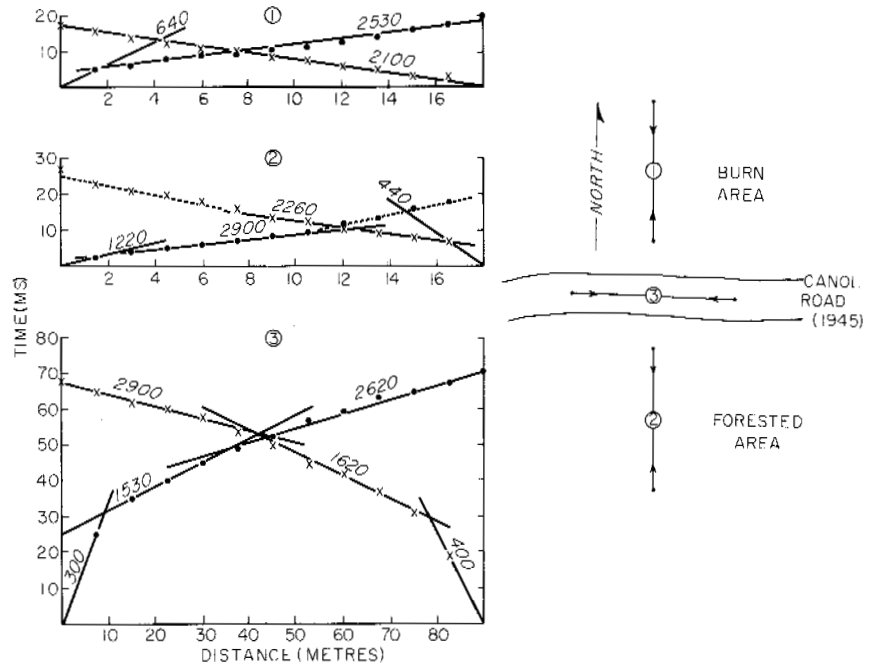


FIGURE 6 A seismic refraction survey at Norman Wells, N.W.T. Profiles 1 and 2 indicate a high velocity (permafrost) close to surface. Profile 3 indicates permafrost at a depth of 17 m.

logical units and the velocity–depth function. The refraction method does not detect the low velocity silts underlying the high velocity sands, since there is a velocity inversion with depth. The dotted line is the predicted velocity–depth function from lithology and temperature measurements (A. S. Judge, personal communication) and the empirical relationship developed by Aptikaev.² Good correlation is shown between the predicted and measured velocity functions.

Large areas of the northern part of the Mackenzie River region are underlain by massive ground ice.¹⁶ A survey was undertaken to determine whether the refraction method could detect the presence of ice at depth. The massive ice is found generally under a layer of till (equal quantities of clay, silt, sand, and gravel), which is generally low in excess ice,¹⁰ and above sands and icy sands. Since the till (or till-like) material should have a velocity less than massive ice in this area, and since frozen saturated sand velocity should be much higher than ice, the refraction method is useful in determining structure at depth. Figure 7 shows a typical velocity depth function from the area. The seismic interpretation and the geological log correlate well. The compressional velocity increases downward from 2 500 km/s in the till. A definite change of slope in the function into 3 050 km/s is observed

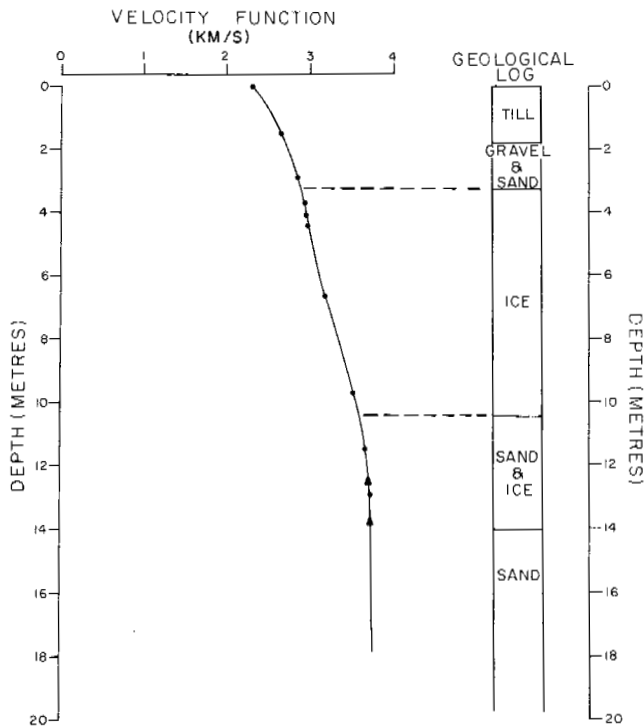


FIGURE 7 A comparison of a velocity function interpretation of a seismic record with borehole lithology in a section containing massive ice. A solid triangle on the plot represents several plotted points indicating refraction from an interface.

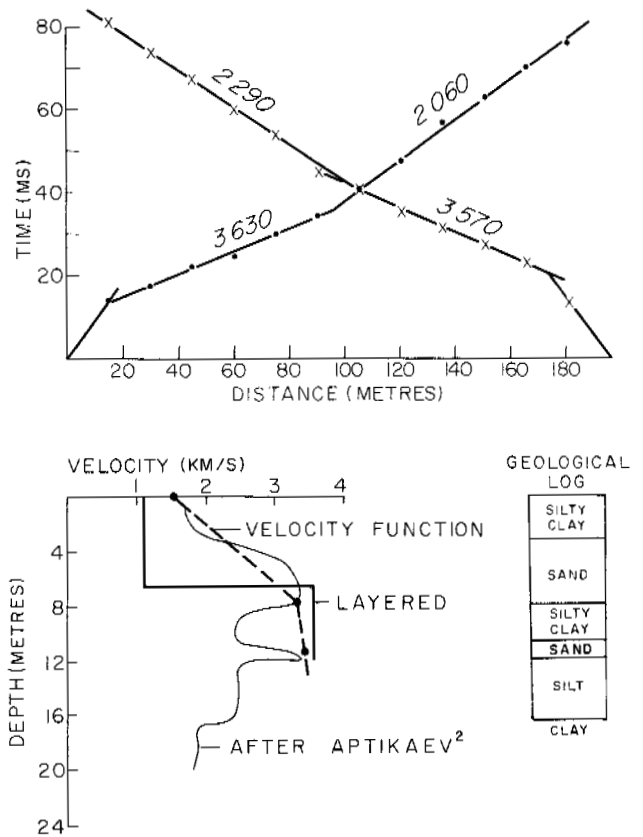


FIGURE 8 (a) A reversed refraction profile from the San Sault area. Apparent velocity inversions result from rapid attenuation of the first arrival. (b) Velocity function and conventional layered-case interpretation of the seismic profile given in (a) compared with the predicted function (following Aptikaev²) from borehole lithology and measured temperatures.

at the top of the massive ice. The bottom of the ice is not denoted as definite velocity increases within the ice to a velocity of 3 960 km/s. This has been correlated with increasing sand content with depth, an effect that has been noted by Mackay¹⁰ in his description of the ice segregation method for the development of massive ice lenses. Similar velocity depth functions have been observed over a considerable area of the Tuktoyaktuk Peninsula. It is suggested that the refraction method can be used to map the distribution of ice lenses in this area in conjunction with some drill- ing control.

MARINE REFRACTION PROFILING

Extensive shallow reflection work in the Beaufort Sea by Shearer¹⁹ has indicated permafrost to be present over large areas offshore. A good discussion of the occurrence of off- shore permafrost has recently been given by Mackay.¹¹ A marine refraction technique was developed to confirm the

existence of permafrost by obtaining velocities (hence material type) from the permafrost zones.

The technique uses a 12-detector array, with 15-m spacing between hydrophones, which is towed behind a small boat. Recording and shooting was done from the same boat with small charges detonated in line with the array. In shallow water, this apparatus was capable of probing up to 60 m below the sea bottom.

Figure 9 shows a cross-sectional profile shot offshore near Tuktoyaktuk on the coast of the Beaufort Sea. Here a high velocity layer has been detected several metres below the sea bottom and has been traced seaward until it either disappears or extends beyond the depth range of the technique. Velocities obtained are similar to those obtained in thick overburden onshore; hence, this high velocity horizon has been interpreted to be the top of the permafrost layer. Since the seacoast recession is prominent along this coastline and since the temperature of the seawater is influenced by the warm Mackenzie River water outpouring 30 km away, the permafrost beneath the sea bottom here is probably relict and is degrading with time. That is, the depth to the top of the permafrost immediately offshore may vary as the time duration of seacoast immersion. It is also interesting to note an apparent correlation between the depth of seawater and the depth to the top of permafrost in the cross section; in particular, the top of permafrost in the shoal area is close to surface.

Not all permafrost occurrences surveyed are confined to areas adjacent to the seacoast. Refraction results in conjunction with reflection surveying have confirmed the presence of high velocity sea bottom sediments 20–30 km offshore, which can be interpreted as permafrost velocities. Surveys are currently under way to examine the areal extent of such occurrences.

MEASUREMENT OF THE THICKNESS OF PERMAFROST

In areas where the thickness of permafrost is variable, the seismic refraction method may be able to detect the presence of thin permafrost zones. Since frozen overburden overlying the equivalent unfrozen material represents a high velocity medium over a low velocity one, refracted seismic waves radiate energy into the low velocity medium, but little energy is radiated upward. Hence, no prominent refracted arrivals from the lower layer will be seen; this was confirmed by the previously mentioned field experiments of Roethlisberger¹⁸ and Bush and Schwarz.⁴ Zaitsev and Parkhomenko²¹ have shown with laboratory models that such refractions do exist as weak later arrivals; however, the interpretation of the event on a seismogram is complicated by the occurrence of higher amplitude events.

Press and Dobrin¹⁵ note that compressional seismic waves travelling in a high-speed surface layer will be rapidly attenuated. Donato⁵ has shown that waves refracted from a thin high-speed layer are attenuated at a rate that varies as a function of the seismic wavelength–layer thickness ratio. Poley and Nootboom¹⁴ showed by model studies that the attenuation of the refracted arrival through high-speed layers may result in the “echeloning” or “shingling” effect of seismic records. They also suggest that arrivals with wavelengths much greater than the thickness of the layer are mostly affected by attenuation. The model studies of Riznechenko and Shamina¹⁷ also demonstrate the rapid attenuation of thin high-velocity layers overlying a thick low-velocity one.

The foregoing discussion suggests that a measurement of the attenuation of the first arrival on seismic refraction records may be a good indication of the presence of a thin

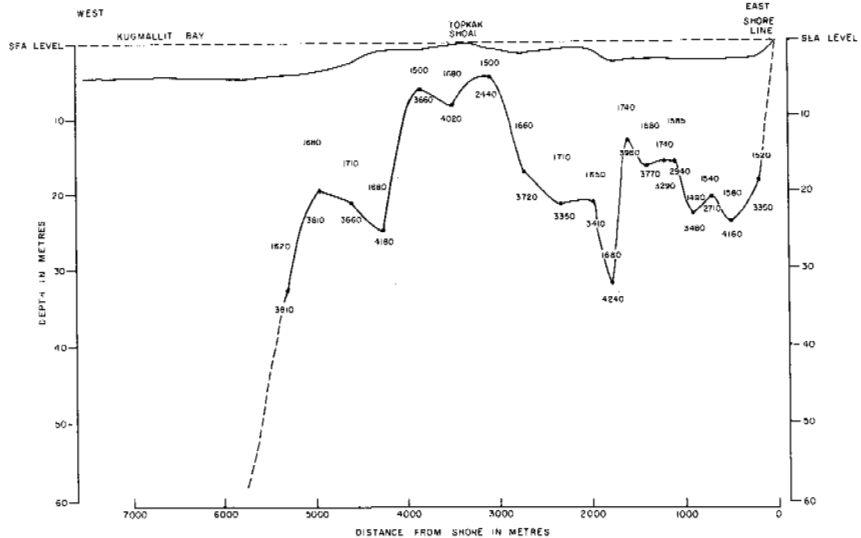


FIGURE 9 A cross section derived from an interpretation of a line of marine refraction profiles in Kugmallit Bay on the Beaufort sea-coast. Velocities in sediments are given in kilometres per second.

high-velocity permafrost layer. However, amplitude measurements of shallow seismic field records are fraught with difficulties such as:

1. unaccounted trace-to-trace variation in amplifier gain settings that may occur at low ambient operating temperatures;
2. variation in detector coupling to ground from geophone to geophone;
3. interference of later arrivals on the record, arriving within one-quarter cycle of the first arrival and contributing a portion of its energy within the measurement interval.

Despite these problems, broad trends in amplitude curves have been obtained for first arrival events in permafrost. Figure 10 plots the variation of amplitudes of first motions against geophone distances for refraction profiles shot in both thin and thick permafrost zones in the Mackenzie Delta region. Curves A, B, and C are from profiles shot in widely separate areas of the Tuktoyaktuk Peninsula in areas of thick permafrost and display similar attenuation rates. Curves 1 and 4 are from profiles shot on recently drained lake bottoms on Richards Island in the Mackenzie Delta. Curves 2 and 3 are from profiles shot on recently drained lake bottoms on the Tuktoyaktuk Peninsula. Curves 1-4 show a variation of attenuation rates, all of which are much higher than in thick permafrost zones. Thickness of permafrost in these areas is known or estimated to be 30 m or less (J. R. Mackay, personal communication). The effect of

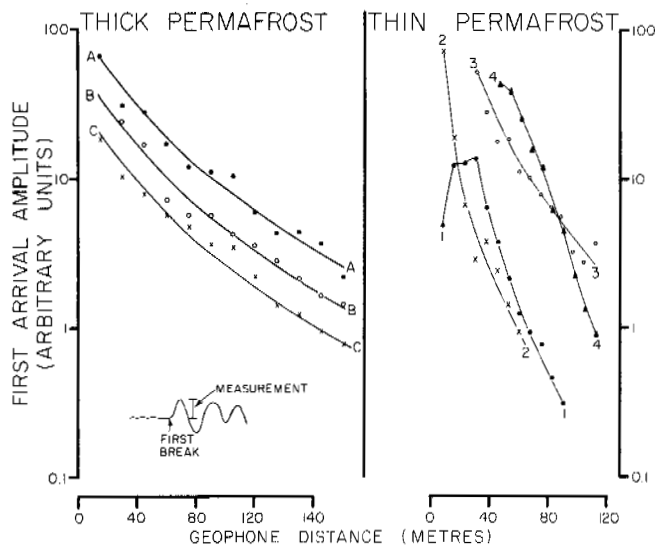


FIGURE 10 A comparison of the attenuation rates of the first arrivals of refraction profiles shot in thick and thin permafrost zones. Curves A, B, and C are on thick permafrost; curves 1-4 are on thin permafrost.

wave-spreading and nonelastic absorption cannot readily account for the anomalous attenuation.

Further studies of the attenuation properties of first arrivals are currently under way with hope that the technique may be made a quantitative one in the future.

SUMMARY

1. Shallow refraction seismic methods have been successfully applied to permafrost studies.
2. Conventional instrumentation used in shallow prospecting can be applied to permafrost in summer or winter for a rapid, economical survey. Refraction spreads are generally much longer than those in permafrost-free areas to obtain the necessary depth information.
3. The refraction method may be used to map the occurrence of permafrost in the discontinuous zone under summertime conditions where a thawed active layer is present, because about a metre of seasonal frost at surface in winter restricts the use of refraction methods.
4. Structure within permafrost can be mapped with the refraction technique in conjunction with borehole control for seismic velocities. Massive ice lenses have been delineated at depth.
5. Marine refraction seismic methods have been used to map the occurrence of permafrost under the sea bottom.
6. Anomalous attenuation of refracted waves has been observed in regions of thin permafrost. This phenomenon may be associated with refraction of seismic waves in a thin high-speed surface layer.

REFERENCES

1. Antsyferov, M. S., N. G. Antsyferova, and Ya. Ya. Kagan. 1964. A study of the propagation velocities and absorption of elastic waves in frozen sand. *Izv. Akad. Nauk, S.S.S.R. Ser. Geofiz.* 1:85-89.
2. Aptikaev, F. F. 1964. Temperature field effect on the distribution of seismic velocities in the permafrost zone. *In Akademiia Nauk SSSR Sibirskoe otd-je. Inst. merzlotovedeniia. Teplove protsessy v merzlykh.* (in Russian)
3. Barnes, D. R. 1966. A review of geophysical methods for delineating permafrost, p. 349-355. *In Permafrost: Proceedings of an international conference.* National Academy of Sciences, Washington, D.C.
4. Bush, B. O., and S. D. Schwarz. 1964. Seismic refraction and electrical measurements over frozen ground, p. 32-37. *In Proceedings of the Canadian regional permafrost conference.* N.R.C. Tech. Mem. No. 86. Ottawa.
5. Donato, R. J. 1965. Measurements on the arrival refracted from a thin high speed layer. *Geophys. Prospec.* 13:387-404.
6. Frolov, A. D. 1961. The propagation of ultrasonic waves in frozen sandy-clayey rock. *Izv. Akad. Nauk, S.S.S.R. Ser. Geofiz.* p. 732-736.
7. Hobson, G. D. 1966. A shallow seismic experiment in permafrost, Klondike area, Yukon Territory, p. 10-14. *In Geological survey of Canada. Paper 66-2.*
8. Hunter, J. A. 1971. A computer method to obtain the velocity

- depth function from seismic refraction data, p. 40-48. *In* Geological Survey of Canada. Paper 71-1 B.
9. Kurfurst, P. J., and M. S. King. 1972. Static and dynamic elastic properties of two sandstones at permafrost temperatures. *Trans. J. Pet. Tech.* 253:495-504.
 10. Mackay, J. R. 1971. The origin of massive icy beds in permafrost, western Arctic Coast, Canada. *Can. J. Earth Sci.* 8:397-422.
 11. Mackay, J. R. 1972. The world of underground ice. *Ann. Assoc. Am. Geogr.* 62(1):1-22.
 12. Nakano, Y., M. Smith, R. Martin, H. Stevens, and K. Knurth. 1971. Determination of the acoustic properties of frozen soils. U.S. Army CRREL Research Rept. Cold Regions Research and Engineering Laboratory, Hanover, New Hampshire.
 13. Ogilvy, A. A. 1970. Geophysical studies in permafrost regions in the U.S.S.R., p. 641-648. *In* Mining Groundwater Geophys. (Geological survey of Canada, Econ. Geol. Rpt.) No. 26.
 14. Poley, J. P. L., and J. J. Nooteboom. 1966. Seismic refraction and screening by thin high-velocity layers. *Geophys. Prospect.* 14(2):184-203.
 15. Press, F., and M. B. Dobrin. 1956. Seismic wave studies over a high-speed surface layer. *Geophysics* 21(2):285-298.
 16. Rampton, V. N., and J. R. Mackay. 1971. Massive ice and icy sediments throughout the Tuktoyaktuk Peninsula, Richards Island and nearby areas, District of Mackenzie. Geological survey of Canada. Paper 71-21.
 17. Riznechenko, Yu. V., and O. G. Shamina. 1957. Elastic waves in a laminated solid medium as investigated on two-dimensional models. *Izv. Akad. Nauk S.S.S.R. Ser. Geofiz* 7:855-873.
 18. Roethlisberger, H. 1961. Seismic refraction soundings in permafrost near Thule, Greenland, p. 970-981. *In* G. O. Naasch [ed.] *Geology of the Arctic*. Vol. 2.
 19. Shearer, J. M., R. F. Macnab, B. R. Pelletier, and T. B. Smith. 1971. Submarine pingos in the Beaufort Sea. *Science* 174: 816-818.
 20. Timur, A. 1968. Velocity of compressional waves in porous media at permafrost temperatures. *Geophysics* 33(4):584-595.
 21. Zaitsev, L. P., and I. S. Parkhomenko. 1964. Continuous head waves in the case of a thin layer lying on a half-space. *Izv. Geofiz. Ser.* 8:1149-1161. (Translation by Am. Geophys. Union)

NOTE

[1] The data for this report were obtained as a result of investigations carried out under the Environmental-Social Program, Northern Pipelines, of the Task Force on Northern Oil Development, Government of Canada.

INVESTIGATION OF SAMPLING PERENNIALY FROZEN ALLUVIAL GRAVEL BY CORE DRILLING

G. Robert Lange

U.S. ARMY COLD REGIONS RESEARCH
AND ENGINEERING LABORATORY
Hanover, New Hampshire

INTRODUCTION

The foundation design of large and important structures to be founded on or in permafrost increases the requirements for quality and quantity of subsurface data over those needed in temperate areas. Both thermally and mechanically "undisturbed" samples may be required.

Good samples of frozen fine-grained soils may be taken by core drilling²⁻⁴ or, in some cases, by drive sampling. However, sites underlain by fine-grained material (which may be ice rich) are not usually considered if other sites underlain by frozen gravel or bedrock are available. Sometimes these frozen gravel and bedrock materials are erroneously thought to suffer negligible consolidation upon thawing, an assumption that has led to such serious problems as intolerable foundation deflections. This paper

is a brief report of an investigation into the problems of core drilling frozen gravel. A more detailed report is currently being prepared.⁵

Some requirements for thermally and mechanically undisturbed samples have arisen in connection with the production and transportation of large petroleum reserves in arctic North America. These include prediction of thaw consolidation around wells producing hot oil through permafrost and problems associated with the design of the trans-Alaska pipeline system. Other anticipated problems are thaw beneath various surface structures, failure of the slopes of open pit mines, caving of drill holes, and failure of tunnel walls in mining and civil works.

Although the rapid development of the north had not yet occurred, in 1958 the Snow, Ice, and Permafrost Research Establishment (SIPRE)—now the U.S. Army Cold

Regions Research and Engineering Laboratory (CRREL) initiated a detailed investigation of the problems of core drilling in frozen silts. In 1959, the problems of core drilling frozen gravel, the subject of this report, were investigated and the results were reported only briefly.³ These investigations were important to, and immediately followed in 1960 by, the core drilling for Project Chariot.⁴ The recently increased need for good samples of all types of perennially frozen earth materials has prompted the reporting at this time of the details of our investigation of the more difficult problem, i.e., coring frozen gravels. The only other known work that has specific reference to coring frozen gravel is Hvorslev and Goode,² who report successfully coring frozen gravel near Thule, Greenland.

The SIPRE trials were conducted in both frozen silt and gravel near Fairbanks, Alaska. They were carried out solely for the purpose of investigating the problem of core drilling in permafrost. One of the chief objectives was to see if close control of the drilling fluid temperature and good core drilling practices would produce uniformly good quality core samples. Other objectives included testing special bit designs and comparing chilled compressed air and diesel fuel as drilling fluids. At the same time, it was thought desirable to find the minimum core size that might be taken from frozen gravel at ground temperatures just below freezing. The concept of using the chilled fluid to stabilize the frozen borehole wall, as opposed to the use of casing, was also tested.

CORE DRILLING OPERATIONS

Two holes, designated GP-1 and GP-2, were drilled in the Tanana Gravels near Fairbanks, Alaska. The holes were cored continuously in frozen granular material below the thawed active layer, one to a depth of 17.3 m and the other to 23.9 m. These materials consisted of well-rounded alluvial gravels and sands generally derived from hard metamorphic and igneous rocks. Permafrost is discontinuous and minimum ground temperatures are only about -1°C . The permafrost bodies are generally less than 30 m thick. While most of the frozen sands and gravels appear to be ice saturated and, consequently, well bonded, this is not always the case.

Equipment, Tools, and Methods

A versatile drill rig and standard tools were used together with special equipment designed for use in permafrost. The Failing Model 1500 SS drill rig was rated for about 152 mm hole to about 460 m depths. The rig, refrigerator, and other special equipment are described elsewhere as are calculations for the refrigerator and pump.^{3,4} Coring bits of only two sizes (78 × 98 mm and 98 × 146 mm) were used since the investigation, in general, was limited to the problems of core drilling for the investigation of foundations

for engineering structures. Some standard diamond core bits were used as well as some of special design (Figure 1).

Both chilled compressed air and diesel fuel with some viscosity additives were used as drilling fluids. Chilled compressed air was supplied by the compressor and refrigerator as has already been described.^{3,4} When liquids were used, arctic-grade diesel fuel along with small amounts of Baragel was used for viscosity control.

Some of the measurements and calculations given in Table I were obtained in the manner described below.

The weight on the bit was calculated from the known weight of the tools, including kelly and swivel, when weight alone was used. When the chuck was tightened for hydraulic feed, the force resulting from the hydraulic pressure was added. The force per point is the total weight on the bit divided by the approximate total number of diamonds in the surface set bits. The pressure on the bit is the total weight on the bit divided by the projected or kerf area of the impregnated bit. The absolute viscosity of the mud was measured with a Baroid rotary viscometer.

Hole GP-1

The details of all the coring operations are given in Table 1. A complete photographic record of all the core was made; representative samples are shown in Figure 2. The work was initiated late in the summer of 1959. Casing, with a 152-mm i.d., was drilled and driven through thawed silt and sand to the top of permafrost at a depth of 2.7 m. Using chilled compressed air and a V contour bottom discharge bit, coring was started with the 70 × 98 mm tools. Results with compressed air were not satisfactory, because thawed balls of silt and cuttings continued to plug the uphole air flow past the core barrel. The same situation had caused difficulty when an attempt was made in previous trials to core frozen silt with compressed air in warm weather. To improve air flow across the bit, the fluid holes of this bit were plugged, modifying it to an internal discharge bit. Even though several types of bits were used, only poor-quality cores of frozen sand with occasional gravel particles were recovered during the first five runs. Some of the core was dropped during run 5 and no further core was obtained, even though the larger 98 × 146 mm bits and core barrels were used during run 9.

Chilled diesel fuel was used starting with run 10. Loose gravel often appeared at the top of cores of frozen sand (Figure 2a) and was found in the sludge barrel. Loose gravel sometimes jammed between the core barrel and the wall, making it difficult to raise the tools. The loose sand and gravel also lodged between the core lifter and the inner tube of the core barrel, which prevented the lifter from opening, caused premature blocking of the core, and often terminated the coring run. This condition was remedied to some extent by modifying the lifter. Thinning the mud to

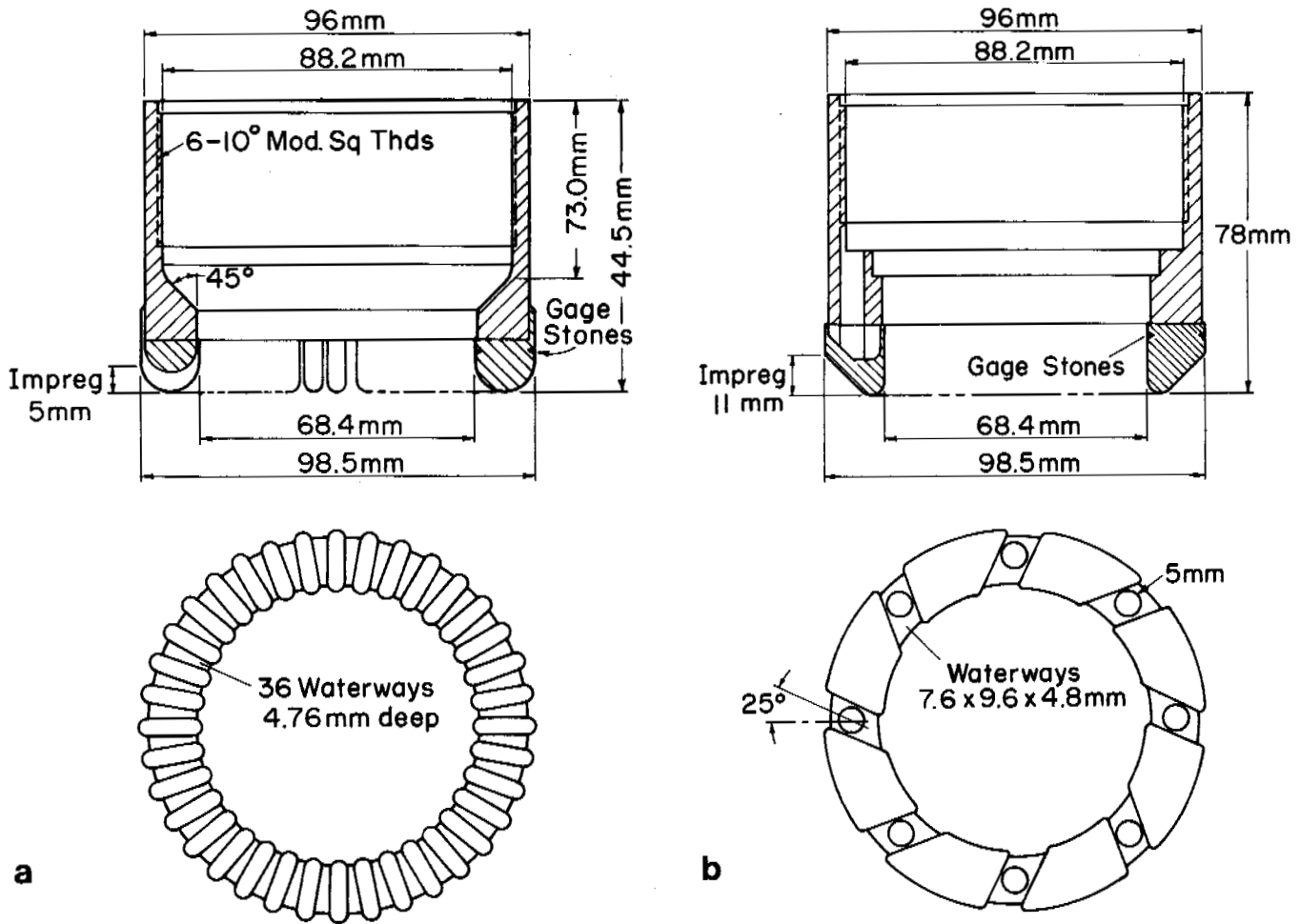


FIGURE 1 (a) Bit No. 4-875: Bottom discharge, impregnated ribbed type, fragmented bort, approximately 48 carats. (b) Bit No. 14-778: Impregnated bottom discharge, V contour, fragmented bort, approximately 118 carats. Fluid holes plugged in field to convert to internal discharge.

nearly clear diesel fuel also reduced this problem. Sometimes loose gravel would appear in the cores between layers of frozen sand, as in Figure 2a. The gravel may not have been well bonded by ice.

From run 23 to run 29, good to excellent cores of well-frozen sandy gravel were obtained using a variety of bits with little or no tearing or plucking of the gravel particles from the core. Figure 2b illustrates the quality of core and material obtained from this portion of hole GP-1. The core was prematurely blocked during run 30 and the resulting grinding of the core prevented its recovery in good condition. It is not known if the partially thawed core taken during run 31 represented the bottom of the permafrost body.

Hole GP-2

It was felt desirable to see if good-quality cores could be consistently taken of frozen sand and gravel using diesel fuel and the smaller (70 × 98 mm) bits and core barrel.

Good cores had been recovered using the smaller bits and core barrels during the coring trials in frozen silt, and they included substantial amounts of soft, weathered gravel.

The rig was moved several metres to the south and 102-mm-i.d. casing was set through thawed sand, silt, and gravel to a depth of 3.4 m. The casing was cemented, and a seal was obtained by freezing water around the casing.

Coring was initiated in mid-October 1959 using diesel fuel with a very small amount of Baragel. Core lifters that presented a smooth inside surface to the core and a splined outside surface to the inner tube extension were used. The refrigerator was run only intermittently due to the low ambient temperatures. Good to excellent cores of well-frozen sand and sandy gravel were taken in most of the length of this hole using a variety of bits. The quality of most of the core from this hole is illustrated in Figure 2c. The materials consisted of frozen sand to depths of 4.3 m and gravel to 9.5 m, followed by layered sand and gravel. Plucking of gravel particles from the core was rare. Frozen gravel that

TABLE 1 Summary of Core Drilling Operations

Run	Bit	Depth, m		Recovery, m			RPM	Penetration rate cm/min	Feed rate, rpm	Weight on bit kN	Force per point kN	Pressure on bit kN/m ²	Bit edge velocity		Drilling fluid			Temperature, °C				Uphole velocity around pipe m/sec.	Remarks
		Start	Stop	Recover	Run	Percent							Outside, m/sec	Inside, m/sec	Pressure, bar	Flow rate m ³ /min	Fluid in	Fluid out	Ambient air	Standpipe			
1	14-778	2.74	3.23	0.30	0.49	61	250	2.5	9.84	1.78		563.27	1.28	.88	6.4	13.31		-2.8	17.4		54	Frozen sand, occasional gravel - 70 mm x 106.5 mm bottom discharge coring bit in 152 mm casing - uphole air flow plugged by thawed cuttings.	
2	14-778	3.20	3.41	0.15	0.21	71	250			1.78		563.27	1.28	.88	6.4	13.30		-3.4	16		53	Bit modified to internal discharge.	
3	14-778	3.41	3.66	0.24	0.24	100	250			1.78		563.27	1.28	.88	6.2	11.33		-3.4	17		46	Frozen sand trace of gravel.	
4	C.J.	3.66	4.60	0.79	0.94	84	300	10.2		1.78			1.55	1.07	5.9	14.72		-2.8	17		60	Loose gravel on top of core-tungsten carbide "cracker-jack" bit.	
5	C.J.	4.60	5.06	0.43	0.46	93	350	12.7 15.2	2.75 2.30	1.78			1.80	1.25	5.9			-2.8	19			Circulation plugged as above - dropped core.	
6	C.J.	5.06	5.52	0	0.46	0	350	5.1 15.2	6.89 2.30	1.78			1.80	1.25	5.5	14.16 15.57		-1.1	17.9		58 64	Tried to pick up core-bit worn - no recovery.	
7	20-890	5.49	5.97	0	0.43	0	350	5.1	6.89	1.78		531.97	1.80	1.25	5.9	14.16		-2.2 -1.1	18.5		58	No recovery - rock bit to 5.5 m to clean hole, standard bit.	
8	20-890	6.92	7.38	0	0.46	0	350	7.6	4.59	1.78		531.97	1.80	1.25	5.2	15.57		-1.1	20.2		64	Reamed to 7.05 m - no recovery.	
9	5-849	7.28	7.96	0	0.67	0	350	3.8	9.19	2.89		662.14	2.68	1.80	4.8	16.99		-2.2	16.8		69	Reamed with 146 mm rock bit to 6.6 m using 88 x 146 mm semi-ribbed bit and large barrel-fragment of frozen wood.	
10	1-709																					Changed to chilled diesel fuel - loose gravel - no core - increased viscosity gravel plugged pump.	
11	1-709	7.96	8.96	.46	1.01	46	350	10.2	3.45	2.89		418.36	2.68	1.80				-1.1	-2.8	20.2		Flat crowned bit - frozen sand and loose gravel.	
12	1-709	7.92	8.90	0.00	0.00	0	350	0.0 5.1	∞ 6.89	3.11		452.90	2.68	1.80				-1.7	-2.8	11.2		Core catcher jammed with coarse cuttings and broke blocking core early.	
13	1-709						350			3.11		452.90	2.68	1.80				-4.5	-4.5	14.0		Core blocked as above.	
14	1-709	8.81	10.18	1.04	1.37	76	375	5.1 6.4	7.38 5.91	3.11		452.90	2.87	1.92	10.3			- .6	-1.7	12.9		Frozen sand and loose gravel - dropped some core.	
15	1-709	10.18	10.21	0.15	0.03		350			3.11		452.90	2.68	1.80	10.3			-4.5	-5.0	12.9		Previous core recovered with loose gravel.	
16	1-709	10.15	10.88	0.24	0.73	33	350	1.3 3.8	27.56 9.19	3.11		452.90	2.68	1.80	3.4 6.9	.114	-1.1	-5.0	14.0	4.5	.14	Frozen sand and loose gravel - core barrel head plugged.	
17	1-709	10.94	11.58	0.61	0.64	96	350	2.5 5.1	13.78 6.89	9.16		1332.81	2.68	1.80	6.9	.227	-5.0 -5.0	-7.8 -6.7	16.0		.29	Frozen sand - sludge barrel full of loose gravel.	
18	1-709	11.55	12.34	0.64	0.79	81	350	2.5 5.1	6.89 13.78				2.68	1.80	3.4 8.6	.303	-6.7 -3.9	-7.3 -5.6	7.0		.38	Some frozen gravel and sand - better core - blocked early.	
19	19-859	12.37	12.83	0.24	0.43	56	350	1.3 5.1	27.56 6.89	7.78		1132.24	2.68	1.80	6.9	.227	-5.6		8.0	-7.8	.29	Core blocked early, standard impregnated bottom discharge bit.	
20	19-859	12.80	13.26	0.46	0.46	100	350	1.3 5.1	27.56 6.89	7.78		1132.24	2.68	1.80	2.8 8.3		-3.4		9.0	-5.6		Frozen gravel, modified lifter - splined inside - smooth outside.	
21	19-859	13.26	14.45	0.85	1.19	71	350 ±			9.56		1391.06	2.68	1.80	2.8 6.9		-4.5		9.0	-7.3		Frozen sand and gravel - good core.	

TABLE I (continued)

Run	Bit	Depth, m		Recovery, m			RPM	Penetration rate cm/min	Feed rate, rpm	Weight on bit kN	Force per point kN	Pressure on bit kN/m ²	Bit edge velocity		Drilling fluid		Temperature, °C				Uphole velocity around pipe m/sec	Remarks
		Start	Stop	Recover	Run	Percent							Outside, m/sec	Inside, m/sec	Pressure, bar	Flow rate m ³ /min	Fluid in	Fluid out	Ambient air	Standpipe		
22	19-859	14.45	14.63	0.18	0.18	100	350			9.56		1391.05	2.68	1.80	4.1 8.3	.227	-3.9		8.0	-6.2	.29	Core blocked early.
23	19-859	14.72	15.85	0.98	1.13	87	350 ±	2.5 5.1	13.78 6.89	8.90		1293.99	2.68	1.80	4.1 8.3	.227	-5.0		10.0	-7.8	.29	Frozen sandy gravel - good core.
24	19-859	15.82	16.98	1.04	1.16	90	350	2.5 5.1	13.78 6.89	9.34		1358.69	2.68	1.80	6.9 12.4	.379	-3.4		11.0	-5.6	.49	Frozen sandy gravel - good core.
25	19-859	16.89	18.17	1.28	1.19		425	2.5 1.3	16.73 33.46	9.56		1391.05	3.26	2.19	5.5 11.0	.303 .379			11.0		.49	Frozen sandy gravel - good core.
26	17-851	18.17	19.42	1.19	1.25	95	350	2.5 5.1	13.78 6.89	9.56 6.67			2.68	1.80	6.9 10.3	.227	-3.9	-3.4	13.0	-3.4 -3.9	.29	Excellent core frozen sandy gravel - standard surface set bottom discharge bit.
27	17-851	19.39	20.60	1.13	1.22	92	350	1.3 2.5	6.89 27.56	8.90	.01		2.68	1.80	3.4 6.9	.189 .151	-5.6	-5.6	13.0	-5.6	.29 .20	Excellent core frozen sandy gravel
28	17-851	20.54	21.34	0.61	0.85	71	300 ±	1.3 10.2	27.56 2.95	8.90	.01		2.29	1.55	1.4	.151	-2.8	-3.4	15.0	-4.5	.20	Chattering - some bit wear on gage stones - hole "sticky".
29	3-845	21.31	22.31	0.91	1.01	91	325	7.6 10.2	4.26 3.20	8.67		818.96	2.50	1.68	3.4 6.9	.227	-5.6	-6.2	12.0	-6.2	.29	Good core frozen sandy gravel - ribbed bit slow in gravel.
30	13-803	22.31	22.74	0.37	0.43	86	350	2.5	13.78	10.23		1488.09	2.68	1.80	6.9 13.8	.308	-3.9	-3.9	7.0	-3.4	.38	Poor core - "v" contour bit - blocked early.
31	13-803	22.74	23.89	1.16	1.16	100	350	2.5 5.1	13.78 6.89	10.23		1488.09	2.68	1.80	13.8 20.7	.379	-3.4	-3.9	7.0	-3.4 -1.1	.49	Thickened mud - full core - partially thawed - not ice saturated (bottom of permafrost?)
1	20-890	3.47	4.69	1.07	1.22	88	200 ±	5.1 10.2	3.94 1.97	6.97		HOLE NO. GP-2		3.4 6.9	.227	-3.9	-2.8	-2.8	-2.2	.93	Diesel fuel and 70 mm x 98 mm barrels - standard impregnated bottom discharge core bit - 102 mm casing to 3.4 m - lifter modified as before - refrigerator needed only intermittently - good core frozen sand.	
2	20-890	4.67	5.79	1.22	1.10		200 ±	2.5 5.1	7.87 3.94	8.01			1.04	.70	3.4 1.89		-3.9 -6.2	-5.0 -7.3	-3.9	-3.4 -6.7	.78	Excellent core frozen sand - frozen sandy gravel 4.3 m to 9.45 m.
3	14-778	5.88	7.10	1.22	1.22	100	200	5.1	3.94	6.97			1.04	.70	3.4 5.5	.189	-6.7	-9.0	-2.2	-9.0	.78	"V" contour surface set modified bit - good core.
4	12-796	7.10	8.35	1.22	1.25	98	200+	10.2	1.97	9.12	.03		1.04	.70	3.4	.189	-7.8 -6.2	-7.3 -5.6	-7.8	-7.8 -6.7	.78	"V" contour bottom discharge bit - good core - not ice saturated.
5	4-875	8.35	9.75	1.34	1.40	96	200+	5.1	3.94	7.78			1.04	.70	6.9	.189	-2.8 -2.8	-2.2	-6.2	-2.8 -4.5	.78	Good core-ribbed bit flattened.
6	18-850	9.57	10.97	1.37	1.40	98	200+	20.3	0.98	7.34	.02		1.04	.70	3.4 6.9	.201 .189	-5.6 -6.7	-6.7 -8.4	-5.6	-6.7 -7.8	.82	Frozen silt with organic material with some sand and gravel - standard bit.
7	18-850	11.00	13.86	2.56	2.65	97	200+	2.5 10.2	7.87 1.97	7.12	.02		1.04	.70	3.4	.165	-7.8	-8.4	-6.2	-7.8	.87	3.0 m barrel - excellent core - 2.54 m frozen coarse sand and sand gravel.
8	14-778	13.66	14.42	0	.76	0	200+	5.1	3.94	7.78			1.04	.70	3.4 6.9	.227	-2.8	-2.2	-6.7	-5.6	.93	Core blocked early - core barrel stuck - dropped core.
9	12-796	14.17	16.15	0.39	1.98	20	200	5.1	3.94	8.45	.03		1.04	.70	2.8 4.1	0.227 0.0379	-6.7	-5.6	-6.7	-5.6 -1.7	.93 1.55	Ran rock bit but hole not cleaned - ground part of core rest good.
10	12-796	16.46	17.25	0.15	0.79	19	200	5.1	3.94	8.23	.03		1.04	.70	6.9	.227	-5.0	-3.9	-8.4	-6.7	.93	Increased viscosity to 20-30 c.p. - ran rock bit to 13.7 m thawed sand and gravel from bottom of hole plugged system (bottom of permafrost?)

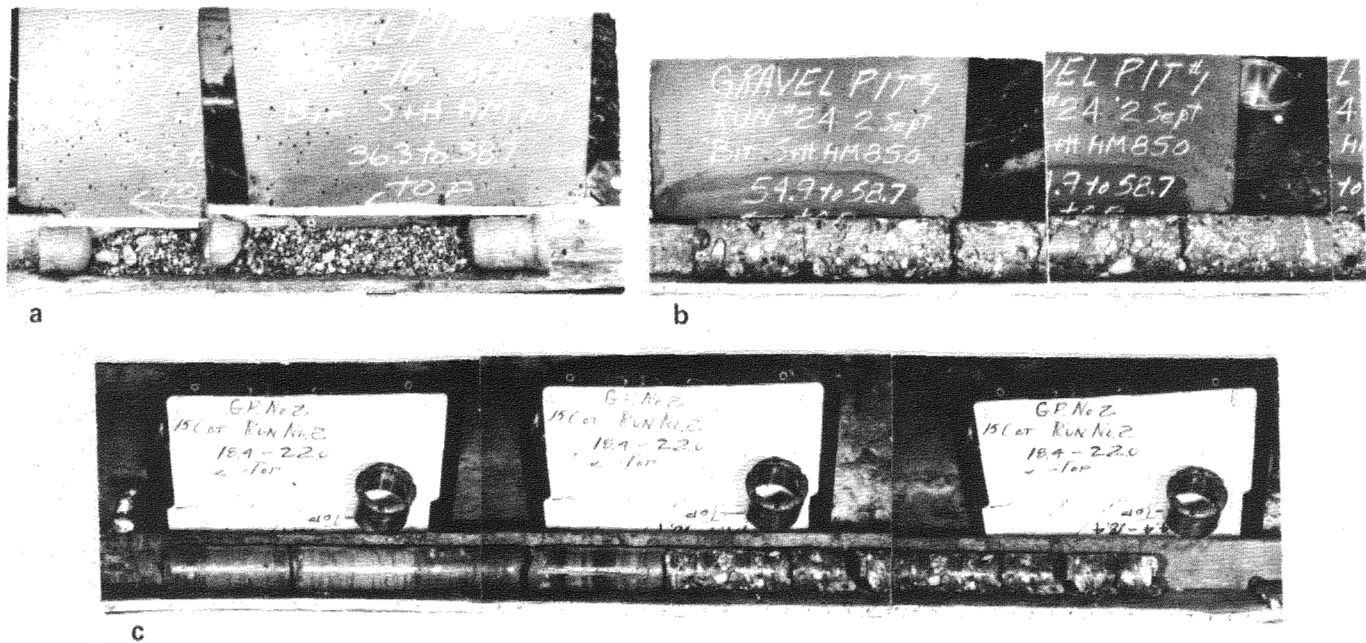


FIGURE 2 Representative core photographs. Chalkboard indicates depths from breakout table. The scale in the photos is in feet and tenths of feet (a) GP-1, run 16 (10.15-10.88 m, 98 mm diam.): loose, thawed gravel with frozen sand. (b) GP-1, run 24 (15.82-16.98 m, 98 mm diam.): good to excellent core typical of most of the recovery of frozen gravel in the lower portion of hole GP-1. (c) GP-2, run 2 (4.67-5.79 m, 70 mm diam.): core representative of the excellent quality obtained from most of hole GP-2.

was not ice saturated was noted during run 4. A secondary mud pit that allowed settlement of silt particles was added to prevent recirculation of coarse particles. A 3-m core barrel was used during run 7, and a 2.6-m core of excellent quality was cut.

The core was blocked prematurely during run 8, and the core barrel stuck in the hole. This led to additional difficulties that precluded further substantial core recovery. Finally, thawed material entered the hole, possibly indicating the bottom of the permafrost body.

DISCUSSION OF RESULTS

Representative results are illustrated in the core photographs (Figure 2). The core shown in Figure 2c represents the quality of a substantial portion of the core that demonstrates better results than any other known attempts in warm permafrost. The quantity is given under the "recovered" column in Table I; the quality is generally shown under "remarks."

In general, poor results were obtained when attempting to core with air when ambient air temperatures were warm, usually because thawed cuttings blocked the flow of return air. This and other difficulties encountered when using compressed air in warm weather occur chiefly because air is a much less effective heat transfer medium. At the mass flow rate required for each of the two different fluid

streams to remove the cuttings from the hole, the diesel fuel has several orders of magnitude greater capacity for heat removal than the compressed air.³ When the ambient air is -4°C or lower, compressed air can be chilled sufficiently with a fan-driven heat exchanger (ambient air to compressed air) to be used to take consistently good cores of perennially frozen rocks and soils. Defrosting problems made the chilling of compressed air by direct mechanical refrigeration very difficult.

The use of diesel fuel brought much better results in terms of quality and amount of core and substantial amounts of good core were taken. Difficulties were experienced when loose sand and gravel or cuttings jammed the core lifter and caused the premature blocking of the core upon entering the barrel. Some of this material was from cuttings and unrecovered core, but some also must have originated in the "dry-frozen" portions of the hole walls, which were eroded by the drilling fluid. It is difficult to conceive of this material being thawed during the use of chilled diesel fuel. Two such zones were noted in the core (runs GP-1-31 and GP-2-4). Modification of the core lifter ameliorated this problem considerably. It is likely that modern mud technology, such as the use of foams,¹ might also reduce the magnitude of this problem if not eliminate it. Desanders or other mechanical means of separation at the surface might also be effective. Mud with the appropriate filtration qualities would probably reduce erosion of these zones.

Proper preparation of the hole before coring runs by use of a noncoring full hole bit, especially one that produces fine cuttings, would have produced better results.

The impregnated ribbed bits cut rapidly in frozen sand but were slow and dulled quickly in gravels containing hard rock types. The V contour bits worked quite well and are to be recommended. Standard bit types with a full round crown were also satisfactory. Surface set bits were fast but were prone to damage and wear when run on loose gravel particles of hard rock types. Impregnated bits were not damaged or worn so easily but tended to cut more slowly. Surface set bits with the V contour probably are a promising design, but were not used often (runs 9 and 10 in GP-2) and then under difficult conditions. Internal discharge or bottom discharge types appeared to work equally well. Over-size kerf dimensions, e.g., 98 × 146 mm, are generally not to be recommended when using diesel fuel. Hvorslev and Goode² found the clearances of the standard 102 × 140 mm bits satisfactory with this size core barrel.

CONCLUSIONS

It is concluded that excellent cores of frozen gravel and frozen, fractured and weathered rock at near-freezing ground temperatures may be taken by circulating a liquid drilling fluid chilled to temperatures just below the ground temperature, even in summer weather, if the material is well bonded by ice. Cooling compressed air is not feasible for core drilling until the ambient air temperature reaches -4°C or cooler. Excellent quality cores as small as 70 mm were

consistently taken. Hvorslev and Goode² were quite successful with NX (55 mm) size core in colder permafrost. Borehole wall stabilization was satisfactorily achieved with the chilled liquids, except possibly where the walls were not well bonded by ice.

ACKNOWLEDGMENTS

This paper presents the results of research performed by the Snow, Ice and Permafrost Research Establishment (now the Cold Regions Research and Engineering Laboratory) under the sponsorship of the U.S. Army Corps of Engineers. The preparation of this report was supported by the Atlantic Richfield Company and USA CRREL. The author is grateful for the assistance of Jack Tedrow and Robert Patenaude during the field work and for the assistance of Specialist Elwood P. Wells in the compilation of the tables and photographs.

REFERENCES

1. Bartlett, L. E. U.S. Patent No. 3,618,681.
2. Hvorslev and Goode. 1966. Core drilling in frozen soil, p. 364-371. *In* Permafrost: Proceedings of an international conference. National Academy of Sciences, Washington, D.C.
3. Lange, G. R. 1966. Refrigerated fluids for drilling and coring in permafrost, p. 375-380. *In* Permafrost: Proceedings of an international conference. National Academy of Sciences, Washington, D.C.
4. Lange, G. R. 1972. Rotary drilling and coring in permafrost, deep core drilling, core analysis and borehole thermometry at Cape Thompson, Alaska. USA CRREL Tech. Rep. 95, Pt. III.
5. Lange, G. R. An investigation of sampling permafrozen gravel and rock by core drilling. USA CRREL Tech. Rep. (In preparation)

POTENTIAL USE OF AIRBORNE DUAL-CHANNEL INFRARED SCANNING TO DETECT MASSIVE ICE IN PERMAFROST

Leonard A. LeSchack, Frederick H. Morse, Wm. R. Brinley, Jr.,
Nancy G. Ryan, and Robert B. Ryan

DEVELOPMENT & RESOURCES TRANSPORTATION CO.
Silver Spring, Maryland

INTRODUCTION

The object of this research was to attempt to develop airborne techniques for ascertaining those areas of permafrost terrain that, owing to inclusions of ice lenses, wedges, strata, etc., in the permafrost, would cause severe engineering problems. While the value of aerial photography is well known, careful examination of photographs taken along the route of the proposed trans-Alaska pipeline showed that there rarely was any way of predicting or detecting massive ice in the permafrost by photographic means, unless polygonal ground patterns were visible.⁶ The specific object of this research, therefore, was to assess the possibility of developing a system to use thermal means for detecting such massive ice in permafrost areas where patterned ground or other photographic indications were otherwise not visible.

The area chosen for this preliminary research was Shaw Creek Flats, about 100 km southeast of Fairbanks, Alaska, along the Richardson Highway. Significant quantities of near-surface ice had been encountered there by the pipeline borehole survey; the near-surface geology was not complicated, there was no significant tree cover, and there were no clear indications of subsurface ice to be seen on the aerial photographs.

It was recognized by the authors at the outset of this research that, to detect massive ice in permafrost by airborne infrared (IR) means, two major conditions had to be met: First, a way had to be found to separate the absolute temperature (T) from the emissive power, $\dot{Q} = [(\epsilon)F(T)]$, recorded by thermal infrared scanner, where ϵ is the surface emissivity. The ice anomalies should primarily influence surface temperature, however, surface emissivity changes, often caused by unrelated phenomena, could easily obscure the desired thermal response and therefore must be separated from it. Additionally, the thermal effects might be so small that ways of enhancing these effects on the imagery might be required. Second, it had to be determined *a priori*, that typical ice inclusions in permafrost could, at some time of the year, produce a thermal effect at the surface that was

of sufficient magnitude to be measurable by present airborne infrared equipment.

THE DUAL-CHANNEL IR SCANNER

In late 1970, the authors conducted preliminary studies that suggested that considerable value would accrue to interpretation of IR scanning imagery obtained in the Arctic if two wavelength channels were scanned simultaneously, rather than one channel as is often done. Present IR scanning equipment is generally sensitive to radiation either in the 2-5 or 8-14 μm range, depending on the sensor utilized. The radiation received at the sensor is the sum of the energy emitted from the surface, the sky radiance reflected by the surface (both of which are modified by atmospheric absorption), and the energy emitted by the atmosphere between the sensor and the surface. Under certain conditions assumed by the authors [1], the dominant energy received at the sensor is that emitted from the surface, which may be represented as

$$\dot{Q} = \epsilon F_{\lambda_1 - \lambda_2}(T), \quad (1)$$

where $F_{\lambda_1 - \lambda_2}(T)$ is the fraction of the total emissive power that is emitted in the wavelength interval $\lambda_1 - \lambda_2$. If two channels are recorded simultaneously, one such equation is produced for each band:

$$\dot{Q}_{4-5} = \epsilon_{4-5} F_{4-5}(T),$$

and

$$\dot{Q}_{8-12} = \epsilon_{8-12} F_{8-12}(T). \quad (2)$$

The emissivity varies as a function of wavelength for each material scanned¹; the function $F_{\lambda_1 - \lambda_2}$ is independent of wavelength. The absolute temperature (T) in both equations would be the same for any given point simultaneously scanned. A ratio of the two signals \dot{Q}_{4-5} and \dot{Q}_{8-12} would, for this simplified model, equal the ratio $\epsilon_{4-5} : \epsilon_{8-12}$; over the temperature range of interest, this emissivity ratio is a

function essentially of the material scanned and not the local temperature [2]. If the ratio signal, rather than either single channel signal, is now plotted, a map of essentially surface emissivity ratios is produced. These data can be enhanced for contour emphasis. Of major significance is the possibility for the separation of the effect of the emissivity of the surface material from the overall radiation response. If the emissivity ratio map is now compared with a map obtained by processing the 8–12- μm signal alone, regions of different surface temperature can be identified and, theoretically, can be related to the presence of massive ice.

A dual-channel scanner that can simultaneously produce the above two functions was constructed specifically for this work.

THERMAL MODELING

When a ground surface is subjected to a significant increase in net solar energy input over a relatively short time, the response of the surface temperatures should reflect the local variations in subsurface composition. There are two such periodic solar energy increases: sunrise (on a daily scale) and springtime (on an annual scale). The response of surface temperatures in the Arctic to daily changes is influenced by a thin subsurface layer ranging in thickness from a few centimetres to approximately a metre, depending on the nature of the material. For example, Weedfall⁹ found that the maximum and minimum diurnal temperature changes do not propagate downward sufficiently far to produce measurable effects at the surface of anomalies of interest in this study. Figure 1, however, shows that, where temperature maxima and minima are recorded over an annual cycle, the warming effect resulting from the onset of spring can be noted at a considerably greater depth, i.e., 2–3 m. This suggests that ice anomalies, which from drillhole data frequently appear

to be found at depths of 0.5–2.5 m, could be expected to influence the annual temperature profile. Therefore, any anomaly of interest in this work must be examined with respect to its response to the *seasonal* increase in net immolation rather than a diurnal increase.

Figure 2 shows the temperature–time response of a uniform media (frozen ground in winter) and that of the same material overlying an ice lens. Initially, after the relatively large solar energy input flux, the increase in the ground temperature in both cases propagates downward at the same rate as the ground thaws. At a time t^* , the temperature disturbance reaches the depth corresponding to the top of the ice lens. Subsequently, the temperature profiles in the two cases will differ. The surface temperature of the uniform media would then rise above the temperature of the surface over the ice lens. The time-dependent surface temperature difference is represented in Figure 3. The time (t^*) at which the temperature increase first reaches the ice lens depends on the depth of the lens, as well as the composition of the material above it, as shown in the following preliminary calculations.

PRELIMINARY HEAT TRANSFER CALCULATIONS

Just prior to the onset of the spring thaw, the temperature throughout the surface material is at its lowest value. The ensuing rapid increase in incoming solar radiation causes the air and surface temperatures to rise. The energy is then propagated downward, causing the temperature profile to rise. The surface temperature depends on a balance among the radiative, convective, and conductive energy transfer rates. The rate and depth of thermal penetration depends on the thermal properties of the surface material. If an ice lens is present, the rate of increase of the temperature profile propagating downward will be slowed when the earth–ice

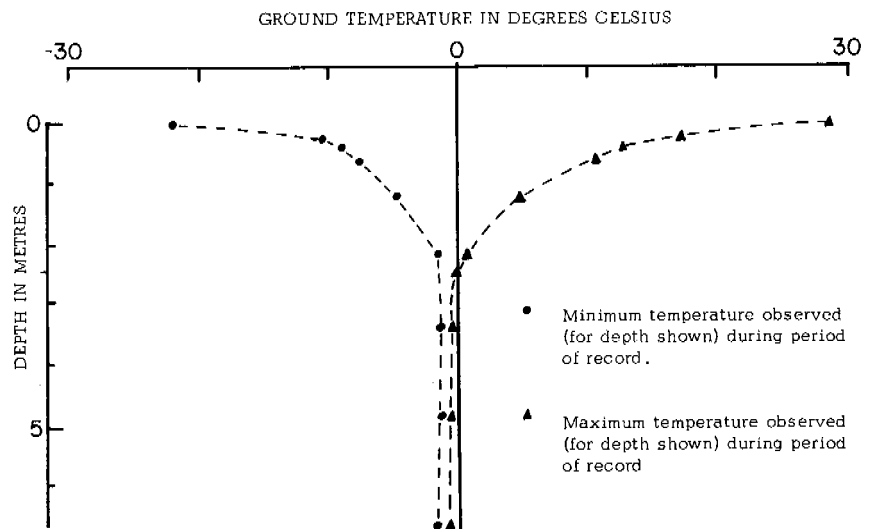


FIGURE 1 Maximum and minimum temperature profiles measured at the Ft. Yukon Test Station, Alaska,⁸ July 1951–April 1952.

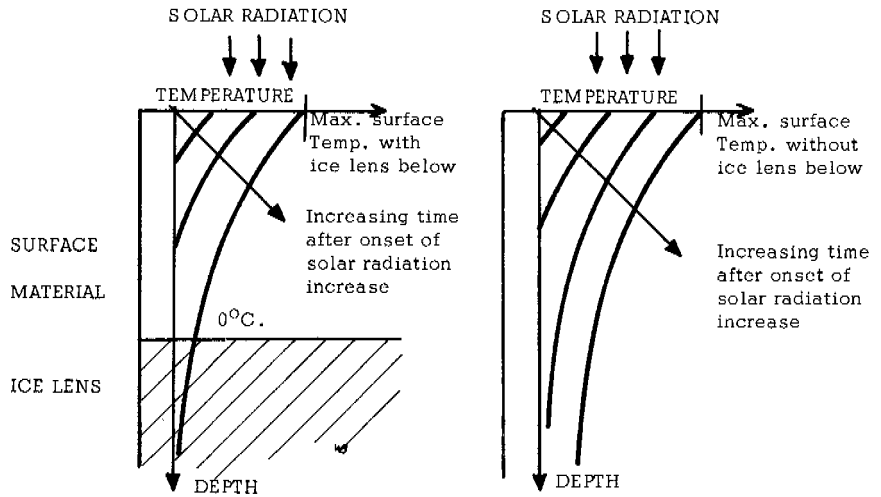


FIGURE 2 Temperature profiles in surface material with and without ice lens present.

interface temperature reaches 0 °C. The surface temperature will then continue to increase, but at a much slower rate as the ice lens melts. For the remainder of the season, the temperature of the surface above the ice-free material will continue to rise at its original rate, while that of the surface above the ice lens will rise more slowly, as shown in Figure 3.

The physical situation described above is approximated by the following model: (a) The solar radiation input will be represented by a constant heat flux equal in magnitude to the average during the peak heating months of June, July, and August; (b) The convection heat transfer coefficient will be taken as zero for the initial calculation of surface temperature. A correction is then made for a finite heat transfer coefficient; (c) The material above the ice lens and the material adjacent to the ice lens is assumed to be homogeneous and to have constant properties. Although a range of materials were studied, only the results for frozen, moderately packed soil

are presented; (d) The ice lens dimensions are assumed to be large relative to its depth below the surface, thereby allowing the edge effects to be neglected; (e) Both the lens-free and lens-containing materials will be treated as semi-infinite solids; and, (f) The initial temperature is uniform throughout the two solids.

The temperature response of a semi-infinite solid after a sudden exposure to a constant heat input at the surface is presented by Schneider.⁷ The surface temperature, T_s , as a function of time after heating, t , is given by

$$T_s = T_0 + (2q\Theta\alpha^{1/2}/K)(t^{1/2}), \quad (3)$$

where T_0 is the initial uniform temperature, q is the radiation energy flux, α and K are the thermal diffusivity and conductivity of the surface material, and Θ is a constant equal to $\pi^{-1/2}$.

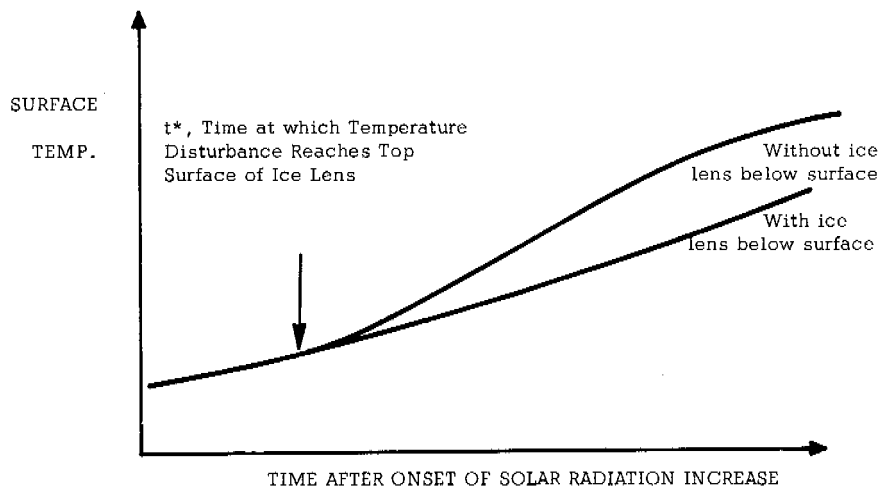


FIGURE 3 Surface temperature as a function of time after onset of springtime solar radiation increase.

For the representative material selected $\alpha = 0.035 \text{ cm}^2/\text{s}$ and $K = 0.031 \text{ cal/s-cm-}^\circ\text{C}$. The radiation energy flux, as measured at Barrow, Alaska,³ was used; $q = 12.6 \text{ mW/cm}^2$. Using these values Eq. (3) becomes:

$$T_s = T_o + 0.021t^{1/2}. \tag{4}$$

The temperature (T_x), which is at any point below the surface (x) at any time (t) is given by

$$T_x = T_o + (2q\Theta\alpha^{1/2}/K)(t^{1/2}). \tag{5}$$

In this case, Θ is a function of X , a dimensionless distance defined as:

$$X = \frac{x}{2\alpha^{1/2}t^{1/2}} \tag{6}$$

The functional relationship between T and X is presented in Nakano and Brown's⁵ Figure 41. By assuming an ice lens at various depths below the surface, Eq. (5) and (6) may be used to find the time, t^* , at which the ice lens temperature rises to 0°C . The surface temperature at that time is calculated using Eq. (4), and this surface temperature is assumed to remain constant during the rest of the 3-month heating period. On the other hand, the surface temperature of the lens-free material continues to rise, according to Eq. (4). At the end of the heating period a maximum temperature difference between the surface above a lens and above the lens-free material is observed:

$$(\Delta T_s)_{\text{max}}^0 \cong T_s(t = 3 \text{ mo}) - T_s(t^*). \tag{7}$$

The superscript ⁰ above ΔT_s indicates that the value so obtained is for a zero convection heat transfer coefficient.

The effect of convection on such a surface temperature difference is to bring the two temperatures closer together and closer to the ambient air temperature. It can be shown that the effect of a finite heat transfer coefficient is to reduce $(\Delta T_s)_{\text{max}}^0$ according to the following approximate relationship:

$$(\Delta T_s)_{\text{max}} = C(\Delta T_s)_{\text{max}}^0/h, \tag{8}$$

where h is the numerical value of the convective heat transfer coefficient (given in $\text{cal/cm}^2 \text{ s }^\circ\text{C}$) and C is a constant equal to 1.4×10^{-4} . For a typical wind speed of 5 m/s, h is approximately $7 \times 10^{-4} \text{ cal/cm}^2 \text{ s }^\circ\text{C}$. Therefore the convection-corrected surface temperature difference is one-fifth that given by Eq. (7).

Using the ice depth values shown below, the following results were obtained:

Ice Lens Depth (m)	t^* (days)	$(\Delta T_s)_{\text{max}}$ ($^\circ\text{C}$)
0.3	38	4.00
0.6	43	3.55
1.2	54	2.55
1.8	70	1.65
2.4	85	0.39

It is to be noted that these results are based on certain simplifying assumptions, made for the purpose of providing the order of magnitude value of the surface temperature difference caused by the subsurface ice lens.

These preliminary calculations indicated that t^* typically would range from 38 to 85 days, and the maximum surface temperature difference would occur shortly after the onset of fall. The maximum surface temperature difference depends primarily on the convective heat transfer rate at the surface, as well as the depth of the ice lens and the composition of the overlying material. The preliminary calculations indicated that anomalies ranging from 4 to 0.4°C could be expected. Temperature differences of this magnitude would be readily sensed by the IR scanning system intended for this project.

The preliminary thermal modeling discussed was conducted in late 1970 to ascertain whether the field program planned for the summer of 1971 would provide meaningful data. The authors chose two geologically simple, but reasonable sections—one with massive ice in permafrost, the other without—to determine whether, under these conditions, a measurable temperature difference on the surface *could* result from different penetration rates of the annual thermal wave because of different thermal characteristics of massive ice and permafrost. It was recognized, as Williams¹⁰ pointed out, that a layer of organic matter at the surface would affect the thermal regimes of these sections, i.e., delay penetration of the annual wave. The consequence of this organic mat covering both model sections would be to delay the annual thermal wave but not to significantly change the predicted surface temperature difference.

A more realistic thermal model was then developed for computer analysis as the field aspects of the experiment got under way. This model accounted for the various energy transfer mechanisms at the surface. The representation of phase change in the freezing or melting zone presented computational difficulties. The melting zone phenomenon, however, has recently been analytically described by Nakano and Brown,⁴ and in a more recent paper⁵ they developed a mathematical model that incorporates this phenomenon. Since their model appears to describe observed thermal profiles in tundra satisfactorily, it is intended to combine their model with the above-described computer model in future work.

PRELIMINARY ANALYSIS

The field party had the advantage of having essentially immediate access to the 8-12- μ m imagery of the Shaw Creek Flats site owing to the utilization of a portable field imagery processing unit. This imagery was taken to the site and used to guide the investigators to features of interest for ground-image correlation. The most significant patterns observed on the predawn imagery of this site were polygonal structures on the ground that were not otherwise visible from available aerial photography or from the ground.

Guided by the imagery, an easily accessible polygon was located, and a series of permafrost probes were conducted along transects spanning the indicated area. At the time that these probes were made (late August), the depth of the active layer actually measured was very close, if not equal, to the depth to permafrost. Since the depth measured is to an isothermal surface, significant variations of it, not attributable to visible surface causes, could be attributed to ice within the permafrost. Thus, when a significant change in depth to permafrost was observed on transect profiles and the depth

anomaly had a ridgelike form located at the area indicated by the imagery, it was believed that massive ice could be found immediately subjacent to this ridge. Consequently, the ridge anomaly was drilled to a depth of 1 m. In spite of considerable melting of the cores during the course of this drilling, significant veins of ice were found at the 50- and 100-cm levels. From their orientation, it appeared that this ice was either horizontal segregations or part of a feeder network leading to deeper massive ice, similar to that found within 100 m of this site at Alyeska test hole 8-45A (Figure 4). Since three other holes were sunk within a radius of 10 m from 8-45A, one of which had significant ice, it is believed that, had other borings been made during the course of the research away from the flanks of the above-mentioned permafrost anomaly, no ice would have been found there either.

IMAGERY ENHANCEMENT

It appears that significant value accrues to imagery that presents a mapping of two simultaneously related parameters over that produced by one. As seen in Figure 5, the ratio

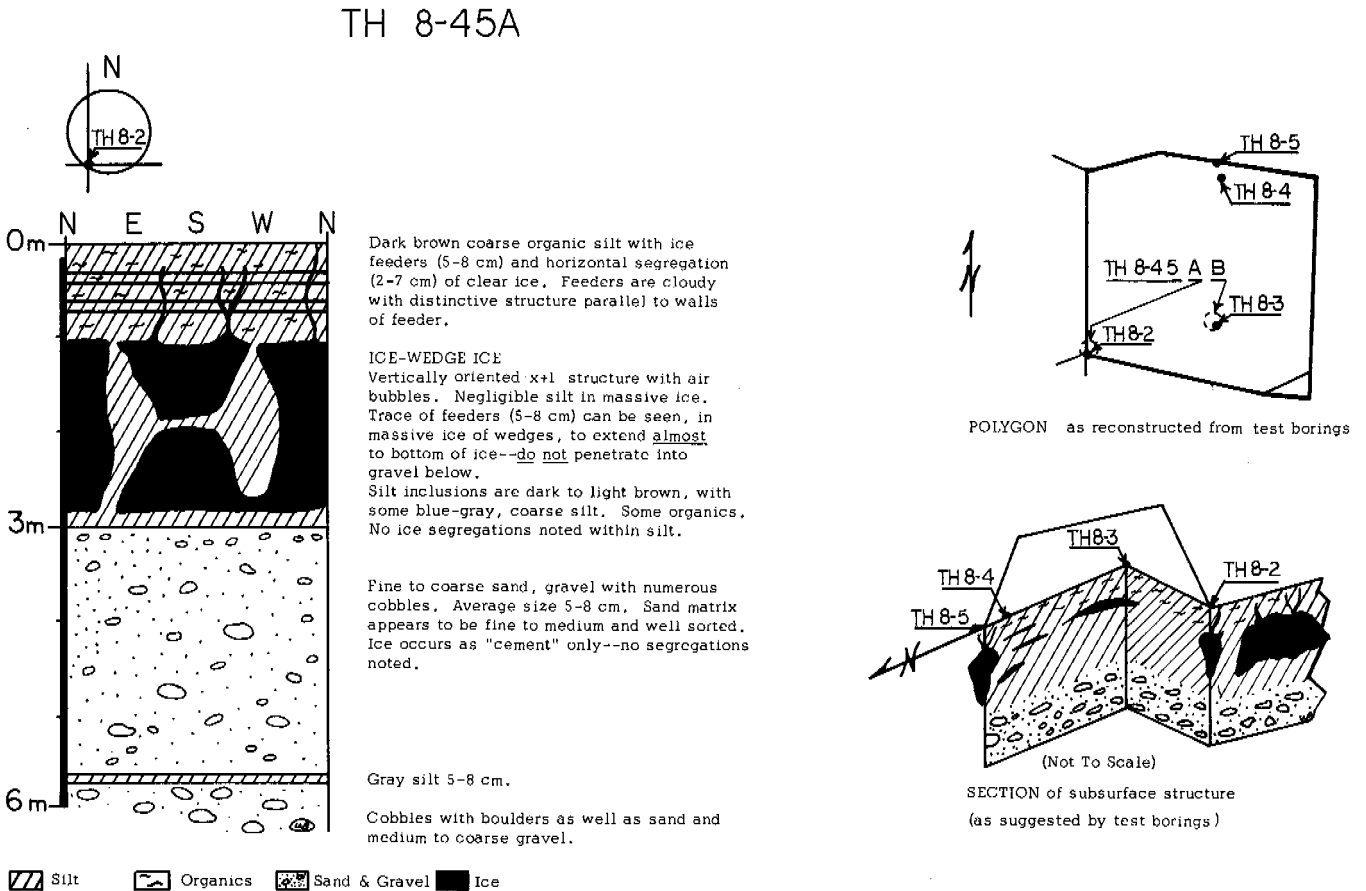


FIGURE 4 A cluster of boreholes were sunk within a visible "freeze polygon" at Shaw Creek Flats (upper right). Hole TH 8-45A at corner of polygon was large enough for an observer to descend into. His notes are reproduced at left. Core data from the other holes permitted drawing section seen at lower right.⁶

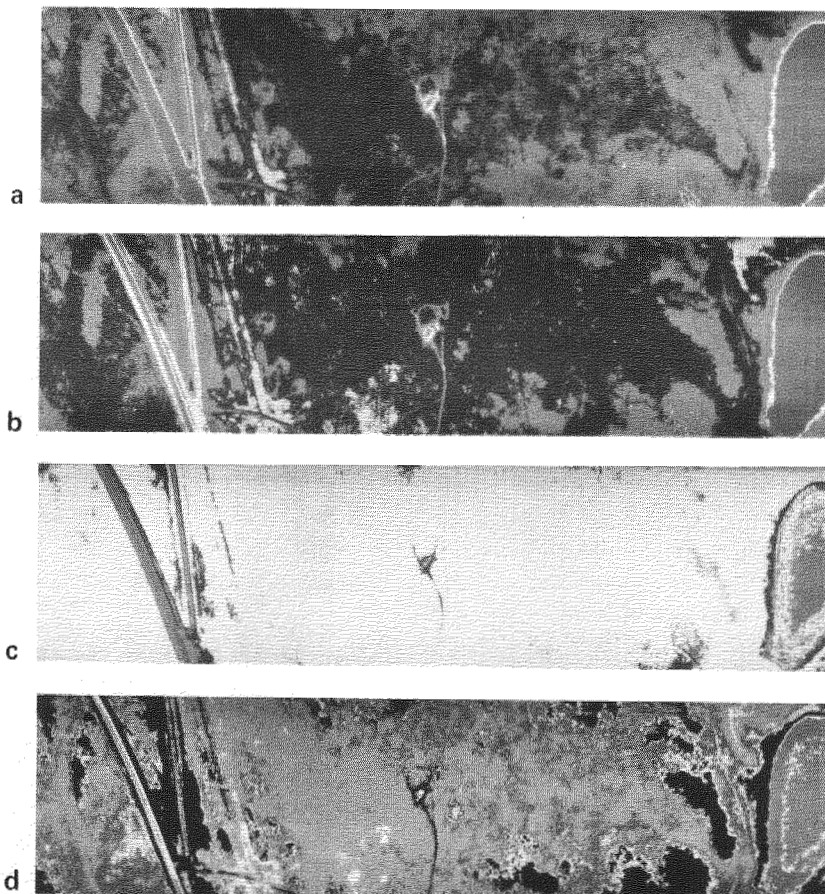


FIGURE 5 Shaw Creek Flats imagery taken at 0450 h on 28 August 1971 from an altitude of 230 m. (a) and (b) are standard 4.5–5.5- μm and 8–12- μm imagery, respectively, obtained with a quantitative scanner; (c) and (d) are the ratio and product imagery, respectively. Open water was used as a datum, i.e., the signal levels over the water for both the (a) and (b) outputs were made equal. It is clear from examination of (c) that the ratio signal does reduce the effect of purely thermal anomalies substantially as can be seen in the large expanse of uniform gray associated with areas of essentially similar emissivities. When this is compared with either (a) or (b) imagery or, especially, with the product imagery (d), anomalies due primarily to thermal differences are revealed. Partial polygonal structures, for example, are obvious in the product imagery whereas on Aerochrome Infrared photography of the same site (not shown) they are not. (Scale 1:9 000)

imagery does appear to map areas of equal emissivity essentially independent of temperature effects. When compared to the single channel imagery and, especially, when compared with the product imagery of the same area, effects due to temperature anomalies are outlined.

In studying both high- and low-altitude Aerochrome Infrared and standard color photography of the area (Figure 6a), little or no evidence of typical ice-wedge polygons is discernible. Standard 8–12- μm thermal infrared imagery (Figure 6b) and product imagery (Figure 6c), however, show partial polygonal structures in the same area. Comparison of product imagery with single-channel 8–2- μm imagery demonstrates that the former enhances polygonal structures.

The polygonal structures evident in the thermal imagery are located in old stream channels. These structures are believed to be surface expressions, in the form of thermal gradients, of near-surface ice-wedge polygons similar to the reconstructed polygon in Figure 4.

CONCLUSION

From the theoretical calculations, the authors believe that, under a limited but reasonable set of natural conditions, it is

possible to sense the thermal effect on the surface of engineeringly significant quantities of ice as they are manifested in the upper 2.5–3 m of permafrost. This appears to be borne out by the field work, from which the following conclusions were drawn.

1. Single-channel IR scanning has a significant but undeveloped potential to locate and identify massive ice in permafrost. Predawn imagery appeared to have the greatest significant information. Polygons undetected by conventional reconnaissance means are, on the basis of these limited experiments, apparently detected by IR scanning. The authors believe that the existence of polygons, with their associated ice wedges, may be determined with greater confidence than heretofore possible in areas of discontinuous permafrost or in areas where there is no visible surface expression, with the techniques herein described.

2. Dual-channel IR scanning offers even greater capabilities of identifying such ice masses. The availability of this capability to engineers who must engage in arctic construction in such areas is considered by the authors to be of value. By obtaining a product of the two signals and mapping the resultant signal, images of polygonal structures appear to

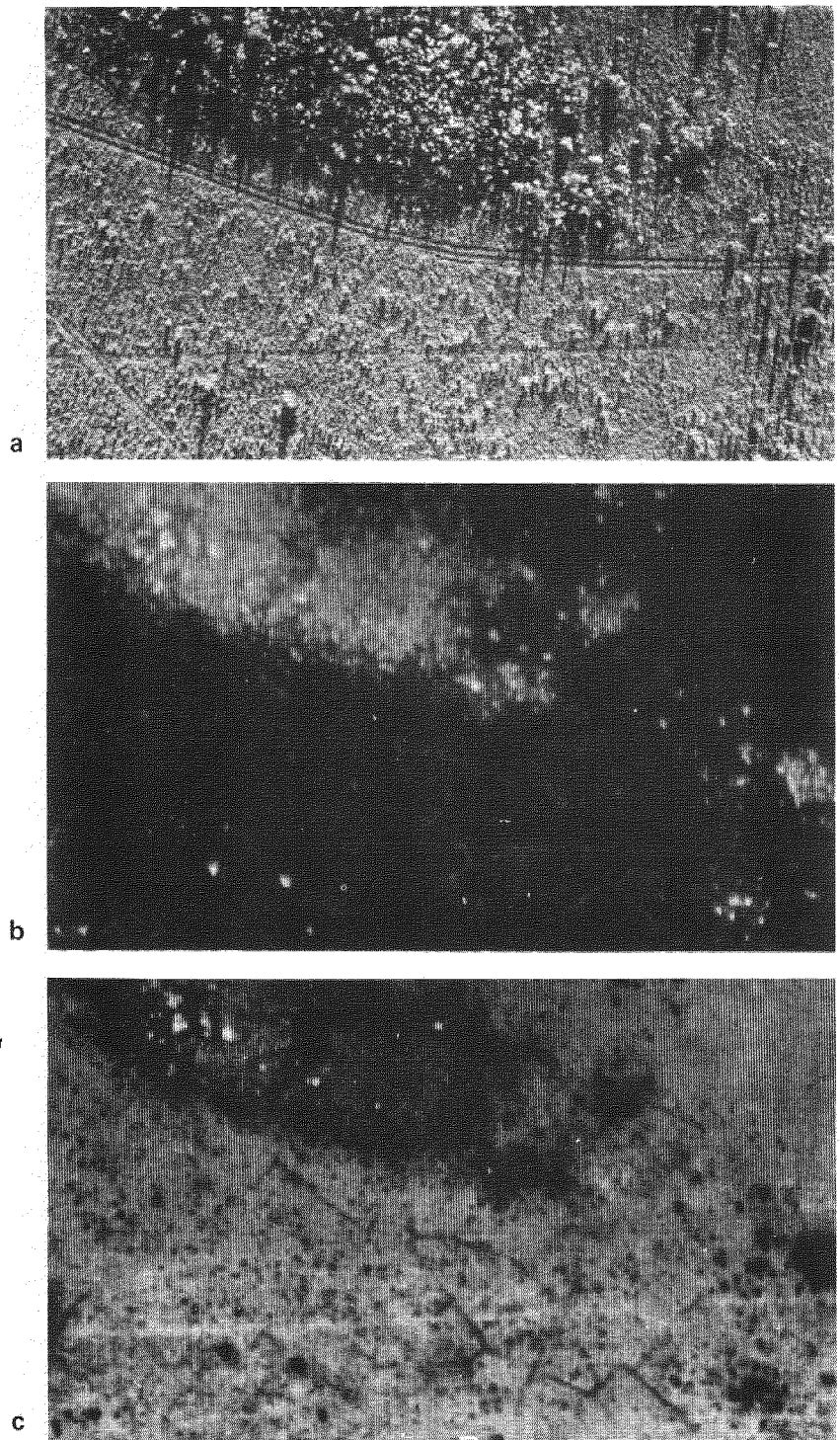


FIGURE 6 (a) Low altitude vertical Kodacolor X (black and white rendition) photograph of an area at Shaw Creek Flats, Alaska, taken on 10 September 1971 at 1600 h (original scale 1:400); (b) standard 8–12- μm thermal imagery taken at 2200 h on 27 August 1971; and (c) product imagery of this same site. The polygonal structures observed in (b) and very much enhanced in (c) are believed to be associated with near-surface ice wedges; these polygons are essentially invisible in (a), although careful examination of the distribution of phreatophytes (*Salix* sp.), seen as gray patterns in the photo, suggest the polygonal structures observed much more clearly on the product imagery.

be enhanced significantly. By taking a ratio of the same two signals, imagery approaching an emissivity ratio map is produced in which the temperature function is significantly attenuated. A comparison of the product and ratio maps suggests that the polygonal structures seen are thermal anomalies and not anomalies due to surface emissivity change.

ACKNOWLEDGMENTS

The authors wish to gratefully acknowledge the help of the following persons who assisted in the program: Ralph Migliaccio and Ray Kreig of R&M Engineering and Geological Consultants, Fairbanks; Frank Whaley, Jr., Alaskan bush pilot extraordinaire, who piloted our instrumented aircraft; and Carl Miller, Executive Vice President of Daedalus Enterprises, Inc., who operated the scanner system and field

processed the imagery for use by the ground party. Additionally, we would like to thank Mr. Gordon W. Greene of the U.S. Geological Survey for copies of that office's Aerochrome Infrared photography and IR imagery of the pipeline route.

This research was supported by the Advanced Research Projects Agency (ARPA order #1722 of 31 March 1971) of the Department of Defense and was monitored by ONR under contract No. N00014-71-C-0396. The views and conclusions contained in this document are those of the authors and should not be interpreted as representing the official policies, either expressed or implied, of the Advanced Research Projects Agency or the U.S. Government. Reproduction in whole or in part is permitted for any purposes of the United States Government.

REFERENCES

1. Buettner, K. J. K., and C. D. Kern. 1965. The determination of infrared emissivities of terrestrial surfaces. *J. Geophys. Res.* 70:6.
2. Hsu, S. T. 1963. *Engineering heat transfer*. Van Nostrand, Princeton, New Jersey. Table A-3.
3. Kelley, J. J., Jr., and D. F. Weaver. 1969. Physical processes at the surface of the arctic tundra. *Arctic* 22:425-437.
4. Nakano, Y., and J. Brown. 1971. Effect of a freezing zone of finite width on the thermal regime of soils. *Water Resour. Res.* 7(5):1226-1233.
5. Nakano, Y., and J. Brown. 1972. Mathematical modeling and validation of the thermal regimes in tundra soils, Barrow, Alaska. *Arctic Alp. Res.* 4(1):19-38.
6. R&M Engineering & Geological Consultants. 1969. Fairbanks, Alaska, soil maps and soil borings data, from Valdez to Prudhoe Bay. Alyeska Pipeline Service Co.
7. Schneider, P. J. 1963. *Temperature response charts*. J. Wiley & Sons, New York.
8. U.S. Army CRREL. 1962. Ground temperature observations, Ft. Yukon, Alaska. Technical Rept. #100. U.S. Army Cold Regions Research and Engineering Laboratory, Hanover, New Hampshire.
9. Weedfall, R. O. 1963. Variation of soil temperatures in Ogotoruk Valley, Alaska. *Arctic* 16:181-195.
10. Williams, G. P. 1968. Thermal regime of a *Sphagnum* peat bog. In *Proceedings of the third international peat congress*. Quebec, Canada.

NOTES

[1] The data presented in this paper were taken from an altitude of 250 m above the terrain; therefore, the atmospheric absorption was assumed to be negligible. The sky radiance reflected by the surface can be expressed as the difference between two terms—one depending on the magnitude of the sky radiance itself, which is invariant during scanning, and the other on the product of the surface emissivity and the sky radiance, which is negligible in comparison with the energy emitted by the surface. This, the energy received at the sensor is the sum of only two terms—the energy emitted by the surface and a constant term related to the sky radiance. Neglecting this constant sky radiance term will not affect the interpretation of spatial patterns formed on the imagery.

[2] Over the temperature range recorded ($\Delta T = 4^\circ\text{C}$), the ratio $F_{4-5}(T) : F_{8-12}(T)$ only varied by approximately 2 percent and, therefore, was assumed to be constant. This constant term will not affect the interpretation of spatial patterns on the imagery.

VII

PRINCIPLES OF CONSTRUCTION IN PERMAFROST REGIONS

Principles of both design and construction; engineering criteria; active and passive construction practices; case histories, environmental protection

ENGINEERING DESIGN AND CONSTRUCTION IN PERMAFROST REGIONS: A Review

Kenneth A. Linell

U.S. ARMY COLD REGIONS RESEARCH AND
ENGINEERING LABORATORY
Hanover, New Hampshire

G. H. Johnston

NATIONAL RESEARCH COUNCIL OF CANADA
Ottawa, Ontario

INTRODUCTION

In North America, development of the permafrost regions is advancing at a rapidly accelerating rate. This creates increasingly intense pressure on the technical community to formulate engineering design and construction principles that will accurately ensure predictable behavior and minimum costs. In North America, research to develop such criteria was started in the 1940's. This has provided an invaluable base and fund of fundamental knowledge to meet this construction need. In the past decade, entirely new construction situations, new and more stringent requirements for structural and environmental stability, and the continuing increase in knowledge of the nature of permafrost have contributed new intensity and scope to the challenge and have provoked especially intense research and investigation efforts. The extent of current activity in applied permafrost research is reflected by the fact that about one third of the total North American papers submitted to the Second International Permafrost Conference appear under Session VII. Also, a large percentage of papers in other sessions are clearly closely supportive of engineering needs.

Because of the large volume of information currently available on construction in permafrost regions, it is impossible to reference all significant literature in this paper. Therefore, references herein have been selected only to be indicative of the current state of the art.

SITE SELECTION AND INVESTIGATION FOR ENGINEERING PURPOSES

The importance of proper selection and investigation of a site or route for construction in permafrost areas, by reconnaissance and detailed site, environmental and material availability studies, cannot be overemphasized. Unfortunately, the fact that rational design requires an adequate base of factual knowledge and that this is doubly important in permafrost regions has sometimes in the past been overlooked or ignored. The record of the past shows many failures of construction on permafrost from lack of this information base. Consequences of encountering unexpected conditions during construction include lost construction time schedules, improvised foundation redesign, carrying of

work unexpectedly into severe fall and winter weather, very large cost increases, delay in beneficial occupancy, heavy repair and maintenance expenses, and disruption of operations. During the last several years, however, recognition of the fundamental need for adequate area, route, and site studies prior to engineering design and construction decisions has increased. Existing and new techniques for obtaining the required surface and subsurface information have been increasingly employed on new construction.

Investigational techniques may be divided into two categories: indirect, including aerial photographic and geophysical methods, and direct, including drilling and sampling and allied techniques.

Use of conventional aerial photographic techniques for terrain and site evaluation in permafrost areas was extensively investigated beginning more than two decades ago and results were reported by Frost.⁵² The U.S. Army Corps of Engineers has included summaries of these techniques in two engineering manuals.^{175,176} The discovery of vast oil and gas and other mineral resources in northern North America in the last few years has greatly spurred the widespread practical use of these aerial photographic techniques. Very extensive application of aerial photographic methods is now being made for both route selection and detailed route and site examination in combination with surface and subsurface investigations on the proposed Alaska pipeline, on several proposed pipelines in northern Canada,¹²⁵ and on associated transportation systems and on other projects. In current practice, airphoto analysis is used not only for reconnaissance evaluation of geological, soils, vegetation, drainage, accessibility, and similar factors but also to assist in detailed layout of roads, buildings and other facilities and in detailed engineering evaluation of permafrost conditions in relation to these projects. Engineering design and construction problems may often be enormously simplified by placing the facility in the most favorable location.

An interesting special case is the use of aerial photographs taken during the thaw-melt period to determine topographic positions of maximum snow accumulation, especially from snow drifting. This approach was used by the Arctic Construction and Frost Effects Laboratory in Greenland in the 1950's for selecting route locations for roads and more recently within the continental United States to minimize

facility snow removal problems. Granberg, in a paper prepared for this conference, describes a technique for indirect mapping of snowcover to aid in predicting localized occurrences of permafrost.⁶³

As outlined by Haugen *et al.*,⁶⁸ the current Earth Resources Terrain Survey (ERTS) program promises to give a wealth of information on terrain and permafrost conditions in Alaska and Canada that will be useful for engineering purposes. Information will be obtained on any given location every 18 days on such surface details as vegetation, snow and ice covers, ground temperatures, and geomorphic and other evidences of permafrost, as well as stream levels and sedimentation patterns, forest fires, etc.

Urgent need exists for new geophysical exploration equipment and techniques that will permit large areas or distances (such as for pipelines and roads) to be covered quickly, conveniently, and economically on a continuous basis, with positive capability to detect problem ice-rich locations and isolated permafrost and ice bodies under specific sites, especially in areas of sporadic permafrost. Electromagnetic sensing systems, both airborne and surface-operated and capable of yielding subsurface information to depths of 15 m or more in frozen soil, have been used on an experimental basis. Hoekstra,⁷¹ Frischknecht and Stanley,⁴⁸ and Bertram *et al.*¹³ have discussed technical approaches in this area. Such equipment is capable of distinguishing, with depth, materials such as soils, ice, and rock having different electrical properties. Although not yet routinely used on major projects, such equipment can be used operationally for some purposes and is in a state of rapid and continuing development. As reported by Garg⁵⁶ and Hunter⁷³ in Session VI, both resistivity and refraction types of conventional seismic systems have utility in permafrost areas. Roethlisberger¹³⁹ has recently summarized the state of the art of seismic exploration in cold regions. Experiments have been performed with acoustic reflection-type sounding equipment with inconclusive results thus far; however, additional research is in progress.

Special equipment and techniques for subsurface exploration and sampling of frozen soil (including clean gravels well bonded by ice), ice, and bedrock by core drilling are available, although improvements over the last decade seem to have been less rapid than in the previous decade. Sellmann and Mellor are summarizing the current state of the art in a monograph.¹⁵¹ The frozen condition may actually offer a distinct advantage in gravels or in fractured or weathered rock provided the material is well ice-bonded. Lange has described for this conference techniques by which these materials can be sampled effectively.¹⁰⁰ Frozen bedrock should never be assumed free of ice if thawing of the rock is possible and if the consequences of undetected ice in the rock would be significant. McAnerney has described a case in which thaw sink holes and subsurface drainage channels

developed in bedrock thought free of ice on basis of non-refrigerated core drilling.¹¹⁷

Though northern development has greatly spurred employment of special equipment and techniques, refrigerated core drilling should be used much more than it is, as undisturbed frozen cores permit visual examinations and accurate measurement and tests of almost completely undisturbed materials. As shown by Smith *et al.*, however, a small degree of disturbance may be present even in frozen cores which has to be taken into account in precise analyses.¹⁶⁰

In fine-grained frozen soils above -4°C drive sampling is feasible, as has been described by Kitze,⁹¹ and is often considerably cheaper, simpler, and more rapid. Samples are structurally disturbed, but still permit accurate detection of ground ice and measurement of moisture content of specimens. Test pits and power-driven augers of various sizes are also widely used to obtain both disturbed and undisturbed samples and for *in situ* examination of the frozen soil profile.

Restrictions against surface movement and operations on the tundra in summer in order to avoid damage to the arctic environment have resulted in use of helicopters to move exploration rigs from location to location. The rigs have even been mounted on the undercarriage of the helicopter itself.

Both thermistors and thermocouples are used for ground temperature measurements, the choice depending on the degree of precision required.¹⁶¹ Diodes have also been used occasionally as sensors to measure ground temperatures. Groundwater table measurements are often difficult to obtain on a routine basis, except in summer. Some experiments have been made with systems that use air displacement (Gilman⁵⁹) or kerosine in the groundwater well to prevent freezeup. Methodology of groundwater measurements in permafrost regions is discussed in greater detail by Williams and van Everdingen in their review paper for Session V. Under the stresses encountered on construction projects, soil moisture cells may not always perform reliably.⁷

In both the United States and Canada an extension of the Unified Soil Classification System is in use in detailed or simplified form for engineering classification of frozen material.^{107,130,182} During the last decade, significant effort has been applied to development of methods of field and laboratory testing of foundations materials for engineering analysis. For example, Crory,³³ Luscher and Afifi,¹¹¹ and Smith *et al.*¹⁶⁰ have reported studies to evaluate thaw-consolidation behavior of foundations. Again, Sayles,¹⁴⁸ Stevens,¹⁶⁴ Ladanyi and Johnston,⁹⁵ and Garg⁵⁶ have carried out studies to measure the mechanical properties of frozen foundation materials useful for engineering analyses, such as strength, creep, and dynamic response characteristics.

For special structures and facilities and where permafrost conditions are particularly complex, full-scale field tests are necessary and should be carried out in advance of construction to provide information for evaluations of the

interaction between the atmosphere, the structure, and the ground.

PRINCIPLES OF ENVIRONMENTAL ENGINEERING AND PROTECTION FOR PERMAFROST TERRAIN

In North America, great public pressure now exists for preservation of the natural environment as well as for correction of pollution and environmental degradation effects where these have been allowed to develop. In the United States, this pressure is backed by laws at the federal level and increasingly at lower governmental levels that require a detailed evaluation and statement of the environmental impact of the construction or facility be submitted to show its acceptability before any new construction is started. In Alaska, these restrictions are further supplemented by a prohibition against operations on the natural tundra surface in summer because experience has shown that even a single vehicle pass may result in uncontrolled permafrost degradation and erosion where conditions are especially fragile. In Canada, similar legislation with regard to pollution and environmental impact is in effect or is being promulgated; Land Use Regulations must be complied with by anyone going anywhere on the lands north of 60° and a specific land use permit is required for every activity that involves going on the surface of the land at any time of the year.

The severe cost and operational penalties that may be encountered if a facility is not environmentally stable serve as further constraints on the engineer. The impact analysis cannot be limited to the structure itself; the total impact of all activities and environmental changes relating to the project must be considered. At a special symposium of the Royal Society of Canada⁶⁷ on "The Tundra Environment" some of the factors to be considered were discussed. The fragile nature of the ground thermal regime and the effects that natural and man-made changes can have on the environmental conditions under which permafrost exists have been described by Watmore,¹⁸⁶ Mackay,¹¹³ and Gold *et al.*⁶⁰ among others. Wein and Bliss¹⁸⁹ have presented a summary of the effects and of methods of coping with them. Changes in vegetation, drainage, and water quality or temperature will affect animal and aquatic life. Erosion may not only destroy utility of land for future generations but may add siltation in streams, which affects aquatic life. Spills of oil or other substances may destroy many types of vegetation. Wildlife migration patterns may be changed.

In the United States, the need to incorporate environmental protective measures into construction on permafrost was recognized by the U.S. Army Corps of Engineers as early as World War II, and positive control requirements began to be incorporated into construction specifications in Alaska many years before the current public pressures and legal restrictions existed. Construction on difficult

permafrost terrain at Kotzebue, Alaska, in 1957 as described by Jensen⁷⁸ is a case example. In Canada the Division of Building Research of the National Research Council, as the primary research agency for the Canadian construction industry, translated the results of research and field experience into technical guidance.

These efforts have led to the current situation as described by J. Brown¹⁵ of greatly accelerated effort by scientists and engineers under sponsorship of both industry and government to develop both better fundamental understanding and better technology for utilization of permafrost terrain.

Much research to develop practical methods for predicting thermal effects in construction has been carried out by many investigators and many of the useful results have been summarized in manual form by the U.S. Army.¹⁷⁸ Sanger¹⁴⁵ has been very active in developing computation methods useful for engineering purposes. Research in use and maintenance of vegetative cover to control degradation of permafrost areas is in its infancy, but some relationships are known, as given in papers by Linell,¹⁰⁵ Heginbottom,⁶⁹ Brown *et al.*,^{16,17} and others. Of particular interest is the indication that in borderline permafrost areas, such as Fairbanks, Alaska, a living cover of low vegetation cannot by itself be relied upon to control permafrost degradation, but in a colder area such as Inuvik, N.W.T., it can be sufficient.

The practical effectiveness of modifying heat exchange at the ground surface on a long-range basis by control of surface color has been demonstrated in pavement applications as reported in papers by Aitken,¹ Fulwider and Aitken,⁵⁴ Berg and Aitken,¹² Wechsler and Glaser,¹⁸⁸ and Kritz and Wechsler.⁹³ In-ground insulation has been found in several Corps of Engineers studies^{9,11,55,159,181} to be effective in slowing or delaying permafrost degradation in marginal permafrost areas, but not in preventing it. Esch,⁴³ in carrying out similar studies, has thus far found similar short-term effectiveness of insulation in degradation control; however, the test duration has not yet been long enough to show long-term behavior.

Numerous research studies have been carried out and/or are currently in progress on environmental engineering for construction of hot and cold pipelines and on effects of, and remedial measures for, oil and gasoline spills in permafrost areas.

FOUNDATION DESIGN AND CONSTRUCTION

Current concepts of foundation design on permafrost are outlined in a manual prepared by the U.S. Army,¹⁷⁷ and Sanger has published a monograph on foundations of structures.¹⁴⁶ On materials identified as thaw-stable under the extension of the Unified Soil Classification System developed for frozen soils,^{107,130,182} foundation design is commonly identical with temperate zone practice, even though founda-

tion soils are frozen below the foundation level. Difficulty sometimes is encountered, however, in determining whether or not clean granular soils containing ice will consolidate after thaw, and elaborate sampling, testing, and compaction experiments have sometimes been conducted in an effort to resolve this question. Terzaghi reported more than 20 years ago that shrinkage or settlement per unit depth of thaw of coarse-grained frozen soils at a site in the vicinity of Fairbanks, Alaska, not containing buried bodies of ice, decreased from an upper limiting value close to the ground surface to almost zero at a depth of about 9 m.¹⁷⁰ He concluded that settlement of the surface under these conditions is by no means necessarily negligible. However, it can also be concluded that settlement of foundations supported at depth in such materials may be entirely tolerable; this is confirmed by observations of thaw settlement of actual construction in the Fairbanks area.¹⁸⁰

On thaw-unstable foundation materials, unlimited challenge and opportunity for design ingenuity are presented. Here design to ensure preservation of the permafrost is by far the most commonly used foundation approach for permanent construction. Normally, acceptance of permafrost degradation, and design therefor, is used only when the foundation materials are thaw stable or where only expedient or short-term construction is involved. Notable exceptions to this approach have been the designs used for the sand fill dikes at the Kelsey and Kettle Generating Stations^{19,82,112,115} and the foundations for several buildings at Thompson in marginal permafrost in northern Manitoba. Removal and replacement of unacceptable materials has been used extensively by the Alaska District of the Corps of Engineers at Fairbanks, Alaska where silts up to about 6 m thick overlay thaw-stable sands and gravels. Similar procedures have been used occasionally in northern Canada to obtain suitable bearing for building foundations.^{65,149} Excavation of ice-rich materials to limit settlements to an acceptable amount was carried out for the Kettle dikes.¹¹⁵ Except for steam or cold water thawing of overburden for gold placer mining operations in Alaska and the Yukon Territory, Canada, no documented case is known to the authors where prethawing to completely eliminate permafrost has been used in North America. However, based on water and steam thaw tests and recommendations by Terzaghi,¹⁷⁰ prethawing of sandy gravels to a depth of 9 m below the original ground surface has been used by the Corps of Engineers in the Fairbanks region with and without blasting as described by Waterhouse and Sills¹⁸⁵ to ensure consolidation of the looser upper strata in advance of foundation construction.

It is widely accepted that structures that cannot tolerate differential movements or seasonal vertical displacements must be supported on permafrost rather than on or in the annual zone of freeze and thaw. However, for structures that have very low movement tolerances, designers should be aware that some seasonal movements may occur in

permafrost to at least as deep as 10 m and placement to as deep as 20 m may be required.¹⁴

The time- and temperature-dependent properties of frozen soils that are subjected to loading are important considerations in foundation design. Creep displacement and decrease in strength with increase in ground temperature may be particularly significant. Long-term strengths may be as much as an order of magnitude less than the strength of a soil subjected to a short-term or instantaneously applied load. These aspects have been covered in Session IV and are referred to in the following sections. From a study of building foundations in Canada's permafrost region, R. J. E. Brown has concluded that "anything can be built in any soil and permafrost conditions, provided the conditions are investigated thoroughly and proper design precautions are taken."¹⁸

Footings

Spread footings, continuous footings, raft or mat foundations, or post and pad construction have been successfully used on thaw-unstable as well as thaw-stable permafrost at such diverse locations as Churchill, Manitoba, Canada³⁹; Fairbanks, Alaska^{34,134,180}; Fort Yukon, Alaska; Pangnirtung, N.W.T., Canada; and Thule, Greenland, with careful planning for structural and thermal stability as appropriate for the foundation conditions. Principles and techniques for design of footings on permafrost have been expressed in manual form by the Corps of Engineers, including such aspects as creep and dynamic response analysis.¹⁷⁷

Thermal control provided for footing-type foundations to maintain permafrost usually consists of either a simple ventilation space between the structure and the ground surface or one of various types of duct systems. Costs of providing ducted foundations easily become excessive unless care is exercised, however. Duct-ventilated gravel fills placed on the ground surface are receiving increasing use in Canada to support slab-on-grade construction, e.g., for aircraft hangars, maintenance garages, and heated oil storage tanks. These vary from simple systems where small diameter pipes are placed in the fill and depend on natural air flow during the winter to remove ground heat, to more complex systems incorporating ventilating fans to ensure adequate air flow. One such system utilizing 1.1-m-diameter pipes on 2.6-m centers has been proposed for a huge railroad maintenance building on Baffin Island.⁶⁴ In the United States, the U.S. Army Corps of Engineers began to investigate and use this type of construction in the later 1940's¹⁰⁸ and has since made numerous installations of many types and magnitudes in areas of both warm and cold permafrost. Experience has shown that duct systems placed below the ground level tend to collect ice and sediment, which block air flow, causing serious maintenance problems.¹⁷⁴ Steam thawing is required to open frozen ducts, which, in turn, may cause serious

ground thermal disturbance. Instead, it is desirable that ducted foundations be sufficiently elevated above, or positioned relative to, the surrounding terrain so as to be self-draining in summer of any accumulation of ice and snow from the preceding winter. It is also essential that ducts be carefully designed to provide proper duct diameter and spacing. Stacks are used when necessary to increase natural airflow or to raise intakes and outlets above snow accumulation levels. Mechanical blower systems to increase volume of air circulation in ducts are generally avoided because of costs, increased mechanical complexity, and the dependence on alertness and care in operation that they introduce. Mechanical refrigeration systems are employed for maintenance of permafrost only in special problem situations or for remedial purposes.

Pile Foundations

Pile foundations incorporating an air space between the structure and ground surface are the most common type of design for permanent construction on thaw-unstable permafrost. Creosoted wood and steel pipe or H-section piles are the most commonly used types. Precast concrete piles are used much less frequently in permafrost in North America and cast-in-place concrete piles only occasionally. Cast-in-place concrete piles have been used at Thompson, Manitoba, where small islands of permafrost were encountered⁶¹; the designs assumed no support to a depth equal to twice the thickness of permafrost and allowance was made for negative skin friction when the permafrost thawed and the soil consolidated. Cast-in-place concrete piles were also used at the Birch Hill Ski Lodge, Fort Wainwright, Fairbanks, Alaska. Where substantial frost heave forces are experienced, concrete piles with conventional amounts of reinforcement are easily cracked in tension, exposing the steel to corrosion. Cast-in-place piles, of course, have to cope with the problems of setting and strength gain of the concrete and of thaw and refreeze of surrounding materials in the permafrost zone.

Piles are placed either by slurring in an auger-drilled hole or by driving. Steam thawing is used only occasionally. Slurry may be the same soil as removed by the auger or concrete sand mixed with water. Use of carefully controlled high-quality backfill around the pile is one approach to increasing effective pile diameter under poor ground conditions. By avoiding excessively wet slurries, freezeback is hastened and made more positive in areas of warm permafrost. When piles exposed to below freezing temperatures are placed by slurring, an ice layer may form on the surface of the pile that may control the allowable tangential shear strength that may be developed. In marginal permafrost areas, circulation of refrigerant through tubing attached to the pile is commonly used to assure expeditious and positive freezeback of slurried piles unless the piles are installed in the

spring months (March through early June) when the ground is sufficiently cold to assure natural freezeback. Artificial refrigeration is not considered necessary where the mean annual ground temperature is -4°C or colder. In fine-grained frozen soils at temperatures down to about -4°C , both steel pipe and H piles have been installed by driving with diesel, vibratory, or other heavy hammers. Very extensive pile loading test programs have been carried out in Alaska by the U.S. Army Corps of Engineers, only part of which have been reported to date.^{7,31,32,35} Newcombe and Rowley *et al.*¹⁴¹ have performed pile tests at Prudhoe Bay, Alaska, and Inuvik, N.W.T., Canada, respectively, which extend available data into new soil and/or ground temperature conditions. The studies reported by Rowley *et al.* include the first results published in North America on lateral load tests of piles imbedded in permafrost.

Since effective adfreeze bond is the major variable affecting the realizable pile bearing capacity of non-end-bearing piles, many methods for increasing the effective skin friction or surface area or for maintaining values at high levels in the critical period of the year have been examined, including use of thermal piles. Thermal piles of various designs are in use, finding their greatest applicability in marginal permafrost areas where extra assurance of freezeback and/or maintenance of design adfreeze bond strength is needed. The most commonly used types have been the two-phase Long thermopile¹⁰⁹ (patented) and the single-phase Balch liquid-filled pile⁸⁰ (patented). Long recommends ring and helix types of thermal piles in combination with ground insulation as methods of maximizing pile capacity at competitive costs.¹¹⁰ Johnson⁸⁰ has studied thermal convection loops, which are thermal pile elements interconnected to provide loop circulation. Babb, Garlid, and Shannon have suggested a "tube-in-tube" concept in which a single phase liquid device is placed within a "cold storage" tube containing ethylene glycol solution in order to increase effectiveness. Reed has demonstrated the potential of forced air circulation piles.¹³⁶ U.S. Army Corps of Engineers practice is to neglect end bearing for piles of about 15 cm tip diameter or less; in larger diameter piles or caissons, end bearing is taken into account.¹⁷⁷

The need for protection of wood and steel piles in permafrost to prevent deterioration has been investigated. Examination of steel pipe and H-piles, installed for periods of 8–11 years at the U.S. Army CRREL, Alaska Field Station, showed that the length of pile imbedded in the permafrost was unaffected by corrosion and only insignificant effects on pile surfaces in the active layer were indicated by metal attack.¹⁴⁰ A study carried out by the Division of Building Research, National Research Council of Canada and the Eastern Forest Products Laboratory, Department of the Environment, Canada, on wood piles installed for a period of at least 10 years at Inuvik, N.W.T., showed that many of the locally cut spruce piles, some untreated and others pro-

tected by a diffusion process applied at the site, had superficial soft rot occurring mainly within the annual thaw zone.¹⁵⁰ All pressure creosoted Douglas fir piles and red cedar poles, treated with creosote by the thermal process, that were examined were in excellent condition. It was concluded that treatment of the local spruce is required and recommendations for improving the on-site treating procedure were made. It was also recommended that all important structures should be supported by pressure creosoted piles with extra heavy creosote treatment. Experience in Alaska and Canada shows that untreated poles used for communication and power lines may be destroyed by decay at the ground line in only a few years, even where the annual precipitation is low. Assuming that the portion of a timber member imbedded in permafrost will last indefinitely without preservative, only the portions extending above permafrost require decay-preventive treatment. However, no method exists for pressure creosoting only part of a member. Therefore entire members must be treated, including the portions to be imbedded in permafrost. Since a coating of creosote reduces the tangential shear stress that can be developed below that which would apply for bare wood, tangential adfreeze working stresses must be reduced accordingly.

Without question, a stable pile foundation can be constructed on any type of frozen soil regardless of the ice content, no matter how borderline the conditions, but each situation must be carefully investigated to ensure that all pertinent factors have been taken into account in order to obtain the most economical designs and satisfactory performance.

Ground Anchors

Construction of anchorages for footings, guyed towers, pipelines (either buried and empty or on slopes), and other facilities subject to uplift, thrust, or overturning forces is difficult and challenging because of the tendency for anchors in frozen ground to yield in creep, the risk of thermal instability in permafrost, and frost heave forces add to the normal structural loading.¹⁷⁷ Both the anchored structure and the anchor may be subject to frost heave and/or thaw settlement but to different degrees; therefore, the structure and the anchor must be analyzed as a system. Anchors for power transmission towers commonly must be very economical to construct because of the large number usually involved, yet adaptable in the field to a wide variety of subsurface conditions; the cost of individual subsurface explorations in advance at each tower location is often prohibitive.

Types of anchors that have been used or investigated for construction in permafrost include gravity, grouted rod, pile (ordinary and corrugated), helical screw, plate (various), belled, and metal expanding. In the 1950's, molten lead was used to grout into frozen bedrock the anchors for a 480-m

radio antenna at Thule, Greenland, because of uncertainty concerning the behavior of Portland cement grout under the very cold ground conditions. Later, gravity anchors relying on the weight of footings and overlying earth fill were used with good results for an antenna in the same region subject to very high wind forces. In the 1960's, anchorage needs for arctic and subarctic transmission lines, oil field developments, and other construction resulted in extensive programs of study by such agencies as CRREL; the Division of Building Research, National Research Council of Canada; Manitoba Hydro and its consulting engineer agent, Teshmont Consultants Limited; Ontario Hydro; and Golden Valley Electric Assn., Fairbanks, Alaska.¹⁶³ These studies were primarily field investigations but also included some laboratory research. Still later, John A. Shuster of Woodward-Lundgren Associates performed field studies in the North Slope area of Alaska, correlated to laboratory triaxial creep tests; these involved six different anchor types in frozen and unfrozen Alaskan soils and included field tests in very cold permafrost. Crory and Tizzard³⁶ have measured rates of creep deformation in field tests extending longer than 1 year, and Tizzard and Lorber¹⁷³ in laboratory studies have shown that failure of plate anchors occurs by punching below a depth equal to six times the plate diameter and by lifting out of a cone of frozen material above this level. This generally agrees with failure behavior observed by Baker and Kondner in unfrozen soils.⁸ Crory and Tizzard have also shown that ordinary commercial screw-in-type anchors cannot be installed by direct screwing into hard-frozen silt without breaking and have developed criteria for long-range holding capacity of anchors.³⁶ Johnston and Ladanyi have investigated in detail the creep performance of grouted rod anchors in marginal permafrost.⁸⁵ Jonassen has described a test program conducted by Manitoba Hydro to evaluate a variety of anchors installed in marginal permafrost, including power-installed screw anchors, grouted rod anchors, belled, Malone, plate, and expanding anchors, for the 880-km-long Nelson River HVDC transmission line.⁸⁶ Reinart reporting on further studies for design of foundations for the Nelson River line concluded that Portland cement grouted anchors provided the most cost-effective solution for the ground conditions there encountered (nonpermafrost to marginal permafrost with subsurface materials varying from bedrock to fat clay containing ice).¹³⁸ However, such factors as the cement type and grout temperature had to be extremely carefully controlled. About 16 000 grouted rod anchors (15 cm diameter) were installed by over burden drilling methods on this project; some were as much as 27 m in length. Construction aspects of the Nelson River line, erected despite formidable climatic, logistic, and terrain problems, are described by Barry and Cormie.¹⁰

Shallow depth expedient anchors for tying down tents or other temporary facilities have also been investigated by Crory and others. A simple light-weight device for inserting

and recovering such anchors has long awaited successful development. Kovacs *et al.* have summarized available information on both expedient and permanent types of anchors for both frozen and unfrozen materials.⁹²

Control of Frost Heave

In field measurements of frost-heaving forces at Fairbanks, Alaska, average maximum adfreeze bond stresses as high as 413.7 kN/m² have been measured on uncoated steel pipe piles in slurried silt backfill.³⁵ The stress would be higher except for relaxation of stress resulting from creep. Since 413.7 kN/m² is an average value over the area of adfreeze within the annual frost zone, higher unit values undoubtedly were developed in the coldest parts of the adfreeze zone. Unless such forces are anticipated in the design, destructive and progressive frost heaving of footings, piles, towers, walls, and other structures may occur. These displacements are often more apparent when an unheated exterior porch, loading slab, or building extension experiences differential frost heave with respect to the main structure.

The U.S. Army Corps of Engineers has summarized available techniques for controlling frost heave and frost thrust.¹⁷⁷ When the structure is supported on top of the annual thaw zone the foundation readily returns each summer to its original position. However, when a fixed foundation is used that might be subject to progressive jacking, frost action effects may be controlled by providing sufficient anchorage in permafrost so that, together with structure loading on the foundation, frost-heaving forces are completely counteracted or by isolating foundation members from uplift forces by various means.

Anchorage of piles or footings may be achieved by providing sufficient imbedment in permafrost. The old engineering rule-of-thumb that the length of piles imbedded in permafrost should be twice the depth of the annual frost zone has been shown to be unreliable. Instead each case is analyzed on its own merits, but a minimum depth of imbedment in permafrost of 3 m is normally considered adequate. When the anchorage approach is used, care should be taken to ensure that structural members (such as concrete piles) will not be cracked or broken. Installing wood piles butt down has been found to limit frost heave movement, but some upward displacement does occur before full resistance is developed. Heave force isolation has been successfully used since 1945 for bench mark and pile isolation^{6,81} and can be applied to footings and other construction. In one of these heave isolation schemes developed in the Arctic Construction and Frost Effects Laboratory, the pile or foundation member is cased, wholly or partly, through the frost zone. The annular space between the pile and casing is then filled with an oil-wax mixture of sufficiently thick consistency to prevent soil, water, or other materials from entering the annular space. To prevent the

casing from being jacked progressively out of the ground by frost action, a plate or flange is attached at the bottom of the casing. To avoid the difficulty and cost involved with use of casings a premixed backfill of soil, oil and wax has also been used by CRREL without casing to reduce transmitted frost heave thrust in the upper part of the annual frost zone to acceptable values. Surface coatings such as heavy creosote or red lead reduce the heave force transmitted but are not relied upon for permanent control of heave. Tar paper or plastic film wrappings do not guarantee even temporary effectiveness, although they have sometimes helped under favorable conditions.

Foundations near and in Water Bodies

Foundations for bridges over water bodies or for port and waterfront construction in permafrost areas tend to involve especially difficult foundation problems because the permafrost conditions are substantially altered near and under the water, especially in borderline permafrost areas. The presence of permafrost may be irregular in such locations and where permafrost does exist its temperature tends to be warmer. Investigations conducted in the Mackenzie River Delta have indicated the distribution of permafrost under and adjacent to water bodies and the effect of channel movements.^{83,84,156} Unfrozen highly saline strata may be encountered, especially in coastal locations. As indicated by the studies reported to this conference by Carlson, Kane and Bowers,²⁴ Sherman,¹⁵² and Kane and Slaughter,⁸⁸ water moving in unfrozen zones beneath and adjacent to the water body may cause a very complex and variable thermal regime pattern. For these reasons highway and railroad bridge and wharf foundations in permafrost areas have been a continuing source of difficulties.

Piles are the most common type of bridge support. Because permafrost conditions tend to be borderline at water bodies, however, little or no capacity for natural freezeback of piles may be available and the effective tangential adfreeze bond strength may be small. Because of uncertain, incomplete, or weak freezeback, the frequency of serious frost heaving of pile bridge foundations has been very high. Péwé and Paige¹²⁹ have reported that frost heave of wood piling on bridges of the Alaska Railroad has reached as much as 35 cm/year, with serious changes in track elevation requiring reduction of train speed to avoid uncoupling of cars or shifting of cargo.

CRREL, the Alaska Department of Highways, and the U.S. Department of Transportation have recently engaged in a cooperative research study of bridge foundations in permafrost near Fairbanks, Alaska. In his analysis to date, Crory has stressed the need to carefully delineate the location of thaw areas in the foundation under the stream for most advantageous selection of bridge pier location.³² However, possible changes over the life of the structure

must also be considered. Other observations in this program have shown that even apparently stable bridge piers are in cyclic seasonal movement as a result of the varying forces acting on the piers. When the design is inadequate, progressive upward or downward displacements occur.

Permanent wharves have been provided at most major settlements along the Mackenzie River. These are usually either timber pile or earth-filled sheet pile structures constructed so that they are submerged by flood waters during spring breakup to avoid ice damage. Piles placed at the shoreline or just inshore penetrate the thin wedge of permafrost occurring at the margins of water bodies. Sheet piling have been anchored to soldier piles installed in permafrost on shore. Although some pile heaving has occurred, no serious problems have been experienced with these structures.

Permafrost is known to occur offshore in northern Alaskan coastal waters and has been reported by Samson and Tordon¹⁴⁴ in the eastern Canadian Arctic and by Mackay¹¹⁴ and others in the Beaufort Sea. Mackay also estimates that permafrost will be encountered extensively in offshore areas of the Canadian Arctic Archipelago. Offshore permafrost in these areas will pose similar problems to those experienced on land, but they will be more serious and difficult to deal with because of the remoteness, severe climate, and usually permanent ice cover. Hwang *et al.*⁷⁵ report on a preliminary study of the thermal regime under a structure forming part of a proposed arctic harbor development in the Beaufort Sea. This structure would support a heated building and consist of a concrete caisson placed on, and retaining, gravel fill on the frozen sea bottom.

Detailed site investigations, including careful subsurface explorations, are especially and absolutely essential when structures are to be built near the edges of, or in, coastal or inland waters. Provided adequate site information has been obtained and the effects of construction and natural changes on site conditions are anticipated and understood, it appears that, in spite of the above-noted difficulties, it is technically feasible to construct stable foundations by fully utilizing available technology, though at the expense of greater initial cost.

ROADS, AIRFIELDS, AND RAILROADS

Roads and airfield pavements constructed on permafrost in North America during World War II encountered difficulties where the subsurface conditions were unfavorable. Since 1950, however, airfield pavements have been constructed on permafrost and operated without problems at various locations such as Thule, Greenland, and Inuvik and Norman Wells, N.W.T., Canada. This good performance is attributable largely to a better understanding of the nature of permafrost and to the greater attention given in design and construction to subsurface exploration and thorough pre-

planning of all operations. Very many kilometres of new road construction on permafrost have also been accomplished successfully in recent years in Alaska and Canada and are anticipated in the future as development of the North continues.

Hennion and Lobacz have summarized current design practices of the U.S. Army Corps of Engineers for pavements on permafrost.⁷⁰ Three basic design approaches for pavements on permafrost are available¹⁰³: (a) design for the reduced strength of the subgrade during the thawing season, accepting whatever pavement roughness may occur from seasonal frost heave and thaw settlement; (b) limited subgrade frost penetration design, in which the primary objective is control of surface roughness caused by seasonal heave and thaw; and (c) full protection against frost heave or thaw settlement above the current permafrost table. Approach (a) is applicable primarily for low to moderate speed roads, parking areas, etc. Approach (b) is applicable for high-speed surfaces such as airfield runways. Method (c) is used over permafrost only in very cold areas, where depth of summer thaw is small enough to make this approach economically feasible.

It has been shown that the total thickness of section required for confinement of thaw penetration within the non-frost-susceptible base course can be reduced by as much as 35 percent and the summer pavement surface temperature reduced by 5 °C by painting the pavement white.^{1,12, 54,93,188} As shown by Berg and Aitken, this technique offers significant potential for controlling permafrost degradation even in a marginal permafrost area such as Fairbanks, Alaska.¹² Perimeter thawing effects also need to be controlled; while a few experiments have been performed to investigate techniques for modifying the albedo of unpaved shoulders, unpaved roads, vegetated areas, and other rough surfaces,⁵ no satisfactory system has been developed.

Experiments by the U.S. Army Corps of Engineers for control of degradation by use of in-ground insulation under pavements were started in 1947.¹⁸¹ Full-scale test installations of various types of insulation in roadways and fills have been made in recent years in northern Canada by the oil industry and the federal government and in Alaska by state and federal agencies and oil companies. Current reports of use of insulation for this purpose by Esch,⁴³ Berg and Aitken,¹² Smith, Berg, and Muller,¹⁵⁹ and others show that in the more northern permafrost areas insulation can be used to replace gravel base course in a ratio that depends on the type of insulation. In the more southern marginal permafrost areas, insulation will delay and may slow the rate of degradation but neither in-ground insulation nor a heat sink material such as compressed peat is capable of preventing thaw degradation.¹²

As reported by Smith¹⁵⁷ and Hennion and Lobacz⁷⁰ investigation is also under way to investigate the potential of "wrapping-up" techniques for control of moisture move-

ments. However, much work is needed before positive conclusions can be drawn.

For ice, the thermal expansion coefficient is about five or six times that of mineral aggregates such as granite or slate; for asphalt, it is more than 20 times.¹⁰⁴ Therefore, the more moisture in the soil or the more asphalt in the paving mix, the greater the shrinkage or expansion with temperature change and the more intense the cracking at low temperatures. This is confirmed by field observations. In the Arctic and Subarctic, pavement cracks may extend a metre or more down into the base course materials. Raveling or spalling of the pavement-wearing surface at edges of cracks produces debris that may be hazardous to aircraft. With age, cracks may become wider and raised or depressed. Water that enters the cracks may freeze and accumulate in the base course, reducing its capacity to function as a drainage course. While the basic phenomena of thermal shrinkage cracking in pavement and earth materials are moderately well understood, technology for minimizing such cracking, except by reduction of moisture and bituminous contents or use of steel reinforcement is minimal.

In recent years, numerous temporary airfields and roads have been built in northern areas with minimum investment of effort, to support oil and mineral exploration activities. Difficulties have arisen, however, due to such problems as ingestion of surface particles into aircraft engines and severe rutting of the surface as the ground thaws and softens when attempts are made to extend operations into the summer season. Use of synthetic insulating materials to provide expedient pavements as described by Smith, Berg, and Muller¹⁵⁹ appears to offer a technically feasible solution to these problems. All temporary or expedient construction, including construction working pads and construction haul roads, must be very carefully designed and controlled to avoid unacceptable environmental effects. Environmental impact may indeed be the controlling factor in the engineering.

For construction on permafrost in general, significant technological gains could accrue from advances in soil modification technology. The potential gains from successful development of an inexpensive system for conversion of frost susceptible soils into non-frost-susceptible materials alone are very large. The Frost Effects Laboratory investigated effects of various additives on frost susceptibility in the 1940's.⁴⁹⁻⁵¹ Lambe and Kaplar^{96,97} continued very extensive studies in this area during the 1950's and early 1960's. They found materials capable of effecting large reductions in ice segregation and frost heave when used in trace amounts. However, these materials have thus far not been widely used in arctic and subarctic construction because available techniques for incorporating such additives are still too costly and some of the materials lack permanence. The possibility of environmental contamination by leachable additives must also be considered.

Placement of embankment material is frequently carried out during the winter months when the frozen surface makes movement most effective.¹⁴⁷ Fills are placed by end dumping, and construction vehicles are prohibited from traveling on or damaging the vegetation mat beyond the limit of the fill itself. Roads are commonly left unpaved either on a permanent basis or for a lengthy period of thermal adjustment; this permits the surface to be maintained at its design grade with a grading machine whenever any thawing of underlying ice may cause settlement. Cutting into the permafrost is avoided whenever possible and pavements are customarily elevated at least 1-2 m above the surrounding terrain, not just to provide bearing capacity and drainage and to aid thermal adjustment under the pavement, or to dampen its effects, but also to minimize snow accumulation and removal problems in winter. Clean sands and gravels are favored for embankments because of their non-frost-heaving qualities, their good subgrade drainage characteristics, and because they can be excavated and placed during freezing weather if they are well drained. Surface and subsurface drainage problems are avoided as far as possible by proper route location. The natural vegetation mat is left in place on the right-of-way and a thick initial layer of fill is normally placed in order to carry the construction vehicles on the soft terrain. As described by Smith and Berg maximum advantage is taken of natural thermal and physical adjustment capabilities of the permafrost terrain.¹⁵⁸

Most railroads constructed in permafrost areas have typically required heavy and continuous maintenance because roadbeds placed on adverse subgrades heave continuously during much of the winter and settle continuously in summer, differential movement occurring not only in the longitudinal direction but also between rails. Serious consideration is being given to the use of high speed, heavy load unit trains for movement of minerals and oil from the North (maximum railroad grades of 0.5 percent and maximum curvature of 2.5°). Pryer concluded in 1963 that railroads that must carry very heavy ore traffic on a year-round basis require design and construction to modern highway standards, with rigid specifications covering the selection and placement of subgrade soils.¹³³ The same basic technical approaches applicable for pavements are also applicable for railroads, that is, control of freeze and thaw penetration, control or modification of soil characteristics, and control of moisture accessibility. Although some studies for control of roadbed frost heave in seasonal frost areas of Canada have been performed in the last decade, no current studies aimed specifically at permafrost conditions are known to the writers.

Improvements in methods of economically ensuring smooth, stable grades and alignments requiring minimum maintenance would have application not only in the permafrost areas, but throughout the cold regions, including especially high-speed transportation systems in the temperate zones.

EXCAVATION AND UNDERGROUND CONSTRUCTION

Ability to effectively and economically excavate and handle frozen materials is a basic requirement for effective year-round construction operations in permafrost regions. Significant laboratory and field work has been done over the past decade to investigate methods of penetration, excavation, and handling of frozen ground and ice, including frozen ore, and of underground construction. In a study to develop fundamental concepts for the rapid disengagement of frozen soil carried out by Foster-Miller Associates^{46,47} for CRREL, the possible methods for penetrating and excavating frozen ground were considered. A separate investigation of methods of conveying snow, ice, and frozen ground from an excavation to a disposal area was also made.⁴⁵ The methods of disengagement studied included such basic processes as the following:

- High-velocity droplet impingement
- High-speed continuous water jets
- High-voltage spark discharge
- High-energy pulsed electron beam
- Laser beam
- Dynamic column unloading
- Cantilever-bending fracture
- Controlled explosive loading
- Shear impacting and vibratory penetration
- Air blasting

It was concluded that the most satisfactory primary processes are shear cutting and indentation cutting and, potentially, high-velocity liquid droplet impingement. The most promising secondary processes included cantilever-bending fracture, brittle ridge fracture, and controlled explosive loading. The novel processes considered were found without exception either very low in effectiveness or not sufficiently developed from an implementation point of view to be of practical interest at this time. It was further concluded that liquid droplet impingement requires advances in the state of the art and extensive development to improve the technology sufficiently to make it practical for large-scale material disengagement. Mellor has more recently reviewed most of the principles that can be conceived of for excavating frozen ground. He has concluded that of the conventional techniques within the realm of existing technology, i.e., ripping, shearing, etc., shear or drag bit cutting offers the best present prospects for work in frozen ground. Of the novel concepts investigated, he has concluded that high-pressure water jets offer the most promise.¹²⁰

The internal jet burner described by Browning and Ordway²⁰ in 1963 has not received wide acceptance for use in frozen ground. Although this burner, which uses kerosine and compressed air, is light enough to be held by two men

during operation, it requires large air compressor capacity. It has penetrated frozen silt to a depth of about 18 m in 30 min.

McAnerney, Hawkes, and Quinn have reported adaptation of coal-mining airblast technology to the excavation of frozen ground in lieu of conventional explosives.¹¹⁹ They have concluded that a tunneling machine incorporating a combined auger-airblast tube is clearly feasible for tunneling in frozen silt. Use of airblasting for trenching is also an efficient technique, as long as it is confined sufficiently to have a surface on which to act. Difficulties were encountered in using the scheme to aid ripping operations because of insufficient confinement of the air blast.

Conventional explosives are, of course, widely employed in every-day construction and mining operations for excavating frozen ground. More or less conventional explosives and drilling and placement procedures are used. In most cases trials are conducted at the site of the work to determine optimum values for amount of explosive and hole spacing to get the best results. However, problems have been encountered in achieving successful stemming of holes in frozen ground and also with failure to achieve complete rupture of the pit face and sufficient fragmentation.^{77,99,171} At Schefferville, Quebec, three times as much powder has been required for blasting frozen iron-ore as for unfrozen¹⁹⁰ and the cost of blasting is more than doubled. Costs increased considerably when blasting frozen ground in open pit operations in permafrost at the Cassiar Mine in northern British Columbia.⁷²

Mellor has found distinct advantages in use of liquid or slurried explosives for excavating frozen materials.¹²¹ Shot drilling is far less expensive since only small holes are required. Also, coupling characteristics of liquid explosives are superior to those of solid explosives. Some sensitive explosives may be unsafe. However, the slurries have not presented any unusual safety problems.

When excavated materials are moisture free, no difficulties are encountered in handling, processing, or transporting the materials regardless of temperature conditions. However, when rock or frozen ground contain moisture the material may freeze to any surface it touches such as power-shovel buckets, loading hoppers, conveyor belts, or railroad car bodies. The problem is most severe at temperatures between about -9 and -1 °C.¹⁹⁰ Methods of coping with the problem have included heating of surfaces with which the material may come in contact and drying the material to moisture content levels low enough to give satisfactory performance. Dubnie has summarized Canadian mining experience.⁴¹

Underground openings, shafts, and tunnels in permafrost have long been used for prospecting, mining, and cold storage of food. Construction methods have included pick and shovel, hydraulic sluicing, and conventional drill and blast techniques. Canadian experience with development

and operation of mines in permafrost areas has been described by Drewe,⁴⁰ Espley,⁴⁴ and Kilgour⁹⁰ and advantages and disadvantages of permafrost in mining operations have been summarized by Pike.¹³¹ One of the advantages is that the frozen condition permits more economical use of the stopeing process by allowing greater height of lifts.

CRREL has constructed three experimental tunnels in glacier ice and two in frozen ground using professional mining techniques. One of the two tunnels in frozen ground was constructed near Thule, Greenland, in -11°C glacial till (approximately 85 percent moisture saturation) by conventional drill and blast techniques.^{165,166} The degree of difficulty was approximately equivalent to tunneling in granite. In a room with about 10 m unsupported span, no measureable closure had occurred after several years. The second tunnel was constructed near Fairbanks, Alaska, in frozen silt of about -1°C mean annual temperature.¹⁶⁷ The original tunnel was cut with an Alkirk tunneling machine equipped with drag-bit cutters. Later, comparative excavation experiments were carried out in the tunnel using a variety of other methods such as conventional drilling and blasting and conventional coal cutting machinery.¹¹⁶ As reported by Pettibone, the Bureau of Mines in 1970 extended a 61-m-long inclined winze down to the gold-bearing gravel and bedrock and constructed a 9 m \times 21 m \times 2.4 m room.¹²⁸ The CRREL and Bureau of Mines studies in this tunnel complex showed that openings in the frozen silt will close progressively by creep at the normal ground temperature of about -1°C . In the 2.4 m \times 4.3 m primary tunnel, the initial rate of closure was about 30 cm/year. It was apparent that the deformation rate of such warm permafrost can be a serious problem.

However, it was found that the closure could be halted by introducing cold air in winter to cool the tunnel walls, using a natural draft system.¹¹⁸ Although Pike¹³¹ has reported no apparent problems from ventilation of mines in rock with heated air, experience with tunnels in snow, ice, and frozen soil containing substantial ice has shown that all heat released in the tunnels by machinery, lights, people, and/or other sources must be very carefully controlled. Pettibone has concluded that simply protecting the tunnel from entrance of summer heat or providing partial roof support with yielding-type supports may be sufficient in frozen soil for purposes such as mining.¹²⁸ However, where substantial amounts of heat are generated or where extended or permanent use of the facility is required, ventilation by circulating cold surface air through the tunnel in winter or by collecting and conducting heated air to the surface with ducts, or mechanical air conditioning or refrigeration systems, are necessary.

Successful techniques have been developed for portal construction to avoid problems of slope instability and moisture infiltration into the tunnel where the tunnel intersects the annual thaw zone. Many frozen soils contain or-

ganic material, including vegetation and animal remains, and underground openings in these materials commonly exhibit a penetrating and unpleasant odor. Techniques for control of this odor and of the dust condition, which results from sublimation of ice in the tunnel walls, need further development. Studies of sublimation by Swinzow^{166,167} have shown that spray painting, lacquering, or coating with a nondrying petroleum product are successful and water-base paint unsuccessful, in inhibiting sublimation. Water sprayed to form an ice film is successful as long as the film lasts, but it sublimates rapidly at lower levels in the tunnel cross section. The organic frozen soils may also contain pockets of methane gas, which present a hazard to tunneling.

Prethaw of materials by use of cold water probe pipes was common practice in the placer mining gold fields in Alaska and Canada when these were active. With the virtual halt of these mining operations, this method of thawing has nearly disappeared. However, the "thaw and scrape" operation that has been commonly used for obtaining borrow materials, making cuts, or preparing foundation surfaces on frozen ground in summer is still widely employed.

DRAINAGE

Poor drainage is a typical condition of permafrost terrain because of the presence of impervious frozen ground at shallow depth, even in the summer. Saturated ground conditions in the summer and the frozen surface in the winter cause infiltration rates from precipitation to drop to as low as zero. When air temperatures drop below 0°C , icings form where water emerges on the surface, in turn, tending to block drainage facilities and cause operational obstacles. Even where precipitation is slight, drainage facilities must be provided to accommodate the large and quickly occurring flow of snow and ice meltwater, possibly combined with precipitation, over the frozen ground surface during a few days of breakup. Subsurface drains are effective only for limited portions of the year or under special conditions, as when a talik (unfrozen zone) exists. Nevertheless, subsurface flow of water within the annual thaw zone may be a very significant factor in the design of engineering structures; even in relatively arid climates of the Far North extensive subsurface flow may occur. Difficulties have been experienced both summer and winter from subsurface flow of water in frost-shattered rock at a seismometer vault placed partially underground at Resolute Bay, N.W.T., Canada. At Thule Air Force Base, studies in 1957-1960 verified the fact that large quantities of water move in summer through the coarse granular materials in the upper soil layers.¹²²⁻¹²⁴ Such water movement is capable of producing greater depth of thaw than would be otherwise experienced. During thaw, ordinary gravity flow is the principal mechanism acting. New supplies of water may be added into the subsurface

flow section both from surface infiltration and from thaw of ground ice. However, when seasonal freezing begins in the fall, strong moisture movements in the soil may also occur toward the planes of freezing. In fine-grained soils, seepage flow in the annual thaw zone is slow and may amount to only a few centimetres per year under gravity effects, but in very coarse cobble or broken rock materials, flow rates as high as 750 m/h¹²³ have been measured. It appears to be within the technological state of the art to control the direction and paths of gravity-induced subsurface flow in the annual thaw zone by controlling depth of subsurface thaw penetration. For example, at Thule, Greenland, painting the airfield pavements white as described by Fulwider and Aitken⁵⁴ raised the permafrost table under the pavements and created barriers to cross-pavement seepage flow.¹²⁴

A case is reported by Linell in which uncontrolled artesian flow from a subpermafrost source caused serious thaw of permafrost together with icing, a frost blister, and surface subsidence.¹⁰⁶ This occurred in a borderline permafrost area, and artificial refreezing of the ground was required to restore stability. In very cold permafrost areas such an upset of the thermal balance is normally rapidly self-correcting after removal of the cause. However, when the thermal disturbance is long range, as under a hot oil pipeline, thawing of permafrost and flow of resulting groundwater may continue indefinitely on a year-round basis. Lachenbruch has presented an analysis of resulting thermal, environmental and structural stability effects.⁹⁴ In their reports on pipeline performance and requirements, Watson *et al.*¹⁸⁷ and Rowley *et al.*¹⁴² have presented some information on groundwater as a factor.

An excellent example of the potential adverse effects of groundwater flow on permafrost stability is the case described by Tobiasson of serious settlement of hangar floors caused by warm groundwater derived from snow infiltrated into cooling ducts, from runoff of snowmelt and rain from pavements roofs, and natural surfaces flowing toward wells installed to keep the groundwater below the foundation cooling system.¹⁷⁴

In a notable case history described by McAnerney, previously mentioned under "Site Selection and Investigation for Engineering Purposes," it was observed that water was disappearing into sink holes that appeared in the bottom of a drainage ditch cut 2.1 m deep into the shale bedrock.¹¹⁷ Investigation disclosed massive ice within the bedrock to a depth of at least 14 m. Subsurface channels were being melted out by the drainage waters. The situation was easily stabilized by rerouting the drainage and backfilling the ditch, which re-established the permafrost conditions. However, if uncorrected, the consequences could have been a major failure.

Other case examples have shown that water from other sources, such as waste or condensate discharges and pipe

leakages, may also contain sufficient heat to degrade permafrost, and it is important that control be sustained not only during construction but for the life of the facility.

As pointed out by Johnson in 1950, Alaskan mineral soils, which usually are medium textured and single-grain structure, are highly susceptible to erosion when thawed.⁷⁹ It is presumed that this may apply in many other parts of the Arctic and Subarctic. Experience shows that merely damaging the natural surface vegetation may be sufficient to lead to catastrophic erosion under adverse conditions.^{69, 113, 186} The damage may be not only to the terrain itself but also to waterways and to fish and wildlife. Where massive terrain adjustments such as described by Smith and Berg are induced by construction,¹⁵⁸ care must be taken to prevent damage to streams by silt-bearing icemelt runoff.

Icings are an engineering and operational problem throughout the cold regions. A bibliography on river, ground, and spring icings has been prepared by Carey,²¹ as well as a monograph on icings developed from surface water and groundwater.²² The latter summarizes current approaches to control icings. Culverts present a special icing problem because of their tendency to become partially or completely blocked with ice during the winter, with the result that flow cannot be handled during thaw runoff. As reported by Carey, Huck, and Gaskin, a cooperative field and laboratory research program to develop methods to improve the control or prevention of icings in culverts has been in progress for several years by CRREL, the Alaska Department of Highways and the U.S. Department of Transportation.²³ Gaskin and Stanley report that carefully controlled applications of electrical heat have been found promising.⁵⁷ Criteria for design of culvert foundations for stability against thawing of underlying foundation materials are discussed in a U.S. Army structure foundation manual.¹⁷⁷ During route selection it is desirable to minimize the number of points where drainage must cross roads or other construction. However, little or no research appears to be in progress to improve techniques for recognizing and predicting icing susceptible locations and conditions during planning, design, and construction.

Experience indicates that in areas of relatively warm permafrost such as Fairbanks, Alaska, road fills can be built of very coarse materials to allow surface water to seep through them in lieu of using culverts, provided the amounts of water involved are relatively small. However, experience in very cold permafrost areas near Thule, Greenland, where the mean annual air temperature is about -11 to -12 °C, shows that in such a climate even the coarsest fills become ice-choked within about 3 years; thereafter, the embankments act as impervious dams rather than drainage fills. As shown by Fulwider, this effect can be exploited to advantage in the design and construction of water supply dams and reservoirs in very cold climates.⁵³

Johnson concluded in 1950 that methods for design of

storm water drains developed for temperate regions are applicable in arctic and subarctic regions if certain specific limitations are observed.⁷⁹ These limitations pertain to such factors as design storm indexes, infiltration rates, and retardance coefficients. The 1950 recommendations were used as the original basis for U.S. Army surface drainage criteria for airfields. These have been supplemented and updated with more recently available information in an Army technical manual.¹⁷⁹

UTILITIES

The construction and operation of reliable water supply, sewage and solid waste, fuel, electric power, heating, communication, and fire protection systems in permafrost areas at reasonable cost is often difficult and complex. Pollution control and environmental disturbance are particularly important factors to be considered even for the smallest communities at remote locations. The factor of reliability is especially important in areas that are very remote and have very severe climatic conditions; Ryan¹⁴³ stresses the need for duplication of equipment, alarm systems, and preventive maintenance for any sanitation facility in the Arctic. Social pressures are constantly increasing for even very small communities to be provided the same water, sewer, and other conveniences as are commonly available in the temperate zones of North America. Ryan has described current efforts of the U.S. Indian Health Service to provide water and sewer facilities to the Alaska natives.¹⁴³ Lawrence has outlined the present situation in northern Canada and has described acceptable practices and guidelines that should be followed including handling of oil spills.¹⁰¹ To best meet needs of the permafrost areas, Clark recommends that particular attention be given to all-purpose, self-contained sanitary facility units capable of shipment to remote places by aircraft.²⁶

Economical provision of a reliable year-round supply of potable water, including its securing, storage, treatment, and distribution is still a difficult problem in many areas, particularly in communities that can tolerate only a small capital investment. Alter has recently summarized the state of the art in a monograph.² Alter has also pointed out that an evolutionary trend is in progress in Alaska toward improved quality, dependability, and availability of water supply services that are engineered to be fully compatible with the Alaskan conditions.⁴ In North America surface sources are the primary means of water supply in permafrost areas, although wells are used at some locations in Alaska and the Yukon Territory, Canada, and seawater is distilled at Kotzebue, Alaska.² At a few places, groundwater aquifers in nonfreezing zones of river beds above permafrost have been developed by means of collection galleries. Sherman has described an excellent example of the latter.¹⁵²

The cost and uncertainties of locating, developing, and providing treatment are definite disadvantages in obtaining water from subpermafrost sources. As pointed out by Alter² advantages of subpermafrost water are in its reliability and temperature. Water from subpermafrost sources is commonly highly mineralized and may be saline and/or associated with methane or other gases. Conventional chemical processes and reverse osmosis have been used for treatment. A major need still exists for simple, reliable, and economical treatment systems for waters from subpermafrost sources, particularly for very small installations or communities.

Alter³ has recently summarized in a monograph the state of the art concerning sewerage and sewage disposal in the cold regions. In recent years, significant research and development has been in progress in the United States by the Environmental Protection Agency, Public Health Service, Bureau of Indian Affairs, U.S. Air Force, U.S. Navy, the U.S. Army Engineer District, Alaska, and the U.S. Army Cold Regions Research and Engineering Laboratory and in Canada by the Canadian Department of National Health and Welfare and Central Mortgage and Housing Corporation, to develop improved sewage treatment systems for cold regions use. The knowledge being gained in these studies is yielding rapid advancement of technology benefiting not only cold regions but also temperate region applications. Since temperature has a marked effect on self-purification processes, the effectiveness of systems that depend on the natural BOD reaction vary greatly with temperature, and, when temperature is near freezing or below, the processes are essentially dormant, including those in natural ground or water or in unaerated waste stabilization ponds (lagoons and similar situations). Dawson and Grainge, based on Canadian and other studies, suggest proposed design criteria for several types of waste water lagoons in arctic and subarctic regions.³⁷ Since numerous waste stabilization ponds are in use in the cold regions of North America, including the permafrost regions, substantial study has been made in recent years for development of mechanical aeration processes for sewage stabilization ponds and other forms of aerobic treatment. Pohl has offered a rational approach to this problem.¹³² Reed was the first to show that extended aeration can operate successfully at temperatures down to just above freezing.¹³⁵ Reed and Buzzell have developed a special, compact, extended aeration activated sludge system using a floating tube settler.¹³⁷ Pohl has under development an inverted tray settler as an alternative way of hastening the settling process.

With increasing development of the Arctic and Subarctic, the need has become pressing for effective systems for disposing of the increasing volumes of solid waste, which tend to resist decomposition under the effects of greatly reduced chemical and biological reaction rates. Cohen²⁷ is currently summarizing the state of the art in solid waste disposal in regions of low temperature in a monograph; in a paper sub-

mitted to this conference, he recommends an incinerator process for disposal of garbage, rubbish, and wastewater sludge.²⁸ The system is claimed to avoid atmospheric pollution while leaving only an inert residue and to be suitable for remote locations with populations up to several thousand people.

Utilidors and pipe systems, such as gas lines, have most commonly been built above ground in permafrost regions because of often difficult combinations of foundation conditions. However, above-ground systems encounter road-crossing problems, require extra insulation, and present physical barriers that are functionally, aesthetically, and psychologically undesirable with communities. Underground systems require favorable subsurface conditions and must be designed to be safe against damage from thermal ground cracking, permafrost degradation, and, possibly, flooding. Systems for distributing water and for collection of waste are moving more and more away from truck transport systems toward highly engineered pipe systems. Simonen and Heinke, in a detailed study of five settlements in the Mackenzie River Delta area of Canada found that water supply and collection and disposal of sewage were the services with the most shortcomings and compared the relative merits and costs of utilidors and tank trucks.¹⁵³ Cooper has described an experimental low-cost utilidor system at Frobisher Bay, N.W.T., and compared it with a similar system installed at Inuvik, N.W.T.²⁹ Leitch and Heinke have described and compared the main, elaborate, and extensive utilidor system at Inuvik with a low-cost utilidor system also in use at this community.¹⁰² Grainge⁶² and Dawson and Slupsky³⁸ have described a sanitary pipeline research installation study carried out at Inuvik to assess the performance of insulated and uninsulated buried and above ground pipelines. They conclude, based on heat loss and cost studies, that where conditions permit, shallow burial (up to 1.2 m) offers the best and cheapest method of constructing water and sewer lines in permafrost. The design and construction of a buried, insulated, and electrically heated, 10-cm-diameter welded steel pipe water supply line, 5.6 km long for a mining community in the Yukon Territory has been described by Cheriton.²⁵ Circulating water distribution systems such as those at Fairbanks, Alaska, offer the distinct advantage over noncirculating systems of being less susceptible to freezeup at points of inadequate frost protection, but they must be carefully engineered and operated. Centralized steam heating systems often go along with the water and sewer-piping systems because they provide a source of heat in utilidors to prevent freezeup. Barrow, Alaska, and Norman Wells, N.W.T., Canada, also have piped community gas systems. There is also a trend toward putting power and communications underground instead of overhead. Some problems have been experienced, however, including difficult excavation, rupture of lines due to thermal cracking of the ground, and

moisture or flooding. One must carefully weigh the advantages and disadvantages and site conditions.

There is a tremendous opportunity for application of ingenuity in design of more reliable and less costly, more easily maintained utility distribution and collection systems. Better solutions to these problems may also contribute to solution of the difficult problem of wintertime fire protection in the Arctic and Subarctic.

EMBANKMENTS AND SLOPES

Hardy and Morrison⁶⁶ and Isaacs and Code⁷⁶ give examples of and discuss the complex stability problems associated with landslides and large-scale sloughing of natural slopes, particularly on river banks. Smith and Berg illustrate problems that may be encountered in cut slopes in permafrost.¹⁵⁸ Creep, sloughing, and solifluction are common on natural and cut slopes in permafrost areas as a result of high-moisture content, reduced shear strength and seepage in the annual thaw zone in summer, seasonal frost raising and lowering, and seasonal thermal shrinkage and expansion effects and must be taken into account by engineers planning construction. Solifluction lobes, stone stripes, and similar forms of patterned ground are easily visible surface evidence of such movements as discussed by Washburn,¹⁸⁴ Frost,⁵² Corte,³⁰ and others. However, existence of such movements is not always so evident. Where structures and facilities must be constructed in areas of such mass wasting, engineering solutions may sometimes be very difficult. A typical example occurs in the gorge of the Nenana River, Alaska, north of McKinley Station where the bed of The Alaska Railroad has had to be reconstructed a number of times at higher elevation as the entire roadbed was gradually displaced down the slope over many years.

Many studies over past decades have demonstrated the large reductions in strength that occur in frost-susceptible soils on thawing.⁸⁹ Some, such as Tauscher,¹⁶⁸ have attempted to explore experimentally the detailed variations of shear strength within the zone of thawed material. Tauscher used a miniature shear vane. A number of analytical efforts have also been made over the past two decades. The consolidation of saturated, frost-loosened soil in the thaw zone differs from the classical Terzaghi consolidation approach in that, as thaw occurs, new water is constantly being released at a moving internal boundary. Nixon and Morgenstern have reviewed this problem and have presented a practical extension of the classical Terzaghi theory applicable to this situation.¹²⁷ Thompson and Lobacz report on an effort to measure thaw shear strength by means of direct shear and triaxial tests.¹⁷²

Embankments are usually relatively well drained and exhibit detrimental slope effects less intensely than natural or cut slopes. However, embankment toes are susceptible to loss of shear strength during thaw, especially where an un-

vegetated embankment contacts the vegetated natural surface, forming a locus of deeper annual thaw penetration into the materials and potential thermal instability, intensified by ponding of surface water as local degradation and settlement occurs. This weakening allows slumping of overlying slope materials. Embankments that are relatively thin may reflect frost heaving and shrinkage cracking of the underlying subgrade.

Maximum advantage should be taken of the existing soil and vegetation mat to assist in providing the protective cover needed for ultimate obtainment of a stable slope. Techniques need to be developed for rapid re-establishment of vegetation cover where this has been destroyed by construction operations. Our knowledge of techniques for rapid vegetation re-establishment under arctic and subarctic conditions is minimal. However, as pointed out by Linell, preservation or re-establishment of a relatively thin cover of living vegetation is not sufficient in marginal permafrost areas to ensure against permafrost degradation.¹⁰⁵

The technique of slope blanketing with granular material used by Lane in seasonal frost areas can be employed as either a supplementary or complete protection measure.⁹⁸ Blanketing with free-draining gravel or similar material not only increases the thickness of mineral cover over the natural slope materials so as to serve as a semi-insulating layer but it also provides surcharge weight to reduce the amount of ice segregation in underlying frost susceptible materials, thus reducing the volume of water to be released from these underlying materials in the spring. It also allows thaw water and seepage to emerge from the underlying soils without erosion or sloughing and through its loading effect serves to assist reconsolidation and rapid regain of strength in frost-loosened materials. This concept was successfully used to stabilize an unstable silt slope at the portal of the experimental tunnel constructed in permafrost by CRREL at Fairbanks, Alaska. Regardless of type of slope cover used, periodic re-dressing of the slope may be needed, if a degrading condition exists.

DAMS AND RESERVOIRS

While the number of dams and reservoirs that have been constructed in permafrost areas of North America is relatively small, our understanding of the technology of such construction is now much more advanced than one or two decades ago. From observations at the Crescent Lake Dam and Reservoir at Thule, Greenland, described by Fulwider,⁵³ we know that in very cold permafrost areas it is entirely feasible to construct thermally and structurally stable watertight dams with permanent reservoir water storage, even with relatively pervious embankment materials, because through seepage is completely sealed off by freezing of the embankment. As Fulwider points out, it may be necessary to consider building larger earth-fill dams in the Arctic in

stages where development of an initial fully frozen condition is needed. The construction of a small, frozen core earth-fill dam for water storage at a new townsite in northern Quebec, Canada, has been proposed⁶⁴ and others have been considered in areas of low temperature permafrost in Alaska. On the other hand, dams in areas of relatively warm permafrost, such as the Hess Creek Dam¹⁵⁴ about 80 km north of Fairbanks, Alaska, and the dikes at the Kelsey and Kettle generating stations in Manitoba,^{112,115} experience through-seepage under permanent reservoir storage, which may lead to eventual complete degradation of permafrost under the barriers. As has been reported by Johnston and Brown^{19,82} for the Kelsey dikes, it is possible to experience rapid thaw settlement of as much as 1.5 m, differentially without failure, but overtopping must be guarded against. This is made possible by employing materials such as sand that can deform as settlement occurs so as to maintain a watertight dam, without occurrence of piping. A system of sand drains in the ice-rich foundation materials was incorporated in the Kelsey and Kettle dikes to assist in maintaining stability during thaw. Adjustment of the structure can only occur, however, when the materials are unfrozen. Failure can occur if the bridging of the frozen outer shell allows the underlying material to separate from it by settlement as was demonstrated by failure of the Loch Alpine Dam near Delhi, Michigan, in 1927.⁴² Significant, longitudinal and transverse cracking to depths of about 3 m due to growth of ice lenses in frost-susceptible core material and thermally induced stresses during the winter have been experienced by some embankments in Canada. Although the cracks usually heal each summer, the cumulative effects over a period of years can become increasingly critical. Such cracking must be anticipated and accounted for in design.

The dams that have been constructed thus far on permafrost in North America, including various community and military installation water supply dams, have all been relatively small (height of Hess Creek Dam equals 24 m). For dams that are significantly higher or have different cross sections, or for climatic conditions intermediate between the borderline and very cold permafrost areas, determination as to whether or not a degrading or watertight situation will result under a permanent reservoir will require special and possibly novel analysis.

The paper submitted by George to this conference describes a type of reservoir project unique for the permafrost regions, in which a dam 38 m high will be used to store flood waters on a very infrequent and temporary basis and, therefore, will not experience the permafrost degrading effects of a permanent reservoir.⁵⁸ The basic plan is to leave the permanently frozen silt under the left side of the dam in place and to design the dam so that the existing permafrost will be protected against thaw. On the other hand, Simoni and Kitzke have concluded that in the Subarctic, large earth-fill embankments do not freeze solidly even dur-

ing extremely cold winters.¹⁵⁴ Although subsurface temperature measurements under the centerline of Hess Creek Dam show that freezing of the embankment occurs annually to a depth of about 8–10 m, permafrost had not developed in the exposed upper part of the embankment 4 years after final emptying of the reservoir (20 years after completion of the earth fill).

PETROLEUM PRODUCTION AND PIPELINES

Although small-scale production of oil and pipeline transmission of oil, gas, and fuel in permafrost areas of North America began as early as World War II,¹⁸ the recent discoveries of major oil and gas resources in Alaska, northern continental Canada, and the Canadian Arctic Archipelago have given major new impetus to development of special technology for petroleum exploration, development, production, and transport in these areas. Construction and operation procedures must be effective and economical under exceptionally adverse conditions, yet protect the environment from possibly irrecoverable damage. The volume of published and unpublished technical information on this subject generated in research, environmental, and engineering studies over the past 5 years is very large. The environmental impact statement prepared by the U.S. Government on the proposed Alaska pipeline alone comprises six volumes with a total of 3204 pages.

Four major technical problem areas are evident:

1. Exploration, drilling, and production of oil from wells through up to 600 m of permafrost, with production oil from depths near 3 000 m typically at a temperature of about 90 °C.
2. Transportation of crude oil at temperatures in the vicinity of 60–70 °C.
3. Transportation of gas in pipelines at temperatures below freezing.
4. Construction and operation of coastal and offshore facilities,¹⁶⁹ including exploratory and production oil wells, terminal and port facilities, and undersea pipelines in ice-filled waters. This problem area potentially surpasses all the others in difficulty.

Specific technical problems are summarized by Kachadoorian and Ferriani in relation to the proposed Alaska pipeline from Prudhoe Bay to Valdez, Alaska, a distance of about 1 270 km.⁸⁷ Many aspects to be considered in the design and construction of pipelines in northern Canada were discussed at the Canadian Northern Pipeline Research Conference in February 1972.¹²⁶

Many of the specific construction problems encountered in petroleum development in permafrost areas, such as foundation design or environmental conservation, have been covered above. However, some of the oil development

aspects of the problems are novel or have special dimensions. Cementing of exploration and production casing to prevent leakage or blowouts at wells in permafrost may pose difficult problems. Thawing and settlement of permafrost around an oil well casing may require special mechanical and installation criteria for the casing and associated well-head structures and equipment to accommodate the anticipated movements, stresses, and pressures without failure. Storage facilities and pipelines carrying hot crude oil at temperatures ranging from 60 to 90 °C require very accurate and reliable analyses of the consequences and costs of various possible construction alternatives. Above-ground hot oil pipelines require far less subsurface design investigation than below-ground pipelines, but require added foundation support systems and thermal insulation, are more easily vandalized or damaged by forest fires, and are less desirable from the point of view of aesthetics and wildlife migration. Lachenbruch has examined some of the potential problems of buried hot pipelines in permafrost.⁹⁴ It is estimated that a buried pipeline carrying oil at 70 °C will thaw frozen ground to a radius of about 15 m in 20 years. Some of the possible serious results of this thawing in thaw-unstable permafrost are overstressing and rupture of the pipe from excessive differential settlement, longitudinal overstressing and buckling of the pipe on slopes from anchorage failure, soil erosion and seepage of heated water along the pipeline axis, slope instability, and adverse effects on vegetation, wildlife, and fish. Provisions must be made for automatic limitation and control of oil spills. Gas pipelines designed to operate at temperatures below freezing offer much simpler design and construction problems than hot oil lines. Some areas, particularly in Alaska, have high seismic activity and possibility of pipe rupture from earthquakes must be considered. The design techniques currently employed for nonfrozen soil conditions for earthquake design are applicable to frozen conditions, but the response of frozen soils to earthquake load may obviously be quite different. Frozen soils have greater stiffness and brittleness and overall rock-like behavior as compared with nonfrozen soil. Wave velocities are much higher in the frozen soil and damping is lower. As reported by the U.S. Geological Survey, a problem may arise from sliding of overlying material at the interface between the frozen and nonfrozen layers. Stream and river crossings are particularly difficult engineering problems because of scarcity of hydrological and scour depth information and the need to avoid damage to aquatic life from increased stream sediment load or from alteration of water temperature. The need for revegetation after construction and after oil spills has been pointed out by Wein and Bliss.¹⁸⁹ Construction, operation, and maintenance activities along the pipeline and at production, pumping, and terminal facilities must be carefully controlled for environmental protection.

While the nature and scope of these problems and their

solutions are reasonably well understood, there has been a deficiency of full-scale experience records and specific quantitative design data. To fill this void, broad programs of laboratory, field, analytical, and theoretical studies have been carried out by government and by industry. These have included full-scale field tests at Barrow, Prudhoe Bay, and Fairbanks, Alaska, and at Inuvik, Sans Sault Rapids, and Norman Wells, N.W.T., Canada. Several recent papers give details of some of these studies. Watson, Rowley, and Slusarchuk have presented results of an experimental determination at Inuvik of the rate of thaw plug development around a buried 61-cm-diameter hot oil pipeline and of the resulting interaction of pipe and ground.¹⁸⁷ Slusarchuk, Watson, and Speer have described the field instrumentation used for these tests.¹⁵⁵ Rowley *et al.* have presented results of performance evaluation of a 1.22-m-diameter warm oil pipeline supported above ground in a gravel fill and on piles.¹⁴² Speer and Watson conclude from field tests in three types of ground that a 1.22-m-diameter by 12.70-mm-thick pipe can tolerate a differential settlement of up to 1 m at a horizontal span of 36 m.¹⁶² Rowley, Watson, and Ladanyi tested permafrost-embedded wood and steel piles both vertically and laterally to obtain specific quantitative criteria for a pile-supported hot oil pipeline.¹⁴¹ Progress reports on gas pipeline test facilities and other studies were presented at the Canadian Northern Pipeline Research Conference by Hurd⁷⁴ and Walker.¹⁸³

It may be concluded that it is within the technological state of the art to develop and make available the petroleum resources of land areas of the Arctic with acceptably low environmental impact. However, much further research and cumulative experience is needed to provide the better understanding and data needed for improved and more economical engineering solutions.

RESEARCH NEEDS

Areas in which this review has shown that further research and development are required for improvement of engineering design and construction are summarized below—not in order of priority.

1. Development is needed of new or improved equipment and technology that will permit rapid, but detailed and economical, determination of permafrost distribution and properties of frozen ground for engineering purposes over both large and small areas or distances. Of special interest are equipment and techniques for:

- a. airborne or remote sensing;
- b. geophysical exploration;
- c. drilling and sampling, including refrigerated systems, and apparatus of minimum weight and maximum portability, to obtain undisturbed cores for examination and testing;

d. *in situ* determination of physical, mechanical (particularly rheological) and thermal properties of frozen ground;

e. transporting and preserving frozen cores in the field and in the laboratory to prevent contamination and thermal and physical disturbance.

2. To improve our capabilities for site evaluation and route selection and to assess the interaction between the atmosphere, the structure, and the ground, there is a need to improve our knowledge of the relationships between surface indicators and subsurface conditions to permit more accurate engineering inferences.

3. Detailed studies are required to define more precisely the heat exchange mechanisms at the ground surface under natural conditions and as a result of engineering or other activities. Of particular importance is the determination of surface characteristics and parameters at the air-ground interface for engineering design, including special surfaces such as rock-fill slopes of dams.

4. There is a need for the development of reliable techniques for estimating site design conditions, e.g., air temperature, precipitation, and wind, at locations widely separated from reporting stations, particularly if they have different elevations and environments, e.g., maritime versus mountainous.

5. Theoretical and experimental studies are needed on the strength and rheology of frozen soils with emphasis on "warm temperature" materials.

6. Further theoretical and experimental studies are needed on the thermal properties of frozen, thawing, and thawed soils in the field and the laboratory.

7. Technology is needed for rapid re-establishment and/or maintenance of thermal stability on surfaces other than pavements including technology for control of albedo of such surfaces and for rapid reestablishment of vegetation on construction surfaces to aid in control of permafrost degradation, erosion, and sloughing. More highly traffic-durable albedo-control surfaces for pavements are also needed.

8. Further field experiments are required to determine the magnitude of frost heave forces that can be encountered and must be incorporated in design of different types of foundations. Procedures are also needed for predicting the amount of frost heave which will be experienced by tower footings or similar unheated foundations imbedded in the annual thaw zone.

9. Research is needed to increase our understanding of seasonal thermal shrinkage and expansion effects in permafrost and to incorporate this information into quantitative engineering design and construction criteria.

10. Further analytical and experimental studies are required to better understand and evaluate the processes involved in the settlement and consolidation of thawing and thawed soils.

11. Present limited information on effects of lateral forces in permafrost foundations needs to be expanded.
12. More economical methods of incorporating air spaces or duct systems in foundations need to be developed.
13. Further investigations are required on pile foundations to improve our knowledge of (a) allowable adfreeze bond stresses, (b) the manner in which stresses are redistributed with time along the length of a pile imbedded in permafrost, (c) methods of reestablishing full adfreeze bond in piles in which the bond has been broken by frost heave or overloading, (d) the full potentials of the many possible variations of conventional, thermal, and specially configured piles, and (e) the feasibility of driving piles into permafrost colder than -4°C . Design procedures should be simplified and more economical designs should be sought with lower factors of safety.
14. Additional study is needed on permanent and expedient anchorages in frozen ground.
15. Technology needs to be developed to permit pavements and railroads to be constructed with minimum added expense to standards of year-round smoothness needed for high-speed transportation systems. This should include research in soil modification technology to improve strength, thermal, frost heaving, and shrinkage-expansion characteristics of pavement and support materials.
16. Continuing research is required to develop faster and more economical methods of excavation, transport, and handling of frozen soil and rock.
17. Research is needed to develop improved techniques for anticipating, evaluating, and coping with thermal, erosional, and icing effects of groundwater flow in and near construction areas and seepage through dams, in permafrost regions.
18. Much more research and investigation are needed to provide simpler, less costly, and more reliable utility systems, in permafrost areas, especially including distribution and collection systems and improved methods of treating and handling water supplies and wastes, with particular attention being given to the economics as well as to the pollution and environmental aspects.
19. Research is needed to develop the most economical methods of controlling embankment and slope stability, and slope deformations, in permafrost regions. This includes research to develop techniques for controlling the localized lowering of the permafrost table at the transition zone between embankment and the natural vegetated surface, with attendant settlement, drainage and slope stability problems.
20. Continuing research is needed for economical design construction and operation of petroleum development systems, especially including those involving hot oil and the Arctic Sea environment.
21. Especially vital to the success of permafrost construction research efforts are feedback data on the actual

performance of facilities and comparison with the design assumptions.

22. The application of utmost ingenuity and persistence is needed to develop design and construction technology that (a) will reduce both the high first costs, including those from construction seasonality constraints, and the high operating and maintenance costs, which are at present major restraints on arctic and subarctic development, and (b) will improve habitability.

REFERENCES

1. Aitken, G. W. Highway test section for passive control of thermal regime in the Subarctic. Tech. Rep., U.S. Army Cold Region Research and Engineering Laboratory, Hanover, New Hampshire. (In preparation)
2. Alter, A. J. 1969. Water supply in cold regions. Monograph III C5a. U.S. Army Cold Regions Research and Engineering Laboratory, Hanover, New Hampshire.
3. Alter, A. J. 1969. Sewerage and sewage disposal in cold regions, Monograph III C5b. U.S. Army Cold Regions Research and Engineering Laboratory, Hanover, New Hampshire.
4. Alter, A. J. Water supply and waste disposal concepts applicable in permafrost regions. This volume.
5. Arctic Construction and Frost Effects Laboratory. 1955. Project 1, approach roads, Greenland 1955 Program, p. 53-61. ACFEL Tech Rep. TR-60. Published by U.S. Army Waterways Experiment Station as Tech. Rep. TR3-505, June 1959.
6. Arctic Construction and Frost Effects Laboratory. 1957. Permanent bench marks in permafrozen soil. Misc. Publ. MP-17, Arctic Construction Frost Effects Laboratory, Boston, Massachusetts.
7. Arctic Construction and Frost Effects Laboratory. 1957. Freeze-back control and pile testing. Kotzebue Air Force Station, Alaska, Tech. Rep. 66. ACFEL, Boston, Massachusetts.
8. Baker, W. H., and R. L. Kondner. 1965. Pullout load capacity of a circular earth anchor buried in sand. Highw. Res. Rec. No. 108.
9. Banfield, A. F., Jr., and H. Csergei. 1966. Results of sampling insulating layers in runway test sections—Alaska field station. Tech. Note. CRREL, Hanover, New Hampshire.
10. Barry, B. L., and J. G. Cormie. 1971. Constructional aspects of the ± 450 KVDC Nelson River transmission line, pp. 459-492. In Proceedings, Manitoba power conference EHV-DC Winnipeg, Canada.
11. Berg, R. L. 1970. Insulation in roads and runways—a bibliography. Tech. Note TN 29. U.S. Army Cold Regions Research and Engineering Laboratory, Hanover, New Hampshire.
12. Berg, R. L., and G. W. Aitken. Passive methods of controlling geocryological conditions in roadway construction. This volume.
13. Bertram, C. L., K. J. Campbell, and S. S. Sandler. 1972. Locating large masses of ground ice with an impulse radar system. In Proceedings 8th International Symposium on Remote Sensing of Environment, University of Michigan, Ann Arbor.
14. Black, R. F. 1957. Some problems in engineering geology caused by permafrost in the Arctic Coastal Plain, northern Alaska. J. Arctic Inst. N. Am. 10:230-240.
15. Brown, J. Environmental strategies for the utilization of permafrost terrain. This volume.
16. Brown, J., W. Richard, and D. Vietor. 1968. Effect of dis-

- turbance on permafrost terrain. Spec. Rep. SR 138. CRREL, Hanover, New Hampshire.
17. Brown, J., and G. C. West. 1970. Tundra biome research in Alaska. The structure and function of cold-dominated ecosystems. Misc. Publ. 87. CRREL, Hanover, New Hampshire.
 18. Brown, R. J. E. 1970. Permafrost in Canada: Its influence on northern development. University of Toronto Press, Toronto. 234 p.
 19. Brown, W. G., and G. H. Johnston. 1970. Dykes on permafrost: Predicting thaw and settlement. *Can. Geotech. J.* 7(4):365-371.
 20. Browning, J. A., and J. F. Ordway. 1966. Use of internal burners for working permafrost and ice, p. 530-534. *In Permafrost: Proceedings of an international conference.* National Academy of Sciences, Washington, D.C.
 21. Carey, K. L. 1970. Icing occurrence, control and prevention, an annotated bibliography. Spec. Rep. SR-151. U.S. Army Cold Regions Research and Engineering Laboratory, Hanover, New Hampshire.
 22. Carey, K. L. 1973. Icings developed from surface water and ground water. Monograph III-D3. U.S. Army Cold Regions Research and Engineering Laboratory, Hanover, New Hampshire.
 23. Carey, K. L., R. L. Huck, and D. A. Gaskin. Prevention and control of culvert icing. Summary report on studies, FY 1966-70. Prepared in cooperation with State of Alaska Department of Highways and U.S. Department of Transportation, Federal Highway Administration, by U.S. Army Cold Regions Research and Engineering Laboratory, Hanover, New Hampshire. (In press)
 24. Carlson, R. F., D. L. Kane, and C. E. Bowers. Groundwater movement adjacent to arctic streams. This volume.
 25. Cheriton, W. R. 1966. Electrical heating of a water supply pipeline under arctic conditions. *J. Eng. Inst. Can.* p. 31-35.
 26. Clark, L. B. A sanitary service complex for villages in permafrost regions. This volume.
 27. Cohen, J. B., and A. J. Alter. Management of solid wastes in cold regions. Monograph III C5c. U.S. Army Cold Regions Research and Engineering Laboratory, Hanover, New Hampshire. (In press)
 28. Cohen, J. B. Solid waste disposal in geocryological areas. This volume.
 29. Cooper, P. F. 1968. Engineering notes on two utilidor. Tech. Note 1. Department of Indian Affairs and Northern Development, Ottawa, Canada. 38 p.
 30. Corte, A. E. 1962. Relationship between four ground patterns, structure of the active layer and type and distribution of ice in the permafrost. Res. Rep. 88. U.S. Army Cold Regions Research and Engineering Laboratory, Hanover, New Hampshire.
 31. Crory, F. E. 1966. Pile foundations in permafrost, p. 467-476. *In Permafrost: Proceedings of an international conference.* National Academy of Sciences, Washington, D.C.
 32. Crory, F. E. 1968. Pile foundations in permafrost areas, Goldstream Creek, Fairbanks, Alaska. Tech. Rep. TR-180. U.S. Army Cold Regions Research and Engineering Laboratory, Hanover, New Hampshire.
 33. Crory, F. E. Settlement associated with thawing of permafrost. This volume.
 34. Crory, F. E. Design of ventilated floor system, Bldg. No. 16, Alaska Field Station. Tech. Rep. U.S. Army Cold Regions Research and Engineering Laboratory, Hanover, New Hampshire. (In press)
 35. Crory, F. E., and R. E. Reed. 1965. Measurement of frost heaving forces on piles. Tech. Rep. 145. U.S. Army Cold Regions Research and Engineering Laboratory, Hanover, New Hampshire.
 36. Crory, F. E., and W. J. Tizzard. Installation and testing of earth anchors at Fairbanks, Alaska. U.S. Army Cold Regions Research and Engineering Laboratory, Hanover, New Hampshire. (In press)
 37. Dawson, R. N., and J. W. Grainge. 1969. Proposed design criteria for wastewater lagoons in arctic and subarctic regions. *J. Water Pollut. Control Fed. Pt. I.* Feb:237-246.
 38. Dawson, R. N., and J. W. Slupsky. 1968. Pipeline research water and sewer lines in permafrost regions. Rep. No. NR-68-8. Department of National Health and Welfare, Edmonton. 78 p.
 39. Dickens, H. B., and D. M. Gray. 1960. Experience with a pier-supported building over permafrost. *J. Soil Mech. Found. Div., (Proc. ASCE)* V. 86(SM5):1-14.
 40. Drewe, J. G. 1969. Design and construction problems at the Clinton Mine of Cassiar Asbestos Corporation Ltd., p. 71-78. *In Proceedings third Canadian conference on permafrost.* Assoc. Com. Geotech. Res. Tech. Memo. No. 96. National Research Council of Canada. Ottawa.
 41. Dubnie, A. 1972. Northern mining problems with particular reference to unit operations in permafrost. *Tech. Bull. TB 148.* Department of Energy, Mines and Resources, Ottawa. 20 p.
 42. *Engineering News-Record.* 1926. Earth dam fails by shrinkage under frost crust. 96(23):942. 10 June 1926. (Loch Alpine Dam)
 43. Esch, D. C. Prevention of thaw degradation of underlying permafrost with roadway subgrade insulation. This volume.
 44. Espley, G. H. 1969. Experience with permafrost in gold mining, p. 59-64. *In Proceedings of third Canadian conference on permafrost.* Assoc. Com. Geotech. Res. Tech. Memo. 96. National Research Council of Canada, Ottawa.
 45. Foster-Miller Associates. 1965. Final phase I report of an investigation of methods of conveying snow, ice and/or frozen ground from an excavation to a disposal area. Intern. Rep. IR 23. U.S. Army Cold Regions Research and Engineering Laboratory, Hanover, New Hampshire.
 46. Foster-Miller Associates. 1967. A study to develop fundamental concepts for the rapid disengagement of frozen soil, phase I. Tech. Rep. TR-233. U.S. Army Cold Regions Research and Engineering Laboratory, Hanover, New Hampshire.
 47. Foster-Miller Associates. 1968. Development of fundamental concepts for the rapid disengagement of frozen soil, final report, phase II. Tech. Rep. TR-234. U.S. Army Cold Regions Research and Engineering Laboratory, Hanover, New Hampshire.
 48. Frischknecht, F. C., and W. D. Stanley. 1971. Airborne and ground electrical resistivity studies along proposed TAPS route. *In Second international symposium on arctic geology,* San Francisco, California. American Association of Petroleum Geologists, Tulsa, Oklahoma.
 49. Frost Effects Laboratory. 1946. Studies on base course treatment to prevent frost action (1945-1946). ACFEL Tech. Rep. TR-4.
 50. Frost Effects Laboratory. 1947. Studies of base course treatment to prevent frost action (1946-1947). ACFEL Tech. Rep. TR-11.
 51. Frost Effects Laboratory. 1949. Addendum No. 1 (1945-1947) to report on frost investigation (1944-1945). ACFEL Tech. Rep. TR-24.
 52. Frost, R. E. 1950. Evaluation of soils and permafrost conditions in the territory of Alaska by means of aerial photographs. Prepared at Purdue University for St. Paul District U.S. Army,

- Corps of Engineers. Tech. Rep. 34. Arctic Construction and Frost Effects Laboratory, Boston, Massachusetts.
53. Fulwider, C. W. Thermal regime in an arctic earth-fill dam. This volume.
 54. Fulwider, C. W., and G. W. Aitken. 1962. Effects of surface color on thaw penetration beneath an asphalt surface in the Arctic, p. 605-610. *In Proceedings, International conference on the structural design of asphalt pavements*, Aug. 20-24, University of Michigan, Ann Arbor.
 55. Fulwider, C. W., and R. L. Berg. Effect of insulating layers on permafrost degradation. Tech. Rep. U.S. Army Cold Regions Research and Engineering Laboratory, Hanover, New Hampshire. (In preparation)
 56. Garg, O. In situ physicomaterial properties of permafrost using geophysical techniques. This volume.
 57. Gaskin, D. A., and L. E. Stanley. Control of culvert icing. This volume.
 58. George, W. Analysis of the proposed Little Chena River, earth-filled nonretention dam, Fairbanks, Alaska. A dam located in a permafrost regime with alternative construction modes. This volume.
 59. Gilman, G. D. 1967. Displacement method for ground water observations during freezing periods. Intern. Rep. 39. CRREL, Hanover, New Hampshire.
 60. Gold, L. W., G. H. Johnston, W. A. Slusarchuk, and L. E. Goodrich. 1972. Thermal effects in permafrost, p. 25-46. *In Proceedings Canadian northern pipeline research conference*. Assoc. Com. Geotech. Res. Tech. Memo. 104. National Research Council of Canada, Ottawa.
 61. Goodman, K. S., and R. M. Hardy. 1962. Permafrost occurrence and associated problems at Thompson, Manitoba, p. 140-148. *In Proceedings 1st Canadian conference on permafrost*. Assoc. Com. Geotech. Res. Tech. Memo. 76. National Research Council of Canada, Ottawa.
 62. Grainge, J. W. 1969. Arctic heated pipe water and waste water systems, p. 47-71. *In Water research*. Vol. 3. Pergamon Press, New York.
 63. Granberg, H. B. Indirect mapping of snowcover for permafrost prediction at Schefferville, Quebec, Canada. This volume.
 64. Hahn, J., and B. Sauer. 1968. Engineering for the Arctic. *J. Eng. Inst. Can.* April:23-28.
 65. Harding, R. G. 1962. Foundation problems at Ft. McPherson, N.W.T., p. 159-166. *In Proceedings 1st Canadian conference on permafrost*. Assoc. Com. Geotech. Res. Tech. Memo. 76. National Research Council of Canada, Ottawa.
 66. Hardy, R. M., and H. L. Morrison. 1972. Slope stability and drainage considerations for arctic pipelines, p. 249-265. *In Proceedings Canadian northern pipeline research conference*. Assoc. Com. Geotech. Res. Tech. Memo. 104. National Research Council of Canada, Ottawa.
 67. Hare, F. K. [ed.]. 1970. The tundra environment. *Trans. Roy. Soc. Can. Sect. III Fourth Ser.*, Vol. VII. Winnipeg.
 68. Haugen, R. K., H. L. McKim, L. W. Gatto, and D. M. Anderson. 1972. Cold regions environmental analysis based on ERTS-1 imagery. *Proceedings, 8th international symposium on remote sensing of environment*, University of Michigan, Ann Arbor. 12 p.
 69. Heginbottom, J. A. Some effects of surface disturbance on the permafrost active layer at Inuvik, Northwest Territories, Canada. This volume.
 70. Hennion, F. B., and E. F. Lobacz. Current Corps of Engineers practices related to design of pavement in areas of permafrost. This volume.
 71. Hoekstra, P. Electromagnetic probing on permafrost. This volume.
 72. Horsley, T. L. 1965. Drilling and blasting at the Cassiar Mine. *Can. Min. Metallurg. Bull. (Montreal)* June:625-627.
 73. Hunter, J. A. The application of shallow seismic methods to mapping of frozen surficial materials. This volume.
 74. Hurd, L. G. 1972. Progress report on gas pipeline research—The Northwest Project Study Group, p. 199-206. *In Proceedings Canadian northern pipeline research conference*. Assoc. Com. Geotech. Res. Tech. Memo. 104. National Research Council of Canada, Ottawa.
 75. Hwang, C. T., D. W. Murray, and E. W. Brooker. 1972. A thermal analysis for structures on permafrost. *Can. Geotech. J.* 9(1):33-46.
 76. Isaacs, R. M., and J. A. Code. 1972. Problems in engineering geology related to pipeline construction, p. 147-178. *In Proceedings Canadian northern pipeline research conference*. Assoc. Com. Geotech. Res. Tech. Memo. 104. National Research Council of Canada, Ottawa.
 77. Ives, J. D. 1961. Iron mining in permafrost, central Labrador-Ungava: A geographical review. *Geogr. Bull. No.* 17.
 78. Jensen, W. C. 1961. Timber piles in permafrost at Alaskan radar station. *Soil Mech. Found. Div. (Proc. ASCE)* 87(SM1): 15-27; discussions by K. Linell *et al.* 1962. 88(SM4):141-153.
 79. Johnson, L. A. 1950. Investigation of airfield drainage, arctic and subarctic regions, in three volumes: Part I, Supplement to Part I, and Part II. Prepared by St. Anthony Falls Laboratory for St. Paul District, U.S. Army, Corps of Engineers. Tech. Rep. 19. Arctic Construction and Frost Effects Laboratory, Boston, Massachusetts.
 80. Johnson, P. R. 1971. Empirical heat transfer rates of small Long and Balch thermal piles and thermal convection loops. Rep. 7102. Institute of Arctic Environmental Engineering, University of Alaska, Fairbanks.
 81. Johnston, G. H. 1962. Bench marks in permafrost areas. *Can. Surv. XVI(1)*:32-41.
 82. Johnston, G. H. 1969. Dykes on permafrost, Kelsey Generating Station, Manitoba. *Can. Geotech. J.* 6(2):139-157.
 83. Johnston, G. H., and R. J. E. Brown. 1964. Some observations on permafrost distribution at a lake in the Mackenzie Delta, N.W.T., Canada. *Arctic* 17(3):162-175.
 84. Johnston, G. H., and R. J. E. Brown. 1966. Occurrence of permafrost at an arctic lake. *Nature* 211(5052):952-953.
 85. Johnston, G. H., and B. Ladanyi. 1972. Field tests of grouted rod anchors in permafrost. *Can. Geotech. J.* 9(2):176-194.
 86. Jonassen, L. P. 1968. Guyed tower anchor research. Paper presented at Meeting of Canadian Electrical Assoc., Transmission Section, Toronto, April. 17 p.
 87. Kachadoorian, R., and O. Ferrians. Permafrost—Related engineering geology problems posed by the trans-Alaska pipeline. This volume.
 88. Kane, D. L., and C. W. Slaughter. Lake and subpermafrost groundwater interaction in a permafrost condition. This volume.
 89. Kaplar, C. W. 1965. Shear strength of a soil after freezing and thawing. *Soil Mech. Found. Div. (Proc. ASCE)* 91(SM2):91-97. Discussion in paper No. 3958 of this title by Bengt, Broms, and Yao, July 1964.
 90. Kilgour, R. J. 1969. Mining experience with permafrost, p. 65-70. *In Proceedings 3rd Canadian conference on permafrost*, Tech. Memo. 96. National Research Council of Canada, Ottawa.
 91. Kitze, F. F. 1967. Soil sampling and drilling near Fairbanks, Alaska. Equipment and procedures. Tech. Rep. 191. U.S. Army Cold Regions Research and Engineering Laboratory, Hanover, New Hampshire.
 92. Kovacs, A., B. McKelvy, and H. Colligan. 1972. Anchor designs

- and anchoring techniques. Intern. Rep. U.S. Army Cold Regions Research and Engineering Laboratory, Hanover, New Hampshire.
93. Kritiz, M. A., and A. E. Wechsler. 1967. Surface characteristics, effect on thermal regime, phase II. Tech. Rep. TR 189. U.S. Army Cold Regions Research and Engineering Laboratory, Hanover, New Hampshire.
 94. Lachenbruch, A. H. 1970. Some estimates of the thermal effects of a heated pipeline in permafrost. Geol. Surv. Circ. 632.
 95. Ladanyi, B., and G. H. Johnston. Evaluation of *in situ* creep properties of frozen soils with the pressuremeter. This volume.
 96. Lambe, T. W., and C. W. Kaplar. 1971. Additives for modifying the frost susceptibility of soils. Tech. Rep. TR-123/1. U.S. Army Cold Regions Research and Engineering Laboratory, Hanover, New Hampshire.
 97. Lambe, T. W., C. W. Kaplar, and T. J. Lambie. 1971. Additives for modifying the frost susceptibility of soils. Tech. Rep. TR-123/2. U.S. Army Cold Regions Research and Engineering Laboratory, Hanover, New Hampshire.
 98. Lane, K. S. 1948. Treatment of frost sloughing slopes. Proc. 2nd Int. Conf. Soil Mech. Found. Eng. (Rotterdam) 3:281-283.
 99. Lang, L. C. 1966. Blasting frozen ore at Knob Lake. Can. Min. J. 87:49-53.
 100. Lange, G. R. Precision sampling of frozen ground and fractured rock by core drilling. This volume.
 101. Lawrence, N. A. 1972. Arctic waste disposal, p. 91-104. *In* Proceedings Canadian northern pipeline research conference. Assoc. Com. Geotech. Res. Tech. Memo. 104. National Research Council of Canada, Ottawa.
 102. Leitch, A. F., and G. W. Heinke. 1970. Comparison of utilidoros in Inuvik, N.W.T. Dep. of Civil Eng., University of Toronto, Toronto. Publ. 70-61.
 103. Linell, K. A. 1960. Frost action and permafrost, p. 13-1-13-35. *In* K. B. Woods [ed.] Highway engineering handbook. McGraw-Hill, New York.
 104. Linell, K. A. 1969. Pavement design for areas of deep frost penetration. Misc. paper. U.S. Army Cold Regions Research and Engineering Laboratory, Hanover, New Hampshire.
 105. Linell, K. A. Long-term effects of vegetative cover on permafrost stability in an area of discontinuous permafrost. This volume.
 106. Linell, K. A. Risks of uncontrolled flow from wells through permafrost. This volume.
 107. Linell, K. A., and C. W. Kaplar. 1966. Description and classification of frozen soils. Tech. Rep. 150. U.S. Army Cold Regions Research and Engineering Laboratory, Hanover, New Hampshire.
 108. Lobacz, E. F., and W. F. Quinn. 1966. Thermal regime beneath buildings constructed on permafrost, p. 247-252. *In* Permafrost: Proceedings of an international conference. National Academy of Sciences, Washington, D.C.
 109. Long, E. L. 1966. The long thermopile, p. 487-491. *In* Permafrost: Proceedings of an international conference. National Academy of Sciences, Washington, D.C.
 110. Long, E. L. Designing friction piles for increased stability at lower cost. This volume.
 111. Luscher, U., and S. S. Affi. Thaw consolidation of Alaskan silts and granular soils. This volume.
 112. MacDonald, D. H. 1966. Design of Kelsey dikes, p. 492-496. *In* Permafrost: Proceedings of an international conference. National Academy of Sciences, Washington, D.C.
 113. Mackay, J. R. 1970. Disturbances to the tundra and forest tundra environment of the western Arctic. Can. Geotech. J. 7(4):420-432.
 114. Mackay, J. R. 1972. Offshore permafrost and ground ice, southern Beaufort Sea, Canada. Can. J. Earth Sci. 9(11): 1150-1561.
 115. MacPherson, J. G., G. H. Watson, and A. Koropatnick. 1970. Dykes on permafrost foundations in northern Manitoba. Can. Geotech. J. 7(4):356-364.
 116. McAnerney, J. M. 1967. Experiments in excavating frozen silt underground. Presented at 1967 Alaska Minerals Conference, University of Alaska, College. 23-26 May 1967.
 117. McAnerney, J. M. 1968. Investigation of subsurface drainage at BMEWS facility, Thule, Greenland. Spec. Rep. SR-111. U.S. Army Cold Regions Research and Engineering Laboratory, Hanover, New Hampshire.
 118. McAnerney, J. M. 1970. Tunneling in a subfreezing environment, p. 378-394. *In* Rapid excavation problems and progress. Proceedings of the tunnel and shaft conference, Minneapolis, Minn., 15-17 May 1968. Society of Mining Engineers of the American Institute of Mining, Metallurgy, and Petroleum Engineers, Inc., New York.
 119. McAnerney, J. M., I. Hawkes, and W. F. Quinn. 1969. Blasting frozen ground with compressed air, p. 39-58. *In* Proceedings of the 3rd Canadian conference on permafrost. Assoc. Com. Geotech. Res. Tech. Memo. 96. National Research Council of Canada, Ottawa.
 120. Mellor, M. 1972. Jet cutting in frozen ground. *In* First international symposium on jet cutting technology, Coventry, England. British Hydromechanical Research Assoc.
 121. Mellor, M. 1972. Use of liquid explosives for excavation of frozen ground. *In* Symposium on military applications of commercial explosives, Valcartier, Quebec, 1972. Defence Research Board of Canada, Ottawa.
 122. Metcalf and Eddy. 1957. Pavement condition report 1957 supplement. Tech. Rep. ENG-445. U.S. Army Corps of Engineers, Eastern Ocean District, North Atlantic Division, New York.
 123. Metcalf and Eddy. 1958. Airfield drainage investigation. Tech. Rep. ENG-455. U.S. Army Corps of Engineers, Eastern Ocean District, North Atlantic Division, New York.
 124. Metcalf and Eddy. 1960. Airfield drainage investigation. Tech. Rep. ENG-465. U.S. Army Corps of Engineers, Eastern Ocean District, North Atlantic Division, New York.
 125. Mollard, J. D. 1972. Airphoto terrain classification and mapping for northern feasibility studies, p. 105-127. *In* Proceedings Canadian northern pipeline research conference. Assoc. Com. Geotech. Res. Tech. Memo. 104. National Research Council of Canada, Ottawa.
 126. National Research Council of Canada. 1972. Proceedings Canadian northern pipeline research conference. Assoc. Com. Geotech. Res. Tech. Memo. 104, NRC, Ottawa, 331 p.
 127. Nixon, J. F., and N. R. Morgenstern. Practical extensions to the theory of consolidation for thawing soils. This volume.
 128. Pettibone, H. C. Placer mining at Fox. This volume.
 129. Péwé, T. L., and R. A. Paige. 1963. Frost heaving of piles with an example from Fairbanks, Alaska. Bull. No. 1111-1. U.S. Geological Survey, Washington, D.C.
 130. Pihlainen, J. A., and G. H. Johnston. 1963. Guide to a field description of permafrost for engineering purposes. Associate Committee on Soil and Snow Mechanics. Tech. Memo. 79. National Research Council, Ottawa.
 131. Pike, A. E. 1966. Mining in permafrost, p. 512-514. *In* Permafrost: Proceedings of an international conference. National Academy of Sciences, Washington, D.C.
 132. Pohl, E. F. 1970. Rational approach to the design of aerated sewage lagoons. Spec. Rep. SR-136. U.S. Army Cold Regions

- Research and Engineering Laboratory, Hanover, New Hampshire.
133. Pryer, R. W. J. 1966. Mine railroads in Labrador-Ungava, p. 503-508. *In* Permafrost: Proceedings of an international conference. National Academy of Sciences, Washington, D.C.
 134. Quinn, W. F. 1965. Design analysis for thickness of ground pad, Bldg. 16, Fairbanks, Alaska. Intern. Rep. U.S. Army Cold Regions Research and Engineering Laboratory, Hanover, New Hampshire.
 135. Reed, S. C. 1966. Interim report, research on extended aeration sewage treatment plant and utility systems at Alaska field station. Intern. Rep. IR-34. U.S. Army Cold Regions Research and Engineering Laboratory, Hanover, New Hampshire.
 136. Reed, R. E. 1966. Refrigeration of a pipe pile by air circulation. Tech. Rep. TR 156. U.S. Army Cold Regions Research and Engineering Laboratory, Hanover, New Hampshire.
 137. Reed, S. C., and T. Buzzell. A sewage treatment concept for permafrost areas. This volume.
 138. Reinart, I. 1971. Nelson River HVDC transmission line foundation design aspects, p. 422-444. *In* Proceedings, Manitoba power conference EHV-DC, Winnipeg, Manitoba, Canada.
 139. Roethlisberger, H. 1972. Seismic exploration in cold regions. Monograph II-A2a. CRREL, Hanover, New Hampshire.
 140. Romanoff, M. 1969. Corrosion evaluation of steel test piles exposed to permafrost soils, p. 6-13. *In* Proc. 25th Conf. National Assoc. of Corrosion Engineers, Houston, Texas.
 141. Rowley, R. K., G. H. Watson, and B. Ladanyi. Vertical and lateral pile load tests in permafrost. This volume.
 142. Rowley, R. K., G. H. Watson, T. M. Wilson, and R. G. Auld. Performance of a 48-inch warm-oil pipeline supported on permafrost. Presented at 25th Can. Geotech. Conf., Ottawa, Dec. 1972.
 143. Ryan, W. L. Design and construction of practical sanitation facilities for small Alaskan communities. This volume.
 144. Samson, L., and F. Tordon. 1969. Experience with engineering site investigations in northern Quebec and northern Baffin Island, p. 21-38. *In* Proceedings 3rd Canadian conference on permafrost. Assoc. Com. Geotech. Res. Tech. Memo. 96. National Research Council of Canada, Ottawa.
 145. Sanger, F. J. 1966. Degree-days and heat conduction in soils, p. 253-262. *In* Permafrost: Proceedings of an international conference. Publ. 1287. National Academy of Sciences, Washington, D.C.
 146. Sanger, F. J. 1969. Foundations of structures in cold regions. Monograph III-C4. CRREL, Hanover, New Hampshire.
 147. Savage, J. E. 1965. Location and construction of roads in the discontinuous permafrost zone, Mackenzie District, Northwest Territories, p. 119-131. *In* Proceedings Canadian regional permafrost conference. Assoc. Com. Geotech. Res. Tech. Memo. 86. National Research Council of Canada, Ottawa.
 148. Sayles, F. H. Triaxial and creep tests on frozen Ottawa sand. This volume.
 149. Sebstyan, G. Y. 1962. Department of Transport procedures for the design of pavement facilities and foundation structures in permafrost subgrade soil areas, p. 167-206. *In* Proceedings 1st Canadian conference on permafrost. Assoc. Com. Geotech. Res. Tech. Memo. 76. National Research Council of Canada, Ottawa.
 150. Sedziak, H. P., J. K. Shields, and G. H. Johnston. Condition of timber foundation piles at Inuvik, N.W.T. Canadian Dept. of the Environment, Ottawa. (In press)
 151. Sellmann, P., and M. Mellor. Drilling in frozen ground. Monograph III C. U.S. Army Cold Regions Research and Engineering Laboratory, Hanover, New Hampshire. (In press)
 152. Sherman, R. G. A groundwater supply for an oil camp near Prudhoe Bay. This volume.
 153. Simonen, E. R., and G. W. Heinke. 1970. An evaluation of municipal services in the Mackenzie River Delta communities. Publ. 70-60. Dep. of Civil Eng., University of Toronto. 119 p.
 154. Simoni, O. W., and F. F. Kitze. 1972. An earth fill dam on permafrost, Hess Creek Dam, Livengood, Alaska. Tech. Rep. TR-196. U.S. Army Cold Regions Research and Engineering Laboratory, Hanover, New Hampshire.
 155. Slusarchuk, W. A., G. H. Watson, and T. L. Speer. Instrumentation around a warm oil pipeline buried in permafrost. Presented at 25th Can. Geotech. Conf., Ottawa, Dec. 1972.
 156. Smith, M. W., and C. T. Hwang. Thermal disturbance due to river shifting, Mackenzie Delta, N.W.T., Canada. This volume.
 157. Smith, N. Membrane-enveloped soil layers, field tests in the Arctic. Tech. Rep. U.S. Army Cold Regions Research and Engineering Laboratory, Hanover, New Hampshire. (In press)
 158. Smith, N., and R. Berg. Massive ground ice formation in road construction in central Alaska. This volume.
 159. Smith, N., R. Berg, and L. Muller. The use of polyurethane insulation in expedient roads on permafrost in central Alaska. This volume.
 160. Smith, W. S., R. E. Smith, J. A. Schuster, and K. Nair. Sample disturbance and thaw consolidation of a deep permafrost. This volume.
 161. Sohlberg, E. T. Subsurface temperature measurements. Tech. Rep. 192. U.S. Army Cold Regions Research and Engineering Laboratory, Hanover, New Hampshire. (In press)
 162. Speer, T. L., G. H. Watson, and R. K. Rowley. Effects of ground ice variability and resulting thaw settlements on a buried warm oil pipeline. This volume.
 163. Stanley Engineering Co. 1965. Preliminary report on installation and testing of power-installed screw anchors in permafrost and thawed silt by the Golden Valley Electric Association, Fairbanks, Alaska.
 164. Stevens, H. W. Viscoelastic properties of frozen soils under vibratory loads. This volume.
 165. Swinzow, G. K. 1966. Tunneling and subsurface installations in permafrost, p. 519-526. *In* Permafrost: Proceedings of an international conference. National Academy of Sciences, Washington, D.C.
 166. Swinzow, G. K. 1964. Tunneling in permafrost, II. Tech. Rep. 91. U.S. Army Cold Regions Research and Engineering Laboratory, Hanover, New Hampshire.
 167. Swinzow, G. K. 1970. Permafrost tunneling by a continuous mechanical method. Tech. Rep. TR-221. U.S. Army Cold Regions Research and Engineering Laboratory, Hanover, New Hampshire.
 168. Tauscher, G. J. 1955. An investigation of the strength and moisture characteristics of a thawing silt. B.S. thesis, Massachusetts Institute of Technology, Cambridge.
 169. Technical University of Norway. 1971. Proceedings of the first international conference on port and ocean engineering under arctic conditions, Aug. 23-30, 1971, Trondheim, Norway.
 170. Terzaghi, K. 1952. Permafrost. *J. Boston Soc. Civ. Eng.* 39(1): 1-50.
 171. Thom, B. G. 1969. Permafrost in the Knob Lake iron mining region, p. 9-20. *In* Proceedings of the third Canadian conference on permafrost. Assoc. Com. Geotech. Res. Tech. Memo. No. 96. National Research Council of Canada, Ottawa.
 172. Thomson, S., and E. F. Lobacz. Shear strength at a thaw interface. This volume.
 173. Tizzard, W., and T. Lorber. Laboratory testing of model anchors.

- Intern. Rep. U.S. Army Cold Regions Research and Engineering Laboratory, Hanover, New Hampshire. (In press)
174. Tobiasson, W. Performance of the Thule hangar soil cooling systems. This volume.
 175. U.S. Army. 1966. Terrain evaluation in arctic and subarctic regions. Tech. Man. TM5-852-8.
 176. U.S. Army/Air Force. 1954. Arctic and subarctic construction, site selection and development. Tech. Man. TM5-852-2/AFM 88-19. Chap. 2.
 177. U.S. Army/Air Force. 1967. Arctic and subarctic construction structure foundations. Tech. Man. TM5-852-4/AFM 88-19. Chap. 4.
 178. U.S. Army/Air Force. 1966. Arctic and subarctic construction, calculation methods for determination of depths of freeze and thaw in soils. Tech. Man. TM5-852-6/AFM 88-19. Chap. 6.
 179. U.S. Army/Air Force. 1965. Arctic and subarctic construction, surface drainage design for airfields and heliports in arctic and subarctic regions. Tech. Man. TM5-852-7/AFM 88-19. Chap. 7.
 180. U.S. Army Cold Regions Research and Engineering Laboratory. 1966. Thaw penetration and subsidence. 500-Man Barracks, Ladd AFB, Alaska. Intern. Rep. 12.
 181. U.S. Army, St. Paul District, Corps of Engineers. 1950. Investigation of military construction in arctic and subarctic regions, comprehensive report 1945-48; Main report, and appendix III-Design and construction studies at Fairbanks research area. ACFEL Tech. Rep. TR-28.
 182. U.S. Department of Defense. 1969. Unified soil classification system for roads, airfields, embankments and foundations. Military Standard MIL-STD-619B (includes system for frozen soils).
 183. Walker, G. W. 1972. Gas Arctic Systems' gas pipeline test facilities. *In* Proceedings Canadian northern pipeline research conference. Assoc. Com. Geotech. Res. Tech. Memo. 104. National Research Council of Canada, Ottawa.
 184. Washburn, A. L. 1965. Classification of patterned ground and review of suggested origins. *Bull. Geol. Soc. Am.* 67(7):823-865.
 185. Waterhouse, R. W., and A. N. Sills. 1952. Thaw-blast method prepares permafrost foundation for Alaskan power plant. *Civ. Eng.* 22(2):126-129.
 186. Watmore, T. G. 1969. Thermal erosion problems in pipelining, p. 142-162. *In* Proceedings of the 3rd Canadian conference on permafrost. Assoc. Com. Geotech. Res. Tech. Memo. 96. National Research Council of Canada, Ottawa.
 187. Watson, G. H., R. K. Rowley, and W. A. Slusarchuk. Performance of a warm oil pipeline buried in permafrost. This volume.
 188. Wechsler, A. E., and P. E. Glaser. 1966. Surface characteristics, effect on thermal regime, phase I. Spec. Rep. SR 88. U.S. Army Cold Regions Research and Engineering Laboratory, Hanover, New Hampshire.
 189. Wein, R., and L. C. Bliss. Biological considerations for construction in the Canadian permafrost regions. This volume.
 190. Woods, K. B., K. A. Linell, and F. E. Crory. 1963. Alaska-Canada trip report. U.S. Army Cold Regions Research and Engineering Laboratory files.

WATER SUPPLY AND WASTE DISPOSAL CONCEPTS APPLICABLE IN PERMAFROST REGIONS

Amos J. Alter

ALASKA DEPARTMENT OF ENVIRONMENTAL
CONSERVATION
Fairbanks, Alaska

INTRODUCTION

At permafrost and cold-dominated sites, water supply and waste disposal systems are especially subject to damage from freezing. Such damage may impair site, processes, and facilities. Several different concepts have been used to reduce the risk of damage. Current technology is adequate to insulate, heat, enclose, monitor, and otherwise provide protection. However, construction and operation costs for most systems appear to be proportional to the protection and reliability sought. Fully reliable systems are the ultimate goal for most communities

Multimillion-dollar government programs for community improvement have been instituted in several communities in Alaska during the last decade. To achieve the overall objectives of these programs, community water supply and sewage disposal services also have been included in improvements. Modern services have been provided in many small villages where permafrost and severe cold climate conditions had made such service no more than a dream previously. Although services have been successfully established, some problems have arisen. This study was initiated to define specific problems and suggest courses of action to solve them.

BACKGROUND

Problems stemming from the provision of water supply and waste disposal services are not all engineering problems, but they are significant to engineers. The issues are social as well as physical. They are economic as well as technical, and they are related and cumulative rather than discrete.

Inadequate transportation and the effects of climate produce logistical problems. Energy is in short supply and expensive. The communities to be served are very small. Skilled manpower for construction, operation, and maintenance is in short supply within the communities and hence often must be imported. Many of the communities to be served exist on a subsistence economy. With little or no industry, many of them appear to be without visible economic base other than welfare payments and hunting and fishing. Materials for construction are unavailable at most community sites and repair

and maintenance services are only available from a distant larger community. Many villages exist as social aggregations of people without corporate structure or local government. Such villages are without local structure for bonding and qualification for certain grants for water and sewage works.

Several agencies of government participate in various aspects of providing water supply and sewage disposal services in Alaska communities. The Governor's Environmental Advisory Board for the Alaska Department of Environmental Conservation recommended that a staff paper be prepared as a result of a collaborative effort among the major participating agencies. Each major agency was invited to consider current problems in providing water supply and waste disposal services and to designate one or more representatives to participate in group analysis of the common problems. Representatives from the agencies met in a seminar in which objectives in service and the most significant problems were identified.

METHODS

Twenty persons, representing the several government agencies and the viewpoints of consumer, planner, developer, builder, operator, maintainer, financier, and supplier of ancillary service or research participated in the seminar. The participants represent a combined total of well over a century of cold region utility service experience, and they considered each problem both as a group and individually. Current practice and problems were examined and discussed in group discussion. Individual analysis was then made of the relative importance of all items considered in group discussion. Priority sheets similar to those shown in Tables I and II were used as an aid to individuals in their analysis. Each respondent was asked to use the priority sheets in identifying established objectives in water supply and waste disposal services and the problems associated with provision of the services. Each of the respondents completed a set of the priority sheets. Data from individually completed priority sheets were compiled and assembled to reflect group response. Analysis of the individual and group response material was used as a basis for the conclusions given below.

TABLE I Problems^a

Item #	(Social)	Priority Assigned	(Physical)	Item #
1	Service unacceptable to consumer	() ()	System freezes	1
2	Operation of facilities not assured	() ()	Proper materials for cold climate use unavailable	2
3	Use of facilities not assured	() ()	Uncertainty of results	3
4	Inadequate finance	() ()	Unfavorable site conditions	4
5	Untrained operators	() ()	Current technology results in excessively complicated system	5
6	Inadequate economic base in community	() ()	Construction schedules flexible	6
7	Systems do not meet fire control needs	() ()	Transportation inadequate	7
8	Systems do not meet industrial needs	() ()	Community configuration not compatible with service system requirements	8
9	Unreliable service	() ()	Repair and maintenance back-up unavailable	9
10	Systems do not conform with current environmental standards	() ()	Need more information on nonfrost susceptible methodology	10
11	No fixed point of responsible management	() ()	Need to know value of cold stress as a utilized resource and how to use cold stress to advantage	11
12	Too expensive to operate	() ()	Inadequate power	12
13	No coordination of effort	() ()	Energy too expensive	13
14	Duplication of facilities	() ()	Systems inefficient	14
15	Unightly structures	() ()	High cost of systems	15
16	Structures create barriers to traffic	()		
17	Acceptable cold region life-style undefined	()		
18	Community utility needs (energy, water, sewer solid waste, heat, communications, etc.) not coordinated	()		
19	Inadequate revenue or tax structure	()		
20	Services must be subsidized	()		
21	Laws inadequate	()		
22	Supervision inadequate	()		
23	Degradation of environment	()		
24	Practice presents potential for spread of disease	()		
25	Establishment doesn't understand objectives	()		

^a This table lists a number of possible problems that an agency may have in connection with the role it plays in meeting Alaskan water supply and sewage disposal needs. Please number each of the items sequentially in descending order of importance.

FINDINGS

The matters of greatest concern were:

1. To prevent the spread of disease in both water supply and waste disposal services;
2. To provide a water supply for domestic use, contrasted with water for both domestic use and other purposes;
3. To maintain environmental excellence in both water supply and waste disposal; and
4. To achieve environmental excellence in waste disposal by removal, stabilization, and control of the wastes.

General discussion among the respondents on current concepts and technology for meeting the above objectives centered around dependability of service, complexity of

facilities, and operation and maintenance experience. Several problems beyond those of site conditions were identified. Both physical and social problems were identified as well as the management and monetary implications of such problems. The following problems were identified as the most significant ones:

1. Excessive costs (ranging from two to ten times the cost for similar services in temperate climates) were cited as the most important problems of current methodology for both water supply and waste disposal;
2. Lack of dependability in both water supply and waste disposal systems, both socially and physically; and
3. Inadequate information on methods and materials for utilization of cold stress itself as a resource and for withstanding the effects of cold stress.

TABLE II Established Objectives^a

Item #	(Water Supply Systems)	Priority Assigned	(Sewage Disposal Systems)	Item #
1	Prevent spread of disease	() ()	Prevent spread of disease	1
2	Provide water for domestic use	() ()	Contribute to comfort	2
3	Provide water under pressure	() ()	Eliminate hand carriage or trucking of wastes	3
4	Meet domestic and fire-flow needs	() ()	Provide flushing type facilities	4
5	Meet domestic, fire and industry needs	() ()	Provide a fluid transport sewerage system	5
6	Finance service	() ()	Remove wastes from immediate living area	6
7	Operate service	() ()	Remove and stabilize wastes	7
8	Regulate service	() ()	Remove and stabilize wastes in an inoffensive manner	8
9	Construct facilities	() ()	Removal, stabilization and control of wastes in a manner to achieve environmental excellence	9
10	Establish standards for service	() ()	Provide adeq. domestic and indust. sewage disposal	10
11	Regulate quality of service	() ()	Provide acceptable non-subsidized sewage disposal	11
12	Facilitate service	() ()	Provide financial support for construction of facilities	12
13	Promote service	() ()	Provide financial support for O&M of facilities	13
14	Advocate	() ()	O&M of sewage disposal facilities	14
15	Monitor service	() ()	Supply support service such as power	15
16	Simplicity	() ()	Provide reliable service	16
17	Reliability	() ()	Provide simple facilities of failsafe nature	17
18	Efficient service	() ()	Provide facilities like those in the South 48	18
19	Low cost service	() ()	Low cost service	19
20	Keep water thawed and available	() ()	Consumer satisfaction	20
21	Consumer satisfaction	() ()	Acceptability to consumer and regulatory bodies	21
22	Acceptability to consumer and regulatory bodies	() ()	Establish standards for service	22
23	Community work program	() ()	Regulate quality of service	23
24	Environmental excellence	() ()	Promote service	24
25	Meet qualifying standards for other but related projects	() ()	Facilitate service	25
		()	Monitor service	26
		()	Advocate service	27
		()	Operate service	28
		()	Efficient service	29
		()	Community work program	30
		()	Environmental excellence	31
		()	Meet qualifying stds. for other related projects	32

^a This table lists a number of possible objectives that an agency may have in connection with the role it plays in meeting Alaskan water supply and waste disposal system needs. Please number each item sequentially in descending order of importance.

Among the alternatives available in meeting the problems, the respondents listed the following:

1. Initiation of research and development necessary to produce simpler, more reliable, and less expensive systems for water supply and waste disposal services. Particular reference was made to the vulnerability of the distribution system in water supply and the collection system in waste disposal, due to cold stress;

2. Placement of greater significance on matching system complexity and dependability with community capabilities

of operation. Thereby, only the simplest concepts and services would be utilized at communities that are very small or predicted to be small, and more complex systems would be utilized in large communities with greater operating capability;

3. Improvement of dependability and reduction of costs through provision of a properly trained and staffed regional or statewide operating and management mechanism;

4. Relaxation of standards for quality of service; and

5. Provision of increased subsidies necessary to make service at all sites feasible and dependable.

DISCUSSION OF FINDINGS

The adequacy of present concepts and methodology to meet all cold region water supply and waste disposal needs is questioned. Engineers have built systems and the intended mission has been accomplished often. But in view of increased demand for service for even very small groups, demand for lower costs for construction and operation of facilities, more stringent environmental constraints, and greater requirements for dependability, physical scientists and engineers are faced with new demands.

Traditionally, reliability in systems has been purchased through increased capital investment, greater complexity in systems, and greater financial outlay for enhanced operational capability. Paradoxically, engineers and physical scientists are now being asked to serve smaller groups and to meet higher standards at reduced capital and operating cost. The two goals are incompatible with present concepts and methodology. Traditional modification of temperate climate systems for cold region use increases cost rather than reduces it. Insulation and heating of conventional facilities wherever they are located or encapsulating them in a favorable micro-environment leads to added cost. Such added costs can be held to a minimum by use of otherwise waste heat and coordination and consolidation of utility systems and services into concepts that combine operations to financial advantage. However, combined services in themselves do not guarantee simpler or more dependable systems.

Fully suitable concepts for cold region use appear to require better use of other resources at hand. Efficiencies probably can be improved with further study and modification of concepts currently in use; but it is doubtful if the required reduction in cost and increase in reliability can be fully achieved by further modification of current concepts.

Cold itself as a resource and further exploitation of natural cold region phenomena remain as the principal relatively untapped resources for further study and potential use. Can the physical attributes of cold climate and attendant permafrost be used to greater advantage in water supply and waste disposal systems? What methodology must be employed in utilizing cold stress to advantage? These questions pose many challenges to the physical scientist and engineer. Inadequate passive concepts were used initially by aborigines and early visitors to polar regions. Passive concepts are well developed for some other types of construction on permafrost, but little has been done to advance and utilize a passive approach and methodology for cold region water supply and waste disposal systems.

Limited experience at hand indicates, conceptually that water and waste water can be processed, stored, and transported effectively by use of cold as a resource (Figure 1). However, insufficient information on modern methodology for full utilization of this concept precludes calling it practical at this time.

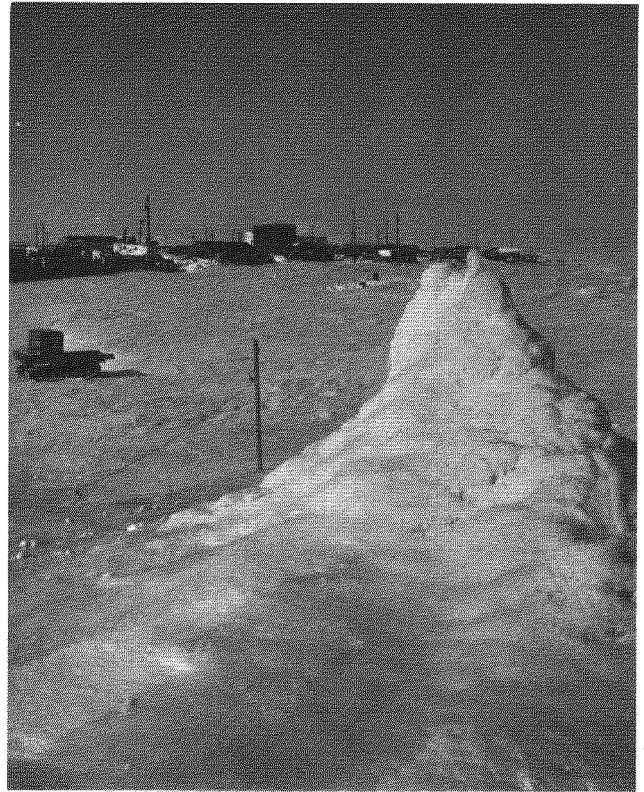


FIGURE 1 Artificially grown ice mound produced near Kotzebue, Alaska, in 1966 as a part of University of Alaska, Arctic Environmental Engineering Laboratory studies. A small pump with hose and discharge nozzle was used to pump saline water that was desalinated by freezing as the water traveled through subzero air to storage in the ice mound.¹

SUMMARY

At present it is difficult, expensive, and possibly impractical at some cold region sites to provide dependable heat-sensitive water supply and waste disposal systems. In the far north the heat-sensitive system concept is out of harmony with the land. Dependability as well as costs for heat-sensitive systems present serious problems. So-called active or passive concepts have been employed to provide foundations on permafrost. Similarly, improved active or passive approaches are indicated in providing water supply and waste disposal services in the far north. Limited experience validates the promise provided by passive concepts. Further research and investigation are indicated in developing a better methodology for application of passive approaches for water supply and waste disposal systems.

Temperate climate concepts require input of heat energy. They are highly susceptible to failure under cold stress. Large imports of fuel to meet the energy needs of conventional systems are unrealistic on a long-term basis. Radical departure from current practice is indicated if costs are to be

reduced significantly and dependability enhanced. Concepts that utilize low temperature or are unaffected by it should be investigated further. Imported energy must be conserved, and cold itself must be exploited as a resource to effectively and efficiently meet demand for water supply and waste disposal service and at the same time maintain environmental excellence on a long-term basis.

REFERENCE

1. Peyton, H. R., P. R. Johnson, and C. E. Behlke. 1967. Saline conversion and ice structures from artificially grown sea ice. Res. Rep. No. 4. University of Alaska, Arctic Environmental Engineering Laboratory and the Institute of Water Resources, College, Alaska.

SOME PASSIVE METHODS OF CONTROLLING GEOCRYOLOGICAL CONDITIONS IN ROADWAY CONSTRUCTION

Richard L. Berg and George W. Aitken

U.S. ARMY COLD REGIONS RESEARCH AND
ENGINEERING LABORATORY
Hanover, New Hampshire

INTRODUCTION

The recent discovery of large deposits of oil and gas in the North American Arctic has provided impetus for rapid development in these areas. To accommodate this and the increased development of other natural resources, a network of roadways will be required. This paper presents some results of one of the testing programs conducted to evaluate passive construction methods to improve design techniques and reduce construction costs of roadways in permafrost areas. The test installation discussed here is located in Fairbanks, Alaska. It compares substantially different design approaches, and two analytical techniques are shown to be applicable for analyzing the thermal performance.

DESCRIPTION OF TEST INSTALLATIONS

The location of the installation is shown in Figure 1, and pertinent climatological data for the site are given in Table I.

The test installation is located at CRREL's Farmers Loop Road facility about 4 km northeast of Fairbanks, at 64°49'N, 147°52'W. The Farmers Loop facility is situated at an elevation of 152.4 m (MSL) on the lower colluvial slopes between the valley fill and the upper colluvial slopes of the rock upland known as Birch Hill. A 98.17-m-long test roadway incorporating five different test sections was constructed by the U.S. Army CRREL over a previously undisturbed, high ice content silt subgrade beginning in

August 1964 (Figure 2). The control (asphaltic concrete) section was built to serve as a base for relative performance evaluation of all the sections.

The white-painted asphaltic concrete section was constructed to evaluate the effectiveness of a pavement surface having relatively high surface reflectivity and to allow comparison of this technique with a similar test program conducted in Thule, Greenland,⁵ and with a smaller test section constructed at the Farmers Loop Road facility in 1947.⁶ The compressed peat subbase section was installed to provide data on the effectiveness of a heat sink constructed of indigenous material in reducing permafrost degradation beneath a paved surface. The treated gravel section (colored black) was included to ascertain if this type of surface treatment would thermally simulate a black asphaltic surface. The untreated gravel section was used to obtain basic data on the thermal effects of this common arctic and subarctic roadway type and to obtain a side-by-side comparison with the treated gravel section.

The site was prepared by stripping the *in situ* organic material from an 11-m-wide area between stations 0+00 and 2+90. The maximum depth of cut was about 0.3 m with the excavated material used to build a small berm about 30 m north of the test sections to minimize infiltration of surface water. The average depth of thaw over the entire area before construction was about 0.9 m and the minimum thickness of the annual thaw zone was 0.3 m at station 1+60. A 0.3- to 0.9-m-thick layer of frozen peat was encountered between

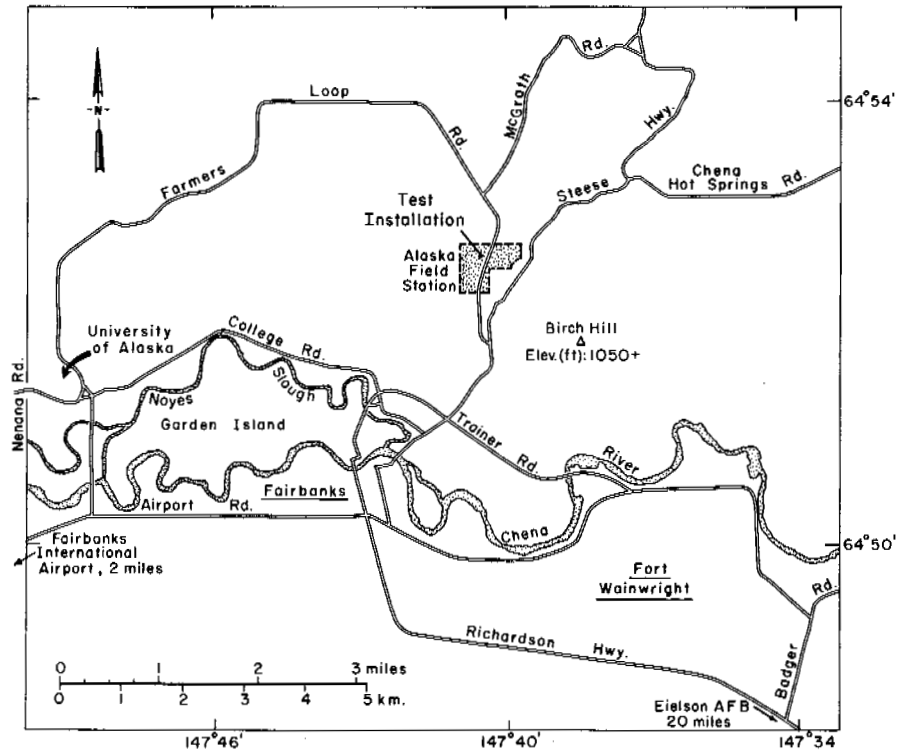


FIGURE 1 Location of test roadways in Alaska.

stations 2+50 and 2+90 and left in place beneath the base course layer. A 0.15- to 0.3-m-thick sand layer and a 0.61-m-thick gravel layer were placed on the subgrade with the sand layer placed almost entirely by hand due to the extremely muddy condition of the thawing silt.

TABLE I Climatological Data^a

Air temperatures (°C)	
Mean annual	-3.44 (36-yr record)
Recorded high	33.9 (25 July 1955)
Recorded low	-54.2 (14 Jan 1934)
Freezing index (°C-days)	
Mean	3 200 (1945-1965)
Design	3 680 (1956)
Thawing index (°C-days)	
Mean	1 844 (1946-1965)
Design	2 040 (1957)
Precipitation (m)	
Mean annual	28.7 (36-yr record)
Max. annual	44.4 (1935)
Max. monthly	17.6 (Aug 1930)
Snowfall (m)	
Mean annual	154 (36-yr record)
Max. annual	297 (1935)
Freezing days	193 (1945-1965)
Thawing days	171 (1946-1965)

^a Data from Fairbanks International Airport about 12.9 km from the test site by the U.S. Weather Service.

The compressed peat subbase section was constructed using preformed bales approximately 0.3 m square by 0.9 m long and weighing about 80 kg each. The bales were compressed at about 193 kN/m² to precompress them to about the maximum stress level anticipated to occur under the traffic and then they were wrapped with steel bands. The dry unit weight of the bales averaged 240 kg/m³, and their average moisture content was 290 percent. A more complete discussion of the equipment and techniques used to fabricate the peat bales is presented by Wilson.¹⁰

The ground temperature assemblies were installed in core-drilled holes in March 1965 (Figure 2). Copper-constantan thermocouples were installed just below the surface and at 0.3-m intervals to a depth of 2.8 m. Additional thermocouples were installed at depths of 3.6, 4.6, and 6.1 m in each section. Data acquisition was initiated in March 1965, utilizing a 300-channel digital data acquisition system with perforated paper tape output.

Final grading of the base course was accomplished in early August 1965, and the asphalt concrete pavement was placed on 24 August. The white paint was applied on 9 September, and the dark gravel section was covered with coal dust on 30 September. The dark gravel section was recovered with coal dust on 2 June 1966 and treated with a coat of MC 2 asphalt on 5 June 1967.

Soil data were obtained from core samples in March 1965. Dry unit weight of the frozen silt ranged from 1 370

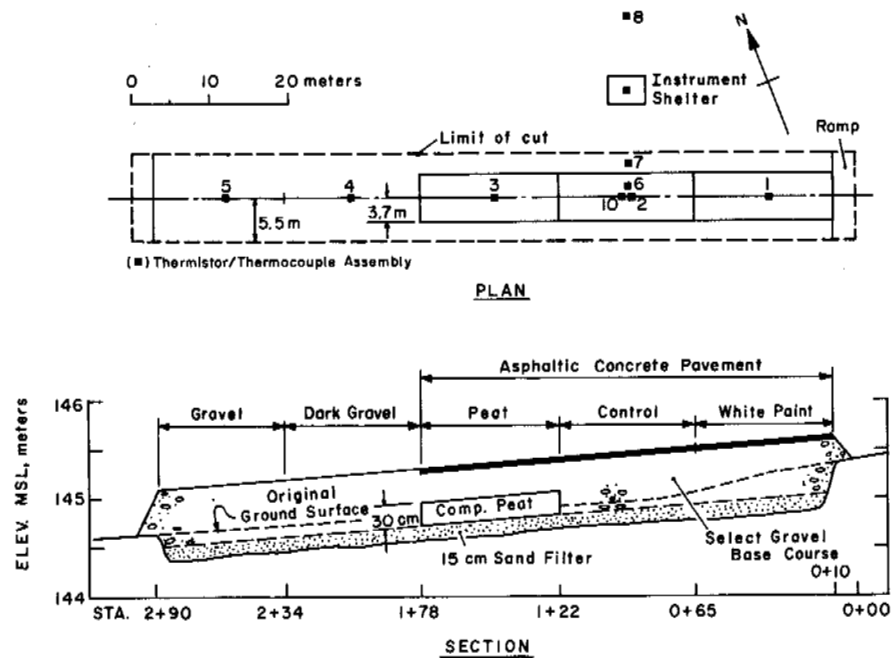


FIGURE 2 Plan and profile, highway test sections.

to $1\,460\text{ kg/m}^3$, and moisture contents (percent by dry weight) ranged from a high of 185 percent down to 32 percent. The average moisture content of the gravel base was 4 percent, and its average dry unit weight was $2\,300\text{ kg/m}^3$. It was non-frost-susceptible with a maximum size of 76 mm and less than 3 percent of the particles smaller than 0.02 mm. During the winter months, the test sections were not trafficked, but snow was removed at irregular intervals.

THERMAL ANALYSIS

The modified Berggren equation² and an explicit one-dimensional finite differencing technique were used to analyze the thermal behavior of the roadway. The finite differencing technique was used to compute and illustrate time-dependent variations of thaw zones and subsurface temperatures. The modified Berggren equation was developed for computing seasonal frost depths in nonpermafrost areas; however, experience has shown that reasonable estimates of thaw depth can also be made with it in permafrost areas. Weaknesses of the modified Berggren equation include the impossibility of studying time-dependent changes of seasonal thaw and the inability to adapt to situations with residual thaw zones.

The general finite differencing method is described by Dusinberre.⁴ Berg and McDougall³ have described this particular computer program in detail. It is a forward differencing technique, and sensitivity analyses have indicated a stability modulus of 2 is adequate. Although temperature-dependent relationships are available for various thermal properties, they are assumed to remain constant in this

program. The method of "excess degrees" described by Dusinberre⁴ is used to account for the latent heat of fusion. Upper boundary temperature variations with time must be specified with subsequent temperatures computed from the initial conditions and upper- and lower-boundary conditions.

A computer program has also been written to solve the modified Berggren equation.¹ It was suitable to use in this study because materials underlying the test sections completely refroze during the preceding winter.

In both computer programs, averages of the frozen and thawed values of thermal conductivity and volumetric heat capacity are used. All soil moisture is assumed to freeze at 0°C and Kersten's⁷ equations relating thermal properties to soil type, dry unit weight, and moisture content are used for both frozen and thawed soils.

DISCUSSION OF RESULTS

Figure 3 shows changes in surface and permafrost elevations that have occurred since the highway test sections were constructed. Permafrost degradation has been greatest beneath the asphaltic concrete surfaced control section and least beneath the white-painted section. Surface subsidence has been greatest in the dark gravel section and essentially no surface settlement has occurred in the white-painted section.

Permafrost degradation has been less in the peat section than in the control section, but surface subsidence has been greater. This was caused by reduction in thaw depths due to the heat sink effects of the peat layer and higher ice content

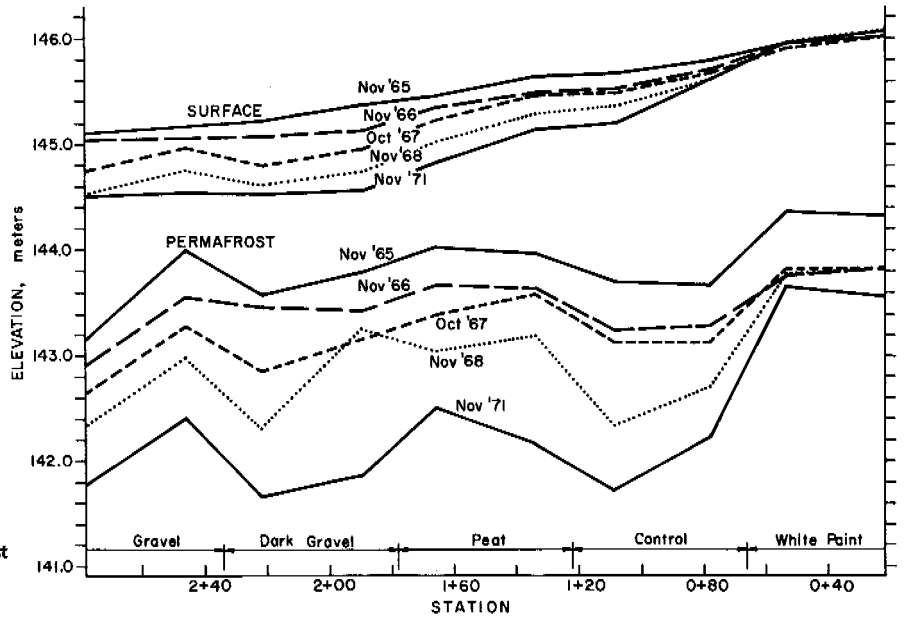


FIGURE 3 Surface subsidence and permafrost degradation, Fairbanks highway test sections, 1965-1971.

natural soils that chanced to occur in the peat section; on thawing, however, consolidation of higher ice content materials was also greater. A much thicker layer of peat would have been necessary to contain the seasonal thaw. However, unless the peat had been compacted to a greater degree than the bales were in this study, surface settlement would undoubtedly have remained significant.

The primary difference in thermal performance between the white-painted section and the control section was the amount of shortwave radiation absorbed at the surface in the summer. Figure 4 shows incident shortwave radiation and reflected shortwave radiation from the white-painted and control sections. The white-painted surface absorbed less than one-half the amount of radiation the control section absorbed. The albedo of the white-painted section was 0.66 and that of the asphaltic concrete control section 0.16.

Due principally to the reduced amount of solar radiation absorbed at its surface, the white-painted test section had the lowest surface temperatures. The "n-factors" (ratios between surface-thawing indexes and air-thawing indexes) measured at the test sections during the 1971 summer are shown in Table II. The n-factors are largest during the early part of the thawing season and decrease after mid-July when the amount of incident solar radiation decreases significantly. Temperature sensors in the gravel section were not functioning properly during this time period; therefore, n-factors for this section are not shown.

The finite difference technique and the modified Berggren equation were used to analyze performance of the test sections. The data from the untreated gravel section for the period from April 1965 through March 1966 were selected

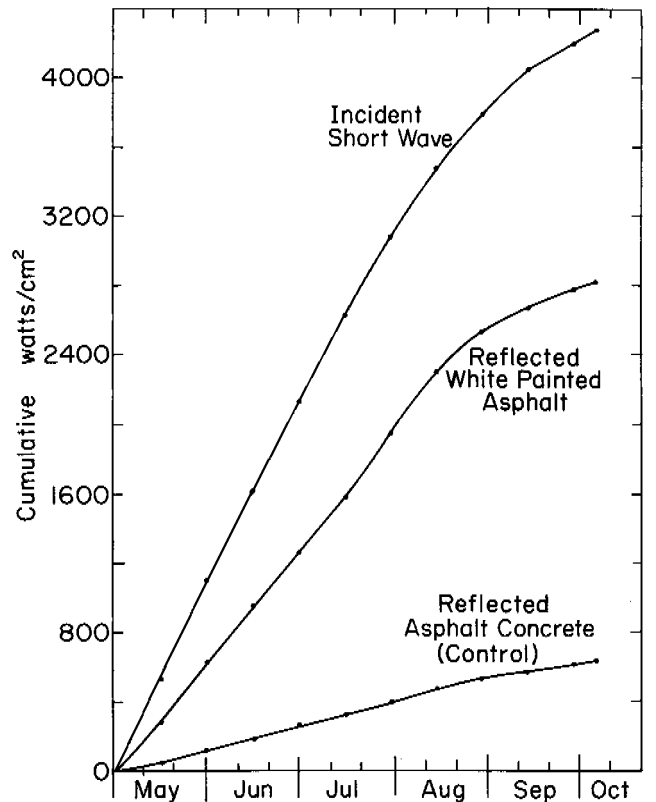


FIGURE 4 Incident and reflected solar radiation, highway test sections 1970.

TABLE II Surface *n*-Factors, 1971

Test Section	May	June	July	August	September	Weighted Average
White painted	—	1.25 ^a	1.11	1.03	0.76	0.98
Control	2.70 ^a	1.88 ^a	1.85	1.79	1.74	1.96
Peat	2.28 ^a	1.75 ^a	1.73	1.61	1.44	1.72
Dark gravel	—	1.79 ^a	1.52	1.39	1.15	1.40

^a Data for only part of month.

as typical to illustrate use of these computational techniques. In this period, the maximum measured depth of thaw at the center of the section was 1.75 m, which occurred near the end of the 1965 thawing season. Upper-boundary temperatures for the finite differencing solution were obtained from hourly temperature records. Thermal properties of the soils were computed using data from the 1965 core samples and the relationships previously discussed.

The maximum depth of thaw computed from the modified Berggren equation was 1.62 m. Using the finite differencing program, the progression of the thawing interface was computed with several time increments. Computed and measured data are in Figure 5 and show very little difference between results using daily or hourly time increments. Considerably more computer time is required for hourly time increments, because the node thickness must be proportion-

ately reduced to provide stability. Both the progression of thaw and the maximum thaw depths are nearly equivalent (1.89 m) using hourly and daily time increments, indicating that hourly time intervals do not substantially increase the accuracy of the computations.

Insulation provides a third alternative passive technique. Although test sections incorporating insulating layers were not included in this test series, such layers have been installed in both test sections and in actual construction over permafrost. The Corps of Engineers made experimental installations as early as 1947. In the 1950's cellular glass insulation was used under pavements in all the hangars at the Thule Air Base. Esch⁵ and Smith, Berg, and Muller⁹ report to this conference on the performance of two foamed plastic test installations. Knight and Condo⁸ have reported on test sections installed near Prudhoe Bay, Alaska, and in 1969 a

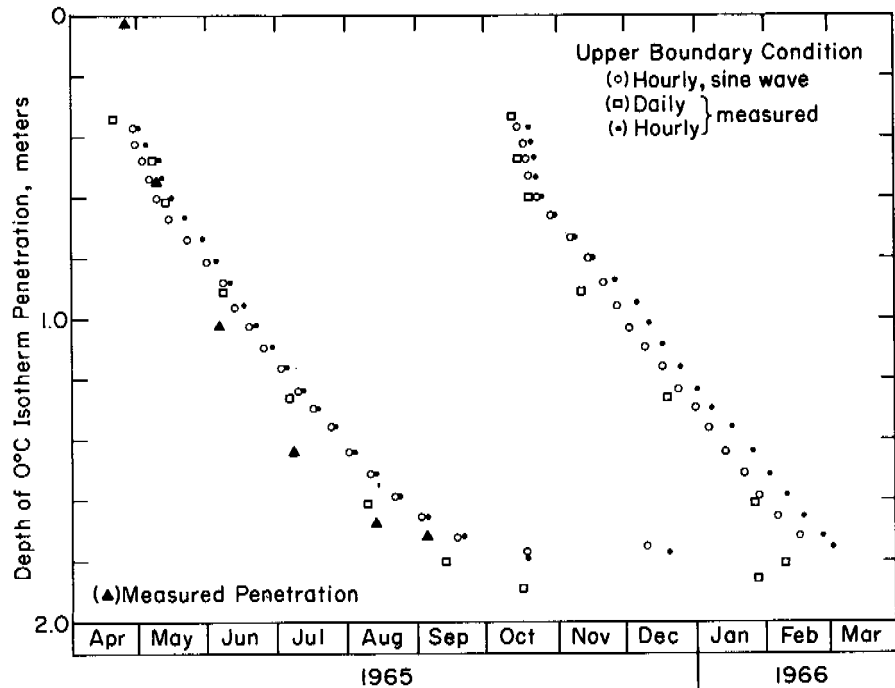


FIGURE 5 Measured and calculated 0 °C isotherm penetration, highway test sections, 1965-1966.

portion of the runway at Kotzebue, Alaska, was insulated prior to laying an asphaltic concrete pavement. Nearly 3 540 m³ of insulation were used on the Kotzebue project, the largest quantity of foamed plastic used to date on a project over permafrost.

SUMMARY

Two different heat transfer computational techniques were shown to be applicable in evaluating thermal designs in permafrost areas. It is believed that the finite difference technique will have more widespread application in the future because of the flexibility it provides with regard to specification of boundary and initial conditions.

In this study, the most effective technique for controlling permafrost degradation was that of painting the pavement surface white. This is in agreement with data obtained from a white-painted runway at Thule, Greenland.⁶ It is unfortunate that the highway test sections were not trafficked so that the effects of abrasion of the paint could have been evaluated. At Thule, repainting every few years has been adequate under aircraft traffic. Undoubtedly, highway traffic and maintenance procedures constitute a more severe environment for the paint, particularly the use of studded snow tires, which would reduce the interval required between repainting to maintain effective albedo control. However, research may yield other still longer lasting techniques for albedo control.

Performance of the baled peat heat sink was not satisfactory and this approach should probably not be considered in an area having a thermal regime similar to that at Fairbanks.

ACKNOWLEDGMENTS

This paper presents the results of research performed by the Cold Regions Research and Engineering Laboratory under the sponsorship of the U.S. Army Corps of Engineers and the Army Materiel Command.

REFERENCES

1. Aitken, G. W., and R. L. Berg. 1968. Digital solution of modified Berggren equation to calculate depth of freeze or thaw in multi-layered systems. Special Report 122. U.S. Army Cold Regions Research and Engineering Laboratory, Hanover, New Hampshire.
2. Aldrich, H. P., and H. M. Paynter. 1953. Analytical studies of freezing and thawing of soils. Technical Report 42. First Interim Report. U.S. Army Corps of Engineers, New England Division, Arctic Construction and Frost Effects Laboratory.
3. Berg, R. L., and J. L. McDougall. 1972. A finite difference program for computing subsurface soil temperatures. USA CRREL Technical Note. (Unpublished)
4. Dusenberre, G. M. 1961. Heat transfer calculations by finite differences. International Textbook Co., Scranton, Pa.
5. Esch, D. Control of permafrost degradation beneath a roadway by subgrade insulation. This volume.
6. Fulwider, C. W., and G. W. Aitken. 1963. Effect of surface color on thaw penetration beneath a pavement in the arctic. *In* Proceedings, First international conference on the structural design of asphalt pavements. Braun-Brumfield, Inc., Ann Arbor, Michigan.
7. Kersten, M. S. 1949. Laboratory research for the determination of the thermal properties of soils. Technical Report 23. Final Report. U.S. Army Corps of Engineers, New England Division.
8. Knight, G. R., and A. C. Condo. 1971. Design and evaluation of insulated and uninsulated roadway embankments for the Arctic. *In* J. L. Burdick [ed.] Proceedings of the symposium on cold regions engineering. Alaska Section, American Society of Civil Engineers and Department of Civil Engineering, University of Alaska, College.
9. Smith, N., R. Berg, and L. Muller. The use of polyurethane foam plastics in the construction of expedient roads on permafrost in Alaska. This volume.
10. Wilson, H. 1965. Construction of a highway test section on permafrost. USA CRREL Technical Note. (Unpublished)

ENVIRONMENTAL CONSIDERATIONS FOR THE UTILIZATION OF PERMAFROST TERRAIN

Jerry Brown

U.S. ARMY COLD REGIONS RESEARCH
AND ENGINEERING LABORATORY
Hanover, New Hampshire

INTRODUCTION

During the elapsed decade since the First International Permafrost Conference,¹⁷ the problems of permafrost and its disruption have become increasingly significant because of the economic development and management of the North American Arctic and Subarctic. Most permafrost terrain, unlike any other terrestrial landscape, contains large volumes of near-surface ice. Passive techniques of construction and exploration require the minimal disturbance of the air-ground interface to prevent thawing of the segregated and massive occurrences of ground ice. The permafrost landscape is therefore an environmentally sensitive surface to travel across and to build upon. For example, in the case of tundra, Ives⁷ suggested that the fragility of this terrain is roughly proportional to the ice content and inversely proportional to the mean annual ground temperature (°C).

In the mid- and late-1960's, renewed and accelerated activities associated with exploration for and development of petroleum reserves in the U.S. Arctic did not consistently reflect the state of engineering and environmental practices available to minimize disturbance of the permafrost.⁸ However, early misconceptions and the lack of proper design, construction, and maintenance techniques have now been largely alleviated. Strict regulatory action, more sophisticated engineering design, increased awareness of problems associated with permafrost, and the environmental concern of industry, government, and private interests are resulting in a concerted effort to minimize both the immediate and long-term consequences of man's activities in the permafrost regions. These problems are not unique to North America; experiences in the Soviet Union appear similar.⁹

Three interrelated activities should be considered in the optimal utilization of permafrost terrain: (a) the development and enforcement of and dissemination of information on regulatory practices and the techniques that minimize man's impact on the permafrost landscape; (b) the development of procedures for the restoration or rehabilitation of permissible and unavoidable disturbance of permafrost to stable and aesthetically acceptable conditions and for keeping the disturbances to an absolute minimum; and (c) the

development of techniques for assessing, predicting, and monitoring short- and long-term and direct and indirect consequences of developmental activities, whether they be for construction, recreation, transportation, or other purposes.

The above activities, taken singly and in combination, are an integral part of land use planning in permafrost as discussed by McVee.¹² The first two—regulation and restoration—are based on past experience, results of applied research, and societal judgments. Responsibility for their successful execution belongs to government agencies and to the potential developers, such as the petroleum industry. The third activity is scientifically far more complex in solution and, ideally, involves a systems analysis approach by which the complex interrelationship of the physical and biological environments is determined and from which computer models are constructed to simulate potential modifications under a range of stresses.

STATUS OF CURRENT ACTIVITIES

The following discussion summarizes recent developments and accomplishments observed by the author during his own research experiences with the U.S. Army Cold Regions Research and Engineering Laboratory and with the interdisciplinary research activities of the Tundra Biome, which is supported by the National Science Foundation, the State of Alaska, the petroleum industry, and the Office of Naval Research. It is not intended to be an all-inclusive review, but is intended to show the extent to which environmental awareness is influencing recent construction and transportation activities in permafrost regions.

Regulation of construction and transportation activities on permafrost is evolving rapidly. In Alaska, for example, both the state and federal governments now regulate the use of many offroad vehicles during the thaw season. At Prudhoe Bay, the scene of major oil development, tracked vehicles are prohibited from the tundra at the time of snowcover melt, during the entire summer, and well into the freezeup season. Special summer permits are required for the operation of low-ground-pressure, nontracked vehicles. Government stipulations on construction tech-

niques in permafrost also have been formulated to guide the construction of the proposed trans-Alaska petroleum pipeline.²⁰ For example, conditions under which the proposed pipeline could be buried or elevated will depend on the thaw stability and ice content of the permafrost. As a result of stipulations, it is likely that burial would not be possible for more than half the proposed 1 300-km route. Although the above-ground design initially satisfies engineering standards, it presents a potential barrier to wildlife movement—principally, the migration of caribou—and ramps or underpasses may be required to permit their relatively unobstructed passage. If required, then the optimal design of the ramps and underpasses, their placement, and the anticipated increased traffic surrounding them must be considered in terms of the vegetative mat, the underlying permafrost, and its susceptibility to thawing.

In situations where some permafrost disturbance cannot be prevented, for instance along right-of-ways, techniques of rehabilitation are required. Generally, it is neither economically nor ecologically feasible or necessary to restore the environment to precisely its original condition. Often, the acceptable solution is to stabilize the disturbed area to prevent further degradation and at the same time optimize ground surface and aesthetic characteristics. In recent years, numerous research projects both in Alaska and Canada have been initiated to establish guidelines for revegetating disturbed construction sites.^{1,2,11,15,21} Several approaches have been employed, including the use of agronomic and native species that use different planting techniques and fertilizer applications. A number of species have been found capable of establishing a well-developed plant cover. Success is generally dependent on availability of nutrients and moisture during the growing season and its length and severity. In the northern zone of continuous permafrost, conditions are generally less favorable for revegetation, whereas in the southern, discontinuous zone longer and warmer growing seasons produce luxuriant growth. Where seedbed conditions are too dry and lack organic matter, peat additives, mulching, and watering techniques are being developed to provide a temporary, more favorable seedbed. On slopes where gully erosion is as likely as permafrost thaws, diking and water bar techniques in conjunction with seeding, fertilizing, and mulching are proving successful.³

The assessment and prediction of short- and long-term consequences of man's activities on the permafrost landscape is the goal of the U.S. Tundra Biome projects of the International Biological Program, a 5-year ecosystem research program in cooperation with other circumpolar countries during the period 1969–1974. The Biome's approach involves acquiring a reasonably complete understanding of the complex interactions that exist in nature among the atmospheric, ecological, and substrate properties and processes; and developing environmental computer models to a point of realism that can, independently of observed data,

replicate natural and stressed phenomena. Once these computer models are developed, various hypothetical perturbed conditions can be simulated. Sensitivity analyses of the input parameters can be performed to identify the most important parameters. These simulations and sensitivity analyses yield time histories (25, 50, 100 years, etc.) of how the stressed system will respond and which parameters are the most important. Although it will be another year before successful models will be available for realistic simulations, several examples can be cited that indicate the types of modeling now under development.

The responses of permafrost to natural and stressed conditions are largely determined by the energy and mass transfers at the air-ground boundary. Figure 1 illustrates the major biological and physical components at the interface. The interaction of vegetative cover or plant canopy, soil temperature and depth of thaw has been initially explored by combining models¹⁴ of radiation and turbulent transfers in tundra vegetation canopies with a model¹⁶ of soil temperatures and heat conduction of tundra soils at Barrow, Alaska. The driving or input variables are the seasonal course of solar radiation, infrared radiation from the sky, turbulent transfer and air temperature and humidity, and soil temperature at the point of zero annual amplitude. Both models require through the season the input of the ground surface temperatures, which are calculated from the energy budget equations for the ground surface under the canopy.¹³ These models then demonstrate the capability of predicting depth of thaw within several centimetres of measured thaw throughout the season. Results of sensitivity analyses to relate change in thaw depth to other environmental variables emphasize the importance of infrared

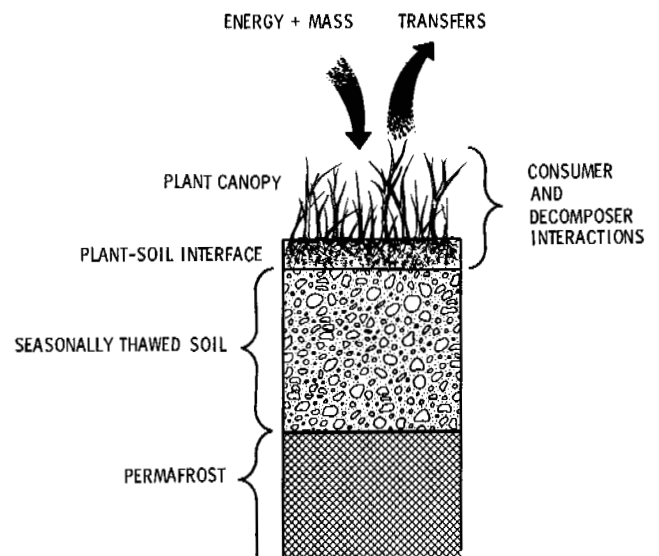


FIGURE 1. Major components active in the energy and mass transfers at the air-ground interface for the arctic tundra ecosystem.

radiation relative to thermal conductivity and air temperature. On a landscape scale, a model of meteorological variations for different habitats such as lakes, wet meadows, and dry uplands realistically produces results similar to the actual observed conditions of permafrost temperatures.¹⁰ Several other models are now being refined or adapted to tundra conditions to allow long-term simulations.^{18,19}

This developing capability to model the vast array of environmental parameters that influence the permafrost will allow ecologists, engineers, and land managers to explore potential long-term adverse impacts that may develop under the cold-dominated permafrost environments. Answers to questions such as the following may be forthcoming:

- How long will it take native vegetation to recolonize disturbed tundra or taiga under climatic conditions which now exist?
- What will be the effect of a given albedo change on the permafrost temperatures over constant or variable climatic conditions for 25, 50, or 100 years?
- How will spacing of road nets and snow drifting influence plant and animal life cycles and soil temperatures over an extended period of time?

An example of how these long-term modeling simulations can directly feed back to regulatory activities concerns the use of low-ground-pressure vehicles during the snow-free period or on light or weak snowcovers. It is an observed fact that whenever the vegetation is pressed into the surface peat layers by a vehicle, it develops a greener tone that persists for many years along the path of the vehicle.^{5,6} This is due to the enhancement of microbial activities that accelerate the decomposition of the dead plant material in the track, which, in turn, gives the appearance of the brighter green belts. In areas where offroad vehicles are permitted random access, even under the protection of light snowcover, a crisscross of such trails across the tundra will develop and persist. Aesthetically, this could be undesirable, and, if the frequency of occurrence is large enough, albedo changes may be expected. The effects of such a seemingly minor disturbance in all its temporal and spatial variations will likely be capable of assessment by modeling. In turn, the results may be in a form that will point out the least desirable time for offroad access, regardless of season, and recommend the best operating conditions such as speed and type terrain to avoid.

CONCLUSION

Current utilization of the permafrost landscape is still relatively low as a result of its vastness, remoteness and inaccessibility, and low population usages. However, where population and industrial centers do exist, the solutions of problems caused by the presence and potential degradation

of permafrost are expensive. Frequently, symptoms of permafrost degradation occur regardless of the care exercised to avoid them. As man increases his activities on the permafrost landscape, increased disruption of the permafrost is likely to occur. These changes are characteristically generated at the ground surface as the energy exchange processes are modified; however, these surface effects are transferred into the permafrost. In many cases, they are cumulative and often lead to adverse consequences. The problem besetting the planner, developer, environmentalist, and others is to define, in advance and under differing permafrost regimes, the types and degrees of modification the permafrost landscape can sustain without adversely affecting its original quality. This definition should include both human or aesthetic values and the physical or thermal constraints imposed by the permafrost. Unsightly vehicle impressions across the uninhabited tundra may be acceptable to some, but an accelerated and headward eroding channel resulting from a poorly designed facility, road, or entrenched vehicle trail is no longer tolerated. The definition of that fine line between permissible and nonpermissible use of the permafrost terrain, both in time and space, should prove to be an excellent point of discussion and cooperation between Northern American, Soviet, and other researchers and planners.

ACKNOWLEDGMENTS

This paper presents the results of observations and research performed by the Cold Regions Research and Engineering Laboratory under the sponsorship of the U.S. Army Corps of Engineers.

REFERENCES

1. Bliss, L. C. 1970. Oil and the ecology of the arctic. *In* The tundra environment. A symposium of section III of the Royal Society of Canada, Winnipeg, 3 June 1970. *Trans. Roy. Soc. Can. Fourth Ser.* 7:1-12.
2. Bliss, L. C., and R. W. Wien. 1972. Plant community responses to disturbance in the western Canadian arctic. *Can. J. Bot.* 50(5):1097-1109.
3. Bolstad, R. 1971. Catline rehabilitation and restoration. p. 107-116. *In* C. W. Slaughter, R. J. Barney, and G. M. Hansen [ed.] Fire in the northern environment. A symposium, College, Alaska, 13-14 April 1971. Pacific Northwest Forest and Range Experiment Station, Portland, Oregon.
4. Burt, G. R. 1970. Travel on thawed tundra. Note 7005. Institute of Arctic Environmental Engineering, University of Alaska, Fairbanks. 23 p.
5. Challinor, J. L. 1971. Vehicle perturbation effects upon a tundra soil-plant system. M.Sc. thesis. University of California, Berkeley. 240 p.
6. Hok, J. R. 1969. A reconnaissance of tractor trails and related phenomena on the North Slope of Alaska. U.S. Department of the Interior, Bureau of Land Management, Washington, D.C. 66 p.

7. Ives, J. D. 1970. Arctic tundra: How fragile? A geomorphologist's point of view. *In* The tundra environment. A symposium of section III of the Royal Society of Canada, Winnipeg, 3 June 1970. *Trans. Roy. Soc. Can. Fourth Ser.* 7:39-42.
8. Klein, D. R. 1970. The impact of oil development in Alaska (a photo essay), p. 209-242. *In* Proceedings of the conference on productivity and conservation in northern circumpolar lands. Edmonton, Canada, 15-17 October 1969. International Union for Conservation of Nature and National Resources, Morges, Switzerland.
9. Kriuchov, V. V. 1968. Soils of the far north should be conserved. *Priroda* No. 12. p. 72-74.
10. Lord, N. W., J. P. Pandolfo, and M. A. Atwater. 1972. Simulations of meteorological variation over arctic coastal tundra under various physical interface conditions. *Arctic Alp. Res.* 4(3):189-209.
11. McCown, B. H. The influence of soil temperature on plant growth and survival in Alaska. *In* Oil resource development and its impact on northern plant communities. A symposium, 17 August 1972. University of Alaska, Fairbanks. (In press)
12. McVee, C. V. Permafrost considerations in land use planning management. This volume.
13. Miller, P. C. 1972. A model of vegetation structure and depth of thaw for the tundra, p. 13-15. *In* Proceedings of the 1972 Tundra Biome symposium, Lake Wilderness Center, University of Washington, Seattle. USA CRREL, Hanover, New Hampshire.
14. Miller, P. C., and L. Tieszen. 1972. A preliminary model of processes affecting primary production in the arctic tundra. *Arctic Alp. Res.* 4(1):1-18.
15. Mitchell, W. W. Adaptation of species and varieties of grasses for potential use in Alaska. *In* Oil resource development and its impact on northern plant communities. A symposium, 17 August 1972, University of Alaska, Fairbanks. (In press)
16. Nakano, Y., and J. Brown. 1972. Mathematical modeling and validation of the thermal regimes in tundra soils, Barrow, Alaska. *Arctic Alp. Res.* 4(1):19-38.
17. National Research Council. 1966. Permafrost: Proceedings of an international conference. Publ. 1287, National Academy of Sciences, Washington, D.C.
18. Outcalt, S. I. 1972. The development and application of a simple digital surface-climate simulator. *J. Appl. Meteorol.* 11(4):629-636.
19. Timin, M. E., B. D. Collier, J. Zich, and D. Walters. 1972. A computer simulation of the arctic tundra ecosystem near Barrow, Alaska, p. 71-79. *In* Proceedings of the 1972 Tundra Biome symposium, Lake Wilderness Center, University of Washington, Seattle. USA CRREL, Hanover, New Hampshire.
20. U.S. Department of the Interior. 1972. Stipulations for proposed trans-Alaskan pipeline. February. 64 p.
21. Van Cleve, K. Revegetation of disturbed tundra and taiga surfaces by introduced and native plant species. *In* Oil resources development and its impact on northern plant communities. A symposium, 17 August 1972, University of Alaska, Fairbanks. (In press)

SOLID WASTE DISPOSAL IN PERMAFROST AREAS

Jules B. Cohen

ARCTIC HEALTH RESEARCH CENTER
Fairbanks, Alaska

INTRODUCTION

The problem of solid waste management is by no means limited to cold regions of the world. A body of literature is growing rapidly that defines problem areas, proposes solutions, and describes the results of research directed toward the problem. However, little progress has been made in applying new technology since Weaver and Keagy¹⁵ completed their 2-year study of sanitary landfills at Mandan, North Dakota, over 20 years ago. In fact, it is estimated by the U.S. Environmental Protection Agency (EPA)³ that only 5 percent of the 16 000 land disposal sites authorized for use by regular collection services meet accepted standards. The others either contribute to water pollution or air pollution,

provide harborage for insects, rodents, and other pests, or deface the landscape. In addition to the sites indicated above, there are perhaps 10 times as many open dumps. Attempts to remedy this situation have resulted in a national program called Mission 5 000, whose purpose is to eliminate open dumps.

In cold regions, the problem of instituting an acceptable solid waste management program is complicated by a variety of interrelated physical, economic, and political considerations. Long, cold winters and seasonally frozen ground or permafrost make earth moving difficult and biological processes inefficient; small, isolated communities make economy of scale and the pooling of resources impossible; the absence of the means and incentives for recovery limit the options that

are available in other regions; and small communities with a weak economic base must assign higher priority to more pressing environmental problems.

In the arctic and subarctic regions of the United States, this leads to open dumping and uncontrolled burning, even in some of the largest communities; abandoning automobiles and fuel drums is commonplace; and the practice of placing garbage and other waste materials on river and sea ice is usual. With environmental awareness becoming a national ethic, the need for improved solid waste disposal procedures is now being recognized in both the Arctic^{1,2} and the Antarctic.^{7,9} This paper discusses the status of solid waste management and the results of several studies conducted by the Arctic Health Research Center into particular solid waste management problems.

In the North, solutions to the problems have been hampered by the lack of basic data that indicate the quantity and type of wastes being generated by the various types of civilian and military communities. Probably the most exhaustive, though geographically limited, surveys conducted in northern Alaska to date on the volume and characteristics of solid waste are those by Smith and Straughn at Murphy Dome Air Force Station,^{10,12} Straughn at Eielson Air Force Base,¹³ and Reid in the Fairbanks-North Star Borough.⁸ Straughn¹² found that the Air Force Station generated about 2.8 kg per capita per day with garbage comprising about 40 percent, combustible rubbish about 48 percent, and noncombustibles the remainder. In another study, Straughn¹³ found that over a 3-week period about 1.0 kg per capita per day was being accumulated, about 18 percent higher than the 0.85 kg per

capita per day reported by Dorogovtsev⁶ for Vorkuta, the Soviet Union. When compacted in a landfill, this material occupied a volume of 350 m³ density of 490 kg/m³. This density was higher than the 420 kg/m³ that would have been the case had the refuse been covered on a daily basis. Reid,⁸ in an aerial survey of scrap disposal in the Fairbanks-North Star Borough (population of 47 600), estimated that 4 000 cars and 1 000 trucks had accumulated as scrap. A mathematical model indicated that the salvage rate was 15.4 percent, over twice the national figure of 7.3 percent for the past 10 years.

STATE OF THE ART

The studies referred to above were conducted as part of an effort to alleviate some of the problems in solid waste management in cold regions. If the nominal components of the management system—storage, collection, transport, treatment, and disposal—are examined individually, it becomes evident that only certain components require modification for cold region operations.

Storage

The storage of solid waste material prior to collection has been adequately solved using the approach taken by the subarctic community of Fairbanks through use of a plastic bag system coupled with once-a-week collection at the curb (Figure 1). The system is economical (\$2.30 U.S. for 50 bags) and has the following advantages: Moist material will



FIGURE 1 Collection of household wastes in plastic bags at Fairbanks, Alaska. Temperature at time of collection was -22°C .

not freeze to the container; as many bags as necessary can be accumulated should poor weather prohibit regular collections; the bags are durable even at -40°C temperatures; and collection can be made in open trucks if necessary. A disadvantage is that the plastic bags do not support very heavy material. For example, at Murphy Dome Air Force Station wet wastes from the dining hall could not be contained in the plastic bags. In addition, when an incinerator was installed at the station the plastic bags tended to flash, thus endangering the operator. These problems were remedied by substituting plastic-lined, heavy paper bags. These provided the necessary characteristics of an acceptable collection system, although at a higher price.

Collection and Transport

With few minor exceptions, the collection and transport of solid wastes from individual households present no particular problems that are directly related to cold regions. The exception is the small village or suburban area where no community system exists. In such areas responsibility for collection and transport rests with the individual, encouraging the use of the backyard burn barrels, small unauthorized dumps, the dumping of refuse along road sides, and a system such as is seen in Figure 2.

The collection and transport of inoperative vehicles and other scrap require a different approach since in many cases weight, volume, or cost may prevent their being removed to an acceptable point of final disposal. Reid estimated that in interior Alaska the cost of transporting an abandoned vehicle

to a final disposal site was about \$8 U.S. Thus, \$38 000 U.S. would be required for the collection of junk vehicles alone in the Fairbanks-North Star Borough.

The removal and disposal of scrap in remote camps and villages is further complicated by unstable soil conditions and the lack of roads. To collect and remove some 8 300 steel drums accumulated over several seasons of exploratory operations at Prudhoe Bay on the North Slope of the Brooks Range, the oil industry found it necessary to use helicopters and vehicles with oversize tires suitable for use on permafrost. These are only a small portion of the drums accumulating throughout the northern regions of the State of Alaska. It has been estimated⁵ that there are over 48 000 in the vicinity of Barrow and 20 000 in the vicinity of Umiat, the remnants of earlier oil exploration. In addition, the Alaskan Air Command estimates that over 350 000 drums are in storage at its sites throughout the state. In the absence of a demand for empty drums, on-site crushing and burying should provide an adequate solution to the scrap disposal problem at remote sites operated by either the military or the oil industry.

Treatment and Disposal

These aspects of the solid waste problems have received the major emphasis, since it is in these parts of the overall system that permafrost becomes a significant and limiting factor. Ultimate disposal, with or without intermediate treatment, must be to the land. It is in this context that several alternatives have been considered in detail.

The most economical and acceptable method of solid



FIGURE 2 Collection of household wastes by snow machine at New Minto, Alaska.

waste disposal is the sanitary landfill. However, in an area where exposed wastes can attract bears and foxes, the need for daily cover material is mandatory, especially since rabies is endemic in the fox population of the American Arctic. The main difficulties with a landfill in permafrost areas are the need for cover material on a daily basis and the possibility that leachate may contaminate surface waters in the vicinity of the landfill. Where coal is burned to develop power, the resulting ash is available for cover material; otherwise, soil must be stockpiled and drained during summer months for use during the winter. Studies of the fate of material introduced into the landfill will be discussed in the following section. The question of whether degradation of wastes is a necessity in permafrost regions is purely political. The Alaska Department of Environmental Conservation at present is considering regulations that would prohibit the use of landfilling for the disposal of putrescible wastes in areas subject to the influence of permafrost conditions. These regulations would also propose incineration as the recommended method for the disposal of solid waste. While incineration is the most feasible alternative to a sanitary landfill, the residue is still subject to final disposal on the land. Incineration, however, does reduce the frequency with which cover material must be applied, since material that was formerly attractive to animals and insect pests will have been reduced to ash. However, it is questionable whether any native villages can ever afford to install or operate incinerators without subsidy from the federal government for capital, operating, and maintenance costs.

Several types of incinerators have been used in cold regions of the United States, but, until the recent activity on the North Slope, these were limited to small units of the single- or multiple-chamber type. These units were used in schools and stores to burn accumulated garbage, or in hospitals and other institutions to consume pathological wastes. Two other events developed almost concurrently with the North Slope explorations that are important here. One was an increased emphasis by the United States Government on the need for better management of solid waste throughout the nation. The policy included solid waste generated by Federal installations. The second event was the impetus for controlling air pollution from federal installations, provided by Executive Order 11 282.⁴ The air pollution regulations developed in support of the executive order applied in part to air pollution from the incineration of solid wastes. The regulations required that the density of emissions from incinerators should not exceed No. 1 on the Ringelmann Scale; that not more than 11.4 kg of waste be burned in a 24-h period in nonurban areas; that refuse be incinerated only in facilities specifically designed for that purpose; and that emissions not exceed 7 g per normal m³ of dry flue gas corrected to 12 percent CO₂ (without the contribution of auxiliary fuel) for installations burning less than 90 kg/h nor more than 4.6 g per normal m³ for installations burning more than 90 kg/h. To meet these

requirements, most incinerators require primary and secondary burners and gas cleaning equipment.

Incinerators that burn over 100 kg/h and meet the four requirements without complex gas cleaning equipment become attractive for remote locations in cold regions. The more sophisticated the equipment in use at a remote site, the greater the manpower that will be required to maintain the equipment and the greater the likelihood that the equipment will be inoperative. In addition, wet scrubbers, while solving the particulate emission problem could add to others, i.e., ice fog and the scarcity of water during winter. A new, simplified design meeting the federal criteria appeared promising and was installed for evaluation at the Murphy Dome Air Force Station.¹⁰ These units, developed to consume 50-1 000 kg/h of rubbish and garbage, are designed on the principle of controlled combustion with less than 100 percent of the air for combustion supplied in the main chamber. These chambers are grateless and generally can be charged from either of two doors, one of which opens to expose the entire end of the chamber for loading large objects prior to firing. The lack of sufficient air for complete combustion, coupled with an overfire burner, pyrolyzes the non-volatile portion of the waste and volatilizes the remainder. The procedure utilizes lower air velocities, thus minimizing the carryover of particulates. The resultant gases pass into an afterburner section where temperatures are maintained at about 700 °C and additional combustion air is provided. In the afterburner section the carbon, carbon monoxide, and unburned hydrocarbons are converted to carbon dioxide and water before discharge to the atmosphere. The residue, an inert material that may be as little as 5 percent of the original waste volume, consists of partially oxidized containers, fused glass, and ash. This residue must still be introduced into the environment for ultimate disposal. The results of our study on the performance of a unit of this type will be discussed.

SOLID WASTE RESEARCH

While nontechnical considerations will generally dictate the manner in which solid waste will be discharged to the environment, the technical manager is still responsible for making certain that the decisions reached considered all available information. The research discussed below was conducted for the purpose of providing additional data on options available to the decision-makers.

Sanitary Landfill Studies

Two questions that are raised regarding the use of the sanitary landfill in the North are whether and to what extent solid wastes decompose after placement in the ground. Sundsbak¹⁴ reported that biological activity enabled temperatures to reach a maximum of 33 °C at one m below the surface in a landfill in the arctic region of Norway. To

answer these questions, the Arctic Health Services Research Center¹³ with support from the Alaskan Air Command installed and instrumented an 18 m² landfill at Eielson Air Force Base near Fairbanks in September 1967. While the experimental cell was being filled, four sampling probes were installed to measure temperature and to sample gases in the cell. In addition, eight well points 2.4 m deep were driven around the site to monitor groundwater quality changes should leaching occur. Gas, water, and temperatures were sampled on a monthly basis during the study, which covered a period of 2½ years. At the end of that period, the landfill was opened to visually determine the extent of decomposition of the waste material.

Carbon dioxide and oxygen concentrations were found to vary according to the season. In the summer the carbon dioxide in the cell reached at least 30 percent; in winter, it dropped to about 10 percent. The concentrations measured are shown in Figure 3. The oxygen concentrations followed an inverse pattern as would be expected; however, while 0 percent oxygen was measured deep in the cell, no traces of methane or hydrogen sulfide were detected. Figure 4 compares temperatures in the cell with the monthly mean ambient temperatures. These temperatures did not appear to reach the values reported by Sundsbak; however, winter temperatures at Fairbanks are colder than those of arctic Norway. Analyses of the well waters showed a seasonal variation that is characteristic of shallow wells, in which hardness, alkali-

linity, and conductance are diluted by the spring melt. However, no significant changes in groundwater quality appeared during the study. When the landfill was opened for visual examination, the top 15 cm in contact with the soil was found to be moist, odoriferous, and covered with mold. Below that level, there was no evidence that decomposition had occurred. These results indicate that wastes discharged to landfills in an arctic or subarctic environment will be preserved for indefinite periods of time. Therefore, landfills should only be considered for areas where future growth is not anticipated or where the land will subsequently be used for parks and recreational areas.

Upon completion of the study described, the site was modified to determine whether aerobic stabilization might be utilized to enhance the rate of waste decomposition. A report by Stone *et al.*¹¹ on the performance of an artificially aerated landfill in California indicated that the process had the potential for decomposing solid waste, reducing volume, and destroying pathogenic organisms in a period of only several months. Adapting this strategy to the Arctic, wastes would be introduced throughout the year following procedures for proper landfill operation. In the spring, well points would be introduced to aerate and add moisture to the cell until temperatures in the cell began to decline. The points would then be removed and the cells recomacted.

In cooperation with the U.S. Army Cold Regions Research and Engineering Laboratory, we applied this strategy

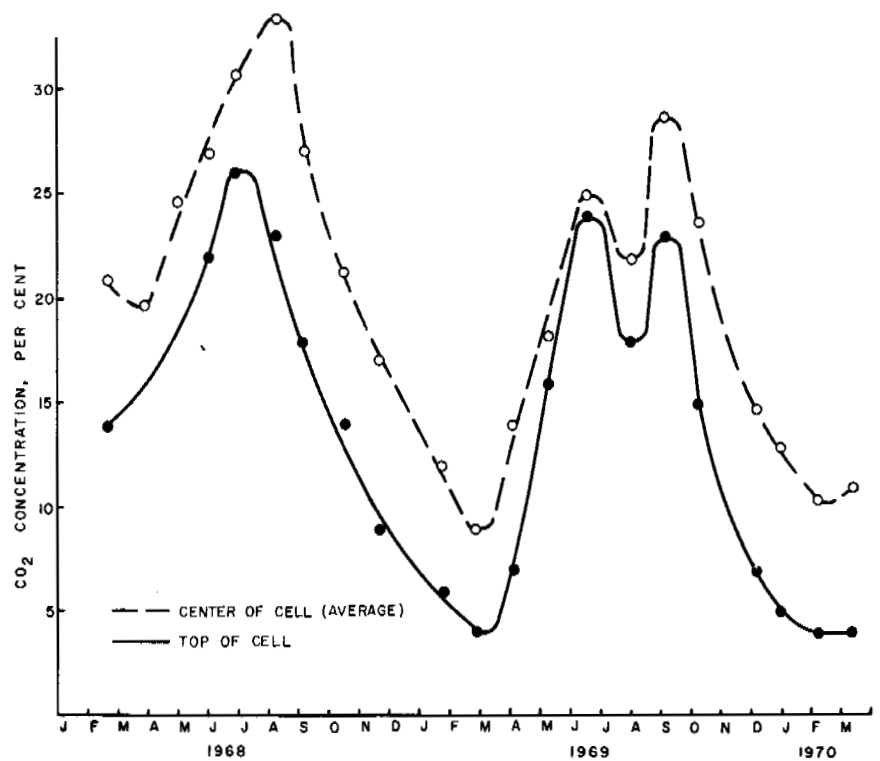


FIGURE 3 Carbon dioxide concentrations measured in experimental landfill.

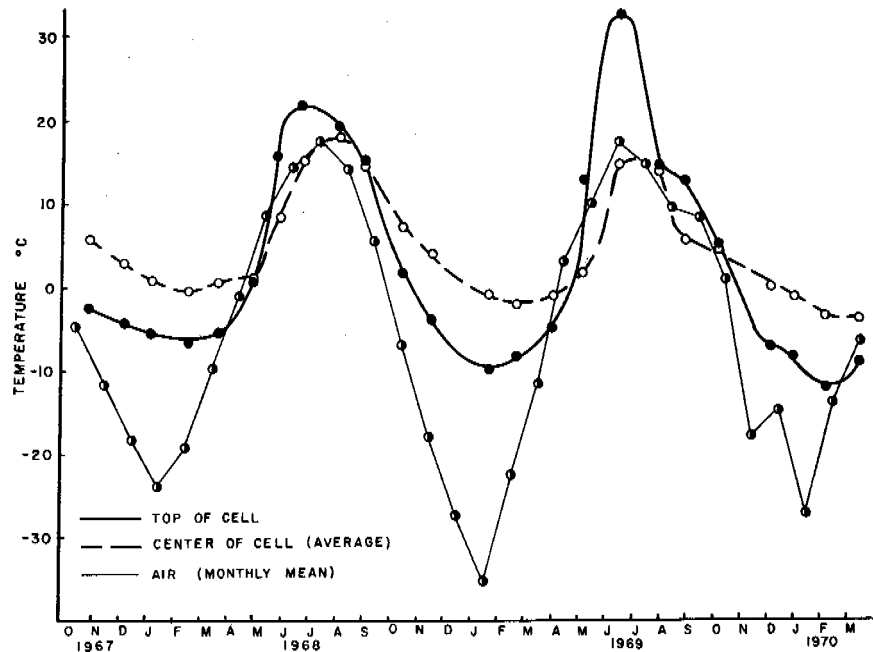


FIGURE 4 Temperatures observed in experimental landfill.

to the site at Eielson Air Force Base. Seven well points were driven into the landfill, one at the center and the remainder equally spaced on a circle 9.4 m in diameter. Approximately 0.38 m^3 of water was pumped down each of the six peripheral well points to provide supplemental moisture. Several weeks later, approximately 0.1 m^3 of sewage sludge was introduced through the same well points in an attempt to add to the microbial population in the cell. Compressed air was introduced by bleeding the contents of an air cylinder (6.3 m^3) into the central well point on a daily basis. Temperatures in the cell were compared with ground temperatures, but little difference was noted during the short period of the study. The study was discontinued when temperatures began declining in September 1971.

The study was continued in June 1972 when ground temperatures began to climb. However, by early August little difference had occurred between landfill and ground temperatures (Figure 5). At that time, sampling of the atmosphere in the cell indicated that the volume of air added was sufficient to maintain an aerobic condition. An attempt was made to improve the performance of the landfill by adding additional heat and moisture to the cell. Twice each week 1.9 m^3 of water at 60°C were added to the peripheral well points. This was continued for about one month. Figure 5 shows that the procedure did little to accelerate the process so the study was terminated. It was apparent to us that in the North large volumes of heat would be required if the decomposition process were to be completed in the ground. An alternative to this would be to operate the system on the surface, which then approximates composting.

Incineration

Where adequate cover material is not available to operate a sanitary landfill, or when governmental policy and regulations prohibit this approach, incineration becomes attractive, even though it is more costly. When incineration was considered for the Murphy Dome Air Force Station, the design of the system was preceded by a study of the characteristics, distribution, and volume of the station's waste. Storage and collection procedures were also examined. The study revealed¹² that the existing system was both unsanitary and cumbersome. Of the 470 kg of solid waste generated on the average, the mess hall contributed over 55 percent. About 47 percent of all station wastes was garbage.

To facilitate the handling and incineration of mess hall wastes, procedures were changed and a paper bag collection system was instituted for the station as a whole. Since the major portion of the station's waste come from the mess hall and was the most difficult to handle, the incinerator was located as close as possible to that source of waste. Four types of paper bag systems were examined, all of which were available in 0.09 and 0.130 m^3 capacities: heavy paper bag, heavy paper bag with a separate plastic liner, wax-impregnated paper bag, and a plastic-lined heavy paper bag. The heavy paper bag was adequate for all but mess hall wastes, whose moisture content caused the bags to lose their strength. Plastic-lined paper bags proved to be the most acceptable. The bags were supported in metal containers and secured at the top by metal flaps. When not in use the containers are covered with metal lids. When full, the bags are stapled

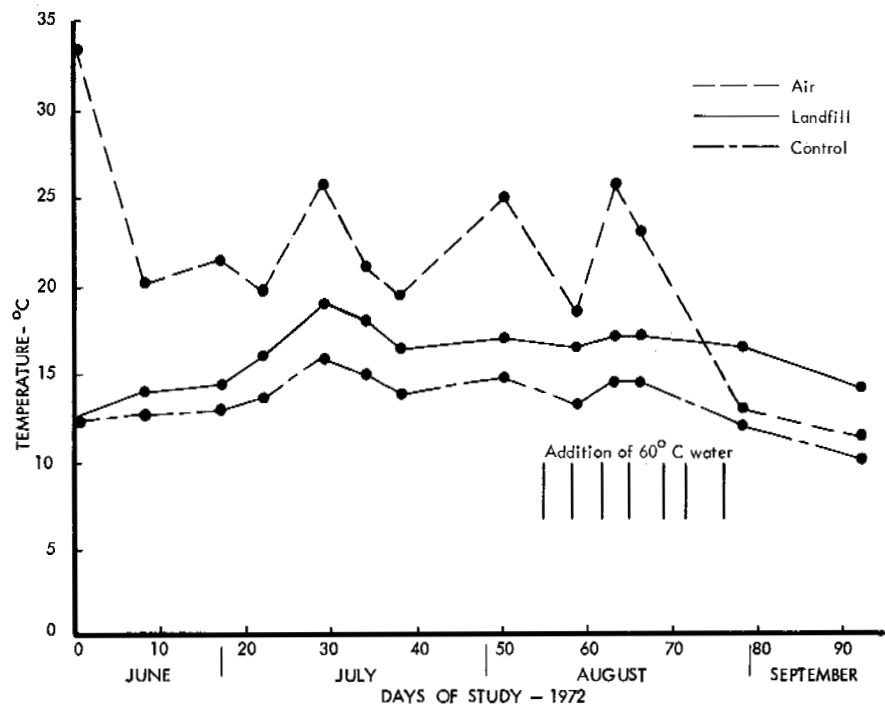


FIGURE 5 Temperatures observed in experimental landfill during aeration.

closed, set aside for collection, thus saving floor space and a new bag inserted. This system reduced the number of containers required and resulted in a more sanitary appearance.

The prototype incinerator chosen was the type described earlier. The unit has a main combustion chamber that is 1.5 m in diameter and 1.8 m long. The unit was rated by the manufacturer to burn 310 kg/h of waste; however, this unit would only meet federal emission standards when burning no more than 190 kg/h. At the time of its purchase, this was the only unit of its type that had used oil rather than natural gas for the auxiliary burners, two of which were provided in the main chamber and one in the afterburner.

The major flaw in the system was the hazard in loading the unit after ignition. The high temperatures in the chamber resulted in the ignition of paper and plastics and the detonation of closed containers and aerosol cans as these were being loaded. These problems required modification of the loading pattern and a change in design of future units. A new loading schedule was adapted, which allowed two charges of about 230 kg to be added safely each workday. The first was added and fired in the morning after the unit was cleaned. The second was added 5 h later—after the first charge had been consumed by a 2-h cycle of the burners in the main chamber, an additional 1-h cycle on the afterburner, followed by a cooling period of 2 h. It was recommended that future designs either include sufficient chamber volume to permit the daily volume of wastes to be loaded as a single charge or that an automatic loading device be added. The

latter choice is not quite as acceptable, since it involves additional mechanical equipment with attendant problems, as well as man-hours for loading since these devices have relatively small capacities. The cost tradeoff between a larger incinerator and a loading device would probably favor the incinerator.

The wastes were well consumed when the incinerator was operated in the manner recommended. The residue from combustibles was a light, fluffy ash, cans were oxidized and brittle, and glass was often melted. The residue from mess hall wastes was generally identifiable as bones, silverware, and plates. Tests to determine weight reduction indicated an average of about 70 percent. Volume reduction averaged 86 percent of the normal wastes; however, the large contribution of cans and bottles was a significant factor. When these were removed a 92 percent weight reduction was observed. Even then, the few cans and bottles that evaded separation comprised a significant fraction of the residue.

Overall, the study indicated that with the design changes suggested above controlled combustion is an acceptable means of meeting requirements for solid waste treatment in the Arctic, particularly when maintenance of air quality is an important consideration.

Combined Systems

Recognizing that individual environmental systems impact on each other—i.e., water and waste water treatment units

producing solid wastes, solid waste systems producing air and water pollution, etc.—more emphasis is being given to combining systems in an effort to minimize this crossover and, in turn, to improve cost effectiveness. Two such combination units have been designed and constructed for use at several recreational camps near King Salmon Airport, Alaska. The units utilize physicochemical waste water treatment in combination with controlled combustion incineration as depicted in Figure 6. Sewage sludge and filter material generated by the waste water treatment process are fed directly to the incinerator, where this and other solid wastes accumulating at the site can be consumed. The performance of these units, which were installed during the spring of 1973, has not yet

been evaluated. While not required in these particular units, future combined units could well use the heat generated by the incinerator to sterilize or pasteurize the waste water before it is discharged to the environment. This would reduce both the cost of purchasing and shipping chemicals and the size of the treatment unit when the holding tank to provide the necessary detention time for disinfection is no longer required.

A more comprehensive system has been developed for the EPA Native Village Demonstration Project. This agency is installing central community facilities to improve living conditions in remote villages in Alaska. Units have been installed at Emmonak in the Yukon Delta and at Wainwright

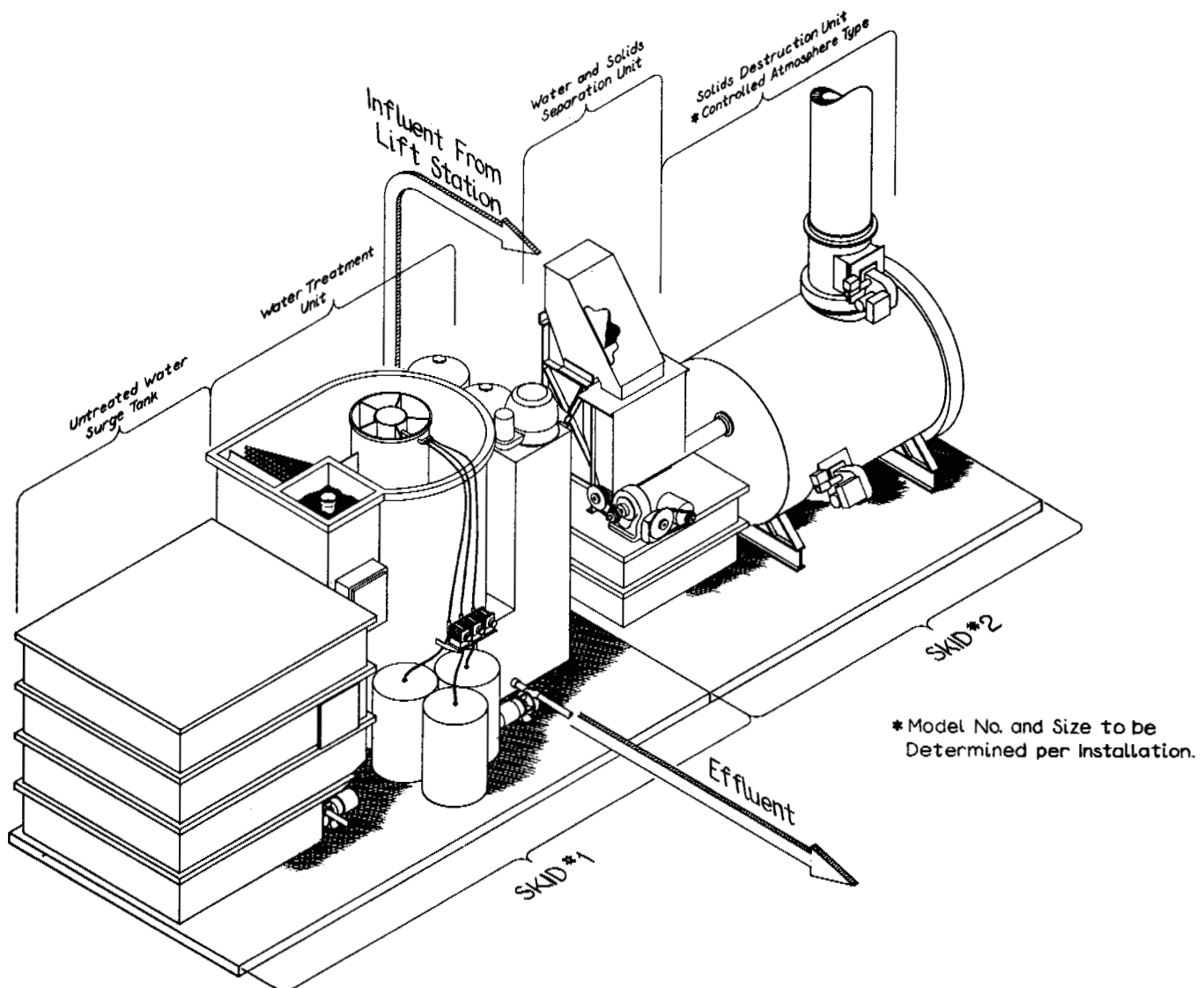


FIGURE 6 Schematic of combined waste water-solid waste treatment unit.

on the coast of the Arctic Ocean. They provide an integrated system of water supply, waste water treatment, and solid waste disposal, along with central showers, sauna, and laundry facilities. Water and waste water are hauled between this facility and storage reservoirs in each home, since water pipes and sewers are not planned for these villages at this time. The facilities are designed to use excess heat from incineration of human wastes and garbage, to provide a portion of the heat required within the facility. New technology has been incorporated into the unit at Emmonak, where a high-efficiency molten-salt catalytic combustor will be used to incinerate all waste material.

Performance data on these units are also lacking due to their recent installation, but the indications are that both communities will require financial assistance from the state or federal government to properly operate and maintain these facilities.

CONCLUSIONS

Communities in the cold climates of the United States must give high priority to a number of environmental problems. While not of the highest priority, solid waste disposal has not been completely neglected. In most cases, the technology exists for solving the problems of solid waste management. The introduction of incinerators in small, remote civil and military communities is evidence that the problem is recognized and is receiving attention. In areas where a solid waste problem still exists, the problem is usually economic rather than technological. However, additional studies are needed to provide more data on the volume and characteristics of solid waste generated in remote villages. In addition, characterizing wastes from seasonal recreation sites and planning for the adequate disposal of these wastes are areas for future consideration.

REFERENCES

1. Alter, A. J. 1972. Arctic environmental health problems. *CRC Crit. Rev. Environ. Control.* 2(4):459-515.
2. Arctic Health Research Center. 1970. Technical information on solid waste management for North Slope activities. Fairbanks, Alaska.
3. U.S. Environmental Protection Agency. 1972. A citizens' solid waste management project—Mission 5000. Publ. No. SW-115ts. Washington, D.C.
4. Code of Federal Regulations. 1969. Prevention, control and abatement of air pollution from federal government activities: Performance standards and techniques of measurement. Title 42, Ch. 4, Part 476. National Archives and Records Service, Office of the U.S. Federal Register. Washington, D.C.
5. Dalton, J. W. 1971. Recommended procedure and cost estimate for clean-up of naval petroleum reserve No. 4, Alaska. Report to: Director, Naval Petroleum and Oil Shale Reserves.
6. Dorogovtsev, V. A. 1969. Garbage disposal in the far north. *G. Sanit.* 34(9).
7. Frederickson, L. H. 1971. Environmental awareness at Hallett Station. *Antarct. J. U.S.* 6(3):57.
8. Reid, L. C., Jr. 1968. A study of scrap disposal in the Fairbanks-North Star Borough, Alaska. Arctic Health Research Center, Fairbanks, Alaska.
9. Thomson, R. B. 1971. United States and New Zealand Cooperation in Environmental Protection. *Antarct. J. U.S.* 6(3):59-61.
10. Smith, D. W., and R. O. Straughn. 1971. Refuse incineration at Murphy Dome Air Force Station. Arctic Health Research Center, Fairbanks, Alaska.
11. Stone, R., E. T. Conrad, and C. Melville. 1968. Land conservation by aerobic landfill stabilization. *Public Works* 99(12):95-98.
12. Straughn, R. O. 1968. Solid wastes characteristics and handling at Murphy Dome Air Force Station. Arctic Health Research Center, Fairbanks, Alaska.
13. Straughn, R. O. 1972. The sanitary landfill in the Subarctic. *Arctic* 25(1):40-48.
14. Sundsbak, H. P. 1971. Temperature measurements in a sanitary landfill in an arctic region. Paper presented at the Second International Symposium on Circumpolar Health, Oulu, Finland.
15. Weaver, L., and D. M. Keagy. 1952. The sanitary landfill in northern states. Publ. No. 226. U.S. Public Health Service, Washington, D.C.

SETTLEMENT ASSOCIATED WITH THE THAWING OF PERMAFROST

Frederick E. Croy

U.S. ARMY COLD REGIONS RESEARCH AND
ENGINEERING LABORATORY
Hanover, New Hampshire

INTRODUCTION

The thawing of permafrost can produce a wide range of volume changes, since the ice volume *in situ* can vary significantly with depth and horizontal distances. Consequently, the settlement on thawing can be quite variable and is often damaging to structures, utilities, roads and airfields. Degradation of the permafrost may be caused in several ways and may occur in a few days or during many years. Whenever permafrost is thawed prior to or after construction, an assessment of the potential volume changes associated with it is essential to solving the engineering problems encountered in the cold regions.

While several papers^{4,5,9,11} in recent years have admirably addressed the combined problems of settlement, heat flow, and pore pressures during the thawing of permafrost, this paper is specifically directed to the development of practical methods of determining the settlement of permafrost on thawing. This is done using common laboratory tests and simple relationships. The purpose of this paper is to provide:

1. A direct, simple and accurate method of predicting the settlements associated with the thawing of permafrost, using the water content and dry unit weight of undisturbed samples of the frozen ground;
2. A greater appreciation for the relationships between water content and dry unit weight of saturated frozen and thawed soils. When the soil is saturated, the potential settlement on thawing can be easily assessed, using only the water content of disturbed or undisturbed samples of the frozen soil; and
3. A settlement prediction method that can be readily integrated with thermal prediction methods in determining the rate of settlement and strength of thawing soils with respect to time. The integration, however, is beyond the scope of the present paper.

BASIC RELATIONSHIPS

Permanently frozen soils have varying amounts of ice, ranging from massive ice, sometimes 10 m or more deep and hundreds of metres wide, to wedges or veins that may be a metre or

only a centimetre thick to frozen soils that have only small ice crystals barely discernible to the naked eye. Usually, the ice in permafrost is heterogeneous, although on a few occasions it may be homogeneous.

The constituents of permanently frozen soils consist of the volume occupied by the soil, ice, water, and air. A frozen sample may have all four constituents present simultaneously or only soil and ice, or—as in the case of many “frozen” clays—soil, ice, and unfrozen water. Assume, as Terzaghi⁷ did in the development of his consolidation theory, that the frozen sample is saturated (i.e., has no air volume). Then we can graphically represent a frozen core sample (Figure 1a) in conventional soil mechanics units (Figure 1b). The volume not occupied by the soil may be ice (in b') or water, having an expansive volume ΔV , in b'' . The dry unit weight of the frozen sample, γ_{d1} , is the weight in grams per cubic centimetre (the unit volume being H^3) while the water content, w_1 , of the frozen sample is the ratio of weight of ice (and any unfrozen water) to the weight of dry soil within the same unit volume. The water content and dry unit weight are the standard units computed for all frozen cores.

If we were to place this unit frozen sample in a consolidometer, we could measure the change in volume of the sample as it thawed, and after thawing was completed, the volume change with increasing axial pressures. Since the sample is constrained laterally, only the one-dimensional consolidation or axial strain (ΔH) is recorded as it is thawed and consolidated. The sample on thawing, however, can expand, experience no change of volume, or consolidate, as depicted in Figure 1c, d, and e.

Should the unit sample expand or heave on thawing (Figure 1c) the amount of expansion, or unit strain, can be termed ΔH . The expanded portion ΔH contains water and soil in the same proportion as the remaining unit H , which we can express as:

$$\Delta H/H = W_{Se}/W_S, \quad (1)$$

where W_{Se} = weight of soil in expanded portion ΔH , and W_S = weight of soil remaining in unit volume, H^3 , equal to γ_{d2} , the thawed dry unit weight of soil.

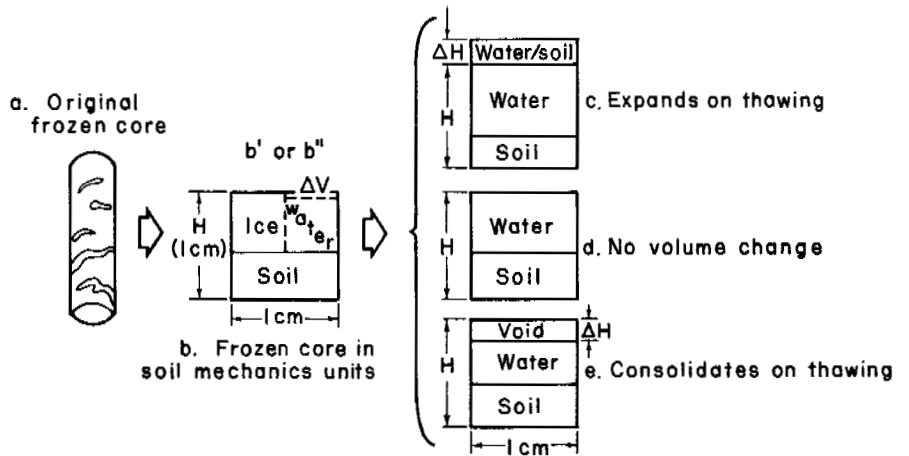


FIGURE 1 The basic volume relationships of frozen core, which, when thawed, might expand, have no volume change, or settle the amount ΔH .

Since the original (frozen) dry unit weight of soil, in the unit volume, H^3 , was γ_{d1} :

$$W_{Se} + W_S = \gamma_{d1}, \tag{2}$$

and since $W_S = \gamma_{d2}$:

$$W_{Se} + \gamma_{d2} = \gamma_{d1},$$

or

$$W_{Se} = \gamma_{d1} - \gamma_{d2}. \tag{3}$$

Substituting in Eq. (1), we now have:

$$\Delta H/H = (\gamma_{d1} - \gamma_{d2})/\gamma_{d2}. \tag{4}$$

Thus, the unit strain in expansion on thawing the frozen sample is expressed with respect to the initial and final dry unit weights only.

However, the original unit volume of frozen soil may experience no volume change on thawing (Figure 1d). This is accomplished by retaining the same unit weight of soil as in b, but providing additional water to compensate for the volume lost during the thawing of ice. Further comments on the amount of water added to the thawed samples in Figures 1c and 1d, as well as unfrozen water, will be given later. For the present discussion, we should merely note that $\Delta H/H = 0$ because $\gamma_{d1} - \gamma_{d2}$ in Eq. (4) is zero.

Should the originally frozen sample contain appreciable amounts of ice, we would experience settlement within the unit sample as shown in Figure 1e. While the volume and weight of soil in Figure 1b and e are the same, the volume that the soil is contained in when thawed is now $(H - \Delta H)H^2$. Accordingly, the thawed dry unit weight is:

$$\gamma_{d2} = W_S/(H - \Delta H)H^2. \tag{5}$$

Since $\gamma_{d1} = W_S/H^3$ or $W_S = H^3 \gamma_{d1}$ by substitution in Eq. (5):

$$\gamma_{d2} = H^3 \gamma_{d1}/(H - \Delta H)H^2, \tag{6}$$

which after rearrangement becomes

$$\Delta H/H = (\gamma_{d2} - \gamma_{d1})/\gamma_{d2}. \tag{7}$$

Thus, Eq. (7) represents the general solution to the unit strain or change in volume of a frozen sample after thawing, the result being positive when the sample settles, zero when there is no volume change, and negative when the soil expands, as in Figure 1c and Eq. (4). Also note that Eq. (7) is solely in terms of dry unit weights; hence, the solution is independent of the initial and final water contents, percent saturation, or amounts of unfrozen water. The equation is valid over the full range of soils, irrespective of the amount of ice present. As shown in the Appendix, Eq. (7) can be shown to be identical to the Terzaghi⁷ equation:

$$\Delta H/H = (e_0 - e_1)/(1 + e_0), \tag{8}$$

where e_0 = the initial void ratio (of the frozen sample), and e_1 = the final void ratio; the void ratio is defined as the ratio of the volume of voids to the volume of solids. The unit strain is a direct function of what condition e_1 represents. If e_1 is the void ratio after thawing under a light seating load, then the unit strain is that which occurred during thawing. If e_1 represents the condition after thawing and consolidation under a known pressure, then the unit strain reflects the entire void ratio change to that condition. Similarly γ_{d2} in Eq. (7) can be the dry unit weight after just thawing or after full consolidation under a known pressure, and the unit strains will reflect the strain to the condition reflected by the γ_{d2} used.

RELATIONSHIP BETWEEN WATER CONTENT AND DRY UNIT WEIGHT

If the frozen sample is saturated, a simple relationship between frozen dry unit weight, water content, and specific gravity (*G*) applies:

$$\gamma_{d1} = \gamma_w / (1/G + 1.09 w_1), \tag{9}$$

where γ_w = unit weight of water, and w_1 = the frozen water content expressed as a ratio of weight of water (ice) to weight of dry soil. Since specific gravity, *G*, normally varies between 2.85 and 2.65 (lower when organics are present), a simple plot of water content versus frozen dry unit weights can be easily prepared (Figure 2). Equation 9 or Figure 2 (drawn to a larger scale) is often used to check field or laboratory computations, but can also be used to estimate γ_{d1} , when only the water content is known and the specific gravity is either known or estimated. This relationship can be particularly useful when only auger cuttings are available or when the conventional samples are badly fractured on drilling or driving. Saturation and specific gravity can be determined by laboratory tests or confirmed by good cores obtained at depths above and below zones in which the hole is advanced by augering. Far too often only selected portions, deemed to be representative, are retained for complete analysis and the rest of the core discarded. If the water content of these

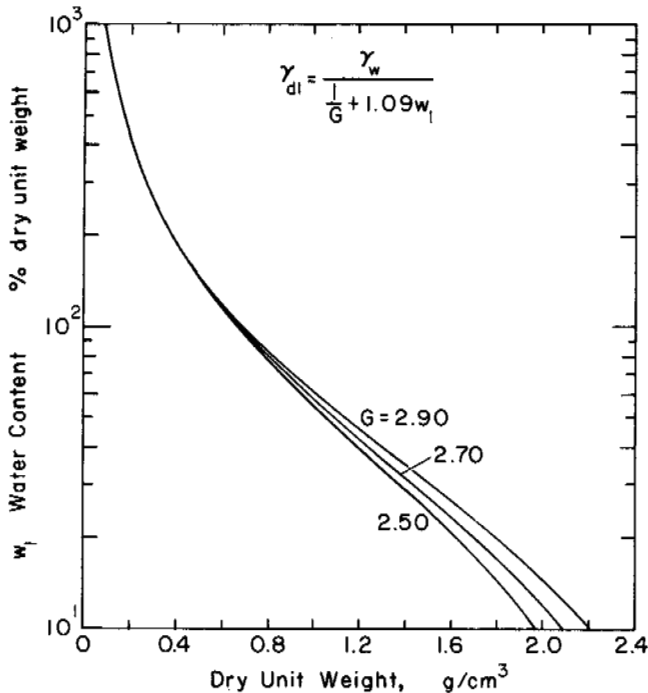


FIGURE 2 Water content versus dry unit weight of frozen soils at several specific gravities.

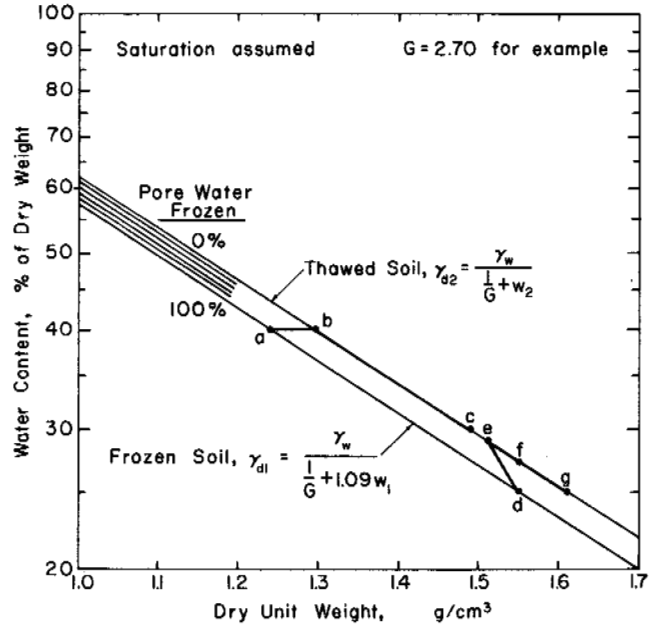


FIGURE 3 Plot of water content (on log scale) versus dry unit weight for frozen and thawed soils and when partially frozen.

discarded portions is taken, a more complete analysis could be made at little cost.

To obtain a better understanding of the change in water content and dry unit weight from the frozen to the thawed and consolidated (or expanded) state, a portion of Figure 2 has been replotted to a larger scale in Figure 3 (for *G* = 2.70 only). Also plotted on Figure 3 is the similar relationship for thawed soils at saturation:

$$\gamma_{d2} = \gamma_w / (1/G + w_2), \tag{10}$$

where w_2 is the thawed water content, expressed as a ratio of weight of water to weight of dry soil. For example, assume a frozen sample having a water content of 0.40 (40 percent) and $\gamma_{d1} = 1.24 \text{ g/cm}^3$, as depicted at point a. After thawing, the sample might have the same or a different water content and dry unit weight, but the coordinates will always fall on the upper (thawed) line, perhaps point b. When the sample is loaded to the overburden pressure and/or appropriate portion of the applied load, it might follow a path from b, along the thawed line, to point c.

A soil with a water content of 25 percent, that expands upon thawing might follow the path d, e, f, g in Figure 3, expanding from d to e during thawing, partially consolidating under applied load to its original dry unit weight and volume from e to f, and consolidating or settling further when proceeding from f to g when the pressure increased. Computations of the unit strains for these two hypothetical cases using Eq. (7) are shown in Table I.

TABLE I Computation of Unit Strains

Point	Water Content (w_2 or w_1)	γ_{d1}	γ_{d2}	$\Delta H/H$ (m/m) ^a	Remarks
a	0.40	1.240			
b	0.40		1.296	0.043 2	from a to b
c	0.30		1.490	0.167 8	from a to c
d	0.25	0.550			
e	0.29		1.510	-0.026 5 ^b	from d to e
f	0.273		1.550	0.000 0	from d to f
g	0.25		1.610	0.037 3	from d to g

^a Equals $(\gamma_{d2} - \gamma_{d1})/\gamma_{d2}$.

^b Expansion.

UNFROZEN WATER

Also shown in Figure 3 (upper left) is the effect of the unfrozen water contained in the originally "frozen" sample. This unfrozen pore water, in equilibrium with the amount of ice at different temperatures and pressures, can be a significant factor when dealing with "frozen" fine-grained soil. As given by Tsytoich,⁸ the relative ice content i_r is the ratio of the weight of ice to the total weight of water (both frozen and thawed) in a "frozen" soil and is calculated by:

$$i_r = (w_1 - w_{un})/w_1, \quad (11)$$

where w_1 is the total water content and w_{un} is the moisture content of the unfrozen portion, both with respect to dry weight of soil. Thus, when the frozen sample has 100 percent of all the water within its voids frozen, $i_r = 1.00$, and, when all the water is thawed, $i_r = 0$. Intermediate values, expressed in Figure 3 as percent, show the effect of the relative ice content on the relationship between water content and dry unit weight.

The relative ice content i_r cannot be multiplied by the frozen water content in Eq. (9) to correct for the unfrozen water, since i_r only influences the 0.09 portion of the water content. To correct for unfrozen water content, Eq. (9) takes the form:

$$\gamma_{d1} = \gamma_w/(1/G + w_1 + 0.09 i_r w_1). \quad (12)$$

Provided the sample is saturated, the unit strain $\Delta H/H$ may be expressed in terms of water contents rather than dry unit weights, by the following substitution:

$$\Delta H/H = (\gamma_{d2} - \gamma_{d1})/\gamma_{d2}, \quad (7)$$

where

$$\gamma_{d2} = \gamma_w/(1/G + w_2), \quad (10)$$

and

$$\gamma_{d1} = \gamma_w/(1/G + 1.09 w_1), \quad (9)$$

to obtain

$$\Delta H/H = (1.09 w_1 - w_2)/(1/G + 1.09 w_1). \quad (13)$$

To compensate for the relative ice content i_r can be incorporated in Eq. (13) and:

$$\Delta H/H = (w_1 + 0.09 i_r w_1 - w_2)/(1/G + w_1 + 0.09 i_r w_1). \quad (14)$$

PORE WATER ON THAWING

Also of interest is the amount of water, ΔW , gained or lost during expansion or consolidation of a frozen sample on thawing. Assuming H and γ_w are both 1.0, the unit amount of water gained or lost is the difference between the strain ΔH and the volume occupied by the expanded (as ice) water ($\Delta V = 0.09 w_1 \gamma_{d1}$) in the original frozen condition, which can be expressed as:

$$\Delta W = \Delta H/H - 0.09 w_1 \gamma_{d1}. \quad (15)$$

In the case of expanding soils, ΔH is negative and ΔW will also be negative, being the sum of the two terms, indicating that additional water (from outside the original sample volume) must be supplied to compensate for both ΔH and $0.09 w_1 \gamma_{d1}$. Pore pressures will be negative until this water is supplied. When ΔH is positive and exactly equals $0.09 w_1 \gamma_{d1}$, as in going from about point a to point b in Figure 3, no water is gained or lost during the thawing and subsequent loading. When ΔH is greater than $0.09 w_1 \gamma_{d1}$ excess water is generated, which must be forced out of the sample and positive pore pressures are generated.

If all of the water is not frozen in the original condition (γ_{d1}), then Eq. (15) should be modified to:

$$\Delta W = \Delta H/H - 0.09 i_r w_1 \gamma_{d1}. \quad (16)$$

Using Eq. (9) and (13), Eq. (15) can also be written solely in terms of initial and final water contents when saturated as:

$$\Delta W = (w_1 - w_2)/(1/G + 1.09 w_1), \quad (17)$$

or when considering unfrozen water as:

$$\Delta W = (w_1 - w_2)/(1/G + w_1 + 0.09 i_r w_1). \quad (18)$$

LABORATORY TESTS

Thaw-consolidation tests conducted at USA CRREL to date have concentrated on the development of standard test pro-

cedures and a thorough understanding of the mechanics involved both in thawing and consolidating or in thawing and expanding. While controlled thawing has been used in the study of the shear strength of soils at the thawed-frozen soil interface, the thaw-consolidation tests to date have been conducted with no attempt to control the rate and direction of thawing, on the assumption that the proposed standard tests could best be accomplished in the standard consolidation apparatus. If the distribution of ice in frozen samples was always homogeneous, thermal controls could be designed to produce a horizontal thaw plane in the sample, as depicted in Figure 4a. Since the ice distribution is seldom uniform, some uneven thawing is inevitable and the thaw front configuration might resemble that shown in Figure 4b. The inaccuracies in remotely measuring the advance of the thaw front with time were a serious handicap in computing the unit strain within the shallow thawing depths, so simple flooding of the device with room temperature de-aired water and initiation of all-around thawing was elected as the test procedure. With all-around thawing, the inner portion of the sample is the last to thaw (Figure 4c), and consolidation reflects the thawing of the inner core rather than the entire sample. Recognizing this, no real use is made of any of the data taken during the thawing process. Only the strain at the end of thawing is utilized. Normally, a seating load of 6.18 or 12.25 kN/m² is applied during the thawing period. After the

sample has completely thawed and no further volume changes are observed, the sample is loaded in the conventional manner employed in testing thawed samples. Figure 5 shows the results of the initial portion of thaw-consolidation tests. Figure 6 shows the swelling pressures associated with the thawing of some of the clay samples. These tests were conducted by adding known weights of lead shot to the loading arm of the consolidation apparatus as the sample thawed, constantly maintaining the original volume (height) of the sample.

Several thaw-consolidation tests are shown in Figure 7. The performance of these real soils is of course similar to that of the hypothetical soils used in Figure 3 and Table I. While coarse-grained soils such as sands have little or no expansion properties, silts and clays can expand on thawing. Accordingly, the strain data in a thaw-consolidation test should always be considered the net strain, being the difference between the consolidation on a macroscale and the swelling on a microscale, or vice versa.

PREDICTION OF SETTLEMENT

While test results on selected samples yield the strains associated with thawing and subsequent pressures, we must also be able to compute the potential settlement of all the soils with depth, without having to test all the cores obtained from the drill hole. To facilitate these computations, a graphical solution of Eq. (7) can be employed (Figure 8). The unit strain is found by entering the original frozen dry unit weight (γ_{d1}) on the horizontal axis (point a) and proceeding vertically, intersecting (point b) the inclined line (or extrapolated line) drawn from 100 percent strain to the final thawed dry unit weight (γ_{d2} , point c). The strain is then read directly at the point of intersection (b). The strain of samples that expanded on thawing ($\gamma_{d2} < \gamma_{d1}$) is computed in a similar manner, using the lower portion of the figure. The assumption is that, regardless of initial dry unit weight, the same soil type will achieve the same final thawed dry unit weight (at the appropriate pressure) as the samples that have been tested in the laboratory consolidometer. Equation 7 can also be re-arranged as:

$$\Delta H/H = (\gamma_{d2} - \gamma_{d1})/\gamma_{d2} = 1 - \gamma_{d1}/\gamma_{d2}, \quad (19)$$

such that the unit strain is quickly found by subtracting from one the ratio of the frozen to the thawed dry unit weight (Figure 9).

The total settlement to be expected when the ground has thawed to a specific depth is computed by a summation of the strains of individual layers, as expressed by,

$$S = \sum_1^n [(\gamma_{d2} - \gamma_{d1})/\gamma_{d2}] h_i \quad (20)$$

where $(\gamma_{d2} - \gamma_{d1})/\gamma_{d2}$ is the unit strain associated with the change in dry unit weight from an initial frozen condition to

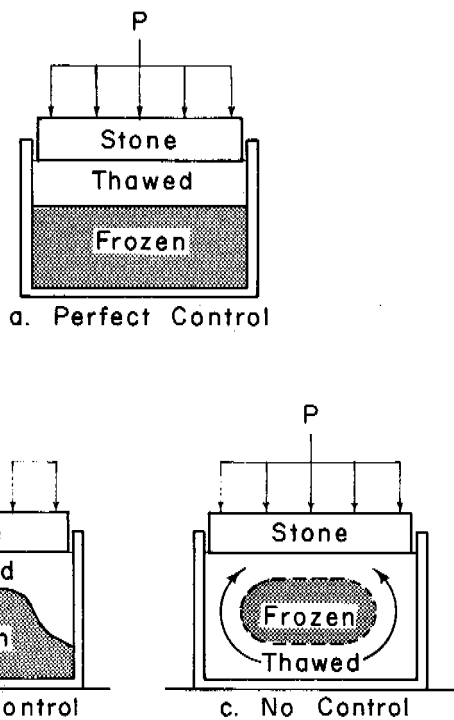


FIGURE 4 Thawing frozen soil sample in consolidometer with perfect and poor thermal control of the thaw front and with no control.

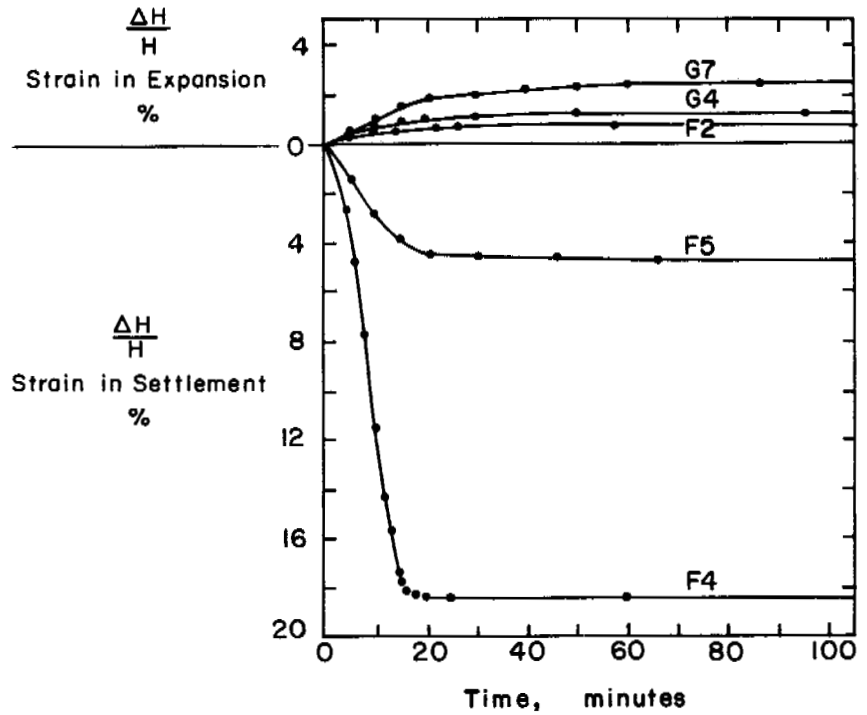


FIGURE 5 Unit strain with time during uncontrolled thawing of soils in consolidometer. Seating load during thawing was 6.25 kN/m² for Glennallen (G) samples, 12.25 kN/m² for Fairbanks (F) samples.

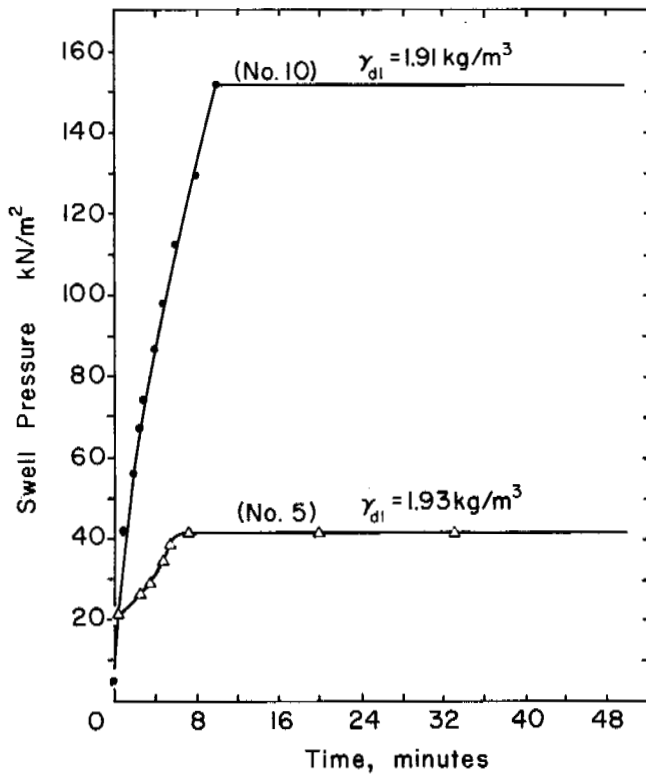


FIGURE 6 Swell pressure generated during the thawing of silty clay from Glennallen, Alaska, as a function of time, additional water being readily available.

a thawed dry unit weight under the overburden and imposed structural pressure of the soil layer of thickness h_i , the individual layers of soils being numbered from 1 to n .

COMPARISON WITH OTHER METHODS

The first experiments to determine the consolidation characteristics of thawing soils were apparently those carried out by Tsytoich (as reported by Bakulin²), as early as 1934. Since that date, Tsytoich and other Soviet researchers have been consistent contributors to the literature available on thaw-consolidation. While recent papers^{9,11} deal with pore pressure and rates of consolidation, the basic predictive method is based on the change in void ratio as shown in Figure 10. A detailed explanation of the method of analysis is also given in a previous paper by Tsytoich.⁸

The compression curve in Figure 10 illustrates the change in void ratio as the frozen soil is initially loaded (point a to b), then allowed to thaw (b to c), and finally to consolidate (c to d) under the application of increasing external pressures. The greatest settlements are depicted as occurring during the thawing stage (from b to c) and are graphically shown as $A_0 = \Delta e/1 + e_0$. The consolidation of the sample after it has completely thawed is regarded as a function of pressure. For small changes in pressure (up to 300-500 kN/m², depending on soil type), the relationship is assumed to be linear, such that $a_0 = \Delta e/1 + e_0 = \tan a$. The complete settlement is calculated by the equation:

$$S = \sum_1^n A_0 h_i + \sum_1^n h_i a_0 \sigma_{zi}, \quad (21)$$

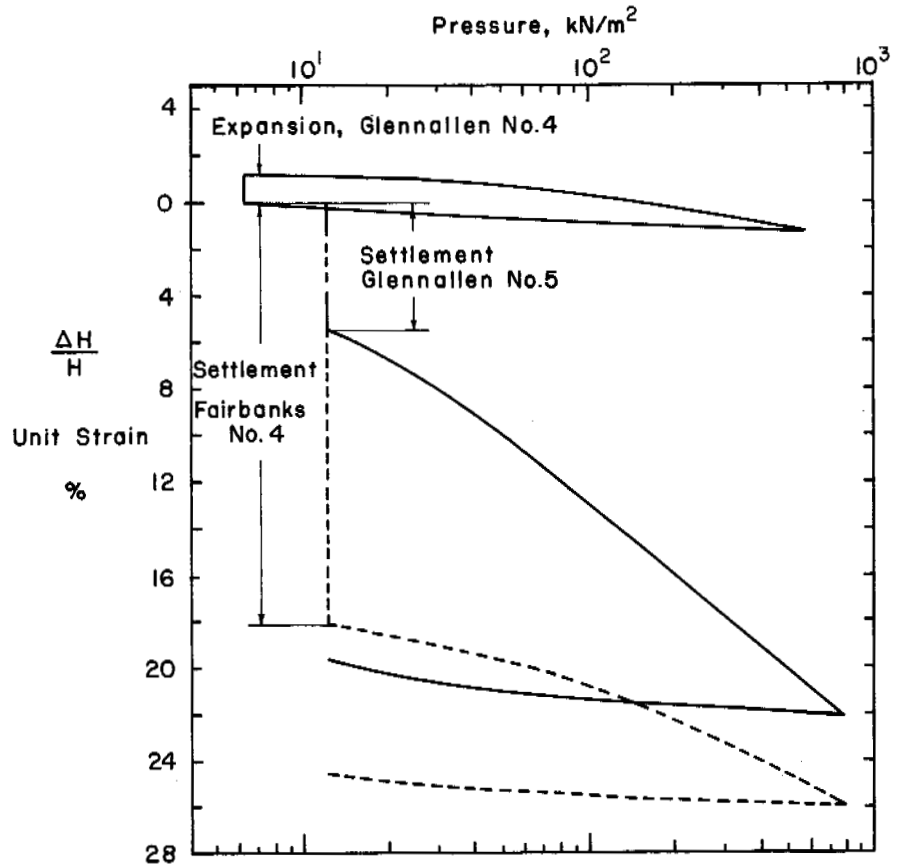


FIGURE 7 Unit strain during thawing and subsequent change of external pressure.

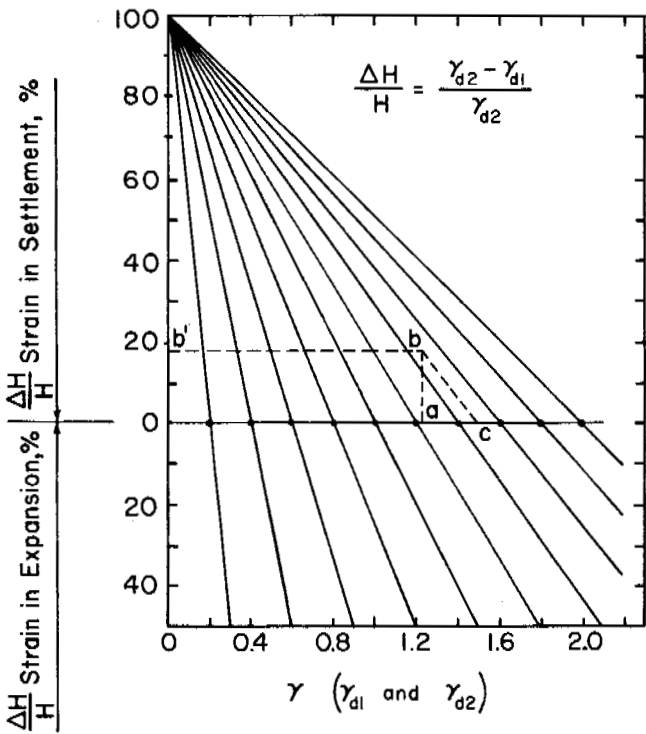


FIGURE 8 Percent unit strain in settlement or expansion when permafrost is thawed, as a function of initial (frozen) and final (thawed) dry unit weights.

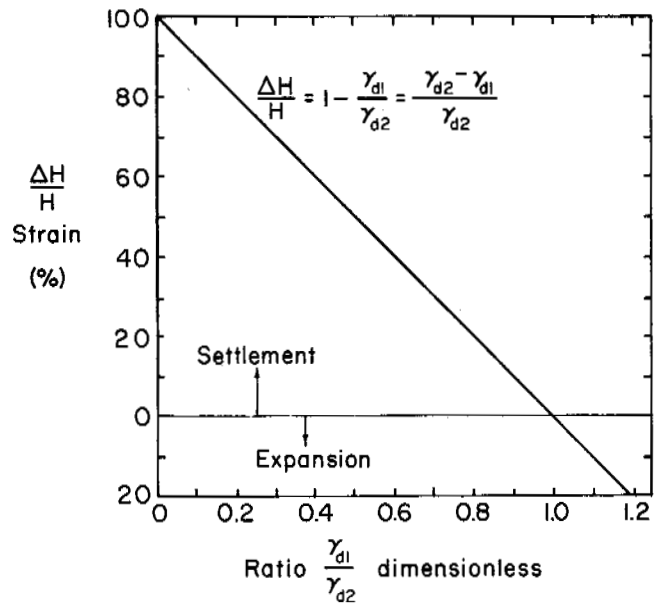


FIGURE 9 Unit strain, in percent, in settlement or expansion when permafrost is thawed as a function of the ratio of initial (frozen) to final (thawed) dry unit weights.

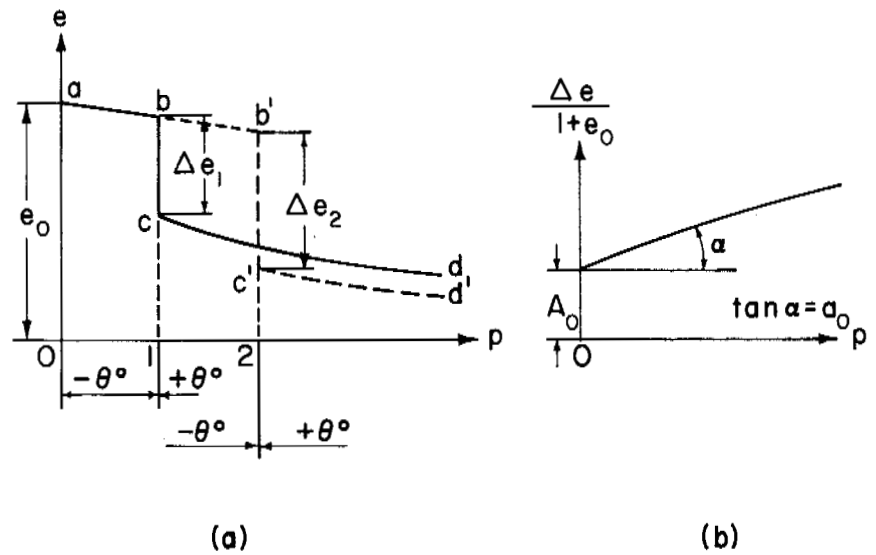


FIGURE 10 Relationship between change of void ratio of frozen soils in the process of thawing and change of external pressure (from Tsytovich *et al.*⁹).

where h_i = the thickness of individual layers of thawed soils, A_0 = the so-called reduced coefficient of thawing, a_0 = the reduced coefficient of consolidation, and σ_{zi} = the average compressive stress in the soil layer under the effect of the external load and the weight of the soil itself. Equation 21 has also been modified to include an equivalent layer, as detailed in Tsytovich⁸ and Ushkalov *et al.*¹⁰

As shown in the Appendix, Eq. (7) is identical to

$$\Delta e / (1 + e_0);$$

thus, there are no discrepancies between Eq. (20) and Eq. (21). Equation 20 is concerned solely with the total change, while Eq. (21) divides the settlement into two components: the amount from just thawing and the amount reflecting the subsequent consolidation with pressure.

Ushkalov *et al.*¹⁰ describe the degree of subsidence of permafrost, e_1 , as being determined from the value of its relative thaw consolidation at a pressure of 98 kN/m² by an equation identical to Eq. (7), given by:

$$e_1 = (\gamma_3 - \gamma_4) / \gamma_3, \tag{22}$$

where γ_3 is the experimentally determined value of dry unit weight of frozen soil g/cm³ after complete thawing under a pressure of 98 kN/m², and γ_4 is the dry unit weight of the same soil in the original frozen condition, equivalent to γ_{d1} , described above.

The soil is considered to be nonsubsident at a value of $e_1 \leq 0.03$, subsident at $0.03 < e_1 \leq 0.1$ and strongly subsident at $e_1 > 0.1$. Kiselev *et al.*³ report that this same equation is used, with no reference to a prescribed test pressure, when computing the settlement potential of only sandy soils. Space does not permit detailed discussion of other Soviet

methods for computing the settlement of fine-grained soils; the reader is referred to papers by Ushkalov *et al.*,¹⁰ Kiselev *et al.*,³ Bakulin,² Bakulin *et al.*,¹ and others.⁶

CONCLUSIONS

Until remote sensing techniques have been developed to the state where the entire vertical and horizontal distribution of ice in frozen ground can be assessed, soil boring remains the primary method of determining the soil-ice condition. The use of the water content and dry unit weight data of frozen samples obtained in the borings appears to be the most convenient method of relating the existing conditions to the potential settlement upon thawing. The dry unit weight of the frozen sample effectively integrates the entire void volume, eliminating the need for calculations of estimations of the quantity or distribution of ice and unfrozen water.

When the final thawed dry unit weight of each soil type has been determined in the laboratory under the appropriate pressure, the ultimate unit settlement can be quickly computed by dividing the difference between the original and final dry unit weights by the final dry unit weight. The unit settlement or strain is applicable to soils that heave, have no volume (axial) change, or settle on thawing and is applicable under conditions of full or partial saturation and over the full range of soil types.

For fully saturated soils (both frozen and thawed), simple equations have been derived to facilitate the computing of unit strain, providing a convenient method when only the water content is known, such as in augering operations. The effect of unfrozen water in "frozen" soils can readily be accounted for and fully appreciated after a thorough study of the relationships between dry unit weight, water content and specific gravity given in Eq. (9) and (10) and Figure 3.

There are no apparent inconsistencies between Tsytoovich's method of computing settlements based on void ratio changes [Eq. (21)] and the method based on changes in dry unit weight [Eq. (20)]. The subdivision of strains during thawing and those under pressure after thawing in Eq. (21) appears to be unnecessary. While the subdivision of strains may not be difficult in analyzing laboratory test results, the extension of these data to include other samples, having a range of ice conditions, may be more difficult. Equation (20) avoids the additional analysis by confining its interest only to the initial and final conditions.

ACKNOWLEDGMENTS

This paper presents the results of research performed by the Cold Regions Research and Engineering Laboratory under the sponsorship of the U.S. Army Corps of Engineers.

REFERENCES

1. Bakulin, F. G., B. A. Savel'yev, and V. F. Zhukov. 1957. Physical processes in thawing ground. USA CRREL Draft Translation 325.
2. Bakulin, F. G. 1960. Settling of frozen ground during thawing at experimental plots. USA CRREL Draft Translation 315.
3. Kiselev, M. F., G. I. Kostinenko, and G. A. Nysovkin. 1965. Calculation of foundation settlements on thawing soils. *In Proceedings 6th international conference on soil mechanics and foundation engineering*. Montreal.
4. Morgenstern, N. R., and J. F. Nixon. 1971. One-dimensional consolidation of thawing soils. *Can. Geotech. J.* No. 8.
5. Morgenstern, N. R. 1972. Untitled paper. *In Proceeding Canadian northern pipeline research conference*, Ottawa.
6. Scientific Research Institute of Foundations and Underground Installation, USSR Academy of Construction and Architecture. 1958. Instructions for determining relative compression in frozen ground thawing under pressure. USA CRREL Draft Translation 291.
7. Terzaghi, K. 1965. *Theoretical soil mechanics*. John Wiley & Sons, New York.
8. Tsytoovich, N. A. 1960. Bases and foundations on frozen soil. *Highw. Res. Board Spec. Rep.* 58.
9. Tsytoovich, N. A., Yu. K. Zaretsky, V. G. Grigoryeva, and Z. G. Ter-Martirosyan. 1965. Consolidation of thawing soils. *In Proceedings 6th international conference on soil mechanics and foundation engineering*. Montreal.
10. Ushkalov, V. P., A. M. Pchelintsev, A. I. Yefimov, and A. I. Dementyev. 1966. Engineering geocryological research, p. 400-

404. *In Permafrost: Proceedings of an international conference*. National Academy of Sciences, Washington, D.C.
11. Zaretskii, Y. K. 1968. Calculation of the settlement of thawing soil. *Soil Mech. Found. Eng.* May-June (3).

APPENDIX

Problem:

Are $(\gamma_{d2} - \gamma_{d1})/\gamma_{d2}$, [Eq. (7)] and $(e_0 - e_1)/(1 + e_0)$ [Eq. (8)] identical?

By definition:

$$\gamma_{d1} = G/(1 + e_1), \text{ and}$$

$$\gamma_{d2} = G/(1 + e_2).$$

Thus,

$$(\gamma_{d2} - \gamma_{d1})/\gamma_{d2} = (G/1 + e_2 - G/1 + e_1)/(G/1 + e_2).$$

Canceling G and multiplying all terms by $1 + e_2$:

$$\frac{[(1 + e_2)/(1 + e_2) - (1 + e_2)/(1 + e_1)]}{[(1 + e_2)/(1 + e_2)],}$$

which is

$$\frac{1 - (1 + e_2)/(1 + e_1) = (1 + e_1)}{(1 + e_1) - (1 + e_2)/(1 + e_1)},$$

which is

$$\frac{[(1 + e_1) - (1 + e_2)]}{(1 + e_1) = (e_1 - e_2)/(1 + e_1)}.$$

Since e_1 (frozen) = e_0 (original) and e_2 (thawed) = e_1 (final) in Terzaghi's equation:

$$(e_1 - e_2)/(1 + e_1) = (e_0 - e_1)/(1 + e_0).$$

Therefore:

$$(\gamma_2 - \gamma_1)/\gamma_2 = (e_0 - e_1)/(1 + e_0), \text{ and}$$

the two expressions are identities.

CONTROL OF PERMAFROST DEGRADATION BENEATH A ROADWAY BY SUBGRADE INSULATION

D. C. Esch

ALASKA DEPARTMENT OF HIGHWAYS
College, Alaska

INTRODUCTION

Newly constructed roadways crossing permafrost terrain originally covered with vegetation have the effect of increasing the amplitude of the seasonal surface and subsurface temperature variations and also of altering the mean annual surface temperature. Readjusting of the permafrost table to the new thermal conditions occurs over a period of years.³ Readjustment is accompanied by roadway surface settlement in areas where permafrost degradation occurs in soils having high frozen moisture contents or segregated ice formations or deposits. The annual cost of maintaining paved roadway surfaces over degrading permafrost in the State of Alaska is very high.

Encouraged by successful installations of foamed plastic insulation materials in controlling seasonal freezing and heaving of subgrade soils in nonpermafrost areas,^{1,6} the Alaska Department of Highways, in 1969, installed two different thicknesses of extruded polystyrene foam insulation boards beneath a newly constructed roadway in a region of relatively warm permafrost. To evaluate the test installations and to provide badly needed data on the thermal regime beneath un-insulated roadway sections, continuing observations are being made on the insulated and adjacent roadway sections. The results of the first 3 years of study are presented herein.

SITE LOCATION AND CONDITIONS

The test sections are located on the Edgerton Highway at a point 10.2 km north of the town of Chitina, Alaska; lat. 60° 35'N, long. 144° 26'W, at an elevation of 287 m (MSL). In this area, the roadway is located in the bottom of a narrow canyon on the north flank of the Chugach Mountains, close to the southern or coastal limit of discontinuous permafrost in this region.

At the test site, the canyon floor is characterized by gently sloping muskeg terrain, with scattered stunted black spruce ranging from 2 to 5 m in height, and with blueberry and willow underbrush. A 25- to 40-cm-thick layer of sphagnum moss covers the ground surface, with the summer water table located near the bottom of the moss. The uppermost soil is a silty peat, perennially frozen below a depth of 40–50 cm, with frozen moisture contents from 150 to 550 percent,

and with organic contents varying from 16 to 40 percent of the dry unit weight. Underlying the peat is a deposit of frozen silt at a depth of 4.8–6.2 m. Borings to a maximum depth of 9.2 m did not penetrate through the permafrost layer.

Weather records from the town of Chitina show an average annual air temperature of -1°C over a 30-year period, with an average precipitation of 0.3 m, including the water equivalent of approximately 1.5 m of annual snowfall. Because of differences in elevation, exposure, and wind velocity between the site and Chitina, the past annual average air temperatures and mean freezing and thawing indices at the test site are not known.

SITE DESIGN AND CONSTRUCTION

The test site chosen was selected because of the uniformity of surface and subsurface conditions, coupled with the occurrence of permafrost at a shallow depth with very high, yet relatively uniform, moisture contents.⁷ It was also required that the site be on a section of fully maintained roadway and subject to routine snow plowing operations; air movement effects of passing vehicles; tire wear of the asphalt pavement, resulting in increased aggregate exposure and changed surface reflectance; and other minor, but perhaps significant, conditions of an operating roadway.

Insulation thicknesses of 5.1 and 10.2 cm of the extruded polystyrene foam (trademark Styrofoam HI) were chosen for installation. This material appeared to present the greatest permanence of insulative properties and resistance to moisture absorption of all available insulations that might be used.^{5,8} The insulation has a minimum compressive strength at 5 percent strain of 2.5 kg/cm², and an initial thermal conductivity of 29 mW/m·K.⁸

Prior to construction, trees and brush were hand cut and cleared from the roadway area without any disturbance to the surface cover—standard Alaska Department of Highways practice for permafrost areas. A layer of gravelly sand, ranging from 0.3 to 0.5 m in thickness, was spread over the moss and leveled in preparation for instrumentation installation and insulation placement. Insulation was supplied as 5.1 cm × 61 cm × 244 cm boards, which were hand placed with joints staggered between adjacent sheets, and pegged into place with small wooden skewers. To prevent thaw beneath

the roadway shoulders and side slopes, the insulation was extended to cover essentially the full width of the embankment, as far as practical. Figure 1 shows a plan view of the installation, which was completed on 8 August 1969. After spreading the initial cover layer of 20–30 cm of gravelly sand with a light crawler-type tractor, normal construction equipment was used to complete the roadway to final grade, resulting in a thickness of approximately 1.55 m of sand and gravel fill above the insulation.

In June 1971, a road-mixed asphaltic pavement was placed over the insulated and adjacent control or uninsulated roadway sections, which had remained gravel-surfaced since construction in 1969. This surface provided an accurate reference for settlement surveys and also provided a more severe test condition due to increased solar heating of the darkened surface.

Instrumentation

Ground temperatures have been measured monthly since construction, by means of a system of 125 copper–constantan thermocouples arranged in 13 vertical strings and installed in borings to a maximum depth of 9.2 m at locations as shown in Figure 1. The strings were located in the insulated and adjacent uninsulated fill sections in a nearby cut section, where excavation into the peat was necessary because of a peat mound, and 27 m west of the roadway centerline in an uncleared area. In insulated areas, strings were located at various points from centerline to toe of slope. Portions of the strings installed in the borings were encased in 1.27 cm i.d. plastic pipe, with the space around the thermocouples filled with heavy oil to retard corrosion and to provide thermal contact with the surrounding soil. Unencased thermocouples were fastened to the top and bottom surfaces of the insulation layer and also located above and beneath the surface moss mat in uninsulated fill areas. Thermocouple extension wires were carried to jack panels enclosed in junction boxes and located on posts at the bottom of the fill slope.

Thermocouples are read with a Leeds and Northrup Model 8 686 portable millivolt potentiometer, using an ice-water bath to provide a 0 °C reference junction temperature. Using the precaution of keeping the potentiometer in a heated vehicle parked on the roadway shoulder while taking readings has resulted in field accuracy on the order of ± 0.2 °C, as determined from the consistency of monthly readings on the deepest thermocouples.

Ambient air temperatures at the site are recorded by a Taylor recording thermograph placed in a U.S. Weather Bureau instrument shelter. The calibration is checked weekly by means of maximum and minimum thermometers.

Since June 1971, ground temperatures have been recorded at four locations at a depth of 3 cm by means of remote recording thermographs. These locations, designated T-1 through T-4, are shown on Figure 1. The units consist of a mercury-filled probe connected by a capillary tube to the recording

mechanism. Three of the probes are located beneath the roadway pavement, and the fourth was placed beneath the gravel surfaced roadway fill slope. The ground temperature recorders were installed to determine the ratio between air and ground surface temperatures for both insulated and uninsulated areas.

Roadway elevation changes are determined by periodic level surveys of the pavement surface, using a bedrock outcrop near the test site as a fixed elevation reference.

Soil Properties of Embankment

The initial leveling layer of gravelly silty sand (Unified Soil Classification SP-SM) was placed at a moisture content of 4 percent. In 1972, samples taken of this material showed an average moisture content of 18 percent, essentially at 100 percent saturation due to the high water table. In-place density of this sand is approximately 1 920 kg/m³. Fill material placed in the first 25 cm above the insulation was similar to that placed in the leveling layer, with an initial moisture content of 4 percent. Above this level, the roadway embankment is composed of gravels, gravelly sands, and broken rock fill from blasting of cuts. The embankment materials are estimated to have an average moisture content of 5 percent and an average dry density of 2 100 kg/m³.

CLIMATOLOGICAL DATA

Air temperatures at the site from October 1969 through September 1972 are shown by Figure 2, plotted for convenience as one-third month average temperatures. Seasonal freezing and thawing indexes have averaged 2 463 and 1 460 °C-days, respectively. The average air temperature over the three freezing and thawing seasons since construction was -2.8 °C.

Snowfall in one-third month periods and snow depths on the ground for the Tonsina weather recording station are also shown by Figure 2. This station, located 40 km west of the test site, is the closest precipitation recording station, and snow depths are generally very similar at the two locations. Total snowfalls for the three winters since construction were 93, 147, and 175 cm.

Wind velocity data are not available, but observations during trips to the site indicate that average wind velocities are quite low, apparently due to the sheltered canyon bottom location.

SURFACE TEMPERATURE DATA

Recorders were installed at four locations in June 1971 to obtain data on the relationships between air and near-surface temperatures (depth of 3 cm). During 1971, data were obtained for only part of the summer and were inadequate for analysis. Due to low-temperature-induced problems with the

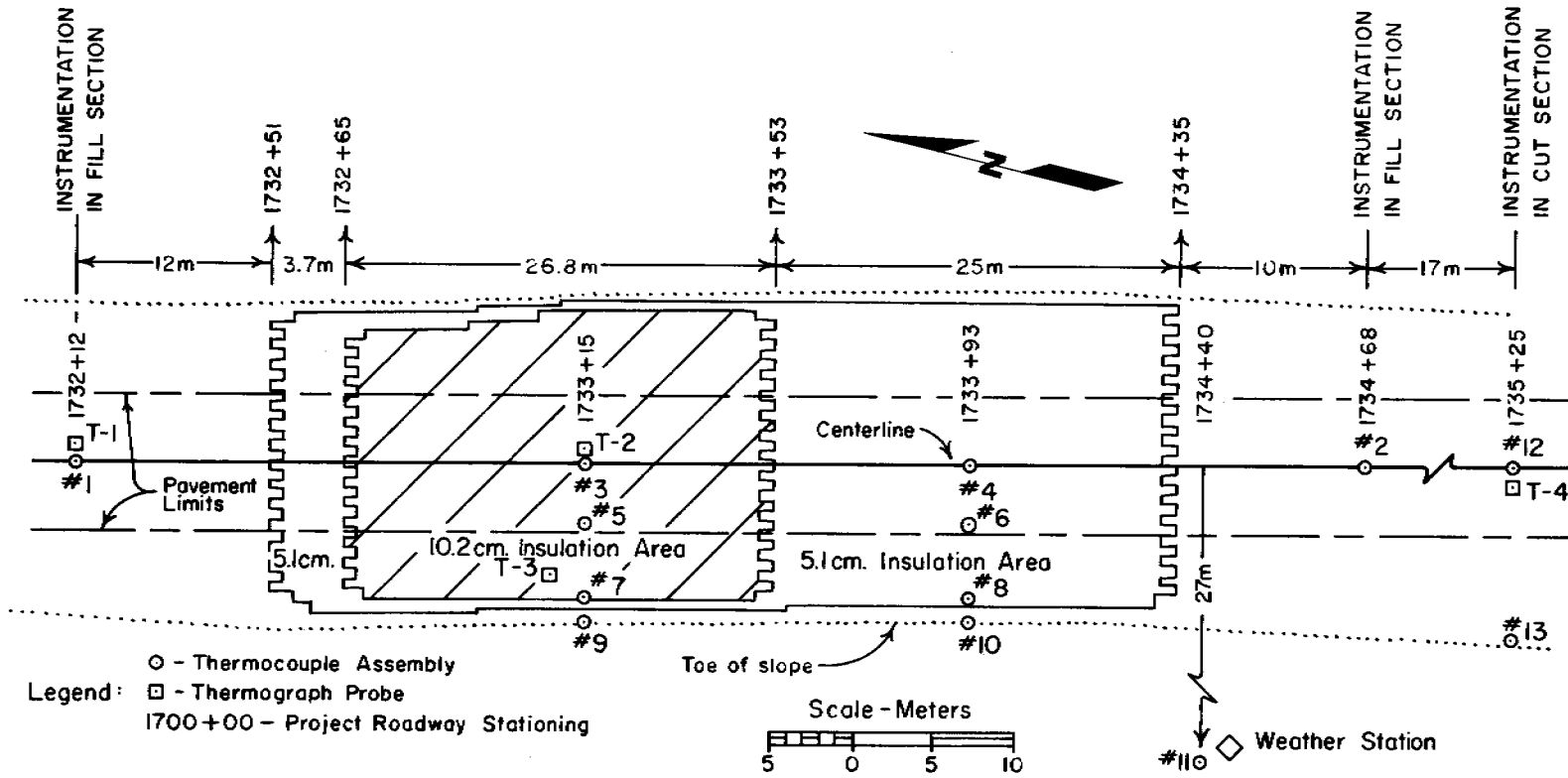


FIGURE 1 Plan view of insulation test sections.

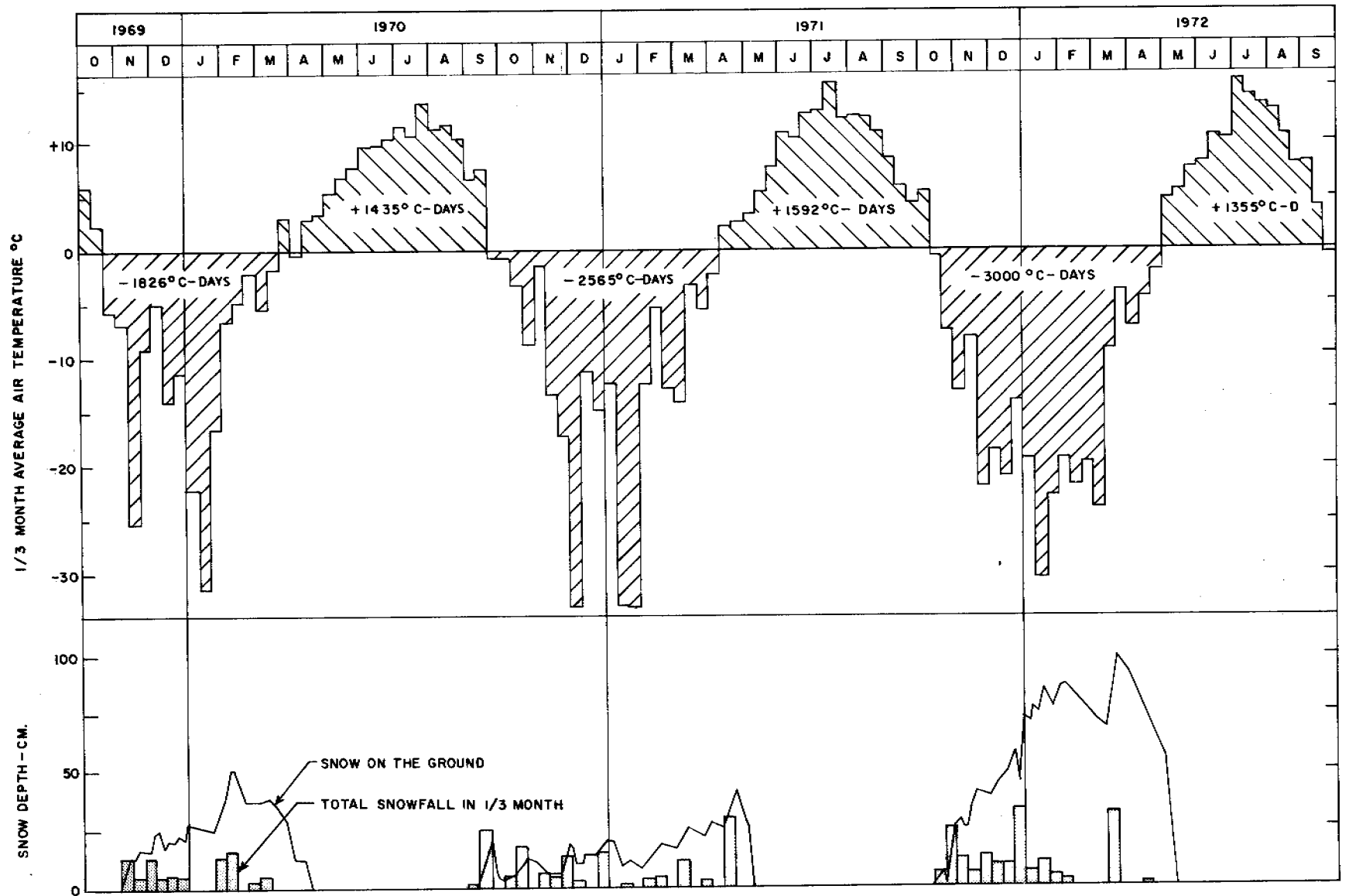


FIGURE 2 Air temperature averages in one-third month periods from the insulation test site. Snowfall and snow on the ground records from Tonsina Weather Recording Station.

chart drives, the 1971–1972 winter data were also incomplete. However, using the available winter records and estimates for the remaining periods gave approximate near-surface to air freezing index ratios, or *n*-factors, of 1.0 for the roadway centerline and 0.7 for the side-slope areas, which received a heavy snowcover due to plowing operations. Records were inadequate to indicate whether significant differences in *n*-factors exist between insulated and uninsulated roadways.

Data from the summer of 1972 are shown in Figure 3. The thawing season *n*-factor near centerline of the 10 cm insulation section, location T-2, was 1.84. Data at T-1, the uninsulated fill section, although incomplete, show surface temperatures very similar to the insulated section.

Surface temperatures for the uninsulated cut section, T-4, were generally lower than at locations T-1 and T-2. This difference is primarily due to the fact that a 5-cm-thick layer of leveling gravel was placed to correct roadway settlements in the cut area early in 1972, and temperatures at T-4 are more indicative of a graveled roadway surface.

The *n*-factor for the roadway fill slope above the 10-cm insulation layer, location T-3, was 1.38. This low factor is due both to the higher surface reflectance of the gravel and to the heavy snowcover that delayed seasonal thaw of the roadway side slopes.

SURFACE SETTLEMENTS

The benefits of installing the subgrade insulation layer are most evident from settlement observations made since the roadway was paved in June 1971 (Figure 4). These data cover settlement during the period from 14 July 1971 through 18 September 1972. Average settlement of the 5- and 10-cm insulation sections over this period were 1.3 and 0.9 cm, respectively. Settlement of adjacent uninsulated areas ranged from 4 to 21 cm, averaging 10 cm. Severe differential settlements occurred over short distances in the uninsulated areas, particularly the vicinity of the cut section.

SEASONAL THAW DEPTHS

Maximum seasonal thaw depths (Figure 5) were determined from the maximum depth of the 0 °C isotherm and from hand probing with a steel rod done each September in the toe of slope areas. Probed thaw depths were generally within ±10 cm of interpolated depths from thermocouple readings. The probe data is believed to be more accurate because of the relatively wide vertical spacing between thermocouples (0.25–0.5 m). Thaw depths, measured from the top of the peat subgrade, were greatest in the uninsulated cut section, reaching a maximum depth of 1.6 m on centerline, compared with centerline thaw depths of 0.6 m beneath the uninsulated fill section, 0.2 m beneath the 5-cm insulation section, and 0.1 m beneath the 10-cm insulation sections. The maximum seasonal thaw depth in undisturbed areas during

this period was 0.2 m beneath the 0.3-m-thick surface moss layer. In insulated areas, thaw depths were greatest near the toe of the fill because of the small area of exposed uninsulated fill at this point.

Thaw and resultant consolidation and settlement of the fill in the toe areas have resulted in the appearance of some longitudinal cracks in the fill side slopes, at distances of 4.3–7.5 m to the right of the roadway centerline. The maximum crack width noted was 10 cm. Some shoulder cracking was noted over approximately 50 percent of both the insulated and uninsulated sections. No cracks extended inward as far as the roadway pavement. Cracks were noted only on the southwest-facing side slopes of the test roadway, which receive the greatest amount of solar radiation. A few probings made beneath the toe of the northeast-facing fill slopes indicated slightly smaller thaw depths than at the toe of the southwest slopes. To date, shoulder cracking does not present a significant problem in this area. However, if steeper side slopes than 3:1 had been used, it appears that cracking might have extended into the pavement area.

SUBSURFACE TEMPERATURES

Temperature envelopes for the four centerline thermocouple strings are shown by Figures 6 through 9, illustrating the maximum and minimum temperatures recorded at various depths as a result of the indicated freezing and thawing seasons. Temperatures from the 1970–1971 winter and the 1971 summer were not plotted on some envelopes for the sake of clarity, because of their intermediate position between the first and third year data.

It was noted that at depths only slightly below the active layer, the soil continues to warm in the fall until refreezing of the active layer is complete. Depending on snowcover, air temperatures, and depth of the active layer, refreezing was completed at the various locations at some time between early December and late February. Thus, at depths below the permafrost table of 1 m or less, the warmest temperatures were observed at 5–7 months after the warmest air temperatures, while the freezing season lag was only 1–2 months. At depths of 6.1–9.2 m, thawing and freezing seasonal lags were normally 6–8 and 4–6 months, respectively.

In summary of Figures 6 through 9, both the uninsulated fill and cut sections had greater seasonal temperature changes within the peat subgrade and deeper seasonal thaw than the undisturbed ground site (Figure 10). In the cut section, temperature variations indicated thaw depths, and resultant settlement were greater than in adjacent fill areas, which, apparently, was due to the absence of the insulating value of the surface moss and cut brush layers remaining beneath the fill sections. However, in some fill areas, settlements were nearly as great as those in the cut section. The reason for the large variations in uninsulated fill area settlement is not known.

Temperature variations at and below the peat surface were

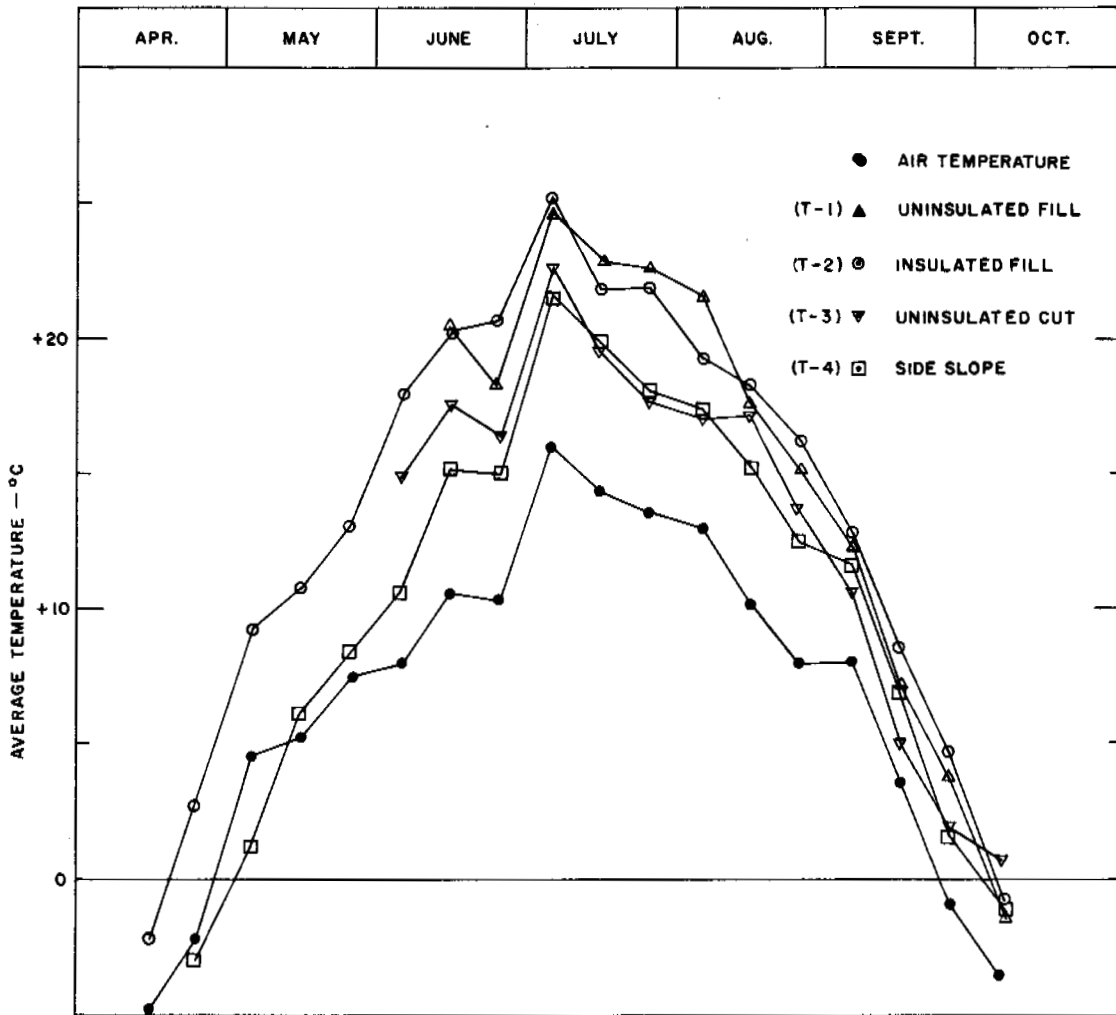


FIGURE 3 Air and near-surface temperature averages in one-third month periods for thawing season of 1972. Surface temperatures are recorded at a depth of 3 cm.

greatly reduced beneath the insulated sections (Figures 8 and 9). The maximum temperature variations recorded in 3 years of centerline observations at 0.5 m below the 5- and 10-cm insulation layers were 2.9 and 1.1 °C, respectively, indicating that the insulation layers were extremely effective in retarding heat exchange between the roadway surface and the subgrade soils.

GROUND TEMPERATURE TRENDS

Table I presents the results of temperature observations made on thermocouples at a depth of 6.1 m below the peat surface in both October 1969 and 1972. These data were selected because they are also indicative of temperature trends noted at other depths. Changes noted are very small and are probably the result of many factors such as air temperature variations, snowcover, slightly differing surface n-factors, and differing

thermal properties of the roadway systems and of the subgrade soils. Perhaps the most significant point to be observed in Table I is the fact that the cut section centerline area was coldest at this depth in 1972 and was the only area to show a decrease in temperatures over this 3-year period.

It is also significant that, although the cut section showed the deepest thaw, it was the first area to completely refreeze in winter. The thermal behavior of the cut section is believed to be primarily the result of the absence of any insulating layer, combined with the fact that the thermal conductivity of this peat, with an average moisture content of approximately 300 percent, can be expected to increase by a factor of two or more with the change of state from thawed to frozen.⁴ This conductivity change would facilitate winter heat loss and retard summer heat gain for sections with peat in the active layer, thus resulting in a significantly lower average temperature at depth than at the surface. By contrast, a

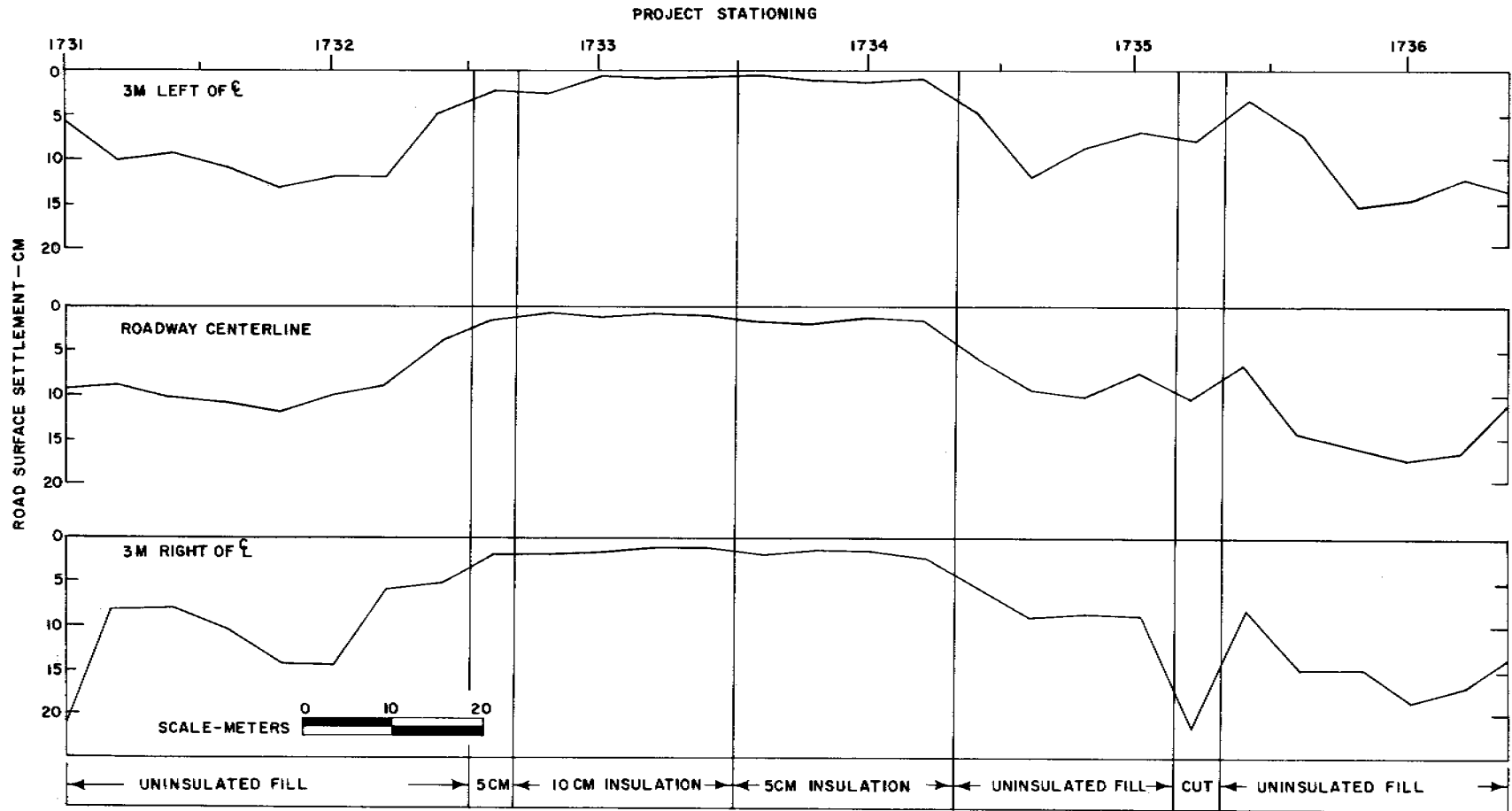


FIGURE 4 Roadway surface settlement profiles, showing elevation changes between 14 July 1971 and 18 September 1972.

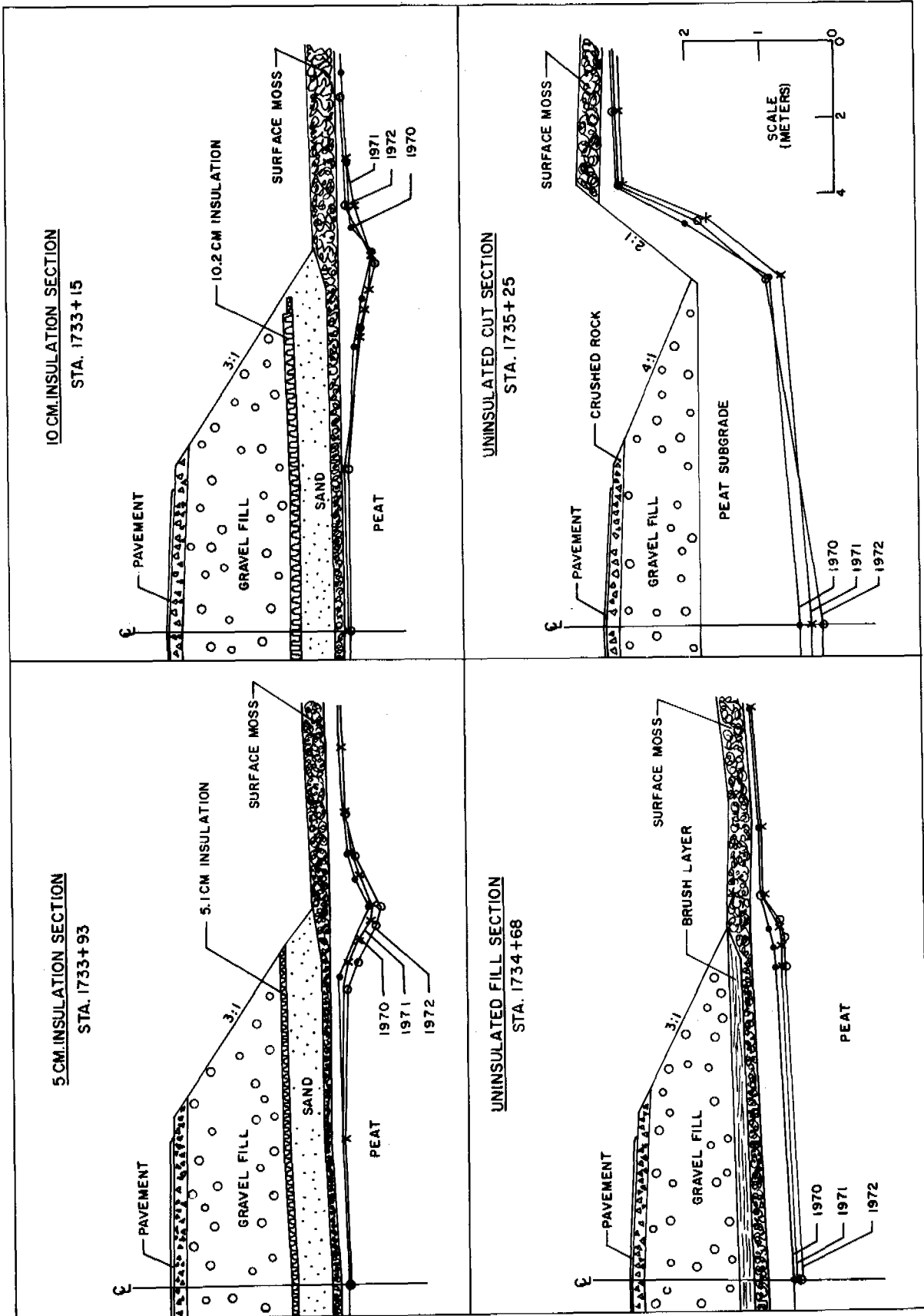


FIGURE 5 Cross sections of insulated and uninsulated roadway sections, showing maximum seasonal thaw depths.

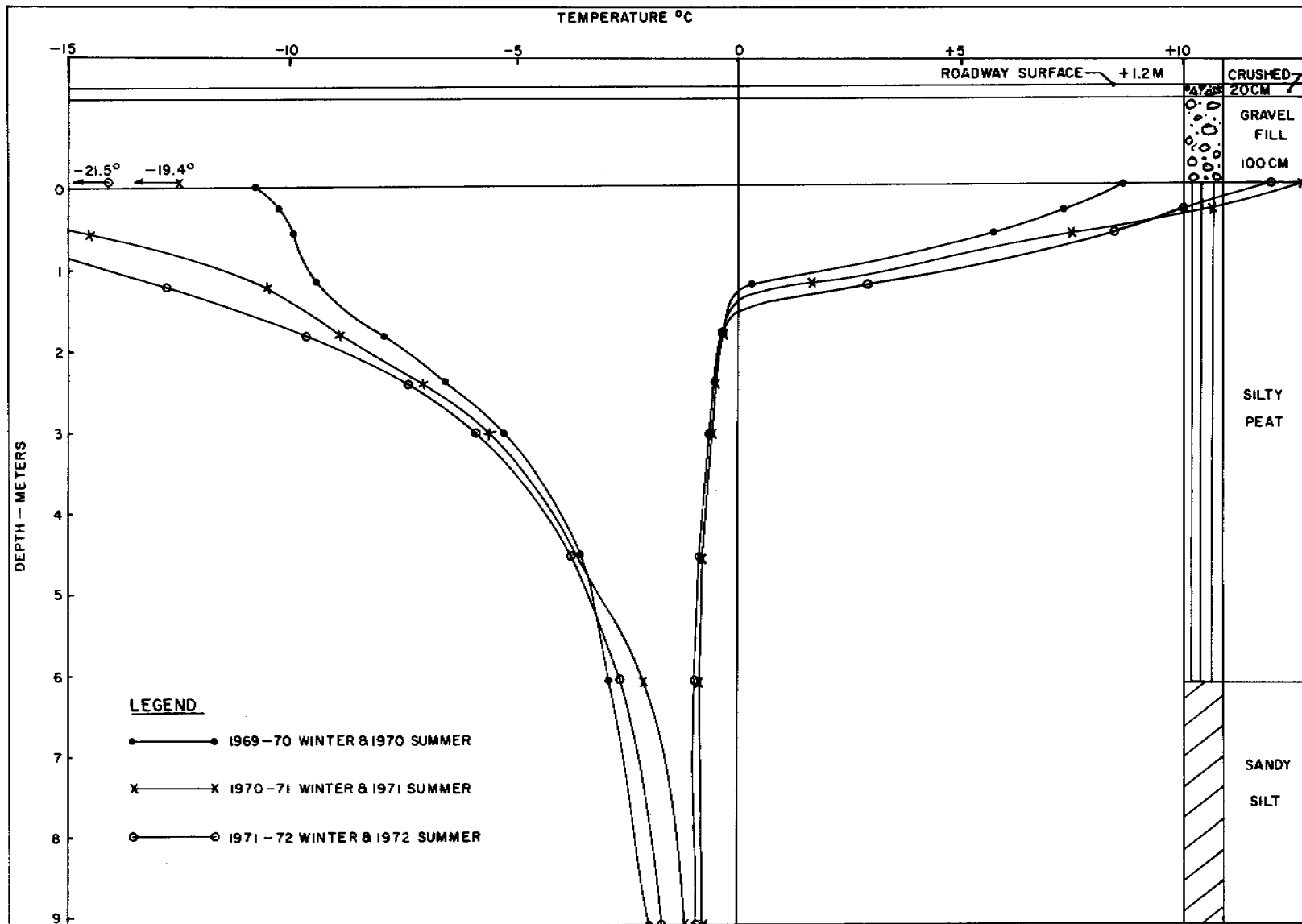


FIGURE 6 Maximum and minimum temperatures observed on centerline, un-insulated cut section, thermocouple string No. 12.

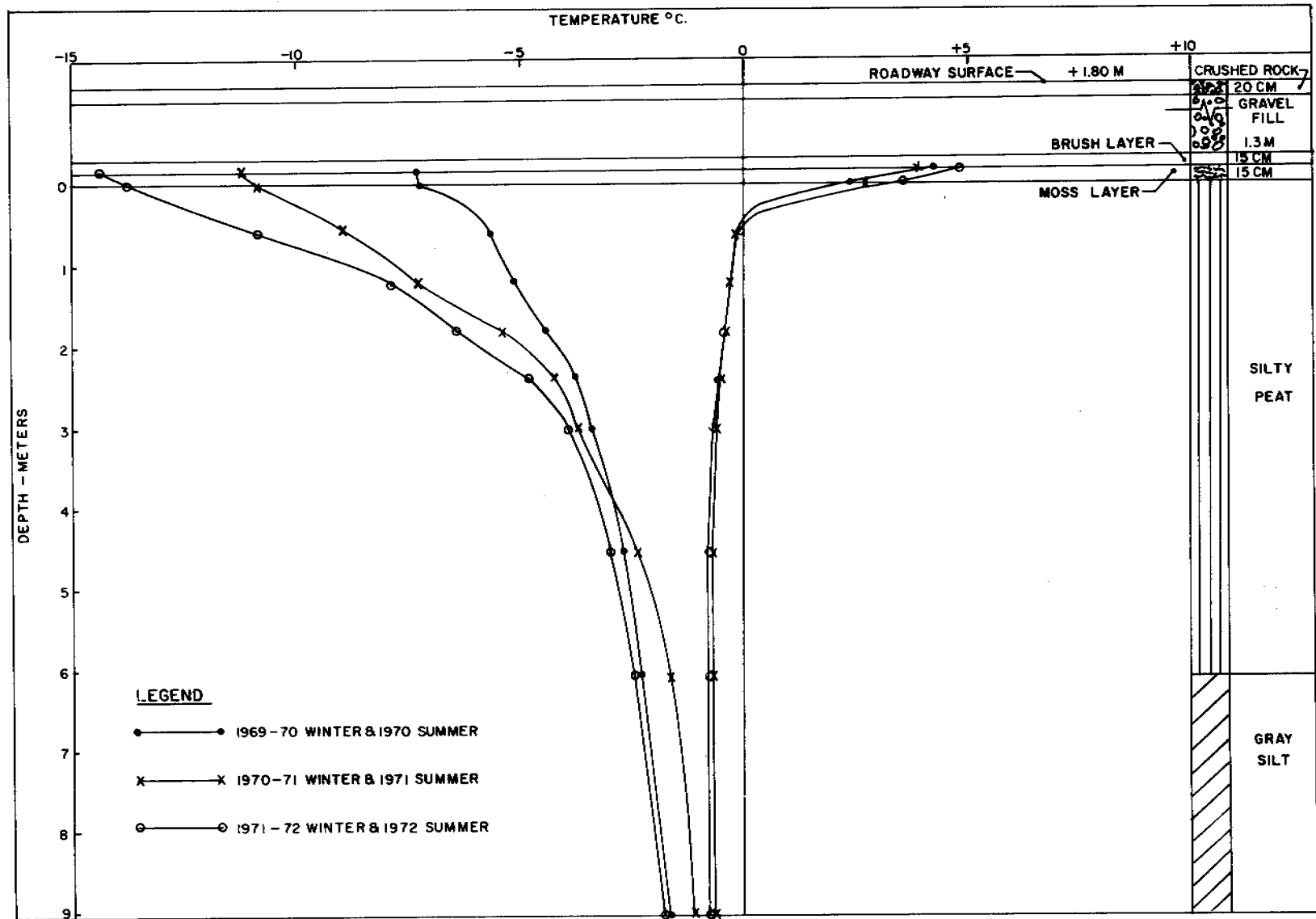


FIGURE 7 Maximum and minimum temperatures observed on centerline, uninsulated fill section, thermocouple string No. 2.

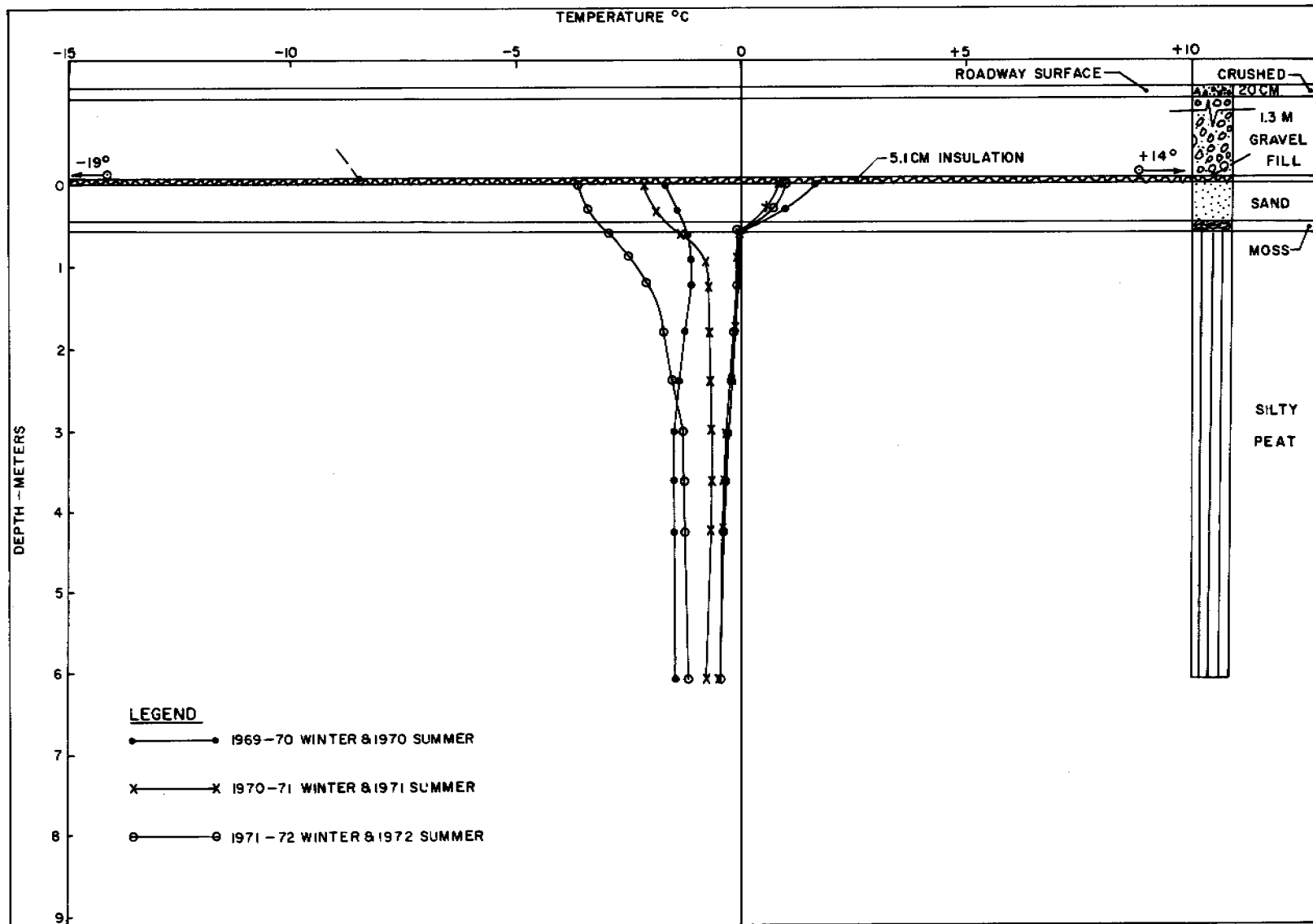


FIGURE 8 Maximum and minimum temperatures observed on centerline, 5.1-cm insulation section, thermocouple string No. 4.

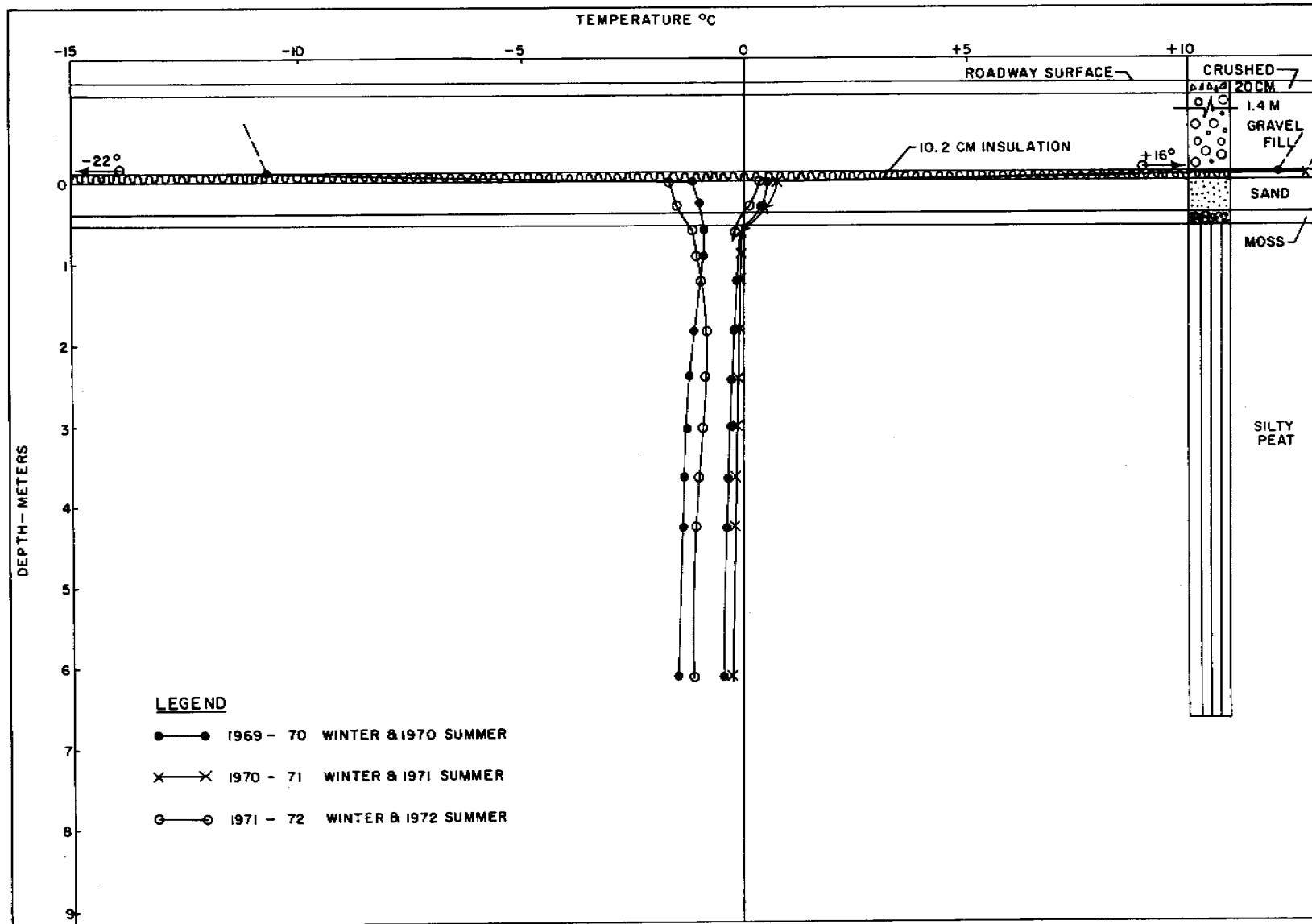


FIGURE 9 Maximum and minimum temperatures observed on centerline, 10.2-cm insulation section, thermocouple string No. 9.

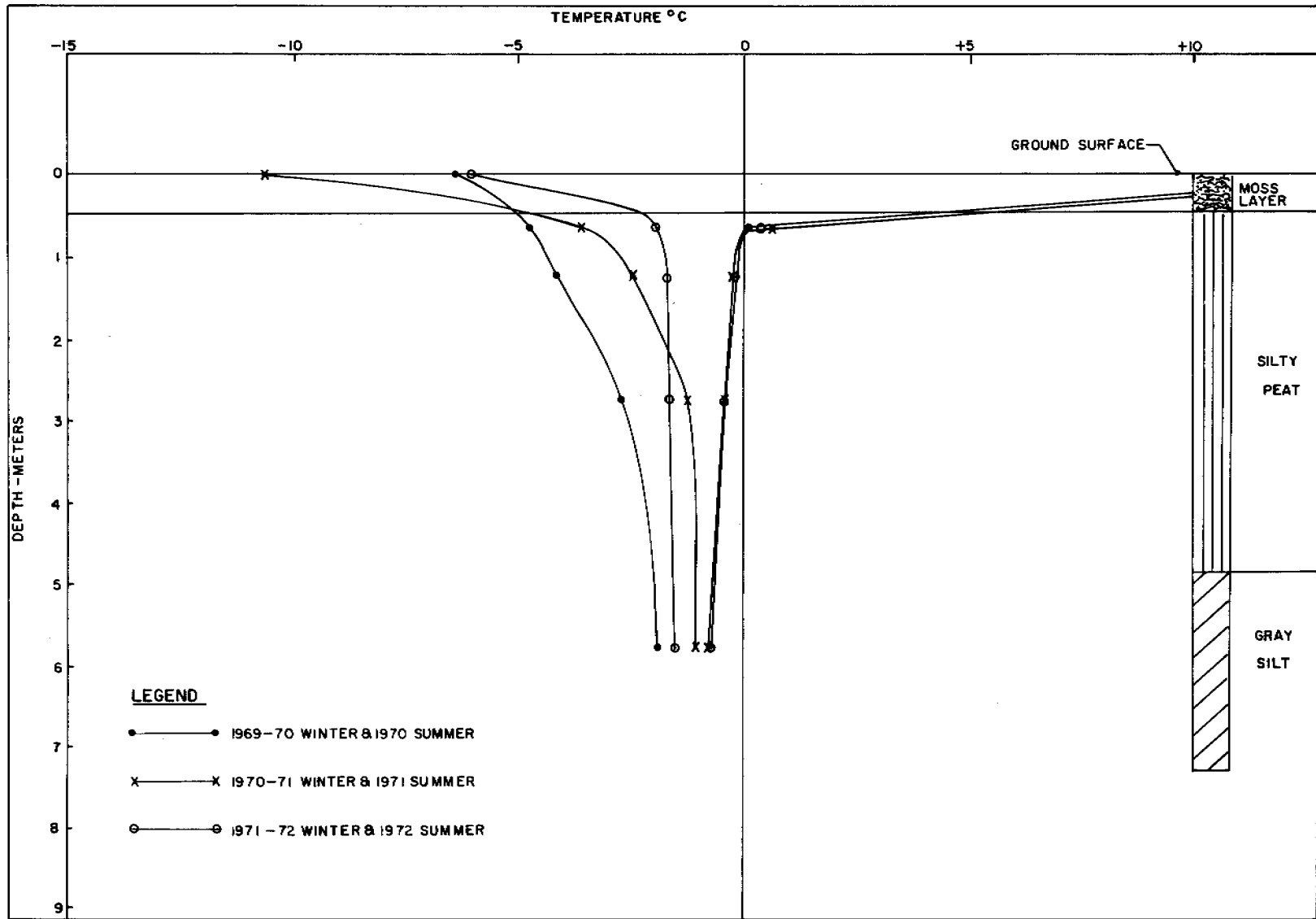


FIGURE 10 Maximum and minimum temperatures observed at undisturbed ground location, thermocouple string No. 11.

TABLE 1 Temperature Comparisons at a Depth of 6.1 m

Condition	Location	Thermocouple String No.	Temperatures (°C)		
			14 Oct. 1969	9 Oct. 1972	Change
Uninsulated fill	Centerline	1	-1.3	-0.8	+0.5
	Centerline	2	-1.2	-1.1	+0.1
10-cm insulation	Centerline	3	-1.1	-0.5	+0.6
	3.7 m right	5	-1.1	-0.4	+0.7
	8.2 m right	7	-1.1	-0.4	+0.7
	9.8 m right (toe)	9	-1.1	-0.5	+0.6
5-cm insulation	Centerline	4	-1.1	-0.6	+0.5
	3.7 m right	6	-1.1	-0.5	+0.6
	8.2 m right	8	-1.1	-0.4	+0.7
	9.8 m right (toe)	10	-1.0	-0.6	+0.4
Undisturbed	27 m right	11	-0.8	-0.6	+0.2
Cut section	Centerline	12	-0.8	-1.2	-0.4
	Ditch bottom	13	-1.1	-0.8	+0.3

foamed plastic insulation layer insulates almost equally against seasonal heat gain and heat loss. Therefore, insulated sections might be expected to have average subsurface temperatures very similar to the average surface temperature. It is recognized that the roadway embankment soils will also increase slightly in conductivity upon freezing,⁴ but this will be offset in insulated areas by a slight decrease in conductivity of the insulation layer at lower temperatures.

The differences noted to date in subsurface temperatures beneath the various sections are very minor. However, in view of the observed roadway surface to air *n*-factors, it appears that residual thaw zones, or taliks, could develop from a combination of a warmer than normal summer and winter and that taliks may develop first beneath the side slopes of the insulated sections.

INSULATION PERFORMANCE

In September 1972, two insulation samples were taken from the 10-cm insulation section and tested for moisture absorption, compressive strength, and thermal conductivity. Test results showed a maximum moisture absorption of 0.42 percent by volume, with no significant changes in insulation thickness or compressive strength. The thermal conductivity of both samples, measured at an average temperature of 22 °C was 29 mW/m·K, indicating no change after 3 years of field exposure.

CONCLUSION

Roadway fill sections constructed over a frozen peat subgrade, with both 5.1- and 10.2-cm-thick insulation layers, have performed very well during the first 3 years after construction, as evidenced by the fact that surface settlement has been very

small and very uniform. Adjacent normally constructed fill sections showed the average settlement to be 8 times greater than the 5-cm insulation section and 11 times greater than the 10-cm section, with severe variations in settlement magnitude. Although air temperatures at the test site have averaged a relatively warm -2.8 °C over the 3 years of observations, no residual thaw zones have developed beneath either insulated or uninsulated sections. All uninsulated roadway sections instrumented in this study have developed progressively deepening active layers since construction, with consolidation of the newly thawed peat resulting in increased surface settlements each year.

Observations of the test site will continue in attempts to determine the ultimate state of equilibrium for all sections and to evaluate the long-term performance of the insulation.

Because of the test installation nature of this study, no valid cost data were obtained. Similarly, the benefits in terms of reduced maintenance costs cannot be determined from observations of short sections of roadway over a relatively short period of time. On the basis of existing data, however, installation of subgrade insulation for controlling permafrost thaw and resultant roadway settlement should be considered where the benefits of reduced settlement appear to justify the increased construction cost.

ACKNOWLEDGMENTS

Investigation of subsurface conditions, construction coordination services for the test sites, and routine temperature observations were performed by personnel of the Valdez District Materials Section of the Alaska Department of Highways.

Appreciation is extended to Dow Chemical Company for supplying the Styrofoam HI insulation.

The research work reported herein was accomplished under the Highway Planning and Research Program in cooperation with the U.S.

Department of Transportation, Federal Highway Administration. The opinions, findings, and conclusions expressed in this paper are those of the author and not necessarily those of the Federal Highway Administration.

REFERENCES

1. Dunphy, W. J., and N. Bigelow. 1966. Experimental insulation of a subgrade in Raymond, Maine—First year evaluation. Soil Mech. Ser. Tech. Paper 66-7. Maine State Highway Commission, Augusta.
2. Esch, D. C. 1971. Subgrade insulation for frost heave control—Summary of second and third winters performance. State of Alaska Department of Highways, Materials Division, Douglas, Alaska.
3. Gold, L. W. 1967. Influence of surface conditions on ground temperature. *Can. J. of Earth Sci.* 4:199–208.
4. Kersten, M. S. 1949. Laboratory research for the determination of the thermal properties of soils. Final Report, ACFEL Tech. Rep. 23. U.S. Army Corps of Engineers, New England Division, Boston.
5. Kritz, M. A., and A. E. Wechsler. 1967. Surface characteristics, effect on thermal regime—Phase II. Tech. Rep. 189. U.S. Army Cold Regions Research and Engineering Laboratory, Hanover, New Hampshire.
6. Penner, E. 1968. Experimental pavement structures insulated with a polyurethane and extruded polystyrene foam. Paper No. 375. National Research Council of Canada, Division of Building Research, Ottawa.
7. Williams, G. P. 1965. Heat balance over sphagnum moss, p. 173–193. *In Proceedings, First Canadian conference on micrometeorology.* (Reprinted as National Research Council Rep. No. 10017), Ottawa.
8. Williams, W. G. 1968. Development and use of plastic foam to prevent frost action damage to highways—A summary of experience in United States. *In International Conference on Highway Insulation, Wurzburg, Germany.*

THERMAL REGIME IN AN ARCTIC EARTHFILL DAM

Charles W. Fulwider

U.S. ARMY COLD REGIONS RESEARCH AND
ENGINEERING LABORATORY
Hanover, New Hampshire

INTRODUCTION

The Crescent Lake Dam is an earthfill embankment constructed near Thule Air Base, Greenland, to impound a dependable water supply for the base. It is one of a very few such structures in the Arctic or Subarctic, and the information presented here on its construction and on the temperature conditions within it during a 6-year period may be of value in the design of future earthfill dams in cold regions.

SITE LOCATION AND CLIMATE

Thule Air Base is located on the west coast of Greenland at 76°33'N and 68°42'W (Figure 1). The climate at Thule is typically arctic with a mean annual temperature of -11.4°C and a mean annual precipitation of 105 mm. Summer temperatures range up to 10°C , and winter temperatures average -30 to -35°C . Thawing usually begins in early June and continues to early September. The average thawing index for the years 1952 through 1959 was 440°C-days and the average freezing index was $4510^{\circ}\text{C-days}$. Indexes for each season are given in Table I.

DESIGN AND CONSTRUCTION

An existing natural reservoir, Crescent Lake, located several km inland from the base, was found from surveys to have a maximum capacity of about 370 000 m^3 . Studies showed that the construction of a dam only 3.6 m high at the south end of the lake and a small auxiliary dike at the north end would increase the reservoir capacity significantly.

The design of the dam and appurtenant structures and supervision of their construction were performed by Metcalf & Eddy and Alfred Hopkins & Associates, Architects-Engineers, under contract with the Northeast District, U.S. Army Corps of Engineers.

The original plans prepared indicate that the fill in the upstream half of the embankment was to be "impervious, unclassified glacial till," but a change prior to construction eliminated this provision and the entire fill was derived from local sidehill borrow with no differentiation in soil type across the profile.

The design of the dam, therefore, was based on the premise that the soil in the central part of the embankment would remain frozen throughout the year, creating an im-

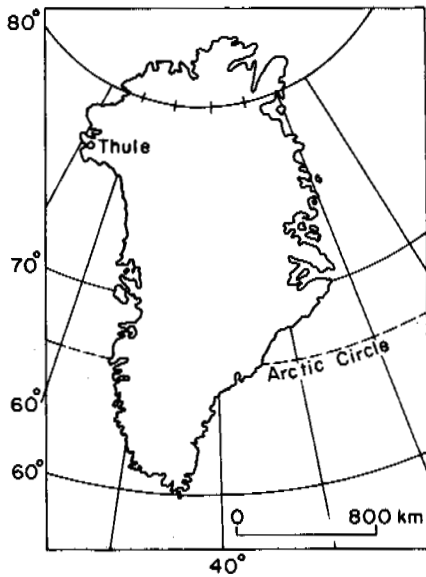


FIGURE 1 Map of Greenland.

pervious core section, and that the water surface elevation would remain below the top of the frozen portion of the dam.

The placement and compaction of the fill for the original dam and auxiliary dike at the north end were performed during the summer of 1952. The top 0.3 m on the reservoir face of the dam was coarse gravel riprap for protection against erosion by wave action. The completed embankment had a length of about 270 m and a maximum height above the original surface of about 3.6 m (crest elevation of 134 m above MSL). An overflow spillway over natural ground was created at the northerly end with coarse gravel riprap to protect the surface against possible erosion.

To increase the storage capacity of the lake reservoir further, the height of the dam was increased to a maximum of about 6 m (crest elevation of 136 m above MSL) in 1954 and early 1955, resulting in an increase in length to about 400 m, mostly on the southeast end. Most of this additional fill was placed in the summer of 1954, with a final 0.3–0.6 m of fill placed in the spring of 1955. At the same time, the existing north end auxiliary dike was increased in height, the spillway raised to about elevation 134.5 m, and an additional small dike constructed at the north end.

Additional fill was placed in the early summer of 1959, raising the dam height by 0.25 m and widening the top of the dam for use as a roadway. Figure 2 is a 1964 photograph illustrating the long, low type of dam. A cross section through the dam (Figure 3) indicates the phases of construction and general soil types used.

INSTALLATION OF THERMOCOUPLE ASSEMBLIES

The study of the temperatures in the Crescent Lake Dam was part of an overall program that included study of the performance of building foundations and pavements at Thule Air Base with the objective of improving design criteria for construction in the Arctic. The program was planned cooperatively by two U.S. Army Corps of Engineers offices, the Northeast (later Eastern Ocean) District and the Arctic Construction and Frost Effects Laboratory (ACFEL) of the New England Division [1].

In late April 1953, assemblies of copper-constantan thermocouples were installed in drilled holes on a cross section through the dam at about its midpoint, at five locations (T1 through T5) as shown in Figure 3. In each assembly, sensing units are at about 0.3-m intervals from the surface to a depth of 3 m, at about 0.6-m intervals to 6.7 m, and at about 1-m spacing below 6.7 m.

TABLE I Freezing and Thawing Indexes and Seasons

Year	Begin Thaw	Begin Freeze	Length of Season (days)		Index (°C-days)	
			Thaw	Freeze	Thaw	Freeze
1952	12 June	11 Sept	91	267	372	4 040
1953	5 June	10 Sept	97	260	361	4 850
1954	28 May	14 Sept	109	263	432	4 900
1955	4 June	3 Sept	91	286	382	4 330
1956	15 June	9 Sept	86	244	414	4 270
1957	11 May	23 Sept	135	242	677	4 480
1958	23 May	28 Aug	97	277	403	4 700
1959	1 June	15 Sept	106		509	
Average	1 June	10 Sept	101	263	440	4 510

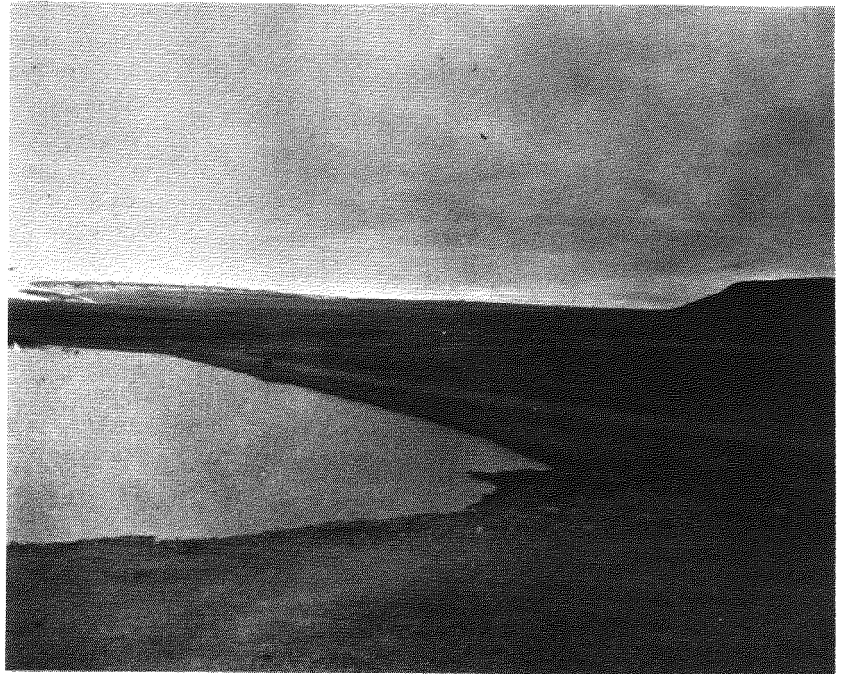
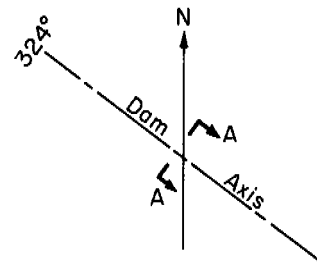


FIGURE 2 Earthfill dam at south end of Crescent Lake, 1964.¹



a. Plan showing orientation of dam axis

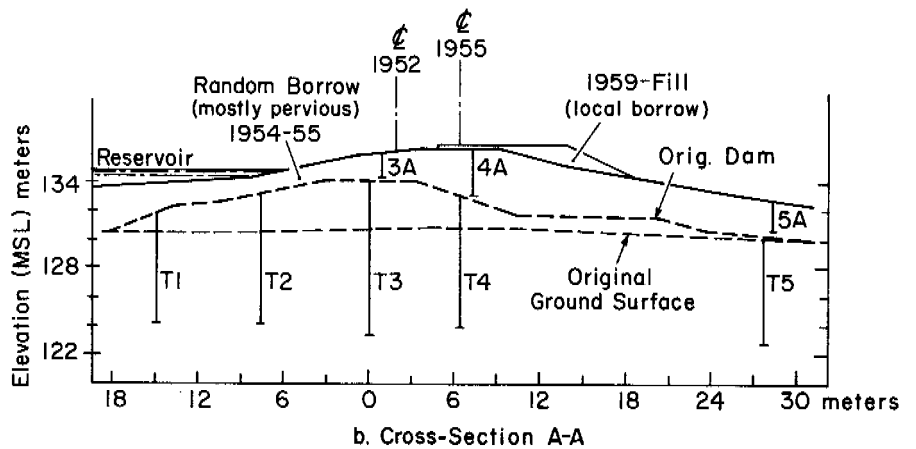


FIGURE 3 Phases of construction and location of temperature assemblies, Crescent Lake dam.

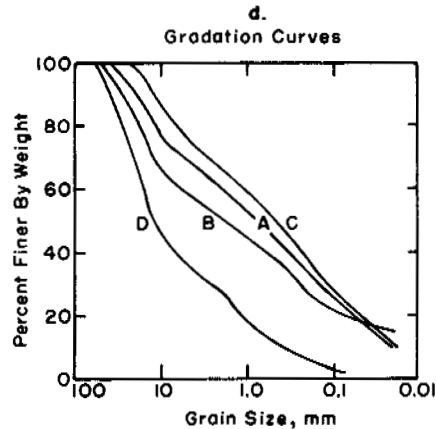
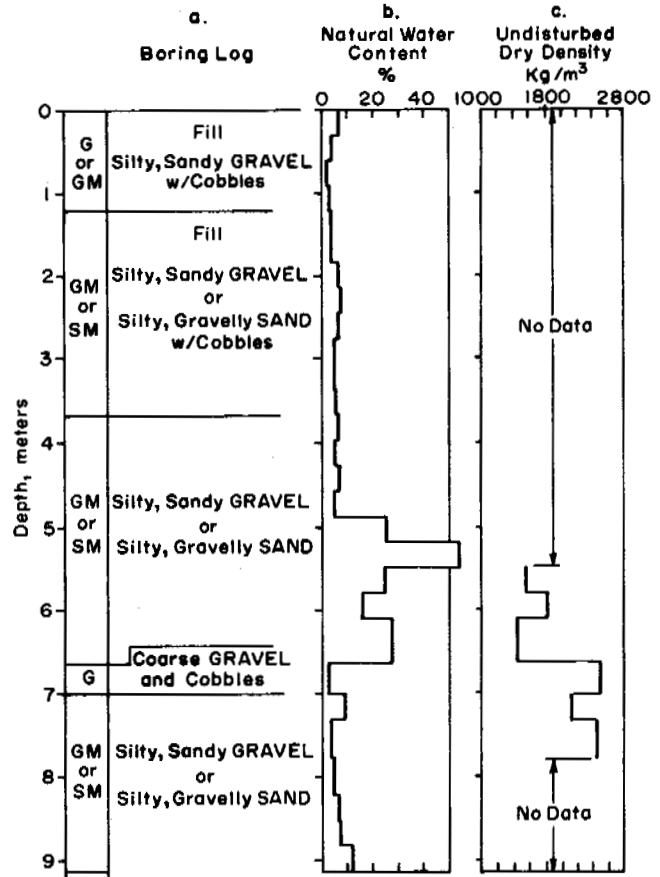
When plans were made to increase the height of the dam to 6 m, the preliminary design did not provide for addition of fill on the reservoir face of the original dam. When the final design did include this addition, the information on the disposition and thickness of the fill was received too late for fabrication of extension temperature assemblies at locations T1 and T2. As a result, short assemblies of the temperature-sensing units were installed only at three locations (3A, 4A, and 5A in Figure 3) in the new fill during the spring of 1955. In each assembly, sensing units are at 0.3-m intervals.

SOILS DATA

The subgrade soil at Thule is predominantly a glacial till and is classified as a silty-sandy gravel or a silty-gravelly sand with 10-45 percent of grains by weight finer than 0.074 mm. Large amounts of ice are present in the permafrost in the Thule area in the form of wedges, lenses, coatings on grains, and as irregular masses up to several feet in thickness.

Holes for the installation of the five temperature assemblies in the original dam were drilled in April 1953 with rotary drilling equipment and produced the only data available to the author on the soils within and under the dam. Previous drilling work at Thule had indicated that satisfactory cores could not be obtained in fill areas, and the holes were advanced through the frozen soil of the embankment fill using a special bit that produced cuttings small enough to be lifted from the hole by compressed air. Cuttings collected for each 0.3 m of hole were sampled for moisture content and the values determined are considered sufficiently reliable for use as approximations and to establish major trends. Core samples were obtained below the fill at all five temperature assembly locations. Figures 4 and 5 present boring logs and soils data for temperature assembly locations T3 and T5. It is assumed that the gradation of the soil used in the embankment was similar to those shown for the upper 3 m of the subgrade. The gradation of a sample taken in the upper 0.3 m or so of the fill at temperature assembly location T2 is also shown in Figure 4. This fill sample does not appear to be representative of material used in the embankment. It is most likely a sample of the lower part of the coarse, gravelly layer placed on the upstream face as riprap for protection against erosion by wave action and is therefore somewhat coarser than the bulk of the embankment fill.

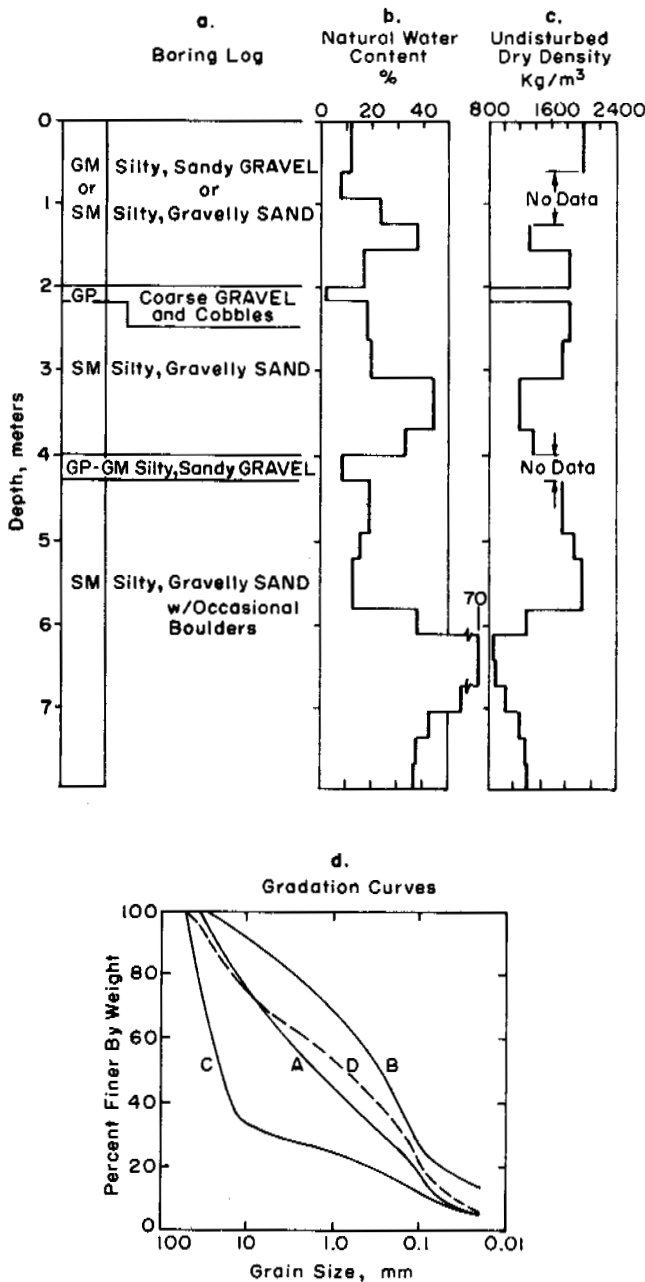
Soils data were not obtained during installation of the short temperature assemblies in the added fill layer at locations T3A, T4A, and T5A in April 1955. Information from the field indicates that the fill placed in 1954 and the spring of 1955 was random borrow, mostly pervious, obtained from nearby side hill areas. It is assumed that the material used was essentially the same as that placed in the original embankment.



Sample Number	Depth meters	Unified Soil Classification
A	4.6-4.9	SM Silty, Gravelly SAND
B	5.4-5.8	GM Silty, Sandy GRAVEL
C	6.2-6.6	SM Silty, Gravelly SAND
D*	-	GW Sandy GRAVEL

*Fill sample, Loc. T2

FIGURE 4 Boring log and soils data, location T3.



Sample Number	Depth meters	Unified Soil Classification	
A	1.5-2.0	SM	Silty, Gravelly SAND
B	3.0-3.7		
C	4.0-4.3	GP-GM	Silty, Sandy GRAVEL
D	5.2-5.7	SM	Silty, Gravelly SAND

FIGURE 5 Boring log and soils data, location T5.

SCHEDULE OF TEMPERATURE OBSERVATIONS AND OTHER DATA

Temperature values were obtained weekly from all temperature assemblies during the period May 1953 through October 1955; thereafter, until observations ceased in mid-October 1959, observations were made only from early May through mid-October each year on about a weekly schedule with single observations made in March, April, and November.

Although water elevations were not recorded on temperature data sheets during the period May 1953 through August 1954, sufficient data were available otherwise to allow a reasonable estimate of the level at various times during the thaw seasons. Beginning in September 1954, water elevations were recorded at the time of each temperature observation.

The thickness of ice that developed on the lake surface was recorded for three winters. Maximum thickness at the end of the 1953-1954 winter was 1.98 m, for 1954-1955 2.16 m, and for 1959-1960 1.8 m.

ANALYSIS OF DATA

As noted previously, the original embankment was placed during the summer of 1952. Although the actual construction schedule is not known, it is likely that fill placement did not begin until about mid-July when thaw had progressed far enough in the area that adequate quantities of unfrozen soil were available to permit continuous placement and compaction of fill. By the beginning of the freezing season in early September, the embankment was completed; based on analysis of data after placement of the 1954 fill, all new fill, plus as much as perhaps 1.2 m of subgrade, was in a thawed condition.

Thermal Regime in the Original Dam

Figure 6a illustrates the temperature conditions in the dam on 30 May 1953, just as thaw was commencing at the crest. Freezeback of the embankment fill and subgrade obviously occurred well before the end of the freezing season. By the end of the thawing season (Figure 6b), thaw had reached a maximum depth of 1.8 m below the crest, with slightly deeper thaw under the downstream slope and 0.3 m or so less under the upstream slope. The temperatures for May 1954 (Figure 6c) are much colder than those of the previous May, indicating that more than one winter was required to establish a stable thermal regime beneath the altered surface. The temperature profile shown in Figure 6d for 30 August 1954 was most certainly affected by the addition of fill in mid-July, but the short period of existence of the original dam makes it difficult to assess the magnitude of this effect. However, the temperatures in the central, or

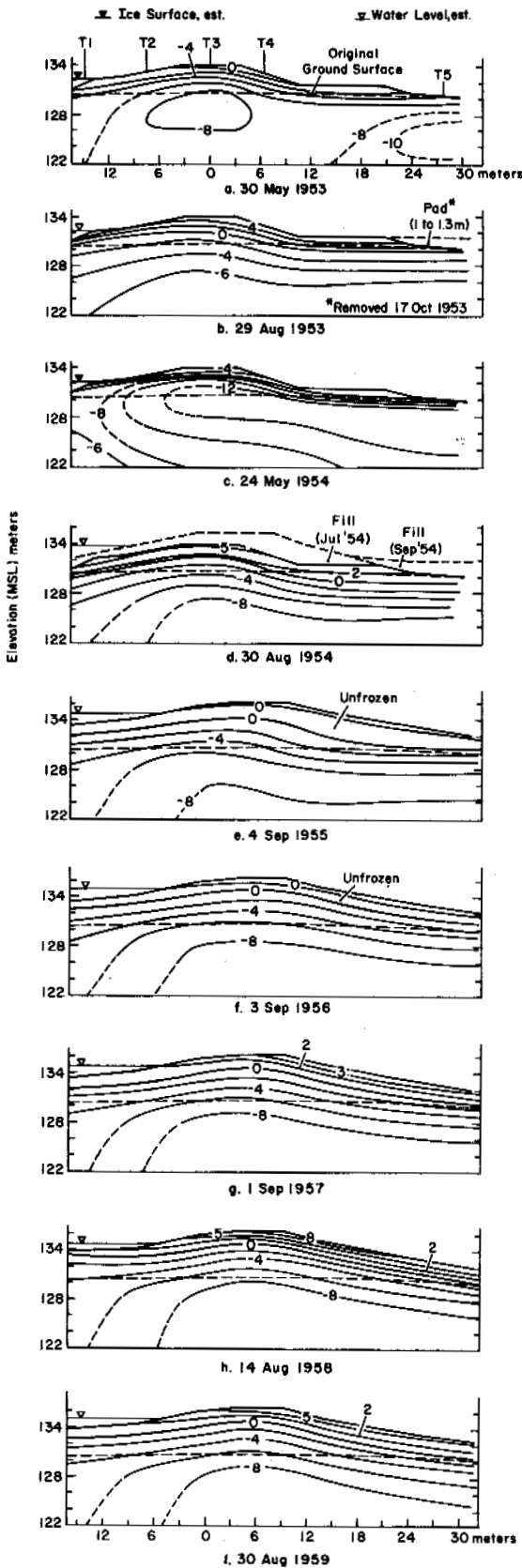


FIGURE 6 Temperature profiles, 1953-1959.

core, section of the embankment are somewhat cooler than those observed at the end of the 1953 thaw season (Figure 6b). It is conjectured that, if the embankment had remained unaltered, temperature profiles for the end of the thaw season for several more years would have shown that temperature stability was established by the end of the 1954 thaw season. This conclusion will be supported in the following discussion of the modified dam.

Thermal Regime in the Modified Dam

The placement of fill in July 1954 was followed in early September by some leakage occurring through the embankment at about midlength, exiting well down the downstream slope. Though the leakage was of some concern and some measures were taken to slow the flow, such as addition of fill on the downstream toe, apparently, it was not a progressively worsening situation. About mid-September freeze-back began and the leakage was sealed off by late October. Probably the main reason for the leakage occurring at all was that the water level of the reservoir was allowed to rise after the placement of fill in July. Data sheets from the field show that the water elevation reached about 134 m by early September, while the top of frozen soil under the crest was at about elevation 132.5 m. An apparent contributing factor was that, since the top of the dam was also a roadway, the top 0.3 m or so of fill at the crest was a gravel with few fines, allowing free flow of water through this section. No significant leakage through the dam has been reported since this occurrence, but some indication of minor seepage has been noted in the last few weeks of a thawing season.

A 0.6-m layer of fill was placed in the spring of 1955 to complete the modified dam, and the temperature profile showed a maximum depth of thaw below the crest of about 1.8 m at the end of the 1955 thaw season (Figure 6e). The temperature conditions shown in Figure 6f for the end of thaw 1956 are the same (with only minor variations) as shown in Figure 6g (end of thaw 1957), Figure 6h (approaching end of thaw 1958) and Figure 6i (end of thaw 1959). Therefore, it may be concluded that by the end of the 1956 thawing season, 2 years after placement of additional fill, a stable thermal regime had been established in the modified dam.

It is of interest to note that the 1957 thaw season was exceptionally warm for the Thule area, with the thawing index more than 1.5 times the average for the 1952-1959 period. However, a comparison of the temperature profile for the end of thaw in 1957 (Figure 6g) with the profile for 1956 (Figure 6f) shows the same depth of thaw beneath the crest and only about 0.2 m greater in 1957 at location T1 and about 0.6 m greater at location T5.

The temperature profiles in Figure 7a-d, along with Figure 6f, illustrate the variations recorded through a typical

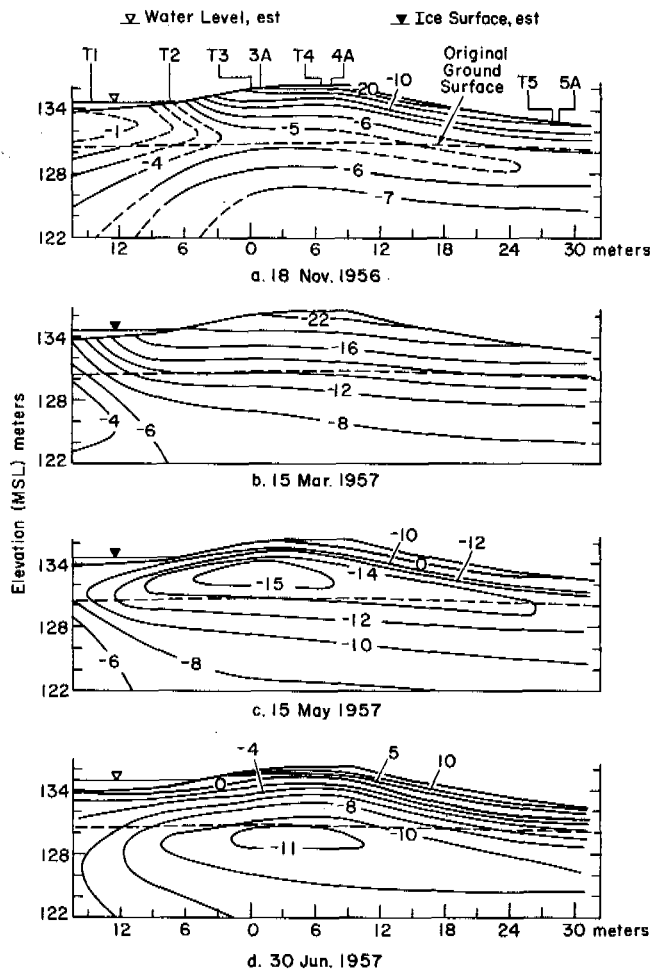


FIGURE 7 Temperature profiles during a typical year.

year after equilibrium was established. Highlights to be noted in these figures are:

Figure 6f: Maximum depth of thaw for the 1956 season, freezeback beginning at the crest and along the downstream slope;

Figure 7a: Freezeback completed, warmest temperatures during the year occurring below about elevation 130 m;

Figure 7b: Coldest temperatures occurring above about elevation 130 m;

Figure 7c: Thaw commencing at the crest and along downstream slope; and

Figure 7d: Thaw has penetrated into dam except for portion under water (ice) of greater than 0.75-m depth.

Lowest temperatures occurring below about elevation 130 m.

CONCLUSION

The studies of the temperature data from Crescent Lake Dam verify the original design premise that the central part of the embankment would remain frozen throughout the year, creating an impervious core section. The data show that two winters were required to establish a stable thermal regime in the original 3.6-m dam and about the same after increasing embankment height by about 2.4 m, although in both instances thawing beneath the crest was limited to about 1.8 m after only one winter. The design provision that the water surface elevation remain below the elevation of the top of the frozen portion of the dam was not strictly adhered to but, with the exception of 1954 and 1955, the lake elevation was within about 0.2 m of the frozen soil surface beneath the crest at the end of each thaw season. In an arctic climate, such as exists in the Thule area, low earth dams, composed of well-graded soil placed at about optimum moisture content, will develop an impermeable frozen core to allow impounding of water after the first winter. The maximum height of embankment to which this might apply is somewhat speculative, but considering the temperatures developed in the original dam after the first winter (Figure 6) the limiting height for complete freezeback in one winter is obviously in excess of 3.6 m, and perhaps as much as 6 m. For an earthfill dam of greater height, it is probable that construction in stages, over several years, would be necessary to ensure dependable natural freezeback of the core section if it is desired to achieve this freezeback before water is impounded.

ACKNOWLEDGMENTS

This paper presents the results of research performed by the Cold Regions Research and Engineering Laboratory under the sponsorship of the U.S. Army Corps of Engineers and the Army Materiel Command. The author wishes to thank Mr. F. E. Crory for his review of the original draft and his constructive comments on it.

REFERENCE

1. Davis, R. M. 1966. Design, construction and performance data of utility systems, Thule Air Base. Spec. Rep. 95. U.S. Army Cold Regions Research and Engineering Laboratory, Hanover, New Hampshire.

NOTE

- [1] ACFEL became a part of the U.S. Army Cold Regions Research and Engineering Laboratory in 1961.

CONTROL OF CULVERT ICING

David A. Gaskin and Leonard E. Stanley

U.S. ARMY COLD REGIONS RESEARCH AND
ENGINEERING LABORATORY
Hanover, New Hampshire

INTRODUCTION

The term *icing* applies to a surface ice mass formed by the freezing of successive sheets of water that originate as ground-water seepage or flow from a spring, stream, or river.¹ As one layer of water freezes, another flows over it, and the icing builds layer by layer, restricted only by the surrounding topography (Figure 1). Icings are a source of serious maintenance problems throughout both permafrost and seasonal frost areas. During thaw periods, for instance, ice-filled drainage structures may cause complete washout of road embankments.

The U.S. Army Cold Regions Research and Engineering Laboratory conducted field and laboratory studies from 1966 to 1971 as a joint research project with the Alaska Department of Highways and the U.S. Department of Transportation on the prevention and control of culvert and road icing. These studies encompassed five major areas of interest: a literature survey to determine methods currently employed for icing prevention and control; evaluation of culvert material and shape; collection of meteorologic, hydrologic, geo-

logic, and ground temperature data in central Alaska; field testing of three icing control techniques; and a laboratory study of culvert icing control using electric heat cables. The first three areas have been previously reported.^{2,3}

FIELD STUDIES

The first field test of electrically heated cables was made at Grenac Creek (Figure 2) during the 1967-1968 winter. During the 1968-1969 winter, three icing control techniques were examined: electric heat cables to maintain the drainage path through the culverts (two sites); channel covers to minimize radiative and convective heat loss (two sites); and channel deepening to obtain better hydraulic conditions (one site).

The electric heat cable technique was most promising in controlling culvert icing, indicating a need for further investigation. The channel covers had to be supplemented by heat (steam) to maintain the drainage path through the winter. The channel deepening reduced the ice severity sufficiently to eliminate bridge deck icing at the site.

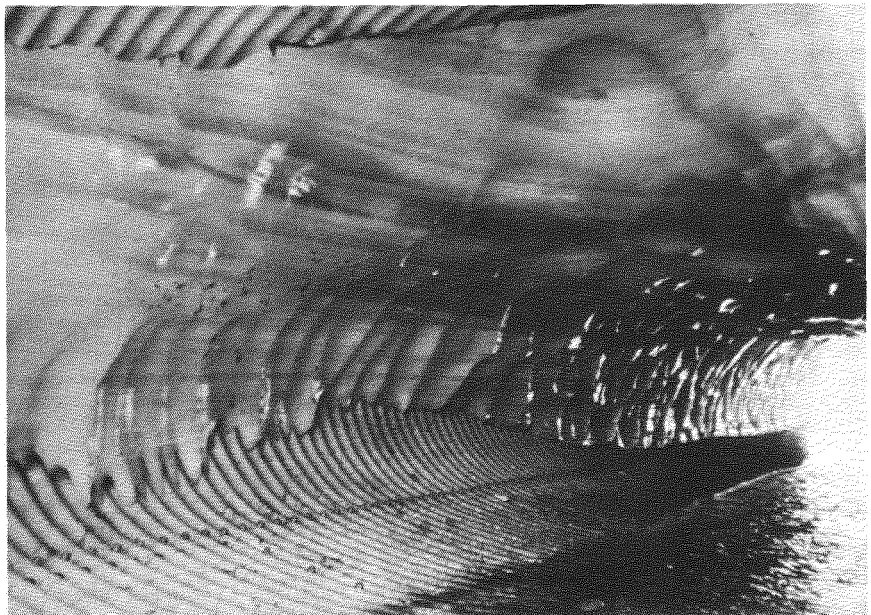


FIGURE 1 Ice remaining in culvert at Big Eldorado Creek near Fairbanks, Alaska, on 8 June 1972. Note ice layering.

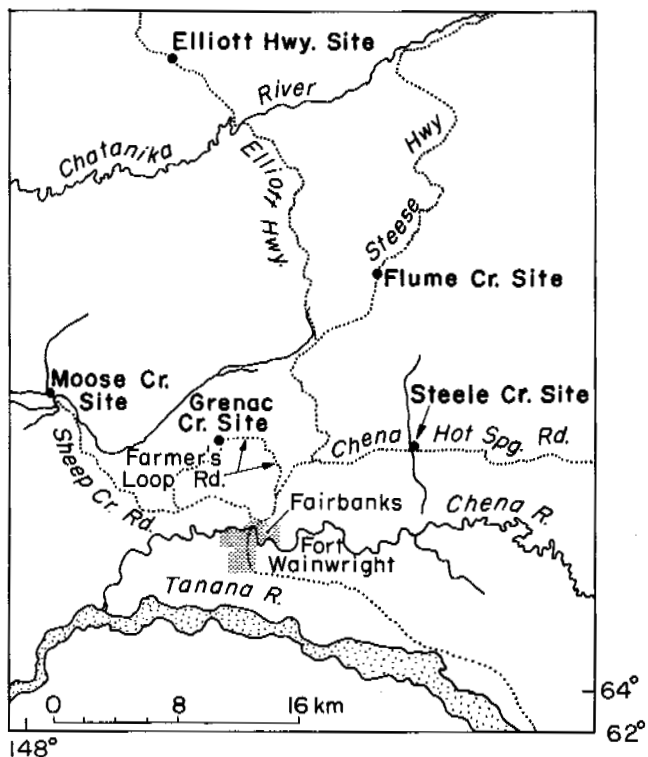


FIGURE 2 General location map.

During the winter seasons of 1969–1970 and 1970–1971, studies were conducted on improved installation and operating procedures for electric heat cables at Grenac and Steele creeks.

Daily icing observations were taken over a 4-year period at three sites near Fairbanks. Observations began when ice started to fill the culverts and extended for 145 days. Icing was considered active for each day that new ice formed above the upstream culvert invert and the ice surface was wet. The active icing ranged from 14.4 percent of the season (1967–1968) to 29.6 percent (1968–1969). The 4-year average was 23.0 percent. Hence, any form of energy used to maintain a

drainage path need be applied for a maximum of 30 percent of the icing season at these three sites.

LABORATORY STUDY

A laboratory study was conducted in 1971 to investigate the electric heat cable method of controlling culvert icing. Specific objectives were to evaluate the energy consumed by an electric heat cable opening a hole in an ice-filled culvert; determine the heat transfer mechanisms involved; investigate the heat distribution; determine the optimum position for the heat cable; evaluate the cyclic application of electrical energy for reducing power to the cable during dormant icing periods; design and test a temperature sensing system to automatically produce and maintain the desired drainage path; and adapt and test an electronic proportional controller⁴ for spring icing conditions to sample water temperature in the culvert and maintain the flowing water above freezing.

MODEL CULVERT

The culvert was modeled by a 196-cm-long wax-coated fiber cylindrical shell with a 30.5-cm diameter and a 6.4-mm wall (Figure 3) and supported on a 5 percent slope. The heat cable was located along the shell's long axis. Bulkheads at each end retained the water during the freeze cycle and were removed to permit collection of the meltwater produced when the heat cable was energized. A group of seven temperature sensors (thermistors), installed on 5-cm centers, monitored the ice temperature.

A cold room was set to -15°C and the bulkheads were closed. The culvert was filled with distilled water chilled to approximately 3°C . Once the water was frozen, the room was set to -5°C and the ice allowed to reach thermal equilibrium. This typified culvert ice temperatures (-7 to -1°C) observed in Alaska. When equilibrium was established, the bulkheads were opened, and each end of the heat cable was supported along the central axis. Power was applied in accordance with the particular test. Upon completion of a test,

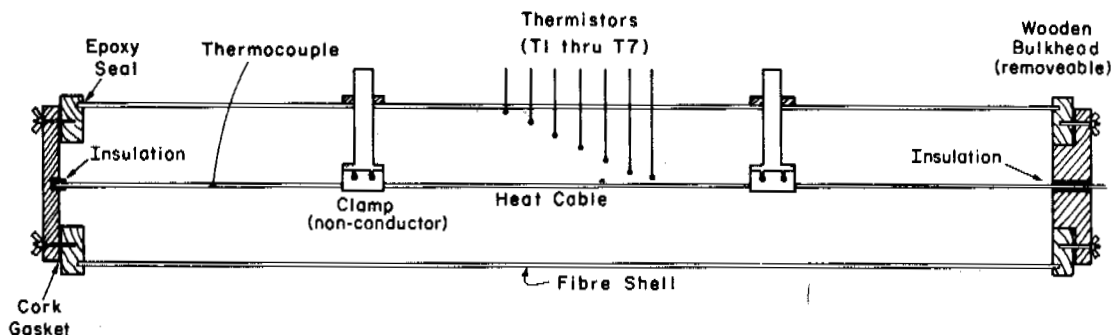


FIGURE 3 The model culvert.

the end supports were removed, the bulkheads closed, and the culvert refrozen.

EXPERIMENTAL PROCEDURE

A series of experiments was designed to evaluate the efficiency of various power levels and systems in melting a tunnel in an ice-filled culvert.

Group 1: Continuous Heating Mode

A group of eight experiments comprised the continuous heating part of the study. Based on the manufacturer's specified maximum allowable sheath temperature (190 °C), the upper power limit was experimentally found to be 262 W/m. Currents of 10, 15, and 20 A were used, corresponding to 49.2, 128, and 262 W/m. The time per test varied from 2.75 to 7.5 h. The factors analyzed were the percentage of energy recovered (to make the hole and heat the unmelted ice) and lost.

Group 2: Equivalent Energy

A second group of three experiments was run to compare pulsed energy (using a 30-s cycle percentage timer) with the same total energy supplied continuously. The continuous power was supplied at power levels of 262 and 128 W/m. For the first test in this group, a percentage timer was set at 53.3 percent. Because the electric power was pulsed, the cable did not get as hot as it would under continuous operation, and only 35 volts was needed to put 20 A through the cable (the maximum current rating for the autotransformer). The cable ran at 230 W/m. The test ran for 5 h; hence, the total energy input was 1 866 W-h. Since only 196 cm of the 305-cm cable was in the culvert, only 64.3 percent (1 200 W-h) of this energy was available to heat and melt the ice.

For the second test in this group, the same total energy was delivered, but continuously at maximum power level (262 W/m). The time for this test was 2.33 h.

For the third test in this group, the power was delivered continuously at a reduced level of 128 W/m. To deliver the same total energy, this test ran for 4.77 h.

Group 3: Automatic System

The third group of tests examined the automatic system. This system uses a temperature sensor and related electronic controls to melt a tunnel of a desired radius and then automatically maintain the tunnel. If the sensor temperature is above the set temperature, the heat cable is energized for only 2 s. If the sensor temperature is at or below the set temperature, the heat cable will remain energized until the sensor temperature rises above the set temperature. At preset intervals, the sensor is interrogated by the timer and sensor control. If the

heat cable is on, no change is made; if the heat cable is off, operation proceeds dependent on sensor temperature as described above.

The diameter of the tunnel is determined by the distance between the sensor and the heat cable and by the temperature setting for which the sensor is to turn off the cable. In this study, the sensor was placed 3.8 cm away from the heat cable in the horizontal plane and the turnoff temperature was set at 0.5 °C. This combination of placement and setting was expected to produce a tunnel approximately 7.6 cm in diameter. The auto-transformer was adjusted to supply 249 W/m to the cable, and the sampling time interval was set to 0.5 h.

The tests in this group consisted of two parts: First, the system was energized to produce a tunnel. The test parameters (power, sensor location, etc.) were as detailed above. This part was considered completed when the first automatic turnoff occurred. The second part, done with the cable in the tunnel produced by the first part, was a series of tests to relate heat cable *on* time in a tunnel to sampling time interval and power level. Two power levels (249 and 135 W/m) and four sampling time intervals (1, 2, 4, and 8 h) were examined.

Proportional System

A fourth system investigated during the laboratory study was a proportional controller with a thermistor temperature sensor and a simulated heat cable. This system delivered power proportional to the difference between the temperature of the sensor and the set point. When the sensor was much colder than the set point, maximum power was delivered. As the sensor warmed, the amount of power was decreased proportionally. When the sensor reached the set point, the power was turned off. As the sensor cooled, the power was turned on slightly. Thus, the system tended to keep the sensor temperature at the set point by providing just enough power to maintain this equilibrium.

Analysis of Energy Distribution

The input power is given by the voltage and current applied to the cable. As noted earlier, only 64.3 percent of the total power was available within the culvert. Consider:

$$q_i = q_1 + q_2 + q_3 + q_4 + q_5 + q_6,$$

where q_i = the input energy available to the ice; q_1 = the energy required to raise that fraction of ice melted to its melting point; q_2 = the energy required to change phase; q_3 = the energy required to raise the water to its exit temperature; q_4 = the energy required to raise the temperature of the unmelted ice; q_5 = the energy lost from the surface of the model culvert to the air in the coldroom; and q_6 = the energy lost to air flow through the hole.

Values for q_1 and q_2 are calculated from the measure-

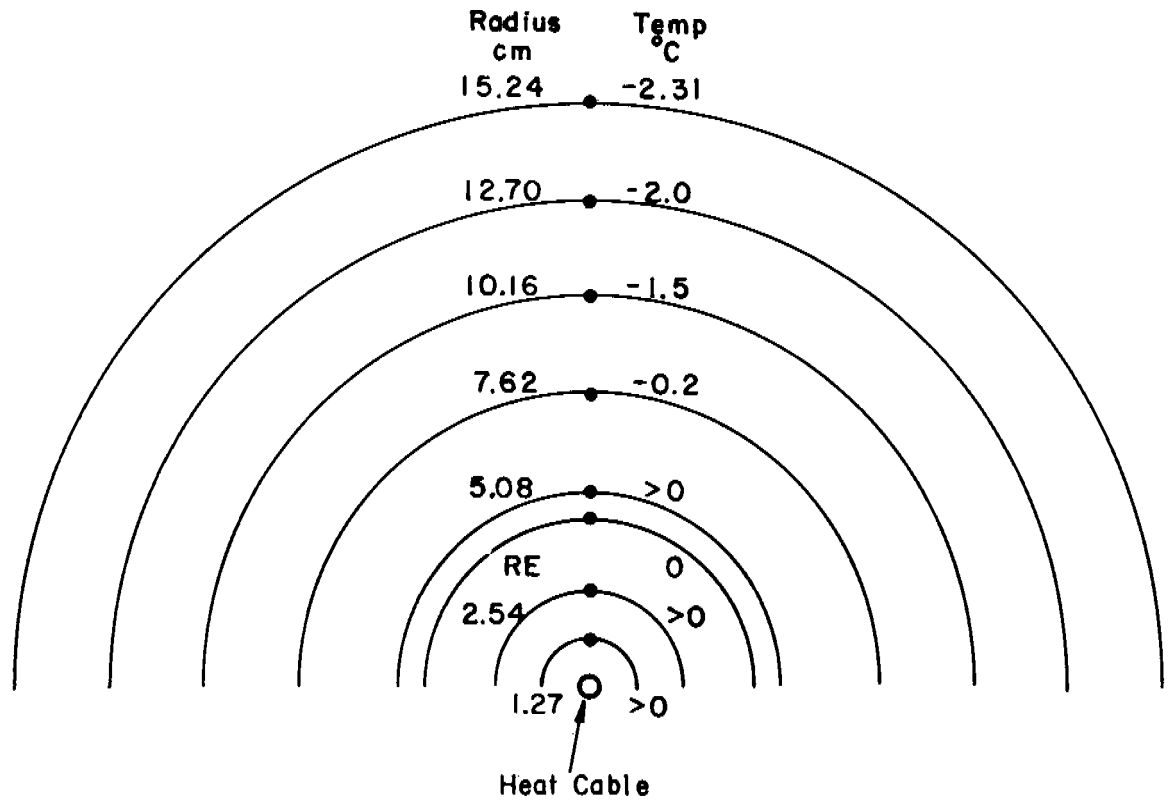


FIGURE 4 Typical cross section through culvert.

ment of the meltwater volume. The quantities q_3 , q_5 , and q_6 were difficult to measure or even estimate and, thus, are lumped together as energy lost. The value for q_4 is estimated by a cylindrical shell method, as follows:

Figure 4 represents a partial cross section through the ice cylinder, in the plane perpendicular to the long axis. Typical temperatures during a run are shown. The RE radius is the effective radius of the hole, determined by the volume of meltwater collected. The nested cylindrical shell method assumes a linear temperature distribution between any two adjacent temperature sensors.

Since the temperature sensors are located at 2.54-cm intervals from the center of the model (except for T1, which is 1.27 cm from the center), shells of 2.54-cm thickness are used. The length of ice is known, so the mass of each shell can be calculated. The amount of heat gained by a shell is:

$$q = cm (t_A - t_I),$$

where q = the heat gained; c = the specific heat of ice; m = the mass of the shell; t_A = the average temperature of the ice in the shell; and t_I = the initial temperature of the shell.

The best representation of the average shell temperature is at the half-volume radius. This radius is:

$$r = [(r_o^2 + r_i^2)/2]^{1/2},$$

where r = the half-volume radius; r_o = the shell outer radius; and r_i = the shell inner radius,

The temperature t at this point is:

$$t = r [(t_i - t_o)/(r_i - r_o)] + [(r_i t_o - r_o t_i)/(r_i - r_o)],$$

where t_i = the temperature at r_i and t_o = the temperature at r_o .

Then the heat q gained by a shell is:

$$q = c \rho L \pi (r_o^2 - r_i^2) (t - t_I),$$

where ρ = the density of ice and L = the length of the cylinder. This expression may be used for all shells when $t_I \leq 0$. When t_I becomes positive, the remaining ice is converted to an equivalent cylindrical shell and its energy gain computed

The above method is complicated by the fact that the hole produced by the cable is elliptical, with its major axis vertical and the heat cable near the lower focus. When the actual elliptical hole is replaced by the virtual equivalent circular hole, an apparent temperature anomaly occurs. However,

enough data exist to replace this ice with an equivalent shell. If V is the volume of meltwater from the ice, then the equivalent radius r_E is:

$$r_E = (r_c^2 + V/\pi L)^{1/2},$$

where r_c = the radius of the heating cable. The heat gained by this shell is:

$$q = c \rho L \pi (r_o^2 - r_E^2) (t - t_1).$$

REDUCTION OF EXPERIMENTAL DATA

A computer program was written to reduce the experimental data into numerical forms more amenable to analysis. The program computes the input power, energy used in melting, energy used to heat unmelted ice, and the radius and cross section of a circular hole equivalent to the actual elliptical hole. The program also computes the percentage of the energy required to make the hole ($q_1 + q_2$), required to heat the unmelted ice (q_4), recovered ($q_1 + q_2 + q_4$), and lost ($q_3 + q_5 + q_6$).

RESULTS

The series of experiments on the continuous system relates the percentage of energy usefully consumed in melting ice

to the watt density. This percentage is the energy required to make the hole divided by the total energy input. The percentage for the 262-W/m tests varied from 66.5 to 69.4 percent (Table I). In the intermediate level (128 W/m), the energy utilized to make the hole varied from 44.6 to 60.6 percent at the low level (49.2 W/m), the range was from 25.7 to 47.2 percent. The warmer (-4.1°C) and colder (-6.6°C) starting temperatures resulted in an increase in energy going to heat unmelted ice: 34.7 percent for the 24 May test and 50.6 percent for the 6 May test (Table I, Group 1). Comparing the efficiency of various power levels operated in the continuous mode, the average cross-section production per unit energy input is $40.6 \text{ cm}^2/\text{kW-h}$ for the high-power level, $33.8 \text{ cm}^2/\text{kW-h}$ for the intermediate level, and $22.2 \text{ cm}^2/\text{kW-h}$ for the low-power level.

All of the experiments indicate that the major heat transfer mechanism for melting a hole in an ice-filled culvert is convection. The 24-h test begun on 8 June developed an elliptical hole that was 20.0 cm high and 15.2 cm wide measured 15 cm in from the downstream face. The cable was 4.4 cm from the bottom of the thaw tunnel. Figure 5 shows a typical plot of sheath temperature versus time. Initially, the sheath temperature is at the ice temperature. When power is applied, the sheath temperature rises to the ice melting point and remains there, losing heat by conduction until the water begins to flow. When the cable-water-ice contact is broken, the

TABLE I Test Results

Line No.	Date	W/m	Current (A)	Voltage (V)	Percent Energy				Ratio Energy To Make Hole to Energy To Heat Unmelted Ice	Initial Starting Temp. ($^\circ\text{C}$)	Cross Section (cm^2)	Total Time of Test (h)	Input Energy (W-h)
					Utilized To Make Hole	To Heat Unmelted Ice	Recovered	Lost					
Group 1: Continuous Heating Mode													
1	6 May	49.2	10	15	25.7	50.6	76.3	23.7	0.51	-6.6	9.10	6.0	578
2	24 May	49.2	10	15	47.2	34.7	81.9	18.1	1.36	-4.1	16.8	6.07	585
3	27 Apr	128	15	26	44.6	31.2	75.8	24.2	1.43	-5.6	22.3	3.33	835
4	8 June	128	15	26	59.7	19.9	79.6	20.4	3.01	-5.5	53.8	6.0	1 500
5	8 June	128	15	26	60.6	17.1	77.7	22.3	3.54	-5.5	68.6	7.5	1 880
6	30 June	128	15	26	59.9	21.2	81.1	18.9	2.83	-5.7	54.5	6.0	1 500
7	3 May	262	20	40	66.8	20.7	87.5	12.5	3.22	-5.4	56.5	2.75	1 410
8	4 June	262	20	40	69.4	15.7	85.1	14.9	4.41	-4.8	64.2	3.0	1 540
9	24 June	262	20	40	66.5	18.5	85.0	15.0	3.60	-6.0	56.5	2.75	1 410
10	24 June	262	20	40	67.1	17.8	84.9	15.1	3.77	-6.0	62.1	3.0	1 540
Group 2: Equivalent Energy													
11	18 June	121	10.7 ^a	35	53.4	21.8	75.2	24.8	2.46	-5.8	38.6	5.0	1 200
12	24 June	262	20	40	66.7	19.4	86.1	13.9	3.43	-6.0	48.1	2.33	1 200
13	30 June	128	15	26	58.0	24.5	82.5	17.5	2.37	-5.7	42.0	4.78	1 200
Group 3: Automatic System													
14	26 July	249	19	40	63.8	17.1	80.9	19.1	3.72	-6.0	53.2	2.83	1 380

^a Equivalent current (53.3 percent of the actual on-time current).

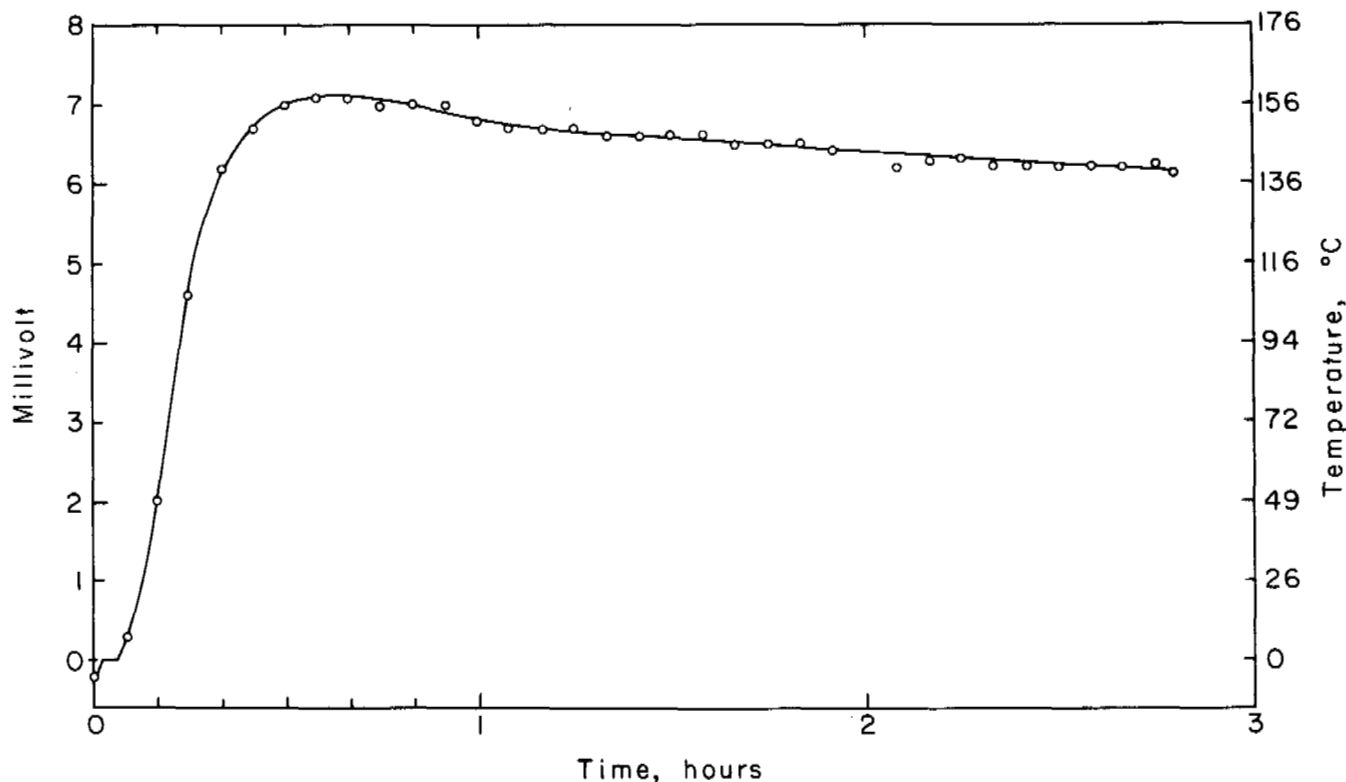


FIGURE 5 Plot of sheath temperature.

sheath temperature rises rapidly, losing heat primarily by radiation. As the hole enlarges, the convective heat transfer mechanism dominates, and the sheath temperature begins to drop.

The test results from evaluation of the short-term percentage timer (pulsed system) are shown in Table I, Group 2. Applying the equivalent amount of energy, as was used in the cycle timer test at 262 W/m resulted in a 24 percent increase in meltwater (8.594 versus 6.909 dm³). Applying this equivalent energy at 128 W/m produced 8 percent more meltwater than the percentage timer test (7.474 versus 6.909 dm³).

The automatic system ran continuously for 2.83 h, then the first automatic shutoff occurred. The system produced an elliptical hole (computed to be 53.2 cm² in cross section). The series of sampling time interval tests did not produce any additional meltwater. The heater-on time varied from a minimum of 10 min per cycle at 249 W/m at the 1-h sampling interval to a maximum of 49 min per cycle at 135 W/m at the 8-h sampling interval. The relationship between power-on time and sampling time intervals is given in Figure 6. From these data, the daily power consumption, as a function of the sampling time interval, was calculated. The results are shown in Figure 7. The curves show that longer sampling time intervals use less power per unit length per day. The curves

also show that a large increase in input power (249 versus 136 W/m) results in a small increase in the daily power consumption.

A pronounced edge effect was observed in all of the experiments. The tunnel exhibited a constriction at both ends where the ice faces were in contact with the circulating cold air. The final measurements made on the downstream end after the 24 June test typify this end constriction. The downstream end measured 6.7 cm high and 5.1 cm wide at the face with the heat cable 1.6 cm off the bottom. Fifteen centimetres in from this end the vertical measurement was 12.1 cm and the horizontal measurement was 8.6 cm.

CONCLUSIONS

The major heat transfer mechanism for melting and/or maintaining an open, freely draining hole in a culvert subject to groundwater icing is convection. This implies that the optimum location for the cable is near the bottom of the culvert, where the largest cross-section hole can be melted without thawing the frozen soil that surrounds the culvert. The cable end risers should be double or triple looped to provide more heat at the ice-air interface where thaw tunnel constrictions occur.

The icing observations taken near Fairbanks averaged 23

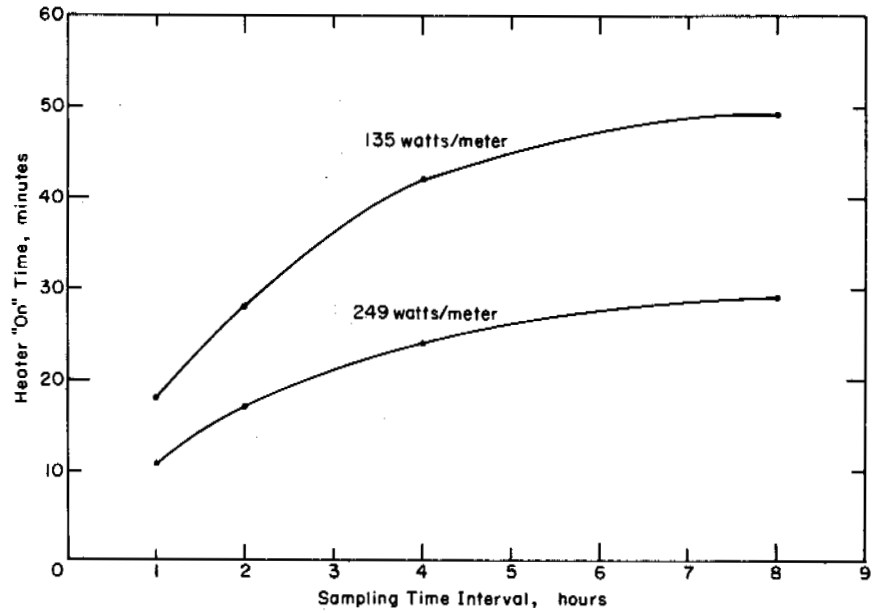


FIGURE 6 Plot of heater-on time as a function of sampling time interval.

percent active icing days of the 145-day season, with a maximum of 29.5 percent over a 4-year span. A flexible system was indicated, so the short-term cycle timer was installed. However, the later laboratory study demonstrated that it is inefficient, primarily because its pulsing mode does not bring the cable to near its maximum power level. The series of continuous heating experiments at three power levels demonstrates that higher power levels are more efficient in

terms of thaw hole cross section produced per unit energy input, i.e., higher power levels tend to distribute a higher percentage of the input energy to hole production. Consider a system that is turned on and off by a long-term (24-h) cycle timer. Such a system, analyzed on a continuous maximum power level basis, will apply about 67 percent of the input energy toward making the hole. This system has the flexibility to adjust input energy levels according to local

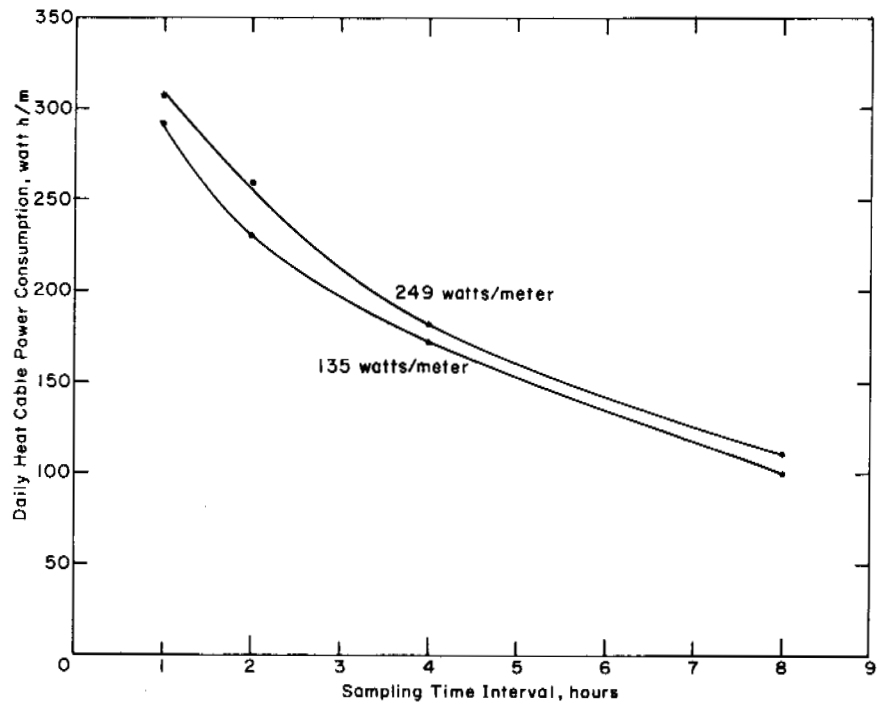


FIGURE 7 Comparison of heater-on time at two power levels.

icing conditions, while operating at high efficiency for melting ice.

The automatic system, developed and tested to evaluate its potential for even better control of groundwater icing, performed well. It produced a 53.2-cm² cross section while the sensor location and temperature setting implied a 46- to 50-cm² hole, predicating a circular hole symmetric about the heat cable. The slightly larger cross section is due to the ellipticity of the hole. The system did not produce any additional meltwater during the 111 sampling intervals, each of which turned the cable on. This system may be too complicated in its present state to be useful as a field system. However, the system definitely has sufficient merit to warrant further development toward simplification of installation and maintenance.

The proportional controller system simulated test demonstrated the feasibility of such an approach to spring icing problems. The sensor can be placed downstream of the problem drainage structure and an electric heat cable installed. When the system is energized, it will keep the water continuously flowing through the drainage structure above the freezing point and so minimize or eliminate the culvert icing blockage.

ACKNOWLEDGMENTS

This paper presents the results of research performed by the Cold Regions Research and Engineering Laboratory under the sponsorship of the U.S. Army Corps of Engineers and the Army Materiel Command. The work was done in cooperation with the Alaska Department of Highways and the U.S. Dept. of Transportation, Federal Highway Administration.

REFERENCES

1. Muller, S. W. 1947. Permafrost or permanently frozen ground and related engineering problems. J. W. Edwards, Inc., Ann Arbor, Michigan.
2. Carey, K. L. 1970. Icing occurrence, control and prevention: Annotated bibliography. Spec. Rep. 151. U.S. Army Cold Regions Research and Engineering Laboratory, Hanover, New Hampshire.
3. Carey, K. L., R. L. Huck, and D. A. Gaskin. Prevention and control of culvert icing: Summary report on studies FY 1966-70. Highways and U.S. Department of Transportation, Federal Highway Administration by USA CRREL. (In press)
4. Codd, B. J., F. E. Neale, and R. E. Thurstans. 1970. A cheap and simple temperature controller. J. Phys. E: Sci. Inst. 3:937-939.

ANALYSIS OF THE PROPOSED LITTLE CHENA RIVER, EARTH FILLED NONRETENTION DAM, FAIRBANKS, ALASKA

Warren George

U.S. ARMY CORPS OF ENGINEERS
Anchorage, Alaska

INTRODUCTION

The Soviet engineers have successfully designed and built a number of dams in permafrost regions; however, construction of such structures in the United States has been limited, and Alaska is probably the only area in the United States that has had or will require such engineering effort. At present, the existing, but not used or maintained, Hess Creek Dam and Reservoir (a privately developed project constructed at latitude 65°30'N to serve as a water supply for a mining venture) was the subject of a paper prepared by E. F. Rice and O. W. Simoni for the First International Permafrost Conference.⁶ Several small dams have been designed and built by this office to provide needed reservoirs for water supply for military in-

stallations at Unalakleet and Indian Mountain, Alaska. Both have performed well and are still functioning. Except for these structures and a smaller structure built by the Department of Health, Education, and Welfare to serve its hospital at Barrow, Alaska, no other known dam situated in a permafrost region has been built in Alaska. One of these structures was briefly described in a paper given on water supply by the author at the First Permafrost Conference.¹

It now becomes important that such construction be given strong consideration in the flood protection works now under analysis and design for the City of Fairbanks, the North Star Borough, and the military post at Fort Wainwright.

One of the important functions and benefits of an international meeting such as the Second Permafrost Conference is to

present studies for such structures that may be of interest to the group and to exchange viewpoints for the attending engineers' mutual understanding and the advancement of the science. It is our firm belief that this paper pertains to a subject of considerable interest to many of the engineers and scientists attending the conference.

The dam discussed herein has special interest because of several unusual circumstances. It will be located in an area in which the permafrost temperature is more marginal than that existing in the areas where such structures have been previously built with permafrost preservation in mind. The same requirements exist, however, to protect the permafrost, and, in fact, these now become even more of a concern. The methods proposed to accomplish this protection have had careful analysis and are discussed in some detail in the paper.

Another circumstance is that probably for the first time such a structure will be used to store waters only temporarily from the recurring storms that would otherwise flood the areas to be protected. The planned built-in drainage conduits running through the dam will allow for the gradual release of these impounded waters. Because of this temporary storage, a moderation and, in fact, control of the heat absorption into the dam from these impounded waters will result. This controlled and limited heat input has been an important factor in even considering the design and construction proposed. This particular circumstance can result in further quite important opportunities that we propose to pursue. By the installation of well-planned instrumentation, covered in more detail below, not only is the safety of the structure assured but, by means of a study program, behavior of the dam in its varying physical environment can be made using the structure as a full-sized field laboratory model, i.e., conducting heat transfer measurements and recording other effects related to the theoretical predictions. Such studies cannot fail to lead to increased understanding of the behavior of such a structure and thereby result in advances in the state of the art and the ability to deal with even more difficult situations of this type, i.e., use as permanent storage reservoirs.

The dam is currently planned⁹ for a height in excess of 31 m and a length between schist rock buttresses of 1 736 m. It will provide for the temporary storage (impoundment) of $128.5 \times 10^6 \text{ m}^3$ of water. An ungated overflow spillway to be provided at the right abutment will handle a probable maximum flood with a peak of $1\,840 \text{ m}^3/\text{s}$ and will result in a spillway discharge of $700 \text{ m}^3/\text{s}$. Total release of the impounded water will occur within 7–24 days, depending on the magnitude of the flood. Hydrologic studies show the relationship of size of average expectancy of flood occurrence, maximum water level, and time period for complete drainout (Table I).

Conservative calculations show that there exists more than a margin of safety from the heat input from such temporary and infrequent impoundments when balanced against heat loss. The more frequent floods will normally

TABLE I Reservoir Impoundment Expectancy

Average Expectancy of Flood Occurrence (years)	Maximum Elevation of Water Level (m)	Drainout Period to Reservoir Bottom (elev. 177.39 m) (days)
2	180.29	7.5
10	184.25	13
25	187.45	15
50	190.04	16.5
100	192.63	18.0
—	202.99	24.0

be of the spring snowmelt type with water temperature quite cold and the duration of the impoundment quite short. The less frequent flood, where water temperatures may be somewhat higher, will not be a problem. Heat input factors from this source will receive further complete computer analysis prior to our completion of the design.

This proposed dam will be one of the important structures in the congressionally authorized major flood protection project under design by the Alaska District, Corps of Engineers. Serious floods of a recurring nature have periodically threatened this area. The last flood of 1967 caused \$98 000 000 damage with a loss of seven lives.

PHYSICAL SETTING

This dam on the Little Chena River would lie in a permafrost area at a location of approximate lat. 65°N and 147°W long. The Little Chena River is a tributary of the larger Chena River, which, in turn, is a tributary of the major Tanana River watershed. Flood waters from each of the streams contribute to the flood threat. Figure 1 shows the general site layout.

The damsite lies in an area of rolling foothills and is geographically situated in the lower confines of the Yukon Tanana uplands. This topography exhibits rounded, maturely dissected, northeast-trending ridges bordered by relatively flat alluvium-filled valleys that result from long-continued, uninterrupted stream erosion and deposition aided by decomposition (chemical) and disintegration (mechanical weathering) of the highly metamorphosed country rock—lower Precambrian Birch Creek schist. The surface is generally covered by a thick mantle of these products of rock disintegration. The stream valleys have reasonably wide floors and gentle gradients. A thick alluvial fill usually exists between the surface features and the underlying rock. The United States Geological Survey maps (Fairbanks Quadrangle)^{5,10} give excellent portrayals of surface distribution and materials content of this regolith.

Typical drilling logs resulting from Becker Hammer drilling equipment operations are shown in Figures 2 and 3.

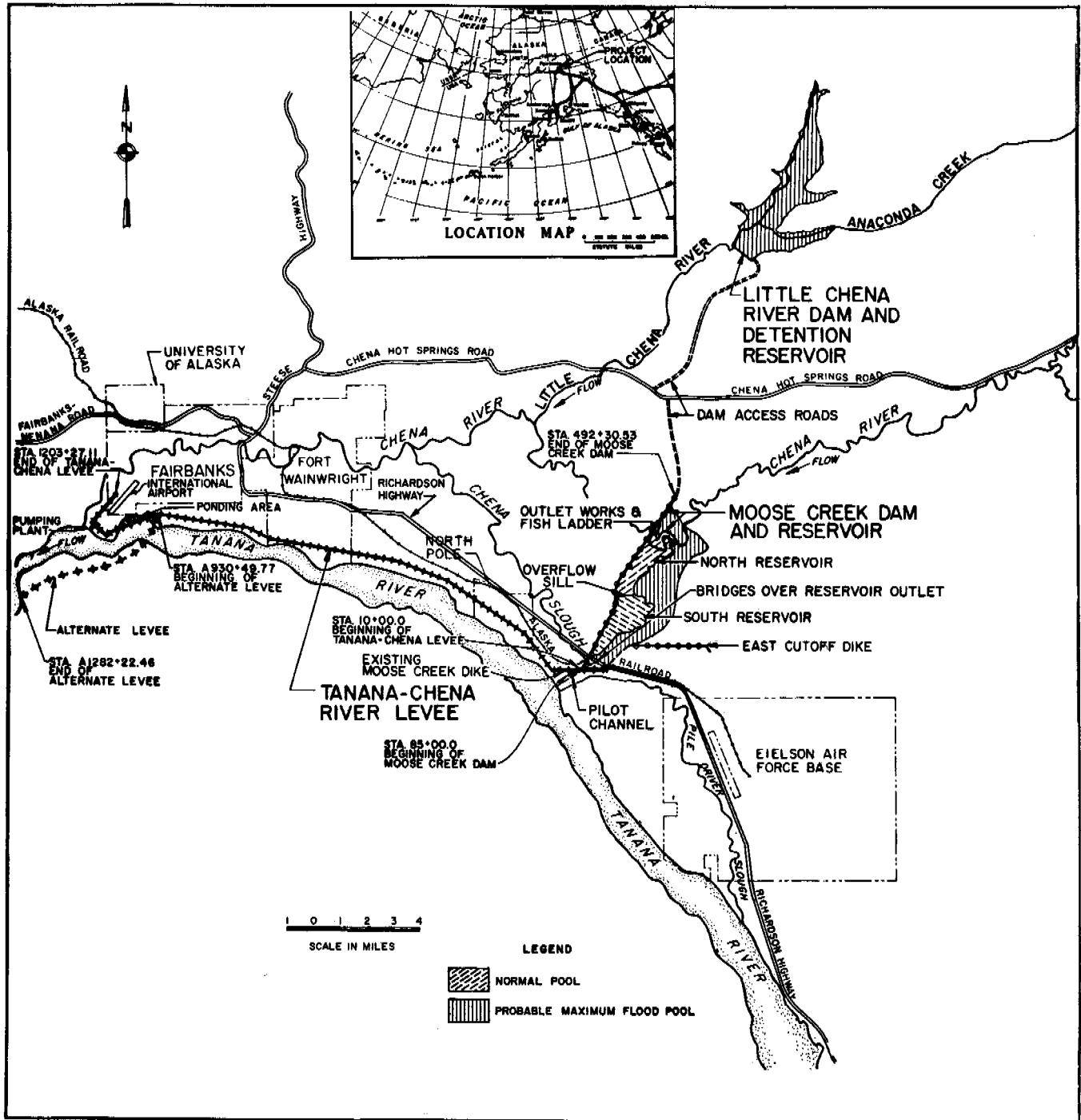


FIGURE 1 Area and location map.

Birch Creek schist, one of the true schists, underlies the surficial mantle and serves as a buttress at each end of the dam. The thickness of this foundation, while unknown, is believed to aggregate several thousand metres. These rocks are among the oldest on the North American continent and have been repeatedly subjected to severe metamorphism, surviving several eras of mountain building; as a result, the

rocks are intricately folded, fractured, jointed, and faulted. Any indication of original rock composition or structures is almost completely obliterated. What can be described as quartzites, quartzitic schists, and quartz mica schists, and intricate patterns of thin dikes, stringers, and veins of quartz are commonly encountered.

The Little Chena damsite occupies a fairly broad valley

DEPARTMENT OF THE ARMY NORTH PACIFIC DIVISION U.S. ARMY ENGINEER DISTRICT, ALASKA		PROJECT Little Chena LOCATION (County or State) N. 4,005-65W E. 334-86S		SHEET 1 OF 2	
EXPLORATION LOG		PERMANENT HOLE NO. DH-96		Bendix Marine Advisors	
FIELD NO. LC-4		PERMANENT HOLE NO. DH-96		DATE 3 Nov 70	
TYPE OF HOLE		DEPTH		TOTAL DEPTH OF HOLE	
TEST PIT	AGEE HOLE	DEPTH	DEPTH	DEPTH	DEPTH
TYPE AND TYPE OF BIT	DATE FOR ELEVATION	SOFT	SOFT	SOFT	SOFT
6 5/8" Crowl-in	Becker Hammer Drill				
TOTAL NO OF SAMPLES	TYPE OF SAMPLES	DATE	DATE	DATE	DATE
30	3 Nov 70	3 Nov 70	3 Nov 70	3 Nov 70	3 Nov 70
DEPTH IN FEET		FORMATION DESCRIPTION		REMARKS	
DEPTH	FORMATION	DEPTH	FORMATION	DEPTH	FORMATION
2	A51 SM	10	Br. silty sand G-0, S-53, Fines-45	6	
4	A65 SM	3 3/4"	Br. silty sand w/ gravel & grav frags G-3, S-77, Fines-20	5	
6			Dry	7	
8				10	
10	A33 GP- GM	1 1/2"	Br. poorly graded silty grav & grav frags G-52, S-42, Fines-6	12	
12			Dry	14	
14				16	
16	A55 GM- GM	2"	Br. well graded silty grav & grav frags G-57, S-36, Fines-7	18	
18			Flowing water 20 GPM between 14' & 15'. Wat	20	
20	J23 SM	1 1/2"	Br. silty sand w/grav & grav frags G-23, S-57, Fines-20	22	
22			Wet	24	
24				26	
26	A48 GM	1 1/2"	Br. silty grav & gravel fragments G-42, S-39, Fines-19	28	
30			Wet	32	
32	A59 GM	1"	Br. well graded grav & grav frags G-54, S-43, Fines-3	34	
34			Moist	36	
36	A54 GP- GM	2 3/4"	Br. poorly graded silty grav & grav frags G-69, S-25, Fines-6	38	
38			Moist	40	
40	A93 GM	1 1/2"	Br. well graded grav & grav frags G-76, S-23, Fines-1	42	
42			Moist	44	
44			Water flowing 75 to 135 GPM between 40' and 42'.	46	
46	A57 SM	1 1/2"	Br. silty sand w/ rock frags G-40, S-47, Fines-13	48	
48			Wet	50	
50	A27 SP- SM	1 1/2"	Br. poorly graded silty sand w/grav & grav frags G-44, S-45, Fines-11	52	
52			Wet	54	
54	A69 GM- GM	2"	Br. well graded silty grav & grav frags G-37, S-33, Fines-10	56	
58			Wet	60	
60	A91 SM- SM	2 1/2"	Br. well graded silty sand w/grav & grav frags G-44, S-44, Fines-12	62	
62			Wet	64	
64	A60 GM- GM	1 1/2"	Br. well graded silty grav & grav frags G-58, S-34, Fines-8	66	
66			Wet	68	
68				70	
70	A90 GP- GM	1 1/2"	Br. poorly graded silty grav & grav frags G-46, S-43, Fines-9	72	
72			Wet	74	
74				76	
76	A61 SM	2"	Br. silty sand w/grav & grav frags G-29, S-47, Fines-24	78	
78			Sample exhibited some dry strength. Atterberg limits attempted.	80	
80	A99 GP- GM	1"	Br. poorly graded silty grav & grav frags G-46, S-42, Fines-12	82	
82			Wet		

DEPARTMENT OF THE ARMY NORTH PACIFIC DIVISION U.S. ARMY ENGINEER DISTRICT, ALASKA		PROJECT Little Chena LOCATION (County or State) N. 4,005-65W E. 334-86S		SHEET 2 OF 2	
EXPLORATION LOG		PERMANENT HOLE NO. DH-96		Bendix Marine Advisors	
FIELD NO. LC-4		PERMANENT HOLE NO. DH-96		DATE 3 Nov 70	
TYPE OF HOLE		DEPTH		TOTAL DEPTH OF HOLE	
TEST PIT	AGEE HOLE	DEPTH	DEPTH	DEPTH	DEPTH
TYPE AND TYPE OF BIT	DATE FOR ELEVATION	SOFT	SOFT	SOFT	SOFT
6 5/8" Crowl-in	Becker Hammer Drill				
TOTAL NO OF SAMPLES	TYPE OF SAMPLES	DATE	DATE	DATE	DATE
30	3 Nov 70	3 Nov 70	3 Nov 70	3 Nov 70	3 Nov 70
DEPTH IN FEET		FORMATION DESCRIPTION		REMARKS	
DEPTH	FORMATION	DEPTH	FORMATION	DEPTH	FORMATION
86	A98 GP- GM	1"	Br. poorly graded silty grav & grav frags G-67, S-46, Fines-8	88	
90	A62 SM	1"	Br. silty sand w/grav & grav frags G-39, S-48, Fines-13	92	
92			Wet	94	
94	A68 SM	2"	Br. silty sand w/rock frags G-23, S-43, Fines-34	96	
96			Wet	98	
98				100	
100	A94 GM- GM	2"	Br. well graded silty grav & grav frags G-45, S-43, Fines-12	102	
102			Wet	104	
104			Sample exhibited some dry strength. Atterberg limits attempted. Sandy Water flow = 7 GPM at 102.5'. Pocket of clean gravel in this zone.	106	
106				108	
108				110	
110	A28 SM	1 1/2"	Br. silty sand w/grav & grav frags G-42, S-44, Fines-14	112	
112			Wet	114	
114				116	
116	A95 GM	1 1/2"	Br. silty grav & grav fragments G-45, S-42, Fines-13	118	
118			Wet	120	
120	J17 GM	2"	Br. silty grav & grav fragments G-66, S-41, Fines-15	122	
122			Moist	124	
124			Attempted to get piez. 41' deep. Too much stick up (69") allowed.	126	
126	A43 SW- SM	3/8"	Br. well graded silty sand w/rock frags G-26, S-63, Fines-#1	128	
128			Wet	130	
130	A85 SM	2"	Br. silty sand w/grav & grav frags G-86, S-47, Fines-17	132	
132			Sample exhibited some dry strength. Atterberg limits attempted.	134	
134	A96 SM	1"	Orenga Br. silty sand w/rock frags G-32, S-51, Fines-17	136	
136			Wet	138	
138				140	
142	A76 SM	1 1/2"	Dr. Br. silty sand w/weathered bedrock frags G-9, S-66, Fines-25	144	
144			Wet	146	
146	A87 SW- SM	1 1/2"	Dr. well graded silty sand w/bedrock frags G-39, S-49, Fines-12	148	
148			Wet	150	
150	A75 GM	1 1/2"	Dr. well graded bed- rock frags G-73, S-22, Fines-5		
			Bottom of hole at 150'.		

FIGURE 2 Little Chena Dam typical drill log.

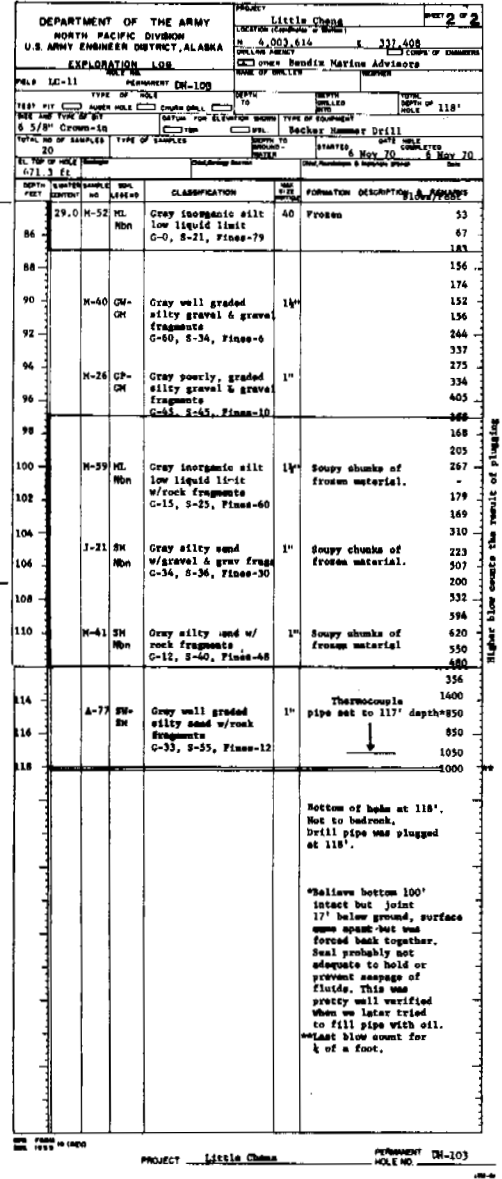
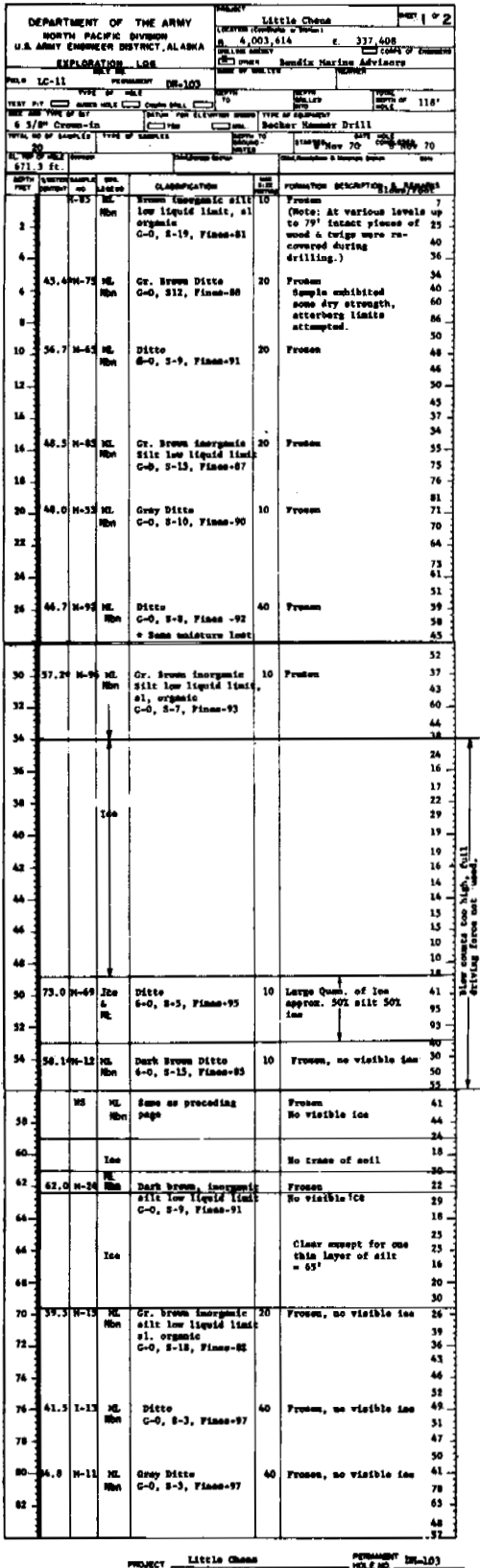


FIGURE 3 Little Chena Dam exploration logs (DH-103).

(Figure 4) in this general geological configuration. The river channel is somewhat tortuous, but it has stabilized itself between banks. Reconnaissance of the area clearly shows old meanders as ponds and bogs. The Birch Creek schist bedrock is exposed on the right abutment. The left abutment ties into a ridge covered with fairly deep deposits of permanently frozen silt. Rock outcrops have not been observed. Sandy gravel has been deposited in the valley floor to a probable maximum depth of 46 m at the center base of the valley diminishing toward the sides (Figure 5).

Foundation materials consist of a frozen silt mass with a thickness of about 31 m at the left abutment. This deposit is in a wedge-shaped configuration and diminishes to a zero thickness about two thirds of the distance across the valley floor toward the right abutment (Figure 5).

The reservoir floor has not been fully explored; however, it is fully expected, through the process of correlation of the topographic features and the deep exploration holes already explored, that the same depositional patterns exist that are present in the foundation materials under the drilled sector of the damsite. Additional check holes are planned to verify this point.

The exposed Birch Creek schist in the right abutment is of the quartz mica variety. This material, a light gray to tan in color, is highly fractured and jointed but appears to be frost riven only to shallow depths. Under the basic approach, as well as the alternate scheme, this dam would be constructed almost entirely within the limits of the regolith. The exception is that some excavation of bedrock material will occur at each abutment and in the construction of the spillway (Figure 6).

While much further subsurface drilling and core drilling on the abutments needs to be done, sufficient work has been accomplished to provide information for the planning concepts now under way. Surface investigations included topographic

mapping, general feature siting, inspection and evaluation of alignments, and reconnaissance for sources of construction materials. Subsurface investigations were made by use of Becker Hammer exploration drill. These holes were drilled in 1970 for identification of subsurface materials and establishing means for permafrost investigation.⁴ The present drilling program includes additional core holes to test rock abutments for the damsite.

In a relatively short distance from the damsite an igneous intrusion identified as granodiorite is available in sufficient quantities for the heavy rock cover for the dam.

CONSTRUCTION PLAN

The basic plan and possible approach for the design and construction as presented in this paper will be to leave the permanently frozen silt in place and to so design the structure as to ensure that the integrity of existing permafrost will not be compromised.²

This approach considered several alternates to surface stripping, one being to strip and excavate the surface organic silts during cold weather and at that time to lay down a gravel working blanket on the stripped surface. The gravel blanket would provide a working pad of sufficient thickness for placement of the dam fill at a later date in milder weather. During this operation, especially careful control and monitoring procedures on temperature changes in the permanently frozen silts are indicated.

Another approach concerning stripping would be to do no stripping other than removing any tree growth, which can be done without the use of heavy equipment and overlaying the existing relatively thin layer (0.3–0.6 m thick) of humus material with the dam-fill material. Such an operation should not affect the dam's structural integrity. The dam's purpose

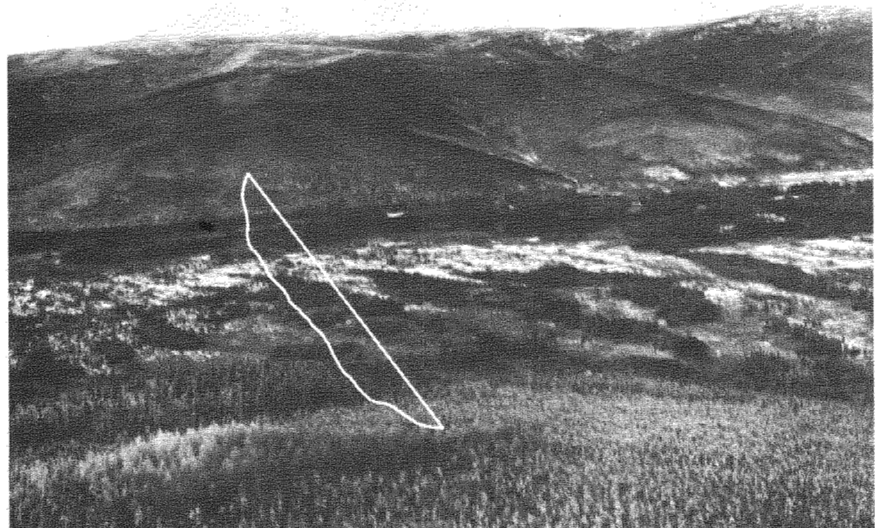


FIGURE 4 General view of proposed site of the Little Chena Dam. The view looks to the west, with the upstream of the river to the right of the picture. Note that the active stream channel lies close to the right abutment at the far side of the valley.

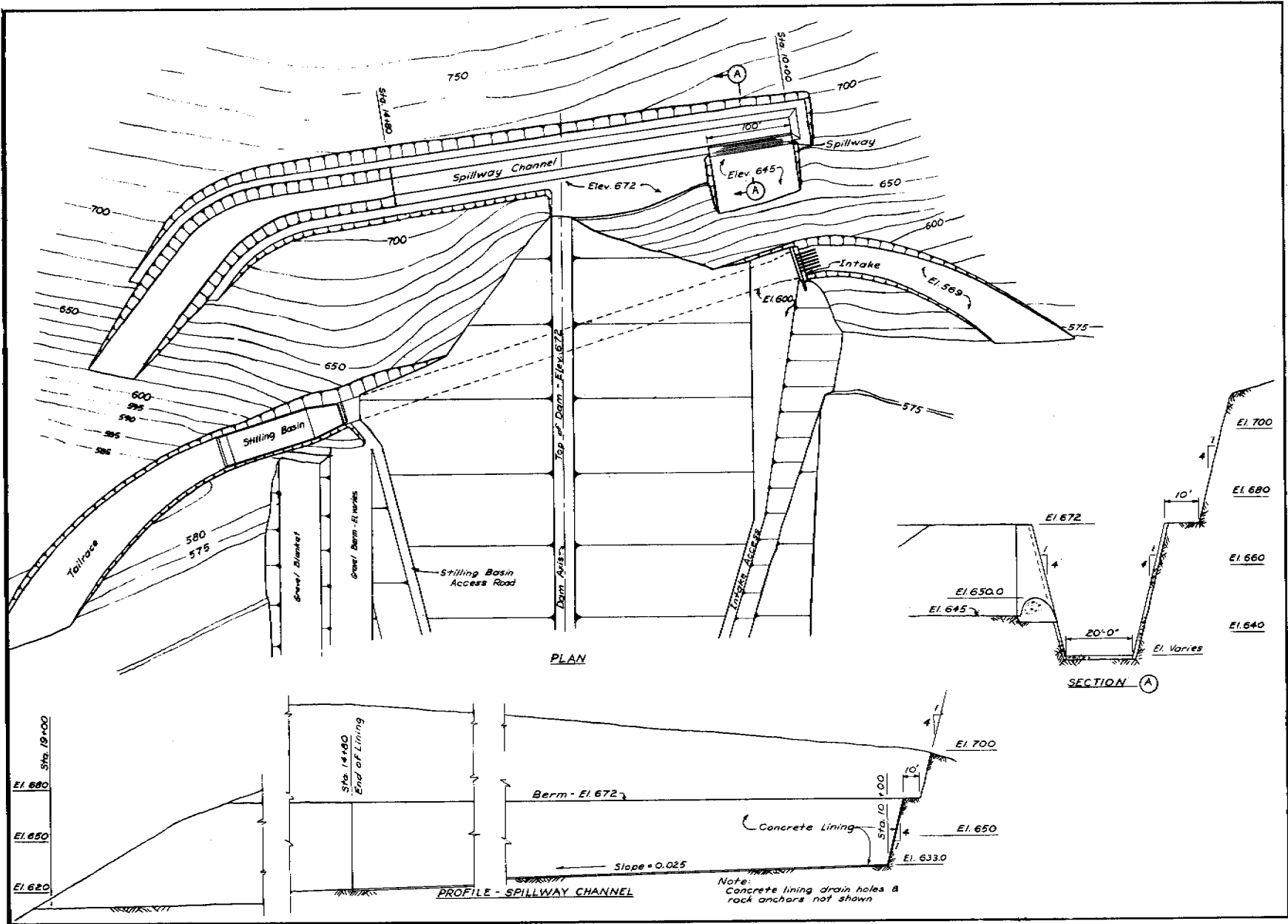


FIGURE 6 Little Chena Dam outlet works and spillway.

being to provide for only temporary storage of floodwaters, seepage control, while important, is somewhat less of a concern. By the use of end-dumping, spreading, and compacting operations in making this fill for the dam, this layer would only be compressed and would not completely lose its insulating effect.

Still another possibility concerning stripping and fill placement that appears to have special merit would be to leave the surficial humus material in place and stockpile the fill material during the warmer season and actually place it in the dam in the cold fall season. Experiences gained from our extensive construction efforts in Alaska have fully demonstrated that winter placement of fill is entirely practicable and in many instances very desirable and appears to be so in this instance. Effective work can be accomplished with equipment presently available and in use at temperatures as low as -31°C . Work has been accomplished in certain cases with temperatures as low as -40°C . Heated cabs for the operators will allow for human comfort. As of now, this office would favor this latter method of placing the dam-fill materials. It is at once evident that maximum control of heat input into the structure favors this approach. Granular materials, such as sand and gravel, are easily handled by stockpiling, draining, and subsequent re-handling. Compaction to and beyond the degree necessary has not presented a problem. In the case of silt, the silt must be obtained from an unfrozen source and kept in that condition during the placement process. This material has also been effectively handled and compaction obtained in such an environment. Compaction equipment used includes vibratory grid rollers and standard rollers of the proper size. Of special importance will be a construction schedule that would permit placement of the embankment prior to river closure, thus allowing the aggradation of the permafrost into the embankment prior to any reservoir impoundment. Careful attention to this type of scheduling will be made.

Figure 7 shows the right side of the structure as conventional design and the left side as the permafrost section; the cross-section configuration is shown in Figure 8 and the centerline profile in Figure 5.

A further natural influence favoring the proposed plan is that the upstream face looks to the north. This, of course, is an optimum configuration. Our observations have noted that slopes in this area in the natural state show a strong nondegrading permafrost condition with a minimum depth of seasonal thaw on slopes of northern exposure.

The principal factor that supports the recommended design is the fact that this region has a mean air freezing index of $3\ 100^{\circ}\text{C}$ -days as opposed to a mean thawing index of $1\ 830^{\circ}\text{C}$ -days and a maximum air thawing of $2\ 135^{\circ}\text{C}$ -days. Reports on other investigations within a relatively close vicinity support these figures, i.e., the paper of Lobacz and Quinn³ reporting on work done at the Cold Regions Research and Engineering Laboratory on building foundations near Fairbanks shows a mean figure of $3\ 160^{\circ}\text{C}$ -days mean minus as opposed to $1\ 845^{\circ}\text{C}$ -days plus.

We realize that there has been a great deal of work done on the subject of heat transfer, i.e., Sanger's⁷ and Scott's⁸ reports to the first permafrost conference in this field, so we will not go into a further analysis, since it appears reasonably certain that, with the safeguards available, the protection of the permafrost can be attained with adequately safe assurance of success. Further analysis, however, will be made to support this reasoning as our design proceeds.

A reduction in heat absorption and conduction to the structure will be provided by the cover contemplated for the dam. Approximately 1 m of large light-colored rock will be spread over the surface of the dam. This rock will optimize the net heat transfer by creating voids that will permit cold air to penetrate below the surface. This configuration will result in a greater depth of freezing during the long winter season. A lesser depth of thawing during the shorter warmer seasons will result from the rock acting as a heat reservoir and radiator and reflecting the sun's rays. These effects in such natural deposits, as compared with those areas devoid of such cover, have been observed in a number of permafrost areas and on moraines by our soils engineers.

The right-hand section of the dam as shown by the plan is generally common to each of the several alternate designs. It is the left-hand section with the underlying frozen silt deposit in which changes in design approach and construction methods vary. Large savings in cost are possible in the recommended design through the careful use of the knowledge and principles developed in working with permafrost and by some of the other concepts proposed herein.

The first alternate approach from the basic considered in our analysis is to remove the permanently frozen silt and replace it with non-frost-susceptible gravels (Figure 9). The second alternative evaluates the merits of thawing and consolidating the existing permafrost and building on this thawed mass in such a way that refreezing will not occur.

Drilling logs (Figures 2 and 3) and the centerline profile (Figure 5) show an upper layer of inorganic silts ranging in depth from zero to about 31 m, overlying silty sandy gravel of varying depth to bedrock. This silty sandy gravel has a maximum thickness of about 46 m. Temperatures in this inorganic silt obtained in the fall of 1972 are shown in Table II. These values agree with other thermal investigations of similar permafrost formations made in this general region.

The present analysis shows that there will be no necessity for installing a cooling system; however, plans will be prepared for such a system in order to have it ready for installation if further development shows that such protection is required. The system is envisioned to be a curtain row of 10 cm o.d. cooling pipes installed in holes drilled in upstream face of the frozen silt, left-hand section of the completed dam. While one row of pipes at appropriate centers is all that appears necessary, additional rows could easily be installed. If artificial cooling proves to be indicated, winter operation should be adequate. This would necessitate only a heat exchange device, which, with the aid of a pumping unit, could supply freezing

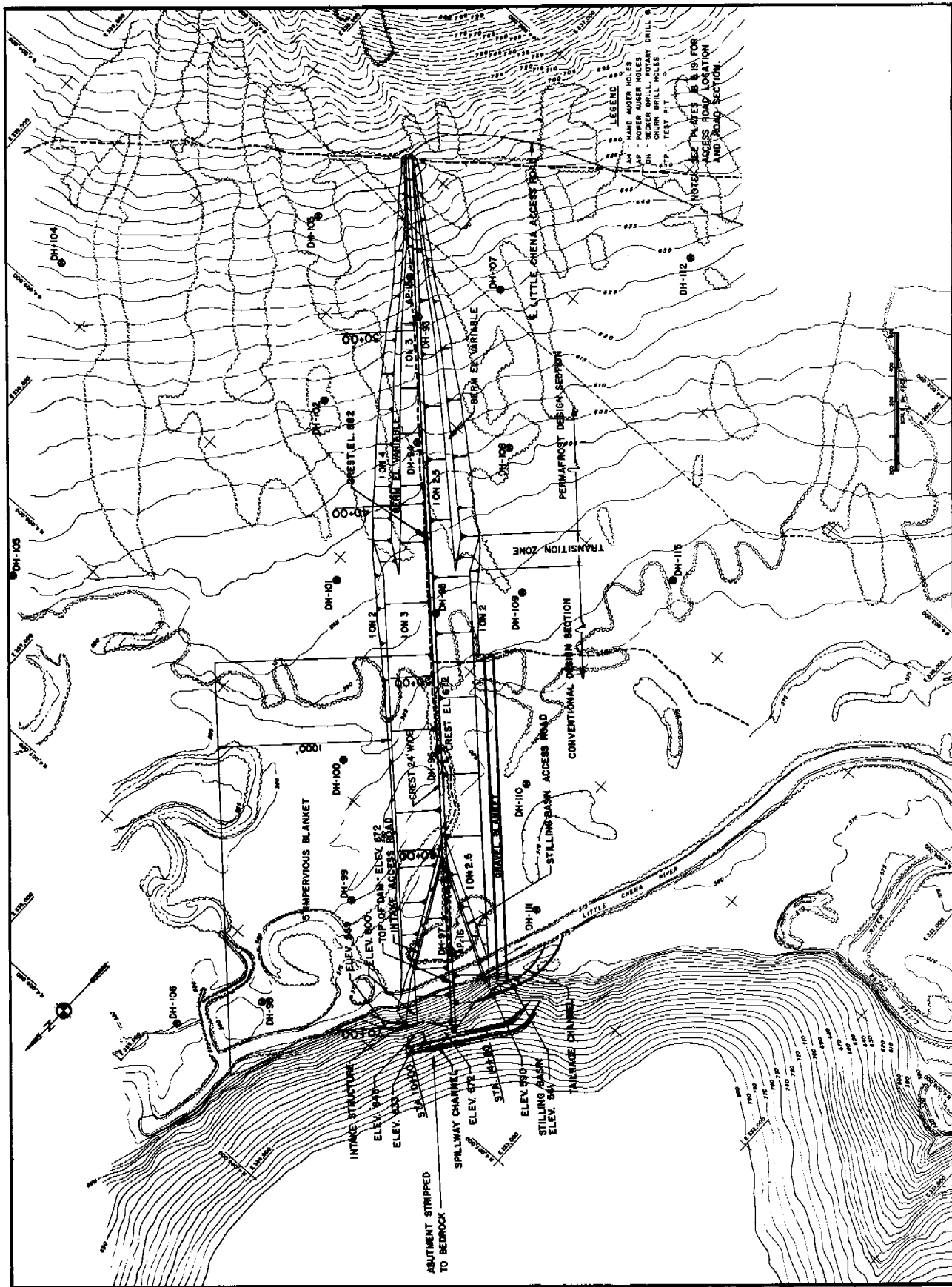


FIGURE 7 Little Chena Dam plan (basic design in this paper).

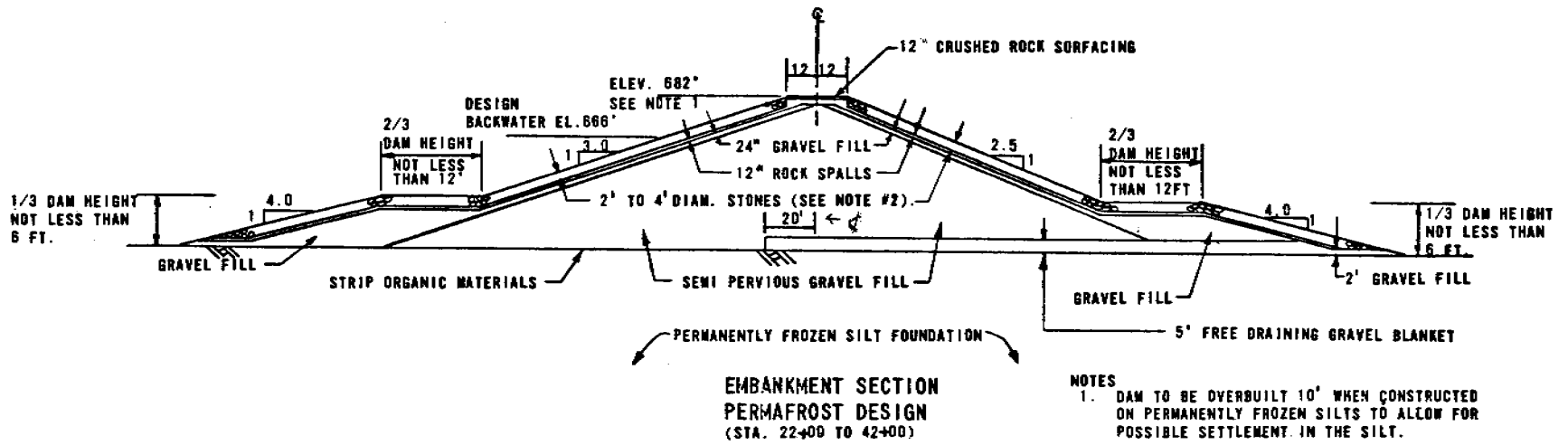
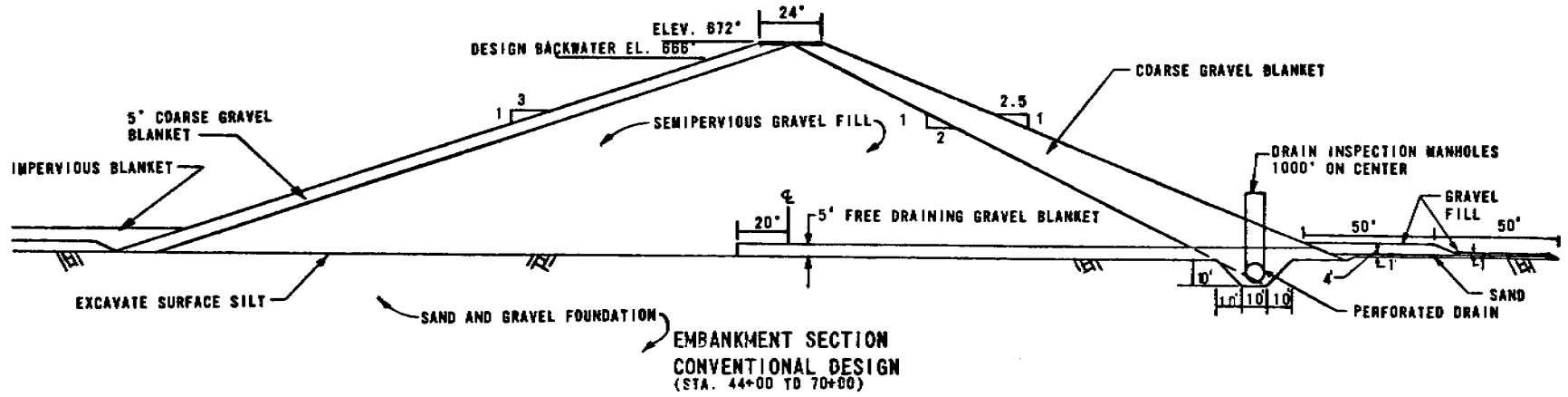


FIGURE 8 Little Chena Dam typical sections (permafrost design basic in this paper and conventional cross-section alternate design in this paper).

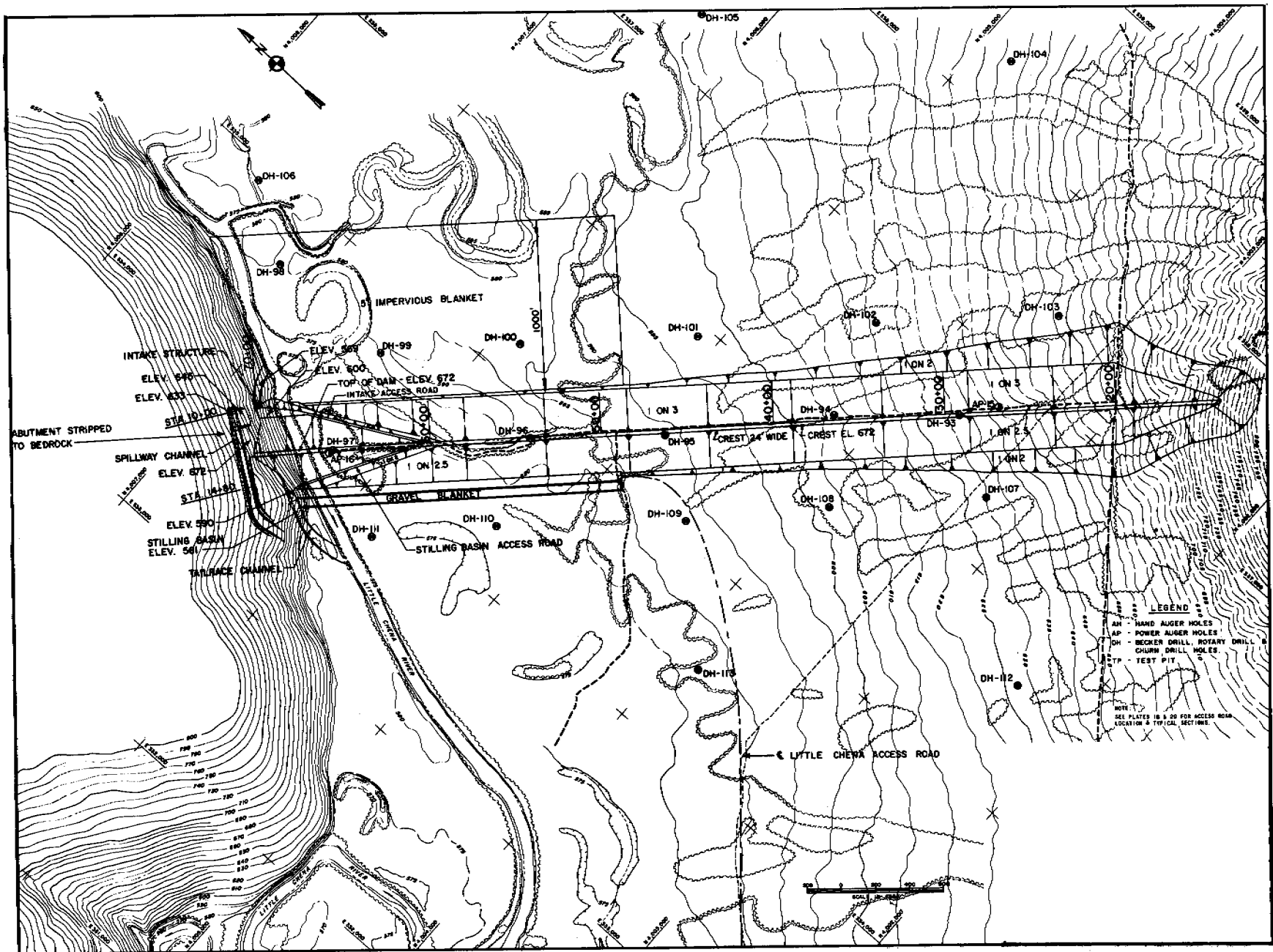


FIGURE 9 Little Chena Dam full excavation of permafrost alternate design.

TABLE II Temperature Gradients

At Depth below Ground Level (m)	Temperature (°C)
21.9	-0.7
18.2	-1.3
15.05	-1.2
12.2	-1.4
8.8	-1.3
3.0	-0.8

fluid to the piping system very economically using the ambient air as a cooling source. If analysis shows that the cooling system must be operated during warm weather, a mechanical freezing unit of appropriate size could be incorporated. Our planning and cost estimates show that such an installation would not only be entirely practical but the added cost would be well within the allowable range.

COSTS

Present cost estimates based on the concepts discussed show that the basic design construction (leaving the frozen silt in place) should cost about \$15 800 000 including \$1 200 000 for an access road or a price for the dam itself of \$14 600 000.

The cost for the alternate dam design construction—removing the frozen silt underlying the left-hand portion of the dam and backfilling it with a suitable non-frost-susceptible material—is estimated at \$24 700 000, including the same \$1 200 000 for the access road or a cost of \$23 500 000 for the dam.

The difference of \$8 900 000 represents the magnitude of possible savings. The cost of the third alternate, i.e., thawing and consolidating the thawed mass, has not been fully analyzed but is expected to be close to the cost of the second alternate. This operation, although feasible, does pose some very difficult

problems such as the drainage and consolidation of the thawed silt, which would be a time-consuming process, and the need to provide a means to ensure that refreezing will not occur. While all of this can be accomplished, further consideration of this approach does not appear to be attractive.

One final point that should be covered is the proposal to include in the dam sufficient instrumentation, perhaps recording types, to allow for study in depth of its behavior. These devices should include thermocouples, strong motion seismic equipment, settlement gages, piezometers, and inclinometers. Information obtained on the behavior of such a structure should, as stated, have great value in advancing the state of the art.

REFERENCES

1. George, W. 1963. Water supply and drainage in Alaska. Alaska District, Corps of Engineers, Anchorage.
2. Kersten, M. S. 1949. Laboratory research for determination of the thermal properties of soils. Corps of Engineers, U.S. Army, St. Paul, Minnesota.
3. Lobacz, E. F., and W. F. Quinn. 1963. Thermal region beneath buildings constructed on permafrost. U.S. Army Cold Regions Research and Engineering Laboratory, Hanover, New Hampshire.
4. Long, E. F. 1963. The long thermopile. Alaska District, Corps of Engineers, Anchorage.
5. Williams, J. R., T. L. Péwé, and R. A. Paige. 1959 and T. L. Péwé, 1958 U.S. Geological Survey Maps, Fairbanks Quadrangle Alaska (D₁) (D₂), respectively.
6. Rice, E. F., and O. W. Simoni. 1966. The Hess Creek Dam, p. 436-439. *In* Permafrost: Proceedings of an international conference. National Academy of Sciences, Washington, D.C.
7. Sanger, F. J. 1963. Degree-days and heat conduction in soils. U.S. Army Cold Regions Research and Engineering Laboratory, Hanover, New Hampshire.
8. Scott, R. F. 1963. Factors affecting freeze or thaw depth in soils. California Institute of Technology, Pasadena.
9. Engineer staff of the Alaska District, Corps of Engineers. 1972. Chena River Lakes project, Fairbanks, Alaska. General Design Memorandum No. 5. Anchorage.

SOME EFFECTS OF SURFACE DISTURBANCE ON THE PERMAFROST ACTIVE LAYER AT INUVIK, N.W.T., CANADA

John Alan Heginbottom

GEOLOGICAL SURVEY OF CANADA
Ottawa, Ontario

INTRODUCTION

Part of the Geological Survey of Canada's continuing programme is the provision of geologic and geomorphologic information on northern terrain as a basis for the sound and rational management of the Canadian north. The importance of this programme was emphasized by the discovery of oil in the western Canadian Arctic, at Atkinson Point, N.W.T., in January 1970. A significant factor in all studies of northern terrain is that the ground is perennially frozen—permafrost—and has a thin upper layer that thaws each summer and freezes each winter—the active layer. Permafrost is reported to underlie about half of Canada²; consequently, studies of the behaviour and properties of frozen ground are just as important as studies of unfrozen materials in other parts of the world.

The study to be described here is part of a continuing investigation of the permafrost active layer in the forest-tundra environment of northern Canada. Particular emphasis is placed on examining the effects of disturbance of the ground surface on the active layer. This information will be used in the production of guidelines and regulations to minimize some of the undesirable effects of land use and northern development.

The data for this report were obtained partly as a result of investigations carried out under the Environmental-Social Program, Northern Pipelines, of the Task Force on Northern Oil Development, Government of Canada, and partly under the general programme of the Geological Survey of Canada.

THE STUDY AREA

The work being reported here has been undertaken in the area of Inuvik, N.W.T., Canada (Figure 1). Intensive studies of disturbed areas and studies of controlled disturbance have been undertaken close to the Inuvik townsite, and less detailed studies have been done at several abandoned oil well sites around the head of the Mackenzie Delta. Only the latter studies will be described here.

The general geology and geography of the Mackenzie Delta area are well described by Mackay,¹¹ with more up-to-date information provided by Fyles, Heginbottom, and

Rampton,⁴ Hughes,⁷ and Kerfoot.¹⁰ Of the eight abandoned oil well sites visited, six are on the Peel and Anderson plains,¹ one is near the northern end of the Peel Plateau, and the eighth is on an alluvial fan between the Richardson Mountains and the Mackenzie Delta. Inuvik is situated on a kame terrace deposit between the south end of the Caribou Hills and the Mackenzie Delta⁴ and the detailed studies have been undertaken in a variety of sites. All are areas of fairly thin clay-silt till, derived largely from the broad expanse of Cretaceous shales to the east. This till variously overlies Palaeozoic dolomites or Cretaceous shales. Some study sites are on low-angle alluvial fans, which are formed of a clay-silt derived from the till, and built on Pleistocene kame terrace gravels. In all cases the subsurface material is rendered impervious by being frozen to depths of more than 100 m.

The structure of the active layer in this area is an important factor. The most obvious feature of the ground surface in the Inuvik area is its hummocky nature. The upper layer of the ground is a complex of mineral soil hummocks separated by shallow, moss-filled trenches. The hummocks are composed of a dense, grey-brown clay-silt, showing little or no soil profile development. In undisturbed areas, some hummocks have mineral soil exposed at the surface, but most are covered with a thin layer (less than 5 cm) of humus, mosses, and lichens. The hummocks are roughly equidimensional on level sites, and generally one to two metres across. On the steeper slopes they elongate downslope and are narrower. The trenches between the hummocks are between 30 and 80 cm wide and about 35 cm deep. The trenches are moss-filled, commonly with bog moss (*Sphagnum*), and underlain by tapering masses or stringers of peat that extend well below the base of the natural active layer.

METHODS AND SOURCES OF DATA AND RESULTS

One of the approaches used in this study has been the examination of sites that have been disturbed, in one way or another at known times in the recent past, to see what effects the disturbance has had on the terrain and the active layer. Work began in 1969 with reference to the forest fire of August 1968 at Inuvik.

In studying previously disturbed sites, the factors that are

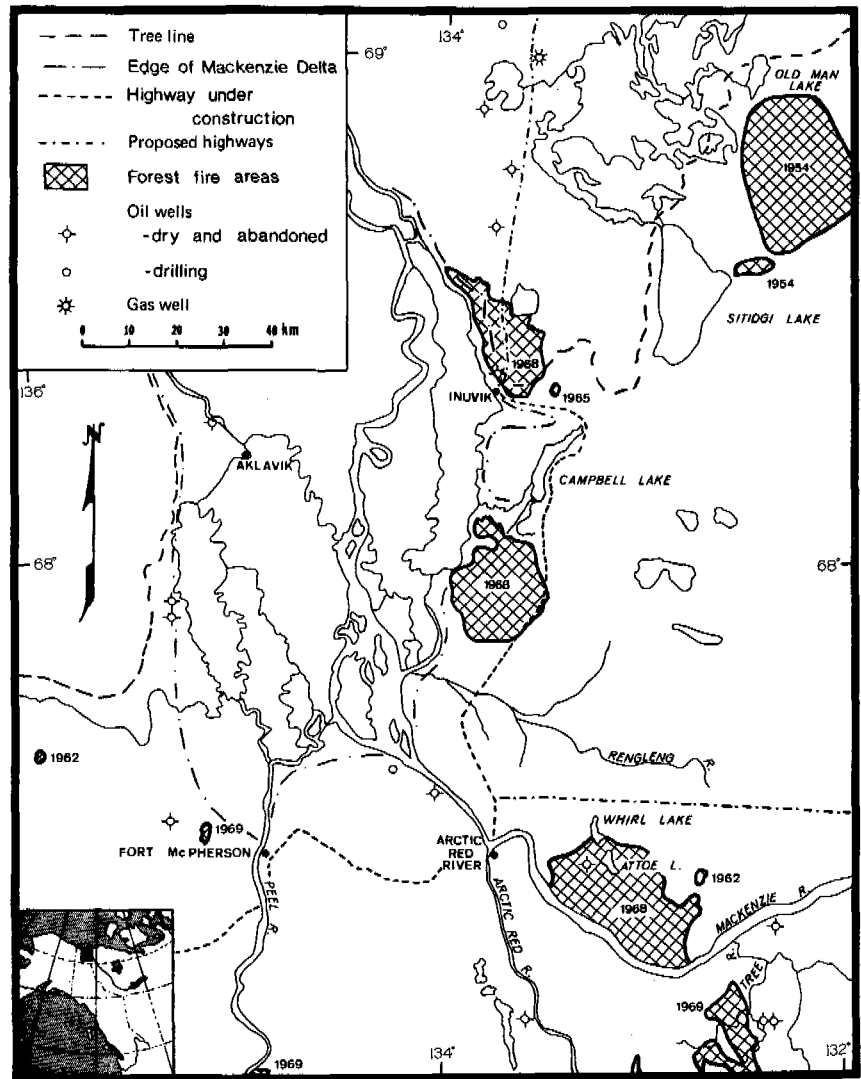


FIGURE 1 General location map of the study area: the Mackenzie Delta area, N.W.T., Canada.

considered may be grouped into (i) those describing the activity, its nature, and its intensity and (ii) those describing the terrain before and after the activity, and thus the effects of the activity on the terrain. As in many other environmental studies, it is necessary to substitute a space variable for the time variable. The details of the terrain before the disturbance are considered to be essentially identical with details of the terrain immediately beyond the area affected by the disturbance.

In the area around the southern Mackenzie Delta, there are three broad groups of activities that can cause terrain disturbance. These comprise settlements and related activities, forest fires, and oil and gas exploration activities. To date, only disturbances resulting from forest fires and oil and gas exploration have been examined. Settlements as such have been excluded from study because the actual activities associated with an observed effect are frequently unknown, and

the occupation of the settlement sites has been relatively long (over 130 years at Fort McPherson). Thus, several of the factors to be considered in the study of a disturbed site cannot be identified or described.

In the case of forest fires, the type of disturbance is known, the area is fairly well defined and, in the case of the more recent ones, the dates of their start and finish are known. Older fires are less well documented and the record is incomplete. The locations of the known, large forest fires that have occurred since 1960 are shown on the map (Figure 1). For this study, "large fires" are fires whose final areal extent was 4 ha or larger.

Detailed studies of the effects of forest fire on the active layer have been concentrated on the 1968 fire around Inuvik. Associated with the disturbance of the forest fires themselves are the effects of the fire-fighting activities. These normally take the form of firebreaks cut by hand or with bulldozers.

In the case of the 1968 Inuvik fire, bulldozers were used widely and some 40 km of firebreak were constructed.⁶ The primary method of studying the effects of the fire and the firebreaks has been by precise levelling of the ground surface and by measuring the thickness of thawed ground with a thin steel probe. The details of the survey procedure are described elsewhere,⁵ and the data are summarized in Table I. The effects of the fire and of the bulldozing of firebreaks are similar—the ground thaws more deeply in summer due to the destruction or removal of the insulating blanket of peat and cryptogams. This deeper thawing allows some of the ice-rich ground below the active layer to thaw and, as this meltwater drains out of the soil mass, the ground subsides. Calculations of the volume of ground lost due to drainage of meltwater suggest that the upper metre of the ground contained about 33 percent by volume excess ice before disturbance. The data presented in Table I show the greatly increased depth of thawing in the area that was bulldozed, compared to the area that was burned.

In 1972 incidental observations were made at the site of a 1954 tundra fire south of Old Man Lake. This area was visited and described by Cody in 1957 and 1963.³ At the location visited in 1972, the terrain had not been severely altered as a result of the fire. Many plants were making a good comeback, with the exception of the cryptogams and black spruce. The depth of thaw was between 15 and 25 cm. No erosion or slope failures were seen.

Other observations in 1969 of the area of the 1968 fire at Inuvik disclosed a number of fresh slope failures of the type referred to by Hughes as active layer "detachment failures."⁷ These have been discussed elsewhere⁵ and will not be described further.

Oil and gas exploration activities have been widespread in the study area for over a decade. The activities have taken the form of surface seismic profiling, followed by the drilling of wildcat wells. Sixteen oil wells are shown on the map (Figure 1); the oldest was completed in 1960, and two are still being drilled. The trails left by the seismic profiling teams are so numerous and widespread that no attempt has been made to map them here.

During the summer of 1972, brief visits were paid to eight of the ten oil well sites in the south half of the area mapped in Figure 1. Of the remaining well sites, one was flooded and the other was still occupied by the drill rig. Most of these oil well sites had a similar layout, a rectangle of land from which the trees had been cleared by bulldozer. These "squares" were generally 120 to 150 m on a side. Running through or beside the square were one or more seismic trails, and a trail led from the square to either a temporary airstrip or to a lake or river on which planes could have landed. The actual wellhead was near the centre of the square with the slush pit beside it and the remainder of the camp facilities around them. The sites were occupied for periods varying between three and seven months, mainly during the winter. The sites that were visited are listed and briefly described in Table II. At each site the observations made covered variations in depth, apparent intensity and type of original disturbance, notes on the original terrain and the present conditions, variations in the depth of thaw and amount of regeneration. Details of the surficial geology are being derived from seismic profile shot-hole drilling logs, but are not available yet.

The effects of the oil rig and well drilling activities are difficult to assess. Near the well-head, gravel and/or wood-chips are frequently spread as an insulating blanket. Wood-

TABLE I Summary of Depth of Thaw Measurement from the Site of the 1968 Forest Fire near Inuvik^a

Line Number Terrain Type	Undisturbed	Burned	Bulldozed
Date of survey ^b	18 Sept. 1969	16 Sept. 1969	17 Sept. 1969
Surface elevation ^c	243	521	428
Depth of thaw ^d	0 - 43 - 75+	18 - 42 - 75+	38 - 65 - 75+
Date of survey	18 Sept. 1971	17 Sept. 1971	18 Sept. 1971
Surface elevation	237	507	407
Depth of thaw	21 - 42 - 77	25 - 55 - 100	38 - 100 - 138
Date of survey	14 Sept. 1972	15 Sept. 1972	14 Sept. 1972
Surface elevation	223	495	399
Depth of thaw	25 - 48 - 85	31 - 61 - 110	36 - 74 - 137 (estimated from 25% sample)

^a The forest fire and the fire fighting (bulldozing of firebreaks) occurred in August 1968.

^b Only fall survey data are shown, as these represent the annual maximum depth of thaw and are thus a measure of the thickness of the active layer.

^c The elevations given are mean elevations, rounded to the nearest centimetre and based on the arbitrary bench mark elevation.

^d The depths given are minimum - median - maximum values, also in centimetres.

TABLE II Details of Oil Well Sites and Seismic Trails Examined, Summer 1972

Well Name	Location	Drilling Date	Numbers and Types of Features Examined					Nature of Other Features	Surficial Geology
			Rig Site	Air-strips	Access Roads	Seismic Trails	Others		
INC - NCO - Mobil Attoe Lake I-06	67° 25'N 133° 15'W	July 69 -Dec. 69	1	1	3	3	No	Till plain and fen	
IOE Tree River H-38	67° 17'N 132° 21'W	Mar. 67 -Apr. 67	1	0	1	2	No	Peat over glacio-lacustrine deposits	
Shell Tree River F-57	67° 06'N 132° 26'W	Nov. 67 -Dec. 67	1	1	1	2	Yes	Borrow pit and river crossing site Peat over outwash gravels	
Shell Tree River East H-57	67° 06'N 132° 26'W		1	0	0	1	No	Peat over glacio-lacustrine deposits	
IOE Swan Lake K-28	67° 08'N 133° 35'W	Jan. 67 -Mar. 67	1	0	1	2	No	Till plain	
IOE Stoney I-50	67° 30'N 135° 23'W	Dec. 65 -May 66	1	0	6	4	Yes	Campsites and staging areas Till plain with thermokarst	
Banff-Aquit-ARCO Treeless Creek I-51	67° 51'N 135° 24'W	Dec. 70 -Jan. 71	1	1	1	1	Yes	Campsite Alluvial fan	
Richfield <i>et al.</i> Point Separation No. 1	67° 34'N 134° 00'W	July 60 -Oct. 60	1	0	1	1	Yes	Campsite Till plain	

Note: Surficial geology is after Hughes, Hodgson & Pilon (Ref. 8).

chips are particularly effective if spread fairly thickly. At Attoe Lake I-06, on 20 June 1972, the ground was thawed for only 10 cm below a 25-cm-thick layer of woodchips, compared with 60 cm under a burned hummock outside the rig square. In general, the depth of thaw was deepest close to the wellhead and decreased towards the edges of the square. This is what one would expect in view of the concentration of activity and of destruction of the vegetation mat in the centre of the area.

Cleared airstrips were examined at three sites. At Attoe Lake the airstrip was formed simply by bulldozing the trees and topmost level of moss off an area of fen, leaving an adequate insulating layer of peat. The airstrip at Shell Tree River was made in a similar manner and was situated on a terrace of glaciofluvial gravels with a cover of peat. Of the three examined, this airstrip exhibited the widest variation in depth of thaw. The third airstrip was on one of the alluvial fans, west of the delta. The surface of the centre of the airstrip was under about 15 cm of water, whereas both ends were waterlogged but not flooded. Sample profiles across these airstrips are shown in Figure 2.

Access roads and seismic trails may be considered together, as their nature is very similar. Numerous examples of each were examined around the eight oil well sites visited. Sample profiles across six seismic lines are presented in Figure 3. The range of conditions seen on the seismic lines and trails was very wide. Apparently, the critical factor controlling the amount of change subsequent to the initial activity is the manner in which the trail was cut. If the trail was cut in summer by bulldozing the trees and the surface vegetation mat aside, then subsequent thawing of the ground proceeds for several years. The effects are the same as those described under the discussion on firebreaks. This is illustrated in profile D at Swan Lake (Figure 3a) where a strip down the centre of the trail was cleared by bulldozing. This strip slumped and the ground is thawed relatively deeply and is completely saturated above the frozen layer. The strips on the sides were cleared of trees, but the vegetation mat was largely undisturbed. The surface is much drier and the depth of thaw is less; in fact it is very similar to conditions in undisturbed areas. Profile E at Swan Lake (Figure 3b) refers to a newer seismic line that crosses the one just described--both profiles were taken 30 m

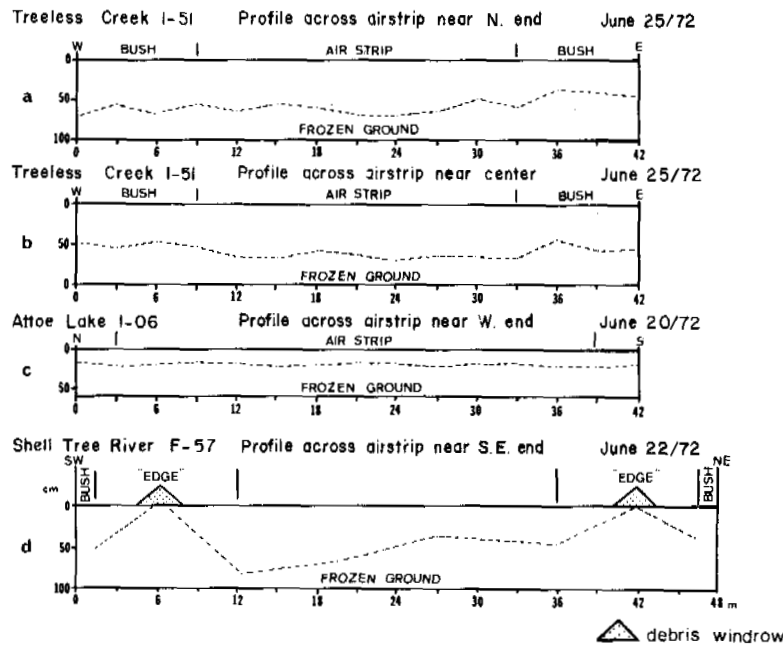


FIGURE 2 Profiles across disturbed areas: airstrips.

from the intersection. This line was constructed by having the bulldozer knock down and push aside only the trees. The only disturbance of the vegetation mat were a few grouser marks. As the profile suggests, conditions in the trail were essentially similar to those off to the side. The contrast between these two seismic trails is further illustrated in Figure 4. Most of the trails examined were in fairly good condition, and no really severe thermokarst effects were seen. Vegetation regeneration on bulldozed trails appears to be slow. An interesting example of erosion being guided by vehicle track marks (Figure 5) was seen on an access trail at Tree River.

DISCUSSION

For the purposes of discussion it is convenient to discard "agency"-centred terms such as forest fire, oil exploration, and bulldozing and to replace them with "process"-centred terms. Thus, the activities and disturbances described in the preceding section may be described as follows: compaction of ground surface, mechanical damage to vegetation, destruction of vegetation, removal of vegetation, removal of vegetation-peat mat, and removal of surface vegetation and soil. Using terms such as these, it is possible to compare the effects of diverse activities and agencies of disturbance. Furthermore, the processes listed above are parts of a continuum that ranges from the very mildest disturbance (a single man walking through the forest once) to the most severe (for ex-

ample, repeated deep bulldozing and soil stripping). As the processes are parts of a continuum, so are their effects, and this is also a convenient framework for discussion. Detailed rankings of agencies, processes and severity are presented in Table III in terms of the intensity of the initial impact.

The general effect of this continuum of processes may be summarized thus: Any compaction alters the thermal transfer properties of the soil material, and removal of any surface vegetation alters the albedo. In most cases both these changes lead to an increase in the downward flux of heat in summer and thus to deeper thawing of the ground and a thicker active layer. Mackay has commented that "The top several feet of the permafrost tends to be an ice-rich zone which is easily affected by a surface disturbance"¹³ and, in the same paper, he outlines an explanation of this observation. A consequence of the ice-rich nature of permafrost immediately below the active layer is that, when the active layer thaws more deeply following surface disturbance, it is this ice-rich material that melts first. If the excess water is able to drain away, there is a permanent subsidence of the ground surface.¹²

On sloping sites other changes can happen in both fine- and coarse-grained materials. These take the form of slope failures, mass movement, and landslides of various kinds. Mention has already been made of the earth flows that occurred after the 1968 fire in Inuvik. Other comments on slope failure following disturbance are given by Isaacs and Code. Figure 6 shows a slope failure in the Inuvik gravel pit following gravel extraction activities.

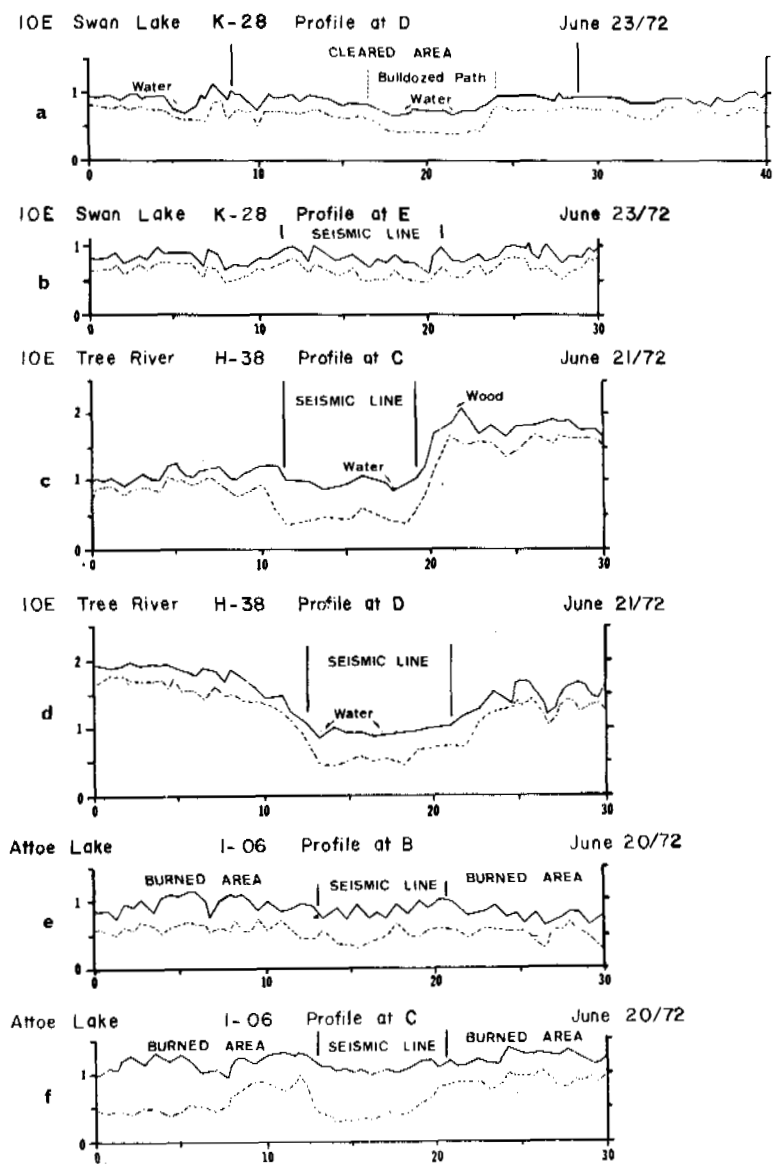


FIGURE 3 Profiles across disturbed areas: seismic trails.

Severity of Initial Disturbance

Most of the field work described in the previous section has been conducted on level sites or on sites with low angles of slope, and the work was designed to consider a range of intensities of terrain disturbance, as outlined in Table III. Not all the agencies and intensities listed in the table have been studied as yet. Thus, no measurements have been made of the effects of minor amounts of compaction such as those produced by varying intensities of foot traffic. Two small examples of the effects of such disturbance are given by Mackay¹² and related work from nonpermafrost areas has been reported.¹⁵ If the various national parks and landmarks sug-

gested for permafrost areas of Canada become popular, measurements of disturbance due to foot traffic may be of considerable importance.

Removal of vegetation without significant compaction can best be accomplished by hand. Preliminary results suggest that the effects of such disturbance are negligible and possibly undetectable. Minor compaction with minimal vegetation removal as shown on the seismic trail illustrated in Figures 3b and 4a, or on air strips (Figure 2) also produce negligible to minor effects.

The effects of mechanical damage to the surface vegetation mat are variable. If the albedo of the surface is sharply reduced, as happens if dark humus or peat is exposed at the sur-

face in place of light-coloured lichens and mosses, then deeper thawing takes place. If the mechanical damage is minor and no colour change is involved, the effects are negligible. Severe mechanical damage, of which no examples were seen, will presumably result in damage similar to that caused by severe compaction or removal of surface vegetation.

Marked effects only appear following disturbances as severe as the more-or-less complete destruction of the vegetation, including the surface vegetation cover, which results from a forest fire. Such effects appear soon, within days in the case of a forest fire,¹⁴ develop over several years (Table I) and persist for several more years.³ The actual time values for the periods of development and persistence are still under investigation.

The more intensive forms of disturbance associated with

severe compaction, removal of all vegetation and removal of soil have been examined in several seismic trails (e.g., Figures 3c-f and 4b). Preliminary observations suggest that the more severe the original disturbance, the more rapidly the effects become apparent. The time required before stabilization or recovery occurs is not known as yet.

Terrain Conditions

Variation in the intensity of the original disturbance is not the only factor that controls the reaction of terrain to disturbance. The properties of the terrain itself are at least as important, and the phenological timing and the time since the disturbance must also be considered. The properties of the terrain that control its reaction to disturbance are slope



FIGURE 4 Seismic trails near Swan Lake ($67^{\circ} 08'N$, $133^{\circ} 35'W$), 23 June 1972. Geological Survey of Canada photographs. (a) Recent trail with minimum of terrain disturbance; (b) older trail with bulldozed central zone.



FIGURE 5 Gullying being guided by vehicle track marks at Tree River (67°06'N, 132°26'W), 22 June 1972. Geological Survey of Canada photograph.

angle, aspect, soil material, vegetation, and the moisture or ice content of the ground. Phenology is important mainly in terms of whether or not the ground is frozen at the time of disturbance. Frozen ground is not normally subject to compaction or to mechanical damage, and thus a higher intensity of activity will produce a lower intensity of disturbance than if the ground is unfrozen. The elapsed time since the disturbance is important only because many of the effects re-

lated to deeper thawing of the active layer take a number of years to develop.

The field observations of forest fires and oil and gas exploration sites provide some information on some of the terrain properties. However, the coverage is neither comprehensive nor detailed for the simple reason that, in studying existing cases of disturbance, they have to be studied *in situ*. Particularly steep slopes or particularly wet areas are usually avoided and thus not represented. Casual observations in the study area suggest that vegetation patterns are controlled in large part by differences in soil moisture or drainage, and by the forest fire history of the area.

As was pointed out in the introduction, the work reported here is part of a continuing investigation, and no discussion is presented of several items described.

TABLE III Ranking of Disturbing Agencies and Processes in Terms of the Intensity of Their Initial Impact

Intensity	Agency	Process
Least intensive	Single to few passes of man on foot	Minor compaction
	Removal of trees by hand	Minor vegetation removal
	Single to few passes of vehicle (with minimal removal of vegetation)	Minor to medium compaction, minor mechanical damage and minor vegetation removal
	Forest fire	Vegetation destruction
	Multiple passes of man on foot	Medium compaction and minor mechanical damage
	Shallow bulldozing	Vegetation and soil removal, compaction
	Multiple passes of vehicles	Severe compaction, vegetation removal, and severe mechanical damage
	Most intensive	Deep bulldozing

Note: Agencies not ranked because data is inadequate or agency impact is too variable:

- Campsites and oilwells
- Alterations of surface and near-surface drainage.

CONCLUSIONS

Most of the sites studied have certain features in common that control the effects of surface disturbance on the permafrost active layer. The sites are generally level or of low slope angle, thus minimizing effects due to slope angle *per se* and effects due to differing aspects. Most are on clay-silt till, with a hummocky surface and a more-or-less continuous mantle of peat, humus and living vegetation, dominated by cryptogams, and with relatively open stands of spruce, alder, birch, and willow. Thus, the one factor that overrides all others in controlling the effects of any terrain disturbance on the permafrost active layer at these sites is the intensity or severity of the original disturbance. Variations in the response of the terrain due to different original terrain conditions are much less. Phenology can be regarded as part of the factor of intensity of the original disturbance.

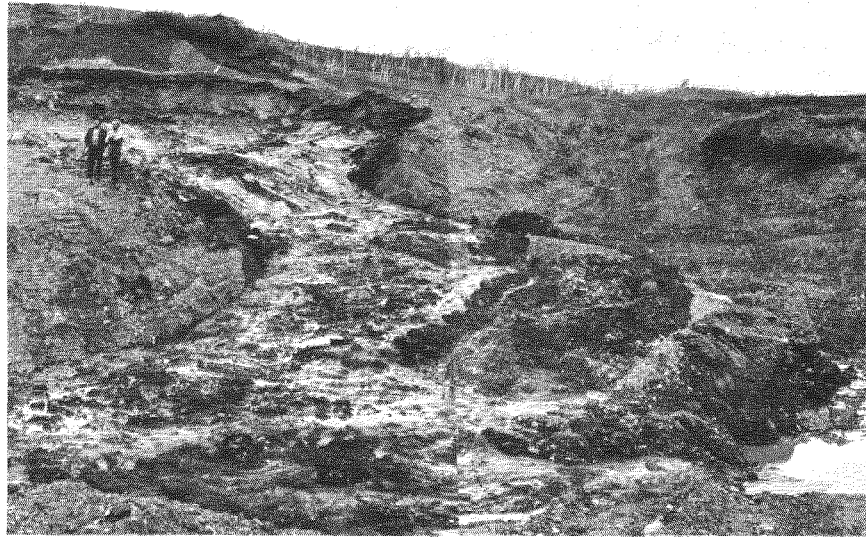


FIGURE 6 Slump in gravels following excavation, Inuvik gravel pit, 27 July 1971. Geological Survey of Canada photograph.

REFERENCES

1. Bostock, H. S. 1970. Physiographic regions of Canada. Canada, Geological Survey, Map 1254A. 1:5 million.
2. Brown, R. J. E. 1970. Permafrost in Canada. The University Press, Toronto. 234 p.
3. Cody, W. J. 1964. Plants of the Mackenzie Delta and reindeer grazing preserve. Plant Research Institute, Ottawa, Canada. 56 p.
4. Fyles, J. G., J. A. Heginbottom, and V. N. Rampton. 1972. Quaternary geology and geomorphology, Mackenzie Delta to Hudson Bay. 24th International Geological Congress. Guidebook for Excursion A-30. 23 p.
5. Heginbottom, J. A. 1971. Some effects of a forest-fire on the permafrost active layer at Inuvik N.W.T. *In* R. J. E. Brown [ed.] Proceedings of a seminar on the permafrost active layer, 4 and 5 May 1971. Canada, NRC/ACGR Tech. Memo. No. 103:31-36.
6. Hill, R. M. 1969. Review of Inuvik forest fire, August 8-18, 1968. Inuvik Research Laboratory. mimeo. Rep. 9 p.
7. Hughes, O. L. 1972. Surficial geology and land classification, Mackenzie Valley Transportation Corridor. *In* R. F. Legget and I. C. Macfarlane [ed.] Proceedings, Canadian northern pipeline research conference, 2-4 February, 1972. Canada NRC/ACGR. Tech. Memo No. 104:17-24.
8. Hughes, O. L., D. A. Hodgson, and J. Pilon. 1972. Surficial geology, N.T.S. sheets 106I, 106M, and 106N, 1:25 000. Canada Geological Survey Open File Report No. 97.
9. Isaacs, R. M., and J. A. Code. 1972. Problems in engineering geology related to pipeline construction. *In* R. F. Legget and I. C. MacFarlane [ed.] Proceedings, Canadian northern pipeline research conference. Canada NRC/ACGR Tech. Memo. No. 104:147-177.
10. Kerfott, D. E. [ed.]. 1972. Mackenzie Delta area monograph. 22nd International Geographical Congress. Brock University, St. Catharines, Ont. 174 p.
11. Mackay, J. R. 1963. The Mackenzie Delta area. Canada, Geographical Branch, Memoir 8:202 p.
12. Mackay, J. R. 1970. Disturbances to the tundra and forest tundra environment of the western Arctic. *Can. Geotech. J.* 7(4):420-432.
13. Mackay, J. R. 1971. Ground ice in the active layer and in the top portion of permafrost. *In* R. J. F. Brown [ed.] Proceedings of a seminar on the permafrost active layer 4 and 5 May 1971. Canada NRC/ACGR Tech. Memo. No. 103:26-30.
14. Watmore, T. G. 1969. Thermal erosion problems in pipelining. *In* R. J. F. Brown [ed.] Proceedings of the third Canadian conference on permafrost, 14 and 15 January 1969. Canada NRC/ACGR Tech. Memo. No. 96:142-162.
15. Watson, A., N. Bayfield, and S. M. Moyes. 1970. Research on human pressures on Scottish mountain tundra soils and animals, p. 256-266. *In* Proceedings conference on the productivity of northern circumpolar lands, Edmonton, Alberta, 15-17 October 1969. *Int. Union for the Conservation of Nature, Publication No. 116* (new series).

CORPS OF ENGINEERS TECHNOLOGY RELATED TO DESIGN OF PAVEMENTS IN AREAS OF PERMAFROST

Frank B. Hennion

OFFICE, CHIEF OF ENGINEERS, U.S. ARMY
Washington, D.C.

Edward F. Lobacz

U.S. ARMY COLD REGIONS RESEARCH AND
ENGINEERING LABORATORY
Hanover, New Hampshire

INTRODUCTION

Pavement Design Concepts

Design of pavements subject to seasonal thaw-freeze cycles is based on either of two basic concepts: control of surface deformation resulting from frost action, or provision of adequate bearing capacity during the most critical climatic period.

In permafrost areas, pavement design must consider not only the effects of seasonal thawing and freezing cycles but also the effect of construction on the existing thermal balance, since changes in the sub-surface thermal regime may cause degradation of the permafrost that result in severe settlements and great reduction in bearing capacity. In arctic regions, with continuous permafrost at shallow depths, satisfactory pavements are best assured by restricting seasonal thawing and freezing to the pavement and a non-frost-susceptible base course, thereby preventing degradation of the permafrost. This method is comparable with the complete protection method in seasonal frost areas; however, the critical factor here is depth of thaw penetration rather than depth of frost penetration. The depth of thaw penetration is estimated based on the design air-thawing index as defined by Sanger.⁷

The limited subgrade frost penetration method described by Linell *et al.*⁴ is impractical for most subarctic areas, because the high freezing index values result in thickness requirements in excess of practical and economical limitations. Therefore design, except in areas of continuous permafrost at shallow depths, is usually based on the reduced subgrade strength method with the added consideration of the effect of construction on the existing thermal regime. In subarctic areas with sporadic permafrost or no permafrost and with horizontally variable, highly frost-susceptible subgrade soil and variable moisture conditions, the limited subgrade frost penetration method or adaptations thereof—for example, the use of insulation—may be applicable for high-speed primary pavements to be used by aircraft, which are especially sensitive to surface roughness.

Temperature Considerations

Air-thawing and air-freezing index values based on long-term air temperature records from a station near the construction site are desirable. In remote northern areas, however, it may be necessary to interpolate records from stations far from the site. Interpolation should consider elevation, wind, topography, and nearness to bodies of water and heavily populated areas, as these factors may cause variation in air indexes over short distances. Also, air temperature records generally are not of sufficient duration in arctic and subarctic regions to permit valid determination of design thawing or freezing indexes.

Freeze-Thaw Penetration

The depth to which freezing temperature will penetrate into granular non-frost-susceptible soils beneath paved areas kept free of snow and ice may be estimated from the curves in Figure 1. These curves are valid only where the permafrost table is deep below the surface, or is nonexistent. The depth to which thawing temperature will penetrate into granular non-frost-susceptible soil beneath paved areas may be estimated from the curves in Figure 2.

Figures 1 and 2 yield maximum depths beneath a pavement surface to which the 0 °C isotherm will penetrate into relatively homogeneous materials under total summer thawing index values or total winter freezing index values. These curves have been computed using the modified Berggren equation and correction factors derived by comparison of theoretical results with field measurements. Prediction of freeze-thaw penetration in nonhomogeneous soils requires the use of numerical calculation techniques.⁷

PAVEMENT DESIGN OVER NON-FROST-SUSCEPTIBLE SUBGRADES

In areas where the soils are not frost-susceptible, or where precipitation and groundwater conditions preclude signifi-

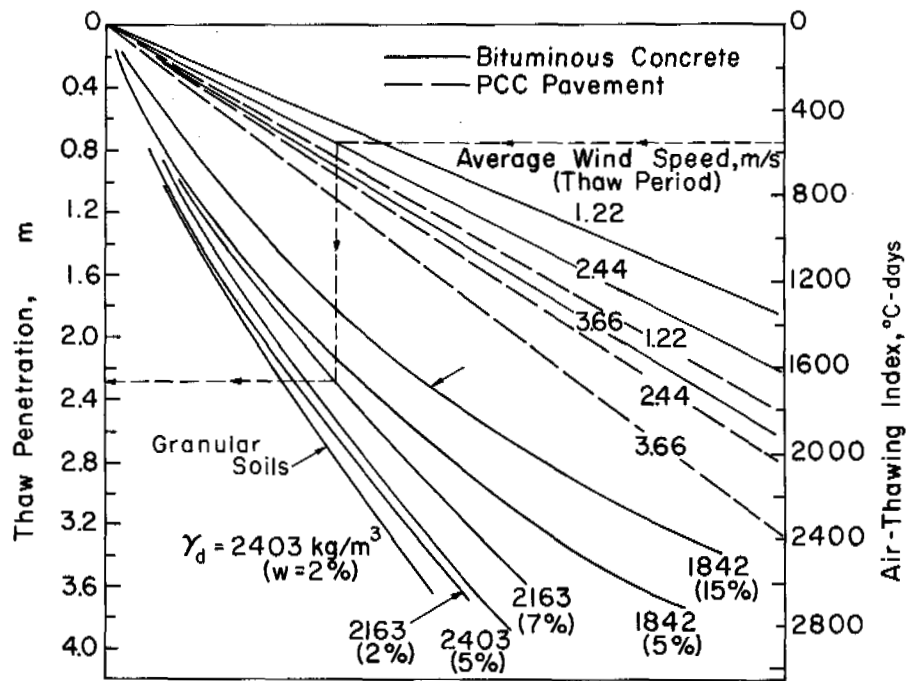


FIGURE 1 Relationship between air-freezing index and frost generation into granular, non-frost-susceptible soil beneath pavements kept free of snow and ice.

cant ice segregation, design principles are the same as in temperate zones. Pockets of frost-susceptible soil should be excavated to the estimated depth of seasonal frost penetration in the subgrade material, and replaced with non-frost-susceptible materials. Such pockets should be large enough to permit feather edging of the backfill.

PAVEMENT DESIGN OVER FROST-SUSCEPTIBLE SUBGRADES

Complete Protection Method

In arctic regions, a design that will limit seasonal thaw to a non-frost-susceptible base course will keep the subgrade frozen and prevent frost heaving or damaging subsidence. The required base course thickness may be approximated from Figure 2 or may be computed using the method given by Sanger.⁷

To use the minimum base course thickness required to restrict seasonal thaw to the pavement and base course, consideration should be given to using relatively high moisture retaining non-frost-susceptible soils, such as uniform sands, in the lower base. After initial freezing, such soils provide considerable resistance to thaw penetration because of their high latent heat. The use of frost-susceptible soils of groups F1 and F2 (Table I) in a subbase course is also permissible if some heaving may be tolerated and if these soils are carefully selected, placed to obtain uniform soil type, and covered with a thickness of non-frost-susceptible base determined by use of the reduced subgrade strength

method as described subsequently. In this event the frost-susceptible subbase course is treated as subgrade in determining the upper-base course thickness. The depth of thaw penetration into such a layered base may be estimated.⁷

For minor and slow speed pavements, where heaving is allowable and where more suitable materials are not available, a group F3 or F4 soil may be used in a subbase course to prevent initial thawing of a high-ice-content subgrade. In such cases, the minimum thickness of the non-frost-susceptible base course over the group F3 or F4 soil should be determined by the reduction in strength method and objectionable frost heaving anticipated. Damage from differential movements can be minimized by ensuring uniformity of placed materials.

The depth of thaw penetration under a bituminous pavement may also be reduced by painting the surface white.³ A reduction in thaw penetration in the order of 35 percent resulted from such surface treatment during one thawing season in an area having an air-thawing index of 433 °C-days. Use of the Portland Cement Concrete (PCC) pavement curves in Figure 2, or the surface transfer coefficient for PCC pavement in the modified Berggren calculation method,⁷ will result in conservative thaw-penetration estimates for white-painted bituminous pavements. Because periodic retreatment is necessary, this method is not recommended except when suitable base and/or subbase materials are unavailable.

In recent years, experimentation has been under way in North America using various rigid insulations placed beneath a base course to prevent subgrade thawing and freezing.² Two foam plastics—polystyrene boards and foamed-in-place

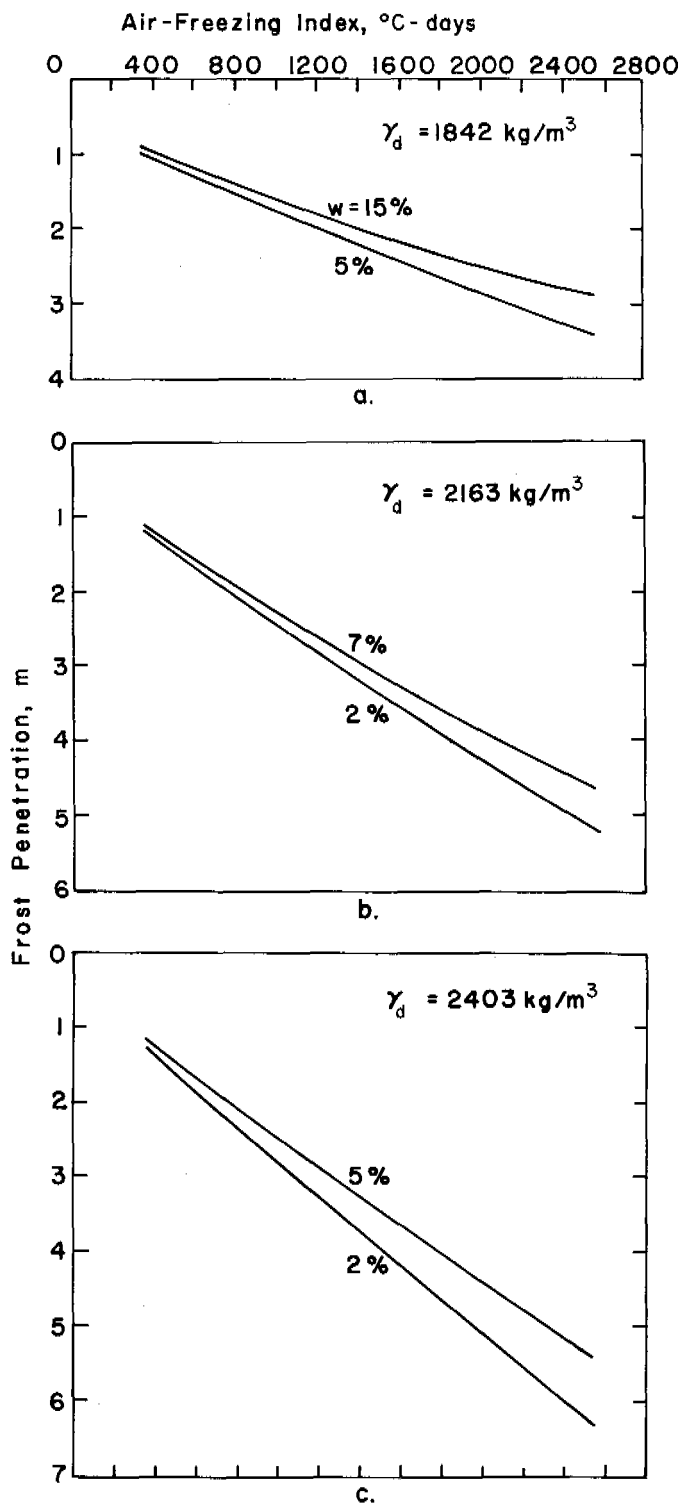


FIGURE 2 Relationship between air-thawing index and thaw penetration into granular, non-frost-susceptible soil beneath pavements.

polyurethane—have been used in experimental pavement sections under varied traffic and climatological conditions in Alaska.¹ Polystyrene demonstrates a low rate of moisture absorption and, in general, its performance is better both thermally and structurally than foamed-in-place polyurethane.⁸ It has been shown that, in the more northern permafrost areas, insulation can be used to replace gravel base course in a ratio that depends on the type of insulation. In the more southern, marginal areas of permafrost, insulation will delay and may slow the rate of degradation, but neither insulation nor heat sink material is capable of preventing thaw degradation entirely. Insulation offers a satisfactory design alternative in areas where non-frost-susceptible granular base course material is unavailable or costs so much that insulation is more economical.

Design Based on Reduced Strength of the Subgrade

Since the combined pavement and base thickness required to prevent seasonal effects in the subgrade is generally greater than 2 m, except in extremely cold areas, design must usually be based on the assumption that thawing and freezing will occur in the subgrade.

This method may be used for flexible pavements on subgrade soils of groups F1, F2, and F3 and rigid pavements over group F1 and F2 soils when subgrade conditions are sufficiently uniform to assure that objectionable differential heaving or subsidence will not occur, or where subgrade variations are correctable to this condition by removal and replacement of pockets of more highly frost-susceptible or high-ice-content soils. The method may also be used for design of minor or slow-speed flexible pavements over all subgrades when appreciable nonuniform heave or subsidence can be tolerated. The reduction in strength method of design should be avoided if at all possible for rigid pavements over F3 and particularly over F4 soils. Thickness requirements for the reduced subgrade strength method of design as herein-after described provide adequate carrying capacity during the period of weakening but may result in objectionable surface roughness and cracking due to heaving or subsidence. In such cases, design studies should include the compilation of frost heaving and settlement experience records from existing airfield or roadway pavements in the vicinity.

The amount, type, and distribution of ice formation in that portion of the existing frozen soil that will be thawed after pavement construction should be determined, and an estimate made of the magnitude and probable unevenness that will result from future subsidence. No general method exists for estimating the subsidence of a pavement due to subgrade thaw. If conditions are uniform, up to a metre of thaw and subsidence of 0.3–0.6 m may result in only small differential settlements. Conversely, differential thawing of the same thickness and the flow of water may result in

TABLE I Frost Design Soil Classification ^{a, b}

Frost Group	Kind of Soil	Percentage by Weight Finer Than 0.02 mm	Typical Soil Types ^c
F1	Gravelly soils	3-10	GW, GP, GW-GM, GP-GM
F2	Gravelly soils Sands	10-20 3-15	GM, GW-GM, GP-GM SW, SP, SM, SW-SM, SP-SM
F3	Gravelly soils Sands, except very fine silty sands Clays, PI>12	Over 20 Over 15	GM, GC SM, SC
F4	All silts Very fine silty sands Clays, PI<12 Varved clays and other fine-grained, banded sediments	Over 15	CL, CH ML, MH SM CL, CL-ML CL and ML: CL, ML, and SM; CL, CH, and ML; CL, CH, ML, and SM

^a Data from Linell *et al.*⁴

^b Soils are listed in approximate order of increasing susceptibility to frost heaving and/or weakening as a result of frost melting. However, the order of listing of subgroups within groups F3 and F4 does not necessarily indicate the order of susceptibility of frost heaving of these subgroups. There is some overlapping of frost susceptibility between groups. The soils in group F4 are of especially high frost susceptibility.

^c Under Unified Soil Classification System (adopted by Corps of Engineers and Bureau of Reclamation, January 1952).

depressions 0.6-0.9 m deep. Most roads in arctic and sub-arctic regions suffer thawing subgrades for some years after construction, because maintenance is more economical than providing adequate initial fill. This method is referred to as "controlled subsidence." An unsurfaced road usually "settles down" after a period of time and paving may be practical. However, the paved surface may alter the thermal balance in the pavement section and underlying materials. The allowable depth of thaw that will hold subsidence within tolerable limits should be based on study of the particular project and on experience in the local area.

For paved areas, base course thicknesses should be increased as necessary over the reduced strength design requirements to provide a surcharge load sufficient to reduce to tolerable limits differential surface heave resulting from seasonal freezing of a frost-susceptible subgrade. Where the subgrade contains intense ice formations, the increased base course thickness will also minimize or prevent excessive subsidence due to thawing. Major maintenance, including periodic resurfacing to maintain a level surface, must otherwise be anticipated.

In addition to the above, all reliable information concerning performance of airfield and roadway pavements constructed in the area being investigated should be considered in developing design requirements. Local experience with

soils of a particular frost design soil group may indicate that assigning the soils to the next higher or lower numerical group would best conform to actual behavior.

FLEXIBLE PAVEMENTS

Design curves⁴ should be used to determine the combined thickness of flexible pavement and non-frost-susceptible base course required for various aircraft wheel loads and gear configurations and for roadways. These curves reflect the reduction in strength of the subgrade soil during the frost-melting period.

Since design thickness computed by this method does not prevent seasonal frost action, or possible permafrost degradation, in the subgrade, depths of freeze and thaw should be estimated using the methods given by Sanger.⁷ If subsoils within the depth of thaw are nonuniform or contain pockets of ice, differential movements can be minimized by removal of such materials. The eventual development of abrupt surface irregularities in the finished pavement may be reduced by tapering excavations and backfills so as to ensure gradual transitions. If annual thaw is greater than freeze, the permafrost will degrade and the depth of thaw may become progressively greater. If the permafrost surface is at some

depth beneath the design pavement sections, pockets of highly frost-susceptible soils within the depth of annual freeze should be removed.

RIGID PAVEMENTS

The thickness of rigid concrete pavements for airfields and roads is determined using the flexural strength of the concrete and the modulus of subgrade reaction for the frost-melting period.

Where thawing and freezing are permitted into a horizontally uniform frost-susceptible subgrade of group F1 or F2 soil beneath a rigid pavement, the differential movement will generally be small. A non-frost-susceptible base course, having a minimum thickness equal to that of the concrete slab, should be used over these soils. The reduced subgrade strength method should be avoided for rigid pavements over F3 and F4 subgrades. Where such construction is required, the following additional requirements apply: Over F3 soils, the non-frost-susceptible base course should be equal to a minimum of one and one-half times the concrete slab thickness. Over F4 soils, the minimum thickness of non-frost-susceptible base course should be equal to one-half the average depth of subgrade that will be subject to annual freezing and thawing. In both cases, reduction of slab size will reduce uncontrolled cracking. In the application of this criterion, the lesser computed depth of freeze or thaw should be employed. In no case should the base course be less than 0.6 m over an F4 soil. The use of insulation should be considered in the design over F3 and F4 soils and the design decision based on initial estimated cost of construction, future maintenance and the operational requirements for the pavement.

UNSURFACED GRAVEL ROADS

Low-cost unsurfaced development roads are common in the Arctic and Subarctic. They suffer a great deal of distortion but are easily regraded. Due to the low precipitation in most of the area, the absence of a waterproof riding surface is not serious. Apart from almost continuous maintenance with a patrol grader, the chief problem is dust control. Roadways are customarily elevated at least 1–2 m above the surrounding terrain not only to aid thermal adjustments beneath the pavement but also to minimize snow accumulation and removal problems in winter. Embankments are generally constructed of clean sands and gravels because of their nonheaving qualities, drainability, and the ability to excavate and place them during freezing weather. Fills should have side slopes of 1½ or 2:1. Occasionally, a very coarse, free-draining bottom layer is used to permit drainage of meltwater in early spring as it flows over the ground surface. Ditches over permafrost must be wide (1.5–3 m) and well clear of the top of the slope.

DRAINAGE

Surface runoff should be carefully controlled, because water flowing over the permafrost table may cause serious permafrost degradation under pavements and facilities.⁵ Runoff is best conveyed in open ditches with culverts provided only where necessary. Subsurface drains are of little value because they are usually blocked by ice when needed most. However, large quantities of water can move underground through granular materials when there is a source of water with access to such materials. This water movement induces a greater than normal thaw.

Water levels in nearby bodies of water should not be permitted to rise above original elevations, owing to the change of subsurface flow. Diversion and control of subsurface flow can be accomplished by inducing buildup of permafrost dams.

CURRENT RESEARCH IN PAVEMENT TECHNOLOGY IN PERMAFROST AREAS

The Corps of Engineers is currently conducting research, field experimentation, and evaluation of pavement systems for both vehicular and aircraft pavements in permafrost areas and areas of seasonal frost. One system utilizes concepts that are not new but offers considerable promise because of recent development of waterproofing membranes that have a high resistance to long-term deterioration. Soils and paving engineers and researchers have experimented over the years with providing a pavement system that would permit substituting low-cost and plentiful fine-grained soils (silts, clays) for the more costly and less plentiful high stability granular aggregates used as base and subbase courses. The lack of success with these systems in the past can be traced to the life of the waterproofing membranes used to protect the encapsulated dry high-density fine-grained soil layers from water infiltration and subsequent loss of strength.

Recent research and field experimentation by the Corps of Engineers Waterways Experiment Station (WES) in encapsulating fine grain soils using two recently developed high durability membranes (0.152 mm-thick polyethylene and polypropylene cloth treated with a cationic emulsified asphalt) indicates a very high potential for use of membrane encapsulated soil layers (MESL) in permanent type pavement systems.⁶

The success of the research at WES, which was aimed at construction in temperate climates, prompted the Corps to initiate research at the U.S. Army CRREL aimed toward the use of the MESL technique for pavement systems in permafrost areas and areas of seasonal frost.

In August 1970, an MESL test section was constructed at the CRREL Alaska Field Station using Fairbanks silt as the embankment encapsulated soil. The section has a length of 76 m, a traffic surface width of 6–6.7 m, and a thickness

from 0 to 0.9 m. Both top and bottom membranes are polypropylene waterproofed with a single hand application of about 2.2 cubic decimeters/m² of RS-2K emulsified asphalt. The emulsion was applied at an ambient temperature of 16–18 °C without prior heating. The average *in situ* moisture content of the silt after placement was 14 percent (optimum was 18 percent by the Standard Proctor Compaction Test).

The section has been used as an approach road mainly in the spring and summer. Traffic testing was conducted with a loaded dump truck during the spring thaw of 1972. The total gross load of the truck was 10 700 kg. The single rear axle (dual wheels) load was 8 000 kg. A total of 106 passes of the loaded dump truck caused no visible distress in the test section.

Moisture contents of frozen cores taken in the spring of 1972 showed the average moisture content to be 18 percent or 4 percent greater than when placed. This indicated slight moisture migration during freezing in the 1971–1972 winter. At 20–30 cm depth, the moisture content was 23 percent. Tests on this section are scheduled to continue over several years.

In addition to the test section at the Alaska Field Station, CRREL is conducting both laboratory and field tests in Hanover. A comprehensive field test facility is currently under construction to assess the performance of membrane encapsulated silt and clay soils under freezing and thawing conditions. The test facility consists of four 3.6 × 3.6 m silt sections, three 3.6 × 3.6 m clay sections, with a 4.8 × 3.6 m transition of 2 cm crushed stone. It is planned by means of artificial refrigeration–heating panels to control the rate of freezing and thawing of such soil systems to determine moisture migration patterns as influenced by freezing and to develop a controllable thaw zone, the strength characteristics of which will be assessed by traffic testing and *in situ* strength tests. This technique will permit freezing and thawing any time throughout the year and will make the study independent of local climate for ground freezing conditions. Instrumentation is provided to obtain comprehensive moisture and density data, tests are scheduled to be initiated early in 1973.

In July 1971, four highway pavement test sections were installed also at CRREL in Hanover, to obtain data for updating the Corps design criteria. The Corps of Engineers designed flexible pavement sections of 76 and 56 cm, which incorporated base courses of crushed rock and underdrains. These are being compared with the designs of about 23 and 13 cm of “full-depth” asphalt with no base course or drains. The sections are instrumented to monitor subsurface moisture content, air and subsurface temperature, asphaltic concrete expansion and contraction, traffic count data, frost heave, and pavement response to loading.

First year results from the frost-melting period tend to show the Corps’ sections perform better than full-depth asphalt, since they showed less deflection under load. They also exhibit less frost heave with 1.2–2.5 cm compared with

5 cm. The heaving was fairly uniform and there was no evidence of failure during thaw consolidation. The winter was relatively mild being about 83 percent of the design index. Monitoring is being continued to permit validation of findings after a few more years of data are available.

SUMMARY

Pavement design procedures outlined are based on approximately 25 years of Corps of Engineers research and design and construction experience in arctic and subarctic areas. Because of broad geographical and climatological application some conservatism is inherent in the procedures.

The Corps research and experimental programs in materials, design, and construction techniques are aimed at reducing conservatism without sacrificing reliability of design. Current research is mainly concentrated in two areas: the MESL concept and stabilized materials. Based on preliminary results to date, the MESL concept appears to be a feasible method of utilizing local, normally unsatisfactory materials as replacements for clean granular base and subbase course materials. Moisture migration in thick silty encapsulated layers presents a design problem; however, indications are that this can be minimized by utilizing horizontal moisture barriers (probably formed in place). Laboratory research is being conducted to classify silts and clays based on moisture migration potential in a closed system subjected to a thermal gradient.

Preliminary data from the “full-depth” asphaltic concrete test facility indicate structural characteristics comparable with a conventional layered flexible pavement system. However, frost heave is greater in the asphaltic concrete sections that have less total thickness than the conventional flexible pavement sections.

Continued observation of test facilities described is required before valid design and construction procedures can be established. A problem with the MESL concept is acceptance by the paving construction industry. Construction of experimental test sections is planned as part of large construction projects to gain acceptance of the required construction techniques.

Areas of needed research to technically advance the design of pavements in areas of permafrost include soil modification technology for conversion of frost-susceptible soils into non-frost-susceptible materials; better techniques for improving the thermal strength and frost heaving and shrinkage characteristics of materials in the annual thaw–freeze zone; and control and elimination of pavement cracking.

ACKNOWLEDGMENTS

This paper presents the results of research performed by the Cold Regions Research and Engineering Laboratory under the sponsorship of the U.S. Army Corps of Engineers.

REFERENCES

1. Berg, R. L. 1972. Thermoinsulating media within embankments on perennially frozen soils. Ph.D. thesis. University of Alaska, Fairbanks.
2. Berg, R. L. 1972. The use of thermal insulating materials in highway construction in the United States. Frost I Jord No. 6. (The Royal Norwegian Council for Scientific and Industrial Research and the Public Roads Administrations Committee on Frost Actions in soils)
3. Fulwider, C. W., and G. W. Aitken. 1962. Effect of surface color on thaw penetration beneath an asphalt surface in the arctic. *In* Proceedings, international conference on structural design of asphalt pavements. University of Michigan, Ann Arbor.
4. Linell, K. A., F. B. Hennion, and E. F. Lobacz. 1963. Corps of Engineers pavement design in areas of seasonal frost. Highw. Res. Board Rec. No. 33. NRC publ. 1153.
5. Metcalf & Eddy, Inc. 1957. Pavement condition report 1957. Suppl. Tech. Rep. ENG-445. U.S. Army Corps of Engineers, Eastern Ocean District, North Atlantic Division, New York.
6. Sale, J. P. 1972. Engineering potentials for membrane encapsulated soil layers. ASCE Annual and National Environmental Engineering Meeting, Session No. 26, Placement and Improvement of Soils, Houston, Texas.
7. Sanger, F. J. 1966. Degree-days and heat conduction in soils, p. 253-262. *In* Permafrost: Proceedings of an international conference. Publ. 1287. National Academy of Sciences, Washington, D.C.
8. Smith, N., R. Berg, and L. Mueller. The use of polyurethane insulation in expedient roads on permafrost in Central Alaska. This volume.

A SANITARY SERVICE COMPLEX FOR VILLAGES IN PERMAFROST REGIONS: A Demonstration Project at Wainwright, Alaska

Charles L. Hoar

WASTECO, INC.
Tualatin, Oregon

Lloyd K. Clark

CLARK & GROFF ENGINEERS, INC.
Salem, Oregon

INTRODUCTION

The United States Federal Water Pollution Control Act of 1970, among other things, called for the "... placement of a prototype community water supply, waste disposal system and laundry facility in a native village of Alaska where such facilities do not presently exist." The purpose of the facility was to demonstrate the use of water supply and waste treatment equipment and procedures for operation and maintenance to benefit the health and welfare of Alaska natives. The location was to be in an arctic or sub-arctic region where permafrost exists.

The implementation of the above Act became the responsibility of the U.S. Environmental Protection Agency, which published the project description in January 1971. EPA also selected three locations where prototype systems would be installed. One of these locations was at Wainwright, Alaska, an Eskimo village of 350 persons situated 145 km southwest of Point Barrow.

PROJECT CHARACTERISTICS

The conditions imposed on the contractor by nature and the federal and state governments were severe and manifold. The major conditions are:

1. The site is underlain with permafrost, with only slight penetration of seasonal thaw. The mean annual temperature is about -11°C , winds are usually prevalent, and violent storms blow in frequently from the west;
2. Heavy shipment by air is limited by weather and air-strip capabilities;
3. Heavy shipment by sea is limited by ice to about 60 days in summer. Off-loading must be by shallow-draft barge or lighter;
4. Mechanical construction equipment at the site was limited and in need of repair;
5. All facilities must meet or exceed state or federal regulations pertaining to health codes, drinking water stan-

dards, sewage and solid waste disposal, air pollution control, and building codes;

6. Facilities must provide safe drinking and bathing water, toilets, showers, wash basins, laundry washers and dryers, and sauna baths in a weatherproof building for year-round use by all the village residents;

7. Facilities must include treatment works for drinking water supply, for gray water wastes from laundry, showers and lavatories, and for sewage and solid wastes. The gray water wastes after treatment must be satisfactory for reuse. Domestic water production must be sufficient for all homes in the village. This water to be delivered by tank trailer and crawler prime mover. Sewage and solid waste handling equipment must be sufficient for disposal of all such wastes in the village. These wastes to be collected by trailer and crawler on a routine basis. Village sewage will be collected from chemical toilets or bucket systems;

8. Operation and repair of facilities must be done by local personnel;

9. Processes requiring highly trained operators or constant attention were not considered satisfactory. Automated procedures were to be eliminated or minimized; and,

10. The building must have protection against fire and a standby power plant for protection against power outage.

Quite obviously, some of the above requirements are contradictory, for example, present technology for treatment of gray waters for reuse in the system calls for knowledgeable operators and a certain amount of automation. Containment of the entire complex in a single building introduces a multiplicity of pipes, pumping and wiring.

The resolution of some of the major problems, prior to construction and manufacture, took the following form:

1. The building would set about 0.9 m above ground on piling placed during freezing weather prior to arrival of the building components.

2. The building would be divided into twelve components or modules each measuring $2.7 \times 5.49 \times 2.43$ m high measured outside.

3. Each module would be completely fabricated, fitted out, and test assembled prior to shipment.

4. The natives who would operate and repair the system would be brought to the plant to assist in the design, manufacture, assembly, and operation of all equipment and controls.

This is truly a prototype and demonstration project. Some features may prove to be impractical. Others may prove to be entirely sound and feasible. One of the advantages in locating the project in Wainwright is that, although the residents are needy in many respects, they are generally well educated and industrious. They have an intense interest

in the development of the project and their cooperation is virtually assured.

DESCRIPTION OF THE COMPLEX

The complex is composed of a building with a drive-through vehicular passageway for the tractor-trailer that delivers domestic water to the homes and also, in another trip, picks up sewage and solid wastes for delivery to the incinerator. The building encloses various handling, treatment, disposal, and personal hygiene facilities that are needed to fulfill the conditions of the law that created the project.

Building Foundation

The foundation consists of pilings set into prebored holes in the permafrost, refrozen in place. Pile cap beams are installed and held in place by either metal saddles or dowel pins. These beams are treated with pentachlorophenol preservative. The top surface of the piling is treated with an asphaltic compound prior to beam placement and beam leveling was accomplished by using shims (cedar shingles). All metallic parts are galvanized mild steel.

Building

The building is composed of 12 modules, joined together on top of the pile cap beams, in such a manner as to form a single building (Figure 1).

The modules are constructed to comply with all existing codes for arctic regions; insulated exterior walls, ceiling, and floors all with a plastic vapor barrier. On top of the modules is a truss and purlin roof structure with plywood sheathing (uninsulated) and aluminum roofing.

The drive-through portion is frame and plywood sheathed (uninsulated) walls with rollup doors at each end. The deck is 7.6 by 15.2 cm tongue-and-groove planking with 1.9 cm exterior plywood cover. This area is approached by a ramp of similar construction. The front entry is provided with a covered porch and steps of frame and plywood sheathing; 5.1 by 15.2 cm deck and steps, with handrails. The interior walls and ceiling are of plywood, finished with fire-retardant coatings suited to the use of the various areas of the building. The floor is finished with suitable material.

All electrical conduit, switches, outlets, and fixtures are surface mounted with materials approved by Underwriters' Laboratories, Inc. (UL) and to existing local and state codes. All plumbing is surface mounted and of material complying with existing local and state codes.

All high-risk fire areas are adequately protected with automatic detection and operating systems. In addition, hand extinguishers are located in accessible areas throughout the building. Hose bibs with attached hoses are located

centimetre asbestos board is placed between the steel bottom and the wood deck.

During the summer season, the tank is filled and held full by pumping as often as is needed to maintain the filled-to-capacity status of the tank until freezeup. During freezeup, water is drawn from the tank. Thus, the entire winter water use is presently held at 3 785 m³.

The supply line from the storage tank to the complex is housed in an insulated and heated utilidor duct and is connected to a manifold upon reaching the building. The manifold provides service to either the interior storage tank for raw water or to an emergency chlorination device that would return water to the outside of the building for pickup by the villagers in case of power failure.

An analysis of this raw water conducted by EPA, Water Quality Office, College, Alaska, is given in Table I.

The interior raw water storage tank, with a capacity of 10.6 m³, is constructed of mild steel, is coated with a nontoxic epoxy coating inside and rust-resistant coating outside, and is fitted with a valve for drainage. Heat transfer coils are attached to the side surfaces of this tank and insulated. A pump provides for transfer from this tank to the potable water treatment system. It also will pump heated water from this tank to the 3 785-m³ tank to prevent freezing.

Potable Water System

Raw water is pumped from the interior raw water storage tank to a treatment tank at 0.32-0.44 dm³/s, where it is hydraulically mixed with automatically proportioned and metred alum and soda ash, coagulated, and settled. The settled water is then filtered, allowed residence time in a

TABLE I Raw Water Analysis

Iron	170 mg/m ³
Manganese	30 mg/m ³
Total dissolved carbon	9.26 mg/m ³
Conductivity	274 μmho
Total hardness	41.0 g/m ³
Turbidity	3.1 jtu
Total solids	132 g/m ³
Total volatile solids	46 g/m ³
Suspended solids	3 g/m ³
Volatile suspended solids	2 g/m ³

clear well compartment, and then chlorinated and transferred to a potable water storage tank. Figure 2 shows a schematic arrangement of this system.

The treatment system includes a multimedia filter bed to provide a filtering rate of 5.36 m/h of bed area at rated capacity. Backwash pumps use clear well water to backwash the filter bed at a rate of 41.4 m/h of filter bed for a period of 5 min. The cycle for backwash is automatically controlled by sensing head loss through the filter and is completed when a predetermined reservoir level has been reached. It is then returned to service. During transfer of water to the storage tank, the water is chlorinated to meet the chlorine demand and beyond the level of a residual of 0.4-0.6 ppm. The tank size assures a holding time of 1 h before distribution

The potable water storage tank is lined and coated similarly to the raw water storage tank, except that it is fitted with a sectioned, removable cover to prevent contamination.

From storage, the potable water is pumped to a cluster

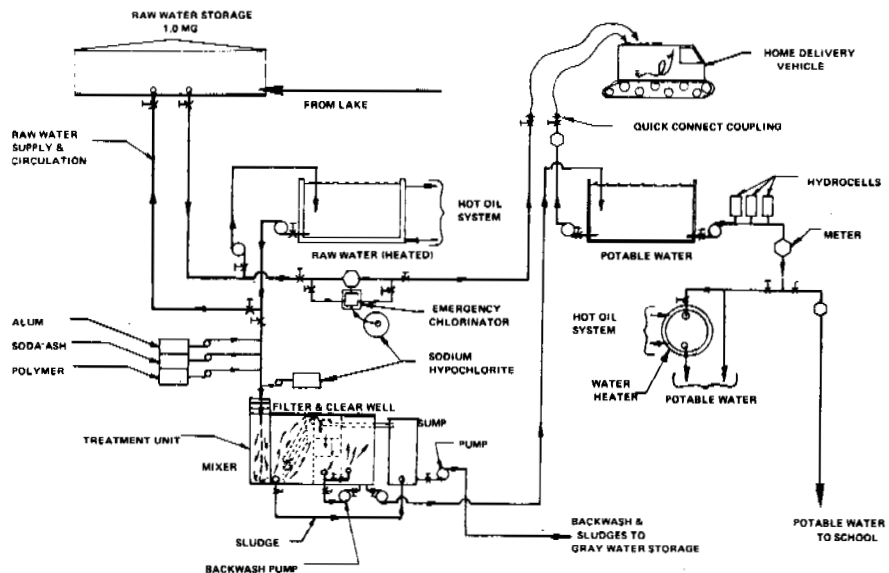


FIGURE 2 Raw water and potable water treatment system.

of hydrocells to ensure constant flow and pressure to the distribution system. From the hydrocells, the water is distributed to the home delivery pickup point, the hot water heater and to the showers, the lavatories, and the drinking fountain. In addition, provision is made to permit connection to a utilidor duct installation to provide potable water to the BIA school.

Gray Water Collection System

Gray water consists of all waste water generated by the personal showers, lavatories, drinking fountains, and laundry washing machines. Laundry machine water comprises about one half of the total gray water flow. Based on documented experience, the analysis of these waters will approximate that given in Table II.

Shower water drains to collection tanks beneath the shower stalls. These tanks also receive drainage from the lavatories. In each tank beneath the showers there is a sump pump to transfer the collected waters to the filter screen. Collection tanks are also fitted with outlets from the pumps and inlet fittings that will allow these tanks to be flushed regularly with recirculated treated waste water. Adequate venting is provided. Pump control is self-contained and a regulated level switch (within the pump) permits cycling of 7- to 10-min on-off operating periods. Access to the sump pump is through a gasketed inspection port in the top surface of the tank between the shower stalls.

Beneath the laundry washers, there is a similar tank capable of collecting all of the waters from the washers, so constructed as to adequately support the loaded washers. The wastes collected are evacuated by an external pump and controlled by a level-sensing device within the tank. The tank is also provided with an inlet fitting that will allow the tank to be flushed with recirculated, treated waste

TABLE II Gray Water Breakdown in g/m³ and pH

Total solids	975-1 420
Suspended solids	100-127
Chloride	120-320
ABS	39-80
BOD	118-284
Chemical oxygen demand	562-662
Phosphate	140-275
pH	6.9-7.0

water. Adequate venting and drain valves are provided. A connection in this system is included for collection of the gray waters of the BIA school, which will be transferred through the utilidor duct.

Gray Water Treatment System

Gray water as collected is delivered to a so-called hydrosieve screen unit (Figure 3). This is a cascading type screen that separates a maximum amount of sludge and lint from the water. It is capable of handling 0.32-1.26 dm³/s with maximum efficiency. The solids slough off the lower portion of the screen into a collection container and then are vacuumed into the sewage waste collection tank.

From the screen, the water is transferred by pump to a centrifuge for removal of minute solids and is then transferred to a storage sump or holding tank. This tank is manufactured of mild steel and protected with appropriate coatings. The tank is fitted with a removable manifold at the bottom of the tank, which will permit aeration during the holding period. A bottom drain is provided.

From the storage-aeration tank, the waters are transferred by pump to an upflow sludge clarifier. At the clarifier,

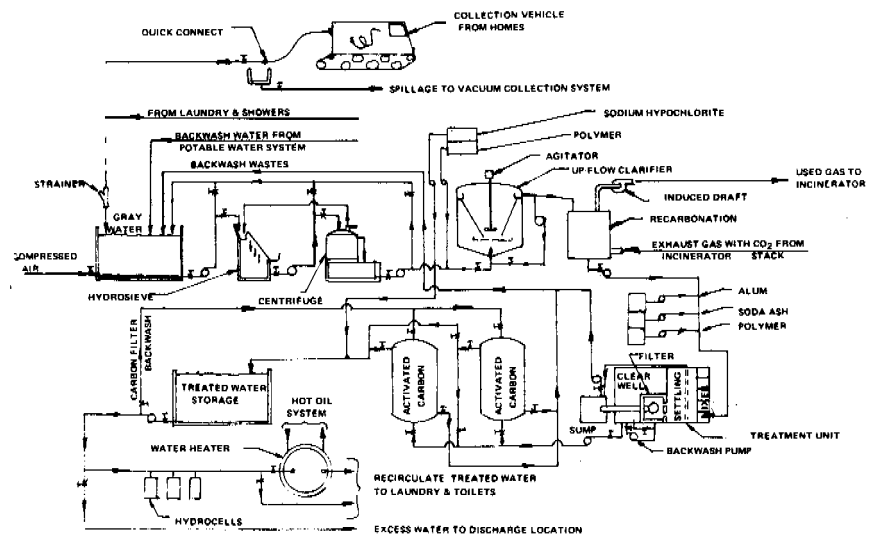


FIGURE 3 Waste (gray) water collection and treatment system.

they are mixed with lime and a cationic quaternary ammonium compound to provide primary chemical coagulation of dissolved solids in the waste water. The clarifier unit is sized to permit 110 min of retention of mixed wastes to allow maximum clarification. The effluent of the unit is expected to have a pH of approximately 11 prior to transfer to a recarbonation chamber.

The recarbonation chamber is designed to utilize the CO₂ contained in the stack gases of the incinerator. Waters cascade down over large pieces of inert plastic material and perforated plates inside of the chamber and are collected at the bottom. The gases from the incinerator stack are ducted to the bottom of the chamber and allowed to pass up through the chamber's perforated plates and plastic material, thus permitting maximum contact of the gases with the cascading waters. A vent from the top of the chamber connects to the upper portion of the incinerator stack. This vent contains an exhaust fan to ensure gas flow through the chamber.

The waters from the recarbonation chamber (pH 8.0–9.0) are pumped to the inlet portion of the water treatment plant at a rate of 0.32–0.44 dm³/s. Here, they are hydraulically mixed with automatically proportioned and metered amounts of alum, polyelectrolyte, and soda ash. They are then allowed to mix, coagulate, and settle for 25–30 min. The clarified water then passes through a multimedia filter bed.

The filter bed area has been designed to provide a filtering rate not exceeding 5.36 m/h of bed area at rated capacity. From the filter bed, the waters are pumped to a clear well reservoir with a capacity for 1-h retention. The water in this reservoir is also utilized to backwash the filter bed.

The backwash pump provides a minimum of 41.4 m/h of filter bed area for a minimum of 5 min and is fitted with controls that start the backwash cycle by sensing head loss through the filter. The pump stops when a predetermined level of the clear well reservoir has been reached. After backwash, the filter bed is returned to service.

After retention in the clear well, the waters are expected to have a chemical oxygen demand value of approximately 10–20 ppm. They then pass on to the achieved carbon columns for final polishing.

Water is circulated through the carbon columns at a rate of 0.32 dm³/s in an upflow mode of circulation and is timed to permit a 30-min contact period of water to carbon. Backwash cleaning of the carbon columns utilizes treated waste water pumped through the carbon bed at rates prescribed by the manufacturer to ensure adequate contaminant removal. At predetermined periods of time, the lower portion of the carbon bed is removed and new carbon, or reactivated carbon, is added to the top portion of the bed. This ensures maximum life at minimal expense.

After contact in the carbon columns, water is transferred

to the treated water storage tank. During transfer, these waters are chlorinated to meet the chlorine demand and beyond that level to a residual of 1.0 ppm and retained in the storage tank for a minimum of 1 h before transfer to the distribution system.

The treated water storage tank is constructed of mild steel and is coated similar to other water storage tanks. A drain valve is provided. The tank is fitted with a sectioned removable cover to prevent surface contamination.

Treated Gray Water Re-Use Distribution System

After the treated water resides in its storage tank, it is pumped to a cluster of hydrocells that ensure constant flow and pressure in the re-use distribution system. From the hydrocells, the water is distributed to a hot water heater and to the laundry to provide hot and cold water for the laundry washer. Re-use water also rinses and recharges each of the commercial airline-type toilet units and rinses shower and laundry collection tanks. Treated gray water is also used for backwashing the carbon columns and for rinsing and backflushing the recarbonation chamber and the upflow sludge clarifier.

To add to the fire protection plan, treated gray water is piped to four hose bibs with lengths of hose attached, located at critical areas in the building. Finally, a hose bib fitting and hose is installed at the sewage collection station in the drive-through area to provide the collection vehicle with hot rinse water and to aid in keeping the collection area clean. The water so used is handled as sewage waste.

Compressed Air System

In an area adjacent to the incinerator, there is located an electrically driven air compressor, mounted on a reservoir tank, with a capacity large enough to fit the needs of the complex. Compressed air is distributed to each of the toilets for operating the flushing mechanisms. Outlets for quick-connect hoses are provided immediately adjacent to the water and waste water treatment systems. Compressed air is also furnished to the waste water storage tank for aeration purposes.

Finally, connections are made to each of the other system lines, so that they may be air evacuated, in the event of total power failure. This is provided to prevent line freezeup. The hot oil heating system is not evacuated, since the oil is not adversely affected by low temperature extremes.

Fire Protection System

Fire protection is composed of three separate subsystems. As previously mentioned, the re-used gray water system serves four hose bibs with hoses. Second, hand-carried

chemical extinguishers are wall-mounted at strategic locations in the building. Finally, in the areas of extreme high fire risk, i.e., incinerator area, auxiliary oil heater area, and around the laundry dryers, a flame-retardant gas extinguisher system is provided. It is controlled by an automatic sensing device.

Emergency doors to allow egress from the dressing rooms adjacent to the saunas have also been provided. These doors have "panic" bars to ensure door opening when activated by pressure against the panic bar.

Sewage Collection System

Collection of all sewage wastes in the toilets in the building is done by a vacuum system (Figure 4). The central collection tank is connected to a vacuum source; as each toilet drain valve is opened, the waste is carried by vacuum to the collection surge tank. While the toilet unit is being evacuated, a rinse valve is opened and the toilet unit is rinsed out. After complete evacuation, the toilet unit is recharged with proper amounts of re-use water and chemical and put back into service.

In the drive-through area, a quick-connect vacuum fitting is provided for evacuating the wastes brought in by the collection vehicle. Provisions are made for a vacuum line in the utilidor duct from the BIA school to eventually collect sewage from that source.

After collecting sewage wastes in the surge tank, they are macerated and pumped into the pathological hearth section of the incinerator for destruction. Thus, human wastes are completely eliminated. There is no further treatment and no effluent waters to be disposed of.

The outlet of the vacuum pump in the system is fitted with a duct that is connected to the secondary burner por-

tion of the incinerator, so that any fumes from the vacuum producing process will be destroyed by incineration. Automatic controls ensure the vacuum process can be started only after the incinerator has been ignited and is in full service.

Incineration System

The incinerator is capable of incinerating the sewage wastes from the project building as described above, as well as the collected wastes from the village homes and the BIA school. This is an estimated daily volume of 0.473 m³, plus all of the type 1 and 2 solid waste generated from these facilities (an estimated daily load of 90-136 kg). In addition, all sludge wastes from the water treatment system, an estimated daily total of 9-13 kg, and all fumes generated by the vacuum system are destroyed in the incinerator. The incinerator is also capable of destroying small loads of pathological waste if the need occurs.

The incinerator burners, one large secondary and one primary in each of two primary hearth areas, are oil fired. Since large coal deposits exist near Wainwright, provisions are made in the design for possible future utilization of coal. The burners are both manually and automatically modulated, to provide optimum operating conditions.

The incinerator is fitted with a heat exchanger to provide the main heat source for the hot oil heat system.

Heating System

The heating system (Figure 5) is composed of two parts. In the first part, hot oil will provide heat required by the: potable water heater; treated water heater; inside raw water tank; saunas; heat tracer lines to utilidor duct to BIA

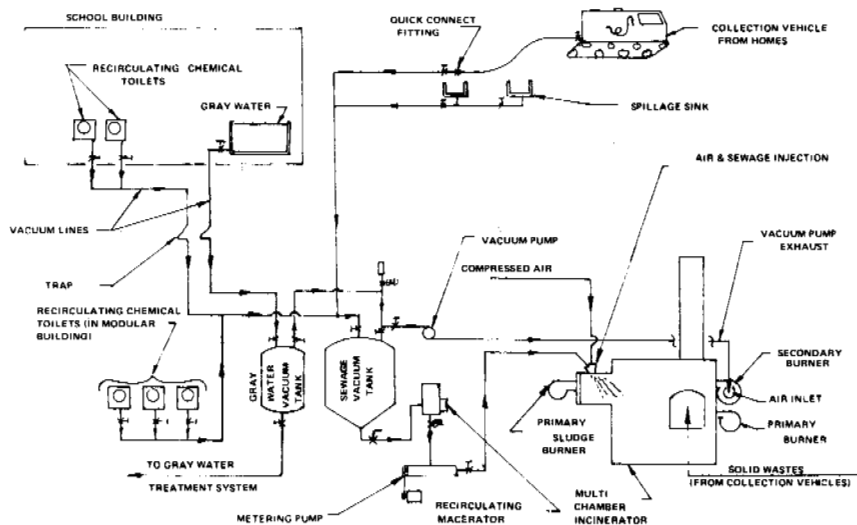


FIGURE 4 Sewage waste collection and disposal system.

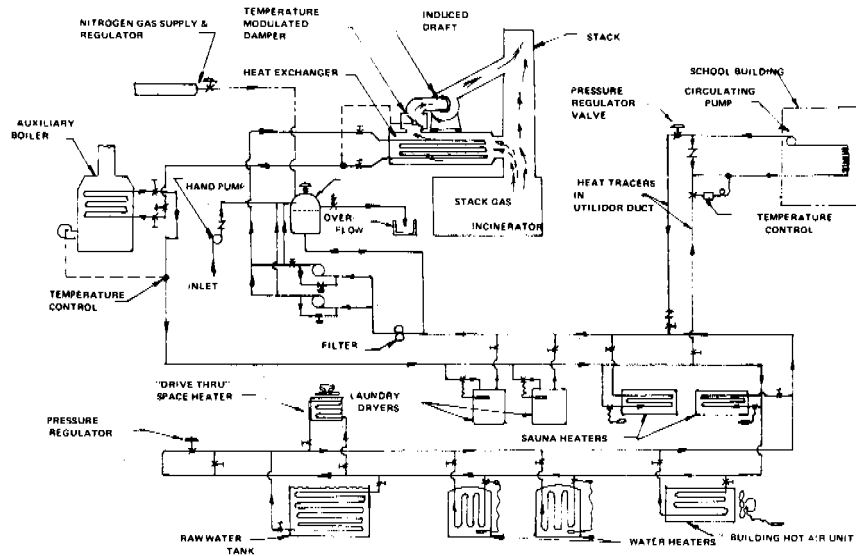


FIGURE 5 Heat transfer medium heating and circulating system.

school; heater tracer lines to raw water and oil supply lines to project building if required; and heat exchanger for hot air circulation system for building.

The oil is heated in a heat-exchanger coil in the incinerator. An auxiliary heater (oil fired) is provided to ensure that adequate input will be available. There is an expansion tank in the system with adequate pumps to maintain flow within the system and makeup of oil from without the system. The exhaust from the auxiliary oil heater is ducted to the incinerator stack.

In the second part of the system, which provides overall building heat, an insulated heat exchanger for fresh air heating and circulating is mounted over the modules and under the roof, to provide circulating, heated, fresh air to the building. Fresh air intake is from the area under the roof that is vented to accept fresh air from outside the building. A blower, sized to provide four air changes per hour, is housed in the heat exchanger enclosure.

The outgoing air is vented by natural aspiration or circulation through the building to the incinerator room by means of backdraft dampers through the walls. This provides preheated air to the incinerator burners. All ventilation and heated air supply ductwork is adequately insulated to ensure minimum heat loss.

A condensate drain pan is provided at the exchanger to collect and drain condensed moisture from the heat exchanger coils to the waste water collection system. Building temperature is modulated by thermostat.

Laundry Facilities

The complex is equipped with four coin-operated automatic washing machines. Two are capable of handling 13.6-kg loads, the other two capable of 5.4- to 6.8-kg loads. There

is also a standard laundry sink for presoaking and other washing. In addition, there are two 13.6-kg tumble dryers (coin-operated). Adjacent to this equipment are tables for folding clothes, etc., and a drinking fountain. This fountain drains to a shower sump.

Personal Hygiene Section

Adjacent to both ends of the laundry facilities are located the washrooms, showers, and sauna. A dressing area is placed outside the sauna-shower area. The showers are coin-operated, i.e., a coin will operate a timing device that will allow a certain period of time of water usage from the shower. The water is manually controlled by regular hot and cold valves and the timer will allow interruptable use of water so that a full measure of timed water usage is given the users.

The saunas, one for each sex, are heated by a portion of the hot-oil heating system and are provided with benches, central light, and thermostatic heat control. A water outlet is available for steam generation from heated peridotite rocks.

There are provisions for a dressing area, with adequate wall hooks installed for use by the natives while in the sauna or showering. In each shower-sauna area there is a lavatory sink with hot and cold water provided. This sink drains to the sump beneath the showers.

Public Hygiene Facilities

At each side of the main entryway and leading from the laundry there is a rest room facility, one for each sex. These contain two toilets and a lavatory sink with hot and cold water. These toilets, similar to the toilet in each of the

personal hygiene sections, are the type previously described. They are also connected to the vacuum sewage collection system.

Additional Information

To ensure reliability of function, a complete spare parts program is provided together with instruction manuals for operation and maintenance. Spare parts are intended to meet the requirements for 1 year. Repair kits and manuals are also provided to reduce the amount of outside repair to a minimum. Sufficient chemicals will be delivered with the unit to provide for a full year of operation. Replacement "lead time" for these materials will be explained in the operating and maintenance manuals.

Power supply to the building is provided by the village. Automatic switchgear is installed for changeover to auxiliary standby equipment in the complex in case the village power is out. Fuel oil supply is stored in five uninsulated steel tanks holding a total of 113.55 m³ and piped into the complex through unheated lines.

COST OF OPERATION

The daily requirements for building heat needs are based on the heat balance study for the building and an assumed efficiency of the heat exchanger of 65 percent and the incinerator operating 8 h per day. Cost is in U.S. dollars.

Potable Water System

Chemicals—Alum, soda ash, polyelectrolyte, sodium hypochlorite \$ 1.18

Waste Water System

Chemicals—Alum, soda ash, polyelectrolyte, lime, cationic ammonium compound, sodium hypochlorite 4.36
Filter Media—Activated carbon replacement 0.20

Toilet Maintenance

Chemicals—MC1000 fluid 1.03
Consumables—Paper towels, toilet paper 0.30

Incinerator System

Fuel Required To Incinerate

a. Sewage and treatment wastes alone 16.12
b. Sewage and treatment wastes plus solid wastes 17.84
c. Sewage and treatment wastes plus additional heat to meet *minimum* building heat needs for occupants 24.00
d. Sewage and treatment wastes, solid wastes, plus heat to meet *minimum* building heat needs for occupants 25.72

e. Sewage and treatment wastes plus heat to meet *average* building heat needs for occupants 28.48
f. Sewage and treatment wastes, solid wastes, plus heat to meet *average* building heat needs for occupants 30.20

The following requirements are based on an auxiliary heater operating at 70 percent efficiency for a period of 16 h per day when it is used with the incinerator or 24 h per day when operated by itself to supply total building heat needs as shown.

Auxiliary Heater

Fuel Required

a. To provide minimal heat with incinerator \$ 13.57
b. To provide average heat with incinerator 15.18
c. To provide minimum heat by itself 39.85
d. To provide average heat by itself 47.90

Building Operation and Maintenance

Labor—Two (2) men 72.00
Electric power costs 8.00

Summary

1. To provide minimum requirements	
a. Incineration and heat	39.85
b. Treatment costs (chemical, etc.)	7.07
c. Electric power	8.00
d. Labor	72.00
	<hr/>
Total Minimum Base Costs	126.92
2. To provide maximum requirements	
a. Incineration and heat	47.90
b. Treatment costs (chemical, etc.)	7.07
c. Electric power	8.00
d. Labor	72.00
	<hr/>
Total Maximum Base Costs	134.97

It must be made clear that the above costs are "best estimates" at the time of this writing. There has not been an opportunity, as yet, to document any of the daily requirements of chemicals, power, fuel, etc.

The cost of operation of the vehicles and vehicles operators for the collection and delivery of water and wastes have not been included in this report since at the time of writing the size and type needed to fulfill requirements had not been determined.

A net cost (the above being gross cost) of operation will result after fees for usage of equipment in the building (washers, dryers and sauna-shower baths) and fees for water pickup have been collected and documented. It is anticipated that some of this documentation will be available by the summer of 1973.

CONCLUSION

Within the north permafrost regions of the world there are many native villages. The hostile environment in these regions and the cultural background of the villagers have delayed the introduction of sanitary amenities enjoyed by residents in more temperate climates.

Recent years have seen significant changes in the native culture. Through the airplane, radio, and greater influx of people from "outside" the native inhabitants find ready-made goods available to replace their handcrafted goods.

Hunting and fishing with rifle and nets, snowmobiles, and outboard engines make their life less strenuous. Governmental programs provide better living quarters, education of the young, and unemployment and welfare payments. The native also is finding employment and a source of cash as a result of increased activity in the Arctic. The acculturation process must eventually include increased attention to personal sanitation in the interest of better health protection.

The health complex prototype described above is one approach at improved sanitation in permafrost regions not only for the individual but for his environment as well.

PERMAFROST PROTECTION FOR PIPELINES

H. O. Jahns, T. W. Miller, L. D. Power,
W. P. Rickey, T. P. Taylor, and J. A. Wheeler

ESSO PRODUCTION RESEARCH CO.
Houston, Texas

INTRODUCTION

Pipeline operations in permafrost regions are faced with unique problems that arise from disturbances of the thermal regime in the ground. The thawing of ice-rich soil can result in a loss of adequate pipeline support. The conventional buried pipeline mode may be inadequate in these soils, particularly if the pipeline is to be operated at temperatures above the freezing point.

Several alternatives that can alleviate this problem are to operate the pipeline at temperatures below 0 °C, to elevate the pipeline above ground on gravel berms or pile foundations, and to provide special means for preventing the thawing of permafrost in the vicinity of the pipeline. The first alternative appears attractive for gas lines, but it may not be feasible for a long oil pipeline when the increased viscosity at low temperatures results in excessive pumping and cooling requirements. Elevating the pipeline solves the problem by removing the heat source from the ground. However, this construction mode is sometimes difficult due to other design constraints, such as earthquakes, certain terrain features (e.g., steep slopes), special hazards (e.g., avalanches), or environmental concerns. Furthermore, placing the pipeline above ground is not always sufficient to guarantee adequate foundation in frozen ground over

the life of the pipeline. Experience in Alaska and other permafrost areas has shown that foundation problems are often encountered even in the absence of an active heat source in the ground. Permafrost thawing may occur as a result of surface disturbances (e.g., removal of vegetation) or from natural causes (e.g., climate changes). These problems are common in the region of discontinuous permafrost where temperatures in the frozen ground are usually near 0 °C, so that even small disturbances of the thermal regime near the surface can result in progressive thawing of the subsoil ("permafrost degradation") with attendant thaw settlement.

Thus, there is a need with both buried and elevated pipelines for special means of preventing the thawing of permafrost. Several systems for permafrost protection have been proposed in the literature.^{2,3,14,20,22} Typically, they utilize natural convection to extract heat from the ground during winter. Some of these devices have been used in practical applications involving various foundation problems in permafrost.^{9,14,16} However, to our knowledge, there is no past experience in connection with large cross-country pipelines. Consequently, there is little quantitative information on which the design engineer can base the selection of particular protection systems for the wide range of environmental conditions that may be encountered by a major arctic pipeline.

This paper presents results of a study aimed at developing such information on the basis of computer simulations of the thermal system of interest. The system includes not only the heat extraction device itself, but also the pipeline or its support, the surrounding soil, and the atmosphere. The emphasis of this work was on the quantitative evaluation of relationships between heat-removal rates and the resulting benefits in terms of permafrost protection. This information allows the designer to determine how much permafrost protection he needs in a given case before he selects the system that can satisfy this need most economically in accord with other design constraints and pipeline operations. The study included laboratory testing of several heat removal devices for large diameter piling. Some test results obtained with a simple "air convection pile," an open-system, natural convection device, are reported in the paper.

The simulation technique developed for this work has been published elsewhere.²³ Only those aspects and modifications that relate to specific boundary conditions, particularly at the soil surface, are discussed in any detail in this paper. The amount and detail of results that could be included are necessarily restricted by space limitations. Thus, only a few typical combinations of climatic and soil conditions are represented as examples of the wide range of conditions that may be encountered in the field. While these examples serve to illustrate the principal characteristics of various permafrost protection systems, more detailed analysis may be required to determine their relative merits in specific applications.

The following discussion addresses only a limited number of permafrost protection systems: insulation and mechanical soil refrigeration for a warm, buried pipeline; natural convection devices for pile supports of an elevated pipeline ("thermal piles"); and, white paint or insulation for gravel berms. This does not imply that other combinations, or other concepts, such as the use of a heat sink for temporary storage of heat during summer,^{2,22} need not be considered for practical applications. However, based on the discussion that follows, we believe that the selection of schemes listed above offer the technical means of providing adequate permafrost protection for both buried and elevated pipelines under most conditions of practical interest.

THERMAL SIMULATIONS

Simulation Technique

The thermal calculations were made with a computer program that simulates two-dimensional heat conduction with a change of state in either rectangular or cylindrical coordinates for a variety of boundary conditions.²³ The program employs a variational technique to obtain approximate piecewise planar temperature solutions to the conduction equation at discrete times. A backward difference implicit

technique is used to relate the solutions at successive points in time. The nonlinear algebraic equations so obtained are solved by Newtonian iteration. Two basic types of boundary conditions can be evaluated by the program: specified temperature as a function of time and location and specified heat flux as a function of time, location, and boundary temperature. The temperature boundary condition can be applied along any line in the calculation grid. The flux boundary condition can be applied only to the exterior of the calculation grid. Specific boundary conditions for the various calculations are described in the appropriate sections below.

The computer model does not account for effects of heat convection in the soil or for soil subsidence. Convection of heat by water draining through a coarse-grained soil on a slope could significantly increase soil temperatures above those calculated. In such situations, the effects of convection must be estimated separately.

Soil Thermal Properties

A hypothetical silt with a moisture content of 45 percent by volume (30 percent of dry weight) is the "standard" soil for the thermal calculations. Alternative soils with higher or lower moisture content (70 percent and 20 percent by volume, respectively) were used in some cases to assess the effect of ice content on predicted results. Gravel in construction pads and berms is assumed to have a moisture content of 19.5 percent by volume. Thermal properties used for these materials are given in Table I. They were estimated on the basis of published correlations.^{10,15}

In most calculations, we assumed that all of the soil moisture freezes or thaws at a discrete freezing point (0 °C). However, the assumption of a discrete freezing point is not always justified. Due to various surface effects, a portion of the moisture may freeze only at temperatures significantly be-

TABLE I Thermal Properties Assumed for Soil and Gravel

Property	Standard Soil	Gravel
Moisture content		
% by volume	45.0	19.5
% Dry weight	30.4	10.1
Thermal conductivity (W/m K)		
Frozen	2.25	2.77
Thawed	1.38	2.42
Heat capacity (10 ⁶ J/m ³ K)		
Frozen	2.01	1.65
Thawed	2.95	2.07
Latent heat content (10 ⁶ J/m ³)	149	65

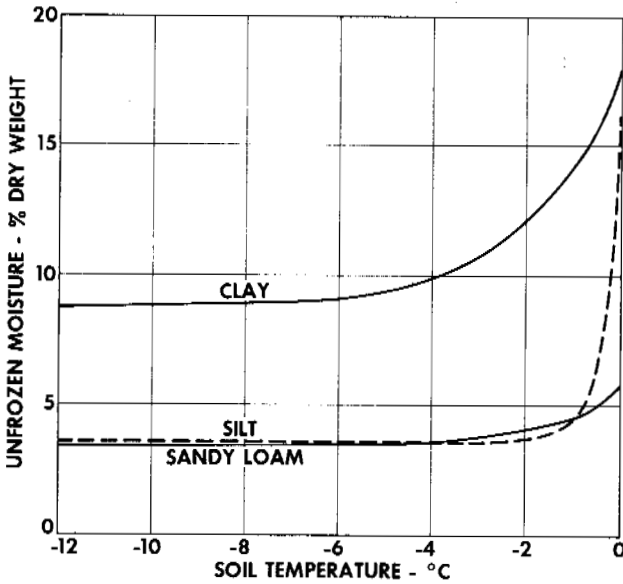


FIGURE 1 Unfrozen moisture content of some typical soils.

low 0 °C. This phenomenon is particularly pronounced in fine-grained soils, and it may affect the performance of thermal protection systems in marginal permafrost. The computer model can take this effect into account if the discrete freezing point is replaced by a "freezing range" where the latent heat content is a function of temperature. Figure 1 shows unfrozen moisture content as a function of temperature for three typical soils. The curves were fitted to experimental data.^{1,17} Soil moisture in excess of the value shown at 0 °C is assumed to freeze precisely at that temperature. These curves were used in several thermal simulations with all other soil properties, including total moisture content, identical to those of the standard soil, so that the effects of the variation in freezing point could be clearly identified.

Boundary Conditions

Boundary conditions at the soil surface play an important role in thermal simulations of the permafrost regime. The degree of detail with which the natural conditions must be represented in the computer model depends on the problem at hand. For instance, a system that relies on mechanical refrigeration to protect permafrost below an insulated buried pipeline is not very sensitive to short-term variations in surface temperature, since its performance is dominated by a strong heat source (the pipeline) and one or more sinks (refrigeration lines) under ground. The benefits of a white-painted gravel surface, on the other hand, depend entirely on the relatively small changes in soil surface temperature that result from a change in radiative properties.

For simulations involving a buried pipeline, soil surface temperatures were specified explicitly as a simple sinusoidal function of time, representing the annual temperature cycle at some nominal depth below the surface vegetation. The mean temperature was varied (from -9.5 to -0.5 °C) to represent a range of climatic conditions, while the amplitude was held constant at 11.1 °C.

Surface temperatures for elevated pipeline modes were based on a rather detailed model of the surface heat balance, taking into account heat conduction in the ground and snow-cover (when present), radiation to and from the surface, heat transfer to and from the atmosphere by convection, and evaporation or melting of precipitation. Our approach here is similar to the methods used by other investigators.^{4,19} Examples of surface temperatures calculated by the model are shown in Figure 2 for three different surface conditions. Surface properties used in these calculations were estimated on the basis of published data^{6,8,11,16,21} and are listed in Table II. We used climatic conditions, i.e., solar radiation, air temperature, wind speed, cloud cover, and snowfall, which are typical for Gulkana, southern Alaska (about 62°N lat.). The calculations assumed permafrost with the standard soil properties (see Table I) and a gravel pad thickness of 60 cm.

The natural surface condition shown in Figure 2 represents a case of warm, but stable, permafrost with an average temperature of -0.5 °C at 9 m depth (" -0.5 °C permafrost") and an active layer thickness of about 1.5 m. The slight increase in summer temperatures for the gravel surface would be sufficient to raise the mean soil temperature above 0 °C. A long-term simulation for this case predicts a thaw depth

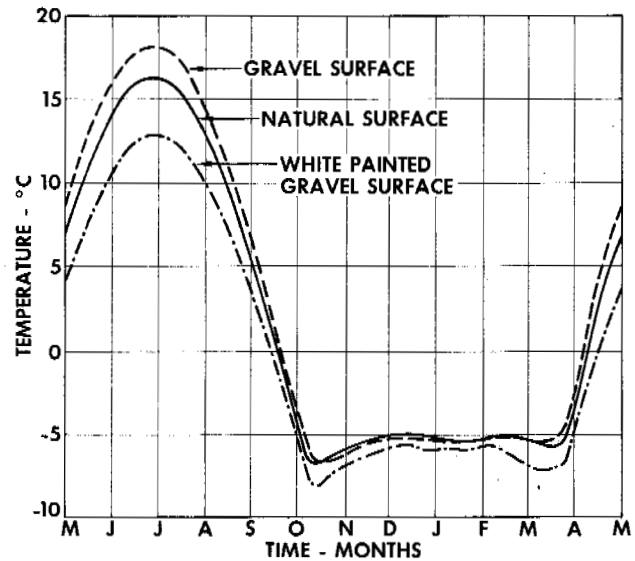


FIGURE 2 Calculated temperatures for natural and gravel surfaces over -0.5 °C permafrost with "standard" soil properties; air temperature mean: -3.4 °C; amplitude: 19.5 °C.

TABLE II List of Assumed Surface Characteristic Parameters

Characteristic	Surface Temperature (°C)	
	Summer	Winter (Snow)
Natural surface		
Heat transfer coefficient (W/m ² K)	71.6	21.0
Longwave emissivity (infrared)	0.90	0.98
Shortwave emissivity (visible)	0.75	0.30
Gravel surface		
Heat transfer coefficient (W/m ² K)	24.4	21.0
Longwave emissivity (infrared)	0.85	0.98
Shortwave emissivity (visible)	0.85	0.30
White-painted gravel surface		
Heat transfer coefficient (W/m ² K)	24.4	21.0
Longwave emissivity (infrared)	0.85	0.98
Shortwave emissivity (visible)	0.30	0.30

of 3.6 m after 20 years. Temperature predictions for the white-painted gravel, on the other hand, indicate a significant reduction in surface temperatures and, therefore, improved permafrost stability in comparison with the natural surface condition.

In our parametric studies of permafrost protection systems, we used simplified representations of the detailed temperature functions obtained from the surface heat balance simulator. Thus, summer temperatures at the soil surface and winter temperatures at the snow surface were approximated by sinusoidal functions of different amplitudes but at the same "median" temperature. In addition, a heat transfer coefficient is used during winter to represent the insulating effect of the snow layer.

Table III lists three sets of surface temperature parameters that were used with the standard soil. The first two sets are both representative of a "warm" (-0.5 °C) perma-

frost, where removal of the surface vegetation or placement of a gravel pad would initiate progressive permafrost degradation. Set I was used for thermal pile simulations, set II for gravel berms. Slightly different values than those shown in Table III had to be used in order to simulate the same ground temperature conditions in one of the alternative soils.

The surface boundary conditions assumed in this study do not necessarily describe accurately any specific locality with given climatic, surface, and soil conditions. Rather, they are considered to be typical for certain permafrost conditions, as characterized by the mean soil temperature below the active layer. This temperature is treated here as the main independent variable that determines applicability and performance requirements for the various permafrost protection schemes.

Other boundary conditions used in the study include a no-flow condition on the right-hand side and an imposed geothermal gradient at the bottom of the grid. We took care to ensure that these boundaries are far enough removed so that they do not significantly affect the temperature distribution near the pipeline. The left-hand side is either a plane of symmetry or a cylindrical surface of small diameter; these are also no-flow boundaries, except where special conditions are imposed to simulate heat removal through piles equipped with thermal convection devices. Pipeline (and refrigerant line) temperatures are specified as "internal" boundary conditions.

All simulations begin in the fall when the active layer is completely thawed ("September startup"). For buried pipeline cases, the initial soil temperature distribution was given by a uniform geothermal gradient of 0.027 K/m. Initial temperatures for elevated pipeline cases were determined by a separate 3-year simulation for the natural, undisturbed condition. In effect, we have assumed that the elevated pipeline, including any gravel pads or berms, is placed instantaneously on previously undisturbed ground, at about the time

TABLE III Assumed Surface Temperatures for Standard Soil

Set	Nominal Soil Temp. ^a (°C)	Air Temp. (°C)		Surface Condition	Surface Temperature (°C)			Snow Heat Transfer Coefficient (W/m ² K)	Permafrost Condition
		Mean	Amplitude		Median	Summer Amplitude	Winter Amplitude (Snow Surface)		
I	-0.5	-3.4	19.5	Undisturbed	-6.1	19.7	22.6	0.32	Stable
				Bare gravel	-5.6	20.8	23.2	0.32	Unstable
II	-0.5	-3.4	19.5	Undisturbed	-3.9	20.2	21.8	0.74	Stable
				Bare gravel	-2.7	20.9	22.9	0.74	Unstable
				Painted gravel	-5.6	17.9	21.3	0.74	Stable
III	-1.7	-3.9	20.0	Undisturbed	-7.2	20.7	22.5	0.32	Stable
				Bare gravel	-6.7	21.6	23.3	0.32	Stable

^a Nominal soil temperature is defined as the average temperature of the soil at 9 m depth with an undisturbed surface.

when the active layer is thawed to its maximum depth. The initial temperature of the gravel is equal to the surface temperature at the time of startup.

Buried Pipelines

The configuration chosen for buried pipeline modes is shown in Figure 3. Because of symmetry, the vertical plane through the pipe centerline is a no-flow boundary.

If the pipe is buried bare, a "thaw plug" will form around it. The numerical simulations indicate that the standard soil would thaw to about 4.5 m and 6.3 m below the pipe, respectively, in "cold" (-10°C) and "warm" (-0.5°C) permafrost, during the first 3 years of operation (Figure 4). In 30 years, the thaw plug may grow to roughly three times the 3-year depth. Soil moisture content has a significant effect on the size of the thaw plug: With an alternate soil of 70 percent water by volume, the predicted values for depth and width of thaw after 3 years were about 35 percent less than the corresponding values for the standard soil. These results are in general agreement with similar calculations reported by Lachenbruch.¹²

INSULATION ONLY

Insulating the pipeline is an effective means of reducing heat transfer from the pipe to the soil. Theoretically, with sufficient insulation, it should be possible to prevent thawing around the pipeline entirely, provided that the pipeline is located below the active layer and that the natural permafrost

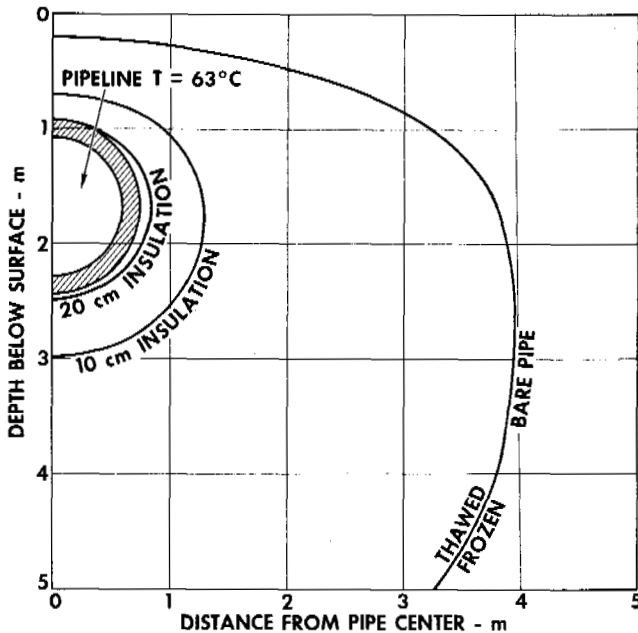


FIGURE 3 Thaw plugs for insulated and bare pipe at 3 years with a mean surface temperature of -9.5°C .

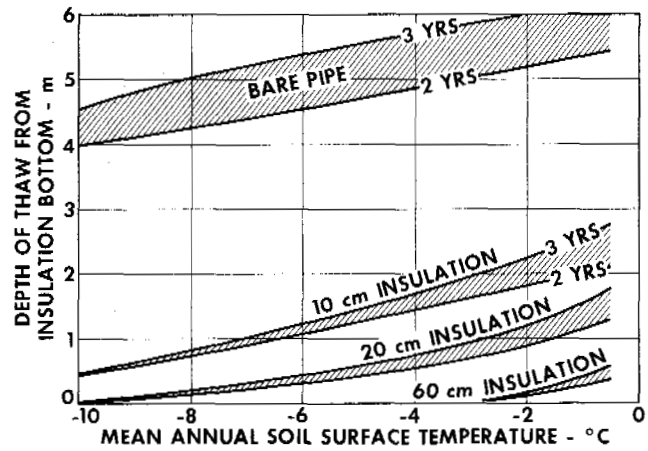


FIGURE 4 Depth of thaw for insulated and bare pipe at 2 and 3 years.

frost temperature is well below 0°C . However, the amount of insulation required to accomplish this increases with both pipeline and permafrost temperature. In warm permafrost, insulation requirements for complete permafrost protection tend to become excessive; but moderate amounts of insulation still result in a significant reduction of the rate of thaw.

Results of sample calculations for an insulating material with a conductivity of 0.035 W/mK , applied in various thicknesses, are shown in Figures 3 and 4. With 10 cm of insulation in cold (-9.5°C) permafrost, the extent of thaw is only about 0.6 m after 3 years (Figure 3). With 20 cm of insulation, the thaw bulb could be essentially eliminated; in this case, the small thawbulb shown in Figure 3 vanishes entirely during the winter and does not merge with the active layer during summer.

Figure 4 shows thaw depths after 2 and 3 years of operation as a function of mean surface temperature. Complete permafrost protection for mean annual surface temperature above -3°C is seen to require more than 60 cm of insulation. Thus, the permafrost protection system would become more massive than the pipeline itself. Apparently, this would also be the case with other proposed schemes,^{2,22} which would make use of heat sinks and natural convection devices to store and remove the excess heat that gets through the insulation.

SOIL REFRIGERATION

Mechanical refrigeration of the soil near a buried pipeline can provide year-round protection in warm permafrost with much less bulk than any of the passive protection systems. This advantage must be weighed against cost and effort required to operate and maintain the refrigeration and pumping equipment. Soil refrigeration has been discussed in considerable detail in another publication.²³ Only a few examples will be presented here. They are for the same gen-

eral soil and surface conditions as the results shown in the previous section.

The refrigeration system considered here consists of two refrigeration lines located below the pipeline on each side of the ditch. A refrigerant (e.g., brine or methanol-water solution) is circulated continuously through these lines from a central refrigeration plant. The particular results shown in Figures 5 and 6 are for refrigeration lines of 15 cm diameter, centered at points about 70 cm to each side and 70 cm below pipe center, and for a constant year-round refrigerant temperature of -5.5°C .

Figure 5 shows the maximum extent of thaw predicted for the end of summer in warm (-0.5°C) permafrost, with 10 cm of insulation around the pipeline. The soil below the lower part of the pipeline remains frozen at all times. The rate of refrigeration, i.e., the amount of thermal energy absorbed by the two refrigeration lines per unit time per unit length of pipeline, is calculated as 62 W/m on an annual basis, with a peak load of 67 W/m during summer.

Refrigeration rate is the primary variable of interest. Figure 6 shows the mean and peak refrigeration rates as a function of mean annual soil surface temperature for 10 and 20 cm of insulation, calculated for 15 cm refrigerant lines at -5.5°C . Also shown is the peak refrigeration rate *required* to prevent thawing below the pipeline during summer. This latter quantity is essentially a function only of surface and soil temperatures, pipeline insulation, and soil properties, while actual refrigeration rates are also a function of refrigerant line size and temperature.

Refrigeration rate decreases with increasing refrigerant temperature. This relationship was found to be approximately linear over the range from -5.5 to -2.0°C . For example, at a mean surface temperature of -2.8°C and with 10 cm of insulation, peak refrigeration rate decreases from 63 to

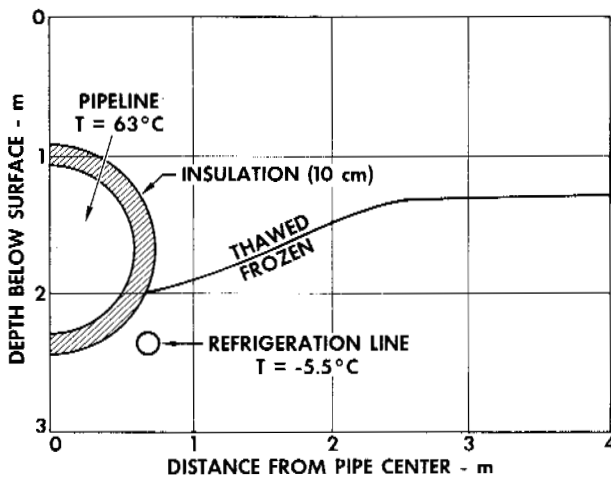


FIGURE 5 Thaw plug for soil refrigeration system in warm (-0.5°C) permafrost.

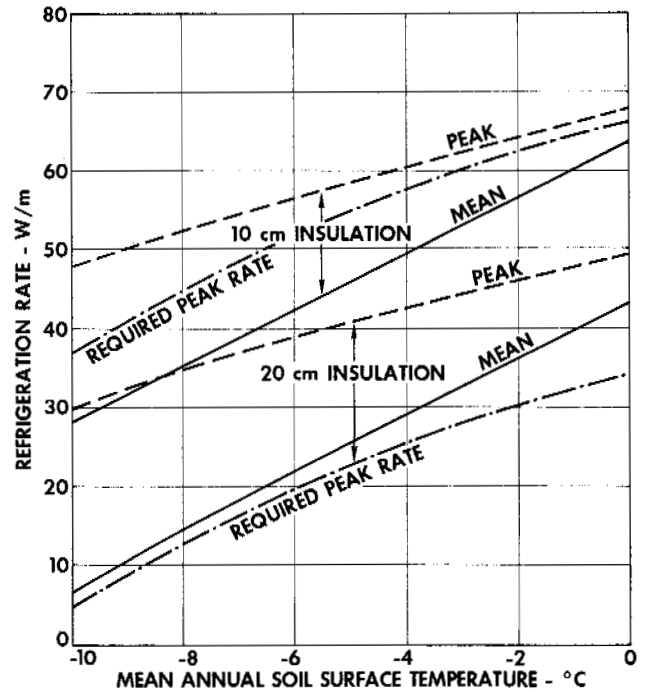


FIGURE 6 Mean and peak annual refrigeration rates with refrigerant temperature of -5.5°C and peak refrigeration rates required to prevent thawing below pipeline.

54 W/m when the refrigerant temperature is raised from -5.5 to -3.9°C . According to Figure 6, the reduced rate would be somewhat below the amount required for complete permafrost protection. In this particular case, a small seasonal thaw plug, about 10 cm deep and 50 cm wide, forms each summer below the pipeline. Refrigeration rates for line diameters other than 15 cm can be estimated by a simple calculation assuming radial, steady-state heat flow in the immediate vicinity of the refrigeration line.

The results presented above are based on the assumption that both refrigeration lines are maintained at the same temperature. In reality, the two lines will be at different temperatures if they are operated in series as the outgoing and return line of a single refrigeration loop. Thus, refrigeration rates will be higher in the outgoing line than in the return line, and the temperature distribution around the pipeline will be asymmetric. Usually, the total refrigeration rate will not differ much from the rate that would be obtained if both lines were operated at a temperature equal to the average of their actual temperatures.

The design of a refrigeration system must ensure that a given minimum refrigeration rate is met or exceeded at all points along the pipeline. There are mainly three variables that can be adjusted to accomplish this objective: refrigeration line size, refrigerant temperature, and refrigerant flow rate. In general, line diameter, flow rate, and the temperature difference between inlet and outlet must all increase

as the length of the refrigeration loop increases. On long loops—in excess of 1 or 2 km—it may be advantageous to place a small amount of insulation around the outgoing branch in order to avoid excessive overrefrigeration from the low-temperature, large-diameter line that will be required. In this fashion, it should be feasible to provide permafrost protection over a distance of 50 km or more from a single refrigeration plant located near the center of the segment. In warm permafrost and for the conditions assumed in this study, the peak refrigeration load for such a plant would be of the order of several thousand kilowatts.

Elevated Pipeline

Two modes of supporting an elevated pipeline will be considered: pile bents and gravel berms. In either case, we will assume that the pipeline is insulated (usually for reasons other than permafrost protection), so that any direct heat transfer from the pipeline to the ground is negligible. Thus, no special means, other than good permafrost construction practices, should be required to prevent permafrost degradation in areas of stable, cold permafrost. Permafrost protection schemes may be needed, however, under more marginal conditions, where the permafrost tends to degrade either from natural causes or as a consequence of construction disturbances of natural surface conditions. The following discussion addresses this condition of marginal permafrost.

PILE SUPPORTS

Several systems have been proposed for the thermal protection of structural piles in permafrost.^{2,14,20} All of these make use of natural convection to remove heat from the ground during winter; they become inactive during summer when the air temperature is above the soil temperature. In our simulations, we used a simplified model of such a device: The below-ground part of the pile surface is coupled to the atmosphere by a heat transfer coefficient, h_p , whose value is a measure of the efficiency of the heat removal system. Reversal of the heat flow during summer is prevented by setting the heat transfer coefficient equal to zero whenever the mean soil temperature along the pile is below the air temperature. The complete set of boundary conditions used in these calculations is shown in Figure 7. The pile diameter of 46 cm defines the inner radius of the cylindrical region ($r_i = 23$ cm). A pile length of 7.6 m was assumed in most calculations, and a no-flow condition was specified at the inner radius below the pile. The small cylindrical volume of soil enclosed by this boundary is neglected.

To examine the expected performance of thermal pile designs under the most adverse conditions, we assumed that the pile would be placed in ground that is initially thawed with a mean annual soil temperature of 0.9 °C. This initial condition corresponds to the long-term steady-state that will be approached as the -0.5 °C permafrost degrades due to

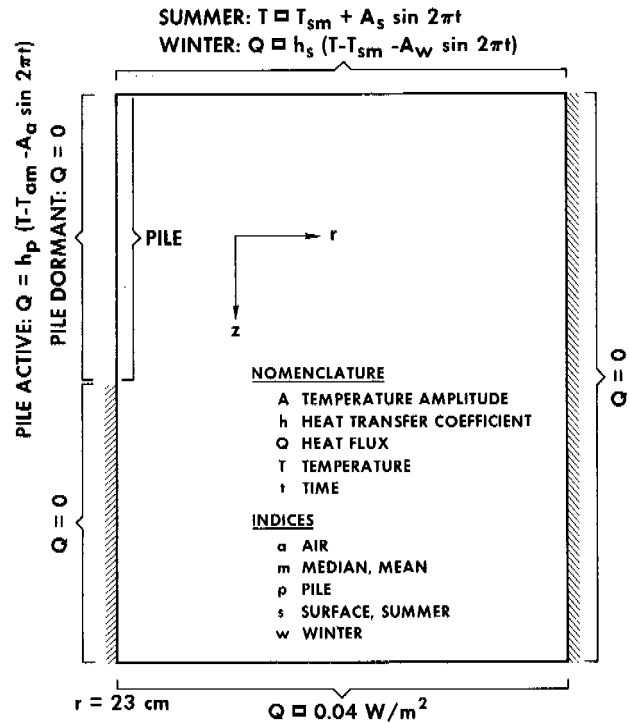


FIGURE 7 Boundary conditions for simulation of thermal piles in cylindrical coordinates. (Time, t , is measured in years from the time in spring, when the seasonal air temperature goes through its mean.)

placement of a gravel pad (see Table III, set I, for specific surface temperature conditions). This case is believed to provide a useful criterion for thermal pile design, since the exact distribution of frozen ground is not always known in advance and some piles intended for permafrost may end up being placed in partially or completely thawed ground. Figure 8 indicates the results obtained for a pile heat transfer coefficient of 3.0 W/m² K (per unit below ground pile surface area). A permanently frozen zone of increasing size is formed around the pile, growing to a radial distance of about 4 m in 30 years. The freeze fronts shown depict conditions at the end of summer, when the active layer is thawed. The size of the frozen zone depends on pile efficiency: a simulation with a smaller heat transfer coefficient (1.5 W/m² K) resulted in a freeze radius of 3 m after 30 years. Increasing the pile efficiency beyond 3.0 W/m² K results in less than proportional benefits in terms of freezing rate.

The dashed line in Figure 8 represents the predicted freeze front after 1 year for a silt with a freezing range as indicated in Figure 1. The radius of the frozen zone is increased by about 30 cm compared with the corresponding results for the standard soil with a discrete freezing point. This is an example of our finding that the existence of unfrozen moisture below 0 °C is generally favorable for permafrost protection. The effect of heat conduction down the pile wall was also included in the calculation represented by

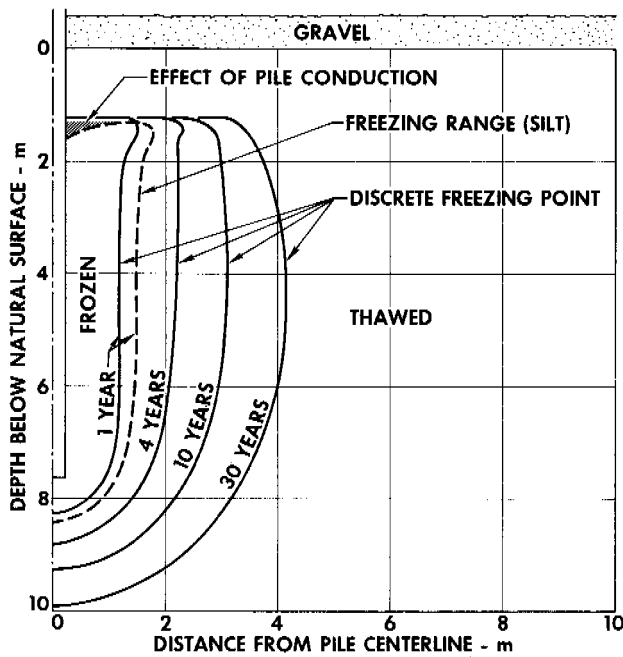


FIGURE 8 Growth of freeze front around a thermal pile with heat transfer coefficient of $3.0 \text{ W/m}^2 \text{ K}$, installed in thawed ground with 60-cm gravel pad.

the dashed line in Figure 8. The calculation grid was refined to model a steel wall 12.5 mm thick, as well as a narrow zone around the pile with sufficient detail. The temperature at the top boundary of the pile was set equal to the air temperature. This calculation indicated a local increase in active layer thickness by about 30 cm, but no “skin melting,” i.e., the freeze front and the pile surface meet at a well-defined line rather than becoming asymptotic to each other.

Soil temperatures at the pile surface are shown in Figure 9 as a function of time for the first year after installation in -0.5°C permafrost and placement of a 60-cm gravel pad. The reference depth is 4.5 m below the original ground surface. The dashed line on top indicates the gradual warming trend that would prevail in the absence of the thermal pile due to increased surface temperatures on the gravel pad. It is significant to note that while pile temperatures are markedly reduced during winter when the heat extraction device is active, the amount of “residual” cooling left at the end of summer is quite small, particularly in soils with a discrete freezing point (solid lines in Figure 9). Most of the heat removed through the pile during its active period is quickly replaced by heat that continues to flow from all sides into the cooled region while the pile is inactive.

The effect of a freezing range in the soil is again seen to be beneficial (see the dashed curve in Figure 9), since the temperature rise during the summer is slower because a considerable amount of heat is required to melt part of the soil moisture as the freezing point is approached. A similar

dampening effect is observed during winter, where soil temperatures remain somewhat above those of the corresponding case with a discrete freezing point, even though more heat is removed: in the example calculation, the pile with $3.0 \text{ W/m}^2 \text{ K}$ removed $5.1 \times 10^9 \text{ J}$ during the first winter from the silt with freezing range, and $4.8 \times 10^9 \text{ J}$ from the standard soil.

Temperatures at the pile-soil interface are an important design criterion for structural piles in permafrost. Adfreeze bond strength, soil shear strength, and long-term creep are functions of soil temperature. In some soils, allowable loads per unit length of pile may be drastically reduced near the freezing point. Thus, the pile length required to carry a given load becomes a function of the temperature profile along the pile-soil interface. Such temperature profiles are shown in Figure 10 for the standard soil and three soils with freezing ranges as given in Figure 1. All other soil properties were left unchanged. The curves show maximum temperatures at the end of the third summer after installation of a thermal pile with 46 cm diameter, 7.6 m length below ground, and a heat transfer coefficient of $3.0 \text{ W/m}^2 \text{ K}$. Slightly lower pile temperatures are predicted for subsequent summers even though the permafrost away from the pile is gradually degrading due to the placement of the gravel pad.

With temperature profiles like those given in Figure 10, pile length requirements for normal pipeline applications are not expected to become excessive. For instance, based on data presented by Croy,⁷ the average “sustained adfreeze strength” for a slurried pile in silt with the temperature profile as given in Figure 10, would be of the order of 9 N/cm^2 for the lower 6 m of pile embedment. Thus, the

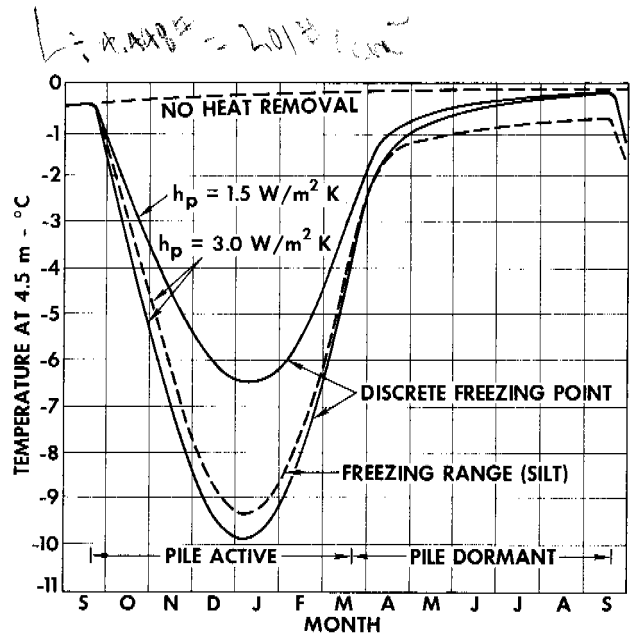


FIGURE 9 Temperature at 4.50-m depth adjacent to thermal pile during first year after installation in -0.5°C permafrost with 60-cm gravel pad.

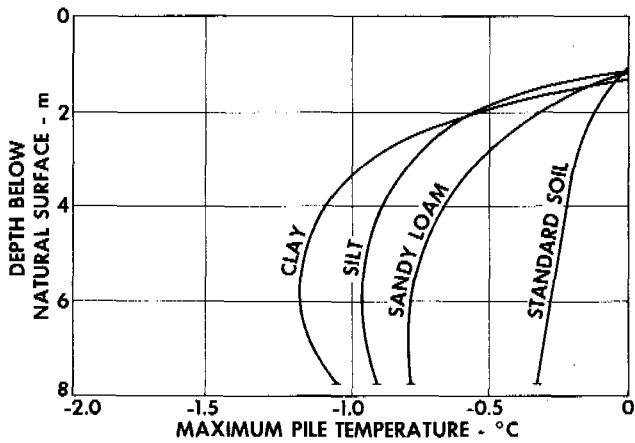


FIGURE 10 Maximum pile temperature profiles after 3 years for -0.5°C permafrost with 60-cm gravel pad; $h_p = 3.0 \text{ W/m}^2 \text{ K}$, pile diameter: 46 cm, length: 7.6 m below natural surface.

pile would be able to carry a nominal load of the order of $78 \times 10^4 \text{ N}$ or about 80 metric tons. Larger pile loads could be accommodated by proportionally longer piles. Increasing thermal pile efficiency beyond the heat transfer coefficient of $3 \text{ W/m}^2 \text{ K}$ produces relatively small benefits in terms of a further reduction of summer temperatures at the pile-soil interface.

GRAVEL BERMS

This section presents results of computer simulations for a continuous gravel berm, 1.8 m thick, 6 m wide at the top, and 13.2 m wide at the bottom, which is placed on warm (-0.5°C) permafrost at the end of the summer season, i.e., when the active layer is thawed. Surface conditions are listed in Table III (set II). Figure 11 shows the berm profile and the predicted meltfront locations for permafrost composed of the standard soil.

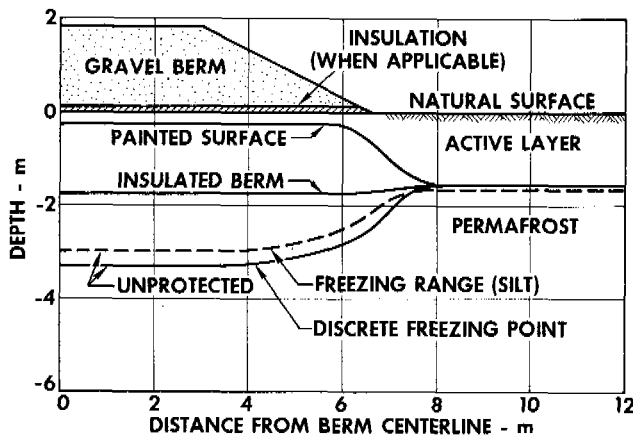


FIGURE 11 Thaw fronts after 20 years for a gravel berm on warm (-0.5°C) permafrost.

Without special means for permafrost protection, the gravel cover is expected to initiate progressive thawing, which is predicted to reach a depth of 3.3 m below the natural surface after 20 years. The dashed line in Figure 11 indicates that the depth of thaw is somewhat reduced (to 3 m) if unfrozen moisture below 0°C is taken into account.

Two means of permafrost protection under the gravel berm have been considered: insulation and white paint. A 5-cm layer of insulation with 0.035 W/mK conductivity placed on the natural surface below the berm would reduce the rate of thaw in the underlying permafrost to essentially zero. However, the active layer below the insulation never refreezes, and the frozen ground below is gradually warming up to 0°C —an indication that the permafrost is unstable. Similar conditions can be expected when the gravel is placed on a layer of insulating organic material, such as peat moss, that may be present under the natural surface.

Significant improvement in permafrost stability is indicated by the curve showing depth of thaw for a white-painted gravel surface. The permafrost level below the berm is raised almost to the level of the original surface, and the average permafrost temperature is lowered by about 1.5°C . Thus, the permafrost regime below the berm would be quite stable. Thawing below the berm could be eliminated entirely if both white paint and insulation were used for thermal protection; however, in this case, it may take several years before the active layer below the insulation freezes back completely if the berm is constructed during the summer.

Radiative surface properties assumed for the white paint are as listed in Table II. They are believed to represent a conservative estimate for a rough gravel surface sprayed with a suitable commercial paint.^{8,11} They do not account for possible long-term degradation from weathering, dust accumulation, or traffic. However, the results presented above would indicate that considerable deterioration of the white surface can be tolerated before repainting will be necessary. In fact, in the example, the permafrost was found to remain stable as long as the short wave emissivity of the painted surface was below 0.50.

EXPERIMENTAL EVALUATION OF THERMAL PILE DESIGNS

This section presents some results of a laboratory study that was carried out to confirm that various types of thermal piles could be designed to achieve the heat removal rates required for structural piles in marginal or degrading permafrost. Test specimens included a single phase device ("Balch" tube) and several two-phase devices (reflux boilers or thermosiphons). The tests indicated that each type could be designed to exceed requirements for thermal pile designs with an effective heat transfer coefficient of $3 \text{ W/m}^2 \text{ K}$ per unit area of below-ground pile surface. Based on the results pre-

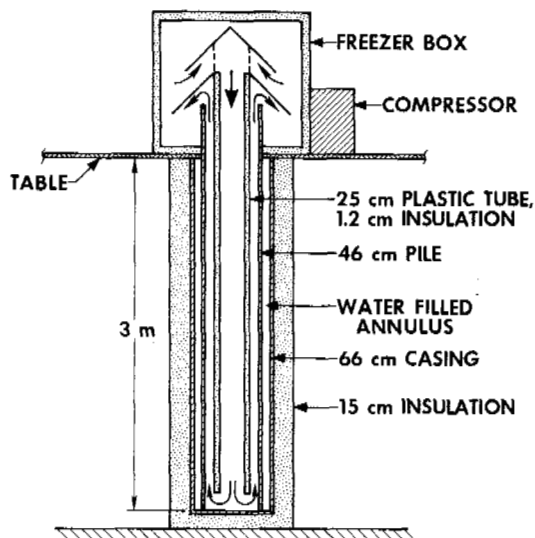


FIGURE 12 Experimental air convection pile.

sented in the preceding section, this value is judged to be adequate for general applications involving large-diameter piles in the zone of discontinuous permafrost. Detailed results of these tests will not be presented here, since more extensive data on each of the systems considered is already available in the literature.^{2,13,14,20}

In addition to the closed systems discussed above, we have also investigated an open system in which ambient air is the convecting fluid. The concept was brought to our attention by W. T. Black and H. R. Peyton.⁵ Natural convection has been observed previously in relatively small piles that were equipped with inner ducts to facilitate forced air circulation.¹⁸ While the efficiency of natural air convection in small piles will be low, the concept may have merits as a permafrost protection scheme in connection with the large-diameter piles considered in this study.

The air convection pile concept was tested with the apparatus shown schematically in Figure 12. For practical applications, some special pile head design will be needed to prevent rain, snow, and wildlife from entering the pile. The conical covers indicated in Figure 12 are only an example of a variety of possible pile head configurations.

Air starts to circulate spontaneously through this pile when the temperature in the freezer box is lowered below the temperature of the water bath. Depending on initial conditions, i.e., temperature distributions in the freezer box, the pile, and the inner tube, the flow may be in either of the two possible directions. However, the direction indicated by arrows in Figure 12 was found to be more stable and more efficient ("normal" flow). Sometimes, when flow had started in the "reverse" direction, it would spontaneously switch to "normal" flow, when a certain temperature difference between the freezer and the water bath was exceeded.

Results of heat flux measurements for the air convection pile are shown in Figure 13. The rate of heat removal was determined from the change in water bath temperature with time and corrected for heat flow through the outer walls of the water bath. The heat flux is plotted as a function of the difference between the average water bath temperature and the freezer box air temperature, measured 15 cm above the box bottom. The two curves in Figure 13 are for an open air convection pile as shown in Figure 12, but with the conical pile covers removed, and for a simple open pile without inner tube. The contrast between the two curves clearly shows the benefits derived from the presence of the inner tube that serves to guide the flow induced by the thermal instability into a single convection loop, extending from the surface to the bottom of the pile. Without the tube, convection takes place in a more irregular and less efficient cellular pattern typical of free convection.

According to Figure 13, the heat flux through the air convection pile is about 400 W at a temperature difference of 20 °C. This corresponds to an effective heat transfer coefficient of 4.6 W/m²K per unit area of pile surface in contact with the water bath, well above the value of 3.0 W/m²K assumed in the numerical simulation of permafrost protection systems. The efficiency of the air convection pile was reduced by about 25 percent when operating in the reverse flow mode and by about 15 percent when the pile head was fitted with conical covers as shown in Figure 12. On the other hand, turbulent mixing of inlet and outlet air streams in the confined freezer box may have resulted in some loss of efficiency that could be avoided in field installations.

More work remains to be done to optimize inner-tube-

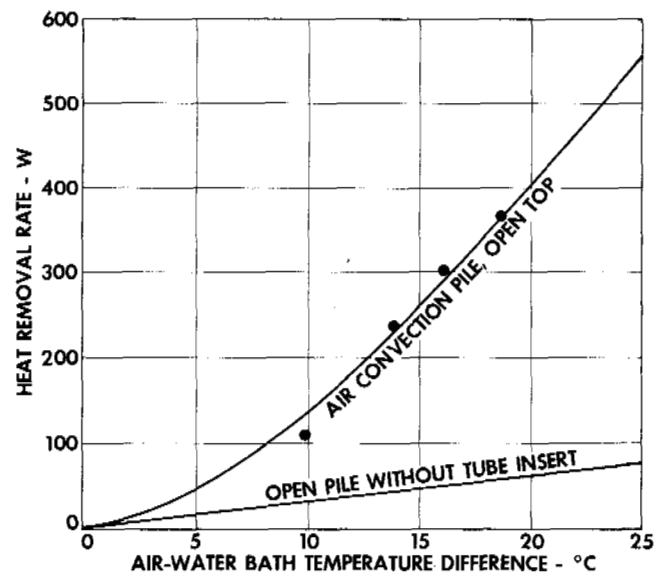


FIGURE 13 Heat removal rates for experimental air convection pile.

diameter and pile-head configuration for the air convection pile and to determine the effect of pile length and insulation. A theoretical model of the device is being developed. Preliminary analysis shows that pile efficiency (in terms of the effective heat transfer coefficient) will be reduced somewhat with increasing pile length and that the benefits of insulating the inner tube are small, especially in long piles. A steel tube made of sheet metal is probably adequate.

The air convection pile may be subject to wind-induced (forced) convection during summer. Special pile head designs may be required to minimize this effect. Or a shutoff device could be provided so that the entry ports or the inner tube can be closed during the summer.

CONCLUSIONS

The following conclusions can be drawn from results presented in this paper for a number of permafrost protection systems.

1. While the various schemes considered differ with respect to thermal efficiency and range of applicability, together they offer the technical means for providing adequate permafrost protection for buried and elevated pipelines in arctic and subarctic regions under most conditions of practical interest.
2. Insulation placed around a warm buried pipeline is an efficient means of reducing heat transfer to the ground and, consequently, reducing the rate of thaw. In cold permafrost, insulation alone can prevent the formation of a permanent thaw plug around the pipeline.
3. Insulation and other passive protection systems for a warm buried pipeline tend to become very bulky in warm permafrost if no thawing is to be allowed below the line.
4. Mechanical refrigeration can provide complete permafrost protection below an insulated buried pipeline under all climatic conditions of interest. Refrigeration rates required in such a system are not excessive.
5. Thermal piles equipped with natural convection devices for heat removal during winter can be designed to prevent permafrost degradation around pile supports for an elevated pipeline. Both single-phase and two-phase closed systems are available for this purpose. In large-diameter piles, an open air convection system can also be used.
6. Temperatures at the pile-soil interface may rise to near the freezing point during the summer when the thermal pile is inactive. In fine-grained soils, the presence of unfrozen moisture below 0 °C has a significant beneficial effect on maximum summer temperatures. Benefits of increasing the thermal efficiency of the convection device are relatively small.
7. White paint and insulation can offer permafrost protection for gravel berms. Painting the gravel surface with a suitable reflective paint will reduce mean annual surface

temperatures and can stabilize permafrost that would otherwise be unstable. An insulating layer below the berm is effective in reducing the rate of permafrost degradation, but its effect on mean ground temperature is small.

8. Latent heat effects play an important role in the thermal performance of permafrost protection systems. These effects are generally beneficial, particularly in fine-grained soils where the total moisture content and the amount of unfrozen moisture below 0 °C tend to be high.

9. The computer model used in this study does not account for effects of convection in the soil. Convection of heat by water draining through coarse-grained soil on a slope could significantly reduce the benefits derived from any of the permafrost protection systems considered.

ACKNOWLEDGEMENTS

This work was partly funded by the Alyeska Pipeline Service Company. The authors wish to thank various Alyeska personnel, in particular H. R. Peyton, for many helpful comments and discussions.

REFERENCES

1. Anderson, D. M., and A. R. Tice. 1972. Predicting unfrozen water contents in frozen soils from surface area measurements. High. Res. Rec. No. 393. p. 12-18.
2. Babb, A. L., D. M. Chow, K. L. Garlid, and R. P. Popovich. 1971. The thermo tube, A natural convection heat transfer device for stabilization of arctic soils in oil producing regions. Paper presented at 46th Annual Fall Meeting, Society of Petroleum Engineers of AIME, New Orleans, Louisiana.
3. Berg, R. L. 1969. Passive methods of thermal control. Tech. Note. U.S. Army Cold Regions Research and Engineering Laboratory, Hanover, New Hampshire. (Unpublished)
4. Berg, R. L. 1968. Energy balance on a paved surface. Tech. Note. U.S. Army Cold Regions Research and Engineering Laboratory, Hanover, New Hampshire. (Unpublished)
5. Black, W. T., and H. R. Peyton. 1971. Personal communication.
6. Buettner, K. J., and C. D. Kern. 1965. The determination of infrared emissivities. J. Geophys. Res. 70(6):1329-1337.
7. Crory, F. E. 1966. Pile foundations in permafrost, p. 467-476. *In* Permafrost: Proceedings of an international conference. National Academy of Sciences, Washington, D.C.
8. Gubareff, G. G., J. E. Janssen, and R. H. Torborg. 1960. Thermal radiation properties survey. 2nd ed. Minneapolis-Honeywell Regulator Co., Minneapolis, Minnesota.
9. Johnson, P. R. 1971. The IAEE heat sink refrigeration system, p. 622-632. *In* Proceedings of the symposium on cold regions engineering. University of Alaska, College.
10. Kersten, M. S. 1949. Laboratory research for the determination of the thermal properties of soils. Eng. Exp. Sta. Univ. Minn. Bull. 28.
11. Kritz, M. A., and A. E. Wechsler. 1967. Surface characteristics effect on thermal regime, phase II. Tech. Rep. 189. U.S. Army Cold Regions Research and Engineering Laboratory, Hanover, New Hampshire.
12. Lachenbruch, A. H. 1970. Some estimates of the thermal effects of a heated pipeline in permafrost. Geol. Surv. Circ. 632.
13. Larkin, B. S. 1970. An experimental study of a two-phase thermosiphon tube. Paper presented at the 84th Annual Meeting of the Engineering Institute of Canada, Ottawa, Ontario.
14. Long, E. L. 1966. The Long thermopile, p. 487-491. *In* Perma-

- frost: Proceedings of an international conference. National Academy of Sciences, Washington, D.C.
15. Lunardini, V. J. 1970. The thermal properties of permafrost. Paper presented at the 23rd Canadian Geotechnical Conference, Banff, Alberta.
 16. Miller, J. M. 1971. Pile foundations in thermally fragile frozen soils, p. 34-72. *In* Proceedings of the symposium on cold regions engineering. University of Alaska, College.
 17. Nersisova, Z. A., and N. A. Tsytoich. 1966. Unfrozen water in frozen soils, p. 230-233. *In* Permafrost: Proceedings of an international conference. National Academy of Sciences, Washington, D.C.
 18. Reed, R. E. 1966. Refrigeration of a pipe pile by air circulation. Tech. Rep. 156. U.S. Army Cold Regions Research and Engineering Laboratory, Hanover, New Hampshire. p. 7.
 19. Scott, R. F. 1964. Heat exchange at the ground surface. Monograph II-A1. U.S. Army Cold Regions Research and Engineering Laboratory, Hanover, New Hampshire.
 20. Waters, E. D. 1973. Stabilization of soil and structures by passive heat transfer devices. Paper to be presented at 74th National Meeting of AIChE, March 11-15, New Orleans, Louisiana.
 21. Wechsler, A. E., and P. E. Glaser. 1966. Surface characteristics effect on thermal regime, phase I. Spec. Rep. 88. U.S. Army Cold Regions Research and Engineering Laboratory, Hanover, New Hampshire.
 22. Weissman, T. 1971. New system to beat permafrost. *Oilweek*, 22(29):23-24.
 23. Wheeler, J. A. 1973. Simulation of heat transfer from a warm pipeline buried in permafrost. Paper to be presented at 74th National Meeting of AIChE, March 11-15, New Orleans, Louisiana.

PERMAFROST-RELATED ENGINEERING GEOLOGY PROBLEMS POSED BY THE TRANS-ALASKA PIPELINE

Reuben Kachadoorian and Oscar J. Ferrians, Jr.

U.S. GEOLOGICAL SURVEY
Menlo Park, California

INTRODUCTION

The proposed trans-Alaska pipeline is designed to transport approximately 318 000 m³ of hot crude oil per day through a 1.219 m diameter pipe from arctic Alaska along a 1 270-km route to Valdez, an ice-free port located on an arm of Prince William Sound in south central Alaska (Figure 1). All but the southern 40 km of the pipeline route is within the permafrost region and much of the pipeline may be buried. The pipeline system also would include pump stations, camp sites, airfields for use during construction and operation of the pipeline, a communications system, access roads, and borrow and quarry sites for construction materials. The marine terminal site at Valdez would consist of a tank farm, a dock, and related facilities. A fleet of tankers would transport crude oil from the terminal to destination ports.

This paper describes the more critical permafrost-related engineering problems that could affect the mechanical integrity of the pipe and the local environment. The solutions to many of the problems are simple. However, the solutions to the more complex problems will require the cooperation of workers in many disciplines such as engineers, geologists, hydrologists, and botanists.

The proposed pipeline originates at Prudhoe Bay on the Arctic Ocean, heads south along the Sagavanirktok and the Atigun rivers, and crosses the Brooks Range through a small pass at an altitude of 1 460 m. The pipeline route continues south, first following the Dietrich River and then the Koyukuk River. The route crosses the Yukon River near the center of Alaska and passes about 12 km east of Fairbanks. From Fairbanks the proposed pipeline route heads southeast several kilometres east of the Tanana River until it crosses it near Delta Junction. From Delta Junction the route follows the Delta River and the Richardson Highway south to Isabel Pass (altitude 1 005 m), in the Alaska Range. From here the route generally parallels and is near the Richardson Highway all the way to the thermal station at Valdez.

Mean annual permafrost temperatures range from about -9 °C on the North Slope to nearly 0 °C at the southern boundary of the permafrost region. Ice in the permafrost ranges from extremely large masses in sediments of the North Slope and fine-grained sediments south of the Brooks Range to essentially none in bedrock and some coarse-grained, well-drained gravels.

The temperature of the crude oil will be about 58 °C when it enters the pipeline. At maximum flow (318 000 m³ per

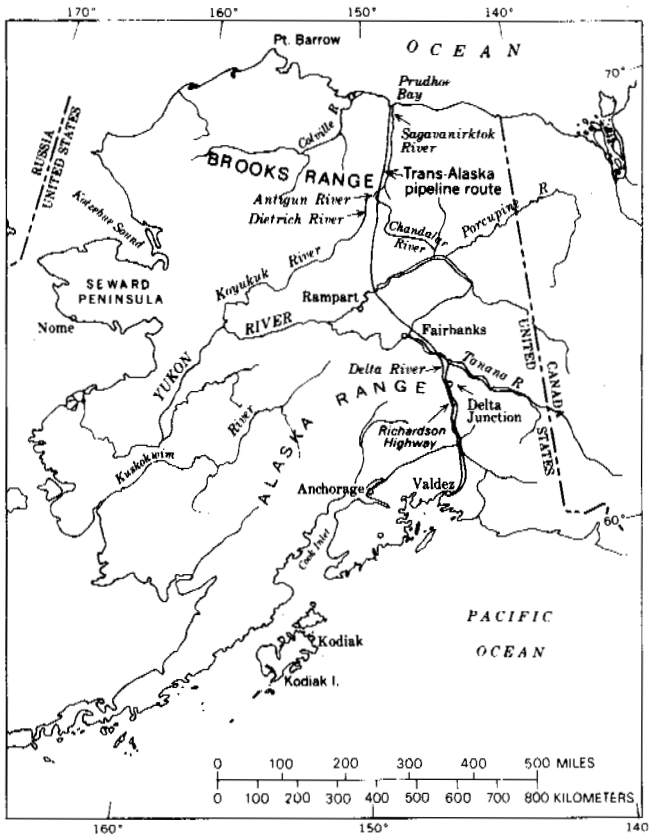


FIGURE 1 Route of the trans-Alaska pipeline.

day), pumping and friction will increase the temperature, and possibly the oil will have to be cooled while in transit so that it will not exceed the pipeline's proposed maximum operating temperature of 63 °C. This maximum operating temperature is limited by the permissible thermal stress on the pipe.

PERMAFROST-RELATED ENGINEERING GEOLOGY PROBLEMS

As proposed, 700 km of the pipeline, or 55 percent, would be buried, and the remaining 570 km, or 45 percent, would be elevated. Approximately 660 km of the buried pipe will be in the permafrost region.

A large hot-oil pipeline buried in permafrost for hundreds of kilometres has no engineering precedent. Unique effects arise primarily from the loss of strength and change in volume of ice-rich soil when it is thawed by heat from the pipe.⁹ These effects can be anticipated and the pipeline system must be designed to minimize the possibility of breaking the pipe because of soil instability and settlement. Secondly, proper construction procedures can minimize the mechanical effects of thawing and heat upon the natural geologic, hydrologic, and biological processes.⁵

Lachenbruch⁹ has estimated that an uninsulated pipe will

cause thawing to a depth of 8–10 m after a few years of near capacity operation in typical materials. The thawing would continue at a progressively decreasing rate, but in most places thermal equilibrium would not be achieved during the life of this system. Insulation will tend to increase pipe temperature, but, if the temperature is controlled, insulation can reduce permafrost thawing substantially. However, the amount of insulation required to eliminate thawing is so large as to make its use impractical. It can be calculated from Lachenbruch's Eq. B-12 and his Figure 6.

In addition to unique effects from thawing permafrost, a pipeline across Alaska whether buried or elevated is beset with potential problems from strong earthquakes, landslides, avalanches, rock slides, glacier surges, and severe seasonal floods. These problems are not new to pipeline engineers, but some may be complicated by the presence of permafrost.

Engineering geology maps of the entire trans-Alaska pipeline route have been prepared.^{1,2,3,4,6,7,8,10,11} These maps, at a scale of 1:125 000, show geologic structure, type of bedrock and surficial deposits, and the engineering characteristics of the mapped units along the route. The maps identify where the various types of engineering geologic problems could be encountered along the route.

Problems associated with permafrost relate primarily to the effects of surface disruption and effects of heat from the hot-oil pipeline once the system is operational. The two types of problems, of course, are not completely independent. For example, if drainage is impeded during construction and the water enters the "thaw plug" developed around the buried hot-oil pipeline, the flowing water can greatly accelerate thawing of permafrost.

Problems Related to Surface Disruption

During both the construction and maintenance phases of the pipeline, damage to the tundra by construction equipment must be minimized. If it is not, underlying permafrost could thaw, and, in ice-rich areas, ponds, small streams, soil flowage, and erosion from surface runoff water might result. These effects, which can be irreversible, could jeopardize the integrity of the pipe whether it were buried or elevated.

A constructed gravel pad up to a metre thick has been proposed to facilitate construction and maintenance of the pipeline. If the pad thickness is not adequate, the permafrost beneath it will thaw and differential settlement or slope failure could result locally, especially where the pad was underlain by ice-rich sediments. This problem could be more severe on slopes and where drainage has been impeded. Locally, where the temperature of the permafrost is close to 0 °C, the thickness of the pad required to prevent thawing of the permafrost could be so great that it would be impractical to construct. In such areas, winter construction can minimize disruption of the protective vegetation cover and limit adverse effects to the surrounding terrain.

Once the pipeline system is completed, surface drainage could be affected by the construction pad, berms, cuts, and other structures associated with the pipeline. These effects caused by disruption of surface drainage could be significant if proper control measures are not taken, and, even with proper measures, these effects cannot be completely eliminated.

After the pipeline is buried and before hot oil is transmitted through it, frost heaving could damage the pipe in areas where the soils surrounding the pipe are frost-susceptible.

Problems Related to Effects of Hot Oil

The most important thermal effects of heat loss from the pipe to the surrounding soil are the loss of strength and change in volume of frozen soil when its ice, particularly if in segregated masses, thaws to water. Instability and differential thaw settlement may follow; the severity naturally depends on the type and ice content of the soil and slope and drainage conditions.

THAW PLUG STABILITY

During and after thawing, ice-rich soils can lose much of their strength, or even liquefy (i.e., go into a quick condition).⁹ As the thaw plug or cylinder grows, excess water will be generated at the thawing interface. If the water drains upward to the ground surface as fast as it is generated, the grains will settle and soil will compact and gain strength. If, however, the permeability of the thawed material is so low the thaw water does not escape as fast as it is generated, part or all of the thaw cylinder will be materially weakened and could behave as a fluid. When such weakening occurs in sloping terrain, soils around the pipe could flow downhill and cause gross pipe deformation and rupture. For anticipated thaw rates, this condition is not likely to occur where the bulk permeability of the thawed material is 10^{-6} cm/s or greater.⁹

Thawed soils can also become liquefied when subjected to seismic vibrations. If this were to occur in sloping terrain, soils around the pipe could flow and damage the pipe.

DIFFERENTIAL SETTLEMENT

Uneven settlement from thawing of inhomogeneous permafrost materials, soil collapse over ice wedges and other ice masses, and differential flotation or sinking in liquefied soils could severely deform the pipe. Sags of 5-10 cm over spans of 15-20 m will require maintenance. If the buckling stresses continue long enough, severe pipe deformation could result. Therefore, it is necessary that a monitoring system be used that will detect deflections in the pipe before they become critical.

DIVERSION OF STREAM CHANNELS

Heat from the pipe buried in a river flood plain would alter seasonal frost distribution and affect formation of river ice. Consequently, in winter the surface and subsurface flow

characteristics could be changed so that major channels could be deflected to the right-of-way, possibly causing disruptive erosion and icings.

OTHER ENGINEERING GEOLOGY PROBLEMS

Although not directly related to permafrost, the effects of seismic activity, corrosion, and problems associated with stream crossings can be accentuated by the presence of permafrost.

Seismic Activity

Any point along the southern two thirds of the proposed trans-Alaska route can be subjected to a large-magnitude earthquake (greater than 7.0 on the Richter scale), and the probability that one or more large-magnitude earthquakes would occur in the vicinity of this portion of the route during the lifetime of the pipeline is extremely high. Because all elements of the proposed pipeline system would be subjected to the effects of strong vibratory ground motion during a large-magnitude earthquake and because large ground displacements could occur along a fault by an earthquake, realistic earthquake-design criteria must be carefully applied to minimize the possibility of pipeline rupture. In addition, at critical localities special contingency plans are needed to limit any potential oil spill that could occur if the pipeline did rupture. An earthquake monitoring system along the pipeline route will be a further aid.

Corrosion

External corrosion is known to cause leaks in existing buried pipelines, and experience with the small diameter pipeline between Haines and Fairbanks, Alaska, indicates that corrosion can be a serious problem in permafrost regions. Coating of the pipe and the installation of an electrical system (cathodic protection) is necessary to eliminate or minimize leaks due to corrosion. For a number of reasons cathodic protection will be more difficult to accomplish in areas underlain by permafrost than it would be in nonpermafrost areas.

Stream Crossings

The proposed pipeline alignment crosses numerous streams, and along many stretches of the route parallels and occurs within stream channels and floodplains. Because of the special engineering geology problems posed in these situations, each stream crossing and floodplain area requires individual study so that special design measures needed to minimize adverse environmental effects can be selected. The most important engineering geologic considerations for floodplains and stream crossings are maximum depth of scour of streams so that the pipe can be buried below this critical depth; maximum limits

of the "Standard Project Flood" so that structures can be located or designed so that they would not be seriously damaged by flooding; potential for bank erosion and for erosion caused by channel changes in areas where the pipeline has steeper gradient than that of the adjacent stream; consequences of auffs not forming where it normally would because of the heat from the buried pipe; and, determining whether or not groundwater, under hydrostatic pressure where confined by seasonal frost, would move upward through the thawed zone around the pipe with enough pressure to liquefy the supporting soils.

SUMMARY

The design, construction, and maintenance of the proposed trans-Alaska pipeline system in the permafrost region of Alaska poses special engineering problems. The severity of problems resulting from soil instability, differential settlement, and erosion of thawed soil depends on the type and ice content of the soil and the slope and drainage conditions. Soil instability, differential settlement, erosion, and disrupted surface and subsurface drainage can result in loss of support and rupture of the pipe. Consequently, the effects of thawing permafrost and of erosion must first be determined and then minimized or controlled by proper design, proper arctic and subarctic construction procedures, and an adequate monitoring system. Some potential effects are so serious that contingency plans must be devised. These actions are necessary in order to maintain the mechanical integrity of the pipeline and to avoid degradation of the adjacent terrain.

REFERENCES

1. Ferrians, O. J., Jr. 1971. Preliminary engineering geologic maps of the proposed trans-Alaska pipeline route—Beechey Point and Sagavanirktok quadrangles. U.S. Geol. Survey open-file report. Scale 1:125 000.
2. Ferrians, O. J., Jr. 1971. Preliminary engineering geologic maps of the proposed trans-Alaska pipeline route—Philip Smith Mountains quadrangle. U.S. Geol. Survey open-file report. Scale 1:125 000.
3. Ferrians, O. J., Jr. 1971. Preliminary engineering geologic maps of the proposed trans-Alaska pipeline route—Gulkana quadrangle. U.S. Geol. Survey open-file report. Scale 1:125 000.
4. Ferrians, O. J., Jr. 1971. Preliminary engineering geologic maps of the proposed trans-Alaska pipeline route—Valdez quadrangle. U.S. Geol. Survey open-file report. Scale 1:125 000.
5. Ferrians, O. J., Jr., R. Kachadoorian, and F. W. Greene. 1969. Permafrost and related engineering problems in Alaska. U.S. Geol. Survey Prof. Paper 678. 37 p.
6. Kachadoorian, R. 1971. Preliminary engineering geologic maps of the proposed trans-Alaska pipeline route—Chandalar and Wiseman quadrangles. U.S. Geol. Survey open-file report. Scale 1:125 000.
7. Kachadoorian, R. 1971. Preliminary engineering geologic maps of the proposed trans-Alaska pipeline route—Bettles and Beaver quadrangles. U.S. Geol. Survey open-file report. Scale 1:125 000.
8. Kachadoorian, R. 1971. Preliminary engineering geologic maps of the proposed trans-Alaska pipeline route—Livengood and Tanana quadrangles. U.S. Geol. Survey open-file report. Scale 1:125 000.
9. Lachenbruch, A. H. 1970. Some estimates of the thermal effects of a heated pipeline in permafrost. U.S. Geol. Survey Circ. 632. 23 p.
10. Weber, F. R. 1971. Preliminary engineering geologic maps of the proposed trans-Alaska pipeline route—Fairbanks and Big Delta quadrangles. U.S. Geol. Survey open-file report. Scale 1:125 000.
11. Weber, F. R. 1971. Preliminary engineering geologic maps of the proposed trans-Alaska pipeline route—Mount Hayes quadrangle. U.S. Geol. Survey open-file report. Scale 1:125 000.

NOTE

- [1] Publication authorized by the Director, U.S. Geological Survey.

LONG-TERM EFFECTS OF VEGETATIVE COVER ON PERMAFROST STABILITY IN AN AREA OF DISCONTINUOUS PERMAFROST

Kenneth A. Linell

U.S. ARMY COLD REGIONS RESEARCH AND
ENGINEERING LABORATORY
Hanover, New Hampshire

INTRODUCTION

In 1946, the U.S. Army Corps of Engineers started a long-term experiment at its Farmers Loop Road Field Station near Fairbanks, Alaska, to investigate the effects of climatic and surface conditions on ground temperatures. This paper presents information obtained as part of these studies, on the relationship between vegetative cover and permafrost degradation. The data extend through 1972, 26 years after the start of the experiment. Previous limited data analyses have not extended beyond 15 years.^{3,6,7}

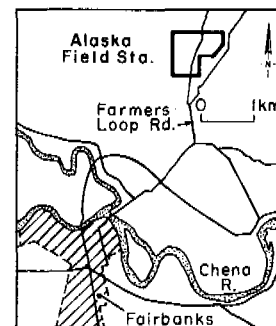
The study site is located about 4 km northeast of Fairbanks (Figure 1). The terrain at the station has a comparatively smooth, gentle slope to the west, providing good surface drainage except at the lowest elevations where swampy conditions exist. The area is located partly on the lower colluvial slopes of the rock upland of Birch Hill to the southeast and partly on the edge of the valley fill. The ground under the station is permanently frozen, with the depth of permafrost approaching 60 m near Farmers Loop Road. The permafrost becomes thinner with increasing elevation on Birch Hill and is absent at the higher elevations.

Fairbanks has a continental climate, being sheltered from maritime influences by surrounding mountain ranges. The mean annual temperature is -3.44°C , with extremes of 33.9°C and -54.2°C . During June, July, and August when the sun is above the horizon over three fourths of the day, the average maximum daily temperatures reach about 22°C . From November to March when the sunshine duration ranges down to less than 4 h a day, temperatures normally fall below -18°C . During December and January maximum temperatures are usually below -18°C .

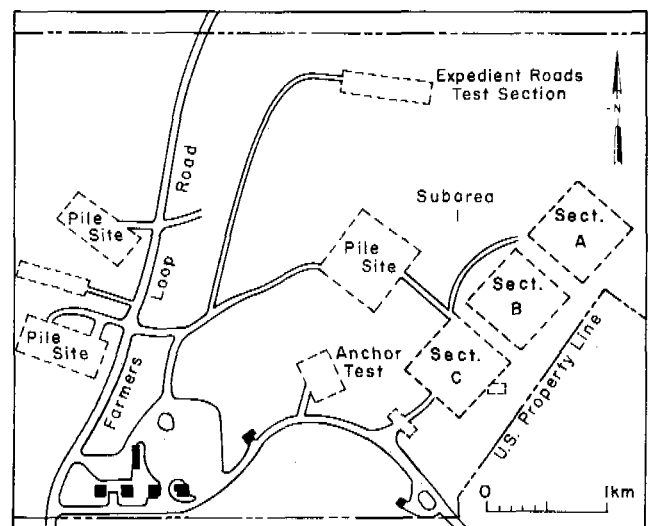
The amount of cloudiness is usually low, particularly between February and April. Wind speeds are particularly low during winter months. Precipitation normally follows a regular pattern and the average annual precipitation is 287 mm. Precipitation increases through the summer months to a maximum in August. Precipitation decreases from September through December. Snowfall begins to increase toward the end of December and reaches a maximum in January.

Average annual snowfall is 1.54 m. April has the lowest monthly precipitation and greatest percentage of sunshine.

The average last day of freezing temperatures in the spring is 21 May and the average first occurrence of freezing temperatures in the fall is 30 August. The mean air freezing and thawing indexes are 3 200 and 1 884 $^{\circ}\text{C}$ -days, respectively.



a. Vicinity Map



b. Alaska Field Station

FIGURE 1 Location of study site.

TEST AREAS

Three 61- by 61-m test areas, designated A, B, and C, were laid out (Figure 1). Permafrost is estimated to extend to a depth of at least 30 m under the test sections. Slope of the ground surface is variable but averages about 4 percent. The soil conditions under the test sites are typical of those over the sloping portion of the Farmers Loop Road test area, consisting of tan silts near the surface and gray silts at depths exceeding 1.4 m, with tan and gray layers at intermediate depths, all classified as ML-Vr and -Vs in the Unified Soil Classification System and Minto silt loam in agricultural terminology.¹⁰ The silt contains layers of peat normally less than 80 mm thick. Organic silt is also encountered, both as distinct layers and as small inclusions. Table I and Figure 2 show a typical boring log, with data on water content and density, and gradation. Soils are identified in accordance with the Unified Soil Classification System.

The organic and inorganic silts with peat layers extend to depths of 15-45 m at the station and sands and gravels are encountered below these materials. Downhill drainage occurs through the annual thaw zone in summer, and the ground is normally saturated to within 0.3 m of the surface or less.

Section A (Figure 1) consists of an undisturbed area with its natural cover of vegetation left intact. The area can be classified as a subarctic taiga forest with a dense growth of white and black spruce attaining heights of 9-15 m. The ground surface is covered by a thick mantle of moss with low-bush cranberries, blueberries, Labrador tea, and other low plant growth. Components of the typical ground cover

TABLE I Boring Log and Soil Properties^a

Depth below Surface (m)	Description of Soil	Moisture Content (%)	Dry Density (kg/m ³)
0.0 -0.25	Pt, peat	258	320
0.25-0.55	ML, V _s -silt with peat (stratified)	26	1 520
0.55-1.2	ML, V _s -silt with peat (stratified)	26	1 420
1.2 -2.5	ML, V _s -silt with peat (stratified)	29	1 455
2.5 -3.9	ML, V _{r,s} -silt with peat (stratified)	37	1 310
3.9 -4.8	ML, V _{r,s} -silt with peat (stratified)	37	1 280
4.8 -6.1	ML, V _{r,s} -silt with peat (stratified)	38	1 280
6.1 -6.5	ML, V _{r,s} -silt with peat (stratified)	41	1 215
6.5 -7.3	ML, V _{r,s} -silt	37	1 280
7.3 -8.6	ML, V _{r,s} -silt	32	1 375
8.6 -9.5	ML, V _{r,s} -silt	33	1 375

^a Surface elevation = 155 m; all soil frozen; hole drilled, March 1946.

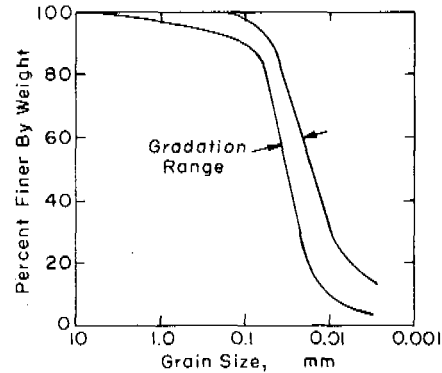


FIGURE 2 Gradation range of silt at Alaska Field Station; boring log and soils data, section C.

in forests of the Fairbanks area have been described by the Soil Conservation Service.¹⁰ The moss, in turn, is directly underlain by a 100- to 230-mm-thick layer of black organic material, not classified in this report as part of the vegetation.

Section B was originally covered by the same type of vegetation as section A, but all trees and brush were removed at the start of the experiment. Trees were cut off about 0.3 m above the moss without disturbing the tree roots. The section has been kept free of trees and high brush during the entire period since 1946. A dense growth of grasses, shrubs such as high-bush cranberries, fire weed, and low-brush shoots (including willow, alder, and dwarf birch) has developed, added to the original ground cover.

In section C, the surface vegetation and soil were stripped off to a depth of about 0.4 m. This area has been periodically restripped with a bulldozer from time to time since 1946 to remove grass and other vegetation whenever it began to become re-established sufficiently to significantly change the surface conditions. Since 1946, snow has been allowed to accumulate and dissipate on the three areas naturally. Surface movements in sections A and B have been restricted to a minimum amount of carefully controlled foot traffic to avoid compaction of snow in winter or damage to moss and other low vegetation in the summer.

At three locations in each of sections A, B and C, sub-surface temperature measurements have been made to a 10-m depth by thermocouples installed in 19-mm-diameter oil-filled pipes; vertical movement observations have also been made. Some groundwater measurements were also obtained at six groundwater wells installed on the perimeter of the sections. Probing to measure the depth of permafrost have been made from time to time at the end of the thaw season as a check on the subsurface temperature information. Only the thermocouple and probing data, relating to the position of the permafrost table, are considered in this paper.

RESULTS

Figure 3 shows the elevation of the permafrost table at the center of each of sections A, B, and C from 1946 through 1972. Also shown in Figure 3 are freezing and thawing indexes for each of these years.

Figure 4 shows a profile on the centerline that runs through the three sections, with the position of the permafrost table detailed at various elapsed times.

DISCUSSION

To better understand and illustrate the information in Figures 3 and 4, the degree-day information in Table II may be examined. The basic data were computed by the Permafrost Division in 1950⁷ and published by Carlson in 1952,³ covering one complete thawing and one complete freezing season. The air temperature data were collected by the U.S. Weather Bureau at Weeks Field, Fairbanks. The surface temperature values were obtained with thermocouples so installed that they were partially imbedded in the surface, below any vegetative cover.

The summertime surface degree-days in section C are nearer to being indicative of the total potentially available summer heat input than the air temperature degree-days because the former include substantial solar radiation input into the ground. The air temperatures were obtained by standard Weather Bureau procedures using shaded instrumentation. In the densely forested section A, surface degree-

days in the summer of 1947 were only about 30 percent of those in the stripped section C. In cleared but not stripped section B they were about 60 percent of those in section C. In the winter of 1947-1948, the freezing days in section A were higher than in section B, but section A was the only one of the three in which the surface freezing degree-days exceeded the thawing degree-days of the previous summer.

It is apparent from both the above data and Figures 3 and 4 that a dense tree cover such as exists in section A, together with its underlying ground cover, is a major factor in maintaining a stable permafrost condition in this area of relatively warm permafrost. Although forests are known to have relatively high absorptivity for incoming solar radiation, it is evident that the net effect of the dense tree cover at this location is to substantially reduce the amount of heat reaching and entering the ground in summer. The cooler, shallower annual thaw zone must, in turn, inhibit the rate of tree growth. These results are contradictory to those reported by Pihlainen⁹ at Inuvik, N.W.T., where after removal of trees and underbrush, but with moss cover left intact, the depth of annual thaw remained unchanged at about 0.6 m. However, mean annual air temperature at Inuvik is 6 °C lower.

It is believed that growth of grass, low shrubs, and small brush shoots that developed in section B after it was cleared, together with the numerous small tree stumps, has partially supported the winter snowcover in section B and reduced its density as compared with either section A or C. Thus, penetration of low temperatures into the ground in winter

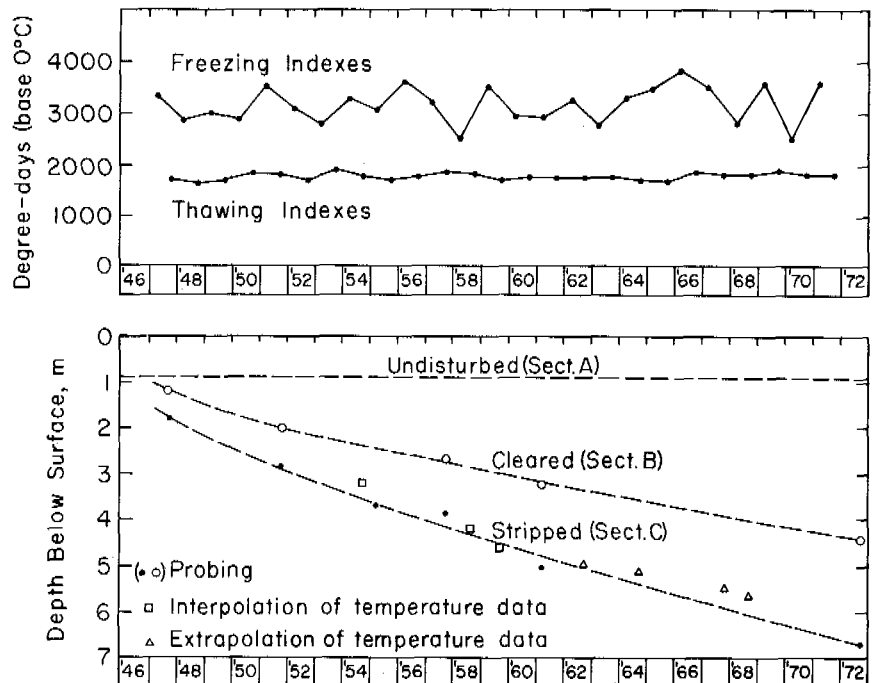


FIGURE 3 Climatic and degradation data versus time (in years).

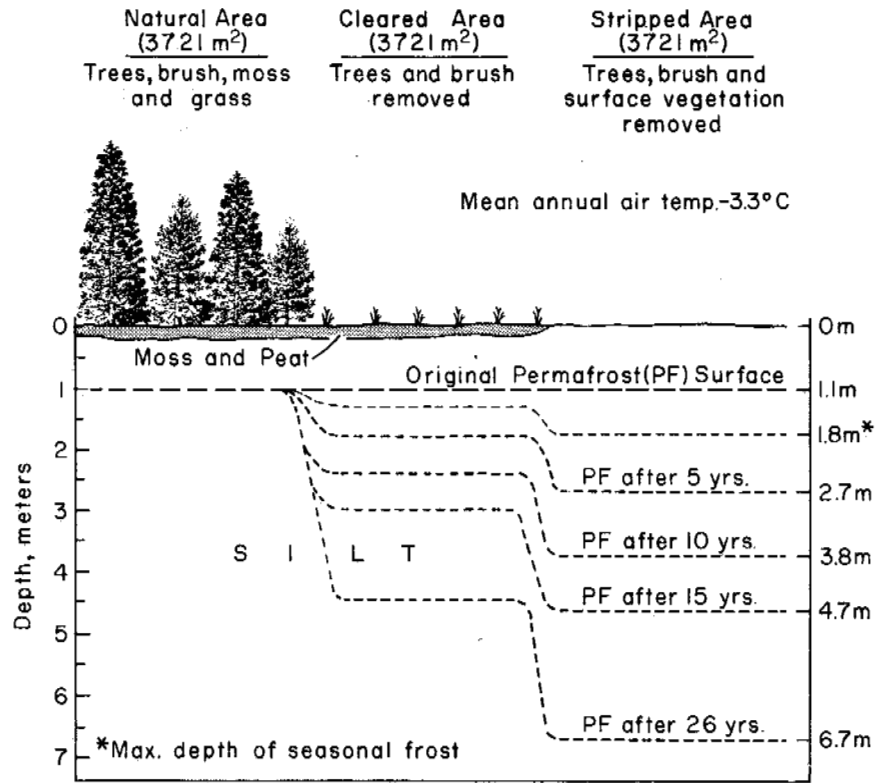


FIGURE 4 Permafrost degradation under different surface treatments over a 26-year period. Mean annual permafrost temperature ranges from about -0.5 °C at a depth of 10 m under natural, forested areas to about -0.2 °C where permafrost is degrading.

is minimized in section B, while at the same time there is better opportunity for heat to reach the ground surface in summer in section B than in section A. The resultant of these two effects is the I/F ratio of 1.78 shown in Table II for section B and permafrost degradation.

In a bare soil section such as C, not only is the albedo under summer conditions low, with maximum opportunity for heating of the ground from both solar input and direct contact with warm air, but at the same time the lower insulating value of the denser snowcover in combination with lack of surface vegetation allows more intense cooling in winter. As indicated in Table II, the surface thawing index

far exceeds the freezing index, with $I/F = 2.24$ and pronounced permafrost degradation occurs.

However, permafrost stability is not a function solely of freezing and thawing indexes. Rigorous analysis will not be attempted here. On the basis of an analysis that assumes that the temperature of soil below the depth of seasonal freezing is 0 °C, Carlson³ has offered as an approximation the criterion that for permafrost to exist the following relationship must be satisfied:

$$K_f/K_u > I/F,$$

TABLE II Degree-Day Data

Data Identification	°C-days		Ratio I/F
	Summer 1947 <i>I</i>	Winter 1947-1948 <i>F</i>	
Air temp. data	1 697 4/13/47 to 9/30/47	2 801 9/30/47 to 5/3/48	0.61
Surface temp. data section A	628 5/12/47 to 10/6/47	-794 10/6/47 to 5/10/48	0.79
Surface temp. data section B	1 233 4/28/47 to 10/6/47	-692 10/6/47 to 4/22/48	1.78
Surface temp. data section C	2 067 4/21/47 to 10/6/47	-922 10/6/47 to 5/3/48	2.24

where K_f = thermal conductivity of the frozen soil; K_u = thermal conductivity of the thawed soil; and I and F = the surface thawing and freezing indexes, respectively.

Kersten⁵ has published results of measurements of thermal conductivity of Fairbanks soils at 25 and 40 °C, at various moisture contents. At a nominal moisture content of 30 percent (compare with Figure 2), he obtained a value of the ratio K_f/K_u of 1.5 for a saturated Fairbanks silty clay. Extrapolation of similar data obtained for a Fairbanks silt from 24.3 to 30 percent moisture would yield a comparable ratio $K_f/K_u = 1.57$. Using either of the latter values, inspection of the I/F values in Table II shows that, under Carlson's approximation, section A with $I/F = 0.79$ should indeed have a stable permafrost condition and sections B and C with I/F values of 1.77 and 2.24, respectively, should be expected to degrade, as was observed.

The significance to construction on permafrost of the results in section B is that simple preservation or re-establishment of low surface vegetation of random, naturally occurring, or naturally developing types cannot by itself be relied upon to prevent long-range degradation of permafrost in a region of relatively warm permafrost temperatures like Fairbanks, Alaska. Other observations have also shown that grass cover over permafrost does not prevent its degradation in the Fairbanks area. For example, some land that was cleared of trees soon after World War I and converted into pasture land experienced such drastic melting of ice in underlying polygons as to become too rough to farm. The land was abandoned and has been reverting to forest conditions.⁸ Inspection of more recently cleared pastures currently in use in the Fairbanks area has revealed evidence of incipient similar development. Kallio and Rieger⁴ found in 1969 that at the University Experiment Station near Fairbanks permafrost had degraded to about 7 m under fields (including grass fields) that had been continually cropped since 1945. Brown² has also reported that ground temperatures measured at Norman Wells, N.W.T., at 0.3-m depth in September 1959 were only slightly lower than air temperatures under a grass surface without moss or peat, but temperatures were significantly lower under other types of cover, such as sedge, moss and peat, and lichen and peat. Mean annual air temperature at Norman Wells is about 2.7 °C lower than at Fairbanks. Kallio and Rieger⁴ concluded from their measurements, which were made with a steel probe, that the permafrost had apparently stabilized at the 7-m depth. However, as illustrated by the curves for sections B and C in Figure 3, the rate change of the permafrost table 20–25 years after clearing is relatively slow and changes over a 3-year period could easily be obscured by normal errors in probe measurements. Similar investigations in interior Alaska, such as those by Brown, Richard, and Vietor,¹ have thus far covered time spans too short to prove long-range trends, though short-range results are comparable.

On the other hand, in low, swampy parts of the Farmers

Loop Road Station, west of Farmers Loop Road, only about 300 m from section B, stable permafrost continues to exist under a relatively low, dense growth of grasses, willows, and shrubs typical of a very wet swamp environment. Dense tree cover like that in section A is absent in these areas. Again, an area located on a north- or northeast-facing slope, receiving significantly less solar radiation in the summer, or a location with a colder climate, would have a significantly more stable permafrost condition. Other variables, such as particular kinds of vegetation and growth characteristics, types of soil and organic mat, and wind, snowfall and cloudiness conditions, can also affect the thermal balance. While there is a large body of literature and general relationships are known, there is a deficiency of specific quantitative information on terrain thermal phenomena in relation to such factors, suitable in scope and form for applied purposes, and much research is still needed. Brown² stated in 1963: "Despite the large number of observations reported in the literature, mechanisms operative in thawing of the active layer and permafrost and causes of variations from one type of vegetation to another are not clearly understood." While there has been much work in the ensuing decade, this statement is still considered valid, particularly from the point of view of applications.

Thus, one *cannot* conclude without exception that the mere absence of trees must necessarily result in permafrost degradation in an area like Fairbanks. Nevertheless, the soil, drainage, vegetative cover, and exposure conditions at test sections A, B, and C are probably representative of a substantial variety of construction situations in the Fairbanks area. A good vegetative cover does have significant value in stabilizing slopes against erosion and, unquestionably, does have an effect on the thermal balance. Continuing research may reveal specific vegetative types and practical procedures most suitable for maximizing these effects. However, simple preservation or re-establishment of nonspecific low vegetative cover on surfaces after construction may exert less control over permafrost degradation than has sometimes been assumed.

CONCLUSION

A comparison of three 61-m square test sections near Fairbanks, Alaska—one kept in its natural tree-covered condition, a second cleared of trees but not stripped, and a third section stripped of all vegetative cover to a depth of about 0.4 m—has shown that only the original densely tree-covered section has remained free from permafrost degradation over an observation period of 26 years. In both the cleared and stripped sections, permafrost degradation is still continuing, though at a distinctly slower rate than in the area that was only cleared. It is concluded that in an environment like that at Fairbanks the maintenance or re-establishment of a random, mixed-type low vegetative cover cannot be counted on to

stop or prevent permafrost degradation in an area subject to surface disturbance. If thermal stability under vegetative cover is to be accurately predictable for engineering purposes on other than an empirical basis, much additional research is still needed to achieve better quantitative information, understanding, and procedures.

ACKNOWLEDGMENTS

This paper presents the results of research performed by the Cold Regions Research and Engineering Laboratory under the sponsorship of the U.S. Army Corps of Engineers and the Army Materiel Command. Particular credit is due the originators of this study in the St. Paul District of the Corps of Engineers and in the Engineering Division, Military Construction Directorate, Office of the Chief of Engineers, as well as the various personnel in the Arctic Construction and Frost Effects Laboratory and at the Cold Regions Research and Engineering Laboratory, especially those stationed at the Farmers Loop Road facility, who have successively helped to carry on the study to the present. The untiring assistance of Mr. Charles W. Fulwider, USA CRREL, during preparation of this paper and review of the completed paper by Messrs. George W. Aitken and Paul V. Sellmann of USA CRREL are also gratefully acknowledged.

REFERENCES

1. Brown, J., W. Rickard, and D. Vietor. 1969. The effect of disturbance on permafrost terrain. U.S. Army Cold Regions Research and Engineering Laboratory Spec. Rep. 138.
2. Brown, R. J. E. 1966. Influence of vegetation on permafrost, p. 20-25. *In* Permafrost: Proceedings of an international conference. National Academy of Sciences, Washington D.C.
3. Carlson, H. 1952. Calculation of depth of thaw in frozen ground, p. 192-223. *In* Frost action in soils. Highw. Res. Board Spec. Rep. No. 2.
4. Kallio, A., and S. Rieger. 1969. Recession of permafrost in a cultivated soil of interior Alaska. *Proc. Soil Sci. Soc. Am.* 33:430-432.
5. Kersten, M. S. 1949. Final report, laboratory research for the determination of the thermal properties of soils. Engineering Experiment Station, University of Minnesota, for Corps of Engineers, U.S. Army, St. Paul District. ACFEL Tech. Rep. 23.
6. Linell, K. A. 1960. Frost action and permafrost, p. 13-1-13-35. *In* K. B. Woods [ed.] Highway engineering handbook. McGraw-Hill, New York.
7. Permafrost Division, U.S. Army Corps of Engineers. 1950. Investigation of military construction in arctic and subarctic regions, comprehensive report 1945-48; Main report, and appendix III-Design and construction studies at Fairbanks research area. ACFEL Tech. Rep. 28.
8. Péwé, T. 1954. Effects of permafrost on cultivated fields, Fairbanks area, Alaska, p. 315-351. *In* Mineral resources of Alaska 1951-53. Bull. 989F. U.S. Geological Survey, Washington, D.C.
9. Pihlainen, J. A. 1962. Inuvik, N.W.T., engineering site information. Tech. Paper No. 135 (NRC6757). National Research Council of Canada, Ottawa.
10. Rieger, S., J. A. Dement, and D. Sanders. 1963. Soil survey of Fairbanks area, Alaska. Ser. 1959. No. 25. Soil Conservation Services, U.S. Dep. of Agriculture, Washington, D.C., in cooperation with Alaska Agricultural Experiment Station.

DESIGNING FRICTION PILES FOR INCREASED STABILITY AT LOWER INSTALLED COST IN PERMAFROST

Erwin L. Long

Anchorage, Alaska

INTRODUCTION

In recent years, considerable knowledge has been gained on the fundamental properties of soils and of frozen soils in particular. This advance in knowledge has provided a greater recognition of the limitations of direct application of experimentally derived properties of soils. The use of test piles to arrive at admissible stresses or to prove a specific design has long been an accepted practice. The recognition of the creep behavior of piles by Tsytoich,¹⁶ Vyalov,^{19,20} Sayles,¹² Scott,¹³ and

Sanger,¹¹ as time-dependent characteristics of the strength properties of frozen soils has presented a difficult and expensive hurdle that designers have attempted to overcome in the use of test piles. This problem is further compounded by the use of piling at stress levels that produce pile compressions that may well exceed the strain to failure of much of the pile's available tangential shear surface and may not represent the pile compression at the pile's design ultimate load. The self-refrigerated ring and helix-type pile installations shown in Figure 1 basically permit the direct use of the frozen

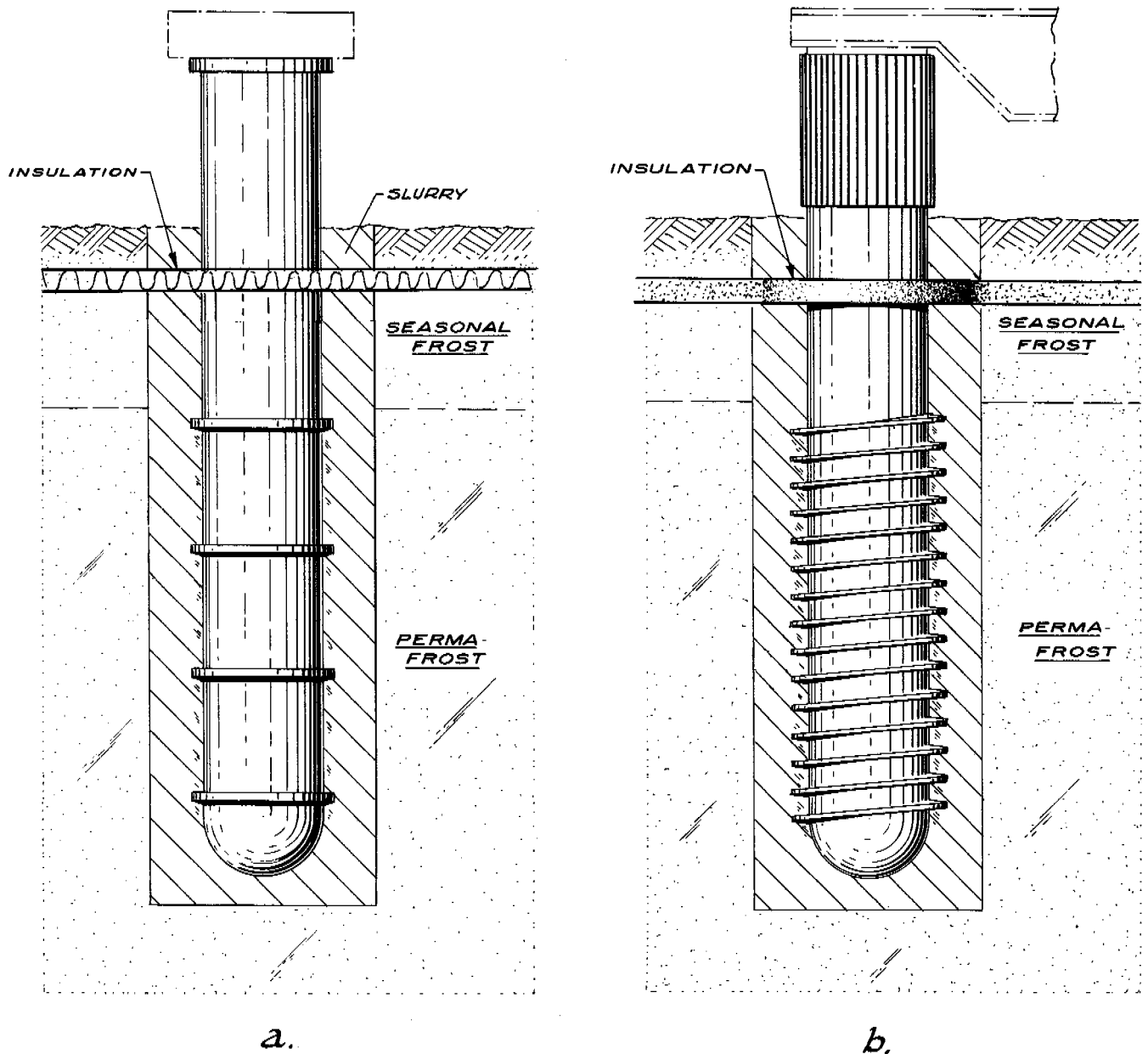


FIGURE 1 (a) Thermal ring pile; (b) thermal blade pile.

soil shear strength in lieu of adfreeze strength with advantages in allowable stress, temperature, stress distribution, length of pile, and allowable bearing during construction.

Structural requirements usually determine the size pile selected, while loads and moments determine the minimum allowable structural column size. Decreasing the depth of thaw can reduce the pile moment and size of pile required. This system has accomplished this by using higher-moisture content soils and by placing insulation approximately 15 cm below the surface (Figure 1).

Frost jacking also can be a problem in normal pile construction. The frost heaving forces⁸ can be reduced or counteracted by lessening depth of thaw, by reducing the friction coefficient of that portion of the pile in the seasonal frost layer, by increasing pile load (decreasing the number of piles) to counteract the heave force, and by increasing the winter temperature of the seasonal zone with a heat-transfer-type pile. The use of a hard vinyl or epoxy surface coating⁹ provides excellent corrosion resistance, can be used in a rutile titanium white paint, and is compatible with above-ground pile surface radi-

ation requirement.⁵ This coating reduces the adfreeze resistance of the pile to one tenth of its normal value.⁹ Ring- or helix-blade-type piles will further reduce the embedded length required to resist frost jacking.

Pile load capacity of a standard pile is obtained by a summation of the allowable adfreeze strength¹¹ added to the allowable pile end bearing strength. Higher allowable strengths permit a reduction in the lengths embedded in the permafrost. Using Vyalov's data¹⁹ it was found that end bearing stress of piles at failure was 5.3–7.9 times the adfreeze stress from laboratory tests and 3.5–10.4 times the adfreeze stress at failure from field tests. Pile tests by Newcombe⁷ give bearing stress at failure equal to from 6.5 to 7.5 times the adfreeze stress at failure, with the lower values reflecting the higher ice content of the underlying gravelly soil. Adfreeze strengths of various pile surfaces and soil types are recorded by Vyalov,^{19,20} Mel'nikov,⁶ Crory,¹ Reed,^{8,9} and Newcombe,⁷ and soil shear strength of various soil types are recorded by Tsytoich,¹⁷ U.S. Dep. Commerce,¹⁵ Kaplar,⁴ and Johnston.²

The ratio of soil shear strength to adfreeze strength was determined for similar temperatures and time to failure by tests of the author and tests by Newcombe,⁷ and Vyalov.¹⁹ This ratio varied from 3 to 7 with 3.0 being a minimum at temperatures below -0.5°C . This ratio may vary for limit strengths at 50–100 years.

A formula that defines time dependent characteristics of frozen soil shear strength is given by Tsytoich¹⁶ as

$$\tau = c_t + \sigma \tan \phi_t, \quad (1)$$

where τ is the shear strength, c is cohesion, σ is normal stress, ϕ is the angle of internal friction, and subscript t represents a time-dependent characteristic. The time-dependent adfreeze and shear strength characteristics at specific temperatures were determined by employing Vyalov's formula:

$$\tau = \beta / \log(tB). \quad (2)$$

where β and B are constants found by plotting results from two or more constant load tests on semilog paper.

Compression data presented by Tsytoich¹⁶ shows differences between instantaneous soil strengths and long-term soil strengths. Long-term strength varied from 13 to 32 percent of instantaneous strength, depending on soil type, moisture content, and temperature, and the degree of loss of strength generally was less for soils tested at lower temperatures and for soils with a greater percent of fines. Sayles¹² shows the long-term strength of Manchester fine sand and Ottawa sand varies from 8 to 17 percent of the instantaneous loading. Field test data from Newcombe⁷ show a value of 17 percent of the 0.01 h test strength compared to the 100-year adfreeze strength of steel friction piles in a silty-sand slurry backfill at -9.4°C .

Stress distribution along a pile has been evaluated by Seed and Reese¹⁴ and others. Pile compression, the very limited strain to failure characteristics of frozen adhesion, and the loss of frozen soil strength following shear combine to reduce the available adfreeze strength along compressible piles. Figure 2 shows the approximate effect of pile compression on adfreeze strength obtained from measurements on 22 cm plain steel friction piles with depths of embedment in permafrost of 1.2–5.4 m with a silt slurry backfill. Field data from Newcombe⁷ show strain to failure varying from 0.20 mm in 0.02 h at -11.4°C to 0.64 mm in 356 h at -8.8°C with 27-cm-diameter plain steel friction piles with embedment of 1.5 m in permafrost with a silty-sand slurry backfill. Pile compression at the top of the permafrost was calculated to be 1.02–0.30 mm. The stress versus strain to failure relationship is shown by Figure 3.

Reheal strengths of three 27-cm friction piles from field data by Newcombe⁷ when evaluated on the basis of identical rates of strain showed strength recovery of 45–55 percent of the initial test strength with plain steel piles in a silty-sand slurry backfill. At lower rates of strain these figures dropped to 26 percent at 0.001 mm/h. Two combined friction and end-bearing piles step loaded after failure provided strengths in each case of 46 percent of the initial strength.

Thermal control of piling is desirable to reduce the heat gain by the soil, to prevent degradation of the permafrost surface, to increase allowable stresses, and to permit the use of ground insulation without danger of long-term warming of the soil. Self-refrigerated pile systems have been discussed by Long,⁵ Reed,¹⁰ and Johnson.³ Figure 4 shows the relationship between maximum and minimum thermopile temperatures for the 1971–1972 season for 16.5-cm-diameter steel thermopiles in a stratified sand and silt subsoil. Johnson³ has completed tests showing the relative heat transfer for small-diameter liquid- and vapor-phase-type self-refrigerated piling. Generally, it is desirable to coat the exposed portion of the pile with hard white vinyl or epoxy paints to minimize absorption of heat during the summers.

Reliability of the heat transfer system is a function of detail design and quality of manufacturer. Licensed pressure vessel manufacturers have provided 100 percent reliability. Earlier thermopile foundations manufactured with less quality control had a 0–5 percent loss of charge from leaks that were easily field repaired to be fully operational.

Slurry placement of piles usually permits higher allowable stresses than driven placement by proper selection of sands for the slurry mixture, by using concrete vibrators to increase soil density, and by eliminating a "failed surface." Ring-type piles are placed with slurry backfill in preaugered holes. Helix-blade-type piles can be similarly placed or can be rotated into the sides of an undersize hole when high torque boring equipment is available. Torque can be minimized with low friction coatings and other means. The greater allowable strengths obtained by the use of ring and blade type piles per-

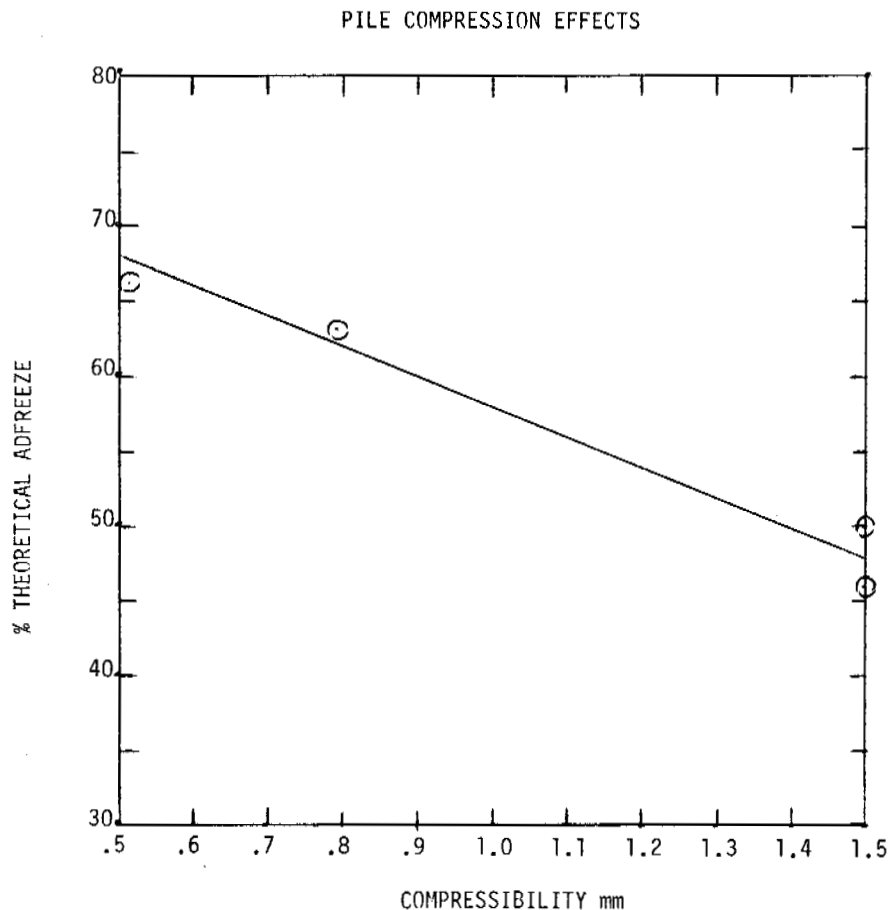


FIGURE 2 Load of test piles at start of plastic flow divided by the theoretical adfreeze in percent versus calculated pile compression at surface of permafrost.

mit a considerable reduction in the length embedded in permafrost. When the construction can justify large capacity cranes, the use of driven piling may be practical. At remote locations with no vehicular access, it is usually more economical to use auger-type boring equipment to minimize heavy equipment mobilization and to place the piling with a consolidated sand or silt slurry. The large capacity drilling rigs available require large cargo aircraft and an adequate airfield for transportation to locations with no vehicular or boat access. Smaller highway-type pole augers with 3.7–4.5 m Kelley bar lengths can be flown in smaller aircraft flying on a scheduled or charter basis into most villages. Adfreeze-type friction piles must be well frozen in before they can be loaded. For this reason, it is common practice for a contractor to fly in his pilings and placement equipment, even in north coastal locations, in late winter so that foundation piling can be in place when barge shipments begin arriving in late June. Ring- and helix-type piles will usually permit construction loads prior to freeze-back of the piling.

Ring-type piles using soil shear in lieu of adfreeze that have been constructed to date make use of 7.6 cm of buried insulation and are constructed on 22 cm o.d. pipe with rings installed from 0.9 to 4 m in depth. Rings are 25.4-mm radial distance and 3.18 cm along the pipe with rings spaced 0.30 m apart. The bore holes were from 3 to 4.5 m deep. Helix-type piles will have 2.5- to 5.0-m-thick blades extending radially 12.7–25.4 mm and spaced 5–15 cm apart with their length, spacing, and thickness being design variables adjusted to the design soil strength. Blades are designed to permit yielding of the blades before the soil exceeds its ultimate shear strength, thus distributing the stresses further along the pile without soil shear. The blades will have progressively less deformation with depth.

Table I compares construction costs at a remote site for 16.5-cm steel pipe ring- and helix-type piles with a typical nonthermal 9-m wood friction pile. An auger system of boring with a sand slurry backfill is assumed. The relative cost of piling is at a typical site that does not have highway access but

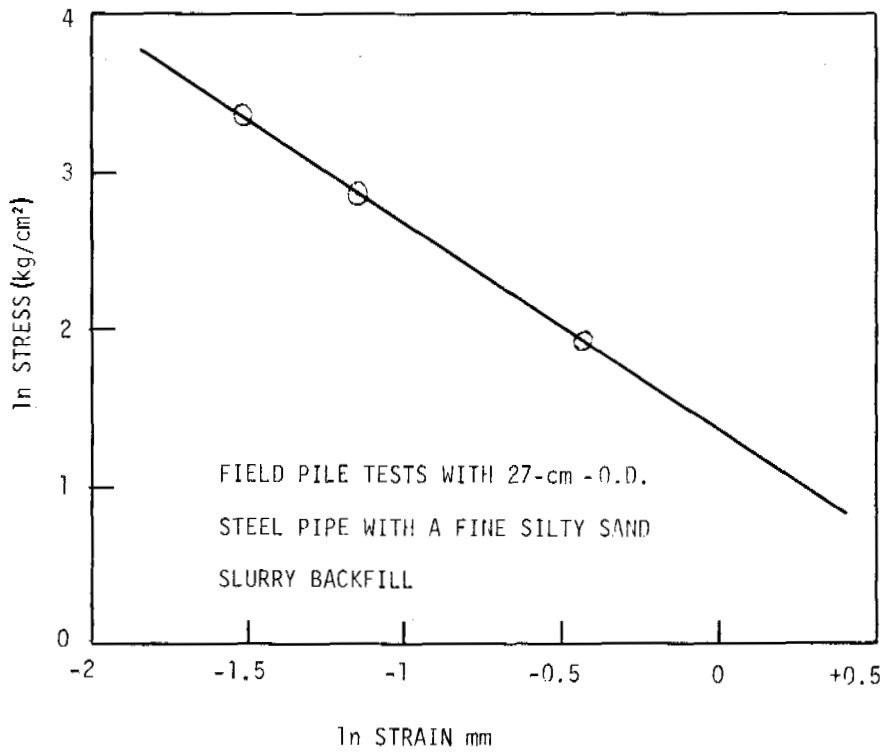


FIGURE 3 Log-log curve of stress versus viscous strain to failure where viscous strain is assumed from the difference between the strain at start of tertiary creep and the intercept of an extension of the secondary creep curve to zero time.

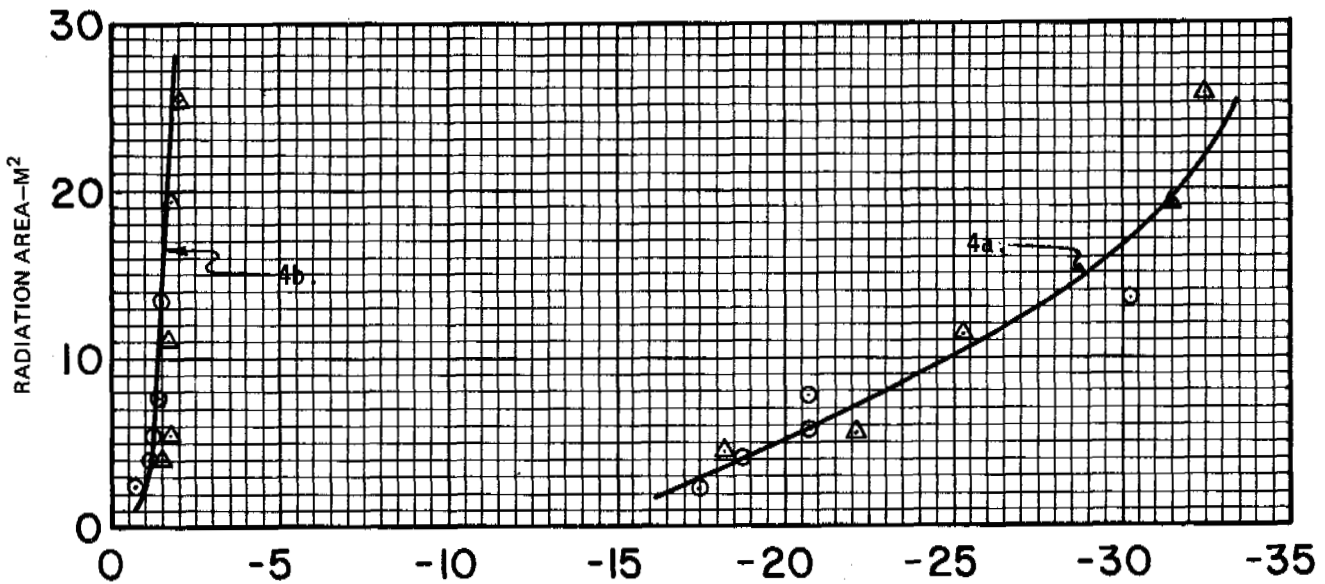


FIGURE 4 Thermopile temperatures (°C) at 4 m depth. (a) Minimum annual temperature, 11 January 1972; (b) maximum annual temperature, 21 September 1972. ○ Perimeter units; Δ nonperimeter units.

TABLE 1 Installed Piling Costs

	Nonthermal Wood Adfreeze Pile	Self-Refrigerated Ring-Type Soil Shear Pile	Self-Refrigerated Helix- Blade-Type Soil Shear Pile
Materials cost	\$ 50.00	\$ 750.00	\$450.00
Pile freight cost	250.00	93.00	117.00
Auger drill	300.00	178.00	178.00
Labor	282.00	141.00	141.00
	<u>\$882.00</u>	<u>\$1 162.00</u>	<u>\$886.00</u>
Design load (kg)	27 000	32 000	45 000
Factor of safety	2	3	2

does have year-round aircraft and summer shallow draft barge access. Freight cost is a combination of boat (from Seattle), rail to Fairbanks, truck to Circle City, and aircraft or shallow draft barge to Fort Yukon.

CONCLUSIONS

The discussion material presented is based on the experience of the author and evaluation of others' works[1].

1. The ability of a pile to utilize the soil shear stresses in lieu of adfreeze stress will permit a significant increase in allowable strength.

2. The allowable soil shear stresses on a pile with blades designed to yield will decrease the effect of pile compression and further increase the ratio of allowable shear strength of a blade pile to allowable adfreeze strength of a plain steel pile.

3. The long-term shear and adfreeze strengths governing a pile in compression or tension may be only 8-32 percent of those strengths as determined by instantaneous loading.

4. Allowable end bearing stresses as determined from combined friction and end-bearing pile tests and friction only pile tests are from 5.3 to 7.9 times the adfreeze stresses at time of failure.

5. Use of buried insulation in combination with self-refrigerated piles and higher-water-content soils near the surface will reduce the depth of thaw and pile structural requirements due to lateral loads.

6. The significantly greater increase in allowable stresses that results from the use of ring- and blade-type piles will permit higher loads, shorter piles, or piles of a lesser diameter where the shear strength of the enveloping natural soil does not further limit the load.

7. Self-refrigerated or thermal type piles can reduce maximum soil temperatures, increase the factor of safety against degradation of the permafrost, as well as permit an increase in allowable stresses.

8. Corrosion protecting coatings can reduce adfreeze resistance to one tenth of their normal value to limit frost jacking and when used with ring- and helix-blade-type piles can be used on the bearing portion of the pile without any loss of pile strength.

9. Increasing the allowable soil stresses and decreasing the depth of thaw and seasonal frost-jacking forces permit the design to utilize shallow depth piles that can greatly reduce transportation, drilling, and placement costs and make this type of foundation fully competitive in cost with plain steel and wood-pile foundations.

REFERENCES

1. Crory, F. E. 1966. Pile foundations in permafrost. *In* Permafrost: Proceedings of an international conference. National Academy of Sciences, Washington, D.C.
2. Johnston, G. H., and B. Ladanyi. 1972. Field tests of grouted rod anchors in permafrost. *Can. Geotech. J.* 9(2).
3. Johnson, P. R. 1971. Imperial heat transfer rates of small Long and Balgh thermal pile and thermal convection loops, IAEE Rep. No. 7102. University of Alaska, Fairbanks.
4. Kaplar, C. W. 1971. Some strength properties of frozen soil and effect of loading rate. Spec. Rep. CRREL, Hanover, New Hampshire.
5. Long, E. L. 1963. The Long thermopile. *In* Permafrost: Proceedings of an international conference. National Academy of Sciences, Washington, D.C.
6. Mel'nikov, P. I., S. S. Vyalov, O. V. Snezhko, and G. F. Shishkanov. 1966. *In* Permafrost: Proceedings of an international conference. National Academy of Sciences, Washington, D.C.
7. Newcombe, T. 1973. B. P. Alaska, Pile Test Program. B. P. North Slope Project, Anchorage, Alaska.
8. Reed, R. E. 1964. Status of investigations to study measures to prevent heave of piles in permafrost (sub-project 36). Tech. Note. CRREL, Hanover, New Hampshire.
9. Reed, R. E. 1965. Status of investigations to study measures to prevent heave of piles in permafrost (sub-project 36). Tech. Note. CRREL, Hanover, New Hampshire.
10. Reed, R. E. 1966. Refrigeration of a pipe pile by air circulation. TR 156. CRREL, Hanover, New Hampshire.
11. Sanger, F. J. 1969. Foundations of structures in cold regions. Monograph III-C4. CRREL, Hanover, New Hampshire.
12. Sayles, F. H. 1968. Creep of frozen sands. CRREL Tech. Rep. 190.
13. Scott, R. F. 1969. The freezing process and mechanics of frozen ground. CRREL Monograph II-D1.
14. Seed, H. B., and L. C. Reese. 1957. The action of soft clay along friction piles. Proc. ASCE.
15. U.S. Dept. of Commerce. 1952. Investigations of descriptions, classification, and strength properties of frozen soils. SIPRE Rep. No. 8. Technical Information Center, Springfield, Virginia.
16. Tsytoich, N. A. 1959. Basic mechanics of freezing, frozen and thawing soils. Moscow. (Translated by V. Poppe, National Science

- Library, National Research Council of Canada, Technical Translation 1239, 1966)
17. Tsytoich, N. A. 1937. An investigation of elastic and plastic deformations in frozen ground. Academy of Sciences, USSR, Committee on Permafrost, Transactions, Vol. X.
 18. Tsytoich, N. A. 1938. On the resistance of frozen ground to load, Tr. Dal'nevost. Kompleksnoj Exped. 2.
 19. Vyalov, S. S. 1959. Rheological properties and bearing capacity of frozen soils. CRREL Transl. 74.
 20. Vyalov, S. S. 1963. The rheology of frozen soil. In Permafrost: Proceedings of an international conference. National Academy of Sciences, Washington, D.C.

NOTE

[1] Detailed data supporting this material and the conclusions are available from the author.

STABILITY OF AN UNDERGROUND ROOM IN FROZEN GRAVEL

Howard C. Pettibone

U.S. BUREAU OF MINES
Spokane, Washington

INTRODUCTION

The economic and technological practicability of mining gold from buried frozen gravel placers in Alaska was investigated by the Bureau of Mines as a part of its Heavy Metals Program. To obtain the necessary engineering data for a feasibility study, the Bureau of Mines needed an underground opening in this material. The most economical procedure was to take advantage of the U.S. Army Cold Regions Research and Engineering Laboratory (CRREL) facilities and adit in frozen silt near Fox, Alaska, about 18 km north of Fairbanks.

To reach the desired gravel area, a crew from the Bureau's Twin Cities Mining Research Center (TCMRC) drove a 2.13-m by 4.57-m winze on a 14-16 percent grade for about 61 m. The final 9.14-m by 21.3-m room (Room A) projects from the right side of the winze near the end (Figure 1a).

GEOLOGY

A geologic section^{5,6} of the test site area (Figure 2) shows the sedimentary formations with reference to bedrock. Bedrock, the floor of Room A, is Birch Creek schist, which is highly altered in the upper 2.74 m (the greatest depth explored). It is overlain by 1.52-4.57 m of early Wisconsin gravels and 15-20 m of silt. The entire section is in the permafrost zone, except the upper 3 m, which thaws during the summer.

The adit, located on the edge of a dredged area on Goldstream Creek, was excavated by CRREL during 1964-1968 in frozen silt characterized by numerous ice wedges. CRREL

found "that underground openings, when remaining at the original temperature (presumably ambient of -1.1 to -0.6 °C) will deform seriously by plastic flow because of the high ice content of the Fairbanks silt."⁷ The use of refrigerated air in the adit during the six warmest months greatly reduced (and even arrested) the vertical deformation rate.

Early Wisconsin gravels form the back and approximately 1.8 m of the 2.44-m walls of Room A. Coarse frozen conglomerate lies immediately above the altered schist bedrock. It is characterized by angular to rounded cobbles and boulders up to 0.61 m in cross section. The space around the coarser rocks is filled with sand, and no ice inclusions were observed. Somewhat interbedded with this coarse formation is a predominantly well-rounded gravel with sand. The frozen silt lenses are very weak and appear to have caved wherever they occurred in the roof although they presented no problem in the walls.

FIELD INSTRUMENTATION—*IN SITU* AND LABORATORY TESTING PROCEDURES

As the excavation of the room progressed, floating points, designed to measure mass subsidence independently from any parting occurring in the first 1.8 m of the adit were installed in the roof, as illustrated by Figure 3. Using an expansion-shell anchor, a 1.8-m studded rock bolt was installed in the roof. The annular space around the bolt at the collar of the hole was caulked with fiber glass insulation. In the floor beneath the 1.8-m bolt, a 0.6-m-long, hex-head machine

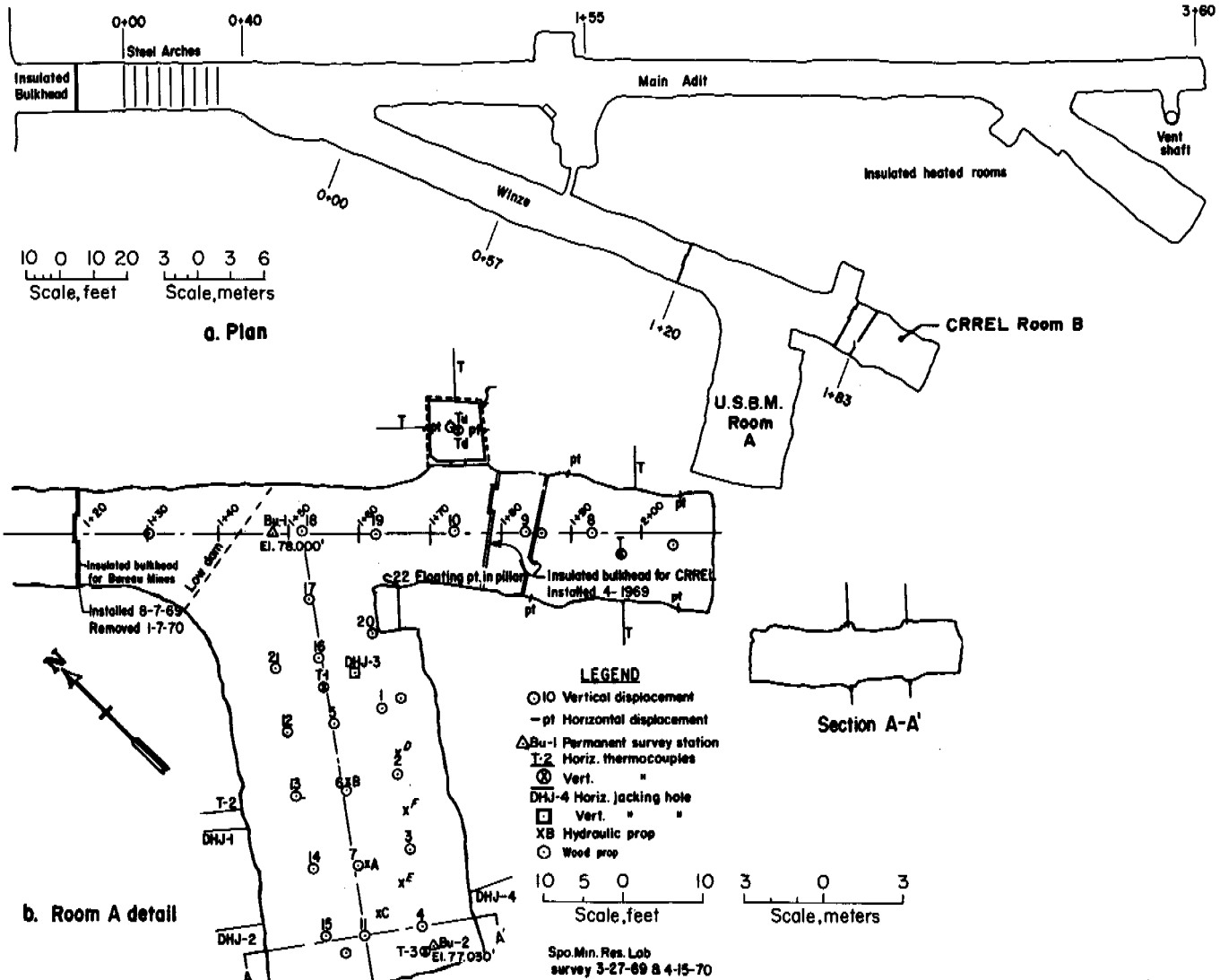


FIGURE 1 Permafrost tunnel plans and section.

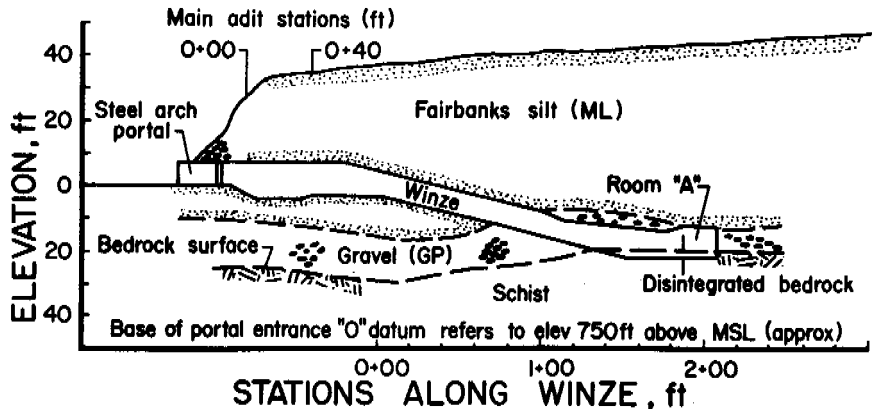


FIGURE 2 Geologic section along winze⁵
(1 foot = 0.304 m).

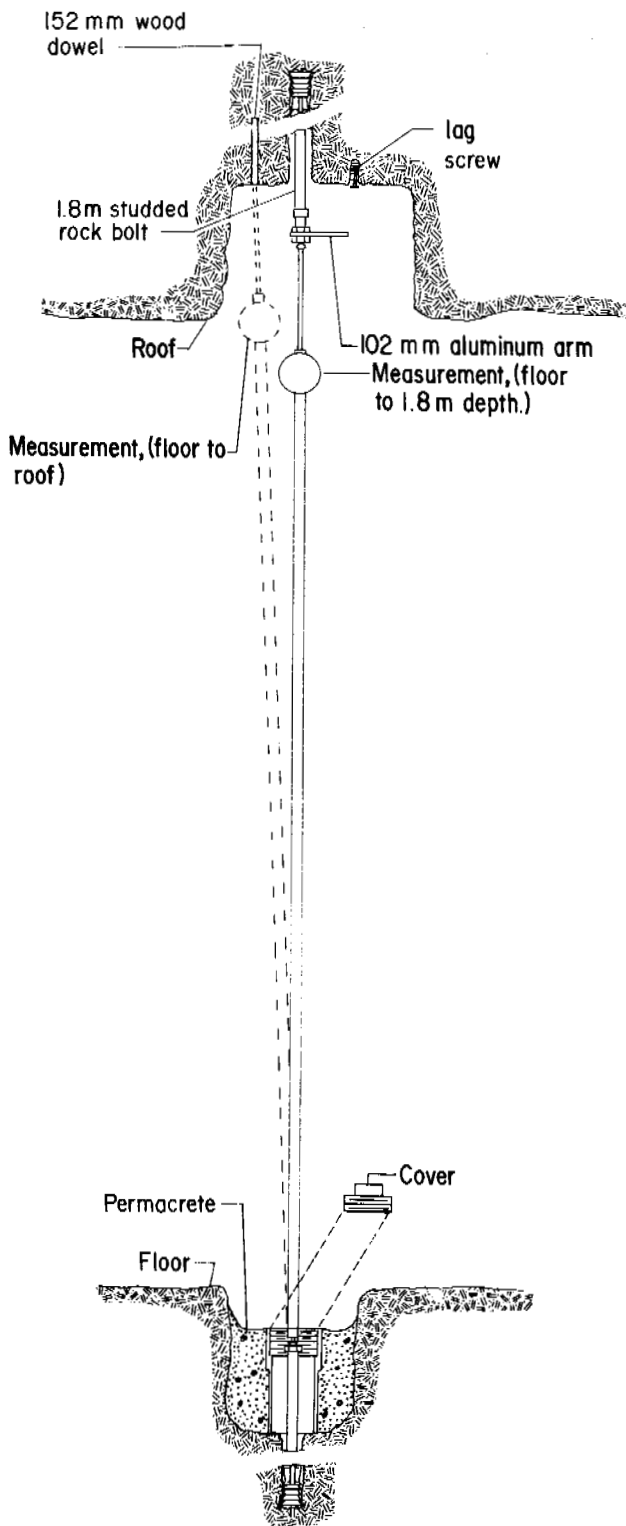


FIGURE 3 Typical closure instrumentation.

bolt was installed employing an expansion-shell anchor. Next, the pipe plug assembly was centered over the head of the 0.6-m bolt and "permacreted" in place using a frozen mixture of water, sand, and gravel. A lag screw was installed in the back, and initial readings were taken on both the closure and the floating points.

During the week of 2 June 1969, eight of the steel bolts in the roof were replaced with 0.6-m-long wood dowels, five were replaced with 1.5-m wood rock bolts, eight of the steel bolts were not changed, a steel pin was driven in the floor under point 21, and all lag screws were replaced with small wood dowels. The steel bolts were replaced with wood dowels, because the data indicated that some bolt slippage was occurring. However, the remaining eight steel bolts performed very well for 2½ years and point 11, discussed later in the report, is a steel bolt.

Two strings of thermocouples, mounted on 1.8-m wood dowels, were installed in the roof and a third string in the right rib of the room as indicated in Figure 1b. Spaced 0.3 m apart, seven thermocouples were mounted on each of the dowels. The thermocouple dowels were anchored into the drill holes with three wood wedges at the collar of the hole; any remaining space around the dowel at the collar was filled with fiber glass insulation. Additionally, CRREL installed several strings of thermocouples in the bulkheaded end of the winze.⁶

Two permanent survey points, designated Bu-1 and Bu-2 (Figure 1b), were installed in Room A. These points are identical to the floor closure points (Figure 3), except that a 1.8-m rock bolt was used, and the annular space around the bolt was filled with arctic transmission grease. These two survey points were tied into the existing survey of the silt tunnel with both horizontal and vertical control. Precise level surveys of all floor and roof closure points, referenced to Bu-1 and Bu-2, were made on 25 March 1969, 19 November 1969, and 14 April 1970. An analysis of the data indicated that the floor points were stable.

Six hydraulic props (nonrigid supports) and two wood posts were placed under some slabby-appearing parts of the roof as a safety provision to protect the men making periodic displacement measurements. Hydraulic prop B was installed in the gravel room 4 March 1969; props A and C were installed 5 March; also, props D, E, and F and two wood posts were installed 15 May. (The locations are specified on Figure 11b.) A Bourdon-tube-gage registers the hydraulic pressure in the prop and gives an indication of its total load.

Two in-place density and moisture tests were performed on chunk samples from the winze between stations 1+80 and 1+92. One was a sample of bedrock; the other, frozen gravel. The chunks, obtained just after a blast, were kept frozen until tested. Another sample of frozen gravel was excavated by hand from the bottom of the Bigelow Bench shaft (located about 1.6 km north of the CRREL tunnel). The densities of the chunks were obtained by the suspended

weight-in-air and water method, using cold water and uncoated samples.

Twelve individual tests were performed with an NX bore-hole plate bearing test device³ (commonly called the Goodman Jack) [1] in percussion drill holes 1.8 m long. A detailed account of these tests is given in Pettibone and Waddell.⁴

On 7 August 1969, a single insulated bulkhead was installed at station 1+20 in the winze to prevent the flow of cool air down the winze and permit observation of the effect of bringing Room A to ambient temperature (-1.7°C). The bulkhead was removed 7 January 1970 in order to determine whether the frigid winter air would retard the creep rate experienced at ambient ground temperature.

The three disturbed samples from the CRREL tunnel site and the one from Bigelow Bench were shipped to Spokane for laboratory testing. Grain-size analysis, Atterberg limits, classification of soils for engineering purposes, specific gravity of No. 4, specific gravity of No. 4, moisture content, and relative density tests were all performed according to the current ASTM designation in 1969.^{1,2}

FIELD TEST RESULTS

Room Size versus Stability

The first room excavated in permafrost gravel was approximately $4.6 \times 12.8 \times 2.4$ m high. When it encountered the overlying frozen-silt formation in the roof, parting took place between the frozen silt and the 0.15–0.91 m of underlying frozen gravel. The parting became apparent from the displacement indicated on points 8 and 9, installed to a 1.8-m depth in the back. On 27 December 1968, the frozen gravel and silt roof in a 4.6- by 4.6-m area at the end of the winze slowly subsided, making a considerable amount of popping noise before finally falling to the floor. Subsequently (1 January 1969 to 29 December 1972), the end of the winze was stable, except for one slab that had to be barred down in early August 1969. In this study, an opening was considered stable if the roof did not require artificial support, the creep rate were too slow to cause a clearance problem, and the strata parting and rock falls were not a problem.

Since the project objective was to determine the stability of frozen gravels, a new room $4.6 \times 15.2 \times 2.4$ m high was excavated south of the inclined winze, where previous drill records indicated a greater thickness of gravel. In effect, a section of the winze became part of the room, giving it a total length of 21.3 m. Closure rate measurements indicated that this room was stable, requiring no artificial support after it was properly barred down. Room temperature during this testing stage averaged about -8.3°C .

By slabbing 2.3 m from each side in successive weeks, the room was then widened to approximately 9 m. The deformation rate increased only slightly with the widening of the roof in and adjacent to the intersection of the room and the winze. However, subsidence all along the roof of the 15.2-m room began at a rate of about 1.9 mm/day, which quickly exceeded the elastic strain calculated for the span. Except for a few thin slabs, the floating rock-bolt extensometers indicated only minor parting (0.25 mm/day additional) in the outer 1.8 m of the roof. In Figure 4 this period is represented by the steep parts of the closure and floating-point curve in February 1969. In March, the first three hydraulic props were installed. Figure 4 presents a plot of the deformation data collected from the closure and floating-point installations at point 11; however, these curves are representative of the data collected from all the points in the gravel room.

Within 2 weeks after the room was enlarged to approximately a 9.1-m width, the subsidence rate began declining. For point 11 (Figure 4), this decreased rate of deformation is evident in both curves (1 March 1969). The subsidence rate continued to decline for the next 3 weeks. The author has no explanation for the apparent expansion at the end of March 1969. Essentially no parting occurred in the outer 1.8 m of the roof, and a steady creep rate of less than 0.25 mm/day developed (average of all points) for the following 3 weeks, during which period the room temperature was approximately -6.7°C . At this temperature, it was concluded that the room was relatively stable and safe without the use of artificial support. Sublimation, however, resulted in accumulation of dust and some loosening of gravel.

From mid-April to mid-June 1969, the temperature in the room was about -3.9°C (an increase of 2.8°C), and

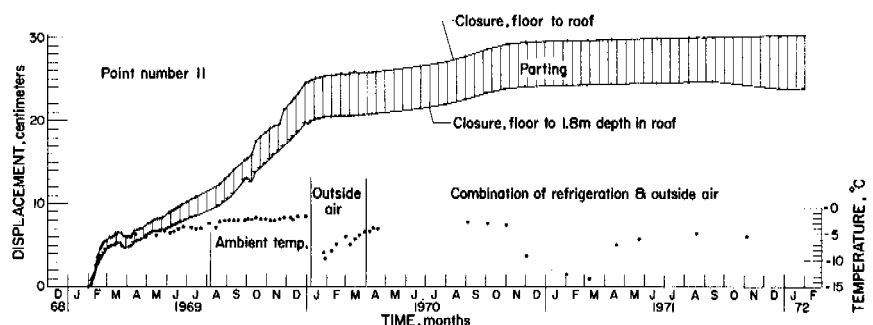


FIGURE 4 Deformation of point 11.

the average roof deformation increased to 0.457 mm/day. Moreover, because thin slabs were loosening in the back, the final five props were installed: three hydraulic props under a low load (454 kg) and the two wood posts. Although the room temperature increased another 0.6 °C from mid-June to 7 August, the average roof deformation remained about the same (0.457 mm/day). On 7 August, the room was isolated from the remainder of the CRREL tunnel by installation of an insulated bulkhead at station 1+20 in the winze (Figure 1). The bulkhead caused a rapid temperature increase to -2.2 °C and an accompanying increase in deformation rate to 0.864 mm/day (Figure 4). The apparent expansion during October 1969 was caused by a damaged dial gage in the extensometer. The sublimation rate seemed to increase, and more frequent barring down was necessary. After the bulkhead was removed on 7 January 1970, the closure rate virtually stopped, becoming 0.051 mm/day. A decrease in the closure rate was anticipated, but this dramatic decline was more than expected.

The hydraulic props were installed under an approximate load of 1 379 kN/m² (about 635 kg total load); over 3 or 4 weeks this weight usually increased to about 6 895 kN/m². The loading rate on the hydraulic props was directly proportional to the closure rate in the room. From 7 August 1969 to 7 January 1970, the load built up very rapidly and had to be released frequently. Maximum load occurred on prop D; it was 11 032 kN/m² or about 5 000 kg total. Installed only to ensure the safety of the men collecting the data in the gravel room, the props did not serve as the major support system. Since the prop, once installed, is loaded by the subsidence creep as well as the weight of the sagging slab, pressure builds rather fast. If the support bore only the weight of the slab, which is all that is necessary, relatively weak supports could be used.

During the author's final inspection of the room in April 1970, 12 cracks in the roof were mapped, ranging in size from hairline width to 15.9 mm. One of the largest cracks (arrowed in Figure 5) passed near closure point 6.

In April 1970, all closure points in the roof of the room were found to be in excellent condition. Some of the bolts and dowels in the roof and floor did wiggle slightly, but no vertical movement was apparent in any of the points. In contrast, point No. 8, located in the CRREL room, was severely corroded. Furthermore, the silt in the roof had flowed down approximately 76.2 mm, completely surrounding the end of the bolt and the top side of the 102-mm aluminum arm attached to the bolt.

For the purpose of this discussion, parting is defined as the expansion or actual vertical separation of the first 1.8 m of the roof. Observation of vertical cracks in the roof of Room A, the roof fall at the end of the winze, and very small horizontal cracks around silt lenses lead to the opinion that vertical separations, as well as expansion of the formation, contribute to the measured parting. A borescope was not

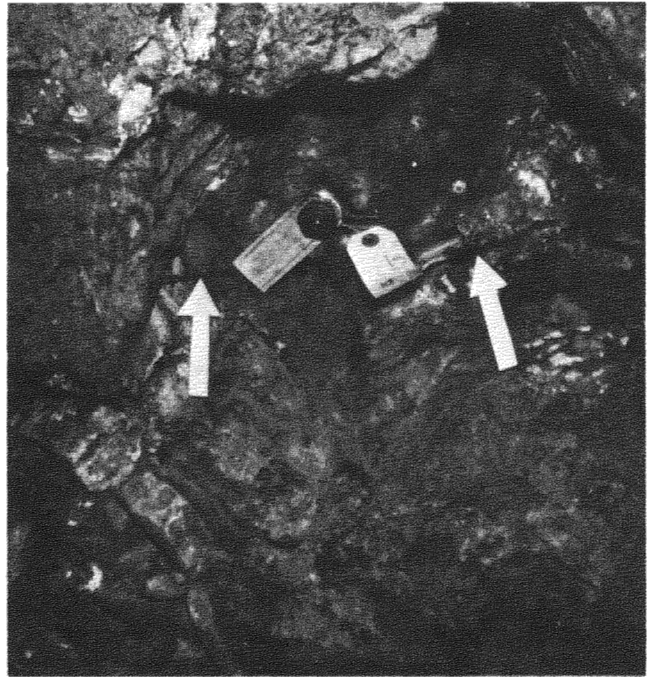


FIGURE 5 Crack in the roof near point 6.

used to determine the percentage of expansion and separation involved.

The amount of parting recorded at point 11 is shown graphically on Figure 4. It is seen that the parting accounts for about 20 percent of the total room closure. The relatively small amount of parting (6 cm) contributing to the large amount of room closure (30 cm) supports the opinion that almost all the closure measured was caused by creeping or flowing of the entire mass of frozen gravel and silt surrounding the room. The room was deemed safe for entry and very stable even after removal of all the hydraulic props on 17 April 1970. CRREL personnel continued to monitor the room until February 1972 and no safety hazards developed.

Microseismic Monitoring

A portable microseismic unit consisting of a geophone, an amplifier, and earphones was briefly tested in an attempt to determine its feasibility in detecting unstable roof conditions. The principle involved is that preliminary failure of the roof might produce subaudible noise, detectable by the unit, and thus afford a warning system for roof failure. Tapping noise 30 m away was easily heard indicating that noise transmits well through the formation. Microseismic noise in the frozen gravel was monitored in March 1969 and again during final removal of the six hydraulic props in April 1970. No microseismic noise at all was detected before, during, or after removal of the props. Although the microseismic study was

TABLE 1 Soil Test Data—Summary of Standard Properties, In-Place Density and Relative Density Tests

Laboratory Sample No.	Identification	Grain-Size Fractions (%)					Atterberg Limits ^a			Classification Symbol (Unified System) Laboratory or Visual ^b	Specific Gravity, —No. 4	Specific Gravity, No. 4	In Place			Laboratory	
		Cobbles (>76.2 mm)	Gravel 76.2 mm to No. 4 Sieve	Sand No. 4—No. 200 Sieve	Silt and Clay <No. 200	Liquid Limit (%)	Plasticity Index (%)	Shrinkage Limit (%)	Dry Density (kg/m ³)				Moisture Content (%)	Relative Density (%)	Maximum Density Dry (kg/m ³)	Minimum Density Dry (kg/m ³)	
1	Winze Sta 1+80 to 1+92. weathered bedrock (Birch Creek schist); well-graded, gravel-sand mixture with silty fines	5	44	42	9	19	4		GW-GM	2.69	2.61	2 019	11.6	73	2 163	1 714	
2	Winze Sta 1+80 to 1+92. placer gravel; poorly graded, gravel-sand mixture	9	64	24	3	Nonplastic			GP	2.72	2.65	2 067	9.7	58	2 339	1 778	
5X	Left and right ribs of 9.1- × 15.2 m gravel room; placer gravel; poorly graded, gravel-sand mixture with silty fines	25	48	22	5	Nonplastic			GP-GM	2.72	2.68				2 371	1 826	
6	Bigelow Bench shaft, top of gravel layer; placer gravel; well-graded, gravel-sand mixture	9	68	20	3	Nonplastic			GW	2.68	2.66	1 874	12.1	10	2 243	1 842	

^a Samples were oven-dried twice before testing.

^b Indicates visual classification by an asterisk.

somewhat inconclusive, the lack of fracture noise is additional evidence that the deformation observed in this room was the result of creep of the ice matrix, and not fracturing of the frozen gravel.

Modulus of Deformation

The modulus of deformation was determined to be 137.9 MN/m². More details of the test results may be found in Pettibone and Waddell.⁴

LABORATORY TEST RESULTS

Table I summarizes the results of the *in situ* density, *in situ* moisture, and laboratory tests. The data show that two of the samples are well-graded, gravel-sand mixtures with small amounts of silty fines. Although the other two samples are classified as poorly graded, they very nearly met the requirements of a well-graded sample. Gradation curves for two of the four samples are given on Figure 6; the other two curves fall either between, or slightly below, those shown. The relative density of the in-place samples indicates that the weathered bedrock is fairly dense (73 percent); whereas the placer gravel ranges from medium dense (53 percent) to very loose (10 percent).

DISCUSSION

In Fairbanks, Alaska, the normal maximum temperatures are below freezing from November through March and, therefore, above freezing during April through October. For 5

months of the year (November through March), an underground room in permafrost gravel at a depth of 15-30 m, 3 m high by 9 m wide by any length (21.3-m length in test), will remain open without artificial support. Most rock falls will occur within a few days after the opening is excavated, and occasional slabs will develop, particularly around silt lenses. Rock falls can be minimized by excavating a smooth roof such as that produced with a continuous miner or with smooth-wall blasting.

A possible method of portal support for operation during the winter months only (November through March) would be continuous support (such as corrugated metal pipe through the active layer), then a sealing off of the portal from April through October. This system would rely on the natural permafrost temperature for mine support during the summer months assuming no work during this period, and supercooling the mine during the winter months with natural cold air. Based on the data at this time (September 1972), the assumption is that the 4.57- by 2.13-m haulageways would stay open, but that a few small rock falls might occur in stope areas with a 9.1-m span.

For year-round operations, the most satisfactory method of ground support would be to keep the ground frozen by maintaining the air temperature in all working areas at -3.9 °C or lower. Circulation of such cold, dry air would aggravate the sublimation problem and increase the frequency of gravel falling from the roof.

To attempt operations during the warm months without refrigeration—i.e., warm air ventilation—continuous support throughout the working and access areas is imperative. In the access areas that must be maintained, possibly for years, cor-

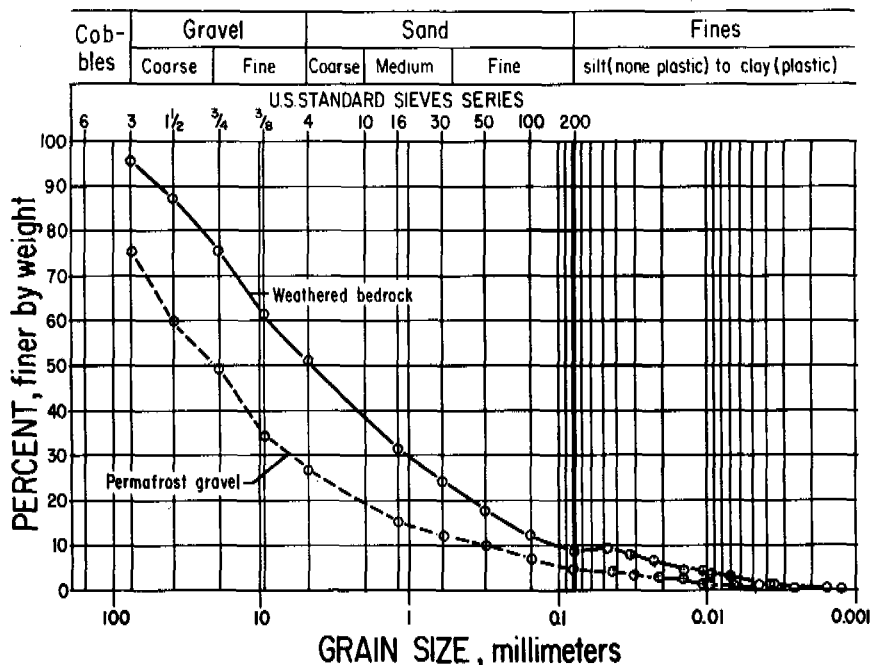


FIGURE 6 Gradation of permafrost gravel, CRREL tunnel site, Fox, Alaska.

rugated metal liner might be essential. The purpose of the support in the stoping or mining areas would be to control surface sloughing, not to bear the load of the subsiding roof. Based on a typical mining cycle, it would be necessary to maintain this area about one month. The support could be a link fence held in place by wood rock bolts, or dowels anchored in the roof. At present, the rate of thaw advance and the time these temporary supports will hold are unknown factors. Thawed material held in place would tend to insulate the frozen ground above. For adequate evaluation, the method should be tested.

CONCLUSIONS

1. When the normal maximum temperatures are below freezing (November through March at Fairbanks, Alaska), an operating mine in permanently frozen gravel would remain open without artificial support.

2. For year-round mining—i.e., when the normal high temperatures are above freezing—the mine must be protected from the heat or else partially supported with yielding-type supports.

3. If it is sealed during the warm months, the mine roof will creep and a few roof falls will occur, but the opening (maximum test span of 9 m) will remain open without artificial support.

4. At an in-place dry density of 2.067 kg/m^3 and a moisture content of 10 percent, the *in situ* modulus of deformation of permanently frozen gravel was found to be 137.9 MN/m^2 at -5°C .

ACKNOWLEDGMENTS

The author is appreciative of assistance rendered by Bruce I. Thomas and Robert W. Carnes of the Bureau of Mines during the excavation, instrumentation, testing, and monitoring of the permafrost room for this project and indebted to Galen G. Waddell for his invaluable help in co-authoring the paper⁴ on which this article is based. The Bureau utilized CRREL's experience and competence in frozen-ground excavation and appreciates their excellent cooperation and the assistance of their personnel.

REFERENCES

1. American Society for Testing and Materials. 1968. Book of ASTM standards. Pt. 10. ASTM, Philadelphia. 636 p.
2. ASTM. 1968. Book of ASTM Standards. Pt. 11. 924 p.
3. Goodman, R. E., and V. K. Tran. 1967. The measurement of rock deformability in bore holes. University of California, Berkeley. 40 p.
4. Pettibone, H. C., and G. G. Waddell. 1971. Stability of an underground room in frozen gravel. *In* Proceedings of the 9th annual engineering geology and soils engineering symposium. Boise, Idaho, April 5, 6, and 7.
5. Sellmann, P. V. 1967. Geology of the USA CRREL permafrost tunnel, Fairbanks, Alaska. CRREL Tech. Rep. TR 199.
6. Thompson, E. G., and F. H. Sayles. 1972. In situ creep analysis of room in frozen soil. *J. Soil Mech. Found. Div. (Proc. ASCE)*, 98(SM9).
7. U.S. Army Materiel Command. 1967. Description of USA CRREL permafrost tunnel at Fox, Alaska. Cold Regions Research and Engineering Laboratory, Hanover, New Hampshire. 7 p.

NOTE

[1] Reference to specific trade names is made for identification only and does not imply endorsement by the Bureau of Mines.

A SEWAGE-TREATMENT CONCEPT FOR PERMAFROST AREAS

Sherwood C. Reed and Timothy D. Buzzell

U.S. ARMY COLD REGIONS RESEARCH AND
ENGINEERING LABORATORY
Hanover, New Hampshire

INTRODUCTION

Standards in the United States and Canada have set water quality goals for the Arctic and Subarctic that are equivalent to water quality requirements for the more populous temperate zone. In general, secondary levels of sewage treatment

are the minimal needs. Constructing and operating such systems in permafrost areas can impose severe engineering, logistic, and economic constraints.

Until recently, the conventional approach was to utilize temperate zone technology and then provide by encapsulation a temperate zone environment for operation of the sys-

tem. Studies have shown that this costly approach is not necessary.^{2,9} The biochemical responses essential to treatment can proceed at relatively low temperatures. However, two major constraints are still imposed on design of the system (a) freezing of the liquid contents or the mechanical equipment must be avoided and (b) the system must not impose deleterious thermal stresses on the supporting permafrost. The concept developed at the U.S. Army Cold Regions Research and Engineering Laboratory (USA CRREL) meets these constraints, provides satisfactory secondary treatment performance, reduces logistic problems, and compared with alternative concepts provides a significant saving in capital costs.

CONCEPT DEVELOPMENT

The objective of the developmental work at USA CRREL was to provide a cost-effective sewage treatment system for isolated small-population communities in the Arctic and Subarctic. Initial efforts included extensive literature searches, field observations, and experimentation with operational treatment systems in Alaska. These investigations indicated that the extended aeration process was the least constrained concept for general application and that the most familiar form of this process in the United States is the prefabricated "packaged" plant. The process is a variation of activated sludge sewage treatment and generally includes a two-step system, the main components of which are an aeration tank to support biological oxidation and a final settling tank or clarifier to separate the solids from discharging before the treated effluent. It is manufactured at the factory, can be delivered to the intended site, and is immediately ready for operation following electrical and hydraulic connections. Other advantages are that the plant is less costly than complex on-site concrete constructions, and that its operational requirements can be managed by relatively unskilled personnel.

Preliminary studies by USA CRREL indicated a number of areas where improvements were possible to optimize use in cold regions: (a) The thin-wall steel or plastic tanks offer little thermal protection and some external housing of the unit is necessary; (b) the prefabricated rigid tank occupies a large volume and often leads to transportation problems for use at remote sites; and (c) some of the materials and mechanical elements used can result in operational and maintenance problems at remote locations.

Thermal Protection

The major area of concern was thermal protection for both the system and its contiguous environment. In temperate regions, it is conventional practice to partially bury the treatment units. However, this approach is not valid in much of the Arctic where thermal degradation of the fine-textured

high-ice-content soils would ultimately lead to structural failure of the treatment system. Construction of the units above ground, therefore, is necessary and this, in turn, requires protection of the system from the extremely cold ambient air temperature encountered. Studies indicated, however, that minimal protection was necessary for the aeration step in these systems. The warm, raw sewage entering the system, combined with continuous agitation of the sewage, permits successful operation with average liquid temperatures at or near the freezing point yet high enough to support biological activity during the 18- to 24-h retention period. Protective elements are required only to maintain the liquid contents of the system in the fluid state and to avoid stress on mechanical elements such as pumps and blowers.

The most critical step in the process is the second when gravity separation of the sludge is necessary prior to discharge of the treated effluent. Usually, this operation is performed in a second tank designed for a 2- to 4-h retention of the material under quiescent conditions.

Design of a clarifier to be compatible with low temperature aeration is difficult, not only because the liquid entering the clarifier is already at or near the freezing point but also because the undisturbed state required during the long retention period is ideal for ice formation. Immersion heaters or other localized heat sources are not possible, since they would induce density currents that oppose the functional intent of the unit. Radiant energy from infrared lamps has been used with partially buried tanks to prevent surface icing, but the energy costs are high. Theoretically, uniform heating of the liquid before it enters the clarifier is possible; however, to allow heat losses during aeration and then reheat the liquid for clarification is not efficient. The need to protect the clarifier has often resulted in both housing and heating the entire treatment unit, which in effect defeats the potential economic advantages of low temperature aeration.

The concept developed at USA CRREL solves the thermal problems by eliminating the separate, exposed clarifier unit, and providing instead a system that will aerate and clarify raw sewage in a single tank. The fundamental element is a floating tube settler, which performs the clarification step.⁸ Utilization of the settler is not limited to the cold regions; however, a summary description of the engineering criteria for the unit is given below since the objective of this paper is to describe the use of the unit as a component in sewage treatment for permafrost areas.

Floating Tube Settler

Clarification requires the removal of suspended solids from the process stream. Most systems are dependent on gravity sedimentation; therefore, retention time becomes dependent on distance of particle travel or depth of the unit. Theoretically

cal advantages of shallow-tray sedimentation systems have been discussed for over 50 years,⁶ but removal of the settled solids has always impeded practical application. Recent papers by Culp,³ Hansen,⁵ and Yao¹⁰ discuss the use of small-diameter, inclined tubes to help implement the benefits of shallow-tray sedimentation. Since settling distance in these tubes is measured in centimetres rather than metres, the time required to provide proper clarification is reduced.

Prefabricated units incorporating fixed tube settlers are commercially available for sewage treatment. But because they are fixed tube settlers and because flow velocity through the tubes is a critical parameter to ensure adequate retention time, they must be designed for diurnal peak flow rates, which may approach 200–300 percent of the daily rates as well as for peak flow velocities that occur during less than 10 percent of the operational life of the system. To accomplish this requires a separate tank or compartment for housing the tubes, thermal protection, and mechanical devices to regularly clean the tubes and to return the sludge to the aeration tank.

The USA CRREL floating tube settler, on the other hand, consists of an inclined bundle of tubes enclosed on top by a collector box (Figure 1). The unit is supported by floats that permit the level of liquid in the containing tank to be slightly higher than the level in the collector box, thus providing a driving force for movement of the liquid-solid mixture into and up the tube units. Laminar conditions rapidly prevail in the small-diameter tubes; and, consequently, effective gravity sedimentation results in only clear effluent appearing in the collector box. The accumulating sludge settling in the tubes slides out of the system and back into the containing tank. A perforated manifold was designed to provide equal flow distribution and to collect the clear effluent for discharge out of the treatment unit through a flexible hose. A recent change, however, in a unit now under evaluation in Fairbanks, Alaska, replaces the perforated manifold with an open trough that contains

small V-notch openings in its sidewalls. Performance of this simpler replacement has been satisfactory to date.

Since the unit floats, it can be designed for a constant steady-state discharge, which is equivalent to the average daily rate and not the diurnal peak. The floating settler, therefore, can be one-third to one-half the size of a unit designed for peak flow conditions which will permit installation directly in the aeration tank, thereby eliminating the need for a separate and exposed clarifier unit.

Additional freeboard in the tank must be provided for temporary storage of the diurnal waste flow peak. This is generally less than 10 percent of the daily flow and would require less than a foot of depth in tanks of conventional design. Many prefabricated treatment units already provide more than a foot of unused freeboard; so this requirement will not add significantly to costs.

In addition to diurnal variations, the design must also consider the peak flow, or maximum day, in which the total flow exceeds the average daily design volume. Design of the tube settler for the average flow rate on the peak days provides control under all conditions. These peak-day flows are often ignored in conventional designs, and washout of solids and deterioration of effluent quality will occur. Consideration of peak-day flows results in a very significant increase in total volume for the entire system.

Since the tube settler floats in the aeration tank, it is exposed to the turbulence produced by the aeration equipment. The USA CRREL unit employs low to moderate turbulence providing adequate oxygen transfer and mixing for the biochemical reactions to occur during aeration. It is a positive advantage to tube settler performance. The slight agitation produced in the unit assists the settled solids to slide out of the tubes and become immediately resuspended in the mixed liquor. This eliminates the need for both frequent cleaning of the unit and the mechanical equipment that returns the sludge to the aeration tank. By comparison, fixed tube settler units in a nonturbulent tank require daily backwashing or cleaning. Although gradual accumulation of biological slime growth may occur on the sides of the tubes of a floating unit, the authors have found that a semiannual cleaning, using air, is satisfactory.

Performance of the tube settler is dependent on a number of physical parameters: flow rate and length, size, cross-sectional shape, and angle of inclination of the settler. Extensive investigations have been undertaken to optimize these parameters and have been reported elsewhere.⁸ The optimum engineering criteria developed from these studies are: individual tubes should be 50.8 mm in diameter, circular in cross section, 0.9 m long, and inclined at an angle of 60° with the horizontal. The hydraulic loading rate should be 41 m³/day/m² of cross-sectional tube area.

Prototype tube settlers fabricated to date have been of all plastic construction, which has the advantage of being both lightweight and resistant to corrosion. The tube ele-

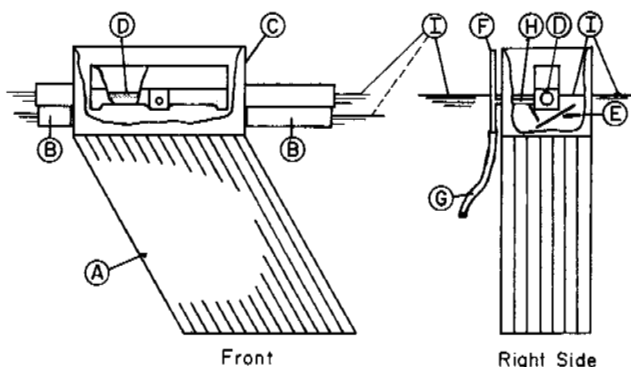


FIGURE 1 Floating tube settler: A, Tubes; B, floats; C, collector box; D, manifold; E, baffles; F, vent; G, flexible hose; H, discharge tube; I, water surface.

ments are thin-wall polyvinyl chloride tubing, and the collector box, floats, and other fittings are made of either Plexiglas or polyethylene. Selection of lightweight elements, consistent with structural requirements, is essential to minimize flotation elements. A unit of the type shown in Figure 1 constructed of these materials requires approximately 0.44 m³ of flotation volume for every square metre of cross-sectional tube area. This unit can be completely fabricated on site with hand tools if necessary. However, better control is better ensured by precutting the components at the manufacturing source and assembling them at the site. Although the entire unit could be prefabricated and assembled prior to shipment, the authors believe that a more efficient package might consist of the prefabricated tube module with all other components pre-cut for on-site assembly.

Long-term sanitary engineering study of system performance^{8,9} verifies the capability of the floating tube settler to produce secondary quality effluents. Table I summarizes typical performance data for the system based on operation of a full-scale 6.4 m³/day treatment unit. As stated previously, the basic treatment approach is the extended aeration process. Use of the floating settler does not change basic design criteria for the extended aeration process or eliminate routine operational requirements such as periodic sludge wasting to maintain effluent quality. Sludge wasting in the USA CRREL system is accomplished by turning off the aeration air supply for approximately 0.5 h to allow the sludge to settle in the aeration tank. A simple air lift can then be used to remove sludge to an adjacent drying bed.

TABLE I Typical Sanitary Engineering Performance Data

Mixed Liquor Concentration (g/m ³)	Tube Settler Effluent ^a			
	Biochemical Oxygen Demand		Suspended Solids	
	g/m ³	% Removal	g/m ³	% Removal
1 436	8	98	14	95
1 810	26	93	17	94
1 830	17	95	32	88
1 812	29	92	14	95
2 262	48	86	63	76
2 324			72	73
2 410	30	92	69	74
2 182	29	92	48	82
2 386	17	96	38	86
2 244	36	90	30	87
2 500			33	87
2 735	61	86	31	88
2 434	29	92	25	90
Average	33.0	92	37.4	86

^a Raw sewage from residential area adjacent to USA CRREL laboratory. Biochemical oxygen demand, 375 g/m³; suspended solids, 263 g/m³.

Basic thermal protection for the tube settler unit is provided by the surrounding liquid contents of the aeration tank. The use of the unit permits realization of the original goal of simple low-temperature aeration with minimal thermal protection. Engineering problems are reduced by employing a single tank that protects both the contents and the contiguous environment from thermal stress.

Tank Design

Desirable tank characteristics are thermal efficiency, minimum operation maintenance, lightweight and small volume for shipping, easy on-site installation, and low capital costs. A survey of available systems and materials indicated that a wood-stave tank of moisture-resistant wood such as redwood is the optimum choice to meet these constraints [1]. Stave thickness and length can be specified within limits, depending on the function and desired depth of the tank. Small-diameter wood pipe is completely prefabricated at the factory. Components for tanks and large-diameter conduits are pre-cut at the factory and shipped unassembled for on-site erection. Logistical problems are minimal since the tanks can be shipped in a compact disassembled state to the site where simple carpentry, instead of welding and other high-skill techniques, can be used for the attachment of required appurtenances.

Dimensions of the 7.6 m³ tank recently installed in Alaska are 2.3-m diameter, 1.8-m depth, and 75-mm nominal thickness (67 mm actual) of tongue-and-groove redwood wall, staves, and floor segments. A certain portion of the inner tank wall becomes saturated when the tank is filled, but the remaining dry segment provides a definite thermal advantage over steel or thin rigid plastics. Operational maintenance is reduced, since painting or other corrosion-control needs are eliminated.

Thermal analysis of any tank used as a sewage treatment system is a complex problem. Superimposed on the variable ambient conditions are the diurnal pattern of waste-flow input, the steady-state discharge from the tube settler, and the nearly continuous agitation and mixing provided by the passage of air bubbles through the system and then by exhaust to the atmosphere.

To simplify the problem, the cooling effect of the aeration bubbles can generally be neglected for these low-intensity aeration systems. Air has little mass and therefore a very small heat transfer from the liquid phase is required to raise the temperature to ambient conditions. It can be assumed that these air bubbles emerge from the liquid with a saturated vapor content that is lost to the atmosphere. When such systems are enclosed in a building, this vapor can be a critical problem resulting in condensation and ice buildup on the walls or ceiling.

Conduction losses through the wooden walls and floor of the tank can be significant. The coefficient of thermal con-

ductivity for redwood is 1.21×10^{-2} W/m K. The tank dimensions described previously give a total of 17.3 m^2 of exposed surface on walls and bottom. A theoretical analysis assuming -51°C ambient air temperature and an average 1°C liquid temperature will show that 1.12×10^3 kW are lost through conduction. By comparison, an equivalent steel tank constructed of 6.3-mm plate would lose over 4.7×10^5 kW under the same ambient conditions.

Convective heat losses from an open liquid surface in an uncovered tank can be even more critical. Assuming a convective heat transfer coefficient of 7.2×10^{-1} W/m K, heat loss from the 4-m^2 surface under the same ambient conditions would be approximately 3.5×10^3 kW. Covering the tank controls convective losses and reduces the problem to conduction through the cover, since the air temperature under the cover equals the liquid temperature in the tank. An uninsulated 12.7-mm-thick plywood cover reduces heat loss to 0.25×10^3 kW. Addition of 50 mm of rigid polystyrene insulation to the cover further reduces heat loss to 62.5 kW. An exhaust vent in such a cover is necessary to displace the volume of air supplied for aeration.

Assuming that an insulated cover is used, the total heat loss from the 7.6 m^3 tank is 1.13×10^3 kW at an average liquid temperature of 1°C and an ambient air temperature of -51°C . The major source of energy to compensate for these losses is the heat contained in the raw sewage entering the tank. At the average design flow of $7.6 \text{ m}^3/\text{day}$, a raw sewage temperature of only 6.7°C would provide the necessary heat input to the system. Raw sewage in the Arctic and Subarctic is usually warmer than this and often approaches $15\text{--}21^\circ\text{C}$ because of the heated transmission pipes and utilidors.¹ Under these conditions, it can be concluded that the wood-stave tank with a simple insulated cover can withstand any ambient temperature conditions that have been experienced in the North American Arctic.

These calculations do not consider the effects of high winds that could induce a much more rapid cooling of the system. Convective losses from the tank surfaces in still air would be quite low since the surface temperature of the tank would be at or very near the ambient air temperature. In accordance with Langmuir's equation,⁷ these convective losses increase by a factor of 7.1 at a wind velocity of 64 km/h. At these and higher velocities, heat losses would be significant but a wind screen around the tank could easily be employed.

The floor of these wood-stave tanks is generally of thinner material than the walls. To provide equivalent thermal characteristics, rigid polystyrene or polyurethane insulation may be attached to the underside of the floor.

Tank foundations are quite simple and require only minor changes for different temperate zones. Above-ground installations usually require a gravel pad whose primary function is to provide load distribution. Its thickness and lateral dimensions will depend on the characteristics of the under-

lying soil. The tank is elevated above the pad on timber cribbing, which, for temperate zone applications, need be only a few centimetres above the pad. For permafrost applications, however, the cribbing height should be increased to approximately 30 cm to allow air to circulate under the tank and to allow heat that might otherwise be transmitted to the supporting permafrost to dissipate.

Aeration System

The motor and blower for the aeration system are the only essential mechanical elements in the USA CRREL treatment concept. Most commercially available systems tend to employ high-capacity blower units that require daily maintenance for at least grease and oil. A typical commercial treatment unit of a size comparable to that of the USA CRREL demonstration in Alaska is equipped with blowers capable of delivering $1 \text{ m}^3/\text{min}$ of air to the system. Part of this air is needed to return the sludge from the separate clarifier to the aeration tank; the remainder still exceeds the oxygen transfer requirements and produces unnecessarily excessive turbulence.

The USA CRREL system uses a low-power direct-drive blower that can deliver at least $0.5 \text{ m}^3/\text{min}$. The blower and drive motor are available preassembled on a common base plate and require only final electrical connection in the field. Routine maintenance for oil and grease are eliminated. When either component fails, it can be easily disconnected and replaced with a spare. A complete standby blower unit should be available at all times.

The blowers are housed in a simple insulated plywood box. Under arctic conditions, an electric light inside the box ensures sufficient protective heat for the motors. This unit can be installed at any convenient location, but a space-saving arrangement is on a wooden walkway spanning the top of the tank that may be reached by ladder.

The aeration system is fabricated of polyvinyl chloride (PVC) pipe rather than the conventional aluminum or other corrosion-resistant metal. It is inexpensive and has the decided advantage that it can be cut with hand tools and assembled in the field to any configuration using solvent cement connections. The systems constructed by USA CRREL employ 3.02-cm-i.d. schedule 40 PVC pipe. One of these systems has been in operation for almost 3 years without problems. Repairs, when required, can be made by unskilled personnel.

The authors have experimented with a variety of air diffusion equipment. Fine bubble diffusers such as ceramic plates and tubes should be avoided; a high-oxygen transfer efficiency is seldom critical in these extended aeration systems, and the fine bubble diffusers lead to clogging problems and maintenance difficulties. In cold weather, when liquid temperatures are low, the aeration system can function without any diffusers and provide adequate treatment with just

an open-ended air pipe terminating near the bottom of the tank. In warm weather, however, oxygen transfer efficiencies are reduced, and at temperatures approaching 15 °C an additional oxygen demand from nitrification reactions is induced, and the open-ended pipe does not maintain satisfactory conditions. High-intensity aeration in most extended aeration systems maintains dissolved oxygen concentrations of from 5 to 9 g/m³. The authors suggest that maintenance of such high oxygen levels is an unnecessary waste of energy. Documentation can be found in the literature⁴ leading to the hypothesis that the microbial reactions involved require only 0.5–1.0 g/m³ oxygen for sustained activity, and the USA CRREL system is designed to maintain these minimal requirements. Some form of coarse bubble diffuser will be required at least in the summer months and it will probably prove more efficient to operate it year around. A number of nonclog, coarse bubble diffusers are commercially available.

SYSTEM COSTS

Although system costs were not the primary objective in initial development of the concept, which up to about 40 m³ are less expensive than steel or rigid plastic, it became apparent that the choice of wood-stave tanks, low-power blowers and plastic piping based on technical requirements would produce a significant saving. The key element in cost savings and operational simplicity is the floating tube settler which replaces the conventional clarifier with all its appurtenant piping and sludge return mechanisms. Fabrication of this complex element may require from one third to one half of the total cost of a treatment unit. Cost analysis for construction of the first USA CRREL prototype showed a total amount of \$2 200 for materials and labor to produce a completely functional system. Delivered price for conventional extended aeration units of comparable volume were at least double this amount.

CONCEPT PERFORMANCE

Two prototype systems based on this concept have been constructed to date. The first unit was erected at the USA CRREL facility in Hanover, New Hampshire, and is in its third year of continuous operation. Sanitary engineering performance was variable during this period because the unit was the basis for criteria development and optimization. Recent performance data (Table I) document the capability of the system to meet treatment goals. Physical performance of the system has been entirely satisfactory. After 2 years, the tank was drained and inspected, and no sign of deterioration was noted. The plastic air piping and blower units have also met all expectations. A second unit was installed by USA CRREL at Fort Wainwright, Alaska, in September 1972 to corroborate performance under actual subarctic

weather conditions and with only the attention of relatively unskilled operators. Performance to date has been successful.

Both units are instrumented with thermocouples to monitor temperatures at various points in the system. Winter data from the USA CRREL system in Hanover, presented in Table II, support the validity of the theoretical thermal analysis discussed above.

CONCLUSIONS

The USA CRREL sewage treatment concept provides a technically viable, cost-effective solution for sewage treatment at small installations in permafrost regions. It can maintain treatment efficiencies comparable with those of conventional extended aeration units with much lower capital costs and significant savings in operation and maintenance. It can be easily erected, operated, and maintained by relatively unskilled personnel. Protective elements required for thermal stress in the cold regions are minimal.

SUMMARY

A treatment concept developed by USA CRREL is described. It is compatible with the permafrost environment and still offers substantial savings in construction costs.

The concept adopts the passive approach to construction in permafrost by protecting the supporting material from thermal stress. The unit is designed to be placed above ground on a gravel pad with the tank slightly elevated on cribbing to permit free air flow underneath. This configuration protects the underlying permafrost from thermal degradation but exposes the tank bottom to the low winter temperatures. A number of protective features are included to prevent freezing of tank contents.

The key element is utilization of a floating tube settler, which provides the essential final clarification of the effluent

TABLE II Typical Thermal Performance (in °C),^a USA CRREL Sewage Treatment System

Ambient Air ^b	Tank Contents ^c	Raw Sewage
-7	18	20
-8	17	19
-10	16	19
-15	15	19
-16	14	20
-18	13	20

^a Measured with copper-constantan thermocouples. Values presented are averages during 2- to 6-h periods during the 1971 winter.

^b Average of three values measured adjacent to exterior of tank. Tank had plywood cover, no insulation.

^c Averages of four values measured at various points in liquid contents. Graphical projection of these data indicate that liquid contents approach 0 °C at an ambient temperature of -51 °C.

prior to discharge. The compact nature of this USA CRREL settler permits installation directly in the aeration tank, thus avoiding the need and costs for separate clarifier tankage. The resulting single-tank-treatment system provides significant thermal and economic advantages for utilization in the permafrost regions of the world.

ACKNOWLEDGMENTS

This paper presents the results of research performed by the Cold Regions Research and Engineering Laboratory under the sponsorship of the U.S. Army Corps of Engineers and the U.S. Air Force.

REFERENCES

1. Alter, A. J. 1969. Sewerage and sewage disposal in cold regions. Cold Regions Science and Engineering Monograph III-C5b. U.S. Army Cold Regions Research and Engineering Laboratory, Hanover, New Hampshire.
2. Clark, S., *et al.* 1970. Design considerations for extended aeration in Alaska. *In* Proceedings, International symposium on water pollution control in cold climates. U.S. Government Printing Office, Washington, D.C.
3. Culp, G. L., *et al.* 1968. High rate sedimentation in water treatment works. *J. Am. Water Works Assoc.* 60:681.
4. Eckenfelder, W., and D. O'Connor. 1961. Biological waste treatment. Pergamon Press, New York.
5. Hansen, S. P., and G. L. Culp. 1967. Applying shallow depth sedimentation theory. *J. Am. Water Works Assoc.* 59:1134.
6. Hazen, A. 1904. On sedimentation. *Trans. Am. Soc. Civ. Eng.* 53:45.
7. Langmuir, I. 1913. Convection and radiation of heat. *Trans. Am. Electrochem. Soc.* 23:299.
8. Reed, S. C., T. Buzzell, and S. Buda. 1972. A floating settler for low cost clarification. *In* Proceedings, Society of engineering science conference on pollution. Engineering and Scientific Solutions, Tel Aviv, Israel.
9. Reed, S. C., and R. S. Murphy. 1969. Low temperature activated sludge settling. *Sanit. Eng. Div. J. Am. Soc. Civ. Eng.* 95:747.
10. Yao, K. M. 1970. Theoretical study of high rate sedimentation. *J. Water Pollut. Control Fed.* 42:218.

NOTE

[1] Wood-stave pipe and tanks were often used during the early period of northern development but in recent construction have been replaced by metal and plastic, which lack thermal efficiency and require large fixed-volume shipment.

VERTICAL AND LATERAL PILE LOAD TESTS IN PERMAFROST

Raymond K. Rowley [1] and George H. Watson [2]

MACKENZIE VALLEY PIPELINE
RESEARCH LIMITED
Calgary, Alberta

Branko Ladanyi

ECOLE POLYTECHNIQUE
Montreal, Quebec

INTRODUCTION

In 1969, Mackenzie Valley Pipe Line Research Limited was formed to investigate problems associated with arctic pipelines. This consortium made a comprehensive study on the technical feasibility and the cost of transporting warm crude oil from Prudhoe Bay, Alaska, across Canada via the Mackenzie River Valley, to midwest and west coast markets in the United States.

A unique feature of the proposed pipeline system was that its route would traverse continuous and discontinuous permafrost, muskeg, and unfrozen terrain. Where direct burial of the pipeline in permafrost was judged impractical, above-ground construction was used in the cost estimates.

Research results and preliminary analytical work indi-

cated that where above-ground construction was contemplated the pipeline should be supported on piles. Above-ground pipeline segments were generally considered to be unrestrained, and preliminary design followed applicable Canadian and United States codes. The pipe was supported intermittently on pile bents and was free to move between restraint points both longitudinally and laterally on these supports. In the horizontal zigzag configuration, however, restraints and anchors were utilized to reduce lateral movement and to limit longitudinal pipe stress. Lateral loads resulting from the pipe sliding sideways on the supports were a major design concern but there was little applicable information on permafrost behaviour under lateral pile loads.

Empirical design capacities were derived from the load-test results. Methods of predicting load-deflection curves and

pile-load capacity were reviewed. A theoretical method for predicting the nonlinear load-deflection curves for permafrost soil in creep was developed and is now being field tested at the pile test site.

SITE CONDITIONS

The site selected was 3 km north of Inuvik, N.W.T., and about 1.5 km east of the Mackenzie River in the Canadian Arctic. The piles were installed in relatively flat ground next to an existing pipeline test facility. The local terrain was a kame terrace overlain with a blanket of silty siltwash sediments.

Large-diameter (30 cm) continuous core samples were recovered from two locations within 8 m of the test pile array.¹⁹ Subsurface conditions were uniform.²⁰

PILE INSTALLATION

An array of 23 piles (18 timber and 5 steel pipe) was installed in early September 1971. Pile dimensions, lengths, embedments, and elevations are summarized in Table I. All test piles were placed in 45-cm-diameter augered holes extending down to the gravel till layer. Each annulus was backfilled with medium to coarse sand with 10–15 percent moisture content and rodded to eliminate bridging. The pipe piles were then filled with sand and those designated for lateral-load tests were filled with concrete from about 0.3 m above

ground surface to the top. End-bearing support for the vertical test piles was eliminated by placing 0.3 m of self-sealing polyurethane foam at the bottom of each hole.

TESTING EQUIPMENT AND PROCEDURES

Three timber and two steel piles were loaded vertically by a 900-kN, hydraulically operated ram. The upward reaction was transferred to the permafrost by a load-transfer beam attached to two 0.5-m-diameter timber tension piles.

Lateral loads were applied to two timber and three steel piles. To provide the required reaction capacity, the timber tension piles were connected to battered reaction piles by heavy gusset plates. Lateral load was applied by means of a 450-kN, hydraulically operated ram.

To reduce the secondary effects of eccentricity for both lateral and vertical tests, the ram loading was applied to the piles through a lubricated ball-and-socket joint.

An unheated, portable structure completely enclosed the test apparatus. Temperature fluctuations were not great and the system components were shaded, so that temperature corrections were reduced to negligible magnitudes.

For the short-term tests, loads were applied in equal increments at 2-h intervals. For the long-term tests, each load increment was maintained on the pile for 24 h, or until displacement had ceased.

LOAD-TEST RESULTS

Thermistors were installed at depths of approximately 1, 2, 3, and 4 m below the ground surface on two timber piles. Daily temperatures were recorded. Permafrost temperatures obtained at the site datum stations and daily mean ambient air temperatures along with the weekly average subsurface temperatures obtained from the thermistors attached to the piles are presented in Figure 1.

Load-test results were plotted as time versus deflection curves (Figures 2, 3, 4). Lateral deflections were taken from the dial gage located nearest the point of load application. Vertical deflections were the geometric averages of the values registered by the dial-gage reference system.

The adfreeze bond strength derived from the vertical-load tests varied from 40.5 to 50.2 kNm⁻². A design value of 43 kNm⁻² at an average ground temperature of -1 °C for the depth of pile embedment was used. The results for pile T-12-V (Figure 2) were considered indicative of the long-term strength that the warm summer-fall conditions would offer.

Allowable working loads were set at 62.3 and 89 kN, respectively, for laterally loaded timber and steel piles. These values were close to the upper limit of terminating creep. Results for pile T-2-L (Figure 3), were considered representative for a timber pile.

In applying the test results, it must be kept in mind that

TABLE I Test Pile Dimensions

Pile Number	Type	Length (m)	Diameter (cm)	Embedment (m)
T-1-L (not tested)	Timber	3.96	33–30	2.44
T-2-L	Timber	4.05	30–28	2.44
T-3-L	Timber	3.90	28–26	2.44
S-4-L	Steel pipe	3.66	27	2.44
S-5-L	Steel pipe	3.66	27	2.44
S-6-L	Steel pipe	3.66	27	2.44
T-7-R	Timber	7.92	46–38	5.49
T-8-B	Timber	4.27	32–29	3.35
T-9-V	Timber	4.42	33–30	3.66
T-10-R	Timber	7.72	46–38	4.88
T-11-B	Timber	4.27	29–25	3.66
T-12-V	Timber	3.44	29–25	2.44
T-13-R	Timber	6.49	48–43	4.27
T-14-B	Timber	4.27	28–25	3.66
T-15-V	Timber	3.35	34–32	2.74
T-16-R	Timber	8.93	44–34	6.10
T-17-B	Timber	3.96	35–31	3.55
S-18-V	Steel pipe	3.51	27	3.05
T-19-R	Timber	8.02	43	5.49
T-20-B	Timber	4.27	33–30	3.66
S-21-V	Steel pipe	4.85	27	4.27
T-22-R	Timber	9.14	43–37	6.10
T-23-B	Timber	4.57	30–25	3.66

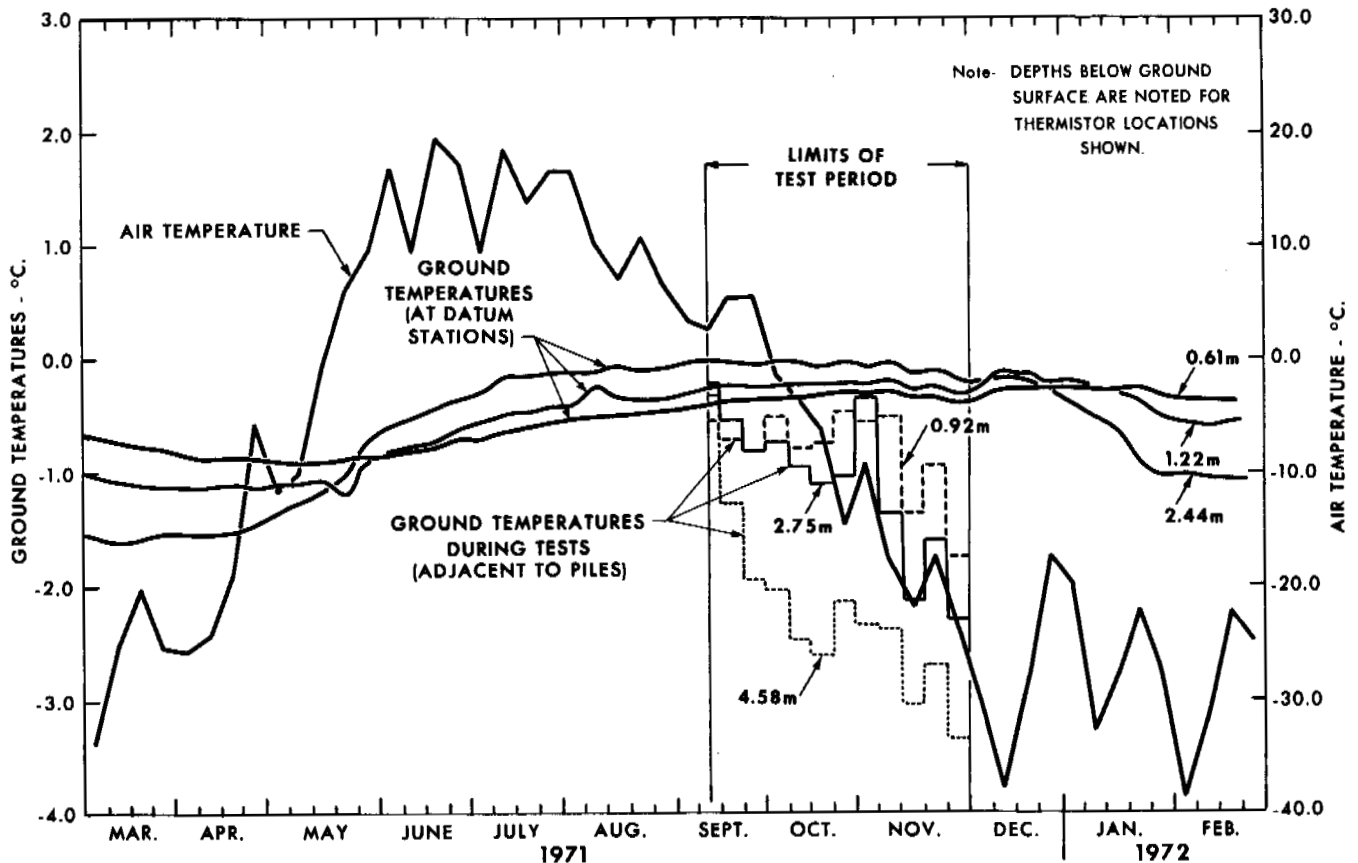


FIGURE 1 Air and ground temperatures.

permafrost temperatures in the active layer were not constant during the load tests. Piles should be designed for the highest permafrost temperatures that would exist for a significant period. Because of the temperature variation, no quantitative comparison of the performance of timber versus steel-pile piles was possible.

ANALYSIS OF VERTICAL-LOAD TEST DATA

The total load capacity of vertically loaded piles in permafrost results from skin friction (between unfrozen soil and the pile), adfreeze bond strength (between frozen soil and the pile), and end bearing. To establish allowable pile capacity, however, the load-deflection curve and the adfreeze bond strength, corresponding to the maximum load at which terminating creep occurs, must also be determined.

As the only unfrozen soil at the test site was the approximately 0.5-m-thick active layer, composed mainly of organic material, the load capacity developed by skin friction was negligible. As explained earlier, the effects of end bearing had been eliminated. This was important for two reasons: uplift or tension piles would depend solely on the load capacity developed through adfreeze bond strength and the

terminating creep phases for adfreeze bond and end bearing might not occur simultaneously for downward loaded piles.^{15,18}

The load applied to the test piles, therefore, was carried almost entirely by the adfreeze bond between the frozen soil and the pile surface. By using the maximum loads at which terminating creep occurred, an average adfreeze strength of 43 kNm^{-2} was obtained from the timber piles.

ANALYSIS OF LATERAL LOAD TEST DATA

Methods for Determining Lateral Load Capacity of Piles

Under normal conditions (thawed soil) the lateral-load capacity of piles can be determined by three basic methods:

1. Using the theory of lateral subgrade reaction (lateral soil resistance), and assuming that the soil resistance at any depth is a linear function of deflection at that depth.⁵
2. Using the theory of elasticity (treating the soil as a semi-infinite, linear-elastic medium).^{3,13,17}
3. Determining experimentally the load-deflection curves

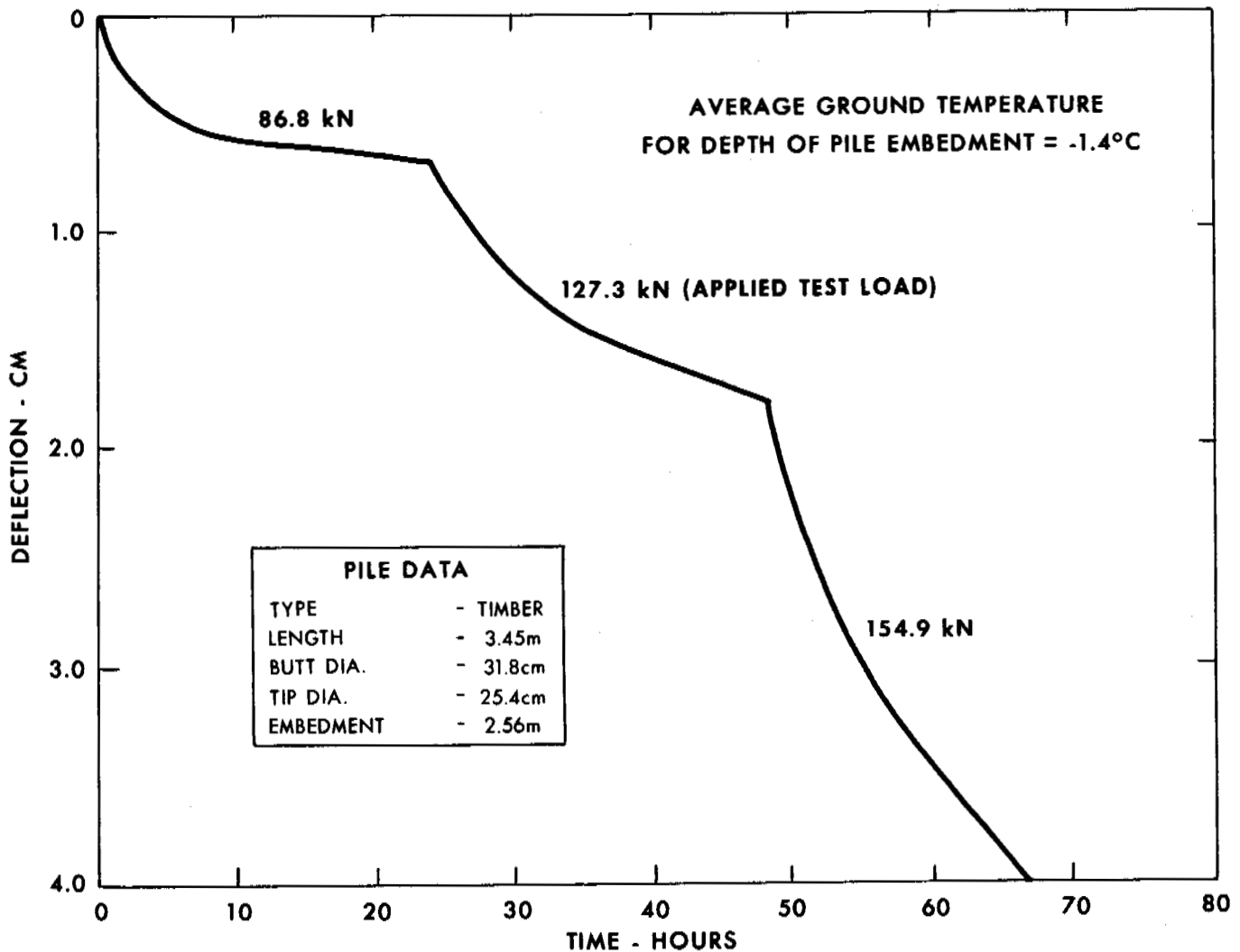


FIGURE 2 Vertical-load test results; pile T-12-V.

of the soil at several levels and using the finite-difference technique to calculate pile behaviour directly from the curves.^{4,14}

The first two methods assume that soil resistance is proportional to load. This assumption is considered valid for relatively stiff soils and for loads in the range of one third to one half of the ultimate bearing capacity of the soils. In weaker soils, and particularly in those showing long-term deformation due to creep, such as frozen soils, the soil response to load is most often nonlinear and an analytical technique able to take this into account is necessary. One technique consists of repeated application of elastic solutions wherein the second modulus is adjusted until it is compatible with the deflection.¹¹ Another described above under point 3 makes direct use of the load deflection curves of the soil. Such curves can be obtained from full-scale lateral pile-load-

ing tests, plate-loading tests,¹⁶ or basic soil properties, as shown in this paper for the case of frozen soil.

Modulus of Lateral Subgrade Reaction from Pile Load Tests

The usual definition of the modulus of subgrade reaction is

$$k = p/y, \quad (1)$$

where p is the applied unit pressure and y is the deflection. If both sides of Eq. (1) are multiplied by the width of the pile, B , another form is obtained:

$$K = P/y, \quad (2)$$

where P is the applied force per unit length of pile.

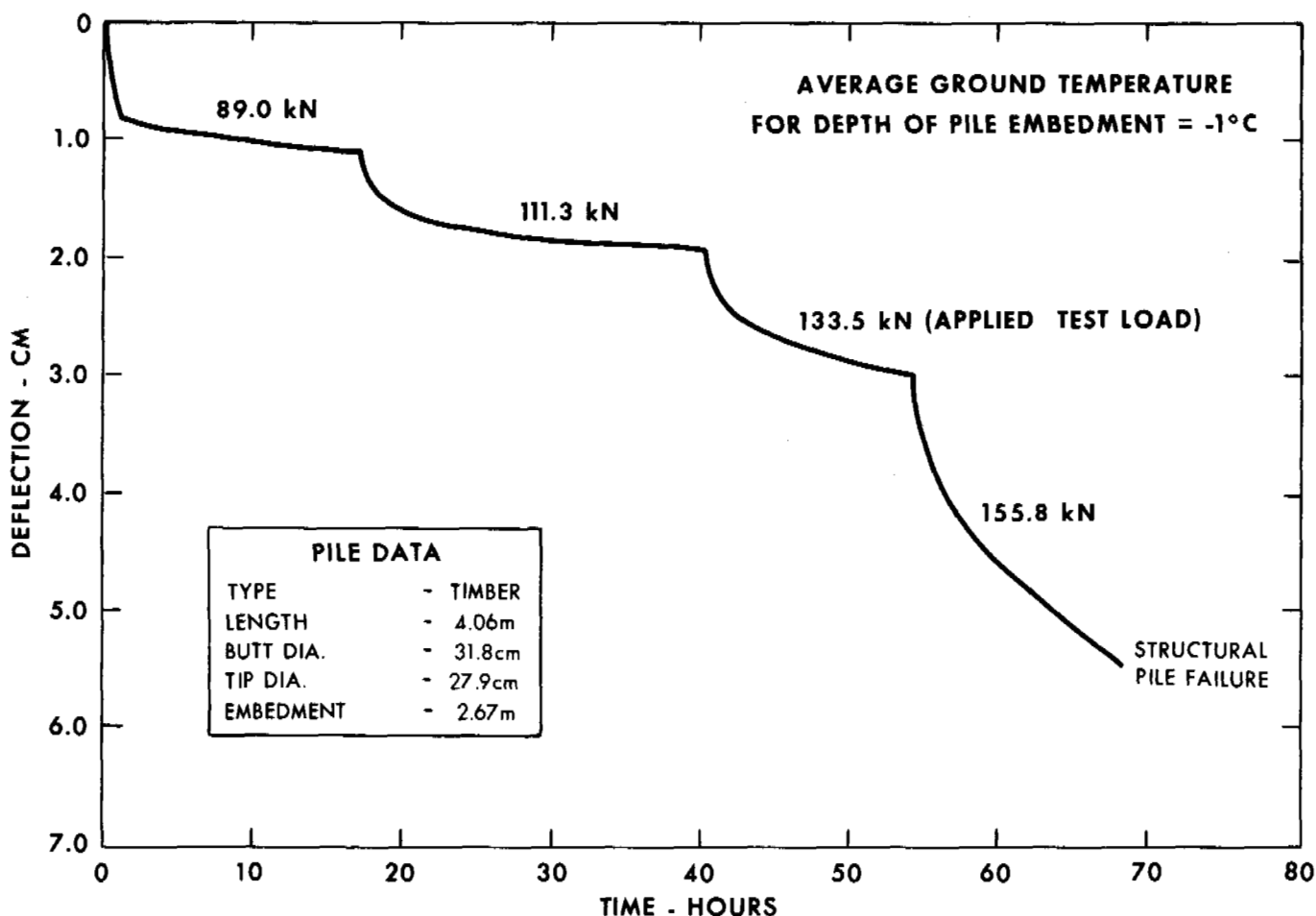


FIGURE 3 Lateral-load test results; pile T-2-L.

For the case where K is constant with depth and independent of pressure, the distribution of lateral deflections, bending moments and soil reactions can be determined analytically.⁵ K depends primarily on the dimensionless ratio L/l_o , where L is the embedment length and l_o denotes the characteristic length given by

$$l_o = (4EI/K)^{0.25}. \quad (3)$$

In this equation, EI represents the pile stiffness, E being the modulus of elasticity of the pile and I the pile moment of inertia, and K is the modulus of subgrade reaction defined by Eq. (2).

According to Broms,² the lateral deflections at the ground surface, for a free-headed pile of length L , loaded laterally by a load Q , acting at a distance e above the ground surface (Figure 5), can be calculated by assuming that the pile is infinitely stiff when the dimensionless length L/l_o is smaller than 1.5. For that case, the lateral deflection at the ground surface, y_o , is given by

$$y_o = (4Q/KL)/(1 + 1.5e/L). \quad (4)$$

On the other hand, the lateral deflection at the ground surface of a free-headed pile can be calculated by assuming that the pile is infinitely long when $(L/l_o) > 2.5$ (> 2.25 according to Vesic¹⁷). The lateral deflection can then be computed from

$$y_o = (2Q/Kl_o)/(1 + e/l_o). \quad (5)$$

For intermediate flexibilities, i.e., for $1.5 < L/l_o < 2.5$, the value of y_o can be deduced from a dimensionless plot as given by Broms.²

Using the above relationships within their respective limits, an average value of the modulus of subgrade reaction, K , can be determined from any lateral pile-loading test in which lateral deflection at the ground surface has been measured.

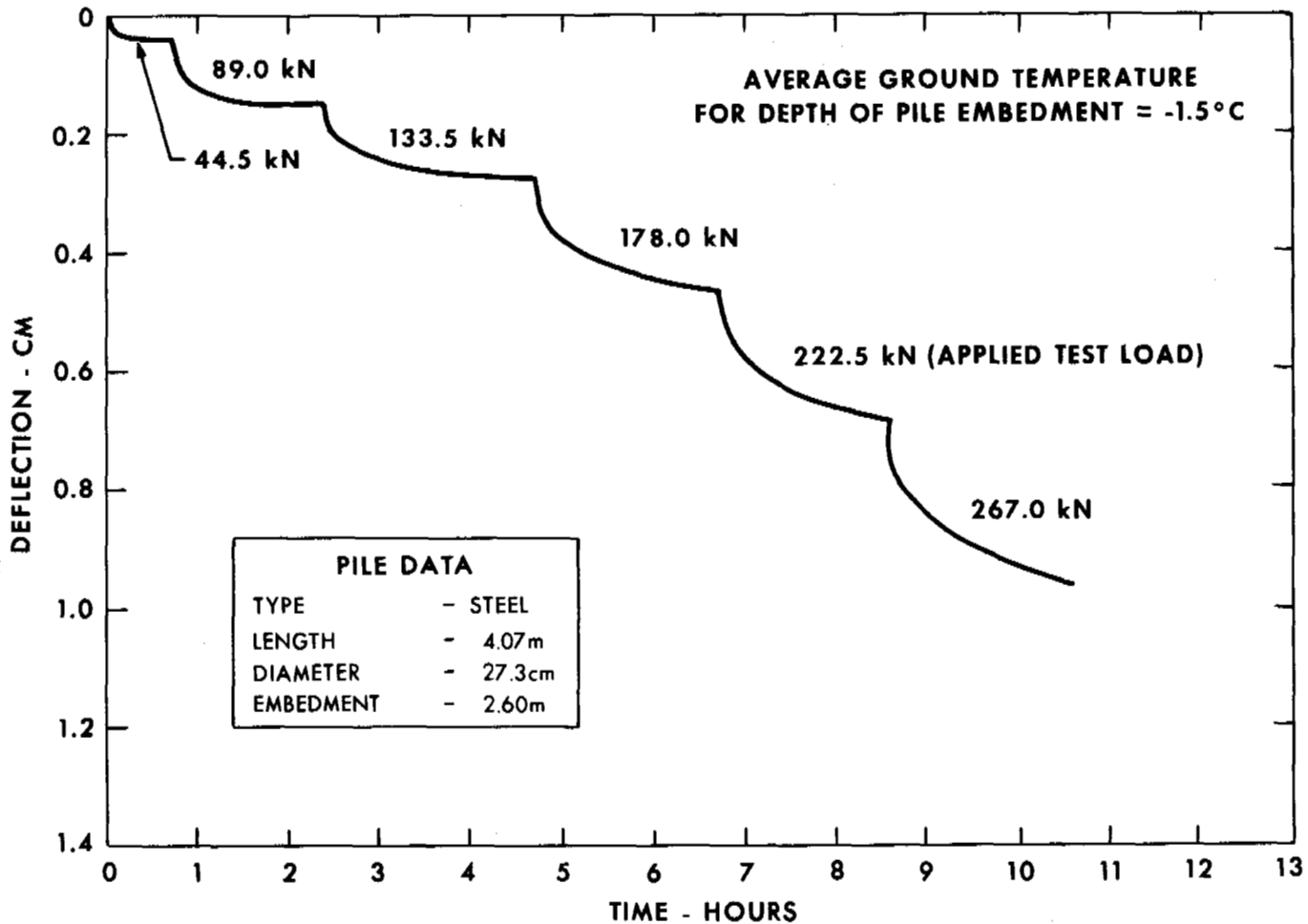


FIGURE 4 Short-term lateral-load test results; pile S-4-L.

Modulus of Lateral Subgrade Reaction from Inuvik Pile Load Tests

In the Inuvik tests, the deflections were measured a little above the ground surface, approximately at the point of load application. The test information can still be used, however, for estimating an approximate value of the secant K modulus and its variation.

The basic data from pile S-4-L were as follows: diameter, $B = 27.35\text{cm}$; wall thickness, 9.5 mm ; moment of inertia, $I = 6\,810\text{ cm}^4$; modulus of elasticity, $E = 273.5\text{ GPa}$. The embedded length of the pile was $L = 261.5\text{ cm}$, and the load Q was applied at the height $e = 53.4\text{ cm}$ above the ground surface. As shown in Figure 4, the pile was loaded up to 267 kN in six equal load increments of 44.5 kN each. After the first increment, the load was held constant for 43 min , while each of the five following steps was 2 h long.

To calculate the modulus of lateral subgrade reaction from the test results, it was necessary to put them in analyti-

cal form. Figure 4 shows that the deflection-time relationship within the first 2 h is approximately parabolic. The load versus instantaneous-creep-rate relationship was found to fit a power law form. The experimental data was, therefore, expressed by the equation

$$y = y_c (Q/\bar{Q})^a (t/t_c)^b, \quad (6)$$

where y is the deflection, Q is the applied load, t is the time, y_c is unit deflection, and t_c is unit time. The three constants to be determined from the test results are the proof load \bar{Q} and the two exponents a and b .

The three constants were determined as follows: First, by plotting y versus t in a log-log plot, a set of nearly parallel straight lines was obtained for which the average slope was equal to b ; second, the values of y at $t/t_c = 1$ are plotted against Q in a log-log plot from which a and \bar{Q} are determined. The following values of the three constants were obtained by this method: $\bar{Q} = 704\text{ kN}$, $a = 1.255$, $b = 0.23$, for the as-

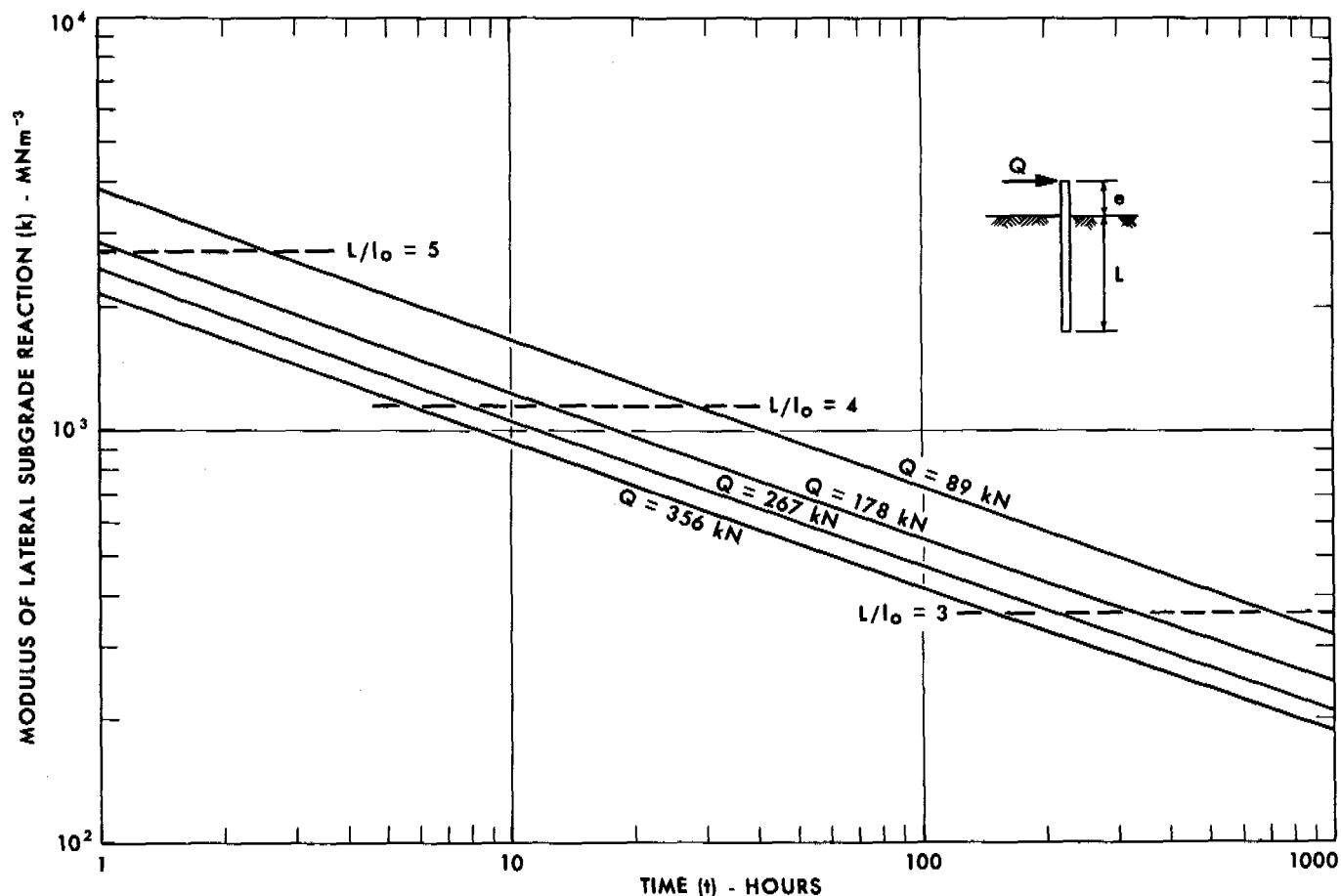


FIGURE 5 Modulus of lateral subgrade reaction values derived from Figure 4.

summed values of unit parameters of $y_c = 1$ cm and $t_c = 1$ h. Substituting these constants in Eq. (6), yields y in cm for Q in kN and t in h, with the deflections y coming close to the observed values.

Values of K were computed for loads of 89, 178, 267, and 356 kN, respectively, and at each load for the time intervals of 1, 10, 100, and 1 000 h. Because the ratio L/l_o was greater than 2.5 for all values of K in the entire domain considered, the computation of K was handled as shown below. Eq. (3) and (5) were combined resulting in the following:

$$(L/l_o)^3 = A[1 + (e/L)(L/l_o)], \quad (7)$$

where A is defined by

$$A = QL^3/2y_o EI. \quad (8)$$

Once L/l_o was known for each previously calculated deflection y_o , the value of K was obtained from the relationship:

$$K = (2Q/Ly_o)(L/l_o)[1 + (e/L)(L/l_o)] \quad (9)$$

Figure 5 shows the result of such a calculation. The modulus of lateral subgrade reaction, k , varied both with load and time over a large interval, ranging from about 4 000 MNm^{-3} at 1 h and the lowest load, to about 185 MNm^{-3} at 1 000 h and the highest load. For a fixed time, k decreases with increasing load, and for a fixed load, k decreases with time because of frozen soil creep.

In Figure 5, the levels of constant L/l_o ratios are also shown on the modulus-time (k - t) curves. L/l_o decreases with time from about 5 at 1 h to less than 3 at 1 000 h. This means that as the frozen soil creeps, the piles slowly lose their fixed support in the soil and become more and more free supported.

The method described permits determination of k for use in design from a pile test. It should, however, be noted that the calculated k values would be approximate, since they are obtained from a theory that assumes there is no lateral bearing capacity failure anywhere around the pile, which is not always true. For example, in the above case, the frozen soils have had to support pressures of up to 9 MNm^{-2} at the surface. This would obviously cause some local bearing failure at the surface and a partial loss of support.²

THEORETICAL PREDICTION OF LOAD-DEFLECTION CURVES

Outline of the Proposed Method

In the range of working loads, the lateral load-deflection curve for a segment of a pile is analogous to the load-settlement curve of a strip load. There have been few attempts to predict the entire pressure-settlement curve of the soil under a given loaded area. Instead, the problem is usually separated into a pressure-settlement portion, in which the soil is considered to be linearly elastic, and a failure portion, in which the soil behaviour is assumed to be perfectly plastic.

The method for pressure-deflection curve prediction proposed here uses, as the starting point, the similarity between the phenomena of deep penetration of punches and the expansion of cavities in soils. The similarity was first observed in deep punching of metals by Bishop,¹ who concluded that "... the pressure required to produce a hole deep in an elastic-plastic medium is proportional to that necessary to expand a cavity of the same volume and under the same conditions. . .". The proposed method assumes that the plastic settlement of a strip load or lateral displacement of a pile, in an amount smaller than half its width can be estimated by equating the displaced volumes at comparable pressures in the two cases. This assumption has already been shown to be valid for concrete⁸ and metals.⁷

The prediction of the load-deflection curve for a laterally loaded pile in frozen soil may, therefore, be achieved by

1. Solving the problem of pressure-creep expansion of a cylindrical cavity;
2. Transforming the pressure-expansion relationship valid for a cylindrical cavity into the pressure-settlement relationship for a strip load; and
3. Determining the final pressure-deflection relationship for the pile.

Creep of a Cylindrical Cavity under Internal Pressure

It is assumed that the frozen soil behaviour under a multiaxial state of stress is governed by the stationary creep rate equation⁶:

$$\dot{\epsilon}_c^{(c)} = d\epsilon_c^{(c)}/d\tau = A \sigma_c^n, \tag{10}$$

where $\dot{\epsilon}_c^{(c)}$ and σ_c are the equivalent creep strain and equivalent creep stress, respectively. The symbol τ denotes the transformed time, related to the real time by:

$$\tau = t^{1/(1+\mu)}, \tag{11}$$

while A denotes

$$A = [\dot{\epsilon}_c (1 + \mu) \sigma_c^{-m}]^{1/(1+\mu)}. \tag{12}$$

The exponent n is given by:

$$n = m/(1 + \mu), \tag{13}$$

where m and μ are creep exponents, σ_c is the creep modulus in units of stress while $\dot{\epsilon}_c$ is an arbitrary, conveniently selected strain rate.

The constitutive equation for frozen soil [Eq. (10)], can be determined from a series of stage-loaded creep tests on frozen soil specimens in the laboratory, or it can be found¹⁰ from the results of *in situ* stage-loaded pressuremeter tests. The latter method furnishes quick large-scale information on soil creep behaviour in the horizontal direction and under essentially plane strain conditions.

According to the solution for stationary creep of a cylindrical cavity under internal pressure,¹² the radial displacement rate of the cavity wall, \dot{u}_i , under a pressure increase of $(p_i - p_o)$ is given by:

$$\dot{u}_i = du_i/d\tau = (\sqrt{3}/2)^{n+1} A r_i [(2/n) (p_i - p_o)]^n, \tag{14}$$

where τ , A , and n are given by Eq. (11), (12), and (13).

For a single-step increase of internal pressure, the radial displacement after the time interval t will then be:

$$u_i(\tau)/r_{i0} = (\sqrt{3}/2)^{n+1} A [(2/n) (p_i - p_o)]^n \tau, \tag{15}$$

where r_{i0} denotes the radius of the cavity at the start of the creep period. Denoting by V_{i0} the corresponding volume of the unit length of cavity, it can be shown from geometrical considerations that the following relationship exists between the initial values r_{i0} , V_{i0} , and the current values r_i and V_i at the time t :

$$V_i/V_{i0} = [1 + u_i(\tau)/r_{i0}]^2. \tag{16}$$

Equation (16), combined with Eq. (15), represents the required creep expansion versus internal pressure relationship to be transformed into a creep settlement versus applied pressure relationship for a strip load.

Transformation of Pressures and Displacements

Based on the above mentioned experience with deep punching of metals, it can be considered that, when a cylindrical pile is pushed laterally into the soil, it generates a soil reaction equal to the cavity expansion pressure p_i . If it is assumed that p_i acts normally on half of the pile circumference and that friction and adhesion mobilized during the lateral movement at the soil-pile interface are small [Eq. (15)], one can replace p_i by the lateral applied pressure q .

Similarly, the amount of lateral displacement of a cylindrical pile in the range of penetrations smaller than half of its diameter, can be evaluated from the cylindrical cavity ex-

pansion displacements by equating the displaced volumes in both cases. This equality gives:

$$y/B = (\pi/8) (V_i/V_{i0} - 1), \quad (17)$$

which is the required displacement transformation formula.

Pressure-Deflection Relationship for the Pile

From the foregoing transformation, the final form of the pressure-deflection relationship for the pile can be found by replacing in Eq. (17) the ratio V_i/V_{i0} from Eq. (16), after having substituted in Eq. (16) the expression for u_r/r_{i0} given by Eq. (15) with p_i replaced by q :

$$y/B = (\pi/8) \left\{ \left(1 + (\sqrt{3}/2)^{n+1} [(2/n)(q - p_0)]^n A \tau \right)^2 - 1 \right\}. \quad (18)$$

The pressure-deflection, or the q - y curve, obtained is not only a nonlinear function of pressure but also a nonlinear function of time [through τ , from Eq. (11)] and temperature [through the creep modulus, σ_c , from Eq. (12)⁹].

A distinct q - y curve can therefore be determined for each given set of time and temperature values. If such q - y curves are determined at different levels along the whole embedded length of the pile for the most unfavourable design conditions (e.g., for a 30-year period) and by assuming the highest probable permafrost temperature along the pile, the design problem of laterally loaded pile could be solved either directly on the basis of the predicted q - y curves or by the conventional subgrade modulus method.

In the latter case, since the q - y plots are nonlinear, an average lateral subgrade modulus can be determined. Its general expression is:

$$K = (q - p_0)/(y/B), \quad (19)$$

where K is the subgrade modulus in the units of stress.

The foregoing analysis is valid if the frozen soil shows only elastic and creep deformations without bearing capacity failure. For failure conditions, the ultimate lateral resistance of the pile can best be estimated by Broms' method for clays in which, however, the cohesion should be made time and temperature dependent.⁹

CONCLUSIONS

1. Results obtained from vertical pile-load tests gave average maximum adhesion values of 43 kNm⁻² at an average temperature of -1 °C.

2. For lateral load tests, the largest load at which terminating creep occurred averaged 110 kN for timber piles and 175 kN for steel piles. Based on these results, the working pile capacities of 62 and 89 kN, respectively, were selected.

3. Using the theory of lateral subgrade reaction, the pile load test data was analyzed. In addition to varying with load due to nonlinearity of the soil pressure-deflection relationship, k decreased with time as a result of soil creep. In the considered case, its value decreased within 1 000 h to less than one tenth of its 1-h value.

4. A theoretical method for predicting the time- and temperature-dependent pressure-deflection curve for the frozen soil using the basic constitutive creep equation of the soil was developed. Preliminary comparisons of predicted and observed pile behaviour have shown promising results.

ACKNOWLEDGMENTS

The authors are grateful for the interest and assistance of their colleagues throughout the project, particularly Mr. R. H. Winn, Jr., Mr. J. J. Termina, and Mr. W. Miller.

This paper is published with the approval of the Research Coordinator of Mackenzie Valley Pipe Line Research Limited.

REFERENCES

1. Bishop, R. F., R. Hill, and N. F. Mott, 1945. The theory of indentation and hardness test. *Proc. Phys. Soc.* 57:147-159.
2. Broms, B. B. 1964. Lateral resistance of piles in cohesive soils. *Proc. ASCE* 90(SM2):27-63.
3. De Beer, E. E. 1948. Computation of beams resulting on soil. *Proc. 2nd Int. Conf. Soil Mech. Found. Eng. (Rotterdam)* 1:119-121.
4. Gleser, S. M. 1953. Lateral load tests on vertical fixed-head and free-head piles. p. 75-101. *Symposium on lateral load tests on piles. STP 154. ASTM, Philadelphia.*
5. Hetenyi, M. 1946. *Beams on elastic foundation.* University of Michigan Press, Ann Arbor. p. 127-140.
6. Hult, J. A. H. 1966. *Creep in engineering structures.* Blaisdell, Waltham, Massachusetts.
7. Johnson, K. L. 1970. The correlation of indentation experiments. *J. Mech. Phys. Solids.* 18:118-126.
8. Ladanyi, B. 1966. Failure mechanism of rock under a plate load. *Proc. 1st Congr. Int. Soc. Rock Mech. (Lisbon)* 1:415-420.
9. Ladanyi, B. 1972. An engineering theory of creep of frozen soils. *Can. Geotech. J.* 9:63-80.
10. Ladanyi, B., and G. H. Johnston. Evaluation of *in situ* creep properties of frozen soils with a pressuremeter. This volume.
11. Matlock, H., and L. C. Reese. 1961. Foundation analysis of offshore pile supported structures. *Proc. 5th Int. Conf. Soil Mech. Found. Eng. (Paris)* 2:91-97.
12. Odquist, F. K. G. 1966. *Mathematical theory of creep and creep rupture.* Clarendon Press, Oxford.
13. Poulos, H. G. 1971. Behaviour of laterally loaded piles: I—Single piles. *Proc. ASCE* 97(SM 5):711-731.
14. Reese, L. G. 1972. The analysis of piles under lateral loading. *In Proceedings, Symposium on the interaction of structure and foundation, University of Birmingham, G.B., 1971.*
15. Sanger, F. J. 1969. *Foundations of structures in cold regions.* Monogr. 111-C4. CRREL, Hanover, New Hampshire.
16. Terzaghi, K. 1955. Evaluation of coefficients of subgrade reaction. *Geotechnique* 5:297-326.
17. Vesic, A. S. 1961. Bending of beams resting on isotropic elastic solid. *Proc. ASCE* 87(EM2):35-53.

18. Vyalov, S. S. 1959. Rheological properties and bearing capacity of frozen soils. Translation 74 UBA. CRREL, Hanover, New Hampshire.
19. Watson, G. H., R. K. Rowley, and W. A. Slusarchuk. Determination of some frozen and thawed properties of permafrost soils. (In preparation)

20. Watson, G. H., R. K. Rowley, and W. A. Slusarchuk. Performance of a warm-oil pipeline buried in permafrost. This volume.

NOTES

- [1] On loan from Standard Oil of California.
[2] On loan from Acres Consulting Services, Calgary, Alberta.

DESIGN AND CONSTRUCTION OF PRACTICAL SANITATION FACILITIES FOR SMALL ALASKAN COMMUNITIES

William L. Ryan

U.S. INDIAN HEALTH SERVICE
Anchorage, Alaska

INTRODUCTION

Alaska is the largest state (1 500 000 km²) of the United States, but has the smallest population (300 000 people). The population includes around 55 000 natives (Indians, Eskimos, and Aleuts) many of whom live in some 200 villages spread throughout the state. These villages range in size from a few families up to 400 families.

Lying at the same latitude, it is slightly larger than the Scandinavian countries of Norway, Sweden, and Finland (Figure 1). However, most of Alaska's climate is colder, since the Aleutian chain deflects the northward flow of the warm Japanese Current, while the Gulf Stream warms Scandinavia's climate. Alaskan construction seasons vary from about 10 months in the southeast panhandle to less than 4 months in the northern sector.

INDIAN HEALTH SERVICE OBJECTIVES

The Alaska Area Sanitation Facilities Construction Branch of the U.S. Indian Health Service (IHS) has the responsibility of raising the health of the natives to the highest possible level through the provision of safe and adequate sources of water and hygienic waste disposal facilities for all villages.

Waterborne and environmentally related diseases are prevalent in the native villages. The provision of an adequate, safe source of water in each home can reduce the incidence of these diseases (Table I). The figures in Table I are estimates since many cases are probably not reported because the nearest hospital may be hundreds of miles away.

Public Health Service studies¹² have shown that the mor-

bidity rates for enteric and other waterborne diseases are reduced by the provision of a safe water source within the community. These studies also indicated that disease levels are reduced considerably more if the water is safely distributed to the individual homes. Three reasons for this follow:

1. People tend to continue using the lake, stream, ice, or snow they have always used (especially during the winter), unless the community watering point is close to their home. However, it is seldom possible to accomplish the latter for all houses within a village;
2. The water often becomes contaminated when it is carried by the individuals to their homes and while stored within the homes; and
3. The quantity of water used within the home has a significant effect on a healthy home environment. When the water must be hauled by the individual, less is used.

Thus, environmental health personnel do not consider the goal of maximum potential health improvement has been met in a given village, unless a safe and adequate supply of running water can be distributed to each house either by vehicle or pipes.

Villages receiving new housing through U.S. Government- or village-supported housing programs receive first priority for IHS sanitation facilities. These housing construction programs will provide an estimated 500 new houses in some 20 different villages each year. Improved housing is an important need, since statistics indicate that the present rural native home consists of 1.5 rooms in which 5.6 people live.

Even though modern trade skills are being developed by

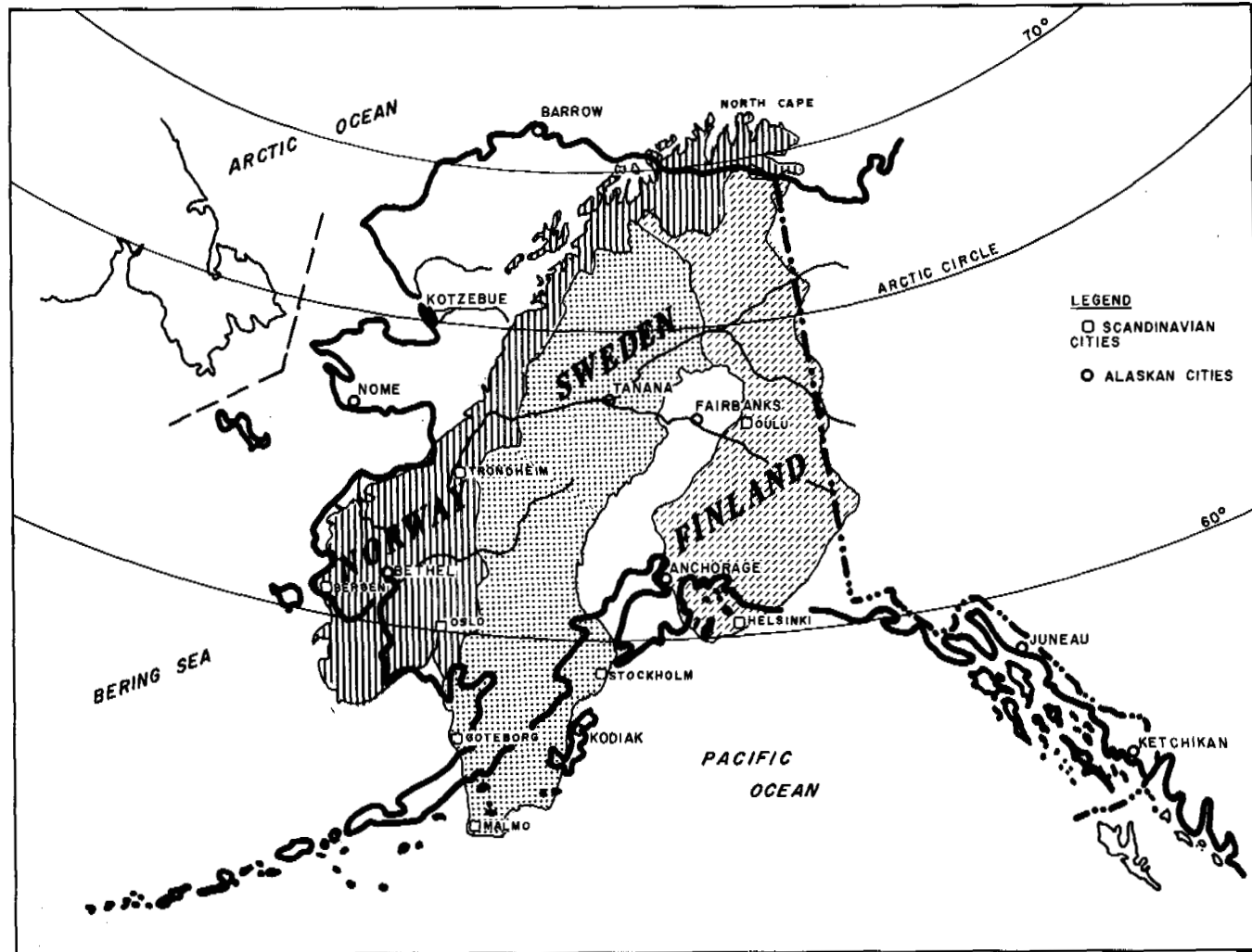


FIGURE 1 Identical latitude comparison between Scandinavia and Alaska.

the natives in the communities, construction foremen and heavy equipment operators usually must be imported from the larger towns at wages of over \$10/h. Part of the IHS program is to develop in the natives the basic skills needed for plumbing and pipe laying, etc., so the community can successfully operate, maintain, and later expand the completed sanitation facilities. In addition, basic bookkeeping and billing

TABLE I Incidence of Diseases Reported by IHS Hospitals in Alaska in 1971

Disease	No. of Cases per 1 000 Alaska Natives
Otitis media	98
Impetigo (severe)	6
Dysentery and diarrhea	14.4
Hepatitis	1.3
Upper respiratory infections	178

procedures must be developed to collect fees from the users for operation and maintenance of the systems.

GENERAL DESIGN CONSIDERATIONS

Design and construction of sanitation facilities in the arctic areas include all the challenges of conventional design and construction as used in the temperate climates plus several additional considerations pertaining to the cold environment. The design of sanitation facilities should consider the conservation and utilization of all available heat sources to reduce the operational expenses of the facilities. In nearly all installations, heat must be added to the water at some point between the source and the consumers.

"Cold" as a Resource

An example of using the cold as a resource is the desalinization of brackish water by freezing. IHS is conducting studies

to determine the feasibility of using large flat rubber "pillow" tanks or open rubber-lined reservoirs for desalinization. The tank or reservoir would be pumped full of brackish water in the fall and allowed to freeze through the winter. Then in early spring the concentrated brine in the center and bottom of the tank would be pumped away. During the summer, the ice will melt and could probably be used for domestic purposes. The cycle may have to be repeated if the meltwater is still brackish.

Locale

Remoteness is a major problem that must be dealt with in arctic construction. All system components, such as pumps, boilers, and electrical generators, are provided with identical standby units. In most cases, it is impossible to send repairmen or parts into a remote village in the winter in time to prevent considerable damage due to freezing of the lines after a component fails. Also, because of a lack of skilled repairmen, it is necessary to keep the controls and facilities as simple as possible so unskilled workmen can be instructed to do all but major repairs. Even though keeping a system simple is important, it must not be simplified to the extent that safeguards, warning devices, etc., are omitted from the design. These safeguards can warn the operator if the circulation should stop in a line, or if the water temperature at the coldest points in the system should drop below a preset value, about 5 °C.

Planning

The increase in new housing and sanitation facility design and construction has highlighted the very real need for community planning in the North. Both the type of sanitation facilities required and the economic feasibility are greatly influenced by the location and layout of the native village. The villages already exist in the majority of the cases, and little planning took place in their original layout and location. However, it must be utilized in the present planning for new houses.

Community planning must take into account the distinct environmental conditions of the North. Some of the problems with possible solutions are as follows:

1. Adequate drainage of the village site is very important in the reduction of diseases, for safety, and for reducing the maintenance costs of all facilities. Villages should be located on sloping ground with roads and walkways constructed with the slope so they do not act as dams to the drainage of water. For roads across the slope, culverts can be installed, but means of keeping them ice-free and open must be provided;
2. Communities should be located on coarse, well-drained soil, if at all possible, to prevent frost heaving problems. Gravel is usually as valuable as gold in permafrost areas;
3. Roadways and building entrances should be located

so the prevailing winter winds in the area will keep them clear of snow;

4. Buildings in the village should be concentrated in one area in order to minimize all utility costs, and parks and school playgrounds should be located on the outskirts of the community rather than in its interior;

5. Communities should be located on south-facing slopes, where possible, to take advantage of solar warming and to provide some protection from the cold northern winds. Also, in discontinuous-permafrost areas, permafrost is usually absent on southern exposure slopes and construction is thereby facilitated;

6. Floodplains must be avoided, unless the houses and utilities can be economically protected from floodwaters and floating ice; and

7. Multifamily housing should be seriously considered, instead of the single family dwellings now being constructed, to reduce utility costs and lower heating costs.

Design Parameters

In many IHS-constructed facilities, heat exchangers are installed on electrical generators to utilize the waste heat from the engine cooling system and/or the exhaust to heat the water to be distributed. In some instances this heat, combined with styrofoam or urethane insulation on the pipelines, is all the heat needed to operate the village utility systems. Nearly all communities contain electrical generators, either in the form of a community-operated facility or to provide electricity to the schools. The availability of electricity is a necessity before one can consider the installation of a piped water distribution system. However, the system must be designed to minimize electrical use because electricity costs vary between 10 and 50¢/kW-h with an average of 20¢/kW-h in Alaskan arctic villages.

Water source and treatment facilities are designed to provide water meeting the U.S. Public Health Service Drinking Water Standards,¹³ where possible. Experience has indicated that arctic villages will use about 0.2 m³ per capita per day when provided with a piped water distribution system and the houses are equipped with sink, lavatory, toilet, and bathtub. Sewage treatment facilities must be designed to treat nearly all the water supplied in arctic native villages because there is little or no lawn watering or car washing, etc. In many villages, an adequate water supply (quality and/or quantity) is difficult to find or expensive to provide and maintain, and ways of reducing water use must be found. Studies³ have shown that 41 percent of the water used in an average home, in the conterminous United States, is used in flushing the toilet (using conventional 20 dm³ per flush toilets) and 37 percent is used for bathing. Thus, low water use toilets, which can flush on 2–6 dm³ of water, and limiting flow valves on showers and sinks should be used in the Arctic. These de-

vices also concentrate and reduce the quantity of sewage that requires treatment and disposal.

Practicality and Social and Economic Acceptability

Approximately 20 percent of the rural Alaskan natives have been served with running water since the IHS sanitation facilities construction program began in 1960. Requests have been received from some 100 additional villages requesting facilities under the program. The rural native people are becoming more aware of the dangers of poor sanitation practices and, because they are doing more and more traveling, they desire the sanitation facilities such as they see in the larger cities of Anchorage, Fairbanks, and Seattle. As can be seen in Table II, the cost to users for piped water and sewers does not have to be beyond their financial capability, and in many cases it is considerably less than what they were previously paying to have a few gallons of drinking and cooking water intermittently delivered by truck. There are other sources of funds to assist individuals and communities in the operation of their facilities also:

1. The State of Alaska has a revenue sharing program that will pay a village \$7 per capita per year if they provide water pollution control facilities and have fire protection capabilities;
2. Individuals receiving welfare, old age pensions, etc., can usually have their payments increased to include the utility costs.
3. Homeowners receiving new houses under Department of Housing and Urban Development housing programs pay nothing additional for utilities as the utility payments are part of the house payment they make. Their house payment is based entirely on their yearly income whether there are utilities or not; and
4. In the case of an emergency, IHS can usually obtain funds to help the village repair their facilities.

To increase the practicality of the sanitation facilities, a "total utility concept" must be considered in each village. This means the water and sewer utilities must be designed and constructed to serve the elementary and high schools, government buildings, health clinics, churches, etc., as well as the individual homes. IHS has received considerable cooperation from the other federal, state, and private agencies and installations in combining sanitation facilities to produce a practical solution instead of each entity developing its own.

Water can be distributed and sewage collected in a native village by two acceptable methods: hauling by vehicle or by using pipelines. IHS presents the alternatives to each village, before facilities are designed, pointing out advantages and disadvantages of each. The final facilities must be fully acceptable to the village because, after completion of the construction, the day-to-day operation and maintenance becomes

their responsibility. All the villages have a very limited or non-existent economic base. This decision, faced jointly by the village and IHS, can be broken down into two main considerations: engineering feasibility and the projected capability of the community to operate and maintain the completed facilities.

The oldest form of water distribution and sewage collection in Alaska is by hauling. Usually vehicles (trucks, if roads are present, or all-terrain vehicles if they are not) are used to deliver water from the source to the houses and to collect the wastes. In the smaller villages, this is usually accomplished by snow vehicles in winter and by hand in the summer. This method of distribution has several disadvantages, three of which were discussed in the introduction. Some additional problems include the following:

1. It is nearly impossible to drive a vehicle in many villages in the summer because of poor soil and drainage conditions;
2. Experience has shown that there is not the same incentive in a village to contribute toward the operation and maintenance of this type of facility that there is when the water is piped into the individual's house and sewage piped away; and
3. Even though initial construction costs are generally lower, operational costs have proven to be higher with the haul systems because of the additional labor necessary to operate and maintain the pickup and delivery equipment.

In cases where the village is extremely spread out or water is very limited, a hauled-type system is a feasible consideration.

WATER SOURCES AND TREATMENT

When a village is placed on the list to receive new houses, one of the first steps in designing the sanitation facilities is to determine the most practicable water source and the quantity and quality of the water it will produce.

Water Source

Subpermafrost wells are drilled for water sources at most village sites having less than 100 m of permafrost, provided treatable water is available. However, dams constructed during the winter and maintained in a frozen condition have been utilized in areas where it is not economical to drill through the permafrost or to treat the water found there. Most of the arctic native villages are located on the western and northern seacoast and brackish groundwater is quite often encountered. Infiltration galleries constructed of perforated pipes buried in the banks or beds of streams that run throughout the year have also been successfully used in villages where wells will not produce a satisfactory source.

TABLE II Sanitation Facilities Now in Operation in Alaska Native Communities

Community and Location (No. of Houses Served)	Type of Facilities	Year Placed in Operation	Approx. Cost to Consumers \$ per Mo. per House	Notes
Barrow on Chukchi Sea (300)	Lake used for source; water hauled by truck; waste collected by truck		\$40 about average	Haul services have had record of failure because of lack of ability to collect adequate amount from consumers
Unalakleet on Norton Sound (120)	Circulating water system; gravity sewer system; infiltration gallery set in stream; facultative lagoon	1966	\$17	Sewer system and lagoon completed in 1972; well-drained soil; buried pipelines
Kaltag on Yukon River (29)	Watering point and batch water treatment; individuals haul own water; privies used for toilet wastes; cesspools used for sink wastes	1966	\$ 5	Operation of watering point has been intermittent; piped water dist. and sewage collection systems now under construction
Grayling on Yukon River (30)	Circulating water system; individual waste disposal; well as water source	1967	\$ 8	Sewer system desirable in future; well was deepened in 1970; buried pipelines
Russian Mission on Yukon River (30)	Well as water source; circulating water source; gravity sewer system; facultative lagoon	1969	\$ 5	Buried pipelines; some flood damage to lagoon in 1971
Holy Cross on Yukon River (40)	Well as water source; circulating water system; gravity sewer system; facultative lagoon	1969	\$ 8	Buried pipelines; well drained soils
Kotzebue on Chukchi Sea (300)	Circulating water system; gravity sewer system; facultative lagoon; dammed creek source	1970	\$15	Buried pipelines; color and taste removal water treatment unit to be added Dec. 1972
Hughes on Koyukuk River (15)	Well as water source; dual main circulating water system; individual septic tanks	1970	\$20	Project cost includes electrical generator which provides a limited amount of electricity for each house; buried pipes
Kipnuk on Bering Sea (45)	Reverse osmosis desalinization unit; individuals haul their water from RO unit	1970	\$50	Generator supplied for power to RO unit has been maintenance problem; ground in village is so soft in summer that boardwalks are a necessity for foot travel
Gulkana on Gulkana River (25)	Well for water source; circulating water system; gravity sewage system; community septic tank with tile field	1970	\$ 8	Well-drained soil; buried pipes
Dot Lake on Alaska Highway (10)	Well for water source; conventional water system and central heat in utilidors; individual septic tanks and tile fields	1970	\$40	Project and cost includes central heat distributed to houses in buried utilidors
Tetlin on Alaska Highway (25)	Well as water supply; central watering point and laundromat from which water is hauled by individuals; lagoon for treatment	1970	\$15	Village has requested piped water dist. and sewage collection system, which is now under design
Shishmaref on Chukchi Sea (44)	Watering point from which individuals haul water; recirculating type recreation vehicle toilets used with wastes discharged to cesspools	1970	\$ 6	Operation of watering point has been intermittent; some maintenance problems have been encountered with the electrically operated toilets
Bethel on Kuskokwim River (200)	Circulating water system; pressure sewer system; subpermafrost well; facultative lagoon	1971	\$25	Houses to be placed on piling in Jan. 1973 because of settlement problems; buried pipelines

TABLE II (Continued)

Community and Location (No. of Houses Served)	Type of Facilities	Year Placed in Operation	Approx. Cost to Consumers \$ per Mo. per House	Notes
Nome on Norton Sound (180)	Circulating water system; gravity sewer system; infiltration gallery; set in spring	1971	\$19	Buried walk; through utilidors; some damage caused to utilidors by frost heave and drainage water
Chistochina on Copper River (10)	Well as water source; circulating water system; individual septic tanks for waste disposal	1971	\$10	Buried pipelines; well-drained soils
Minto west of Fairbanks (40)	Well as water source; circulating water system; gravity sewer system; facultative lagoon for treatment	1971	\$16	Problems have been encountered because of undependable electrical power and inability of village to reliably maintain facilities; buried pipelines
Lower Kalskag on Kuskokwim River (40)	Well as water source; circulating water system; gravity sewer system; community septic tank and tile field	1971	\$ 6	Well-drained soil; buried pipes; permafrost not present at edge of river where tile field is located
Kiana on Kobuk River (50)	Well as water source; circulating water system; gravity sewage system; extended aeration sewage treatment plant	1972	\$25	Buried pipelines; not room for lagoon without expensive pumping equipment
Wainwright on Chukchi Sea (55)	Large storage tank filled in summer from lake; tracked vehicles to deliver water and collect sewage; central water and sewage treatment facility with incinerator funded and constructed by U.S. Environmental Protection Agency as a demonstration project	1972	\$45 est.	To be operational by Nov. 1972 and in complete operation in summer 1973; capacity of tank will allow usage through winter without pumping from the shallow lake

IHS operates three small cable-tool (churn-type) well-drilling rigs. These units are slower than the larger rotary drilling rigs, but they can be dismantled and transported to isolated villages with a small bush airplane.

Water Treatment

The type of water treatment provided for the villages varies from simple chlorination and fluoridation to desalinization. All sources are chlorinated as the last treatment step to provide a chlorine residual that protects the water from future contamination in the distribution system.

Natural fluorides are absent in nearly all water sources in arctic Alaska. Thus, fluoride is added at the recommendation of the IHS dentists, to prevent tooth decay. Fluoride saturators are generally used for fluoride addition, since they essentially eliminate the possibility of an overdose.

Probably the most common treatment problem encountered (but also the most easily solved) is the removal of iron. Concentrations vary up to 50 ppm with an average of about

5 ppm. IHS has used several different iron-removal processes such as lime-alum addition, with flocculation and settling, and aeration and filtration. Filtration through ion-exchange resins with potassium permanganate continuously fed to recharge the resin has proven to be the most trouble-free and economical treatment. However, an economical method has not been found for removing iron on an individual house basis in remote villages where the houses are widely scattered and individual wells are provided. Several small package units have been tried, but all have presented operational and maintenance problems and thus are not satisfactory for use in a remote native village.

The most difficult treatment problem encountered is the treatment of brackish water on the small scale needed to provide potable water for a native village. At present, reverse osmosis units seem to offer the most practical treatment method, but membranes have not yet been perfected to treat sea water. Several 4 m³/day units have been tried with varying degrees of success. Vapor compression distillation units have been used to treat seawater at IHS hospitals

at Kotzebue and Barrow. These units have been a continuous and expensive operation and maintenance problem, even at these installations where highly paid and trained maintenance people are available. They would impose far too great a financial and technical burden on a small native village.

Frequently, color and tastes must be removed from water. This problem is nearly always encountered when a surface source is developed in a tundra area. The water absorbs tannins and lignins as it drains through the moss and lichens. There are treatment methods under investigation at this time, such as oxidation using ozone and flocculation, settling, and filtration after feeding polyelectrolytes, to assist floc formation. A polyelectrolyte feed-filtration unit is being installed at present to treat the surface water source for the City of Kotzebue.

Nitrate removal has been a problem in some isolated cases, and no practical solution has been found short of distillation.

WATER DISTRIBUTION AND SEWAGE COLLECTION

Different approaches, such as pressure and vacuum sewage collection systems and circulating water distribution systems, have been and are being constructed in arctic Alaska to provide the native communities with sanitation facilities and to protect the arctic environment. In nearly all cases, the quantity of water is limited or it must be treated, and economics prevent using conventional type systems that waste water in order to prevent the lines from freezing. Another disadvantage of bypassing water is the large quantities of wastewater that require treatment and disposal.

Circulating Water System

The most widely used water system design in arctic Alaska is a single main circulating system using "pitofices" (Figure 2) for circulation in the house service lines.¹⁰ A small circulating pump or venturi can also be used for service line circulation. A single main circulating water system is installed in a loop beginning and ending at a pumping station where heat can be added to the circulating water as needed to maintain a water temperature of about 5 °C. The main lines must lie within 20 m of each house served if pitofices are to be effective for circulation in the service lines, and the velocity in the service line will be roughly one tenth of that in the main. All mains are sloped to low points where T-based fire hydrants are located directly over the line. The lines can be quickly pumped dry through the hydrants to prevent freezing in the event circulation must be stopped.

Sewage Collection Systems

In most villages conventional gravity sewage collection systems are used with several alterations added to reduce

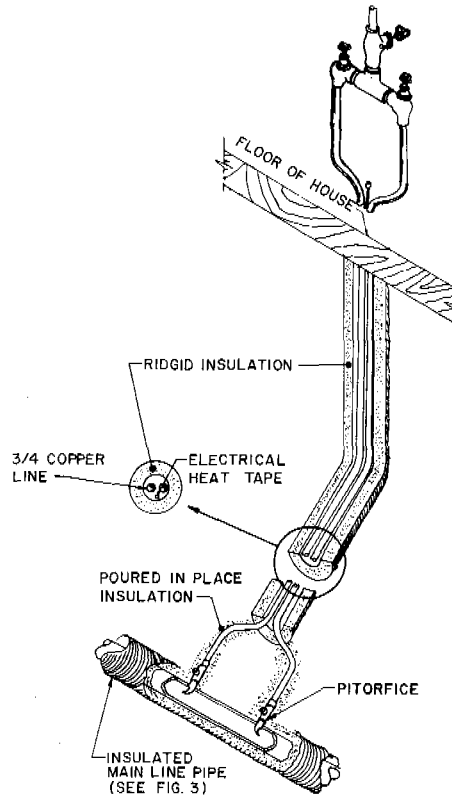


FIGURE 2 Typical pitofice service line insulation.

freezing problems. All lines and manholes are well insulated and dead ends are constructed so they can be flushed with warm water during periods of low flow. Very little pipe movement can be tolerated with gravity sewers. If soil and drainage conditions indicate frost heaving or settling, other sewage collection systems not relying on gravity must be considered. One type that IHS has used is a pressure system. The sewage is pumped from each house, or small cluster of houses, through pressurized mains to the sewage treatment facility. The pressure lines do not have to be graded, and smaller lines can be used. However, the pumping increases the operational and maintenance costs. Studies are in progress at present to develop more reliable pump-grinder units for the individual houses served with pressure sewer systems.

Another type of collection system that can be used in locations where frost heaving is a problem is the vacuum sewer system. This system was originally developed in Sweden and utilizes a central collection tank that is held under a vacuum. The main lines (smaller in size like those in a pressure system) connect the individual houses to the collection tank and are also under vacuum. The plumbing fixtures in the houses are equipped with vacuum breaking valves, which, when opened, allow the contents to be drawn through the

lines to the collection tank. Again, grading of the lines is not critical and as an added advantage, the toilets only use 1.2 dm³ per flush. Vacuum sewage collection systems are currently in operation in Sweden and Bermuda, and IHS plans to have a system in operation in the Arctic by August 1973. It will be closely monitored, and information will be gathered for future designs. In locations where the sewage collection lines must be installed above ground in utilidors, a pressure or vacuum system approach is very inviting because, if one relies on gravity and the terrain is level, many houses may have to be elevated high off the ground.

Materials and Methods

There are three primary methods of constructing water distribution and sewage collection lines in arctic areas: insulated pipes buried directly in the soil, buried utilidors, and above-ground utilidors. All three have been used by IHS, with buried pipelines proving to be the most successful and economical to construct and maintain. IHS has developed an insulated pipe consisting of a polyvinylchloride plastic carrier pipe surrounded by a corrugated aluminum culvert with the annular space filled with urethane insulation (Figure 3) which is used for essentially all water distribution and sewage collection lines. The sizes of the inner carrier pipe and outer protective pipe can be varied to provide the needed flow capacity and correct amount of insulation. Above-ground utilidors on piling are the preferred construction method under high-soil-moisture (frost-heave) conditions. If central heating facilities are provided, utilidors are usually more economical, regardless of soil conditions. Utilidors are expensive to construct (around \$900/m compared with \$60/m for buried pipelines) and maintain, and the houses served must be closely spaced to reduce total utilidor footage. Any above-ground facilities are subject to vandalism, greatly increased heat losses because of colder outside temperatures, and drifting snow, and they tend to hinder foot and vehicular traffic around the village. Above-ground utilidors do have the advan-

tage that access can be gained any time of the year for repairs.

SEWAGE TREATMENT

Because of the high cost of electricity and lack of maintenance personnel and equipment, sewage treatment facilities must be designed to operate as simply as possible.

Lagoons

A facultative lagoon is the first consideration if local conditions permit. Near most villages in the Arctic, there are small shallow ponds that freeze to the bottom in the winter. In many cases, the outlets of these ponds can be dammed to increase their depth to the point they can be used as a facultative sewage treatment pond. There can be an odor given off for a short period of time when the ice melts in the spring but with the long periods of sunlight in the summer, treatment efficiency is high. Thus, they should be designed to retain the entire flow during the winter months. Facultative lagoons should be located downwind and at least 300 m from the nearest dwelling. The lagoons must be designed to prevent the incoming sewage from thawing the permafrost beneath it to the extent the lagoon structure will be jeopardized.

If there is not sufficient area available for a facultative lagoon, an aerated lagoon can be considered. Aeration is usually accomplished with air distribution tubing laid on the floor of the lagoon. In some cases where reindeer processings or other industrial waste is present only in the summer, a surface aerator is used in the village lagoon to temporarily increase the treatment capacity.

Treatment Plants

The topography of some villages prevents the use of even an aerated lagoon without the requirement of expensive pumping. In many of these places, however, there is room for a small

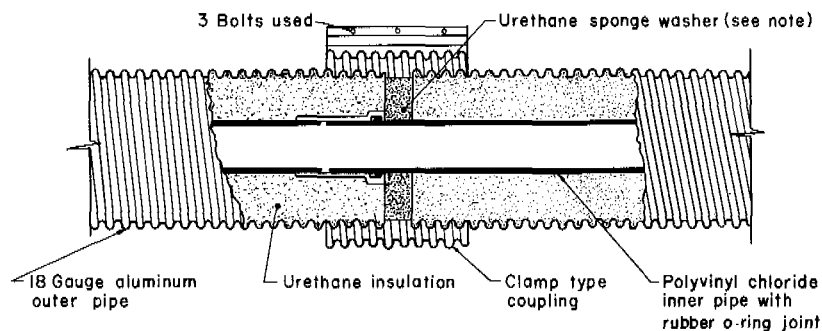


FIGURE 3 IHS insulated pipe. Sponge washer is 7.6 cm thick and compressed to 5.1 cm when pipe is jointed.

extended aeration plant. These package-type plants must be completely housed in a heated, ventilated building. Two of the disadvantages of these plants are that skilled operators are needed; and that they are more expensive to operate and maintain. If operated properly, however, they provide a higher degree of treatment than a lagoon.

Physicochemical package treatment plants have been used by oil exploration camps on the North Slope of Alaska with very good results; because of high operating costs, however, IHS has not used them in the native villages. They are essentially a water treatment plant and can handle intermittent flows because they do not depend on biological action. Physicochemical plants require considerable amounts of chemicals during operation and produce sludge that requires disposal.

Community Septic Tanks

Large community septic tanks with drain fields have been installed in small villages where room was not available for a lagoon and the village could not economically operate and maintain a package-type plant. The drain field must be installed in beach sand or gravel along the ocean or a river where permafrost is absent. As with all treatment solutions, equipment and training must be provided for the operation and maintenance of the septic tanks.

CONCLUSIONS

Table I summarizes many of the IHS installations currently in arctic Alaska. There are also about six village sanitation facilities in different stages of construction and some 30 under design. Several conclusions can be drawn from the work IHS has done in rural Alaska:

1. Piped water distribution and sewage collection facilities can be designed so they will be successfully operated and maintained by the native villages;
2. Piped facilities are usually more costly to construct but less expensive to operate and maintain than haul-type facilities relying on vehicles;
3. Morbidity rates for enteric and other waterborne diseases are reduced considerably further with the provision of safe water distribution and sewage collection systems than they are if a watering point only is provided in a community;
4. The native people have a definite desire to improve their environment;
5. Heat should be conserved, and "cold" used as a resource in the design of facilities in any cold climate;
6. All vital components, such as pumps and boilers, must be provided with identical standby units and equipped with devices that warn the operator if they fail;
7. Good community planning practices are absent in most

existing villages, but must be considered when laying out new villages or expanding old ones;

8. Promising new and innovative ideas should definitely be considered in the design and construction of sanitation facilities in the Arctic;
9. Desalinization of brackish water is the most expensive and least desirable solution to a village's water problems;
10. A practical and economical substitute is needed for the conventional gravity sewage collection system in small Alaskan villages;
11. In most native villages, a utilidor-type system is very expensive to construct and maintain. If ground conditions permit, buried insulated lines are a much more satisfactory solution; and
12. Sanitation facilities should be kept as uncomplicated as possible, but still accomplish the basic objective of improving the health of the native people.

The Indian Health Service has considerable work yet to accomplish to reach the goal of providing an adequate, safe source of running water and hygienic waste disposal for each native home in Alaska. At present, there is an unmet need of some 4 000 existing houses that lack adequate sanitation facilities plus the new houses being built each year.

REFERENCES

1. Alter, A. J. 1969. Sewerage and sewage disposal in cold regions. Cold Regions Science and Engineering Monograph III-C5b, U.S. Army CRREL, Hanover, New Hampshire.
2. Alter, A. J. 1969. Water supply in cold regions. Cold Regions Science and Engineering Monograph III-C5a, U.S. Army CRREL, Hanover, New Hampshire.
3. Bailey, J. R., *et al.* 1969. A study of flow reduction and treatment of wastewater from households. Water Pollut. Control Res. Ser. No. 11050 FKE. U.S. Government Printing Office, Washington, D.C.
4. Crum, J. A. 1971. Environmental aspects of native village habitat improvement in Alaska. Rep. No. EEP-46. Stanford University, Palo Alto, California.
5. Grainge, J. W. 1969. Arctic heated pipe water and wastewater systems. *Water Res.* 3:47-71.
6. Grainge, J. W., and J. W. Shaw. 1971. Community planning for satisfactory sewage disposal in permafrost regions. Paper presented at the Second International Symposium on Circumpolar Health, Oulu, Finland.
7. National Research Council. 1966. Permafrost: Proceedings of an international conference. National Academy of Sciences, Washington, D.C.
8. Proceedings, Symposium on cold regions engineering. Vol. I and II. University of Alaska, College. March 1971.
9. Ryan, W. L. 1970. Effectiveness of urethane pipe insulation in the arctic environment. Unpublished rep. Indian Health Service, Anchorage, Alaska.
10. Ryan, W. L., and K. C. Lauster. 1966. Design and operation of Unalakleet, Alaska water system. *J. Am. Water Works Assoc.* 58:1045.

11. Ryan, W. L. 1971. Sanitation facilities for communities in Alaska's Arctic. Paper presented at the Second International Symposium on Circumpolar Health, Oulu, Finland.
12. U.S. Public Health Service Monograph No. 54-1958. PHS Publ. No. 591. 1958. U.S. Government Printing Office, Washington, D.C.
13. U.S. Public Health Service Drinking Water Standards. PHS Publ. No. 956. 1962. U.S. Government Printing Office, Washington, D.C.

ENCOUNTERING MASSIVE GROUND ICE DURING ROAD CONSTRUCTION IN CENTRAL ALASKA

North Smith and Richard Berg

U.S. ARMY COLD REGIONS RESEARCH AND
ENGINEERING LABORATORY
Hanover, New Hampshire

INTRODUCTION

After confirmation of the presence of large oil resources on Alaska's North Slope, a consortium of oil companies proposed to construct a pipeline from Prudhoe Bay on the north coast to Valdez on the south coast. To aid in construction of the pipeline a gravel haul road was also planned¹ (Figure 1). The immediate purpose of the road was to provide access for construction of the northern section of the planned 1 270-km pipeline. The road was later to become part of the state highway system [1].

Work on the first 90 km of the road, from Livengood to the Yukon River, commenced in September 1969. By early November, the contractor had completed two sections, one 40 km long and another 19 km long. The entire 90 km of roadway was passable early in 1970, although many sections had not been constructed to final grade. Embankment construction was completed in July 1970.

DISCUSSION

Due to a very tight time schedule, preliminary subsurface soil exploration was limited and aerial photography was used as the primary tool in selecting the route and borrow areas. Permafrost was anticipated under most of the route but the extent of the ice-rich soils actually encountered was unexpected.⁴ The roadway alignment and grade restrictions required several cuts. Many of these were less than 3 m deep, but others exceeded 9 m.

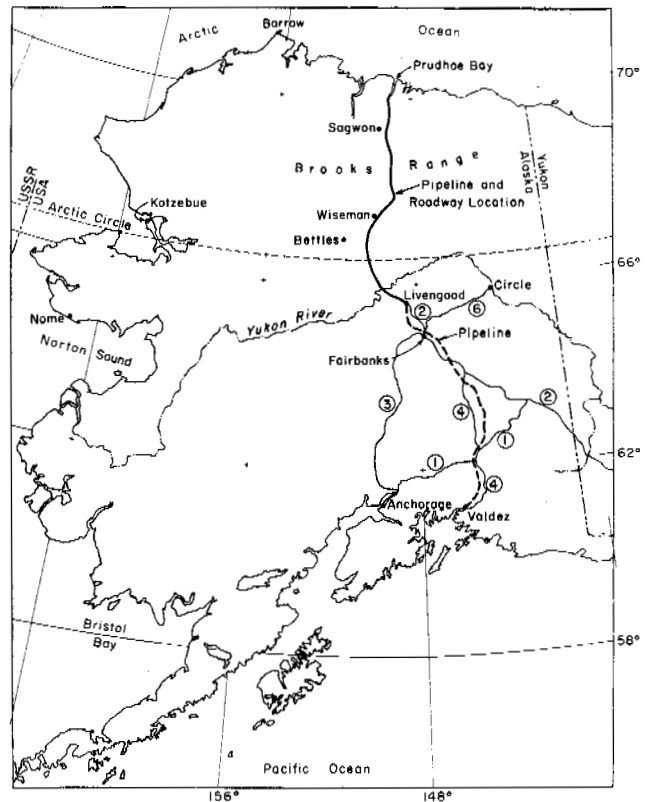


FIGURE 1 Map of Alaska, showing proposed pipeline and roadway route. Circled numbers identify Alaska State Highways.

Kovacs² traveled the road in early 1970 to make observations on the ice bridge across the Yukon River. He reported that several cuts along the roadway had exposed massive ice inclusions and wedges. On 23 April 1970 the authors made the first of several trips over the road.

Ice-rich soils were encountered in several cuts in the southern 30 km of the road; however, most of these cuts were too shallow to present major construction and maintenance problems. Eight relatively deep cuts were made in high ice content soils from about 31 km to Hess Creek at about 39 km. From Figure 2, showing the locations of four of the eight cuts (diamond km markers), it is apparent that these were made in north-facing terrain. It is generally established that permafrost is nearer the surface and more prevalent in north-facing slopes throughout arctic regions with discontinuous-permafrost conditions. When large volumes of ice were first encountered in the road alignment approaching Hess Creek, relocation of the route was considered. But since geologic features in the immediate vicinity were sim-

ilar to those containing the large ice inclusions it was not done.

The first major cut, at 31.6 km, was made at the normal 1:1 backslope. When other similar high-ice-content materials were encountered, nearly vertical backslopes were used. It was hoped that the vertical slopes would "heal" more rapidly and require less maintenance than the sloping backslopes; it was reasoned that less exposure would result and the vegetative cover would remain intact and slowly slump over to cover and insulate the receding cut surface. Wide ditches were made in these cuts to allow removal of thawed debris with heavy earth-moving equipment, if necessary. The areas were also undercut and backfilled with approximately 1.6 m of crushed rock to reduce anticipated differential settlement in the roadway.

Considerable maintenance has been required due to differential settlement of the roadbed and sloughing of the high-ice-content backslopes. The owners of the roadway were aware of these problems at the time of construction, but



FIGURE 2 Locations of cuts in high-ice-content soils along roadway.¹ The solid line is the alignment of the proposed 1.22-m pipeline; soil test holes are indicated by the T.H. followed by numerals.



FIGURE 3 Frozen 1:1 backslope, 31.6 km, 23 April 1970.

they estimated that maintenance costs would be lower than the construction cost of designs necessary to eliminate these problems. The backslopes may currently be considered an "eyesore" by some people, but in most instances they appear to be rapidly approaching a stabilized condition. The roadbed in these locations may take longer to stabilize than the



FIGURE 4 Thawing backslope, 31.6 km, 26 June 1970.



FIGURE 5 Backslope erosion into parallel ditch, 31.6 km, 26 June 1970.

backslopes, but the driving surface is gravel, which can be maintained relatively easily and inexpensively.

The series of photos (Figures 3-8) taken at 31.6 km illustrates the performance of the only relatively high backslope cut at 1:1 slope. The gray areas where the snow had melted (Figure 3) were massive ice inclusions in April 1970. In



FIGURE 6 Seeded backslope and broken rock revetment, 31.6 km, 11 August 1970.



FIGURE 7 Receding backslopes and stabilized ditch sediments, 31.6 km, 28 May 1971.

June 1970, noticeable thawing and erosion had taken place (Figures 4 and 5). The material in the ditch was not stable enough to support a small rock tossed from the shoulder. Between June and August 1970, the ditch had been cleaned out and a broken rock revetment installed (Figure 6). Rapid melting was still apparent, however, and material in the ditch was still very unstable. Both sides of the roadway had been hydroseeded in this time interval and grass was growing on the most stable positions of the backslope in August 1970. In May 1971, material in the ditch had stabilized sufficiently to support a man's weight and the backslope appeared fairly dry (Figure 7). Little additional slope degradation occurred during the 1971 thawing season and material in the ditch contained several desiccation cracks in August 1971 (Figure 8). At this time, it appeared that the slope was fairly stable and that possibly reseeding would provide complete stabilization.

The series of photographs of the left slope at 32.6 km shows the typical performance of a vertical cut with massive ice inclusions. The April 1970 photos (Figures 9 and 10) show several large areas of essentially pure ice. The June 1970 photo (Figure 11) shows the change after a period of only about 2 months. Note the vegetative mat overhanging the slope and the large areas on top of the slope where the trees and brush had been cleared. Hand clearing was conducted on top of many of the cuts in an effort to lower their height slightly by promoting melting from the top. Clearing also prevented rupture of the organic mat by the uprooting effect of falling trees at the face of the slope. The organic mat has



FIGURE 8 Desiccation of ditch sediments and continued slope recession, 31.6 km, 17 August 1971.

remained essentially intact as the face receded and has promoted more rapid stabilization by its shading and insulating effects. In August 1970, part of the overhanging organic mat had been torn by its own weight and that of stumps, brush, and cut trees (Figures 12 and 13). Some grass had grown as a result of hydroseeding. In May 1971, some additional flattening of the slope was observed, but the spring runoff had little adverse effect upon the slope (Figures 14 and 15). This was generally true at all the slopes. The August 1971 photographs (Figures 16 and 17) show additional slumping near the top of the slope but it appeared that the material



FIGURE 9 Frozen vertical backslope, 32.6 km, 23 April 1970.



FIGURE 10 Frozen vertical backslope, 32.6 km, 23 April 1970.



FIGURE 11 Overhanging mat and clearing atop backslope, 32.6 km, 26 June 1970.

may have been at its natural angle of repose, thus providing a nearly stable slope. The slope had a very untidy appearance due to tree trunks and stumps having fallen onto it. Reseeding this slope would minimize the possibilities of environmental damage due to erosion by surface water and would also make it look better.

Although the behavior of only two of the high-ice-content cuts has been discussed in this paper, their performance has been typical of nearly all of the similarly constructed slopes in this 90 km of roadway. Observations made during summer 1972 showed that stabilization was proceeding but still not complete. The original vegetation mat at the top of the cuts had slumped forward and no near-vertical exposures were seen while the lower slopes were somewhat greater amounts of grass. As might be expected, the processes proceeded more slowly during the third thaw season than during the

second. The environmental impacts of such construction activities have been adequately enumerated and discussed by Lotspeich.³

Observations on the performance of these slopes have led the authors to recommend the following guidelines for making cuts through ice-rich soils:

1. Avoid north-facing slopes when possible.
2. Make vertical backslopes on cuts.
3. Provide a wide ditch at the base of the cut to allow removal of material if necessary and to allow deposition of some overlying material during the stabilization process.
4. Clear trees and brush from the top of the slope for a distance about equal to the height of the slope. Although it was not done on any of these slopes, nailing a coarse wire mesh to the stumps may provide additional tensile strength



FIGURE 12 Slope has receded to edge of clearing in Figure 11, 32.6 km, 11 August 1970.



FIGURE 13 Massive ice under overhang, 32.6 km, 11 August 1970.



FIGURE 14 Additional slumping of backslope, 32.6 km, 28 May 1971.

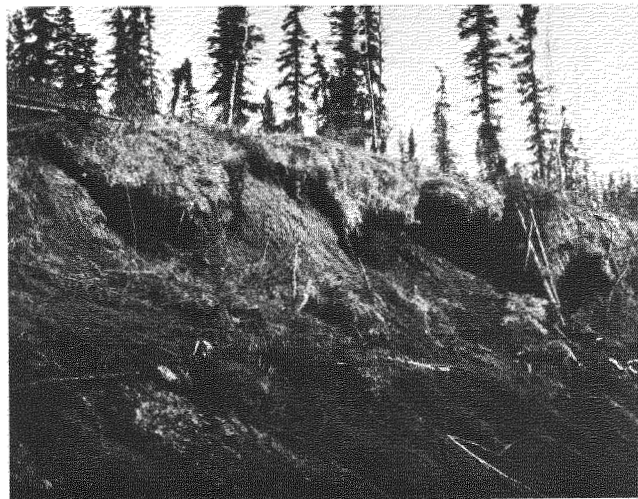


FIGURE 15 Natural burial of ground ice, 32.6 km, 28 May 1971.

to the organic mat and reduce the amount of tearing of the organic mat, especially on higher backslopes. As melting and erosion occur during the stabilization process, it may be necessary to remove additional trees from the top of the slope. This cutting, as well as the initial cutting, should be accomplished with hand tools. Heavy construction equipment should not be used outside the excavation area.

5. Vegetative reseeding should not be attempted until slope stabilization has commenced. A large portion of the seed originally sowed did not grow on these slopes because it was quickly covered with a thick layer of cold, wet soil. Had reseeding been accomplished during the second summer,

more of the seed would have grown and the slopes probably would now be more stable and picturesque.

CONCLUSION

Development of oil and gas resources in the Alaskan and Canadian Arctic will open up these areas for additional growth of other industries. In the next decade the Canadian and Alaskan governments both plan to construct hundreds of kilometres of roads in the Arctic and Subarctic. Railroads will also be extended into these areas. Many hundreds of kilometres of permafrost will be crossed by these transportation networks, and the alignment and grades on these



FIGURE 16 More stable backslope, 32.6 km, 17 August 1971.



FIGURE 17 Untidy appearance and continued thawing of backslope, 32.6 km, 17 August 1971.

roads and railroads may be more restricted than on the road discussed in this paper. It is probable that cuts into ice-rich permafrost will be necessary. The observed construction techniques using these high-ice-content cuts appear to have been successful and should also be applicable to similar problems in other permafrost regions.

ACKNOWLEDGMENTS

This paper presents the results of research performed by the Cold Regions Research and Engineering Laboratory under the sponsorship of the U.S. Army Corps of Engineers. During most of the time the roadway was being observed, Alyeska Pipeline Service Company (and its predecessor the Trans-Alaska Pipeline System) controlled access to it. The authors and other USA CRREL personnel were allowed to make essentially uncontrolled visits to the road.

REFERENCES

1. Alyeska Pipeline Service Company. Project description of the trans-Alaska pipeline system, Appendix—Road drawings. Vol. 3, Appendices—Vol. 18 and 20.
2. Kovacs, A. 1970. An informal note on the TAPS road and ice bridge. U.S. Army Cold Regions Research and Engineering Laboratory Hanover, New Hampshire. (Unpublished manuscript)
3. Lotspeich, F. B. 1971. Environmental guidelines for road construction in Alaska. Rep. No. 1610 GOI 08/71. Environmental Protection Agency, Alaska Water Laboratory, College.
4. Trans-Alaska Pipeline System. 1969. Proposal documents for construction of road from Livengood to Yukon River.

NOTE

[1] The design and construction of the road was the responsibility of the Alyeska Pipeline Service Company (formerly Trans-Alaska Pipeline Service).

THE USE OF POLYURETHANE FOAM PLASTICS IN THE CONSTRUCTION OF EXPEDIENT ROADS ON PERMAFROST IN CENTRAL ALASKA

North Smith, Richard Berg, and Larry Muller

U.S. ARMY COLD REGIONS RESEARCH AND
ENGINEERING LABORATORY
Hanover, New Hampshire

INTRODUCTION

In the cold regions of the world, seasonally and permanently frozen soils present severe road construction and maintenance problems during winter and the thawing period. At present, the use of as much as 1.0–3.0 m of granular materials to minimize or prevent deleterious freezing and thawing actions is common practice. In general, for expedient roads designed for short lives, such as those required for lumbering, mining and oil explorations, and military operations, this method is too time-consuming; also, many areas lack sufficient quantities of granular materials for this practice. The recent emphasis on environmental damage has highlighted the inadequacies of established design and construction practices. Recent developments in materials and improvements in application techniques indicate that environmental damage, as well as time and effort, might be minimized by the partial or complete substitution of synthetic thermal insulations for granular materials. This paper describes the construction and traffic

testing of expedient road test sections incorporating foamed-in-place polyurethane insulation of two densities over a subgrade containing seasonally and permanently frozen high-moisture-content silt and evaluates the thermal performance of these test sections. The foamed-in-place polyurethane insulation was selected for testing rather than factory-produced board-type panels because of the advantage of less bulk in the shipment of materials. Also, it was felt that the subgrade or leveling course preparation would be less time-consuming for the foamed-in-place insulation. A prefabricated aluminum airfield landing mat was used as a traffic wearing surface.

SITE SELECTION AND CONSTRUCTION

Early in November 1969, a test area with an average annual frost zone depth of less than 50 cm was located by probing the soil in an undisturbed area at the USA CRREL Alaska Field Station, near Fairbanks, Alaska (Figure 1). The results of the soil probing are presented in Table I. The variable

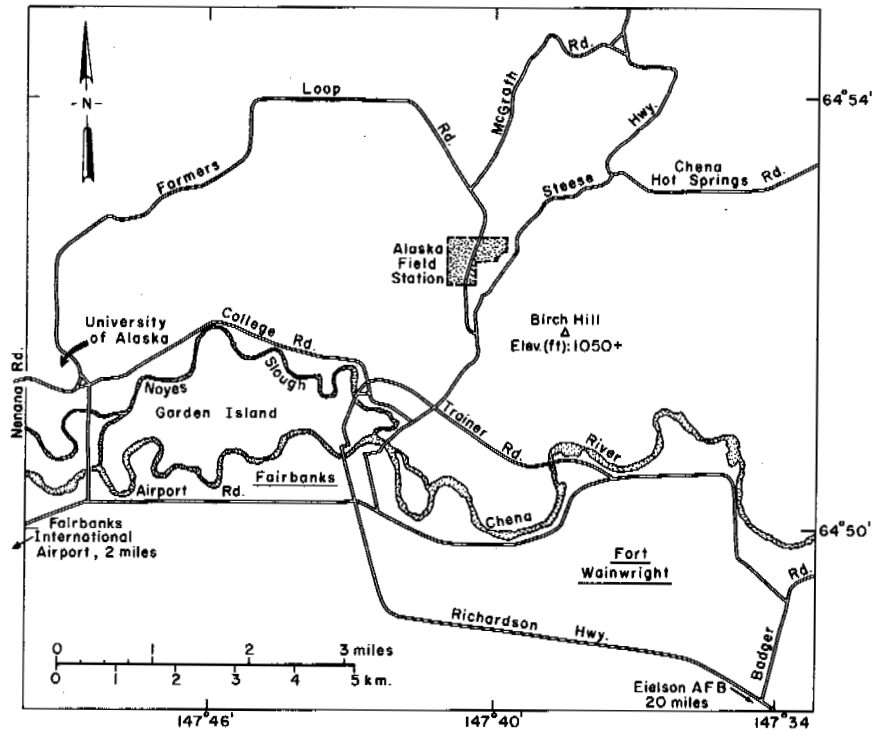


FIGURE 1 Location of test site.

depths to permafrost are felt to be due primarily to variations in vegetative cover. The area between stations 0+00 and 0+40 had been previously cleared many years ago for a communications line, which is now abandoned. The test area was cleared of spruce trees, bird's-eye willow, and underbrush with hand tools, thereby leaving the natural insulating surface vegetative mat essentially undisturbed. The annual frost zone, which had

a maximum thaw depth of approximately 62 cm under the insulation test sections area, was allowed to refreeze completely during the 1969-1970 freezing season. Snowfall during the ensuing winter was light and soil probings made in March and April 1970 established that the subgrade had completely frozen.

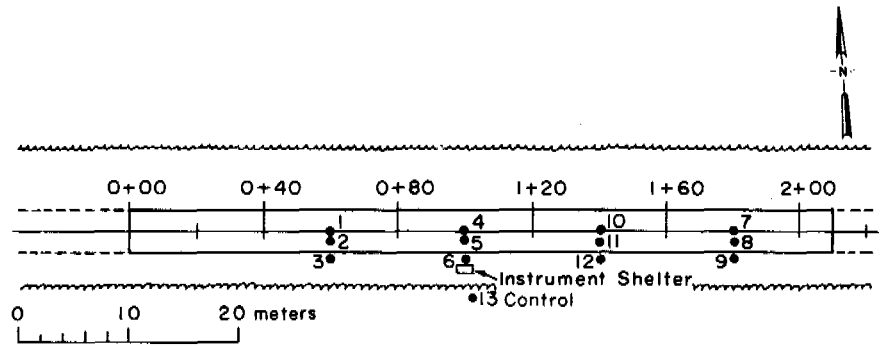
Twelve thermocouple assemblies, having eight temperature probe points each, were installed in the test areas in holes augered with the 10-cm-diameter USA CRREL core auger. Three assemblies were installed in each of four test sections having different thicknesses of insulation. Five of the temperature probe points of each assembly were spaced in the 1.5-m-deep auger holes and three were placed above the original ground surface in the test sections. A control thermocouple assembly was installed in another auger hole to a depth of about 3 m in a relatively undisturbed area adjacent to the test area. A plan view of the test area showing the locations of the thermocouple assemblies and profiles of the assemblies is shown in Figure 2.

Mechanical and hydrometer gradation analyses were conducted, and *in situ* moisture contents, densities, and Atterberg limits were determined for the cores from the thermocouple holes. The entire test area is underlain by soil ranging from slightly plastic to nonplastic silt and organic silt. Moisture contents ranged from about 40 percent to about 350 percent by dry weight, and densities ranged from about 224 to 1 234 kg/m³. The surface organic layer was about 5.0 cm thick.

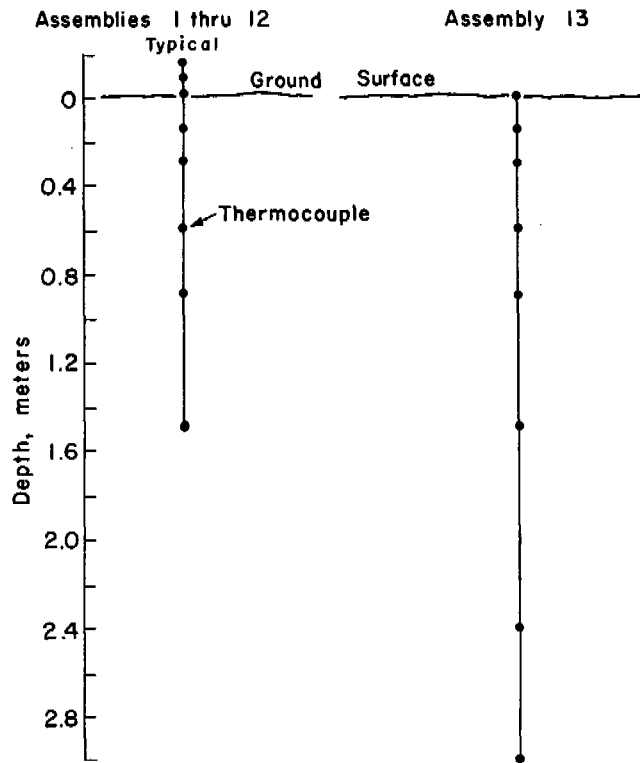
After installation of the thermocouple assemblies, the

TABLE 1 Original Depth to Permafrost in Test Area (11 November 1969)

Station No.	Depth in cm of Probe Point Locations from Centerline (m)				
	4.5 Left	3.0 Left	0	3.0 Right	4.5 Right
0 + 40	68.6	64.0	67.0	59.5	67.0
0 + 60	55.0	45.8	50.3	38.1	42.7
0 + 80	38.1	36.6	51.8	62.5	41.1
1 + 00	39.6	38.1	48.8	39.6	45.8
1 + 20	30.5	38.1	42.7	38.1	36.6
1 + 40	45.8	42.7	57.9	48.8	44.2
1 + 60	51.8	51.8	61.0	41.2	48.8
1 + 80	38.1	47.3	50.3	32.0	38.1
2 + 00	59.5	53.4	42.7	36.6	38.1
2 + 20	45.8	45.8	47.3	44.2	35.0
Thermocouple assembly 13 (undisturbed area)			45.8		



a. Plan



b. Profiles

FIGURE 2 Locations and profiles of thermocouple assemblies.

area was undisturbed until early April 1970, when the test sections were constructed. Before construction started, a snowcover approximately 10 cm thick was removed. The annual frost zone was completely frozen at this time.

The underbrush and smaller spruce trees and limbs resulting from the clearing operation were mechanically chopped (Figure 3), and the chips were spread about 15 cm deep over an area 12.2 m long and 6.1 m wide as a test leveling course material on which to spray the foam insulation. On the remainder of the test area, gravel was end-dumped from

trucks and spread to an average depth of 15 cm with a bulldozer.

Before the insulating layer was placed, measurements of *in situ* moisture content, density, and CBR were made on the wood chips and gravel leveling courses. Results are given in Table II.

Two polyurethane, spray-in-place formulations were used on the project. One formulation had a nominal density of 32.04 kg/m³ and the other a nominal density of 96.12 kg/m³. The foam formulator indicated that it was necessary



FIGURE 3 Woodchips prior to leveling.

TABLE II Properties of Construction Materials

Material	Station Location	Moisture Content (%)	Density (kg/m ³)	CBR at 0.5 cm Deflection ^a (%)	Unconfined Compressive Strength at 5% Strain (N/m ²)	Flexural Strength at 10% Strain (N/m ²)	Thermal Conductivity ^b (kcal-m/m ² -h-°C)
Wood chips	1 + 23	37	264				0.118 at 23.9 °C
	1 + 65			0.7		0.088 at 4.4 °C	
Gravel leveling course	1 + 20	3.9	2 226.78	12.5			
	0 + 90	3.8	2 226.78	8.7			
	0 + 70	3.5	2 210.76	12.0			
Low-density polyurethane foam on wood chip base	1 + 70		32.04	1.2			
				1.3			
Low-density polyurethane foam on gravel base	1 + 30		32.04	1.8	12.4 × 10 ⁴	10.3 × 10 ⁴	0.0196 at 24.4 °C
	0 + 65			2.1			0.0185 at 7.2 °C
High-density polyurethane foam on gravel base	1 + 20		80.1	5.7	51.7 × 10 ⁴	70.3 × 10 ⁴	0.0211 at 23.9 °C
							0.0205 at 7.2 °C
High-density foam on low-density foam	1 + 00			7.8			

^a 0.5 cm deflection on the CBR test is considered appropriate for expedient facilities.

^b One kcal m/m² h °C = 1.165 W/m² K.

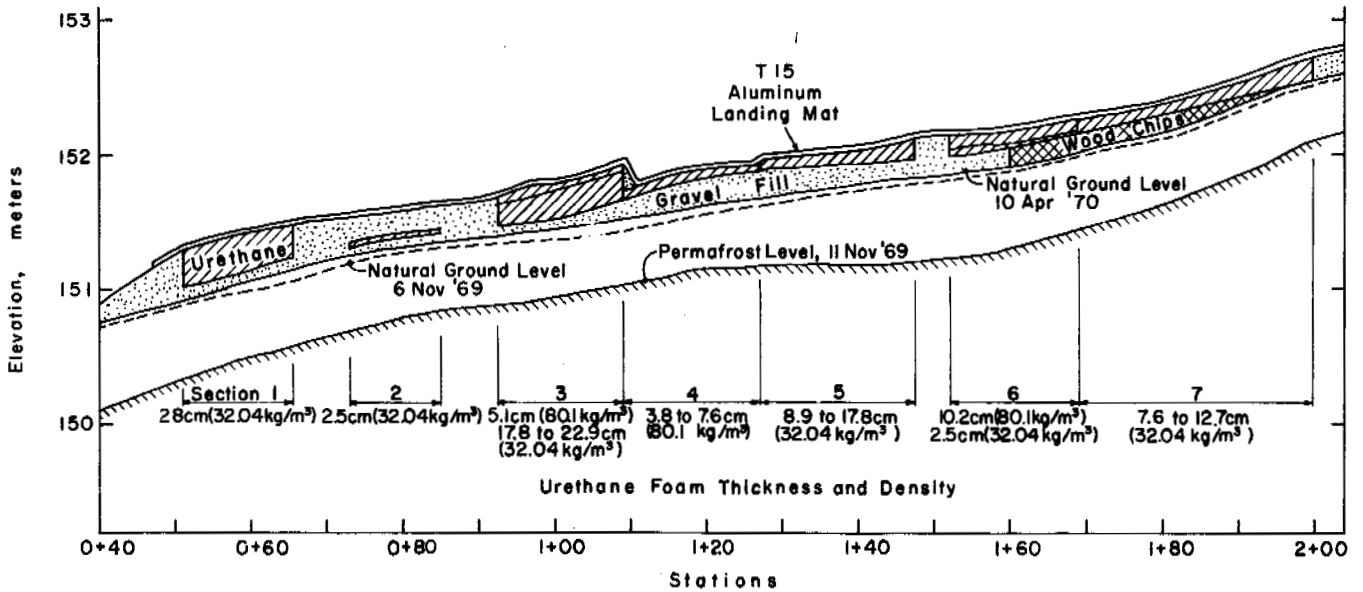


FIGURE 4 As-built centerline profile of test sections.

to apply the higher density formulation in very thin layers to achieve this density. During application, the layers were slightly thicker than desired and the resulting foam had a density of 80.10 kg/m^3 . These materials were placed in various combinations, as shown in Figure 4 and Table III. When all of the insulation had been placed, CBR tests were performed at several locations and samples of sections were removed for shipment to CRREL. Density, unconfined compressive strength, flexural strength, and thermal conductivity tests were conducted on these samples. Results from the tests are also shown in Table II.

The spraying operation was started at the rear of the area on section 7 to allow easy access for materials and equipment. A typical spraying operation is shown in Figure 5. The sections with two layers having different densities are indicated on

Figure 4. However, the layers of the same density material were sprayed in multiple applications of approximately 10 cm each; these are omitted on the drawing for clarity.

Sections 5 and 7 were intended to provide a comparison of the leveling course materials by spraying approximately the same thickness of the lower-density foam insulation on approximately 15 cm of gravel and wood chips, respectively. Sections 4 and 5 were intended to provide a comparison of approximately the same thicknesses of insulation, with higher and lower densities, respectively, on the same type and thickness of leveling course material. The hand-spraying operations did not give as precise thickness control as desired. Composite sections 3 and 6 were attempts to increase the load-supporting qualities of the test section by covering the lower-density foam with the higher-density foam. The question of the re-

TABLE III Test Section Leveling Materials and Foam Insulation Thicknesses

Section	Material and Leveling Course Thickness (cm)	Thickness 32.04 kg/m^3 Insulation (cm)	Thickness 80.10 kg/m^3 Insulation (cm)	Total Foam Insulation Thickness (cm)
1	10.2, gravel	28		28
2	10.2, gravel	2.5		2.5
3	12.7, gravel	17.8-22.9	5.1	22.9-28.0
4	17.8, gravel		3.8-7.6	3.8-7.6
5	15.2, gravel	8.9-17.8		8.9-17.8
6	Half sections on 15.2, gravel and woodchips	2.5	10.2	12.7
7	15.2, woodchips	7.6-12.7		7.6-12.7



FIGURE 5 Foam insulation spraying.

quired or optimum thickness of insulation was addressed by making sections with several insulation thicknesses. These included sections 1 and 2 with the two extremes of thicknesses.

During placement of the insulation, maximum daily air temperatures ranged from about 9 to 12 °C. Minimum daily air temperatures over this same period ranged from about -9 to -5 °C. The cool nighttime temperatures caused frost formation on the gravel, wood chips, and previously sprayed insulation surfaces. Early morning melting of this frost resulted in damp surfaces on which the insulation was sprayed.

These moisture and temperature conditions notwithstanding, no major difficulties were experienced in spraying the lower-density foam formulation. The spray apparatus, chemical drums, and most of the lengths of hoses to the spray gun were housed in a 227-kg carryall heated by the heaters used for vehicle personnel. Considerable differential shrinkage between the top and bottom surfaces of the insulation layer caused an upward curling at the edges of the foam slabs (Figures 6 and 7). The low overnight curing temperatures and the presence of surface moisture during spraying were thought to have contributed to the curling phenomenon. Also, as a result of an error in the instruction manual for the equipment, the volumetric mixing ratio of the chemicals for this formulation was incorrect. Later laboratory studies established relationships between curling and curing temperatures and curling and surface moisture of the substrate. A full report on these studies was given by Sayward and Smith.¹

The heating procedures used for the lower-density foam material were unsatisfactory when spraying the formulation for the higher-density material. This was evidenced by the

fact that an improper mix of the two chemicals was producing a collapsible froth rather than a foam insulation. It was necessary to use a large oil-fired space heater to heat the chemical drums during these spraying operations. Although the actual temperatures of the chemicals were not monitored, the outside surfaces of the drums were heated to approximately 49 °C. A small amount of shrinkage occurred in the higher-density insulation; however, overnight temperatures during curing did not go below about -4 °C, and the mixing ratio of the foam chemicals was correct for this formulation.

TEST RESULTS

During the 1970 and 1971 thawing seasons, more than 1 000 passes of rubber-tired vehicles of various types traveled over the test sections. Throughout this time the performance of the test sections was continuously monitored and observed.

Prior to covering the roadway with surfacing material, a four-wheel-drive utility vehicle with a gross weight of 1 540 kg was driven over the lower-density foam of section 1 to observe the effect of wheel loads directly on the foam. As expected, the foam easily held the vehicle, leaving only a 0.3- to 0.6-cm indentation in the foam surface. However, the outer skin of the foam was broken, exposing the inner cells to easy access by moisture and thus more rapid deterioration. Therefore, prefabricated panels of aluminum matting were placed over all of the sections with surfaces of the lower-density foam. Each panel was approximately 3.58 m long by 0.56 m wide and constructed of 0.64-cm-thick aluminum with 3.8-cm-deep ribs (spaced approximately 12.7 cm center to center) extending the length of the panel. The panels were

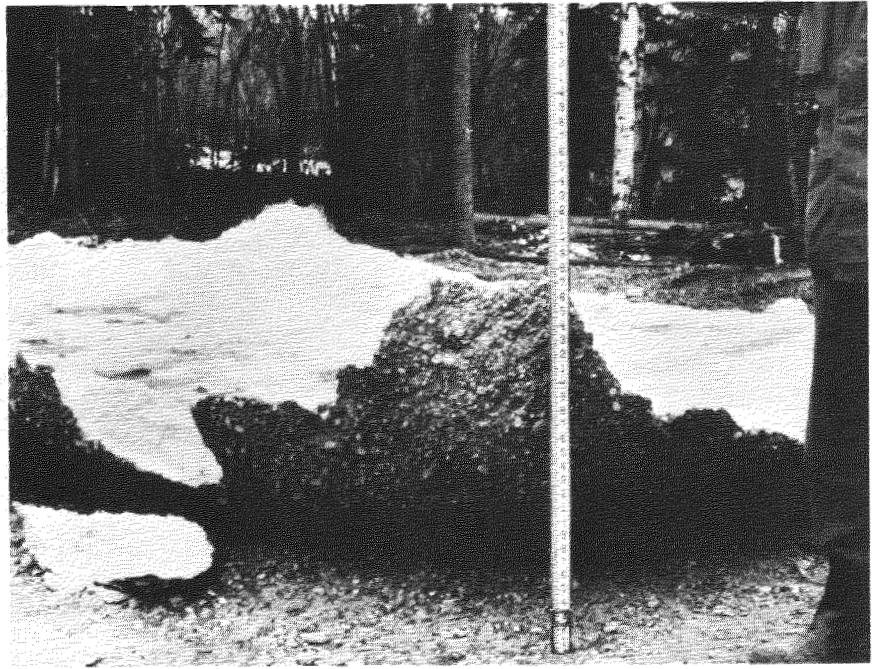


FIGURE 6 Curling on gravel base.

connected to each other when installed by an open hinge-type connection along the length of the panel. The higher-density foam was not covered at this time because its surface was undamaged by trafficking with an empty dump truck having a gross weight of 6 114 kg.

Since all the test sections withstood several passes of the empty dump truck and other unloaded vehicles, the dump

truck that was to be the test vehicle was loaded with gravel for further trafficking (Figure 8). The total gross weight of the loaded dump truck was 12 270 kg resulting in a maximum single wheel load of 2 415 kg. After only eight passes with the loaded test vehicle, the higher-density foam surface began to fracture; therefore, these sections were also covered with the matting before trafficking was continued.

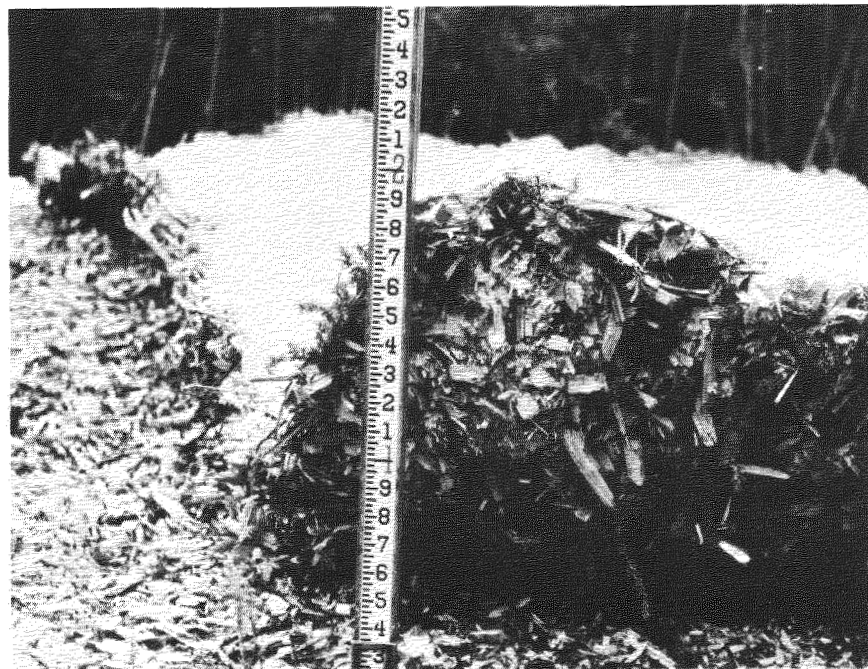


FIGURE 7 Curling on woodchip base.



FIGURE 8 Loaded test vehicle.

Settlements of the sections during trafficking were determined at regular intervals from engineering level measurements made on top of the matting. Figure 9 shows the centerline profiles from those measurements.

In 1970, the air thawing index was 1 964 °C-days and the thawing season was 171 days. The air freezing index for the

1970-1971 freezing season was 3 652 °C-days and the freezing season was 194 days. The 1971 air-thawing index was 1 974 °C-days and the thawing season was 189 days.

Thermocouple observations were made on a weekly basis throughout the thawing seasons and until the subgrade had completely refrozen during the freezing season. The observa-

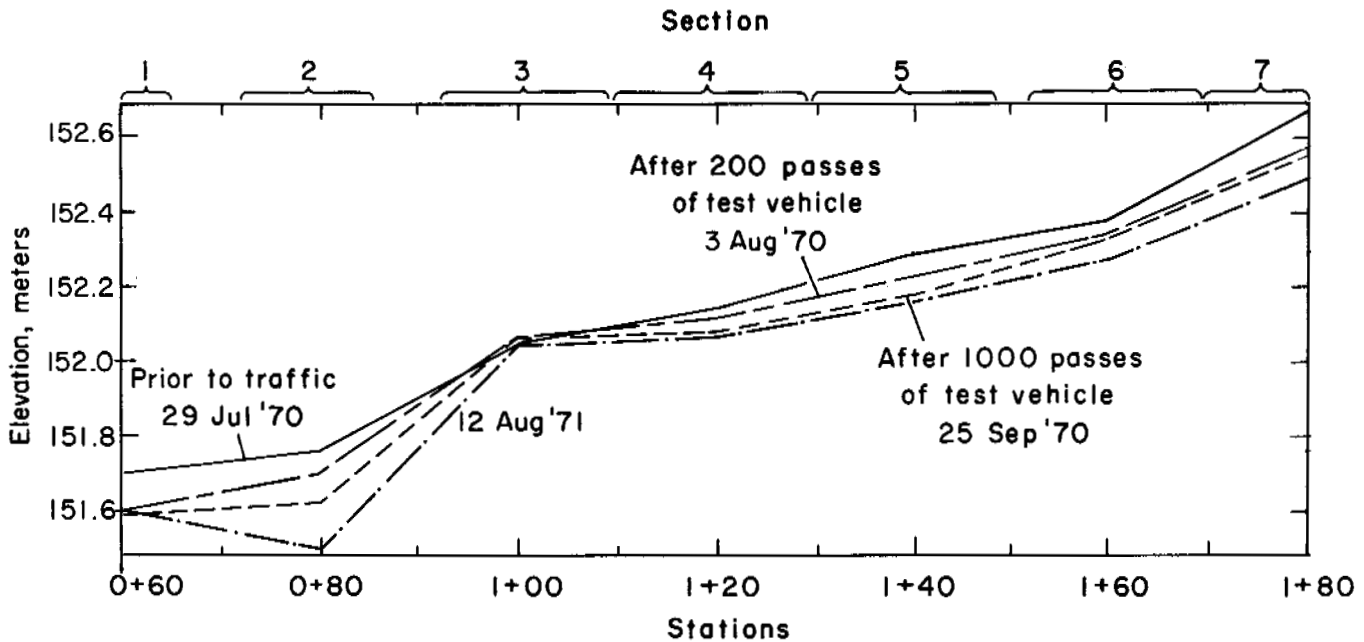


FIGURE 9 Centerline profile of test sections during thaw season and traffic testing.

tions were made to determine the effects of the insulated test sections on the thermal regime of the subgrade. As expected, the insulation did not completely prevent the thawing of the subgrade. However, in 1970 the depths of subgrade thaw beneath sections 1, 3, 5, and 7, which were instrumented with thermocouples, were calculated as 54 cm less than the recorded thaw depth at thermocouple assembly 13 in the undisturbed area adjacent to the test site in 1970 and 67 cm less in 1971. However, it is believed that the installation of the thermocouple string in the undisturbed area caused a localized change in the highly sensitive subsurface thermal regime in the succeeding years. Nearby soil probings at other test sections indicate the maximum thaw depths for undisturbed areas to be about 0.5 m. These data along with the settlements for each of the four test sections are given in Table IV. Comparisons of these data indicate that settlements were generally greater with greater thaw depths.

DISCUSSION

Section 3 settled the least of all of the test sections during the two thawing seasons. The subgrade also thawed the least at this section, which had a total insulation thickness of 22.9 to 28.0 cm. Table IV shows that the settlements and thaw depths were greater at the left or north wheel tracks; this was partially caused by edge effects and greater exposure to sun because of tree shading on the right or south side. A 91.4-cm thaw depth was measured through the gravel on the left side of the sections and is indicative of what can be expected after one thawing season with about 30–40 cm of gravel placed on the vegetative mat. This uninsulated gravel berm was nearly impassable after a few passes with a light, track-mounted front-end loader (Figure 10). Environmental damage of this (and worse) nature is evident throughout the Arctic and Subarctic from similar expedient operations.

Section 1 experienced considerably more thaw and settlement than section 3 although the insulation thicknesses of the two sections were nearly the same. This is attributed to

the lack of insulation on the approach end of section 1 and the presence of only 5.1 cm of insulation in section 2.

The overall settlements of sections 1, 5, and 7 during the first thawing season were essentially the same although the maximum subgrade thaw depths were significantly different. The relatively smaller settlements of section 1, which had the greatest thaw depths, are attributed to the greater area distribution of the load on the subgrade because of the thicker foam insulation layer. This same comparative phenomenon is apparent to a lesser degree between section 5 and 7. The greater thaw depth at section 5 than at section 7 in 1970, although the foam insulation averaged 3.0 cm thicker on section 5, seems to indicate that the woodchips under section 7 provided a greater insulating value than the gravel and the additional foam insulation in section 5.

During the second thawing season, section 1 again had the greatest average thaw depth but the least average settlement of all the sections, which reaffirms the greater load distribution on the subgrade resulting in less consolidation of the subgrade soil. Sections 5 and 7 had essentially the same average thaw depths, but section 7 had significantly more settlement. The greater settlement at section 7 is attributed to continued consolidation of the woodchips and a higher average moisture content of the subgrade soils. These settlements would not be excessive, however, for service limited to one or two thawing seasons. The limited amount of vegetative materials available for chipping in the arctic and subarctic regions and the time limitation for expedient road construction do not make the widespread use of wood chips attractive.

Sections 2, 4 and 6, which were not instrumented with thermocouples, were monitored for settlements and were probed at the edges for thaw depths. Sections 4 and 6 performed essentially the same as section 5; because of its higher-strength foam insulation and thicker leveling gravel course, section 4 had slightly less overall settlement than section 5. Section 2 performed most poorly of all the sections because of its thin layer of insulation and the continued rutting and consolidation of the overlying gravel layer.

TABLE IV Maximum Subgrade Thaw Depths and Test Section Settlements, 1970 and 1971

Section	1970 Depth (m)						1971 Depth (m)								
	North Wheel		Centerline		South Wheel		North Wheel		Centerline		South Wheel				
	Thaw	Settlement	Thaw	Settlement	Thaw	Settlement	Thaw	Settlement	Thaw	Settlement	Thaw	Settlement			
1	0.78	0.14	0.60	0.14	0.66	0.12	0.99	0.04	0.58	0.02	0.64	0.03			
3	0.40	0.06	0.29	0.02	0.33	0.00	0.69	0.01	0.24	0.03	0.33	0.09			
5	0.65	0.14	0.60	0.12	0.58	0.10	0.92	0.06	0.52	0.03	0.56	0.07			
7	0.50	0.14	0.48	0.13	0.52	0.12	0.78	0.07	0.62	0.08	0.56	0.12			
Maximum thaw at thermocouple assembly 13				0.83								0.91			



FIGURE 10 Thawing on north side of the test sections.

CONCLUSIONS

All the sections, except section 2, which had a total settlement after 2 years of 0.28 m, provided an acceptable roadway throughout both thawing seasons. The lower-density foam insulation was crushed under the ribs of the aluminum matting. However, after the matting had "seated" to the depth of the ribs, no additional crushing occurred. The sections incorporating the higher-density foam insulation provided a more durable surface that did not crush under the aluminum matting.

An optimum thickness of foam insulation having these strength and thermal properties cannot be determined directly from these test data. It is apparent, however, that the greater thickness of foam insulation in section 3 did not proportionally improve its performance, under these loading conditions, over sections 5 and 7.

It is considered that for this type of expedient road construction on permafrost terrain similar to central Alaska that 10 cm of foam insulation with these strength and thermal properties is sufficient thickness to withstand 1 000 passes of a loaded dump truck having a maximum single wheel load

of 2 415 kg. Additional use as an access road for lumbering, mining, and oil explorations, and military operations with wheel loads up to 5 000 kg could be handled for a minimum of one thaw season.

This approach to expedient road construction provides considerable advantage for minimizing environmental damage over previously established expedient practices.

Wood chips as a leveling course provided some insulation advantage over the gravel leveling course of approximately equal thickness. This might also be an expedient method of disposal of clearing material.

ACKNOWLEDGMENTS

This paper presents the results of research performed by the Cold Regions Research and Engineering Laboratory under the sponsorship of the U.S. Army Corps of Engineers.

REFERENCE

1. Sayward, J. M., and N. Smith. 1971. Curling of urethane foam insulation. Intern. Rep. 230. U.S. Army Cold Regions Research and Engineering Laboratory, Hanover, New Hampshire.

EFFECTS OF GROUND-ICE VARIABILITY AND RESULTING THAW SETTLEMENTS ON BURIED WARM-OIL PIPELINES

T. L. Speer [1], G. H. Watson [2], and R. K. Rowley [3]

MACKENZIE VALLEY PIPELINE RESEARCH
LIMITED
Calgary, Alberta

INTRODUCTION

During 1971 and 1972, Mackenzie Valley Pipe Line Research Limited completed comprehensive feasibility studies on oil pipeline routes extending from arctic regions of Canada and the United States to existing pipelines in western Canada. The routes investigated originate at Prudhoe Bay, Alaska, and Tuktoyaktuk, Northwest Territories, and terminate in Edmonton, Alberta, Canada. Two routings from Prudhoe Bay into Canada were considered.

In these studies the proposed warm pipeline was considered to be buried wherever permafrost conditions permitted. Below-ground construction was considered to offer more reliable and economic transportation in the isolated North than would an elevated pipeline. The decision to bury the line was based on a comprehensive set of geotechnical criteria. Extensive research was needed to determine the engineering properties of permafrost and its behaviour while thawing.

The amount of ice, its distribution in the thawed zone and the depth of thaw below a buried pipeline determine the final configuration of the trench bottom after settlement. Resulting differential foundation settlement could produce curvature in a buried pipeline and be one of several sources causing pipe stress. The horizontal settlement variability is of major significance because the pipe has a limiting radius of curvature for buckling and a limited, safe, unsupported, spanning capability under operating conditions.

Field and laboratory studies were undertaken to determine the type and variability of ground ice occurring in clay and silt permafrost soils and to establish limiting pipe burial criteria. Specific objectives of these studies follow:

1. To derive a general relationship between frozen bulk density and thaw settlement for permafrost mineral soils;
2. To determine the ice variation for specific terrains in which the proposed pipeline might be buried;
3. To determine the representative potential total and differential settlements for these specific terrains; and

4. To establish a method of using both the frozen bulk density and thaw settlement data (total and differential) obtained to establish practical design limits for a warm buried pipeline.

PHOTOGEOLOGIC INTERPRETATION

Detailed airphoto-interpretive studies along possible pipeline route corridors were completed early in the study. As a result of this work, geologic map units were defined in terms of topographic conditions, geologic origin, and general environmental factors. The studies were supplemented by a field reconnaissance consisting of widely spaced drilling, sampling, and laboratory testing.

Engineering application of the photogeologic data is based on the premise that map units can be defined and their boundaries delineated with confidence. Once the areal boundaries, stratigraphic position, and gross lithology were established, it then became necessary to express quantitatively the range of engineering properties to be expected in each unit.³

Engineering characterization of geologic map units based on stratigraphic and lithologic interpretation from exposures and scattered borings has not, in general, been successful. The primary reason for this is that the expected range of a given variable (thaw settlement, for example) is often so broad that the data are of little use for engineering decisions. The ice variability studies overcame this difficulty by assessing (using closely spaced sampling and testing of two-dimensional arrays) thaw settlement of representative areas of geologic map units.

The first three such arrays studied and reported in this paper represented the following geologic situations:

1. Massive to thickly bedded silt and clay, deposited in proglacial lakes (arrays 1 and 2),
2. Dense massive lodgement till (silty sand and sandy silt) overlain by a veneer of fine-grained lake-deposited material or reworked till (array 3).

Ground ice at the three sites is both segregated and non-segregated. The ice is of epigenetic origin.² Massive ice, such as ice wedges, is not present.

SITE DESCRIPTIONS

Site 1—Norman Wells

Array 1 is located approximately 3 km northwest of Norman Wells and 1 km south of the confluence of Bosworth Creek and the Mackenzie River. The terrain is essentially flat. The south margin of the site slopes very gently to the northwest. Small shallow lakes are scattered throughout the general area. Vegetation consists of moderately dense black spruce and occasional birch and alder. The area immediately north-east of the site is muskeg, with scattered tamarack (larch).

The site is underlain by a sequence of massive or thickly bedded, lake-deposited silt and clay, about 9 m thick. The organic cover is only a few centimetres thick. The silt and clay contain occasional lenses and inclusions of organic silt and wood fragments. Dense granular soil or till underlies the silt and clay.

Ice in the silt and clay occurs generally as random inclusions and irregular lenses that range in thickness up to 5 cm. Occasionally, zones of mixed ice and soil are found.

Site 2—Landing Lake

Array 2 is located approximately 53 km northwest of Norman Wells and 3 km from the east bank of the Mackenzie River. The terrain slopes very gently to the southeast at a gradient of 1–3 percent. Vegetation consists of moderately dense black spruce and occasional tamarack, with an undergrowth of young conifers and sparse brush. A small shallow lake lies along the east margin of the site.

The site is underlain by a sequence of late glacial, lake-deposited, silty clay and clayey silt, ranging in thickness from 10 to 13 m, and mantled with a surficial veneer of peat and organic silt. Occasional thin lenses of sand or gravel are distributed throughout the silt and clay. Sporadic organic inclusions and wood fragments are also present. The silt and clay sequence is underlain by dense till, dominantly silty sand.

Ice in the organic veneer occurs generally as irregular, horizontal and subhorizontal lenses mixed with irregular ice inclusions. The lenses and inclusions are generally less than 2.5 cm in thickness. In the clay and silt strata, random inclusions and crystals are the dominant ice form. Visible ice is rare in the underlying till.

Site 3—Campbell Lake

Array 3 is located approximately 23 km southeast of Inuvik. It lies on a broad featureless plain, which slopes to the

northwest at about 20 m/km. The area is forested with a moderately dense stand of black spruce and occasional tamarack.

Below a depth of 2–4 m, the site is underlain by dense till (sandy silt with some clay and occasional gravel). The till is of relatively low ice content, with ice occurring as thin and irregular lenses, inclusions, and crystals. The overlying silt, clay and organic soil contain lenses commonly up to 2.5 cm in thickness.

SITE INVESTIGATION

The sites selected represented one geologic map unit in which it was expected that the quantity and distribution of ice would be low enough to permit conventional pipe burial, one unit in which burial would be marginal, and one unit in which the ice content would be sufficiently high to be potentially detrimental when thawed to a conventional buried pipeline.

The lateral variation of the soil and ice was studied in rectangular arrays of borings. Holes were taken to a depth of 13 m or until the ice content was such that thaw settlement would be negligible. The borehole layout was slightly different for each array (Figures 1–3).

Two methods of obtaining continuous core from the holes were used. At site 1, the drill rig consisted of a diesel-powered, hydraulically driven, vibratory coring unit. Sam-

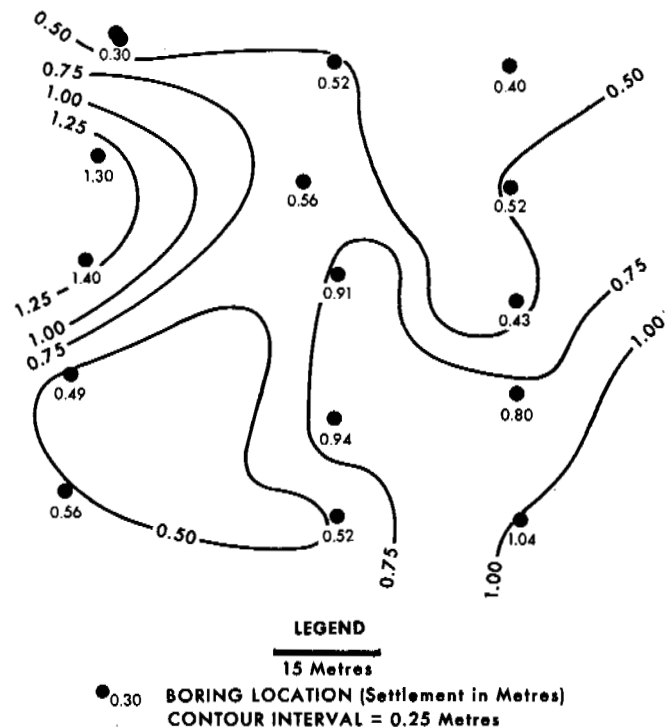


FIGURE 1 Estimated thaw settlements (depth, 2-13 m); site 1, Norman Wells, N.W.T.

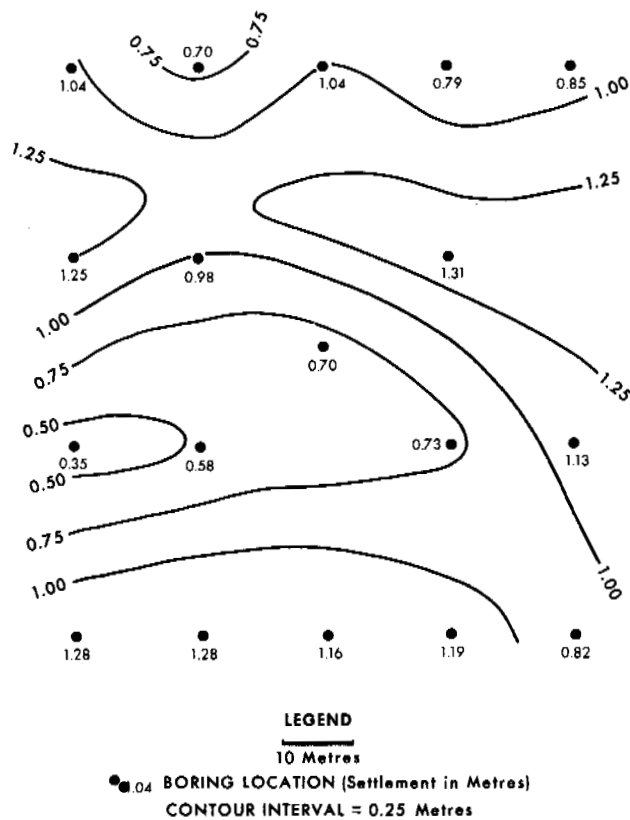


FIGURE 2 Estimated thaw settlements (depth, 2-13 m); site 2, Landing Lake, N.W.T.

ples were recovered in a 10-cm-diameter pipe. Sample runs were approximately 1.5 m in length. The sample tube was vibrated into the ground under the load of the drilling unit. Vertical oscillations at resonant frequency caused the pipe to penetrate the permafrost easily to the desired depth. The sample tube was then retracted and the samples recovered by vibrating the sample tube while it was in a vertical position.

At sites 2 and 3, continuous core was obtained by use of a conventional rotary air rig. The sample tube consisted of a 7.6- or 10.2-cm-diameter fluted hollow-stem auger. The cutting head contained 2 or 4 replaceable, angled, tungsten-carbide-tipped, cutting teeth. As the sample tube was slowly rotated, the cuttings were carried up the external flutes to the top of the sampler. The inside diameter of the sample tube was slightly greater than that of the cutting head, thus ensuring easy extraction of the sample from the tube.

LABORATORY TESTING

To obtain a general relationship for thaw settlement in terms of an easily measured soil property (the *in situ* frozen bulk density), thaw consolidation tests were run on several hundred samples representing a broad spectrum of soil types

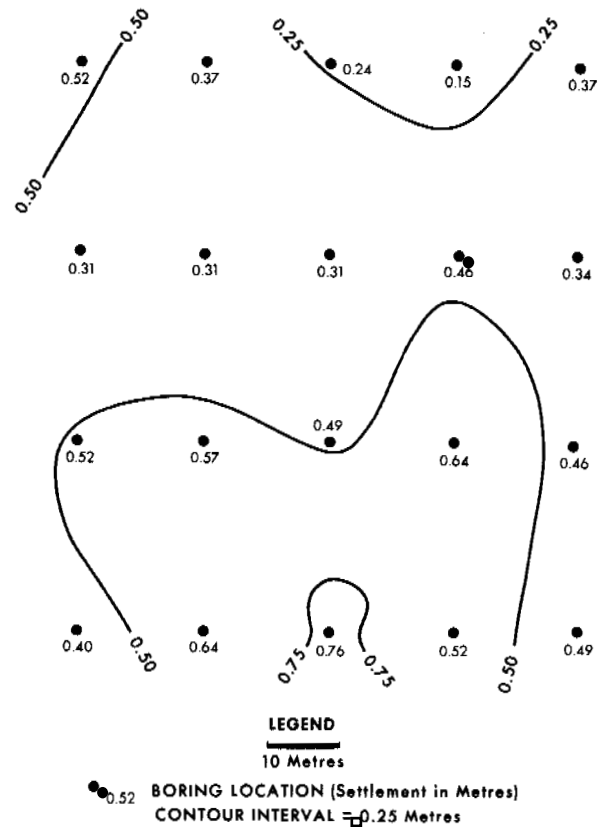


FIGURE 3 Estimated thaw settlements (depth, 2-13 m); site 3, Campbell Lake, N.W.T.

and ice contents. Samples used in these tests were from the three test arrays previously described and from a test site near Inuvik.⁵

After initial sample inspection, including photographing, the frozen bulk density of each sample was determined using a sand displacement method. Subsequent testing determined the uniaxial strain of ice-rich soil when thawed under load. Most of the samples were thawed under a load equivalent to the total overburden pressure at sample depth. Methods of sample preparation and test procedures are described elsewhere.⁶

In addition to the frozen-bulk density and thaw-settlement tests, measurements were made of thawed strength, grain-size distribution, Atterberg limits, and thermal conductivity (of both frozen and thawed samples). Typical classification results are shown in Table I for the ice-rich soils at each site.

ANALYSIS

Results of the thaw-settlement tests were plotted in terms of thaw settlement versus frozen bulk density (Figure 4). A least-squares curve was fitted to these data to give the equation:

TABLE 1 Typical Classification Test Values for the Array Sites

Test Site No.	Soil Description	Range of Water Content (%)	Grain Size			Liquid Limit	Plastic Limit
			Sand (%)	Silt (%)	Clay (%)		
1. Norman Wells	Clayey silt	30-60	10	70	20	35-55	25-30
2. Landing Lake	Clayey silt	10-60	10	60	30	40-50	20-30
3. Campbell Lake	Silt	10-45	5	90	5	35-40	10-15

$$S = 73.60 - 101.8 \ln \gamma,$$

where S = settlement in percent and γ = frozen bulk density in g cm^{-3} . The residual standard variation was 7.01 percent.

Because samples covering a broad range of frozen bulk densities were used, it was possible to establish an average

curve from which thaw settlement could be estimated. A close examination of the data points indicates that there may be a unique curve for each soil type. This is particularly evident in the case of site 3, where thaw settlement appears to be about 5 percent greater for a given frozen bulk density than at the other sites. For settlement analysis at this site,

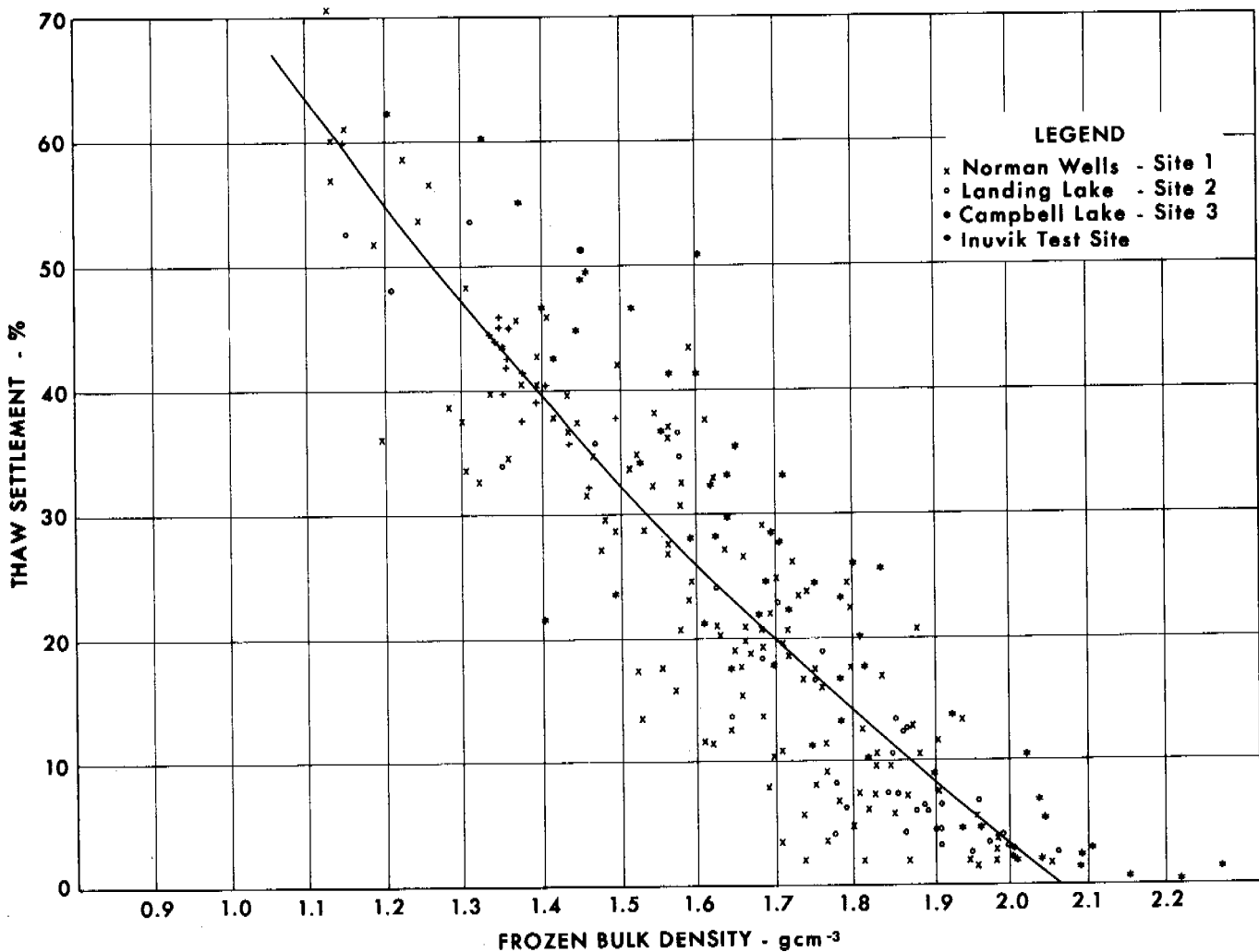


FIGURE 4 Thaw settlement versus frozen bulk density relationship.

however, it was not too important as most of the material had a density indicating settlement of less than 10 percent.

The limits of the equation defining the relationship are 1.09 g cm^{-3} and 2.05 g cm^{-3} . In the few cases where densities were less than 1.09 g cm^{-3} , thaw settlement was assumed to be 68 percent, unless pure ice was present and a settlement of 100 percent used. For densities between 2.05 and 2.16 g cm^{-3} , the thaw settlement value was assumed constant at 2 percent. For values greater than 2.16 g cm^{-3} , the thaw settlement was assumed to be negligible. In addition, all samples with a high organic content were omitted in defining the thaw settlement versus frozen bulk density relationship. Omitting the organic samples was of little significance in calculating the thaw settlement values as existing codes of practice indicated that the proposed study pipe should be founded at a depth of approximately 2–3 m below ground level. At the sites investigated, the majority of the organic material was found within 1.5 m of ground surface.

On the basis of the thaw settlement relationship and analytical results,⁴ which indicated that (over the useful life of the pipeline) the thaw front would extend to approximately 13 m below ground surface, a settlement value was obtained at each hole. Settlement contours were drawn on the array grid to indicate the typical differential foundation settlement for the geologic map units. Settlement ranges and the average settlement for each site are shown in Table II.

From these results, preliminary data were obtained on the total settlement and the settlement range that might be anticipated within a specific map unit.

APPLICATION

Foundation settlement, beneath a pipeline buried in permafrost, can be estimated from the density–settlement curve (Figure 4) if the soil density profile and depth of thaw are known. The total settlement is the sum of the settlements of the various soil strata within the thawed zone. To demonstrate the validity of the density–settlement curve, total settlement predictions were made for two experimental pipeline installations and compared with the field performance data. Predicted settlements agreed well with measured values.

TABLE II Estimated Total Settlements for Test Arrays

Site No. and Location	Settlement		
	Maximum (m)	Minimum (m)	Average (m)
1. Norman Wells	1.4	0.30	0.78
2. Landing Lake	1.31	0.35	0.98
3. Campbell Lake	0.76	0.15	0.44

The field test facilities installed near Inuvik^{4,5} consisted of a 1.22-m-diameter, 610-m-long, above-ground pipeline loop and a 0.61-m-diameter, 27.4-m-long, buried test section. Data on frozen bulk density were obtained from a few core holes drilled near the two pipes. Although test data were not extensive enough to prepare a contoured settlement plot similar to Figure 1, settlements estimated from nearby holes were compared with the observed pipe settlement.

Half of the above-ground loop was placed in a continuous gravel berm. Observed settlements of the thawed permafrost foundation under the berm exceeded estimated settlements by an average 7 percent (ranging from –5 to 17 percent).

The buried test section was placed in a ditch, and the excavation backfilled with sand. The observed settlements exceeded the estimated average downward movement by about 9 percent (1 percent at the east and 18 percent at the west ends, respectively).

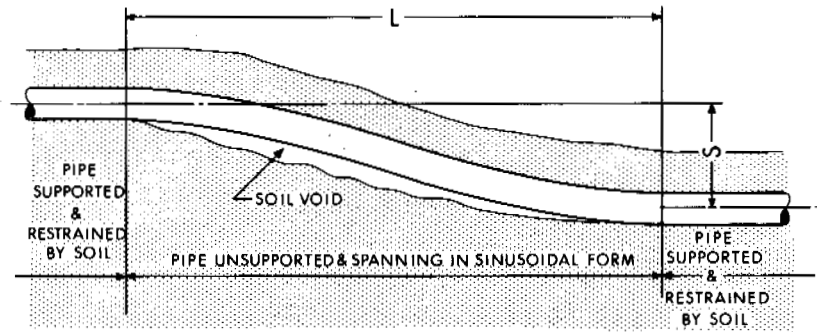
The more direct application of total and differential thaw settlement and its variability to pipeline design can be illustrated by a hypothetical example. Consider the proposed burial of a warm-oil pipeline in permafrost terrain. Assume the steel pipe is 1.22 m in diameter by 1.27 cm in wall thickness and has a specified minimum yield strength of $4\,570 \text{ kg cm}^{-2}$.

Further assume that other design conditions are (a) bottom of pipe 2 m below ground surface; (b) normal internal operating pressure of 63.6 kg cm^{-2} ; (c) no-flow (shutdown) internal pressure of 0 kg cm^{-2} ; and (d) residual axial compressive stress resulting from a temperature differential of 58°C (the temperature differential being the difference between maximum operating and minimum operating or installation temperature).

One important design limit is pipe buckling. For the pipe in the example, assume that the limiting radius of curvature is 232 m for the no-flow condition. The limiting radius can be determined either analytically or experimentally.¹ The maximum differential settlement that the pipe can withstand without buckling will be the amount that results in the minimum radius of curvature.

Assuming that the resulting geometric deformation of the pipe is sinusoidal, the spanning distance, L , across which the pipe deflection, S , occurs, can be calculated for varying values of S while maintaining a constant $R_0 = 232 \text{ m}$. The resulting curve is plotted in Figure 5.

If sites 1, 2, and 3 are representative of specific terrains in which the pipeline might be buried, then the pipe could cross any site at random. The profile of the ditch bottom for any crossing can be plotted from the settlement contours. This profile would show the anticipated differential settlement along the crossing. If, for example, the settlement profile indicates combinations of L and S values equal to or less than L_{max} that plot above the curve, then pipe burial would be safe because the resulting radius of curva-



L = HORIZONTAL SPANNING DISTANCE - M WITH
 MINIMUM RADIUS OF CURVATURE = 232 M

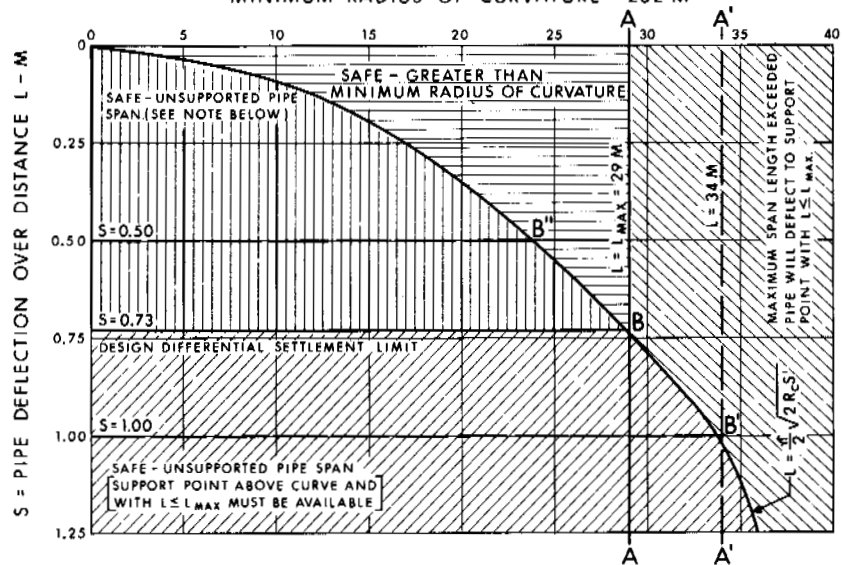


FIGURE 5 Pipe spanning capability versus differential settlement.

ture would exceed the minimum at which pipe buckling would occur. No values of $L > L_{max}$ can be considered because the pipe will not support a span longer than L_{max} .

If the L and S values plot below the curve, then pipe burial would not necessarily be safe, and the free-spanning capability of the pipe would have to be considered. If the settlement profile contained a support point that was above the curve with $L \leq L_{max}$, then the pipe would span those points below the curve.

The design differential settlement criterion limit for this example is 0.73 m and is illustrated in Figure 5 by the vertical line B-B. If a geologic map unit were encountered in which this differential-settlement limit was exceeded, the pipeline would be installed above ground in that location, unless cost considerations indicated a better solution.

Horizontal lines B'-B' and B''-B'' represent differential settlements of 1.0 and 0.5 m, respectively. Because construction cost is such a dominant factor, it might be advantageous to bury the pipeline in a terrain with S 1.0 m. In this case, the free-spanning capability of the pipe would

have to be increased to 34 m (vertical line A'-A') by increasing the pipe wall thickness, for example.

Similarly, it might be advantageous to reduce the differential settlement to $S = 0.5$ m in order to reduce soil subsidence above the pipe and future ditch backfill and right-of-way maintenance costs. In this case, the design safety factor against pipe buckling would be increased if the pipe wall thickness was not reduced.

The final selection of a burial criterion (differential-settlement limitation) should be determined by the optimum combination of technical and cost considerations. However, based on a limiting differential settlement of $S = 0.73$ m in this example, with a 1.22-m-diameter pipe, site 1 would be marginal, site 2 unsuitable, and site 3 favourable for pipeline burial.

CONCLUSIONS

1. By using the relationship between frozen bulk-density and thaw settlement, total and differential settlements can

be estimated. The estimates can be used to express the range of settlement variability within geologic map units. The degree of representation depends on the success with which map units can be identified.

2. Initial results reported herein indicate that there may be a unique relationship between frozen bulk density and thaw settlement for each different soil type. For practical purposes, the average curve presented appears adequate. Further work is needed to define a relationship for organic soils.

3. Within the limitations expressed in conclusion 1, differential settlements can be presented in the form of contoured settlement. This information is a valuable aid to pipeline design in thawing permafrost and may have application to other structures on frozen soils.

ACKNOWLEDGMENTS

The authors are grateful for the interest and assistance of their colleagues throughout the project, particularly J. W. Gorman, J. M. Blackwell, and W. Miller.

This paper is published with the approval of the Research Coordinator of Mackenzie Valley Pipe Line Research Limited.

REFERENCES

1. Bouwkamp, J. G. 1972. Structural behaviour of a large diameter pipeline under combined loading. *In* 23rd annual pipeline conference, Dallas, Texas.
2. Mackay, J. R. 1972. The world of underground ice. *Assoc. Am. Geogr.* 62(1).
3. Mollard, J. D. 1972. Airphoto terrain classification and mapping for northern feasibility studies. *In* Canadian northern pipeline research conference, Ottawa.
4. Rowley, R. K., G. H. Watson, T. M. Wilson, and R. G. Auld. 1972. Performance of a 48-inch warm-oil pipeline supported on permafrost. 25th Annual Canadian geotechnical conference, Ottawa.
5. Watson, G. H., R. K. Rowley, and W. A. Slusarchuk. The performance of a warm-oil pipeline buried in permafrost. This volume.
6. Watson, G. H., W. A. Slusarchuk, and R. K. Rowley. Determination of some frozen and thawed properties of permafrost soils. (In preparation)

NOTES

- [1] On loan from AMOCO Oil Company, Chicago, Illinois.
- [2] On loan from Acres Consulting Services, Calgary, Alberta.
- [3] On loan from Standard Oil of California.

PERFORMANCE OF THE THULE HANGAR SOIL COOLING SYSTEMS

Wayne Tobiasson

U.S. ARMY COLD REGIONS RESEARCH AND
ENGINEERING LABORATORY
Hanover, New Hampshire

INTRODUCTION

Thule Air Base is located on the northwest coast of Greenland about 1 100 km north of the Arctic Circle. The 10 hangars at Thule are among the largest heated structures built on permafrost in North America. The soil cooling techniques used for these hangars have received considerable attention: Soviet and North American authors have used the hangars to illustrate state of the art ducted foundation design. However, several operational difficulties have occurred and localized floor settlements have resulted. To illustrate these difficulties, hangar performance over the past two decades will be discussed.

THE HANGARS

Of the 10 hangars at Thule the six larger hangars, which are 90.6 m by 59.2 m in plan, are discussed in this paper. The soil cooling systems for the four smaller hangars differ in detail from those of the large hangars but are the same in principle.

Because of heavy live loads, the floors are not elevated but are placed on non-frost-susceptible gravel pads. The pads vary in thickness from 1.5 to 8.2 m; their average thickness is 3.7 m. Winter freezing of the pads and cooling of the ice-rich native soils below are accomplished by directing air into 63 corrugated metal ducts spaced 92 cm

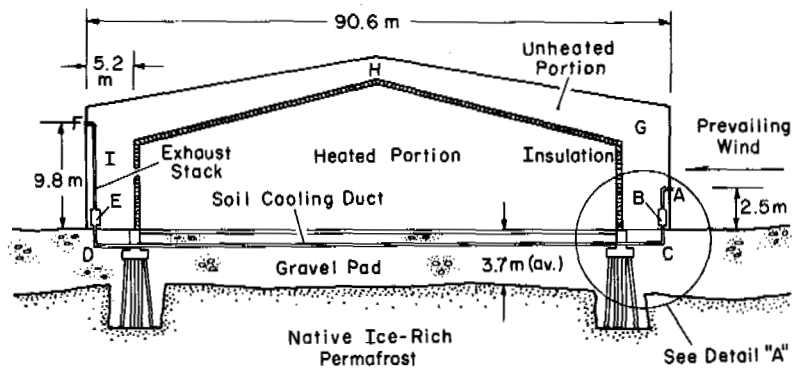
apart, 163 cm below the insulated floor. These ducts are not water tight. At the east end of the hangar a horizontal manifold tunnel provides a transition between the 63 ducts and 9 intake stacks. The stacks rise from the manifold and penetrate the hangar wall about 2.5 m above grade. A similar manifold exists at the west end of the ducts. From it, nine exhaust stacks rise 9.8 m above grade before penetrating the west endwall. The exhaust stacks are higher in order to create a natural convective draft (chimney draft) through the soil cooling system. All stacks contain dampers so that the system can be closed between May and October to prevent entry of warm summer air. Details of the soil cooling system are given in Figure 1.

The steel frame superstructure of each hangar rests on 20 piers supported by butt-down timber piles bearing on permafrost (Figure 1).

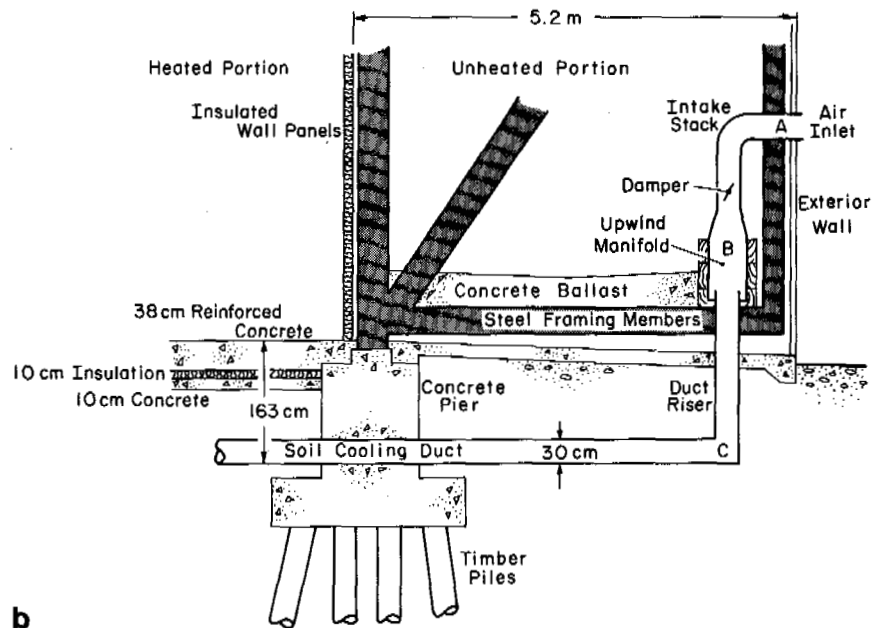
CLIMATE AND SOILS

The mean annual air temperature is -11°C , and the extremes range from -43°C to 18°C .³ The design air-thawing index equals 550°C-days and the design freezing index equals $4\,860^{\circ}\text{C-days}$.¹³ The thawing season begins in May or June, and the freezing season begins in late August or September. Prevailing winds are from the east off the ice cap. The average wind speed is 3.5 m/s with winter winds averaging about 4.0 m/s.¹⁰ Monthly peak gusts are consistently above 22 m/s. Winter storms from the southeast transport quantities of fine dry snow, creating a significant snow control problem.

Up to 22 m of ice-rich sandy silt overlies the highly fractured sedimentary bedrock. Excavations and soil borings have uncovered large ice layers and wedges as well as ice



a (Not to Scale)



b

FIGURE 1 Details of soil cooling system.

dispersed among soil particles. It is estimated that the upper 7 m of soil contains 50 percent ice by volume.⁸ Permafrost extends to an estimated depth of 490 m.² The annual thaw zone varies in thickness from 0.3 to 1.8 m and is usually refrozen by late September.

HANGAR PERFORMANCE

Two of the large hangars were built in 1951, the other four in 1953. As early as 1954 it was apparent that the "critical zone" for the soil cooling system was about three fourths of the way to the downwind end of each hangar: Soil in these areas was not refreezing. Ducts were inspected and found to be clear, with winter air velocities averaging about 0.8 m/s. In 1955, a theoretical study of the system¹¹ indicated that the soil-cooling capability of the ducts was used up in the upwind three fourths of the ducts. That study indicated that about 96 percent of the available chimney draft was lost to friction, with 40 percent of the frictional loss occurring at the inlet, outlet, and bends. Although it was suggested that acceptable system performance could be achieved by reconfiguring the inlets, no modifications were made.

By 1956, thaw was deepening beneath the critical zone and ducts were becoming blocked with ice, snow, and, to a lesser degree, silt. During the winter of 1956-1957 ducts were steam cleaned, but they were again blocked by ice the following spring. During the summer of 1957, ducts were again steam cleaned, water wells were installed in the hangars, and an extensive study of groundwater flow was undertaken using fluorescent dye.⁵ Vast quantities of subsurface waterflow were detected within the non-frost-susceptible material used for hangar pads and pavement bases. Although groundwater was considered the root of the duct icing problem, it was recommended that snow should no longer be piled alongside the hangars and that paved aprons be placed east and west of each hangar to divert roof runoff. These recommendations were implemented. Infiltrating snow was seen to enter both intake and exhaust stacks, but its contribution to duct blockage was considered relatively minor.

In 1958 groundwater flow was again studied.⁶ In 1959 control of groundwater was attempted by lowering the elevation of a nearby lake 2.5 m by pumping, and by pumping water from wells previously installed within the hangars. Pumping was conducted throughout the summer to maintain the water table at least 2.3 m below hangar floors. In this operation, many cubic metres of water were pumped from beneath each hangar. In 1960 the lake was lowered an additional 1.2 m, and again a hangar dewatering program was conducted.⁷ Notwithstanding all this effort, steam cleaning of ducts was required before winter. Thus, pumping and steam cleaning became an annual operation. The small size of the manifolds and ducts complicated cleaning. More effective inspection and cleaning could have been achieved

if the soil-cooling system components had been large enough to permit entry by operation and maintenance personnel.

In 1962 localized settlement was noticed in one hangar. Although specific details of steam cleaning between 1964 and 1968 are lacking, records refer to "attempts" at steam cleaning rather than to successfully completed programs. In 1968 the center of the settled area was depressed 6 cm in one hangar, 28 cm in three other hangars, 69 cm in hangar 10, and 107 cm in hangar 2. The diameters of the two largest settlement depressions exceeded 30 m.

During 1969 a comprehensive investigation¹² was made and it was concluded that: (a) thawing of ice-rich native soil was the basic cause of floor settlement; (b) maximum depth of thaw was consistently located in the vicinity of the well from which water had been pumped; (c) duct blockages significantly decreased the effectiveness of the soil-cooling systems; therefore, clearing of blocked ducts would be required each fall; (d) more soil cooling was needed than the soil cooling systems could provide in their present condition; and (e) although hangar floors had settled, there had been no distress to the pile-supported superstructures.

The October 1970 settlement depression in hangar 10 and several positions of the 0 °C isotherm since 1953 for that hangar are shown in Figure 2. In 1970 pumping of water from wells within the hangars was terminated. Since that time, portions of some ducts have been submerged, but ducts have generally been above the groundwater table.

Unfortunately, ducts were not steam cleaned during the winters of 1969-1970, 1970-1971, and 1971-1972, and during that period about 70 percent of all ducts were blocked with ice. Settlement records through 1971 suggested that the thaw bulb below each hangar had stabilized. However, a settlement survey conducted in October 1972 indicated that settlement had begun once again in four of the hangars. During the fall of 1972 ducts were steam cleaned and air leaks in the manifolds were reduced. As of this writing, the effectiveness of the 1972 steam cleaning and manifold sealing is not known.

EVALUATION

The Basic Soil Cooling System

Even before duct icings occurred, the soil cooling systems were not consistently capable of refreezing the gravel pad in the critical zone three fourths of the way to the downwind end of each hangar. Analysis of performance data suggests that several relatively minor changes would significantly improve the system.

Chimney Draft

The system was designed to utilize the chimney draft to create air flow through the ducts. However, the chimney

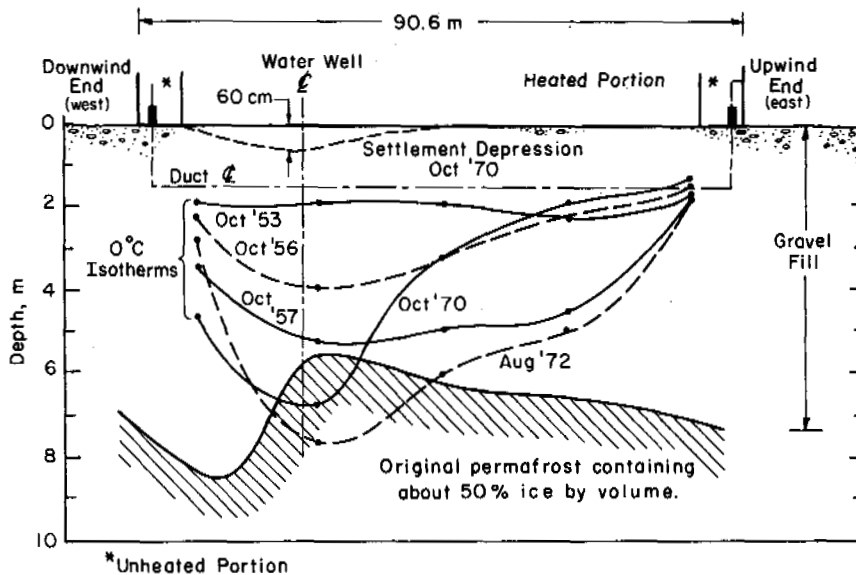


FIGURE 2 Thaw and settlement, 19.6 m south of north wall, hangar 10.

draft is reduced by the cooling of the air rising in the chimneys since they are located in the cold, unheated portion of each hangar and are constructed of uninsulated sheet metal. Using the U.S. Army calculation method,⁴ a 10 percent increase in soil cooling capability could be achieved if the average temperature in the chimney were increased 2 °C.

Use of Wind Forces

When the door between the heated portion of a hangar and the unheated portion is unlatched, excess air pressure in the unheated area swings the door forcefully into the hangar. Under average outside wind conditions (3.5 m/s from the east) an individual can close the door, but during periods of high winds he may require assistance. Since the upwind and downwind unheated areas are interconnected over the top of the heated portion of the hangar, this situation is present at the doors leading into both the downwind and upwind unheated areas.

The source of pressurization is clearly evident when a cover of the upwind manifold is lifted: Cold air blows out of the manifold and into the unheated area. Even with covers in place, enough air leaks out of gaps in the manifold to pressurize the unheated area. Consequently, parallel air-flow paths exist: one through the soil cooling ducts (path A, B, C, D, E, F; Figure 1), and the other through the unheated portion of the hangar (path A, B, G, H, I, E, F; Figure 1).

It has been observed that when ducts are clear and the system is operating under a significant chimney draft on a cold winter day (-30 °C), with below-average winds of about 3 m/s, there is still a significant overpressure in the

unheated areas. Consequently, even when chimney draft potential is high and the wind-induced draft is below average, the wind-induced draft exceeds the chimney draft.

Although American design methods call attention to the importance of air-tight construction in soil-cooling systems and suggest cowled intakes to take advantage of wind forces,⁹ wind-induced drafts are ignored in design calculations since these drafts are "highly erratic and unpredictable."⁴ On the other hand, Soviet practice considers both chimney and wind-induced drafts quantitatively in design calculations.¹

In some geographical areas, winter winds may not be intense enough to contribute much to system performance. In other areas, such as Thule, wind-induced drafts may exceed chimney drafts.

Because manifolds are not air tight and inspection covers are not always in place, much of the wind effect never reaches the ducts. If the manifolds were air tight, flow through the ducts would increase and the thermal efficiency of the soil cooling system would be improved.

Suction along the lee side of the hangars, as well as pressure on the windward side, contributes to the wind effect. A more consistent and somewhat greater suction could be developed by terminating the chimney above the roof. This should also reduce downwind snow infiltration problems since downwind stacks now exit the hangars in an area where snow eddies during storms.¹²

Dampers

As shown in Figure 3, the average monthly outside air temperature is warmer than duct temperatures in the critical

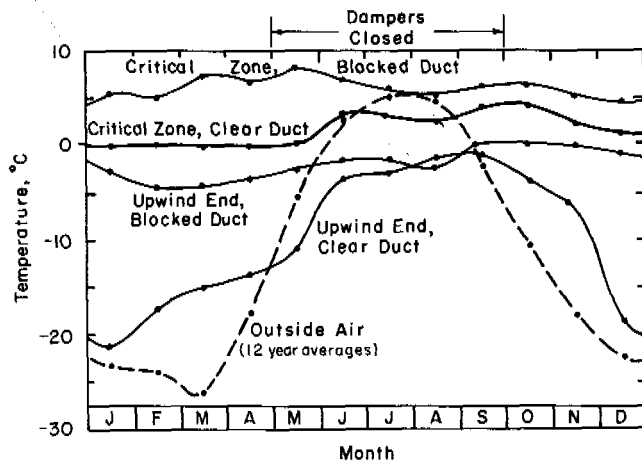


FIGURE 3 Outside air and duct temperature.

zone only during July and August. By having the duct open in late August and September, significant cooling will be achieved.

On several occasions, dampers have inadvertently been allowed to remain closed throughout the winter. The soil cooling system relies on winter cooling; if dampers were removed, operational errors would be reduced, and reliability would increase. A preliminary comparison of the present October to May operation with year-round operation suggests that with dampers removed the soil warming in July and early August would be offset by cooling achieved in late August and September during an average summer. However, during an exceptionally warm summer the depth of thaw under a hangar with dampers removed would increase perhaps as much as 0.5 m over the depth of thaw expected for a closed system.

The existing system contains dampers on both upwind and downwind stacks. In the summer, with the upwind damper blocking flow of air through the system but with the downwind damper open or removed, natural convection would tend to replace warm air in the ducts with outside air if the outside air is colder.

Duct Blockages

The soil cooling systems are considered only marginally effective when ducts are clear, but they are totally incapable of functioning as designed when ducts are blocked. The variations in performance of a system when ducts are first clear and then blocked is shown in Figure 4.

Periodic observation of ducts has shown that although infiltrating snow contributes to duct blockages infiltrating groundwater is the principal cause of blockages. Groundwater need not rise to the level of ducts below the hangar floor to create blockages. It is evident from Figure 2 that

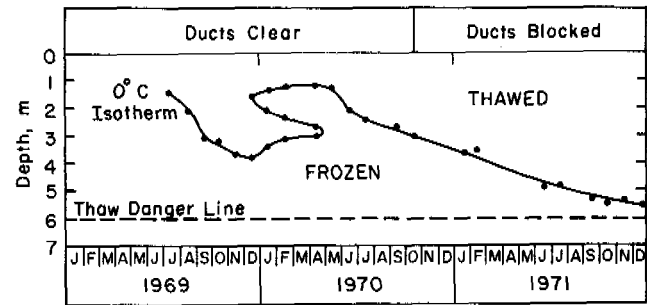


FIGURE 4 Effect of duct blockage on thaw under center of hangar 10.

the ducts cannot be blocked with ice under the heated portion of the hangar since they are within the thaw bulb in that area. Blockages are confined to the portion of each duct under the unheated ends of the hangar. Soils in this location are cold and do not thaw as rapidly during the summer as the soil surrounding the hangar. Meltwater in the active layer flows to this cold area, enters the duct risers, and then refreezes within the duct. Unless the soil-cooling systems are modified to bypass the portion of each duct under the unheated areas, annual duct blockages by infiltrating groundwater appear inevitable.

Pumping

It is certainly no coincidence that the settlement depressions in all hangars are centered at the well from which groundwater has been pumped. The vigorous pumping programs conducted in the 1960's caused a tremendous amount of warm surface water to flow into hangar pads. Heat introduced into the pads by this water caused localized deepening of the thaw bulb and settlements resulted. The localized deepening of the October 1970 thaw bulb adjacent to the well (as shown in Figure 2) was the result of pumping. The August 1972 thaw bulb was influenced more by duct blockages than by pumping and localized deepening was not as noticeable.

Pumping may be necessary in some hangars to lower the groundwater table below the ducts before winter soil cooling begins. Such pumping should be attempted only after the active layer surrounding the hangar has refrozen. At that time, the pump would draw from an isolated pocket of water within the thaw bulb and a minimal amount of pumping would produce surface drawdown since no inflow would occur. It is estimated that the removal of 31 m³ of water would lower the water table 10 cm. With the pumping equipment used previously at Thule, this would amount to a 1- or 2-day maintenance task per hangar rather than a summer-long operation as in the past.

If pumping is required to lower the groundwater table

below the ducts, dampers in the upwind stacks should be closed until after the pumping operation to prevent formation of ice within the ducts. Therefore, it seems advisable to retain the upwind dampers.

Lowering the water table below each hangar a metre or more just prior to the winter soil-cooling season would increase the rate of soil cooling. Perhaps in an emergency this procedure could be followed, but it is not considered necessary for routine operation of the soil cooling systems at Thule.

FUTURE PLANS

For the existing hangars at Thule several alternatives have been investigated, ranging from complete abandonment of the soil cooling systems to the installation of sophisticated mechanical refrigeration equipment. Based on technical economic considerations two alternative plans for the future have been developed. Which alternative will be adopted has yet to be determined.

Plan A

Duct deicing would be required annually. Manifolds would be sealed to more effectively use chimney and wind drafts. Downwind dampers would be removed and upwind dampers would be closed in June of each year. In the fall, once the active layer surrounding a hangar had refrozen, the depth to water below the hangar floor would be determined. If water were within 20 cm of duct inverts, pumping would begin from wells below the hangar to lower the water table at least 30 cm below duct inverts. Ducts would be steam

cleaned at their upwind and downwind ends. After steam cleaning the ducts, the depth to water would be remeasured and, if necessary, additional pumping would be conducted. With all ducts clean, upwind dampers would be opened to allow winter cooling of supporting soils. Plan A would be a viable choice only if ducts were effectively steam cleaned before each winter.

Plan B

The requirement for annual duct deicing would be eliminated by removing the portion of the soil cooling system that become blocked with ice. New manifolds would be constructed under the east and west ends of the heated portion of each hangar as shown in Figure 5. Insulated intake structures would be installed above the upwind manifold. The new intakes would end in the unheated upwind end of the hangar. Existing intake stacks would be removed so that the upwind portion of the hangar could serve as a stilling basin to remove snow from the air before it enters the soil cooling system (Figure 5). Insulated exhaust stacks would be installed above the downwind manifold. The stacks would be located within the warm hangar to increase chimney draft. They would end a metre or more above the roof.

This system would be operated from late August to June, or perhaps year-round to increase reliability. For year-round operation, it would be necessary to temporarily block air-flow each fall in certain hangars until after the groundwater table is lowered by pumping. Pumping would not be conducted until the active layer surrounding the hangar had frozen.

In the event that chimney and wind drafts prove to be

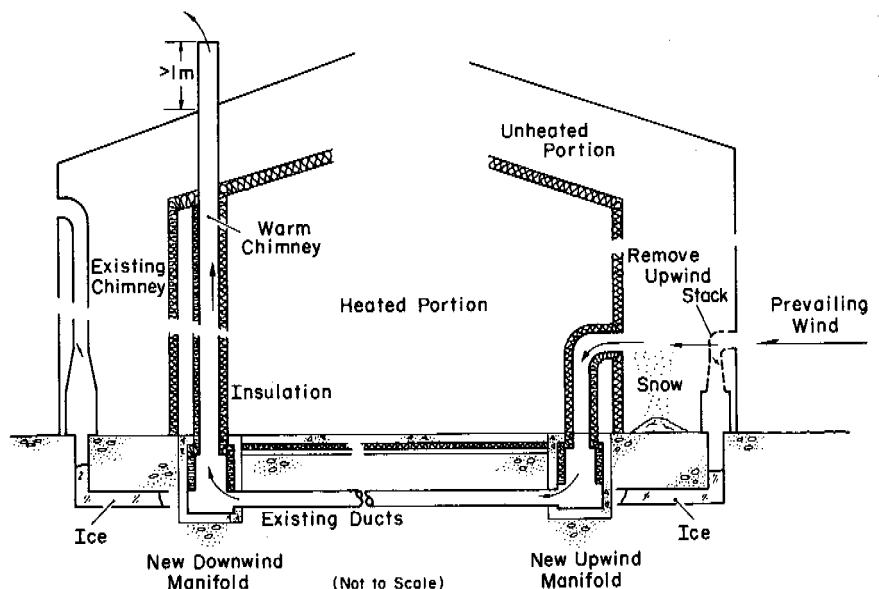


FIGURE 5 Plan B—new intakes, manifolds, and chimneys.

insufficient for either plan A or plan B, fans could be installed to increase airflow through the soil cooling system. Hopefully, fans will not be necessary.

CONCLUSIONS

Although ducted soil cooling systems can effectively prevent permafrost degradation below on-grade heated buildings, the experience gained at Thule indicates that ducted systems can be sensitive. The Thule experience emphasizes that:

1. Potential problems caused by groundwater in the active layer should be carefully investigated.
2. Manifolds, and perhaps the ducts themselves, should be large enough to permit entry of maintenance personnel for inspection and removal of blockages.
3. Provisions should be incorporated to minimize the amount of snow infiltration and to remove any drift snow that enters the soil cooling ducts.
4. The ends of exhaust stacks should be located a metre or more above the roof rather than high on the lee side of the building, where snow eddies.
5. A significant draft can be created by each chimney, but if the air cools as it rises up the chimney, the chimney effect will be diminished. Where possible, therefore, building heat should be utilized to help warm the chimney.
6. The wind can be a very important force in causing air flow in a soil cooling system. Whether or not wind-induced drafts are considered quantitatively in the design, the use of wind forces should be an important design objective. In some geographical areas, winter winds may not be intense enough to contribute much to system performance. In other areas, such as Thule, wind-induced drafts may exceed chimney drafts.
7. The system should be airtight. Air intakes should point into the wind and the exhaust end of the system should be configured to use wind-induced suction.
8. Soil warming that might result if a soil cooling system is operated year round should be evaluated against the increase in system reliability achieved by eliminating the requirement for annual opening and closing of dampers.
9. If dampers are installed, they should be placed only on upwind stacks. Eliminating downwind dampers allows convection currents to remove warm air from ducts even with the upwind damper closed.

ACKNOWLEDGMENTS

This paper presents the results of research performed by the Cold Regions Research and Engineering Laboratory under the sponsorship

of the U.S. Army Corps of Engineers and the U.S. Air Force Aerospace Defense Command. The hangars at Thule Air Base, Greenland, were designed for the U.S. Air Force by Metcalf and Eddy, Engineers, and Alfred Hopkins and Associates, Architects, under contract with the Northeast District, U.S. Army Corps of Engineers. The hangars were built by the joint-venture, North Atlantic Constructors. The Civil Engineering Division of the 4683D Air Base Group, Aerospace Defense Command, U.S. Air Force, operates and maintains the facilities at Thule. Performance information has been collected by Metcalf and Eddy personnel, military personnel and Danish nationals employed by the Base Civil Engineering Division, and by USA CRREL personnel.

REFERENCES

1. Academy of Construction and Architecture, USSR, Research Institute of Foundations and Underground Structures. 1962. Instructions for designing bearing media and foundations in the southern zone of the permafrost region. (translated by V. Poppe) Tech. Translation TT 1298. National Research Council of Canada, Ottawa.
2. Ball, D. G., and I. H. Call. 1966. U.S. sanitary and hydraulic engineering practice in Greenland, p. 409-412. *In* Permafrost: Proceedings of an international conference. National Academy of Sciences, Washington, D.C.
3. Davis, R. M. 1966. Design, construction and performance data of utility systems, Thule Air Base. U.S. Army Cold Regions Research and Engineering Laboratory. Spec. Rep. 95.
4. U.S. Army/U.S. Air Force. 1966. Arctic and subarctic construction, calculation methods for determination of depths of freeze and thaw in soils. U.S. Army Tech. Man. TM5-852-6.
5. Metcalf and Eddy, Inc. 1957. Pavement condition report 1957 supplement. Tech. Rep. No. ENG-445. U.S. Army Corps of Engineers, Eastern Ocean District, Boston, Massachusetts.
6. Metcalf and Eddy, Inc. 1958. Airfield drainage investigation. Tech. Rep. No. ENG-455. U.S. Army Corps of Engineers, Eastern Ocean District, Boston, Massachusetts.
7. Metcalf and Eddy, Inc. 1960. Airfield drainage investigation. Tech. Rep. No. ENG-465. U.S. Army Corps of Engineers, Eastern Ocean District, Boston, Massachusetts.
8. Metcalf and Eddy, Inc. (N.D.) Greenland completion report, 1951-1955. Spec. Rep. prepared for the U.S. Army Corps of Engineers.
9. Sanger, F. J. 1969. Foundations of structures in cold regions. USA CRREL Cold Regions Science and Engineering Monograph III-C4.
10. Stehly, N. S. 1965. Polar weather limitations on construction--Preliminary arctic survey. Tech. Rep. R391. U.S. Naval Civil Engineering Laboratory, Port Hueneme, California.
11. Takahashi, Y. 1966. Study of air duct cooling systems under a heated building on permafrost (Hangar 7A-4, Thule AB, Greenland). USA CRREL Intern. Rep. 16.
12. Tobiasson, W., and J. Lowry, III. 1970. Hangar floor settlements at Thule Air Base, Greenland. Tech. Rep. No. AFWL-TR-69-122. U.S. Air Force Weapons Laboratory, Albuquerque, New Mexico.
13. Tobiasson, W., and D. Flax. 1972. Instructions for monitoring instrumentation in the Thule hangars. USA CRREL Report to USAF.

PERFORMANCE OF A WARM-OIL PIPELINE BURIED IN PERMAFROST

George H. Watson [1] and Raymond K. Rowley [2]

William A. Slusarchuk

MACKENZIE VALLEY PIPELINE RESEARCH
LIMITED
Calgary, Alberta

NATIONAL RESEARCH COUNCIL
OF CANADA
Ottawa, Ontario

INTRODUCTION

To study the behavior of permafrost as a foundation material for a warm-oil pipeline, Mackenzie Valley Pipe Line Research Limited, with technical assistance from the Division of Building Research, National Research Council of Canada, installed a 27-m test section of 0.61-m-diameter pipe near Inuvik, N.W.T. The surrounding foundation material (ice-rich silty clay) was thawed by circulating oil at 71 °C.

The principal objectives of the field test, which began in July 1971 and concluded in January 1972, were to

1. Measure pore pressure within the foundation during thawing and assess its effect on shear-strength values for analyses of slope stability;
2. Measure temperature within the foundation and determine the location and rate of movement of the thaw front;
3. Monitor settlement of both foundation and pipe during thawing and freezeback; and
4. Determine representative frozen bulk densities for each soil layer within the foundation, predict values of pipe settlement, and compare these values with the measured movements.

SITE CONDITIONS

The Inuvik test site is located in the continuous permafrost zone (at about lat. 68°20' N, long. 133°45' W) adjacent to the Mackenzie River Delta.

The buried test section was located adjacent to existing oil-circulating facilities. A gravel work pad had been built on the site previously but not used. The greatest depth of ice-rich silt was found at this location. It was also an economical location because of its proximity to the existing support facilities.

A generalized soil profile, obtained from large-diameter (30 cm) cores, is given in Table I.

INSTALLATION OF TEST FACILITY

The 0.61-m pipe was installed during the first week of July 1971. A small backhoe was used to remove the 1.21-m thicknesses of gravel pad and dig a trench approximately 1 m deep into the virgin soil. The pipe was bedded on sand and the ditch backfilled with sand to the bottom of the gravel fill. The gravel fill was then restored.

Settlement rods were attached to the pipe at the centre and

TABLE I Generalized Soil Profile of Inuvik Test Site

Depth below Surface (m)	Stratum Designation	Description of Soil Stratum	Bulk Frozen Density (g cm ⁻³)	Strain on Thawing (%)
0-1.37		Gravel fill	—	—
1.37-1.52		Compressed organics	—	—
1.52-1.82	A	Silty clay (organic)	1.137	40 ^a
1.82-1.98	B	Ice (trace of silt)	0.945	90 ^b
1.98-2.74	C	Ice with silt inclusions	1.233	56 ^a
2.74-3.96	D	Silt and ice	1.426	40 ^a
3.96 and Below	E	Gravelly till	2.002	Nil

^a Estimated from laboratory tests at *in situ* overburden pressure

^b Estimated from field frozen bulk density, measured on core samples.

both ends, and temperature sensing points installed within it. Protective sleeves were installed around the settlement rods to prevent damage.

TEST SECTION OPERATION

The flow of warm oil through it began on 22 July 1971. The oil temperature was maintained at approximately 71 °C until 1 October 1971 when the heaters broke down and circulation was stopped. The oil temperature gradually decreased, until by 3 November 1971 it was down to 3 °C. Warm oil circulation was then resumed and continued until January 1972.

Pore pressure and thermistor readings were taken daily and a settlement survey was made at least twice weekly. Grid surveys were also taken before, during, and after the test to define surface settlement.

INSTRUMENT SELECTION AND INSTALLATION

Although development of instruments for measuring soil properties in unfrozen soils is well advanced, only limited progress had been made in instrumentation for measuring pore pressures in frozen soils during thaw. It was recognized that to instrument the frozen foundation of the proposed facility, some development work would be necessary, especially for pore pressure measurement, to ensure that the instruments would perform adequately and be sturdy enough to withstand arctic conditions. Details of the instrumentation used are described elsewhere.⁶

Selecting the piezometer was the most difficult task. The unit had to be sensitive in the low range of pore pressure values anticipated in the test, yet rugged enough to withstand possible high freezeback pressures. A rapid response was also required.

Standpipe, closed hydraulic, electrical diaphragm, and pneumatic units were considered. The pneumatic unit was chosen because it met the requirements of sensitivity plus ruggedness and also had been used successfully in frozen dyke foundations.² This instrument functions by the application of gas pressure through a closed-loop system to balance the pore pressure acting against the sensing element. For use in impervious soils, this type of piezometer has a single bellows to minimize time lag. Any change in pore pressure results in minute movement of the bellows, requiring displacement of only a very small amount of pore water.

Instrument locations in the ground around the pipe were selected on the basis of thermal simulator predictions, experience gained from a previous test loop,⁵ and known soil and ice conditions (Figure 1). Four piezometer-thermistor probes, anchored at depth, were used to monitor the cross-section locations and were placed close to the centre of the test section. These multiple sensor probes contained a total

of 11 piezometers and 28 thermistors. A second series of "floating" (i.e., not anchored) single-sensor piezometer probes was installed as an auxiliary system for the rigid anchored assemblies. A series of standpipes was installed to monitor the groundwater levels across and along the pipe during thaw.

Installation of the instruments started on 10 July 1971. Standard piezometer installation procedures were followed with minor changes because of the permafrost. Each piezometer-thermistor unit was placed in the hole with the sensor openings surrounded by a plug of sand at least 45 cm long. The sand was saturated with a glycol mixture to ensure a "hard" system. A 45-cm (minimum) compacted bentonite seal was then placed above each sand plug.

The chambers around the piezometers in both single- and multiple-sensor probes were saturated with a mixture of water and glycol. Their calibration was re-checked before installation. In assembling the probes, an extra length of casing was provided at the bottom. Just before placement, the depth of the instrument hole was measured accurately and the extra casing cut off as necessary to allow the probe to be set at the correct elevation.

A small heated hut was built close to the instrumented area to house all the reading equipment and readout points for the piezometers. All thermistor leads were run to the existing instrument trailer and connected to the readout equipment.

For measuring temperature, thermocouples, resistance-temperature devices (RTD's) and thermistors were considered. Thermistors were chosen because they had been used successfully at the Inuvik site and could be easily incorporated into the existing digital readout system. The existing datum stations, used to monitor the soil-temperature profile to supply data for a thermal simulator, consisted of a series of thermistors to a depth of 7.5 m.

In view of the limitations of the conductive model used for predicting thaw-front location,⁵ additional instrumentation was installed (e.g., ground surface temperature sensors) to upgrade the input data so that the buried test section's thermal effects on the foundation could be simulated later. Field-measured soil thermal conductivities are being used in continuing analytical studies. Convection effects in this case were minimal as the level site made for little groundwater flow.

The National Research Council of Canada has developed settlement gages for use in permafrost and their spiral foot gage was selected for use in this study.^{1,3}

As pore pressures were expected to be small, the elevation of the groundwater level in the thaw bulb had to be accurately defined. For this purpose, data from the standpipes were supplemented by direct measurements of the water table elevation in the trench, at the centre and end settlement points of the buried pipe. A well-established water

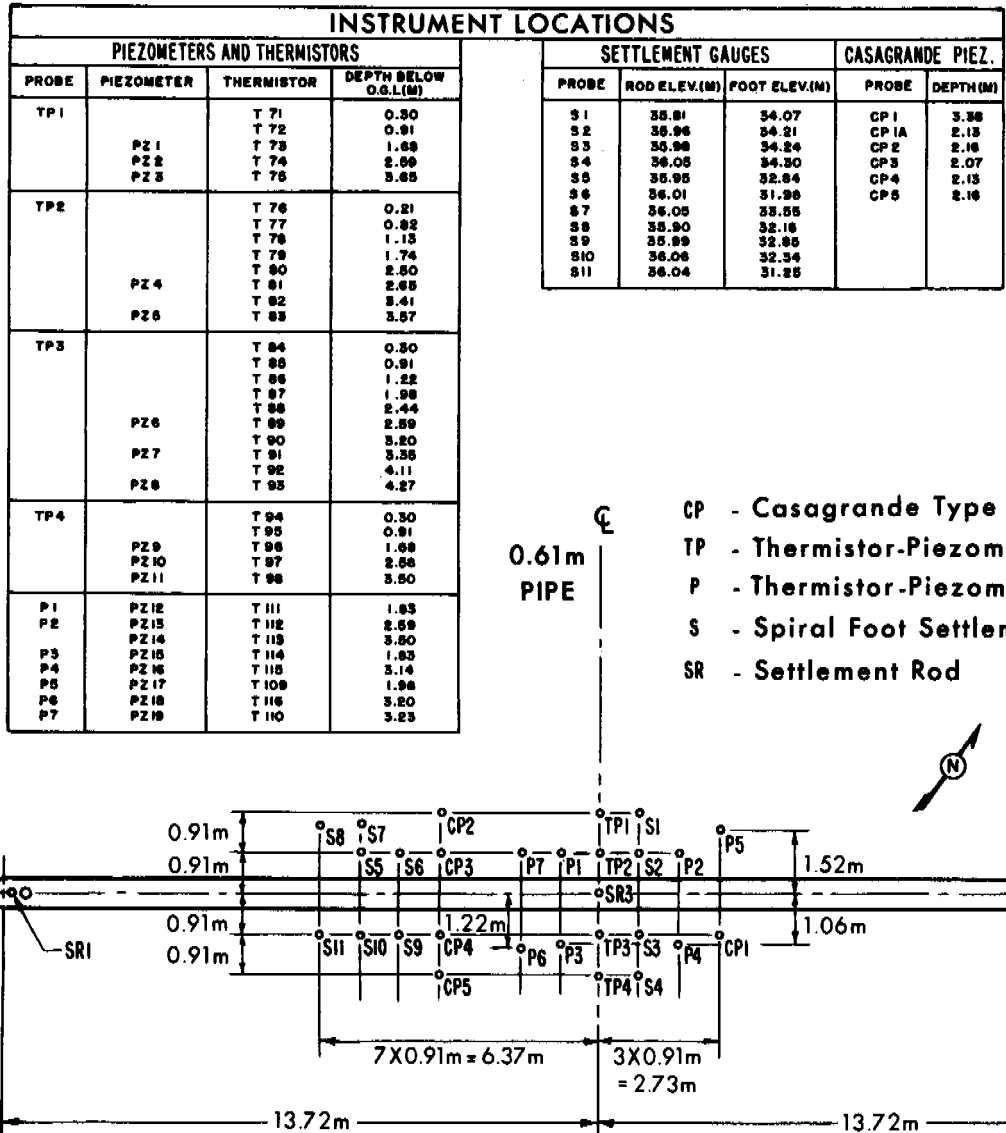


FIGURE 1 Plan of instrumentation around buried pipe.

table elevation was defined with 5 of 6 Casagrande tips being in good agreement with the directly measured elevations in the trench.

Elevation control was maintained on the Casagrande tips during the period of severe ground movement by measuring from a predetermined elevation to the water table with a standard electrical probe.

During the initial stages of the test, the ice layer close to the bottom of the pipe melted and most of the support cribbing at the north end of the oil flow lines had to be removed. A flexible hose connection was installed in the 15-cm supply line to ensure that it would not be overstressed and that settlement would not be impeded at this end of the buried section.

FOUNDATION AND PIPE PERFORMANCE

Pore Pressure

Pore water pressures within the thaw bulb were measured to determine if excess pore pressures existed during thawing. It was also hoped to trace the path of the melt water as it flowed from the thaw front. The anchored piezometer probes provided the most useful data for pore pressure analysis, as both the distance between piezometers on a probe and their elevations were known at all times. Hydraulic gradients, reflecting the amount of excess pore pressure and, therefore, the extent of the loss of the frictional component of the soil strength can be readily calculated from probe readings.

Over 90 percent of the piezometers appeared to function satisfactorily. The deeper ones indicated an increase in pore pressure during the initial freezeback period immediately after installation. This increase was probably the result of pressures generated by the volume expansion of freezing water. In some cases these pressures were large as evidenced by values obtained from one tip that were greater than the capacity of the readout equipment (21 m of water). After initial freezeback and before thawing, the high pressures dissipated, and in most cases negative pore pressures were recorded. These negative pressures were possibly due to the lensing action and associated contraction in the ice-rich silty clay as the soil was gradually restored to equilibrium conditions.

As the thaw front advanced toward each piezometer unit, a rapid rise in pore pressure was recorded. The maximum readings for each of the tips in the anchored probes are shown on Table II. The maximum pressures occurred at different times, and every functioning tip recorded a pressure in excess of the hydrostatic head.

In near-surface areas and close to the trench, pore pressures dissipated rapidly. At depth they were sustained for much longer, and in some cases no dissipation was observed during the test (Figures 2 and 3).

The excess pore pressures developed during the test did not approach the value of the total overburden pressure, so that a significant effective stress was always present within the thaw plug in spite of the existence of hydraulic gradients. A large portion of the overburden pressure came from the gravel pad that extended above the water table.

TABLE II Date and Magnitude of Maximum Pore Pressures

Probe	Initial Depth of Unit (m)	Maximum Pore Pressure (m of water)	Approximate Maximum Excess Pore Pressure (m of water)	Date of Maximum Pore Pressure
TP 1	1.67	0	0	^a
	2.59	2.01	0.64	3 Oct.
	3.66	3.17	0.73	20 Nov.
TP 2	2.65	1.67	0.30	12 Aug.
	3.56	3.17	0.88	20 Nov.
TP 3	2.59	2.01	0.76	5 Aug.
	3.35	2.44	0.42	5 Sept.
	4.27	3.41	0.49	10 Sept.
TP 4	1.65	1.25	0.85	19 Nov.
	2.59	1.74	0.43	28 Sept.
	3.50	3.41	1.19	23 Nov.

^a Not functioning.

The pore pressure results revealed two general trends: First, the maximum value recorded by each piezometer indicated an excess of hydrostatic pressure. Second, for each of the multiple piezometer strings, the excess pore pressures always increased with depth, showing that hydraulic gradients existed by which water was moved away from the thaw front.

Although it is difficult to establish a flow net for conditions within the thaw plug, measured pressures indicate that the water released by thawing flowed upward toward the trench.

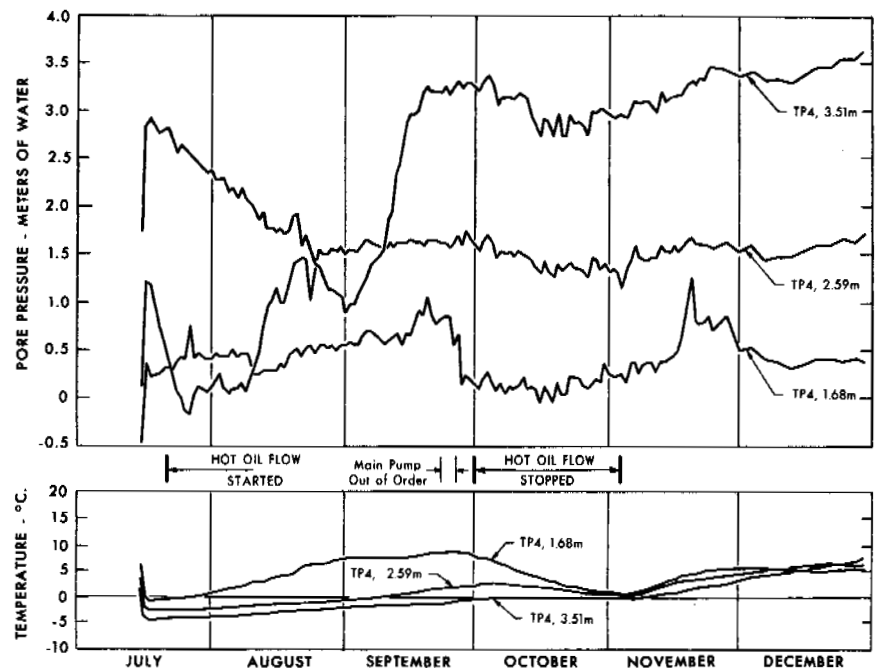


FIGURE 2 Pore pressure and temperature readings (TP 4).

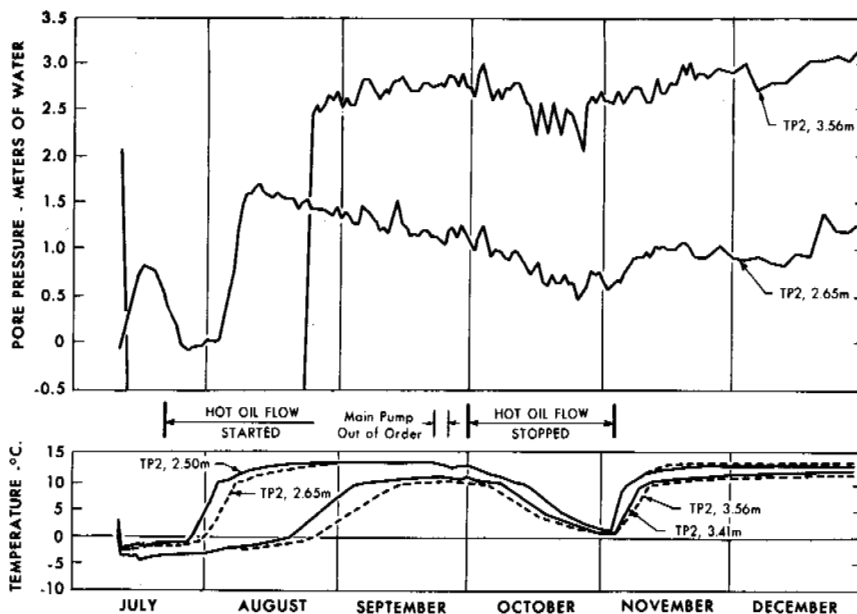


FIGURE 3 Pore pressure and temperature readings (TP 2)

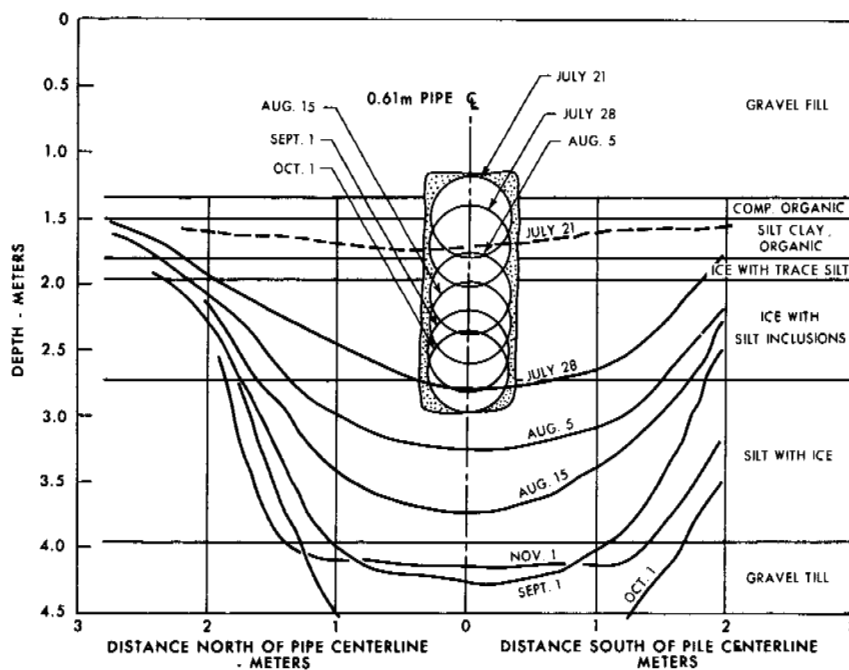


FIGURE 4 Position of 0°C isotherm during the test.

Temperature

To monitor the location and rate of movement of the thaw front, temperatures were recorded at 46 points around the buried pipe (Figure 4). The thaw rate was found to be more rapid than had been predicted by a thermal simulator, as pipe settlement had not been incorporated in the simulator program.

Initially, the thaw front advanced rapidly both downward and to either side of the pipe, but the rate slowed down

with increasing distance between the pipe and the 0°C isotherm. In the early stages of the test, the thawed zone assumed the shape of a shallow bowl, but as the pipe (heat source) settled, the thaw front advanced more rapidly downward than horizontally, and the shape of the thawed zone became that of a deep bowl.

The vertical distance from the bottom of the pipe to the 0°C isotherm followed the square-root-of-time law defined as follows:

$$x = \beta t^{1/2}$$

where x = the vertical distance from the bottom of the pipe to the 0°C isotherm in metres; β = a constant in $\text{m h}^{1/2}$; and t = time in h.

The value of β determined from the field test was $0.046 \text{ m h}^{1/2}$. Computing the constant β from Stefan's equation gives a value of $0.057 \text{ m h}^{1/2}$. This result indicates that, even though the pipe settled more than 1.3 m, the square-root-of-time law can be used to predict the location of the thaw front beneath it.

Settlement

Figure 5 shows surface profiles across the centre of the buried section on 19 July 1971 (before the test), 1 September 1971

(immediately after the thaw front below the pipe passed out of the ice-rich permafrost layers), and 11 July 1972 (after the test was completed). Almost all the settlement resulted from the thawing of the upper ice-rich, permafrost layers. The till was dense and settled very little on thawing. When the thaw front first penetrated the till, the maximum settlement of the ground surface (and the pipe) was approximately 0.98 m or 80 percent of the total settlement during the test.

Settlement was measured at 11 points at various depths within the foundation (Figure 6). Elevations were taken from the tops of steel rods with spiral foot gages attached to their bases. This method works well when foundation movement takes place parallel to the axis of the rod. Thawing around the pipe resulted in two-dimensional movement. In addition

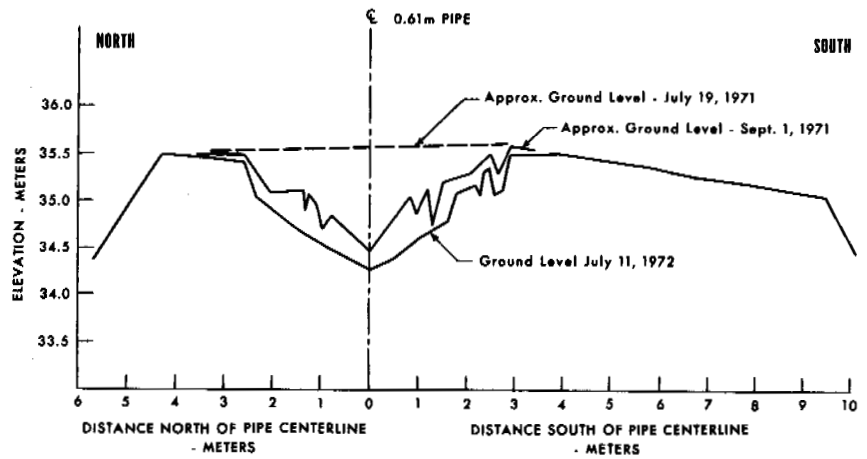


FIGURE 5 Surface profile 14 m from east end of test section.

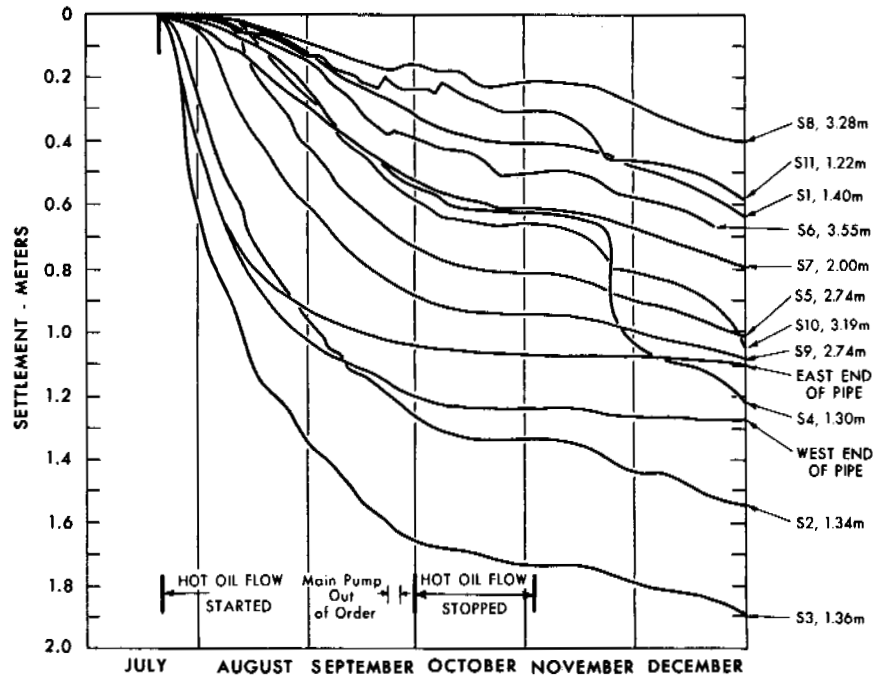


FIGURE 6 Time versus settlement plot for foot gages and pipe.

to moving downward, the thawed material tended to slough inward toward the pipe, causing the adjacent settlement rods to bow.

As elevation readings were taken from the tops of the bowed rods, settlement values were from 0.09 to 0.21 m too high. Corrections to these values were incorporated in the analysis of the pipe performance.

Three groups of gages were installed to determine settlement within the different layers of ice-rich permafrost as it thawed. The gages in each group were located at the same distance from the pipe centreline but at different elevations. Although the amount of rod bowing was slightly different for each group, it was practically the same for the individual gages within each group. Consequently, the error introduced by bowing was essentially eliminated when the difference in settlement between gages in the same group were calculated. Figure 7 shows the settlement-difference plots for one group, including the date at which the thaw front passed each gage foot. The group consisted of gages S2, S5, and S6, which were located 1 m away from the pipe centreline. Originally, S2 was located at an elevation of 34.21 m, S5 at 32.84 m, and S6 at 31.98 m.

S2 began to settle shortly after the warm oil started circulating. The curves for S2-S5 and S2-S6 are identical until approximately 5 August when the thaw front passed S5. The S2-S5 curve then started to level off and became almost horizontal in about 2 weeks. The S2-S6 and S5-S6 curves also started to level off after the thaw front passed the lower gage, and became horizontal after 2 weeks.

Approximately 80 percent of the settlement between any two gages had occurred by the time the thaw front reached the bottom gage, and most of the remaining 20 percent took place within the next 2 weeks.

Elevation measurements were taken on the steel rods attached to the pipe to monitor its settlement. As these rods were protected from bending by a 30-cm sleeve, pipe settlement was determined accurately.

Measured and predicted settlement values are presented in Table III. The predicted values are based on laboratory thaw-settlement tests and the soil profile determined from the borings used for instrument installation. The frozen bulk density versus thaw settlement relationship used to predict these values is presented elsewhere.⁷

CONCLUSIONS

1. During thawing of the foundation, excess pore pressures were recorded. In the upper layers, two of three piezometers indicated that the pore pressures dissipated rapidly. At greater depths, pore pressure rose to a maximum value and remained nearly constant during the testing period. Although the values of excess pore pressures are small, a hydraulic gradient was developed at depth. This factor should be considered in slope-stability calculations.
2. Comparison of computed and measured locations of the thaw front indicate that the square-root-of-time law can be used to predict the thaw front location beneath the pipe.
3. Settlement measurements show variability over short

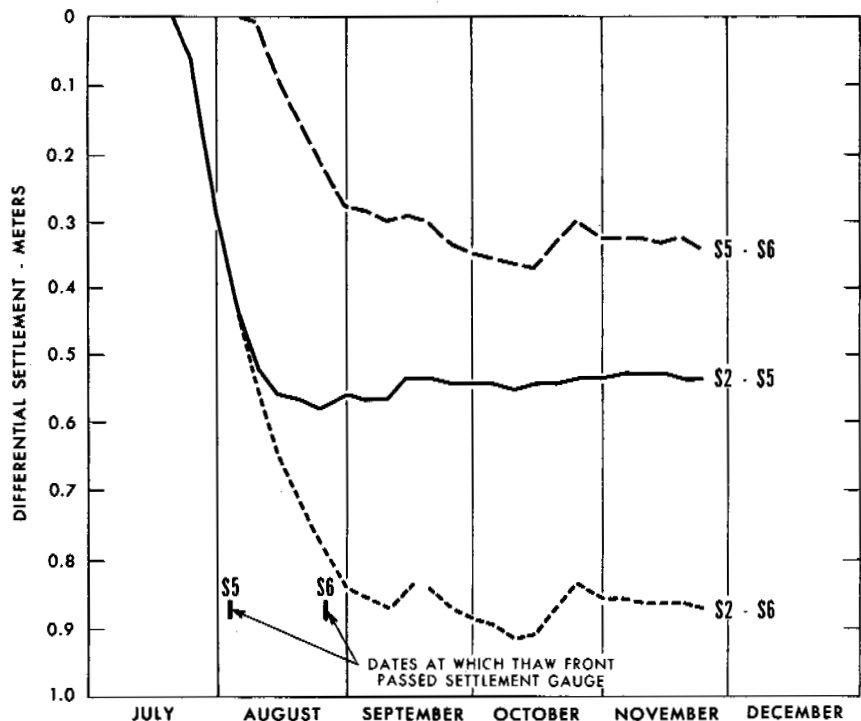


FIGURE 7 Differential settlement versus time.

TABLE III Differential Settlement Summary

Gage Numbers	Original Layer Thickness (m)	Layer Designation and Thickness (m)		Predicted Strain (%)	Predicted Settlement of Each Layer (m)	Predicted Settlement (m)	Measured Settlement (m)
S7-S8	1.36	C	0.67	56	0.37	0.65	0.43
		D	0.70	40	0.28		
S5-S6	0.86	D	0.85	40	0.34	0.34	0.33
S2-S5	1.37	A	0.12	40	0.05	0.67	0.53
		B	0.15	90	0.14		
		C	0.75	56	0.42		
		D	0.15	40	0.06		
S2-S6	2.23	A	0.12	40	0.05	1.01	0.85
		B	0.15	90	0.14		
		C	0.75	56	0.42		
		D	1.00	40	0.40		
S9-S10	0.51	D	0.51	40	0.21	0.21	0.27
S10-S11	1.09	D	0.70	40	0.28	0.28	0.33
		E	0.40	0	0		
S3-S9	1.38	A	0.33	40	0.13	0.75	0.79
		B	0.15	90	0.14		
		C	0.76	56	0.42		
		D	0.12	40	0.05		
S3-S10	1.89	A	0.33	40	0.13	1.00	1.06
		B	0.15	90	0.14		
		C	0.76	56	0.43		
		D	0.64	40	0.30		
Pipe	2.13 (bottom of pipe to top of gravel)	B	0.15	90	0.14	1.05	1.06 (west)
		C	0.76	56	0.43		1.24 (east)
		D	1.21	40	0.48		

distances. However, the amount of settlement was predicted within practical accuracy by using average values obtained from laboratory thaw-settlement tests.

4. Settlement followed thawing closely and continued after the 0 °C isotherm had passed. This could indicate a high initial permeability after thawing, which decreased substantially with time.

5. The conditions that promoted thawing were accelerated in terms of the proposed pipeline conditions. For the test section, oil was circulated at 71 °C from the start of the test, whereas for the pipeline a buildup from 38 to 60 °C in 5 years is proposed. Under full-scale operation, the slower heat buildup would result in lower pore pressures and slower settlement rates.

ACKNOWLEDGMENTS

The authors are grateful for the interest and assistance of their colleagues throughout the project, particularly L. W. Gold, T. L. Speer, and W. Miller.

This paper is a joint contribution of Mackenzie Valley Pipe Line Research Limited and the Division of Building Research, National Research Council of Canada and is published with the approval of the Research Coordinator of Mackenzie Valley Pipe Line Research Limited and the Director of the Division of Building Research.

REFERENCES

- Bozozuk, M., G. H. Johnston, and J. J. Hamilton. 1963. Deep benchmarks in clay and permafrost areas. Field testing of soils. ASTM Spec. Tech. Publ. No. 322. p. 265-275.
- Gupta, R. C., R. G. Marshall, and D. Badke. 1972. Instrumentation of dykes on permafrost—Kettle generating station. 25th Can. Geotech. Conf.
- Johnston, G. H. 1965. Permafrost studies at Kelsey hydroelectric generating station—Research and instrumentation. NRC Div. Bldg. Res. Tech. Paper No. 178. 35 p.
- Morgenstern, N. R., and J. F. Nixon. 1972. One-dimensional consolidation of thawing soils. Can. Geotech. J. 8(4).
- Rowley, R. K., G. H. Watson, R. G. Auld, and T. M. Wilson. 1972. Permafrost of a 48-inch warm-oil pipeline supported on permafrost. 25th Can. Geotech. Conf.
- Slusarchuk, W. A., G. H. Watson, and T. L. Speer. 1972. Instrumentation around a warm-oil pipeline buried in permafrost. 25th Can. Geotech. Conf.
- Watson, G. H., R. K. Rowley, and W. A. Slusarchuk. Determination of some frozen and thawed properties of permafrost soils. (In preparation)

NOTES

- [1] On loan from Acres Consulting Services, Calgary, Alberta, Canada.
- [2] On loan from Standard Oil of California.

BIOLOGICAL CONSIDERATIONS FOR CONSTRUCTION IN THE CANADIAN PERMAFROST REGION [1]

Ross W. Wein

UNIVERSITY OF NEW BRUNSWICK
Fredericton, New Brunswick

L. C. Bliss

UNIVERSITY OF ALBERTA
Edmonton, Alberta

INTRODUCTION

Announcement of petroleum discoveries in Alaska and the Canadian Mainland Arctic and the Arctic islands precipitated many questions about the biological consequences of northern developments, and there was an immediate search for background data. Unfortunately, little was known about mammal, fish, and bird population numbers, the magnitude of population fluctuations, or even the regions of importance that required protection. Neither was there much information on plant communities, or their relationship to soils, topography, and regeneration after disturbance. A recent bibliography has been compiled to assess the available research information,³⁰ and a series of maps, tentatively indicating important wildlife habitats, is now available for large areas of the Arctic.¹⁰ This paper considers biological problems that are related to northern construction in light of recent studies. These studies have been sponsored by government (National Research Council of Canada-International Biological Program, Arctic Land Use Research Programme of the Department of Indian and Northern Affairs, Canadian Wildlife Service, Polar Continental Shelf Project of the Department of Energy, Mines and Resources), industry (Arctic Petroleum Operators Association, Canadian Arctic Gas Study Ltd.), and the University of Alberta.

MAINLAND ARCTIC

The mainland Arctic can be divided into three major physiographic regions: upland tundra, coastal lowlands, and mountains and foothills. Each region has inherently different biological problems with regard to construction activities.

Permafrost conditions, geological substrates, and vegetation-soil units can be related closely to these regions. Non-migratory animals such as barren-ground grizzly bear, dall sheep, moose, nesting birds, and lake-bound fish populations can also be related to physiographic regions but migratory organisms such as caribou, wolves, nonnesting birds, and river-dwelling fish run freely across land units. Sensitive habitat areas of both migratory and nonmigratory species must be avoided during certain seasons by modifying construction schedules and procedures.

Upland Tundra

This physiographic region is considered to be the gently rolling terrain that has lakes of thermokarst origin,²⁵ where the distribution and abundance of underground ice is little understood,²⁷ and where a change in the thermal balance over ice-rich areas will cause thermokarst topography.

Summer seismic operations, for instance, caused thermokarst to develop along these lines.^{17,19} Under the disturbed area the active layer increased, but Hernandez¹⁷ found no major soil erosion. *Arctophila fulva*, *Carex aquatilis*, *Arctagrostis latifolia*, *Calamagrostis canadensis*, *Poa lanata* and *Luzula confusa* were the most successful pioneers.¹⁷ These are the same plants that colonize naturally occurring mudflows²⁴ and are the species that should be used in vegetation programmes where possible.

Subsequent to 1965, seismic activity was shifted to winter when the moss and low shrub layer is protected by snow. Winter damage is so slight in the wet sedge communities that it is difficult to find the path in the summer. In the shrub tundra and tree covered areas, the woody vegetation is broken, but regrowth of many species starts the following spring.¹⁷

Winter snow roads constructed for continuous winter transportation produce similar disturbance. Over hummock terrain the use of snow-ice roads preserves the microtopography and vegetation to a greater degree than roads of only compacted snow.

Revegetation research on disturbed areas has shown that several of the native species mentioned above and agronomic species (*Festuca rubra*, *Phleum pratense* and *Poa pratensis*) produce good growth and overwinter well.^{17,34,40} The invasion and establishment of the agronomic species in the undisturbed communities, based on the present available data, seem unlikely.¹⁸

Growth of these species can be increased by additional nutrients and, although nitrogen is usually the limiting element in undisturbed tundra,¹⁵ there is a greater response to phosphorus fertilizers on disturbed areas.⁴⁰ During large construction projects, such as in pipelining, soil must be held in place until the vegetation cover has been established. Large quantities of silt released into rivers at pipeline cross-

ings could damage fish populations, especially if this coincides with critical stages of fish life cycles such as migration and spawning.³² This will be most important in streams that have low sediment loads. Another biological problem related to seismic operations in the upland tundra is that of changing caribou migrations. Little evidence has been gathered to date to support this criticism. More major obstructions, such as roads, telecommunication lines, and pipelines, may affect caribou movements as in Scandinavia,²² but Calef and Lortie concluded that bermed or buried pipelines would likely be crossed by caribou during migration.⁹ Concern has also been expressed that wildfires will increase during northern development, but we must remember that northern biomes have evolved under a fire regime. In studies of upland tundra fires, Cody^{11,12} indicated that revegetation was favorable after 9 years. Brown *et al.*,⁶ Mackay,²⁶ and Wein and Bliss³⁷ showed that after fire the active layer increased up to 50 percent or more. Wein and Bliss noted that regrowth, as measured by above-ground production, equalled that on the unburned areas after 2 years, and it was estimated that the above-ground plant material would be replaced within 7–17 years.³⁷

This rapid regrowth was attributed to warmer soils, accelerated microbial activity, and increased nutrient cycling. In areas of high ice content soil, such as near Inuvik, N.W.T., slumps have been triggered by wildfire but the percentage of the landscape affected is very small and has not yet been documented.

One of the most important biological concerns associated with the petroleum industry is that of oil spills. Experimental crude oil spills on upland tundra have shown that the capacity for these landscape types to hold spilled oil is high in summer (up to 76 500 m³/km²) and although the contaminated vascular vegetation was killed, the underground plants survived^{29,36} and gave 20–50 percent recovery. Lichens did not recover and only *Polytrichum juniperinum* of the mosses showed regrowth. Spills should not be disturbed mechanically because oil does decompose even in these cold soils,¹⁴ and “seeding” with microorganisms or addition of nitrogen fertilizers may be useful.

Disturbances of the vegetation surface, whether by oil spills, fire, or winter roads, caused decreased albedo and latent heat fluxes with an increased soil heat flux.¹⁶ The peat layer was important initially because of its high moisture content and, secondarily, because of decreased thermal conductivity as water is lost by latent heat flux. Any activity that disrupts or destroys the peat layer will lead to increased active layer and melt-out of ice inclusions.

Coastal Lowlands

These areas have particularly high ice content soils and slumps triggered by wave action or river bank erosion are common along the 500 km Yukon Territory coastline.²⁵ Summer seismic operations proved very detrimental to these

areas and water now stands in these lines.¹⁷ Current winter seismic operations and winter roads cause no damage, because the high ice content of the frozen soils prevents soil compaction or damage to underground plant parts. Fire hazard is not great in these wet sedge communities; however, oil spills could be particularly damaging to water fowl, because high water tables keep the oil on the surface.³⁶ Care must be taken to prevent spills in this area because oil will quickly move into streams or lakes; this could be disastrous if a spill occurred when waterfowl, such as snow geese, were gathered on open waters during migration.³⁹

Mountains and Foothills

The foothills of the British and Richardson mountains also have high ice contents, especially in the more silty soils; coupled with the generally steeper slopes, more erosional problems would be expected. Solifluction lobes in the mountains and slumps along river banks are expressions of this instability.³⁵

Fire is just as important in this region as in the uplands if the biomass is sufficiently great and with the updraft caused by fires they can sweep up into the alpine tundra to drastically reduce ranges such as those of dall sheep.³⁸

Pipelines across mountainous areas would follow river valleys and in many cases may be buried in river gravels. Little is presently known about the spawning runs or spawning areas of northern fish but the silting of streams may repel spawning runs, may kill fish by clogging their gills with silt, and may drastically change downstream spawning beds. If gravel is used for road or pipeline construction, spawning beds will be destroyed,³² although the magnitude of this problem has not as yet been determined. Oil spills in this area would quickly become an aquatic problem and are yet to be studied.

Mainland Forest-Tundra

To the south of the true tundra, tree and shrub biomass rapidly increases.³⁸ With the increased number of thunderstorms,²¹ the probability of fires becomes greater. In the forest-tundra, fires are a major ecological agent, and the required degree of fire protection is not yet known. Moose habitat is improved after fire but caribou, which rely on lichen growth, lose suitable winter habitat for many years.³¹ More recent information on caribou food habitats, however, suggests that fire is of somewhat less significance because lichens are not as essential.^{20,33} Terrestrial fur bearers such as marten and aquatic fur-bearers, such as beaver, muskrat, and mink, may also suffer from a lack of suitable habitat following fire.⁹

Since the forest-tundra zone lies within the discontinuous-permafrost zone, where unfrozen areas occur, ground ice is not as prevalent⁷ and seismic operations are permitted in summer and winter. These lines through the trees provide caribou

with corridors of easy access,⁹ although the ultimate effects of these lines on migration are not known.

Oil spills would be just as damaging to the aquatic system as in more northern areas but in the upland the greater active layer in the June to September period would hold more oil and runoff into the aquatic system would be slower. During the remainder of the year runoff would be similar to more northern areas.

ARCTIC ISLANDS

The Canadian Arctic Archipelago consists of ca. 1.42 million km² or 56 percent of the Canadian Arctic. Physiographically, the eastern islands of Baffin, Devon, Ellesmere, and Axel Heiberg contain mountains of Precambrian granite and large glaciers, while the western islands are much lower in elevation and contain younger sediments of Mesozoic and Cenozoic age. Plateau areas and mountain slopes above 250–300 m contain few plants and little animal life. These areas are polar deserts, and, other than increasing silt loads of streams flowing from them, little biological damage results from well drilling and haul roads or pipeline construction should that occur.

Coastal lowlands and fiord valleys on Axel Heiberg and Ellesmere islands and inland areas at low elevation on Banks and Victoria islands have a relatively lush sedge-grass-moss cover more comparable with the mainland coastal lowlands. Slopes and low elevation plateaus and ridges (50–300 m) have a partial plant cover and limited animal populations; these areas are called polar semi-deserts.

Lowlands

Coastal lowlands and fiord valleys occupy less than 3 percent of the Queen Elizabeth Islands, which lie north of 75°. These separated areas, often no more than 25–100 km², contain a nearly complete cover of sedge-grass-moss communities and provide prime habitat for muskox, especially for winter grazing. Numerous lakes make these areas important waterfowl nesting habitat. These lowlands are literally oases in a nearly barren landscape.

Use of tracked vehicles in these areas in summer is as detrimental as in the lowlands of the mainland Arctic.¹ Babb¹ also found that in most areas surface rutting or soil compaction resulted in less than a 15 percent increase in depth of the active layer, indicating that plant cover has far less influence on energy dissipation than in the mainland Arctic. In simulated surface blading in these lowland sites, albedo increased about 50 percent, latent heat and sensible heat losses increased, but soil energy flux increased only slightly.¹ This probably results from the much lower permafrost temperatures⁷ and reduced net radiation at these latitudes.

Natural revegetation of these lowlands will be difficult because the native flora has few pioneering species. Seed production, seedling establishment, and seedling growth of native species is tenuous, and there is no indication that introduced species would be more successful.^{1,4,5}

Diesel fuel sprayed on *Carex stans* vegetation killed the vascular plants on contact, just as with crude oil. One year later vascular plant cover was reduced about 50 percent while lichens and mosses showed little effect at an application rate of 0.25 dm³ m⁻².¹

Ice wedge polygons are widespread in the Arctic and are particularly common in gravel beaches. Only recently has this massive ice been recognized in many of these high latitude regions.⁸

Slopes and Uplands (Polar Semideserts)

These sites with a 20 to over 50 percent cover of low vascular plants, lichens, and mosses are preferred summer and winter habitat of Peary's caribou, lemming, jaeger, and several other species of birds. While these polar semideserts or polar steppes contain much less plant cover and less animal activity than the lowlands, they occupy vast areas. Surface soils remain moist only where there is a cover of crustose lichens. This contrasts to sites having mosses, fruticose lichens, and scattered vascular plants. Revegetation programs will meet with little success because of competition in the first case and drought in the second case.

In many of these areas there is little, if any, indication of ice-rich permafrost, yet on slopes, small to massive slumps occur.^{1,3,8} The cold soils act as a point of condensation for moisture accumulation at the permafrost table and result in a lubricated and unstable site.¹ Once the rolling upland surface soils have dried after spring snowmelt, little rutting occurs with offroad seismic and other vehicles.²

Mass wasting is a common natural feature in these High Arctic environments, though 90 percent of annual runoff occurs with spring snowmelt.²⁹ With little plant cover and surface soils ranging from sands to clay, headward erosion of small and large streams appears rapid. This also manifests itself in accelerated soil erosion along scraped airstrips and rutted roads on gentle to steep slopes. Observations show that gullies 1–2 m deep and 2–4 m wide can develop in only two summers, yet water erosion from snowmelt occurred for only 2–3 weeks each June. Accelerated sheet and gully erosion from changed drainages and deeper snowpack on the leeward side of storage areas, airstrips, buildings, etc., may prove to be a major environmental problem in building and maintaining gas pipeline facilities in the arctic archipelago.

It should be emphasized that for future management and protection of these physiographic regions, research must be linked to vegetation-soils-permafrost units to be effective. Plant community classifications in sufficient detail have been advanced by Corns,¹³ Hernandez,¹⁷ Lambert,²³ and Wein

*et al.*³⁸ for the mainland Arctic, but for the arctic islands this work is just starting.

REFERENCES

- Babb, T. A. 1972. High arctic manipulation and disturbance studies, p. 369-391. In L. C. Bliss [ed.] Devon Island IBP project, high arctic ecosystem project report 1970 and 1971. University of Alberta Printing Ser., Edmonton.
- Barnett, D. M., and M. Kuc. 1972. Terrain performance, Melville Island, District of Franklin. Pt. A, Paper 72-1. Geological Survey of Canada, Ottawa. p. 137-139.
- Beschel, R. E. 1963. Hummocks and their vegetation in the high arctic, p. 13-20. In Permafrost: Proceedings of an international conference. National Academy of Sciences, Washington, D.C.
- Bliss, L. C., and R. W. Wein. 1972. Plant community responses to disturbances in the western Canadian Arctic. Can. J. Bot. 50:1097-1109.
- Bliss, L. C., and R. W. Wein. 1972. Ecological problems associated with arctic oil and gas development, p. 65-77. In R. F. Legget and I. C. MacFarlane [ed.] Proceedings of the Canadian northern pipeline research conference. NRCC Tech. Mem. 104. Ottawa.
- Brown, J., W. Rickard, and D. Vietor. 1969. The effect of disturbance on permafrost terrain. U.S. ARMY CRREL Spec. Rep. 138. 13 p.
- Brown, R. J. E. 1970. Permafrost in Canada. University of Toronto Press, Toronto. 234 p.
- Brown, R. J. E. 1972. Permafrost in the Canadian Arctic Archipelago. Z. Geomorphol. N.F. Suppl. 13:102-130.
- Calef, G. W., and G. M. Lortie. 1971. Appendix I, Observations of the Porcupine Caribou Herd. April 1-September 22, 1971. In Towards an environmental impact assessment of a gas pipeline from Prudhoe Bay, Alaska to Alberta. Environmental Protection Board, Winnipeg.
- Canadian Wildlife Service. 1972. The arctic ecology map series. 2nd ed. Dept. of Environment, Wildlife Serv. Ottawa.
- Cody, W. J. 1964. Reindeer range survey 1957 and 1963. Plant Res. Inst., Can. Dep. Agric., Ottawa. 15 p.
- Cody, W. J. 1965. Plants of the Mackenzie River Delta and reindeer grazing preserve. Plant Res. Inst. Can. Dep. Agric., Ottawa. 56 p.
- Corns, I. G. W. 1972. Plant communities in the Mackenzie Delta Region, p. 1-46. In L. C. Bliss and R. W. Wein [ed.] Botanical Studies of Natural and Man Modified Habitats in the Eastern Mackenzie Delta region and the Arctic Islands, ALUR, Dep. Indian and Northern Affairs, Ottawa. 288 p.
- Gossen, R. G., and D. Parkinson. The effect of crude oil spills on the microbial populations of selected Arctic soils. I. Biomass and respiration. Can. J. Microbiol. Vol. 19. (In press)
- Haag, R. W. 1972. Mineral nutrition and primary production in native tundra communities of the Mackenzie Delta Region, N.W.T. M.Sc. thesis. University of Alberta, Edmonton. 89 p.
- Haag, R. W. Energy budget changes following surface disturbance to upland tundra vegetation. In L. C. Bliss [ed.] Botanical studies of natural and man Modified habitats in the Mackenzie Valley, eastern Mackenzie Delta region, and the Arctic Islands. ALUR, Dep. Indian and Northern Affairs, Ottawa. (In press)
- Hernandez, H. 1972. Surficial disturbance and natural plant recolonization in the Tuktoyaktuk Peninsula Region, N.W.T. M.Sc. thesis. University of Alberta, Edmonton. 99 p.
- Hernandez, H. 1973. Revegetation studies: Norman Wells, Inuvik and Tuktoyaktuk, N.W.T. and Prudhoe Bay, Alaska; a report to the E.P.B. and ALUR. Interim Rep. No. 3. Environ. Protec. Board, Winnipeg and ALUR (see Haag, 1973)
- Hok, J. R. 1969. A reconnaissance of tractor trails and related phenomena on the North Slope of Alaska. U.S. Dep. Interior, Bureau Land Manage. 66 p.
- Kelsall, J. P. 1968. The migratory barren-ground caribou of Canada. Dep. Indian and Northern Affairs Can. Wildlife Serv., Ottawa. 340 p.
- Kendrew, W. G., and D. Kerr. 1955. The climate of British Columbia and the Yukon Territory. Meteorol. Div. Dep. Transport., Toronto. 222 p.
- Klein, D. R. 1971. Action of reindeer to obstructions and disturbances. Science 173:393-398.
- Lambert, J. D. H. 1968. The ecology and successional trends of tundra plant communities in the Low Arctic Subalpine zone of the Richardson and British Mountains of the Canadian Western Arctic. Ph.D. thesis. University of British Columbia, Vancouver. 164 p.
- Lambert, J. D. H. 1972. Plant succession on tundra mudflows: preliminary observations. Arctic 25:99-106.
- Mackay, J. R. 1963. The Mackenzie Delta area, N.W.T. Geogr. Branch, Dep. Mines Tech. Surv., Ottawa. Mem. 8. 202 p.
- Mackay, J. R. 1970. Disturbances to the tundra and forest tundra environment of the western arctic. Can. Geotech. J. 7:420-432.
- Mackay, J. R. 1972. The world of underground ice. Ann. Assoc. Am. Geogr. 62:1-22.
- McCann, S. B., P. J. Howarth, and J. G. Cogley. 1972. Fluvial processes in a periglacial environment, Queen Elizabeth Islands, N.W.T., Canada. Trans. Inst. Br. Geogr. 55:69-82.
- McCown, B. H., J. Brown, and R. P. Murrmann. 1971. Effect of oil seepages and spills on the ecology and biochemistry in cold dominated environments. Ann. Rep. U.S. Army CRREL. 18 p.
- Roberts-Pichette, P. 1972. Annotated bibliography of permafrost-vegetation-wildlife-landform relationships. For. Manage. Inst. Inform. Rep. FMR-X43, Can. For. Serv., Dep. Environment. 350 p.
- Scotter, G. W. 1964. Effects of forest fires on the winter range of the barren ground caribou in northern Saskatchewan. Wildlife Serv., Wildlife Manage. Bull. Ser. 1 No. 8. 111 p.
- Shotton, R. T. 1971. Appendix II. The nature and mechanisms of problems that might arise to fish from pipeline construction activities. (See Calef and Lortie, 1971.)
- Skoog, R. O. 1968. Ecology of the caribou (*Rangifer tarandus grantii*) in Alaska. Ph.D. thesis. University of California, Berkeley. 699 p.
- Wein, R. W. 1971. Appendix IV. A preliminary report on revegetation trials related to the proposed Gas Arctic Pipeline. (See Calef and Lortie, 1971.)
- Wein, R. W. 1971. Appendix III. Report on a vegetation survey along the proposed gas pipeline route—Peel Plateau to Old Crow Mountains. (See Calef and Lortie, 1971.)
- Wein, R. W., and L. C. Bliss. 1973. Experimental crude oil spills on arctic plant communities. J. appl. Ecol. 10:699-680.
- Wein, R. W., and L. C. Bliss. Changes in arctic Eriophorum tussock communities following fire. Ecology 54. (In press)
- Wein, R. W., L. R. Hettinger, and A. J. Janz. Plant community-soils relationships in the northern Yukon Territory. (In preparation)
- Woodford, J. 1972. The violated vision. McClelland and Stewart Ltd., Toronto. 136 p.
- Younkin, W. E. 1971. Revegetation studies of disturbances in the Mackenzie Delta region, p. 175-229 (See Corns, 1972).

NOTE

[1] Paper No. 6, Mackenzie Delta Region.

APPENDIXES

UNITED STATES PLANNING COMMITTEE

TROY L. PÉWÉ (*Chairman*), Professor and Chairman, Department of Geology, Arizona State University, Tempe, Arizona 85285

AMOS J. ALTER, Environmental Research Engineer, Office of Research and Academic Coordination, Alaska Department of Environmental Conservation, Fairbanks, Alaska 99701

JERRY BROWN, Research Soil Scientist, U.S. Army Cold Regions Research and Engineering Laboratory, Hanover, New Hampshire 03755

MAX CLIFTON BREWER, Commissioner of the Environment, Alaska State Office Building, Juneau, Alaska 99801

GEORGE FILLER, Architect, Juneau, Alaska 99801

GEORGE C. HOWARD, Research Group, Supervisor Engineering, Amoco Production Company, Tulsa, Oklahoma 74102

JOHN R. KIELY, Director, Bechtel Corporation, San Francisco, California 94105

ARTHUR H. LACHENBRUCH, Research Geophysics Branch, U.S. Geological Survey, Menlo Park, California 94025

G. A. LEONARDS, Head, School of Civil Engineering, Purdue University, Lafayette, Indiana 47907

KENNETH A. LINELL, Chief, Experimental Engineering Division, U.S. Army Cold Regions Research and Engineering Laboratory, Hanover, New Hampshire 03755

JOHN W. MARR, Professor of Biology, Department of Environmental, Population and Organismic Biology, University of Colorado, Boulder, Colorado 80304

FREDERICK J. SANGER, Senior Technical Advisor, Office of the Under Secretary, U.S. Department of the Interior, Washington, D.C. 20240

MORT D. TURNER, Interagency Arctic Research Committee, National Science Foundation, Washington, D.C. 20550

A. LINCOLN WASHBURN, Director, Quaternary Research Center and Professor, Geological Sciences, University of Washington, Seattle, Washington 98105

HARRY B. ZACHRISON, SR. (deceased), Arlington, Virginia 22203

Staff

ROBERT N. DILLON, Secretary, Executive Director, Building Research Advisory Board, National Research Council, Washington, D.C. 20418

JOAN D. FINCH, Planning Secretary, Staff Officer, Building Research Advisory Board, National Research Council, Washington, D.C. 20418

CLARET M. HEIDER, Associate Editor, Building Research Advisory Board, National Research Council, Washington, D.C. 20418

Consultants

JOHN E. SATER, Technical Editor, Arctic Institute of North America, Washington, D.C. 20009

RICHARD H. RAGLE, Technical Editor, Arctic Institute of North America, Washington, D.C. 20009

FREDERICK J. SANGER, Honorary Technical Advisor, Washington, D.C.

SPONSORS OF THE UNITED STATES PLANNING COMMITTEE

ATLANTIC RICHFIELD COMPANY, Los Angeles, California
BP ALASKA INC., New York, New York
EL PASO NATURAL GAS COMPANY, El Paso, Texas
HUMBLE OIL AND REFINING COMPANY, Houston, Texas
NATIONAL SCIENCE FOUNDATION, Washington, D.C.
PHILLIPS PETROLEUM COMPANY, Bartlesville, Oklahoma
SHELL OIL COMPANY, Houston, Texas
STANDARD OIL COMPANY OF CALIFORNIA, San Francisco, California
UNION OIL COMPANY OF CALIFORNIA, Brea, California
U.S. ARMY CORPS OF ENGINEER, Washington, D.C.

ORGANIZING COMMITTEE OF CANADA

J. R. MACKAY (*Chairman*), Department of Geography, University of British Columbia, Vancouver, 8, B.C.
R. J. E. BROWN, Research Advisor, Division of Building Research, National Research Council, Ottawa, Ontario KIA OR6
O. L. HUGHES, Quaternary Research & Geomorphology Division, Department of Energy, Mines and Resources, Calgary
44, Alberta
A. M. JESSOP, Earth Physics Branch, Department of Energy, Mines and Resources, Ottawa, Ontario
W. O. KUPSCH, Director, Institute for Northern Studies, University of Saskatchewan, Saskatoon, Saskatchewan
O. LØKEN, Hydrologic Sciences Division, Environment Canada, Ottawa, Canada, KIA OE7
L. NICHOLS, Geotechnical Research Group, Iron Ore Company of Canada Limited, Schefferville, P.Q.
J. Y. C. QUONG, Whitehorse District Office, Department of Public Works, Whitehorse, Y.T.
G. REMPEL, Imperial Oil Limited, Calgary, Alberta
M. C. RINGHAM, Engineering Design Division, Construction, Engineering & Architectural Branch, Ministry of Transport,
Ottawa, Ontario
L. SAMSON, General Manager, Terratech Limited, Saint Laurent, P.Q.
J. D. MOLLARD, J. D. Mollard & Associates Ltd., Regina, Saskatchewan
H. A. THOMPSON, Head, Arctic Climatology Unit, Atmospheric Environment Service, Downsview, Ontario

Sponsor

NATIONAL RESEARCH COUNCIL OF CANADA, Ottawa, Ontario

AUTHORS OF SUMMARY REVIEW PAPERS

Session I

L. W. GOLD Head, Geotechnical Section, Division of Building Research, National Research Council of Canada, Ottawa, Ontario, Canada KIA OR6

ARTHUR H. LACHENBRUCH, Research Geophysicist, U.S. Geological Survey, Geothermal Studies, Menlo Park, California 94025

Session II

ROGER J. E. BROWN, Research Advisor, National Research Council, Ottawa 7, Ontario, Canada KIA OR6

TROY L. PÉWÉ, Professor and Chairman, Department of Geology, Arizona State University, Tempe, Arizona 95285

Session III

J. ROSS MACKAY, Professor, Department of Geography, Vancouver 8, British Columbia, Canada

ROBERT F. BLACK, Department of Geology, University of Connecticut, Storrs, Connecticut 06268

Session IV

DUWAYNE M. ANDERSON, Chief, Earth Sciences Branch, U.S. Army Cold Regions Research and Engineering Laboratory, Hanover, New Hampshire 03755

N. R. MORGENSTERN, Professor of Civil Engineering, Department of Civil Engineering, The University of Alberta, Edmonton, Alberta, Canada

Session V

JOHN R. WILLIAMS, Central N.E. District Office, Water Resources Division, U.S. Geological Survey, Boston, Massachusetts 02203

ROBERT O. VAN EVERDINGEN, Research Scientist, Inland Water Directorate, Hydrology Research Division, Water Resources Branch, Calgary, Alberta, Canada T2L 2A7

Session VI

OSCAR J. FERRIANS, JR., U.S. Geological Survey, Menlo Park, California 94025

G. D. HOBSON, Geophysicist, Geological Survey of Canada, and A/Coordinator, Polar Continental Shelf Project, Department of Energy, Mines and Resources, Ottawa, Ontario, Canada KIA OE4

Session VII

KENNETH A. LINELL, Chief, Experimental Engineering Division, U.S. Army Cold Regions Research and Engineering Laboratory, Hanover, New Hampshire 03755

G. H. JOHNSTON, Northern Research, Geotechnical Section, Division of Building Research, National Research Council of Canada, Ottawa, Ontario, Canada KIA OR6

AUTHORS OF THE UNITED STATES PAPERS

- AFIFI, SHERIF S. (Session IV), Woodward-Lundgren & Associates, Oakland, California
- AITKEN, GEORGE W. (Session VII), U.S. Army Cold Regions Research and Engineering Laboratory, Hanover, New Hampshire
- ALTER, AMOS J. (Session VII), Environmental Research Engineer, Office of Research and Academic Coordination, Alaska Department of Environmental Conservation, Fairbanks, Alaska
- ANDERSON, D. M. (Sessions III, IV, and VI), Chief, Earth Sciences Branch, U.S. Army Cold Regions Research and Engineering Laboratory, Hanover, New Hampshire
- BEARSON, GLENN D. (Session IV), Lawrence Livermore Laboratory, University of California, Livermore, California
- BERG, RICHARD L. (Session VII), Research Civil Engineer, Northern Engineering Branch, U.S. Army Cold Regions Research and Engineering Laboratory, Hanover, New Hampshire
- BLACK, ROBERT F. (Session III), Professor of Geology, Department of Geology and Geography, University of Connecticut, Storrs, Connecticut
- BOCKHEIM, J. G. (Session III), University of British Columbia, Vancouver, British Columbia, Canada
- BOWERS, C. EDWARD (Session V), Professor of Civil Engineering, University of Minnesota, Minneapolis, Minnesota
- BRINLEY, WM. R., JR. (Session VI), Development & Resources Transportation Co., Silver Spring, Maryland
- BROWN, JERRY (Sessions II and VII), Research Soil Scientist, U.S. Army Cold Regions Research and Engineering Laboratory, Hanover, New Hampshire
- BUZZELL, TIMOTHY D. (Session VII), U.S. Army Cold Regions Research and Engineering Laboratory, Hanover, New Hampshire
- CARLSON, ROBERT F. (Session V), Director, Institute of Water Resources, University of Alaska, Fairbanks, Alaska
- CHAMBERLAIN, EDWIN (Session IV), Research Civil Engineer, Foundations and Materials Research Branch, Experimental Engineering Division, U.S. Army Cold Regions Research and Engineering Laboratory, Hanover, New Hampshire
- CLARK, C. C. (Session II), Department of Geology, Northern Illinois University, Dekalb, Illinois
- CLARK, LLOYD K. (Session VII), Clark & Groff Engineers, Inc., Salem, Oregon
- COHEN, JULES B. (Session VII), Chief, Environmental Sciences Branch, Arctic Health Research Center, Fairbanks, Alaska
- CRORY, FREDERICK E. (Session VII), Chief, Foundations and Materials Research Branch, Experimental Engineering Division, U.S. Army Cold Regions Research and Engineering Laboratory, Hanover, New Hampshire
- DINGMAN, S. LAWRENCE (Session V), Chief of Research, DuBois & King, Inc., Randolph, Vermont
- ESCH, D. C. (Session VII), Engineer of Tests, Alaska Department of Highways, College, Alaska
- FERRIANS, OSCAR J. (Session VII), Geologist, Branch of Alaskan Geology, U.S. Geological Survey, Menlo Park, California
- FROULA, NILSON H. (Session IV), Systems, Science and Software, LaJolla, California
- FULWIDER, CHARLES W. (Session VII), U.S. Army Cold Regions Research and Engineering Laboratory, Hanover, New Hampshire
- GASKIN, DAVID A. (Session VII), Research Geologist, Northern Engineering Research Branch, U.S. Army Cold Regions Research and Engineering Laboratory, Hanover, New Hampshire
- GATTO, LAWRENCE W. (Session VI), U.S. Army Cold Regions Research and Engineering Laboratory, Hanover, New Hampshire
- GEORGE, WARREN (Session VII), Chief, Pipeline Division, Alaska District, U.S. Army Corps of Engineers, Anchorage, Alaska
- HENNION, FRANK B. (Session VII), Chief, Civil Engineering Section, Advanced Technology Branch, Engineering Division Military Construction, Department of the Army, Office, Chief of Engineers, Washington, D.C.
- HOAR, CHARLES L. (Session VII), Project Engineer, Wasteco, Inc., Tualatin, Oregon
- HOEKSTRA, PIETER (Session VI), Research Physicist, Physical Sciences Branch, U.S. Army Cold Regions Research and Engineering Laboratory, Hanover, New Hampshire
- HUGHES, T. (Session III), Research Associate, Institute of Polar Studies, The Ohio State University, Columbus, Ohio
- IVES, JACK D. (Session II), Director, Institute of Arctic and Alpine Research, and Professor of Geography, University of Colorado, Boulder, Colorado

780 Authors of the United States Papers

- JAHNS, H. O. (Session VII), Esso Production Research Co., Houston, Texas
- JUMIKIS, ALFREDS R. (Session IV), Professor, Thermal Soil Mechanics and Foundation Engineering, Department of Civil and Environmental Engineering, College of Engineering, Rutgers University—The State University of New Jersey, New Brunswick, New Jersey
- KACHADOORIAN, REUBEN (Session VII), U.S. Geological Survey, Menlo Park, California
- KANE, DOUGLAS L. (Session V), Research Hydrologist, Institute of Water Resources, University of Alaska, Fairbanks, Alaska
- KLIEWER, RAYMOND MILTON (Session I), Brown & Root, Inc., Houston, Texas
- LANGE, G. ROBERT (Session VI), Geologist, Northern Engineering Branch, U.S. Army Cold Regions Research and Engineering Laboratory, Hanover, New Hampshire
- LARSON, DONALD B. (Session IV), Lawrence Livermore Laboratory, University of California, Livermore, California
- LeSCHACK, LEONARD A. (Session VI), President, Development & Resources Transportation Co., Silver Spring, Maryland
- LEWELLEN, ROBERT I. (Session II), Littleton, Colorado
- LINELL, KENNETH A. (Sessions V and VII), Chief, Experimental Engineering Division, U.S. Army Cold Regions Research and Engineering Laboratory, Hanover, New Hampshire
- LOBACZ, EDWARD F. (Sessions IV and VII), Chief, Construction Engineering Branch, U.S. Army Cold Regions Research and Engineering Laboratory, Hanover, New Hampshire
- LONG, ERWIN L. (Session VII), Anchorage, Alaska
- LUSCHER, ULRICH (Session IV), Associate, Woodward-Lundgren & Associates, Oakland, California
- McGINNIS, L. D. (Session II), Coordinator, Dry Valley Drilling Project, Department of Geology, Northern Illinois University, Dekalb, Illinois
- McKIM, HARLAN L. (Session IV), U.S. Army Cold Regions Research and Engineering Laboratory, Hanover, New Hampshire
- McNEILL, DUNCAN (Session VI), Barringer Research Ltd., Toronto, Ontario, Canada
- McVEE, CURTIS V. (Session II), State Director, Bureau of Land Management, Anchorage, Alaska
- MELLOR, MALCOLM (Session IV), U.S. Army Cold Regions Research and Engineering Laboratory, Hanover, New Hampshire
- MILLER, ROBERT D. (Session IV), Professor of Soil Physics, Department of Agronomy, Cornell University, Ithaca, New York
- MILLER, T. W. (Session VII), Esso Production Research Co., Houston, Texas
- MORSE, FREDERICK H. (Session VI), Development & Resources Transportation Co., Silver Spring, Maryland
- MULLER, LARRY (Session VII), U.S. Army Cold Regions Research and Engineering Laboratory, Hanover, New Hampshire
- MURRMANN, RICHARD P. (Session IV), Research Chemist, Earth Sciences Branch, U.S. Army Cold Regions Research and Engineering Laboratory, Hanover, New Hampshire
- NAIR, KESHAVAN (Session IV), Vice President, Woodward-Lundgren & Associates, Oakland, California
- NAKANO, YOSHISUKE (Session IV), Research Chemical Engineer, Foundations and Materials Research Branch, U.S. Army Cold Regions Research and Engineering Laboratory, Hanover, New Hampshire
- NAKAO, K. (Session II), Department of Geophysics, Hokkaido University, Sapporo, Japan
- OERTLE, D. H. (Session IV), Continental Oil Company, Ponca City, Oklahoma
- OUTCALT, SAMUEL I. (Session III), Assistant Professor, Department of Geography, University of Michigan, Ann Arbor, Michigan
- PETTIBONE, HOWARD C. (Session VII), Research Civil Engineer, U.S. Bureau of Mines, Spokane, Washington
- PÉWÉ, TROY L. (Session II), Professor and Chairman, Department of Geology, University of Arizona, Tempe, Arizona
- POWER, L. D. (Session VII), Esso Production Research Co., Houston, Texas
- PRICE, LARRY W. (Session III), Associate Professor of Geography, Department of Geography, Portland State University, Portland, Oregon
- RADD, F. J. (Session IV), Senior Research Associate, Central Research Division, Research and Development Department, Continental Oil Company, Ponca City, Oklahoma
- REED, SHERWOOD C. (Session VII), Research Sanitary Engineer, U.S. Army Cold Regions Research and Engineering Laboratory, Hanover, New Hampshire
- RICKEY, W. P. (Session VII), Esso Production Research Co., Houston, Texas
- RYAN, NANCY G. (Session VI), Development & Resources Transportation Co., Silver Spring, Maryland
- RYAN, ROBERT B. (Session VI), Development & Resources Transportation Co., Silver Spring, Maryland
- RYAN, WILLIAM L. (Session VII), Chief, Sanitation Facilities, U.S. Indian Health Service, Anchorage, Alaska

- SAYLES, FRANCIS H. (Session IV), Research Civil Engineer, U.S. Army Cold Regions Research and Engineering Laboratory, Hanover, New Hampshire
- SELLMANN, PAUL V. (Session II), Geologist, Northern Engineering Research Branch, U.S. Army Cold Regions Research and Engineering Laboratory, Hanover, New Hampshire
- SHERMAN, RICHARD G. (Session V), Chief Geologist, Metcalf & Eddy, Inc., Boston, Massachusetts
- SLAUGHTER, CHARLES W. (Session V), U.S. Army Cold Regions Research and Engineering Laboratory, Hanover, New Hampshire
- SMITH, NORTH (Session VII), Research Civil Engineer, Northern Engineering Research Branch, U.S. Army Cold Regions Research and Engineering Laboratory, Hanover, New Hampshire
- SMITH, ROBERT E. (Session IV), Staff Civil Engineer, Atlantic Richfield Company, Dallas, Texas
- SMITH, WAYNE S. (Session IV), Staff Engineer, Woodward-Lundgren & Associates, Oakland, California
- STANLEY, LEONARD E. (Session VII), Research Physicist, Technical Services Division, U.S. Army Cold Regions Research and Engineering Laboratory, Hanover, New Hampshire
- STEVENS, HENRY W. (Session IV), U.S. Army Cold Regions Research and Engineering Laboratory, Hanover, New Hampshire
- TAYLOR, JAMES R. (Session IV), Lawrence Livermore Laboratory, University of California, Livermore, California
- TAYLOR, T. P. (Session VII), Esso Production Research Co., Houston, Texas
- THOMSON, STANLEY (Session IV), Professor of Civil Engineering, Department of Civil Engineering, University of Alberta, Edmonton, Alberta
- TICE, ALLEN R. (Session IV), U.S. Army Cold Regions Research and Engineering Laboratory, Hanover, New Hampshire
- TOBIASSON, WAYNE (Session VII), Research Civil Engineer, Experimental Engineering Division, U.S. Army Cold Regions Research and Engineering Laboratory, Hanover, New Hampshire
- UGOLINI, F. C. (Sessions III and VI), Associate Professor, College of Forest Resources, University of Washington, Seattle, Washington
- VIERECK, LESLIE A. (Session I), Principal Plant Ecologist, Institute of Northern Forestry, U.S. Forest Service, Fairbanks, Alaska
- WALKER, H. J. (Session V), Professor, Louisiana State University, Baton Rouge, Louisiana
- WHEELER, J. A. (Session VII), Esso Production Research Co., Houston, Texas

AUTHORS OF THE CANADIAN PAPERS

- BLISS, L. C. (Session VII), Department of Botany, University of Alberta, Edmonton, Alberta
- BROWN, ROGER J. E. (Session I), Northern Research, Geotechnical Section, Division of Building Research, National Research Council of Canada, Ottawa, Ontario
- CRAMPTON, C. B. (Session II), Department of the Environment, Edmonton, Alberta
- EGGINTON, P. (Session III), Department of Geography, University of Ottawa, Ontario
- FRENCH, H. M. (Session III), Professor, Department of Geography, University of Ottawa, Ottawa, Ontario
- GARG, OM P. (Session VI), Geotechnical Engineer, Iron Ore Company of Canada, Schefferville, Quebec
- GASKIN, PAUL N. (Session IV), Queen's University, Kingston, Ontario
- GILL, DON (Session II), Professor, Department of Geography, University of Alberta, Edmonton, Alberta
- GRANBERG, HARDY B. (Session II), McGill Sub-Arctic Research Laboratory, Schefferville, Quebec
- HEGINBOTTOM, JOHN ALAN (Session VII), Terrain Sciences Division, Geological Survey of Canada, Ottawa, Ontario
- HUNTER, J. A. M. (Session VI), A/Head, Seismic Section, Resources, Geophysics and Geochemistry Division, Geological Survey of Canada, Ottawa, Ontario
- HWANG, C. T. (Session I), E. W. Brooker & Associates, Edmonton, Alberta
- JANIGA, PAUL V. (Session IV), McGill University, Montreal, Quebec

782 Authors of the Canadian Papers

- JOHNSTON, G. H. (Session IV), Northern Research, Geotechnical Section, Division of Building Research, National Research Council of Canada, Ottawa, Ontario
- JUDGE, A. S. (Session I), Earth Physics Branch No. 437, Department of Energy, Mines and Resources, Ottawa, Ontario
- LADANYI, BRANKO (Sessions IV and VII), Professor, Department of Mining Engineering, and Director, Northern Engineering Centre, Ecole Polytechnique, Montréal, Québec
- LAGAREC, DANIEL (Session II), Centre d'Etudes Nordiques, Université Laval, Québec City, Québec
- MACKAY, J. ROSS (Session III), Professor, Department of Geography, University of British Columbia, Vancouver, British Columbia
- MORGENSTERN, N. R. (Session IV), Professor, Department of Civil Engineering, University of Alberta, Edmonton, Alberta
- NICHOLSON, FRANK H. (Session II), McGill Sub-Arctic Research Laboratory, Schefferville, Québec
- NIXON, J. F. (Session IV), Department of Civil Engineering, University of Alberta, Edmonton, Alberta
- OSLER, JOHN C. (Session IV), McGill University, Montreal, Québec
- ROWLEY, RAYMOND K. (Session VII), Mackenzie Valley Pipeline Research Limited, Calgary, Alberta (Standard Oil of California, U.S.A.)
- RUTTER, N. W. (Session II), Geological Survey of Canada, Department of Energy, Mines and Resources, Calgary, Alberta
- SLUSARCHUK, WILLIAM A. (Session VII), National Research Council of Canada, Ottawa, Ontario
- SMITH, M. W. (Session I), Assistant Professor, Department of Geography, Carleton University, Ottawa, Ontario
- SPEER, T. L. (Session VII), Mackenzie Valley Pipeline Research Limited, Calgary, Alberta (AMOCO Oil Company, Chicago, Illinois, U.S.A.)
- SUTHERLAND, HUGH B. (Session IV), Cormack Professor of Civil Engineering, Department of Civil Engineering, University of Glasgow, Glasgow, Scotland
- THOM, BRUCE G. (Session II), Department of Biogeography and Geomorphology, Australian National University, Canberra, Australia
- WATSON, GEORGE H. (Session VII), Mackenzie Valley Pipeline Research Limited, Calgary, Alberta (Acres Consulting Services, Calgary, Alberta)
- WEIN, ROSS W. (Session VII), Assistant Professor, Department of Biology, University of New Brunswick, Fredericton, New Brunswick
- YONG, RAYMOND, N. (Session IV), Professor of Civil Engineering and Applied Mechanics and Director, Soil Mechanics Laboratory, McGill University, Montreal, Québec

STANDARD SYMBOLS AND UNITS, SELECTED METRIC CONVERSIONS

Throughout the contributed papers, standard symbols (where established) have been used. In some cases where confusion might be caused because of an admixture of scientific disciplines, symbols have been defined in the text. In the case of *soil mechanics* the standard adopted is *Technical Terms, Symbols and Definitions*. International Society of Soil Mechanics and Foundation Engineering, 1967.

To the extent possible, units are expressed in metric units with a preference toward the S. I. (Système Internationale), except for well-known expressions when conversion would be unfamiliar to the reader. Selected metric conversions that have been identified as such deviations are presented below.

Partial List of Conversions to S.I. Units

(From ASTM Metric Practice Guide. E 380-72)

<i>To convert from</i>	<i>to</i>	<i>Multiply by</i>
angstrom (Å)	metre (m)	1.00×10^{-10}
atmosphere (atm) (technical)	pascal (Pa)	1.00×10^5
bar	Pa	1.00×10^5
barrel (42 U.S. gal-oil)	m ³	1.59×10^{-1}
calorie (cal)	joule (J)	4.19
cal/cm ²	J/m ²	4.19×10^4
cal/cm ² /s	watt/metre ² (W/m ²)	4.19×10^4
cal/cm ² ·s·°C	watt/metre kelvin (W/m ² ·K)	4.19×10^2
cal/g	J/kg	4.19×10^3
cal/g·°C	J/kg·K	4.19×10^3
cal/s	W	4.19
foot (ft)	m	3.05×10^{-1}
galileo (gal)	m/s ²	1.00×10^{-2}
gauss (G)	tesla (T)	1.00×10^{-4}
g/cm ³	kg/m ³	1.00×10^3
hectare (ha)	km ²	1.00×10^{-2}
kgf	newton (N)	9.81
kgf/cm ²	pascal (Pa)	9.81×10^4
kilowatt-hour (kW·h)	J	3.60×10^6
litre	m ³	1.00×10^{-3}
litre	dm ³	1.00
mg/l	g/m ³	1.00
mho	siemens (S)	1.00
mile	km	1.61
newton/m ²	pascal (Pa)	1.00
tonne/m ³ (t/m ³)	kg/m ³	1.00×10^3